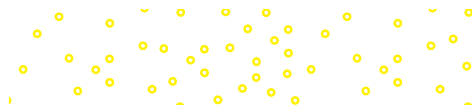SIXTH EDITION

Heat and Mass
Transfer | FUNDAMENTALS
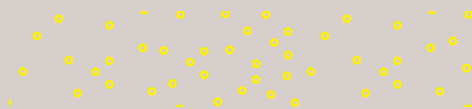## & APPLICATIONS

McGraw Hill Education

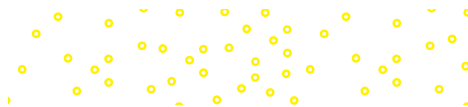**YUNUS A. ÇENGEL** | **AFSHIN J. GHAJAR**

HEAT AND MASS TRANSFER

FUNDAMENTALS & APPLICATIONS

Quotes on Ethics

Without ethics, everything happens as if we were all five billion passengers on a big machinery and nobody is driving the machinery. And it's going faster and faster, but we don't know where.
—Jacques Cousteau

Because you're able to do it and because you have the right to do it doesn't mean it's right to do it.
—Laura Schlessinger

A man without ethics is a wild beast loosed upon this world.
—Manly Hall

The concern for man and his destiny must always be the chief interest of all technical effort. Never forget it among your diagrams and equations.
—Albert Einstein

To educate a man in mind and not in morals is to educate a menace to society.
—Theodore Roosevelt

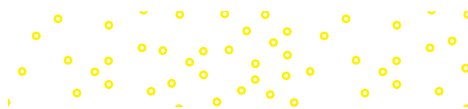*Politics which revolves around benefit is savagery.*
—Said Nursi

The true test of civilization is, not the census, nor the size of the cities, nor the crops, but the kind of man that the country turns out.
—Ralph W. Emerson

The measure of a man's character is what he would do if he knew he never would be found out.
—Thomas B. Macaulay

HEAT AND MASS TRANSFER

FUNDAMENTALS & APPLICATIONS

SIXTH EDITION

YUNUS A. ÇENGEL
University of Nevada, Reno

AFSHIN J. GHAJAR
Oklahoma State University, Stillwater

Mc
Graw
Hill
Education

HEAT AND MASS TRANSFER: FUNDAMENTALS AND APPLICATIONS, SIXTH EDITION

Library of Congress Cataloging-in-Publication Data

The Internet addresses listed in the text were accurate at the time of publication. The inclusion of a website does not indicate an endorsement by the authors or McGraw-Hill Education, and McGraw-Hill Education does not guarantee the accuracy of the information presented at these sites.

ABOUT THE AUTHORS

Yunus A. Çengel is Professor Emeritus of Mechanical Engineering at the University of Nevada, Reno. He received his B.S. in mechanical engineering from Istanbul Technical University and his M.S. and Ph.D. in mechanical engineering from North Carolina State University. His areas of interest are renewable energy, energy efficiency, energy policies, heat transfer enhancement, and engineering education. He served as the director of the Industrial Assessment Center (IAC) at the University of Nevada, Reno, from 1996 to 2000. He has led teams of engineering students to numerous manufacturing facilities in Northern Nevada and California to perform industrial assessments and has prepared energy conservation, waste minimization, and productivity enhancement reports for them. He has also served as an advisor for various government organizations and corporations.
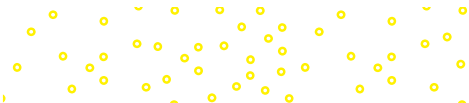
Dr. Çengel is also the author or coauthor of the widely adopted textbooks *Thermodynamics: An Engineering Approach* (9th ed., 2019), *Fluid Mechanics: Fundamentals and Applications* (4th ed., 2018), *Fundamentals of Thermal-Fluid Sciences* (5th ed., 2017), and *Differential Equations for Engineers and Scientists* (1st ed., 2013), all published by McGraw-Hill. Some of his textbooks have been translated into Chinese, Japanese, Korean, Thai, Spanish, Portuguese, Turkish, Italian, Greek, French and Basq.

Dr. Çengel is the recipient of several outstanding teacher awards, and he received the ASEE Meriam/Wiley Distinguished Author Award for excellence in authorship in 1992 and again in 2000. Dr. Çengel is a registered Professional Engineer in the State of Nevada, and he is a member of the American Society of Mechanical Engineers (ASME) and the American Society for Engineering Education (ASEE).

Afshin J. Ghajar is Regents Professor and John Brammer Professor in the School of Mechanical and Aerospace Engineering at Oklahoma State University, Stillwater, Oklahoma, and an Honorary Professor of Xi'an Jiaotong University, Xi'an, China. He received his B.S., M.S., and Ph.D. degrees, all in mechanical engineering, from Oklahoma State University. His expertise is in experimental heat transfer/fluid mechanics and the development of practical engineering correlations. Dr. Ghajar has made significant contributions to the field of thermal sciences through his experimental, empirical, and numerical works in heat transfer and stratification in sensible heat storage systems, heat transfer to non-Newtonian fluids, heat transfer in the transition region, and non-boiling heat transfer in two-phase flow. His current research is in two-phase flow heat transfer/pressure drop studies in pipes with different orientations, heat transfer/pressure drop in mini/micro tubes, and mixed convective heat transfer/pressure drop in the transition region (plain and enhanced tubes). Dr. Ghajar has been a Summer Research Fellow at Wright Patterson AFB (Dayton, Ohio) and Dow Chemical Company (Freeport, Texas). He and his co-workers have published over 200 reviewed research papers. He has delivered numerous keynote and invited lectures at major technical conferences and institutions.
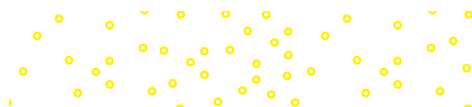
He has received several outstanding teaching, research, advising, and service awards from the College of Engineering at Oklahoma State University. His latest significant awards are the 75th Anniversary Medal of the ASME Heat Transfer Division "in recognition of his service to the heat transfer community and contributions to the field," awarded in 2013. He received the ASME ICNMM 2016 Outstanding Leadership Award, which recognizes a person whose service within the ICNMM (International Conference on Nanochannels, Microchannels, and Minichannels) is exemplary. He also received the 2017 Donald Q. Kern Award "in recognition of his outstanding leadership in the field of heat exchangers and two-phase flow, book and archival publications, and service to the academic and industrial professionals." Dr. Ghajar is a Fellow of the American Society of Mechanical Engineers (ASME), Heat Transfer Series Editor for CRC Press/Taylor & Francis, and Editor-in-Chief of *Heat Transfer Engineering,* an international journal aimed at practicing engineers and specialists in heat transfer published by Taylor and Francis.

BRIEF CONTENTS

CONTENTS

C H A P T E R   T H I R T E E N
RADIATION HEAT TRANSFER   799

C H A P T E R   F O U R T E E N
MASS TRANSFER   871

C H A P T E R   F I F T E E N
COOLING OF ELECTRONIC EQUIPMENT
(Online Chapter)

CHAPTER SIXTEEN

HEATING AND COOLING OF BUILDINGS (Online Chapter)

CHAPTER SEVENTEEN

REFRIGERATION AND FREEZING OF FOODS (Online Chapter)

APPENDIX 1

PROPERTY TABLES AND CHARTS (SI UNITS)   945

APPENDIX 2

PROPERTY TABLES AND CHARTS (ENGLISH UNITS)   973

PREFACE

BACKGROUND

Heat and mass transfer is a basic science that deals with the rate of transfer of thermal energy. It is an exciting and fascinating subject with unlimited practical applications ranging from biological systems to common household appliances, residential and commercial buildings, industrial processes, electronic devices, and food processing. Students are assumed to have an adequate background in calculus and physics. The completion of first courses in thermodynamics, fluid mechanics, and differential equations prior to taking heat transfer is desirable. However, relevant concepts from these topics are introduced and reviewed as needed.

OBJECTIVES

This book is intended for undergraduate engineering students in their sophomore or junior year and as a reference book for practicing engineers. The objectives of this text are

- To present the *basic principles* and *equations* of heat transfer.
- To show numerous and diverse real-world *engineering examples* to help students develop the intuition they need to correctly apply heat transfer principles in engineering.
- To develop an *intuitive understanding* of heat transfer by emphasizing the physics and physical arguments.

It is our hope that this book, through its careful explanations of concepts and its use of many practical examples and figures, helps students to develop the skills they need to bridge the gap between gaining knowledge and confidently applying that knowledge.

In engineering practice, an understanding of the mechanisms of heat transfer is becoming increasingly important since heat transfer plays a crucial role in the design of vehicles, power plants, refrigerators, electronic devices, buildings, and bridges, among other things. Even a chef needs an intuitive understanding of heat transfer in order to cook the food "right" by adjusting the rate of heat transfer. We may not be aware of it, but we already use the principles of heat transfer when we seek thermal comfort. We insulate our bodies by putting on heavy coats in winter, and we minimize heat gain by radiation by staying in shady places in summer. We speed up the cooling of hot food by blowing on it and keep warm in cold weather by cuddling up and thus minimizing our exposed surface area. That is, we already use heat transfer whether we realize it or not.

PHILOSOPHY AND GOAL

This text is the outcome of an attempt to have a textbook for a practically oriented heat transfer course for engineering students. The text covers the standard topics of heat transfer with an emphasis on physics and real-world

applications. This approach is more in line with students' intuition and makes learning the subject matter enjoyable.

The philosophy that contributed to the overwhelming popularity of the prior editions of this book has remained unchanged in this edition. Our goal has been to offer an engineering textbook that

- Communicates directly with tomorrow's engineers in a *simple yet precise* manner.
- Leads students toward a clear understanding and a firm grasp of the *basic principles* of heat transfer.
- Encourages *creative thinking* and development of a *deeper understanding* and *intuitive feel* for heat transfer.
- Is *read* by students with *interest* and *enthusiasm* rather than being used as a guide to solve problems.

Special effort has been made to appeal to students' natural curiosity and to help them explore the various facets of the exciting subject area of heat transfer. The enthusiastic response we received from the users of prior editions—from small colleges to large universities all over the world—indicates that our objectives have largely been achieved. It is our philosophy that the best way to learn is by practice. Therefore, special effort is made throughout the book to reinforce material that was presented earlier (in each chapter as well as in material from previous chapters). Many of the illustrated example problems and end-of-chapter problems are comprehensive and encourage students to review and revisit concepts and intuitions gained previously.

Yesterday's engineer spent a major portion of his or her time substituting values into formulas and obtaining numerical results. However, now formula manipulations and number crunching are being left mainly to the computers. Tomorrow's engineer will have to have a clear understanding and a firm grasp of the *basic principles* so that he or she can understand even the most complex problems, formulate them, and interpret the results. A conscious effort is made to emphasize these basic principles while also enabling students to see how computational tools are used in engineering practice.

NEW TO THE SIXTH EDITION

One of the primary changes in the sixth edition of this text is the effective use of full color to enhance the learning experience of students and to make it more enjoyable. Another significant change is the inclusion of a new section in Chap. 1 on Engineering Codes and Standards (C&S). A knowledge of heat and mass transfer, along with adherence to the relevant codes and standards, allow engineers to analyze, design, and build components and systems to function within the design conditions. Throughout the text, as appropriate, example problems and end-of-chapter problems related to engineering codes and standards have been presented to introduce this concept to tomorrow's engineers. The third important change has been in Chap. 4 where the graphical representation of the one-dimensional transient conduction solutions (Heisler charts) have been eliminated, and the emphasis has been placed on the solution with more accurate approximate or exact analytical expressions. Other important changes have been the addition of five new sections or subsections: "Aerogel—A Remarkable Superinsulating Material," "Equation Solvers," and

"Accuracy, Precision and Significant Digits" to Chap. 1, "General Solutions for Simultaneously Moving Plates and Fluids" to Chap. 7, and "Analogies Between Momentum and Heat Transfer in the Transition Region" to Chap. 8.

We have also incorporated 20 new solved example problems in the text, modified over 450 of the existing end-of-chapter problems, and added over 150 new end-of-chapter problems. A significant number of the new problems are on the concept of Engineering Codes and Standards (C&S). All the popular features of the previous editions have been retained, while new ones have been added. Updates and changes for clarity and readability have been made throughout the text.

ENGINEERING CODES AND STANDARDS (C&S) PROBLEMS

A recent study done by ASME Vision 2030 Project reveals that almost 50 percent of engineers in their early careers are unfamiliar with engineering codes and standards. As companies and manufacturers are expanding operations globally, there is a greater interest in harmonizing codes and standards across jurisdictions and disciplines. The need for engineers to have the knowledge about codes and standards is growing, and having this knowledge allows engineers to innovate and manufacture competitive products. In the subject of heat and mass transfer, there are several engineering codes and standards that are relevant. These codes and standards have been issued and published by professional associations, such as the ASME and the ASHRAE, and standards organizations, such as ASTM International, ANSI, and the ISO. The Engineering Codes and Standards (C&S) concept is first introduced in Chap. 1. The engineering C&S concept complements the Prevention through Design (PtD) concept that was introduced in the fifth edition of this book to emphasize safety in designs. The example problems and end-of-chapter problems in each chapter not only offer perspectives on interesting real-world applications but also introduce the concepts of engineering C&S to tomorrow's engineers so they may influence a change in the culture toward a greater emphasis on codes and standards. The knowledge of heat and mass transfer, along with adherence to the relevant codes and standards, allow engineers to analyze, design, and build components and systems to function within their design conditions.

CONTENT CHANGES AND REORGANIZATION

With the exception of the changes already mentioned, several updates and changes for clarity and readability have been made in the text. In this edition, we have introduced 20 new example problems and over 600 new and modified end-of-chapter problems. The noteworthy changes are summarized here for those who are familiar with the previous edition.

- In Chap. 1, four new sections or subsections have been added: "Aerogel—A Remarkable Superinsulating Material" by Dr. Ann M. Anderson of Union College, "Engineering Codes and Standards (C&S)" by Dr. Clement C. Tang of the University of North Dakota, "Equation Solver," and "Accuracy, Precision and Significant Digits." Also, the Topic of Special Interest on "Thermal Comfort" has been expanded.

- In Chap. 3, the section on "Bioheat Transfer Equation" has been expanded.

- In Chap. 4, the graphical representation of the one-dimensional transient conduction solutions (Heisler charts) have been eliminated, and the emphasis has been placed on the solution with more accurate approximate or exact analytical expressions. Based on the input we have received from instructors, very few students use the graphical representations of the one-dimensional, transient conduction solutions (Heisler charts); most prefer to solve the approximate or exact analytical expressions. In addition, all the example problems using the graphical solution have been updated.

- In Chap. 7, a new subsection on "General Solutions for Simultaneously Moving Plates and Fluids" has been added. In addition, new equations for the flat plate average Nusselt number with unheated starting length for laminar and turbulent flows have been added. We have also updated Table 7-1 with several additional correlations for noncircular geometries.

- In Chap. 8, a new subsection on "Analogies Between Momentum and Heat Transfer in the Transition Region" has been added. Also, we have updated/expanded internal forced convection heat transfer correlations in laminar, transitional, and turbulent flows.

- In Chap. 10, the coverage of the Topic of Special Interest on "Non-Boiling Two-Phase Flow Heat Transfer" has been expanded.

- In Chap. 11, the coverage of the Topic of Special Interest on "The Human Cardiovascular System as a Countercurrent Heat Exchanger" has been expanded.

- In Chap. 13, the section on view factors was updated. We have also updated and added a few view factor relations.

LEARNING TOOLS

EMPHASIS ON PHYSICS

A distinctive feature of this book is its emphasis on the physical aspects of the subject matter in addition to mathematical representations and manipulations. The authors believe that the emphasis in undergraduate education should remain on *developing a sense of underlying physical mechanisms* and a *mastery of solving practical problems* that an engineer is likely to face in the real world. Developing an intuitive understanding should also make the course a more motivating and worthwhile experience for the students.

EFFECTIVE USE OF ASSOCIATION

An observant mind should have no difficulty understanding engineering sciences. After all, the principles of engineering sciences are based on our *everyday experiences and experimental observations.* Therefore, a physical, intuitive approach is used throughout this text. Frequently, *parallels are drawn* between the subject matter and students' everyday experiences so that they can relate the subject matter to what they already know. The process of cooking, for example, serves as an excellent vehicle to demonstrate the basic principles of heat transfer.

SELF-INSTRUCTING

The material in the text is introduced at a level that an average student can follow comfortably. It speaks *to* students, not *over* students. In fact, it is *self-instructive.* The order of coverage is from *simple* to *general.* That is, it starts with the simplest case and adds complexities gradually. In this way, the basic principles are repeatedly applied to different systems, and students master how to apply the principles instead of how to simplify a general formula. Noting that principles of science are based on experimental observations, all the derivations in this text are based on physical arguments, and thus they are easy to follow and understand.

EXTENSIVE USE OF ARTWORK

Figures are important learning tools that help the students "get the picture," and the text makes effective use of graphics. It contains more figures and illustrations than any other book in this category. This sixth edition of *Heat and Mass Transfer: Fundamentals & Applications,* features an enhanced art program done in four colors to provide more realism and pedagogical understanding. Further, a large number of figures have been upgraded to become three-dimensional and thus more real-life. Figures attract attention and stimulate curiosity and interest. Most of the figures in this text are intended to serve as a means of emphasizing some key concepts that would otherwise go unnoticed; some serve as summaries.

LEARNING OBJECTIVES AND SUMMARIES

Each chapter begins with an *Overview* of the material to be covered and chapter-specific *Learning Objectives.* A *Summary* is included at the end of each chapter, providing a quick review of basic concepts and important relations, and pointing out the relevance of the material.

NUMEROUS WORKED-OUT EXAMPLES WITH A SYSTEMATIC SOLUTIONS PROCEDURE

Each chapter contains several worked-out *examples* that both clarify the material and illustrate the use of the basic principles in a context that helps develop student's intuition. An *intuitive* and *systematic* approach is used in the solution of all example problems. The solution methodology starts with a statement of the problem, and all objectives are identified. The assumptions and approximations are then stated together with their justifications. Any properties needed to solve the problem are listed separately. Numerical values are used together with their units to emphasize that numbers without units are meaningless, and that unit manipulations are as important as manipulating the numerical values with a calculator. The significance of each example's result is discussed following the solution. This methodical approach is also followed and provided in the solutions to the end-of-chapter problems, available to the instructors.

A WEALTH OF REALISTIC END-OF-CHAPTER PROBLEMS

The end-of-chapter problems are grouped under specific topics to make problem selection easier for both instructors and students. Within each group of problems are:

- *Concept Questions,* indicated by "C," to check the students' level of understanding of basic concepts.

- *Prevention through Design Problems,* designated by the icon PtD. These problems introduce the concepts of PtD to the minds of tomorrow's engineers whereby they may influence a change in culture toward more emphasis on safe designs.

- *Engineering Codes and Standards Problems,* designated by the icon C&S. These problems introduce the concepts of C&S to engineering students. The knowledge of heat and mass transfer, along with adherence to the relevant engineering codes and standards, allow tomorrow's engineers to analyze, design, and build components and systems to function within the design conditions.

- *Computer-Oriented Problems,* designated by the icon. These problems are comprehensive in nature and are intended to be solved with a computer, using appropriate software.

- *Review Problems* are more comprehensive in nature and are not directly tied to any specific section of a chapter—in some cases they require review of material learned in previous chapters. These problems are placed under the heading "Review Problems."

- *Fundamentals of Engineering (FE) Exam Problems* are designed to help students prepare for the *Fundamentals of Engineering* exam, as they prepare for their Professional Engineering license. These are *multiple-choice problems,* and they are intended to check the readers' understanding of fundamentals and to help them avoid common pitfalls. These problems are placed under the heading "Fundamentals of Engineering (FE) Exam Problems."

- *Design and Essay Problems* are intended to encourage students to make engineering judgments, to conduct independent exploration of topics of interest, and to communicate their findings in a professional manner. These problems are placed under the heading "Design and Essay Problems."

- *Problems Designated by an "E"* are in English units, and SI users can ignore them.

Several economics- and safety-related problems are incorporated throughout to enhance cost and safety awareness among engineering students. Answers to selected problems are listed immediately following the problem for convenience to students.

USE OF COMMON NOTATION

The use of different notation for the same quantities in different engineering courses has long been a source of discontent and confusion. A student taking both heat transfer and fluid mechanics, for example, has to use notation Q for heat transfer in one course and for volume flow rate in the other. In this text, we have made a conscious effort to minimize this conflict by adopting the familiar thermodynamic notation $\dot{V}$ for volume flow rate, thus reserving the notation Q for heat transfer. This type of effort has been made in all the other engineering texts by lead author Yunus Çengel. We think that both students and instructors will appreciate this effort to promote a common notation.

A CHOICE OF SI ALONE OR SI/ENGLISH UNITS

In recognition of the fact that English units are still widely used in some industries, both SI and English units are used in this text, with an emphasis on SI. The material in this text can be covered using combined SI/English units or SI units alone, depending on the preference of the instructor. The property tables and charts in the appendices are presented in both units, except the ones that involve dimensionless quantities. Problems, tables, and charts in English units are designated by "**E**" after the number for easy recognition, and they can be ignored by SI users.

TOPICS OF SPECIAL INTEREST

Most chapters contain a real-world application, end-of-chapter optional section called "Topic of Special Interest" where interesting applications of heat transfer are discussed. Examples include *Thermal Comfort* in Chap. 1, *Heat Transfer Through Walls and Roofs* in Chap. 3, *Microscale Heat Transfer* in Chap. 6, *Transitional Flow in Tubes* in Chap. 8, *Heat Transfer Through Windows* in Chap. 9, *Non-Boiling Two-Phase Flow Heat Transfer* in Chap. 10, *Human Cardiovascular System as a Countercurrent Heat Exchanger* in Chap. 11, and *Heat Transfer from the Human Body* in Chap. 13. The topics selected for these sections provide intriguing extensions to heat transfer, but they can be ignored without a loss in continuity.

IMPORTANT HEAT TRANSFER TERMS

Through the chapters, when an important key term or concept is introduced and defined, it appears in **red** boldface type.

CONVERSION FACTORS

Frequently used conversion factors and physical constants are listed at the very end of the book for easy reference.

NOMENCLATURE

A list of the major symbols, subscripts, and superscripts are also listed at the very end of the book for easy reference.

SUPPLEMENTS

The following supplements are available to the users of the book.

TEXT WEBSITE

Visit the website for several instructor resources including Lecture PowerPoints, the text's images in PowerPoint form, Solution's Manual, and helpful web links for students.

THREE ONLINE APPLICATION CHAPTERS

The application chapters "Cooling of Electronic Equipment" (Chap. 15), "Heating and Cooling of Buildings" (Chap. 16), and "Refrigeration and Freezing of Foods" (Chap. 17) are available via the text website.

Affordability & Outcomes = Academic Freedom!

You deserve choice, flexibility and control. You know what's best for your students and selecting the course materials that will help them succeed should be in your hands.

Thats why providing you with a wide range of options that lower costs and drive better outcomes is our highest priority.

connect®

Students—study more efficiently, retain more and achieve better outcomes. Instructors—focus on what you love—teaching.
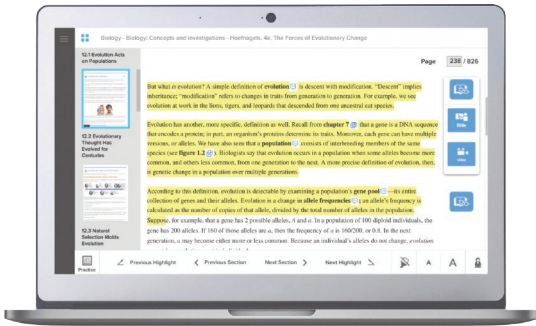
They'll thank you for it.

Study resources in Connect help your students be better prepared in less time. You can transform your class time from dull definitions to dynamic discussion. Hear from your peers about the benefits of Connect at **www.mheducation.com/highered/connect**

Study anytime, anywhere.

Download the free ReadAnywhere app and access your online eBook when it's convenient, even if you're offline. And since the app automatically syncs with your eBook in Connect, all of your notes are available every time you open it. Find out more at **www.mheducation.com/readanywhere**

Learning for everyone.

McGraw-Hill works directly with Accessibility Services Departments and faculty to meet the learning needs of all students. Please contact your Accessibility Services office and ask them to email accessibility@mheducation.com, or visit **www.mheducation.com/about/accessibility.html** for more information.

A full array of affordable & effective solutions

- Digital Courseware
- Digital Print Bundles
- Inclusive Access
- Print/eBook Rentals
- Discount Print Purchase
- Mobile Apps
- OER

Learn more at: www.mheducation.com/realvalue

Rent It

Affordable print and digital rental options through our partnerships with leading textbook distributors including Amazon, Barnes & Noble, Chegg, Follett, and more.

Go Digital

A full and flexible range of affordable digital solutions ranging from Connect, ALEKS, inclusive access, mobile apps, OER and more.

Get Print

Students who purchase digital materials can get a loose-leaf print version at a significantly reduced rate to meet their individual preferences and budget.

HEAT AND MASS TRANSFER

FUNDAMENTALS & APPLICATIONS

INTRODUCTION AND BASIC CONCEPTS

The science of thermodynamics deals with the *amount* of heat transfer as a system undergoes a process from one equilibrium state to another, and it makes no reference to *how long* the process will take. But in engineering, we are often interested in the *rate* of heat transfer, which is the topic of the science of *heat transfer*.

We start this chapter with a review of the fundamental concepts of thermodynamics that form the framework for heat transfer. We first present the relation of heat to other forms of energy and review the energy balance. We then present the three basic mechanisms of heat transfer, which are conduction, convection, and radiation, and we discuss thermal conductivity. *Conduction* is the transfer of energy from the more energetic particles of a substance to the adjacent, less energetic ones as a result of interactions between the particles. *Convection* is the mode of heat transfer between a solid surface and the adjacent liquid or gas that is in motion, and it involves the combined effects of conduction and fluid motion. *Radiation* is the energy emitted by matter in the form of electromagnetic waves (or photons) as a result of the changes in the electronic configurations of the atoms or molecules. We close this chapter with a discussion of simultaneous heat transfer.

OBJECTIVES

When you finish studying this chapter, you should be able to:

- Understand how thermodynamics and heat transfer are related to each other,
- Distinguish thermal energy from other forms of energy and heat transfer from other forms of energy transfer,
- Perform general energy balances as well as surface energy balances,
- Understand the basic mechanisms of heat transfer, which are conduction, convection, and radiation, and Fourier's law of heat conduction, Newton's law of cooling, and the Stefan–Boltzmann law of radiation,
- Identify the mechanisms of heat transfer that occur simultaneously in practice,
- Develop an awareness of the cost associated with heat losses, and
- Solve various heat transfer problems encountered in practice.

1–1 ▪ THERMODYNAMICS AND HEAT TRANSFER

We all know from experience that a cold canned drink left in a room warms up and a warm canned drink left in a refrigerator cools down. This is accomplished by the transfer of *energy* from the warm medium to the cold one. The energy transfer is always from the higher temperature medium to the lower temperature one, and the energy transfer stops when the two media reach the same temperature.

You will recall from thermodynamics that energy exists in various forms. In this text we are primarily interested in **heat**, which is *the form of energy that can be transferred from one system to another as a result of temperature difference.* The science that deals with the determination of the *rates* of such energy transfers is **heat transfer**.

You may be wondering why we need to undertake a detailed study on heat transfer. After all, we can determine the amount of heat transfer for any system undergoing any process using a thermodynamic analysis alone. The reason is that thermodynamics is concerned with the *amount* of heat transfer as a system undergoes a process from one equilibrium state to another, and it gives no indication about *how long* the process will take. A thermodynamic analysis simply tells us how much heat must be transferred to realize a specified change of state to satisfy the conservation of energy principle.

FIGURE 1–1
We are normally interested in how long it takes for the hot coffee in a thermos bottle to cool to a certain temperature, which cannot be determined from a thermodynamic analysis alone.

In practice we are more concerned about the rate of heat transfer (heat transfer per unit time) than we are with the amount of it. For example, we can determine the amount of heat transferred from a thermos bottle as the hot coffee inside cools from 90°C to 80°C by a thermodynamic analysis alone. But a typical user or designer of a thermos bottle is primarily interested in *how long* it will be before the hot coffee inside cools to 80°C, and a thermodynamic analysis cannot answer this question. Determining the rates of heat transfer to or from a system and thus the times of heating or cooling, as well as the variation of the temperature, is the subject of heat transfer (Fig. 1–1).

Thermodynamics deals with equilibrium states and changes from one equilibrium state to another. Heat transfer, on the other hand, deals with systems that lack thermal equilibrium, and thus it is a *nonequilibrium* phenomenon. Therefore, the study of heat transfer cannot be based on the principles of thermodynamics alone. However, the laws of thermodynamics lay the framework for the science of heat transfer. The *first law* requires that the rate of energy transfer into a system be equal to the rate of increase of the energy of that system. The *second law* requires that heat be transferred in the direction of decreasing temperature (Fig. 1–2). This is like saying that a car parked on an inclined road must go downhill in the direction of decreasing elevation when its brakes are released. It is also analogous to the electric current flowing in the direction of decreasing voltage or the fluid flowing in the direction of decreasing total pressure.

FIGURE 1–2
Heat flows in the direction of decreasing temperature.

The basic requirement for heat transfer is the presence of a *temperature difference.* There can be no net heat transfer between two bodies that are at the same temperature. The temperature difference is the *driving force* for heat transfer, just as the *voltage difference* is the driving force for electric current flow and *pressure difference* is the driving force for fluid flow. The rate of heat transfer in a certain direction depends on the magnitude of the *temperature gradient* (the temperature difference per unit length or the rate of change of temperature) in that direction. The larger the temperature gradient, the higher the rate of heat transfer.

Application Areas of Heat Transfer

Heat transfer is commonly encountered in engineering systems and other aspects of life, and one does not need to go very far to see some application areas of heat transfer. In fact, one does not need to go anywhere. The human body is constantly rejecting heat to its surroundings, and human comfort is closely tied to the rate of this heat rejection. We try to control this heat transfer rate by adjusting our clothing to the environmental conditions.

Many ordinary household appliances are designed, in whole or in part, by using the principles of heat transfer. Some examples include the electric or gas range, the heating and air-conditioning system, the refrigerator and freezer, the water heater, the iron, and even the computer, the TV, and the DVD player. Of course, energy-efficient homes are designed on the basis of minimizing heat loss in winter and heat gain in summer. Heat transfer plays a major role in the design of many other devices, such as car radiators, solar collectors, various components of power plants, and even spacecraft (Fig. 1–3). The optimal insulation thickness in the walls and roofs of houses, on hot water or steam pipes, or on water heaters is again determined on the basis of a heat transfer analysis with economic considerations.

Historical Background

Heat has always been perceived to be something that produces in us a sensation of warmth, and one would think that the nature of heat was one of the first things understood by humankind. But it was only in the middle of the

The human body
©Andrew Olney/age fotostock
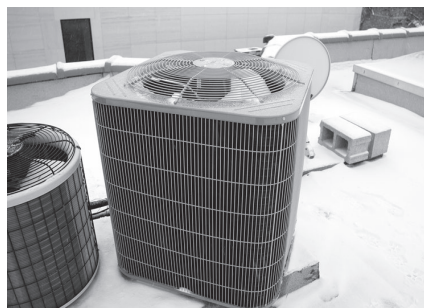
Air-conditioning systems
©McGraw-Hill Education/Jill Braaten, photographer

Heating systems
©Comstock Images/ Getty Images
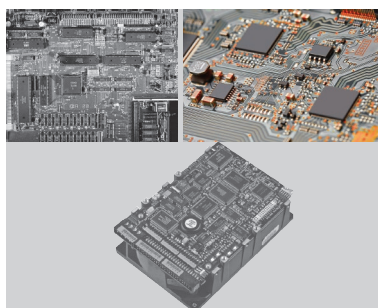
Electronic equipment
©Eric Tormey/Alamy
©Raimundas/Shutterstock
©Brand X Pictures/Jupiter Images

Power plants
©Malcom Fife/age fotostock

Refrigeration systems
©McGraw-Hill Education/ Jill Braaten, photographer

FIGURE 1–3
Some application areas of heat transfer.
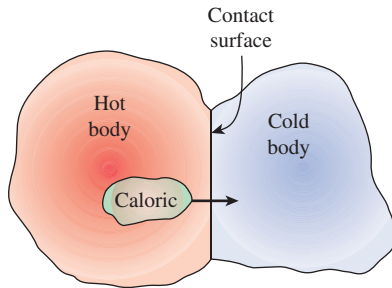
FIGURE 1–4
In the early 19th century, heat was thought to be an invisible fluid called *caloric* that flowed from warmer bodies to cooler ones.

19th century that we had a true physical understanding of the nature of heat, thanks to the development at that time of the **kinetic theory**, which treats molecules as tiny balls that are in motion and thus possess kinetic energy. Heat is then defined as the energy associated with the random motion of atoms and molecules. Although it was suggested in the 18th and early 19th centuries that heat is the manifestation of motion at the molecular level (called the *live force*), the prevailing view of heat until the middle of the 19th century was based on the **caloric theory** proposed by the French chemist Antoine Lavoisier (1743–1794) in 1789. The caloric theory asserts that heat is a fluid-like substance called **caloric** that is a massless, colorless, odorless, and tasteless substance that can be poured from one body into another (Fig. 1–4). When caloric was added to a body, its temperature increased; and when caloric was removed from a body, its temperature decreased. When a body could not contain any more caloric, much the same way as when a glass of water could not dissolve any more salt or sugar, the body was said to be saturated with caloric. This interpretation gave rise to the terms *saturated liquid* and *saturated vapor* that are still in use today.

The caloric theory came under attack soon after its introduction. It maintained that heat was a substance that could not be created or destroyed. Yet it was known that heat could be generated indefinitely by rubbing one's hands together or rubbing two pieces of wood together. In 1798, the American Benjamin Thompson (Count Rumford) (1753–1814) showed in his papers that heat can be generated continuously through friction. The validity of the caloric theory was also challenged by several others. But it was the careful experiments of the Englishman James P. Joule (Fig. 1–5) published in 1843 that finally convinced the skeptics that heat was not a substance after all, thus putting the caloric theory to rest. Although the caloric theory was totally abandoned in the middle of the 19th century, it contributed greatly to the development of thermodynamics and heat transfer.

1–2 ■ ENGINEERING HEAT TRANSFER

Heat transfer equipment such as heat exchangers, boilers, condensers, radiators, heaters, furnaces, refrigerators, and solar collectors are designed primarily on the basis of heat transfer analysis. The heat transfer problems encountered in practice can be considered in two groups: (1) *rating* and (2) *sizing* problems. The rating problems deal with the determination of the heat transfer rate for an existing system at a specified temperature difference. The sizing problems deal with the determination of the size of a system in order to transfer heat at a specified rate for a specified temperature difference.

An engineering device or process can be studied either *experimentally* (testing and taking measurements) or *analytically* (by analysis or calculations). The experimental approach has the advantage that we deal with the actual physical system, and the desired quantity is determined by measurement, within the limits of experimental error. However, this approach is expensive, time-consuming, and often impractical. Besides, the system we are analyzing may not even exist. For example, the heating and plumbing systems of a building must usually be sized *before* the building is actually built on the basis of the specifications given. The analytical approach (including the numerical approach) has the advantage that it is fast and inexpensive, but the results

obtained are subject to the accuracy of the assumptions, approximations, and idealizations made in the analysis. In engineering studies, often a good compromise is reached by reducing the choices to just a few by analysis, and then verifying the findings experimentally.

Modeling in Engineering

The descriptions of most scientific problems involve equations that relate the changes in some key variables to each other. Usually the smaller the increment chosen in the changing variables, the more general and accurate the description. In the limiting case of infinitesimal or differential changes in variables, we obtain differential equations that provide precise mathematical formulations for the physical principles and laws by representing the rates of change as derivatives. Therefore, differential equations are used to investigate a wide variety of problems in sciences and engineering (Fig. 1–6). However, many problems encountered in practice can be solved without resorting to differential equations and the complications associated with them.

The study of physical phenomena involves two important steps. In the first step, all the variables that affect the phenomena are identified, reasonable assumptions and approximations are made, and the interdependence of these variables is studied. The relevant physical laws and principles are invoked, and the problem is formulated mathematically. The equation itself is very instructive because it shows the degree of dependence of some variables on others and the relative importance of various terms. In the second step, the problem is solved using an appropriate approach, and the results are interpreted.

Many processes that seem to occur in nature randomly and without any order are, in fact, being governed by some visible or not-so-visible physical laws. Whether we notice them or not, these laws are there, governing consistently and predictably what seem to be ordinary events. Most of these laws are well defined and well understood by scientists. This makes it possible to predict the course of an event before it actually occurs, or to study various aspects of an event mathematically without actually running expensive and time-consuming experiments. This is where the power of analysis lies. Very accurate results to meaningful practical problems can be obtained with relatively little effort by using a suitable and realistic mathematical model. The preparation of such models requires an adequate knowledge of the natural phenomena involved and the relevant laws, as well as sound judgment. An unrealistic model will obviously give inaccurate and thus unacceptable results.

An analyst working on an engineering problem often finds himself or herself in a position to make a choice between a very accurate but complex model and a simple but not-so-accurate model. The right choice depends on the situation at hand. The right choice is usually the simplest model that yields adequate results. For example, the process of baking potatoes or roasting a round chunk of beef in an oven can be studied analytically in a simple way by modeling the potato or the roast as a spherical solid ball that has the properties of water (Fig. 1–7). The model is quite simple, but the results obtained are sufficiently accurate for most practical purposes. As another example, when we analyze the heat losses from a building in order to select the right size for a heater, we determine the heat losses under anticipated worst conditions and select a
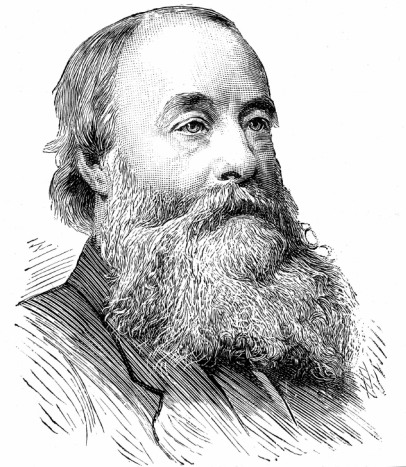
FIGURE 1–5
James Prescott Joule (1818–1889) was a British physicist born in Salford, Lancashire, England. Joule is best known for his work on the conversion of electrical and mechanical energy into heat and the first law of thermodynamics. The energy unit joule (J) is named after him. The Joule's law of electric heating that he formulated states that the rate of heat production in a conducting wire is proportional to the product of the resistance of the wire and the square of the electric current. Through his experiments, Joule demonstrated the mechanical equivalence of heat—the conversion of mechanical energy into an equivalent amount of thermal energy—which laid the foundation for the conservation of energy principle. Joule, together with William Thomson (later Lord Kelvin), discovered the temperature drop of a substance during free expansion, a phenomenon known as the Joule-Thomson effect, which provides the basis of operation for modern-day vapor-compression refrigeration and air-conditioning systems.
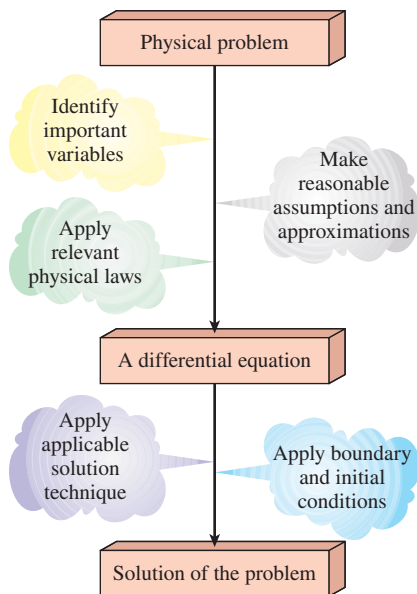
FIGURE 1–6
Mathematical modeling of physical problems.
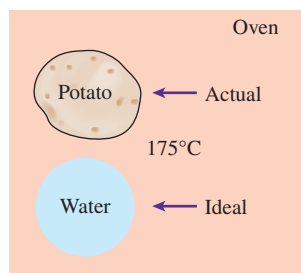
FIGURE 1–7
Modeling is a powerful engineering tool that provides great insight and simplicity at the expense of some accuracy.

furnace that will provide sufficient energy to make up for those losses. Often we tend to choose a larger furnace in anticipation of some future expansion or just to provide a factor of safety. A very simple analysis is adequate in this case.

When selecting heat transfer equipment, it is important to consider the actual operating conditions. For example, when purchasing a heat exchanger that will handle hard water, we must consider that some calcium deposits will form on the heat transfer surfaces over time, causing fouling and thus a gradual decline in performance. The heat exchanger must be selected on the basis of operation under these adverse conditions instead of under new conditions.

Preparing very accurate but complex models is usually not so difficult. But such models are not much use to an analyst if they are very difficult and time-consuming to solve. At the minimum, the model should reflect the essential features of the physical problem it represents. There are many significant real-world problems that can be analyzed with a simple model. But it should always be kept in mind that the results obtained from an analysis are as accurate as the assumptions made in simplifying the problem. Therefore, the solution obtained should not be applied to situations for which the original assumptions do not hold.

A solution that is not quite consistent with the observed nature of the problem indicates that the mathematical model used is too crude. In that case, a more realistic model should be prepared by eliminating one or more of the questionable assumptions. This will result in a more complex problem that, of course, is more difficult to solve. Thus any solution to a problem should be interpreted within the context of its formulation.

1–3 ▪ HEAT AND OTHER FORMS OF ENERGY

Energy can exist in numerous forms such as thermal, mechanical, kinetic, potential, electrical, magnetic, chemical, and nuclear, and their sum constitutes the **total energy** E (or e on a unit mass basis) of a system. The forms of energy related to the molecular structure of a system and the degree of the molecular activity are referred to as the *microscopic energy*. The sum of all microscopic forms of energy is called the **internal energy** of a system and is denoted by U (or u on a unit mass basis).

The international unit of energy is *joule* (J) or *kilojoule* (1 kJ = 1000 J). In the English system, the unit of energy is the *British thermal unit* (Btu), which is defined as the energy needed to raise the temperature of 1 lbm of water at 60°F by 1°F. The magnitudes of kJ and Btu are almost identical (1 Btu = 1.055056 kJ). Another well-known unit of energy is the *calorie* (1 cal = 4.1868 J), which is defined as the energy needed to raise the temperature of 1 gram of water at 14.5°C by 1°C.

Internal energy may be viewed as the sum of the kinetic and potential energies of the molecules. The portion of the internal energy of a system associated with the kinetic energy of the molecules is called **sensible energy** or **sensible heat**. The average velocity and the degree of activity of the molecules are proportional to the temperature. Thus, at higher temperatures the molecules possess higher kinetic energy, and as a result, the system has a higher internal energy.

The internal energy is also associated with the intermolecular forces between the molecules of a system. These are the forces that bind the molecules to

each other, and, as one would expect, they are strongest in solids and weakest in gases. If sufficient energy is added to the molecules of a solid or liquid, they will overcome these molecular forces and simply break away, turning the system to a gas. This is a *phase change* process, and because of this added energy, a system in the gas phase is at a higher internal energy level than it is in the solid or the liquid phase. The internal energy associated with the phase of a system is called **latent energy** or **latent heat**.

The changes mentioned above can occur without a change in the chemical composition of a system. Most heat transfer problems fall into this category, and one does not need to pay any attention to the forces binding the atoms in a molecule together. The internal energy associated with the atomic bonds in a molecule is called **chemical** (or **bond**) **energy**, whereas the internal energy associated with the bonds within the nucleus of the atom itself is called **nuclear energy**. The chemical and nuclear energies are absorbed or released during chemical or nuclear reactions, respectively.

In the analysis of systems that involve fluid flow, we often encounter the combination of properties u and Pv. For the sake of simplicity and convenience, this combination is defined as **enthalpy** h. That is, $h = u + Pv$ where the term Pv represents the *flow energy* of the fluid (also called the *flow work*), which is the energy needed to push a fluid and to maintain flow. In the energy analysis of flowing fluids, it is convenient to treat the flow energy as part of the energy of the fluid and to represent the microscopic energy of a fluid stream by enthalpy h (Fig. 1–8).
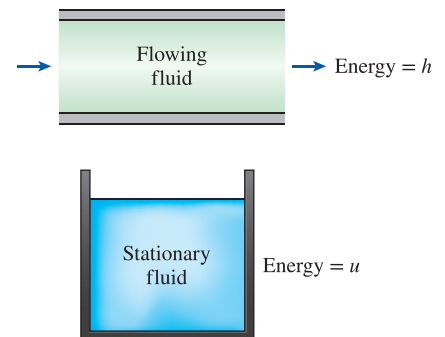
FIGURE 1–8
The *internal energy u* represents the microscopic energy of a nonflowing fluid, whereas *enthalpy h* represents the microscopic energy of a flowing fluid.

Specific Heats of Gases, Liquids, and Solids

You may recall that an **ideal gas** is defined as a gas that obeys the relation

$$Pv = RT \ \text{ or } \ P = \rho RT \tag{1–1}$$

where P is the absolute pressure, v is the specific volume, T is the thermodynamic (or absolute) temperature, ρ is the density, and R is the gas constant. It has been experimentally observed that the ideal gas relation given above closely approximates the P-v-T behavior of real gases at low densities. At low pressures and high temperatures, the density of a gas decreases, and the gas behaves like an ideal gas. In the range of practical interest, many familiar gases such as air, nitrogen, oxygen, hydrogen, helium, argon, neon, and carbon dioxide and even heavier gases such as krypton can be treated as ideal gases with negligible error (often less than 1 percent). Dense gases such as water vapor in steam power plants and refrigerant vapor in refrigerators, however, should not always be treated as ideal gases since they usually exist at a state near saturation.

You may also recall that **specific heat** is defined as *the energy required to raise the temperature of a unit mass of a substance by one degree* (Fig. 1–9). In general, this energy depends on how the process is executed. We are usually interested in two kinds of specific heats: specific heat at constant volume c_v and specific heat at constant pressure c_p. The **specific heat at constant volume** c_v can be viewed as the energy required to raise the temperature of a unit mass of a substance by one degree as the volume is held constant. The energy required to do the same as the pressure is held constant is the
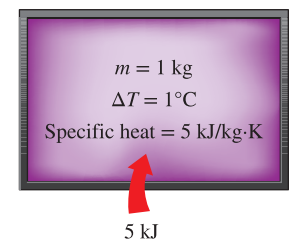
FIGURE 1–9
Specific heat is the energy required to raise the temperature of a unit mass of a substance by one degree in a specified way.

specific heat at constant pressure c_p. The specific heat at constant pressure c_p is greater than c_v because at constant pressure the system is allowed to expand, and the energy for this expansion work must also be supplied to the system. For ideal gases, these two specific heats are related to each other by $c_p = c_v + R$.

A common unit for specific heats is kJ/kg·°C or kJ/kg·K. Notice that these two units are *identical* since $\Delta T(°C) = \Delta T(K)$, and a 1°C change in temperature is equivalent to a change of 1 K. Also,

$$1 \text{ kJ/kg·°C} \equiv 1 \text{ J/g·°C} \equiv 1 \text{ kJ/kg·K} \equiv 1 \text{ J/g·K}$$

FIGURE 1–10
The specific heat of a substance changes with temperature.

The specific heats of a substance, in general, depend on two independent properties such as temperature and pressure. For an *ideal gas,* however, they depend on *temperature* only (Fig. 1–10). At low pressures all real gases approach ideal gas behavior, and therefore their specific heats depend on temperature only.

The differential changes in the internal energy u and enthalpy h of an ideal gas can be expressed in terms of the specific heats as

$$du = c_v \, dT \text{ and } dh = c_p \, dT \tag{1–2}$$

The finite changes in the internal energy and enthalpy of an ideal gas during a process can be expressed approximately by using specific heat values at the average temperature as

$$\Delta u = c_{v,\text{ avg}} \Delta T \quad \text{and} \quad \Delta h = c_{p,\text{ avg}} \Delta T \quad \text{(J/g)} \tag{1–3}$$

or

$$\Delta U = m c_{v,\text{ avg}} \Delta T \quad \text{and} \quad \Delta H = m c_{p,\text{ avg}} \Delta T \quad \text{(J)} \tag{1–4}$$

FIGURE 1–11
The c_v and c_p values of incompressible substances are identical and are denoted by c.

where m is the mass of the system.

A substance whose specific volume (or density) does not change with temperature or pressure is called an **incompressible substance**. The specific volumes of solids and liquids essentially remain constant during a process, and thus they can be approximated as incompressible substances without sacrificing much in accuracy.

The constant-volume and constant-pressure specific heats are identical for incompressible substances (Fig. 1–11). Therefore, for solids and liquids the subscripts on c_v and c_p can be dropped and both specific heats can be represented by a single symbol, c. That is, $c_p \cong c_v \cong c$. This result could also be deduced from the physical definitions of constant-volume and constant-pressure specific heats. Specific heats of several common gases, liquids, and solids are given in the Appendix.

The specific heats of incompressible substances depend on temperature only. Therefore, the change in the internal energy of solids and liquids can be expressed as

$$\Delta U = m c_{\text{avg}} \Delta T \quad \text{(J)} \tag{1–5}$$

where c_{avg} is the average specific heat evaluated at the average temperature. Note that the internal energy change of the systems that remain in a single phase (liquid, solid, or gas) during the process can be determined very easily using average specific heats.

Energy Transfer

Energy can be transferred to or from a given mass by two mechanisms: *heat transfer Q* and *work W.* An energy interaction is heat transfer if its driving force is a temperature difference. Otherwise, it is work. A rising piston, a rotating shaft, and an electrical wire crossing the system boundaries are all associated with work interactions. Work done *per unit time* is called **power** and is denoted by $\dot{W}$. The unit of power is W or hp (1 hp = 746 W). Car engines and hydraulic, steam, and gas turbines produce work; compressors, pumps, and mixers consume work. Notice that the energy of a system decreases as it does work and increases as work is done on it.

In daily life, we often refer to the sensible and latent forms of internal energy as **heat**, and we talk about the heat content of bodies (Fig. 1–12). In thermodynamics, however, those forms of energy are usually referred to as **thermal energy** to prevent any confusion with *heat transfer.*

The term *heat* and the associated phrases such as *heat flow, heat addition, heat rejection, heat absorption, heat gain, heat loss, heat storage, heat generation, electrical heating, latent heat, body heat,* and *heat source* are in common use today, and the attempt to replace *heat* in these phrases with *thermal energy* has had only limited success. These phrases are deeply rooted in our vocabulary, and they are used by both ordinary people and scientists without causing any misunderstanding. For example, the phrase *body heat* is understood to mean the *thermal energy content* of a body. Likewise, *heat flow* is understood to mean the *transfer of thermal energy,* not the flow of a fluid-like substance called *heat,* although the latter incorrect interpretation, based on the caloric theory, is the origin of this phrase. Also, the transfer of heat into a system is frequently referred to as *heat addition* and the transfer of heat out of a system as *heat rejection.*

Keeping in line with current practice, we will refer to the thermal energy as *heat* and the transfer of thermal energy as *heat transfer.* The amount of heat transferred during the process is denoted by *Q.* The amount of heat transferred per unit time is called the **heat transfer rate** and is denoted by $\dot{Q}$. The overdot stands for the time derivative, or "per unit time." The heat transfer rate $\dot{Q}$ has the unit J/s, which is equivalent to W.

When the *rate* of heat transfer $\dot{Q}$ is available, then the total amount of heat transfer *Q* during a time interval Δt can be determined from

$$Q = \int_0^{\Delta t} \dot{Q} \; dt \quad \text{(J)} \tag{1–6}$$

provided that the variation of $\dot{Q}$ with time is known. For the special case of $\dot{Q}$ = constant, Eq. 1–6 reduces to

$$Q = \dot{Q} \Delta t \quad \text{(J)} \tag{1–7}$$

Vapor
80°C

Liquid
80°C

Heat
transfer

25°C
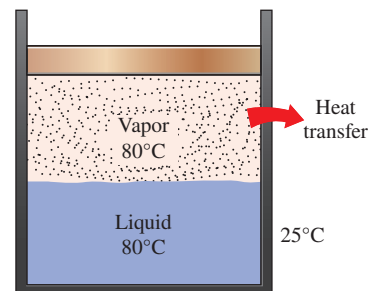
FIGURE 1–12

The sensible and latent forms of internal energy can be transferred as a result of a temperature difference, and they are referred to as *heat* or *thermal energy.*

$$\dot{q} = \frac{\dot{Q}}{A} = \frac{24 \text{ W}}{6 \text{ m}^2} = 4 \text{ W/m}^2$$
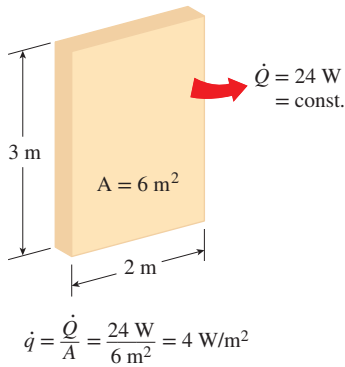
FIGURE 1–13

Heat flux is heat transfer *per unit time* and *per unit area,* and is equal to $\dot{q} = \dot{Q}/A$ when $\dot{Q}$ is uniform over the area A.
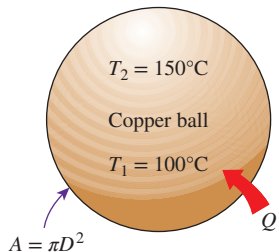
FIGURE 1–14
Schematic for Example 1–1.

The rate of heat transfer per unit area normal to the direction of heat transfer is called **heat flux**, and the average heat flux is expressed as (Fig. 1–13)

$$\dot{q} = \frac{\dot{Q}}{A} \quad (\text{W/m}^2) \tag{1–8}$$

where A is the heat transfer area. The unit of heat flux in English units is Btu/h·ft². Note that heat flux may vary with time as well as position on a surface.

EXAMPLE 1–1   Heating of a Copper Ball

A 10-cm-diameter copper ball is to be heated from 100°C to an average temperature of 150°C in 30 min (Fig. 1–14). Taking the average density and specific heat of copper in this temperature range to be $\rho = 8950$ kg/m³ and $c_p = 0.395$ kJ/kg·°C, respectively, determine (*a*) the total amount of heat transfer to the copper ball, (*b*) the average rate of heat transfer to the ball, and (*c*) the average heat flux.

SOLUTION   The copper ball is to be heated from 100°C to 150°C. The total heat transfer, the average rate of heat transfer, and the average heat flux are to be determined.

Assumptions   Constant properties can be used for copper at the average temperature.

Properties   The average density and specific heat of copper are given to be $\rho = 8950$ kg/m³ and $c_p = 0.395$ kJ/kg·°C.

Analysis   (*a*) The amount of heat transferred to the copper ball is simply the change in its internal energy and is determined from

$$\text{Energy transfer to the system} = \text{Energy increase of the system}$$
$$Q = \Delta U = mc_{\text{avg}}(T_2 - T_1)$$

where

$$m = \rho V = \frac{\pi}{6}\rho D^3 = \frac{\pi}{6}(8950 \text{ kg/m}^3)(0.1 \text{ m})^3 = 4.686 \text{ kg}$$

Substituting,

$$Q = (4.686 \text{ kg})(0.395 \text{ kJ/kg·°C})(150 - 100)°C = \textbf{92.6 kJ}$$

Therefore, 92.6 kJ of heat needs to be transferred to the copper ball to heat it from 100°C to 150°C.

(*b*) The rate of heat transfer normally changes during a process with time. However, we can determine the *average* rate of heat transfer by dividing the total amount of heat transfer by the time interval. Therefore,

$$\dot{Q}_{\text{avg}} = \frac{Q}{\Delta t} = \frac{92.6 \text{ kJ}}{1800 \text{ s}} = 0.0514 \text{ kJ/s} = \textbf{51.4 W}$$

(*c*) Heat flux is defined as the heat transfer per unit time per unit area, or the rate of heat transfer per unit area. Therefore, the average heat flux in this case is

$$\dot{q}_{\text{avg}} = \frac{\dot{Q}_{\text{avg}}}{A} = \frac{\dot{Q}_{\text{avg}}}{\pi D^2} = \frac{51.4 \text{ W}}{\pi(0.1 \text{ m})^2} = \textbf{1636 W/m}^2$$

Discussion   Note that heat flux may vary with location on a surface. The value calculated here is the *average* heat flux over the entire surface of the ball.

1−4 ▪ THE FIRST LAW OF THERMODYNAMICS

The **first law of thermodynamics**, also known as the **conservation of energy principle**, states that *energy can neither be created nor destroyed during a process; it can only change forms.* Therefore, every bit of energy must be accounted for during a process. The conservation of energy principle (or the energy balance) for *any system* undergoing *any process* may be expressed as follows: *The net change (increase or decrease) in the total energy of the system during a process is equal to the difference between the total energy entering and the total energy leaving the system during that process.* That is,

$$\begin{pmatrix} \text{Total energy} \\ \text{entering the} \\ \text{system} \end{pmatrix} - \begin{pmatrix} \text{Total energy} \\ \text{leaving the} \\ \text{system} \end{pmatrix} = \begin{pmatrix} \text{Change in the} \\ \text{total energy of} \\ \text{the system} \end{pmatrix} \qquad \textbf{(1−9)}$$

Noting that energy can be transferred to or from a system by *heat, work,* and *mass flow,* and that the total energy of a simple compressible system consists of internal, kinetic, and potential energies, the **energy balance** for any system undergoing any process can be expressed as

$$\underbrace{E_{\text{in}} - E_{\text{out}}}_{\substack{\text{Net energy transfer} \\ \text{by heat, work, and mass}}} = \underbrace{\Delta E_{\text{system}}}_{\substack{\text{Change in internal, kinetic,} \\ \text{potential, etc., energies}}} \quad \text{(J)} \qquad \textbf{(1−10)}$$

or, in the **rate form**, as

$$\underbrace{\dot{E}_{\text{in}} - \dot{E}_{\text{out}}}_{\substack{\text{Rate of net energy transfer} \\ \text{by heat, work, and mass}}} = \underbrace{dE_{\text{system}}/dt}_{\substack{\text{Rate of change in internal} \\ \text{kinetic, potential, etc., energies}}} \quad \text{(W)} \qquad \textbf{(1−11)}$$

Energy is a property, and the value of a property does not change unless the state of the system changes. Therefore, the energy change of a system is zero ($\Delta E_{\text{system}} = 0$) if the state of the system does not change during the process, that is, the process is steady. The energy balance in this case reduces to (Fig. 1–15)

Steady, rate form:
$$\underbrace{\dot{E}_{\text{in}}}_{\substack{\text{Rate of net energy transfer in} \\ \text{by heat, work, and mass}}} = \underbrace{\dot{E}_{\text{out}}}_{\substack{\text{Rate of net energy transfer out} \\ \text{by heat, work, and mass}}} \qquad \textbf{(1−12)}$$

In the absence of significant electric, magnetic, motion, gravity, and surface tension effects (i.e., for stationary simple compressible systems), the change in the *total energy* of a system during a process is simply the change in its *internal energy.* That is, $\Delta E_{\text{system}} = \Delta U_{\text{system}}$.

In heat transfer analysis, we are usually interested only in the forms of energy that can be transferred as a result of a temperature difference, that is, heat or thermal energy. In such cases it is convenient to write a **heat balance** and to treat the conversion of nuclear, chemical, mechanical, and electrical energies into thermal energy as *heat generation.* The *energy balance* in that case can be expressed as

$$\underbrace{Q_{\text{in}} - Q_{\text{out}}}_{\substack{\text{Net heat} \\ \text{transfer}}} + \underbrace{E_{\text{gen}}}_{\substack{\text{Heat} \\ \text{generation}}} = \underbrace{\Delta E_{\text{thermal, system}}}_{\substack{\text{Change in thermal} \\ \text{energy of the system}}} \quad \text{(J)} \qquad \textbf{(1−13)}$$
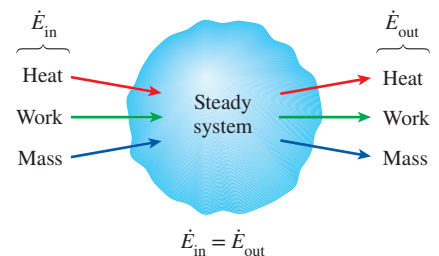
FIGURE 1−15

In steady operation, the rate of energy transfer to a system is equal to the rate of energy transfer from the system.
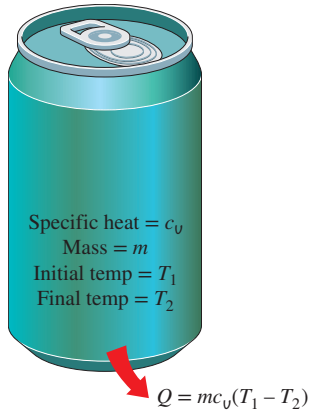
FIGURE 1–16
In the absence of any work interactions, the change in the energy content of a closed system is equal to the net heat transfer.

Energy Balance for Closed Systems *(Fixed Mass)*

A closed system consists of a *fixed mass.* The total energy E for most systems encountered in practice consists of the internal energy U. This is especially the case for stationary systems since they don't involve any changes in their velocity or elevation during a process. The energy balance relation in that case reduces to

Stationary closed system: $\qquad E_{in} - E_{out} = \Delta U = m c_v \Delta T \qquad$ (J) **(1–14)**

where we expressed the internal energy change in terms of mass m, the specific heat at constant volume c_v, and the temperature change ΔT of the system. When the system involves heat transfer only and no work interactions across its boundary, the energy balance relation further reduces to (Fig. 1–16)

Stationary closed system, no work: $\qquad Q = m c_v \Delta T \qquad$ (J) **(1–15)**

where Q is the net amount of heat transfer to or from the system. This is the form of the energy balance relation we will use most often when dealing with a fixed mass.

Energy Balance for Steady-Flow Systems

A large number of engineering devices such as water heaters and car radiators involve mass flow in and out of a system, and they are modeled as *control volumes.* Most control volumes are analyzed under steady operating conditions. The term *steady* means *no change with time* at a specified location. The opposite of steady is *unsteady* or *transient.* Also, the term *uniform* implies *no change with position* throughout a surface or region at a specified time. These meanings are consistent with their everyday usage (steady girlfriend, uniform distribution, etc.). The total energy content of a control volume during a *steady-flow process* remains constant (E_{CV} = constant). That is, the change in the total energy of the control volume during such a process is zero ($\Delta E_{CV} = 0$). Thus the amount of energy entering a control volume in all forms (heat, work, mass transfer) for a steady-flow process must be equal to the amount of energy leaving it.

The amount of mass flowing through a cross section of a flow device per unit time is called the **mass flow rate**, and it is denoted by $\dot{m}$. A fluid may flow in and out of a control volume through pipes or ducts. The mass flow rate of a fluid flowing in a pipe or duct is proportional to the cross-sectional area A_c of the pipe or duct, the density ρ, and the velocity V of the fluid. The mass flow rate through a differential area dA_c can be expressed as $\Delta \dot{m} = \rho V_n dA_c$ where V_n is the velocity component normal to dA_c. The mass flow rate through the entire cross-sectional area is obtained by integration over A_c.

The flow of a fluid through a pipe or duct can often be approximated to be *one-dimensional.* That is, the properties can be assumed to vary in one direction only (the direction of flow). As a result, all properties are assumed to be uniform at any cross section normal to the flow direction, and the properties are assumed to have *bulk average values* over the entire cross section. Under the one-dimensional flow approximation, the mass flow rate of a fluid flowing in a pipe or duct can be expressed as (Fig. 1–17)

$$\dot{m} = \rho V A_c \qquad \text{(kg/s)} \qquad \textbf{(1–16)}$$
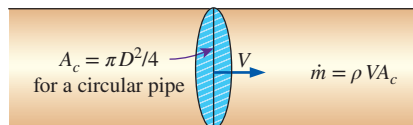
FIGURE 1–17
The mass flow rate of a fluid at a cross section is equal to the product of the fluid density, average fluid velocity, and the cross-sectional area.

where ρ is the fluid density, V is the average fluid velocity in the flow direction, and A_c is the cross-sectional area of the pipe or duct.

The volume of a fluid flowing through a pipe or duct per unit time is called the **volume flow rate** $\dot{V}$ and is expressed as

$$\dot{V} = V A_c = \frac{\dot{m}}{\rho} \quad (\text{m}^3/\text{s}) \tag{1–17}$$

Note that the mass flow rate of a fluid through a pipe or duct remains constant during steady flow. This is not the case for the volume flow rate, however, unless the density of the fluid remains constant.

For a steady-flow system with one inlet and one exit, the rate of mass flow into the control volume must be equal to the rate of mass flow out of it. That is, $\dot{m}_{in} = \dot{m}_{out} = \dot{m}$. When the changes in kinetic and potential energies are negligible, which is usually the case, and there is no work interaction, the energy balance for such a steady-flow system reduces to (Fig. 1–18)

$$\dot{Q} = \dot{m}\,\Delta h = \dot{m}\,c_p \Delta T \quad (\text{kJ/s}) \tag{1–18}$$

where $\dot{Q}$ is the rate of net heat transfer into or out of the control volume. This is the form of the energy balance relation that we will use most often for steady-flow systems.

FIGURE 1–18
Under steady conditions, the net rate of energy transfer to a fluid in a control volume is equal to the rate of increase in the energy of the fluid stream flowing through the control volume.

Surface Energy Balance

As mentioned in the chapter opener, heat is transferred by the mechanisms of conduction, convection, and radiation, and heat often changes vehicles as it is transferred from one medium to another. For example, the heat conducted to the outer surface of the wall of a house in winter is convected away by the cold outdoor air while being radiated to the cold surroundings. In such cases, it may be necessary to keep track of the energy interactions at the surface, and this is done by applying the conservation of energy principle to the surface.

A surface contains no volume or mass and thus no energy. Therefore, a surface can be viewed as a fictitious system whose energy content remains constant during a process (just like a steady-state or steady-flow system). Then the energy balance for a surface can be expressed as

Surface energy balance: $\qquad \dot{E}_{in} = \dot{E}_{out} \tag{1–19}$

This relation is valid for both steady and transient conditions, and the surface energy balance does not involve heat generation since a surface does not have a volume. The energy balance for the outer surface of the wall in Fig. 1–19, for example, can be expressed as

$$\dot{Q}_1 = \dot{Q}_2 + \dot{Q}_3 \tag{1–20}$$

where $\dot{Q}_1$ is conduction through the wall to the surface, $\dot{Q}_2$ is convection from the surface to the outdoor air, and $\dot{Q}_3$ is net radiation from the surface to the surroundings.

When the directions of interactions are not known, all energy interactions can be assumed to be toward the surface, and the surface energy balance can be expressed as $\Sigma \dot{E}_{in} = 0$. Note that the interactions in the opposite direction will end up having negative values, and balance this equation.
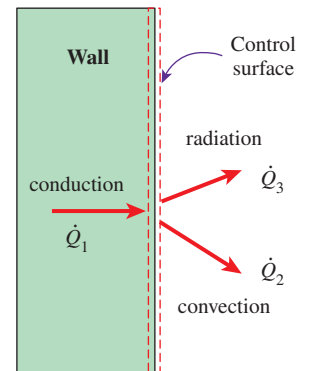
FIGURE 1–19
Energy interactions at the outer wall surface of a house.

AISI 304
stainless
steel sheet

$\dot{Q}_{loss}$

$V = 1$ cm/s

$T_{in} = 500$ K $T_{out} = 300$ K
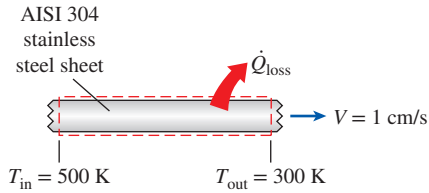
FIGURE 1–20
Schematic for Example 1–2.

EXAMPLE 1–2   **Cooling of Stainless Steel Sheets**

A heated continuous AISI 304 stainless steel sheet is being conveyed at a constant speed of 1 cm/s into a chamber to be cooled (Fig. 1–20). The stainless steel sheet is 5 mm thick and 2 m wide, and it enters and exits the chamber at 500 K and 300 K, respectively. Determine the rate of heat loss from the stainless steel sheet inside the chamber.

SOLUTION   The rate of heat loss from a stainless steel sheet being conveyed inside a chamber is to be determined.
Assumptions   **1** Steady operating conditions exist. **2** The stainless steel sheet has constant properties. **3** Changes in potential and kinetic energy are negligible.
Properties   The constant-pressure specific heat of AISI 304 stainless steel at the average temperature of $(500 + 300)/2 = 400$ K is 515 J/kg·K. The density of AISI 304 stainless steel is 7900 kg/m^3 (Table A–3).
Analysis   The mass of the stainless steel sheet being conveyed enters and exits the chamber at a rate of

$$\dot{m} = \rho V w t$$
$$= (7900 \text{ kg/m}^3)(0.01 \text{ m/s})(2 \text{ m})(0.005 \text{ m})$$
$$= 0.79 \text{ kg/s}$$

The rate of heat loss from the stainless steel sheet in the chamber can be determined as follows:

$$\dot{Q}_{loss} = \dot{m} c_p (T_{in} - T_{out})$$
$$= (0.79 \text{ kg/s})(515 \text{ J/kg·K})(500 - 300)\text{K} = 81,370 \text{ J/s}$$
$$= \mathbf{81.4 \text{ kW}}$$

Discussion   The stainless steel sheet being conveyed in and out of the chamber is treated as a control volume.

5 m

20 cm

25 cm

54°C

Hot air
100 kPa
60°C
5 m/s

$\dot{Q}_{loss}$
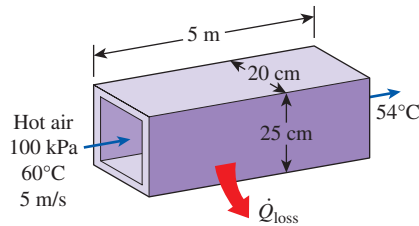
FIGURE 1–21
Schematic for Example 1–3.

EXAMPLE 1–3   **Heat Loss from Heating Ducts in a Basement**

A 5-m-long section of an air heating system of a house passes through an unheated space in the basement (Fig. 1–21). The cross section of the rectangular duct of the heating system is 20 cm × 25 cm. Hot air enters the duct at 100 kPa and 60°C at an average velocity of 5 m/s. The temperature of the air in the duct drops to 54°C as a result of heat loss to the cool space in the basement. Determine the rate of heat loss from the air in the duct to the basement under steady conditions. Also, determine the cost of this heat loss per hour if the house is heated by a natural gas furnace that has an efficiency of 80 percent and the cost of the natural gas in that area is $1.60/therm (1 therm = 100,000 Btu = 105,500 kJ).

SOLUTION   The temperature of the air in the heating duct of a house drops as a result of heat loss to the cool space in the basement. The rate of heat loss from the hot air and its cost are to be determined.
Assumptions   **1** Steady operating conditions exist. **2** Air can be treated as an ideal gas with constant properties at room temperature.
Properties   The constant-pressure specific heat of air at the average temperature of $(54 + 60)/2 = 57°C$ is 1.007 kJ/kg·K (Table A–15).
Analysis   We take the basement section of the heating system as our system, which is a steady-flow system. The rate of heat loss from the air in the duct can be determined from

$$\dot{Q} = \dot{m} c_p \Delta T$$

where $\dot{m}$ is the mass flow rate and ΔT is the temperature drop. The density of air at the inlet conditions is

$$\rho = \frac{P}{RT} = \frac{100 \text{ kPa}}{(0.287 \text{ kPa} \cdot \text{m}^3/\text{kg} \cdot \text{K})(60 + 273)\text{K}} = 1.046 \text{ kg/m}^3$$

The cross-sectional area of the duct is

$$A_c = (0.20 \text{ m})(0.25 \text{ m}) = 0.05 \text{ m}^2$$

Then the mass flow rate of air through the duct and the rate of heat loss become

$$\dot{m} = \rho V A_c = (1.046 \text{ kg/m}^3)(5 \text{ m/s})(0.05 \text{ m}^2) = 0.2615 \text{ kg/s}$$

and

$$\begin{aligned}
\dot{Q}_{\text{loss}} &= \dot{m} c_p (T_{\text{in}} - T_{\text{out}}) \\
&= (0.2615 \text{ kg/s})(1.007 \text{ kJ/kg} \cdot °\text{C})(60 - 54)°\text{C} \\
&= \textbf{1.58 kJ/s}
\end{aligned}$$

or 5688 kJ/h. The cost of this heat loss to the homeowner is

$$\begin{aligned}
\text{Cost of heat loss} &= \frac{(\text{Rate of heat loss})(\text{Unit cost of energy input})}{\text{Furnace efficiency}} \\
&= \frac{(5688 \text{ kJ/h})(\$1.60/\text{therm})}{0.80}\left(\frac{1 \text{ therm}}{105{,}500 \text{ kJ}}\right) \\
&= \textbf{\$0.108/h}
\end{aligned}$$

Discussion The heat loss from the heating ducts in the basement is costing the homeowner 10.8 cents per hour. Assuming the heater operates 2000 hours during a heating season, the annual cost of this heat loss adds up to $216. Most of this money can be saved by insulating the heating ducts in the unheated areas.

EXAMPLE 1–4 **Electric Heating of a House at High Elevation**

Consider a house that has a floor space of 2000 ft² and an average height of 9 ft at 5000 ft elevation where the standard atmospheric pressure is 12.2 psia (Fig. 1–22). Initially the house is at a uniform temperature of 50°F. Now the electric heater is turned on, and the heater runs until the air temperature in the house rises to an average value of 70°F. Determine the amount of energy transferred to the air assuming (*a*) the house is airtight and thus no air escapes during the heating process and (*b*) some air escapes through the cracks as the heated air in the house expands at constant pressure. Also determine the cost of this heat for each case if the cost of electricity in that area is $0.075/kWh.

SOLUTION The air in the house is heated by an electric heater. The amount and cost of the energy transferred to the air are to be determined for constant-volume and constant-pressure cases.
Assumptions **1** Air can be treated as an ideal gas with constant properties. **2** Heat loss from the house during heating is negligible. **3** The volume occupied by the furniture and other things is negligible.
Properties The specific heats of air at the average temperature of $(50 + 70)/2 = 60°\text{F}$ are $c_p = 0.240$ Btu/lbm·R and $c_v = c_p - R = 0.171$ Btu/lbm·R (Tables A–1E and A–15E).
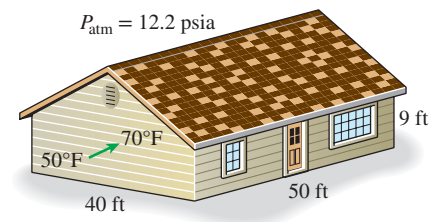
FIGURE 1–22
Schematic for Example 1–4.

$P_{\text{atm}} = 12.2$ psia

70°F
50°F
9 ft
40 ft
50 ft

Analysis   The volume and the mass of the air in the house are

$$V = \text{(Floor area)(Height)} = (2000 \text{ ft}^2)(9 \text{ ft}) = 18{,}000 \text{ ft}^3$$

$$m = \frac{PV}{RT} = \frac{(12.2 \text{ psia})(18{,}000 \text{ ft}^3)}{(0.3704 \text{ psia·ft}^3/\text{lbm·R})(50 + 460)\text{R}} = 1162 \text{ lbm}$$

(*a*) The amount of energy transferred to air at constant volume is simply the change in its internal energy and is determined from

$$E_\text{in} - E_\text{out} = \Delta E_\text{system}$$

$$\begin{aligned}
E_\text{in, constant volume} &= \Delta U_\text{air} = mc_v \Delta T \\
&= (1162 \text{ lbm})(0.171 \text{ Btu/lbm·°F})(70 - 50)\text{°F} \\
&= \textbf{3974 Btu}
\end{aligned}$$

At a unit cost of $0.075/kWh, the total cost of this energy is

$$\begin{aligned}
\text{Cost of energy} &= \text{(Amount of energy)(Unit cost of energy)} \\
&= (3974 \text{ Btu})(\$0.075/\text{kWh})\left(\frac{1 \text{ kWh}}{3412 \text{ Btu}}\right) \\
&= \textbf{\$0.087}
\end{aligned}$$

(*b*) The amount of energy transferred to air at constant pressure is the change in its enthalpy and is determined from

$$\begin{aligned}
E_\text{in,constant pressure} &= \Delta H_\text{air} = mc_p \Delta T \\
&= (1162 \text{ lbm})(0.240 \text{ Btu/lbm·°F})(70 - 50)\text{°F} \\
&= \textbf{5578 Btu}
\end{aligned}$$

At a unit cost of $0.075/kWh, the total cost of this energy is

$$\begin{aligned}
\text{Cost of energy} &= \text{(Amount of energy)(Unit cost of energy)} \\
&= (5578 \text{ Btu})(\$0.075/\text{kWh})\left(\frac{1 \text{ kWh}}{3412 \text{ Btu}}\right) \\
&= \textbf{\$0.123}
\end{aligned}$$

Discussion   It costs about 9 cents in the first case and 12 cents in the second case to raise the temperature of the air in this house from 50°F to 70°F. The second answer is more realistic since every house has cracks, especially around the doors and windows, and the pressure in the house remains essentially constant during a heating process. Therefore, the second approach is used in practice. This conservative approach somewhat overpredicts the amount of energy used, however, since some of the air escapes through the cracks before it is heated to 70°F.

1–5 ▪ HEAT TRANSFER MECHANISMS

In Sec. 1–1, we defined *heat* as the form of energy that can be transferred from one system to another as a result of temperature difference. A thermodynamic analysis is concerned with the *amount* of heat transfer as a system undergoes a process from one equilibrium state to another. The science that deals with

the determination of the *rates* of such energy transfers is the science of *heat transfer.* The transfer of energy as heat is always from the higher-temperature medium to the lower-temperature one, and heat transfer stops when the two media reach the same temperature.

Heat can be transferred in three different modes: *conduction, convection,* and *radiation.* All modes of heat transfer require the existence of a temperature difference, and all modes are from the high-temperature medium to a lower-temperature one. Next we give a brief description of each mode. A detailed study of these modes is given in later chapters of this text.

1−6 ▪ CONDUCTION

Conduction is the transfer of energy from the more energetic particles of a substance to the adjacent less energetic ones as a result of interactions between the particles. Conduction can take place in solids, liquids, or gases. In gases and liquids, conduction is due to the *collisions* and *diffusion* of the molecules during their random motion. In solids, it is due to the combination of *vibrations* of the molecules in a lattice and the energy transport by *free electrons.* A cold canned drink in a warm room, for example, eventually warms up to the room temperature as a result of heat transfer from the room to the drink through the aluminum can by conduction.

The *rate* of heat conduction through a medium depends on the *geometry* of the medium, its *thickness,* and the *material* of the medium, as well as the *temperature difference* across the medium. We know that wrapping a hot water tank with glass wool (an insulating material) reduces the rate of heat loss from the tank. The thicker the insulation, the smaller the heat loss. We also know that a hot water tank loses heat at a higher rate when the temperature of the room housing the tank is lowered. Further, the larger the tank, the larger the surface area and thus the rate of heat loss.

Consider steady heat conduction through a large plane wall of thickness $\Delta x = L$ and area A, as shown in Fig. 1–23. The temperature difference across the wall is $\Delta T = T_2 - T_1$. Experiments have shown that the rate of heat transfer $\dot{Q}$ through the wall is *doubled* when the temperature difference ΔT across the wall or the area A normal to the direction of heat transfer is doubled, but is *halved* when the wall thickness L is doubled. Thus we conclude that *the rate of heat conduction through a plane layer is proportional to the temperature difference across the layer and the heat transfer area but is inversely proportional to the thickness of the layer.* That is,

$$\text{Rate of heat conduction} \propto \frac{(\text{Area})(\text{Temperature difference})}{\text{Thickness}}$$

or,

$$\dot{Q}_{\text{cond}} = kA\frac{T_1 - T_2}{\Delta x} = -kA\frac{\Delta T}{\Delta x} \quad (\text{W}) \tag{1–21}$$

where the constant of proportionality k is the **thermal conductivity** of the material, which is a *measure of the ability of a material to conduct heat* (Fig. 1–24). In the limiting case of $\Delta x \to 0$, Eq. 1–21 reduces to the differential form

$$\dot{Q}_{\text{cond}} = -kA\frac{dT}{dx} \quad (\text{W}) \tag{1–22}$$
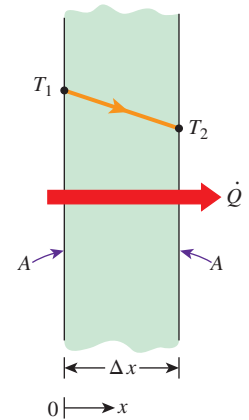
FIGURE 1−23
Heat conduction through a large plane wall of thickness Δx and area A.
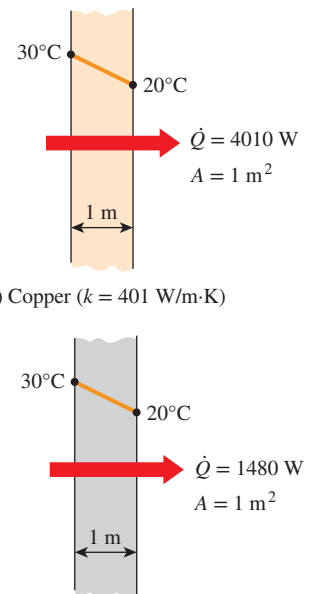
(*a*) Copper ($k = 401$ W/m·K)

(*b*) Silicon ($k = 148$ W/m·K)

FIGURE 1−24
The rate of heat conduction through a solid is directly proportional to its thermal conductivity.

FIGURE 1–25
Jean Baptiste Joseph Fourier
(1768–1830) was a French mathematician and physicist born in Auxerre, France. He is best known for his work on the infinite series of trigonometric functions that bear his name and for his development of the mathematical theory of heat conduction. Fourier established the partial differential equation governing heat diffusion, and he solved it by using the Fourier series. The Fourier transform, Fourier number, and Fourier's law of heat conduction are named in his honor. Fourier is also credited with the discovery of the greenhouse effect in 1824.

©Stock Montage/Getty Images
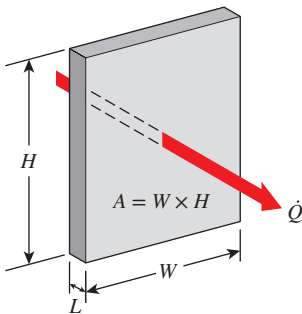
FIGURE 1–26
In heat conduction analysis, *A* represents the area *normal* to the direction of heat transfer.

which is called **Fourier's law of heat conduction** after J. Fourier (Fig. 1–25), who expressed it first in his heat transfer text in 1822. Here dT/dx is the **temperature gradient**, which is the slope of the temperature curve on a *T-x* diagram (the rate of change of *T* with *x*), at location *x*. Equation 1–22 indicates that the rate of heat conduction in a given direction is proportional to the temperature gradient in that direction. Heat is conducted in the direction of decreasing temperature, and the temperature gradient becomes negative when temperature decreases with increasing *x*. The *negative sign* in Eq. 1–22 ensures that heat transfer in the positive *x* direction is a positive quantity.

The heat transfer area *A* is always *normal* to the direction of heat transfer. For heat loss through a 5-m-long, 3-m-high, and 25-cm-thick wall, for example, the heat transfer area is $A = 15$ m². Note that the thickness of the wall has no effect on *A* (Fig. 1–26).

EXAMPLE 1–5   **The Cost of Heat Loss Through a Roof**

The roof of an electrically heated home is 6 m long, 8 m wide, and 0.25 m thick, and it is made of a flat layer of concrete whose thermal conductivity is $k = 0.8$ W/m·K (Fig. 1–27). The temperatures of the inner and the outer surfaces of the roof one night are measured to be 15°C and 4°C, respectively, for a period of 10 h. Determine (*a*) the rate of heat loss through the roof that night and (*b*) the cost of that heat loss to the homeowner if the cost of electricity is \$0.08/kWh.

SOLUTION   The inner and outer surfaces of the flat concrete roof of an electrically heated home are maintained at specified temperatures during a night. The heat loss through the roof and its cost that night are to be determined.
Assumptions   **1** Steady operating conditions exist during the entire night since the surface temperatures of the roof remain constant at the specified values. **2** Constant properties can be used for the roof.
Properties   The thermal conductivity of the roof is given to be $k = 0.8$ W/m·K.
Analysis   (*a*) Noting that heat transfer through the roof is by conduction and the area of the roof is $A = 6$ m × 8 m = 48 m², the steady rate of heat transfer through the roof is

$$\dot{Q} = kA\frac{T_1 - T_2}{L} = (0.8 \text{ W/m·K})(48 \text{ m}^2)\frac{(15 - 4)°C}{0.25 \text{ m}} = \textbf{1690 W = 1.69 kW}$$

(*b*) The amount of heat lost through the roof during a 10-h period and its cost are

$$Q = \dot{Q}\,\Delta t = (1.69 \text{ kW})(10 \text{ h}) = 16.9 \text{ kWh}$$
$$\text{Cost} = (\text{Amount of energy})(\text{Unit cost of energy})$$
$$= (16.9 \text{ kWh})(\$0.08/\text{kWh}) = \textbf{\$1.35}$$

Discussion   The cost to the homeowner of the heat loss through the roof that night was \$1.35. The total heating bill of the house will be much larger since the heat losses through the walls are not considered in these calculations.

Thermal Conductivity

We have seen that different materials store heat differently, and we have defined the property specific heat c_p as a measure of a material's ability to store thermal energy. For example, $c_p = 4.18$ kJ/kg·°C for water and $c_p = 0.45$ kJ/kg·°C

for iron at room temperature, which indicates that water can store almost 10 times the energy that iron can per unit mass. Likewise, the thermal conductivity k is a measure of a material's ability to conduct heat. For example, $k = 0.607$ W/m·K for water and $k = 80.2$ W/m·K for iron at room temperature, which indicates that iron conducts heat more than 100 times faster than water can. Thus we say that water is a poor heat conductor relative to iron, although water is an excellent medium for storing thermal energy.

Equation 1–21 for the rate of conduction heat transfer under steady conditions can also be viewed as the defining equation for thermal conductivity. Thus the **thermal conductivity** of a material can be defined as *the rate of heat transfer through a unit thickness of the material per unit area per unit temperature difference.* The thermal conductivity of a material is a measure of the ability of the material to conduct heat. A high value for thermal conductivity indicates that the material is a good heat conductor, and a low value indicates that the material is a poor heat conductor or *insulator.* The thermal conductivities of some common materials at room temperature are given in Table 1–1. The thermal conductivity of pure copper at room temperature is $k = 401$ W/m·K, which indicates that a 1-m-thick copper wall will conduct heat at a rate of 401 W per m² area per K temperature difference across the wall. Note that materials such as copper and silver that are good electric conductors are also good heat conductors and have high values of thermal conductivity. Materials such as rubber, wood, and Styrofoam are poor conductors of heat and have low conductivity values.

A layer of material of known thickness and area can be heated from one side by an electric resistance heater of known output. If the outer surfaces of the heater are well insulated, all the heat generated by the resistance heater will be transferred through the material whose conductivity is to be determined. Then measuring the two surface temperatures of the material when steady heat transfer is reached and substituting them into Eq. 1–21 together with other known quantities give the thermal conductivity (Fig. 1–28).

The thermal conductivities of materials vary over a wide range, as shown in Fig. 1–29. The thermal conductivities of gases such as air vary by a factor of 10^4 from those of pure metals such as copper. Note that pure crystals and metals have the highest thermal conductivities, and gases and insulating materials have the lowest. Aside from the typical insulators listed in Fig. 1–29, one of the best solid insulators with the lowest thermal conductivity compared to the conventional insulators (Table 1–1) is **aerogel**. See Sec. 1–10 for more details about aerogels.

Temperature is a measure of the kinetic energies of the particles such as the molecules or atoms of a substance. In a liquid or gas, the kinetic energy of the molecules is due to their random translational motion as well as their vibrational and rotational motions. When two molecules possessing different kinetic energies collide, part of the kinetic energy of the more energetic (higher-temperature) molecule is transferred to the less energetic (lower-temperature) molecule, much the same as when two elastic balls of the same mass at different velocities collide and part of the kinetic energy of the faster ball is transferred to the slower one. The higher the temperature, the faster the molecules move, and the higher the number of such collisions, the better the heat transfer.

The *kinetic theory* of gases predicts, and the experiments confirm, that the thermal conductivity of gases is proportional to the *square root of the*
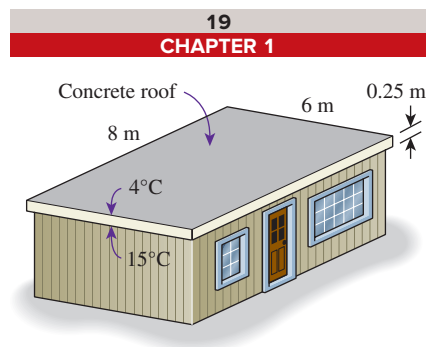
FIGURE 1–27
Schematic for Example 1–5.

TABLE 1–1

The thermal conductivities of some materials at room temperature

Material	k,W/m·K*
Diamond	2300
Silver	429
Copper	401
Gold	317
Aluminum	237
Iron	80.2
Mercury (*l*)	8.54
Glass	0.78
Brick	0.72
Water (*l*)	0.607
Human skin	0.37
Wood (oak)	0.17
Helium (*g*)	0.152
Soft rubber	0.13
Glass fiber	0.043
Air (*g*)	0.026
Urethane, rigid foam	0.026

*Multiply by 0.5778 to convert to Btu/h·ft·°F.

$$k = \frac{L}{A(T_1 - T_2)} \dot{Q}$$
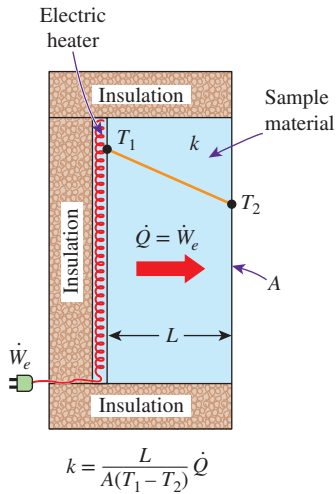
FIGURE 1–28

A simple experimental setup to determine the thermal conductivity of a material.

thermodynamic temperature T and inversely proportional to the *square root of the molar mass M.* Therefore, for a particular gas (fixed *M*), the thermal conductivity increases with increasing temperature, and at a fixed temperature the thermal conductivity decreases with increasing *M.* For example, at a fixed temperature of 1000 K, the thermal conductivity of helium ($M = 4$) is 0.343 W/m·K, and that of air ($M = 29$) is 0.0667 W/m·K, which is much lower than that of helium.

The thermal conductivities of *gases* at 1 atm pressure are listed in Table A-16. However, they can also be used at pressures other than 1 atm since the thermal conductivity of gases is *independent of pressure* in a wide range of pressures encountered in practice.

The mechanism of heat conduction in a *liquid* is complicated by the fact that the molecules are more closely spaced, and they exert a stronger intermolecular force field. The thermal conductivities of liquids usually lie between those of solids and gases. The thermal conductivity of a substance is normally highest in the solid phase and lowest in the gas phase. The thermal conductivity of liquids is generally insensitive to pressure except near the thermodynamic critical point. Unlike gases, the thermal conductivities of most liquids decrease with increasing temperature, with water being a notable exception. Like gases, the conductivity of liquids decreases with increasing molar mass. Liquid metals such as mercury and sodium have high thermal conductivities and are very suitable for use in applications where a high heat transfer rate to a liquid is desired, as in nuclear power plants.
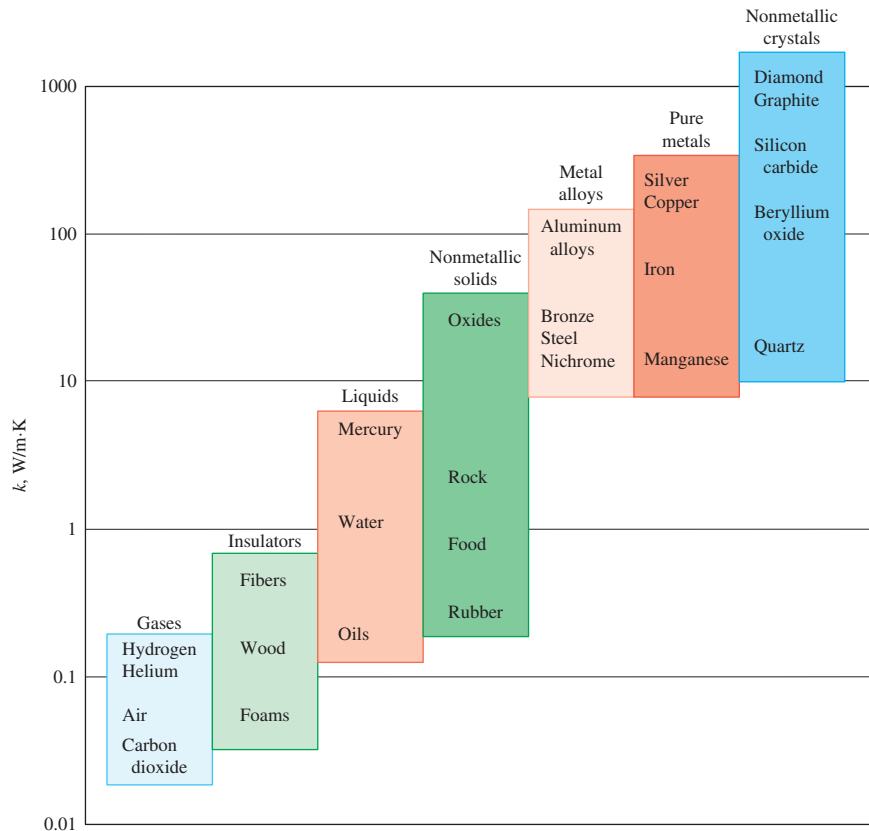
FIGURE 1–29

The range of thermal conductivity of various materials at room temperature.

In *solids,* heat conduction is due to two effects: (1) the *lattice vibrational waves* induced by the vibrational motions of the molecules positioned at relatively fixed positions in a periodic manner called a lattice and (2) the energy transported via the *free flow of electrons* in the solid (Fig. 1–30). The thermal conductivity of a solid is obtained by adding the lattice and electronic components. The relatively high thermal conductivities of pure metals are primarily due to the electronic component. The lattice component of thermal conductivity strongly depends on the way the molecules are arranged. For example, diamond, which is a highly ordered crystalline solid, has the highest known thermal conductivity at room temperature.

Unlike metals, which are good electrical and heat conductors, *crystalline solids* such as diamond and semiconductors such as silicon are good heat conductors but poor electrical conductors. As a result, such materials find widespread use in the electronics industry. Despite their higher price, diamond heat sinks are used in the cooling of sensitive electronic components because of the excellent thermal conductivity of diamond. Silicon oils and gaskets are commonly used in the packaging of electronic components because they provide both good thermal contact and good electrical insulation.

Pure metals have high thermal conductivities, and one would think that *metal alloys* should also have high conductivities. One would expect an alloy made of two metals of thermal conductivities k_1 and k_2 to have a conductivity k between k_1 and k_2. But this turns out not to be the case. The thermal conductivity of an alloy of two metals is usually much lower than that of either metal, as shown in Table 1–2. Even small amounts in a pure metal of "foreign" molecules that are good conductors themselves seriously disrupt the transfer of heat in that metal. For example, the thermal conductivity of steel containing just 1 percent of chrome is 62 W/m·K, while the thermal conductivities of iron and chromium are 83 and 95 W/m·K, respectively.

The thermal conductivities of materials vary with temperature (Table 1–3). The variation of thermal conductivity over certain temperature ranges is negligible for some materials but significant for others, as shown in Fig. 1–31. The thermal conductivities of certain solids exhibit dramatic increases at temperatures near absolute zero, when these solids become *superconductors.* For example, the conductivity of copper reaches a maximum value of about 20,000 W/m·K at 20 K, which is about 50 times the conductivity at room temperature. The thermal conductivities and other thermal properties of various materials are given in Tables A–3 to A–17.

As shown in Table 1–1 and Fig. 1–31, most liquids have relatively low thermal conductivities when compared to the thermal conductivity of solids. The thermal conductivity of commonly used heat transfer fluids (such as water or oil) can be considerably increased by adding small solid particles to the fluid. The name **nanofluid** refers to the suspension of nanometer-sized particles (with typical length scales of 1 to 100 nm), called nanoparticles, in conventional fluids. The nanoparticles used in nanofluids are typically made of metals, oxides, carbides, or carbon nanotubes. Common base fluids include water, ethylene glycol, and oil. Nanofluids have been shown to enhance the thermal conductivity and convective heat transfer performance of the working (base) liquids.

Values of thermal conductivity given in Tables A–3 to A–17 are appropriate when the physical dimensions of the material under consideration are
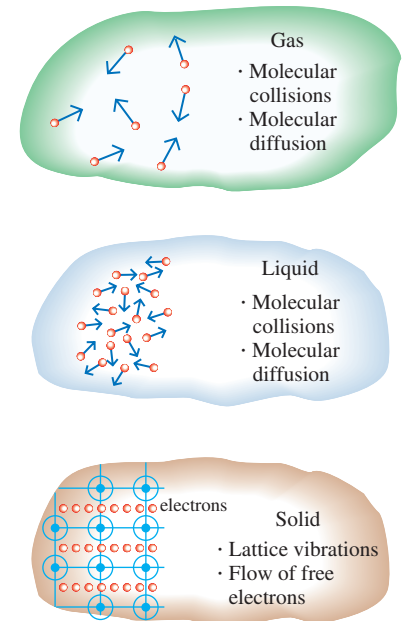
FIGURE 1–30
The mechanisms of heat conduction in different phases of a substance.

TABLE 1–2

The thermal conductivity of an alloy is usually much lower than the thermal conductivity of either metal of which it is composed

Pure Metal or Alloy	k, W/m·K, at 300 K
Copper	401
Nickel	91
Constantan	
(55% Cu, 45% Ni)	23
Copper	401
Aluminum	237
Commercial bronze	
(90% Cu, 10% Al)	52

TABLE 1–3

Thermal conductivities of materials vary with temperature

T, K	k, W/m·K	
	Copper	Aluminum
100	482	302
200	413	237
300	401	237
400	393	240
600	379	231
800	366	218

FIGURE 1–31

The variation of the thermal conductivity of various solids, liquids, and gases with temperature.
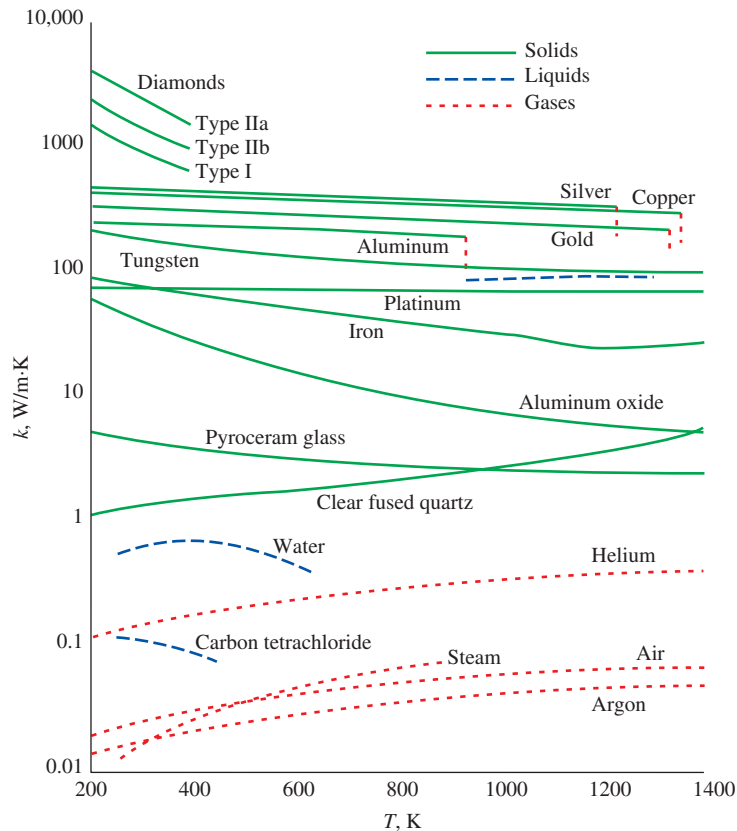
relatively large. In some of the emerging areas of technology, such as microelectronics, the physical dimensions are typically in the order of micro or nanometers. For these applications the small physical dimensions most likely will influence the value of thermal conductivity in the solid and liquid states. In these situations, as the physical dimensions decrease, the average net distance traveled by the energy carriers typically decreases, and this reduces the value of thermal conductivity.

The temperature dependence of thermal conductivity causes considerable complexity in conduction analysis. Therefore, it is common practice to evaluate the thermal conductivity k at the *average temperature* and treat it as a *constant* in calculations.

In heat transfer analysis, a material is normally assumed to be *isotropic;* that is, to have uniform properties in all directions. This assumption is realistic for most materials, except those that exhibit different structural characteristics in different directions, such as laminated composite materials and wood. The thermal conductivity of wood across the grain, for example, is different than that parallel to the grain.

Thermal Diffusivity

The product ρc_p, which is often encountered in heat transfer analysis, is called the **heat capacity** of a material. Both the specific heat c_p and the heat capacity ρc_p represent the heat storage capability of a material. But c_p expresses it *per*

unit mass, whereas ρc_p expresses it *per unit volume,* as can be noticed from their units J/kg·K and J/m³·K, respectively.

Another material property that appears in the transient heat conduction analysis is the **thermal diffusivity**, which represents how fast heat diffuses through a material and is defined as

$$\alpha = \frac{\text{Heat conduction}}{\text{Heat storage}} = \frac{k}{\rho c_p} \quad (\text{m}^2/\text{s}) \tag{1–23}$$

Note that the thermal conductivity k represents how well a material conducts heat, and the heat capacity ρc_p represents how much energy a material stores per unit volume. Therefore, the thermal diffusivity of a material can be viewed as the ratio of the *heat conducted* through the material to the *heat stored* per unit volume. A material that has a high thermal conductivity or a low heat capacity will obviously have a large thermal diffusivity. The larger the thermal diffusivity, the faster the propagation of heat into the medium. A small value of thermal diffusivity means that heat is mostly absorbed by the material and a small amount of heat is conducted further.

The thermal diffusivities of some common materials at 20°C are given in Table 1–4. Note that the thermal diffusivity ranges from $\alpha = 0.14 \times 10^{-6}$ m²/s for water to 149×10^{-6} m²/s for silver, which is a difference of more than a thousand times. Also note that the thermal diffusivities of beef and water are the same. This is not surprising, since meat as well as fresh vegetables and fruits are mostly water, and thus they possess the thermal properties of water.

TABLE 1–4

The thermal diffusivities of some materials at room temperature

Material	α, m²/s*
Silver	149×10^{-6}
Gold	127×10^{-6}
Copper	113×10^{-6}
Aluminum	97.5×10^{-6}
Iron	22.8×10^{-6}
Mercury (*l*)	4.7×10^{-6}
Marble	1.2×10^{-6}
Ice	1.2×10^{-6}
Concrete	0.75×10^{-6}
Brick	0.52×10^{-6}
Heavy soil (dry)	0.52×10^{-6}
Glass	0.34×10^{-6}
Glass wool	0.23×10^{-6}
Water (*l*)	0.14×10^{-6}
Beef	0.14×10^{-6}
Wood (oak)	0.13×10^{-6}

*Multiply by 10.76 to convert to ft²/s.

EXAMPLE 1–6 Measuring the Thermal Conductivity of a Material

A common way of measuring the thermal conductivity of a material is to sandwich an electric thermofoil heater between two identical samples of the material, as shown in Fig. 1–32. The thickness of the resistance heater, including its cover, which is made of thin silicon rubber, is usually less than 0.5 mm. A circulating fluid such as tap water keeps the exposed ends of the samples at constant temperature. The lateral surfaces of the samples are well insulated to ensure that heat transfer through the samples is one-dimensional. Two thermocouples are embedded into each sample some distance L apart, and a differential thermometer reads the temperature drop ΔT across this distance along each sample. When steady operating conditions are reached, the total rate of heat transfer through both samples becomes equal to the electric power drawn by the heater.

In a certain experiment, cylindrical samples of diameter 5 cm and length 10 cm are used. The two thermocouples in each sample are placed 3 cm apart. After initial transients, the electric heater is observed to draw 0.4 A at 110 V, and both differential thermometers read a temperature difference of 15°C. Determine the thermal conductivity of the sample.

SOLUTION The thermal conductivity of a material is to be determined by ensuring one-dimensional heat conduction and by measuring temperatures when steady operating conditions are reached.

Assumptions **1** Steady operating conditions exist since the temperature readings do not change with time. **2** Heat losses through the lateral surfaces of the apparatus are negligible since those surfaces are well insulated, and thus all heat generated by the heater is conducted through the samples. **3** The apparatus possesses thermal symmetry.
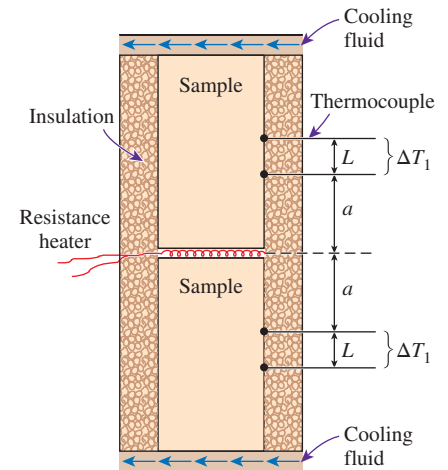
FIGURE 1–32
Apparatus to measure the thermal conductivity of a material using two identical samples and a thin resistance heater (Example 1–6).

Analysis   The electrical power consumed by the resistance heater and converted to heat is

$$\dot{W}_e = \mathrm{V}I = (110 \text{ V})(0.4 \text{ A}) = 44 \text{ W}$$

The rate of heat flow through each sample is

$$\dot{Q} = \frac{1}{2}\dot{W}_e = \frac{1}{2} \times (44 \text{ W}) = 22 \text{ W}$$

since only half of the heat generated flows through each sample because of symmetry. Reading the same temperature difference across the same distance in each sample also confirms that the apparatus possesses thermal symmetry. The heat transfer area is the area normal to the direction of heat transfer, which is the cross-sectional area of the cylinder in this case:

$$A = \frac{1}{4}\pi D^2 = \frac{1}{4}\pi (0.05 \text{ m})^2 = 0.001963 \text{ m}^2$$

Noting that the temperature drops by 15°C within 3 cm in the direction of heat flow, the thermal conductivity of the sample is determined to be

$$\dot{Q} = kA\frac{\Delta T}{L} \rightarrow k = \frac{\dot{Q}L}{A\Delta T} = \frac{(22 \text{ W})(0.03 \text{ m})}{(0.001963 \text{ m}^2)(15°C)} = \textbf{22.4 W/m·K}$$

Discussion   Perhaps you are wondering if we really need to use two samples in the apparatus, since the measurements on the second sample do not give any additional information. It seems like we can replace the second sample with insulation. Indeed, we do not need the second sample; however, it enables us to verify the temperature measurements on the first sample and provides thermal symmetry, which reduces experimental error.

EXAMPLE 1–7   Conversion Between SI and English Units

An engineer who is working on the heat transfer analysis of a brick building in English units needs the thermal conductivity of brick. But the only value he can find from his handbooks is 0.72 W/m·°C, which is in SI units. To make matters worse, the engineer does not have a direct conversion factor between the two unit systems for thermal conductivity. Can you help him out?

SOLUTION   The situation this engineer is facing is not unique, and most engineers often find themselves in a similar position. When converting units, one must be careful to avoid some common pitfalls that lead to costly mistakes. Although unit conversion is a simple process, it requires care and careful reasoning.

   The conversion factors for W and m are straightforward and are given in conversion tables to be

$$1 \text{ W} = 3.41214 \text{ Btu/h}$$
$$1 \text{ m} = 3.2808 \text{ ft}$$

But the conversion of °C into °F is not so simple, and it can be a source of error if one is not careful. Perhaps the first thought that comes to mind is to replace °C by (°F − 32)/1.8 since $T(°C) = [T(°F)−32]/1.8$. But this will be wrong since the °C in the unit W/m·°C represents per *°C change in temperature.* Noting that 1°C change in temperature corresponds to 1.8°F, so the proper conversion factor is

$$1°C = 1.8°F$$

Substituting, we get

$$1 \text{ W/m·°C} = \frac{3.41214 \text{ Btu/h}}{(3.2808 \text{ ft})(1.8°F)} = 0.5778 \text{ Btu/h·ft·°F}$$

which is the desired conversion factor. Therefore, the thermal conductivity of the brick in English units is

$$k_{\text{brick}} = 0.72 \text{ W/m·°C}$$
$$= 0.72 \times (0.5778 \text{ Btu/h·ft·°F})$$
$$= \textbf{0.42 Btu/h·ft·°F}$$

Discussion Note that the thermal conductivity value of a material in English units is about half that in SI units (Fig. 1–33). Also note that we rounded the result to two significant digits (the same number in the original value) since expressing the result in more significant digits (such as 0.4160 instead of 0.42) would falsely imply a more accurate value than the original one.

$k = 0.72$ W/m·°C
$= 0.42$ Btu/h·ft·°F
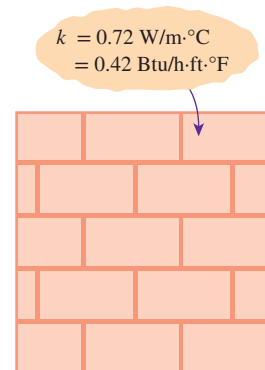
FIGURE 1–33
The thermal conductivity value in English units is obtained by multiplying the value in SI units by 0.5778.

1–7 ▪ CONVECTION

Convection is the mode of energy transfer between a solid surface and the adjacent liquid or gas that is in motion, and it involves the combined effects of *conduction* and *fluid motion.* The faster the fluid motion, the greater the convection heat transfer. In the absence of any bulk fluid motion, heat transfer between a solid surface and the adjacent fluid is by pure conduction. The presence of bulk motion of the fluid enhances the heat transfer between the solid surface and the fluid, but it also complicates the determination of heat transfer rates.

Consider the cooling of a hot block by blowing cool air over its top surface (Fig. 1–34). Heat is first transferred to the air layer adjacent to the block by conduction. This heat is then carried away from the surface by convection, that is, by the combined effects of conduction within the air that is due to the random motion of air molecules and the bulk or macroscopic motion of the air that removes the heated air near the surface and replaces it with the cooler air.

Convection is called **forced convection** if the fluid is forced to flow over the surface by external means such as a fan, pump, or the wind. In contrast, convection is called **natural** (or **free**) **convection** if the fluid motion is caused by buoyancy forces that are induced by density differences due to the variation of temperature in the fluid (Fig. 1–35). For example, in the absence of a fan, heat transfer from the surface of the hot block in Fig. 1–34 is by natural convection since any motion in the air in this case is due to the rise of the warmer (and thus lighter) air near the surface and the fall of the cooler (and thus heavier) air to fill its place. Heat transfer between the block and the surrounding air is by conduction if the temperature difference between the air and the block is not large enough to overcome the resistance of air to movement and thus to initiate natural convection currents.

Heat transfer processes that involve *change of phase* of a fluid are also considered to be convection because of the fluid motion induced during the process, such as the rise of the vapor bubbles during boiling or the fall of the liquid droplets during condensation.
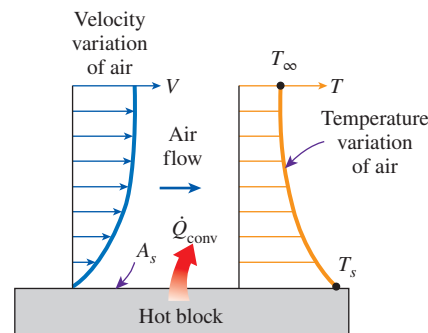
FIGURE 1–34
Heat transfer from a hot surface to air by convection.
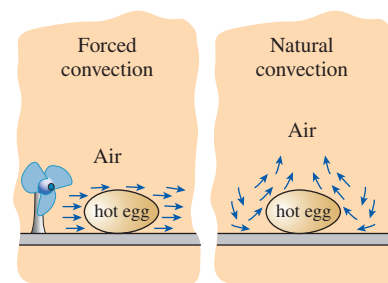
FIGURE 1–35
The cooling of a boiled egg by forced and natural convection.

FIGURE 1–36
Sir Isaac Newton (1642–1727) was an English mathematician, physicist, and astronomer, born in Lincolnshire, England. Newton is regarded as one of the greatest scientists and mathematicians in history. His contributions to mathematics include the development of the binomial theorem, the differential calculus, and the integral calculus. He is said to have conceived the idea of the law of gravity upon observing the fall of an apple in 1665. With the three fundamental laws that bear his name and are described in *Philosophiae Naturalis Principia Mathematica,* Newton is known as the father of classical mechanics. Newton showed that each of Kepler's three laws on the motion of planets and stars could be derived from the single law of gravity. Newton is also credited for the discovery of the composite nature of white light and the separation of different colors by a prism. The law of cooling that governs the rate of heat transfer from a hot surface to a cooler surrounding fluid is also attributed to Newton.

©Pixtal/age fotostock

Despite the complexity of convection, the rate of *convection heat transfer* is observed to be proportional to the temperature difference, and it is conveniently expressed by **Newton's law of cooling** as (Fig. 1–36)

$$\dot{Q}_{\text{conv}} = hA_s(T_s - T_\infty) \quad \text{(W)} \tag{1–24}$$

where h is the *convection heat transfer coefficient* in W/m²·K or Btu/h·ft²·°F, A_s is the surface area through which convection heat transfer takes place, T_s is the surface temperature, and T_∞ is the temperature of the fluid sufficiently far from the surface. Note that at the surface, the fluid temperature equals the surface temperature of the solid.

The convection heat transfer coefficient h is not a property of the fluid. It is an experimentally determined parameter whose value depends on all the variables influencing convection such as the surface geometry, the nature of fluid motion, the properties of the fluid, and the bulk fluid velocity. Typical values of h are given in Table 1–5.

Some people do not consider convection to be a fundamental mechanism of heat transfer since it is essentially heat conduction in the presence of fluid motion. But we still need to give this combined phenomenon a name, unless we are willing to keep referring to it as "conduction with fluid motion." Thus, it is practical to recognize convection as a separate heat transfer mechanism despite the valid arguments to the contrary.

EXAMPLE 1–8 **Measuring Convection Heat Transfer Coefficient**

A 2-m-long, 0.3-cm-diameter electrical wire extends across a room at 15°C, as shown in Fig. 1–37. Heat is generated in the wire as a result of resistance heating, and the surface temperature of the wire is measured to be 152°C in steady operation. Also, the voltage drop and electric current through the wire are measured to be 60 V and 1.5 A, respectively. Disregarding any heat transfer by radiation, determine the convection heat transfer coefficient for heat transfer between the outer surface of the wire and the air in the room.

SOLUTION The convection heat transfer coefficient for heat transfer from an electrically heated wire to air is to be determined by measuring temperatures when steady operating conditions are reached and the electric power consumed.

Assumptions **1** Steady operating conditions exist since the temperature readings do not change with time. **2** Radiation heat transfer is negligible.

Analysis When steady operating conditions are reached, the rate of heat loss from the wire equals the rate of heat generation in the wire as a result of resistance heating. That is,

$$\dot{Q} = \dot{E}_{\text{generated}} = VI = (60 \text{ V})(1.5 \text{ A}) = 90 \text{ W}$$

The surface area of the wire is

$$A_s = \pi DL = \pi(0.003 \text{ m})(2 \text{ m}) = 0.01885 \text{ m}^2$$

Newton's law of cooling for convection heat transfer is expressed as

$$\dot{Q}_{\text{conv}} = hA_s(T_s - T_\infty)$$

Disregarding any heat transfer by radiation and thus assuming all the heat loss from the wire occurs by convection, the convection heat transfer coefficient is determined to be

$$h = \frac{\dot{Q}_{\text{conv}}}{A_s(T_s - T_\infty)} = \frac{90 \text{ W}}{(0.01885 \text{ m}^2)(152 - 15)^\circ\text{C}} = \textbf{34.9 W/m}^2\cdot\textbf{K}$$

Discussion   Note that the simple setup described above can be used to determine the average heat transfer coefficients from a variety of surfaces in air. Also, heat transfer by radiation can be eliminated by keeping the surrounding surfaces at the temperature of the wire.

1–8 ▪ RADIATION

Radiation is the energy emitted by matter in the form of *electromagnetic waves* (or *photons*) as a result of the changes in the electronic configurations of the atoms or molecules. Unlike conduction and convection, the transfer of heat by radiation does not require the presence of an *intervening medium.* In fact, heat transfer by radiation is fastest (it occurs at the speed of light), and it suffers no attenuation in a vacuum. This is how the energy of the sun reaches the earth.

In heat transfer studies we are interested in *thermal radiation,* which is the form of radiation emitted by bodies because of their temperature. It differs from other forms of electromagnetic radiation such as X-rays, gamma rays, microwaves, radio waves, and television waves that are not related to temperature. All bodies at a temperature above absolute zero emit thermal radiation.

Radiation is a *volumetric phenomenon,* and all solids, liquids, and gases emit, absorb, or transmit radiation to varying degrees. However, radiation is usually considered to be a *surface phenomenon* for solids that are opaque to thermal radiation such as metals, wood, and rocks since the radiation emitted by the interior regions of such material can never reach the surface, and the radiation incident on such bodies is usually absorbed within a few microns from the surface.

The maximum rate of radiation that can be emitted from a surface at a thermodynamic temperature T_s (in K or R) is given by the **Stefan–Boltzmann law** as

$$\dot{Q}_{\text{emit, max}} = \sigma A_s T_s^4 \quad \text{(W)} \tag{1–25}$$

where $\sigma = 5.670 \times 10^{-8}$ W/m^2·K^4 or 0.1714×10^{-8} Btu/h·ft^2·R^4 is the *Stefan–Boltzmann constant.* The idealized surface that emits radiation at this maximum rate is called a **blackbody**, and the radiation emitted by a blackbody is called **blackbody radiation** (Fig. 1–38). The radiation emitted by all real surfaces is less than the radiation emitted by a blackbody at the same temperature and is expressed as

$$\dot{Q}_{\text{emit}} = \varepsilon\sigma A_s T_s^4 \quad \text{(W)} \tag{1–26}$$

where ε is the **emissivity** of the surface. The property emissivity, whose value is in the range $0 \leq \varepsilon \leq 1$, is a measure of how closely a surface approximates a blackbody for which $\varepsilon = 1$. The emissivities of some surfaces are given in Table 1–6.

TABLE 1–5

Typical values of convection heat transfer coefficient

Type of Convection	h, W/m^2·K*
Free convection of gases	2–25
Free convection of liquids	10–1000
Forced convection of gases	25–250
Forced convection of liquids	50–20,000
Boiling and condensation	2500–100,000

*Multiply by 0.176 to convert to Btu/h·ft^2·°F.
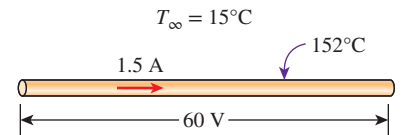
FIGURE 1–37
Schematic for Example 1–8.
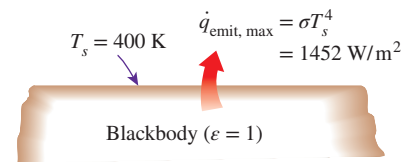
FIGURE 1–38
Blackbody radiation represents the *maximum amount of radiation that can be emitted from a surface at a specified temperature.*

TABLE 1−6

Emissivities of some materials at 300 K

Material	Emissivity
Aluminum foil	0.07
Anodized aluminum	0.82
Polished copper	0.03
Polished gold	0.03
Polished silver	0.02
Polished stainless steel	0.17
Black paint	0.98
White paint	0.90
White paper	0.92–0.97
Asphalt pavement	0.85–0.93
Red brick	0.93–0.96
Human skin	0.95
Wood	0.82–0.92
Soil	0.93–0.96
Water	0.96
Vegetation	0.92–0.96

FIGURE 1−39
The absorption of radiation incident on an opaque surface of absorptivity α.

FIGURE 1−40
Radiation heat transfer between a surface and the surfaces surrounding it.

Another important radiation property of a surface is its **absorptivity** α, which is the fraction of the radiation energy incident on a surface that is absorbed by the surface. Like emissivity, its value is in the range $0 \leq \alpha \leq 1$. A blackbody absorbs all radiation incident on it. That is, a blackbody is a perfect absorber ($\alpha = 1$) as well as a perfect emitter.

In general, both ε and α of a surface depend on the temperature and the wavelength of the radiation. **Kirchhoff's law** of radiation states that the emissivity and the absorptivity of a surface at a given temperature and wavelength are equal. In many practical applications, the surface temperature and the temperature of the source of incident radiation are of the same order of magnitude, and the average absorptivity of a surface is taken to be equal to its average emissivity. The rate at which a surface absorbs radiation is determined from (Fig. 1–39)

$$\dot{Q}_{\text{absorbed}} = \alpha \dot{Q}_{\text{incident}} \quad (\text{W}) \tag{1–27}$$

where $\dot{Q}_{\text{incident}}$ is the rate at which radiation is incident on the surface and α is the absorptivity of the surface. For opaque (nontransparent) surfaces, the portion of incident radiation not absorbed by the surface is reflected back.

The difference between the rates of radiation emitted by the surface and the radiation absorbed is the *net* radiation heat transfer. If the rate of radiation absorption is greater than the rate of radiation emission, the surface is said to be *gaining* energy by radiation. Otherwise, the surface is said to be *losing* energy by radiation. In general, the determination of the net rate of heat transfer by radiation between two surfaces is a complicated matter since it depends on the properties of the surfaces, their orientation relative to each other, and the interaction of the medium between the surfaces with radiation.

When a surface of emissivity ε and surface area A_s at a *thermodynamic temperature* T_s is *completely enclosed* by a much larger (or black) surface at thermodynamic temperature T_{surr} separated by a gas (such as air) that does not intervene with radiation, the net rate of radiation heat transfer between these two surfaces is given by (Fig. 1–40)

$$\dot{Q}_{\text{rad}} = \varepsilon \sigma A_s (T_s^4 - T_{\text{surr}}^4) \quad (\text{W}) \tag{1–28}$$

In this special case, the emissivity and the surface area of the surrounding surface do not have any effect on the net radiation heat transfer.

Radiation heat transfer to or from a surface surrounded by a gas such as air occurs *parallel* to conduction (or convection, if there is bulk gas motion) between the surface and the gas. Thus the total heat transfer is determined by *adding* the contributions of both heat transfer mechanisms. For simplicity and convenience, this is often done by defining a **combined heat transfer coefficient** h_{combined} that includes the effects of both convection and radiation. Then the *total* heat transfer rate to or from a surface by convection and radiation is expressed as

$$\dot{Q}_{\text{total}} = \dot{Q}_{\text{conv}} + \dot{Q}_{\text{rad}} = h_{\text{conv}} A_s (T_s - T_{\text{surr}}) + \varepsilon \sigma A_s (T_s^4 - T_{\text{surr}}^4)$$

$$\dot{Q}_{\text{total}} = h_{\text{combined}} A_s (T_s - T_{\text{surr}}) \quad (\text{W}) \tag{1–29}$$

$$h_{\text{combined}} = h_{\text{conv}} + h_{\text{rad}} = h_{\text{conv}} + \varepsilon \sigma (T_s + T_{\text{surr}})(T_s^2 + T_{\text{surr}}^2)$$
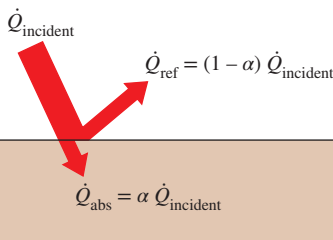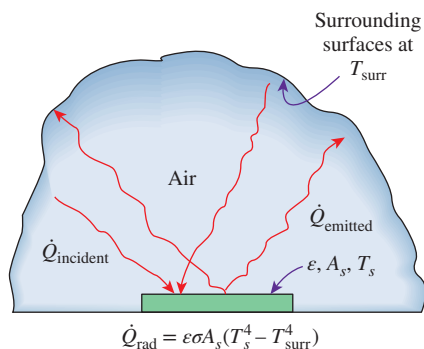
Note that the combined heat transfer coefficient is essentially a convection heat transfer coefficient modified to include the effects of radiation.

Radiation is usually significant relative to conduction or natural convection, but negligible relative to forced convection. Thus radiation in forced convection applications is usually disregarded, especially when the surfaces involved have low emissivities and low to moderate temperatures.

EXAMPLE 1–9   Radiation Effect on Thermal Comfort

It is a common experience to feel chilly in winter and warm in summer in our homes even when the thermostat setting is kept the same. This is due to the so-called radiation effect resulting from radiation heat exchange between our bodies and the surrounding surfaces of the walls and the ceiling.

Consider a person standing in a room maintained at 22°C at all times. The inner surfaces of the walls, floors, and the ceiling of the house are at an average temperature of 10°C in winter and 25°C in summer. Determine the rate of radiation heat transfer between this person and the surrounding surfaces if the exposed surface area and the average outer surface temperature of the person are $1.4\,\text{m}^2$ and 30°C, respectively (Fig. 1–41).

SOLUTION   The rates of radiation heat transfer between a person and the surrounding surfaces at specified temperatures are to be determined in summer and winter.
Assumptions   **1** Steady operating conditions exist. **2** Heat transfer by convection is not considered. **3** The person is completely surrounded by the interior surfaces of the room. **4** The surrounding surfaces are at a uniform temperature.
Properties   The emissivity of a person is $\varepsilon = 0.95$ (Table 1–6).
Analysis   The net rates of radiation heat transfer from the body to the surrounding walls, ceiling, and floor in winter and summer are

$$\dot{Q}_{\text{rad, winter}} = \varepsilon\sigma A_s\,(T_s^4 - T_{\text{surr, winter}}^4)$$
$$= (0.95)(5.67 \times 10^{-8}\ \text{W/m}^2\cdot\text{K}^4)(1.4\,\text{m}^2)$$
$$\times \left[(30 + 273)^4 - (10 + 273)^4\right]\,\text{K}^4$$
$$= \textbf{152 W}$$

and

$$\dot{Q}_{\text{rad, summer}} = \varepsilon\sigma A_s\,(T_s^4 - T_{\text{surr, summer}}^4)$$
$$= (0.95)(5.67 \times 10^{-8}\ \text{W/m}^2\cdot\text{K}^4)(1.4\,\text{m}^2)$$
$$\times \left[(30 + 273)^4 - (25 + 273)^4\right]\text{K}^4$$
$$= \textbf{40.9 W}$$

Discussion   Note that we must use *thermodynamic (i.e., absolute) temperatures* in radiation calculations. Also note that the rate of heat loss from the person by radiation is almost four times as large in winter as it is in summer, which explains the chill we feel in winter even if the thermostat setting is kept the same.
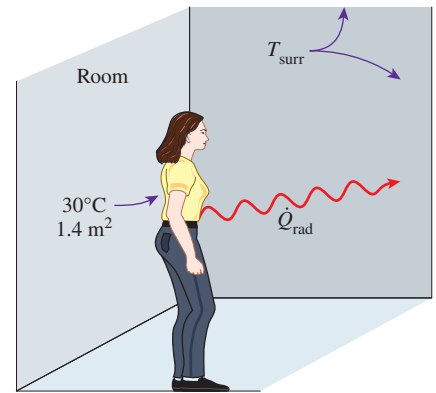
FIGURE 1–41
Schematic for Example 1–9.

1–9 ▪ SIMULTANEOUS HEAT TRANSFER MECHANISMS

We mentioned that there are three mechanisms of heat transfer, but not all three can exist simultaneously in a medium. For example, heat transfer is only by conduction in *opaque solids,* but by conduction and radiation in *semitransparent solids.* Thus, a solid may involve conduction and radiation but not
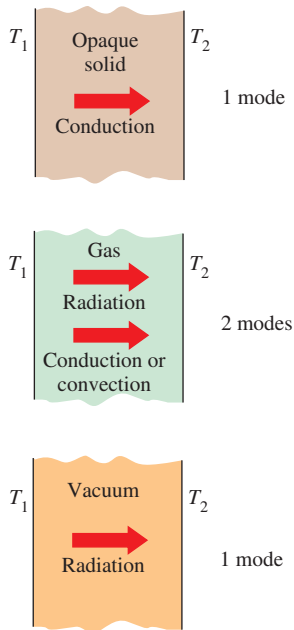
FIGURE 1–42
Although there are three mechanisms of heat transfer, a medium may involve only two of them simultaneously.
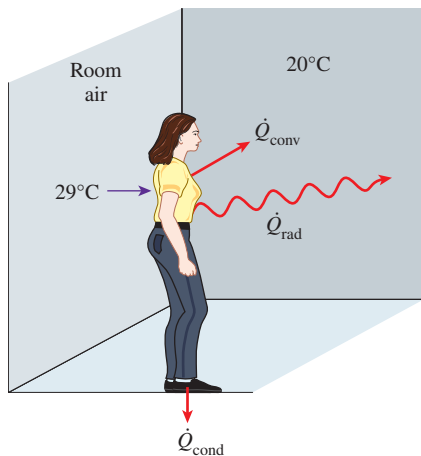
FIGURE 1–43
Heat transfer from the person described in Example 1–10.

convection. However, a solid may involve heat transfer by convection and/ or radiation on its surfaces exposed to a fluid or other surfaces. For example, the outer surfaces of a cold piece of rock will warm up in a warmer environment as a result of heat gain by convection (from the air) and radiation (from the sun or the warmer surrounding surfaces). But the inner parts of the rock will warm up as this heat is transferred to the inner region of the rock by conduction.

Heat transfer is by conduction and possibly by radiation in a *still fluid* (no bulk fluid motion) and by convection and radiation in a *flowing fluid.* In the absence of radiation, heat transfer through a fluid is either by conduction or convection, depending on the presence of any bulk fluid motion. Convection can be viewed as combined conduction and fluid motion, and conduction in a fluid can be viewed as a special case of convection in the absence of any fluid motion (Fig. 1–42).

Thus, when we deal with heat transfer through a *fluid,* we have either *conduction* or *convection,* but not both. Also, gases are practically transparent to radiation, except that some gases are known to absorb radiation strongly at certain wavelengths. Ozone, for example, strongly absorbs ultraviolet radiation. But in most cases, a gas between two solid surfaces does not interfere with radiation, and it acts effectively as a vacuum. Liquids, on the other hand, are usually strong absorbers of radiation.

Finally, heat transfer through a *vacuum* is by radiation only since conduction or convection requires the presence of a material medium.

EXAMPLE 1–10   Heat Loss from a Person

Consider a person standing in a breezy room at 20°C. Determine the total rate of heat transfer from this person if the exposed surface area and the average outer surface temperature of the person are 1.6 m^2 and 29°C, respectively, and the convection heat transfer coefficient is 6 W/m^2·K (Fig. 1–43).

SOLUTION   The total rate of heat transfer from a person by both convection and radiation to the surrounding air and surfaces at specified temperatures is to be determined.

Assumptions   **1** Steady operating conditions exist. **2** The person is completely surrounded by the interior surfaces of the room. **3** The surrounding surfaces are at the same temperature as the air in the room. **4** Heat conduction to the floor through the feet is negligible.

Properties   The emissivity of a person is $\varepsilon = 0.95$ (Table 1–6).

Analysis   The heat transfer between the person and the air in the room is by convection (instead of conduction) since it is conceivable that the air in the vicinity of the skin or clothing warms up and rises as a result of heat transfer from the body, initiating natural convection currents. It appears that the experimentally determined value for the rate of convection heat transfer in this case is 6 W per unit surface area (m^2) per unit temperature difference (in K or °C) between the person and the air away from the person. Thus, the rate of convection heat transfer from the person to the air in the room is

$$\dot{Q}_{conv} = hA_s (T_s - T_\infty)$$
$$= (6 \text{ W/m}^2\text{·K})(1.6 \text{ m}^2)(29 - 20)°C$$
$$= 86.4 \text{ W}$$

The person also loses heat by radiation to the surrounding wall surfaces. We take the temperature of the surfaces of the walls, ceiling, and floor to be equal to the air temperature in this case for simplicity, but we recognize that this does not need to be the case. These surfaces may be at a higher or lower temperature than the average temperature of the room air, depending on the outdoor conditions and the structure of the walls. Considering that air does not intervene with radiation and the person is completely enclosed by the surrounding surfaces, the net rate of radiation heat transfer from the person to the surrounding walls, ceiling, and floor is

$$\dot{Q}_{rad} = \varepsilon \sigma A_s (T_s^4 - T_{surr}^4)$$
$$= (0.95)(5.67 \times 10^{-8} \text{ W/m}^2 \cdot \text{K}^4)(1.6 \text{ m}^2)$$
$$\times [(29 + 273)^4 - (20 + 273)^4] \text{K}^4$$
$$= 81.7 \text{ W}$$

Note that we must use *thermodynamic* temperatures in radiation calculations. Also note that we used the emissivity value for the skin and clothing at room temperature since the emissivity is not expected to change significantly at a slightly higher temperature.

Then the rate of total heat transfer from the body is determined by adding these two quantities:

$$\dot{Q}_{total} = \dot{Q}_{conv} + \dot{Q}_{rad} = (86.4 + 81.7) \text{ W} \cong \mathbf{168 \text{ W}}$$

Discussion The heat transfer would be much higher if the person were not dressed since the exposed surface temperature would be higher. Thus, an important function of the clothes is to serve as a barrier against heat transfer.

In these calculations, heat transfer through the feet to the floor by conduction, which is usually very small, is neglected. Heat transfer from the skin by perspiration, which is the dominant mode of heat transfer in hot environments, is not considered here.

Also, the units W/m²·°C and W/m²·K for heat transfer coefficient are equivalent and can be interchanged.

EXAMPLE 1–11   Heat Transfer Between Two Isothermal Plates

Consider steady heat transfer between two large parallel plates at constant temperatures of $T_1 = 300$ K and $T_2 = 200$ K that are $L = 1$ cm apart, as shown in Fig. 1–44. Assuming the surfaces to be black (emissivity $\varepsilon = 1$), determine the rate of heat transfer between the plates per unit surface area, assuming the gap between the plates is (*a*) filled with atmospheric air, (*b*) evacuated, (*c*) filled with urethane insulation, and (*d*) filled with superinsulation that has an apparent thermal conductivity of 0.00002 W/m·K.

SOLUTION The total rate of heat transfer between two large parallel plates at specified temperatures is to be determined for four different cases.
Assumptions **1** Steady operating conditions exist. **2** There are no natural convection currents in the air between the plates. **3** The surfaces are black, and thus $\varepsilon = 1$.
Properties The thermal conductivity at the average temperature of 250 K is $k = 0.0219$ W/m·K for air (Table A–15), 0.026 W/m·K for urethane insulation (Table A–6), and 0.00002 W/m·K for the superinsulation.
Analysis (*a*) The rates of conduction and radiation heat transfer between the plates through the air layer are

$$\dot{Q}_{cond} = kA\frac{T_1 - T_2}{L} = (0.0219 \text{ W/m·K})(1 \text{ m}^2)\frac{(300 - 200)\text{K}}{0.01 \text{ m}} = 219 \text{ W}$$

$T_1 = 300$ K $\dot{Q}$ $T_2 = 200$ K

$L = 1$ cm

$\varepsilon = 1$
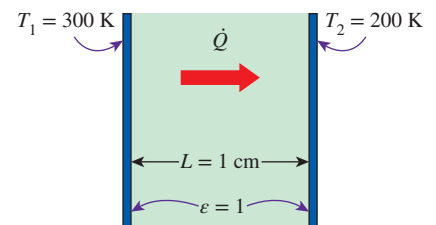
FIGURE 1–44
Schematic for Example 1–11.

and

$$\dot{Q}_{rad} = \varepsilon\sigma A(T_1^4 - T_2^4)$$
$$= (1)(5.67 \times 10^{-8}\ \text{W/m}^2\cdot\text{K}^4)(1\ \text{m}^2)\big[(300\ \text{K})^4 - (200\ \text{K})^4\big] = 369\ \text{W}$$

Therefore,

$$\dot{Q}_{total} = \dot{Q}_{cond} + \dot{Q}_{rad} = 219 + 369 = \textbf{588 W}$$

The heat transfer rate in reality will be higher because of the natural convection currents that are likely to occur in the airspace between the plates.

(*b*) When the airspace between the plates is evacuated, there will be no conduction or convection, and the only heat transfer between the plates will be by radiation. Therefore,

$$\dot{Q}_{total} = \dot{Q}_{rad} = \textbf{369 W}$$

(*c*) An opaque solid material placed between two plates blocks direct radiation heat transfer between the plates. Also, the thermal conductivity of an insulating material accounts for the radiation heat transfer that may be occurring through the voids in the insulating material. The rate of heat transfer through the urethane insulation is

$$\dot{Q}_{total} = \dot{Q}_{cond} = kA\frac{T_1 - T_2}{L} = (0.026\ \text{W/m}\cdot\text{K})(1\ \text{m}^2)\frac{(300 - 200)\ \text{K}}{0.01\ \text{m}} = \textbf{260 W}$$

Note that heat transfer through the urethane material is less than the heat transfer through the air determined in (*a*), although the thermal conductivity of the insulation is higher than that of air. This is because the insulation blocks the radiation, whereas air transmits it.

(*d*) The layers of the superinsulation prevent any direct radiation heat transfer between the plates. However, radiation heat transfer between the sheets of superinsulation does occur, and the apparent thermal conductivity of the superinsulation accounts for this effect. Therefore,

$$\dot{Q}_{total} = kA\frac{T_1 - T_2}{L} = (0.00002\ \text{W/m}\cdot\text{K})(1\ \text{m}^2)\frac{(300 - 200)\ \text{K}}{0.01\ \text{m}} = \textbf{0.2 W}$$

which is $\frac{1}{1845}$ of the heat transfer through the vacuum. The results of this example are summarized in Fig. 1–45 to put them into perspective.

Discussion This example demonstrates the effectiveness of superinsulations and explains why they are the insulation of choice in critical applications despite their high cost.
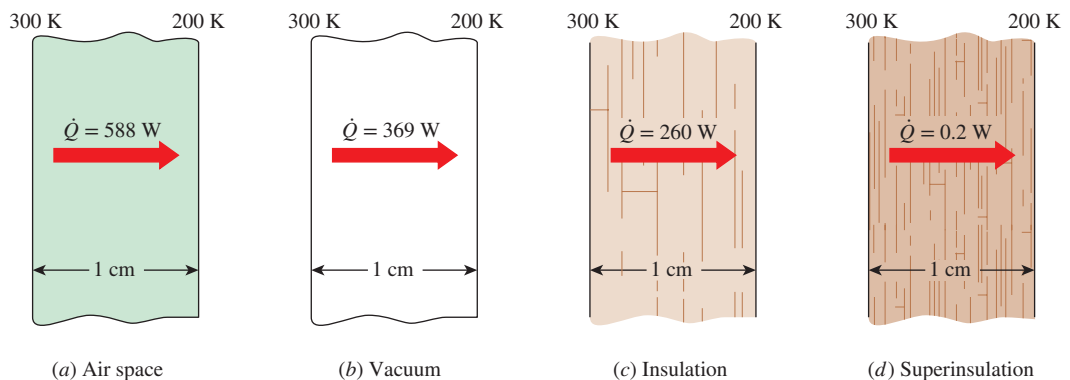
FIGURE 1–45
Different ways of reducing heat transfer between two isothermal plates, and their effectiveness.

(*a*) Air space (*b*) Vacuum (*c*) Insulation (*d*) Superinsulation

FIGURE 1–46
A chicken being cooked in a
microwave oven (Example 1–12).

EXAMPLE 1–12 Heat Transfer in Conventional and Microwave Ovens

The fast and efficient cooking of microwave ovens has made them one of the essential appliances in modern kitchens (Fig. 1–46). Discuss the heat transfer mechanisms associated with the cooking of a chicken in microwave and conventional ovens, and explain why cooking in a microwave oven is more efficient.

SOLUTION Food is cooked in a microwave oven by absorbing the electromagnetic radiation energy generated by the microwave tube, called the magnetron. The radiation emitted by the magnetron is not thermal radiation since its emission is not due to the temperature of the magnetron; rather, it is due to the conversion of electrical energy into electromagnetic radiation at a specified wavelength. The wavelength of the microwave radiation is such that it is *reflected* by metal surfaces; *transmitted* by the cookware made of glass, ceramic, or plastic; and *absorbed* and converted to internal energy by food (especially the water, sugar, and fat) molecules.

In a microwave oven, the *radiation* that strikes the chicken is absorbed by the skin of the chicken and the outer parts. As a result, the temperature of the chicken at and near the skin rises. Heat is then *conducted* toward the inner parts of the chicken from its outer parts. Of course, some of the heat absorbed by the outer surface of the chicken is lost to the air in the oven by *convection.*

In a conventional oven, the air in the oven is first heated to the desired temperature by the electric or gas heating element. This preheating may take several minutes. The heat is then transferred from the air to the skin of the chicken by *natural convection* in older ovens or by *forced convection* in the newer convection ovens that utilize a fan. The air motion in convection ovens increases the convection heat transfer coefficient and thus decreases the cooking time. Heat is then *conducted* toward the inner parts of the chicken from its outer parts as in microwave ovens.

Microwave ovens replace the slow convection heat transfer process in conventional ovens by the instantaneous radiation heat transfer. As a result, microwave ovens transfer energy to the food at full capacity the moment they are turned on, and thus they cook faster while consuming less energy.
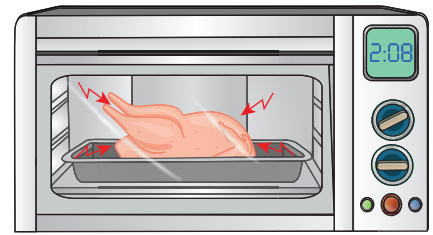
EXAMPLE 1–13 Heating of a Plate by Solar Energy

A thin metal plate is insulated on the back and exposed to solar radiation at the front surface (Fig. 1–47). The exposed surface of the plate has an absorptivity of 0.6 for solar radiation. If solar radiation is incident on the plate at a rate of 700 W/m^2 and the surrounding air temperature is 25°C, determine the surface temperature of the plate when the heat loss by convection and radiation equals the solar energy absorbed by the plate. Assume the combined convection and radiation heat transfer coefficient to be 50 W/m^2·K.

SOLUTION The back side of the thin metal plate is insulated, and the front side is exposed to solar radiation. The surface temperature of the plate is to be determined when it stabilizes.
Assumptions **1** Steady operating conditions exist. **2** Heat transfer through the insulated side of the plate is negligible. **3** The heat transfer coefficient remains constant.
Properties The solar absorptivity of the plate is given to be $\alpha = 0.6$.
Analysis The absorptivity of the plate is 0.6, and thus 60 percent of the solar radiation incident on the plate is absorbed continuously. As a result, the temperature of the plate
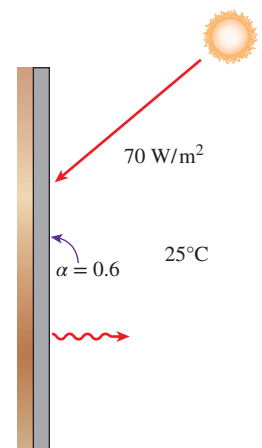
FIGURE 1–47
Schematic for Example 1–13.

70 W/m^2

25°C

$\alpha = 0.6$

rises, and the temperature difference between the plate and the surroundings increases. This increasing temperature difference causes the rate of heat loss from the plate to the surroundings to increase. At some point, the rate of heat loss from the plate equals the rate of solar energy absorbed, and the temperature of the plate no longer changes. The temperature of the plate when steady operation is established is determined from

$$\dot{E}_{\text{gained}} = \dot{E}_{\text{lost}} \quad \text{or} \quad \alpha A_s \, \dot{q}_{\text{incident, solar}} = h_{\text{combined}} A_s (T_s - T_\infty)$$

Solving for T_s and substituting, the plate surface temperature is determined to be

$$T_s = T_\infty + \alpha \frac{\dot{q}_{\text{incident, solar}}}{h_{\text{combined}}} = 25°C + \frac{0.6 \times (700 \text{ W/m}^2)}{50 \text{ W/m}^2 \cdot \text{K}} = \textbf{33.4°C}$$

Discussion Note that the heat losses prevent the plate temperature from rising above 33.4°C. Also, the combined heat transfer coefficient accounts for the effects of both convection and radiation, and thus it is very convenient to use in heat transfer calculations when its value is known with reasonable accuracy.

1–10 ▪ AEROGEL—A REMARKABLE SUPERINSULATING MATERIAL*

Aerogels—often called "frozen smoke"—are lightweight and have an ethereal blue haze. An aerogel in your hand feels like a piece of air—but it is a solid. What makes them so interesting is their unique nanoporous structure. This structure is formed through the sol-gel process, whereby a sol (a particulate-containing solution) undergoes a polymerization reaction to form a nanoporous wet gel. The key to making an aerogel is to carefully dry the wet gel. This can be difficult because, unless care is taken, capillary forces due to surface tension will cause the nanoporous structure to collapse as it dries. Supercritical extraction is commonly used to make aerogels. If the wet gel is heated and pressurized to a state above the critical point of the solvent that is in the wet gel, surface tension can be eliminated and the wet gel can be dried to form an aerogel. Aerogels can be made from many different precursor materials. The most common type of aerogel is the silica aerogel. Figure 1–48, a famous aerogel picture from the NASA Stardust site, demonstrates the insulating properties of silica aerogel.

When an aerogel is made by the sol-gel method, it forms a nanoporous structure comprised of clusters of silica spheres on the order of 5–10 nm that connect and form long, chain-like connecting structures with pores that range from 5 to 100 nm in size, as shown in Fig. 1–49. Because of this structure, silica aerogels are very porous (90–99 percent air) and have low density (0.05–0.4 g/cm^3) and large surface areas (500–1400 m^2/g). They are also highly translucent and have low thermal conductivity (0.01–0.3 W/m·K, which is lower than the thermal conductivity of most of the insulators shown in Fig. 1–29).
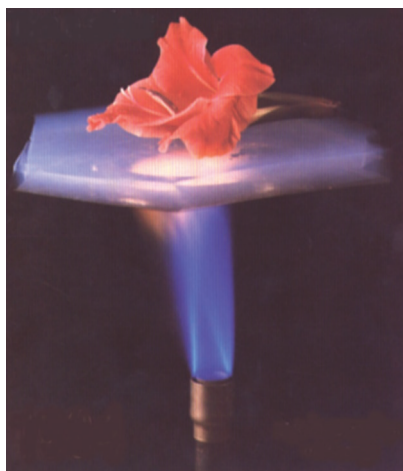
FIGURE 1–48
A silica aerogel insulates a flower from the heat of a Bunsen burner.
Source: JPL/NASA

---

*This section is contributed by Professor Ann M. Anderson, Mechanical Engineering Department, Union College, Schenectady, NY.

10–20 nm

5 nm
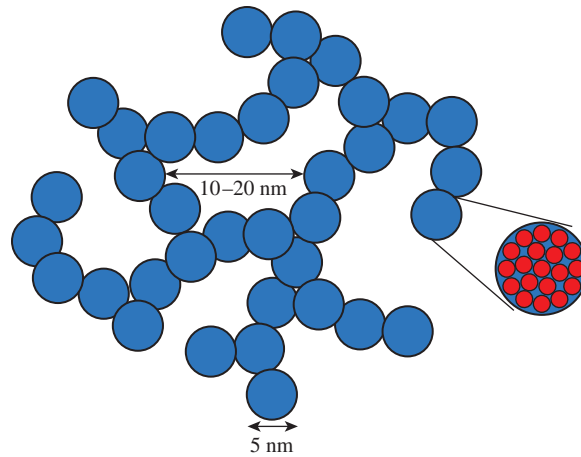
FIGURE 1–49
Schematic representation of
an aerogel nanostructure.
©*Ann M. Anderson*

In general, heat is transferred by conduction, convection, and radiation. Convection through an aerogel is hindered by the small pore size, and at low temperatures radiation is not significant. Therefore, the primary method for heat transfer through an aerogel is by conduction in both the solid and gaseous phases. Solid phase conduction is related to the thermal conductivity of the solid and the amount of that solid. Since aerogels are so porous, there is very little solid material, and what is there follows a tortuous path with many dead ends (formed by the original sol-gel process). For these reasons, the thermal conductivity of an aerogel is very low.

Aerogels are commercially available in an impregnated blanket form, as granules, or as monolithic pieces. They are used in a variety of applications, including comet dust collectors, oil spill clean-up material, and chemical sensors. The most common application for aerogels is as insulation where, for example, they are used in daylighting products (insulating windows), high-performance clothing, and pipe insulation.

A monolithic aerogel under slight vacuum can have a thermal conductivity as low as 0.01 W/m·K. Because they are also translucent, aerogels can be used in daylighting and window applications. For example, consider a 6-mm-thick single-pane glass window ($k = 1.0$ W/m·K) that is 25 cm × 16 cm with an inside temperature of 30°C and an outside temperature of 10°C. The heat loss through the window can be calculated as:

$$\dot{Q} = kA\frac{\Delta T}{\Delta x} = \left(1.0\,\frac{\text{W}}{\text{m·K}}\right)(0.25\,\text{m} \times 0.16\,\text{m})\frac{(30 - 10)°\text{C}}{0.006\,\text{m}} = 133.3\,\text{W}$$

If we could make the window pane out of a monolithic aerogel under slight vacuum, the heat loss would be:

$$\dot{Q} = kA\frac{\Delta T}{\Delta x} = \left(0.01\,\frac{\text{W}}{\text{m·K}}\right)(0.25\,\text{m} \times 0.16\,\text{m})\frac{(30 - 10)°\text{C}}{0.006\,\text{m}} = 1.3\,\text{W}$$

The use of aerogel would reduce the heat loss by a factor of 100!

So why don't we have more aerogel windows? There are two major limiting factors to the more widespread use of aerogels: cost and fragility. Supercritical

extraction involves expensive equipment, which drives up the cost of aerogels. The unique nanoporous structure of the aerogel that gives it the remarkable insulating properties is also very fragile. Much of the current research in the aerogel community is focused on developing methods that reduce the cost of aerogels and make them stronger.

1–11 ▪ PREVENTION THROUGH DESIGN*

The emphasis on safety is not unusual in the fields of engineering. It is not surprising that the first of the fundamental canons of ethics for engineers is to "hold paramount the safety, health, and welfare of the public" when fulfilling their professional duties (*Code of Ethics for Engineers,* 2007). In 2007, the National Institute for Occupational Safety and Health (NIOSH) launched the National Prevention through Design (PtD) initiative, with the mission to prevent or reduce work-related injuries, illnesses, and fatalities by including prevention considerations in all circumstances that affect people in their workplaces (*Prevention Through Design: Plan for the National Initiative,* 2010). PtD involves applying the means of reducing risks and preventing hazards in the design of equipment, tools, processes, and work facilities. We present example problems and end-of-chapter problems on PtD throughout this text not only to provide discussions of interesting real-world applications, but also to introduce the concepts of PtD to the minds of tomorrow's engineers so that they may influence a change in culture toward more emphasis on safe designs.

The National PtD Initiative is largely being discussed in the context of preventing hazards in working environments. Nevertheless, the concepts of PtD can also be rationally applied to preventing failures and damages to devices, products, and systems. Failures and damages often have negative impacts on the environment, profitability, and the society at large. Within the context of heat and mass transfer, the PtD concepts can be presented along with the physical mechanisms involved and their practical applications. Issues such as prevention of thermal burn, fire hazard, and thermal failure in systems are topics that can relate the concepts of PtD with the basic science of heat and mass transfer. The process of solving heat and mass transfer problems, along with the application of PtD concepts, involves incorporating prescribed PtD criteria, be it the prevention of burn injury, fire hazard, or system failure, to the solutions (Fig. 1–50). To successfully arrive at a solution that satisfies prescribed PtD criteria requires understanding how the physical mechanisms of heat and mass transfer interrelate with the concepts of PtD.

Thermal burn occurs when skin tissues are exposed to temperatures that are higher than their physiological temperature. When this happens, the protein and cellular structures of skin tissues are altered as the higher temperatures cause thermal shocks and disrupt the skin cells. The degree of injury as a result of thermal burn is influenced by the temperature to which the
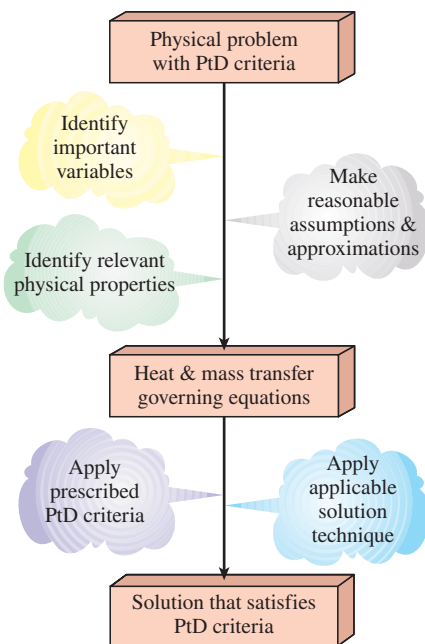
FIGURE 1–50
Process of solving problems with application of PtD concepts.

*This section is contributed by Professor Clement C. Tang, Mechanical Engineering Department, University of North Dakota, Grand Forks, ND.

skin is exposed and the duration of exposure. The skin reaction to thermal burn is dependent upon the heat transfer rate from the hot medium to the skin. When exposed to temperatures above approximately 43°C, the human skin can begin to feel discomfort and pain; damage can occur if the exposure is sufficiently long. Exposure to a temperature of about 48°C can cause human skin to receive a first-degree burn injury, and temperatures above 70°C can cause instantaneous damage to human skin (ASTM Standard C1055-03, 2009).

Injury from thermal burn can result from all three modes of heat transfer: conduction, convection, and radiation. Thermal burn by conduction heat transfer occurs when the skin is in contact with a hot solid surface. The thermal properties, roughness, and temperature of the hot solid surface, along with the contact duration and the nature of the skin, all influence the degree of this thermal burn injury. Scalding of skin from hot fluid is a thermal burn caused by convection heat transfer to the skin. Scalding on skin tissue can occur through spilling of hot liquid or accidental immersion into hot liquid. Thermal burn injuries from convection heat transfer of hot gas are not only external but also can be internal, affecting the upper respiratory tract and even the lungs. Thermal burn by radiation can be caused from laser or other sources such as nuclear explosion. Although human skin can reflect much of the incident energy from radiation, exposure to high-energy laser beams can cause thermal burn on skin. The severity of thermal burn from laser is influenced by the range of wavelength that allows the laser beam to penetrate into the skin tissue and the duration of exposure.

In the prevention of fire hazard, the understanding of flash point is important. Flash point is the lowest temperature at which a liquid can vaporize and form a mixture with air to become ignitable. When a liquid reaches its flash point, a source of ignition (e.g., open flame, spark, static electricity, and hot object) will cause the liquid to ignite. Therefore, designs for fire hazard prevention must be in place when storing, handling, or transporting a liquid above its flash point so that it is not exposed to an ignition source. The lower the flash point of a liquid, the more susceptible it is to a fire hazard. Flash point is also used for characterizing liquids into fire hazard categories, such as combustible and flammable liquids. The National Fire Protection Association (NFPA) has classified a liquid with a flash point of 37.8°C (100°F) or higher as a combustible liquid. A liquid with a flash point below 37.8°C is classified as flammable liquid. Another concept important to fire hazard prevention is the autoignition temperature (AIT), which is the minimum temperature at which a substance will spontaneously ignite without an ignition source. A substance is autoignited when it is heated above a temperature at which the rate of heat release from the exothermic oxidation reaction becomes significantly greater than the rate of heat lost to the surroundings. Factors influencing the autoignition temperature include atmospheric pressure, humidity, and oxygen concentration.

The science of heat and mass transfer can be coupled with the concepts of PtD to mitigate the risks of thermal failure in systems. Thermal stress can compromise the integrity of parts and components in a system. Extreme temperature can alter the physical properties of a material, which can cause a component to lose its functionality. Cold temperature on the morning of January 28, 1986,
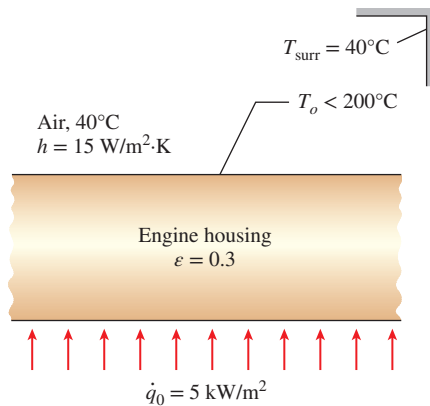
affected the elasticity of the O-ring on a solid rocket booster of the space shuttle *Challenger*. The loss of the O-ring's elasticity and ability to seal allowed hot combustion gas to leak through a solid rocket booster, which led to the tragic disaster.

PtD **EXAMPLE 1–14** **Fire Hazard Prevention of Oil Leakage on Hot Engine Surface**

Oil leakage and spillage on hot engine surfaces can create fire hazards. Some engine oils have an autoignition temperature above 250°C. When oil leakage comes in contact with a hot engine surface that has a higher temperature than its autoignition temperature, the oil can ignite spontaneously. Consider the outer surface of an engine situated in a place where there is a possibility of being in contact with oil leakage. The engine surface has an emissivity of 0.3, and when it is in operation, its inner surface is subjected to 5 kW/m² of heat flux (Fig. 1–51). The engine is in an environment where the ambient air and surrounding temperature is 40°C, while the convection heat transfer coefficient is 15 W/m²·K. To prevent a fire hazard, the temperature of the engine surface should be kept below 200°C. Determine whether oil on the engine surface is at a risk of autoignition. If there is a risk of autoignition, discuss a possible prevention measure that can be implemented.

SOLUTION In this example, the concepts of PtD are applied with the basic understanding of simultaneous heat transfer mechanisms via convection and radiation. The inner surface of an engine is subject to a heat flux of 5 kW/m². We must determine whether the engine surface temperature is below 200°C to prevent spontaneous ignition in the event of oil leakage onto the engine surface.

Assumptions **1** Steady operating conditions exist. **2** The surrounding surfaces are at the same temperature as the ambient air. **3** Heat conduction through the engine housing is one-dimensional. **4** The engine inner surface is subjected to uniform heat flux.

Properties Emissivity of the engine surface is given as $\varepsilon = 0.3$.

Analysis When in operation, the inner surface of the engine is subjected to a uniform heat flux, which is equal to the sum of heat fluxes transferred by convection and radiation on the outer surface. Therefore,

$$\dot{q}_0 = h(T_o - T_\infty) + \varepsilon\sigma\,(T_o^4 - T_{surr}^4)$$
$$5000 \text{ W/m}^2 = (15 \text{ W/m}^2\cdot\text{K})\,[\,T_o - (40 + 273)]\text{K}$$
$$+(0.3)(5.67 \times 10^{-8} \text{ W/m}^2\cdot\text{K}^4)[\,T_o^4 - (40 + 273)^4]\,\text{K}^4$$

Using appropriate software and solving implicitly for the engine outer surface temperature (T_o), the result is $T_o = 552$ K = **279°C**.

Discussion The solution reveals that the engine outer surface temperature is greater than 200°C, which presents the risk of autoignition in the event of oil leakage onto the engine outer surface. To mitigate the risk of fire hazards, the outer surface of the engine should be insulated. In practice, the engine surface temperature is not uniform; instead, high local surface temperatures result in hot spots on the engine surface. Engine housings generally come in irregular shapes, thus making the prediction of hot spots on the engine surface difficult. However, using handheld infrared thermometers, engine operators can quickly identify the areas that are prone to hot spots and take proper prevention measures.

$T_{surr} = 40°C$

$T_o < 200°C$

Air, 40°C
$h = 15 \text{ W/m}^2\cdot\text{K}$

Engine housing
$\varepsilon = 0.3$

$\dot{q}_0 = 5 \text{ kW/m}^2$

FIGURE 1–51
Schematic for Example 1–14.

1−12 ▪ ENGINEERING CODES AND STANDARDS*

Engineering codes and standards are ubiquitous. When we consider any given device that we use daily, the path, from the design to the prototype and finally to the production of the final product is guided by standards and regulated by codes. A product that has been manufactured to meet certain standards tells the user about the product's quality and that it has met certain levels of scrutiny set forth by those standards. In essence, engineering standards communicate to the user that the product is expected to function safely and meets quality objectives. At the industrial level, engineering codes and standards provide efficiency in engineering processes (from design to manufacturing), maintain safety and uniformity of products that allows interchangeability, and improve commerce. Engineering codes and standards are evolutionary—they are continually revised to reflect technical advances, such as new technologies, new designs, new procedures, and new materials.

The development of engineering codes and standards is rooted in the engineers' code of ethics to "hold paramount the safety, health, and welfare of the public" in their professions (*Code of Ethics for Engineers,* 2007). The founding of the American Society of Mechanical Engineers (ASME) in 1880 provided a forum for engineers, designers, and machine shop managers to discuss and collaborate to solve issues brought on by the industrial age. Within four years, the first ASME standard, "Code for the Conduct of Trials of Steam Boilers," was issued. This was the first ASME Performance Test Code (PTC). Today, there are close to 50 ASME PTCs, and they cover components, systems, and facilities. Performance test codes are used by manufacturers to ensure the reliability of their products, and users can use the PTCs to protect themselves from products that function poorly.

Some of the very first engineering codes and standards were needed because of engineering failures that caused the loss of life and property. In 1905, a boiler exploded in a shoe factory in Brockton, Massachusetts. In the next year, a similar incident happened in another shoe factory in Lynn, Massachusetts. Within a decade, the first edition of the Boiler and Pressure Vessel Code (BPVC) was issued by the ASME in 1914 and published in 1915. Today, the ASME BPVC has been adopted by the United States and Canada, and it is being used in over 100 countries around the world (*ASME Boiler & Pressure Vessel Code,* 2015).

A recent study done by ASME Vision 2030 Project reveals that almost 50 percent of engineers in their early career are unfamiliar with engineering codes and standards (ASME Vision 2030 Project, n.d.). As companies and manufacturers expand operations globally, there is a greater need to harmonize codes and standards across jurisdictions and disciplines. The need for engineers to know about codes and standards is growing, and having this knowledge allows engineers to innovate and manufacture competitive products.

In the subject of heat and mass transfer, there are several engineering codes and standards that are relevant. These codes and standards have been issued and published by professional associations, such as the ASME and

*This section is contributed by Professor Clement C. Tang, Mechanical Engineering Department, University of North Dakota, Grand Forks, ND.

the ASHRAE, and standards organizations, such as ASTM International, the ANSI, and the ISO. For instance, the 2015 ASME Boiler & Pressure Vessel Code, Section IV (ASME BPVC.IV-2015) provided the permitted O-ring materials and their temperature limits for water tube attachments in hot water boilers (*ASME Boiler & Pressure Vessel Code,* 2015). Another example is the standard specification issued by ASTM International for polyethylene insulation used on electrical cable (ASTM D1351-14, 2014), which is important as overheating can rapidly deteriorate the insulation. Extreme temperatures and thermal cycles can cause materials to deteriorate and thereby affect the functionality of components. The knowledge of heat and mass transfer, along with adherence to the relevant codes and standards, allow engineers to analyze, design, and build components and systems to function within the design conditions. Throughout the text, as appropriate, example problems and end-of-chapter problems related to codes and standards will be presented to introduce this concept to tomorrow's engineers.
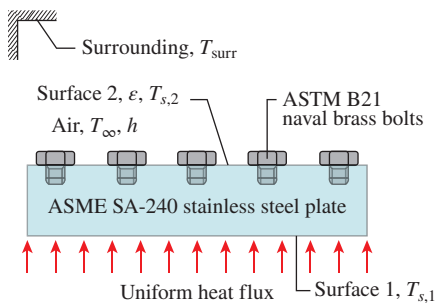
FIGURE 1–52
Schematic for Example 1–15.

C & S *EXAMPLE 1–15*   **Compliance of ASME Codes for a Component Experiencing Simultaneous Heat Transfer Mechanisms**

A component consists of a series of ASTM B21 naval brass bolts bolted on the upper surface of an ASME SA-240 stainless steel plate ($k = 15$ W/m·K) with a thickness of 10 cm (Fig. 1–52). One side of the stainless steel plate is subjected to a uniform heat flux of 2.2 kW/m², while another side experiences convection and thermal radiation with ambient air at 30°C and surroundings at 40°C. The plate surface has an emissivity of 0.3, and the convection heat transfer coefficient is 5 W/m²·K. The maximum use temperature for the B21 bolts permitted by the ASME Code for Process Piping (ASME B31.3-2014) is 149°C. Also, the ASME Boiler and Pressure Vessel Code (ASME BPVC.IV-2015, HF-300) limits the maximum use temperature for the SA-240 plate to 260°C. An engineer is tasked to ensure that both the B21 bolts and the SA-240 plate comply with the ASME codes. What would be the engineer's conclusion?

SOLUTION   In this example, the engineering codes developed by the ASME are incorporated in a problem that involves simultaneous heat transfer mechanisms. To ensure compliance with the ASME Boiler and Pressure Vessel Code and the ASME Code for Process Piping, it becomes necessary to first determine the surface temperature of the plate on the side that is subjected to convection and thermal radiation. By inspection, one can conclude that the minimum temperature of the plate occurs at surface 2, while the maximum temperature occurs at surface 1.
Assumptions   **1** Heat transfer is steady. **2** One-dimensional heat conduction through the metal plate. **3** Uniform heat flux at bottom surface. **4** Uniform surface temperature at the upper plate surface. **5** The temperature of the bolts is equal to the upper surface temperature of the plate.
Properties   Emissivity of the engine surface is given as $\varepsilon = 0.3$.
Analysis   The uniform heat flux subjected on the bottom plate surface is equal to the heat flux transferred by convection and radiation on the upper surface.

$$\dot{q}_o = \dot{q}_{\text{cond}} = \dot{q}_{\text{conv}} + \dot{q}_{\text{rad}} = 2200 \text{ W/m}^2$$

For the convection and radiation heat transfer, we have

$$\dot{q}_{\text{conv}} + \dot{q}_{\text{rad}} = h(T_{s,2} - T_\infty) + \varepsilon\,\sigma\,(T_{s,2}^4 - T_{\text{surr}}^4) = 2200\ \text{W/m}^2$$

Assuming the temperature of the bolts is equal to the upper surface temperature of the plate, with $T_\infty = 303$ K and $T_{\text{surr}} = 313$ K, we determine

$$T_{\text{bolt}} = T_{s,2} = \textbf{522 K} = \textbf{249°C} > 149°C$$

To ensure that the entire plate is below 260°C, the temperature at the plate surface subjected to the uniform heat flux needs to be determined. From Fourier's law of heat conduction, we have

$$\dot{q}_o = k\frac{T_{s,1} - T_{s,2}}{L} = 2200\ \text{W/m}^2 \quad \rightarrow \quad T_{s,1} = \dot{q}_o\frac{L}{k} + T_{s,2}$$

Thus

$$T_{s,1} = \dot{q}_o\frac{L}{k} + T_{s,2} = (2200\ \text{W/m}^2)\,\frac{0.1\ m}{15\ \text{W/m·K}} + 249°C$$

$$= \textbf{264°C} > 260°C$$

Discussion   The temperature of the B21 bolts exceeds the maximum allowable use temperature by 100°C. Although surface 2 is below the permitted temperature for the SA-240 plate, surface 1 exceeds the maximum allowable use temperature by 4°C. Thus, under the given conditions, both the ASTM B21 bolts and the ASME SA-240 plate are not suitable for this component.

1–13 ▪ PROBLEM-SOLVING TECHNIQUE

The first step in learning any science is to grasp the fundamentals. The next step is to master the fundamentals by testing this knowledge. This is done by solving significant real-world problems. Solving such problems, especially complicated ones, requires a systematic approach. By using a step-by-step approach, an engineer can reduce the solution of a complicated problem into the solution of a series of simple problems (Fig. 1–53). When you are solving a problem, we recommend that you use the following steps zealously as applicable. This will help you to avoid some of the common pitfalls associated with problem solving.

Step 1: Problem Statement

In your own words, briefly state the problem, the key information given, and the quantities to be found. This is to make sure that you understand the problem and the objectives before you attempt to solve the problem.

Step 2: Schematic

Draw a realistic sketch of the physical system involved, and list the relevant information on the figure. The sketch does not have to be something elaborate,
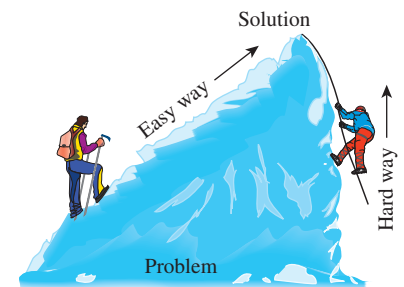
FIGURE 1–53
A step-by-step approach can greatly simplify problem solving.

Given: Air temperature in Denver

To be found: Density of air

Missing information: Atmospheric pressure

Assumption #1: Take $P = 1$ atm (Inappropriate. Ignores effect of altitude. Will cause more than 15% error.)

Assumption #2: Take $P = 0.83$ atm (Appropriate. Ignores only minor effects such as weather.)

FIGURE 1–54
The assumptions made while solving an engineering problem must be reasonable and justifiable.

Energy use: $80/yr

Energy saved by insulation: $200/yr

IMPOSSIBLE!

FIGURE 1–55
The results obtained from an engineering analysis must be checked for reasonableness.

but it should resemble the actual system and show the key features. Indicate any energy and mass interactions with the surroundings. Listing the given information on the sketch helps one to see the entire problem at once.

Step 3: Assumptions and Approximations

State any appropriate assumptions and approximations made to simplify the problem to make it possible to obtain a solution. Justify the questionable assumptions. Assume reasonable values for missing quantities that are necessary. For example, in the absence of specific data for atmospheric pressure, it can be taken to be 1 atm. However, it should be noted in the analysis that the atmospheric pressure decreases with increasing elevation. For example, it drops to 0.83 atm in Denver (elevation 1610 m) (Fig. 1–54).

Step 4: Physical Laws

Apply all the relevant basic physical laws and principles (such as the conservation of energy), and reduce them to their simplest form by utilizing the assumptions made. However, the region to which a physical law is applied must be clearly identified first.

Step 5: Properties

Determine the unknown properties necessary to solve the problem from property relations or tables. List the properties separately, and indicate their source, if applicable.

Step 6: Calculations

Substitute the known quantities into the simplified relations and perform the calculations to determine the unknowns. Pay particular attention to the units and unit cancellations, and remember that a dimensional quantity without a unit is meaningless. Also, don't give a false implication of high precision by copying all the digits from the calculator—round the results to an appropriate number of significant digits (see Sec. 1–15).

Step 7: Reasoning, Verification, and Discussion

Check to make sure that the results obtained are reasonable and intuitive, and verify the validity of the questionable assumptions. Repeat the calculations that resulted in unreasonable values. For example, insulating a water heater that uses $80 worth of natural gas a year cannot result in savings of $200 a year (Fig. 1–55).

Also, point out the significance of the results, and discuss their implications. State the conclusions that can be drawn from the results and any recommendations that can be made from them. Emphasize the limitations under which the results are applicable, and caution against any possible misunderstandings and using the results in situations where the underlying assumptions do not apply. For example, if you determined that wrapping a water heater with a $20 insulation jacket will reduce the energy cost by $30 a year, indicate that the insulation will pay for itself from the energy it saves in less than a year. However, also indicate that the analysis does not consider labor costs and that this will be the case if you install the insulation yourself.

Keep in mind that the solutions you present to your instructors, and any engineering analysis presented to others, are a form of communication. Therefore neatness, organization, completeness, and visual appearance are of utmost importance for maximum effectiveness (Fig. 1–56). Besides, neatness also serves as a great checking tool since it is very easy to spot errors and inconsistencies in neat work. Carelessness and skipping steps to save time often end up costing more time and unnecessary anxiety.

The approach described here is used in the solved example problems without explicitly stating each step, and it is also used in the Solutions Manual for this text. For some problems, some of the steps may not be applicable or necessary. However, we cannot overemphasize the importance of a logical and orderly approach to problem solving. Most difficulties encountered while solving a problem are not due to a lack of knowledge; rather, they are due to a lack of organization. You are strongly encouraged to follow these steps in problem solving until you develop your own approach that works best for you.

FIGURE 1–56
Neatness and organization are highly valued by employers.

1–14 ▪ ENGINEERING SOFTWARE PACKAGES

You may be wondering why we are about to undertake an in-depth study of the fundamentals of another engineering science. After all, almost all problems we are likely to encounter in practice can be solved using one of several sophisticated software packages readily available today. These software packages not only give the desired numerical results, but they also supply the outputs in graphical form for impressive presentations. It is unthinkable to practice engineering today without using some of these packages. This tremendous computing power available to us at the touch of a button is both a blessing and a curse. It certainly enables engineers to solve problems easily and quickly, but it also opens the door for abuses and misinformation. In the hands of poorly educated people, these software packages are as dangerous as sophisticated, powerful weapons in the hands of poorly trained soldiers.

Thinking that a person who can use engineering software without proper training on fundamentals can practice engineering is like thinking that a person who can use a wrench can work as a mechanic. If it were true that engineering students no longer need fundamentals courses because of computers, then it would also be true that employers would no longer need high-salaried engineers since any person who knows how to use a word-processing program can also learn how to use the software. However, the statistics show that the need for engineers is on the rise, not on the decline, despite the availability of software.

We should always remember that the computing power and the engineering software available today are just tools, and tools have meaning only in the hands of masters. Having the best word-processing program does not make a person a good writer, but it certainly makes the job of a good writer much easier and makes the writer more productive (Fig. 1–57). Hand calculators did not eliminate the need to teach our children how to add or subtract, and sophisticated medical software did not take the place of medical school training. Neither will engineering software replace the traditional engineering education. It will simply cause a shift in emphasis in the courses from mathematics to physics. That is, more time will be spent in the classroom discussing the physical aspects of the problems in greater detail, and less time on the mechanics of solution procedures.
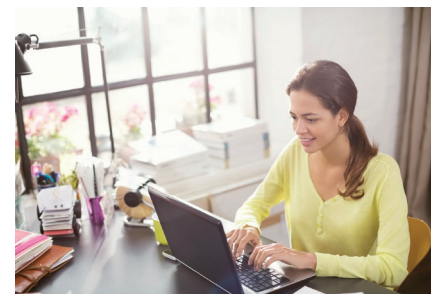
FIGURE 1–57
An excellent word-processing program does not make a person a good writer; it simply makes a good writer a better and more efficient writer.

©Caia Images/Glow Images

All these marvelous and powerful tools available today put an extra burden on today's engineers. They must still have a thorough understanding of the fundamentals, develop a "feel" for the physical phenomena, be able to put the data into proper perspective, and make sound engineering judgments, just like their predecessors. However, they must do it much better, and much faster, using more realistic models because of the powerful tools available today. The engineers in the past had to rely on hand calculations, slide rules, and later hand calculators and computers. Today they rely on software packages. The easy access to such power and the possibility of a simple misunderstanding or misinterpretation causing great damage make it more important today than ever to have solid training in the fundamentals of engineering. In this text we make an extra effort to put the emphasis on developing an intuitive and physical understanding of natural phenomena instead of on the mathematical details of solution procedures.

Equation Solvers

You are probably familiar with the equation solving capabilities of spreadsheets such as Microsoft Excel. Despite its simplicity, Excel is commonly used in solving systems of equations in engineering as well as finance. It enables the user to conduct parametric studies, plot the results, and ask "what if" questions. It can also solve simultaneous equations if properly set up. There are also numerous sophisticated equation solvers commonly used in engineering practice, such as the Engineering Equation Solver (EES), which is a program that easily solves systems of linear or nonlinear algebraic or differential equations numerically. It has a large library of built-in thermodynamic property functions as well as mathematical functions, and it allows the user to supply additional property data.

Unlike some software packages, equation solvers do not solve engineering problems; they only solve the equations supplied by the user. Therefore, the user must understand the problem and formulate it by applying any relevant physical laws and relations. Equation solvers save the user considerable time and effort by simply solving the resulting mathematical equations. This makes it possible to attempt significant engineering problems not suitable for hand calculations and to conduct parametric studies quickly and conveniently.

EXAMPLE 1–16   Solving a System of Equations Numerically

The difference of two numbers is 4, and the sum of the squares of these two numbers is equal to the sum of the numbers plus 20. Determine these two numbers.

SOLUTION   Relations are given for the difference and the sum of the squares of two numbers. The two numbers are to be determined.

Analysis   We first solve the problem using EES. We start the EES program by double-clicking on its icon, open a new file, and type the following on the blank screen that appears:

$$x - y = 4$$
$$x^2 + y^2 = x + y + 20$$

which is an exact mathematical expression of the problem statement with x and y denoting the unknown numbers. The solution to this system of equations (one linear and one nonlinear) with two unknowns is obtained by a single click on the "calculator" icon on the taskbar. It gives (Fig. 1–58)

$$x = 5 \text{ and } y = 1$$

We now solve the same problem using Excel. Start Excel. File/Options/Add-Ins/Solver Add-In/OK, where the underline means to click on that option and the slash separates each sequential option. Choose a cell for x and a cell for y and enter initial guesses there (we chose cells C25 and D25 and guessed 0.5 and 0.5). We must rewrite the two equations so that no variables are on the right-hand side (RHS): $x - y = 4$ and $x^2 + y^2 - x - y = 20$. Choose a cell for the RHS of each equation and enter the formula there (we chose cells D20 and D21; see the equations in Fig. 1–59a). Data/Solver. Set the cell for the RHS of the first equation (D20) as the "Objective" with a value of 4, set the cells for x and y (C25:D25) as those subject to constraints, and set the constraint such that the cell for the RHS of the second equation (D21) must equal 20. Solve/OK. The solution iterates to the correct final values of $x = 5$ and $y = 1$, respectively (Fig. 1–59b). *Note:* For better convergence, the precision, number of allowed iterations, etc., can be changed in Data/Solver/Options.

Discussion Note that all we did was formulate the problem as we would on paper; EES or Excel took care of all the mathematical details of the solution. Also note that equations can be linear or nonlinear, and they can be entered in any order with unknowns on either side. Friendly equation solvers such as EES allow the user to concentrate on the physics of the problem without worrying about the mathematical complexities associated with the solution of the resulting system of equations.

FIGURE 1–58
EES screen images for Example 1–16.
Source: Engineering Equation Solver

1–15 ▪ ACCURACY, PRECISION, AND SIGNIFICANT DIGITS

In engineering calculations, the supplied information is not known to more than a certain number of significant digits, usually three digits. Consequently, the results obtained cannot possibly be precise to more significant digits. Reporting results in more significant digits falsely implies greater precision than exists, and it should be avoided.

Regardless of the system of units employed, engineers must be aware of three principles that govern the proper use of numbers: accuracy, precision, and significant digits. For engineering measurements, they are defined as follows:

- **Accuracy error** (*inaccuracy*) is the value of one reading minus the true value. In general, the accuracy of a set of measurements refers to the closeness of the average reading to the true value. Accuracy is generally associated with repeatable, fixed errors.
- **Precision error** is the value of one reading minus the average of readings. In general, the precision of a set of measurements refers to the fineness of the resolution and the repeatability of the instrument. Precision is generally associated with unrepeatable, random errors.
- **Significant digits** are digits that are relevant and meaningful.

FIGURE 1–59
Excel screen images for Example 1–16. (*a*) Equations, with initial guesses highlighted. (*b*) Final results after using Excel's Solver, with converged values highlighted.
Source: Microsoft Excel
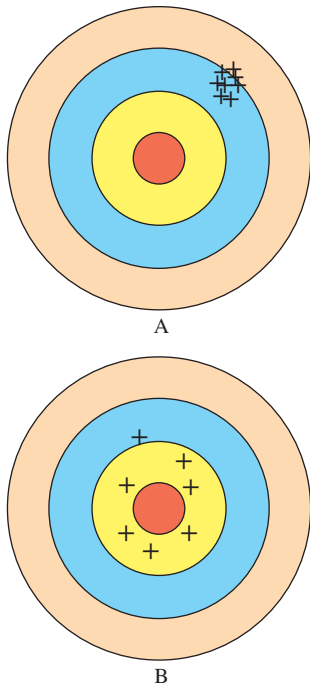
FIGURE 1–60
Illustration of accuracy versus precision. Shooter A is more precise, but less accurate, while shooter B is more accurate, but less precise.

TABLE 1–7

Significant digits

Number	Exponential Notation	Number of Significant Digits
12.3	1.23×10^1	3
123,000	1.23×10^5	3
0.00123	1.23×10^{-3}	3
40,300	4.03×10^4	3
40,300	4.0300×10^4	5
0.005600	5.600×10^{-3}	4
0.0056	5.6×10^{-3}	2
0.006	$6. \times 10^{-3}$	1

A measurement or calculation can be very precise without being very accurate, and vice versa. For example, suppose the true value of the temperature is 25.00°C. Two thermocouples A and B take five temperature readings each:

Thermocouple A: 25.50, 25.69, 25.52, 25.58, and 25.61°C. Average of all readings = 25.58°C.

Thermocouple B: 26.3, 24.5, 23.9, 26.8, and 23.6°C. Average of all readings = 25.02°C.

Clearly, thermocouple A is more precise, since none of the readings differs by more than 0.11°C from the average. However, the average is 25.58°C, 0.58°C greater than the true temperature; this indicates significant **bias error**, also called **constant error** or **systematic error**. On the other hand, thermocouple B is not very precise, since its readings swing wildly from the average; but its overall average is much closer to the true value. Hence, thermocouple B is more accurate than thermocouple A, at least for this set of readings, even though it is less precise. The difference between accuracy and precision can be illustrated effectively by analogy to shooting arrows at a target, as sketched in Fig. 1–60. Shooter A is very precise, but not very accurate, while shooter B has better overall accuracy, but less precision.

Many engineers do not pay proper attention to the number of significant digits in their calculations. The least significant numeral in a number implies the precision of the measurement or calculation. For example, a result written as 1.23 (three significant digits) *implies* that the result is precise to within one digit in the second decimal place; i.e., the number is somewhere between 1.22 and 1.24. Expressing this number with any more digits would be misleading. The number of significant digits is most easily evaluated when the number is written in exponential notation; the number of significant digits can then simply be counted, including zeroes. Alternatively, the least significant digit can be underlined to indicate the author's intent. Some examples are shown in Table 1–7.

When performing calculations or manipulations of several parameters, the final result is generally only as precise as the least precise parameter in the problem. For example, suppose A and B are multiplied to obtain C. If $A = 2.3601$ (five significant digits), and $B = 0.34$ (two significant digits), then $C = 0.80$ (only two digits are significant in the final result). Note that most students are tempted to write $C = 0.802434$, with six significant digits, since that is what is displayed on a calculator after multiplying these two numbers.

Let's analyze this simple example carefully. Suppose the exact value of B is 0.33501, which is read by the instrument as 0.34. Also suppose A is exactly 2.3601, as measured by a more accurate and precise instrument. In this case, $C = A \times B = 0.79066$ to five significant digits. Note that our first answer, $C = 0.80$, is off by one digit in the second decimal place. Likewise, if B is 0.34499 and is read by the instrument as 0.34, the product of A and B would be 0.81421 to five significant digits. Our original answer of 0.80 is again off by one digit in the second decimal place. The main point here is that 0.80 (to two significant digits) is the best one can expect from this multiplication since, to begin with, one of the values had only two significant digits.

Another way of looking at this is to say that beyond the first two digits in the answer, the rest of the digits are meaningless or not significant. For example, if one reports what the calculator displays, 2.3601 times 0.34 equals 0.802434, the last four digits are *meaningless.* As shown, the final result may lie between 0.79 and 0.81—any digits beyond the two significant digits are not only meaningless, but *misleading,* since they imply to the reader more precision than is really there.

As another example, consider a 3.75-L container filled with gasoline whose density is 0.845 kg/L, and determine its mass. Probably the first thought that comes to your mind is to multiply the volume and density to obtain 3.16875 kg for the mass, which falsely implies that the mass so determined is precise to six significant digits. In reality, however, the mass cannot be more precise than three significant digits since both the volume and the density are precise to three significant digits only. Therefore, the result should be rounded to three significant digits, and the mass should be reported to be 3.17 kg instead of what the calculator displays (Fig. 1–61). The result, 3.16875 kg, would be correct only if the volume and density were given to be 3.75000 L and 0.845000 kg/L, respectively. The value 3.75 L implies that we are fairly confident that the volume is precise within ± 0.01 L, and it cannot be 3.74 or 3.76 L. However, the volume can be 3.746, 3.750, 3.753, etc., since they all round to 3.75 L.

You should also be aware that sometimes we knowingly introduce small errors in order to avoid the trouble of searching for more accurate data. For example, when dealing with liquid water, we often use the value of 1000 kg/m^3 for density, which is the density value of pure water at 0°C. Using this value at 75°C will result in an error of 2.5 percent since the density at this temperature is 975 kg/m^3. The minerals and impurities in the water will introduce additional error. This being the case, you should have no reservation in rounding the final results to a reasonable number of significant digits. Besides, having a few percent uncertainty in the results of engineering analysis is usually the norm, not the exception.

When writing intermediate results in a computation, it is advisable to keep several "extra" digits to avoid round-off errors; however, the final result should be written with the number of significant digits taken into consideration. You must also keep in mind that a certain number of significant digits of precision in the result does not necessarily imply the same number of digits of overall *accuracy.* Bias error in one of the readings may, for example, significantly reduce the overall accuracy of the result, perhaps even rendering the last significant digit meaningless and reducing the overall number of reliable digits by one. Experimentally determined values are subject to measurement errors, and such errors are reflected in the results obtained. For example, if the density of a substance has an uncertainty of 2 percent, then the mass determined using this density value will also have an uncertainty of 2 percent.

Finally, when the number of significant digits is unknown, the accepted engineering standard is three significant digits. Therefore, if the length of a pipe is given to be 40 m, we will assume it to be 40.0 m in order to justify using three significant digits in the final results.

Given: Volume: $V = 3.75$ L

Density: $\rho = 0.845$ kg/L

(3 significant digits)

Also, $3.75 \times 0.845 = 3.16875$

Find: Mass: $m = \rho V = 3.16875$ kg

Rounding to 3 significant digits:
$m = 3.17$ kg

FIGURE 1–61
A result with more significant digits than that of given data falsely implies more accuracy.

TOPIC OF SPECIAL INTEREST*
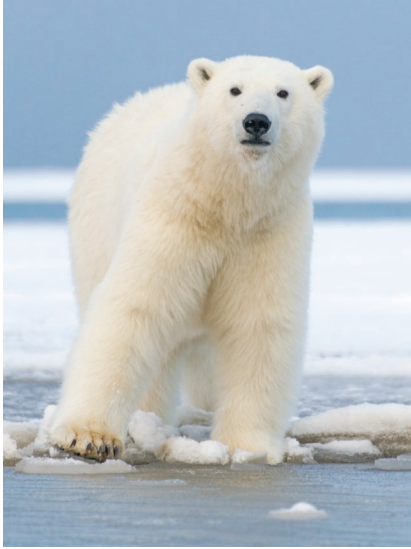
FIGURE 1–62
Most animals come into this world with fur, but human beings come with a delicate skin that provides little thermal insulation.

©Dawn Wilson Photography/Getty Images
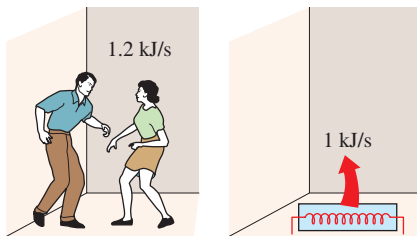
FIGURE 1–63
Two fast-dancing people supply more heat to a room than a 1-kW resistance heater.

Thermal Comfort

Unlike animals such as a fox or a bear that are born with fur, human beings come into this world with little protection against harsh environmental conditions (Fig. 1–62). Therefore, we can claim that the search for thermal comfort dates back to the beginning of human history. It is believed that early human beings lived in caves that provided shelter as well as protection from extreme thermal conditions. Probably the first form of heating system used was *open fire,* followed by fire in dwellings through the use of a *chimney* to vent out the combustion gases. The concept of *central heating* dates back to the times of the Romans, who heated homes by utilizing double-floor construction techniques and passing the fire's fumes through the opening between the two floor layers. The Romans were also the first to use *transparent windows* made of mica or glass to keep the wind and rain out while letting the light in. Wood and coal were the primary energy sources for heating, and oil and candles were used for lighting. The ruins of south-facing houses indicate that the value of *solar heating* was recognized early in our history.

The term **air-conditioning** is usually used in a restricted sense to imply cooling, but in its broad sense it means *to condition* the air to the desired level by heating, cooling, humidifying, dehumidifying, cleaning, and/or deodorizing. The purpose of the air-conditioning system of a building is to provide *complete thermal comfort* for its occupants. Therefore, we need to understand the thermal aspects of the *human body* in order to design an effective air-conditioning system.

The building blocks of living organisms are *cells,* which resemble miniature factories performing various functions necessary for the survival of organisms. The human body contains about 100 trillion cells with an average diameter of 0.01 mm. In a typical cell, thousands of chemical reactions occur every second during which some molecules are broken down (catabolic pathways). Energy is released in the form of heat, and some energy is stored in usable forms and some new molecules are formed (anabolic pathways) using the stored energy. The high level of chemical activity in all cells helps to maintain the human body temperature of 37.0°C (98.6°F) while performing the necessary bodily functions to sustain life. The combination of all of these processes is called the **metabolism**. In simple terms, metabolism refers to the burning of foods such as carbohydrates, fat, and protein. The metabolizable energy content of foods is usually expressed by nutritionists in terms of the capitalized Calorie. One Calorie is equivalent to 1 Cal = 1 kcal = 4.1868 kJ. Excess consumed Calories are stored in the body for potential use at a later time. Interestingly, these excess stored Calories alter the thermal properties and thus thermal comfort of the human body.

---

*This section can be skipped without loss in continuity.

The rate of metabolism at the resting state is called the *basal metabolic rate,* which is the rate of metabolism required to keep a body performing the necessary bodily functions such as breathing and blood circulation at zero external activity level. The metabolic rate can also be interpreted as the energy consumption rate for a body. For an *average man* (30 years old, 70 kg, 1.73 m high, 1.8 m^2 surface area), the basal metabolic rate is 84 W. That is, the body converts chemical energy of the food (or of the body fat if the person had not eaten) into heat at a rate of 84 J/s, which is then dissipated to the surroundings. The metabolic rate increases with the *level of activity,* and it may exceed 10 times the basal metabolic rate when someone is doing strenuous exercise. That is, two people doing heavy exercising in a room may be supplying more energy to the room than a 1-kW resistance heater (Fig. 1–63). An average man generates heat at a rate of 108 W while reading, writing, typing, or listening to a lecture in a classroom in a seated position. The maximum metabolic rate of an average man is 1250 W at age 20 and 730 at age 70. The corresponding rates for women are about 30 percent lower. Maximum metabolic rates of trained athletes can exceed 2000 W.

Metabolic rates during various activities are given in Table 1–8 per unit body surface area. The **surface area** of a nude body was given by D. DuBois in 1916 as

$$A_s = 0.202\, m^{0.425}\, h^{0.725} \quad (\text{m}^2) \tag{1–30}$$

where *m* is the mass of the body in kg and *h* is the height in m. *Clothing* increases the surface area of a person by up to about 50 percent and may provide additional resistance to dissipation of heat. The metabolic rates given in the table are sufficiently accurate for most purposes, but there is considerable uncertainty at high activity levels, and these values are dependent on the tissue composition of the body (e.g., fat vs. lean muscle). More accurate values can be determined by measuring the rate of respiratory *oxygen consumption,* which ranges from about 0.25 L/min for an average resting man to more than 2 L/min during extremely heavy work. All energy released during metabolism can be assumed to be released as *heat* (in sensible or latent forms) since the external mechanical work done by the muscles is very small. Besides, the work done during most activities such as walking or riding an exercise bicycle is eventually converted to heat through friction.

The comfort of the human body depends primarily on three environmental factors: the temperature, relative humidity, and air motion. The temperature of the environment is the single most important index of comfort. Extensive research is done on human subjects to determine the "**thermal comfort zone**" and to identify the conditions under which the body feels comfortable in an environment. It has been observed that most normally clothed people resting or doing light work feel comfortable in the *operative temperature* (roughly, the average temperature of air and surrounding surfaces) range of 23°C to 27°C or 73°F to 80°F (Fig. 1–64). For unclothed people, this range is 29°C to 31°C. Interestingly, the operative temperature

TABLE 1–8

Metabolic rates during various activities

Activity	Metabolic Rate* W/m^2
Resting:	
Sleeping	40
Reclining	45
Seated, quiet	60
Standing, relaxed	70
Walking (on the level):	
2 mph (0.89 m/s)	115
3 mph (1.34 m/s)	150
4 mph (1.79 m/s)	220
Office Activities:	
Reading, seated	55
Writing	60
Typing	65
Filing, seated	70
Filing, standing	80
Walking about	100
Lifting/packing	120
Driving/Flying:	
Car	60–115
Aircraft, routine	70
Heavy vehicle	185
Miscellaneous Occupational Activities:	
Cooking	95–115
Cleaning house	115–140
Machine work:	
Light	115–140
Heavy	235
Handling 50-kg bags	235
Pick and shovel work	235–280
Miscellaneous Leisure Activities:	
Dancing, social	140–255
Calisthenics/exercise	175–235
Tennis, singles	210–270
Basketball	290–440
Wrestling, competitive	410–505

*Multiply by 1.8 m^2 to obtain metabolic rates for an average man. Multiply by 0.3171 to convert to Btu/h·ft^2.

From American Society of Heating, Refrigeration, and Air-Conditioning Engineers, Handbook of Fundamentals, *2017, Chap. 9, Table 4.*
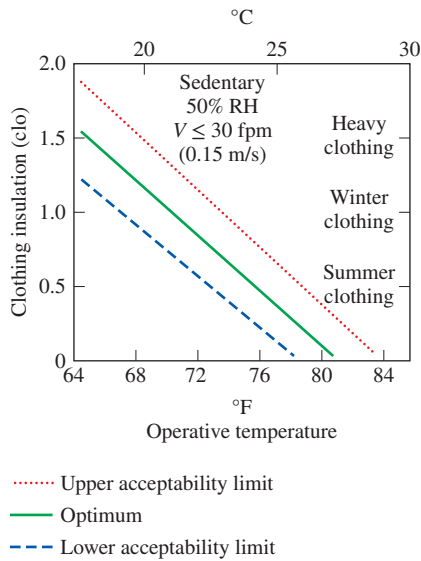
FIGURE 1–64

The effect of clothing on the environmental temperature that feels comfortable (1 col = 0.155 m²·°C/W = 0.880 ft²·°F·h/Btu).

From ASHRAE Standard 55-1981
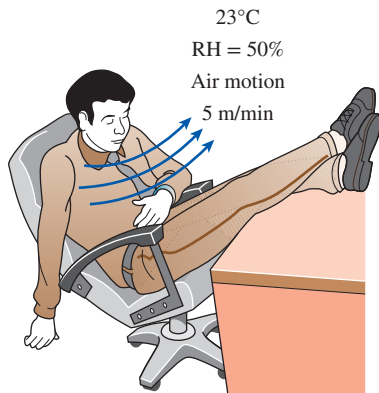
FIGURE 1–65

A thermally comfortable environment.

is higher than the average temperature of many highly populated areas in the world, which tend to have an average yearly temperature in the range of 15°C to 20°C or 59°F to 68°F (Table 1–9). Relative humidity also has a considerable effect on comfort since it is a measure of air's ability to absorb moisture, and thus it affects the amount of heat a body can dissipate by evaporation. High relative humidity slows down heat rejection by evaporation, especially at high temperatures, and low relative humidity speeds it up. The desirable level of *relative humidity* is the broad range of 30 to 70 percent, with 50 percent being the most desirable level. Most people at these conditions feel neither hot nor cold, and the body does not need to activate any of the defense mechanisms to maintain the normal body temperature (Fig. 1–65).

Another factor that has a major effect on thermal comfort is **excessive air motion** or **draft**, which causes undesired local cooling of the human body. Draft is identified by many as a most annoying factor in work places, automobiles, and airplanes. Experiencing discomfort by draft is most common among people wearing indoor clothing and doing light sedentary work and least common among people with high activity levels. The air velocity should be kept below 9 m/min (30 ft/min) in winter and 15 m/min (50 ft/min) in summer to minimize discomfort by draft, especially when the air is cool. A low level of air motion is desirable as it removes the warm, moist air that builds around the body and replaces it with fresh air. Therefore, air motion should be strong enough to remove heat and moisture from the vicinity of the body but gentle enough to be unnoticed. High-speed air motion causes discomfort outdoors as well. For example, an environment at 10°C (50°F) with 48 km/h winds feels as cold as an environment at −7°C (20°F) with 3 km/h winds because of the chilling effect of the air motion (the wind-chill factor).

A comfort system should provide *uniform conditions* throughout the living space to avoid discomfort caused by nonuniformities such as *drafts, asymmetric thermal radiation, hot or cold floors,* and *vertical temperature stratification.* **Asymmetric thermal radiation** is caused by the *cold surfaces* of large windows, uninsulated walls, or cold products and the *warm surfaces* of gas or electric radiant heating panels on the walls or ceiling, solar-heated masonry walls or ceilings, and warm machinery. Asymmetric radiation causes discomfort by exposing different sides of the body to surfaces at different temperatures and thus to different heat loss or gain by radiation. A person whose left side is exposed to a cold window, for example, will feel like heat is being drained from that side of his or her body (Fig. 1–66). For thermal comfort, the radiant temperature asymmetry should not exceed 5°C in the vertical direction and 10°C in the horizontal direction. The unpleasant effect of radiation asymmetry can be minimized by properly sizing and installing heating panels, using double-pane windows, and providing generous insulation at the walls and the roof.

Direct contact with **cold** or **hot floor surfaces** also causes localized discomfort in the feet. The temperature of the floor depends on the way it is *constructed* (being directly on the ground or on top of a heated room,

being made of wood or concrete, the use of insulation, etc.) as well as the *floor covering used* such as pads, carpets, rugs, and linoleum. A floor temperature of 23 to 25°C is comfortable to most people. The floor asymmetry loses its significance for people with footwear. An effective and economical way of raising the floor temperature is to use radiant heating panels instead of turning the thermostat up. Another nonuniform condition that causes discomfort is **temperature stratification** in a room that exposes the head and the feet to different temperatures. For thermal comfort, the temperature difference between the head and foot levels should not exceed 5°C. This effect can be minimized by using destratification fans.

It should be noted that no thermal environment will please everyone. No matter what we do, some people will express some discomfort. The thermal comfort zone is based on a 90 percent acceptance rate. That is, an environment is deemed comfortable if only 10 percent of the people are dissatisfied with it. Metabolism decreases somewhat with *age,* but it has no effect on the comfort zone. Research indicates that there is no appreciable difference between the environments preferred by old and young people. Experiments also show that *men* and *women* prefer almost the same environment. The metabolism rate of women is somewhat lower, but this is compensated by their slightly lower skin temperature, lower surface area, and lower evaporative loss as compared with men. Also, there is no significant variation in the comfort zone from one part of the world to another and from winter to summer even though large environmental temperature differences may exist in different parts of the world and even within the same region during different seasons (Table 1–9). Therefore, the same thermal comfort conditions can be used *throughout the world* in any season. Also, people cannot *acclimatize* themselves to prefer different comfort conditions since these preferences are based on factors that are difficult to control, such as basal metabolic rate.

In a **cold environment**, the rate of heat loss from the body may exceed the rate of metabolic heat generation. Average specific heat of the human body is 3.49 kJ/kg·°C, and thus each 1°C drop in body temperature corresponds to a deficit of 244 kJ in body heat content for an average 70-kg man. A drop of 0.5°C in mean body temperature causes noticeable but acceptable discomfort. A drop of 2.6°C causes extreme discomfort. A sleeping person wakes up when his or her mean body temperature drops by 1.3°C (which normally shows up as a 0.5°C drop in the core body and 3°C in the skin area). The drop of core body temperature below 35°C may damage the body temperature regulation mechanism, while a core below 28°C may be fatal and a drop to 23°C will be fatal (Table 1–9). Sedentary people report feeling *comfortable* at a *mean skin temperature* of 33.3°C, *uncomfortably cold* at 31°C, *shivering cold* at 30°C, and *extremely cold* at 29°C. People doing heavy work report feeling comfortable at much lower temperatures, which shows that the activity level and thus metabolism rate affects human performance and comfort. The extremities of the body such as hands and feet are most easily affected by cold weather, and their temperature is a better indication of comfort and performance. The extremities

TABLE 1–9

Comparison of biologically relevant and environmental temperatures

Location or Activity	Temperature °C
Record high world temperature, Death Valley, California, USA	57
Death (due to proteins denaturing)	44
Normal core body temperature	37
Average yearly temperature in Singapore	28
Average yearly temperature in Corumba, Brazil	25
Death (due to hypothermia)	23
Nominal interior temperature	22
Average yearly temperature in Los Angeles, California, USA	19
Average yearly temperature in Shanghai, China	16
Average yearly temperature in New York, New York, USA	13
Average yearly temperature in Anchorage, Alaska, USA	2
Record low world temperature, Vostok Station, Antarctica	−89
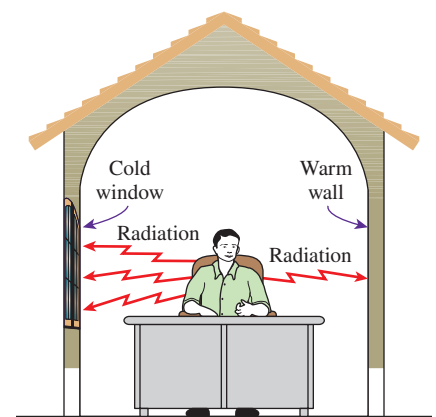
FIGURE 1–66

Cold surfaces cause excessive heat loss from the body by radiation, and thus discomfort on the affected side of the body.

FIGURE 1–67
The rate of metabolic heat generation may go up by six times the resting level during total body shivering in cold weather.

FIGURE 1–68
In hot environments, a body can dissipate a large amount of metabolic heat by sweating since the sweat absorbs the body heat and evaporates.

can and normally do experience more drastic changes in temperature as compared with the core temperature or skin temperature closer to the core. A hand-skin temperature of 20°C is perceived to be uncomfortably cold, 15°C to be extremely cold, and 5°C to be painfully cold. Useful work can be performed by hands without difficulty as long as the skin temperature of fingers remains above 16°C (American Society of Heating, Refrigeration, and Air-Conditioning Engineers, 2017, Chapter 9).

The first line of defense of the body against excessive heat loss in a cold environment is *to reduce the skin temperature* and thus the rate of heat loss from the skin by constricting the arteries, thus decreasing the blood flow to the skin. This measure decreases the temperature of the tissues subjacent to the skin but maintains the core body temperature. The next preventive measure is increasing the rate of *metabolic heat generation* in the body by *shivering,* unless the person does it voluntarily by increasing his or her level of activity or puts on additional clothing. Shivering begins slowly in small muscle groups and may double the rate of metabolic heat production of the body at its initial stages. In the extreme case of total body shivering, the rate of heat production may reach six times the resting levels (Fig. 1–67). Shivering converts stored chemical energy into mechanical work and dissipated heat. If this measure also proves inadequate, the core body temperature starts *falling.* Body parts farthest away from the core such as the hands and feet are at greatest danger for tissue damage.

In **hot environments**, the rate of heat loss from the body may drop below the metabolic heat generation rate. This time the body activates the opposite mechanisms. First the body increases the *blood flow* and thus heat transport to the skin, causing the temperature of the skin and the subjacent tissues to rise and approach the deep body temperature. Under extreme heat conditions, the *heart rate* may reach 150 beats per minute in order to maintain adequate blood supply to the brain and the skin. At higher heart rates, the *volumetric efficiency* of the heart drops because the very short time between heartbeats does not allow for complete filling of the heart chambers, and thus the blood supply to the skin, and more importantly to the brain, drops. This causes the person to faint as a result of *heat exhaustion.* Dehydration makes the problem worse, since physiological mechanisms will activate to reduce blood flow to the extremities and skin. A similar thing happens when a person working very hard for a long time stops suddenly and becomes sedentary. The blood that has flooded the skin and other tissues that were in use (e.g., muscles) has difficulty returning to the heart in this case since the relaxed muscles no longer force the blood back to the heart, and thus there is less blood available for pumping to the brain. Therefore, a "cooling down" period after exercising is just as important as a "warming up" period.

The next line of defense is releasing water from sweat glands and resorting to *evaporative cooling,* unless the person removes some clothing and reduces the activity level (Fig. 1–68). The body can maintain its core temperature at 37°C in this evaporative cooling mode indefinitely, even

in environments at higher temperatures (as high as 200°C during military endurance tests), if the person drinks plenty of liquids to replenish his or her water reserves and the ambient air is sufficiently dry to allow the sweat to evaporate instead of rolling down the skin. If this measure proves inadequate, the body will have to start absorbing the metabolic heat and the deep body temperature will rise. A person can tolerate a temperature rise of 1.4°C without major discomfort but may *collapse* when the core body temperature rise reaches 2.8°C. People feel sluggish and their efficiency drops considerably when the core body temperature rises above 39°C. A core temperature above 41°C may damage most innate proteins, resulting in cessation of sweating, increased heat production by shivering, and a *heat stroke* with irreversible and life-threatening damage. Death can occur above 43°C (Table 1–9).

A surface temperature of 46°C causes pain on the skin. Therefore, direct contact with a metal block at this temperature or above is painful. However, a person can stay in a room at 100°C for up to 30 min without any damage or pain on the skin because of the convective resistance at the skin surface and evaporative cooling. We can even put our hands into an oven at 200°C for a short time without getting burned as long as the skin does not touch a hot surface. This is also because the thermal conductivity of air to skin is much lower than metal to skin.

The processes that have been described in the previous few paragraphs fall into a category of physiology termed *thermoregulation.* The body has mechanisms to act as a thermostat, when the core body temperature deviates from the normal resting value. With an increase in temperature, skin blood vessels dilate and sweat is produced, while a decrease in temperature induces skin blood vessel constriction and shivering. It is also important to point out that not all living beings use these same mechanisms to regulate the temperature of their bodies. A dog, which is an endotherm similar to humans, loses heat by panting because sweat evaporation would be minimal since the fluid particles would be trapped by the fur. Ectotherms must derive heat from the environment—for example, a lizard warms up by standing on a sun-heated rock. It is also important to note that the metabolisms of endotherms are not dependent on the surrounding environment, whereas ectotherm metabolism is highly dependent on the environment. Thermoregulation in the human body is achieved by keeping a tight balance between heat gain and heat loss. The bioheat transfer equation introduced in Chap. 3 is used to calculate the heat transfer between a human body and its surroundings.

Thermoregulation can be adjusted by both behavioral changes and physiological changes. We have discussed many behavioral changes, such as relocating to a more desirable environment within the structure or putting on more clothing. Physiological changes include blood vessel diameter changes and the production of sweat. However, under normal conditions, few of these changes are needed because of the efficient organization of arteries and veins; they are arranged as a countercurrent heat exchanger (for more information, refer to Chap. 11 Topic of Special

Interest, "The Human Cardiovascular System as a Countercurrent Heat Exchanger"). The primary function of this countercurrent heat exchanger in the human body is to minimize the loss of heat to the external environment. In nearly all systems, an artery, which delivers "warm" blood from the body core, is located directly adjacent to a vein, which returns "cool" blood to the core of the body. Recall that the extremities may be at a very different temperature than the core, and this would be manifested directly in the blood returning from the limb. However, since the vein runs adjacent to an artery, there is a continual conduction of heat along the entire blood vessel length from the artery to the vein. This acts to prevent cool blood from entering the core of the body and reducing the core temperature.

Another factor that affects thermal comfort, health, and productivity is **ventilation**. Fresh outdoor air can be provided to a building *naturally* by doing nothing, or *forcefully* by a mechanical ventilation system. In the first case, which is the norm in residential buildings, the necessary ventilation is provided by *infiltration through cracks and leaks* in the living space and by the opening of the windows and doors. The additional ventilation needed in the bathrooms and kitchens is provided by *air vents with dampers* or *exhaust fans* due to the high humidity/smoke generated in these rooms. With this kind of uncontrolled ventilation, however, the fresh air supply will be either too high, wasting energy, or too low, causing poor indoor air quality. But the current practice is not likely to change for residential buildings since there is not a public outcry about energy waste or air quality, and thus it is difficult to justify the cost and complexity of mechanical ventilation systems.

Mechanical ventilation systems are part of any heating and air conditioning system in *commercial buildings,* providing the necessary amount of fresh outdoor air and distributing it uniformly throughout the building. This is not surprising since many rooms in large commercial buildings have no windows and thus rely on mechanical ventilation. Even the rooms with windows are in the same situation since the windows are tightly sealed and cannot be opened in most buildings. It is not a good idea to oversize the ventilation system just to be on the "safe side" since exhausting the heated or cooled indoor air wastes energy. On the other hand, reducing the ventilation rates below the required minimum to conserve energy should also be avoided so that the indoor air quality can be maintained at the required levels. The minimum fresh air ventilation requirements are listed in Table 1–10. The values are based on controlling CO_2 and other contaminants with an adequate margin of safety, which requires each person be supplied with at least 7.5 L/s (15 ft^3/min) of fresh air.

Another function of the mechanical ventilation system is to **clean** the air by filtering it as it enters the building. Various types of filters are available for this purpose, depending on the cleanliness requirements and the allowable pressure drop.

TABLE 1–10

Minimum fresh air requirements in buildings

Application	Requirement (per person) L/s	Requirement (per person) ft³/min
Classrooms, libraries, supermarkets	8	15
Dining rooms, conference rooms, offices	10	20
Hospital rooms	13	25
Hotel rooms	15 (per room)	30 (per room)
Smoking lounges	30	60
Retail stores	1.0–1.5 (per m²)	0.2–0.3 (per ft²)
Residential buildings	0.35 air change per hour, but not less than 7.5 L/s (or 15 ft³/min) per person	

From ASHRAE Standard 62–1989

SUMMARY

In this chapter, the basics of heat transfer are introduced and discussed. The science of *thermodynamics* deals with the amount of heat transfer as a system undergoes a process from one equilibrium state to another, whereas the science of *heat transfer* deals with the rate of heat transfer, which is the main focus of interest in the design and evaluation of heat transfer equipment. The sum of all forms of energy of a system is called *total energy,* and it includes the internal, kinetic, and potential energies. The *internal energy* represents the molecular energy of a system, and it consists of sensible, latent, chemical, and nuclear forms. The sensible and latent forms of internal energy can be transferred from one medium to another as a result of a temperature difference, and they are referred to as *heat* or *thermal energy.* Thus, *heat transfer* is the exchange of the sensible and latent forms of internal energy between two media as a result of a temperature difference. The amount of heat transferred per unit time is called the *heat transfer rate* and is denoted by $\dot{Q}$. The rate of heat transfer per unit area is called *heat flux, $\dot{q}$.*

A system of fixed mass is called a *closed system,* and a system that involves mass transfer across its boundaries is called an *open system* or *control volume.* The *first law of thermodynamics* or the *energy balance* for any system undergoing any process can be expressed as

$$E_{in} - E_{out} = \Delta E_{system}$$

When a stationary closed system involves heat transfer only and no work interactions across its boundary, the energy balance relation reduces to

$$Q = mc_v\Delta T$$

where Q is the amount of net heat transfer to or from the system. When heat is transferred at a constant rate of $\dot{Q}$, the amount of heat transfer during a time interval Δt can be determined from $Q = \dot{Q}\Delta t$.

Under steady conditions and in the absence of any work interactions, the conservation of energy relation for a control volume with one inlet and one exit with negligible changes in kinetic and potential energies can be expressed as

$$\dot{Q} = \dot{m}c_p\Delta T$$

where $\dot{m} = \rho V A_c$ is the mass flow rate and $\dot{Q}$ is the rate of net heat transfer into or out of the control volume.

Heat can be transferred in three different modes: conduction, convection, and radiation. *Conduction* is the transfer of heat from the more energetic particles of a substance to the adjacent less energetic ones as a result of interactions between the particles and is expressed by *Fourier's law of heat conduction* as

$$\dot{Q}_{cond} = -kA\frac{dT}{dx}$$

where k is the *thermal conductivity* of the material in W/m·K or Btu/h·ft·R, A is the *area* normal to the direction of heat transfer, and dT/dx is the *temperature gradient.* The magnitude of the rate of heat conduction across a plane layer of thickness L is given by

$$\dot{Q}_{cond} = kA\frac{\Delta T}{L}$$

where ΔT is the temperature difference across the layer.

Convection is the mode of heat transfer between a solid surface and the adjacent liquid or gas that is in motion, and it involves the combined effects of conduction and fluid motion. The rate of convection heat transfer is expressed by *Newton's law of cooling* as

$$\dot{Q}_{convection} = hA_s(T_s - T_\infty)$$

where h is the *convection heat transfer coefficient* in W/m²·K or Btu/h·ft²·R, A_s is the *surface area* through which convection heat transfer takes place, T_s is the *surface temperature,* and T_∞ is the *temperature of the fluid* sufficiently far from the surface.

Radiation is the energy emitted by matter in the form of electromagnetic waves (or photons) as a result of the changes in the electronic configurations of the atoms or molecules. The maximum rate of radiation that can be emitted from a surface at a thermodynamic temperature T_s is given by the *Stefan–Boltzmann law* as $\dot{Q}_{emit, max} = \sigma A_s T_s^4$, where $\sigma = 5.67 \times 10^{-8}$ W/m²·K⁴ or 0.1714×10^{-8} Btu/h·ft²·R⁴ is the *Stefan–Boltzmann constant.*

When a surface of emissivity ε and surface area A_s at a temperature T_s is completely enclosed by a much larger (or black) surface at a temperature T_{surr} separated by a gas (such as air) that does not block radiation, the net rate of radiation heat transfer between these two surfaces is given by

$$\dot{Q}_{rad} = \varepsilon\sigma A_s(T_s^4 - T_{surr}^4)$$

In this case, the emissivity (ε) and the surface area of the surrounding surface do not have any effect on the net radiation heat transfer.

The rate at which a surface absorbs radiation is determined from $\dot{Q}_{absorbed} = \alpha\dot{Q}_{incident}$ where $\dot{Q}_{incident}$ is the rate at which radiation is incident on the surface and α is the absorptivity of the surface.

REFERENCES AND SUGGESTED READING

1. American Society of Heating, Refrigeration, and Air-Conditioning Engineers. The latest version says: *ASHRAE Handbook-Fundamentals.* Atlanta, GA: ASHRAE, 2017.

2. *ASME Boiler & Pressure Vessel Code,* Section IV, "Rules for Construction of Heating Boilers." New York: ASME, 2015.

3. ASME Vision 2030 Project, "Creating the Future of Mechanical Engineering Education," no date. Available at http://community.asme.org/board_education/w/wiki/7883. asme-vision-2030-project.aspx.

4. ASTM D1351-14, "Standard Specification for Thermoplastic Polyethylene Insulation for Electrical Wire and Cable." West Conshohocken, PA, 2014, available at www.astm.org.

5. ASTM Standard C1055-03, "Standard Guide for Heated System Surface Conditions that Produce Contact Burn Injuries," ASTM International, West Conshohocken, PA: ASTM International, 2009.

6. Y. A. Çengel, J. M. Cimbala, and R. H. Turner. *Fundamentals of Thermal-Fluid Sciences.* 5th ed. New York: McGraw-Hill, 2017.

7. Y. A. Çengel, M. A. Boles, and M. Kanoglu. *Thermodynamics—An Engineering Approach.* 9th ed. New York: McGraw-Hill, 2019.

8. *Code of Ethics for Engineers*, National Society of Professional Engineers (NSPE) Publication Number 1102, 2007, available at http://www.nspe.org/Ethics/CodeofEthics/index.html.

9. K.R. Rao (ed.). *Continuing & Changing Priorities of ASME Boiler & Pressure Vessel Codes and Standards.* New York: ASME Press, 2014.

10. *Prevention through Design: Plan for the National Initiative*, National Institute for Occupational Safety and Health (NIOSH) Publication Number 2011-121, 2010, available at http://www.cdc.gov/niosh/docs/2011-121/.

11. R. J. Ribando. *Heat Transfer Tools.* New York: McGraw-Hill, 2002.

PROBLEMS*

Thermodynamics and Heat Transfer

1–1C How does the science of heat transfer differ from the science of thermodynamics?

1–2C What is the driving force for (*a*) heat transfer, (*b*) electric current flow, and (*c*) fluid flow?

1–3C How do rating problems in heat transfer differ from the sizing problems?

1–4C What is the difference between the analytical and experimental approaches to heat transfer? Discuss the advantages and disadvantages of each approach.

1–5C What is the importance of modeling in engineering? How are the mathematical models for engineering processes prepared?

1–6C When modeling an engineering process, how is the right choice made between a simple but crude and a complex but accurate model? Is the complex model necessarily a better choice since it is more accurate?

---

*Problems designated by a "C" are concept questions, and students are encouraged to answer them all. Problems designated by an "E" are in English units, and the SI users can ignore them. Problems with the 🖥 icon are comprehensive in nature and are intended to be solved with appropriate software. Problems with the 🅿🆃🅳 icon are Prevention through Design problems. Problems with the 🄲🅂🅂 icon are Codes and Standards problems.

1–7C On a hot summer day, a student turns his fan on when he leaves his room in the morning. When he returns in the evening, will his room be warmer or cooler than the neighboring rooms? Why? Assume all the doors and windows are kept closed.

1–8C Consider two identical rooms, one with a refrigerator in it and the other without one. If all the doors and windows are closed, will the room that contains the refrigerator be cooler or warmer than the other room? Why?

1–9C It is often claimed that you should leave the heating system in your house on all the time rather than turning it off when you are not home because it takes more energy to heat the house back to its normal temperature. What do you think?

1–10C Someone claims that turning the thermostat of the central air conditioning of a warm house to the lowest level will cool the house a lot faster. Is there any truth to this claim?

1–11C Consider a perfectly insulated (no heat loss from the skin) 80-L electric water heater set at 60°C. Observing that one tank of hot water is sufficient to meet the hot water needs of a family for an entire day, someone suggests using a timer to heat the water once a day to the set temperature and then turning it off to save energy and money. Do you think the family should take this advice and invest in a timer? Assume there is a single tariff for electricity for all hours of the day.

1–12C An ideal gas is heated from 50°C to 80°C (*a*) at constant volume and (*b*) at constant pressure. For which case do you think the energy required will be greater? Why?

1–13C What is heat flux? How is it related to the heat transfer rate?

1–14C What are the mechanisms of energy transfer to a closed system? How is heat transfer distinguished from the other forms of energy transfer?

1–15E A logic chip used in a computer dissipates 3 W of power in an environment at 120°F and has a heat transfer surface area of 0.08 in². Assuming the heat transfer from the surface to be uniform, determine (*a*) the amount of heat this chip dissipates during an eight-hour workday in kWh and (*b*) the heat flux on the surface of the chip in W/in².

1–16 Consider a 150-W incandescent lamp. The filament of the lamp is 5 cm long and has a diameter of 0.5 mm. The diameter of the glass bulb of the lamp is 8 cm. Determine the heat flux in W/m² (*a*) on the surface of the filament and (*b*) on the surface of the glass bulb, and (*c*) calculate how much it will cost per year to keep that lamp on for eight hours a day every day if the unit cost of electricity is $0.08/kWh.
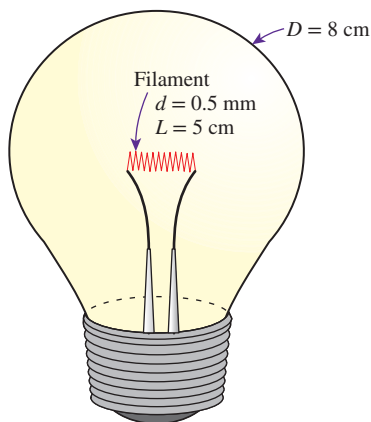
FIGURE P1−16

1–17 A 15-cm-diameter aluminum ball is to be heated from 80°C to an average temperature of 200°C. Taking the average density and specific heat of aluminum in this temperature range to be $\rho = 2700$ kg/m³ and $c_p = 0.90$ kJ/kg·K, respectively, determine the amount of energy that needs to be transferred to the aluminum ball. *Answer: 515 kJ*

1–18E A 60-gallon water heater is initially filled with water at 50°F. Determine how much energy (in Btu) needs to be transferred to the water to raise its temperature to 120°F. Evaluate the water properties at an average water temperature of 85°F.

1–19 Infiltration of cold air into a warm house during winter through the cracks around doors, windows, and other openings is a major source of energy loss since the cold air that enters

needs to be heated to the room temperature. The infiltration is often expressed in terms of ACH (air changes per hour). An ACH of 2 indicates that all air in the house is replaced twice every hour by the cold air outside.

Consider an electrically heated house that has a floor space of 200 m² and an average height of 3 m at 1000 m elevation, where the standard atmospheric pressure is 89.6 kPa. The house is maintained at a temperature of 22°C, and the infiltration losses are estimated to amount to 0.7 ACH. Assuming the pressure and the temperature in the house remain constant, determine the amount of energy loss from the house due to infiltration for a day during which the average outdoor temperature is 5°C. Also, determine the cost of this energy loss for that day if the unit cost of electricity in that area is $0.082/kWh. *Answers: 53.8 kWh/day, $4.41/day*

1–20 [PtD] Liquid ethanol is a flammable fluid and can release vapors that form explosive mixtures at temperatures above its flash point at 16.6°C. In a chemical plant, liquid ethanol ($c_p = 2.44$ kJ/kg·K, $\rho = 789$ kg/m³) is being transported in a pipe with an inside diameter of 5 cm. The pipe is located in a hot area with the presence of an ignition source, where an estimated 20 kW of heat is added to the ethanol. Your task as an engineer is to design a pumping system to transport the ethanol safely and to prevent fire hazard. If the inlet temperature of the ethanol is 10°C, determine the volume flow rate that is necessary to keep the temperature of the ethanol in the pipe below its flash point.
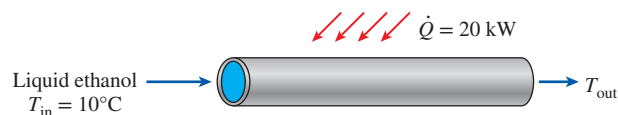
FIGURE P1−20

1–21 [PtD] In many manufacturing plants, individuals are often working around high-temperature surfaces. Exposed hot surfaces that can cause thermal burns on human skin are considered hazards in the workplace. Metallic surfaces above 70°C can instantly damage skin that touches them. Consider an AISI 1010 carbon steel strip ($\rho = 7832$ kg/m³) 2 mm thick and 3 cm wide that is conveyed into a chamber to be cooled at a constant speed of 1 m/s. The steel strip enters the cooling chamber at 597°C. Determine the rate at which heat needs to be removed so that the steel strip exits the chamber at 47°C. Discuss how the conveyance speed can affect the required rate of heat removal.
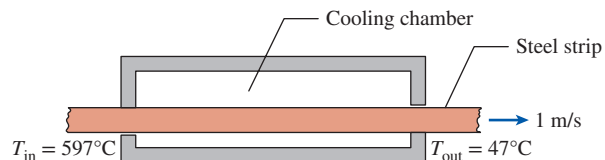
FIGURE P1−21

1–22 1.2 kg of liquid water initially at 15°C is to be heated to 95°C in a teapot equipped with a 1200-W electric heating element inside. The teapot is 0.5 kg and has an average specific heat of 0.7 kJ/kg·K. Taking the specific heat of water to be 4.18 kJ/kg·K and disregarding any heat loss from the teapot, determine how long it will take for the water to be heated.

Water
15°C

Electric
heating
element

1200 W
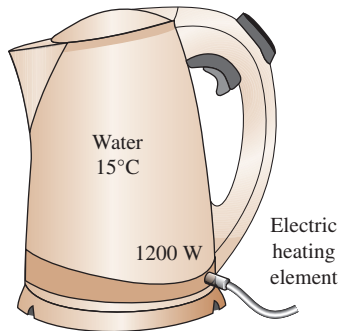
FIGURE P1–22

1–23 C&S A water heater uses 100 kW to heat 60 gallons of liquid water from an initial temperature of 20°C. The average density and specific heat of the water are 970 kg/m³ and 4.18 kJ/kg·K, respectively. According to the service restrictions of the ASME Boiler and Pressure Vessel Code (ASME BPVC.IV-2015, HG-101), water heaters should not be operating at temperatures exceeding 120°C at or near the heater outlet. Determine the heating duration such that the final water temperature that would exit the water heater would be in compliance with the ASME Boiler and Pressure Vessel Code.

1–24 C&S A boiler with a mass of 10 kg uses 50 kW to heat 20 gallons of liquid water initially at 15°C. The average specific heats for the boiler material and the water are 0.48 kJ/kg·K and 4.18 kJ/kg·K, respectively. The average density of the water is 850 kg/m³. According to the service restrictions of the ASME Boiler and Pressure Vessel Code (ASME BPVC.IV-2015, HG-101), hot water boilers should not be operating at temperatures exceeding 120°C at or near the boiler outlet. Determine whether the final water temperature that would exit the boiler after 30 min of heating at 50 kW would be in compliance with the ASME Boiler and Pressure Vessel Code.

1–25 Water is heated in an insulated, constant diameter tube by a 7-kW electric resistance heater. If the water enters the heater steadily at 15°C and leaves at 70°C, determine the mass flow rate of the water.

Water
15°C

70°C

Resistance
heater, 7 kW
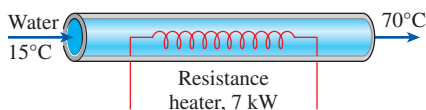
FIGURE P1–25

1–26 A room is heated by a baseboard resistance heater. When the heat losses from the room on a winter day amount to 7000 kJ/h, it is observed that the air temperature in the room remains constant even though the heater operates continuously. Determine the power rating of the heater in kW.

1–27 A 5-m × 6-m × 8-m room is to be heated by an electrical resistance heater placed in a short duct in the room. Initially, the room is at 15°C, and the local atmospheric pressure is 98 kPa. The room is losing heat steadily to the outside at a rate of 200 kJ/min. A 300-W fan circulates the air steadily through the duct and the electric heater at an average mass flow rate of 50 kg/min. The duct can be assumed to be adiabatic, and there is no air leaking in or out of the room. If it takes 18 min for the room air to reach an average temperature of 25°C, find (*a*) the power rating of the electric heater and (*b*) the temperature rise that the air experiences each time it passes through the heater.

1–28 A hair dryer is basically a duct in which a few layers of electric resistors are placed. A small fan pulls the air in and forces it to flow over the resistors, where it is heated. Air enters a 1200-W hair dryer at 100 kPa and 22°C and leaves at 47°C. The cross-sectional area of the hair dryer at the exit is 60 cm². Neglecting the power consumed by the fan and the heat losses through the walls of the hair dryer, determine (*a*) the volume flow rate of air at the inlet and (*b*) the velocity of the air at the exit.

$T_2 = 47°C$
$A_2 = 60$ cm²

$P_1 = 100$ kPa
$T_1 = 22°C$

$\dot{W}_e = 1200$ W
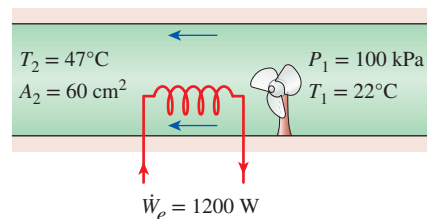
FIGURE P1–28

1–29E Air enters the duct of an air-conditioning system at 15 psia and 50°F at a volume flow rate of 450 ft³/min. The diameter of the duct is 10 in, and heat is transferred to the air in the duct from the surroundings at a rate of 2 Btu/s. Determine (*a*) the velocity of the air at the duct inlet and (*b*) the temperature of the air at the exit. *Answers:* (*a*) 825 ft/min, (*b*) 64°F

1–30 C&S Liquid water with a specific heat of 4.18 kJ/kg·K is heated in a circular tube by an electrical heater at 10 kW. The water enters the tube at 10°C with a mass flow rate of 10 g/s. The inner surface of the tube is lined with polyvinylidene chloride (PVDC) lining. According to the ASME Code for Process Piping (ASME B31.3-2014, A323), the recommended maximum temperature for PVDC lining is 79°C.

Determine whether the water exiting the tube would be in compliance with the ASME Code for Process Piping. What is the minimum mass flow rate of the water needed to keep the exit temperature from exceeding the recommended maximum temperature for PVDC lining?

Heat Transfer Mechanisms

1–31C Define thermal conductivity, and explain its significance in heat transfer.

1–32C Which is a better heat conductor, diamond or silver?

1–33C How do the thermal conductivity of gases and liquids vary with temperature?

1–34C Why is the thermal conductivity of superinsulation orders of magnitude lower than the thermal conductivity of ordinary insulation?

1–35C Why do we characterize the heat conduction ability of insulators in terms of their apparent thermal conductivity instead of their ordinary thermal conductivity?

1–36C What are the mechanisms of heat transfer? How are they distinguished from each other?

1–37C Write down the expressions for the physical laws that govern each mode of heat transfer, and identify the variables involved in each relation.

1–38C How does heat conduction differ from convection?

1–39C Does any of the energy of the sun reach the earth by conduction or convection?

1–40C How does forced convection differ from natural convection?

1–41C What is the physical mechanism of heat conduction in a solid, a liquid, and a gas?

1–42C Consider heat transfer through a windowless wall of a house on a winter day. Discuss the parameters that affect the rate of heat conduction through the wall.

1–43C Consider heat loss through two walls of a house on a winter night. The walls are identical except that one of them has a tightly fit glass window. Through which wall will the house lose more heat? Explain.

1–44C Consider two houses that are identical except that the walls are built using bricks in one house and wood in the other. If the walls of the brick house are twice as thick, which house do you think will be more energy efficient?

1–45C Consider two walls of a house that are identical except that one is made of 10-cm-thick wood while the other is made of 25-cm-thick brick. Through which wall will the house lose more heat in winter?

1–46C Define emissivity and absorptivity. What is Kirchhoff's law of radiation?

1–47C What is a blackbody? How do real bodies differ from blackbodies?

1–48 A wood slab with a thickness of 0.05 m is subjected to a heat flux of 40 W/m². The left and right surface temperatures of the wood slab are kept at constant temperatures of 40°C and 20°C, respectively. What is the thermal conductivity of the wood slab?

1–49 The inner and outer surfaces of a 4-m × 7-m brick wall of thickness 30 cm and thermal conductivity 0.69 W/m·K are maintained at temperatures of 20°C and 5°C, respectively. Determine the rate of heat transfer through the wall in W.
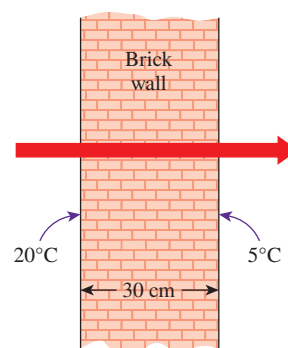
FIGURE P1–49

1–50E The inner and outer glasses of a 4-ft × 4-ft double-pane window are at 60°F and 48°F, respectively. If the 0.25-in space between the two glasses is filled with still air, determine the rate of heat transfer through the window. *Answer:* 131 Btu/h

1–51 The inner and outer surfaces of a 0.5-cm thick 2-m × 2-m window glass in winter are 10°C and 3°C, respectively. If the thermal conductivity of the glass is 0.78 W/m·K, determine the amount of heat loss through the glass over a period of 5 h. What would your answer be if the glass were 1 cm thick? *Answers:* 78.6 MJ, 39.3 MJ

1–52 Reconsider Prob. 1–51. Using appropriate software, plot the amount of heat loss through the glass as a function of the window glass thickness in the range of 0.1 cm to 1.0 cm. Discuss the results.

1–53 An aluminum pan whose thermal conductivity is 237 W/m·K has a flat bottom with diameter 15 cm and thickness 0.4 cm. Heat is transferred steadily to boiling water in the pan through its bottom at a rate of 800 W. If the inner surface of the bottom of the pan is at 105°C, determine the temperature of the outer surface of the bottom of the pan.

105°C

0.4 cm

800 W
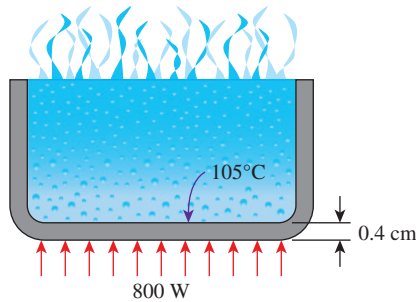
FIGURE P1–53

1–54E The north wall of an electrically heated home is 20 ft long, 10 ft high, and 1 ft thick and is made of brick whose thermal conductivity is $k = 0.42$ Btu/h·ft·°F. On a certain winter night, the temperatures of the inner and the outer surfaces of the wall are measured to be at about 62°F and 25°F, respectively, for a period of 8 h. Determine (a) the rate of heat loss through the wall that night and (b) the cost of that heat loss to the homeowner if the cost of electricity is $0.07/kWh.

1–55 In a certain experiment, cylindrical samples of diameter 4 cm and length 7 cm are used (see Fig. 1–32). The two thermocouples in each sample are placed 3 cm apart. After initial transients, the electric heater is observed to draw 0.6 A at 110 V, and both differential thermometers read a temperature difference of 10°C. Determine the thermal conductivity of the sample. *Answer:* 78.8 W/m·K

1–56 One way of measuring the thermal conductivity of a material is to sandwich an electric thermofoil heater between two identical rectangular samples of the material and to heavily insulate the four outer edges, as shown in Fig. P1-56. Thermocouples attached to the inner and outer surfaces of the samples record the temperatures.

During an experiment, two 0.5-cm-thick samples 10 cm × 10 cm in size are used. When steady operation is reached, the heater is observed to draw 25 W of electric power, and the temperature of each sample is observed to drop from 82°C at the inner surface to 74°C at the outer surface. Determine the thermal conductivity of the material at the average temperature.

Samples — Insulation

Wattmeter

Insulation

Source

0.5 cm

Resistance heater
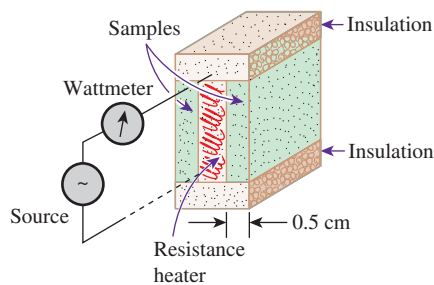
FIGURE P1–56

1–57 [PtD] Silicon wafer is susceptible to warping when the wafer is subjected to a temperature difference across its thickness. Thus, steps needed to be taken to prevent the temperature gradient across the wafer thickness from getting large. As an engineer in a semiconductor company, your task is to determine the maximum allowable heat flux on the bottom surface of the wafer while maintaining the upper surface temperature at 27°C. To prevent the wafer from warping, the temperature difference across its thickness of 500 μm cannot exceed 1°C.

$L = 500$ μm

T_{up}

Silicon wafer

T_{bot}

$\dot{q}$
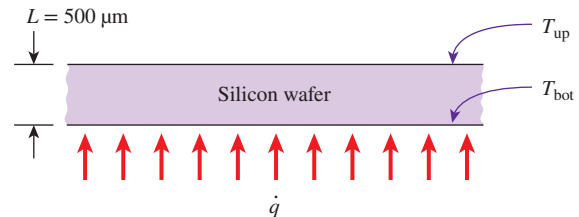
FIGURE P1–57

1–58 A concrete wall with a surface area of 20 m^2 and a thickness of 0.30 m separates conditioned room air from ambient air. The temperature of the inner surface of the wall (T_1) is maintained at 25°C. (a) Determine the heat loss $\dot{Q}$(W) through the concrete wall for three thermal conductivity values of 0.75, 1, and 1.25 W/m·K and outer wall surface temperatures of $T_2 = -15, -10, -5, 0, 5, 10, 15, 20, 25, 30,$ and 38°C (a total of 11 data points for each thermal conductivity value). Tabulate the results for all three cases in one table. Also provide a computer-generated graph [Heat loss, $\dot{Q}$(W) vs. Outside wall temperature, T_2(°C)] for the display of your results. The results for all three cases should be plotted on the same graph. (b) Discuss your results for the three cases.

1–59 A hollow spherical iron container with outer diameter 20 cm and thickness 0.2 cm is filled with iced water at 0°C. If the outer surface temperature is 5°C, determine the approximate rate of heat gain by the iced water in kW and the rate at which ice melts in the container. The heat of fusion of water is 333.7 kJ/kg. Treat the spherical shell as a plain wall, and use the outer area.

5°C

Iced water

0.2 cm

FIGURE P1–59

1–60 Reconsider Prob. 1–59. Using appropriate software, plot the rate at which ice melts as a function of the container thickness in the range of 0.1 cm to 1.0 cm. Discuss the results.

1–61 C&S A heating cable is embedded in a concrete slab to melt snow on a 5-m × 5-m surface area. The heating cable is heated electrically with joule heating. The concrete has a thermal conductivity of 1.4 W/m·K, and the layer between the slab surface and the heater surface is 50 mm. When the surface is covered with snow, the heat generated from the heating cable can melt snow at a rate of 0.1 kg/s. According to the National Electrical Code (NFPA 70), the power density (heat flux) for embedded snow-melting equipment should not exceed 1300 W/m^2. Under the given conditions, does the concrete slab with the embedded heating cable operate in compliance with the NFPA 70 code? Also, to minimize thermal stress in the concrete, the temperature difference between the heater surface (T_1) and the slab surface (T_2) should not exceed 21°C (2015 ASHRAE Handbook—HVAC Applications, Chap. 51). Do the current operating conditions allow $T_1 - T_2 \leq 21$°C?

Snow
Concrete slab
Slab surface, T_2
Heater surface, T_1
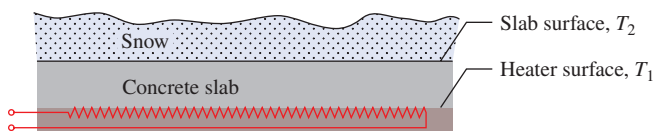
FIGURE P1–61

1–62E An engineer who is working on the heat transfer analysis of a house in English units needs the convection heat transfer coefficient on the outer surface of the house. But the only value he can find from his handbooks is 14 W/m^2·K, which is in SI units. The engineer does not have a direct conversion factor between the two unit systems for the convection heat transfer coefficient. Using the conversion factors between W and Btu/h, m and ft, and °C and °F, express the given convection heat transfer coefficient in Btu/h·ft^2·°F. *Answer:* 2.47 Btu/h·ft^2·°F

1–63 Air at 20°C with a convection heat transfer coefficient of 20 W/m^2·K blows over a pond. The surface temperature of the pond is at 40°C. Determine the heat flux between the surface of the pond and the air.

1–64 C&S A series of ASME SA-193 carbon steel bolts are bolted to the upper surface of a metal plate. The bottom surface of the plate is subjected to a uniform heat flux of 5 kW/m^2. The upper surface of the plate is exposed to ambient air with a temperature of 30°C and a convection heat transfer coefficient of 10 W/m^2·K. The ASME Boiler and Pressure Vessel Code (ASME BPVC.IV-2015, HF-300) limits the maximum allowable use temperature to 260°C for the SA-193

bolts. Determine whether the use of these SA-193 bolts complies with the ASME code under these conditions. If the temperature of the bolts exceeds the maximum allowable use temperature of the ASME code, discuss a possible solution to lower the temperature of the bolts.

Air, T_∞, h
Bolt
Metal plate
Uniform heat flux
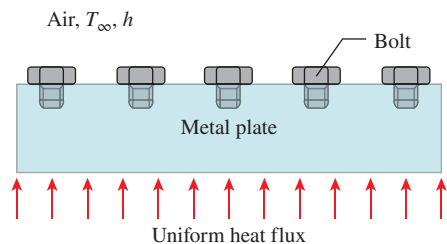
FIGURE P1–64

1–65 In a power plant, pipes transporting superheated vapor are very common. Superheated vapor is flowing at a rate of 0.3 kg/s inside a pipe 5 cm in diameter and 10 m in length. The pipe is located in a power plant at 20°C and has a uniform surface temperature of 100°C. If the temperature drop between the inlet and exit of the pipe is 30°C, and the specific heat of the vapor is 2190 J/kg·K, determine the heat transfer coefficient as a result of convection between the pipe surface and the surroundings.

Air, 20°C
$T_s = 100$°C
$D = 5$ cm
Superheated vapor 0.3 kg/s
$L = 10$ m
$T_{in} - T_{out} = 30$°C
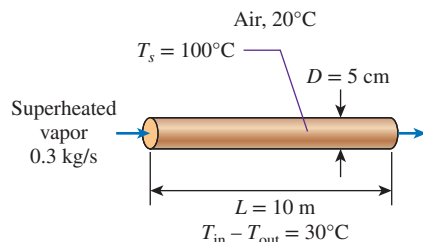
FIGURE P1–65

1–66 C&S A boiler supplies hot water to a commercial dishwasher through a pipe with a surface temperature of 50°C. The hot water exits the boiler at 95°C, and it is transported in a pipe that has an outside diameter of 20 mm. The distance between the boiler and the dishwasher is 20 m. The section of the pipe between the boiler and the dishwater is exposed to convection with a heat transfer coefficient of 100 W/m^2·K at an ambient temperature of 20°C. The hot water flows steadily in the pipe at 60 g/s, and its average specific heat is 4.20 kJ/kg·K. The National Sanitation Foundation standard for commercial warewashing equipment (ANSI/NSF 3)

requires the final rinse water temperature to be at least 82°C. Under these conditions, does the hot water entering the dishwasher meet the ANSI/NSF 3 standard? If not, discuss some possible ways to increase the water temperature entering the dishwasher.

1–67 C&S Hot liquid is flowing in a steel pipe with a 22-mm inner diameter and a 27-mm outer diameter. The pipe outer surface is subjected to a uniform flux of 1200 W/m² for a length of 1 m. The pipe inner surface is coated with a thin polyvinylidene fluoride (PVDF) lining. The hot liquid flowing inside the pipe has a mean temperature of 120°C and a convection heat transfer coefficient of 50 W/m²·K. The ASME Code for Process Piping (ASME B31.3-2014, A323) recommends a maximum temperature for PVDF lining to be 135°C. Does the surface temperature of the PVDF lining comply with the recommendation of the code?

1–68 An electric current of 5 A passing through a resistor has a measured voltage of 6 V across the resistor. The resistor is cylindrical with a diameter of 2.5 cm and length of 15 cm. The resistor has a uniform temperature of 90°C, and the room air temperature is 20°C. Assuming that heat transfer by radiation is negligible, determine the heat transfer coefficient by convection.

1–69 C&S An electric current of 1 A passing through a cable has a measured voltage of 30 V across the cable. The cable is covered with polyethylene insulation, and convection occurs at the outer surface of the insulation. The ambient temperature is 20°C with a convection heat transfer coefficient of 5 W/m²·K, and the surface area subjected to the convection is 0.1 m². The ASTM D1351 standard specifies that thermoplastic polyethylene insulation is suitable for use on electrical cable with operation at temperatures up to 75°C. Under these conditions, will the polyethylene insulation for the cable meet the ASTM D1351 standard? If the polyethylene insulation does not meet the ASTM D1351 standard, then discuss possible solutions to meet the standard.

1–70 PtD An AISI 316 stainless steel spherical container is used for storing chemicals undergoing exothermic reaction that provides a uniform heat flux of 60 kW/m² to the container's inner surface. The container has an inner diameter of 1 m and a wall thickness of 5 cm. To prevent thermal burns on individuals working around the container, it is necessary to keep the container's outer surface temperature below 50°C. If the ambient temperature is 23°C, determine the necessary convection heat transfer coefficient to keep the container's outer surface temperature below 50°C. Is the necessary convection heat transfer coefficient feasible with free convection of air? If not, discuss other options to prevent the container's outer surface temperature from causing thermal burns.
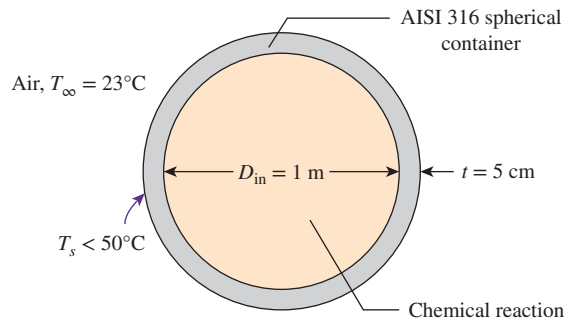
FIGURE P1−70

1–71 A transistor with a height of 0.4 cm and a diameter of 0.6 cm is mounted on a circuit board. The transistor is cooled by air flowing over it with an average heat transfer coefficient of 30 W/m²·K. If the air temperature is 55°C and the transistor case temperature is not to exceed 70°C, determine the amount of power this transistor can dissipate safely. Disregard any heat transfer from the transistor base.
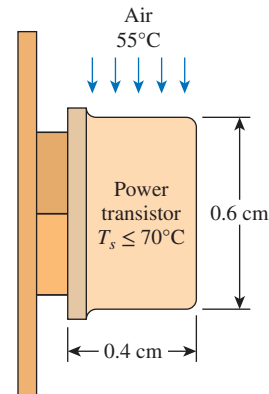
FIGURE P1−71

1–72E A 200-ft-long section of a steam pipe whose outer diameter is 4 in passes through an open space at 50°F. The average temperature of the outer surface of the pipe is measured to be 280°F, and the average heat transfer coefficient on that surface is determined to be 6 Btu/h·ft²·°F. Determine (*a*) the rate of heat loss from the steam pipe and (*b*) the annual cost of this energy loss if steam is generated in a natural gas furnace having an efficiency of 86 percent and the price of natural gas is $1.10/therm (1 therm = 100,000 Btu). *Answers:* (*a*) 289,027 Btu/h, (*b*) $32,384/yr

1–73 The boiling temperature of nitrogen at atmospheric pressure at sea level (1 atm) is −196°C. Therefore, nitrogen is commonly used in low-temperature scientific studies

since the temperature of liquid nitrogen in a tank open to the atmosphere remains constant at −196°C until the liquid nitrogen in the tank is depleted. Any heat transfer to the tank results in the evaporation of some liquid nitrogen, which has a heat of vaporization of 198 kJ/kg and a density of 810 kg/m³ at 1 atm.

Consider a 4-m-diameter spherical tank initially filled with liquid nitrogen at 1 atm and −196°C. The tank is exposed to 20°C ambient air with a heat transfer coefficient of 25 W/m²·K. The temperature of the thin-shelled spherical tank is observed to be almost the same as the temperature of the nitrogen inside. Disregarding any radiation heat exchange, determine the rate of evaporation of the liquid nitrogen in the tank as a result of the heat transfer from the ambient air.
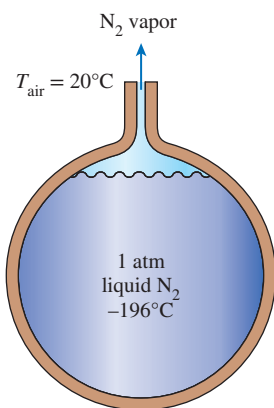
FIGURE P1−73

1–74 A series of experiments were conducted by passing 40°C air over a long 25-mm-diameter cylinder with an embedded electrical heater. The objective of these experiments was to determine the power per unit length required ($\dot{W}/L$) to maintain the surface temperature of the cylinder at 300°C for different air velocities (V). The results of these experiments are given in the following table:

V (m/s)	1	2	4	8	12
$\dot{W}/L$ (W/m)	450	658	983	1507	1963

(a) Assuming a uniform temperature over the cylinder, negligible radiation between the cylinder surface and surroundings, and steady-state conditions, determine the convection heat transfer coefficient (h) for each velocity (V). Plot the results in terms of h (W/m²·K) vs. V (m/s). Provide a computer-generated graph for the display of your results, and tabulate the data used for the graph.

(b) Assume that the heat transfer coefficient and velocity can be expressed in the form $h = CV^n$. Determine the values of the constants C and n from the results of part (a) by plotting h vs. V on log-log coordinates and choosing a C value that assures a match at V = 1 m/s and then varying n to get the best fit.

1–75 A 1.4-m-long, 0.2-cm-diameter electrical wire extends across a room that is maintained at 20°C. Heat is generated in the wire as a result of resistance heating, and the surface temperature of the wire is measured to be 240°C in steady operation. Also, the voltage drop and electric current through the wire are measured to be 110 V and 3 A, respectively. Disregarding any heat transfer by radiation, determine the convection heat transfer coefficient for heat transfer between the outer surface of the wire and the air in the room. *Answer:* 170.5 W/m²·K
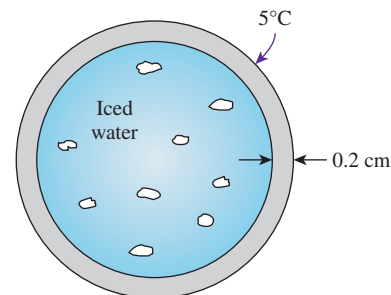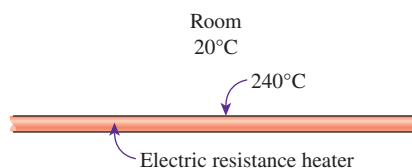

FIGURE P1−75

1–76 Reconsider Prob. 1–75. Using appropriate software, plot the convection heat transfer coefficient as a function of the wire surface temperature in the range of 100°C to 300°C. Discuss the results.

1–77E Using the conversion factors between W and Btu/h, m and ft, and K and R, express the Stefan–Boltzmann constant $\sigma = 5.67 \times 10^{-8}$ W/m²·K⁴ in the English unit Btu/h·ft²·R⁴.

1–78 The outer surface of a spacecraft in space has an emissivity of 0.8 and a solar absorptivity of 0.3. If solar radiation is incident on the spacecraft at a rate of 950 W/m², determine the surface temperature of the spacecraft when the radiation emitted equals the solar energy absorbed.

1–79 Consider a person whose exposed surface area is 1.7 m², emissivity is 0.5, and surface temperature is 32°C. Determine the rate of heat loss from that person by radiation in a large room having walls at a temperature of (a) 300 K and (b) 280 K. *Answers:* (a) 26.7 W, (b) 121 W

1–80 Consider a sealed 20-cm-high electronic box whose base dimensions are 40 cm × 40 cm placed in a vacuum chamber. The emissivity of the outer surface of the box is 0.95. If the electronic components in the box dissipate a total of 100 W of power and the outer surface temperature of the box is not to exceed 55°C, determine the temperature at which the surrounding surfaces must be kept if this box is to be cooled by radiation alone. Assume the heat transfer from the bottom surface of the box to the stand to be negligible.
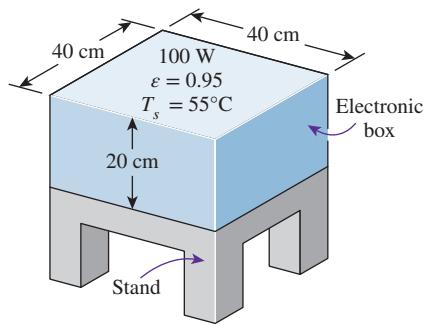
FIGURE P1–80

1–81 Two surfaces, one highly polished and the other heavily oxidized, are found to be emitting the same amount of energy per unit area. The highly polished surface has an emissivity of 0.1 at 1070°C, while the emissivity of the heavily oxidized surface is 0.78. Determine the temperature of the heavily oxidized surface.

1–82 A spherical interplanetary probe with a diameter of 2 m is sent out into the solar system. The probe surface is made of material having an emissivity of 0.9 and an absorptivity of 0.1. Signals from the sensors monitoring the probe surface temperatures are indicating an average value of −40°C for a space temperature of 0 K. If the electronics inside the probe are generating heat at a rate of 100 W/m³, determine the incident radiation rate on the probe surface.

1–83 An electronic package in the shape of a sphere with an outer diameter of 100 mm is placed in a large laboratory room. The surface emissivity of the package can assume three different values (0.2, 0.25, and 0.3). The walls of the room are maintained at a constant temperature of 77 K. The electronics in this package can only operate in the surface temperature range of $40°C \leq T_s \leq 85°C$. Determine the range of power dissipation ($\dot{W}$) for the electronic package over this temperature range for the three surface emissivity values (ε). Plot the results in terms of $\dot{W}(W)$ vs. $T_s(°C)$ for the three different values of emissivity over a surface temperature range of 40 to 85°C with temperature increments of 5°C (total of 10 data points for each ε value). Provide a computer-generated graph for the display of your results, and tabulate the data used for the graph. Comment on the results obtained.

Simultaneous Heat Transfer Mechanisms

1–84C Can all three modes of heat transfer occur simultaneously (in parallel) in a medium?

1–85C Can a medium involve (*a*) conduction and convection, (*b*) conduction and radiation, or (*c*) convection and radiation simultaneously? Give examples for the "yes" answers.

1–86C The deep human body temperature of a healthy person remains constant at 37°C while the temperature and the humidity of the environment change with time. Discuss the heat transfer mechanisms between the human body and the environment in both summer and winter, and explain how a person can keep cooler in summer and warmer in winter.

1–87C We often turn the fan on in summer to help us cool. Explain how a fan makes us feel cooler in the summer. Also explain why some people use ceiling fans also in winter.

1–88 Consider a 20-cm-thick granite wall with a thermal conductivity of 2.79 W/m·K. The temperature of the left surface is held constant at 50°C, whereas the right face is exposed to a flow of 22°C air with a convection heat transfer coefficient of 15 W/m²·K. Neglecting heat transfer by radiation, find the right wall surface temperature and the heat flux through the wall.
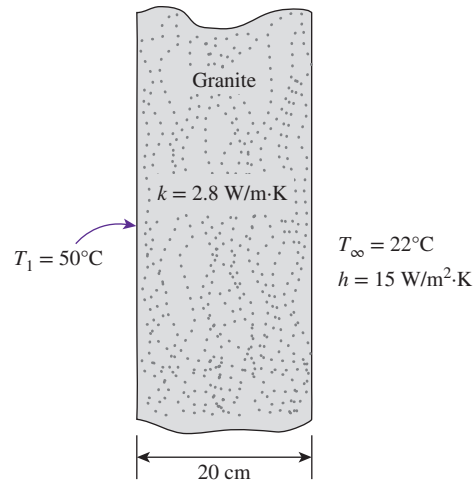
FIGURE P1–88

1–89 A solid plate, with a thickness of 15 cm and a thermal conductivity of 80 W/m·K, is being cooled at the upper surface by air. The air temperature is 10°C, while the temperatures at the upper and lower surfaces of the plate are 50 and 60°C, respectively. Determine the convection heat transfer coefficient of air at the upper surface, and discuss whether the value is reasonable or not for forced convection of air.
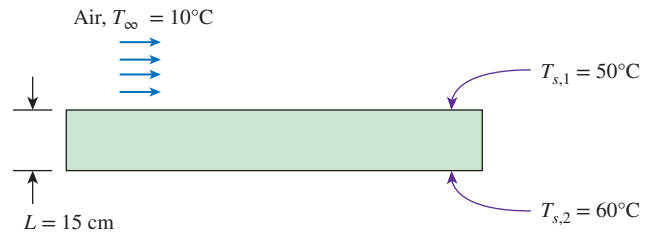
FIGURE P1–89

1–90 Air at 20°C with a convection heat transfer coefficient of 25 W/m²·K blows over a horizontal steel hot plate ($k = 43$ W/m·K). The surface area of the plate is 0.38 m² with a thickness of 2 cm. The plate surface is maintained at a constant temperature

of $T_s = 250°C$, and the plate loses 300 W from its surface by radiation. Calculate the inside plate temperature (T_i).
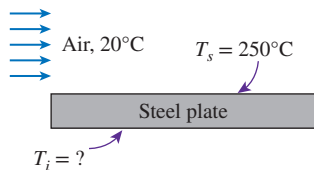
FIGURE P1–90

1–91 An electronic package with a surface area of 1 m² placed in an orbiting space station is exposed to space. The electronics in this package dissipate all 1 kW of its power to the space through its exposed surface. The exposed surface has an emissivity of 1.0 and an absorptivity of 0.25. Determine the steady-state exposed surface temperature of the electronic package (*a*) if the surface is exposed to a solar flux of 750 W/m², and (*b*) if the surface is not exposed to the sun.

1–92 Consider steady heat transfer between two large parallel plates at constant temperatures of $T_1 = 290$ K and $T_2 = 150$ K that are $L = 2$ cm apart. Assuming the surfaces to be black (emissivity $\varepsilon = 1$), determine the rate of heat transfer between the plates per unit surface area assuming the gap between the plates is (*a*) filled with atmospheric air, (*b*) evacuated, (*c*) filled with fiberglass insulation, and (*d*) filled with superinsulation having an apparent thermal conductivity of 0.00015 W/m·K.

1–93 Heat treatment is common in processing of semiconductor material. A 200-mm-diameter silicon wafer with thickness of 725 μm is being heat treated in a vacuum chamber by infrared heat. The surrounding walls of the chamber have a uniform temperature of 310 K. The infrared heater provides an incident radiation flux of 200 kW/m² on the upper surface of the wafer, and the emissivity and absorptivity of the wafer surface are 0.70. Using a pyrometer, the lower surface temperature of the wafer is measured to be 1000 K. Assuming there is no radiation exchange between the lower surface of the wafer and the surroundings, determine the upper surface temperature of the wafer. (*Note:* A *pyrometer* is a noncontacting device that intercepts and measures thermal radiation. This device can be used to determine the temperature of an object's surface.)
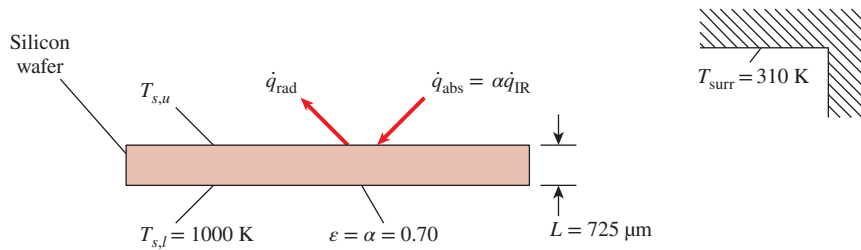
1–94 Consider a person standing in a room at 23°C. Determine the total rate of heat transfer from this person if the exposed surface area and the skin temperature of the person are 1.7 m² and 32°C, respectively, and the convection heat transfer coefficient is 5 W/m²·K. Take the emissivity of the skin and the clothes to be 0.9, and assume the temperature of the inner surfaces of the room to be the same as the air temperature.

1–95E A 2-in-diameter spherical ball whose surface is maintained at a temperature of 170°F is suspended in the middle of a room at 70°F. If the convection heat transfer coefficient is 15 Btu/h·ft²·°F and the emissivity of the surface is 0.8, determine the total rate of heat transfer from the ball.

1–96 A 1000-W iron is left on an ironing board with its base exposed to the air at 20°C. The convection heat transfer coefficient between the base surface and the surrounding air is 35 W/m²·K. If the base has an emissivity of 0.6 and a surface area of 0.02 m², determine the temperature of the base of the iron. *Answer:* 674°C
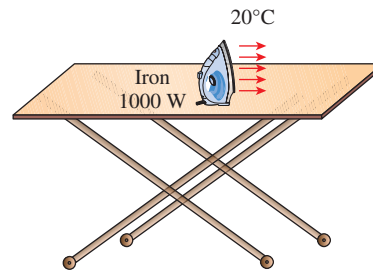
FIGURE P1–96

1–97 ⟨C&S⟩ The upper surface of a plate is bolted with ASTM B21 naval brass bolts. The bottom surface of the plate is fully insulated. The upper plate surface is exposed to convection at an air temperature of 50°C and a convection heat transfer coefficient of 5 W/m²·K. Also, thermal radiation exchange occurs between the upper plate surface and the surrounding surface temperature of 300°C. The emissivity of the plate surface and the bolts is 0.3. The ASME Code for Process Piping (ASME B31.3-2014) limits the maximum use

FIGURE P1–93

temperature of B21 bolts to 149°C. Determine whether the ASTM B21 bolts on the plate comply with the ASME code.
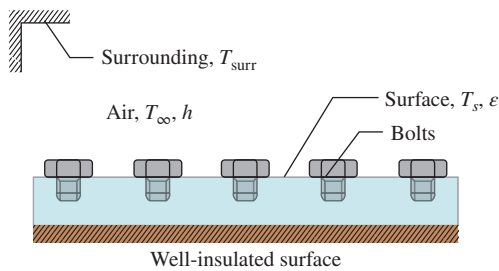
FIGURE P1–97

1–98 A 3-m-internal-diameter spherical tank made of 1-cm-thick stainless steel is used to store iced water at 0°C. The tank is located outdoors at 25°C. Assuming the entire steel tank to be at 0°C and thus the thermal resistance of the tank to be negligible, determine (*a*) the rate of heat transfer to the iced water in the tank and (*b*) the amount of ice at 0°C that melts during a 24-h period. The heat of fusion of water at atmospheric pressure is $h_{if} = 333.7$ kJ/kg. The emissivity of the outer surface of the tank is 0.75, and the convection heat transfer coefficient on the outer surface can be taken to be 30 W/m²·K. Assume the average surrounding surface temperature for radiation exchange to be 15°C. *Answers: (a)* 23.1 kW, (*b*) 5980 kg

1–99 In the metal processing industry, heat treatment of metals is commonly done using electrically heated draw batch furnaces. Consider a furnace that is situated in a room with surrounding air temperature of 30°C and an average convection heat transfer coefficient of 12 W/m²·K. The furnace front is made of a steel plate with thickness of 20 mm and a thermal conductivity of 25 W/m·K. The outer furnace front surface has an emissivity of 0.23, and the inside surface is subjected to a heat flux of 8 kW/m². Determine the outside surface temperature of the furnace front.
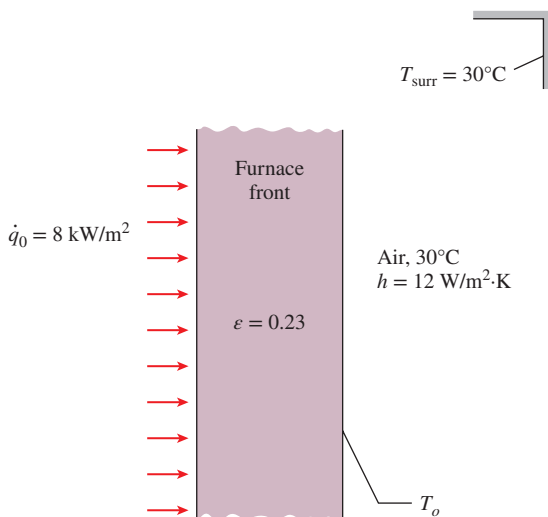
FIGURE P1–99

1–100 Solar radiation is incident on a 5-m² solar absorber plate surface at a rate of 800 W/m². Ninety-three percent of the solar radiation is absorbed by the absorber plate, while the remaining 7 percent is reflected away. The solar absorber plate has a surface temperature of 40°C with an emissivity of 0.9 that experiences radiation exchange with the surrounding temperature of −5°C. In addition, convective heat transfer occurs between the absorber plate surface and the ambient air of 20°C with a convection heat transfer coefficient of 7 W/m²·K. Determine the efficiency of the solar absorber, which is defined as the ratio of the usable heat collected by the absorber to the incident solar radiation on the absorber.

1–101 A flat-plate solar collector is used to heat water by having water flow through tubes attached at the back of the thin solar absorber plate. The absorber plate has a surface area of 2 m² with emissivity and absorptivity of 0.9. The surface temperature of the absorber is 35°C, and solar radiation is incident on the absorber at 500 W/m² with a surrounding temperature of 0°C. The convection heat transfer coefficient at the absorber surface is 5 W/m²·K, while the ambient temperature is 25°C. Net heat absorbed by the solar collector heats the water from an inlet temperature (T_{in}) to an outlet temperature (T_{out}). If the water flow rate is 5 g/s with a specific heat of 4.2 kJ/kg·K, determine the temperature rise of the water.
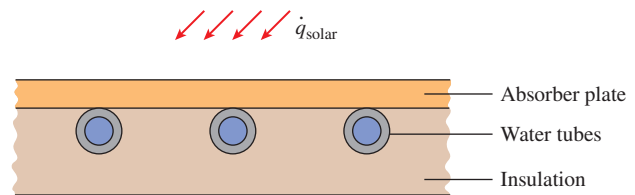
FIGURE P1–101

1–102 **PtD** Heat treatment of metals is commonly done using electrically heated draw batch furnaces. Consider a furnace that is situated in a room with a surrounding air temperature of 30°C and an average convection heat transfer coefficient of 15 W/m²·K. The outer furnace front surface has an emissivity of 0.7, and the inside surface is subjected to a heat flux of 5 kW/m². To ensure safety and avoid thermal burns to people working around the furnace, the outer front surface of the furnace should be kept below 50°C. Based on the information given about the furnace, does the furnace front surface require insulation to prevent thermal burns?
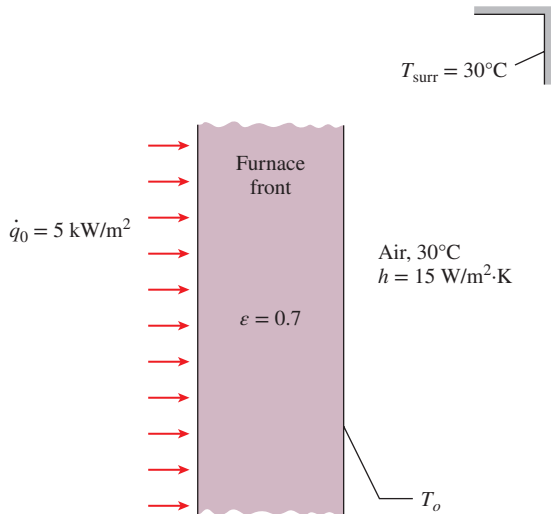
FIGURE P1–102

1–103E Consider a flat-plate solar collector placed horizontally on the flat roof of a house. The collector is 5 ft wide and 15 ft long, and the average temperature of the exposed surface of the collector is 100°F. The emissivity of the exposed surface of the collector is 0.9. Determine the rate of heat loss from the collector by convection and radiation during a calm day when the ambient air temperature is 70°F and the effective sky temperature for radiation exchange is 50°F. Take the convection heat transfer coefficient on the exposed surface to be 2.5 Btu/h.ft^2·°F.
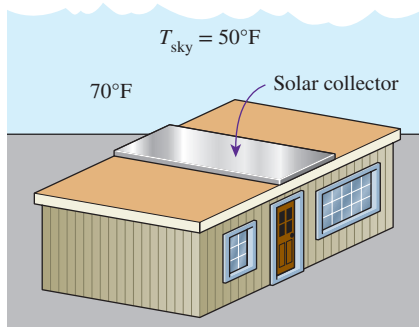
FIGURE P1–103E

1–104 An AISI 304 stainless steel sheet is going through an annealing process inside an electrically heated oven. The ambient air inside the oven is 600°C, while the surrounding surfaces of the oven are at a uniform temperature of 750°C. If the emissivity of the stainless steel sheet is 0.40 and the average convection heat transfer coefficient is 10 W/m^2·K, determine the temperature of the stainless steel sheet.

1–105 The roof of a house consists of a 15-cm-thick concrete slab ($k = 2$ W/m·K) that is 15 m wide and 20 m long.

The emissivity of the outer surface of the roof is 0.9, and the convection heat transfer coefficient on that surface is estimated to be 15 W/m^2·K. The inner surface of the roof is maintained at 15°C. On a clear winter night, the ambient air is reported to be at 10°C, while the night sky temperature for radiation heat transfer is 255 K. Considering both radiation and convection heat transfer, determine the outer surface temperature and the rate of heat transfer through the roof.

If the house is heated by a furnace burning natural gas with an efficiency of 85 percent, and the unit cost of natural gas is $0.60/therm (1 therm = 105,500 kJ of energy content), determine the money lost through the roof that night during a 14-h period.

1–106 **C&S** A nonmetal plate ($k = 0.05$ W/m·K) and an ASME SA-240 stainless steel plate ($k = 15$ W/m·K) are bolted together by ASTM B21 naval brass bolts. Both plates have a thickness of 38 mm, and the brass bolts are bolted through both plates. The bottom steel plate surface (surface 1) is subjected to a uniform heat flux of 200 W/m^2. The top nonmetal plate surface (surface 2) is exposed to convection at an air temperature of 20°C and a convection heat transfer coefficient of 5 W/m^2·K. Also, thermal radiation exchange occurs between the upper plate surface and the surrounding surface temperature of 30°C. The emissivity of the plate surface and the bolts is 0.3. The ASME Boiler and Pressure Vessel Code (ASME BPVC.IV-2015, HF-300) limits the maximum use temperature to 260°C for the SA-240 steel plate. The ASME Code for Process Piping (ASME B31.3-2014) limits the maximum use temperature of B21 bolts to 149°C. Determine whether both ASME codes are being complied with under these conditions.
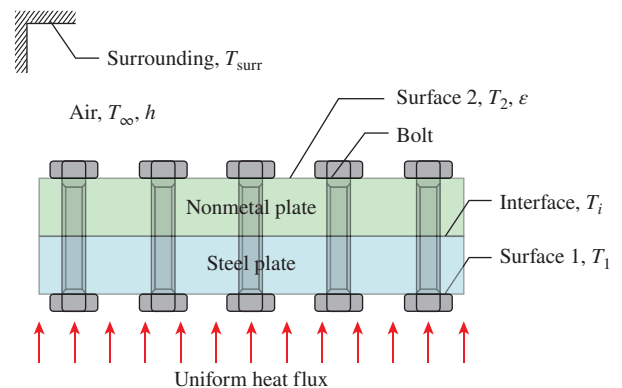
FIGURE P1–106

1–107 The inner and outer surfaces of a 25-cm-thick wall in summer are at 27°C and 44°C, respectively. The outer surface of the wall exchanges heat by radiation with surrounding surfaces at 40°C and by convection with ambient air also at 40°C with a convection heat transfer coefficient of 8 W/m^2·K. Solar radiation is

incident on the surface at a rate of 150 W/m². If both the emissivity and the solar absorptivity of the outer surface are 0.8, determine the effective thermal conductivity of the wall.
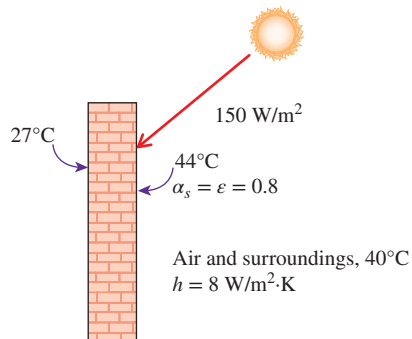
FIGURE P1−107

Solving Engineering Problems

1–108C   What is the value of the engineering software packages in (*a*) engineering education and (*b*) engineering practice?

1–109   Determine a positive real root of this equation using appropriate software:

$$3.5\,x^3 - 10\,x^{0.5} - 3x = -4$$

1–110   Solve this system of two equations with two unknowns using appropriate software:

$$x^3 - y^2 = 10.5$$
$$3xy + y = 4.6$$

1–111   Solve this system of three equations with three unknowns using appropriate software:

$$2x - y + z = 5$$
$$3x^2 + 2y = z + 2$$
$$xy + 2z = 8$$

1–112   Solve this system of three equations with three unknowns using appropriate software:

$$x^2 y - z = 1.5$$
$$x - 3\,y^{0.5} + xz = -2$$
$$x + y - z = 4.2$$

Special Topic: Thermal Comfort

1–113C   What is metabolism? What is the range of metabolic rate for an average man? Why are we interested in the metabolic rate of the occupants of a building when we deal with heating and air conditioning?

1–114C   Why is the metabolic rate of women, in general, lower than that of men? What is the effect of clothing on the environmental temperature that feels comfortable?

1–115C   What is asymmetric thermal radiation? How does it cause thermal discomfort in the occupants of a room?

1–116C   How do (*a*) draft and (*b*) cold floor surfaces cause discomfort for a room's occupants?

1–117C   What is stratification? Is it more likely to occur at places with low ceilings or places with high ceilings? How does it cause thermal discomfort for a room's occupants? How can stratification be prevented?

1–118C   Why is it necessary to ventilate buildings? What is the effect of ventilation on energy consumption for heating in winter and for cooling in summer? Is it a good idea to keep the bathroom fans on all the time? Explain.

1–119   Consider a house in Atlanta, Georgia, that is maintained at 22°C and has a total of 20 m² of window area. The windows are double-door type with wood frames and metal spacers and have a *U*-factor of 2.5 W/m²·K (see Prob. 1–120 for the definition of *U*-factor). The winter average temperature of Atlanta is 11.3°C. Determine the average rate of heat loss through the windows in winter.

1–120   The rate of heat loss through a unit surface area of a window per unit temperature difference between the indoors and the outdoors is called the *U*-factor. The value of the *U*-factor ranges from about 1.25 W/m²·K (or 0.22 Btu/h·ft²·°F) for low-*e* coated, argon-filled, quadruple-pane windows to 6.25 W/m²·K (or 1.1 Btu/h·ft²·°F) for a single-pane window with aluminum frames. Determine the range for the rate of heat loss through a 1.2-m × 1.8-m window of a house that is maintained at 20°C when the outdoor air temperature is −8°C.
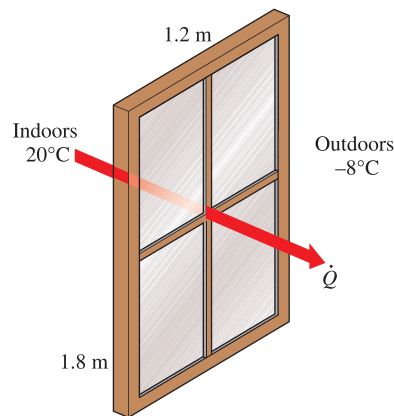
FIGURE P1−120

Review Problems

1–121   A 4-m × 5-m × 6-m room is to be heated by one ton (1000 kg) of liquid water contained in a tank placed in the room. The room is losing heat to the outside at an average rate of 10,000 kJ/h. The room is initially at 20°C and 100 kPa and

is maintained at an average temperature of 20°C at all times. If the hot water is to meet the heating requirements of this room for a 24-h period, determine the minimum temperature of the water when it is first brought into the room. Assume constant specific heats for both air and water at room temperature.   *Answer: 77.4°C*

1–122   Engine valves ($c_p = 440$ J/kg·K and $\rho = 7840$ kg/m³) are to be heated from 40°C to 800°C in 5 min in the heat treatment section of a valve manufacturing facility. The valves have a cylindrical stem with a diameter of 8 mm and a length of 10 cm. The valve head and the stem may be assumed to be of equal surface area, with a total mass of 0.0788 kg. For a single valve, determine (*a*) the amount of heat transfer, (*b*) the average rate of heat transfer, (*c*) the average heat flux, and (*d*) the number of valves that can be heat treated per day if the heating section can hold 25 valves and it is used 10 h per day.

1–123   A cylindrical resistor element on a circuit board dissipates 0.8 W of power. The resistor is 2 cm long and has a diameter of 0.4 cm. Assuming heat to be transferred uniformly from all surfaces, determine (*a*) the amount of heat this resistor dissipates during a 24-h period, (*b*) the heat flux, and (*c*) the fraction of heat dissipated from the top and bottom surfaces.

1–124   The heat generated in the circuitry on the surface of a silicon chip ($k = 130$ W/m·K) is conducted to the ceramic substrate to which it is attached. The chip is 6 mm × 6 mm in size and 0.5 mm thick and dissipates 3 W of power. Disregarding any heat transfer through the 0.5-mm-high side surfaces, determine the temperature difference between the front and back surfaces of the chip in steady operation.
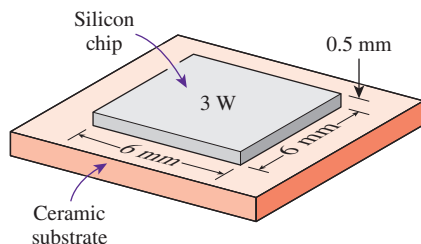
FIGURE P1–124

1–125   A 0.3-cm-thick, 12-cm-high, and 18-cm-long circuit board houses 80 closely spaced logic chips on one side, each dissipating 0.06 W. The board is impregnated with copper fillings and has an effective thermal conductivity of 16 W/m·K. All the heat generated in the chips is conducted across the circuit board and is dissipated from the back side of the board to the ambient air. Determine the temperature difference between the two sides of the circuit board.   *Answer: 0.042°C*

1–126   A 40-cm-long, 800-W electric resistance heating element with diameter 0.5 cm and surface temperature 120°C is immersed in 75 kg of water initially at 20°C. Determine how

long it will take for this heater to raise the water temperature to 80°C. Also, determine the convection heat transfer coefficients at the beginning and at the end of the heating process.

1–127   It is well known that wind makes the cold air feel much colder as a result of the *wind-chill effect* that is due to the increase in the convection heat transfer coefficient with increasing air velocity. The wind-chill effect is usually expressed in terms of the *wind-chill temperature* (WCT), which is the apparent temperature felt by exposed skin. For an outdoor air temperature of 0°C, for example, the wind-chill temperature is −5°C with 20 km/h winds and −9°C with 60 km/h winds. That is, a person exposed to 0°C windy air at 20 km/h will feel as cold as a person exposed to −5°C calm air (air motion under 5 km/h).

For heat transfer purposes, a standing man can be modeled as a 30-cm-diameter, 170-cm-long vertical cylinder with both the top and bottom surfaces insulated and with the side surface at an average temperature of 34°C. For a convection heat transfer coefficient of 15 W/m²·K, determine the rate of heat loss from this man by convection in still air at 20°C. What would your answer be if the convection heat transfer coefficient is increased to 30 W/m²·K as a result of winds? What is the wind-chill temperature in this case?   *Answers: 336 W, 672 W, 6°C*

1–128   An engine block with a surface area measured to be 0.95 m² generates a power output of 50 kW with a net engine efficiency of 35 percent. The engine block operates inside a compartment at 157°C, and the average convection heat transfer coefficient is 50 W/m²·K. If convection is the only heat transfer mechanism occurring, determine the engine block surface temperature.   *Answer: 841°C*

1–129   Consider an electrical wire submerged in liquid water at atmospheric conditions. The wire has a diameter of 1 mm and a length of 15 cm. The current through the wire is increased until the water reaches a temperature of 100°C. For this situation (boiling water) use an average value of the upper and lower values of the convection heat transfer coefficients given in Table 1–5. The wire surface temperature is to be maintained at 115°C. How much electric power is required for this case?
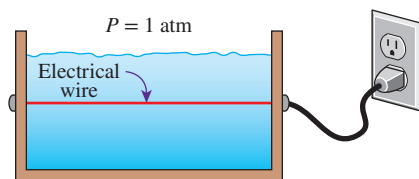
FIGURE P1–129

1–130   A cylindrical fuel rod 2 cm in diameter is encased in a concentric tube and cooled by water. The fuel generates heat uniformly at a rate of 150 MW/m³. The convection heat transfer coefficient on the fuel rod is 5000 W/m²·K, and the average

temperature of the cooling water, sufficiently far from the fuel rod, is 70°C. Determine the surface temperature of the fuel rod, and discuss whether the value of the given convection heat transfer coefficient on the fuel rod is reasonable.
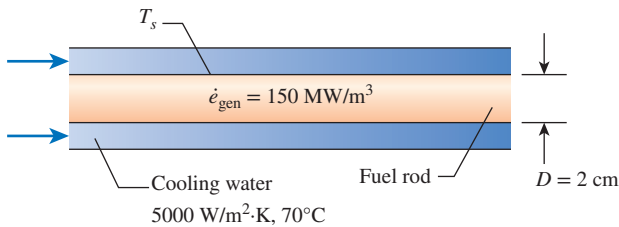
FIGURE P1−130

1–131 [PtD] The critical heat flux (CHF) is a thermal limit at which a boiling crisis occurs whereby an abrupt rise in temperature causes overheating on a fuel rod surface that leads to damage. A cylindrical fuel rod 2 cm in diameter is encased in a concentric tube and cooled by water. The fuel generates heat uniformly at a rate of $150 \ MW/m^3$. The average temperature of the cooling water, sufficiently far from the fuel rod, is 80°C. The operating pressure of the cooling water is such that the surface temperature of the fuel rod must be kept below 300°C to prevent the cooling water from reaching the critical heat flux. Determine the necessary convection heat transfer coefficient to prevent the critical heat flux from occurring.
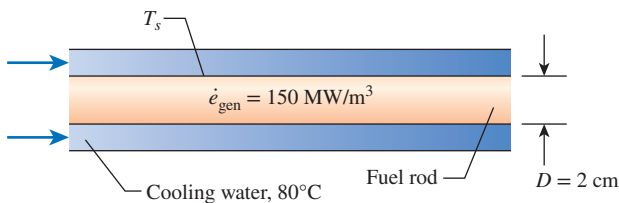
FIGURE P1−131

1–132 Consider a person standing in a room maintained at 20°C at all times. The inner surfaces of the walls, floors, and ceiling of the house are observed to be at an average temperature of 12°C in winter and 23°C in summer. Determine the rates of radiation heat transfer between this person and the surrounding surfaces in both summer and winter if the exposed surface area, emissivity, and the average outer surface temperature of the person are $1.6 \ m^2$, 0.95, and 32°C, respectively.

1–133 Consider a 3-m × 3-m × 3-m cubical furnace whose top and side surfaces closely approximate black surfaces at a temperature of 1200 K. The base surface has an emissivity of

$\varepsilon = 0.7$, and is maintained at 800 K. Determine the net rate of radiation heat transfer to the base surface from the top and side surfaces. *Answer:* 594 kW

1–134 A soldering iron has a cylindrical tip of 2.5 mm in diameter and 20 mm in length. With age and usage, the tip has oxidized and has an emissivity of 0.80. Assuming that the average convection heat transfer coefficient over the soldering iron tip is $25 \ W/m^2 \cdot K$ and the surrounding air temperature is 20°C, determine the power required to maintain the tip at 400°C.
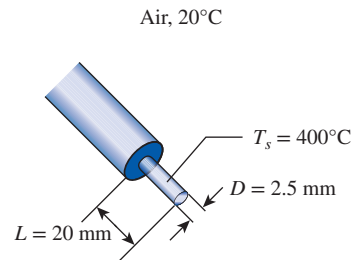
FIGURE P1−134

1–135 A thin metal plate is insulated on the back and exposed to solar radiation on the front surface. The exposed surface of the plate has an absorptivity of 0.7 for solar radiation. If solar radiation is incident on the plate at a rate of $550 \ W/m^2$ and the surrounding air temperature is 10°C, determine the surface temperature of the plate when the heat loss by convection equals the solar energy absorbed by the plate. Take the convection heat transfer coefficient to be $25 \ W/m^2 \cdot K$, and disregard any heat loss by radiation.
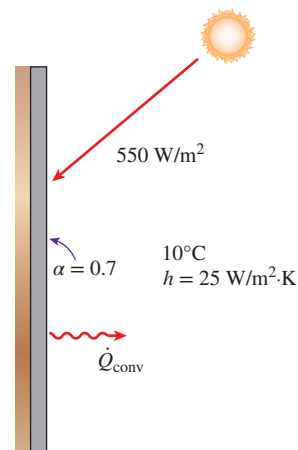
FIGURE P1−135

1–136 Consider a flat-plate solar collector placed on the roof of a house. The temperatures at the inner and outer surfaces of the glass cover are measured to be 28°C and 25°C,

respectively. The glass cover has a surface area of 2.5 m², a thickness of 0.6 cm, and a thermal conductivity of 0.7 W/m·K. Heat is lost from the outer surface of the cover by convection and radiation with a convection heat transfer coefficient of 10 W/m²·K and an ambient temperature of 15°C. Determine the fraction of heat lost from the glass cover by radiation.

1–137 An electric heater with the total surface area of 0.25 m² and emissivity 0.75 is in a room where the air has a temperature of 20°C and the walls are at 10°C. When the heater consumes 500 W of electric power, its surface has a steady temperature of 120°C. Determine the temperature of the heater surface when it consumes 700 W. Solve the problem (*a*) assuming negligible radiation and (*b*) taking radiation into consideration. Based on your results, comment on the assumption made in part (*a*).
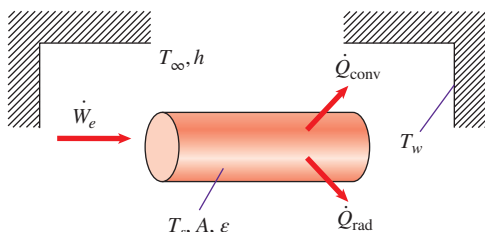
FIGURE P1–137

1–138 An ice skating rink is located in a building where the air is at $T_{air} = 20$°C and the walls are at $T_w = 25$°C. The convection heat transfer coefficient between the ice and the surrounding air is $h = 10$ W/m²·K. The emissivity of ice is $\varepsilon = 0.95$. The latent heat of fusion of ice is $h_{if} = 333.7$ kJ/kg, and its density is 920 kg/m³. (*a*) Calculate the refrigeration load of the system necessary to maintain the ice at $T_s = 0$°C for an ice rink of 12 m by 40 m. (*b*) How long would it take to melt $\delta = 3$ mm of ice from the surface of the rink if no cooling is supplied and the surface is considered insulated on the back side?
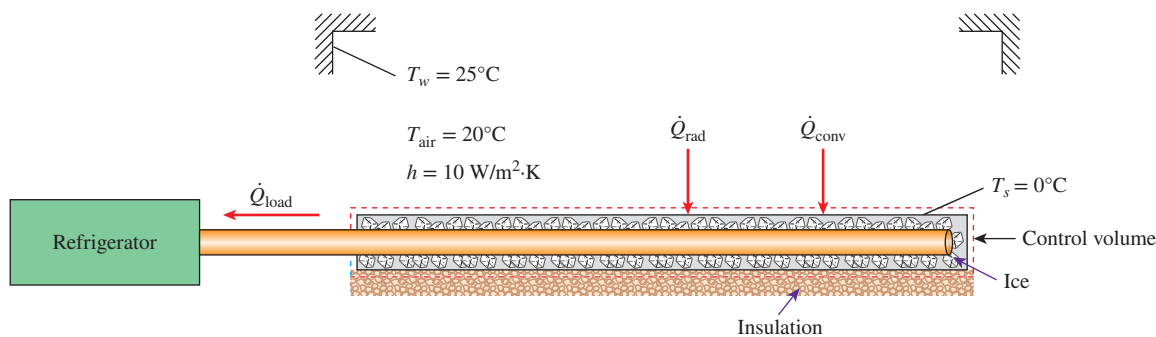
Fundamentals of Engineering (FE) Exam Problems

1–139 Which expression is used to determine the heat flux for conduction?

(*a*) $-kA\dfrac{dT}{dx}$ (*b*) $-k$ grad T (*c*) $h(T_2 - T_1)$

(*d*) $\varepsilon\sigma T^4$ (*e*) None of them

1–140 Which expression is used to determine the heat flux for convection?

(*a*) $-kA\dfrac{dT}{dx}$ (*b*) $-k$ grad T (*c*) $h(T_2 - T_1)$

(*d*) $\varepsilon\sigma T^4$ (*e*) None of them

1–141 Which expression is used to determine the heat flux emitted by thermal radiation from a surface?

(*a*) $-kA\dfrac{dT}{dx}$ (*b*) $-k$ grad T (*c*) $h(T_2 - T_1)$

(*d*) $\varepsilon\sigma T^4$ (*e*) None of them

1–142 A 1-kW electric resistance heater in a room is turned on and kept on for 50 min. The amount of energy transferred to the room by the heater is

(*a*) 1 kJ   (*b*) 50 kJ   (*c*) 3000 kJ

(*d*) 3600 kJ   (*e*) 6000 kJ

1–143 A 2-kW electric resistance heater submerged in 30-kg water is turned on and kept on for 10 min. During the process, 500 kJ of heat is lost from the water. The temperature rise of the water is

(*a*) 5.6°C   (*b*) 9.6°C   (*c*) 13.6°C

(*d*) 23.3°C   (*e*) 42.5°C

1–144 Eggs with a mass of 0.15 kg per egg and a specific heat of 3.32 kJ/kg·°C are cooled from 32°C to 10°C at a rate of 300 eggs per minute. The rate of heat removal from the eggs is

(*a*) 11 kW   (*b*) 80 kW   (*c*) 25 kW

(*d*) 657 kW   (*e*) 55 kW

1–145 A cold bottled drink ($m = 2.5$ kg, $c_p = 4200$ J/kg·K) at 5°C is left on a table in a room. The average temperature of

FIGURE P1–138

the drink is observed to rise to 15°C in 30 min. The average rate of heat transfer to the drink is
(a) 23 W   (b) 29 W   (c) 58 W
(d) 88 W   (e) 122 W

1–146 Water enters a pipe at 20°C at a rate of 0.25 kg/s and is heated to 60°C. The rate of heat transfer to the water is
(a) 10 kW   (b) 20.9 kW   (c) 41.8 kW
(d) 62.7 kW   (e) 167.2 kW

1–147 Air enters a 12-m-long, 7-cm-diameter pipe at 50°C at a rate of 0.06 kg/s. The air is cooled at an average rate of 400 W per square meter surface area of the pipe. The air temperature at the exit of the pipe is
(a) 4.3°C   (b) 17.5°C   (c) 32.5°C
(d) 43.4°C   (e) 45.8°C

1–148 Heat is lost steadily through a 0.5-cm thick, 2-m × 3-m window glass whose thermal conductivity is 0.7 W/m·K. The inner and outer surface temperatures of the glass are measured to be 12°C to 9°C. The rate of heat loss by conduction through the glass is
(a) 420 W   (b) 5040 W   (c) 17,600 W
(d) 1256 W   (e) 2520 W

1–149 Steady heat conduction occurs through a 0.3-m-thick, 9-m × 3-m composite wall at a rate of 1.2 kW. If the inner and outer surface temperatures of the wall are 15°C and 7°C, the effective thermal conductivity of the wall is
(a) 0.61 W/m·K   (b) 0.83 W/m·K   (c) 1.7 W/m·K
(d) 2.2 W/m·K   (e) 5.1 W/m·K

1–150 Heat is lost through a brick wall ($k = 0.72$ W/m·K), which is 4 m long, 3 m wide, and 25 cm thick at a rate of 500 W. If the inner surface of the wall is at 22°C, the temperature at the midplane of the wall is
(a) 0°C   (b) 7.5°C   (c) 11.0°C
(d) 14.8°C   (e) 22°C

1–151 A 10-cm-high and 20-cm-wide circuit board houses on its surface 100 closely spaced chips, each generating heat at a rate of 0.08 W and transferring it by convection and radiation to the surrounding medium at 40°C. Heat transfer from the back surface of the board is negligible. If the combined convection and radiation heat transfer coefficient on the surface of the board is 22 W/m²·K, the average surface temperature of the chips is
(a) 72.4°C   (b) 66.5°C   (c) 40.4°C
(d) 58.2°C   (e) 49.1°C

1–152 A 40-cm-long, 0.4-cm-diameter electric resistance wire submerged in water is used to determine the convection heat transfer coefficient in water during boiling at 1 atm pressure. The surface temperature of the wire is measured to be 114°C when a wattmeter indicates the electric power consumption to be 7.6 kW. The heat transfer coefficient is
(a) 108 kW/m²·K   (b) 13.3 kW/m²·K
(c) 68.1 kW/m²·K   (d) 0.76 kW/m²·K
(e) 256 kW/m²·K

1–153 While driving down a highway early in the evening, the airflow over an automobile establishes an overall heat transfer coefficient of 25 W/m²·K. The passenger cabin of this automobile exposes 8 m² of surface to the moving ambient air. On a day when the ambient temperature is 33°C, how much cooling must the air-conditioning system supply to maintain a temperature of 20°C in the passenger cabin?
(a) 0.65 MW   (b) 1.4 MW   (c) 2.6 MW
(d) 3.5 MW   (e) 0.94 MW

1–154 A room is heated by a 1.2-kW electric resistance heater whose wires have a diameter of 4 mm and a total length of 3.4 m. The air in the room is at 23°C, and the interior surfaces of the room are at 17°C. The convection heat transfer coefficient on the surface of the wires is 8 W/m²·K. If the rates of heat transfer from the wires to the room by convection and by radiation are equal, the surface temperature of the wire is
(a) 3534°C   (b) 1778°C   (c) 1772°C
(d) 98°C   (e) 25°C

1–155 Over 90 percent of the energy dissipated by an incandescent lightbulb is in the form of heat, not light. What is the temperature of a vacuum-enclosed tungsten filament with an exposed surface area of 2.03 cm² in a 100-W incandescent lightbulb? The emissivity of tungsten at the anticipated high temperatures is about 0.35. Note that the lightbulb consumes 100 W of electrical energy and dissipates all of it by radiation.
(a) 1870 K   (b) 2230 K   (c) 2640 K
(d) 3120 K   (e) 2980 K

1–156 On a still, clear night, the sky appears to be a blackbody with an equivalent temperature of 250 K. What is the air temperature when a strawberry field cools to 0°C and freezes if the heat transfer coefficient between the plants and air is 6 W/m²·K because of a light breeze and the plants have an emissivity of 0.9?
(a) 14°C   (b) 7°C   (c) 3°C
(d) 0°C   (e) −3°C

1–157 A 30-cm-diameter black ball at 120°C is suspended in air. It is losing heat to the surrounding air at 25°C by convection with a heat transfer coefficient of 12 W/m²·K and by radiation to the surrounding surfaces at 15°C. The total rate of heat transfer from the black ball is
(a) 322 W   (b) 595 W   (c) 234 W
(d) 472 W   (e) 2100 W

1–158 A 3-m² black surface at 140°C is losing heat to the surrounding air at 35°C by convection with a heat transfer coefficient of 16 W/m²·K and by radiation to the surrounding surfaces at 15°C. The total rate of heat loss from the surface is
(a) 5105 W   (b) 2940 W   (c) 3779 W
(d) 8819 W   (e) 5040 W

1–159 A person's head can be approximated as a 25-cm-diameter sphere at 35°C with an emissivity of 0.95. Heat is lost from the head to the surrounding air at 25°C by convection with a heat transfer coefficient of 11 W/m²·K and by radiation

to the surrounding surfaces at 10°C. Disregarding the neck, determine the total rate of heat loss from the head.

(*a*) 22 W   (*b*) 27 W   (*c*) 49 W
(*d*) 172 W   (*e*) 249 W

1–160 A person standing in a room loses heat to the air in the room by convection and to the surrounding surfaces by radiation. Both the air in the room and the surrounding surfaces are at 20°C. The exposed surface of the person is $1.5\,\text{m}^2$ and has an average temperature of 32°C and an emissivity of 0.90. If the rates of heat transfer from the person by convection and by radiation are equal, the combined heat transfer coefficient is

(*a*) $0.008\ \text{W/m}^2\text{·K}$ (*b*) $3.0\ \text{W/m}^2\text{·K}$
(*c*) $5.5\ \text{W/m}^2\text{·K}$ (*d*) $8.3\ \text{W/m}^2\text{·K}$
(*e*) $10.9\ \text{W/m}^2\text{·K}$

Design and Essay Problems

1–161 Write an essay on how microwave ovens work, and explain how they cook much faster than conventional ovens. Discuss whether conventional electric or microwave ovens consume more electricity for the same task.

1–162 Using information from the utility bills for the coldest month last year, estimate the average rate of heat loss from your house for that month. In your analysis, consider the contribution of the internal heat sources such as people, lights, and appliances. Identify the primary sources of heat loss from your house, and propose ways of improving the energy efficiency of your house.

1–163 Conduct this experiment to determine the combined heat transfer coefficient between an incandescent lightbulb and the surrounding air and surfaces using a 60-W lightbulb. You will need a thermometer, which can be purchased in a hardware store, and metal glue. You will also need a piece of string and a ruler to calculate the surface area of the lightbulb. First,

measure the air temperature in the room, and then glue the tip of the thermocouple wire of the thermometer to the glass of the lightbulb. Turn the light on and wait until the temperature reading stabilizes. The temperature reading will give the surface temperature of the lightbulb. Assuming 10 percent of the rated power of the bulb is converted to light and is transmitted by the glass, calculate the heat transfer coefficient from Newton's law of cooling.

1–164 It is well known that at the same outdoor air temperature a person is cooled at a faster rate under windy conditions than under calm conditions due to the higher convection heat transfer coefficients associated with windy air. The phrase *wind-chill* is used to relate the rate of heat loss from people under windy conditions to an equivalent air temperature for calm conditions (considered to be a wind or walking speed of 3 mph or 5 km/h). The hypothetical *wind-chill temperature* (WCT), called the *wind-chill temperature index* (WCTI), is an air temperature equivalent to the air temperature needed to produce the same cooling effect under calm conditions. A 2003 report on wind-chill temperature by the U.S. National Weather Service gives the WCTI in metric units as

$$\text{WCTI (°C)} = 13.12 + 0.6215T - 11.37\,V^{0.16} + 0.3965\,TV^{0.16}$$

where T is the air temperature in °C and V the wind speed in km/h at 10 m elevation. Show that this relation can be expressed in English units as

$$\text{WCTI (°F)} = 35.74 + 0.6215T - 35.75\,V^{0.16} + 0.4275\,TV^{0.16}$$

where T is the air temperature in °F and V the wind speed in mph at 33 ft elevation. Also, prepare a table for WCTI for air temperatures ranging from 10 to -60°C and wind speeds ranging from 10 to 80 km/h. Comment on the magnitude of the cooling effect of the wind and the danger of frostbite.

Design Element: "C&S icon ©McGraw-Hill Education; PtD icon ©McGraw-Hill Education; laptop art ©McGraw-Hill Education".

HEAT CONDUCTION EQUATION

Heat transfer has *direction* as well as *magnitude.* The rate of heat conduction in a specified direction is proportional to the *temperature gradient,* which is the rate of change in temperature with distance in that direction. Heat conduction in a medium, in general, is three-dimensional and time dependent, and the temperature in a medium varies with position as well as time, that is, $T = T(x, y, z, t)$. Heat conduction in a medium is said to be *steady* when the temperature does not vary with time, and *unsteady* or *transient* when it does. Heat conduction in a medium is said to be *one-dimensional* when conduction is significant in one dimension only and negligible in the other two primary dimensions, *two-dimensional* when conduction in the third dimension is negligible, and *three-dimensional* when conduction in all dimensions is significant.

We start this chapter with a description of steady, unsteady, and multidimensional heat conduction. Then we derive the differential equation that governs heat conduction in a large plane wall, a long cylinder, and a sphere, and generalize the results to three-dimensional cases in rectangular, cylindrical, and spherical coordinates. Following a discussion of the boundary conditions, we present the formulation of heat conduction problems and their solutions. Finally, we consider heat conduction problems with variable thermal conductivity.

This chapter deals with the theoretical and mathematical aspects of heat conduction, and it can be covered selectively, if desired, without causing a significant loss in continuity. The more practical aspects of heat conduction are covered in the following two chapters.

OBJECTIVES

When you finish studying this chapter, you should be able to:

- Understand multidimensionality and time dependence of heat transfer and the conditions under which a heat transfer problem can be approximated as being one-dimensional,

- Obtain the differential equation of heat conduction in various coordinate systems, and simplify it for the steady one-dimensional case,

- Identify the thermal conditions on surfaces, and express them mathematically as boundary and initial conditions,

- Solve one-dimensional heat conduction problems and obtain the temperature distributions within a medium and the heat flux,

- Analyze one-dimensional heat conduction in solids that involve heat generation, and

- Evaluate heat conduction in solids with temperature-dependent thermal conductivity.
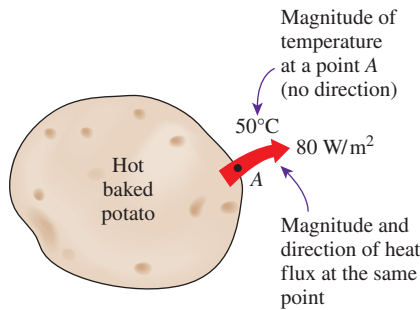
FIGURE 2–1
Heat transfer has direction as well
as magnitude, and thus it is
a *vector* quantity.
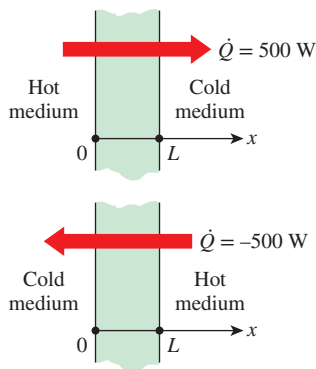
FIGURE 2–2
Indicating direction for heat transfer
(positive in the positive direction;
negative in the negative direction).

2–1 ▪ INTRODUCTION

In Chapter 1, heat conduction was defined as the transfer of thermal energy
from the more energetic particles of a medium to the adjacent less energetic
ones. It was stated that conduction can take place in liquids and gases as well
as solids provided that there is no bulk motion involved.

Although heat transfer and temperature are closely related, they are of a dif-
ferent nature. Unlike temperature, heat transfer has direction as well as mag-
nitude, and thus it is a *vector* quantity (Fig. 2–1). Therefore, we must specify
both direction and magnitude in order to describe heat transfer completely
at a point. For example, saying that the temperature on the inner surface of
a wall is 18°C describes the temperature at that location fully. But saying
that the heat flux on that surface is 50 W/m^2 immediately prompts the ques-
tion "in what direction?" We can answer this question by saying that heat
conduction is toward the inside (indicating heat gain) or toward the outside
(indicating heat loss).

To avoid such questions, we can work with a coordinate system and indicate
direction with plus or minus signs. The generally accepted convention is that
heat transfer in the positive direction of a coordinate axis is positive, and in
the opposite direction it is negative. Therefore, a positive quantity indicates
heat transfer in the positive direction, and a negative quantity indicates heat
transfer in the negative direction (Fig. 2–2).

The driving force for any form of heat transfer is the *temperature differ-
ence,* and the larger the temperature difference, the larger the rate of heat
transfer. Some heat transfer problems in engineering require the determina-
tion of the *temperature distribution* (the variation of temperature) throughout
the medium in order to calculate some quantities of interest such as the local
heat transfer rate, thermal expansion, and thermal stress at some critical loca-
tions at specified times. The specification of the temperature at a point in a
medium first requires the specification of the location of that point. This can
be done by choosing a suitable coordinate system such as the *rectangular,
cylindrical,* or *spherical* coordinates, depending on the geometry involved,
and a convenient reference point (the origin).

The *location* of a point is specified as (x, y, z) in rectangular coordinates,
as (r, ϕ, z) in cylindrical coordinates, and as (r, ϕ, θ) in spherical coordinates,
where the distances *x, y, z,* and *r* and the angles ϕ and θ are as shown in
Fig. 2–3. Then the temperature at a point (x, y, z) at time *t* in rectangular
coordinates is expressed as $T(x, y, z, t)$. The best coordinate system for a
given geometry is the one that describes the surfaces of the geometry best.
For example, a parallelepiped is best described in rectangular coordinates
since each surface can be described by a constant value of the *x-, y-,* or
z-coordinates. A cylinder is best suited for cylindrical coordinates since its
lateral surface can be described by a constant value of the radius. Similarly,
the entire outer surface of a spherical body can best be described by a con-
stant value of the radius in spherical coordinates. For an arbitrarily shaped
body, we normally use rectangular coordinates since it is easier to deal with
distances than with angles.

The notation just described is also used to identify the variables involved
in a heat transfer problem. For example, the notation $T(x, y, z, t)$ implies that
the temperature varies with the space variables *x, y,* and *z* as well as time.

(a) Rectangular coordinates   (b) Cylindrical coordinates   (c) Spherical coordinates
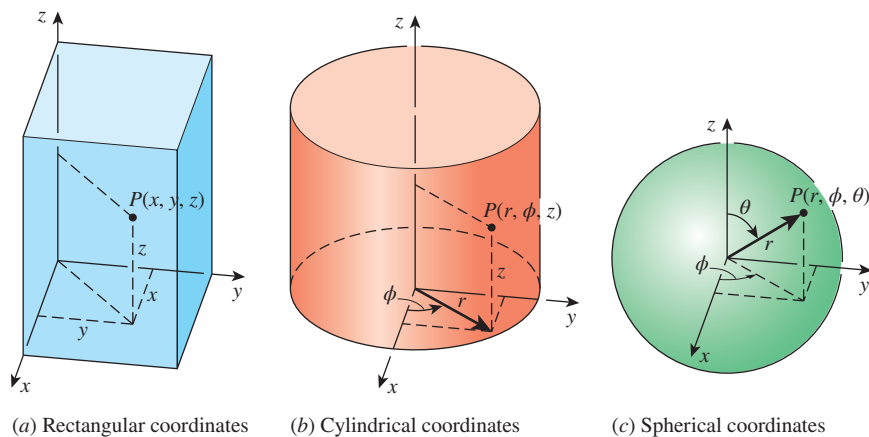
FIGURE 2–3
The various distances and angles involved when describing the location of a point in different coordinate systems.

The notation $T(x)$, on the other hand, indicates that the temperature varies in the x-direction only, and there is no variation with the other two space coordinates or time.

Steady Versus Transient Heat Transfer

Heat transfer problems are often classified as being **steady** (also called *steady-state*) or **transient** (also called *unsteady*). The term *steady* implies *no change with time* at any point within the medium, while *transient* implies *variation with time* or *time dependence*. Therefore, the temperature or heat flux remains unchanged with time during steady heat transfer through a medium at any location, although both quantities may vary from one location to another (Fig. 2–4). For example, heat transfer through the walls of a house is steady when the conditions inside the house and the outdoors remain constant for several hours. But even in this case, the temperatures on the inner and outer surfaces of the wall will be different unless the temperatures inside and outside the house are the same. The cooling of an apple in a refrigerator, on the other hand, is a transient heat transfer process since the temperature at any fixed point within the apple will change with time during cooling. During transient heat transfer, the temperature normally varies with time as well as position. In the special case of variation with time but not with position, the temperature of the medium changes *uniformly* with time. Such heat transfer systems are called **lumped systems**. A small metal object such as a thermocouple junction or a thin copper wire, for example, can be analyzed as a lumped system during a heating or cooling process.

Most heat transfer problems encountered in practice are *transient* in nature, but they are usually analyzed under some presumed *steady* conditions since steady processes are easier to analyze, and they provide the answers to our questions. For example, heat transfer through the walls and ceiling of a typical house is never steady since the outdoor conditions such as the temperature, the speed and direction of the wind, the location of the sun, and so on, change constantly. The conditions in a typical house are not so steady, either. Therefore, it is almost impossible to perform a heat transfer analysis of a house accurately. But then, do we really need an in-depth heat transfer analysis?

Time = 2 PM   Time = 5 PM
15°C   7°C   15°C   7°C

$\dot{Q}_1$ $\dot{Q}_2 = \dot{Q}_1$

(a) Steady

15°C   7°C   12°C   5°C

$\dot{Q}_1$ $\dot{Q}_2 \neq \dot{Q}_1$
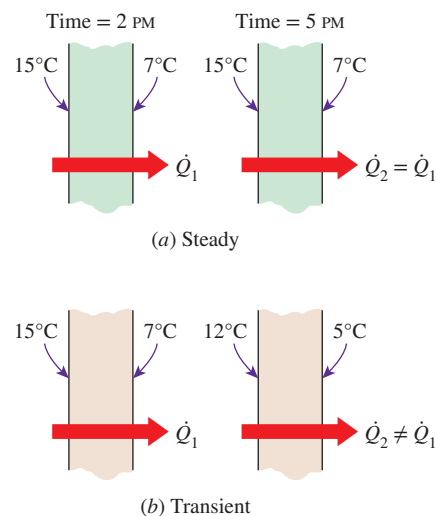
(b) Transient

FIGURE 2–4
Transient and steady heat conduction in a plane wall.

If the purpose of a heat transfer analysis of a house is to determine the proper size of a heater, which is usually the case, we need to know the *maximum* rate of heat loss from the house, which is determined by considering the heat loss from the house under *worst* conditions for an extended period of time, that is, during *steady* operation under worst conditions. Therefore, we can get the answer to our question by doing a heat transfer analysis under steady conditions. If the heater is large enough to keep the house warm under the most demanding conditions, it is large enough for all conditions. The approach described above is a common practice in engineering.

Multidimensional Heat Transfer

Heat transfer problems are also classified as being *one-dimensional, two-dimensional,* or *three-dimensional,* depending on the relative magnitudes of heat transfer rates in different directions and the level of accuracy desired. In the most general case, heat transfer through a medium is **three-dimensional**. That is, the temperature varies along all three primary directions within the medium during the heat transfer process. The temperature distribution throughout the medium at a specified time as well as the heat transfer rate at any location in this general case can be described by a set of three coordinates such as the *x, y,* and *z* in the rectangular (or Cartesian) coordinate system; the *r, ϕ,* and *z* in the cylindrical coordinate system; and the *r, ϕ,* and *θ* in the spherical (or polar) coordinate system. The temperature distribution in this case is expressed as $T(x, y, z, t)$, $T(r, \phi, z, t)$, and $T(r, \phi, \theta, t)$ in the respective coordinate systems.

The temperature in a medium, in some cases, varies mainly in two primary directions, and the variation of temperature in the third direction (and thus heat transfer in that direction) is negligible. A heat transfer problem in that case is said to be **two-dimensional**. For example, the steady temperature distribution in a long bar of rectangular cross section can be expressed as $T(x, y)$ if the temperature variation in the *z*-direction (along the bar) is negligible and there is no change with time (Fig. 2–5).

A heat transfer problem is said to be **one-dimensional** if the temperature in the medium varies in one direction only and thus heat is transferred in one direction, and the variation of temperature and thus heat transfer in other directions are negligible or zero. For example, heat transfer through the glass of a window can be considered to be one-dimensional since heat transfer through the glass occurs predominantly in one direction (the direction normal to the surface of the glass) and heat transfer in other directions (from one side edge to the other and from the top edge to the bottom) is negligible (Fig. 2–6). Likewise, heat transfer through a hot water pipe can be considered to be one-dimensional since heat transfer through the pipe occurs predominantly in the radial direction from the hot water to the ambient, and heat transfer along the pipe and along the circumference of a cross section (*z*- and *ϕ*-directions) is typically negligible. Heat transfer to an egg dropped into boiling water is also nearly one-dimensional because of symmetry. Heat is transferred to the egg in this case in the radial direction, that is, along straight lines passing through the midpoint of the egg.

We mentioned in Chap. 1 that the rate of heat conduction through a medium in a specified direction (say, in the *x*-direction) is proportional to the temperature difference across the medium and the area normal to the direction of heat
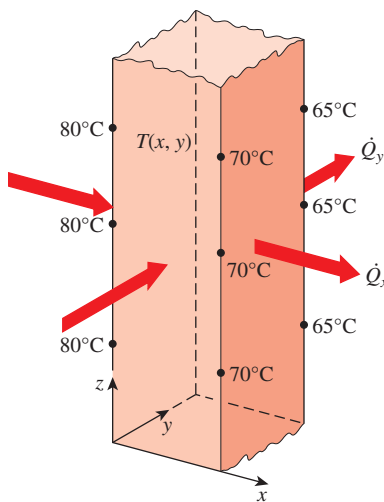
FIGURE 2–5
Two-dimensional heat transfer in a long rectangular bar.
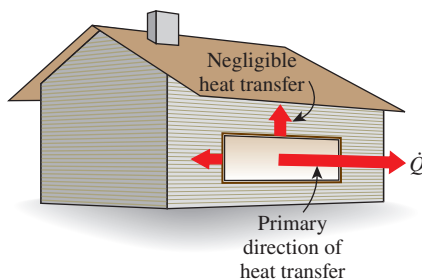
FIGURE 2–6
Heat transfer through the window of a house can be taken to be one-dimensional.

transfer but is inversely proportional to the distance in that direction. This was expressed in the differential form by **Fourier's law of heat conduction** for one-dimensional heat conduction as

$$\dot{Q}_{\text{cond}} = -kA\frac{dT}{dx} \quad \text{(W)} \tag{2–1}$$

where k is the *thermal conductivity* of the material, which is a measure of the ability of a material to conduct heat, and dT/dx is the *temperature gradient,* which is the slope of the temperature curve on a *T-x* diagram (Fig. 2–7). The thermal conductivity of a material, in general, varies with temperature. But sufficiently accurate results can be obtained by using a constant value for thermal conductivity at the *average* temperature.

Heat is conducted in the direction of decreasing temperature, and thus the temperature gradient is negative when heat is conducted in the positive *x*-direction. The *negative sign* in Eq. 2–1 ensures that heat transfer in the positive *x*-direction is a positive quantity.

To obtain a general relation for Fourier's law of heat conduction, consider a medium in which the temperature distribution is three-dimensional. Figure 2–8 shows an isothermal surface in that medium. The heat transfer vector at a point *P* on this surface must be perpendicular to the surface, and it must point in the direction of decreasing temperature. If *n* is the normal of the isothermal surface at point *P,* the rate of heat conduction at that point can be expressed by Fourier's law as

$$\dot{Q}_n = -kA\frac{\partial T}{\partial n} \quad \text{(W)} \tag{2–2}$$

In rectangular coordinates, the heat conduction vector can be expressed in terms of its components as

$$\vec{\dot{Q}}_n = \dot{Q}_x\vec{i} + \dot{Q}_y\vec{j} + \dot{Q}_z\vec{k} \tag{2–3}$$

where $\vec{i}, \vec{j},$ and $\vec{k}$ are the unit vectors, and $\dot{Q}_x, \dot{Q}_y$ and $\dot{Q}_z$ are the magnitudes of the heat transfer rates in the *x*-, *y*-, and *z*-directions, which again can be determined from Fourier's law as

$$\dot{Q}_x = -kA_x\frac{\partial T}{\partial x}, \quad \dot{Q}_y = -kA_y\frac{\partial T}{\partial y}, \quad \text{and} \quad \dot{Q}_z = -kA_z\frac{\partial T}{\partial z} \tag{2–4}$$

Here A_x, A_y and A_z are heat conduction areas normal to the *x*-, *y*-, and *z*-directions, respectively (Fig. 2–8).

Most engineering materials are *isotropic* in nature, and thus they have the same properties in all directions. For such materials we do not need to be concerned about the variation of properties with direction. But in *anisotropic* materials, such as the fibrous or composite materials, the properties may change with direction. For example, some of the properties of wood along the grain are different than those in the direction normal to the grain. In such cases, the thermal conductivity may need to be expressed as a tensor quantity to account for the variation with direction. The treatment of such advanced topics is beyond the scope of this text, and we will assume the thermal conductivity of a material to be independent of direction.
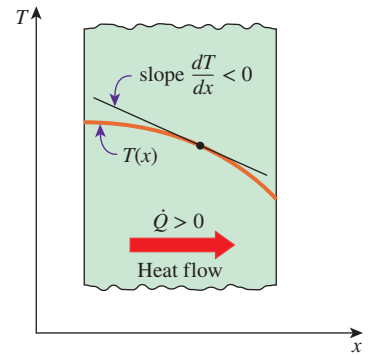
FIGURE 2–7
The temperature gradient dT/dx is simply the slope of the temperature curve on a *T-x* diagram.
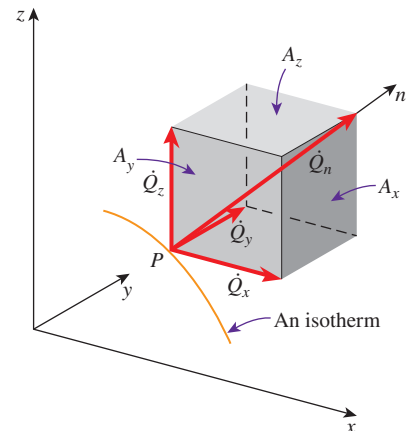
FIGURE 2–8
The heat transfer vector is always normal to an isothermal surface and can be resolved into its components like any other vector.
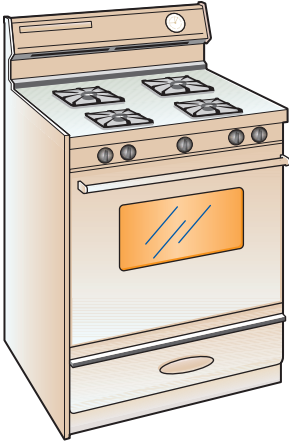
FIGURE 2–9
Heat is generated in the heating coils
of an electric range as a result of the
conversion of electrical energy to heat.
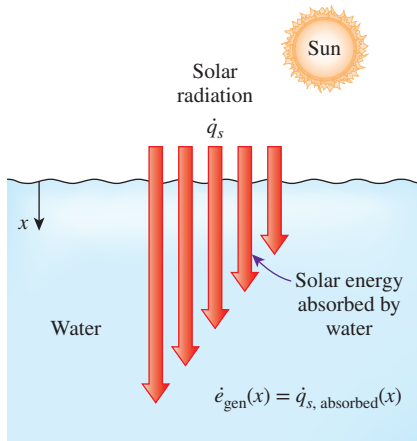
FIGURE 2–10
The absorption of solar radiation
by water can be treated as heat
generation.

Heat Generation

A medium through which heat is conducted may involve the conversion of mechanical, electrical, nuclear, or chemical energy into heat (or thermal energy). In heat conduction analysis, such conversion processes are characterized as **heat** (or **thermal energy**) **generation**.

For example, the temperature of a resistance wire rises rapidly when electric current passes through it as a result of the electrical energy being converted to heat at a rate of I^2R, where I is the current and R is the electrical resistance of the wire (Fig. 2–9). The safe and effective removal of this heat away from the sites of heat generation (the electronic circuits) is the subject of *electronics cooling,* which is one of the modern application areas of heat transfer.

Likewise, a large amount of heat is generated in the fuel elements of nuclear reactors as a result of nuclear fission that serves as the *heat source* in nuclear power plants. The natural disintegration of radioactive elements in nuclear waste or other radioactive material also results in the generation of heat. The heat generated in the sun as a result of the fusion of hydrogen into helium makes the sun a large nuclear reactor that supplies heat to the earth.

Another source of heat generation in a medium is exothermic chemical reactions that may occur throughout the medium. The chemical reaction in this case serves as a *heat source* for the medium. In the case of endothermic reactions, however, heat is absorbed instead of being released during reaction, and thus the chemical reaction serves as a *heat sink*. The heat generation term becomes a negative quantity in this case.

Often it is also convenient to model the absorption of radiation such as solar energy or gamma rays as heat generation when these rays penetrate deep into the body while being absorbed gradually. For example, the absorption of solar energy in large bodies of water can be treated as heat generation throughout the water at a rate equal to the rate of absorption, which varies with depth (Fig. 2–10). But the absorption of solar energy by an opaque body occurs within a few microns of the surface, and the solar energy that penetrates into the medium in this case can be treated as specified heat flux on the surface.

Note that heat generation is a *volumetric phenomenon.* That is, it occurs throughout the body of a medium. Therefore, the rate of heat generation in a medium is usually specified *per unit volume* and is denoted by $\dot{e}_{gen}$, whose unit is W/m^3 or $Btu/h \cdot ft^3$.

The rate of heat generation in a medium may vary with time as well as position within the medium. When the variation of heat generation with position is known, the *total* rate of heat generation in a medium of volume V can be determined from

$$\dot{E}_{gen} = \int_V \dot{e}_{gen} \, dV \quad \text{(W)} \tag{2–5}$$

In the special case of *uniform* heat generation, as in the case of electric resistance heating throughout a homogeneous material, the relation in Eq. 2–5 reduces to $\dot{E}_{gen} = \dot{e}_{gen} V$, where $\dot{e}_{gen}$ is the constant rate of heat generation per unit volume.

■ **EXAMPLE 2–1**   **Heat Generation in a Hair Dryer**

The resistance wire of a 1200-W hair dryer is 80 cm long and has a diameter of $D = 0.3$ cm (Fig. 2–11). Determine the rate of heat generation in the wire per unit volume, in W/cm^3, and the heat flux on the outer surface of the wire as a result of this heat generation.

SOLUTION   The power consumed by the resistance wire of a hair dryer is given. The heat generation and the heat flux are to be determined.
Assumptions   Heat is generated uniformly in the resistance wire.
Analysis   A 1200-W hair dryer converts electrical energy into heat in the wire at a rate of 1200 W. Therefore, the rate of heat generation in a resistance wire is equal to the power consumption of a resistance heater. Then the rate of heat generation in the wire per unit volume is determined by dividing the total rate of heat generation by the volume of the wire,

$$\dot{e}_{gen} = \frac{\dot{E}_{gen}}{V_{wire}} = \frac{\dot{E}_{gen}}{(\pi D^2/4)L} = \frac{1200 \text{ W}}{[\pi(0.3 \text{ cm})^2/4](80 \text{ cm})} = \textbf{212 W/cm}^3$$

Similarly, heat flux on the outer surface of the wire as a result of this heat generation is determined by dividing the total rate of heat generation by the surface area of the wire,

$$\dot{Q}_s = \frac{\dot{E}_{gen}}{A_{wire}} = \frac{\dot{E}_{gen}}{\pi DL} = \frac{1200 \text{ W}}{\pi(0.3 \text{ cm})(80 \text{ cm})} = \textbf{15.9 W/cm}^2$$

Discussion   Note that heat generation is expressed per unit volume in W/cm^3 or $Btu/h \cdot ft^3$, whereas heat flux is expressed per unit surface area in W/cm^2 or $Btu/h \cdot ft^2$.

Hair dryer
1200 W
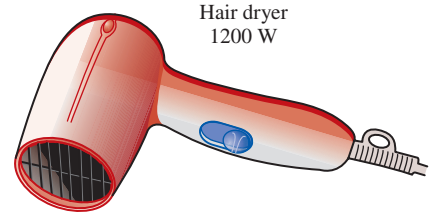
FIGURE 2–11
Schematic for Example 2–1.

2–2 ▪ ONE-DIMENSIONAL HEAT CONDUCTION EQUATION

Consider heat conduction through a large plane wall such as the wall of a house, the glass of a single-pane window, the metal plate at the bottom of a pressing iron, a cast-iron steam pipe, a cylindrical nuclear fuel element, an electrical resistance wire, the wall of a spherical container, or a spherical metal ball that is being quenched or tempered. Heat conduction in these and many other geometries can be approximated as being *one-dimensional* since heat conduction through these geometries is dominant in one direction and negligible in other directions. Next we develop the one-dimensional heat conduction equation in rectangular, cylindrical, and spherical coordinates.

Heat Conduction Equation in a Large Plane Wall

Consider a thin element of thickness Δx in a large plane wall, as shown in Fig. 2–12. Assume the density of the wall is ρ, the specific heat is c, and the area of the wall normal to the direction of heat transfer is A. An *energy balance* on this thin element during a small time interval Δt can be expressed as

$A_x = A_{x+\Delta x} = A$
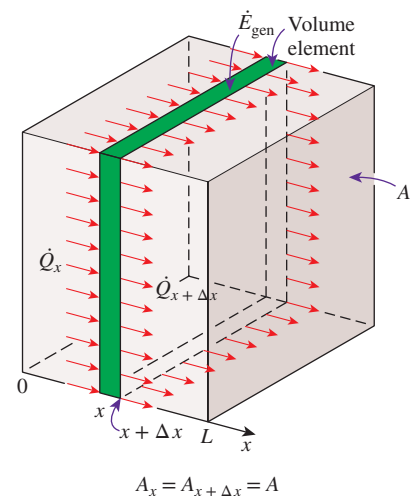
FIGURE 2–12
One-dimensional heat conduction through a volume element in a large plane wall.

$$\begin{pmatrix} \text{Rate of heat} \\ \text{conduction} \\ \text{at } x \end{pmatrix} - \begin{pmatrix} \text{Rate of heat} \\ \text{conduction} \\ \text{at } x + \Delta x \end{pmatrix} + \begin{pmatrix} \text{Rate of heat} \\ \text{generation} \\ \text{inside the} \\ \text{element} \end{pmatrix} = \begin{pmatrix} \text{Rate of change} \\ \text{of the energy} \\ \text{content of the} \\ \text{element} \end{pmatrix}$$

or

$$\dot{Q}_x - \dot{Q}_{x + \Delta x} + \dot{E}_{\text{gen, element}} = \frac{\Delta E_{\text{element}}}{\Delta t} \tag{2–6}$$

But the change in the energy content of the element and the rate of heat generation within the element can be expressed as

$$\Delta E_{\text{element}} = E_{t + \Delta t} - E_t = mc(T_{t + \Delta t} - T_t) = \rho c A \Delta x (T_{t + \Delta t} - T_t) \tag{2–7}$$

$$\dot{E}_{\text{gen, element}} = \dot{e}_{\text{gen}} V_{\text{element}} = \dot{e}_{\text{gen}} A \Delta x \tag{2–8}$$

Substituting into Eq. 2–6, we get

$$\dot{Q}_x - \dot{Q}_{x + \Delta x} + \dot{e}_{\text{gen}} A \Delta x = \rho c A \Delta x \frac{T_{t + \Delta t} - T_t}{\Delta t} \tag{2–9}$$

Dividing by $A\Delta x$ gives

$$-\frac{1}{A} \frac{\dot{Q}_{x + \Delta x} - \dot{Q}_x}{\Delta x} + \dot{e}_{\text{gen}} = \rho c \frac{T_{t + \Delta t} - T_t}{\Delta t} \tag{2–10}$$

Taking the limit as $\Delta x \to 0$ and $\Delta t \to 0$ yields

$$\frac{1}{A} \frac{\partial}{\partial x}\left(kA\frac{\partial T}{\partial x}\right) + \dot{e}_{\text{gen}} = \rho c \frac{\partial T}{\partial t} \tag{2–11}$$

since, from the definition of the derivative and Fourier's law of heat conduction,

$$\lim_{\Delta x \to 0} \frac{\dot{Q}_{x + \Delta x} - \dot{Q}_x}{\Delta x} = \frac{\partial \dot{Q}}{\partial x} = \frac{\partial}{\partial x}\left(-kA\frac{\partial T}{\partial x}\right) \tag{2–12}$$

Noting that the area A is constant for a plane wall, the one-dimensional transient heat conduction equation in a plane wall becomes

Variable conductivity: $\qquad \frac{\partial}{\partial x}\left(k\frac{\partial T}{\partial x}\right) + \dot{e}_{\text{gen}} = \rho c \frac{\partial T}{\partial t}$ (2–13)

The thermal conductivity k of a material, in general, depends on the temperature T (and therefore x), and thus it cannot be taken out of the derivative. However, the *thermal conductivity* in most practical applications can be assumed to remain *constant* at some average value. Equation 2–13 in that case reduces to

Constant conductivity: $\qquad \frac{\partial^2 T}{\partial x^2} + \frac{\dot{e}_{\text{gen}}}{k} = \frac{1}{\alpha}\frac{\partial T}{\partial t}$ (2–14)

where the property $\alpha = k/\rho c$ is the **thermal diffusivity** of the material and represents how fast heat propagates through a material. It reduces to the following forms under specified conditions (Fig. 2–13):

General, one-dimensional:

No generation   Steady-state

$$\frac{\partial^2 T}{\partial x^2} + \cancel{\frac{\dot{e}_{\text{gen}}}{k}}^{\,0} = \cancel{\frac{1}{\alpha}\frac{\partial T}{\partial t}}^{\,0}$$

Steady, one-dimensional:
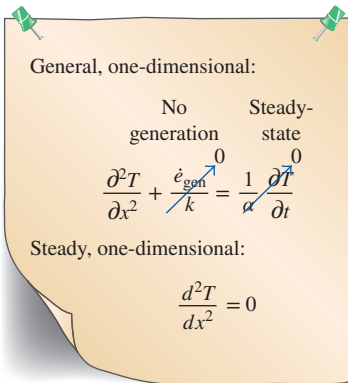
$$\frac{d^2 T}{dx^2} = 0$$

FIGURE 2–13
The simplification of the one-dimensional heat conduction equation in a plane wall for the case of constant conductivity for steady conduction with no heat generation.

(1) *Steady-state:*
  ($\partial/\partial t = 0$)

$$\frac{d^2 T}{dx^2} + \frac{\dot{e}_{gen}}{k} = 0 \qquad \textbf{(2–15)}$$

(2) *Transient, no heat generation:*
  ($\dot{e}_{gen} = 0$)

$$\frac{\partial^2 T}{\partial x^2} = \frac{1}{\alpha} \frac{\partial T}{\partial t} \qquad \textbf{(2–16)}$$

(3) *Steady-state, no heat generation:*
  ($\partial/\partial t = 0$ and $\dot{e}_{gen} = 0$)

$$\frac{d^2 T}{dx^2} = 0 \qquad \textbf{(2–17)}$$

Note that we replaced the partial derivatives with ordinary derivatives in the one-dimensional steady heat conduction case since the partial and ordinary derivatives of a function are identical when the function depends on a single variable only [$T = T(x)$ in this case]. For the general solution of Eqs. 2–15 and 2–17, refer to the Topic of Special Interest ("A Brief Review of Differential Equations") at the end of this chapter.

Heat Conduction Equation in a Long Cylinder

Now consider a thin cylindrical shell element of thickness Δr in a long cylinder, as shown in Fig. 2–14. Assume the density of the cylinder is ρ, the specific heat is c, and the length is L. The area of the cylinder normal to the direction of heat transfer at any location is $A = 2\pi r L$ where r is the value of the radius at that location. Note that the heat transfer area A depends on r in this case, and thus it varies with location. An *energy balance* on this thin cylindrical shell element during a small time interval Δt can be expressed as

$$\begin{pmatrix} \text{Rate of heat} \\ \text{conduction} \\ \text{at } r \end{pmatrix} - \begin{pmatrix} \text{Rate of heat} \\ \text{conduction} \\ \text{at } r + \Delta r \end{pmatrix} + \begin{pmatrix} \text{Rate of heat} \\ \text{generation} \\ \text{inside the} \\ \text{element} \end{pmatrix} = \begin{pmatrix} \text{Rate of change} \\ \text{of the energy} \\ \text{content of the} \\ \text{element} \end{pmatrix}$$

or

$$\dot{Q}_r - \dot{Q}_{r+\Delta r} + \dot{E}_{gen,\,element} = \frac{\Delta E_{element}}{\Delta t} \qquad \textbf{(2–18)}$$

The change in the energy content of the element and the rate of heat generation within the element can be expressed as

$$\Delta E_{element} = E_{t+\Delta t} - E_t = mc(T_{t+\Delta t} - T_t) = \rho c A \Delta r (T_{t+\Delta t} - T_t) \qquad \textbf{(2–19)}$$

$$\dot{E}_{gen,\,element} = \dot{e}_{gen} V_{element} = \dot{e}_{gen} A \Delta r \qquad \textbf{(2–20)}$$

Substituting into Eq. 2–18, we get

$$\dot{Q}_r - \dot{Q}_{r+\Delta r} + \dot{e}_{gen} A \Delta r = \rho c A \Delta r \frac{T_{t+\Delta t} - T_t}{\Delta t} \qquad \textbf{(2–21)}$$

where $A = 2\pi r L$. You may be tempted to express the area at the *middle* of the element using the *average* radius as $A = 2\pi(r + \Delta r/2)L$. But there is nothing we can gain from this complication since later in the analysis we will take the limit as $\Delta r \to 0$, and thus the term $\Delta r/2$ will drop out. Now dividing Eq. 2–21 by $A\Delta r$ gives

$$-\frac{1}{A} \frac{\dot{Q}_{r+\Delta r} - \dot{Q}_r}{\Delta r} + \dot{e}_{gen} = \rho c \frac{T_{t+\Delta t} - T_t}{\Delta t} \qquad \textbf{(2–22)}$$
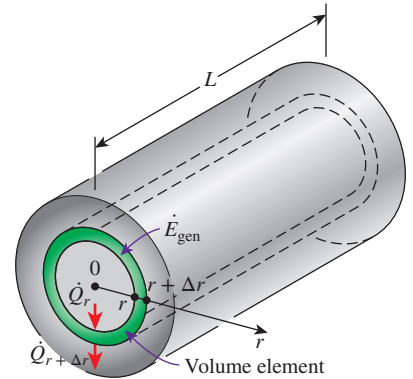
FIGURE 2–14
One-dimensional heat conduction through a volume element in a long cylinder.

(*a*) The form that is ready to integrate

$$\frac{d}{dr}\left(r\frac{dT}{dr}\right) = 0$$

(*b*) The equivalent alternative form

$$r\frac{d^2T}{dr^2} + \frac{dT}{dr} = 0$$
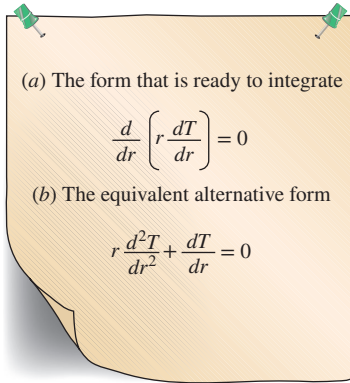
FIGURE 2–15
Two equivalent forms of the differential equation for the one-dimensional steady heat conduction in a cylinder with no heat generation.

Taking the limit as $\Delta r \to 0$ and $\Delta t \to 0$ yields

$$\frac{1}{A}\frac{\partial}{\partial r}\left(kA\frac{\partial T}{\partial r}\right) + \dot{e}_{gen} = \rho c\frac{\partial T}{\partial t} \tag{2–23}$$

since, from the definition of the derivative and Fourier's law of heat conduction,

$$\lim_{\Delta r \to 0}\frac{\dot{Q}_{r+\Delta r} - \dot{Q}_r}{\Delta r} = \frac{\partial \dot{Q}}{\partial r} = \frac{\partial}{\partial r}\left(-kA\frac{\partial T}{\partial r}\right) \tag{2–24}$$

Noting that the heat transfer area in this case is $A = 2\pi rL$, the one-dimensional transient heat conduction equation in a cylinder becomes

Variable conductivity: $$\frac{1}{r}\frac{\partial}{\partial r}\left(rk\frac{\partial T}{\partial r}\right) + \dot{e}_{gen} = \rho c\frac{\partial T}{\partial t} \tag{2–25}$$

For the case of constant thermal conductivity, the previous equation reduces to

Constant conductivity: $$\frac{1}{r}\frac{\partial}{\partial r}\left(r\frac{\partial T}{\partial r}\right) + \frac{\dot{e}_{gen}}{k} = \frac{1}{\alpha}\frac{\partial T}{\partial t} \tag{2–26}$$

where again the property $\alpha = k/\rho c$ is the thermal diffusivity of the material. Eq. 2–26 reduces to the following forms under specified conditions (Fig. 2–15):

(1) *Steady-state:*
   ($\partial/\partial t = 0$) $$\frac{1}{r}\frac{d}{dr}\left(r\frac{dT}{dr}\right) + \frac{\dot{e}_{gen}}{k} = 0 \tag{2–27}$$

(2) *Transient, no heat generation:*
   ($\dot{e}_{gen} = 0$) $$\frac{1}{r}\frac{\partial}{\partial r}\left(r\frac{\partial T}{\partial r}\right) = \frac{1}{\alpha}\frac{\partial T}{\partial t} \tag{2–28}$$

(3) *Steady-state, no heat generation:*
   ($\partial/\partial t = 0$ and $\dot{e}_{gen} = 0$) $$\frac{d}{dr}\left(r\frac{dT}{dr}\right) = 0 \tag{2–29}$$

Note that we again replaced the partial derivatives with ordinary derivatives in the one-dimensional steady heat conduction case since the partial and ordinary derivatives of a function are identical when the function depends on a single variable only [$T = T(r)$ in this case]. For the general solution of Eqs. 2–27 and 2–29, refer to the Topic of Special Interest ("A Brief Review of Differential Equations") at the end of this chapter.

Heat Conduction Equation in a Sphere

Now consider a sphere with density ρ, specific heat c, and outer radius R. The area of the sphere normal to the direction of heat transfer at any location is $A = 4\pi r^2$, where r is the value of the radius at that location. Note that the heat transfer area A depends on r in this case also, and thus it varies with location. By considering a thin spherical shell element of thickness Δr and repeating the approach described previously for the cylinder by using $A = 4\pi r^2$ instead of $A = 2\pi rL$, the one-dimensional transient heat conduction equation for a sphere is determined to be (Fig. 2–16)

Variable conductivity: $$\frac{1}{r^2}\frac{\partial}{\partial r}\left(r^2 k\frac{\partial T}{\partial r}\right) + \dot{e}_{gen} = \rho c\frac{\partial T}{\partial t} \tag{2–30}$$

which, in the case of constant thermal conductivity, reduces to

Constant conductivity: $$\frac{1}{r^2}\frac{\partial}{\partial r}\left(r^2\frac{\partial T}{\partial r}\right) + \frac{\dot{e}_{gen}}{k} = \frac{1}{\alpha}\frac{\partial T}{\partial t} \tag{2–31}$$
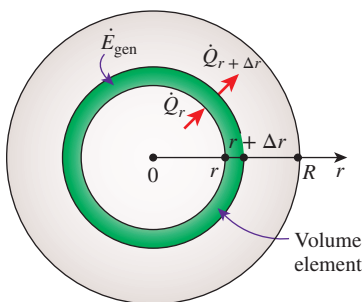
FIGURE 2–16
One-dimensional heat conduction through a volume element in a sphere.

where again the property $\alpha = k/\rho c$ is the thermal diffusivity of the material. It reduces to the following forms under specified conditions:

(1) *Steady-state:*
    ($\partial/\partial t = 0$)

$$\frac{1}{r^2}\frac{d}{dr}\left(r^2\frac{dT}{dr}\right) + \frac{\dot{e}_{gen}}{k} = 0 \tag{2-32}$$

(2) *Transient,*
    no heat generation:
    ($\dot{e}_{gen} = 0$)

$$\frac{1}{r^2}\frac{\partial}{\partial r}\left(r^2\frac{\partial T}{\partial r}\right) = \frac{1}{\alpha}\frac{\partial T}{\partial t} \tag{2-33}$$

(3) *Steady-state,*
    no heat generation:
    ($\partial/\partial t = 0$ and $\dot{e}_{gen} = 0$)

$$\frac{d}{dr}\left(r^2\frac{dT}{dr}\right) = 0 \quad \text{or} \quad r\frac{d^2T}{dr^2} + 2\frac{dT}{dr} = 0 \tag{2-34}$$

where again we replaced the partial derivatives with ordinary derivatives in the one-dimensional steady heat conduction case. For the general solution of Eqs. 2–32 and 2–34, refer to the Topic of Special Interest ("A Brief Review of Differential Equations") at the end of this chapter.

Combined One-Dimensional Heat Conduction Equation

An examination of the one-dimensional transient heat conduction equations for the plane wall, cylinder, and sphere reveals that all three equations can be expressed in a compact form as

$$\frac{1}{r^n}\frac{\partial}{\partial r}\left(r^n k\frac{\partial T}{\partial r}\right) + \dot{e}_{gen} = \rho c\frac{\partial T}{\partial t} \tag{2-35}$$

where $n = 0$ for a plane wall, $n = 1$ for a cylinder, and $n = 2$ for a sphere. In the case of a plane wall, it is customary to replace the variable r with x. This equation can be simplified for steady-state or no heat generation cases as described before.

EXAMPLE 2–2   **Heat Conduction Through the Bottom of a Pan**

Consider a steel pan placed on top of an electric range to cook spaghetti (Fig. 2–17). The bottom section of the pan is 0.4 cm thick and has a diameter of 18 cm. The electric heating unit on the range top consumes 800 W of power during cooking, and 80 percent of the heat generated in the heating element is transferred uniformly to the pan. Assuming constant thermal conductivity, obtain the differential equation that describes the variation of the temperature in the bottom section of the pan during steady operation.

SOLUTION   A steel pan placed on top of an electric range is considered. The differential equation for the variation of temperature in the bottom of the pan is to be obtained.

Analysis   The bottom section of the pan has a large surface area relative to its thickness and can be approximated as a large plane wall. Heat flux is applied to the bottom surface of the pan uniformly, and the conditions on the inner surface are also uniform. Therefore, we expect the heat transfer through the bottom section of the pan to be from the bottom surface toward the top, and heat transfer in this case can reasonably be approximated as being one-dimensional. Taking the direction normal to the bottom surface of the pan to be the x-axis, we will have $T = T(x)$ during steady operation since the temperature in this case will depend on x only.

800 W
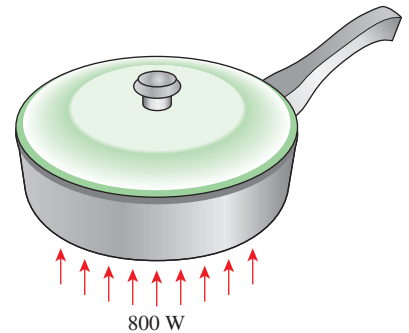
FIGURE 2–17
Schematic for Example 2–2.

The thermal conductivity is given to be constant, and there is no heat generation in the medium (within the bottom section of the pan). Therefore, the differential equation governing the variation of temperature in the bottom section of the pan in this case is simply Eq. 2–17,

$$\frac{d^2T}{dx^2} = 0$$

which is the steady one-dimensional heat conduction equation in rectangular coordinates under the conditions of constant thermal conductivity and no heat generation.
Discussion Note that the conditions at the surface of the medium have no effect on the differential equation.
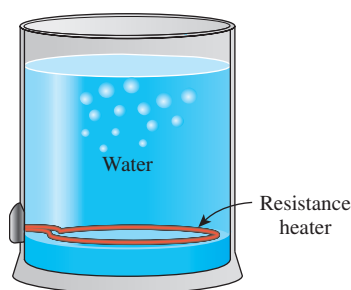
FIGURE 2–18
Schematic for Example 2–3.

EXAMPLE 2–3 **Heat Conduction in a Resistance Heater**

A 2-kW resistance heater wire with thermal conductivity $k = 15$ W/m·K, diameter $D = 0.4$ cm, and length $L = 50$ cm is used to boil water by immersing it in water (Fig. 2–18). Assuming the variation of the thermal conductivity of the wire with temperature to be negligible, obtain the differential equation that describes the variation of the temperature in the wire during steady operation.

SOLUTION The resistance wire of a water heater is considered. The differential equation for the variation of temperature in the wire is to be obtained.
Analysis The resistance wire can be considered to be a very long cylinder since its length is more than 100 times its diameter. Also, heat is generated uniformly in the wire, and the conditions on the outer surface of the wire are uniform. Therefore, it is reasonable to expect the temperature in the wire to vary in the radial r-direction only, and thus the heat transfer is one-dimensional. Then we have $T = T(r)$ during steady operation since the temperature in this case depends on r only.

The rate of heat generation in the wire per unit volume can be determined from

$$\dot{e}_{gen} = \frac{\dot{E}_{gen}}{V_{wire}} = \frac{\dot{E}_{gen}}{(\pi D^2/4)L} = \frac{2000\,\text{W}}{[\pi(0.004\,\text{m})^2/4](0.5\,\text{m})} = 0.318 \times 10^9\,\text{W/m}^3$$

Noting that the thermal conductivity is given to be constant, the differential equation that governs the variation of temperature in the wire is simply Eq. 2–27,

$$\frac{1}{r}\frac{d}{dr}\left(r\frac{dT}{dr}\right) + \frac{\dot{e}_{gen}}{k} = 0$$

which is the steady one-dimensional heat conduction equation in cylindrical coordinates for the case of constant thermal conductivity.
Discussion Note again that the conditions at the surface of the wire have no effect on the differential equation.

EXAMPLE 2–4   Cooling of a Hot Metal Ball in Air

A spherical metal ball of radius R is heated in an oven to a temperature of 600°F throughout and is then taken out of the oven and allowed to cool in ambient air at $T_\infty = 75°F$ by convection and radiation (Fig. 2–19). The thermal conductivity of the ball material is known to vary linearly with temperature. Assuming the ball is cooled uniformly from the entire outer surface, obtain the differential equation that describes the variation of the temperature in the ball during cooling.

SOLUTION   A hot metal ball is allowed to cool in ambient air. The differential equation for the variation of temperature within the ball is to be obtained.

Analysis   The ball is initially at a uniform temperature and is cooled uniformly from the entire outer surface. Also, the temperature at any point in the ball changes with time during cooling. Therefore, this is a one-dimensional transient heat conduction problem since the temperature within the ball changes with the radial distance r and the time t. That is, $T = T(r, t)$.

The thermal conductivity is given to be variable, and there is no heat generation in the ball. Therefore, the differential equation that governs the variation of temperature in the ball in this case is obtained from Eq. 2–30 by setting the heat generation term equal to zero. We obtain

$$\frac{1}{r^2} \frac{\partial}{\partial r}\left(r^2 k \frac{\partial T}{\partial r} \right) = \rho c \frac{\partial T}{\partial t}$$

which is the one-dimensional transient heat conduction equation in spherical coordinates under the conditions of variable thermal conductivity and no heat generation.

Discussion   Note again that the conditions at the outer surface of the ball have no effect on the differential equation.
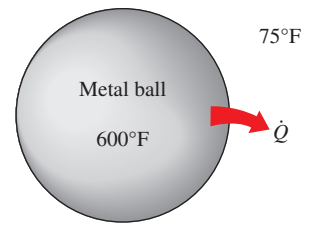
FIGURE 2–19
Schematic for Example 2–4.

2–3 ▪ GENERAL HEAT CONDUCTION EQUATION

In Sec. 2-2 we considered one-dimensional heat conduction and assumed heat conduction in other directions to be negligible. Most heat transfer problems encountered in practice can be approximated as being one-dimensional, and we mostly deal with such problems in this text. However, this is not always the case, and sometimes we need to consider heat transfer in other directions as well. In such cases, heat conduction is said to be *multidimensional,* and in this section we develop the governing differential equation in rectangular, cylindrical, and spherical coordinate systems.

Rectangular Coordinates

Consider a small rectangular element of length Δx, width Δy, and height Δz, as shown in Fig. 2–20. Assume the density of the body is ρ and the specific heat is c. An *energy balance* on this element during a small time interval Δt can be expressed as

$$\begin{pmatrix} \text{Rate of heat} \\ \text{conduction} \\ \text{at } x, y, \text{ and } z \end{pmatrix} - \begin{pmatrix} \text{Rate of heat} \\ \text{conduction} \\ \text{at } x + \Delta x \\ y + \Delta y \text{ and } z + \Delta z \end{pmatrix} + \begin{pmatrix} \text{Rate of heat} \\ \text{generation} \\ \text{inside the} \\ \text{element} \end{pmatrix} = \begin{pmatrix} \text{Rate of change} \\ \text{of the energy} \\ \text{content of the} \\ \text{element} \end{pmatrix}$$
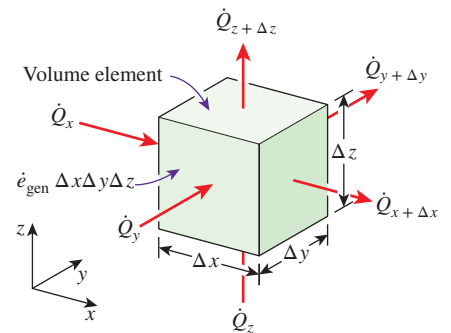
FIGURE 2–20
Three-dimensional heat conduction through a rectangular volume element.

or

$$\dot{Q}_x + \dot{Q}_y + \dot{Q}_z - \dot{Q}_{x+\Delta x} - \dot{Q}_{y+\Delta y} - \dot{Q}_{z+\Delta z} + \dot{E}_{\text{gen, element}} = \frac{\Delta E_{\text{element}}}{\Delta t} \quad \textbf{(2–36)}$$

Noting that the volume of the element is $V_{\text{element}} = \Delta x \Delta y \Delta z$, the change in the energy content of the element and the rate of heat generation within the element can be expressed as

$$\Delta E_{\text{element}} = E_{t+\Delta t} - E_t = mc(T_{t+\Delta t} - T_t) = \rho c \Delta x \Delta y \Delta z (T_{t+\Delta t} - T_t)$$

$$\dot{E}_{\text{gen, element}} = \dot{e}_{\text{gen}} V_{\text{element}} = \dot{e}_{\text{gen}} \Delta x \Delta y \Delta z$$

Substituting into Eq. 2–36, we get

$$\dot{Q}_x + \dot{Q}_y + \dot{Q}_z - \dot{Q}_{x+\Delta x} - \dot{Q}_{y+\Delta y} - \dot{Q}_{z+\Delta z} + \dot{e}_{\text{gen}} \Delta x \Delta y \Delta z = \rho c \Delta x \Delta y \Delta z \frac{T_{t+\Delta t} - T_t}{\Delta t}$$

Dividing by $\Delta x \Delta y \Delta z$ gives

$$-\frac{1}{\Delta y \Delta z} \frac{\dot{Q}_{x+\Delta x} - \dot{Q}_x}{\Delta x} - \frac{1}{\Delta x \Delta z} \frac{\dot{Q}_{y+\Delta y} - \dot{Q}_y}{\Delta y} - \frac{1}{\Delta x \Delta y} \frac{\dot{Q}_{z+\Delta z} - \dot{Q}_z}{\Delta z} + \dot{e}_{\text{gen}} =$$

$$\rho c \frac{T_{t+\Delta t} - T_t}{\Delta t} \quad \textbf{(2–37)}$$

Noting that the heat transfer areas of the element for heat conduction in the *x, y,* and *z* directions are $A_x = \Delta y \Delta z$, $A_y = \Delta x \Delta z$, and $A_z = \Delta x \Delta y$, respectively, and taking the limit as $\Delta x, \Delta y, \Delta z$ and $\Delta t \rightarrow 0$ yields

$$\frac{\partial}{\partial x}\left(k\frac{\partial T}{\partial x}\right) + \frac{\partial}{\partial y}\left(k\frac{\partial T}{\partial y}\right) + \frac{\partial}{\partial z}\left(k\frac{\partial T}{\partial z}\right) + \dot{e}_{\text{gen}} = \rho c \frac{\partial T}{\partial t} \quad \textbf{(2–38)}$$

since, from the definition of the derivative and Fourier's law of heat conduction,

$$\lim_{\Delta x \rightarrow 0} \frac{1}{\Delta y \Delta z} \frac{\dot{Q}_{x+\Delta x} - \dot{Q}_x}{\Delta x} = \frac{1}{\Delta y \Delta z} \frac{\partial Q_x}{\partial x} = \frac{1}{\Delta y \Delta z} \frac{\partial}{\partial x}\left(-k\Delta y \Delta z \frac{\partial T}{\partial x}\right) = -\frac{\partial}{\partial x}\left(k\frac{\partial T}{\partial x}\right)$$

$$\lim_{\Delta y \rightarrow 0} \frac{1}{\Delta x \Delta z} \frac{\dot{Q}_{y+\Delta y} - \dot{Q}_y}{\Delta y} = \frac{1}{\Delta x \Delta z} \frac{\partial Q_y}{\partial y} = \frac{1}{\Delta x \Delta z} \frac{\partial}{\partial y}\left(-k\Delta x \Delta z \frac{\partial T}{\partial y}\right) = -\frac{\partial}{\partial y}\left(k\frac{\partial T}{\partial y}\right)$$

$$\lim_{\Delta z \rightarrow 0} \frac{1}{\Delta x \Delta y} \frac{\dot{Q}_{z+\Delta z} - \dot{Q}_z}{\Delta z} = \frac{1}{\Delta x \Delta y} \frac{\partial Q_z}{\partial z} = \frac{1}{\Delta x \Delta y} \frac{\partial}{\partial z}\left(-k\Delta x \Delta y \frac{\partial T}{\partial z}\right) = -\frac{\partial}{\partial z}\left(k\frac{\partial T}{\partial z}\right)$$

Equation 2–38 is the general heat conduction equation in rectangular coordinates. In the case of constant thermal conductivity, it reduces to

$$\frac{\partial^2 T}{\partial x^2} + \frac{\partial^2 T}{\partial y^2} + \frac{\partial^2 T}{\partial z^2} + \frac{\dot{e}_{\text{gen}}}{k} = \frac{1}{\alpha} \frac{\partial T}{\partial t} \quad \textbf{(2–39)}$$

where the property $\alpha = k/\rho c$ is again the *thermal diffusivity* of the material. Equation 2–39 is known as the **Fourier-Biot equation**, and it reduces to these forms under specified conditions:

(1) *Steady-state:*
(called the **Poisson equation**)

$$\frac{\partial^2 T}{\partial x^2} + \frac{\partial^2 T}{\partial y^2} + \frac{\partial^2 T}{\partial z^2} + \frac{\dot{e}_{gen}}{k} = 0 \qquad \text{(2–40)}$$

(2) *Transient, no heat generation:*
(called the **diffusion equation**)

$$\frac{\partial^2 T}{\partial x^2} + \frac{\partial^2 T}{\partial y^2} + \frac{\partial^2 T}{\partial z^2} = \frac{1}{\alpha}\frac{\partial T}{\partial t} \qquad \text{(2–41)}$$

(3) *Steady-state, no heat generation:*
(called the **Laplace equation**)

$$\frac{\partial^2 T}{\partial x^2} + \frac{\partial^2 T}{\partial y^2} + \frac{\partial^2 T}{\partial z^2} = 0 \qquad \text{(2–42)}$$

Note that in the special case of one-dimensional heat transfer in the *x*-direction, the derivatives with respect to *y* and *z* drop out, and the preceding equations reduce to the ones developed in the previous section for a plane wall (Fig. 2–21).
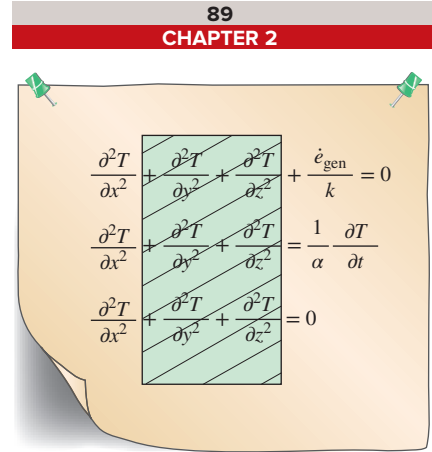
FIGURE 2–21
The three-dimensional heat conduction equations reduce to the one-dimensional ones when the temperature varies in one dimension only.

Cylindrical Coordinates

The general heat conduction equation in cylindrical coordinates can be obtained from an energy balance on a volume element in cylindrical coordinates, shown in Fig. 2–22, by following the steps just outlined. It can also be obtained directly from Eq. 2–38 by coordinate transformation using the following relations between the coordinates of a point in rectangular and cylindrical coordinate systems:

$$x = r\cos\phi, \quad y = r\sin\phi, \quad \text{and} \quad z = z$$

After lengthy manipulations, we obtain

$$\frac{1}{r}\frac{\partial}{\partial r}\left(kr\frac{\partial T}{\partial r}\right) + \frac{1}{r^2}\frac{\partial}{\partial \phi}\left(k\frac{\partial T}{\partial \phi}\right) + \frac{\partial}{\partial z}\left(k\frac{\partial T}{\partial z}\right) + \dot{e}_{gen} = \rho c\frac{\partial T}{\partial t} \qquad \text{(2–43)}$$

where the heat flux components in the radial, circumferential, and axial directions, respectively, are:

$$\dot{q}_r = -k\frac{\partial T}{\partial r}, \quad \dot{q}_\phi = -\frac{k}{r}\frac{\partial T}{\partial \phi}, \quad \dot{q}_z = -k\frac{\partial T}{\partial z}$$
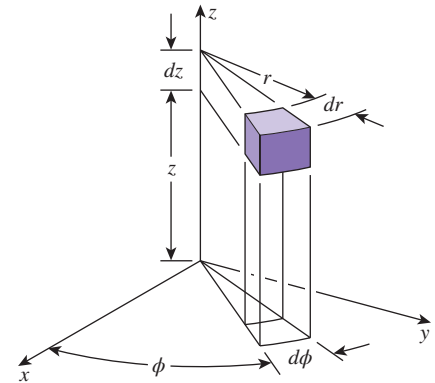
FIGURE 2–22
A differential volume element in cylindrical coordinates.

Spherical Coordinates

The general heat conduction equations in spherical coordinates can be obtained from an energy balance on a volume element in spherical coordinates, shown in Fig. 2–23, by following the steps outlined above. It can also be obtained directly from Eq. 2–38 by coordinate transformation using the following relations between the coordinates of a point in rectangular and spherical coordinate systems:

$$x = r\cos\phi\sin\theta, \quad y = r\sin\phi\sin\theta, \quad \text{and} \quad z = r\cos\theta$$

Again after lengthy manipulations, we obtain

$$\frac{1}{r^2}\frac{\partial}{\partial r}\left(kr^2\frac{\partial T}{\partial r}\right) + \frac{1}{r^2\sin^2\theta}\frac{\partial}{\partial \phi}\left(k\frac{\partial T}{\partial \phi}\right) + \frac{1}{r^2\sin\theta}\frac{\partial}{\partial \theta}\left(k\sin\theta\frac{\partial T}{\partial \theta}\right) + \dot{e}_{gen} = \rho c\frac{\partial T}{\partial t} \qquad \text{(2–44)}$$

where the heat flux components in the radial, polar, and azimuthal directions, respectively, are:

$$\dot{q}_r = -k\frac{\partial T}{\partial r}, \quad \dot{q}_\theta = -\frac{k}{r}\frac{\partial T}{\partial \theta}, \quad \dot{q}_\phi = -\frac{k}{r\sin\theta}\frac{\partial T}{\partial \phi}$$

Obtaining analytical solutions to these differential equations requires a knowledge of the solution techniques of partial differential equations, which is beyond the scope of this introductory text. Here we limit our consideration to one-dimensional steady-state cases since they result in ordinary differential equations.
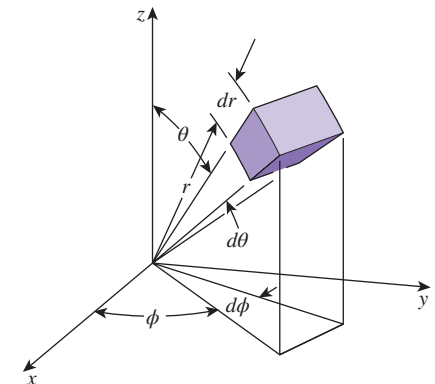
FIGURE 2–23
A differential volume element in spherical coordinates.
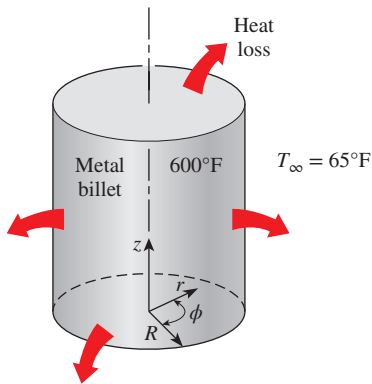
FIGURE 2–24
Schematic for Example 2–5.

EXAMPLE 2–5   **Heat Conduction in a Short Cylinder**

A short cylindrical metal billet of radius R and height h is heated in an oven to a temperature of 600°F throughout and is then taken out of the oven and allowed to cool in ambient air at $T_\infty = 65°F$ by convection and radiation. Assuming the billet is cooled uniformly from all outer surfaces and the variation of the thermal conductivity of the material with temperature is negligible, obtain the differential equation that describes the variation of the temperature in the billet during this cooling process.

SOLUTION   A short cylindrical billet is cooled in ambient air. The differential equation for the variation of temperature is to be obtained.
Analysis   The billet shown in Fig. 2–24 is initially at a uniform temperature and is cooled uniformly from the top and bottom surfaces in the z-direction as well as the lateral surface in the radial r-direction. Also, the temperature at any point in the ball changes with time during cooling. Therefore, this is a two-dimensional transient heat conduction problem since the temperature within the billet changes with the radial and axial distances r and z and with time t. That is, $T = T(r, z, t)$.

The thermal conductivity is given to be constant, and there is no heat generation in the billet. Therefore, the differential equation that governs the variation of temperature in the billet in this case is obtained from Eq. 2–43 by setting the heat generation term and the derivatives with respect to ϕ equal to zero. We obtain

$$\frac{1}{r}\frac{\partial}{\partial r}\left(kr\frac{\partial T}{\partial r}\right) + \frac{\partial}{\partial z}\left(k\frac{\partial T}{\partial z}\right) = \rho c\frac{\partial T}{\partial t}$$

In the case of constant thermal conductivity, it reduces to

$$\frac{1}{r}\frac{\partial}{\partial r}\left(r\frac{\partial T}{\partial r}\right) + \frac{\partial^2 T}{\partial z^2} = \frac{1}{\alpha}\frac{\partial T}{\partial t}$$

which is the desired equation.
Discussion   Note that the boundary and initial conditions have no effect on the differential equation.

2–4 ▪ BOUNDARY AND INITIAL CONDITIONS

The heat conduction equations above were developed using an energy balance on a differential element inside the medium, and they remain the same regardless of the *thermal conditions* on the *surfaces* of the medium. That is, the differential equations do not incorporate any information related to the conditions on the surfaces such as the surface temperature or a specified heat flux. Yet we know that the heat flux and the temperature distribution in a medium depend on the conditions at the surfaces, and the description of a heat transfer problem in a medium is not complete without a full description of the thermal conditions at the bounding surfaces of the medium. The *mathematical expressions* of the thermal conditions at the boundaries are called the **boundary conditions**.

From a mathematical point of view, solving a differential equation is essentially a process of *removing derivatives,* or an *integration* process, and thus the solution of a differential equation typically involves arbitrary constants (Fig. 2–25). It follows that to obtain a unique solution to a problem, we need to specify more than just the governing differential equation. We need to specify some conditions (such as the value of the function or its derivatives at some value of the independent variable) so that forcing the solution to satisfy these conditions at specified points will result in unique values for the arbitrary constants and thus a *unique solution.* But since the differential equation has no place for the additional information or conditions, we need to supply them separately in the form of boundary or initial conditions.

Consider the variation of temperature along the wall of a brick house in winter. The temperature at any point in the wall depends on, among other things, the conditions at the two surfaces of the wall such as the air temperature of the house, the velocity and direction of the winds, and the solar energy incident on the outer surface. That is, the temperature distribution in a medium depends on the conditions at the boundaries of the medium as well as the heat transfer mechanism inside the medium. To describe a heat transfer problem completely, *two boundary conditions* must be given for *each direction* of the coordinate system along which heat transfer is significant (Fig. 2–26). Therefore, we need to specify *two boundary conditions* for one-dimensional problems, *four boundary conditions* for two-dimensional problems, and *six boundary conditions* for three-dimensional problems. In the case of the wall of a house, for example, we need to specify the conditions at two locations (the inner and the outer surfaces) of the wall since heat transfer in this case is one-dimensional. But in the case of a parallelepiped, we need to specify six boundary conditions (one at each face) when heat transfer in all three dimensions is significant.

The physical argument presented above is consistent with the mathematical nature of the problem since the heat conduction equation is second order (i.e., involves second derivatives with respect to the space variables) in all directions along which heat conduction is significant, and the general solution of a second-order linear differential equation involves two arbitrary constants for each direction. That is, the number of boundary conditions that need to be specified in a direction are equal to the order of the differential equation in that direction.

Reconsider the brick wall already discussed. The temperature at any point on the wall at a specified time also depends on the condition of the wall at the beginning of the heat conduction process. Such a condition, which is usually specified at time $t = 0$, is called the **initial condition**, which is a mathematical expression for the temperature distribution of the medium initially. Note that we need only one initial condition for a heat conduction problem regardless of the dimension since the conduction equation is first order in time (it involves the first derivative of temperature with respect to time).

In rectangular coordinates, the initial condition can be specified in the general form as

$$T(x, y, z, 0) = f(x, y, z) \qquad \textbf{(2–45)}$$

where the function $f(x, y, z)$ represents the temperature distribution throughout the medium at time $t = 0$. When the medium is initially at a uniform

FIGURE 2–25
The general solution of a typical differential equation involves arbitrary constants, and thus an infinite number of solutions.
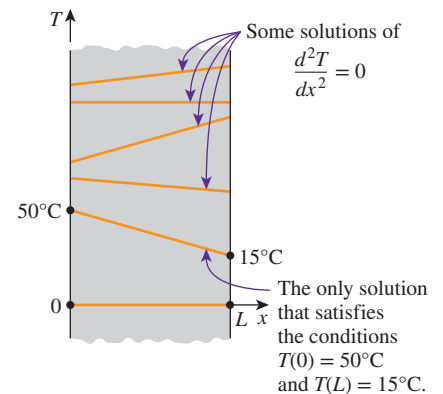
FIGURE 2–26
To describe a heat transfer problem completely, two boundary conditions must be given for each direction along which heat transfer is significant.

temperature of T_i, the initial condition in Eq. 2–45 can be expressed as $T(x, y, z, 0) = T_i$. Note that under *steady* conditions, the heat conduction equation does not involve any time derivatives, and thus we do not need to specify an initial condition.

The heat conduction equation is first order in time, and thus the initial condition cannot involve any derivatives (it is limited to a specified temperature). However, the heat conduction equation is second order in space coordinates, and thus a boundary condition may involve first derivatives at the boundaries as well as specified values of temperature. Boundary conditions most commonly encountered in practice are the *specified temperature, specified heat flux, convection,* and *radiation* boundary conditions.

1 Specified Temperature Boundary Condition

The *temperature* of an exposed surface can usually be measured directly and easily. Therefore, one of the easiest ways to specify the thermal conditions on a surface is to specify the temperature. For one-dimensional heat transfer through a plane wall of thickness *L,* for example, the specified temperature boundary conditions can be expressed as (Fig. 2–27)

$$T(0, t) = T_1$$
$$T(L, t) = T_2 \tag{2-46}$$

where T_1 and T_2 are the specified temperatures at surfaces at $x = 0$ and $x = L$, respectively. The specified temperatures can be constant, which is the case for steady heat conduction, or they may vary with time.

FIGURE 2–27
Specified temperature boundary
conditions on both surfaces
of a plane wall.

In the figure: 150°C, $T(x, t)$, 70°C, 0, L, x

$T(0, t) = 150°C$
$T(L, t) = 70°C$

2 Specified Heat Flux Boundary Condition

When there is sufficient information about energy interactions at a surface, it may be possible to determine the rate of heat transfer and thus the *heat flux $\dot{q}$* (heat transfer rate per unit surface area, W/m^2) on that surface, and this information can be used as one of the boundary conditions. The heat flux in the positive *x*-direction anywhere in the medium, including the boundaries, can be expressed by *Fourier's law* of heat conduction as

$$\dot{q} = -k\frac{\partial T}{\partial x} = \left(\begin{array}{c} \text{Heat flux in the} \\ \text{positive } x - \text{direction} \end{array} \right) \quad (W/m^2) \tag{2-47}$$

Then the boundary condition at a boundary is obtained by setting the specified heat flux equal to $-k(\partial T/\partial x)$ at that boundary. The sign of the specified heat flux is determined by inspection: *positive* if the heat flux is in the positive direction of the coordinate axis, and *negative* if it is in the opposite direction. Note that it is extremely important to have the *correct sign* for the specified heat flux since the wrong sign will invert the direction of heat transfer and cause the heat gain to be interpreted as heat loss (Fig. 2–28).

For a plate of thickness *L* subjected to heat flux of 50 W/m^2 into the medium from both sides, for example, the specified heat flux boundary conditions can be expressed as

$$-k\frac{\partial T(0, t)}{\partial x} = 50 \quad \text{and} \quad -k\frac{\partial T(L, t)}{\partial x} = -50 \tag{2-48}$$
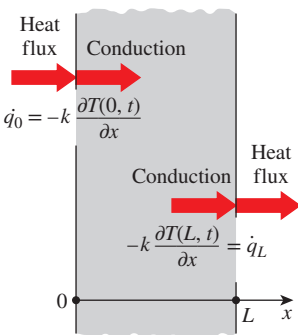
FIGURE 2–28
Specified heat flux boundary
conditions on both surfaces
of a plane wall.

In the figure: Heat flux, Conduction, $\dot{q}_0 = -k\frac{\partial T(0, t)}{\partial x}$, Conduction, Heat flux, $-k\frac{\partial T(L, t)}{\partial x} = \dot{q}_L$, 0, L, x

Note that the heat flux at the surface at $x = L$ is in the *negative x*-direction, and thus it is $-50\ \text{W/m}^2$. The direction of heat flux arrows at $x = L$ in Fig. 2–28 in this case would be reversed.

Special Case: Insulated Boundary

Some surfaces are commonly insulated in practice in order to minimize heat loss (or heat gain) through them. Insulation reduces heat transfer but does not totally eliminate it unless its thickness is infinity. However, heat transfer through a properly insulated surface can be taken to be zero since adequate insulation reduces heat transfer through a surface to negligible levels. Therefore, a well-insulated surface can be modeled as a surface with a specified heat flux of zero. Then the boundary condition on a perfectly insulated surface (at $x = 0$, for example) can be expressed as (Fig. 2–29)

$$k\frac{\partial T(0,t)}{\partial x} = 0 \quad \text{or} \quad \frac{\partial T(0,t)}{\partial x} = 0 \tag{2–49}$$

That is, *on an insulated surface, the first derivative of temperature with respect to the space variable (the temperature gradient) in the direction normal to the insulated surface is zero.* This also means that the temperature function must be perpendicular to an insulated surface since the slope of temperature at the surface must be zero.

$$\frac{\partial T(0,t)}{\partial x} = 0$$

$$T(L, t) = 60°\text{C}$$

FIGURE 2–29
A plane wall with insulation and specified temperature boundary conditions.

Another Special Case: Thermal Symmetry

Some heat transfer problems possess *thermal symmetry* as a result of the symmetry in imposed thermal conditions. For example, the two surfaces of a large hot plate of thickness L suspended vertically in air are subjected to the same thermal conditions, and thus the temperature distribution in one half of the plate is the same as that in the other half. That is, the heat transfer problem in this plate possesses thermal symmetry about the center plane at $x = L/2$. Also, the direction of heat flow at any point in the plate is toward the surface closer to the point, and there is no heat flow across the center plane. Therefore, the center plane can be viewed as an insulated surface, and the thermal condition at this plane of symmetry can be expressed as (Fig. 2–30)

$$\frac{\partial T(L/2, t)}{\partial x} = 0 \tag{2–50}$$

which resembles the *insulation* or *zero heat flux* boundary condition. This result can also be deduced from a plot of temperature distribution with a maximum, and thus zero slope, at the center plane.

In the case of cylindrical (or spherical) bodies having thermal symmetry about the centerline (or midpoint), the thermal symmetry boundary condition requires that the first derivative of temperature with respect to r (the radial variable) be zero at the centerline (or the midpoint).

$$\frac{\partial T(L/2, t)}{\partial x} = 0$$

FIGURE 2–30
Thermal symmetry boundary condition at the center plane of a plane wall.
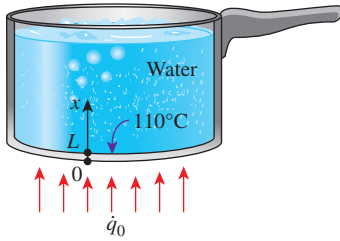
FIGURE 2–31
Schematic for Example 2–6.

EXAMPLE 2–6   **Heat Flux Boundary Condition**

Consider an aluminum pan used to cook beef stew on top of an electric range. The bottom section of the pan is $L = 0.3$ cm thick and has a diameter of $D = 20$ cm. The electric heating unit on the range top consumes 800 W of power during cooking, and 90 percent of the heat generated in the heating element is transferred to the pan. During steady operation, the temperature of the inner surface of the pan is measured to be 110°C. Express the boundary conditions for the bottom section of the pan during this cooking process.

SOLUTION   An aluminum pan on an electric range top is considered. The boundary conditions for the bottom of the pan are to be obtained.
Analysis   The heat transfer through the bottom section of the pan is from the bottom surface toward the top and can reasonably be approximated as being one-dimensional. We take the direction normal to the bottom surfaces of the pan as the x-axis with the origin at the outer surface, as shown in Fig. 2–31. Then the inner and outer surfaces of the bottom section of the pan can be represented by $x = 0$ and $x = L$, respectively. During steady operation, the temperature will depend on x only, and thus $T = T(x)$.

The boundary condition on the outer surface of the bottom of the pan at $x = 0$ can be approximated as being specified heat flux since it is stated that 90 percent of the 800 W (i.e., 720 W) is transferred to the pan at that surface. Therefore,

$$-k\frac{dT(0)}{dx} = \dot{q}_0$$

where

$$\dot{q}_0 = \frac{\text{Heat transfer rate}}{\text{Bottom surface area}} = \frac{0.720 \text{ kW}}{\pi(0.1 \text{ m})^2} = 22.9 \text{ kW/m}^2$$

The temperature at the inner surface of the bottom of the pan is specified to be 110°C. Then the boundary condition on this surface can be expressed as

$$T(L) = 110°C$$

where $L = 0.003$ m.
Discussion   Note that the determination of the boundary conditions may require some reasoning and approximations.

3   Convection Boundary Condition

Convection is probably the most common boundary condition encountered in practice since most heat transfer surfaces are exposed to an environment at a specified temperature. The convection boundary condition is based on a *surface energy balance* expressed as

$$\begin{pmatrix} \text{Heat conduction} \\ \text{at the surface in a} \\ \text{selected direction} \end{pmatrix} = \begin{pmatrix} \text{Heat convection} \\ \text{at the surface in} \\ \text{the same direction} \end{pmatrix}$$

For one-dimensional heat transfer in the *x*-direction in a plate of thickness *L,* the convection boundary conditions on both surfaces can be expressed as

$$-k\frac{\partial T(0, t)}{\partial x} = h_1[T_{\infty 1} - T(0, t)] \tag{2-51a}$$

and

$$-k\frac{\partial T(L, t)}{\partial x} = h_2[T(L, t) - T_{\infty 2}] \tag{2-51b}$$

where h_1 and h_2 are the convection heat transfer coefficients and $T_{\infty 1}$ and $T_{\infty 2}$ are the temperatures of the surrounding media on the two sides of the plate, as shown in Fig. 2–32.

In writing Eqs. 2–51 for convection boundary conditions, we have selected the direction of heat transfer to be the positive *x*-direction at both surfaces. But those expressions are equally applicable when heat transfer is in the opposite direction at one or both surfaces since reversing the direction of heat transfer at a surface simply reverses the signs of *both* conduction and convection terms at that surface. This is equivalent to multiplying an equation by -1, which has no effect on the equality (Fig. 2–33). Being able to select either direction as the direction of heat transfer is certainly a relief since often we do not know the surface temperature and thus the direction of heat transfer at a surface in advance. This argument is also valid for other boundary conditions, such as the radiation and combined boundary conditions to be discussed shortly.

Note that a surface has zero thickness and thus no mass, and it cannot store any energy. Therefore, the entire net heat entering the surface from one side must leave the surface from the other side. The convection boundary condition simply states that heat continues to flow from a body to the surrounding medium at the same rate, and it just changes vehicles at the surface from conduction to convection (or vice versa in the other direction). This is analogous to people traveling on buses on land and transferring to ships at the shore. If the passengers are not allowed to wander around at the shore, then the rate at which the people are unloaded at the shore from the buses must equal the rate at which they board the ships. We may call this the "conservation of people" principle.

Also note that the surface temperatures $T(0, t)$ and $T(L, t)$ are not known (if they were known, we would simply use them as the specified temperature boundary conditions and not bother with convection). But a surface temperature can be determined once the solution $T(x, t)$ is obtained by substituting the value of *x* at that surface into the solution.
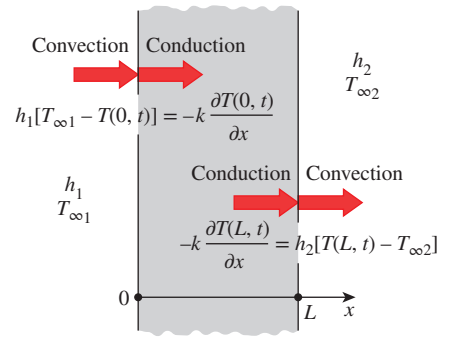
FIGURE 2–32
Convection boundary conditions on the two surfaces of a plane wall.
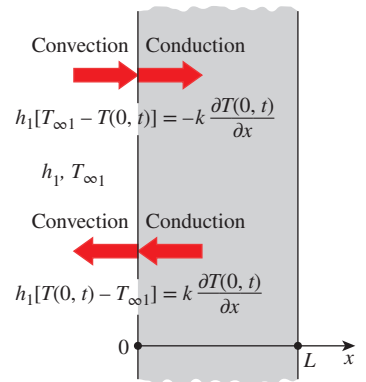
FIGURE 2–33
The assumed direction of heat transfer at a boundary has no effect on the boundary condition expression.

EXAMPLE 2–7   Convection and Insulation Boundary Conditions

Steam flows through a pipe shown in Fig. 2–34 at an average temperature of $T_\infty = 200°C$. The inner and outer radii of the pipe are $r_1 = 8$ cm and $r_2 = 8.5$ cm, respectively, and the outer surface of the pipe is heavily insulated. If the convection heat transfer coefficient on the inner surface of the pipe is $h = 65$ W/m²·K, express the boundary conditions on the inner and outer surfaces of the pipe during transient periods.
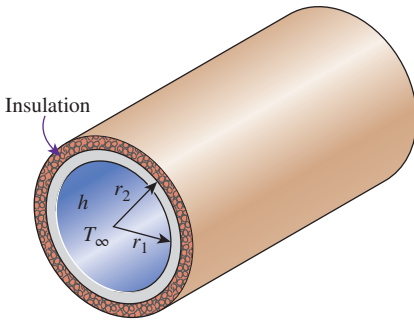
FIGURE 2–34
Schematic for Example 2–7.

SOLUTION The flow of steam through an insulated pipe is considered. The boundary conditions on the inner and outer surfaces of the pipe are to be obtained.

Analysis During initial transient periods, heat transfer through the pipe material predominantly is in the radial direction, and thus it can be approximated as being one-dimensional. Then the temperature within the pipe material changes with the radial distance r and the time t. That is, $T = T(r, t)$.

It is stated that heat transfer between the steam and the pipe at the inner surface is by convection. Then taking the direction of heat transfer to be the positive r-direction, the boundary condition on that surface can be expressed as

$$-k\frac{\partial T(r_1, t)}{\partial r} = h[T_\infty - T(r_1)]$$

The pipe is said to be well insulated on the outside, and thus heat loss through the outer surface of the pipe can be assumed to be negligible. Then the boundary condition at the outer surface can be expressed as

$$\frac{\partial T(r_2, t)}{\partial r} = 0$$

Discussion Note that the temperature gradient must be zero on the outer surface of the pipe at all times.

4 Radiation Boundary Condition

In some cases, such as those encountered in space and cryogenic applications, a heat transfer surface is surrounded by an evacuated space, and thus there is no convection heat transfer between a surface and the surrounding medium. In such cases, *radiation* becomes the only mechanism of heat transfer between the surface under consideration and the surroundings. Using an energy balance, the radiation boundary condition on a surface can be expressed as

$$\begin{pmatrix} \text{Heat conduction} \\ \text{at the surface in a} \\ \text{selected direction} \end{pmatrix} = \begin{pmatrix} \text{Radiation exchange} \\ \text{at the surface in} \\ \text{the same direction} \end{pmatrix}$$

For one-dimensional heat transfer in the x-direction in a plate of thickness L, the radiation boundary conditions on both surfaces can be expressed as (Fig. 2–35)

$$-k\frac{\partial T(0, t)}{\partial x} = \varepsilon_1\sigma[T_{\text{surr},1}^4 - T(0, t)^4] \qquad \textbf{(2–52a)}$$

and

$$-k\frac{\partial T(L, t)}{\partial x} = \varepsilon_2\sigma[T(L, t)^4 - T_{\text{surr},2}^4] \qquad \textbf{(2–52b)}$$

FIGURE 2–35
Radiation boundary conditions on both surfaces of a plane wall.

where ε_1 and ε_2 are the emissivities of the boundary surfaces, $\sigma = 5.67 \times 10^{-8}$ W/m^2·K^4 is the Stefan–Boltzmann constant, and $T_{\text{surr},1}$ and $T_{\text{surr},2}$ are the average temperatures of the surfaces surrounding the two sides of the plate, respectively. Note that the temperatures in radiation calculations must be expressed in K or R (not in °C or °F).

The radiation boundary condition involves the fourth power of temperature, and thus it is a *nonlinear* condition. As a result, the application of this boundary condition results in powers of the unknown coefficients, which makes it difficult

to determine them. Therefore, it is tempting to ignore radiation exchange at a surface during a heat transfer analysis in order to avoid the complications associated with nonlinearity. This is especially the case when heat transfer at the surface is dominated by convection, and the role of radiation is minor.

5 Interface Boundary Conditions

Some bodies are made up of layers of different materials, and the solution of a heat transfer problem in such a medium requires the solution of the heat transfer problem in each layer. This, in turn, requires the specification of the boundary conditions at each *interface.*

The boundary conditions at an interface are based on the requirements that (1) two bodies in contact must have the *same temperature* at the area of contact and (2) an interface (which is a surface) cannot store any energy, and thus the *heat flux* on the two sides of an interface *must be the same.* The boundary conditions at the interface of two bodies A and B in perfect contact at $x = x_0$ can be expressed as (Fig. 2–36)

$$T_A(x_0, t) = T_B(x_0, t) \tag{2–53}$$

and

$$-k_A \frac{\partial T_A(x_0, t)}{\partial x} = -k_B \frac{\partial T_B(x_0, t)}{\partial x} \tag{2–54}$$

where k_A and k_B are the thermal conductivities of the layers A and B, respectively. The case of imperfect contact results in thermal contact resistance, which is considered in Chap. 3.

6 Generalized Boundary Conditions

So far we have considered surfaces subjected to *single mode* heat transfer, such as the specified heat flux, convection, or radiation for simplicity. In general, however, a surface may involve convection, radiation, *and* specified heat flux simultaneously. The boundary condition in such cases is again obtained from a surface energy balance, expressed as

$$\begin{pmatrix} \text{Heat transfer} \\ \text{to the surface} \\ \text{in all modes} \end{pmatrix} = \begin{pmatrix} \text{Heat transfer} \\ \text{from the surface} \\ \text{in all modes} \end{pmatrix} \tag{2–55}$$

This is illustrated in Examples 2–8 and 2–9.

FIGURE 2–36
Boundary conditions at the interface of two bodies in perfect contact.

EXAMPLE 2–8   Combined Convection and Radiation Condition

A spherical metal ball of radius r_0 is heated in an oven to a temperature of 600°F throughout and is then taken out of the oven and allowed to cool in ambient air at $T_\infty = 78°F$, as shown in Fig. 2–37. The thermal conductivity of the ball material is $k = 8.3$ Btu/h·ft·R, and the average convection heat transfer coefficient on the outer surface of the ball is evaluated to be $h = 4.5$ Btu/h·ft²·R. The emissivity of the outer surface of the ball is $\varepsilon = 0.6$, and the average temperature of the surrounding surfaces is $T_{surr} = 525$ R. Assuming the ball is cooled uniformly from the entire outer surface, express the initial and boundary conditions for the cooling process of the ball.

FIGURE 2–37
Schematic for Example 2–8.

SOLUTION The cooling of a hot spherical metal ball is considered. The initial and boundary conditions are to be obtained.

Analysis The ball is initially at a uniform temperature and is cooled uniformly from the entire outer surface. Therefore, this is a one-dimensional transient heat transfer problem since the temperature within the ball changes with the radial distance r and the time t. That is, $T = T(r, t)$. Taking the moment the ball is removed from the oven to be $t = 0$, the initial condition can be expressed as

$$T(r, 0) = T_i = 600°F$$

The problem possesses symmetry about the midpoint ($r = 0$) since the isotherms in this case are concentric spheres, and thus no heat is crossing the midpoint of the ball. Then the boundary condition at the midpoint can be expressed as

$$\frac{\partial T(0, t)}{\partial r} = 0$$

The heat conducted to the outer surface of the ball is lost to the environment by convection and radiation. Then taking the direction of heat transfer to be the positive r-direction, the boundary condition on the outer surface can be expressed as

$$-k\frac{\partial T(r_0, t)}{\partial r} = h[T(r_0) - T_\infty] + \varepsilon\sigma[T(r_0)^4 - T_{surr}^4]$$

Discussion All of the quantities in the above relations are known except the temperatures and their derivatives at $r = 0$ and r_0. Also, the radiation part of the boundary condition is often ignored for simplicity by modifying the convection heat transfer coefficient to account for the contribution of radiation. The convection coefficient h in that case becomes the combined heat transfer coefficient.

EXAMPLE 2–9   Combined Convection, Radiation, and Heat Flux

Consider the south wall of a house that is $L = 0.2$ m thick. The outer surface of the wall is exposed to solar radiation and has an absorptivity of $\alpha = 0.5$ for solar energy. The interior of the house is maintained at $T_{\infty 1} = 20°C$, while the ambient air temperature outside remains at $T_{\infty 2} = 5°C$. The sky, the ground, and the surfaces of the surrounding structures at this location can be modeled as a surface at an effective temperature of $T_{sky} = 255$ K for radiation exchange on the outer surface. The radiation exchange between the inner surface of the wall and the surfaces of the walls, floor, and ceiling it faces is negligible. The convection heat transfer coefficients on the inner and the outer surfaces of the wall are $h_1 = 6$ W/m²·K and $h_2 = 25$ W/m²·K, respectively. The thermal conductivity of the wall material is $k = 0.7$ W/m·K, and the emissivity of the outer surface is $\varepsilon_2 = 0.9$. Assuming the heat transfer through the wall to be steady and one-dimensional, express the boundary conditions on the inner and the outer surfaces of the wall.

SOLUTION The wall of a house subjected to solar radiation is considered. The boundary conditions on the inner and outer surfaces of the wall are to be obtained.

Analysis We take the direction normal to the wall surfaces as the *x*-axis with the origin at the inner surface of the wall, as shown in Fig. 2–38. The heat transfer through the wall is given to be steady and one-dimensional, and thus the temperature depends on *x* only and not on time. That is, $T = T(x)$.

The boundary condition on the inner surface of the wall at $x = 0$ is a typical convection condition since it does not involve any radiation or specified heat flux. Taking the direction of heat transfer to be the positive *x*-direction, the boundary condition on the inner surface can be expressed as

$$-k\frac{dT(0)}{dx} = h_1[T_{\infty 1} - T(0)]$$

The boundary condition on the outer surface at $x = L$ is quite general as it involves conduction, convection, radiation, and specified heat flux. Again taking the direction of heat transfer to be the positive *x*-direction, the boundary condition on the outer surface can be expressed as

$$-k\frac{dT(L)}{dx} = h_2[T(L) - T_{\infty 2}] + \varepsilon_2\sigma[T(L)^4 - T_{sky}^4] - \alpha\dot{q}_{solar}$$

where $\dot{q}_{solar}$ is the incident solar heat flux.

Discussion Assuming the opposite direction for heat transfer would give the same result multiplied by -1, which is equivalent to the relation here. All the quantities in these relations are known except the temperatures and their derivatives at the two boundaries.
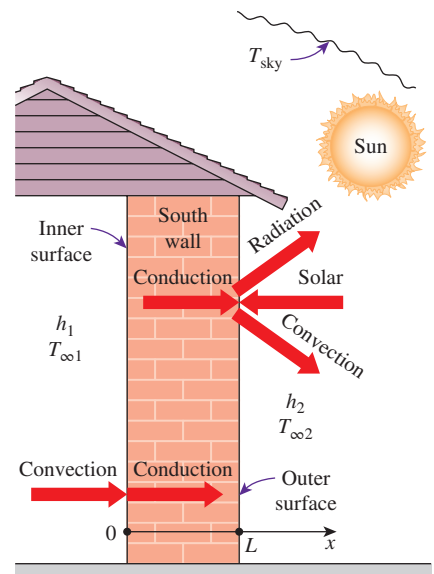
FIGURE 2–38
Schematic for Example 2–9.

Note that a heat transfer problem may involve different kinds of boundary conditions on different surfaces. For example, a plate may be subject to *heat flux* on one surface while losing or gaining heat by *convection* from the other surface. Also, the two boundary conditions in a direction may be specified *at the same boundary,* while no condition is imposed on the other boundary. For example, specifying the temperature and heat flux at $x = 0$ of a plate of thickness *L* will result in a unique solution for the one-dimensional steady temperature distribution in the plate, including the value of temperature at the surface $x = L$. Although not necessary, there is nothing wrong with specifying more than two boundary conditions in a specified direction, provided that there is no contradiction. The extra conditions in this case can be used to verify the results.

2–5 ▪ SOLUTION OF STEADY ONE-DIMENSIONAL HEAT CONDUCTION PROBLEMS

So far we have derived the differential equations for heat conduction in various coordinate systems and discussed the possible boundary conditions. A heat conduction problem can be formulated by specifying the applicable differential equation and a set of proper boundary conditions.

In this section we will solve a wide range of heat conduction problems in rectangular, cylindrical, and spherical geometries. We will limit our attention to problems that result in *ordinary differential equations* such as the *steady one-dimensional* heat conduction problems. We will also assume *constant thermal conductivity,* but we will consider variable conductivity later in this

chapter. If you feel rusty on differential equations or haven't taken differential equations yet, no need to panic. *Simple integration* is all you need to solve the steady one-dimensional heat conduction problems.

The solution procedure for solving heat conduction problems can be summarized as (1) *formulate* the problem by obtaining the applicable differential equation in its simplest form and specifying the boundary conditions, (2) obtain the *general solution* of the differential equation, and (3) apply the *boundary conditions* and determine the arbitrary constants in the general solution (Fig. 2–39). This is demonstrated with examples.

FIGURE 2–39
Basic steps involved in the solution of heat transfer problems.
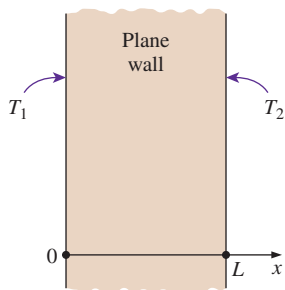
FIGURE 2–40
Schematic for Example 2–10.

EXAMPLE 2–10   Heat Conduction in a Plane Wall

Consider a large plane wall of thickness $L = 0.2$ m, thermal conductivity $k = 1.2$ W/m·K, and surface area A = 15 m^2. The two sides of the wall are maintained at constant temperatures of $T_1 = 120$°C and $T_2 = 50$°C, respectively, as shown in Fig. 2–40. Determine (*a*) the variation of temperature within the wall and the value of temperature at $x = 0.1$ m and (*b*) the rate of heat conduction through the wall under steady conditions.

SOLUTION   A plane wall with specified surface temperatures is given. The variation of temperature and the rate of heat transfer are to be determined.
Assumptions   **1** Heat conduction is steady. **2** Heat conduction is one-dimensional since the wall is large relative to its thickness, and the thermal conditions on both sides are uniform. **3** Thermal conductivity is constant. **4** There is no heat generation.
Properties   The thermal conductivity is given to be $k = 1.2$ W/m·K.
Analysis   (*a*) Taking the direction normal to the surface of the wall to be the *x*-direction, the differential equation for this problem can be expressed as

$$\frac{d^2T}{dx^2} = 0$$

with boundary conditions

$$T(0) = T_1 = 120°C$$
$$T(L) = T_2 = 50°C$$

The differential equation is linear and second order, and a quick inspection of it reveals that it has a single term involving derivatives and no terms involving the unknown function *T* as a factor. Thus, it can be solved by direct integration. Noting that an integration reduces the order of a derivative by one, the general solution to the preceding differential equation can be obtained by two simple successive integrations, each of which introduces an integration constant.

Integrating the differential equation once with respect to *x* yields

$$\frac{dT}{dx} = C_1$$

where C_1 is an arbitrary constant. Notice that the order of the derivative went down by one as a result of integration. As a check, if we take the derivative of this equation, we will obtain the original differential equation. This equation is not the solution yet since it involves a derivative.

Integrating one more time, we obtain

$$T(x) = C_1 x + C_2$$

which is the general solution to the differential equation (Fig. 2–41). The general solution in this case resembles the general formula of a straight line whose slope is C_1 and whose value at $x = 0$ is C_2. This is not surprising since the second derivative represents the change in the slope of a function, and a zero second derivative indicates that the slope of the function remains constant. Therefore, *any straight line* is a solution to this differential equation.

The general solution contains two unknown constants C_1 and C_2, and thus we need two equations to determine them uniquely and obtain the specific solution. These equations are obtained by forcing the general solution to satisfy the specified boundary conditions. The application of each condition yields one equation, and thus we need to specify two conditions to determine the constants C_1 and C_2.

When applying a boundary condition to an equation, *all occurrences of the dependent and independent variables and any derivatives are replaced by the specified values.* Thus the only unknowns in the resulting equations are the arbitrary constants.

The first boundary condition can be interpreted as *in the general solution, replace all the x's with zero and T(x) with T_1.* That is (Fig. 2–42),

$$T(0) = C_1 \times 0 + C_2 \quad \rightarrow \quad C_2 = T_1$$

The second boundary condition can be interpreted as *in the general solution, replace all the x's with L and T(x) with T_2.* That is,

$$T(L) = C_1 L + C_2 \quad \rightarrow \quad T_2 = C_1 L + T_1 \quad \rightarrow \quad C_1 = \frac{T_2 - T_1}{L}$$

Substituting the C_1 and C_2 expressions into the general solution, we obtain

$$T(x) = \frac{T_2 - T_1}{L} x + T_1 \qquad \text{(2–56)}$$

which is the desired solution since it satisfies not only the differential equation but also the two specified boundary conditions. That is, differentiating Eq. 2–56 with respect to x twice will give $d^2 T/dx^2$, which is the given differential equation, and substituting $x = 0$ and $x = L$ into Eq. 2–56 gives $T(0) = T_1$ and $T(L) = T_2$, respectively, which are the specified conditions at the boundaries.

Substituting the given information, the value of the temperature at $x = 0.1$ m is determined to be

$$T(0.1 \text{ m}) = \frac{(50 - 120)°\text{C}}{0.2 \text{ m}}(0.1 \text{ m}) + 120°\text{C} = \textbf{85°C}$$

(*b*) The rate of heat conduction anywhere in the wall is determined from Fourier's law to be

$$\dot{Q}_{\text{wall}} = -kA\frac{dT}{dx} = -kAC_1 = -kA\frac{T_2 - T_1}{L} = kA\frac{T_1 - T_2}{L} \qquad \text{(2–57)}$$

The numerical value of the rate of heat conduction through the wall is determined by substituting the given values to be

$$\dot{Q} = kA\frac{T_1 - T_2}{L} = (1.2 \text{ W/m·K})(15 \text{ m}^2)\frac{(120 - 50)°\text{C}}{0.2 \text{ m}} = \textbf{6300 W}$$

Discussion Note that under steady conditions, the rate of heat conduction through a plane wall is constant.
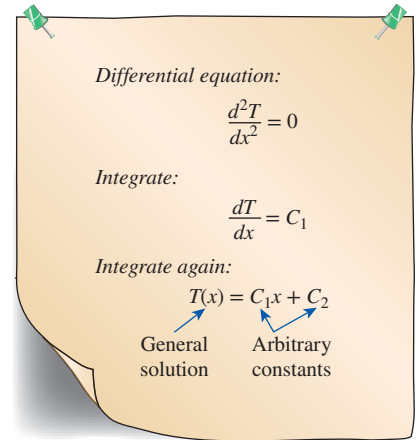
FIGURE 2–41
Obtaining the general solution to a simple second-order differential equation by integration.
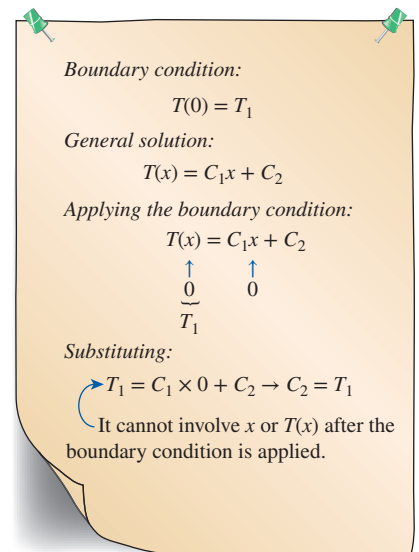
FIGURE 2–42
When applying a boundary condition to the general solution at a specified point, all occurrences of the dependent and independent variables should be replaced by their specified values at that point.

EXAMPLE 2–11 **A Wall with Various Sets of Boundary Conditions**

Consider steady one-dimensional heat conduction in a large plane wall of thickness L and constant thermal conductivity k with no heat generation. Obtain expressions for the variation of temperature within the wall for the following pairs of boundary conditions (Fig. 2–43):

$(a) \ -k\frac{dT(0)}{dx} = \dot{q}_0 = 40 \text{ W/cm}^2$ and $T(0) = T_0 = 15°\text{C}$

$(b) \ -k\frac{dT(0)}{dx} = \dot{q}_0 = 40 \text{ W/cm}^2$ and $-k\frac{dT(L)}{dx} = \dot{q}_L = -25 \text{ W/cm}^2$

$(c) \ -k\frac{dT(0)}{dx} = \dot{q}_0 = 40 \text{ W/cm}^2$ and $-k\frac{dT(L)}{dx} = \dot{q}_L = \dot{q}_0 = 40 \text{ W/cm}^2$

SOLUTION Steady one-dimensional heat conduction in a large plane wall is considered. The variation of temperature is to be determined for different sets of boundary conditions.

Analysis This is a steady one-dimensional heat conduction problem with constant thermal conductivity and no heat generation in the medium, and the heat conduction equation in this case can be expressed as (Eq. 2–17)

$$\frac{d^2T}{dx^2} = 0$$

whose general solution was determined in the previous example by direct integration to be

$$T(x) = C_1 x + C_2$$

where C_1 and C_2 are two arbitrary integration constants. The specific solutions corresponding to each specified pair of boundary conditions are determined as follows:

(a) In this case, both boundary conditions are specified at the same boundary at $x = 0$, and no boundary condition is specified at the other boundary at $x = L$. Noting that

$$\frac{dT}{dx} = C_1$$

the application of the boundary conditions gives

$$-k\frac{dT(0)}{dx} = \dot{q}_0 \quad \rightarrow \quad -kC_1 = \dot{q}_0 \quad \rightarrow \quad C_1 = -\frac{\dot{q}_0}{k}$$

and

$$T(0) = T_0 \quad \rightarrow \quad T_0 = C_1 \times 0 + C_2 \quad \rightarrow \quad C_2 = T_0$$

Substituting, the specific solution in this case is determined to be

$$T(x) = -\frac{\dot{q}_0}{k}x + T_0$$
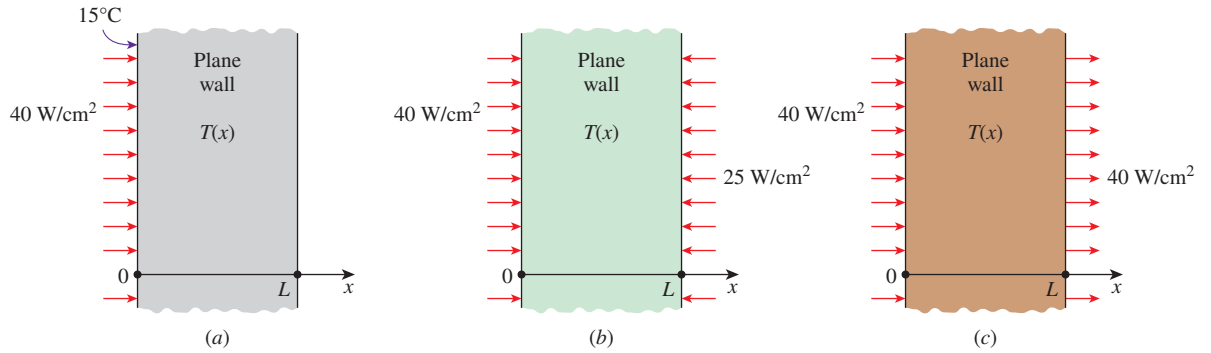
FIGURE 2–43
Schematic for Example 2–11.

Therefore, the two boundary conditions can be specified at the same boundary, and it is not necessary to specify them at different locations. In fact, the fundamental theorem of linear ordinary differential equations guarantees that a unique solution exists when both conditions are specified at the same location. But no such guarantee exists when the two conditions are specified at different boundaries, as you will see below.

(*b*) In this case, different heat fluxes are specified at the two boundaries. The application of the boundary conditions gives

$$-k\frac{dT(0)}{dx} = \dot{q}_0 \quad \rightarrow \quad -kC_1 = \dot{q}_0 \quad \rightarrow \quad C_1 = -\frac{\dot{q}_0}{k}$$

and

$$-k\frac{dT(L)}{dx} = \dot{q}_L \quad \rightarrow \quad -kC_1 = \dot{q}_L \quad \rightarrow \quad C_1 = -\frac{\dot{q}_L}{k}$$

Since $\dot{q}_0 \neq \dot{q}_L$ and the constant C_1 cannot be equal to two different things at the same time, there is no solution in this case. This is not surprising since this case corresponds to supplying heat to the plane wall from both sides and expecting the temperature of the wall to remain steady (not to change with time). This is impossible.

(*c*) In this case, the same values for heat flux are specified at the two boundaries. The application of the boundary conditions gives

$$-k\frac{dT(0)}{dx} = \dot{q}_0 \quad \rightarrow \quad -kC_1 = \dot{q}_0 \quad \rightarrow \quad C_1 = -\frac{\dot{q}_0}{k}$$

and

$$-k\frac{dT(L)}{dx} = \dot{q}_0 \quad \rightarrow \quad -kC_1 = \dot{q}_0 \quad \rightarrow \quad C_1 = -\frac{\dot{q}_0}{k}$$

Thus, both conditions result in the same value for the constant C_1, but no value for C_2. Substituting, the specific solution in this case is determined to be

$$T(x) = -\frac{\dot{q}_0}{k}x + C_2$$

which is not a unique solution since C_2 is arbitrary.

Differential equation:
$$T''(x) = 0$$

General solution:
$$T(x) = C_1 x + C_2$$

(*a*) *Unique solution:*
$$\left.\begin{array}{r} -kT'(0) = \dot{q}_0 \\ T'(0) = T_0 \end{array}\right\} \; T(x) = -\frac{\dot{q}_0}{k} x + T_0$$

(*b*) *No solution:*
$$\left.\begin{array}{r} -kT'(0) = \dot{q}_0 \\ -kT'(L) = \dot{q}_L \end{array}\right\} \; T(x) = \text{None}$$

(*c*) *Multiple solutions:*
$$\left.\begin{array}{r} -kT'(0) = \dot{q}_0 \\ -kT'(L) = \dot{q}_0 \end{array}\right\} \; T(x) = -\frac{\dot{q}_0}{k} x + C_2$$
$$\uparrow$$
Arbitrary

FIGURE 2–44
A boundary-value problem may have a unique solution, infinitely many solutions, or no solutions at all.
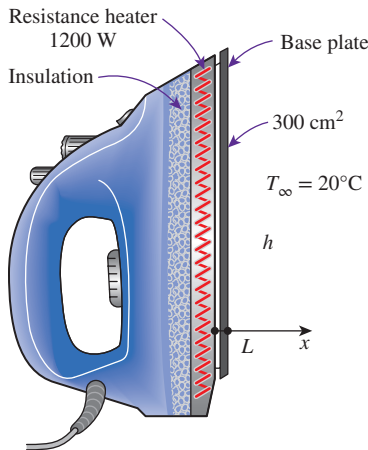
FIGURE 2–45
Schematic for Example 2–12.

Discussion The last solution represents a family of straight lines whose slope is $-\dot{q}_0/k$. Physically, this problem corresponds to requiring the rate of heat supplied to the wall at $x = 0$ to be equal to the rate of heat removal from the other side of the wall at $x = L$. But this is a consequence of the heat conduction through the wall being steady, and thus the second boundary condition does not provide any new information. So it is not surprising that the solution of this problem is not unique. The three cases we have discussed are summarized in Fig. 2–44.

EXAMPLE 2–12   Heat Conduction in the Base Plate of an Iron

Consider the base plate of a 1200-W household iron that has a thickness of $L = 0.5$ cm, base area of $A = 300$ cm^2, and thermal conductivity of $k = 15$ W/m·K. The inner surface of the base plate is subjected to uniform heat flux generated by the resistance heaters inside, and the outer surface loses heat to the surroundings at $T_\infty = 20°$C by convection, as shown in Fig. 2–45. Taking the convection heat transfer coefficient to be $h = 80$ W/m^2·K and disregarding heat loss by radiation, obtain an expression for the variation of temperature in the base plate, and evaluate the temperatures at the inner and the outer surfaces.

SOLUTION The base plate of an iron is considered. The variation of temperature in the plate and the surface temperatures are to be determined.
Assumptions **1** Heat transfer is steady since there is no change with time. **2** Heat transfer is one-dimensional since the surface area of the base plate is large relative to its thickness, and the thermal conditions on both sides are uniform. **3** Thermal conductivity is constant. **4** There is no heat generation in the medium. **5** Heat transfer by radiation is negligible. **6** The upper part of the iron is well insulated, so all heat generated in the resistance wires is transferred to the base plate through its inner surface.
Properties The thermal conductivity is given to be $k = 15$ W/m·K.
Analysis The inner surface of the base plate is subjected to uniform heat flux at a rate of

$$\dot{q}_0 = \frac{\dot{Q}_0}{A_{\text{base}}} = \frac{1200 \text{ W}}{0.03 \text{ m}^2} = 40{,}000 \text{ W/m}^2$$

The outer side of the plate is subjected to the convection condition. Taking the direction normal to the surface of the wall as the *x*-direction with its origin on the inner surface, the differential equation for this problem can be expressed as (Fig. 2–46)

$$\frac{d^2 T}{dx^2} = 0$$

with the boundary conditions

$$-k\frac{dT(0)}{dx} = \dot{q}_0 = 40{,}000 \text{ W/m}^2$$

$$-k\frac{dT(L)}{dx} = h[T(L) - T_\infty]$$

The general solution to the differential equation is again obtained by two successive integrations to be

$$\frac{dT}{dx} = C_1$$

and

$$T(x) = C_1 x + C_2 \qquad \textbf{(a)}$$

where C_1 and C_2 are arbitrary constants. Applying the first boundary condition,

$$-k\frac{dT(0)}{dx} = \dot{q}_0 \quad \rightarrow \quad -kC_1 = \dot{q}_0 \quad \rightarrow \quad C_1 = -\frac{\dot{q}_0}{k}$$

Noting that $dT/dx = C_1$ and $T(L) = C_1 L + C_2$, the application of the second boundary condition gives

$$-k\frac{dT(L)}{dx} = h[T(L) - T_\infty] \quad \rightarrow \quad -kC_1 = h[(C_1 L + C_2) - T_\infty]$$

Substituting $C_1 = -\dot{q}_0/k$ and solving for C_2, we obtain

$$C_2 = T_\infty + \frac{\dot{q}_0}{h} + \frac{\dot{q}_0}{k}L$$

Now substituting C_1 and C_2 into the general solution (a) gives

$$T(x) = T_\infty + \dot{q}_0\left(\frac{L-x}{k} + \frac{1}{h}\right) \qquad \textbf{(b)}$$

which is the solution for the variation of the temperature in the plate. The temperatures at the inner and outer surfaces of the plate are determined by substituting $x = 0$ and $x = L$, respectively, into the relation (b):

$$T(0) = T_\infty + \dot{q}_0\left(\frac{L}{k} + \frac{1}{h}\right)$$
$$= 20°C + (40,000 \text{ W/m}^2)\left(\frac{0.005 \text{ m}}{15 \text{ W/m·K}} + \frac{1}{80 \text{ W/m}^2\text{·K}}\right) = \textbf{533°C}$$

and

$$T(L) = T_\infty + \dot{q}_0\left(0 + \frac{1}{h}\right) = 20°C + \frac{40,000 \text{ W/m}^2}{80 \text{ W/m}^2\text{·K}} = \textbf{520°C}$$

Discussion Note that the temperature of the inner surface of the base plate is 13°C higher than the temperature of the outer surface when steady operating conditions are reached. Also note that this heat transfer analysis enables us to calculate the temperatures of surfaces that we cannot even reach. This example demonstrates how the heat flux and convection boundary conditions are applied to heat transfer problems.
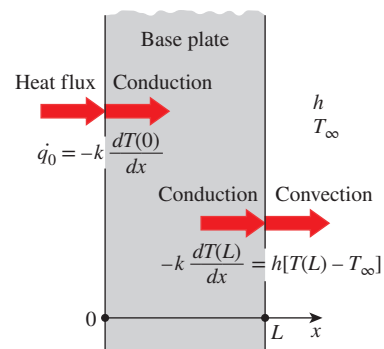
FIGURE 2–46
The boundary conditions on the base plate of the iron discussed in Example 2–12.
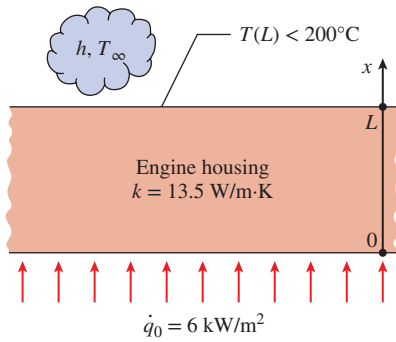
FIGURE 2–47
Schematic for Example 2–13.

PtD **EXAMPLE 2–13** **Fire Hazard Prevention of Oil Leakage on Hot Engine Surface**

The outer surface of an engine is situated in a place where oil leakage can occur. Some oils have autoignition temperatures of approximately 250°C. When oil comes in contact with a hot engine surface that has a higher temperature than its autoignition temperature, the oil can ignite spontaneously. Treating the engine housing as a plane wall, the inner surface ($x = 0$) is subjected to a heat flux of 6 kW/m^2, as shown in Fig. 2–47. The engine housing ($k = 13.5$ W/m·k) has a thickness of 1 cm, and the outer surface ($x = L$) is exposed to an environment where the ambient air is 35°C with a convection heat transfer coefficient of 20 W/m^2·K. To prevent fire hazard in the event the leaked oil comes in contact with the hot engine surface, the temperature of the engine surface should be kept below 200°C. Determine the variation of temperature in the engine housing and the temperature of the inner and outer surfaces. Is the outer surface temperature of the engine below the autoignition temperature?

SOLUTION In this example, the concepts of prevention through design (PtD) are applied in conjunction with the solution of a steady one-dimensional heat conduction problem. The outer surface of the engine is exposed to an environment where the ambient air is 35°C with a convection heat transfer coefficient of 20 W/m^2·K. The inner surface of the engine is subjected to a heat flux of 6 kW/m^2. The variation of temperature in the engine housing and the temperature of the inner and outer surfaces of the engine are to be determined. To prevent fire hazard in the event the leaked oil comes in contact with the hot engine surface, the outer surface temperature of the engine should be kept below 200°C.

Assumptions **1** Heat conduction is steady and one-dimensional. **2** Thermal conductivity is constant. **3** There is no heat generation in the engine housing (plane wall). **4** The inner surface at $x = 0$ is subjected to uniform heat flux while the outer surface at $x = L$ is subjected to convection.

Properties The thermal conductivity of the engine housing is given to be $k = 13.5$ W/m·K.

Analysis Taking the direction normal to the surface of the wall to be the x-direction with $x = 0$ at the inner surface, the mathematical formulation can be expressed as

$$\frac{d^2T}{dx^2} = 0$$

with boundary conditions

$$-k\frac{dT(0)}{dx} = \dot{q}_0$$

$$-k\frac{dT(L)}{dx} = h[T(L) - T_\infty]$$

Integrating the differential equation twice with respect to x yields

$$\frac{dT}{dx} = C_1$$

$$T(x) = C_1x + C_2$$

where C_1 and C_2 are arbitrary constants. Applying the first boundary condition yields

$$-k\frac{dT(0)}{dx} = \dot{q}_0 \quad \rightarrow \quad -kC_1 = \dot{q}_0 \quad \rightarrow \quad C_1 = -\frac{\dot{q}_0}{k}$$

The application of the second boundary condition gives

$$-k\frac{dT(L)}{dx} = h[T(L) - T_\infty] \quad \rightarrow \quad -kC_1 = h(C_1L + C_2 - T_\infty)$$

Substituting for $C_1 = -\dot{q}_0/k$ and solving for C_2, we obtain

$$C_2 = -C_1\left(\frac{k}{h} + L\right) + T_\infty = \frac{\dot{q}_0}{k}\left(\frac{k}{h} + L\right) + T_\infty$$

Now substituting C_1 and C_2 into the general solution, the variation of temperature becomes

$$T(x) = \frac{\dot{q}_0}{k}\left(\frac{k}{h} + L - x\right) + T_\infty$$

The temperature at $x = 0$ (the inner surface) is:

$$T(0) = \frac{\dot{q}_0}{k}\left(\frac{k}{h} + L\right) + T_\infty = \frac{6000 \text{ W/m}^2}{13.5 \text{ W/m·K}}\left(\frac{13.5 \text{ W/m·K}}{20 \text{ W/m}^2\text{·K}} + 0.010 \text{ m}\right) + 35°\text{C}$$

$$= \mathbf{339°C}$$

The temperature at $x = L = 0.01$ m (the outer surface) is:

$$T(L) = \frac{\dot{q}_0}{h} + T_\infty = \frac{6000 \text{ W/m}^2}{20 \text{ W/m}^2\text{·K}} + 35°\text{C} = \mathbf{335°C}$$

Discussion The outer surface temperature of the engine is 135°C higher than the safe temperature of 200°C. The outer surface of the engine should be covered with protective insulation to prevent a fire hazard in the event of oil leakage.

EXAMPLE 2–14   **Heat Conduction in a Solar Heated Wall**

Consider a large plane wall of thickness $L = 0.06$ m and thermal conductivity $k = 1.2$ W/m·K in space. The wall is covered with white porcelain tiles that have an emissivity of $\varepsilon = 0.85$ and a solar absorptivity of $\alpha = 0.26$, as shown in Fig. 2–48. The inner surface of the wall is maintained at $T_1 = 300$ K at all times, while the outer surface is exposed to solar radiation that is incident at a rate of $\dot{q}_{\text{solar}} = 800$ W/m². The outer surface is also losing heat by radiation to deep space at 0 K. Determine the temperature of the outer surface of the wall and the rate of heat transfer through the wall when steady operating conditions are reached. What would your response be if no solar radiation were incident on the surface?

SOLUTION   A plane wall in space is subjected to a specified temperature on one side and solar radiation on the other side. The outer surface temperature and the rate of heat transfer are to be determined.
Assumptions   **1** Heat transfer is steady since there is no change with time. **2** Heat transfer is one-dimensional since the wall is large relative to its thickness, and the thermal conditions on both sides are uniform. **3** Thermal conductivity is constant. **4** There is no heat generation.
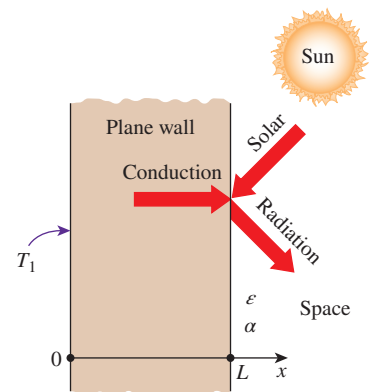
FIGURE 2–48
Schematic for Example 2–14.

Properties The thermal conductivity is given to be $k = 1.2\,\text{W/m·K}$.

Analysis Taking the direction normal to the surface of the wall as the x-direction with its origin on the inner surface, the differential equation for this problem can be expressed as

$$\frac{d^2T}{dx^2} = 0$$

with boundary conditions

$$T(0) = T_1 = 300\ \text{K}$$

$$-k\frac{dT(L)}{dx} = \varepsilon\sigma[T(L)^4 - T_{\text{space}}^4] - \alpha\dot{q}_{\text{solar}}$$

where $T_{\text{space}} = 0$. The general solution to the differential equation is again obtained by two successive integrations to be

$$T(x) = C_1 x + C_2 \qquad\qquad (a)$$

where C_1 and C_2 are arbitrary constants. Applying the first boundary condition yields

$$T(0) = C_1 \times 0 + C_2 \;\rightarrow\; C_2 = T_1$$

Noting that $dT/dx = C_1$ and $T(L) = C_1 L + C_2 = C_1 L + T_1$, the application of the second boundary condition gives

$$-k\frac{dT(L)}{dx} = \varepsilon\sigma T(L)^4 - \alpha\dot{q}_{\text{solar}} \;\rightarrow\; -kC_1 = \varepsilon\sigma(C_1 L + T_1)^4 - \alpha\dot{q}_{\text{solar}}$$

Although C_1 is the only unknown in this equation, we cannot get an explicit expression for it because the equation is nonlinear, and thus we cannot get a closed-form expression for the temperature distribution. This should explain why we do our best to avoid nonlinearities in the analysis, such as those associated with radiation.

Let us back up a little and denote the outer surface temperature by $T(L) = T_L$ instead of $T(L) = C_1 L + T_1$. The application of the second boundary condition in this case gives

$$-k\frac{dT(L)}{dx} = \varepsilon\sigma T(L)^4 - \alpha\dot{q}_{\text{solar}} \;\rightarrow\; -kC_1 = \varepsilon\sigma T_L^4 - \alpha\dot{q}_{\text{solar}}$$

Solving for C_1 gives

$$C_1 = \frac{\alpha\dot{q}_{\text{solar}} - \varepsilon\sigma T_L^4}{k} \qquad\qquad (b)$$

Now substituting C_1 and C_2 into the general solution (a), we obtain

$$T(x) = \frac{\alpha\dot{q}_{\text{solar}} - \varepsilon\sigma T_L^4}{k}x + T_1 \qquad\qquad (c)$$

which is the solution for the variation of the temperature in the wall in terms of the unknown outer surface temperature T_L. At $x = L$, it becomes

$$T_L = \frac{\alpha\dot{q}_{\text{solar}} - \varepsilon\sigma T_L^4}{k}L + T_1 \qquad\qquad (d)$$

which is an implicit relation for the outer surface temperature T_L. Substituting the given values, we get

$$T_L = \frac{0.26 \times (800 \text{ W/m}^2) - 0.85 \times (5.67 \times 10^{-8} \text{ W/m}^2\cdot\text{K}^4)T_L^4}{1.2 \text{ W/m}\cdot\text{K}}(0.06 \text{ m}) + 300 \text{ K}$$

which simplifies to

$$T_L = 310.4 - 0.240975\left(\frac{T_L}{100}\right)^4$$

This equation can be solved by one of the several nonlinear equation solvers available (or by the old fashioned trial-and-error method) to give (Fig. 2–49)

$$T_L = \textbf{292.7 K}$$

Knowing the outer surface temperature and knowing that it must remain constant under steady conditions, the temperature distribution in the wall can be determined by substituting this T_L value into Eq. (c):

$$T(x) = \frac{0.26 \times (800 \text{ W/m}^2) - 0.85 \times (5.67 \times 10^{-8} \text{ W/m}^2\cdot\text{K}^4)(292.7 \text{ K})^4}{1.2 \text{ W/m}\cdot\text{K}}x + 300 \text{ K}$$

which simplifies to

$$T(x) = (-121.5 \text{ K/m})x + 300 \text{ mK}$$

Note that the outer surface temperature turned out to be lower than the inner surface temperature. Therefore, the heat transfer through the wall is toward the outside despite the absorption of solar radiation by the outer surface. Knowing both the inner and outer surface temperatures of the wall, the steady rate of heat conduction through the wall can be determined from

$$\dot{q} = k\frac{T_1 - T_L}{L} = (1.2 \text{ W/m}\cdot\text{K})\frac{(300 - 292.7) \text{ K}}{0.06 \text{ m}} = \textbf{146 W/m}^2$$

Discussion   In the case of no incident solar radiation, the outer surface temperature, determined from Eq. (d) by setting $\dot{q}_{solar} = 0$, is $T_L = \textbf{284.3 K.}$ It is interesting to note that the solar energy incident on the surface causes the surface temperature to increase by about 8 K only when the inner surface temperature of the wall is maintained at 300 K.

(1) *Rearrange the equation to be solved:*

$$T_L = 310.4 - 0.240975\left(\frac{T_L}{100}\right)^4$$

The equation is in the proper form since the left side consists of T_L only.

(2) *Guess the value of T_L, say 300 K, and substitute into the right side of the equation. It gives*

$$T_L = 290.2 \text{ K}$$

(3) *Now substitute this value of T_L into the right side of the equation and get*

$$T_L = 293.1 \text{ K}$$

(4) *Repeat step* (3) *until convergence to desired accuracy is achieved. The subsequent iterations give*

$$T_L = 292.6 \text{ K}$$
$$T_L = 292.7 \text{ K}$$
$$T_L = 292.7 \text{ K}$$

Therefore, the solution is $T_L = 292.7$ K. The result is independent of the initial guess.

FIGURE 2–49
A simple method of solving a nonlinear equation is to arrange the equation such that the unknown is alone on the left side while everything else is on the right side, and to iterate after an initial guess until convergence.

EXAMPLE 2–15   Heat Loss Through a Steam Pipe

Consider a steam pipe of length $L = 20$ m, inner radius $r_1 = 6$ cm, outer radius $r_2 = 8$ cm, and thermal conductivity $k = 20$ W/m·K, as shown in Fig. 2–50. The inner and outer surfaces of the pipe are maintained at average temperatures of $T_1 = 150°C$ and $T_2 = 60°C$, respectively. Obtain a general relation for the temperature distribution inside the pipe under steady conditions, and determine the rate of heat loss from the steam through the pipe.

SOLUTION   A steam pipe is subjected to specified temperatures on its surfaces. The variation of temperature and the rate of heat transfer are to be determined.

FIGURE 2–50
Schematic for Example 2–14.

Differential equation:

$$\frac{d}{dr}\left(r\frac{dT}{dr}\right) = 0$$

Integrate:

$$r\frac{dT}{dr} = C_1$$

Divide by r ($r \neq 0$):

$$\frac{dT}{dr} = \frac{C_1}{r}$$

Integrate again:

$$T(r) = C_1 \ln r + C_2$$

which is the general solution.
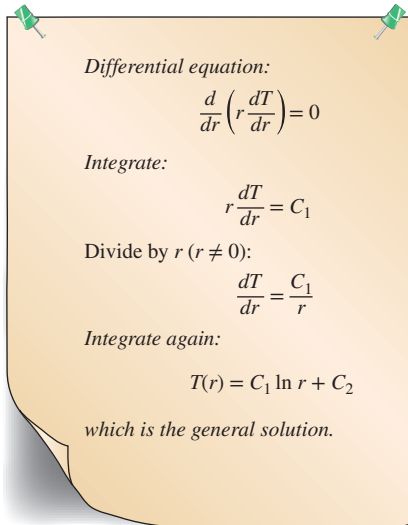
FIGURE 2–51
Basic steps involved in the solution of the steady one-dimensional heat conduction equation in cylindrical coordinates.

Assumptions **1** Heat transfer is steady since there is no change with time. **2** Heat transfer is one-dimensional since there is thermal symmetry about the centerline and no variation in the axial direction, and thus $T = T(r)$. **3** Thermal conductivity is constant. **4** There is no heat generation.

Properties The thermal conductivity is given to be $k = 20\,\text{W/m·K}$.

Analysis The mathematical formulation of this problem can be expressed as

$$\frac{d}{dr}\left(r\frac{dT}{dr}\right) = 0$$

with boundary conditions

$$T(r_1) = T_1 = 150°C$$
$$T(r_2) = T_2 = 60°C$$

Integrating the differential equation once with respect to r gives

$$r\frac{dT}{dr} = C_1$$

where C_1 is an arbitrary constant. We now divide both sides of this equation by r to bring it to a readily integrable form,

$$\frac{dT}{dr} = \frac{C_1}{r}$$

Again integrating with respect to r gives (Fig. 2–51)

$$T(r) = C_1 \ln r + C_2 \tag{a}$$

We now apply both boundary conditions by replacing all occurrences of r and $T(r)$ in Eq. (a) with the specified values at the boundaries. We get

$$T(r_1) = T_1 \quad \rightarrow \quad C_1 \ln r_1 + C_2 = T_1$$
$$T(r_2) = T_2 \quad \rightarrow \quad C_1 \ln r_2 + C_2 = T_2$$

which are two equations in two unknowns, C_1 and C_2. Solving them simultaneously gives

$$C_1 = \frac{T_2 - T_1}{\ln(r_2/r_1)} \quad \text{and} \quad C_2 = T_1 - \frac{T_2 - T_1}{\ln(r_2/r_1)}\ln r_1$$

Substituting them into Eq. (a) and rearranging, the variation of temperature within the pipe is determined to be

$$T(r) = \frac{\ln(r/r_1)}{\ln(r_2/r_1)}(T_2 - T_1) + T_1 \tag{2–58}$$

The rate of heat loss from the steam is simply the total rate of heat conduction through the pipe and is determined from Fourier's law to be

$$\dot{Q}_{\text{cylinder}} = -kA\frac{dT}{dr} = -k(2\pi rL)\frac{C_1}{r} = -2\pi kL\,C_1 = 2\pi kL\frac{T_1 - T_2}{\ln(r_2/r_1)} \tag{2–59}$$

The numerical value of the rate of heat conduction through the pipe is determined by substituting the given values

$$\dot{Q} = 2\pi(20\ \text{W/m·K})(20\ \text{m})\frac{(150 - 60)°C}{\ln(0.08/0.06)} = \mathbf{786\ kW}$$

Discussion Note that the total rate of heat transfer through a pipe is constant, but the heat flux $\dot{q} = \dot{Q}/(2\pi rL)$ is not since it decreases in the direction of heat transfer with increasing radius.

■ *EXAMPLE 2–16* Heat Conduction Through a Spherical Shell

Consider a spherical container of inner radius $r_1 = 8$ cm, outer radius $r_2 = 10$ cm, and thermal conductivity $k = 45$ W/m·K, as shown in Fig. 2–52. The inner and outer surfaces of the container are maintained at constant temperatures of $T_1 = 200°C$ and $T_2 = 80°C$, respectively, as a result of some chemical reactions occurring inside. Obtain a general relation for the temperature distribution inside the shell under steady conditions, and determine the rate of heat loss from the container.

SOLUTION A spherical container is subjected to specified temperatures on its surfaces. The variation of temperature and the rate of heat transfer are to be determined.

Assumptions **1** Heat transfer is steady since there is no change with time. **2** Heat transfer is one-dimensional since there is thermal symmetry about the midpoint, and thus $T = T(r)$. **3** Thermal conductivity is constant. **4** There is no heat generation.

Properties The thermal conductivity is given to be $k = 45$ W/m·K.

Analysis The mathematical formulation of this problem can be expressed as

$$\frac{d}{dr}\left(r^2 \frac{dT}{dr}\right) = 0$$

with boundary conditions

$$T(r_1) = T_1 = 200°C$$
$$T(r_2) = T_2 = 80°C$$

Integrating the differential equation once with respect to r yields

$$r^2 \frac{dT}{dr} = C_1$$

where C_1 is an arbitrary constant. We now divide both sides of this equation by r^2 to bring it to a readily integrable form,

$$\frac{dT}{dr} = \frac{C_1}{r^2}$$

Again integrating with respect to r gives

$$T(r) = -\frac{C_1}{r} + C_2 \qquad (a)$$

We now apply both boundary conditions by replacing all occurrences of r and $T(r)$ in the preceding relation with the specified values at the boundaries. We get

$$T(r_1) = T_1 \quad \rightarrow \quad -\frac{C_1}{r_1} + C_2 = T_1$$

$$T(r_2) = T_2 \quad \rightarrow \quad -\frac{C_1}{r_2} + C_2 = T_2$$
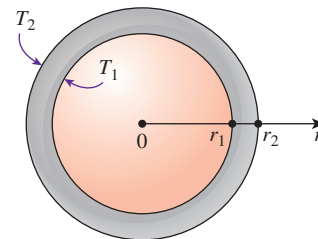
FIGURE 2–52
Schematic for Example 2–16.

FIGURE 2−53
During steady one-dimensional heat conduction in a spherical (or cylindrical) container, the total rate of heat transfer remains constant, but the heat flux decreases with increasing radius.
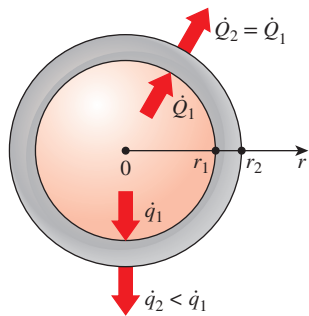
$$\dot{q}_1 = \frac{\dot{Q}_1}{A_1} = \frac{27.1 \text{ kW}}{4\pi \, (0.08 \text{ m})^2} = 337 \text{ kW/m}^2$$

$$\dot{q}_2 = \frac{\dot{Q}_2}{A_2} = \frac{27.1 \text{ kW}}{4\pi \, (0.10 \text{ m})^2} = 216 \text{ kW/m}^2$$

which are two equations in two unknowns, C_1 and C_2. Solving them simultaneously gives

$$C_1 = -\frac{r_1 r_2}{r_2 - r_1}(T_1 - T_2) \quad \text{and} \quad C_2 = \frac{r_2 T_2 - r_1 T_1}{r_2 - r_1}$$

Substituting into Eq. (*a*), the variation of temperature within the spherical shell is determined to be

$$T(r) = \frac{r_1 r_2}{r(r_2 - r_1)}(T_1 - T_2) + \frac{r_2 T_2 - r_1 T_1}{r_2 - r_1} \tag{2–60}$$

The rate of heat loss from the container is simply the total rate of heat conduction through the container wall and is determined from Fourier's law

$$\dot{Q}_{\text{sphere}} = -kA\frac{dT}{dr} = -k(4\pi r^2)\frac{C_1}{r^2} = -4\pi k C_1 = 4\pi k r_1 r_2 \frac{T_1 - T_2}{r_2 - r_1} \tag{2–61}$$

The numerical value of the rate of heat conduction through the wall is determined by substituting the given values to be

$$\dot{Q} = 4\pi(45 \text{ W/m·K})(0.08 \text{ m})(0.10 \text{ m})\frac{(200 - 80)°\text{C}}{(0.10 - 0.08) \text{ m}} = \textbf{27.1 kW}$$

Discussion   Note that the total rate of heat transfer through a spherical shell is constant, but the heat flux $\dot{q} = \dot{Q}/4\pi r^2$ is not since it decreases in the direction of heat transfer with increasing radius as shown in Fig. 2–53.

2−6 ▪ HEAT GENERATION IN A SOLID

Many practical heat transfer applications involve the conversion of some form of energy into *thermal* energy in the medium. Such media are said to involve internal *heat generation,* which manifests itself as a rise in temperature throughout the medium. Some examples of heat generation are *resistance heating* in wires, exothermic *chemical reactions* in a solid, and *nuclear reactions* in nuclear fuel rods where electrical, chemical, and nuclear energies are converted to heat, respectively (Fig. 2–54). The absorption of radiation throughout the volume of a semitransparent medium such as water can also be considered to be heat generation within the medium, as explained earlier.

Heat generation is usually expressed *per unit volume* of the medium and is denoted by $\dot{e}_{\text{gen}}$, whose unit is W/m^3. For example, heat generation in an electrical wire of outer radius r_o and length L can be expressed as

$$\dot{e}_{\text{gen}} = \frac{\dot{E}_{\text{gen, electric}}}{V_{\text{wire}}} = \frac{I^2 R_e}{\pi r_o^2 L} \qquad \text{(W/m}^3) \tag{2–62}$$

FIGURE 2−54
Heat generation in solids is commonly encountered in practice.

where I is the electric current and R_e is the electrical resistance of the wire.

The temperature of a medium *rises* during heat generation as a result of the absorption of the generated heat by the medium during the transient start-up period. As the temperature of the medium increases, so does the heat transfer from the medium to its surroundings. This continues until steady operating

conditions are reached and the rate of heat generation equals the rate of heat transfer to the surroundings. Once steady operation has been established, the temperature of the medium at any point no longer changes.

The *maximum temperature* T_{max} in a solid that involves uniform heat generation occurs at a location *farthest away* from the outer surface when the outer surface of the solid is maintained at a constant temperature T_s. For example, the maximum temperature occurs at the *midplane* in a plane wall, at the *centerline* in a long cylinder, and at the *midpoint* in a sphere. The temperature distribution within the solid in these cases is *symmetrical* about the center of symmetry.

The quantities of major interest in a medium with heat generation are the surface temperature T_s and the maximum temperature T_{max} that occurs in the medium in *steady* operation. Next we develop expressions for these two quantities for common geometries for the case of *uniform* heat generation ($\dot{e}_{gen}$ = constant) within the medium.

Consider a solid medium of surface area A_s, volume V, and constant thermal conductivity k, where heat is generated at a constant rate of $\dot{e}_{gen}$ per unit volume. Heat is transferred from the solid to the surrounding medium at T_∞, with a constant heat transfer coefficient of h. All the surfaces of the solid are maintained at a common temperature T_s. Under *steady* conditions, the energy balance for this solid can be expressed as (Fig. 2–55)

FIGURE 2–55
At steady conditions, all heat generated in a solid must leave the solid through its outer surface.

$$\begin{pmatrix} \text{Rate of} \\ \textit{heat transfer} \\ \text{from the solid} \end{pmatrix} = \begin{pmatrix} \text{Rate of} \\ \textit{energy generation} \\ \text{within the solid} \end{pmatrix} \qquad \textbf{(2–63)}$$

or

$$\dot{Q} = \dot{e}_{gen}V \qquad \text{(W)} \qquad \textbf{(2–64)}$$

Disregarding radiation (or incorporating it in the heat transfer coefficient h), the heat transfer rate can also be expressed from Newton's law of cooling as

$$\dot{Q} = hA_s(T_s - T_\infty) \qquad \text{(W)} \qquad \textbf{(2–65)}$$

Combining Eqs. 2–64 and 2–65 and solving for the surface temperature T_s gives

$$T_s = T_\infty + \frac{\dot{e}_{gen}V}{hA_s} \qquad \textbf{(2–66)}$$

For a large *plane wall* of thickness $2L$ ($A_s = 2A_{wall}$ and $V = 2LA_{wall}$) with both sides of the wall maintained at the same temperature T_s, a long solid *cylinder* of radius r_o ($A_s = 2\pi r_o L$ and $V = \pi r_o^2 L$), and a solid *sphere* of radius r_o ($A_s = 4\pi r_o^2$ and $V = \frac{4}{3}\pi r_o^3$), Eq. 2–66 reduces to

$$T_{s,\,\text{plane wall}} = T_\infty + \frac{\dot{e}_{gen}L}{h} \qquad \textbf{(2–67)}$$

$$T_{s,\,\text{cylinder}} = T_\infty + \frac{\dot{e}_{gen}r_o}{2h} \qquad \textbf{(2–68)}$$

$$T_{s,\,\text{sphere}} = T_\infty + \frac{\dot{e}_{gen}r_o}{3h} \qquad \textbf{(2–69)}$$

FIGURE 2–56
Heat conducted through a cylindrical shell of radius r is equal to the heat generated within a shell.
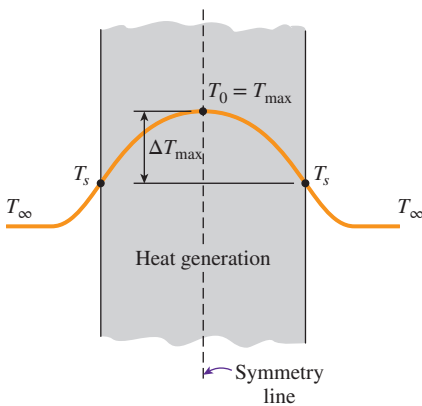
FIGURE 2–57
The maximum temperature in a symmetrical solid with uniform heat generation occurs at its center.

Note that the rise in surface temperature T_s is due to heat generation in the solid.

Reconsider heat transfer from a long solid cylinder with heat generation. We mentioned that, under *steady* conditions, all heat generated within the medium is conducted through the outer surface of the cylinder. Now consider an imaginary inner cylinder of radius r within the cylinder (Fig. 2–56). Again the *heat generated* within this inner cylinder must be equal to the *heat conducted* through its outer surface. That is, from Fourier's law of heat conduction,

$$-kA_r\frac{dT}{dr} = \dot{e}_{gen}V_r \qquad (2\text{–}70)$$

where $A_r = 2\pi rL$ and $V_r = \pi r^2 L$ at any location r. Substituting these expressions into Eq. 2–70 and separating the variables, we get

$$-k(2\pi rL)\frac{dT}{dr} = \dot{e}_{gen}(\pi r^2 L) \quad \rightarrow \quad dT = -\frac{\dot{e}_{gen}}{2k}r\,dr$$

Integrating from $r = 0$ where $T(0) = T_0$ to $r = r_o$ where $T(r_o) = T_s$ yields

$$\Delta T_{max,\,cylinder} = T_0 - T_s = \frac{\dot{e}_{gen}r_o^2}{4k} \qquad (2\text{–}71)$$

where T_0 is the centerline temperature of the cylinder, which is the *maximum temperature,* and ΔT_{max} is the difference between the centerline and the surface temperatures of the cylinder, which is the *maximum temperature rise* in the cylinder above the surface temperature. Once ΔT_{max} is available, the centerline temperature can easily be determined from (Fig. 2–57)

$$T_{center} = T_0 = T_s + \Delta T_{max} \qquad (2\text{–}72)$$

The approach outlined here can also be used to determine the *maximum temperature rise* in a plane wall of thickness $2L$ with both sides of the wall maintained at the same temperature T_s and a solid sphere of radius r_o, with these results:

$$\Delta T_{max,\,plane\,wall} = \frac{\dot{e}_{gen}L^2}{2k} \qquad (2\text{–}73)$$

$$\Delta T_{max,\,sphere} = \frac{\dot{e}_{gen}r_o^2}{6k} \qquad (2\text{–}74)$$

Again the maximum temperature at the center can be determined from Eq. 2–72 by adding the maximum temperature rise to the surface temperature of the solid.

EXAMPLE 2–17   **Centerline Temperature of a Resistance Heater**

A 2-kW resistance heater wire whose thermal conductivity is $k = 15$ W/m·K has a diameter of $D = 4$ mm and a length of $L = 0.5$ m, and it is used to boil water (Fig. 2–58). If the outer surface temperature of the resistance wire is $T_s = 105°C$, determine the temperature at the center of the wire.

FIGURE 2–58
Schematic for Example 2–17.

SOLUTION The center temperature of a resistance heater submerged in water is to be determined.

Assumptions **1** Heat transfer is steady since there is no change with time. **2** Heat transfer is one-dimensional since there is thermal symmetry about the centerline and no change in the axial direction. **3** Thermal conductivity is constant. **4** Heat generation in the heater is uniform.

Properties The thermal conductivity is given to be $k = 15$ W/m·K.

Analysis The 2-kW resistance heater converts electric energy into heat at a rate of 2 kW. The heat generation per unit volume of the wire is

$$\dot{e}_{gen} = \frac{\dot{E}_{gen}}{V_{wire}} = \frac{\dot{E}_{gen}}{\pi r_o^2 L} = \frac{2000 \text{ W}}{\pi (0.002 \text{ m})^2 (0.5 \text{ m})} = 0.318 \times 10^9 \text{ W/m}^3$$

Then the center temperature of the wire is determined from Eq. 2–71 to be

$$T_0 = T_s + \frac{\dot{e}_{gen} r_o^2}{4k} = 105°C + \frac{(0.318 \times 10^9 \text{ W/m}^3)(0.002 \text{ m})^2}{4 \times (15 \text{ W/m·°C})} = \mathbf{126°C}$$

Discussion Note that the temperature difference between the center and the surface of the wire is 21°C. Also, the thermal conductivity units W/m·°C and W/m·K are equivalent.

We have developed these relations using the intuitive *energy balance* approach. However, we could have obtained the same relations by setting up the appropriate *differential equations* and solving them, as illustrated in Examples 2–18 and 2–19.

EXAMPLE 2–18 **Variation of Temperature in a Resistance Heater**

A long, homogeneous resistance wire of radius $r_o = 0.2$ in and thermal conductivity $k = 7.8$ Btu/h·ft·°F is being used to boil water at atmospheric pressure by the passage of electric current, as shown in Fig. 2–59. Heat is generated in the wire uniformly as a result of resistance heating at a rate of $\dot{e}_{gen} = 2400$ Btu/h·in³. If the outer surface temperature of the wire is measured to be $T_s = 226°F$, obtain a relation for the temperature distribution, and determine the temperature at the centerline of the wire when steady operating conditions are reached.

SOLUTION This heat transfer problem is similar to Example 2–17, except that we need to obtain a relation for the variation of temperature within the wire with *r*. Differential equations are well suited for this purpose.

Assumptions **1** Heat transfer is steady since there is no change with time. **2** Heat transfer is one-dimensional since there is no thermal symmetry about the centerline and no change in the axial direction. **3** Thermal conductivity is constant. **4** Heat generation in the wire is uniform.

Properties The thermal conductivity is given to be $k = 7.8$ Btu/h·ft·°F.

Analysis The differential equation which governs the variation of temperature in the wire is simply Eq. 2–27,

$$\frac{1}{r}\frac{d}{dr}\left(r\frac{dT}{dr}\right) + \frac{\dot{e}_{gen}}{k} = 0$$
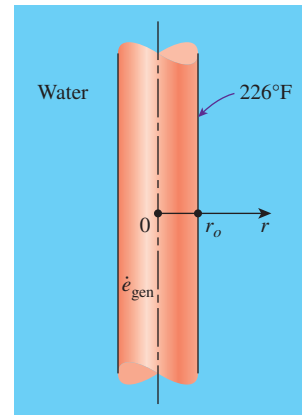
FIGURE 2–59
Schematic for Example 2–18.
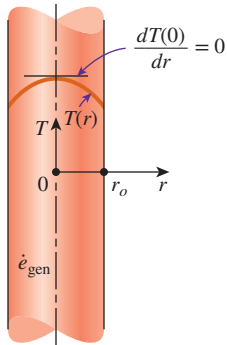
FIGURE 2–60
The thermal symmetry condition at the centerline of a wire in which heat is generated uniformly.

This is a second-order linear ordinary differential equation, and thus its general solution contains two arbitrary constants. The determination of these constants requires the specification of two boundary conditions, which can be taken to be

$$T(r_o) = T_s = 226°F$$

and

$$\frac{dT(0)}{dr} = 0$$

The first boundary condition simply states that the temperature of the outer surface of the wire is 226°F. The second boundary condition is the symmetry condition at the centerline, and it states that the maximum temperature in the wire occurs at the centerline, and thus the slope of the temperature at $r = 0$ must be zero (Fig. 2–60). This completes the mathematical formulation of the problem.

Although not immediately obvious, the differential equation is in a form that can be solved by direct integration. Multiplying both sides of the equation by r and rearranging, we obtain

$$\frac{d}{dr}\left(r\frac{dT}{dr}\right) = -\frac{\dot{e}_{gen}}{k}r$$

Integrating with respect to r gives

$$r\frac{dT}{dr} = -\frac{\dot{e}_{gen}}{k}\frac{r^2}{2} + C_1 \tag{a}$$

since the heat generation is constant, and the integral of a derivative of a function is the function itself. That is, integration removes a derivative. It is convenient at this point to apply the second boundary condition, since it is related to the first derivative of the temperature, by replacing all occurrences of r and dT/dr in Eq. (a) with zero. It yields

$$0 \times \frac{dT(0)}{dr} = -\frac{\dot{e}_{gen}}{2k} \times 0 + C_1 \rightarrow C_1 = 0$$

Thus C_1 cancels from the solution. We now divide Eq. (a) by r to bring it to a readily integrable form,

$$\frac{dT}{dr} = -\frac{\dot{e}_{gen}}{2k}r$$

Again integrating with respect to r gives

$$T(r) = -\frac{\dot{e}_{gen}}{4k}r^2 + C_2 \tag{b}$$

We now apply the first boundary condition by replacing all occurrences of r with r_0 and all occurrences of T with T_s. We get

$$T_s = -\frac{\dot{e}_{gen}}{4k}r_o^2 + C_2 \rightarrow C_2 = T_s + \frac{\dot{e}_{gen}}{4k}r_o^2$$

Substituting this C_2 relation into Eq. (*b*) and rearranging give

$$T(r) = T_s + \frac{\dot{e}_{gen}}{4k}(r_o^2 - r^2) \qquad \text{(c)}$$

which is the desired solution for the temperature distribution in the wire as a function of r. The temperature at the centerline ($r = 0$) is obtained by replacing r in Eq. (*c*) with zero and substituting the known quantities,

$$T(0) = T_s + \frac{\dot{e}_{gen}}{4k}r_o^2 = 226°F + \frac{2400 \text{ Btu/h·in}^3}{4 \times (7.8 \text{ Btu/h·ft·°F})}\left(\frac{12 \text{ in}}{1 \text{ ft}}\right)(0.2 \text{ in})^2 = \mathbf{263°F}$$

Discussion The temperature of the centerline is 37°F above the temperature of the outer surface of the wire. Note that the expression above for the centerline temperature is identical to Eq. 2–71, which was obtained using an energy balance on a control volume.

EXAMPLE 2–19   Heat Conduction in a Two-Layer Medium

Consider a long resistance wire of radius $r_1 = 0.2$ cm and thermal conductivity $k_{wire} = 15$ W/m·K in which heat is generated uniformly as a result of resistance heating at a constant rate of $\dot{e}_{gen} = 50$ W/cm^3 (Fig. 2–61). The wire is embedded in a 0.5-cm-thick layer of ceramic whose thermal conductivity is $k_{ceramic} = 1.2$ W/m·K. If the outer surface temperature of the ceramic layer is measured to be $T_s = 45°C$, determine the temperatures at the center of the resistance wire and the interface of the wire and the ceramic layer under steady conditions.

SOLUTION The surface and interface temperatures of a resistance wire covered with a ceramic layer are to be determined.
Assumptions **1** Heat transfer is steady since there is no change with time. **2** Heat transfer is one-dimensional since this two-layer heat transfer problem possesses symmetry about the centerline and involves no change in the axial direction, and thus $T = T(r)$. **3** Thermal conductivities are constant. **4** Heat generation in the wire is uniform.
Properties It is given that $k_{wire} = 15$ W/m·K and $k_{ceramic} = 1.2$ W/m·K.
Analysis Letting T_1 denote the unknown interface temperature, the heat transfer problem in the wire can be formulated as

$$\frac{1}{r}\frac{d}{dr}\left(r\frac{dT_{wire}}{dr}\right) + \frac{\dot{e}_{gen}}{k} = 0$$

with

$$T_{wire}(r_1) = T_1$$
$$\frac{dT_{wire}(0)}{dr} = 0$$

This problem was solved in Example 2–18, and its solution was determined to be

$$T_{wire}(r) = T_1 + \frac{\dot{e}_{gen}}{4k_{wire}}(r_1^2 - r^2) \qquad \text{(a)}$$

Interface

Wire r_1

r_2

$T_s = 45°C$

r
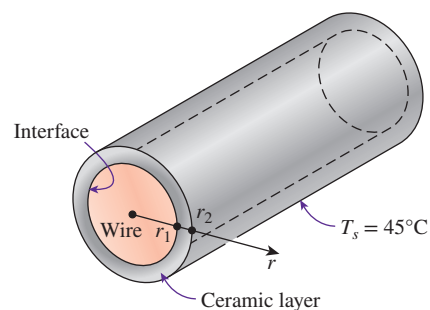
Ceramic layer

FIGURE 2–61
Schematic for Example 2–19.

Noting that the ceramic layer does not involve any heat generation and its outer surface temperature is specified, the heat conduction problem in that layer can be expressed as

$$\frac{d}{dr}\left(r\frac{dT_{\text{ceramic}}}{dr}\right) = 0$$

with

$$T_{\text{ceramic}}(r_1) = T_1$$
$$T_{\text{ceramic}}(r_2) = T_s = 45°\text{C}$$

This problem was solved in Example 2–16, and its solution was determined to be

$$T_{\text{ceramic}}(r) = \frac{\ln(r/r_1)}{\ln(r_2/r_1)}(T_s - T_1) + T_1 \qquad \textbf{(b)}$$

We have already utilized the first interface condition by setting the wire and ceramic layer temperatures equal to T_1 at the interface $r = r_1$. The interface temperature T_1 is determined from the second interface condition that the heat flux in the wire and the ceramic layer at $r = r_1$ must be the same:

$$-k_{\text{wire}}\frac{dT_{\text{wire}}(r_1)}{dr} = -k_{\text{ceramic}}\frac{dT_{\text{ceramic}}(r_1)}{dr} \quad \rightarrow \quad \frac{\dot{e}_{\text{gen}}r_1}{2} = -k_{\text{ceramic}}\frac{T_s - T_1}{\ln(r_2/r_1)}\left(\frac{1}{r_1}\right)$$

Solving for T_1 and substituting the given values, the interface temperature is determined to be

$$T_1 = \frac{\dot{e}_{\text{gen}}r_1^2}{2k_{\text{ceramic}}}\ln\frac{r_2}{r_1} + T_s$$

$$= \frac{(50 \times 10^6 \text{ W/m}^3)(0.002 \text{ m})^2}{2(1.2 \text{ W/m·K})} \ln\frac{0.007 \text{ m}}{0.002 \text{ m}} + 45°\text{C} = \textbf{149.4°C}$$

Knowing the interface temperature, the temperature at the centerline $(r = 0)$ is obtained by substituting the known quantities into Eq. (a),

$$T_{\text{wire}}(0) = T_I + \frac{\dot{e}_{\text{gen}}r_1^2}{4k_{\text{wire}}} = 149.4°\text{C} + \frac{(50 \times 10^6 \text{ W/m}^3)(0.002 \text{ m})^2}{4 \times (15 \text{ W/m·K})} = \textbf{152.7°C}$$

Thus the temperature of the centerline is slightly above the interface temperature.

Discussion   This example demonstrates how steady one-dimensional heat conduction problems in composite media can be solved. We could also solve this problem by determining the heat flux at the interface by dividing the total heat generated in the wire by the surface area of the wire and then using this value as the specified heat flux boundary condition for both the wire and the ceramic layer. This way the two problems are decoupled and can be solved separately.

EXAMPLE 2–20 Heat Conduction in a Plane Wall with Heat Generation

A large plane wall of thickness $2L$ experiences uniform heat generation (Fig. 2–62). Determine the expression for the variation of temperature within the wall, if (*a*) $T_1 > T_2$ and (*b*) $T_1 = T_2$.

SOLUTION A large plane wall experiences uniform heat generation. The expressions for the variation of temperature within the wall for $T_1 > T_2$ and $T_1 = T_2$ are to be determined.

Assumptions **1** Heat conduction is steady. **2** Heat conduction is one-dimensional. **3** Thermal conductivity is constant. **4** Heat generation is uniform.

Analysis We begin with the general heat conduction equation for rectangular coordinates,

$$\frac{\partial}{\partial x}\left(k\frac{\partial T}{\partial x}\right) + \frac{\partial}{\partial y}\left(k\frac{\partial T}{\partial y}\right) + \frac{\partial}{\partial z}\left(k\frac{\partial T}{\partial z}\right) + \dot{e}_{gen} = \rho c \frac{\partial T}{\partial t}$$

For steady one-dimensional heat conduction and constant thermal conductivity, the general heat conduction equation is simplified to

$$\frac{d^2T}{dx^2} + \frac{\dot{e}_{gen}}{k} = 0$$

Integrating twice gives the general solution to this second-order differential equation as

$$T(x) = -\frac{\dot{e}_{gen}}{2k}x^2 + C_1 x + C_2$$

(*a*) For the case of asymmetrical boundary conditions with $T_1 > T_2$, applying the boundary conditions gives

$$x = -L: \quad T(-L) = T_1 = -\frac{\dot{e}_{gen}}{2k}L^2 - C_1 L + C_2$$

$$x = L: \quad T(L) = T_2 = -\frac{\dot{e}_{gen}}{2k}L^2 + C_1 L + C_2$$

Note that in this problem the coordinate system is placed at the middle of the plane wall ($x = 0$), and x to the right of the centerline is considered positive and to the left negative. In analyzing plane wall problems with heat generation, this notation is usually adopted in order to better capture the effect of heat generation on the temperature profile. Solving for the constants C_1 and C_2 yields

$$C_1 = \frac{T_2 - T_1}{2L} \quad \text{and} \quad C_2 = \frac{\dot{e}_{gen}}{2k}L^2 + \frac{T_1 + T_2}{2}$$

Substituting C_1 and C_2 expressions into the general solution, the variation of temperature within the wall is determined to be

$$T(x) = \frac{\dot{e}_{gen}L^2}{2k}\left(1 - \frac{x^2}{L^2}\right) + \frac{T_2 - T_1}{2}\left(\frac{x}{L}\right) + \frac{T_1 + T_2}{2} \qquad \text{(a)}$$
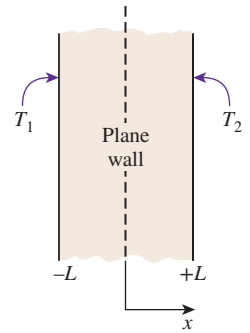
FIGURE 2–62
Schematic for Example 2–20.

(*b*) For the case of symmetrical boundary conditions, substituting $T_2 = T_1$ into Eq. (*a*) gives

$$T(x) = \frac{\dot{e}_{gen}L^2}{2k}\left(1 - \frac{x^2}{L^2}\right) + T_1 \qquad \qquad \textbf{(b)}$$

Discussion Equation (*a*) shows that the variation of temperature within the wall for the case of asymmetrical boundary conditions with $T_1 > T_2$ is not symmetric, and the maximum temperature occurs to the left of the centerline. Note that Eq. (*a*) reduces to the temperature solution of Example 2–10 (Eq. 2–56) for heat conduction in a plane wall with no heat generation by setting $\dot{e}_{gen} = 0$ and making the appropriate coordinate transformation. In the case of symmetrical boundary conditions ($T_1 = T_2$), Eq. (*b*) shows that the variation of temperature within the wall is symmetric, and the maximum temperature occurs at the centerline. This is comparable to the results shown in Example 2–17 for temperature variation in a cylindrical resistance heater.
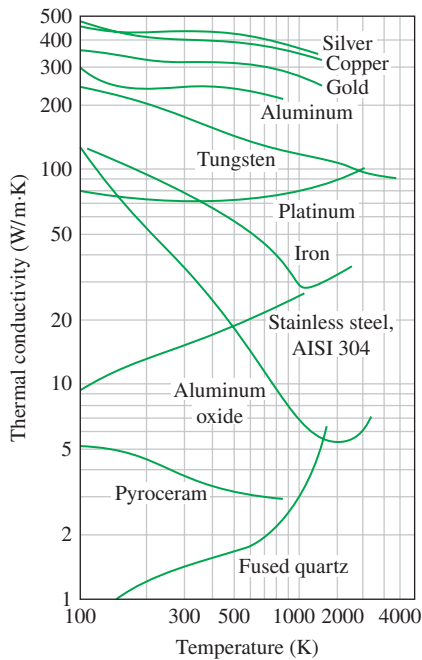
FIGURE 2–63
Variation of the thermal conductivity of some solids with temperature.

2–7 ▪ VARIABLE THERMAL CONDUCTIVITY, *k*(*T*)

You will recall from Chap. 1 that the thermal conductivity of a material, in general, varies with temperature (Fig. 2–63). However, this variation is mild for many materials in the range of practical interest and can be disregarded. In such cases, we can use an average value for the thermal conductivity and treat it as a constant, as we have been doing so far. This is also common practice for other temperature-dependent properties such as the density and specific heat.

When the variation of thermal conductivity with temperature in a specified temperature interval is large, however, it may be necessary to account for this variation to minimize the error. Accounting for the variation of the thermal conductivity with temperature, in general, complicates the analysis. But in the case of simple one-dimensional cases, we can obtain heat transfer relations in a straightforward manner.

When the variation of thermal conductivity with temperature $k(T)$ is known, the average value of the thermal conductivity in the temperature range between T_1 and T_2 can be determined from

$$k_{avg} = \frac{\int_{T_1}^{T_2} k(T)\,dT}{T_2 - T_1} \qquad \qquad \textbf{(2–75)}$$

This relation is based on the requirement that the rate of heat transfer through a medium with constant average thermal conductivity k_{avg} equals the rate of heat transfer through the same medium with variable conductivity $k(T)$. Note that in the case of constant thermal conductivity $k(T) = k$, Eq. 2–75 reduces to $k_{avg} = k$, as expected.

Then the rate of steady heat transfer through a plane wall, cylindrical layer, or spherical layer for the case of variable thermal conductivity can be

determined by replacing the constant thermal conductivity k in Eqs. 2–57, 2–59, and 2–61 with the k_{avg} expression (or value) from Eq. 2–75:

$$\dot{Q}_{\text{plane wall}} = k_{\text{avg}} A \frac{T_1 - T_2}{L} = \frac{A}{L} \int_{T_2}^{T_1} k(T) dT \qquad \text{(2–76)}$$

$$\dot{Q}_{\text{cylinder}} = 2\pi k_{\text{avg}} L \frac{T_1 - T_2}{\ln(r_2/r_1)} = \frac{2\pi L}{\ln(r_2/r_1)} \int_{T_2}^{T_1} k(T) dT \qquad \text{(2–77)}$$

$$\dot{Q}_{\text{sphere}} = 4\pi k_{\text{avg}} r_1 r_2 \frac{T_1 - T_2}{r_2 - r_1} = \frac{4\pi r_1 r_2}{r_2 - r_1} \int_{T_2}^{T_1} k(T) dT \qquad \text{(2–78)}$$

The variation in thermal conductivity of a material with temperature in the temperature range of interest can often be approximated as a linear function and expressed as

$$k(T) = k_0(1 + \beta T) \qquad \text{(2–79)}$$

where β is called the **temperature coefficient of thermal conductivity**. The *average* value of thermal conductivity in the temperature range T_1 to T_2 in this case can be determined from

$$k_{\text{avg}} = \frac{\int_{T_1}^{T_2} k_0(1 + \beta T) dT}{T_2 - T_1} = k_0 \left(1 + \beta \frac{T_2 + T_1}{2}\right) = k(T_{\text{avg}}) \qquad \text{(2–80)}$$

Note that the *average thermal conductivity* in this case is equal to the thermal conductivity value at the *average temperature.*

We mentioned earlier that in a plane wall the temperature varies linearly during steady one-dimensional heat conduction when the thermal conductivity is constant. But this is no longer the case when the thermal conductivity changes with temperature, even linearly, as shown in Fig. 2–64.
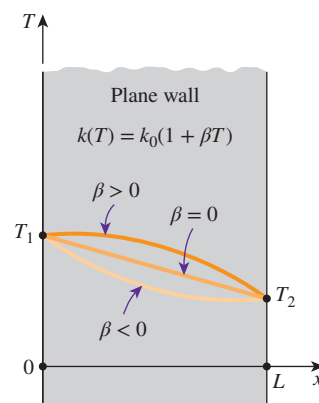
FIGURE 2–64
The variation of temperature in a plane wall during steady one-dimensional heat conduction for the cases of constant and variable thermal conductivity.

FIGURE 2–65
Schematic for Example 2–21.

■ **EXAMPLE 2–21**   **Variation of Temperature in a Wall with $k(T)$**

Consider a plane wall of thickness L whose thermal conductivity varies linearly in a specified temperature range as $k(T) = k_0(1 + \beta T)$ where k_0 and β are constants. The wall surface at $x = 0$ is maintained at a constant temperature of T_1 while the surface at $x = L$ is maintained at T_2, as shown in Fig. 2–65. Assuming steady one-dimensional heat transfer, obtain a relation for (*a*) the heat transfer rate through the wall and (*b*) the temperature distribution $T(x)$ in the wall.

SOLUTION   A plate with variable conductivity is subjected to specified temperatures on both sides. The variation of temperature and the rate of heat transfer are to be determined.
Assumptions   **1** Heat transfer is given to be steady and one-dimensional. **2** Thermal conductivity varies linearly. **3** There is no heat generation.
Properties   The thermal conductivity is given to be $k(T) = k_0(1 + \beta T)$.
Analysis   (*a*) The rate of heat transfer through the wall can be determined from

$$\dot{Q} = k_{\text{avg}} A \frac{T_1 - T_2}{L}$$

where A is the heat conduction area of the wall and

$$k_{\text{avg}} = k(T_{\text{avg}}) = k_0\left(1 + \beta\frac{T_2 + T_1}{2}\right)$$

is the average thermal conductivity (Eq. 2–80).

(*b*) To determine the temperature distribution in the wall, we begin with Fourier's law of heat conduction, expressed as

$$\dot{Q} = -k(T)\,A\frac{dT}{dx}$$

where the rate of conduction heat transfer $\dot{Q}$ and the area A are constant. Separating variables and integrating from $x = 0$ where $T(0) = T_1$ to any x where $T(x) = T$, we get

$$\int_0^x \dot{Q}dx = -A\int_{T_1}^T k(T)dT$$

Substituting $k(T) = k_0(1 + \beta T)$ and performing the integrations, we obtain

$$\dot{Q}x = -Ak_0[(T - T_1) + \beta(T^2 - T_1^2)/2]$$

Substituting the $\dot{Q}$ expression from part (*a*) and rearranging give

$$T^2 + \frac{2}{\beta}T + \frac{2k_{\text{avg}}}{\beta k_0}\frac{x}{L}(T_1 - T_2) - T_1^2 - \frac{2}{\beta}T_1 = 0$$

which is a *quadratic* equation in the unknown temperature T. Using the quadratic formula, the temperature distribution $T(x)$ in the wall is determined to be

$$T(x) = -\frac{1}{\beta} \pm \sqrt{\frac{1}{\beta^2} - \frac{2k_{\text{avg}}}{\beta k_0}\frac{x}{L}(T_1 - T_2) + T_1^2 + \frac{2}{\beta}T_1}$$

Discussion The proper sign of the square root term (+ or −) is determined from the requirement that the temperature at any point within the medium must remain between T_1 and T_2. This result explains why the temperature distribution in a plane wall is no longer a straight line when the thermal conductivity varies with temperature.
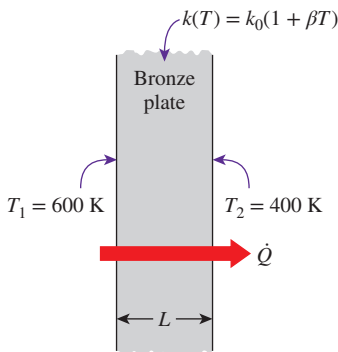
FIGURE 2–66
Schematic for Example 2–22.

EXAMPLE 2–22   Heat Conduction Through a Wall with *k*(*T*)

Consider a 2-m-high and 0.7-m-wide bronze plate whose thickness is 0.1 m. One side of the plate is maintained at a constant temperature of 600 K while the other side is maintained at 400 K, as shown in Fig. 2–66. The thermal conductivity of the bronze plate can be assumed to vary linearly in that temperature range as $k(T) = k_0(1 + \beta T)$ where $k_0 = 38$ W/m·K and $\beta = 9.21 \times 10^{-4}$ K^{-1}. Disregarding the edge effects and assuming steady one-dimensional heat transfer, determine the rate of heat conduction through the plate.

SOLUTION   A plate with variable conductivity is subjected to specified temperatures on both sides. The rate of heat transfer is to be determined.
Assumptions   **1** Heat transfer is given to be steady and one-dimensional. **2** Thermal conductivity varies linearly. **3** There is no heat generation.

Properties   The thermal conductivity is given to be $k(T) = k_0(1 + \beta T)$.

Analysis   The average thermal conductivity of the medium in this case is simply the value at the average temperature and is determined from

$$k_{avg} = k(T_{avg}) = k_0\left(1 + \beta\frac{T_2 + T_1}{2}\right)$$

$$= (38 \text{ W/m·K})\left[1 + (9.21 \times 10^{-4}\text{ K}^{-1})\frac{(600 + 400)\text{ K}}{2}\right]$$

$$= 55.5 \text{ W/m·K}$$

Then the rate of heat conduction through the plate can be determined from Eq. 2–76 to be

$$\dot{Q} = k_{avg}A\frac{T_1 - T_2}{L}$$

$$= (55.5 \text{ W/m·K})(2 \text{ m} \times 0.7 \text{ m})\frac{(600 - 400)\text{K}}{0.1 \text{ m}} = \textbf{155 kW}$$

Discussion   We would have obtained the same result by substituting the given $k(T)$ relation into the second part of Eq. 2–76 and performing the indicated integration.

TOPIC OF SPECIAL INTEREST*

A Brief Review of Differential Equations

As we mentioned in Chap. 1, the description of most scientific problems involves relations that involve changes in some key variables with respect to each other. Usually the smaller the increment chosen in the changing variables, the more general and accurate the description. In the limiting case of infinitesimal or differential changes in variables, we obtain *differential equations,* which provide precise mathematical formulations for the physical principles and laws by representing the rates of change as *derivatives.* Therefore, differential equations are used to investigate a wide variety of problems in sciences and engineering, including heat transfer.

Differential equations arise when relevant *physical laws* and *principles* are applied to a problem by considering infinitesimal changes in the variables of interest. Therefore, obtaining the governing differential equation for a specific problem requires an adequate knowledge of the nature of the problem, the variables involved, appropriate simplifying assumptions, and the applicable physical laws and principles involved, as well as a careful analysis.

An equation, in general, may involve one or more variables. As the name implies, a **variable** is a quantity that may assume various values during a study. A quantity whose value is fixed during a study is called a **constant**. Constants are usually denoted by the earlier letters of the alphabet, such as *a, b, c,* and *d,* whereas variables are usually denoted by the later ones, such

* This section can be skipped without a loss in continuity.
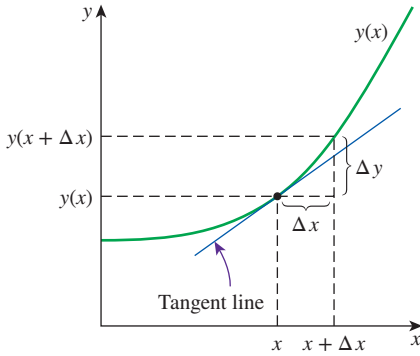
FIGURE 2–67
The derivative of a function at a point represents the slope of the tangent line of the function at that point.

as t, x, y, and z. A variable whose value can be changed arbitrarily is called an **independent variable** (or argument). A variable whose value depends on the value of other variables and thus cannot be varied independently is called a **dependent variable** (or a function).

A dependent variable y that depends on a variable x is usually denoted as $y(x)$ for clarity. However, this notation becomes very inconvenient and cumbersome when y is repeated several times in an expression. In such cases it is desirable to denote $y(x)$ simply as y when it is clear that y is a function of x. This shortcut in notation improves the appearance and the readability of the equations. The value of y at a fixed number a is denoted by $y(a)$.

The **derivative** of a function $y(x)$ at a point is equivalent to the *slope* of the tangent line to the graph of the function at that point and is defined as (Fig. 2–67)

$$y'(x) = \frac{dy(x)}{dx} = \lim_{\Delta x \to 0} \frac{\Delta y}{\Delta x} = \lim_{\Delta x \to 0} \frac{y(x + \Delta x) - y(x)}{\Delta x} \qquad \textbf{(2–81)}$$

Here Δx represents a (small) change in the independent variable x and is called an *increment* of x. The corresponding change in the function y is called an increment of y and is denoted by Δy. Therefore, the derivative of a function can be viewed as the ratio of the increment Δy of the function to the increment Δx of the independent variable for very small Δx. Note that Δy and thus $y'(x)$ are zero if the function y does not change with x.

Most problems encountered in practice involve quantities that change with time t, and their first derivatives with respect to time represent the rate of change of those quantities with time. For example, if $N(t)$ denotes the population of a bacteria colony at time t, then the first derivative $N' = dN/dt$ represents the rate of change of the population, which is the amount the population increases or decreases per unit time.

The derivative of the first derivative of a function y is called the *second derivative* of y and is denoted by y'' or d^2y/dx^2. In general, the derivative of the $(n-1)$st derivative of y is called the nth derivative of y and is denoted by $y^{(n)}$ or $d^n y/dx^n$. Here, n is a positive integer and is called the *order* of the derivative. The order n should not be confused with the *degree* of a derivative. For example, y''' is the third-order derivative of y, but $(y')^3$ is the third degree of the first derivative of y. Note that the first derivative of a function represents the *slope* or the *rate of change* of the function with the independent variable, and the second derivative represents the *rate of change of the slope* of the function with the independent variable.

When a function y depends on two or more independent variables such as x and t, it is sometimes of interest to examine the dependence of the function on only one of the variables. This is done by taking the derivative of the function with respect to that variable while holding the other variables constant. Such derivatives are called **partial derivatives**. The first partial derivatives of the function $y(x, t)$ with respect to x and t are defined as (Fig. 2–68)

$$\frac{\partial y}{\partial x} = \lim_{\Delta x \to 0} \frac{y(x + \Delta x, t) - y(x, t)}{\Delta x} \qquad \textbf{(2–82)}$$
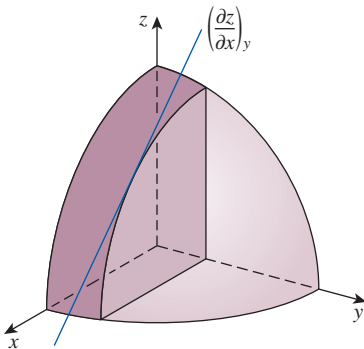
FIGURE 2–68
Graphical representation of partial derivative $\partial z/\partial x$.

$$\frac{\partial y}{\partial t} = \lim_{\Delta x \to 0} \frac{y(x, t + \Delta t) - y(x, t)}{\Delta t} \tag{2-83}$$

Note that when finding $\partial y/\partial x$ we treat t as a constant and differentiate y with respect to x. Likewise, when finding $\partial y/\partial t$ we treat x as a constant and differentiate y with respect to t.

Integration can be viewed as the inverse of differentiation. Integration is commonly used in solving differential equations since solving a differential equation is essentially a process of removing the derivatives from the equation. Differentiation is the process of finding $y'(x)$ when a function $y(x)$ is given, whereas integration is the process of finding the function $y(x)$ when its derivative $y'(x)$ is given. The integral of this derivative is expressed as

$$\int y'(x)dx = \int dy = y(x) + C \tag{2-84}$$

since $y'(x)dx = dy$ and the integral of the differential of a function is the function itself (plus a constant, of course). In Eq. 2–84, x is the integration variable and C is an arbitrary constant called the **integration constant**.

The derivative of $y(x) + C$ is $y'(x)$ no matter what the value of the constant C is. Therefore, two functions that differ by a constant have the same derivative, and we always add a constant C during integration to recover this constant that is lost during differentiation. The integral in Eq. 2–84 is called an **indefinite integral** since the value of the arbitrary constant C is indefinite. The described procedure can be extended to higher-order derivatives (Fig. 2–69). For example,

$$\int y''(x)\,dx = y'(x) + C \tag{2-85}$$

This can be proved by defining a new variable $u(x) = y'(x)$, differentiating it to obtain $u'(x) = y''(x)$, and then applying Eq. 2–84. Therefore, the order of a derivative decreases by one each time it is integrated.

Classification of Differential Equations

A differential equation that involves only ordinary derivatives is called an **ordinary differential equation**, and a differential equation that involves partial derivatives is called a **partial differential equation**. Then it follows that problems that involve a single independent variable result in ordinary differential equations, and problems that involve two or more independent variables result in partial differential equations. A differential equation may involve several derivatives of various orders of an unknown function. The order of the highest derivative in a differential equation is the order of the equation. For example, the order of $y''' + (y'')^4 = 7x^5$ is 3 since it contains no fourth or higher order derivatives.

You will remember from algebra that the equation $3x - 5 = 0$ is much easier to solve than the equation $x^4 + 3x - 5 = 0$ because the first equation is linear whereas the second one is nonlinear. This is also true for differential equations. Therefore, before we start solving a differential equation,

$$\int dy = y + C$$
$$\int y'dx = y + C$$
$$\int y''dx = y' + C$$
$$\int y'''dx = y'' + C$$
$$\int y^{(n)}dx = y^{(n-1)} + C$$
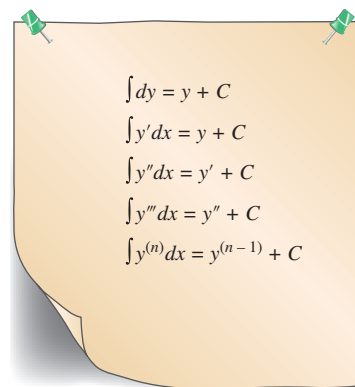
FIGURE 2–69
Some indefinite integrals that involve derivatives.
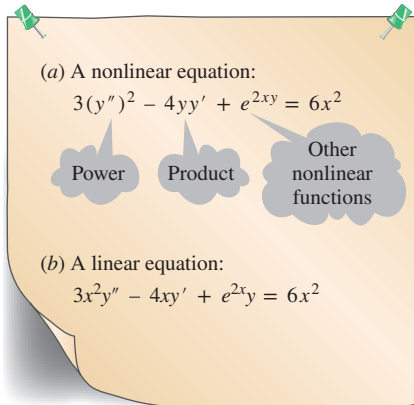
FIGURE 2–70
A differential equation that is
(*a*) nonlinear and (*b*) linear. When
checking for linearity, we examine
the dependent variable only.
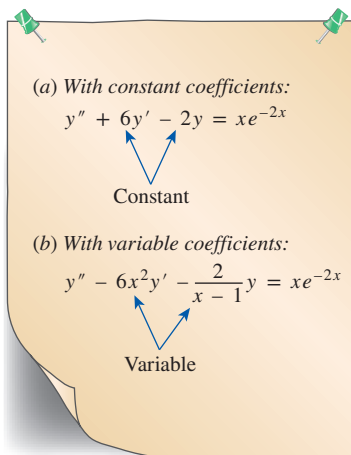
FIGURE 2–71
A differential equation with
(*a*) constant coefficients and
(*b*) variable coefficients.

we usually check for linearity. A differential equation is said to be **linear** if the dependent variable and all of its derivatives are of the first degree and their coefficients depend on the independent variable only. In other words, a differential equation is linear if it can be written in a form that does not involve (1) any powers of the dependent variable or its derivatives such as y^3 or $(y')^2$, (2) any products of the dependent variable or its derivatives such as $y y'$ or $y' y'''$, and (3) any other nonlinear functions of the dependent variable such as $\sin y$ or e^y. If any of these conditions apply, it is **nonlinear** (Fig. 2–70).

A linear differential equation, however, may contain (1) powers or non-linear functions of the independent variable, such as x^2 and $\cos x$ and (2) products of the dependent variable (or its derivatives) and functions of the independent variable, such as $x^3 y'$, $x^2 y$, and $e^{-2x} y''$. A linear differential equation of order n can be expressed in the most general form as

$$y^{(n)} + f_1(x)y^{(n-1)} + \cdots + f_{n-1}(x)y' + f_n(x)y = R(x) \qquad \textbf{(2–86)}$$

A differential equation that cannot be put into this form is nonlinear. A linear differential equation in y is said to be **homogeneous** as well if $R(x) = 0$. Otherwise, it is nonhomogeneous. That is, each term in a linear homogeneous equation contains the dependent variable or one of its derivatives after the equation is cleared of any common factors. The term $R(x)$ is called the *nonhomogeneous term.*

Differential equations are also classified by the nature of the coefficients of the dependent variable and its derivatives. A differential equation is said to have **constant coefficients** if the coefficients of all the terms that involve the dependent variable or its derivatives are constants. If, after clearing any common factors, any of the terms with the dependent variable or its derivatives involve the independent variable as a coefficient, that equation is said to have **variable coefficients** (Fig. 2–71). Differential equations with constant coefficients are usually much easier to solve than those with variable coefficients.

Solutions of Differential Equations

Solving a differential equation can be as easy as performing one or more integrations, but such simple differential equations are usually the exception rather than the rule. There is no single general solution method applicable to all differential equations. There are different solution techniques, each being applicable to different classes of differential equations. Sometimes solving a differential equation requires the use of two or more techniques as well as ingenuity and mastery of solution methods. Some differential equations can be solved only by using some very clever tricks. Some cannot be solved analytically at all.

In algebra, we usually seek discrete values that satisfy an algebraic equation such as $x^2 - 7x - 10 = 0$. When dealing with differential equations, however, we seek functions that satisfy the equation in a specified interval. For example, the algebraic equation $x^2 - 7x - 10 = 0$ is satisfied by two

numbers only: 2 and 5. But the differential equation $y' - 7y = 0$ is satisfied by the function e^{7x} for any value of x (Fig. 2–72).

Consider the algebraic equation $x^3 - 6x^2 + 11x - 6 = 0$. Obviously, $x = 1$ satisfies this equation, and thus it is a solution. However, it is not the only solution to this equation. We can easily show by direct substitution that $x = 2$ and $x = 3$ also satisfy this equation, and thus they are solutions as well. But there are no other solutions to this equation. Therefore, we say that the set 1, 2, and 3 forms the complete solution to this algebraic equation.

The same line of reasoning also applies to differential equations. Typically, differential equations have multiple solutions that contain at least one arbitrary constant. Any function that satisfies the differential equation on an interval is called a *solution* to that differential equation in that interval. A solution that involves one or more arbitrary constants represents a family of functions that satisfy the differential equation and is called a **general solution** to that equation. Not surprisingly, a differential equation may have more than one general solution. A general solution is usually referred to as the **general solution** or the **complete solution** if every solution to the equation can be obtained from it as a special case. A solution that can be obtained from a general solution by assigning particular values to the arbitrary constants is called a **specific solution**.

You will recall from algebra that a number is a solution to an algebraic equation if it satisfies the equation. For example, 2 is a solution to the equation $x^3 - 8 = 0$ because the substitution of 2 for x yields zero. Likewise, a function is a solution to a differential equation if that function satisfies the differential equation. In other words, a solution function yields identity when substituted into the differential equation. For example, it can be shown by direct substitution that the function $3e^{-2x}$ is a solution for $y'' - 4y = 0$ (Fig. 2–73).

General Solution to Selected Differential Equations

This section provides general solution to the differential equations presented in Chaps. 2 and 3. First the general solution to the one-dimensional steady-state, constant properties heat conduction equations with and without heat generation in three coordinate systems (rectangular, cylindrical, and spherical) presented in Chap. 2 are listed, followed by the general solution to the fin and the bioheat transfer equations of Chap. 3.

- 1-D steady-state heat conduction equation with constant heat generation—rectangular coordinates (Eq. 2–15)

$$\frac{d^2y}{dx^2} + S = 0$$

Solution: $y(x) = C_1x + C_2 - \frac{1}{2}Sx^2$

(*a*) *An algebraic equation:*
$$y^2 - 7y - 10 = 0$$
Solution: $y = 2$ and $y = 5$

(*b*) *A differential equation:*
$$y' - 7y = 0$$
Solution: $y = e^{7x}$
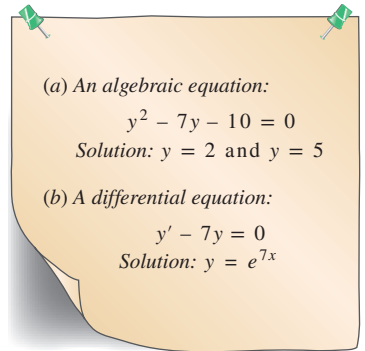
FIGURE 2–72
Unlike those of algebraic equations, the solutions of differential equations are typically functions instead of discrete values.

Function: $f = 3e^{-2x}$

Differential equation: $y'' - 4y = 0$

Derivatives of f:
$$f' = -6e^{-2x}$$
$$f'' = 12e^{-2x}$$

Substituting into $y'' - 4y = 0$:
$$f'' - 4f \overset{?}{=} 0$$
$$12e^{-2x} - 4 \times 3e^{-2x} \overset{?}{=} 0$$
$$0 = 0$$

Therefore, the function $3e^{-2x}$ is a solution for the differential equation $y'' - 4y = 0$.
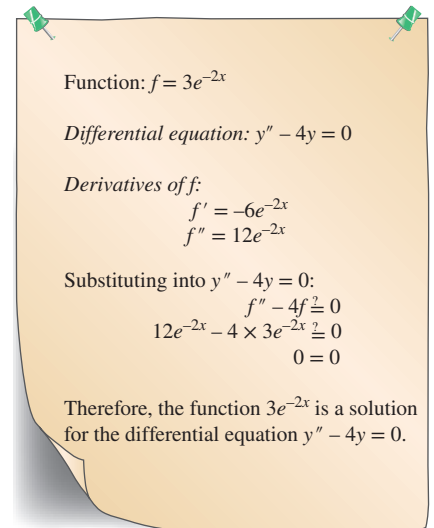
FIGURE 2–73
Verifying that a given function is a solution for a differential equation.

- 1-D steady-state heat conduction equation without heat generation—rectangular coordinates (Eq. 2–17)

$$\frac{d^2 y}{dx^2} = 0$$

Solution: $y(x) = C_1 x + C_2$

- 1-D steady-state heat conduction equation with constant heat generation—cylindrical coordinates (Eq. 2–27)

$$\frac{1}{r}\frac{d}{dr}\left(r\frac{dy}{dr}\right) + S = 0$$

Solution: $y(r) = C_1 \ln r + C_2 - \frac{1}{4}S r^2$

- 1-D steady-state heat conduction equation without heat generation—cylindrical coordinates (Eq. 2–29)

$$\frac{1}{r}\frac{d}{dr}\left(r\frac{dy}{dr}\right) = 0$$

Solution: $y(r) = C_1 \ln r + C_2$

- 1-D steady-state heat conduction equation with constant heat generation—spherical coordinates (Eq. 2–32)

$$\frac{1}{r^2}\frac{d}{dr}\left(r^2\frac{dy}{dr}\right) + S = 0$$

Solution: $y(r) = -\frac{C_1}{r} + C_2 - \frac{1}{6}S r^2$

- 1-D steady-state heat conduction equation without heat generation—spherical coordinates (Eq. 2–34)

$$\frac{d}{dr}\left(r^2\frac{dy}{dr}\right) = 0$$

Solution: $y(r) = -\frac{C_1}{r} + C_2$

- 1-D steady-state fin or bioheat transfer equations for uniform cross section with constant coefficients—rectangular coordinates (Eq. 3–56 or Eq. 3–88)

$$\frac{d^2 y}{dx^2} - \lambda^2 y = 0$$

Solution: $y(x) = C_1 e^{+\lambda x} + C_2 e^{-\lambda x}$

- Modified Bessel equation of order zero with constant coefficients (bioheat transfer equation)—cylindrical coordinates (Eq. 3–90)

$$\frac{1}{r}\frac{d}{dr}\left(r\frac{dy}{dr}\right) - B^2 y = 0$$

Solution: $y(r) = C_1 I_0(Br) + C_2 K_0(Br)$

where I_0 and K_0 are modified, zero-order Bessel functions of the first and second kinds, respectively. The values of I_0 and K_0 are given in Table 3–4.

SUMMARY

In this chapter we have studied the heat conduction equation and its solutions. Heat conduction in a medium is said to be *steady* when the temperature does not vary with time and *unsteady* or *transient* when it does. Heat conduction in a medium is said to be *one-dimensional* when conduction is significant in one dimension only and negligible in the other two dimensions. It is said to be *two-dimensional* when conduction in the third dimension is negligible and *three-dimensional* when conduction in all dimensions is significant. In heat transfer analysis, the conversion of electrical, chemical, or nuclear energy into heat (or thermal) energy is characterized as *heat generation.*

The heat conduction equation can be derived by performing an energy balance on a differential volume element. The one-dimensional heat conduction equations in rectangular, cylindrical, and spherical coordinate systems for the case of constant thermal conductivities are expressed as

$$\frac{\partial^2 T}{\partial x^2} + \frac{\dot{e}_{\text{gen}}}{k} = \frac{1}{\alpha}\frac{\partial T}{\partial t}$$

$$\frac{1}{r}\frac{\partial}{\partial r}\left(r\frac{\partial T}{\partial r}\right) + \frac{\dot{e}_{\text{gen}}}{k} = \frac{1}{\alpha}\frac{\partial T}{\partial t}$$

$$\frac{1}{r^2}\frac{\partial}{\partial r}\left(r^2\frac{\partial T}{\partial r}\right) + \frac{\dot{e}_{\text{gen}}}{k} = \frac{1}{\alpha}\frac{\partial T}{\partial t}$$

where the property $\alpha = k/\rho c$ is the *thermal diffusivity* of the material.

The solution of a heat conduction problem depends on the conditions at the surfaces, and the mathematical expressions for the thermal conditions at the boundaries are called the *boundary conditions.* The solution of transient heat conduction problems also depends on the condition of the medium at the beginning of the heat conduction process. Such a condition, which is usually specified at time $t = 0$, is called the *initial condition,* which is a mathematical expression for the temperature distribution of the medium initially. Complete mathematical description of a heat conduction problem requires the specification of two boundary conditions for each dimension along which heat conduction is significant and an initial condition when the problem is transient. The most common boundary conditions are the *specified temperature, specified heat flux, convection,* and *radiation* boundary conditions. A boundary surface, in general, may involve specified heat flux, convection, and radiation at the same time.

For steady one-dimensional heat transfer through a plate of thickness *L,* the various types of boundary conditions at the surfaces at $x = 0$ and $x = L$ can be expressed as

Specified temperature:

$$T(0) = T_1 \quad \text{and} \quad T(L) = T_2$$

where T_1 and T_2 are the specified temperatures at surfaces at $x = 0$ and $x = L$.

Specified heat flux:

$$-k\frac{dT(0)}{dx} = \dot{q}_0 \quad \text{and} \quad -k\frac{dT(L)}{dx} = \dot{q}_L$$

where $\dot{q}_0$ and $\dot{q}_L$ are the specified heat fluxes at surfaces at $x = 0$ and $x = L$.

Insulation or thermal symmetry:

$$\frac{dT(0)}{dx} = 0 \quad \text{and} \quad \frac{dT(L)}{dx} = 0$$

Convection:

$$-k\frac{dT(0)}{dx} = h_1[T_{\infty 1} - T(0)] \quad \text{and} \quad -k\frac{dT(L)}{dx} = h_2[T(L) - T_{\infty 2}]$$

where h_1 and h_2 are the convection heat transfer coefficients and $T_{\infty 1}$ and $T_{\infty 2}$ are the temperatures of the surrounding media on the two sides of the plate.

Radiation:

$$-k\frac{dT(0)}{dx} = \varepsilon_1\sigma[T_{\text{surr},1}^4 - T(0)^4] \quad \text{and}$$

$$-k\frac{dT(L)}{dx} = \varepsilon_2\sigma[T(L)^4 - T_{\text{surr},2}^4]$$

where ε_1 and ε_2 are the emissivities of the boundary surfaces, $\sigma = 5.67 \times 10^{-8}$ W/m²·K⁴ is the Stefan–Boltzmann constant, and $T_{\text{surr},1}$ and $T_{\text{surr},2}$ are the average temperatures of the surfaces surrounding the two sides of the plate. In radiation calculations, the temperatures must be in K or R.

Interface of two bodies A and B in perfect contact at $x = x_0$:

$$T_A(x_0) = T_B(x_0) \quad \text{and} \quad -k_A\frac{dT_A(x_0)}{dx} = -k_B\frac{dT_B(x_0)}{dx}$$

where k_A and k_B are the thermal conductivities of the layers *A* and *B.*

Heat generation is usually expressed *per unit volume* of the medium and is denoted by $\dot{e}_{\text{gen}}$, whose unit is W/m³. Under steady conditions, the surface temperature T_s of a plane wall of thickness 2L, a cylinder of outer radius r_0, and a sphere of radius

r_0 in which heat is generated at a constant rate of $\dot{e}_{\text{gen}}$ per unit volume in a surrounding medium at T_∞ can be expressed as

$$T_{s,\text{plane wall}} = T_\infty + \frac{\dot{e}_{\text{gen}}L}{h}$$

$$T_{s,\text{cylinder}} = T_\infty + \frac{\dot{e}_{\text{gen}}r_o}{2h}$$

$$T_{s,\text{sphere}} = T_\infty + \frac{\dot{e}_{\text{gen}}r_o}{3h}$$

where h is the convection heat transfer coefficient. The maximum temperature rise between the surface and the midsection of a medium is given by

$$\Delta T_{\text{max,plane wall}} = \frac{\dot{e}_{\text{gen}}L^2}{2k}$$

$$\Delta T_{\text{max,cylinder}} = \frac{\dot{e}_{\text{gen}}r_o^2}{4k}$$

$$\Delta T_{\text{max,sphere}} = \frac{\dot{e}_{\text{gen}}r_o^2}{6k}$$

When the variation of thermal conductivity with temperature $k(T)$ is known, the average value of the thermal conductivity in the temperature range between T_1 and T_2 can be determined from

$$k_{\text{avg}} = \frac{\displaystyle\int_{T_1}^{T_2} k(T)dT}{T_2 - T_1}$$

Then the rate of steady heat transfer through a plane wall, cylindrical layer, or spherical layer can be expressed as

$$\dot{Q}_{\text{plane wall}} = k_{\text{avg}}A\frac{T_1 - T_2}{L} = \frac{A}{L}\int_{T_2}^{T_1} k(T)dT$$

$$\dot{Q}_{\text{cylinder}} = 2\pi k_{\text{avg}}L\frac{T_1 - T_2}{\ln(r_2/r_1)} = \frac{2\pi L}{\ln(r_2/r_1)}\int_{T_2}^{T_1} k(T)dT$$

$$\dot{Q}_{\text{sphere}} = 4\pi k_{\text{avg}}r_1 r_2\frac{T_1 - T_2}{r_2 - r_1} = \frac{4\pi r_1 r_2}{r_2 - r_1}\int_{T_2}^{T_1} k(T)dT$$

The variation of thermal conductivity of a material with temperature can often be approximated as a linear function and expressed as

$$k(T) = k_0(1 + \beta T)$$

where β is called the *temperature coefficient of thermal conductivity.*

REFERENCES AND SUGGESTED READINGS

1. W. E. Boyce and R. C. Diprima. *Elementary Differential Equations and Boundary Value Problems,* 4th ed. New York: John Wiley & Sons, 1986.

2. S. S. Kutateladze. *Fundamentals of Heat Transfer.* New York: Academic Press, 1963.

PROBLEMS*

Introduction

2–1C How does transient heat transfer differ from steady heat transfer? How does one-dimensional heat transfer differ from two-dimensional heat transfer?

2–2C Is heat transfer a scalar or a vector quantity? Explain. Answer the same question for temperature.

2–3C Does a heat flux vector at a point P on an isothermal surface of a medium have to be perpendicular to the surface at that point? Explain.

---

* Problems designated by a "C" are concept questions, and students are encouraged to answer them all. Problems designated by an "E" are in English units, and the SI users can ignore them. Problems with the ☑ icon are comprehensive in nature and are intended to be solved with appropriate software. Problems with the 🅿️ᵗᴰ icon are Prevention through Design problems. Problems with the 🅲&🆂 icon are Codes and Standards problems.

2–4C From a heat transfer point of view, what is the difference between isotropic and anisotropic materials?

2–5C What is heat generation in a solid? Give examples.

2–6C Heat generation is also referred to as energy generation or thermal energy generation. What do you think of these phrases?

2–7C In order to size the compressor of a new refrigerator, we wish to determine the rate of heat transfer from the kitchen air into the refrigerated space through the walls, door, and the top and bottom sections of the refrigerator. In your analysis, would you treat this as a transient or as a steady-state heat transfer problem? Also, would you consider the heat transfer to be one-dimensional or multidimensional? Explain.

2–8C In order to determine the size of the heating element of a new oven, we wish to determine the rate of heat loss through the walls, door, and the top and bottom sections of the oven. In your analysis, would you consider this to be a steady or

a transient heat transfer problem? Also, would you consider the heat transfer to be one-dimensional or multidimensional? Explain.

2–9C Consider a round potato being baked in an oven. Would you model the heat transfer to the potato as one-, two-, or three-dimensional? Would the heat transfer be steady or transient? Also, which coordinate system would you use to solve this problem, and where would you place the origin? Explain.

2–10C Consider an egg being cooked in boiling water in a pan. Would you model the heat transfer to the egg as one-, two-, or three-dimensional? Would the heat transfer be steady or transient? Also, which coordinate system would you use to solve this problem, and where would you place the origin? Explain.

2–11C Consider a hot dog being cooked in boiling water in a pan. Would you model the heat transfer to the hot dog as one-, two-, or three-dimensional? Would the heat transfer be steady or transient? Also, which coordinate system would you use to solve this problem, and where would you place the origin? Explain.

2–12C Consider the cooking process of a roast beef in an oven. Would you consider this to be a steady or a transient heat transfer problem? Also, would you consider this to be one-, two-, or three-dimensional? Explain.

2–13C Consider heat loss from a 200-L cylindrical hot water tank in a house to the surrounding medium. Would you consider this to be a steady or a transient heat transfer problem? Also, would you consider this heat transfer problem to be one-, two-, or three-dimensional? Explain.

2–14C Consider a cold canned drink left on a dinner table. Would you model the heat transfer to the drink as one-, two-, or three-dimensional? Would the heat transfer be steady or transient? Also, which coordinate system would you use to analyze this heat transfer problem, and where would you place the origin? Explain.

2–15 Heat flux meters use a very sensitive device known as a thermopile to measure the temperature difference across a thin, heat conducting film made of kapton ($k = 0.345$ W/m·K). If the thermopile can detect temperature differences of $0.1°C$ or more and the film thickness is 2 mm, what is the minimum heat flux this meter can detect? *Answer:* 17.3 W/m^2

2–16 A stainless steel cylindrical rod with a diameter $D = 18$ mm and length $L = 110$ mm is insulated on its exterior surface except for the ends. The mass of the rod is 0.221 kg. The steady one-dimensional temperature distribution in the rod is $T(x) = 310\,\text{K} - 20\,\text{K}\,(x/L)$. Determine the heat flux along the rod.

2–17 Consider a large 3-cm-thick stainless steel plate in which heat is generated uniformly at a rate of 5×10^6 W/m^3. Assuming the plate is losing heat from both sides, determine the heat flux on the surface of the plate during steady operation. *Answer:* 75 kW/m^2

2–18 In a nuclear reactor, heat is generated uniformly in the 5-cm-diameter cylindrical uranium rods at a rate of 7×10^7 W/m^3. If the length of the rods is 1 m, determine the rate of heat generation in each rod. *Answer:* 137 kW

2–19 In a solar pond, the absorption of solar energy can be modeled as heat generation and can be approximated by $\dot{e}_{gen} = \dot{e}_0 e^{-bx}$, where $\dot{e}_0$ is the rate of heat absorption at the top surface per unit volume and b is a constant. Obtain a relation for the total rate of heat generation in a water layer of surface area A and thickness L at the top of the pond.
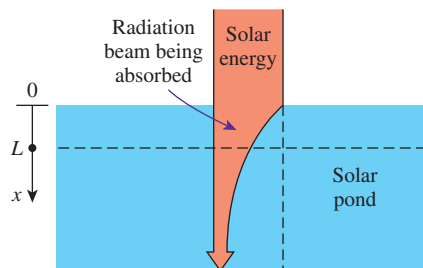
FIGURE P2–19

2–20E The resistance wire of a 1000-W iron is 15 in long and has a diameter of $D = 0.08$ in. Determine the rate of heat generation in the wire per unit volume in Btu/h·ft^3 and the heat flux on the outer surface of the wire in Btu/h·ft^2 as a result of this heat generation.
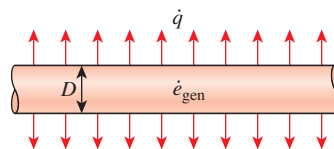
FIGURE P2–20E

Heat Conduction Equation

2–21C Write down the one-dimensional transient heat conduction equation for a plane wall with constant thermal conductivity and heat generation in its simplest form, and indicate what each variable represents.

2–22C Write down the one-dimensional transient heat conduction equation for a long cylinder with constant thermal conductivity and heat generation, and indicate what each variable represents.

2–23 Starting with an energy balance on a rectangular volume element, derive the one-dimensional transient heat conduction equation for a plane wall with constant thermal conductivity and no heat generation.

2–24 Starting with an energy balance on a cylindrical shell volume element, derive the steady one-dimensional heat conduction equation for a long cylinder with constant thermal conductivity in which heat is generated at a rate of $\dot{e}_{gen}$.
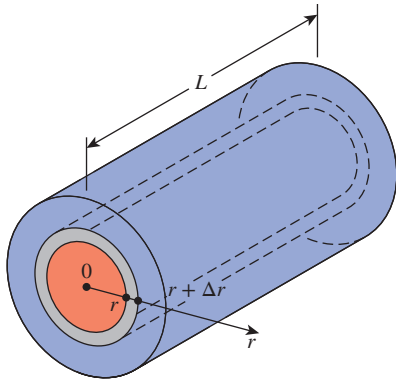
FIGURE P2–24

2–25 Starting with an energy balance on a spherical shell volume element, derive the one-dimensional transient heat conduction equation for a sphere with constant thermal conductivity and no heat generation.
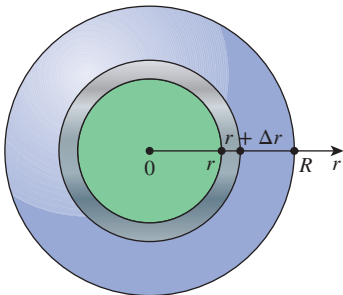
FIGURE P2–25

2–26 Consider a medium in which the heat conduction equation is given in its simplest form as

$$\frac{\partial^2 T}{\partial x^2} = \frac{1}{\alpha} \frac{\partial T}{\partial t}$$

(a) Is heat transfer steady or transient?
(b) Is heat transfer one-, two-, or three-dimensional?
(c) Is there heat generation in the medium?
(d) Is the thermal conductivity of the medium constant or variable?

2–27 Consider a medium in which the heat conduction equation is given in its simplest form as

$$\frac{\partial^2 T}{\partial x^2} + \frac{\partial^2 T}{\partial y^2} = \frac{1}{\alpha} \frac{\partial T}{\partial t}$$

(a) Is heat transfer steady or transient?
(b) Is heat transfer one-, two-, or three-dimensional?
(c) Is there heat generation in the medium?
(d) Is the thermal conductivity of the medium constant or variable?

2–28 Consider a medium in which the heat conduction equation is given in its simplest form as

$$\frac{1}{r} \frac{d}{dr}\left(rk\frac{dT}{dr}\right) + \dot{e}_{\text{gen}} = 0$$

(a) Is heat transfer steady or transient?
(b) Is heat transfer one-, two-, or three-dimensional?
(c) Is there heat generation in the medium?
(d) Is the thermal conductivity of the medium constant or variable?

2–29 Consider a medium in which the heat conduction equation is given in its simplest form as

$$\frac{1}{r} \frac{\partial}{\partial r}\left(kr\frac{\partial T}{\partial r}\right) + \frac{\partial}{\partial z}\left(k\frac{\partial T}{\partial z}\right) + \dot{e}_{\text{gen}} = 0$$

(a) Is heat transfer steady or transient?
(b) Is heat transfer one-, two-, or three-dimensional?
(c) Is there heat generation in the medium?
(d) Is the thermal conductivity of the medium constant or variable?

2–30 Consider a medium in which the heat conduction equation is given in its simplest form as

$$r\frac{d^2 T}{dr^2} + 2\frac{dT}{dr} = 0$$

(a) Is heat transfer steady or transient?
(b) Is heat transfer one-, two-, or three-dimensional?
(c) Is there heat generation in the medium?
(d) Is the thermal conductivity of the medium constant or variable?

2–31 Consider a medium in which the heat conduction equation is given in its simplest form as

$$\frac{1}{r^2} \frac{\partial}{\partial r}\left(r^2\frac{\partial T}{\partial r}\right) = \frac{1}{\alpha} \frac{\partial T}{\partial t}$$

(a) Is heat transfer steady or transient?
(b) Is heat transfer one-, two-, or three-dimensional?
(c) Is there heat generation in the medium?
(d) Is the thermal conductivity of the medium constant or variable?

2–32 Consider a medium in which the heat conduction equation is given in its simplest form as

$$\frac{1}{r^2} \frac{\partial}{\partial r}\left(r^2\frac{\partial T}{\partial r}\right) + \frac{1}{r^2\sin^2\theta} \frac{\partial^2 T}{\partial \phi^2} = \frac{1}{\alpha} \frac{\partial T}{\partial t}$$

(a) Is heat transfer steady or transient?
(b) Is heat transfer one-, two-, or three-dimensional?
(c) Is there heat generation in the medium?
(d) Is the thermal conductivity of the medium constant or variable?

2–33 Starting with an energy balance on a volume element, derive the two-dimensional transient heat conduction equation in rectangular coordinates for $T(x, y, t)$ for the case of constant thermal conductivity and no heat generation.

2–34 Starting with an energy balance on a ring-shaped volume element, derive the two-dimensional steady heat conduction equation in cylindrical coordinates for $T(r, z)$ for the case of constant thermal conductivity and no heat generation.
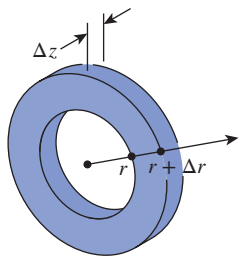
FIGURE P2–34

2–35 Starting with an energy balance on a disk volume element, derive the one-dimensional transient heat conduction equation for $T(z, t)$ in a cylinder of diameter D with an insulated side surface for the case of constant thermal conductivity with heat generation.
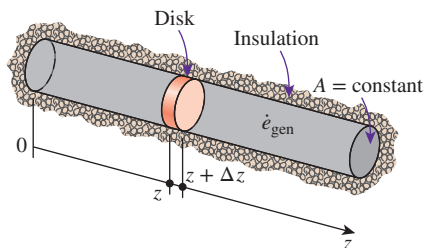
FIGURE P2–35

Boundary and Initial Conditions; Formulation of Heat Conduction Problems

2–36C What is a boundary condition? How many boundary conditions do we need to specify for a two-dimensional heat conduction problem?

2–37C What is an initial condition? How many initial conditions do we need to specify for a two-dimensional heat conduction problem?

2–38C What is a thermal symmetry boundary condition? How is it expressed mathematically?

2–39C How is the boundary condition on an insulated surface expressed mathematically?

2–40C It is claimed that the temperature profile in a medium must be perpendicular to an insulated surface. Is this a valid claim? Explain.

2–41C Why do we try to avoid the radiation boundary conditions in heat transfer analysis?

2–42 Consider an aluminum pan used to cook stew on top of an electric range. The bottom section of the pan is $L = 0.25$ cm thick and has a diameter of $D = 18$ cm. The electric heating unit on the range top consumes 900 W of power during cooking, and 90 percent of the heat generated in the heating element is transferred to the pan. During steady operation, the temperature of the inner surface of the pan is measured to be 108°C. Assuming temperature-dependent thermal conductivity and one-dimensional heat transfer, express the mathematical formulation (the differential equation and the boundary conditions) of this heat conduction problem during steady operation. Do not solve.

2–43 Consider a steel pan used to boil water on top of an electric range. The bottom section of the pan is $L = 0.5$ cm thick and has a diameter of $D = 20$ cm. The electric heating unit on the range top consumes 1250 W of power during cooking, and 85 percent of the heat generated in the heating element is transferred uniformly to the pan. Heat transfer from the top surface of the bottom section to the water is by convection with a heat transfer coefficient of h. Assuming constant thermal conductivity and one-dimensional heat transfer, express the mathematical formulation (the differential equation and the boundary conditions) of this heat conduction problem during steady operation. Do not solve.
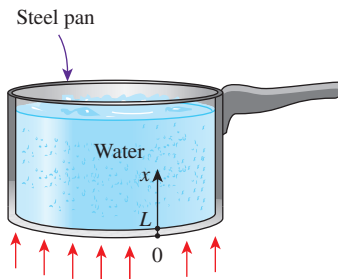
FIGURE P2–43

2–44 Consider the east wall of a house that has a thickness of L. The outer surface of the wall exchanges heat by both convection and radiation. The interior of the house is maintained at $T_{\infty 1}$, while the ambient air temperature outside remains at $T_{\infty 2}$. The sky, the ground, and the surfaces of the surrounding structures at this location can be modeled as a surface at an effective temperature of T_{sky} for radiation exchange on the outer surface. The radiation exchange between the inner surface of the wall and the surfaces of the walls, floor, and ceiling it faces is negligible. The convection heat transfer coefficients on the inner and outer surfaces of the wall are h_1 and h_2, respectively. The thermal conductivity of the wall material is k and the emissivity of the outer surface is ε_2. Assuming the heat transfer through the wall to be steady and one-dimensional, express the mathematical formulation (the differential equation and the boundary and initial conditions) of this heat conduction problem. Do not solve.
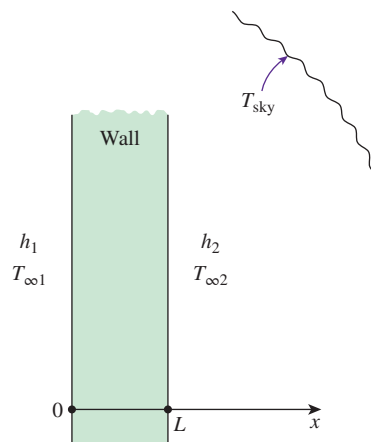
FIGURE P2–44

2–45 Heat is generated in a long wire of radius r_o at a constant rate of $\dot{e}_{gen}$ per unit volume. The wire is covered with a plastic insulation layer. Express the heat flux boundary condition at the interface in terms of the heat generated.

2–46 Consider a long pipe of inner radius r_1, outer radius r_2, and thermal conductivity k. The outer surface of the pipe is subjected to convection to a medium at T_∞ with a heat transfer coefficient of h, but the direction of heat transfer is not known. Express the convection boundary condition on the outer surface of the pipe.

2–47E A 2-kW resistance heater wire whose thermal conductivity is $k = 10.4$ Btu/h·ft·R has a radius of $r_o = 0.06$ in and a length of $L = 15$ in, and it is used for space heating. Assuming constant thermal conductivity and one-dimensional heat transfer, express the mathematical formulation (the differential equation and the boundary conditions) of this heat conduction problem during steady operation. Do not solve.

2–48 Water flows through a pipe at an average temperature of $T_\infty = 70°C$. The inner and outer radii of the pipe are $r_1 = 6$ cm and $r_2 = 6.5$ cm, respectively. The outer surface of the pipe is wrapped with a thin electric heater that consumes 300 W per m length of the pipe. The exposed surface of the heater is heavily insulated so that all heat generated in the heater is transferred to the pipe. Heat is transferred from the inner surface of the pipe to the water by convection with a heat transfer coefficient of $h = 85$ W/m²·K. Assuming constant thermal conductivity and one-dimensional heat transfer, express the mathematical formulation (the differential equation and the boundary conditions) of the heat conduction in the pipe during steady operation. Do not solve.
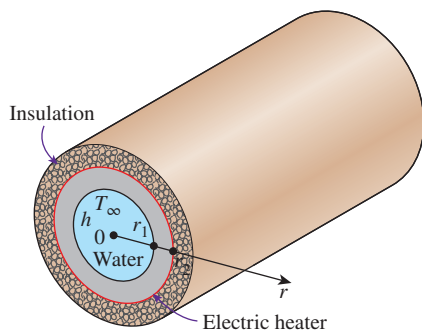
FIGURE P2–48

2–49 Consider a spherical container of inner radius r_1, outer radius r_2, and thermal conductivity k. Express the boundary condition on the inner surface of the container for steady one-dimensional conduction for the following cases: (*a*) specified temperature of 50°C, (*b*) specified heat flux of 30 W/m² toward the center, (*c*) convection to a medium at T_∞ with a heat transfer coefficient of h.
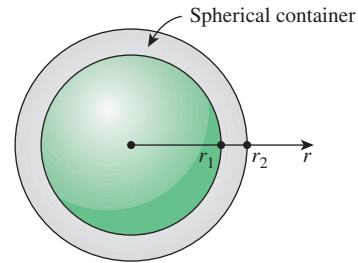
FIGURE P2–49

2–50 Consider a spherical shell of inner radius r_1, outer radius r_2, thermal conductivity k, and emissivity ε. The outer surface of the shell is subjected to radiation to surrounding surfaces at T_{surr}, but the direction of heat transfer is not known. Express the radiation boundary condition on the outer surface of the shell.

2–51 A container consists of two spherical layers, *A* and *B*, that are in perfect contact. If the radius of the interface is r_o, express the boundary conditions at the interface.

2–52 A spherical metal ball of radius r_o is heated in an oven to a temperature of T_i throughout and is then taken out of the oven and dropped into a large body of water at T_∞, where it is cooled by convection with an average convection heat transfer coefficient of h. Assuming constant thermal conductivity and transient one-dimensional heat transfer, express the mathematical formulation (the differential equation and the boundary and initial conditions) of this heat conduction problem. Do not solve.

2–53 A spherical metal ball of radius r_o is heated in an oven to a temperature of T_i throughout and is then taken out of the oven and allowed to cool in ambient air at T_∞ by convection and radiation. The emissivity of the outer surface of the cylinder is ε, and the temperature of the surrounding surfaces is T_{surr}. The average convection heat transfer coefficient is estimated to be h. Assuming variable thermal conductivity and transient one-dimensional heat transfer, express the mathematical formulation (the differential equation and the boundary and initial conditions) of this heat conduction problem. Do not solve.
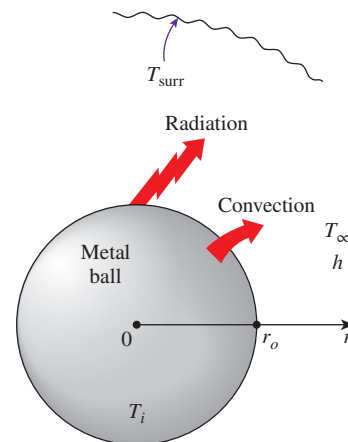
FIGURE P2–53

Solution of Steady One-Dimensional Heat Conduction Problems

2–54C   It is stated that the temperature in a plane wall with constant thermal conductivity and no heat generation varies linearly during steady one-dimensional heat conduction. Will this still be the case when the wall loses heat by radiation from its surfaces?

2–55C   Consider one-dimensional heat conduction through a large plane wall with no heat generation that is perfectly insulated on one side and is subjected to convection and radiation on the other side. It is claimed that under steady conditions, the temperature in a plane wall must be uniform (the same everywhere). Do you agree with this claim? Why?

2–56C   Consider a solid cylindrical rod whose side surface is maintained at a constant temperature while the end surfaces are perfectly insulated. The thermal conductivity of the rod material is constant, and there is no heat generation. It is claimed that the temperature in the radial direction within the rod will not vary during steady heat conduction. Do you agree with this claim? Why?

2–57C   Consider a solid cylindrical rod whose ends are maintained at constant but different temperatures while the side surface is perfectly insulated. There is no heat generation. It is claimed that the temperature along the axis of the rod varies linearly during steady heat conduction. Do you agree with this claim? Why?

2–58   Consider a large plane wall of thickness $L = 0.3$ m, thermal conductivity $k = 2.5$ W/m·K, and surface area $A = 12$ m^2. The left side of the wall at $x = 0$ is subjected to a net heat flux of $\dot{q}_0 = 700$ W/m^2, while the temperature at that surface is measured to be $T_1 = 80°C$. Assuming constant thermal conductivity and no heat generation in the wall, (a) express the differential equation and the boundary conditions for steady one-dimensional heat conduction through the wall, (b) obtain a relation for the variation of temperature in the wall by solving the differential equation, and (c) evaluate the temperature of the right surface of the wall at $x = L$.   *Answer:* (c) −4°C
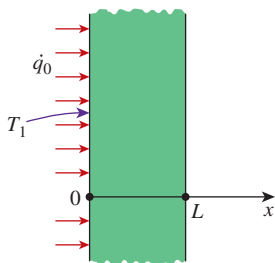
FIGURE P2–58

2–59   Consider the base plate of an 800-W household iron with a thickness of $L = 0.6$ cm, base area of $A = 160$ cm^2, and thermal conductivity of $k = 20$ W/m·K. The inner surface of the base plate is subjected to uniform heat flux generated by the resistance heaters inside. When steady operating conditions are reached, the outer surface temperature of the plate is measured to be 85°C. Disregarding any heat loss through the upper part of the iron, (a) express the differential equation and the boundary conditions for steady one-dimensional heat conduction through the plate, (b) obtain a relation for the variation of temperature in the base plate by solving the differential equation, and (c) evaluate the inner surface temperature.   *Answer:* (c) 100°C
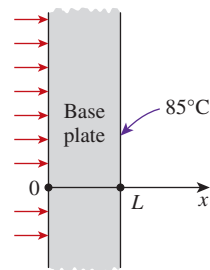
FIGURE P2–59

2–60   C & S   A heating cable is embedded in a concrete slab for snow melting. The heating cable is heated electrically with joule heating to provide the concrete slab with a uniform heat of 1200 W/m^2. The concrete has a thermal conductivity of 1.4 W/m·K. To minimize thermal stress in the concrete, the temperature difference between the heater surface (T_1) and the slab surface (T_2) should not exceed 21°C (2015 ASHRAE Handbook—HVAC Applications, Chap. 51). Formulate the temperature profile in the concrete slab, and determine the thickness of the concrete slab (L) so that $T_1 - T_2 \leq 21°C$.
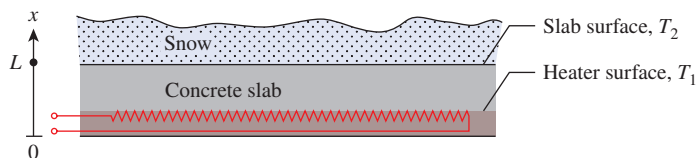
FIGURE P2–60

2–61   Consider a large plane wall of thickness $L = 0.4$ m, thermal conductivity $k = 2.3$ W/m·K, and surface area $A = 30$ m^2. The left side of the wall is maintained at a constant temperature of $T_1 = 90°C$, while the right side loses heat by convection to the surrounding air at $T_\infty = 25°C$ with a heat transfer coefficient of $h = 24$ W/m^2·K. Assuming constant thermal conductivity and no heat generation in the wall, (a) express the differential equation and the boundary conditions for steady one-dimensional heat conduction through the wall, (b) obtain a relation for the variation of temperature in the wall by solving the differential equation, and (c) evaluate the rate of heat transfer through the wall.   *Answer:* (c) 9045 W

2–62 Consider a 20-cm-thick concrete plane wall ($k = 0.77$ W/m·K) subjected to convection on both sides with $T_{\infty 1} = 27°C$ and $h_1 = 5$ W/m²·K on the inside and $T_{\infty 2} = 8°C$ and $h_2 = 12$ W/m²·K on the outside. Assuming constant thermal conductivity with no heat generation and negligible radiation, (*a*) express the differential equation and the boundary conditions for steady one-dimensional heat conduction through the wall, (*b*) obtain a relation for the variation of temperature in the wall by solving the differential equation, and (*c*) evaluate the temperatures at the inner and outer surfaces of the wall.

2–63 **PtD** In metal processing plants, workers often operate near hot metal surfaces. Exposed hot surfaces are hazards that can potentially cause thermal burns on human skin. Metallic surfaces above 70°C are considered extremely hot. Damage to skin can occur instantaneously upon contact with metallic surfaces at that temperature. In a plant that processes metal plates, a plate is conveyed through a series of fans to cool its surface in an ambient temperature of 30°C. The plate is 25 mm thick and has a thermal conductivity of 13.5 W/m²·K. The temperature at the bottom surface of the plate is monitored by an infrared (IR) thermometer. Obtain an expression for the variation of temperature in the metal plate. The IR thermometer measures the bottom surface of the plate to be 60°C. Determine the minimum value of the convection heat transfer coefficient needed to keep the top surface below 47°C.
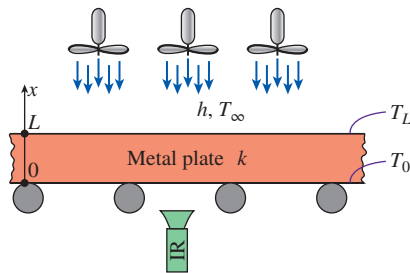
FIGURE P2–63

2–64 **C & S** A metal plate with a thickness of 5 cm and a thermal conductivity of 15 W/m·K has its bottom surface subjected to a uniform heat flux of 2250 W/m². The upper surface of the plate is exposed to ambient air with a temperature of 30°C and a convection heat transfer coefficient of 10 W/m²·K. A series of ASME SA-193 carbon steel bolts are bolted onto the upper surface of a metal plate. The ASME Boiler and Pressure Vessel Code (ASME BPVC.IV-2015, HF-300) limits the maximum allowable use temperature to 260°C for the SA-193 bolts. Formulate the temperature profile in the metal plate, and determine the location in the plate where the temperature begins to exceed 260°C. If the thread length of the bolts is 1 cm, would the SA-193 bolts comply with the ASME code?
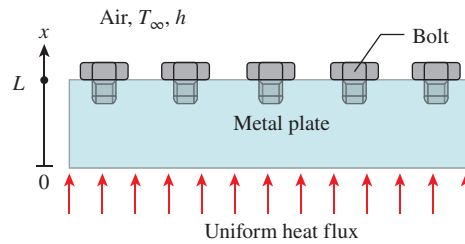
FIGURE P2–64

2–65 A large plane wall has a thickness $L = 50$ cm and thermal conductivity $k = 25$ W/m·K. On the left surface ($x = 0$), it is subjected to a uniform heat flux $\dot{q}_0$ while the surface temperature T_0 is constant. On the right surface, it experiences convection and radiation heat transfer while the surface temperature is $T_L = 225°C$ and the surrounding temperature is 25°C. The emissivity and the convection heat transfer coefficient on the right surface are 0.7 and 15 W/m²·K, respectively. (*a*) Show that the variation of temperature in the wall can be expressed as $T(x) = (\dot{q}_0/k)(L - x) + T_L$, (*b*) calculate the heat flux $\dot{q}_0$ on the left face of the wall, and (*c*) determine the temperature of the left surface of the wall at $x = 0$.
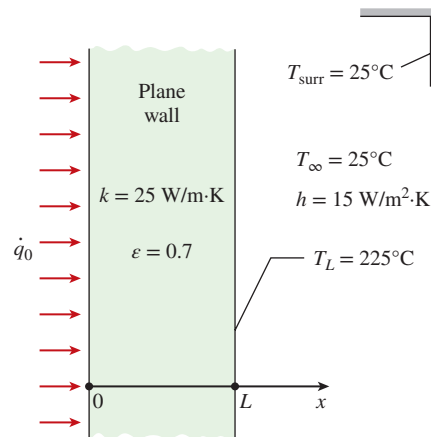
FIGURE P2–65

2–66 A flat-plate solar collector is used to heat water by having water flow through tubes attached at the back of the thin solar absorber plate. The absorber plate has an emissivity and an absorptivity of 0.9. The top surface ($x = 0$) temperature of the absorber is $T_0 = 35°C$, and solar radiation is incident on the absorber at 500 W/m² with a surrounding temperature of 0°C. The convection heat transfer coefficient at the absorber surface is 5 W/m²·K, while the ambient temperature is 25°C. Show that the variation of temperature in the absorber plate can be expressed as $T(x) = -(\dot{q}_0/k)x + T_0$, and determine net heat flux $\dot{q}_0$ absorbed by the solar collector.
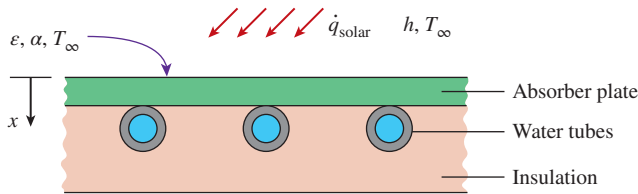
FIGURE P2–66

2–67 Electrically heated draw batch furnaces are commonly used in the heat treatment industry. Consider a draw batch furnace front made of a 20-mm-thick steel plate with a thermal conductivity of 25 W/m·K. The furnace is situated in a room with a surrounding air temperature of 20°C and an average convection heat transfer coefficient of 10 W/m^2·K. If the inside surface of the furnace front is subjected to uniform heat flux of 5 kW/m^2 and the outer surface has an emissivity of 0.30, determine the inside surface temperature of the furnace front.
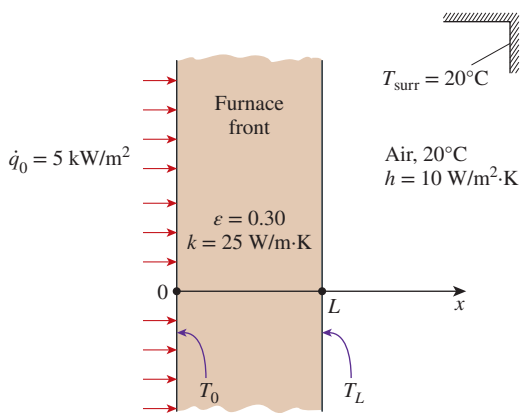
FIGURE P2–67

2–68E A large steel plate having a thickness of $L = 4$ in, thermal conductivity of $k = 7.2$ Btu/h·ft·°F, and an emissivity of $\varepsilon = 0.7$ is lying on the ground. The exposed surface of the plate at $x = L$ is known to exchange heat by convection with the ambient air at $T_\infty = 90$°F with an average heat transfer coefficient of $h = 12$ Btu/h·ft^2·°F as well as by radiation with the open sky with an equivalent sky temperature of $T_{sky} = 480$ R. Also, the temperature of the upper surface of the plate is measured to be 75°F. Assuming steady one-dimensional heat transfer, (a) express the differential equation and the boundary conditions for heat conduction through the plate, (b) obtain a relation for the variation of temperature in the plate by solving the differential equation, and (c) determine the value of the lower surface temperature of the plate at $x = 0$.
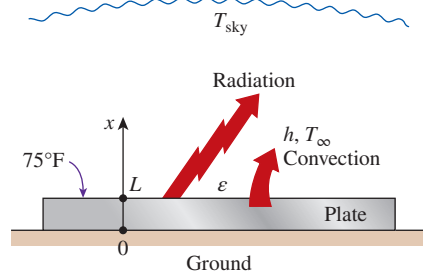
FIGURE P2–68E

2–69 A plate has its upper surface exposed to natural convection at an air temperature of 50°C , and it has a convection heat transfer coefficient of 2 W/m^2·K. Also, thermal radiation exchange occurs between the upper plate surface and the surrounding surface temperature of 200°C. The bottom surface of the plate is fully insulated. The upper surface of the plate is bolted with ASTM B21 naval brass bolts. The emissivity of the plate surface and the bolts is 0.3. The ASME Code for Process Piping (ASME B31.3-2014) limits the maximum use temperature of B21 bolts to 149°C. Determine the temperature profile in the plate. Would the ASTM B21 bolts on the plate comply with the ASME code? If not, propose a solution to keep the plate temperature below the maximum use temperature.
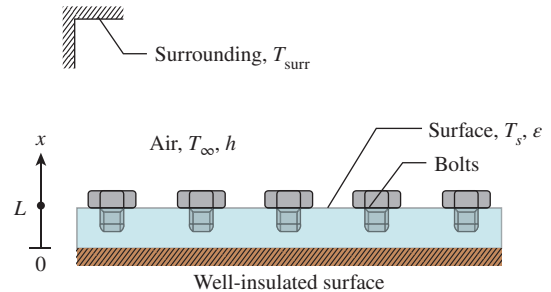
FIGURE P2–69

2–70 Consider a chilled-water pipe of length L, inner radius r_1, outer radius r_2, and thermal conductivity k. Water flows in the pipe at a temperature T_f, and the heat transfer coefficient at the inner surface is h. If the pipe is well insulated on the outer surface, (a) express the differential equation and the boundary conditions for steady one-dimensional heat conduction through the pipe, and (b) obtain a relation for the variation of temperature in the pipe by solving the differential equation.

2–71E Consider a steam pipe of length $L = 30$ ft, inner radius $r_1 = 2$ in, outer radius $r_2 = 2.4$ in, and thermal conductivity $k = 7.2$ Btu/h·ft·°F. Steam is flowing through the pipe at an average temperature of 250°F, and the average convection heat transfer coefficient on the inner surface is given to be

$h = 12$ Btu/h·ft^2·°F. If the average temperature on the outer surfaces of the pipe is $T_2 = 160$°F, (*a*) express the differential equation and the boundary conditions for steady one-dimensional heat conduction through the pipe, (*b*) obtain a relation for the variation of temperature in the pipe by solving the differential equation, and (*c*) evaluate the rate of heat loss from the steam through the pipe. *Answer:* (*c*) 33,600 Btu/h
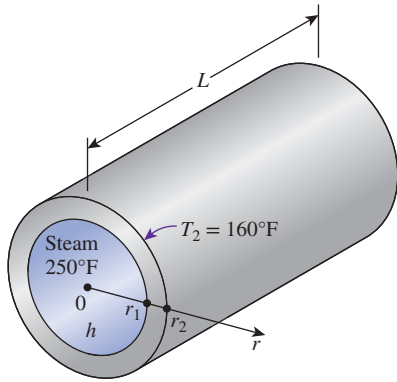
FIGURE P2–71E

2–72 A pipe in a manufacturing plant is transporting superheated vapor at a mass flow rate of 0.3 kg/s. The pipe is 10 m long and has an inner diameter of 5 cm and a wall thickness of 6 mm. The pipe has a thermal conductivity of 17 W/m·K, and the inner pipe surface is at a uniform temperature of 120°C. The temperature drop between the inlet and exit of the pipe is 7°C, and the constant pressure specific heat of vapor is 2190 J/kg·°C. If the air temperature in the manufacturing plant is 25°C, determine the heat transfer coefficient as a result of convection between the outer pipe surface and the surrounding air.
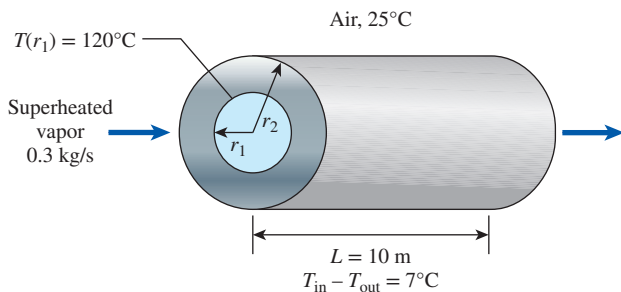
FIGURE P2–72

2–73 In subsea oil and natural gas production, hydrocarbon fluids may leave the reservoir with a temperature of 70°C and flow in subsea surroundings of 5°C. Because of the temperature difference between the reservoir and the subsea environment, the knowledge of heat transfer is critical to prevent gas hydrate and wax deposition blockages. Consider a subsea pipeline with inner diameter of 0.5 m and wall thickness of 8 mm is used

for transporting liquid hydrocarbon at an average temperature of 70°C, and the average convection heat transfer coefficient on the inner pipeline surface is estimated to be 250 W/m^2·K. The subsea has a temperature of 5°C, and the average convection heat transfer coefficient on the outer pipeline surface is estimated to be 150 W/m^2·K. If the pipeline is made of material with thermal conductivity of 60 W/m·K, use the heat conduction equation to (*a*) obtain the temperature variation in the pipeline wall, (*b*) determine the inner surface temperature of the pipeline, (*c*) obtain the mathematical expression for the rate of heat loss from the liquid hydrocarbon in the pipeline, and (*d*) determine the heat flux through the outer pipeline surface.
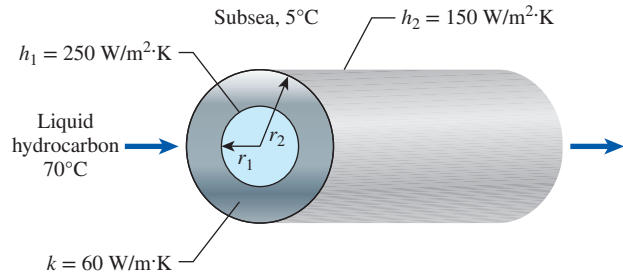
FIGURE P2–73

2–74 **PtD** Liquid ethanol is a flammable fluid that has a flash point at 16.6°C. At temperatures above the flash point, ethanol can release vapors that form explosive mixtures, which could ignite when a source of ignition is present. In a chemical plant, liquid ethanol is being transported in a pipe ($k = 15$ W/m·K) with an inside diameter of 3 cm and a wall thickness of 3 mm. The pipe passes through areas where an ignition source can occasionally occur, and the pipe's outer surface is subjected to a heat flux of 1 kW/m^2. The ethanol flowing in the pipe has an average temperature of 10°C with an average convection heat transfer coefficient of 50 W/m^2·K. Your task as an engineer is to ensure that the ethanol is transported safely and to prevent fire hazard. Determine the variation of temperature in the pipe wall and the temperatures of the inner and outer surfaces of the pipe. Are both surface temperatures safely below the flash point of liquid ethanol?
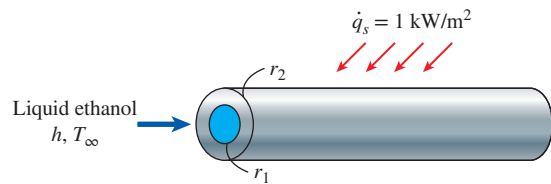
FIGURE P2–74

2–75 [C&S] Liquid water flows in a tube with the inner surface lined with polyvinylidene chloride (PVDC). The inner diameter of the tube is 24 mm, and its wall thickness is 5 mm. The thermal conductivity of the tube wall is 15 W/m·K. The water flowing in the tube has a temperature of 20°C, and the convection heat transfer coefficient with the inner tube surface is 50 W/m²·K. The outer surface of the tube is subjected to a uniform heat flux of 2300 W/m². According to the ASME Code for Process Piping (ASME B31.3-2014, A323), the recommended maximum temperature for PVDC lining is 79°C. Formulate the temperature profile in the tube wall. Use the temperature profile to determine if the tube inner surface is in compliance with the ASME Code for Process Piping.
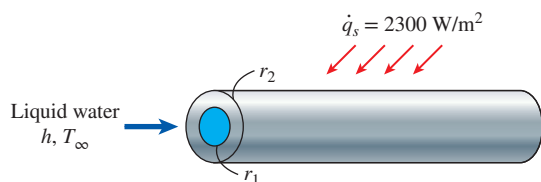
FIGURE P2–75

2–76 [C&S] Liquid water flows in a tube with the inner surface lined with polytetrafluoroethylene (PTFE). The inner diameter of the tube is 24 mm, and its wall thickness is 5 mm. The thermal conductivity of the tube wall is 15 W/m·K. The water flowing in the tube has a temperature of 50°C, and the convection heat transfer coefficient with the inner tube surface is 50 W/m²·K. The outer surface of the tube is exposed to convection with superheated steam at 600°C with a convection heat transfer coefficient of 50 W/m²·K. According to the ASME Code for Process Piping (ASME B31.3-2014, A323), the recommended maximum temperature for PTFE lining is 260°C. Formulate the temperature profile in the tube wall. Use the temperature profile to determine if the tube inner surface is in compliance with the ASME Code for Process Piping.
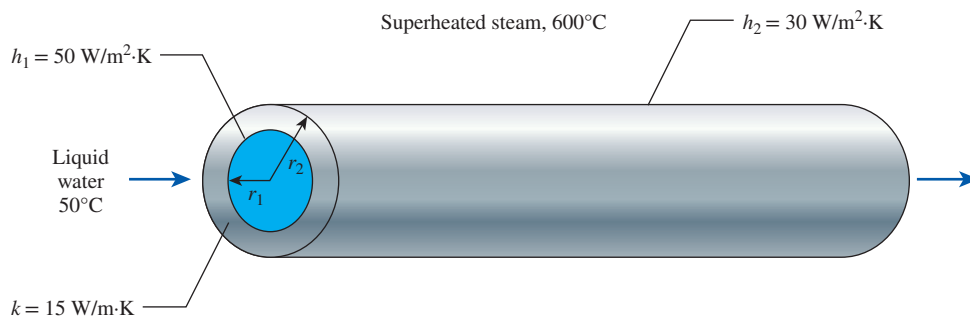
2–77 A spherical container with an inner radius $r_1 = 1$ m and an outer radius $r_2 = 1.05$ m has its inner surface subjected to a uniform heat flux of $\dot{q}_1 = 7$ kW/m². The outer surface of the container has a temperature $T_2 = 25°C$, and the container wall thermal conductivity is $k = 1.5$ W/m·K. Show that the variation of temperature in the container wall can be expressed as $T(r) = (\dot{q}_1 r_1^2/k)(1/r - 1/r_2) + T_2$ and determine the temperature of the inner surface of the container at $r = r_1$.
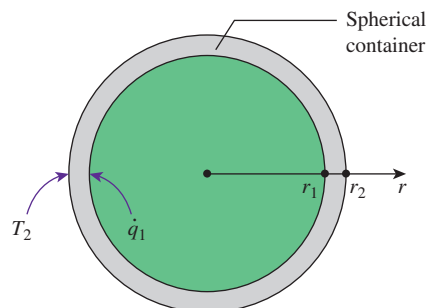
FIGURE P2–77

2–78 A spherical shell with thermal conductivity k has inner and outer radii of r_1 and r_2, respectively. The inner surface of the shell is subjected to a uniform heat flux of $\dot{q}_1$, while the outer surface of the shell is exposed to convection heat transfer with a coefficient h and an ambient temperature T_∞. Determine the variation of temperature in the shell wall, and show that the outer surface temperature of the shell can be expressed as $T(r_2) = (\dot{q}_1/h)(r_1/r_2)^2 + T_\infty$.
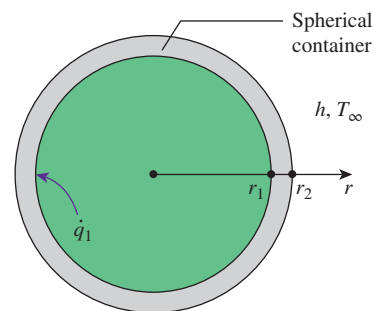
FIGURE P2–78

FIGURE P2–76

2–79 A spherical container of inner radius $r_1 = 2$ m, outer radius $r_2 = 2.1$ m, and thermal conductivity $k = 30$ W/m·K is filled with iced water at 0°C. The container is gaining heat by convection from the surrounding air at $T_\infty = 25$°C with a heat transfer coefficient of $h = 18$ W/m²·K. Assuming the inner surface temperature of the container to be 0°C, (*a*) express the differential equation and the boundary conditions for steady one-dimensional heat conduction through the container, (*b*) obtain a relation for the variation of temperature in the container by solving the differential equation, and (*c*) evaluate the rate of heat gain to the iced water.

2–80 **PtD** A stainless steel spherical container with $k = 15$ W/m·K is used for storing chemicals undergoing exothermic reaction. The reaction provides a uniform heat flux of 60 kW/m² to the container's inner surface. The container has an inner radius of 50 cm and a wall thickness of 5 cm and is situated in a surrounding with an ambient temperature of 23°C. The container's outer surface is subjected to convection heat transfer with a coefficient of 1000 W/m²·K. To prevent thermal burns to individuals working around the container, it is necessary to keep the container's outer surface temperature below 50°C. Determine the variation of temperature in the container wall and the temperatures of the inner and outer surfaces of the container. Is the outer surface temperature of the container cool enough to prevent thermal burns?
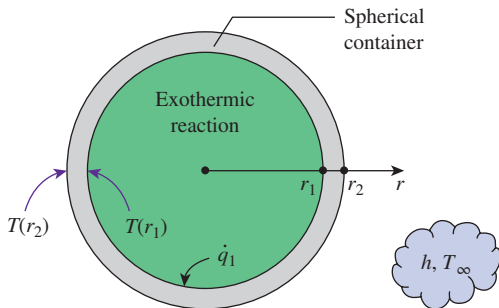
FIGURE P2–80

2–81 In a food processing facility, a spherical container of inner radius $r_1 = 40$ cm, outer radius $r_2 = 41$ cm, and thermal conductivity $k = 1.5$ W/m·K is used to store hot water and to keep it at 100°C at all times. To accomplish this, the outer surface of the container is wrapped with a 500-W electric strip heater and then insulated. The temperature of the inner surface of the container is observed to be nearly 100°C at all times. Assuming 10 percent of the heat generated in the heater is lost through the insulation, (*a*) express the differential equation and the boundary conditions for steady one-dimensional heat conduction through the container, (*b*) obtain a relation for the variation of temperature in the container material by solving the differential equation, and (*c*) evaluate the outer surface temperature of the container. Also determine how much water at 100°C this tank can supply steadily if the cold water enters at 20°C.
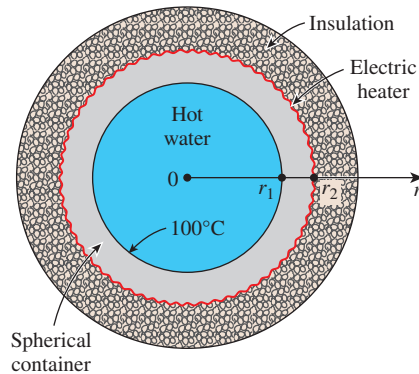
FIGURE P2–81

Heat Generation in a Solid

2–82C What is heat generation? Give some examples.

2–83C Does heat generation in a solid violate the first law of thermodynamics, which states that energy cannot be created or destroyed? Explain.

2–84C Consider uniform heat generation in a cylinder and in a sphere of equal radius made of the same material in the same environment. Which geometry will have a higher temperature at its center? Why?

2–85C An iron is left unattended, and its base temperature rises as a result of resistance heating inside. When will the rate of heat generation inside the iron be equal to the rate of heat loss from the iron?

2–86C Consider the uniform heating of a plate in an environment at a constant temperature. Is it possible for part of the heat generated in the left half of the plate to leave the plate through the right surface? Explain.

2–87 Consider a large 5-cm-thick brass plate ($k = 111$ W/m·K) in which heat is generated uniformly at a rate of 2×10^5 W/m³. One side of the plate is insulated, while the other side is exposed to an environment at 25°C with a heat transfer coefficient of 44 W/m²·K. Explain where in the plate the highest and the lowest temperatures will occur, and determine their values.
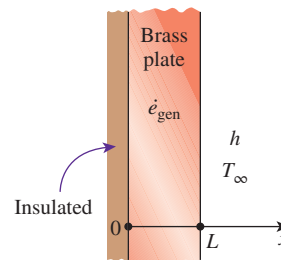
FIGURE P2–87

2–88 Reconsider Prob. 2–87. Using appropriate software, investigate the effect of the heat transfer coefficient on the highest and lowest temperatures in the plate. Let the heat transfer coefficient vary from 20 W/m²·K to 100 W/m²·K. Plot the highest and lowest temperatures as a function of the heat transfer coefficient, and discuss the results.

2–89 Consider a large 3-cm-thick stainless steel plate ($k = 15.1$ W/m·K) in which heat is generated uniformly at a rate of 5×10^5 W/m³. Both sides of the plate are exposed to an environment at 30°C with a heat transfer coefficient of 60 W/m²·K. Explain where in the plate the highest and the lowest temperatures will occur, and determine their values.

2–90 Consider a large plate of thickness L and thermal conductivity k in which heat is generated uniformly at a rate of $\dot{e}_{gen}$. One side of the plate is insulated, while the other side is exposed to an environment at T_∞ with a heat transfer coefficient of h. (a) Express the differential equation and the boundary conditions for steady one-dimensional heat conduction through the plate, (b) determine the variation of temperature in the plate, and (c) obtain relations for the temperatures on both surfaces and the maximum temperature rise in the plate in terms of given parameters.
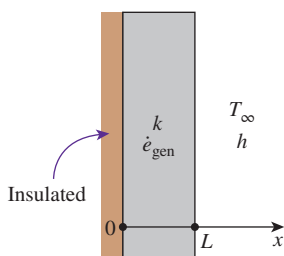
FIGURE P2–90

2–91E Consider a large plane wall of thickness L and constant thermal conductivity k. The left side of the wall ($x = 0$) is maintained at a constant temperature T_0, while the right surface at $x = L$ is insulated. Heat is generated in the wall at the rate of $\dot{e}_{gen} = ax^2$ Btu/h·ft³. Assuming steady one-dimensional heat transfer: (a) Express the differential equation and the boundary conditions for heat conduction through the wall. (b) By solving the differential equation, obtain a relation for the variation of temperature in the wall $T(x)$ in terms of x, L, k, a, and T_0. (c) What is the highest temperature (°C) in the plane wall when: $L = 1$ ft, $k = 5$ Btu/h·ft·°F, $a = 1200$ Btu/h·ft⁵, and $T_0 = 700°F$?
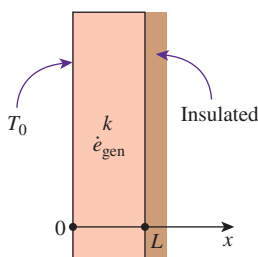
FIGURE P2–91E

2–92 Consider a large plane wall of thickness $L = 0.05$ m. The wall surface at $x = 0$ is insulated, while the surface at $x = L$ is maintained at a temperature of 30°C. The thermal conductivity of the wall is $k = 30$ W/m·K, and heat is generated in the wall at a rate of $\dot{e}_{gen} = \dot{e}_0 \dot{e}^{-0.5x/L}$ W/m³ where $\dot{e}_{gen} = 8 \times 10^6$ W/m³. Assuming steady one-dimensional heat transfer, (a) express the differential equation and the boundary conditions for heat conduction through the wall, (b) obtain a relation for the variation of temperature in the wall by solving the differential equation, and (c) determine the temperature of the insulated surface of the wall. *Answer: (c) 314°C*

2–93 Reconsider Prob. 2–92. Using the relation given for the heat generation in the wall, plot the heat generation as a function of the distance x in the range of $x = 0$ to $x = L$, and discuss the results. Use appropriate software.

2–94 In a nuclear reactor, 1-cm-diameter cylindrical uranium rods cooled by water from outside serve as the fuel. Heat is generated uniformly in the rods ($k = 29.5$ W/m·K) at a rate of 4×10^7 W/m³. If the outer surface temperature of rods is 220°C, determine the temperature at their center.
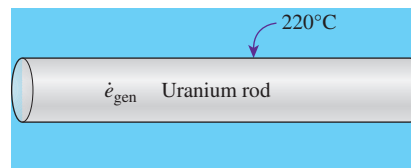
FIGURE P2–94

2–95E Heat is generated uniformly at a rate of 3 kW per ft length in a 0.08-in-diameter electric resistance wire made of nickel steel ($k = 5.8$ Btu/h·ft·°F). Determine the temperature difference between the centerline and the surface of the wire.

2–96 A 2-kW resistance heater wire with thermal conductivity of $k = 20$ W/m·K, a diameter of $D = 4$ mm, and a length of $L = 0.9$ m is used to boil water. If the outer surface temperature of the resistance wire is $T_s = 110°C$, determine the temperature at the center of the wire.
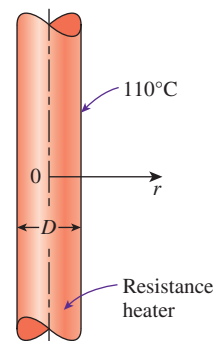
FIGURE P2–96

2–97 Consider a long solid cylinder of radius $r_o = 4$ cm and thermal conductivity $k = 25$ W/m·K. Heat is generated in the cylinder uniformly at a rate of $\dot{e}_{gen} = 35$ W/cm³. The side surface of the cylinder is maintained at a constant temperature of $T_s = 80°C$. The variation of temperature in the cylinder is given by

$$T(r) = \frac{\dot{e}_{gen} r_o^2}{k}\left[1 - \left(\frac{r}{r_o}\right)^2\right] + T_s$$

Based on this relation, determine (*a*) if the heat conduction is steady or transient, (*b*) if it is one-, two-, or three-dimensional, and (*c*) the value of heat flux on the side surface of the cylinder at $r = r_o$.

2–98 🖥 Reconsider Prob. 2–97. Using the relation obtained for the variation of temperature in the cylinder, plot the temperature as a function of the radius r in the range of $r = 0$ to $r = r_o$, and discuss the results. Use appropriate software.

2–99 A cylindrical nuclear fuel rod 1 cm in diameter is encased in a concentric tube 2 cm in diameter, where cooling water flows through the annular region between the fuel rod ($k = 30$ W/m·K) and the concentric tube. Heat is generated uniformly in the rod at a rate of 50 MW/m³. The convection heat transfer coefficient for the concentric tube surface is 2000 W/m²·K. If the surface temperature of the concentric tube is 40°C, determine the average temperature of the cooling water. Can one use the given information to determine the surface temperature of the fuel rod? Explain. *Answer:* 71.3°C
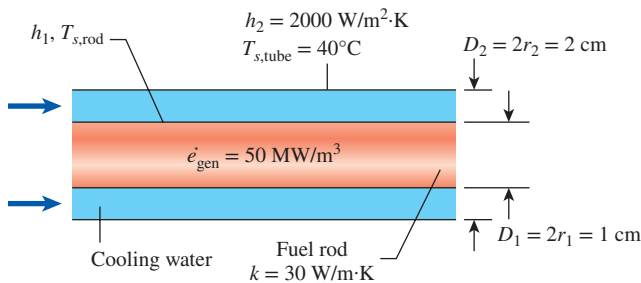
FIGURE P2–99

2–100 Consider a solid stainless steel wire with a thermal conductivity of 14 W/m·K. The wire has a diameter of 1 mm, has a resistivity of 45×10^{-8} Ω·m, and carries a current of 120 A. (*a*) Determine the rate of heat generated within the wire (W/m³), and (*b*) calculate the maximum temperature rise in the wire.
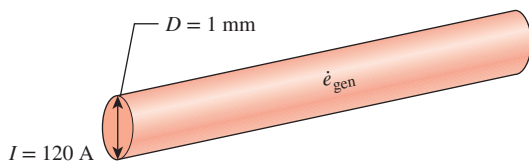
FIGURE P2–100

2–101 A long homogeneous resistance wire of radius $r_o = 5$ mm is being used to heat the air in a room by the passage of electric current. Heat is generated in the wire uniformly at a rate of 5×10^7 W/m³ as a result of resistance heating. If the temperature of the outer surface of the wire remains at 180°C, determine the temperature at $r = 3.5$ mm after steady operation conditions are reached. Take the thermal conductivity of the wire to be $k = 8$ W/m·K. *Answer:* 200°C
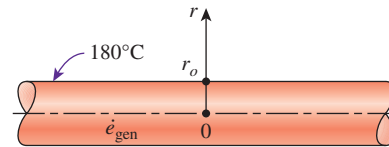
FIGURE P2–101

2–102 A long homogeneous resistance wire of radius $r_o = 0.6$ cm and thermal conductivity $k = 15.2$ W/m·K is being used to boil water at atmospheric pressure by the passage of electric current. Heat is generated in the wire uniformly as a result of resistance heating at a rate of 16.4 W/cm³. The heat generated is transferred to water at 100°C by convection with an average heat transfer coefficient of $h = 3200$ W/m²·K. Assuming steady one-dimensional heat transfer, (*a*) express the differential equation and the boundary conditions for heat conduction through the wire, (*b*) obtain a relation for the variation of temperature in the wire by solving the differential equation, and (*c*) determine the temperature at the centerline of the wire. *Answer:* (*c*) 125°C
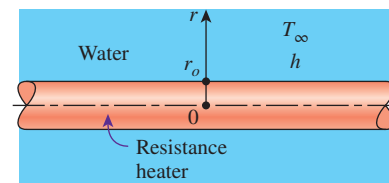
FIGURE P2–102

2–103 A 6-m-long, 2-kW electrical resistance wire is made of 0.2-cm-diameter stainless steel ($k = 15.1$ W/m·K). The resistance wire operates in an environment at 20°C with a heat transfer coefficient of 175 W/m²·K at the outer surface. Determine the surface temperature of the wire (*a*) by using the applicable relation and (*b*) by setting up the proper differential equation and solving it. *Answers:* (*a*) 323°C, (*b*) 323°C

2–104 🔲PtD A cylindrical fuel rod ($k = 30$ W/m·K) 2 cm in diameter is encased in a concentric tube and cooled by water. The fuel rod generates heat uniformly at a rate of 100 MW/m³, and the average temperature of the cooling water is 75°C with a convection heat transfer coefficient of 2500 W/m²·K. The operating pressure of the cooling water is such that the surface temperature of the fuel rod must be kept below 200°C to prevent the cooling water from reaching the critical heat flux (CHF). The critical heat flux is a thermal

limit at which a boiling crisis can occur that causes overheating on the fuel rod surface and leads to damage. Determine the variation of temperature in the fuel rod and the temperature of the fuel rod surface. Is the surface of the fuel rod adequately cooled?
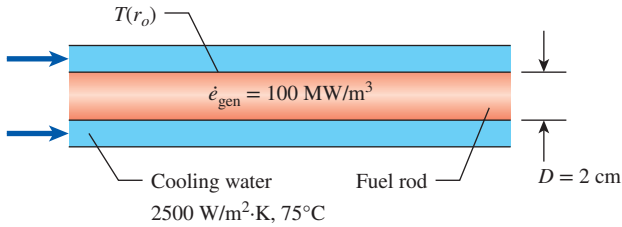
FIGURE P2–104

2–105 **C&S** A long electrical resistance wire of radius $r_1 = 0.2$ cm has a thermal conductivity $k_{wire} = 15$ W/m·K. Heat is generated uniformly in the wire as a result of resistance heating at a constant rate of 1.2 W/cm³. The wire is covered with polyethylene insulation with a thickness of 0.5 cm and thermal conductivity of $k_{ins} = 0.4$ W/m·K. The outer surface of the insulation is subjected to convection and radiation with the surroundings at 20°C. The combined convection and radiation heat transfer coefficients is 7 W/m²·K. Formulate the temperature profiles for the wire and the polyethylene insulation. Use the temperature profiles to determine the temperature at the interface of the wire and the insulation and the temperature at the center of the wire. The ASTM D1351 standard specifies that thermoplastic polyethylene insulation is suitable for use on electrical wire with operation at temperatures up to 75°C. Under these conditions, does the polyethylene insulation for the wire meet the ASTM D1351 standard?
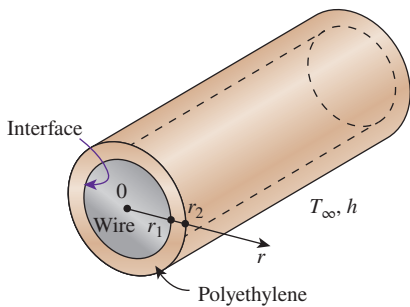
FIGURE P2–105

2–106 Consider a homogeneous spherical piece of radioactive material of radius $r_o = 0.04$ m that is generating heat at a constant rate of $\dot{e}_{gen} = 4 \times 10^7$ W/m³. The heat generated is dissipated to the environment steadily. The outer surface of the sphere is maintained at a uniform temperature of 80°C, and the thermal conductivity of the sphere is $k = 15$ W/m·K. Assuming steady one-dimensional heat transfer, (a) express

the differential equation and the boundary conditions for heat conduction through the sphere, (b) obtain a relation for the variation of temperature in the sphere by solving the differential equation, and (c) determine the temperature at the center of the sphere.
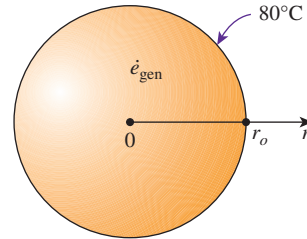
FIGURE P2–106

2–107 Reconsider Prob. 2–106. Using the relation obtained for the variation of temperature in the sphere, plot the temperature as a function of the radius r in the range of $r = 0$ to $r = r_o$. Also, plot the center temperature of the sphere as a function of the thermal conductivity in the range of 10 W/m·K to 400 W/m·K. Discuss the results. Use appropriate software.

2–108 A spherical communication satellite with a diameter of 2.5 m is orbiting the earth. The outer surface of the satellite in space has an emissivity of 0.75 and a solar absorptivity of 0.10, while solar radiation is incident on the spacecraft at a rate of 1000 W/m². If the satellite is made of material with an average thermal conductivity of 5 W/m·K and the midpoint temperature is 0°C, determine the heat generation rate and the surface temperature of the satellite.
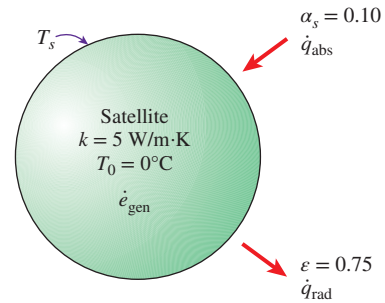
FIGURE P2–108

Variable Thermal Conductivity

2–109C Is the thermal conductivity of a medium, in general, constant or does it vary with temperature?

2–110C When the thermal conductivity of a medium varies linearly with temperature, is the average thermal conductivity always equivalent to the conductivity value at the average temperature?

2–111C The temperature of a plane wall during steady one-dimensional heat conduction varies linearly when the thermal conductivity is constant. Is this still the case when the thermal conductivity varies linearly with temperature?

2–112C Consider steady one-dimensional heat conduction in a plane wall in which the thermal conductivity varies linearly. The error involved in heat transfer calculations by assuming constant thermal conductivity at the average temperature is (*a*) none, (*b*) small, or (*c*) significant.

2–113C Consider steady one-dimensional heat conduction in a plane wall, a long cylinder, and a sphere with constant thermal conductivity and no heat generation. Will the temperature in any of these media vary linearly? Explain.

2–114 A silicon wafer with thickness of 925 μm is being heated with a uniform heat flux at the lower surface. The silicon wafer has a thermal conductivity that varies with temperature and can be expressed as $k(T) = (a + bT + cT^2)$ W/m·K, where $a = 437$, $b = -1.29$, and $c = 0.00111$. To avoid warping, the temperature difference across the wafer thickness cannot exceed 2°C. If the upper surface of the silicon wafer is at a uniform temperature of 600 K, determine the maximum allowable heat flux.
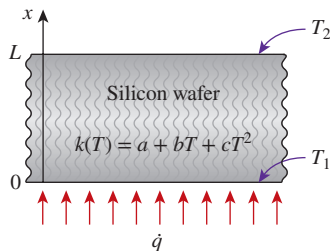
FIGURE P2–114

2–115 Consider a 1.5-m-high and 0.6-m-wide plate whose thickness is 0.15 m. One side of the plate is maintained at a constant temperature of 500 K, while the other side is maintained at 350 K. The thermal conductivity of the plate can be assumed to vary linearly in that temperature range as $k(T) = k_0(1 + \beta T)$ where $k_0 = 25$ W/m·K and $\beta = 8.7 \times 10^{-4}$K^{-1}. Disregarding the edge effects and assuming steady one-dimensional heat transfer, determine the rate of heat conduction through the plate. *Answer: 30.8 kW*

2–116 On the left side, a steel plate is subjected to a uniform heat flux of 50 kW/m^2 and maintained at a constant temperature of 800 K. On the right side, the temperature is maintained at 600 K. The steel plate has a variable thermal conductivity given as $k(T) = k_0(1 + \beta T)$, where $k_0 = 9.14$ W/m·K, $\beta = 0.0023$ K^{-1}, and T is in K. Determine the thickness of the steel plate (in m).

2–117 Consider a plane wall of thickness L whose thermal conductivity varies in a specified temperature range as $k(T) = k_0(1 + \beta T^2)$ where k_0 and β are two specified constants.

The wall surface at $x = 0$ is maintained at a constant temperature of T_1, while the surface at $x = L$ is maintained at T_2. Assuming steady one-dimensional heat transfer, obtain a relation for the heat transfer rate through the wall.

2–118 The thermal conductivity of stainless steel has been characterized experimentally to vary with temperature as $k(T) = 9.14 + 0.021T$ for $273 < T < 1500$ K, where k is in W/m·K and T is in K. Determine the average thermal conductivity between 300 and 1200 K, and express $k(T)$ in the form of $k(T) = k_0(1 + \beta T)$, where k_0 is in W/m·K and β is in K^{-1}.

2–119 A circular metal pipe has a wall thickness of 10 mm and an inner diameter of 10 cm. The pipe's outer surface is subjected to a uniform heat flux of 5 kW/m^2 and has a temperature of 500°C. The metal pipe has a variable thermal conductivity given as $k(T) = k_0(1 + \beta T)$, where $k_0 = 7.5$ W/m·K, $\beta = 0.0012$ K^{-1}, and T is in K. Determine the inner surface temperature of the pipe.
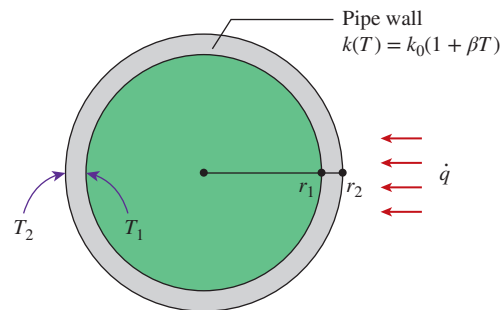
FIGURE P2–119

2–120 PtD A pipe is used for transporting boiling water in which the inner surface is at 100°C. The pipe is situated in surroundings where the ambient temperature is 10°C and the convection heat transfer coefficient is 70 W/m^2·K. The wall thickness of the pipe is 3 mm, and its inner diameter is 30 mm. The pipe wall has a variable thermal conductivity given as $k(T) = k_0(1 + \beta T)$, where $k_0 = 1.23$ W/m·K, $\beta = 0.002$ K^{-1}, and T is in K. For safety reasons and to protect workers from thermal burns, the outer surface temperature of the pipe should be kept below 50°C. Determine whether the outer surface temperature of the pipe is at a low enough temperature to avoid thermal burns.

2–121 A pipe is used for transporting hot fluid in which the inner surface is at 150°C. The pipe has a wall thickness of 5 mm and an inner diameter of 15 cm. The pipe wall has a variable thermal conductivity given as $k(T) = k_0(1 + \beta T)$, where $k_0 = 8.5$ W/m·K, $\beta = 0.001$ K^{-1}, and T is in K. The pipe is situated in surroundings of freezing air at 0°C with a convection heat transfer coefficient of 60 W/m^2·K on the pipe's outer surface. Solar radiation is incident on the pipe's outer surface at a rate of 100 W/m^2, and both the emissivity and solar absorptivity of the outer surface are 0.9. Determine the outer surface temperature of the pipe.
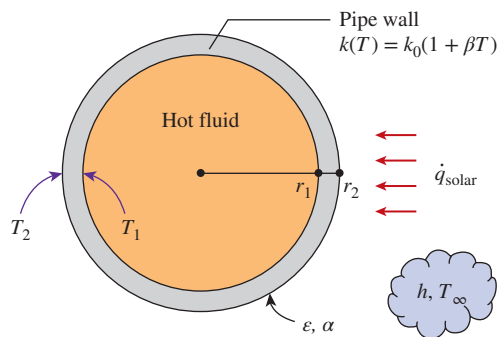
FIGURE P2–121

2–122 A spherical container with an inner radius of 1 m and a wall thickness of 5 mm has its inner surface subjected to a uniform heat flux of 7 kW/m^2. The outer surface of the container is maintained at 20°C. The container wall is made of a material with a thermal conductivity given as $k(T) = k_0(1 + \beta T)$, where $k_0 = 1.33$ W/m·K, $\beta = 0.0023$ K^{-1}, and T is in K. Determine the temperature drop across the container wall thickness.
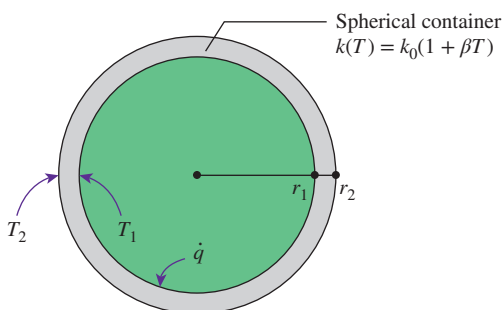
FIGURE P2–122

2–123 Consider a spherical shell of inner radius r_1 and outer radius r_2 whose thermal conductivity varies linearly in a specified temperature range as $k(T) = k_0(1 + \beta T)$ where k_0 and β are two specified constants. The inner surface of the shell is maintained at a constant temperature of T_1, while the outer surface is maintained at T_2. Assuming steady one-dimensional heat transfer, obtain a relation for (*a*) the heat transfer rate through the shell and (*b*) the temperature distribution $T(r)$ in the shell.

2–124 **PtD** A spherical vessel is filled with chemicals undergoing an exothermic reaction. The reaction provides a uniform heat flux on the inner surface of the vessel. The inner diameter of the vessel is 5 m and its inner surface temperature is at 120°C. The wall of the vessel has a variable thermal conductivity given as $k(T) = k_0(1 + \beta T)$, where $k_0 = 1.01$ W/m·K, $\beta = 0.0018$ K^{-1}, and T is in K. The vessel is situated in a surrounding with an ambient temperature of

15°C, and the vessel's outer surface experiences convection heat transfer with a coefficient of 80 W/m^2·K. To prevent thermal burns to workers who touch the vessel, the outer surface temperature of the vessel should be kept below 50°C. Determine the minimum wall thickness of the vessel so that the outer surface temperature is 50°C or lower.

2–125 A spherical tank is filled with ice slurry, where its inner surface is at 0°C. The tank has an inner diameter of 9 m, and its wall thickness is 20 mm. The tank wall is made of a material with a thermal conductivity given as $k(T) = k_0(1 + \beta T)$, where $k_0 = 0.33$ W/m·K, $\beta = 0.0025$ K^{-1}, and T is in K. The temperature outside the tank is 35°C, and the convection heat transfer coefficient is 70 W/m^2·K. Solar radiation is incident on the tank's outer surface at a rate of 150 W/m^2, where the emissivity and solar absorptivity of the outer surface are 0.75. Determine the outer surface temperature of the tank.

Special Topic: Review of Differential Equations

2–126C Why do we often utilize simplifying assumptions when we derive differential equations?

2–127C What is a variable? How do you distinguish a dependent variable from an independent one in a problem?

2–128C Can a differential equation involve more than one independent variable? Can it involve more than one dependent variable? Give examples.

2–129C What is the geometrical interpretation of a derivative? What is the difference between partial derivatives and ordinary derivatives?

2–130C What is the difference between the degree and the order of a derivative?

2–131C Consider a function $f(x, y)$ and its partial derivative $\partial f/\partial x$. Under what conditions will this partial derivative be equal to the ordinary derivative df/dx?

2–132C Consider a function $f(x)$ and its derivative df/dx. Does this derivative have to be a function of x?

2–133C How is integration related to derivation?

2–134C What is the difference between an algebraic equation and a differential equation?

2–135C What is the difference between an ordinary differential equation and a partial differential equation?

2–136C How is the order of a differential equation determined?

2–137C How do you distinguish a linear differential equation from a nonlinear one?

2–138C How do you recognize a linear homogeneous differential equation? Give an example and explain why it is linear and homogeneous.

2–139C How do differential equations with constant coefficients differ from those with variable coefficients? Give an example for each type.

2–140C What kinds of differential equations can be solved by direct integration?

2–141C Consider a third-order linear and homogeneous differential equation. How many arbitrary constants will its general solution involve?

Review Problems

2–142 A large plane wall, with a thickness L and a thermal conductivity k, has its left surface ($x = 0$) exposed to a uniform heat flux $\dot{q}_0$. On the right surface ($x = L$), convection and radiation heat transfer occur in a surrounding temperature of T_∞. The emissivity and the convection heat transfer coefficient on the right surface are ε and h, respectively. Express the boundary conditions and the differential equation of this heat conduction problem during steady operation.

2–143 Consider a long rectangular bar of length a in the x-direction and width b in the y-direction that is initially at a uniform temperature of T_i. The surfaces of the bar at $x = 0$ and $y = 0$ are insulated, while heat is lost from the other two surfaces by convection to the surrounding medium at temperature T_∞ with a heat transfer coefficient of h. Assuming constant thermal conductivity and transient two-dimensional heat transfer with no heat generation, express the mathematical formulation (the differential equation and the boundary and initial conditions) of this heat conduction problem. Do not solve.
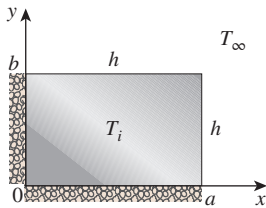
FIGURE P2–143

2–144E Consider a large plane wall of thickness $L = 0.8$ ft and thermal conductivity $k = 1.2$ Btu/h·ft·°F. The wall is covered with a material that has an emissivity of $\varepsilon = 0.80$ and a solar absorptivity of $\alpha = 0.60$. The inner surface of the wall is maintained at $T_1 = 520$ R at all times, while the outer surface is exposed to solar radiation that is incident at a rate of $\dot{q}_{solar} = 300$ Btu/h·ft^2. The outer surface is also losing heat by radiation to deep space at 0 K. Determine the temperature of the outer surface of the wall and the rate of heat transfer through the wall when steady operating conditions are reached. *Answers: 554 R, 50.9 Btu/h·ft^2*
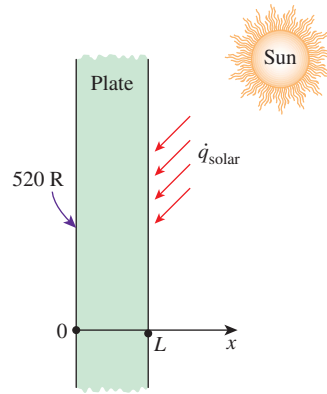
FIGURE P2–144E

2–145 A spherical vessel has an inner radius r_1 and an outer radius r_2. The inner surface ($r = r_1$) of the vessel is subjected to a uniform heat flux $\dot{q}_1$. The outer surface ($r = r_2$) is exposed to convection and radiation heat transfer in a surrounding temperature of T_∞. The emissivity and the convection heat transfer coefficient on the outer surface are ε and h, respectively. Express the boundary conditions and the differential equation of this heat conduction problem during steady operation.

2–146 Consider a short cylinder of radius r_o and height H in which heat is generated at a constant rate of $\dot{e}_{gen}$. Heat is lost from the cylindrical surface at $r = r_o$ by convection to the surrounding medium at temperature T_∞ with a heat transfer coefficient of h. The bottom surface of the cylinder at $z = 0$ is insulated, while the top surface at $z = H$ is subjected to uniform heat flux $\dot{q}_H$. Assuming constant thermal conductivity and steady two-dimensional heat transfer, express the mathematical formulation (the differential equation and the boundary conditions) of this heat conduction problem. Do not solve.

2–147 Consider a small hot metal object of mass m and specific heat c that is initially at a temperature of T_i. Now the object is allowed to cool in an environment at T_∞ by convection with a heat transfer coefficient of h. The temperature of the metal object is observed to vary uniformly with time during cooling. Writing an energy balance on the entire metal object, derive the differential equation that describes the variation of temperature of the ball with time, $T(t)$. Assume constant thermal conductivity and no heat generation in the object. Do not solve.
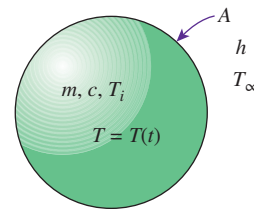
FIGURE P2–147

2–148 Consider a 20-cm-thick large concrete plane wall ($k = 0.77$ W/m·K) subjected to convection on both sides with $T_{\infty 1} = 22°C$ and $h_1 = 8$ W/m²·K on the inside and $T_{\infty 2} = 8°C$ and $h_2 = 12$ W/m²·K on the outside. Assuming constant thermal conductivity with no heat generation and negligible radiation, (a) express the differential equations and the boundary conditions for steady one-dimensional heat conduction through the wall, (b) obtain a relation for the variation of temperature in the wall by solving the differential equation, and (c) evaluate the temperatures at the inner and outer surfaces of the wall.

2–149 A 1000-W iron is left on the ironing board with its base exposed to ambient air at 26°C. The base plate of the iron has a thickness of $L = 0.5$ cm, base area of $A = 150$ cm², and thermal conductivity of $k = 18$ W/m·K. The inner surface of the base plate is subjected to uniform heat flux generated by the resistance heaters inside. The outer surface of the base plate, whose emissivity is $\varepsilon = 0.7$, loses heat by convection to ambient air with an average heat transfer coefficient of $h = 30$ W/m²·K as well as by radiation to the surrounding surfaces at an average temperature of $T_{surr} = 295$ K. Disregarding any heat loss through the upper part of the iron, (a) express the differential equation and the boundary conditions for steady one-dimensional heat conduction through the plate, (b) obtain a relation for the temperature of the outer surface of the plate by solving the differential equation, and (c) evaluate the outer surface temperature.
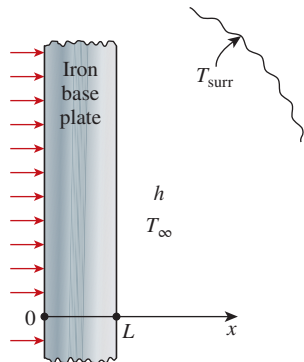
FIGURE P2–149

2–150 [C&S] A heating cable is embedded in a concrete slab for snow melting on a 30 m² surface area. The heating cable is heated electrically with joule heating. When the surface is covered with snow, the heat generated from the heating cable can melt snow at a rate of 0.1 kg/s. According to the National Electrical Code (NFPA 70), the power density for embedded snow-melting equipment should not exceed 1300 W/m². Formulate the temperature profile in the concrete slab in terms of the snow melt rate. Determine whether melting snow at 0.1 kg/s would be in compliance with the NFPA 70 code.
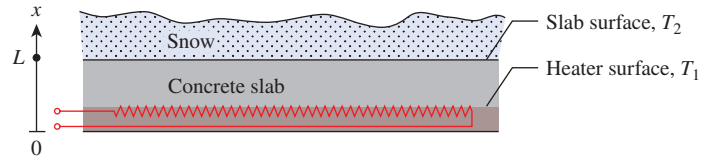
FIGURE P2–150

2–151 [C&S] A series of ASME SA-193 carbon steel bolts are bolted onto the upper surface of a metal plate. The metal plate has a thickness of 3 cm, and its thermal conductivity is 15 W/m·K. The bottom surface of the plate is subjected to a uniform heat flux of 5 kW/m². The upper surface of the plate is exposed to ambient air with a temperature of 30°C and a convection heat transfer coefficient of 10 W/m²·K. The ASME Boiler and Pressure Vessel Code (ASME BPVC.IV-2015, HF-300) limits the maximum allowable use temperature to 260°C for the SA-193 bolts. Formulate the variation of temperature in the metal plate, and determine the temperatures at $x = 0$, 1.5, and 3.0 cm. Would the SA-193 bolts comply with the ASME code?
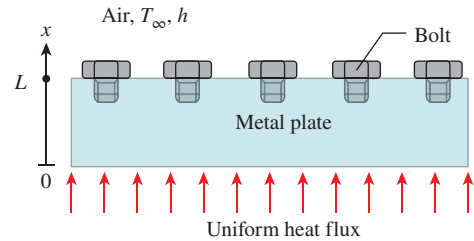
FIGURE P2–151

2–152 Consider a steam pipe of length L, inner radius r_1, outer radius r_2, and constant thermal conductivity k. Steam flows inside the pipe at an average temperature of T_i with a convection heat transfer coefficient of h_i. The outer surface of the pipe is exposed to convection to the surrounding air at a temperature of T_0 with a heat transfer coefficient of h_o. Assuming steady one-dimensional heat conduction through the pipe, (a) express the differential equation and the boundary conditions for heat conduction through the pipe material, (b) obtain a relation for the variation of temperature in the pipe material by solving the differential equation, and (c) obtain a relation for the temperature of the outer surface of the pipe.
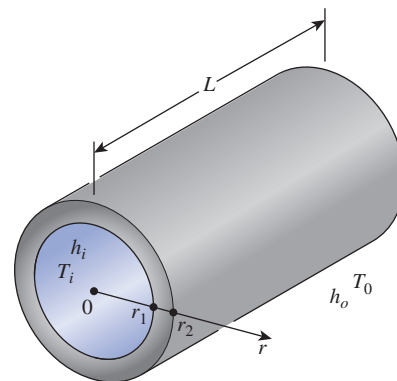
FIGURE P2–152

2–153 Exhaust gases from a manufacturing plant are being discharged through a 10-m-tall exhaust stack with outer diameter of 1 m, wall thickness of 10 cm, and thermal conductivity of 40 W/m·K. The exhaust gases are discharged at a rate of 1.2 kg/s, while the temperature drop between the inlet and exit of the exhaust stack is 30°C, and the constant pressure specific heat of the exhaust gases is 1600 J/kg·K. On a particular day, the outer surface of the exhaust stack experiences radiation with the surrounding at 27°C and convection with the ambient air at 27°C also, with an average convection heat transfer coefficient of 8 W/m²·K. Solar radiation is incident on the exhaust stack outer surface at a rate of 150 W/m², and both the emissivity and solar absorptivity of the outer surface are 0.9. Assuming steady one-dimensional heat transfer, (a) obtain the variation of temperature in the exhaust stack wall and (b) determine the inner surface temperature of the exhaust stack.
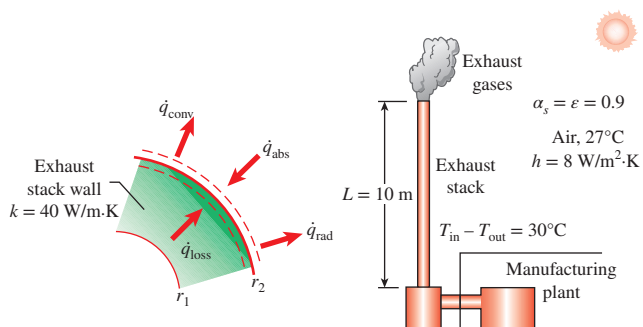
FIGURE P2–153

2–154E Consider a steam pipe of length $L = 35$ ft, inner radius $r_1 = 2$ in, outer radius $r_2 = 24$ in, and thermal conductivity $k = 8$ Btu/h·ft·°F. Steam is flowing through the pipe at an average temperature of 250°F, and the average convection heat transfer coefficient on the inner surface is given to be $h = 15$ Btu/h·ft²·°F. If the average temperature on the outer surfaces of the pipe is $T_2 = 160°F$, (a) express the differential equation and the boundary conditions for steady one-dimensional heat conduction through the pipe, (b) obtain a relation for the variation of temperature in the pipe by solving the differential equation, and (c) evaluate the rate of heat loss from the steam through the pipe.
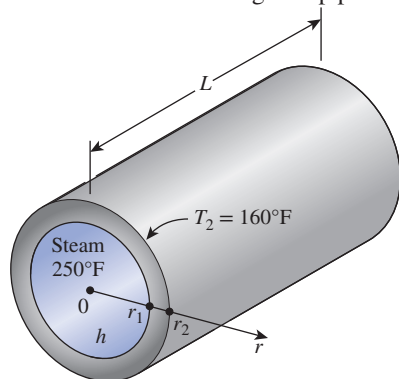
FIGURE P2–154E

2–155 When a long section of a compressed air line passes through the outdoors, the moisture in the compressed air freezes in cold weather, disrupting and even completely blocking the airflow in the pipe. To avoid this problem, the outer surface of the pipe is wrapped with electric strip heaters and then insulated. Consider a compressed air pipe of length $L = 6$ m, inner radius $r_1 = 3.7$ cm, outer radius $r_2 = 4.0$ cm, and thermal conductivity $k = 14$ W/m·K equipped with a 300-W strip heater. Air is flowing through the pipe at an average temperature of $-10°C$, and the average convection heat transfer coefficient on the inner surface is $h = 30$ W/m²·K. Assuming 15 percent of the heat generated in the strip heater is lost through the insulation, (a) express the differential equation and the boundary conditions for steady one-dimensional heat conduction through the pipe, (b) obtain a relation for the variation of temperature in the pipe material by solving the differential equation, and (c) evaluate the inner and outer surface temperatures of the pipe.
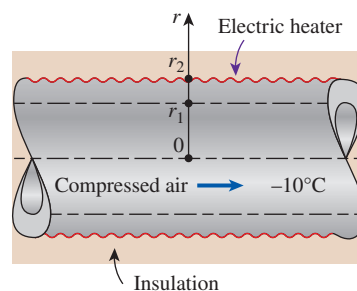
FIGURE P2–155

2–156 Consider a water pipe of length $L = 17$ m, inner radius $r_1 = 15$ cm, outer radius $r_2 = 20$ cm, and thermal conductivity $k = 14$ W/m·K. Heat is generated in the pipe material uniformly by a 25-kW electric resistance heater. The inner and outer surfaces of the pipe are at $T_1 = 60°C$ and $T_2 = 80°C$, respectively. Obtain a general relation for temperature distribution inside the pipe under steady conditions and determine the temperature at the center plane of the pipe.

2–157 A long electrical resistance wire of radius $r_1 = 0.25$ cm has a thermal conductivity $k_{wire} = 15$ W/m·K. Heat is generated uniformly in the wire as a result of resistance heating at a constant rate of 0.5 W/cm³. The wire is covered with polyethylene insulation with a thickness of 0.25 cm and thermal conductivity of $k_{ins} = 0.4$ W/m·K. The outer surface of the insulation is subjected to free convection in air at 20°C and a convection heat transfer coefficient of 2 W/m²·K. Formulate the temperature profiles for the wire and the polyethylene insulation. Use the temperature profiles to determine the temperature at the interface of the wire and the insulation and the temperature at the center of the wire. The ASTM D1351 standard specifies that thermoplastic polyethylene insulation is suitable for use on electrical wire that operates at temperatures up to 75°C. Under these conditions, does the polyethylene insulation for the wire meet the ASTM D1351 standard?
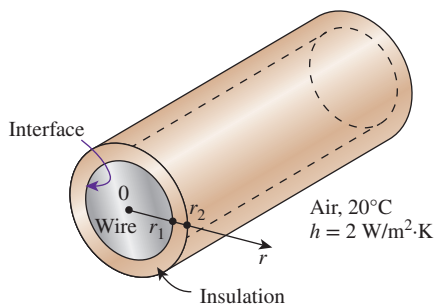
FIGURE P2–157

2–158 In a manufacturing plant, a quench hardening process is used to treat steel ball bearings ($c = 500$ J/kg·K, $k = 60$ W/m·K, $\rho = 7900$ kg/m^3) of 25 mm in diameter. After being heated to a prescribed temperature, the steel ball bearings are quenched. Determine the rate of heat loss if the rate of temperature decrease in the ball bearings at a given instant during the quenching process is 50 K/s. *Answer:* 1.62 kW

2–159 Consider a spherical reactor of 5-cm diameter operating at steady conditions with a temperature variation that can be expressed in the form of $T(r) = a - br^2$, where $a = 850°C$ and $b = 5 \times 10^5$ K/m^2. The reactor is made of material with $c = 200$ J/kg·°C, $k = 40$ W/m·K, $\rho = 9000$ kg/m^3. If the heat generation of the reactor is suddenly set to 9 MW/m^3, determine the time rate of temperature change in the reactor. Is the heat generation of the reactor suddenly increased or decreased to 9 MW/m^3 from its steady operating condition?

2–160 Consider a cylindrical shell of length L, inner radius r_1, and outer radius r_2 whose thermal conductivity varies in a specified temperature range as $k(T) = k_0(1 + \beta T^2)$ where k_0 and β are two specified constants. The inner surface of the shell is maintained at a constant temperature of T_1 while the outer surface is maintained at T_2. Assuming steady one-dimensional heat transfer, obtain a relation for the heat transfer rate through the shell.

2–161 A pipe is used for transporting boiling water in which the inner surface is at 100°C. The pipe is situated where the ambient temperature is 20°C and the convection heat transfer coefficient is 50 W/m^2·K. The pipe has a wall thickness of 3 mm and an inner diameter of 25 mm, and it has a variable thermal conductivity given as $k(T) = k_0(1 + \beta T)$, where $k_0 = 1.5$ W/m·K, $\beta = 0.003$ K^{-1}, and T is in K. Determine the outer surface temperature of the pipe.

2–162 A metal spherical tank is filled with chemicals undergoing an exothermic reaction. The reaction provides a uniform heat flux on the inner surface of the tank. The tank has an inner diameter of 5 m, and its wall thickness is 10 mm. The tank wall has a variable thermal conductivity given as $k(T) = k_0(1 + \beta T)$, where $k_0 = 9.1$ W/m·K, $\beta = 0.0018$ K^{-1}, and T is in K. The area surrounding the tank has an ambient temperature of 15°C, the tank's outer surface experiences

convection heat transfer with a coefficient of 80 W/m^2·K. Determine the heat flux on the tank's inner surface if the inner surface temperature is 120°C.

Fundamentals of Engineering (FE) Exam Problems

2–163 The heat conduction equation in a medium is given in its simplest form as

$$\frac{1}{r}\frac{d}{dr}\left(rk\frac{dT}{dr}\right) + \dot{e}_{\text{gen}} = 0$$

Select the wrong statement below.
   (*a*) The medium is of cylindrical shape.
   (*b*) The thermal conductivity of the medium is constant.
   (*c*) Heat transfer through the medium is steady.
   (*d*) There is heat generation within the medium.
   (*e*) Heat conduction through the medium is one-dimensional.

2–164 Consider a medium in which the heat conduction equation is given in its simplest forms as

$$\frac{1}{r^2}\frac{\partial}{\partial r}\left(r^2\frac{\partial T}{\partial r}\right) = \frac{1}{\alpha}\frac{\partial T}{\partial t}$$

   (*a*) Is heat transfer steady or transient?
   (*b*) Is heat transfer one-, two-, or three-dimensional?
   (*c*) Is there heat generation in the medium?
   (*d*) Is the thermal conductivity of the medium constant or variable?
   (*e*) Is the medium a plane wall, a cylinder, or a sphere?
   (*f*) Is this differential equation for heat conduction linear or nonlinear?

2–165 Consider a large plane wall of thickness L, thermal conductivity k, and surface area A. The left surface of the wall is exposed to the ambient air at T_∞ with a heat transfer coefficient of h while the right surface is insulated. The variation of temperature in the wall for steady one-dimensional heat conduction with no heat generation is

(*a*) $T(x) = \dfrac{h(L-x)}{k}T_\infty$ (*b*) $T(x) = \dfrac{k}{h(x+0.5L)}T_\infty$

(*c*) $T(x) = \left(1 - \dfrac{xh}{k}\right)T_\infty$ (*d*) $T(x) = (L-x)T_\infty$

(*e*) $T(x) = T_\infty$

2–166 A solar heat flux $\dot{q}_s$ is incident on a sidewalk whose thermal conductivity is k, solar absorptivity is α_s, and convective heat transfer coefficient is h. Taking the positive x-direction to be toward the sky and disregarding radiation exchange with the surrounding surfaces, the correct boundary condition for this sidewalk surface is

(*a*) $-k\dfrac{dT}{dx} = \alpha_s \dot{q}_s$ (*b*) $-k\dfrac{dT}{dx} = h(T - T_\infty)$

(*c*) $-k\dfrac{dT}{dx} = h(T - T_\infty) - \alpha_s \dot{q}_s$ (*d*) $h(T - T_\infty) = \alpha_s \dot{q}_s$

(*e*) None of them

2–167 A plane wall of thickness L is subjected to convection at both surfaces with ambient temperature $T_{\infty 1}$ and heat transfer coefficient h_1 at the inner surface and corresponding $T_{\infty 2}$ and h_2 values at the outer surface. Taking the positive direction of x to be from the inner surface to the outer surface, the correct expression for the convection boundary condition is

(a) $k\dfrac{dT(0)}{dx} = h_1[T(0) - T_{\infty 1}]$ (b) $k\dfrac{dT(L)}{dx} = h_2[T(L) - T_{\infty 2}]$

(c) $-k\dfrac{dT(0)}{dx} = h_1(T_{\infty 1} - T_{\infty 2})$ (d) $-k\dfrac{dT(L)}{dx} = h_2(T_{\infty 1} - T_{\infty 2})$

(e) None of them

2–168 Consider steady one-dimensional heat conduction through a plane wall, a cylindrical shell, and a spherical shell of uniform thickness with constant thermophysical properties and no thermal energy generation. The geometry in which the variation of temperature in the direction of heat transfer will be linear is

(a) plane wall   (b) cylindrical shell   (c) spherical shell
(d) all of them   (e) none of them

2–169 The conduction equation boundary condition for an adiabatic surface with direction n being normal to the surface is

(a) $T = 0$ (b) $dT/dn = 0$ (c) $d^2T/dn^2 = 0$
(d) $d^3T/dn^3 = 0$ (e) $-kdT/dn = 1$

2–170 The variation of temperature in a plane wall is determined to be $T(x) = 65x + 25$ where x is in m and T is in °C. If the temperature at one surface is 38°C, the thickness of the wall is

(a) 2 m   (b) 0.4 m   (c) 0.2 m
(d) 0.1 m   (e) 0.05 m

2–171 The variation of temperature in a plane wall is determined to be $T(x) = 110x - 48x$ where x is in m and T is in °C. If the thickness of the wall is 0.75 m, the temperature difference between the inner and outer surfaces of the wall is

(a) 110°C   (b) 74°C   (c) 55°C   (d) 36°C   (e) 18°C

2–172 The temperatures at the inner and outer surfaces of a 15-cm-thick plane wall are measured to be 40°C and 28°C, respectively. The expression for steady, one-dimensional variation of temperature in the wall is

(a) $T(x) = 28x + 40$ (b) $T(x) = -40x + 28$
(c) $T(x) = 40x + 28$ (d) $T(x) = -80x + 40$
(e) $T(x) = 40x - 80$

2–173 The thermal conductivity of a solid depends upon the solid's temperature as $k = aT + b$ where a and b are constants. The temperature in a planar layer of this solid as it conducts heat is given by

(a) $aT + b = x + C_2$ (b) $aT + b = C_1 x^2 + C_2$
(c) $aT^2 + bT = C_1 x + C_2$ (d) $aT^2 + bT = C_1 x^2 + C_2$
(e) None of them

2–174 Hot water flows through a PVC ($k = 0.092$ W/m·K) pipe whose inner diameter is 2 cm and whose outer diameter is 2.5 cm. The temperature of the interior surface of this pipe is 35°C, and the temperature of the exterior surface is 20°C. The rate of heat transfer per unit of pipe length is

(a) 22.8 W/m   (b) 38.9 W/m   (c) 48.7 W/m
(d) 63.6 W/m   (e) 72.6 W/m

2–175 Heat is generated in a long 0.3-cm-diameter cylindrical electric heater at a rate of 150 W/m³. The heat flux at the surface of the heater in steady operation is

(a) 42.7 W/cm²   (b) 159 W/cm²   (c) 150 W/cm²
(d) 10.6 W/cm²   (e) 11.3 W/cm²

2–176 Heat is generated uniformly in a 4-cm-diameter, 16-cm-long solid bar ($k = 2.4$ W/m·K). The temperatures at the center and at the surface of the bar are measured to be 210°C and 45°C, respectively. The rate of heat generation within the bar is

(a) 240 W   (b) 796 W   (c) 1013 W
(d) 79,620 W   (e) 3.96×10^6 W

2–177 Heat is generated in an 8-cm-diameter spherical radioactive material whose thermal conductivity is 25 W/m·K uniformly at a rate of 15 W/cm³. If the surface temperature of the material is measured to be 120°C, the center temperature of the material during steady operation is

(a) 160°C   (b) 280°C   (c) 212°C
(d) 360°C   (e) 600°C

2–178 Heat is generated in a 3-cm-diameter spherical radioactive material uniformly at a rate of 15 W/cm³. Heat is dissipated to the surrounding medium at 25°C with a heat transfer coefficient of 120 W/m²·K. The surface temperature of the material in steady operation is

(a) 56°C   (b) 84°C   (c) 494°C
(d) 650°C   (e) 108°C

Design and Essay Problems

2–179 Write an essay on heat generation in nuclear fuel rods. Obtain information on the ranges of heat generation, the variation of heat generation with position in the rods, and the absorption of emitted radiation by the cooling medium.

2–180 Write an interactive computer program to calculate the heat transfer rate and the value of temperature anywhere in the medium for steady one-dimensional heat conduction in a long cylindrical shell for any combination of specified temperature, specified heat flux, and convection boundary conditions. Run the program for five different sets of specified boundary conditions.

2–181 Write an interactive computer program to calculate the heat transfer rate and the value of temperature anywhere in the medium for steady one-dimensional heat conduction in a spherical shell for any combination of specified temperature, specified heat flux, and convection boundary conditions. Run the program for five different sets of specified boundary conditions.

Design Element: "C&S icon ©McGraw-Hill Education; PtD icon ©McGraw-Hill Education; laptop art ©McGraw-Hill Education".

STEADY HEAT CONDUCTION

I n heat transfer analysis, we are often interested in the rate of heat transfer through a medium under steady conditions and surface temperatures. Such problems can be solved easily without involving any differential equations by the introduction of the *thermal resistance concept* in a manner analogous to electrical circuit problems. In this case, the thermal resistance corresponds to electrical resistance, temperature difference corresponds to voltage, and the heat transfer rate corresponds to electric current.

We start this chapter with *one-dimensional steady heat conduction* in a plane wall, a cylinder, and a sphere, and we develop relations for *thermal resistances* in these geometries. We also develop thermal resistance relations for convection and radiation conditions at the boundaries. We apply this concept to heat conduction problems in *multilayer* plane walls, cylinders, and spheres and generalize it to systems that involve heat transfer in two or three dimensions. We also discuss the *thermal contact resistance* and the *overall heat transfer coefficient* and develop relations for the critical radius of insulation for a cylinder and a sphere. Finally, we discuss steady heat transfer from *finned surfaces* and some complex geometrics commonly encountered in practice through the use of *conduction shape factors*.

OBJECTIVES

When you finish studying this chapter, you should be able to:

- Understand the concept of thermal resistance and its limitations, and develop thermal resistance networks for practical heat conduction problems,

- Solve steady conduction problems that involve multilayer rectangular, cylindrical, or spherical geometries,

- Develop an intuitive understanding of thermal contact resistance and circumstances under which it may be significant,

- Identify applications in which insulation may actually increase heat transfer,

- Analyze finned surfaces, and assess how efficiently and effectively fins enhance heat transfer, and

- Solve multidimensional practical heat conduction problems using conduction shape factors.

FIGURE 3–1
Heat transfer through a wall is one-dimensional when the temperature of the wall varies in one direction only.

FIGURE 3–2
Under steady conditions, the temperature distribution in a plane wall is a straight line.
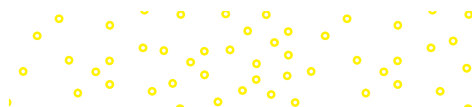
3–1 ▪ STEADY HEAT CONDUCTION IN PLANE WALLS

Consider steady heat conduction through the walls of a house during a winter day. We know that heat is continuously lost to the outdoors through the wall. We intuitively feel that heat transfer through the wall is in the *normal direction* to the wall surface, and no significant heat transfer takes place in the wall in other directions (Fig. 3–1).

Recall that heat transfer in a certain direction is driven by the *temperature gradient* in that direction. There is no heat transfer in a direction in which there is no change in temperature. Temperature measurements at several locations on the inner or outer wall surface will confirm that a wall surface is nearly *isothermal.* That is, the temperatures at the top and bottom of a wall surface as well as at the right and left ends are almost the same. Therefore, there is no heat transfer through the wall from the top to the bottom, or from left to right, but there is considerable temperature difference between the inner and the outer surfaces of the wall, and thus significant heat transfer in the direction from the inner surface to the outer one.

The small thickness of the wall causes the temperature gradient in that direction to be large. Further, if the air temperatures inside and outside the house remain constant, then heat transfer through the wall of a house can be modeled as *steady* and *one-dimensional.* The temperature of the wall in this case depends on one direction only (say the *x*-direction) and can be expressed as $T(x)$.

Noting that heat transfer is the only energy interaction involved in this case and there is no heat generation, the *energy balance* for the wall can be expressed as

$$\begin{pmatrix} \text{Rate of} \\ \text{heat transfer} \\ \text{into the wall} \end{pmatrix} - \begin{pmatrix} \text{Rate of} \\ \text{heat transfer} \\ \text{out of the wall} \end{pmatrix} = \begin{pmatrix} \text{Rate of change} \\ \text{of the energy} \\ \text{of the wall} \end{pmatrix}$$

or

$$\dot{Q}_{\text{in}} - \dot{Q}_{\text{out}} = \frac{dE_{\text{wall}}}{dt} \tag{3–1}$$

But $dE_{\text{wall}}/dt = 0$ for *steady* operation, since there is no change in the temperature of the wall with time at any point. Therefore, the rate of heat transfer into the wall must be equal to the rate of heat transfer out of it. In other words, *the rate of heat transfer through the wall must be constant,* $\dot{Q}_{\text{cond, wall}} = $ constant.

Consider a plane wall of thickness L and average thermal conductivity k. The two surfaces of the wall are maintained at constant temperatures of T_1 and T_2. For one-dimensional steady heat conduction through the wall, we have $T(x)$. Then Fourier's law of heat conduction for the wall can be expressed as

$$\dot{Q}_{\text{cond, wall}} = -kA\frac{dT}{dx} \quad \text{(W)} \tag{3–2}$$

where the rate of conduction heat transfer $\dot{Q}_{\text{cond, wall}}$ and the wall area A are constant. Thus $dT/dx = $ constant, which means that *the temperature through the wall varies linearly with x.* That is, the temperature distribution in the wall under steady conditions is a *straight line* (Fig. 3–2).
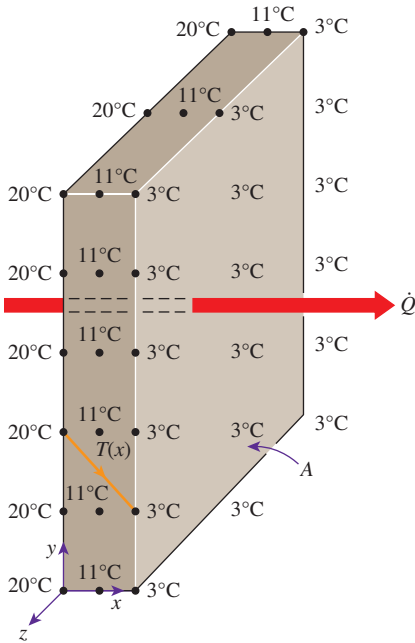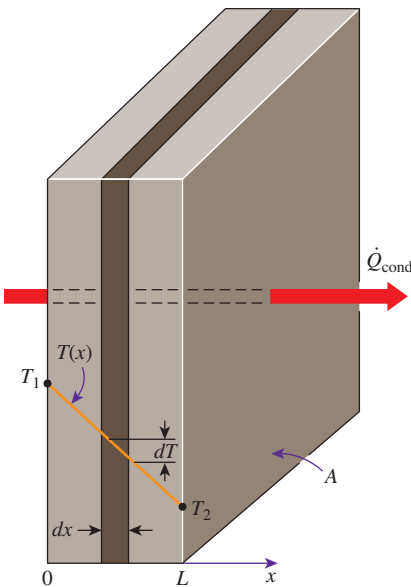
Separating the variables in the preceding equation and integrating from $x = 0$, where $T(0) = T_1$, to $x = L$, where $T(L) = T_2$, we get

$$\int_{x=0}^{L} \dot{Q}_{\text{cond, wall}} \, dx = -\int_{T=T_1}^{T_2} kA \, dT$$

Performing the integrations and rearranging gives

$$\dot{Q}_{\text{cond, wall}} = kA \frac{T_1 - T_2}{L} \quad (\text{W}) \tag{3–3}$$

which is identical to Eq. 1–21. Again, *the rate of heat conduction through a plane wall is proportional to the average thermal conductivity, the wall area, and the temperature difference, but is inversely proportional to the wall thickness.* Also, once the rate of heat conduction is available, the temperature $T(x)$ at any location x can be determined by replacing T_2 in Eq. 3–3 with T and L with x.

Thermal Resistance Concept

Equation 3–3 for heat conduction through a plane wall can be rearranged as

$$\dot{Q}_{\text{cond, wall}} = \frac{T_1 - T_2}{R_{\text{wall}}} \quad (\text{W}) \tag{3–4}$$

where

$$R_{\text{wall}} = \frac{L}{kA} \quad (\text{K/W}) \tag{3–5}$$

is the *thermal resistance* of the wall against heat conduction or simply the **conduction resistance** of the wall. Note that the thermal resistance of a medium depends on the *geometry* and the *thermal properties* of the medium. Note that thermal resistance can also be expressed as $R_{\text{wall}} = \Delta T / \dot{Q}_{\text{cond, wall}}$, which is the ratio of the driving potential ΔT to the corresponding transfer rate $\dot{Q}_{\text{cond, wall}}$.

This equation for heat transfer is analogous to the relation for *electric current flow I,* expressed as

$$I = \frac{V_1 - V_2}{R_e} \tag{3–6}$$

where $R_e = L / \sigma_e A$ is the *electrical resistance* and $V_1 - V_2$ is the *voltage difference* across the resistance (σ_e is the electrical conductivity). Thus, the *rate of heat transfer* through a layer corresponds to the *electric current,* the *thermal resistance* corresponds to *electrical resistance,* and the *temperature difference* corresponds to *voltage difference* across the layer (Fig. 3–3).

Consider convection heat transfer from a solid surface of area A_s and temperature T_s to a fluid whose temperature sufficiently far from the surface is T_∞, with a convection heat transfer coefficient h. Newton's law of cooling for convection heat transfer rate $\dot{Q}_{\text{conv}} = hA_s(T_s - T_\infty)$ can be rearranged as

$$\dot{Q}_{\text{conv}} = \frac{T_s - T_\infty}{R_{\text{conv}}} \quad (\text{W}) \tag{3–7}$$

$$\dot{Q} = \frac{T_1 - T_2}{R}$$

$T_1 \bullet$ —⋀⋀⋀— $\bullet T_2$
R
(*a*) Heat flow

$$I = \frac{V_1 - V_2}{R_e}$$

$V_1 \bullet$ —⋀⋀⋀— $\bullet V_2$
R_e
(*b*) Electric current flow
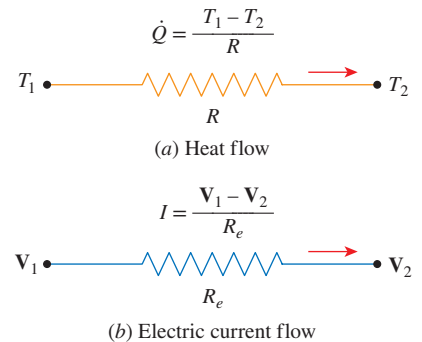
FIGURE 3–3

Analogy between thermal and electrical resistance concepts.
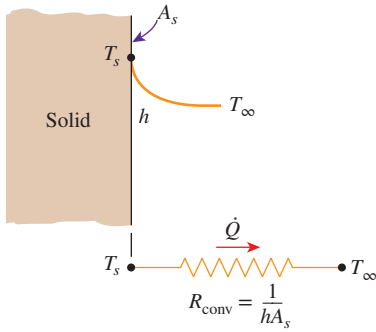
FIGURE 3–4
Schematic for convection resistance at a surface.

where

$$R_{\text{conv}} = \frac{1}{hA_s} \quad \text{(K/W)} \tag{3–8}$$

is the *thermal resistance* of the surface against heat convection, or simply the **convection resistance** of the surface (Fig. 3–4). Note that when the convection heat transfer coefficient is very large ($h \rightarrow \infty$), the convection resistance becomes *zero* and $T_s \approx T_\infty$. That is, the surface offers *no resistance to convection,* and thus it does not slow down the heat transfer process. This situation is approached in practice at surfaces where boiling and condensation occur. Also note that the surface does not have to be a plane surface. Equation 3–8 for convection resistance is valid for surfaces of any shape, provided that the assumption of $h =$ constant and uniform is reasonable.

When the wall is surrounded by a gas, the *radiation effects,* which we have ignored so far, can be significant and may need to be considered. The rate of radiation heat transfer between a surface of emissivity ε and area A_s at temperature T_s and the surrounding surfaces at some average temperature T_{surr} can be expressed as

$$\dot{Q}_{\text{rad}} = \varepsilon\sigma A_s(T_s^4 - T_{\text{surr}}^4) = h_{\text{rad}} A_s(T_s - T_{\text{surr}}) = \frac{T_s - T_{\text{surr}}}{R_{\text{rad}}} \quad \text{(W)} \tag{3–9}$$

where

$$R_{\text{rad}} = \frac{1}{h_{\text{rad}}A_s} \quad \text{(K/W)} \tag{3–10}$$

is the *thermal resistance* of a surface against radiation, or the **radiation resistance**, and

$$h_{\text{rad}} = \frac{\dot{Q}_{\text{rad}}}{A_s(T_s - T_{\text{surr}})} = \varepsilon\sigma(T_s^2 + T_{\text{surr}}^2)(T_s + T_{\text{surr}}) \quad \text{(W/m}^2\cdot\text{K)} \tag{3–11}$$

is the **radiation heat transfer coefficient**. Note that both T_s and T_{surr} *must* be in K in the evaluation of h_{rad}. The definition of the radiation heat transfer coefficient enables us to express radiation conveniently in a manner analogous to convection in terms of a temperature difference. But h_{rad} depends strongly on temperature, while h_{conv} usually does not.

A surface exposed to the surrounding air involves convection and radiation simultaneously, and the total heat transfer at the surface is determined by adding (or subtracting, if in the opposite direction) the radiation and convection components. The convection and radiation resistances are parallel to each other, as shown in Fig. 3–5, and they may cause some complication in the thermal resistance network. When $T_{\text{surr}} \approx T_\infty$, the radiation effect can properly be accounted for by replacing h in the convection resistance relation (Eq. 3–8) with

$$h_{\text{combined}} = h_{\text{conv}} + h_{\text{rad}} \quad \text{(W/m}^2\cdot\text{K)} \tag{3–12}$$
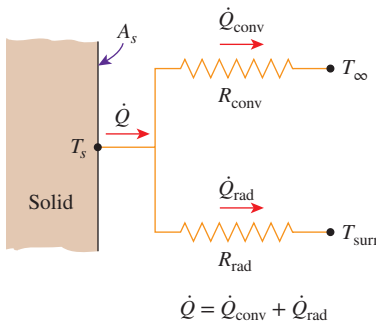
FIGURE 3–5
Schematic for convection and radiation resistances at a surface.

where h_{combined} is the **combined heat transfer coefficient** discussed in Chap. 1. This way all complications associated with radiation are avoided.

$$\dot{Q} = \frac{T_{\infty 1} - T_{\infty 2}}{R_{\text{conv},1} + R_{\text{wall}} + R_{\text{conv},2}}$$

Thermal network

$$I = \frac{\mathbf{V}_1 - \mathbf{V}_2}{R_{e,1} + R_{e,2} + R_{e,3}}$$

Electrical analogy
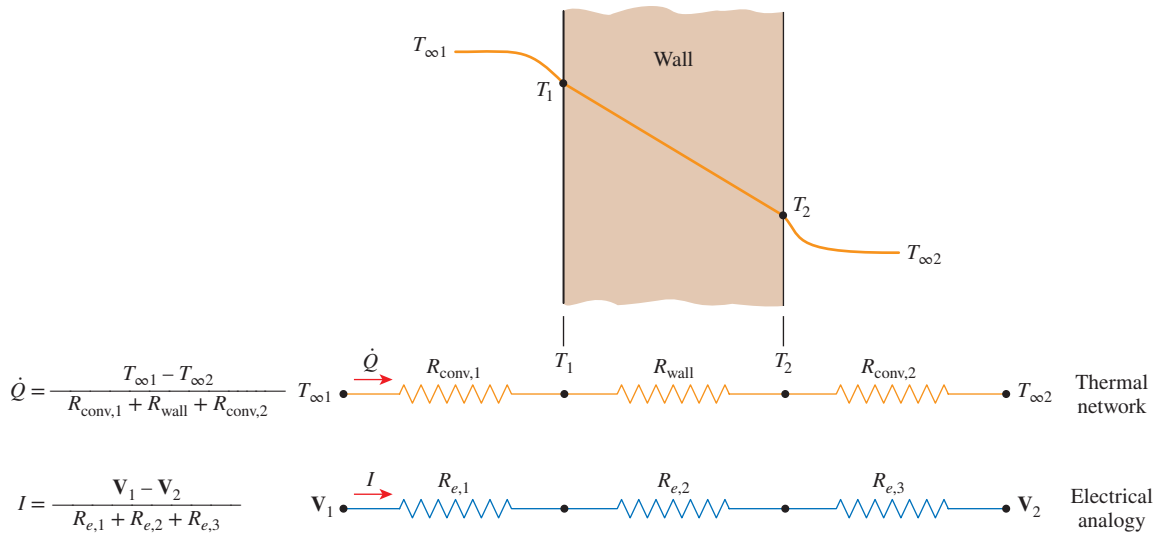
FIGURE 3–6

The thermal resistance network for heat transfer through a plane wall subjected to convection on both sides, and the electrical analogy.

Thermal Resistance Network

Now consider steady one-dimensional heat transfer through a plane wall of thickness L, area A, and thermal conductivity k that is exposed to convection on both sides to fluids at temperatures $T_{\infty 1}$ and $T_{\infty 2}$ with heat transfer coefficients h_1 and h_2, respectively, as shown in Fig. 3–6. Assuming $T_{\infty 2} < T_{\infty 1}$, the variation of temperature will be as shown in the figure. Note that the temperature varies linearly in the wall and asymptotically approaches $T_{\infty 1}$ and $T_{\infty 2}$ in the fluids as we move away from the wall.

Under steady conditions we have

$$\begin{pmatrix} \text{Rate of} \\ \textit{heat convection} \\ \text{into the wall} \end{pmatrix} = \begin{pmatrix} \text{Rate of} \\ \textit{heat conduction} \\ \text{through the wall} \end{pmatrix} = \begin{pmatrix} \text{Rate of} \\ \textit{heat convection} \\ \text{from the wall} \end{pmatrix}$$

or

$$\dot{Q} = h_1 A(T_{\infty 1} - T_1) = kA\frac{T_1 - T_2}{L} = h_2 A(T_2 - T_{\infty 2}) \tag{3–13}$$

which can be rearranged as

$$\dot{Q} = \frac{T_{\infty 1} - T_1}{1/h_1 A} = \frac{T_1 - T_2}{L/kA} = \frac{T_2 - T_{\infty 2}}{1/h_2 A}$$

$$= \frac{T_{\infty 1} - T_1}{R_{\text{conv, 1}}} = \frac{T_1 - T_2}{R_{\text{wall}}} = \frac{T_2 - T_{\infty 2}}{R_{\text{conv, 2}}} \tag{3–14}$$

If
$$\frac{a_1}{b_1} = \frac{a_2}{b_2} = \cdots = \frac{a_n}{b_n} = c$$

then
$$\frac{a_1 + a_2 + \cdots + a_n}{b_1 + b_2 + \cdots + b_n} = c$$

For example,
$$\frac{1}{4} = \frac{2}{8} = \frac{5}{20} = 0.25$$

and
$$\frac{1 + 2 + 5}{4 + 8 + 20} = 0.25$$
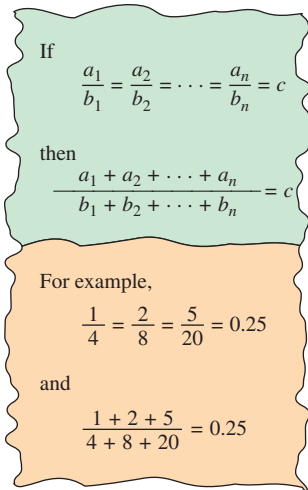
FIGURE 3–7
A useful mathematical identity.

Once the rate of heat transfer is calculated, Eq. 3–14 can also be used to determine the intermediate temperatures T_1 or T_2. Adding the numerators and denominators yields (Fig. 3–7)

$$\dot{Q} = \frac{T_{\infty 1} - T_{\infty 2}}{R_{total}} \quad \text{(W)} \tag{3–15}$$

where

$$R_{total} = R_{conv,\,1} + R_{wall} + R_{conv,\,2} = \frac{1}{h_1 A} + \frac{L}{kA} + \frac{1}{h_2 A} \quad \text{(K/W)} \tag{3–16}$$

Note that the heat transfer area A is constant for a plane wall, and the rate of heat transfer through a wall separating two media is equal to the overall temperature difference $(T_{\infty 1} - T_{\infty 2})$ divided by the total thermal resistance between the media. Also note that the thermal resistances are in *series,* and the equivalent thermal resistance is determined by simply *adding* the individual resistances, just like the electrical resistances connected in series. Thus, the electrical analogy still applies. We summarize this as *the rate of steady heat transfer between two surfaces is equal to the temperature difference divided by the total thermal resistance between those two surfaces.*

Another observation that can be made from Eq. 3–15 is that the ratio of the temperature drop to the thermal resistance across any layer is constant, and thus the temperature drop across any layer is proportional to the thermal resistance of the layer. The larger the resistance, the larger the temperature drop. In fact, the equation $\dot{Q} = \Delta T/R$ can be rearranged as

$$\Delta T = \dot{Q} R \quad \text{(°C)} \tag{3–17}$$

which indicates that the *temperature drop* across any layer is equal to the *rate of heat transfer* times the *thermal resistance* across that layer (Fig. 3–8). You may recall that this is also true for voltage drop across an electrical resistance when the electric current is constant.

It is sometimes convenient to express heat transfer through a medium in an manner analogous to Newton's law of cooling as

$$\dot{Q} = UA\,\Delta T \quad \text{(W)} \tag{3–18}$$

where U is the **overall heat transfer coefficient** with the unit $W/m^2 \cdot K$. The overall heat transfer coefficient is usually used in heat transfer calculations associated with heat exchangers (Chap. 11). It is also used in heat transfer calculations through windows (Chap. 9), commonly referred to as U-factor. A comparison of Eqs. 3–15 and 3–18 reveals that

$$UA = \frac{1}{R_{total}} \quad \text{(W/K)} \tag{3–19}$$

Therefore, for a unit area, the overall heat transfer coefficient is equal to the inverse of the total thermal resistance.

Note that we do not need to know the surface temperatures of the wall in order to evaluate the rate of steady heat transfer through it. All we need to know is the convection heat transfer coefficients and the fluid temperatures
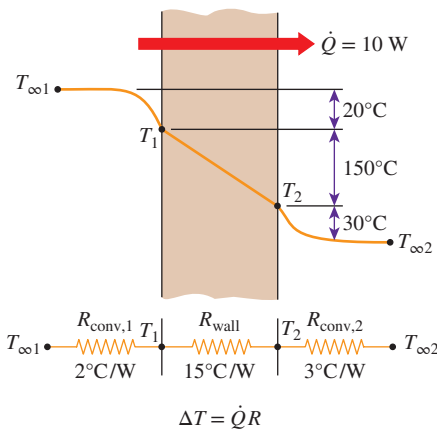
FIGURE 3–8
The temperature drop across a layer is proportional to its thermal resistance.

on both sides of the wall. The *surface temperature* of the wall can be determined as described above using the thermal resistance concept, but by taking the surface at which the temperature is to be determined as one of the terminal surfaces. For example, once $\dot{Q}$ is evaluated, the surface temperature T_1 can be determined from

$$\dot{Q} = \frac{T_{\infty 1} - T_1}{R_{\text{conv, 1}}} = \frac{T_{\infty 1} - T_1}{1/h_1 A} \qquad \text{(3–20)}$$

Multilayer Plane Walls

In practice, we often encounter plane walls that consist of several layers of different materials. The thermal resistance concept can still be used to determine the rate of steady heat transfer through such *composite* walls. As you may have already guessed, this is done by simply noting that the conduction resistance of each wall is *L/kA* connected in series, and using the electrical analogy—that is, by dividing the *temperature difference* between two surfaces at known temperatures by the *total thermal resistance* between them.

Consider a plane wall that consists of two layers (such as a brick wall with a layer of insulation). The rate of steady heat transfer through this two-layer composite wall can be expressed as (Fig. 3–9)

$$\dot{Q} = \frac{T_{\infty 1} - T_{\infty 2}}{R_{\text{total}}} \qquad \text{(3–21)}$$

where R_{total} is the *total thermal resistance,* expressed as

$$R_{\text{total}} = R_{\text{conv, 1}} + R_{\text{wall, 1}} + R_{\text{wall, 2}} + R_{\text{conv, 2}}$$

$$= \frac{1}{h_1 A} + \frac{L_1}{k_1 A} + \frac{L_2}{k_2 A} + \frac{1}{h_2 A} \qquad \text{(3–22)}$$
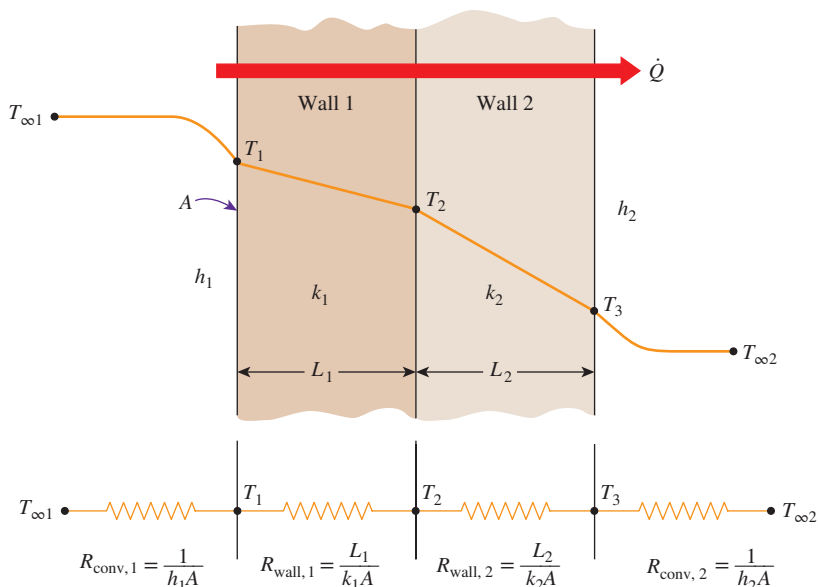
FIGURE 3–9

The thermal resistance network for heat transfer through a two-layer plane wall subjected to convection on both sides.
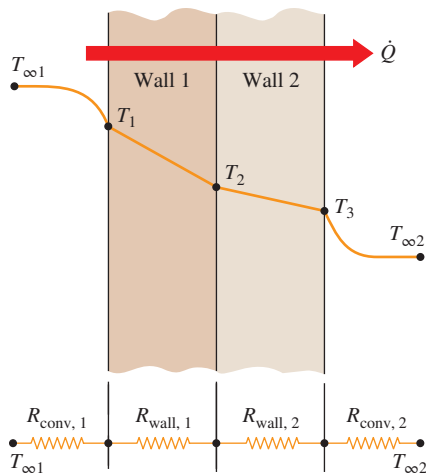
To find T_1: $\dot{Q} = \dfrac{T_{\infty 1} - T_1}{R_{\text{conv, 1}}}$

To find T_2: $\dot{Q} = \dfrac{T_{\infty 1} - T_2}{R_{\text{conv, 1}} + R_{\text{wall, 1}}}$

To find T_3: $\dot{Q} = \dfrac{T_3 - T_{\infty 2}}{R_{\text{conv, 2}}}$

FIGURE 3–10

The evaluation of the surface and interface temperatures when $T_{\infty 1}$ and $T_{\infty 2}$ are given and $\dot{Q}$ is calculated.

The subscripts 1 and 2 in the R_{wall} relations indicate the first and the second layers, respectively. We could also obtain this result by following the approach already used for the single-layer case by noting that the rate of steady heat transfer $\dot{Q}$ through a multilayer medium is constant, and thus it must be the same through each layer. Note from the thermal resistance network that the resistances are *in series,* and thus the *total thermal resistance* is simply the *arithmetic sum* of the individual thermal resistances in the path of heat transfer.

This result for the *two-layer* case is analogous to the *single-layer* case, except that an *additional resistance* is added for the *additional layer.* This result can be extended to plane walls that consist of *three* or *more layers* by adding an *additional resistance* for each *additional layer.*

Once $\dot{Q}$ is *known,* an unknown surface temperature T_j at any surface or interface j can be determined from

$$\dot{Q} = \frac{T_i - T_j}{R_{\text{total, } i-j}} \tag{3–23}$$

where T_i is a *known* temperature at location i and $R_{\text{total, } i-j}$ is the total thermal resistance between locations i and j. For example, when the fluid temperatures $T_{\infty 1}$ and $T_{\infty 2}$ for the two-layer case shown in Fig. 3–9 are available and $\dot{Q}$ is calculated from Eq. 3–21, the interface temperature T_2 between the two walls can be determined from (Fig. 3–10)

$$\dot{Q} = \frac{T_{\infty 1} - T_2}{R_{\text{conv, 1}} + R_{\text{wall, 1}}} = \frac{T_{\infty 1} - T_2}{\dfrac{1}{h_1 A} + \dfrac{L_1}{k_1 A}} \tag{3–24}$$

The temperature drop across a layer is easily determined from Eq. 3–17 by multiplying $\dot{Q}$ by the thermal resistance of that layer.

The thermal resistance concept is widely used in practice because it is intuitively easy to understand and it has proven to be a powerful tool in the solution of a wide range of heat transfer problems. But its use is limited to systems through which the rate of heat transfer $\dot{Q}$ remains *constant;* that is, to systems involving *steady* heat transfer with *no heat generation* (such as resistance heating or chemical reactions) within the medium.

FIGURE 3–11
Schematic for Example 3–1.

EXAMPLE 3–1   **Heat Loss Through a Wall**

Consider a 3-m-high, 5-m-wide, and 0.3-m-thick wall whose thermal conductivity is $k = 0.9$ W/m·K (Fig. 3–11). On a certain day, the temperatures of the inner and the outer surfaces of the wall are measured to be 16°C and 2°C, respectively. Determine the rate of heat loss through the wall on that day.

SOLUTION The two surfaces of a wall are maintained at specified temperatures. The rate of heat loss through the wall is to be determined.

Assumptions **1** Heat transfer through the wall is steady since the surface temperatures remain constant at the specified values. **2** Heat transfer is one-dimensional since any significant temperature gradients exist in the direction from the indoors to the outdoors. **3** Thermal conductivity is constant.

Properties The thermal conductivity is given to be $k = 0.9$ W/m·K.

Analysis Noting that heat transfer through the wall is by conduction and the area of the wall is $A = 3$ m $\times$ 5 m $= 15$ m^2, the steady rate of heat transfer through the wall can be determined from Eq. 3–3 to be

$$\dot{Q} = kA\frac{T_1 - T_2}{L} = (0.9 \text{ W/m·°C})(15 \text{ m}^2)\frac{(16 - 2)\text{°C}}{0.3 \text{ m}} = \textbf{630 W}$$

We could also determine the steady rate of heat transfer through the wall by making use of the thermal resistance concept from

$$\dot{Q} = \frac{\Delta T_{\text{wall}}}{R_{\text{wall}}}$$

where

$$R_{\text{wall}} = \frac{L}{kA} = \frac{0.3 \text{ m}}{(0.9 \text{ W/m·°C})(15 \text{ m}^2)} = 0.02222\text{°C/W}$$

Substituting, we get

$$\dot{Q} = \frac{(16 - 2)\text{°C}}{0.02222\text{°C/W}} = 630 \text{ W}$$

Discussion This is the same result obtained earlier. Note that heat conduction through a plane wall with specified surface temperatures can be determined directly and easily without utilizing the thermal resistance concept. However, the thermal resistance concept serves as a valuable tool in more complex heat transfer problems, as you will see in the following examples. Also, the units W/m·°C and W/m·K for thermal conductivity are equivalent, and thus interchangeable. This is also the case for °C and K for temperature differences.

EXAMPLE 3–2   **Heat Loss Through a Single-Pane Window**

Consider a 0.8-m-high and 1.5-m-wide glass window with a thickness of 8 mm and a thermal conductivity of $k = 0.78$ W/m·K. Determine the steady rate of heat transfer through this glass window and the temperature of its inner surface for a day during which the room is maintained at 20°C while the temperature of the outdoors is -10°C. Take the heat transfer coefficients on the inner and outer surfaces of the window to be $h_1 = 10$ W/m^2·K and $h_2 = 40$ W/m^2·K, which includes the effects of radiation.

SOLUTION Heat loss through a window glass is considered. The rate of heat transfer through the window and the inner surface temperature are to be determined.
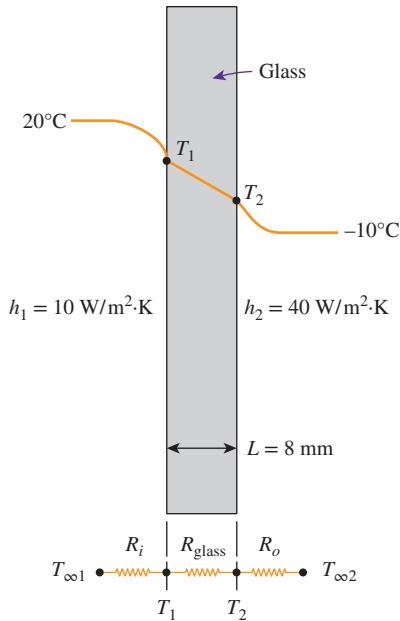
FIGURE 3–12
Schematic for Example 3–2.

Assumptions **1** Heat transfer through the window is steady since the surface temperatures remain constant at the specified values. **2** Heat transfer through the wall is one-dimensional since any significant temperature gradients exist in the direction from the indoors to the outdoors. **3** Thermal conductivity is constant.

Properties The thermal conductivity is given to be $k = 0.78$ W/m·K.

Analysis This problem involves conduction through the glass window and convection at its surfaces, and it can best be handled by making use of the thermal resistance concept and drawing the thermal resistance network, as shown in Fig. 3–12. Noting that the area of the window is $A = 0.8$ m $\times$ 1.5 m $= 1.2$ m^2, the individual resistances are evaluated from their definitions to be

$$R_i = R_{conv,\,1} = \frac{1}{h_1 A} = \frac{1}{(10 \text{ W/m}^2\cdot\text{K})(1.2 \text{ m}^2)} = 0.08333°\text{C/W}$$

$$R_{glass} = \frac{L}{kA} = \frac{0.008 \text{ m}}{(0.78 \text{ W/m·K})(1.2 \text{ m}^2)} = 0.00855°\text{C/W}$$

$$R_o = R_{conv,\,2} = \frac{1}{h_2 A} = \frac{1}{(40 \text{ W/m}^2\cdot\text{K})(1.2 \text{ m}^2)} = 0.02083°\text{C/W}$$

Noting that all three resistances are in series, the total resistance is

$$R_{total} = R_{conv,\,1} + R_{glass} + R_{conv,\,2} = 0.08333 + 0.00855 + 0.02083$$
$$= 0.1127°\text{C/W}$$

Then the steady rate of heat transfer through the window becomes

$$\dot{Q} = \frac{T_{\infty 1} - T_{\infty 2}}{R_{total}} = \frac{[20 - (-10)]°\text{C}}{0.1127°\text{C/W}} = \textbf{266 W}$$

Knowing the rate of heat transfer, the inner surface temperature of the window glass can be determined from

$$\dot{Q} = \frac{T_{\infty 1} - T_1}{R_{conv,\,1}} \rightarrow T_1 = T_{\infty 1} - \dot{Q}R_{conv,\,1}$$
$$= 20°\text{C} - (266 \text{ W})(0.08333°\text{C/W})$$
$$= \textbf{-2.2°C}$$

Discussion Note that the inner surface temperature of the window glass is $-2.2°$C even though the temperature of the air in the room is maintained at 20°C. Such low surface temperatures are highly undesirable since they cause the formation of fog or even frost on the inner surfaces of the glass when the humidity in the room is high.

EXAMPLE 3–3 **Heat Loss Through Double-Pane Windows**

Consider a 0.8-m-high and 1.5-m-wide double-pane window consisting of two 4-mm-thick layers of glass ($k = 0.78$ W/m·K) separated by a 10-mm-wide stagnant airspace ($k = 0.026$ W/m·K). Determine the steady rate of heat transfer through this

double-pane window and the temperature of its inner surface for a day during which the room is maintained at 20°C while the temperature of the outdoors is −10°C. Take the convection heat transfer coefficients on the inner and outer surfaces of the window to be $h_1 = 10$ W/m²·K and $h_2 = 40$ W/m²·K, which includes the effects of radiation.

SOLUTION A double-pane window is considered. The rate of heat transfer through the window and the inner surface temperature are to be determined.

Analysis This example problem is identical to the previous one except that the single 8-mm-thick window glass is replaced by two 4-mm-thick glasses that enclose a 10-mm-wide stagnant airspace. Therefore, the thermal resistance network of this problem involves two additional conduction resistances corresponding to the two additional layers, as shown in Fig. 3–13. Noting that the area of the window is again $A = 0.8$ m × 1.5 m = 1.2 m², the individual resistances are evaluated from their definitions to be

$$R_i = R_{\text{conv, 1}} = \frac{1}{h_1 A} = \frac{1}{(10 \text{ W/m}^2\cdot\text{K})(1.2 \text{ m}^2)} = 0.08333°\text{C/W}$$

$$R_1 = R_3 = R_{\text{glass}} = \frac{L_1}{k_1 A} = \frac{0.004 \text{ m}}{(0.78 \text{ W/m}\cdot\text{K})(1.2 \text{ m}^2)} = 0.00427°\text{C/W}$$

$$R_2 = R_{\text{air}} = \frac{L_2}{k_2 A} = \frac{0.01 \text{ m}}{(0.026 \text{ W/m}\cdot\text{K})(1.2 \text{ m}^2)} = 0.3205°\text{C/W}$$

$$R_o = R_{\text{conv, 2}} = \frac{1}{h_2 A} = \frac{1}{(40 \text{ W/m}^2\cdot\text{K})(1.2 \text{ m}^2)} = 0.02083°\text{C/W}$$

Noting that all three resistances are in series, the total resistance is

$$R_{\text{total}} = R_{\text{conv, 1}} + R_{\text{glass, 1}} + R_{\text{air}} + R_{\text{glass, 2}} + R_{\text{conv, 2}}$$
$$= 0.08333 + 0.00427 + 0.3205 + 0.00427 + 0.02083$$
$$= 0.4332°\text{C/W}$$

Then the steady rate of heat transfer through the window becomes

$$\dot{Q} = \frac{T_{\infty1} - T_{\infty2}}{R_{\text{total}}} = \frac{[20 - (-10)]°\text{C}}{0.4332°\text{C/W}} = \textbf{69.2 W}$$

which is about one-fourth of the result obtained in Example 3–3. This explains the popularity of the double- and even triple-pane windows in cold climates. The drastic reduction in the heat transfer rate in this case is due to the large thermal resistance of the air layer between the glasses.

The inner surface temperature of the window in this case will be

$$T_1 = T_{\infty1} - \dot{Q} R_{\text{conv, 1}} = 20°\text{C} - (69.2 \text{ W})(0.08333°\text{C/W}) = \textbf{14.2°C}$$

which is considerably higher than the −2.2°C obtained in Example 3–2. Therefore, a double-pane window will rarely get fogged. A double-pane window will also reduce the heat gain in summer and thus reduce the air-conditioning costs.
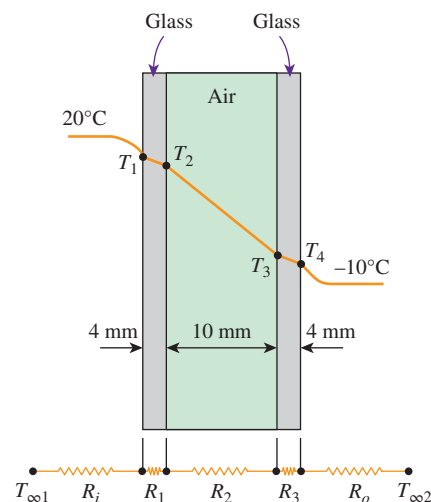
FIGURE 3–13
Schematic for Example 3–3.

(a) Ideal (perfect) thermal contact   (b) Actual (imperfect) thermal contact
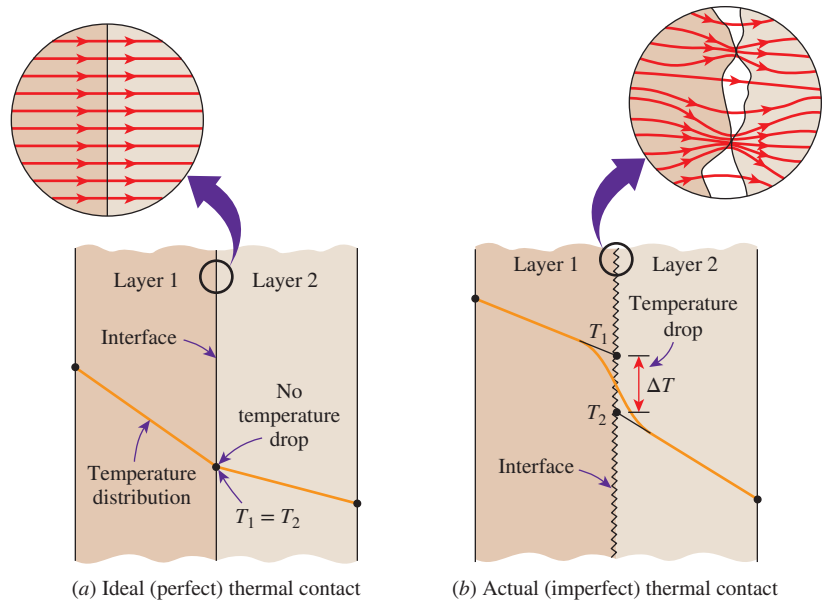
FIGURE 3–14
Temperature distribution and heat flow lines along two solid plates pressed against each other for the case of perfect and imperfect contact.

FIGURE 3–15
A typical experimental setup for the determination of thermal contact resistance.
Source: Song et al., 1993.

3–2 ▪ THERMAL CONTACT RESISTANCE

In the analysis of heat conduction through multilayer solids, we assumed "perfect contact" at the interface of two layers, and thus no temperature drop at the interface. This would be the case when the surfaces are perfectly smooth and they produce a perfect contact at each point. In reality, however, even flat surfaces that appear smooth to the eye turn out to be rather rough when examined under a microscope, as shown in Fig. 3–14, with numerous peaks and valleys. That is, a surface is *microscopically rough* no matter how smooth it appears to be.

When two such surfaces are pressed against each other, the peaks form good material contact but the valleys form voids filled with air in most cases. As a result, an interface contains numerous *air gaps* of varying sizes that act as *insulation* because of the low thermal conductivity of air. Thus, an interface offers some resistance to heat transfer, and this resistance for a unit interface area is called the **thermal contact resistance**, R_c. The value of R_c is determined experimentally using a setup like the one shown in Fig. 3–15, and as expected, there is considerable scatter of data because of the difficulty in characterizing the surfaces.

Consider heat transfer through two metal rods of cross-sectional area A that are pressed against each other. Heat transfer through the interface of these two rods is the sum of the heat transfers through the *solid contact spots* (solid-to-solid conduction) and the *gaps* (conduction and/or radiation across the gaps) in the noncontact areas (which is a major contributor to heat transfer) and can be expressed as

$$\dot{Q} = \dot{Q}_{\text{contact}} + \dot{Q}_{\text{gap}} \tag{3–25}$$

It can also be expressed in an manner analogous to Newton's law of cooling as

$$\dot{Q} = h_c A \, \Delta T_{\text{interface}} \tag{3–26}$$
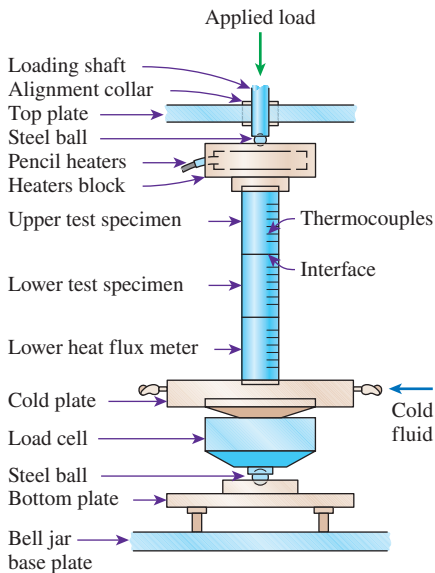
where A is the apparent interface area (which is the same as the cross-sectional area of the rods) and $\Delta T_{\text{interface}}$ is the effective temperature difference at the interface. The quantity h_c, which corresponds to the convection heat transfer coefficient, is called the **thermal contact conductance** and is expressed as

$$h_c = \frac{\dot{Q}/A}{\Delta T_{\text{interface}}} \quad (\text{W/m}^2 \cdot \text{K}) \tag{3-27}$$

It is related to thermal contact resistance by

$$R_c = \frac{1}{h_c} = \frac{\Delta T_{\text{interface}}}{\dot{Q}/A} \quad (\text{m}^2 \cdot \text{K/W}) \tag{3-28}$$

That is, thermal contact resistance is the inverse of thermal contact conductance. Usually, thermal contact conductance is reported in the literature, but the concept of thermal contact resistance serves as a better vehicle for explaining the effect of interface on heat transfer. Note that R_c represents thermal contact resistance for a *unit area.* The thermal resistance for the entire interface is obtained by dividing R_c by the apparent interface area A.

The thermal contact resistance can be determined from Eq. 3–28 by measuring the temperature drop at the interface and dividing it by the heat flux under steady conditions. The value of thermal contact resistance depends on the *surface roughness* and the *material properties* as well as the *temperature* and *pressure* at the interface and the *type of fluid* trapped at the interface. The situation becomes more complex when plates are fastened by bolts, screws, or rivets since the interface pressure in this case is nonuniform. The thermal contact resistance in that case also depends on the plate thickness, the bolt radius, and the size of the contact zone. Thermal contact resistance is observed to *decrease* with *decreasing surface roughness* and *increasing interface pressure,* as expected. Most experimentally determined values of the thermal contact resistance fall between 0.000005 and 0.0005 m²·K/W (the corresponding range of thermal contact conductance is 2000 to 200,000 W/m²·K).

When we analyze heat transfer in a medium consisting of two or more layers, the first thing we need to know is whether the thermal contact resistance is *significant* or not. We can answer this question by comparing the magnitudes of the thermal resistances of the layers with typical values of thermal contact resistance. For example, the thermal resistance of a 1-cm-thick layer of an insulating material for a unit surface area is

$$R_{c,\text{ insulation}} = \frac{L}{k} = \frac{0.01 \text{ m}}{0.04 \text{ W/m} \cdot \text{K}} = 0.25 \text{ m}^2 \cdot \text{K/W}$$

whereas for a 1-cm-thick layer of copper, it is

$$R_{c,\text{ copper}} = \frac{L}{k} = \frac{0.01 \text{ m}}{386 \text{ W/m} \cdot \text{K}} = 0.000026 \text{ m}^2 \cdot \text{K/W}$$

Comparing the values preceding with typical values of thermal contact resistance, we conclude that thermal contact resistance is significant and can even dominate the heat transfer for good heat conductors such as metals, but it can

TABLE 3–1

Thermal contact conductance for aluminum plates with different fluids at the interface for a surface roughness of 10 μm and interface pressure of 1 atm

Fluid at the Interface	Contact Conductance, h_c, W/m²·K
Air	3640
Helium	9520
Hydrogen	13,900
Silicone oil	19,000
Glycerin	37,700

Source: E. Fried. "Thermal Conduction Contribution to Heat Transfer at Contacts." Thermal Conductivity, *vol. 2, ed. R. P. Tye. London: Academic Press, 1969.*
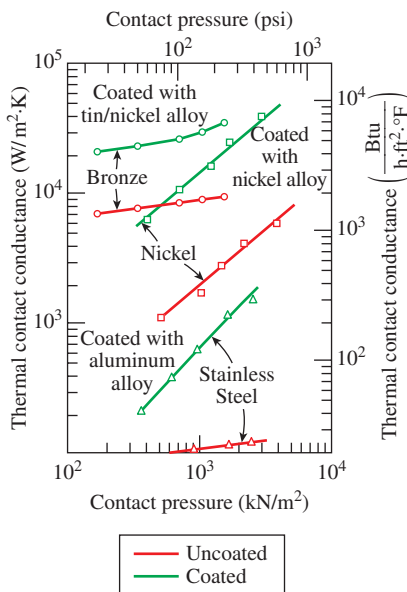
FIGURE 3–16
Effect of metallic coatings on thermal contact conductance.
Source: Peterson, 1987.

be disregarded for poor heat conductors such as insulations. This is not surprising since insulating materials consist mostly of airspace just like the interface itself.

The thermal contact resistance can be minimized by applying a thermally conducting liquid called a *thermal grease* such as silicon oil on the surfaces before they are pressed against each other. This is commonly done when attaching electronic components such as power transistors to heat sinks. The thermal contact resistance can also be reduced by replacing the air at the interface with a *better conducting gas* such as helium or hydrogen, as shown in Table 3–1.

Another way to minimize the contact resistance is to insert a *soft metallic foil* such as tin, silver, copper, nickel, or aluminum between the two surfaces. Experimental studies show that the thermal contact resistance can be reduced by a factor of up to 7 by a metallic foil at the interface. For maximum effectiveness, the foils must be very thin. The effect of metallic coatings on thermal contact conductance is shown in Fig. 3–16 for various metal surfaces.

There is considerable uncertainty in the contact conductance data reported in the literature, and care should be exercised when using them. In Table 3–2, some experimental results are given for the contact conductance between similar and dissimilar metal surfaces for use in preliminary design calculations. Note that the *thermal contact conductance* is *highest* (and thus the contact resistance is lowest) for *soft metals* with *smooth surfaces* at *high pressure.*

EXAMPLE 3–4   Equivalent Thickness for Contact Resistance

The thermal contact conductance at the interface of two 1-cm-thick copper plates is measured to be 18,000 W/m²·K. Determine the thickness of the copper plate whose thermal resistance is equal to the thermal resistance of the interface between the plates (Fig. 3–17).

SOLUTION The thickness of the copper plate whose thermal resistance is equal to the thermal contact resistance is to be determined.
Properties The thermal conductivity of copper at room temperature is $k = 401$ W/m·K (Table A–3).
Analysis Noting that thermal contact resistance is the inverse of thermal contact conductance, the thermal contact resistance is

$$R_c = \frac{1}{h_c} = \frac{1}{18,000 \text{ W/m}^2\text{·K}} = 5.556 \times 10^{-5} \text{ m}^2\text{·K/W}$$

For a unit surface area, the thermal resistance of a flat plate is defined as

$$R = \frac{L}{k}$$

where L is the thickness of the plate and k is the thermal conductivity. Setting $R = R_c$, the equivalent thickness is determined from the relation above to be

$$L = kR_c = (401 \text{ W/m·K})(5.556 \times 10^{-5} \text{ m}^2\text{·K/W}) = 0.0223 \text{ m} = \textbf{2.23 cm}$$

TABLE 3–2

Thermal contact conductance of some metal surfaces in air (from various sources)

Material	Surface Condition	Roughness, μm	Temperature, °C	Pressure, MPa	h_c,* W/m²·K
Identical Metal Pairs					
416 Stainless steel	Ground	2.54	90–200	0.17–2.5	3,800
304 Stainless steel	Ground	1.14	20	4–7	1,900
Aluminum	Ground	2.54	150	1.2–2.5	11,400
Copper	Ground	1.27	20	1.2–20	143,000
Copper	Milled	3.81	20	1–5	55,500
Copper (vacuum)	Milled	0.25	30	0.17–7	11,400
Dissimilar Metal Pairs					
Stainless steel–				10	2,900
Aluminum		20–30	20	20	3,600
Stainless steel–				10	16,400
Aluminum		1.0–2.0	20	20	20,800
Steel Ct-30–				10	50,000
Aluminum	Ground	1.4–2.0	20	15–35	59,000
Steel Ct-30–				10	4,800
Aluminum	Milled	4.5–7.2	20	30	8,300
				5	42,000
Aluminum-Copper	Ground	1.17–1.4	20	15	56,000
				10	12,000
Aluminum-Copper	Milled	4.4–4.5	20	20–35	12,000

*Divide the given values by 5.678 to convert to Btu/h·ft²·°F.

Discussion   Note that the interface between the two plates offers as much resistance to heat transfer as a 2.23-cm-thick copper plate. It is interesting that the thermal contact resistance in this case is greater than the sum of the thermal resistances of both plates.

FIGURE 3–17
Schematic for Example 3–4.

EXAMPLE 3–5   Contact Resistance of Transistors

Four identical power transistors with aluminum casing are attached on one side of a 1-cm-thick 20-cm × 20-cm square copper plate ($k = 386$ W/m·K) by screws that exert an average pressure of 6 MPa (Fig. 3–18). The base area of each transistor is 8 cm², and each transistor is placed at the center of a 10-cm × 10-cm quarter section of the plate. The interface roughness is estimated to be about 1.5 μm. All transistors are covered by a thick Plexiglas layer, which is a poor conductor of heat, and thus all the heat generated at the junction of the transistor must be dissipated to the ambient at 20°C through the back surface of the copper plate. The combined convection/radiation heat transfer coefficient at the back surface can be taken to be 25 W/m²·K. If the case temperature of the transistor is not to exceed 70°C, determine the maximum power each transistor can dissipate safely and the temperature jump at the case/plate interface.

FIGURE 3–18
Schematic for Example 3–5.

SOLUTION Four identical power transistors are attached on a copper plate. For a maximum case temperature of 70°C, the maximum power dissipation and the temperature jump at the interface are to be determined.

Assumptions **1** Steady operating conditions exist. **2** Heat transfer can be approximated as being one-dimensional, although it is recognized that heat conduction in some parts of the plate will be two-dimensional since the plate area is much larger than the base area of the transistor. But the large thermal conductivity of copper will minimize this effect. **3** All the heat generated at the junction is dissipated through the back surface of the plate since the transistors are covered by a thick Plexiglas layer. **4** Thermal conductivities are constant.

Properties The thermal conductivity of copper is given to be $k = 386$ W/m·K. The contact conductance is obtained from Table 3–2 to be $h_c = 42,000$ W/m²·K, which corresponds to a copper/aluminum interface for the case of $1.17 - 1.4$ μm roughness and 5 MPa pressure, which is sufficiently close to what we have.

Analysis The contact area between the case and the plate is given to be 8 cm², and the plate area for each transistor is 100 cm². The thermal resistance network of this problem consists of three resistances in series (interface, plate, and convection), which are determined to be

$$R_{\text{interface}} = \frac{1}{h_c A_c} = \frac{1}{(42,000 \text{ W/m}^2\text{·K})(8 \times 10^{-4} \text{m}^2)} = 0.030°\text{C/W}$$

$$R_{\text{plate}} = \frac{L}{kA} = \frac{0.01 \text{ m}}{(386 \text{ W/m·K})(0.01 \text{ m}^2)} = 0.0026°\text{C/W}$$

$$R_{\text{conv}} = \frac{1}{h_o A} = \frac{1}{(25 \text{ W/m}^2\text{·K})(0.01 \text{ m}^2)} = 4.0°\text{C/W}$$

The total thermal resistance is then

$$R_{\text{total}} = R_{\text{interface}} + R_{\text{plate}} + R_{\text{ambient}} = 0.030 + 0.0026 + 4.0 = 4.0326°\text{C/W}$$

Note that the thermal resistance of a copper plate is very small and can be ignored altogether. Then the rate of heat transfer is determined to be

$$\dot{Q} = \frac{\Delta T}{R_{\text{total}}} = \frac{(70 - 20)°\text{C}}{4.0326°\text{C/W}} = \textbf{12.4 W}$$

Therefore, the power transistor should not be operated at power levels greater than 12.4 W if the case temperature is not to exceed 70°C.

The temperature jump at the interface is determined from

$$\Delta T_{\text{interface}} = \dot{Q} R_{\text{interface}} = (12.4 \text{ W})(0.030°\text{C/W}) = \textbf{0.37°C}$$

which is not very large. Therefore, even if we eliminate the thermal contact resistance at the interface completely, we lower the operating temperature of the transistor in this case by less than 0.4°C.

3–3 ▪ GENERALIZED THERMAL RESISTANCE NETWORKS

The *thermal resistance* concept or the *electrical analogy* can also be used to solve steady heat transfer problems that involve parallel layers or combined series-parallel arrangements. Although such problems are often two- or even three-dimensional, approximate solutions can be obtained by assuming one-dimensional heat transfer and using the thermal resistance network.

Consider the composite wall shown in Fig. 3–19, which consists of two parallel layers. The thermal resistance network, which consists of two parallel resistances, can be represented as shown in the figure. Noting that the total heat transfer is the sum of the heat transfers through each layer, we have

$$\dot{Q} = \dot{Q}_1 + \dot{Q}_2 = \frac{T_1 - T_2}{R_1} + \frac{T_1 - T_2}{R_2} = (T_1 - T_2)\left(\frac{1}{R_1} + \frac{1}{R_2}\right) \tag{3–29}$$

Utilizing the electrical analogy, we get

$$\dot{Q} = \frac{T_1 - T_2}{R_{\text{total}}} \tag{3–30}$$

where

$$\frac{1}{R_{\text{total}}} = \frac{1}{R_1} + \frac{1}{R_2} \quad \rightarrow \quad R_{\text{total}} = \frac{R_1 R_2}{R_1 + R_2} \tag{3–31}$$

since the resistances are in parallel.

Now consider the combined series-parallel arrangement shown in Fig. 3–20. The total rate of heat transfer through this composite system can again be expressed as

$$\dot{Q} = \frac{T_1 - T_\infty}{R_{\text{total}}} \tag{3–32}$$

where

$$R_{\text{total}} = R_{12} + R_3 + R_{\text{conv}} = \frac{R_1 R_2}{R_1 + R_2} + R_3 + R_{\text{conv}} \tag{3–33}$$

and

$$R_1 = \frac{L_1}{k_1 A_1} \quad R_2 = \frac{L_2}{k_2 A_2} \quad R_3 = \frac{L_3}{k_3 A_3} \quad R_{\text{conv}} = \frac{1}{h A_3} \tag{3–34}$$

Once the individual thermal resistances are evaluated, the total resistance and the total rate of heat transfer can easily be determined from the relations above.

The result obtained is somewhat approximate, since the surfaces of the third layer are probably not isothermal, and heat transfer between the first two layers is likely to occur.

Two assumptions commonly used in solving complex multidimensional heat transfer problems by treating them as one-dimensional (say, in the *x*-direction) using the thermal resistance network are (1) any plane wall normal to the *x*-axis is *isothermal* (i.e., assumes the temperature varies in
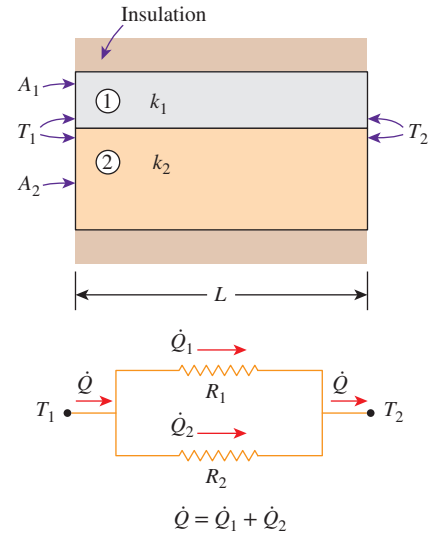
FIGURE 3–19
Thermal resistance network for two parallel layers.
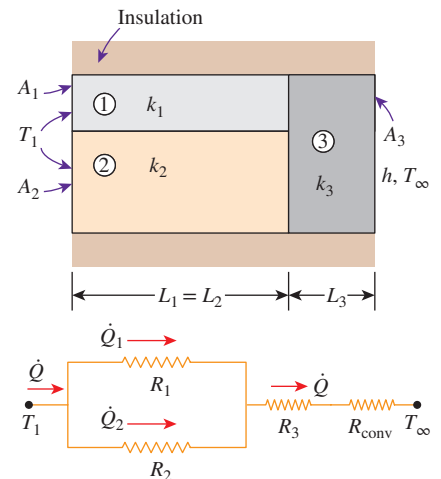
FIGURE 3–20
Thermal resistance network for combined series-parallel arrangement.

the *x*-direction only) and (2) any plane parallel to the *x*-axis is *adiabatic* (i.e., assumes heat transfer occurs in the *x*-direction only). These two assumptions result in different resistance networks, and thus different (but usually close) values for the total thermal resistance and thus heat transfer. The actual result lies between these two values. In geometries in which heat transfer occurs predominantly in one direction, either approach gives satisfactory results.

Foam   Plaster

h_2
$T_{\infty 2}$

1.5 cm

Brick

h_1
$T_{\infty 1}$

22 cm

1.5 cm

$\longrightarrow x$

3 2   16 cm   2

R_3

R_i R_1 R_2 R_4 R_6 R_o
$T_{\infty 1}$ •———————————————• $T_{\infty 2}$
                R_5
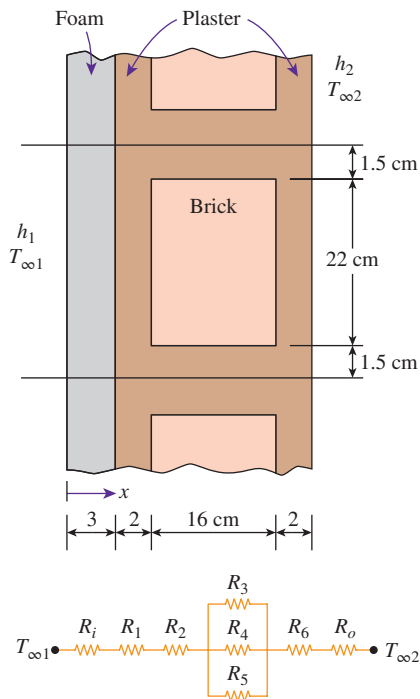
FIGURE 3–21
Schematic for Example 3–6.

EXAMPLE 3–6   **Heat Loss Through a Composite Wall**

A 3-m-high and 5-m-wide wall consists of long 16-cm × 22-cm cross section horizontal bricks ($k = 0.72$ W/m·K) separated by 3-cm-thick plaster layers ($k = 0.22$ W/m·K). There are also 2-cm-thick plaster layers on each side of the brick and a 3-cm-thick rigid foam ($k = 0.026$ W/m·K) on the inner side of the wall, as shown in Fig. 3–21. The indoor and the outdoor temperatures are 20°C and −10°C, respectively, and the convection heat transfer coefficients on the inner and the outer sides are $h_1 = 10$ W/m²·K and $h_2 = 25$ W/m²·K, respectively. Assuming one-dimensional heat transfer and disregarding radiation, determine the rate of heat transfer through the wall.

SOLUTION   The composition of a composite wall is given. The rate of heat transfer through the wall is to be determined.

Assumptions   **1** Heat transfer is steady since there is no indication of change with time. **2** Heat transfer can be approximated as being one-dimensional since it is predominantly in the *x*-direction. **3** Thermal conductivities are constant. **4** Heat transfer by radiation is negligible.

Properties   The thermal conductivities are given to be $k = 0.72$ W/m·K for bricks, $k = 0.22$ W/m·K for plaster layers, and $k = 0.026$ W/m·K for the rigid foam.

Analysis   There is a pattern in the construction of this wall that repeats itself every 25-cm distance in the vertical direction. There is no variation in the horizontal direction. Therefore, we consider a 1-m-deep and 0.25-m-high portion of the wall, since it is representative of the entire wall.

Assuming any cross section of the wall normal to the *x*-direction to be *isothermal*, the thermal resistance network for the representative section of the wall becomes as shown in Fig. 3–21. The individual resistances are evaluated as:

$$R_i = R_{\text{conv, 1}} = \frac{1}{h_1 A} = \frac{1}{(10 \text{ W/m}^2\cdot\text{K})(0.25 \times 1 \text{ m}^2)} = 0.40°\text{C/W}$$

$$R_1 = R_{\text{foam}} = \frac{L}{kA} = \frac{0.03 \text{ m}}{(0.026 \text{ W/m}\cdot\text{K})(0.25 \times 1 \text{ m}^2)} = 4.62°\text{C/W}$$

$$R_2 = R_6 = R_{\text{plaster, side}} = \frac{L}{kA} = \frac{0.02 \text{ m}}{(0.22 \text{ W/m}\cdot\text{K})(0.25 \times 1 \text{ m}^2)}$$
$$= 0.36°\text{C/W}$$

$$R_3 = R_5 = R_{\text{plaster, center}} = \frac{L}{kA} = \frac{0.16 \text{ m}}{(0.22 \text{ W/m}\cdot\text{K})(0.015 \times 1 \text{ m}^2)}$$
$$= 48.48°\text{C/W}$$

$$R_4 = R_{\text{brick}} = \frac{L}{kA} = \frac{0.16 \text{ m}}{(0.72 \text{ W/m}\cdot\text{K})(0.22 \times 1 \text{ m}^2)} = 1.01°\text{C/W}$$

$$R_o = R_{\text{conv, 2}} = \frac{1}{h_2 A} = \frac{1}{(25 \text{ W/m}^2\cdot\text{K})(0.25 \times 1 \text{ m}^2)} = 0.16°\text{C/W}$$

The three resistances R_3, R_4, and R_5 in the middle are parallel, and their equivalent resistance is determined from

$$\frac{1}{R_{\text{mid}}} = \frac{1}{R_3} + \frac{1}{R_4} + \frac{1}{R_5} = \frac{1}{48.48} + \frac{1}{1.01} + \frac{1}{48.48} = 1.03 \text{ W/°C}$$

which gives

$$R_{\text{mid}} = 0.97°\text{C/W}$$

Now all the resistances are in series, and the total resistance is

$$R_{\text{total}} = R_i + R_1 + R_2 + R_{\text{mid}} + R_6 + R_o$$
$$= 0.40 + 4.62 + 0.36 + 0.97 + 0.36 + 0.16$$
$$= 6.87°\text{C/W}$$

Then the steady rate of heat transfer through the wall becomes

$$\dot{Q} = \frac{T_{\infty 1} - T_{\infty 2}}{R_{\text{total}}} = \frac{[20 - (-10)]°\text{C}}{6.87°\text{C/W}} = 4.37 \text{ W} \quad \text{(per 0.25 m}^2 \text{ surface area)}$$

or 4.37/0.25 = 17.5 W per m² area. The total area of the wall is $A = 3 \text{ m} \times 5 \text{ m} = 15 \text{ m}^2$. Then the rate of heat transfer through the entire wall becomes

$$\dot{Q}_{\text{total}} = (1.75 \text{ W/m}^2)(15 \text{ m}^2) = \textbf{263 W}$$

Of course, this result is approximate, since we assumed the temperature within the wall to vary in one direction only and ignored any temperature change (and thus heat transfer) in the other two directions.

Discussion In the preceding solution, we assumed the temperature at any cross section of the wall normal to the *x*-direction was *isothermal*. We could also solve this problem by going to the other extreme and assuming the surfaces parallel to the *x*-direction are *adiabatic*. The thermal resistance network in this case will be as shown in Fig. 3–22. By following the approach outlined above, the total thermal resistance in this case is determined to be $R_{\text{total}} = 6.97°\text{C/W}$, which is very close to the value 6.85°C/W obtained before. Thus, either approach gives roughly the same result in this case. This example demonstrates that either approach can be used in practice to obtain satisfactory results.
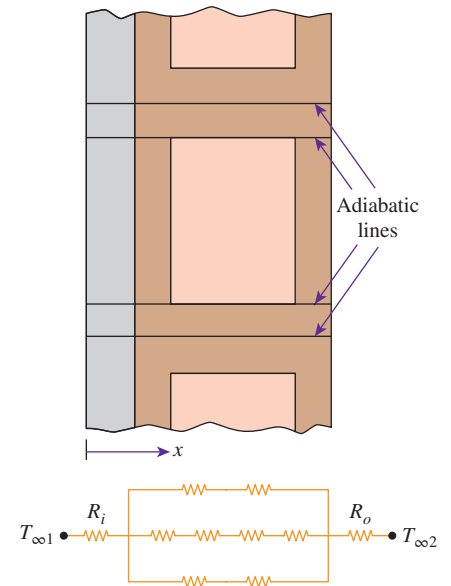
FIGURE 3–22
Alternative thermal resistance network for Example 3–6 for the case of surfaces parallel to the primary direction of heat transfer being adiabatic.

3–4 • HEAT CONDUCTION IN CYLINDERS AND SPHERES

Consider steady heat conduction through a hot-water pipe. Heat is continuously lost to the outdoors through the wall of the pipe, and we intuitively feel that heat transfer through the pipe is in the normal direction to the pipe
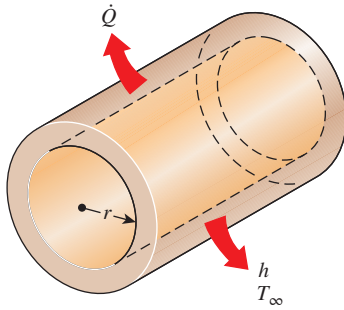
FIGURE 3–23
Heat is lost from a hot-water pipe to the air outside in the radial direction, and thus heat transfer from a long pipe is one-dimensional.
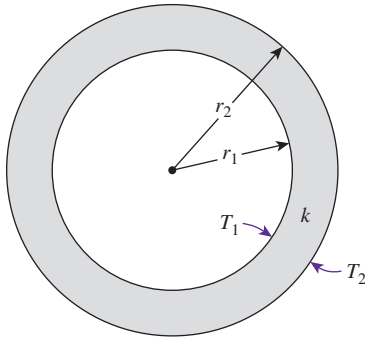
FIGURE 3–24
A long cylindrical pipe (or spherical shell) with specified inner and outer surface temperatures T_1 and T_2.

surface and that no significant heat transfer takes place in the pipe in other directions (Fig. 3–23). The wall of the pipe, whose thickness is rather small, separates two fluids at different temperatures, and thus the temperature gradient in the radial direction is relatively large. Further, if the fluid temperatures inside and outside the pipe remain constant, then heat transfer through the pipe is *steady*. Thus heat transfer through the pipe can be modeled as *steady* and *one-dimensional*. The temperature of the pipe in this case depends on one direction only (the radial r-direction) and can be expressed as $T = T(r)$. The temperature is independent of the azimuthal angle or the axial distance. This situation is approximated in practice in long cylindrical pipes and spherical containers.

In *steady* operation, there is no change in the temperature of the pipe with time at any point. Therefore, the rate of heat transfer into the pipe must be equal to the rate of heat transfer out of it. In other words, heat transfer through the pipe must be constant, $\dot{Q}_{cond,\,cyl} = \text{constant}$.

Consider a long cylindrical layer (such as a circular pipe) of inner radius r_1, outer radius r_2, length L, and average thermal conductivity k (Fig. 3–24). The two surfaces of the cylindrical layer are maintained at constant temperatures T_1 and T_2. There is no heat generation in the layer, and the thermal conductivity is constant. For one-dimensional heat conduction through the cylindrical layer, we have $T(r)$. Then Fourier's law of heat conduction for heat transfer through the cylindrical layer can be expressed as

$$\dot{Q}_{cond,\,cyl} = -kA\frac{dT}{dr} \quad \text{(W)} \tag{3–35}$$

where $A = 2\pi rL$ is the heat transfer area at location r. Note that A depends on r, and thus it *varies* in the direction of heat transfer. Separating the variables in Eq. 3–35 and integrating from $r = r_1$, where $T(r_1) = T_1$, to $r = r_2$, where $T(r_2) = T_2$, gives

$$\int_{r=r_1}^{r_2} \frac{\dot{Q}_{cond,\,cyl}}{A}dr = -\int_{T=T_1}^{T_2} k\,dT \tag{3–36}$$

Substituting $A = 2\pi rL$ and performing the integrations give

$$\dot{Q}_{cond,\,cyl} = 2\pi Lk \frac{T_1 - T_2}{\ln(r_2/r_1)} \quad \text{(W)} \tag{3–37}$$

since $\dot{Q}_{cond,\,cyl} = \text{constant}$. This equation can be rearranged as

$$\dot{Q}_{cond,\,cyl} = \frac{T_1 - T_2}{R_{cyl}} \quad \text{(W)} \tag{3–38}$$

where

$$R_{cyl} = \frac{\ln(r_2/r_1)}{2\pi Lk} = \frac{\ln(\text{Outer radius/Inner radius})}{2\pi \times \text{Length} \times \text{Thermal conductivity}} \tag{3–39}$$

is the *thermal resistance* of the cylindrical layer against heat conduction, or simply the *conduction resistance* of the cylinder layer. Note that Eq. 3–37 is identical to Eq. 2–59 which was obtained by using the "standard" approach by first solving the heat conduction equation in cylindrical coordinates, Eq. 2–29, to obtain the temperature distribution, Eq. 2–58, and then using the Fourier's law to obtain the heat transfer rate. The method used in obtaining Eq. 3–37 can be considered an "alternative" approach. However, it is restricted to one-dimensional steady heat conduction with no heat generation.

We can repeat the analysis for a *spherical layer* by taking $A = 4\pi r^2$ and performing the integrations in Eq. 3–36. The result can be expressed as

$$\dot{Q}_{\text{cond, sph}} = \frac{T_1 - T_2}{R_{\text{sph}}} \tag{3–40}$$

where

$$R_{\text{sph}} = \frac{r_2 - r_1}{4\pi r_1 r_2 k} = \frac{\text{Outer radius} - \text{Inner radius}}{4\pi(\text{Outer radius})(\text{Inner radius})(\text{Thermal conductivity})} \tag{3–41}$$

is the *thermal resistance* of the spherical layer against heat conduction, or simply the *conduction resistance* of the spherical layer. Note also that Eq. 3–40 is identical to Eq. 2–61, which was obtained by solving the heat conduction equation in spherical coordinates.

Now consider steady one-dimensional heat transfer through a cylindrical or spherical layer that is exposed to convection on both sides to fluids at temperatures $T_{\infty 1}$ and $T_{\infty 2}$ with heat transfer coefficients h_1 and h_2, respectively, as shown in Fig. 3–25. The thermal resistance network in this case consists of one conduction and two convection resistances in series, just like the one for the plane wall, and the rate of heat transfer under steady conditions can be expressed as

$$\dot{Q} = \frac{T_{\infty 1} - T_{\infty 2}}{R_{\text{total}}} \tag{3–42}$$

where

$$R_{\text{total}} = R_{\text{conv, 1}} + R_{\text{cyl}} + R_{\text{conv, 2}}$$
$$= \frac{1}{(2\pi r_1 L)h_1} + \frac{\ln r_2/r_1}{2\pi Lk} + \frac{1}{(2\pi r_2 L)h_2} \tag{3–43}$$

for a *cylindrical* layer, and

$$R_{\text{total}} = R_{\text{conv, 1}} + R_{\text{sph}} + R_{\text{conv, 2}}$$
$$= \frac{1}{(4\pi r_1^2)h_1} + \frac{r_2 - r_1}{4\pi r_1 r_2 k} + \frac{1}{(4\pi r_2^2)h_2} \tag{3–44}$$

for a spherical layer. Note that A in the convection resistance relation $R_{\text{conv}} = 1/hA$ is the *surface area at which convection occurs.* It is equal to $A = 2\pi rL$ for a cylindrical surface and $A = 4\pi r^2$ for a spherical surface of radius r. Also note that the thermal resistances are in series, and thus the total thermal resistance is determined by simply adding the individual resistances, just like the electrical resistances connected in series.

$$R_{\text{total}} = R_{\text{conv,1}} + R_{\text{cyl}} + R_{\text{conv,2}}$$
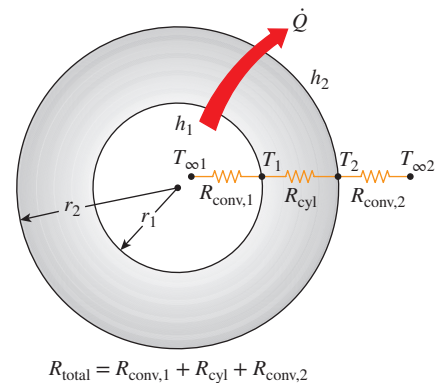
FIGURE 3–25

The thermal resistance network for a cylindrical (or spherical) shell subjected to convection from both the inner and the outer sides.

Multilayered Cylinders and Spheres

Steady heat transfer through multilayered cylindrical or spherical shells can be handled just like multilayered plane walls discussed earlier by simply adding an *additional resistance* in series for each *additional layer.* For example, the steady heat transfer rate through the three-layered composite cylinder of length L shown in Fig. 3–26 with convection on both sides can be expressed as

$$\dot{Q} = \frac{T_{\infty 1} - T_{\infty 2}}{R_{\text{total}}} \tag{3–45}$$

where R_{total} is the *total thermal resistance,* expressed as

$$
\begin{aligned}
R_{\text{total}} &= R_{\text{conv, 1}} + R_{\text{cyl, 1}} + R_{\text{cyl, 2}} + R_{\text{cyl, 3}} + R_{\text{conv, 2}} \\
&= \frac{1}{h_1 A_1} + \frac{\ln(r_2/r_1)}{2\pi L k_1} + \frac{\ln(r_3/r_2)}{2\pi L k_2} + \frac{\ln(r_4/r_3)}{2\pi L k_3} + \frac{1}{h_2 A_4}
\end{aligned} \tag{3–46}
$$

where $A_1 = 2\pi r_1 L$ and $A_4 = 2\pi r_4 L$. Equation 3–46 can also be used for a three-layered spherical shell by replacing the thermal resistances of cylindrical layers with the corresponding spherical ones. Again, note from the thermal resistance network that the resistances are in series, and thus the total thermal resistance is simply the *arithmetic sum* of the individual thermal resistances in the path of heat flow.

Once $\dot{Q}$ is known, we can determine any intermediate temperature T_j by applying the relation $\dot{Q} = (T_i - T_j)/R_{\text{total, } i-j}$ across any layer or layers such that T_i is a *known* temperature at location i and $R_{\text{total, } i-j}$ is the total thermal resistance between locations i and j (Fig. 3–27). For example, once $\dot{Q}$ has been calculated, the interface temperature T_2 between the first and second cylindrical layers can be determined from
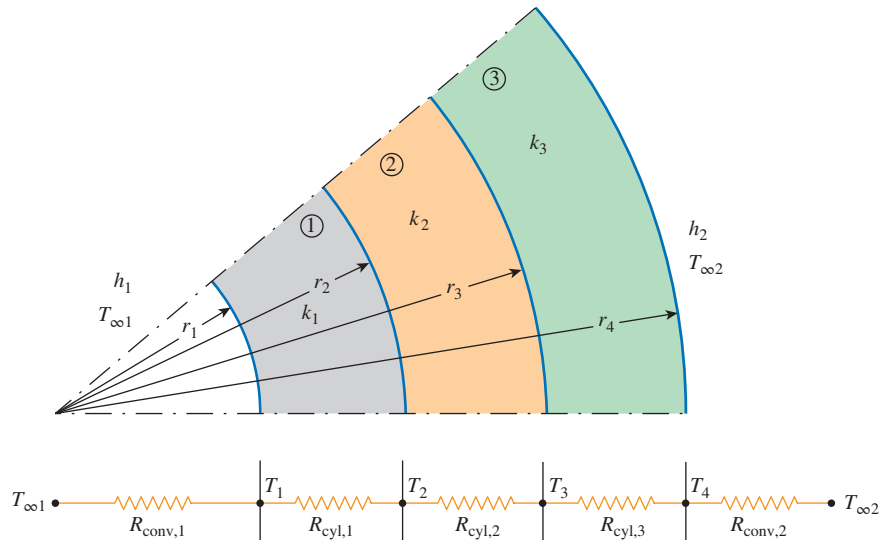
FIGURE 3–26

The thermal resistance network for heat transfer through a three-layered composite cylinder subjected to convection on both sides.

$$\dot{Q} = \frac{T_{\infty 1} - T_2}{R_{\text{conv, 1}} + R_{\text{cyl, 1}}} = \frac{T_{\infty 1} - T_2}{\dfrac{1}{h_1(2\pi r_1 L)} + \dfrac{\ln(r_2/r_1)}{2\pi L k_1}} \tag{3–47}$$

We could also calculate T_2 from

$$\dot{Q} = \frac{T_2 - T_{\infty 2}}{R_2 + R_3 + R_{\text{conv, 2}}} = \frac{T_2 - T_{\infty 2}}{\dfrac{\ln(r_3/r_2)}{2\pi L k_2} + \dfrac{\ln(r_4/r_3)}{2\pi L k_3} + \dfrac{1}{h_o(2\pi r_4 L)}} \tag{3–48}$$

Although both relations give the same result, we prefer the first one since it involves fewer terms and thus less work.

The thermal resistance concept can also be used for *other geometries,* provided that the proper conduction resistances and the proper surface areas in convection resistances are used.

$$\dot{Q} = \frac{T_{\infty 1} - T_1}{R_{\text{conv,1}}}$$
$$= \frac{T_{\infty 1} - T_2}{R_{\text{conv,1}} + R_1}$$
$$= \frac{T_1 - T_3}{R_1 + R_2}$$
$$= \frac{T_2 - T_3}{R_2}$$
$$= \frac{T_2 - T_{\infty 2}}{R_2 + R_{\text{conv,2}}}$$
$$= \cdots$$

FIGURE 3–27
The ratio $\Delta T/R$ across any layer is equal to $\dot{Q}$, which remains constant in one-dimensional steady conduction.

EXAMPLE 3–7   Heat Transfer to a Spherical Container

A 3-m internal diameter spherical tank made of 2-cm-thick stainless steel ($k = 15$ W/m·K) is used to store iced water at $T_{\infty 1} = 0°C$. The tank is located in a room whose temperature is $T_{\infty 2} = 22°C$. The walls of the room are also at 22°C. The outer surface of the tank is black, and heat transfer between the outer surface of the tank and the surroundings is by natural convection and radiation. The convection heat transfer coefficients at the inner and the outer surfaces of the tank are $h_1 = 80$ W/m²·K and $h_2 = 10$ W/m²·K, respectively. Determine (*a*) the rate of heat transfer to the iced water in the tank and (*b*) the amount of ice at 0°C that melts during a 24-h period.

SOLUTION   A spherical container filled with iced water is subjected to convection and radiation heat transfer at its outer surface. The rate of heat transfer and the amount of ice that melts per day are to be determined.
Assumptions   **1** Heat transfer is steady since the specified thermal conditions at the boundaries do not change with time. **2** Heat transfer is one-dimensional since there is thermal symmetry about the midpoint. **3** Thermal conductivity is constant.
Properties   The thermal conductivity of steel is given to be $k = 15$ W/m·K. The heat of fusion of water at atmospheric pressure is $h_{if} = 333.7$ kJ/kg. The outer surface of the tank is black, and thus its emissivity is $\varepsilon = 1$.
Analysis   (*a*) The thermal resistance network for this problem is given in Fig. 3–28. Noting that the inner diameter of the tank is $D_1 = 3$ m and the outer diameter is $D_2 = 3.04$ m, the inner and the outer surface areas of the tank are

$$A_1 = \pi D_1^2 = \pi (3 \text{ m})^2 = 28.2 \text{ m}^2$$
$$A_2 = \pi D_2^2 = \pi (3.04 \text{ m})^2 = 29.0 \text{ m}^2$$

Also, the radiation heat transfer coefficient is given by

$$h_{\text{rad}} = \varepsilon \sigma (T_2^2 + T_{\infty 2}^2)(T_2 + T_{\infty 2})$$

But we do not know the outer surface temperature T_2 of the tank, and thus we cannot calculate h_{rad}. Therefore, we need to assume a T_2 value now and check the accuracy
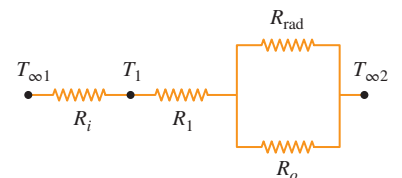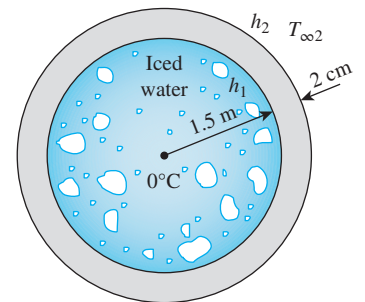
FIGURE 3–28
Schematic for Example 3–7.

of this assumption later. We will repeat the calculations if necessary using a revised value for T_2.

We note that T_2 must be between 0°C and 22°C, but it must be closer to 0°C, since the heat transfer coefficient inside the tank is much larger. Taking $T_2 = 5°C = 278$ K, the radiation heat transfer coefficient is determined to be

$$h_{rad} = (1)(5.67 \times 10^{-8} \text{ W/m}^2 \cdot \text{K}^4) [(295 \text{ K})^2 + (278 \text{ K})^2][(295 + 278) \text{ K}]$$
$$= 5.34 \text{ W/m}^2 \cdot \text{K} = 5.34 \text{ W/m}^2 \cdot °\text{C}$$

Then the individual thermal resistances become

$$R_i = R_{conv, 1} = \frac{1}{h_1 A_1} = \frac{1}{(80 \text{ W/m}^2 \cdot \text{K})(28.3 \text{ m}^2)} = 0.000442°\text{C/W}$$

$$R_1 = R_{sphere} = \frac{r_2 - r_1}{4\pi k r_1 r_2} = \frac{(1.52 - 1.50) \text{ m}}{4\pi(15 \text{ W/m}\cdot\text{K})(1.52 \text{ m})(1.50 \text{ m})}$$
$$= 0.000047°\text{C/W}$$

$$R_o = R_{conv, 2} = \frac{1}{h_2 A_2} = \frac{1}{(10 \text{ W/m}^2 \cdot \text{K})(29.0 \text{ m}^2)} = 0.00345°\text{C/W}$$

$$R_{rad} = \frac{1}{h_{rad} A_2} = \frac{1}{(5.34 \text{ W/m}^2 \cdot \text{K})(29.0 \text{ m}^2)} = 0.00646°\text{C/W}$$

The two parallel resistances R_o and R_{rad} can be replaced by an equivalent resistance R_{equiv} determined from

$$\frac{1}{R_{equiv}} = \frac{1}{R_o} + \frac{1}{R_{rad}} = \frac{1}{0.00345} + \frac{1}{0.00646} = 444.7 \text{ W/°C}$$

which gives

$$R_{equiv} = 0.00225°\text{C/W}$$

Now all the resistances are in series, and the total resistance is

$$R_{total} = R_i + R_1 + R_{equiv} = 0.000442 + 0.000047 + 0.00225 = 0.00274°\text{C/W}$$

Then the steady rate of heat transfer to the iced water becomes

$$\dot{Q} = \frac{T_{\infty 2} - T_{\infty 1}}{R_{total}} = \frac{(22 - 0)°\text{C}}{0.00274°\text{C/W}} = \textbf{8029 W} \quad \text{(or } \dot{Q} = 8.029 \text{ kJ/s)}$$

To check the validity of our original assumption, we now determine the outer surface temperature from

$$\dot{Q} = \frac{T_{\infty 2} - T_2}{R_{equiv}} \longrightarrow T_2 = T_{\infty 2} - \dot{Q} R_{equiv}$$
$$= 22°\text{C} - (8029 \text{ W})(0.00225°\text{C/W}) = 4°\text{C}$$

which is sufficiently close to the 5°C assumed in the determination of the radiation heat transfer coefficient. Therefore, there is no need to repeat the calculations using 4°C for T_2.

(b) The total amount of heat transfer during a 24-h period is

$$Q = \dot{Q}\,\Delta t = (8.029 \text{ kJ/s})(24 \times 3600 \text{ s}) = 693{,}700 \text{ kJ}$$

Noting that it takes 333.7 kJ of energy to melt 1 kg of ice at 0°C, the amount of ice that will melt during a 24-h period is

$$m_{\text{ice}} = \frac{Q}{h_{if}} = \frac{693{,}700 \text{ kJ}}{333.7 \text{ kJ/kg}} = \textbf{2079 kg}$$

Therefore, about 2 metric tons of ice will melt in the tank every day.

Discussion   An easier way to deal with combined convection and radiation at a surface when the surrounding medium and surfaces are at the same temperature is to add the radiation and convection heat transfer coefficients and to treat the result as the convection heat transfer coefficient. That is, to take $h = 10 + 5.34 = 15.34$ W/m²·K in this case. This way, we can ignore radiation since its contribution is accounted for in the convection heat transfer coefficient. The convection resistance of the outer surface in this case would be

$$R_{\text{combined}} = \frac{1}{h_{\text{combined}}A_2} = \frac{1}{(15.34 \text{ W/m}^2\text{·K})(29.0 \text{ m}^2)} = 0.00225°\text{C/W}$$

which is identical to the value obtained for equivalent resistance for the parallel convection and the radiation resistances.

EXAMPLE 3–8   Heat Loss Through an Insulated Steam Pipe

Steam at $T_{\infty 1} = 320°$C flows in a cast iron pipe ($k = 80$ W/m·K) whose inner and outer diameters are $D_1 = 5$ cm and $D_2 = 5.5$ cm, respectively. The pipe is covered with 3-cm-thick glass wool insulation with $k = 0.05$ W/m·K. Heat is lost to the surroundings at $T_{\infty 2} = 5°$C by natural convection and radiation, with a combined heat transfer coefficient of $h_2 = 18$ W/m²·K. Taking the heat transfer coefficient inside the pipe to be $h_1 = 60$ W/m²·K, determine the rate of heat loss from the steam per unit length of the pipe. Also determine the temperature drops across the pipe shell and the insulation.

SOLUTION   A steam pipe covered with glass wool insulation is subjected to convection on its surfaces. The rate of heat transfer per unit length and the temperature drops across the pipe and the insulation are to be determined.

Assumptions   **1** Heat transfer is steady since there is no indication of any change with time. **2** Heat transfer is one-dimensional since there is thermal symmetry about the centerline and no variation in the axial direction. **3** Thermal conductivities are constant. **4** The thermal contact resistance at the interface is negligible.

Properties   The thermal conductivities are given to be $k = 80$ W/m·K for cast iron and $k = 0.05$ W/m·K for glass wool insulation.
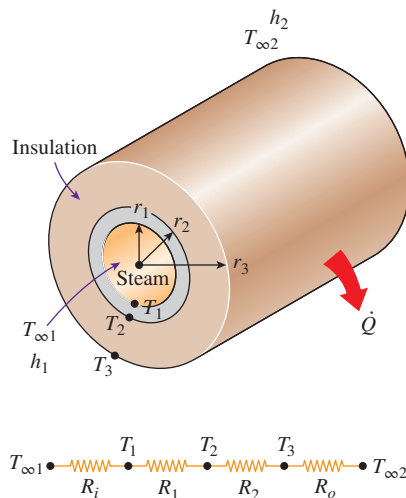
FIGURE 3–29
Schematic for Example 3–8.

Analysis The thermal resistance network for this problem involves four resistances in series and is given in Fig. 3–29. Taking $L = 1$ m, the areas of the surfaces exposed to convection are determined to be

$$A_1 = 2\pi r_1 L = 2\pi(0.025 \text{ m})(1 \text{ m}) = 0.157 \text{ m}^2$$
$$A_3 = 2\pi r_3 L = 2\pi(0.0575 \text{ m})(1 \text{ m}) = 0.361 \text{ m}^2$$

Then the individual thermal resistances become

$$R_i = R_{\text{conv, 1}} = \frac{1}{h_1 A_1} = \frac{1}{(60 \text{ W/m}^2\cdot\text{K})(0.157 \text{ m}^2)} = 0.106°\text{C/W}$$

$$R_1 = R_{\text{pipe}} = \frac{\ln(r_2/r_1)}{2\pi k_1 L} = \frac{\ln(2.75/2.5)}{2\pi(80 \text{ W/m}\cdot\text{K})(1 \text{ m})} = 0.0002°\text{C/W}$$

$$R_2 = R_{\text{insulation}} = \frac{\ln(r_3/r_2)}{2\pi k_2 L} = \frac{\ln(5.75/2.75)}{2\pi(0.05 \text{ W/m}\cdot\text{K})(1 \text{ m})} = 2.35°\text{C/W}$$

$$R_o = R_{\text{conv, 2}} = \frac{1}{h_2 A_3} = \frac{1}{(18 \text{ W/m}^2\cdot\text{K})(0.361 \text{ m}^2)} = 0.154°\text{C/W}$$

Noting that all resistances are in series, the total resistance is determined to be

$$R_{\text{total}} = R_i + R_1 + R_2 + R_o = 0.106 + 0.0002 + 2.35 + 0.154 = 2.61°\text{C/W}$$

Then the steady rate of heat loss from the steam becomes

$$\dot{Q} = \frac{T_{\infty 1} - T_{\infty 2}}{R_{\text{total}}} = \frac{(320 - 5)°\text{C}}{2.61°\text{C/W}} = \textbf{121 W} \quad \text{(per m pipe length)}$$

The heat loss for a given pipe length can be determined by multiplying the preceding quantity by the pipe length L.

The temperature drops across the pipe and the insulation are determined from Eq. 3–17 to be

$$\Delta T_{\text{pipe}} = \dot{Q} R_{\text{pipe}} = (121 \text{ W})(0.0002°\text{C/W}) = \textbf{0.02°C}$$

$$\Delta T_{\text{insulation}} = \dot{Q} R_{\text{insulation}} = (121 \text{ W})(2.35°\text{C/W}) = \textbf{284°C}$$

That is, the temperatures between the inner and the outer surfaces of the pipe differ by 0.02°C, whereas the temperatures between the inner and the outer surfaces of the insulation differ by 284°C.

Discussion Note that the thermal resistance of the pipe is too small relative to the other resistances and can be neglected without causing any significant error. Also note that the temperature drop across the pipe is practically zero, and thus the pipe can be assumed to be isothermal. The resistance to heat flow in insulated pipes is primarily due to insulation.

3–5 ▪ CRITICAL RADIUS OF INSULATION

We know that adding more insulation to a wall or to the attic always decreases heat transfer. The thicker the insulation, the lower the heat transfer rate. This is expected, since the heat transfer area A is constant, and adding insulation always increases the thermal resistance of the wall without increasing the convection resistance.

Adding insulation to a cylindrical pipe or a spherical shell, however, is a different matter. The additional insulation increases the conduction resistance

of the insulation layer but decreases the convection resistance of the surface because of the increase in the outer surface area for convection. The heat transfer from the pipe may increase or decrease, depending on which effect dominates.

Consider a cylindrical pipe of outer radius r_1 whose outer surface temperature T_1 is kept constant (Fig. 3–30). The pipe is now insulated with a material whose thermal conductivity is k and whose outer radius is r_2. Heat is lost from the pipe to the surrounding medium at temperature T_∞, with a convection heat transfer coefficient h. The rate of heat transfer from the insulated pipe to the surrounding air can be expressed as (Fig. 3–31)

$$\dot{Q} = \frac{T_1 - T_\infty}{R_{\text{ins}} + R_{\text{conv}}} = \frac{T_1 - T_\infty}{\dfrac{\ln(r_2/r_1)}{2\pi L k} + \dfrac{1}{h(2\pi r_2 L)}} \tag{3–49}$$

The variation of $\dot{Q}$ with the outer radius of the insulation r_2 is plotted in Fig. 3–31. The value of r_2 at which $\dot{Q}$ reaches a maximum is determined from the requirement that $d\dot{Q}/dr_2 = 0$ (zero slope). Performing the differentiation and solving for r_2 yields the **critical radius of insulation** for a cylindrical body:

$$r_{\text{cr, cylinder}} = \frac{k}{h} \qquad \text{(m)} \tag{3–50}$$

Note that the critical radius of insulation depends on the thermal conductivity of the insulation k and the external convection heat transfer coefficient h. The rate of heat transfer from the cylinder increases with the addition of insulation for $r_2 < r_{\text{cr}}$, reaches a maximum when $r_2 = r_{\text{cr}}$, and starts to decrease for $r_2 > r_{\text{cr}}$. Thus, insulating the pipe may actually increase the rate of heat transfer from the pipe instead of decreasing it when $r_2 < r_{\text{cr}}$.

The important question to answer at this point is whether we need to be concerned about the critical radius of insulation when insulating hot-water pipes or even hot-water tanks. Should we always check and make sure that the outer radius of insulation sufficiently exceeds the critical radius before we install any insulation? Probably not, as explained here.

The value of the critical radius r_{cr} is largest when k is large and h is small. Noting that the lowest value of h encountered in practice is about 5 W/m²·K for the case of natural convection of gases, and that the thermal conductivity of common insulating materials is about 0.05 W/m·K, the largest value of the critical radius we are likely to encounter is

$$r_{\text{cr, max}} = \frac{k_{\text{max, insulation}}}{h_{\text{min}}} \approx \frac{0.05 \text{ W/m·K}}{5 \text{ W/m}^2\text{·K}} = 0.01 \text{ m} = 1 \text{ cm}$$

This value would be even smaller when the radiation effects are considered. The critical radius would be much less in forced convection, often less than 1 mm, because of much larger h values associated with forced convection. Therefore, we can insulate hot-water or steam pipes freely without worrying about the possibility of increasing the heat transfer by insulating the pipes.

The radius of electric wires may be smaller than the critical radius. Therefore, the plastic electrical insulation may actually *enhance* the heat
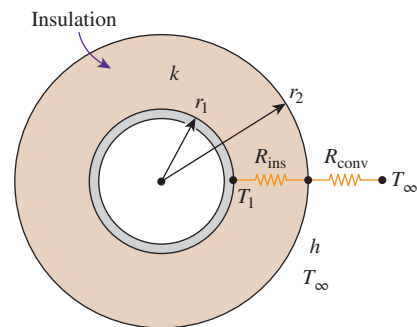
FIGURE 3–30
An insulated cylindrical pipe exposed to convection from the outer surface and the thermal resistance network associated with it.
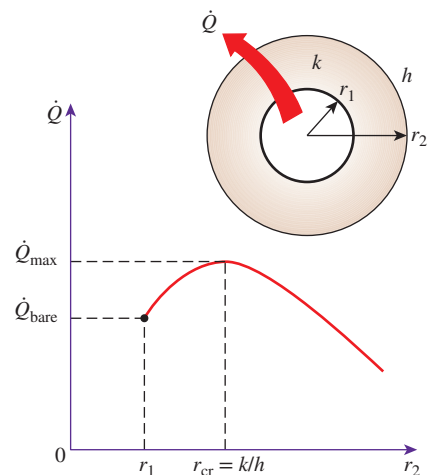
FIGURE 3–31
The variation of heat transfer rate with the outer radius of the insulation r_2 when $r_1 < r_{\text{cr}}$.

transfer from electric wires and thus keep their steady operating temperatures at lower and thus safer levels.

The discussions above can be repeated for a sphere, and it can be shown in a similar manner that the critical radius of insulation for a spherical shell is

$$r_{cr, \, sphere} = \frac{2k}{h} \qquad\qquad \textbf{(3–51)}$$

where k is the thermal conductivity of the insulation and h is the convection heat transfer coefficient on the outer surface.

EXAMPLE 3–9   Heat Loss from an Insulated Electric Wire

A 3-mm-diameter and 5-m-long electric wire is tightly wrapped with a 2-mm-thick plastic cover whose thermal conductivity is $k = 0.15$ W/m·K. Electrical measurements indicate that a current of 10 A passes through the wire, and there is a voltage drop of 8 V along the wire. If the insulated wire is exposed to a medium at $T_\infty = 30°C$ with a heat transfer coefficient of $h = 12$ W/m^2·K, determine the temperature at the interface of the wire and the plastic cover in steady operation. Also determine whether doubling the thickness of the plastic cover will increase or decrease this interface temperature.

SOLUTION   An electric wire is tightly wrapped with a plastic cover. The interface temperature and the effect of doubling the thickness of the plastic cover on the interface temperature are to be determined.

Assumptions   **1** Heat transfer is steady since there is no indication of any change with time. **2** Heat transfer is one-dimensional since there is thermal symmetry about the centerline and no variation in the axial direction. **3** Thermal conductivities are constant. **4** The thermal contact resistance at the interface is negligible. **5** Heat transfer coefficient incorporates the radiation effects, if any.

Properties   The thermal conductivity of plastic is given to be $k = 0.15$ W/m·K.

Analysis   Heat is generated in the wire, and its temperature rises as a result of resistance heating. We assume heat is generated uniformly throughout the wire and is transferred to the surrounding medium in the radial direction. In steady operation, the rate of heat transfer becomes equal to the heat generated within the wire, which is determined to be

$$\dot{Q} = \dot{W}_e = \mathbf{V}I = (8 \text{ V})(10 \text{ A}) = 80 \text{ W}$$

The thermal resistance network for this problem involves a conduction resistance for the plastic cover and a convection resistance for the outer surface in series, as shown in Fig. 3–32. The values of these two resistances are

$$A_2 = (2\pi r_2)\, L = 2\pi(0.0035 \text{ m})(5 \text{ m}) = 0.110 \text{ m}^2$$

$$R_{conv} = \frac{1}{hA_2} = \frac{1}{(12 \text{ W/m}^2\text{·K})(0.110 \text{ m}^2)} = 0.76°C/W$$

$$R_{plastic} = \frac{\ln(r_2/r_1)}{2\pi kL} = \frac{\ln(3.5/1.5)}{2\pi(0.15 \text{ W/m·K})(5 \text{ m})} = 0.18°C/W$$

$\dot{Q}$

k

r_1 r_2

T_1

T_2

h
T_∞

$\dot{Q} \rightarrow$ T_1 —wwww— T_2 —wwww— T_∞
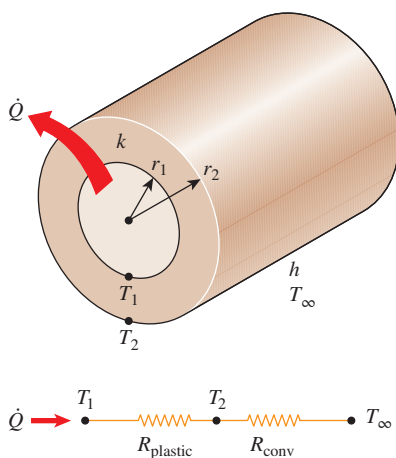
$R_{plastic}$ R_{conv}

FIGURE 3–32
Schematic for Example 3–9.

and therefore

$$R_{\text{total}} = R_{\text{plastic}} + R_{\text{conv}} = 0.76 + 0.18 = 0.94°\text{C/W}$$

Then the interface temperature can be determined from

$$\dot{Q} = \frac{T_1 - T_\infty}{R_{\text{total}}} \quad \longrightarrow \quad T_1 = T_\infty + \dot{Q}R_{\text{total}}$$
$$= 30°\text{C} + (80\text{ W})(0.94°\text{C/W}) = \mathbf{105°C}$$

Note that we did not involve the electrical wire directly in the thermal resistance network, since the wire involves heat generation.

To answer the second part of the question, we need to know the critical radius of insulation of the plastic cover. It is determined from Eq. 3–50 to be

$$r_{\text{cr}} = \frac{k}{h} = \frac{0.15\text{ W/m·K}}{12\text{ W/m}^2\text{·K}} = 0.0125\text{ m} = 12.5\text{ mm}$$

which is larger than the radius of the plastic cover. Therefore, increasing the thickness of the plastic cover will *enhance* heat transfer until the outer radius of the cover reaches 12.5 mm. As a result, the rate of heat transfer $\dot{Q}$ will *increase* when the interface temperature T_1 is held constant, or T_1 will *decrease* when $\dot{Q}$ is held constant, which is the case here.

Discussion It can be shown by repeating the calculations for a 4-mm-thick plastic cover that the interface temperature drops to 90.6°C when the thickness of the plastic cover is doubled. It can also be shown in a similar manner that the interface reaches a minimum temperature of 83°C when the outer radius of the plastic cover equals the critical radius.

3–6 · HEAT TRANSFER FROM FINNED SURFACES

The rate of heat transfer from a surface at a temperature T_s to the surrounding medium at T_∞ is given by Newton's law of cooling as

$$\dot{Q}_{\text{conv}} = hA_s(T_s - T_\infty)$$

where A_s is the heat transfer surface area and h is the convection heat transfer coefficient. When the temperatures T_s and T_∞ are fixed by design considerations, as is often the case, there are *two ways* to increase the rate of heat transfer: to increase the *convection heat transfer coefficient h* or to increase the *surface area A_s*. Increasing h may require the installation of a pump or fan, or replacing the existing one with a larger one, but this approach may or may not be practical. Besides, it may not be adequate. The alternative is to increase the surface area by attaching to the surface *extended surfaces* called *fins* made of highly conductive materials such as aluminum. Finned surfaces are manufactured by extruding, welding, or wrapping a thin metal sheet on a surface. Fins enhance heat transfer from a surface by exposing a larger surface area to convection and radiation.

An interesting application of fins from about 150 million years ago, the Jurassic era, is shown in Fig. 3–33. The dinosaur stegosaurus lived during

FIGURE 3–33
Presumed cooling fins on dinosaur stegosaurus.
©Christian Darkin/Alamy

FIGURE 3–34
The thin plate fins of a car radiator greatly increase the rate of heat transfer to the air.

Left: ©James Kleiser/Yunus Cengel
right: ©McGraw-Hill Education/Christopher Kerrigan, photographer
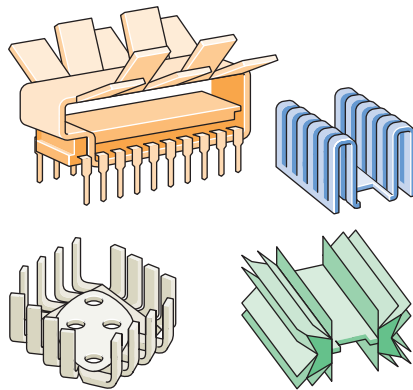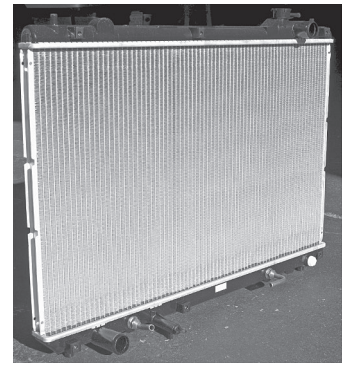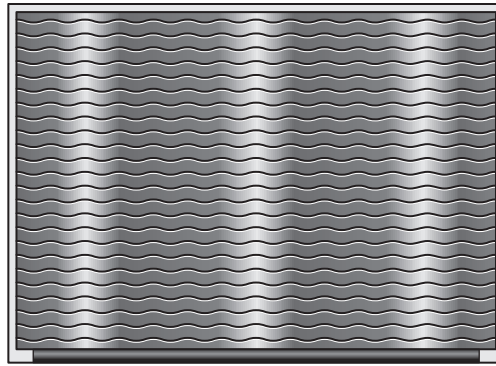
FIGURE 3–35
Some innovative fin designs.
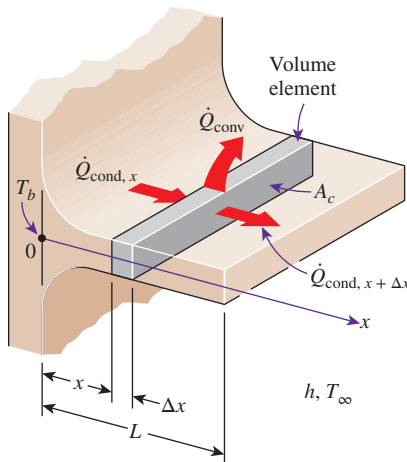
FIGURE 3–36
Volume element of a fin at location x having a length of Δx, cross-sectional area of A_c, and perimeter of p.

this era, and it had two rows of big (and bizarre) bony plates down its back. For a long time, scientists thought that the plates were some kind of armor to protect the vegetarian from predators. We now know that a lot of blood flowed through the plates, and they may have acted like a car radiator. The heart pumped blood through the plates, and the plates acted like cooling fins to cool the blood down.

Finned surfaces are commonly used in practice to enhance heat transfer, and they often increase the rate of heat transfer from a surface severalfold. The car radiator shown in Fig. 3–34 is an example of a finned surface. The closely packed thin metal sheets attached to the hot-water tubes increase the surface area for convection and thus the rate of convection heat transfer from the tubes to the air many times. There are a variety of innovative fin designs available in the market, and they seem to be limited only by imagination (Fig. 3–35).

In the analysis of fins, we consider *steady* operation with *no heat generation* in the fin, and we assume the thermal conductivity k of the material to remain constant. We also assume the convection heat transfer coefficient h to be *constant* and *uniform* over the entire surface of the fin for convenience in the analysis. We recognize that the convection heat transfer coefficient h, in general, varies along the fin as well as along its circumference, and its value at a point is a strong function of the *fluid motion* at that point. The value of h is usually much lower at the *fin base* than it is at the *fin tip* because the fluid is surrounded by solid surfaces near the base, which seriously disrupt its motion to the point of "suffocating" it, while the fluid near the fin tip has little contact with a solid surface and thus encounters little resistance to flow. Therefore, adding too many fins on a surface may actually decrease the overall heat transfer when the decrease in h offsets any gain resulting from the increase in the surface area.

Fin Equation

Consider a volume element of a fin at location x having a length of Δx, a cross-sectional area of A_c, and a perimeter of p, as shown in Fig. 3–36. Under steady conditions, the energy balance on this volume element can be expressed as

$$
\begin{pmatrix} \text{Rate of } heat \\ conduction\ into \\ \text{the element at } x \end{pmatrix} = \begin{pmatrix} \text{Rate of } heat \\ conduction\ from\ \text{the} \\ \text{element at } x + \Delta x \end{pmatrix} + \begin{pmatrix} \text{Rate of } heat \\ convection\ from \\ \text{the element} \end{pmatrix}
$$

or

$$\dot{Q}_{\text{cond, }x} = \dot{Q}_{\text{cond, }x+\Delta x} + \dot{Q}_{\text{conv}}$$

where

$$\dot{Q}_{\text{conv}} = h(p\,\Delta x)(T - T_\infty)$$

Substituting and dividing by Δx, we obtain

$$\frac{\dot{Q}_{\text{cond, }x+\Delta x} - \dot{Q}_{\text{cond, }x}}{\Delta x} + hp(T - T_\infty) = 0 \tag{3–52}$$

Taking the limit as $\Delta x \to 0$ gives

$$\frac{d\dot{Q}_{\text{cond}}}{dx} + hp(T - T_\infty) = 0 \tag{3–53}$$

From Fourier's law of heat conduction we have

$$\dot{Q}_{\text{cond}} = -kA_c \frac{dT}{dx} \tag{3–54}$$

where A_c is the cross-sectional area of the fin at location x. Substitution of this relation into Eq. 3–53 gives the differential equation governing heat transfer in fins,

$$\frac{d}{dx}\left(kA_c \frac{dT}{dx}\right) - hp(T - T_\infty) = 0 \tag{3–55}$$

In general, the cross-sectional area A_c and the perimeter p of a fin vary with x, which makes this differential equation difficult to solve. In the special case of *constant cross section* and *constant thermal conductivity,* the differential equation Eq. 3–55 reduces to

$$\frac{d^2T}{dx^2} - \frac{hp}{kA_c}(T - T_\infty) = 0 \quad \text{or} \quad \frac{d^2\theta}{dx^2} - m^2\theta = 0 \tag{3–56}$$

where

$$m^2 = \frac{hp}{kA_c} \tag{3–57}$$

and $\theta = T - T_\infty$ is the *temperature excess.* At the fin base we have $\theta_b = T_b - T_\infty$.

Equation 3–56 is a linear, homogeneous, second-order differential equation with constant coefficients. A fundamental theory of differential equations states that such an equation has two linearly independent solution functions, and its general solution is the linear combination of those two solution functions. A careful examination of the differential equation reveals that subtracting a constant multiple of the solution function θ from its second derivative yields zero. Thus we conclude that the function θ and its second derivative must be *constant multiples* of each other. The only functions whose derivatives are constant multiples of the functions themselves are the *exponential functions* (or a linear combination of exponential functions such as sine and cosine hyperbolic functions). Therefore, the solution functions of the preceding differential equation are the exponential functions e^{-mx} or e^{mx} or constant multiples of them. This can be verified by direct substitution. For example, the second derivative of e^{-mx} is m^2e^{-mx}, and its substitution into Eq. 3–56
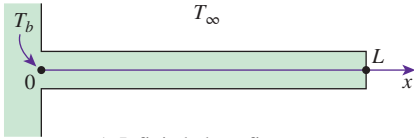
1. Infinitely long fin
2. Negligible heat loss (adiabatic tip)
3. Specified temperature
4. Convection

FIGURE 3–37
Boundary conditions at the fin base and the fin tip.

yields zero. Therefore, the general solution of the differential equation Eq. 3–56 is

$$\theta(x) = C_1 e^{mx} + C_2 e^{-mx} \tag{3–58}$$

where C_1 and C_2 are arbitrary constants whose values are to be determined from the boundary conditions at the base and at the tip of the fin. Note that we need only two conditions to determine C_1 and C_2 uniquely.

The temperature of the plate to which the fins are attached is normally known in advance. Therefore, at the fin base we have a *specified temperature* boundary condition, expressed as

Boundary condition at fin base: $\qquad \theta(0) = \theta_b = T_b - T_\infty \tag{3–59}$

At the fin tip we have several possibilities, including infinitely long fins, negligible heat loss (idealized as an adiabatic tip), specified temperature, and convection (Fig. 3–37). Next, we consider each case separately.

1 Infinitely Long Fin ($T_{\text{fin tip}} = T_\infty$)

For a sufficiently long fin of *uniform* cross section (A_c = constant), the temperature of the fin at the fin tip approaches the environment temperature T_∞ and thus θ approaches zero. That is,

Boundary condition at fin tip: $\qquad \theta(L) = T(L) - T_\infty = 0 \quad \text{as} \quad L \to \infty$

This condition is satisfied by the function e^{-mx}, but not by the other prospective solution function e^{mx} since it tends to infinity as x gets larger. Therefore, the general solution in this case will consist of a constant multiple of e^{-mx}. The value of the constant multiple is determined from the requirement that at the fin base where $x = 0$, the value of θ is θ_b. Noting that $e^{-mx} = e^0 = 1$, the proper value of the constant is θ_b, and the solution function we are looking for is $\theta(x) = \theta_b e^{-mx}$. This function satisfies the differential equation as well as the requirements that the solution reduce to θ_b at the fin base and approach zero at the fin tip for large x. Noting that $\theta = T - T_\infty$ and $m = \sqrt{hp/kA_c}$, the variation of temperature along the fin in this case can be expressed as

Very long fin: $\qquad \dfrac{T(x) - T_\infty}{T_b - T_\infty} = e^{-mx} = e^{-x\sqrt{hp/kA_c}} \tag{3–60}$

$T(x) = T_\infty + (T_b - T_\infty)e^{-x\sqrt{\frac{hp}{kA_c}}}$

T_b, h, T_∞, k, D, $A_b = A_c$

($p = \pi D$, $A_c = \pi D^2/4$ for a cylindrical fin)

FIGURE 3–38
A long circular fin of uniform cross section and the variation of temperature along it.

Note that the temperature along the fin in this case decreases *exponentially* from T_b to T_∞, as shown in Fig. 3–38. The steady rate of *heat transfer* from the entire fin can be determined from Fourier's law of heat conduction

Very long fin: $\qquad \dot{Q}_{\text{long fin}} = -kA_c \dfrac{dT}{dx}\bigg|_{x=0} = \sqrt{hpkA_c}\,(T_b - T_\infty) \tag{3–61}$

where p is the perimeter, A_c is the cross-sectional area of the fin, and x is the distance from the fin base. Alternatively, the rate of heat transfer from the fin could also be determined by considering heat transfer from a differential volume element of the fin and integrating it over the entire surface of the fin:

$$\dot{Q}_{\text{fin}} = \int_{A_{\text{fin}}} h[T(x) - T_\infty]\,dA_{\text{fin}} = \int_{A_{\text{fin}}} h\theta(x)\,dA_{\text{fin}} \tag{3–62}$$

The two approaches described are equivalent and give the same result since, under steady conditions, the heat transfer from the exposed surfaces of the fin is equal to the heat transfer to the fin at the base (Fig. 3–39).

FIGURE 3–39

Under steady conditions, heat transfer from the exposed surfaces of the fin is equal to heat conduction to the fin at the base.

2   Negligible Heat Loss from the Fin Tip (Adiabatic fin tip, $\dot{Q}_{\text{fin tip}} = 0$)

Fins are not likely to be so long that their temperature approaches the surrounding temperature at the tip. A more realistic situation is for heat transfer from the fin tip to be negligible since the heat transfer from the fin is proportional to its surface area, and the surface area of the fin tip is usually a negligible fraction of the total fin area. Then the fin tip can be assumed to be adiabatic, and the condition at the fin tip can be expressed as

Boundary condition at fin tip:
$$\left.\frac{d\theta}{dx}\right|_{x=L} = 0 \tag{3–63}$$

The condition at the fin base remains the same as expressed in Eq. 3–59. The application of the boundary conditions given by Eqs. 3–59 and 3–63 on the general solution (Eq. 3–58) requires that $\theta(0) = \theta_b = C_1 + C_2$ and $mC_1 e^{mL} - mC_2 e^{-mL} = 0$, respectively. Solving these two equations simultaneously for C_1 and C_2 yields $C_1 = \theta_b/(1 + e^{2mL})$ and $C_2 = \theta_b/(1 + e^{-2mL})$. Substituting the relations for C_1 and C_2 into Eq. 3–58 and using the definition of the hyperbolic cosine function $\cosh x = (e^x + e^{-x})/2$ gives the desired relation for the temperature distribution:

Adiabatic fin tip:
$$\frac{T(x) - T_\infty}{T_b - T_\infty} = \frac{\cosh m(L - x)}{\cosh mL} \tag{3–64}$$

The rate of heat transfer from the fin can be determined again from Fourier's law of heat conduction:

Adiabatic fin tip:
$$\dot{Q}_{\text{adiabatic tip}} = -kA_c \left.\frac{dT}{dx}\right|_{x=0} = \sqrt{hpkA_c}\,(T_b - T_\infty)\tanh mL \tag{3–65}$$

where the equation for the hyperbolic tangent function is

$$\tanh x = \sinh x/\cosh x = (e^x - e^{-x})/(e^x + e^{-x}).$$

Note that the heat transfer relations for the very long fin and the fin with negligible heat loss at the tip differ by the factor tanh mL, which approaches 1 as L becomes very large.

3   Specified Temperature ($T_{\text{fin, tip}} = T_L$)

In this case the temperature at the end of the fin (the fin tip) is fixed at a specified temperature T_L. This case could be considered as a generalization of the case of *Infinitely Long Fin* where the fin tip temperature was fixed at T_∞. The condition at the fin tip for this case is

Boundary condition at fin tip:
$$\theta(L) = \theta_L = T_L - T_\infty \tag{3–66}$$

The fin base boundary condition remains the same as given in Eq. 3–59. Applying the boundary conditions given by Eqs. 3–59 and 3–66 on the general solution (Eq. 3–58) gives, after some lengthy algebra and using the
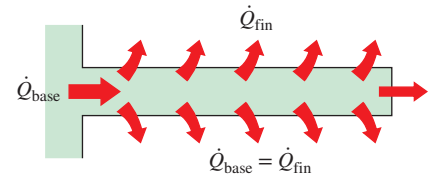
definition of the hyperbolic sine function, $\sinh x = (e^x - e^{-x})/2$, the desired temperature distribution:

Specified fin tip temperature:

$$\frac{T(x) - T_\infty}{T_b - T_\infty} = \frac{[(T_L - T_\infty)/(T_b - T_\infty)] \sinh mx + \sinh m(L - x)}{\sinh mL} \tag{3–67}$$

Using the Fourier's law of heat conduction, the *rate of heat transfer* from the fin is

Specified fin tip temperature:

$$\dot{Q}_{\text{specified temp.}} = -kA_c \frac{dT}{dx}\bigg|_{x=0}$$

$$= \sqrt{hpkA_c}(T_b - T_\infty) \frac{\cosh mL - [(T_L - T_\infty)/(T_b - T_\infty)]}{\sinh mL} \tag{3–68}$$

Note that Eqs. 3–67 and 3–68 reduce to Eqs. 3–60 and 3–61 for the case of *infinitely long fin* ($L \to \infty$).

4 Convection from Fin Tip

The fin tips, in practice, are exposed to the surroundings, and thus the proper boundary condition for the fin tip is convection that may also include the effects of radiation. Consider the case of convection only at the tip. The condition at the fin tip can be obtained from an energy balance at the fin tip ($\dot{Q}_{\text{cond}} = \dot{Q}_{\text{conv}}$) That is,

Boundary condition at fin tip: $\qquad -kA_c \frac{dT}{dx}\bigg|_{x=L} = hA_c[T(L) - T_\infty]$ $\tag{3–69}$

The boundary condition at the fin base is Eq. 3–59, which is the same as the three previous cases. Substituting the two boundary conditions given by Eqs. 3–59 and 3–69 into the general solution (Eq. 3–58), it may be shown after some lengthy manipulation that the temperature distribution is

Convection from fin tip: $\quad \dfrac{T(x) - T_\infty}{T_b - T_\infty} = \dfrac{\cosh m(L - x) + (h/mk) \sinh m(L - x)}{\cosh mL + (h/mk) \sinh mL}$ $\tag{3–70}$

The *rate of heat transfer* from the fin can be found by substituting the temperature gradient at the base of the fin, obtained from Eq. 3–70, into Fourier's law of heat conduction. The result is

Convection from fin tip:

$$\dot{Q}_{\text{convection}} = -kA_c \frac{dT}{dx}\bigg|_{x=0}$$

$$= \sqrt{hpkA_c}(T_b - T_\infty) \frac{\sinh mL + (h/mk) \cosh mL}{\cosh mL + (h/mk) \sinh mL} \tag{3–71}$$

The solution to the general fin equation for the case of *convection from fin tip* is rather complex. An approximate, yet practical and accurate, way of accounting for the loss from the fin tip is to replace the *fin length L* in the relation for the *insulated tip* case with a **corrected fin length** defined as (Fig. 3–40)

Corrected fin length: $\qquad\qquad L_c = L + \dfrac{A_c}{p}$ $\tag{3–72}$

(a) Actual fin with convection at the tip

(b) Equivalent fin with insulated tip
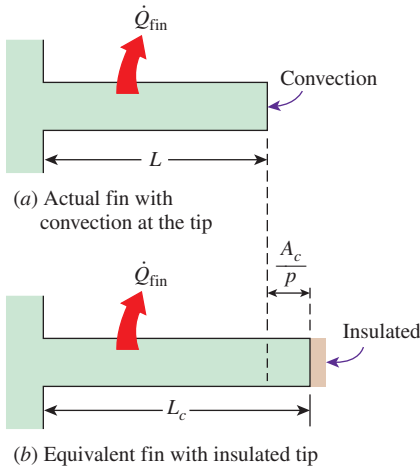
FIGURE 3–40
Corrected fin length L_c is defined such that heat transfer from a fin of length L_c with insulated tip is equal to heat transfer from the actual fin of length L with convection at the fin tip.

where A_c is the cross-sectional area and p is the perimeter of the fin at the tip. Multiplying the preceding relation by the perimeter gives $A_{\text{corrected}} = A_{\text{fin(lateral)}} + A_{\text{tip}}$, which indicates that the fin area determined using the corrected length is equivalent to the sum of the lateral fin area plus the fin tip area.

The corrected length approximation gives very good results when the variation of temperature near the fin tip is small (which is the case when $mL \geq 1$) and the heat transfer coefficient at the fin tip is about the same as that at the lateral surface of the fin. Therefore, *fins subjected to convection at their tips can be treated as fins with insulated tips by replacing the actual fin length with the corrected length in Eqs. 3–64 and 3–65.*

Using the proper relations for A_c and p, the corrected lengths for rectangular and cylindrical fins are easily determined to be

$$L_{c, \text{rectangular fin}} = L + \frac{t}{2} \quad \text{and} \quad L_{c, \text{cylindrical fin}} = L + \frac{D}{4}$$

where t is the thickness of the rectangular fins and D is the diameter of the cylindrical fins.

Fin Efficiency

Consider the surface of a *plane wall* at temperature T_b exposed to a medium at temperature T_∞. Heat is lost from the surface to the surrounding medium by convection with a heat transfer coefficient of h. Disregarding radiation or accounting for its contribution in the convection coefficient h, heat transfer from a surface area A_s is expressed as $\dot{Q} = hA_s(T_s - T_\infty)$.

Now let us consider a fin of constant cross-sectional area $A_c = A_b$ and length L that is attached to the surface with a perfect contact (Fig. 3–41). This time heat is transferred from the surface to the fin *by conduction* and from the fin to the surrounding medium *by convection* with the same heat transfer coefficient h. The temperature of the fin is T_b at the fin base and gradually decreases toward the fin tip. Convection from the fin surface causes the temperature at any cross section to drop somewhat from the midsection toward the outer surfaces. However, the cross-sectional area of the fins is usually very small, and thus the temperature at any cross section can be considered to be uniform. Also, the fin tip can be assumed for convenience and simplicity to be adiabatic by using the corrected length for the fin instead of the actual length.

In the limiting case of *zero thermal resistance* or *infinite thermal conductivity* ($k \rightarrow \infty$), the temperature of the fin is uniform at the base value of T_b. The heat transfer from the fin is *maximum* in this case and can be expressed as

$$\dot{Q}_{\text{fin, max}} = hA_{\text{fin}}(T_b - T_\infty) \tag{3–73}$$

In reality, however, the temperature of the fin drops along the fin, and thus the heat transfer from the fin is less because of the decreasing temperature difference $T(x) - T_\infty$ toward the fin tip, as shown in Fig. 3–42. To account for the effect of this decrease in temperature on heat transfer, we define a **fin efficiency** as

$$\eta_{\text{fin}} = \frac{\dot{Q}_{\text{fin}}}{\dot{Q}_{\text{fin, max}}} = \frac{\text{Actual heat transfer rate from the fin}}{\begin{array}{c}\text{Ideal heat transfer rate from the fin}\\\text{if the entire fin were at base temperature}\end{array}} \tag{3–74}$$

(a) Surface without fins

(b) Surface with a fin

$A_{\text{fin}} = 2 \times w \times L + w \times t$
$\cong 2 \times w \times L$
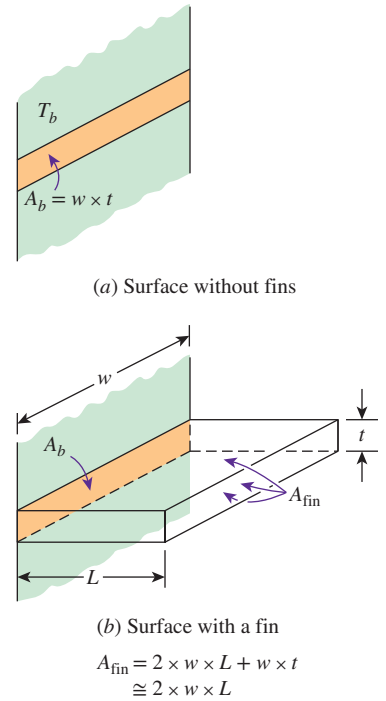
FIGURE 3–41

Fins enhance heat transfer from a surface by enhancing surface area.
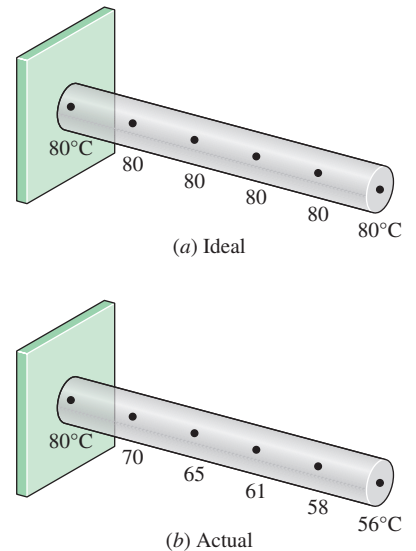
(a) Ideal

(b) Actual

FIGURE 3–42

Ideal and actual temperature distribution along a fin.

TABLE 3–3

Efficiency and surface areas of common fin configurations

Straight rectangular fins

$m = \sqrt{2h/kt}$
$L_c = L + t/2$
$A_{\text{fin}} = 2wL_c$

$\eta_{\text{fin}} = \dfrac{\tanh mL_c}{mL_c}$
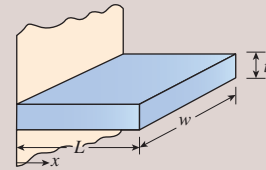
Straight triangular fins

$m = \sqrt{2h/kt}$
$A_{\text{fin}} = 2w\sqrt{L^2 + (t/2)^2}$

$\eta_{\text{fin}} = \dfrac{1}{mL}\dfrac{I_1(2mL)}{I_0(2mL)}$
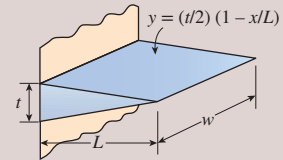
Straight parabolic fins

$m = \sqrt{2h/kt}$
$A_{\text{fin}} = wL[C_1 + (L/t)\ln(t/L + C_1)]$
$C_1 = \sqrt{1 + (t/L)^2}$

$\eta_{\text{fin}} = \dfrac{2}{1 + \sqrt{(2mL)^2 + 1}}$
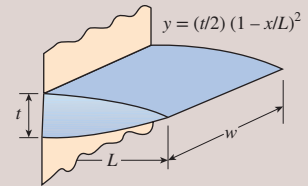
Circular fins of rectangular profile

$m = \sqrt{2h/kt}$
$r_{2c} = r_2 + t/2$
$A_{\text{fin}} = 2\pi(r_{2c}^2 - r_1^2)$

$\eta_{\text{fin}} = C_2 \dfrac{K_1(mr_1)I_1(mr_{2c}) - I_1(mr_1)K_1(mr_{2c})}{I_0(mr_1)K_1(mr_{2c}) + K_0(mr_1)I_1(mr_{2c})}$

$C_2 = \dfrac{2r_1/m}{r_{2c}^2 - r_1^2}$
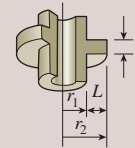
Pin fins of rectangular profile

$m = \sqrt{4h/kD}$
$L_c = L + D/4$
$A_{\text{fin}} = \pi D L_c$

$\eta_{\text{fin}} = \dfrac{\tanh mL_c}{mL_c}$
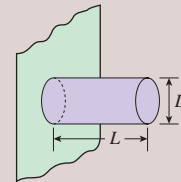
Pin fins of triangular profile

$m = \sqrt{4h/kD}$
$A_{\text{fin}} = \dfrac{\pi D}{2}\sqrt{L^2 + (D/2)^2}$

$\eta_{\text{fin}} = \dfrac{2}{mL}\dfrac{I_2(2mL)}{I_1(2mL)}$
$I_2(x) = I_0(x) - (2/x)\,I_1(x)$ where $x = 2mL$
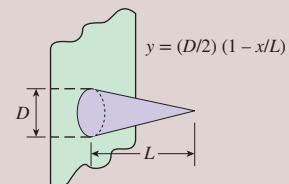
Pin fins of parabolic profile

$m = \sqrt{4h/kD}$
$A_{\text{fin}} = \dfrac{\pi L^3}{8D}\left[C_3 C_4 - \dfrac{L}{2D}\ln[(2DC_4/L) + C_3]\right]$
$C_3 = 1 + 2(D/L)^2$
$C_4 = \sqrt{1 + (D/L)^2}$

$\eta_{\text{fin}} = \dfrac{2}{1 + \sqrt{(2mL/3)^2 + 1}}$
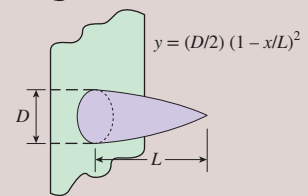
Pin fins of parabolic profile (blunt tip)

$m = \sqrt{4h/kD}$
$A_{\text{fin}} = \dfrac{\pi D^4}{96L^2}\{[16(L/D)^2 + 1]^{3/2} - 1\}$

$\eta_{\text{fin}} = \dfrac{3}{2mL}\dfrac{I_1(4mL/3)}{I_0(4mL/3)}$
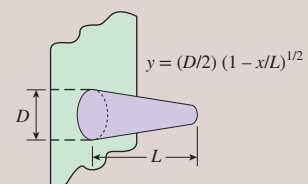
or

$$\dot{Q}_{\text{fin}} = \eta_{\text{fin}} \dot{Q}_{\text{fin, max}} = \eta_{\text{fin}} h A_{\text{fin}}(T_b - T_\infty) \tag{3-75}$$

where A_{fin} is the total surface area of the fin. This relation enables us to determine the heat transfer from a fin when its efficiency is known. For the cases of constant cross section of *very long fins* and *fins with adiabatic tips,* the fin efficiency can be expressed as

$$\eta_{\text{long fin}} = \frac{\dot{Q}_{\text{fin}}}{\dot{Q}_{\text{fin, max}}} = \frac{\sqrt{hpkA_c}(T_b - T_\infty)}{hA_{\text{fin}}(T_b - T_\infty)} = \frac{1}{L}\sqrt{\frac{kA_c}{hp}} = \frac{1}{mL} \tag{3-76}$$

and

$$\eta_{\text{adiabatic tip}} = \frac{\dot{Q}_{\text{fin}}}{\dot{Q}_{\text{fin, max}}} = \frac{\sqrt{hpkA_c}(T_b - T_\infty)\tanh mL}{hA_{\text{fin}}(T_b - T_\infty)} = \frac{\tanh mL}{mL} \tag{3-77}$$

since $A_{\text{fin}} = pL$ for fins with constant cross section. Equation 3–77 can also be used for fins subjected to convection provided that the fin length L is replaced by the corrected length L_c.

Table 3–3 provides fin efficiency relations for fins with uniform and nonuniform cross section. For fins with nonuniform profile, Eq. 3–56 is no longer valid, and the general form of the differential equation governing heat transfer in fins of arbitrary shape, Eq. 3–55, must be used. For these cases the solution is no longer in the form of simple exponential or hyperbolic functions. The mathematical functions I and K that appear in some of these relations are the *modified Bessel functions,* and their values are given in Table 3–4. Efficiencies are plotted in Fig. 3–43 for fins on a *plain surface* and in Fig. 3–44 for *circular fins* of constant thickness. For most fins of constant thickness encountered in practice, the fin thickness t is too small relative to the fin length $L,$ and thus the fin tip area is negligible.

Note that fins with triangular and parabolic profiles contain less material and are more efficient than the ones with rectangular profiles, and thus are more suitable for applications requiring minimum weight such as space applications.

An important consideration in the design of finned surfaces is the selection of the proper *fin length L.* Normally the *longer* the fin, the *larger* the heat transfer area and thus the *higher* the rate of heat transfer from the fin. But also the larger the fin, the bigger the mass, the higher the price, and the larger the fluid friction. Therefore, increasing the length of the fin beyond a certain value cannot be justified unless the added benefits outweigh the added cost. Also, the fin efficiency decreases with increasing fin length because of the decrease in fin temperature with length. Fin lengths that cause the fin efficiency to drop below 60 percent usually cannot be justified economically and should be avoided. The efficiency of most fins used in practice is above 90 percent.

Fin Effectiveness

Fins are used to *enhance* heat transfer, and the use of fins on a surface cannot be recommended unless the enhancement in heat transfer justifies the added cost and complexity associated with the fins. In fact, there is no assurance that

TABLE 3–4

Modified Bessel functions of the first and second kinds*

x	$e^{-x}I_0(x)$	$e^{-x}I_1(x)$	$e^{-x}K_0(x)$	$e^{-x}K_1(x)$
0.0	1.0000	0.0000	∞	∞
0.2	0.8269	0.0823	2.1408	5.8334
0.4	0.6974	0.1368	1.6627	3.2587
0.6	0.5993	0.1722	1.4167	2.3739
0.8	0.5241	0.1945	1.2582	1.9179
1.0	0.4658	0.2079	1.1445	1.6362
1.2	0.4198	0.2153	1.0575	1.4429
1.4	0.3831	0.2185	0.9881	1.3011
1.6	0.3533	0.2190	0.9309	1.1919
1.8	0.3289	0.2177	0.8828	1.1048
2.0	0.3085	0.2153	0.8416	1.0335
2.2	0.2913	0.2121	0.8057	0.9738
2.4	0.2766	0.2085	0.7740	0.9229
2.6	0.2639	0.2047	0.7459	0.8790
2.8	0.2528	0.2007	0.7206	0.8405
3.0	0.2430	0.1968	0.6978	0.8066
3.2	0.2343	0.1930	0.6770	0.7763
3.4	0.2264	0.1892	0.6580	0.7491
3.6	0.2193	0.1856	0.6405	0.7245
3.8	0.2129	0.1821	0.6243	0.7021
4.0	0.2070	0.1788	0.6093	0.6816
4.2	0.2016	0.1755	0.5953	0.6627
4.4	0.1966	0.1725	0.5823	0.6454
4.6	0.1919	0.1695	0.5701	0.6292
4.8	0.1876	0.1667	0.5586	0.6143
5.0	0.1835	0.1640	0.5478	0.6003
5.2	0.1797	0.1614	0.5376	0.5872
5.4	0.1762	0.1589	0.5280	0.5749
5.6	0.1728	0.1565	0.5188	0.5634
5.8	0.1697	0.1542	0.5101	0.5525
6.0	0.1667	0.1521	0.5019	0.5422
6.5	0.1598	0.1469	0.4828	0.5187
7.0	0.1537	0.1423	0.4658	0.4981
7.5	0.1483	0.1380	0.4505	0.4797
8.0	0.1434	0.1341	0.4366	0.4631
8.5	0.1390	0.1305	0.4239	0.4482
9.0	0.1350	0.1272	0.4123	0.4346
9.5	0.1313	0.1241	0.4016	0.4222
10.0	0.1278	0.1213	0.3916	0.4108

*Evaluated from EES using the mathematical functions Bessel_I(x) and Bessel_K(x)
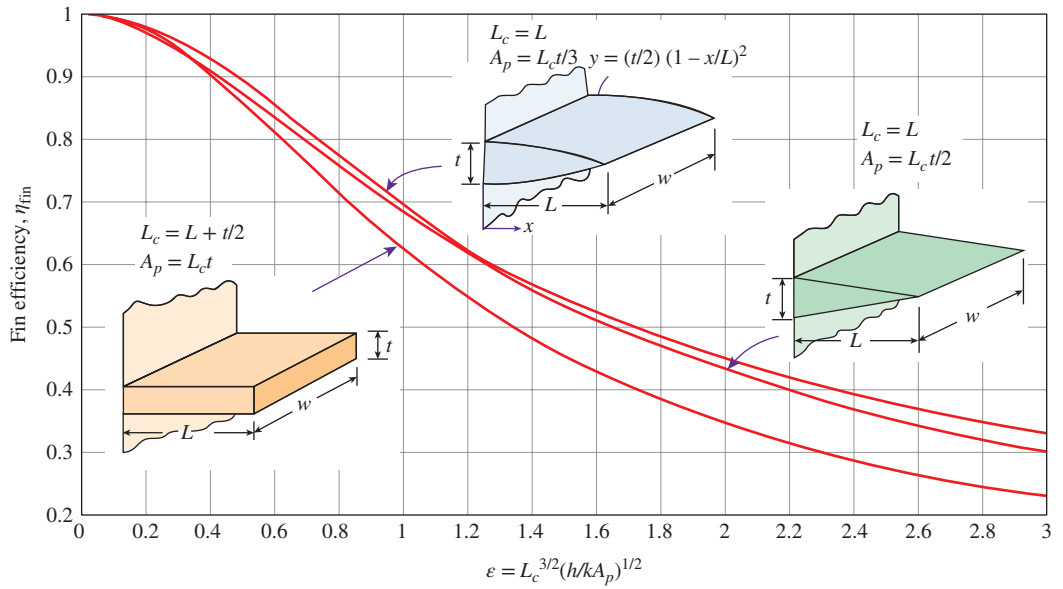
FIGURE 3–43
Efficiency of straight fins of rectangular, triangular, and parabolic profiles.
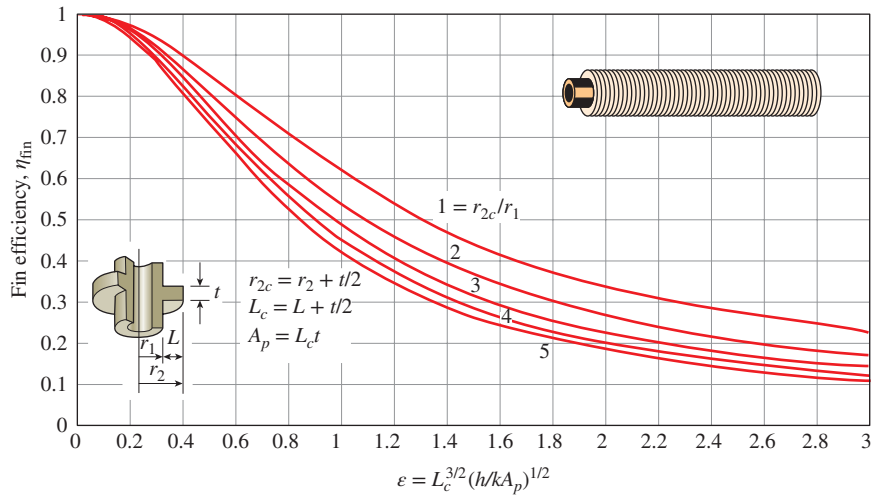
FIGURE 3–44
Efficiency of annular fins of constant thickness t.

adding fins on a surface will *enhance* heat transfer. The performance of the fins is judged on the basis of the enhancement in heat transfer relative to the no-fin case. The performance of fins is expressed in terms of the *fin effectiveness* ε_{fin} defined as (Fig. 3–45)

$$\varepsilon_{\text{fin}} = \frac{\dot{Q}_{\text{fin}}}{\dot{Q}_{\text{no fin}}} = \frac{\dot{Q}_{\text{fin}}}{hA_b(T_b - T_\infty)} = \frac{\text{Heat transfer rate from the fin of \textit{base area} } A_b}{\text{Heat transfer rate from the surface of \textit{area} } A_b} \qquad \textbf{(3–78)}$$

Hence, A_b is the cross-sectional area of the fin at the base and $\dot{Q}_{\text{no fin}}$ represents the rate of heat transfer from this area if no fins are attached to the surface. An effectiveness of $\varepsilon_{\text{fin}} = 1$ indicates that the addition of fins to the surface does not affect heat transfer at all. That is, heat conducted to the fin through the base area A_b is equal to the heat transferred from the same area A_b to the surrounding medium. An effectiveness of $\varepsilon_{\text{fin}} < 1$ indicates that the fin actually acts as *insulation,* slowing down the heat transfer from the surface. This situation can occur when fins made of low thermal conductivity materials are used. An effectiveness of $\varepsilon_{\text{fin}} > 1$ indicates that fins are *enhancing* heat transfer from the surface, as they should. However, the use of fins cannot be justified unless ε_{fin} is sufficiently larger than 1. Finned surfaces are designed on the basis of *maximizing* effectiveness for a specified cost or *minimizing* cost for a desired effectiveness.

Note that both the fin efficiency and fin effectiveness are related to the performance of the fin, but they are different quantities. However, they are related to each other by

$$\varepsilon_{\text{fin}} = \frac{\dot{Q}_{\text{fin}}}{\dot{Q}_{\text{no fin}}} = \frac{\dot{Q}_{\text{fin}}}{hA_b(T_b - T_\infty)} = \frac{\eta_{\text{fin}}hA_{\text{fin}}(T_b - T_\infty)}{hA_b(T_b - T_\infty)} = \frac{A_{\text{fin}}}{A_b}\eta_{\text{fin}} \qquad \textbf{(3–79)}$$

Therefore, the fin effectiveness can be determined easily when the fin efficiency is known, or vice versa.

The rate of heat transfer from a sufficiently *long* fin of *uniform* cross section under steady conditions is given by Eq. 3–61. Substituting this relation into Eq. 3–78, the effectiveness of such a long fin is determined to be

$$\varepsilon_{\text{long fin}} = \frac{\dot{Q}_{\text{fin}}}{\dot{Q}_{\text{no fin}}} = \frac{\sqrt{hpkA_c}(T_b - T_\infty)}{hA_b(T_b - T_\infty)} = \sqrt{\frac{kp}{hA_c}} \qquad \textbf{(3–80)}$$

since $A_c = A_b$ in this case. We can draw several important conclusions from the fin effectiveness relation above for consideration in the design and selection of the fins:

- The *thermal conductivity k* of the fin material should be as high as possible. Thus it is no coincidence that fins are made from metals, with copper, aluminum, and iron being the most common ones. Perhaps the most widely used fins are made of aluminum because of its low cost and weight and its resistance to corrosion.

- The ratio of the *perimeter* to the *cross-sectional area* of the fin p/A_c should be as high as possible. This criterion is satisfied by *thin* plate fins and *slender* pin fins.

- The use of fins is *most effective* in applications involving a *low convection heat transfer coefficient.* Thus, the use of fins is more easily justified when the medium is a *gas* instead of a liquid and the heat transfer is by *natural convection* instead of by forced convection. Therefore, it is no coincidence that in liquid-to-gas heat exchangers such as the car radiator, fins are placed on the *gas* side.

When determining the rate of heat transfer from a finned surface, we must consider the *unfinned portion* of the surface as well as the *fins.* Therefore, the rate of heat transfer for a surface containing n fins can be expressed as
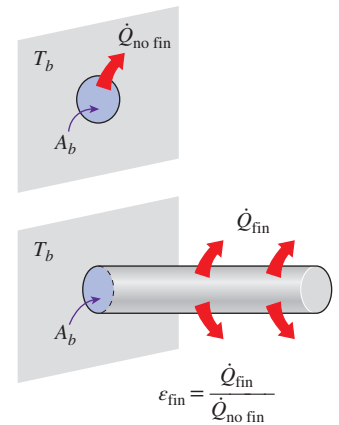
$$\varepsilon_{\text{fin}} = \frac{\dot{Q}_{\text{fin}}}{\dot{Q}_{\text{no fin}}}$$

FIGURE 3–45
The effectiveness of a fin.
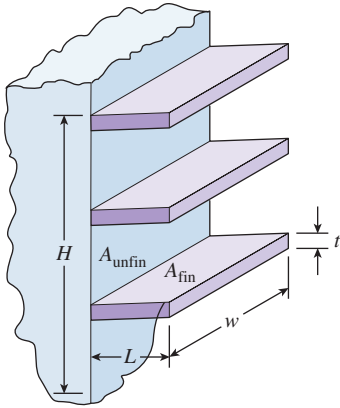
$A_{\text{no fin}} = w \times H$
$A_{\text{unfin}} = w \times H - 3 \times (t \times w)$
$A_{\text{fin}} = 2 \times L \times w + t \times w$
$\cong 2 \times L \times w$ (one fin)

FIGURE 3–46
Various surface areas associated with a rectangular surface with three fins.

FIGURE 3–47
Because of the gradual temperature drop along the fin, the region near the fin tip makes little or no contribution to heat transfer.

$$\dot{Q}_{\text{total, fin}} = \dot{Q}_{\text{unfin}} + \dot{Q}_{\text{fin}}$$
$$= hA_{\text{unfin}}(T_b - T_\infty) + \eta_{\text{fin}}hA_{\text{fin}}(T_b - T_\infty) \qquad \textbf{(3–81)}$$
$$= h(A_{\text{unfin}} + \eta_{\text{fin}}A_{\text{fin}})(T_b - T_\infty)$$

We can also define an **overall effectiveness** for a finned surface as the ratio of the total heat transfer from the finned surface to the heat transfer from the same surface if there were no fins,

$$\varepsilon_{\text{fin, overall}} = \frac{\dot{Q}_{\text{total, fin}}}{\dot{Q}_{\text{total, no fin}}} = \frac{h(A_{\text{unfin}} + \eta_{\text{fin}}A_{\text{fin}})(T_b - T_\infty)}{hA_{\text{no fin}}(T_b - T_\infty)} = \frac{A_{\text{unfin}} + \eta_{\text{fin}}A_{\text{fin}}}{A_{\text{no fin}}} \qquad \textbf{(3–82)}$$

where $A_{\text{no fin}}$ is the area of the surface when there are no fins, A_{fin} is the total surface area of all the fins on the surface, and A_{unfin} is the area of the unfinned portion of the surface (Fig. 3–46). Note that the overall fin effectiveness depends on the fin density (number of fins per unit length) as well as the effectiveness of the individual fins. The overall effectiveness is a better measure of the performance of a finned surface than the effectiveness of the individual fins.

Proper Length of a Fin

An important step in the design of a fin is the determination of the appropriate length of the fin once the fin material and the fin cross section are specified. You may be tempted to think that the longer the fin, the larger the surface area and thus the higher the rate of heat transfer. Therefore, for maximum heat transfer, the fin should be infinitely long. However, the temperature drops along the fin exponentially and reaches the environment temperature at some length. The part of the fin beyond this length does not contribute to heat transfer since it is at the temperature of the environment, as shown in Fig. 3–47. Therefore, designing such an "extra long" fin is out of the question since it results in material waste, excessive weight, and increased size and thus increased cost with no benefit in return (in fact, such a long fin will hurt performance since it will suppress fluid motion and thus reduce the convection heat transfer coefficient). Fins that are so long that the temperature approaches the environment temperature cannot be recommended either since the little increase in heat transfer at the tip region cannot justify the disproportionate increase in the weight and cost.

To get a sense of the proper length of a fin, we compare heat transfer from a fin of finite length to heat transfer from an infinitely long fin under the same conditions. The ratio of these two heat transfers is
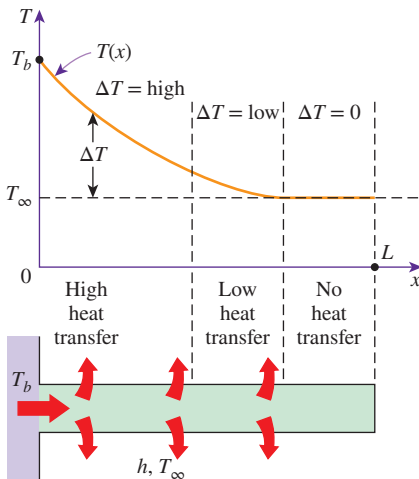
Heat transfer ratio:
$$\frac{\dot{Q}_{\text{fin}}}{\dot{Q}_{\text{long fin}}} = \frac{\sqrt{hpkA_c}(T_b - T_\infty)\tanh mL}{\sqrt{hpkA_c}(T_b - T_\infty)} = \tanh mL \qquad \textbf{(3–83)}$$

Using a hand calculator, the values of tanh mL are evaluated for some values of mL, and the results are given in Table 3–5. We observe from the table that heat transfer from a fin increases with mL almost linearly at first, but the curve reaches a plateau later and reaches a value for the infinitely long fin at about $mL = 5$. Therefore, a fin whose length is $L = 5/m$ can be considered to be an infinitely long fin. We also observe that reducing the fin length by half in that case (from $mL = 5$ to $mL = 2.5$) causes a drop of just 1 percent in heat transfer. We certainly would not hesitate sacrificing 1 percent in heat transfer performance in return for 50 percent reduction in the size and possibly

the cost of the fin. In practice, a fin length that corresponds to about $mL = 1$ will transfer 76.2 percent of the heat that can be transferred by an infinitely long fin, and thus it should offer a good compromise between heat transfer performance and the fin size.

A common approximation used in the analysis of fins is to assume the fin temperature to vary in one direction only (along the fin length) and the temperature variation along other directions is negligible. Perhaps you are wondering if this one-dimensional approximation is a reasonable one. This is certainly the case for fins made of thin metal sheets such as the fins on a car radiator, but we wouldn't be so sure for fins made of thick materials. Studies have shown that the error involved in one-dimensional fin analysis is negligible (less than about 1 percent) when

$$\frac{h\delta}{k} < 0.2$$

where δ is the characteristic thickness of the fin, which is taken to be the plate thickness t for rectangular fins and the diameter D for cylindrical ones.

Specially designed finned surfaces called *heat sinks,* which are commonly used in the cooling of electronic equipment, involve one-of-a-kind complex geometries, as shown in Table 3–6. The heat transfer performance of heat sinks is usually expressed in terms of their *thermal resistances R* in °C/W, which is defined as

$$\dot{Q}_{fin} = \frac{T_b - T_\infty}{R} = hA_{fin}\eta_{fin}(T_b - T_\infty) \tag{3-84}$$

A small value of thermal resistance indicates a small temperature drop across the heat sink, and thus a high fin efficiency.

TABLE 3–5

The variation of heat transfer from a fin relative to that from an infinitely long fin

mL	$\dfrac{\dot{Q}_{fin}}{\dot{Q}_{long\ fin}} = \tanh\ mL$
0.1	0.100
0.2	0.197
0.5	0.462
1.0	0.762
1.5	0.905
2.0	0.964
2.5	0.987
3.0	0.995
4.0	0.999
5.0	1.000

EXAMPLE 3–10   Maximum Power Dissipation of a Transistor

Power transistors that are commonly used in electronic devices consume large amounts of electric power. The failure rate of electronic components increases almost exponentially with operating temperature. As a rule of thumb, the failure rate of electronic components is halved for each 10°C reduction in the junction operating temperature. Therefore, the operating temperature of electronic components is kept below a safe level to minimize the risk of failure.

The sensitive electronic circuitry of a power transistor at the junction is protected by its case, which is a rigid metal enclosure. Heat transfer characteristics of a power transistor are usually specified by the manufacturer in terms of the case-to-ambient thermal resistance, which accounts for both the natural convection and radiation heat transfers.

The case-to-ambient thermal resistance of a power transistor that has a maximum power rating of 10 W is given to be 20°C/W. If the case temperature of the transistor is not to exceed 85°C, determine the power at which this transistor can be operated safely in an environment at 25°C.

SOLUTION   The maximum power rating of a transistor whose case temperature is not to exceed 85°C is to be determined.
Assumptions   **1** Steady operating conditions exist. **2** The transistor case is isothermal at 85°C.
Properties   The case-to-ambient thermal resistance is given to be 20°C/W.

TABLE 3–6

Combined natural convection and radiation thermal resistance of various heat sinks used in the cooling of electronic devices between the heat sink and the surroundings. All fins are made of aluminum 6063T-5, are black anodized, and are 76 mm (3 in) long.

HS 5030
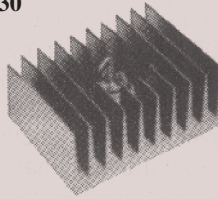
$R = 0.9°C/W$ (vertical)
$R = 1.2°C/W$ (horizontal)

Dimensions: 76 mm × 105 mm × 44 mm
Surface area: 677 cm^2

HS 6065
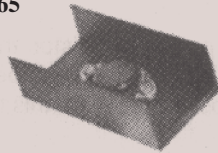
$R = 5°C/W$

Dimensions: 76 mm × 38 mm × 24 mm
Surface area: 387 cm^2

HS 6071
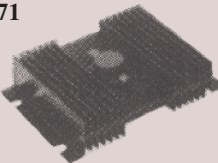
$R = 1.4°C/W$ (vertical)
$R = 1.8°C/W$ (horizontal)

Dimensions: 76 mm × 92 mm × 26 mm
Surface area: 968 cm^2

HS 6105
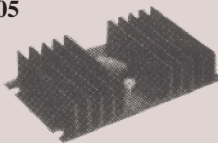
$R = 1.8°C/W$ (vertical)
$R = 2.1°C/W$ (horizontal)

Dimensions: 76 mm × 127 mm × 91 mm
Surface area: 677 cm^2

HS 6115

$R = 1.1°C/W$ (vertical)
$R = 1.3°C/W$ (horizontal)

Dimensions: 76 mm × 102 mm × 25 mm
Surface area: 929 cm^2

HS 7030
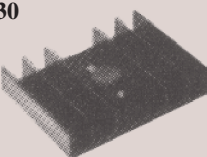
$R = 2.9°C/W$ (vertical)
$R = 3.1°C/W$ (horizontal)

Dimensions: 76 mm × 97 mm × 19 mm
Surface area: 290 cm^2

Analysis The power transistor and the thermal resistance network associated with it are shown in Fig. 3–48. We notice from the thermal resistance network that there is a single resistance of 20°C/W between the case at $T_c = 85$°C and the ambient at $T_\infty = 22$°C, and thus the rate of heat transfer is

$$\dot{Q} = \left(\frac{\Delta T}{R}\right)_{\text{case-ambient}} = \frac{T_c - T_\infty}{R_{\text{case-ambient}}} = \frac{(85 - 25)°C}{20°C/W} = \textbf{3 W}$$

Therefore, this power transistor should not be operated at power levels above 3 W if its case temperature is not to exceed 85°C.

Discussion This transistor can be used at higher power levels by attaching it to a heat sink (which lowers the thermal resistance by increasing the heat transfer surface area, as discussed in the next example) or by using a fan (which lowers the thermal resistance by increasing the convection heat transfer coefficient).
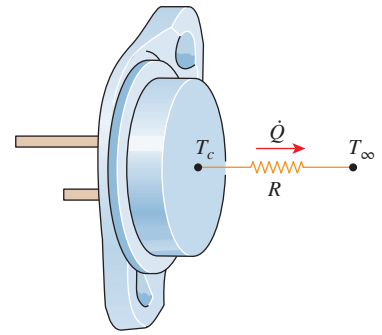
FIGURE 3–48
Schematic for Example 3–10.

EXAMPLE 3–11   Selecting a Heat Sink for a Transistor

A 25-W power transistor is to be cooled by attaching it to one of the commercially available heat sinks shown in Table 3–6. Select a heat sink that will allow the case temperature of the transistor not to exceed 55°C in the ambient air at 18°C.

SOLUTION A commercially available heat sink from Table 3–6 is to be selected to keep the case temperature of a transistor below 55°C.

Assumptions **1** Steady operating conditions exist. **2** The transistor case is isothermal at 55°C. **3** The contact resistance between the transistor and the heat sink is negligible.

Analysis The rate of heat transfer from a 25-W transistor at full power is $\dot{Q} = 25$ W. The thermal resistance between the transistor attached to the heat sink and the ambient air for the specified temperature difference is determined to be

$$\dot{Q} = \frac{\Delta T}{R} \longrightarrow R = \frac{\Delta T}{\dot{Q}} = \frac{(55 - 18)°C}{25\ W} = 1.5°C/W$$

Therefore, the thermal resistance of the heat sink should be below 1.5°C/W. An examination of Table 3–6 reveals that the HS 5030 in both horizontal and vertical positions, HS 6071 in vertical position, and HS 6115 in both horizontal and vertical positions can be selected.

EXAMPLE 3–12   Heat Transfer from Fins of Variable Cross Section

Aluminum pin fins of parabolic profile with blunt tips are attached on a plane wall with surface temperature of 200°C (Fig. 3–49). Each fin has a length of 20 mm and a base diameter of 5 mm. The fins are exposed to an ambient air condition of 25°C and the convection heat transfer coefficient is 50 W/m²·K. If the thermal conductivity of the fins is 240 W/m·K, determine the efficiency, heat transfer rate, and effectiveness of each fin.

SOLUTION The efficiency, heat transfer rate, and effectiveness of a pin fin of parabolic profile with a blunt tip is to be determined.
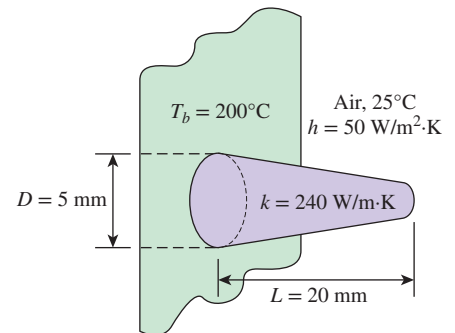
FIGURE 3–49
Schematic for Example 3–12.

Assumptions **1** Heat conduction is steady and one-dimensional. **2** Thermal properties are constant. **3** Heat transfer by radiation is negligible.

Properties The thermal conductivity of the fin is given as 240 W/m·K.

Analysis From Table 3–3, for pin fins of parabolic profile (blunt tip), we have

$$mL = \sqrt{\frac{4h}{kD}}L = \sqrt{\frac{4(50 \text{ W/m}^2\cdot\text{K})}{(240 \text{ W/m}\cdot\text{K})(0.005 \text{ m})}}(0.020 \text{ m}) = 0.2582$$

$$A_{\text{fin}} = \frac{\pi D^4}{96L^2}\left\{\left[16\left(\frac{L}{D}\right)^2 + 1\right]^{3/2} - 1\right\} = \frac{\pi(0.005 \text{ m})^4}{96(0.020 \text{ m})^2}\left\{\left[16\left(\frac{0.020 \text{ m}}{0.005 \text{ m}}\right)^2 + 1\right]^{3/2} - 1\right\}$$

$$= 2.106 \times 10^{-4} \text{ m}^2$$

$$\eta_{\text{fin}} = \frac{3}{2mL}\frac{I_1(4mL/3)}{I_0(4\text{m}L/3)} = \frac{3}{2(0.2582)}\frac{I_1[4(0.2582)/3]}{I_0[4(0.2582)/3]} = 5.8095\frac{I_1[0.3443]}{I_0[0.3443]}$$

The values of the Bessel functions corresponding to $x = 0.3443$ are determined from Table 3–4 to be $I_0 = 1.0350$ and $I_1 = 0.1716$. Substituting, the fin efficiency is determined to be

$$\eta_{\text{fin}} = 5.8095\frac{0.1716}{1.0350} = \mathbf{0.9632}$$

The heat transfer rate for a single fin is

$$\dot{Q}_{\text{fin}} = \eta_{\text{fin}}hA_{\text{fin}}(T_b - T_\infty)$$
$$= (0.9632)(50 \text{ W/m}^2\cdot\text{K})(2.106 \times 10^{-4}\text{ m}^2)(200 - 25)°\text{C} = \mathbf{1.77 \text{ W}}$$

The fin effectiveness is

$$\varepsilon_{\text{fin}} = \frac{\dot{Q}_{\text{fin}}}{hA_b(T_b - T_\infty)} = \frac{\dot{Q}_{\text{fin}}}{h(\pi D^2/4)(T_b - T_\infty)}$$
$$= \frac{1.77 \text{ W}}{(50 \text{ W/m}^2\cdot\text{K})\,[\pi(0.005 \text{ m})^2/4](200 - 25)°\text{C}}$$
$$= \mathbf{10.3}$$

That is, over a tenfold increase in heat transfer is achieved by using a pin fin in this case.

Discussion The fin efficiency can be determined more accurately by avoiding the interpolation error by using an equation solver with built-in mathematical functions such as EES. Copying the line

eta_fin = 3/(2*0.2582)*Bessel_|1(4*0.2582/3)/Bessel_|0 (4*0.2582/3)

on a blank EES screen and hitting the 'solve' button gives the fin efficiency to be $\eta_{\text{fin}} = 0.9855$, which is about 2 percent higher than the result obtained above using the tables.

4 cm

2 mm × 2 mm

$T_b = 85°C$

$T_\infty = 25°C$
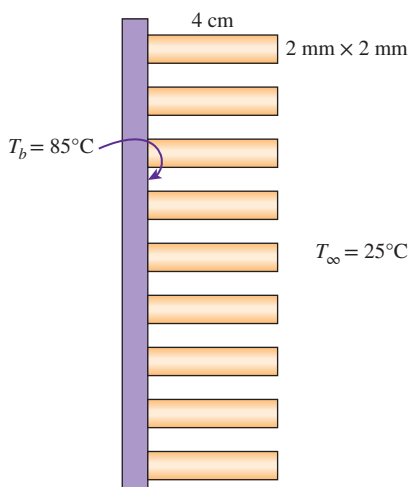
FIGURE 3–50
Schematic for Example 3–13.

PtD **EXAMPLE 3–13** **Preventing Circuit Board Surface from Overheating**

A 15-cm × 20-cm integrated circuit board is to be cooled by attaching 4-cm-long aluminum ($k = 237$ W/m·K) fins on one side of it (Fig. 3–50). Each fin has a 2-mm × 2-mm square cross section. The surrounding ambient temperature is 25°C and the convection heat transfer coefficient on each fin surface is 20 W/m²·K. To prevent the circuit board

from overheating, the upper surface of the circuit board needs to be at 85°C or cooler. Design a finned surface having the appropriate number of fins, with an overall effectiveness of 3 that can keep the circuit board surface from overheating.

SOLUTION In this example, the concepts of Prevention through Design (PtD) are applied in conjunction with the fin analysis. An integrated circuit board is to be cooled by attaching aluminum fins of square cross section on one side. The number of fins needed to keep the circuit board surface cooler than 85°C, while having an overall effectiveness of 3, is to be determined.

Assumptions **1** Steady operating conditions exist. **2** Heat conduction is one-dimensional. **3** Heat transfer from the fin tips is negligible. **4** Fins are very long. **5** The heat transfer coefficient is constant and uniform over the entire fin surface. **6** The thermal properties of the fins are constant.

Properties The thermal conductivity of the aluminum fins is given to be $k = 237$ W/m·K.

Analysis Noting that the cross-sectional areas of the fins are constant, the efficiency of the square cross-section fins that are assumed to be very long with adiabatic tips can be determined to be

$$m = \sqrt{\frac{hp}{kA_c}} = \sqrt{\frac{4ha}{ka^2}} = \sqrt{\frac{4(20 \text{ W/m}^2\text{·K})(0.02 \text{ m})}{(237 \text{ W/m·K})(0.02 \text{ m})^2}} = 12.99 \text{ m}^{-1}$$

where a is the length of each side of the square fin.

$$\eta_{\text{fin}} = \frac{\tanh mL}{mL} = \frac{\tanh(12.99 \text{ m}^{-1} \times 0.04 \text{ m})}{12.99 \text{ m}^{-1} \times 0.04 \text{ m}} = 0.919$$

The finned and unfinned surface areas, and heat transfer rates from these areas are

$$A_{\text{fin}} = n_{\text{fin}} \times 4 \times (0.002 \text{ m})(0.04 \text{ m}) = 0.00032 n_{\text{fin}} \text{ m}^2$$

$$A_{\text{unfinned}} = (0.15 \text{ m})(0.20 \text{ m}) - n_{\text{fin}}(0.002 \text{ m})(0.002 \text{ m})$$
$$= 0.03 - 0.000004 n_{\text{fin}} \text{ m}^2$$

$$\dot{Q}_{\text{finned}} = \eta_{\text{fin}}\dot{Q}_{\text{fin, max}} = \eta_{\text{fin}}hA_{\text{fin}}(T_b - T_\infty)$$
$$= 0.919(20 \text{ W/m}^2\text{·K})(0.00032 n_{\text{fin}} \text{ m}^2)(85 - 25)°C$$
$$= 0.3529 n_{\text{fin}} \text{ W}$$

$$\dot{Q}_{\text{unfinned}} = hA_{\text{unfinned}}(T_b - T_\infty) = (20 \text{ W/m}^2\text{·K})(0.03 - 0.000004 n_{\text{fin}} \text{ m}^2)(85 - 25)°C$$
$$= 36 - 0.0048 n_{\text{fin}} \text{ W}$$

Then the total heat transfer from the finned surface (circuit board) becomes

$$\dot{Q}_{\text{total, fin}} = \dot{Q}_{\text{finned}} + \dot{Q}_{\text{unfinned}} = 0.3529\, n_{\text{fin}} + 36 - 0.0048\, n_{\text{fin}} \text{ W}$$

The rate of heat transfer if there were no fins attached to the plate would be

$$A_{\text{no fin}} = (0.15 \text{ m})(0.20 \text{ m}) = 0.03 \text{ m}^2$$

$$\dot{Q}_{\text{no fin}} = hA_{\text{no fin}}(T_b - T_\infty) = (20 \text{ W/m}^2\text{·K})(0.03 \text{ m}^2)(85 - 25)°C = 36 \text{ W}$$

The number of fins can be determined from the overall fin effectiveness equation

$$\varepsilon_{\text{fin}} = \frac{\dot{Q}_{\text{fin}}}{\dot{Q}_{\text{no fin}}}$$

$$3 = \frac{0.3529\, n_{\text{fin}} + 36 - 0.0048\, n_{\text{fin}}}{36}$$

$$n_{\text{fin}} = \mathbf{207}$$

3−7 ▪ BIOHEAT TRANSFER EQUATION

The study of heat transfer in biological systems is referred to as *bioheat transfer*. It is the study of heat transfer within the human body or external to the body. Bioheat transfer can be considered a subfield of biomedical engineering with its foundation in heat transfer engineering. Heat transfer within the human body, in particular in adverse environments, is an active area of research for the development of new medical treatments or devices to minimize the effects of the adverse conditions.

The transport of thermal energy in living tissues is a very complex process. It involves multiple mechanisms such as conduction, convection, radiation, evaporation, phase change, metabolic heat generation (heat generated by the body through the digestion of food, work, and exercise), and perfusion (exchange of thermal energy between flowing blood and the surrounding tissue). The addition of varied metabolic heat generation rates throughout the body is what typically complicates the study of bioheat transfer. Recall that the human body is a remarkably good insulator (see Topic of Special Interest: "Thermal Comfort") and that the heat transfer properties can be altered based on the clothing worn or the conditions of the environment (e.g., wind speed, humidity, etc.). Also, some of the considerations based on blood perfusion will be discussed in Topic of Special Interest: "The Human Cardiovascular System as a Counter-Current Heat Exchanger" (Chap. 11).

A simple yet fairly accurate bioheat transfer equation or model was proposed by Harry Pennes in 1948 and published in Volume 1 of the *Journal of Applied Physiology.* For the development of his model, Pennes measured temperature distributions as a function of radial position in the forearms of nine human subjects. His data showed a temperature differential of 3 to 4°C between the skin and the interior of the arm. Pennes attributed this temperature difference to the effects of metabolic heat generation and perfusion in the arm. Based on his experimental results, Pennes proposed a model, now known as Pennes' bioheat transfer equation, to describe the effects of metabolism and blood perfusion on the energy balance within living tissue. Pennes' model was considered a major introductory effort in quantifying the heat transfer contribution of perfusion in tissue. His model is a modified version of the heat conduction equation introduced in Chap. 2 which accounts for the effects of metabolic heat generation and perfusion.

During the past decade, Pennes' bioheat transfer model has been widely used but also criticized for various reasons. To gain a better understanding of one of the most influential articles ever published in the *Journal of Applied Physiology,* Pennes' 1948 paper was republished for the 50th anniversary of the journal and was revisited in great depth by Wissler. Wissler reevaluated Pennes' work by revisiting his original experimental data and analysis. Wissler in his concluding remarks states that "much of the criticism directed toward Pennes' model is not justified and those who base their theoretical

model calculations on the Pennes' model can be somewhat more confident that their starting equations are valid."

In this section a simplified version of the bioheat transfer equation for the case of steady-state, constant properties, one-dimensional heat transfer in rectangular coordinates is introduced. Following Pennes' model, modifying Eq. 2–15 to account for the effects of metabolic heat generation and perfusion heat sources results in

$$\frac{d^2T}{dx^2} + \frac{\dot{e}_m + \dot{e}_p}{k} = 0 \qquad \text{(3–85)}$$

where $\dot{e}_m$ and $\dot{e}_p$ are the *metabolic* and *perfusion* heat source terms (W/m³).

A simple expression for the perfusion term was proposed by Pennes. Pennes suggested that the rate of heat transfer from blood to tissue per unit volume of tissue ($\dot{e}_p$) is proportional to the perfusion rate $\dot{p}$ (volumetric blood flow rate per unit volume of tissue or 1/s) and the difference between the blood temperature entering small capillaries (on the order of 8 μm in diameter) at an arterial inlet temperature of T_a and a perfusate of blood (consisting of mostly water and ions) exiting through the capillary wall at the local tissue temperature of T. It was difficult for Pennes to measure the temperature of the blood perfusate exiting the capillary, and he thus assumed that the temperature, T, would be the same as the temperature of blood exiting the capillary and entering the venous circulation. It is important to note that under normal physiological conditions blood can only leave the capillary through the venous end, but some perfusate of blood leaves through the wall. The perfusate that leaves the capillary is to help provide nutrients to the surrounding tissue. The expression proposed by Pennes for the exchange of thermal energy between flowing blood and the surrounding tissue (perfusion) is

$$\dot{e}_p = \dot{p}\rho_b c_b (T_a - T) \qquad (\text{W/m}^3) \qquad \text{(3–86)}$$

where ρ_b (kg/m³) is the density of blood and c_b (J/kg·K) is the specific heat of blood.

Substituting the Pennes' perfusion heat source term expression, Eq. 3–86, into Eq. 3–85 results in

$$\frac{d^2T}{dx^2} + \frac{\dot{e}_m + \dot{p}\rho_b c_b (T_a - T)}{k} = 0 \qquad \text{(3–87)}$$

Following the procedure that led to Eq. 3–56 for extended surfaces and assuming constant $\dot{e}_m, \dot{p}, \rho_b, c_b$, and T_a, the differential Eq. 3–87 reduces to

$$\frac{d^2\theta}{dx^2} - B^2\theta = 0 \qquad \text{(3–88)}$$

where $B^2 = \dot{p}\rho_b c_b/k$ has units of (1/m) and $\theta = T - T_a - \dot{e}_m/\dot{p}\rho_b c_b$ is the *temperature excess.* Equation 3–88 is in form identical to Eq. 3–56, and the solutions presented in the text for the different boundary conditions could be used. It should be noted that the density of blood, specific heat of blood, and arterial temperature are reasonably constant with respect to time and space. However, the metabolic heat source term is rarely constant, and the perfusion rate will have a small temporal variation in the capillaries. If the time duration of your problem is small, the variation in these terms would be negligible.

One of the applications of Eq. 3–88 is in a process called *thermoregulation.* Thermoregulation is the ability of an organism to regulate its body temperature within certain boundaries, even when the surrounding temperature is very different than the body temperature. Recall that when we discussed thermal comfort, we noted that most individuals live in areas that have an average temperature lower than both the core body temperature and the temperature that an average human finds comfortable. Thermoregulation in the human body is achieved by keeping a tight balance between heat gain and heat loss. Humans' temperature regulation system is similar to the operation of a home furnace. The human body regulates heat generation and preservation to maintain the internal body temperature or core temperature. Normal core temperature at rest varies between 36.5 and 37.5°C (97.7 and 99.5°F). However, the temperature at the extremities is not regulated as tightly as the core temperature, and it can vary significantly from the core temperature (imagine having a snowball fight without wearing gloves); under normal external operating temperatures it is in the range of 33–34°C. It is also important to note that the temperature of the extremities can fluctuate rather quickly depending on the activity level and the external environment.

A more realistic approach to the study of heat transfer within the human body is to solve the bioheat transfer equation in cylindrical coordinates as shown in the following equations. The one-dimensional steady-state bioheat transfer differential equation in cylindrical coordinates with constant properties is

$$\frac{1}{r}\frac{d}{dr}\left(r\frac{dT}{dr}\right) + \frac{\dot{e}_m + \dot{e}_p}{k} = 0 \tag{3–89}$$

Following the same procedure that led to the development of Eq. 3–88, the bioheat transfer equation in cylindrical coordinates in terms of excess temperature θ is

$$\frac{1}{r}\frac{d}{dr}\left(r\frac{d\theta}{dr}\right) - B^2\theta = 0 \tag{3–90}$$

Equation 3–90 is a *modified Bessel equation* of order zero, and its general solution is of the form

$$\theta(r) = C_1 I_0(Br) + C_2 K_0(Br) \tag{3–91}$$

where I_0 and K_0 are modified, zero-order Bessel functions of the first and second kinds, respectively. The values of I_0 and K_0 are given in Table 3–4.

One of the applications of Eq. 3–90 would be, for example, in the analysis of the steady-state heat transfer from a human forearm subjected to certain environmental conditions. One of the end-of-chapter problems will be on this subject. The following example demonstrates the use of Eq. 3–88 in calculating heat transfer between a human body and its surroundings.

EXAMPLE 3–14　　**Application of Bioheat Transfer Equation**

We are interested in heat transfer analysis from a human body subjected to certain environmental conditions. For this purpose, consider a region of muscle with a skin/fat layer over it under steady-state conditions as shown in Fig. 3–51. For simplicity,

approximate this region as a one-dimensional plane wall with surface area A. The muscle thickness is L_m covered by a layer of skin/fat with a thickness L_{sf}. The metabolic heat generation rate ($\dot{e}_m$) and perfusion rate ($\dot{p}$) are both constant throughout the muscle. The blood density and specific heat are ρ_b and c_b, respectively. The core body temperate (T_c) and the arterial blood temperature (T_a) are both assumed to be the same and constant. The muscle and the skin/fat layer thermal conductivities are k_m and k_{sf}, respectively. The skin has an emissivity of ε and the body is subjected to an air environment with a temperature of T_∞, a convection heat transfer coefficient of h_{conv}, and a radiation heat transfer coefficient of h_{rad}. Assuming blood properties and thermal conductivities are all constant, (*a*) develop an expression for the interface temperature (T_i) between the muscle and the outer skin/fat layer, and (*b*) determine the temperature T_i and the rate of heat loss from the body ($\dot{Q}_b$), and the skin temperature (T_s) for the following conditions:

$A = 1.8$ m², $L_m = 0.03$ m, $L_{sf} = 0.003$ m, $\dot{e}_m = 700$ W/m³, $\dot{p} = 0.0005$ 1/s,
$T_c = T_a = 37°C$, $T_\infty = T_{surr} = 24°C$, $\varepsilon = 0.95$, $\rho_b = 1000$ kg/m³, $c_b = 3600$ J/kg·K,
$k_m = 0.5$ W/m·K, $k_{sf} = 0.3$ W/m·K, $h_{conv} = 2$ W/m²·K, $h_{rad} = 5.9$ W/m²·K

SOLUTION A region of muscle with a skin/fat layer over it for a human body is subjected to certain environmental conditions. An expression for the interface temperature, the value of the interface temperature, the rate of heat loss from the body, and the skin temperature for a set of conditions are to be determined.

Assumptions **1** Muscle and skin/fat layer considered as a 1-D plain wall. **2** Steady-state conditions. **3** Blood properties, thermal conductivities, arterial temperature, core body temperature, metabolic heat generation rate, and perfusion rate are all constant. **4** Radiation exchange between the skin surface and the surroundings is between a small surface and a large enclosure at the air temperature. **5** Solar radiation is negligible.
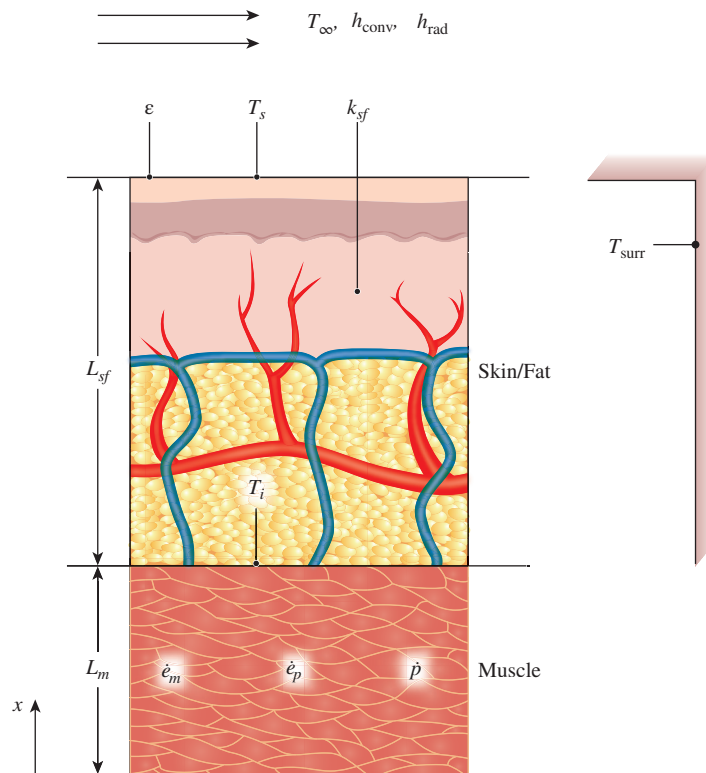
FIGURE 3–51
Schematic for Example 3–14.

Properties Muscle thermal conductivity $k_m = 0.5$ W/m·K, skin/fat layer thermal conductivity $k_{sf} = 0.3$ W/m·K, blood density $\rho_b = 1000$ kg/m^3 and blood specific heat $c_b = 3600$ J/kg·K.

Analysis (*a*) Solve the bioheat transfer differential equation, Eq. 3–88, along with the appropriate boundary conditions to develop an expression for the interface temperature (T_i) between the muscle and the outer skin/fat layer. The bioheat differential equation is

$$\frac{d^2\theta}{dx^2} - B^2\theta = 0$$

where $B^2 = \dot{p}\rho_b c_b/k$ has units of (1/m) and $\theta = T - T_a - \dot{e}_m/\dot{p}\rho_b c_b$. The boundary conditions for the problem in terms of temperature excess θ are:

$$\theta(0) = T_c - T_a - \dot{e}_m/\dot{p}\rho_b c_b = \theta_c \quad \text{and} \quad \theta(L_m) = T_i - T_a - \dot{e}_m/\dot{p}\rho_b c_b = \theta_i$$

The solution to Eq. 3–88 with the two specified temperature boundary conditions θ_c and θ_i, is given by Eq. 3–67 developed for fins (case 3 – specified temperature). For our case Eq. 3–67 becomes

$$\frac{\theta}{\theta_c} = \frac{(\theta_i/\theta_c)\sinh Bx + \sinh B(L_m - x)}{\sinh BL_m} \tag{3–92}$$

Note that T_i that appears in θ_i in Eq. 3–92 is unknown. In order to find T_i, use Eq. 3–92 to calculate the rate at which heat leaves the muscle and enters the skin/fat layer at $x = L_m$ and equate it with the rate at which heat is transferred through the skin/fat layer and into the environment.

Using the Fourier's law of heat conduction, the rate of heat transfer that leaves the muscle at $x = L_m$ and enters the skin/fat layer is

$$\dot{Q}_{\text{specified temp.}} = -k_m A \frac{dT}{dx}\bigg|_{x=L_m} = -k_m A \frac{d\theta}{dx}\bigg|_{x=L_m} = -k_m A B\theta_c \frac{(\theta_i/\theta_c)\cosh BL_m - 1}{\sinh BL_m}$$

The rate at which heat is transferred through the skin/fat layer and into the environment is obtained by using the thermal resistance network concept (see Sec. 3–1). In this case the thermal resistance is a combined series-parallel arrangement. Heat is transferred through the skin/fat layer by conduction in series and is in parallel with heat transfer by convection and radiation. The total rate of heat transfer through the skin/fat layer and into the environment (the rate of heat loss from the body) is

$$\dot{Q}_b = \frac{T_i - T_\infty}{R_{\text{total}}}$$

where the total resistance is $R_{\text{total}} = R_{sf} + R_{\text{conv} - \text{rad}} = R_{sf} + \dfrac{R_{\text{conv}} R_{\text{rad}}}{R_{\text{conv}} + R_{\text{rad}}}$

and the individual resistances are $R_{sf} = \dfrac{L_{sf}}{k_{sf} A}, R_{\text{conv}} = \dfrac{1}{h_{\text{conv}} A}$ and $R_{\text{rad}} = \dfrac{1}{h_{\text{rad}} A}$

Equating the rate of heat transfer that leaves the muscle at $x = L_m$ and enters the skin/fat layer with the rate at which heat is transferred through the skin/fat layer and into the environment yields

$$-k_m A B\theta_c \frac{(\theta_i/\theta_c)\cosh BL_m - 1}{\sinh BL_m} = \frac{T_i - T_\infty}{R_{\text{total}}}$$

The above equation can be solved for T_i; the final expression is

$$T_i = \frac{T_\infty \sinh BL_m + k_m A B R_{\text{total}}\left[\theta_c + \left(T_a + \dfrac{\dot{e}_m}{\dot{p}\rho_b c_b}\right)\cosh BL_m\right]}{\sinh BL_m + k_m A B R_{\text{total}}\cosh BL_m}$$

(*b*) Using the data given in the problem statement and the expression for the interface temperature (T_i) between the muscle and the outer skin/fat layer, the interface temperature between the muscle and the outer skin/fat layer is

$$T_i = \mathbf{34.8°C}$$

Using the calculated value of T_i and the equation for the total rate of heat transfer through the skin/fat layer and into the environment, the heat loss from the body is

$$\dot{Q}_b = \mathbf{142\ W}$$

The skin temperature (T_s) can be calculated by applying Fourier's law of heat conduction to the skin/fat layer

$$\dot{Q}_b = k_{sf}A\frac{T_i - T_s}{L_{sf}}$$

Solving the preceding equation for T_s,

$$T_s = T_i - \frac{\dot{Q}_b L_{sf}}{k_{sf}A} \approx \mathbf{34°C}$$

Discussion   The skin temperature of 34°C is comfortable. However, if the environmental conditions change, our bodies will adjust. For example, if the temperatures of the air and the surroundings were lowered considerably, we would shiver. Shivering can increase the metabolic heat generation rate by up to six times the resting metabolic rate. If the air and the surroundings temperatures were increased considerably, we would sweat. Sweating will cause an increase in the perfusion rate near the skin surface, which causes an increase in the heat loss to the surroundings via evaporation.

3–8 ▪ HEAT TRANSFER IN COMMON CONFIGURATIONS

So far, we have considered heat transfer in *simple* geometries such as large plane walls, long cylinders, and spheres. This is because heat transfer in such geometries can be approximated as *one-dimensional,* and simple analytical solutions can be obtained easily. But many problems encountered in practice are two- or three-dimensional and involve rather complicated geometries for which no simple solutions are available.

An important class of heat transfer problems for which simple solutions are obtained encompasses those involving two surfaces maintained at *constant* temperatures T_1 and T_2. The steady rate of heat transfer between these two surfaces is expressed as

$$\dot{Q} = Sk(T_1 - T_2) \tag{3–93}$$

where *S* is the **conduction shape factor**, which has the dimension of *length,* and *k* is the thermal conductivity of the medium between the surfaces. The conduction shape factor depends on the *geometry* of the system only.

Conduction shape factors have been determined for a number of configurations encountered in practice and are given in Table 3–7 for some common cases. More comprehensive tables are available in the literature. Once the value of the shape factor is known for a specific geometry, the total steady heat transfer rate can be determined from Eq. 3–93 using the specified two

TABLE 3–7

Conduction shape factors S for several configurations for use in $\dot{Q} = kS(T_1 - T_2)$ to determine the steady rate of heat transfer through a medium of thermal conductivity k between the surfaces at temperatures T_1 and T_2
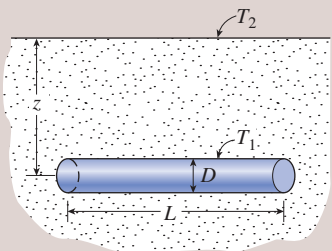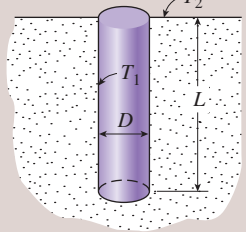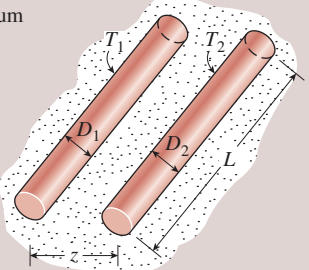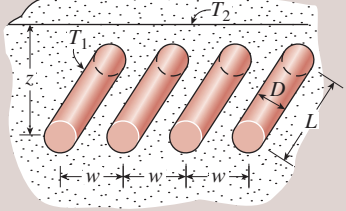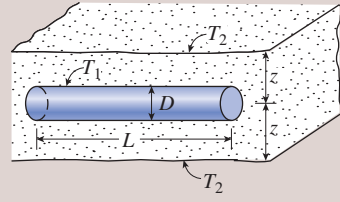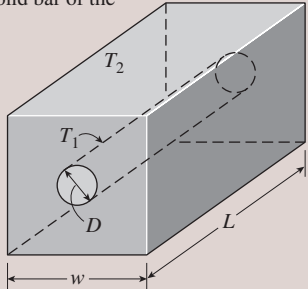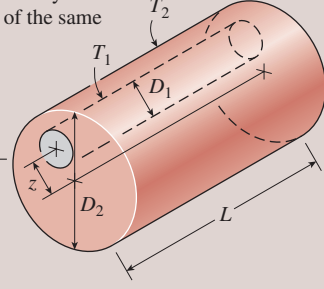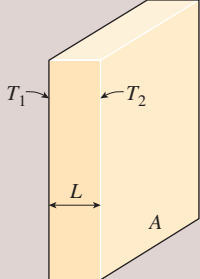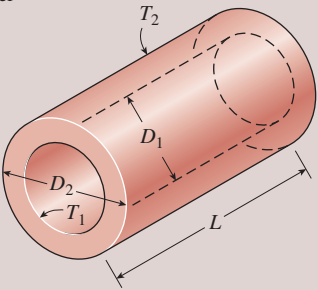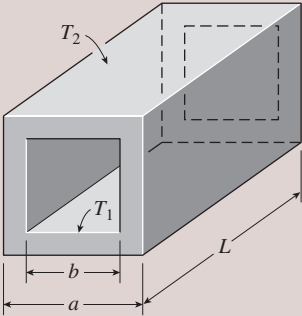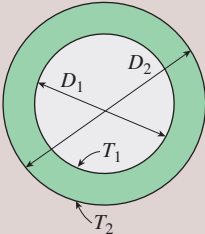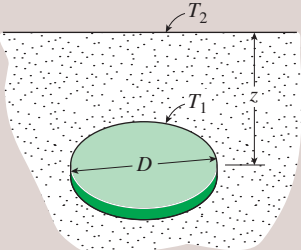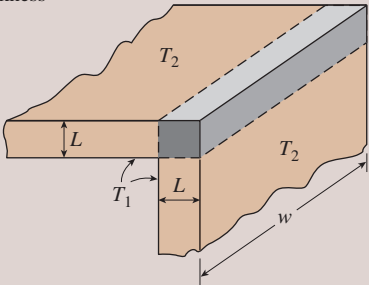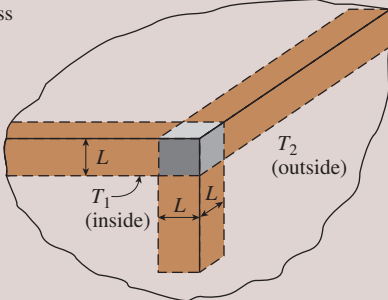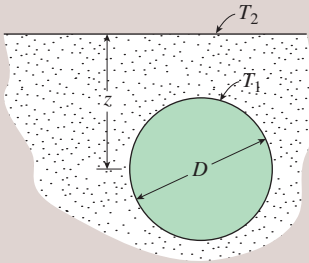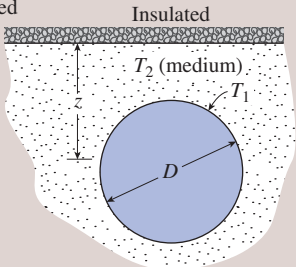
(1) Isothermal cylinder of length L buried in a semi-infinite medium ($L \gg D$ and $z > 1.5D$)

$$S = \frac{2\pi L}{\ln(4z/D)}$$

(2) Vertical isothermal cylinder of length L buried in a semi-infinite medium ($L \gg D$)

$$S = \frac{2\pi L}{\ln(4L/D)}$$

(3) Two parallel isothermal cylinders placed in an infinite medium ($L \gg D_1, D_2, z$)

$$S = \frac{2\pi L}{\cosh^{-1}\left(\dfrac{4z^2 - D_1^2 - D_2^2}{2D_1 D_2}\right)}$$

(4) A row of equally spaced parallel isothermal cylinders buried in a semi-infinite medium ($L \gg D, z,$ and $w > 1.5D$)

$$S = \frac{2\pi L}{\ln\left(\dfrac{2w}{\pi D} \sinh \dfrac{2\pi z}{w}\right)}$$
(per cylinder)

(5) Circular isothermal cylinder of length L in the midplane of an infinite wall ($z > 0.5D$)

$$S = \frac{2\pi L}{\ln(8z/\pi D)}$$

(6) Circular isothermal cylinder of length L at the center of a square solid bar of the same length

$$S = \frac{2\pi L}{\ln(1.08w/D)}$$

(7) Eccentric circular isothermal cylinder of length L in a cylinder of the same length ($L > D_2$)

$$S = \frac{2\pi L}{\cosh^{-1}\left(\dfrac{D_1^2 + D_2^2 - 4z^2}{2D_1 D_2}\right)}$$

(8) Large plane wall

$$S = \frac{A}{L}$$

TABLE 3–7 (*CONTINUED*)

(9) A long cylindrical layer

$$S = \frac{2\pi L}{\ln (D_2/D_1)}$$

(10) A square flow passage

(*a*) For $a/b > 1.4$,

$$S = \frac{2\pi L}{0.93 \ln (0.948 a/b)}$$

(*b*) For $a/b < 1.4$,

$$S = \frac{2\pi L}{0.785 \ln (a/b)}$$

(11) A spherical layer

$$S = \frac{2\pi D_1 D_2}{D_2 - D_1}$$

(12) Disk buried parallel to the surface in a semi-infinite medium ($z \gg D$)

$$S = 4D$$

($S = 2D$ when $z = 0$)

(13) The edge of two adjoining walls of equal thickness

$$S = 0.54 w$$

(14) Corner of three walls of equal thickness

$$S = 0.15 L$$

(15) Isothermal sphere buried in a semi-infinite medium

$$S = \frac{2\pi D}{1 - 0.25D/z}$$

(16) Isothermal sphere buried in a semi-infinite medium at T_2 whose surface is insulated

$$S = \frac{2\pi D}{1 + 0.25D/z}$$

constant temperatures of the two surfaces and the thermal conductivity of the medium between them. Note that conduction shape factors are applicable only when heat transfer between the two surfaces is by *conduction.* Therefore, they cannot be used when the medium between the surfaces is a liquid or gas, which involves natural or forced convection currents.

A comparison of Eqs. 3–4 and 3–93 reveals that the conduction shape factor S is related to the thermal resistance R by $R = 1/kS$ or $S = 1/kR$. Thus, these two quantities are the inverse of each other when the thermal conductivity of the medium is unity. The use of the conduction shape factors is illustrated with Examples 3–15 and 3–16.

It is well known that insulation reduces heat transfer and saves energy and money. Decisions on the right amount of insulation are based on a heat transfer analysis, followed by an economic analysis to determine the "monetary value" of energy loss. This is illustrated with Example 3–17.
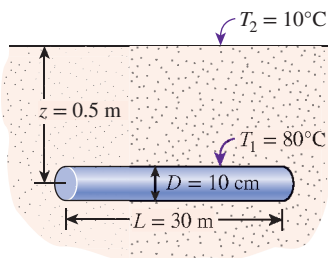
FIGURE 3–52
Schematic for Example 3–15.

FIGURE 3–53
Schematic for Example 3–16.

EXAMPLE 3–15   Heat Loss from Buried Steam Pipes

A 30-m-long, 10-cm-diameter hot-water pipe of a district heating system is buried in the soil 50 cm below the ground surface, as shown in Fig. 3–52. The outer surface temperature of the pipe is 80°C. Taking the surface temperature of the earth to be 10°C and the thermal conductivity of the soil at that location to be 0.9 W/m·K, determine the rate of heat loss from the pipe.

SOLUTION   The hot-water pipe of a district heating system is buried in the soil. The rate of heat loss from the pipe is to be determined.
Assumptions   **1** Steady operating conditions exist. **2** Heat transfer is two-dimensional (no change in the axial direction). **3** Thermal conductivity of the soil is constant.
Properties   The thermal conductivity of the soil is given to be $k = 0.9$ W/m·K.
Analysis   The shape factor for this configuration is given in Table 3–7 to be

$$S = \frac{2\pi L}{\ln(4z/D)}$$

since $z > 1.5D$, where z is the distance of the pipe from the ground surface, and D is the diameter of the pipe. Substituting,

$$S = \frac{2\pi \times (30 \text{ m})}{\ln (4 \times 0.5/0.1)} = 62.9 \text{ m}$$

Then the steady rate of heat transfer from the pipe becomes

$$\dot{Q} = Sk(T_1 - T_2) = (62.9 \text{ m})(0.9 \text{ W/m·K})(80 - 10)°C = \textbf{3963 W}$$

Discussion   Note that this heat is conducted from the pipe surface to the surface of the earth through the soil and then transferred to the atmosphere by convection and radiation.

EXAMPLE 3–16   Heat Transfer Between Hot- and Cold-Water Pipes

A 5-m-long section of hot- and cold-water pipes run parallel to each other in a thick concrete layer, as shown in Fig. 3–53. The diameters of both pipes are 5 cm, and the distance between the centerline of the pipes is 30 cm. The surface temperatures of the hot and cold pipes are 70°C and 15°C, respectively. Taking the thermal conductivity of the concrete to be $k = 0.75$ W/m·K, determine the rate of heat transfer between the pipes.

SOLUTION Hot- and cold-water pipes run parallel to each other in a thick concrete layer. The rate of heat transfer between the pipes is to be determined.

Assumptions **1** Steady operating conditions exist. **2** Heat transfer is two-dimensional (no change in the axial direction). **3** Thermal conductivity of the concrete is constant.

Properties The thermal conductivity of concrete is given to be $k = 0.75$ W/m·K.

Analysis The shape factor for this configuration is given in Table 3–7 to be

$$S = \frac{2\pi L}{\cosh^{-1}\left(\dfrac{4z^2 - D_1^2 - D_2^2}{2D_1 D_2}\right)}$$

where z is the distance between the centerlines of the pipes and L is their length. Substituting,

$$S = \frac{2\pi \times (5 \text{ m})}{\cosh^{-1}\left(\dfrac{4 \times 0.3^2 - 0.05^2 - 0.05^2}{2 \times 0.05 \times 0.05}\right)} = 6.34 \text{ m}$$

Then the steady rate of heat transfer between the pipes becomes

$$\dot{Q} = Sk(T_1 - T_2) = (6.34 \text{ m})(0.75 \text{ W/m·K})(70 - 15°) \text{ C} = \textbf{262 W}$$

Discussion We can reduce this heat loss by placing the hot- and cold-water pipes farther away from each other.

EXAMPLE 3–17 Cost of Heat Loss Through Walls in Winter

Consider an electrically heated house whose walls are 9 ft high and have an *R*-value of insulation of 13 (i.e., a thickness-to-thermal conductivity ratio of $L/k = 13$ h·ft²·°F/Btu). Two of the walls of the house are 40 ft long and the others are 30 ft long. The house is maintained at 75°F at all times, while the temperature of the outdoors varies. Determine the amount of heat lost through the walls of the house on a certain day during which the average temperature of the outdoors is 45°F. Also, determine the cost of this heat loss to the homeowner if the unit cost of electricity is $0.075/kWh. For combined convection and radiation heat transfer coefficients, use the ASHRAE (American Society of Heating, Refrigeration, and Air Conditioning Engineers) recommended values of $h_i = 1.46$ Btu/h·ft²·°F for the inner surface of the walls and $h_o = 6.0$ Btu/h·ft²·°F for the outer surface of the walls under 15 mph wind conditions in winter.

SOLUTION An electrically heated house with *R*-13 insulation is considered. The amount of heat lost through the walls and its cost are to be determined.

Assumptions **1** The indoor and outdoor air temperatures have remained at the given values for the entire day so that heat transfer through the walls is steady. **2** Heat transfer through the walls is one-dimensional since any significant temperature gradients in this case exist in the direction from the indoors to the outdoors. **3** The radiation effects are accounted for in the heat transfer coefficients.

Analysis This problem involves conduction through the wall and convection at its surfaces and can best be handled by making use of the thermal resistance concept and drawing the thermal resistance network, as shown in Fig. 3–54. The heat transfer area of the walls is

$$A = \text{Circumference} \times \text{Height} = (2 \times 30 \text{ ft} + 2 \times 40 \text{ ft})(9 \text{ ft}) = 1260 \text{ ft}^2$$
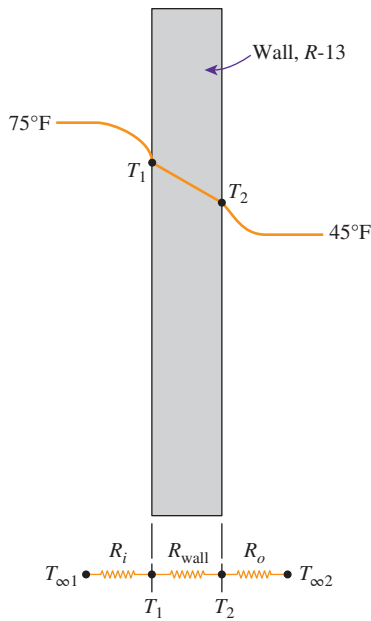
FIGURE 3–54
Schematic for Example 3–17.

Then the individual resistances are evaluated from their definitions to be

$$R_i = R_{\text{conv}, i} = \frac{1}{h_i A} = \frac{1}{(1.46 \text{ Btu/h·ft}^2\text{·°F})(1260 \text{ ft}^2)} = 0.00054 \text{ h·°F/Btu}$$

$$R_{\text{wall}} = \frac{L}{kA} = \frac{R\text{-value}}{A} = \frac{13 \text{ h·ft}^2\text{·°F/Btu}}{1260 \text{ ft}^2} = 0.01032 \text{ h·°F/Btu}$$

$$R_o = R_{\text{conv}, o} = \frac{1}{h_o A} = \frac{1}{(6.0 \text{ Btu/h·ft}^2\text{·°F})(1260 \text{ ft}^2)} = 0.00013 \text{ h·°F/Btu}$$

Noting that all three resistances are in series, the total resistance is

$$R_{\text{total}} = R_i + R_{\text{wall}} + R_o = 0.00054 + 0.01032 + 0.00013 = 0.01099 \text{ h·°F/Btu}$$

Then the steady rate of heat transfer through the walls of the house becomes

$$\dot{Q} = \frac{T_{\infty 1} - T_{\infty 2}}{R_{\text{total}}} = \frac{(75 - 45)\text{°F}}{0.01099 \text{ h·°F/Btu}} = 2730 \text{ Btu/h}$$

Finally, the total amount of heat lost through the walls during a 24-h period and its cost to the homeowner are

$$Q = \dot{Q}\,\Delta t = (2730 \text{ Btu/h})(24\text{-h/day}) = \textbf{65,514 Btu/day} = \textbf{19.2 kWh/day}$$

since 1 kWh = 3412 Btu, and

Heating cost = (Energy lost)(Cost of energy) = (19.2 kWh/day)($0.075/kWh)
= **$1.44/day**

Discussion The heat losses through the walls of the house that day cost the home-owner $1.44 worth of electricity. Most of this loss can be saved by insulation.

Heat Transfer Through Walls and Roofs

Under steady conditions, the rate of heat transfer through any section of a building wall or roof can be determined from

$$\dot{Q} = UA(T_i - T_o) = \frac{A(T_i - T_o)}{R} \tag{3–94}$$

where T_i and T_o are the indoor and outdoor air temperatures, A is the heat transfer area, U is the overall heat transfer coefficient (the U-factor), and

* This section can be skipped without a loss in continuity.

$R = 1/U$ is the overall unit thermal resistance (the R-value). Walls and roofs of buildings consist of various layers of materials, and the structure and operating conditions of the walls and the roofs may differ significantly from one building to another. Therefore, it is not practical to list the R-values (or U-factors) of different kinds of walls or roofs under different conditions. Instead, the overall R-value is determined from the thermal resistances of the individual components using the thermal resistance network. The overall thermal resistance of a structure can be determined most accurately in a lab by actually assembling the unit and testing it as a whole, but this approach is usually very time consuming and expensive. The analytical approach described here is fast and straightforward, and the results are usually in good agreement with the experimental values.

The unit thermal resistance of a plane layer of thickness L and thermal conductivity k can be determined from $R = L/k$. The thermal conductivity and other properties of common building materials are given in the appendix. The unit thermal resistances of various components used in building structures are listed in Table 3–8 for convenience.

Heat transfer through a wall or roof section is also affected by the convection and radiation heat transfer coefficients at the exposed surfaces. The effects of convection and radiation on the inner and outer surfaces of walls and roofs are usually combined into the *combined convection and radiation heat transfer coefficients* (also called *surface conductances*) h_i and h_o,

TABLE 3–8

Unit thermal resistance (the R-value) of common components used in buildings

Component	R-value m²·°C/W	ft²·h·°F/Btu	Component	R-value m²·°C/W	ft²·h·°F/Btu
Outside surface (winter)	0.030	0.17	Wood stud, nominal 2 in × 6 in		
Outside surface (summer)	0.044	0.25	(5.5 in or 140 mm wide)	0.98	5.56
Inside surface, still air	0.12	0.68	Clay tile, 100 mm (4 in)	0.18	1.01
Plane airspace, vertical, ordinary surfaces ($\varepsilon_{eff} = 0.82$):			Acoustic tile	0.32	1.79
13 mm ($\frac{1}{2}$ in)	0.16	0.90	Asphalt shingle roofing	0.077	0.44
20 mm ($\frac{3}{4}$ in)	0.17	0.94	Building paper	0.011	0.06
40 mm (1.5 in)	0.16	0.90	Concrete block, 100 mm (4 in):		
90 mm (3.5 in)	0.16	0.91	Lightweight	0.27	1.51
Insulation, 25 mm (1 in) :			Heavyweight	0.13	0.71
Glass fiber	0.70	4.00	Plaster or gypsum board,		
Mineral fiber batt	0.66	3.73	13 mm ($\frac{1}{2}$ in)	0.079	0.45
Urethane rigid foam	0.98	5.56	Wood fiberboard, 13 mm ($\frac{1}{2}$ in)	0.23	1.31
Stucco, 25 mm (1 in)	0.037	0.21	Plywood, 13 mm ($\frac{1}{2}$ in)	0.11	0.62
Face brick, 100 mm (4 in)	0.075	0.43	Concrete, 200 mm (8 in) :		
Common brick, 100 mm (4 in)	0.12	0.79	Lightweight	1.17	6.67
Steel siding	0.00	0.00	Heavyweight	0.12	0.67
Slag, 13 mm ($\frac{1}{2}$ in)	0.067	0.38	Cement mortar, 13 mm ($\frac{1}{2}$ in)	0.018	0.10
Wood, 25 mm (1 in)	0.22	1.25	Wood bevel lapped siding,		
Wood stud, nominal 2 in × 4 in			13 mm × 200 mm		
(3.5 in or 90 mm wide)	0.63	3.58	($\frac{1}{2}$ in × 8 in)	0.14	0.81

TABLE 3–9

Combined convection and radiation heat transfer coefficients at window, wall, or roof surfaces (from ASHRAE *Handbook of Fundamentals,* Chap. 22, Table 1).

Position	Direction of Heat Flow	h, W/m²·K* Surface Emittance, ε		
		0.90	0.20	0.05
Still air (both indoors and outdoors)				
Horiz.	Up ↑	9.26	5.17	4.32
Horiz.	Down ↓	6.13	2.10	1.25
45° slope	Up ↑	9.09	5.00	4.15
45° slope	Down ↓	7.50	3.41	2.56
Vertical	Horiz. →	8.29	4.20	3.35
Moving air (any position, any direction)				
Winter condition (winds at 15 mph or 24 km/h)		34.0	—	—
Summer condition (winds at 7.5 mph or 12 km/h)		22.7	—	—

*Multiply by 0.176 to convert to Btu/h·ft²·°F. Surface resistance can be obtained from $R = 1/h$.

respectively, whose values are given in Table 3–9 for ordinary surfaces ($\varepsilon = 0.9$) and reflective surfaces ($\varepsilon = 0.2$ or 0.05). Note that surfaces having a low emittance also have a low surface conductance due to the reduction in radiation heat transfer. The values in the table are based on a surface temperature of $21°C(72°F)$ and a surface–air temperature difference of $5.5°C$ ($10°F$). Also, the equivalent surface temperature of the environment is assumed to be equal to the ambient air temperature. Despite the convenience it offers, this assumption is not quite accurate because of the additional radiation heat loss from the surface to the clear sky. The effect of sky radiation can be accounted for approximately by taking the outside temperature to be the average of the outdoor air and sky temperatures.

The inner surface heat transfer coefficient h_i remains fairly constant throughout the year, but the value of h_o varies considerably because of its dependence on the orientation and wind speed, which can vary from less than 1 km/h in calm weather to over 40 km/h during storms. The commonly used values of h_i and h_o for peak load calculations are

$$h_i = 8.29 \text{ W/m}^2\cdot\text{K} = 1.46 \text{ Btu/h·ft}^2\cdot°\text{F} \quad \text{(winter and summer)}$$

$$h_o = \begin{cases} 34.0 \text{ W/m}^2\cdot\text{K} = 6.0 \text{ Btu/h·ft}^2\cdot°\text{F} & \text{(winter)} \\ 22.7 \text{ W/m}^2\cdot\text{K} = 4.0 \text{ Btu/h·ft}^2\cdot°\text{F} & \text{(summer)} \end{cases}$$

which correspond to design wind conditions of 24 km/h (15 mph) for winter and 12 km/h (7.5 mph) for summer. The corresponding surface thermal resistances (R-values) are determined from $R_i = 1/h_i$ and $R_o = 1/h_o$. The surface conductance values under still air conditions can be used for interior surfaces as well as exterior surfaces in calm weather.

Building components often involve *trapped airspaces* between various layers. Thermal resistances of such airspaces depend on the thickness of the layer, the temperature difference across the layer, the mean air temperature, the emissivity of each surface, the orientation of the air layer, and the direction of heat transfer. The emissivities of surfaces commonly encountered in buildings are given in Table 3–10. The **effective emissivity** of a plane-parallel airspace is given by

$$\frac{1}{\varepsilon_{\text{effective}}} = \frac{1}{\varepsilon_1} + \frac{1}{\varepsilon_2} - 1 \tag{3–95}$$

where ε_1 and ε_2 are the emissivities of the surfaces of the airspace. Table 3–10 also lists the effective emissivities of airspaces for the cases where (1) the emissivity of one surface of the airspace is ε while the emissivity of the other surface is 0.9 (a building material) and (2) the emissivity of both surfaces is ε. Note that the effective emissivity of an airspace between building materials is $0.82/0.03 = 27$ times that of an airspace between surfaces covered with aluminum foil. For specified surface temperatures, radiation heat transfer through an airspace is proportional to effective emissivity, and thus the rate of radiation heat transfer in the ordinary surface case is 27 times that of the reflective surface case.

Table 3–11 lists the thermal resistances of 20-mm-, 40-mm-, and 90-mm-(0.75-in, 1.5-in, and 3.5-in) thick airspaces under various conditions. The

thermal resistance values in the table are applicable to airspaces of uniform thickness bounded by plane, smooth, parallel surfaces with no air leakage. Thermal resistances for other temperatures, emissivities, and airspaces can be obtained by interpolation and moderate extrapolation. Note that the presence of a low-emissivity surface reduces radiation heat transfer across an airspace and thus significantly increases the thermal resistance. The thermal effectiveness of a low-emissivity surface will decline, however, if the condition of the surface changes as a result of some effects such as condensation, surface oxidation, and dust accumulation.

The *R*-value of a wall or roof structure that involves layers of uniform thickness is determined easily by simply adding up the unit thermal resistances of the layers that are in series. But when a structure involves components such as wood studs and metal connectors, then the thermal resistance network involves parallel connections and possible two-dimensional effects. The overall *R*-value in this case can be determined by assuming (1) parallel heat flow paths through areas of different construction or (2) isothermal planes normal to the direction of heat transfer. The first approach usually overpredicts the overall thermal resistance, whereas the second approach usually underpredicts it. The parallel heat flow path approach is more suitable for wood frame walls and roofs, whereas the isothermal planes approach is more suitable for masonry or metal frame walls.

The thermal contact resistance between different components of building structures ranges between 0.01 and 0.1 m²·°C/W, which is negligible in most cases. However, it may be significant for metal building components such as steel framing members.

The construction of wood frame flat ceilings typically involves 2-in × 6-in joists on 400-mm (16-in) or 600-mm (24-in) centers. The fraction of framing is usually taken to be 0.10 for joists on 400-mm centers and 0.07 for joists on 600-mm centers.

Most buildings have a combination of a ceiling and a roof with an attic space in between, and the determination of the *R*-value of the roof–attic–ceiling combination depends on whether the attic is vented or not. For adequately ventilated attics, the attic air temperature is practically the same as the outdoor air temperature, and thus heat transfer through the roof is governed by the *R*-value of the ceiling only. However, heat is also transferred between the roof and the ceiling by radiation, and it needs to be considered (Fig. 3–55). The major function of the roof in this case is to serve as a radiation shield by blocking off solar radiation. Effectively ventilating the attic in summer should not lead one to believe that heat gain to the building through the attic is greatly reduced. This is because most of the heat transfer through the attic is by radiation.

Radiation heat transfer between the ceiling and the roof can be minimized by covering at least one side of the attic (the roof or the ceiling side) with a reflective material, called *radiant barrier,* such as aluminum foil or aluminum-coated paper. Tests on houses with *R*-19 attic floor insulation have shown that radiant barriers can reduce summer ceiling heat gains by 16 to 42 percent compared to an attic with the same insulation level and no radiant barrier. Considering that the ceiling heat gain represents about

TABLE 3–10

Emissivities ε of various surfaces and the effective emissivity of airspaces

Surface	ε	Effective Emissivity of Airspace	
		$\varepsilon_1 = \varepsilon$ $\varepsilon_2 = 0.9$	$\varepsilon_1 = \varepsilon$ $\varepsilon_2 = \varepsilon$
Aluminum foil, bright	0.05*	0.05	0.03
Aluminum sheet	0.12	0.12	0.06
Aluminum-coated paper, polished	0.20	0.20	0.11
Steel, galvanized, bright	0.25	0.24	0.15
Aluminum paint	0.50	0.47	0.35
Building materials: Wood, paper, masonry, nonmetallic paints	0.90	0.82	0.82
Ordinary glass	0.84	0.77	0.72

From ASHRAE Handbook of Fundamentals, *Chap. 22, Table 3.*
*Surface emissivity of aluminum foil increases to 0.30 with barely visible condensation, and to 0.70 with clearly visible condensation.
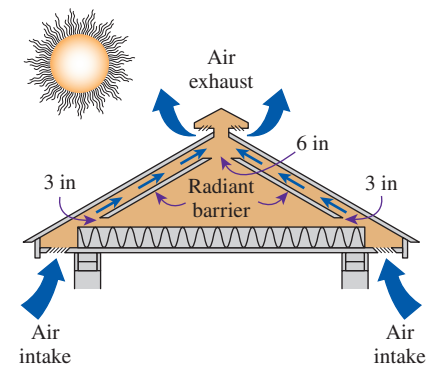
FIGURE 3–55

Ventilation paths for a naturally ventilated attic and the appropriate size of the flow areas around the radiant barrier for proper air circulation.

From DOE/CE-0335P, U.S. Dept. of Energy.

TABLE 3–11

Unit thermal resistances (R-values) of well-sealed plane airspaces

(*a*) SI units (in m²·°C/W)

Position of Airspace	Direction of Heat Flow	Mean Temp., °C	Temp. Diff., °C	20-mm Airspace Effective Emissivity, ε_{eff}				40-mm Airspace Effective Emissivity, ε_{eff}				90-mm Airspace Effective Emissivity, ε_{eff}			
				0.03	0.05	0.5	0.82	0.03	0.05	0.5	0.82	0.03	0.05	0.5	0.82
Horizontal	Up ↑	32.2	5.6	0.41	0.39	0.18	0.13	0.45	0.42	0.19	0.14	0.50	0.47	0.20	0.14
		10.0	16.7	0.30	0.29	0.17	0.14	0.33	0.32	0.18	0.14	0.27	0.35	0.19	0.15
		10.0	5.6	0.40	0.39	0.20	0.15	0.44	0.42	0.21	0.16	0.49	0.47	0.23	0.16
		−17.8	11.1	0.32	0.32	0.20	0.16	0.35	0.34	0.22	0.17	0.40	0.38	0.23	0.18
45° slope	Up ↑	32.2	5.6	0.52	0.49	0.20	0.14	0.51	0.48	0.20	0.14	0.56	0.52	0.21	0.14
		10.0	16.7	0.35	0.34	0.19	0.14	0.38	0.36	0.20	0.15	0.40	0.38	0.20	0.15
		10.0	5.6	0.51	0.48	0.23	0.17	0.51	0.48	0.23	0.17	0.55	0.52	0.24	0.17
		17.8	11.1	0.37	0.36	0.23	0.18	0.40	0.39	0.24	0.18	0.43	0.41	0.24	0.19
Vertical	Horizontal →	32.2	5.6	0.62	0.57	0.21	0.15	0.70	0.64	0.22	0.15	0.65	0.60	0.22	0.15
		10.0	16.7	0.51	0.49	0.23	0.17	0.45	0.43	0.22	0.16	0.47	0.45	0.22	0.16
		10.0	5.6	0.65	0.61	0.25	0.18	0.67	0.62	0.26	0.18	0.64	0.60	0.25	0.18
		−17.8	11.1	0.55	0.53	0.28	0.21	0.49	0.47	0.26	0.20	0.51	0.49	0.27	0.20
45° slope	Down ↓	32.2	5.6	0.62	0.58	0.21	0.15	0.89	0.80	0.24	0.16	0.85	0.76	0.24	0.16
		10.0	16.7	0.60	0.57	0.24	0.17	0.63	0.59	0.25	0.18	0.62	0.58	0.25	0.18
		10.0	5.6	0.67	0.63	0.26	0.18	0.90	0.82	0.28	0.19	0.83	0.77	0.28	0.19
		−17.8	11.1	0.66	0.63	0.30	0.22	0.68	0.64	0.31	0.22	0.67	0.64	0.31	0.22
Horizontal	Down ↓	32.2	5.6	0.62	0.58	0.21	0.15	1.07	0.94	0.25	0.17	1.77	1.44	0.28	0.18
		10.0	16.7	0.66	0.62	0.25	0.18	1.10	0.99	0.30	0.20	1.69	1.44	0.33	0.21
		10.0	5.6	0.68	0.63	0.26	0.18	1.16	1.04	0.30	0.20	1.96	1.63	0.34	0.22
		−17.8	11.1	0.74	0.70	0.32	0.23	1.24	1.13	0.39	0.26	1.92	1.68	0.43	0.29

(b) English units (in h·ft²·°F/Btu)

Position of Airspace	Direction of Heat Flow	Mean Temp., °F	Temp. Diff., °F	0.75-in Airspace Effective Emissivity, ε_{eff}				1.5-in Airspace Effective Emissivity, ε_{eff}				3.5-in Airspace Effective Emissivity, ε_{eff}			
				0.03	0.05	0.5	0.82	0.03	0.05	0.5	0.82	0.03	0.05	0.5	0.82
Horizontal	Up ↑	90	10	2.34	2.22	1.04	0.75	2.55	2.41	1.08	0.77	2.84	2.66	1.13	0.80
		50	30	1.71	1.66	0.99	0.77	1.87	1.81	1.04	0.80	2.09	2.01	1.10	0.84
		50	10	2.30	2.21	1.16	0.87	2.50	2.40	1.21	0.89	2.80	2.66	1.28	0.93
		0	20	1.83	1.79	1.16	0.93	2.01	1.95	1.23	0.97	2.25	2.18	1.32	1.03
45° slope	Up ↓	90	10	2.96	2.78	1.15	0.81	2.92	2.73	1.14	0.80	3.18	2.96	1.18	0.82
		50	30	1.99	1.92	1.08	0.82	2.14	2.06	1.12	0.84	2.26	2.17	1.15	0.86
		50	10	2.90	2.75	1.29	0.94	2.88	2.74	1.29	0.94	3.12	2.95	1.34	0.96
		0	20	2.13	2.07	1.28	1.00	2.30	2.23	1.34	1.04	2.42	2.35	1.38	1.06
Vertical	Horizontal →	90	10	3.50	3.24	1.22	0.84	3.99	3.66	1.27	0.87	3.69	3.40	1.24	0.85
		50	30	2.91	2.77	1.30	0.94	2.58	2.46	1.23	0.90	2.67	2.55	1.25	0.91
		50	10	3.70	3.46	1.43	1.01	3.79	3.55	1.45	1.02	3.63	3.40	1.42	1.01
		0	20	3.14	3.02	1.58	1.18	2.76	2.66	1.48	1.12	2.88	2.78	1.51	1.14
45° slope	Down ↓	90	10	3.53	3.27	1.22	0.84	5.07	4.55	1.36	0.91	4.81	4.33	1.34	0.90
		50	30	3.43	3.23	1.39	0.99	3.58	3.36	1.42	1.00	3.51	3.30	1.40	1.00
		50	10	3.81	3.57	1.45	1.02	5.10	4.66	1.60	1.09	4.74	4.36	1.57	1.08
		0	20	3.75	3.57	1.72	1.26	3.85	3.66	1.74	1.27	3.81	3.63	1.74	1.27
Horizontal	Down ↓	90	10	3.55	3.29	1.22	0.85	6.09	5.35	1.43	0.94	10.07	8.19	1.57	1.00
		50	30	3.77	3.52	1.44	1.02	6.27	5.63	1.70	1.14	9.60	8.17	1.88	1.22
		50	10	3.84	3.59	1.45	1.02	6.61	5.90	1.73	1.15	11.15	9.27	1.93	1.24
		0	20	4.18	3.96	1.81	1.30	7.03	6.43	2.19	1.49	10.90	9.52	2.47	1.62

From ASHRAE Handbook of Fundamentals, *Chap. 22, Table 2.*

(a) Under the roof deck   (b) At the bottom of rafters   (c) On top of attic floor insulation
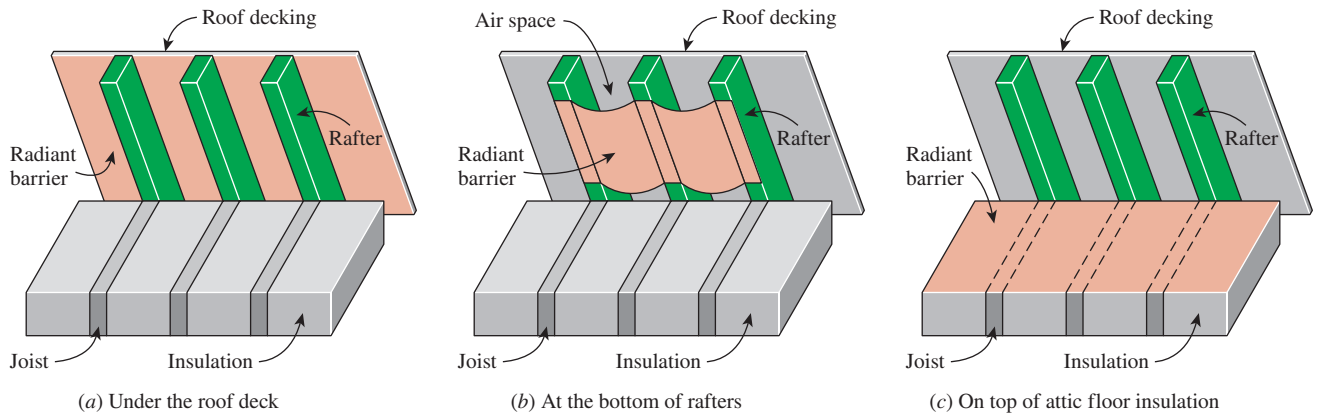
FIGURE 3–56

Three possible locations for an attic radiant barrier.

From DOE/CE-0335P, U.S. Dept. of Energy.

15 to 25 percent of the total cooling load of a house, radiant barriers will reduce the air conditioning costs by 2 to 10 percent. Radiant barriers also reduce the heat loss in winter through the ceiling, but tests have shown that the percentage reduction in heat losses is less. As a result, the percentage reduction in heating costs will be less than the reduction in the air-conditioning costs. Also, the values given are for new and undusted radiant barrier installations, and percentages will be lower for aged or dusty radiant barriers.

Some possible locations for attic radiant barriers are given in Fig. 3–56. In whole house tests on houses with R-19 attic floor insulation, radiant barriers have reduced the ceiling heat gain by an average of 35 percent when the radiant barrier is installed on the attic floor, and by 24 percent when it is attached to the bottom of roof rafters. Test cell tests also demonstrated that the best location for radiant barriers is the attic floor, provided that the attic is not used as a storage area and is kept clean.

For unvented attics, any heat transfer must occur through (1) the ceiling, (2) the attic space, and (3) the roof (Fig. 3–57). Therefore, the overall R-value of the roof–ceiling combination with an unvented attic depends on the combined effects of the R-value of the ceiling and the R-value of the roof as well as the thermal resistance of the attic space. The attic space can be treated as an air layer in the analysis. But a more practical way of accounting for its effect is to consider surface resistances on the roof and ceiling surfaces facing each other. In this case, the R-values of the ceiling and the roof are first determined separately (by using convection resistances for the still-air case for the attic surfaces). Then it can be shown that the overall R-value of the ceiling–roof combination per unit area of the ceiling can be expressed as

$$R = R_{\text{ceiling}} + R_{\text{roof}} \left(\frac{A_{\text{ceiling}}}{A_{\text{roof}}} \right) \qquad (3\text{–}96)$$
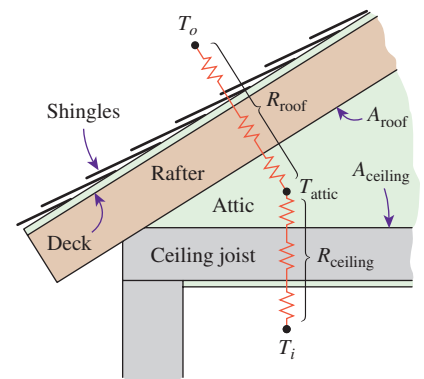
FIGURE 3–57

Thermal resistance network for a pitched roof–attic–ceiling combination for the case of an unvented attic.

where A_{ceiling} and A_{roof} are the ceiling and roof areas, respectively. The area ratio is equal to 1 for flat roofs and is less than 1 for pitched roofs. For a 45° pitched roof, the area ratio is $A_{\text{ceiling}}/A_{\text{roof}} = 1/\sqrt{2} = 0.707$. Note that the pitched roof has a greater area for heat transfer than the flat ceiling, and the area ratio accounts for the reduction in the unit R-value of the roof when expressed per unit area of the ceiling. Also, the direction of heat flow is up in winter (heat loss through the roof) and down in summer (heat gain through the roof).

The R-value of a structure determined by analysis assumes that the materials used and the quality of workmanship meet the standards. Poor workmanship and substandard materials used during construction may result in R-values that deviate from predicted values. Therefore, some engineers use a safety factor in their designs based on experience in critical applications.

EXAMPLE 3–18   The *R*-Value of a Wood Frame Wall

Determine the overall unit thermal resistance (the R-value) and the overall heat transfer coefficient (the U-factor) of a wood frame wall that is built around 38-mm × 90-mm (2 × 4 nominal) wood studs with a center-to-center distance of 400 mm. The 90-mm-wide cavity between the studs is filled with glass fiber insulation. The inside is finished with 13-mm gypsum wallboard and the outside with 13-mm wood fiberboard and 13-mm × 200-mm wood bevel lapped siding. The insulated cavity constitutes 75 percent of the heat transmission area while the studs, plates, and sills constitute 21 percent. The headers constitute 4 percent of the area, and they can be treated as studs.

Also, determine the rate of heat loss through the walls of a house whose perimeter is 50 m and wall height is 2.5 m in Las Vegas, Nevada, whose winter design temperature is −2°C. Take the indoor design temperature to be 22°C and assume 20 percent of the wall area is occupied by glazing.

SOLUTION   The R-value and the U-factor of a wood frame wall as well as the rate of heat loss through such a wall in Las Vegas are to be determined.
Assumptions   **1** Steady operating conditions exist. **2** Heat transfer through the wall is one-dimensional. **3** Thermal properties of the wall and the heat transfer coefficients are constant.
Properties   The R-values of different materials are given in Table 3–8.
Analysis   The schematic of the wall as well as the different elements used in its construction are shown here. Heat transfer through the insulation and through the studs meets different resistances, and thus we need to analyze the thermal resistance for each path separately. Once the unit thermal resistances and the U-factors for the insulation and stud sections are available, the overall average thermal resistance for the entire wall can be determined from

$$R_{\text{overall}} = 1/U_{\text{overall}}$$

where

$$U_{\text{overall}} = (U \times f_{\text{area}})_{\text{insulation}} + (U \times f_{\text{area}})_{\text{stud}}$$

and the value of the area fraction f_{area} is 0.75 for the insulation section and 0.25 for the stud section since the headers that constitute a small part of the wall are to be treated as studs. Using the available R-values from Table 3–8 and calculating others, the total R-values for each section can be determined in a systematic manner in the following table.
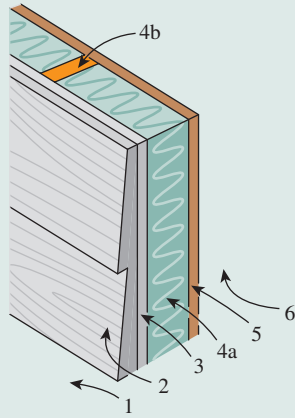
Schematic			R-value, m²·°C/W	
		Construction	Between Studs	At Studs
	1.	Outside surface, 24 km/h wind	0.030	0.030
	2.	Wood bevel lapped siding	0.14	0.14
	3.	Wood fiberboard sheeting, 13 mm	0.23	0.23
	4a.	Glass fiber insulation, 90 mm	2.45	—
	4b.	Wood stud, 38 mm × 90 mm	—	0.63
	5.	Gypsum wallboard, 13 mm	0.079	0.079
	6.	Inside surface, still air	0.12	0.12

	Between Studs	At Studs
Total unit thermal resistance of each section, R (in m²·°C/W)	3.05	1.23
The U-factor of each section, $U = 1/R$, in W/m²·K	0.328	0.813
Area fraction of each section, f_{area}	0.75	0.25

Overall U-factor: $U = \Sigma f_{area,\,i} U_i = 0.75 \times 0.328 + 0.25 \times 0.813$
$$= \textbf{0.449 W/m}^2\textbf{·K}$$
Overall unit thermal resistance: $\qquad\qquad R = 1/U = \textbf{2.23 m}^2\textbf{·°C/W}$

We conclude that the overall unit thermal resistance of the wall is 2.23 m²·°C/W, and this value accounts for the effects of the studs and headers. It corresponds to an R-value of $2.23 \times 5.68 = 12.7$ (or nearly R-13) in English units. Note that if there were no wood studs and headers in the wall, the overall thermal resistance would be 3.05 m²·°C/W, which is 37 percent greater than 2.23 m²·°C/W. Therefore, the wood studs and headers in this case serve as thermal bridges in wood frame walls, and their effect must be considered in the thermal analysis of buildings.

The perimeter of the building is 50 m, and the height of the walls is 2.5 m. Noting that glazing constitutes 20 percent of the walls, the total wall area is

$$A_{wall} = 0.80(\text{Perimeter})(\text{Height}) = 0.80(50 \text{ m})(2.5 \text{ m}) = 100 \text{ m}^2$$

Then the rate of heat loss through the walls under design conditions becomes

$$\begin{aligned}\dot{Q}_{wall} &= (UA)_{wall}(T_i - T_o) \\ &= (0.449 \text{ W/m}^2\text{·K})(100 \text{ m}^2)[22 - (-2)°\text{C}] \\ &= \textbf{1078 W}\end{aligned}$$

Discussion Note that a 1-kW resistance heater in this house will make up almost all the heat lost through the walls, except through the doors and windows, when the outdoor air temperature drops to −2°C.

EXAMPLE 3–19   The *R*-Value of a Wall with Rigid Foam

The 13-mm-thick wood fiberboard sheathing of the wood stud wall discussed in the previous example is replaced by a 25-mm-thick rigid foam insulation. Determine the percent increase in the *R*-value of the wall as a result.

SOLUTION   The overall *R*-value of the existing wall was determined in Example 3–18 to be 2.23 m²·°C/W. Noting that the *R*-values of the fiberboard and the foam insulation are 0.23 m²·°C/W and 0.98 m²·°C/W, respectively, and the added and removed thermal resistances are in series, the overall *R*-value of the wall after modification becomes

$$R_{new} = R_{old} - R_{removed} + R_{added}$$
$$= 2.23 - 0.23 + 0.98$$
$$= 2.98 \text{ m}^2 \cdot {}^\circ\text{C/W}$$

This represents an increase of $(2.98 - 2.23)/2.23 = 0.34$ or **34 percent** in the *R*-value of the wall. This example demonstrates how to evaluate the new *R*-value of a structure when some structural members are added or removed.

EXAMPLE 3–20   The *R*-Value of a Masonry Wall

Determine the overall unit thermal resistance (the *R*-value) and the overall heat transfer coefficient (the *U*-factor) of a masonry cavity wall that is built around 6-in-thick concrete blocks made of lightweight aggregate with three cores filled with perlite ($R = 4.2$ h·ft²·°F/Btu). The outside is finished with 4-in face brick with $\frac{1}{2}$-in cement mortar between the bricks and concrete blocks. The inside finish consists of $\frac{1}{2}$-in gypsum wallboard separated from the concrete block by $\frac{3}{4}$-in-thick (1-in × 3-in nominal) vertical furring ($R = 4.2$ h·ft²·°F/Btu) whose center-to-center distance is 16 in. Both sides of the $\frac{1}{2}$-in-thick airspace between the concrete block and the gypsum board are coated with reflective aluminum foil ($\varepsilon = 0.05$) so that the effective emissivity of the airspace is 0.03. For a mean temperature of 50°F and a temperature difference of 30°F, the *R*-value of the airspace is 2.91 h·ft²·°F/Btu. The reflective airspace constitutes 80 percent of the heat transmission area, while the vertical furring constitutes 20 percent.

SOLUTION   The *R*-value and the *U*-factor of a masonry cavity wall are to be determined.
Assumptions   **1** Steady operating conditions exist. **2** Heat transfer through the wall is one-dimensional. **3** Thermal properties of the wall and the heat transfer coefficients are constant.
Properties   The *R*-values of different materials are given in Table 3–8.
Analysis   The schematic of the wall as well as the different elements used in its construction are shown below. Following the approach described here and using the available *R*-values from Table 3–8, the overall *R*-value of the wall is determined in the following table.
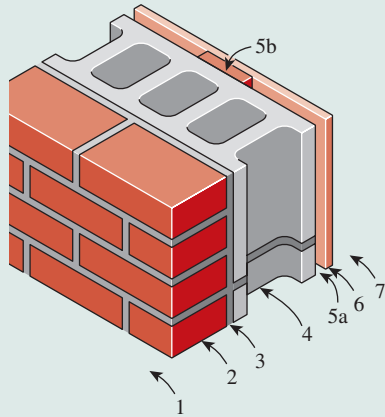
	Construction	R-value, h·ft²·°F/Btu	
Schematic		Between Furring	At Furring
	1. Outside surface, 15 mph wind	0.17	0.17
	2. Face brick, 4 in	0.43	0.43
	3. Cement mortar, 0.5 in	0.10	0.10
	4. Concrete block, 6 in	4.20	4.20
	5a. Reflective airspace, $\frac{3}{4}$ in	2.91	—
	5b. Nominal 1 × 3 vertical furring	—	0.94
	6. Gypsum wallboard, 0.5 in	0.45	0.45
	7. Inside surface, still air	0.68	0.68

Total unit thermal resistance of each section, R 8.94   6.97

The U-factor of each section, $U = 1/R$, in Btu/h·ft²·°F   0.112   0.143

Area fraction of each section, f_{area} 0.80   0.20

Overall U-factor: $U = \Sigma f_{area,\,i} U_i = 0.80 \times 0.112 + 0.20 \times 0.413$

$\qquad\qquad\qquad = \textbf{0.118 Btu/h·ft}^2\textbf{·°F}$

Overall unit thermal resistance: $\qquad\qquad R = 1/U = \textbf{8.46 h·ft}^2\textbf{·°F/Btu}$

Therefore, the overall unit thermal resistance of the wall is 8.46 h·ft²·°F/Btu and the overall U-factor is 0.118 Btu/h·ft²·°F. These values account for the effects of the vertical furring.

EXAMPLE 3–21   The R-Value of a Pitched Roof

Determine the overall unit thermal resistance (the R-value) and the overall heat transfer coefficient (the U-factor) of a 45° pitched roof built around nominal 2-in × 4-in wood studs with a center-to-center distance of 16 in. The 3.5-in-wide airspace between the studs does not have any reflective surface and thus its effective emissivity is 0.84. For a mean temperature of 90°F and a temperature difference of 30°F, the R-value of the airspace is 0.86 h·ft²·°F/Btu. The lower part of the roof is finished with $\frac{1}{2}$-in gypsum wallboard and the upper part with $\frac{5}{8}$-in plywood, building paper, and asphalt shingle roofing. The airspace constitutes 75 percent of the heat transmission area, while the studs and headers constitute 25 percent.

SOLUTION   The R-value and the U-factor of a 45° pitched roof are to be determined.

Assumptions   **1** Steady operating conditions exist. **2** Heat transfer through the roof is one-dimensional. **3** Thermal properties of the roof and the heat transfer coefficients are constant.

Properties The R-values of different materials are given in Table 3–8.
Analysis The schematic of the pitched roof as well as the different elements used in its construction are shown below. Following the approach described above and using the available R-values from Table 3–8, the overall R-value of the roof can be determined in the table here.

Schematic
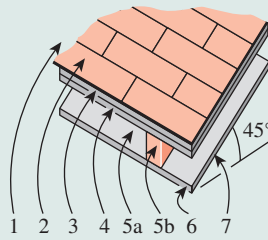
Construction	R-value, h·ft²·°F/Btu	
	Between Studs	At Studs
1. Outside surface, 15 mph wind	0.17	0.17
2. Asphalt shingle roofing	0.44	0.44
3. Building paper	0.06	0.06
4. Plywood deck, $\frac{5}{8}$in	0.78	0.78
5a. Nonreflective airspace, 3.5 in	0.86	—
5b. Wood stud, 2 in × 4 in	—	3.58
6. Gypsum wallboard, 0.5 in	0.45	0.45
7. Inside surface, 45° slope, still air	0.63	0.63
Total unit thermal resistance of each section, R	3.39	6.11
The U-factor of each section, $U = 1/R$, in Btu/h·ft²·°F	0.292	0.163
Area fraction of each section, f_{area}	0.75	0.25

Overall U-factor: $U = \Sigma f_{area, i}\, U_i = 0.75 \times 0.292 + 0.25 \times 0.163$
$= $ **0.260 Btu/h·ft²·°F**
Overall unit thermal resistance: $\qquad\qquad R = 1/U = $ **3.85 h·ft²·°F/Btu**

Therefore, the overall unit thermal resistance of this pitched roof is 3.85 h·ft²·°F/Btu, and the overall U-factor is 0.260 Btu/h·ft²·°F. Note that the wood studs offer much larger thermal resistance to heat flow than the airspace between the studs.

SUMMARY

One-dimensional heat transfer through a simple or composite body exposed to convection from both sides to media at temperatures $T_{\infty 1}$ and $T_{\infty 2}$ can be expressed as

$$\dot{Q} = \frac{T_{\infty 1} - T_{\infty 2}}{R_{total}}$$

where R_{total} is the total thermal resistance between the two media. For a plane wall exposed to convection on both sides, the total resistance is expressed as

$$R_{total} = R_{conv, 1} + R_{wall} + R_{conv, 2} = \frac{1}{h_1 A} + \frac{L}{kA} + \frac{1}{h_2 A}$$

This relation can be extended to plane walls that consist of two or more layers by adding an additional resistance for each additional layer. The elementary thermal resistance relations can be expressed as follows:

Conduction resistance (plane wall): $\quad R_{wall} = \dfrac{L}{kA}$

Conduction resistance (cylinder): $\quad R_{cyl} = \dfrac{\ln(r_2/r_1)}{2\pi Lk}$

Conduction resistance (sphere): $\quad R_{sph} = \dfrac{r_2 - r_1}{4\pi r_1 r_2 k}$

Convection resistance: $\quad R_{conv} = \dfrac{1}{hA}$

Interface resistance: $\quad R_{interface} = \dfrac{1}{h_c A} = \dfrac{R_c}{A}$

Radiation resistance: $\quad R_{rad} = \dfrac{1}{h_{rad} A}$

where h_c is the thermal contact conductance, R_c is the thermal contact resistance, and the radiation heat transfer coefficient is defined as

$$h_{rad} = \varepsilon\sigma(T_s^2 + T_{surr}^2)(T_s + T_{surr})$$

Once the rate of heat transfer is available, the *temperature drop* across any layer can be determined from

$$\Delta T = \dot{Q}R$$

The thermal resistance concept can also be used to solve steady heat transfer problems involving parallel layers or combined series-parallel arrangements.

Adding insulation to a cylindrical pipe or a spherical shell increases the rate of heat transfer if the outer radius of the insulation is less than the *critical radius of insulation,* defined as

$$r_{cr, cylinder} = \frac{k_{ins}}{h}$$

$$r_{cr, sphere} = \frac{2k_{ins}}{h}$$

The effectiveness of an insulation is often given in terms of its *R-value,* the thermal resistance of the material for a unit surface area, expressed as

$$R\text{-value} = \frac{L}{k} \qquad \text{(flat insulation)}$$

where L is the thickness and k is the thermal conductivity of the material.

Finned surfaces are commonly used in practice to enhance heat transfer. Fins enhance heat transfer from a surface by exposing a larger surface area to convection. The temperature distribution along the fin is given by

Very long fin:
$$\frac{T(x) - T_\infty}{T_b - T_\infty} = e^{-x\sqrt{hp/kA_c}}$$

Adiabatic fin tip:
$$\frac{T(x) - T_\infty}{T_b - T_\infty} = \frac{\cosh m(L - x)}{\cosh mL}$$

Specified temperature at fin tip:

$$\frac{T(x) - T_\infty}{T_b - T_\infty} = \frac{[(T_L - T_\infty)/(T_b - T_\infty)]\sinh mx + \sinh m(L - x)}{\sinh mL}$$

Convection from fin tip:

$$\frac{T(x) - T_\infty}{T_b - T_\infty} = \frac{\cosh m(L - x) + (h/mk)\sinh m(L - x)}{\cosh mL + (h/mk)\sinh mL}$$

where $m = \sqrt{hp/kA_c}$, p is the perimeter, and A_c is the cross-sectional area of the fin. The rates of heat transfer for these cases are given to be

Very long fin:

$$\dot{Q}_{long\,fin} = -kA_c\frac{dT}{dx}\bigg|_{x=0} = \sqrt{hpkA_c}(T_b - T_\infty)$$

Adiabatic fin tip:

$$\dot{Q}_{adiabatic\,tip} = -kA_c\frac{dT}{dx}\bigg|_{x=0} = \sqrt{hpkA_c}(T_b - T_\infty)\tanh mL$$

Specified temperature at fin tip:

$$\dot{Q}_{specified\,temp.} = \sqrt{hpkA_c}(T_b - T_\infty)\frac{\cosh mL - [(T_L - T_\infty)/(T_b - T_\infty)]}{\sinh mL}$$

Convection from the fin tip:

$$\dot{Q}_{convection} = \sqrt{hpkA_c}(T_b - T_\infty)\frac{\sinh mL + (h/mk)\cosh mL}{\cosh mL + (h/mk)\sinh mL}$$

Fins exposed to convection at their tips can be treated as fins with adiabatic tips by using the corrected length $L_c = L + A_c/p$ instead of the actual fin length.

The temperature of a fin drops along the fin, and thus the heat transfer from the fin is less because of the decreasing temperature difference toward the fin tip. To account for the effect of this decrease in temperature on heat transfer, we define *fin efficiency* as

$$\eta_{fin} = \frac{\dot{Q}_{fin}}{\dot{Q}_{fin,\,max}} = \frac{\text{Actual heat transfer rate from the fin}}{\substack{\text{Ideal heat transfer rate from the fin if}\\ \text{the entire fin were at base temperature}}}$$

When the fin efficiency is available, the rate of heat transfer from a fin can be determined from

$$\dot{Q}_{fin} = \eta_{fin}\dot{Q}_{fin,\,max} = \eta_{fin}hA_{fin}(T_b - T_\infty)$$

The performance of the fins is judged on the basis of the enhancement in heat transfer relative to the no-fin case and is expressed in terms of the *fin effectiveness* ε_{fin}, defined as

$$\varepsilon_{fin} = \frac{\dot{Q}_{fin}}{\dot{Q}_{no\,fin}} = \frac{\dot{Q}_{fin}}{hA_b(T_b - T_\infty)} = \frac{\substack{\text{Heat transfer rate from}\\ \text{the fin of } base\ area\ A_b}}{\substack{\text{Heat transfer rate from}\\ \text{the surface of } area\ A_b}}$$

Here, A_b is the cross-sectional area of the fin at the base, and $\dot{Q}_{no\,fin}$ represents the rate of heat transfer from this area if no fins are attached to the surface. The *overall effectiveness* for a finned surface is defined as the ratio of the total heat transfer from the finned surface to the heat transfer from the same surface if there were no fins,

$$\varepsilon_{fin,\,overall} = \frac{\dot{Q}_{total,\,fin}}{\dot{Q}_{total,\,no\,fin}} = \frac{h(A_{unfin} + \eta_{fin}A_{fin})(T_b - T_\infty)}{hA_{no\,fin}(T_b - T_\infty)}$$

Fin efficiency and fin effectiveness are related to each other by

$$\varepsilon_{fin} = \frac{A_{fin}}{A_b}\eta_{fin}$$

Certain multidimensional heat transfer problems involve two surfaces maintained at constant temperatures T_1 and T_2. The steady rate of heat transfer between these two surfaces is expressed as

$$\dot{Q} = Sk(T_1 - T_2)$$

where S is the *conduction shape factor* that has the dimension of *length* and k is the thermal conductivity of the medium between the surfaces.

REFERENCES AND SUGGESTED READING

1. American Society of Heating, Refrigeration, and Air Conditioning Engineers. *Handbook of Fundamentals.* Atlanta: ASHRAE, 1993.

2. R. V. Andrews. "Solving Conductive Heat Transfer Problems with Electrical-Analogue Shape Factors." *Chemical Engineering Progress* 5 (1955), p. 67.

3. R. Barron. *Cryogenic Systems.* New York: McGraw-Hill, 1967.

4. W. M. Edmunds. "Residential Insulation." *ASTM Standardization News* (Jan. 1989), pp. 36–39.

5. L. S. Fletcher. "Recent Developments in Contact Conductance Heat Transfer." *Journal of Heat Transfer* 110, no. 4B (1988), pp. 1059–79.

6. E. Fried. "Thermal Conduction Contribution to Heat Transfer at Contacts." *Thermal Conductivity,* vol. 2, ed. R. P. Tye. London: Academic Press, 1969.

7. K. A. Gardner. "Efficiency of Extended Surfaces." *Trans. ASME* 67 (1945), pp. 621–31. Reprinted by permission of ASME International.

8. D. Q. Kern and A. D. Kraus. *Extended Surface Heat Transfer.* New York: McGraw-Hill, 1972.

9. H. H. Pennes, "Analysis of Tissue and Arterial Blood Temperatures in the Resting Human Forearm." *Journal of Applied Physiology* 1 (1948), pp. 93–122.

10. H. H. Pennes, "Analysis of Tissue and Arterial Blood Temperatures in the Resting Human Forearm." *Journal of Applied Physiology* 85 (1998), pp. 5–34 (Pennes 1948 article republished for the 50th anniversary of the *Journal of Applied Physiology*).

11. G. P. Peterson. "Thermal Contact Resistance in Waste Heat Recovery Systems." *Proceedings of the 18th ASME/ ETCE Hydrocarbon Processing Symposium,* Dallas, TX, 1987, pp. 45–51. Reprinted by permission of ASME International.

12. S. Song, M. M. Yovanovich, and F. O. Goodman. "Thermal Gap Conductance of Conforming Surfaces in Contact." *Journal of Heat Transfer* 115 (1993), p. 533.

13. J. E. Sunderland and K. R. Johnson. "Shape Factors for Heat Conduction through Bodies with Isothermal or Convective Boundary Conditions." *Trans. ASME* 10 (1964), pp. 2317–41.

14. E. H. Wissler, "Pennes' 1948 Paper Revisited." *Journal of Applied Physiology* 85 (1998), pp. 35–41.

PROBLEMS*

Steady Heat Conduction in Plane Walls

3–1C Consider heat conduction through a wall of thickness *L* and area *A*. Under what conditions will the temperature distributions in the wall be a straight line?

3–2C Consider heat conduction through a plane wall. Does the energy content of the wall change during steady heat conduction? How about during transient conduction? Explain.

3–3C What does the thermal resistance of a medium represent?

3–4C Can we define the convection resistance for a unit surface area as the inverse of the convection heat transfer coefficient?

3–5C Consider steady heat transfer through the wall of a room in winter. The convection heat transfer coefficient at the outer surface of the wall is three times that of the inner surface as a result of the winds. On which surface of the wall do you think the temperature will be closer to the surrounding air temperature? Explain.

3–6C How is the combined heat transfer coefficient defined? What convenience does it offer in heat transfer calculations?

3–7C Why are the convection and the radiation resistances at a surface in parallel instead of being in series?

3–8C Consider steady one-dimensional heat transfer through a plane wall exposed to convection from both sides to environments at known temperatures $T_{\infty 1}$ and $T_{\infty 2}$ with known heat transfer coefficients h_1 and h_2. Once the rate of heat transfer $\dot{Q}$ has been evaluated, explain how you would determine the temperature of each surface.

3–9C Someone comments that a microwave oven can be viewed as a conventional oven with zero convection resistance at the surface of the food. Is this an accurate statement?

3–10C Consider two cold canned drinks, one wrapped in a blanket and the other placed on a table in the same room. Which drink will warm up faster?

*Problems designated by a "C" are concept questions, and students are encouraged to answer them all. Problems designated by an "E" are in English units, and the SI users can ignore them. Problems with the ⌨ icon are comprehensive in nature and are intended to be solved with appropriate software. Problems with the **PtD** icon are Prevention through Design problems. Problems with the **C&S** icon are Codes and Standards problems.

3–11C The bottom of a pan is made of a 4-mm-thick aluminum layer. In order to increase the rate of heat transfer through the bottom of the pan, someone proposes a design for the bottom that consists of a 3-mm-thick copper layer sandwiched between two 2-mm-thick aluminum layers. Will the new design conduct heat better? Explain. Assume perfect contact between the layers.

2 mm
3 mm
2 mm

Aluminum   Copper
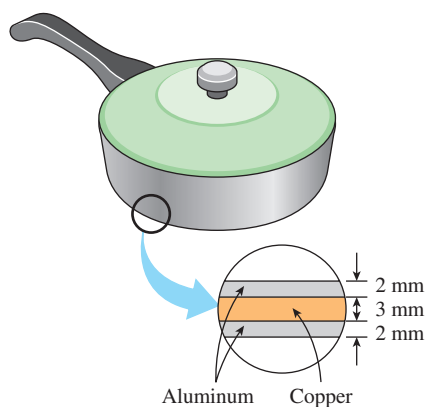
FIGURE P3–11C

3–12C Consider a surface of area A at which the convection and radiation heat transfer coefficients are h_{conv} and h_{rad}, respectively. Explain how you would determine (a) the single equivalent heat transfer coefficient, and (b) the equivalent thermal resistance. Assume the medium and the surrounding surfaces are at the same temperature.

3–13C How does the thermal resistance network associated with a single-layer plane wall differ from the one associated with a five-layer composite wall?

3–14C Consider steady one-dimensional heat transfer through a multilayer medium. If the rate of heat transfer $\dot{Q}$ is known, explain how you would determine the temperature drop across each layer.

3–15C Consider a window glass consisting of two 4-mm-thick glass sheets pressed tightly against each other. Compare the heat transfer rate through this window with that of one consisting of a single 8-mm-thick glass sheet under identical conditions.

3–16 Consider a 3-m-high, 6-m-wide, and 0.25-m-thick brick wall whose thermal conductivity is $k = 0.8$ W/m·K. On a certain day, the temperatures of the inner and the outer surfaces of the wall are measured to be 14°C and 5°C, respectively. Determine the rate of heat loss through the wall on that day.

3–17 Consider a person standing in a room at 20°C with an exposed surface area of 1.7 m². The deep body temperature of the human body is 37°C, and the thermal conductivity of the human tissue near the skin is about 0.3 W/m·K. The body is losing heat at a rate of 150 W by natural convection and radiation to the surroundings. Taking the body temperature 0.5 cm beneath the skin to be 37°C, determine the skin temperature of the person. *Answer:* 35.5°C

3–18E Consider an electrically heated brick house ($k = 0.40$ Btu/h·ft·°F) whose walls are 9 ft high and 1 ft thick. Two of the walls of the house are 50 ft long and the others are 35 ft long. The house is maintained at 70°F at all times while the temperature of the outdoors varies. On a certain day, the temperature of the inner surface of the walls is measured to be at 55°F while the average temperature of the outer surface is observed to remain at 45°F during the day for 10 h and at 35°F at night for 14 h. Determine the amount of heat lost from the house that day. Also determine the cost of that heat loss to the homeowner for an electricity price of \$0.09/kWh.

$T_{in} = 70°F$

9 ft

50 ft

35 ft
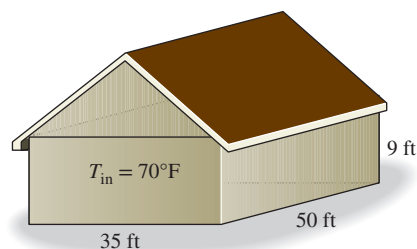
FIGURE P3–18E

3–19 A 12-cm × 18-cm circuit board houses on its surface 100 closely spaced logic chips, each dissipating 0.06 W in an environment at 40°C. The heat transfer from the back surface of the board is negligible. If the heat transfer coefficient on the surface of the board is 10 W/m²·K, determine (a) the heat flux on the surface of the circuit board, in W/m²; (b) the surface temperature of the chips; and (c) the thermal resistance between the surface of the circuit board and the cooling medium, in °C/W.

3–20 Water is boiling in a 25-cm-diameter aluminum pan ($k = 237$ W/m·K) at 95°C. Heat is transferred steadily to the boiling water in the pan through its 0.5-cm-thick flat bottom at a rate of 800 W. If the inner surface temperature of the bottom of the pan is 108°C, determine (a) the boiling heat transfer coefficient on the inner surface of the pan and (b) the outer surface temperature of the bottom of the pan.

3–21 A cylindrical resistor element on a circuit board dissipates 0.15 W of power in an environment at 35°C. The resistor is 1.2 cm long and has a diameter of 0.3 cm. Assuming heat to be transferred uniformly from all surfaces, determine (a) the amount of heat this resistor dissipates during a 24-h period; (b) the heat flux on the surface of the resistor, in W/m²; and (c) the surface temperature of the resistor for a combined convection and radiation heat transfer coefficient of 9 W/m²·K.

3–22 Consider a power transistor that dissipates 0.15 W of power in an environment at 30°C. The transistor is 0.4 cm long and has a diameter of 0.5 cm. Assuming heat to be transferred uniformly from all surfaces, determine (*a*) the amount of heat this resistor dissipates during a 24-h period, in kWh; (*b*) the heat flux on the surface of the transistor, in W/m²; and (*c*) the surface temperature of the resistor for a combined convection and radiation heat transfer coefficient of 18 W/m²·K.

30°C

Power transistor 0.15 W

0.5 cm

0.4 cm
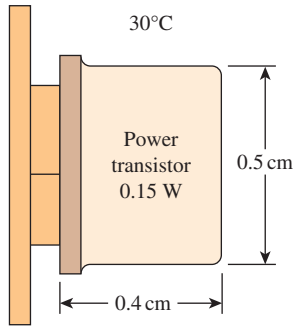
FIGURE P3–22

3–23 A 1.0 m × 1.5 m double-pane window consists of two 4-mm-thick layers of glass ($k = 0.78$ W/m·K) that are separated by a 5-mm air gap ($k_{air} = 0.025$ W/m·K). The heat flow through the air gap is assumed to be by conduction. The inside and outside air temperatures are 20°C and −20°C, respectively, and the inside and outside heat transfer coefficients are 40 and 20 W/m²·K. Determine (*a*) the daily rate of heat loss through the window in steady operation and (*b*) the temperature difference across the largest thermal resistance.

3–24 Consider a 1.5-m-high and 2.4-m-wide glass window whose thickness is 6 mm and thermal conductivity is $k = 0.78$ W/m·K. Determine the steady rate of heat transfer through this glass window and the temperature of its inner surface for a day during which the room is maintained at 24°C while the temperature of the outdoors is −5°C. Take the convection heat transfer coefficients on the inner and outer surfaces of the window to be $h_1 = 10$ W/m²·K and $h_2 = 25$ W/m²·K, and disregard any heat transfer by radiation.

3–25 Consider a 1.5-m-high and 2.4-m-wide double-pane window consisting of two 3-mm-thick layers of glass ($k = 0.78$ W/m·K) separated by a 12-mm-wide stagnant airspace ($k = 0.026$ W/m·K). Determine the steady rate of heat transfer through this double-pane window and the temperature of its inner surface for a day during which the room is maintained at 21°C while the temperature of the outdoors is −5°C. Take the convection heat transfer coefficients on the inner and outer surfaces of the window to be $h_1 = 10$ W/m²·K and $h_2 = 25$ W/m²·K, and disregard any heat transfer by radiation.
Answers: 154 W, 16.7°C

Glass

3   12   3 mm

Frame
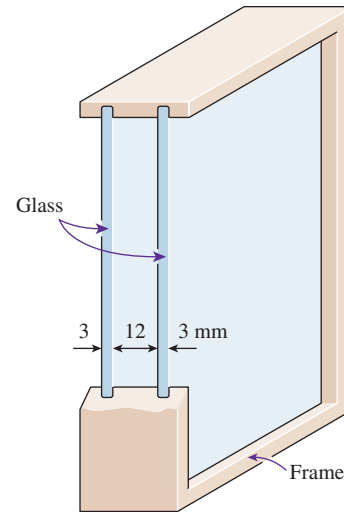
FIGURE P3–25

3–26 Repeat Prob. 3–25, assuming the space between the two glass layers is evacuated.

3–27 Reconsider Prob. 3–25. Using appropriate software, plot the rate of heat transfer through the window as a function of the width of airspace in the range of 2 mm to 20 mm, assuming pure conduction through the air. Discuss the results.

3–28E A wall is constructed of two layers of 0.6-in-thick sheetrock ($k = 0.10$ Btu/h·ft·°F), which is a plasterboard made of two layers of heavy paper separated by a layer of gypsum, placed 7 in apart. The space between the sheetrocks is filled with fiberglass insulation ($k = 0.020$ Btu/h·ft·°F). Determine (*a*) the thermal resistance of the wall and (*b*) its *R*-value of insulation in English units.

Fiberglass insulation

Sheetrock

0.6 in   7 in   0.6 in
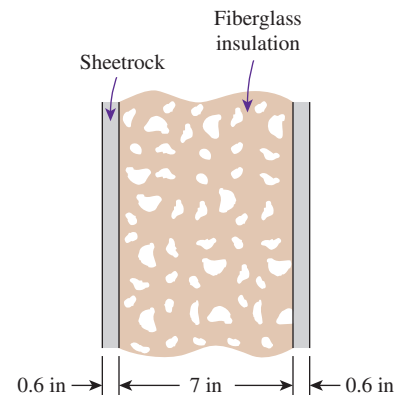
FIGURE P3–28E

3–29 To defog the rear window of an automobile, a very thin transparent heating element is attached to the inner surface of

the window. A uniform heat flux of 1300 W/m² is provided to the heating element for defogging a rear window with thickness of 5 mm. The interior temperature of the automobile is 22°C, and the convection heat transfer coefficient is 15 W/m²·K. The outside ambient temperature is −5°C, and the convection heat transfer coefficient is 100 W/m²·K. If the thermal conductivity of the window is 1.2 W/m·K, determine the inner surface temperature of the window.

Heating element
$\dot{q}_h = 1300$ W/m²

Inside air, 22°C
$h_i = 15$ W/m²·K

Rear window
$k = 1.2$ W/m·K

Outside air, −5°C
$h_o = 100$ W/m²·K

T_1

$L = 5$ mm
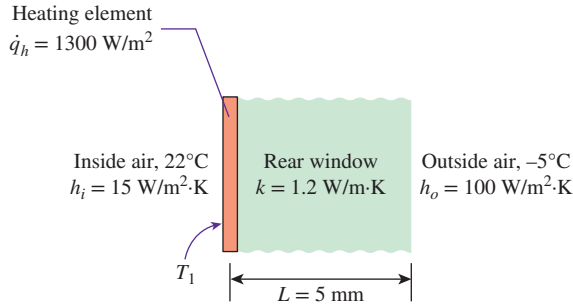
FIGURE P3−29

3–30 A transparent film is to be bonded onto the top surface of a solid plate inside a heated chamber. For the bond to cure properly, a temperature of 70°C is to be maintained at the bond, between the film and the solid plate. The transparent film has a thickness of 1 mm and thermal conductivity of 0.05 W/m·K, while the solid plate is 13 mm thick and has a thermal conductivity of 1.2 W/m·K. Inside the heated chamber, the convection heat transfer coefficient is 70 W/m²·K. If the bottom surface of the solid plate is maintained at 52°C, determine the temperature inside the heated chamber and the surface temperature of the transparent film. Assume thermal contact resistance is negligible.

T_1
Air, $h = 70$ W/m²·K
Transparent film
$k_f = 0.05$ W/m·K

$L_f = 1$ mm
$L_s = 13$ mm

Solid plate
$k_s = 1.2$ W/m·K

$T_b = 70°C$

$T_2 = 52°C$
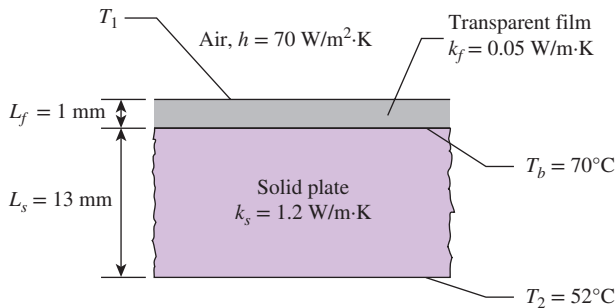
FIGURE P3−30

3–31 To defrost ice accumulated on the outer surface of an automobile windshield, warm air is blown over the inner surface of the windshield. Consider an automobile windshield with thickness of 5 mm and thermal conductivity of

1.4 W/m·K. The outside ambient temperature is −10°C and the convection heat transfer coefficient is 200 W/m²·K, while the ambient temperature inside the automobile is 25°C. Determine the value of the convection heat transfer coefficient for the warm air blowing over the inner surface of the windshield necessary to cause the accumulated ice to begin melting.

$L = 5$ mm

Outside air, −10°C
$h_o = 200$ W/m²·K

Windshield
$k = 1.4$ W/m·K

Inside air, 25°C

$T_1 = 0°C$
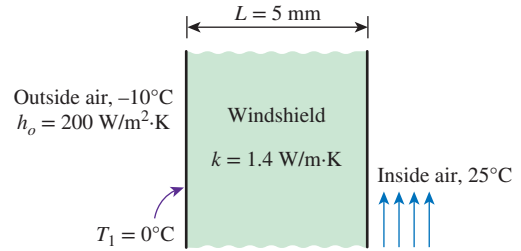
FIGURE P3−31

3–32 The roof of a house consists of a 15-cm-thick concrete slab ($k = 2$ W/m·K) that is 15 m wide and 20 m long. The convection heat transfer coefficients on the inner and outer surfaces of the roof are 5 and 12 W/m²·K, respectively. On a clear winter night, the ambient air is reported to be at 10°C, while the night sky temperature is 100 K. The house and the interior surfaces of the wall are maintained at a constant temperature of 20°C. The emissivity of both surfaces of the concrete roof is 0.9. Considering both radiation and convection heat transfers, determine the rate of heat transfer through the roof, and the inner surface temperature of the roof.

If the house is heated by a furnace burning natural gas with an efficiency of 80 percent, and the price of natural gas is $1.20/therm (1 therm = 105,500 kJ of energy content), determine the money lost through the roof that night during a 14-h period.

$T_{sky} = 100$ K

$T_{air} = 10°C$

Concrete roof

15 cm

20 m

15 m

$T_{in} = 20°C$
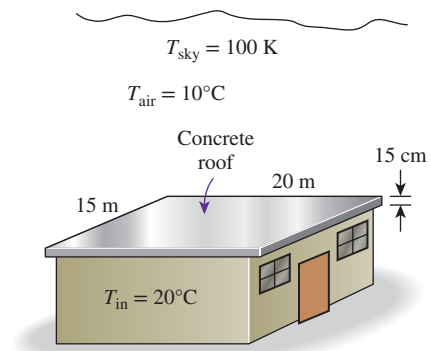
FIGURE P3−32

3–33 A 2-m × 1.5-m section of wall of an industrial furnace burning natural gas is not insulated, and the temperature at the outer surface of this section is measured to be 110°C. The temperature of the furnace room is 32°C, and the combined

convection and radiation heat transfer coefficient at the surface of the outer furnace is 10 W/m²·K. It is proposed to insulate this section of the furnace wall with glass wool insulation ($k = 0.038$ W/m·K) in order to reduce the heat loss by 90 percent. Assuming the outer surface temperature of the metal section remains at about 110°C, determine the thickness of the insulation that needs to be used.

The furnace operates continuously and has an efficiency of 78 percent. The price of the natural gas is $1.10/therm (1 therm = 105,500 kJ of energy content). If the installation of the insulation will cost $250 for materials and labor, determine how long it will take for the insulation to pay for itself from the energy it saves.

3–34 The wall of a refrigerator is constructed of fiberglass insulation ($k = 0.035$ W/m·K) sandwiched between two layers of 1-mm-thick sheet metal ($k = 15.1$ W/m·K). The refrigerated space is maintained at 2°C, and the average heat transfer coefficients at the inner and outer surfaces of the wall are 4 W/m²·K and 9 W/m²·K, respectively. The kitchen temperature averages 24°C. It is observed that condensation occurs on the outer surfaces of the refrigerator when the temperature of the outer surface drops to 20°C. Determine the minimum thickness of fiberglass insulation that needs to be used in the wall in order to avoid condensation on the outer surfaces.
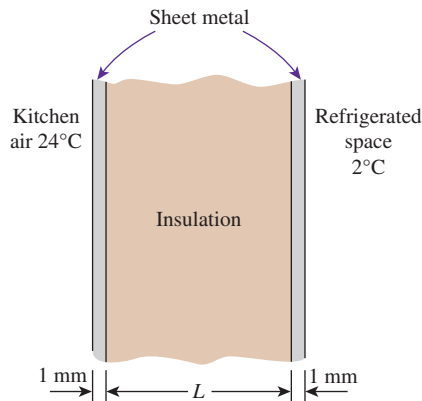
FIGURE P3–34

3–35 Reconsider Prob. 3–34. Using appropriate software, investigate the effects of the thermal conductivities of the insulation material and the sheet metal on the thickness of the insulation. Let the thermal conductivity vary from 0.02 W/m·K to 0.08 W/m·K for insulation and 10 W/m·K to 400 W/m·K for sheet metal. Plot the thickness of the insulation as the functions of the thermal conductivities of the insulation and the sheet metal, and discuss the results.

3–36 Heat is to be conducted along a circuit board that has a copper layer on one side. The circuit board is 15 cm long and 15 cm wide, and the thicknesses of the copper and epoxy layers are 0.1 mm and 1.2 mm, respectively. Disregarding heat transfer from side surfaces, determine the percentages of heat

conduction along the copper ($k = 386$ W/m·K) and epoxy ($k = 0.26$ W/m·K) layers. Also determine the effective thermal conductivity of the board. *Answers:* 0.8 percent, 99.2 percent, and 29.9 W/m·K

3–37E A 0.05-in-thick copper plate ($k = 223$ Btu/h·ft·°F) is sandwiched between two 0.15-in-thick epoxy boards ($k = 0.15$ Btu/h·ft·°F) that are 7 in × 9 in in size. Determine the effective thermal conductivity of the board along its 9-in-long side. What fraction of the heat conducted along that side is conducted through copper?
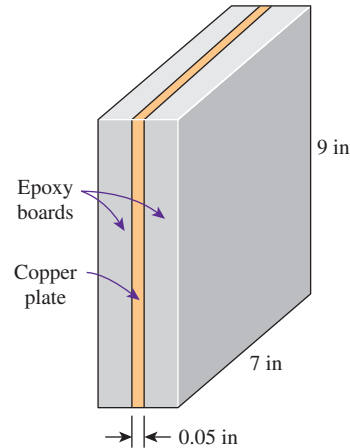
FIGURE P3–37E

3–38 Consider a house that has a 10-m × 20-m base and a 4-m-high wall. All four walls of the house have an *R*-value of 2.31 m²·°C/W. The two 10-m × 4-m walls have no windows. The third wall has five windows made of 0.5-cm-thick glass ($k = 0.78$ W/m·K), 1.2 m × 1.8 m in size. The fourth wall has the same size and number of windows, but they are double-paned with a 1.5-cm-thick stagnant airspace ($k = 0.026$ W/m·K) enclosed between two 0.5-cm-thick glass layers. The thermostat in the house is set at 24°C, and the average temperature outside at that location is 8°C during the seven-month-long heating season. Disregarding any direct radiation gain or loss through the windows and taking the heat transfer coefficients at the inner and outer surfaces of the house to be 7 and 18 W/m²·K, respectively, determine the average rate of heat transfer through each wall.

If the house is electrically heated and the price of electricity is $0.08/kWh, determine the amount of money this household will save per heating season by converting the single-pane windows to double-pane windows.

3–39E Consider a house whose walls are 12 ft high and 40 ft long. Two of the walls of the house have no windows, while each of the other two walls has four windows made of 0.25-in-thick glass ($k = 0.45$/Btu·h·ft°F), 3 ft × 5 ft in size. The walls are certified to have an *R*-value of 19 (i.e., an *L/k* value of 19 h·ft²·°F/Btu). Disregarding any direct radiation gain or loss

through the windows and taking the heat transfer coefficients at the inner and outer surfaces of the house to be 2 and 4 Btu/h·ft²·°F, respectively, determine the ratio of the heat transfer through the walls with and without windows.
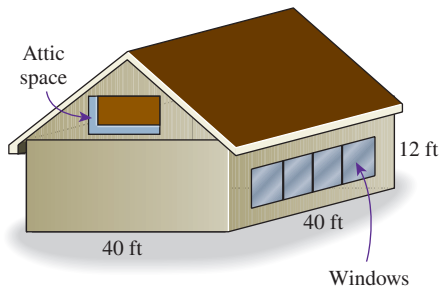
FIGURE P3–39E

3–40 PtD The outer surface of an engine is situated in a place where oil leakage can occur. When leaked oil comes in contact with a hot surface that has a temperature above its autoignition temperature, the oil can ignite spontaneously. Consider an engine cover that is made of a stainless steel plate with a thickness of 1 cm and a thermal conductivity of 14 W/m·K. The inner surface of the engine cover is exposed to hot air with a convection heat transfer coefficient of 7 W/m²·K at 333°C. The outer surface is exposed to an environment where the ambient air is 69°C with a convection heat transfer coefficient of 7 W/m²·K. To prevent fire hazard in the event of oil leak on the engine cover, a layer of thermal barrier coating (TBC) with a thermal conductivity of 1.1 W/m·K is applied on the engine cover outer surface. Would a TBC layer of 4 mm in thickness be sufficient to keep the engine cover surface below the autoignition temperature of 200°C to prevent a fire hazard?
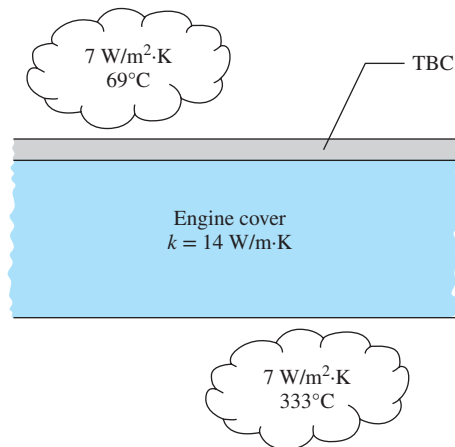
FIGURE P3–40

3–41 PtD Heat dissipated from a machine in operation can cause hot spots on its surface. Exposed hot spots can cause thermal burns when in contact with human skin

tissue and are considered to be hazards at the workplace. Consider a machine surface that is made of 5-mm-thick aluminum with a thermal conductivity of 237 W/m·K. During operation the machine dissipates about 300 W/m² of heat to the surroundings, and the inner aluminum surface is at 150°C. To protect machine operators from thermal burns, the machine surface can be covered with insulation. The aluminum/insulation interface has a thermal contact conductance of 3000 W/m²·K. What is the thickness required for the insulation layer with a thermal conductivity of 0.06 W/m·K in order to maintain the surface temperature at 45°C or lower?
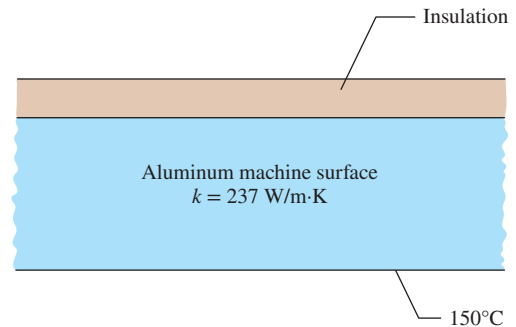
FIGURE P3–41

3–42 C&S A nonmetal plate ($k = 0.05$ W/m·K) is attached on the upper surface of an ASME SB-96 copper–silicon plate ($k = 36$ W/m·K). The nonmetal plate and the ASME SB-96 plate have thicknesses of 20 mm and 35 mm, respectively. The bottom surface of the ASME-SB-96 plate (surface 1) is subjected to a uniform heat flux of 200 W/m². The top nonmetal plate surface (surface 2) is exposed to convection at an air temperature of 15°C and a convection heat transfer coefficient of 10 W/m²·K. Copper–silicon alloys are not always suitable for applications where they are exposed to certain median and high temperatures. Therefore, the ASME Boiler and Pressure Vessel Code (ASME BPVC.IV-2015, HF-300) limits equipment constructed with ASME SB-96 plate to be operated at a temperature not exceeding 93°C. Determine the temperature at the bottom surface of the ASME SB-96 plate and the temperature at the interface. Would the use of the ASME SB-96 plate under these conditions be in compliance with the ASME Boiler and Pressure Vessel Code?
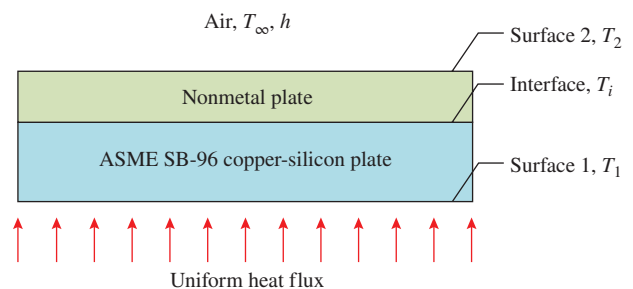
FIGURE P3–42

3–43 [C&S] An ASME SB-96 copper–silicon plate ($k = 36$ W/m·K) is attached on an ASTM A240 904L stainless steel plate ($k = 13$ W/m·K). Both plates are 25 mm thick. A series of ASTM B21 naval brass bolts are attached on the upper surface of the copper–silicon plate. The bottom surface of the stainless steel plate is exposed to convection with steam at 260°C and a convection heat transfer coefficient of 500 W/m²·K. The upper surface of the copper–silicon plate is exposed to convection with steam at 80°C and a convection heat transfer coefficient of 300 W/m²·K. According to the ASME Boiler and Pressure Vessel Code (ASME BPVC. IV-2015, HF-300), components constructed with ASME SB-96 plates should not be operated at temperatures above 93°C. According to the ASME Code for Process Piping (ASME B31.3-2014, Table A-2M), the maximum use temperature for the B21 bolts is 149°C, while the maximum use temperature for the ASTM A240 904L stainless steel plate is 260°C (ASME B31.3-2014, Table A-1M). Determine the temperatures at the upper surface of the stainless steel plate, at the bottom surface of the copper–silicon plate, and at the interface. Would the use of the copper–silicon plate, stainless steel plate, and ASTM B21 bolts be in compliance with the ASME Boiler and Pressure Vessel Code and the ASME Code for Process Piping?
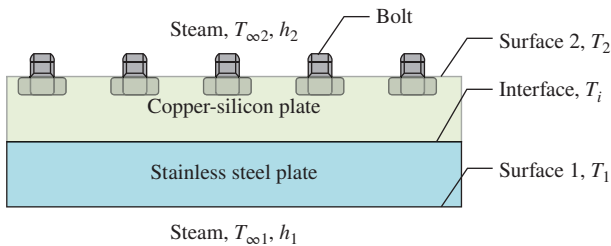
FIGURE P3–43

Thermal Contact Resistance

3–44C What is thermal contact resistance? How is it related to thermal contact conductance?

3–45C Will the thermal contact resistance be greater for smooth or rough plain surfaces?

3–46C Explain how the thermal contact resistance can be minimized.

3–47C A wall consists of two layers of insulation pressed against each other. Do we need to be concerned about the thermal contact resistance at the interface in a heat transfer analysis or can we just ignore it?

3–48C A plate consists of two thin metal layers pressed against each other. Do we need to be concerned about the thermal contact resistance at the interface in a heat transfer analysis or can we just ignore it?

3–49C Consider two surfaces pressed against each other. Now the air at the interface is evacuated. Will the thermal contact resistance at the interface increase or decrease as a result?

3–50 The thermal contact conductance at the interface of two 1-cm-thick aluminum plates is measured to be 11,000 W/m²·K. Determine the thickness of the aluminum plate whose thermal resistance is equal to the thermal resistance of the interface between the plates.
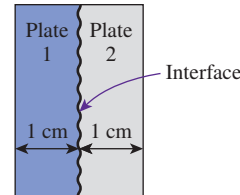
FIGURE P3–50

3–51 Two 5-cm-diameter, 15-cm-long aluminum bars ($k = 176$ W/m·K) with ground surfaces are pressed against each other with a pressure of 20 atm. The bars are enclosed in an insulation sleeve and, thus, heat transfer from the lateral surfaces is negligible. If the top and bottom surfaces of the two-bar system are maintained at temperatures of 150°C and 20°C, respectively, determine (*a*) the rate of heat transfer along the cylinders under steady conditions and (*b*) the temperature drop at the interface. *Answers: (a)* 142.4 W, *(b)* 6.4°C

3–52 A 1-mm-thick copper plate ($k = 401$ W/m·K) is sandwiched between two 7-mm-thick epoxy boards ($k = 0.26$ W/m·K) that are 15 cm × 20 cm in size. If the thermal contact conductance on both sides of the copper plate is estimated to be 6000 W/m·K, determine the error involved in the total thermal resistance of the plate if the thermal contact conductances are ignored.
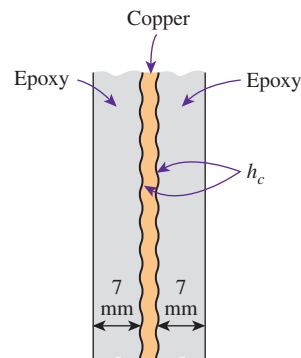
FIGURE P3–52

3–53 Two identical aluminum plates with thickness of 30 cm are pressed against each other at an average pressure of 1 atm. The interface, sandwiched between the two plates, is filled with glycerin. On the left outer surface, it is subjected to

a uniform heat flux of 7800 W/m² at a constant temperature of 50°C. On the right outer surface, the temperature is maintained constant at 30°C. Determine the thermal contact conductance of the glycerin at the interface if the thermal conductivity of the aluminum plates is 237 W/m·K. Discuss whether the value of the thermal contact conductance is reasonable or not.

3–54   A two-layer wall is made of two metal plates, with surface roughness of about 25 μm, pressed together at an average pressure of 10 MPa. The first layer is a stainless steel plate with a thickness of 5 mm and a thermal conductivity of 14 W/m·K. The second layer is an aluminum plate with a thickness of 15 mm and a thermal conductivity of 237 W/m·K. On the stainless steel side of the wall, the surface is subjected to a heat flux of 800 W/m². On the aluminum side of the wall, the surface experiences convection heat transfer at an ambient temperature of 20°C, where the convection coefficient is 12 W/m²·K. Determine the surface temperature of the stainless steel plate.

3–55   An aluminum plate 25 mm thick ($k = 235$ W/m·K) is attached to a copper plate with thickness of 10 mm. The copper plate is heated electrically to dissipate a uniform heat flux of 5300 W/m². The upper surface of the aluminum plate is exposed to convection heat transfer in a condition such that the convection heat transfer coefficient is 67 W/m²·K and the surrounding room temperature is 20°C. Other surfaces of the two attached plates are insulated such that heat only dissipates through the upper surface of the aluminum plate. If the surface of the copper plate that is attached to the aluminum plate has a temperature of 100°C, determine the thermal contact conductance of the aluminum/copper interface.
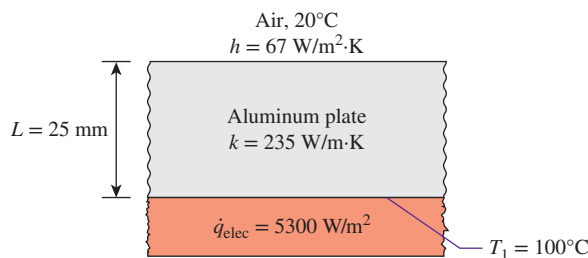
FIGURE P3–55

3–56   An aluminum plate and a stainless steel plate are pressed against each other at an average pressure of 20 MPa. Both plates have a surface roughness of 2 μm. Determine the impact on the temperature drop at the interface if the surface roughness of the plates is increased tenfold.

3–57   A thin electronic component with a surface area of 950 cm² is cooled by having a heat sink attached on its top surface. The thermal contact conductance of the interface between the electronic component and the heat sink is 2000 W/m²·K.

According to the manufacturer, the heat sink has combined convection and radiation thermal resistance of 0.3 K/W. If the electronic component dissipates 45 W of heat through the heat sink in a surrounding temperature of 30°C, determine the temperature of the electronic component. Does the contact resistance at the interface of the electronic component and the heat sink play a significant role in the heat dissipation?

3–58   Consider an engine cover that is made with two layers of metal plates. The inner layer is stainless steel ($k_1 = 14$ W/m·K) with a thickness of 10 mm, and the outer layer is aluminum ($k_2 = 237$ W/m·K) with a thickness of 5 mm. Both metal plates have a surface roughness of about 23 μm. The aluminum plate is attached on the stainless steel plate by screws that exert an average pressure of 20 MPa at the interface. The inside stainless steel surface of the cover is exposed to heat from the engine with a convection heat transfer coefficient of 10 W/m²·K at an ambient temperature of 150°C. The outside aluminum surface is exposed to a convection heat transfer coefficient of 25 W/m²·K at an ambient temperature of 40°C. Determine the heat flux through the engine cover.

3–59   Inconel® refers to a class of nickel-chromium-based superalloys that are used in high-temperature applications, such as gas turbine blades. For further improvement in the performance of gas turbine engines, the outer blade surface is coated with ceramic-based thermal barrier coating (TBC). A flat Inconel® plate with a thickness of 12 mm is coated with a layer of TBC with a thickness of 300 μm on its surface. At the interface between the Inconel® and the TBC, the thermal contact conductance is 3500 W/m²·K. The thermal conductivities of the Inconel® and the TBC are 25 W/m·K and 1.5 W/m·K, respectively. The plate is in a surrounding of hot combustion gasses at 1500°C, and the convection heat transfer coefficient is 750 W/m²·K. Determine the temperature at the mid-plane of the Inconel® plate if the outer surface temperature is 1200°C.

3–60   ⌗⌗⌗ A composite wall is made of stainless steel ($k = 13$ W/m·K, 30 mm thick), copper–silicon ($k = 36$ W/m·K, 30 mm thick), and nonmetal ($k = 0.1$ W/m·K, 15 mm thick) plates. The copper–silicon plate is sandwiched between the stainless steel plate at the bottom and the nonmetal plate at the top. A series of ASTM B21 naval brass bolts are bolted to the nonmetal plate, and the upper surface of the plate is exposed to convection heat transfer with air at 20°C and $h = 20$ W/m²·K. At the bottom surface, the stainless steel plate is subjected to a uniform heat flux of 2000 W/m². Thermal contact resistances exist at the plate interfaces. The thermal contact conductance between the stainless steel and copper–silicon plates is 20,000 W/m²·K; and the thermal contact conductance between the copper–silicon and nonmetal plates is 10,000 W/m²·K. The ASME Code for Process Piping (ASME B31.3-2014, Table A-2M) limits the maximum use temperature for the ASTM B21 bolts to 149°C. Determine the total thermal resistance of the

wall for an area of 1 m², between T_1 and T_∞. Would the ASTM B21 bolts in the nonmetal plate comply with the ASME code?
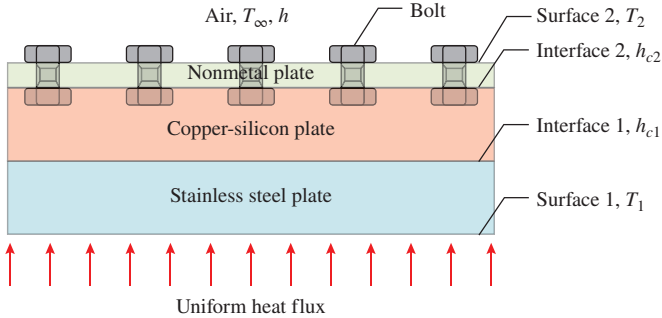
FIGURE P3–60

3–61 [C&S] A nonmetal plate ($k = 3$ W/m·K) is attached on an ASTM A240 904L stainless steel plate ($k = 13$ W/m·K). The nonmetal plate and the stainless steel plate have thicknesses of 10 mm and 30 mm, respectively. The nonmetal plate is bolted to the stainless steel plate with a series of ASTM B211 6061 aluminum alloy bolts. The upper surface of the nonmetal plate is exposed to convection heat transfer with air at 20°C and $h = 50$ W/m²·K. The bottom surface of the stainless steel plate is exposed to convection with steam at 260°C and $h = 500$ W/m²·K. The thermal contact conductance between the stainless steel and nonmetal plates is 10,000 W/m²·K. According to the ASME Code for Process Piping (ASME B31.3-2014, Table A-2M), the maximum use temperature for the B211 6061 bolts is 204°C, while the maximum use temperature for the ASTM A240 904L plate is 260°C (ASME B31.3-2014, Table A-1M). Would the use of the ASTM A240 904L plate and ASTM B211 6061 bolts be in compliance with the ASME Code for Process Piping?
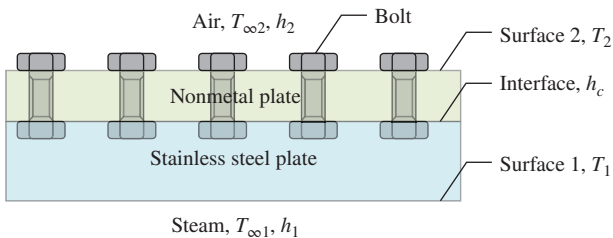
FIGURE P3–61

Generalized Thermal Resistance Networks

3–62C What are the two approaches used in the development of the thermal resistance network for two-dimensional problems?

3–63C The thermal resistance networks can also be used approximately for multidimensional problems. For what kind of multidimensional problems will the thermal resistance approach give adequate results?

3–64C When plotting the thermal resistance network associated with a heat transfer problem, explain when two resistances are in series and when they are in parallel.

3–65 A 10-cm-thick wall is to be constructed with 2.5-m-long wood studs ($k = 0.11$ W/m·K) that have a cross section of 10 cm × 10 cm. At some point the builder ran out of those studs and started using pairs of 2.5-m-long wood studs that have a cross section of 5 cm × 10 cm nailed to each other instead. The manganese steel nails ($k = 50$ W/m·K) are 10 cm long and have a diameter of 0.4 cm. A total of 50 nails are used to connect the two studs, which are mounted to the wall such that the nails cross the wall. The temperature difference between the inner and outer surfaces of the wall is 8°C. Assuming the thermal contact resistance between the two layers to be negligible, determine the rate of heat transfer (*a*) through a solid stud and (*b*) through a stud pair of equal length and width nailed to each other. (*c*) Also determine the effective conductivity of the nailed stud pair.

3–66E Consider a 10-in × 12-in epoxy glass laminate ($k = 0.10$ Btu/h·ft·°F) whose thickness is 0.05 in. In order to reduce the thermal resistance across its thickness, cylindrical copper fillings ($k = 223$ Btu/h·ft·°F) of 0.02 in diameter are to be planted throughout the board, with a center-to-center distance of 0.06 in. Determine the new value of the thermal resistance of the epoxy board for heat conduction across its thickness as a result of this modification. *Answer: 0.000256 h·°F/Btu*
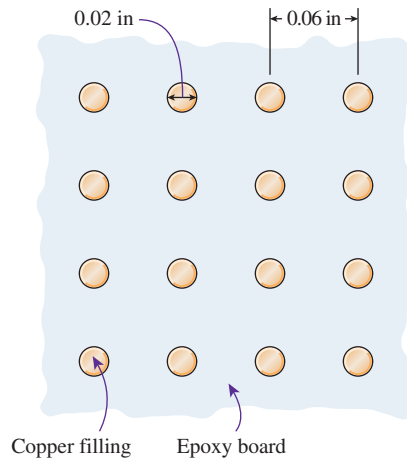
FIGURE P3–66E

3–67 Clothing made of several thin layers of fabric with trapped air in between, often called ski clothing, is commonly used in cold climates because it is light, fashionable, and a very effective thermal insulator. So it is no surprise that such clothing has largely replaced thick and heavy old-fashioned coats.

Consider a jacket made of five layers of 0.15-mm-thick synthetic fabric ($k = 0.13$ W/m·K) with 1.5-mm-thick air-space ($k = 0.026$ W/m·K) between the layers. Assuming the inner surface temperature of the jacket to be 25°C and the surface area to be 1.25 m^2, determine the rate of heat loss through the jacket when the temperature of the outdoors is 0°C and the heat transfer coefficient at the outer surface is 25 W/m^2·K.

What would your response be if the jacket is made of a single layer of 0.75-mm-thick synthetic fabric? What should be the thickness of a wool fabric ($k = 0.035$ W/m·K) if the person is to achieve the same level of thermal comfort wearing a thick wool coat instead of a five-layer ski jacket?

3–68 A 5-m-wide, 4-m-high, and 40-m-long kiln used to cure concrete pipes is made of 20-cm-thick concrete walls and ceiling ($k = 0.9$ W/m·K). The kiln is maintained at 40°C by injecting hot steam into it. The two ends of the kiln, 4 m × 5 m in size, are made of a 3-mm-thick sheet metal covered with 2-cm-thick Styrofoam ($k = 0.033$ W/m·K). The convection heat transfer coefficients on the inner and the outer surfaces of the kiln are 3000 W/m^2·K and 25 W/m^2·K, respectively. Disregarding any heat loss through the floor, determine the rate of heat loss from the kiln when the ambient air is at −4°C.
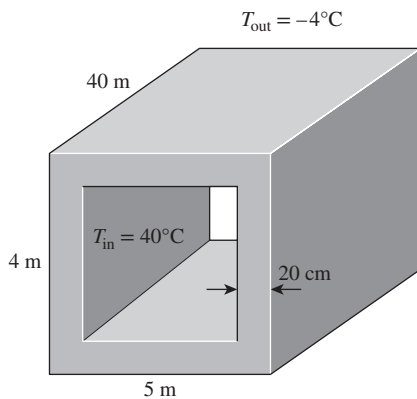
FIGURE P3–68

3–69 Reconsider Prob. 3–68. Using appropriate software, investigate the effects of the thickness of the wall and the convection heat transfer coefficient on the outer surface on the rate of heat loss from the kiln. Let the thickness vary from 10 cm to 30 cm and the convection heat transfer coefficient from 5 W/m^2·K to 50 W/m^2·K. Plot the rate of heat transfer as functions of wall thickness and the convection heat transfer coefficient, and discuss the results.

3–70 A typical section of a building wall is shown in Fig. P3–70. This section extends in and out of the page and is repeated in the vertical direction. The wall support members are made of steel ($k = 50$ W/m·K). The support members are 8 cm(t_{23}) × 0.5 cm(L_B). The remainder of the inner wall space

is filled with insulation ($k = 0.03$ W/m·K) and measures 8 cm (t_{23}) × 60 cm (L_B). The inner wall is made of gypsum board ($k = 0.5$ W/m·K) that is 1 cm thick (t_{12}) and the outer wall is made of brick ($k = 1.0$ W/m·K) that is 10 cm thick (t_{34}). What is the average heat flux through this wall when $T_1 = 20$°C and $T_4 = 35$°C?
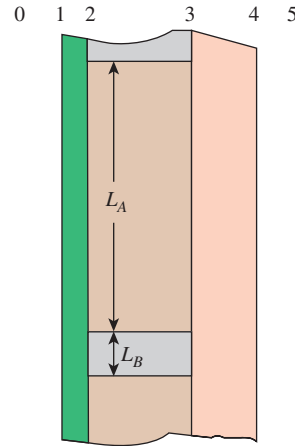
FIGURE P3–70

3–71 A 4-m-high and 6-m-wide wall consists of a long 15-cm × 25-cm cross section of horizontal bricks ($k = 0.72$ W/m·K) separated by 3-cm-thick plaster layers ($k = 0.22$ W/m·K). There are also 2-cm-thick plaster layers on each side of the wall, and a 2-cm-thick rigid foam ($k = 0.026$ W/m·K) on the inner side of the wall. The indoor and the outdoor temperatures are 22°C and −4°C, and the convection heat transfer coefficients on the inner and the outer sides are $h_1 = 10$ W/m^2·K and $h_2 = 20$ W/m^2·K, respectively. Assuming one-dimensional heat transfer and disregarding radiation, determine the rate of heat transfer through the wall.
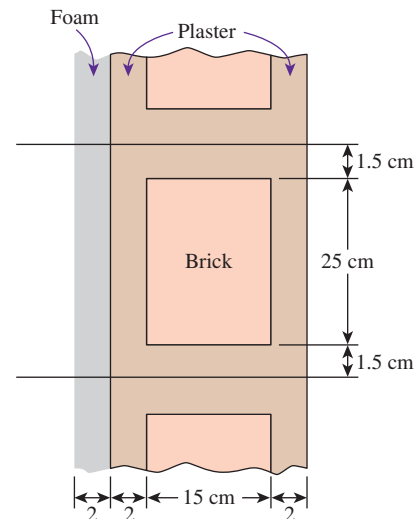
FIGURE P3–71

3–72 Reconsider Prob. 3–71. Using appropriate software, plot the rate of heat transfer through the wall as a function of the thickness of the rigid foam in the range of 1 cm to 10 cm. Discuss the results.

3–73 A 12-m-long and 5-m-high wall is constructed of two layers of 1-cm-thick sheetrock ($k = 0.17$ W/m·K) spaced 16 cm by wood studs ($k = 0.11$ W/m·K) whose cross section is 16 cm × 5 cm. The studs are placed vertically 60 cm apart, and the space between them is filled with fiberglass insulation ($k = 0.034$ W/m·K). The house is maintained at 20°C and the ambient temperature outside is −9°C. Taking the heat transfer coefficients at the inner and outer surfaces of the house to be 8.3 and 34 W/m²·K, respectively, determine (a) the thermal resistance of the wall considering a representative section of it and (b) the rate of heat transfer through the wall.

3–74E A 10-in-thick, 30-ft-long, and 10-ft-high wall is to be constructed using 9-in-long solid bricks ($k = 0.40$ Btu/h·ft·°F) of cross section 7 in × 7 in, or identical-size bricks with nine square air holes ($k = 0.015$ Btu/h·ft·°F) that are 9 in long and have a cross section of 1.5 in × 1.5 in. There is a 0.5-in-thick plaster layer ($k = 0.10$ Btu/h·ft·°F) between two adjacent bricks on all four sides and on both sides of the wall. The house is maintained at 80°F and the ambient temperature outside is 35°F. Taking the heat transfer coefficients at the inner and outer surfaces of the wall to be 1.5 and 6 Btu/h·ft²·°F, respectively, determine the rate of heat transfer through the wall constructed of (a) solid bricks and (b) bricks with air holes.
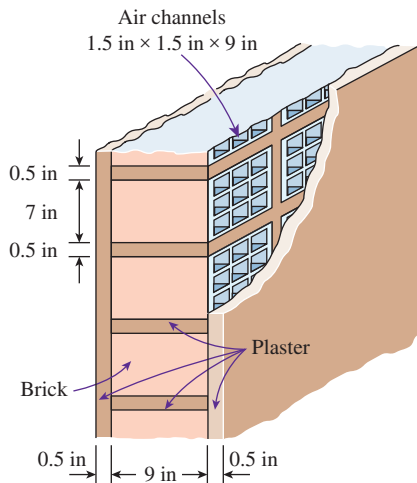
FIGURE P3−74E

3–75 Consider a 5-m-high, 8-m-long, and 0.22-m-thick wall whose representative cross section is as given in the figure. The thermal conductivities of various materials used, in W/m·K, are $k_A = k_F = 2$, $k_B = 8$, $k_C = 20$, $k_D = 15$, and $k_E = 35$. The left and right surfaces of the wall are maintained at uniform temperatures of 300°C and 100°C, respectively. Assuming heat transfer through the wall to be one-dimensional, determine

(a) the rate of heat transfer through the wall; (b) the temperature at the point where the sections B, D, and E meet; and (c) the temperature drop across the section F. Disregard any contact resistances at the interfaces.
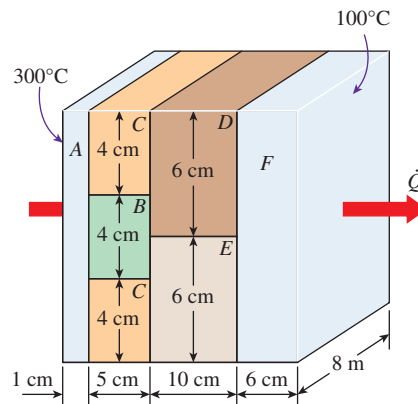
FIGURE P3−75

3–76 In an experiment to measure convection heat transfer coefficients, a very thin metal foil of very low emissivity (e.g., highly polished copper) is attached on the surface of a slab of material with very low thermal conductivity. The other surface of the metal foil is exposed to convection heat transfer by flowing fluid over the foil surface. This setup diminishes heat conduction through the slab and radiation on the metal foil surface, while heat convection plays the prominent role. The slab to which the metal foil is attached has a thickness of 25 mm and a thermal conductivity of 0.023 W/m·K. In a condition where the surrounding room temperature is 20°C, the metal foil is heated electrically with a uniform heat flux of 5000 W/m². If the bottom surface of the slab is 20°C and the metal foil has an emissivity of 0.02, determine (a) the convection heat transfer coefficient if air is flowing over the metal foil and the surface temperature of the foil is 150°C; and (b) the convection heat transfer coefficient if water is flowing over the metal foil and the surface temperature of the foil is 30°C.
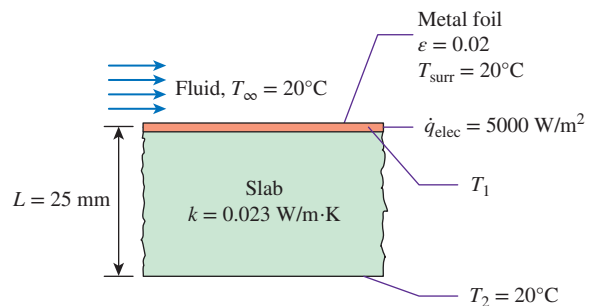
FIGURE P3−76

3–77 C&S A stainless steel plate ($k = 13$ W/m·K, 1 cm thick) is attached on an ASME SB-96 copper–silicon plate ($k = 36$ W/m·K, 3 cm thick) to form a plane wall. The bottom surface of the ASME SB-96 plate (surface 1) is subjected to a uniform heat flux of 750 W/m². The top surface of the stainless steel plate (surface 2) is exposed to convection heat transfer with air, at $T_\infty = 20°C$ and $h = 5$ W/m²·K, and thermal radiation with the surroundings at $T_{surr} = 20°C$. The stainless steel surface has an emissivity of 0.3. The thermal contact conductance at the interface of stainless steel and copper–silicon plates is 5000 W/m²·K. The ASME Boiler and Pressure Vessel Code (ASME BPVC.IV-2015, HF-300) limits equipment constructed with ASME SB-96 plate to be operated at a temperature not exceeding 93°C. Determine the total thermal resistance of the wall for an area of 1 m², between T_1 and T_∞. Would the use of the ASME SB-96 plate under these conditions be in compliance with the ASME Boiler and Pressure Vessel Code?
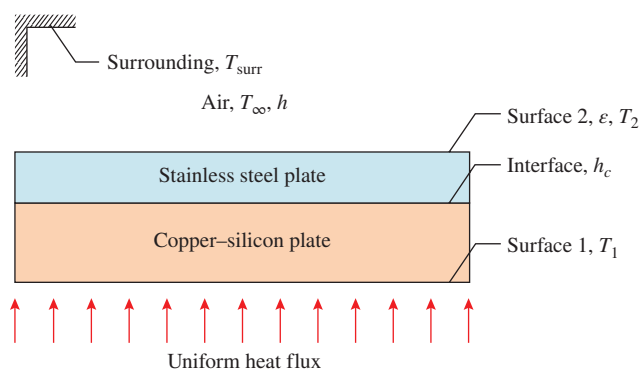
FIGURE P3–77

Heat Conduction in Cylinders and Spheres

3–78C What is an infinitely long cylinder? When is it proper to treat an actual cylinder as being infinitely long, and when is it not?

3–79C Can the thermal resistance concept be used for a solid cylinder or sphere in steady operation? Explain.

3–80C Consider a short cylinder whose top and bottom surfaces are insulated. The cylinder is initially at a uniform temperature T_i and is subjected to convection from its side surface to a medium at temperature T_∞, with a heat transfer coefficient of h. Is the heat transfer in this short cylinder one- or two-dimensional? Explain.

3–81 Steam at 280°C flows in a stainless steel pipe ($k = 15$ W/m·K) whose inner and outer diameters are 5 cm and 5.5 cm, respectively. The pipe is covered with 3-cm-thick glass wool insulation ($k = 0.038$ W/m·K). Heat is lost to the surroundings at 5°C by natural convection and radiation, with a combined natural convection and radiation heat transfer

coefficient of 22 W/m²·K. Taking the heat transfer coefficient inside the pipe to be 80 W/m²·K, determine the rate of heat loss from the steam per unit length of the pipe. Also determine the temperature drops across the pipe shell and the insulation.

3–82 Reconsider Prob. 3–81. Using appropriate software, investigate the effect of the thickness of the insulation on the rate of heat loss from the steam and the temperature drop across the insulation layer. Let the insulation thickness vary from 1 cm to 10 cm. Plot the rate of heat loss and the temperature drop as a function of insulation thickness, and discuss the results.

3–83 A 50-m-long section of a steam pipe whose outer diameter is 10 cm passes through an open space at 15°C. The average temperature of the outer surface of the pipe is measured to be 150°C. If the combined heat transfer coefficient on the outer surface of the pipe is 20 W/m²·K, determine (a) the rate of heat loss from the steam pipe; (b) the annual cost of this energy lost if steam is generated in a natural gas furnace that has an efficiency of 75 percent and the price of natural gas is $0.52/therm (1 therm = 105,500 kJ); and (c) the thickness of fiberglass insulation ($k = 0.035$ W/m·K) needed in order to save 90 percent of the heat lost. Assume the pipe temperature remains constant at 150°C.
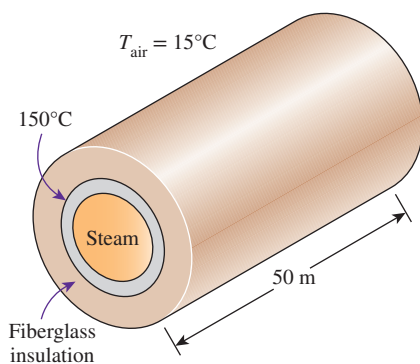
FIGURE P3–83

3–84 Superheated steam at an average temperature 200°C is transported through a steel pipe ($k = 50$ W/m·K, $D_o = 8.0$ cm, $D_i = 6.0$ cm, and $L = 20.0$ m). The pipe is insulated with a 4-cm-thick layer of gypsum plaster ($k = 0.5$ W/m·K). The insulated pipe is placed horizontally inside a warehouse where the average air temperature is 10°C. The steam and the air heat transfer coefficients are estimated to be 800 and 200 W/m²·K, respectively. Calculate (a) the daily rate of heat transfer from the superheated steam, and (b) the temperature on the outside surface of the gypsum plaster insulation.

3–85 C&S Hot liquid is flowing in a steel pipe with an inner diameter of $D_1 = 22$ mm and an outer diameter of $D_2 = 27$ mm. The inner surface of the pipe is coated with a thin fluorinated ethylene propylene (FEP) lining. The thermal conductivity of the pipe wall is 15 W/m·K. The pipe outer surface is

subjected to a uniform flux of 1200 W/m² for a length of 1 m. The hot liquid flowing inside the pipe has a mean temperature of 180°C and a convection heat transfer coefficient of 50 W/m²·K. The interface between the FEP lining and the steel surface has a thermal contact conductance of 1500 W/m²·K. Determine the temperatures at the lining and at the pipe outer surface for the pipe length subjected to the uniform heat flux. What is the total thermal resistance between the two temperatures? The ASME Code for Process Piping (ASME B31.3-2014, A323) recommends a maximum temperature for FEP lining to be 204°C. Does the FEP lining comply with the recommendation of the code?

3–86 C&S Hot water flows in a 1-m-long section of a pipe that is made of acrylonitrile butadiene styrene (ABS) thermoplastic. The ABS pipe section has an inner diameter of $D_1 = 22$ mm and an outer diameter of $D_2 = 27$ mm. The thermal conductivity of the ABS pipe wall is 0.1 W/m·K. The outer pipe surface is exposed to convection heat transfer with air at 20°C and $h = 10$ W/m²·K. The water flowing inside the pipe has a convection heat transfer coefficient of 50 W/m²·K. According to the ASME Code for Process Piping (ASME B31.3-2014, Table B-1), the maximum recommended temperature for ABS pipe is 80°C. Determine the maximum temperature of the water flowing in the pipe, such that the ABS pipe is operating at the recommended temperature or lower. What is the temperature at the outer pipe surface when the water is at maximum temperature?

3–87E Steam exiting the turbine of a steam power plant at 100°F is to be condensed in a large condenser by cooling water flowing through copper pipes ($k = 223$ Btu/h·ft·°F) of inner diameter 0.4 in and outer diameter 0.6 in at an average temperature of 70°F. The heat of vaporization of water at 100°F is 1037 Btu/lbm. The heat transfer coefficients are 2400 Btu/h·ft²·F° on the steam side and 35 Btu/h·ft²·F° on the water side. Determine the length of the tube required to condense steam at a rate of 250 lbm/h. *Answer:* 2380 ft

Steam, 100°F
250 lbm/h

Cooling water

Liquid water
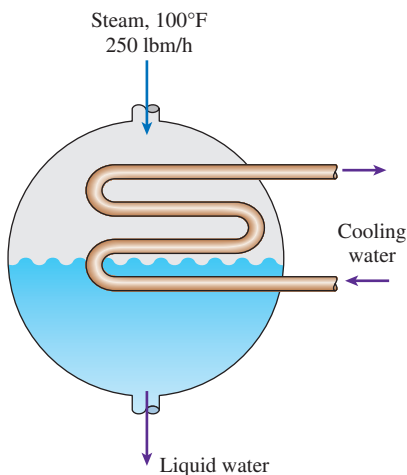
FIGURE P3–87E

3–88E Repeat Prob. 3–87E, assuming that a 0.01-in-thick layer of mineral deposit ($k = 0.5$ Btu/h·ft·°F) has formed on the inner surface of the pipe.

3–89E Reconsider Prob. 3–87E. Using appropriate software, investigate the effects of the thermal conductivity of the pipe material and the outer diameter of the pipe on the length of the tube required. Let the thermal conductivity vary from 10 Btu/h·ft·°F to 400 Btu/h·ft·°F and the outer diameter from 0.5 in to 1.0 in. Plot the length of the tube as functions of pipe conductivity and the outer pipe diameter, and discuss the results.

3–90 A 2.2-mm-diameter and 14-m-long electric wire is tightly wrapped with a 1-mm-thick plastic cover whose thermal conductivity is $k = 0.15$ W/m·K. Electrical measurements indicate that a current of 13 A passes through the wire, and there is a voltage drop of 8 V along the wire. If the insulated wire is exposed to a medium at $T_\infty = 30°C$ with a heat transfer coefficient of $h = 24$ W/m²·K, determine the temperature at the interface of the wire and the plastic cover in steady operation. Also determine if doubling the thickness of the plastic cover will increase or decrease this interface temperature.

Electrical wire $T_\infty = 30°C$
Insulation
14 m
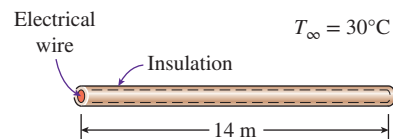
FIGURE P3–90

3–91 Consider a 1.5-m-high electric hot-water heater that has a diameter of 40 cm and maintains the hot water at 60°C. The tank is located in a small room whose average temperature is 27°C, and the heat transfer coefficients on the inner and outer surfaces of the heater are 50 and 12 W/m²·K, respectively. The tank is placed in another 46-cm-diameter sheet metal tank of negligible thickness, and the space between the two tanks is filled with foam insulation ($k = 0.03$ W/m·K). The thermal resistances of the water tank and the outer thin sheet metal shell are very small and can be neglected. The price of electricity is $0.08/kWh, and the homeowner pays $280 a year for water heating. Determine the fraction of the hot-water energy cost of this household that is due to the heat loss from the tank.

Hot-water tank insulation kits consisting of 3-cm-thick fiberglass insulation ($k = 0.035$ W/m·K) large enough to wrap the entire tank are available in the market for about $30. If such an insulation is installed on this water tank by the homeowner himself, how long will it take for this additional insulation to pay for itself? *Answers:* 15.2 percent, 21 months
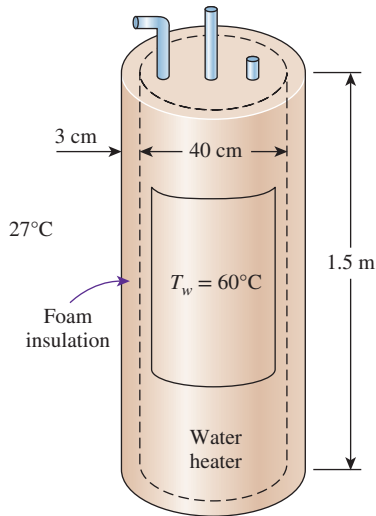
FIGURE P3–91

3–92 Chilled water enters a thin-shelled 4-cm-diameter, 200-m-long pipe at 7°C at a rate of 0.98 kg/s and leaves at 8°C. The pipe is exposed to ambient air at 30°C with a heat transfer coefficient of 9 W/m²·K. If the pipe is to be insulated with glass wool insulation ($k = 0.05$ W/m·K) in order to decrease the temperature rise of water to 0.25°C, determine the required thickness of the insulation.

3–93E Steam at 450°F is flowing through a steel pipe ($k = 8.7$ Btu/h·ft·°F) whose inner and outer diameters are 3.5 in and 4.0 in, respectively, in an environment at 55°F. The pipe is insulated with 2-in-thick fiberglass insulation ($k = 0.020$ Btu/h·ft·°F). If the heat transfer coefficients on the inside and the outside of the pipe are 30 and 5 Btu/h·ft²·°F, respectively, determine the rate of heat loss from the steam per foot length of the pipe. What is the error involved in neglecting the thermal resistance of the steel pipe in calculations?

3–94 Hot water at an average temperature of 90°C is flowing through a 15-m section of a cast iron pipe ($k = 52$ W/m·K) whose inner and outer diameters are 4 cm and 4.6 cm, respectively. The outer surface of the pipe, whose emissivity is 0.7, is exposed to the cold air at 10°C in the basement, with a heat transfer coefficient of 15 W/m²·K. The heat transfer coefficient at the inner surface of the pipe is 120 W/m²·K. Taking the walls of the basement to be at 10°C also, determine the rate of heat loss from the hot water. Also, determine the average velocity of the water in the pipe if the temperature of the water drops by 3°C as it passes through the basement.

3–95 **C&S** Liquid flows in a metal pipe with an inner diameter of $D_1 = 22$ mm and an outer diameter of $D_2 = 32$ mm. The thermal conductivity of the pipe wall is 12 W/m·K. The inner surface of the pipe is coated with a thin polyvinylidene chloride (PVDC) lining. Along a length of 1 m,

the pipe outer surface is exposed to convection heat transfer with hot gas, at $T_\infty = 100$°C and $h = 5$ W/m²·K, and thermal radiation with a surrounding at $T_{surr} = 100$°C. The emissivity at the pipe outer surface is 0.3. The liquid flowing inside the pipe has a convection heat transfer coefficient of 50 W/m²·K. If the outer surface of the pipe is at 85°C, determine the temperature at the PVDC lining and the temperature of the liquid. The ASME Code for Process Piping (ASME B31.3-2014, A323) recommends a maximum temperature for PVDC lining to be 79°C. Does the PVDC lining comply with the recommendation of the code?

3–96 In a pharmaceutical plant, a copper pipe ($k_c = 400$ W/m·K) with inner diameter of 20 mm and wall thickness of 2.5 mm is used for carrying liquid oxygen to a storage tank. The liquid oxygen flowing in the pipe has an average temperature of −200°C and a convection heat transfer coefficient of 120 W/m²·K. The condition surrounding the pipe has an ambient air temperature of 20°C and a combined heat transfer coefficient of 20 W/m²·K. If the dew point is 10°C, determine the thickness of the insulation ($k_i = 0.05$ W/m·K) around the copper pipe to avoid condensation on the outer surface. Assume thermal contact resistance is negligible.
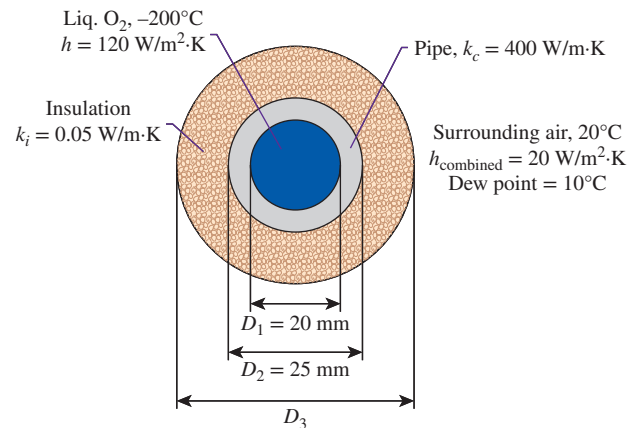
FIGURE P3–96

3–97 [laptop icon] Liquid hydrogen is flowing through an insulated pipe ($k = 23$ W/m·K, $D_i = 3$ cm, $D_o = 4$ cm, and $L = 20$ m). The pipe is situated in a chemical plant, where the average air temperature is 40°C. The convection heat transfer coefficients of the liquid hydrogen and the ambient air are 200 W/m²·K and 50 W/m²·K, respectively. If the outer surface temperature of the insulated pipe is 5°C, determine the thickness of the pipe insulation ($k = 0.6$ W/m·K) in order to keep the liquid hydrogen flowing at an average temperature of −300°C.

3–98 **PtD** [laptop icon] Exposure to high concentrations of gaseous ammonia can cause lung damage. To prevent gaseous ammonia from leaking out, ammonia is transported in

its liquid state through a pipe ($k = 25$ W/m·K, $D_i = 2.5$ cm, $D_o = 4$ cm, and $L = 10$ m). Since liquid ammonia has a normal boiling point of $-33.3°C$, the pipe needs to be properly insulated to prevent the surrounding heat from causing the ammonia to boil. The pipe is situated in a laboratory, where the average ambient air temperature is $20°C$. The convection heat transfer coefficients of the liquid ammonia and the ambient air are 100 W/m²·K and 20 W/m²·K, respectively. Determine the insulation thickness for the pipe using a material with $k = 0.75$ W/m·K to keep the liquid ammonia flowing at an average temperature of $-35°C$, while maintaining the insulated pipe outer surface temperature at $10°C$.

3–99 **PtD** A mixture of chemicals is flowing in a pipe ($k = 14$ W/m·K, $D_i = 2.5$ cm, $D_o = 3$ cm, and $L = 10$ m). During the transport, the mixture undergoes an exothermic reaction having an average temperature of $135°C$ and a convection heat transfer coefficient of 150 W/m²·K. To prevent any incident of thermal burn, the pipe needs to be insulated. However, due to the vicinity of the pipe, there is only enough room to fit a 2.5-cm-thick layer of insulation over the pipe. The pipe is situated in a plant where the average ambient air temperature is $20°C$ and the convection heat transfer coefficient is 25 W/m²·K. Determine the insulation for the pipe such that the thermal conductivity of the insulation is sufficient to maintain the outside surface temperature at $45°C$ or lower.

3–100 **PtD** Ice slurry is being transported in a pipe ($k = 15$ W/m·K, $D_i = 2.5$ cm, $D_o = 3$ cm, and $L = 5$ m) with an inner surface temperature of $0°C$. The ambient condition surrounding the pipe has a temperature of $20°C$, a convection heat transfer coefficient of 10 W/m²·K, and a dew point of $10°C$. If the outer surface temperature of the pipe drops below the dew point, condensation can occur on the surface. Since this pipe is located in a vicinity of high-voltage devices, water droplets from the condensation can create an electrical hazard. To prevent an electrical accident, the pipe surface needs to be insulated. Determine the insulation thickness for the pipe using a material with $k = 0.95$ W/m·K to prevent the outer surface temperature from dropping below the dew point.

3–101 An 8-m-internal-diameter spherical tank made of 1.5-cm-thick stainless steel ($k = 15$ W/m·K) is used to store iced water at $0°C$. The tank is located in a room whose temperature is $25°C$. The walls of the room are also at $25°C$. The outer surface of the tank is black (emissivity $\varepsilon = 1$), and heat transfer between the outer surface of the tank and the surroundings is by natural convection and radiation. The convection heat transfer coefficients at the inner and the outer surfaces of the tank are 80 W/m²·K and 10 W/m²·K, respectively. Determine (*a*) the rate of heat transfer to the iced water in the tank and (*b*) the amount of ice at $0°C$ that melts during a 24-h period. The heat of fusion of water at atmospheric pressure is $h_{if} = 333.7$ kJ/kg.

$T_{room} = 25°C$

Iced water

$D_i = 8$ m

1.5 cm

$T_{in} = 0°C$
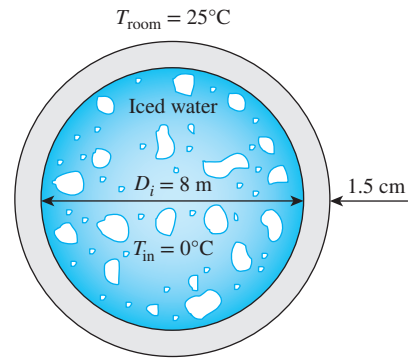
FIGURE P3–101

3–102 The boiling temperature of nitrogen at atmospheric pressure at sea level (1 atm pressure) is $-196°C$. Therefore, nitrogen is commonly used in low-temperature scientific studies since the temperature of liquid nitrogen in a tank open to the atmosphere will remain constant at $-196°C$ until it is depleted. Any heat transfer to the tank will result in the evaporation of some liquid nitrogen, which has a heat of vaporization of 198 kJ/kg and a density of 810 kg/m³ at 1 atm.

Consider a 3-m-diameter spherical tank that is initially filled with liquid nitrogen at 1 atm and $-196°C$. The tank is exposed to ambient air at $15°C$, with a combined convection and radiation heat transfer coefficient of 35 W/m²·K. The temperature of the thin-shelled spherical tank is observed to be almost the same as the temperature of the nitrogen inside. Determine the rate of evaporation of the liquid nitrogen in the tank as a result of the heat transfer from the ambient air if the tank is (*a*) not insulated, (*b*) insulated with 5-cm-thick fiberglass insulation ($k = 0.035$ W/m·K), and (*c*) insulated with 2-cm-thick superinsulation which has an effective thermal conductivity of 0.00005 W/m·K.

N₂ vapor

$T_{air} = 15°C$

1 atm
Liquid N₂
$-196°C$
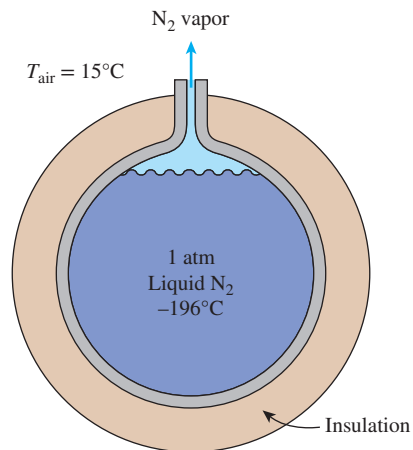
Insulation

FIGURE P3–102

3–103 Repeat Prob. 3–102 for liquid oxygen, which has a boiling temperature of −183°C, a heat of vaporization of 213 kJ/kg, and a density of 1140 kg/m³ at 1 atm pressure.

Critical Radius of Insulation

3–104C What is the critical radius of insulation? How is it defined for a cylindrical layer?

3–105C Consider an insulated pipe exposed to the atmosphere. Will the critical radius of insulation be greater on calm days or on windy days? Why?

3–106C A pipe is insulated to reduce the heat loss from it. However, measurements indicate that the rate of heat loss has increased instead of decreasing. Can the measurements be right?

3–107C Consider a pipe at a constant temperature whose radius is greater than the critical radius of insulation. Someone claims that the rate of heat loss from the pipe has increased when some insulation is added to the pipe. Is this claim valid?

3–108C A pipe is insulated such that the outer radius of the insulation is less than the critical radius. Now the insulation is taken off. Will the rate of heat transfer from the pipe increase or decrease for the same pipe surface temperature?

3–109E A 0.083-in-diameter electrical wire at 90°F is covered by 0.02-in-thick plastic insulation ($k = 0.075$ Btu/h·ft·°F). The wire is exposed to a medium at 50°F, with a combined convection and radiation heat transfer coefficient of 2.5 Btu/h·ft²·°F. Determine if the plastic insulation on the wire will increase or decrease heat transfer from the wire.   *Answer:* It helps

3–110E Repeat Prob. 3–109E, assuming a thermal contact resistance of 0.01 h·ft²·°F/Btu at the interface of the wire and the insulation.

3–111 A 4-mm-diameter spherical ball at 50°C is covered by a 1-mm-thick plastic insulation ($k = 0.13$ W/m·K). The ball is exposed to a medium at 15°C, with a combined convection and radiation heat transfer coefficient of 20 W/m²·K. Determine if the plastic insulation on the ball will help or hurt heat transfer from the ball.

Plastic insulation

4 mm   1 mm
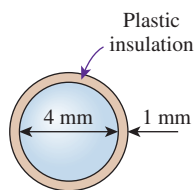
FIGURE P3–111

3–112 Reconsider Prob. 3–111. Using appropriate software, plot the rate of heat transfer from the ball as a function of the plastic insulation thickness in the range of 0.5 mm to 20 mm. Discuss the results.

Heat Transfer from Finned Surfaces

3–113C Hot air is to be cooled as it is forced to flow through the tubes exposed to atmospheric air. Fins are to be added in order to enhance heat transfer. Would you recommend attaching the fins inside or outside the tubes? Why? When would you recommend attaching fins both inside and outside the tubes?

3–114C What is the reason for the widespread use of fins on surfaces?

3–115C What is the difference between the fin effectiveness and the fin efficiency?

3–116C The fins attached to a surface are determined to have an effectiveness of 0.9. Do you think the rate of heat transfer from the surface has increased or decreased as a result of the addition of these fins?

3–117C Explain how the fins enhance heat transfer from a surface. Also, explain how the addition of fins may actually decrease heat transfer from a surface.

3–118C How does the overall effectiveness of a finned surface differ from the effectiveness of a single fin?

3–119C Hot water is to be cooled as it flows through the tubes exposed to atmospheric air. Fins are to be attached in order to enhance heat transfer. Would you recommend attaching the fins inside or outside the tubes? Why?

3–120C Consider two finned surfaces that are identical except that the fins on the first surface are formed by casting or extrusion, whereas they are attached to the second surface afterwards by welding or tight fitting. For which case do you think the fins will provide greater enhancement in heat transfer? Explain.

3–121C The heat transfer surface area of a fin is equal to the sum of all surfaces of the fin exposed to the surrounding medium, including the surface area of the fin tip. Under what conditions can we neglect heat transfer from the fin tip?

3–122C Does the (*a*) efficiency and (*b*) effectiveness of a fin increase or decrease as the fin length is increased?

3–123C Two pin fins are identical, except that the diameter of one of them is twice the diameter of the other. For which fin is the (*a*) fin effectiveness and (*b*) fin efficiency higher? Explain.

3–124C Two plate fins of constant rectangular cross section are identical, except that the thickness of one of them is twice the thickness of the other. For which fin is the (*a*) fin effectiveness and (*b*) fin efficiency higher? Explain.

3–125C Two finned surfaces are identical, except that the convection heat transfer coefficient of one of them is twice that of the other. For which finned surface is the (*a*) fin effectiveness and (*b*) fin efficiency higher? Explain.

3–126 Obtain a relation for the fin efficiency for a fin of constant cross-sectional area A_c, perimeter p, length L, and

thermal conductivity k exposed to convection to a medium at T_∞ with a heat transfer coefficient h. Assume the fins are sufficiently long so that the temperature of the fin at the tip is nearly T_∞. Take the temperature of the fin at the base to be T_b and neglect heat transfer from the fin tips. Simplify the relation for (*a*) a circular fin of diameter D and (*b*) rectangular fins of thickness t.

3–127 A 4-mm-diameter and 10-cm-long aluminum fin ($k = 237$ W/m·K) is attached to a surface. If the heat transfer coefficient is 12 W/m²·K, determine the percent error in the rate of heat transfer from the fin when the infinitely long fin assumption is used instead of the adiabatic fin tip assumption.
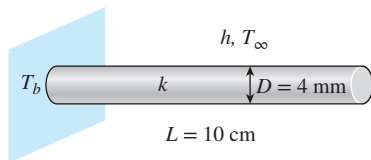
FIGURE P3–127

3–128 Consider a very long rectangular fin attached to a flat surface such that the temperature at the end of the fin is essentially that of the surrounding air, i.e., 20°C. Its width is 5.0 cm; thickness is 1.0 mm; thermal conductivity is 200 W/m·K; and base temperature is 40°C. The heat transfer coefficient is 20 W/m²·K. Estimate the fin temperature at a distance of 5.0 cm from the base and the rate of heat loss from the entire fin.

3–129 Consider a very long, slender rod. One end of the rod is attached to a base surface maintained at T_b, while the surface of the rod is exposed to an air temperature of 400°C. Thermocouples imbedded in the rod at locations 25 and 120 mm from the base surface register temperatures of 325°C and 375°C, respectively. (*a*) Calculate the rod base temperature (°C). (*b*) Determine the rod length (mm) for the case where the ratio of the heat transfer from a finite length fin to the heat transfer from a very long fin under the same conditions is 99 percent.
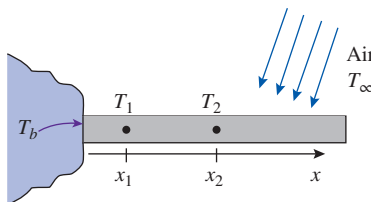
FIGURE P3–129

3–130 Two very long, slender rods of the same diameter and length are given. One rod (Rod 1) is made of aluminum and has a thermal conductivity $k_1 = 200$ W/m·K, but the thermal conductivity of Rod 2, k_2, is not known. To determine the thermal conductivity of Rod 2, both rods at one end are thermally attached to a metal surface which is maintained at a constant

temperature T_b. Both rods are losing heat by convection, with a convection heat transfer coefficient h into the ambient air at T_∞. The surface temperature of each rod is measured at various distances from the hot base surface. The measurements reveal that the temperature of the aluminum rod (Rod 1) at $x_1 = 40$ cm from the base is the same as that of the rod of unknown thermal conductivity (Rod 2) at $x_2 = 20$ cm from the base. Determine the thermal conductivity k_2 of the second rod (W/m·K).
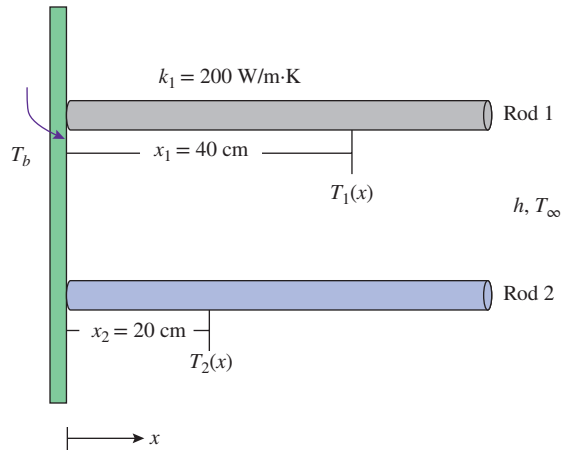
FIGURE P3–130

3–131 A turbine blade made of a metal alloy ($k = 17$ W/m·K) has a length of 5.3 cm, a perimeter of 11 cm, and a cross-sectional area of 5.13 cm². The turbine blade is exposed to hot gas from the combustion chamber at 973°C with a convection heat transfer coefficient of 538 W/m²·K. The base of the turbine blade maintains a constant temperature of 450°C, and the tip is adiabatic. Determine the heat transfer rate to the turbine blade and the temperature at the tip.
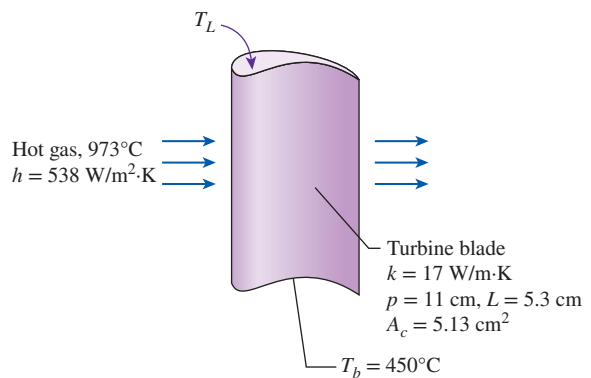
FIGURE P3–131

3–132 An ASTM B209 5154 aluminum alloy plate is connected to an insulation plate by long metal bolts 4.8 mm in diameter. The portion of the bolts exposed to convection heat transfer with air is 5 cm long. The thermal

conductivity of the bolt is known to be 15 W/m·K. The ambient condition of the air is at 20°C with a convection heat transfer coefficient of 20 W/m²·K. According to the ASME Code for Process Piping (ASME B31.3-2014, Table A-1M), the maximum use temperature for the ASTM B209 5154 aluminum alloy plate is 65°C. If the temperature of the bolt at midlength (2.5 cm from the upper surface of the aluminum plate) is 50°C, determine the temperature T_b at the upper surface of the aluminum plate. What is the rate of heat loss from each bolt to convection? Is the use of the ASTM B209 5154 plate in compliance with the ASME Code for Process Piping?
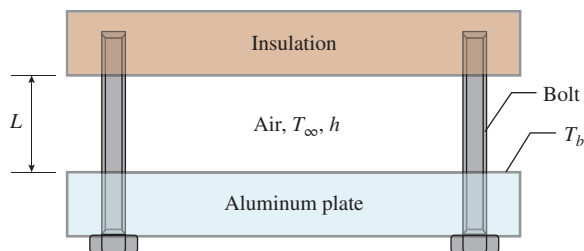
FIGURE P3−132

3–133E Consider a stainless steel spoon ($k = 8.7$ Btu/h·ft²·°F) partially immersed in boiling water at 200°F in a kitchen at 75°F. The handle of the spoon has a cross section of 0.08 in × 0.5 in and extends 7 in in the air from the free surface of the water. If the heat transfer coefficient at the exposed surfaces of the spoon handle is 3 Btu/h·ft²·°F, determine the temperature difference across the exposed surface of the spoon handle. State your assumptions.   *Answer:* 124.6°F
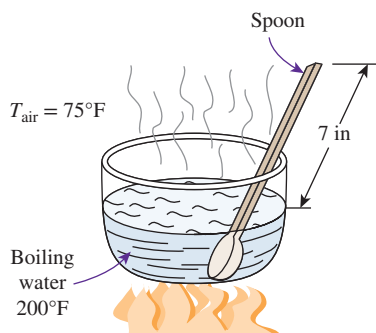
FIGURE P3−133E

3–134E Reconsider Prob. 3–133E. Using appropriate software, investigate the effects of the thermal conductivity of the spoon material and the length of its extension in the air on the temperature difference across the exposed surface of the spoon handle. Let the thermal conductivity vary from 5 Btu/h·ft²·°F to 225 Btu/h·ft²·°F and the length from 5 in to 12 in. Plot the temperature difference as the function of thermal conductivity and length, and discuss the results.

3–135 A DC motor delivers mechanical power to a rotating stainless steel shaft ($k = 15.1$ W/m·K) with a length of 25 cm and a diameter of 25 mm. In a surrounding with ambient air temperature of 20°C and convection heat transfer coefficient of 25 W/m²·K, the surface area of the motor housing that is exposed to the ambient air is 0.075 m². The motor uses 300 W of electrical power and delivers 55 percent of it as mechanical power to rotate the stainless steel shaft. If the tip of the stainless steel shaft has a temperature of 22°C, determine the surface temperature of the motor housing. Assume the base temperature of the shaft is equal to the surface temperature of the motor housing.
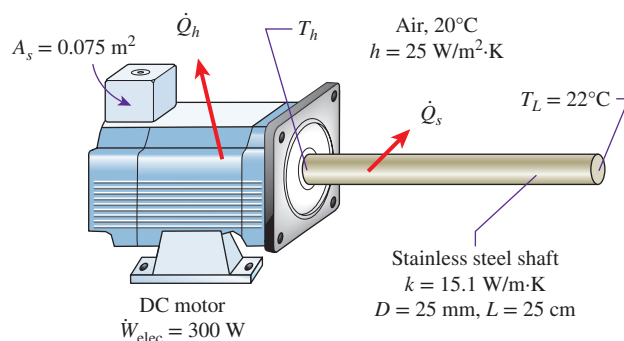
FIGURE P3−135

3–136 [C&S] A stainless steel plate is connected to a copper plate by long ASTM B98 copper–silicon bolts of 9.5 mm in diameter. The portion of the bolts exposed to convection heat transfer with air is 5 cm long. The air temperature for convection is at 20°C with a convection heat transfer coefficient of 5 W/m²·K. The thermal conductivity of the bolt is known to be 36 W/m·K. The copper plate has a uniform temperature of 70°C. If each bolt is estimated to have a rate of heat loss to convection of 5 W, determine the temperature T_b at the upper surface of the stainless steel plate. According to the ASME Code for Process Piping (ASME B31.3-2014, Table A-2M), the maximum use temperature for the ASTM B98 copper–silicon bolt is 149°C. Does the use of the ASTM B98 bolts in this condition comply with the ASME code?
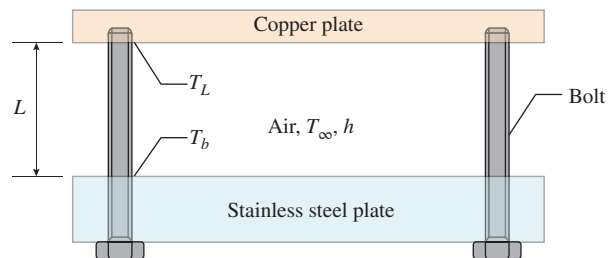
FIGURE P3−136

3–137 A plane wall with surface temperature of 350°C is attached with straight rectangular fins ($k = 235$ W/m·K). The fins are exposed to an ambient air condition of 25°C, and the convection heat transfer coefficient is 154 W/m²·K. Each fin has a length of 50 mm, a base 5 mm thick, and a width of 100 mm. Determine the efficiency, heat transfer rate, and effectiveness of each fin, using (*a*) Table 3–3 and (*b*) Figure 3–43.
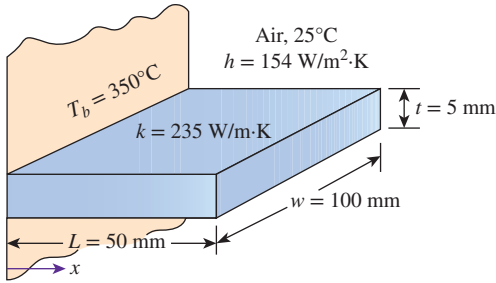
FIGURE P3–137

3–138 Two 4-m-long and 0.4-cm-thick cast iron ($k = 52$ W/m·K) steam pipes of outer diameter 10 cm are connected to each other through two 1-cm-thick flanges of outer diameter 18 cm. The steam flows inside the pipe at an average temperature of 200°C with a heat transfer coefficient of 180 W/m²·K. The outer surface of the pipe is exposed to an ambient at 12°C, with a heat transfer coefficient of 25 W/m²·K. (*a*) Disregarding the flanges, determine the average outer surface temperature of the pipe. (*b*) Using this temperature for the base of the flange and treating the flanges as the fins, determine the fin efficiency and the rate of heat transfer from the flanges. (*c*) What length of pipe is the flange section equivalent to for heat transfer purposes?
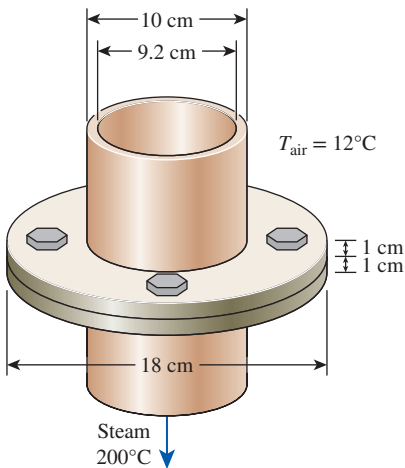
FIGURE P3–138

3–139 Pipes with inner and outer diameters of 50 mm and 60 mm, respectively, are used for transporting superheated vapor in a manufacturing plant. The pipes with thermal conductivity of

16 W/m·K are connected together by flanges with combined thickness of 20 mm and outer diameter of 90 mm. Air condition surrounding the pipes has a temperature of 25°C and a convection heat transfer coefficient of 10 W/m²·K. If the inner surface temperature of the pipe is maintained at a constant temperature of 150°C, determine the temperature at the base of the flange and the rate of heat loss through the flange.
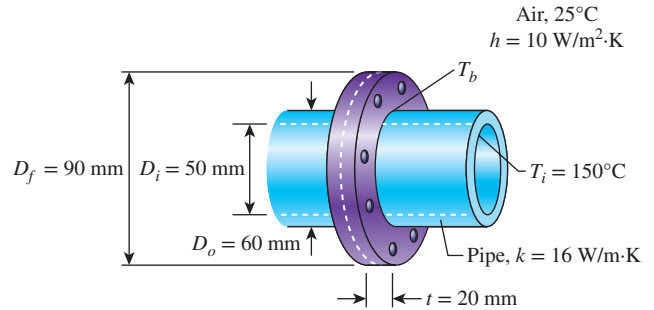
FIGURE P3–139

3–140 Steam in a heating system flows through tubes whose outer diameter is 5 cm and whose walls are maintained at a temperature of 130°C. Circular aluminum alloy 2024-T6 fins ($k = 186$ W/m·K) of outer diameter 6 cm and constant thickness 1 mm are attached to the tube. The space between the fins is 3 mm, and thus there are 250 fins per meter length of the tube. Heat is transferred to the surrounding air at $T_\infty = 25$°C, with a heat transfer coefficient of 40 W/m²·K. Determine the increase in heat transfer from the tube per meter of its length as a result of adding fins.   *Answer:* 1788 W
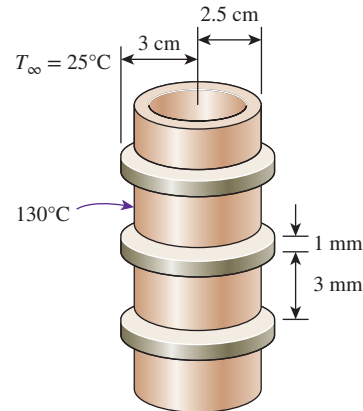
FIGURE P3–140

3–141 A 0.4-cm-thick, 12-cm-high, and 18-cm-long circuit board houses 80 closely spaced logic chips on one side, each dissipating 0.04 W. The board is impregnated with copper fillings and has an effective thermal conductivity of 30 W/m·K. All the heat generated in the chips is conducted across the circuit board and is dissipated from the back side of the board to a medium at 40°C, with a heat transfer coefficient of

52 W/m²·K. (*a*) Determine the temperatures on the two sides of the circuit board. (*b*) Now a 0.2-cm-thick, 12-cm-high, and 18-cm-long aluminum plate ($k = 237$ W/m·K) with 864 2-cm-long aluminum pin fins of diameter 0.25 cm is attached to the back side of the circuit board with a 0.02-cm-thick epoxy adhesive ($k = 1.8$ W/m·K). Determine the new temperatures on the two sides of the circuit board.

3–142 A hot surface at 100°C is to be cooled by attaching 3-cm-long, 0.25-cm-diameter aluminum pin fins ($k = 237$ W/m·K) to it, with a center-to-center distance of 0.6 cm. The temperature of the surrounding medium is 30°C, and the heat transfer coefficient on the surfaces is 35 W/m²·K. Determine the rate of heat transfer from the surface for a 1-m × 1-m section of the plate. Also determine the overall effectiveness of the fins.
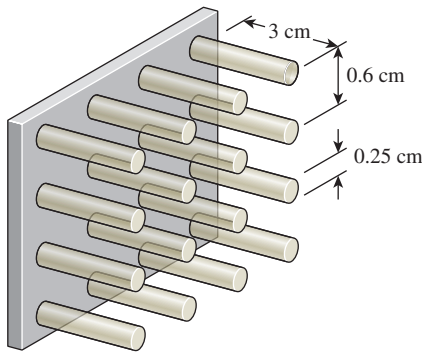
FIGURE P3–142

3–143 Reconsider Prob. 3–142. Using appropriate software, investigate the effect of the center-to-center distance of the fins on the rate of heat transfer from the surface and the overall effectiveness of the fins. Let the center-to-center distance vary from 0.4 cm to 2.0 cm. Plot the rate of heat transfer and the overall effectiveness as a function of the center-to-center distance, and discuss the results.

3–144 Circular cooling fins of diameter $D = 1$ mm and length $L = 30$ mm, made of copper ($k = 380$ W/m·K), are used to enhance heat transfer from a surface that is maintained at temperature $T_{s1} = 132°C$. Each rod has one end attached to this surface ($x = 0$), while the opposite end ($x = L$) is joined to a second surface, which is maintained at $T_{s2} = 0°C$. The air flowing between the surfaces and the rods is also at $T_\infty = 0°C$, and the convection coefficient is $h = 100$ W/m²·K.

(*a*) Express the function $\theta(x) = T(x) - T_\infty$ along a fin, and calculate the temperature at $x = L/2$.

(*b*) Determine the rate of heat transferred from the hot surface through each fin and the fin effectiveness. Is the use of fins justified? Why?

(*c*) What is the total rate of heat transfer from a 10-cm by 10-cm section of the wall, which has 625 uniformly distributed fins? Assume the same convection coefficient for the fin and for the unfinned wall surface.
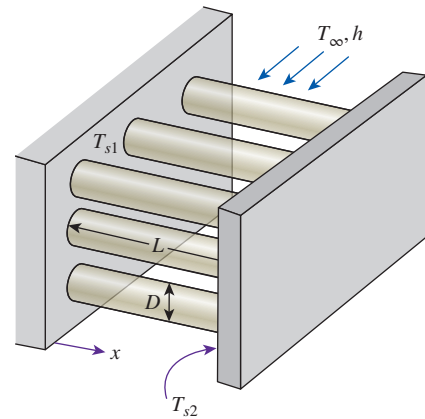
FIGURE P3–144

3–145 A 40-W power transistor is to be cooled by attaching it to one of the commercially available heat sinks shown in Table 3–6. Select a heat sink that will allow the case temperature of the transistor not to exceed 90°C in the ambient air at 20°C.
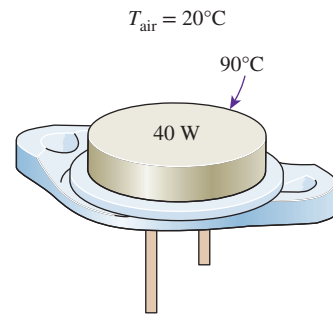
FIGURE P3–145

3–146 A 60-W power transistor is to be cooled by attaching it to one of the commercially available heat sinks shown in Table 3–6. Select a heat sink that will allow the case temperature of the transistor not to exceed 90°C in the ambient air at 30°C.

Bioheat Transfer Equation

3–147 The human body is adaptable to extreme climatic conditions and keeps the body core and skin temperatures within the comfort zone by regulating the metabolic heat generation rate. For example, in extreme cold conditions, the human body will maintain the body temperature by increasing metabolic heat generation, while in very hot conditions, the body will sweat and release heat. To understand this effect of ambient conditions on the human body, repeat Example 3–14 in the text and consider a case where climatic conditions change from −20°C and 20°C. For this change in ambient air temperature, calculate the metabolic heat generation rate required with

skin/fat thicknesses of 0.0075, 0.005, and 0.0025 m to maintain the skin temperature at 34°C. Assume that in spite of the change in ambient air temperature, the perspiration rate remains constant at 0.0005 s^{-1}. Plot a graph of metabolic heat generation rate against the ambient temperature with temperature increments of 5°C.

3–148 Consider the conditions of Example 3–14 in the text for two different environments of air and water with convective heat transfer coefficient of 2 W/m^2·K and 20 W/m^2·K, respectively. The ambient (T_∞) and surrounding temperature (T_{surr}) for both air and water may be assumed to be 15°C. What would be the metabolic heat generation rate required to maintain the skin temperature at 34°C?

3–149 Consider the conditions of Example 3–14 in the text except that the ambient air is at a temperature of 30°C. A person with skin/fat layer thickness of 0.003 m is doing vigorous exercise which raises the metabolic heat generation rate from 700 to 7000 W/m^3 over a period of time. Calculate the perspiration rate required in L/s so as to maintain the skin temperature at 34°C. Assume that perspiration properties are the same as those of liquid water at the average surface skin temperature of 35.5°C.

3–150 We are interested in steady-state heat transfer analysis from a human forearm subjected to certain environmental conditions. For this purpose, consider the forearm to be made up of muscle with thickness r_m with a skin/fat layer of thickness t_{sf} over it, as shown in Figure P3–150. For simplicity, approximate the forearm as a one-dimensional cylinder and ignore the presence of bones. The metabolic heat generation rate ($\dot{e}_m$) and perfusion rate ($\dot{p}$) are both constant throughout the muscle. The blood density and specific heat are ρ_b and c_b, respectively. The core body temperate (T_c) and the arterial blood temperature (T_a) are both assumed to be the same and constant. The muscle and the skin/fat layer thermal conductivities are k_m and k_{sf}, respectively. The skin has an emissivity of ε, and the forearm is subjected to an air environment with a temperature of T_∞, a convection heat transfer coefficient of h_{conv}, and a radiation heat transfer coefficient of h_{rad}. Assuming blood properties and thermal conductivities are all constant, (a) write the bioheat transfer equation in radial coordinates. The boundary conditions for the forearm are specified constant temperature at the outer surface of the muscle (T_i) and temperature symmetry at the centerline of the forearm. (b) Solve the differential equation and apply the boundary conditions to develop an expression for the temperature distribution in the forearm. (c) Determine the temperature at the outer surface of the muscle (T_i) and the maximum temperature in the forearm (T_{max}) for the following conditions:

$r_m = 0.05$ m, $t_{sf} = 0.003$ m, $\dot{e}_m = 700$ W/m^3, $\dot{p} = 0.0005$ 1/s,
$T_a = 37°C$, $T_\infty = T_{surr} = 24°C$, $\varepsilon = 0.95$,
$\rho_b = 1000$ kg/m^3, $c_b = 3600$ J/kg·K, $k_m = 0.5$ W/m·K,
$k_{sf} = 0.3$ W/m·K, $h_{conv} = 2$ W/m^2·K, $h_{rad} = 5.9$ W/m^2·K
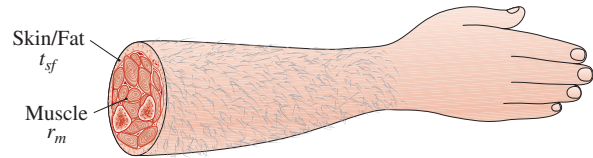
FIGURE P3–150

Heat Transfer in Common Configurations

3–151C What is a conduction shape factor? How is it related to the thermal resistance?

3–152C What is the value of conduction shape factors in engineering?

3–153 A 12-m-long and 8-cm-diameter hot-water pipe of a district heating system is buried in the soil 80 cm below the ground surface. The outer surface temperature of the pipe is 60°C. Taking the surface temperature of the earth to be 2°C and the thermal conductivity of the soil at that location to be 0.9 W/m·K, determine the rate of heat loss from the pipe.
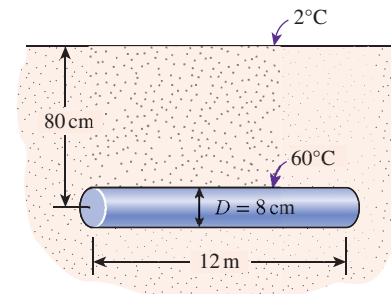
FIGURE P3–153

3–154 A thin-walled cylindrical container is placed horizontally on snow-covered ground. The container is 1.5 m long and has a diameter of 10 cm. The container contains chemicals undergoing an exothermic reaction and generating heat at 900 W/m^3. After a severe winter storm, the container is covered with approximately 30 cm of fresh snow. At the surface, the snow has a temperature of −5°C. Determine the surface temperature of the container. Discuss whether or not the snow around the container will begin to melt.

3–155 Hot water at an average temperature of 53°C and an average velocity of 0.4 m/s is flowing through a 5-m section of a thin-walled hot-water pipe that has an outer diameter of 2.5 cm. The pipe passes through the center of a 14-cm-thick wall filled with fiberglass insulation ($k = 0.035$ W/m·K). If the surfaces of the wall are at 18°C, determine (a) the rate of heat transfer from the pipe to the air in the rooms and (b) the temperature drop of the hot water as it flows through this 5-m-long section of the wall. *Answers:* 19.6 W, 0.024°C
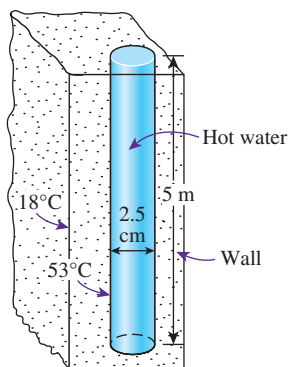
FIGURE P3–155

3–156 Hot- and cold-water pipes 12 m long run parallel to each other in a thick concrete layer. The diameters of both pipes are 6 cm, and the distance between the centerlines of the pipes is 40 cm. The surface temperatures of the hot and cold pipes are 60°C and 15°C, respectively. Taking the thermal conductivity of the concrete to be $k = 0.75$ W/m·K, determine the rate of heat transfer between the pipes. *Answer:* 492 W

3–157 Reconsider Prob. 3–156. Using appropriate software, plot the rate of heat transfer between the pipes as a function of the distance between the centerlines of the pipes in the range of 10 cm to 1.0 m. Discuss the results.

3–158E A row of 3-ft-long and 1-in-diameter used uranium fuel rods that are still radioactive are buried in the ground parallel to each other with a center-to-center distance of 8 in at a depth of 15 ft from the ground surface at a location where the thermal conductivity of the soil is 0.6 Btu/h·ft·°F. If the surface temperatures of the rods and the ground are 350°F and 60°F, respectively, determine the rate of heat transfer from the fuel rods to the atmosphere through the soil.
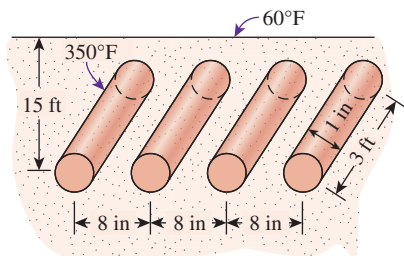
FIGURE P3–158E

3–159 Hot water at an average temperature of 80°C and an average velocity of 1.5 m/s is flowing through a 25-m section of a pipe that has an outer diameter of 5 cm. The pipe extends 2 m in the ambient air above the ground, dips into the ground ($k = 1.5$ W/m·K) vertically for 3 m, and continues horizontally at this depth for 20 m more before it enters the next building.

The first section of the pipe is exposed to the ambient air at 5°C, with a heat transfer coefficient of 22 W/m²·K. If the surface of the ground is covered with snow at −3°C, determine (*a*) the total rate of heat loss from the hot water and (*b*) the temperature drop of the hot water as it flows through this 25-m-long section of the pipe.
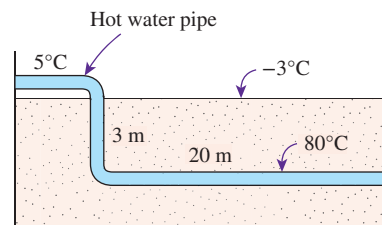
FIGURE P3–159

3–160 Hot water at an average temperature of 90°C passes through a row of eight parallel pipes that are 4 m long and have an outer diameter of 3 cm, located vertically in the middle of a concrete wall ($k = 0.75$ W/m·K) that is 4 m high, 8 m long, and 15 cm thick. If the surfaces of the concrete walls are exposed to a medium at 32°C, with a heat transfer coefficient of 12 W/m²·K, determine the rate of heat loss from the hot water and the surface temperature of the wall.

3–161 Two flow passages with different cross-sectional shapes, one circular another square, are each centered in a square solid bar of the same dimension and thermal conductivity. Both configurations have the same length, T_1, and T_2. Determine which configuration has the higher rate of heat transfer through the square solid bar for (*a*) $a = 1.2b$ and (*b*) $a = 2b$.
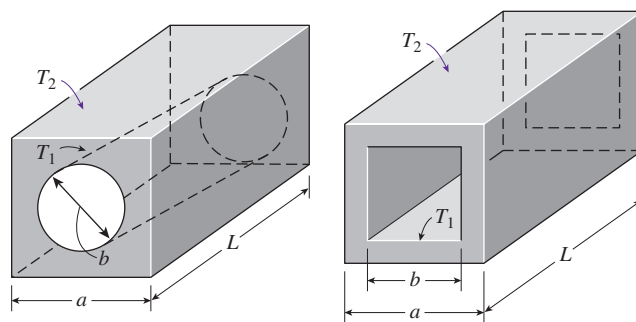
FIGURE P3–161

3–162 Consider a tube for transporting steam that is not centered properly in a cylindrical insulation material ($k = 0.73$ W/m·K). The tube diameter is $D_1 = 20$ cm and the insulation diameter is $D_2 = 40$ cm. The distance between the center of the tube and the center of the insulation is $z = 5$ mm. If the surface of the tube maintains a temperature of 100°C and the outer surface temperature of the insulation is constant at 30°C,

determine the rate of heat transfer per unit length of the tube through the insulation.
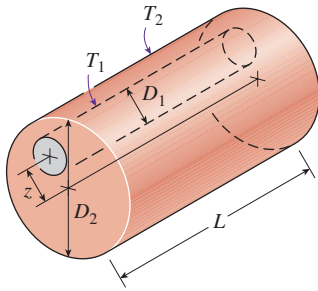
FIGURE P3–162

3–163 Consider two tubes of the same diameter ($D_1 = 20$ cm), length, and surface temperature (T_1). One tube is properly centered in a cylindrical insulation of $D_2 = 40$ cm; the other tube is placed in eccentric with the same diameter cylindrical insulation, where the distance between the center of the tube and the center of the insulation is $z = 5$ mm. If both configurations have the same outer surface temperature T_2, determine which configuration has the higher rate of heat transfer through the insulation.
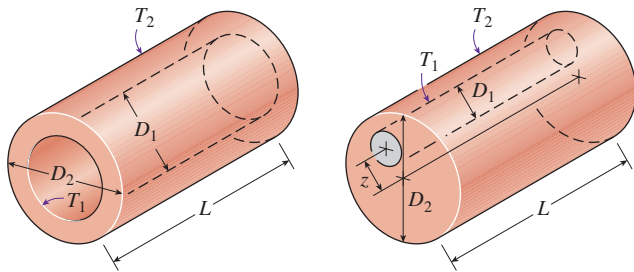
FIGURE P3–163

3–164 Consider a 25-m-long thick-walled concrete duct ($k = 0.75$ W/m·K) of square cross section. The outer dimensions of the duct are 20 cm × 20 cm, and the thickness of the duct wall is 2 cm. If the inner and outer surfaces of the duct are at 100°C and 30°C, respectively, determine the rate of heat transfer through the walls of the duct. *Answer:* 47.1 kW
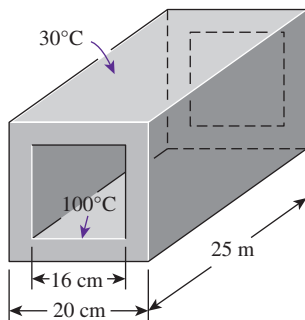
FIGURE P3–164

3–165 Consider a house with a flat roof whose outer dimensions are 12 m × 12 m. The outer walls of the house are 6 m high. The walls and the roof of the house are made of 20-cm-thick concrete ($k = 0.75$ W/m·K). The temperatures of the inner and outer surfaces of the house are 15°C and 3°C, respectively. Accounting for the effects of the edges of adjoining surfaces, determine the rate of heat loss from the house through its walls and the roof. What is the error involved in ignoring the effects of the edges and corners and treating the roof as a 12-m × 12-m surface and the walls as 6-m × 12-m surfaces for simplicity?

3–166 A 3-m-diameter spherical tank containing some radioactive material is buried in the ground ($k = 1.4$ W/m·K). The distance between the top surface of the tank and the ground surface is 4 m. If the surface temperatures of the tank and the ground are 140°C and 15°C, respectively, determine the rate of heat transfer from the tank.

3–167 Radioactive material, stored in a spherical vessel of diameter $D = 3.5$ m, is buried underground at a depth of 10 m. The radioactive material inside the vessel releases heat at a rate of 1000 W/m³. The surface temperature of the vessel is constant at 480°C, and the thermal conductivity of the ground is 2 W/m·K. When it snows in the winter, will the area directly above the spherical vessel be covered with snow?

Special Topics: Heat Transfer Through the Walls and Roofs

3–168C What is the *R*-value of a wall? How does it differ from the unit thermal resistance of the wall? How is it related to the *U*-factor?

3–169C What is effective emissivity for a plane-parallel airspace? How is it determined? How is radiation heat transfer through the airspace determined when the effective emissivity is known?

3–170C The unit thermal resistances (*R*-values) of both 40-mm and 90-mm vertical airspaces are given in Table 3–9 to be 0.22 m²·C/W, which implies that more than doubling the thickness of airspace in a wall has no effect on heat transfer through the wall. Do you think this is a typing error? Explain.

3–171C What is a radiant barrier? What kinds of materials are suitable for use as radiant barriers? Is it worthwhile to use radiant barriers in the attics of homes?

3–172C Consider a house whose attic space is ventilated effectively so that the air temperature in the attic is the same as the ambient air temperature at all times. Will the roof still have any effect on heat transfer through the ceiling? Explain.

3–173 Determine the summer *R*-value and the *U*-factor of a wood frame wall that is built around 38-mm × 140-mm wood studs with a center-to-center distance of 400 mm. The 140-mm-wide cavity between the studs is filled with mineral fiber batt insulation. The inside is finished with 13-mm gypsum wallboard and the outside with 13-mm wood fiberboard and 13-mm × 200-mm wood bevel lapped siding. The insulated cavity constitutes 80 percent of the heat transmission area, while the studs, headers, plates, and sills constitute 20 percent. *Answers:* 3.213 m²·K/W, 0.311 W/m²·K
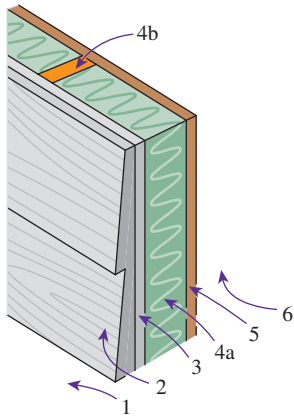
FIGURE P3–173

3–174 The 13-mm-thick wood fiberboard sheathing of the wood stud wall in Prob. 3–173 is replaced by a 25-mm-thick rigid foam insulation. Determine the percent increase in the R-value of the wall as a result.

3–175 The overall heat transfer coefficient (the U-value) of a wall under winter design conditions is $U = 2.25$ W/m²·K. Now a layer of 100-mm face brick is added to the outside, leaving a 20-mm airspace between the wall and the bricks. Determine the new U-value of the wall. Also, determine the rate of heat transfer through a 3-m-high, 7-m-long section of the wall after modification when the indoor and outdoor temperatures are 22°C and −25°C, respectively.
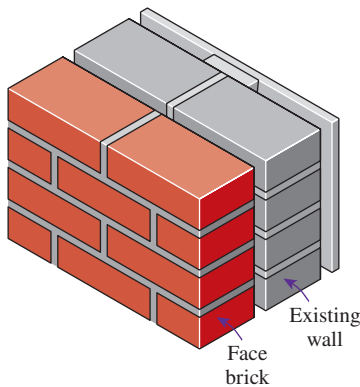
FIGURE P3–175

3–176 Consider a flat ceiling that is built around 38-mm × 90-mm wood studs with a center-to-center distance of 400 mm. The lower part of the ceiling is finished with 13-mm gypsum wallboard, while the upper part consists of a wood sub-floor ($R = 0.166$ m²·°C/W), a 13-mm plywood layer, a layer of felt ($R = 0.011$ m²·°C/W), and linoleum ($R = 0.009$ m²·°C/W). Both sides of the ceiling are exposed to still air. The airspace constitutes 82 percent of the heat transmission area, while the studs and headers constitute 18 percent. Determine the winter R-value and the U-factor of the ceiling assuming the 90-mm-wide airspace

between the studs (*a*) does not have any reflective surface, (*b*) has a reflective surface with $\varepsilon = 0.05$ on one side, and (*c*) has reflective surfaces with $\varepsilon = 0.05$ on both sides. Assume a mean temperature of 10°C and a temperature difference of 5.6°C for the airspace.
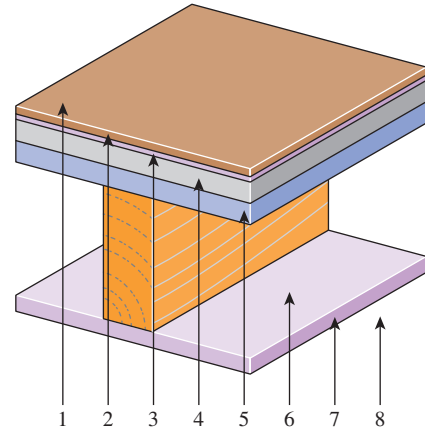
FIGURE P3–176

3–177 Determine the winter R-value and the U-factor of a masonry cavity wall that consists of 100-mm common bricks, a 90-mm airspace, 100-mm concrete blocks made of lightweight aggregate, 20-mm airspace, and 13-mm gypsum wallboard separated from the concrete block by 20-mm-thick (1-in × 3-in nominal) vertical furring whose center-to-center distance is 400 mm. Neither side of the two airspaces is coated with any reflective films. When determining the R-value of the airspaces, the temperature difference across them can be taken to be 16.7°C with a mean air temperature of 10°C. The airspace constitutes 84 percent of the heat transmission area, while the vertical furring and similar structures constitute 16 percent. *Answers:* 1.02 m²·°C/W, 0.978 W/m²·K
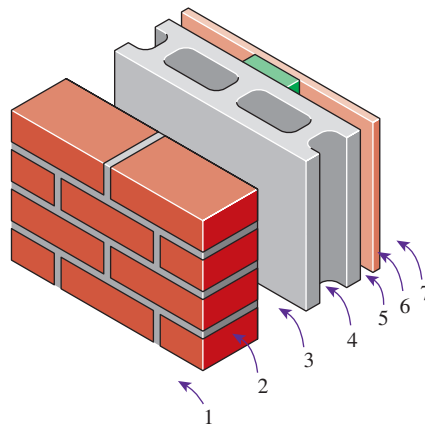
FIGURE P3–177

3–178 Repeat Prob. 3–177 assuming one side of both air-spaces is coated with a reflective film of $\varepsilon = 0.05$.

3–179 Determine the winter R-value and the U-factor of a masonry wall that consists of the following layers: 100-mm

face bricks, 100-mm common bricks, 25-mm urethane rigid foam insulation, and 13-mm gypsum wallboard. *Answers: 1.404 m²·°C/W, 0.712 W/m²·K*

3–180 The overall heat transfer coefficient (the U-value) of a wall under winter design conditions is $U = 1.40$ W/m²·K. Determine the U-value of the wall under summer design conditions.

3–181E Determine the winter R-value and the U-factor of a masonry cavity wall that is built around 4-in-thick concrete blocks made of lightweight aggregate. The outside is finished with 4-in face brick with $\frac{1}{2}$-in cement mortar between the bricks and concrete blocks. The inside finish consists of $\frac{1}{2}$-in gypsum wallboard separated from the concrete block by $\frac{3}{4}$-in-thick (1-in by 3-in nominal) vertical furring whose center-to-center distance is 16 in. Neither side of the $\frac{3}{4}$-in-thick airspace between the concrete block and the gypsum board is coated with any reflective film. When determining the R-value of the airspace, the temperature difference across it can be taken to be 30°F with a mean air temperature of 50°F. The airspace constitutes 80 percent of the heat transmission area, while the vertical furring and similar structures constitute 20 percent.
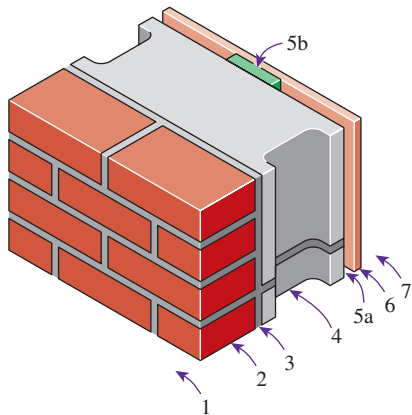
FIGURE P3–181E

3–182 Determine the summer and winter R-values, in m²·°C/W, of a masonry wall that consists of 100-mm face bricks, 13 mm of cement mortar, 100-mm lightweight concrete block, 40-mm airspace, and 20-mm plasterboard. *Answers: 0.809 and 0.795 m²·°C/W*

3–183E The overall heat transfer coefficient of a wall is determined to be $U = 0.075$ Btu/h·ft²·°F under the conditions of still air inside and winds of 7.5 mph outside. What will the U-factor be when the wind velocity outside is doubled? *Answer: 0.0755 Btu/h·ft²·°F*

3–184 Two homes are identical, except that the walls of one house consist of 200-mm lightweight concrete blocks, 20-mm airspace, and 20-mm plasterboard, while the walls of the other house involve the standard R-2.4 m²·°C/W frame wall construction. Which house do you think is more energy efficient?

3–185 Determine the R-value of a ceiling that consists of a layer of 19-mm acoustical tiles whose top surface is covered with a highly reflective aluminum foil for winter conditions. Assume still air below and above the tiles.
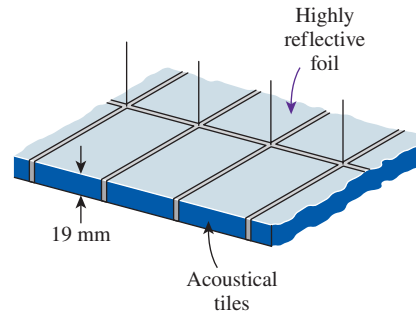
FIGURE P3–185

Review Problems

3–186 Consider two identical people each generating 60 W of metabolic heat steadily while doing sedentary work and dissipating it by convection and perspiration. The first person is wearing clothes made of 1-mm-thick leather ($k = 0.159$ W/m·K) that covers half of the body, while the second one is wearing clothes made of 1-mm-thick synthetic fabric ($k = 0.13$ W/m·K) that covers the body completely. The ambient air is at 30°C, the heat transfer coefficient at the outer surface is 15 W/m²·K, and the inner surface temperature of the clothes can be taken to be 32°C. Treating the body of each person as a 25-cm-diameter, 1.7-m-long cylinder, determine the fractions of heat lost from each person by perspiration.

3–187 Cold conditioned air at 12°C is flowing inside a 1.5-cm-thick square aluminum ($k = 237$ W/m·K) duct of inner cross section 22 cm × 22 cm at a mass flow rate of 0.8 kg/s. The duct is exposed to air at 33°C with a combined convection-radiation heat transfer coefficient of 13 W/m²·K. The convection heat transfer coefficient at the inner surface is 75 W/m²·K. If the air temperature in the duct should not increase by more than 1°C, determine the maximum length of the duct.

3–188 Hot water is flowing at an average velocity of 1.5 m/s through a cast iron pipe ($k = 52$ W/m·K) whose inner and outer diameters are 3 cm and 3.5 cm, respectively. The pipe passes through a 15-m-long section of a basement whose temperature is 15°C. If the temperature of the water drops from 70°C to 67°C as it passes through the basement and the heat transfer coefficient on the inner surface of the pipe is 400 W/m²·K, determine the combined convection and radiation heat transfer coefficient at the outer surface of the pipe. *Answer: 272.5 W/m²·K*

3–189 The plumbing system of a house involves a 0.5-m section of a plastic pipe ($k = 0.16$ W/m·K) of inner diameter 2 cm and outer diameter 2.4 cm exposed to the ambient air. During a cold and windy night, the ambient air temperature remains at about −5°C for a period of 14 h. The combined convection and radiation heat transfer coefficient on the outer surface of the

pipe is estimated to be 40 W/m²·K, and the heat of fusion of water is 333.7 kJ/kg. Assuming the pipe to contain stationary water initially at 0°C, determine if the water in that section of the pipe will completely freeze that night.
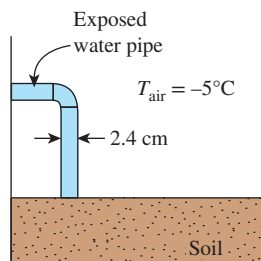
FIGURE P3–189

3–190 A cylindrical nuclear fuel rod of 15 mm in diameter is encased in a concentric hollow ceramic cylinder with inner diameter of 35 mm and outer diameter of 110 mm. This created an air gap between the fuel rod and the hollow ceramic cylinder with a convection heat transfer coefficient of 10 W/m²·K. The hollow ceramic cylinder has a thermal conductivity of 0.07 W/m·K, and its outer surface maintains a constant temperature of 30°C. If the fuel rod generates heat at a rate of 1 MW/m³, determine the temperature at the surface of the fuel rod. *Answer:* 1026°C
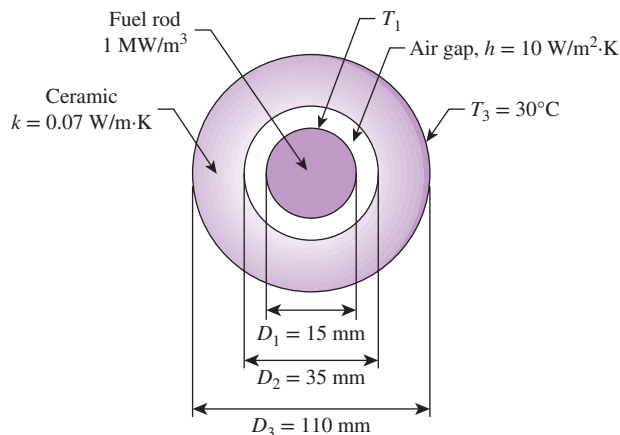
FIGURE P3–190

3–191 Steam at 260°C is flowing inside a steel pipe ($k = 61$ W/m·K) whose inner and outer diameters are 10 cm and 12 cm, respectively, in an environment at 20°C. The heat transfer coefficients inside and outside the pipe are 120 W/m²·K and 14 W/m²·K, respectively. Determine (*a*) the thickness of the insulation ($k = 0.038$ W/m·K) needed to reduce the heat loss by 95 percent and (*b*) the thickness of the insulation needed to reduce the exposed surface temperature of insulated pipe to 40°C for safety reasons.

3–192 A spherical vessel, 3.0 m in diameter (and negligible wall thickness), is used for storing a fluid at a temperature of 0°C. The vessel is covered with a 5.0-cm-thick layer of an insulation ($k = 0.20$ W/m·K). The surrounding air is at 22°C. The inside and outside heat transfer coefficients are 40 and 10 W/m²·K, respectively. Calculate (*a*) all thermal resistances, in K/W, (*b*) the steady rate of heat transfer, and (*c*) the temperature difference across the insulation layer.

3–193 One wall of a refrigerated warehouse is 10.0 m high and 5.0 m wide. The wall is made of three layers: 1.0-cm-thick aluminum ($k = 200$ W/m·K), 8.0-cm-thick fiberglass ($k = 0.038$ W/m·K), and 3.0-cm-thick gypsum board ($k = 0.48$ W/m·K). The warehouse inside and outside temperatures are -10°C and 20°C, respectively, and the average value of both inside and outside heat transfer coefficients is 40 W/m²·K.

(*a*) Calculate the rate of heat transfer across the warehouse wall in steady operation.
(*b*) Suppose that 400 metal bolts ($k = 43$ W/m·K), each 2.0 cm in diameter and 12.0 cm long, are used to fasten (i.e., hold together) the three wall layers. Calculate the rate of heat transfer for the "bolted" wall.
(*c*) What is the percent change in the rate of heat transfer across the wall due to metal bolts?

3–194 A 4-m-high and 6-m-long wall is constructed of two large 0.8-cm-thick steel plates ($k = 15$ W/m·K) separated by 1-cm-thick and 22-cm-wide steel bars placed 99 cm apart. The remaining space between the steel plates is filled with fiberglass insulation ($k = 0.035$ W/m·K). If the temperature difference between the inner and the outer surfaces of the walls is 22°C, determine the rate of heat transfer through the wall. Can we ignore the steel bars between the plates in heat transfer analysis since they occupy only 1 percent of the heat transfer surface area?
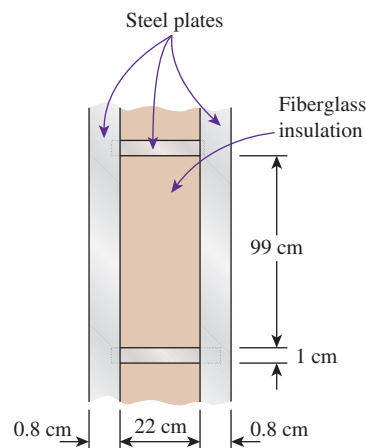
FIGURE P3–194

3–195 A typical section of a building wall is shown in Fig. P3–195. This section extends in and out of the page and is repeated in the vertical direction. The wall support members are made of steel ($k = 50$ W/m·K). The support members

are 8 cm $(t_{23}) \times 0.5$ cm (L_B). The remainder of the inner wall space is filled with insulation $(k = 0.03$ W/m·K) and measures 8 cm $(t_{23}) \times 60$ cm (L_B). The inner wall is made of gypsum board $(k = 0.5$ W/m·K) that is 1 cm thick (t_{12}), and the outer wall is made of brick $(k = 1.0$ W/m·K) that is 10 cm thick (t_{34}). What is the temperature on the interior brick surface, 3, when $T_1 = 20°$C and $T_4 = 35°$C?
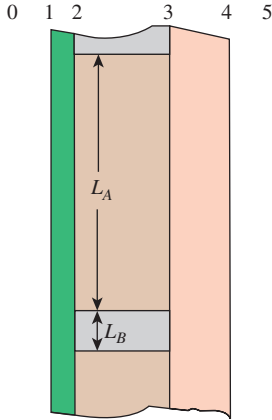
FIGURE P3–195

3–196 A 12-cm-long bar with a square cross section, as shown in Fig. P3–196, consists of a 1-cm-thick copper layer $(k = 380$ W/m·K) and a 1-cm-thick epoxy composite layer $(k = 0.4$ W/m·K). Calculate the rate of heat transfer under a thermal driving force of 50°C when the direction of steady one-dimensional heat transfer is (a) from front to back (i.e., along its length), (b) from left to right, and (c) from top to bottom.
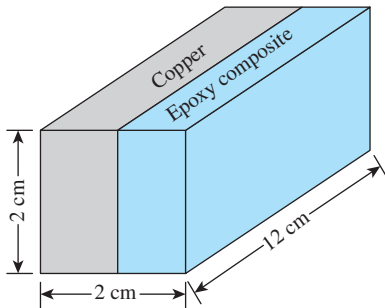
FIGURE P3–196

3–197 Circular fins of uniform cross section, with diameter of 10 mm and length of 50 mm, are attached to a wall with surface temperature of 350°C. The fins are made of material with thermal conductivity of 240 W/m·K, they are exposed to an ambient air condition of 25°C, and the convection heat transfer coefficient is 250 W/m²·K. Determine the heat transfer rate and plot the temperature variation of a single fin for the following boundary conditions:
 (a) Infinitely long fin
 (b) Adiabatic fin tip
 (c) Fin with tip temperature of 250°C
 (d) Convection from the fin tip
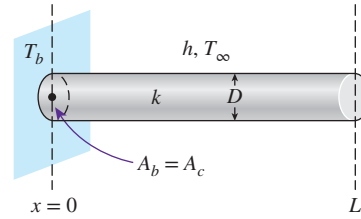
FIGURE P3–197

3–198 A total of 10 rectangular aluminum fins $(k = 203$ W/m·K) are placed on the outside flat surface of an electronic device. Each fin is 100 mm wide, 20 mm high, and 4 mm thick. The fins are located parallel to each other at a center-to-center distance of 8 mm. The temperature at the outside surface of the electronic device is 72°C. The air is at 20°C, and the heat transfer coefficient is 80 W/m²·K. Determine (a) the rate of heat loss from the electronic device to the surrounding air and (b) the fin effectiveness.

3–199 A plane wall with surface temperature of 300°C is attached with straight aluminum triangular fins $(k = 236$ W/m·K). The fins are exposed to an ambient air condition of 25°C, and the convection heat transfer coefficient is 25 W/m²·K. Each fin has a length of 55 mm, a base 4 mm thick, and a width of 110 mm. Using Table 3–3, determine the efficiency, heat transfer rate, and effectiveness of each fin.
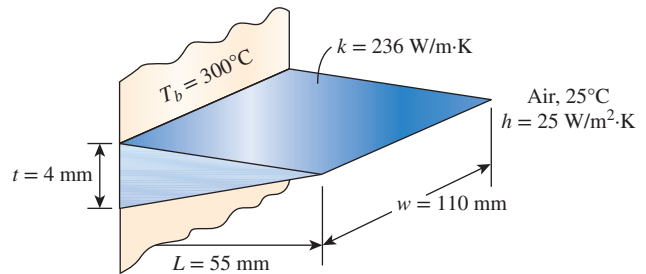
FIGURE P3–199

3–200 A plane wall surface at 200°C is to be cooled with aluminum pin fins of parabolic profile with blunt tips. Each fin has a length of 25 mm and a base diameter of 4 mm. The fins are exposed to ambient air at 25°C, and the heat transfer coefficient is 45 W/m²·K. If the thermal conductivity of the fins is 230 W/m·K, determine the heat transfer rate from a single fin and the increase in the rate of heat transfer per m² surface area as a result of attaching fins. Assume there are 100 fins per m² surface area.

3–201 Steam in a heating system flows through tubes whose outer diameter is 3 cm and whose walls are maintained at a temperature of 120°C. Circular aluminum alloy fins $(k = 180$ W/m·K) of outer diameter 6 cm and constant thickness $t = 2$ mm are attached to the tube, as shown in Fig. P3–201. The space between the fins is 3 mm, and thus there are 200 fins per meter length of the tube. Heat is transferred to the surrounding air at 25°C, with a combined heat transfer coefficient of 60 W/m²·K. Determine the increase in heat transfer from the tube per meter of its length as a result of adding fins.
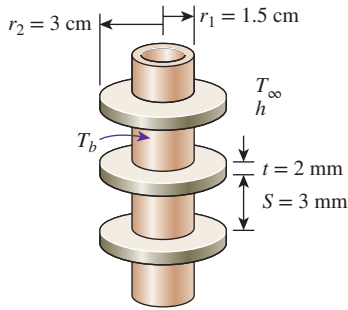
FIGURE P3–201

3–202 A 0.2-cm-thick, 10-cm-high, and 15-cm-long circuit board houses electronic components on one side that dissipate a total of 15 W of heat uniformly. The board is impregnated with conducting metal fillings and has an effective thermal conductivity of 12 W/m·K. All the heat generated in the components is conducted across the circuit board and is dissipated from the back side of the board to a medium at 37°C, with a heat transfer coefficient of 45 W/m^2·K. (*a*) Determine the surface temperatures on the two sides of the circuit board. (*b*) Now a 0.1-cm-thick, 10-cm-high, and 15-cm-long aluminum plate ($k = 237$ W/m·K) with 20 0.2-cm-thick, 2-cm-long, and 15-cm-wide aluminum fins of rectangular profile are attached to the back side of the circuit board with a 0.03-cm-thick epoxy adhesive ($k = 1.8$ W/m·K). Determine the new temperatures on the two sides of the circuit board.
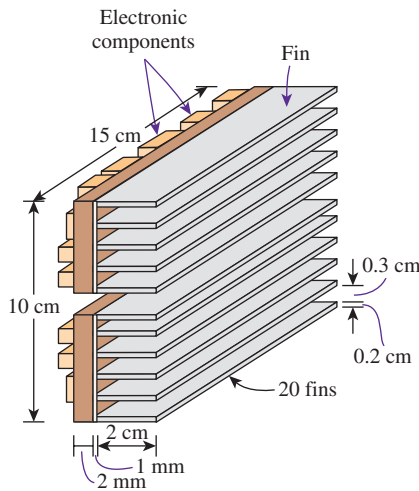
FIGURE P3–202

3–203 **PtD** In a manufacturing plant, 100-mm by 40-mm thin rectangular electronic devices are assembled in mass quantity. The top surface of the electronic device is made of aluminum and is attached with an HS 5030 aluminum heat sink positioned horizontally. The electronic device dissipates 45 W of heat through the heat sink. Both aluminum surfaces have a roughness of about 10 μm and an average interface pressure of 1 atm. To prevent the electronic device from overheating,

the top surface temperature should be kept below 85°C in an ambient surrounding of 30°C. Your task as a product engineer is to ensure that the heat sink attached on the device's top surface is able to keep the device from overheating. Determine whether or not the top surface temperature of the electronic device, with an HS 5030 heat sink attached, is higher than 85°C. If so, what action can be taken to reduce the surface temperature to below 85°C? Since your company has a vast quantity of the HS 5030 heat sinks in inventory, replacing the heat sinks with more effective ones is too costly and is not a viable solution.

3–204 A row of 10 parallel pipes that are 5 m long and have an outer diameter of 6 cm are used to transport steam at 145°C through the concrete floor ($k = 0.75$ W/m·K) of a 10-m × 5-m room that is maintained at 24°C. The combined convection and radiation heat transfer coefficient at the floor is 12 W/m^2·K. If the surface temperature of the concrete floor is not to exceed 38°C, determine how deep the steam pipes should be buried below the surface of the concrete floor.
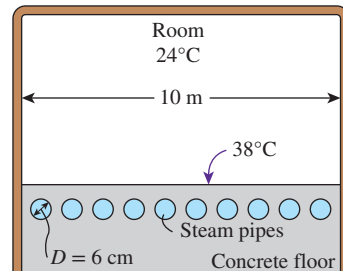
FIGURE P3–204

3–205 A 0.6-m-diameter, 1.9-m-long cylindrical tank containing liquefied natural gas (LNG) at −160°C is placed at the center of a 1.9-m-long 1.4-m × 1.4-m square solid bar made of an insulating material with $k = 0.0002$ W/m·K. If the outer surface temperature of the bar is 12°C, determine the rate of heat transfer to the tank. Also, determine the LNG temperature after one month. Take the density and the specific heat of LNG to be 425 kg/m^3 and 3.475 kJ/kg·°C, respectively.

3–206 In a combined heat and power (CHP) generation process, by-product heat is used for domestic or industrial heating
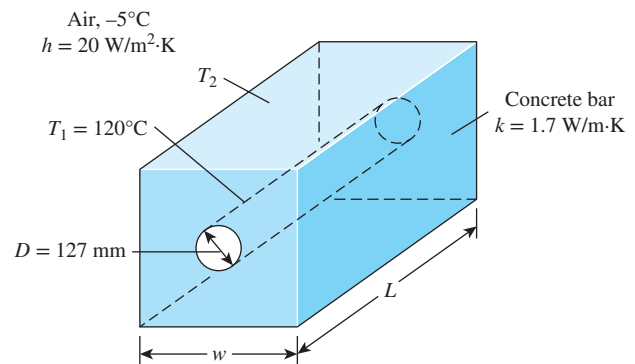
FIGURE P3–206

purposes. Hot steam is carried from a CHP generation plant by a tube with diameter of 127 mm centered at a square cross-section solid bar made of concrete with thermal conductivity of 1.7 W/m·K. The surface temperature of the tube is constant at 120°C, while the square concrete bar is exposed to air with temperature of −5°C and convection heat transfer coefficient of 20 W/m²·K. If the temperature difference between the outer surface of the square concrete bar and the ambient air is to be maintained at 5°C, determine the width of the square concrete bar and the rate of heat loss per meter length. *Answers:* 1.32 m, 530 W/m

3–207 A 2.2-m-diameter spherical steel tank filled with iced water at 0°C is buried underground at a location where the thermal conductivity of the soil is $k = 0.55$ W/m·K. The distance between the tank center and the ground surface is 2.4 m. For a ground surface temperature of 18°C, determine the rate of heat transfer to the iced water in the tank. What would your answer be if the soil temperature were 18°C and the ground surface were insulated?

3–208 A thin-walled spherical tank is buried in the ground at a depth of 3 m. The tank has a diameter of 1.5 m, and it contains chemicals undergoing exothermic reaction that provides a uniform heat flux of 1 kW/m² to the tank's inner surface. From soil analysis, the ground has a thermal conductivity of 1.3 W/m·K and a temperature of 10°C. Determine the surface temperature of the tank. Discuss the effect of the ground depth on the surface temperature of the tank.

Fundamentals of Engineering (FE) Exam Problems

3–209 Heat is lost at a rate of 275 W per m² area of a 15-cm-thick wall with a thermal conductivity of $k = 1.1$ W/m·K. The temperature drop across the wall is

(*a*) 37.5°C (*b*) 27.5°C (*c*) 16.0°C
(*d*) 8.0°C (*e*) 4.0°C

3–210 Consider a wall that consists of two layers, *A* and *B,* with the following values: $k_A = 1.2$ W/m·K, $L_A = 8$ cm, $k_B = 0.2$ W/m·K, $L_B = 5$ cm. If the temperature drop across the wall is 18°C, the rate of heat transfer through the wall per unit area of the wall is

(*a*) 56.8 W/m² (*b*) 72.1 W/m² (*c*) 114 W/m²
(*d*) 201 W/m² (*e*) 270 W/m²

3–211 Heat is generated steadily in a 3-cm-diameter spherical ball. The ball is exposed to ambient air at 26°C with a heat transfer coefficient of 7.5 W/m²·K. The ball is to be covered with a material of thermal conductivity 0.15 W/m·K. The thickness of the covering material that will maximize heat generation within the ball while keeping ball surface temperature constant is

(*a*) 0.5 cm (*b*) 1.0 cm (*c*) 1.5 cm (*d*) 2.0 cm (*e*) 2.5 cm

3–212 Consider a 1.5-m-high and 2-m-wide triple pane window. The thickness of each glass layer ($k = 0.80$ W/m·K) is 0.5 cm, and the thickness of each airspace ($k = 0.025$ W/m·K) is 1.2 cm. If the inner and outer surface temperatures of the

window are 10°C and 0°C, respectively, the rate of heat loss through the window is

(*a*) 3.4 W (*b*) 10.2 W (*c*) 30.7 W (*d*) 61.7 W (*e*) 86.8 W

3–213 Consider two metal plates pressed against each other. Other things being equal, which of the measures below will cause the thermal contact resistance to increase?

(*a*) Cleaning the surfaces to make them shinier.
(*b*) Pressing the plates against each other with a greater force.
(*c*) Filling the gap with a conducting fluid.
(*d*) Using softer metals.
(*e*) Coating the contact surfaces with a thin layer of soft metal such as tin.

3–214 A 10-m-long, 8-cm-outer-radius cylindrical steam pipe is covered with 3-cm-thick cylindrical insulation with a thermal conductivity of 0.05 W/m·K. If the rate of heat loss from the pipe is 1000 W, the temperature drop across the insulation is

(*a*) 58°C (*b*) 101°C (*c*) 143°C (*d*) 282°C (*e*) 600°C

3–215 A 5-m-diameter spherical tank is filled with liquid oxygen ($\rho = 1141$ kg/m³, $c_p = 1.71$ kJ/kg·°C) at −184°C. It is observed that the temperature of oxygen increases to −183°C in a 144-hour period. The average rate of heat transfer to the tank is

(*a*) 124 W (*b*) 185 W (*c*) 246 W (*d*) 348 W (*e*) 421 W

3–216 A 2.5-m-high, 4-m-wide, and 20-cm-thick wall of a house has a thermal resistance of 0.025°C/W. The thermal conductivity of the wall is

(*a*) 0.8 W/m·K (*b*) 1.2 W/m·K (*c*) 3.4 W/m·K
(*d*) 5.2 W/m·K (*e*) 8.0 W/m·K

3–217 Consider two walls, *A* and *B,* with the same surface areas and the same temperature drops across their thicknesses. The ratio of thermal conductivities is $k_A/k_B = 4$ and the ratio of the wall thicknesses is $L_A/L_B = 2$. The ratio of heat transfer rates through the walls $\dot{Q}_A/\dot{Q}_B$ is

(*a*) 0.5 (*b*) 1 (*c*) 2 (*d*) 4 (*e*) 8

3–218 A hot plane surface at 100°C is exposed to air at 25°C with a combined heat transfer coefficient of 20 W/m²·K. The heat loss from the surface is to be reduced by half by covering it with sufficient insulation with a thermal conductivity of 0.10 W/m·K. Assuming the heat transfer coefficient to remain constant, the required thickness of insulation is

(*a*) 0.1 cm (*b*) 0.5 cm (*c*) 1.0 cm (*d*) 2.0 cm (*e*) 5 cm

3–219 A room at 20°C air temperature is losing heat to the outdoor air at 0°C at a rate of 1000 W through a 2.5-m-high and 4-m-long wall. Now the wall is insulated with 2-cm-thick insulation with a conductivity of 0.02 W/m·K. Determine the rate of heat loss from the room through this wall after insulation. Assume the heat transfer coefficients on the inner and outer surfaces of the wall, the room air temperature, and the outdoor air temperature remain unchanged. Also, disregard radiation.

(*a*) 20 W (*b*) 561 W (*c*) 388 W (*d*) 167 W (*e*) 200 W

3–220 A 1-cm-diameter, 30-cm-long fin made of aluminum ($k = 237$ W/m·K) is attached to a surface at 80°C. The surface is exposed to ambient air at 22°C with a heat transfer coefficient of 18 W/m²·K. If the fin can be assumed to be very long, the rate of heat transfer from the fin is

(*a*) 2.0 W (*b*) 3.2 W   (*c*) 4.4 W   (*d*) 5.5 W   (*e*) 6.0 W

3–221 A 1-cm-diameter, 30-cm-long fin made of aluminum ($k = 237$ W/m·K) is attached to a surface at 80°C. The surface is exposed to ambient air at 22°C with a heat transfer coefficient of 11 W/m²·K. If the fin can be assumed to be very long, its efficiency is

(*a*) 0.60   (*b*) 0.67   (*c*) 0.72   (*d*) 0.77   (*e*) 0.88

3–222 A hot surface at 80°C in air at 20°C is to be cooled by attaching 10-cm-long and 1-cm-diameter cylindrical fins. The combined heat transfer coefficient is 30 W/m²·K, and heat transfer from the fin tip is negligible. If the fin efficiency is 0.75, the rate of heat loss from 100 fins is

(*a*) 325 W (*b*) 707 W   (*c*) 566 W   (*d*) 424 W   (*e*) 754 W

3–223 A cylindrical pin fin of diameter 0.6 cm and length of 3 cm with negligible heat loss from the tip has an efficiency of 0.7. The effectiveness of this fin is

(*a*) 0.3   (*b*) 0.7   (*c*) 2   (*d*) 8   (*e*) 14

3–224 A 3-cm-long, 2-mm × 2-mm rectangular cross-section aluminum fin ($k = 237$ W/m·K) is attached to a surface. If the fin efficiency is 65 percent, the effectiveness of this single fin is

(*a*) 39   (*b*) 30   (*c*) 24   (*d*) 18   (*e*) 7

3–225 Two finned surfaces with long fins are identical, except that the convection heat transfer coefficient for the first finned surface is twice that of the second one. Which of the following conditions is accurate for the efficiency and effectiveness of the first finned surface relative to the second one?

(*a*) Higher efficiency and higher effectiveness
(*b*) Higher efficiency but lower effectiveness
(*c*) Lower efficiency but higher effectiveness
(*d*) Lower efficiency and lower effectiveness
(*e*) Equal efficiency and equal effectiveness

3–226 A 20-cm-diameter hot sphere at 120°C is buried in the ground with a thermal conductivity of 1.2 W/m·K. The distance between the center of the sphere and the ground surface is 0.8 m, and the ground surface temperature is 15°C. The rate of heat loss from the sphere is

(*a*) 169 W (*b*) 20 W   (*c*) 217 W   (*d*) 312 W (*e*) 1.8 W

3–227 A 25-cm-diameter, 2.4-m-long vertical cylinder containing ice at 0°C is buried right under the ground. The cylinder is thin-shelled and is made of a high-thermal-conductivity material. The surface temperature and the thermal conductivity of the ground are 18°C and 0.85 W/m·K, respectively. The rate of heat transfer to the cylinder is

(*a*) 37.2 W   (*b*) 63.2 W   (*c*) 158 W
(*d*) 480 W   (*e*) 1210 W

3–228 Hot water ($c_p = 4.179$ kJ/kg·K) flows through an 80-m-long PVC ($k = 0.092$ W/m·K) pipe whose inner diameter is 2 cm and outer diameter is 2.5 cm at a rate of 1 kg/s, entering at 40°C. If the entire interior surface of this pipe is maintained at 35°C and the entire exterior surface at 20°C, the outlet temperature of water is

(*a*) 35°C   (*b*) 36°C   (*c*) 37°C   (*d*) 38°C   (*e*) 39°C

3–229 The walls of a food storage facility are made of a 2-cm-thick layer of wood ($k = 0.1$ W/m·K) in contact with a 5-cm-thick layer of polyurethane foam ($k = 0.03$ W/m·K). If the temperature of the surface of the wood is −10°C and the temperature of the surface of the polyurethane foam is 20°C, the temperature of the surface where the two layers are in contact is

(*a*) −7°C (*b*) −2°C   (*c*) 3°C   (*d*) 8°C   (*e*) 11°C

3–230 The equivalent thermal resistance for the thermal circuit shown here is
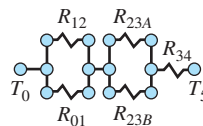
(*a*) $R_{12}R_{01} + R_{23A} + R_{23B} + R_{34}$

(*b*) $R_{12}R_{01} + \left(\dfrac{R_{23A}R_{23B}}{R_{23A} + R_{23B}} \right) + R_{34}$

(*c*) $\left(\dfrac{R_{12}R_{01}}{R_{12} + R_{01}} \right) + \left(\dfrac{R_{23A}R_{23B}}{R_{23A} + R_{23B}} \right) + \dfrac{1}{R_{34}}$

(*d*) $\left(\dfrac{R_{12}R_{01}}{R_{12} + R_{01}} \right) + \left(\dfrac{R_{23A}R_{23B}}{R_{23A} + R_{23B}} \right) + R_{34}$

(*e*) None of them

3–231 The 700 m² ceiling of a building has a thermal resistance of 0.52 m²·K/W. The rate at which heat is lost through this ceiling on a cold winter day when the ambient temperature is −10°C and the interior is at 20°C is

(*a*) 23.1 kW   (*b*) 40.4 kW   (*c*) 55.6 kW
(*d*) 68.1 kW   (*e*) 88.6 kW

3–232 A 1-m-inner-diameter liquid-oxygen storage tank at a hospital keeps the liquid oxygen at 90 K. The tank consists of a 0.5-cm-thick aluminum ($k = 170$ W/m·K) shell whose exterior is covered with a 10-cm-thick layer of insulation ($k = 0.02$ W/m·K). The insulation is exposed to the ambient air at 20°C, and the heat transfer coefficient on the exterior side of the insulation is 5 W/m²·K. The rate at which the liquid oxygen gains heat is

(*a*) 141 W (*b*) 176 W   (*c*) 181 W   (*d*) 201 W (*e*) 221 W

3–233 A 1-m-inner-diameter liquid-oxygen storage tank at a hospital keeps the liquid oxygen at 90 K. The tank consists of a 0.5-cm-thick aluminum ($k = 170$ W/m·K) shell whose exterior

is covered with a 10-cm-thick layer of insulation ($k = 0.02$ W/m·K). The insulation is exposed to the ambient air at 20°C, and the heat transfer coefficient on the exterior side of the insulation is 5 W/m^2·K. The temperature of the exterior surface of the insulation is

(a) 13°C   (b) 9°C   (c) 2°C   (d) −3°C   (e) −12°C

3–234   The fin efficiency is defined as the ratio of the actual heat transfer from the fin to

(a) The heat transfer from the same fin with an adiabatic tip
(b) The heat transfer from an equivalent fin which is infinitely long
(c) The heat transfer from the same fin if the temperature along the entire length of the fin is the same as the base temperature
(d) The heat transfer through the base area of the same fin
(e) None of the above

3–235   Computer memory chips are mounted on a finned metallic mount to protect them from overheating. A 152-MB memory chip dissipates 5 W of heat to air at 25°C. If the temperature of this chip is not to exceed 60°C, the overall heat transfer coefficient–area product of the finned metal mount must be at least

(a) 0.14 W/°C   (b) 0.20 W/°C   (c) 0.32 W/°C
(d) 0.48 W/°C   (e) 0.76 W/°C

3–236   In the United States, building insulation is specified by the R-value (thermal resistance in h·ft^2·°F/Btu units). A homeowner decides to save on the cost of heating the home by adding additional insulation in the attic. If the total R-value is increased from 15 to 25, the homeowner can expect the heat loss through the ceiling to be reduced by

(a) 25%   (b) 40%   (c) 50%   (d) 60%   (e) 75%

3–237   A triangular-shaped fin on a motorcycle engine is 0.5 cm thick at its base and 3 cm long (normal distance between the base and the tip of the triangle), and is made of aluminum ($k = 150$ W/m·K). This fin is exposed to air with a convective heat transfer coefficient of 30 W/m^2·K acting on its surfaces. The efficiency of the fin is 75 percent. If the fin base temperature is 130°C and the air temperature is 25°C, the heat transfer from this fin per unit width is

(a) 32 W/m   (b) 57 W/m   (c) 102 W/m
(d) 124 W/m   (e) 142 W/m

3–238   A plane brick wall ($k = 0.7$ W/m·K) is 10 cm thick. The thermal resistance of this wall per unit of wall area is

(a) 0.143 m^2·K/W   (b) 0.250 m^2·K/W
(c) 0.327 m^2·K/W   (d) 0.448 m^2·K/W
(e) 0.524 m^2·K/W

Design and Essay Problems

3–239   The temperature in deep space is close to absolute zero, which presents thermal challenges for the astronauts who do space walks. Propose a design for the clothing of the astronauts that will be most suitable for the thermal environment in space. Defend the selections in your design.

3–240   In the design of electronic components, it is desirable to attach the electronic circuitry to a substrate material that is a very good thermal conductor but also a very effective electrical insulator. If high cost is not a major concern, what material would you propose for the substrate?

3–241   Using cylindrical samples of the same material, devise an experiment to determine the thermal contact resistance. Cylindrical samples are available at any length, and the thermal conductivity of the material is known.

3–242   Find out about the wall construction of the cabins of large commercial airplanes, the range of ambient conditions under which they operate, typical heat transfer coefficients on the inner and outer surfaces of the wall, and the heat generation rates inside. Determine the size of the heating and air-conditioning system that will be able to maintain the cabin at 20°C at all times for an airplane capable of carrying 400 people.

3–243   Repeat Prob. 3–242 for a submarine with a crew of 60 people.

3–244   A house with 200-m^2 floor space is to be heated with geothermal water flowing through pipes laid in the ground under the floor. The walls of the house are 4 m high, and there are 10 single-paned windows in the house that are 1.2 m wide and 1.8 m high. The house has R-19 (in h·ft^2·°F/Btu) insulation in the walls and R-30 in the ceiling. The floor temperature is not to exceed 40°C. Hot geothermal water is available at 90°C, and the inner and outer diameters of the pipes to be used are 2.4 cm and 3.0 cm. Design such a heating system for this house in your area.

3–245   Using a timer (or watch) and a thermometer, conduct this experiment to determine the rate of heat gain of your refrigerator. First, make sure that the door of the refrigerator is not opened for at least a few hours to make sure that steady operating conditions are established. Start the timer when the refrigerator stops running, and measure the time Δt_1 it stays off before it kicks in. Then measure the time Δt_2 it stays on. Noting that the heat removed during Δt_2 is equal to the heat gain of the refrigerator during $\Delta t_1 + \Delta t_2$ and using the power consumed by the refrigerator when it is running, determine the average rate of heat gain for your refrigerator, in watts. Take the COP (coefficient of performance) of your refrigerator to be 1.3 if it is not available.

Now, clean the condenser coils of the refrigerator and remove any obstacles in the way of airflow through the coils. Then determine the improvement in the COP of the refrigerator.

4

TRANSIENT HEAT CONDUCTION

The temperature of a body, in general, varies with time as well as position. In rectangular coordinates, this variation is expressed as $T(x, y, z, t)$, where (x, y, z) indicate variation in the x-, y-, and z-directions, and t indicates variation with time. In the preceding chapter, we considered heat conduction under *steady* conditions, for which the temperature of a body at any point does not change with time. This certainly simplified the analysis, especially when the temperature varied in one direction only, and we were able to obtain analytical solutions. In this chapter, we consider the variation of temperature with *time* as well as *position* in one- and multidimensional systems.

We start this chapter with the analysis of *lumped systems* in which the temperature of a body varies with time but remains uniform throughout at any time. Then we consider the variation of temperature with time as well as position for one-dimensional heat conduction problems such as those associated with a large plane wall, a long cylinder, a sphere, and a semi-infinite medium using *analytical solutions.* Finally, we consider transient heat conduction in multidimensional systems by utilizing the *product solution.*

OBJECTIVES

When you finish studying this chapter, you should be able to:

- Assess when the spatial variation of temperature is negligible and temperature varies nearly uniformly with time, making the simplified lumped system analysis applicable,

- Obtain analytical solutions for transient one-dimensional conduction problems in rectangular, cylindrical, and spherical geometries using the method of separation of variables, and understand why a one-term solution is usually a reasonable approximation,

- Solve the transient conduction problem in large media using the similarity variable, and predict the variation of temperature with time and distance from the exposed surface, and

- Construct solutions for multidimensional transient conduction problems using the product solution approach.
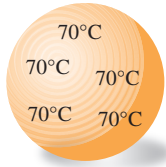
(*a*) Copper ball
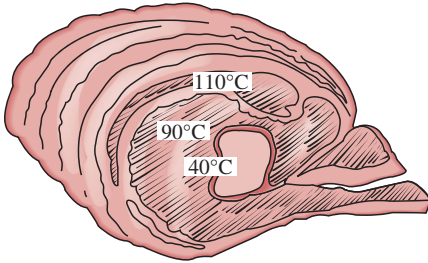
(*b*) Roast beef

FIGURE 4–1

A small copper ball can be modeled as a lumped system, but a roast beef cannot.
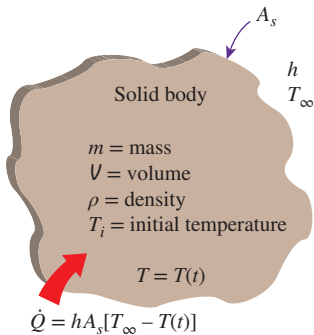
FIGURE 4–2

The geometry and parameters involved in the lumped system analysis.

4–1 ▪ LUMPED SYSTEM ANALYSIS

In heat transfer analysis, some bodies are observed to behave like a "lump" whose interior temperature remains essentially uniform at any time during a heat transfer process. The temperature of such bodies can be taken to be a function of time only, $T(t)$. Heat transfer analysis that utilizes this idealization is known as **lumped system analysis**, which provides great simplification in certain classes of heat transfer problems without much sacrifice from accuracy.

Consider a small hot copper ball coming out of an oven (Fig. 4–1). Measurements indicate that the temperature of the copper ball changes with time, but it does not change much with position at any given time. Thus the temperature of the ball remains nearly uniform at all times, and we can talk about the temperature of the ball with no reference to a specific location.

Now let us go to the other extreme and consider a large roast in an oven. If you have done any roasting, you must have noticed that the temperature distribution within the roast is not even close to being uniform. You can easily verify this by taking the roast out before it is completely done and cutting it in half. You will see that the outer parts of the roast are well done while the center part is barely warm. Thus, lumped system analysis is not applicable in this case. Before presenting a criterion about the applicability of lumped system analysis, we develop the formulation associated with it.

Consider a body of arbitrary shape of mass m, volume V, surface area A_s, density ρ, and specific heat c_p initially at a uniform temperature T_i (Fig. 4–2). At time $t = 0$, the body is placed into a medium at temperature T_∞, and heat transfer takes place between the body and its environment, with a heat transfer coefficient h. For the sake of discussion, we assume that $T_\infty > T_i$, but the analysis is equally valid for the opposite case. We assume lumped system analysis to be applicable, so that the temperature remains uniform within the body at all times and changes with time only, $T = T(t)$.

During a differential time interval dt, the temperature of the body rises by a differential amount dT. An energy balance of the solid for the time interval dt can be expressed as

$$\begin{pmatrix} \text{Heat transfer into the body} \\ \text{during } dt \end{pmatrix} = \begin{pmatrix} \text{The increase in} \\ \text{the of the body} \\ \text{energy during } dt \end{pmatrix}$$

or

$$hA_s(T_\infty - T)\,dt = mc_p\,dT \qquad (4\text{–}1)$$

Noting that $m = \rho V$ and $dT = d(T - T_\infty)$ since $T_\infty =$ constant, Eq. 4–1 can be rearranged as

$$\frac{d(T - T_\infty)}{T - T_\infty} = \frac{hA_s}{\rho V c_p}\,dt \qquad (4\text{–}2)$$

Integrating from $t = 0$, at which $T = T_i$, to any time t, at which $T = T(t)$, gives

$$\ln\frac{T(t) - T_\infty}{T_i - T_\infty} = -\frac{hA_s}{\rho V c_p}t \qquad (4\text{–}3)$$

Taking the exponential of both sides and rearranging, we obtain

$$\frac{T(t) - T_\infty}{T_i - T_\infty} = e^{-bt} \qquad \textbf{(4–4)}$$

where

$$b = \frac{hA_s}{\rho V c_p} \qquad (1/s) \qquad \textbf{(4–5)}$$

is a positive quantity whose dimension is (time)$^{-1}$. The reciprocal of b has time units (usually s) and is called the **time constant**. Equation 4–4 is plotted in Fig. 4–3 for different values of b. There are two observations that can be made from this figure and the relation above:

1. Equation 4–4 enables us to determine the temperature $T(t)$ of a body at time t, or alternatively, the time t required for the temperature to reach a specified value $T(t)$.

2. The temperature of a body approaches the ambient temperature T_∞ exponentially. The temperature of the body changes rapidly at the beginning, but rather slowly later on. A large value of b indicates that the body approaches the environment temperature in a short time. The larger the value of the exponent b, the higher the rate of decay in temperature. Note that b is proportional to the surface area but inversely proportional to the mass and the specific heat of the body. This is not surprising since it takes longer to heat or cool a larger mass, especially when it has a large specific heat.

Once the temperature $T(t)$ at time t is available from Eq. 4–4, the *rate* of convection heat transfer between the body and its environment at that time can be determined from Newton's law of cooling as

$$\dot{Q}(t) = hA_s[T(t) - T_\infty] \qquad (W) \qquad \textbf{(4–6)}$$

The *total amount* of heat transfer between the body and the surrounding medium over the time interval $t = 0$ to t is simply the change in the energy content of the body:

$$Q = mc_p[T(t) - T_i] \qquad (kJ) \qquad \textbf{(4–7)}$$

The amount of heat transfer reaches its upper limit when the body reaches the surrounding temperature T_∞. Therefore, the *maximum* heat transfer between the body and its surroundings is (Fig. 4–4)

$$Q_{max} = mc_p(T_\infty - T_i) \qquad (kJ) \qquad \textbf{(4–8)}$$

We could also obtain this equation by substituting the $T(t)$ relation from Eq. 4–4 into the $\dot{Q}(t)$ relation in Eq. 4–6 and integrating it from $t = 0$ to $t \to \infty$.

Criteria for Lumped System Analysis

The lumped system analysis certainly provides great convenience in heat transfer analysis, and naturally we would like to know when it is appropriate
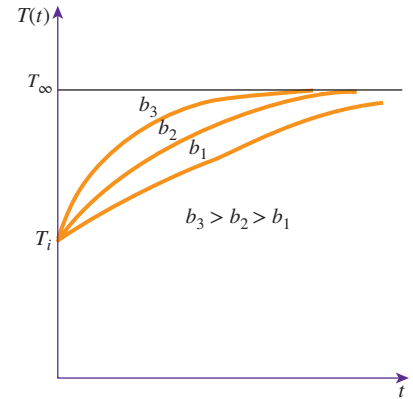
FIGURE 4–3
The temperature of a lumped system approaches the environment temperature as time gets larger.
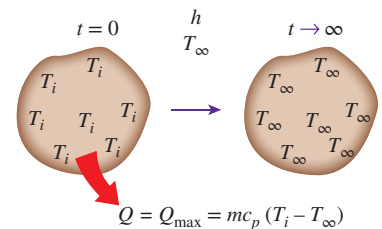
FIGURE 4–4
Heat transfer to or from a body reaches its maximum value when the body reaches the environment temperature.

FIGURE 4–5
Jean-Baptiste Biot (1774–1862) was a French physicist, astronomer, and mathematician born in Paris, France. Although younger, Biot worked on the analysis of heat conduction even earlier than Fourier did (1802 or 1803) and attempted, unsuccessfully, to deal with the problem of incorporating external convection effects in heat conduction analysis. Fourier read Biot's work and by 1807 had determined for himself how to solve the elusive problem. In 1804, Biot accompanied Gay Lussac on the first balloon ascent undertaken for scientific purposes. In 1820, with Felix Savart, he discovered the law known as "Biot and Savart's Law." He was especially interested in questions relating to the polarization of light, and for his achievements in this field he was awarded the Rumford Medal of the Royal Society in 1840. The dimensionless **Biot number (Bi)** used in transient heat transfer calculations is named after him.

©World History Archive/Alamy

to use it. The first step in establishing a criterion for the applicability of the lumped system analysis is to define a **characteristic length** as

$$L_c = \frac{V}{A_s}$$

and a dimensionless **Biot number** (Fig. 4–5) Bi as

$$\mathrm{Bi} = \frac{hL_c}{k} \qquad\qquad (4\text{–}9)$$

The characteristic length L_c to be used in the Biot number for simple geometries in which heat transfer is one-dimensional, such as a large plane wall of thickness $2L$, a long cylinder of radius r_o, and a sphere of radius r_o, becomes L (half thickness), $r_o/2$, and $r_o/3$, respectively. Equation 4–9 can also be expressed as (Fig. 4–6)

$$\mathrm{Bi} = \frac{h}{k/L_c}\frac{\Delta T}{\Delta T} = \frac{\text{Convection at the surface of the body}}{\text{Conduction within the body}}$$

or

$$\mathrm{Bi} = \frac{L_c/k}{1/h} = \frac{\text{Conduction resistance within the body}}{\text{Convection resistance at the surface of the body}}$$

When a solid body is being heated by the hotter fluid surrounding it (such as a potato being baked in an oven), heat is first *convected* to the body and subsequently *conducted* within the body. The Biot number is the *ratio* of the internal resistance of a body to *heat conduction* to its external resistance to *heat convection*. Therefore, a small Biot number represents small resistance to heat conduction, and thus small temperature gradients within the body.

Lumped system analysis assumes a *uniform* temperature distribution throughout the body, which is the case only when the thermal resistance of the body to heat conduction (the *conduction resistance*) is zero. Thus, lumped system analysis is *exact* when $\mathrm{Bi} = 0$ and *approximate* when $\mathrm{Bi} > 0$. Of course, the smaller the Bi number, the more accurate the lumped system analysis. Then the question we must answer is, how much accuracy are we willing to sacrifice for the convenience of the lumped system analysis?

Before answering this question, we should mention that a 15 percent uncertainty in the convection heat transfer coefficient h in most cases is considered normal and expected. Assuming h to be *constant* and *uniform* is also an approximation of questionable validity, especially for irregular geometries. Therefore, in the absence of sufficient experimental data for the specific geometry under consideration, we cannot claim our results to be better than ± 15 percent, even when $\mathrm{Bi} = 0$. This being the case, introducing another source of uncertainty in the problem will not have much effect on the overall uncertainty, provided that it is minor. It is generally accepted that lumped system analysis is *applicable* if

$$\mathrm{Bi} \leq 0.1$$

When this criterion is satisfied, the temperatures within the body relative to the surroundings (i.e., $T - T_\infty$) remain within 5 percent of each other even for well-rounded geometries such as a spherical ball. Thus, when $\mathrm{Bi} < 0.1$,

the variation of temperature with location within the body is slight and can reasonably be approximated as being uniform.

The first step in the application of lumped system analysis is the calculation of the *Biot number* and the assessment of the applicability of this approach. One may still wish to use lumped system analysis even when the criterion Bi < 0.1 is not satisfied if high accuracy is not a major concern.

Note that the Biot number is the ratio of the *convection* at the surface to *conduction* within the body, and this number should be as small as possible for lumped system analysis to be applicable. Therefore, *small bodies* with *high thermal conductivity* are good candidates for lumped system analysis, especially when they are in a medium that is a poor conductor of heat (such as air or another gas) and motionless. Thus, the hot small copper ball placed in quiescent air, discussed earlier, is most likely to satisfy the criterion for lumped system analysis (Fig. 4–7).

Convection

Conduction

h
T_∞

Solid body

$$Bi = \frac{\text{heat convection}}{\text{heat conduction}}$$

FIGURE 4–6
The Biot number can be viewed as the ratio of the convection at the surface to conduction within the body.

Some Remarks on Heat Transfer in Lumped Systems

To understand the heat transfer mechanism during the heating or cooling of a solid by the fluid surrounding it, and the criterion for lumped system analysis, consider this analogy (Fig. 4–8). People from the mainland are to go *by boat* to an island whose entire shore is a harbor, and from the harbor to their destinations on the island *by bus.* The overcrowding of people at the harbor depends on the boat traffic to the island and the ground transportation system on the island. If there is an excellent ground transportation system with plenty of buses, there will be no overcrowding at the harbor, especially when the boat traffic is light. But when the opposite is true, there will be a huge overcrowding at the harbor, creating a large difference between the populations at the harbor and inland. The chance of overcrowding is much lower in a small island with plenty of fast buses.

In heat transfer, a poor ground transportation system corresponds to poor heat conduction in a body, and overcrowding at the harbor to the accumulation of thermal energy and the subsequent rise in temperature near the surface of the body relative to its inner parts. Lumped system analysis is obviously not applicable when there is overcrowding at the surface. Of course, we have disregarded radiation in this analogy and thus the air traffic to the island. Like passengers at the harbor, heat changes *vehicles* at the surface from *convection* to *conduction.* Noting that a surface has zero thickness and thus cannot store any energy, heat reaching the surface of a body by convection must continue its journey within the body by conduction.

Consider heat transfer from a hot body to its cooler surroundings. Heat is transferred from the body to the surrounding fluid as a result of a temperature difference. But this energy comes from the region near the surface, and thus the temperature of the body near the surface will drop. This creates a *temperature gradient* between the inner and outer regions of the body and initiates heat transfer by conduction from the interior of the body toward the outer surface.

When the convection heat transfer coefficient h and thus the rate of convection from the body are high, the temperature of the body near the surface drops quickly (Fig. 4–9). This creates a larger temperature difference between the inner and outer regions unless the body is able to transfer heat from the inner to the outer regions just as fast. Thus, the magnitude of the maximum
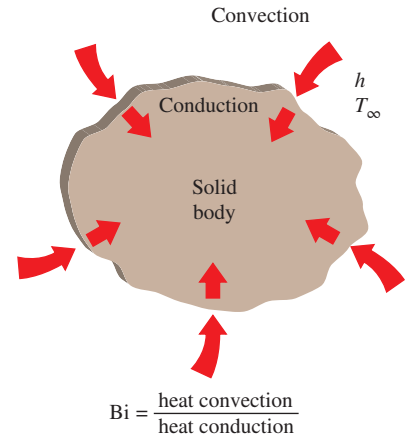
$h = 15$ W/m²·K

Spherical copper ball

$k = 401$ W/m·K

$D = 12$ cm

$$L_c = \frac{V}{A_s} = \frac{\frac{1}{6}\pi D^3}{\pi D^2} = \frac{1}{6}D = 0.02 \text{ m}$$

$$Bi = \frac{hL_c}{k} = \frac{15 \times 0.02}{401} = 0.00075 < 1$$
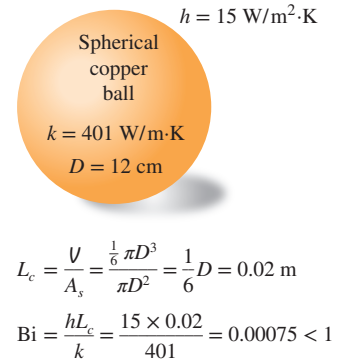
FIGURE 4–7
Small bodies with high thermal conductivities and low convection coefficients are most likely to satisfy the criterion for lumped system analysis.

Boat

Bus
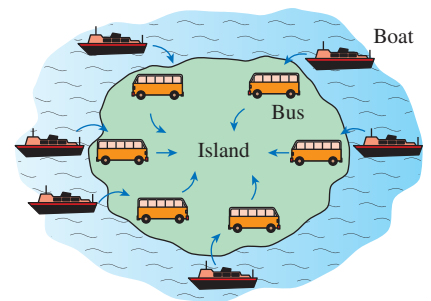
Island

FIGURE 4–8
Analogy between heat transfer to a solid and passenger traffic to an island.
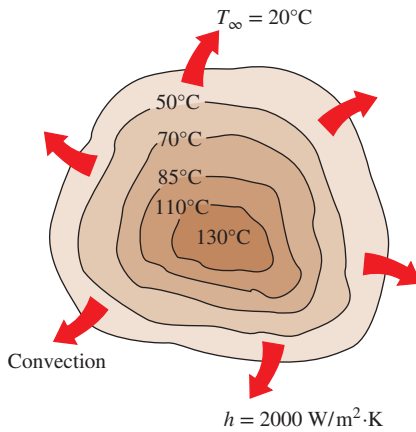
FIGURE 4–9
When the convection coefficient h is high and k is low, large temperature differences occur between the inner and outer regions of a large solid.
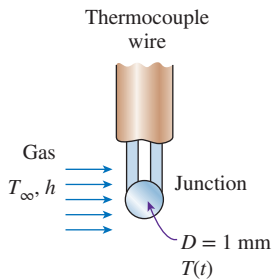
FIGURE 4–10
Schematic for Example 4–1.

temperature difference within the body depends strongly on the ability of a body to conduct heat toward its surface relative to the ability of the surrounding medium to convect heat away from the surface. The Biot number is a measure of the relative magnitudes of these two competing effects.

Recall that heat conduction in a specified direction n per unit surface area is expressed as $\dot{q} = -k\,\partial T/\partial n$, where $\partial T/\partial n$ is the temperature gradient and k is the thermal conductivity of the solid. Thus, the temperature distribution in the body will be *uniform* only when its thermal conductivity is *infinite,* and no such material is known to exist. Therefore, temperature gradients and thus temperature differences must exist within the body, no matter how small, in order for heat conduction to take place. Of course, the temperature gradient and the thermal conductivity are inversely proportional for a given heat flux. Therefore, the larger the thermal conductivity, the smaller the temperature gradient.

EXAMPLE 4–1   **Temperature Measurement by Thermocouples**

The temperature of a gas stream is to be measured by a thermocouple whose junction can be approximated as a 1-mm-diameter sphere, as shown in Fig. 4–10. The properties of the junction are $k = 35$ W/m·K, $\rho = 8500$ kg/m^3, and $c_p = 320$ J/kg·K, and the convection heat transfer coefficient between the junction and the gas is $h = 210$ W/m^2·K. Determine how long it will take for the thermocouple to read 99 percent of the initial temperature difference.

SOLUTION   The temperature of a gas stream is to be measured by a thermocouple. The time it takes to register 99 percent of the initial ΔT is to be determined.
Assumptions   **1** The junction is spherical in shape with a diameter of $D = 0.001$ m. **2** The thermal properties of the junction and the heat transfer coefficient are constant. **3** Radiation effects are negligible.
Properties   The properties of the junction are given in the problem statement.
Analysis   The characteristic length of the junction is

$$L_c = \frac{V}{A_s} = \frac{\frac{1}{6}\pi D^3}{\pi D^2} = \frac{1}{6}D = \frac{1}{6}(0.001 \text{ m}) = 1.67 \times 10^{-4} \text{ m}$$

Then the Biot number becomes

$$\text{Bi} = \frac{hL_c}{k} = \frac{(210 \text{ W/m}^2\text{·K})(1.67 \times 10^{-4} \text{ m})}{35 \text{ W/m·K}} = 0.001 < 0.1$$

Therefore, lumped system analysis is applicable, and the error involved in this approximation is negligible.

In order to read 99 percent of the initial temperature difference $T_i - T_\infty$ between the junction and the gas, we must have

$$\frac{T(t) - T_\infty}{T_i - T_\infty} = 0.01$$

For example, when $T_i = 0°C$ and $T_\infty = 100°C$, a thermocouple is considered to have read 99 percent of this applied temperature difference when its reading indicates $T(t) = 99°$ C.

The value of the exponent b is

$$b = \frac{hA_s}{\rho c_p V} = \frac{h}{\rho c_p L_c} = \frac{210 \text{ W/m}^2 \cdot \text{K}}{(8500 \text{ kg/m}^3)(320 \text{ J/kg} \cdot \text{K})(1.67 \times 10^{-4} \text{ m})} = 0.462 \text{ s}^{-1}$$

We now substitute these values into Eq. 4–4 and obtain

$$\frac{T(t) - T_\infty}{T_i - T_\infty} = e^{-bt} \quad \longrightarrow \quad 0.01 = e^{-(0.462 \text{ s}^{-1})t}$$

which yields

$$t = \textbf{10 s}$$

Therefore, we must wait at least 10 s for the temperature of the thermocouple junction to approach within 99 percent of the initial junction-gas temperature difference.

Discussion   Note that conduction through the wires and radiation exchange with the surrounding surfaces affect the result, and they should be considered in a more refined analysis.

PtD *EXAMPLE 4–2*   **Air Cooling of Metal Plates**

Metal plates ($k = 180$ W/m·K, $\rho = 2800$ kg/m³, and $c_p = 880$ J/kg·K) with a thickness of 2 cm exiting an oven are conveyed through a 10-m-long cooling chamber at a speed of 4 cm/s (Fig. 4–11). The plates enter the cooling chamber at an initial temperature of 700°C. The air temperature in the cooling chamber is 15°C, and the plates are cooled with blowing air. The convection heat transfer coefficient is given as a function of the air velocity $h = 33V^{0.8}$, where h is in W/m²·K and V is in m/s. To prevent any incident of thermal burn, it is necessary to design the cooling process such that the plates exit the cooling chamber at a relatively safe temperature of 50°C or less. Determine the air velocity and the heat transfer coefficient such that the temperature of the plates exiting the cooling chamber is at 50°C.

SOLUTION   In this example, the concepts of Prevention through Design (PtD) are applied in conjunction with lumped system analysis. Metal plates exiting an oven are being cooled by air in a cooling chamber. The air velocity and convection heat transfer coefficient that are required to cool the plates so that they exit the cooling chamber at 50°C are to be determined.

Assumptions   **1** The thermal properties of metal plates are constant. **2** Convection heat transfer coefficient is uniform. **3** Heat transfer by radiation is negligible. **4** The Biot number is Bi < 0.1 so that the lumped system analysis is applicable (this assumption will be verified).

Properties   The properties of the metal plates are given as $k = 180$ W/m·K, $\rho = 2800$ kg/m³, and $c_p = 880$ J/kg·K.

Analysis   With a metal plate thickness of $2L = 2$ cm, the characteristic length of the plate is

$$L_c = \frac{V}{A_s} = \frac{2LA}{2A} = L = \frac{20 \text{ mm}}{2} = 10 \text{ mm}$$

Cooling chamber, 15°C

4 cm/s

2 cm

Metal plate

Blowing air
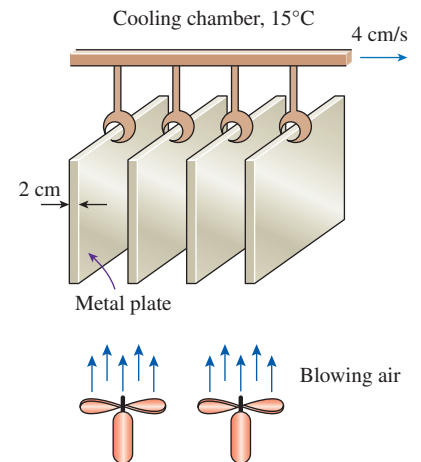
FIGURE 4–11
Schematic for Example 4–2.

Using the lumped system analysis,

$$b = \frac{hA_s}{\rho c_p V} = \frac{h}{\rho c_p L_c} = \frac{33V_{\text{air}}^{0.8}}{\rho c_p L_c} = \frac{33V_{\text{air}}^{0.8}}{(2800 \text{ kg/m}^3)(880 \text{ J/kg·K})(0.010 \text{ m})}$$

The duration of cooling can be determined from the cooling chamber length and the speed of the plates,

$$t = \frac{10 \text{ m}}{0.04 \text{ m/s}} = 250 \text{ s}$$

$$\frac{T(t) - T_\infty}{T_i - T_\infty} = e^{-bt} \quad \rightarrow \quad b = -\frac{1}{t} \ln\left[\frac{T(t) - T_\infty}{T_i - T_\infty}\right]$$

$$= -\frac{1}{250 \text{ s}} \ln\left(\frac{50 - 15}{700 - 15}\right) = 0.0119 \text{ s}^{-1}$$

Thus, the air velocity and convection heat transfer coefficient necessary to cool the plates to 50°C as they exit the cooling chamber is

$$b = \frac{33V_{\text{air}}^{0.8}}{\rho c_p L_c} = 0.01195 \text{ s}^{-1}$$

$$V_{\text{air}} = \left[\frac{(0.0119 \text{ s}^{-1})(2800 \text{ kg/m}^3)(880 \text{ J/kg·K})(0.010 \text{ m})}{33}\right]^{1/0.8} = \textbf{15.3 m/s}$$

$$h = 33V_{\text{air}}^{0.8} = 33(15.3 \text{ m/s})^{0.8} = \textbf{293 W/m}^2\textbf{·K}$$

This analysis was carried out under the assumption that it is a lumped system, and for this assumption to be applicable, the condition Bi < 0.1 needs to be satisfied.

$$\text{Bi} = \frac{hL_c}{k} = \frac{(293 \text{ W/m}^2\text{·K})(0.010 \text{ m})}{180 \text{ W/m·K}} = 0.0163 < 0.1$$

Discussion The effect of the air velocity on the temperature of the plates exiting the cooling chamber is plotted in Fig. 4–12. The figure shows that for air velocities greater than 15.3 m/s, the temperature of the plates stays well below 50°C, which should prevent any incident of thermal burn.
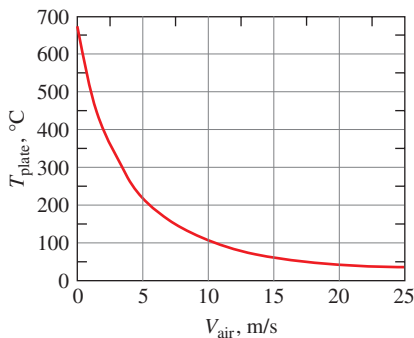
FIGURE 4–12
Variation of plate temperature with the air velocity at the exit of the cooling chamber.

4–2 ▪ TRANSIENT HEAT CONDUCTION IN LARGE PLANE WALLS, LONG CYLINDERS, AND SPHERES WITH SPATIAL EFFECTS

In Sec. 4–1, we considered bodies in which the variation of temperature within the body is negligible; that is, bodies that remain nearly *isothermal* during a process. Relatively small bodies of highly conductive materials approximate this behavior. In general, however, the temperature within a body changes from point to point as well as with time. In this section, we consider the variation of temperature with *time* and *position* in one-dimensional problems such as those associated with a large plane wall, a long cylinder, and a sphere.

Consider a plane wall of thickness 2L, a long cylinder of radius r_o, and a sphere of radius r_o initially at a *uniform temperature T_i*, as shown in Fig. 4–13. At time $t = 0$, each geometry is placed in a large medium that is at a constant

(a) A large plane wall   (b) A long cylinder   (c) A sphere
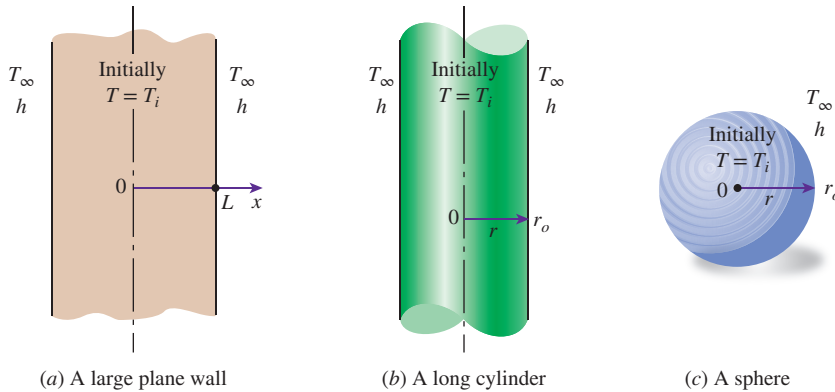
FIGURE 4–13
Schematic of the simple geometries in which heat transfer is one-dimensional.

temperature T_∞ and kept in that medium for $t > 0$. Heat transfer takes place between these bodies and their environments by convection with a *uniform* and *constant* heat transfer coefficient *h*. Note that all three cases possess geometric and thermal symmetry: the plane wall is symmetric about its *center plane* ($x = 0$), the cylinder is symmetric about its *centerline* ($r = 0$), and the sphere is symmetric about its *center point* ($r = 0$). We neglect *radiation* heat transfer between these bodies and their surrounding surfaces, or we incorporate the radiation effect into the convection heat transfer coefficient *h*.

The variation of the temperature profile with *time* in the plane wall is illustrated in Fig. 4–14. When the wall is first exposed to the surrounding medium at $T_\infty < T_i$ at $t = 0$, the entire wall is at its initial temperature T_i. But the wall temperature at and near the surfaces starts to drop as a result of heat transfer from the wall to the surrounding medium. This creates a *temperature gradient* in the wall and initiates heat conduction from the inner parts of the wall toward its outer surfaces. Note that the temperature at the center of the wall remains at T_i until $t = t_2$, and that the temperature profile within the wall remains symmetric at all times about the center plane. The temperature profile gets flatter and flatter as time passes as a result of heat transfer, and it eventually becomes uniform at $T = T_\infty$. That is, the wall reaches *thermal equilibrium* with its surroundings. At that point, heat transfer stops since there is no longer a temperature difference. Similar discussions can be given for the long cylinder or sphere.
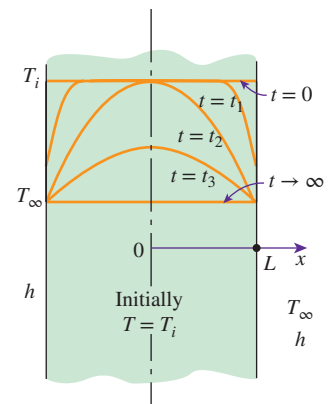
FIGURE 4–14
Transient temperature profiles in a plane wall exposed to convection from its surfaces for $T_i > T_\infty$.

Nondimensionalized One-Dimensional Transient Conduction Problem

The formulation of heat conduction problems for the determination of the one-dimensional transient temperature distribution in a plane wall, a cylinder, or a sphere results in a partial differential equation whose solution typically involves infinite series and transcendental equations, which are inconvenient to use. But the analytical solution provides valuable insight into the physical problem, and thus it is important to go through the steps involved. Next we demonstrate the solution procedure for the case of plane wall.

Consider a plane wall of thickness 2*L* initially at a uniform temperature of T_i, as shown in Fig. 4–13*a*. At time $t = 0$, the wall is immersed in a fluid at temperature T_∞ and is subjected to convection heat transfer from both sides with a convection coefficient of *h*. The height and the width of the wall are large relative to its thickness, and thus heat conduction in the wall can be

approximated to be one-dimensional. Also, there is thermal symmetry about the midplane passing through $x = 0$, and thus the temperature distribution must be symmetrical about the midplane. Therefore, the value of temperature at any $-x$ value in $-L \leq x \leq 0$ at any time t must be equal to the value at $+x$ in $0 \leq x \leq L$ at the same time. This means we can formulate and solve the heat conduction problem in the positive half domain $0 \leq x \leq L$, and then apply the solution to the other half.

Under the conditions of constant thermophysical properties, no heat generation, thermal symmetry about the midplane, uniform initial temperature, and constant convection coefficient, the one-dimensional transient heat conduction problem in the half-domain $0 \leq x \leq L$ of the plane wall can be expressed as (see Chap. 2)

Differential equation: $\quad \dfrac{\partial^2 T}{\partial x^2} = \dfrac{1}{\alpha} \dfrac{\partial T}{\partial t}$ **(4–10a)**

Boundary conditions: $\quad \dfrac{\partial T(0, t)}{\partial x} = 0 \quad \text{and} \quad -k \dfrac{\partial T(L, t)}{\partial x} = h[T(L, t) - T_\infty]$ **(4–10b)**

Initial condition: $\quad T(x, 0) = T_i$ **(4–10c)**

where the property $\alpha = k/\rho c_p$ is the thermal diffusivity of the material.

We now attempt to nondimensionalize the problem by defining a dimensionless space variable $X = x/L$ and dimensionless temperature $\theta(x, t) = [T(x, t) - T_\infty]/[T_i - T_\infty]$. These are convenient choices since both X and θ vary between 0 and 1. However, there is no clear guidance for the proper form of the dimensionless time variable and the h/k ratio, so we will let the analysis indicate them. We note that

$$\frac{\partial \theta}{\partial X} = \frac{\partial \theta}{\partial (x/L)} = \frac{L}{T_i - T_\infty} \frac{\partial T}{\partial x}, \ \frac{\partial^2 \theta}{\partial X^2} = \frac{L^2}{T_i - T_\infty} \frac{\partial^2 T}{\partial x^2} \ \text{and} \ \frac{\partial \theta}{\partial t} = \frac{1}{T_i - T_\infty} \frac{\partial T}{\partial t}$$

Substituting into Eqs. 4–10a and 4–10b and rearranging give

$$\frac{\partial^2 \theta}{\partial X^2} = \frac{L^2}{\alpha} \frac{\partial \theta}{\partial t} \quad \text{and} \quad \frac{\partial \theta(1, t)}{\partial X} = \frac{-hL}{k} \theta(1, t) \qquad \textbf{(4–11)}$$

Therefore, the proper form of the dimensionless time is $\tau = \alpha t/L^2$, which is called the **Fourier number** Fo (named after Jean Baptiste Joseph Fourier, *see* Fig. 1–27), and we recognize Bi $= hL/k$ as the Biot number defined in Sec. 4–1. Then the formulation of the one-dimensional transient heat conduction problem in a plane wall can be expressed in nondimensional form as

Dimensionless differential equation: $\quad \dfrac{\partial^2 \theta}{\partial X^2} = \dfrac{\partial \theta}{\partial \tau}$ **(4–12a)**

Dimensionless BC's: $\quad \dfrac{\partial \theta(0, \tau)}{\partial X} = 0 \quad \text{and} \quad \dfrac{\partial \theta(1, \tau)}{\partial X} = -\text{Bi}\theta(1, \tau)$ **(4–12b)**

Dimensionless initial condition: $\quad \theta(X, 0) = 1$ **(4–12c)**

where

$$\theta(X, \tau) = \frac{T(x, t) - T_\infty}{T_i - T_\infty} \qquad \textit{Dimensionless temperature}$$

$$X = \frac{x}{L} \qquad \textit{Dimensionless distance from the center}$$

$$\text{Bi} = \frac{hL}{k} \qquad \textit{Dimensionless heat transfer coefficient (Biot number)}$$

$$\tau = \frac{\alpha t}{L^2} = \text{Fo} \qquad \textit{Dimensionless time (Fourier number)}$$

The heat conduction equation in cylindrical or spherical coordinates can be nondimensionalized in a similar way. Note that nondimensionalization reduces the number of independent variables and parameters from 8 to 3—from x, L, t, k, α, h, T_i, and T_∞ to X, Bi, and Fo (Fig. 4–15). That is,

$$\theta = f(X, \text{Bi, Fo}) \qquad \textbf{(4–13)}$$

This makes it very practical to conduct parametric studies and avoid results in graphical form. Equation 4–13 is the generalized version of Eq. 4–4 for the lumped system analysis (no space variables). This can be shown by using the definitions of θ, α, L_c, Bi, and Fo in Eq. 4–4. The final result is

$$\theta = \frac{T(t) - T_\infty}{T_i - T_\infty} = e^{-bt} = e^{-\frac{hA_s t}{\rho V c_p}} = e^{-\text{BiFo}}$$

or $\theta = f(\text{Fo, Bi})$ which is the special case of Eq. 4–13 with no space variable.

Exact Solution of One-Dimensional Transient Conduction Problem*

The nondimensionalized partial differential equation given in Eqs. 4–12 together with its boundary and initial conditions can be solved using several analytical and numerical techniques, including the Laplace or other transform methods, the method of separation of variables, the finite difference method, and the finite element method. Here we use the method of **separation of variables** developed by J. Fourier in the 1820s, which is based on expanding an arbitrary function (including a constant) in terms of Fourier series. The method is applied by assuming the dependent variable to be a product of a number of functions, each being a function of a single independent variable. This reduces the partial differential equation to a system of ordinary differential equations, each being a function of a single independent variable. In the case of transient conduction in a plane wall, for example, the dependent variable is the solution function $\theta(X, \tau)$, which is expressed as $\theta(X, \tau) = F(X)G(\tau)$, and the application of the method results in two ordinary differential equation, one in X and the other in τ.

The method is applicable if (1) the geometry is simple and finite (such as a rectangular block, a cylinder, or a sphere) so that the boundary surfaces can be described by simple mathematical functions, and (2) the differential equation and the boundary and initial conditions in their most simplified form are linear (no terms that involve products of the dependent variable or its derivatives) and involve only one nonhomogeneous term (a term without the dependent variable or its derivatives). If the formulation involves a number of nonhomogeneous terms, the problem can be split up into an equal number of simpler problems each involving only one nonhomogeneous term, and then combining the solutions by superposition.

Now we demonstrate the use of the method of separation of variables by applying it to the one-dimensional transient heat conduction problem given in

(*a*) Original heat conduction problem:

$$\frac{\partial^2 T}{\partial x^2} = \frac{1}{\alpha} \frac{\partial T}{\partial x}, \; T(x, 0) = T_i$$

$$\frac{\partial T(0, t)}{\partial x} = 0, \; -k\frac{\partial T(L, t)}{\partial x} = h[T(L, t) - T_\infty]$$

$$T = F(x, L, t, k, \alpha, h, T_i, T_\infty)$$

(*b*) Nondimensionalized problem:

$$\frac{\partial^2 \theta}{\partial X^2} = \frac{\partial \theta}{\partial \tau}, \; \theta(X, 0) = 1$$

$$\frac{\partial \theta(0, \tau)}{\partial X} = 0, \; \frac{\partial \theta(1, \tau)}{\partial X} = -\text{Bi}\theta(1, \tau)$$

$$\theta = f(X, \text{Bi}, \tau)$$

FIGURE 4–15

Nondimensionalization reduces the number of independent variables in one-dimensional transient conduction problems from 8 to 3, offering great convenience in the presentation of results.

---

*This section can be skipped if desired without a loss of continuity.

Eqs. 4–12. First, we express the dimensionless temperature function $\theta(X, \tau)$ as a product of a function of X only and a function of τ only as

$$\theta(X, \tau) = F(X)G(\tau) \tag{4–14}$$

Substituting Eq. 4–14 into Eq. 4–12a and dividing by the product FG gives

$$\frac{1}{F}\frac{d^2F}{dX^2} = \frac{1}{G}\frac{dG}{d\tau} \tag{4–15}$$

Observe that all the terms that depend on X are on the left-hand side of the equation and all the terms that depend on τ are on the right-hand side. That is, the terms that are functions of different variables are *separated* (and thus the name *separation of variables*). The left-hand side of this equation is a function of X only, and the right-hand side is a function of only τ. Considering that both X and τ can be varied independently, the equality in Eq. 4–15 can hold for any value of X and τ only if Eq. 4–15 is equal to a constant. Further, it must be a *negative* constant that we will indicate by $-\lambda^2$ since a positive constant will cause the function $G(\tau)$ to increase indefinitely with time (to be infinite), which is unphysical, and a value of zero for the constant means no time dependence, which is again inconsistent with the physical problem. Setting Eq. 4–15 equal to $-\lambda^2$ gives

$$\frac{d^2F}{dX^2} + \lambda^2 F = 0 \quad \text{and} \quad \frac{dG}{d\tau} + \lambda^2 G = 0 \tag{4–16}$$

whose general solutions are

$$F = C_1\cos(\lambda X) + C_2\sin(\lambda X) \quad \text{and} \quad G = C_3 e^{-\lambda^2\tau} \tag{4–17}$$

and

$$\theta = FG = C_3 e^{-\lambda^2\tau}[C_1\cos(\lambda X) + C_2\sin(\lambda X)] = e^{-\lambda^2\tau}[A\cos(\lambda X) + B\sin(\lambda X)] \tag{4–18}$$

where $A = C_1 C_3$ and $B = C_2 C_3$ are arbitrary constants. Note that we need to determine only A and B to obtain the solution of the problem.

Applying the boundary conditions in Eq. 4–12b gives

$$\frac{\partial\theta(0, \tau)}{\partial X} = 0 \rightarrow e^{-\lambda^2\tau}(-A\lambda\sin 0 + B\lambda\cos 0) = 0 \rightarrow B = 0 \rightarrow \theta = Ae^{-\lambda^2\tau}\cos(\lambda X)$$

$$\frac{\partial\theta(1, \tau)}{\partial X} = -\text{Bi}\theta(1, \tau) \rightarrow -Ae^{-\lambda^2\tau}\lambda\sin\lambda = -\text{Bi}Ae^{-\lambda^2\tau}\cos\lambda \rightarrow \lambda\tan\lambda = \text{Bi}$$

But tangent is a periodic function with a period of π, and the equation $\lambda\tan\lambda = \text{Bi}$ has the root λ_1 between 0 and π, the root λ_2 between π and 2π, the root λ_n between $(n - 1)\pi$ and $n\pi$, etc. To recognize that the transcendental equation $\lambda\tan\lambda = \text{Bi}$ has an infinite number of roots, it is expressed as

$$\lambda_n\tan\lambda_n = \text{Bi} \tag{4–19}$$

Eq. 4–19 is called the **characteristic equation** or **eigenfunction**, and its roots are called the **characteristic values** or **eigenvalues**. The characteristic equation is implicit in this case, and thus the characteristic values need to be determined numerically. Then it follows that there are an infinite number of solutions of the form $Ae^{-\lambda^2\tau}\cos(\lambda X)$, and the solution of this linear heat conduction problem is a linear combination of them,

$$\theta = \sum_{n=1}^{\infty} A_n e^{-\lambda_n^2\tau}\cos(\lambda_n X) \tag{4–20}$$

The constants A_n are determined from the initial condition, Eq. 4–12c,

$$\theta(X, 0) = 1 \quad \rightarrow \quad 1 = \sum_{n=1}^{\infty} A_n \cos(\lambda_n X) \tag{4–21}$$

This is a Fourier series expansion that expresses a constant in terms of an infinite series of cosine functions. Now we multiply both sides of Eq. 4–21 by $\cos(\lambda_m X)$ and integrate from $X = 0$ to $X = 1$. The right-hand side involves an infinite number of integrals of the form $\int_0^1 \cos(\lambda_m X) \cos(\lambda_n X) dX$. It can be shown that all of these integrals vanish except when $n = m$, and the coefficient A_n becomes

$$\int_0^1 \cos(\lambda_n X) dX = A_n \int_0^1 \cos^2(\lambda_n X) dX \rightarrow A_n = \frac{4 \sin \lambda_n}{2\lambda_n + \sin(2\lambda_n)} \tag{4–22}$$

This completes the analysis for the solution of a one-dimensional transient heat conduction problem in a plane wall. Solutions in other geometries such as a long cylinder and a sphere can be determined using the same approach. The long cylinder approximation allows the assumption of one-dimensional conduction in the radial direction. It is a reasonable approximation for cylinders having length (L) to radius (r_o) ratio, $L/r_o \geq 10$. The results for all three geometries are summarized in Table 4–1. The solution for the plane wall is also applicable for a plane wall of thickness L whose left surface at $x = 0$ is insulated and the right surface at $x = L$ is subjected to convection since this is precisely the mathematical problem we solved.

The analytical solutions of transient conduction problems typically involve infinite series, and thus the evaluation of an infinite number of terms to determine the temperature at a specified location and time. This may look intimidating at first, but there is no need to worry. As demonstrated in Fig. 4–16, the terms in the summation decline rapidly as n and thus λ_n increase because of the exponential decay function $e^{-\lambda_n^2 \tau}$. This is especially the case when the dimensionless time τ is large. Therefore, the evaluation of the first few terms of the infinite series (in this case just the first term) is usually adequate to determine the dimensionless temperature θ.

$$\theta_n = A_n e^{-\lambda_n^2 \tau} \cos(\lambda_n X)$$
$$A_n = \frac{4 \sin \lambda_n}{2\lambda_n + \sin(2\lambda_n)}$$
$$\lambda_n \tan \lambda_n = \text{Bi}$$

For Bi = 5, X = 1, and $\tau = 0.2$:

n	λ_n	A_n	θ_n
1	1.3138	1.2402	0.22321
2	4.0336	−0.3442	0.00835
3	6.9096	0.1588	0.00001
4	9.8928	−0.876	0.00000
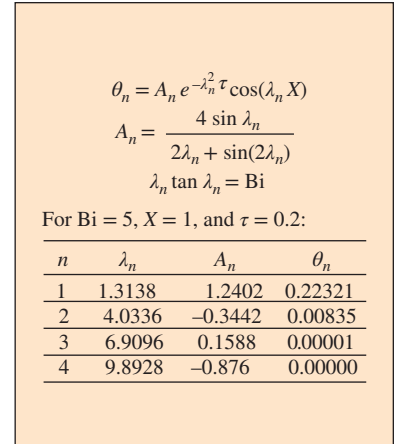
FIGURE 4–16

The term in the series solution of transient conduction problems decline rapidly as n and thus λ_n increase because of the exponential decay function with the exponent $-\lambda_n \tau$.

TABLE 4–1

Summary of the solutions for one-dimensional transient conduction in a plane wall of thickness $2L$, a cylinder of radius r_o, and a sphere of radius r_o subjected to convection from all surfaces.*

Geometry	Solution	λ_n's are the roots of
Plane wall	$\theta = \sum_{n=1}^{\infty} \frac{4 \sin \lambda_n}{2\lambda_n + \sin(2\lambda_n)} e^{-\lambda_n^2 \tau} \cos(\lambda_n x/L)$	$\lambda_n \tan \lambda_n = \text{Bi}$
Cylinder	$\theta = \sum_{n=1}^{\infty} \frac{2}{\lambda_n} \frac{J_1(\lambda_n)}{J_0^2(\lambda_n) + J_1^2(\lambda_n)} e^{-\lambda_n^2 \tau} J_0(\lambda_n r/r_o)$	$\lambda_n \frac{J_1(\lambda_n)}{J_0(\lambda_n)} = \text{Bi}$
Sphere	$\theta = \sum_{n=1}^{\infty} \frac{4(\sin \lambda_n - \lambda_n \cos \lambda_n)}{2\lambda_n - \sin(2\lambda_n)} e^{-\lambda_n^2 \tau} \frac{\sin(\lambda_n r/r_o)}{\lambda_n r/r_o}$	$1 - \lambda_n \cot \lambda_n = \text{Bi}$

*Here $\theta = (T - T_\infty)/(T_i - T_\infty)$ is the dimensionless temperature, Bi $= hL/k$ or hr_o/k is the Biot number, Fo $= \tau = \alpha t/L^2$ or $\alpha t/r_o^2$ is the Fourier number, and J_0 and J_1 are the Bessel functions of the first kind whose values are given in Table 4–3. Note that the characteristic length used for each geometry in the equations for the Biot and Fourier numbers is different for the exact (analytical) solution than the one used for the lumped system analysis.

Approximate Analytical Solutions

The analytical solution we obtained for one-dimensional transient heat conduction in a plane wall involves infinite series and implicit equations, which are difficult to evaluate. Therefore, we have an incentive to simplify the analytical solutions and to present the solutions in *tabular* form using simple relations.

The dimensionless quantities defined above for a plane wall can also be used for a *cylinder* or *sphere* by replacing the space variable x with r and the half-thickness L with the outer radius r_o. Note that the characteristic length in the definition of the Biot number is taken to be the *half-thickness L* for the plane wall and the *radius r_o* for the long cylinder and sphere instead of V/A used in lumped system analysis.

We mentioned earlier that the terms in the series solutions in Table 4–1 converge rapidly with increasing time, and for $\tau > 0.2$, keeping the first term and neglecting all the remaining terms in the series results in an error under 2 percent. We are usually interested in the solution for times with $\tau > 0.2$, and thus it is very convenient to express the solution using this **one-term approximation**, given as

Plane wall: $\quad \theta_{\text{wall}} = \dfrac{T(x, t) - T_\infty}{T_i - T_\infty} = A_1 e^{-\lambda_1^2 \tau} \cos(\lambda_1 x/L), \; \tau > 0.2$ $\qquad$ **(4–23)**

Cylinder: $\quad \theta_{\text{cyl}} = \dfrac{T(r, t) - T_\infty}{T_i - T_\infty} = A_1 e^{-\lambda_1^2 \tau} J_0(\lambda_1 r/r_o), \; \tau > 0.2$ $\qquad$ **(4–24)**

Sphere: $\quad \theta_{\text{sph}} = \dfrac{T(r, t) - T_\infty}{T_i - T_\infty} = A_1 e^{-\lambda_1^2 \tau} \dfrac{\sin(\lambda_1 r/r_o)}{\lambda_1 r/r_o}, \; \tau > 0.2$ $\qquad$ **(4–25)**

where the constants A_1 and λ_1 are functions of the Bi number only, and their values are listed in Table 4–2 against the Bi number for all three geometries. The function J_0 is the zeroth-order Bessel function of the first kind, whose value can be determined from Table 4–3. Noting that $\cos(0) = J_0(0) = 1$ and the limit of $(\sin x)/x$ is also 1, these relations simplify to the next ones at the center of a plane wall, cylinder, or sphere:

Center of plane wall (x = 0): $\qquad \theta_{0, \text{wall}} = \dfrac{T_0 - T_\infty}{T_i - T_\infty} = A_1 e^{-\lambda_1^2 \tau}$ $\qquad$ **(4–26)**

Center of cylinder (r = 0): $\qquad \theta_{0, \text{cyl}} = \dfrac{T_0 - T_\infty}{T_i - T_\infty} = A_1 e^{-\lambda_1^2 \tau}$ $\qquad$ **(4–27)**

Center of sphere (r = 0): $\qquad \theta_{0, \text{sph}} = \dfrac{T_0 - T_\infty}{T_i - T_\infty} = A_1 e^{-\lambda_1^2 \tau}$ $\qquad$ **(4–28)**

Comparing the two sets of equations above, we notice that the dimensionless temperatures anywhere in a plane wall, cylinder, and sphere are related to the center temperature by

$$\frac{\theta_{\text{wall}}}{\theta_{0, \text{wall}}} = \cos\left(\frac{\lambda_1 x}{L}\right), \quad \frac{\theta_{\text{cyl}}}{\theta_{0, \text{cyl}}} = J_0\left(\frac{\lambda_1 r}{r_o}\right), \quad \text{and} \quad \frac{\theta_{\text{sph}}}{\theta_{0, \text{sph}}} = \frac{\sin(\lambda_1 r/r_o)}{\lambda_1 r/r_o} \quad \textbf{(4–29)}$$

which shows that time dependence of dimensionless temperature within a given geometry is the same throughout. That is, if the dimensionless center temperature θ_0 drops by 20 percent at a specified time, so does the dimensionless temperature θ_0 anywhere else in the medium at the same time.

TABLE 4–2

Coefficients used in the one-term approximate solution of transient one-dimensional heat conduction in plane walls, cylinders, and spheres (Bi $= hL/k$ for a plane wall of thickness $2L$, and Bi $= hr_o/k$ for a cylinder or sphere of radius r_o)

	Plane Wall		Cylinder		Sphere	
Bi	λ_1(rad)	A_1	λ_1(rad)	A_1	λ_1(rad)	A_1
0.01	0.0998	1.0017	0.1412	1.0025	0.1730	1.0030
0.02	0.1410	1.0033	0.1995	1.0050	0.2445	1.0060
0.04	0.1987	1.0066	0.2814	1.0099	0.3450	1.0120
0.06	0.2425	1.0098	0.3438	1.0148	0.4217	1.0179
0.08	0.2791	1.0130	0.3960	1.0197	0.4860	1.0239
0.1	0.3111	1.0161	0.4417	1.0246	0.5423	1.0298
0.2	0.4328	1.0311	0.6170	1.0483	0.7593	1.0592
0.3	0.5218	1.0450	0.7465	1.0712	0.9208	1.0880
0.4	0.5932	1.0580	0.8516	1.0931	1.0528	1.1164
0.5	0.6533	1.0701	0.9408	1.1143	1.1656	1.1441
0.6	0.7051	1.0814	1.0184	1.1345	1.2644	1.1713
0.7	0.7506	1.0918	1.0873	1.1539	1.3525	1.1978
0.8	0.7910	1.1016	1.1490	1.1724	1.4320	1.2236
0.9	0.8274	1.1107	1.2048	1.1902	1.5044	1.2488
1.0	0.8603	1.1191	1.2558	1.2071	1.5708	1.2732
2.0	1.0769	1.1785	1.5995	1.3384	2.0288	1.4793
3.0	1.1925	1.2102	1.7887	1.4191	2.2889	1.6227
4.0	1.2646	1.2287	1.9081	1.4698	2.4556	1.7202
5.0	1.3138	1.2403	1.9898	1.5029	2.5704	1.7870
6.0	1.3496	1.2479	2.0490	1.5253	2.6537	1.8338
7.0	1.3766	1.2532	2.0937	1.5411	2.7165	1.8673
8.0	1.3978	1.2570	2.1286	1.5526	2.7654	1.8920
9.0	1.4149	1.2598	2.1566	1.5611	2.8044	1.9106
10.0	1.4289	1.2620	2.1795	1.5677	2.8363	1.9249
20.0	1.4961	1.2699	2.2880	1.5919	2.9857	1.9781
30.0	1.5202	1.2717	2.3261	1.5973	3.0372	1.9898
40.0	1.5325	1.2723	2.3455	1.5993	3.0632	1.9942
50.0	1.5400	1.2727	2.3572	1.6002	3.0788	1.9962
100.0	1.5552	1.2731	2.3809	1.6015	3.1102	1.9990
∞	1.5708	1.2732	2.4048	1.6021	3.1416	2.0000

TABLE 4–3

The zeroth- and first-order Bessel functions of the first kind

η	$J_0(\eta)$	$J_1(\eta)$
0.0	1.0000	0.0000
0.1	0.9975	0.0499
0.2	0.9900	0.0995
0.3	0.9776	0.1483
0.4	0.9604	0.1960
0.5	0.9385	0.2423
0.6	0.9120	0.2867
0.7	0.8812	0.3290
0.8	0.8463	0.3688
0.9	0.8075	0.4059
1.0	0.7652	0.4400
1.1	0.7196	0.4709
1.2	0.6711	0.4983
1.3	0.6201	0.5220
1.4	0.5669	0.5419
1.5	0.5118	0.5579
1.6	0.4554	0.5699
1.7	0.3980	0.5778
1.8	0.3400	0.5815
1.9	0.2818	0.5812
2.0	0.2239	0.5767
2.1	0.1666	0.5683
2.2	0.1104	0.5560
2.3	0.0555	0.5399
2.4	0.0025	0.5202
2.6	−0.0968	0.4708
2.8	−0.1850	0.4097
3.0	−0.2601	0.3391
3.2	−0.3202	0.2613

Once the Bi number is known, these relations can be used to determine the temperature anywhere in the medium. The determination of the constants A_1 and λ_1 from Table 4–2 usually requires interpolation.

Graphical representation of the one-term approximation solutions for a large plane wall, long cylinder, and sphere were presented by M. P. Heisler in 1947 and are called transient temperature charts or **Heisler charts**. They were supplemented in 1961 with transient heat transfer charts by H. Gröber. The charts are sometimes difficult to read, and they are subject to reading errors. Therefore, the one-term approximate expressions should be preferred to the charts and will be used in this chapter.

Note that the case Bi $= \infty$ in Table 4–2 corresponds to $h \to \infty$, which corresponds to the case of *specified surface temperature* T_∞. That is, the case in which the surfaces of the body are suddenly brought to the temperature T_∞ at $t = 0$ and kept at T_∞ at all times can be handled by setting h to infinity (Fig. 4.17).

The temperature of the body changes from the initial temperature T_i to the temperature of the surroundings T_∞ at the end of the transient heat conduction
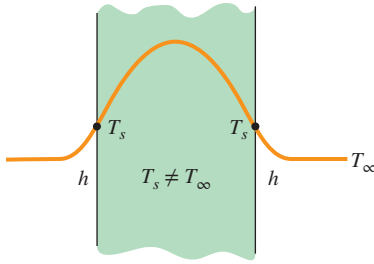
(*a*) Finite convection coefficient
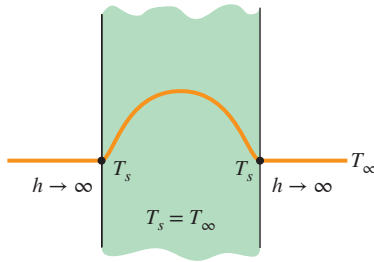
(*b*) Infinite convection coefficient

FIGURE 4–17
The specified surface temperature corresponds to the case of convection to an environment at T_∞ with a convection coefficient h that is *infinite*.

process. Thus, the *maximum* amount of heat that a body can gain (or lose if $T_i > T_\infty$) is simply the *change* in the *energy content* of the body. That is,

$$Q_{max} = mc_p(T_\infty - T_i) = \rho V c_p(T_\infty - T_i) \quad \text{(kJ)} \tag{4–30}$$

where m is the mass, V is the volume, ρ is the density, and c_p is the specific heat of the body. Thus, Q_{max} represents the amount of heat transfer for $t \to \infty$. The amount of heat transfer Q at a finite time t is obviously less than this maximum, and it can be expressed as the sum of the internal energy changes throughout the entire geometry as

$$Q = \int_V \rho c_p [T(x, t) - T_i] dV \tag{4–31}$$

where $T(x, t)$ is the temperature distribution in the medium at time t. Assuming constant properties, the ratio of Q/Q_{max} becomes

$$\frac{Q}{Q_{max}} = \frac{\int_V \rho c_p [T(x, t) - T_i] dV}{\rho c_p (T_\infty - T_i) V} = \frac{1}{V} \int_V (1 - \theta) dV \tag{4–32}$$

Using the appropriate nondimensional temperature relations based on the one-term approximation for the plane wall, cylinder, and sphere, and performing the indicated integrations, we obtain the following relations for the fraction of heat transfer in those geometries:

Plane wall: $$\left(\frac{Q}{Q_{max}} \right)_{wall} = 1 - \theta_{0, \text{ wall}} \frac{\sin \lambda_1}{\lambda_1} \tag{4–33}$$

Cylinder: $$\left(\frac{Q}{Q_{max}} \right)_{cyl} = 1 - 2\theta_{0, \text{ cyl}} \frac{J_1(\lambda_1)}{\lambda_1} \tag{4–34}$$

Sphere: $$\left(\frac{Q}{Q_{max}} \right)_{sph} = 1 - 3\theta_{0, \text{ sph}} \frac{\sin \lambda_1 - \lambda_1 \cos \lambda_1}{\lambda_1^3} \tag{4–35}$$

Note that once the *fraction* of heat transfer Q/Q_{max} based on the one-term approximation relations given above has been determined for the given t, the actual amount of heat transfer by that time can be evaluated by multiplying this fraction by Q_{max} given by Eq. 4–30. A *negative* sign for Q_{max} indicates that the body is *rejecting* heat.

The use of the one-term approximate solutions already discussed is limited to the conditions specified at the beginning of this section: the body is initially at a *uniform* temperature, the temperature of the medium surrounding the body and the convection heat transfer coefficient are *constant* and *uniform,* and there is no *heat generation* in the body.

We discussed the physical significance of the *Biot number* earlier and indicated that it is a measure of the relative magnitudes of the two heat transfer mechanisms: *convection* at the surface and *conduction* through the solid. A *small* value of Bi indicates that the inner resistance of the body to heat conduction is *small* relative to the resistance to convection between the surface and the fluid. As a result, the temperature distribution within the solid becomes fairly uniform, and lumped system analysis becomes applicable.

Recall that when Bi < 0.1, the error in assuming the temperature within the body to be *uniform* is negligible.

To understand the physical significance of the *Fourier number τ* (or Fo), we express it as (Fig 4.18)

$$\tau = \frac{\alpha t}{L^2} = \frac{kL^2(1/L)}{\rho c_p L^3/t} \frac{\Delta T}{\Delta T} = \frac{\text{The rate at which heat is } \textit{conducted}}{\text{across a body of thickness } L \text{ and}} \quad \text{(4–36)}$$

Therefore, the Fourier number is a measure of *heat conducted* through a body relative to *heat stored*. Thus, a large value of the Fourier number indicates faster propagation of heat through a body.

Perhaps you are wondering about what constitutes an infinitely large plate or an infinitely long cylinder. After all, nothing in this world is infinite. A plate whose thickness is small relative to the other dimensions can be modeled as an infinitely large plate, except very near the outer edges. But the edge effects on large bodies are usually negligible, and thus a large plane wall such as the wall of a house can be modeled as an infinitely large wall for heat transfer purposes. Similarly, a long cylinder whose diameter is small relative to its length can be analyzed as an infinitely long cylinder. The use of the one-term approximate solutions is illustrated in Examples 4–3, 4–4, and 4–5.
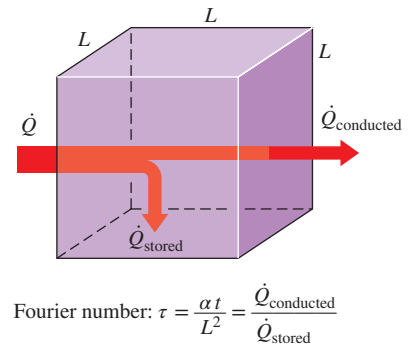
Fourier number: $\tau = \dfrac{\alpha t}{L^2} = \dfrac{\dot{Q}_{\text{conducted}}}{\dot{Q}_{\text{stored}}}$

FIGURE 4–18
Fourier number at time *t* can be viewed as the ratio of the rate of heat conducted to the rate of heat stored at that time.

EXAMPLE 4–3   Heating of Brass Plates in an Oven

In a production facility, large brass plates of 4-cm thickness that are initially at a uniform temperature of 20°C are heated by passing them through an oven that is maintained at 500°C (Fig. 4.19). The plates remain in the oven for a period of 7 min. Taking the combined convection and radiation heat transfer coefficient to be $h = 120$ W/m²·K, determine the surface temperature of the plates when they come out of the oven.

SOLUTION   Large brass plates are heated in an oven. The surface temperature of the plates leaving the oven is to be determined.
Assumptions   1 Heat conduction in the plate is one-dimensional since the plate is large relative to its thickness and there is thermal symmetry about the center plane. 2 The thermal properties of the plate and the heat transfer coefficient are constant. 3 The Fourier number is $\tau > 0.2$ so the one-term approximate solutions are applicable.
Properties   The properties of brass at room temperature are $k = 110$ W/m·K, $\rho = 8530$ kg/m³, $c_p = 380$ J/kg·K, and $\alpha = 33.9 \times 10^{-6}$ m²/s (Table A–3). More accurate results are obtained by using properties at average temperature.
Analysis   The temperature at a specified location at a given time can be determined from the one-term solutions. Noting that the half-thickness of the plate is $L = 0.02$ m, the Biot number for this problem is

$$\text{Bi} = \frac{hL}{k} = \frac{(120 \text{ W/m}^2\text{·K}) (0.02 \text{ m})}{52 \text{ W/m·K}} = 0.022$$

The coefficients λ_1 and A_1 for a plane wall corresponding to this Bi are determined from Table 4–2 to be

$$\lambda_1 = 0.1468, \quad A_1 = 1.0036$$

$T_\infty = 500°C$
$h = 120$ W/m²·K

$2L = 4$ cm
Brass plate
$T_i = 20°C$
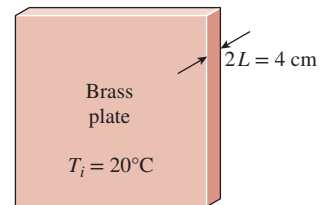
FIGURE 4–19
Schematic for Example 4–3.

The Fourier number is

$$\tau = \frac{\alpha t}{L^2} = \frac{(33.9 \times 10^{-6} \text{ m}^2/\text{s}) \, (7 \times 60 \text{ s})}{(0.02 \text{ m})^2} = 35.6$$

which is greater than 0.2, and thus the one-term approximate solution is applicable.

The surface $(x = L)$ temperature of the plates is determined by substituting these and other values into Eq. 4–23 and solving for $T(L, t)$

$$\frac{T(x, t) - T_\infty}{T_i - T_\infty} = A_1 e^{-\lambda_1^2 \tau} \cos(\lambda_1 x/L) \rightarrow \frac{T(L, t) - T_\infty}{T_i - T_\infty} = A_1 e^{-\lambda_1^2 \tau} \cos(\lambda_1)$$

$$T(L, t) = (T_i - T_\infty) \, A_1 e^{-\lambda_1^2 \tau} \cos(\lambda_1) + T_\infty$$

and thus

$$T(L, t) = (20 - 500) \, (1.0036) e^{-(0.1468)^2 (35.6)} \cos(0.1468) - 500 = \textbf{279°C}$$

Therefore, the surface temperature of the plates will be 279°C when they leave the oven.

Discussion We notice that the Biot number in this case is Bi = 0.022, which is much less than 0.1. Therefore, we expect the lumped system analysis to be applicable, and the lumped system analysis in this case may yield just as accurate results with less effort.

The heat transfer surface area of the plate is $2A$, where A is the face area of the plate (the plate transfers heat through both of its surfaces), and the volume of the plate is $V = (2L) \, A$, where L is the half-thickness of the plate. The exponent b used in the lumped system analysis is

$$b = \frac{hA_s}{\rho c_p V} = \frac{h(2A)}{\rho c_p (2LA)} = \frac{h}{\rho c_p L}$$

$$= \frac{120 \text{ W/m}^2 \cdot \text{K}}{(8530 \text{ kg/m}^3) \, (380 \text{ J/kg} \cdot \text{K}) \, (0.02 \text{ m})} = 0.00185 \text{ s}^{-1}$$

Then the temperature of the plate at $t = 7 \text{ min} = 420 \text{ s}$ is determined from

$$\frac{T(t) - T_\infty}{T_i - T_\infty} = e^{-bt} \quad \longrightarrow \quad \frac{T(t) - 500}{20 - 500} = e^{-(0.00185 \text{ s}^{-1})(420 \text{ s})}$$

It yields

$$T(t) = 279°C$$

which is identical to the result obtained above using the one-term approximate solution. Therefore, we can use lumped system analysis with confidence when the Biot number is sufficiently small.

$T_\infty = 200°C$
$h = 80 \text{ W/m}^2 \cdot \text{K}$

Stainless steel shaft

$D = 20 \text{ cm}$

$T_i = 600°C$
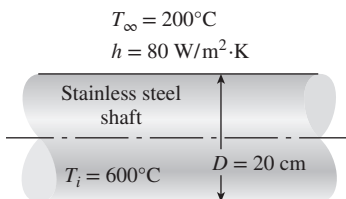
FIGURE 4–20
Schematic for Example 4–4.

EXAMPLE 4–4   **Cooling of a Long Stainless Steel Cylindrical Shaft**

A long 20-cm-diameter cylindrical shaft made of stainless steel 304 comes out of an oven at a uniform temperature of 600°C (Fig. 4–20). The shaft is then allowed to cool slowly in an environment chamber at 200°C with an average heat transfer coefficient of $h = 80 \text{ W/m}^2 \cdot \text{K}$. Determine the temperature at the center of the shaft 45 min after

the start of the cooling process. Also, determine the heat transfer per unit length of the shaft during this time period.

SOLUTION A long cylindrical shaft is allowed to cool slowly. The center temperature and the heat transfer per unit length are to be determined.

Assumptions **1** Heat conduction in the shaft is one-dimensional since it is long and it has thermal symmetry about the centerline. **2** The thermal properties of the shaft and the heat transfer coefficient are constant. **3** The Fourier number is $\tau > 0.2$, so the one-term approximate solutions are applicable.

Properties The properties of stainless steel 304 at room temperature are $k = 14.9$ W/m·K, $\rho = 7900$ kg/m^3, $c_p = 477$ J/kg·K, and $\alpha = 3.95 \times 10^{-6}$ m^2/s (Table A–3). More accurate results can be obtained by using properties at average temperature.

Analysis The temperature within the shaft may vary with the radial distance r as well as with time, and the temperature at a specified location at a given time can be determined from the one-term approximate solutions. Noting that the radius of the shaft is $r_o = 0.1$ m, the Biot and Fourier numbers for this problem are

$$\text{Bi} = \frac{hr_o}{k} = \frac{(80 \text{ W/m}^2\text{·K}) (0.1\text{m})}{14.9 \text{ W/m·K}} = 0.537$$

$$\tau = \frac{\alpha t}{r_o^2} = \frac{(3.95 \times 10^{-5} \text{ m}^2/\text{s}) (45 \times 60 \text{ s})}{(0.1 \text{ m})^2} = 1.07$$

The coefficients λ_1 and A_1 for a cylinder corresponding to this Bi are determined from Table 4–2 to be

$$\lambda_1 = 0.970, \quad A_1 = 1.122$$

Substituting these values into Eq. 4–27 gives

$$\theta_0 = \frac{T_0 - T_\infty}{T_i - T_\infty} = A_1 e^{-\lambda_1^2 \tau} = 1.122 e^{-(0.970)^2(1.07)} = 0.41$$

and thus the temperature at the center of the shaft is

$$T_0 = T_\infty + 0.41(T_i - T_\infty) = 200 + 0.41(600 - 200) = \mathbf{364°C}$$

To determine the actual heat transfer, we first need to calculate the maximum heat that can be transferred from the cylinder, which is the sensible energy of the cylinder relative to its environment. Taking $L = 1$ m,

$$m = \rho V = \rho \pi r_o^2 L = (7900 \text{ kg/m}^3)\pi(0.1 \text{ m})^2(1 \text{ m}) = 248.2 \text{ kg}$$

$$Q_{\text{max}} = mc_p(T_i - T_\infty) = (248.2 \text{ kg})(0.477 \text{ kJ/kg·K})(600 - 200)°C$$
$$= 47,350 \text{ kJ}$$

Then the fractional heat transfer (Q/Q_{max}) for the cylinder is determined from Eq. 4–34 to be

$$\frac{Q}{Q_{\text{max}}} = 1 - 2\theta_0\frac{J_1(\lambda_1)}{\lambda_1} = 1 - 2 \times 0.41\frac{0.430}{0.970} = 0.636$$

where the value of $J_1(\lambda_1)$ for $\lambda_1 = 0.970$ is determined from Table 4–3 to be 0.430.

The total heat transfer from the shaft during the first 45 min of the cooling is

$$Q = 0.636 Q_{\text{max}} = 0.636 \times (47,350 \text{ kJ}) = \mathbf{30,120 \text{ kJ}}$$

Discussion During the 45 minutes of the cooling period, the center temperature drops by 236°C, and the heat transferred from the shaft to the environment during this cooling process is about 64 percent of the maximum heat that can be transferred from the shaft.
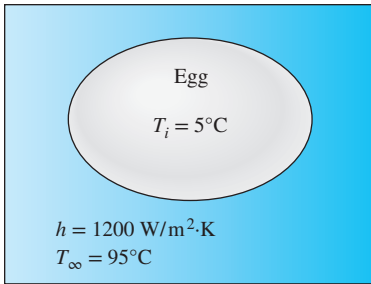
FIGURE 4–21
Schematic for Example 4–5.

EXAMPLE 4–5 Boiling Eggs

An ordinary egg can be approximated as a 5-cm-diameter sphere (Fig. 4–21). The egg is initially at a uniform temperature of 5°C and is dropped into boiling water at 95°C. Taking the convection heat transfer coefficient to be $h = 1200$ W/m^2·K, determine how long it will take for the center of the egg to reach 70°C.

SOLUTION An egg is cooked in boiling water. The cooking time of the egg is to be determined.

Assumptions **1** The egg is spherical in shape with a radius of $r_o = 2.5$ cm. **2** Heat conduction in the egg is one-dimensional because of thermal symmetry about the midpoint. **3** The thermal properties of the egg and the heat transfer coefficient are constant. **4** The Fourier number is $\tau > 0.2$, so the one-term approximate solutions are applicable.

Properties The water content of eggs is about 74 percent, and thus the thermal conductivity and diffusivity of eggs can be approximated by those of water at the average temperature of $(5 + 70)/2 = 37.5$°C; $k = 0.627$ W/m·K and $\alpha = k/\rho c_p = 0.151 \times 10^{-6}$ m^2/s (Table A–9).

Analysis Egg white begins to thicken at 63°C and turns solid at 65°C. The yolk begins to thicken at 65°C and sets at 70°C. The whole egg sets at temperatures above 70°C. Therefore, the egg in this case will qualify as hard boiled. The temperature within the egg varies with radial distance as well as time, and the temperature at a specified location at a given time can be determined from the one-term approximate solution. The Biot number for this problem is

$$\text{Bi} = \frac{hr_o}{k} = \frac{(1200 \text{ W/m}^2\text{·K})(0.025 \text{ m})}{0.627 \text{ W/m·K}} = 47.8$$

which is much greater than 0.1, and thus the lumped system analysis is not applicable. The coefficients λ_1 and A_1 for a sphere corresponding to this Bi are, from Table 4–2,

$$\lambda_1 = 3.0754, \quad A_1 = 1.9958$$

Substituting these and other values into Eq. 4–28 and solving for τ gives

$$\frac{T_0 - T_\infty}{T_i - T_\infty} = A_1 e^{-\lambda_1^2 \tau} \longrightarrow \frac{70 - 95}{5 - 95} = 1.9958 e^{-(3.0754)^2 \tau} \longrightarrow \tau = 0.209$$

which is greater than 0.2, and thus the one-term approximate solution is applicable with an error of less than 2 percent. Then the cooking time is determined from the definition of the Fourier number to be

$$t = \frac{\tau r_o^2}{\alpha} = \frac{(0.209)(0.025 \text{ m})^2}{0.151 \times 10^{-6} \text{ m}^2/\text{s}} = 865 \text{ s} \approx \textbf{14.4 min}$$

Therefore, it will take about 15 min for the center of the egg to be heated from 5°C to 70°C.

Discussion Note that the Biot number in lumped system analysis was defined differently as $\text{Bi} = hL_c/k = h(r_o/3)/k$. However, either definition can be used in determining the applicability of the lumped system analysis unless $\text{Bi} \approx 0.1$.

   Also note that the cooking time depends on many parameters such as the size of the egg, its temperature before cooking, the boiling temperature of water (and thus altitude), and the heat transfer coefficient (and thus the level of bubble motion during boiling). Therefore, there is a considerable amount of science or a good amount of experience behind boiling eggs to the correct amount of doneness.

4–3 ▪ TRANSIENT HEAT CONDUCTION IN SEMI-INFINITE SOLIDS

A semi-infinite solid is an idealized body that has a *single plane surface* and extends to infinity in all directions, as shown in Fig. 4–22. This idealized body is used to indicate that the temperature change in the part of the body in which we are interested (the region close to the surface) is due to the thermal conditions on a single surface. The earth, for example, can be considered to be a semi-infinite medium in determining the variation of temperature near its surface. Also, a thick wall can be modeled as a semi-infinite medium if all we are interested in is the variation of temperature in the region near one of the surfaces, and the other surface is too far away to have any impact on the region of interest during the time of observation. The temperature in the core region of the wall remains unchanged in this case.

For short periods of time, most bodies can be modeled as semi-infinite solids since heat does not have sufficient time to penetrate deep into the body, and the thickness of the body does not enter into the heat transfer analysis. A steel piece of any shape, for example, can be treated as a semi-infinite solid when it is quenched rapidly to harden its surface. A body whose surface is heated by a laser pulse can be treated the same way.

Consider a semi-infinite solid with constant thermophysical properties, no internal heat generation, uniform thermal conditions on its exposed surface, and initially a uniform temperature of T_i throughout. Heat transfer in this case occurs only in the direction normal to the surface (the x direction), and thus it is one-dimensional. Differential equations are independent of the boundary or initial conditions, and thus Eq. 4–10a for one-dimensional transient conduction in Cartesian coordinates applies. The depth of the solid is large ($x \rightarrow \infty$) compared to the depth that heat can penetrate, and these phenomena can be expressed mathematically as a boundary condition as $T(x \rightarrow \infty, t) = T_i$.

Heat conduction in a semi-infinite solid is governed by the thermal conditions imposed on the exposed surface, and thus the solution depends strongly on the boundary condition at $x = 0$. Below we present a detailed analytical solution for the case of constant temperature T_s on the surface and give the results for other more complicated boundary conditions. When the surface temperature is changed to T_s at $t = 0$ and held constant at that value at all times, the formulation of the problem can be expressed as

Differential equation:
$$\frac{\partial^2 T}{\partial x^2} = \frac{1}{\alpha} \frac{\partial T}{\partial t} \qquad \text{(4–37a)}$$

Boundary conditions: $T(0, t) = T_s$ and $T(x \rightarrow \infty, t) = T_i$ (4–37b)

Initial condition:
$$T(x, 0) = T_i \qquad \text{(4–37c)}$$

The separation of variables technique does not work in this case since the medium is infinite. But another clever approach that converts the partial differential equation into an ordinary differential equation by combining the two independent variables x and t into a single variable η, called the **similarity variable**, works well. For transient conduction in a semi-infinite medium, it is defined as

Similarity variable:
$$\eta = \frac{x}{\sqrt{4\alpha t}} \qquad \text{(4–38)}$$
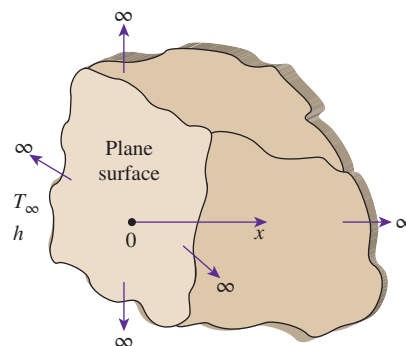
FIGURE 4–22
Schematic of a semi-infinite body.

$$\frac{\partial^2 T}{\partial x^2} = \frac{1}{\alpha} \frac{\partial T}{\partial t} \quad \text{and} \quad \eta = \frac{x}{\sqrt{4\alpha t}}$$

$$\frac{\partial T}{\partial t} = \frac{dT}{d\eta} \frac{\partial \eta}{\partial t} = \frac{-x}{2t\sqrt{4\alpha t}} \frac{dT}{d\eta}$$

$$\frac{\partial T}{\partial x} = \frac{dT}{d\eta} \frac{\partial \eta}{\partial x} = \frac{1}{\sqrt{4\alpha t}} \frac{dT}{d\eta}$$

$$\frac{\partial^2 T}{\partial x^2} = \frac{d}{d\eta}\left(\frac{\partial T}{\partial x}\right)\frac{\partial \eta}{\partial x} = \frac{1}{4\alpha t} \frac{d^2 T}{d\eta^2}$$

FIGURE 4–23
Transformation of variables in the derivatives of the heat conduction equation by the use of chain rule.

Assuming $T = T(\eta)$ (to be verified) and using the chain rule, all derivatives in the heat conduction equation can be transformed into the new variable, as shown in Fig. 4–23. Noting that $\eta = 0$ at $x = 0$ and $\eta \to \infty$ as $x \to \infty$ (and also at $t = 0$) and substituting into Eqs. 4–37 give, after simplification,

$$\frac{d^2 T}{d\eta^2} = -2\eta\frac{dT}{d\eta} \tag{4–39a}$$

$$T(0) = T_s \quad \text{and} \quad T(\eta \to \infty) = T_i \tag{4–39b}$$

Note that the second boundary condition and the initial condition result in the same boundary condition. Both the transformed equation and the boundary conditions depend on η only and are independent of x and t. Therefore, transformation is successful, and η is indeed a similarity variable.

To solve the second-order ordinary differential equation in Eqs. 4–39, we define a new variable w as $w = dT/d\eta$. This reduces Eq. 4–39a into a first-order differential equation than can be solved by separating variables,

$$\frac{dw}{d\eta} = -2\eta w \quad \to \quad \frac{dw}{w} = -2\eta d\eta \quad \to \quad \ln w = -\eta^2 + C_0 \to w = C_1 e^{-\eta^2}$$

where $C_1 = \ln C_0$. Back substituting $w = dT/d\eta$ and integrating again,

$$T = C_1 \int_0^\eta e^{-u^2}\,du + C_2 \tag{4–40}$$

where u is a dummy integration variable. The boundary condition at $\eta = 0$ gives $C_2 = T_s$, and the one for $\eta \to \infty$ gives

$$T_i = C_1 \int_0^\infty e^{-u^2}\,du + C_2 = C_1\frac{\sqrt{\pi}}{2} + T_s \to C_1 = \frac{2(T_i - T_s)}{\sqrt{\pi}} \tag{4–41}$$

Substituting the C_1 and C_2 expressions into Eq. 4–40 and rearranging, the variation of temperature becomes

$$\frac{T - T_s}{T_i - T_s} = \frac{2}{\sqrt{\pi}}\int_0^\eta e^{-u^2}\,du = \text{erf}(\eta) = 1 - \text{erfc}(\eta) \tag{4–42}$$

where the mathematical functions

$$\text{erf}(\eta) = \frac{2}{\sqrt{\pi}}\int_0^\eta e^{-u^2}\,du \quad \text{and} \quad \text{erfc}(\eta) = 1 - \text{erf}(\eta) = 1 - \frac{2}{\sqrt{\pi}}\int_0^\eta e^{-u^2}\,du \tag{4–43}$$

FIGURE 4–24
Error function is a standard mathematical function, just like the sinus and tangent functions, whose value varies between 0 and 1.

are called the **error function** and the **complementary error function**, respectively, of argument η (Fig. 4–24). Despite its simple appearance, the integral in the definition of the error function cannot be performed analytically. Therefore, the function $\text{erfc}(\eta)$ is evaluated numerically for different values of η, and the results are listed in Table 4–4.

TABLE 4–4

The complementary error function

η	erfc (η)	η	erfc (η)	η	erfc (η)	η	erfc (η)	η	erfc (η)	η	erfc (η)
0.00	1.00000	0.38	0.5910	0.76	0.2825	1.14	0.1069	1.52	0.03159	1.90	0.00721
0.02	0.9774	0.40	0.5716	0.78	0.2700	1.16	0.10090	1.54	0.02941	1.92	0.00662
0.04	0.9549	0.42	0.5525	0.80	0.2579	1.18	0.09516	1.56	0.02737	1.94	0.00608
0.06	0.9324	0.44	0.5338	0.82	0.2462	1.20	0.08969	1.58	0.02545	1.96	0.00557
0.08	0.9099	0.46	0.5153	0.84	0.2349	1.22	0.08447	1.60	0.02365	1.98	0.00511
0.10	0.8875	0.48	0.4973	0.86	0.2239	1.24	0.07950	1.62	0.02196	2.00	0.00468
0.12	0.8652	0.50	0.4795	0.88	0.2133	1.26	0.07476	1.64	0.02038	2.10	0.00298
0.14	0.8431	0.52	0.4621	0.90	0.2031	1.28	0.07027	1.66	0.01890	2.20	0.00186
0.16	0.8210	0.54	0.4451	0.92	0.1932	1.30	0.06599	1.68	0.01751	2.30	0.00114
0.18	0.7991	0.56	0.4284	0.94	0.1837	1.32	0.06194	1.70	0.01612	2.40	0.00069
0.20	0.7773	0.58	0.4121	0.96	0.1746	1.34	0.05809	1.72	0.01500	2.50	0.00041
0.22	0.7557	0.60	0.3961	0.98	0.1658	1.36	0.05444	1.74	0.01387	2.60	0.00024
0.24	0.7343	0.62	0.3806	1.00	0.1573	1.38	0.05098	1.76	0.01281	2.70	0.00013
0.26	0.7131	0.64	0.3654	1.02	0.1492	1.40	0.04772	1.78	0.01183	2.80	7.5E-05
0.28	0.6921	0.66	0.3506	1.04	0.1413	1.42	0.04462	1.80	0.01091	2.90	4.1E-05
0.30	0.6714	0.68	0.3362	1.06	0.1339	1.44	0.04170	1.82	0.01006	3.00	2.2E-05
0.32	0.6509	0.70	0.3222	1.08	0.1267	1.46	0.03895	1.84	0.00926	3.20	6.0E-06
0.34	0.6306	0.72	0.3086	1.10	0.1198	1.48	0.03635	1.86	0.00853	3.40	1.5E-06
0.36	0.6107	0.74	0.2953	1.12	0.1132	1.50	0.03390	1.88	0.00784	3.60	3.6E-07

Knowing the temperature distribution, the heat flux at the surface can be determined from Fourier's law to be

$$\dot{q}_s = -k\frac{\partial T}{\partial x}\Big|_{x=0} = -k\frac{dT}{d\eta}\frac{\partial \eta}{\partial x}\Big|_{\eta=0} = -kC_1 e^{-\eta^2}\frac{1}{\sqrt{4\alpha t}}\Big|_{\eta=0} = \frac{k(T_s - T_i)}{\sqrt{\pi\alpha t}} \quad \text{(4–44)}$$

The solutions in Eqs. 4–42 and 4–44 correspond to the case when the temperature of the exposed surface of the medium is suddenly raised (or lowered) to T_s at $t = 0$ and is maintained at that value at all times. The specified surface temperature case is closely approximated in practice when condensation or boiling takes place on the surface. Using a similar approach or the Laplace transform technique, analytical solutions can be obtained for other boundary conditions on the surface, with the following results.

Case 1: Specified Surface Temperature, T_s = constant (Fig. 4–25).

$$\frac{T(x, t) - T_i}{T_s - T_i} = \text{erfc}\left(\frac{x}{2\sqrt{\alpha t}}\right) \quad \text{and} \quad \dot{q}_s(t) = \frac{k(T_s - T_i)}{\sqrt{\pi\alpha t}} \quad \text{(4–45)}$$

Case 2: Specified Surface Heat Flux, $\dot{q}_s$ = constant.

$$T(x, t) - T_i = \frac{\dot{q}_s}{k}\left[\sqrt{\frac{4\alpha t}{\pi}}\exp\left(-\frac{x^2}{4\alpha t}\right) - x\,\text{erfc}\left(\frac{x}{2\sqrt{\alpha t}}\right)\right] \quad \text{(4–46)}$$
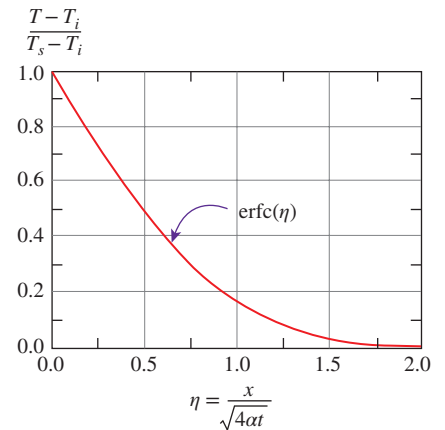
FIGURE 4–25

Dimensionless temperature distribution for transient conduction in a semi-infinite solid whose surface is maintained at a constant temperature T_s.

Case 3: Convection on the Surface, $\dot{q}_s(t) = h[T_\infty - T(0, t)]$.

$$\frac{T(x, t) - T_i}{T_\infty - T_i} = \mathrm{erfc}\left(\frac{x}{2\sqrt{\alpha t}}\right) - \exp\left(\frac{hx}{k} + \frac{h^2\alpha t}{k^2}\right)\mathrm{erfc}\left(\frac{x}{2\sqrt{\alpha t}} + \frac{h\sqrt{\alpha t}}{k}\right)$$

(4–47)

Case 4: Energy Pulse at Surface, e_s = constant.
Energy in the amount of e_s per unit surface area (in J/m^2) is supplied to the semi-infinite body instantaneously at time $t = 0$ (by a laser pulse, for example), and all energy is assumed to enter the body, with no heat loss from the surface.

$$T(x, t) - T_i = \frac{e_s}{k\sqrt{\pi t/\alpha}}\exp\left(-\frac{x^2}{4\alpha t}\right)$$

(4–48)

Note that Cases 1 and 3 are closely related. In Case 1, the surface $x = 0$ is brought to a temperature T_s at time $t = 0$ and kept at that value at all times. In Case 3, the surface is exposed to convection by a fluid at a constant temperature T_∞ with a heat transfer coefficient h.

The solutions for all four cases are plotted in Fig. 4–26 for a representative case using a large cast iron block initially at 0°C throughout. In Case 1, the surface temperature remains constant at the specified value of T_s, and temperature increases gradually within the medium as heat penetrates deeper into the solid. Note that during initial periods only a thin slice near the surface is affected by heat transfer. Also, the temperature gradient at the surface and thus the rate of heat transfer into the solid decreases with time. In Case 2, heat is continually supplied to the solid, and thus the temperature within the solid, including the surface, increases with time. This is also the case with convection (Case 3), except that the surrounding fluid temperature T_∞ is the highest temperature that the solid body can rise to. In Case 4, the surface is subjected to an instant burst of heat supply at time $t = 0$, such as heating by a laser pulse, and then the surface is covered with insulation. The result is an instant rise in surface temperature, followed by a temperature drop as heat is conducted deeper into the solid. Note that the temperature profile is always normal to the surface at all times. (Why?)

The variation of temperature with position and time in a semi-infinite solid subjected to convection heat transfer is plotted in Fig. 4–27 for the nondimensionalized temperature against the dimensionless similarity variable $\eta = x/\sqrt{4\alpha t}$ for various values of the parameter $h\sqrt{\alpha t}/k$. Although the graphical solution given in Fig. 4–27 is simply a plot of the exact analytical solution, it is subject to reading errors, and thus is of limited accuracy compared to the analytical solution. Also, the values on the vertical axis of Fig. 4–27 correspond to $x = 0$, and thus represent the surface temperature. The curve $h\sqrt{\alpha t}/k = \infty$ corresponds to $h \to \infty$, which corresponds to the case of *specified temperature* T_∞ at the surface at $x = 0$. That is, the case in which the surface of the semi-infinite body is suddenly brought to temperature T_∞ at $t = 0$ and kept at T_∞ at all times can be handled by setting h to infinity. For a *finite* heat transfer coefficient h, the surface temperature approaches the fluid temperature T_∞ as the time t approaches infinity.
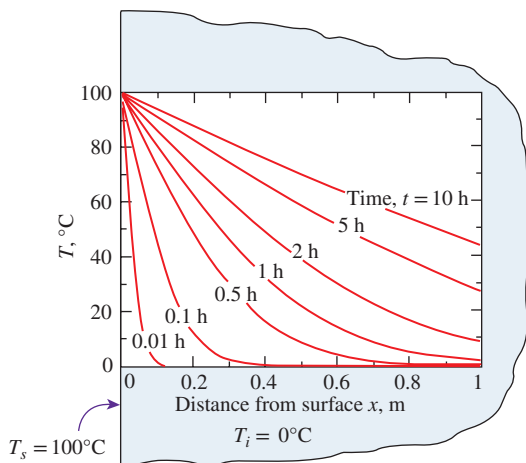
(a) Specified surface temperature, $T_s =$ constant
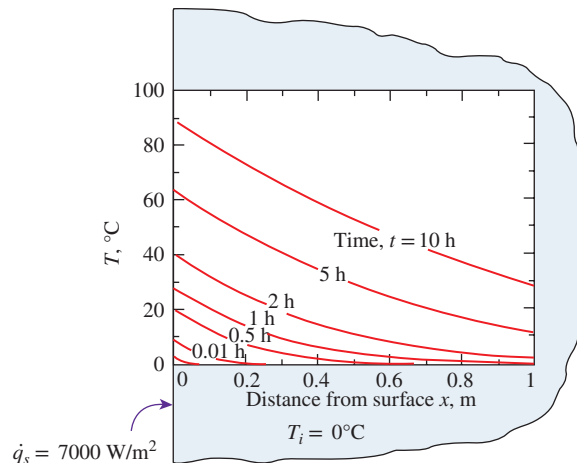
(b) Specified surface heat flux, $\dot{q}_s =$ constant
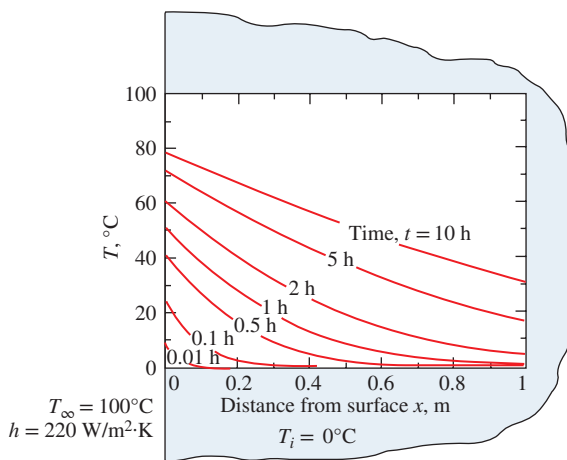
(c) Convection at the surface
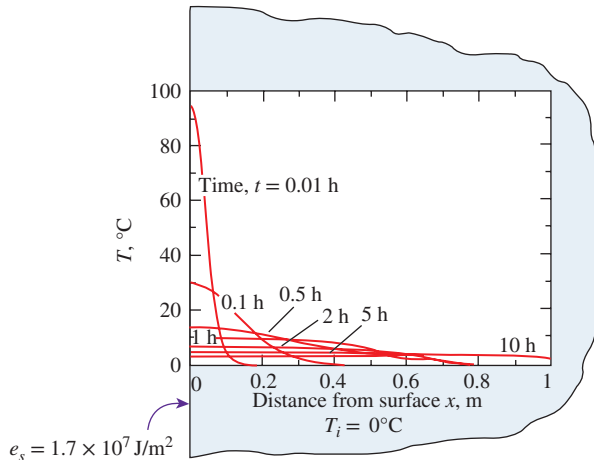
(d) Energy pulse at the surface, $e_s =$ constant

FIGURE 4–26
Variations of temperature with position and time in a large cast iron block ($\alpha = 2.31 \times 10^{-5}$ m^2/s, $k = 80.2$ W/m·K) initially at 0°C under different thermal conditions on the surface.

Contact of Two Semi-Infinite Solids

When two large bodies *A* and *B*, initially at uniform temperatures $T_{A,i}$ and $T_{B,i}$ are brought into contact, they instantly achieve temperature equality at the contact surface (temperature equality is achieved over the entire surface if the contact resistance is negligible). If the two bodies are of the same material with constant properties, thermal symmetry requires the contact surface temperature to be the arithmetic average, $T_s = (T_{A,i} + T_{B,i})/2$, and to remain constant at that value at all times.
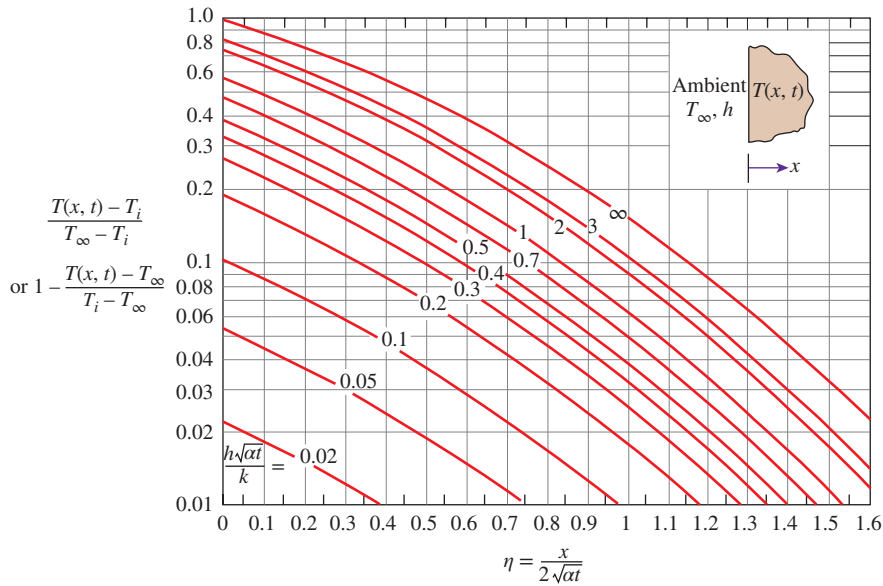
FIGURE 4–27

Variation of temperature with position and time in a semi-infinite solid initially at temperature T_i subjected to convection to an environment at T_∞ with a convection heat transfer coefficient of h (plotted using EES).

FIGURE 4–28

Contact of two semi-infinite solids of different initial temperatures.

If the bodies are of different materials, they still achieve a temperature equality, but the surface temperature T_s in this case will be different than the arithmetic average. Noting that both bodies can be treated as semi-infinite solids with the same specified surface temperature, the energy balance on the contact surface gives, from Eq. 4–45,

$$\dot{q}_{s,A} = \dot{q}_{s,B} \rightarrow -\frac{k_A(T_s - T_{A,i})}{\sqrt{\pi\alpha_A t}} = \frac{k_B(T_s - T_{B,i})}{\sqrt{\pi\alpha_B t}} \rightarrow \frac{T_{A,i} - T_s}{T_s - T_{B,i}} = \sqrt{\frac{(k\rho c_p)_B}{(k\rho c_p)_A}}$$
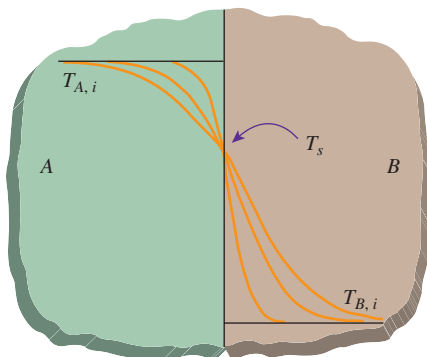
Then T_s is determined to be (Fig. 4–28)

$$T_s = \frac{\sqrt{(k\rho c_p)_A}\, T_{A,i} + \sqrt{(k\rho c_p)_B}\, T_{B,i}}{\sqrt{(k\rho c_p)_A} + \sqrt{(k\rho c_p)_B}} \tag{4–49}$$

Therefore, the interface temperature of two bodies brought into contact is dominated by the body with the larger $k\rho c_p$. This also explains why a metal at room temperature feels colder than wood at the same temperature. At room temperature, the $\sqrt{k\rho c_p}$ value is 24 kJ/m²·K for aluminum, 0.38 kJ/m²·K for wood, and 1.1 kJ/m²·K for human flesh. Using Eq. 4–49, it can be shown that when a person with a skin temperature of 35°C touches an aluminum block and then a wood block both at 15°C, the contact surface temperature will be 15.9°C in the case of aluminum and 30°C in the case of wood.

EXAMPLE 4–6   **Minimum Burial Depth of Water Pipes to Avoid Freezing**

In areas where the air temperature remains below 0°C for prolonged periods of time, the freezing of water in underground pipes is a major concern. Fortunately, the soil remains relatively warm during those periods, and it takes weeks for the subfreezing temperatures to reach the water mains in the ground. Thus, the soil effectively serves as insulation to protect the water from subfreezing temperatures in winter.

The ground at a particular location is covered with snowpack at $-10°C$ for a continuous period of three months, and the average soil properties at that location are $k = 0.4$ W/m·K and $\alpha = 0.15 \times 10^{-6}$ m²/s (Fig. 4–29). Assuming an initial uniform temperature of 15°C for the ground, determine the minimum burial depth to prevent the water pipes from freezing.

SOLUTION   The water pipes are buried in the ground to prevent freezing. The minimum burial depth at a particular location is to be determined.

Assumptions   **1** The temperature in the soil is affected by the thermal conditions at one surface only, and thus the soil can be considered to be a semi-infinite medium. **2** The thermal properties of the soil are constant.

Properties   The properties of the soil are as given in the problem statement.

Analysis   The temperature of the soil surrounding the pipes will be 0°C after three months in the case of minimum burial depth. Therefore, from Fig. 4–27, we have

$$\left.\begin{array}{l} \dfrac{h\sqrt{\alpha t}}{k} = \infty \quad \text{(since } h \to \infty) \\[2mm] \dfrac{T(x, t) - T_i}{T_\infty - T_i} = \dfrac{0 - 15}{-10 - 15} = 0.6 \end{array}\right\} \eta = \dfrac{x}{2\sqrt{\alpha t}} = 0.36$$

We note that

$$t = (90 \text{ days})(24 \text{ h/day})(3600 \text{ s/h}) = 7.78 \times 10^6 \text{ s}$$

and thus

$$x = 2\eta\sqrt{\alpha t} = 2 \times 0.36\sqrt{(0.15 \times 10^{-6} \text{ m}^2/\text{s})(7.78 \times 10^6 \text{ s})} = \textbf{0.78 m}$$

Therefore, the water pipes must be buried to a depth of at least 78 cm to avoid freezing under the specified harsh winter conditions.

ALTERNATIVE SOLUTION   The solution of this problem could also be determined from Eq. 4–45:

$$\frac{T(x, t) - T_i}{T_s - T_i} = \text{erfc}\left(\frac{x}{2\sqrt{\alpha t}}\right) \quad \longrightarrow \quad \frac{0 - 15}{-10 - 15} = \text{erfc}\left(\frac{x}{2\sqrt{\alpha t}}\right) = 0.60$$

The argument that corresponds to this value of the complementary error function is determined from Table 4–4 to be $\eta = 0.37$. Therefore,

$$x = 2\eta\sqrt{\alpha t} = 2 \times 0.37\sqrt{(0.15 \times 10^{-6} \text{ m}^2/\text{s})(7.78 \times 10^6 \text{ s})} = \textbf{0.80 m}$$

Again, the slight difference is due to the reading error of the chart.
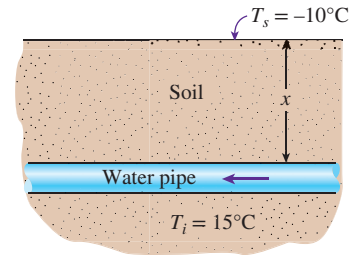
FIGURE 4–29
Schematic for Example 4–6.

$\dot{q}_s = 1250$ W/m^2

Wood block

$T_i = 20°C$
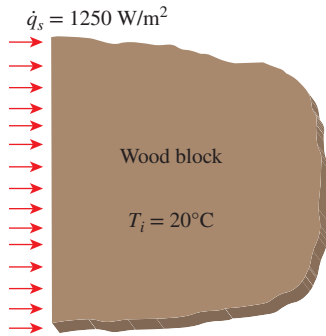
FIGURE 4–30
Schematic for Example 4–7.
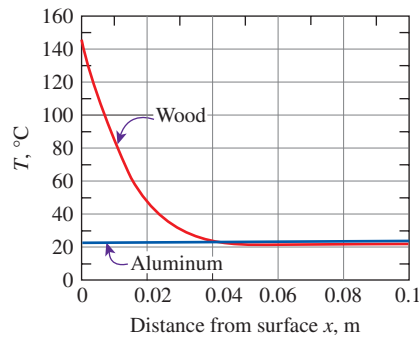
FIGURE 4–31
Variation of temperature within
the wood and aluminum blocks at
$t = 20$ min.

Cryogenic fluid, T_∞, h

L

Metal plate

x

Bolt
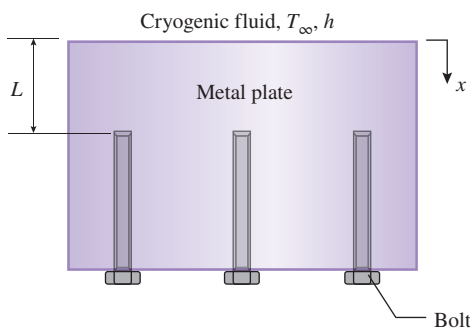
FIGURE 4–32
Schematic for Example 4–8.

EXAMPLE 4–7   **Surface Temperature Rise of Heated Blocks**

A thick, black-painted wood block at 20°C is subjected to constant solar heat flux of
1250 W/m^2 (Fig. 4–30). Determine the exposed surface temperature of the block after
20 minutes. What would your answer be if the block were made of aluminum?

SOLUTION   A wood block is subjected to solar heat flux. The surface temperature
of the block is to be determined and compared to the value for an aluminum block.
Assumptions   **1** All incident solar radiation is absorbed by the block. **2** Heat loss from
the block is disregarded (and thus the result obtained is the maximum temperature). **3** The
block is sufficiently thick to be treated as a semi-infinite solid, and the properties of the
block are constant.
Properties   Thermal conductivity and diffusivity values at room temperature are
$k = 0.159$ W/m·K and $\alpha = k/\rho c_p = 1.75 \times 10^{-7}$ m^2/s for hardwoods (Table A–5) and
$k = 237$ W/m·K and $\alpha = 9.71 \times 10^{-5}$ m^2/s for pure aluminum (Table A–3).
Analysis   This is a transient conduction problem in a semi-infinite medium subjected to
constant surface heat flux, and the surface temperature can be expressed from Eq. 4–46 as

$$T_s = T(0, t) = T_i + \frac{\dot{q}_s}{k}\sqrt{\frac{4\alpha t}{\pi}}$$

Substituting the given values, the surface temperatures for both the wood and alumi-
num blocks are determined to be

$$T_{s,\text{ wood}} = 20°C + \frac{1250 \text{ W/m}^2}{0.159 \text{ W/m·K}}\sqrt{\frac{4(1.75 \times 10^{-7} \text{ m}^2/\text{s})(20 \times 60 \text{ s})}{\pi}} = \mathbf{149°C}$$

$$T_{s,\text{ Al}} = 20°C + \frac{1250 \text{ W/m}^2}{237 \text{ W/m·K}}\sqrt{\frac{4(9.71 \times 10^{-5} \text{ m}^2/\text{s})(20 \times 60 \text{ s})}{\pi}} = \mathbf{22.0°C}$$

Note that thermal energy supplied to the wood accumulates near the surface because
of the low conductivity and diffusivity of wood, causing the surface temperature to
rise to high values. Metals, on the other hand, conduct the heat they receive to inner
parts of the block because of their high conductivity and diffusivity, resulting in mini-
mal temperature rise at the surface. In reality, both temperatures will be lower because
of heat losses.
Discussion   The temperature profiles for both wood and aluminum blocks at
$t = 20$ min are evaluated and plotted in Fig. 4–31 using appropriate software. At a depth of
$x = 0.044$ m the temperature in both blocks is 21.8°C. At a depth of 0.08 m, the tempera-
tures become 20.0°C for wood and 21.6°C for aluminum block, which confirms that heat
penetrates faster and further in metals than in nonmetals.

C&S *EXAMPLE 4–8*   **Compliance of ASME Codes for Bolts
Exposed to Cryogenic Fluid**

A series of long stainless steel bolts (ASTM A437 B4B) are fastened into a thick
metal plate (Fig. 4–32). The metal plate has a thermal conductivity of 16.3 W/m·K,
a specific heat of 500 J/kg·K, and a density of 8 g/cm^3. The upper surface of the plate
is occasionally exposed to cryogenic fluid at $-70°C$ with a convection heat transfer

coefficient of 300 W/m²·K. The bolts are fastened into the metal plate from the bottom surface, and the distance measured from the plate's upper surface to the bolt tips is $L = 1$ cm. The ASME Code for Process Piping limits the minimum suitable temperature for ASTM A437 B4B stainless steel bolt to $-30°C$ (ASME B31.3-2014, Table A-2M). If the initial temperature of the plate is $10°C$ and the plate's upper surface is exposed to the cryogenic fluid for 30 minutes, would the bolts fastened in the plate still comply with the ASME code?

SOLUTION ASTM A437 B4B stainless steel bolts are fastened in a metal plate from the bottom surface, while the plate's upper surface is subjected to convection with cryogenic fluid at $T_\infty = -70°C$ and $h = 300$ W/m²·K. The plate has an initial temperature of $10°C$. Would the bolts comply with the ASME Code for Process Piping if the plate's upper surface is exposed to the cold fluid for 30 min?

Assumptions **1** The plate is thick and is considered a semi-infinite solid. **2.** Heat conduction is transient in the semi-infinite solid. **3** Thermal properties are constant. **4** Radiation effects are negligible. **5** The convection heat transfer coefficient is constant.

Properties The thermal properties of the metal plate are $c_p = 500$ J/kg·K, $k = 16.3$ W/m·K, and $\rho = 8000$ kg/m³.

Analysis This is a transient conduction problem in a semi-infinite medium subjected to convection at the surface; use Eq. 4–47 to calculate the plate temperature at a depth of $x = 1$ cm. So we have

$$\frac{T(x, t) - T_i}{T_\infty - T_i} = \text{erfc}\left(\frac{x}{2\sqrt{\alpha t}}\right) - \exp\left(\frac{hx}{k} + \frac{h^2\alpha t}{k^2}\right)\text{erfc}\left(\frac{x}{2\sqrt{\alpha t}} + \frac{h\sqrt{\alpha t}}{k}\right)$$

where $x = L = 0.01$ m and $t = 1800$ s. First we determine the various quantities in parentheses in Eq. 4–47:

$$\alpha = \frac{k}{\rho c_p} = \frac{16.3 \text{ W/m·K}}{(8000 \text{ kg/m}^3)(500 \text{ J/kg·K})} = 4.075 \times 10^{-6} \text{ m}^2/\text{s}$$

$$\frac{x}{2\sqrt{\alpha t}} = \frac{0.01 \text{ m}}{2\sqrt{(4.075 \times 10^{-6} \text{ m}^2/\text{s})(1800 \text{ s})}} = 0.058381$$

$$\frac{x}{2\sqrt{\alpha t}} + \frac{h\sqrt{\alpha t}}{k} = 0.58381 + \frac{(300 \text{ W/m}^2\text{·K})\sqrt{(4.075 \times 10^{-6} \text{ m}^2/\text{s})(1800 \text{ s})}}{16.3 \text{ W/m·K}} = 1.6347$$

$$\frac{hx}{k} = \frac{(300 \text{ W/m}^2\text{·K})(0.01 \text{ m})}{16.3 \text{ W/m·K}} = 0.18405$$

$$\frac{h^2\alpha t}{k^2} = \frac{(300 \text{ W/m}^2\text{·K})^2 (4.075 \times 10^{-6} \text{ m}^2/\text{s})(1800 \text{ s})}{(16.3 \text{ W/m·K})^2} = 2.48466$$

$$\text{erfc}\left(\frac{x}{2\sqrt{\alpha t}}\right) = \text{erfc}(0.058381) = 0.9342$$

$$\text{erfc}\left(\frac{x}{2\sqrt{\alpha t}} + \frac{h\sqrt{\alpha t}}{k}\right) = \text{erfc}(1.6347) = 0.020791$$

Thus

$$\frac{T(L, t) - T_i}{T_\infty - T_i} = 0.9342 - \exp(0.18405 + 2.48466)(0.020791) = 0.63437$$
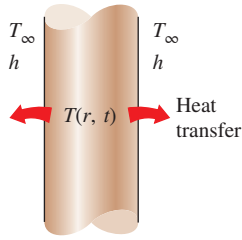
(*a*) Long cylinder
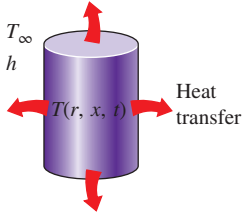
(*b*) Short cylinder (two-dimensional)

FIGURE 4–33
The temperature in a short cylinder exposed to convection from all surfaces varies in both the radial and axial directions, and thus heat is transferred in both directions.
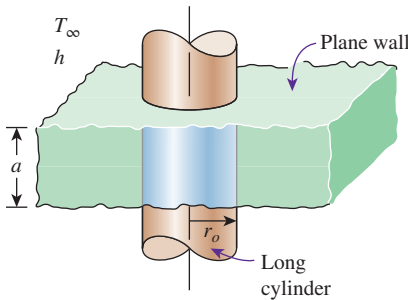
FIGURE 4–34
A short cylinder of radius r_o and height *a* is the *intersection* of a long cylinder of radius r_o and a plane wall of thickness *a*.

and

$$T(L, t) = (-70 - 10)°C(0.63437) + 10°C = \mathbf{-40.7°C} < -30°C$$

Discussion After 30 minutes of subjecting the upper surface to convection with the cryogenic fluid, the plate temperature at a depth of $x = 1$ cm from the upper surface is $-40.7°C$. This means that the bolt tips are at a temperature that is below the minimum suitable temperature specified by the ASME Code for Process Piping. Therefore, the bolts would not be in compliance.

4–4 · TRANSIENT HEAT CONDUCTION IN MULTIDIMENSIONAL SYSTEMS

The analytical solutions presented earlier can be used to determine the temperature distribution and heat transfer in *one-dimensional* heat conduction problems associated with a large plane wall, a long cylinder, a sphere, and a semi-infinite medium. Using a superposition approach called the **product solution**, these solutions can also be used to construct solutions for the *two-dimensional* transient heat conduction problems encountered in geometries such as a short cylinder, a long rectangular bar, or a semi-infinite cylinder or plate, and even *three-dimensional* problems associated with geometries such as a rectangular prism or a semi-infinite rectangular bar, provided that *all* surfaces of the solid are subjected to convection to the *same* fluid at temperature T_∞, with the *same* heat transfer coefficient *h,* and the body involves no heat generation (Fig. 4–33). The solution in such multidimensional geometries can be expressed as the *product* of the solutions for the one-dimensional geometries whose intersection is the multidimensional geometry.

Consider a *short cylinder* of height *a* and radius r_o initially at a uniform temperature T_i. There is no heat generation in the cylinder. At time $t = 0$, the cylinder is subjected to convection from all surfaces to a medium at temperature T_∞ with a heat transfer coefficient *h*. The temperature within the cylinder will change with *x* as well as *r* and time *t* since heat transfer occurs from the top and bottom of the cylinder as well as its side surfaces. That is, $T = T(r, x, t)$, and thus this is a two-dimensional transient heat conduction problem. When the properties are assumed to be constant, it can be shown that the solution to this two-dimensional problem can be expressed as

$$\left(\frac{T(r, x, t) - T_\infty}{T_i - T_\infty}\right)_{\substack{\text{short} \\ \text{cylinder}}} = \left(\frac{T(x, t) - T_\infty}{T_i - T_\infty}\right)_{\substack{\text{plane} \\ \text{wall}}} \left(\frac{T(r, t) - T_\infty}{T_i - T_\infty}\right)_{\substack{\text{infinite} \\ \text{cylinder}}} \quad \textbf{(4–50)}$$

That is, the solution for the two-dimensional short cylinder of height *a* and radius r_o is equal to the *product* of the nondimensionalized solutions for the one-dimensional plane wall of thickness *a* and the long cylinder of radius r_o, which are the two geometries whose intersection is the short cylinder, as shown in Fig. 4–34. We generalize this as follows: *the solution*

for a multidimensional geometry is the product of the solutions of the one-dimensional geometries whose intersection is the multidimensional body.

For convenience, the one-dimensional solutions are denoted by

$$\theta_{\text{wall}}(x, t) = \left(\frac{T(x, t) - T_\infty}{T_i - T_\infty} \right)_{\substack{\text{plane} \\ \text{wall}}}$$

$$\theta_{\text{cyl}}(r, t) = \left(\frac{T(r, t) - T_\infty}{T_i - T_\infty} \right)_{\substack{\text{infinite} \\ \text{cylinder}}} \qquad \textbf{(4–51)}$$

$$\theta_{\text{semi-inf}}(x, t) = \left(\frac{T(x, t) - T_\infty}{T_i - T_\infty} \right)_{\substack{\text{semi-infinite} \\ \text{solid}}}$$

For example, the solution for a long, solid bar whose cross section is an $a \times b$ rectangle is the intersection of the two infinite plane walls of thicknesses a and b, as shown in Fig. 4–35, and thus the transient temperature distribution for this rectangular bar can be expressed as

$$\left(\frac{T(x, y, t) - T_\infty}{T_i - T_\infty} \right)_{\substack{\text{rectangular} \\ \text{bar}}} = \theta_{\text{wall}}(x, t)\theta_{\text{wall}}(y, t) \qquad \textbf{(4–52)}$$

The proper forms of the product solutions for some other geometries are given in Table 4–5. It is important to note that the *x*-coordinate is measured from the *surface* in a semi-infinite solid and from the *midplane* in a plane wall. The radial distance *r* is always measured from the centerline.

Note that the solution of a *two-dimensional* problem involves the product of *two* one-dimensional solutions, whereas the solution of a *three-dimensional* problem involves the product of *three* one-dimensional solutions.

A modified form of the product solution can also be used to determine the total transient heat transfer to or from a multidimensional geometry by using the one-dimensional values, as shown by L. S. Langston in 1982. The transient heat transfer for a two-dimensional geometry formed by the intersection of two one-dimensional geometries 1 and 2 is

$$\left(\frac{Q}{Q_{\text{max}}} \right)_{\text{total, 2D}} = \left(\frac{Q}{Q_{\text{max}}} \right)_1 + \left(\frac{Q}{Q_{\text{max}}} \right)_2 \left[1 - \left(\frac{Q}{Q_{\text{max}}} \right)_1 \right] \qquad \textbf{(4–53)}$$

Transient heat transfer for a three-dimensional body formed by the intersection of three one-dimensional bodies 1, 2, and 3 is given by

$$\left(\frac{Q}{Q_{\text{max}}} \right)_{\text{total, 3D}} = \left(\frac{Q}{Q_{\text{max}}} \right)_1 + \left(\frac{Q}{Q_{\text{max}}} \right)_2 \left[1 - \left(\frac{Q}{Q_{\text{max}}} \right)_1 \right]$$

$$+ \left(\frac{Q}{Q_{\text{max}}} \right)_3 \left[1 - \left(\frac{Q}{Q_{\text{max}}} \right)_1 \right] \left[1 - \left(\frac{Q}{Q_{\text{max}}} \right)_2 \right] \qquad \textbf{(4–54)}$$

The use of the product solution in transient two- and three-dimensional heat conduction problems is illustrated in the following examples.
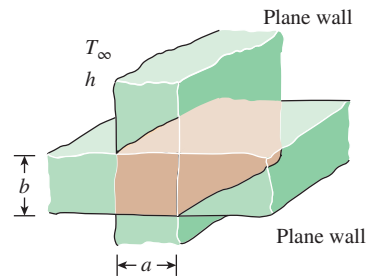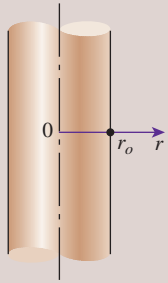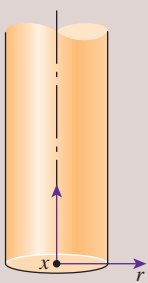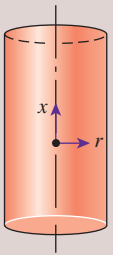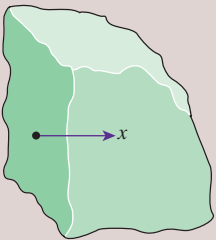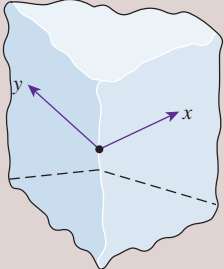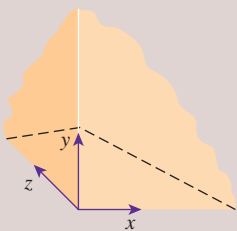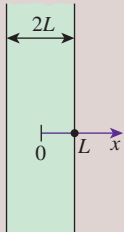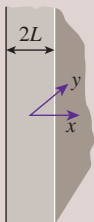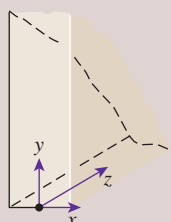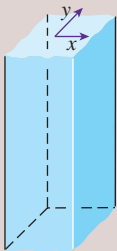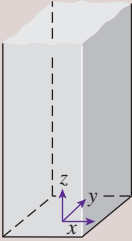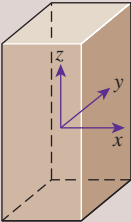
FIGURE 4–35

A long, solid bar of rectangular profile $a \times b$ is the *intersection* of two plane walls of thicknesses *a* and *b*.

TABLE 4–5

Multidimensional solutions expressed as products of one-dimensional solutions for bodies that are initially at a uniform temperature T_i and exposed to convection from all surfaces to a medium at T_∞

$\theta(r, t) = \theta_{\text{cyl}}(r, t)$
Infinite cylinder

$\theta(x, r, t) = \theta_{\text{cyl}}(r, t)\, \theta_{\text{semi-inf}}(x, t)$
Semi-infinite cylinder

$\theta(x, r, t) = \theta_{\text{cyl}}(r, t)\, \theta_{\text{wall}}(x, t)$
Short cylinder

$\theta(x, t) = \theta_{\text{semi-inf}}(x, t)$
Semi-infinite medium

$\theta(x, y, t) = \theta_{\text{semi-inf}}(x, t)\, \theta_{\text{semi-inf}}(y, t)$
Quarter-infinite medium

$\theta(x, y, z, t) =$
$\theta_{\text{semi-inf}}(x, t)\, \theta_{\text{semi-inf}}(y, t)\, \theta_{\text{semi-inf}}(z, t)$
Corner region of a large medium

$\theta(x, t) = \theta_{\text{wall}}(x, t)$
Infinite plate (or plane wall)

$\theta(x, y, t) = \theta_{\text{wall}}(x, t)\, \theta_{\text{semi-inf}}(y, t)$
Semi-infinite plate

$\theta(x, y, z, t) =$
$\theta_{\text{wall}}(x, t)\, \theta_{\text{semi-inf}}(y, t)\, \theta_{\text{semi-inf}}(z, t)$
Quarter-infinite plate

$\theta(x, y, t) = \theta_{\text{wall}}(x, t)\, \theta_{\text{wall}}(y, t)$
Infinite rectangular bar

$\theta(x, y, z, t) =$
$\theta_{\text{wall}}(x, t)\, \theta_{\text{wall}}(y, t)\, \theta_{\text{semi-inf}}(z, t)$
Semi-infinite rectangular bar

$\theta(x, y, z, t) =$
$\theta_{\text{wall}}(x, t)\, \theta_{\text{wall}}(y, t)\, \theta_{\text{wall}}(z, t)$
Rectangular parallelepiped

EXAMPLE 4–9   Cooling of a Short Brass Cylinder

A short brass cylinder of diameter $D = 10$ cm and height $H = 12$ cm is initially at a uniform temperature $T_i = 120°C$. The cylinder is now placed in atmospheric air at 25°C, where heat transfer takes place by convection, with a heat transfer coefficient of $h = 60$ W/m²·K. Calculate the temperature at (a) the center of the cylinder and (b) the center of the top surface of the cylinder 15 min after the start of the cooling.

SOLUTION   A short cylinder is allowed to cool in atmospheric air. The temperatures at the centers of the cylinder and the top surface are to be determined.

Assumptions   **1** Heat conduction in the short cylinder is two-dimensional, and thus the temperature varies in both the axial x- and the radial r-directions. **2** The thermal properties of the cylinder and the heat transfer coefficient are constant. **3** The Fourier number is $\tau > 0.2$ so that the one-term approximate solutions are applicable.

Properties   The properties of brass at room temperature are $k = 110$ W/m·K and $\alpha = 33.9 \times 10^{-6}$ m²/s (Table A–3). More accurate results can be obtained by using properties at average temperature.

Analysis   (a) This short cylinder can physically be formed by the intersection of a long cylinder of radius $r_o = 5$ cm and a plane wall of thickness $2L = 12$ cm, as shown in Fig. 4–36. The dimensionless temperature at the center of the plane wall is determined from Eq. 4–26.

First we find the Biot and Fourier numbers for the plane wall

$$\text{Bi} = \frac{hL}{k} = \frac{(60 \text{ W/m}^2\text{·K}) (0.06 \text{ m})}{110 \text{ W/m·K}} = 0.0327$$

$$\tau = \frac{\alpha t}{L^2} = \frac{(3.39 \times 10^{-5} \text{ m}^2\text{/s}) (15 \times 60 \text{ s})}{(0.06 \text{ m})^2} = 8.48$$

The coefficients λ_1 and A_1 for a plane wall corresponding to Bi = 0.0327 are determined from Table 4–2 to be $\lambda_1 = 0.1776$ and $A_1 = 1.0054$.

Substituting these and other values into Eq. 4–26 gives

$$\theta_{0, \text{wall}} = \frac{T_0 - T_\infty}{T_i - T_\infty} = A_1 e^{-\lambda_1^2 \tau} = 1.0054 \, e^{-(0.1776)^2(8.48)} = 0.77$$

Similarly, the temperature at the center of the cylinder is determined from the one-term approximate solutions Eq. 4–27. First we find the Biot and Fourier numbers for the cylinder

$$\text{Bi} = \frac{hr_o}{k} = \frac{(60 \text{ W/m}^2\text{·K}) (0.05 \text{ m})}{110 \text{ W/m·K}} = 0.0273$$

$$\tau = \frac{\alpha t}{L^2} = \frac{(3.39 \times 10^{-5} \text{ m}^2\text{/s})(15 \times 60 \text{ s})}{(0.05 \text{ m})^2} = 12.2$$

The coefficients λ_1 and A_1 for a cylinder corresponding to Bi = 0.0273 are determined from Table 4–2 to be $\lambda_1 = 0.2294$ and $A_1 = 1.0068$.

Substituting these and other values into Eq. 4–27 gives

$$\theta_{0, \text{cyl}} = \frac{T_0 - T_\infty}{T_i - T_\infty} = A_1 e^{-\lambda_1^2 \tau} = 1.0068 e^{-(0.2294)^2(12.2)} = 0.53$$

Therefore,

$$\left(\frac{T(0, 0, t) - T_\infty}{T_i - T_\infty} \right)_{\substack{\text{short} \\ \text{cylinder}}} = \theta_{0, \text{wall}}(0, t) \times \theta_{0, \text{cyl}}(0, t) = 0.77 \times 0.53 = 0.41$$

$T_\infty = 25°C$
$h = 60$ W/m²·K
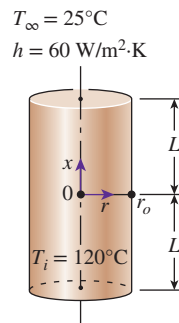
FIGURE 4–36
Schematic for Example 4–9.

and

$$T(0, 0, t) = T_\infty + 0.41(T_i - T_\infty) = 25 + 0.41(120 - 25) = \mathbf{64°C}$$

This is the temperature at the center of the short cylinder, which is also the center of both the long cylinder and the plate.

(*b*) The center of the top surface of the cylinder is still at the center of the long cylinder ($r = 0$), but at the outer surface of the plane wall ($x = L$). Therefore, we first need to find the surface temperature of the wall using the one-term approximate solutions Eq. 4–23. Noting that $x = L = 0.06$ m, the values of the Biot number, Fourier number, and the constants λ_1 and A_1 remain the same as was determined in part (*a*) for the plane wall. Substituting these and other values into Eq. 4–23 gives

$$\theta_{wall} = \frac{T(x, t) - T_\infty}{T_i - T_\infty} = A_1 e^{-\lambda_1^2 \tau} \cos(\lambda_1 x/L)$$

$$\theta_{wall} = \frac{T(x, L) - T_\infty}{T_i - T_\infty} = A_1 e^{-\lambda_1^2 \tau} \cos(\lambda_1) = 1.0054 e^{-(0.1776)^2 (8.48)} \cos(0.1776) = 0.757$$

Therefore,

$$\left(\frac{T(L, 0, t) - T_\infty}{T_i - T_\infty} \right)_{\substack{\text{short} \\ \text{cylinder}}} = \theta_{wall}(L, t)\, \theta_{0, \text{cyl}}(0, t) = 0.757 \times 0.53 = 0.40$$

and

$$T(L, 0, t) = T_\infty + 0.40(T_i - T_\infty) = 25 + 0.40(120 - 25) = \mathbf{63°C}$$

which is the temperature at the center of the top surface of the cylinder.

EXAMPLE 4–10   Heat Transfer from a Short Cylinder

Determine the total heat transfer from the short brass cylinder ($\rho = 8530$ kg/m³, $c_p = 0.380$ kJ/kg·K) discussed in Example 4–9.

SOLUTION   We first determine the maximum heat that can be transferred from the cylinder, which is the sensible energy content of the cylinder relative to its environment:

$$m = \rho V = \rho \pi r_o^2 H = (8530 \text{ kg/m}^3)\pi(0.05 \text{ m})^2(0.12 \text{ m}) = 8.04 \text{ kg}$$

$$Q_{max} = mc_p(T_i - T_\infty) = (8.04 \text{ kg})(0.380 \text{ kJ/kg·K})(120 - 25)°C = 290.2 \text{ kJ}$$

Then we determine the dimensionless heat transfer ratios for both geometries. For the plane wall, it is determined from the one-term approximate solutions Eq. 4–33 to be

$$\left(\frac{Q}{Q_{max}} \right)_{wall} = 1 - \theta_{0, \text{wall}} \frac{\sin(\lambda_1)}{\lambda_1} = 1 - (0.77) \frac{\sin(0.1776)}{0.1776} = 0.23$$

Similarly, for the cylinder using the one-term approximate relation Eq. 4–34, we have

$$\left(\frac{Q}{Q_{max}} \right)_{cyl} = 1 - 2\theta_{0, \text{cyl}} \frac{J_1(\lambda_1)}{\lambda_1} = 1 - 2(0.53) \frac{0.11385}{0.2294} = 0.47$$

since $J_1(0.2294) = 0.11385$ from Table 4–3. The heat transfer ratio for the short cylinder is, from Eq. 4–53,

$$\left(\frac{Q}{Q_{max}}\right)_{short\ cyl} = \left(\frac{Q}{Q_{max}}\right)_{plane\ wall} + \left(\frac{Q}{Q_{max}}\right)_{long\ cyl}\left[1 - \left(\frac{Q}{Q_{max}}\right)_{plane\ wall}\right]$$
$$= 0.23 + 0.47(1 - 0.23) = 0.592$$

Therefore, the total heat transfer from the cylinder during the first 15 min of cooling is

$$Q = 0.592\,Q_{max} = 0.592 \times (290.2 \text{ kJ}) = \textbf{172 kJ}$$

TOPIC OF SPECIAL INTEREST *

Refrigeration and Freezing of Foods

Control of Microorganisms in Foods

Microorganisms such as *bacteria, yeasts, molds,* and *viruses* are widely encountered in air, water, soil, living organisms, and unprocessed food items, and cause *off-flavors* and *odors, slime production, changes* in texture and appearance, and the eventual *spoilage* of foods. Holding perishable foods at warm temperatures is the primary cause of spoilage, and the prevention of food spoilage and the premature degradation of quality due to microorganisms is the largest application area of refrigeration. The first step in controlling microorganisms is to understand what they are and the factors that affect their transmission, growth, and destruction.

Of the various kinds of microorganisms, *bacteria* are mainly responsible for the spoilage of foods, especially moist foods. Dry and acidic foods create an undesirable environment for the growth of bacteria, but not for the growth of yeasts and molds. *Molds* are also encountered on moist surfaces, cheese, and spoiled foods. Specific *viruses* are encountered in certain animals and humans, and poor sanitation practices, such as keeping processed foods in the same area as the uncooked ones and being careless about handwashing, can cause the contamination of food products.

When *contamination* occurs, the microorganisms start to adapt to the new environmental conditions. This initial slow or no-growth period is called the **lag phase**, and the shelf life of a food item is directly proportional to the length of this phase (Fig. 4–37). The adaptation period is followed by an *exponential growth* period during which the population of microorganisms can double two or more times every hour under favorable conditions unless drastic sanitation measures are taken. The depletion of nutrients and the accumulation of toxins slow down the growth and start the *death* period.

The *rate of growth* of microorganisms in a food item depends on the characteristics of the food itself such as the chemical structure, pH level, presence of inhibitors and competing microorganisms, and water activity as well as the environmental conditions such as the temperature and relative humidity of the environment and the air motion (Fig. 4–38).
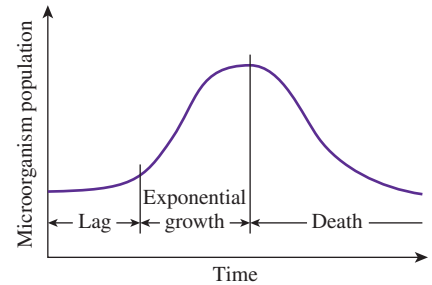
FIGURE 4–37
Typical growth curve of microorganisms.
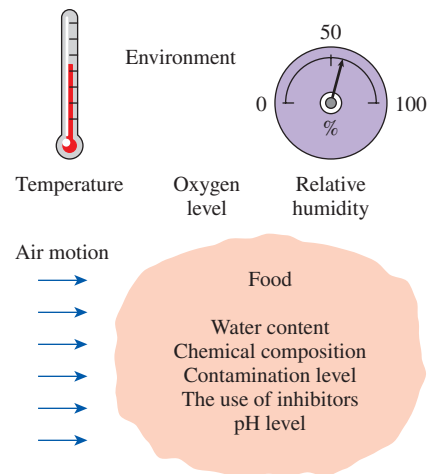
FIGURE 4–38
The factors that affect the rate of growth of microorganisms.

---

*This section can be skipped without a loss of continuity.
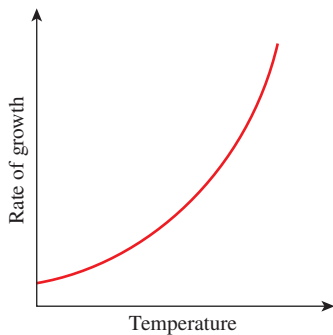
Microorganisms need *food* to grow and multiply, and their nutritional needs are readily provided by the carbohydrates, proteins, minerals, and vitamins in a food. Different types of microorganisms have different nutritional needs, and the types of nutrients in a food determine the types of microorganisms that may dwell on them. The preservatives added to the food may also inhibit the growth of certain microorganisms. Different kinds of microorganisms that exist compete for the same food supply, and thus the composition of microorganisms in a food at any time depends on the *initial make-up* of the microorganisms.

All living organisms need *water* to grow, and microorganisms cannot grow in foods that are not sufficiently moist. Microbiological growth in refrigerated foods such as fresh fruits, vegetables, and meats starts at the *exposed surfaces* where contamination is most likely to occur. Fresh meat in a package left in a room will spoil quickly, as you may have noticed. A meat carcass hung in a controlled environment, on the other hand, will age healthily as a result of *dehydration* on the outer surface, which inhibits microbiological growth there and protects the carcass.

Microorganism growth in a food item is governed by the combined effects of the *characteristics of the food* and the *environmental factors*. We cannot do much about the characteristics of the food, but we certainly can alter the environmental conditions to more desirable levels through *heating, cooling, ventilating, humidification, dehumidification,* and control of the *oxygen* levels. The growth rate of microorganisms in foods is a strong function of temperature, and temperature control is the single most effective mechanism for controlling the growth rate.

Microorganisms grow best at "warm" temperatures, usually between 20 and 60°C. The growth rate *declines* at high temperatures, and *death* occurs at still higher temperatures, usually above 70°C for most microorganisms. *Cooling* is an effective and practical way of reducing the growth rate of microorganisms and thus extending the *shelf life* of perishable foods. A temperature of 4°C or lower is considered to be a safe refrigeration temperature. Sometimes a small increase in refrigeration temperature may cause a large increase in the growth rate, and thus a considerable decrease in shelf life of the food (Fig. 4–39). The growth rate of some microorganisms, for example, doubles for each 3°C rise in temperature.

Another factor that affects microbiological growth and transmission is the *relative humidity* of the environment, which is a measure of the water content of the air. High humidity in *cold rooms* should be avoided since condensation that forms on the walls and ceiling creates the proper environment for *mold growth* and buildups. The drip of contaminated condensate onto food products in the room poses a potential health hazard.

Different microorganisms react differently to the presence of oxygen in the environment. Some microorganisms such as molds require oxygen for growth, while some others cannot grow in the presence of oxygen. Some grow best in low-oxygen environments, while others grow in environments regardless of the amount of oxygen. Therefore, the growth of certain microorganisms can be controlled by controlling the *amount of oxygen* in the environment. For example, vacuum packaging inhibits the growth of

FIGURE 4–39
The rate of growth of microorganisms in a food product increases exponentially with increasing environmental temperature.

microorganisms that require oxygen. Also, the storage life of some fruits can be extended by reducing the oxygen level in the storage room.

Microorganisms in food products can be controlled by (1) *preventing* contamination by following strict sanitation practices, (2) *inhibiting* growth by altering the environmental conditions, and (3) *destroying* the organisms by heat treatment or chemicals. The best way to minimize contamination in food processing areas is to use fine air filters in ventilation systems to capture the *dust particles* that transport the bacteria in the air. Of course, the filters must remain dry since microorganisms can grow in wet filters. Also, the ventilation system must maintain a positive pressure in the food processing areas to prevent any airborne contaminants from entering inside by infiltration. The elimination of *condensation* on the walls and the ceiling of the facility and the diversion of *plumbing* condensation drip pans of refrigerators to the drain system are two other preventive measures against contamination. Drip systems must be cleaned regularly to prevent microbiological growth in them. Also, any *contact* between raw and cooked food products should be minimized, and cooked products must be stored in rooms with positive pressures. Frozen foods must be kept at −18°C or below, and utmost care should be exercised when food products are packaged after they are frozen to avoid contamination during packaging.

The growth of microorganisms is best controlled by keeping the *temperature* and *relative humidity* of the environment in the desirable range. Keeping the relative humidity below 60 percent, for example, prevents the growth of all microorganisms on the surfaces. Microorganisms can be destroyed by *heating* the food product to high temperatures (usually above 70°C), by treating them with *chemicals,* or by exposing them to *ultraviolet light* or solar radiation.

Distinction should be made between *survival* and *growth* of microorganisms. A particular microorganism that may not grow at some low temperature may be able to survive at that temperature for a very long time (Fig. 4–40). Therefore, freezing is not an effective way of killing microorganisms. In fact, some microorganism cultures are preserved by freezing them at very low temperatures. The *rate of freezing* is also an important consideration in the refrigeration of foods since some microorganisms adapt to low temperatures and grow at those temperatures when the cooling rate is very low.

Refrigeration and Freezing of Foods

The *storage life* of fresh perishable foods such as meats, fish, vegetables, and fruits can be extended by several days by storing them at temperatures just above freezing, usually between 1 and 4°C. The storage life of foods can be extended by several months by freezing and storing them at subfreezing temperatures, usually between −18 and −35°C, depending on the particular food (Fig. 4–41).

Refrigeration *slows down* the chemical and biological processes in foods, and the accompanying deterioration and loss of quality and nutrients. Sweet corn, for example, may lose half of its initial sugar content in one day at 21°C, but only 5 percent of it at 0°C. Fresh asparagus may lose 50 percent of its vitamin C content in one day at 20°C, but in 12 days
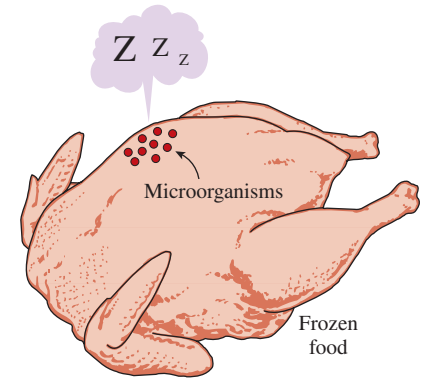
FIGURE 4–40
Freezing may stop the growth of microorganisms, but it may not necessarily kill them.
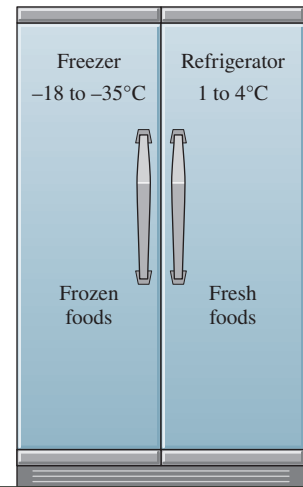
FIGURE 4–41
Recommended refrigeration and freezing temperatures for most perishable foods.
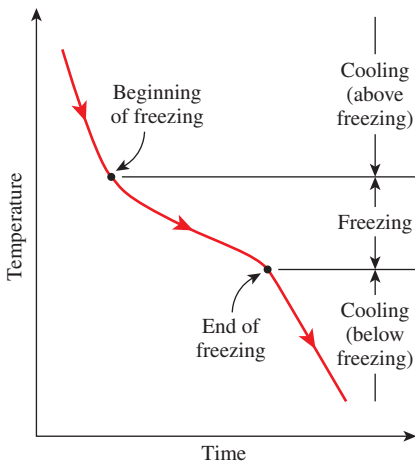
FIGURE 4–42
Typical freezing curve of a food item.

TABLE 4–6

Thermal properties of beef

Quantity	Typical Value
Average density	1070 kg/m^3
Specific heat:	
Above freezing	3.14 kJ/kg·K
Below freezing	1.70 kJ/kg·K
Freezing point	−2.7°C
Latent heat of fusion	249 kJ/kg
Thermal	0.41 W/m·K
conductivity	(at 6°C)

at 0°C. Refrigeration also extends the shelf life of products. The first appearance of unsightly yellowing of broccoli, for example, may be delayed by three or more days by refrigeration.

Early attempts to freeze food items resulted in poor-quality products because of the large ice crystals that formed. It was determined that the *rate of freezing* has a major effect on the size of ice crystals and the quality, texture, and nutritional and sensory properties of many foods. During *slow freezing,* ice crystals can grow to a large size, whereas during *fast freezing* a large number of ice crystals start forming at once and are much smaller in size. Large ice crystals are not desirable since they can *puncture* the walls of the cells, causing a degradation of texture and a loss of natural juices during thawing. A *crust* forms rapidly on the outer layer of the product and seals in the juices, aromatics, and flavoring agents. The product quality is also affected adversely by temperature fluctuations of the storage room.

The ordinary refrigeration of foods involves *cooling* only without any phase change. The *freezing* of foods, on the other hand, involves three stages: *cooling* to the freezing point (removing the sensible heat), *freezing* (removing the latent heat), and *further cooling* to the desired subfreezing temperature (removing the sensible heat of frozen food), as shown in Fig. 4–42.

Beef Products

Meat carcasses in slaughterhouses should be cooled *as fast as possible* to a uniform temperature of about 1.7°C to reduce the growth rate of microorganisms that may be present on carcass surfaces, and thus minimize spoilage. The right level of *temperature, humidity,* and *air motion* should be selected to prevent excessive shrinkage, toughening, and discoloration.

The deep body temperature of an animal is about 39°C, but this temperature tends to rise a couple of degrees in the midsections after slaughter as a result of the *heat generated* during the biological reactions that occur in the cells. The temperature of the exposed surfaces, on the other hand, tends to drop as a result of heat losses. The thickest part of the carcass is the *round,* and the center of the round is the last place to cool during chilling. Therefore, the cooling of the carcass can best be monitored by inserting a thermometer deep into the central part of the round.

About 70 percent of the beef carcass is water, and the carcass is cooled mostly by *evaporative cooling* as a result of moisture migration toward the surface where evaporation occurs. But this shrinking translates into a loss of salable mass that can amount to 2 percent of the total mass during an overnight chilling. To prevent *excessive* loss of mass, carcasses are usually washed or sprayed with water prior to cooling. With adequate care, spray chilling can eliminate carcass cooling shrinkage almost entirely.

The average total mass of dressed beef, which is normally split into two sides, is about 300 kg, and the average specific heat of the carcass is about 3.14 kJ/kg·K (Table 4–6). The *chilling room* must have a capacity equal to the daily kill of the slaughterhouse, which may be several hundred. A beef carcass is washed before it enters the chilling room and absorbs a large amount of water (about 3.6 kg) at its surface during the washing process. This does not represent a net mass gain, however, since it is lost
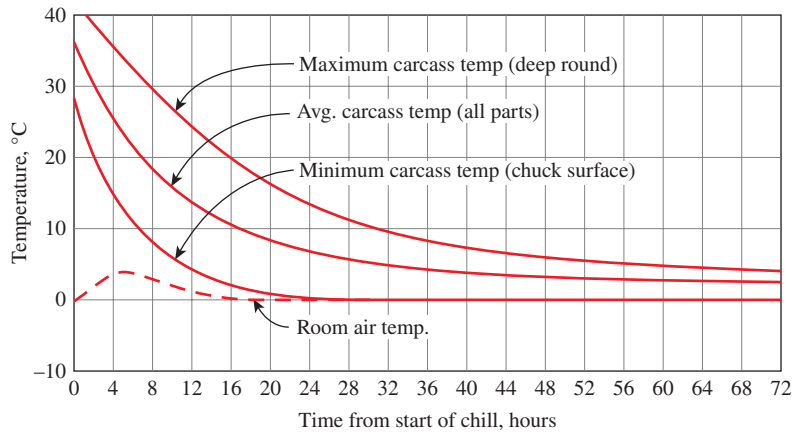
FIGURE 4–43

Typical cooling curve of a beef carcass in the chilling and holding rooms at an average temperature of 0°C.

From ASHRAE Handbook: Refrigeration, Chap. 11, Fig. 2.

by dripping or evaporation in the chilling room during cooling. Ideally, the carcass does not lose or gain any net weight as it is cooled in the chilling room. However, it does lose about 0.5 percent of the total mass in the *holding room* as it continues to cool. The actual product loss is determined by first weighing the dry carcass before washing and then weighing it again after it is cooled.

The refrigerated air temperature in the chilling room of beef carcasses must be sufficiently high to avoid *freezing* and *discoloration* on the outer surfaces of the carcass. This means a long residence time for the massive beef carcasses in the chilling room to cool to the desired temperature. Beef carcasses are only partially cooled at the end of an overnight stay in the chilling room. The temperature of a beef carcass drops to 1.7 to 7°C at the surface and to about 15°C in middle parts of the round in 10 h. It takes another day or two in the *holding room* maintained at 1 to 2°C to complete *chilling* and *temperature equalization.* But hog carcasses are fully chilled during that period because of their smaller size. The *air circulation* in the holding room is kept at minimum levels to avoid excessive moisture loss and discoloration. The refrigeration load of the holding room is much smaller than that of the chilling room, and thus it requires a smaller refrigeration system.

Beef carcasses intended for distant markets are shipped the day after slaughter in refrigerated trucks, where the rest of the cooling is done. This practice makes it possible to deliver fresh meat long distances in a timely manner.

The variation in temperature of the beef carcass during cooling is given in Fig. 4–43. Initially, the cooling process is dominated by *sensible* heat transfer. Note that the average temperature of the carcass is reduced by about 28°C (from 36 to 8°C) in 20 h. The cooling rate of the carcass could be increased by *lowering* the refrigerated air temperature and *increasing* the air velocity, but such measures also increase the risk of *surface freezing.*

Most meats are judged on their **tenderness**, and the preservation of tenderness is an important consideration in the refrigeration and freezing of meats. Meat consists primarily of bundles of tiny *muscle fibers* bundled together inside long strings of *connective tissues* that hold it together. The
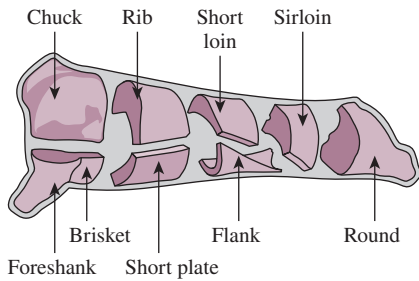
FIGURE 4–44
Various cuts of beef.
From National Livestock and Meat Board.
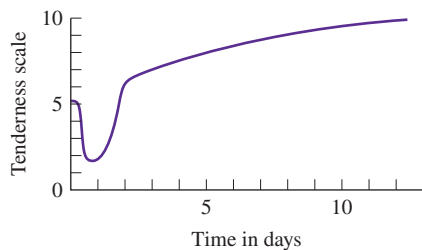
FIGURE 4–45
Variation of tenderness of meat stored at 2°C with time after slaughter.
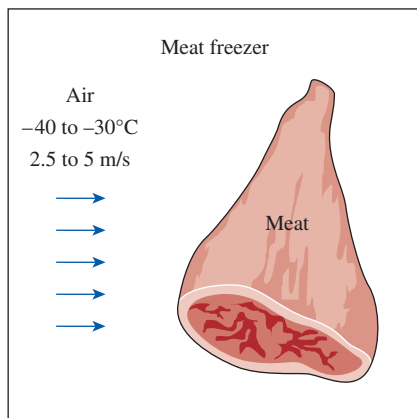
FIGURE 4–46
The freezing time of meat can be reduced considerably by using low-temperature air at high velocity.

tenderness of a certain cut of beef depends on the location of the cut, the age, and the activity level of the animal. Cuts from the relatively inactive mid-backbone section of the animal such as short loins, sirloin, and prime ribs are more tender than the cuts from the active parts such as the legs and the neck (Fig. 4–44). The more active the animal, the more the connective tissue, and the tougher the meat. The meat of an older animal is more flavorful, however, and is preferred for stewing since the toughness of the meat does not pose a problem for moist-heat cooking such as boiling. The protein *collagen,* which is the main component of the connective tissue, softens and dissolves in hot and moist environments and gradually transforms into *gelatin,* and tenderizes the meat.

The old saying "one should either cook an animal immediately after slaughter or wait at least two days" has a lot of truth in it. The biomechanical reactions in the muscle continue after the slaughter until the energy supplied to the muscle to do work diminishes. The muscle then stiffens and goes into *rigor mortis.* This process begins several hours after the animal is slaughtered and continues for 12 to 36 h until an enzymatic action sets in and tenderizes the connective tissue, as shown in Fig. 4–45. It takes about seven days to complete tenderization naturally in storage facilities maintained at 2°C. Electrical stimulation also causes the meat to be tender. To avoid toughness, fresh meat should not be frozen before rigor mortis has passed.

You have probably noticed that steaks are tender and rather tasty when they are hot but toughen as they cool. This is because the gelatin that formed during cooking thickens as it cools, and meat loses its tenderness. So it is no surprise that first-class restaurants serve their steak on hot thick plates that keep the steaks warm for a long time. Also, cooking *softens* the connective tissue but *toughens* the tender muscle fibers. Therefore, barbecuing on *low heat* for a long time results in a tough steak.

Variety meats intended for long-term storage must be frozen rapidly to reduce spoilage and preserve quality. Perhaps the first thought that comes to mind to freeze meat is to place the meat packages into the *freezer* and wait. But the freezing time is *too long* in this case, especially for large boxes. For example, the core temperature of a 4-cm-deep box containing 32 kg of variety meat can be as high as 16°C 24 h after it is placed into a −30°C freezer. The freezing time of large boxes can be shortened considerably by adding some *dry ice* into it.

A more effective method of freezing, called *quick chilling,* involves the use of lower air temperatures, −40 to −30°C, with higher velocities of 2.5 m/s to 5 m/s over the product (Fig. 4–46). The internal temperature should be lowered to −4°C for products to be transferred to a storage freezer and to −18°C for products to be shipped immediately. The *rate of freezing* depends on the *package material* and its insulating properties, the *thickness* of the largest box, the *type* of meat, and the *capacity* of the refrigeration system. Note that the air temperature will rise excessively during initial stages of freezing and increase the freezing time if the capacity of the system is inadequate. A smaller refrigeration system will be adequate if dry ice is to be used in packages. Shrinkage during freezing varies from about 0.5 to 1 percent.

Although the average freezing point of lean meat can be taken to be $-2°C$ with a latent heat of 249 kJ/kg, it should be remembered that freezing occurs over a *temperature range,* with most freezing occurring between -1 and $-4°C$. Therefore, cooling the meat through this temperature range and removing the latent heat takes the most time during freezing.

Meat can be kept at an internal temperature of -2 to $-1°C$ for local use and storage for *under a week.* Meat must be frozen and stored at much lower temperatures for *long-term storage.* The lower the storage temperature, the longer the storage life of meat products, as shown in Table 4–7.

The *internal temperature* of carcasses entering the cooling sections varies from 38 to 41°C for hogs and from 37 to 39°C for lambs and calves. It takes about 15 h to cool the hogs and calves to the recommended temperature of 3 to 4°C. The cooling-room temperature is maintained at -1 to 0°C, and the temperature difference between the refrigerant and the cooling air is kept at about 6°C. Air is circulated at a rate of about 7 to 12 air changes per hour. *Lamb carcasses* are cooled to an internal temperature of 1 to 2°C, which takes about 12 to 14 h, and are held at that temperature with 85 to 90 percent relative humidity until shipped or processed. The recommended rate of *air circulation* is 50 to 60 air changes per hour during the first 4 to 6 h, which is reduced to 10 to 12 changes per hour afterward.

Freezing does not seem to affect the *flavor* of meat much, but it affects the *quality* in several ways. The *rate* and *temperature* of freezing may influence color, tenderness, and drip. Rapid freezing increases tenderness and reduces the tissue damage and the amount of drip after thawing. Storage at low freezing temperatures causes significant changes in *animal fat.* Frozen pork experiences more undesirable changes during storage because of its fat structure, and thus its acceptable storage period is shorter than that of beef, veal, or lamb.

Meat storage facilities usually have a *refrigerated shipping dock* where the orders are assembled and shipped out. Such docks save valuable storage space from being used for shipping purposes and provide a more acceptable working environment for the employees. Packing plants that ship whole or half carcasses in bulk quantities may not need a shipping dock; a load-out door is often adequate for such cases.

A refrigerated *shipping dock,* as shown in Fig. 4–47, reduces the *refrigeration load* of freezers or coolers and prevents *temperature fluctuations* in the storage area. It is often adequate to maintain the shipping docks at 4 to 7°C for the coolers and about 1.5°C for the freezers. The dew point of the dock air should be below the product temperature to avoid condensation on the surface of the products and loss of quality. The rate of *airflow* through the loading doors and other openings is proportional to the *square root* of the temperature difference, and thus reducing the temperature difference at the opening by half by keeping the shipping dock at the average temperature reduces the rate of airflow into the dock and thus into the freezer by $1 - \sqrt{0.5} \cong 0.3$, or 30 percent. Also, the air that flows into the freezer is already cooled to about 1.5°C by the refrigeration unit of the dock, which represents about 50 percent of the cooling load of the incoming air. Thus, the net effect of the refrigerated shipping dock is a reduction of the *infiltration load* of the freezer by about 65 percent since

TABLE 4–7

Storage life of frozen meat products at different storage temperatures

Product	Storage Life, Months		
	Temperature		
	$-12°C$	$-18°C$	$-23°C$
Beef	4–12	6–18	12–24
Lamb	3–8	6–16	12–18
Veal	3–4	4–14	8
Pork	2–6	4–12	8–15
Chopped beef	3–4	4–6	8
Cooked foods	2–3	2–4	

From ASHRAE Handbook: Refrigeration*, Chap. 10, Table 7.*
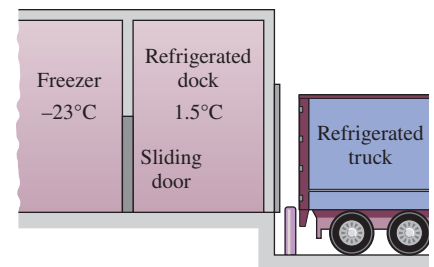
FIGURE 4–47
A refrigerated truck dock for loading frozen items to a refrigerated truck.
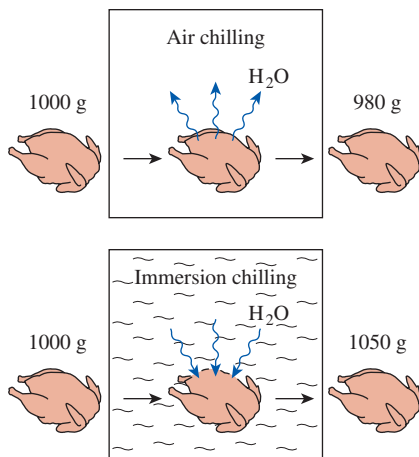
$1 - 0.7 \times 0.5 = 0.65$. The net gain is equal to the difference between the reduction of the infiltration load of the freezer and the refrigeration load of the shipping dock. Note that the dock refrigerators operate at much higher temperatures ($1.5°C$ instead of about $-23°C$), and thus they consume much less power for the same amount of cooling.

Poultry Products

Poultry products can be preserved by *ice-chilling* to 1 to 2°C or *deep chilling* to about $-2°C$ for short-term storage, or by *freezing* them to $-18°C$ or below for long-term storage. Poultry processing plants are completely *automated,* and the small size of the birds makes continuous conveyor line operation feasible.

The birds are first electrically stunned before cutting to prevent struggling. Following a 90- to 120-s bleeding time, the birds are *scalded* by immersing them in a tank of warm water, usually at 51 to 55°C, for up to 120 s to loosen the feathers. Then the feathers are removed by feather-picking machines, and the eviscerated carcass is *washed* thoroughly before chilling. The internal temperature of the birds ranges from 24 to 35°C after washing, depending on the temperatures of the ambient air and the washing water as well as the extent of washing.

To control the microbial growth, the USDA regulations require that poultry be chilled to 4°C or below in less than 4 h for carcasses of less than 1.8 kg, in less than 6 h for carcasses of 1.8 to 3.6 kg, and in less than 8 h for carcasses more than 3.6 kg. Meeting these requirements today is not difficult since slow *air chilling* is largely replaced by rapid *immersion chilling* in tanks of slush ice. Immersion chilling has the added benefit that it not only prevents dehydration, but it causes a *net absorption of water* and thus increases the mass of salable product. Cool air chilling of unpacked poultry can cause a moisture loss of 1 to 2 percent, while water immersion chilling can cause a moisture absorption of 4 to 15 percent (Fig. 4–48). Water spray chilling can cause a moisture absorption of up to 4 percent. Most water absorbed is held between the flesh and the skin and the connective tissues in the skin. In immersion chilling, some soluble solids are lost from the carcass to the water, but the loss has no significant effect on flavor.

Many slush ice tank chillers today are replaced by *continuous* flow-type immersion slush ice chillers. Continuous slush ice-chillers can reduce the internal temperature of poultry from 32 to 4°C in about 30 minutes at a rate up to 10, 000 birds per hour. Ice requirements depend on the inlet and exit temperatures of the carcass and the water, but 0.25 kg of ice per kg of carcass is usually adequate. However, *bacterial contamination* such as salmonella remains a concern with this method, and it may be necessary to chloride the water to control contamination.

Tenderness is an important consideration for poultry products just as it is for red meat, and preserving tenderness is an important consideration in the cooling and freezing of poultry. Birds cooked or frozen before passing through rigor mortis remain very tough. Natural tenderization begins soon after slaughter and is completed within 24 h when birds are held at 4°C.

FIGURE 4–48
Air chilling causes dehydration and thus weight loss for poultry, whereas immersion chilling causes a weight gain as a result of water absorption.

Tenderization is rapid during the first three hours and slows down there-after. Immersion in hot water and cutting into the muscle adversely affect tenderization. Increasing the *scalding temperature* or the scalding time has been observed to increase toughness, and decreasing the scalding time has been observed to increase tenderness. The *beating action* of mechanical feather-picking machines causes considerable toughening. Therefore, it is recommended that any cutting be done after tenderization. *Cutting up* the bird into pieces before natural tenderization is completed reduces tender-ness considerably. Therefore, it is recommended that any cutting be done after tenderization. *Rapid chilling* of poultry can also have a toughening effect. It is found that the tenderization process can be speeded up consid-erably by a patented *electrical stunning* process.

Poultry products are *highly perishable,* and thus they should be kept at the *lowest* possible temperature to maximize their shelf life. Studies have shown that the populations of certain bacteria double every 36 h at −2°C, 14 h at 0°C, 7 h at 5°C, and less than 1 h at 25°C (Fig. 4–49). Studies have also shown that the total bacterial counts on birds held at 2°C for 14 days are equivalent to those held at 10°C for 5 days or 24°C for 1 day. It has also been found that birds held at −1°C had 8 days of additional shelf life over those held at 4°C.

The growth of microorganisms on the *surfaces* of the poultry causes the development of an *off-odor* and *bacterial slime.* The higher the ini-tial amount of bacterial contamination, the faster the sliming occurs. Therefore, good sanitation practices during processing such as cleaning the equipment frequently and washing the carcasses are as important as the storage temperature in extending shelf life.

Poultry must be frozen *rapidly* to ensure a light, pleasing appearance. Poultry that is frozen slowly appears dark and develops large ice crys-tals that damage the tissue. The ice crystals formed during rapid freezing are small. Delaying freezing of poultry causes the ice crystals to become larger. Rapid freezing can be accomplished by forced air at temperatures of −23 to −40°C and velocities of 1.5 to 5 m/s in *air-blast tunnel freezers.* Most poultry is frozen this way. Also, the packaged birds freeze much faster on open shelves than they do in boxes. If poultry packages must be frozen in boxes, then it is very desirable to leave the boxes open or to cut holes on the boxes in the direction of airflow during freezing. For best results, the blast tunnel should be fully loaded across its cross-section with even spacing between the products to assure uniform airflow around all sides of the packages. The freezing time of poultry as a function of refrig-erated air temperature is given in Fig. 4–50. Thermal properties of poultry are given in Table 4–8.

Other freezing methods for poultry include sandwiching between *cold plates, immersion* into a refrigerated liquid such as glycol or calcium chloride brine, and *cryogenic cooling* with liquid nitrogen. Poultry can be frozen in several hours by cold plates. Very high freezing rates can be obtained by *immersing* the packaged birds into a low-temperature brine. The freezing time of birds in −29°C brine can be as low as 20 min, depend-ing on the size of the bird (Fig. 4–51). Also, immersion freezing produces a very appealing light appearance, and the high rates of heat transfer make
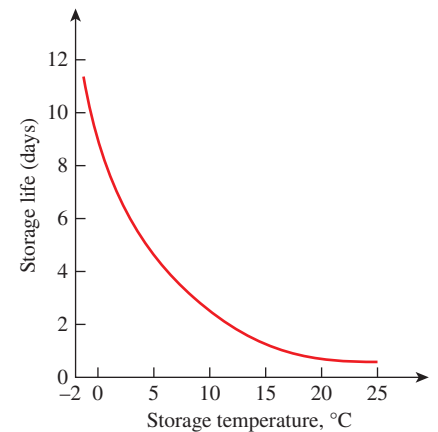
FIGURE 4–49
The storage life of fresh poultry decreases exponentially with increasing storage temperature.
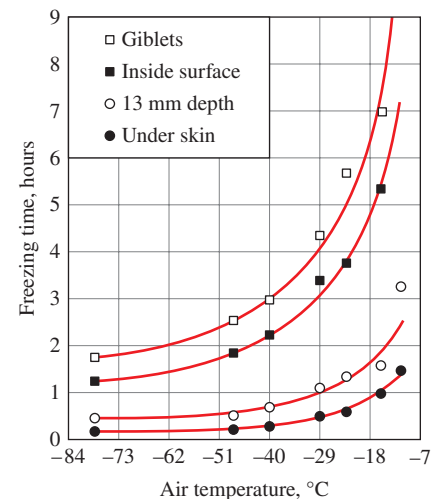
Note: Freezing time is the time required for temperature to fall from 0 to –4°C. The values are for 2.3 to 3.6 kg chickens with initial temperature of 0 to 2°C and with air velocity of 2.3 to 2.8 m/s.

FIGURE 4–50
The variation of freezing time of poultry with air temperature.

FIGURE 4–51

The variation of temperature of the breast of 6.8-kg turkeys initially at 1°C with depth during immersion cooling at −29°C.

From van der Berg and Lentz, 1958.
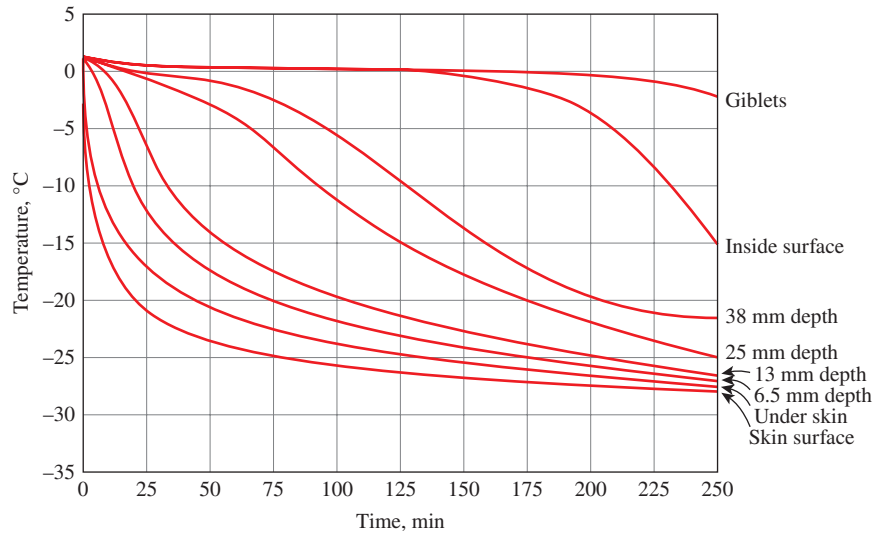
TABLE 4–8

Thermal properties of poultry

Quantity	Typical Value
Average density:	
Muscle	1070 kg/m³
Skin	1030 kg/m³
Specific heat:	
Above freezing	2.94 kJ/kg·K
Below freezing	1.55 kJ/kg·K
Freezing point	−2.8°C
Latent heat of fusion	247 kJ/kg
Thermal conductivity:	(in W/m·K)
Breast muscle	0.502 at 20°C
	1.384 at −20°C
	1.506 at −40°C
Dark muscle	1.557 at −40°C

continuous line operation feasible. It also has lower initial and maintenance costs than forced air, but *leaks* into the packages through some small holes or cracks remain a concern. The convection heat transfer coefficient is 17 W/m²·K for air at −29°C and 2.5 m/s, whereas it is 170 W/m²·K for sodium chloride brine at −18°C and a velocity of 0.02 m/s. Sometimes liquid nitrogen is used to crust freeze the poultry products to −73°C. The freezing is then completed with air in a holding room at −23°C.

Properly packaged poultry products can be *stored* frozen for up to about a year at temperatures of −18°C or lower. The storage life drops considerably at higher (but still below-freezing) temperatures. Significant changes occur in flavor and juiciness when poultry is frozen for too long, and a stale rancid odor develops. Frozen poultry may become dehydrated and experience **freezer burn**, which may reduce the eye appeal of the product and cause toughening of the affected area. Dehydration and thus freezer burn can be controlled by *humidification, lowering* the storage temperature, and packaging the product in essentially *impermeable* film. The storage life can be extended by packing the poultry in an *oxygen-free* environment. The bacterial counts in precooked frozen products must be kept at safe levels since bacteria may not be destroyed completely during the reheating process at home.

Frozen poultry can be *thawed* in ambient air, water, refrigerator, or oven without any significant difference in taste. Big birds like turkey should be thawed safely by holding them in a refrigerator at 2 to 4°C for two to four days, depending on the size of the bird. They can also be thawed by immersing them in cool water in a large container for 4 to 6 h, or holding them in a paper bag. Care must be exercised to keep the bird's surface *cool* to minimize *microbiological growth* when thawing in air or water.

EXAMPLE 4–11   Chilling of Beef Carcasses in a Meat Plant

The chilling room of a meat plant is 18 m × 20 m × 5.5 m in size and has a capacity of 450 beef carcasses. The power consumed by the fans and the lights of the chilling room are 26 and 3 kW, respectively, and the room gains heat through its envelope at a rate of 13 kW. The average mass of beef carcasses is 285 kg. The carcasses enter the chilling room at 36°C after they are washed to facilitate evaporative cooling and are cooled to 15°C in 10 h. The water is expected to evaporate at a rate of 0.080 kg/s. The air enters the evaporator section of the refrigeration system at 0.7°C and leaves at −2°C. The air side of the evaporator is heavily finned, and the overall heat transfer coefficient of the evaporator based on the air side is 20 W/m²·K. Also, the average temperature difference between the air and the refrigerant in the evaporator is 5.5°C. Determine (*a*) the refrigeration load of the chilling room, (*b*) the volume flow rate of air, and (*c*) the heat transfer surface area of the evaporator on the air side, assuming all the vapor and the fog in the air freezes in the evaporator.

SOLUTION   The chilling room of a meat plant with a capacity of 450 beef carcasses is considered. The cooling load, the airflow rate, and the heat transfer area of the evaporator are to be determined.

Assumptions   **1** Water evaporates at a rate of 0.080 kg/s. **2** All the moisture in the air freezes in the evaporator.

Properties   The heat of fusion and the heat of vaporization of water at 0°C are 333.7 kJ/kg and 2501 kJ/kg (Table A–9). The density and specific heat of air at 0°C are 1.292 kg/m³ and 1.006 kJ/kg·K (Table A–15). Also, the specific heat of beef carcass is determined from the relation in Table A–7*b* to be

$$c_p = 1.68 + 2.51 \times (\text{water content}) = 1.68 + 2.51 \times 0.58 = 3.14 \text{ kJ/kg·K}$$

Analysis   (*a*) A sketch of the chilling room is given in Fig. 4–52. The amount of beef mass that needs to be cooled per unit time is

$$\dot{m}_{\text{beef}} = (\text{Total beef mass cooled})/(\text{Cooling time})$$
$$= (450 \text{ carcasses})(285 \text{ kg/carcass})(10 \times 3600 \text{ s}) = 3.56 \text{ kg/s}$$

The product refrigeration load can be viewed as the energy that needs to be removed from the beef carcass as it is cooled from 36 to 15°C at a rate of 3.56 kg/s and is determined to be

$$\dot{Q}_{\text{beef}} = (\dot{m}c_p\Delta T)_{\text{beef}} = (3.56 \text{ kg/s})(3.14 \text{ kJ/kg·K})(36 - 15)°\text{C} = 235 \text{ kW}$$

Then the total refrigeration load of the chilling room becomes

$$\dot{Q}_{\text{total, chillroom}} = \dot{Q}_{\text{beef}} + \dot{Q}_{\text{fan}} + \dot{Q}_{\text{lights}} + \dot{Q}_{\text{heat gain}} = 235 + 26 + 3 + 13$$
$$= \mathbf{277 \text{ kW}}$$

The amount of carcass cooling due to evaporative cooling of water is

$$\dot{Q}_{\text{beef, evaporative}} = (\dot{m}h_{fg})_{\text{water}} = (0.080 \text{ kg/s})(2501 \text{ kJ/kg}) = 200 \text{ kW}$$

which is 200/235 = 0.85 = 85 percent of the total product cooling load. The remaining 15 percent of the heat is transferred by convection and radiation.

Lights, 3 kW

13 kW

Beef carcass

Evaporation 0.080 kg/s

36°C 285 kg

Refrigerated air

Fans, 26 kW

0.7°C   Evaporator   −2°C

$\dot{Q}_{\text{evap}}$
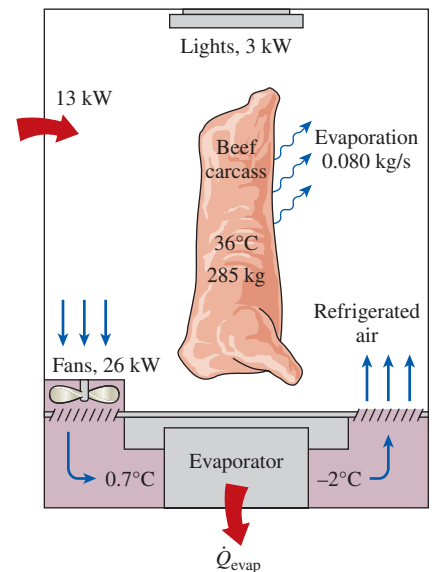
FIGURE 4–52
Schematic for Example 4–11.

(*b*) Heat is transferred to air at the rate determined above, and the temperature of the air rises from $-2°C$ to $0.7°C$ as a result. Therefore, the mass flow rate of air is

$$\dot{m}_{\text{air}} = \frac{\dot{Q}_{\text{air}}}{(c_p \Delta T_{\text{air}})} = \frac{277 \text{ kW}}{(1.006 \text{ kJ/kg·K})[0.7 - (-2)°C]} = 102.0 \text{ kg/s}$$

Then the volume flow rate of air becomes

$$\dot{V}_{\text{air}} = \frac{\dot{m}_{\text{air}}}{\rho_{\text{air}}} = \frac{102 \text{ kg/s}}{1.292 \text{ kg/m}^3} = \mathbf{78.9 \ m^3/s}$$

(*c*) Normally the heat transfer load of the evaporator is the same as the refrigeration load. But in this case the water that enters the evaporator as a liquid is frozen as the temperature drops to $-2°C$, and the evaporator must also remove the latent heat of freezing, which is determined from

$$\dot{Q}_{\text{freezing}} = (\dot{m} h_{\text{latent}})_{\text{water}} = (0.080 \text{ kg/s})(333.7 \text{ kJ/kg}) = 27 \text{ kW}$$

Therefore, the total rate of heat removal at the evaporator is

$$\dot{Q}_{\text{evaporator}} = \dot{Q}_{\text{total, chill room}} + \dot{Q}_{\text{freezing}} = 277 + 27 = 304 \text{ kW}$$

Then the heat transfer surface area of the evaporator on the air side is determined from $\dot{Q}_{\text{evaporator}} = (UA)_{\text{air side}} \Delta T$,

$$A = \frac{\dot{Q}_{\text{evaporator}}}{U \Delta T} = \frac{304{,}000 \text{ W}}{(20 \text{ W/m}^2\text{·K})(5.5°C)} = \mathbf{2764 \ m^2}$$

Obviously, a finned surface must be used to provide such a large surface area on the air side.

SUMMARY

In this chapter, we considered the variation of temperature with time as well as position in one- or multidimensional systems. We first considered the *lumped systems* in which the temperature varies with time but remains uniform throughout the system at any time. The temperature of a lumped body of arbitrary shape of mass m, volume V, surface area A_s, density ρ, and specific heat c_p initially at a uniform temperature T_i that is exposed to convection at time $t = 0$ in a medium at temperature T_∞ with a heat transfer coefficient h is expressed as

$$\frac{T(t) - T_\infty}{T_i - T_\infty} = e^{-bt}$$

where

$$b = \frac{hA_s}{\rho c_p V} = \frac{h}{\rho c_p L_c}$$

is a positive quantity whose dimension is $(\text{time})^{-1}$. This relation can be used to determine the temperature $T(t)$ of a body at time t or, alternatively, the time t required for the temperature to reach a specified value $T(t)$. Once the temperature $T(t)$ at time t is available, the *rate* of convection heat transfer between the body and its environment at that time can be determined from Newton's law of cooling as

$$\dot{Q}(t) = hA_s[T(t) - T_\infty]$$

The *total amount* of heat transfer between the body and the surrounding medium over the time interval $t = 0$ to t is simply the change in the energy content of the body,

$$Q = mc_p[T(t) - T_i]$$

The *maximum* heat transfer between the body and its surroundings is

$$Q_{\text{max}} = mc_p(T_\infty - T_i)$$

The error involved in lumped system analysis is negligible when

$$\text{Bi} = \frac{hL_c}{k} < 0.1$$

where Bi is the *Biot number* and $L_c = V/A_s$ is the *characteristic length*.

When the lumped system analysis is not applicable, the variation of temperature with position as well as time can be determined using the *one-term approximation solutions* for a large plane wall, a long cylinder, and a sphere, respectively. These solutions are applicable for one-dimensional heat transfer in those geometries. Therefore, their use is limited to situations in which the body is initially at a uniform temperature, all surfaces are subjected to the same thermal conditions, and the body does not involve any heat generation. These solutions can also be used to determine the total heat transfer from the body up to a specified time *t*.

Using the *one-term approximation,* the solutions of one-dimensional transient heat conduction problems are expressed analytically as

Plane wall: $\quad \theta_{\text{wall}} = \dfrac{T(x, t) - T_\infty}{T_i - T_\infty} = A_1 e^{-\lambda_1^2 \tau} \cos(\lambda_1 x/L)$

Cylinder: $\quad \theta_{\text{cyl}} = \dfrac{T(r, t) - T_\infty}{T_i - T_\infty} = A_1 e^{-\lambda_1^2 \tau} J_0(\lambda_1 r/r_o)$

Sphere: $\quad \theta_{\text{sph}} = \dfrac{T(r, t) - T_\infty}{T_i - T_\infty} = A_1 e^{-\lambda_1^2 \tau} \dfrac{\sin(\lambda_1 r/r_o)}{\lambda_1 r/r_o}$

where the constants A_1 and λ_1 are functions of the Bi number only, and their values are listed in Table 4–2 against the Bi number for all three geometries. The error involved in one-term solutions is less than 2 percent when $\tau > 0.2$.

Using the one-term solutions, the fractional heat transfers in different geometries are expressed as

Plane wall: $\quad \left(\dfrac{Q}{Q_{\max}}\right)_{\text{wall}} = 1 - \theta_{0, \text{wall}} \dfrac{\sin \lambda_1}{\lambda_1}$

Cylinder: $\quad \left(\dfrac{Q}{Q_{\max}}\right)_{\text{cyl}} = 1 - 2\theta_{0, \text{cyl}} \dfrac{J_1(\lambda_1)}{\lambda_1}$

Sphere: $\quad \left(\dfrac{Q}{Q_{\max}}\right)_{\text{sph}} = 1 - 3\theta_{0, \text{sph}} \dfrac{\sin \lambda_1 - \lambda_1 \cos \lambda_1}{\lambda_1^3}$

The solutions of transient heat conduction in a semi-infinite solid with constant properties under various boundary conditions at the surface are given as follows:

Specified Surface Temperature, T_s = constant:

$$\frac{T(x, t) - T_i}{T_s - T_i} = \text{erfc}\left(\frac{x}{2\sqrt{\alpha t}}\right) \text{ and } \dot{q}_s(t) = \frac{k(T_s - T_i)}{\sqrt{\pi \alpha t}}$$

Specified Surface Heat Flux, $\dot{q}_s$ = constant:

$$T(x, t) - T_i = \frac{\dot{q}_s}{k}\left[\sqrt{\frac{4\alpha t}{\pi}} \exp\left(-\frac{x^2}{4\alpha t}\right) - x\,\text{erfc}\left(\frac{x}{2\sqrt{\alpha t}}\right)\right]$$

Convection on the Surface, $\dot{q}_s(t) = h[T_\infty - T(0, t)]$:

$$\frac{T(x, t) - T_i}{T_\infty - T_i} = \text{erfc}\left(\frac{x}{2\sqrt{\alpha t}}\right) - \exp\left(\frac{hx}{k} + \frac{h^2\alpha t}{k^2}\right)$$
$$\times \text{erfc}\left(\frac{x}{2\sqrt{\alpha t}} + \frac{h\sqrt{\alpha t}}{k}\right)$$

Energy Pulse at Surface, e_s = constant:

$$T(x, t) - T_i = \frac{e_s}{k\sqrt{\pi t/\alpha}} \exp\left(-\frac{x^2}{4\alpha t}\right)$$

where erfc (η) is the *complementary error function* of argument η.

Using a superposition principle called the *product solution,* these one-term approximate solutions can also be used to construct solutions for the *two-dimensional* transient heat conduction problems encountered in geometries such as a short cylinder, a long rectangular bar, or a semi-infinite cylinder or plate, and even *three-dimensional* problems associated with geometries such as a rectangular prism or a semi-infinite rectangular bar, provided that all surfaces of the solid are subjected to convection to the same fluid at temperature T_∞, with the same convection heat transfer coefficient *h,* and the body involves no heat generation. The solution in such multidimensional geometries can be expressed as the product of the solutions for the one-dimensional geometries whose intersection is the multidimensional geometry.

The total heat transfer to or from a multidimensional geometry can also be determined by using the one-dimensional values. The transient heat transfer for a two-dimensional geometry formed by the intersection of two one-dimensional geometries 1 and 2 is

$$\left(\frac{Q}{Q_{\max}}\right)_{\text{total, 2D}} = \left(\frac{Q}{Q_{\max}}\right)_1 + \left(\frac{Q}{Q_{\max}}\right)_2\left[1 - \left(\frac{Q}{Q_{\max}}\right)_1\right]$$

Transient heat transfer for a three-dimensional body formed by the intersection of three one-dimensional bodies 1, 2, and 3 is given by

$$\left(\frac{Q}{Q_{\max}}\right)_{\text{total, 3D}} = \left(\frac{Q}{Q_{\max}}\right)_1 + \left(\frac{Q}{Q_{\max}}\right)_2\left[1 - \left(\frac{Q}{Q_{\max}}\right)_1\right]$$
$$+ \left(\frac{Q}{Q_{\max}}\right)_3\left[1 - \left(\frac{Q}{Q_{\max}}\right)_1\right]\left[1 - \left(\frac{Q}{Q_{\max}}\right)_2\right]$$

REFERENCES AND SUGGESTED READING

1. ASHRAE. *Handbook: Refrigeration.* SI version. Atlanta, GA: American Society of Heating, Refrigerating, and Air-Conditioning Engineers, Inc., 1994.

2. H. S. Carslaw and J. C. Jaeger. *Conduction of Heat in Solids*, 2nd ed. London: Oxford University Press, 1959.

3. H. Gröber, S. Erk, and U. Grigull. *Fundamentals of Heat Transfer.* New York: McGraw-Hill, 1961.

4. M. P. Heisler. "Temperature Charts for Induction and Constant Temperature Heating." *ASME Transactions* 69 (1947), pp. 227–36.

5. H. Hillman. *Kitchen Science.* Mount Vernon, NY: Consumers Union, 1981.

6. S. Kakaç and Y. Yener, *Heat Conduction.* New York: Hemisphere Publishing Co., 1985.

7. L. S. Langston. "Heat Transfer from Multidimensional Objects Using One-Dimensional Solutions for Heat Loss." *International Journal of Heat and Mass Transfer* 25 (1982), pp. 149–50.

8. P. J. Schneider. *Conduction Heat Transfer.* Reading, MA: Addison-Wesley, 1955.

9. L. van der Berg and C. P. Lentz. "Factors Affecting Freezing Rate and Appearance of Eviscerated Poultry Frozen in Air." *Food Technology* 12 (1958).

PROBLEMS*

Lumped System Analysis

4–1C What is the physical significance of the Biot number? Is the Biot number more likely to be larger for highly conducting solids or poorly conducting ones?

4–2C What is lumped system analysis? When is it applicable?

4–3C In what medium is the lumped system analysis more likely to be applicable: in water or in air? Why?

4–4C For which solid is the lumped system analysis more likely to be applicable: an actual apple or a golden apple of the same size? Why?

4–5C For which kinds of bodies made of the same material is the lumped system analysis more likely to be applicable: slender ones or well-rounded ones of the same volume? Why?

4–6C Consider heat transfer between two identical hot solid bodies and the air surrounding them. The first solid is being cooled by a fan while the second one is allowed to cool naturally. For which solid is the lumped system analysis more likely to be applicable? Why?

4–7C Consider heat transfer between two identical hot solid bodies and their environments. The first solid is dropped in a large container filled with water, while the second one is allowed to cool naturally in the air. For which solid is the lumped system analysis more likely to be applicable? Why?

4–8C Consider a hot baked potato on a plate. The temperature of the potato is observed to drop by 4°C during the first minute. Will the temperature drop during the second minute be less than, equal to, or more than 4°C? Why?
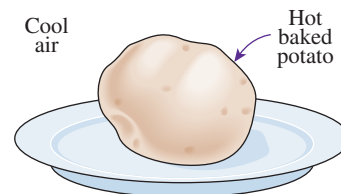
FIGURE P4–8C

4–9C Consider a potato being baked in an oven that is maintained at a constant temperature. The temperature of the potato is observed to rise by 5°C during the first minute. Will the temperature rise during the second minute be less than, equal to, or more than 5°C? Why?

4–10C Consider two identical 4-kg pieces of roast beef. The first piece is baked as a whole, while the second is baked after being cut into two equal pieces in the same oven. Will there be any difference between the cooking times of the whole and cut roasts? Why?

---

*Problems designated by a "C" are concept questions, and students are encouraged to answer them all. Problems designated by an "E" are in English units, and the SI users can ignore them. Problems with the 🖥 icon are comprehensive in nature and are intended to be solved with appropriate software. Problems with the **PtD** icon are Prevention through Design problems. Problems with the **C&S** icon are Codes and Standards problems.

4–11C Consider a sphere and a cylinder of equal volume made of copper. Both the sphere and the cylinder are initially at the same temperature and are exposed to convection in the same environment. Which do you think will cool faster, the cylinder or the sphere? Why?

4–12 Obtain relations for the characteristic lengths of a large plane wall of thickness $2L$, a very long cylinder of radius r_o, and a sphere of radius r_o.

4–13 Obtain a relation for the time required for a lumped system to reach the average temperature $\frac{1}{2}(T_i + T_\infty)$, where T_i is the initial temperature and T_∞ is the temperature of the environment.

4–14 A brick of $203 \times 102 \times 57$ mm in dimension is being burned in a kiln to $1100°C$ and then allowed to cool in a room with ambient air temperature of $30°C$ and convection heat transfer coefficient of 5 W/m²·K. If the brick has properties of $\rho = 1920$ kg/m³, $c_p = 790$ J/kg·K, and $k = 0.90$ W/m·K, determine the time required to cool the brick to a temperature difference of $5°C$ from the ambient air temperature.

4–15 C&S In a device for cryogenic process, a section of an ASTM A203 B steel plate is occasionally exposed to very cold fluid. The plate has a thickness of 1 cm with a thermal conductivity of 52 W/m·K, a specific heat of 470 J/kg·K, and a density of 7.9 g/cm³. The plate is situated such that both surfaces are exposed to cryogenic fluid at $-50°C$ with a convection heat transfer coefficient of 50 W/m²·K. The minimum temperature suitable for the ASTM A203 B steel plate is $-30°C$ (ASME Code for Process Piping, B31.3-2014, Table A-1M). If the plate has an initial temperature of $20°C$, determine how long it will take to reach the minimum suitable temperature stipulated by the ASME Code for Process Piping.

$T_\infty = -50°C$
$h = 50$ W/m²·K

Steel plate

$L = 1$ cm

$T_i = 20°C$
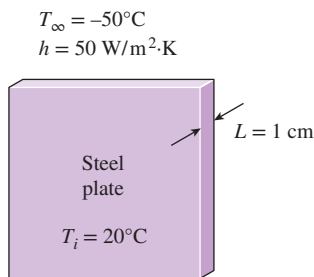
FIGURE P4–15

4–16 Consider an 800-W iron whose base plate is made of 0.5-cm-thick aluminum alloy 2024–T6 ($\rho = 2770$ kg/m³, $c_p = 875$ J/kg·K, $\alpha = 7.3 \times 10^{-5}$ m²/s). The base plate has a surface area of 0.03 m². Initially, the iron is in thermal equilibrium with the ambient air at $22°C$. Taking the heat transfer coefficient at the surface of the base plate to be 12 W/m²·K and assuming 85 percent of the heat generated in the resistance wires is transferred to the plate, determine how long it will take for the plate temperature to reach $140°C$. Is it realistic to assume the plate temperature to be uniform at all times?

Air 22°C

800 W iron
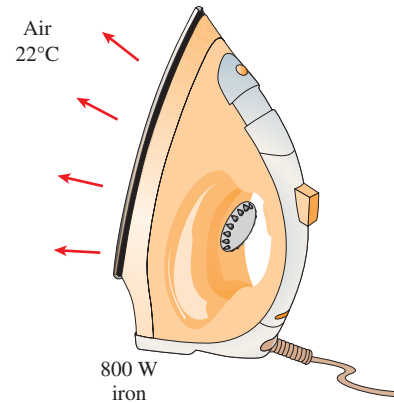
FIGURE P4–16

4–17 Reconsider Prob. 4–16. Using appropriate software, investigate the effects of the heat transfer coefficient and the final plate temperature on the time it will take for the plate to reach this temperature. Let the heat transfer coefficient vary from 5 W/m²·K to 25 W/m²·K and the temperature from $30°C$ to $200°C$. Plot the time as functions of the heat transfer coefficient and the temperature, and discuss the results.

4–18 Metal plates ($k = 180$ W/m·K, $\rho = 2800$ kg/m³, and $c_p = 880$ J/kg·K) with a thickness of 1 cm are being heated in an oven for 2 min. Air in the oven is maintained at $800°C$ with a convection heat transfer coefficient of 200 W/m²·K. If the initial temperature of the plates is $20°C$, determine the temperature of the plates when they are removed from the oven.

4–19 A 5-mm-thick stainless steel strip ($k = 21$ W/m·K, $\rho = 8000$ kg/m³, and $c_p = 570$ J/kg·K) is being heat treated as it moves through a furnace at a speed of 1 cm/s. The air temperature in the furnace is maintained at $900°C$ with a convection heat transfer coefficient of 80 W/m²·K. If the furnace length is 3 m and the stainless steel strip enters it at $20°C$, determine the temperature of the strip as it exits the furnace.

Furnace
900°C

1 cm/s

3 m

Stainless steel
20°C
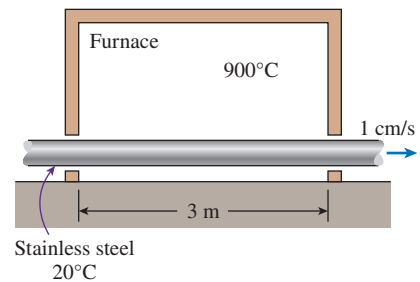
FIGURE P4–19

4–20 C&S Two plates are held together by square stainless steel (ASTM A479 904L) bars with thickness of 12 mm. Each bar has a thermal conductivity of 12 W/m·K, a specific heat of 500 J/kg·K, and a density of 7.9 g/cm³.

The bars are situated in between the two plates, and they are occasionally submerged in hot liquid at 300°C with a convection heat transfer coefficient of 96 W/m²·K. The length of each bar that is exposed to the hot liquid is 25 mm with an initial temperature of 20°C. The maximum use temperature allowed for ASTM A479 904L bars is 260°C (ASME Code for Process Piping, ASME B31.3-2014, Table A-1M). If the bars are submerged in the hot liquid for 5 min, will they be in compliance with the ASME code? How long will it take for the bars to reach the maximum use temperature?

4–21 A batch of 2-cm-thick stainless steel plates ($k = 21$ W/m·K, $\rho = 8000$ kg/m³, and $c_p = 570$ J/kg·K) are conveyed through a furnace to be heat treated. The plates enter the furnace at 18°C, and they travel a distance of 3 m inside the furnace. The air temperature in the furnace is maintained at 950°C with a convection heat transfer coefficient of 150 W/m²·K. Using appropriate software, determine how the velocity of the plates affects the temperature of the plates at the end of the heat treatment. Let the velocity of the plates vary from 5 to 60 mm/s, and plot the temperature of the plates at the furnace exit as a function of the velocity.

Furnace, 950°C

5 to 60 mm/s

2 cm

Stainless steel plate
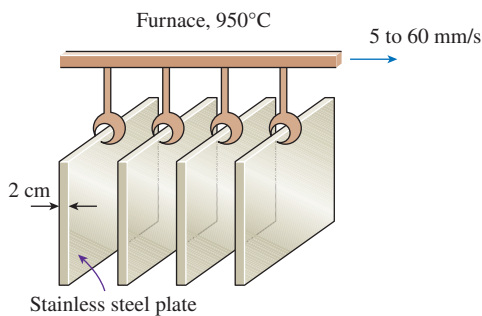
FIGURE P4–21

4–22 A 6-mm-thick stainless steel strip ($k = 21$ W/m·K, $\rho = 8000$ kg/m³, and $c_p = 570$ J/kg·K) exiting an oven at a temperature of 500°C is allowed to cool within a buffer zone distance of 5 m. To prevent thermal burns to workers who are handling the strip at the end of the buffer zone, the surface temperature of the strip should be cooled to 45°C. If the air temperature in the buffer zone is 15°C and the convection heat transfer coefficient is 120 W/m²·K, determine the maximum speed of the stainless steel strip.

4–23 After heat treatment, the 2-cm-thick metal plates ($k = 180$ W/m·K, $\rho = 2800$ kg/m³, and $c_p = 880$ J/kg·K) are conveyed through a cooling chamber with a length of 10 m. The plates enter the cooling chamber at an initial temperature of 500°C. The cooling chamber maintains a temperature of 10°C, and the convection heat transfer coefficient is given as a function of the air velocity blowing over the plates $h = 33\,V^{0.8}$, where h is in W/m²·K and V is in m/s. To prevent any incident of thermal burn, it is necessary for the

plates to exit the cooling chamber at a temperature below 50°C. In designing the cooling process to meet this safety criterion, use appropriate software to investigate the effect of the air velocity on the temperature of the plates at the exit of the cooling chamber. Let the air velocity vary from 0 to 40 m/s, and plot the temperatures of the plates exiting the cooling chamber as a function of air velocity at the moving plate speed of 2, 5, and 8 cm/s.

4–24 A long copper rod of diameter 2.0 cm is initially at a uniform temperature of 100°C. It is now exposed to an airstream at 20°C with a heat transfer coefficient of 200 W/m²·K. How long would it take for the copper rod to cool to an average temperature of 25°C?

4–25 Springs in automobile suspension systems are made of steel rods heated and wound into coils while ductile. Consider steel rods ($\rho = 7832$ kg/m³, $c_p = 434$ J/kg·K, and $k = 63.9$ W/m·K) with diameter of 2.5 cm and length of 1.27 m. The steel rods are heated in an oven with a uniform convection heat transfer coefficient of 20 W/m²·K. The steel rods were heated from an initial temperature of 20°C to the desired temperature of 450°C before being wound into coils. Determine the ambient temperature in the oven if the steel rods were to be heated to the desired temperature within 10 min.

4–26 Steel rods ($\rho = 7832$ kg/m³, $c_p = 434$ J/kg·K, and $k = 63.9$ W/m·K) are heated in a furnace to 850°C and then quenched in a water bath at 50°C for a period of 40 s as part of a hardening process. The convection heat transfer coefficient is 650 W/m²·K. If the steel rods have diameter of 40 mm and length of 2 m, determine their average temperature when they are taken out of the water bath.

4–27 Two plates are held together by bolts made of ASTM B98 (UNS C65500) copper–silicon. The bolts are 3 mm in diameter; they have a thermal conductivity of 36 W/m·K, a specific heat of 377 J/kg·K, and a density of 8.55 g/cm³. The bolts are situated in between the two plates, and they are occasionally exposed to hot steam at 200°C with a convection heat transfer coefficient of 50 W/m²·K. The length of each bolt exposed to the steam is 25 mm. According to the ASME Code for Process Piping (ASME B31.3-2014, Table A-2M), the maximum temperature allowed for ASTM B98 bolts is 149°C. If the initial temperature of the bolts is 20°C, how long can the bolts be in the hot steam before the maximum use temperature is reached?

4–28 Two components in cryogenic equipment are held together by stainless steel (ASTM A437 B4B) bolts with diameter of 25 mm. The bolts have a thermal conductivity of 23.9 W/m·K, a specific heat of 460 J/kg·K, and a density of 7.8 g/cm³. When the cryogenic fluid flows between the two components, the bolts are submerged in the cold fluid. The length of each bolt submerged in the cryogenic fluid is 5 cm, and the initial temperature of the bolts is 10°C. The cryogenic fluid has a temperature of −40°C with a convection heat transfer coefficient of 40 W/m²·K. The ASME Code for

Process Piping limits the minimum suitable temperature for ASTM A437 B4B bolts to $-30°C$ (ASME B31.3-2014, Table A-2M). If the bolts are exposed to the cold fluid for 12 min, will they still comply with the ASME code? How long will it take for the bolts to reach the minimum suitable temperature?

4–29 To warm up some milk for a baby, a mother pours milk into a thin-walled cylindrical container whose diameter is 6 cm. The height of the milk in the container is 7 cm. She then places the container into a large pan filled with hot water at 70°C. The milk is stirred constantly so that its temperature is uniform at all times. If the heat transfer coefficient between the water and the container is 120 W/m²·K, determine how long it will take for the milk to warm up from 3°C to 38°C. Assume the entire surface area of the cylindrical container (including the top and bottom) is in thermal contact with the hot water. Take the properties of the milk to be the same as those of water. Can the milk in this case be treated as a lumped system? Why? *Answer:* 4.50 min

4–30 A person is found dead at 5 p.m. in a room whose temperature is 20°C. The temperature of the body is measured to be 25°C when found, and the heat transfer coefficient is estimated to be 8 W/m²·K. Modeling the body as a 30-cm-diameter, 1.70-m-long cylinder and using the lumped system analysis as a rough approximation, estimate the time of death of that person.

4–31 The temperature of a gas stream is to be measured by a thermocouple whose junction can be approximated as a 1.2-mm-diameter sphere. The properties of the junction are $k = 35$ W/m·K, $\rho = 8500$ kg/m³, and $c_p = 320$ J/kg·K, and the heat transfer coefficient between the junction and the gas is $h = 110$ W/m²·K. Determine how long it will take for the thermocouple to read 99 percent of the initial temperature difference. *Answer:* 22.8 s

4–32 In an experiment, the temperature of a hot gas stream is to be measured by a thermocouple with a spherical junction. Due to the nature of this experiment, the response time of the thermocouple to register 99 percent of the initial temperature difference must be within 5 s. The properties of the thermocouple junction are $k = 35$ W/m·K, $\rho = 8500$ kg/m³, and $c_p = 320$ J/kg·K. If the heat transfer coefficient between the thermocouple junction and the gas is 250 W/m²·K, determine the diameter of the junction.

4–33 A thermocouple with a spherical junction diameter of 0.5 mm is used for measuring the temperature of hot airflow in a circular duct. The convection heat transfer coefficient of the airflow can be related with the diameter (D) of the spherical junction and the average airflow velocity (V) as $h = 2.2(V/D)^{0.5}$, where D, h, and V are in m, W/m²·K, and m/s, respectively. The properties of the thermocouple junction are $k = 35$ W/m·K, $\rho = 8500$ kg/m³, and $c_p = 320$ J/kg·K. Determine the minimum airflow velocity that the thermocouple can use, if the maximum response time of the thermocouple to register 99 percent of the initial temperature difference is 5 s.

Airflow, V
T_∞, h Thermocouple junction
$D = 0.5$ mm
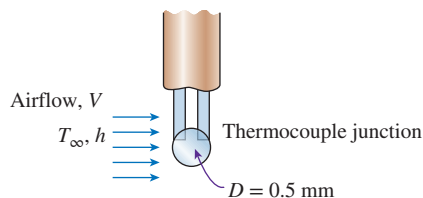
FIGURE P4–33

4–34 Pulverized coal particles are used in oxy-fuel combustion power plants for electricity generation. Consider a situation where coal particles are suspended in hot air flowing through a heated tube, where the convection heat transfer coefficient is 100 W/m²·K. If the average surface area and volume of the coal particles are 3.1 mm² and 0.5 mm³, respectively, determine how much time it would take to heat the coal particles to two-thirds of the initial temperature difference.

4–35 Oxy-fuel combustion power plants use pulverized coal particles as fuel to burn in a pure oxygen environment to generate electricity. Before entering the furnace, pulverized spherical coal particles with an average diameter of 300 μm are transported at 2 m/s through a 3-m-long heated tube while suspended in hot air. The air temperature in the tube is 900°C, and the average convection heat transfer coefficient is 250 W/m²·K. Determine the temperature of the coal particles at the exit of the heated tube if the initial temperature of the particles is 20°C.

4–36 Plasma spraying is a process used for coating a material surface with a protective layer to prevent the material from degradation. In a plasma spraying process, the protective layer in powder form is injected into a plasma jet. The powder is then heated to molten droplets and propelled onto the material surface. Once deposited on the material surface, the molten droplets solidify and form a layer of protective coating. Consider a plasma spraying process using alumina ($k = 30$ W/m·K, $\rho = 3970$ kg/m³, and $c_p = 800$ J/kg·K) powder that is injected into a plasma jet at $T_\infty = 15,000°C$ and $h = 10,000$ W/m²·K. The alumina powder is made of spherical particles with an average diameter of 60 μm and a melting point at 2300°C. Determine the amount of time it would take for the particles, with an initial temperature of 20°C, to reach their melting point from the moment they are injected into the plasma jet.

4–37 Consider a spherical shell satellite with outer diameter of 4 m and shell thickness of 10 mm that is reentering the atmosphere. The shell satellite is made of stainless steel with properties of $\rho = 8238$ kg/m³, $c_p = 468$ J/kg·K, and $k = 13.4$ W/m·K. During the reentry, the effective atmosphere temperature surrounding the satellite is 1250°C with a convection heat transfer coefficient of 130 W/m²·K. If the initial temperature of the shell is 10°C, determine the shell temperature after 5 min of reentry. Assume heat transfer occurs only on the satellite shell.

4–38 Carbon steel balls ($\rho = 7833$ kg/m³, $k = 54$ W/m·K, $c_p = 0.465$ kJ/kg·°C, and $\alpha = 1.474 \times 10^{-6}$ m²/s) 8 mm in diameter are annealed by heating them first to 900°C in a furnace

and then allowing them to cool slowly to 100°C in ambient air at 35°C. If the average heat transfer coefficient is 75 W/m²·K, determine how long the annealing process will take. If 2500 balls are to be annealed per hour, determine the total rate of heat transfer from the balls to the ambient air.
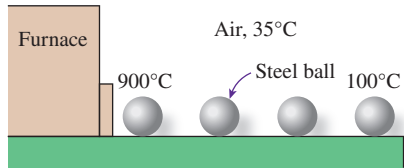
FIGURE P4–38

4–39 Reconsider Prob. 4–38. Using appropriate software, investigate the effect of the initial temperature of the balls on the annealing time and the total rate of heat transfer. Let the temperature vary from 500°C to 1000°C. Plot the time and the total rate of heat transfer as a function of the initial temperature, and discuss the results.

4–40E In a manufacturing facility, 2-in-diameter brass balls ($k = 64.1$ Btu/h·ft·°F, $\rho = 532$ lbm/ft³, and $c_p = 0.092$ Btu/lbm·°F) initially at 250°F are quenched in a water bath at 120°F for a period of 2 min at a rate of 120 balls per minute. If the convection heat transfer coefficient is 42 Btu/h·ft²·°F, determine (*a*) the temperature of the balls after quenching and (*b*) the rate at which heat needs to be removed from the water in order to keep its temperature constant at 120°F.
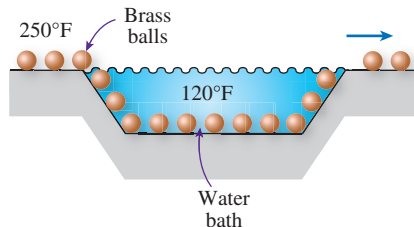
FIGURE P4–40E

4–41 Consider a sphere of diameter 5 cm, a cube of side length 5 cm, and a rectangular prism of dimension 4 cm × 5 cm × 6 cm, all initially at 0°C and all made of silver ($k = 429$ W/m·K, $\rho = 10{,}500$ kg/m³, $c_p = 0.235$ kJ/kg·K). Now all three of these geometries are exposed to ambient air at 33°C on all of their surfaces with a heat transfer coefficient of 12 W/m²·K. Determine how long it will take for the temperature of each geometry to rise to 25°C.

4–42 An electronic device dissipating 18 W has a mass of 20 g, a specific heat of 850 J/kg·K, and a surface area of 4 cm². The device is lightly used, and it is on for 5 min and then off for several hours, during which it cools to the ambient temperature of 25°C. Taking the heat transfer coefficient to be 12 W/m²·K, determine the temperature of the device at the end of the 5-min operating period. What would your answer be if the device were attached to an aluminum heat sink having a mass of 200 g and a surface area of 80 cm²? Assume the device and the heat sink to be nearly isothermal.

Transient Heat Conduction in Large Plane Walls, Long Cylinders, and Spheres with Spatial Effects

4–43C An egg is to be cooked to a certain level of doneness by being dropped into boiling water. Can the cooking time be shortened by turning up the heat and bringing water to a more rapid boiling?

4–44C What is an infinitely long cylinder? When is it proper to treat an actual cylinder as being infinitely long, and when is it not? For example, is it proper to use this model when finding the temperatures near the bottom or top surfaces of a cylinder? Explain.

4–45C What is the physical significance of the Fourier number? Will the Fourier number for a specified heat transfer problem double when the time is doubled?

4–46C Can the one-term approximate solutions for a plane wall exposed to convection on both sides be used for a plane wall with one side exposed to convection while the other side is insulated? Explain.

4–47C How can we use the one-term approximate solutions when the surface temperature of the geometry is specified instead of the temperature of the surrounding medium and the convection heat transfer coefficient?

4–48C The Biot number during a heat transfer process between a sphere and its surroundings is determined to be 0.02. Would you use lumped system analysis or the one-term approximate solutions when determining the midpoint temperature of the sphere? Why?

4–49C A body at an initial temperature of T_i is brought into a medium at a constant temperature of T_∞. How can you determine the maximum possible amount of heat transfer between the body and the surrounding medium?

4–50 A hot brass plate is having its upper surface cooled by an impinging jet of air at temperature of 15°C and convection heat transfer coefficient of 220 W/m²·K. The 10-cm-thick brass plate ($\rho = 8530$ kg/m³, $c_p = 380$ J/kg·K, $k = 110$ W/m·K, and $\alpha = 33.9 \times 10^{-6}$ m²/s) has a uniform initial temperature of 650°C, and the bottom surface of the plate is insulated. Determine the temperature at the center plane of the brass plate after 3 min of cooling. Solve this problem using the analytical one-term approximation method.
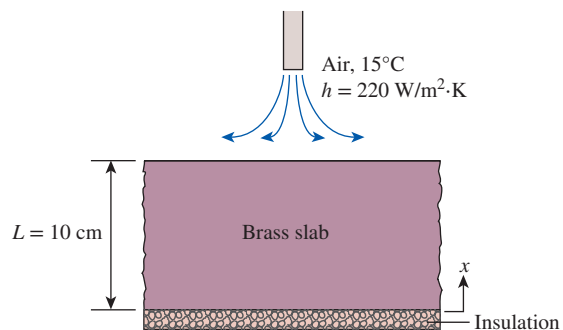
FIGURE P4–50

4–51 In a meat processing plant, 2-cm-thick steaks ($k = 0.45$ W/m·K and $\alpha = 0.91 \times 10^{-7}$ m²/s) that are initially at 25°C are to be cooled by passing them through a refrigeration room at -11°C. The heat transfer coefficient on both sides of the steaks is 9 W/m²·K. If both surfaces of the steaks are to be cooled to 2°C, determine how long the steaks should be kept in the refrigeration room. Solve this problem using the analytical one-term approximation method.

4–52 [C&S] A large plate made of stainless steel (ASTM A240 410S) that has a thickness of 5 cm is part of the equipment for a fluid flow process at high temperature. The plate has a thermal conductivity of 26.9 W/m·K, a specific heat of 460 J/kg·K, and a density of 7.73 g/cm³. Both surfaces of the plate are occasionally exposed to hot fluid at 700°C with a convection heat transfer coefficient of 323 W/m²·K. The maximum use temperature for the ASTM A240 410S stainless steel plate is 649°C (ASME Code for Process Piping, ASME B31.3-2014, Table A-1M). If the plate has an initial temperature of 20°C, how long can the plate be exposed to the hot fluid before reaching its maximum use temperature?

$T_\infty = 700$°C
$h = 323$ W/m²·K

Stainless steel plate

$2L = 5$ cm

$T_i = 20$°C
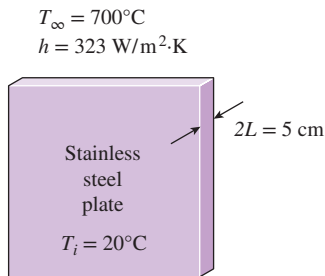
FIGURE P4–52

4–53 A 10-cm-thick aluminum plate ($\alpha = 97.1 \times 10^{-6}$ m²/s) is being heated in liquid with temperature of 500°C. The aluminum plate has a uniform initial temperature of 25°C. If the surface temperature of the aluminum plate is approximately the liquid temperature, determine the temperature at the center plane of the aluminum plate after 15 s of heating. Solve this problem using the analytical one-term approximation method.

4–54 In a production facility, 3-cm-thick large brass plates ($k = 110$ W/m·K, $\rho = 8530$ kg/m³, $c_p = 380$ J/kg·K, and $\alpha = 33.9 \times 10^{-6}$ m²/s) that are initially at a uniform temperature of 25°C are heated by passing them through an oven maintained at 700°C. The plates remain in the oven for a period of 10 min. Taking the convection heat transfer coefficient to be $h = 80$ W/m²·K, determine the surface temperature of the plates when they come out of the oven. Solve this problem using the analytical one-term approximation method. Can this problem be solved using lumped system analysis? Justify your answer.

Furnace, 700°C

3 cm

Brass plate
25°C
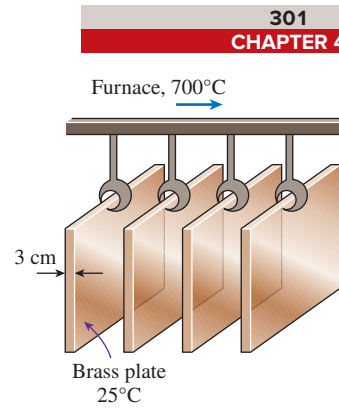
FIGURE P4–54

4–55 [computer icon] Reconsider Prob. 4–54. Using appropriate software, investigate the effects of the temperature of the oven and the heating time on the final surface temperature of the plates. Let the oven temperature vary from 500°C to 900°C and the time from 2 min to 30 min. Plot the surface temperature as the functions of the oven temperature and the time, and discuss the results.

4–56 Layers of 23-cm-thick meat slabs ($k = 0.47$ W/m·K and $\alpha = 0.13 \times 10^{-6}$ m²/s) initially at a uniform temperature of 7°C are to be frozen by refrigerated air at -30°C flowing at a velocity of 1.4 m/s. The average heat transfer coefficient between the meat and the air is 20 W/m²·K. Assuming the size of the meat slabs to be large relative to their thickness, determine how long it will take for the center temperature of the slabs to drop to -18°C. Also, determine the surface temperature of the meat slab at that time.

4–57 [C&S] A large ASTM A203 B steel plate, with a thickness of 7 cm, in a cryogenic process is suddenly exposed to very cold fluid at -50°C with $h = 594$ W/m²·K. The plate has a thermal conductivity of 52 W/m·K, a specific heat of 470 J/kg·K, and a density of 7.9 g/cm³. The ASME Code for Process Piping limits the minimum suitable temperature for ASTM A203 B steel plate to -30°C (ASME B31.3-2014, Table A-1M). If the initial temperature of the plate is 20°C and the plate is exposed to the cryogenic fluid for 6 min, would it still comply with the ASME code?

$T_\infty = -50$°C
$h = 594$ W/m²·K

Steel plate

$2L = 7$ cm

$T_i = 20$°C
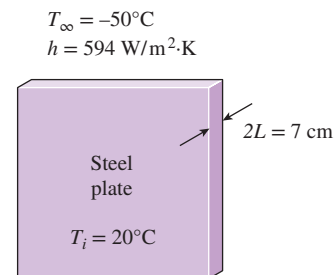
FIGURE P4–57

4–58 A heated 6-mm-thick Pyroceram plate ($\rho = 2600$ kg/m³, $c_p = 808$ J/kg·K, $k = 3.98$ W/m·K, and $\alpha = 1.89 \times 10^{-6}$ m²/s) is being cooled in a room with air temperature of 25°C and convection heat transfer coefficient of 13.3 W/m²·K. The heated Pyroceram plate had an initial temperature of 500°C, and it is allowed to cool for 286 s. If the mass of the Pyroceram plate is 10 kg, determine the heat transfer from the Pyroceram plate during the cooling process using the analytical one-term approximation method.

4–59 After a long, hard week on the books, you and your friend are ready to relax and enjoy the weekend. You take a steak 50 mm thick from the freezer. (*a*) How long (in hours) do you have to let the good times roll before the steak has thawed? Assume that the steak is initially at −8°C, that it thaws when the temperature at the center of the steak reaches 4°C, and that the room temperature is 22°C with a convection heat transfer coefficient of 10 W/m²·K. Neglect the heat of fusion associated with the melting phase change. Treat the steak as a one-dimensional plane wall having the following properties: $\rho = 1000$ kg/m³, $c_p = 4472$ J/kg·K, and $k = 0.625$ W/m·K. (*b*) How much energy per unit area (in J/m²) has been removed from the steak during this period of thawing? (*c*) Show whether or not the thawing of this steak can be analyzed by neglecting the internal thermal resistance of the steak.

4–60 A long Pyroceram rod ($\rho = 2600$ kg/m³, $c_p = 808$ J/kg·K, $k = 3.98$ W/m·K, and $\alpha = 1.89 \times 10^{-6}$ m²/s) with diameter of 10 mm has an initial uniform temperature of 1000°C. The Pyroceram rod is allowed to cool in an ambient temperature of 25°C and convection heat transfer coefficient of 80 W/m²·K. If the Pyroceram rod is allowed to cool for 3 min, determine the temperature at the center of the rod using the analytical one-term approximation method.

4–61 A long cylindrical wood log ($k = 0.17$ W/m·K and $\alpha = 1.28 \times 10^{-7}$ m²/s) is 10 cm in diameter and is initially at a uniform temperature of 25°C. It is exposed to hot gases at 525°C in a fireplace with a heat transfer coefficient of 13.6 W/m²·K on the surface. If the ignition temperature of the wood is 375°C, determine how long it will be before the log ignites. Solve this problem using the analytical one-term approximation method.

4–62E Long cylindrical AISI stainless steel rods ($k = 7.74$ Btu/h·ft·°F and $\alpha = 0.135$ ft²/h) of 4-in diameter are
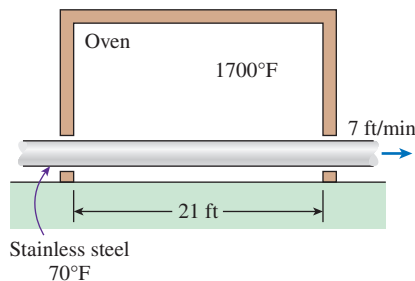
FIGURE P4–62E

heat treated by drawing them at a velocity of 7 ft/min through a 21-ft-long oven maintained at 1700°F. The heat transfer coefficient in the oven is 20 Btu/h·ft²·°F. If the rods enter the oven at 70°F, determine their centerline temperature when they leave. Solve this problem using the analytical one-term approximation method.

4–63 A long iron rod ($\rho = 7870$ kg/m³, $c_p = 447$ J/kg·K, $k = 80.2$ W/m·K, and $\alpha = 23.1 \times 10^{-6}$ m²/s) with diameter of 25 mm is initially heated to a uniform temperature of 700°C. The iron rod is then quenched in a large water bath that is maintained at constant temperature of 50°C and with a convection heat transfer coefficient of 128 W/m²·K. Determine the time required for the iron rod surface temperature to cool to 200°C. Solve this problem using the analytical one-term approximation method.

Water, 50°C
$h = 128$ W/m²·K
Iron rod
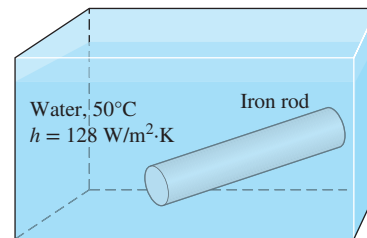
FIGURE P4–63

4–64 A 2-cm-diameter plastic rod has a thermocouple inserted to measure temperature at the center of the rod. The plastic rod ($\rho = 1190$ kg/m³, $c_p = 1465$ J/kg·K, and $k = 0.19$ W/m·K) was initially heated to a uniform temperature of 70°C and allowed to be cooled in ambient air at 25°C. After 1388 s of cooling, the thermocouple measured the temperature at the center of the rod to be 30°C. Determine the convection heat transfer coefficient for this process. Solve this problem using the analytical one-term approximation method.

Air, 25°C
Plastic rod
Thermocouple wires
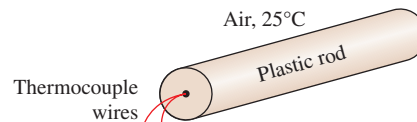
FIGURE P4–64

4–65 A 65-kg beef carcass ($k = 0.47$ W/m·K and $\alpha = 0.13 \times 10^{-6}$ m²/s) initially at a uniform temperature of 37°C is to be cooled by refrigerated air at −10°C flowing at a velocity of 1.2 m/s. The average heat transfer coefficient between the carcass and the air is 22 W/m²·K. Treating the carcass as a cylinder of diameter 24 cm and height 1.4 m and disregarding heat transfer from the base and top surfaces, determine how long it will take for the center temperature of the carcass to drop to 4°C. Also, determine if any part of the carcass will freeze during this process. Solve this problem using the analytical one-term approximation method. *Answer:* 12.2 h
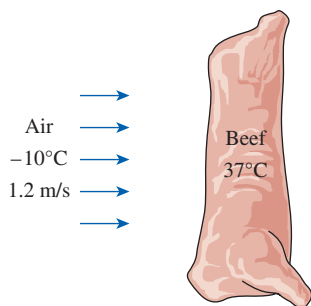
FIGURE P4–65

4–66 A long nickel alloy (ASTM B335) cylindrical rod is used as a component in high-temperature process equipment. The rod has a diameter of 5 cm; its thermal conductivity, specific heat, and density are 11 W/m·K, 380 J/kg·K, and 9.3 g/cm³, respectively. Occasionally, the rod is submerged in hot fluid for several minutes, where the fluid temperature is 500°C with a convection heat transfer coefficient of 440 W/m²·K. The ASME Code for Process Piping limits the maximum use temperature for ASTM B335 rod to 427°C (ASME B31.3-2014, Table A-1M). If the initial temperature of the rod is 20°C, how long can the rod be submerged in the hot fluid before reaching its maximum use temperature?
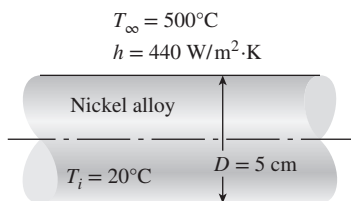
FIGURE P4–66

4–67 A 30-cm-diameter, 4-m-high cylindrical column of a house made of concrete ($k = 0.79$ W/m·K, $\alpha = 5.94 \times 10^{-7}$ m²/s, $\rho = 1600$ kg/m³, and $c_p = 0.84$ kJ/kg·K) cooled to 14°C during a cold night is heated again during the day by being exposed to ambient air at an average temperature of 28°C with an average heat transfer coefficient of 14 W/m²·K. Using the analytical one-term approximation method, determine (*a*) how long it will take for the column surface temperature to rise to 27°C, (*b*) the amount of heat transfer until the center temperature reaches to 28°C, and (*c*) the amount of heat transfer until the surface temperature reaches 27°C.

4–68 A long 35-cm-diameter cylindrical shaft made of stainless steel 304 ($k = 14.9$ W/m·K, $\rho = 7900$ kg/m³, $c_p = 477$ J/kg·K, and $\alpha = 3.95 \times 10^{-6}$ m²/s) comes out of an oven at a uniform temperature of 500°C. The shaft is then allowed to cool slowly in a chamber at 150°C with an average convection heat transfer coefficient of $h = 60$ W/m²·K. Determine the temperature at the center of the shaft 20 min after the start of the cooling process. Also, determine the heat transfer per unit length of the shaft

during this time period. Solve this problem using the analytical one-term approximation method. *Answers:* 486°C, 22,270 kJ

4–69 Reconsider Prob. 4–68. Using appropriate software, investigate the effect of the cooling time on the final center temperature of the shaft and the amount of heat transfer. Let the time vary from 5 min to 60 min. Plot the center temperature and the heat transfer as a function of the time, and discuss the results.

4–70 Steel rods, 2 m in length and 60 mm in diameter, are being drawn through an oven that maintains a temperature of 800°C and convection heat transfer coefficient of 128 W/m²·K. The steel rods ($\rho = 7832$ kg/m³, $c_p = 434$ J/kg·K, $k = 63.9$ W/m·K, and $\alpha = 18.8 \times 10^{-6}$ m²/s) were initially in uniform temperature of 30°C. Using the analytical one-term approximation method, determine the amount of heat transferred to the steel rod after 133 s of heating.

4–71 For heat transfer purposes, an egg can be considered to be a 5.5-cm-diameter sphere having the properties of water. An egg that is initially at 4.3°C is dropped into boiling water at 100°C. The heat transfer coefficient at the surface of the egg is estimated to be 800 W/m²·K. If the egg is considered cooked when its center temperature reaches 71°C, determine how long the egg should be kept in the boiling water. Solve this problem using the analytical one-term approximation method.

4–72 Citrus fruits are very susceptible to cold weather, and extended exposure to subfreezing temperatures can destroy them. Consider an 8-cm-diameter orange that is initially at 15°C. A cold front moves in one night, and the ambient temperature suddenly drops to −6°C, with a heat transfer coefficient of 15 W/m²·K. Using the properties of water for the orange and assuming the ambient conditions remain constant for 4 h before the cold front moves out, determine if any part of the orange will freeze that night. Solve this problem using the analytical one-term approximation method.

4–73 Chickens with an average mass of 1.7 kg ($k = 0.45$ W/m·K and $\alpha = 0.13 \times 10^{-6}$ m²/s) initially at a uniform temperature of 15°C are to be chilled in agitated brine at −7°C. The average heat transfer coefficient between the chicken and the brine is determined experimentally to be 440 W/m²·K. Taking the average density of the chicken to be 0.95 g/cm³ and treating the chicken as a spherical lump, determine the center and the surface temperatures of the chicken in 2 h and 45 min. Also, determine if any part of the chicken will freeze during this process. Solve this problem using the analytical one-term approximation method.

4–74 Hailstones are formed in high-altitude clouds at 253 K. Consider a hailstone with diameter of 20 mm that is falling through air at 15°C with convection heat transfer coefficient of 163 W/m²·K. Assuming the hailstone can be modeled as a sphere and has properties of ice at 253 K, determine how long it takes to reach melting point at the surface of the falling hailstone. Solve this problem using the analytical one-term approximation method.

4–75 An ordinary egg can be approximated as a 5.5-cm-diameter sphere whose properties are roughly $k = 0.6$ W/m·K and $\alpha = 0.14 \times 10^{-6}$ m²/s. The egg is initially at a uniform temperature of 4°C and is dropped into boiling water at 97°C. Taking the convection heat transfer coefficient to be $h = 1400$ W/m²·K, determine how long it will take for the center of the egg to reach 70°C. Solve this problem using the analytical one-term approximation method.

Boiling water   97°C

Egg

$T_i = 4°C$

FIGURE P4–75

4–76 Reconsider Prob. 4–75. Using appropriate software, investigate the effect of the final center temperature of the egg on the time it will take for the center to reach this temperature. Let the temperature vary from 50°C to 95°C. Plot the time versus the temperature, and discuss the results.

4–77E Oranges of 2.5-in-diameter ($k = 0.26$ Btu/h·ft·°F and $\alpha = 1.4 \times 10^{-6}$ ft²/s) initially at a uniform temperature of 78°F are to be cooled by refrigerated air at 25°F flowing at a velocity of 1 ft/s. The average heat transfer coefficient between the oranges and the air is experimentally determined to be 4.6 Btu/h·ft²·°F. Determine how long it will take for the center temperature of the oranges to drop to 40°F. Also, determine if any part of the oranges will freeze during this process. Solve this problem using the analytical one-term approximation method.

4–78 White potatoes ($k = 0.50$ W/m·K and $\alpha = 0.13 \times 10^{-6}$ m²/s) that are initially at a uniform temperature of 20°C and have an average diameter of 6 cm are to be cooled by refrigerated air at 2°C flowing at a velocity of 4 m/s. The average heat transfer coefficient between the potatoes and the air is experimentally determined to be 19 W/m²·K. Determine how long it will take for the center temperature of the potatoes to drop to 6°C. Also, determine if any part of the potatoes will experience chilling injury during this process. Solve this problem using the analytical one-term approximation method.

Air
2°C
4 m/s

Potato
$T_i = 20°C$
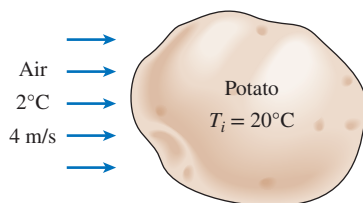
FIGURE P4–78

4–79 An experiment is to be conducted to determine the heat transfer coefficient on the surfaces of tomatoes that are placed in cold water at 7°C. The tomatoes ($k = 0.59$ W/m·K, $\alpha = 0.141 \times 10^{-6}$ m²/s, $\rho = 999$ kg/m³, $c_p = 3.99$ kJ/kg·K) with an initial uniform temperature of 30°C are spherical with a diameter of 8 cm. After 2 h, the temperatures at the center and the surface of the tomatoes are measured to be 10.0°C and 7.1°C, respectively. Using the analytical one-term approximation method, determine the heat transfer coefficient and the amount of heat transfer during this period if there are eight such tomatoes in water.

4–80 A person puts a few apples into the freezer at −15°C to cool them quickly for guests who are about to arrive. Initially, the apples are at a uniform temperature of 25°C, and the heat transfer coefficient on the surfaces is 8 W/m²·K. Treating the apples as 9-cm-diameter spheres and taking their properties to be $\rho = 840$ kg/m³, $c_p = 3.81$ kJ/kg·K, $k = 0.418$ W/m·K, and $\alpha = 1.3 \times 10^{-7}$ m²/s, determine the center and surface temperatures of the apples in 1 h. Also, determine the amount of heat transfer from each apple. Solve this problem using the analytical one-term approximation method.

4–81 Reconsider Prob. 4–80. Using appropriate software, investigate the effect of the initial temperature of the apples on the final center and surface temperatures and the amount of heat transfer. Let the initial temperature vary from 2°C to 30°C. Plot the center temperature, the surface temperature, and the amount of heat transfer as a function of the initial temperature, and discuss the results.

4–82 A 9-cm-diameter potato ($\rho = 1100$ kg/m³, $c_p = 3900$ J/kg·K, $k = 0.6$ W/m·K, and $\alpha = 1.4 \times 10^{-7}$ m²/s) that is initially at a uniform temperature of 25°C is baked in an oven at 170°C until a temperature sensor inserted into the center of the potato indicates a reading of 70°C. The potato is then taken out of the oven and wrapped in thick towels so that almost no heat is lost from the baked potato. Assuming the heat transfer coefficient in the oven to be 40 W/m²·K, determine (a) how long the potato is baked in the oven and (b) the final equilibrium temperature of the potato after it is wrapped. Solve this problem using the analytical one-term approximation method.

4–83 In *Betty Crocker's Cookbook,* it is stated that it takes 2 h 45 min to roast a 3.2-kg rib initially at 4.5°C to "rare" in an oven maintained at 163°C. It is recommended that a meat thermometer be used to monitor the cooking, and the rib is considered rare when the thermometer inserted into the center of the thickest part of the meat registers 60°C. The rib can be treated as a homogeneous spherical object with the properties $\rho = 1200$ kg/m³, $c_p = 4.1$ kJ/kg·K, $k = 0.45$ W/m·K, and $\alpha = 0.91 \times 10^{-7}$ m²/s. Determine (a) the heat transfer coefficient at the surface of the rib; (b) the temperature of the outer surface of the rib when it is done; and (c) the amount of heat transferred to the rib. (d) Using the values obtained, predict how long it will take to roast this rib to "medium" level, which occurs when the innermost temperature of the rib reaches 71°C. Compare your result to the listed value of 3 h 20 min.

If the roast rib is to be set on the counter for about 15 min before it is sliced, it is recommended that the rib be taken out of the oven when the thermometer registers about 4°C below the indicated value because the rib will continue cooking even after it is taken out of the oven. Do you agree with this recommendation? Solve this problem using the analytical one-term approximation method. *Answers:* (*a*) 156.9 W/m^2.K, (*b*) 159.5°C, (*c*) 1629 kJ, (*d*) 3.0 h

4–84 Repeat Prob. 4–83 for a roast rib that is to be "well-done" instead of "rare." A rib is considered to be well-done when its center temperature reaches 77°C, and the roasting in this case takes about 4 h 15 min.

Transient Heat Conduction in Semi-Infinite Solids

4–85C Under what conditions can a plane wall be treated as a semi-infinite mediaum?

4–86C What is a semi-infinite medium? Give examples of solid bodies that can be treated as semi-infinite media for heat transfer purposes.

4–87C Consider a hot semi-infinite solid at an initial temperature of T_i that is exposed to convection to a cooler medium at a constant temperature of T_∞, with a heat transfer coefficient of h. Explain how you can determine the total amount of heat transfer from the solid up to a specified time t_o.

4–88E The walls of a furnace are made of 1.5-ft-thick concrete ($k = 0.64$ Btu/h·ft·°F and $\alpha = 0.023$ ft^2/h). Initially, the furnace and the surrounding air are in thermal equilibrium at 70°F. The furnace is then fired, and the inner surfaces of the furnace are subjected to hot gases at 1800°F with a very large heat transfer coefficient. Determine how long it will take for the temperature of the outer surface of the furnace walls to rise to 70.1°F. *Answer:* 3.0 h

4–89 Consider a curing kiln whose walls are made of 30-cm-thick concrete with a thermal diffusivity of $\alpha = 0.23 \times 10^{-5}$ m^2/s. Initially, the kiln and its walls are in equilibrium with the surroundings at 6°C. Then all the doors are closed and the kiln is heated by steam so that the temperature of the inner surface of the walls is raised to 42°C and the temperature is maintained at that level for 2.5 h. The curing kiln is then opened and exposed to the atmospheric air after the steam flow is turned off. If the
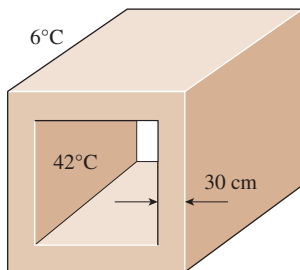
outer surfaces of the walls of the kiln were insulated, would it save any energy that day during the period the kiln was used for curing for 2.5 h only, or would it make no difference? Base your answer on calculations.

4–90 In areas where the air temperature remains below 0°C for prolonged periods of time, the freezing of water in underground pipes is a major concern. Fortunately, the soil remains relatively warm during those periods, and it takes weeks for the subfreezing temperatures to reach the water mains in the ground. Thus, the soil effectively serves as an insulation to protect the water from the freezing atmospheric temperatures in winter.

The ground at a particular location is covered with snow-pack at −8°C for a continuous period of 60 days, and the average soil properties at that location are $k = 0.35$ W/m·K and $\alpha = 0.15 \times 10^{-6}$ m^2/s. Assuming an initial uniform temperature of 8°C for the ground, determine the minimum burial depth to prevent the water pipes from freezing.

4–91 A large cast iron container ($k = 52$ W/m·K and $\alpha = 1.70 \times 10^{-5}$ m^2/s) with 4-cm-thick walls is initially at a uniform temperature of 0°C and is filled with ice at 0°C. Now the outer surfaces of the container are exposed to hot water at 55°C with a very large heat transfer coefficient. Determine how long it will be before the ice inside the container starts melting. Also, taking the heat transfer coefficient on the inner surface of the container to be 250 W/m^2·K, determine the rate of heat transfer to the ice through a 1.2-m-wide and 2-m-high section of the wall when steady operating conditions are reached. Assume the ice starts melting when its inner surface temperature rises to 0.1°C.
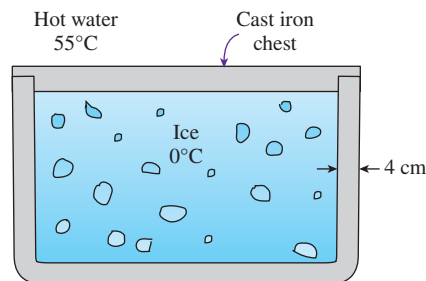
FIGURE P4–91

4–92 A highway made of asphalt is initially at a uniform temperature of 55°C. Suddenly the highway surface temperature is reduced to 25°C by rain. Determine the temperature at the depth of 3 cm from the highway surface and the heat flux transferred from the highway after 60 min. Assume the highway surface temperature is maintained at 25°C. *Answers:* 53.6°C, 98 W/m^2

4–93 A thick aluminum block initially at 20°C is subjected to constant heat flux of 4000 W/m^2 by an electric resistance heater whose top surface is insulated. Determine how much the surface temperature of the block will rise after 30 min.

FIGURE P4–89

4–94 Refractory bricks are used as linings for furnaces, and they generally have low thermal conductivity to minimize heat loss through the furnace walls. Consider a thick furnace wall lined with refractory bricks ($k = 1.0$ W/m·K and $\alpha = 5.08 \times 10^{-7}$ m²/s), where initially the wall has a uniform temperature of 15°C. If the wall surface is subjected to uniform heat flux of 20 kW/m², determine the temperature at the depth of 10 cm from the surface after an hour of heating time.

$\dot{q}_s = 20{,}000$ W/m²

Thick refractory brick wall

$T_i = 15°C$
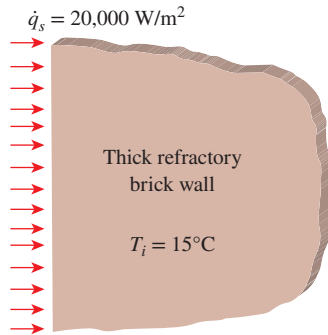
FIGURE P4–94

4–95 A thick wall made of refractory bricks ($k = 1.0$ W/m·K and $\alpha = 5.08 \times 10^{-7}$ m²/s) has a uniform initial temperature of 15°C. The wall surface is subjected to uniform heat flux of 20 kW/m². Using appropriate software, investigate the effect of heating time on the temperature at the wall surface and at $x = 1$ cm and $x = 5$ cm from the surface. Let the heating time vary from 10 to 3600 s, and plot the temperatures at $x = 0$, 1, and 5 cm from the wall surface as a function of heating time.

4–96 A stainless steel slab ($k = 14.9$ W/m·K and $\alpha = 3.95 \times 10^{-6}$ m²/s) and a copper slab ($k = 401$ W/m·K and $\alpha = 117 \times 10^{-6}$ m²/s) are subjected to uniform heat flux of 10 kW/m² at the surface. Both slabs have a uniform initial temperature of 20°C. Using appropriate software, investigate the effect of time on the temperatures of both materials at the depth of 8 cm from the surface. By varying the time of exposure to the heat flux from 5 to 300 s, plot the temperatures at a depth of $x = 8$ cm from the surface as a function of time.

4–97 Thick slabs of stainless steel ($k = 14.9$ W/m·K and $\alpha = 3.95 \times 10^{-6}$ m²/s) and copper ($k = 401$ W/m·K and $\alpha = 117 \times 10^{-6}$ m²/s) are subjected to uniform heat flux of 8 kW/m² at the surface. The two slabs have a uniform initial temperature of 20°C. Determine the temperatures of both slabs, at 1 cm from the surface, after 60 s of exposure to the heat flux.

$\dot{q}_s = 8000$ W/m²

x

Stainless steel slab

Copper slab
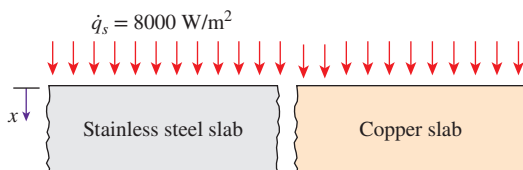
FIGURE P4–97

4–98 A thick wood slab ($k = 0.17$ W/m·K and $\alpha = 1.28 \times 10^{-7}$ m²/s) that is initially at a uniform temperature of 25°C is exposed to hot gases at 550°C for a period of 5 min. The heat transfer coefficient between the gases and the wood slab is 35 W/m²·K. If the ignition temperature of the wood is 450°C, determine if the wood will ignite.

4–99 **C&S** An ASTM F441 chlorinated polyvinyl chloride (CPVC) tube is embedded in a thick metal plate. The metal plate has a thermal conductivity of 26.9 W/m·K, a specific heat of 460 J/kg·K, and a density of 7.73 g/cm³. The upper surface of the plate is occasionally exposed to hot fluid at 300°C with a convection heat transfer coefficient of 200 W/m²·K. The distance measured from the plate's upper surface to the tube surface is $L = 2$ cm. The ASME Code for Process Piping limits the maximum use temperature for ASTM F441 CPVC tube to 93.3°C (ASME B31.3-2014, Table B-1). If the initial temperature of the plate is 20°C and the plate's upper surface is exposed to the hot fluid for 10 min, would the CPVC tube embedded in the plate still comply with the ASME code?

Hot fluid, T_∞, h

L

Metal plate

x

Tube
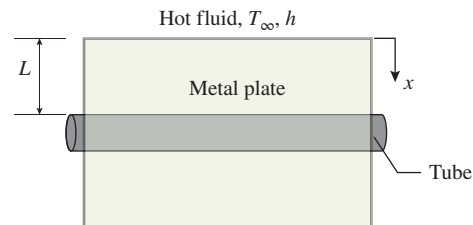
FIGURE P4–99

4–100 The soil temperature in the upper layers of the earth varies with the variations in the atmospheric conditions. Before a cold front moves in, the earth at a location is initially at a uniform temperature of 15°C. Then the area is subjected to a temperature of −8°C and high winds that result in a convection heat transfer coefficient of 40 W/m²·K on the earth's surface for a period of 10 h. Taking the properties of the soil at that location to be $k = 0.9$ W/m·K and $\alpha = 1.6 \times 10^{-5}$ m²/s, determine the soil temperature at distances 0, 10, 20, and 50 cm from the earth's surface at the end of this 10-h period.

Winds, −8°C

Soil

15°C
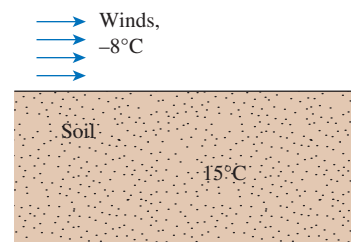
FIGURE P4–100

4–101 Reconsider Prob. 4–100. Using appropriate software, plot the soil temperature as a function of the distance from the earth's surface as the distance varies from 0 m to 1 m, and discuss the results.

4–102 We often cut a watermelon in half and put it into the freezer to cool it quickly. But usually we forget to check on it and end up having a watermelon with a frozen layer on the top. To avoid this potential problem, a person wants to set a timer so that it will go off when the temperature of the exposed surface of the watermelon drops to 3°C. Consider a 25-cm-diameter spherical watermelon that is cut into two equal parts and put into a freezer at −12°C. Initially, the entire watermelon is at a uniform temperature of 25°C, and the heat transfer coefficient on the surfaces is 22 W/m²·K. Assuming the watermelon to have the properties of water, determine how long it will take for the center of the exposed cut surfaces of the watermelon to drop to 3°C.

4–103 In a vacuum chamber, a thick slab is placed under an array of laser diodes with an output constant pulse. A thermocouple is inserted inside the slab at 25 mm from the surface, and the slab has an initial uniform temperature of 20°C. The known properties of the slab are $k = 63.9$ W/m·K and $a = 18.8 \times 10^{-6}$ m²/s. If the thermocouple measured a temperature of 130°C after the slab surface has been exposed to the laser pulse, for 30 s, determine (*a*) the amount of energy per unit surface area directed on the slab surface and (*b*) the thermocouple reading after 60 s has elapsed.
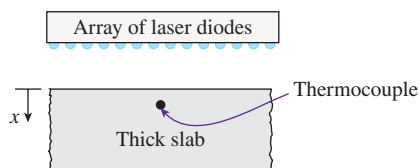
FIGURE P4−103

4–104 Thick slabs of stainless steel ($k = 14.9$ W/m·K and $\alpha = 3.95 \times 10^{-6}$ m²/s) and copper ($k = 401$ W/m·K and $\alpha = 117 \times 10^{-6}$ m²/s) are placed under an array of laser diodes, which supply an energy pulse of 5×10^7 J/m² instantaneously at $t = 0$ to both materials. The two slabs have a uniform initial temperature of 20°C. Determine the temperatures of both slabs at 5 cm from the surface and 60 s after receiving an energy pulse from the laser diodes.
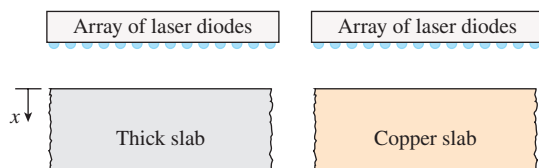
FIGURE P4−104

4–105 A stainless steel slab ($k = 14.9$ W/m·K and $\alpha = 3.95 \times 10^{-6}$ m²/s) and a copper slab ($k = 401$ W/m·K and $\alpha = 117 \times 10^{-6}$ m²/s) are placed under an array of laser diodes, which supply an energy pulse of 5×10^7 J/m² instantaneously at $t = 0$ to both materials. The two slabs have a uniform initial temperature of 20°C. Using appropriate software, investigate the effect of time on the temperatures of both materials at the depth of 5 cm from the surface. By varying the time from 1 to 80 s after the slabs have received the energy pulse, plot the temperatures at 5 cm from the surface as a function of time.

4–106 A barefooted person whose feet are at 32°C steps on a large aluminum block at 20°C. Treating both the feet and the aluminum block as semi-infinite solids, determine the contact surface temperature. What would your answer be if the person stepped on a wood block instead? At room temperature, the $\sqrt{k\rho c_p}$ value is 24 kJ/m²·°C for aluminum, 0.38 kJ/m²·°C for wood, and 1.1 kJ/m²·°C for human flesh.

Transient Heat Conduction in Multidimensional Systems

4–107C What is the product solution method? How is it used to determine the transient temperature distribution in a two-dimensional system?

4–108C How is the product solution used to determine the variation of temperature with time and position in three-dimensional systems?

4–109C A short cylinder initially at a uniform temperature T_i is subjected to convection from all of its surfaces to a medium at temperature T_∞. Explain how you can determine the temperature of the midpoint of the cylinder at a specified time t.

4–110C Consider a short cylinder whose top and bottom surfaces are insulated. The cylinder is initially at a uniform temperature T_i and is subjected to convection from its side surface to a medium at temperature T_∞ with a heat transfer coefficient of h. Is the heat transfer in this short cylinder one- or two-dimensional? Explain.

4–111 Consider a cubic block whose sides are 5 cm long and a cylindrical block whose height and diameter are also 5 cm. Both blocks are initially at 20°C and are made of
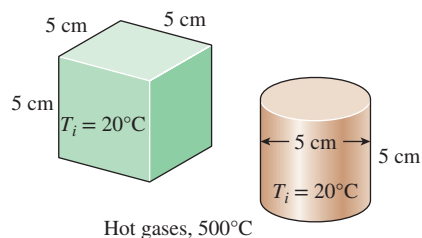
FIGURE P4−111

granite ($k = 2.5$ W/m·K and $\alpha = 1.15 \times 10^{-6}$ m²/s). Now both blocks are exposed to hot gases at 500°C in a furnace on all of their surfaces with a heat transfer coefficient of 40 W/m²·K. Determine the center temperature of each geometry after 10, 20, and 60 min. Solve this problem using the analytical one-term approximation method.

4–112 Repeat Prob. 4–111 with the heat transfer coefficient at the top and the bottom surfaces of each block being doubled to 80 W/m²·K.

4–113 C&S A long square stainless steel (ASTM A479 904L) bar is part of a component in high-temperature process equipment. The bar has a thickness of 5 cm, and its specific heat, thermal conductivity, and density are 500 J/kg·K, 12 W/m·K, and 7.9 g/cm³, respectively. Occasionally, the bar is submerged in hot fluid at 300°C with a convection heat transfer coefficient of 288 W/m²·K. According to the ASME Code for Process Piping, the maximum use temperature for ASTM A479 904L bar is 260°C (ASME B31.3-2014, Table A-1M). If the initial temperature of the bar is 20°C and the bar is submerged in the hot fluid for 7 min, would it be in compliance with the ASME code? How long will it take for the bar to reach the maximum use temperature? Solve this problem using the analytical one-term approximation method.
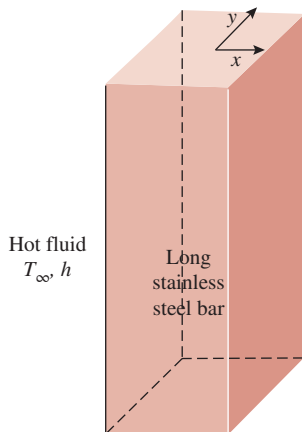
FIGURE P4–113

4–114E A hot dog can be considered to be a cylinder 5 in long and 0.8 in in diameter whose properties are $\rho = 61.2$ lbm/ft³, $c_p = 0.93$ Btu/lbm·°F, $k = 0.44$ Btu/h·ft·°F, and $\alpha = 0.0077$ ft²/h. A hot dog initially at 40°F is dropped into boiling water at 212°F. If the heat transfer coefficient at the surface of the hot dog is estimated to be 120 Btu/h·ft²·°F, determine the center temperature of the hot dog after 5, 10, and 15 min by treating the hot dog as (*a*) a finite cylinder and (*b*) an infinitely long cylinder. Solve this problem using the analytical one-term approximation method.

4–115 A 6-cm-high rectangular ice block ($k = 2.22$ W/m·K and $\alpha = 0.124 \times 10^{-7}$ m²/s) initially at −18°C is placed on a table on its square base 4 cm × 4 cm in size in a room at 18°C. The heat transfer coefficient on the exposed surfaces of the ice block is 12 W/m²·K. Disregarding any heat transfer from the base to the table, determine how long it will be before the ice block starts melting. Where on the ice block will the first liquid droplets appear? Solve this problem using the analytical one-term approximation method.
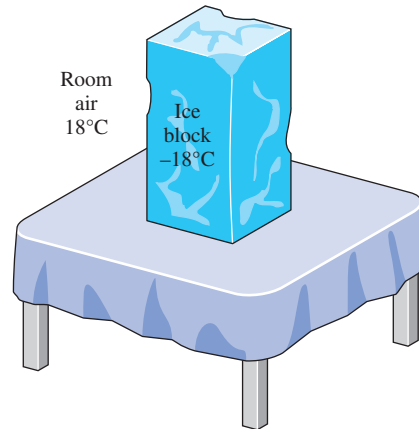
FIGURE P4–115

4–116 Reconsider Prob. 4–115. Using appropriate software, investigate the effect of the initial temperature of the ice block on the time period before the ice block starts melting. Let the initial temperature vary from −26°C to −4°C. Plot the time versus the initial temperature, and discuss the results.

4–117 A 2-cm-high cylindrical ice block ($k = 2.22$ W/m·K and $\alpha = 0.124 \times 10^{-7}$ m²/s) is placed on a table on its base of diameter 2 cm in a room at 24°C. The heat transfer coefficient on the exposed surfaces of the ice block is 13 W/m²·K, and heat transfer from the base of the ice block to the table is negligible. If the ice block is not to start melting at any point for at least 3 h, determine what the initial temperature of the ice block should be. Solve this problem using the analytical one-term approximation method.

4–118 A short brass cylinder ($\rho = 8530$ kg/m³, $c_p = 0.389$ kJ/kg·K, $k = 110$ W/m·K, and $\alpha = 3.39 \times 10^{-5}$ m²/s) of diameter 4 cm and height 20 cm is initially at a uniform temperature of 150°C. The cylinder is now placed in atmospheric air at 20°C, where heat transfer takes place by convection with a heat transfer coefficient of 40 W/m²·K. Calculate (*a*) the center temperature of the cylinder; (*b*) the center temperature of the top surface of the cylinder; and (*c*) the total heat transfer from the cylinder 15 min after the start of the cooling. Solve this problem using the analytical one-term approximation method.

Ambient air 20°C

Brass cylinder

20 cm

4 cm

150°C
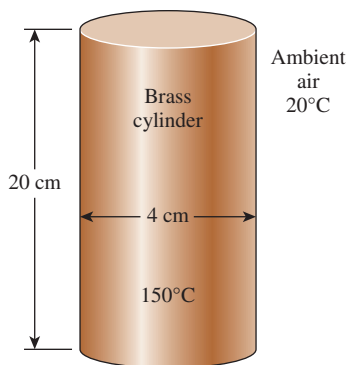
FIGURE P4–118

4–119 Reconsider Prob. 4–118. Using appropriate software, investigate the effect of the cooling time on the center temperature of the cylinder, the center temperature of the top surface of the cylinder, and the total heat transfer. Let the time vary from 5 min to 60 min. Plot the center temperature of the cylinder, the center temperature of the top surface, and the total heat transfer as a function of the time, and discuss the results.

4–120 A semi-infinite aluminum cylinder ($k = 237$ W/m·K, $\alpha = 9.71 \times 10^{-5}$ m²/s) of diameter $D = 15$ cm is initially at a uniform temperature of $T_i = 115°C$. The cylinder is now placed in water at 10°C, where heat transfer takes place by convection with a heat transfer coefficient of $h = 140$ W/m²·K. Determine the temperature at the center of the cylinder 5 cm from the end surface 8 min after the start of cooling. Solve this problem using the analytical one-term approximation method.

4–121 A 30-cm-long cylindrical aluminum block ($\rho = 2702$ kg/m³, $c_p = 0.896$ kJ/kg·K, $k = 236$ W/m·K, and $\alpha = 9.75 \times 10^{-5}$ m²/s), 15 cm in diameter, is initially at a uniform temperature of 20°C. The block is to be heated in a furnace at 1200°C until its center temperature rises to 300°C. If the heat transfer coefficient on all surfaces of the block is 80 W/m²·K, determine how long the block should be kept in the furnace. Also, determine the amount of heat transfer from the aluminum block if it is allowed to cool in the room until its temperature drops to 20°C throughout. Solve this problem using the analytical one-term approximation method.

4–122 Repeat Prob. 4–121 for the case where the aluminum block is inserted into the furnace on a low-conductivity material so that the heat transfer to or from the bottom surface of the block is negligible.
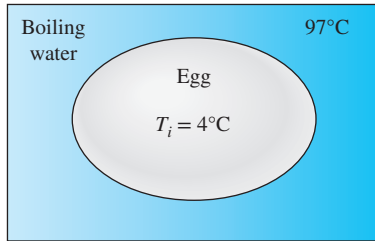
4–123 Reconsider Prob. 4–121. Using appropriate software, investigate the effect of the final center temperature of the block on the heating time and the amount of heat transfer. Let the final center temperature vary from 50°C to 1000°C. Plot the time and the heat transfer as a function of the final center temperature, and discuss the results.

Special Topic: Refrigeration and Freezing of Foods

4–124C What are the common kinds of microorganisms? What undesirable changes do microorganisms cause in foods?

4–125C How does refrigeration prevent or delay the spoilage of foods? Why does freezing extend the storage life of foods for months?

4–126C What are the environmental factors that affect the growth rate of microorganisms in foods?

4–127C What is the effect of cooking on the microorganisms in foods? Why is it important that the internal temperature of a roast in an oven be raised above 70°C?

4–128C How can the contamination of foods with microorganisms be prevented or minimized? How can the growth of microorganisms in foods be retarded? How can the microorganisms in foods be destroyed?

4–129C How does (*a*) the air motion and (*b*) the relative humidity of the environment affect the growth of microorganisms in foods?

4–130C The cooling of a beef carcass from 37°C to 5°C with refrigerated air at 0°C in a chilling room takes about 48 h. To reduce the cooling time, it is proposed to cool the carcass with refrigerated air at −10°C. How would you evaluate this proposal?

4–131C Consider the freezing of packaged meat in boxes with refrigerated air. How do (*a*) the temperature of air, (*b*) the velocity of air, (*c*) the capacity of the refrigeration system, and (*d*) the size of the meat boxes affect the freezing time?

4–132C How does the rate of freezing affect the tenderness, color, and the drip of meat during thawing?

4–133C It is claimed that beef can be stored for up to two years at −23°C but no more than one year at −12°C. Is this claim reasonable? Explain.

4–134C What is a refrigerated shipping dock? How does it reduce the refrigeration load of the cold storage rooms?

4–135C How does immersion chilling of poultry compare to forced-air chilling with respect to (*a*) cooling time, (*b*) moisture loss of poultry, and (*c*) microbial growth?

4–136C What is the proper storage temperature of frozen poultry? What are the primary methods of freezing for poultry?

4–137C What are the factors that affect the quality of frozen fish?

4–138 The chilling room of a meat plant is 15 m × 18 m × 5.5 m in size and has a capacity of 350 beef carcasses. The power consumed by the fans and the lights in the chilling room are 22 and 2 kW, respectively, and the room gains heat through its envelope at a rate of 14 kW. The average mass of beef carcasses is 220 kg. The carcasses enter the chilling room at 35°C, after they are washed to facilitate evaporative cooling, and are cooled to 16°C in 12 h. The air enters the chilling room at −2.2°C and leaves at 0.5°C. Determine (*a*) the refrigeration

load of the chilling room and (*b*) the volume flow rate of air. The average specific heats of beef carcasses and air are 3.14 and 1.0 kJ/kg·°C, respectively, and the density of air can be taken to be 1.28 kg/m³.

4–139 Chickens with an average mass of 2.2 kg and average specific heat of 3.54 kJ/kg·°C are to be cooled by chilled water that enters a continuous-flow-type immersion chiller at 0.5°C. Chickens are dropped into the chiller at a uniform temperature of 15°C at a rate of 500 chickens per hour and are cooled to an average temperature of 3°C before they are taken out. The chiller gains heat from the surroundings at a rate of 210 kJ/min. Determine (*a*) the rate of heat removal from the chicken, in kW, and (*b*) the mass flow rate of water, in kg/s, if the temperature rise of water is not to exceed 2°C.

4–140E Chickens with a water content of 74 percent, an initial temperature of 32°F, and a mass of about 7.5 lbm are to be frozen by refrigerated air at −40°F. Using Fig. 4–50, determine how long it will take to reduce the inner surface temperature of chickens to 25°F. What would your answer be if the air temperature were −80°F?

4–141 Turkeys with a water content of 64 percent that are initially at 1°C and have a mass of about 7 kg are to be frozen by submerging them into brine at −29°C. Using Fig. 4–51, determine how long it will take to reduce the temperature of the turkey breast at a depth of 3.8 cm to −18°C. If the temperature at a depth of 3.8 cm in the breast represents the average temperature of the turkey, determine the amount of heat transfer per turkey assuming (*a*) the entire water content of the turkey is frozen and (*b*) only 90 percent of the water content of the turkey is frozen at −18°C. Take the specific heats of turkey to be 2.98 and 1.65 kJ/kg·°C above and below the freezing point of −2.8°C, respectively, and the latent heat of fusion of turkey to be 214 kJ/kg. *Answers: (a)* 1753 kJ, *(b)* 1617 kJ
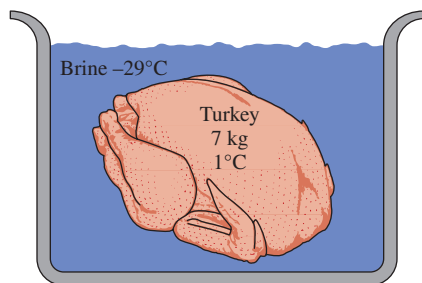
FIGURE P4–141

Review Problems

4–142 Large steel plates 1.0 cm in thickness are quenched from 600°C to 100°C by submerging them in an oil reservoir held at 30°C. The average heat transfer coefficient for both faces of steel plates is 400 W/m²·K. Average steel properties are $k = 45$ W/m·K, $\rho = 7800$ kg/m³, and $c_p = 470$ J/kg·K. Calculate the quench time for steel plates.

4–143 A long roll of 2-m-wide and 0.5-cm-thick 1-Mn manganese steel plate coming off a furnace at 820°C is to be quenched in an oil bath ($c_p = 2.0$ kJ/kg·K) at 45°C. The metal sheet is moving at a steady velocity of 20 m/min, and the oil bath is 9 m long. Taking the convection heat transfer coefficient on both sides of the plate to be 860 W/m²·K, determine the temperature of the sheet metal when it leaves the oil bath. Also, determine the required rate of heat removal from the oil to keep its temperature constant at 45°C.
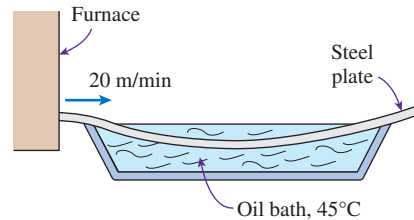
FIGURE P4–143

4–144 Long aluminum wires of diameter 3 mm ($\rho = 2702$ kg/m³, $c_p = 0.896$ kJ/kg·K, $k = 236$ W/m·K, and $\alpha = 9.75 \times 10^{-5}$ m²/s) are extruded at a temperature of 350°C and exposed to atmospheric air at 30°C with a heat transfer coefficient of 35 W/m²·K. (*a*) Determine how long it will take for the wire temperature to drop to 50°C. (*b*) If the wire is extruded at a velocity of 10 m/min, determine how far the wire travels after extrusion by the time its temperature drops to 50°C. What change in the cooling process would you propose to shorten this distance? (*c*) Assuming the aluminum wire leaves the extrusion room at 50°C, determine the rate of heat transfer from the wire to the extrusion room. *Answers: (a)* 144 s, *(b)* 24 m, *(c)* 856 W
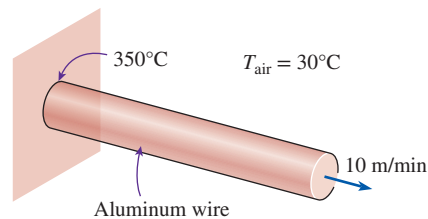
FIGURE P4–144

4–145 Repeat Prob. 4–144 for a copper wire ($\rho = 8950$ kg/m³, $c_p = 0.383$ kJ/kg·K, $k = 386$ W/m·K, and $\alpha = 1.13 \times 10^{-4}$ m²/s).

4–146 Aluminum wires 4 mm in diameter are produced by extrusion. The wires leave the extruder at an average temperature of 350°C and at a linear rate of 10 m/min. Before leaving the extrusion room, the wires are cooled to an average temperature of 50°C by transferring heat to the surrounding air at 25°C with a heat transfer coefficient of 50 W/m²·K. Calculate the necessary length of the wire cooling section in the extrusion room.

4–147E During a picnic on a hot summer day, the only available drinks were those at the ambient temperature of 90°F. In an effort to cool a 12-fluid-oz drink in a can, which is 5 in high and has a diameter of 2.5 in, a person grabs the can and starts

shaking it in the iced water of the chest at 32°F. The temperature of the drink can be assumed to be uniform at all times, and the heat transfer coefficient between the iced water and the aluminum can is 30 Btu/h·ft²·°F . Using the properties of water for the drink, estimate how long it will take for the canned drink to cool to 40°F. Solve this problem using lumped system analysis. Is the lumped system analysis applicable to this problem? Why?

4–148   Two metal rods are being heated in an oven with uniform ambient temperature of 1000°C and convection heat transfer coefficient of 25 W/m²·K. Rod A is made of aluminum ($\rho = 2702$ kg/m³, $c_p = 903$ J/kg·K, and $k = 237$ W/m·K) and rod B is made of stainless steel ($\rho = 8238$ kg/m³, $c_p = 468$ J/kg·K, and $k = 13.4$ W/m·K). Both rods have a diameter of 25 mm and a length of 1 m. If the initial temperature of both rods is 15°C, determine the average temperatures of both rods after 5 min.

4–149   Stainless steel ball bearings ($\rho = 8085$ kg/m³, $k = 15.1$ W/m·°C, $c_p = 0.480$ KJ/kg·°C, and $\alpha = 3.91 \times 10^{-6}$ m²/s) having a diameter of 1.2 cm are to be quenched in water. The balls leave the oven at a uniform temperature of 900°C and are exposed to air at 30°C for a while before they are dropped into the water. If the temperature of the balls is not to fall below 850°C prior to quenching and the heat transfer coefficient in the air is 125 W/m²·°C, determine how long they can stand in the air before being dropped into the water.

4–150   In an annealing process, a 50-mm-thick stainless steel plate ($\rho = 8238$ kg/m³, $c_p = 468$ J/kg·K, $k = 13.4$ W/m·K, and $\alpha = 3.48 \times 10^{-6}$ m²/s) was reheated in a furnace from an initial uniform temperature of 230°C. The ambient temperature inside the furnace is uniform at 1000°C, and the convection heat transfer coefficient is 215 W/m²·K. If the entire stainless steel plate is to be heated to at least 600°C, determine the time that the plate should be heated in the furnace using the analytical one-term approximation method.

4–151   During a fire, the trunks of some dry oak trees ($k = 0.17$ W/m·K and $\alpha = 1.28 \times 10^{-7}$ m²/s) that are initially at a uniform temperature of 30°C are exposed to hot gases at 600°C for a period of 4 h, with a heat transfer coefficient of 65 W/m²·K on the surface. The ignition temperature of the trees is 410°C. Treating the trunks of the trees as long cylindrical rods of diameter 20 cm, determine if these dry trees will ignite as the fire sweeps through them. Solve this problem using the analytical one-term approximation method.

Hot gases
30°C
600°C

20 cm
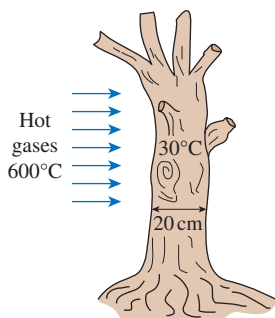
FIGURE P4–151

4–152E   In *Betty Crocker's Cookbook,* it is stated that it takes 5 h to roast a 14-lb stuffed turkey initially at 40°F in an oven maintained at 325°F. It is recommended that a meat thermometer be used to monitor the cooking, and the turkey is considered done when the thermometer inserted deep into the thickest part of the breast or thigh without touching the bone registers 185°F. The turkey can be treated as a homogeneous spherical object with the properties $\rho = 75$ lbm/ft³, $c_p = 0.98$ Btu/lbm·°F, $k = 0.26$ Btu/h·ft·°F, and $\alpha = 0.0035$ ft²/h. Assuming the tip of the thermometer is at one-third radial distance from the center of the turkey, determine (*a*) the average heat transfer coefficient at the surface of the turkey, (*b*) the temperature of the skin of the turkey when it is done, and (*c*) the total amount of heat transferred to the turkey in the oven. Will the reading of the thermometer be more or less than 185°F 5 min after the turkey is taken out of the oven?

4–153   A watermelon initially at 35°C is to be cooled by dropping it into a lake at 15°C. After 4 h and 40 min of cooling, the center temperature of the watermelon is measured to be 20°C. Treating the watermelon as a 20-cm-diameter sphere and using the properties $k = 0.618$ W/m·K, $\alpha = 0.15 \times 10^{-6}$ m²/s, $\rho = 995$ kg/m³, and $c_p = 4.18$ kJ/kg·K, determine the average heat transfer coefficient and the surface temperature of the watermelon at the end of the cooling period. Solve this problem using the analytical one-term approximation method.

4–154   Spherical glass beads coming out of a kiln are allowed to cool in a room temperature of 30°C. A glass bead with a diameter of 10 mm and an initial temperature of 400°C is allowed to cool for 3 min. If the convection heat transfer coefficient is 28 W/m²·K, determine the temperature at the center of the glass bead using the analytical one-term approximation method. The glass bead has properties of $\rho = 2800$ kg/m³, $c_p = 750$ J/kg·K, and $k = 0.7$ W/m·K.

4–155   Water mains must be placed at sufficient depth below the earth's surface to avoid freezing during extended periods of subfreezing temperatures. Determine the minimum depth at which the water main must be placed at a location where the soil is initially at 15°C and the earth's surface temperature under the worst conditions is expected to remain at $-10°C$ for 75 days. Take the properties of soil at that location to be $k = 0.7$ W/m·K and $\alpha = 1.4 \times 10^{-5}$ m²/s.   *Answer:* 7.05 m

4–156   A 40-cm-thick brick wall ($k = 0.72$ W/m·K, and $\alpha = 1.6 \times 10^{-6}$ m²/s) is heated to an average temperature of 18°C by the heating system and the solar radiation incident on it during the day. During the night, the outer surface of the wall is exposed to cold air at $-3°C$ with an average heat transfer coefficient of 20 W/m²·K. Determine the wall temperatures at distances 15, 30, and 40 cm from the outer surface for a period of 2 h.

4–157   In a volcano eruption, lava at 1200°C is found flowing on the ground. The ground was initially at 15°C, and the lava flow has a convection heat transfer coefficient of 3500 W/m²·K. Determine the ground surface (*a*) temperature and (*b*) heat flux after 2 s of lava flow. Assume the ground has properties of dry soil.

4–158 A large heated steel block ($\rho = 7832$ kg/m^3, $c_p = 434$ J/kg·K, $k = 63.9$ W/m·K, and $\alpha = 18.8 \times 10^{-6}$ m^2/s) is allowed to cool in a room at 25°C. The steel block has an initial temperature of 450°C, and the convection heat transfer coefficient is 25 W/m^2·K. Assuming that the steel block can be treated as a quarter-infinite medium, determine the temperature at the edge of the steel block after 10 min of cooling.

4–159 A large iron slab ($\rho = 7870$ kg/m^3, $c_p = 447$ J/kg·K, and $k = 80.2$ W/m·K) was initially heated to a uniform temperature of 150°C and then placed on a concrete floor ($\rho = 1600$ kg/m^3, $c_p = 840$ J/kg·K, and $k = 0.79$ W/m·K). The concrete floor was initially at a uniform temperature of 30°C. Determine (*a*) the surface temperature between the iron slab and concrete floor and (*b*) the temperature of the concrete floor at the depth of 25 mm, if the surface temperature remains constant after 15 min.
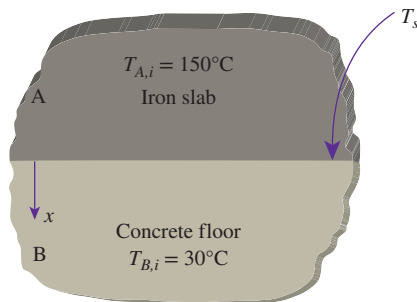
FIGURE P4–159

4–160 A hot dog can be considered to be a 12-cm-long cylinder whose diameter is 2 cm and whose properties are $\rho = 980$ kg/m^3, $c_p = 3.9$ kJ/kg·K, $k = 0.76$ W/m·K, and $\alpha = 2 \times 10^{-7}$ m^2/s. A hot dog initially at 5°C is dropped into boiling water at 100°C. The heat transfer coefficient at the surface of the hot dog is estimated to be 600 W/m^2·K. If the hot dog is considered cooked when its center temperature reaches 80°C, determine how long it will take to cook it in the boiling water. Solve this problem using the analytical one-term approximation method.

4–161 Consider the engine block of a car made of cast iron ($k = 52$ W/m·K and $\alpha = 1.7 \times 10^{-5}$ m^2/s). The engine can be considered to be a rectangular block whose sides are 80 cm, 40 cm, and 40 cm. The engine is at a temperature of 150°C when it is turned off. The engine is then exposed to atmospheric air at 17°C with a heat transfer coefficient of 6 W/m^2·K. Determine (*a*) the center temperature of the top surface whose sides are 80 cm and 40 cm and (*b*) the corner temperature after 45 min of cooling. Solve this problem using the analytical one-term approximation method.

4–162 A man is found dead in a room at 12°C. The surface temperature on his waist is measured to be 23°C, and the heat transfer coefficient is estimated to be 9 W/m^2·K. Modeling the body as a 28-cm diameter, 1.80-m-long cylinder, estimate how long it has been since he died. Take the properties of the body

to be $k = 0.62$ W/m·K and $\alpha = 0.15 \times 10^{-6}$ m^2/s, and assume the initial temperature of the body to be 36°C. Solve this problem using the analytical one-term approximation method.

Fundamentals of Engineering (FE) Exam Problems

4–163 The Biot number can be thought of as the ratio of
(*a*) the conduction thermal resistance to the convective thermal resistance
(*b*) the convective thermal resistance to the conduction thermal resistance
(*c*) the thermal energy storage capacity to the conduction thermal resistance
(*d*) the thermal energy storage capacity to the convection thermal resistance
(*e*) none of the above

4–164 Lumped system analysis of transient heat conduction situations is valid when the Biot number is
(*a*) very small   (*b*) approximately one
(*c*) very large   (*d*) any real number
(*e*) cannot say unless the Fourier number is also known

4–165 Polyvinylchloride automotive body panels ($k = 0.092$ W/m·K, $c_p = 1.05$ kJ/kg·K, $\rho = 1714$ kg/m^3), 1 mm thick, emerge from an injection molder at 120°C. They need to be cooled to 40°C by exposing both sides of the panels to 20°C air before they can be handled. If the convective heat transfer coefficient is 15 W/m^2·K and radiation is not considered, the time that the panels must be exposed to air before they can be handled is
(*a*) 0.8 min   (*b*) 1.6 min   (*c*) 2.4 min
(*d*) 3.1 min   (*e*) 5.6 min

4–166 A steel casting cools to 90 percent of the original temperature difference in 30 min in still air. The time it takes to cool this same casting to 90 percent of the original temperature difference in a moving air stream whose convective heat transfer coefficient is 5 times that of still air is
(*a*) 3 min   (*b*) 6 min   (*c*) 9 min
(*d*) 12 min   (*e*) 15 min

4–167 An 18-cm-long, 16-cm-wide, and 12-cm-high hot iron block ($\rho = 7870$ kg/m^3, $c_p = 447$ J/kg·K) initially at 20°C is placed in an oven for heat treatment. The heat transfer coefficient on the surface of the block is 100 W/m^2·K. If the temperature of the block must rise to 750°C in a 25-min period, the oven must be maintained at
(*a*) 750°C   (*b*) 830°C   (*c*) 875°C
(*d*) 910°C   (*e*) 1000°C

4–168 A 10-cm-inner-diameter, 30-cm-long can filled with water initially at 25°C is put into a household refrigerator at 3°C. The heat transfer coefficient on the surface of the can is 14 W/m^2·K. Assuming that the temperature of the water remains uniform during the cooling process, the time it takes for the water temperature to drop to 5°C is
(*a*) 0.55 h   (*b*) 1.17 h   (*c*) 2.09 h
(*d*) 3.60 h   (*e*) 4.97 h

4–169 A 6-cm-diameter, 13-cm-high canned drink ($\rho = 977$ kg/m^3, $k = 0.607$ W/m·K, $c_p = 4180$ J/kg·K) initially at 25°C is to be cooled to 5°C by dropping it into iced water at 0°C. Total surface area and volume of the drink are $A_s = 301.6$ cm^2 and $V = 367.6$ cm^3. If the heat transfer coefficient is 120 W/m^2·K, determine how long it will take for the drink to cool to 5°C. Assume the can is agitated in water, and thus the temperature of the drink changes uniformly with time.
(a) 1.5 min (b) 8.7 min (c) 11.1 min
(d) 26.6 min (e) 6.7 min

4–170 Copper balls ($\rho = 8933$ kg/m^3, $k = 401$ W/m·K, $c_p = 385$ J/kg·°C, $\alpha = 1.166 \times 10^{-4}$ m^2/s) initially at 180°C are allowed to cool in air at 30°C for a period of 2 min. If the balls have a diameter of 2 cm and the heat transfer coefficient is 80 W/m^2·K, the center temperature of the balls at the end of cooling is
(a) 78°C (b) 95°C (c) 118°C
(d) 134°C (e) 151°C

4–171 Carbon steel balls ($\rho = 7830$ kg/m^3, $k = 64$ W/m·K, $c_p = 434$ J/kg·K) initially at 200°C are quenched in an oil bath at 20°C for a period of 3 min. If the balls have a diameter of 5 cm and the convection heat transfer coefficient is 450 W/m^2·K, the center temperature of the balls after quenching will be (*Hint:* Check the Biot number.)
(a) 30.3°C (b) 46.1°C (c) 55.4°C
(d) 68.9°C (e) 79.4°C

4–172 In a production facility, large plates made of stainless steel ($k = 15$ W/m·K, $\alpha = 3.91 \times 10^{-6}$ m^2/s) of 40 cm thickness are taken out of an oven at a uniform temperature of 750°C. The plates are placed in a water bath that is kept at a constant temperature of 20°C with a heat transfer coefficient of 600 W/m^2·K. The time it takes for the surface temperature of the plates to drop to 120°C is
(a) 0.6 h (b) 0.8 h (c) 1.4 h
(d) 2.6 h (e) 3.2 h

4–173 A long 18-cm-diameter bar made of hardwood ($k = 0.159$ W/m·K, $\alpha = 1.75 \times 10^{-7}$ m^2/s) is exposed to air at 30°C with a heat transfer coefficient of 8.83 W/m^2·K. If the center temperature of the bar is measured to be 15°C after 3 h, the initial temperature of the bar is
(a) 11.9°C (b) 4.9°C (c) 1.7°C
(d) 0°C (e) −9.2°C

4–174 Consider a 7.6-cm-long and 3-cm-diameter cylindrical lamb meat chunk ($\rho = 1030$ kg/m^3, $c_p = 3.49$ kJ/kg·K, $k = 0.456$ W/m·K, $\alpha = 1.3 \times 10^{-7}$ m^2/s). Fifteen such meat chunks initially at 2°C are dropped into boiling water at 95°C with a heat transfer coefficient of 1200 W/m^2·K. The amount of heat transfer during the first 8 min of cooking is
(a) 71 kJ (b) 227 kJ (c) 238 kJ
(d) 269 kJ (e) 307 kJ

4–175 Consider a 7.6-cm-diameter cylindrical lamb meat chunk ($\rho = 1030$ kg/m^3, $c_p = 3.49$ kJ/kg·K, $k = 0.456$ W/m·K,

$\alpha = 1.3 \times 10^{-7}$ m^2/s). Such a meat chunk initially at 2°C is dropped into boiling water at 95°C with a heat transfer coefficient of 1200 W/m^2·K. The time it takes for the center temperature of the meat chunk to rise to 75°C is
(a) 136 min (b) 21.2 min (c) 13.6 min
(d) 11.0 min (e) 8.5 min

4–176 A potato may be approximated as a 5.7-cm solid sphere with the properties $\rho = 910$ kg/m^3, $c_p = 4.25$ kJ/kg·K, $k = 0.68$ W/m·K, and $\alpha = 1.76 \times 10^{-7}$ m^2/s. Twelve such potatoes initially at 25°C are to be cooked by placing them in an oven maintained at 250°C with a heat transfer coefficient of 95 W/m^2·K. The amount of heat transfer to the potatoes by the time the center temperature reaches 90°C is
(a) 1012 kJ (b) 1366 kJ (c) 1788 kJ
(d) 2046 kJ (e) 3270 kJ

4–177 A small chicken ($k = 0.45$ W/m·K, $\alpha = 0.15 \times 10^{-6}$ m^2/s) can be approximated as an 11.25-cm-diameter solid sphere. The chicken is initially at a uniform temperature of 8°C and is to be cooked in an oven maintained at 220°C with a heat transfer coefficient of 80 W/m^2·K. With this idealization, the temperature at the center of the chicken after a 90-min period is
(a) 25°C (b) 61°C (c) 89°C
(d) 122°C (e) 168°C

4–178 A potato may be approximated as a 5.7-cm-diameter solid sphere with the properties $\rho = 910$ kg/m^3, $c_p = 4.25$ kJ/kg·K, $k = 0.68$ W/m·K, and $\alpha = 1.76 \times 10^{-7}$ m^2/s. Twelve such potatoes initially at 25°C are to be cooked by placing them in an oven maintained at 250°C with a heat transfer coefficient of 95 W/m^2·K. The amount of heat transfer to the potatoes during a 30-min period is
(a) 77 kJ (b) 483 kJ (c) 927 kJ
(d) 970 kJ (e) 1012 kJ

4–179 When water, as in a pond or lake, is heated by warm air above it, it remains stable, does not move, and forms a warm layer of water on top of a cold layer. Consider a deep lake ($k = 0.6$ W/m·K, $c_p = 4.179$ kJ/kg·K) that is initially at a uniform temperature of 2°C and has its surface temperature suddenly increased to 20°C by a spring weather front. The temperature of the water 1 m below the surface 400 h after this change is
(a) 2.1°C (b) 4.2°C (c) 6.3°C
(d) 8.4°C (e) 10.2°C

4–180 A large chunk of tissue at 35°C with a thermal diffusivity of 1×10^{-7} m^2/s is dropped into iced water. The water is well-stirred so that the surface temperature of the tissue drops to 0°C at time zero and remains at 0°C at all times. The temperature of the tissue after 4 min at a depth of 1 cm is
(a) 5°C (b) 30°C (c) 25°C
(d) 20°C (e) 10°C

4–181 The 35-cm-thick roof of a large room made of concrete ($k = 0.79$ W/m·K, $\alpha = 5.88 \times 10^{-7}$ m^2/s) is initially at a uniform temperature of 15°C. After a heavy snowstorm, the

outer surface of the roof remains covered with snow at $-5°C$. The roof temperature at 12 cm distance from the outer surface after 2 h is

(*a*) 13°C   (*b*) 11°C   (*c*) 7°C
(*d*) 3°C   (*e*) $-5°C$

Design and Essay Problems

4–182 Conduct the following experiment at home to determine the combined convection and radiation heat transfer coefficient at the surface of an apple exposed to the room air. You will need two thermometers and a clock.

First, weigh the apple and measure its diameter. You can measure its volume by placing it in a large measuring cup halfway filled with water, and measuring the change in volume when it is completely immersed in the water. Refrigerate the apple overnight so that it is at a uniform temperature in the morning, and measure the air temperature in the kitchen. Then take the apple out and stick one of the thermometers to its middle and the other just under the skin. Record both temperatures every 5 min for an hour. Using these two temperatures, calculate the heat transfer coefficient for each interval and take their average. The result is the combined convection and radiation heat transfer coefficient for this heat transfer process. Using your experimental data, also calculate the thermal conductivity and thermal diffusivity of the apple and compare them to the values given above.

4–183 Repeat Prob. 4–182 using a banana instead of an apple. The thermal properties of bananas are practically the same as those of apples.

4–184 Conduct the following experiment to determine the time constant for a can of soda and then predict the temperature of the soda at different times. Leave the soda in the refrigerator overnight. Measure the air temperature in the kitchen and the temperature of the soda while it is still in the refrigerator by taping the sensor of the thermometer to the outer surface of the can. Then take the soda out and measure its temperature again in 5 min. Using these values, calculate the exponent *b*. Using this *b*-value, predict the temperatures of the soda in 10, 15, 20, 30, and 60 min and compare the results with the actual temperature measurements. Do you think the lumped system analysis is valid in this case?

4–185 Citrus trees are very susceptible to cold weather, and extended exposure to subfreezing temperatures can destroy the crop. In order to protect the trees from occasional cold fronts with subfreezing temperatures, tree growers in Florida usually install water sprinklers on the trees. When the temperature drops below a certain level, the sprinklers spray water on the trees and their fruits to protect them against the damage the subfreezing temperatures can cause. Explain the basic mechanism behind this protection measure, and write an essay on how the system works in practice.

NUMERICAL METHODS IN HEAT CONDUCTION

So far we have mostly considered relatively simple heat conduction problems involving *simple geometries* with simple boundary conditions because only such simple problems can be solved *analytically.* But many problems encountered in practice involve *complicated geometries* with complex boundary conditions or variable properties, and cannot be solved analytically. In such cases, sufficiently accurate approximate solutions can be obtained by computers using a *numerical method.*

Analytical solution methods such as those presented in Chap. 2 are based on solving the governing differential equation together with the boundary conditions. They result in solution functions for the temperature at *every point* in the medium. Numerical methods, on the other hand, are based on replacing the differential equation by a set of *n* algebraic equations for the unknown temperatures at *n* selected points in the medium, and the simultaneous solution of these equations results in the temperature values at those *discrete points.*

There are several ways of obtaining the numerical formulation of a heat conduction problem, such as the *finite difference* method, the *finite element* method, the *boundary element* method, and the *energy balance* (or control volume) method. Each method has its own advantages and disadvantages, and each is used in practice. In this chapter, we use primarily the *energy balance* approach since it is based on the familiar energy balances on control volumes instead of heavy mathematical formulations, and thus it gives a better physical feel for the problem. Besides, it results in the same set of algebraic equations as the finite difference method. In this chapter, the numerical formulation and solution of heat conduction problems are demonstrated for both steady and transient cases in various geometries.

OBJECTIVES

When you finish studying this chapter, you should be able to:

■ Understand the limitations of analytical solutions of conduction problems, and the need for computation-intensive numerical methods,

■ Express derivatives as differences, and obtain finite difference formulations,

■ Solve steady one- or two-dimensional conduction problems numerically using the finite difference method, and

■ Solve transient one- or two-dimensional conduction problems using the finite difference method.
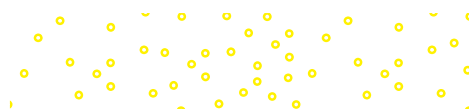
5–1 ■ WHY NUMERICAL METHODS?

The ready availability of high-speed computers and easy-to-use powerful software packages has had a major impact on engineering education and practice in recent years. Engineers in the past had to rely on *analytical skills* to solve significant engineering problems, and thus they had to undergo a rigorous training in mathematics. Today's engineers, on the other hand, have access to a tremendous amount of *computation power* under their fingertips, and they mostly need to understand the physical nature of the problem and interpret the results. But they also need to understand how calculations are performed by the computers to develop an awareness of the processes involved and the limitations, while avoiding any possible pitfalls.

In Chap. 2, we solved various heat conduction problems in various geometries in a systematic but highly mathematical manner by (1) deriving the governing differential equation by performing an energy balance on a differential volume element, (2) expressing the boundary conditions in the proper mathematical form, and (3) solving the differential equation and applying the boundary conditions to determine the integration constants. This resulted in a solution function for the temperature distribution in the medium, and the solution obtained in this manner is called the analytical solution of the problem. For example, the mathematical formulation of one-dimensional steady heat conduction in a sphere of radius r_o whose outer surface is maintained at a uniform temperature of T_1 with uniform heat generation at a rate of $\dot{e}$ was expressed as (Fig. 5–1)

$$\frac{1}{r^2}\frac{d}{dr}\left(r^2\frac{dT}{dr}\right) + \frac{\dot{e}}{k} = 0$$

$$\frac{dT(0)}{dr} = 0 \quad \text{and} \quad T(r_o) = T_1 \tag{5–1}$$

whose (analytical) solution is

$$T(r) = T_1 + \frac{\dot{e}}{6k}(r_o^2 - r^2) \tag{5–2}$$

This is certainly a very desirable form of solution since the temperature at any point within the sphere can be determined simply by substituting the *r*-coordinate of the point into the analytical solution function above. The analytical solution of a problem is also referred to as the exact solution since it satisfies the differential equation and the boundary conditions. This can be verified by substituting the solution function into the differential equation and the boundary conditions. Further, the *rate of heat transfer* at any location within the sphere or its surface can be determined by taking the derivative of the solution function $T(r)$ and substituting it into Fourier's law as

$$\dot{Q}(r) = -kA\frac{dT}{dr} = -k(4\pi r^2)\left(-\frac{\dot{e}\,r}{3k}\right) = \frac{4\pi r^3\dot{e}}{3} \tag{5–3}$$

The analysis preceding did not require any mathematical sophistication beyond the level of *simple integration,* and you are probably wondering why anyone

$$\frac{1}{r^2}\frac{d}{dr}\left(r^2\frac{dT}{dr}\right) + \frac{\dot{e}}{k} = 0$$

Sphere

$$\frac{dT(0)}{dr} = 0$$

$$T(r_o) = T_1$$

Solution:

$$T(r) = T_1 + \frac{\dot{e}}{6k}(r_o^2 - r^2)$$

$$\dot{Q}(r) = -kA\frac{dT}{dr} = \frac{4\pi r^3\dot{e}}{3}$$

FIGURE 5–1
The analytical solution of a problem requires solving the governing differential equation and applying the boundary conditions.

would ask for something else. After all, the solutions obtained are exact and easy to use. Besides, they are instructive since they show clearly the functional dependence of temperature and heat transfer on the independent variable *r*. Well, there are several reasons for searching for alternative solution methods.

1 Limitations

Analytical solution methods are limited to *highly simplified problems* in *simple geometries* (Fig. 5–2). The geometry must be such that its entire surface can be described mathematically in a coordinate system by setting the variables equal to constants. That is, it must fit into a coordinate system *perfectly* with nothing sticking out or in. In the case of one-dimensional heat conduction in a solid sphere of radius r_o, for example, the entire outer surface can be described by $r = r_o$. Likewise, the surfaces of a finite solid cylinder of radius r_o and height H can be described by $r = r_o$ for the side surface and $z = 0$ and $z = H$ for the bottom and top surfaces, respectively. Even minor complications in geometry can make an analytical solution impossible. For example, a spherical object with an extrusion like a *handle* at some location is impossible to handle analytically since the boundary conditions in this case cannot be expressed in any familiar coordinate system.

Even in simple geometries, heat transfer problems cannot be solved analytically if the *thermal conditions* are not sufficiently simple. For example, the consideration of the variation of thermal conductivity with temperature, the variation of the heat transfer coefficient over the surface, or the radiation heat transfer on the surfaces can make it impossible to obtain an analytical solution. Therefore, analytical solutions are limited to problems that are simple or can be simplified with reasonable approximations.

2 Better Modeling

We mentioned earlier that analytical solutions are exact solutions since they do not involve any approximations. But this statement needs some clarification. Distinction should be made between an *actual real-world problem* and the *mathematical model* that is an idealized representation of it. The solutions we get are the solutions of mathematical models, and the degree of applicability of these solutions to the actual physical problems depends on the accuracy of the model. An "approximate" solution of a realistic model of a physical problem is usually more accurate than the "exact" solution of a crude mathematical model (Fig. 5–3).

When attempting to get an analytical solution to a physical problem, there is always the tendency to *oversimplify* the problem to make the mathematical model sufficiently simple to warrant an analytical solution. Therefore, it is common practice to ignore any effects that cause mathematical complications such as nonlinearities in the differential equation or the boundary conditions. So it comes as no surprise that *nonlinearities* such as temperature dependence of thermal conductivity and the radiation boundary conditions are seldom considered in analytical solutions. A mathematical model intended for a numerical solution is likely to represent the actual problem better. Therefore, the numerical solution of engineering problems has now become the norm rather than the exception even when analytical solutions are available.
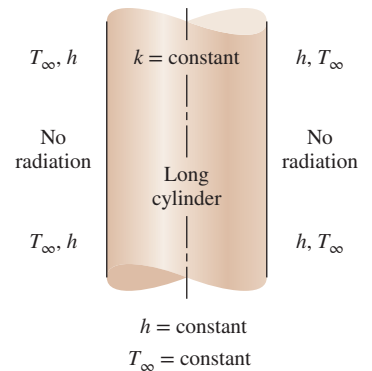
FIGURE 5–2

Analytical solution methods are limited to simplified problems in simple geometries.
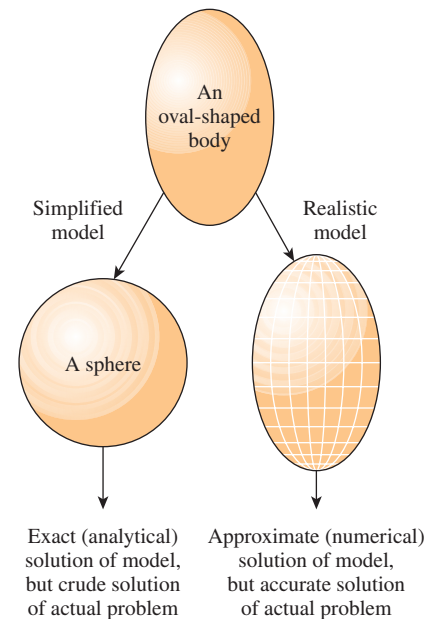
FIGURE 5–3

The approximate numerical solution of a real-world problem may be more accurate than the exact (analytical) solution of an oversimplified model of that problem.
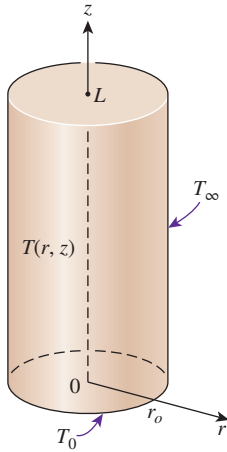
Analytical solution:

$$\frac{T(r, z) - T_\infty}{T_0 - T_\infty} = \sum_{n=1}^{\infty} \frac{J_0(\lambda_n r)}{\lambda_n J_1(\lambda_n r_o)} \frac{\sinh \lambda_n (L - z)}{\sinh (\lambda_n L)}$$

where λ_n's are roots of $J_0(\lambda_n r_o) = 0$

FIGURE 5–4
Some analytical solutions are very complex and difficult to use.

FIGURE 5–5
The ready availability of high-powered computers with sophisticated software packages has made numerical solution the norm rather than the exception.

3 Flexibility

Engineering problems often require extensive *parametric studies* to understand the influence of some variables on the solution in order to choose the right set of variables and to answer some "what-if" questions. This is an *iterative process* that is extremely tedious and time-consuming if done by hand. Computers and numerical methods are ideally suited for such calculations, and a wide range of related problems can be solved by minor modifications in the code or input variables. Today it is almost unthinkable to perform any significant optimization studies in engineering without the power and flexibility of computers and numerical methods.

4 Complications

Some problems can be solved analytically, but the solution procedure is so complex and the resulting solution expressions so complicated that it is not worth all that effort. With the exception of steady one-dimensional or transient lumped system problems, all heat conduction problems result in *partial* differential equations. Solving such equations usually requires mathematical sophistication beyond that acquired at the undergraduate level, such as orthogonality, eigenvalues, Fourier and Laplace transforms, Bessel and Legendre functions, and infinite series. In such cases, the evaluation of the solution, which often involves double or triple summations of infinite series at a specified point, is a challenge in itself (Fig. 5–4). Therefore, even when the solutions are available in some handbooks, they are intimidating enough to scare prospective users away.

5 Human Nature

As human beings, we like to sit back and make wishes, and we like our wishes to come true without much effort. The invention of TV remote controls made us feel like kings in our homes since the commands we give in our comfortable chairs by pressing buttons are immediately carried out by the obedient TV sets. After all, what good is cable TV without a remote control? We certainly would love to continue being the king in our little cubicle in the engineering office by solving problems at the press of a button on a computer (until they invent a remote control for the computers, of course). Well, this might have been a fantasy yesterday, but it is a reality today. Practically all engineering offices today are equipped with *high-powered computers* with *sophisticated software packages,* with impressive presentation-style colorful output in graphical and tabular form (Fig. 5–5). Besides, the results are as accurate as the analytical results for all practical purposes. The computers have certainly changed the way engineering is practiced.

This discussion should not lead you to believe that analytical solutions are unnecessary and that they should be discarded from the engineering curriculum. On the contrary, insight into the *physical phenomena* and *engineering wisdom* is gained primarily through analysis. The "feel" that engineers develop during the analysis of simple but fundamental problems serves as an invaluable tool when interpreting a huge pile of results obtained from a computer when solving a complex problem. A simple analysis by hand for a limiting case can be used to check whether the results are in the proper range.

Also, nothing can take the place of getting "ballpark" results on a piece of paper during preliminary discussions. The calculators made the basic arithmetic operations by hand a thing of the past, but they did not eliminate the need for instructing grade school children how to add or multiply.

In this chapter, you will learn how to *formulate* and *solve* heat transfer problems numerically using one or more approaches. In your professional life, you will probably solve the heat transfer problems you come across using a professional software package, and you are highly unlikely to write your own programs to solve such problems. (Besides, people will be highly skeptical of the results obtained using your own program instead of using a well-established commercial software package that has stood the test of time.) The insight you gain in this chapter by formulating and solving some heat transfer problems will help you better understand the available software packages and be an informed and responsible user.

5–2 ■ FINITE DIFFERENCE FORMULATION OF DIFFERENTIAL EQUATIONS

The numerical methods for solving differential equations are based on replacing the *differential equations* with *algebraic equations*. In the case of the popular **finite difference** method, this is done by replacing the *derivatives* with *differences*. Below we demonstrate this with both first- and second-order derivatives. But first we give a motivational example.

Consider a man who deposits his money in the amount of $A_0 = \$100$ in a savings account at an annual interest rate of 18 percent, and let us try to determine the amount of money he will have after one year if interest is compounded continuously (or instantaneously). In the case of simple interest, the money will earn $18 interest, and the man will have $100 + 100 \times 0.18 = \$118.00$ in his account after one year. But in the case of compounding, the interest earned during a compounding period will also earn interest for the remaining part of the year, and the year-end balance will be greater than $118. For example, if the money is compounded twice a year, the balance will be $100 + 100 \times (0.18/2) = \$109$ after six months, and $109 + 109 \times (0.18/2) = \$118.81$ at the end of the year. We could also determine the balance A directly from

$$A = A_0(1 + i)^n = (\$100)(1 + 0.09)^2 = \$118.81 \tag{5-4}$$

where i is the interest rate for the compounding period and n is the number of periods. Using the same formula, the year-end balance is determined for monthly, daily, hourly, minutely, and even secondly compounding, and the results are given in Table 5–1.

Note that in the case of daily compounding, the year-end balance will be $119.72, which is $1.72 more than the simple interest case. (So it is no wonder that the credit card companies usually charge interest compounded daily when determining the balance.) Also note that compounding at smaller time intervals, even at the end of each second, does not change the result, and we suspect that instantaneous compounding using "differential" time intervals dt will give the same result. This suspicion is confirmed by obtaining

TABLE 5–1

Year-end balance of a $100 account earning interest at an annual rate of 18 percent for various compounding periods

Compounding period	Number of periods, n	Year-end balance
1 year	1	$118.00
6 months	2	118.81
1 month	12	119.56
1 week	52	119.68
1 day	365	119.72
1 hour	8760	119.72
1 minute	525,600	119.72
1 second	31,536,000	119.72
Instantaneous	∞	119.72
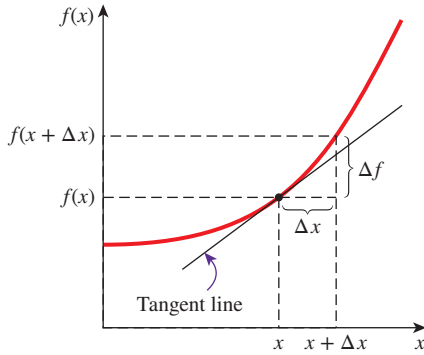
FIGURE 5–6
The derivative of a function at a point represents the slope of the function at that point.

FIGURE 5–7
Schematic of the nodes and the nodal temperatures used in the development of the finite difference formulation of heat transfer in a plane wall.

the differential equation $dA/dt = iA$ for the balance A, whose solution is $A = A_0 \exp(it)$. Substitution yields

$$A = (\$100) \exp(0.18 \times 1) = \$119.72$$

which is identical to the result for daily compounding. Therefore, replacing a differential time interval dt with a finite time interval of $\Delta t = 1$ day gave the same result when rounded to the second decimal place for cents, which leads us into believing that *reasonably accurate results can be obtained by replacing differential quantities with sufficiently small differences.*

Next, we develop the finite difference formulation of heat conduction problems by replacing the derivatives in the differential equations with differences. In the following section we do it using the energy balance method, which does not require any knowledge of differential equations.

Derivatives are the building blocks of differential equations, and thus we first give a brief review of derivatives. Consider a function f that depends on x, as shown in Fig. 5–6. The **first derivative** of $f(x)$ at a point is equivalent to the *slope* of a line tangent to the curve at that point and is defined as

$$\frac{df(x)}{dx} = \lim_{\Delta x \to 0} \frac{\Delta f}{\Delta x} = \lim_{\Delta x \to 0} \frac{f(x + \Delta x) - f(x)}{\Delta x} \tag{5–5}$$

which is the ratio of the increment Δf of the function to the increment Δx of the independent variable as $\Delta x \to 0$. If we don't take the indicated limit, we will have the following *approximate* relation for the derivative:

$$\frac{df(x)}{dx} \cong \frac{f(x + \Delta x) - f(x)}{\Delta x} \tag{5–6}$$

This approximate expression of the derivative in terms of differences is the **finite difference form** of the first derivative. The equation above can also be obtained by writing the *Taylor series expansion* of the function f about the point x,

$$f(x + \Delta x) = f(x) + \Delta x \frac{df(x)}{dx} + \frac{1}{2} \Delta x^2 \frac{d^2 f(x)}{dx^2} + \cdots \tag{5–7}$$

and neglecting all the terms in the expansion except the first two. The first term neglected is proportional to Δx^2, and thus the *error* involved in each step of this approximation is also proportional to Δx^2. However, the *commutative error* involved after M steps in the direction of length L is proportional to Δx since $M \Delta x^2 = (L/\Delta x)\Delta x^2 = L\Delta x$. Therefore, the smaller the Δx, the smaller the error, and thus the more accurate the approximation.

Now consider steady one-dimensional heat conduction in a plane wall of thickness L with heat generation. The wall is subdivided into M sections of equal thickness $\Delta x = L/M$ in the x-direction, separated by planes passing through $M + 1$ points 0, 1, 2, . . . , $m - 1$, m, $m + 1$, . . . , M called **nodes** or **nodal points**, as shown in Fig. 5–7. The x-coordinate of any point m is simply $x_m = m\Delta x$, and the temperature at that point is simply $T(x_m) = T_m$.

The heat conduction equation involves the second derivatives of temperature with respect to the space variables, such as d^2T/dx^2, and the finite difference formulation is based on replacing the second derivatives with appropriate
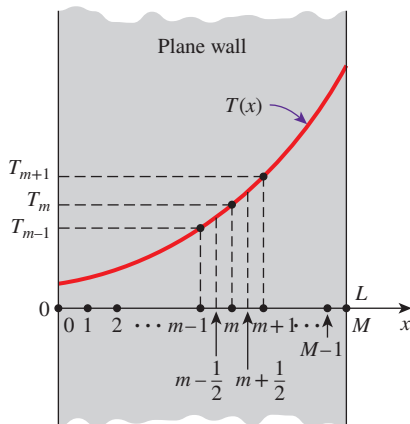
differences. But we need to start the process with first derivatives. The first derivative of temperature dT/dx at the midpoints $m - \frac{1}{2}$ and $m + \frac{1}{2}$ of the sections surrounding the node m can be expressed as

$$\frac{dT}{dx}\bigg|_{m-\frac{1}{2}} \cong \frac{T_m - T_{m-1}}{\Delta x} \quad \text{and} \quad \frac{dT}{dx}\bigg|_{m+\frac{1}{2}} \cong \frac{T_{m+1} - T_m}{\Delta x} \tag{5-8}$$

Noting that the second derivative is simply the derivative of the first derivative, the second derivative of temperature at node m can be expressed as

$$\frac{d^2T}{dx^2}\bigg|_m \cong \frac{\dfrac{dT}{dx}\bigg|_{m+\frac{1}{2}} - \dfrac{dT}{dx}\bigg|_{m-\frac{1}{2}}}{\Delta x} = \frac{\dfrac{T_{m+1} - T_m}{\Delta x} - \dfrac{T_m - T_{m-1}}{\Delta x}}{\Delta x} = \frac{T_{m-1} - 2T_m + T_{m+1}}{\Delta x^2} \tag{5-9}$$

which is the *finite difference representation* of the *second derivative* at a general internal node m. Note that the second derivative of temperature at a node m is expressed in terms of the temperatures at node m and its two neighboring nodes. Then the differential equation

$$\frac{d^2T}{dx^2} + \frac{\dot{e}}{k} = 0 \tag{5-10}$$

which is the governing equation for *steady one-dimensional* heat transfer in a plane wall with heat generation and constant thermal conductivity, can be expressed in the *finite difference* form as (Fig. 5–8)

$$\frac{T_{m-1} - 2T_m + T_{m+1}}{\Delta x^2} + \frac{\dot{e}_m}{k} = 0, \qquad m = 1, 2, 3, \ldots, M-1 \tag{5-11}$$

where $\dot{e}_m$ is the rate of heat generation per unit volume at node m. For the case of no heat generation ($\dot{e}_m = 0$), Eq. 5–11 reduces to $T_m = \frac{1}{2}(T_{m-1} + T_{m+1})$, which is the most simplified form of the one-dimensional finite difference formulation. The equation simply implies that the temperature of each interior node is the arithmetic average of the temperatures of the two neighboring nodes. If the surface temperatures T_0 and T_M are specified, the application of this equation to each of the $M-1$ interior nodes results in $M-1$ equations for the determination of $M-1$ unknown temperatures at the interior nodes. Solving these equations simultaneously gives the temperature values at the nodes. If the temperatures at the outer surfaces are not known, then we need to obtain two more equations in a similar manner using the specified boundary conditions. Then the unknown temperatures at $M+1$ nodes are determined by solving the resulting system of $M+1$ equations in $M+1$ unknowns simultaneously.

Note that the *boundary conditions* have no effect on the finite difference formulation of interior nodes of the medium. This is not surprising since the control volume used in the development of the formulation does not involve any part of the boundary. You may recall that the boundary conditions had no effect on the differential equation of heat conduction in the medium, either.

The finite difference formulation above can easily be extended to two- or three-dimensional heat transfer problems by replacing each second derivative with a difference equation in that direction. For example, the *finite difference*

Plane wall

Differential equation:

$$\frac{d^2T}{dx^2} + \frac{\dot{e}}{k} = 0$$

Valid at every point

Finite difference equation:

$$\frac{T_{m-1} - 2T_m + T_{m+1}}{\Delta x^2} + \frac{\dot{e}_m}{k} = 0$$

Valid at discrete points

$|\leftarrow \Delta x \rightarrow|$
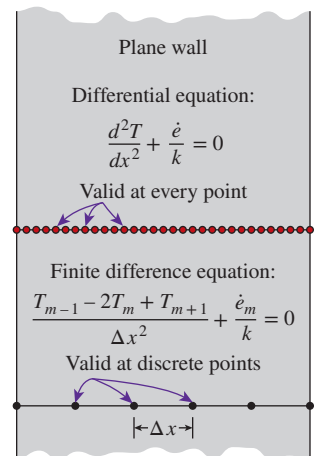
FIGURE 5–8

The differential equation is valid at every point of a medium, whereas the finite difference equation is valid at discrete points (the nodes) only.
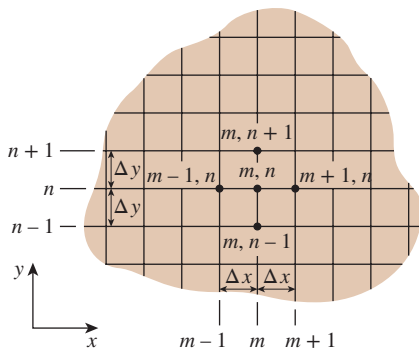
FIGURE 5–9
Finite difference mesh for
two-dimensional conduction in
rectangular coordinates.

formulation for **steady two-dimensional heat conduction** in a region with
heat generation and constant thermal conductivity can be expressed in rectangular coordinates as (Fig. 5–9)

$$\frac{T_{m+1,n} - 2T_{m,n} + T_{m-1,n}}{\Delta x^2} + \frac{T_{m,n+1} - 2T_{m,n} + T_{m,n-1}}{\Delta y^2} + \frac{\dot{e}_{m,n}}{k} = 0 \quad (5\text{–}12)$$

for $m = 1, 2, 3, \ldots, M - 1$ and $n = 1, 2, 3, \ldots, N - 1$ at any interior node
(m, n). Note that a rectangular region that is divided into M equal subregions
in the x-direction and N equal subregions in the y-direction has a total of
$(M + 1)(N + 1)$ nodes, and Eq. 5–12 can be used to obtain the finite difference equations at $(M - 1)(N - 1)$ of these nodes (i.e., all nodes except those
at the boundaries).

The finite difference formulation given above to demonstrate how difference equations are obtained from differential equations. However, we use the
energy balance approach in the following sections to obtain the numerical
formulation because it is more *intuitive* and can handle *boundary conditions*
more easily. Besides, the energy balance approach does not require having the
differential equation before the analysis.

5–3 · ONE-DIMENSIONAL STEADY HEAT CONDUCTION

In this section we develop the finite difference formulation of heat conduction in a plane wall using the energy balance approach and discuss how to
solve the resulting equations. The **energy balance method** is based on *subdividing* the medium into a sufficient number of volume elements and then
applying an *energy balance* on each element. This is done by first *selecting*
the nodal points (or nodes) at which the temperatures are to be determined
and then *forming elements* (or control volumes) over the nodes by drawing
lines through the midpoints between the nodes. This way, the interior nodes
remain at the middle of the elements, and the properties *at the node* such as
the temperature and the rate of heat generation represent the *average* properties of the element. Sometimes it is convenient to think of temperature as
varying *linearly* between the nodes, especially when expressing heat conduction between the elements using Fourier's law.

To demonstrate the approach, again consider steady one-dimensional heat
transfer in a plane wall of thickness L with heat generation $\dot{e}(x)$ and constant
conductivity k. The wall is now subdivided into M equal regions of thickness $\Delta x = L/M$ in the x-direction, and the divisions between the regions are
selected as the nodes. Therefore, we have $M + 1$ nodes labeled 0, 1, 2, . . . ,
$m - 1, m, m + 1, \ldots, M$, as shown in Fig. 5–10. The x-coordinate of any
node m is simply $x_m = m\Delta x$, and the temperature at that point is $T(x_m) = T_m$.
Elements are formed by drawing vertical lines through the midpoints between
the nodes. Note that all interior elements represented by interior nodes are
full-size elements (they have a thickness of Δx), whereas the two elements at
the boundaries are half-sized.

To obtain a general difference equation for the interior nodes, consider the
element represented by node m and the two neighboring nodes $m - 1$ and
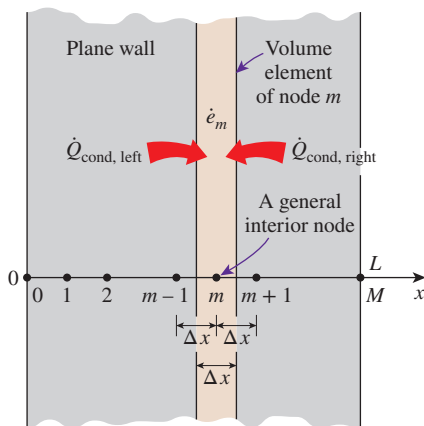
FIGURE 5–10
The nodal points and volume
elements for the finite difference
formulation of one-dimensional
conduction in a plane wall.

$m + 1$. Assuming the heat conduction to be *into* the element on all surfaces, an energy balance on the element can be expressed as

$$\begin{pmatrix} \text{Rate of heat} \\ \text{conduction} \\ \text{at the left} \\ \text{surface} \end{pmatrix} + \begin{pmatrix} \text{Rate of heat} \\ \text{conduction} \\ \text{at the right} \\ \text{surface} \end{pmatrix} + \begin{pmatrix} \text{Rate of heat} \\ \text{generation} \\ \text{inside the} \\ \text{element} \end{pmatrix} = \begin{pmatrix} \text{Rate of change} \\ \text{of the energy} \\ \text{content of} \\ \text{the element} \end{pmatrix}$$

or

$$\dot{Q}_{\text{cond, left}} + \dot{Q}_{\text{cond, right}} + \dot{E}_{\text{gen, element}} = \frac{\Delta E_{\text{element}}}{\Delta t} = 0 \qquad \textbf{(5–13)}$$

since the energy content of a medium (or any part of it) does not change under *steady* conditions, and thus $\Delta E_{\text{element}} = 0$. The rate of *heat generation* within the element can be expressed as

$$\dot{E}_{\text{gen, element}} = \dot{e}_m V_{\text{element}} = \dot{e}_m A \Delta x \qquad \textbf{(5–14)}$$

where $\dot{e}_m$ is the rate of heat generation per unit volume in W/m^3 evaluated at node m and treated as a constant for the entire element, and A is heat transfer area, which is simply the inner (or outer) surface area of the wall.

Recall that when temperature varies *linearly,* the steady rate of heat conduction across a plane wall of thickness L can be expressed as

$$\dot{Q}_{\text{cond}} = kA\frac{\Delta T}{L} \qquad \textbf{(5–15)}$$

where ΔT is the temperature change across the wall and the direction of heat transfer is from the high temperature side to the low temperature. In the case of a plane wall with heat generation, the variation of temperature is not linear, and thus the relation above is not applicable. However, the variation of temperature between the nodes can be *approximated* as being linear in the determination of heat conduction across a thin layer of thickness Δx between two nodes (Fig. 5–11). Obviously the smaller the distance Δx between two nodes, the more accurate is this approximation. (In fact, such approximations are the reason for classifying the numerical methods as approximate solution methods. In the limiting case of Δx approaching zero, the formulation becomes exact, and we obtain a differential equation.) Noting that the direction of heat transfer on both surfaces of the element is assumed to be *toward* the node $m,$ the rate of heat conduction at the left and right surfaces can be expressed as

$$\dot{Q}_{\text{cond, left}} = kA\frac{T_{m-1} - T_m}{\Delta x} \quad \text{and} \quad \dot{Q}_{\text{cond, right}} = kA\frac{T_{m+1} - T_m}{\Delta x} \qquad \textbf{(5–16)}$$

Substituting Eqs. 5–14 and 5–16 into Eq. 5–13 gives

$$kA\frac{T_{m-1} - T_m}{\Delta x} + kA\frac{T_{m+1} - T_m}{\Delta x} + \dot{e}_m A \Delta x = 0 \qquad \textbf{(5–17)}$$

which simplifies to

$$\frac{T_{m-1} - 2T_m + T_{m+1}}{\Delta x^2} + \frac{\dot{e}_m}{k} = 0, \qquad m = 1, 2, 3, \ldots, M - 1 \qquad \textbf{(5–18)}$$
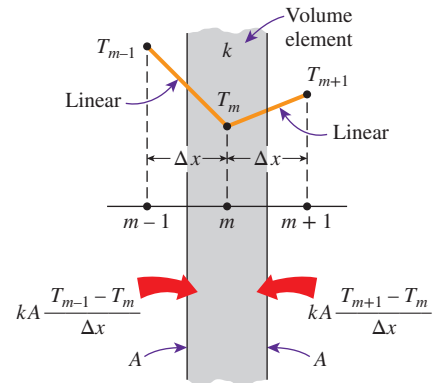
FIGURE 5–11
In finite difference formulation, the temperature is assumed to vary linearly between the nodes.
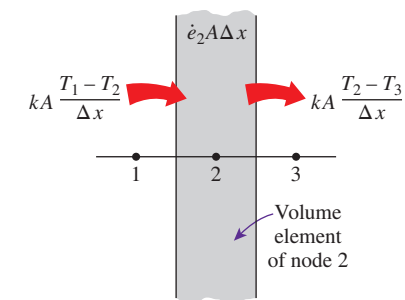
$$kA \frac{T_1 - T_2}{\Delta x} - kA \frac{T_2 - T_3}{\Delta x} + \dot{e}_2 A \Delta x = 0$$

or

$$T_1 - 2T_2 + T_3 + \dot{e}_2 A \Delta x^2 / k = 0$$

(*a*) Assuming heat transfer to be out of the volume element at the right surface.
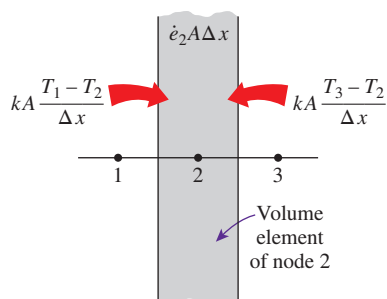
$$kA \frac{T_1 - T_2}{\Delta x} + kA \frac{T_3 - T_2}{\Delta x} + \dot{e}_2 A \Delta x = 0$$

or

$$T_1 - 2T_2 + T_3 + \dot{e}_2 A \Delta x^2 / k = 0$$

(*b*) Assuming heat transfer to be into the volume element at all surfaces.

FIGURE 5–12
The assumed direction of heat transfer at surfaces of a volume element has no effect on the finite difference formulation.

which is *identical* to the difference equation (Eq. 5–11) obtained earlier. Again, this equation is applicable to each of the $M - 1$ interior nodes, and its application gives $M - 1$ equations for the determination of temperatures at $M + 1$ nodes. The two additional equations needed to solve for the $M + 1$ unknown nodal temperatures are obtained by applying the energy balance on the two elements at the boundaries (unless, of course, the boundary temperatures are specified).

You are probably thinking that if heat is conducted into the element from both sides, as assumed in the formulation, the temperature of the medium will have to rise and thus heat conduction cannot be steady. Perhaps a more realistic approach would be to assume the heat conduction to be *into* the element on the left side and *out of* the element on the right side. If you repeat the formulation using this assumption, you will again obtain the same result since the heat conduction term on the right side in this case involves $T_m - T_{m+1}$ instead of $T_{m+1} - T_m$, which is subtracted instead of being added. Therefore, the assumed direction of heat conduction at the surfaces of the volume elements has no effect on the formulation, as shown in Fig. 5–12. (Besides, the actual direction of heat transfer is usually not known.) However, it is convenient to assume heat conduction to be into the element at all surfaces and not worry about the sign of the conduction terms. Then all temperature differences in conduction relations are expressed as the temperature of the neighboring node minus the temperature of the node under consideration, and all conduction terms are added.

Boundary Conditions

Above we have developed a general relation for obtaining the finite difference equation for each interior node of a plane wall. This relation is not applicable to the nodes on the boundaries, however, since it requires the presence of nodes on both sides of the node under consideration, and a boundary node does not have a neighboring node on at least one side. Therefore, we need to obtain the finite difference equations of boundary nodes separately. This is best done by applying an *energy balance* on the volume elements of boundary nodes.

Boundary conditions most commonly encountered in practice are the *specified temperature, specified heat flux, convection,* and *radiation* boundary conditions, and here we develop the finite difference formulations for them for the case of steady one-dimensional heat conduction in a plane wall of thickness L as an example. The node number at the left surface at $x = 0$ is 0, and at the right surface at $x = L$ it is M. Note that the width of the volume element for either boundary node is $\Delta x / 2$.

The **specified temperature** boundary condition is the simplest boundary condition to deal with. For one-dimensional heat transfer through a plane wall of thickness L, the *specified temperature boundary conditions* on both the left and right surfaces can be expressed as (Fig. 5–13)

$$T(0) = T_0 = \text{Specified value}$$

$$T(L) = T_M = \text{Specified value}$$

(5–19)

where T_0 and T_M are the specified temperatures at surfaces at $x = 0$ and $x = L$, respectively. Therefore, the specified temperature boundary conditions

are incorporated by simply assigning the given surface temperatures to the boundary nodes. We do not need to write an energy balance in this case unless we decide to determine the rate of heat transfer into or out of the medium after the temperatures at the interior nodes are determined.

When other boundary conditions such as the *specified heat flux, convection, radiation,* or *combined convection and radiation* conditions are specified at a boundary, the finite difference equation for the node at that boundary is obtained by writing an *energy balance* on the volume element at that boundary. The energy balance is again expressed as

$$\sum_{\text{All sides}} \dot{Q} + \dot{E}_{\text{gen, element}} = 0 \qquad \text{(5–20)}$$

for heat transfer under *steady* conditions. Again we assume all heat transfer to be *into* the volume element from all surfaces for convenience in formulation, except for specified heat flux since its direction is already specified. Specified heat flux is taken to be a *positive* quantity if into the medium and a *negative* quantity if out of the medium. Then the finite difference formulation at the node $m = 0$ (at the left boundary where $x = 0$) of a plane wall of thickness L during steady one-dimensional heat conduction can be expressed as (Fig. 5–14)

$$\dot{Q}_{\text{left surface}} + kA\frac{T_1 - T_0}{\Delta x} + \dot{e}_0(A\Delta x/2) = 0 \qquad \text{(5–21)}$$

where $A\Delta x/2$ is the *volume* of the volume element (note that the boundary element has half thickness), $\dot{e}_0$ is the rate of heat generation per unit volume (in W/m³) at $x = 0$, and A is the heat transfer area, which is constant for a plane wall. Note that we have Δx in the denominator of the second term instead of $\Delta x/2$. This is because the ratio in that term involves the temperature difference between nodes 0 and 1, and thus we must use the distance between those two nodes, which is Δx.

The finite difference form of various boundary conditions can be obtained from Eq. 5–21 by replacing $\dot{Q}_{\text{left surface}}$ with a suitable expression. Next this is done for various boundary conditions at the left boundary.

1. Specified Heat Flux Boundary Condition

$$\dot{q}_0 A + kA\frac{T_1 - T_0}{\Delta x} + \dot{e}_0(A\Delta x/2) = 0 \qquad \text{(5–22)}$$

Special case: **Insulated Boundary** ($\dot{q}_0 = 0$)

$$kA\frac{T_1 - T_0}{\Delta x} + \dot{e}_0(A\Delta x/2) = 0 \qquad \text{(5–23)}$$

2. Convection Boundary Condition

$$hA(T_\infty - T_0) + kA\frac{T_1 - T_0}{\Delta x} + \dot{e}_0(A\Delta x/2) = 0 \qquad \text{(5–24)}$$
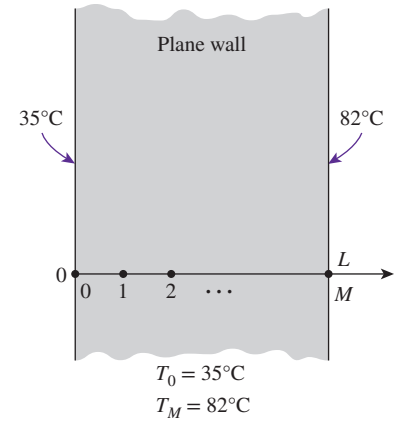
FIGURE 5–13
Finite difference formulation of specified temperature boundary conditions on both surfaces of a plane wall.

$$\dot{Q}_{\text{left surface}} + kA\frac{T_1 - T_0}{\Delta x} + \dot{e}_0 A\frac{\Delta x}{2} = 0$$
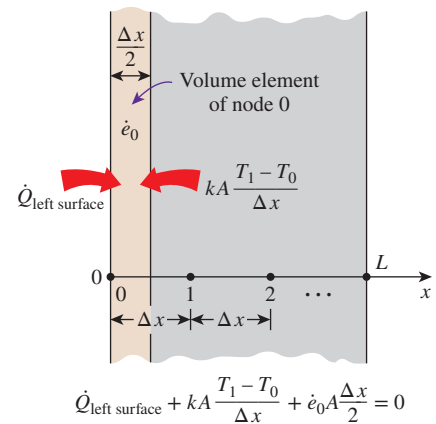
FIGURE 5–14
Schematic for the finite difference formulation of the left boundary node of a plane wall.

$$hA(T_\infty - T_0) + \varepsilon\sigma A(T_{surr}^4 - T_0^4)$$
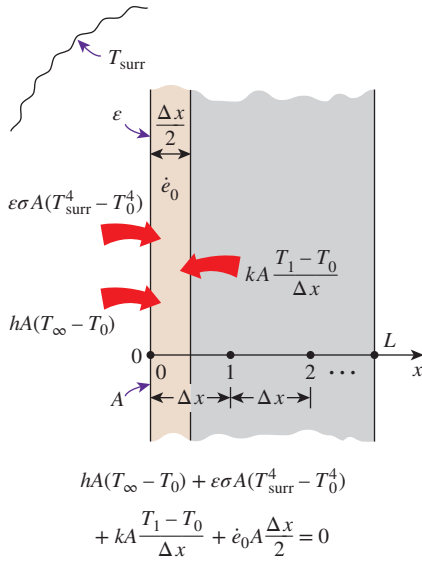
$$+ kA\frac{T_1 - T_0}{\Delta x} + \dot{e}_0 A\frac{\Delta x}{2} = 0$$

FIGURE 5–15
Schematic for the finite difference formulation of combined convection and radiation on the left boundary of a plane wall.

3. **Radiation Boundary Condition**

$$\varepsilon\sigma A(T_{surr}^4 - T_0^4) + kA\frac{T_1 - T_0}{\Delta x} + \dot{e}_0(A\Delta x/2) = 0 \tag{5–25}$$

4. **Combined Convection and Radiation Boundary Condition** (Fig. 5–15)

$$hA(T_\infty - T_0) + \varepsilon\sigma A(T_{surr}^4 - T_0^4) + kA\frac{T_1 - T_0}{\Delta x} + \dot{e}_0(A\Delta x/2) = 0 \tag{5–26}$$

or

$$h_{combined}A(T_\infty - T_0) + kA\frac{T_1 - T_0}{\Delta x} + \dot{e}_0(A\Delta x/2) = 0 \tag{5–27}$$

5. **Combined Convection, Radiation, and Heat Flux Boundary Condition**

$$\dot{q}_0 A + hA(T_\infty - T_0) + \varepsilon\sigma A(T_{surr}^4 - T_0^4) + kA\frac{T_1 - T_0}{\Delta x} + \dot{e}_0(A\Delta x/2) = 0 \tag{5–28}$$

6. **Interface Boundary Condition** Two different solid media A and B are assumed to be in perfect contact, and thus at the same temperature at the interface at node m (Fig. 5–16). Subscripts A and B indicate properties of media A and B, respectively.

$$k_A A\frac{T_{m-1} - T_m}{\Delta x} + k_B A\frac{T_{m+1} - T_m}{\Delta x} + \dot{e}_{A,m}(A\Delta x/2) + \dot{e}_{B,m}(A\Delta x/2) = 0 \tag{5–29}$$

$$k_A A\frac{T_{m-1} - T_m}{\Delta x} + k_B A\frac{T_{m+1} - T_m}{\Delta x}$$

$$+ \dot{e}_{A,m}A\frac{\Delta x}{2} + \dot{e}_{B,m}A\frac{\Delta x}{2} = 0$$
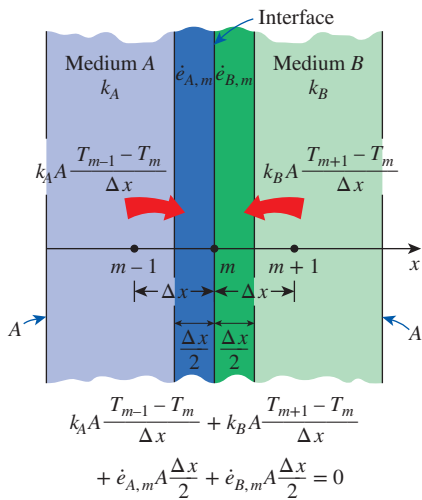
FIGURE 5–16
Schematic for the finite difference formulation of the interface boundary condition for two media A and B that are in perfect thermal contact.

In these relations, $\dot{q}_0$ is the specified heat flux in W/m², h is the convection coefficient, $h_{combined}$ is the combined convection and radiation coefficient, T_∞ is the temperature of the surrounding medium, T_{surr} is the temperature of the surrounding surfaces, ε is the emissivity of the surface, and σ is the Stefan–Boltzmann constant. The relations above can also be used for node M on the right boundary by replacing the subscript 0 with M and the subscript 1 with $M - 1$.

Note that *thermodynamic temperatures* must be used in radiation heat transfer calculations, and all temperatures should be expressed in K or R when a boundary condition involves radiation to avoid mistakes. We usually try to avoid the *radiation boundary condition* even in numerical solutions since it causes the finite difference equations to be *nonlinear,* which are more difficult to solve.

Treating Insulated Boundary Nodes as Interior Nodes: The Mirror Image Concept

One way of obtaining the finite difference formulation of a node on an insulated boundary is to treat insulation as "zero" heat flux and to write an energy balance, as is done in Eq. 5–23. Another and more practical way is to treat the node on an insulated boundary as an interior node. Conceptually this is done

by replacing the insulation on the boundary with a *mirror* and considering the reflection of the medium as its extension (Fig. 5–17). This way the node next to the boundary node appears on both sides of the boundary node because of symmetry, converting it into an interior node. Then using the general formula (Eq. 5–18) for an interior node, which involves the sum of the temperatures of the adjoining nodes minus twice the node temperature, the finite difference formulation of a node $m = 0$ on an insulated boundary of a plane wall can be expressed as

$$\frac{T_{m+1} - 2T_m + T_{m-1}}{\Delta x^2} + \frac{\dot{e}_m}{k} = 0 \quad \rightarrow \quad \frac{T_1 - 2T_0 + T_1}{\Delta x^2} + \frac{\dot{e}_0}{k} = 0 \qquad \textbf{(5–30)}$$

which is equivalent to Eq. 5–23 obtained by the energy balance approach.

The mirror image approach can also be used for problems that possess thermal symmetry by replacing the plane of symmetry with a mirror. Alternately, we can replace the plane of symmetry with insulation and consider only half of the medium in the solution. The solution in the other half of the medium is simply the mirror image of the solution obtained.
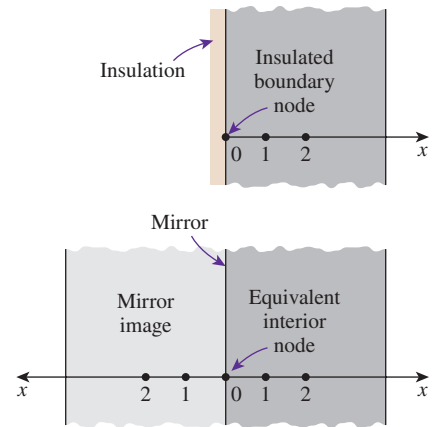
FIGURE 5–17
A node on an insulated boundary can be treated as an interior node by replacing the insulation with a mirror.

EXAMPLE 5–1   Steady Heat Conduction in a Large Uranium Plate

Consider a large uranium plate of thickness $L = 4$ cm and thermal conductivity $k = 28$ W/m·K in which heat is generated uniformly at a constant rate of $\dot{e} = 5 \times 10^6$ W/m³. One side of the plate is maintained at 0°C by iced water, while the other side is subjected to convection to an environment at $T_\infty = 30$°C with a heat transfer coefficient of $h = 45$ W/m²·K, as shown in Fig. 5–18. Considering a total of three equally spaced nodes in the medium, two at the boundaries and one at the middle, estimate the exposed surface temperature of the plate under steady conditions using the finite difference approach.

SOLUTION A uranium plate is subjected to specified temperature on one side and convection on the other. The unknown surface temperature of the plate is to be determined numerically using three equally spaced nodes.

Assumptions 1 Heat transfer through the wall is steady since there is no indication of any change with time. 2 Heat transfer is one-dimensional since the plate is large relative to its thickness. 3 Thermal conductivity is constant. 4 Radiation heat transfer is negligible.

Properties The thermal conductivity is given to be $k = 28$ W/m·K.

Analysis The number of nodes is specified to be $M = 3$, and they are chosen to be at the two surfaces of the plate and the midpoint, as shown in the figure. Then the nodal spacing Δx becomes

$$\Delta x = \frac{L}{M-1} = \frac{0.04 \text{ m}}{3-1} = 0.02 \text{ m}$$

We number the nodes 0, 1, and 2. The temperature at node 0 is given to be $T_0 = 0$°C, and the temperatures at nodes 1 and 2 are to be determined. This problem involves only two unknown nodal temperatures, and thus we need to have only two equations to determine them uniquely. These equations are obtained by applying the finite difference method to nodes 1 and 2.
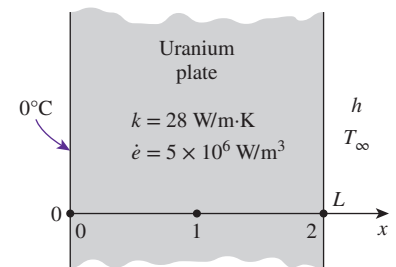
FIGURE 5–18
Schematic for Example 5–1.

Node 1 is an interior node, and the finite difference formulation at that node is obtained directly from Eq. 5–18 by setting $m = 1$:

$$\frac{T_0 - 2T_1 + T_2}{\Delta x^2} + \frac{\dot{e}_1}{k} = 0 \rightarrow \frac{0 - 2T_1 + T_2}{\Delta x^2} + \frac{\dot{e}_1}{k} = 0 \rightarrow 2T_1 - T_2 = \frac{\dot{e}_1 \Delta x^2}{k} \quad \textbf{(1)}$$

Node 2 is a boundary node subjected to convection, and the finite difference formulation at that node is obtained by writing an energy balance on the volume element of thickness $\Delta x/2$ at that boundary by assuming heat transfer to be into the medium at all sides:

$$hA(T_\infty - T_2) + kA\frac{T_1 - T_2}{\Delta x} + \dot{e}_2(A\Delta x/2) = 0$$

Canceling the heat transfer area A and rearranging give

$$T_1 - \left(1 + \frac{h\Delta x}{k}\right)T_2 = -\frac{h\Delta x}{k}T_\infty - \frac{\dot{e}_2 \Delta x^2}{2k} \quad \textbf{(2)}$$

Equations (1) and (2) form a system of two equations in two unknowns T_1 and T_2. Substituting the given quantities and simplifying gives

$$2T_1 - T_2 = 71.43 \qquad \text{(in °C)}$$
$$T_1 - 1.032T_2 = -36.68 \qquad \text{(in °C)}$$

This is a system of two algebraic equations in two unknowns and can be solved easily by the elimination method. Solving the first equation for T_1 and substituting into the second equation result in an equation in T_2 whose solution is

$$T_2 = \mathbf{136.1°C}$$

This is the temperature of the surface exposed to convection, which is the desired result. Substitution of this result into the first equation gives $T_1 = 103.8°C$, which is the temperature at the middle of the plate.

Discussion The purpose of this example is to demonstrate the use of the finite difference method with minimal calculations, and the accuracy of the result was not a major concern. But you might still be wondering how accurate the result obtained above is. After all, we used a mesh of only three nodes for the entire plate, which seems to be rather crude. This problem can be solved analytically as described in Chap. 2, and the analytical (exact) solution can be shown to be

$$T(x) = \frac{0.5\dot{e}\,hL^2/k + \dot{e}L + T_\infty h}{hL + k}x - \frac{\dot{e}x^2}{2k}$$

Substituting the given quantities, the temperature of the exposed surface of the plate at $x = L = 0.04$ m is determined to be 136.0°C, which is almost identical to the result obtained here with the approximate finite difference method (Fig. 5–19). Therefore, highly accurate results can be obtained with numerical methods by using a limited number of nodes.
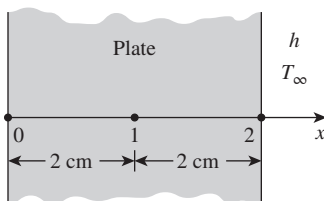
Finite difference solution:

$$T_2 = 136.1°C$$

Exact solution:

$$T_2 = 136.0°C$$

FIGURE 5–19

Despite being approximate in nature, highly accurate results can be obtained by numerical methods.

EXAMPLE 5–2   Heat Transfer from Triangular Fins

Consider an aluminum alloy fin ($k = 180$ W/m·K) of triangular cross section with length $L = 5$ cm, base thickness $b = 1$ cm, and very large width w, as shown in Fig. 5–20. The base of the fin is maintained at a temperature of $T_0 = 200°$C. The fin is losing heat to the surrounding medium at $T_\infty = 25°$C with a heat transfer coefficient of $h = 15$ W/m^2·K. Using the finite difference method with six equally spaced nodes along the fin in the x-direction, determine (*a*) the temperatures at the nodes, (*b*) the rate of heat transfer from the fin for $w = 1$ m, and (*c*) the fin efficiency.

SOLUTION A long triangular fin attached to a surface is considered. The nodal temperatures, the rate of heat transfer, and the fin efficiency are to be determined numerically using six equally spaced nodes.

Assumptions **1** Heat transfer is steady since there is no indication of any change with time. **2** The temperature along the fin varies in the x direction only. **3** Thermal conductivity is constant. **4** Radiation heat transfer is negligible.

Properties The thermal conductivity is given to be $k = 180$ W/m·K.

Analysis (*a*) The number of nodes in the fin is specified to be $M = 6$, and their location is as shown in the figure. Then the nodal spacing Δx becomes

$$\Delta x = \frac{L}{M - 1} = \frac{0.05 \text{ m}}{6 - 1} = 0.01 \text{ m}$$

The temperature at node 0 is given to be $T_0 = 200°$C, and the temperatures at the remaining five nodes are to be determined. Therefore, we need to have five equations to determine them uniquely. Nodes 1, 2, 3, and 4 are interior nodes, and the finite difference formulation for a general interior node m is obtained by applying an energy balance on the volume element of this node. Noting that heat transfer is steady and that there is no heat generation in the fin, and assuming heat transfer to be into the medium at all sides, the energy balance can be expressed as

$$\sum_{\text{All sides}} \dot{Q} = 0 \rightarrow kA_{\text{left}}\frac{T_{m-1} - T_m}{\Delta x} + kA_{\text{right}}\frac{T_{m+1} - T_m}{\Delta x} + hA_{\text{conv}}(T_\infty - T_m) = 0$$

Note that heat transfer areas are different for each node in this case, and using geometrical relations, they can be expressed as

$$A_{\text{left}} = (\text{Height} \times \text{Width})_{@m-\frac{1}{2}} = 2w[L - (m - 1/2)\Delta x]\tan\theta$$
$$A_{\text{right}} = (\text{Height} \times \text{Width})_{@m+\frac{1}{2}} = 2w[L - (m + 1/2)\Delta x]\tan\theta$$
$$A_{\text{conv}} = 2 \times \text{Length} \times \text{Width} = 2w(\Delta x/\cos\theta)$$

Substituting,

$$2kw[L - (m - \tfrac{1}{2})\Delta x]\tan\theta\frac{T_{m-1} - T_m}{\Delta x}$$

$$+ 2kw[L - (m + \tfrac{1}{2})\Delta x]\tan\theta\frac{T_{m+1} - T_m}{\Delta x} + h\frac{2w\Delta x}{\cos\theta}(T_\infty - T_m) = 0$$
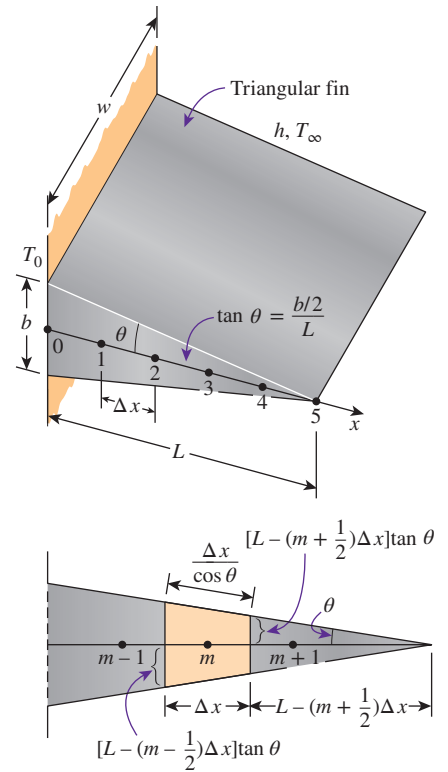
FIGURE 5–20
Schematic for Example 5–2 and the volume element of a general interior node of the fin.

Dividing each term by $2kwL \tan \theta / \Delta x$ gives

$$\left[1 - (m - \tfrac{1}{2})\frac{\Delta x}{L}\right](T_{m-1} - T_m) + \left[1 - (m + \tfrac{1}{2})\frac{\Delta x}{L}\right](T_{m+1} - T_m)$$

$$+ \frac{h(\Delta x)^2}{kL \sin \theta}(T_\infty - T_m) = 0$$

Note that

$$\tan \theta = \frac{b/2}{L} = \frac{0.5 \text{ cm}}{5 \text{ cm}} = 0.1 \quad \rightarrow \quad \theta = \tan^{-1} 0.1 = 5.71°$$

Also, $\sin 5.71° = 0.0995$. Then the substitution of known quantities gives

$$(5.5 - m)T_{m-1} - (10.008 - 2m)T_m + (4.5 - m)T_{m+1} = -0.209$$

Now substituting 1, 2, 3, and 4 for m results in these finite difference equations for the interior nodes:

$$m = 1: \quad -8.008T_1 + 3.5T_2 = -900.209 \tag{1}$$
$$m = 2: \quad 3.5T_1 - 6.008T_2 + 2.5T_3 = -0.209 \tag{2}$$
$$m = 3: \quad 2.5T_2 - 4.008T_3 + 1.5T_4 = -0.209 \tag{3}$$
$$m = 4: \quad 1.5T_3 - 2.088T_4 + 0.5T_5 = -0.209 \tag{4}$$

The finite difference equation for the boundary node 5 is obtained by writing an energy balance on the volume element of length $\Delta x/2$ at that boundary, again by assuming heat transfer to be into the medium at all sides (Fig. 5–21):

$$kA_{\text{left}}\frac{T_4 - T_5}{\Delta x} + hA_{\text{conv}}(T_\infty - T_5) = 0$$

where

$$A_{\text{left}} = 2w\frac{\Delta x}{2}\tan \theta \quad \text{and} \quad A_{\text{conv}} = 2w\frac{\Delta x/2}{\cos \theta}$$

Canceling w in all terms and substituting the known quantities gives

$$T_4 - 1.008T_5 = -0.209 \tag{5}$$

Equations (1) through (5) form a linear system of five algebraic equations in five unknowns. Solving them simultaneously using an equation solver gives

$$T_1 = \mathbf{198.6°C} \quad T_2 = \mathbf{197.1°C} \quad T_3 = \mathbf{195.7°C}$$
$$T_4 = \mathbf{194.3°C} \quad T_5 = \mathbf{192.9°C}$$

which is the desired solution for the nodal temperatures.

(*b*) The total rate of heat transfer from the fin is simply the sum of the heat transfer from each volume element to the ambient, and for $w = 1$ m it is determined from

FIGURE 5–21
Schematic of the volume element of node 5 at the tip of a triangular fin.

$$\dot{Q}_{\text{fin}} = \sum_{m=0}^{5} \dot{Q}_{\text{element, } m} = \sum_{m=0}^{5} hA_{\text{conv, } m}(T_m - T_\infty)$$

Noting that the heat transfer surface area is $w\Delta x/\cos\theta$ for the boundary nodes 0 and 5, and twice as large for the interior nodes 1, 2, 3, and 4, we have

$$\dot{Q}_{\text{fin}} = h\frac{w\Delta x}{\cos\theta}[(T_0 - T_\infty) + 2(T_1 - T_\infty) + 2(T_2 - T_\infty) + 2(T_3 - T_\infty)$$

$$+ 2(T_4 - T_\infty) + (T_5 - T_\infty)]$$

$$= h\frac{w\Delta x}{\cos\theta}[T_0 + 2(T_1 + T_2 + T_3 + T_4) + T_5 - 10\,T_\infty]°C$$

$$= (15\text{ W/m}^2\cdot\text{K})\frac{(1\text{ m})(0.01\text{ m})}{\cos 5.71°}[200 + 2 \times 785.7$$

$$+ 192.9 - 10 \times 25]°C$$

$$= \textbf{258.4 W}$$

(c) If the entire fin were at the base temperature of $T_o = 200°C$, the total rate of heat transfer from the fin for $w = 1$ m would be

$$\dot{Q}_{\text{max}} = hA_{\text{fin, total}}(T_0 - T_\infty) = h(2wL/\cos\theta)(T_0 - T_\infty)$$

$$= (15\text{ W/m}^2\cdot\text{K})[2(1\text{ m})(0.05\text{ m})/\cos 5.71°](200 - 25)°C$$

$$= 263.8\text{ W}$$

Then the fin efficiency is determined from

$$\eta_{\text{fin}} = \frac{\dot{Q}_{\text{fin}}}{\dot{Q}_{\text{max}}} = \frac{258.4\text{ W}}{263.8\text{ W}} = \textbf{0.98}$$

which is less than 1, as expected. We could also determine the fin efficiency in this case from the proper fin efficiency curve in Chap. 3, which is based on the analytical solution. We would read 0.98 for the fin efficiency, which is identical to the value determined above numerically.

The finite difference formulation of steady heat conduction problems usually results in a system of N algebraic equations in N unknown nodal temperatures that need to be solved simultaneously. When N is small (such as 2 or 3), we can use the elementary *elimination method* to eliminate all unknowns except one and then solve for that unknown (see Example 5–1). The other unknowns are then determined by back substitution. When N is large, which is usually the case, the elimination method is not practical, and we need to use a more systematic approach that can be adapted to computers.

There are numerous systematic approaches available in the literature, and they are broadly classified as **direct** and **iterative** methods. The direct methods are based on a fixed number of well-defined steps that result in the solution in a systematic manner. The iterative methods, on the other hand, are based on an initial guess for the solution that is refined by iteration until a

Direct methods:
   Solve in a systematic manner following a
   series of well-defined steps.

Iterative methods:
   Start with an initial guess for the solution,
   and iterate until solution converges.

FIGURE 5–22
Two general categories of solution
methods for solving systems of
algebraic equations.

specified convergence criterion is satisfied (Fig. 5–22). The direct methods usually require a large amount of computer memory and computation time, and they are more suitable for systems with a relatively small number of equations. The computer memory requirements for iterative methods are minimal, and thus they are usually preferred for large systems. The convergence of iterative methods to the desired solution, however, may pose a problem.

One of the simplest iterative methods is the *Gauss-Seidel* iteration. The method applied to a system of *N* algebraic equations in *N* unknown nodal temperatures proceeds as follows: (1) write the finite difference equations explicitly for each node (the nodal temperature on the left-hand side and all other terms on the right-hand side of the equation), (2) make a reasonable initial guess for each unknown nodal temperature, (3) use the explicit equations to calculate new values for each nodal temperature—*always use the most recent values of the temperature for each node on the right-hand side of the explicit finite difference equation,* and (4) repeat the process until convergence within some tolerable error (specified convergence criterion) is achieved. The method is illustrated in Table 5–2 by solving the five finite difference equations given in Example 5–2 for the five nodal temperatures. As shown in Table 5–2, the first row is the initial guess for the nodal temperatures. Substituting into the explicit equations yields the results displayed in the second row, and so on. The nodal temperatures are considered converged by the fifth iteration, since the successive sixth and seventh iterations do not bring any changes to the temperatures. Comparing with the temperatures calculated in Example 5–2(*a*), the temperatures obtained using the Gauss-Seidel iterative method are within 0.3°C agreement. The small discrepancy between the two methods is due to *round-off error* (retaining a limited number of digits during the calculations).

TABLE 5–2

Application of the *Gauss-Seidel* iterative method to the finite difference equations of Example 5–2.

Finite difference equations in explicit form

$T_1 = 0.4371T_2 + 112.4137$
$T_2 = 0.5826T_1 + 0.4161T_3 + 0.0348$
$T_3 = 0.6238T_2 + 0.3743T_4 + 0.0521$
$T_4 = 0.7470T_3 + 0.2490T_5 + 0.1041$
$T_5 = 0.9921T_4 + 0.2073$

Iteration	Nodal Temperature, °C				
	T_1	T_2	T_3	T_4	T_5
Initial Guess	195.0	195.0	195.0	195.0	195.0
1	197.6	196.3	195.5	194.7	193.4
2	198.2	196.9	195.8	194.5	193.2
3	198.5	197.2	195.9	194.5	193.2
4	198.6	197.3	195.9	194.5	193.2
5	198.7	197.3	195.9	194.5	193.2
6	198.7	197.3	195.9	194.5	193.2
7	198.7	197.3	195.9	194.5	193.2

FIGURE 5–23
The nodal network for the finite difference formulation of two-dimensional conduction in rectangular coordinates.

5–4 ▪ TWO-DIMENSIONAL STEADY HEAT CONDUCTION

In Sec. 5–3, we considered one-dimensional heat conduction and assumed heat conduction in other directions to be negligible. Many heat transfer problems encountered in practice can be approximated as being one-dimensional, but this is not always the case. Sometimes we need to consider heat transfer in other directions as well when the variation of temperature in other directions is significant. In this section we consider the numerical formulation and solution of two-dimensional steady heat conduction in rectangular coordinates using the finite difference method. The approach presented here can be extended to three-dimensional cases.

Consider a *rectangular region* in which heat conduction is significant in the x- and y-directions. Now divide the x-y plane of the region into a rectangular mesh of nodal points spaced Δx and Δy apart in the x- and y-directions, respectively, as shown in Fig. 5–23, and consider a unit depth of $\Delta z = 1$ in the z-direction. Our goal is to determine the temperatures at the nodes, and it is convenient to number the nodes and describe their position by the numbers instead of actual coordinates. A logical numbering scheme for two-dimensional problems is the *double subscript notation* (m, n) where $m = 0, 1, 2, \ldots, M$ is the node count in the x-direction and $n = 0, 1, 2, \ldots, N$ is the node count in the y-direction. The coordinates of the node (m, n) are simply $x = m\Delta x$ and $y = n\Delta y$, and the temperature at the node (m, n) is denoted by $T_{m,n}$.

Now consider a *volume element* of size $\Delta x \times \Delta y \times 1$ centered about a general interior node (m,n) in a region in which heat is generated at a rate of $\dot{e}$ and the thermal conductivity k is constant, as shown in Fig. 5–24. Again assuming the direction of heat conduction to be *toward* the node under consideration at all surfaces, the energy balance on the volume element can be expressed as

$$\begin{pmatrix} \text{Rate of heat conduction} \\ \text{at the left, top , right,} \\ \text{and bottom surfaces} \end{pmatrix} + \begin{pmatrix} \text{Rate of heat} \\ \text{generation inside} \\ \text{the element} \end{pmatrix} = \begin{pmatrix} \text{Rate of change of} \\ \text{the energy content} \\ \text{of the element} \end{pmatrix}$$

or

$$\dot{Q}_{\text{cond, left}} + \dot{Q}_{\text{cond, top}} + \dot{Q}_{\text{cond, right}} + \dot{Q}_{\text{cond, bottom}} + \dot{E}_{\text{gen, element}} = \frac{\Delta E_{\text{element}}}{\Delta t} = 0 \quad \textbf{(5–31)}$$

FIGURE 5–24
The volume element of a general interior node (m, n) for two-dimensional conduction in rectangular coordinates.

for the *steady* case. Again assuming the temperatures between the adjacent nodes to vary linearly and noting that the heat transfer area is $A_x = \Delta y \times 1 = \Delta y$ in the x-direction and $A_y = \Delta x \times 1 = \Delta x$ in the y-direction, the energy balance relation above becomes

$$k\Delta y \frac{T_{m-1, n} - T_{m, n}}{\Delta x} + k\Delta x \frac{T_{m, n+1} - T_{m, n}}{\Delta y} + k\Delta y \frac{T_{m+1, n} - T_{m, n}}{\Delta x}$$
$$+ k\Delta x \frac{T_{m, n-1} - T_{m, n}}{\Delta y} + \dot{e}_{m, n} \Delta x \Delta y = 0 \quad \textbf{(5–32)}$$

Dividing each term by $\Delta x \times \Delta y$ and simplifying gives

$$\frac{T_{m-1, n} - 2T_{m, n} + T_{m+1, n}}{\Delta x^2} + \frac{T_{m, n-1} - 2T_{m, n} + T_{m, n+1}}{\Delta y^2} + \frac{\dot{e}_{m, n}}{k} = 0 \quad \textbf{(5–33)}$$

for $m = 1, 2, 3, \ldots, M - 1$ and $n = 1, 2, 3, \ldots, N - 1$. This equation is identical to Eq. 5–12 obtained earlier by replacing the derivatives in the differential equation with differences for an interior node (m, n). Again a rectangular region of M equally spaced nodes in the x-direction and N equally spaced nodes in the y-direction has a total of $(M + 1)(N + 1)$ nodes, and Eq. 5–33 can be used to obtain the finite difference equations at all interior nodes.

In finite difference analysis, usually a **square mesh** is used for simplicity (except when the magnitudes of temperature gradients in the x- and y-directions are very different), and thus Δx and Δy are taken to be the same. Then $\Delta x = \Delta y = l$, and the preceding relation simplifies to

$$T_{m-1, n} + T_{m+1, n} + T_{m, n+1} + T_{m, n-1} - 4T_{m, n} + \frac{\dot{e}_{m, n}l^2}{k} = 0 \qquad \textbf{(5–34)}$$

That is, the finite difference formulation of an interior node is obtained by *adding the temperatures of the four nearest neighbors of the* node*, subtracting four times the temperature of the* node *itself, and adding the heat generation term.* It can also be expressed in this form, which is easy to remember:

$$T_{\text{left}} + T_{\text{top}} + T_{\text{right}} + T_{\text{bottom}} - 4T_{\text{node}} + \frac{\dot{e}_{\text{node}}l^2}{k} = 0 \qquad \textbf{(5–35)}$$

When there is no heat generation in the medium, the finite difference equation for an interior node further simplifies to $T_{\text{node}} = (T_{\text{left}} + T_{\text{top}} + T_{\text{right}} + T_{\text{bottom}})/4$, *which has the interesting interpretation that the temperature of each interior* node *is the arithmetic average of the temperatures of the four neighboring* nodes. This statement is also true for the three-dimensional problems except that the interior nodes in that case will have six neighboring nodes instead of four.

Boundary Nodes

The development of finite difference formulation of *boundary* node*s* in two- (or three-) dimensional problems is similar to the development in the one-dimensional case discussed earlier. Again, the region is partitioned between the nodes by forming *volume elements* around the nodes, and an *energy balance* is written for each boundary node. Various boundary conditions can be handled as discussed for a plane wall, except that the volume elements in the two-dimensional case involve heat transfer in the *y-direction* as well as the *x-direction.* Insulated surfaces can still be viewed as "mirrors," and the mirror image concept can be used to treat nodes on insulated boundaries as interior nodes.

For heat transfer under *steady* conditions, the basic equation to keep in mind when writing an *energy balance* on a volume element is (Fig. 5–25)

$$\sum_{\text{All sides}} \dot{Q} + \dot{e}V_{\text{element}} = 0 \qquad \textbf{(5–36)}$$

whether the problem is one-, two-, or three-dimensional. Again we assume, for convenience in formulation, all heat transfer to be *into* the volume element from all surfaces except for specified heat flux, whose direction is already specified. This is demonstrated in Example 5–3 for various boundary conditions.

$$\dot{Q}_{\text{left}} + \dot{Q}_{\text{top}} + \dot{Q}_{\text{right}} + \dot{Q}_{\text{bottom}} + \dot{e}_2 V_2 = 0$$
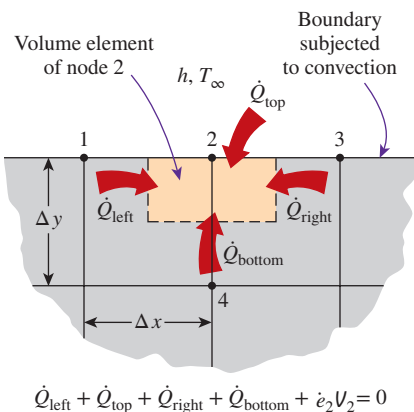
FIGURE 5–25
The finite difference formulation of a boundary node is obtained by writing an energy balance on its volume element.

EXAMPLE 5–3 Steady Two-Dimensional Heat Conduction in L-Bars

Consider steady heat transfer in an L-shaped solid body whose cross section is given in Fig. 5–26. Heat transfer in the direction normal to the plane of the paper is negligible, and thus heat transfer in the body is two-dimensional. The thermal conductivity of the body is $k = 15$ W/m·K, and heat is generated in the body at a rate of $\dot{e} = 2 \times 10^6$ W/m^3. The left surface of the body is insulated, and the bottom surface is maintained at a uniform temperature of 90°C. The entire top surface is subjected to convection to ambient air at $T_\infty = 25$°C with a convection coefficient of $h = 80$ W/m^2·K, and the right surface is subjected to heat flux at a uniform rate of $\dot{q}_R = 5000$ W/m^2. The nodal network of the problem consists of 15 equally spaced nodes with $\Delta x = \Delta y = 1.2$ cm, as shown in the figure. Five of the nodes are at the bottom surface, and thus their temperatures are known. Obtain the finite difference equations at the remaining nine nodes and determine the nodal temperatures by solving them.

SOLUTION Heat transfer in a long L-shaped solid bar with specified boundary conditions is considered. The nine unknown nodal temperatures are to be determined with the finite difference method.

Assumptions **1** Heat transfer is steady and two-dimensional, as stated. **2** Thermal conductivity is constant. **3** Heat generation is uniform. **4** Radiation heat transfer is negligible.

Properties The thermal conductivity is given to be $k = 15$ W/m·K.

Analysis We observe that all nodes are boundary nodes except node 5, which is an interior node. Therefore, we have to rely on energy balances to obtain the finite difference equations. But first we form the volume elements by partitioning the region among the nodes equitably by drawing dashed lines between the nodes. If we consider the volume element represented by an interior node to be *full size* (i.e., $\Delta x \times \Delta y \times 1$), then the element represented by a regular boundary node such as node 2 becomes *half size* (i.e., $\Delta x \times \Delta y/2 \times 1$), and a corner node such as node 1 is *quarter size* (i.e., $\Delta x/2 \times \Delta y/2 \times 1$). Keeping Eq. 5–36 in mind for the energy balance, the finite difference equations for each of the nine nodes are obtained as follows:

(*a*) Node 1. The volume element of this corner node is insulated on the left and subjected to convection at the top and to conduction at the right and bottom surfaces. An energy balance on this element gives (Fig. 5–27*a*)

$$0 + h\frac{\Delta x}{2}(T_\infty - T_1) + k\frac{\Delta y}{2}\frac{T_2 - T_1}{\Delta x} + k\frac{\Delta x}{2}\frac{T_4 - T_1}{\Delta y} + \dot{e}_1\frac{\Delta x}{2}\frac{\Delta y}{2} = 0$$

Taking $\Delta x = \Delta y = l$, it simplifies to

$$-\left(2 + \frac{hl}{k}\right)T_1 + T_2 + T_4 = -\frac{hl}{k}T_\infty - \frac{\dot{e}_1 l^2}{2k}$$

(*b*) Node 2. The volume element of this boundary node is subjected to convection at the top and to conduction at the right, bottom, and left surfaces. An energy balance on this element gives (Fig. 5–27*b*)

$$h\Delta x(T_\infty - T_2) + k\frac{\Delta y}{2}\frac{T_3 - T_2}{\Delta x} + k\Delta x\frac{T_5 - T_2}{\Delta y} + k\frac{\Delta y}{2}\frac{T_1 - T_2}{\Delta x} + \dot{e}_2\Delta x\frac{\Delta y}{2} = 0$$
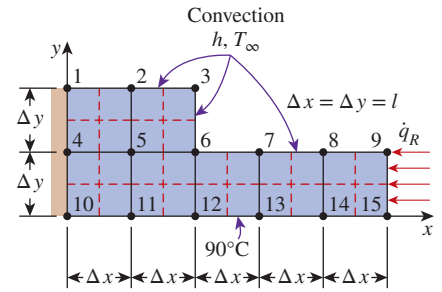
FIGURE 5–26
Schematic for Example 5–3 and the nodal network (the boundaries of volume elements of the nodes are indicated by dashed lines).

(*a*) Node 1   (*b*) Node 2
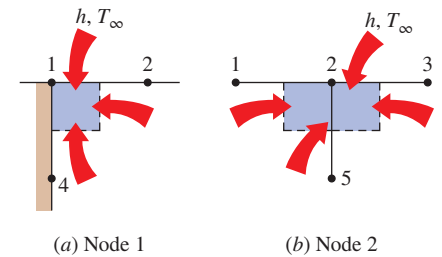
FIGURE 5–27
Schematics for energy balances on the volume elements of nodes 1 and 2.
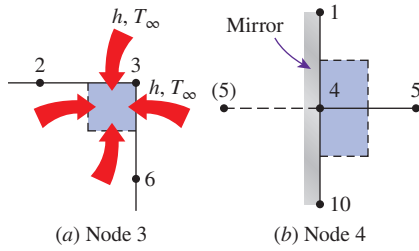
FIGURE 5–28
Schematics for energy balances on the volume elements of nodes 3 and 4.

FIGURE 5–29
Schematics for energy balances on the volume elements of nodes 5 and 6.

Taking $\Delta x = \Delta y = l$, it simplifies to

$$T_1 - \left(4 + \frac{2hl}{k}\right)T_2 + T_3 + 2T_5 = -\frac{2hl}{k}T_\infty - \frac{\dot{e}_2 l^2}{k}$$

(*c*) Node 3. The volume element of this corner node is subjected to convection at the top and right surfaces and to conduction at the bottom and left surfaces. An energy balance on this element gives (Fig. 5–28*a*)

$$h\left(\frac{\Delta x}{2} + \frac{\Delta y}{2}\right)(T_\infty - T_3) + k\frac{\Delta x}{2}\frac{T_6 - T_3}{\Delta y} + k\frac{\Delta y}{2}\frac{T_2 - T_3}{\Delta x} + \dot{e}_3\frac{\Delta x}{2}\frac{\Delta y}{2} = 0$$

Taking $\Delta x = \Delta y = l$, it simplifies to

$$T_2 - \left(2 + \frac{2hl}{k}\right)T_3 + T_6 = -\frac{2hl}{k}T_\infty - \frac{\dot{e}_3 l^2}{2k}$$

(*d*) Node 4. This node is on the insulated boundary and can be treated as an interior node by replacing the insulation with a mirror. This puts a reflected image of node 5 to the left of node 4. Noting that $\Delta x = \Delta y = l$, the general interior node relation for the steady two-dimensional case (Eq. 5–35) gives (Fig. 5–28*b*)

$$T_5 + T_1 + T_5 + T_{10} - 4T_4 + \frac{\dot{e}_4 l^2}{k} = 0$$

or, noting that $T_{10} = 90°C$,

$$T_1 - 4T_4 + 2T_5 = -90 - \frac{\dot{e}_4 l^2}{k}$$

(*e*) Node 5. This is an interior node, and noting that $\Delta x = \Delta y = l$, the finite difference formulation of this node is obtained directly from Eq. 5–35 to be (Fig. 5–29*a*)

$$T_4 + T_2 + T_6 + T_{11} - 4T_5 + \frac{\dot{e}_5 l^2}{k} = 0$$

or, noting that $T_{11} = 90°C$,

$$T_2 + T_4 - 4T_5 + T_6 = -90 - \frac{\dot{e}_5 l^2}{k}$$

(*f*) Node 6. The volume element of this inner corner node is subjected to convection at the L-shaped exposed surface and to conduction at other surfaces. An energy balance on this element gives (Fig. 5–29*b*)

$$h\left(\frac{\Delta x}{2} + \frac{\Delta y}{2}\right)(T_\infty - T_6) + k\frac{\Delta y}{2}\frac{T_7 - T_6}{\Delta x} + k\Delta x\frac{T_{12} - T_6}{\Delta y}$$

$$+ k\Delta y\frac{T_5 - T_6}{\Delta x} + k\frac{\Delta x}{2}\frac{T_3 - T_6}{\Delta y} + \dot{e}_6\frac{3\Delta x\Delta y}{4} = 0$$

Taking $\Delta x = \Delta y = l$ and noting that $T_{12} = 90°C$, it simplifies to

$$T_3 + 2T_5 - \left(6 + \frac{2hl}{k}\right)T_6 + T_7 = -180 - \frac{2hl}{k}T_\infty - \frac{3\dot{e}_6 l^2}{2k}$$

(*g*) Node 7. The volume element of this boundary node is subjected to convection at the top and to conduction at the right, bottom, and left surfaces. An energy balance on this element gives (Fig. 5–30*a*)

$$h\Delta x(T_\infty - T_7) + k\frac{\Delta y}{2}\frac{T_8 - T_7}{\Delta x} + k\Delta x\frac{T_{13} - T_7}{\Delta y}$$
$$+ k\frac{\Delta y}{2}\frac{T_6 - T_7}{\Delta x} + \dot{e}_7\Delta x\frac{\Delta y}{2} = 0$$

Taking $\Delta x = \Delta y = l$ and noting that $T_{13} = 90°C$, it simplifies to

$$T_6 - \left(4 + \frac{2hl}{k}\right)T_7 + T_8 = -180 - \frac{2hl}{k}T_\infty - \frac{\dot{e}_7 l^2}{k}$$

(*h*) Node 8. This node is identical to node 7, and the finite difference formulation of this node can be obtained from that of node 7 by shifting the node numbers by 1 (i.e., replacing subscript *m* with *m* + 1). It gives

$$T_7 - \left(4 + \frac{2hl}{k}\right)T_8 + T_9 = -180 - \frac{2hl}{k}T_\infty - \frac{\dot{e}_8 l^2}{k}$$

(*i*) Node 9. The volume element of this corner node is subjected to convection at the top surface, to heat flux at the right surface, and to conduction at the bottom and left surfaces. An energy balance on this element gives (Fig. 5–30*b*)

$$h\frac{\Delta x}{2}(T_\infty - T_9) + \dot{q}_R\frac{\Delta y}{2} + k\frac{\Delta x}{2}\frac{T_{15} - T_9}{\Delta y} + k\frac{\Delta y}{2}\frac{T_8 - T_9}{\Delta x} + \dot{e}_9\frac{\Delta x}{2}\frac{\Delta y}{2} = 0$$

Taking $\Delta x = \Delta y = l$ and noting that $T_{15} = 90°C$, it simplifies to

$$T_8 - \left(2 + \frac{hl}{k}\right)T_9 = -90 - \frac{\dot{q}_R l}{k} - \frac{hl}{k}T_\infty - \frac{\dot{e}_9 l^2}{2k}$$

This completes the development of the finite difference formulation for this problem. Substituting the given quantities, the system of nine equations for the determination of nine unknown nodal temperatures becomes

$$-2.064T_1 + T_2 + T_4 = -11.2$$
$$T_1 - 4.128T_2 + T_3 + 2T_5 = -22.4$$
$$T_2 - 2.128T_3 + T_6 = -12.8$$
$$T_1 - 4T_4 + 2T_5 = -109.2$$
$$T_2 + T_4 - 4T_5 + T_6 = -109.2$$
$$T_3 + 2T_5 - 6.128T_6 + T_7 = -212.0$$
$$T_6 - 4.128T_7 + T_8 = -202.4$$
$$T_7 - 4.128T_8 + T_9 = -202.4$$
$$T_8 - 2.064T_9 = -105.2$$

(*a*) Node 7   (*b*) Node 9
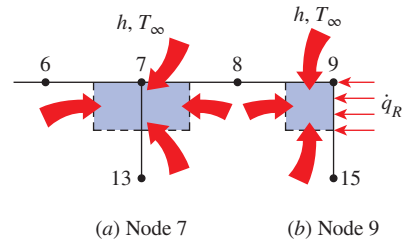
FIGURE 5–30

Schematics for energy balances on the volume elements of nodes 7 and 9.

which is a system of nine algebraic equations with nine unknowns. Using an equation solver, its solution is determined to be

$$T_1 = 112.1°C \quad T_2 = 110.8°C \quad T_3 = 106.6°C$$
$$T_4 = 109.4°C \quad T_5 = 108.1°C \quad T_6 = 103.2°C$$
$$T_7 = 97.3°C \quad T_8 = 96.3°C \quad T_9 = 97.6°C$$

Note that the temperature is the highest at node 1 and the lowest at node 8. This is consistent with our expectations since node 1 is the farthest away from the bottom surface, which is maintained at 90°C and has one side insulated, and node 8 has the largest exposed area relative to its volume while being close to the surface at 90°C.
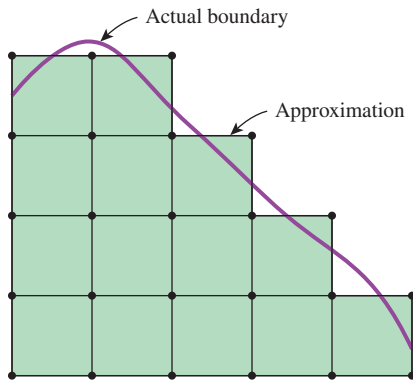
FIGURE 5–31
Approximating an irregular boundary with a rectangular mesh.

Irregular Boundaries

In problems with simple geometries, we can fill the entire region using simple volume elements such as strips for a plane wall and rectangular elements for two-dimensional conduction in a rectangular region. We can also use cylindrical or spherical shell elements to cover the cylindrical and spherical bodies entirely. However, many geometries encountered in practice, such as turbine blades or engine blocks, do not have simple shapes, and it is difficult to fill such geometries having irregular boundaries with simple volume elements. A practical way of dealing with such geometries is to replace the irregular geometry with a series of simple volume elements, as shown in Fig. 5–31. This simple approach is often satisfactory for practical purposes, especially when the nodes are closely spaced near the boundary. More sophisticated approaches are available for handling irregular boundaries, and they are commonly incorporated into the commercial software packages.

EXAMPLE 5–4   **Heat Loss Through Chimneys**

Hot combustion gases of a furnace are flowing through a square chimney made of concrete ($k = 1.4$ W/m·K). The flow section of the chimney is 20 cm $\times$ 20 cm, and the thickness of the wall is 20 cm. The average temperature of the hot gases in the chimney is $T_i = 300°C$, and the average convection heat transfer coefficient inside the chimney is $h_i = 70$ W/m²·K. The chimney is losing heat from its outer surface to the ambient air at $T_o = 20°C$ by convection with a heat transfer coefficient of $h_o = 21$ W/m²·K and to the sky by radiation. The emissivity of the outer surface of the wall is $\varepsilon = 0.9$, and the effective sky temperature is estimated to be 260 K. Using the finite difference method with $\Delta x = \Delta y = 10$ cm and taking full advantage of symmetry, determine the temperatures at the nodal points of a cross section and the rate of heat loss for a 1-m-long section of the chimney.

SOLUTION   Heat transfer through a square chimney is considered. The nodal temperatures and the rate of heat loss per unit length are to be determined with the finite difference method.

Assumptions **1** Heat transfer is steady since there is no indication of change with time. **2** Heat transfer through the chimney is two-dimensional since the height of the chimney is large relative to its cross section, and thus heat conduction through the chimney in the axial direction is negligible. It is tempting to simplify the problem further by considering heat transfer in each wall to be one-dimensional, which would be the case if the walls were thin and thus the corner effects were negligible. This assumption cannot be justified in this case since the walls are very thick and the corner sections constitute a considerable portion of the chimney structure. **3** Thermal conductivity is constant.

Properties The properties of the chimney are given to be $k = 1.4$ W/m·K and $\varepsilon = 0.9$.

Analysis The cross section of the chimney is given in Fig. 5–32. The most striking aspect of this problem is the apparent symmetry about the horizontal and vertical lines passing through the midpoint of the chimney as well as the diagonal axes, as indicated on the figure. Therefore, we need to consider only one-eighth of the geometry in the solution whose nodal network consists of nine equally spaced nodes.

No heat can cross a symmetry line, and thus symmetry lines can be treated as insulated surfaces and thus "mirrors" in the finite difference formulation. Then the nodes in the middle of the symmetry lines can be treated as interior nodes by using mirror images. Six of the nodes are boundary nodes, so we have to write energy balances to obtain their finite difference formulations. First we partition the region among the nodes equitably by drawing dashed lines between the nodes through the middle. Then the region around a node surrounded by the boundary or the dashed lines represents the volume element of the node. Considering a unit depth and using the energy balance approach for the boundary nodes (again assuming all heat transfer into the volume element for convenience) and the formula for the interior nodes, the finite difference equations for the nine nodes are determined as follows:

(*a*) Node 1. On the inner boundary, subjected to convection, Fig. 5–33*a*

$$0 + h_i \frac{\Delta x}{2}(T_i - T_1) + k\frac{\Delta y}{2}\frac{T_2 - T_1}{\Delta x} + k\frac{\Delta x}{2}\frac{T_3 - T_1}{\Delta y} + 0 = 0$$

Taking $\Delta x = \Delta y = l$, it simplifies to

$$-\left(2 + \frac{h_i l}{k}\right)T_1 + T_2 + T_3 = -\frac{h_i l}{k}T_i$$

(*b*) Node 2. On the inner boundary, subjected to convection, Fig. 5–33*b*

$$k\frac{\Delta y}{2}\frac{T_1 - T_2}{\Delta x} + h_i\frac{\Delta x}{2}(T_i - T_2) + 0 + k\Delta x\frac{T_4 - T_2}{\Delta y} = 0$$

Taking $\Delta x = \Delta y = l$, it simplifies to

$$T_1 - \left(3 + \frac{h_i l}{k}\right)T_2 + 2T_4 = -\frac{h_i l}{k}T_i$$
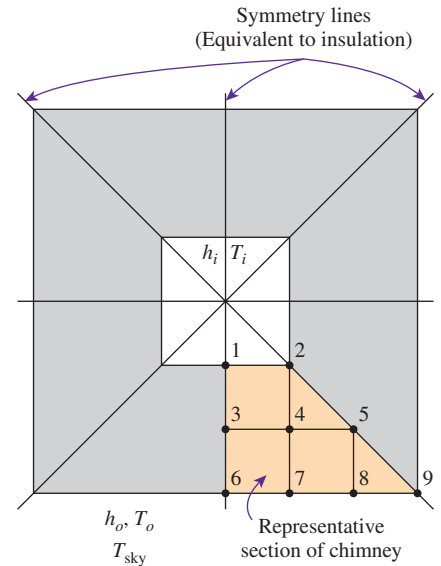
FIGURE 5–32
Schematic of the chimney discussed in Example 5–4 and the nodal network for a representative section.
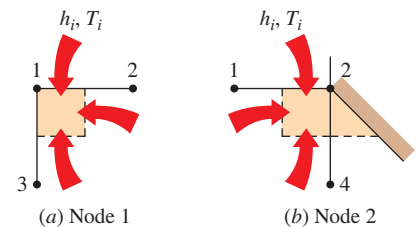
FIGURE 5–33
Schematics for energy balances on the volume elements of nodes 1 and 2.
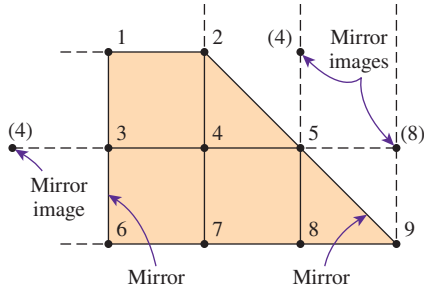
FIGURE 5–34
Converting the boundary nodes 3 and 5
on symmetry lines to interior nodes by
using mirror images.
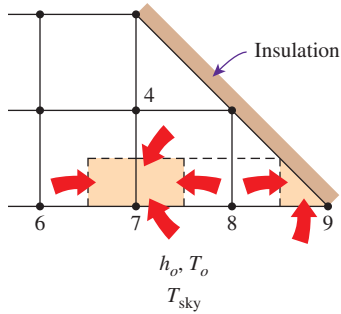
FIGURE 5–35
Schematics for energy balances on the
volume elements of nodes 7 and 9.

(*c*) Nodes 3, 4, and 5. (Interior nodes, Fig. 5–34)

$$\text{Node 3: } T_4 + T_1 + T_4 + T_6 - 4T_3 = 0$$
$$\text{Node 4: } T_3 + T_2 + T_5 + T_7 - 4T_4 = 0$$
$$\text{Node 5: } T_4 + T_4 + T_8 + T_8 - 4T_5 = 0$$

(*d*) Node 6. (On the outer boundary, subjected to convection and radiation)

$$0 + k\frac{\Delta x}{2}\frac{T_3 - T_6}{\Delta y} + k\frac{\Delta y}{2}\frac{T_7 - T_6}{\Delta x}$$
$$+ h_o\frac{\Delta x}{2}(T_o - T_6) + \varepsilon\sigma\frac{\Delta x}{2}(T_{sky}^4 - T_6^4) = 0$$

Taking $\Delta x = \Delta y = l$, it simplifies to

$$T_2 + T_3 - \left(2 + \frac{h_o l}{k}\right) T_6 = -\frac{h_o l}{k}T_o - \frac{\varepsilon\sigma l}{k}(T_{sky}^4 - T_6^4)$$

(*e*) Node 7. (On the outer boundary, subjected to convection and radiation, Fig. 5–35)

$$k\frac{\Delta y}{2}\frac{T_6 - T_7}{\Delta x} + k\Delta x\frac{T_4 - T_7}{\Delta y} + k\frac{\Delta y}{2}\frac{T_8 - T_7}{\Delta x}$$
$$+ h_o\Delta x(T_o - T_7) + \varepsilon\sigma\Delta x(T_{sky}^4 - T_7^4) = 0$$

Taking $\Delta x = \Delta y = l$, it simplifies to

$$2T_4 + T_6 - \left(4 + \frac{2h_o l}{k}\right) T_7 + T_8 = -\frac{2h_o l}{k}T_o - \frac{2\varepsilon\sigma l}{k}(T_{sky}^4 - T_7^4)$$

(*f*) Node 8. Same as node 7, except shift the node numbers up by 1 (replace 4 with 5, 6 with 7, 7 with 8, and 8 with 9 in the last relation)

$$2T_5 + T_7 - \left(4 + \frac{2h_o l}{k}\right) T_8 + T_9 = -\frac{2h_o l}{k}T_o - \frac{2\varepsilon\sigma l}{k}(T_{sky}^4 - T_8^4)$$

(*g*) Node 9. (On the outer boundary, subjected to convection and radiation, Fig. 5–35)

$$k\frac{\Delta y}{2}\frac{T_8 - T_9}{\Delta x} + 0 + h_o\frac{\Delta x}{2}(T_o - T_9) + \varepsilon\sigma\frac{\Delta x}{2}(T_{sky}^4 - T_9^4) = 0$$

Taking $\Delta x = \Delta y = l$, it simplifies to

$$T_8 - \left(1 + \frac{h_o l}{k}\right) T_9 = -\frac{h_o l}{k}T_o - \frac{\varepsilon\sigma l}{k}(T_{sky}^4 - T_9^4)$$

This problem involves radiation, which requires the use of absolute temperature, and
thus all temperatures should be expressed in Kelvin. Alternately, we could use °C
for all temperatures provided that the four temperatures in the radiation terms are

expressed in the form $(T + 273)^4$. Substituting the given quantities, the system of nine equations for the determination of nine unknown nodal temperatures in a form suitable for use with an iteration method becomes

$$T_1 = (T_2 + T_3 + 2865)/7$$
$$T_2 = (T_1 + 2T_4 + 2865)/8$$
$$T_3 = (T_1 + 2T_4 + T_6)/4$$
$$T_4 = (T_2 + T_3 + T_5 + T_7)/4$$
$$T_5 = (2T_4 + 2T_8)/4$$
$$T_6 = (T_2 + T_3 + 456.2 - 0.3645 \times 10^{-9} T_6^4)/3.5$$
$$T_7 = (2T_4 + T_6 + T_8 + 912.4 - 0.729 \times 10^{-9} T_7^4)/7$$
$$T_8 = (2T_5 + T_7 + T_9 + 912.4 - 0.729 \times 10^{-9} T_8^4)/7$$
$$T_9 = (T_8 + 456.2 - 0.3645 \times 10^{-9} T_9^4)/2.5$$

which is a system of *nonlinear* equations. Using the Gauss-Seidel iteration method or an equation solver, its solution is determined to be

$T_1 = 545.7$ K $= 272.6°$C	$T_2 = 529.2$ K $= 256.1°$C	$T_3 = 425.2$ K $= 152.1°$C
$T_4 = 411.2$ K $= 138.0°$C	$T_5 = 362.1$ K $= 89.0°$C	$T_6 = 332.9$ K $= 59.7°$C
$T_7 = 328.1$ K $= 54.9°$C	$T_8 = 313.1$ K $= 39.9°$C	$T_9 = 296.5$ K $= 23.4°$C

The variation of temperature in the chimney is shown in Fig. 5–36.

Note that the temperatures are highest at the inner wall (but less than 300°C) and lowest at the outer wall (but more that 260 K), as expected.

The average temperature at the outer surface of the chimney weighed by the surface area is

$$T_{\text{wall, out}} = \frac{(0.5T_6 + T_7 + T_8 + 0.5T_9)}{(0.5 + 1 + 1 + 0.5)}$$

$$= \frac{0.5 \times 332.9 + 328.1 + 313.1 + 0.5 \times 296.5}{3} = 318.6 \text{ K}$$

Temperature, °C

FIGURE 5–36
The variation of temperature in the chimney.

Then the rate of heat loss through the 1-m-long section of the chimney can be determined approximately from

$$\dot{Q}_{\text{chimney}} = h_o A_o (T_{\text{wall, out}} - T_o) + \varepsilon \sigma A_o (T_{\text{wall, out}}^4 - T_{\text{sky}}^4)$$
$$= (21 \text{ W/m}^2 \cdot \text{K})[4 \times (0.6 \text{ m})(1 \text{ m})](318.6 - 293)\text{K}$$
$$+ 0.9(5.67 \times 10^{-8} \text{ W/m}^2 \cdot \text{K}^4)$$
$$[4 \times (0.6 \text{ m})(1 \text{ m})](318.6 \text{ K})^4 - (260 \text{ K})^4$$
$$= 1291 + 702 = \mathbf{1993 \text{ W}}$$

We could also determine the heat transfer by finding the average temperature of the inner wall, which is $(272.6 + 256.1)/2 = 264.4°$C, and applying Newton's law of cooling at that surface:

$$\dot{Q}_{\text{chimney}} = h_i A_i (T_i - T_{\text{wall, in}})$$
$$= (70 \text{ W/m}^2 \cdot \text{K})[4 \times (0.2 \text{ m})(1 \text{ m})](300 - 264.4)°\text{C} = 1994 \text{ W}$$

The difference between the two results is due to the approximate nature of the numerical analysis.

Discussion We used a relatively crude numerical model to solve this problem to keep the complexities at a manageable level. The accuracy of the solution obtained can be improved by using a finer mesh and thus a greater number of nodes. Also, when radiation is involved, it is more accurate (but more laborious) to determine the heat losses for each node and add them up instead of using the average temperature.

5–5 · TRANSIENT HEAT CONDUCTION

So far in this chapter we have applied the finite difference method to *steady* heat transfer problems. In this section we extend the method to solve *transient* problems.

We applied the finite difference method to steady problems by *discretizing* the problem in the space variables and solving for temperatures at *discrete* points called the nodes. The solution obtained is valid for any time since under steady conditions the temperatures do not change with time. In transient problems, however, the temperatures change with time as well as position, and thus the finite difference solution of transient problems requires *discretization in time* in addition to discretization in space, as shown in Fig. 5–37. This is done by selecting a suitable time step Δt and solving for the unknown nodal temperatures repeatedly for each Δt until the solution at the desired time is obtained. For example, consider a hot metal object that is taken out of the oven at an initial temperature of T_i at time $t = 0$ and is allowed to cool in ambient air. If a time step of $\Delta t = 5$ min is chosen, the determination of the temperature distribution in the metal piece after 3 h requires the determination of the temperatures $3 \times 60/5 = 36$ times, or in 36 time steps. Therefore, the computation time of this problem is 36 times that of a steady problem. Choosing a smaller Δt increases the accuracy of the solution, but it also increases the computation time.

In transient problems, the *superscript i* is used as the *index* or *counter* of time steps, with $i = 0$ corresponding to the specified initial condition. In the case of the hot metal piece discussed above, $i = 1$ corresponds to $t = 1 \times \Delta t = 5$ min, $i = 2$ corresponds to $t = 2 \times \Delta t = 10$ min, and a general time step i corresponds to $t_i = i\Delta t$. The notation T_m^i is used to represent the temperature at the node m at time step i.

The formulation of transient heat conduction problems differs from that of steady ones in that the transient problems involve an *additional term* representing the *change in the energy content* of the medium with time. This additional term appears as a first derivative of temperature with respect to time in the differential equation and as a change in the internal energy content during Δt in the energy balance formulation. The nodes and the volume elements in transient problems are selected as they are in the steady case, and, again assuming all heat transfer is *into* the element for convenience, the energy balance on a volume element during a time interval Δt can be expressed as

$$\begin{pmatrix} \text{Heat transferred into} \\ \text{the volume element} \\ \text{from all of its surfaces} \\ \text{during } \Delta t \end{pmatrix} + \begin{pmatrix} \text{Heat generated} \\ \text{within the} \\ \text{volume element} \\ \text{during } \Delta t \end{pmatrix} = \begin{pmatrix} \text{The change in the} \\ \text{energy content of} \\ \text{the volume element} \\ \text{during } \Delta t \end{pmatrix}$$
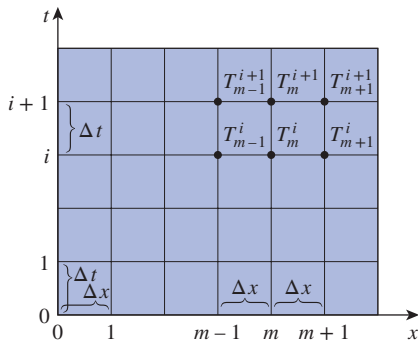
FIGURE 5–37

Finite difference formulation of time-dependent problems involves discrete points in time as well as space.

or

$$\Delta t \times \sum_{\text{All sides}} \dot{Q} + \Delta t \times \dot{E}_{\text{gen, element}} = \Delta E_{\text{element}} \qquad \textbf{(5–37)}$$

where the rate of heat transfer $\dot{Q}$ normally consists of conduction terms for interior nodes but may involve convection, heat flux, and radiation for boundary nodes.

Noting that $\Delta E_{\text{element}} = mc_p \Delta T = \rho V_{\text{element}} c_p \Delta T$, where ρ is density and c_p is the specific heat of the element, dividing the earlier relation by Δt gives

$$\sum_{\text{All sides}} \dot{Q} + \dot{E}_{\text{gen, element}} = \frac{\Delta E_{\text{element}}}{\Delta t} = \rho V_{\text{element}} c_p \frac{\Delta T}{\Delta t} \qquad \textbf{(5–38)}$$

or, for any node m in the medium and its volume element,

$$\sum_{\text{All sides}} \dot{Q} + \dot{E}_{\text{gen, element}} = \rho V_{\text{element}} c_p \frac{T_m^{i+1} - T_m^i}{\Delta t} \qquad \textbf{(5–39)}$$

where T_m^i and T_m^{i+1} are the temperatures of node m at times $t_i = i\Delta t$ and $t_{i+1} = (i+1)\Delta t$, respectively, and $T_m^{i+1} - T_m^i$ represents the temperature change of the node during the time interval Δt between the time steps i and $i+1$ (Fig. 5–38).

Note that the ratio $(T_m^{i+1} - T_m^i)/\Delta t$ is simply the finite difference approximation of the partial derivative $\partial T/\partial t$ that appears in the differential equations of transient problems. Therefore, we would obtain the same result for the finite difference formulation if we followed a strict mathematical approach instead of the energy balance approach used above. Also note that the finite difference formulations of steady and transient problems differ by the single term on the right side of the equal sign, and the format of that term remains the same in all coordinate systems regardless of whether heat transfer is one-, two-, or three-dimensional. For the special case of $T_m^{i+1} = T_m^i$ (i.e., no change in temperature with time), the formulation reduces to that of the steady case, as expected.

The nodal temperatures in transient problems normally change during each time step, and you may be wondering whether to use temperatures at the *previous* time step i or the *new* time step $i+1$ for the terms on the left side of Eq. 5–39. Well, both are reasonable approaches, and both are used in practice. The finite difference approach is called the **explicit method** in the first case and the **implicit method** in the second case, and they are expressed in the general form as (Fig. 5–39)

Explicit method: $$\sum_{\text{All sides}} \dot{Q}^i + \dot{E}_{\text{gen, element}}^i = \rho V_{\text{element}} c_p \frac{T_m^{i+1} - T_m^i}{\Delta t} \qquad \textbf{(5–40)}$$

Implicit method: $$\sum_{\text{All sides}} \dot{Q}^{i+1} + \dot{E}_{\text{gen, element}}^{i+1} = \rho V_{\text{element}} c_p \frac{T_m^{i+1} - T_m^i}{\Delta t} \qquad \textbf{(5–41)}$$

It appears that the time derivative is expressed in *forward difference* form in the explicit case and *backward difference* form in the implicit case. Of course, it is also possible to mix the two fundamental formulations of Eqs. 5–40

Volume element (can be any shape)

ρ = density
V = volume
ρV = mass
c_p = specific heat
ΔT = temperature change

Node m

$$\Delta U = \rho V c_p \Delta T = \rho V c_p (T_m^{i+1} - T_m^i)$$
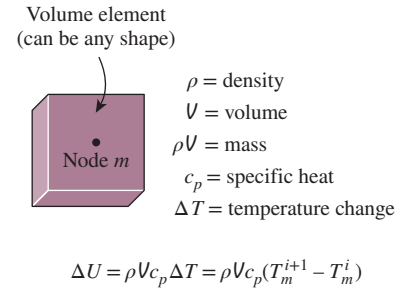
FIGURE 5–38
The change in the energy content of the volume element of a node during a time interval Δt.

If expressed at $i+1$: Implicit method

$$\sum_{\text{All sides}} \dot{Q} + \dot{E}_{\text{gen, element}} = \rho V_{\text{element}} c_p \frac{T_m^{i+1} - T_m^i}{\Delta t}$$

If expressed at i: Explicit method
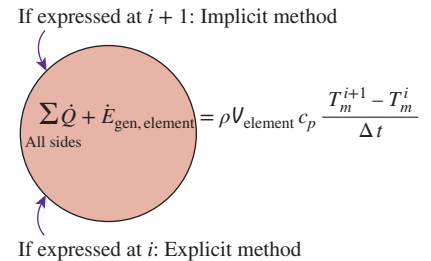
FIGURE 5–39
The formulation of explicit and implicit methods differs at the time step (previous or new) at which the heat transfer and heat generation terms are expressed.

and 5–41 and come up with more elaborate formulations, but such formulations offer little insight and are beyond the scope of this text. Note that both formulations are simply expressions between the nodal temperatures before and after a time interval and are based on determining the new temperatures T_m^{i+1} using the *previous* temperatures T_m^i. *The explicit and implicit formulations given here are quite general and can be used in any coordinate system regardless of the dimension of heat transfer.* The volume elements in multidimensional cases simply have more surfaces and thus involve more terms in the summation.

The explicit and implicit methods have their advantages and disadvantages, and one method is not necessarily better than the other one. Next you will see that the *explicit method* is easy to implement but imposes a limit on the allowable time step to avoid instabilities in the solution, and the *implicit method* requires the nodal temperatures to be solved simultaneously for each time step but imposes no limit on the magnitude of the time step. We limit the discussion to one- and two-dimensional cases to keep the complexities at a manageable level, but the analysis can readily be extended to three-dimensional cases and other coordinate systems.

Transient Heat Conduction in a Plane Wall

Consider transient one-dimensional heat conduction in a plane wall of thickness L with heat generation $\dot{e}(x, t)$ that may vary with time and position and constant conductivity k with a mesh size of $\Delta x = L/M$ and nodes 0, 1, 2, . . . , M in the x-direction, as shown in Fig. 5–40. Noting that the volume element of a general interior node m involves heat conduction from two sides, and the volume of the element is $V_{\text{element}} = A\Delta x$, the transient finite difference formulation for an interior node can be expressed on the basis of Eq. 5–39 as

$$kA\frac{T_{m-1} - T_m}{\Delta x} + kA\frac{T_{m+1} - T_m}{\Delta x} + \dot{e}_m A\Delta x = \rho A\Delta x c_p\frac{T_m^{i+1} - T_m^i}{\Delta t} \tag{5–42}$$

Canceling the surface area A and multiplying by $\Delta x/k$, it simplifies to

$$T_{m-1} - 2T_m + T_{m+1} + \frac{\dot{e}_m\Delta x^2}{k} = \frac{\Delta x^2}{\alpha\Delta t}(T_m^{i+1} - T_m^i) \tag{5–43}$$

where $\alpha = k/\rho c_p$ is the *thermal diffusivity* of the wall material. We now define a dimensionless **mesh Fourier number** as

$$\tau = \frac{\alpha\Delta t}{\Delta x^2} \tag{5–44}$$

Then Eq. 5–43 reduces to

$$T_{m-1} - 2T_m + T_{m+1} + \frac{\dot{e}_m\Delta x^2}{k} = \frac{T_m^{i+1} - T_m^i}{\tau} \tag{5–45}$$

Note that the left side of this equation is simply the finite difference formulation of the problem for the steady case. This is not surprising since the formulation must reduce to the steady case for $T_m^{i+1} = T_m^i$. Also, we are still not

FIGURE 5–40
The nodal points and volume elements for the transient finite difference formulation of one-dimensional conduction in a plane wall.

committed to explicit or implicit formulation since we did not indicate the time step on the left side of the equation. We now obtain the *explicit* finite difference formulation by expressing the left side at time step i as

$$T_{m-1}^i - 2T_m^i + T_{m+1}^i + \frac{\dot{e}_m^i \Delta x^2}{k} = \frac{T_m^{i+1} - T_m^i}{\tau} \quad \text{(explicit)} \tag{5–46}$$

This equation can be solved *explicitly* for the new temperature T_m^{i+1} (and thus the name *explicit* method) to give

$$T_m^{i+1} = \tau(T_{m-1}^i + T_{m+1}^i) + (1 - 2\tau)\,T_m^i + \tau\frac{\dot{e}_m^i \Delta x^2}{k} \tag{5–47}$$

for all interior nodes $m = 1, 2, 3, \ldots, M - 1$ in a plane wall. Expressing the left side of Eq. 5–45 at time step $i + 1$ instead of i would give the *implicit* finite difference formulation as

$$T_{m-1}^{i+1} - 2T_m^{i+1} + T_{m+1}^{i+1} + \frac{\dot{e}_m^{i+1} \Delta x^2}{k} = \frac{T_m^{i+1} - T_m^i}{\tau} \quad \text{(implicit)} \tag{5–48}$$

which can be rearranged as

$$\tau T_{m-1}^{i+1} - (1 + 2\tau)T_m^{i+1} + \tau T_{m+1}^{i+1} + \tau\frac{\dot{e}_m^{i+1} \Delta x^2}{k} + T_m^i = 0 \tag{5–49}$$

The application of either the explicit or the implicit formulation to each of the $M - 1$ interior nodes gives $M - 1$ equations. The remaining two equations are obtained by applying the same method to the two boundary nodes unless, of course, the boundary temperatures are specified as constants (invariant with time). For example, the formulation of the convection boundary condition at the left boundary (node 0) for the explicit case can be expressed as (Fig. 5–41)

$$hA(T_\infty - T_0^i) + kA\frac{T_1^i - T_0^i}{\Delta x} + \dot{e}_0^i A\frac{\Delta x}{2} = \rho A\frac{\Delta x}{2}c_p\frac{T_0^{i+1} - T_0^i}{\Delta t} \tag{5–50}$$

which simplifies to

$$T_0^{i+1} = \left(1 - 2\tau - 2\tau\frac{h\Delta x}{k}\right)T_0^i + 2\tau T_1^i + 2\tau\frac{h\Delta x}{k}T_\infty + \tau\frac{\dot{e}_0^i \Delta x^2}{k} \tag{5–51}$$

Note that in the case of no heat generation and $\tau = 0.5$, which is the upper limit of the stability criterion for the one-dimensional explicit method (discussed in the next subsection), the explicit finite difference formulation for a general interior node reduces to $[T_m^{i+1} = (T_{m-1}^i + T_{m+1}^i)/2]$, which has the interesting interpretation that *the temperature of an interior* node *at the new time step is simply the average of the temperatures of its neighboring* node*s at the previous time step.*

Once the formulation (explicit or implicit) is complete and the initial condition is specified, the solution of a transient problem is obtained by *marching* in time using a step size of Δt as follows: select a suitable time step Δt and determine the nodal temperatures from the initial condition. Taking the initial temperatures as the *previous* solution T_m^i at $t = 0$, obtain the new solution
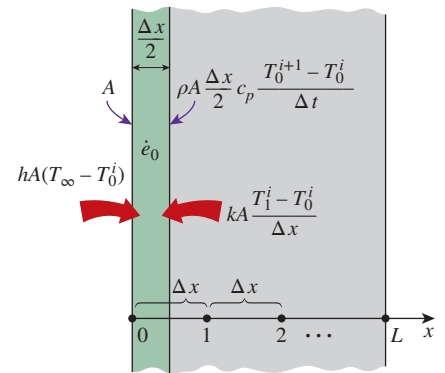
FIGURE 5–41
Schematic for the explicit finite difference formulation of the convection condition at the left boundary of a plane wall.

Explicit formulation:

$$T_0^{i+1} = a_0 T_0^i + \cdots$$
$$T_1^{i+1} = a_1 T_1^i + \cdots$$
$$\vdots$$
$$T_m^{i+1} = a_m T_m^i + \cdots$$
$$\vdots$$
$$T_M^{i+1} = a_M T_M^i + \cdots$$

Stability criterion:

$$a_m \geq 0, \, m = 0, 1, 2, \ldots m, \ldots M$$
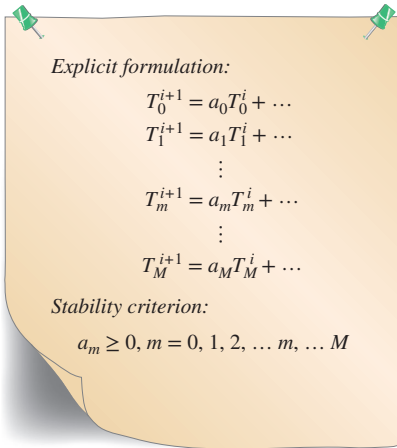
FIGURE 5–42
The stability criterion of the explicit method requires all primary coefficients to be positive or zero.

T_m^{i+1} at all nodes at time $t = \Delta t$ using the transient finite difference relations. Now using the solution just obtained at $t = \Delta t$ as the *previous* solution T_m^i, obtain the new solution T_m^{i+1} at $t = 2\Delta t$ using the same relations. Repeat the process until the solution at the desired time is obtained.

Stability Criterion for Explicit Method: Limitation on Δt

The explicit method is easy to use, but it suffers from an undesirable feature that severely restricts its utility: the explicit method is not unconditionally stable, and the largest permissible value of the time step Δt is limited by the stability criterion. If the time step Δt is not sufficiently small, the solutions obtained by the explicit method may oscillate wildly and diverge from the actual solution. To avoid such divergent oscillations in nodal temperatures, the value of Δt must be maintained below a certain upper limit established by the **stability criterion**. It can be shown mathematically or by a physical argument based on the second law of thermodynamics that *the stability criterion is satisfied if the coefficients of all T_m^i in the T_m^{i+1} expressions (called the* **primary coefficients**) *are greater than or equal to zero for all* nodes *m* (Fig. 5–42). Of course, all the terms involving T_m^i for a particular node must be grouped together before this criterion is applied.

Different equations for different nodes may result in different restrictions on the size of the time step Δt, and the criterion that is most restrictive should be used in the solution of the problem. A practical approach is to identify the equation with the *smallest primary coefficient* since it is the most restrictive and to determine the allowable values of Δt by applying the stability criterion to that equation only. A Δt value obtained this way also satisfies the stability criterion for all other equations in the system.

For example, in the case of transient one-dimensional heat conduction in a plane wall with specified surface temperatures, the explicit finite difference equations for all the nodes (which are *interior nodes*) are obtained from Eq. 5–47. The coefficient of T_m^i in the T_m^{i+1} expression is $1 - 2\tau$, which is independent of the node number m, and thus the stability criterion for all nodes in this case is $1 - 2\tau \geq 0$ or

$$\tau = \frac{\alpha \Delta t}{\Delta x^2} \leq \frac{1}{2} \begin{pmatrix} \text{interior nodes, one-dimensional heat} \\ \text{transfer in rectangular coordinates} \end{pmatrix} \quad \textbf{(5–52)}$$

When the material of the medium and thus its thermal diffusivity α is known and the value of the mesh size Δx is specified, the largest allowable value of the time step Δt can be determined from this relation. For example, in the case of a brick wall ($\alpha = 0.45 \times 10^{-6}\,\text{m}^2/\text{s}$) with a mesh size of $\Delta x = 0.01$ m, the upper limit of the time step is

$$\Delta t \leq \frac{1}{2}\frac{\Delta x^2}{\alpha} = \frac{(0.01\,\text{m})^2}{2(0.45 \times 10^{-6}\,\text{m}^2/\text{s})} = 111\,\text{s} = 1.85\,\text{min}$$

The boundary nodes involving convection and/or radiation are more restrictive than the interior nodes and thus require smaller time steps. Therefore, the most restrictive boundary node should be used in the determination of the maximum allowable time step Δt when a transient problem is solved with

the explicit method. For example, the explicit finite difference formulation for the convection boundary condition at the left boundary (node 0) of the plane wall shown in Fig. 5–41 expressed by Eq. 5–51 is more restrictive than the explicit finite difference formulation for the interior nodes presented by Eq. 5–47. Therefore, in this case the stability criterion for all nodes becomes

$$1 - 2\tau - 2\tau\frac{h\Delta x}{k} \geq 0 \quad \text{or} \quad \tau \leq \frac{1}{2(1 + h\Delta x/k)}$$

To gain a better understanding of the stability criterion, consider the explicit finite difference formulation for an interior node of a plane wall (Eq. 5–47) for the case of no heat generation,

$$T_m^{i+1} = \tau(T_{m-1}^i + T_{m+1}^i) + (1 - 2\tau)T_m^i$$

Assume that at some time step i the temperatures T_{m-1}^i and T_{m+1}^i are equal but less than T_m^i (say, $T_{m-1}^i = T_{m+1}^i = 50°C$ and $T_m^i = 80°C$). At the next time step, we expect the temperature of node m to be between the two values (say, 70°C). However, if the value of τ exceeds 0.5 (say, $\tau = 1$), the temperature of node m at the next time step will be less than the temperature of the neighboring nodes (it will be 20°C), which is physically impossible and violates the second law of thermodynamics (Fig. 5–43). Requiring the new temperature of node m to remain above the temperature of the neighboring nodes is equivalent to requiring the value of τ to remain below 0.5.

The implicit method is *unconditionally stable,* and thus we can use any time step we please with that method (of course, the smaller the time step, the better the accuracy of the solution). The disadvantage of the implicit method is that it results in a set of equations that must be solved *simultaneously* for each time step. Both methods are used in practice.
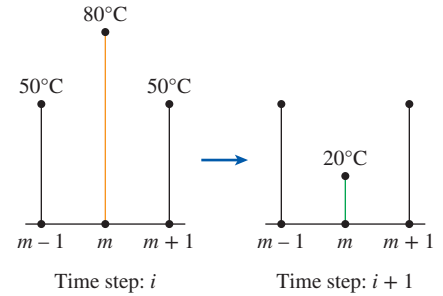
FIGURE 5–43

The violation of the stability criterion in the explicit method may result in the violation of the second law of thermodynamics and thus divergence of solution.

EXAMPLE 5–5   **Transient Heat Conduction in a Large Uranium Plate**

Consider a large uranium plate of thickness $L = 4$ cm, thermal conductivity $k = 28$ W/m·K, and thermal diffusivity $\alpha = 12.5 \times 10^{-6}$ m^2/s that is initially at a uniform temperature of 200°C. Heat is generated uniformly in the plate at a constant rate of $\dot{e} = 5 \times 10^6$ W/m^3. At time $t = 0$, one side of the plate is brought into contact with iced water and is maintained at 0°C at all times, while the other side is subjected to convection to an environment at $T_\infty = 30°C$ with a heat transfer coefficient of $h = 45$ W/m^2·K, as shown in Fig. 5–44. Considering a total of three equally spaced nodes in the medium, two at the boundaries and one at the middle, estimate the exposed surface temperature of the plate 2.5 min after the start of cooling using (*a*) the explicit method and (*b*) the implicit method.

SOLUTION   We have solved this problem in Example 5–1 for the steady case, and here we repeat it for the transient case to demonstrate the application of the transient finite difference methods. Again we assume one-dimensional heat transfer in rectangular coordinates and constant thermal conductivity. The number of nodes is
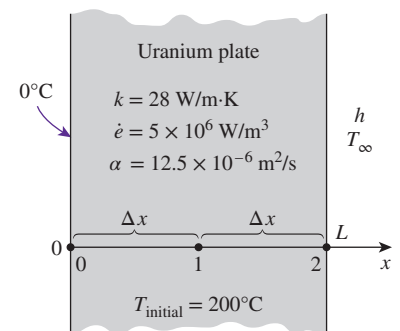
FIGURE 5–44
Schematic for Example 5–5.
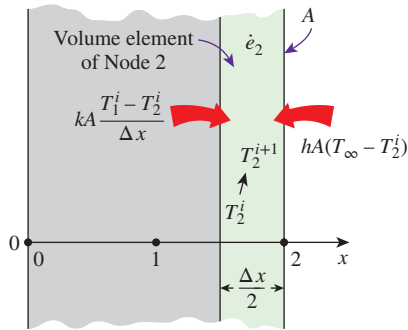
FIGURE 5–45
Schematic for the explicit finite difference formulation of the convection condition at the right boundary of a plane wall.

specified to be $M = 3$, and they are chosen to be at the two surfaces of the plate and at the middle, as shown in the figure. Then the nodal spacing Δx becomes

$$\Delta x = \frac{L}{M-1} = \frac{0.04 \text{ m}}{3-1} = 0.02 \text{ m}$$

We number the nodes as 0, 1, and 2. The temperature at node 0 is given to be $T_0 = 0°\text{C}$ at all times, and the temperatures at nodes 1 and 2 are to be determined. This problem involves only two unknown nodal temperatures, and thus we need to have only two equations to determine them uniquely. These equations are obtained by applying the finite difference method to nodes 1 and 2.

(*a*) Node 1 is an interior node, and the *explicit* finite difference formulation at that node is obtained directly from Eq. 5–47 by setting $m = 1$:

$$T_1^{i+1} = \tau(T_0 + T_2^i) + (1 - 2\tau)T_1^i + \tau\frac{\dot{e}_1 \Delta x^2}{k} \qquad (a)$$

Node 2 is a boundary node subjected to convection, and the finite difference formulation at that node is obtained by writing an energy balance on the volume element of thickness $\Delta x/2$ at that boundary by assuming heat transfer to be into the medium at all sides (Fig. 5–45):

$$hA(T_\infty - T_2^i) + kA\frac{T_1^i - T_2^i}{\Delta x} + \dot{e}_2 A\frac{\Delta x}{2} = \rho A\frac{\Delta x}{2}c_p\frac{T_2^{i+1} - T_2^i}{\Delta t}$$

Dividing by $kA/2\Delta x$ and using the definitions of thermal diffusivity $\alpha = k/\rho c_p$ and the dimensionless mesh Fourier number $\tau = \alpha \Delta t/\Delta x^2$ gives

$$\frac{2h\Delta x}{k}(T_\infty - T_2^i) + 2(T_1^i - T_2^i) + \frac{\dot{e}_2 \Delta x^2}{k} = \frac{T_2^{i+1} - T_2^i}{\tau}$$

which can be solved for T_2^{i+1} to give

$$T_2^{i+1} = \left(1 - 2\tau - 2\tau\frac{h\Delta x}{k}\right)T_2^i + \tau\left(2T_1^i + 2\frac{h\Delta x}{k}T_\infty + \frac{\dot{e}_2 \Delta x^2}{k}\right) \qquad (b)$$

Note that we did not use the superscript i for quantities that do not change with time. Next we need to determine the upper limit of the time step Δt from the stability criterion, which requires the coefficient of T_1^i in Eq. (*a*) and the coefficient of T_2^i in the second equation to be greater than or equal to zero. The coefficient of T_2^i is smaller in this case, and thus the stability criterion for this problem can be expressed as

$$1 - 2\tau - 2\tau\frac{h\Delta x}{k} \geq 0 \rightarrow \tau \leq \frac{1}{2(1 + h\Delta x/k)} \rightarrow \Delta t \leq \frac{\Delta x^2}{2\alpha(1 + h\Delta x/k)}$$

since $\tau = \alpha \Delta t/\Delta x^2$. Substituting the given quantities, the maximum allowable value of the time step is determined to be

$$\Delta t \leq \frac{(0.02 \text{ m})^2}{2(12.5 \times 10^{-6} \text{ m}^2/\text{s})[1 + (45 \text{ W/m}^2\cdot\text{K})(0.02 \text{ m})/28 \text{ W/m}\cdot\text{K}]} = 15.5 \text{ s}$$

Therefore, any time step less than 15.5 s can be used to solve this problem. For convenience, let us choose the time step to be $\Delta t = 15$ s. Then the mesh Fourier number becomes

$$\tau = \frac{\alpha \Delta t}{\Delta x^2} = \frac{(12.5 \times 10^{-6} \text{ m}^2/\text{s})(15 \text{ s})}{(0.02 \text{ m})^2} = 0.46875 \quad \text{(for } \Delta t = 15 \text{ s)}$$

Substituting this value of τ and other quantities, the explicit finite difference Eqs. (*a*) and (*b*) reduce to

$$T_1^{i+1} = 0.0625 T_1^i + 0.46875 T_2^i + 33.482$$
$$T_2^{i+1} = 0.9375 T_1^i + 0.032366 T_2^i + 34.386$$

The initial temperature of the medium at $t = 0$ and $i = 0$ is given to be $200°C$ throughout, and thus $T_1^0 = T_2^0 = 200°C$. Then the nodal temperatures at T_1^1 and T_2^1 at $t = \Delta t = 15$ s are determined from these equations to be

$$T_1^1 = 0.0625 T_1^0 + 0.46875 T_2^0 + 33.482$$
$$= 0.0625 \times 200 + 0.46875 \times 200 + 33.482 = 139.7°C$$
$$T_2^1 = 0.9375 T_1^0 + 0.032366 T_2^0 + 34.386$$
$$= 0.9375 \times 200 + 0.032366 \times 200 + 34.386 = 228.4°C$$

Similarly, the nodal temperatures T_1^2 and T_2^2 at $t = 2\Delta t = 2 \times 15 = 30$ s are

$$T_1^2 = 0.0625 T_1^1 + 0.46875 T_2^1 + 33.482$$
$$= 0.0625 \times 139.7 + 0.46875 \times 228.4 + 33.482 = 149.3°C$$
$$T_2^2 = 0.9375 T_1^1 + 0.032366 T_2^1 + 34.386$$
$$= 0.9375 \times 139.7 + 0.032366 \times 228.4 + 34.386 = 172.8°C$$

Continuing in the same manner, the temperatures at nodes 1 and 2 are determined for $i = 1, 2, 3, 4, 5, \ldots, 40$ and are given in Table 5–3. Therefore, the temperature at the exposed boundary surface 2.5 min after the start of cooling is

$$T_L^{2.5 \text{ min}} = T_2^{10} = \mathbf{139.0°C}$$

(*b*) Node 1 is an interior node, and the *implicit* finite difference formulation at that node is obtained directly from Eq. 5–49 by setting $m = 1$:

$$\tau T_0 - (1 + 2\tau) T_1^{i+1} + \tau T_2^{i+1} + \tau \frac{\dot{e}_0 \Delta x^2}{k} + T_1^i = 0 \quad \text{(c)}$$

Node 2 is a boundary node subjected to convection, and the implicit finite difference formulation at that node can be obtained from this formulation by expressing the left side of the equation at time step $i + 1$ instead of i as

$$\frac{2h\Delta x}{k}(T_\infty - T_2^{i+1}) + 2(T_1^{i+1} - T_2^{i+1}) + \frac{\dot{e}_2 \Delta x^2}{k} = \frac{T_2^{i+1} - T_2^i}{\tau}$$

TABLE 5–3

The variation of the nodal temperatures in Example 5–5 with time obtained by the *explicit* method

Time Step, i	Time, s	Node Temperature, °C T_1^i	T_2^i
0	0	200.0	200.0
1	15	139.7	228.4
2	30	149.3	172.8
3	45	123.8	179.9
4	60	125.6	156.3
5	75	114.6	157.1
6	90	114.3	146.9
7	105	109.5	146.3
8	120	108.9	141.8
9	135	106.7	141.1
10	150	106.3	139.0
20	300	103.8	136.1
30	450	103.7	136.0
40	600	103.7	136.0

which can be rearranged as

$$2\tau T_1^{i+1} - \left(1 + 2\tau + 2\tau\frac{h\Delta x}{k}\right)T_2^{i+1} + 2\tau\frac{h\Delta x}{k}T_\infty + \tau\frac{\dot{e}_2\Delta x^2}{k} + T_2^i = 0 \qquad \textbf{(d)}$$

Again we did not use the superscript i or $i+1$ for quantities that do not change with time. The implicit method imposes no limit on the time step, and thus we can choose any value we want. However, we again choose $\Delta t = 15$ s, and thus $\tau = 0.46875$, to make a comparison with part (a) possible. Substituting this value of τ and other given quantities, the two implicit finite difference equations developed here reduce to

$$-1.9375T_1^{i+1} + 0.46875T_2^{i+1} + T_1^i + 33.482 = 0$$

$$0.9375T_1^{i+1} - 1.9676T_2^{i+1} + T_2^i + 34.386 = 0$$

Again $T_1^0 = T_2^0 = 200°C$ at $t = 0$ and $i = 0$ because of the initial condition, and for $i = 0$, these two equations reduce to

$$-1.9375T_1^1 + 0.46875T_2^1 + 200 + 33.482 = 0$$

$$0.9375T_1^1 - 1.9676T_2^1 + 200 + 34.386 = 0$$

The unknown nodal temperatures T_1^1 and T_2^1 at $t = \Delta t = 15$ s are determined by solving these two equations simultaneously to be

$$T_1^1 = 168.8°C \quad \text{and} \quad T_2^1 = 199.6°C$$

Similarly, for $i = 1$, these equations reduce to

$$-1.9375T_2^1 + 0.46875T_2^2 + 168.8 + 33.482 = 0$$

$$0.9375T_1^2 - 1.9676T_2^2 + 199.6 + 34.386 = 0$$

The unknown nodal temperatures T_1^2 and T_2^2 at $t = \Delta t = 2 \times 15 = 30$ s are determined by solving these two equations simultaneously to be

$$T_1^2 = 150.5°C \quad \text{and} \quad T_2^2 = 190.6°C \, T_1^2$$

Continuing in this manner, the temperatures at nodes 1 and 2 are determined for $i = 2, 3, 4, 5, \ldots, 40$ and are listed in Table 5–4, and the temperature at the exposed boundary surface (node 2) 2.5 min after the start of cooling is obtained to be

$$T_L^{2.5\,\text{min}} = T_2^{10} = \textbf{143.9°C}$$

which is close to the result obtained by the explicit method. Note that either method could be used to obtain satisfactory results to transient problems, except, perhaps, for the first few time steps. The implicit method is preferred when it is desirable to use large time steps, and the explicit method is preferred when one wishes to avoid the simultaneous solution of a system of algebraic equations.

TABLE 5−4

The variation of the nodal temperatures in Example 5–5 with time obtained by the *implicit* method

Time Step, i	Time, s	Node Temperature, °C	
		T_1^i	T_2^i
0	0	200.0	200.0
1	15	168.8	199.6
2	30	150.5	190.6
3	45	138.6	180.4
4	60	130.3	171.2
5	75	124.1	163.6
6	90	119.5	157.6
7	105	115.9	152.8
8	120	113.2	149.0
9	135	111.0	146.1
10	150	109.4	143.9
20	300	104.2	136.7
30	450	103.8	136.1
40	600	103.8	136.1

EXAMPLE 5–6   Solar Energy Storage in Trombe Walls

Dark-painted thick masonry walls called Trombe walls are commonly used on south sides of passive solar homes to absorb solar energy, store it during the day, and release it to the house during the night (Fig. 5–46). The idea was proposed by E. L. Morse of Massachusetts in 1881 and is named after Professor Felix Trombe of France, who used it extensively in his designs in the 1970s. Usually a single or double layer of glazing is placed outside the wall; it transmits most of the solar energy while blocking heat losses from the exposed surface of the wall to the outside. Also, air vents are commonly installed at the bottom and top of the Trombe walls so that the house air enters the parallel flow channel between the Trombe wall and the glazing, rises as it is heated, and enters the room through the top vent.

Consider a house in Reno, Nevada, whose south wall consists of a 1-ft-thick Trombe wall whose thermal conductivity is $k = 0.40$ Btu/h·ft·°F and whose thermal diffusivity is $\alpha = 4.78 \times 10^{-6}$ ft^2/s. The variation of the ambient temperature T_{out} and the solar heat flux $\dot{q}_{\text{solar}}$ incident on a south-facing vertical surface throughout the day for a typical day in January is given in Table 5–5 in 3-h intervals. The Trombe wall has single glazing with an absorptivity-transmissivity product of $\kappa = 0.77$ (that is, 77 percent of the solar energy incident is absorbed by the exposed surface of the Trombe wall), and the average combined heat transfer coefficient for heat loss from the Trombe wall to the ambient is determined to be $h_{\text{out}} = 0.7$ Btu/h·ft^2·°F. The interior of the house is maintained at $T_{\text{in}} = 70$°F at all times, and the heat transfer coefficient at the interior surface of the Trombe wall is $h_{\text{in}} = 1.8$ Btu/h·ft^2·°F. Also, the vents on the Trombe wall are kept closed, and thus the only heat transfer between the air in the house and the Trombe wall is through the interior surface of the wall. Assuming the temperature of the Trombe wall varies linearly between 70°F at the interior surface and 30°F at the exterior surface at 7 a.m. and using the explicit finite difference method with a uniform nodal spacing of $\Delta x = 0.2$ ft, determine the temperature distribution along the thickness of the Trombe wall after 12, 24, 36, and 48 h. Also, determine the net amount of heat transferred to the house from the Trombe wall during the first day and the second day. Assume the wall is 10 ft high and 25 ft long.

SOLUTION   The passive solar heating of a house through a Trombe wall is considered. The temperature distribution in the wall in 12-h intervals and the amount of heat transfer during the first and second days are to be determined.

Assumptions   **1** Heat transfer is one-dimensional since the exposed surface of the wall is large relative to its thickness. **2** Thermal conductivity is constant. **3** The heat transfer coefficients are constant.

Properties   The wall properties are given to be $k = 0.40$ Btu/h·ft·°F, $\alpha = 4.78 \times 10^{-6}$ ft^2/s, and $\kappa = 0.77$.

Analysis   The nodal spacing is given to be $\Delta x = 0.2$ ft, and thus the total number of nodes along the Trombe wall is

$$M = \frac{L}{\Delta x} + 1 = \frac{1 \text{ ft}}{0.2 \text{ ft}} + 1 = 6$$

We number the nodes as 0, 1, 2, 3, 4, and 5, with node 0 on the interior surface of the Trombe wall and node 5 on the exterior surface, as shown in Fig. 5–47. Nodes 1 through 4 are interior nodes, and the explicit finite difference formulations of these nodes are obtained directly from Eq. 5–47 to be
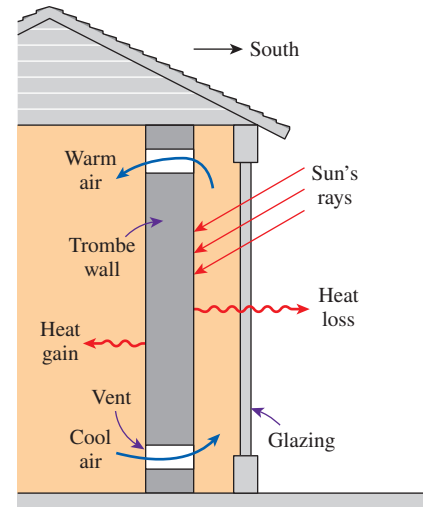
FIGURE 5–46
Schematic of a Trombe wall
(Example 5–6).

TABLE 5–5

The hourly variation of monthly average ambient temperature and solar heat flux incident on a vertical surface for January in Reno, Nevada

Time of Day	Ambient Temperature, °F	Solar Radiation, Btu/h·ft^2
7 a.m.–10 a.m.	33	114
10 a.m.–1 p.m.	43	242
1 p.m.–4 p.m.	45	178
4 p.m.–7 p.m.	37	0
7 p.m.–10 p.m.	32	0
10 p.m.–1 a.m.	27	0
1 a.m.–4 a.m.	26	0
4 a.m.–7 a.m.	25	0
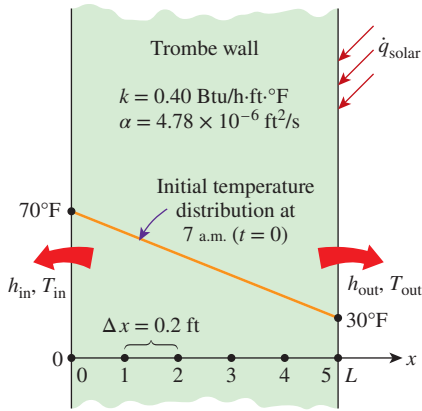
FIGURE 5–47
The nodal network for the Trombe wall discussed in Example 5–6.

Node 1 $(m = 1)$: $\quad T_1^{i+1} = \tau(T_0^i + T_2^i) + (1 - 2\tau)T_1^i$ **(1)**

Node 2 $(m = 2)$: $\quad T_2^{i+1} = \tau(T_1^i + T_3^i) + (1 - 2\tau)T_2^i$ **(2)**

Node 3 $(m = 3)$: $\quad T_3^{i+1} = \tau(T_2^i + T_4^i) + (1 - 2\tau)T_3^i$ **(3)**

Node 4 $(m = 4)$: $\quad T_4^{i+1} = \tau(T_3^i + T_5^i) + (1 - 2\tau)T_4^i$ **(4)**

The interior surface is subjected to convection, and thus the explicit formulation of node 0 can be obtained directly from Eq. 5–51 to be

$$T_0^{i+1} = \left(1 - 2\tau - 2\tau\frac{h_{in}\Delta x}{k}\right)T_0^i + 2\tau T_1^i + 2\tau\frac{h_{in}\Delta x}{k}T_{in}$$

Substituting the quantities h_{in}, Δx, k, and T_{in}, which do not change with time, into this equation gives

$$T_0^{i+1} = (1 - 3.80\tau)T_0^i + \tau(2T_1^i + 126.0) \tag{5}$$

The exterior surface of the Trombe wall is subjected to convection as well as to heat flux. The explicit finite difference formulation at that boundary is obtained by writing an energy balance on the volume element represented by node 5,

$$h_{out}A(T_{out}^i - T_5^i) + \kappa A\dot{q}_{solar}^i + kA\frac{T_4^i - T_5^i}{\Delta x} = \rho A\frac{\Delta x}{2}c_p\frac{T_5^{i+1} - T_5^i}{\Delta t} \tag{5-53}$$

which simplifies to

$$T_5^{i+1} = \left(1 - 2\tau - 2\tau\frac{h_{out}\Delta x}{k}\right)T_5^i + 2\tau T_4^i + 2\tau\frac{h_{out}\Delta x}{k}T_{out}^i + 2\tau\frac{\kappa\dot{q}_{solar}^i\Delta x}{k} \tag{5-54}$$

where $\tau = \alpha\Delta t/\Delta x^2$ is the dimensionless mesh Fourier number. Note that we kept the superscript i for quantities that vary with time. Substituting the quantities h_{out}, Δx, k, and κ, which do not change with time, into this equation gives

$$T_5^{i+1} = (1 - 2.70\tau)T_5^i + \tau(2T_4^i + 0.70T_{out}^i + 0.770\dot{q}_{solar}^i) \tag{6}$$

where the unit of $\dot{q}_{solar}^i$ is Btu/h·ft².

Next we need to determine the upper limit of the time step Δt from the stability criterion since we are using the explicit method. This requires the identification of the smallest primary coefficient in the system. We know that the boundary nodes are more restrictive than the interior nodes, and thus we examine the formulations of the boundary nodes 0 and 5 only. The smallest and thus the most restrictive primary coefficient in this case is the coefficient of T_0^i in the formulation of node 0 since $1 - 3.8\tau < 1 - 2.7\tau$, and thus the stability criterion for this problem can be expressed as

$$1 - 3.80\,\tau \geq 0 \rightarrow \tau = \frac{\alpha\Delta x}{\Delta x^2} \leq \frac{1}{3.80}$$

Substituting the given quantities, the maximum allowable value of the time step is determined to be

$$\Delta t \leq \frac{\Delta x^2}{3.80\alpha} = \frac{(0.2\ \text{ft})^2}{3.80 \times (4.78 \times 10^{-6}\ \text{ft}^2/\text{s})} = 2202\ \text{s}$$

Therefore, any time step less than 2202 s can be used to solve this problem. For convenience, let us choose the time step to be $\Delta t = 900$ s $= 15$ min. Then the mesh Fourier number becomes

$$\tau = \frac{\alpha \Delta t}{\Delta x^2} = \frac{(4.78 \times 10^{-6}\,\text{ft}^2/\text{s})(900\,\text{s})}{(0.2\,\text{ft})^2} = 0.10755 \quad \text{(for } \Delta t = 15\ \text{min)}$$

Initially (at 7 a.m. or $t = 0$), the temperature of the wall is said to vary linearly between 70°F at node 0 and 30°F at node 5. Noting that there are five nodal spacings of equal length, the temperature change between two neighboring nodes is $(70 - 30)°\text{F}/5 = 8°\text{F}$. Therefore, the initial nodal temperatures are

$$T_0^0 = 70°\text{F}, \quad T_1^0 = 62°\text{F}, \quad T_2^0 = 54°\text{F},$$
$$T_3^0 = 46°\text{F}, \quad T_4^0 = 38°\text{F}, \quad T_5^0 = 30°\text{F}$$

Then the nodal temperatures at $t = \Delta t = 15$ min (at 7:15 a.m.) are determined from these equations to be

$$T_0^1 = (1 - 3.80\tau)\,T_0^0 + \tau(2T_1^0 + 126.0)$$
$$\quad = (1 - 3.80 \times 0.10755)\,70 + 0.10755(2 \times 62 + 126.0) = 68.3°\text{F}$$
$$T_1^1 = \tau(T_0^0 + T_2^0) + (1 - 2\tau)T_1^0$$
$$\quad = 0.10755(70 + 54) + (1 - 2 \times 0.10755)62 = 62°\text{F}$$
$$T_2^1 = \tau(T_1^0 + T_3^0) + (1 - 2\tau)T_2^0$$
$$\quad = 0.10755(62 + 46) + (1 - 2 \times 0.10755)54 = 54°\text{F}$$
$$T_3^1 = \tau(T_2^0 + T_4^0) + (1 - 2\tau)T_3^0$$
$$\quad = 0.10755(54 + 38) + (1 - 2 \times 0.10755)46 = 46°\text{F}$$
$$T_4^1 = \tau(T_3^0 + T_5^0) + (1 - 2\tau)T_4^0$$
$$\quad = 0.10755(46 + 30) + (1 - 2 \times 0.10755)38 = 38°\text{F}$$
$$T_5^1 = (1 - 2.70\tau)\,T_5^0 + \tau(2T_4^0 + 0.70\,T_{\text{out}}^0 + 0.770\,\dot{q}_{\text{solar}}^0)$$
$$\quad = (1 - 2.70 \times 0.10755)\,30 + 0.10755(2 \times 38 + 0.70 \times 33 + 0.770 \times 114)$$
$$\quad = 41.4°\text{F}$$

Note that the inner surface temperature of the Trombe wall dropped by 1.7°F and the outer surface temperature rose by 11.4°F during the first time step, while the temperatures at the interior nodes remained the same. This is typical of transient problems in media that involve no heat generation. The nodal temperatures at the following time steps are determined similarly with the help of a computer. Note that the data for ambient temperature and the incident solar radiation change every 3 h, which corresponds to 12 time steps, and this must be reflected in the computer program. For example, the value of $\dot{q}_{\text{solar}}^i$ must be taken to be $\dot{q}_{\text{solar}}^i = 114$ for $i = 1 - 12$, $\dot{q}_{\text{solar}}^i = 242$ for $i = 13 - 24$, $\dot{q}_{\text{solar}}^i = 178$ for $i = 25 - 36$, and $\dot{q}_{\text{solar}}^i = 0$ for $i = 37 - 96$.

The results after 6, 12, 18, 24, 30, 36, 42, and 48 h are given in Table 5–6 and are plotted in Fig. 5–48 for the first day. Note that the interior temperature of the Trombe wall drops in early morning hours but then rises as the solar energy absorbed by the exterior surface diffuses through the wall. The exterior surface temperature of the Trombe wall rises from 30 to 142°F in just 6 h because of the solar energy absorbed, but it then drops to 53°F by next morning as a result of heat loss at night. Therefore, it may be worthwhile to cover the outer surface at night to minimize the heat losses.
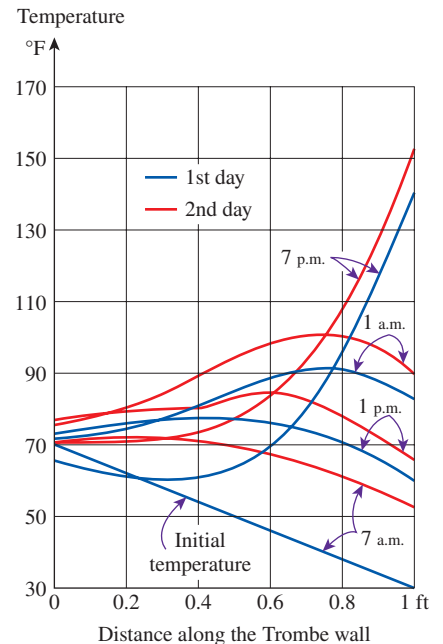
FIGURE 5–48

The variation of temperatures in the Trombe wall discussed in Example 5–6.

TABLE 5–6

The temperatures at the nodes of a Trombe wall at various times

Time	Time Step, i	Nodal Temperatures, °F					
		T_0	T_1	T_2	T_3	T_4	T_5
0 h (7 a.m.)	0	70.0	62.0	54.0	46.0	38.0	30.0
6 h (1 a.m.)	24	65.3	61.7	61.5	69.7	94.1	142.0
12 h (7 a.m.)	48	71.6	74.2	80.4	88.4	91.7	82.4
18 h (1 a.m.)	72	73.3	75.9	77.4	76.3	71.2	61.2
24 h (7 a.m.)	96	71.2	71.9	70.9	67.7	61.7	53.0
30 h (1 a.m.)	120	70.3	71.1	74.3	84.2	108.3	153.2
36 h (7 a.m.)	144	75.4	81.1	89.4	98.2	101.0	89.7
42 h (1 a.m.)	168	75.8	80.7	83.5	83.0	77.4	66.2
48 h (7 a.m.)	192	73.0	75.1	72.2	66.0	66.0	56.3

The rate of heat transfer from the Trombe wall to the interior of the house during each time step is determined from Newton's law using the average temperature at the inner surface of the wall (node 0) as

$$Q_{\text{Trombe wall}}^i = \dot{Q}_{\text{Trombe wall}}^i \, \Delta t = h_{\text{in}} A (T_0^i - T_{\text{in}}) \, \Delta t = h_{\text{in}} A [(T_0^i + T_0^{i-1})/2 - T_{\text{in}}] \Delta t$$

Therefore, the amount of heat transfer during the first time step ($i = 1$) or during the first 15-min period is

$$\begin{aligned} Q_{\text{Trombe wall}}^1 &= h_{\text{in}} A [(T_0^1 + T_0^0)/2 - T_{\text{in}}] \Delta t \\ &= (1.8 \text{ Btu/h·ft}^2\text{·°F})(10 \times 25 \text{ ft}^2)[(68.3 + 70)/2 - 70\text{°F}](0.25 \text{ h}) \\ &= -95.6 \text{ Btu} \end{aligned}$$

The negative sign indicates that heat is transferred to the Trombe wall from the air in the house, which represents a heat loss. Then the total heat transfer during a specified time period is determined by adding the heat transfer amounts for each time step as

$$Q_{\text{Trombe wall}} = \sum_{i=1}^{I} Q_{\text{Trombe wall}}^i = \sum_{i=1}^{I} h_{\text{in}} A [(T_0^i + T_0^{i-1})/2 - T_{\text{in}}] \Delta t \tag{5–55}$$

where I is the total number of time intervals in the specified time period. In this case $I = 48$ for 12 h, 96 for 24 h, and so on. Following the approach described here using a computer, the amount of heat transfer between the Trombe wall and the interior of the house is determined to be

$$Q_{\text{Trombe wall}} = -17{,}048 \text{ Btu after 12 h} \quad \text{(17,048 Btu loss during the first 12 h)}$$
$$Q_{\text{Trombe wall}} = -2483 \text{ Btu after 24 h} \quad \text{(14,565 Btu gain during the second 12 h)}$$
$$Q_{\text{Trombe wall}} = 5610 \text{ Btu after 36 h} \quad \text{(8093 Btu gain during the third 12 h)}$$
$$Q_{\text{Trombe wall}} = 34{,}400 \text{ Btu after 48 h} \quad \text{(28,790 Btu gain during the fourth 12 h)}$$

Therefore, the house loses 2483 Btu through the Trombe wall the first day as a result of the low start-up temperature but delivers a total of 36,883 Btu of heat to the house the second day. It can be shown that the Trombe wall will deliver even more heat to the house during the third day since it will start the day at a higher average temperature.

Two-Dimensional Transient Heat Conduction

Consider a rectangular region in which heat conduction is significant in the x- and y-directions, and consider a unit depth of $\Delta z = 1$ in the z-direction. Heat may be generated in the medium at a rate of $\dot{e}(x, y, t)$, which may vary with time and position, with the thermal conductivity k of the medium assumed to be constant. Now divide the x-y plane of the region into a *rectangular mesh* of nodal points spaced Δx and Δy apart in the x- and y-directions, respectively, and consider a general interior node (m, n) whose coordinates are $x = m\Delta x$ and $y = n\Delta y$, as shown in Fig. 5–49. Noting that the volume element centered about the general interior node (m, n) involves heat conduction from four sides (right, left, top, and bottom) and the volume of the element is $V_{\text{element}} = \Delta x \times \Delta y \times 1 = \Delta x \Delta y$, the transient finite difference formulation for a general interior node can be expressed on the basis of Eq. 5–39 as

$$k\Delta y \frac{T_{m-1, n} - T_{m, n}}{\Delta x} + k\Delta x \frac{T_{m, n+1} - T_{m, n}}{\Delta y} + k\Delta y \frac{T_{m+1, n} - T_{m, n}}{\Delta x}$$

$$+ k\Delta x \frac{T_{m, n-1} - T_{m, n}}{\Delta y} + \dot{e}_{m, n} \Delta x \Delta y = \rho \Delta x \Delta y \, c_p \frac{T_m^{i+1} - T_m^i}{\Delta t} \quad \textbf{(5–56)}$$

Taking a square mesh ($\Delta x = \Delta y = l$) and dividing each term by k gives, after simplifying,

$$T_{m-1, n} + T_{m+1, n} + T_{m, n+1} + T_{m, n-1} - 4T_{m, n} + \frac{\dot{e}_{m, n} l^2}{k} = \frac{T_m^{i+1} - T_m^i}{\tau} \quad \textbf{(5–57)}$$

where again $\alpha = k/\rho c_p$ is the thermal diffusivity of the material and $\tau = \alpha \Delta t/l^2$ is the dimensionless mesh Fourier number. It can also be expressed in terms of the temperatures at the neighboring nodes in the following easy-to-remember form:

$$T_{\text{left}} + T_{\text{top}} + T_{\text{right}} + T_{\text{bottom}} - 4T_{\text{node}} + \frac{\dot{e}_{\text{node}} l^2}{k} = \frac{T_{\text{node}}^{i+1} - T_{\text{node}}^i}{\tau} \quad \textbf{(5–58)}$$

Again the left side of this equation is simply the finite difference formulation of the problem for the *steady case,* as expected. Also, we are still not committed to explicit or implicit formulation since we did not indicate the time step on the left side of the equation. We now obtain the *explicit* finite difference formulation by expressing the left side at time step i as

$$T_{\text{left}}^i + T_{\text{top}}^i + T_{\text{right}}^i + T_{\text{bottom}}^i - 4T_{\text{node}}^i + \frac{\dot{e}_{\text{node}}^i l^2}{k} = \frac{T_{\text{node}}^{i+1} - T_{\text{node}}^i}{\tau} \quad \textbf{(5–59)}$$

Expressing the left side at time step $i + 1$ instead of i would give the implicit formulation. Equation 5–59 can be solved *explicitly* for the new temperature T_{node}^{i+1} to give

$$T_{\text{node}}^{i+1} = \tau(T_{\text{left}}^i + T_{\text{top}}^i + T_{\text{right}}^i + T_{\text{bottom}}^i) + (1 - 4\tau)T_{\text{node}}^i + \tau \frac{\dot{e}_{\text{node}}^i l^2}{k} \quad \textbf{(5–60)}$$

for all interior nodes (m, n) where $m = 1, 2, 3, \ldots, M - 1$ and $n = 1, 2, 3, \ldots, N - 1$ in the medium. In the case of no heat generation and $\tau = 1/4$, which is the upper limit of the stability criterion for the two-dimensional explicit
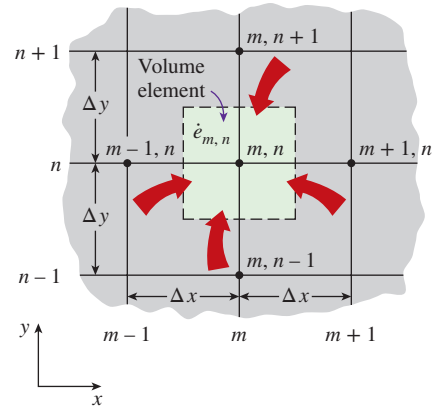
FIGURE 5–49
The volume element of a general interior node (m, n) for two-dimensional transient conduction in rectangular coordinates.

Time step *i*:
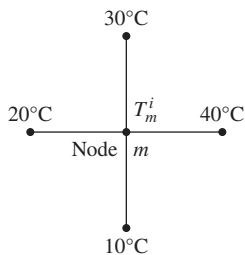
Time step *i* + 1:
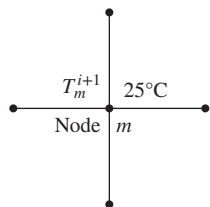
FIGURE 5–50

In the case of no heat generation and $\tau = \frac{1}{4}$, the temperature of an interior node at the new time step is the average of the temperatures of its neighboring nodes at the previous time step.

method (see Eq. 5–61), the explicit finite difference formulation for a general interior node reduces to $T_{node}^{i+1} = (T_{left}^i + T_{top}^i + T_{right}^i + T_{bottom}^i)/4$, which has the interpretation that *the temperature of an interior* node *at the new time step is simply the average of the temperatures of its neighboring node*s *at the previous time step* (Fig. 5–50).

The stability criterion that requires the coefficient of T_m^i in the T_m^{i+1} expression to be greater than or equal to zero for all nodes is equally valid for two- or three-dimensional cases and severely limits the size of the time step Δt that can be used with the explicit method. In the case of transient two-dimensional heat transfer in rectangular coordinates, the coefficient of T_m^i in the T_m^{i+1} expression is $1 - 4\tau$, and thus the stability criterion for all interior nodes in this case is $1 - 4\tau > 0$, or

$$\tau = \frac{\alpha\Delta t}{l^2} \leq \frac{1}{4} \quad \text{(interior nodes, two-dimensional heat transfer in rectangular coordinates)} \tag{5–61}$$

where $\Delta x = \Delta y = l$. When the material of the medium and thus its thermal diffusivity α are known and the value of the mesh size l is specified, the largest allowable value of the time step Δt can be determined from the relation above. Again the boundary nodes involving convection and/or radiation are more restrictive than the interior nodes and thus require smaller time steps. Therefore, the most restrictive boundary node should be used in the determination of the maximum allowable time step Δt when a transient problem is solved with the explicit method.

The application of Eq. 5–60 to each of the $(M - 1) \times (N - 1)$ interior nodes gives $(M - 1) \times (N - 1)$ equations. The remaining equations are obtained by applying the method to the boundary nodes unless, of course, the boundary temperatures are specified as being constant. The development of the transient finite difference formulation of boundary nodes in two- (or three-) dimensional problems is similar to the development in the one-dimensional case discussed earlier. Again the region is partitioned between the nodes by forming volume elements around the nodes, and an energy balance is written for each boundary node on the basis of Eq. 5–39. This is illustrated in Example 5–7.
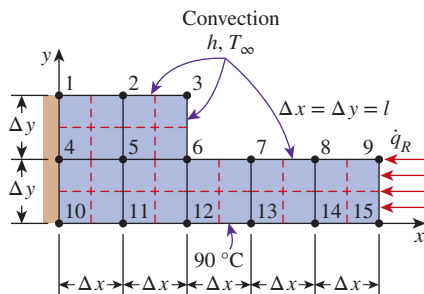
FIGURE 5–51
Schematic and nodal network for Example 5–7.

EXAMPLE 5–7 **Transient Two-Dimensional Heat Conduction in L-Bars**

Consider two-dimensional transient heat transfer in an L-shaped solid body that is initially at a uniform temperature of 90°C and whose cross section is given in Fig. 5–51. The thermal conductivity and diffusivity of the body are $k = 15$ W/m·K and $\alpha = 3.2 \times 10^{-6}$ m²/s, respectively, and heat is generated in the body at a rate of $\dot{e} = 2 \times 10^6$ W/m³. The left surface of the body is insulated, and the bottom surface is maintained at a uniform temperature of 90°C at all times. At time $t = 0$, the entire top surface is subjected to convection to ambient air at $T_\infty = 25$°C with a convection coefficient of $h = 80$ W/m²·K, and the right surface is subjected to heat flux at a uniform rate of $\dot{q}_R = 5000$ W/m². The nodal network of the problem consists of 15 equally spaced nodes with $\Delta x = \Delta y = 1.2$ cm, as shown in the figure. Five of the nodes are at the bottom surface, and thus their temperatures are known. Using the explicit method, determine the temperature at the top corner (node 3) of the body after 1, 3, 5, 10, and 60 min.

SOLUTION This is a transient two-dimensional heat transfer problem in rectangular coordinates, and it was solved in Example 5–3 for the steady case. Therefore, the solution of this transient problem should approach the solution for the steady case when the time is sufficiently large. The thermal conductivity and heat generation rate are given to be constants. We observe that all nodes are boundary nodes except node 5, which is an interior node. Therefore, we have to rely on energy balances to obtain the finite difference equations. The region is partitioned among the nodes equitably as shown in the figure, and the explicit finite difference equations are determined on the basis of the energy balance for the transient case expressed as

$$\sum_{\text{All sides}} \dot{Q}^i + \dot{e} V_{\text{element}} = \rho V_{\text{element}} c_p \frac{T_m^{i+1} - T_m^i}{\Delta t}$$

The quantities h, T_∞, $\dot{e}$, and $\dot{q}_R$ do not change with time, and thus we do not need to use the superscript i for them. Also, the energy balance expressions are simplified using the definitions of thermal diffusivity $\alpha = k/\rho c_p$ and the dimensionless mesh Fourier number $\tau = \alpha \Delta t / l^2$, where $\Delta x = \Delta y = l$.

(*a*) Node 1. (Boundary node subjected to convection and insulation, Fig. 5–52*a*)

$$h\frac{\Delta x}{2}(T_\infty - T_1^i) + k\frac{\Delta y}{2}\frac{T_2^i - T_1^i}{\Delta x} + k\frac{\Delta x}{2}\frac{T_4^i - T_1^i}{\Delta y}$$

$$+ \dot{e}_1\frac{\Delta x}{2}\frac{\Delta y}{2} = \rho\frac{\Delta x}{2}\frac{\Delta y}{2}c_p\frac{T_1^{i+1} - T_1^i}{\Delta t}$$

Dividing by $k/4$ and simplifying,

$$\frac{2hl}{k}(T_\infty - T_1^i) + 2(T_2^i - T_1^i) + 2(T_4^i - T_1^i) + \frac{\dot{e}_1 l^2}{k} = \frac{T_1^{i+1} - T_1^i}{\tau}$$

which can be solved for T_1^{i+1} to give

$$T_1^{i+1} = \left(1 - 4\tau - 2\tau\frac{hl}{k}\right)T_1^i + 2\tau\left(T_2^i + T_4^i + \frac{hl}{k}T_\infty + \frac{\dot{e}_1 l^2}{2k}\right)$$

(*b*) Node 2. (Boundary node subjected to convection, Fig. 5–52*b*)

$$h\Delta x(T_\infty - T_2^i) + k\frac{\Delta y}{2}\frac{T_3^i - T_2^i}{\Delta x} + k\Delta x\frac{T_5^i - T_2^i}{\Delta y}$$

$$+ k\frac{\Delta y}{2}\frac{T_1^i - T_2^i}{\Delta x} + \dot{e}_2\Delta x\frac{\Delta y}{2} = \rho\Delta x\frac{\Delta y}{2}c_p\frac{T_2^{i+1} - T_2^i}{\Delta t}$$

Dividing by $k/2$, simplifying, and solving for T_2^{i+1} gives

$$T_2^{i+1} = \left(1 - 4\tau - 2\tau\frac{hl}{k}\right)T_2^i + \tau\left(T_1^i + T_3^i + 2T_5^i + \frac{2hl}{k}T_\infty + \frac{\dot{e}_2 l^2}{k}\right)$$

(*a*) Node 1   (*b*) Node 2
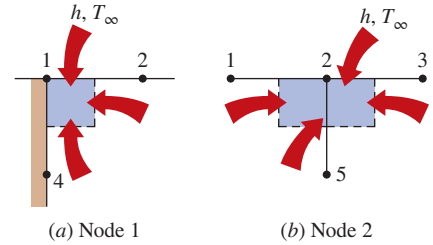
FIGURE 5–52
Schematics for energy balances on the volume elements of nodes 1 and 2.
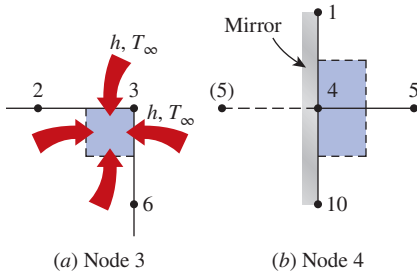
FIGURE 5–53
Schematics for energy balances on the volume elements of nodes 3 and 4.
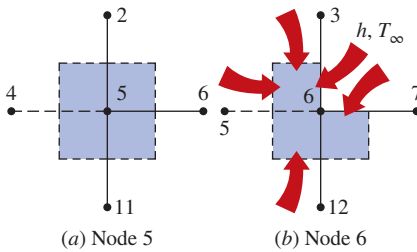
FIGURE 5–54
Schematics for energy balances on the volume elements of nodes 5 and 6.
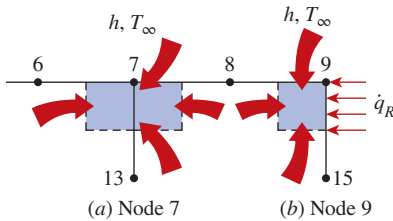
FIGURE 5–55
Schematics for energy balances on the volume elements of nodes 7 and 9.

(*c*) Node 3. (Boundary node subjected to convection on two sides, Fig. 5–53*a*)

$$h\left(\frac{\Delta x}{2} + \frac{\Delta y}{2}\right)(T_\infty - T_3^i) + k\frac{\Delta x}{2}\frac{T_6^i - T_3^i}{\Delta y}$$

$$+ k\frac{\Delta y}{2}\frac{T_2^i - T_3^i}{\Delta x} + \dot{e}_3\frac{\Delta x}{2}\frac{\Delta y}{2} = \rho\frac{\Delta x}{2}\frac{\Delta y}{2}c_p\frac{T_3^{i+1} - T_3^i}{\Delta t}$$

Dividing by $k/4$, simplifying, and solving for T_3^{i+1} gives

$$T_3^{i+1} = \left(1 - 4\tau - 4\tau\frac{hl}{k}\right)T_3^i + 2\tau\left(T_2^i + T_6^i + 2\frac{hl}{k}T_\infty + \frac{\dot{e}_3 l^2}{2k}\right)$$

(*d*) Node 4. (On the insulated boundary, and can be treated as an interior node, Fig. 5–53*b*). Noting that $T_{10} = 90°C$, Eq. 5–60 gives

$$T_4^{i+1} = (1 - 4\tau)T_4^i + \tau\left(T_1^i + 2T_5^i + 90 + \frac{\dot{e}_4 l^2}{k}\right)$$

(*e*) Node 5. (Interior node, Fig. 5–54*a*). Noting that $T_{11} = 90°C$, Eq. 5–60 gives

$$T_5^{i+1} = (1 - 4\tau)T_5^i + \tau\left(T_2^i + T_4^i + T_6^i + 90 + \frac{\dot{e}_5 l^2}{k}\right)$$

(*f*) Node 6. (Boundary node subjected to convection on two sides, Fig. 5–54*b*)

$$h\left(\frac{\Delta x}{2} + \frac{\Delta y}{2}\right)(T_\infty - T_6^i) + k\frac{\Delta y}{2}\frac{T_7^i - T_6^i}{\Delta x} + k\Delta x\frac{T_{12}^i - T_6^i}{\Delta y} + k\Delta y\frac{T_5^i - T_6^i}{\Delta x}$$

$$+ \frac{\Delta x}{2}\frac{T_3^i - T_6^i}{\Delta y} + \dot{e}_6\frac{3\Delta x\Delta y}{4} = \rho\frac{3\Delta x\Delta y}{4}c_p\frac{T_6^{i+1} - T_6^i}{\Delta t}$$

Dividing by $3k/4$, simplifying, and solving for T_6^{i+1} gives

$$T_6^{i+1} = \left(1 - 4\tau - 4\tau\frac{hl}{3k}\right)T_6^i$$

$$+ \frac{\tau}{3}\left(2T_3^i + 4T_5^i + 2T_7^i + 4 \times 90 + 4\frac{hl}{k}T_\infty + 3\frac{\dot{e}_6 l^2}{k}\right)$$

(*g*) Node 7. (Boundary node subjected to convection, Fig. 5–55*a*)

$$h\Delta x(T_\infty - T_7^i) + k\frac{\Delta y}{2}\frac{T_8^i - T_7^i}{\Delta x} + k\Delta x\frac{T_{13}^i - T_7^i}{\Delta y}$$

$$+ k\frac{\Delta y}{2}\frac{T_6^i - T_7^i}{\Delta x} + \dot{e}_7\Delta x\frac{\Delta y}{2} = \rho\Delta x\frac{\Delta y}{2}c_p\frac{T_7^{i+1} - T_7^i}{\Delta t}$$

Dividing by $k/2$, simplifying, and solving for T_7^{i+1} gives

$$T_7^{i+1} = \left(1 - 4\tau - 2\tau\frac{hl}{k}\right)T_7^i + \tau\left(T_6^i + T_8^i + 2 \times 90 + \frac{2hl}{k}T_\infty + \frac{\dot{e}_2 l^2}{k}\right)$$

(*h*) Node 8. This node is identical to node 7, and the finite difference formulation of this node can be obtained from that of node 7 by shifting the node numbers by 1 (i.e., replacing subscript *m* with subscript *m* + 1). It gives

$$T_8^{i+1} = \left(1 - 4\tau - 2\tau\frac{hl}{k}\right)T_8^i + \tau\left(T_7^i + T_9^i + 2\times 90 + \frac{2hl}{k}T_\infty + \frac{\dot{e}_8 l^2}{k}\right)$$

(*i*) Node 9. (Boundary node subjected to convection on two sides, Fig. 5–55*b*)

$$h\frac{\Delta x}{2}(T_\infty - T_9^i) + \dot{q}_R\frac{\Delta y}{2} + k\frac{\Delta x}{2}\frac{T_{15}^i - T_9^i}{\Delta y}$$

$$+ \frac{k\Delta y}{2}\frac{T_8^i - T_9^i}{\Delta x} + \dot{e}_9\frac{\Delta x}{2}\frac{\Delta y}{2} = \rho\frac{\Delta x}{2}\frac{\Delta y}{2}c_p\frac{T_9^{i+1} - T_9^i}{\Delta t}$$

Dividing by *k*/4, simplifying, and solving for T_9^{i+1} gives

$$T_9^{i+1} = \left(1 - 4\tau - 2\tau\frac{hl}{k}\right)T_9^i + 2\tau\left(T_8^i + 90 + \frac{\dot{q}_R l}{k} + \frac{hl}{k}T_\infty + \frac{\dot{e}_9 l^2}{2k}\right)$$

This completes the finite difference formulation of the problem. Next we need to determine the upper limit of the time step Δt from the stability criterion, which requires the coefficient of T_m^i in the T_m^{i+1} expression (the primary coefficient) to be greater than or equal to zero for all nodes. The smallest primary coefficient in the nine equations here is the coefficient of T_3^i in the T_3^{i+1} expression, and thus the stability criterion for this problem can be expressed as

$$1 - 4\tau - 4\tau\frac{hl}{k} \geq 0 \quad \rightarrow \quad \tau \leq \frac{1}{4(1 + hl/k)} \quad \rightarrow \quad \Delta t \leq \frac{l^2}{4\alpha(1 + hl/k)}$$

since $\tau = \alpha\Delta t/l^2$. Substituting the given quantities, the maximum allowable value of the time step is determined to be

$$\Delta t \leq \frac{(0.012 \text{ m})^2}{4(3.2 \times 10^{-6} \text{ m}^2/\text{s})\left[1 + (80 \text{ W/m}^2\cdot\text{K})(0.012 \text{ m})/(15 \text{ W/m}\cdot\text{K})\right]} = 10.6 \text{ s}$$

Therefore, any time step less than 10.6 s can be used to solve this problem. For convenience, let us choose the time step to be $\Delta t = 10$ s. Then the mesh Fourier number becomes

$$\tau = \frac{\alpha\Delta t}{l^2} = \frac{(3.2 \times 10^{-6} \text{ m}^2/\text{s})(10 \text{ s})}{(0.012 \text{ m})^2} = 0.222 \text{ (for } \Delta t = 10 \text{ s)}$$

Substituting this value of τ and other given quantities, the developed transient finite difference equations simplify to

$$T_1^{i+1} = 0.0836T_1^i + 0.444(T_2^i + T_4^i + 11.2)$$
$$T_2^{i+1} = 0.0836T_2^i + 0.222(T_1^i + T_3^i + 2T_5^i + 22.4)$$
$$T_3^{i+1} = 0.0552T_3^i + 0.444(T_2^i + T_6^i + 12.8)$$
$$T_4^{i+1} = 0.112T_4^i + 0.222(T_1^i + 2T_5^i + 109.2)$$
$$T_5^{i+1} = 0.112T_5^i + 0.222(T_2^i + T_4^i + T_6^i + 109.2)$$
$$T_6^{i+1} = 0.0931T_6^i + 0.074(2T_3^i + 4T_5^i + 2T_7^i + 424)$$
$$T_7^{i+1} = 0.0836T_7^i + 0.222(T_6^i + T_8^i + 202.4)$$
$$T_8^{i+1} = 0.0836T_8^i + 0.222(T_7^i + T_9^i + 202.4)$$
$$T_9^{i+1} = 0.0836T_9^i + 0.444(T_8^i + 105.2)$$

Using the specified initial condition as the solution at time $t = 0$ (for $i = 0$), sweeping through these nine equations gives the solution at intervals of 10 s. The solution at the upper corner node (node 3) is determined to be 100.2, 105.9, 106.5, 106.6, and 106.6°C at 1, 3, 5, 10, and 60 min, respectively. Note that the last three solutions are practically identical to the solution for the steady case obtained in Example 5–3. This indicates that steady conditions are reached in the medium after about 5 min.

Controlling the Numerical Error

A comparison of the numerical results with the exact results for temperature distribution in a cylinder would show that the results obtained by a numerical method are approximate, and they may or may not be sufficiently close to the exact (true) solution values. The difference between a numerical solution and the exact solution is the **error** involved in the numerical solution, and it is primarily due to two sources:

- The **discretization error** (also called the *truncation* or *formulation* error), which is caused by the approximations used in the formulation of the numerical method.

- The **round-off error**, which is caused by the computer's use of a limited number of significant digits and continuously rounding (or chopping) off the digits it cannot retain.

Below we discuss both types of errors.

Discretization Error

The discretization error involved in numerical methods is due to replacing the *derivatives* with *differences* in each step, or the actual temperature distribution between two adjacent nodes with a straight line segment.

Consider the variation of the solution of a transient heat transfer problem with time at a specified nodal point. Both the numerical and actual (exact) solutions coincide at the beginning of the first time step, as expected, but the numerical solution deviates from the exact solution as the time t increases. The difference between the two solutions at $t = \Delta t$ is due to the approximation at the first time step only and is called the *local discretization error*. One would expect the situation to get worse with each step since the second step uses the erroneous result of the first step as its starting point and adds a second local discretization error on top of it, as shown in Fig. 5–56. The accumulation of the local discretization errors continues with the increasing number of time steps, and the total discretization error at any step is called the *global* or *accumulated discretization error*. Note that the local and global discretization errors are identical for the first time step. The global discretization error usually increases with the increasing number of steps, but the opposite may occur when the solution function
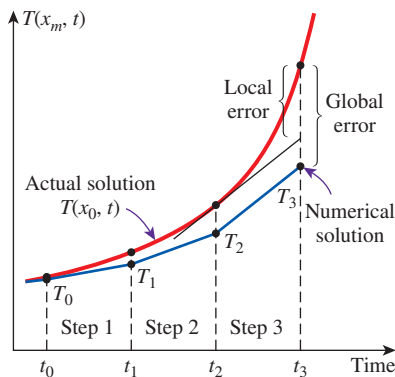
FIGURE 5–56
The local and global discretization errors of the finite difference method at the third time step at a specified nodal point.

---

*This section can be skipped without a loss of continuity.

changes direction frequently, giving rise to local discretization errors of opposite signs, which tend to cancel each other.

To have an idea about the magnitude of the local discretization error, consider the Taylor series expansion of the temperature at a specified nodal point m about time t_i,

$$T(x_m, t_i + \Delta t) = T(x_m, t_i) + \Delta t \frac{\partial T(x_m, t_i)}{\partial t} + \frac{1}{2} \Delta t^2 \frac{\partial^2 T(x_m, t_i)}{\partial t^2} + \ldots \qquad \textbf{(5–62)}$$

The finite difference formulation of the time derivative at the same nodal point is expressed as

$$\frac{\partial T(x_m, t_i)}{\partial t} \cong \frac{T(x_m, t_i + \Delta t) - T(x_m, t_i)}{\Delta t} = \frac{T_m^{i+1} - T_m^i}{\Delta t} \qquad \textbf{(5–63)}$$

or

$$T(x_m, t_i + \Delta t) \cong T(x_m, t_i) + \Delta t \frac{\partial T(x_m, t_i)}{\partial t} \qquad \textbf{(5–64)}$$

which resembles the *Taylor series expansion* terminated after the first two terms. Therefore, the third and later terms in the Taylor series expansion represent the error involved in the finite difference approximation. For a sufficiently small time step, these terms decay rapidly as the order of derivative increases, and their contributions become smaller and smaller. The first term neglected in the Taylor series expansion is proportional to Δt^2, and thus the local discretization error of this approximation, which is the error involved in each step, is also proportional to Δt^2.

The local discretization error is the formulation error associated with a single step and gives an idea about the accuracy of the method used. However, the solution results obtained at every step except the first one involve the *accumulated error* up to that point, and the local error alone does not have much significance. What we really need to know is the global discretization error. In the worst case, the accumulated discretization error after I time steps during a time period t_0 is $i(\Delta t)^2 = (t_0/\Delta t)(\Delta t)^2 = t_0 \Delta t$, which is proportional to Δt. Thus, we conclude that the local discretization error is proportional to the square of the step size Δt^2 while the global discretization error is proportional to the step size Δt itself. Therefore, the smaller the mesh size (or the size of the time step in transient problems), the smaller the error, and thus the more accurate is the approximation. For example, halving the step size will reduce the global discretization error by half. It should be clear from the previous discussions that the discretization error can be minimized by decreasing the step size in space or time as much as possible. The discretization error approaches zero as the difference quantities such as Δx and Δt approach the differential quantities such as dx and dt.

Round-Off Error

If we had a computer that could retain an infinite number of digits for all numbers, the difference between the exact solution and the approximate (numerical) solution at any point would entirely be due to discretization error. But we know that every computer (or calculator) represents numbers
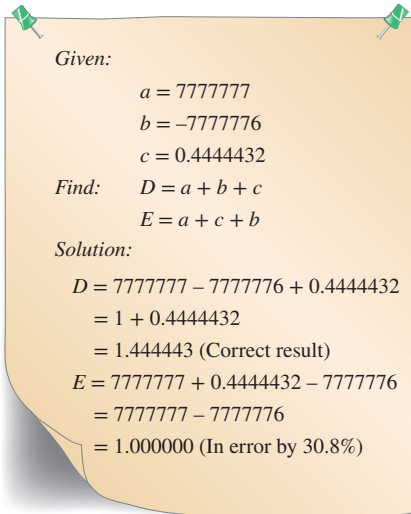
FIGURE 5–57
A simple arithmetic operation
performed with a computer in single
precision using seven significant
digits, which results in 30.8 percent
error when the order of operation is
reversed.
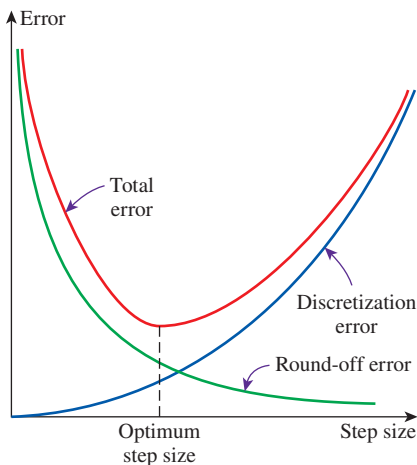
FIGURE 5–58
As the mesh or time step size
decreases, the discretization error
decreases but the round-off error
increases.

using a finite number of significant digits. The default value of the number of significant digits for many computers is seven, which is referred to as *single precision.* But the user may perform the calculations using 15 significant digits for the numbers, if he or she wishes, which is referred to as *double precision.* Of course, performing calculations in double precision will require more computer memory and a longer execution time.

In single precision mode with seven significant digits, a computer registers the number 44444.666666 as 44444.67 or 44444.66, depending on the method of rounding the computer uses. In the first case, the excess digits are said to be *rounded* to the closest integer, whereas in the second case they are said to be *chopped off.* Therefore, the numbers $a = 44444.12345$ and $b = 44444.12032$ are equivalent for a computer that performs calculations using seven significant digits. Such a computer would give $a - b = 0$ instead of the true value 0.00313.

The error due to retaining a limited number of digits during calculations is called the **round-off error**. This error is random in nature, and there is no easy and systematic way of predicting it. It depends on the number of calculations, the method of rounding off, the type of computer, and even the sequence of calculations.

In algebra you learned that $a + b + c = a + c + b$, which seems quite reasonable. But this is not necessarily true for calculations performed with a computer, as demonstrated in Fig. 5–57. Note that changing the sequence of calculations results in an error of 30.8 percent in just two operations. Considering that any significant problem involves thousands or even millions of such operations performed in sequence, we realize that the accumulated round-off error has the potential to cause serious error without giving any warning signs. Experienced programmers are very much aware of this danger, and they structure their programs to prevent any buildup of the round-off error. For example, it is much safer to multiply a number by 10 than to add it 10 times. Also, it is much safer to start any addition process with the smallest numbers and continue with larger numbers. This rule is particularly important when evaluating series with a large number of terms with alternating signs.

The round-off error is proportional to the *number of computations* performed during the solution. In the finite difference method, the number of calculations increases as the mesh size or the time step size decreases. Halving the mesh or time step size, for example, doubles the number of calculations and thus the accumulated round-off error.

Controlling the Error in Numerical Methods

The total error in any result obtained by a numerical method is the sum of the *discretization error,* which decreases with decreasing step size, and the *round-off error,* which increases with decreasing step size, as shown in Fig. 5–58. Therefore, decreasing the step size too much in order to get more accurate results may actually backfire and give less accurate results because of a faster increase in the round-off error. We should be careful not to let round-off error get out of control by avoiding a large number of computations with very small numbers.

In practice, we do not know the exact solution of the problem, and thus we cannot determine the magnitude of the error involved in the numerical

method. Knowing that the global discretization error is proportional to the step size is not much help, either, since there is no easy way of determining the value of the proportionality constant. Besides, the global discretization error alone is meaningless without a true estimate of the round-off error. Therefore, we recommend the following practical procedures to assess the accuracy of the results obtained by a numerical method.

- Start the calculations with a reasonable mesh size Δx (and time step size Δt for transient problems) based on experience. Then repeat the calculations using a mesh size of $\Delta x/2$. If the results obtained by halving the mesh size do not differ significantly from the results obtained with the full mesh size, we conclude that the discretization error is at an acceptable level. But if the difference is larger than we can accept, then we have to repeat the calculations using a mesh size $\Delta x/4$ or even a smaller one at regions of high temperature gradients. We continue in this manner until halving the mesh size does not cause any significant change in the results, which indicates that the discretization error is reduced to an acceptable level.

- Repeat the calculations using double precision holding the mesh size (and the size of the time step in transient problems) constant. If the changes are not significant, we conclude that the round-off error is not a problem. But if the changes are too large to accept, then we may try reducing the total number of calculations by increasing the mesh size or changing the order of computations. But if the increased mesh size gives unacceptable discretization errors, then we may have to find a reasonable compromise.

It should always be kept in mind that the results obtained by numerical method may not reflect trouble spots in certain problems that require special consideration, such as hot spots or areas of high temperature gradients. The results that seem quite reasonable overall may be in considerable error at certain locations. This is another reason for always repeating the calculations at least twice with different mesh sizes before accepting them as the solution of the problem. Most commercial software packages have built-in routines that vary the mesh size as necessary to obtain highly accurate solutions. But it is a good engineering practice to be aware of any potential pitfalls of numerical methods and to examine the results obtained with a critical eye.

SUMMARY

Analytical solution methods are limited to highly simplified problems in simple geometries, and it is often necessary to use a numerical method to solve real-world problems with complicated geometries or nonuniform thermal conditions. The numerical *finite difference method* is based on replacing derivatives with differences, and the finite difference formulation of a heat transfer problem is obtained by selecting a sufficient number of points in the region, called the *nodal points* or node*s,* and writing *energy balances* on the volume elements centered about the nodes.

For *steady* heat transfer, the *energy balance* on a volume element can be expressed in general as

$$\sum_{\text{All sides}} \dot{Q} + \dot{e}\, V_{\text{element}} = 0$$

whether the problem is one-, two-, or three-dimensional. For convenience in formulation, we always assume all heat transfer to be *into* the volume element from all surfaces toward the node under consideration, except for specified heat flux whose direction is already specified. The finite difference

formulations for a general interior node under *steady* conditions are expressed for some geometries as follows:

One-dimensional steady conduction in a plane wall:

$$\frac{T_{m-1} - 2T_m + T_{m+1}}{(\Delta x)^2} + \frac{\dot{e}_m}{k} = 0$$

Two-dimensional steady conduction in rectangular coordinates:

$$T_{\text{left}} + T_{\text{top}} + T_{\text{right}} + T_{\text{bottom}} - 4T_{\text{node}} + \frac{\dot{e}_{\text{node}}l^2}{k} = 0$$

where Δx is the nodal spacing for the plane wall and $\Delta x = \Delta y = l$ is the nodal spacing for the two-dimensional case. Insulated boundaries can be viewed as mirrors in formulation, and thus the nodes on insulated boundaries can be treated as interior nodes by using mirror images.

The finite difference formulation at node 0 at the left boundary of a plane wall for steady one-dimensional heat conduction can be expressed as

$$\dot{Q}_{\text{left surface}} + kA\frac{T_1 - T_0}{\Delta x} + \dot{e}_0(A\Delta x/2) = 0$$

where $A\Delta x/2$ is the volume of the volume, $\dot{e}_0$ is the rate of heat generation per unit volume at $x = 0$, and A is the heat transfer area. The form of the first term depends on the boundary condition at $x = 0$ (convection, radiation, specified heat flux, etc.).

The finite difference formulation of heat conduction problems usually results in a system of N algebraic equations in N unknown nodal temperatures that need to be solved simultaneously.

The finite difference formulation of *transient* heat conduction problems is based on an energy balance that also accounts for the variation of the energy content of the volume element during a time interval Δt. The heat transfer and heat generation terms are expressed at the previous time step i in the *explicit method*, and at the new time step $i + 1$ in the *implicit method*. For a general node m, the finite difference formulations are expressed as

Explicit method:

$$\sum_{\text{All sides}} \dot{Q}^i + \dot{e}_m^i V_{\text{element}} = \rho V_{\text{element}} c_p \frac{T_m^{i+1} - T_m^i}{\Delta t}$$

Implicit method:

$$\sum_{\text{All sides}} \dot{Q}^{i+1} + \dot{e}_m^{i+1} V_{\text{element}} = \rho V_{\text{element}} c_p \frac{T_m^{i+1} - T_m^i}{\Delta t}$$

where T_m^i and T_m^{i+1} are the temperatures of node m at times $t_i = i\Delta t$ and $t_{i+1} = (i+1)\Delta t$, respectively, and $T_m^{i+1} - T_m^i$ represents the temperature change of the node during the time interval Δt between the time steps i and $i + 1$. The explicit and implicit formulations given here are quite general and can be used in any coordinate system regardless of heat transfer being one-, two-, or three-dimensional.

The explicit formulation of a general interior node for one- and two-dimensional heat transfer in rectangular coordinates can be expressed as

One-dimensional case:

$$T_m^{i+1} = \tau(T_{m-1}^i + T_{m+1}^i) + (1 - 2\tau)T_m^i + \tau\frac{\dot{e}_m^i \Delta x^2}{k}$$

Two-dimensional case:

$$T_{\text{node}}^{i+1} = \tau(T_{\text{left}}^i + T_{\text{top}}^i + T_{\text{right}}^i + T_{\text{bottom}}^i)$$

$$+ (1 - 4\tau)T_{\text{node}}^i + \tau\frac{\dot{e}_{\text{node}}^i l^2}{k}$$

where $\tau = \alpha\Delta t/\Delta x^2$ is the dimensionless *mesh Fourier number* and $\alpha = k/\rho c_p$ is the *thermal diffusivity* of the medium.

The implicit method is inherently stable, and any value of Δt can be used with that method as the time step. The largest value of the time step Δt in the explicit method is limited by the *stability criterion*, expressed as: *the coefficients of all T_m^i in the T_m^{i+1} expressions (called the primary coefficients) must be greater than or equal to zero for all nodes m.* The maximum value of Δt is determined by applying the stability criterion to the equation with the smallest primary coefficient since it is the most restrictive. For problems with specified temperatures or heat fluxes at all the boundaries, the stability criterion can be expressed as $\tau \leq \frac{1}{2}$ for one-dimensional problems and $\tau \leq \frac{1}{4}$ for the two-dimensional problems in rectangular coordinates.

REFERENCES AND SUGGESTED READING

1. D. A. Anderson, J. C. Tannehill, and R. H. Pletcher. *Computational Fluid Mechanics and Heat Transfer.* New York: Hemisphere, 1984.

2. C. A. Brebbia. *The Boundary Element Method for Engineers.* New York: Halsted Press, 1978.

3. G. E. Forsythe and W. R. Wasow. *Finite Difference Methods for Partial Differential Equations.* New York: John Wiley & Sons, 1960.

4. B. Gebhart. *Heat Conduction and Mass Diffusion.* New York: McGraw-Hill, 1993.

5. K. H. Huebner and E. A. Thornton. *The Finite Element Method for Engineers.* 2nd ed. New York: John Wiley & Sons, 1982.

6. Y. Jaluria and K. E. Torrance. *Computational Heat Transfer.* New York: Hemisphere, 1986.

7. W. J. Minkowycz, E. M. Sparrow, G. E. Schneider, and R. H. Pletcher. *Handbook of Numerical Heat Transfer.* New York: John Wiley & Sons, 1988.

8. G. E. Myers. *Analytical Methods in Conduction Heat Transfer.* New York: McGraw-Hill, 1971.

9. D. H. Norrie and G. DeVries. *An Introduction to Finite Element Analysis.* New York: Academic Press, 1978.

10. M. N. Özişik. *Finite Difference Methods in Heat Transfer.* Boca Raton, FL: CRC Press, 1994.

11. S. V. Patankhar. *Numerical Heat Transfer and Fluid Flow.* New York: Hemisphere, 1980.

12. T. M. Shih. *Numerical Heat Transfer.* New York: Hemisphere, 1984.

PROBLEMS *

Why Numerical Methods?

5–1C With powerful computers and software packages readily available, do you think obtaining analytical solutions to engineering problems will eventually disappear from engineering curricula?

5–2C What are the limitations of the analytical solution methods?

5–3C Consider a heat conduction problem that can be solved both analytically, by solving the governing differential equation and applying the boundary conditions, and numerically, by a software package available on your computer. Which approach would you use to solve this problem? Explain your reasoning.

5–4C What is the basis of the energy balance method? How does it differ from the formal finite difference method? For a specified nodal network, will these two methods result in the same or a different set of equations?

5–5C How do numerical solution methods differ from analytical ones? What are the advantages and disadvantages of numerical and analytical methods?

5–6C Two engineers are to solve an actual heat transfer problem in a manufacturing facility. Engineer A makes the necessary simplifying assumptions and solves the problem analytically, while Engineer B solves it numerically using a powerful software package. Engineer A claims he solved the problem exactly and thus his results are better, while Engineer B claims that he used a more realistic model and thus his results are better. To resolve the dispute, you are asked to solve the problem experimentally in a lab. Which engineer do you think the experiments will prove right? Explain.

Finite Difference Formulation of Differential Equations

5–7C Define these terms used in the finite difference formulation: node, nodal network, volume element, nodal spacing, and difference equation.

*Problems designated by a "C" are concept questions, and students are encouraged to answer them all. Problems designated by an "E" are in English units, and the SI users can ignore them. Problems with the 🖥 icon are comprehensive in nature and are intended to be solved with appropriate software. Problems with the 🅿ᴴᴰ icon are Prevention through Design problems. Problems with the 🄲&🅂 icon are Codes and Standards problems.

5–8 The finite difference formulation of steady two-dimensional heat conduction in a medium with heat generation and constant thermal conductivity is given by

$$\frac{T_{m-1,n} - 2T_{m,n} + T_{m+1,n}}{\Delta x^2} + \frac{T_{m,n-1} - 2T_{m,n} + T_{m,n+1}}{\Delta y^2}$$
$$+ \frac{\dot{e}_{m,n}}{k} = 0$$

in rectangular coordinates. Modify this relation for the three-dimensional case.

5–9 For a one-dimensional, steady-state, variable thermal conductivity heat conduction with uniform internal heat generation, develop a generalized finite difference formulation for the interior nodes, with the left surface boundary node exposed to constant heat flux and the right surface boundary node exposed to a convective environment. The variable conductivity is modeled such that the thermal conductivity varies linearly with the temperature as $k(T) = k_o(1 + \beta T)$ where T is the average temperature between the two nodes.

5–10 In many engineering applications variation in thermal properties is significant, especially when there are large temperature gradients or the material is not homogeneous. To account for these variations in thermal properties, develop a finite difference formulation for an internal node in the case of a three-dimensional, steady-state heat conduction equation with variable thermal conductivity.

5–11 Consider steady one-dimensional heat conduction in a plane wall with variable heat generation and constant thermal conductivity. The nodal network of the medium consists of nodes 0, 1, 2, 3, and 4 with a uniform nodal spacing of Δx. Using the finite difference form of the first derivative (*not* the energy balance approach), obtain the finite difference formulation of the boundary nodes for the case of uniform heat flux $\dot{q}_0$ at the left boundary (node 0) and convection at the right boundary (node 4) with a convection coefficient of h and an ambient temperature of T_∞.

5–12 Consider steady one-dimensional heat conduction in a plane wall with variable heat generation and constant thermal conductivity, as shown in Fig. P5–12. The nodal network of the medium consists of nodes 0, 1, 2, 3, 4, and 5 with a uniform nodal spacing of Δx. Using the finite difference form of the first derivative (*not* the energy balance approach), obtain the finite difference formulation of the boundary nodes for the

case of insulation at the left boundary (node 0) and radiation at the right boundary (node 5) with an emissivity of ε and surrounding temperature of T_{surr}.

FIGURE P5–12

One-Dimensional Steady Heat Conduction

5–13C Explain how the finite difference form of a heat conduction problem is obtained by the energy balance method.

5–14C What are the basic steps involved in solving a system of equations with the Gauss-Seidel method?

5–15C Consider a medium in which the finite difference formulation of a general interior node is given in its simplest form as

$$\frac{T_{m-1} - 2T_m + T_{m+1}}{\Delta x^2} + \frac{\dot{e}_m}{k} = 0$$

(a) Is heat transfer in this medium steady or transient?
(b) Is heat transfer one-, two-, or three-dimensional?
(c) Is there heat generation in the medium?
(d) Is the nodal spacing constant or variable?
(e) Is the thermal conductivity of the medium constant or variable?

5–16C How is an insulated boundary handled in the finite difference formulation of a problem? How does a symmetry line differ from an insulated boundary in the finite difference formulation?

5–17C How can a node on an insulated boundary be treated as an interior node in the finite difference formulation of a plane wall? Explain.

5–18C In the energy balance formulation of the finite difference method, it is recommended that all heat transfer at the boundaries of the volume element be assumed to be into the volume element even for steady heat conduction. Is this a valid recommendation even though it seems to violate the conservation of energy principle?

5–19 Consider steady heat conduction in a plane wall whose left surface (node 0) is maintained at 40°C while the right surface (node 8) is subjected to a heat flux of 3000 W/m². Express the finite difference formulation of the boundary nodes 0 and 8 for the case of no heat generation. Also obtain the finite difference formulation for the rate of heat transfer at the left boundary.
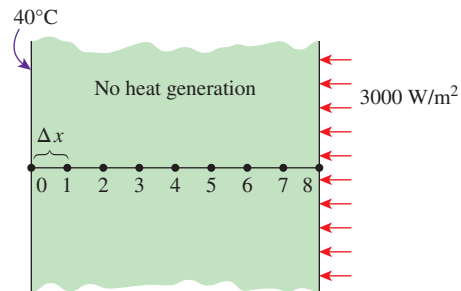
FIGURE P5–19

5–20 Consider steady heat conduction in a plane wall with variable heat generation and constant thermal conductivity. The nodal network of the medium consists of nodes 0, 1, 2, 3, and 4 with a uniform nodal spacing of Δx. Using the energy balance approach, obtain the finite difference formulation of the boundary nodes for the case of uniform heat flux $\dot{q}_0$ at the left boundary (node 0) and convection at the right boundary (node 4) with a convection coefficient of h and an ambient temperature of T_∞.

5–21 Consider steady one-dimensional heat conduction in a plane wall with variable heat generation and constant thermal conductivity. The nodal network of the medium consists of nodes 0, 1, 2, 3, 4, and 5 with a uniform nodal spacing of Δx. Using the energy balance approach, obtain the finite difference formulation of the boundary nodes for the case of insulation at the left boundary (node 0) and radiation at the right boundary (node 5) with an emissivity of ε and surrounding temperature of T_{surr}.

5–22 Consider steady one-dimensional heat conduction in a composite plane wall consisting of two layers A and B in perfect contact at the interface. The wall involves no heat generation. The nodal network of the medium consists of nodes 0, 1 (at the interface), and 2 with a uniform nodal spacing of Δx. Using the energy balance approach, obtain the finite difference formulation of this problem for the case of insulation at the left boundary (node 0) and radiation at the right boundary (node 2) with an emissivity of ε and surrounding temperature of T_{surr}.

5–23 Consider steady one-dimensional heat conduction in a pin fin of constant diameter D with constant thermal conductivity. The fin is losing heat by convection to the ambient air at T_∞ with a convection coefficient of h, and by radiation to the surrounding surfaces at an average temperature of T_{surr}. The nodal network of the fin consists of nodes 0 (at the base), 1 (in the middle), and 2 (at the fin tip) with a uniform nodal spacing of Δx. Using the energy balance approach, obtain the finite difference formulation of this problem to determine T_1 and T_2 for the case of specified temperature at the fin base and negligible heat transfer at the fin tip. All temperatures are in °C.
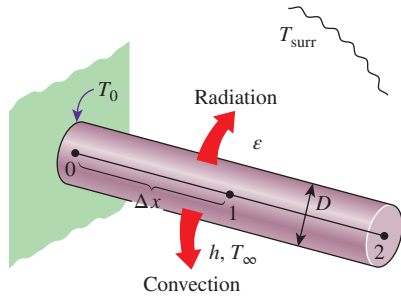
FIGURE P5–23

5–24 Consider steady one-dimensional heat conduction in a plane wall with variable heat generation and variable thermal conductivity. The nodal network of the medium consists of nodes 0, 1, and 2 with a uniform nodal spacing of Δx. Using the energy balance approach, obtain the finite difference formulation of this problem for the case of specified heat flux $\dot{q}_0$ to the wall and convection at the left boundary (node 0) with a convection coefficient of h and ambient temperature of T_∞, and radiation at the right boundary (node 2) with an emissivity of ε and surrounding surface temperature of T_{surr}.
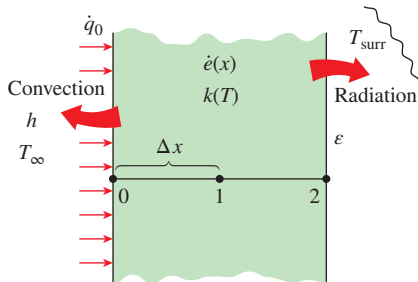
FIGURE P5–24

5–25 Consider steady one-dimensional heat conduction in a pin fin of constant diameter D with constant thermal conductivity. The fin is losing heat by convection to the ambient air at T_∞ with a heat transfer coefficient of h. The nodal network of the fin consists of nodes 0 (at the base), 1 (in the middle), and 2 (at the fin tip) with a uniform nodal spacing of Δx. Using the energy balance approach, obtain the finite difference formulation of this problem to determine T_1 and T_2 for the case of specified temperature at the fin base and negligible heat transfer at the fin tip. All temperatures are in °C.

5–26 Consider steady one-dimensional heat conduction in a plane wall with variable heat generation and constant thermal conductivity. The nodal network of the medium consists of nodes 0, 1, 2, 3, 4, and 5 with a uniform nodal spacing of Δx. The temperature at the right boundary (node 5) is specified. Using the energy balance approach, obtain the finite difference formulation of the boundary node 0 on the left boundary for the case of combined convection, radiation, and heat flux at the left boundary with an emissivity of ε, convection coefficient of h, ambient temperature of T_∞, surrounding temperature of T_{surr},

and uniform heat flux of $\dot{q}_0$. Also, obtain the finite difference formulation for the rate of heat transfer at the right boundary.
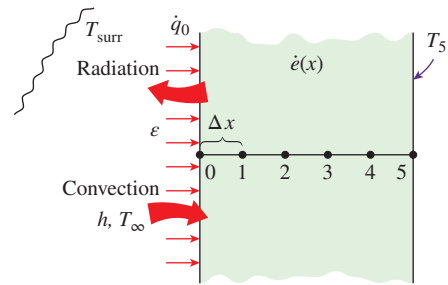
FIGURE P5–26

5–27 Consider the base plate of an 800-W household iron having a thickness of $L = 0.6$ cm, base area of $A = 160$ cm^2, and thermal conductivity of $k = 20$ W/m·K. The inner surface of the base plate is subjected to uniform heat flux generated by the resistance heaters inside. When steady operating conditions are reached, the outer surface temperature of the plate is measured to be 85°C. Disregarding any heat loss through the upper part of the iron and taking the nodal spacing to be 0.2 cm, (*a*) obtain the finite difference formulation for the nodes and (*b*) determine the inner surface temperature of the plate by solving those equations. *Answer:* (*b*) 100°C
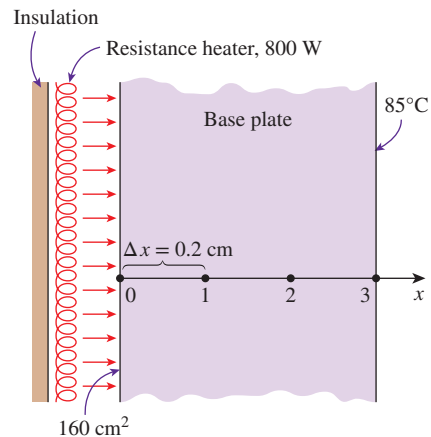
FIGURE P5–27

5–28 Consider a large plane wall of thickness $L = 0.3$ m, thermal conductivity $k = 1.8$ W/m·K, and surface area $A = 24$ m^2. The left side of the wall is subjected to a heat flux of $\dot{q}_0 = 350$ W/m^2, while the temperature at that surface is measured to be $T_0 = 60$°C. Assuming steady one-dimensional heat transfer and taking the nodal spacing to be 6 cm, (*a*) obtain the finite difference formulation for the six nodes and (*b*) determine the temperature of the other surface of the wall by solving those equations.

5–29 Consider a large plane wall of thickness $L = 0.4$ m, thermal conductivity $k = 2.3$ W/m·K, and surface area $A = 20$ m^2. The left side of the wall is maintained at a constant temperature of 95°C, while the right side loses heat by convection to

the surrounding air at $T_\infty = 15°C$ with a heat transfer coefficient of $h = 18$ W/m²·K. Assuming steady one-dimensional heat transfer and taking the nodal spacing to be 10 cm, (*a*) obtain the finite difference formulation for all nodes, (*b*) determine the nodal temperatures by solving those equations, and (*c*) evaluate the rate of heat transfer through the wall.

5–30E A large steel plate having a thickness of $L = 5$ in, thermal conductivity of $k = 7.2$ Btu/h·ft·°F, and an emissivity of $\varepsilon = 0.6$ is lying on the ground. The exposed surface of the plate exchanges heat by convection with the ambient air at $T_\infty = 80°F$ with an average heat transfer coefficient of $h = 3.5$ Btu/h·ft²·°F as well as by radiation with the open sky at an equivalent sky temperature of $T_{sky} = 510$ R. The ground temperature below a certain depth (say, 3 ft) is not affected by the weather conditions outside and remains fairly constant at 50°F at that location. The thermal conductivity of the soil can be taken to be $k_{soil} = 0.49$ Btu/h·ft·°F, and the steel plate can be assumed to be in perfect contact with the ground. Assuming steady one-dimensional heat transfer and taking the nodal spacings to be 1 in in the plate and 0.6 ft in the ground, (*a*) obtain the finite difference formulation for all 11 nodes shown in Fig. P5–30E and (*b*) determine the top and bottom surface temperatures of the plate by solving those equations.
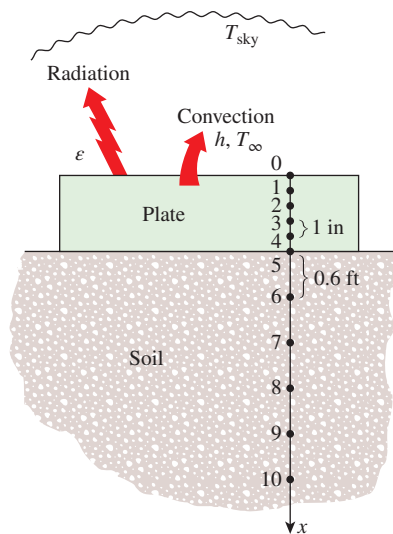
FIGURE P5–30E

5–31E Repeat Prob. 5–30E by disregarding radiation heat transfer from the upper surface.   *Answers:* (*b*) 78.7°F, 78.4°F

5–32 A 1-m-long and 0.1-m-thick steel plate of thermal conductivity 35 W/m·K is well insulated on both sides, while the top surface is exposed to a uniform heat flux of 5500 W/m². The bottom surface is convectively cooled by a fluid at 10°C having a convective heat transfer coefficient of 150 W/m²·K. Assuming one-dimensional heat conduction in the lateral direction, find the temperature at the midpoint of the plate. Discretize the plate thickness into four equal parts.

5–33 [C&S] A nonmetal plate ($k = 3$ W/m·K) is attached to an ASTM A240 904L stainless steel plate ($k = 13$ W/m·K). The nonmetal plate and the stainless steel plate have thicknesses of 1 cm and 3 cm, respectively. The nonmetal plate is bolted to the stainless steel plate with a series of ASTM B211 6061 aluminum alloy bolts. The upper surface of the nonmetal plate is exposed to convection heat transfer with air at 20°C and $h = 50$ W/m²·K. The bottom surface of the stainless steel plate is exposed to convection with steam at 260°C and $h = 300$ W/m²·K. According to the ASME Code for Process Piping (ASME B31.3-2014, Table A-2M), the maximum use temperature for the B211 6061 bolts is 204°C, while the maximum use temperature for the ASTM A240 904L plate is 260°C (ASME B31.3-2014, Table A-1M). Using the finite difference method with a uniform nodal spacing of $\Delta x = 5$ mm along the plate thicknesses, determine the temperature at each node. Plot the temperature distribution as a function of *x*. Would the use of the ASTM A240 904L plate and ASTM B211 6061 bolts be in compliance with the ASME Code for Process Piping?
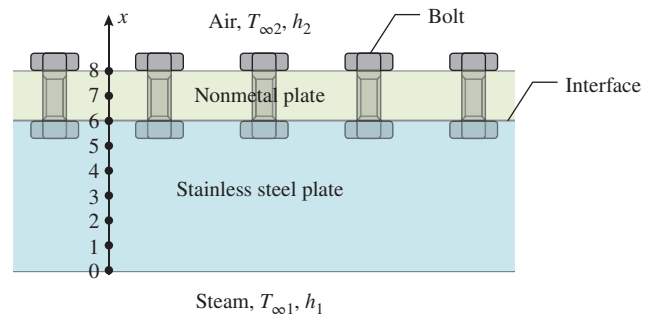
FIGURE P5–33

5–34 [C&S] A nonmetal plate ($k = 0.05$ W/m·K) is attached on the upper surface of an ASME SB-96 copper–silicon plate ($k = 36$ W/m·K). The nonmetal plate and the ASME SB-96 plate have thicknesses of 20 mm and 30 mm, respectively. The bottom surface of the ASME SB-96 plate (surface 1) is subjected to a uniform heat flux of 150 W/m². The top nonmetal plate surface (surface 2) is exposed to convection at an air temperature of 15°C and a convection heat transfer coefficient of 5 W/m²·K. Copper–silicon alloys are not always suitable for applications where they are exposed to certain median and high temperatures. Therefore, the ASME Boiler and Pressure Vessel Code (ASME BPVC.IV-2015, HF-300) limits equipment constructed with ASME SB-96 plate to be operated at a temperature not exceeding 93°C. Using the finite difference method with a uniform nodal spacing of $\Delta x = 5$ mm along the plate thicknesses, determine the temperature at each node. Plot the temperature distribution as a function of *x*. Would the use of the ASME SB-96 plate under these conditions be in compliance with the ASME Boiler and Pressure Vessel Code? What is the lowest value of the convection heat transfer coefficient for the air so that the ASME SB-96 plate is below 93°C?
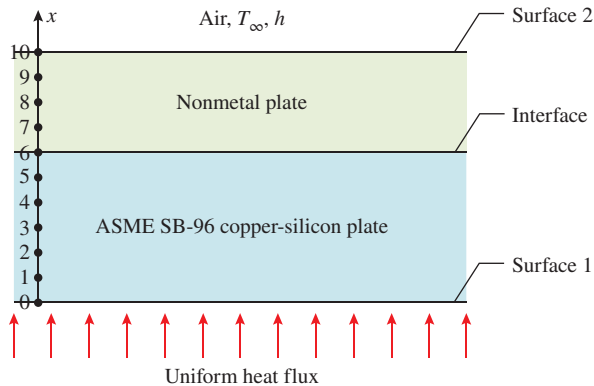
FIGURE P5–34

5–35 `C & S` A stainless steel plate ($k = 13$ W/m·K, 1 cm thick) is attached to an ASME SB-96 copper–silicon plate ($k = 36$ W/m·K, 3 cm thick) to form a plane wall. The bottom surface of the ASME SB-96 plate (surface 1) is subjected to a uniform heat flux of 750 W/m². The top surface of the stainless steel plate (surface 2) is exposed to convection heat transfer with air at $T_\infty = 20$°C, and thermal radiation with the surroundings at $T_{surr} = 20$°C. The combined heat transfer coefficient for convection and radiation is $h_{comb} = 7.76$ W/m²·K. The ASME Boiler and Pressure Vessel Code (ASME BPVC.IV-2015, HF-300) limits equipment constructed with ASME SB-96 plate to be operated at a temperature not exceeding 93°C. Using the finite difference method with a uniform nodal spacing of $\Delta x = 5$ mm along the plate thicknesses, determine the temperature at each node. Would the use of the ASME SB-96 plate under these conditions be in compliance with the ASME Boiler and Pressure Vessel Code? What is the highest heat flux that the bottom surface can be subjected to such that the ASME SB-96 plate is still operating below 93°C?
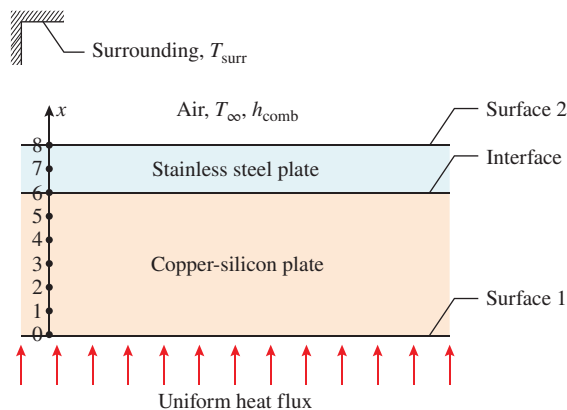
FIGURE P5–35

5–36 `C & S` A composite wall is made of stainless steel ($k_1 = 13$ W/m·K, 30 mm thick), concrete ($k_2 = 1.1$ W/m·K, 30 mm thick), and nonmetal ($k_3 = 0.1$ W/m·K, 15 mm thick) plates. The concrete plate is sandwiched between the stainless steel plate at the bottom and the nonmetal plate at the top. A series of ASTM B21 naval brass bolts are bolted to the nonmetal plate, and the upper surface of the plate is exposed to convection heat transfer with air at 20°C and $h = 20$ W/m²·K. At the bottom surface, the stainless steel plate is subjected to a uniform heat flux of 2000 W/m². The ASME Code for Process Piping (ASME B31.3-2014, Table A-2M) limits the maximum use temperature for the ASTM B21 bolts to 149°C. Using the finite difference method with a uniform nodal spacing of $\Delta x_1 = 10$ mm for the stainless steel and concrete plates, and $\Delta x_2 = 5$ mm for the nonmetal plate, determine the temperature at each node. Plot the temperature distribution as a function of x along the plate thicknesses. Would the ASTM B21 bolts in the nonmetal plate comply with the ASME code?
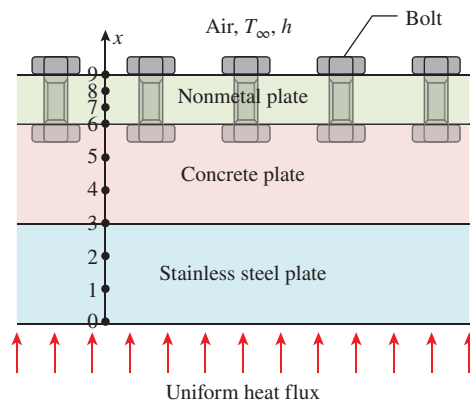
FIGURE P5–36

5–37 Consider a large uranium plate of thickness 5 cm and thermal conductivity $k = 34$ W/m·K in which heat is generated uniformly at a constant rate of $\dot{e} = 6 \times 10^5$ W/m³. One side of the plate is insulated, while the other side is subjected to convection to an environment at 30°C with a heat transfer coefficient of $h = 60$ W/m²·K. Considering six equally spaced nodes with a nodal spacing of 1 cm, (*a*) obtain the finite difference formulation of this problem and (*b*) determine the nodal temperatures under steady conditions by solving those equations.

5–38 Repeat Prob. 5–37 using appropriate software.

5–39 Consider one-dimensional steady-state heat conduction in a composite wall made up of two different materials A ($k = 45$ W/m·K) and B ($k = 28$ W/m·K). There is a heating element passing through the material A that causes uniform heat generation at a rate of 70,000 W/m³. The total thickness of the wall is 20 cm with equal thickness of material A and material B. Using a uniform nodal spacing of 2.5 cm, (*a*) obtain a finite difference formulation for the case of constant uniform heat

flux of 4500 W/m² at the wall inner (left) surface while the outer (right) surface is exposed to combined radiation ($\varepsilon = 0.9$) and convection boundary condition ($h = 70$ W/m²·K). Assume the surrounding temperature is equal to that of the ambient temperature at 10°C, and determine (*b*) the temperature distribution across the wall thickness using boundary conditions in part (*a*).

5–40 A stainless steel plane wall ($k = 15.1$ W/m·K) of thickness 1 m experiences a uniform heat generation of 1000 W/m³. The left side of the wall is maintained at a constant temperature of 70°C, and the right side of the wall is exposed to ambient air temperature of 0°C with a convection heat transfer coefficient of 250 W/m²·K. Using a uniform nodal spacing of 0.2 m, (*a*) obtain the finite difference equations and (*b*) determine the nodal temperatures by solving those equations.

5–41 Consider a 2-m-long and 0.7-m-wide stainless steel plate whose thickness is 0.1 m. The left surface of the plate is exposed to a uniform heat flux of 2000 W/m², while the right surface of the plate is exposed to a convective environment at 0°C with $h = 400$ W/m²·K. The thermal conductivity of the stainless steel plate can be assumed to vary linearly with temperature range as $k(T) = k_o(1 + \beta T)$ where $k_o = 48$ W/m·K and $\beta = 9.21 \times 10^{-4}\,°C^{-1}$. The stainless steel plate experiences a uniform volumetric heat generation at a rate of 8×10^5 W/m³. Assuming steady-state one-dimensional heat transfer, determine the temperature distribution along the plate thickness.

5–42 A plane wall with surface temperature of 350°C is attached with straight rectangular fins ($k = 235$ W/m·K). The fins are exposed to an ambient air condition of 25°C, and the convection heat transfer coefficient is 154 W/m²·K. Each fin has a length of 50 mm, a base 5 mm thick, and a width of 100 mm. For a single fin, using a uniform nodal spacing of 10 mm, determine (*a*) the finite difference equations, (*b*) the nodal temperatures by solving the finite difference equations, and (*c*) the heat transfer rate and compare the result with the analytical solution.
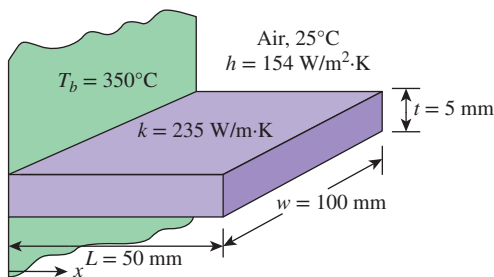
FIGURE P5–42

5–43 Consider a stainless steel spoon ($k = 15.1$ W/m·K, $\varepsilon = 0.6$) that is partially immersed in boiling water at 100°C in a kitchen at 32°C. The handle of the spoon has a cross section of about 0.2 cm × 1 cm and extends 18 cm in the air from

the free surface of the water. The spoon loses heat by convection to the ambient air with an average heat transfer coefficient of $h = 13$ W/m²·K as well as by radiation to the surrounding surfaces at an average temperature of $T_{surr} = 295$ K. Assuming steady one-dimensional heat transfer along the spoon and taking the nodal spacing to be 3 cm, (*a*) obtain the finite difference formulation for all nodes, (*b*) determine the temperature of the tip of the spoon by solving those equations, and (*c*) determine the rate of heat transfer from the exposed surfaces of the spoon.

5–44 A circular fin of uniform cross section, with diameter of 10 mm and length of 50 mm, is attached to a wall with a surface temperature of 350°C. The fin is made of material with thermal conductivity of 240 W/m·K, it is exposed to an ambient air condition of 25°C, and the convection heat transfer coefficient is 250 W/m²·K. Assume steady one-dimensional heat transfer along the fin and the nodal spacing to be uniformly 10 mm. (*a*) Using the energy balance approach, obtain the finite difference equations to determine the nodal temperatures. (*b*) Determine the nodal temperatures along the fin by solving those equations, and compare the results with the analytical solution. (*c*) Calculate the heat transfer rate, and compare the result with the analytical solution.
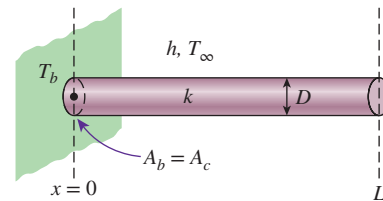
FIGURE P5–44

5–45 A cylindrical aluminum fin with adiabatic tip is attached to a wall with surface temperature of 300°C, and it is exposed to an ambient air condition of 15°C with convection heat transfer coefficient of 150 W/m²·K. The fin has a uniform cross section with diameter of 1 cm, length of 5 cm, and thermal conductivity of 237 W/m·K. Assuming steady one-dimensional heat transfer along the fin and the nodal spacing to be uniformly 10 mm, (*a*) obtain the finite difference equations for use with the Gauss-Seidel iterative method, and (*b*) determine the nodal temperatures using the Gauss-Seidel iterative method, and compare the results with the analytical solution.

5–46 [C&S] A stainless steel plate is connected to an insulation plate by square ASTM A479 904L stainless steel bars. Each square bar has a thickness of 1 cm and a length of 5 cm. The bars are exposed to convection heat transfer with a hot gas. The temperature of the hot gas is 300°C with a convection heat transfer coefficient of 25 W/m²·K. The thermal conductivity for ASTM A479 904L stainless steel is known to be 12 W/m·K. The stainless steel plate maintains a uniform temperature of 100°C. According to the ASME Code for Process Piping (ASME B31.3-2014, Table A-1M), the maximum use temperature for ASTM A479 904L stainless steel bar

is 260°C. Using the finite difference method with a uniform nodal spacing of $\Delta x = 5$ mm along the bar, determine the temperature at each node. Compare the numerical results with the analytical solution. Plot the temperature distribution along the bar. Would any part of the ASTM A479 904L bars be above the maximum use temperature of 260°C?
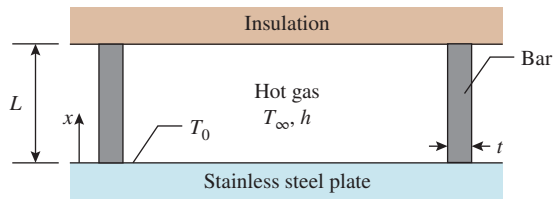
FIGURE P5–46

5–47 A circular fin ($k = 240$ W/m·K) of uniform cross section, with diameter of 10 mm and length of 50 mm, is attached to a wall with surface temperature of 350°C. The fin tip has a temperature of 200°C, it is exposed to an ambient air condition of 25°C, and the convection heat transfer coefficient is 250 W/m²·K. Assuming steady one-dimensional heat transfer along the fin and the nodal spacing to be uniformly 10 mm, (*a*) using the energy balance approach, obtain the finite difference equations to determine the nodal temperatures, and (*b*) determine the nodal temperatures along the fin by solving those equations, and compare the results with the analytical solution.

5–48 C & S A stainless steel plate is connected to a copper plate by long ASTM B98 copper–silicon bolts 9.5 mm in diameter. The portion of the bolts exposed to convection heat transfer with hot gas is 5 cm long. The gas temperature for convection is at 500°C with a convection heat transfer coefficient of 50 W/m²·K. The thermal conductivity of the bolt is known to be 36 W/m·K. The stainless steel plate has a uniform temperature of 100°C, and the copper plate has a uniform temperature of 80°C. According to the ASME Code for Process Piping (ASME B31.3-2014, Table A-2M), the maximum use temperature for an ASTM B98 copper–silicon bolt is 149°C. Using the finite difference method with a uniform nodal spacing of $\Delta x = 5$ mm along the bolt, determine the temperature at each node. Plot the temperature distribution along the bolt. Compare the numerical results with the analytical solution. Would any part of the ASTM B98 bolts be above the maximum use temperature of 149°C?
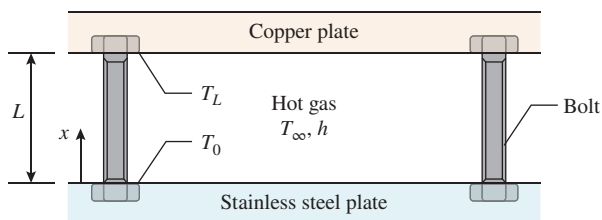
FIGURE P5–48

5–49 C & S A nonmetal plate is connected to a stainless steel plate by long ASTM A437 B4B stainless steel bolts 9.5 mm in diameter. The portion of the bolts exposed to convection heat transfer with a cryogenic fluid is 5 cm long. The fluid temperature for convection is at −50°C with a convection heat transfer coefficient of 100 W/m²·K. The thermal conductivity of the bolts is known to be 23.9 W/m·K. Both the nonmetal and stainless steel plates maintain a uniform temperature of 0°C. According to the ASME Code for Process Piping (ASME B31.3-2014, Table A-2M), the minimum temperature suitable for ASTM A437 B4B stainless steel bolts is −30°C. Using the finite difference method with a uniform nodal spacing of $\Delta x = 5$ mm along the bolt, determine the temperature at each node. Compare the numerical results with the analytical solution. Plot the temperature distribution along the bolt. Would any part of the ASTM A437 B4B bolts be lower than the minimum suitable temperature of −30°C?
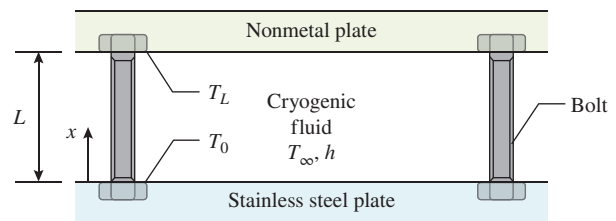
FIGURE P5–49

5–50 A DC motor delivers mechanical power to a rotating stainless steel shaft ($k = 15.1$ W/m·K) with a length of 25 cm and a diameter of 25 mm. The DC motor is in a surrounding with ambient air temperature of 20°C and convection heat transfer coefficient of 25 W/m²·K, and the base temperature of the motor shaft is 90°C. Using a uniform nodal spacing of 5 cm along the motor shaft, determine the finite difference equations and the nodal temperatures by solving those equations.
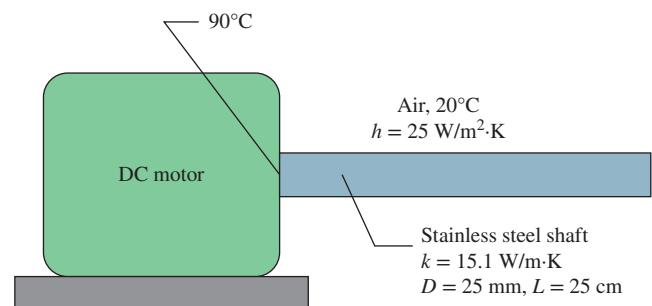
FIGURE P5–50

5–51 One side of a 2-m-high and 3-m-wide vertical plate at 80°C is to be cooled by attaching aluminum fins ($k = 237$ W/m·K) of rectangular profile in an environment at 35°C. The fins are 2 cm long, 0.3 cm thick, and 0.4 cm apart, as shown in Fig. P5–51. The heat transfer coefficient between the fins and

the surrounding air for combined convection and radiation is estimated to be 30 W/m²·K. Assuming steady one-dimensional heat transfer along the fin and taking the nodal spacing to be 0.5 cm, determine (a) the finite difference formulation of this problem, (b) the nodal temperatures along the fin by solving these equations, (c) the rate of heat transfer from a single fin, and (d) the rate of heat transfer from the entire finned surface of the plate.
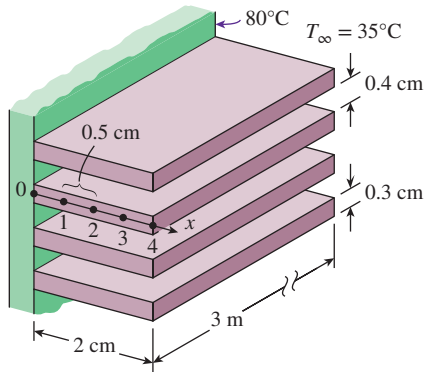
FIGURE P5–51

5–52 A hot surface at 100°C is to be cooled by attaching 3-cm-long, 0.25-cm-diameter aluminum pin fins ($k = 237$ W/m·K) with a center-to-center distance of 0.6 cm. The temperature of the surrounding medium is 30°C, and the combined heat transfer coefficient on the surfaces is 35 W/m²·K. Assuming steady one-dimensional heat transfer along the fin and taking the nodal spacing to be 0.5 cm, determine (a) the finite difference formulation of this problem, (b) the nodal temperatures along the fin by solving these equations, (c) the rate of heat transfer from a single fin, and (d) the rate of heat transfer from a 1-m × 1-m section of the plate.
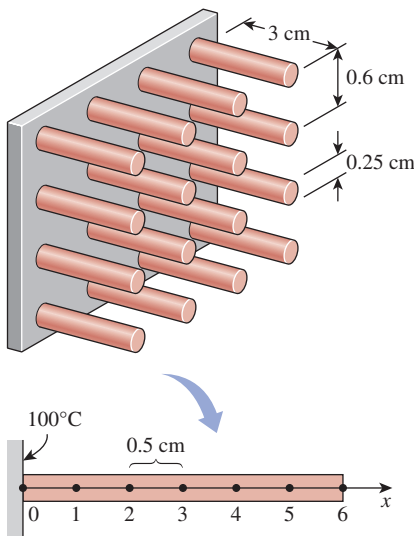
FIGURE P5–52

5–53 Repeat Prob. 5–52 using copper fins ($k = 386$ W/m·K) instead of aluminum ones. *Answers:* (b) 98.6°C, 97.5°C, 96.7°C, 96.0°C, 95.7°C, 95.5°C

5–54 Consider an aluminum alloy fin ($k = 180$ W/m·K) of triangular cross section whose length is $L = 5$ cm, base thickness is $b = 1$ cm, and width w in the direction normal to the plane of paper is very large. The base of the fin is maintained at a temperature of $T_0 = 180$°C. The fin is losing heat by convection to the ambient air at $T_\infty = 25$°C with a heat transfer coefficient of $h = 25$ W/m²·K and by radiation to the surrounding surfaces at an average temperature of $T_{surr} = 290$ K. Using the finite difference method with six equally spaced nodes along the fin in the x-direction, determine (a) the temperatures at the nodes and (b) the rate of heat transfer from the fin for $w = 1$ m. Take the emissivity of the fin surface to be 0.9 and assume steady one-dimensional heat transfer in the fin. *Answers:* (a) 177.0°C, 174.1°C, 171.2°C, 168.4°C, 165.5°C; (b) 537 W
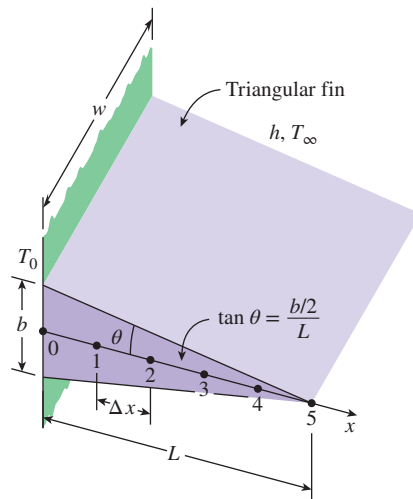
FIGURE P5–54

5–55 📖 Reconsider Prob. 5–54. Using appropriate software, investigate the effect of the fin base temperature on the fin tip temperature and the rate of heat transfer from the fin. Let the temperature at the fin base vary from 100°C to 200°C. Plot the fin tip temperature and the rate of heat transfer as a function of the fin base temperature, and discuss the results.

5–56 Two 3-m-long and 0.4-cm-thick cast iron ($k = 52$ W/m·K, $\varepsilon = 0.8$) steam pipes of outer diameter 10 cm are connected to each other through two 1-cm-thick flanges of outer diameter 20 cm. The steam flows inside the pipe at an average temperature of 250°C with a heat transfer coefficient of 180 W/m²·K. The outer surface of the pipe is exposed to convection with ambient air at 12°C with a heat transfer coefficient of 25 W/m²·K as well as radiation with the surrounding surfaces at an average temperature of $T_{surr} = 290$ K. Assuming steady one-dimensional heat conduction along the flanges and taking

the nodal spacing to be 1 cm along the flange, (*a*) obtain the finite difference formulation for all nodes, (*b*) determine the temperature at the tip of the flange by solving those equations, and (*c*) determine the rate of heat transfer from the exposed surfaces of the flange.
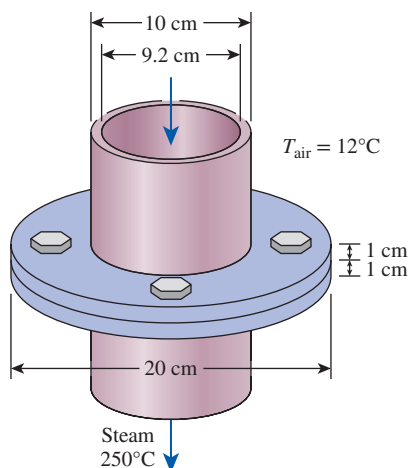
FIGURE P5–56

5–57 Reconsider Prob. 5–56. Using appropriate software, investigate the effects of the steam temperature and the outer heat transfer coefficient on the flange tip temperature and the rate of heat transfer from the exposed surfaces of the flange. Let the steam temperature vary from 150°C to 300°C and the heat transfer coefficient from 15 W/m²·K to 60 W/m²·K. Plot the flange tip temperature and the heat transfer rate as functions of steam temperature and heat transfer coefficient, and discuss the results.

5–58 Using appropriate software, solve these systems of algebraic equations.

(*a*) $\quad 3x_1 - x_2 + 3x_3 = 0$
$\quad\quad -x_1 + 2x_2 + x_3 = 3$
$\quad\quad 2x_1 - x_2 - x_3 = 2$

(*b*) $\quad 4x_1 - 2x_2^2 + 0.5x_3 = -2$
$\quad\quad\quad x_1^3 - x_2 + x_3 = 11.964$
$\quad\quad\quad x_1 + x_2 + x_3 = 3$

Answers: (*a*) $x_1 = 2$, $x_2 = 3$, $x_3 = -1$, (*b*) $x_1 = 2.33$, $x_2 = 2.29$, $x_3 = -1.62$

5–59 Using appropriate software, solve these systems of algebraic equations.

(*a*) $\quad 3x_1 + 2x_2 - x_3 + x_4 = 6$
$\quad\quad\quad\quad x_1 + 2x_2 - x_4 = -3$
$\quad\quad -2x_1 + x_2 + 3x_3 + x_4 = 2$
$\quad\quad\quad 3x_2 + x_3 - 4x_4 = -6$

(*b*) $\quad 3x_1 + x_2^2 + 2x_3 = 8$
$\quad\quad -x_1^2 + 3x_2 + 2x_3 = -6.293$
$\quad\quad 2x_1 - x_2^4 + 4x_3 = -12$

5–60 Using appropriate software, solve these systems of algebraic equations.

(*a*) $\quad 4x_1 - x_2 + 2x_3 + x_4 = -6$
$\quad\quad x_1 + 3x_2 - x_3 + 4x_4 = -1$
$\quad\quad\quad -x_1 + 2x_2 + 5x_4 = 5$
$\quad\quad\quad 2x_2 - 4x_3 - 3x_4 = -5$

(*b*) $\quad 2x_1 + x_2^4 - 2x_3 + x_4 = 1$
$\quad\quad x_1^2 + 4x_2 + 2x_3^2 - 2x_4 = -3$
$\quad\quad\quad -x_1 + x_2^4 + 5x_3 = 10$
$\quad\quad\quad 3x_1 - x_3^2 + 8x_4 = 15$

Two-Dimensional Steady Heat Conduction

5–61C What is an irregular boundary? What is a practical way of handling irregular boundary surfaces with the finite difference method?

5–62C Consider a medium in which the finite difference formulation of a general interior node is given in its simplest form as

$$T_{\text{node}} = (T_{\text{left}} + T_{\text{top}} + T_{\text{right}} + T_{\text{bottom}})/4$$

(*a*) Is heat transfer in this medium steady or transient?
(*b*) Is heat transfer one-, two-, or three-dimensional?
(*c*) Is there heat generation in the medium?
(*d*) Is the nodal spacing constant or variable?
(*e*) Is the thermal conductivity of the medium constant or variable?

5–63C Consider a medium in which the finite difference formulation of a general interior node is given in its simplest form as

$$T_{\text{left}} + T_{\text{top}} + T_{\text{right}} + T_{\text{bottom}} - 4T_{\text{node}} + \frac{\dot{e}_{\text{node}}l^2}{k} = 0$$

(*a*) Is heat transfer in this medium steady or transient?
(*b*) Is heat transfer one-, two-, or three-dimensional?
(*c*) Is there heat generation in the medium?
(*d*) Is the nodal spacing constant or variable?
(*e*) Is the thermal conductivity of the medium constant or variable?

5–64 Starting with an energy balance on a volume element, obtain the steady two-dimensional finite difference equation for a general interior node in rectangular coordinates for $T(x, y)$ for the case of variable thermal conductivity and uniform heat generation.

5–65 Consider steady two-dimensional heat transfer in a square cross section (3 cm × 3 cm) with the prescribed

temperatures at the top, right, bottom, and left surfaces to be 100°C, 200°C, 300°C, and 500°C, respectively. Using a uniform mesh size $\Delta x = \Delta y$, determine (a) the finite difference equations and (b) the nodal temperatures with the Gauss-Seidel iterative method.
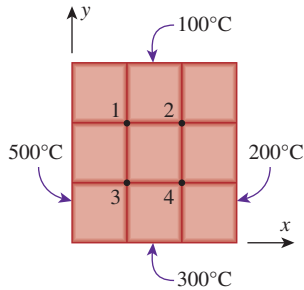
FIGURE P5–65

5–66 Consider steady two-dimensional heat transfer in a long solid body whose cross section is given in the figure. The measured temperatures at selected points of the outer surfaces are as shown. The thermal conductivity of the body is $k = 45$ W/m·K, and there is no heat generation. Using the finite difference method with a mesh size of $\Delta x = \Delta y = 2.0$ cm, determine the temperatures at the indicated points in the medium. *Hint:* Take advantage of symmetry.
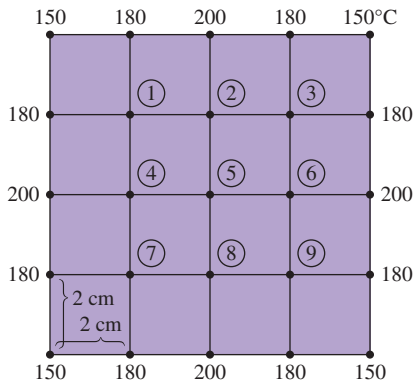
FIGURE P5–66

5–67 Consider steady two-dimensional heat transfer in a long solid bar of (a) square and (b) rectangular cross sections as shown in the figure. The measured temperatures at selected points of the outer surfaces are as shown. The thermal conductivity of the body is $k = 20$ W/m·K, and there is no heat generation. Using the finite difference method with a mesh size of $\Delta x = \Delta y = 1.0$ cm, determine the temperatures at the indicated points in the medium. *Answers:* (a) $T_1 = 185$°C, $T_2 = T_3 = T_4 = 190$°C
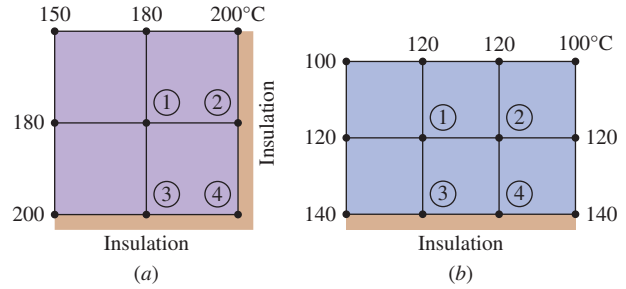
FIGURE P5–67

5–68 Consider steady two-dimensional heat conduction in a square cross section (3 cm × 3 cm, $k = 20$ W/m·K, $\alpha = 6.694 \times 10^{-6}$ m²/s) with constant prescribed temperature of 100°C and 300°C at the top and bottom surfaces, respectively. The left surface is exposed to a constant heat flux of 1000 W/m², while the right surface is in contact with a convective environment ($h = 45$ W/m²·K) at 20°C. Using a uniform mesh size of $\Delta x = \Delta y$, determine (a) finite difference equations and (b) the nodal temperatures using the Gauss-Seidel iteration method.
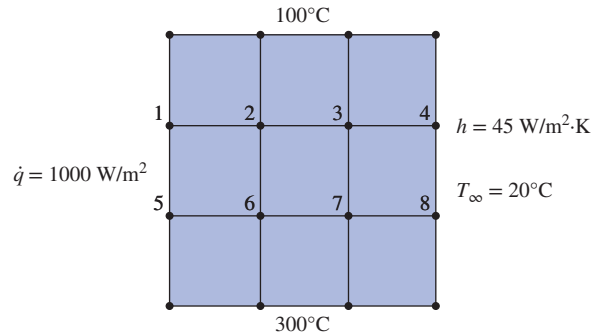
FIGURE P5–68

5–69 Consider steady two-dimensional heat transfer in a rectangular cross section (60 cm × 30 cm) with the prescribed temperatures at the left, right, and bottom surfaces to be 0°C, and the top surface is given as $100 \sin(\pi x/60)$. Using a uniform mesh size $\Delta x = \Delta y$, determine (a) the finite difference equations and (b) the nodal temperatures.
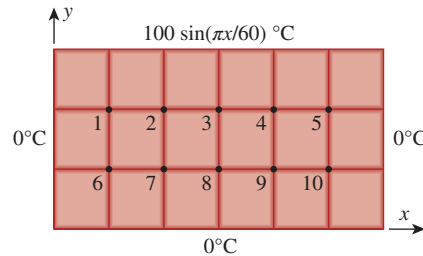
FIGURE P5–69

5–70 Consider a rectangular metal block ($k = 35$ W/m·K) of dimensions 100 cm × 75 cm subjected to a sinusoidal temperature variation at its top surface while its bottom surface is insulated. The two sides of the metal block are exposed to a convective environment at 15°C and have a heat transfer coefficient of 50 W/m²·K. The sinusoidal temperature distribution at the top surface is given as $100 \sin(\pi x/L)$. Using a uniform mesh size of $\Delta x = \Delta y = 25$ cm, determine (a) finite difference equations and (b) the nodal temperatures.
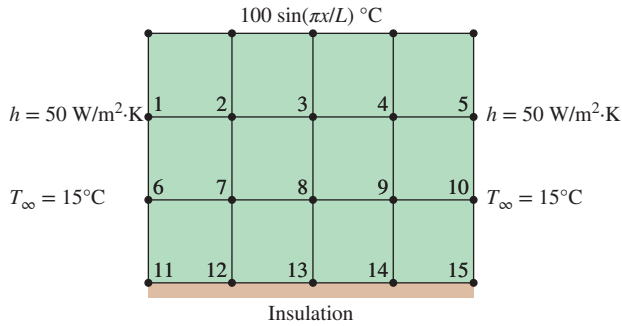
FIGURE P5–70

5–71 Consider a long bar of rectangular cross section (60 mm by 90 mm on a side) and of thermal conductivity 1 W/m·K. The top surface is exposed to a convection process with air at 100°C and a convection heat transfer coefficient of 100 W/m²·K, while the remaining surfaces are maintained at 50°C. Using a grid spacing of 30 mm and the Gauss-Seidel iteration method, determine the temperatures at nodes 1, 2, and 3 shown in Fig. P5–71. Use an initial estimate of 0°C for all the nodal temperatures and a 0.35°C convergence criterion.
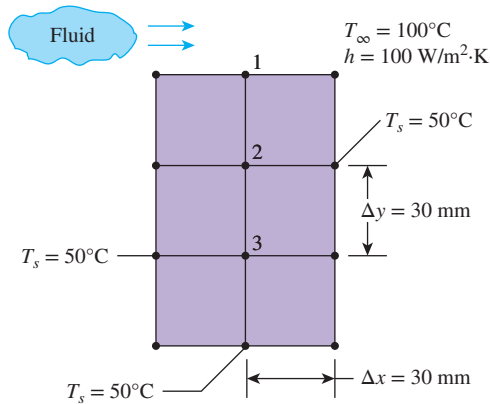
FIGURE P5–71

5–72 Consider steady two-dimensional heat transfer in a long solid body whose cross section is given in Fig. P5–72. The temperatures at the selected nodes and the thermal conditions on the boundaries are as shown. The thermal conductivity of the body

is $k = 150$ W/m·K, and heat is generated in the body uniformly at a rate of $\dot{e} = 3 \times 10^7$ W/m³. Using the finite difference method with a mesh size of $\Delta x = \Delta y = 10$ cm, determine (a) the temperatures at nodes 1, 2, 3, and 4 and (b) the rate of heat loss from the top surface through a 1-m-long section of the body.
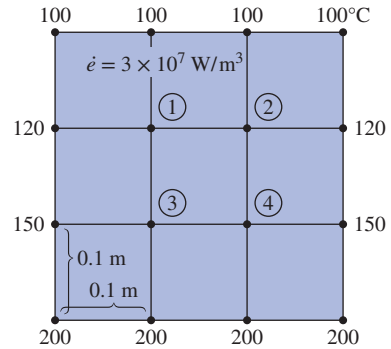
FIGURE P5–72

5–73 Repeat Prob. 5–72 using appropriate software.

5–74 Reconsider Prob. 5–72. Using appropriate software, investigate the effects of the thermal conductivity and the heat generation rate on the temperatures at nodes 1 and 3 and the rate of heat loss from the top surface. Let the thermal conductivity vary from 10 W/m·K to 400 W/m·K and the heat generation rate from 10^5 W/m³ to 10^8 W/m³. Plot the temperatures at nodes 1 and 3 and the rate of heat loss as functions of thermal conductivity and heat generation rate, and discuss the results.

5–75 Steady-state temperatures (K) at three nodal points of a two-dimensional system with a thermal conductivity of $k = 20$ W/m·K are shown in Fig. P5–75. The grid spacing is 5 mm. The 2-D system experiences a uniform volumetric heat generation rate of 5×10^7 W/m³. The top and right sides of the system are insulated, while the left and the bottom sides are maintained at a constant temperature of 300 K. Determine T_1, T_2, and T_3 (K).
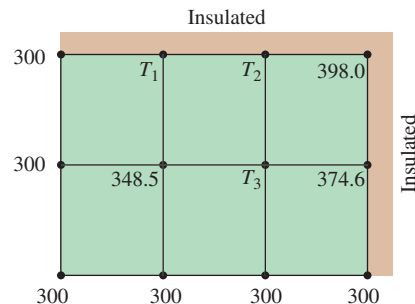
FIGURE P5–75

5–76 Consider steady two-dimensional heat transfer in a long solid body whose cross section is given in Fig. P5–76. The temperatures at the selected nodes and the thermal conditions at the

boundaries are as shown. The thermal conductivity of the body is $k = 45$ W/m·K, and heat is generated in the body uniformly at a rate of $\dot{e} = 4 \times 10^6$ W/m^3. Using the finite difference method with a mesh size of $\Delta x = \Delta y = 4$ cm, determine (a) the temperatures at nodes 1, 2, and 3 and (b) the rate of heat loss from the bottom surface through a 1-m-long section of the body.
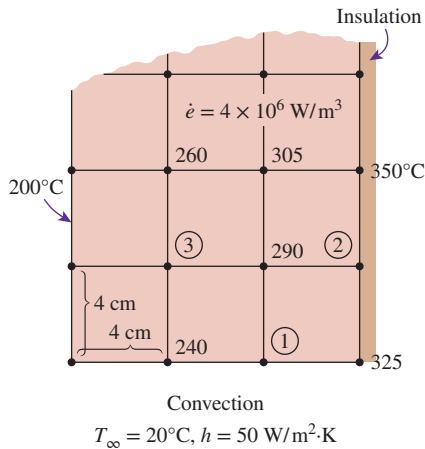
FIGURE P5–76

5–77 Repeat Prob. 5–76 using appropriate software.

5–78 Consider a 5-m-long constantan block ($k = 23$ W/m·K) 30 cm high and 50 cm wide (Fig. P5–78). The block is completely submerged in iced water at 0°C that is well stirred, and the heat transfer coefficient is so high that the temperatures on both sides of the block can be taken to be 0°C. The bottom surface of the bar is covered with a low-conductivity material so that heat transfer through the bottom surface is negligible. The top surface of the block is heated uniformly by an 8-kW resistance heater. Using the finite difference method with a mesh size of $\Delta x = \Delta y = 10$ cm and taking advantage of symmetry, (a) obtain the finite difference formulation of this problem for steady two-dimensional heat transfer, (b) determine the unknown nodal temperatures by solving those equations, and (c) determine the rate of heat transfer from the block to the iced water.
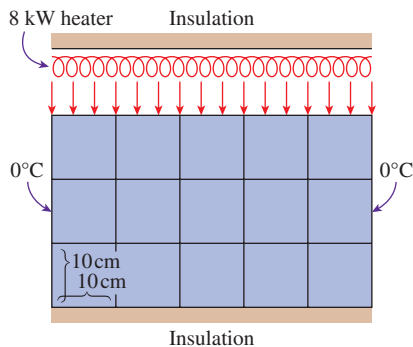
FIGURE P5–78

5–79 Consider steady two-dimensional heat transfer in a long solid bar ($k = 25$ W/m·K) of square cross section (3 cm × 3 cm) with the prescribed temperatures at the top, right, bottom, and left surfaces to be 100°C, 200°C, 300°C, and 500°C, respectively. Heat is generated in the bar uniformly at a rate of $\dot{e} = 5 \times 10^6$ W/m^3. Using a uniform mesh size $\Delta x = \Delta y = 1$ cm, determine (a) the finite difference equations and (b) the nodal temperatures with the Gauss-Seidel iterative method.
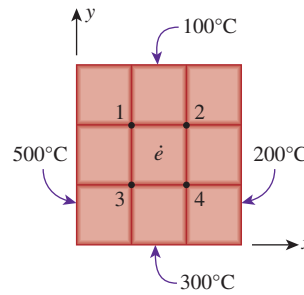
FIGURE P5–79

5–80E Consider steady two-dimensional heat transfer in a long solid bar of square cross section in which heat is generated uniformly at a rate of $\dot{e} = 0.19 \times 10^5$ Btu/h·ft^3. The cross section of the bar is 0.5 ft × 0.5 ft in size, and its thermal conductivity is $k = 16$ Btu/h·ft·°F. All four sides of the bar are subjected to convection with the ambient air at $T_\infty = 70$°F with a heat transfer coefficient of $h = 7.9$ Btu/h·ft^2·°F. Using the finite difference method with a mesh size of $\Delta x = \Delta y = 0.25$ ft, determine (a) the temperatures at the nine nodes and (b) the rate of heat loss from the bar through a 1-ft-long section. *Answers:* (b) 4750 Btu/h
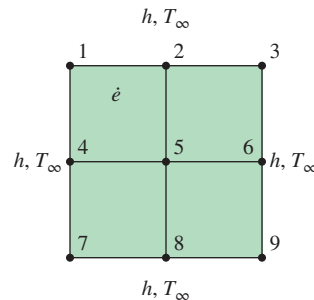
FIGURE P5–80E

5–81 Hot combustion gases of a furnace are flowing through a concrete chimney ($k = 1.4$ W/m·K) of rectangular cross section. The flow section of the chimney is 20 cm × 40 cm, and

the thickness of the wall is 10 cm. The average temperature of the hot gases in the chimney is $T_i = 280°C$, and the average convection heat transfer coefficient inside the chimney is $h_i = 75$ W/m²·K. The chimney is losing heat from its outer surface to the ambient air at $T_0 = 15°C$ by convection with a heat transfer coefficient of $h_o = 18$ W/m²·K and to the sky by radiation. The emissivity of the outer surface of the wall is $\varepsilon = 0.9$, and the effective sky temperature is estimated to be 250 K.

Using the finite difference method with $\Delta x = \Delta y = 10$ cm and taking full advantage of symmetry, (a) obtain the finite difference formulation of this problem for steady two-dimensional heat transfer, (b) determine the temperatures at the nodal points of a cross section, and (c) evaluate the rate of heat loss for a 1-m-long section of the chimney.
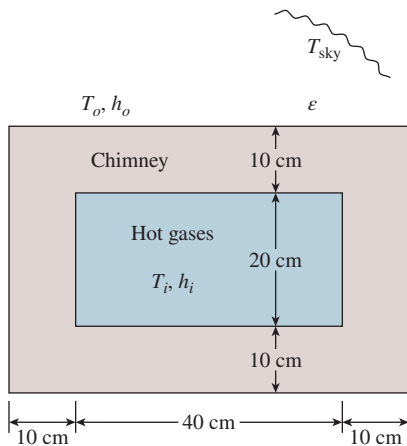
FIGURE P5–83

FIGURE P5–81

5–82 Repeat Prob. 5–81 by disregarding radiation heat transfer from the outer surfaces of the chimney.

5–83 A thin-film 500-W electrical heater of negligible thickness and dimensions 100 mm × 100 mm is sandwiched between two slabs made of copper alloy ($k = 120$ W/m·K) and stainless steel (15 W/m·K). The two plates, copper and stainless steel with thickness 50 mm and 50 mm, are surrounded by air with heat transfer coefficients of 75 W/m²·K and 25 W/m²·K, respectively. The plates are subjected to a constant temperature of 50°C and 30°C at the top and the bottom surface, respectively, as shown in Fig. P5–83. The temperature of the surrounding air is maintained at 20°C. Determine (a) the finite difference formulation at each node and (b) the location of maximum temperature.
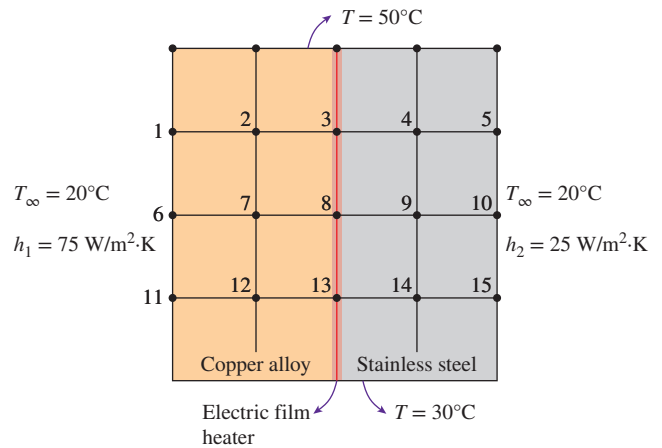
5–84 The wall of a heat exchanger separates hot water at $T_A = 90°C$ from cold water at $T_B = 10°C$. To extend the heat transfer area, two-dimensional ridges are machined on the cold side of the wall, as shown in Fig. P5–84. This geometry causes nonuniform thermal stresses, which may become critical for crack initiation along the lines between two ridges. To predict thermal stresses, the temperature field inside the wall must be determined. Convection coefficients are high enough so that the surface temperature is equal to that of the water on each side of the wall.

(a) Identify the smallest section of the wall that can be analyzed in order to find the temperature field in the whole wall.

(b) For the domain found in part (a), construct a two-dimensional grid with $\Delta x = \Delta y = 5$ mm and write the matrix equation $AT = C$ (elements of matrices A and C must be numbers). Do not solve for T.

(c) A thermocouple mounted at point M reads 46.9°C. Determine the other unknown temperatures in the grid defined in part (b).
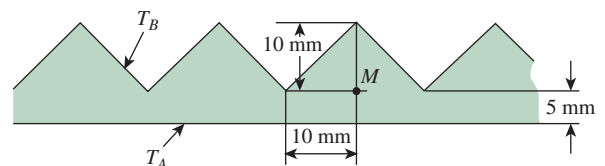
FIGURE P5–84

5–85 Consider steady two-dimensional heat transfer in two long solid bars whose cross sections are given in Fig. P5–85. The measured temperatures at selected points on the outer surfaces are as shown. The thermal conductivity of the body is $k = 20$ W/m·K, and there is no heat generation. Using the finite

difference method with a mesh size of $\Delta x = \Delta y = 1.0$ cm, determine the temperatures at the indicated points in the medium. *Hint:* Take advantage of symmetry. *Answers:* (*b*) $T_1 = T_4 = 93°C$, $T_2 = T_3 = 86°C$
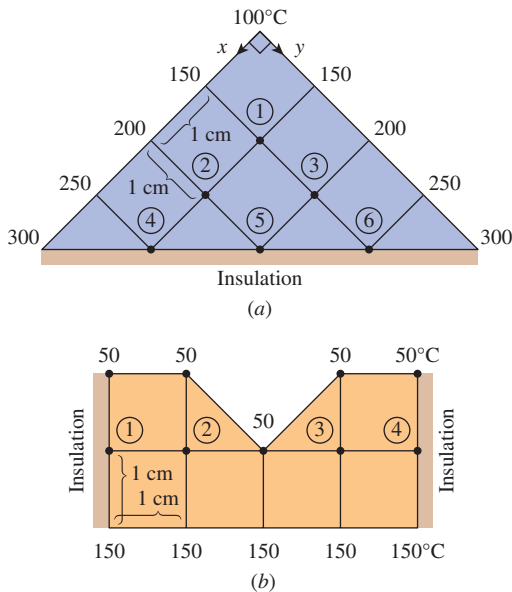
FIGURE P5–85

5–86 Consider a long concrete dam ($k = 0.6$ W/m·K, $\alpha_s = 0.7$) of triangular cross section whose exposed surface is subjected to solar heat flux of $\dot{q}_s = 800$ W/m² and to convection and radiation to the environment at 25°C with a combined heat transfer coefficient of 30 W/m²·K. The 2-m-high vertical section of the dam is subjected to convection by water at 15°C with a heat transfer coefficient of 150 W/m²·K, and heat transfer through the 2-m-long base is considered to be negligible. Using the finite difference method with a mesh size of $\Delta x = \Delta y = 1$ m and assuming steady two-dimensional heat transfer, determine the temperature of the top, middle, and bottom of the exposed surface of the dam. *Answers:* 21.3°C, 43.2°C, 43.6°C
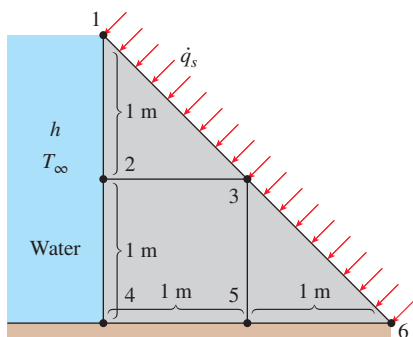
FIGURE P5–86

5–87 Consider a long solid bar whose thermal conductivity is $k = 5$ W/m·K and whose cross section is given in Fig. P5–87. The top surface of the bar is maintained at 50°C, while the bottom surface is maintained at 120°C. The left surface is insulated, and the remaining three surfaces are subjected to convection with ambient air at $T_\infty = 25°C$ with a heat transfer coefficient of $h = 40$ W/m²·K. Using the finite difference method with a mesh size of $\Delta x = \Delta y = 10$ cm, (*a*) obtain the finite difference formulation of this problem for steady two-dimensional heat transfer and (*b*) determine the unknown nodal temperatures by solving those equations. *Answers:* (*b*) 78.8°C, 72.7°C, 64.6°C
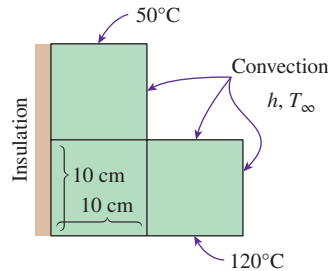
FIGURE P5–87

5–88 Consider steady two-dimensional heat transfer in an L-shaped solid body whose cross section is given in Fig. P5–88. The thermal conductivity of the body is $k = 45$ W/m·K, and heat is generated in the body at a rate of $\dot{e} = 5 \times 10^6$ W/m³. The right surface of the body is insulated, and the bottom surface is maintained at a uniform temperature of 180°C. The entire top surface is subjected to convection with ambient air at $T_\infty = 30°C$ with a heat transfer coefficient of $h = 55$ W/m²·K, and the left surface is subjected to heat flux at a uniform rate of $\dot{q}_L = 8000$ W/m². The nodal network of the problem consists of 13 equally spaced nodes with $\Delta x = \Delta y = 1.5$ cm. Five of the nodes are at the bottom surface, and thus their temperatures are known. (*a*) Obtain the finite difference equations at the remaining eight nodes, and (*b*) determine the nodal temperatures by solving those equations.
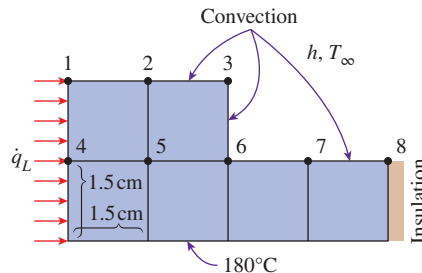
FIGURE P5–88

5–89 As shown in Fig. P5–89, a T-shaped bar ($k = 28$ W/m·K) in inverted position is attached to a surface maintained at 200°C. The two sides of the bottom portion of the T bar are insulated, while the rest of the sides are subjected to a

convective environment with $h = 30$ W/m²·K and ambient temperature of 10°C. The mesh size is uniform for the long portion of the bar while it is doubled in the *x*-direction for the bottom portion of the T bar. Assuming steady-state conditions and no internal heat generation, determine (*a*) the finite difference formulation for each node and (*b*) the nodal temperatures. *Hint:* Take advantage of symmetry.
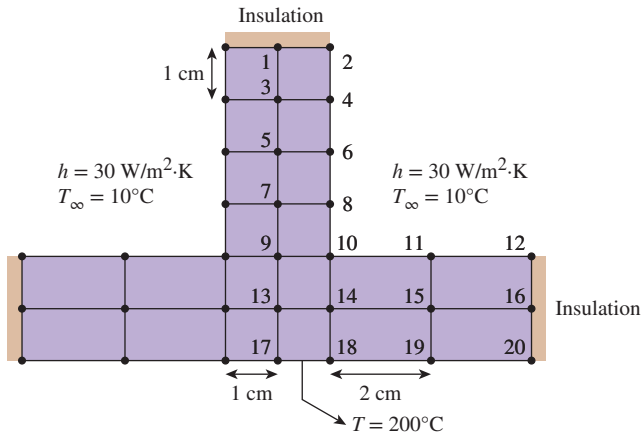
FIGURE P5–89

5–90 Sintering is a metallurgical process used to create metal objects with better physical properties by holding powdered material in a mold and heating it to a temperature slightly below its melting point. Two materials, nickel ($k = 90.7$ W/m·K) and copper ($k = 401$ W/m·K), are embedded in a mold made of stainless steel ($k = 15.1$ W/m·K), as shown in Fig. P5–90. The bottom surface of stainless steel is maintained at a nonuniform temperature while its two sides are insulated. The upper surface of nickel and copper is exposed to a convective environment with $h = 125$ W/m²·K and ambient temperature of 15°C. Assuming steady-state heat conduction and a mesh size of 1.5 cm, develop finite difference equations for different nodes and determine the nodal temperatures. The density of the powdered material after sintering is about 99 percent of the original metal density and hence may be considered a continuous solid material for all practical purposes. *Hint:* Use the mirror image concept for the nodes at the insulated boundary.
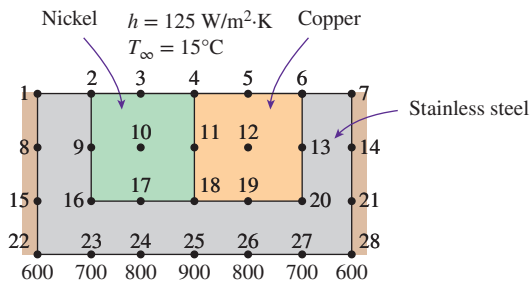
FIGURE P5–90

5–91E Consider steady two-dimensional heat transfer in a V-grooved solid body whose cross section is given in Fig. P5–91E. The top surfaces of the groove are maintained at 32°F while the bottom surface is maintained at 212°F. The side surfaces of the groove are insulated. Using the finite difference method with a mesh size of $\Delta x = \Delta y = 1$ ft and taking advantage of symmetry, determine the temperatures at the middle of the insulated surfaces.
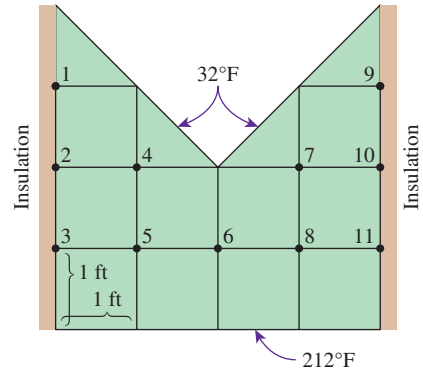
FIGURE P5–91E

5–92E Reconsider Prob. 5–91E. Using appropriate software, and investigate the effects of the temperatures at the top and bottom surfaces on the temperature in the middle of the insulated surface. Let the temperatures at the top and bottom surfaces vary from 32°F to 212°F. Plot the temperature in the middle of the insulated surface as functions of the temperatures at the top and bottom surfaces, and discuss the results.

Transient Heat Conduction

5–93C How does the finite difference formulation of a transient heat conduction problem differ from that of a steady heat conduction problem? What does the term $\rho A \Delta x\, c_p (T_m^{i+1} - T_m^i)/\Delta t$ represent in the transient finite difference formulation?

5–94C What are the two basic methods of solution of transient problems based on finite differencing? How do heat transfer terms in the energy balance formulation differ in the two methods?

5–95C The explicit finite difference formulation of a general interior node for transient heat conduction in a plane wall is given by

$$T_{m-1}^i - 2T_m^i + T_{m+1}^i + \frac{\dot{e}_m^i \Delta x^2}{k} = \frac{T_m^{i+1} - T_m^i}{\tau}$$

Obtain the finite difference formulation for the steady case by simplifying the preceding relation.

5–96C Consider transient one-dimensional heat conduction in a plane wall that is to be solved by the explicit method. If both sides of the wall are at specified temperatures, express the stability criterion for this problem in its simplest form.

5–97C Consider transient one-dimensional heat conduction in a plane wall that is to be solved by the explicit method. If both sides of the wall are subjected to specified heat flux, express the stability criterion for this problem in its simplest form.

5–98C The explicit finite difference formulation of a general interior node for transient two-dimensional heat conduction is given by

$$T^{i+1}_{\text{node}} = \tau(T^i_{\text{left}} + T^i_{\text{top}} + T^i_{\text{right}} + T^i_{\text{bottom}})$$

$$+(1 - 4\tau)T^i_{\text{node}} + \tau\frac{\dot{e}^i_{\text{node}}l^2}{k}$$

Obtain the finite difference formulation for the steady case by simplifying the preceding relation.

5–99C Is there any limitation on the size of the time step Δt in the solution of transient heat conduction problems using (*a*) the explicit method and (*b*) the implicit method?

5–100C Express the general stability criterion for the explicit method of solution of transient heat conduction problems.

5–101C Consider transient two-dimensional heat conduction in a rectangular region that is to be solved by the explicit method. If all boundaries of the region are either insulated or at specified temperatures, express the stability criterion for this problem in its simplest form.

5–102C The implicit method is unconditionally stable and thus any value of time step Δt can be used in the solution of transient heat conduction problems. To minimize the computation time, someone suggests using a very large value of Δt since there is no danger of instability. Do you agree with this suggestion? Explain.

5–103 Starting with an energy balance on a volume element, obtain the two-dimensional transient explicit finite difference equation for a general interior node in rectangular coordinates for $T(x, y, t)$ for the case of constant thermal conductivity and no heat generation.

5–104 Starting with an energy balance on a volume element, obtain the two-dimensional transient implicit finite difference equation for a general interior node in rectangular coordinates for $T(x, y, t)$ for the case of constant thermal conductivity and no heat generation.

5–105 Starting with an energy balance on a disk volume element, derive the one-dimensional transient explicit finite difference equation for a general interior node for $T(z, t)$ in a cylinder whose side surface is insulated for the case of constant thermal conductivity with uniform heat generation.

5–106 Consider transient heat conduction in a plane wall whose left surface (node 0) is maintained at 80°C while the right surface (node 6) is subjected to a solar heat flux of 600 W/m². The wall is initially at a uniform temperature of 50°C. Express the explicit finite difference formulation

of the boundary nodes 0 and 6 for the case of no heat generation. Also, obtain the finite difference formulation for the total amount of heat transfer at the left boundary during the first three time steps.

5–107 Consider transient heat conduction in a plane wall with variable heat generation and constant thermal conductivity. The nodal network of the medium consists of nodes 0, 1, 2, 3, and 4 with a uniform nodal spacing of Δx. The wall is initially at a specified temperature. Using the energy balance approach, obtain the explicit finite difference formulation of the boundary nodes for the case of uniform heat flux $\dot{q}_0$ at the left boundary (node 0) and convection at the right boundary (node 4) with a convection coefficient of h and an ambient temperature of T_∞. Do not simplify.
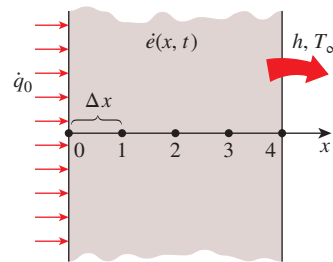
FIGURE P5–107

5–108 Repeat Prob. 5–107 for the case of implicit formulation.

5–109 Consider transient heat conduction in a plane wall with variable heat generation and constant thermal conductivity. The nodal network of the medium consists of nodes 0, 1, 2, 3, 4, and 5 with a uniform nodal spacing of Δx. The wall is initially at a specified temperature. Using the energy balance approach, obtain the explicit finite difference formulation of the boundary nodes for the case of insulation at the left boundary (node 0) and radiation at the right boundary (node 5) with an emissivity of ε and surrounding temperature of T_{surr}.

5–110 Consider transient heat conduction in a plane wall with variable heat generation and constant thermal conductivity. The nodal network of the medium consists of nodes 0, 1, 2, 3, and 4 with a uniform nodal spacing of Δx. The wall is initially at a specified temperature. The temperature at the right boundary (node 4) is specified. Using the energy balance approach, obtain the explicit finite difference formulation of the boundary node 0 for the case of combined convection, radiation, and heat flux at the left boundary with an emissivity of ε, convection coefficient of h, ambient temperature of T_∞, surrounding temperature of T_{surr}, and uniform heat flux of $\dot{q}_0$ toward the wall. Also, obtain the finite difference formulation for the total amount of heat transfer at the right boundary for the first 20 time steps.
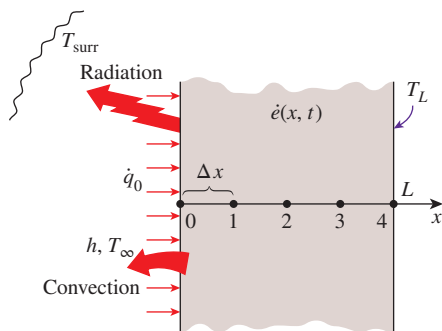
FIGURE P5–110

5–111 Consider one-dimensional transient heat conduction in a composite plane wall that consists of two layers A and B with perfect contact at the interface. The wall involves no heat generation and initially is at a specified temperature. The nodal network of the medium consists of nodes 0, 1 (at the interface), and 2 with a uniform nodal spacing of Δx. Using the energy balance approach, obtain the explicit finite difference formulation of this problem for the case of insulation at the left boundary (node 0) and radiation at the right boundary (node 2) with an emissivity of ε and surrounding temperature of T_{surr}.
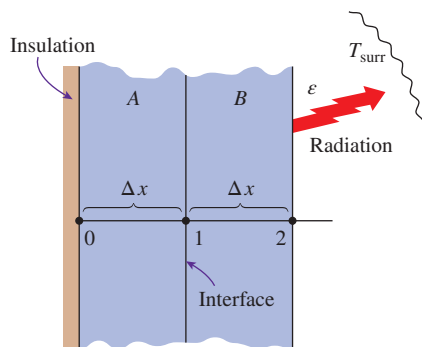
FIGURE P5–111

5–112 Consider transient one-dimensional heat conduction in a pin fin of constant diameter D with constant thermal conductivity. The fin is losing heat by convection to the ambient air at T_∞ with a heat transfer coefficient of h and by radiation to the surrounding surfaces at an average temperature of T_{surr}. The nodal network of the fin consists of nodes 0 (at the base), 1 (in the middle), and 2 (at the fin tip) with a uniform nodal spacing of Δx. Using the energy balance approach, obtain the explicit finite difference formulation of this problem for the case of a specified temperature at the fin base and negligible heat transfer at the fin tip.

5–113 Repeat Prob. 5–112 for the case of implicit formulation.

5–114 A hot brass plate is having its upper surface cooled by an impinging jet of air at a temperature of 15°C and convection heat transfer coefficient of 220 W/m²·K. The 10-cm-thick brass plate ($\rho = 8530$ kg/m³, $c_p = 380$ J/kg·K, $k = 110$ W/m·K, and $\alpha = 33.9 \times 10^{-6}$ m²/s) had a uniform initial temperature of 650°C, and the lower surface of the plate is insulated. Using a uniform nodal spacing of $\Delta x = 2.5$ cm and time step of $\Delta t = 10$ s, determine (*a*) the implicit finite difference equations and (*b*) the nodal temperatures of the brass plate after 10 seconds of cooling.
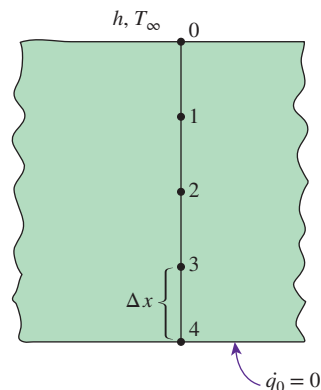
FIGURE P5–114

5–115 Consider a large uranium plate of thickness $L = 9$ cm, thermal conductivity $k = 28$ W/m·K, and thermal diffusivity $\alpha = 12.5 \times 10^{-6}$ m²/s that is initially at a uniform temperature of 100°C. Heat is generated uniformly in the plate at a constant rate of $\dot{e} = 10^6$ W/m³. At time $t = 0$, the left side of the plate is insulated while the other side is subjected to convection with an environment at $T_\infty = 20$°C with a heat transfer coefficient of $h = 35$ W/m²·K. Using the explicit finite difference approach with a uniform nodal spacing of $\Delta x = 1.5$ cm, determine (*a*) the temperature distribution in the plate after 5 min and (*b*) how long it will take for steady conditions to be reached in the plate.

5–116 Reconsider Prob. 5–115. Using appropriate software, investigate the effect of the cooling time on the temperatures of the left and right sides of the plate. Let the time vary from 5 min to 60 min. Plot the temperatures at the left and right surfaces as a function of time, and discuss the results.

5–117E Consider a house whose windows are made of 0.375-in-thick glass ($k = 0.48$ Btu/h·ft·°F and $\alpha = 4.2 \times 10^{-6}$ ft²/s). Initially, the entire house, including the walls and the windows, is at the outdoor temperature of $T_o = 35$°F. It is observed that the windows are fogged because the indoor temperature is below the dew-point temperature of 54°F. Now the heater is turned on, and the air temperature in the house is raised to $T_i = 72$°F at a rate of 2°F rise per minute. The heat transfer coefficients at the inner and outer surfaces of the wall can be taken to be $h_i = 1.2$ and $h_o = 2.6$ Btu/h·ft²·°F, respectively, and the outdoor temperature can be assumed to remain constant.

Using the explicit finite difference method with a mesh size of $\Delta x = 0.125$ in, determine how long it will take for the fog on the windows to clear up (i.e., for the inner surface temperature of the window glass to reach 54°F).
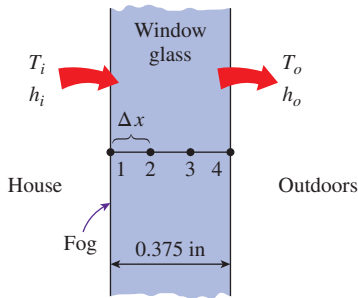
FIGURE P5–117E

5–118 A series of long stainless steel bolts (ASTM A437 B4B) are fastened into a metal plate with a thickness of 4 cm. The bolts have a thermal conductivity of 23.9 W/m·K, a specific heat of 460 J/kg·K, and a density of 7.8 g/cm³. For the metal plate, the specific heat, thermal conductivity, and density are 500 J/kg·K, 16.3 W/m·K, and 8 g/cm³, respectively. The upper surface of the plate is occasionally exposed to cryogenic fluid at −70°C with a convection heat transfer coefficient of 300 W/m²·K. The lower surface of the plate is exposed to convection with air at 10°C and a convection heat transfer coefficient of 10 W/m²·K. The bolts are fastened into the metal plate from the bottom surface, and the distance measured from the plate's upper surface to the bolt tips is 1 cm. The ASME Code for Process Piping limits the minimum suitable temperature for ASTM A437 B4B stainless steel bolt to −30°C (ASME B31.3-2014, Table A-2M). If the initial temperature of the plate is 10°C and the plate's upper surface is exposed to the cryogenic fluid for 9 min, would the bolts fastened in the plate still comply with the ASME code? Using the explicit finite difference formulations with a uniform nodal spacing of $\Delta x = 1$ cm, determine the temperature at each node for the duration of the upper surface being exposed to the cryogenic fluid. Plot the nodal temperatures as a function of time.
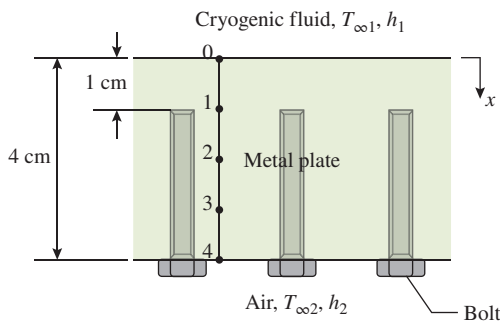
FIGURE P5–118

5–119 An ASTM F441 chlorinated polyvinyl chloride (CPVC) tube is embedded in a metal plate with a thickness of 4 cm. The metal plate has a thermal conductivity of 26.9 W/m·K, a specific heat of 460 J/kg·K, and a density of 7.73 g/cm³. The upper surface of the plate is occasionally exposed to hot fluid at 300°C with a convection heat transfer coefficient of 200 W/m²·K. The lower surface of the plate is well insulated. The distance measured from the plate's upper surface to the tube surface is 1 cm. The ASME Code for Process Piping limits the maximum use temperature for ASTM F441 CPVC tube to 93.3°C (ASME B31.3-2014, Table B-1). If the initial temperature of the plate is 20°C and the plate's upper surface is exposed to the hot fluid for 5 min, would the CPVC tube embedded in the plate still comply with the ASME code? Using the explicit finite difference formulations with a uniform nodal spacing of $\Delta x = 1$ cm, determine the temperature at each node for the duration of the upper surface being exposed to the hot fluid. Plot the nodal temperatures as a function of time.
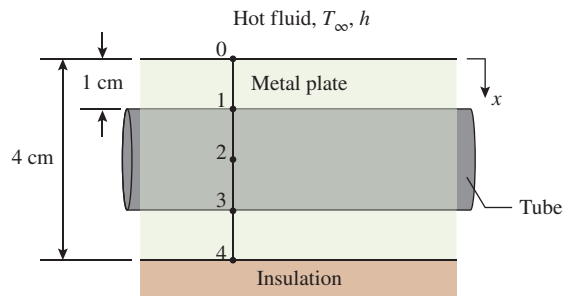
FIGURE P5–119

5–120 The roof of a house consists of a 15-cm-thick concrete slab ($k = 1.4$ W/m·K and $\alpha = 0.69 \times 10^{-6}$ m²/s) that is 18 m wide and 32 m long. One evening at 6 p.m., the slab is observed to be at a uniform temperature of 18°C. The average ambient air and the night sky temperatures for the entire night are predicted to be 6°C and 260 K, respectively. The convection heat transfer coefficients at the inner and outer surfaces of the roof can be taken to be $h_i = 5$ W/m²·K and $h_o = 12$ W/m²·K, respectively. The house and the interior surfaces of the walls and the floor are maintained at a constant temperature of 20°C during the night, and the emissivity of both surfaces of the concrete roof is 0.9. Considering both radiation and convection heat transfers and using the explicit finite difference method with a time step of $\Delta t = 5$ min and a mesh size of $\Delta x = 3$ cm, determine the temperatures of the inner and outer surfaces of the roof at 6 a.m. Also, determine the average rate of heat transfer through the roof during that night.

FIGURE P5–120

coefficient of $h = 80$ W/m²·K, and the left surface is subjected to uniform heat flux at a rate of $\dot{q}_L = 8000$ W/m². The nodal network of the problem consists of 13 equally spaced nodes with $\Delta x = \Delta y = 1.5$ cm. Using the explicit method, determine the temperature at the top corner (node 3) of the body after 2, 5, and 30 min.
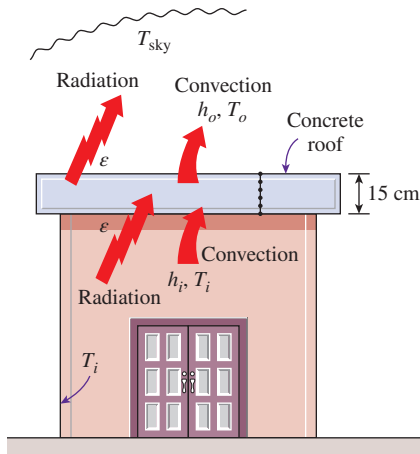
FIGURE P5–123

5–121 Consider a refrigerator whose outer dimensions are 1.80 m × 0.8 m × 0.7 m. The walls of the refrigerator are constructed of 3-cm-thick urethane insulation ($k = 0.026$ W/m·K and $\alpha = 0.36 \times 10^{-6}$ m²/s) sandwiched between two layers of sheet metal with negligible thickness. The refrigerated space is maintained at 3°C, and the average heat transfer coefficients at the inner and outer surfaces of the wall are 6 W/m²·K and 9 W/m²·K, respectively. Heat transfer through the bottom surface of the refrigerator is negligible. The kitchen temperature remains constant at about 25°C. Initially, the refrigerator contains 15 kg of food items at an average specific heat of 3.6 kJ/kg·K. Now a malfunction occurs, and the refrigerator stops running for 6 h as a result. Assuming the temperature of the contents of the refrigerator, including the air inside, rises uniformly during this period, predict the temperature inside the refrigerator after 6 h when the repairman arrives. Use the explicit finite difference method with a time step of $\Delta t = 1$ min and a mesh size of $\Delta x = 1$ cm, and disregard corner effects (i.e., assume one-dimensional heat transfer in the walls).

5–122 Reconsider Prob. 5–121. Using appropriate software, plot the temperature inside the refrigerator as a function of heating time as time varies from 1 h to 10 h, and discuss the results.

5–123 Consider two-dimensional transient heat transfer in an L-shaped solid bar that is initially at a uniform temperature of 140°C and whose cross section is given in Fig. P5–123. The thermal conductivity and diffusivity of the body are $k = 15$ W/m·K and $\alpha = 3.2 \times 10^{-6}$ m²/s, respectively, and heat is generated in the body at a rate of $\dot{e} = 2 \times 10^7$ W/m³. The right surface of the body is insulated, and the bottom surface is maintained at a uniform temperature of 140°C at all times. At time $t = 0$, the entire top surface is subjected to convection with ambient air at $T_\infty = 25°$C with a heat transfer

5–124 Reconsider Prob. 5–123. Using appropriate software, plot the temperature at the top corner as a function of heating time as it varies from 2 min to 30 min, and discuss the results.

5–125 Consider a long solid bar ($k = 28$ W/m·K and $\alpha = 12 \times 10^{-6}$ m²/s) of square cross section that is initially at a uniform temperature of 32°C. The cross section of the bar is 20 cm × 20 cm in size, and heat is generated in it uniformly at a rate of $\dot{e} = 8 \times 10^5$ W/m³. All four sides of the bar are subjected to convection to the ambient air at $T_\infty = 30°$C with a heat transfer coefficient of $h = 45$ W/m²·K. Using the explicit finite difference method with a mesh size of $\Delta x = \Delta y = 10$ cm, determine the centerline temperature of the bar (a) after 20 min and (b) after steady conditions are established.
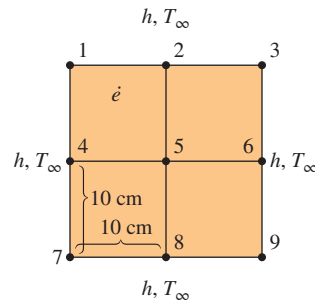
FIGURE P5–125

5–126 A long square stainless steel (ASTM A479 904L) bar is part of a component in high-temperature process equipment. The bar has a thickness of 5 cm, and its

specific heat, thermal conductivity, and density are 500 J/kg·K, 12 W/m·K, and 7.9 g/cm³, respectively. Occasionally, the bar is submerged in hot fluid at 300°C with a convection heat transfer coefficient of 288 W/m²·K. According to the ASME Code for Process Piping, the maximum use temperature for ASTM A479 904L bar is 260°C (ASME B31.3-2014, Table A-1M). If the initial temperature of the bar is 20°C and it is submerged in the hot fluid for 7 min, would it be in compliance with the ASME code? How long will it take for the bar to reach the maximum use temperature? Using the explicit finite difference formulations with a uniform nodal spacing of $\Delta x = \Delta y = 2.5$ cm, determine the temperature at each node for the duration of the bar being submerged in the hot fluid. Plot the nodal temperatures as a function of time
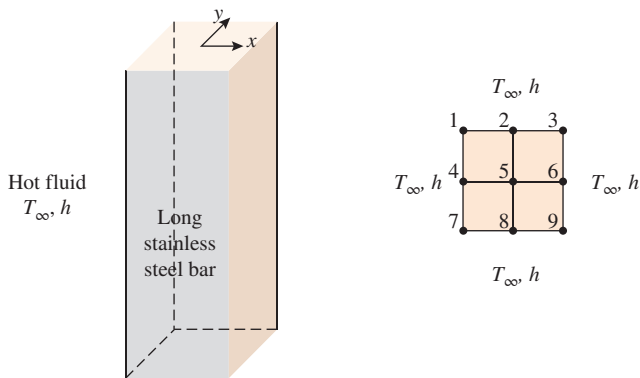
FIGURE P5–126

5–127 A common annoyance in cars in winter months is the formation of fog on the glass surfaces that blocks the view. A practical way of solving this problem is to blow hot air or to attach electric resistance heaters to the inner surfaces. Consider the rear window of a car that consists of a 0.4-cm-thick glass ($k = 0.84$ W/m·K and $\alpha = 0.39 \times 10^{-6}$ m²/s). Strip heater wires of negligible thickness are attached to the inner surface of the glass, 4 cm apart. Each wire generates heat at a rate of 25 W/m length. Initially the entire car, including its windows, is at the outdoor temperature of $T_o = -3$°C. The heat transfer coefficients at the inner and outer surfaces of the glass can be taken to be $h_i = 6$ W/m²·K and $h_o = 20$ W/m²·K, respectively. Using the explicit finite difference method with a mesh size of $\Delta x = 0.2$ cm along the thickness and $\Delta y = 1$ cm in the direction normal to the heater wires, determine the temperature distribution throughout the glass 15 min after the strip heaters are turned on. Also, determine the temperature distribution when steady conditions are reached.
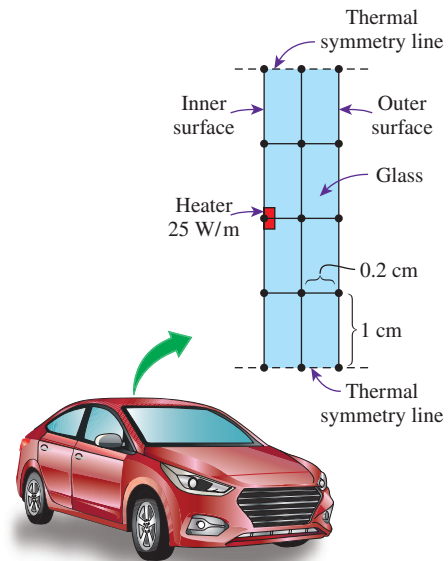
FIGURE P5–127

5–128 Repeat Prob. 5–127 using the implicit method with a time step of 1 min.

5–129 Revisit Prob. 5–68 of two-dimensional heat conduction in a square cross section. (*a*) Develop an explicit finite difference formulation for a two-dimensional transient heat conduction case and (*b*) find the nodal temperatures after 15 s.

5–130 Quench hardening is a mechanical process in which the ferrous metals or alloys are first heated and then quickly cooled down to improve their physical properties and avoid phase transformation. Consider a 40-cm × 20-cm block of copper alloy ($k = 120$ W/m·K, $\alpha = 3.91 \times 10^{-6}$ m²/s) being heated uniformly until it reaches a temperature of 800°C. It is then suddenly immersed into the water bath maintained at 15°C with $h = 100$ W/m²·K for quenching process. However, the upper surface of the metal is not submerged in the water and is exposed to air at 15°C with a convective heat transfer
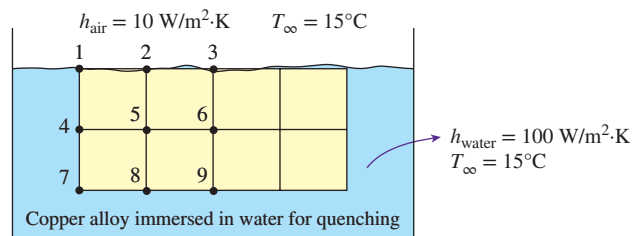
FIGURE P5–130

coefficient of 10 W/m²·K. Using an explicit finite difference formulation, calculate the temperature distribution in the copper alloy block after 10 min have elapsed using $\Delta t = 10$ s and a uniform mesh size of $\Delta x = \Delta y = 10$ cm.

5–131 Consider a 2-cm × 4-cm ceramic strip ($k = 3$ W/m·K, $\rho = 1600$ kg/m³, and $c_p = 800$ J/kg·K) embedded in very high conductivity material as shown in Fig. P5–131. The two sides of the ceramic strip are maintained at a constant temperature of 300°C. The bottom surface of the strip is insulated, while the top surface is exposed to a convective environment with $h = 200$ W/m²·K and ambient temperature of 50°C. Initially at $t = 0$, the ceramic strip is at a uniform temperature of 300°C. Using the implicit finite difference formulation and a time step of 2 s, determine the nodal temperatures after 12 s for a uniform mesh size of 1 cm.
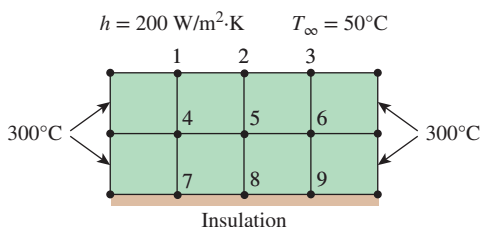
FIGURE P5–131

Special Topic: Controlling the Numerical Error

5–132C Why do the results obtained using a numerical method differ from the exact results obtained analytically? What are the causes of this difference?

5–133C What is the cause of the discretization error? How does the global discretization error differ from the local discretization error?

5–134C Can the global (accumulated) discretization error be less than the local error during a step? Explain.

5–135C How is the finite difference formulation for the first derivative related to the Taylor series expansion of the solution function?

5–136C Explain why the local discretization error of the finite difference method is proportional to the square of the step size. Also explain why the global discretization error is proportional to the step size itself.

5–137C What causes the round-off error? What kinds of calculations are most susceptible to round-off error?

5–138C What happens to the discretization and the round-off errors as the step size is decreased?

5–139C Suggest some practical ways of reducing the round-off error.

5–140C What is a practical way of checking if the round-off error has been significant in calculations?

5–141C What is a practical way of checking if the discretization error has been significant in calculations?

Review Problems

5–142 Starting with an energy balance on the volume element, obtain the steady three-dimensional finite difference equation for a general interior node in rectangular coordinates for $T(x, y, z)$ for the case of constant thermal conductivity and uniform heat generation.

5–143 Starting with an energy balance on the volume element, obtain the three-dimensional transient explicit finite difference equation for a general interior node in rectangular coordinates for $T(x, y, z, t)$ for the case of constant thermal conductivity and no heat generation.

5–144 Consider steady one-dimensional heat conduction in a plane wall with variable heat generation and constant thermal conductivity. The nodal network of the medium consists of nodes 0, 1, 2, and 3 with a uniform nodal spacing of Δx. The temperature at the left boundary (node 0) is specified. Using the energy balance approach, obtain the finite difference formulation of boundary node 3 at the right boundary for the case of combined convection and radiation with an emissivity of ε, convection coefficient of h, ambient temperature of T_∞, and surrounding temperature of T_{surr}. Also, obtain the finite difference formulation for the rate of heat transfer at the left boundary.
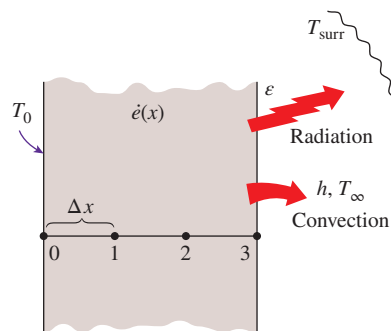
FIGURE P5–144

5–145 Consider one-dimensional transient heat conduction in a plane wall with variable heat generation and variable thermal conductivity. The nodal network of the medium consists of nodes 0, 1, and 2 with a uniform nodal spacing of Δx. Using the energy balance approach, obtain the explicit finite difference formulation of this problem for the case of specified heat flux $\dot{q}_0$ and convection at the left boundary (node 0) with a convection coefficient of h and ambient temperature of T_∞, and radiation at the right boundary (node 2) with an emissivity of ε and surrounding temperature of T_{surr}.

5–146 Repeat Prob. 5–145 for the case of implicit formulation.

5–147 Consider steady one-dimensional heat conduction in a pin fin of constant diameter D with constant thermal conductivity. The fin is losing heat by convection with the ambient air at T_∞ (in °C) with a convection coefficient of h, and by radiation to the surrounding surfaces at an average temperature of T_{surr} (in K). The nodal network of the fin consists of nodes 0 (at the base), 1 (in the middle), and 2 (at the fin tip) with a uniform nodal spacing of Δx. Using the energy balance approach, obtain the finite difference formulation of this problem for the case of a specified temperature at the fin base and convection and radiation heat transfer at the fin tip.
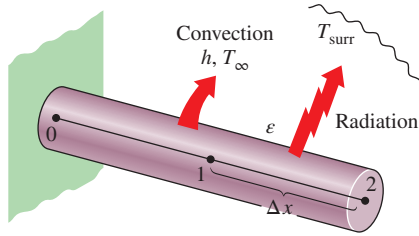
FIGURE P5–147

5–148E Consider a large plane wall of thickness $L = 0.3$ ft and thermal conductivity $k = 1.2$ Btu/h·ft·°F in space. The wall is covered with a material having an emissivity of $\varepsilon = 0.80$ and a solar absorptivity of $\alpha_s = 0.60$. The inner surface of the wall is maintained at 520 R at all times, while the outer surface is exposed to solar radiation that is incident at a rate of $\dot{q}_s = 350$ Btu/h·ft^2. The outer surface is also losing heat by radiation to deep space at 0 R. Using a uniform nodal spacing of $\Delta x = 0.1$ ft, (a) obtain the finite difference formulation for steady one-dimensional heat conduction and (b) determine the nodal temperatures by solving those equations. *Answer:* (b) 528 R, 535 R, 543 R
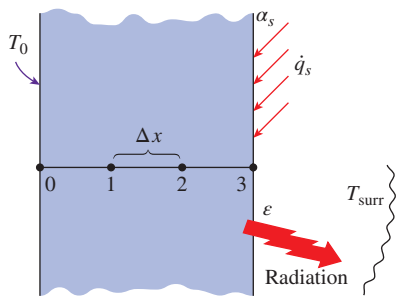
FIGURE P5–148E

5–149 Consider a nuclear fuel element ($k = 57$ W/m·K) that can be modeled as a plane wall with thickness of 4 cm. The fuel element generates 3×10^7 W/m^3 of heat uniformly. Both side surfaces of the fuel element are cooled by liquid with temperature of 80°C and convection heat transfer coefficient of 8000 W/m^2·K. Using a uniform nodal spacing of 8 mm,

(a) obtain the finite difference equations, (b) determine the nodal temperatures by solving those equations, and (c) compare the surface temperatures of both sides of the fuel element with the analytical solution.
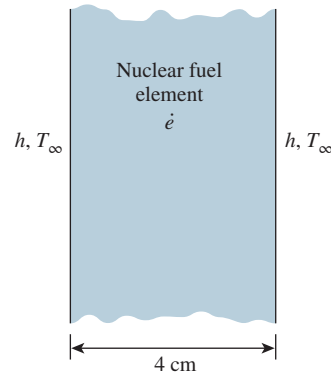
FIGURE P5–149

5–150 A fuel element ($k = 67$ W/m·K) that can be modeled as a plane wall has a thickness of 4 cm. The fuel element generates 5×10^7 W/m^3 of heat uniformly. Both side surfaces of the fuel element are cooled by liquid with temperature of 90°C and convection heat transfer coefficient of 5000 W/m^2·K. Use a uniform nodal spacing of 4 mm and make use of the symmetry line at the center of the plane wall to determine (a) the finite difference equations and (b) the nodal temperatures by solving those equations.

5–151 Consider steady two-dimensional heat transfer in a long solid bar ($k = 25$ W/m·K) of square cross section (2 cm × 2 cm) with heat generated in the bar uniformly at a rate of $\dot{e} = 3 \times 10^6$ W/m^3. The left and bottom surfaces maintain a constant temperature of 200°C. The top and right surfaces are subjected to convection with an ambient air temperature of 100°C and heat transfer coefficient of 250 W/m^2·K. Using a uniform mesh size $\Delta x = \Delta y = 1$ cm, determine (a) the finite difference equations and (b) the nodal temperatures with the Gauss-Seidel iterative method.
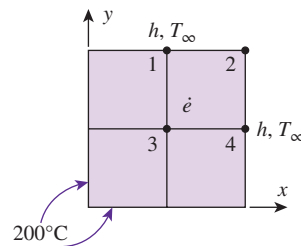
FIGURE P5–151

5–152 A two-dimensional bar has the geometry shown in Fig. P5–152 with specified temperature T_A on the upper surface and T_B on the lower surfaces, and insulation on the sides.

The thermal conductivity of the upper part of the bar is k_A, while that of the lower part is k_B. For a grid defined by $\Delta x = \Delta y = l$, write the simplest form of the matrix equation, $AT = C$, used to find the steady-state temperature field in the cross section of the bar. Identify on the figure the grid nodes where you write the energy balance.
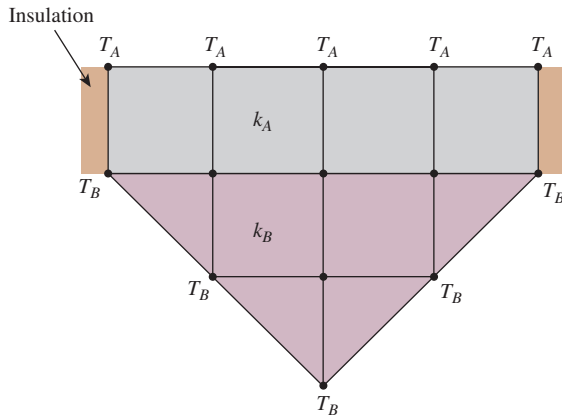
FIGURE P5–152

5–153 Starting with an energy balance on a disk volume element, derive the one-dimensional transient implicit finite difference equation for a general interior node for $T(z, t)$ in a cylinder whose side surface is subjected to convection with a convection coefficient of h and an ambient temperature of T_∞ for the case of constant thermal conductivity with uniform heat generation.

5–154 A hot surface at 120°C is to be cooled by attaching 8-cm-long, 0.8-cm- diameter aluminum pin fins ($k = 237$ W/m·K and $\alpha = 97.1 \times 10^{-6}$ m²/s) to it with a center-to-center distance of 1.6 cm. The temperature of the surrounding medium is 15°C, and the heat transfer coefficient on the surfaces is 35 W/m²·K. Initially, the fins are at a uniform temperature of 30°C, and at time $t = 0$, the temperature of the hot surface is raised to 120°C. Assuming one-dimensional heat conduction along the fin and taking the nodal spacing to be $\Delta x = 2$ cm and a time step to be $\Delta t = 0.5$ s, determine the nodal temperatures after 10 min by using the explicit finite difference method. Also, determine how long it will take for steady conditions to be reached.
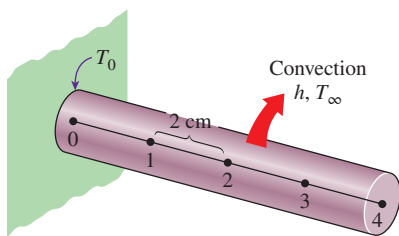
FIGURE P5–154

5–155 Solar radiation incident on a large body of clean water ($k = 0.61$ W/m·K and $\alpha = 0.15 \times 10^{-6}$ m²/s) such as a lake, a river, or a pond is mostly absorbed by water, and the amount of absorption varies with depth. For solar radiation incident at a 45° angle on a 1-m-deep large pond whose bottom surface is black (zero reflectivity), for example, 2.8 percent of the solar energy is reflected back to the atmosphere, 37.9 percent is absorbed by the bottom surface, and the remaining 59.3 percent is absorbed by the water body. If the pond is considered to be four layers of equal thickness (0.25 m in this case), it can be shown that 47.3 percent of the incident solar energy is absorbed by the top layer, 6.1 percent by the upper mid layer, 3.6 percent by the lower mid layer, and 2.4 percent by the bottom layer [for more information, see Çengel and Özişik, *Solar Energy,* 33, no. 6 (1984), pp. 581–591]. The radiation absorbed by the water can be treated conveniently as heat generation in the heat transfer analysis of the pond.

Consider a large 1-m-deep pond that is initially at a uniform temperature of 15°C throughout. Solar energy is incident on the pond surface at 45° at an average rate of 500 W/m² for a period of 4 h. Assuming no convection currents in the water and using the explicit finite difference method with a mesh size of $\Delta x = 0.25$ m and a time step of $\Delta t = 15$ min, determine the temperature distribution in the pond under the most favorable conditions (i.e., no heat losses from the top or bottom surfaces of the pond). The solar energy absorbed by the bottom surface of the pond can be treated as a heat flux to the water at that surface in this case.
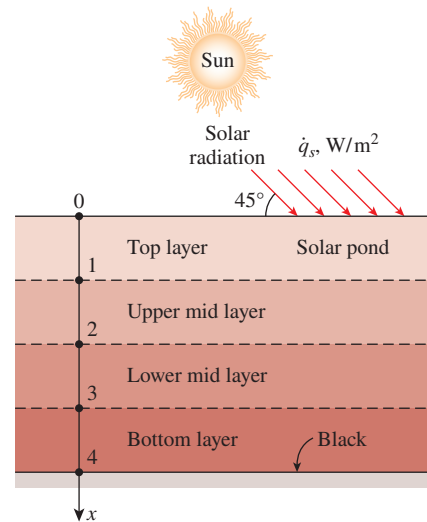
FIGURE P5–155

5–156 Reconsider Prob. 5–155. The absorption of solar radiation in that case can be expressed more accurately as a fourth-degree polynomial as

$$\dot{e}(x) = \dot{q}_s(0.859 - 3.415x + 6.704x^2 - 6.339x^3 + 2.278x^4), \text{ W/m}^3$$

where $\dot{q}_s$ is the solar flux incident on the surface of the pond in W/m^2 and x is the distance from the free surface of the pond in m. Solve Prob. 5–155 using this relation for the absorption of solar radiation.

5–157 A hot brass plate is having its upper surface cooled by an impinging jet of air at a temperature of 15°C and convection heat transfer coefficient of 220 W/m^2·K. The 10-cm-thick brass plate ($\rho = 8530$ kg/m^3, $c_p = 380$ J/kg·K, $k = 110$ W/m·K, and $\alpha = 33.9 \times 10^{-6}$ m^2/s) had a uniform initial temperature of 650°C, and the lower surface of the plate is insulated. Using a uniform nodal spacing of $\Delta x = 2.5$ cm, determine (*a*) the explicit finite difference equations, (*b*) the maximum allowable value of the time step, and (*c*) the temperature at the center plane of the brass plate after 1 min of cooling, and (*d*) compare the result in (*c*) with the approximate analytical solution from Chap. 4.

Air, 15°C
$h = 220$ W/m^2·K

Brass slab

$L = 10$ cm

x

Insulation
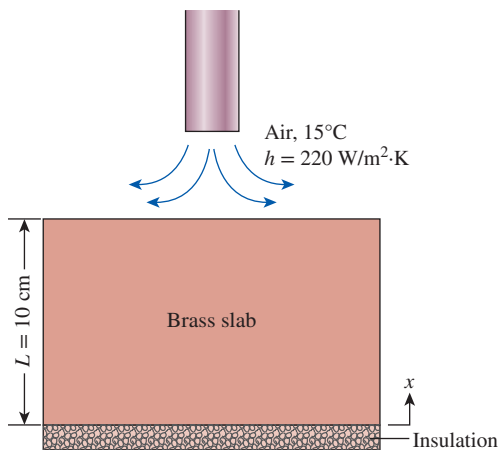
FIGURE P5−157

5–158 Consider a uranium nuclear fuel element ($k = 35$ W/m·K, $\rho = 19{,}070$ kg/m^3, and $c_p = 116$ J/kg·K) of radius 10 cm that experiences a volumetric heat generation at a rate of 4×10^5 W/m^3 because of the nuclear fission reaction. The nuclear fuel element initially at a temperature of 500°C is enclosed inside a cladding made of stainless steel material ($k = 15$ W/m·K, $\rho = 8055$ kg/m^3, and $c_p = 480$ J/kg·K) of thickness 4 cm. The fuel element is cooled by passing pressurized heavy water over the cladding surface. The pressurized water has a bulk temperature of 50°C, and the convective heat transfer coefficient is 1000 W/m^2·K. Assuming one-dimensional transient heat conduction in Cartesian coordinates, determine the temperature in the fuel rod and in the cladding after 10, 20, and 30 min. Use the implicit finite difference formulation with a uniform mesh size of 2 cm and a time step of 1 min.

$h = 1000$ W/m^2·K

$T_\infty = 50$°C

Uranium fuel rod   Stainless steel cladding
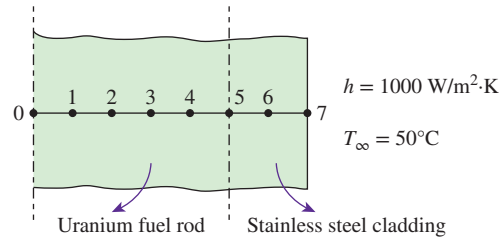
FIGURE P5−158

5–159 Starting with an energy balance on the volume element, obtain the two-dimensional transient explicit finite difference equation for a general interior node in rectangular coordinates for $T(x, y, t)$ for the case of constant thermal conductivity and uniform heat generation.

5–160 A long steel bar has the cross section shown in Fig. P5–160. The bar is removed from a heat treatment oven at $T_i = 700$°C and placed on the bottom of a tank filled with water at 10°C. To intensify the heat transfer, the water is vigorously circulated, which creates a virtually constant temperature $T_s = 10$°C on all sides of the bar, except for the bottom side, which is adiabatic. The properties of the bar are $c_p = 430$ J/kg·K, $k = 40$ W/m·K, and $\rho = 8000$ kg/m^3.

(*a*) Write the finite difference equations for the unknown temperatures in the grid using the explicit method. Group all constant quantities in one term. Identify dimensionless parameters such as Bi and Fo if applicable.

(*b*) Determine the range of time steps for which the explicit scheme is numerically stable.

(*c*) For $\Delta t = 10$ s, determine the temperature field at $t = 10$ s and $t = 20$ s. Fill in the table below.

Node	$T(10$ s$)$	$T(20$ s$)$
1	_____	_____
2	_____	_____
3	_____	_____
4	_____	_____
5	_____	_____
6	_____	_____
7	_____	_____

$T_s = 10$°C

5 cm

5 cm
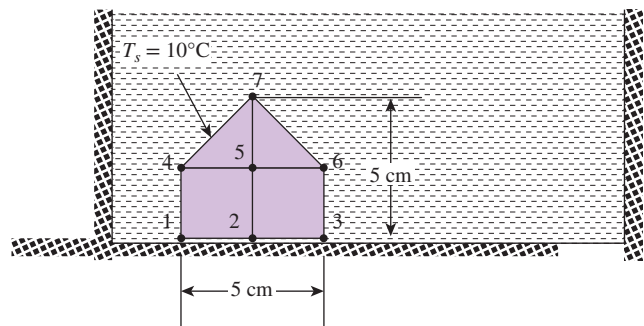
FIGURE P5−160

Fundamentals of Engineering (FE) Exam Problems

5–161 The unsteady forward-difference heat conduction for a constant-area (A) pin fin with perimeter p, when exposed to air whose temperature is T_0 with a convection heat transfer coefficient of h, is

$$T_m^{*+1} = \frac{k}{\rho c_p \Delta x^2}\left[T_{m-1}^* + T_{m+1}^* + \frac{hp\Delta x^2}{A}T_0\right]$$
$$- \left[1 - \frac{2k}{\rho c_p \Delta x^2} - \frac{hp}{\rho c_p A}\right]T_m^*$$

In order for this equation to produce a stable solution, the quantity $\dfrac{2k}{\rho c_p \Delta x^2} + \dfrac{hp}{\rho c_p A}$ must be

(*a*) negative   (*b*) zero   (*c*) positive
(*d*) greater than 1   (*e*) less than 1

5–162 Air at T_0 acts on the top surface of the rectangular solid shown in Fig. P5–162 with a convection heat transfer coefficient of h. The correct steady-state finite difference heat conduction equation for node 3 of this solid is

(*a*) $T_3 = [(k/2\Delta)(T_2 + T_4 + T_7) + hT_0]/[(k/\Delta) + h]$
(*b*) $T_3 = [(k/2\Delta)(T_2 + T_4 + 2T_7) + hT_0]/[(2k/\Delta) + h]$
(*c*) $T_3 = [(k/\Delta)(T_2 + T_4) + hT_0]/[(2k/\Delta) + h]$
(*d*) $T_3 = [(k/\Delta)(T_2 + T_4 + T_7) + hT_0]/[(k/\Delta) + h]$
(*e*) $T_3 = [(k/\Delta)(2T_2 + 2T_4 + T_7) + hT_0]/[(k/\Delta) + h]$
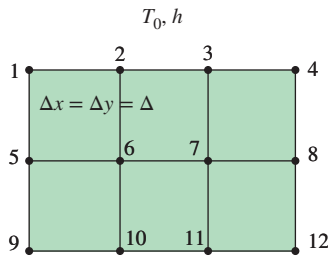
FIGURE P5–162

5–163 What is the correct unsteady forward-difference heat conduction equation of node 6 of the rectangular solid shown in Fig. P5–163 if its temperature at the previous time (Δt) is T_6^*?

(*a*) $T_6^{i+1} = [k\Delta t/(\rho c_p\Delta^2)](T_5^* + T_2^* + T_7^* + T_{10}^*)$
  $+ [1 - 4k\Delta t/(\rho c_p\Delta^2)]T_6^*$

(*b*) $T_6^{i+1} = [k\Delta t/(\rho c_p\Delta^2)](T_5^* + T_2^* + T_7^* + T_{10}^*)$
  $+ [1 - k\Delta t/(\rho c_p\Delta^2)]T_6^*$

(*c*) $T_6^{i+1} = [k\Delta t/(\rho c_p\Delta^2)](T_5^* + T_2^* + T_7^* + T_{10}^*)$
  $+ [2k\Delta t/(\rho c_p\Delta^2)]T_6^*$

(*d*) $T_6^{i+1} = [2k\Delta t/(\rho c_p\Delta^2)](T_5^* + T_2^* + T_7^* + T_{10}^*)$
  $+ [1 - 2k\Delta t/(\rho c_p\Delta^2)]T_6^*$

(*e*) $T_6^{i+1} = [2k\Delta t/(\rho c_p\Delta^2)](T_5^* + T_2^* + T_7^* + T_{10}^*)$
  $+ [1 - 4k\Delta t/(\rho c_p\Delta^2)]T_6^*$
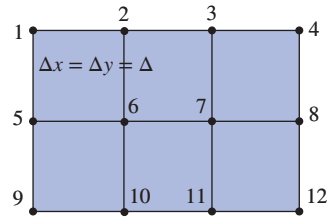
FIGURE P5–163

5–164 What is the correct steady-state finite difference heat conduction equation of node 6 of the rectangular solid shown in Fig. P5–164?

(*a*) $T_6 = (T_1 + T_3 + T_9 + T_{11})/2$
(*b*) $T_6 = (T_5 + T_7 + T_2 + T_{10})/2$
(*c*) $T_6 = (T_1 + T_3 + T_9 + T_{11})/4$
(*d*) $T_6 = (T_2 + T_5 + T_7 + T_{10})/4$
(*e*) $T_6 = (T_1 + T_2 + T_9 + T_{10})/4$
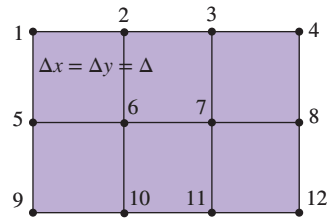
FIGURE P5–164

5–165 The height of the cells for a finite difference solution of the temperature in the rectangular solid shown in Fig. P5–165 is one-half the cell width to improve the accuracy of the solution. The correct steady-state finite difference heat conduction equation for cell 6 is

(*a*) $T_6 = 0.1(T_5 + T_7) + 0.4(T_2 + T_{10})$
(*b*) $T_6 = 0.25(T_5 + T_7) + 0.25(T_2 + T_{10})$
(*c*) $T_6 = 0.5(T_5 + T_7) + 0.5(T_2 + T_{10})$
(*d*) $T_6 = 0.4(T_5 + T_7) + 0.1(T_2 + T_{10})$
(*e*) $T_6 = 0.5(T_5 + T_7) + 0.5(T_2 + T_{10})$
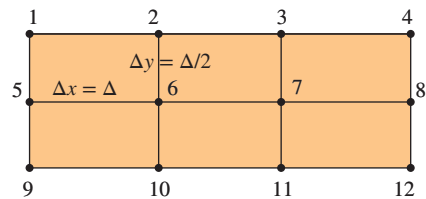
FIGURE P5–165

5–166 The height of the cells for a finite difference solution of the temperature in the rectangular solid shown in Fig. P5–166 is one-half the cell width to improve the accuracy of the solution. If the left surface is exposed to air at T_0 with a heat transfer coefficient of h, the correct finite difference heat conduction energy balance for node 5 is

(a) $2T_1 + 2T_9 + T_6 - T_5 + h\Delta/k(T_0 - T_5) = 0$

(b) $2T_1 + 2T_9 + T_6 - 2T_5 + h\Delta/k(T_0 - T_5) = 0$

(c) $2T_1 + 2T_9 + T_6 - 3T_5 + h\Delta/k(T_0 - T_5) = 0$

(d) $2T_1 + 2T_9 + T_6 - 4T_5 + h\Delta/k(T_0 - T_5) = 0$

(e) $2T_1 + 2T_9 + T_6 - 5T_5 + h\Delta/k(T_0 - T_5) = 0$
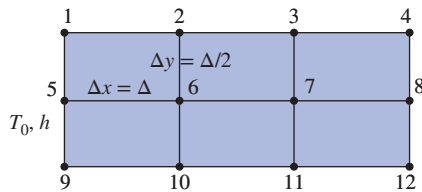
FIGURE P5–166

Design and Essay Problems

5–167 Write a two-page essay on the finite element method, and explain why it is used in most commercial engineering software packages. Also explain how it compares to the finite difference method.

5–168 Numerous professional software packages are available in the market for performing heat transfer analysis, and they are widely advertised in professional magazines such as the *Mechanical Engineering* magazine published by the American Society of Mechanical Engineers (ASME). Your company decides to purchase such a software package and asks you to prepare a report on the available packages, their costs, capabilities, ease of use, and compatibility with the available hardware and other software as well as the reputation of the software company, their history, financial health, customer support, training, and future prospects, among other things. After a preliminary investigation, select the top three packages and prepare a full report on them.

5–169 Design a defrosting plate to speed up defrosting of flat food items such as frozen steaks and packaged vegetables, and evaluate its performance using the finite difference method. Compare your design to the defrosting plates currently available on the market. The plate must perform well, and it must be suitable for purchase and use as a household utensil, durable, easy to clean, easy to manufacture, and affordable. The frozen food is expected to be at an initial temperature of $-18°C$ at the beginning of the thawing process and $0°C$ at the end with all the ice melted. Specify the material, shape, size, and thickness of the proposed plate. Justify your recommendations by calculations. Take the ambient and surrounding surface temperatures to be $20°C$ and the convection heat transfer coefficient to be 15 W/m²·K in your analysis. For a typical case, determine the defrosting time with and without the plate.

5–170 Design a fire-resistant safety box whose outer dimensions are 0.5 m $\times$ 0.5 m $\times$ 0.5 m that will protect its combustible contents from fire which may last up to 2 h. Assume the box will be exposed to an environment at an average temperature of $700°C$ with a combined heat transfer coefficient of 70 W/m²·K, and the temperature inside the box must be below $150°C$ at the end of 2 h. The cavity of the box must be as large as possible while meeting the design constraints, and the insulation material selected must withstand the high temperatures to which it will be exposed. Cost, durability, and strength are also important considerations in the selection of insulation materials.

FUNDAMENTALS OF CONVECTION

So far, we have considered *conduction,* which is the mechanism of heat transfer through a solid or a quiescent fluid. We now consider *convection,* which is the mechanism of heat transfer through a fluid in the presence of bulk fluid motion.

Convection is classified as *natural* (or *free*) and *forced convection,* depending on how the fluid motion is initiated. In forced convection, the fluid is forced to flow over a surface or in a pipe by external means such as a pump or a fan. In natural convection, any fluid motion is caused by natural means such as the buoyancy effect, which manifests itself as the rise of warmer fluid and the fall of the cooler fluid. Convection is also classified as *external* and *internal,* depending on whether the fluid is forced to flow over a surface or in a pipe.

We start this chapter with a general physical description of the convection mechanism. We then discuss the *velocity* and *thermal boundary layers* and *laminar and turbulent flows.* We continue with the discussion of the dimensionless *Reynolds, Prandtl,* and *Nusselt numbers* and their physical significance. Next we derive the *convection equations* on the basis of mass, momentum, and energy conservation, and we obtain solutions for *flow over a flat plate.* We then nondimensionalize the convection equations and obtain functional forms of friction and convection coefficients. Finally, we present analogies between momentum and heat transfer.

OBJECTIVES

When you finish studying this chapter, you should be able to:

- Understand the physical mechanism of convection and its classification,

- Visualize the development of velocity and thermal boundary layers during flow over surfaces,

- Gain a working knowledge of the dimensionless Reynolds, Prandtl, and Nusselt numbers,

- Distinguish between laminar and turbulent flows, and gain an understanding of the mechanisms of momentum and heat transfer in turbulent flow,

- Derive the differential equations that govern convection on the basis of mass, momentum, and energy balances, and solve these equations for some simple cases such as laminar flow over a flat plate,

- Nondimensionalize the convection equations and obtain the functional forms of friction and heat transfer coefficients, and

- Use analogies between momentum and heat transfer, and determine heat transfer coefficient from your knowledge of friction coefficient.
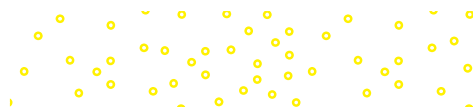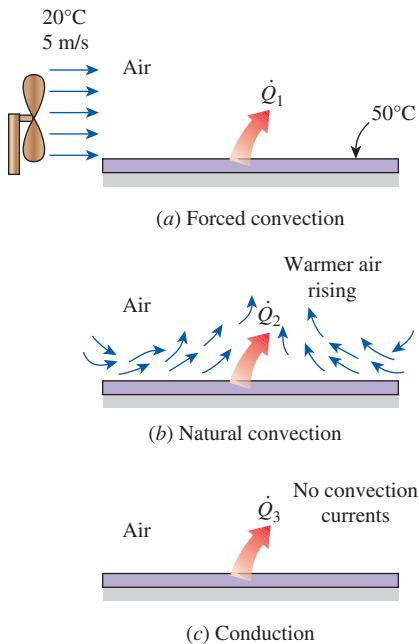
FIGURE 6–1
Heat transfer from a hot surface to the surrounding fluid by convection and conduction.
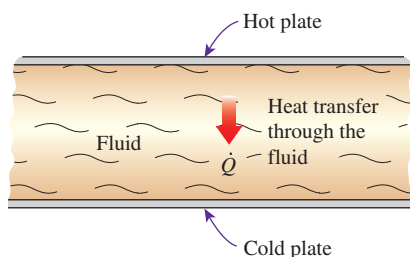
6–1 ▪ PHYSICAL MECHANISM OF CONVECTION

We mentioned in Chap. 1 that there are three basic mechanisms of heat transfer: conduction, convection, and radiation. Conduction and convection are similar in that both mechanisms require the presence of a material medium. But they are different in that convection requires the presence of fluid motion.

Heat transfer through a solid is always by conduction, since the molecules of a solid remain at relatively fixed positions. Heat transfer through a liquid or gas, however, can be by conduction or convection, depending on the presence of any bulk fluid motion. Heat transfer through a fluid is by convection in the presence of bulk fluid motion and by conduction in the absence of it. Therefore, conduction in a fluid can be viewed as the limiting case of convection, corresponding to the case of quiescent fluid (Fig. 6–1).

Convection heat transfer is complicated by the fact that it involves fluid motion as well as heat conduction. The fluid motion enhances heat transfer, since it brings warmer and cooler chunks of fluid into contact, initiating higher rates of conduction at a greater number of sites in a fluid. Therefore, the rate of heat transfer through a fluid is much higher by convection than it is by conduction. In fact, the higher the fluid velocity, the higher the rate of heat transfer.

To clarify this point further, consider steady heat transfer through a fluid contained between two parallel plates maintained at different temperatures, as shown in Fig. 6–2. The temperatures of the fluid and the plate are the same at the points of contact because of the continuity of temperature. Assuming no fluid motion, the energy of the hotter fluid molecules near the hot plate is transferred to the adjacent cooler fluid molecules. This energy is then transferred to the next layer of the cooler fluid molecules. This energy is then transferred to the next layer of the cooler fluid, and so on, until it is finally transferred to the other plate. This is what happens during conduction through a fluid. Now let us use a syringe to draw some fluid near the hot plate and inject it next to the cold plate repeatedly. You can imagine that this will speed up the heat transfer process considerably, since some energy is carried to the other side as a result of fluid motion.

Consider the cooling of a hot block with a fan blowing air over its top surface. We know that heat is transferred from the hot block to the surrounding cooler air, and the block eventually cools. We also know that the block cools faster if the fan is switched to a higher speed. Replacing air with water enhances the convection heat transfer even more.

Experience shows that convection heat transfer strongly depends on the fluid properties *dynamic viscosity μ*, *thermal conductivity k, density ρ*, and *specific heat c_p*, as well as the *fluid velocity V.* It also depends on the *geometry* and the *roughness* of the solid surface, in addition to the *type of fluid flow* (such as being streamlined or turbulent). Thus, we expect the convection heat transfer relations to be rather complex because of the dependence of convection on so many variables. This is not surprising, since convection is the most complex mechanism of heat transfer.

Despite the complexity of convection, the rate of convection heat transfer is observed to be proportional to the temperature difference and is conveniently expressed by **Newton's law of cooling** as

$$\dot{q}_{\text{conv}} = h(T_s - T_\infty) \quad (\text{W/m}^2) \tag{6–1}$$

FIGURE 6–2
Heat transfer through a fluid sandwiched between two parallel plates.

or

$$\dot{Q}_{conv} = hA_s(T_s - T_\infty) \qquad (W) \qquad \textbf{(6–2)}$$

where

h = convection heat transfer coefficient, W/m²·K

A_s = heat transfer surface area, m²

T_s = temperature of the surface, °C

T_∞ = temperature of the fluid sufficiently far from the surface, °C

Judging from its units, the **convection heat transfer coefficient** h can be defined as *the rate of heat transfer between a solid surface and a fluid per unit surface area per unit temperature difference.*

You should not be deceived by the simple appearance of this relation, because the convection heat transfer coefficient h depends on several of the mentioned variables, and thus is difficult to determine.

Fluid flow is often confined by solid surfaces, and it is important to understand how the presence of solid surfaces affects fluid flow. Consider the flow of a fluid in a stationary pipe or over a solid surface that is nonporous (i.e., impermeable to the fluid). All experimental observations indicate that a fluid in motion comes to a complete stop at the surface and assumes a zero velocity relative to the surface. That is, a fluid in direct contact with a solid "sticks" to the surface due to viscous effects, and there is no slip. This is known as the **no-slip condition**.

Figure 6–3, obtained from a video clip, clearly shows the evolution of a velocity gradient as a result of the fluid sticking to the surface of a blunt nose. The layer that sticks to the surface slows the adjacent fluid layer because of viscous forces between the fluid layers, which slows the next layer, and so on. Therefore, the no-slip condition is responsible for the development of the velocity profile. The flow region adjacent to the wall in which the viscous effects (and thus the velocity gradients) are significant is called the **boundary layer**. The fluid property responsible for the no-slip condition and the development of the boundary layer is *viscosity* and is discussed briefly in Sec. 6–2.

A fluid layer adjacent to a moving surface has the same velocity as the surface. A consequence of the no-slip condition is that all velocity profiles must have zero values with respect to the surface at the points of contact between a fluid and a solid surface (Fig. 6–4). Another consequence of the no-slip condition is the *surface drag,* which is the force a fluid exerts on a surface in the flow direction.

An implication of the no-slip condition is that heat transfer from the solid surface to the fluid layer adjacent to the surface is by *pure conduction,* since the fluid layer is motionless, and it can be expressed as

$$\dot{q}_{conv} = \dot{q}_{cond} = -k_{fluid} \frac{\partial T}{\partial y}\bigg|_{y=0} \qquad (W/m^2) \qquad \textbf{(6–3)}$$

where T represents the temperature distribution in the fluid and $(\partial T/\partial y)_{y=0}$ is the *temperature gradient* at the surface. Heat is then *convected away* from the surface as a result of fluid motion. Note that convection heat transfer from a solid surface to a fluid is merely the conduction heat transfer from the solid surface to the fluid layer adjacent to the surface. Therefore, we can equate Eqs. 6–1 and 6–3 for the heat flux to obtain

$$h = \frac{-k_{fluid}(\partial T/\partial y)_{y=0}}{T_s - T_\infty} \qquad (W/m^2·K) \qquad \textbf{(6–4)}$$

FIGURE 6–3
The development of a velocity profile due to the no-slip condition as a fluid flows over a blunt nose.
Courtesy of IIHR-Hydroscience & Engineering

FIGURE 6–4
A fluid flowing over a stationary surface comes to a complete stop at the surface because of the no-slip condition.

for the determination of the *convection heat transfer coefficient* when the temperature distribution within the fluid is known.

The convection heat transfer coefficient, in general, varies along the flow (or *x*-) direction. The *average* or *mean* convection heat transfer coefficient for a surface in such cases is determined by properly averaging the *local* convection heat transfer coefficients over the entire surface.

Nusselt Number

In convection studies, it is common practice to nondimensionalize the governing equations and combine the variables, which group together into *dimensionless numbers* in order to reduce the number of total variables. It is also common practice to nondimensionalize the heat transfer coefficient h with the Nusselt number, defined as

$$\text{Nu} = \frac{hL_c}{k} \tag{6–5}$$

where k is the thermal conductivity of the fluid and L_c is the *characteristic length.* The Nusselt number is named after Wilhelm Nusselt (Fig. 6–5), who made significant contributions to convective heat transfer in the first half of the 20th century, and it is viewed as the *dimensionless convection heat transfer coefficient.*

To understand the physical significance of the Nusselt number, consider a fluid layer of thickness L and temperature difference $\Delta T = T_2 - T_1$, as shown in Fig. 6–6. Heat transfer through the fluid layer is by *convection* when the fluid involves some motion and by *conduction* when the fluid layer is motionless. Heat flux (the rate of heat transfer per unit surface area) in either case is

$$\dot{q}_{\text{conv}} = h\Delta T \tag{6–6}$$

and

$$\dot{q}_{\text{cond}} = k\frac{\Delta T}{L} \tag{6–7}$$

Taking their ratio gives

$$\frac{\dot{q}_{\text{conv}}}{\dot{q}_{\text{cond}}} = \frac{h\Delta T}{k\Delta T/L} = \frac{hL}{k} = \text{Nu} \tag{6–8}$$

which is the Nusselt number. Therefore, the Nusselt number represents the enhancement of heat transfer through a fluid layer as a result of convection relative to conduction across the same fluid layer. The larger the Nusselt number, the more effective the convection. A Nusselt number of $\text{Nu} = 1$ for a fluid layer represents heat transfer across the layer by pure conduction.

We use forced convection in daily life more often than you might think (Fig. 6–7). We resort to forced convection whenever we want to increase the rate of heat transfer from a hot object. For example, we turn on the fan on hot summer days to help our bodies to cool more effectively. The higher the fan speed, the better we feel. We *stir* our soup and *blow* on a hot slice of pizza to make them cool faster. The air on windy winter days feels much colder than it actually is. The simplest solution to heating problems in electronics packaging is to use a large enough fan.

FIGURE 6–5
Wilhelm Nusselt (1882–1957), was a German engineer, born in Nuremberg, Germany. He studied machinery at the Technical Universities of Berlin-Charlottenburg and Munchen and conducted advanced studies in mathematics and physics. His doctoral thesis was on the "Conductivity of Insulating Materials," which he completed in 1907. In 1915, Nusselt published his pioneering paper: "The Basic Laws of Heat Transfer," in which he first proposed the dimensionless groups now known as the principal parameters in the similarity theory of heat transfer. His other famous works were concerned with the film condensation of steam on vertical surfaces, the combustion of pulverized coal, and the analogy between heat and mass transfer in evaporation. Among his well-known mathematical works are the solutions for laminar heat transfer in the entrance region of tubes and for heat exchange in crossflow, and the basic theory of regenerators.
Source: Wikipedia

EXAMPLE 6–1   **Heat Transfer Calculation from Temperature Profile**

During the flow of air at $T_\infty = 20°C$ over a plate surface maintained at a constant temperature of $T_s = 160°C$, the dimensionless temperature profile within the air layer over the plate is determined to be

$$\frac{T(y) - T_\infty}{T_s - T_\infty} = e^{-ay}$$

where $a = 3200$ m^{-1} and y is the vertical distance measured from the plate surface in m (Fig. 6–8). Determine the heat flux on the plate surface and the convection heat transfer coefficient.

SOLUTION   Airflow over a flat plate has a given temperature profile. The heat flux on the plate surface and the convection heat transfer coefficient are to be determined.

Assumptions   **1** The given nondimensional temperature profile is representative of the variation of temperature over the entire plate. **2** Heat transfer by radiation is negligible.

Properties   The thermal conductivity of air at the film temperature of $T_f = (T_s + T_\infty)/2 = (160°C + 20°C)/2 = 90°C$ is $k = 0.03024$ W/m·K (Table A–15).

Analysis   Noting that heat transfer from the plate to air at the surface is by conduction, heat flux from the solid surface to the fluid layer adjacent to the surface is determined from

$$\dot{q} = \dot{q}_{cond} = -k_{fluid} \frac{\partial T}{\partial y}\bigg|_{y=0}$$

where the temperature gradient at the plate surface is

$$\frac{\partial T}{\partial y}\bigg|_{y=0} = (T_s - T_\infty)a[e^{-ay}]_{y=0} = (T_s - T_\infty)(-a)$$

$$= (160°C - 20°C)(-3200 \text{ m}^{-1}) = -4.48 \times 10^5 \, °C/m$$

Substituting, the heat flux is determined to be

$$\dot{q} = -(0.03024 \text{ W/m·K})(-4.48 \times 10^5 \, °C/m) = \mathbf{1.35 \times 10^4 \text{ W/m}^2}$$

Then the convection heat transfer coefficient becomes

$$h = \frac{-k_{fluid}(\partial T/\partial y)_{y=0}}{T_s - T_\infty}$$

$$= \frac{-(0.03024 \text{ W/m·K})(-4.48 \times 10^5 \, °C/m)}{(160°C - 20°C)} = \mathbf{96.8 \text{ W/m}^2\text{·K}}$$

Discussion   The convection heat transfer coefficient could also be determined from Newton's law of cooling, $\dot{q} = h(T_s - T_\infty)$.
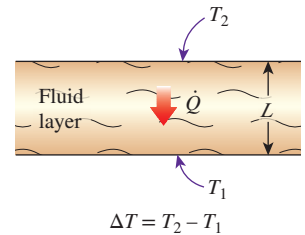
FIGURE 6–6
Heat transfer through a fluid layer of thickness L and temperature difference ΔT.
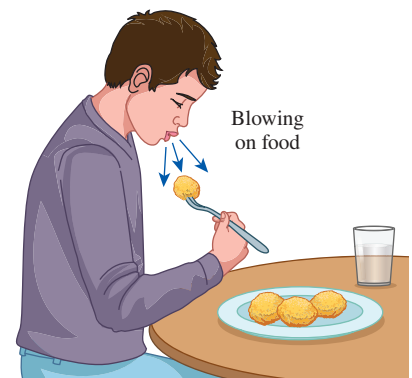
FIGURE 6–7
We resort to forced convection whenever we need to increase the rate of heat transfer.
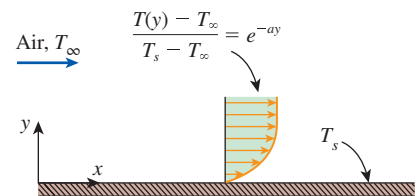
FIGURE 6–8
Schematic for Example 6–1.

6–2 ▪ CLASSIFICATION OF FLUID FLOWS

Convection heat transfer is closely tied with fluid mechanics, which is the science that deals with the behavior of fluids at rest or in motion, and the interaction of fluids with solids or other fluids at the boundaries. A wide variety of fluid flow problems is encountered in practice, and it is usually convenient to classify them on the basis of some common characteristics to make it feasible to study them in groups. There are many ways to classify fluid flow problems, and here we present some general categories.

Viscous Versus Inviscid Regions of Flow

When two fluid layers move relative to each other, a friction force develops between them, and the slower layer tries to slow down the faster layer. This internal resistance to flow is quantified by the fluid property *viscosity,* which is a measure of internal stickiness of the fluid. Viscosity is caused by cohesive forces between the molecules in liquids and by molecular collisions in gases. There is no fluid with zero viscosity, and thus all fluid flows involve viscous effects to some degree. Flows in which the frictional effects are significant are called **viscous flows**. However, in many flows of practical interest, there are *regions* (typically regions not close to solid surfaces) where viscous forces are negligibly small compared to inertial or pressure forces. Neglecting the viscous terms in such **inviscid flow regions** greatly simplifies the analysis without much loss in accuracy.

The development of viscous and inviscid regions of flow as a result of inserting a flat plate parallel into a fluid stream of uniform velocity is shown in Fig. 6–9. The fluid sticks to the plate on both sides because of the no-slip condition, and the thin boundary layer in which the viscous effects are significant near the plate surface is the *viscous flow region.* The region of flow on both sides away from the plate and unaffected by the presence of the plate is the *inviscid flow region.*
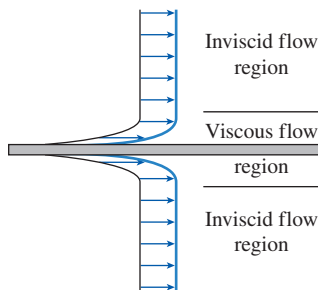
FIGURE 6–9
Flow of an originally uniform fluid stream over a flat plate, and the regions of viscous flow (next to the plate on both sides) and inviscid flow (away from the plate).

Internal Versus External Flow

A fluid flow is classified as being internal or external, depending on whether the fluid is forced to flow in a confined channel or over a surface. The flow of an unbounded fluid over a surface such as a plate, a wire, or a pipe is **external flow**. The flow in a pipe or duct is **internal flow** if the fluid is completely bounded by solid surfaces. Water flow in a pipe, for example, is internal flow, and airflow over a ball or over an exposed pipe during a windy day is external flow (Fig. 6–10). The flow of liquids in a duct is called *open-channel flow* if the duct is only partially filled with the liquid and there is a free surface. The flows of water in rivers and irrigation ditches are examples of such flows.

Internal flows are dominated by the influence of viscosity throughout the flow field. In external flows, the viscous effects are limited to boundary layers near solid surfaces and to wake regions downstream of bodies.

FIGURE 6–10
External flow over a tennis ball, and the turbulent wake region behind.

Courtesy NASA Ames Research Center and Cislunar Aerospace, Inc.

Compressible Versus Incompressible Flow

A flow is classified as being *compressible* or *incompressible,* depending on the level of variation of density during flow. Incompressibility is an approximation, and a flow is said to be **incompressible** if the density remains nearly

constant throughout. Therefore, the volume of every portion of fluid remains unchanged over the course of its motion when the flow (or the fluid) is incompressible.

The densities of liquids are essentially constant, and thus the flow of liquids is typically incompressible. Therefore, liquids are usually referred to as *incompressible substances.* A pressure of 210 atm, for example, causes the density of liquid water at 1 atm to change by just 1 percent. Gases, on the other hand, are highly compressible. A pressure change of just 0.01 atm, for example, causes a change of 1 percent in the density of atmospheric air.

Liquid flows are incompressible to a high level of accuracy, but the level of variation in density in gas flows and the consequent level of approximation made when modeling gas flows as incompressible depends on the Mach number, defined as $Ma = V/c$, where c is the **speed of sound** whose value is 346 m/s in air at room temperature at sea level. Gas flows can often be approximated as incompressible if the density changes are under about 5 percent, which is usually the case when $Ma < 0.3$. Therefore, the compressibility effects of air can be neglected at speeds under about 100 m/s. Note that the flow of a gas is not necessarily a compressible flow.

Small density changes of liquids corresponding to large pressure changes can still have important consequences. The irritating "water hammer" in a water pipe, for example, is caused by the vibrations of the pipe generated by the reflection of pressure waves following the sudden closing of the valves.

Laminar Versus Turbulent Flow

Some flows are smooth and orderly while others are rather chaotic. The highly ordered fluid motion characterized by smooth layers of fluid is called **laminar**. The word *laminar* comes from the movement of adjacent fluid particles together in "laminates." The flow of high-viscosity fluids such as oils at low velocities is typically laminar. The highly disordered fluid motion that typically occurs at high velocities and is characterized by velocity fluctuations is called **turbulent** (Fig. 6–11). The flow of low-viscosity fluids such as air at high velocities is typically turbulent. The flow regime greatly influences the required power for pumping. A flow that alternates between being laminar and turbulent is called **transitional**.

Natural (or Unforced) Versus Forced Flow

A fluid flow is said to be natural or forced, depending on how the fluid motion is initiated. In **forced flow**, a fluid is forced to flow over a surface or in a pipe by external means such as a pump or a fan. In **natural flows**, any fluid motion is due to natural means such as the buoyancy effect, which manifests itself as the rise of the warmer (and thus lighter) fluid and the fall of cooler (and thus denser) fluid (Fig. 6–12). In solar hot-water systems, for example, the thermosiphoning effect is commonly used to replace pumps by placing the water tank sufficiently above the solar collectors.

Steady Versus Unsteady Flow

The terms *steady* and *uniform* are used frequently in engineering, and thus it is important to have a clear understanding of their meanings. The term **steady** implies *no change at a point with time.* The opposite of steady is **unsteady**.

Laminar

Transitional
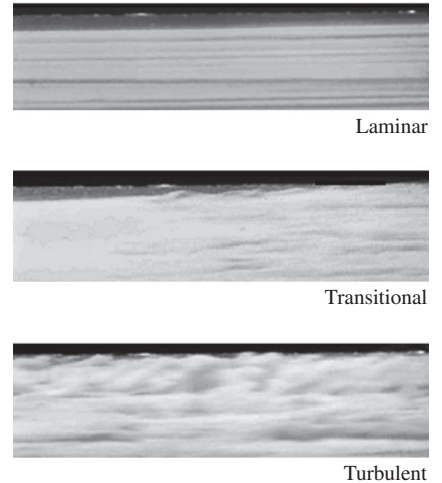
Turbulent

FIGURE 6–11
Laminar, transitional, and turbulent flows.
©Henri Werlé–ONERA, the French Aerospace Lab

$L = 0.2$ m

$V_0 = 0.2$ m/s

$Re = 3 \times 10^3$
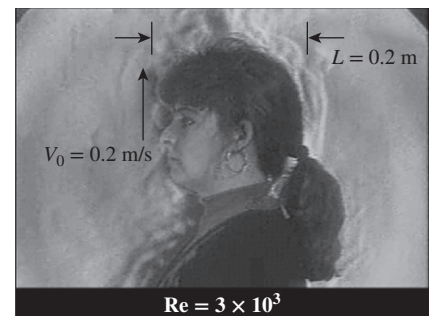
FIGURE 6–12
In this schlieren image, the rise of lighter, warmer air adjacent to the person's body indicates that humans and warm-blooded animals are surrounded by thermal plumes of rising warm air.
G.S. Settles, Gas Dynamics Lab, Penn State University. Used by permission.

The term **uniform** implies *no change with location* over a specified region. These meanings are consistent with their everyday use (steady girlfriend, uniform distribution, etc.).

The terms *unsteady* and *transient* are often used interchangeably, but these terms are not synonyms. In fluid mechanics, *unsteady* is the most general term that applies to any flow that is not steady, but **transient** is typically used for developing flows. When a rocket engine is fired up, for example, there are transient effects (the pressure builds up inside the rocket engine, the flow accelerates, etc.) until the engine settles down and operates steadily. The term **periodic** refers to the kind of unsteady flow in which the flow oscillates about a steady mean.

Many devices such as turbines, compressors, boilers, condensers, and heat exchangers operate for long periods of time under the same conditions, and they are classified as *steady-flow devices.* (Note that the flow field near the rotating blades of a turbomachine is of course unsteady, but we consider the overall flow field rather than the details at some localities when we classify devices.) During steady flow, the fluid properties can change from point to point within a device, but at any fixed point they remain constant. Therefore, the volume, the mass, and the total energy content of a steady-flow device or flow section remain constant in steady operation.

Steady-flow conditions can be closely approximated by devices that are intended for continuous operation such as turbines, pumps, boilers, condensers, and heat exchangers of power plants or refrigeration systems. Some cyclic devices, such as reciprocating engines or compressors, do not satisfy the steady-flow conditions since the flow at the inlets and the exits is pulsating and not steady. However, the fluid properties vary with time in a periodic manner, and the flow through these devices can still be analyzed as a steady-flow process by using time-averaged values for the properties.

One-, Two-, and Three-Dimensional Flows

A flow field is best characterized by the velocity distribution, and thus a flow is said to be one-, two-, or three-dimensional if the flow velocity varies in one, two, or three primary dimensions, respectively. A typical fluid flow involves a three-dimensional geometry, and the velocity may vary in all three dimensions, rendering the flow three-dimensional [$\vec{V}(x, y, z)$ in rectangular or $\vec{V}(r, \theta, z)$ in cylindrical coordinates]. However, the variation of velocity in certain directions can be small relative to the variation in other directions and can be ignored with negligible error. In such cases, the flow can be modeled conveniently as being one- or two-dimensional, which is easier to analyze.

Consider steady flow of a fluid through a circular pipe attached to a large tank. The fluid velocity everywhere on the pipe surface is zero because of the no-slip condition, and the flow is two-dimensional in the entrance region of the pipe since the velocity changes in both the *r*- and *z*-directions. The velocity profile develops fully and remains unchanged after some distance from the inlet (about 10 pipe diameters in turbulent flow, and less in laminar pipe flow, as in Fig. 6–13), and the flow in this region is said to be *fully developed.* The fully developed flow in a circular pipe is *one-dimensional* since the velocity varies in the radial *r*-direction but not in the angular *θ*- or axial *z*-directions, as shown in Fig. 6–13. That is, the velocity profile is the same at any axial *z*-location, and it is symmetric about the axis of the pipe.

FIGURE 6–13
The development of the velocity profile in a circular pipe. $V = V(r, z)$ and thus the flow is two-dimensional in the entrance region, and it becomes one-dimensional downstream when the velocity profile fully develops and remains unchanged in the flow direction, $V = V(r)$.
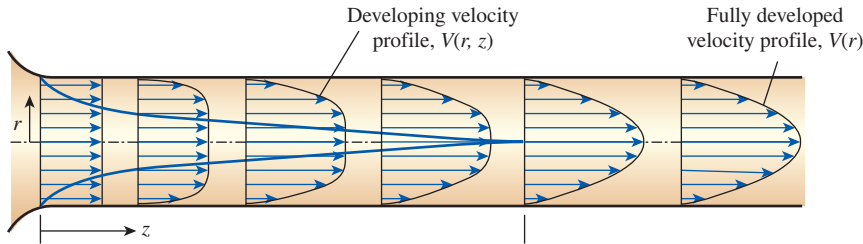
Note that the dimensionality of the flow also depends on the choice of coordinate system and its orientation. The pipe flow discussed, for example, is one-dimensional in cylindrical coordinates, but two-dimensional in Cartesian coordinates—illustrating the importance of choosing the most appropriate coordinate system. Also note that even in this simple flow, the velocity cannot be uniform across the cross section of the pipe because of the no-slip condition. However, at a well-rounded entrance to the pipe, the velocity profile may be approximated as being nearly uniform across the pipe, since the velocity is nearly constant at all radii except very close to the pipe wall.

6–3 ▪ VELOCITY BOUNDARY LAYER

Consider the parallel flow of a fluid over a *flat plate,* as shown in Fig. 6–14. Surfaces that are slightly contoured such as turbine blades can also be approximated as flat plates with reasonable accuracy. The *x*-coordinate is measured along the plate surface from the *leading edge* of the plate in the direction of the flow, and *y* is measured from the surface in the normal direction. The fluid approaches the plate in the *x*-direction with a uniform velocity *V,* which is practically identical to the free-stream velocity over the plate away from the surface (this would not be the case for crossflow over blunt bodies such as a cylinder).

For the sake of discussion, we can consider the fluid to consist of adjacent layers piled on top of each other. The velocity of the particles in the first fluid
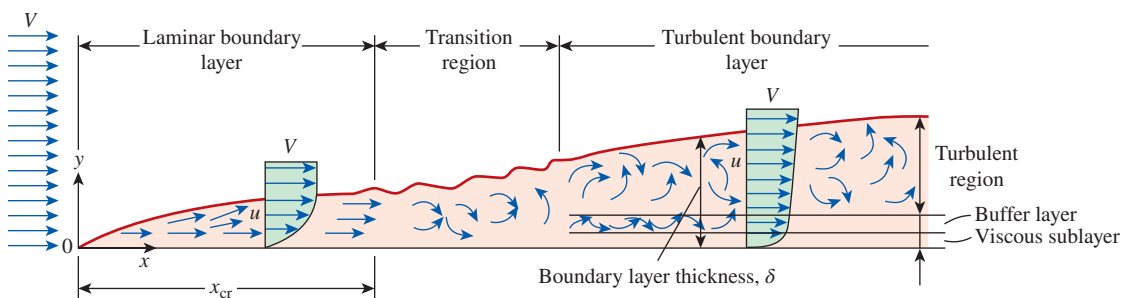
FIGURE 6–14
The development of the boundary layer for flow over a flat plate, and the different flow regimes.
Courtesy of University of Delaware.
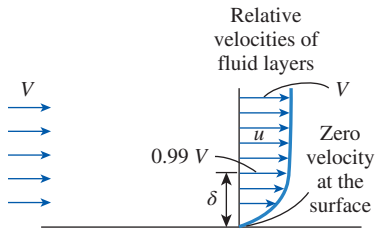
FIGURE 6–15
The development of a boundary layer on a surface is due to the no-slip condition and friction.

FIGURE 6–16
The viscosity of liquids decreases and the viscosity of gases increases with temperature.

layer adjacent to the plate becomes zero because of the no-slip condition. This motionless layer slows down the particles of the neighboring fluid layer as a result of friction between the particles of these two adjoining fluid layers at different velocities. This fluid layer then slows down the molecules of the next layer, and so on. Thus, the presence of the plate is felt up to some normal distance δ from the plate beyond which the free-stream velocity remains essentially unchanged. As a result, the x-component of the fluid velocity, u, varies from 0 at $y = 0$ to nearly V at $y = \delta$ (Fig. 6–15).

The region of the flow above the plate bounded by δ in which the effects of the viscous shearing forces caused by fluid viscosity are felt is called the **velocity boundary layer**. The *boundary layer thickness, δ*, is typically defined as the distance y from the surface at which $u = 0.99V$.

The hypothetical line of $u = 0.99V$ divides the flow over a plate into two regions: the **boundary layer region**, in which the viscous effects and the velocity changes are significant, and the **irrotational flow region**, in which the frictional effects are negligible and the velocity remains essentially constant.

Wall Shear Stress

Consider the flow of a fluid over the surface of a plate. The fluid layer in contact with the surface tries to drag the plate along via friction, exerting a *friction force* on it. Likewise, a faster fluid layer tries to drag the adjacent slower layer and exert a friction force because of the friction between the two layers. Friction force per unit area is called **shear stress** and is denoted by τ. Experimental studies indicate that the shear stress for most fluids is proportional to the *velocity gradient,* and the shear stress at the wall surface is expressed as

$$\tau_w = \mu \frac{\partial u}{\partial y}\bigg|_{y=0} \qquad (\text{N/m}^2) \qquad \text{(6–9)}$$

where the constant of proportionality μ is the **dynamic viscosity** of the fluid, whose unit is kg/m·s (or equivalently, N·s/m^2, or Pa·s, or poise = 0.1 Pa·s).

The fluids that obey the linear relationship above are called **Newtonian fluids**, after Sir Isaac Newton, who expressed it first in 1687 (Fig. 1–36). Most common fluids such as water, air, gasoline, and oils are Newtonian fluids. Blood and liquid plastics are examples of non-Newtonian fluids. In this text we consider Newtonian fluids only.

In fluid flow and heat transfer studies, the ratio of dynamic viscosity to density appears frequently. For convenience, this ratio is given the name **kinematic viscosity** ν and is expressed as $\nu = \mu/\rho$. Two common units of kinematic viscosity are m^2/s and *stoke* (1 stoke = 1 cm^2/s = 0.0001 m^2/s).

The viscosity of a fluid is a measure of its *resistance to deformation,* and it is a strong function of temperature. The viscosities of liquids *decrease* with temperature, whereas the viscosities of gases *increase* with temperature (Fig. 6–16). The viscosities of some fluids at 20°C are listed in Table 6–1. Note that the viscosities of different fluids differ by several orders of magnitude.
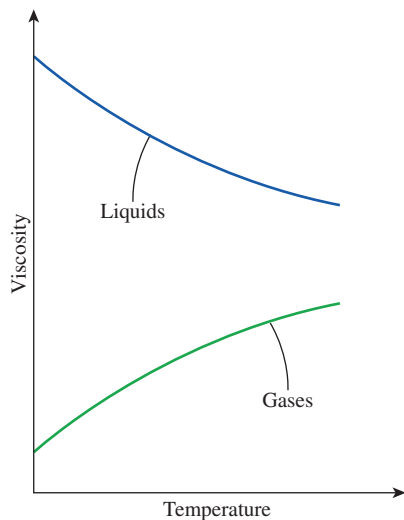
The determination of the wall shear stress τ_w from Eq. 6–9 is not practical since it requires a knowledge of the flow velocity profile. A more practical approach in external flow is to relate τ_w to the upstream velocity V as

$$\tau_w = C_f \frac{\rho V^2}{2} \quad (\text{N/m}^2) \tag{6–10}$$

where C_f is the dimensionless **friction coefficient** or **skin friction coefficient**, whose value in most cases is determined experimentally, and ρ is the density of the fluid. Note that the friction coefficient, in general, varies with location along the surface. Once the average friction coefficient over a given surface is available, the friction force over the entire surface is determined from

$$F_f = C_f A_s \frac{\rho V^2}{2} \quad (\text{N}) \tag{6–11}$$

where A_s is the surface area.

The friction coefficient is an important parameter in heat transfer studies since it is directly related to the heat transfer coefficient and the power requirements of the pump or fan.

6–4 ▪ THERMAL BOUNDARY LAYER

We have seen that a velocity boundary layer develops when a fluid flows over a surface as a result of the fluid layer adjacent to the surface assuming the surface velocity (i.e., zero velocity relative to the surface). Also, we defined the velocity boundary layer as the region in which the fluid velocity varies from zero to $0.99V$. Likewise, a *thermal boundary layer* develops when a fluid at a specified temperature flows over a surface that is at a different temperature, as shown in Fig. 6–17.

Consider the flow of a fluid at a uniform temperature of T_∞ over an isothermal flat plate at temperature T_s. The fluid particles in the layer adjacent to the surface reach thermal equilibrium with the plate and assume the surface temperature T_s. These fluid particles then exchange energy with the particles in the adjoining fluid layer, and so on. As a result, a temperature profile develops in the flow field that ranges from T_s at the surface to T_∞ sufficiently far from the surface. The flow region over the surface in which the temperature variation in the direction normal to the surface is significant is the **thermal boundary layer**. The *thickness* of the thermal boundary layer δ_t at any location along the surface is defined as *the distance from the surface at which the temperature difference* $T - T_s$ *equals* $0.99(T_\infty - T_s)$. Note that for the special case of $T_s = 0$, we have $T = 0.99T_\infty$ at the outer edge of the thermal boundary layer, which is analogous to $u = 0.99V$ for the velocity boundary layer.

The thickness of the thermal boundary layer increases in the flow direction, since the effects of heat transfer are felt at greater distances from the surface further downstream.

The convection heat transfer rate anywhere along the surface is directly related to the temperature gradient at that location. Therefore, the shape of the temperature profile in the thermal boundary layer dictates the convection heat transfer between a solid surface and the fluid flowing over it. In flow over a heated (or cooled) surface, both velocity and thermal boundary layers develop

TABLE 6–1

Dynamic viscosities of some fluids at 1 atm and 20°C (unless otherwise stated)

Fluid	Dynamic Viscosity μ, kg/m·s
Glycerin:	
−20°C	134.0
0°C	10.5
20°C	1.52
40°C	0.31
Engine oil:	
SAE 10W	0.10
SAE 10W30	0.17
SAE 30	0.29
SAE 50	0.86
Mercury	0.0015
Ethyl alcohol	0.0012
Water:	
0°C	0.0018
20°C	0.0010
100°C (liquid)	0.00028
100°C (vapor)	0.000012
Blood, 37°C	0.00040
Gasoline	0.00029
Ammonia	0.00015
Air	0.000018
Hydrogen, 0°C	0.0000088
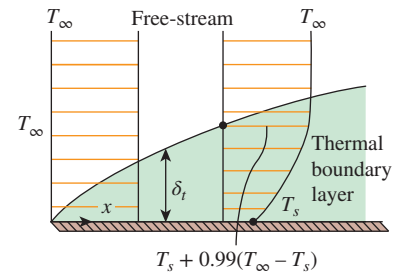
FIGURE 6–17
Thermal boundary layer on a flat plate (the fluid is hotter than the plate surface).

FIGURE 6–18
Ludwig Prandtl (1875–1953), was a German physicist famous for his work in aeronautics, born in Freising, Bavaria. His discovery in 1904 of the boundary layer which adjoins the surface of a body moving in a fluid led to an understanding of skin friction drag and of the way in which streamlining reduces the drag of airplane wings and other moving bodies. Prandtl's work and decisive advances in boundary layer and wing theories became the basic material of aeronautics. He also made important contributions to the theories of supersonic flow and of turbulence, and he contributed much to the development of wind tunnels and other aerodynamic equipment. The dimensionless **Prandtl number** was named after him.

©ullstein bild Dtl./Getty Images

TABLE 6–2

Typical ranges of Prandtl numbers for common fluids

Fluid	Pr
Liquid metals	0.004–0.030
Gases	0.7–1.0
Water	1.7–13.7
Light organic fluids	5–50
Oils	50–100,000
Glycerin	2000–100,000

simultaneously. Noting that the fluid velocity has a strong influence on the temperature profile, the development of the velocity boundary layer relative to the thermal boundary layer will have a strong effect on the convection heat transfer.

Prandtl Number

The relative thickness of the velocity and the thermal boundary layers is best described by the *dimensionless* parameter **Prandtl number**, defined as

$$\text{Pr} = \frac{\text{Molecular diffusivity of momentum}}{\text{Molecular diffusivity of heat}} = \frac{\nu}{\alpha} = \frac{\mu c_p}{k} \tag{6–12}$$

It is named after Ludwig Prandtl (Fig. 6–18), who introduced the concept of boundary layer in 1904 and made significant contributions to boundary layer theory. The Prandtl numbers of fluids range from less than 0.01 for liquid metals to more than 100,000 for heavy oils (Table 6–2). Note that the Prandtl number is in the order of 10 for water.

The Prandtl numbers of gases are about 1, which indicates that both momentum and heat dissipate through the fluid at about the same rate. Heat diffuses very quickly in liquid metals ($\text{Pr} \ll 1$) and very slowly in oils ($\text{Pr} \gg 1$) relative to momentum. Consequently the thermal boundary layer is much thicker for liquid metals and much thinner for oils relative to the velocity boundary layer.

Liquid metals are a special class of fluids with very low Prandtl numbers (Table 6–2). The very low Prandtl number is due to the high thermal conductivity of these fluids, since the specific heat and viscosity of liquid metals are very comparable to other common fluids. Considerable interest has been placed on liquid metals as coolants in applications where large amounts of heat must be removed from a relatively small space, as in a nuclear reactor. Liquid metals, aside from having high thermal conductivity values, have high thermal capacity, low vapor pressure, and low melting point. They remain in the liquid state at higher temperatures than conventional fluids. This makes them more attractive for use in compact heat exchangers. However, liquid metals are corrosive in nature, and their contact with air or water may result in violent action. Suitable measures for handling them have been developed.

6–5 ▪ LAMINAR AND TURBULENT FLOWS

If you have been around smokers, you probably noticed that the cigarette smoke rises in a smooth plume for the first few centimeters and then starts fluctuating randomly in all directions as it continues its rise. Other plumes behave similarly (Fig. 6–19). Likewise, a careful inspection of flow in a pipe reveals that the fluid flow is streamlined at low velocities but turns chaotic as the velocity is increased above a critical value, as shown in Fig. 6–20. The flow regime in the first case is said to be **laminar**, characterized by *smooth streamlines* and *highly ordered motion,* and **turbulent** in the second case, where it is characterized by *velocity fluctuations* and *highly disordered motion.* The **transition** from laminar to turbulent flow does not occur suddenly; rather, it occurs over some region in which the flow fluctuates between laminar and turbulent flows before it becomes fully turbulent. Most flows encountered in practice are turbulent. Laminar flow is encountered when highly viscous fluids such as oils flow in small pipes or narrow passages.

We can verify the existence of these laminar, transitional, and turbulent flow regimes by injecting some dye streak into the flow in a glass tube, as the British scientist Osborn Reynolds (Fig. 6–21) did over a century ago. We observe that the dye streak forms a *straight and smooth line* at low velocities when the flow is laminar (we may see some blurring because of molecular diffusion), has *bursts of fluctuations* in the transitional regime, and *zigzags rapidly and randomly* when the flow becomes fully turbulent. These zigzags and the dispersion of the dye are indicative of the fluctuations in the main flow and the rapid mixing of fluid particles from adjacent layers.

Typical average velocity profiles in laminar and turbulent flow are also given in Fig. 6–14. Note that the velocity profile in turbulent flow is much fuller than that in laminar flow, with a sharp drop near the surface. The turbulent boundary layer can be considered to consist of four regions, characterized by the distance from the wall. The very thin layer next to the wall where viscous effects are dominant is the **viscous sublayer**. The velocity profile in this layer is very nearly *linear,* and the flow is streamlined. Next to the viscous sublayer is the **buffer layer**, in which turbulent effects are becoming significant, but the flow is still dominated by viscous effects. Above the buffer layer is the **overlap layer**, in which the turbulent effects are much more significant, but still not dominant. Above that is the **turbulent layer**, in which turbulent effects dominate over viscous effects.

The *intense mixing* of the fluid in turbulent flow as a result of rapid fluctuations enhances heat and momentum transfer between fluid particles, which increases the friction force on the surface and the convection heat transfer rate. It also causes the boundary layer to enlarge. Both the friction and heat transfer coefficients reach maximum values when the flow becomes *fully turbulent.* So it will come as no surprise that a special effort is made in the design of heat transfer coefficients associated with turbulent flow. The enhancement in heat transfer in turbulent flow does not come for free, however. It may be necessary to use a larger pump to overcome the larger friction forces accompanying the higher heat transfer rate.

Reynolds Number

The transition from laminar to turbulent flow depends on the *surface geometry, surface roughness, flow velocity, surface temperature,* and *type of fluid,* among other things. After exhaustive experiments in the 1880s, Osborne Reynolds discovered that the flow regime depends mainly on the ratio of the *inertia forces* to *viscous forces* in the fluid. This ratio is called the **Reynolds number** (Fig. 6–21), which is a *dimensionless* quantity, and which is expressed for external flow as (Fig. 6–22)

$$\mathrm{Re} = \frac{\text{Inertia forces}}{\text{Viscous forces}} = \frac{VL_c}{\nu} = \frac{\rho VL_c}{\mu} \tag{6–13}$$

where V is the upstream velocity (equivalent to the free-stream velocity for a flat plate), L_c is the characteristic length of the geometry, and $\nu = \mu/\rho$ is the kinematic viscosity of the fluid. For a flat plate, the characteristic length is the distance x from the leading edge. Note that kinematic viscosity has the unit m²/s, which is identical to the unit of thermal diffusivity and which can be viewed as *viscous diffusivity* or *diffusivity for momentum.*
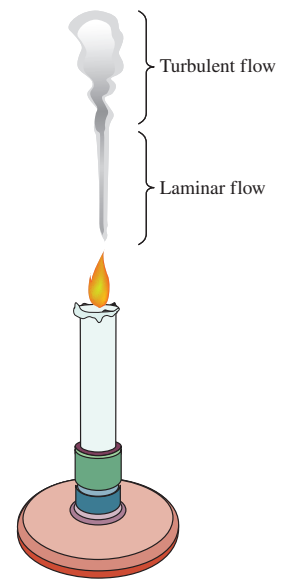
FIGURE 6−19
Laminar and turbulent flow regimes of candle smoke.
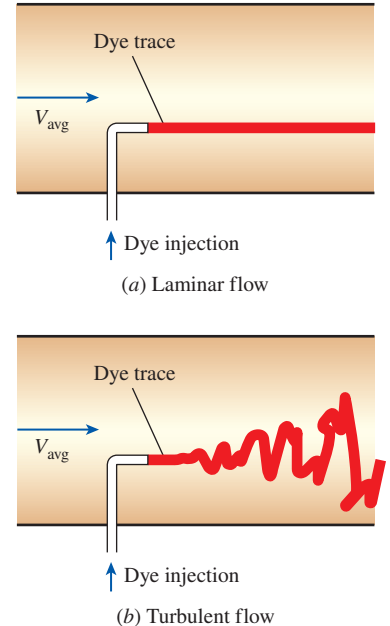
FIGURE 6−20
The behavior of colored fluid injected into the flow in laminar and turbulent flows in a pipe.

FIGURE 6–21
Osborne Reynolds (1842–1912), an English engineer and physicist best known for his work in the fields of hydraulics and hydrodynamics, was born in Belfast, Ireland. Reynolds' studies of condensation and the transfer of heat between solids and fluids brought about radical revisions in boiler and condenser design, and his work on turbine pumps laid the foundation for their rapid development. His classical paper on "The Law of Resistance in Parallel Channels" (1883) investigated the transition from smooth, or laminar, to turbulent flow. In 1886 he also formulated "The Theory of Lubrication," and later in 1889, he developed a mathematical framework which became the standard in turbulence work. His other work included the explanation of the radi-ometer and an early absolute determi-nation of the mechanical equivalent of heat. The dimensionless **Reynolds number**, which provides a criterion for dynamic similarity and for correct modeling in many fluid flow experi-ments, is named after him.
©Paul Fearn/Alamy

At *large* Reynolds numbers, the inertia forces, which are proportional to the density and the velocity of the fluid, are large relative to the viscous forces, and thus the viscous forces cannot prevent the random and rapid fluctuations of the fluid. At *small* or *moderate* Reynolds numbers, however, the viscous forces are large enough to suppress these fluctuations and to keep the fluid "in line." Thus the flow is *turbulent* in the first case and *laminar* in the second.

The Reynolds number at which the flow becomes turbulent is called the **critical Reynolds number**. The value of the critical Reynolds number is dif-ferent for different geometries and flow conditions. For flow over a flat plate, the generally accepted value of the critical Reynolds number is $\text{Re}_{cr} = V x_{cr}/v = 5 \times 10^5$, where x_{cr} is the distance from the leading edge of the plate at which transition from laminar to turbulent flow occurs. The value of Re_{cr} may change substantially, however, depending on the level of turbulence in the free stream.

6–6 ▪ HEAT AND MOMENTUM TRANSFER IN TURBULENT FLOW

Most flows encountered in engineering practice are turbulent, and thus it is important to understand how turbulence affects wall shear stress and heat transfer. However, turbulent flow is a complex mechanism dominated by fluctuations, and despite tremendous amounts of work done in this area by researchers, the theory of turbulent flow is still not fully understood. Therefore, we must rely on experiments and the empirical or semi-empirical correlations developed for various situations.

Turbulent flow is characterized by disorderly and rapid fluctuations of swirling regions of fluid, called **eddies**, throughout the flow. These fluctuations provide an additional mechanism for momentum and energy transfer. In laminar flow, fluid particles flow in an orderly manner along pathlines, and momentum and energy are transferred across streamlines by molecular diffusion. In turbulent flow, the swirling eddies transport mass, momentum, and energy to other regions of flow much more rapidly than molecular diffusion, greatly enhancing mass, momen-tum, and heat transfer. As a result, turbulent flow is associated with much higher values of friction, heat transfer, and mass transfer coefficients (Fig. 6–23).

Even when the average flow is steady, the eddy motion in turbulent flow causes significant fluctuations in the values of velocity, temperature, pressure, and even density (in compressible flow). Figure 6–24 shows the variation of the instantaneous velocity component u with time at a specified location, as can be measured with a hot-wire anemometer probe or other sensitive device. We observe that the instantaneous values of the velocity fluctuate about an average value, which suggests that the velocity can be expressed as the sum of an *average value* $\bar{u}$ and a *fluctuating component u'*,

$$u = \bar{u} + u' \tag{6–14}$$

This is also the case for other properties such as the velocity component v in the y-direction, and thus $v = \bar{v} + v'$, $P = \bar{P} + P'$, and $T = \bar{T} + T'$. The aver-age value of a property at some location is determined by averaging it over a time interval that is sufficiently large so that the time average levels off to a constant. Therefore, the time average of fluctuating components is zero, e.g., $\overline{u'} = 0$. The magnitude of u' is usually just a few percent of $\bar{u}$, but the high frequencies of eddies (in the order of a thousand per second) makes

them very effective for the transport of momentum, thermal energy, and mass. In time-averaged *stationary* turbulent flow, the average values of properties (indicated by an overbar) are independent of time. The chaotic fluctuations of fluid particles play a dominant role in pressure drop, and these random motions must be considered in analyses together with the average velocity.

Perhaps the first thought that comes to mind is to determine the shear stress in an analogous manner to laminar flow from $\tau = -\mu \, d\bar{u}/dr$, where $\bar{u}(r)$ is the average velocity profile for turbulent flow. But the experimental studies show that this is not the case, and the shear stress is much larger due to the turbulent fluctuations. Therefore, it is convenient to think of the turbulent shear stress as consisting of two parts: the *laminar component,* which accounts for the friction between layers in the flow direction (expressed as $\tau_{lam} = \mu(d\bar{u}/dr)$), and the *turbulent component,* which accounts for the friction between the fluctuating fluid particles and the fluid body (denoted as τ_{turb} and is related to the fluctuation components of velocity).

Consider turbulent flow in a horizontal pipe and the upward eddy motion of fluid particles in a layer of lower velocity to an adjacent layer of higher velocity through a differential area dA as a result of the velocity fluctuation v', as shown in Fig. 6–25. The mass flow rate of the fluid particles rising through dA is $\rho v' \, dA$, and its net effect on the layer above dA is a reduction in its average flow velocity because of momentum transfer to the fluid particles with lower average flow velocity. This momentum transfer causes the horizontal velocity of the fluid particles to increase by u', and thus causes its momentum in the horizontal direction to increase at a rate of $(\rho v' dA)u'$, which must be equal to the decrease in the momentum of the upper fluid layer.

Noting that force in a given direction is equal to the rate of change of momentum in that direction, the horizontal force acting on a fluid element above dA due to the passing of fluid particles through dA is $\delta F = (\rho v' dA)(-u') = -\rho u' v' dA$. Therefore, the shear force per unit area due to the eddy motion of fluid particles $\delta F/dA = -\rho u' v'$ can be viewed as the instantaneous turbulent shear stress. Then the **turbulent shear stress** can be expressed as $\tau_{turb} = -\rho \overline{u' v'}$ where $\overline{u' v'}$ is the time average of the product of the fluctuating velocity components u' and v'. Similarly, considering that $h = c_p T$ represents the energy of the fluid and T' is the eddy temperature relative to the mean value, the rate of thermal energy transport by turbulent eddies is $\dot{q}_{turb} = \rho c_p \overline{v' T'}$. Note that $\overline{u' v'} \neq 0$, even though $\overline{u'} = 0$ and $\overline{v'} = 0$ (and thus $\overline{u'} \, \overline{v'} = 0$), and experimental results show that $\overline{u' v'}$ is usually a negative quantity. Terms such as $-\rho \overline{u' v'}$ or $-\rho \overline{u'^2}$ are called **Reynolds stresses** or **turbulent stresses**.

The random eddy motion of groups of particles resembles the random motion of molecules in a gas—colliding with each other after traveling a certain distance and exchanging momentum and heat in the process. Therefore, momentum and heat transport by eddies in turbulent boundary layers is analogous to the molecular momentum and heat diffusion. Then turbulent wall shear stress and turbulent heat transfer can be expressed in an analogous manner as

$$\tau_{turb} = -\rho \overline{u'v'} = \mu_t \frac{\partial \bar{u}}{\partial y} \qquad \text{and} \qquad \dot{q}_{turb} = \rho c_p \overline{v' T'} = -k_t \frac{\partial T}{\partial y} \tag{6-15}$$

where μ_t is called the **turbulent** (or **eddy**) **viscosity**, which accounts for momentum transport by turbulent eddies, and k_t is called the **turbulent** (or **eddy**) **thermal conductivity**, which accounts for thermal energy transport by
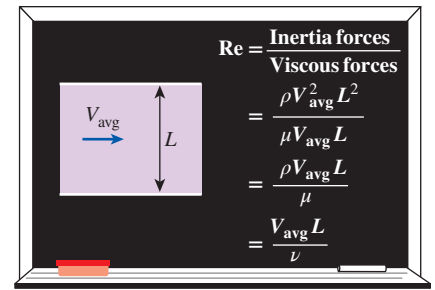
FIGURE 6–22
The Reynolds number can be viewed as the ratio of inertial forces to viscous forces acting on a fluid element.

(*a*) Before turbulence   (*b*) After turbulence
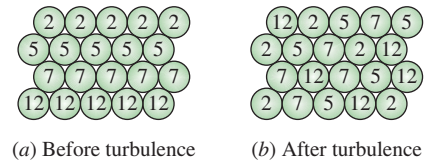
FIGURE 6–23
The intense mixing in turbulent flow brings fluid particles at different temperatures into close contact and thus enhances heat transfer.
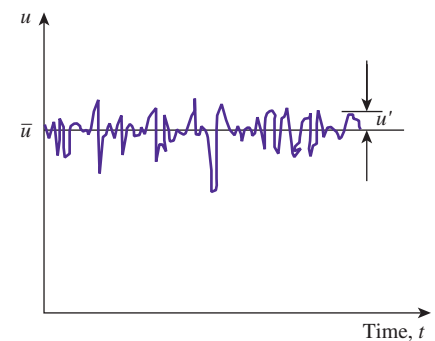
FIGURE 6–24
Fluctuations of the velocity component *u* with time at a specified location in turbulent flow.
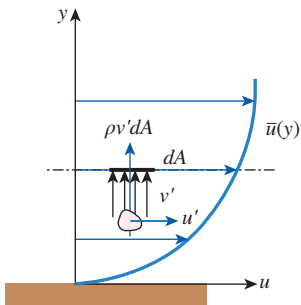
FIGURE 6–25
Fluid particle moving upward through a differential area dA as a result of the velocity fluctuation v'.

Laminar flow
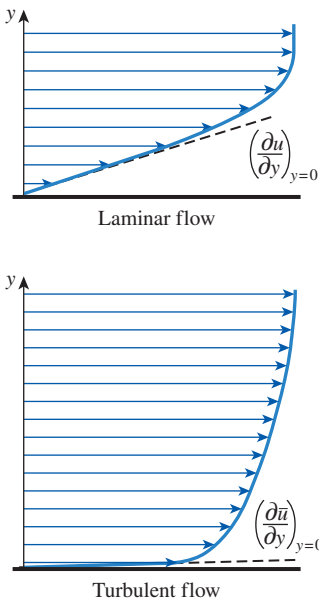
Turbulent flow

FIGURE 6–26
The velocity gradients at the wall, and thus the wall shear stress, are much larger for turbulent flow than they are for laminar flow, even though the turbulent boundary layer is thicker than the laminar one for the same value of free-stream velocity.

turbulent eddies. Then the total shear stress and total heat flux can be expressed conveniently as

$$\tau_{\text{total}} = (\mu + \mu_t)\frac{\partial \overline{u}}{\partial y} = \rho(\nu + \nu_t)\frac{\partial \overline{u}}{\partial y} \qquad (6\text{–}16)$$

and

$$\dot{q}_{\text{total}} = -(k + k_t)\frac{\partial \overline{T}}{\partial y} = -\rho c_p(\alpha + \alpha_t)\frac{\partial \overline{T}}{\partial y} \qquad (6\text{–}17)$$

where $\nu_t = \mu_t/\rho$ is the **kinematic eddy viscosity** (or **eddy diffusivity of momentum**) and $\alpha_t = k_t/\rho c_p$ is the **eddy thermal diffusivity** (or **eddy diffusivity of heat**).

Eddy motion and thus eddy diffusivities are much larger than their molecular counterparts in the core region of a turbulent boundary layer. The eddy motion loses its intensity close to the wall and diminishes at the wall because of the no-slip condition. Therefore, the velocity and temperature profiles are very slowly changing in the core region of a turbulent boundary layer, but they are very steep in the thin layer adjacent to the wall, resulting in large velocity and temperature gradients at the wall surface. So it is no surprise that the wall shear stress and wall heat flux are much larger in turbulent flow than they are in laminar flow (Fig. 6–26).

Note that molecular diffusivities v and α (as well as μ and k) are fluid properties, and their values can be found listed in fluid handbooks. Eddy diffusivities ν_t and α_t (as well as μ_t and k_t), however, are *not* fluid properties, and their values depend on flow conditions. Eddy diffusivities ν_t and α_t decrease toward the wall, becoming zero at the wall. Their values range from zero at the wall to several thousand times the values of molecular diffusivities in the core region.

6–7 ▪ DERIVATION OF DIFFERENTIAL CONVECTION EQUATIONS*

In this section we derive the governing equations of fluid flow in the boundary layers. To keep the analysis at a manageable level, we assume the flow to be steady and two-dimensional and the fluid to be Newtonian with constant properties (density, viscosity, thermal conductivity, etc.).

Consider the parallel flow of a fluid over a surface. We take the flow direction along the surface to be x and the direction normal to the surface to be $y,$ and we choose a differential volume element of length dx, height dy, and unit depth in the z-direction (normal to the paper) for analysis (Fig. 6–27). The fluid flows over the surface with a uniform free-stream velocity $V,$ but the velocity within the boundary layer is two-dimensional: the x-component of the velocity is $u,$ and the y-component is $v.$ Note that $u = u(x, y)$ and $v = v(x, y)$ in steady two-dimensional flow.

Next we apply three fundamental laws to this fluid element: Conservation of mass, conservation of momentum, and conservation of energy to obtain the continuity, momentum, and energy equations for laminar flow in boundary layers.

*This and the upcoming sections of this chapter deal with theoretical aspects of convection, and can be skipped and be used as a reference if desired without a loss in continuity.

The Continuity Equation

The conservation of mass principle is simply a statement that mass cannot be created or destroyed during a process and all the mass must be accounted for during an analysis. In steady flow, the amount of mass within the control volume remains constant, and thus the conservation of mass can be expressed as

$$\left(\begin{array}{c}\text{Rate of mass flow}\\\text{into the control volume}\end{array}\right) = \left(\begin{array}{c}\text{Rate of mass flow}\\\text{out of the control volume}\end{array}\right) \qquad \textbf{(6–18)}$$

Noting that mass flow rate is equal to the product of density, average velocity, and cross-sectional area normal to flow, the rate at which fluid enters the control volume from the left surface is $\rho u(dy \cdot 1)$. The rate at which the fluid leaves the control volume from the right surface can be expressed as

$$\rho\left(u + \frac{\partial u}{\partial x}dx\right)(dy \cdot 1) \qquad \textbf{(6–19)}$$

Repeating this for the y direction and substituting the results into Eq. 6–18, we obtain

$$\rho u(dy \cdot 1) + \rho v(dx \cdot 1) = \rho\left(u + \frac{\partial u}{\partial x}dx\right)(dy \cdot 1) + \rho\left(v + \frac{\partial v}{\partial y}dy\right)(dx \cdot 1) \qquad \textbf{(6–20)}$$

Simplifying and dividing by $dx \cdot dy \cdot 1$ gives

$$\frac{\partial u}{\partial x} + \frac{\partial v}{\partial y} = 0 \qquad \textbf{(6–21)}$$

This is the *conservation of mass* relation in differential form, which is also known as the **continuity equation** or **mass balance** for steady two-dimensional flow of a fluid with constant density.

The Momentum Equations

The differential forms of the equations of motion in the velocity boundary layer are obtained by applying Newton's second law of motion to a differential control volume element in the boundary layer. Newton's second law is an expression for momentum balance and can be stated as *the net force acting on the control volume is equal to the mass times the acceleration of the fluid element within the control volume, which is also equal to the net rate of momentum outflow from the control volume.*

The forces acting on the control volume consist of *body forces* that act throughout the entire body of the control volume (such as gravity, electric, and magnetic forces) and are proportional to the volume of the body, and *surface forces* that act on the control surface (such as the pressure forces due to hydrostatic pressure and shear stresses due to viscous effects) and are proportional to the surface area. The surface forces appear as the control volume is isolated from its surroundings for analysis, and the effect of the detached body is replaced by a force at that location. Note that pressure represents the compressive force applied on the fluid element by the surrounding fluid, and it is always directed to the surface.

We express Newton's second law of motion for the control volume as

$$(\text{Mass})\left(\begin{array}{c}\text{Acceleration}\\\text{in a specified direction}\end{array}\right) = \left(\begin{array}{c}\text{Net force (body and surface)}\\\text{acting in that direction}\end{array}\right) \qquad \textbf{(6–22)}$$
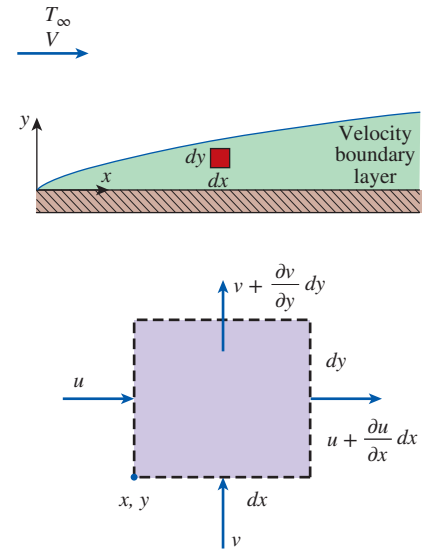
FIGURE 6–27

Differential control volume used in the derivation of mass balance in velocity boundary layer in two-dimensional flow over a surface.

or

$$\delta m \cdot a_x = F_{\text{surface}, x} + F_{\text{body}, x} \tag{6–23}$$

where the mass of the fluid element within the control volume is

$$\delta m = \rho(dx \cdot dy \cdot 1) \tag{6–24}$$

Noting that flow is steady and two-dimensional and thus $u = u(x, y)$, the total differential of u is

$$du = \frac{\partial u}{\partial x} dx + \frac{\partial u}{\partial y} dy \tag{6–25}$$

Then the acceleration of the fluid element in the x-direction becomes

$$a_x = \frac{du}{dt} = \frac{\partial u}{\partial x} \frac{dx}{dt} + \frac{\partial u}{\partial y} \frac{dy}{dt} = u\frac{\partial u}{\partial x} + v\frac{\partial u}{\partial y} \tag{6–26}$$
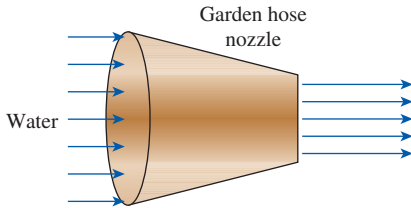
FIGURE 6–28
During steady flow, a fluid may not accelerate in time at a fixed point, but it may accelerate in space.

You may be tempted to think that acceleration is zero in steady flow since acceleration is the rate of change of velocity with time, and in steady flow there is no change with time. Well, a garden hose nozzle tells us that this understanding is not correct. Even in steady flow and thus constant mass flow rate, water accelerates through the nozzle (Fig. 6–28). *Steady* simply means no change with time at a specified location (and thus $\partial u/\partial t = 0$), but the value of a quantity may change from one location to another (and thus $\partial u/\partial x$ and $\partial u/\partial y$ may be different from zero). In the case of a nozzle, the velocity of water remains constant at a specified point, but it changes from the inlet to the exit (water accelerates along the nozzle, which is the reason for attaching a nozzle to the garden hose in the first place).

The forces acting on a surface are due to pressure and viscous effects. In two-dimensional flow, the *viscous stress* at any point on an imaginary surface within the fluid can be resolved into two perpendicular components: one normal to the surface called *normal stress* (which should not be confused with pressure) and another along the wall surface called *shear stress.* The normal stress is related to the velocity gradients $\partial u/\partial x$ and $\partial v/\partial y,$ which are much smaller than $\partial u/\partial y,$ to which shear stress is related. Neglecting the normal stresses for simplicity, the surface forces acting on the control volume in the x-direction are as shown in Fig. 6–29. Then the net surface force acting in the x-direction becomes

FIGURE 6–29
Differential control volume used in the derivation of x-momentum equation in velocity boundary layer in two-dimensional flow over a surface.

$$F_{\text{surface}, x} = \left(\frac{\partial \tau}{\partial y} dy\right)(dx \cdot 1) - \left(\frac{\partial P}{\partial x} dx\right)(dy \cdot 1) = \left(\frac{\partial \tau}{\partial y} - \frac{\partial P}{\partial x}\right)(dx \cdot dy \cdot 1)$$
$$= \left(\mu\frac{\partial^2 u}{\partial y^2} - \frac{\partial P}{\partial x}\right)(dx \cdot dy \cdot 1) \tag{6–27}$$

since $\tau = \mu(\partial u/\partial y)$. Substituting Eqs. 6–24, 6–26, and 6–27 into Eq. 6–23 and dividing by $dx \cdot dy \cdot 1$ gives

$$\rho\left(u\frac{\partial u}{\partial x} + v\frac{\partial u}{\partial y}\right) = \mu\frac{\partial^2 u}{\partial y^2} - \frac{\partial P}{\partial x} \tag{6–28}$$

This is the relation for the **momentum balance** in the x-direction, and it is known as the **x-momentum equation**. Note that we would obtain the same result if we used momentum flow rates for the left-hand side of this equation instead of mass times acceleration. If there is a body force acting in the x-direction, it can be added to the right side of the equation, provided that it is expressed per unit volume of the fluid.

In a boundary layer, the velocity component in the flow direction is much larger than that in the normal direction, and thus $u \gg v$, and $\partial v / \partial x$ and $\partial v / \partial y$ are negligible. Also, u varies greatly with y in the normal direction from zero at the wall surface to nearly the free-stream value across the relatively thin boundary layer, while the variation of u with x along the flow is typically small. Therefore, $\partial u / \partial y \gg \partial u / \partial x$. Similarly, if the fluid and the wall are at different temperatures and the fluid is heated or cooled during flow, heat conduction occurs primarily in the direction normal to the surface, and thus $\partial T / \partial y \gg \partial T / \partial x$. That is, the velocity and temperature gradients normal to the surface are much greater than those along the surface. These simplifications are known as the **boundary layer approximations**. These approximations greatly simplify the analysis, usually with little loss in accuracy, and they make it possible to obtain analytical solutions for certain types of flow problems (Fig. 6–30).

When gravity effects and other body forces are negligible and the boundary layer approximations are valid, applying Newton's second law of motion on the volume element in the y-direction gives the *y-momentum equation* to be

$$\frac{\partial P}{\partial y} = 0 \qquad\qquad \textbf{(6–29)}$$

That is, *the variation of pressure in the direction normal to the surface is negligible,* and thus $P = P(x)$ and $\partial P / \partial x = dP / dx$. Then it follows that for a given x, the pressure in the boundary layer is equal to the pressure in the free stream, and the pressure determined by a separate analysis of fluid flow in the free stream (which is typically easier because of the absence of viscous effects) can readily be used in the boundary layer analysis.

The velocity components in the free stream region of a flat plate are $u = V = $ constant and $v = 0$. Substituting these into the x-momentum equations (Eq. 6–28) gives $\partial P / \partial x = 0$. Therefore, for flow over a flat plate, the pressure remains constant over the entire plate (both inside and outside the boundary layer).

Conservation of Energy Equation

The energy balance for any system undergoing any process is expressed as $E_{in} - E_{out} = \Delta E_{system}$, which states that the change in the energy content of a system during a process is equal to the difference between the energy input and the energy output. During a *steady-flow process,* the total energy content of a control volume remains constant (and thus $\Delta E_{system} = 0$), and the amount of energy entering a control volume in all forms must be equal to the amount of energy leaving it. Then the rate form of the general energy equation reduces for a steady-flow process to $\dot{E}_{in} - \dot{E}_{out} = 0$.

Noting that energy can be transferred by heat, work, and mass only, the energy balance for a steady-flow control volume can be written explicitly as

$$(\dot{E}_{in} - \dot{E}_{out})_{by\ heat} + (\dot{E}_{in} - \dot{E}_{out})_{by\ work} + (\dot{E}_{in} - \dot{E}_{out})_{by\ mass} = 0 \qquad \textbf{(6–30)}$$

The total energy of a flowing fluid stream per unit mass is $e_{stream} = h + ke + pe$ where h is the enthalpy (which is the sum of internal energy and flow energy), $pe = gz$ is the potential energy, and $ke = V^2/2 = (u^2 + v^2)/2$ is the kinetic energy of the fluid per unit mass. The kinetic and potential energies are usually very small relative to enthalpy, and therefore it is common practice to neglect them (besides, it can be shown that if kinetic energy is included in the
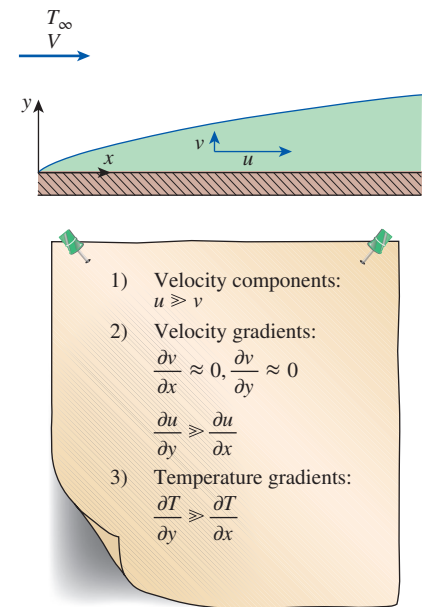
FIGURE 6–30
Boundary layer approximations.
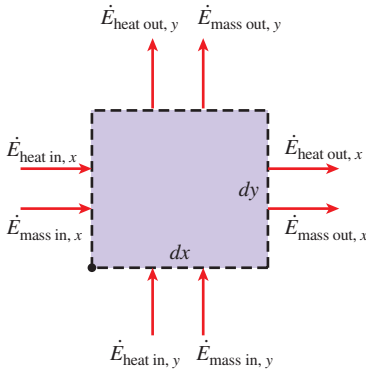
FIGURE 6–31

The energy transfers by heat and mass flow associated with a differential control volume in the thermal boundary layer in steady two-dimensional flow.

following analysis, all the terms due to this inclusion cancel each other). We assume the density ρ, specific heat c_p, viscosity μ, and the thermal conductivity k of the fluid to be constant. Then the energy of the fluid per unit mass can be expressed as $e_{\text{stream}} = h = c_p T$.

Energy is a scalar quantity, and thus energy interactions in all directions can be combined in one equation. Noting that the mass flow rate of the fluid entering the control volume from the left is $\rho u (dy \cdot 1)$, the rate of energy transfer to the control volume by mass in the x-direction is, from Fig. 6–31,

$$(\dot{E}_{\text{in}} - \dot{E}_{\text{out}})_{\text{by mass, }x} = (\dot{m}e_{\text{stream}})_x - \left[(\dot{m}e_{\text{stream}})_x + \frac{\partial(\dot{m}e_{\text{stream}})_x}{\partial x} dx \right]$$

$$= -\frac{\partial[\rho u(dy\cdot 1)c_p T]}{\partial x} dx = -\rho c_p \left(u\frac{\partial T}{\partial x} + T\frac{\partial u}{\partial x} \right) dxdy \quad \text{(6–31)}$$

Repeating this for the y-direction and adding the results, the net rate of energy transfer to the control volume by mass is determined to be

$$(\dot{E}_{\text{in}} - \dot{E}_{\text{out}})_{\text{by mass}} = -\rho c_p \left(u\frac{\partial T}{\partial x} + T\frac{\partial u}{\partial x} \right) dxdy - \rho c_p \left(v\frac{\partial T}{\partial y} + T\frac{\partial v}{\partial y} \right) dxdy$$

$$= -\rho c_p \left(u\frac{\partial T}{\partial x} + v\frac{\partial T}{\partial x} \right) dxdy \quad \text{(6–32)}$$

since $\partial u/\partial x + \partial v/\partial y = 0$ from the continuity equation.

The net rate of heat conduction to the volume element in the x-direction is

$$(\dot{E}_{\text{in}} - \dot{E}_{\text{out}})_{\text{by heat, }x} = \dot{Q}_x - \left(\dot{Q}_x + \frac{\partial \dot{Q}_x}{\partial x} dx \right) = -\frac{\partial}{\partial x}\left(-k(dy\cdot 1)\frac{\partial T}{\partial x} \right) dx$$

$$= k\frac{\partial^2 T}{\partial x^2} dxdy \quad \text{(6–33)}$$

Repeating this for the y-direction and adding the results, the net rate of energy transfer to the control volume by heat conduction becomes

$$(\dot{E}_{\text{in}} - \dot{E}_{\text{out}})_{\text{by heat}} = k\frac{\partial^2 T}{\partial x^2} dxdy + k\frac{\partial^2 T}{\partial y^2} dxdy = k\left(\frac{\partial^2 T}{\partial x^2} + \frac{\partial^2 T}{\partial y^2} \right) dxdy \quad \text{(6–34)}$$

Another mechanism of energy transfer to and from the fluid in the control volume is the work done by the body and surface forces. The work done by a body force is determined by multiplying this force by the velocity in the direction of the force and the volume of the fluid element, and this work needs to be considered only in the presence of significant gravitational, electric, or magnetic effects. The surface forces consist of the forces due to fluid pressure and the viscous shear stresses. The work done by pressure (the flow work) is already accounted for in the analysis above by using enthalpy for the microscopic energy of the fluid instead of internal energy. The shear stresses that result from viscous effects are usually very small and can be neglected in many cases. This is especially the case for applications that involve low or moderate velocities.

Then the energy equation for the steady two-dimensional flow of a fluid with constant properties and negligible shear stresses is obtained by substituting Eqs. 6–32 and 6–34 into 6–30 to be

$$\rho c_p \left(u\frac{\partial T}{\partial x} + v\frac{\partial T}{\partial y} \right) = k\left(\frac{\partial^2 T}{\partial x^2} + \frac{\partial^2 T}{\partial y^2} \right) \quad \text{(6–35)}$$

which states that *the net energy convected by the fluid out of the control volume is equal to the net energy transferred into the control volume by heat conduction.*

When the viscous shear stresses are not negligible, their effect is accounted for by expressing the energy equation as

$$\rho c_p \left(u \frac{\partial T}{\partial x} + v \frac{\partial T}{\partial y} \right) = k \left(\frac{\partial^2 T}{\partial x^2} + \frac{\partial^2 T}{\partial y^2} \right) + \mu \Phi \qquad \text{(6–36)}$$

where the *viscous dissipation function* Φ is obtained after a lengthy analysis [see an advanced book such as the one by *Schlichting* (1979) for details] to be

$$\Phi = 2 \left[\left(\frac{\partial u}{\partial x} \right)^2 + \left(\frac{\partial v}{\partial y} \right)^2 \right] + \left(\frac{\partial u}{\partial y} + \frac{\partial v}{\partial x} \right)^2 \qquad \text{(6–37)}$$

Viscous dissipation may play a dominant role in high-speed flows, especially when the viscosity of the fluid is high (like the flow of oil in journal bearings). This manifests itself as a significant rise in fluid temperature due to the conversion of the kinetic energy of the fluid to thermal energy. Viscous dissipation is also significant for high-speed flights of aircraft.

For the special case of a stationary fluid, $u = v = 0$, the energy equation reduces, as expected, to the steady two-dimensional heat conduction equation,

$$\frac{\partial^2 T}{\partial x^2} + \frac{\partial^2 T}{\partial y^2} = 0 \qquad \text{(6–38)}$$

EXAMPLE 6–2   Temperature Rise of Oil in a Journal Bearing

The flow of oil in a journal bearing can be approximated as parallel flow between two large plates with one plate moving and the other stationary. Such flows are known as Couette flow.

Consider two large isothermal plates separated by 2-mm-thick oil film. The upper plate moves at a constant velocity of 12 m/s, while the lower plate is stationary. Both plates are maintained at 20°C. (*a*) Obtain relations for the velocity and temperature distributions in the oil. (*b*) Determine the maximum temperature in the oil and the heat flux from the oil to each plate (Fig. 6–32).

SOLUTION   Parallel flow of oil between two plates is considered. The velocity and temperature distributions, the maximum temperature, and the total heat transfer rate are to be determined.

Assumptions   **1** Steady operating conditions exist. **2** Oil is an incompressible substance with constant properties. **3** Body forces such as gravity are negligible. **4** The plates are large, so there is no variation in the *z*-direction.

Properties   The properties of oil at 20°C are (Table A–13):

$$k = 0.145 \text{ W/m·K} \quad \text{and} \quad \mu = 0.8374 \text{ kg/m·s} = 0.8374 \text{ N·s/m}^2$$

Analysis   (*a*) We take the *x-axis* to be the flow direction and *y* to be the normal direction. This is parallel flow between two plates, and thus $v = 0$. Then the continuity equation (Eq. 6–21) reduces to

Continuity: $\dfrac{\partial u}{\partial x} + \dfrac{\partial v}{\partial y} = 0 \rightarrow \dfrac{\partial u}{\partial x} = 0 \quad \rightarrow u = u(y)$
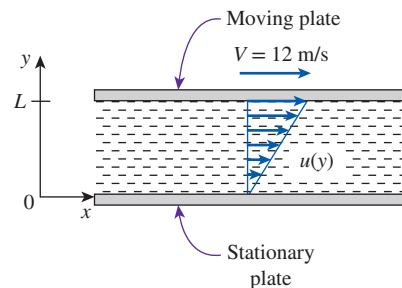
FIGURE 6–32
Schematic for Example 6–2.

Therefore, the *x*-component of velocity does not change in the flow direction (i.e., the velocity profile remains unchanged). Noting that $u = u(y)$, $v = 0$, and $\partial P/\partial x = 0$ (flow is maintained by the motion of the upper plate rather than the pressure gradient), the *x*-momentum equation (Eq. 6–28) reduces to

x-momentum:
$$\rho\left(u\frac{\partial u}{\partial x} + v\frac{\partial u}{\partial y}\right) = \mu\frac{\partial^2 u}{\partial y^2} - \frac{\partial P}{\partial x} \quad \rightarrow \quad \frac{d^2 u}{dy^2} = 0$$

This is a second-order ordinary differential equation, and integrating it twice gives

$$u(y) = C_1 y + C_2$$

The fluid velocities at the plate surfaces must be equal to the velocities of the plates because of the no-slip condition. Therefore, the boundary conditions are $u(0) = 0$ and $u(L) = V$, and applying them gives the velocity distribution to be

$$u(y) = \frac{y}{L}V$$

Frictional heating due to viscous dissipation in this case is significant because of the high viscosity of oil and the large plate velocity. The plates are isothermal, and there is no change in the flow direction, and thus the temperature depends on *y* only, $T = T(y)$. Also, $u = u(y)$ and $v = 0$. Then the energy equation with dissipation (Eqs. 6–36 and 6–37) reduce to

Energy:
$$0 = k\frac{\partial^2 T}{\partial y^2} + \mu\left(\frac{\partial u}{\partial y}\right)^2 \quad \rightarrow \quad k\frac{d^2 T}{dy^2} = -\mu\left(\frac{V}{L}\right)^2$$

since $\partial u/\partial y = V/L$. Dividing both sides by k and integrating twice give

$$T(y) = -\frac{\mu}{2k}\left(\frac{y}{L}V\right)^2 + C_3 y + C_4$$

Applying the boundary conditions $T(0) = T_0$ and $T(L) = T_0$ gives the temperature distribution to be

$$T(y) = T_0 + \frac{\mu V^2}{2k}\left(\frac{y}{L} - \frac{y^2}{L^2}\right)$$

(*b*) The temperature gradient is determined by differentiating $T(y)$ with respect to *y*,

$$\frac{dT}{dy} = \frac{\mu V^2}{2kL}\left(1 - 2\frac{y}{L}\right)$$

The location of maximum temperature is determined by setting $dT/dy = 0$ and solving for *y*,

$$\frac{dT}{dy} = \frac{\mu V^2}{2kL}\left(1 - 2\frac{y}{L}\right) = 0 \quad \rightarrow \quad y = \frac{L}{2}$$

Therefore, maximum temperature occurs at midplane, which is not surprising since both plates are maintained at the same temperature. The maximum temperature is the value of temperature at $y = L/2$,

$$T_{max} = T\left(\frac{L}{2}\right) = T_0 + \frac{\mu V^2}{2k}\left(\frac{L/2}{L} - \frac{(L/2)^2}{L^2}\right) = T_0 + \frac{\mu V^2}{8k}$$

$$= 20 + \frac{(0.8374 \text{ N·s/m}^2)(12 \text{ m/s})^2}{8(0.145 \text{ W/m·K})}\left(\frac{1 \text{ W}}{1 \text{ N·m/s}}\right) = \textbf{124°C}$$

Heat flux at the plates is determined from the definition of heat flux,

$$\dot{q}_0 = -k\frac{dT}{dy}\bigg|_{y=0} = -k\frac{\mu V^2}{2kL}\bigg|(1-0) = -\frac{\mu V^2}{2L}$$

$$= -\frac{(0.8374\text{ N·s/m}^2)(12\text{ m/s})^2}{2(0.002\text{ m})}\left(\frac{1\text{ kW}}{1000\text{ N·m/s}}\right) = \mathbf{-30.1\text{ kW/m}^2}$$

$$\dot{q}_L = -k\frac{dT}{dy}\bigg|_{y=L} = -k\frac{\mu V^2}{2kL}(1-2) = \frac{\mu V^2}{2L} = -\dot{q}_0 = \mathbf{30.1\text{ kW/m}^2}$$

Therefore, heat fluxes at the two plates are equal in magnitude but opposite in sign.

Discussion A temperature rise of 104°C confirms our suspicion that viscous dissipation is very significant. Also, the heat flux is equivalent to the rate of mechanical energy dissipation. Therefore, mechanical energy is being converted to thermal energy at a rate of 60.2 kW/m² of plate area to overcome friction in the oil. Finally, calculations are done using oil properties at 20°C, but the oil temperature turned out to be much higher. Therefore, knowing the strong dependence of viscosity on temperature, calculations should be repeated using properties at the average temperature of 72°C to improve accuracy.

6–8 ▪ SOLUTIONS OF CONVECTION EQUATIONS FOR A FLAT PLATE

Consider laminar flow of a fluid over a *flat plate,* as shown in Fig. 6–33. Surfaces that are slightly contoured such as turbine blades can also be approximated as flat plates with reasonable accuracy. The *x*-coordinate is measured along the plate surface from the leading edge of the plate in the direction of the flow, and *y* is measured from the surface in the normal direction. The fluid approaches the plate in the *x*-direction with a uniform upstream velocity, which is equivalent to the free stream velocity *V*.

When viscous dissipation is negligible, the continuity, momentum, and energy equations (Eqs. 6–21, 6–28, and 6–35) reduce for steady, incompressible, laminar flow of a fluid with constant properties over a flat plate to

FIGURE 6–33
Boundary conditions for flow over a flat plate.

Continuity:
$$\frac{\partial u}{\partial x} + \frac{\partial v}{\partial y} = 0 \tag{6–39}$$

Momentum:
$$u\frac{\partial u}{\partial x} + v\frac{\partial u}{\partial y} = \nu\frac{\partial^2 u}{\partial y^2} \tag{6–40}$$

Energy:
$$u\frac{\partial T}{\partial x} + v\frac{\partial T}{\partial y} = \alpha\frac{\partial^2 T}{\partial y^2} \tag{6–41}$$

with the boundary conditions (Fig. 6–25)

At $x = 0$: $u(0, y) = V$, $T(0, y) = T_\infty$
At $y = 0$: $u(x, 0) = 0$, $v(x, 0) = 0, T(x, 0) = T_w$ (6–42)
As $y \to \infty$: $u(x, \infty) = V$, $T(x, \infty) = T_\infty$

When fluid properties are assumed to be constant and thus independent of temperature, the first two equations can be solved separately for the velocity

components u and v. Once the velocity distribution is available, we can determine the friction coefficient and the boundary layer thickness using their definitions. Also, knowing u and v, the temperature becomes the only unknown in the last equation, and it can be solved for temperature distribution.

The continuity and momentum equations were first solved in 1908 by the German engineer H. Blasius, a student of L. Prandtl. This was done by transforming the two partial differential equations into a single ordinary differential equation by introducing a new independent variable, called the **similarity variable**. The finding of such a variable, assuming it exists, is more of an art than science, and it requires to have a good insight into the problem.

Noticing that the general shape of the velocity profile remains the same along the plate, Blasius reasoned that the nondimensional velocity profile u/V should remain unchanged when plotted against the nondimensional distance y/δ, where δ is the thickness of the local velocity boundary layer at a given x. That is, although both δ and u at a given y vary with x, the velocity u at a fixed y/δ remains constant. Blasius was also aware from the work of Stokes that δ is proportional to $\sqrt{\nu x/V}$, and thus he defined a *dimensionless similarity variable* as

$$\eta = y\sqrt{\frac{V}{\nu x}} \tag{6–43}$$

and thus $u/V =$ function(η). He then introduced a *stream function $\psi(x, y)$* as

$$u = \frac{\partial \psi}{\partial y} \quad \text{and} \quad v = -\frac{\partial \psi}{\partial x} \tag{6–44}$$

so that the continuity equation (Eq. 6–39) is automatically satisfied and thus eliminated (this can be verified easily by direct substitution). Next he defined a function $f(\eta)$ as the dependent variable as

$$f(\eta) = \frac{\psi}{V\sqrt{\nu x/V}} \tag{6–45}$$

Then the velocity components become

$$u = \frac{\partial \psi}{\partial y} = \frac{\partial \psi}{\partial \eta}\frac{\partial \eta}{\partial y} = V\sqrt{\frac{\nu x}{V}}\frac{df}{d\eta}\sqrt{\frac{V}{\nu x}} = V\frac{df}{d\eta} \tag{6–46}$$

$$v = -\frac{\partial \psi}{\partial x} = -V\sqrt{\frac{\nu x}{V}}\frac{df}{d\eta} - \frac{V}{2}\sqrt{\frac{\nu}{Vx}}f = \frac{1}{2}\sqrt{\frac{V\nu}{x}}\left(\eta\frac{df}{d\eta} - f\right) \tag{6–47}$$

By differentiating these u and v relations, the derivatives of the velocity components can be shown to be

$$\frac{\partial u}{\partial x} = -\frac{V}{2x}\eta\frac{d^2f}{d\eta^2}, \quad \frac{\partial u}{\partial y} = V\sqrt{\frac{V}{\nu x}}\frac{d^2f}{d\eta^2}, \quad \frac{\partial^2 u}{\partial y^2} = \frac{V^2}{\nu x}\frac{d^3f}{d\eta^3} \tag{6–48}$$

Substituting these relations into the momentum equation and simplifying, we obtain

$$2\frac{d^3f}{d\eta^3} + f\frac{d^2f}{d\eta^2} = 0 \tag{6–49}$$

which is a third-order nonlinear differential equation. Therefore, the system of two partial differential equations is transformed into a single ordinary differential equation by the use of a similarity variable. Using the definitions of

f and η, the boundary conditions in terms of the similarity variables can be expressed as

$$f(0) = 0, \quad \frac{df}{d\eta}\bigg|_{\eta=0} = 0, \quad \text{and} \quad \frac{df}{d\eta}\bigg|_{\eta=\infty} = 1 \qquad \textbf{(6–50)}$$

The transformed equation with its associated boundary conditions cannot be solved analytically, and thus an alternative solution method is necessary. The problem was first solved by Blasius in 1908 using a power series expansion approach, and this original solution is known as the *Blasius solution.* The problem is later solved more accurately using different numerical approaches, and results from such a solution are given in Table 6–3. The nondimensional velocity profile can be obtained by plotting u/V against η. The results obtained by this simplified analysis are in excellent agreement with experimental results.

Recall that we defined the boundary layer thickness as the distance from the surface for which $u/V = 0.99$. We observe from Table 6–3 that the value of η corresponding to $u/V = 0.99$ is $\eta = 4.91$. Substituting $\eta = 4.91$ and $y = \delta$ into the definition of the similarity variable (Eq. 6–43) gives $4.91 = \delta\sqrt{V/\nu x}$. Then the velocity boundary layer thickness becomes

$$\delta = \frac{4.91}{\sqrt{V/\nu x}} = \frac{4.91x}{\sqrt{\text{Re}_x}} \qquad \textbf{(6–51)}$$

since $\text{Re}_x = Vx/\nu$, where x is the distance from the leading edge of the plate. Note that the boundary layer thickness increases with increasing kinematic viscosity ν and with increasing distance from the leading edge x, but it decreases with increasing free-stream velocity V. Therefore, a large free-stream velocity suppresses the boundary layer and causes it to be thinner.

The shear stress on the wall can be determined from its definition and the $\partial u/\partial y$ relation in Eq. 6–48:

$$\tau_w = \mu\frac{\partial u}{\partial y}\bigg|_{y=0} = \mu V\sqrt{\frac{V}{\nu x}}\frac{d^2f}{d\eta^2}\bigg|_{\eta=0} \qquad \textbf{(6–52)}$$

Substituting the value of the second derivative of f at $\eta = 0$ from Table 6–3 gives

$$\tau_w = 0.332V\sqrt{\frac{\rho\mu V}{x}} = \frac{0.332\rho V^2}{\sqrt{\text{Re}_x}} \qquad \textbf{(6–53)}$$

Then the local friction coefficient becomes

$$C_{f,x} = \frac{\tau_w}{\rho V^2/2} = 0.664\,\text{Re}_x^{-1/2} \qquad \textbf{(6–54)}$$

Note that unlike the boundary layer thickness, wall shear stress and the skin friction coefficient decrease along the plate as $x^{-1/2}$.

The Energy Equation

Knowing the velocity profile, we are now ready to solve the energy equation for temperature distribution for the case of constant wall temperature T_s. First we introduce the dimensionless temperature θ as

$$\theta(x, y) = \frac{T(x, y) - T_s}{T_\infty - T_s} \qquad \textbf{(6–55)}$$

TABLE 6–3

Similarity function f and its derivatives for laminar boundary layer along a flat plate

η	f	$\dfrac{df}{d\eta}=\dfrac{u}{V}$	$\dfrac{d^2f}{d\eta^2}$
0	0	0	0.332
0.5	0.042	0.166	0.331
1.0	0.166	0.330	0.323
1.5	0.370	0.487	0.303
2.0	0.650	0.630	0.267
2.5	0.996	0.751	0.217
3.0	1.397	0.846	0.161
3.5	1.838	0.913	0.108
4.0	2.306	0.956	0.064
4.5	2.790	0.980	0.034
5.0	3.283	0.992	0.016
5.5	3.781	0.997	0.007
6.0	4.280	0.999	0.002
∞	∞	1	0

Noting that both T_s and T_∞ are constant, substitution into the energy equation Eq. 6–41 gives

$$u\frac{\partial\theta}{\partial x} + v\frac{\partial\theta}{\partial y} = \alpha\frac{\partial^2\theta}{\partial y^2} \qquad \textbf{(6–56)}$$

Temperature profiles for flow over an isothermal flat plate are similar, just like the velocity profiles, and thus we expect a similarity solution for temperature to exist. Further, the thickness of the thermal boundary layer is proportional to $\sqrt{vx/V}$, just like the thickness of the velocity boundary layer, and thus the similarity variable is also η, and $\theta = \theta(\eta)$. Using the chain rule and substituting the u and v expressions from Eqs. 6–46 and 6–47 into the energy equation gives

$$V\frac{df}{d\eta}\frac{d\theta}{d\eta}\frac{\partial\eta}{\partial x} + \frac{1}{2}\sqrt{\frac{Vy}{x}}\left(\eta\frac{df}{d\eta}f\right)\frac{d\theta}{d\eta}\frac{\partial\eta}{\partial y} = \alpha\frac{d^2\theta}{d\eta^2}\left(\frac{\partial\eta}{\partial y}\right)^2 \qquad \textbf{(6–57)}$$

Simplifying and noting that $\mathrm{Pr} = v/\alpha$ gives

$$2\frac{d^2\theta}{d\eta^2} + \mathrm{Pr}\, f\frac{d\theta}{d\eta} = 0 \qquad \textbf{(6–58)}$$

FIGURE 6–34

When $\mathrm{Pr} = 1$, the velocity and thermal boundary layers coincide, and the nondimensional velocity and temperature profiles are identical for steady, incompressible, laminar flow over a flat plate.

with the boundary conditions $\theta(0) = 0$ and $\theta(\infty) = 1$. Obtaining an equation for θ as a function of η alone confirms that the temperature profiles are similar, and thus a similarity solution exists. Again a closed-form solution cannot be obtained for this boundary value problem, and it must be solved numerically.

It is interesting to note that for $\mathrm{Pr} = 1$, this equation reduces to Eq. 6–49 when θ is replaced by $df/d\eta$, which is equivalent to u/V (see Eq. 6–46). The boundary conditions for θ and $df/d\eta$ are also identical. Thus we conclude that the velocity and thermal boundary layers coincide, and the nondimensional velocity and temperature profiles (u/V and θ) are identical for steady, incompressible, laminar flow of a fluid with constant properties and $\mathrm{Pr} = 1$ over an isothermal flat plate (Fig. 6–34). The value of the temperature gradient at the surface ($y = 0$ or $\eta = 0$) in this case is, from Table 6–3, $d\theta/d\eta = d^2f/d\eta^2 = 0.332$.

Equation 6–58 is solved for numerous values of Prandtl numbers. For $\mathrm{Pr} > 0.6$, the nondimensional temperature gradient at the surface is found to be proportional to $\mathrm{Pr}^{1/3}$ and is expressed as

$$\left.\frac{d\theta}{d\eta}\right|_{\eta=0} = 0.332\,\mathrm{Pr}^{1/3} \qquad \textbf{(6–59)}$$

The temperature gradient at the surface is

$$\left.\frac{\partial T}{\partial y}\right|_{y=0} = (T_\infty - T_s)\left.\frac{\partial\theta}{\partial y}\right|_{y=0} = (T_\infty - T_s)\left.\frac{d\theta}{d\eta}\right|_{\eta=0}\left.\frac{\partial\eta}{\partial y}\right|_{y=0}$$

$$= 0.332\,\mathrm{Pr}^{1/3}(T_\infty - T_s)\sqrt{\frac{V}{vx}} \qquad \textbf{(6–60)}$$

Then the local convection coefficient and Nusselt number become

$$h_x = \frac{\dot{q}_s}{T_s - T_\infty} = \frac{-k(\partial T/\partial y)|_{y=0}}{T_s - T_\infty} = 0.332\,\mathrm{Pr}^{1/3}k\sqrt{\frac{V}{vx}} \qquad \textbf{(6–61)}$$

and

$$\mathrm{Nu}_x = \frac{h_x x}{k} = 0.332 \, \mathrm{Pr}^{1/3} \mathrm{Re}_x^{1/2} \quad \mathrm{Pr} > 0.6 \tag{6–62}$$

The Nu_x values obtained from this relation agree well with measured values.

Solving Eq. 6–58 numerically for the temperature profile for different Prandtl numbers, and using the definition of the thermal boundary layer, it is determined that $\delta/\delta_t \cong \mathrm{Pr}^{1/3}$. Then the thermal boundary layer thickness becomes

$$\delta_t = \frac{\delta}{\mathrm{Pr}^{1/3}} = \frac{4.91x}{\mathrm{Pr}^{1/3}\sqrt{\mathrm{Re}_x}} \tag{6–63}$$

Note that these relations are valid only for laminar flow over an isothermal flat plate. Also, the effect of variable properties can be accounted for by evaluating all such properties at the film temperature defined as $T_f = (T_s + T_\infty)/2$.

The Blasius solution gives important insights, but its value is largely historical because of the limitations it involves. Today both laminar and turbulent flows over surfaces are routinely analyzed using numerical methods.

6–9 ▪ NONDIMENSIONALIZED CONVECTION EQUATIONS AND SIMILARITY

When viscous dissipation is negligible, the continuity, momentum, and energy equations for steady, laminar flow of a fluid with constant properties are given by Eqs. 6–21, 6–28, and 6–35.

These equations and the boundary conditions can be nondimensionalized by dividing all dependent and independent variables by relevant and meaningful constant quantities: all lengths by a characteristic length L (which is the length for a plate), all velocities by a reference velocity V (which is the free stream velocity for a plate), pressure by ρV^2 (which is twice the free stream dynamic pressure for a plate), and temperature by a suitable temperature difference (which is $T_\infty - T_s$ for a plate). We get

$$x^* = \frac{x}{L}, \quad y^* = \frac{y}{L}, \quad u^* = \frac{u}{V}, \quad v^* = \frac{v}{V}, \quad P^* = \frac{P}{\rho V^2} \quad \text{and} \quad T^* = \frac{T - T_s}{T_\infty - T_s}$$

where the asterisks are used to denote nondimensional variables. Introducing these variables into Eqs. 6–21, 6–28, and 6–41 and simplifying give

Continuity:
$$\frac{\partial u^*}{\partial x^*} + \frac{\partial v^*}{\partial y^*} = 0 \tag{6–64}$$

Momentum:
$$u^* \frac{\partial u^*}{\partial x^*} + v^* \frac{\partial u^*}{\partial y^*} = \frac{1}{\mathrm{Re}_L} \frac{\partial^2 u^*}{\partial y^{*2}} - \frac{dP^*}{dx^*} \tag{6–65}$$

Energy:
$$u^* \frac{\partial T^*}{\partial x^*} + v^* \frac{\partial T^*}{\partial y^*} = \frac{1}{\mathrm{Re}_L \mathrm{Pr}} \frac{\partial^2 T^*}{\partial y^{*2}} \tag{6–66}$$

with the boundary conditions

$$u^*(0, y^*) = 1, \quad u^*(x^*, 0) = 0, \quad u^*(x^*, \infty) = 1, \quad v^*(x^*, 0) = 0,$$
$$T^*(0, y^*) = 1, \quad T^*(x^*, 0) = 0, \quad T^*(x^*, \infty) = 1 \tag{6–67}$$

Parameters before nondimensionalizing:
$L, V, T_\infty, T_s, \nu, \alpha$
Parameters after nondimensionalizing:
Re, Pr

FIGURE 6–35
The number of parameters is reduced greatly by nondimensionalizing the convection equations.

where $Re_L = VL/\nu$ is the dimensionless Reynolds number and $Pr = \nu/\alpha$ is the Prandtl number. For a given type of geometry, the solutions to problems with the same Re and Pr numbers are similar, and thus Re and Pr numbers serve as *similarity parameters*. Two physical phenomena are *similar* if they have the same dimensionless forms of governing differential equations and boundary conditions (see Example 6–3).

A major advantage of nondimensionalizing is the significant reduction in the number of parameters. The original problem involves six parameters ($L, V, T_\infty, T_s \nu, \alpha$), but the nondimensionalized problem involves just two parameters (Re_L and Pr). For a given geometry, problems that have the same values for the similarity parameters have identical solutions. For example, determining the convection heat transfer coefficient for flow over a given surface requires numerical solutions or experimental investigations for several fluids, with several sets of velocities, surface lengths, wall temperatures, and free stream temperatures. The same information can be obtained with far fewer investigations by grouping data into the dimensionless Re and Pr numbers. Another advantage of similarity parameters is that they enable us to group the results of a large number of experiments and to report them conveniently in terms of such parameters (Fig. 6–35).

FIGURE 6–36
Schematic for Example 6–3.

EXAMPLE 6–3 **Finding Rate of Heat Transfer Using Similarity Parameters**

An airfoil with a characteristic length of 0.15 m and a surface temperature of 325°C is placed in airflow at 37°C with free stream velocity of 100 m/s. The rate of heat transfer from the airfoil is 1600 W. If a second airfoil with a characteristic length of 0.3 m and a surface temperature of 425°C is placed in the airflow at 37°C with free stream velocity of 50 m/s, determine the rate of heat transfer from the second airfoil. The surface area of the airfoil may be assumed to be directly proportional to its characteristic length (Fig. 6–36).

SOLUTION Two airfoils with different characteristic lengths and surface temperatures are placed in airflow of different free stream velocities at 37°C. The rate of heat transfer from the second airfoil is to be determined.
Assumptions **1** Steady operating conditions exist. **2** Properties are constant. **3** Both airfoils are geometrically similar. **4** Surface area A is directly proportional to characteristic length L.
Analysis The relation for Nusselt, Prandtl, and Reynolds numbers is given as

$$Nu = g(Re, Pr)$$

where $\quad Nu = \dfrac{hL}{k}, \quad Pr = \dfrac{c_p\mu}{k}, \quad Re = \dfrac{VL}{\nu}$

Then, for airfoils 1 and 2 we have

$$Re_1 = \frac{V_1 L_1}{\nu} = \frac{(100 \text{ m/s})(0.15 \text{ m})}{\nu} = \frac{15 \text{ m}^2/\text{s}}{\nu} \quad \text{and} \quad Pr_1 = \frac{c_p\mu}{k}$$

$$Re_2 = \frac{V_2 L_2}{\nu} = \frac{(50 \text{ m/s})(0.3 \text{ m})}{\nu} = \frac{15 \text{ m}^2/\text{s}}{\nu} \quad \text{and} \quad Pr_2 = \frac{c_p\mu}{k}$$

Since the fluid properties are constant, we have $Re_1 = Re_2$ and $Pr_1 = Pr_2$, which implies

$$Nu_1 = g(Re_1, Pr_1) = Nu_2 = g(Re_2, Pr_2) \rightarrow Nu_1 = Nu_2$$

Hence

$$\frac{h_1 L_1}{k} = \frac{h_2 L_2}{k} \rightarrow h_2 = h_1 \frac{L_1}{L_2} = \frac{\dot{Q}_1}{A_1(T_{s,1} - T_\infty)} \frac{L_1}{L_2}$$

$$\dot{Q}_2 = h_2 A_2(T_{s,2} - T_\infty) = \frac{L_1}{L_2} \frac{A_2}{A_1} \frac{(T_{s,2} - T_\infty)}{(T_{s,1} - T_\infty)} \dot{Q}_1$$

$$\dot{Q}_2 = \frac{(T_{s,2} - T_\infty)}{(T_{s,1} - T_\infty)} \dot{Q}_1 = \frac{(425 - 37)°C}{(325 - 37)°C} (1600 \text{ W}) = \textbf{2156 W}$$

Discussion The relation for the Nusselt numbers $Nu_1 = Nu_2$ is valid due to $Re_1 = Re_2$ and $Pr_1 = Pr_2$. Slight variation of ν from airfoil 1 to airfoil 2 would cause Re_2 to differ from Re_1. However, for the given conditions, the variable property effect is small.

6–10 ▪ FUNCTIONAL FORMS OF FRICTION AND CONVECTION COEFFICIENTS

The three nondimensionalized boundary layer equations (Eqs. 6–64, 6–65, and 6–66) involve three unknown functions u^*, v^*, and T^*, two independent variables x^* and y^*, and two parameters Re_L and Pr. The pressure $P^*(x^*)$ depends on the geometry involved (it is constant for a flat plate), and it has the same value inside and outside the boundary layer at a specified x^*. Therefore, it can be determined separately from the free stream conditions, and dP^*/dx^* in Eq. 6–65 can be treated as a known function of x^*. Note that the boundary conditions do not introduce any new parameters.

For a given geometry, the solution for u^* can be expressed as

$$u^* = f_1(x^*, y^*, Re_L) \tag{6–68}$$

Then the shear stress at the surface becomes

$$\tau_w = \mu \frac{\partial u}{\partial y}\bigg|_{y=0} = \frac{\mu V}{L} \frac{\partial u^*}{\partial y^*}\bigg|_{y^*=0} = \frac{\mu V}{L} f_2(x^*, Re_L) \tag{6–69}$$

Substituting into its definition gives the local friction coefficient,

$$C_{f,x} = \frac{\tau_w}{\rho V^2/2} = \frac{\mu V/L}{\rho V^2/2} f_2(x^*, Re_L) = \frac{2}{Re_L} f_2(x^*, Re_L) = f_3(x^*, Re_L) \tag{6–70}$$

Thus we conclude that the friction coefficient for a given geometry can be expressed in terms of the Reynolds number Re and the dimensionless space variable x^* alone (instead of being expressed in terms of x, L, V, ρ, and μ). This is a very significant finding, and it shows the value of nondimensionalized equations.

Similarly, the solution of Eq. 6–66 for the dimensionless temperature T^* for a given geometry can be expressed as

$$T^* = g_1(x^*, y^*, \text{Re}_L, \text{Pr}) \tag{6–71}$$

Using the definition of T^*, the convection heat transfer coefficient becomes

$$h_x = \frac{-k(\partial T/\partial y)|_{y=0}}{T_s - T_\infty} = \frac{-k(T_\infty - T_s)}{L(T_s - T_\infty)} \frac{\partial T^*}{\partial y^*}\bigg|_{y^*=0} = \frac{k}{L} \frac{\partial T^*}{\partial y^*}\bigg|_{y^*=0} \tag{6–72}$$

Substituting this into the Nusselt number relation gives [or alternately, we can rearrange the relation above in dimensionless form as $hL/k = (\partial T^*/\partial y^*)|_{y^*=0}$ and define the dimensionless group hL/k as the Nusselt number]

$$\text{Nu}_x = \frac{h_x x}{k} = \frac{\partial T^*}{\partial y^*}\bigg|_{y^*=0} = g_2(x^*, \text{Re}_x, \text{Pr}) \tag{6–73}$$

FIGURE 6–37
The Nusselt number is equivalent to the dimensionless temperature gradient at the surface.

Note that the Nusselt number is equivalent to the *dimensionless temperature gradient at the surface,* and thus it is properly referred to as the dimensionless heat transfer coefficient (Fig. 6–37). Also, the Nusselt number for a given geometry can be expressed in terms of the Reynolds number Re, the Prandtl number Pr, and the space variable x^*, and such a relation can be used for different fluids flowing at different velocities over similar geometries of different lengths.

The average friction and heat transfer coefficients are determined by integrating $C_{f,x}$ and Nu_x over the surface of the given body with respect to x^* from 0 to 1. Integration removes the dependence on x^*, and the average friction coefficient and Nusselt number can be expressed as

$$C_f = f_4(\text{Re}_L) \quad \text{and} \quad \text{Nu} = g_3(\text{Re}_L, \text{Pr}) \tag{6–74}$$

Local Nusselt number:
$$\text{Nu}_x = \text{function } (x^*, \text{Re}_x, \text{Pr})$$
Average Nusselt number:
$$\text{Nu} = \text{function } (\text{Re}_L, \text{Pr})$$
A common form of Nusselt number:
$$\text{Nu} = C \, \text{Re}_L^m \text{Pr}^n$$

FIGURE 6–38
For a given geometry, the average Nusselt number is a function of Reynolds and Prandtl numbers.

These relations are extremely valuable as they state that for a given geometry, the friction coefficient can be expressed as a function of Reynolds number alone, and the Nusselt number as a function of Reynolds and Prandtl numbers alone (Fig. 6–38). Therefore, experimentalists can study a problem with a minimum number of experiments, and report their friction and heat transfer coefficient measurements conveniently in terms of Reynolds and Prandtl numbers. For example, a friction coefficient relation obtained with air for a given surface can also be used for water at the same Reynolds number. But it should be kept in mind that the validity of these relations is limited by the limitations on the boundary layer equations used in the analysis.

The experimental data for heat transfer is often represented with reasonable accuracy by a simple power-law relation of the form

$$\text{Nu} = C \, \text{Re}_L^m \, \text{Pr}^n \tag{6–75}$$

where m and n are constant exponents (usually between 0 and 1), and the value of the constant C depends on geometry. Sometimes more complex relations are used for better accuracy.

6–11 ■ ANALOGIES BETWEEN MOMENTUM AND HEAT TRANSFER

In forced convection analysis, we are primarily interested in the determination of the quantities C_f (to calculate shear stress at the wall) and Nu (to calculate heat transfer rates). Therefore, it is very desirable to have a relation between

C_f and Nu so that we can calculate one when the other is available. Such relations are developed on the basis of the similarity between momentum and heat transfers in boundary layers and are known as the *Reynolds analogy* (Fig. 6–20) and the *Chilton–Colburn analogy*.

Reconsider the nondimensionalized momentum and energy equations for steady, incompressible, laminar flow of a fluid with constant properties and negligible viscous dissipation (Eqs. 6–65 and 6–66). When Pr = 1 (which is approximately the case for gases) and $\partial P^*/\partial x^* = 0$ (which is the case when, $u = V =$ constant in the free stream, as in flow over a flat plate), these equations simplify to

$$\text{Momentum:} \qquad u^* \frac{\partial u^*}{\partial x^*} + v^* \frac{\partial u^*}{\partial y^*} = \frac{1}{\text{Re}_L} \frac{\partial^2 u^*}{\partial y^{*2}} \qquad \text{(6–76)}$$

$$\text{Energy:} \qquad u^* \frac{\partial T^*}{\partial x^*} + v^* \frac{\partial T^*}{\partial y^*} = \frac{1}{\text{Re}_L} \frac{\partial^2 T^*}{\partial y^{*2}} \qquad \text{(6–77)}$$

which are exactly of the same form for the dimensionless velocity u^* and temperature T^*. The boundary conditions for u^* and T^* are also identical. Therefore, the functions u^* and T^* must be identical, and thus the first derivatives of u^* and T^* at the surface must be equal to each other,

$$\left.\frac{\partial u^*}{\partial y^*}\right|_{y^*=0} = \left.\frac{\partial T^*}{\partial y^*}\right|_{y^*=0} \qquad \text{(6–78)}$$

Then from Eqs. 6–69, 6–70, and 6–73 we have

$$C_{f,x} \frac{\text{Re}_x}{2} = \text{Nu}_x \quad (\text{Pr} = 1) \qquad \text{(6–79)}$$

which is known as the **Reynolds analogy** (Fig. 6–39). This is an important analogy since it allows us to determine the heat transfer coefficient for fluids with Pr ≈ 1 from a knowledge of the friction coefficient, which is easier to measure. The Reynolds analogy is also expressed alternately as

$$\frac{C_{f,x}}{2} = \text{St}_x \quad (\text{Pr} = 1) \qquad \text{(6–80)}$$

where

$$\text{St} = \frac{h}{\rho c_p V} = \frac{\text{Nu}}{\text{Re}_L \text{Pr}} \qquad \text{(6–81)}$$

which is the **Stanton number** (Fig. 6–40), which is also a dimensionless heat transfer coefficient.

Reynolds analogy is of limited use because of the restrictions Pr = 1 and $\partial P^*/\partial x^* = 0$ on it, and it is desirable to have an analogy that is applicable over a wide range of Pr. This is done by adding a Prandtl number correction.

The friction coefficient and Nusselt number for a flat plate were determined in Section 6–8 to be

$$C_{f,x} = 0.664 \,\text{Re}_x^{-1/2} \qquad \text{and} \qquad \text{Nu}_x = 0.332 \,\text{Pr}^{1/3}\,\text{Re}_x^{1/2} \qquad \text{(6–82)}$$

Taking their ratio and rearranging give the desired relation, known as the **modified Reynolds analogy** or **Chilton–Colburn analogy**,

$$C_{f,x} \frac{\text{Re}_x}{2} = \text{Nu}_x \,\text{Pr}^{-1/3} \qquad \text{or} \qquad \frac{C_{f,x}}{2} = \text{St}_x \,\text{Pr}^{2/3} = j_H \qquad \text{(6–83)}$$

Profiles:	$u^* = T^*$
Gradients:	$\left.\dfrac{\partial u^*}{\partial y^*}\right|_{y^*=0} = \left.\dfrac{\partial T^*}{\partial y^*}\right|_{y^*=0}$
Analogy:	$C_{f,x} \dfrac{\text{Re}_x}{2} = \text{Nu}_x$

FIGURE 6–39
When Pr = 1 and $\partial P^*/\partial x^* \approx 0$, the nondimensional velocity and temperature profiles become identical, and Nu is related to C_f by the Reynolds analogy.
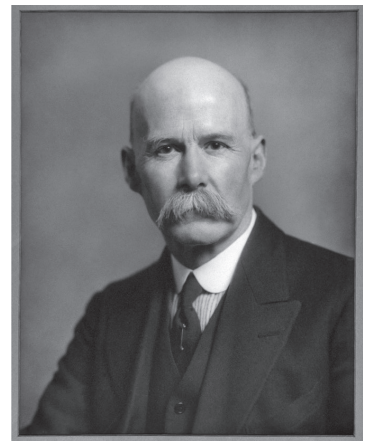
FIGURE 6–40
Sir Thomas Edward Stanton (1865–1931), was a British engineer, born at Atherstone in Warwickshire, England. From 1891 to 1896 he worked in Osborne Reynolds' laboratory at Owens College, Manchester, England. Stanton's main field of interest was fluid flow and friction and the related problem of heat transmission. From 1902 to 1907 he executed a large research program concerning wind forces on structures, such as bridges and roofs. After 1908, the year when the Wright Brothers made their first airplane flights in Europe, Stanton was devoted to problems of airplane and airship design and the dissipation of heat from air-cooled engines. The dimensionless heat transfer coefficient **Stanton number** is named after him.
Courtesy of University of Bristol, Faculty of Engineering

FIGURE 6–41
Allan Philip Colburn (1904–1955), an American engineer, was born in Madison, Wisconsin. His research was on condensation of water vapor from saturated airstreams. He brought together for the first time in American engineering work the fundamentals of momentum, heat and mass transfer, and thermodynamic principles to deal with this complex problem. The dimensionless empirical parameter **Colburn j-factor** ($j_H = St_x Pr^{2/3}$) is named after him.
Courtesy of University of Delaware
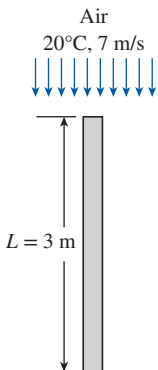
FIGURE 6–42
Schematic for Example 6–4.

for $0.6 < Pr < 60$. Here j_H is called the *Colburn j-factor* (Fig. 6–41). Although this relation is developed using relations for laminar flow over a flat plate (for which $\partial P^*/\partial x^* = 0$), experimental studies show that it is also applicable approximately for turbulent flow over a surface, even in the presence of pressure gradients. For laminar flow, however, the analogy is not applicable unless $\partial P^*/\partial x^* \approx 0$. Therefore, it does not apply to laminar flow in a pipe. Analogies between C_f and Nu that are more accurate are also developed, but they are more complex and beyond the scope of this book. The analogies given above can be used for both local and average quantities.

EXAMPLE 6–4   **Finding Convection Coefficient from Drag Measurement**

A 2-m × 3-m flat plate is suspended in a room and is subjected to airflow parallel to its surfaces along its 3-m-long side. The free stream temperature and velocity of air are 20°C and 7 m/s. The total drag force acting on the plate is measured to be 0.86 N. Determine the average convection heat transfer coefficient for the plate (Fig. 6–42).

SOLUTION   A flat plate is subjected to airflow, and the drag force acting on it is measured. The average convection coefficient is to be determined.
Assumptions   **1** Steady operating conditions exist. **2** The edge effects are negligible. **3** The local atmospheric pressure is 1 atm.
Properties   The properties of air at 20°C and 1 atm are (Table A–15):

$$\rho = 1.204 \text{ kg/m}^3, \qquad c_p = 1.007 \text{ kJ/kg·K}, \qquad Pr = 0.7309$$

Analysis   The flow is along the 3-m side of the plate, and thus the characteristic length is $L = 3$ m. Both sides of the plate are exposed to airflow, and thus the total surface area is

$$A_s = 2WL = 2(2 \text{ m})(3 \text{ m}) = 12 \text{ m}^2$$

For flat plates, the drag force is equivalent to friction force. The average friction coefficient C_f can be determined from Eq. 6–11,

$$F_f = C_f A_s \frac{\rho V^2}{2}$$

Solving for C_f and substituting,

$$C_f = \frac{F_f}{\rho A_s V^2/2} = \frac{0.86 \text{ N}}{(1.204 \text{ kg/m}^3)(12 \text{ m}^2)(7 \text{ m/s})^2/2} \left(\frac{1 \text{ kg·m/s}^2}{1 \text{ N}} \right) = 0.00243$$

Then the average heat transfer coefficient can be determined from the modified Reynolds analogy (Eq. 6–83) to be

$$h = \frac{C_f \rho V c_p}{2 \, Pr^{2/3}} = \frac{0.00243}{2} \frac{(1.204 \text{ kg/m}^3)(7 \text{ m/s})(1007 \text{ J/kg·K})}{0.7309^{2/3}} = \textbf{12.7 W/m}^2\textbf{·K}$$

Discussion   This example shows the great utility of momentum-heat transfer analogies in that the convection heat transfer coefficient can be obtained from a knowledge of the friction coefficient, which is easier to determine.

TOPIC OF SPECIAL INTEREST

Microscale Heat Transfer*

Heat transfer considerations play a crucial role in the design and operation of many modern devices. New approaches and methods of analyses have been developed to understand and modulate (enhance or suppress) such energy interactions. Modulation typically occurs through actively controlling the surface phenomena, or focusing of the volumetric energy. In this section we discuss one such example—microscale heat transfer.

Recent inventions in micro ($\sim 10^{-6}$ m) and nano ($\sim 10^{-9}$ m) scale systems have shown tremendous benefits in fluid flow and heat transfer processes. These devices are extremely tiny and are only visible through electron microscopes. The detailed understanding of the governing mechanism of these systems will be at the heart of realizing many future technologies. Examples include chemical and biological sensors, hydrogen storage, space exploration devices, and drug screening. Micro-nanoscale device development also poses several new challenges, however. For example, the classical heat transfer knowledge originates from the thermal equilibrium approach, and the equations are derived for material continua. As the length scale of the system becomes minuscule, the heat transfer through these particles in nanoscale systems is no longer an equilibrium process, and the continuum-based equilibrium approach is no longer valid. Thus, a more general understanding of the concept of heat transfer becomes essential.

Both length and time scales are crucial in micro- and nanoscale heat transfer. The significance of length scale becomes evident from the fact that the surface area per unit volume of an object increases as the length scale of the object shrinks. This means the heat transfer through the surface becomes orders of magnitude more important in microscale than in large everyday objects. Transport of thermal energy in electronic and thermoelectric equipment often occurs at a range of length scales from millimeters to nanometers. For example, in a microelectronic chip (such as the MOSFET in Fig. 6–43) heat is generated in a nanometer-size drain region and ultimately conducted to the surroundings through substrates whose thickness is of the order of a millimeter. Clearly energy transport and conversion mechanisms in devices involve a wide range of length scales and are quite difficult to model.

Small time scales also play an important role in energy transport mechanisms. For example, ultra-short (pico-second and femto-second) pulse lasers are extremely useful for material processing industries. Here the tiny time scales permit localized laser-material interaction beneficial for high-energy deposition and transport.

The applicability of the continuum model is determined by the local value of the nondimensional Knudsen number (Kn), which is defined as the ratio of the mean free path (mfp) of the heat-carrier medium to the

---

*This section is contributed by Subrata Roy, Computational Plasma Dynamics Laboratory, Mechanical Engineering, Kettering University, Flint, MI.

FIGURE 6–43
Metal-oxide semiconductor field-effect transistor (MOSFET) used in microelectronics.

Photo: *©Ferenc Szelepcsenyi/Alamy*
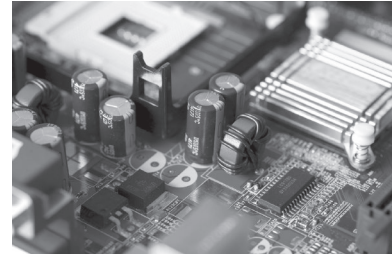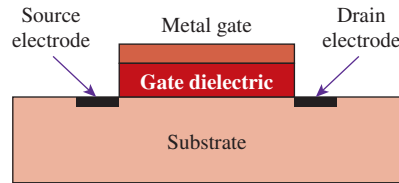
system reference length scale (say thermal diffusion length). Microscale effects become important when the mfp becomes comparable to or greater than the reference length of the device, say at Kn > 0.001. As a result, thermophysical properties of materials become dependent on structure, and heat conduction processes are no longer local phenomena, but rather exhibit long-range radiative effects.

The conventional macroscopic Fourier conduction model violates this nonlocal feature of microscale heat transfer, and alternative approaches are necessary for analysis. The most suitable model to date is the concept of *phonon.* The thermal energy in a uniform solid material can be interpreted as the vibrations of a regular lattice of closely bound atoms inside. These atoms exhibit collective modes of sound waves (phonons) which transport energy at the speed of sound in a material. Following quantum mechanical principles, phonons exhibit particle-like properties of bosons with zero spin (wave-particle duality). Phonons play an important role in many of the physical properties of solids, such as the thermal and the electrical conductivities. In insulating solids, phonons are also the primary mechanism by which heat conduction takes place.

The variation of temperature near the bounding wall continues to be a major determinant of heat transfer though the surface. However, when the continuum approach breaks down, the conventional Newton's law of cooling using wall and bulk fluid temperature needs to be modified. Specifically, unlike in macroscale objects where the wall and adjacent fluid temperatures are equal ($T_w = T_g$), in a micro device there is a temperature slip and the two values are different. One well-known relation for calculating the temperature jump at the wall of a microgeometry was derived by von Smoluchowski in 1898,

$$T_g - T_w = \frac{2 - \sigma_T}{\sigma_T}\left[\frac{2\gamma}{\gamma + 1}\right]\frac{\lambda}{\text{Pr}}\left(\frac{\partial T}{\partial y}\right)_w \tag{6–84}$$

where T is the temperature in K, σ_T is the thermal accommodation coefficient and indicates the molecular fraction reflected diffusively from the wall, γ is the specific heat ratio, and Pr is the Prandtl number. Once this value is known, the heat transfer rate may be calculated from:

$$-k\left(\frac{\partial T}{\partial y}\right)_w = \frac{\sigma_T\sqrt{2\pi RT}}{2 - \sigma_T}\left[\frac{\gamma + 1}{2\gamma}\right]\frac{5\rho\, c_p}{16}(T_w - T_g) \tag{6–85}$$

As an example, the temperature distribution and Mach number contours inside a microtube of width $H = 1.2\ \mu$m are plotted in Fig. 6–44 for

(a) Nitrogen gas temperature in K for Kn = 0.062

(b) Nitrogen gas velocity relative to the speed of sound (Mach number)

(c) Helium gas temperature in K for Kn = 0.14

(d) Helium gas velocity relative to the speed of sound (Mach number)
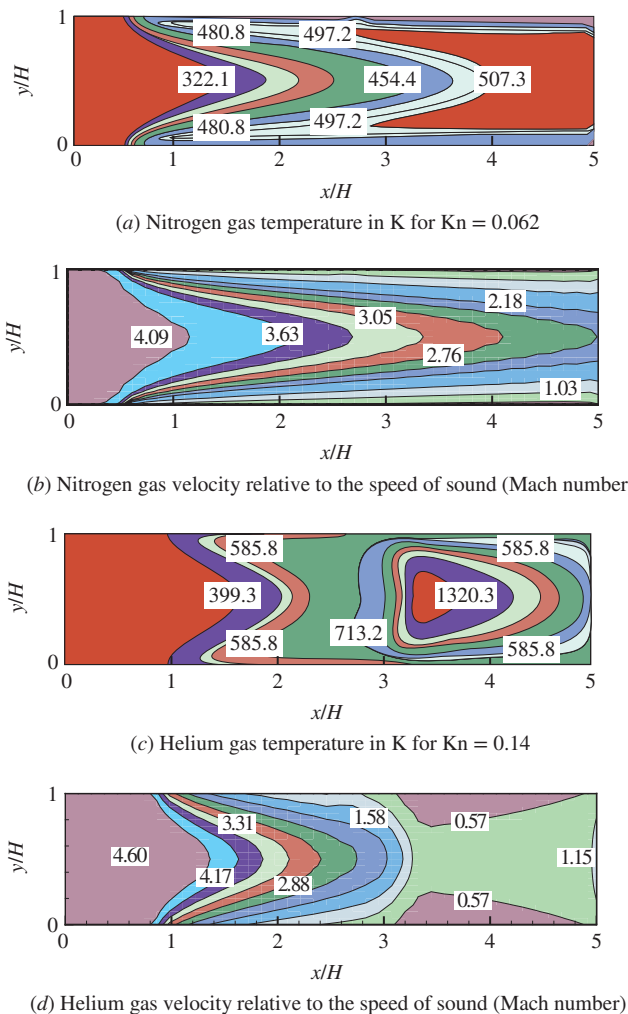
FIGURE 6–44

Fluid-thermal characteristics inside a microchannel.

From Raju and Roy, 2005.

supersonic flow of nitrogen and helium. For nitrogen gas with an inlet Kn = 0.062, the gas temperature (T_g) adjacent to the wall differs substantially from the fixed wall temperature, as shown in Fig. 6–44a, where T_w is 323 K and T_g is almost 510 K. The effect of this wall heat transfer is to reduce the Mach number, as shown in Figure 6–44b, but the flow remains supersonic. For helium gas with inlet Kn = 0.14 and a lower wall temperature of 298 K, the gas temperature immediately adjacent to the wall is even higher—up to 586 K, as shown in the Fig. 6–44c. This creates very high wall heat flux that is unattainable in macroscale applications. In this case, shown in Fig. 6–44d, heat transfer is large enough to choke the flow.

1. D. G. Cahill, W. K. Ford, K. E. Goodson, *et al.*, "Nanoscale Thermal Transport."*Journal of Applied Physics* 93, no. 2 (2003), pp. 793–817.

2. R. Raju and S. Roy, "Hydrodynamic Study of High Speed Flow and Heat Transfer Through a Microchannel."*Journal of Thermophysics and Heat Transfer* 19, no.1 (2005), pp. 106–113.

3. S. Roy, R. Raju, H. Chuang, B. Kruden and M. Meyyappan, "Modeling Gas Flow Through Microchannels and Nanopores." *Journal of Applied Physics* 93, no. 8 (2003), pp. 4870–79.

4. M. von Smoluchowski, "Ueber Wärmeleitung in Verdünnten Gasen,"*Annalen der Physik und Chemi.* 64 (1898), pp. 101–130.

5. C. L. Tien, A. Majumdar, and F. Gerner. *Microscale Energy Transport.* New York: Taylor & Francis Publishing, 1998.

SUMMARY

Convection heat transfer is expressed by *Newton's law of cooling* as

$$\dot{Q}_{\text{conv}} = hA_s(T_s - T_\infty)$$

where h is the convection heat transfer coefficient, T_s is the surface temperature, and T_∞ is the free-stream temperature. The convection coefficient is also expressed as

$$h = \frac{-k_{\text{fluid}}(\partial T/\partial y)_{y=0}}{T_s - T_\infty}$$

The *Nusselt number,* which is the dimensionless heat transfer coefficient, is defined as

$$\text{Nu} = \frac{hL_c}{k}$$

where k is the thermal conductivity of the fluid and L_c is the characteristic length.

The highly ordered fluid motion characterized by smooth streamlines is called *laminar.* The highly disordered fluid motion that typically occurs at high velocities characterized by velocity fluctuations is called *turbulent.* The random and rapid fluctuations of groups of fluid particles, called *eddies,* provide an additional mechanism for momentum and heat transfer.

The region of the flow above the plate bounded by δ in which the effects of the viscous shearing forces caused by fluid viscosity are felt is called the *velocity boundary layer.* The *boundary layer thickness, δ,* is defined as the distance from the surface at which $u = 0.99V$. The hypothetical line of $u = 0.99V$ divides the flow over a plate into the *boundary layer region* in which the viscous effects and the velocity changes are significant, and the *irrotational flow region,* in which the frictional effects are negligible.

The friction force per unit area is called *shear stress,* and the shear stress at the wall surface is expressed as

$$\tau_w = \mu \frac{\partial u}{\partial y}\bigg|_{y=0} \quad \text{or} \quad \tau_w = C_f \frac{\rho V^2}{2}$$

where μ is the dynamic viscosity, V is the upstream velocity, and C_f is the dimensionless *friction coefficient.* The property $\nu = \mu/\rho$ is the *kinematic viscosity.* The friction force over the entire surface is determined from

$$F_f = C_f A_s \frac{\rho V^2}{2}$$

The flow region over the surface in which the temperature variation in the direction normal to the surface is significant is the *thermal boundary layer.* The *thickness* of the thermal boundary layer δ_t at any location along the surface is the distance from the surface at which the temperature difference $T - T_s$ equals $0.99(T_\infty - T_s)$. The relative thickness of the velocity and the thermal boundary layers is best described by the dimensionless *Prandtl number,* defined as

$$\text{Pr} = \frac{\text{Molecular diffusivity of momentum}}{\text{Molecular diffusivity of heat}} = \frac{\nu}{\alpha} = \frac{\mu c_p}{k}$$

For external flow, the dimensionless *Reynolds number* is expressed as

$$\text{Re} = \frac{\text{Inertia forces}}{\text{Viscous forces}} = \frac{VL_c}{\nu} = \frac{\rho VL_c}{\mu}$$

For a flat plate, the characteristic length is the distance x from the leading edge. The Reynolds number at which the flow becomes turbulent is called the *critical Reynolds number.* For flow over a flat plate, its value is taken to be $\text{Re}_{\text{cr}} = Vx_{\text{cr}}/\nu = 5 \times 10^5$.

The continuity, momentum, and energy equations for steady two-dimensional incompressible flow with constant properties are determined from mass, momentum, and energy balances to be

Continuity: $\quad \dfrac{\partial u}{\partial x} + \dfrac{\partial v}{\partial y} = 0$

x-momentum: $\rho\left(u\dfrac{\partial u}{\partial x} + v\dfrac{\partial u}{\partial y}\right) = \mu\dfrac{\partial^2 u}{\partial y^2} - \dfrac{\partial P}{\partial x}$

Energy: $\quad \rho c_p\left[u\dfrac{\partial T}{\partial x} + v\dfrac{\partial T}{\partial y}\right] = k\left(\dfrac{\partial^2 T}{\partial x^2} + \dfrac{\partial^2 T}{\partial y^2}\right) + \mu\Phi$

where the *viscous dissipation function Φ* is

$$\Phi = 2\left[\left(\frac{\partial u}{\partial x}\right)^2 + \left(\frac{\partial v}{\partial y}\right)^2\right] + \left(\frac{\partial u}{\partial y} + \frac{\partial v}{\partial x}\right)^2$$

Using the boundary layer approximations and a similarity variable, these equations can be solved for parallel steady incompressible flow over a flat plate, with the following results:

Velocity boundary layer thickness: $\quad \delta = \dfrac{4.91}{\sqrt{V/\nu x}} = \dfrac{4.91x}{\sqrt{\mathrm{Re}_x}}$

Local friction coefficient: $\quad C_{f,x} = \dfrac{\tau_w}{\rho V^2/2} = 0.664\,\mathrm{Re}_x^{-1/2}$

Local Nusselt number: $\quad \mathrm{Nu}_x = \dfrac{h_x x}{k} = 0.332\,\mathrm{Pr}^{1/3}\,\mathrm{Re}_x^{1/2}$

Thermal boundary layer thickness: $\quad \delta_t = \dfrac{\delta}{\mathrm{Pr}^{1/3}} = \dfrac{4.91x}{\mathrm{Pr}^{1/3}\sqrt{\mathrm{Re}_x}}$

The average friction coefficient and Nusselt number are expressed in functional form as

$$C_f = f(\mathrm{Re}_L) \quad \text{and} \quad \mathrm{Nu} = g(\mathrm{Re}_L, \mathrm{Pr})$$

The Nusselt number can be expressed by a simple power-law relation of the form

$$\mathrm{Nu} = C\,\mathrm{Re}_L^m\,\mathrm{Pr}^n$$

where m and n are constant exponents, and the value of the constant C depends on geometry. The *Reynolds analogy* relates the convection coefficient to the friction coefficient for fluids with $\mathrm{Pr} \approx 1$ and is expressed as

$$C_{f,x}\frac{\mathrm{Re}_x}{2} = \mathrm{Nu}_x \qquad \text{or} \qquad \frac{C_{f,x}}{2} = \mathrm{St}_x$$

where

$$\mathrm{St} = \frac{h}{\rho c_p V} = \frac{\mathrm{Nu}}{\mathrm{Re}_L\,\mathrm{Pr}}$$

is the *Stanton number.* The analogy is extended to other Prandtl numbers by the *modified Reynolds analogy* or *Chilton–Colburn analogy,* expressed as

$$C_{f,x}\frac{\mathrm{Re}_x}{2} = \mathrm{Nu}_x\,\mathrm{Pr}^{-1/3}$$

or

$$\frac{C_{f,x}}{2} = \mathrm{St}_x\,\mathrm{Pr}^{2/3} = j_H\,(0.6 < \mathrm{Pr} < 60)$$

These analogies are also applicable approximately for turbulent flow over a surface, even in the presence of pressure gradients.

REFERENCES AND SUGGESTED READING

1. H. Blasius. "The Boundary Layers in Fluids with Little Friction (in German)." *Z. Math. Phys.* 56, no.1 (1908); pp. 1–37; English translation in National Advisory Committee for Aeronautics Technical Memo No. 1256, February 1950.

2. Y. A. Çengel and J. M. Cimbala. *Fluid Mechanics: Fundamentals and Applications.* 4th ed. New York: McGraw-Hill Education, 2018.

3. W. M. Kays, M. E. Crawford and B. Weigand. *Convective Heat and Mass Transfer.* 4th ed. New York: McGraw-Hill, 2005.

4. O. Reynolds. "On the Experimental Investigation of the Circumstances Which Determine Whether the Motion of Water Shall Be Direct or Sinuous, and the Law of Resistance in Parallel Channels." *Philosophical Transactions of the Royal Society of London* 174 (1883), pp. 935–82.

5. H. Schlichting. *Boundary Layer Theory.* 7th ed. New York: McGraw-Hill, 1979.

6. G. G. Stokes. "On the Effect of the Internal Friction of Fluids on the Motion of Pendulums." *Cambridge Philosophical Transactions,* IX, 8, 1851.

PROBLEMS*

Mechanism and Types of Convection

6–1C Define incompressible flow and incompressible fluid. Must the flow of a compressible fluid necessarily be treated as compressible?

6–2C What is forced convection? How does it differ from natural convection? Is convection that is caused by winds forced or natural convection?

6–3C What is external forced convection? How does it differ from internal forced convection? Can a heat transfer system involve both internal and external convection at the same time? Give an example.

6–4C In which mode of heat transfer is the convection heat transfer coefficient usually higher, natural convection or forced convection? Why?

6–5C Consider a hot baked potato. Will the potato cool faster or slower when we blow the warm air coming from our lungs on it instead of letting it cool naturally in the cooler air in the room? Explain.

6–6C What is the physical significance of the Nusselt number? How is it defined?

6–7C When is heat transfer through a fluid conduction and when is it convection? For what case is the rate of heat transfer higher? How does the convection heat transfer coefficient differ from the thermal conductivity of a fluid?

6–8 An average man has a body surface area of 1.8 m^2 and a skin temperature of 33°C. The convection heat transfer coefficient for a clothed person walking in still air is expressed as $h = 8.6V^{0.53}$ for $0.5 < V < 2$ m/s, where V is the walking velocity in m/s. Assuming the average surface temperature of the clothed person to be 30°C, determine the rate of heat loss from an average man walking in still air at 7°C by convection at a walking velocity of (*a*) 0.5 m/s, (*b*) 1.0 m/s, (*c*) 1.5 m/s, and (*d*) 2.0 m/s.

6–9 The convection heat transfer coefficient for a clothed person standing in moving air is expressed as $h = 14.8V^{0.69}$ for $0.15 < V < 1.5$ m/s, where V is the air velocity. For a person with a body surface area of 1.7 m^2 and an average surface temperature of 29°C, determine the rate of heat loss from the person in windy air at 10°C by convection for air velocities of (*a*) 0.5 m/s, (*b*) 1.0 m/s, and (*c*) 1.5 m/s.

*Problems designated by a "C" are concept questions, and students are encouraged to answer them all. Problems designated by an "E" are in English units, and the SI users can ignore them. Problems with the 🖳 icon are comprehensive in nature and are intended to be solved with appropriate software. Problems with the 🄿🅃🄳 icon are Prevention through Design problems. Problems with the 🄲🅂 icon are Codes and Standards problems.

6–10 During air cooling of potatoes, the heat transfer coefficient for combined convection, radiation, and evaporation is determined experimentally to be as shown:

Air Velocity, m/s	Heat Transfer Coefficient, W/m^2·K
0.66	14.0
1.00	19.1
1.36	20.2
1.73	24.4

Consider an 8-cm-diameter potato initially at 20°C. Potatoes are cooled by refrigerated air at 5°C at a velocity of 1 m/s. Determine the initial rate of heat transfer from a potato, and the initial value of the temperature gradient in the potato at the surface.

6–11 The upper surface of a 50-cm-thick solid plate ($k = 237$ W/m·K) is being cooled by water with temperature of 20°C. The upper and lower surfaces of the solid plate maintained at constant temperatures of 60°C and 120°C, respectively. Determine the water convection heat transfer coefficient and the water temperature gradient at the upper plate surface.
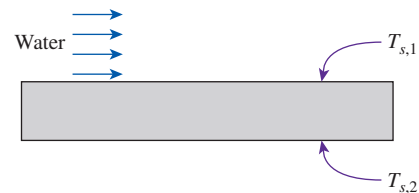
FIGURE P6–11

6–12 Consider airflow over a plate surface maintained at a temperature of 220°C. The temperature profile of the airflow is given as

$$T(y) = T_\infty - (T_\infty - T_s)\exp\left(-\frac{V}{\alpha_{\text{fluid}}}y\right)$$

The airflow at 1 atm has a free stream velocity and temperature of 0.08 m/s and 20°C, respectively. Determine the heat flux on the plate surface and the convection heat transfer coefficient of the airflow.

6–13 During air cooling of oranges, grapefruit, and tangelos, the heat transfer coefficient for combined convection, radiation, and evaporation for air velocities of $0.11 < V < 0.33$ m/s is determined experimentally and is expressed as $h = 5.05\,k_{\text{air}}\,\text{Re}^{1/3}/D$, where the diameter D is the characteristic length. Oranges are cooled by refrigerated air at 3°C and 1 atm at a velocity of 0.3 m/s. Determine (*a*) the initial rate of heat transfer from a 7-cm-diameter orange initially at 15°C with a thermal

conductivity of 0.7 W/m·K, (*b*) the value of the initial temperature gradient inside the orange at the surface, and (*c*) the value of the Nusselt number.
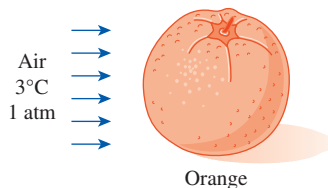
FIGURE P6–13

6–14 During air cooling of steel balls, the convection heat transfer coefficient is determined experimentally as a function of air velocity to be $h = 17.9V^{0.54}$ for $0.5 < V < 2$ m/s, where *h* and *V* are in W/m²·K and m/s, respectively. Consider a 24-mm-diameter steel ball initially at 300°C with a thermal conductivity of 15 W/m·K. The steel balls are cooled in air at 10°C and a velocity of 1.5 m/s. Determine the initial values of the heat flux and the temperature gradient in the steel ball at the surface.

6–15 **C & S** The upper surface of a 1-m × 1-m ASTM B152 copper plate is being cooled by air at 20°C. The air is flowing parallel over the plate surface at a velocity of 0.5 m/s. The local convection heat transfer coefficient along the plate surface is correlated with the correlation $h_x = 1.36\, x^{-0.5}$, where h_x and *x* have the units W/m²·K and m, respectively. The maximum use temperature for the ASTM B152 copper plate is 260°C (ASME Code for Process Piping, ASME B31.3-2014, Table A-1M). Evaluate the average convection heat transfer coefficient *h* for the entire plate. If the rate of convection heat transfer from the plate surface is 700 W, would the use of ASTM B152 plate be in compliance with the ASME Code for Process Piping?

6–16 **C & S** In cryogenic equipment, cold gas flows in parallel over the surface of a 1-m × 1-m ASTM A240 410S stainless steel plate. The average convection heat transfer coefficient for the plate surface is correlated with the gas velocity as $h = 6.5V^{0.8}$, where *h* and *V* have the units W/m²·K and m/s, respectively. The temperature of the cold gas is −50°C. The minimum temperature suitable for the ASTM A240 410S plate is −30°C (ASME Code for Process Piping, ASME B31.3-2014, Table A-1M). To keep the plate's temperature from going below −30°C, the plate is heated at a rate of 840 W. Determine the maximum velocity that the gas can achieve without cooling the plate below the suitable temperature set by the ASME Code for Process Piping.

6–17 **C & S** Two metal plates are connected by a long ASTM B98 copper–silicon bolt. A hot gas at 200°C flows between the plates and across the cylindrical bolt. The diameter of the bolt is 9.5 mm, and the length of the bolt exposed to the hot gas is 10 cm. The average convection heat transfer coefficient for the bolt in crossflow is correlated with the gas

velocity as $h = 24.6V^{0.62}$, where *h* and *V* have the units W/m²·K and m/s, respectively. The maximum use temperature for the ASTM B98 bolt is 149°C (ASME Code for Process Piping, ASME B31.3-2014, Table A-2M). If the gas velocity is 10.4 m/s, determine the minimum heat removal rate required to keep the bolt surface from going above the maximum use temperature.

6–18 **C & S** Two metal plates are connected by a long ASTM A479 904L stainless steel bar. A hot gas, at 400°C, flows between the plates and across the bar. The bar has a square cross section with a width of 2 cm, and the length of the bar exposed to the hot gas is 10 cm. The average convection heat transfer coefficient for the bar in crossflow is correlated with the gas velocity as $h = 13.6V^{0.675}$, where *h* and *V* have the units W/m²·K and m/s, respectively. The maximum use temperature for the ASTM A479 904L is 260°C (ASME Code for Process Piping, ASME B31.3-2014, Table A-1M). The temperature of the bar is maintained by a cooling mechanism with the capability of removing heat at a rate of 100 W. Determine the maximum velocity that the gas can achieve without heating the stainless steel bar above the maximum use temperature set by the ASME Code for Process Piping.

6–19 A ball bearing manufacturing plant is using air to cool chromium steel balls ($k = 40$ W/m·K). The convection heat transfer coefficient for the cooling is determined experimentally as a function of air velocity to be $h = 18.05V^{0.56}$, where *h* and *V* are in W/m²·K and m/s, respectively. At a given moment during the cooling process with the air temperature at 5°C, a chromium steel ball has a surface temperature of 450°C. Using appropriate software, determine the effect of the air velocity (*V*) on the temperature gradient in the chromium steel ball at the surface. By varying the air velocity from 0.2 to 2.4 m/s with increments of 0.2 m/s, plot the temperature gradient in the chromium steel ball at the surface as a function of air velocity.

6–20 Consider the surface of a metal plate being cooled by forced convection. Determine the ratio of the temperature gradient in the fluid to the temperature gradient in the metal plate at the surface.

6–21 A metal plate is being cooled by air ($k_{\text{fluid}} = 0.259$ W/m·K) at the upper surface while the lower surface is subjected to a uniform heat flux of 1000 W/m². Determine the temperature gradient in the air at the upper surface of the metal plate.
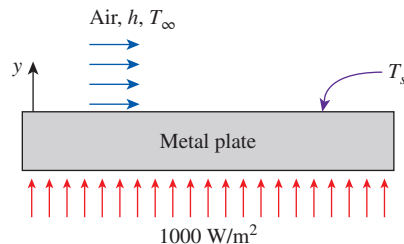
FIGURE P6–21

6–22 The top surface of a metal plate ($k_{plate} = 237$ W/m·K) is being cooled by air ($k_{air} = 0.243$ W/m·K) while the bottom surface is exposed to a hot steam at 100°C with a convection heat transfer coefficient of 30 W/m²·K. If the bottom surface temperature of the plate is 80°C, determine the temperature gradient in the air and the temperature gradient in the plate at the top surface of the plate.

Air, h_{air}, $T_{\infty 2}$

y

T_2

Solid plate

T_1

Hot steam, h_{steam}, $T_{\infty 1}$
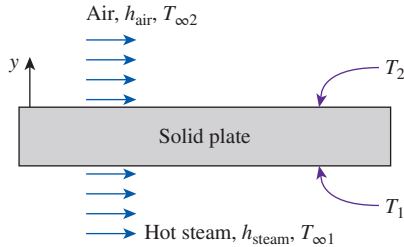
FIGURE P6−22

6–23 During air cooling of a flat plate ($k = 1.4$ W/m·K), the convection heat transfer coefficient is given as a function of air velocity to be $h = 27V^{0.85}$, where h and V are in W/m²·K and m/s, respectively. At a given moment, the surface temperature of the plate is 75°C and the air ($k = 0.0266$ W/m·K) temperature is 5°C. Using appropriate software, determine the effect of the air velocity (V) on the air temperature gradient at the plate surface. By varying the air velocity from 0 to 1.2 m/s with increments of 0.1 m/s, plot the air temperature and plate temperature gradients at the plate surface as a function of air velocity.

6–24 A metal plate ($k = 180$ W/m·K, $\rho = 2800$ kg/m³, and $c_p = 880$ J/kg·K) with a thickness of 1 cm is being cooled by air at 5°C with a convection heat transfer coefficient of 30 W/m²·K. If the initial temperature of the plate is 300°C, determine the plate temperature gradient at the surface after 2 minutes of cooling. *Hint:* Use the lumped system analysis to calculate the plate surface temperature. Make sure to verify the application of this method to this problem.

6–25 Air at 5°C, with a convection heat transfer coefficient of 30 W/m²·K, is used for cooling metal plates coming out of a heat treatment oven at an initial temperature of 300°C. The plates ($k = 180$ W/m·K, $\rho = 2800$ kg/m³, and $c_p = 880$ J/kg·K) have a thickness of 10 mm. Using appropriate software, determine the effect of cooling time on the temperature gradient in the metal plates at the surface. By varying the cooling time from 0 to 3000 s, plot the temperature gradient in the plates at the surface as a function of cooling time. *Hint:* Use the lumped system analysis to calculate the plate surface temperature. Make sure to verify the application of this method to this problem.

6–26 A 5-mm-thick stainless steel strip ($k = 21$ W/m·K, $\rho = 8000$ kg/m³, and $c_p = 570$ J/kg·K) is being heat treated as it moves through a furnace at a speed of 1 cm/s. The air

temperature in the furnace is maintained at 900°C with a convection heat transfer coefficient of 80 W/m²·K. If the furnace length is 3 m and the stainless steel strip enters it at 20°C, determine the surface temperature gradient of the strip at mid-length of the furnace. *Hint:* Use the lumped system analysis to calculate the plate surface temperature. Make sure to verify the application of this method to this problem.

6–27 A long steel strip is being conveyed through a 3-m-long furnace to be heat treated at a speed of 0.01 m/s. The steel strip ($k = 21$ W/m·K, $\rho = 8000$ kg/m³, and $c_p = 570$ J/kg·K) has a thickness of 5 mm, and it enters the furnace at an initial temperature of 20°C. Inside the furnace, the air temperature is maintained at 900°C with a convection heat transfer coefficient of 80 W/m²·K. Using appropriate software, determine the surface temperature gradient of the steel strip as a function of location inside the furnace. By varying the location in the furnace for $0 \leq x \leq 3$ m with increments of 0.2 m, plot the surface temperature gradient of the strip as a function of furnace location. *Hint:* Use the lumped system analysis to calculate the plate surface temperature. Make sure to verify the application of this method to this problem.

Furnace

Steel strip

y

0.01 m/s

$x = 0$ $x = 3$ m
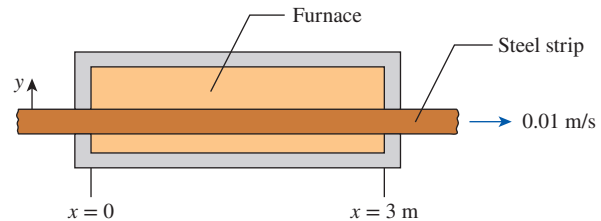
FIGURE P6−27

Boundary Layers and Flow Regimes

6–28C What is the no-slip condition? What causes it?

6–29C What is Newtonian fluid? Is water a Newtonian fluid?

6–30C What is viscosity? What causes viscosity in liquids and in gases? Is dynamic viscosity typically higher for a liquid or for a gas?

6–31C Consider two identical small glass balls dropped into two identical containers, one filled with water and the other with oil. Which ball will reach the bottom of the container first? Why?

6–32C How does the dynamic viscosity of (*a*) liquids and (*b*) gases vary with temperature?

6–33C What fluid property is responsible for the development of the velocity boundary layer? For what kinds of fluids will there be no velocity boundary layer on a flat plate?

6–34C What is the physical significance of the Prandtl number? Does the value of the Prandtl number depend on the type of flow or the flow geometry? Does the Prandtl number of air change with pressure? Does it change with temperature?

6–35C Will a thermal boundary layer develop in flow over a surface even if both the fluid and the surface are at the same temperature?

6–36C What is the physical significance of the Reynolds number? How is it defined for external flow over a plate of length L?

6–37C How does turbulent flow differ from laminar flow? For which flow is the heat transfer coefficient higher?

6–38C What does the friction coefficient represent in flow over a flat plate? How is it related to the drag force acting on the plate?

6–39C What is the physical mechanism that causes the friction factor to be higher in turbulent flow?

6–40C What is turbulent viscosity? What is it caused by?

6–41C What is turbulent thermal conductivity? What is it caused by?

6–42 Consider fluid flow over a surface with a velocity profile given as

$$u(y) = 100(y + 2y^2 - 0.5y^3) \text{ m/s}$$

Determine the shear stress at the wall surface, if the fluid is (*a*) air at 1 atm and (*b*) liquid water, both at 20°C. Also calculate the wall shear stress ratio for the two fluids, and interpret the result.

6–43 Consider a flow over a surface with the velocity and temperature profiles given as

$$u(y) = C_1(y + y^2 - y^3)$$
$$T(y) = C_2 - e^{-2C_2 y}$$

where the coefficients C_1 and C_2 are constants. Determine the expressions for the friction coefficient (C_f) and the convection heat transfer coefficient (h).

6–44 Air flowing over a 1-m-long flat plate at a velocity of 7 m/s has a friction coefficient given as $C_f = 0.664(Vx/\nu)^{-0.5}$, where x is the location along the plate. Determine the wall shear stress and the air velocity gradient on the plate surface at mid-length of the plate. Evaluate the air properties at 20°C and 1 atm.

6–45 💻 The friction coefficient of air flowing over a flat plate is given as $C_f = 0.664(Vx/\nu)^{-0.5}$, where x is the location along the plate. Using appropriate software, determine the effect of the air velocity (V) on the wall shear stress (τ_w) at the plate locations of $x = 0.5$ m and 1 m. By varying the air velocity from 0.5 to 6 m/s with increments of 0.5 m/s, plot the wall shear stress as a function of air velocity at $x = 0.5$ m and 1 m. Evaluate the air properties at 20°C and 1 atm.

6–46 💻 Air flowing over a flat plate at 5 m/s has a friction coefficient given as $C_f = 0.664(Vx/\nu)^{-0.5}$, where x is the location along the plate. Using appropriate software, determine the effect of the location along the plate (x) on

the wall shear stress (τ_w). By varying x from 0.01 to 1 m, plot the wall shear stress as a function of x. Evaluate the air properties at 20°C and 1 atm.

6–47 Consider a flat plate positioned inside a wind tunnel, and air at 1 atm and 20°C is flowing with a free stream velocity of 60 m/s. What is the minimum length of the plate necessary for the Reynolds number to reach 2×10^7? If the critical Reynolds number is 5×10^5, what type of flow regime would the airflow experience at 0.2 m from the leading edge?

6–48 Air flows over a flat plate at 40 m/s, 25°C, and 1 atm pressure. (*a*) What plate length should be used to achieve a Reynolds number of 1×10^8 at the end of the plate? (*b*) If the critical Reynolds number is 5×10^5, at what distance from the leading edge of the plate would transition occur?

6–49 Consider fluid flowing with a free stream velocity of 5 m/s over a flat plate, where the critical Reynolds number is 5×10^5. Determine the distance from the leading edge at which the transition from laminar to turbulent flow occurs for air (at 1 atm), liquid water, methanol, and engine oil, all at 20°C, and mercury at 25°C.

6–50E Consider fluid flowing with a free stream velocity of 1 ft/s over a flat plate, where the critical Reynolds number is 5×10^5. Determine the distance from the leading edge at which the transition from laminar to turbulent flow occurs for air (at 1 atm), liquid water, isobutane, and engine oil, and mercury. Evaluate all properties at 50°F.

Convection Equations and Similarity Solutions

6–51C Consider steady, laminar, two-dimensional, incompressible flow with constant properties and a Prandtl number of unity. For a given geometry, is it correct to say that both the average friction and heat transfer coefficients depend on the Reynolds number only?

6–52C Express the continuity equation for steady two-dimensional flow with constant properties, and explain what each term represents.

6–53C Is the acceleration of a fluid particle necessarily zero in steady flow? Explain.

6–54C For steady two-dimensional flow, what are the boundary layer approximations?

6–55C For what types of fluids and flows is the viscous dissipation term in the energy equation likely to be significant?

6–56C For steady two-dimensional flow over an isothermal flat plate in the x-direction, express the boundary conditions for the velocity components u and v and the temperature T at the plate surface and at the edge of the boundary layer.

6–57C What is a similarity variable, and what is it used for? For what kinds of functions can we expect a similarity solution for a set of partial differential equations to exist?

6–58C Consider steady, laminar, two-dimensional flow over an isothermal plate. Does the thickness of the velocity boundary layer increase or decrease with (*a*) distance from the leading edge, (*b*) free-stream velocity, and (*c*) kinematic viscosity?

6–59C Consider steady, laminar, two-dimensional flow over an isothermal plate. Does the wall shear stress increase, decrease, or remain constant with distance from the leading edge?

6–60C What are the advantages of nondimensionalizing the convection equations?

6–61C Under what conditions can a curved surface be treated as a flat plate in fluid flow and convection analysis?

6–62 Consider a 5-cm-diameter shaft rotating at 5600 rpm in a 25-cm-long bearing with a clearance of 0.5 mm. Determine the power required to rotate the shaft if the fluid in the gap is (*a*) air, (*b*) water, and (*c*) oil at 40°C and 1 atm.

6–63 Oil flow in a journal bearing can be treated as parallel flow between two large isothermal plates with one plate moving at a constant velocity of 8 m/s and the other stationary. Consider such a flow with a uniform spacing of 0.7 mm between the plates. The temperatures of the upper and lower plates are 40°C and 15°C, respectively. By simplifying and solving the continuity, momentum, and energy equations, determine (*a*) the velocity and temperature distributions in the oil, (*b*) the maximum temperature and where it occurs, and (*c*) the heat flux from the oil to each plate.
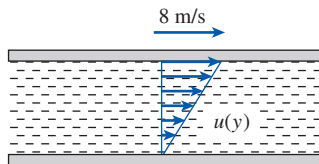
FIGURE P6–63

6–64 Repeat Prob. 6–63 for a spacing of 0.5 mm.

6–65 Consider the flow of fluid between two large parallel isothermal plates separated by a distance *L*. The upper plate is moving at a constant velocity of *V* and maintained at temperature T_0 while the lower plate is stationary and insulated. By simplifying and solving the continuity, momentum, and energy equations, obtain relations for the maximum temperature of fluid, the location where it occurs, and heat flux at the upper plate.

6–66 Reconsider Prob. 6–65. Using the results of this problem, obtain a relation for the volumetric heat generation rate $\dot{e}_{gen}$, in W/m³. Then express the convection problem as an equivalent conduction problem in the oil layer. Verify your model by solving the conduction problem and obtaining a relation for the maximum temperature, which should be identical to the one obtained in the convection analysis.

6–67 A 6-cm-diameter shaft rotates at 3000 rpm in a 20-cm-long bearing with a uniform clearance of 0.2 mm. At

steady operating conditions, both the bearing and the shaft in the vicinity of the oil gap are at 50°C, and the viscosity and thermal conductivity of lubricating oil are 0.05 N·s/m² and 0.17 W/m·K. By simplifying and solving the continuity, momentum, and energy equations, determine (*a*) the maximum temperature of oil, (*b*) the rates of heat transfer to the bearing and the shaft, and (*c*) the mechanical power wasted by the viscous dissipation in the oil. Treat this problem as parallel flow between two large plates with one plate moving at constant velocity and the other stationary. *Answers: (a) 53.3°C, (b) 419 W, (c) 838 W*
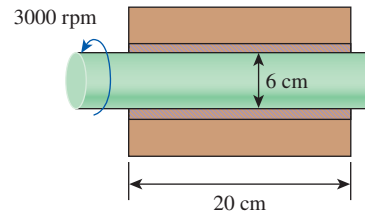
FIGURE P6–67

6–68 Repeat Prob. 6–67 by assuming the shaft to have reached peak temperature and thus heat transfer to the shaft to be negligible, and the bearing surface still to be maintained at 50°C.

6–69 Reconsider Prob. 6–67. Using appropriate software, investigate the effect of shaft velocity on the mechanical power wasted by viscous dissipation. Let the shaft rotation vary from 0 rpm to 6000 rpm. Plot the power wasted versus the shaft rpm, and discuss the results.

6–70 A 4-cm-diameter shaft rotates at 5200 rpm in a 15-cm-long, 8-cm-outer-diameter cast iron bearing ($k = 70$ W/m·K) with a uniform clearance of 0.6 mm filled with lubricating oil ($\mu = 0.03$ N·s/m² and $k = 0.14$ W/m·K). The bearing is cooled externally by a liquid, and its outer surface is maintained at 40°C. Disregarding heat conduction through the shaft and assuming one-dimensional heat transfer, determine (*a*) the rate of heat transfer to the coolant, (*b*) the surface temperature of the shaft, and (*c*) the mechanical power wasted by the viscous dissipation in oil. Treat this problem as parallel flow between two large plates with one plate moving at constant velocity and the other stationary.
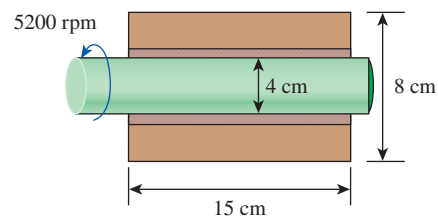
FIGURE P6–70

6–71 Repeat Prob. 6–70 for a clearance of 1 mm.

6–72E Glycerin at 50°F is flowing over a flat plate at a free stream velocity of 6 ft/s. Determine the velocity and thermal boundary layer thicknesses at a distance of 0.5 ft from the leading edge. Also calculate the ratio of the velocity boundary thickness to the thermal boundary layer thickness for this flow, and interpret the result.

6–73 Water at 20°C is flowing with velocity of 0.5 m/s between two parallel flat plates placed 1 cm apart. Determine the distances from the entrance at which the velocity and thermal boundary layers meet.
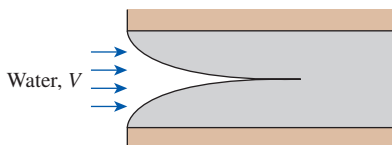
FIGURE P6–73

6–74E Consider a laminar boundary layer flow over a flat plate. Determine the δ/δ_t ratios for air (at 1 atm), liquid water, isobutane, engine oil, and mercury. Evaluate all properties at 50°F.

6–75 For laminar boundary layers, it is reasonable to expect that $\delta/\delta_t \approx \mathrm{Pr}^n$, where n is a positive exponent. Consider laminar boundary layer flow over a flat plate with air at 100°C and 1 atm, where the thermal boundary layer thickness is approximately 15% larger than the velocity boundary layer thickness. Determine the ratio of δ/δ_t if the fluid is engine oil (unused) under the same flow conditions.

6–76 Air at 10°C and 1 atm is flowing over a 0.3-m-long plate at 70°C at velocity of 3.0 m/s. Using appropriate software, plot the following on a combined graph for the range of $x = 0.0$ m to $x = x_{cr}$.
(*a*) The hydrodynamic boundary layer as a function of *x*.
(*b*) The thermal boundary layer as a function of *x*.

6–77 Liquid water at 15°C is flowing over a 0.3-m-wide plate at 65°C at a velocity of 3.0 m/s. Using appropriate software, plot (*a*) the hydrodynamic boundary layer and (*b*) the thermal boundary layer as a function of *x* on the same graph for the range of $x = 0.0$ m to $x = x_{cr}$. Use a critical Reynolds number of 500,000.

6–78 Saturated liquid water at 5°C is flowing over a flat plate at a velocity of 1 m/s. Using appropriate software, determine the effect of the location along the plate (*x*) on the velocity and thermal boundary layer thicknesses. By varying *x* for $0 < x \le 0.5$ m, plot the velocity and thermal boundary layer thicknesses as a function of *x*. Discuss the results.

6–79 Mercury at 0°C is flowing over a flat plate at a velocity of 0.1 m/s. Using appropriate software, determine the effect of the location along the plate (*x*) on the velocity and thermal boundary layer thicknesses. By varying *x* for $0 < x \le 0.5$ m, plot the velocity and thermal boundary layer thicknesses as a function of *x*. Discuss the results.

6–80 Water vapor at 0°C and 1 atm is flowing over a flat plate at a velocity of 10 m/s. Using appropriate software, determine the effect of the location along the plate (*x*) on the velocity and thermal boundary layer thicknesses. By varying *x* for $0 < x \le 0.5$ m, plot the velocity and thermal boundary layer thicknesses as a function of *x*. Discuss the results.

6–81 Consider a laminar ideal gas flow over a flat plate, where the local Nusselt number can be expressed as $\mathrm{Nu}_x = 0.332\,\mathrm{Re}_x^{1/2}\,\mathrm{Pr}^{1/3}$. Using the expression for the local Nusselt number, show that it can be rewritten in terms of local convection heat transfer coefficient as $h_x = C[V/(xT)]^m$, where *C* and *m* are constants.

6–82 Consider air flowing over a 1-m-long flat plate at a velocity of 3 m/s. Determine the convection heat transfer coefficients and the Nusselt numbers at $x = 0.5$ m and 0.75 m. Evaluate the air properties at 40°C and 1 atm.

6–83 A cryogenic gas flows at 5 m/s in parallel over the surface of an ASTM A240 410S stainless steel plate. The temperature of the cold gas is −50°C, and the plate length is 1 m. The minimum temperature suitable for the ASTM A240 410S plate is −30°C (ASME Code for Process Piping, ASME B31.3-2014, Table A-1M). In the interest of designing a heater, determine the total heat flux on the plate surface necessary to maintain the surface temperature at −30°C. Use the following gas properties for the analysis: $c_p = 1.002$ kJ/kg·K, $k = 0.02057$ W/m·K, $\mu = 1.527 \times 10^{-5}$ kg/m·s, and $\rho = 1.514$ kg/m³.

6–84 The upper surface of an ASME SB-96 copper–silicon plate is subjected to convection with hot air flowing at 7.5 m/s parallel over the plate surface. The length of the plate is 1 m, and the temperature of the hot air is 200°C. The ASME Boiler and Pressure Vessel Code (ASME BPVC.IV-2015, HF-300) limits equipment constructed with ASME SB-96 plate to be operated at a temperature not exceeding 93°C. In the interest of designing a cooling mechanism to keep the plate surface temperature from exceeding 93°C, determine the variation of the local heat flux on the plate surface for $0 < x \le 1$ m. Plot the local heat flux on the plate surface for $0 < x \le 1$ m. Use the following air properties for the analysis: $c_p = 1.016$ kJ/kg·K, $k = 0.03419$ W/m·K, $\mu = 2.371 \times 10^{-5}$ kg/m·s, and $\rho = 0.8412$ kg/m³.

6–85 The upper surface of an ASTM B152 copper plate is subjected to convection with hot air flowing at 6 m/s parallel over the plate surface. The length of the plate is 1 m, and the temperature of the hot air is 400°C. The maximum use temperature for the ASTM B152 copper plate is 260°C (ASME Code for Process Piping, ASME B31.3-2014, Table A-1M). Determine the variation of the local heat flux with the

thermal boundary layer thickness on the plate surface for $0 < x \leq 1$ m:

   (*a*) Plot the thermal boundary layer thickness on the plate surface for $0 < x \leq 1$ m.

   (*b*) Plot the local heat flux as a function of the thermal boundary layer thickness on the plate surface.

Discuss the results. Use the following air properties for the analysis: $c_p = 1.052$ kJ/kg·K, $k = 0.04601$ W/m·K, $\mu = 3.035 \times 10^{-5}$ kg/m·s, and $\rho = 0.5852$ kg/m^3.

6–86 Air with a temperature of 20°C is flowing over a flat plate ($k = 15$ W/m·K) at a velocity of 3 m/s. The plate surface temperature is maintained at 60°C. Using appropriate software, determine the effect of the location along the plate (x) on the heat transfer coefficient and the surface temperature gradient of the plate. By varying x for $0 < x \leq 0.5$ m, plot the heat transfer coefficient and the surface temperature gradient of the plate as a function of x. Evaluate the air properties at 40°C and 1 atm.

6–87 For laminar flow over a flat plate, the local heat transfer coefficient varies as $h_x = Cx^{-0.5}$, where x is measured from the leading edge of the plate and C is a constant. Determine the ratio of the average convection heat transfer coefficient over the entire plate of length L to the local convection heat transfer coefficient at the end of the plate.

6–88E An airfoil with a characteristic length of 0.2 ft is placed in airflow at 1 atm and 60°F with free stream velocity of 150 ft/s and convection heat transfer coefficient of 21 Btu/h·ft^2·°F. If a second airfoil with a characteristic length of 0.4 ft is placed in the airflow at 1 atm and 60°F with free stream velocity of 75 ft/s, determine the heat flux from the second airfoil. Both airfoils are maintained at a constant surface temperature of 180°F.
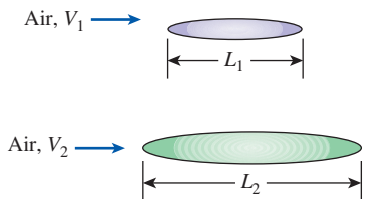
FIGURE P6–88E

6–89 Consider two irregularly shaped objects with different characteristic lengths. The characteristic length of the first object is $L_1 = 0.5$ m, and it is maintained at a uniform surface temperature of $T_{s,1} = 350$ K. The first object is placed in atmospheric air at a temperature of $T_{\infty,1} = 250$ K and an air velocity of $V_1 = 20$ m/s. The average heat flux from the first object under these conditions is 8000 W/m^2. The second object has a characteristic length of $L_2 = 2.5$ m, is maintained at a uniform surface temperature of $T_{s,2} = 350$ K, and is placed in atmospheric air at a temperature of $T_{\infty,2} = 250$ K and an air velocity of $V_2 = 4$ m/s. Determine the average convection heat transfer coefficient for the second object.

Momentum and Heat Transfer Analogies

6–90C How is the Reynolds analogy expressed? What is the value of it? What are its limitations?

6–91C How is the modified Reynolds analogy expressed? What is the value of it? What are its limitations?

6–92 Consider an airplane cruising at an altitude of 10 km where standard atmospheric conditions are −50°C and 26.5 kPa at a speed of 800 km/h. Each wing of the airplane can be modeled as a 25-m × 3-m flat plate, and the friction coefficient of the wings is 0.0016. Using the momentum–heat transfer analogy, determine the heat transfer coefficient for the wings at cruising conditions. *Answer:* 89.6 W/m^2·K

6–93 A metallic airfoil of elliptical cross section has a mass of 50 kg, surface area of 12m^2, and a specific heat of 0.50 kJ/kg·K. The airfoil is subjected to airflow at 1 atm, 25°C, and 5 m/s along its 3-m-long side. The average temperature of the airfoil is observed to drop from 160°C to 150°C within 2 min of cooling. Assuming the surface temperature of the airfoil to be equal to its average temperature and using the momentum–heat transfer analogy, determine the average friction coefficient of the airfoil surface. Evaluate the air properties at 25°C and 1 atm. *Answer:* 0.000363

6–94 Repeat Prob. 6–93 for an airflow velocity of 10 m/s.

6–95 The electrically heated 0.6-m-high and 1.8-m-long windshield of a car is subjected to parallel winds at 1 atm, 0°C, and 80 km/h. The electric power consumption is observed to be 70 W when the exposed surface temperature of the windshield is 4°C. Disregarding radiation and heat transfer from the inner surface and using the momentum–heat transfer analogy, determine drag force the wind exerts on the windshield. Evaluate the air properties at 2°C and 1 atm.

6–96 A 5-m × 5-m flat plate maintained at a constant temperature of 80°C is subjected to parallel flow of air at 1 atm, 20°C, and 10 m/s. The total drag force acting on the upper surface of the plate is measured to be 2.4 N. Using the momentum–heat transfer analogy, determine the average convection heat transfer coefficient and the rate of heat transfer between the upper surface of the plate and the air. Evaluate the air properties at 50°C and 1 atm.

6–97 Air (1 atm, 5°C) with free stream velocity of 2 m/s is flowing in parallel to a stationary thin 1-m × 1-m flat plate over the top and bottom surfaces. The flat plate has a uniform surface temperature of 35°C. If the friction force asserted on the flat plate is 0.1 N, determine the rate of heat transfer from the plate. Evaluate the air properties at 20°C and 1 atm. *Answer:* 1862 W

FIGURE P6–97

6–98 Air at 1 atm and 20°C is flowing over the top surface of a 0.2-m × 0.5-m-thin metal foil. The airstream velocity is 100 m/s and the metal foil is heated electrically with a uniform heat flux of 6100 W/m². If the friction force on the metal foil surface is 0.3 N, determine the surface temperature of the metal foil. Evaluate the air properties at 100°C and 1 atm. Is this a good assumption?
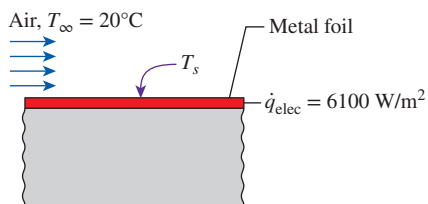
Air, $T_\infty = 20°C$ — Metal foil

T_s

$\dot{q}_{elec} = 6100$ W/m²

FIGURE P6–98

6–99 **C&S** The upper surface of an ASME SB-96 copper–silicon plate is subjected to convection with hot air flowing at 6.5 m/s parallel over the plate surface. The plate is square with a length of 1 m, and the temperature of the hot air is 200°C. The ASME Boiler and Pressure Vessel Code (ASME BPVC.IV-2015, HF-300) limits equipment constructed with ASME SB-96 plate to be operated at a temperature not exceeding 93°C. From a wind tunnel experiment, the average friction coefficient for the upper surface of the plate was found to be 0.0023. In the interest of designing a cooling mechanism to keep the plate surface temperature from exceeding 93°C, determine the minimum heat removal rate required to keep the plate surface from going above 93°C. Use the following air properties for the analysis: $c_p = 1.016$ kJ/kg·K, $k = 0.03419$ W/m·K, $\mu = 2.371 \times 10^{-5}$ kg/m·s, and $\rho = 0.8412$ kg/m³.

6–100 Air at 1 atm is flowing over a flat plate with a free stream velocity of 70 m/s. If the convection heat transfer coefficient can be correlated by $\mathrm{Nu}_x = 0.03 \, \mathrm{Re}_x^{0.8} \, \mathrm{Pr}^{1/3}$, determine the friction coefficient and wall shear stress at a location 2 m from the leading edge. Evaluate air properties at 20°C and 1 atm.

6–101 Metal plates are being cooled with air blowing in parallel over each plate. The average friction coefficient over each plate is given as $C_f = 1.33 \, (\mathrm{Re}_L)^{-0.5}$ for $\mathrm{Re}_L < 5 \times 10^5$. Each metal plate length parallel to the airflow is 1 m. Determine the average convection heat transfer coefficient for the plate if the air velocity is 5 m/s. Evaluate the air properties at 20°C and 1 atm.

6–102 A flat plate is subject to airflow parallel to its surface. The average friction coefficient over the plate is given as

$$C_f = 1.33 \, (\mathrm{Re}_L)^{-1/2} \quad \text{for } \mathrm{Re}_L < 5 \times 10^5 \text{ (laminar flow)}$$

$$C_f = 0.074 \, (\mathrm{Re}_L)^{-1/5} \quad \text{for } 5 \times 10^5 \le \mathrm{Re}_L \le 10^7 \text{ (turbulent flow)}$$

The plate length parallel to the airflow is 1 m. Using appropriate software, determine the effect of air velocity on the average convection heat transfer coefficient for the plate. By varying the air velocity for $0 < V \le 20$ m/s, plot the average convection heat transfer coefficient as a function of air velocity. Evaluate the air properties at 20°C and 1 atm.

Special Topic: Microscale Heat Transfer

6–103 Using a cylinder, a sphere, and a cube as examples, show that the rate of heat transfer is inversely proportional to the nominal size of the object. That is, heat transfer per unit area increases as the size of the object decreases.

(a) Cylinder (b) Sphere (c) Cube
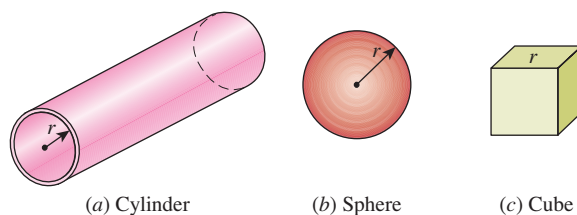
FIGURE P6–103

6–104 Determine the heat flux at the wall of a microchannel of width 1 μm if the wall temperature is 50°C and the average gas temperature near the wall is 100°C for the cases of
(a) $\sigma_T = 1.0, \gamma = 1.667, k = 0.15$ W/m·K, $\lambda/\mathrm{Pr} = 0.5$
(b) $\sigma_T = 0.8, \gamma = 2, k = 0.1$ W/m·K, $\lambda/\mathrm{Pr} = 5$

6–105 If $(\partial T/\partial y)_w = 65$ K/m, calculate the Nusselt number for a microchannel of width 1.2 μm if the wall temperature is 50°C and it is surrounded by (a) ambient air at temperature 30°C, (b) nitrogen gas at temperature −100°C.

Review Problems

6–106E Evaluate the Prandtl number from the following data: $c_p = 0.5$ Btu/lbm·R, $k = 2$ Btu/h·ft·R, $\mu = 0.3$ lbm/ft·s.

6–107 A fluid flows at 5 m/s over a wide flat plate 15 cm long. For each substance from the following list, calculate the Reynolds number at the downstream end of the plate. Indicate whether the flow at that point is laminar or turbulent. Assume all fluids are at 50°C. (a) Air, (b) CO_2, (c) Water, (d) Engine oil (unused).

6–108E Consider a fluid flowing over a flat plate at a constant free stream velocity. The critical Reynolds number is 5×10^5, and the distance from the leading edge at which the transition from laminar to turbulent flow occurs is $x_{cr} = 7$ ft. Determine the characteristic length (L_c) at which the Reynolds number is 1×10^5.

6–109 Consider the Couette flow of a fluid with a viscosity of $\mu = 0.8$ N·s/m² and thermal conductivity of $k_f = 0.145$ W/m·K. The lower plate is stationary and made of a material of thermal conductivity $k_p = 1.5$ W/m·K and thickness $b = 3$ mm. Its outer surface is maintained at $T_s = 50°C$. The upper plate

is insulated and moves with a uniform speed $V = 7$ m/s. The distance between plates is $L = 5$ mm.

(a) Determine the temperature distribution function, $T(y)$, in the fluid $(0 < y < L)$.

(b) Calculate the maximum temperature of the fluid, as well as the temperature of the fluid at the contact surfaces with the lower and upper plates.
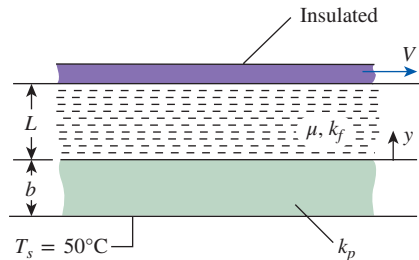
FIGURE P6–109

6–110 Engine oil at 15°C is flowing over a 0.3-m-wide plate at 65°C at a velocity of 3.0 m/s. Using appropriate software, plot (a) the hydrodynamic boundary layer and (b) the thermal boundary layer as a function of x on the same graph for the range of $x = 0.0$ m to $x = x_{cr}$. Use a critical Reynolds number of 500,000.

6–111 Object 1 with a characteristic length of 0.5 m is placed in airflow at 1 atm and 20°C with free stream velocity of 50 m/s. The heat flux transfer from object 1 when placed in the airflow is measured to be 12,000 W/m². If object 2 has the same shape and geometry as object 1 (but with a characteristic length of 5 m) and it is placed in the airflow at 1 atm and 20°C with free stream velocity of 5 m/s, determine the average convection heat transfer coefficient for object 2. Both objects are maintained at a constant surface temperature of 120°C.

6–112 A rectangular bar with a characteristic length of 0.5 m is placed in a free stream flow where the convection heat transfer coefficients were found to be 100 W/m²·K and 50 W/m²·K when the free stream velocities were 25 m/s and 5 m/s, respectively. If the Nusselt number can be expressed as Nu $= C \mathrm{Re}^m \mathrm{Pr}^n$, where C, m, and n are constants, determine the convection heat transfer coefficients for similar bars with (a) $L = 1$ m and $V = 5$ m/s, and (b) $L = 2$ m and $V = 50$ m/s.

6–113 In an effort to prevent the formation of ice on the surface of a wing, electrical heaters are embedded inside the wing. With a characteristic length of 2.5 m, the wing has a friction coefficient of 0.001. If the wing is moving at a speed of 200 m/s through air at 1 atm and −20°C, determine the heat flux necessary to keep the wing surface above 0°C. Evaluate the air properties at −10°C and 1 atm.

6–114 A 15-cm × 20-cm circuit board is being cooled by forced convection of air at 1 atm. The heat from the circuit board is estimated to be 1000 W/m². If the airstream velocity is 3 m/s and the shear stress of the circuit board surface is 0.075 N/m², determine the temperature difference between the circuit board surface temperature and the airstream temperature. Evaluate the air properties at 40°C and 1 atm.
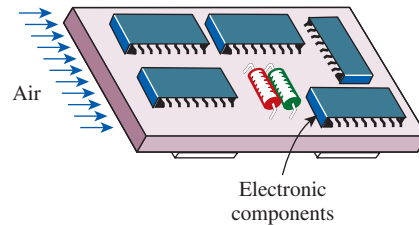
FIGURE P6–114

6–115 Atmospheric air with a velocity of 10 m/s and a temperature of 20°C is in parallel flow over a flat heater surface which is maintained at 80°C. The surface area of the heater is 0.30 m². The drag force induced by the airflow on the heater is measured to be 0.2 N. Using the momentum–heat transfer analogy, determine the electrical power needed to maintain the prescribed heater surface temperature of 80°C. Evaluate the air properties at 50°C and 1 atm.

Fundamentals of Engineering (FE) Exam Problems

6–116 The transition from laminar flow to turbulent flow in a forced convection situation is determined by which one of the following dimensionless numbers?

(a) Grasshof   (b) Nusselt   (c) Reynolds
(d) Stanton   (e) Mach

6–117 The _____ number is a significant dimensionless parameter for forced convection, and the _____ number is a significant dimensionless parameter for natural convection.

(a) Reynolds, Grashof   (b) Reynolds, Mach
(c) Reynolds, Eckert   (d) Reynolds, Schmidt
(e) Grashof, Sherwood

6–118 In any forced or natural convection situation, the velocity of the flowing fluid is zero where the fluid wets any stationary surface. The magnitude of heat flux where the fluid wets a stationary surface is given by

(a) $k(T_{\text{fluid}} - T_{\text{wall}})$ (b) $k\dfrac{dT}{dy}\Big|_{\text{wall}}$

(c) $k\dfrac{d^2T}{dy^2}\Big|_{\text{wall}}$ (d) $h\dfrac{dT}{dy}\Big|_{\text{wall}}$

(e) None of them

6–119 The coefficient of friction C_f for a fluid flowing across a surface in terms of the surface shear stress, τ_w, is given by

(a) $2\rho V^2/\tau_w$ (b) $2\tau_w/\rho V^2$ (c) $2\tau_w/\rho V^2 \Delta T$
(d) $4\tau_w/\rho V^2$ (e) None of them

6–120 Most correlations for the convection heat transfer coefficient use the dimensionless Nusselt number, which is defined as

(a) h/k (b) k/h (c) hL_c/k

(d) kL_c/h (e) $k/\rho c_p$

6–121 For the same initial conditions, one can expect the laminar thermal and momentum boundary layers on a flat plate to have the same thickness when the Prandtl number of the flowing fluid is

(a) Close to zero   (b) Small   (c) Approximately one

(d) Large   (e) Very large

6–122 One can expect the heat transfer coefficient for turbulent flow to be _____ for laminar flow.

(a) less than   (b) same as   (c) greater than

6–123 An electrical water ($k = 0.61$ W/m·K) heater uses natural convection to transfer heat from a 1-cm-diameter by 0.65-m-long, 110 V electrical resistance heater to the water. During operation, the surface temperature of this heater is 120°C while the temperature of the water is 35°C, and the Nusselt number (based on the diameter) is 6. Considering only the side surface of the heater (and thus $A = \pi DL$), the current passing through the electrical heating element is

(a) 3.2 A   (b) 3.7 A   (c) 4.6 A   (d) 5.8 A   (e) 6.6 A

6–124 In turbulent flow, one can estimate the Nusselt number using the analogy between heat and momentum transfer (Colburn analogy). This analogy relates the Nusselt number to the coefficient of friction, C_f, as

(a) $\text{Nu} = 0.5\, C_f \text{Re Pr}^{1/3}$ (b) $\text{Nu} = 0.5\, C_f \text{Re Pr}^{2/3}$

(c) $\text{Nu} = C_f \text{Re Pr}^{1/3}$ (d) $\text{Nu} = C_f \text{Re Pr}^{2/3}$

(e) $\text{Nu} = C_f \text{Re}^{1/2}\ \text{Pr}^{1/3}$

Design and Essay Problems

6–125 Design an experiment to measure the viscosity of liquids using a vertical funnel with a cylindrical reservoir of height h and a narrow flow section of diameter D and length L. Making appropriate assumptions, obtain a relation for viscosity in terms of easily measurable quantities such as density and volume flow rate.

6–126 A facility is equipped with a wind tunnel and can measure the friction coefficient for flat surfaces and airfoils. Design an experiment to determine the mean heat transfer coefficient for a surface using friction coefficient data.

EXTERNAL FORCED CONVECTION

I n Chap. 6, we considered the general and theoretical aspects of forced convection, with emphasis on differential formulation and analytical solutions. In this chapter, we consider the practical aspects of forced convection to or from flat or curved surfaces subjected to *external flow,* characterized by the freely growing boundary layers surrounded by a free flow region that involves no velocity and temperature gradients.

We start this chapter with an overview of external flow, with emphasis on friction and pressure drag, flow separation, and the evaluation of average drag and convection coefficients. We continue with *parallel flow over flat plates.* In Chap. 6, we solved the boundary layer equations for steady, laminar, parallel flow over a flat plate, and we obtained relations for the local friction coefficient and the Nusselt number. Using these relations as the starting point, we determine the average friction coefficient and Nusselt number. We then extend the analysis to turbulent flow over flat plates with and without an unheated starting length.

Next, we consider *crossflow over cylinders and spheres,* and we present graphs and empirical correlations for the drag coefficients and the Nusselt numbers and discuss their significance. Finally, we consider *crossflow over tube banks* in aligned and staggered configurations, and we present correlations for the pressure drop and the average Nusselt number for both configurations.

OBJECTIVES

When you finish studying this chapter, you should be able to:

- Distinguish between internal and external flow,

- Develop an intuitive understanding of friction drag and pressure drag, and evaluate the average drag and convection coefficients in external flow,

- Evaluate the drag and heat transfer associated with flow over a flat plate for both laminar and turbulent flow,

- Calculate the drag force exerted on cylinders and spheres during crossflow, and the average heat transfer coefficient, and

- Determine the pressure drop and the average heat transfer coefficient associated with flow across a tube bank for both in-line and staggered configurations.
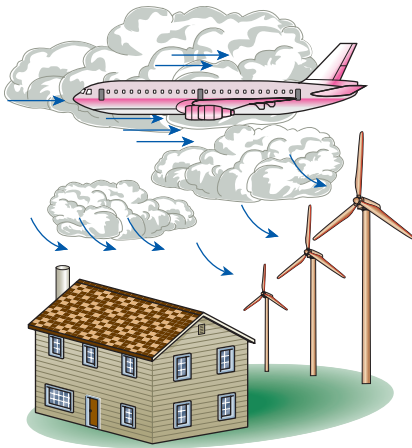
FIGURE 7–1
Flow over bodies is commonly
encountered in practice.

7–1 ■ DRAG AND HEAT TRANSFER IN EXTERNAL FLOW

Fluid flow over solid bodies often occurs in practice, and it is responsible for many physical phenomena such as the *drag force* acting on automobiles, power lines, trees, and underwater pipelines; the *lift* developed by airplane wings; the *upward draft* of rain, snow, hail, and dust particles in high winds; and the *cooling* of metal or plastic sheets, steam and hot water pipes, and extruded wires (Fig. 7–1). Therefore, developing a good understanding of external flow and external forced convection is important in the mechanical and thermal design of many engineering systems such as aircraft, automobiles, buildings, electronic components, and turbine blades.

The flow fields and geometries for most external flow problems are too complicated to be solved analytically, and thus we have to rely on correlations based on experimental data. The availability of high-speed computers has made it possible to conduct series of "numerical experimentations" quickly by solving the governing equations numerically and then to resort to expensive and time-consuming testing and experimentation only in the final stages of design. In this chapter, we mostly rely on relations developed experimentally.

The velocity of the fluid relative to an immersed solid body sufficiently far from the body (outside the boundary layer) is called the **free-stream velocity**. It is usually taken to be equal to the **upstream velocity** *V*, also called the **approach velocity**, which is the velocity of the approaching fluid far ahead of the body. This idealization is nearly exact for very thin bodies, such as a flat plate parallel to flow, but approximate for blunt bodies such as a large cylinder. The fluid velocity ranges from zero at the surface (the no-slip condition) to the free-stream value away from the surface, and the subscript "infinity" serves as a reminder that this is the value at a distance where the presence of the body is not felt. The upstream velocity, in general, may vary with location and time (e.g., the wind blowing past a building). But in the design and analysis, the upstream velocity is usually assumed to be *uniform* and *steady* for convenience, and this is what we will do in this chapter.

Friction and Pressure Drag

It is common experience that a body meets some resistance when it is forced to move through a fluid, especially a liquid. You may have seen high winds knocking down trees, power lines, and even trailers, and have felt the strong "push" the wind exerts on your body. You experience the same feeling when you extend your arm out of the window of a moving car. The force a flowing fluid exerts on a body in the flow direction is called **drag** (Fig. 7–2).

A stationary fluid exerts only normal pressure forces on the surface of a body immersed in it. A moving fluid, however, also exerts tangential shear forces on the surface because of the no-slip condition caused by viscous effects. Both of these forces, in general, have components in the direction of flow, and thus the drag force is due to the combined effects of pressure and wall shear forces in the flow direction. The components of the pressure and wall shear forces in the *normal* direction to flow tend to move the body in that direction, and their sum is called **lift**.

In general, both the skin friction (wall shear) and pressure contribute to the drag and the lift. In the special case of a thin, flat plate aligned parallel to the

FIGURE 7–2
Schematic for measuring the drag force acting on a car in a wind tunnel.

flow direction, the drag force depends on the wall shear only and is independent of pressure. When the flat plate is placed normal to the flow direction, however, the drag force depends on the pressure only and is independent of the wall shear since the shear stress in this case acts in the direction normal to flow (Fig. 7–3). For slender bodies such as wings, the shear force acts nearly parallel to the flow direction. The drag force for such slender bodies is mostly due to shear forces (the skin friction).

The drag force F_D depends on the density ρ of the fluid, the upstream velocity V, and the size, shape, and orientation of the body, among other things. The drag characteristics of a body are represented by the dimensionless **drag coefficient** C_D defined as

Drag coefficient:
$$C_D = \frac{F_D}{\frac{1}{2}\rho V^2 A}$$
(7–1)

where A is the *frontal area* (the area projected on a plane normal to the direction of flow) for blunt bodies—bodies that tend to block the flow. The frontal area of a cylinder of diameter D and length L, for example, is $A = LD$. For parallel flow over flat plates or thin airfoils, A is the surface area. The drag coefficient is primarily a function of the shape of the body, but it may also depend on the Reynolds number and the surface roughness.

The drag force is the net force exerted by a fluid on a body in the direction of flow due to the combined effects of wall shear and pressure forces. The part of drag that is due directly to wall shear stress τ_w is called the **skin friction drag** (or just *friction drag*) since it is caused by frictional effects, and the part that is due directly to pressure P is called the **pressure drag** (also called the *form drag* because of its strong dependence on the form or shape of the body). When the friction and pressure drag coefficients are available, the total drag coefficient is determined by simply adding them,

$$C_D = C_{D,\,\text{friction}} + C_{D,\,\text{pressure}}$$
(7–2)

The *friction drag* is the component of the wall shear force in the direction of flow, and thus it depends on the orientation of the body as well as the magnitude of the wall shear stress τ_w. The friction drag is *zero* for a surface normal to flow and *maximum* for a surface parallel to flow since the friction drag in this case equals the total shear force on the surface. Therefore, for parallel flow over a flat plate, the drag coefficient is equal to the *friction drag coefficient,* or simply the *friction coefficient* (Fig. 7–4). That is,

Flat plate:
$$C_D = C_{D,\,\text{friction}} = C_f$$
(7–3)

Once the average friction coefficient C_f is available, the drag (or friction) force over the surface can be determined from Eq. 7–1. In this case, A is the surface area of the plate exposed to fluid flow. When both sides of a thin plate are subjected to flow, A becomes the total area of the top and bottom surfaces. Note that the friction coefficient, in general, varies with location along the surface.

Friction drag is a strong function of viscosity, and an "idealized" fluid with zero viscosity would produce zero friction drag since the wall shear stress would be zero. The pressure drag would also be zero in this case during steady flow regardless of the shape of the body since there are no pressure losses. For flow in the horizontal direction, for example, the pressure along a horizontal
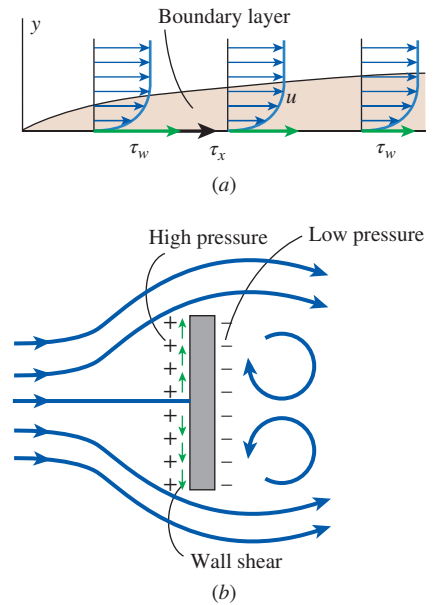
FIGURE 7–3
(*a*) Drag force acting on a flat plate parallel to the flow depends on wall shear only. (*b*) Drag force acting on a flat plate normal to the flow depends on the pressure only and is independent of the wall shear, which acts normal to the free-stream flow.
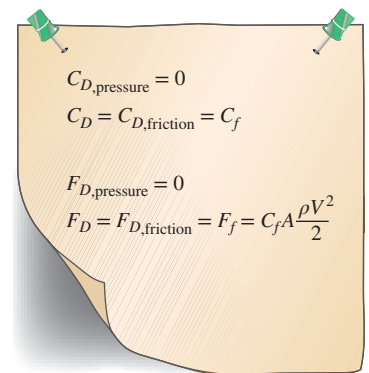
FIGURE 7–4
For parallel flow over a flat plate, the pressure drag is zero, and thus the drag coefficient is equal to the friction coefficient, and the drag force is equal to the friction force.

line is constant (just like stationary fluids) since the upstream velocity is constant, and thus there is no net pressure force acting on the body in the horizontal direction. Therefore, the total drag is zero for the case of ideal inviscid fluid flow.

At low Reynolds numbers, most drag is due to friction drag. This is especially the case for highly streamlined bodies such as airfoils. The friction drag is also proportional to the surface area. Therefore, bodies with a larger surface area experience a larger friction drag. Large commercial airplanes, for example, reduce their total surface area and thus drag by retracting their wing extensions when they reach the cruising altitudes to save fuel. The friction drag coefficient is independent of *surface roughness* in laminar flow, but it is a strong function of surface roughness in turbulent flow due to surface roughness elements protruding further into the boundary layer.

The pressure drag is proportional to the frontal area and to the *difference* between the pressures acting on the front and back of the immersed body. Therefore, the pressure drag is usually dominant for blunt bodies, negligible for streamlined bodies such as airfoils, and zero for thin, flat plates parallel to the flow.

When a fluid separates from a body, it forms a separated region between the body and the fluid stream. This low-pressure region behind the body where recirculating and backflows occur is called the **separated region**. The larger the separated region, the larger the pressure drag. The effects of flow separation are felt far downstream in the form of reduced velocity (relative to the upstream velocity). The region of flow trailing the body where the effects of the body on velocity are felt is called the **wake** (Fig. 7–5). The separated region comes to an end when the two flow streams reattach. Therefore, the separated region is an enclosed volume, whereas the wake keeps growing behind the body until the fluid in the wake region regains its velocity and the velocity profile becomes nearly flat again. Viscous and rotational effects are the most significant in the boundary layer, the separated region, and the wake.

Heat Transfer

The phenomena that affect drag force also affect heat transfer, and this effect appears in the Nusselt number. By nondimensionalizing the boundary layer equations, it was shown in Chap. 6 that the local and average Nusselt numbers have the functional form

$$\text{Nu}_x = f_1(x^*, \text{Re}_x, \text{Pr}) \quad \text{and} \quad \text{Nu} = f_2(\text{Re}_L, \text{Pr}) \tag{7–4a, b}$$

The experimental data for heat transfer are often represented conveniently with reasonable accuracy by a simple power-law relation of the form

$$\text{Nu} = C\,\text{Re}_L^m\,\text{Pr}^n \tag{7–5}$$

where m and n are constant exponents, and the value of the constant C depends on geometry and flow.

The fluid temperature in the thermal boundary layer varies from T_s at the surface to about T_∞ at the outer edge of the boundary. The fluid properties also

FIGURE 7–5
Separation during flow over a tennis ball and the wake region.
Courtesy NASA Ames Research Center and Cislunar Aerospace, Inc.

vary with temperature, and thus with position across the boundary layer. In order to account for the variation of the properties with temperature, the fluid properties are usually evaluated at the so-called **film temperature**, defined as

$$T_f = \frac{T_s + T_\infty}{2} \tag{7–6}$$

which is the *arithmetic average* of the surface and the free-stream temperatures. The fluid properties are then assumed to remain constant at those values during the entire flow. An alternative way of accounting for the variation of properties with temperature is to evaluate all properties at the free-stream temperature and to multiply the Nusselt number relation in Eq. 7–5 by $(Pr_\infty/Pr_s)^r$ or $(\mu_\infty/\mu_s)^r$ where r is an experimentally determined constant.

The local drag and convection coefficients vary along the surface as a result of the changes in the velocity boundary layers in the flow direction. We are usually interested in the drag force and the heat transfer rate for the *entire* surface, which can be determined using the *average* friction and convection coefficient. Therefore, we present correlations for both local (identified with the subscript x) and average friction and convection coefficients. When relations for local friction and convection coefficients are available, the *average* friction and convection coefficients for the entire surface can be determined by integration from

$$C_f = \frac{1}{L} \int_0^L C_{f,x} \, dx \tag{7–7}$$

and

$$h = \frac{1}{L} \int_0^L h_x \, dx \tag{7–8}$$

When the average drag and convection coefficients are available, the drag force can be determined from Eq. 7–1, and the rate of heat transfer to or from an isothermal surface can be determined from

$$\dot{Q} = hA_s(T_s - T_\infty) \tag{7–9}$$

where A_s is the surface area.

7–2 · PARALLEL FLOW OVER FLAT PLATES

Consider the parallel flow of a fluid over a flat plate of length L in the flow direction, as shown in Fig. 7–6. The x-coordinate is measured along the plate surface from the leading edge in the direction of the flow. The fluid approaches the plate in the x-direction with a uniform velocity V and temperature T_∞. The flow in the velocity boundary layers starts out as laminar, but if the plate is sufficiently long, the flow becomes turbulent at a distance x_{cr} from the leading edge where the Reynolds number reaches its critical value for transition.

The transition from laminar to turbulent flow depends on the *surface geometry, surface roughness, upstream velocity, surface temperature,* and the *type of fluid,* among other things, and it is best characterized by the Reynolds number.
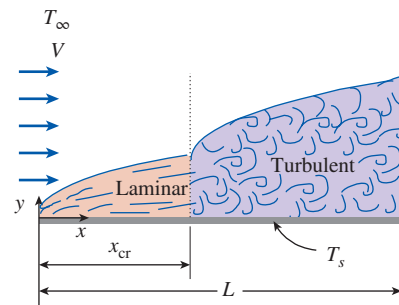
FIGURE 7–6
Laminar and turbulent regions of the boundary layer during flow over a flat plate.

The Reynolds number at a distance x from the leading edge of a flat plate is expressed as

$$\text{Re}_x = \frac{\rho V x}{\mu} = \frac{V x}{\nu} \tag{7-10}$$

Note that the value of the Reynolds number varies for a flat plate along the flow, reaching $\text{Re}_L = V L / \nu$ at the end of the plate.

For flow over a flat plate, the transition from laminar to turbulent begins at about $\text{Re} \cong 1 \times 10^5$, but it does not become fully turbulent before the Reynolds number reaches much higher values, typically around 3×10^6. In engineering analysis, a generally accepted value for the critical Reynolds number is

$$\text{Re}_{\text{cr}} = \frac{\rho V x_{\text{cr}}}{\mu} = 5 \times 10^5 \tag{7-11}$$

The actual value of the engineering critical Reynolds number for a flat plate may vary somewhat from 10^5 to 3×10^6, depending on the surface roughness, the turbulence level, and the variation of pressure along the surface.

Friction Coefficient

Based on analysis, the boundary layer thickness and the local friction coefficient at location x for laminar flow over a flat plate were determined in Chap. 6 to be

Laminar: $\qquad \delta = \dfrac{4.91x}{\text{Re}_x^{1/2}}$ and $\qquad C_{f,x} = \dfrac{0.664}{\text{Re}_x^{1/2}}, \qquad \text{Re}_x < 5 \times 10^5 \tag{7-12a, b}$

From experiments, the corresponding relations for turbulent flow are

Turbulent: $\qquad \delta = \dfrac{0.38x}{\text{Re}_x^{1/5}}$ and $\qquad C_{f,x} = \dfrac{0.059}{\text{Re}_x^{1/5}}, \qquad 5 \times 10^5 \le \text{Re}_x \le 10^7 \tag{7-13a, b}$

where x is the distance from the leading edge of the plate and $\text{Re}_x = V x / \nu$ is the Reynolds number at location x. Note that $C_{f,x}$ is proportional to $\text{Re}_x^{-1/2}$ and thus to $x^{-1/2}$ for laminar flow. Therefore, $C_{f,x}$ is supposedly *infinite* at the leading edge ($x = 0$) and decreases by a factor of $x^{-1/2}$ in the flow direction. The local friction coefficients are higher in turbulent flow than they are in laminar flow because of the intense mixing that occurs in the turbulent boundary layer. Note that $C_{f,x}$ reaches its highest values when the flow becomes fully turbulent, and it then decreases by a factor of $x^{-1/5}$ in the flow direction.

The *average* friction coefficient over the entire plate is determined by substituting the preceding relations into Eq. 7–7 and performing the integrations (Fig. 7–7). We get

Laminar: $\qquad\qquad C_f = \dfrac{1.33}{\text{Re}_L^{1/2}} \qquad \text{Re}_L < 5 \times 10^5 \tag{7-14}$

Turbulent: $\qquad\qquad C_f = \dfrac{0.074}{\text{Re}_L^{1/5}} \qquad 5 \times 10^5 \le \text{Re}_L \le 10^7 \tag{7-15}$

The first relation gives the average friction coefficient for the entire plate when the flow is *laminar* over the *entire* plate. Note that the average friction coefficient over the entire plate in case of laminar flow is twice the value of the local friction coefficient at the end of the plate, $C_f = 2C_{f,x=L}$. The second relation gives the average friction coefficient for the entire plate only when

$$C_f = \frac{1}{L} \int_0^L C_{f,x}\, dx$$

$$= \frac{1}{L} \int_0^L \frac{0.664}{\text{Re}_x^{1/2}}\, dx$$

$$= \frac{0.664}{L} \int_0^L \left(\frac{Vx}{\nu} \right)^{-1/2} dx$$

$$= \frac{0.664}{L} \left(\frac{V}{\nu} \right)^{-1/2} \frac{x^{1/2}}{\frac{1}{2}} \Big|_0^L$$

$$= \frac{2 \times 0.664}{L} \left(\frac{V}{\nu L} \right)^{-1/2}$$

$$= \frac{1.33}{\text{Re}_L^{1/2}}$$

FIGURE 7–7
The average friction coefficient over a surface is determined by integrating the local friction coefficient over the entire surface. The values shown here are for a laminar flat plate boundary layer.

the flow is *turbulent* over the *entire* plate, or when the laminar flow region of the plate is too small relative to the turbulent flow region (that is, $x_{cr} \ll L$).

In some cases, a flat plate is sufficiently long for the flow to become turbulent, but not long enough to disregard the laminar flow region. In such cases, the *average* friction coefficient over the entire plate is determined by performing the integration in Eq. 7–7 over two parts: use Eq. 7–12*b* for the laminar region $0 \le x \le x_{cr}$ and Eq. 7–13*b* for the turbulent region $x_{cr} < x \le L$ as

$$C_f = \frac{1}{L}\left(\int_0^{x_{cr}} C_{f,x\,\text{laminar}}\, dx + \int_{x_{cr}}^{L} C_{f,x,\,\text{turbulent}}\, dx\right) \qquad \textbf{(7–16)}$$

Note that we included the transition region with the turbulent region. Again taking the critical Reynolds number to be $Re_{cr} = 5 \times 10^5$ and performing the integrations of Eq. 7–16 after substituting the indicated expressions, the *average* friction coefficient over the entire plate is determined to be

$$C_f = \frac{0.074}{Re_L^{1/5}} - \frac{1742}{Re_L} \qquad 5 \times 10^5 \le Re_L \le 10^7 \qquad \textbf{(7–17)}$$

For a completely turbulent boundary layer ($Re_{cr} = 0$) or a very short x_{cr} ($L \gg x_{cr}$ or $Re_L \gg Re_{cr}$), Eq. 7–17 simplifies to the equation for turbulent flow, Eq. 7–15. The constants in Eq. 7–17 will be different for different critical Reynolds numbers. Also, the surfaces are assumed to be *smooth* and the free stream to be *turbulence free*. For laminar flow, the friction coefficient depends on only the Reynolds number, and the surface roughness has no effect. For turbulent flow, however, surface roughness causes the friction coefficient to increase severalfold, to the point that in fully turbulent regime the friction coefficient is a function of surface roughness alone and is independent of the Reynolds number (Fig. 7–8). This is also the case in pipe flow.

A curve fit of experimental data for the average friction coefficient in this regime is given by Schlichting (1979) as

Rough surface, turbulent: $\quad C_f = \left(1.89 - 1.62 \log\frac{\varepsilon}{L}\right)^{-2.5} \qquad \textbf{(7–18)}$

where ε is the surface roughness and L is the length of the plate in the flow direction. In the absence of a better relation, the relation above can be used for turbulent flow on rough surfaces for $Re > 10^6$, especially when $\varepsilon/L > 10^{-4}$.

Heat Transfer Coefficient
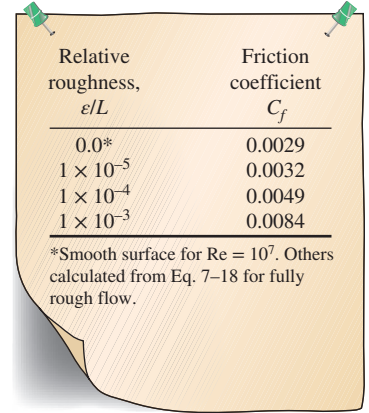
The local Nusselt number at a location x for laminar flow over a flat plate for the case of constant wall temperature was determined in Chap. 6 by solving the differential energy equation to be

Laminar: $\quad Nu_x = \frac{h_x x}{k} = 0.332\, Re_x^{0.5} Pr^{1/3} \qquad Pr > 0.6, \quad Re_x < 5 \times 10^5 \qquad \textbf{(7–19)}$

From experiments, the corresponding relation for turbulent flow is

Turbulent: $\quad Nu_x = \frac{h_x x}{k} = 0.0296\, Re_x^{0.8} Pr^{1/3} \qquad \begin{array}{l} 0.6 \le Pr \le 60 \\ 5 \times 10^5 \le Re_x \le 10^7 \end{array} \qquad \textbf{(7–20)}$

Note that h_x is proportional to $Re_x^{0.5}$ and thus to $x^{-0.5}$ for laminar flow. Therefore, h_x is *infinite* at the leading edge ($x = 0$) and decreases by a factor of $x^{-0.5}$ in the

Relative roughness, ε/L	Friction coefficient C_f
0.0*	0.0029
1×10^{-5}	0.0032
1×10^{-4}	0.0049
1×10^{-3}	0.0084

*Smooth surface for $Re = 10^7$. Others calculated from Eq. 7–18 for fully rough flow.

FIGURE 7–8
For turbulent flow, surface roughness may cause the friction coefficient to increase severalfold.
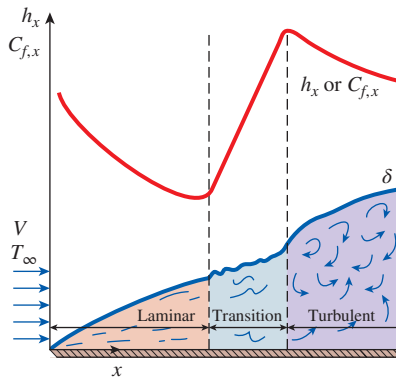
FIGURE 7–9
The variation of the local friction and heat transfer coefficients for flow over a flat plate.
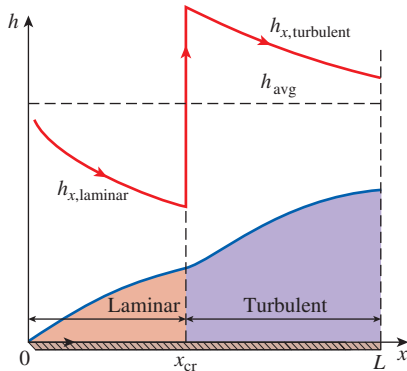
FIGURE 7–10
Graphical representation of the average heat transfer coefficient for a flat plate with combined laminar and turbulent flow.

flow direction. The variation of the boundary layer thickness δ and the friction and heat transfer coefficients along an isothermal flat plate are shown in Fig. 7–9. The local friction and heat transfer coefficients are higher in turbulent flow than they are in laminar flow. Also, h_x reaches its highest values when the flow becomes fully turbulent, and then decreases by a factor of $x^{-0.2}$ in the flow direction, as shown in the figure.

The *average* Nusselt number over the entire plate is determined by substituting the relations above into Eq. 7–8 and performing the integrations. We get

Laminar: $\quad \text{Nu} = \dfrac{hL}{k} = 0.664\, \text{Re}_L^{0.5}\, \text{Pr}^{1/3} \quad \text{Re}_L < 5 \times 10^5,\ \text{Pr} > 0.6$ **(7–21)**

Turbulent: $\quad \text{Nu} = \dfrac{hL}{k} = 0.037\, \text{Re}_L^{0.8}\, \text{Pr}^{1/3} \quad \begin{array}{l} 0.6 \leq \text{Pr} \leq 60 \\ 5 \times 10^5 \leq \text{Re}_L \leq 10^7 \end{array}$ **(7–22)**

The first relation gives the average heat transfer coefficient for the entire plate when the flow is *laminar* over the *entire* plate. Note that the average Nusselt number over the entire plate in case of laminar flow is twice the value of the local Nusselt number at the end of the plate, $\text{Nu} = 2\text{Nu}_{x=L}$ or $h = 2h_{x=L}$. This is only true for laminar flow and does not carry over to the turbulent flow. The second relation gives the average heat transfer coefficient for the entire plate only when the flow is *turbulent* over the *entire* plate, or when the laminar flow region of the plate is too small relative to the turbulent flow region.

In some cases, a flat plate is sufficiently long for the flow to become turbulent, but not long enough to disregard the laminar flow region. In such cases, the *average* heat transfer coefficient over the entire plate is determined by performing the integration in Eq. 7–8 over two parts: use Eq. 7–19 for the laminar region $0 \leq x \leq x_{cr}$ and Eq. 7–20 for the turbulent region $x_{cr} \leq x \leq L$ as

$$h = \frac{1}{L} \left(\int_0^{x_{cr}} h_{x,\,\text{laminar}}\, dx + \int_{x_{cr}}^{L} h_{x,\,\text{turbulent}}\, dx \right)$$ **(7–23)**

Again taking the critical Reynolds number to be $\text{Re}_{cr} = 5 \times 10^5$ and performing the integrations in Eq. 7–23 after substituting the indicated expressions, the *average* Nusselt number over the *entire* plate is determined to be (Fig. 7–10)

$$\text{Nu} = \frac{hL}{k} = (0.037\, \text{Re}_L^{0.8} - 871)\text{Pr}^{1/3} \quad \begin{array}{l} 0.6 \leq \text{Pr} \leq 60 \\ 5 \times 10^5 \leq \text{Re}_L \leq 10^7 \end{array}$$ **(7–24)**

For a completely turbulent boundary layer ($\text{Re}_{cr} = 0$) or a very short $x_{cr}(L \gg x_{cr}$ or $\text{Re}_L \gg \text{Re}_{cr}$), Eq. 7–24 simplifies to the equation for turbulent flow, Eq. 7–22. The constants in Eq. 7–24 will be different for different critical Reynolds numbers.

Liquid metals such as mercury have high thermal conductivities, and they are commonly used in applications that require high heat transfer rates. Liquid metals have very small Prandtl numbers, and Eq. 7–19 does not apply. However, for this case the thermal boundary layer develops much faster than the velocity boundary layer. Then we can assume the velocity in the thermal boundary layer to be constant at the free stream value and solve the energy equation. It gives

$$\text{Nu}_x = 0.565(\text{Re}_x\, \text{Pr})^{1/2} = 0.565\, \text{Pe}_x^{1/2} \quad \text{Pr} \leq 0.05,\ \text{Pe}_x \geq 100$$ **(7–25)**

where $\text{Pe}_x = \text{Re}_x\text{Pr}$ is the dimensionless **Peclet number** (Fig. 7–11).

It is desirable to have a single correlation that applies to *all fluids*, including liquid metals. By curve-fitting existing data, Churchill and Ozoe (1973) proposed the following relation for laminar flow over an isothermal flat plate which is applicable for *all Prandtl numbers* and is claimed to be accurate to ±1 percent,

$$\text{Nu}_x = \frac{h_x x}{k} = \frac{0.3387 \, \text{Pr}^{1/3} \, \text{Re}_x^{1/2}}{[1 + (0.0468/\text{Pr})^{2/3}]^{1/4}} \quad \text{Re}_x \, \text{Pr} \geq 100 \quad \textbf{(7–26)}$$

with $\text{Nu} = 2\text{Nu}_{x=L}$. For the *uniform heat flux* case, 0.3387 is changed to 0.4637 and 0.0468 is changed to 0.02052. Properties are still evaluated at the film temperature.

These relations have been obtained for the case of *isothermal* surfaces, but they could also be used approximately for the case of nonisothermal surfaces by assuming the surface temperature to be constant at some average value. Also, the surfaces are assumed to be *smooth,* and the free stream to be *turbulent free*. The effect of variable properties can be accounted for by evaluating all properties at the film temperature.

Flat Plate with Unheated Starting Length

So far we have limited our consideration to situations for which the entire plate is heated from the leading edge. But many practical applications involve surfaces with an unheated starting section of length ξ, shown in Fig. 7–12, and thus there is no heat transfer for $0 < x < \xi$. In such cases, the velocity boundary layer starts to develop at the leading edge ($x = 0$), but the thermal boundary layer starts to develop where heating starts ($x = \xi$).

Consider a flat plate whose heated section is maintained at a constant temperature ($T = T_s$ constant for $x > \xi$). Using integral solution methods, the local Nusselt numbers for both laminar and turbulent flows are determined to be

Laminar: $$\text{Nu}_x = \frac{\text{Nu}_{x\,(\text{for } \xi=0)}}{[1 - (\xi/x)^{3/4}]^{1/3}} = \frac{0.332 \, \text{Re}_x^{0.5} \, \text{Pr}^{1/3}}{[1 - (\xi/x)^{3/4}]^{1/3}} \quad \textbf{(7–27)}$$

Turbulent: $$\text{Nu}_x = \frac{\text{Nu}_{x\,(\text{for } \xi=0)}}{[1 - (\xi/x)^{9/10}]^{1/9}} = \frac{0.0296 \, \text{Re}_x^{0.8} \, \text{Pr}^{1/3}}{[1 - (\xi/x)^{9/10}]^{1/9}} \quad \textbf{(7–28)}$$

for $x > \xi$. Note that for $\xi = 0$, these Nu_x relations reduce to $\text{Nu}_{x(\text{for } \xi=0)}$, which is the Nusselt number relation for a flat plate without an unheated starting length. Therefore, the terms in brackets in the denominator serve as correction factors for plates with unheated starting lengths.

The determination of the average Nusselt number for the heated section of a plate requires the integration of the local Nusselt number relations above, which cannot be done analytically. Therefore, integrations must be done numerically. The results of numerical integrations have been correlated for the average Nusselt number (Ameel, 1997) as

Laminar: $$\text{Nu} = \text{Nu}_{(\text{for } \xi=0)} \frac{L}{L - \xi}[1 - (\xi/L)^{3/4}]^{2/3} \quad \textbf{(7–29)}$$

Turbulent: $$\text{Nu} = \text{Nu}_{(\text{for } \xi=0)} \frac{L}{L - \xi}[1 - (\xi/L)^{9/10}]^{8/9} \quad \textbf{(7–30)}$$

The quantity $\text{Nu}_{(\text{for } \xi=0)}$ is the average Nusselt number for a plate of length L when heating starts at the leading edge of the plate. For laminar flow,

FIGURE 7–11
Jean Claude Eugene Peclet
(1793–1857), a French physicist, was born in Besancon, France. He was one of the first scholars of the Ecole Normale at Paris. His publications were famous for their clarity of style, sharp-minded views, and well-performed experiments. The dimensionless **Peclet number** is named after him.
©Classic Image/Alamy
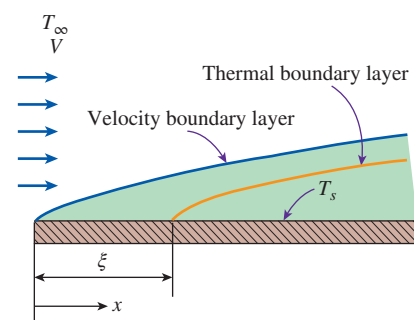
FIGURE 7–12
Flow over a flat plate with an unheated starting length.

it can be obtained from Eq. 7–21; for turbulent flow, it is obtained from Eq. 7–22 (assuming turbulent flow over the entire surface). Note that Nu is equal to hL/k, where h is averaged over the heated portion of the plate only, which has the length $(L - \xi)$. To determine the total rate of heat transfer from the plate, the averaged value of h over the heated portion of the plate must be multiplied by the area of the heated section.

Uniform Heat Flux

When a flat plate is subjected to *uniform heat flux* instead of uniform temperature, the local Nusselt number is given by

$$\text{Laminar:} \quad \text{Nu}_x = 0.453 \, \text{Re}_x^{0.5} \, \text{Pr}^{1/3} \qquad \text{Pr} > 0.6, \qquad \text{Re}_x < 5 \times 10^5 \tag{7–31}$$

$$\text{Turbulent:} \quad \text{Nu}_x = 0.0308 \, \text{Re}_x^{0.8} \, \text{Pr}^{1/3} \quad 0.6 \le \text{Pr} \le 60, \quad 5 \times 10^5 \le \text{Re}_x \le 10^7 \tag{7–32}$$

These relations give values that are 36 percent higher for laminar flow and 4 percent higher for turbulent flow relative to the isothermal plate case. When the plate involves an unheated starting length, the relations developed for the uniform surface temperature case can still be used provided that Eqs. 7–31 and 7–32 are used for $\text{Nu}_{x(\text{for } \xi=0)}$ in Eqs. 7–27 and 7–28, respectively. To obtain the *average* Nusselt number for a flat plate subjected to *uniform heat flux*, it is sufficiently accurate to use the average Nusselt number equations developed for the case of isothermal surfaces for laminar flow (Eq. 7–21) and turbulent flow (Eq. 7–22).

When heat flux $\dot{q}_s$ is prescribed, the rate of heat transfer to or from the plate and the surface temperature at a distance x are determined from

$$\dot{Q} = \dot{q}_s A_s \tag{7–33}$$

and

$$\dot{q}_s = h_x[T_s(x) - T_\infty] \rightarrow T_s(x) = T_\infty + \frac{\dot{q}_s}{h_x} \tag{7–34}$$

where A_s is the heat transfer surface area.

General Solutions for Simultaneously Moving Plates and Fluids

The results presented so far in this chapter primarily correspond to the case of fluid passing over a stationary plate. However, in some circumstances, both the plate and the fluid are in motion. For example, in the thermal processing of sheetlike material such as paper, linoleum, polymeric sheets, roofing shingles, insulating materials, and fine-fiber matts, the sheet moves parallel to its own plane. The moving sheet may induce motion in the neighboring fluid or, alternatively, the fluid may have an independent forced convection motion that is parallel to that of the sheet. The generalized solutions for this scenario are available by correlations developed in Sparrow and Abraham (2005).

EXAMPLE 7–1   Flow of Hot Oil Over a Flat Plate

Engine oil at 60°C flows over the upper surface of a 5-m-long flat plate whose temperature is 20°C with a velocity of 2 m/s (Fig. 7–13). Determine the total drag force and the rate of heat transfer per unit width of the entire plate.

SOLUTION   Engine oil flows over a flat plate. The total drag force and the rate of heat transfer per unit width of the plate are to be determined.

Assumptions   **1** The flow is steady and incompressible. **2** The critical Reynolds number is $Re_{cr} = 5 \times 10^5$.

Properties   The properties of engine oil at the film temperature of $T_f = (T_s + T_\infty)/2 = (20 + 60)/2 = 40°C$ are (Table A–13)

$$\rho = 876 \text{ kg/m}^3 \qquad Pr = 2962$$
$$k = 0.1444 \text{ W/m·K} \qquad \nu = 2.485 \times 10^{-4} \text{ m}^2/\text{s}$$

Analysis   Noting that $L = 5$ m, the Reynolds number at the end of the plate is

$$Re_L = \frac{VL}{\nu} = \frac{(2 \text{ m/s})(5 \text{ m})}{2.485 \times 10^{-4} \text{ m}^2/\text{s}} = 4.024 \times 10^4$$

which is less than the critical Reynolds number. Thus we have *laminar flow* over the entire plate, and the average friction coefficient is

$$C_f = 1.33 \, Re_L^{-0.5} = 1.33 \times (4.024 \times 10^4)^{-0.5} = 0.00663$$

Noting that the pressure drag is zero and thus $C_D = C_f$ for parallel flow over a flat plate, the drag force acting on the plate per unit width becomes

$$F_D = C_f A \frac{\rho V^2}{2} = 0.00663(5 \times 1 \text{ m}^2) \frac{(876 \text{ kg/m}^3)(2 \text{ m/s})^2}{2} \left(\frac{1 \text{ N}}{1 \text{ kg·m/s}^2}\right) = \textbf{58.1 N}$$

The total drag force acting on the entire plate can be determined by multiplying the value obtained above by the width of the plate.

This force per unit width corresponds to the weight of a mass of about 6 kg. Therefore, a person who applies an equal and opposite force to the plate to keep it from moving will feel like he or she is using as much force as is necessary to hold a 6-kg mass from dropping.

Similarly, the Nusselt number is determined using the laminar flow relations for a flat plate,

$$Nu = \frac{hL}{k} = 0.664 \, Re_L^{0.5} Pr^{1/3} = 0.664 \times (4.024 \times 10^4)^{0.5} \times 2962^{1/3} = 1913$$

Then,

$$h = \frac{k}{L}Nu = \frac{0.144 \text{ W/m·K}}{5 \text{ m}}(1913) = 55.25 \text{ W/m}^2\text{·K}$$

and

$$\dot{Q} = hA_s(T_\infty - T_s) = (55.25 \text{ W/m}^2\text{·K})(5 \times 1 \text{ m}^2)(60 - 20)°C = \textbf{11,050 W}$$

Discussion   Note that heat transfer is always from the higher-temperature medium to the lower-temperature one. In this case, it is from the oil to the plate. The heat transfer rate is per meter width of the plate. The heat transfer for the entire plate can be obtained by multiplying the value obtained by the actual width of the plate.

$T_\infty = 60°C$
$V = 2$ m/s
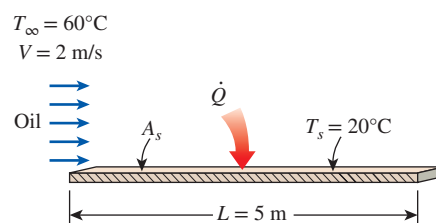
FIGURE 7–13
Schematic for Example 7–1.
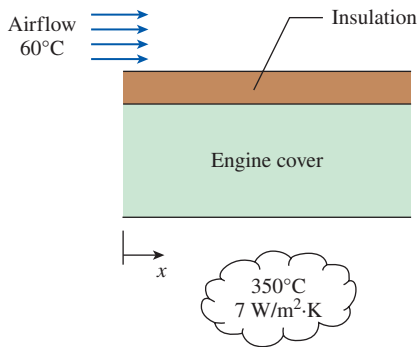
FIGURE 7–14
Schematic for Example 7–2.

Airflow 60°C — Insulation — Engine cover — x — 350°C 7 W/m²·K

PtD **EXAMPLE 7–2**   **Prevention of Fire Hazard in the Event of Oil Leakage**

Heat dissipated from an engine in operation can cause hot spots on its surface. If the outer surface of an engine is situated in a place where oil leakage is possible, then when leaked oil comes in contact with hot spots above the oil's autoignition temperature, it can ignite spontaneously. Consider an engine cover that is made of a stainless steel plate with a thickness of 1 cm and a thermal conductivity of 14 W/m·K. The stainless steel plate is covered with a 5-mm-thick insulation ($k = 0.5$ W/m·K). The inner surface of the engine cover is exposed to hot air at 350°C with a convection heat transfer coefficient of 7 W/m²·K (Fig. 7–14). The 2-m-long engine outer surface is cooled by air blowing in parallel over it at 7 m/s in an environment where the ambient air is at 60°C. To prevent fire hazard in the event of oil leak on the engine cover, the engine cover surface should be kept below 180°C. It has been determined that the 5-mm-thick insulation layer is not sufficient to keep the engine cover surface below 180°C. To solve this problem, one of the plant supervisors suggested adjusting the blower capacity to provide an increase in the cooling air velocity by 10 percent. Determine if this is a viable method for keeping the engine cover surface below 180°C. Evaluate the air properties at 120°C.

SOLUTION   In this example, the concepts of prevention through design (PtD) are applied in conjunction with external forced convection and thermal resistance analysis. An engine cover with a layer of insulation is subjected to convection heat transfer on the inner and outer surfaces. To prevent a fire hazard by keeping the engine outer surface temperature below 180°C, it is suggested to increase the cooling air velocity by 10 percent. The effectiveness of this method is to be evaluated.

Assumptions   **1** The thermal properties of the plate and insulation are constant. **2** One-dimensional heat conduction through the plate. **3** Uniform plate surface temperature. **4** Thermal contact resistance at interface is negligible. **5** Radiation effects are negligible. **6** Local atmospheric pressure is 1 atm. **7** The critical Reynolds number is $\text{Re}_{cr} = 5 \times 10^5$.

Properties   The thermal conductivities of the stainless steel and the insulation are given to be $k_{ss} = 14$ W/m·K and $k_{ins} = 0.5$ W/m·K, respectively. The properties of air are evaluated at $T_f = 120°C$: $k = 0.03235$ W/m·K, $\nu = 2.522 \times 10^{-5}$ m²/s, and $\text{Pr} = 0.7073$ (from Table A–15).

Analysis   When the cooling air velocity is increased by 10 percent (7.7 m/s), the Reynolds number for the 2-m-long plate is

$$\text{Re}_L = \frac{VL}{\nu} = \frac{(7.7 \text{ m/s})(2 \text{ m})}{2.522 \times 10^{-5} \text{ m}^2/\text{s}} = 610{,}626 > 5 \times 10^5$$

With the Reynolds number between $5 \times 10^5 < \text{Re}_L < 10^7$, the proper equation is the combined laminar and turbulent relation for the Nusselt number:

$$\text{Nu} = \frac{hL}{k} = (0.037 \text{Re}_L^{0.8} - 871)\text{Pr}^{1/3}$$
$$= [0.037(610{,}626)^{0.8} - 871](0.7073)^{1/3}$$
$$= 625.77$$

The convection heat transfer coefficient on the engine outer surface is

$$h = \text{Nu}\frac{k}{L} = 625.77\left(\frac{0.03235 \text{ W/m·K}}{2 \text{ m}}\right) = 10.122 \text{ W/m}^2\text{·K}$$

From Chap. 3, the thermal resistances of different layers are

$R_{\text{conv}, i} = \dfrac{1}{h_i A}$ (inside surface convection resistance),

$R_{ss} = \dfrac{L_{ss}}{k_{ss} A}$ (stainless steel layer resistance),

$R_{\text{ins}} = \dfrac{L_{\text{ins}}}{k_{\text{ins}} A}$ (insulation layer resistance),

$R_{\text{conv}, o} = \dfrac{1}{h_o A}$ (outside surface convection resistance)

Then,

$$A R_{\text{total}} = A(R_{\text{conv}, i} + R_{ss} + R_{\text{ins}} + R_{\text{conv}, o}) = \frac{1}{h_i} + \frac{L_{ss}}{k_{ss}} + \frac{L_{\text{ins}}}{k_{\text{ins}}} + \frac{1}{h_o}$$

$$= \frac{1}{7 \text{ W/m}^2\cdot\text{K}} + \frac{0.01 \text{ m}}{14 \text{ W/m}\cdot\text{K}} + \frac{0.005 \text{ m}}{0.5 \text{ W/m}\cdot\text{K}} + \frac{1}{10.122 \text{ W/m}^2\cdot\text{K}}$$

$$= 0.25237 \text{ m}^2\cdot\text{K/W}$$

and

$$AR_{\text{conv}, o} = \frac{1}{h_o} = \frac{1}{10.122 \text{ W/m}^2\cdot\text{K}} = 0.09879 \text{ m}^2\cdot\text{K/W}$$

The heat flux through the layers is

$$\dot{q} = \frac{\dot{Q}}{A} = \frac{T_{\infty, i} - T_{\infty, o}}{AR_{\text{total}}} = \frac{T_{s, o} - T_{\infty, o}}{AR_{\text{conv}, o}} \rightarrow T_{s, o} = \frac{R_{\text{conv}, o}}{R_{\text{total}}}(T_{\infty, i} - T_{\infty, o}) + T_{\infty, o}$$

The outer surface temperature is

$$T_{s, o} = \frac{0.09879 \text{ m}^2\cdot\text{K/W}}{0.25237 \text{ m}^2\cdot\text{K/W}}(350 - 60)°\text{C} + 60°\text{C} = \textbf{173.5°C}$$

Yes, the suggested method is a viable method.

Discussion Increasing the cooling air velocity from 7 m/s to 7.7 m/s (by only 10 percent), kept the engine outer surface temperature below the fire hazard limit of 180°C. Another method that could be explored would be to increase the insulation thickness.

EXAMPLE 7–3   Cooling of Plastic Sheets by Forced Air

The forming section of a plastics plant puts out a continuous sheet of plastic that is 4 ft wide and 0.04 in thick at a velocity of 30 ft/min. The temperature of the plastic sheet is 200°F when it is exposed to the surrounding air, and a 2-ft-long section of the plastic sheet is subjected to airflow at 80°F at a velocity of 10 ft/s on both sides along its surfaces normal to the direction of motion of the sheet, as shown in Fig. 7–15. Determine (*a*) the rate of heat transfer from the plastic sheet to air by forced convection and radiation and (*b*) the temperature of the plastic sheet at the end of the cooling section. Take the density, specific heat, and emissivity of the plastic sheet to be $\rho = 75$ lbm/ft^3, $c_p = 0.4$ Btu/lbm·°F, and $\varepsilon = 0.9$.

SOLUTION Plastic sheets are cooled as they leave the forming section of a plastics plant. The rate of heat loss from the plastic sheet by convection and radiation and the exit temperature of the plastic sheet are to be determined.
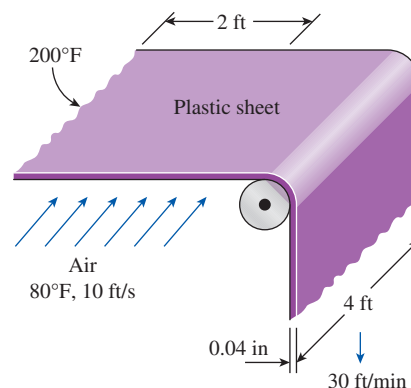
FIGURE 7–15
Schematic for Example 7–3.

Assumptions **1** Steady operating conditions exist. **2** The critical Reynolds number is $Re_{cr} = 5 \times 10^5$. **3** Air is an ideal gas. **4** The local atmospheric pressure is 1 atm. **5** The surrounding surfaces are at the temperature of the room air.

Properties The properties of the plastic sheet are given in the problem statement. The properties of air at the film temperature of $T_f = (T_s + T_\infty)/2 = (200 + 80)/2 = 140°F$ and 1 atm pressure are (Table A–15E)

$$k = 0.01623 \text{ Btu/h·ft·°F} \qquad Pr = 0.7202$$
$$\nu = 0.204 \times 10^{-3} \text{ ft}^2/\text{s}$$

Analysis (*a*) We expect the temperature of the plastic sheet to drop somewhat as it flows through the 2-ft-long cooling section, but at this point we do not know the magnitude of that drop. Therefore, we assume the plastic sheet to be isothermal at 200°F to get started. We will repeat the calculations if necessary to account for the temperature drop of the plastic sheet.

Noting that $L = 4$ ft, the Reynolds number at the end of the airflow across the plastic sheet is

$$\text{Re}_L = \frac{VL}{\nu} = \frac{(10 \text{ ft/s})(4 \text{ ft})}{0.204 \times 10^{-3} \text{ ft}^2/\text{s}} = 1.961 \times 10^5$$

which is less than the critical Reynolds number. Thus, we have *laminar flow* over the entire sheet, and the Nusselt number is determined from the laminar flow relations for a flat plate to be

$$\text{Nu} = \frac{hL}{k} = 0.664 \, \text{Re}_L^{0.5} \, Pr^{1/3} = 0.664 \times (1.961 \times 10^5)^{0.5} \times (0.7202)^{1/3} = 263.6$$

Then,

$$h = \frac{k}{L}\text{Nu} = \frac{0.01623 \text{ Btu/h·ft·°F}}{4 \text{ ft}}(263.6) = 1.07 \text{ Btu/h·ft}^2\text{·°F}$$

$$A_s = (2 \text{ ft})(4 \text{ ft})(2 \text{ sides}) = 16 \text{ ft}^2$$

and

$$\begin{aligned}
\dot{Q}_{\text{conv}} &= hA_s(T_s - T_\infty) \\
&= (1.07 \text{ Btu/h·ft}^2\text{·°F})(16 \text{ ft}^2)(200 - 80)°F \\
&= 2054 \text{ Btu/h} \\
\dot{Q}_{\text{rad}} &= \varepsilon\sigma A_s(T_s^4 - T_{\text{surr}}^4) \\
&= (0.9)(0.1714 \times 10^{-8} \text{ Btu/h·ft}^2\text{·R}^4)(16 \text{ ft}^2)[(660 \text{ R})^4 - (540 \text{ R})^4] \\
&= 2585 \text{ Btu/h}
\end{aligned}$$

Therefore, the rate of cooling of the plastic sheet by combined convection and radiation is

$$\dot{Q}_{\text{total}} = \dot{Q}_{\text{conv}} + \dot{Q}_{\text{rad}} = 2054 + 2585 = \textbf{4639 Btu/h}$$

(*b*) To find the temperature of the plastic sheet at the end of the cooling section, we need to know the mass of the plastic rolling out per unit time (or the mass flow rate), which is determined from

$$\dot{m} = \rho A_c V_{\text{plastic}} = (75 \text{ lbm/ft}^3)\left(\frac{4 \times 0.04}{12}\text{ft}^2\right)\left(\frac{30}{60}\text{ft/s}\right) = 0.5 \text{ lbm/s}$$

Then, an energy balance on the cooled section of the plastic sheet yields

$$\dot{Q} = \dot{m}c_p(T_2 - T_1) \rightarrow T_2 = T_1 + \frac{\dot{Q}}{\dot{m}c_p}$$

Noting that $\dot{Q}$ is a negative quantity (heat loss) for the plastic sheet and substituting, the temperature of the plastic sheet as it leaves the cooling section is determined to be

$$T_2 = 200°F + \frac{-4639 \text{ Btu/h}}{(0.5 \text{ lbm/s})(0.4 \text{ Btu/lbm·°F})}\left(\frac{1 \text{ h}}{3600 \text{ s}}\right) = \mathbf{193.6°F}$$

Discussion The average temperature of the plastic sheet drops by about 6.4°F as it passes through the cooling section. The calculations now can be repeated by taking the average temperature of the plastic sheet to be 196.8°F instead of 200°F for better accuracy, but the change in the results will be insignificant because of the small change in temperature.

EXAMPLE 7–4 **Heat Transfer from a Flat Plate with Unheated Starting Length**

An airstream at 1 atm flows, with a velocity of 4 m/s, in parallel over a 2-m-long flat plate where there is an unheated starting length of 0.5 m. The airstream has a temperature of 20°C, and the heated section of the flat plate is maintained at a constant temperature of 80°C. Determine (*a*) the average Nusselt number and convection heat transfer coefficient for the heated section and (b) the rate of heat transfer per unit width for the heated section.

SOLUTION An airstream flows in parallel over a flat plate where there is an unheated starting length. The average Nusselt number, the average convection heat transfer coefficient, and the rate of heat transfer per unit width for the heated section are to be determined.

Assumptions **1** Steady operating conditions exist. **2** Surface temperature is uniform throughout the heated section. **3** Thermal properties are constant. **4** The critical Reynolds number is $Re_{cr} = 5 \times 10^5$.

Properties The properties of air at the film temperature of $T_f = (T_s + T_\infty)/2 = (80 + 20)/2 = 50°C$ and 1 atm pressure are (Table A–15E)

$$k = 0.02735 \text{ W/m·K} \qquad Pr = 0.7228 \qquad \nu = 1.798 \times 10^{-5} \text{ m}^2/\text{s}$$

Analysis (*a*) The Reynolds number at $L = 2$ m is

$$Re_L = \frac{VL}{\nu} = \frac{(4 \text{ m/s})(2 \text{ m})}{1.798 \times 10^{-5} \text{ m}^2/\text{s}} = 4.449 \times 10^5$$

Since $Re_L < 5 \times 10^5$, the flow over the entire plate is laminar. Using the proper relation for Nusselt number, the average Nusselt number over the heated section can be determined:

$$Nu = Nu_{(\text{for } \xi=0)}\frac{L}{L - \xi}[1 - (\xi/L)^{3/4}]^{2/3}$$

where

$$Nu_{(\text{for } \xi=0)} = 0.664 \text{ Re}_L^{0.5} \text{ Pr}^{1/3} = 0.664(4.449 \times 10^5)^{0.5}(0.7228)^{1/3} = 397.5$$

then

$$Nu = (397.5)\frac{2 \text{ m}}{2 \text{ m} - 0.5 \text{ m}}[1 - (0.5 \text{ m}/2 \text{ m})^{3/4}]^{2/3} = \mathbf{396.2}$$

The average convection heat transfer coefficient over the heated section is

$$h = Nu\frac{k}{L} = 396.2\left(\frac{0.02735 \text{ W/m·K}}{2 \text{ m}}\right) = \mathbf{5.42 \text{ W/m}^2\text{·K}}$$

(*b*) The rate of heat transfer per unit width (*w*) for the heated section is

$$\dot{Q} = hA(T_s - T_\infty) = h(L - \xi)w(T_s - T_\infty)$$

$$\dot{Q}/w = (5.42 \text{ W/m}^2\cdot\text{K})(2 \text{ m} - 0.5 \text{ m})(80 - 20)\text{K} = \textbf{487.8 W/m}$$

Discussion   The heat transfer in this case is from the surface to the airsteam (from the higher temperature to the lower temperature). Once the actual width of the plate is known, the heat transfer for the entire plate can be determined. For the plate with unheated starting length, the thermal boundary layer does not begin to grow until the heated section, while the velocity boundary layer begins at the leading edge.

7–3 ▪ FLOW ACROSS CYLINDERS AND SPHERES

Flow across cylinders and spheres is frequently encountered in practice. For example, the tubes in a shell-and-tube heat exchanger involve both *internal flow* through the tubes and *external flow* over the tubes, and both flows must be considered in the analysis of the heat exchanger. Also, many sports such as soccer, tennis, and golf involve flow over spherical balls.

The characteristic length for a circular cylinder or sphere is taken to be the *external diameter D*. Thus, the Reynolds number is defined as $\text{Re} = \text{Re}_D = VD/\nu$ where *V* is the uniform velocity of the fluid as it approaches the cylinder or sphere. The critical Reynolds number for flow across a circular cylinder or sphere is about $\text{Re}_{cr} \cong 2 \times 10^5$. That is, the boundary layer remains laminar for about $\text{Re} \lesssim 2 \times 10^5$ and becomes turbulent for $\text{Re} \gtrsim 2 \times 10^5$.

Crossflow over a cylinder exhibits complex flow patterns, as shown in Fig. 7–16. The fluid approaching the cylinder branches out and encircles the cylinder, forming a boundary layer that wraps around the cylinder. The fluid particles on the midplane strike the cylinder at the stagnation point, bringing the fluid to a complete stop and thus raising the pressure at that point. The pressure decreases in the flow direction while the fluid velocity increases.

At very low upstream velocities ($\text{Re} \lesssim 1$), the fluid completely wraps around the cylinder, and the two arms of the fluid meet on the rear side of the cylinder in an orderly manner. Thus, the fluid follows the curvature of the cylinder. At higher velocities, the fluid still hugs the cylinder on the frontal side, but it is too fast to remain attached to the surface as it approaches the top (or bottom) of the cylinder. As a result, the boundary layer detaches from the surface, forming a separation region behind the cylinder. Flow in the wake region is characterized by periodic vortex formation and pressures much lower than the stagnation point pressure.
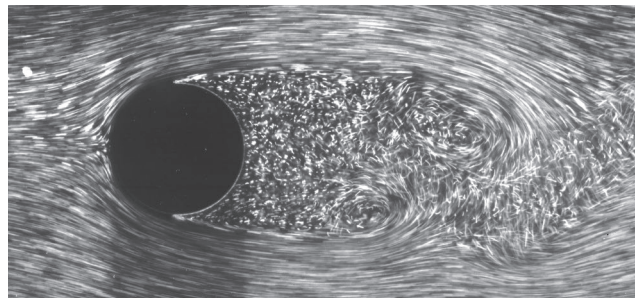
FIGURE 7–16
Laminar boundary layer separation with a turbulent wake; flow over a circular cylinder at Re = 2000.
©Henri Werlé—ONERA, the French Aerospace Lab

The nature of the flow across a cylinder or sphere strongly affects the total drag coefficient C_D. Both the *friction drag* and the *pressure drag* can be significant. The high pressure in the vicinity of the stagnation point and the low pressure on the opposite side in the wake produce a net force on the body in the direction of flow. The drag force is primarily due to friction drag at low Reynolds numbers (Re < 10) and to pressure drag at high Reynolds numbers (Re > 5000). Both effects are significant at intermediate Reynolds numbers.

From dimensional analysis it can be shown that the average drag coefficients C_D for a smooth single circular cylinder and a sphere is a function of Reynolds number, $C_D = f(\text{Re}_D)$, as shown in Fig. 7–17. The curves exhibit different behaviors in different ranges of Reynolds numbers:

- For Re $\lesssim$ 1, we have creeping flow, and the drag coefficient decreases with increasing Reynolds number. For a sphere, it is $C_D = 24/\text{Re}$. There is no flow separation in this regime.

- At about Re = 10, separation starts occurring on the rear of the body with vortex shedding starting at about Re $\cong$ 90. The region of separation increases with increasing Reynolds number up to about Re = 10^3. At this point, the drag is mostly (about 95 percent) due to pressure drag. The drag coefficient continues to decrease with increasing Reynolds number in this range of $10 < \text{Re} < 10^3$. (A decrease in the drag coefficient does not necessarily indicate a decrease in drag. The drag force is proportional to the square of the velocity, and the increase in velocity at higher Reynolds numbers usually more than offsets the decrease in the drag coefficient.)

- In the moderate range of $10^3 < \text{Re} < 10^5$, the drag coefficient remains relatively constant. This behavior is characteristic of blunt bodies. The flow in the boundary layer is laminar in this range, but the flow in the separated region past the cylinder or sphere is highly turbulent, with a wide, turbulent wake.

- There is a sudden drop in the drag coefficient somewhere in the range of $10^5 < \text{Re} < 10^6$ (usually, at about 2×10^5). This large reduction in C_D is due to the flow in the boundary layer becoming *turbulent,* which moves the separation point further toward the rear of the body, reducing the size
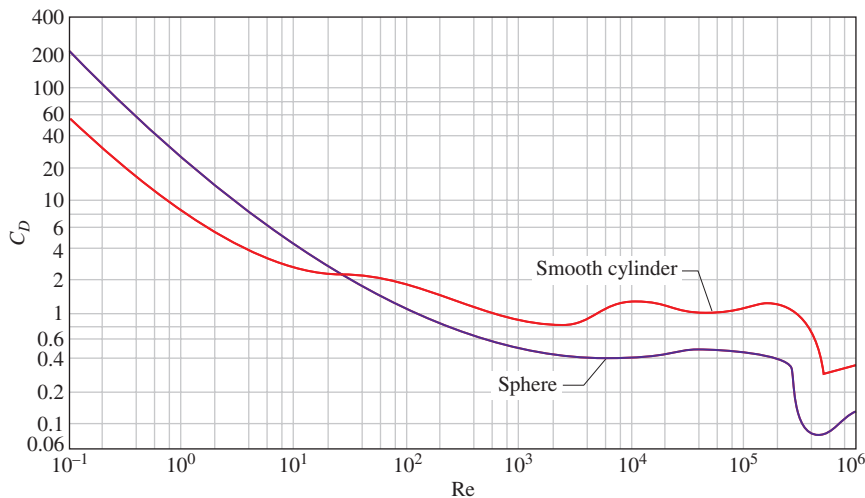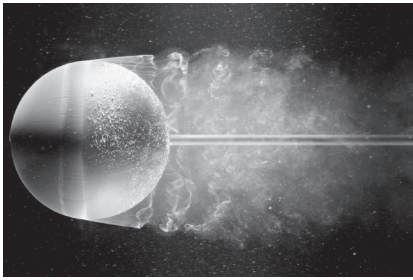
(a)
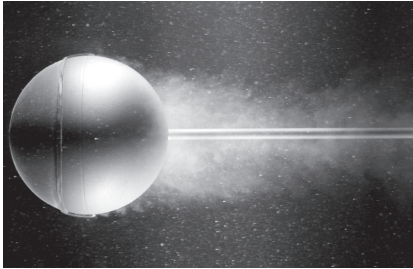
(b)

FIGURE 7–18

Flow visualization of flow over (a) a smooth sphere at Re = 15,000 and (b) a sphere at Re = 30,000 with a trip wire. The delay of boundary layer separation is clearly seen by comparing the two photographs.

©*Henri Werlé—ONERA, the French Aerospace Lab*

of the wake and thus the magnitude of the pressure drag. This is in contrast to streamlined bodies, which experience an increase in the drag coefficient (mostly due to friction drag) when the boundary layer becomes turbulent.

Flow separation occurs at about $\theta \cong 80°$ (measured from the front stagnation point of a cylinder) when the boundary layer is *laminar* and at about $\theta \cong 140°$ when it is *turbulent* (Fig. 7–18). The delay of separation in turbulent flow is caused by the rapid fluctuations of the fluid in the transverse direction, which enable the turbulent boundary layer to travel farther along the surface before separation occurs, resulting in a narrower wake and a smaller pressure drag. Keep in mind that turbulent flow has a fuller velocity profile than in the laminar case, and thus it requires a stronger adverse pressure gradient to overcome the additional momentum close to the wall. In the range of Reynolds numbers where the flow changes from laminar to turbulent, even the drag force F_D decreases as the velocity (and thus the Reynolds number) increases. This results in a sudden decrease in drag of a flying body (sometimes called the *drag crisis*) and instabilities in flight.

Effect of Surface Roughness

We mentioned earlier that *surface roughness,* in general, increases the drag coefficient in turbulent flow. This is especially the case for streamlined bodies. For blunt bodies such as a circular cylinder or sphere, however, an increase in the surface roughness may actually *decrease* the drag coefficient, as shown in Fig. 7–19 for a sphere. This is done by tripping the boundary layer into turbulence at a lower Reynolds number and thus causing the fluid to close in behind the body, narrowing the wake and reducing pressure drag considerably. This results in a much smaller drag coefficient and thus drag force for a rough-surfaced cylinder or sphere in a certain range of Reynolds number compared to a smooth one of identical size at the same velocity. At Re = 2×10^5, for example, $C_D \cong 0.1$ for a rough sphere with $\varepsilon/D = 0.0015$, whereas $C_D \cong 0.5$ for a smooth one. Therefore, the drag coefficient in this case is reduced by a factor of 5 by simply roughening the surface. Note, however, that
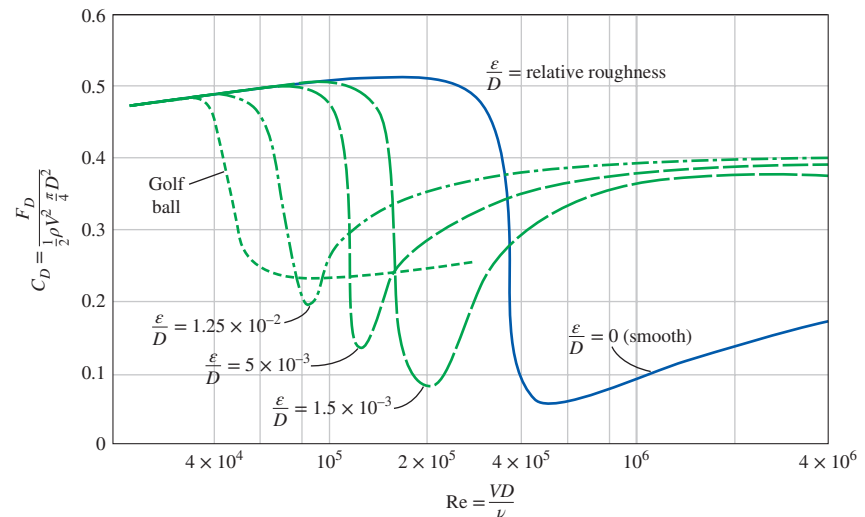
FIGURE 7–19

The effect of surface roughness on the drag coefficient of a sphere.

Source: Blevins, 1984.

at Re $= 10^6$, $C_D \cong 0.4$ for a very rough sphere while $C_D \cong 0.1$ for the smooth one. Obviously, roughening the sphere in this case will increase the drag by a factor of 4 (Fig. 7–20).

The preceding discussion shows that roughening the surface can be used to great advantage in reducing drag, but it can also backfire on us if we are not careful—specifically, if we do not operate in the right range of the Reynolds number. With this consideration, golf balls are intentionally roughened to induce *turbulence* at a lower Reynolds number to take advantage of the sharp *drop* in the drag coefficient at the onset of turbulence in the boundary layer (the typical velocity range of golf balls is 15 to 150 m/s, and the Reynolds number is less than 4×10^5). The critical Reynolds number of dimpled golf balls is about 4×10^4. The occurrence of turbulent flow at this Reynolds number reduces the drag coefficient of a golf ball by about half, as shown in Fig. 7–19. For a given hit, this means a longer distance for the ball. Experienced golfers also give the ball a spin during the hit, which helps the rough ball develop a lift and thus travel higher and farther. A similar argument can be given for a tennis ball. For a table tennis ball, however, the distances are very short, and the balls never reach the speeds in the turbulent range. Therefore, the surfaces of table tennis balls are made smooth.

Once the drag coefficient is available, the drag force acting on a body in crossflow can be determined from Eq. 7–1 where A is the *frontal area* ($A = LD$ for a cylinder of length L and $A = \pi D^2/4$ for a sphere). It should be kept in mind that free-stream turbulence and disturbances by other bodies in the flow (such as flow over tube bundles) may affect the drag coefficients significantly.

	C_D	
Re	Smooth Surface	Rough Surface, $\varepsilon/D = 0.0015$
2×10^5	0.5	0.1
10^6	0.1	0.4

FIGURE 7–20
Surface roughness may increase or decrease the drag coefficient of a spherical object, depending on the value of the Reynolds number.

■ **EXAMPLE 7–5** **Drag Force Acting on a Pipe in a River**

A 2.2-cm-outer-diameter pipe is to span a river at a 30-m-wide section while being completely immersed in water (Fig. 7–21). The average flow velocity of water is 4 m/s, and the water temperature is 15°C. Determine the drag force exerted on the pipe by the river.

SOLUTION A pipe is submerged in a river. The drag force that acts on the pipe is to be determined.
Assumptions **1** The outer surface of the pipe is smooth so that Fig. 7–17 can be used to determine the drag coefficient. **2** Water flow in the river is steady. **3** The direction of water flow is normal to the pipe. **4** Turbulence in river flow is not considered.
Properties The density and dynamic viscosity of water at 15°C are $\rho = 999.1$ kg/m³ and $\mu = 1.138 \times 10^{-3}$ kg/m·s (Table A–9).
Analysis Noting that $D = 0.022$ m, the Reynolds number is

$$\text{Re} = \frac{VD}{\nu} = \frac{\rho VD}{\mu} = \frac{(999.1 \text{ kg/m}^3)(4 \text{ m/s})(0.022 \text{ m})}{1.138 \times 10^{-3} \text{ kg/m·s}} = 7.73 \times 10^4$$

The drag coefficient corresponding to this value is, from Fig. 7–17, $C_D = 1.0$. Also, the frontal area for flow past a cylinder is $A = LD$. Then the drag force acting on the pipe becomes

$$F_D = C_D A \frac{\rho V^2}{2} = 1.0(30 \times 0.022 \text{ m}^2) \frac{(999.1 \text{ kg/m}^3)(4 \text{ m/s})^2}{2} \left(\frac{1 \text{ N}}{1 \text{ kg·m/s}^2} \right)$$

$$= 5275 \text{ N} \cong \textbf{5.30 kN}$$
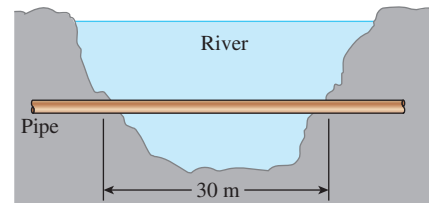
FIGURE 7–21
Schematic for Example 7–5.

> ***Discussion*** Note that this force is equivalent to the weight of a mass over 500 kg. Therefore, the drag force the river exerts on the pipe is equivalent to hanging a total of over 500 kg in mass on the pipe supported at its ends 30 m apart. The necessary precautions should be taken if the pipe cannot support this force. If the river were to flow at a faster speed or if turbulent fluctuations in the river were more significant, the drag force would be even larger. *Unsteady* forces on the pipe might then be significant.
>
> Reading C_D values from Fig. 7–17 for a smooth cylinder in crossflow could at times be difficult. Hooman and Dukhan (2013) proposed a simple correlation, $C_D = 1 + (6/\text{Re})$ for the Reynolds number range of $10^2 < \text{Re} < 10^5$.
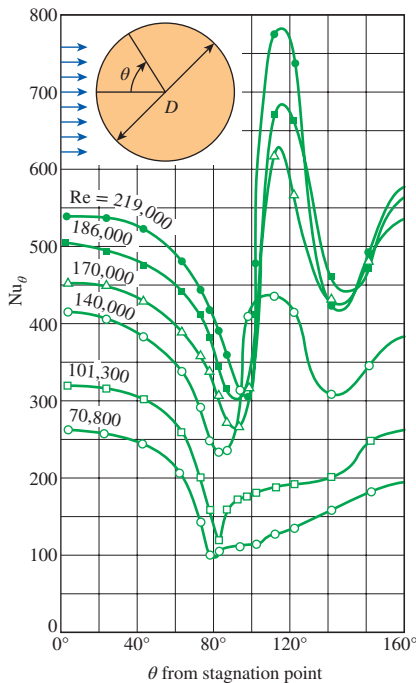
Heat Transfer Coefficient

Flows across cylinders and spheres, in general, involve *flow separation,* which is difficult to handle analytically. Therefore, such flows must be studied experimentally or numerically. Indeed, flow across cylinders and spheres has been studied experimentally by many investigators, and several empirical correlations have been developed for the heat transfer coefficient.

The complicated flow pattern across a cylinder greatly influences heat transfer. The variation of the local Nusselt number Nu_θ around the periphery of a cylinder subjected to crossflow of air is given in Fig. 7–22. Note that, for all cases, the value of Nu_θ starts out relatively high at the stagnation point ($\theta = 0°$) but decreases with increasing θ as a result of the thickening of the laminar boundary layer. On the two curves at the bottom corresponding to $\text{Re} = 70,800$ and 101,300, Nu_θ reaches a minimum at $\theta \approx 80°$, which is the separation point in laminar flow. Then Nu_θ increases with increasing θ as a result of the intense mixing in the separated flow region (the wake). The curves at the top corresponding to $\text{Re} = 140,000$ to 219,000 differ from the first two curves in that they have *two* minima for Nu_θ. The sharp increase in Nu_θ at about $\theta \approx 90°$ is due to the transition from laminar to turbulent flow. The later decrease in Nu_θ is again due to the thickening of the boundary layer. Nu_θ reaches its second minimum at about $\theta \approx 140°$, which is the flow separation point in turbulent flow, and increases with θ as a result of the intense mixing in the turbulent wake region.

The preceding discussions on the local heat transfer coefficients are insightful; however, they are of limited value in heat transfer calculations since the calculation of heat transfer requires the *average* heat transfer coefficient over the entire surface. Of the several such relations available in the literature for the average Nusselt number for crossflow over a cylinder, we present the one proposed by Churchill and Bernstein (1977):

$$\text{Nu}_{\text{cyl}} = \frac{hD}{k} = 0.3 + \frac{0.62\,\text{Re}^{1/2}\,\text{Pr}^{1/3}}{[1 + (0.4/\text{Pr})^{2/3}]^{1/4}}\left[1 + \left(\frac{\text{Re}}{282,000}\right)^{5/8}\right]^{4/5} \quad \textbf{(7–35)}$$

This relation is quite comprehensive in that it correlates available data well for $\text{RePr} > 0.2$. The fluid properties are evaluated at the *film temperature* $T_f = \frac{1}{2}(T_\infty + T_s)$, which is the average of the free-stream and surface temperatures.

For flow over a *sphere,* Whitaker (1972) recommends the following comprehensive correlation:

$$\text{Nu}_{\text{sph}} = \frac{hD}{k} = 2 + [0.4\,\text{Re}^{1/2} + 0.06\,\text{Re}^{2/3}]\text{Pr}^{0.4}\left(\frac{\mu_\infty}{\mu_s}\right)^{1/4} \quad \textbf{(7–36)}$$

which is valid for $3.5 \leq \text{Re} \leq 8 \times 10^4$, $0.7 \leq \text{Pr} \leq 380$ and $1.0 \leq (\mu_\infty/\mu_s) \leq 3.2$. The fluid properties in this case are evaluated at the free-stream temperature

FIGURE 7–22
Variation of the local heat transfer coefficient along the circumference of a circular cylinder in crossflow of air.
Source: Giedt, 1949.

T_∞, except for μ_s, which is evaluated at the surface temperature T_s. Although the two relations above are considered to be quite accurate, the results obtained from them can be off by as much as 30 percent.
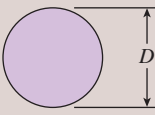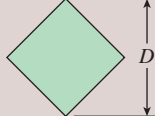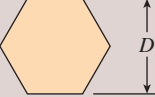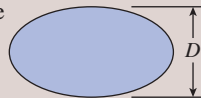
The average Nusselt number for flow across cylinders can be expressed compactly as

$$\mathrm{Nu}_{\mathrm{cyl}} = \frac{hD}{k} = C\,\mathrm{Re}^m\,\mathrm{Pr}^n \qquad \textbf{(7–37)}$$

where $n = \frac{1}{3}$ and the experimentally determined constants C and m are given in Table 7–1 for circular as well as various noncircular cylinders. The characteristic length D for use in the calculation of the Reynolds and the Nusselt numbers for different geometries is as indicated on the figure. All fluid properties are evaluated at the film temperature. Note that the values presented in Table 7–1 for noncircular geometries have been updated based on the recommendations of Sparrow et al. (2004). Correlations for square and chamfered cylinders for all possible directions of incoming fluid are available in Tong et al. (2016).

TABLE 7–1

Empirical correlations for the average Nusselt number for forced convection over circular and noncircular cylinders in crossflow

Cross-Section of the Cylinder	Fluid	Range of Re	Nusselt Number
Circle	Gas or liquid	0.4–4 4–40 40–4000 4000–40,000 40,000–400,000	$\mathrm{Nu} = 0.989\,\mathrm{Re}^{0.330}\,\mathrm{Pr}^{1/3}$ $\mathrm{Nu} = 0.911\,\mathrm{Re}^{0.385}\,\mathrm{Pr}^{1/3}$ $\mathrm{Nu} = 0.683\,\mathrm{Re}^{0.466}\,\mathrm{Pr}^{1/3}$ $\mathrm{Nu} = 0.193\,\mathrm{Re}^{0.618}\,\mathrm{Pr}^{1/3}$ $\mathrm{Nu} = 0.027\,\mathrm{Re}^{0.805}\,\mathrm{Pr}^{1/3}$
Square	Gas	3900–79,000 32,000–1,600,000	$\mathrm{Nu} = 0.094\,\mathrm{Re}^{0.675}\,\mathrm{Pr}^{1/3}$ $\mathrm{Nu} = 0.0249\,\mathrm{Re}^{0.811}\,\mathrm{Pr}^{1/3}$
Square (tilted 45°)	Gas	5600–111,000 46,000–2,300,000	$\mathrm{Nu} = 0.258\,\mathrm{Re}^{0.588}\,\mathrm{Pr}^{1/3}$ $\mathrm{Nu} = 0.0260\,\mathrm{Re}^{0.839}\,\mathrm{Pr}^{1/3}$
Hexagon	Gas	4500–90,700	$\mathrm{Nu} = 0.148\,\mathrm{Re}^{0.638}\,\mathrm{Pr}^{1/3}$
Hexagon (tilted 45°)	Gas	5200–20,400 20,400–105,000	$\mathrm{Nu} = 0.162\,\mathrm{Re}^{0.638}\,\mathrm{Pr}^{1/3}$ $\mathrm{Nu} = 0.039\,\mathrm{Re}^{0.782}\,\mathrm{Pr}^{1/3}$
Vertical plate	Gas	6300–23,600	$\mathrm{Nu} = 0.257\,\mathrm{Re}^{0.731}\,\mathrm{Pr}^{1/3}$
Ellipse	Gas	1400–8200	$\mathrm{Nu} = 0.197\,\mathrm{Re}^{0.612}\,\mathrm{Pr}^{1/3}$

Source: Zukauskas, 1972, Jakob 1949, Sparrow et al., 2004, and Tong et al., 2016.

The relations for cylinders presented here are for *single* cylinders or cylinders oriented such that the flow over them is not affected by the presence of others. Also, they are applicable to *smooth* surfaces. *Surface roughness* and the *free-stream turbulence* may affect the drag and heat transfer coefficients significantly. Eq. 7–37 provides a simpler alternative to Eq. 7–35 for flow over cylinders. However, Eq. 7–35 is more accurate, and thus it should be preferred in calculations whenever possible.

FIGURE 7–23
Schematic for Example 7–6.

EXAMPLE 7–6   **Heat Loss from a Steam Pipe in Windy Air**

A long 10-cm-diameter steam pipe whose external surface temperature is 110°C passes through some open area that is not protected against the winds (Fig. 7–23). Determine the rate of heat loss from the pipe per unit of its length when the air is at 1 atm pressure and 10°C and the wind is blowing across the pipe at a velocity of 8 m/s.

SOLUTION A steam pipe is exposed to windy air. The rate of heat loss from the steam is to be determined.

Assumptions **1** Steady operating conditions exist. **2** Radiation effects are negligible. **3** Air is an ideal gas.

Properties The properties of air at the average film temperature of $T_f = (T_s + T_\infty)/2 = (110 + 10)/2 = 60°C$ and 1 atm pressure are (Table A–15)

$$k = 0.02808 \text{ W/m·K} \qquad \text{Pr} = 0.7202 \qquad \nu = 1.896 \times 10^{-5} \text{ m}^2/\text{s}$$

Analysis The Reynolds number is

$$\text{Re} = \frac{VD}{\nu} = \frac{(8 \text{ m/s})(0.1 \text{ m})}{1.896 \times 10^{-5} \text{ m}^2/\text{s}} = 4.219 \times 10^4$$

The Nusselt number can be determined from

$$\text{Nu} = \frac{hD}{k} = 0.3 + \frac{0.62 \, \text{Re}^{1/2} \, \text{Pr}^{1/3}}{[1 + (0.4/\text{Pr})^{2/3}]^{1/4}} \left[1 + \left(\frac{\text{Re}}{282,000} \right)^{5/8} \right]^{4/5}$$

$$= 0.3 + \frac{0.62(4.219 \times 10^4)^{1/2}(0.7202)^{1/3}}{[1 + (0.4/0.7202)^{2/3}]^{1/4}} \left[1 + \left(\frac{4.219 \times 10^4}{282,000} \right)^{5/8} \right]^{4/5}$$

$$= 124$$

and

$$h = \frac{k}{D}\text{Nu} = \frac{0.02808 \text{ W/m·K}}{0.1 \text{ m}}(124) = 34.8 \text{ W/m}^2\text{·K}$$

Then, the rate of heat transfer from the pipe per unit of its length becomes

$$A_s = pL = \pi DL = \pi(0.1 \text{ m})(1 \text{ m}) = 0.314 \text{ m}^2$$

$$\dot{Q} = hA_s(T_s - T_\infty) = (34.8 \text{ W/m}^2\text{·K})(0.314 \text{ m}^2)(110 - 10)°C = \textbf{1093 W}$$

The rate of heat loss from the entire pipe can be obtained by multiplying the value above by the length of the pipe in m.

Discussion The simpler Nusselt number relation in Table 7–1 in this case would give Nu = 128, which is 3 percent higher than the value obtained above using Eq. 7–35.

Air

$T_\infty = 25°C$
$V = 3$ m/s

Steel
ball
300°C

FIGURE 7–24
Schematic for Example 7–7.

EXAMPLE 7–7   Cooling of a Steel Ball by Forced Air

A 25-cm-diameter stainless steel ball ($\rho = 8055$ kg/m^3, $c_p = 480$ J/kg·K) is removed from the oven at a uniform temperature of 300°C (Fig. 7–24). The ball is then subjected to the flow of air at 1 atm pressure and 25°C with a velocity of 3 m/s. The surface temperature of the ball eventually drops to 200°C. Determine the average convection heat transfer coefficient during this cooling process, and estimate how long the process will take.

SOLUTION A hot stainless steel ball is cooled by forced air. The average convection heat transfer coefficient and the cooling time are to be determined.

Assumptions **1** Steady operating conditions exist. **2** Radiation effects are negligible. **3** Air is an ideal gas. **4** The outer surface temperature of the ball is uniform at all times. **5** The surface temperature of the ball during cooling is changing. Therefore, the convection heat transfer coefficient between the ball and the air will also change. To avoid this complexity, we take the surface temperature of the ball to be constant at the average temperature of $(300 + 200)/2 = 250°C$ in the evaluation of the heat transfer coefficient and use the value obtained for the entire cooling process.

Properties The dynamic viscosity of air at the average surface temperature is $\mu_s = \mu_{@ 250°C} = 2.76 \times 10^{-5}$ kg/m·s. The properties of air at the free-stream temperature of 25°C and 1 atm are (Table A–15)

$$k = 0.02551 \text{ W/m·K} \qquad \nu = 1.562 \times 10^{-5} \text{ m}^2\text{/s}$$
$$\mu = 1.849 \times 10^{-5} \text{ kg/m·s} \qquad \text{Pr} = 0.7296$$

Analysis The Reynolds number is determined from

$$\text{Re} = \frac{VD}{\nu} = \frac{(3 \text{ m/s}) (0.25 \text{ m})}{1.562 \times 10^{-5} \text{ m}^2\text{/s}} = 4.802 \times 10^4$$

The Nusselt number is

$$\text{Nu} = \frac{hD}{k} = 2 + [0.4 \text{ Re}^{1/2} + 0.06 \text{ Re}^{2/3}] \text{ Pr}^{0.4} \left(\frac{\mu_\infty}{\mu_s}\right)^{1/4}$$
$$= 2 + [0.4 (4.802 \times 10^4)^{1/2} + 0.06 (4.802 \times 10^4)^{2/3}](0.7296)^{0.4}$$
$$\times \left(\frac{1.849 \times 10^{-5}}{2.76 \times 10^{-5}}\right)^{1/4}$$
$$= 135$$

Then the average convection heat transfer coefficient becomes

$$h = \frac{k}{D}\text{Nu} = \frac{0.02551 \text{ W/m·K}}{0.25 \text{ m}}(135) = \textbf{13.8 W/m}^2\textbf{·K}$$

In order to estimate the time of cooling of the ball from 300°C to 200°C, we determine the *average* rate of heat transfer from Newton's law of cooling by using the *average* surface temperature. That is,

$$A_s = \pi D^2 = \pi(0.25 \text{ m})^2 = 0.1963 \text{ m}^2$$

$$\dot{Q}_{avg} = hA_s(T_{s, avg} - T_\infty) = (13.8 \text{ W/m}^2\text{·K})(0.1963 \text{ m}^2)(250 - 25)°C = 610 \text{ W}$$
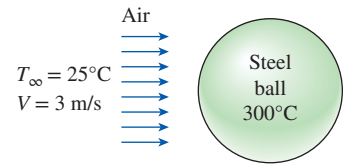
Next we determine the *total* heat transferred from the ball, which is simply the change in the energy of the ball as it cools from 300°C to 200°C:

$$m = \rho V = \rho \tfrac{1}{6}\pi D^3 = (8055 \text{ kg/m}^3) \tfrac{1}{6}\pi(0.25 \text{ m})^3 = 65.9 \text{ kg}$$

$$Q_{\text{total}} = mc_p(T_2 - T_1) = (65.9 \text{ kg})(480 \text{ J/kg·K})(300 - 200)°C = 3,163,000 \text{ J}$$

In this calculation, we assumed that the entire ball is at 200°C, which is not necessarily true. The inner region of the ball will probably be at a higher temperature than its surface. With this assumption, the time of cooling is determined to be

$$\Delta t \approx \frac{Q}{\dot{Q}_{\text{avg}}} = \frac{3,163,000 \text{ J}}{610 \text{ J/s}} = 5185 \text{ s} = \textbf{1 h 26 min}$$

Discussion The time of cooling could also be determined more accurately using the relations introduced in Chap. 4. But the simplifying assumptions we made above can be justified if all we need is a ballpark value. It will be naive to expect the time of cooling to be exactly 1 h 26 min, but, using our engineering judgment, it is realistic to expect the time of cooling to be somewhere between one and two hours.
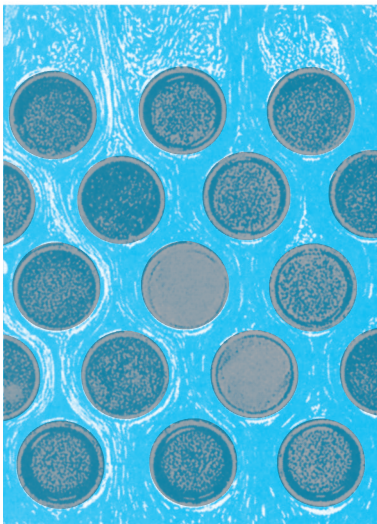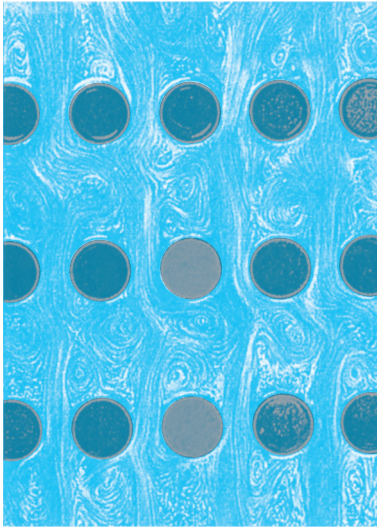
7−4 ▪ FLOW ACROSS TUBE BANKS

Crossflow over tube banks is commonly encountered in practice in heat transfer equipment such as the condensers and evaporators of power plants, refrigerators, and air conditioners. In such equipment, one fluid moves through the tubes while the other moves over the tubes in a perpendicular direction.

In a heat exchanger that involves a tube bank, the tubes are usually placed in a *shell* (and thus the name *shell-and-tube heat exchanger*), especially when the fluid is a liquid, and the fluid flows through the space between the tubes and the shell. There are many types of shell-and-tube heat exchangers, some of which are considered in Chap. 11. In this section we consider the general aspects of flow over a tube bank, and we try to develop a better and more intuitive understanding of the performance of heat exchangers that involve a tube bank.

Flow *through* the tubes can be analyzed by considering flow through a single tube and multiplying the results by the number of tubes. This is not the case for flow *over* the tubes, however, since the tubes affect the flow pattern and turbulence level downstream, and thus heat transfer to or from them, as shown in Fig. 7–25. Therefore, when analyzing heat transfer from a tube bank in crossflow, we must consider all the tubes in the bundle at once.

The tubes in a tube bank are usually arranged either *in-line* or *staggered* in the direction of flow, as shown in Fig. 7–26. The outer tube diameter D is taken as the characteristic length. The arrangement of the tubes in the tube bank is characterized by the *transverse pitch* S_T, the *longitudinal pitch* S_L, and the *diagonal pitch* S_D between tube centers. The diagonal pitch is determined from

$$S_D = \sqrt{S_L^2 + (S_T/2)^2} \tag{7–38}$$

Flow
direction

FIGURE 7–25
Flow patterns for in-line and staggered tube banks.

As the fluid enters the tube bank, the flow area decreases from $A_1 = S_T L$ to $A_T = (S_T - D) L$ between the tubes, and thus flow velocity increases. In staggered arrangement, the velocity may increase further in the diagonal region if the tube rows are very close to each other. In tube banks, the flow characteristics are dominated by the maximum velocity V_{max} that occurs within the tube bank rather than the approach velocity V. Therefore, the Reynolds number is defined on the basis of maximum velocity as

$$\text{Re}_D = \frac{\rho V_{max} D}{\mu} = \frac{V_{max} D}{\nu} \tag{7–39}$$

The maximum velocity is determined from the conservation of mass requirement for steady incompressible flow. For *in-line* arrangement, the maximum velocity occurs at the minimum flow area between the tubes, and the conservation of mass can be expressed as (see Fig. 7–26a) $\rho V A_1 = \rho V_{max} A_T$ or $V S_T = V_{max}(S_T - D)$, Then the maximum velocity becomes

$$V_{max} = \frac{S_T}{S_T - D} V \tag{7–40}$$

In *staggered* arrangement, the fluid approaching through area A_1 in Fig. 7–26b passes through area A_T and then through area $2A_D$ as it wraps around the pipe in the next row. If $2A_D > A_T$, maximum velocity still occurs at A_T between the tubes, and thus the V_{max} relation Eq. 7–40 can also be used for staggered tube banks. But if $2A_D < A_T$ [or, if $2(S_D - D) < (S_T - D)$], maximum velocity occurs at the diagonal cross sections, and the maximum velocity in this case becomes

Staggered and $S_D < (S_T + D)/2$: $\qquad V_{max} = \frac{S_T}{2(S_D - D)} V \tag{7–41}$

since $\rho V A_1 = \rho V_{max}(2A_D)$ or $V S_T = 2V_{max}(S_D - D)$.

The nature of flow around a tube in the first row resembles flow over a single tube discussed in Section 7–3, especially when the tubes are not too close to each other. Therefore, each tube in a tube bank that consists of a single transverse row can be treated as a single tube in crossflow. The nature of flow around a tube in the second and subsequent rows is very different, however, because of wakes formed and the turbulence caused by the tubes upstream. The level of turbulence, and thus the heat transfer coefficient, increases with row number because of the combined effects of upstream rows. But there is no significant change in turbulence level after the first few rows, and thus the heat transfer coefficient remains constant.

Flow through tube banks is studied experimentally since it is too complex to be treated analytically. We are primarily interested in the average heat transfer coefficient for the entire tube bank, which depends on the number of tube rows along the flow as well as the arrangement and the size of the tubes.

Several correlations, all based on experimental data, have been proposed for the average Nusselt number for crossflow over tube banks. More recently, Zukauskas (1987) has proposed correlations whose general form is

$$\text{Nu}_D = \frac{hD}{k} = C \, \text{Re}_D^m \, \text{Pr}^n \, (\text{Pr}/\text{Pr}_s)^{0.25} \tag{7–42}$$

$A_1 = S_T L$
$A_T = (S_T - D)L$ (b) Staggered
$A_D = (S_D - D)L$
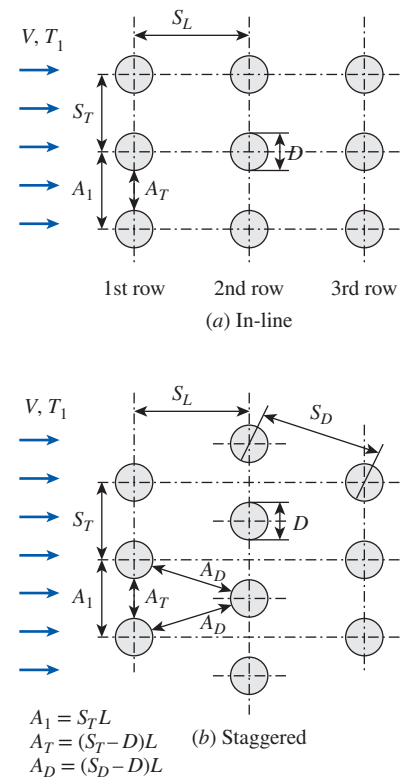
FIGURE 7–26

Arrangement of the tubes in in-line and staggered tube banks (A_1, A_T, and A_D are flow areas at indicated locations, and L is the length of the tubes).

where the values of the constants *C*, *m*, and *n* depend on Reynolds number. Such correlations are given in Table 7–2 for tube banks with more than 16 rows ($N_L > 16$), $0.7 < \text{Pr} < 500$ and $0 < \text{Re}_D < 2 \times 10^6$. The uncertainty in the values of Nusselt number obtained from these relations is ± 15 percent. Note that all properties except Pr_s are to be evaluated at the arithmetic mean temperature of the fluid determined from

$$T_m = \frac{T_i + T_e}{2} \tag{7-43}$$

where T_i and T_e are the fluid temperatures at the inlet and the exit of the tube bank, respectively.

The average Nusselt number relations in Table 7–2 are for tube banks with more than 16 rows. Those relations can also be used for tube banks with $N_L < 16$, provided that they are modified as

$$\text{Nu}_{D,\,N_L<16} = F\text{Nu}_D \tag{7-44}$$

where *F* is a *correction factor F* whose values are given in Table 7–3. For $\text{Re}_D > 1000$, the correction factor is independent of Reynolds number.

Once the Nusselt number and thus the average heat transfer coefficient for the entire tube bank is known, the heat transfer rate can be determined from

TABLE 7–2

Nusselt number correlations for crossflow over tube banks for $N_L > 16$, $0 < \text{Re}_D < 2 \times 10^6$ and $0.7 < \text{Pr} < 500$*

Arrangement	Range of Re_D	Correlation
In-line	0–100	$\text{Nu}_D = 0.9\,\text{Re}_D^{0.4}\text{Pr}^{0.36}(\text{Pr}/\text{Pr}_s)^{0.25}$
	100–1000	$\text{Nu}_D = 0.52\,\text{Re}_D^{0.5}\text{Pr}^{0.36}(\text{Pr}/\text{Pr}_s)^{0.25}$
	1000–2×10^5	$\text{Nu}_D = 0.27\,\text{Re}_D^{0.63}\text{Pr}^{0.36}(\text{Pr}/\text{Pr}_s)^{0.25}$
	2×10^5–2×10^6	$\text{Nu}_D = 0.333\,\text{Re}_D^{0.8}\text{Pr}^{0.4}(\text{Pr}/\text{Pr}_s)^{0.25}$
Staggered	0–500	$\text{Nu}_D = 1.04\,\text{Re}_D^{0.4}\text{Pr}^{0.36}(\text{Pr}/\text{Pr}_s)^{0.25}$
	500–1000	$\text{Nu}_D = 0.71\,\text{Re}_D^{0.5}\text{Pr}^{0.36}(\text{Pr}/\text{Pr}_s)^{0.25}$
	1000–2×10^5	$\text{Nu}_D = 0.35(S_T/S_L)^{0.2}\text{Re}_D^{0.6}\text{Pr}^{0.36}(\text{Pr}/\text{Pr}_s)^{0.25}$
	2×10^5–2×10^6	$\text{Nu}_D = 0.031(S_T/S_L)^{0.2}\text{Re}_D^{0.8}\text{Pr}^{0.36}(\text{Pr}/\text{Pr}_s)^{0.25}$

Source: Zukauskas, 1987.

*All properties except Pr_s are to be evaluated at the arithmetic mean of the inlet and outlet temperatures of the fluid (Pr_s is to be evaluated at T_s).

TABLE 7–3

Correction factor *F* to be used in $\text{Nu}_{D,\,N_L<16} = F\text{Nu}_D$ for $N_L < 16$ and $\text{Re}_D > 1000$

N_L	1	2	3	4	5	7	10	13
In-line	0.70	0.80	0.86	0.90	0.93	0.96	0.98	0.99
Staggered	0.64	0.76	0.84	0.89	0.93	0.96	0.98	0.99

Source: Zukauskas, 1987.

Newton's law of cooling using a suitable temperature difference ΔT. The first thought that comes to mind is to use $\Delta T = T_s - T_{avg} = T_s - (T_i + T_e)/2$. But this, in general, overpredicts the heat transfer rate. We show in Chap. 8 that the proper temperature difference for internal flow (flow over tube banks is still internal flow through the shell) is the *log mean temperature difference* ΔT_{lm}, defined as

$$\Delta T_{lm} = \frac{(T_s - T_e) - (T_s - T_i)}{\ln[(T_s - T_e)/(T_s - T_i)]} = \frac{\Delta T_e - \Delta T_i}{\ln(\Delta T_e/\Delta T_i)} \qquad \textbf{(7–45)}$$

We also show that the exit temperature of the fluid T_e can be determined from

$$T_e = T_s - (T_s - T_i) \exp\left(-\frac{A_s h}{\dot{m} c_p}\right) \qquad \textbf{(7–46)}$$

where $A_s = N\pi DL$ is the heat transfer surface area and $\dot{m} = \rho V(N_T S_T L)$ is the mass flow rate of the fluid. Here N is the total number of tubes in the bank, which is the product of N_T (number of tubes in the transverse plane) and N_L (number of rows in the flow direction), L is the length of the tubes, and V is the velocity of the fluid just before entering the tube bank. Then the heat transfer rate can be determined from

$$\dot{Q} = hA_s\Delta T_{lm} = \dot{m}c_p(T_e - T_i) \qquad \textbf{(7–47)}$$

The second relation is usually more convenient to use since it does not require the calculation of ΔT_{lm}.

Pressure Drop

Another quantity of interest associated with tube banks is the *pressure drop* ΔP, which is the irreversible pressure loss between the inlet and the exit of the tube bank. It is a measure of the resistance the tubes offer to flow over them and is expressed as

$$\Delta P = N_L f \chi \frac{\rho V_{max}^2}{2} \qquad \textbf{(7–48)}$$

where f is the friction factor and χ is the correction factor, both plotted in Figs. 7–27a and 7–27b against the Reynolds number based on the maximum velocity V_{max}. The friction factor in Fig. 7–27a is for a *square* in-line tube bank $(S_T = S_L)$, and the correction factor given in the insert is used to account for the effects of deviation of rectangular in-line arrangements from square arrangement. Similarly, the friction factor in Fig. 7–27b is for an *equilateral* staggered tube bank $(S_T = S_D)$, and the correction factor is to account for the effects of deviation from equilateral arrangement. Note that $\chi = 1$ for both square and equilateral triangle arrangements. Also, pressure drop occurs in the flow direction, and thus we used N_L (the number of rows) in the ΔP relation.

The power required to move a fluid through a tube bank is proportional to the pressure drop, and when the pressure drop is available, the pumping power required to overcome flow resistance can be determined from

$$\dot{W}_{\text{pump}} = \dot{V}\Delta P = \frac{\dot{m}\Delta P}{\rho} \tag{7-49}$$

where $\dot{V} = V(N_T S_T L)$ is the volume flow rate and $\dot{m} = \rho\dot{V} = \rho V(N_T S_T L)$ is the mass flow rate of the fluid through the tube bank. Note that the power required to keep a fluid flowing through the tube bank (and thus the operating cost) is proportional to the pressure drop. Therefore, the benefits of enhancing heat transfer in a tube bank via rearrangement should be weighed against the cost of additional power requirements.

In this section we limited our consideration to tube banks with base surfaces (no fins). Tube banks with finned surfaces are also commonly used in practice, especially when the fluid is a gas, and heat transfer and pressure drop correlations can be found in the literature for tube banks with pin fins, plate fins, strip fins, etc.
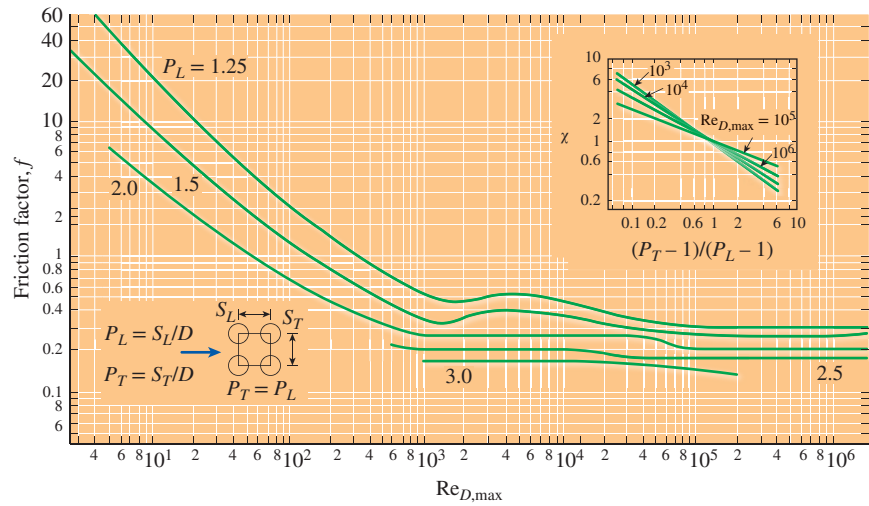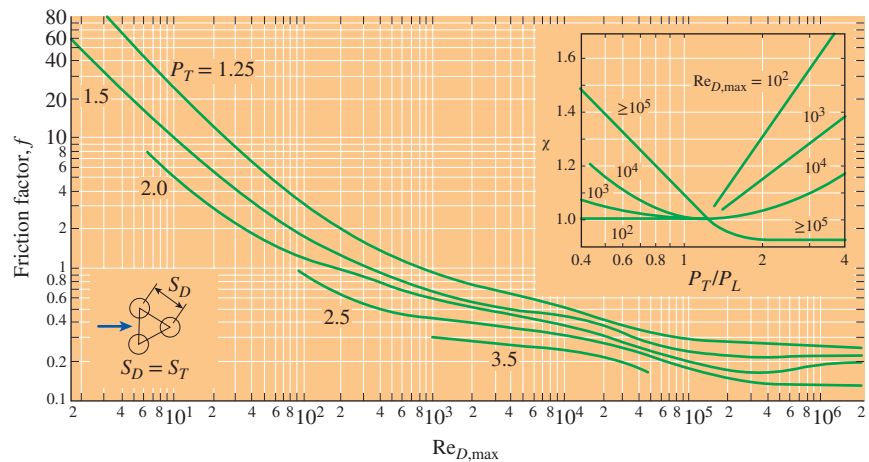
FIGURE 7-27

Friction factor f and correction factor χ for tube banks.

Source: From Zukauskas and Ulinskas (1985).

EXAMPLE 7–8   Preheating Air by Geothermal Water in a Tube Bank

In an industrial facility, air is to be preheated before entering a furnace by geothermal water at 120°C flowing through the tubes of a tube bank located in a duct. Air enters the duct at 20°C and 1 atm with a mean velocity of 4.5 m/s and flows over the tubes in normal direction. The outer diameter of the tubes is 1.5 cm, and the tubes are arranged in-line with longitudinal and transverse pitches of $S_L = S_T = 5$ cm. There are 6 rows in the flow direction with 10 tubes in each row, as shown in Fig. 7–28. Determine the rate of heat transfer per unit length of the tubes and the pressure drop across the tube bank.

SOLUTION   Air is heated by geothermal water in a tube bank. The rate of heat transfer to air and the pressure drop of air are to be determined.

Assumptions   **1** Steady operating conditions exist. **2** The surface temperature of the tubes is equal to the temperature of geothermal water.

Properties   The exit temperature of air, and thus the mean temperature, is not known. We evaluate the air properties at the assumed mean temperature of 60°C (will be checked later) and 1 atm (Table A–15):

$$k = 0.02808 \text{ W/m·K} \qquad\qquad \rho = 1.059 \text{ kg/m}^3$$

$$c_p = 1.007 \text{ kJ/kg·K} \qquad\qquad \text{Pr} = 0.7202$$

$$\mu = 2.008 \times 10^{-5} \text{ kg/m·s} \qquad \text{Pr}_s = \text{Pr}_{@120°C} = 0.7073$$

Also, the density of air at the inlet temperature of 20°C (for use in the mass flow rate calculation at the inlet) is $\rho_1 = 1.204 \text{ kg/m}^3$.

Analysis   It is given that $D = 0.015$ m, $S_L = S_T = 0.05$ m, and $V = 4.5$ m/s. Then the maximum velocity and the Reynolds number based on the maximum velocity become

$$V_{max} = \frac{S_T}{S_T - D} V = \frac{0.05}{0.05 - 0.015}(4.5 \text{ m/s}) = 6.43 \text{ m/s}$$

$$\text{Re}_D = \frac{\rho V_{max} D}{\mu} = \frac{(1.059 \text{ kg/m}^3)(6.43 \text{ m/s})(0.015 \text{ m})}{2.008 \times 10^{-5} \text{ kg/m·s}} = 5086$$

The average Nusselt number is determined using the proper relation from Table 7–2 to be

$$\text{Nu}_D = 0.27 \, \text{Re}_D^{0.63} \, \text{Pr}^{0.36} (\text{Pr}/\text{Pr}_s)^{0.25}$$

$$= 0.27 \, (5086)^{0.63}(0.7202)^{0.36}(0.7202/0.7073)^{0.25} = 52.1$$

This Nusselt number is applicable to tube banks with $N_L > 16$. In our case, the number of rows is $N_L = 6$, and the corresponding correction factor from Table 7–3 is $F = 0.945$. Then the average Nusselt number and heat transfer coefficient for all the tubes in the tube bank become

$$\text{Nu}_{D, N_L<16} = F\text{Nu}_D = (0.945)(52.1) = 49.3$$

Air
$V = 4.5$ m/s
$T_1 = 20$°C
$T_s = 120$°C

S_T

$S_L = S_T = 5$ cm

$D = 1.5$ cm
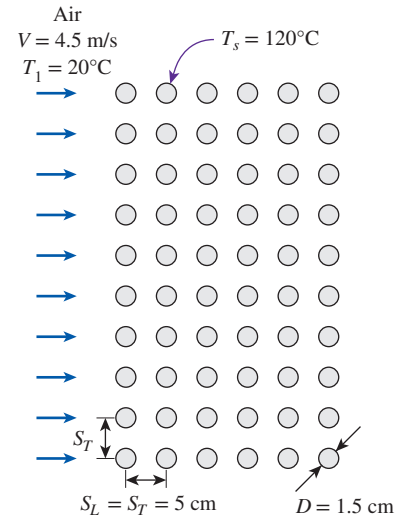
FIGURE 7–28
Schematic for Example 7–8.

$$h = \frac{\text{Nu}_{D, N_L < 16} k}{D} = \frac{49.3(0.02808 \text{ W/m·K})}{0.015 \text{ m}} = 92.2 \text{ W/m}^2\text{·K}$$

The total number of tubes is $N = N_L \times N_T = 6 \times 10 = 60$. For a unit tube length ($L = 1$ m), the heat transfer surface area and the mass flow rate of air (evaluated at the inlet) are

$$A_s = N\pi DL = 60\pi(0.015 \text{ m})(1 \text{ m}) = 2.827 \text{ m}^2$$

$$\dot{m} = \dot{m}_1 = \rho_1 V(N_T S_T L)$$

$$= (1.204 \text{ kg/m}^3)(4.5 \text{ m/s})(10)(0.05 \text{ m})(1 \text{ m}) = 2.709 \text{ kg/s}$$

Then the fluid exit temperature, the log mean temperature difference, and the rate of heat transfer become

$$T_e = T_s - (T_s - T_i) \exp\left(-\frac{A_s h}{\dot{m} c_p}\right)$$

$$= 120 - (120 - 20) \exp\left[-\frac{(2.827 \text{ m}^2)(92.2 \text{ W/m}^2\text{·K})}{(2.709 \text{ kg/s})(1007 \text{ J/kg·K})}\right] = 29.11°C$$

$$\Delta T_{\text{lm}} = \frac{(T_s - T_e) - (T_s - T_i)}{\ln[(T_s - T_e)/(T_s - T_i)]} = \frac{(120 - 29.11) - (120 - 20)}{\ln[(120 - 29.11)/(120 - 20)]} = 95.4°C$$

$$\dot{Q} = hA_s\Delta T_{\text{lm}} = (92.2 \text{ W/m}^2\text{·K})(2.827 \text{ m}^2)(95.4°C) = \mathbf{2.49 \times 10^4 \text{ W}}$$

The rate of heat transfer can also be determined in a simpler way from

$$\dot{Q} = hA_s\Delta T_{\text{lm}} = \dot{m}c_p(T_e - T_i)$$

$$= (2.709 \text{ kg/s})(1007 \text{ J/kg·K})(29.11 - 20)°C = 2.49 \times 10^4 \text{ W}$$

For this square in-line tube bank, the friction coefficient corresponding to $\text{Re}_D = 5086$ and $S_L/D = 5/1.5 = 3.33$ is, from Fig. 7–27a, $f = 0.16$. Also, $\chi = 1$ for the square arrangements. Then the pressure drop across the tube bank becomes

$$\Delta P = N_L f\chi\frac{\rho V_{\text{max}}^2}{2}$$

$$= 6(0.16)(1)\frac{(1.059 \text{ kg/m}^3)(6.43 \text{ m/s})^2}{2}\left(\frac{1 \text{ N}}{1 \text{ kg·m/s}^2}\right) = \mathbf{21 \text{ Pa}}$$

Discussion The arithmetic mean fluid temperature is $(T_i + T_e)/2 = (20 + 29.11)/2 = 24.6°C$, which is not close to the assumed value of 60°C. Repeating calculations for 25°C gives 2.57×10^4 W for the rate of heat transfer and 23.5 Pa for the pressure drop.

SUMMARY

The force a flowing fluid exerts on a body in the flow direction is called *drag*. The part of drag that is due directly to wall shear stress τ_w is called the *skin friction drag* since it is caused by frictional effects, and the part that is due directly to pressure is called the *pressure drag* or *form drag* because of its strong dependence on the form or shape of the body.

The *drag coefficient C_D* is a dimensionless number that represents the drag characteristics of a body, and it is defined as

$$C_D = \frac{F_D}{\frac{1}{2}\rho V^2 A}$$

where *A* is the *frontal area* for blunt bodies and the surface area for parallel flow over flat plates or thin airfoils. For flow over a flat plate, the Reynolds number is

$$\text{Re}_x = \frac{\rho V x}{\mu} = \frac{V x}{\nu}$$

Transition from laminar to turbulent occurs at the *critical Reynolds number* of

$$\text{Re}_{x,\,cr} = \frac{\rho V x_{cr}}{\mu} = 5 \times 10^5$$

For parallel flow over an isothermal flat plate, the local friction coefficent and Nusselt number are

Laminar: $\quad C_{f,x} = \dfrac{0.664}{\text{Re}_x^{1/2}} \quad \text{Re}_x < 5 \times 10^5$

$$\text{Nu}_x = \frac{h_x x}{k} = 0.332 \text{Re}_x^{0.5}\,\text{Pr}^{1/3} \quad \text{Pr} > 0.6$$

Turbulent:

$$C_{f,x} = \frac{0.059}{\text{Re}_x^{1/5}} \quad 5 \times 10^5 \le \text{Re}_x \le 10^7$$

$$\text{Nu}_x = \frac{h_x x}{k} = 0.0296 \text{Re}_x^{0.8}\,\text{Pr}^{1/3} \quad \begin{array}{l} 0.6 \le \text{Pr} \le 60 \\ 5 \times 10^5 \le \text{Re}_x \le 10^7 \end{array}$$

The *average* friction coefficient relations for flow over a flat plate are:

Laminar: $\quad C_f = \dfrac{1.33}{\text{Re}_L^{1/2}} \quad \text{Re}_L < 5 \times 10^5$

Turbulent: $\quad C_f = \dfrac{0.074}{\text{Re}_L^{1/5}} \quad 5 \times 10^5 \le \text{Re}_L \le 10^7$

Combined: $\quad C_f = \dfrac{0.074}{\text{Re}_L^{1/5}} - \dfrac{1742}{\text{Re}_L} \quad 5 \times 10^5 \le \text{Re}_L \le 10^7$

Rough surface, turbulent: $\quad C_f = \left(1.89 - 1.62 \log\dfrac{\varepsilon}{L}\right)^{-2.5}$

The average Nusselt number relations for flow over an isothermal flat plate are:

Laminar: $\quad \text{Nu} = \dfrac{hL}{k} = 0.664\,\text{Re}_L^{0.5}\,\text{Pr}^{1/3} \quad \begin{array}{l} \text{Pr} > 0.6 \\ \text{Re}_L < 5 \times 10^5 \end{array}$

Turbulent:

$$\text{Nu} = \frac{hL}{k} = 0.037\,\text{Re}_L^{0.8}\,\text{Pr}^{1/3} \quad \begin{array}{l} 0.6 \le \text{Pr} \le 60 \\ 5 \times 10^5 \le \text{Re}_L \le 10^7 \end{array}$$

Combined:

$$\text{Nu} = \frac{hL}{k} = (0.037\,\text{Re}_L^{0.8} - 871)\,\text{Pr}^{1/3} \quad \begin{array}{l} 0.6 \le \text{Pr} \le 60 \\ 5 \times 10^5 \le \text{Re}_L \le 10^7 \end{array}$$

For isothermal surfaces with an unheated starting section of length ξ, the local and average Nusselt number relations are

Laminar: $\quad \text{Nu}_x = \dfrac{\text{Nu}_{x\,(\text{for}\,\xi=0)}}{[1 - (\xi/x)^{3/4}]^{1/3}} = \dfrac{0.332\,\text{Re}_x^{0.5}\,\text{Pr}^{1/3}}{[1 - (\xi/x)^{3/4}]^{1/3}}$

Turbulent: $\quad \text{Nu}_x = \dfrac{\text{Nu}_{x\,(\text{for}\,\xi=0)}}{[1 - (\xi/x)^{9/10}]^{1/9}} = \dfrac{0.0296\,\text{Re}_x^{0.8}\,\text{Pr}^{1/3}}{[1 - (\xi/x)^{9/10}]^{1/9}}$

Laminar: $\quad \text{Nu} = \text{Nu}_{(\text{for}\,\xi=0)}\dfrac{L}{L-\xi}\,[1 - (\xi/L)^{3/4}]^{2/3}$

Turbulent: $\quad \text{Nu} = \text{Nu}_{(\text{for}\,\xi=0)}\dfrac{L}{L-\xi}\,[1 - (\xi/L)^{9/10}]^{8/9}$

These relations are for the case of *isothermal* surfaces. When a flat plate is subjected to *uniform heat flux,* the local Nusselt number is given by

Laminar: $\quad \text{Nu}_x = 0.453\,\text{Re}_x^{0.5}\,\text{Pr}^{1/3} \quad \begin{array}{l} \text{Pr} > 0.6 \\ \text{Re}_x < 5 \times 10^5 \end{array}$

Turbulent: $\quad \text{Nu}_x = 0.0308\,\text{Re}_x^{0.8}\,\text{Pr}^{1/3} \quad \begin{array}{l} 0.6 \le \text{Pr} \le 60 \\ 5 \times 10^5 \le \text{Re}_x \le 10^7 \end{array}$

The average Nusselt numbers for crossflow over a *cylinder* and *sphere* are

$$\mathrm{Nu}_{\mathrm{cyl}} = \frac{hD}{k} = 0.3 + \frac{0.62 \, \mathrm{Re}^{1/2} \, \mathrm{Pr}^{1/3}}{[1 + (0.4/\mathrm{Pr})^{2/3}]^{1/4}} \left[1 + \left(\frac{\mathrm{Re}}{282{,}000} \right)^{5/8} \right]^{4/5}$$

which is valid for Re Pr > 0.2, and

$$\mathrm{Nu}_{\mathrm{sph}} = \frac{hD}{k} = 2 + [0.4 \, \mathrm{Re}^{1/2} + 0.06 \, \mathrm{Re}^{2/3}]\mathrm{Pr}^{0.4} \left(\frac{\mu_\infty}{\mu_s} \right)^{1/4}$$

which is valid for $3.5 \le \mathrm{Re} \le 8 \times 10^4$, $0.7 \le \mathrm{Pr} \le 380$ and $1.0 \le (\mu_\infty/\mu_s) \le 3.2$. The fluid properties are evaluated at the film temperature $T_f = (T_\infty + T_s)/2$ in the case of a cylinder, and at the free-stream temperature T_∞ (except for μ_s, which is evaluated at the surface temperature T_s) in the case of a sphere.

In tube banks, the Reynolds number is based on the maximum velocity $V_{\max}$ that is related to the approach velocity V as

In-line and *Staggered* with $S_D < (S_T + D)/2$:

$$V_{\max} = \frac{S_T}{S_T - D} V$$

Staggered with $S_D < (S_T + D)/2$:

$$V_{\max} = \frac{S_T}{2(S_D - D)} V$$

where S_T is the transverse pitch and S_D is the diagonal pitch. The average Nusselt number for crossflow over tube banks is expressed as

$$\mathrm{Nu}_D = \frac{hD}{k} = C \, \mathrm{Re}_D^m \, \mathrm{Pr}^n \, (\mathrm{Pr}/\mathrm{Pr}_s)^{0.25}$$

where the values of the constants C, m, and n depend on Reynolds number. Such correlations are given in Table 7–2. All properties except Pr_s are to be evaluated at the arithmetic mean of the inlet and exit temperatures of the fluid defined as $T_m = (T_i + T_e)/2$.

The average Nusselt number for tube banks with less than 16 rows is expressed as

$$\mathrm{Nu}_{D, \, N_L < 16} = F\mathrm{Nu}_D$$

where F is the *correction factor* whose values are given in Table 7–3. The heat transfer rate to or from a tube bank is determined from

$$\dot{Q} = hA_s \Delta T_{\mathrm{lm}} = \dot{m} c_p (T_e - T_i)$$

where ΔT_{lm} is the logarithmic mean temperature difference defined as

$$\Delta T_{\mathrm{lm}} = \frac{(T_s - T_e) - (T_s - T_i)}{\ln[(T_s - T_e)/(T_s - T_i)]} = \frac{\Delta T_e - \Delta T_i}{\ln(\Delta T_e / \Delta T_i)}$$

and the exit temperature of the fluid T_e is

$$T_e = T_s - (T_s - T_i) \exp\left(-\frac{A_s h}{\dot{m} c_p} \right)$$

where $A_s = N\pi DL$ is the heat transfer surface area and $\dot{m} = \rho V(N_T S_T L)$ is the mass flow rate of the fluid. The pressure drop ΔP for a tube bank is expressed as

$$\Delta P = N_L f \chi \frac{\rho V_{\max}^2}{2}$$

where f is the friction factor and χ is the correction factor, both given in Fig. 7–27.

REFERENCES AND SUGGESTED READING

1. T. A. Ameel. "Average Effects of Forced Convection Over a Flat Plate with an Unheated Starting Length." *International Communications in Heat and Mass Transfer* 24, no. 8 (1997), pp. 1113–1120.

2. R. D. Blevin. *Applied Fluid Dynamics Handbook*. New York: Van Nostrand Reinhold, 1984.

3. S. W. Churchill and M. Bernstein. "A Correlating Equation for Forced Convection from Gases and Liquids to a Circular Cylinder in Cross Flow." *Journal of Heat Transfer* 99 (1977), pp. 300–306.

4. S. W. Churchill and H. Ozoe. "Correlations for Laminar Forced Convection in Flow over an Isothermal Flat Plate and in Developing and Fully Developed Flow in an Isothermal Tube." *Journal of Heat Transfer* 95 (Feb. 1973), pp. 78–84.

5. W. M. Edmunds. "Residential Insulation." *ASTM Standardization News* (Jan. 1989), pp. 36–39.

6. W. H. Giedt. "Investigation of Variation of Point Unit-Heat Transfer Coefficient Around a Cylinder Normal to an Air Stream." *Transactions of the ASME* 71 (1949), pp. 375–381.

7. "Green and Clean: The Economic, Energy, and Environmental Benefits of Insulation," *Alliance to Save Energy,* April 2001.

8. K. Hooman and N. Dukhan. "A Theoretical Model with Experimental Verification to Predict Hydrodynamics of Foams." *Transport in Porous Media* 100 (2013), pp. 393–406.

9. M. Jakob. *Heat Transfer.* Vol. l. New York: John Wiley & Sons, 1949.

10. W. M. Kays, M. E. Crawford, and B. Weigand. *Convective Heat and Mass Transfer.* 4th ed. New York: McGraw-Hill, 2005.

11. H. Schlichting. *Boundary Layer Theory,* 7th ed. New York, McGraw-Hill, 1979.

12. E. M. Sparrow and J. P. Abraham. "Universal Solutions for the Streamwise Variation of the Temperature of a Moving Sheet in the Presence of a Moving Fluid." *International Journal of Heat and Mass Transfer* 48 (2005), pp. 3047–3056.

13. E. M. Sparrow, J. P. Abraham, and J. C. K. Tong. "Archival Correlations for Average Heat Transfer Coefficients for Non-Circular and Circular Cylinders and for Spheres in Crossflow." *International Journal of Heat and Mass Transfer* 47 (2004), pp. 5285–5296.

14. J. C. K. Tong, J. P. Abraham, W. J. Minkowycz, and E. M. Sparrow. "A New Archive of Heat Transfer Coefficients

from Square and Chamfered Cylinders at Angles of Attack in Crossflow." *International Journal of Thermal Sciences* 105 (2016), pp. 218-223.

15. S. Whitaker. "Forced Convection Heat Transfer Correlations for Flow in Pipe, Past Flat Plates, Single Cylinders, Single Spheres, and for Flow in Packed Beds and Tube Bundles." *AIChE Journal* 18 (1972), pp. 361–371.

16. R. D. Willis. "Photographic Study of Fluid Flow Between Banks of Tubes." *Engineering* (1934), pp. 423–425.

17. A. Zukauskas. "Convection Heat Transfer in Cross Flow." In *Advances in Heat Transfer,* J. P. Hartnett and T. F. Irvine, Jr., (Eds.). Vol. 8. New York: Academic Press, 1972, pp. 93–106.

18. A. Zukauskas. "Heat Transfer from Tubes in Cross Flow." In *Advances in Heat Transfer,* J. P. Hartnett and T. F. Irvine, Jr. (Eds.). Vol. 8. New York: Academic Press, 1972.

19. A. Zukauskas. "Heat Transfer from Tubes in Cross Flow." In *Handbook of Single Phase Convective Heat Transfer,* S. Kakac, R. K. Shah, and Win Aung (Eds.). New York: Wiley Interscience, 1987.

20. A. Zukauskas and R. Ulinskas. "Efficiency Parameters for Heat Transfer in Tube Banks." *Heat Transfer Engineering* 6 (1985), pp. 19–25.

PROBLEMS*

Drag Force and Heat Transfer in External Flow

7–1C What is the difference between the upstream velocity and the free-stream velocity? For what types of flow are these two velocities equal to each other?

7–2C What is drag? What causes it? Why do we usually try to minimize it?

7–3C What is lift? What causes it? Does wall shear contribute to the lift?

7–4C During flow over a given body, the drag force, the upstream velocity, and the fluid density are measured. Explain

how you would determine the drag coefficient. What area would you use in calculations?

7–5C Define the frontal area of a body subjected to external flow. When is it appropriate to use the frontal area in drag and lift calculations?

7–6C What is the difference between skin friction drag and pressure drag? Which is usually more significant for slender bodies such as airfoils?

7–7C What is the difference between streamlined and blunt bodies? Is a tennis ball a streamlined or blunt body?

7–8C What is the effect of streamlining on (*a*) friction drag and (*b*) pressure drag? Does the total drag acting on a body necessarily decrease as a result of streamlining? Explain.

7–9C What is the effect of surface roughness on the friction drag coefficient in laminar and turbulent flows?

7–10C What is flow separation? What causes it? What is the effect of flow separation on the drag coefficient?

* Problems designated by a "C" are concept questions, and students are encouraged to answer them all. Problems designated by an "E" are in English units, and the SI users can ignore them. Problems with the 🖥 icon are comprehensive in nature and are intended to be solved with appropriate software. Problems with the 🅟🅣🅓 icon are Prevention through Design problems. Problems with the 🄲🄰🅂 icon are Codes and Standards problems.

Flow Over Flat Plates

7–11C What does the friction coefficient represent in flow over a flat plate? How is it related to the drag force acting on the plate?

7–12C Consider laminar flow over a flat plate. Will the friction coefficient change with distance from the leading edge? How about the heat transfer coefficient?

7–13C How are the average friction and heat transfer coefficients determined in flow over a flat plate?

7–14 Air at 25°C and 1 atm is flowing over a long flat plate with a velocity of 8 m/s. Determine the distance from the leading edge of the plate where the flow becomes turbulent and the thickness of the boundary layer at that location.

7–15 Repeat Prob. 7–14 for water.

7–16 The weight of a thin flat plate 50-cm × 50-cm is balanced by a counterweight that has a mass of 2 kg, as shown in the figure. Now a fan is turned on, and air at 1 atm and 25°C flows downward over both surfaces of the plate with a free-stream velocity of 8 m/s. Determine the mass of the counterweight that needs to be added in order to balance the plate in this case.
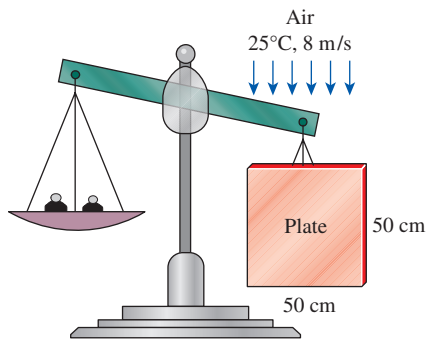
FIGURE P7–16

7–17 Air at 15°C and 1 atm flows over a 0.3-m-wide plate at 65°C at a velocity of 3.0 m/s. Compute the following quantities at $x = 0.3$ m:
 (a) Hydrodynamic boundary layer thickness, m
 (b) Local friction coefficient
 (c) Average friction coefficient
 (d) Total drag force due to friction, N
 (e) Local convection heat transfer coefficient, W/m²·K
 (f) Average convection heat transfer coefficient, W/m²·K
 (g) Rate of convective heat transfer, W

7–18 Engine oil at 85°C flows over a 10-m-long flat plate whose temperature is 35°C with a velocity of 2.5 m/s. Determine the total drag force and the rate of heat transfer over the entire plate per unit width.

7–19E Air at 60°F flows over a 10-ft-long flat plate at 7 ft/s. Determine the local friction and heat transfer coefficients at intervals of 1 ft, and plot the results against the distance from the leading edge.

7–20E Reconsider Prob. 7–19E. Using appropriate software, evaluate the local friction and heat transfer coefficients along the plate at intervals of 0.1 ft, and plot them against the distance from the leading edge.

7–21 Consider laminar flow of a fluid over a flat plate maintained at a constant temperature. Now the free-stream velocity of the fluid is doubled. Determine the change in the drag force on the plate and the rate of heat transfer between the fluid and the plate. Assume the flow to remain laminar.

7–22 In an experiment, the local heat transfer over a flat plate was correlated in the form of the local Nusselt number as expressed by the following correlation

$$\text{Nu}_x = 0.035\text{Re}_x^{0.8}\text{Pr}^{1/3}$$

Determine the ratio of the average convection heat transfer coefficient (h) over the entire plate length to the local convection heat transfer coefficient (h_x) at $x = L$.

7–23 Hot water vapor flows in parallel over the upper surface of a 1-m-long plate. The velocity of the water vapor is 10 m/s at a temperature of 450°C. A copper–silicon (ASTM B98) bolt is embedded in the plate at midlength. The maximum use temperature for the ASTM B98 copper–silicon bolt is 149°C (ASME Code for Process Piping, ASME B31.3-2014, Table A-2M). To devise a cooling mechanism to keep the bolt from getting above the maximum use temperature, it becomes necessary to determine the local heat flux at the location where the bolt is embedded. If the plate surface is kept at the maximum use temperature of the bolt, what is the local heat flux from the hot water vapor at the location of the bolt?

FIGURE P7–23

7–24 Water at 43.3°C flows over a large plate at a velocity of 30.0 cm/s. The plate is 1.0-m long (in the flow direction), and its surface is maintained at a uniform temperature of 10.0°C. Calculate the steady rate of heat transfer per unit width of the plate.

7–25 The forming section of a plastics plant puts out a continuous sheet of plastic that is 1.2-m wide and 2-mm thick at a rate of 15 m/min. The temperature of the plastic sheet is

90°C when it is exposed to the surrounding air, and the sheet is subjected to airflow at 30°C at a velocity of 3 m/s on both sides along its surfaces normal to the direction of motion of the sheet. The width of the air cooling section is such that a fixed point on the plastic sheet passes through that section in 2 s. Determine the rate of heat transfer from the plastic sheet to the air.
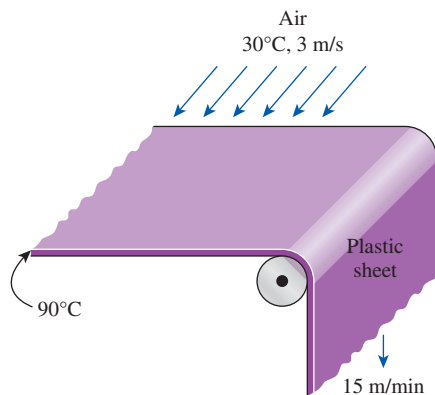
FIGURE P7–25

7–26 Hot carbon dioxide exhaust gas at 1 atm is being cooled by flat plates. The gas at 220°C flows in parallel over the upper and lower surfaces of a 1.5-m-long flat plate at a velocity of 3 m/s. If the flat plate surface temperature is maintained at 80°C, determine (*a*) the local convection heat transfer coefficient at 1 m from the leading edge, (*b*) the average convection heat transfer coefficient over the entire plate, and (*c*) the total heat flux transfer to the plate.

7–27 **C&S** The upper surface of a 1-m × 1-m ASTM B152 copper plate is being cooled by air at 20°C. The air is flowing parallel over the plate surface at a velocity of 0.5 m/s. The maximum use temperature for the ASTM B152 copper plate is 260°C (ASME Code for Process Piping, ASME B31.3-2014, Table A-1M). Determine the average convection heat transfer rate from the plate surface that is required to keep the plate surface temperature from going higher than the maximum use temperature.

7–28 A transformer that is 10-cm long, 6.2-cm wide, and 5-cm high is to be cooled by attaching a 10-cm × 6.2-cm-wide polished aluminum heat sink (emissivity = 0.03) to its top surface. The heat sink has seven fins, which are 5-mm high, 2-mm thick, and 10-cm long. A fan blows air at 25°C parallel to the passages between the fins. The heat sink is to dissipate 12 W of heat, and the base temperature of the heat sink is not to exceed 60°C. Assuming the fins and the base plate to be nearly isothermal and the radiation heat transfer to be negligible, determine the minimum free-stream velocity the fan needs to supply to avoid overheating. Assume the flow is laminar over the entire finned surface of the transformer.
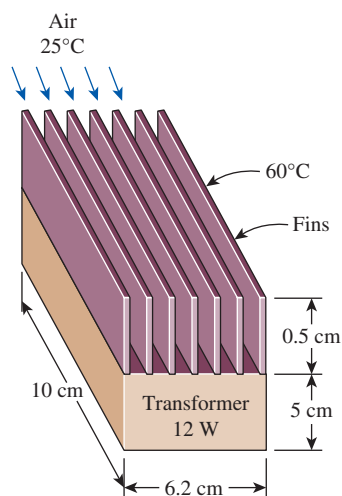
FIGURE P7–28

7–29 Repeat Prob. 7–28 assuming the heat sink to be black-anodized and thus to have an effective emissivity of 0.90. Note that in radiation calculations the base area (10-cm × 6.2-cm) is to be used, not the total surface area.

7–30 Hot engine oil at 150°C is flowing in parallel over a flat plate at a velocity of 2 m/s. Surface temperature of the 0.5-m-long flat plate is constant at 50°C. Determine (*a*) the local convection heat transfer coefficient at 0.2 m from the leading edge and the average convection heat transfer coefficient, and (*b*) repeat part (*a*) using the Churchill and Ozoe (1973) relation.

7–31 Parallel plates form a solar collector that covers a roof, as shown in the figure. The plates are maintained at 15°C, while ambient air at 10°C flows over the roof with $V = 2$ m/s. Determine the rate of convective heat loss from (*a*) the first plate and (*b*) the third plate.
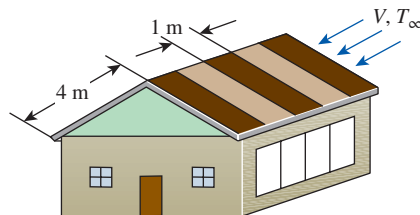
FIGURE P7–31

7–32 Hydrogen gas at 1 atm is flowing in parallel over the upper and lower surfaces of a 3-m-long flat plate at a velocity of 2.5 m/s. The gas temperature is 120°C, and the surface temperature of the plate is maintained at 30°C. Using appropriate software, investigate the local convection heat transfer coefficient and the local total convection heat flux

along the plate. By varying the location along the plate for $0.2 \leq x \leq 3$ m, plot the local convection heat transfer coefficient and the local total convection heat flux as functions of x. Assume flow is laminar, but make sure to verify this assumption.

7–33 Carbon dioxide and hydrogen as ideal gases at 1 atm and $-20°C$ flow in parallel over a flat plate. The flow velocity of each gas is 1 m/s, and the surface temperature of the 3-m-long plate is maintained at $20°C$. Using appropriate software, evaluate the local Reynolds number, the local Nusselt number, and the local convection heat transfer coefficient along the plate for each gas. By varying the location along the plate for $0.2 \leq x \leq 3$ m, plot the local Reynolds number, the local Nusselt number, and the local convection heat transfer coefficient for each gas as functions of x. Discuss which gas has a higher local Nusselt number and which gas has a higher convection heat transfer coefficient along the plate. Assume flow is laminar, but make sure to verify this assumption.

7–34 An array of power transistors, dissipating 5 W of power each, are to be cooled by mounting them on a 25-cm × 25-cm-square aluminum plate and blowing air at $35°C$ over the plate with a fan at a velocity of 4 m/s. The average temperature of the plate is not to exceed $65°C$. Assuming the heat transfer from the back side of the plate to be negligible and disregarding radiation, determine the number of transistors that can be placed on this plate.
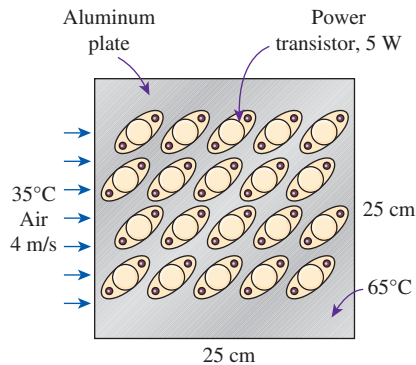
FIGURE P7–34

7–35 Repeat Prob. 7–34 for a location at an elevation of 1610 m where the atmospheric pressure is 83.4 kPa. *Answer:* 5

7–36 Air flows in parallel over the upper surface of a 2-m-long plate. The velocity of the air is 20 m/s at a temperature of $250°C$. Two copper–silicon (ASTM B98) bolts are embedded in the plate: the first bolt at 0.25 m from the leading edge, and the second bolt at 1.75 m from the leading edge. The maximum use temperature for the ASTM B98 copper–silicon bolt is $149°C$ (ASME Code for Process Piping, ASME B31.3-2014, Table A-2M). To devise a cooling mechanism to keep the bolts from heating above the maximum use

temperature, it becomes necessary to determine the local heat fluxes at the locations where the bolts are embedded. If the plate surface is kept at the maximum use temperature of the bolts, what are the local heat fluxes from the air at the locations of both bolts?
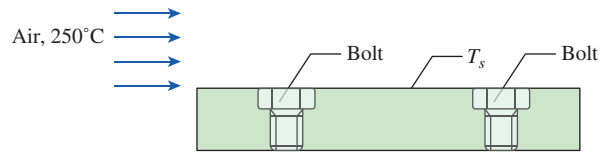
FIGURE P7–36

7–37E Consider a refrigeration truck traveling at 70 mph at a location where the air temperature is $80°F$. The refrigerated compartment of the truck can be considered to be a 9-ft-wide, 7-ft-high, and 20-ft-long rectangular box. The refrigeration system of the truck can provide 3 tons of refrigeration (i.e., it can remove heat at a rate of 600 Btu/min). The outer surface of the truck is coated with a low-emissivity material, and thus radiation heat transfer is very small. Determine the average temperature of the outer surface of the refrigeration compartment of the truck if the refrigeration system is observed to be operating at half the capacity. Assume the airflow over the entire outer surface to be turbulent and the heat transfer coefficient at the front and rear surfaces to be equal to that on side surfaces. For air properties evaluations, assume a film temperature of $80°F$. Is this a good assumption?
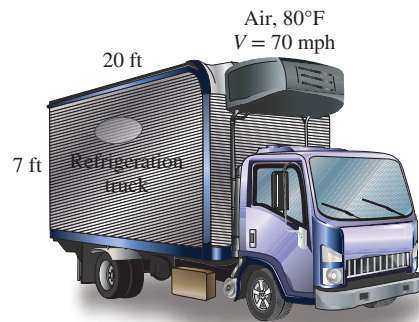
FIGURE P7–37E

7–38 Consider a hot automotive engine, which can be approximated as a 0.5-m-high, 0.40-m-wide, and 0.8-m-long rectangular block. The bottom surface of the block is at a temperature of $100°C$ and has an emissivity of 0.95. The ambient air is at $20°C$, and the road surface is at $25°C$. Determine the rate of heat transfer from the bottom surface of the engine block by convection and radiation as the car travels at a velocity of 80 km/h. Assume the flow to be turbulent over the entire surface because of the constant agitation of the engine block.

7–39 Air at 1 atm is flowing in parallel over a 3-m-long flat plate with a velocity of 7 m/s. The air has a free-stream temperature of 120°C, and the surface temperature of the plate is maintained at 20°C. Determine the distance x from the leading edge of the plate where the critical Reynolds number ($Re_{cr} = 5 \times 10^5$) is reached. Then, using appropriate software, evaluate the local convection heat transfer coefficient along the plate. By varying the location along the plate for $0.2 \leq x \leq 3$ m, plot the local convection heat transfer coefficient as a function of x, and discuss the results.

7–40 **PtD** Heat dissipated from a machine in operation can cause hot spots on its surface. Exposed hot spots that can cause thermal burns on human skin are considered to be hazards in the workplace. Consider a 1.5-m × 1.5-m flat machine surface that is made of 5-mm-thick aluminum ($k = 237$ W/m·K). During operation, the machine's inner aluminum surface temperature can be as high as 90°C, while the outer surface is cooled with 30°C air flowing in parallel over it at 10 m/s. To protect machine operators from thermal burns, the machine surface can be covered with insulation. The aluminum/insulation interface has a thermal contact conductance of 3000 W/m²·K. What is the thickness of insulation (with a thermal conductivity of 0.06 W/m·K) needed to keep the local outer surface temperature at 45°C or lower? Using appropriate software, plot the required insulation thickness and the local convection heat transfer coefficient along the outer surface in parallel with the airflow.
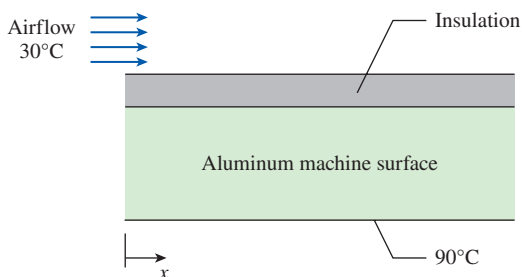
FIGURE P7–40

7–41 Air at 1 atm and 20°C is flowing over the top surface of a 0.5-m-long thin flat plate. The airstream velocity is 50 m/s, and the plate is maintained at a constant surface temperature of 180°C. Determine (*a*) the average friction coefficient and (*b*) the average convection heat transfer coefficient, and (*c*) repeat part (*b*) using the modified Reynolds analogy.

FIGURE P7–41

7–42 **C&S** In cryogenic equipment, cold air flows in parallel over the surface of a 2-m × 2-m ASTM A240 410S stainless steel plate. The air velocity is 5 m/s at a temperature of −70°C. The minimum temperature suitable for the ASTM A240 410S plate is −30°C (ASME Code for Process Piping, ASME B31.3-2014, Table A-1M). The plate is heated to keep its surface temperature from going below −30°C. Determine the average heat transfer rate required to keep the plate surface from getting below the minimum suitable temperature.

7–43 A 5-m-long strip of sheet metal is being transported on a conveyor at a velocity of 5 m/s, while the coating on the upper surface is being cured by infrared lamps. The coating on the upper surface of the metal strip has an absorptivity of 0.6 and an emissivity of 0.7, while the surrounding ambient air temperature is 25°C. Radiation heat transfer occurs only on the upper surface, while convection heat transfer occurs on both upper and lower surfaces of the sheet metal. If the infrared lamps supply a constant heat flux of 5000 W/m², determine the surface temperature of the sheet metal. Evaluate the properties of air at 80°C.
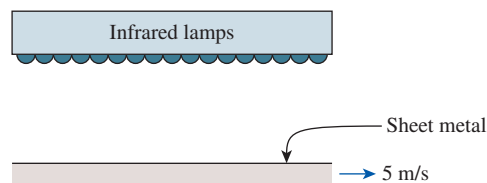
FIGURE P7–43

7–44 Reconsider Prob. 7–43. Using appropriate software, evaluate the effect of the sheet metal velocity on its surface temperature. By varying the sheet metal velocity from 3 to 30 m/s, plot the surface temperature of the sheet metal as a function of velocity. If the surface temperature of the sheet metal should be maintained above 100°C, determine the minimum velocity that is necessary to satisfy this condition. Evaluate the properties of air at 80°C.

7–45 The local atmospheric pressure in Denver, Colorado (elevation 1610 m), is 83.4 kPa. Air at this pressure and at 30°C flows with a velocity of 6 m/s over a 2.5-m × 8-m flat plate whose temperature is 120°C. Determine the rate of heat transfer from the plate if the air flows parallel to the (*a*) 8-m-long side and (*b*) the 2.5-m side.

7–46 During a cold winter day, wind at 42 km/h is blowing parallel to a 6-m-high and 10-m-long wall of a house. If the air outside is at 5°C and the surface temperature of the wall is 12°C, determine the rate of heat loss from that wall by convection. What would your answer be if the wind velocity was doubled? *Answers:* 10.8 kW, 19.4 kW
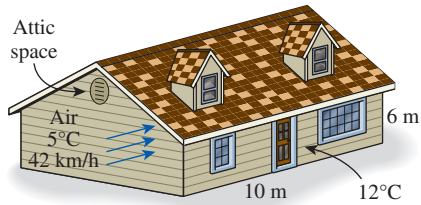
FIGURE P7–46

7–47 Reconsider Prob. 7–46. Using appropriate software, investigate the effects of wind velocity and outside air temperature on the rate of heat loss from the wall by convection. Let the wind velocity vary from 10 km/h to 80 km/h and the outside air temperature from 0°C to 10°C. Plot the rate of heat loss as a function of the wind velocity and of the outside temperature, and discuss the results.

7–48E Warm air is blown over the inner surface of an automobile windshield to defrost ice accumulated on the outer surface of the windshield. Consider an automobile windshield ($k_w = 0.8$ Btu/h·ft·R) with an overall height of 20 in and thickness of 0.2 in. The outside air (1 atm) ambient temperature is 8°F, and the average airflow velocity over the outer windshield surface is 50 mph, while the ambient temperature inside the automobile is 77°F. Determine the value of the convection heat transfer coefficient for the warm air blowing over the inner surface of the windshield that is needed to cause the accumulated ice to begin melting. Assume the windshield surface can be treated as a flat-plate surface.

7–49 The top surface of the passenger car of a train moving at a velocity of 95 km/h is 2.8-m wide and 8-m long. The top surface is absorbing solar radiation at a rate of 380 W/m^2, and the temperature of the ambient air is 30°C. Assuming the roof of the car to be perfectly insulated and the radiation heat exchange with the surroundings to be small relative to convection, determine the equilibrium temperature of the top surface of the car. *Answer:* 37.5°C

FIGURE P7–49

7–50 Reconsider Prob. 7–49. Using appropriate software, investigate the effects of the train velocity and the rate of absorption of solar radiation on the equilibrium temperature of the top surface of the car. Let the train velocity vary from 10 km/h to 120 km/h and the rate of solar absorption from 100 W/m^2 to 500 W/m^2. Plot the equilibrium temperature as functions of train velocity and solar radiation absorption rate, and discuss the results.

7–51 Solar radiation is incident on the glass cover of a solar collector at a rate of 700 W/m^2. The glass transmits 88 percent of the incident radiation and has an emissivity of 0.90. The entire hot water needs of a family in summer can be met by two collectors 1.2-m high and 1-m wide. The two collectors are attached to each other on one side so that they appear like a single collector 1.2-m × 2-m in size. The temperature of the glass cover is measured to be 35°C on a day when the surrounding air temperature is 25°C and the wind is blowing at 30 km/h. The effective sky temperature for radiation exchange between the glass cover and the open sky is −40°C. Water enters the tubes attached to the absorber plate at a rate of 1 kg/min. Assuming the back surface of the absorber plate to be heavily insulated and the only heat loss to occur through the glass cover, determine (*a*) the total rate of heat loss from the collector, (*b*) the collector efficiency, which is the ratio of the amount of heat transferred to the water to the solar energy incident on the collector, and (*c*) the temperature rise of water as it flows through the collector.
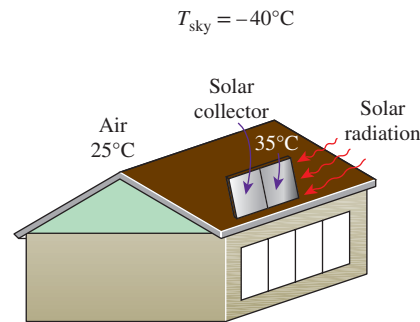
FIGURE P7–51

7–52 Reconsider Example 7–2. Another method that could be explored to keep the engine outer surface temperature below the fire hazard limit of 180°C is to increase the insulation thickness. Increase the insulation thickness by threefold and verify if this method would keep the temperature below the required limit for the safe operation of the engine. Compare the effectiveness of this method with the one used in Example 7–2.

7–53 The outer surface of an engine is situated in a place where oil leakage can occur. When leaked oil comes in contact with a hot surface that has a temperature above

its autoignition temperature, the oil can ignite spontaneously. Consider an engine cover that is made of a stainless steel plate with a thickness of 1 cm and a thermal conductivity of 14 W/m·K. The inner surface of the engine cover is exposed to hot air with a convection heat transfer coefficient of 7 W/m²·K at a temperature of 333°C. The engine outer surface is cooled by air blowing in parallel over the 2-m-long surface at 7.1 m/s, in an environment where the ambient air is at 60°C. To prevent fire hazard in the event of an oil leak on the engine cover, a layer of thermal barrier coating (TBC) with a thermal conductivity of 1.1 W/m·K is applied on the engine cover outer surface. Would a TBC layer with a thickness of 4 mm in conjunction with 7.1 m/s air cooling be sufficient to keep the engine cover surface from going above 180°C to prevent fire hazard? Evaluate the air properties at 120°C.

7–54 PtD Metal plates ($k = 180$ W/m·K, $\rho = 2800$ kg/m³, and $c_p = 880$ J/kg·K) with a length of 1 m and a thickness of 2 cm exiting an oven are then conveyed through a 10-m-long cooling chamber at a speed of 5 mm/s. The plates enter the cooling chamber at an initial temperature of 155°C. In the cooling chamber, the plates are cooled with 10°C air blowing in parallel over them. To prevent thermal burns, it is necessary to design the cooling process so that the plates exit the cooling chamber at a relatively safe temperature. Determine the air velocity such that the temperature of the plates exiting the cooling chamber is 45°C or less. Assume combined laminar and turbulent flow (verify this assumption). *Hint:* Use lumped system analysis to determine the required cooling time (verify the application of this method to this problem).
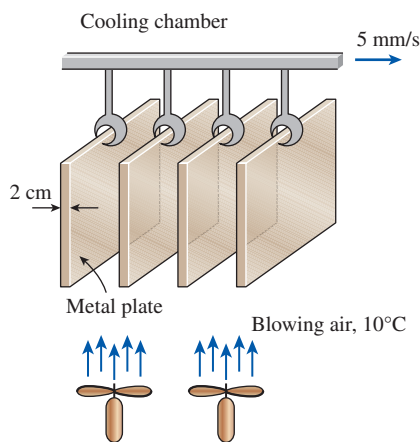
FIGURE P7–54

7–55 Mercury at 25°C flows over a 3-m-long and 2-m-wide flat plate maintained at 75°C with a velocity of 0.01 m/s. Determine the rate of heat transfer from the entire plate.
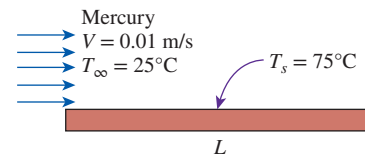
FIGURE P7–55

7–56 Liquid mercury at 250°C is flowing in parallel over a flat plate at a velocity of 0.3 m/s. Surface temperature of the 0.1-m-long flat plate is constant at 50°C. Determine (a) the local convection heat transfer coefficient at 5 cm from the leading edge and (b) the average convection heat transfer coefficient over the entire plate.

7–57 Water vapor at 250°C is flowing with a velocity of 5 m/s in parallel over a 2-m-long flat plate where there is an unheated starting length of 0.5 m. The heated section of the flat plate is maintained at a constant temperature of 50°C. Determine (a) the local convection heat transfer coefficient at the trailing edge, (b) the average convection heat transfer coefficient for the heated section, and (c) the rate of heat transfer per unit width for the heated section.

7–58 A 15-mm × 15-mm silicon chip is mounted such that the edges are flush in a substrate. The chip dissipates 1.4 W of power uniformly, while air at 20°C (1 atm) with a velocity of 25 m/s is used to cool the upper surface of the chip. If the substrate provides an unheated starting length of 15 mm, determine the surface temperature at the trailing edge of the chip. Evaluate the air properties at 50°C.

7–59 C&S In cryogenic equipment, cold gas flows in parallel over the surface of a 1-m-long plate. The gas velocity is 4 m/s at a temperature of −70°C. The gas has a thermal conductivity of 0.01979 W/m·K, a kinematic viscosity of 9.319×10^{-6} m²/s, and a Prandtl number of 0.7440. A stainless steel (ASTM A437 B4B) bolt is embedded in the plate at midlength. The minimum temperature suitable for the ASTM A437 B4B stainless steel bolt is −30°C (ASME Code for Process Piping, ASME B31.3-2014, Table A-2M). To keep the bolt from getting below its minimum suitable temperature, the plate is subjected to a uniform heat flux of 250 W/m². Determine whether the heat flux to the plate is sufficient to keep the bolt above the minimum suitable temperature of −30°C.
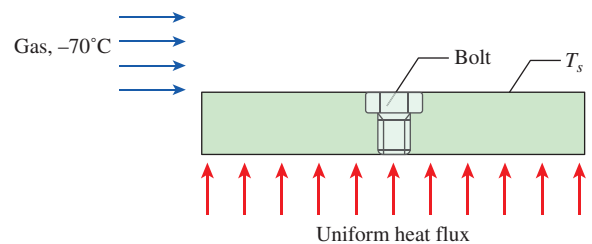
FIGURE P7–59

7–60 The upper surface of a metal plate is being cooled with parallel airflow while its lower surface is subjected to a uniform heat flux of 810 W/m². The air has a free-stream velocity and temperature of 2.5 m/s and 15°C, respectively. Determine the surface temperature of the plate at $x = 1.5$ m from the leading edge. *Hint:* The surface temperature has to be found iteratively. Start the iteration process with an initial guess of 45°C for the surface temperature.
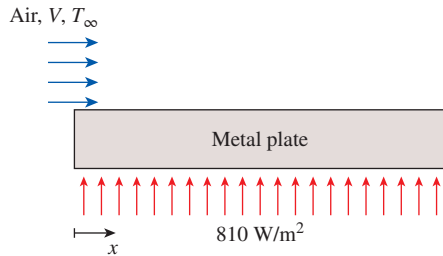
FIGURE P7–60

7–61 Reconsider Prob. 7–60. Using appropriate software, evaluate the local convection heat transfer coefficient, the local surface temperature, and the local film temperature along the plate. By varying the location along the plate for $0.2 \leq x \leq 3$ m, plot the local convection heat transfer coefficient, the local surface temperature, and the local film temperature as functions of x.

7–62 Air is flowing in parallel over the upper surface of a flat plate with a length of 4 m. The first half of the plate length, from the leading edge, has a constant surface temperature of 50°C. The second half of the plate length is subjected to a uniform heat flux of 86 W/m². The air has a free-stream velocity and temperature of 2 m/s and 10°C, respectively. Determine the local convection heat transfer coefficients at 1 m and 3 m from the leading edge. As a first approximation, assume the boundary layer over the second portion of the plate with uniform heat flux has not been affected by the first half of the plate with constant surface temperature. Evaluate the air properties at a film temperature of 30°C. Is the film temperature $T_f = 30$°C applicable at $x = 3$ m?
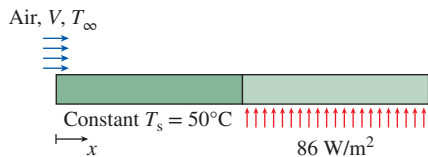
FIGURE P7–62

7–63 Reconsider Prob. 7–62. Using appropriate software, evaluate the local convection heat transfer coefficient, the local surface temperature, and the local film

temperature along the plate. By varying the location along the plate for $0.2 \leq x \leq 4$ m, plot the local convection heat transfer coefficient, the local surface temperature, and the local film temperature as functions of x.

7–64 **C&S** Hot gas flows in parallel over the upper surface of a 2-m-long plate. The velocity of the gas is 17 m/s at a temperature of 250°C. The gas has a thermal conductivity of 0.03779 W/m·K, a kinematic viscosity of 3.455×10^{-5} m²/s, and a Prandtl number of 0.6974. Two copper–silicon (ASTM B98) bolts are embedded in the plate: the first bolt at 0.5 m from the leading edge, and the second bolt at 1.5 m from the leading edge. The maximum use temperature for the ASTM B98 copper–silicon bolt is 149°C (ASME Code for Process Piping, ASME B31.3-2014, Table A-2M). A cooling device removes the heat from the plate uniformly at 2000 W/m². Determine whether the heat being removed from the plate is sufficient to keep the bolts below the maximum use temperature of 149°C.
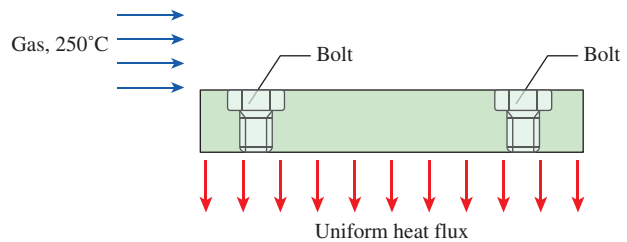
FIGURE P7–64

7–65 A 15-cm × 15-cm circuit board dissipating 20 W of power uniformly is cooled by air, which approaches the circuit board at 20°C with a velocity of 6 m/s. Disregarding any heat transfer from the back surface of the board, determine the surface temperature of the electronic components (*a*) at the leading edge and (*b*) at the end of the board. Assume the flow to be turbulent since the electronic components are expected to act as turbulators. For air properties evaluations, assume a film temperature of 35°C. Is this a good assumption?

Flow Across Cylinders and Spheres

7–66C In flow over blunt bodies such as a cylinder, how does the pressure drag differ from the friction drag?

7–67C In flow over cylinders, why does the drag coefficient suddenly drop when the flow becomes turbulent? Isn't turbulence supposed to increase the drag coefficient instead of decreasing it?

7–68C Why is flow separation in flow over cylinders delayed in turbulent flow?

7–69C Consider laminar flow of air across a hot circular cylinder. At what point on the cylinder will the heat transfer be highest? What would your answer be if the flow were turbulent?

7–70 Consider the flow of a fluid across a cylinder maintained at a constant temperature. Now the free-stream velocity of the fluid is doubled. Determine the change in the drag force on the cylinder and the rate of heat transfer between the fluid and the cylinder.

7–71 A long 12-cm-diameter steam pipe whose external surface temperature is 90°C passes through some open area that is not protected against the winds. Determine the rate of heat loss from the pipe per unit of its length when the air is at 1 atm pressure and 7°C and the wind is blowing across the pipe at a velocity of 65 km/h.

7–72 C&S Two metal plates are connected by a long ASTM B98 copper–silicon bolt. Air, at 250°C, flows at 17 m/s between the plates and across the cylindrical bolt. The diameter of the bolt is 9.5 mm, and the length of the bolt exposed to the air is 10 cm. The maximum use temperature for the ASTM B98 bolt is 149°C (ASME Code for Process Piping, ASME B31.3-2014, Table A-2M). The temperature of the bolt is maintained by a cooling mechanism with the capability of removing heat at a rate of 30 W. Determine whether the heat removed from the bolt is sufficient to keep the bolt at 149°C or lower.

7–73 A heated long cylindrical rod is placed in a crossflow of air at 20°C (1 atm) with velocity of 10 m/s. The rod has a diameter of 5 mm, and its surface has an emissivity of 0.95. If the surrounding temperature is 20°C and the heat flux dissipated from the rod is 16,000 W/m², determine the surface temperature of the rod. Evaluate the air properties at 70°C.

7–74E A person extends his uncovered arms into the windy air outside at 54°F and 30 mph in order to feel nature closely (Fig. P7–74E). Initially, the skin temperature of the arm is 84°F. Treating the arm as a 2-ft-long and 3-in-diameter cylinder, determine the rate of heat loss from the arm.
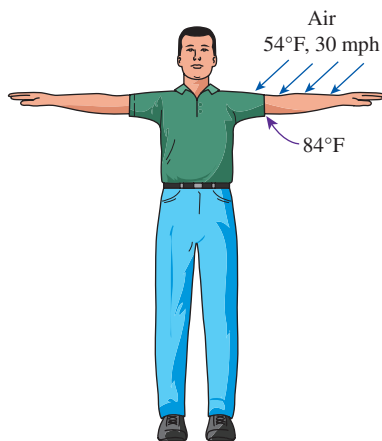
7–75E Reconsider Prob. 7–74E. Using appropriate software, investigate the effects of air temperature and wind velocity on the rate of heat loss from the arm. Let the air temperature vary from 20°F to 80°F and the wind velocity from 10 mph to 40 mph. Plot the rate of heat loss as a function of air temperature and of wind velocity, and discuss the results.

7–76 In a geothermal power plant, the used geothermal water at 80°C enters a 15-cm-diameter and 400-m-long uninsulated pipe at a rate of 8.5 kg/s and leaves at 70°C before being reinjected back to the ground. Windy air at 15°C flows normal to the pipe. Disregarding radiation, determine the average wind velocity in km/h.
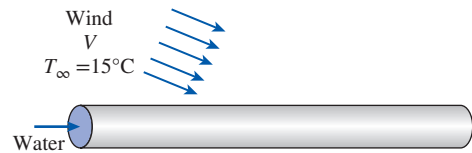
FIGURE P7–76

7–77 C&S In a piece of cryogenic equipment, two metal plates are connected by a long ASTM A437 B4B stainless steel bolt. Cold gas, at −70°C, flows between the plates and across the cylindrical bolt. The gas has a thermal conductivity of 0.02 W/m·K, a kinematic viscosity of 9.3×10^{-6} m²/s, and a Prandtl number of 0.74. The diameter of the bolt is 9.5 mm, and the length of the bolt exposed to the gas is 10 cm. The minimum temperature suitable for the ASTM A437 B4B stainless steel bolt is −30°C (ASME Code for Process Piping, ASME B31.3-2014, Table A-2M). The temperature of the bolt is maintained by a heating mechanism capable of providing heat at 15 W. Determine the maximum velocity that the gas can achieve without cooling the bolt below the minimum suitable temperature of −30°C.

7–78 A 5-mm-diameter electrical transmission line carries an electric current of 50 A and has a resistance of 0.002 ohm per meter length. Determine the surface temperature of the wire during a windy day when the air temperature is 10°C and the wind is blowing across the transmission line at 50 km/h.
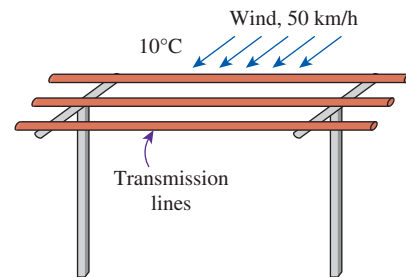
FIGURE P7–74E

FIGURE P7–78

7–79 Reconsider Prob. 7–78. Using appropriate software, investigate the effect of the wind velocity on the surface temperature of the wire. Let the wind velocity vary from 10 km/h to 80 km/h. Plot the surface temperature as a function of wind velocity, and discuss the results.

7–80 A long aluminum wire of diameter 3 mm is extruded at a temperature of 280°C. The wire is subjected to cross airflow at 20°C at a velocity of 6 m/s. Determine the rate of heat transfer from the wire to the air per meter length when it is first exposed to the air.
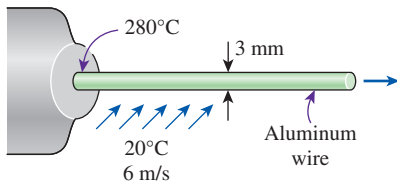
FIGURE P7–80

7–81E Consider a person who is trying to keep cool on a hot summer day by turning a fan on and exposing his entire body to airflow. The air temperature is 85°F, and the fan is blowing air at a velocity of 6 ft/s. If the person is doing light work and generating sensible heat at a rate of 300 Btu/h, determine the average temperature of the outer surface (skin or clothing) of the person. The average human body can be treated as a 1-ft-diameter cylinder with an exposed surface area of 18 ft². Disregard any heat transfer by radiation. What would your answer be if the air velocity were doubled? Evaluate the air properties at 100°F. *Answers: 95.1°F, 91.6°F*
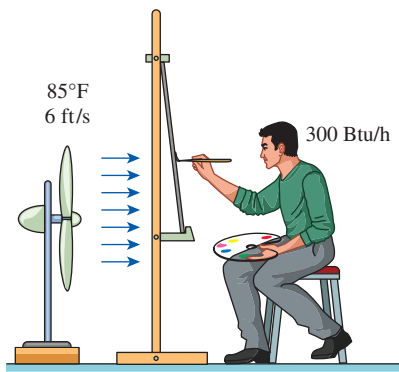
FIGURE P7–81E

7–82E A 12-ft-long, 1.5-kW electrical resistance wire is made of 0.1-in-diameter stainless steel ($k = 8.7$ Btu/h·ft·°F). The resistance wire operates in an environment at 85°F. Determine the surface temperature of the wire if it is cooled by

a fan blowing air at a velocity of 20 ft/s. For evaluations of the air properties, the film temperature has to be found iteratively. As an initial guess, assume the film temperature to be 200°F.
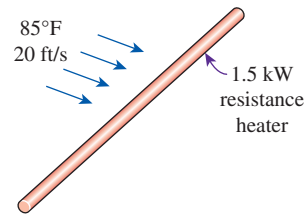
FIGURE P7–82E

7–83 A 0.4-W cylindrical electronic component with diameter 0.3 cm and length 1.8 cm and mounted on a circuit board is cooled by air flowing across it at a velocity of 240 m/min. If the air temperature is 35°C, determine the surface temperature of the component. For air properties evaluations, assume a film temperature of 50°C. Is this a good assumption?

7–84 Consider a 50-cm-diameter and 95-cm-long hot water tank. The tank is placed on the roof of a house. The water inside the tank is heated to 80°C by a flat-plate solar collector during the day. The tank is then exposed to windy air at 18°C with an average velocity of 40 km/h during the night. Estimate the temperature of the tank after a 45-min period. Assume the tank surface to be at the same temperature as the water inside and the heat transfer coefficient on the top and bottom surfaces to be the same as that on the side surface. Evaluate the air properties at 50°C.

7–85 Reconsider Prob. 7–84. Using appropriate software, plot the temperature of the tank as a function of the cooling time as the time varies from 30 min to 5 h, and discuss the results.

7–86 During a plant visit, it was noticed that a 12-m-long section of a 12-cm-diameter steam pipe is completely exposed to the ambient air. The temperature measurements indicate that the average temperature of the outer surface of the steam pipe is 75°C when the ambient temperature is 5°C. There are also light winds in the area at 25 km/h. The emissivity of the outer surface of the pipe is 0.8, and the average temperature of the surfaces surrounding the pipe, including the sky, is estimated to be 0°C. Determine the amount of heat lost from the steam during a 10-h-long workday.

Steam is supplied by a gas-fired steam generator that has an efficiency of 80 percent, and the plant pays $1.05/therm of natural gas. If the pipe is insulated and 90 percent of the heat loss is saved, determine the amount of money this facility will save a year as a result of insulating the steam pipes. Assume the plant operates every day of the year for 10 h. State your assumptions.

$T_{surr} = 0°C$ $\varepsilon = 0.8$
   75°C

12 cm   Steam pipe

5°C
25 km/h
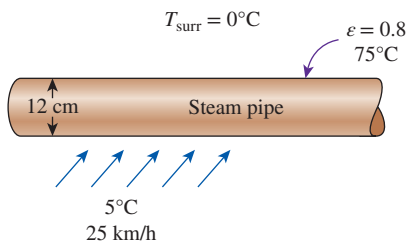
FIGURE P7–86

7–87 Reconsider Prob. 7–86. There seems to be some uncertainty about the average temperature of the surfaces surrounding the pipe used in radiation calculations, and you are asked to determine if it makes any significant difference in overall heat transfer. Repeat the calculations for average surrounding surface temperatures of −20°C and 25°C, respectively, and determine the change in the values obtained.

7–88 A 10-cm-diameter, 30-cm-high cylindrical bottle contains cold water at 3°C. The bottle is placed in windy air at 27°C. The water temperature is measured to be 11°C after 45 min of cooling. Disregarding radiation effects and heat transfer from the top and bottom surfaces, estimate the average wind velocity.

7–89 Exhaust gases from a manufacturing plant are being discharged through a 10-m-tall exhaust stack with outer diameter of 1 m. The exhaust gases are discharged at a rate of 1.2 kg/s, while temperature drop between inlet and exit of the exhaust stack is 30°C, and the constant pressure specific heat of the exhaust gases is 1600 J/kg·K. On a particular day, wind at 27°C is blowing across the exhaust stack with a velocity of 10 m/s, while the outer surface of the exhaust stack experiences radiation with the surroundings at 27°C. Solar radiation is incident on the exhaust stack outer surface at a rate of 1400 W/m², and both the emissivity and solar absorptivity of the outer surface are 0.9. Determine the exhaust stack outer surface temperature. Evaluate the air properties at 80°C.
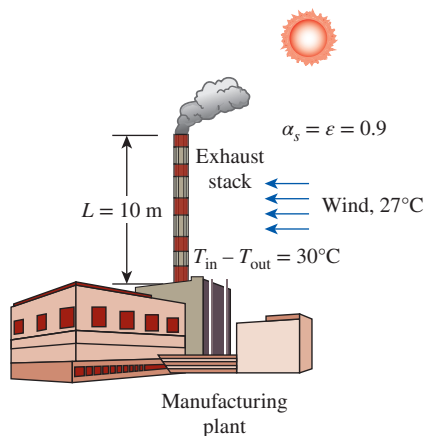
$\alpha_s = \varepsilon = 0.9$
Exhaust stack
Wind, 27°C
$L = 10$ m
$T_{in} - T_{out} = 30°C$
Manufacturing plant

FIGURE P7–89

7–90 PtD Exposure to high concentration of gaseous ammonia can cause lung damage. To prevent gaseous ammonia from leaking out, ammonia is transported in its liquid state through a pipe ($k = 25$ W/m·K, $D_{i, pipe} = 2.5$ cm, $D_{o, pipe} = 4$ cm, and $L = 10$ m). Since liquid ammonia has a normal boiling point of −33.3°C, the pipe needs to be properly insulated to prevent the surrounding heat from causing the ammonia to boil. The pipe is situated in a laboratory, where air at 20°C is blowing across it with a velocity of 7 m/s. The convection heat transfer coefficient of the liquid ammonia is 100 W/m²·K. Calculate the minimum insulation thickness for the pipe using a material with $k = 0.75$ W/m·K to keep the liquid ammonia flowing at an average temperature of −35°C, while maintaining the insulated pipe outer surface temperature at 10°C.

7–91 PtD Ice slurry is being transported in a pipe ($k = 15$ W/m·K, $D_i = 2.5$ cm, $D_o = 3$ cm, and $L = 5$ m) with an inner surface temperature of 0°C. The ambient condition surrounding the pipe has a temperature of 20°C and a dew point at 10°C. A blower is located near the pipe, which provides blowing air across the pipe at a velocity of 2 m/s. If the outer surface temperature of the pipe drops below the dew point, condensation can occur on the surface. Since this pipe is located near high-voltage devices, water droplets from the condensation can cause an electrical hazard. To prevent accidents, the pipe surface needs to be insulated. Calculate the minimum insulation thickness for the pipe using a material with $k = 0.95$ W/m·K to prevent the outer surface temperature from dropping below the dew point.

7–92 Air at 20°C (1 atm) is flowing over a 5-cm-diameter sphere with a velocity of 3.5 m/s. If the surface temperature of the sphere is constant at 80°C, determine (*a*) the average drag coefficient on the sphere and (*b*) the heat transfer rate from the sphere.

7–93 A stainless steel ball ($\rho = 8055$ kg/m³, $c_p = 480$ J/kg·K) of diameter $D = 15$ cm is removed from the oven at a uniform temperature of 125°C. The ball is then subjected to the flow of air at 1 atm pressure and 30°C with a velocity of 6 m/s. The surface temperature of the ball eventually drops to 75°C. Determine the average convection heat transfer coefficient during this cooling process, and estimate how long this process has taken.

7–94 Reconsider Prob. 7–93. Using appropriate software, investigate the effect of air velocity on the average convection heat transfer coefficient and the cooling time. Let the air velocity vary from 1 m/s to 10 m/s. Plot the heat transfer coefficient and the cooling time as a function of air velocity, and discuss the results.

7–95 An average person generates heat at a rate of 84 W while resting. Assuming one-quarter of this heat is lost from the head and disregarding radiation, determine the average surface temperature of the head when it is not covered and

is subjected to winds at 10°C and 12 km/h. The head can be approximated as a 30-cm-diameter sphere. Assume a surface temperature of 15°C for evaluation of μ_s. Is this a good assumption? *Answer:* 14.9°C

7–96 An incandescent lightbulb is an inexpensive but highly inefficient device that converts electrical energy into light. It converts about 10 percent of the electrical energy it consumes into light while converting the remaining 90 percent into heat. (A fluorescent lightbulb will give the same amount of light while consuming only one-fourth of the electrical energy, and it will last 10 times longer than an incandescent lightbulb.) The glass bulb of the lamp heats up very quickly as a result of absorbing all that heat and dissipating it to the surroundings by convection and radiation.

Consider a 10-cm-diameter, 100-W lightbulb cooled by a fan that blows air at 30°C to the bulb at a velocity of 2 m/s. The surrounding surfaces are also at 30°C, and the emissivity of the glass is 0.9. Assuming 10 percent of the energy passes through the glass bulb as light with negligible absorption and the rest of the energy is absorbed and dissipated by the bulb itself, determine the equilibrium temperature of the glass bulb. Assume a surface temperature of 100°C for evaluation of μ_s. Is this a good assumption?

Air
30°C
2 m/s

100 W

$\varepsilon = 0.9$

Light, 10 W
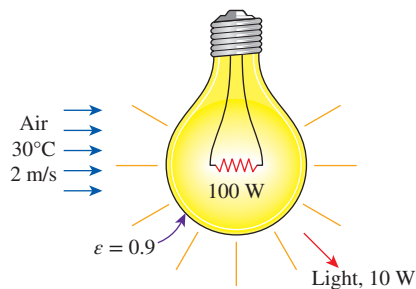
FIGURE P7–96

7–97 A 0.4-m-diameter spherical tank of negligible thickness contains iced water at 0°C. Air at 25°C flows over the tank with a velocity of 3 m/s. Determine the rate of heat transfer to the tank and the rate at which ice melts. The heat of fusion of water at 0°C is 333.7 kJ/kg.

7–98 In an experiment, the temperature of a hot airstream is to be measured by a thermocouple with a spherical junction. Due to the nature of this experiment, the response time of the thermocouple to register 99 percent of the initial temperature difference must be within 5 s. The properties of the thermocouple junction are $k = 35$ W/m·K, $\rho = 8500$ kg/m³, and $c_p = 320$ J/kg·K. The hot air has a free-stream velocity and temperature of 3 m/s and 140°C, respectively. If the initial temperature of the thermocouple junction is 20°C, determine the thermocouple junction diameter that would satisfy the required response time of 5 s. *Hint:* Use lumped system analysis to determine the time required for the

thermocouple to register 99 percent of the initial temperature difference (verify the application of this method to this problem).

Airflow, V

T_∞, h

Thermocouple junction

D
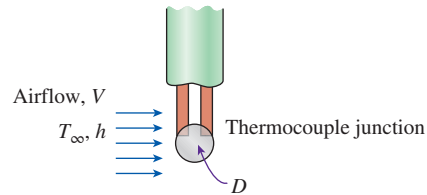
FIGURE P7–98

7–99 Reconsider Prob. 7–98. Using appropriate software, evaluate the effect of the hot air velocity on the thermocouple junction diameter that would satisfy the required response time of 5 s. By varying the hot air velocity from 1 to 10 m/s, plot the thermocouple junction diameter as a function of air velocity.

7–100 A thermocouple with a spherical junction diameter of 1 mm is used for measuring the temperature of a hydrogen gas stream. The properties of the thermocouple junction are $k = 35$ W/m·K, $\rho = 8500$ kg/m³, and $c_p = 320$ J/kg·K. The hydrogen gas, behaving as an ideal gas at 1 atm, has a free-stream temperature of 200°C. If the initial temperature of the thermocouple junction is 10°C, evaluate the time for the thermocouple to register 99 percent of the initial temperature difference at different free-stream velocities of the hydrogen gas. Using appropriate software, perform the evaluation by varying the free-stream velocity from 1 to 100 m/s. Then, plot the thermocouple response time and the convection heat transfer coefficient as a function of free-stream velocity. *Hint:* Use the lumped system analysis to determine the time required for the thermocouple to register 99 percent of the initial temperature difference (verify the application of this method to this problem).

H₂ gas flow, V

T_∞, h

Thermocouple junction

$D = 1$ mm
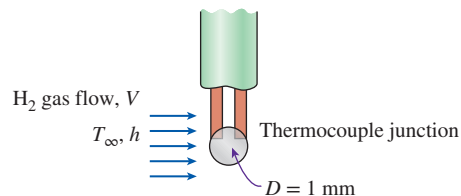
FIGURE P7–100

7–101 PtD A glass ($k = 1.1$ W/m·K) spherical tank is filled with chemicals undergoing exothermic reaction. The reaction keeps the inner surface temperature of the tank at 80°C. The tank has an inner radius of 0.5 m, and its wall thickness is 10 mm. Situated in surroundings with an ambient temperature of 15°C and a convection heat transfer

coefficient of 70 W/m²·K, the tank's outer surface is being cooled by air flowing across it at 5 m/s. In order to prevent thermal burn on individuals working around the container, it is necessary to keep the tank's outer surface temperature below 50°C. Determine whether or not the tank's outer surface temperature is safe from thermal burn hazards.
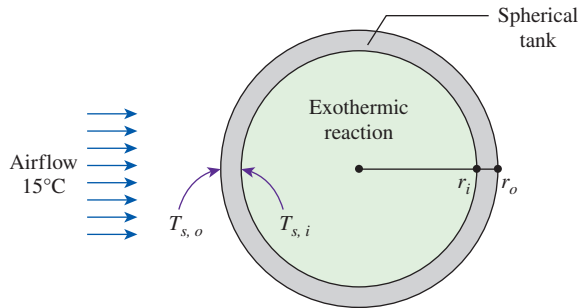
FIGURE P7–101

7–102 The components of an electronic system are located in a 1.5-m-long horizontal duct whose cross section is 20 cm × 20 cm. The components in the duct are not allowed to come into direct contact with cooling air, and thus they are cooled by air at 30°C flowing over the duct with a velocity of 200 m/min. If the surface temperature of the duct is not to exceed 65°C, determine the total power rating of the electronic devices that can be mounted into the duct.
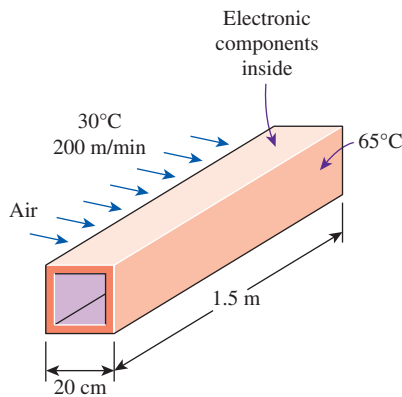
FIGURE P7–102

7–103 Repeat Prob. 7–102 for a location at a 3000-m altitude where the atmospheric pressure is 70.12 kPa.

7–104 **C&S** Two metal plates are connected by a long ASTM A479 904L stainless steel bar. Air, at 340°C, flows at 25 m/s between the plates and across the bar. The bar has a square cross section with a width of 10 mm, and the length of the bar exposed to the hot air is 10 cm. The maximum use temperature for the ASTM A479 904L is

260°C (ASME Code for Process Piping, ASME B31.3-2014, Table A-1M). The temperature of the bar is maintained by a cooling mechanism capable of removing heat at a rate of 50 W. Determine whether the heat removed from the bar is sufficient to keep the bar at 260°C or lower.

7–105 A 0.2-m × 0.2-m street sign surface has an absorptivity of 0.6 and an emissivity of 0.7, while the street sign is subjected to a crossflow wind at 20°C with a velocity of 1 m/s. Solar radiation is incident on the street sign at a rate of 1100 W/m², and the surrounding temperature is 20°C. Determine the surface temperature of the street sign. Evaluate the air properties at 30°C. Treat the sign surface as a vertical plate in crossflow.
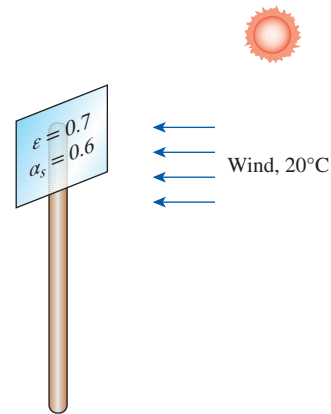
FIGURE P7–105

7–106 A coated sheet is being dried with hot air blowing in cross flow on the sheet surface. The surface temperature of the sheet is constant at 90°C, while the air velocity and temperature are 0.3 m/s and 110°C, respectively. The length of the sheet subjected to the blowing hot air is 1-m long. Determine the convection heat transfer coefficient and the heat flux added to the sheet surface. Treat the coated sheet as a vertical plate in crossflow.
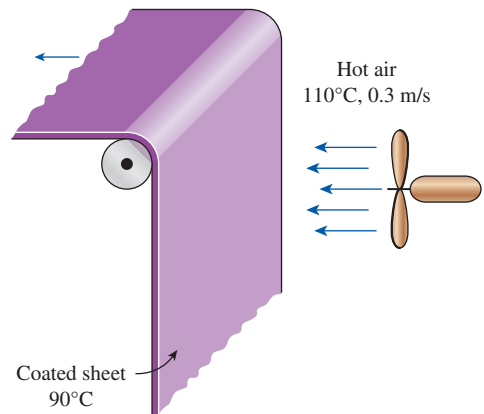
FIGURE P7–106

7–107 Reconsider Prob. 7–106. Using appropriate software, evaluate the hot air velocity on the convection heat transfer coefficient. By varying the hot air velocity from 0.15 to 0.35 m/s, plot the convection heat transfer coefficient as a function of air velocity.

Flow Across Tube Banks

7–108C In flow across tube banks, how does the heat transfer coefficient vary with the row number in the flow direction? How does it vary in the transverse direction for a given row number?

7–109C In flow across tube banks, why is the Reynolds number based on the maximum velocity instead of the uniform approach velocity?

7–110 A tube bank consists of 300 tubes at a distance of 6 cm between the centerlines of any two adjacent tubes. Air approaches the tube bank in the normal direction at 20°C and 1 atm with a mean velocity of 6 m/s. There are 20 rows in the flow direction with 15 tubes in each row with an average surface temperature of 140°C. For an outer tube diameter of 2 cm, determine the average heat transfer coefficient. Evaluate the air properties at an assumed mean temperature of 70°C and 1 atm.

7–111 Water at 15°C is to be heated to 65°C by passing it over a bundle of 4-m-long, 1-cm-diameter resistance heater rods maintained at 90°C. Water approaches the heater rod bundle in the normal direction at a mean velocity of 0.8 m/s. The rods are arranged in-line with longitudinal and transverse pitches of $S_L = 4$ cm and $S_T = 3$ cm. Determine the number of tube rows N_L in the flow direction needed to achieve the indicated temperature rise.
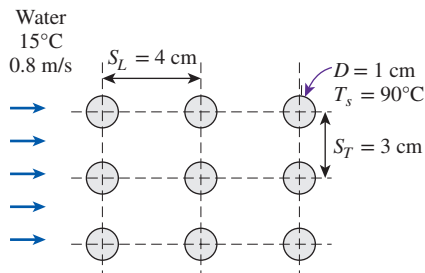
FIGURE P7–111

7–112 Air is to be heated by passing it over a bank of 3-m-long tubes inside which steam is condensing at 100°C. Air approaches the tube bank in the normal direction at 20°C and 1 atm with a mean velocity of 5.2 m/s. The outer diameter of the tubes is 1.6 cm, and the tubes are staggered with longitudinal and transverse pitches of $S_L = S_T = 4$ cm. There are 20 rows in the flow direction with 10 tubes in each row. Determine (*a*) the rate of heat transfer, (*b*) the pressure drop across the tube bank,

and (*c*) the rate of condensation of steam inside the tubes. Evaluate the air properties at an assumed mean temperature of 35°C and 1 atm. Is this a good assumption?

7–113 Repeat Prob. 7–112 for in-line arrangement with $S_L = S_T = 6$ cm.

7–114 Exhaust gases at 1 atm and 300°C are used to preheat water in an industrial facility by passing them over a bank of tubes through which water is flowing at a rate of 6 kg/s. The mean tube wall temperature is 80°C. Exhaust gases approach the tube bank in the normal direction at 4.5 m/s. The outer diameter of the tubes is 2.1 cm, and the tubes are arranged in-line with longitudinal and transverse pitches of $S_L = S_T = 8$ cm. There are 16 rows in the flow direction with eight tubes in each row. Using the properties of air for exhaust gases, determine (*a*) the rate of heat transfer per unit length of tubes, (*b*) pressure drop across the tube bank, and (*c*) the temperature rise of water flowing through the tubes per unit length of tubes. Evaluate the air properties at an assumed mean temperature of 250°C and 1 atm. Is this a good assumption?

7–115 Air is to be cooled in the evaporator section of a refrigerator by passing it over a bank of 0.8-cm-outer-diameter and 0.8-m-long tubes inside which the refrigerant is evaporating at −20°C. Air approaches the tube bank in the normal direction at 0°C and 1 atm with a mean velocity of 5 m/s. The tubes are arranged in-line with longitudinal and transverse pitches of $S_L = S_T = 1.5$ cm. There are 25 rows in the flow direction with 15 tubes in each row. Determine (*a*) the refrigeration capacity of this system and (*b*) pressure drop across the tube bank. Evaluate the air properties at an assumed mean temperature of −5°C and 1 atm. Is this a good assumption?
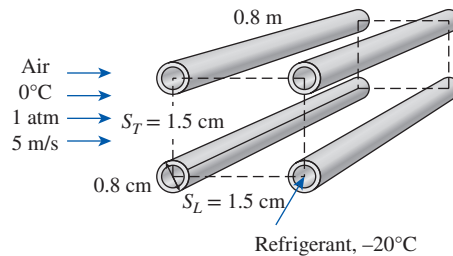
FIGURE P7–115

7–116 Repeat Prob. 7–115 by solving it for staggered arrangement with $S_L = S_T = 1.5$ cm, and compare the performance of the evaporator for the in-line and staggered arrangements.

7–117 Combustion air in a manufacturing facility is to be preheated before entering a furnace by hot water at 90°C flowing through the tubes of a tube bank located in a duct. Air enters the duct at 15°C and 1 atm with a mean velocity of 4.5 m/s, and it flows over the tubes in the normal direction. The outer diameter of the tubes is 2.2 cm, and the tubes

are arranged in-line with longitudinal and transverse pitches of $S_L = S_T = 5$ cm. There are eight rows in the flow direction with eight tubes in each row. Determine the rate of heat transfer per unit length of the tubes and the pressure drop across the tube bank. Evaluate the air properties at an assumed mean temperature of 20°C and 1 atm. Is this a good assumption?

7–118 Repeat Prob. 7–117 for staggered arrangement with $S_L = S_T = 6$ cm.

Review Problems

7–119 Air at 15°C and 1 atm flows over a 0.3-m-wide plate at 65°C at a velocity of 3.0 m/s. Compute the following quantities at $x = x_{cr}$:
  (a) Hydrodynamic boundary layer thickness, m
  (b) Local friction coefficient
  (c) Average friction coefficient
  (d) Total drag force due to friction, N
  (e) Local convection heat transfer coefficient, W/m²·K
  (f) Average convection heat transfer coefficient, W/m²·K
  (g) Rate of convective heat transfer, W

7–120 Air (1 atm, 5°C) with a free-stream velocity of 2 m/s flows in parallel with a stationary thin 1-m × 1-m flat plate over the top and bottom surfaces. The flat plate has a uniform surface temperature of 35°C. Determine (a) the average friction coefficient, (b) the average convection heat transfer coefficient, and (c) the average convection heat transfer coefficient using the modified Reynolds analogy, and compare with the result obtained in (b).

FIGURE P7–120

7–121 Four power transistors, each dissipating 10 W, are mounted on a thin vertical aluminum plate ($k = 237$ W/m·K) 22 cm × 22 cm in size. The heat generated by the transistors is to be dissipated by both surfaces of the plate to the surrounding air at 20°C, which is blown over the plate by a fan at a velocity of 5 m/s. The entire plate can be assumed to be nearly isothermal, and the exposed surface area of the transistor can be taken to be equal to its base area. Determine the temperature of the aluminum plate. Evaluate the air properties at a film temperature of 40°C and 1 atm.

7–122 Oil at 60°C flows at a velocity of 20 cm/s over a 5.0-m-long and 1.0-m-wide flat plate maintained at a constant temperature of 20°C. Determine the rate of heat transfer from the oil to the plate if the average oil properties are $\rho = 880$ kg/m³, $\mu = 0.005$ kg/m·s, $k = 0.15$ W/m·K, and $c_p = 2.0$ kJ/kg·K.

7–123E The passenger compartment of a minivan traveling at 70 mph can be modeled as a 3.2-ft-high, 6-ft-wide, and 12-ft-long rectangular box whose walls have an insulating value of R-3 (i.e., a wall thickness-to-thermal conductivity ratio of 3 h·ft²·°F/Btu). The interior of a minivan is maintained at an average temperature of 70°F during a trip at night while the outside air temperature is 90°F.

The average heat transfer coefficient on the interior surfaces of the van is 1.2 Btu/h·ft²·°F. The airflow over the exterior surfaces can be assumed to be turbulent because of the intense vibrations involved, and the heat transfer coefficient on the front and back surfaces can be taken to be equal to that on the top surface. Disregarding any heat gain or loss by radiation, determine the rate of heat transfer from the ambient air to the van. Assume the airflow to be entirely turbulent because of the intense vibrations involved. Use a film temperature of 80°F for evaluations of air properties at 1 atm.
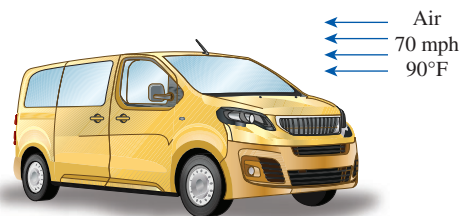
FIGURE P7–123E

7–124 A thin, square, flat plate has 1.2 m on each side. Air at 10°C flows over the top and bottom surfaces of a very rough plate in a direction parallel to one edge, with a velocity of 48 m/s. The surface of the plate is maintained at a constant temperature of 54°C. The plate is mounted on a scale that measures a drag force of 1.5 N. Determine the total heat transfer rate from the plate to the air.

7–125 Consider a house that is maintained at a constant temperature of 22°C. One of the walls of the house has three single-pane glass windows that are 1.5 m high and 1.8 m long. The glass ($k = 0.78$ W/m·K) is 0.5 cm thick, and the heat transfer coefficient on the inner surface of the glass is 8 W/m²·K. Now winds at 35 km/h start to blow parallel to the surface of this wall. If the air temperature outside is −2°C, determine the rate of heat loss through the windows of this wall. Assume radiation heat transfer to be negligible. Evaluate the air properties at a film temperature of 5°C and 1 atm.

7–126 An automotive engine can be approximated as a 0.4-m-high, 0.60-m-wide, and 0.7-m-long rectangular block. The bottom surface of the block is at a temperature of 75°C and has an emissivity of 0.92. The ambient air is at 5°C, and the road surface is at 10°C. Determine the rate of heat transfer from the bottom surface of the engine block by convection and radiation as the car travels at a velocity of 60 km/h. Assume the flow to be turbulent over the entire surface because of the constant agitation of the engine block. How will the heat transfer be affected when a 2-mm-thick layer of gunk ($k = 3$ W/m·K)

has formed at the bottom surface as a result of the dirt and oil collected at that surface over time? Assume the metal temperature under the gunk is still 75°C.
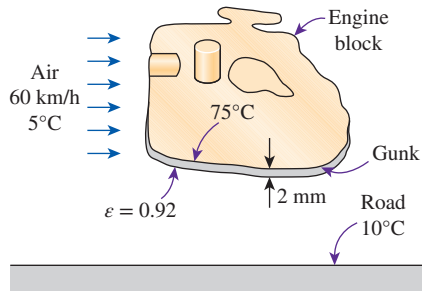
FIGURE P7−126

7–127E A 15-ft-long strip of sheet metal is being transported on a conveyor at a velocity of 16 ft/s. To cure the coating on the upper surface of the sheet metal, infrared lamps providing a constant radiant flux of 1500 Btu/h·ft² are used. The coating on the upper surface of the metal strip has an absorptivity of 0.6 and an emissivity of 0.7, while the surrounding ambient air temperature is 77°F. Radiation heat transfer occurs only on the upper surface, while convection heat transfer occurs on both upper and lower surfaces of the sheet metal. Determine the surface temperature of the sheet metal. Evaluate the properties of air at 180°F.
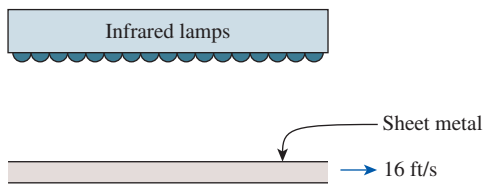
FIGURE P7−127E

7–128 To defrost ice accumulated on the outer surface of an automobile windshield, warm air is blown over the inner surface of the windshield. Consider an automobile windshield ($k_w = 1.4$ W/m·K) with an overall height of 0.5 m and thickness of 5 mm. The outside air (1 atm) ambient temperature is −20°C, and the average airflow velocity over the outer windshield surface is 80 km/h, while the ambient temperature inside the automobile is 25°C. Determine the value of the convection heat transfer coefficient for the warm air blowing over the inner surface of the windshield that is needed to cause the accumulated ice to begin melting. Assume the windshield surface can be treated as a flat plate surface.
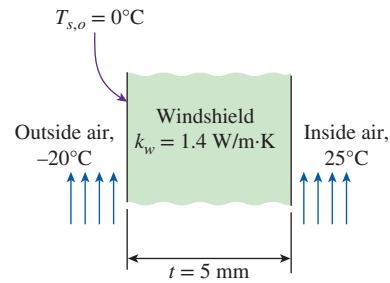
FIGURE P7−128

7–129 The local atmospheric pressure in Denver, Colorado (elevation 1610 m), is 83.4 kPa. Air at this pressure and 20°C flows with a velocity of 8 m/s over a 1.5-m × 6-m flat plate whose temperature is 140°C. Determine the rate of heat transfer from the plate if the air flows parallel to (*a*) the 6-m-long side and (*b*) the 1.5-m side.
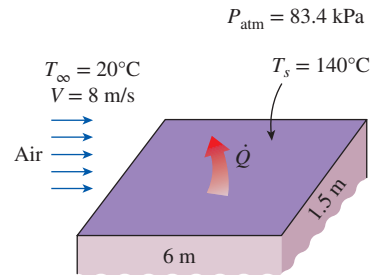
FIGURE P7−129

7–130 A 20-mm × 20-mm silicon chip is mounted such that the edges are flush in a substrate. The substrate provides an unheated starting length of 20 mm that acts as a turbulator. A turbulator is a device that trips the velocity boundary layer to turbulence. Hence the flow is turbulent over the chip. Airflow at 25°C (1 atm) with a velocity of 25 m/s is used to cool the upper surface of the chip. If the maximum surface temperature of the chip cannot exceed 75°C, determine the maximum allowable power dissipation on the chip surface.

7–131 An airstream at 1 atm flows, with a velocity of 15 m/s, in parallel over a 3-m-long flat plate where there is an unheated starting length of 1 m. The airstream has a temperature of 20°C, and the heated section of the flat plate is maintained at a constant temperature of 80°C. Determine (*a*) the local convection heat transfer coefficient at the trailing edge and (*b*) the average convection heat transfer coefficient for the heated section.

7–132 In the effort to increase the removal of heat from a hot surface at 120°C, a cylindrical pin fin ($k_f = 237$ W/m·K) with a diameter of 5 mm is attached to the hot surface. Air at 20°C (1 atm) is flowing across the pin fin with a velocity of 10 m/s.

Determine the maximum possible rate of heat transfer from the pin fin. Evaluate the air properties at 70°C.
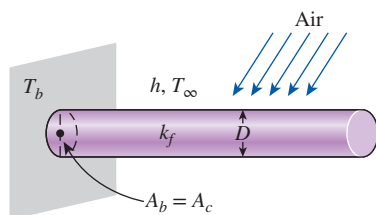
FIGURE P7–132

7–133 Consider a person who is trying to keep cool on a hot summer day by turning a fan on and exposing his body to airflow. The air temperature is 32°C, and the fan is blowing air at a velocity of 5 m/s. The surrounding surfaces are at 40°C, and the emissivity of the person can be taken to be 0.9. If the person is doing light work and generating sensible heat at a rate of 90 W, determine the average temperature of the outer surface (skin or clothing) of the person. The average human body can be treated as a 30-cm-diameter cylinder with an exposed surface area of 1.7 m². Evaluate the air properties at a film temperature of 35°C and 1 atm. *Answer:* 36.2°C

7–134E A transistor with a height of 0.32 in and a diameter of 0.22 in is mounted on a circuit board. The transistor is cooled by air flowing over it at a velocity of 600 ft/min. If the air temperature is 120°F and the transistor case temperature is not to exceed 180°F, determine the amount of power this transistor can dissipate safely.
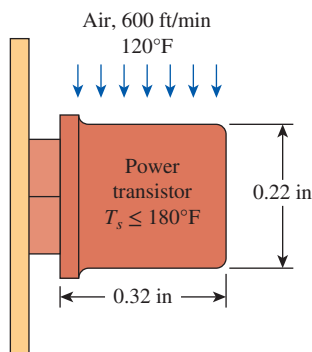
FIGURE P7–134E

7–135 Steam at 250°C flows in a stainless steel pipe ($k = 15$ W/m·K) whose inner and outer diameters are 4 cm and 4.6 cm, respectively. The pipe is covered with 3.5-cm-thick glass wool insulation ($k = 0.038$ W/m·K) whose outer surface has an emissivity of 0.3. Heat is lost to the surrounding air and surfaces at 3°C by convection and radiation. Taking the heat transfer coefficient inside the pipe to be 80 W/m²·K, determine

the rate of heat loss from the steam per unit length of the pipe when air is flowing across the pipe at 4 m/s. Evaluate the air properties at a film temperature of 10°C and 1 atm.

7–136 A cylindrical rod is placed in a crossflow of air at 20°C (1 atm) with velocity of 10 m/s. The rod has a diameter of 5 mm and a constant surface temperature of 120°C. Determine (*a*) the average drag coefficient, (*b*) the convection heat transfer coefficient using the Churchill and Bernstein relation, and (*c*) the convection heat transfer coefficient using Table 7–1.

7–137 A 0.55-m-internal-diameter spherical tank made of 1-cm-thick stainless steel ($k = 15$ W/m·K) is used to store iced water at 0°C. The tank is located outdoors at 30°C and is subjected to winds at 8 km/h. Assuming the entire steel tank to be at 0°C and thus its thermal resistance to be negligible, determine (*a*) the rate of heat transfer to the iced water in the tank and (*b*) the amount of ice at 0°C that melts during a 24-h period. The heat of fusion of water at atmospheric pressure is $h_{if} = 333.7$ kJ/kg. Disregard any heat transfer by radiation.
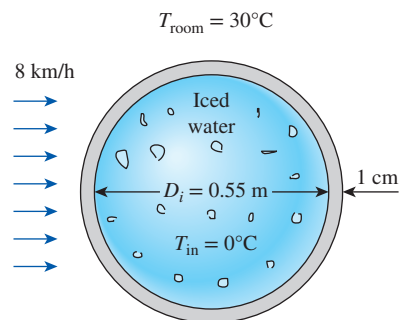
FIGURE P7–137

7–138 Repeat Prob. 7–137, assuming the inner surface of the tank to be at 0°C but by taking the thermal resistance of the tank and heat transfer by radiation into consideration. Assume the average surrounding surface temperature for radiation exchange to be 25°C and the outer surface of the tank to have an emissivity of 0.75. *Answers:* (*a*) 379 W, (*b*) 98.1 kg

7–139 An array of electrical heating elements is used in an air-duct heater as shown in Fig. P7–139. Each element has a length of 200 mm and a uniform surface temperature of 350°C. Atmospheric air enters the heater with a velocity of 8 m/s and a temperature of 25°C. Determine the total heat transfer rate and the temperature of the air leaving the heater. Neglect the change in air properties as a result of temperature change across the heater. Evaluate the air properties at an assumed mean temperature of 35°C and 1 atm. Is this a good assumption?

Air
$T_i = 25°C$
$V = 8$ m/s

24 mm

$T_s = 350°C$

$D = 12$ mm
$(L = 200$ mm$)$

24 mm

T_o
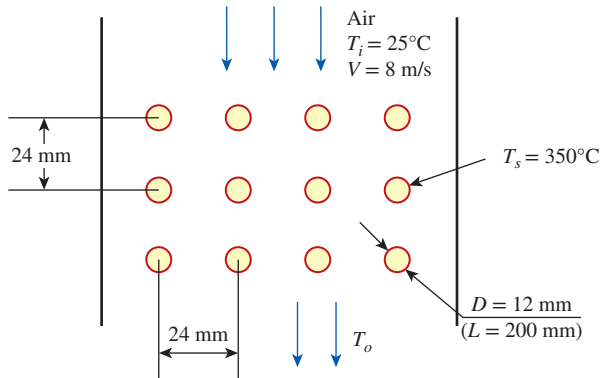
FIGURE P7−139

Fundamentals of Engineering (FE) Exam Problems

7–140   For laminar flow of a fluid along a flat plate, one would expect the largest local convection heat transfer coefficient for the same Reynolds and Prandl numbers when

(*a*) The same temperature is maintained on the surface
(*b*) The same heat flux is maintained on the surface
(*c*) The plate has an unheated section
(*d*) The plate surface is polished
(*e*) None of the above

7–141   Air at 20°C flows over a 4-m-long and 3-m-wide surface of a plate whose temperature is 80°C with a velocity of 7 m/s. The length of the surface for which the flow remains laminar is

(*a*) 0.9 m   (*b*) 1.3 m   (*c*) 1.8 m
(*d*) 2.2 m   (*e*) 3.7 m

(For air, use $k = 0.02735$ W/m·K, Pr $= 0.7228$, $\nu = 1.798 \times 10^{-5}$ m²/s)

7–142   Air at 20°C flows over a 4-m-long and 3-m-wide surface of a plate whose temperature is 80°C with a velocity of 5 m/s. The rate of heat transfer from the laminar flow region of the surface is

(*a*) 950 W   (*b*) 1037 W   (*c*) 2074 W
(*d*) 2640 W   (*e*) 3075 W

(For air, use $k = 0.02735$ W/m·K, Pr $= 0.7228$, $\nu = 1.798 \times 10^{-5}$ m²/s)

7–143   Engine oil at 105°C flows over the surface of a flat plate whose temperature is 15°C with a velocity of 1.5 m/s. The local drag force per unit surface area 0.8 m from the leading edge of the plate is

(*a*) 21.8 N/m²   (*b*) 14.3 N/m²   (*c*) 10.9 N/m²
(*d*) 8.5 N/m²   (*e*) 5.5 N/m²

(For oil, use $\nu = 8.565 \times 10^{-5}$ m²/s, $\rho = 864$ kg/m³)

7–144   Air ($k = 0.028$ W/m·K, Pr $= 0.7$) at 50°C flows along a 1-m-long flat plate whose temperature is maintained at 20°C with a velocity such that the Reynolds number at the end of the plate is 10,000. The heat transfer per unit width between the plate and air is

(*a*) 20 W/m   (*b*) 30 W/m   (*c*) 40 W/m
(*d*) 50 W/m   (*e*) 60 W/m

7–145   Air at 15°C flows over a flat plate subjected to a uniform heat flux of 240 W/m² with a velocity of 3.5 m/s. The surface temperature of the plate 6 m from the leading edge is

(*a*) 40.5°C   (*b*) 41.5°C   (*c*) 58.2°C
(*d*) 95.4°C   (*e*) 134°C

(For air, use $k = 0.02551$ W/m·K, Pr $= 0.7296$, $\nu = 1.562 \times 10^{-5}$ m²/s)

7–146   Air at 20°C flows over a 4-m-long and 3-m-wide surface of a plate whose temperature is 80°C with a velocity of 5 m/s. The rate of heat transfer from the surface is

(*a*) 7383 W   (*b*) 8985 W   (*c*) 11,231 W
(*d*) 14,672 W   (*e*) 20,402 W

(For air, use $k = 0.02735$ W/m·K, Pr $= 0.7228$, $\nu = 1.798 \times 10^{-5}$ m²/s)

7–147   Water at 75°C flows over a 2-m-long, 2-m-wide surface of a plate whose temperature is 5°C with a velocity of 1.5 m/s. The total drag force acting on the plate is

(*a*) 2.8 N   (*b*) 12.3 N   (*c*) 13.7 N
(*d*) 15.4 N   (*e*) 20.0 N

(For water, use $\nu = 0.658 \times 10^{-6}$ m²/s, $\rho = 992$ kg/m³)

7–148   Air at 25°C flows over a 5-cm-diameter, 1.7-m-long smooth pipe with a velocity of 4 m/s. A refrigerant at −15°C flows inside the pipe, and the surface temperature of the pipe is essentially the same as the refrigerant temperature inside. The drag force exerted on the pipe by the air is

(*a*) 0.4 N   (*b*) 1.1 N   (*c*) 8.5 N
(*d*) 13 N   (*e*) 18 N

(For air, use $\nu = 1.382 \times 10^{-5}$ m²/s, $\rho = 1.269$ kg/m³)

7–149   Air at 25°C flows over a 4-cm-diameter, 1.7-m-long pipe with a velocity of 4 m/s. A refrigerant at −15°C flows inside the pipe, and the surface temperature of the pipe is essentially the same as the refrigerant temperature inside. Air properties at the average temperature are $k = 0.0240$ W/m·K, Pr $= 0.735$, $\nu = 1.382 \times 10^{-5}$ m²/s. The rate of heat transfer to the pipe is

(*a*) 126 W   (*b*) 245 W   (*c*) 302 W
(*d*) 415 W   (*e*) 556 W

7–150   Kitchen water at 10°C flows over a 10-cm-diameter pipe with a velocity of 1.1 m/s. Geothermal water enters the pipe at 90°C at a rate of 1.25 kg/s. For calculation purposes, the surface temperature of the pipe may be assumed to be 70°C. If the geothermal water is to leave the pipe at 50°C, the required length of the pipe is

(a) 1.1 m (b) 1.8 m (c) 2.9 m

(d) 4.3 m (e) 7.6 m

(For both water streams, use $k = 0.631$ W/m·K, Pr = 4.32, $\nu = 0.658 \times 10^{-6}$ m²/s, $c_p = 4179$ J/kg·K)

7–151 Wind at 30°C flows over a 0.5-m-diameter spherical tank containing iced water at 0°C with a velocity of 25 km/h. If the tank is thin-shelled with a high thermal conductivity material, the rate at which ice melts is

(a) 4.78 kg/h (b) 6.15 kg/h (c) 7.45 kg/h

(d) 11.8 kg/h (e) 16.0 kg/h

(Take $h_{if} = 333.7$ kJ/kg, and use the following for air: $k = 0.02588$ W/m·K, Pr = 0.7282, $\nu = 1.608 \times 10^{-5}$ m²/s, $\mu_{\infty} = 1.872 \times 10^{-5}$ kg/m·s, $\mu_s = 1.729 \times 10^{-5}$ kg/m·s)

7–152 Ambient air at 20°C flows over a 30-cm-diameter hot spherical object with a velocity of 4.2 m/s. If the average surface temperature of the object is 200°C, the average convection heat transfer coefficient during this process is

(a) 8.6 W/m·K (b) 15.7 W/m·K (c) 18.6 W/m·K

(d) 21.0 W/m·K (e) 32.4 W/m·K

(For air, use $k = 0.2514$ W/m·K, Pr = 0.7309, $\nu = 1.516 \times 10^{-5}$ m²/s, $\mu_{\infty} = 1.825 \times 10^{-5}$ kg/m·s, $\mu_s = 2.577 \times 10^{-5}$ kg/m·s)

7–153 Jakob (1949) suggests the following correlation be used for square tubes in a liquid crossflow situation:

$$Nu = 0.102 \, Re^{0.675} \, Pr^{1/3}$$

Water ($k = 0.61$ W/m·K, Pr = 6) at 50°C flows across a 1-cm-square tube with a Reynolds number of 10,000 and surface temperature of 75°C. If the tube is 3 m long, the rate of heat transfer between the tube and water is

(a) 9.8 kW (b) 12.4 kW (c) 17.0 kW

(d) 19.6 kW (e) 24.0 kW

7–154 Air (Pr = 0.7, $k = 0.026$ W/m·K) at 200°C flows across 3-cm-diameter tubes whose surface temperature is 50°C with a Reynolds number of 8000. The Churchill and Bernstein (1977) convective heat transfer correlation for the average Nusselt number in this situation is

$$Nu = 0.3 + \frac{0.62 \, Re^{0.5} \, Pr^{0.33}}{[1 + (0.4/Pr)^{0.67}]^{0.25}}$$

(a) 1.3 kW/m² (b) 2.4 kW/m² (c) 4.1 kW/m²

(d) 5.7 kW/m² (e) 8.2 kW/m²

7–155 Jakob (1949) suggests the following correlation be used for square tubes in a liquid crossflow situation:

$$Nu = 0.102 \, Re^{0.625} \, Pr^{1/3}$$

Water ($k = 0.61$ W/m·K, Pr = 6) flows across a 1-cm-square tube with a Reynolds number of 10,000. The convection heat transfer coefficient is

(a) 5.7 kW/m²·K (b) 8.3 kW/m²·K (c) 11.2 kW/m²·K

(d) 15.6 kW/m²·K (e) 18.1 kW/m²·K

Design and Essay Problems

7–156 On average, superinsulated homes use just 15 percent of the fuel required to heat the same size conventional home built before the energy crisis in the 1970s. Write an essay on superinsulated homes, and identify the features that make them so energy efficient as well as the problems associated with them. Do you think superinsulated homes will be economically attractive in your area?

7–157 Conduct this experiment to determine the heat loss coefficient of your house or apartment in W/°C or Btu/h·°F. First make sure that the conditions in the house are steady and the house is at the set temperature of the thermostat. Use an outdoor thermometer to monitor outdoor temperature. One evening, using a watch or timer, determine how long the heater was on during a 3-h period and the average outdoor temperature during that period. Then using the heat output rating of your heater, determine the amount of heat supplied. Also, estimate the amount of heat generation in the house during that period by noting the number of people, the total wattage of lights that were on, and the heat generated by the appliances and equipment. Using that information, calculate the average rate of heat loss from the house and the heat loss coefficient.

7–158 The decision whether to invest in an energy-saving measure is made on the basis of the length of time needed for it to pay for itself in projected energy (and thus cost) savings. The easiest way to decide is to calculate the simple payback period by simply dividing the installed cost of the measure by the annual cost savings and comparing it to the lifetime of the installation. This approach is adequate for short payback periods (less than five years) in stable economies with low interest rates (under 10 percent) since the error involved is no larger than the uncertainties. However, if the payback period is long, it may be necessary to consider the *interest rate* if the money is to be borrowed, or the *rate of return* if the money is invested elsewhere instead of the energy conservation measure. For example, a simple payback period of five years corresponds to 5.0, 6.12, 6.64, 7.27, 8.09, 9.919, 10.84, and 13.91 for an interest rate (or return on investment) of 0, 6, 8, 10, 12, 14, 16, and 18 percent, respectively. Finding out the proper relations from engineering economics books, determine the payback periods for the interest rates given above corresponding to simple payback periods of 1 to 10 years.

Design Element: "C&S icon ©McGraw-Hill Education; PtD icon ©McGraw-Hill Education; laptop art ©McGraw-Hill Education".

INTERNAL FORCED CONVECTION

L iquid or gas flow through pipes or ducts is commonly used in heating and cooling applications. The fluid in such applications is forced to flow by a fan or pump through a flow section that is sufficiently long to accomplish the desired heat transfer. In this chapter, we pay particular attention to the determination of the *friction factor* and *convection coefficient* since they are directly related to the *pressure drop* and *heat transfer rate,* respectively. These quantities are then used to determine the pumping power requirement and the required tube length.

There is a fundamental difference between external and internal flows. In *external flow,* considered in Chap. 7, the fluid has a free surface, and thus the boundary layer over the surface is free to grow indefinitely. In *internal flow,* however, the fluid is completely confined by the inner surfaces of the tube, and thus there is a limit on how much the boundary layer can grow.

We start this chapter with a general physical description of internal flow, and the *average velocity* and *average temperature*. We continue with the discussion of the *hydrodynamic* and *thermal entry lengths, developing flow,* and *fully developed flow.* We then obtain the velocity and temperature profiles for fully developed laminar flow and develop relations for the friction factor and Nusselt number. Finally, we present empirical relations for developing and fully developed flows and demonstrate their use.

Circular pipe

Water
50 atm

Rectangular
duct

Air
1.2 atm
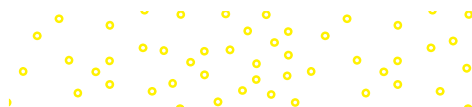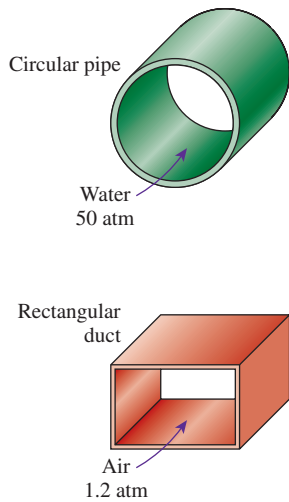
FIGURE 8–1
Circular pipes can withstand large
pressure differences between the
inside and the outside without
undergoing any significant distortion,
but noncircular pipes cannot.

V_{avg} V_{max}
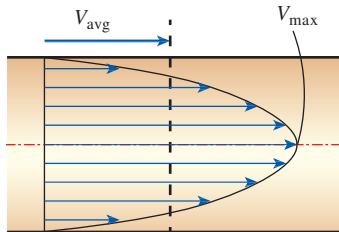
FIGURE 8–2
Average velocity V_{avg} is defined as the
average speed through a cross section.
For fully developed laminar pipe flow,
V_{avg} is half of the maximum velocity.

8–1 ▪ INTRODUCTION

The terms *pipe, duct,* and *conduit* are usually used interchangeably for flow
sections. In general, flow sections of circular cross section are referred to as
pipes (especially when the fluid is a liquid) and flow sections of noncircular
cross section as *ducts* (especially when the fluid is a gas). Small-diameter
pipes are usually referred to as *tubes.* Given this uncertainty, we will use more
descriptive phrases (such as *a circular pipe* or *a rectangular duct*) whenever
necessary to avoid any misunderstandings.

You have probably noticed that most fluids, especially liquids, are trans-
ported in *circular pipes.* This is because pipes with a circular cross section
can withstand large pressure differences between the inside and the outside
without undergoing significant distortion. *Noncircular pipes* are usually used
in applications such as the heating and cooling systems of buildings where
the pressure difference is relatively small, the manufacturing and installation
costs are lower, and the available space is limited for ductwork (Fig. 8–1). For
a fixed surface area, the circular tube gives the most heat transfer for the least
pressure drop, which explains the overwhelming popularity of circular tubes
in heat transfer equipment.

Although the theory of fluid flow is reasonably well understood, theo-
retical solutions are obtained only for a few simple cases such as fully
developed laminar flow in a circular pipe. Therefore, we must rely on
experimental results and empirical relations for most fluid flow problems
rather than closed-form analytical solutions. Noting that the experimental
results are obtained under carefully controlled laboratory conditions and
that no two systems are exactly alike, we must not be so naive as to view
the results obtained as exact. An error of 10 percent (or more) in friction
factors calculated using the relations in this chapter is the norm rather than
the exception.

The fluid velocity in a pipe changes from *zero* at the wall because of the no-
slip condition to a maximum at the pipe center. In fluid flow, it is convenient
to work with an *average* velocity V_{avg}, which remains constant in incompress-
ible flow when the cross-sectional area of the pipe is constant (Fig. 8–2). The
average velocity in heating and cooling applications may change somewhat
because of changes in density with temperature. But in practice we evaluate
the fluid properties at some average temperature and treat them as constants.
The convenience of working with constant properties usually more than justi-
fies the slight loss in accuracy.

Also, the friction between the fluid particles in a pipe does cause a
slight rise in fluid temperature as a result of the mechanical energy being
converted to sensible thermal energy. But this temperature rise due to
frictional heating is usually too small to warrant any consideration in cal-
culations and thus is disregarded. For example, in the absence of any heat
transfer, no noticeable difference can be detected between the inlet and
outlet temperatures of water flowing in a pipe. The primary consequence
of friction in fluid flow is pressure drop, and thus any significant tem-
perature change in the fluid is due to heat transfer. But frictional heating
must be considered for flows that involve highly viscous fluids with large
velocity gradients.

8–2 ■ AVERAGE VELOCITY AND TEMPERATURE

In external flow, the free-stream velocity served as a convenient reference velocity for use in the evaluation of the Reynolds number and the friction coefficient. In internal flow, there is no free stream, and thus we need an alternative. The fluid velocity in a tube changes from zero at the surface because of the no-slip condition to a maximum at the tube center. Therefore, it is convenient to work with an **average** or **mean velocity** V_{avg}, which remains constant for incompressible flow when the cross-sectional area of the tube is constant.

The value of the average velocity V_{avg} at some streamwise cross section is determined from the requirement that the *conservation of mass* principle be satisfied (Fig. 8–2). That is,

$$\dot{m} = \rho V_{avg} A_c = \int_{A_c} \rho u(r) \, dA_c \tag{8–1}$$

where $\dot{m}$ is the mass flow rate, ρ is the density, A_c is the cross-sectional area, and $u(r)$ is the velocity profile. Then, the average velocity for incompressible flow in a circular pipe of radius R is expressed as

$$V_{avg} = \frac{\int_{A_c} \rho u(r) \, dA_c}{\rho A_c} = \frac{\int_0^R \rho u(r) 2\pi r \, dr}{\rho \pi R^2} = \frac{2}{R^2} \int_0^R u(r) r \, dr \tag{8–2}$$

Therefore, when we know the flow rate or the velocity profile, the average velocity can be determined easily.

When a fluid is heated or cooled as it flows through a tube, the temperature of the fluid at any cross section changes from T_s at the surface of the wall to some maximum (or minimum in the case of heating) at the tube center. In fluid flow, it is convenient to work with an **average** or **mean temperature** T_m, which remains constant at a cross section. Unlike the mean velocity, the mean temperature T_m *changes* in the flow direction whenever the fluid is heated or cooled.

The value of the mean temperature T_m is determined from the requirement that the *conservation of energy* principle be satisfied. That is, the energy transported by the fluid through a cross section in actual flow must be equal to the energy that would be transported through the same cross section if the fluid were at a constant temperature T_m. This can be expressed mathematically as (Fig. 8–3)

$$\dot{E}_{fluid} = \dot{m} c_p T_m = \int_{\dot{m}} c_p T(r) \delta \dot{m} = \int_{A_c} \rho c_p T(r) u(r) dA_c \tag{8–3}$$

where c_p is the specific heat of the fluid. Note that the product $\dot{m} c_p T_m$ at any cross section along the tube represents the *energy flow* with the fluid at that cross section. Then, the mean temperature of a fluid with constant density and specific heat flowing in a circular pipe of radius R can be expressed as

$$T_m = \frac{\int_{\dot{m}} c_p T(r) \delta \dot{m}}{\dot{m} c_p} = \frac{\int_0^R c_p T(r) \rho u(r) 2\pi r dr}{\rho V_{avg} (\pi R^2) c_p} = \frac{2}{V_{avg} R^2} \int_0^R T(r) u(r) \, r dr \tag{8–4}$$

Note that the mean temperature T_m of a fluid changes during heating or cooling. Also, the fluid properties in internal flow are usually evaluated at the *bulk*

FIGURE 8–3

Actual and idealized temperature profiles for flow in a tube (the rate at which energy is transported with the fluid is the same for both cases).
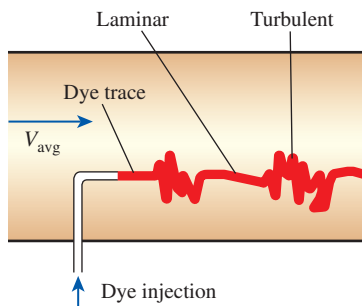
mean fluid temperature, which is the arithmetic average of the mean temperatures at the inlet and the exit. That is, $T_b = (T_i + T_e)/2$.

Laminar and Turbulent Flow in Tubes

Flow in a tube can be laminar or turbulent, depending on the flow conditions. Fluid flow is streamlined and thus laminar at low velocities, but turns turbulent as the velocity is increased beyond a critical value. Transition from laminar to turbulent flow does not occur suddenly; rather, it occurs over some range of velocity where the flow fluctuates between laminar and turbulent flows before it becomes fully turbulent. Most pipe flows encountered in practice are turbulent. Laminar flow is encountered when highly viscous fluids such as oils flow in small-diameter tubes or narrow passages.

For flow in a circular tube, the Reynolds number is defined as

$$\text{Re} = \frac{V_{\text{avg}}D}{\nu} = \frac{\rho V_{\text{avg}}D}{\mu} = \frac{\rho D}{\mu}\left(\frac{\dot{m}}{\rho \pi D^2/4}\right) = \frac{4\dot{m}}{\mu \pi D} \tag{8-5}$$

where V_{avg} is the average flow velocity, D is the diameter of the tube, and $\nu = \mu/\rho$ is the kinematic viscosity of the fluid.

For flow through noncircular tubes, the Reynolds number as well as the Nusselt number, and the friction factor are based on the **hydraulic diameter** D_h defined as (Fig. 8–4)

$$D_h = \frac{4A_c}{p} \tag{8-6}$$

where A_c is the cross-sectional area of the tube and p is its wetted perimeter. The hydraulic diameter is defined such that it reduces to ordinary diameter D for circular tubes since

Circular tubes:
$$D_h = \frac{4A_c}{p} = \frac{4\pi D^2/4}{\pi D} = D$$

It certainly is desirable to have precise values of Reynolds numbers for laminar, transitional, and turbulent flows, but this is not the case in practice. This is because the transition from laminar to turbulent flow also depends on the degree of disturbance of the flow by *surface roughness, pipe vibrations,* and the *fluctuations in the flow.* Under most practical conditions, the flow in a tube is laminar for Re < 2300, fully turbulent for Re > 10,000, and transitional in between. But it should be kept in mind that in many cases the flow becomes fully turbulent for Re > 4000, as discussed in the Topic of Special Interest later in this chapter. When designing piping networks and determining pumping power, a conservative approach is taken, and flows with Re > 4000 are assumed to be turbulent.

In transitional flow, the flow switches between laminar and turbulent in a disorderly fashion (Fig. 8–5). It should be kept in mind that laminar flow can be maintained at much higher Reynolds numbers in very smooth pipes by avoiding flow disturbances and tube vibrations. In such carefully controlled experiments, laminar flow has been maintained at Reynolds numbers of up to 100,000.

Circular tube:
$$D_h = \frac{4(\pi D^2/4)}{\pi D} = D$$

Square duct:
$$D_h = \frac{4a^2}{4a} = a$$

Rectangular duct:
$$D_h = \frac{4ab}{2(a+b)} = \frac{2ab}{a+b}$$

Channel:
$$D_h = \frac{4ab}{2a+b}$$

FIGURE 8–4
The hydraulic diameter $D_h = 4A_c/p$ is defined such that it reduces to ordinary diameter for circular tubes. When there is a free surface, such as in open-channel flow, the wetted perimeter includes only the walls in contact with the fluid.

FIGURE 8–5
In the transitional flow region of the flow switches between laminar and turbulent somewhat randomly.

8–3 ▪ THE ENTRANCE REGION

Consider a fluid entering a circular pipe at a uniform velocity. Because of the no-slip condition, the fluid particles in the layer in contact with the wall of the pipe come to a complete stop. This layer also causes the fluid particles in the adjacent layers to slow down gradually as a result of friction. To make up for this velocity reduction, the velocity of the fluid at the midsection of the pipe has to increase to keep the mass flow rate through the pipe constant. As a result, a velocity gradient develops along the pipe.

The region of the flow in which the effects of the viscous shearing forces caused by fluid viscosity are felt is called the **velocity boundary layer** or just the **boundary layer**. The hypothetical boundary surface divides the flow in a pipe into two regions: the **boundary layer region**, in which the viscous effects and the velocity changes are significant, and the **irrotational** (**core**) **flow region**, in which the frictional effects are negligible and the velocity remains essentially constant in the radial direction.

The thickness of this boundary layer increases in the flow direction until the boundary layer reaches the pipe center and thus fills the entire pipe, as shown in Fig. 8–6, and the velocity becomes fully developed a little further downstream. The region from the pipe inlet to the point at which the velocity profile is fully developed is called the **hydrodynamic entrance region**, and the length of this region is called the **hydrodynamic entry length** L_h. Flow in the entrance region is called *hydrodynamically developing flow* since this is the region where the velocity profile develops. The region beyond the entrance region in which the velocity profile is fully developed and remains unchanged is called the **hydrodynamically fully developed region**. The velocity profile in the fully developed region is *parabolic* in laminar flow and somewhat *flatter* or fuller in turbulent flow due to eddy motion and more vigorous mixing in a radial direction.

Now consider a fluid at a uniform temperature entering a circular tube whose surface is maintained at a different temperature. This time, the fluid particles in the layer in contact with the surface of the tube assume the surface temperature. This initiates convection heat transfer in the tube and the development of a *thermal boundary layer* along the tube. The thickness of this boundary layer also increases in the flow direction until the boundary layer reaches the tube center and thus fills the entire tube, as shown in Fig. 8–7.
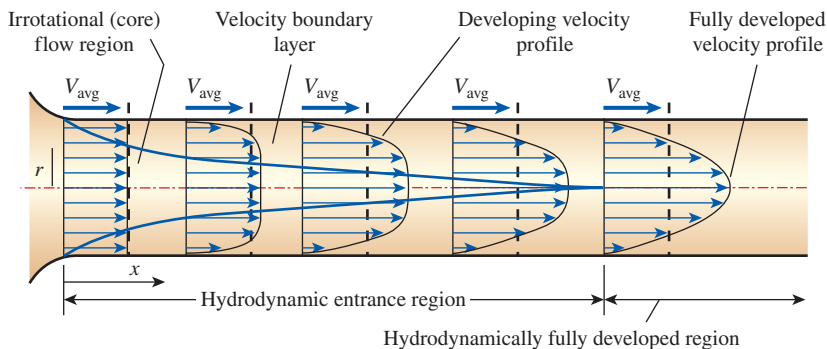
FIGURE 8–6

The development of the velocity boundary layer in a pipe. (The developed average velocity profile is parabolic in laminar flow, as shown, but much flatter or fuller in turbulent flow.)
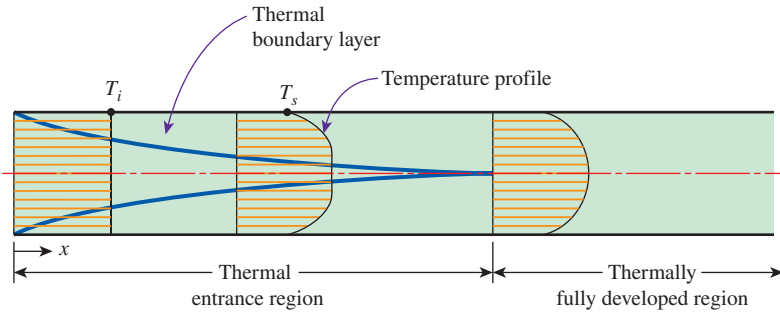
FIGURE 8–7
The development of the thermal boundary layer in a tube. (The fluid in the tube is being cooled.)

The region of flow over which the thermal boundary layer develops and reaches the tube center is called the **thermal entrance region**, and the length of this region is called the **thermal entry length** L_t. Flow in the thermal entrance region is called *thermally developing flow* since this is the region where the temperature profile develops. The region beyond the thermal entrance region in which the dimensionless temperature profile expressed as $(T_s - T)/(T_s - T_m)$ remains unchanged is called the **thermally fully developed region**. The region in which the flow is both hydrodynamically and thermally developed and thus both the velocity and dimensionless temperature profiles remain unchanged is called *fully developed flow.* That is,

Hydrodynamically fully developed:
$$\frac{\partial u(r, x)}{\partial x} = 0 \longrightarrow u = u(r) \qquad \textbf{(8–7)}$$

Thermally fully developed:
$$\frac{\partial}{\partial x}\left[\frac{T_s(x) - T(r, x)}{T_s(x) - T_m(x)}\right] = 0 \qquad \textbf{(8–8)}$$

The shear stress at the tube wall τ_w is related to the slope of the velocity profile at the surface. Noting that the velocity profile remains unchanged in the hydrodynamically fully developed region, the wall shear stress also remains constant in that region. A similar argument can be given for the heat transfer coefficient in the thermally fully developed region.

In a thermally fully developed region, the derivative of $(T_s - T)/(T_s - T_m)$ with respect to x is zero by definition, and thus $(T_s - T)/(T_s - T_m)$ is independent of x. Then, the derivative of $(T_s - T)/(T_s - T_m)$ with respect to r must also be independent of x. That is,

$$\frac{\partial}{\partial r}\left(\frac{T_s - T}{T_s - T_m}\right)\bigg|_{r = R} = \frac{-(\partial T/\partial r)|_{r = R}}{T_s - T_m} \neq f(x) \qquad \textbf{(8–9)}$$

Surface heat flux can be expressed as

$$\dot{q}_s = h_x(T_s - T_m) = k\frac{\partial T}{\partial r}\bigg|_{r = R} \longrightarrow h_x = \frac{k(\partial T/\partial r)|_{r = R}}{T_s - T_m} \qquad \textbf{(8–10)}$$

FIGURE 8–8
Variation of the friction factor and the convection heat transfer coefficient in the flow direction for flow in a tube $(Pr > 1)$.

which, from Eq. 8–9, is independent of x. Thus, we conclude that *in the thermally fully developed region of a tube, the local convection coefficient is constant* (does not vary with x). Therefore, both *the local friction factor f_x* (*which is related to the local wall shear stress*) and the local convection coefficient h_x remain constant in the hydrodynamically and thermally fully developed regions, respectively, as shown in Fig. 8–8 for $Pr > 1$.

Note that the *temperature profile* in the thermally fully developed region may vary with *x* in the flow direction. That is, unlike the velocity profile, the temperature profile can be different at different cross sections of the tube in the developed region, and it usually is. However, the dimensionless temperature profile defined previously remains unchanged in the thermally developed region when the temperature or heat flux at the tube surface remains constant.

During laminar flow in a tube, the magnitude of the dimensionless Prandtl number Pr is a measure of the relative growth of the velocity and thermal boundary layers. For fluids with Pr ≈ 1, such as gases, the two boundary layers essentially coincide with each other. For fluids with Pr ≫ 1, such as oils, the velocity boundary layer outgrows the thermal boundary layer. As a result, the hydrodynamic entry length is smaller than the thermal entry length. The opposite is true for fluids with Pr ≪ 1 such as liquid metals.

Consider a fluid that is being heated (or cooled) in a tube as it flows through it. The wall shear stress and the heat transfer coefficient are *highest* at the tube inlet where the thickness of the boundary layers is smallest, and they decrease gradually to the fully developed values, as shown in Fig. 8–8. Therefore, the pressure drop and heat flux are *higher* in the entrance regions of a tube, and the effect of the entrance region is always to *increase* the average friction factor and heat transfer coefficient for the entire tube. This enhancement can be significant for short tubes but negligible for long ones.

Entry Lengths

The hydrodynamic entry length is usually taken to be the distance from the tube entrance where the wall shear stress (and thus the friction factor) reaches within about 2 percent of the fully developed value. In *laminar flow,* the hydrodynamic and thermal entry lengths are given approximately as [see Kays and Crawford (1993) and Shah and Bhatti (1987)]

$$L_{h,\,\text{laminar}} \approx 0.05 \text{ Re } D \qquad\qquad \textbf{(8–11)}$$

$$L_{t,\,\text{laminar}} \approx 0.05 \text{ Re Pr } D = \text{Pr } L_{h,\,\text{laminar}} \qquad\qquad \textbf{(8–12)}$$

For Re = 20, the hydrodynamic entry length is about the size of the diameter, but it increases linearly with velocity. In the limiting case of Re = 2300, the hydrodynamic entry length is 115*D.* When the flow is simultaneously hydrodynamically and thermally developing, a longer thermal entrance length is required than for hydrodynamically fully developed flow. Meyer and Everts (2018a) suggest replacing the coefficient of 0.05 used in Eq. 8–12 with 0.12 for simultaneously hydrodynamically and thermally developing forced convection laminar flow.

In *turbulent flow,* the intense mixing during random fluctuations usually overshadows the effects of molecular diffusion, and therefore the hydrodynamic and thermal entry lengths are of about the same size and independent of the Prandtl number.

The entry length is much shorter in turbulent flow, as expected, and its dependence on the Reynolds number is weaker. In many tube flows of practical interest, the entrance effects become insignificant beyond a tube length of 10 diameters, and the hydrodynamic and thermal entry lengths are approximately taken to be

$$L_{h,\,\text{turbulent}} \approx L_{t,\,\text{turbulent}} \approx 10D \qquad\qquad \textbf{(8–13)}$$

The variation of local Nusselt number along a tube in turbulent flow for both constant surface temperature and constant surface heat flux is given
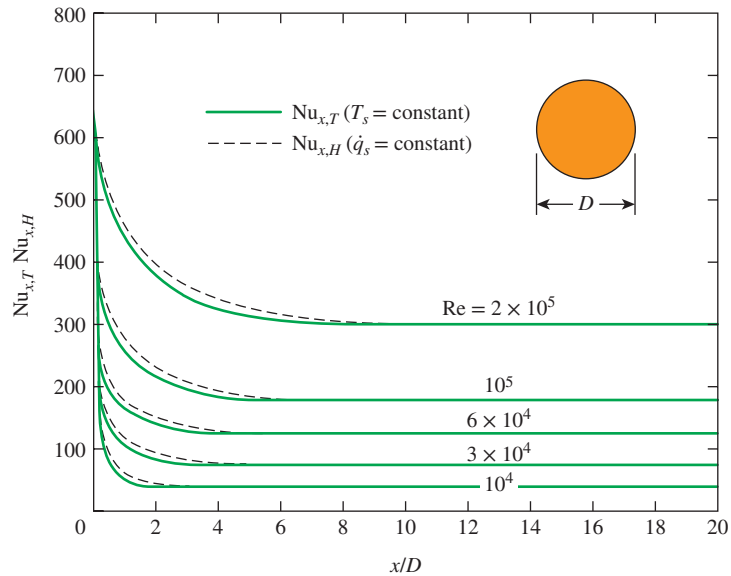
FIGURE 8–9
Variation of local Nusselt number along a tube in turbulent flow for both constant surface temperature and constant surface heat flux
Source: Deissler, 1953.

in Fig. 8–9 for the range of Reynolds numbers encountered in heat transfer equipment. We make these important observations from this figure:

- The Nusselt numbers and thus the convection heat transfer coefficients are much higher in the entrance region.
- The Nusselt number reaches a constant value at a distance of less than 10 diameters, and thus the flow can be assumed to be fully developed for $x > 10D$.
- The Nusselt numbers for the constant surface temperature and constant surface heat flux conditions are identical in the fully developed regions and nearly identical in the entrance regions. Therefore, Nusselt number is insensitive to the type of thermal boundary condition, and the turbulent flow correlations can be used for either type of boundary condition.

Precise correlations for the friction and heat transfer coefficients for the entrance regions are available in the literature. However, the tubes used in practice in forced convection are usually several times the length of either entrance region, and thus the flow through the tubes is often assumed to be fully developed for the entire length of the tube. This simplistic approach gives *reasonable* results for the rate of heat transfer for long tubes and *conservative* results for short ones.

It should be noted that the above observations are only valid for turbulent flow. In laminar flow Nusselt number values are much lower than turbulent flow values, the distance for the Nusselt number to reach a constant value is typically much longer, and the flow is sensitive to the thermal boundary conditions imposed on the flow.

Energy balance:
$$\dot{Q} = \dot{m}c_p(T_e - T_i)$$
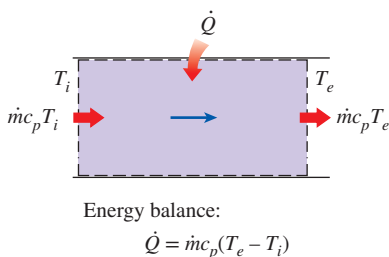
FIGURE 8–10
The heat transfer to a fluid flowing in a tube is equal to the increase in the energy of the fluid.

8–4 ■ GENERAL THERMAL ANALYSIS

In the absence of any work interactions (such as electric resistance heating), the conservation of energy equation for the steady flow of a fluid in a tube can be expressed as (Fig. 8–10)

$$\dot{Q} = \dot{m}c_p(T_e - T_i) \quad \text{(W)} \tag{8–14}$$

where T_i and T_e are the mean fluid temperatures at the inlet and exit of the tube, respectively, and $\dot{Q}$ is the rate of heat transfer to or from the fluid. Note that the temperature of a fluid flowing in a tube remains constant in the absence of any energy interactions through the wall of the tube.

The thermal conditions at the surface can usually be approximated with reasonable accuracy to be *constant surface temperature* ($T_s = $ constant) or *constant surface heat flux* ($\dot{q}_s = $ constant). For example, the constant surface temperature condition is realized when a phase change process such as boiling or condensation occurs at the outer surface of a tube. The constant surface heat flux condition is realized when the tube is subjected to radiation or electric resistance heating uniformly from all directions.

Surface heat flux is expressed as

$$\dot{q}_s = h_x(T_s - T_m) \qquad (\text{W/m}^2) \tag{8-15}$$

where h_x is the *local* heat transfer coefficient and T_s and T_m are the surface and the mean fluid temperatures at that location. Note that the mean fluid temperature T_m of a fluid flowing in a tube must change during heating or cooling. Therefore, when $h_x = h = $ constant, the surface temperature T_s must change when $\dot{q}_s = $ constant, and the surface heat flux $\dot{q}_s$ must change when $T_s = $ constant. Thus we may have either $T_s = $ constant or $\dot{q}_s = $ constant at the surface of a tube, but not both. Next we consider convection heat transfer for these two common cases.

Constant Surface Heat Flux ($\dot{q}_s = $ constant)

In the case of $\dot{q}_s = $ constant, the rate of heat transfer can also be expressed as

$$\dot{Q} = \dot{q}_s A_s = \dot{m}c_p(T_e - T_i) \qquad (\text{W}) \tag{8-16}$$

Then the mean fluid temperature at the tube exit becomes

$$T_e = T_i + \frac{\dot{q}_s A_s}{\dot{m}c_p} \tag{8-17}$$

Note that the mean fluid temperature increases *linearly* in the flow direction in the case of constant surface heat flux, since the surface area increases linearly in the flow direction (A_s is equal to the perimeter, which is constant, times the tube length).

The surface temperature in the case of constant surface heat flux $\dot{q}_s$ can be determined from

$$\dot{q}_s = h(T_s - T_m) \quad \longrightarrow \quad T_s = T_m + \frac{\dot{q}_s}{h} \tag{8-18}$$

In the fully developed region, the surface temperature T_s will also increase linearly in the flow direction since h is constant and thus $T_s - T_m = $ constant (Fig. 8–11). Of course this is true when the fluid properties remain constant during flow.

The slope of the mean fluid temperature T_m on a T-x diagram can be determined by applying the steady-flow energy balance to a tube slice of thickness dx shown in Fig. 8–12. It gives

$$\dot{m}c_p dT_m = \dot{q}_s(p\,dx) \quad \longrightarrow \quad \frac{dT_m}{dx} = \frac{\dot{q}_s p}{\dot{m}c_p} = \text{constant} \tag{8-19}$$

where p is the perimeter of the tube.
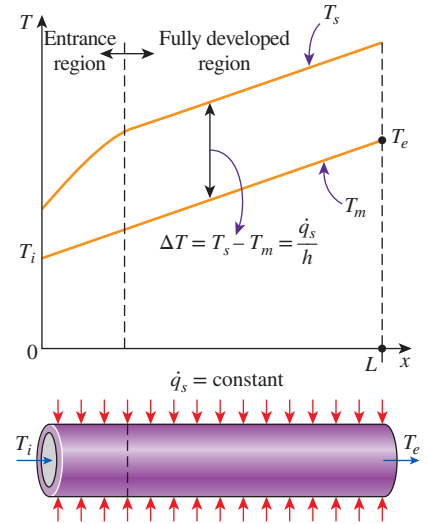
FIGURE 8–11
Variation of the *tube surface* and the *mean fluid* temperatures along the tube for the case of constant surface heat flux.
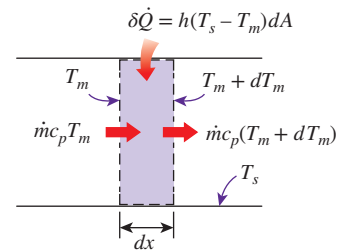
FIGURE 8–12
Energy interactions for a differential control volume in a tube.

Noting that both $\dot{q}_s$ and h are constants, the differentiation of Eq. 8–18 with respect to x gives

$$\frac{dT_m}{dx} = \frac{dT_s}{dx} \tag{8–20}$$

Also, the requirement that the dimensionless temperature profile remains unchanged in the fully developed region gives

$$\frac{\partial}{\partial x}\left(\frac{T_s - T}{T_s - T_m}\right) = 0 \quad \longrightarrow \quad \frac{1}{T_s - T_m}\left(\frac{\partial T_s}{\partial x} - \frac{\partial T}{\partial x}\right) = 0 \quad \longrightarrow \quad \frac{\partial T}{\partial x} = \frac{dT_s}{dx} \tag{8–21}$$

since $T_s - T_m = $ constant. Combining Eqs. 8–19, 8–20, and 8–21 gives

$$\frac{\partial T}{\partial x} = \frac{dT_s}{dx} = \frac{dT_m}{dx} = \frac{\dot{q}_s P}{\dot{m}c_p} = \text{constant} \tag{8–22}$$

Then we conclude that *in fully developed flow in a tube subjected to constant surface heat flux, the temperature gradient is independent of x, and thus the shape of the temperature profile does not change along the tube* (Fig. 8–13).

Integrating Eq. 8–22 from $x = 0$ (tube inlet where $T_m = T_i$) we obtain an expression for the variation of mean temperature along the tube

$$T_m = T_i + \frac{\dot{q}_s P}{\dot{m}c_p}x \tag{8–23}$$

We evaluate this equation at $x = L$ (tube exit where $T_m = T_e$). Then when we recognize that $A_s = pL$, Eq. 8–17 is obtained. From Eq. 8–23 we can conclude again that the mean temperature varies linearly with x along the tube for the case of constant heat flux.

For a circular tube, $p = 2\pi R$ and $\dot{m} = \rho V_{avg}A_c = \rho V_{avg}(\pi R^2)$. Then Eq. 8–22 becomes

Circular tube: $\qquad \dfrac{\partial T}{\partial x} = \dfrac{dT_s}{dx} = \dfrac{dT_m}{dx} = \dfrac{2\dot{q}_s}{\rho V_{avg}c_p R} = \text{constant} \tag{8–24}$

where V_{avg} is the mean velocity of the fluid.

Constant Surface Temperature (T_s = constant)

From Newton's law of cooling, the rate of heat transfer to or from a fluid flowing in a tube can be expressed as

$$\dot{Q} = hA_s\Delta T_{avg} = hA_s(T_s - T_m)_{avg} \qquad (\text{W}) \tag{8–25}$$

where h is the average convection heat transfer coefficient, A_s is the heat transfer surface area (it is equal to πDL for a circular pipe of length L), and ΔT_{avg} is some appropriate *average* temperature difference between the fluid and the surface. Below we discuss two suitable ways of expressing ΔT_{avg}.

In the constant surface temperature (T_s = constant) case, ΔT_{avg} can be expressed *approximately* by the **arithmetic mean temperature difference** ΔT_{am} as

$$\Delta T_{avg} \approx \Delta T_{am} = \frac{\Delta T_i + \Delta T_e}{2} = \frac{(T_s - T_i) + (T_s - T_e)}{2} = T_s - \frac{T_i + T_e}{2}$$
$$= T_s - T_b \tag{8–26}$$

where $T_b = (T_i + T_e)/2$ is the *bulk mean fluid temperature,* which is the *arithmetic average* of the mean fluid temperatures at the inlet and the exit of the tube.
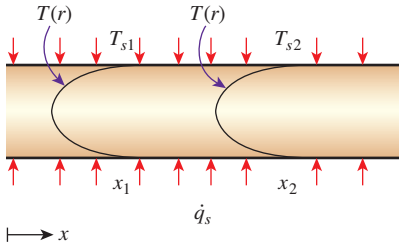
FIGURE 8–13

The shape of the temperature profile remains unchanged in the fully developed region of a tube subjected to constant surface heat flux.

Note that the *arithmetic mean temperature difference* ΔT_{am} is simply the *average* of the *temperature differences* between the surface and the fluid at the inlet and the exit of the tube. Inherent in this definition is the assumption that the mean fluid temperature varies linearly along the tube, which is hardly ever the case when T_s = constant. This simple approximation often gives acceptable results, but not always. Therefore, we need a better way to evaluate ΔT_{avg}.

Consider the heating of a fluid in a tube of constant cross section whose inner surface is maintained at a constant temperature of T_s. We know that the mean temperature of the fluid T_m increases in the flow direction as a result of heat transfer. The energy balance on a differential control volume shown in Fig. 8–12 gives

$$\dot{m}c_p \, dT_m = h(T_s - T_m)dA_s \tag{8-27}$$

That is, the increase in the energy of the fluid (represented by an increase in its mean temperature by dT_m) is equal to the heat transferred to the fluid from the tube surface by convection. Noting that the differential surface area is $dA_s = pdx$, where p is the perimeter of the tube, and that $dT_m = -d(T_s - T_m)$, since T_s is constant, the relation above can be rearranged as

$$\frac{d(T_s - T_m)}{T_s - T_m} = -\frac{hp}{\dot{m}c_p}dx \tag{8-28}$$

Integrating from $x = 0$ (tube inlet where $T_m = T_i$) to $x = L$ (tube exit where $T_m = T_e$) gives

$$\ln\frac{T_s - T_e}{T_s - T_i} = -\frac{hA_s}{\dot{m}c_p} \tag{8-29}$$

where $A_s = pL$ is the surface area of the tube and h is the constant *average* convection heat transfer coefficient. Taking the exponential of both sides and solving for T_e gives the following relation, which is very useful for the determination of the *mean fluid temperature at the tube exit:*

$$T_e = T_s - (T_s - T_i)\exp(-hA_s/\dot{m}c_p) \tag{8-30}$$

This relation can also be used to determine the mean fluid temperature $T_m(x)$ at any x by replacing $A_s = pL$ with px.

Note that the temperature difference between the fluid and the surface *decays exponentially* in the flow direction, and the rate of decay depends on the magnitude of the exponent $hA_s/\dot{m}c_p$, as shown in Fig. 8–14. This dimensionless parameter is called the *number of transfer units,* denoted by NTU, and is a measure of the effectiveness of the heat transfer systems. For NTU > 5, the exit temperature of the fluid becomes almost equal to the surface temperature, $T_e \approx T_s$ (Fig. 8–15). Noting that the fluid temperature can approach the surface temperature but cannot cross it, an NTU of about 5 indicates that the limit is reached for heat transfer, and the heat transfer does not increase no matter how much we extend the length of the tube. A small value of NTU, on the other hand, indicates more opportunities for heat transfer, and the heat transfer continues to increase as the tube length is increased. A large NTU and thus a large heat transfer surface area (which means a large tube) may be desirable from a heat transfer point of view, but it may be unacceptable from an economic point of view. The selection of heat transfer equipment usually reflects a compromise between heat transfer performance and cost.
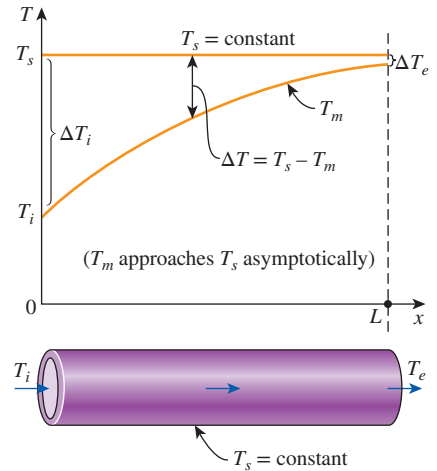
FIGURE 8–14
The variation of the *mean fluid* temperature along the tube for the case of constant temperature.
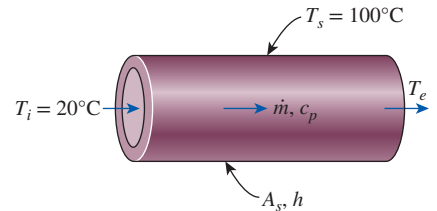
NTU = $hA_s/\dot{m}c_p$	T_e, °C
0.01	20.8
0.05	23.9
0.10	27.6
0.50	51.5
1.00	70.6
5.00	99.5
10.00	100.0

FIGURE 8–15
An NTU greater than 5 indicates that the fluid flowing in a tube will reach the surface temperature at the exit regardless of the inlet temperature.

Solving Eq. 8–29 for $\dot{m}c_p$ gives

$$\dot{m}c_p = -\frac{hA_s}{\ln[(T_s - T_e)/(T_s - T_i)]}$$ (8–31)

Substituting this into Eq. 8–14, we obtain

$$\dot{Q} = hA_s\Delta T_{lm}$$ (8–32)

where

$$\Delta T_{lm} = \frac{T_i - T_e}{\ln[(T_s - T_e)/(T_s - T_i)]} = \frac{\Delta T_e - \Delta T_i}{\ln(\Delta T_e/\Delta T_i)}$$ (8–33)

is the **log mean temperature difference**. Note that $\Delta T_i = T_s - T_i$ and $\Delta T_e = T_s - T_e$ are the temperature differences between the surface and the fluid at the inlet and the exit of the tube, respectively. This ΔT_{lm} relation appears to be prone to misuse, but it is practically fail-safe, since using T_i in place of T_e and vice versa in the numerator and/or the denominator will, at most, affect the sign, not the magnitude. Also, it can be used for both heating ($T_s > T_i$ and T_e) and cooling ($T_s < T_i$ and T_e) of a fluid in a tube.

The log mean temperature difference ΔT_{lm} is obtained by tracing the actual temperature profile of the fluid along the tube and is an *exact* representation of the *average temperature difference* between the fluid and the surface. It truly reflects the exponential decay of the local temperature difference. When ΔT_e differs from ΔT_i by no more than 40 percent, the error in using the arithmetic mean temperature difference is less than 1 percent. But the error increases to undesirable levels when ΔT_e differs from ΔT_i by greater amounts. Therefore, we should always use the log mean temperature difference when determining the convection heat transfer in a tube whose surface is maintained at a constant temperature T_s.
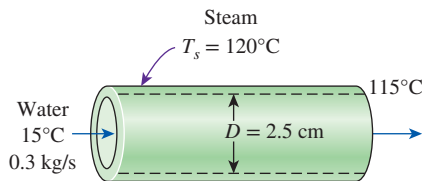
FIGURE 8–16
Schematic for Example 8–1.

EXAMPLE 8–1   **Heating of Water in a Tube by Steam**

Water enters a 2.5-cm-internal-diameter thin copper tube of a heat exchanger at 15°C at a rate of 0.3 kg/s, and is heated by steam condensing outside at 120°C. If the average heat transfer coefficient is 800 W/m²·K, determine the length of the tube required in order to heat the water to 115°C (Fig. 8–16).

SOLUTION   Water is heated by steam in a circular tube. The tube length required to heat the water to a specified temperature is to be determined.
Assumptions   **1** Steady operating conditions exist. **2** Fluid properties are constant. **3** The convection heat transfer coefficient is constant. **4** The conduction resistance of copper tube is negligible, so the inner surface temperature of the tube is equal to the condensation temperature of steam.
Properties   The specific heat of water at the bulk mean temperature of $(15 + 115)/2 = 65°C$ is 4187 J/kg·K. The heat of condensation of steam at 120°C is 2203 kJ/kg (Table A–9).
Analysis   Knowing the inlet and exit temperatures of water, the rate of heat transfer is determined to be

$$\dot{Q} = \dot{m}c_p(T_e - T_i) = (0.3\ \text{kg/s})(4.187\ \text{kJ/kg·K})(115°C - 15°C)$$
$$= 125.6\ \text{kW}$$

The log mean temperature difference is

$$\Delta T_e = T_s - T_e = 120°C - 115°C = 5°C$$

$$\Delta T_i = T_s - T_i = 120°C - 15°C = 105°C$$

$$\Delta T_{lm} = \frac{\Delta T_e - T_i}{\ln(\Delta T_e/\Delta T_i)} = \frac{5 - 105}{\ln(5/105)} = 32.85°C$$

The heat transfer surface area is

$$\dot{Q} = hA_s \Delta T_{lm} \longrightarrow A_s = \frac{\dot{Q}}{h\Delta T_{lm}} = \frac{125.6 \text{ kW}}{(0.8 \text{ kW/m}^2\cdot\text{K})(32.85°C)} = 4.78 \text{ m}^2$$

Then the required tube length becomes

$$A_s = \pi DL \longrightarrow L = \frac{A_s}{\pi D} = \frac{4.78 \text{ m}^2}{\pi(0.025 \text{ m})} = \textbf{61 m}$$

Discussion   The bulk mean temperature of water during this heating process is 65°C, and thus the *arithmetic* mean temperature difference is $\Delta T_{am} = 120 - 65 = 55°C$. Using ΔT_{am} instead of ΔT_{lm} would give $L = 36$ m, which is grossly in error. This shows the importance of using the log mean temperature in calculations.

8–5 · LAMINAR FLOW IN TUBES

We mentioned in Sec. 8–2 that flow in tubes is laminar for $\text{Re} \lesssim 2300$ and that the flow is fully developed if the tube is sufficiently long (relative to the entry length) so that the entrance effects are negligible. In this section we consider steady, laminar, incompressible flow of a fluid with constant properties in the fully developed region of a straight circular pipe. We obtain the momentum equation by applying a force balance to a differential volume element, and we obtain the velocity profile by solving it. Then we use it to obtain a relation for the friction factor. An important aspect of the analysis here is that it is one of the few available for viscous flow.

In fully developed laminar flow, each fluid particle moves at a constant axial velocity along a streamline, and the velocity profile $u(r)$ remains unchanged in the flow direction. There is no motion in the radial direction, and thus the velocity component in the direction normal to the pipe axis is everywhere zero. There is no acceleration since the flow is steady and fully developed.

Now consider a ring-shaped differential volume element of radius r, thickness dr, and length dx oriented coaxially with the tube, as shown in Fig. 8–17. The volume element involves only pressure and viscous effects, and thus the pressure and shear forces must balance each other. The pressure force acting on a submerged plane surface is the product of the pressure at the centroid of the surface and the surface area. A force balance on the volume element in the flow direction gives

$$(2\pi r \, dr \, P)_x - (2\pi r \, dr \, P)_{x+dx} + (2\pi r \, dx \, \tau)_r - (2\pi r \, dx \, \tau)_{r+dr} = 0 \qquad \textbf{(8–34)}$$
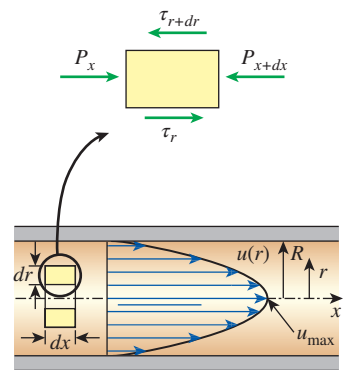
FIGURE 8–17
Free-body diagram of a ring-shaped differential fluid element of radius r, thickness dr, and length dx oriented coaxially with a horizontal tube in fully developed laminar flow.

$2\pi R\, dx\, \tau_w$

$\pi R^2 P \longrightarrow$ $\longleftarrow \pi R^2(P + dP)$

r

R

x

dx
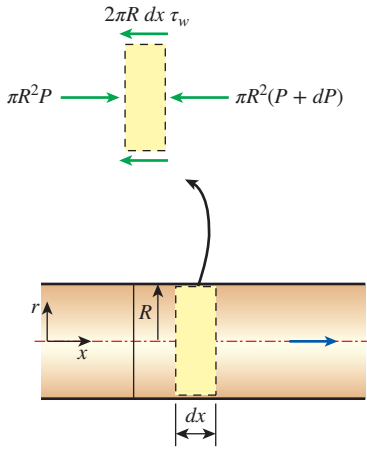
Force balance:

$$\pi R^2 P - \pi R^2(P + dP) - 2\pi R\, dx\, \tau_w = 0$$

Simplifying:

$$\frac{dP}{dx} = -\frac{2\tau_w}{R}$$

FIGURE 8–18

Free-body diagram of a fluid disk element of radius R and length dx in fully developed laminar flow in a horizontal tube.

which indicates that in fully developed flow in a horizontal tube, the viscous and pressure forces balance each other. Dividing by $2\pi dr dx$ and rearranging,

$$r\frac{P_{x+dx} - P_x}{dx} + \frac{(r\tau)_{r+dr} - (r\tau)_r}{dr} = 0 \qquad \textbf{(8–35)}$$

Taking the limit as $dr, dx \longrightarrow 0$ gives

$$r\frac{dP}{dr} + \frac{d(r\tau)}{dr} = 0 \qquad \textbf{(8–36)}$$

Substituting $\tau = -\mu(du/dr)$ and taking $\mu = $ constant gives the desired equation,

$$\frac{\mu}{r}\frac{d}{dr}\left(r\frac{du}{dr}\right) = \frac{dP}{dx} \qquad \textbf{(8–37)}$$

The quantity du/dr is negative in pipe flow, and the negative sign is included to obtain positive values for τ. (Or, $du/dr = -du/dy$ since $y = R - r$.) The left side of Eq. 8–37 is a function of r, and the right side is a function of x. The equality must hold for any value of r and x, and an equality of the form $f(r) = g(x)$ can be satisfied only if both $f(r)$ and $g(x)$ are equal to the same constant. Thus we conclude that $dP/dx = $ constant. This can be verified by writing a force balance on a volume element of radius R and thickness dx (a slice of the tube), which gives (Fig. 8–18)

$$\frac{dP}{dx} = -\frac{2\tau_w}{R}$$

Here τ_w is constant since the viscosity and the velocity profile are constants in the fully developed region. Therefore, $dP/dx = $ constant.

Equation 8–37 is solved by rearranging and integrating it twice to give

$$u(r) = \frac{1}{4\mu}\left(\frac{dP}{dx}\right) + C_1 \ln r + C_2 \qquad \textbf{(8–38)}$$

The velocity profile $u(r)$ is obtained by applying the boundary conditions $\partial u/\partial r = 0$ at $r = 0$ (because of symmetry about the centerline) and $u = 0$ at $r = R$ (the no-slip condition at the tube wall). We get

$$u(r) = -\frac{R^2}{4\mu}\left(\frac{dP}{dx}\right)\left(1 - \frac{r^2}{R^2}\right) \qquad \textbf{(8–39)}$$

Therefore, the velocity profile in fully developed laminar flow in a tube is *parabolic* with a maximum at the centerline and a minimum (zero) at the tube wall. Also, the axial velocity u is positive for any r, and thus the axial pressure gradient dP/dx must be negative (i.e., pressure must decrease in the flow direction because of viscous effects).

The average velocity is determined from its definition by substituting Eq. 8–39 into Eq. 8–2 and performing the integration, yielding

$$V_{\text{avg}} = \frac{2}{R^2}\int_0^R u(r)\, r\, dr = \frac{-2}{R^2}\int_0^R \frac{R^2}{4\mu}\left(\frac{dP}{dx}\right)\left(1 - \frac{r^2}{R^2}\right) r\, dr = -\frac{R^2}{8\mu}\left(\frac{dP}{dx}\right) \qquad \textbf{(8–40)}$$

Combining the last two equations, the velocity profile is rewritten as

$$u(r) = 2V_{avg}\left(1 - \frac{r^2}{R^2}\right) \tag{8-41}$$

This is a convenient form for the velocity profile since V_{avg} can be determined easily from the flow rate information.

The maximum velocity occurs at the centerline and is determined from Eq. 8–41 by substituting $r = 0$,

$$u_{max} = 2V_{avg} \tag{8-42}$$

Therefore, *the average velocity in fully developed laminar pipe flow is one-half of the maximum velocity.*

Pressure Drop

A quantity of interest in the analysis of pipe flow is the *pressure drop* ΔP since it is directly related to the power requirements of the fan or pump to maintain flow. We note that $dP/dx = $ constant, and integrating from $x = x_1$ where the pressure is P_1 to $x = x_1 + L$ where the pressure is P_2 gives

$$\frac{dP}{dx} = \frac{P_2 - P_1}{L} \tag{8-43}$$

Substituting Eq. 8–43 into the V_{avg} expression in Eq. 8–40, the pressure drop is expressed as

Laminar flow: $\quad \Delta P = P_1 - P_2 = \dfrac{8\mu L V_{avg}}{R^2} = \dfrac{32\mu L V_{avg}}{D^2}$ $\tag{8-44}$

The symbol Δ is typically used to indicate the difference between the final and initial values, like $\Delta y = y_2 - y_1$. But in fluid flow, ΔP is used to designate pressure drop, and thus it is $P_1 - P_2$. A pressure drop due to viscous effects represents an irreversible pressure loss, and it is called **pressure loss** ΔP_L to emphasize that it is a *loss* (just like the head loss h_L, which as we shall see is proportional to ΔP).

Note from Eq. 8–44 that the pressure drop is proportional to the viscosity μ of the fluid, and ΔP would be zero if there were no friction. Therefore, the drop of pressure from P_1 to P_2 in this case is due entirely to viscous effects, and Eq. 8–44 represents the pressure loss ΔP_L when a fluid of viscosity μ flows through a pipe of constant diameter D and length L at average velocity V_{avg}.

In practice, it is convenient to express the pressure loss for all types of fully developed internal flows (laminar or turbulent flows, circular or noncircular pipes, smooth or rough surfaces, horizontal or inclined pipes) as (Fig. 8–19)

Pressure loss: $\quad \Delta P_L = f\dfrac{L}{D}\dfrac{\rho V_{avg}^2}{2}$ $\tag{8-45}$

where $\rho V_{avg}^2/2$ is the *dynamic pressure* and f is the **Darcy friction factor**,

$$f = \frac{8\tau_w}{\rho V_{avg}^2}$$

It is also called the **Darcy–Weisbach friction factor**, named after the Frenchman Henry Darcy (1803–1858) and the German Julius Weisbach (1806–1871), the two engineers who provided the greatest contribution in its
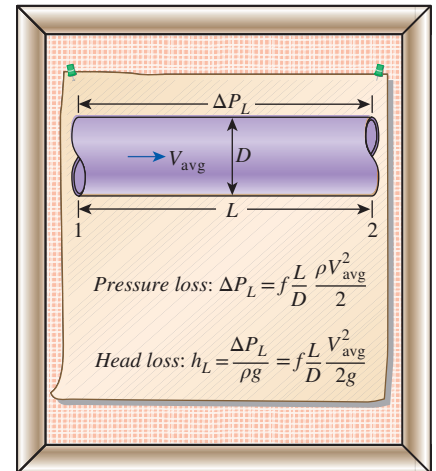
FIGURE 8–19

The relation for pressure loss (and head loss) is one of the most general relations in fluid mechanics, and it is valid for laminar or turbulent flows, circular or noncircular tubes, and pipes with smooth or rough surfaces.

development. It should not be confused with the *friction coefficient* C_f [also called the *Fanning friction factor,* named after the American engineer John Fanning (1837–1911)], which is defined as $C_f = 2\tau_w/(\rho V_{avg}^2) = f/4$.

Setting Eqs. 8–44 and 8–45 equal to each other and solving for f gives the friction factor for fully developed laminar flow in a circular tube,

Circular tube, laminar:
$$f = \frac{64\mu}{\rho D V_{avg}} = \frac{64}{Re} \qquad \textbf{(8–46)}$$

This equation shows that *in laminar flow, the friction factor is a function of the Reynolds number only and is independent of the roughness of the pipe surface.*

In the analysis of piping systems, pressure losses are commonly expressed in terms of the *equivalent fluid column height,* called the **head loss** h_L. Noting from fluid statics that $\Delta P = \rho g h$ and thus a pressure difference of ΔP corresponds to a fluid height of $h = \Delta P/\rho g$, the *pipe head loss* is obtained by dividing ΔP_L by ρg to give

$$h_L = \frac{\Delta P_L}{\rho g} = f \frac{L}{D} \frac{V_{avg}^2}{2g}$$

The head loss h_L represents *the additional height that the fluid needs to be raised by a pump in order to overcome the frictional losses in the pipe.* The head loss is caused by viscosity, and it is directly related to the wall shear stress. Equation 8–45 is valid for both laminar and turbulent flows in both circular and noncircular tubes, but Eq. 8–46 is valid only for fully developed laminar flow in circular pipes.

Once the pressure loss (or head loss) is known, the required pumping power *to overcome the pressure loss* is determined from

$$\dot{W}_{pump, L} = \dot{V}\Delta P_L = \dot{V}\rho g h_L = \dot{m} g h_L \qquad \textbf{(8–47)}$$

where $\dot{V}$ is the volume flow rate and $\dot{m}$ is the mass flow rate.

The average velocity for laminar flow in a horizontal tube is, from Eq. 8–44,

Horizontal tube:
$$V_{avg} = \frac{(P_1 - P_2)R^2}{8\mu L} = \frac{(P_1 - P_2)D^2}{32\mu L} = \frac{\Delta P \, D^2}{32\mu L}$$

Then the volume flow rate for laminar flow through a horizontal tube of diameter D and length L becomes

$$\dot{V} = V_{avg}A_c = \frac{(P_1 - P_2)R^2}{8\mu L} \pi R^2 = \frac{(P_1 - P_2)\pi D^4}{128\mu L} = \frac{\Delta P \, \pi D^4}{128\mu L} \qquad \textbf{(8–48)}$$

This equation is known as **Poiseuille's law**, and this flow is called *Hagen–Poiseuille flow* in honor of the works of G. Hagen (1797–1884) and J. Poiseuille (1799–1869) on the subject. Note from Eq. 8–48 that *for a specified flow rate, the pressure drop and thus the required pumping power is proportional to the length of the pipe and the viscosity of the fluid, but it is inversely proportional to the fourth power of the radius (or diameter) of the pipe.* Therefore, the pumping power requirement for a piping system can be reduced by a factor of 16 by doubling the tube diameter (Fig. 8–20). Of course the benefits of the reduction in the energy costs must be weighed against the increased cost of construction due to using a larger-diameter tube.

The pressure drop ΔP equals the pressure loss ΔP_L in the case of a horizontal tube, but this is not the case for inclined pipes or pipes with variable cross-sectional area because of the changes in elevation and velocity.
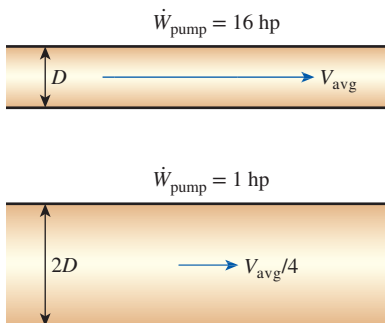
FIGURE 8–20
The pumping power requirement for a laminar flow piping system can be reduced by a factor of 16 by doubling the tube diameter.

Temperature Profile and the Nusselt Number

In the previous analysis, we have obtained the velocity profile for fully developed flow in a circular tube from a force balance applied on a volume element and determined the friction factor and the pressure drop. Next we obtain the energy equation by applying the energy balance on a differential volume element and solve it to obtain the temperature profile for the constant surface temperature and the constant surface heat flux cases.

Reconsider steady laminar flow of a fluid in a circular tube of radius R. The fluid properties ρ, k, and c_p are constant, and the work done by viscous forces is negligible. The fluid flows along the x-axis with velocity u. The flow is fully developed so that u is independent of x and thus $u = u(r)$. Noting that energy is transferred by mass in the x-direction and by conduction in the r-direction (heat conduction in the x-direction is assumed to be negligible), the steady-flow energy balance for a cylindrical shell element of thickness dr and length dx can be expressed as (Fig. 8–21)

FIGURE 8–21
The differential volume element used in the derivation of energy balance relation.

$$\dot{m}c_p T_x - \dot{m}c_p T_{x+dx} + \dot{Q}_r - \dot{Q}_{r+dr} = 0 \qquad \text{(8–49)}$$

where $\dot{m} = \rho u A_c = \rho u(2\pi r dr)$. Substituting and dividing by $2\pi r dr dx$ gives, after rearranging,

$$\rho c_p u \frac{T_{x+dx} - T_x}{dx} = -\frac{1}{2\pi r dx} \frac{\dot{Q}_{r+dr} - \dot{Q}_r}{dr} \qquad \text{(8–50)}$$

or

$$u\frac{\partial T}{\partial x} = -\frac{1}{2\rho c_p \pi r dx} \frac{\partial \dot{Q}}{\partial r} \qquad \text{(8–51)}$$

But from Fourier's law of heat conduction in the radial direction,

$$\frac{\partial \dot{Q}}{\partial r} = \frac{\partial}{\partial r}\left(-2\pi r k dx \frac{\partial T}{\partial r}\right) = -2\pi k dx \frac{\partial}{\partial r}\left(r\frac{\partial T}{\partial r}\right) \qquad \text{(8–52)}$$

Substituting and using $\alpha = k/\rho c_p$ gives

$$u\frac{\partial T}{\partial x} = \frac{\alpha}{r} \frac{\partial}{\partial r}\left(r\frac{\partial T}{\partial r}\right) \qquad \text{(8–53)}$$

which states that *the rate of net energy transfer to the control volume by mass flow is equal to the net rate of heat conduction in the radial direction.*

Constant Surface Heat Flux

For fully developed flow in a circular tube subjected to constant surface heat flux, we have, from Eq. 8–24,

$$\frac{\partial T}{\partial x} = \frac{dT_s}{dx} = \frac{dT_m}{dx} = \frac{2\dot{q}_s}{\rho V_{\text{avg}} c_p R} = \text{constant} \qquad \text{(8–54)}$$

If heat conduction in the x-direction were considered in the derivation of Eq. 8–53, it would give an additional term $\alpha \partial^2 T/\partial x^2$, which would be equal to zero since $\partial T/\partial x = $ constant and thus $T = T(r)$. Therefore, the assumption that there is no axial heat conduction is satisfied exactly in this case.

Substituting Eq. 8–54 and the relation for velocity profile (Eq. 8–41) into Eq. 8–53 gives

$$\frac{4\dot{q}_s}{kR}\left(1 - \frac{r^2}{R^2}\right) = \frac{1}{r}\frac{d}{dr}\left(r\frac{dT}{dr}\right) \tag{8–55}$$

which is a second-order ordinary differential equation. Its general solution is obtained by separating the variables and integrating twice to be

$$T = \frac{\dot{q}_s}{kR}\left(r^2 - \frac{r^4}{4R^2}\right) + C_1\ln r + C_2 \tag{8–56}$$

The desired solution to the problem is obtained by applying the boundary conditions $\partial T/\partial r = 0$ at $r = 0$ (because of symmetry) and $T = T_s$ at $r = R$. We get

$$T = T_s - \frac{\dot{q}_sR}{k}\left(\frac{3}{4} - \frac{r^2}{R^2} + \frac{r^4}{4R^4}\right) \tag{8–57}$$

The mean temperature T_m is determined by substituting the velocity and temperature profile relations (Eqs. 8–41 and 8–57) into Eq. 8–4 and performing the integration. It gives

$$T_m = T_s - \frac{11}{24}\frac{\dot{q}_sR}{k} \tag{8–58}$$

Combining this relation with $\dot{q}_s = h(T_s - T_m)$ gives

$$h = \frac{24}{11}\frac{k}{R} = \frac{48}{11}\frac{k}{D} = 4.36\frac{k}{D} \tag{8–59}$$

or

Circular tube, laminar ($\dot{q}_s =$ constant): $\text{Nu} = \dfrac{hD}{k} = 4.36$ $\tag{8–60}$

Therefore, for fully developed laminar flow in a circular tube subjected to constant surface heat flux, the Nusselt number is a constant. There is no dependence on the Reynolds or the Prandtl numbers.

Constant Surface Temperature

A similar analysis can be performed for fully developed laminar flow in a circular tube for the case of constant surface temperature T_s. The solution procedure in this case is more complex than the constant surface heat flux case, but the resulting Nusselt number relation obtained is equally simple. This problem has been solved iteratively as reported by Kays and Crawford (1993) and more recently by Shokouhmand and Hooman (2003) using an exact analytical procedure. The resulting Nusselt number relation obtained is (Fig. 8–22):

Circular tube, laminar ($T_s =$ constant): $\text{Nu} = \dfrac{hD}{k} = 3.66$ $\tag{8–61}$

Comparison of Eqs. 8–60 and 8–61 shows that the Nusselt number for the case of constant surface heat flux is 16 percent higher than the case of constant surface temperature for the fully developed laminar pipe flow. This shows that laminar flow is sensitive to the applied surface thermal boundary condition and for applications requiring higher rates of heat transfer, whenever possible; the constant surface heat flux boundary condition should be used. This is contrary to the results shown in Fig. 8–9 for the turbulent flow, which showed

$T_s =$ constant

$f = \dfrac{64}{\text{Re}}$ $u(r)$

$\text{Nu} = 3.66$

Fully developed laminar flow
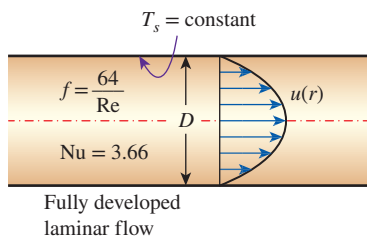
FIGURE 8–22
In laminar flow in a tube with constant surface temperature, both the *friction factor* and the *heat transfer coefficient* remain constant in the fully developed region.

no sensitivity to the different surface thermal boundary conditions in the fully developed region.
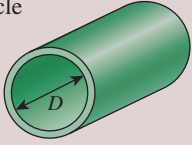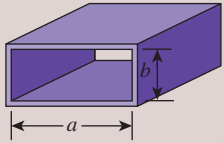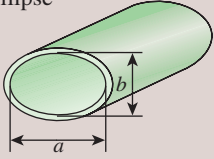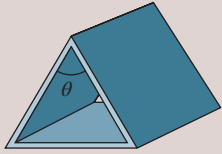
The thermal conductivity k for use in the Nu relations above should be evaluated at the bulk mean fluid temperature, which is the arithmetic average of the mean fluid temperatures at the inlet and the exit of the tube. For laminar flow, the effect of *surface roughness* on the friction factor and the heat transfer coefficient is negligible.

Laminar Flow in Noncircular Tubes

The friction factor f and the Nusselt number relations are given in Table 8–1 for *fully developed laminar flow* in tubes of various cross sections. The Reynolds and Nusselt numbers for flow in these tubes are based on the hydraulic diameter $D_h = 4A_c/p$, where A_c is the cross-sectional area of the tube and p is its perimeter. Once the Nusselt number is available, the convection heat transfer coefficient is determined from $h = k\text{Nu}/D_h$.

TABLE 8–1

Nusselt number and friction factor for fully developed laminar flow in tubes of various cross sections ($D_h = 4A_c/p$, Re = $V_{avg}D_h/\nu$, and Nu = hD_h/k)

Tube Geometry	a/b or $\theta°$	Nusselt Number T_s = Const.	Nusselt Number $\dot{q}_s$ = Const.	Friction Factor f
Circle	—	3.66	4.36	64.00/Re
Rectangle	a/b			
	1	2.98	3.61	56.92/Re
	2	3.39	4.12	62.20/Re
	3	3.96	4.79	68.36/Re
	4	4.44	5.33	72.92/Re
	6	5.14	6.05	78.80/Re
	8	5.60	6.49	82.32/Re
	∞	7.54	8.24	96.00/Re
Ellipse	a/b			
	1	3.66	4.36	64.00/Re
	2	3.74	4.56	67.28/Re
	4	3.79	4.88	72.96/Re
	8	3.72	5.09	76.60/Re
	16	3.65	5.18	78.16/Re
Isosceles triangle	θ			
	10°	1.61	2.45	50.80/Re
	30°	2.26	2.91	52.28/Re
	60°	2.47	3.11	53.32/Re
	90°	2.34	2.98	52.60/Re
	120°	2.00	2.68	50.96/Re

FIGURE 8–23
Leo Graetz (1856–1941), a German physicist, was born at Breslau (then in Germany, now called Wroclaw and in Poland). His scientific work was first concerned with the fields of heat conduction, radiation, friction, and elasticity. He was one of the first to investigate the propagation of electromagnetic energy. The dimensionless **Graetz number** describing heat transfer is named after him.

©Art Collection 2/Alamy

Developing Laminar Flow in the Entrance Region

The heat transfer analysis presented so far has been for hydrodynamically and thermally developed (fully developed) laminar flow in a circular tube where conditions given by Eqs. 8–7 and 8–8 were valid. However, in the entrance region, the energy equation Eq. 8–53 is no longer valid since in this region there is motion in the radial direction and the velocity profile $u(r)$ changes in the flow direction. In addition, for example for the case of constant surface heat flux, the axial temperature gradient $\partial T/\partial x$ can no longer be simplified through Eq. 8–54. Therefore, the solution to the energy equation in the entrance region is more complicated than the fully developed region, and the energy equation is solved numerically. The local values of Nusselt number are typically presented either graphically or in tabular form in terms of the inverse of a dimensionless parameter called the Graetz number (Fig. 8–23) which is defined as $Gz = (D/x)Re\ Pr$. As shown in Fig. 8–24, the fully developed conditions for both cases of constant surface heat flux and constant surface temperature are reached for $1/Gz = (x/D)/Re\ Pr \approx 0.05$, which is consistent with the results given by Eq. 8–12 for laminar thermal entry length. Therefore, when the inverse of the Graetz number is greater than 0.05, the local Nusselt numbers approach their fully developed values of 4.36 for constant surface heat flux and 3.66 for constant surface temperature. Excellent treatments of this subject are contained in Shah and London (1978) and Shah and Bhatti (1987). Two different solutions are obtained in the literature. The simplest case is for hydrodynamically developed flow and thermally developing flow. The more complicated case is for hydrodynamically and thermally developing flow. In this case the solution is a function of the Prandtl number, and for each case the value of the Prandtl number must be specified a priori.

There are a limited number of empirical correlations available in the literature for the average Nusselt number under constant surface temperature boundary conditions. For example, for a circular tube of length L subjected to constant surface temperature, the average Nusselt number for the *thermal entrance region* can be determined from (Edwards et al., 1979)

Entry region, laminar: $\qquad Nu = 3.66 + \dfrac{0.065(D/L)\ Re\ Pr}{1 + 0.04[(D/L)\ Re\ Pr]^{2/3}}$ **(8–62)**

Note that the average Nusselt number is larger at the entrance region, as expected, and it approaches asymptotically to the fully developed value of 3.66 as $L \to \infty$. This relation assumes that the flow is hydrodynamically developed when the fluid enters the heating section, but it can also be used for flow developing hydrodynamically when $Pr \geq 5$.

When the difference between the surface and the fluid temperatures is large, it may be necessary to account for the variation of viscosity with temperature.

The average Nusselt number for hydrodynamically and thermally developing laminar flow in a circular tube in that case can be determined from (Sieder and Tate, 1936)

Entry region, laminar: $\qquad Nu = 1.86\left(\dfrac{Re\ Pr D}{L}\right)^{1/3}\left(\dfrac{\mu_b}{\mu_s}\right)^{0.14}$ **(8–63)**

The preceding equation is recommended for $0.60 \leq \mathrm{Pr} \leq 5$ and $0.0044 \leq (\mu_b/\mu_s) \leq 9.75$. Note that the term $(D/L)\mathrm{RePr}$ in both Eqs. 8–62 and 8–63 is the Graetz number for a circular tube of length L. All properties appearing in Eqs. 8–62 and 8–63 should be evaluated at the bulk mean fluid temperature, $T_b = (T_i + T_e)/2$, except for μ_s, which is evaluated at the surface temperature.

The average Nusselt number for the thermal entrance region of flow between *isothermal parallel plates* of length L is expressed as (Edwards et al., 1979)

Entry region, laminar: $\quad \mathrm{Nu} = 7.54 + \dfrac{0.03(D_h/L)\mathrm{Re\,Pr}}{1 + 0.016[(D_h/L)\mathrm{Re\,Pr}]^{2/3}}$ **(8–64)**

where D_h is the hydraulic diameter, which is twice the spacing of the plates. This relation can be used for $\mathrm{Re} \leq 2800$.

FIGURE 8–24

Local Nusselt numbers in the entry and fully developed regions for laminar flow in a circular tube for hydrodynamically developed and thermally developing flow.

EXAMPLE 8–2 Average Velocity and Temperature in Laminar Tube Flow

The velocity and temperature profiles for a fluid flowing in a circular tube of inner radius $R = 4$ cm (Fig. 8–25) are given as

$$u(r) = 0.2[1 - (r/R)^2] \quad \text{(in m/s)}$$

$$T(r) = 250 + 200(r/R)^3 \quad \text{(in K)}$$

Determine the average flow velocity and the average fluid temperature in the tube.

SOLUTION Using the given velocity and temperatures profiles in a tube, the average flow velocity and the average fluid temperature are to be determined.

Assumptions **1** Steady operating conditions exist. **2** Properties are constant.

Analysis On the basis of the conservation of mass principle, the average velocity in a circular tube of inner radius R is expressed as

$$V_{\mathrm{avg}} = \frac{2}{R^2}\int_0^R u(r)\,r\,dr$$

Substituting the known quantities and performing the integration, the average velocity is determined to be

$$V_{\mathrm{avg}} = \frac{2}{R^2}\int_0^R 0.2\left(r - \frac{r^3}{R^2}\right)dr = \frac{2 \times 0.2}{R^2}\left(\frac{r^2}{2} - \frac{r^4}{4R^2}\right)_0^R = \frac{2 \times 0.2}{R^2}\left(\frac{R^2}{4}\right) = \textbf{0.1 m/s}$$

On the basis of the conservation of energy principle, the average (or mean) fluid temperature at a cross section is expressed as

$$T_m = \frac{2}{V_{\mathrm{avg}}R^2}\int_0^R T(r)u(r)\,r\,dr$$

FIGURE 8–25

Schematic for Example 8–2.

Substituting the known quantities and performing the integration, the average temperature is determined to be

$$T_m = \frac{2}{V_{avg}R^2}\int_0^R 0.2\left(1 - \frac{r^2}{R^2}\right)\left(250 + 200\frac{r^3}{R^3}\right)r\,dr$$

$$= \frac{2 \times 0.2}{V_{avg}R^2}\left(250\frac{r^2}{2} - 250\frac{r^4}{4R^2} + 200\frac{r^5}{5R^3} - 200\frac{r^7}{7R^5}\right)\Bigg|_0^R$$

$$= \frac{2 \times 0.2}{V_{avg}R^2}\left(\frac{250R^2}{2} - \frac{250R^2}{4} + \frac{200R^2}{5} - \frac{200R^2}{7}\right) = \frac{2 \times 0.2 \times 73.93}{0.1} = \textbf{295.7 K}$$

Discussion The velocity profile for laminar flow is expressed as $u(r) = 2V_{avg}[1 - (r/R)^2]$. Comparing this with the given profile $u(r) = 0.2[1 - (r/R)^2]$, we could obtain the same value of average velocity directly by observation. Also, the parabolic velocity profile indicates that this is a fully developed laminar flow.
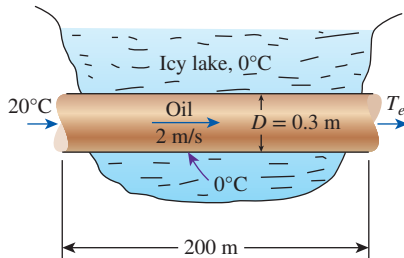
FIGURE 8–26
Schematic for Example 8–3.

EXAMPLE 8–3   **Flow of Oil in a Pipeline Through a Lake**

Consider the flow of oil at 20°C in a 30-cm-diameter pipeline at an average velocity of 2 m/s (Fig. 8–26). A 200-m-long section of the horizontal pipeline passes through icy waters of a lake at 0°C. Measurements indicate that the surface temperature of the pipe is very nearly 0°C. Disregarding the thermal resistance of the pipe material, determine (*a*) the temperature of the oil when the pipe leaves the lake, (*b*) the rate of heat transfer from the oil, and (*c*) the pumping power required to overcome the pressure losses and to maintain the flow of the oil in the pipe.

SOLUTION Oil flows in a pipeline that passes through icy waters of a lake at 0°C. The exit temperature of the oil, the rate of heat loss, and the pumping power needed to overcome pressure losses are to be determined.
Assumptions **1** Steady operating conditions exist. **2** The surface temperature of the pipe is very nearly 0°C. **3** The thermal resistance of the pipe is negligible. **4** The inner surfaces of the pipeline are smooth. **5** The flow is hydrodynamically developed when the pipeline reaches the lake.
Properties We do not know the exit temperature of the oil, and thus we cannot determine the bulk mean temperature, which is the temperature at which the properties of oil are to be evaluated. The mean temperature of the oil at the inlet is 20°C, and we expect this temperature to drop somewhat as a result of heat loss to the icy waters of the lake. We evaluate the properties of the oil at the inlet temperature, but we will repeat the calculations, if necessary, using properties at the evaluated bulk mean temperature. At 20°C we read (Table A–13)

$$\rho = 888.1 \text{ kg/m}^3 \qquad \nu = 9.429 \times 10^{-4} \text{ m}^2/\text{s}$$
$$k = 0.145 \text{ W/m·K} \qquad c_p = 1880 \text{ J/kg·K} \qquad \text{Pr} = 10{,}863$$

Analysis (*a*) The Reynolds number is

$$\text{Re} = \frac{V_{avg}D}{\nu} = \frac{(2 \text{ m/s})(0.3 \text{ m})}{9.429 \times 10^{-4} \text{ m}^2/\text{s}} = 636$$

which is less than the critical Reynolds number of 2300. Therefore, the flow is laminar, and the thermal entry length in this case is roughly

$$L_t \approx 0.05 \, \text{Re Pr} \, D = 0.05 \times 636 \times 10{,}863 \times (0.3 \, \text{m}) \approx 103{,}600 \, \text{m}$$

which is much greater than the total length of the pipe. This is typical of fluids with high Prandtl numbers. Therefore, we assume thermally developing flow and determine the Nusselt number from

$$\text{Nu} = \frac{hD}{k} = 3.66 + \frac{0.065(D/L) \, \text{Re Pr}}{1 + 0.04 \, [(D/L) \, \text{Re Pr}]^{2/3}}$$

$$= 3.66 + \frac{0.065(0.3/200) \times 636 \times 10{,}863}{1 + 0.04 \, [(0.3/200) \times 636 \times 10{,}863]^{2/3}}$$

$$= 33.7$$

Note that this Nusselt number is considerably higher than the fully developed value of 3.66. Then,

$$h = \frac{k}{D}\text{Nu} = \frac{0.145 \, \text{W/m·K}}{0.3 \, \text{m}}(33.7) = 16.3 \, \text{W/m}^2\text{·K}$$

Also,

$$A_s = \pi D L = \pi(0.3 \, \text{m})(200 \, \text{m}) = 188.5 \, \text{m}^2$$

$$\dot{m} = \rho A_c V_{\text{avg}} = (888.1 \, \text{kg/m}^3)[\tfrac{1}{4}\pi(0.3 \, \text{m})^2](2 \, \text{m/s}) = 125.6 \, \text{kg/s}$$

Next we determine the exit temperature of oil,

$$T_e = T_s - (T_s - T_i) \exp(-hA_s/\dot{m}c_p)$$

$$= 0°\text{C} - [(0 - 20)°\text{C}] \exp\left[-\frac{(16.3 \, \text{W/m}^2\text{·K})(188.5 \, \text{m}^2)}{(125.6 \, \text{kg/s})(1881 \, \text{J/kg·K})}\right]$$

$$= \mathbf{19.74°C}$$

Thus, the mean temperature of oil drops by a mere 0.26°C as it crosses the lake. This makes the bulk mean oil temperature 19.87°C, which is practically identical to the inlet temperature of 20°C. Therefore, we do not need to reevaluate the properties.

(*b*) The log mean temperature difference and the rate of heat loss from the oil are

$$\Delta T_{\text{lm}} = \frac{T_i - T_e}{\ln \dfrac{T_s - T_e}{T_s - T_i}} = \frac{20 - 19.74}{\ln \dfrac{0 - 19.74}{0 - 20}} = -19.87°\text{C}$$

$$\dot{Q} = hA_s \, \Delta T_{\text{lm}} = (16.3 \, \text{W/m}^2\text{·K})(188.5 \, \text{m}^2)(-19.87°\text{C}) = \mathbf{-6.11 \times 10^4 \, W}$$

Therefore, the oil will lose heat at a rate of 61.1 kW as it flows through the pipe in the icy waters of the lake. Note that ΔT_{lm} is identical to the arithmetic mean temperature in this case, since $\Delta T_i \approx \Delta T_e$.

(*c*) The laminar flow of oil is hydrodynamically developed. Therefore, the friction factor can be determined from

$$f = \frac{64}{\text{Re}} = \frac{64}{636} = 0.1006$$

Then the pressure drop in the pipe and the required pumping power become

$$\Delta P = f\frac{L}{D}\frac{\rho V_{avg}^2}{2} = 0.1006\frac{200 \text{ m}}{0.3 \text{ m}}\frac{(888.1 \text{ kg/m}^3)(2 \text{ m/s})^2}{2} = 1.19 \times 10^5 \text{ N/m}^2$$

$$\dot{W}_{pump} = \frac{\dot{m}\Delta P}{\rho} = \frac{(125.6 \text{ kg/s})(1.19 \times 10^5 \text{ N/m}^2)}{888.1 \text{ kg/m}^3} = \textbf{16.8 kW}$$

Discussion We need a 16.8-kW pump just to overcome the friction in the pipe as the oil flows in the 200-m-long pipe through the lake.

8–6 ▪ TURBULENT FLOW IN TUBES

We mentioned earlier that flow in smooth tubes is usually fully turbulent for Re > 10,000. Turbulent flow is commonly used in practice because of the higher heat transfer coefficients associated with it. Most correlations for the friction and heat transfer coefficients in turbulent flow are based on experimental studies because of the difficulty in dealing with turbulent flow theoretically.

For *smooth* tubes, the friction factor in turbulent flow can be determined from the explicit *first Petukhov equation* (Petukhov, 1970), given as

$$\textit{Smooth tubes:} \quad f = (0.790 \ln \text{Re} - 1.64)^{-2} \qquad 3000 < \text{Re} < 5 \times 10^6 \qquad \textbf{(8–65)}$$

The Nusselt number in turbulent flow is related to the friction factor through the *Chilton–Colburn analogy,* expressed as

$$\text{Nu} = 0.125 f \text{RePr}^{1/3} \qquad \textbf{(8–66)}$$

Once the friction factor is available, this equation can be used conveniently to evaluate the Nusselt number for both smooth and rough tubes.

For fully developed turbulent flow in *smooth tubes,* a simple relation for the Nusselt number can be obtained by substituting the simple power law relation $f = 0.184 \text{ Re}^{-0.2}$ for the friction factor into Eq. 8–66. It gives

$$\text{Nu} = 0.023 \text{ Re}^{0.8} \text{Pr}^{1/3} \qquad \begin{pmatrix} 0.7 \leq \text{Pr} \leq 160 \\ \text{Re} > 10,000 \end{pmatrix} \qquad \textbf{(8–67)}$$

which is known as the *Colburn equation.* The accuracy of this equation can be improved by modifying it as

$$\text{Nu} = 0.023 \text{ Re}^{0.8} \text{Pr}^n \qquad \textbf{(8–68)}$$

where $n = 0.4$ for *heating* and 0.3 for *cooling* of the fluid flowing through the tube. This equation is known as the *Dittus–Boelter equation* (Dittus and Boelter, 1930), and it is preferred over the Colburn equation.

The preceding equations can be used when the temperature difference between the fluid and wall surface is not large by evaluating all fluid properties at the *bulk mean fluid temperature* $T_b = (T_i + T_e)/2$. When the variation in properties is large due to a large temperature difference, the following equation due to Sieder and Tate (1936) can be used:

$$\text{Nu} = 0.027 \text{ Re}^{0.8} \text{Pr}^{1/3}\left(\frac{\mu_b}{\mu_s}\right)^{0.14} \qquad \begin{pmatrix} 0.7 \leq \text{Pr} \leq 16,700 \\ \text{Re} \geq 10,000 \end{pmatrix} \qquad \textbf{(8–69)}$$

Here all properties are evaluated at T_b except μ_s, which is evaluated at T_s.

The preceding Nusselt number relations are fairly simple, but they may give errors as large as 25 percent. This error can be reduced considerably to less than 10 percent by using more complex but accurate relations, such as the *second Petukhov equation*, expressed as

$$\text{Nu} = \frac{(f/8)\text{Re Pr}}{1.07 + 12.7(f/8)^{0.5}(\text{Pr}^{2/3} - 1)} \quad \binom{0.5 \leq \text{Pr} \leq 2000}{10^4 < \text{Re} < 5 \times 10^6} \tag{8–70}$$

The accuracy of this relation at lower Reynolds numbers is improved by modifying it as (Gnielinski, 1976)

$$\text{Nu} = \frac{(f/8)(\text{Re} - 1000)\text{Pr}}{1 + 12.7(f/8)^{0.5}(\text{Pr}^{2/3} - 1)} \quad \binom{0.5 \leq \text{Pr} \leq 2000}{3 \times 10^3 < \text{Re} < 5 \times 10^6} \tag{8–71}$$

where the friction factor f can be determined from an appropriate relation such as the first Petukhov equation. Gnielinski's equation should be preferred in calculations. Again properties should be evaluated at the bulk mean fluid temperature.

The preceding relations are not very sensitive to the *thermal conditions* at the tube surfaces, and they can be used for both $T_s = $ constant and $\dot{q}_s = $ constant cases. Despite their simplicity, the correlations already presented give sufficiently accurate results for most engineering purposes. They can also be used to obtain rough estimates of the friction factor and the heat transfer coefficients in the transition region.

The relations given so far do not apply to liquid metals because of their very low Prandtl numbers. For liquid metals ($0.004 < \text{Pr} < 0.01$), the following relations are recommended by Sleicher and Rouse (1975) for $10^4 < \text{Re} < 10^6$:

$$\textit{Liquid metals, } T_s = \text{constant:} \quad \text{Nu} = 4.8 + 0.0156 \, \text{Re}^{0.85} \, \text{Pr}_s^{0.93} \tag{8–72}$$

$$\textit{Liquid metals, } \dot{q}_s = \text{constant:} \quad \text{Nu} = 6.3 + 0.0167 \, \text{Re}^{0.85} \, \text{Pr}_s^{0.93} \tag{8–73}$$

where the subscript s indicates that the Prandtl number is to be evaluated at the surface temperature.

Fully Developed Transitional Flow Heat Transfer

As mentioned in Section 8–2, there is a regime of fluid flow which is neither fully laminar nor fully turbulent. Generally, internal flows with Reynolds numbers less than 2300 are considered fully laminar. As the Reynolds number rises, it contains increasingly more turbulent motion until $\text{Re} \sim 4000$; at this point, it is mostly turbulent. By the time the Reynolds number is increased to ~10,000, it is normally fully turbulent.

The methods to handle fully laminar and fully turbulent heat transfer have already been discussed, but in some cases the flow is in this transitional zone. Fortunately, the methods for handling fully developed turbulent flow can easily be adapted to deal with flow in this region. A simple approach is discussed in detail in Abraham et al. (2011). The recommendation is to continue to use Gnielinski's (1976) correlation (Eq. 8–71) for fully developed turbulent flow along with f values determined from the following expressions for two common flow geometries, the round tube and the parallel-plate channel. These

correlations can be applied over the Reynolds number ranges listed and are reasonably accurate for any thermal boundary condition, including the uniform wall temperature and uniform wall heat flux cases. A slightly more accurate approach is available for transitional flows in round tubes (Abraham et al., 2009) but for most engineering applications, the following expressions are suitable.

Smooth round pipe:

$$f = 3.03 \times 10^{-12}\,\text{Re}^3 - 3.67 \times 10^{-8}\,\text{Re}^2 + 1.46 \times 10^{-4}\,\text{Re} - 0.151 \qquad \textbf{(8–74)}$$

which is valid for $2300 < \text{Re} < 4500$

Smooth, parallel-plate channel:

$$f = -6.38 \times 10^{-13}\,\text{Re}^3 + 1.17 \times 10^{-8}\,\text{Re}^2 - 6.69 \times 10^{-5}\,\text{Re} + 0.147 \qquad \textbf{(8–75)}$$

which is valid for $2300 < \text{Re} < 8000$

The calculation of Nusselt number or heat transfer coefficient in the transition region was further studied in detail by Gnielinski (2013). According to his study, the equations used to calculate the Nusselt number in tubes do not agree in the transition region between laminar and turbulent flow. There is a gap at $\text{Re} = 2300$. He developed a linear interpolation in the transition region between the Nusselt numbers at $\text{Re} = 2300$ and $\text{Re} = 4000$. His proposed linear interpolation connects the laminar flow equation at $\text{Re} = 2300$ with the turbulent flow equation at $\text{Re} = 4000$ and avoids the gap between the equations for laminar and turbulent flows and leads to a method of calculation providing heat transfer coefficients for all flow regimes in tubes.

As discussed in the Topic of Special Interest later in this chapter, a very detailed discussion is provided for transitional flows with particular emphasis on the entrance geometry and on the development region. That discussion also handles flows which may experience buoyant motion and property variations.

Rough Surfaces

Any irregularity or roughness on the surface disturbs the laminar sublayer and affects the flow. Therefore, unlike laminar flow, the friction factor and the convection coefficient in turbulent flow are strong functions of surface roughness.

The friction factor in fully developed turbulent pipe flow depends on the Reynolds number and the **relative roughness** ε/D, which is the ratio of the mean height of roughness of the pipe to the pipe diameter. The functional form of this dependence cannot be obtained from a theoretical analysis, and all available results are obtained from painstaking experiments using artificially roughened surfaces (usually by gluing sand grains of a known size on the inner surfaces of the pipes). Most such experiments were conducted by Prandtl's student J. Nikuradse in 1933, followed by the works of others. The friction factor was calculated from the measurements of the flow rate and the pressure drop.

The experimental results obtained are presented in tabular, graphical, and functional forms obtained by curve-fitting experimental data. In 1939, Cyril F. Colebrook (1910–1997) combined the available data for transition and turbulent flow in smooth as well as rough pipes into the following implicit relation known as the **Colebrook equation**:

$$\frac{1}{\sqrt{f}} = -2.0 \log\!\left(\frac{\varepsilon/D}{3.7} + \frac{2.51}{\text{Re}\sqrt{f}} \right) \qquad \text{(turbulent flow)} \qquad \textbf{(8–76)}$$

Relative Roughness, ε/D	Friction Factor, f
0.0*	0.0119
0.00001	0.0119
0.0001	0.0134
0.0005	0.0172
0.001	0.0199
0.005	0.0305
0.01	0.0380
0.05	0.0716

*Smooth surface. All values are for Re = 10^6, and are calculated from Eq. 8–76.

FIGURE 8–27
The friction factor is minimum for a smooth pipe and increases with roughness.

We note that the logarithm in Eq. 8–76 is a base 10 rather than a natural logarithm. In 1942, the American engineer Hunter Rouse (1906–1996) verified Colebrook's equation and produced a graphical plot of f as a function of Re and the product $\text{Re}\sqrt{f}$. He also presented the laminar flow relation and a table of commercial pipe roughness. Two years later, Lewis F. Moody (1880–1953) redrew Rouse's diagram into the form commonly used today. The now famous **Moody chart** is given in the appendix as Fig. A–20. It presents the Darcy friction factor for pipe flow as a function of the Reynolds number and ε/D over a wide range. It is probably one of the most widely accepted and used charts in engineering. Although it was developed for circular pipes, it can also be used for noncircular pipes by replacing the diameter with the hydraulic diameter.

For smooth pipes, the agreement between the Petukhov and Colebrook equations is very good. The friction factor is minimum for a smooth pipe (but still not zero because of the no-slip condition), and it increases with roughness (Fig. 8–27).

Commercially available pipes are specified according to a **nominal diameter**. The nominal diameter does not necessarily indicate the actual inside diameter of the pipe (Table 8–2). Therefore, in calculations we should make sure to use the actual inside diameter of the pipe. For example, a 2-inch nominal size steel pipe has an actual inside diameter of 2.067 inches. Another specification is **pipe schedule**. Schedule is the thickness of the inside diameter of the pipe. Schedule 40 is usually a standard thickness for most applications, which is normally a 1/4-inch wall (Table 8–2). As the schedule number increases or decreases, so does the wall thickness. However, the outside diameter remains the same. Standard piping schedules are 10, 40, 80, 120, and 160.

Commercially available pipes differ from those used in the experiments in that the roughness of pipes in the market is not uniform, and it is difficult to give a precise description of it. Equivalent roughness values for some commercial pipes are given in Table 8–3 as well as in the Moody chart. But it should be kept in mind that these values are for new pipes, and the relative roughness of pipes may increase with use as a result of corrosion, scale buildup, and precipitation. As a result, the friction factor may increase by a factor of 5 to 10. Actual operating conditions must be considered in the design of piping systems. Also, the Moody chart and its equivalent Colebrook equation involve several uncertainties (the roughness size, experimental error, curve fitting of data, etc.), and thus the results obtained should not be treated as exact. They are usually considered to be accurate to ±15 percent over the entire range in the figure.

The Colebrook equation is implicit in f, and thus the determination of the friction factor requires iteration. An approximate explicit relation for f was given by S. E. Haaland in 1983 as

$$\frac{1}{\sqrt{f}} \cong -1.8 \log \left[\frac{6.9}{\text{Re}} + \left(\frac{\varepsilon/D}{3.7} \right)^{1.11} \right] \tag{8–77}$$

The results obtained from this relation are within 2 percent of those obtained from the Colebrook equation. If more accurate results are desired, Eq. 8–77 can be used as a good *first guess* in a Newton iteration when using a programmable calculator or a spreadsheet to solve for f with Eq. 8–76.

In turbulent flow, wall roughness increases the heat transfer coefficient h by a factor of 2 or more (Dipprey and Sabersky, 1963). The convection heat transfer coefficient for rough tubes can be calculated approximately from

TABLE 8–2

Standard sizes for Schedule 40 steel pipes

Nominal Size, in	Actual Inside Diameter, in
⅛	0.269
¼	0.364
⅜	0.493
½	0.622
¾	0.824
1	1.049
1½	1.610
2	2.067
2½	2.469
3	3.068
5	5.047
10	10.02

TABLE 8–3

Equivalent roughness values for new commercial pipes*

Material	Roughness, ε	
	ft	mm
Glass, plastic	0 (smooth)	
Concrete	0.003–0.03	0.9–9
Wood stave	0.0016	0.5
Rubber, smoothed	0.000033	0.01
Copper or brass tubing	0.000005	0.0015
Cast iron	0.00085	0.26
Galvanized iron	0.0005	0.15
Wrought iron	0.00015	0.046
Stainless steel	0.000007	0.002
Commercial steel	0.00015	0.045

*The uncertainty in these values can be as much as ±60 percent.
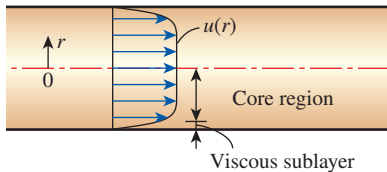
FIGURE 8–28
In turbulent flow, the velocity profile is nearly a straight line in the core region, and any significant velocity gradients occur in the viscous sublayer.
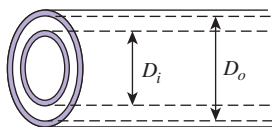
FIGURE 8–29
A double-tube heat exchanger that consists of two concentric tubes.

the Nusselt number relations such as Eq. 8–71 by using the friction factor determined from the Moody chart or the Colebrook equation. However, this approach is not very accurate since there is no further increase in h with f for $f > 4f_{\text{smooth}}$ (Norris, 1970), and correlations developed specifically for rough tubes should be used when more accuracy is desired.

Developing Turbulent Flow in the Entrance Region

The entry lengths for turbulent flow are typically short, often just 10 tube diameters long, and thus the Nusselt number determined for fully developed turbulent flow can be used approximately for the entire tube. This simple approach gives reasonable results for pressure drop and heat transfer for long tubes and conservative results for short ones. Correlations for the friction and heat transfer coefficients for the entrance regions are available in the literature for better accuracy.

Turbulent Flow in Noncircular Tubes

The velocity and temperature profiles in turbulent flow are nearly straight lines in the core region, and any significant velocity and temperature gradients occur in the viscous sublayer (Fig. 8–28). Despite the small thickness of the viscous sublayer (usually much less than 1 percent of the pipe diameter), the characteristics of the flow in this layer are very important since they set the stage for flow in the rest of the pipe. Therefore, pressure drop and heat transfer characteristics of turbulent flow in tubes are dominated by the very thin viscous sublayer next to the wall surface, and the shape of the core region is not of much significance. Consequently, the turbulent flow relations given above for circular tubes can also be used for noncircular tubes with reasonable accuracy by replacing the diameter D in the evaluation of the Reynolds number by the hydraulic diameter $D_h = 4A_c/p$.

Flow Through Tube Annulus

Some simple heat transfer devices consist of two concentric tubes and are properly called *double-tube heat exchangers* (Fig. 8–29). In such devices, one fluid flows through the tube while the other flows through the annular space. The governing differential equations for both flows are identical. Therefore, steady laminar flow through an annulus can be studied analytically by using suitable boundary conditions.

Consider a concentric annulus of inner diameter D_i and outer diameter D_o. The hydraulic diameter of the annulus is

$$D_h = \frac{4A_c}{p} = \frac{4\pi(D_o^2 - D_i^2)/4}{\pi(D_o + D_i)} = D_o - D_i$$

Annular flow is associated with two Nusselt numbers—Nu_i on the inner tube surface and Nu_o on the outer tube surface—since it may involve heat transfer on both surfaces. The Nusselt numbers for fully developed laminar flow with one surface isothermal and the other adiabatic are given in Table 8–4. When Nusselt numbers are known, the convection heat transfer coefficients for the inner and the outer surfaces are determined from

$$Nu_i = \frac{h_i D_h}{k} \quad \text{and} \quad Nu_o = \frac{h_o D_h}{k} \tag{8–78}$$

For fully developed turbulent flow, the inner and outer convection heat transfer coefficients are approximately equal to each other, and the tube

annulus can be treated as a noncircular duct with a hydraulic diameter of $D_h = D_o - D_i$. The Nusselt number in this case can be determined from a suitable turbulent flow relation such as the Gnielinski equation (Eq. 8–71). To improve the accuracy of Nusselt numbers obtained from these relations for annular flow, Petukhov and Roizen (1964) recommend multiplying them by the following correction factors when one of the tube walls is adiabatic and heat transfer is through the other wall:

$$F_i = 0.86 \left(\frac{D_i}{D_o} \right)^{-0.16} \text{ (outer wall adiabatic)} \quad \textbf{(8–79)}$$

$$F_o = 1 - 0.14 \left(\frac{D_i}{D_o} \right)^{0.6} \text{ (inner wall adiabatic)} \quad \textbf{(8–80)}$$

Gnielinski (2015), on the basis of a large amount of recent experimental data from the literature, improved his earlier heat transfer correlations for turbulent annular flow (Gnielinski, 2009) and developed a single comprehensive correlation for the calculation of the heat transfer coefficient for turbulent flow in tubes and concentric annular ducts. Only different correlations for the friction factor are required, and the appropriate hydraulic diameter must be used. Specific additional factors are needed that take into consideration the effect of the diameter ratio of the annulus and the different boundary conditions for heating and cooling. Examples include heat transfer at the inner wall with the outer wall insulated and heat transfer at the outer wall with the inner wall insulated. No experimental data were found for heat transfer from both walls to the annular flow.

Heat Transfer Enhancement

Tubes with rough surfaces have much higher heat transfer coefficients than tubes with smooth surfaces. Therefore, tube surfaces are often intentionally *roughened, corrugated,* or *finned* in order to *enhance* the convection heat transfer coefficient and thus the convection heat transfer rate (Fig. 8–30). Heat transfer in turbulent flow in a tube has been increased by as much as 400 percent by roughening the surface. Roughening the surface, of course, also increases the friction factor and thus the power requirement for the pump or the fan.

The convection heat transfer coefficient can also be increased by inducing pulsating flow by pulse generators, by inducing swirl by inserting a twisted tape into the tube, or by inducing secondary flows by coiling the tube.

TABLE 8–4

Nusselt number for fully developed laminar flow in an annulus with one surface isothermal and the other adiabatic

D_i/D_o	Nu_i	Nu_o
0	—	3.66
0.05	17.46	4.06
0.10	11.56	4.11
0.25	7.37	4.23
0.50	5.74	4.43
1.00	4.86	4.86

Source: Kays and Perkins, 1972

(*a*) Finned surface

(*b*) Roughened surface
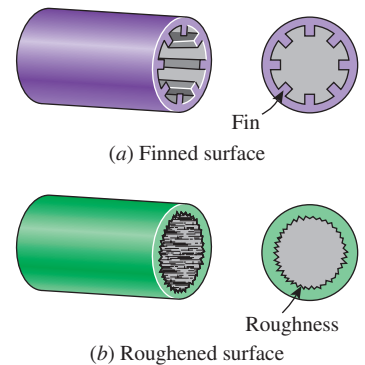
FIGURE 8–30
Tube surfaces are often *roughened, corrugated,* or *finned* in order to *enhance* convection heat transfer.

FIGURE 8–31
Schematic for Example 8–4.

EXAMPLE 8–4   **Pressure Drop in a Water Tube**

Water at 60°F ($\rho = 62.36$ lbm/ft³ and $\mu = 7.536 \times 10^{-4}$ lbm/ft·s) is flowing steadily in a 2-in-internal-diameter horizontal tube made of stainless steel at a rate of 0.2 ft³/s (Fig. 8–31). Determine the pressure drop and the required pumping power input for flow through a 200-ft-long section of the tube.

SOLUTION   The flow rate through a specified water tube is given. The pressure drop and the pumping power requirements are to be determined.
Assumptions   **1** The flow is steady and incompressible. **2** The entrance effects are negligible, and thus the flow is fully developed. **3** The tube involves no components such as

bends, valves, and connectors. **4** The piping section involves no work devices such as a pump or a turbine.

Properties The density and dynamic viscosity of water are given to be $\rho = 62.36$ lbm/ft^3 and $\mu = 7.536 \times 10^{-4}$ lbm/ft·s. For stainless steel, $\varepsilon = 0.000007$ ft (Table 8–3).

Analysis First we calculate the mean velocity and the Reynolds number to determine the flow regime:

$$V = \frac{\dot{V}}{A_c} = \frac{\dot{V}}{\pi D^2/4} = \frac{0.2 \text{ ft}^3/\text{s}}{\pi (2/12 \text{ ft})^2/4} = 9.17 \text{ ft/s}$$

$$\text{Re} = \frac{\rho V D}{\mu} = \frac{(62.36 \text{ lbm/ft}^3)(9.17 \text{ ft/s})(2/12 \text{ ft})}{7.536 \times 10^{-4} \text{ lbm/ft·s}} = 126{,}400$$

Since Re is greater than 10,000, the flow is turbulent. The relative roughness of the tube is

$$\varepsilon/D = \frac{0.000007 \text{ ft}}{2/12 \text{ ft}} = 0.000042$$

The friction factor corresponding to this relative roughness and Reynolds number can simply be determined from the Moody chart. To avoid the reading error, we determine it from the Colebrook equation:

$$\frac{1}{\sqrt{f}} = -2.0 \log\left(\frac{\varepsilon/D}{3.7} + \frac{2.51}{\text{Re}\sqrt{f}}\right) \rightarrow \frac{1}{\sqrt{f}} = -2.0 \log\left(\frac{0.000042}{3.7} + \frac{2.51}{126{,}400\sqrt{f}}\right)$$

Using an equation solver or an iterative scheme, the friction factor is determined to be $f = 0.0174$. Then the pressure drop and the required power input become

$$\Delta P = f\frac{L}{D}\frac{\rho V^2}{2} = 0.0174\frac{200 \text{ ft}}{2/12 \text{ ft}}\frac{(62.36 \text{ lbm/ft}^3)(9.17 \text{ ft/s})^2}{2}\left(\frac{1 \text{ lbf}}{32.174 \text{ lbm·ft/s}^2}\right)$$

$$= \textbf{1700 lbf/ft}^2 = \textbf{11.8 psi}$$

$$\dot{W}_{\text{pump}} = \dot{V}\Delta P = (0.2 \text{ ft}^3/\text{s})(1700 \text{ lbf/ft}^2)\left(\frac{1 \text{ W}}{0.73756 \text{ lbf·ft/s}}\right) = \textbf{461 W}$$

Therefore, power input in the amount of 461 W is needed to overcome the frictional losses in the tube.

Discussion The friction factor could also be determined easily from the explicit Haaland relation. It would give $f = 0.0172$, which is sufficiently close to 0.0174. Also, the friction factor corresponding to $\varepsilon = 0$ in this case is 0.0170, which indicates that this stainless-steel pipe can be assumed to be smooth with negligible error.
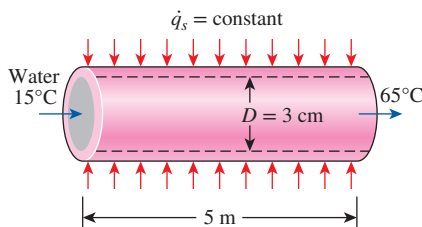
FIGURE 8–32
Schematic for Example 8–5.

EXAMPLE 8–5 **Heating of Water by Resistance Heaters with Turbulent Flow in a Tube**

Water is to be heated from 15°C to 65°C as it flows through a 3-cm-internal-diameter 5-m-long tube (Fig. 8–32). The tube is equipped with an electric resistance heater that provides uniform heating throughout the surface of the tube. The outer surface of the heater is well insulated, so in steady operation, all the heat generated in the heater is transferred to the water in the tube. If the system is to provide hot water at a rate of 10 L/min, determine the power rating of the resistance heater. Also estimate the inner surface temperature of the tube at the exit.

SOLUTION Water is to be heated in a tube equipped with an electric resistance heater on its surface. The power rating of the heater and the inner surface temperature at the exit are to be determined.

Assumptions **1** Steady flow conditions exist. **2** The surface heat flux is uniform. **3** The inner surfaces of the tube are smooth.

Properties The properties of water at the bulk mean temperature of $T_b = (T_i + T_e)/2 = (15 + 65)/2 = 40°C$ are (Table A–9)

$$\rho = 992.1 \text{ kg/m}^3 \qquad\qquad c_p = 4179 \text{ J/kg·K}$$

$$k = 0.631 \text{ W/m·K} \qquad\qquad \text{Pr} = 4.32$$

$$\nu = \mu/\rho = 0.658 \times 10^{-6} \text{ m}^2/\text{s}$$

Analysis The cross-sectional and heat transfer surface areas are

$$A_c = \tfrac{1}{4}\pi D^2 = \tfrac{1}{4}\pi(0.03 \text{ m})^2 = 7.069 \times 10^{-4} \text{ m}^2$$

$$A_s = \pi D L = \pi(0.03 \text{ m})(5 \text{ m}) = 0.471 \text{ m}^2$$

The volume flow rate of water is given as $\dot{V} = 10$ L/min $= 0.01$ m³/min. Then the mass flow rate becomes

$$\dot{m} = \rho\,\dot{V} = (992.1 \text{ kg/m}^3)(0.01 \text{ m}^3/\text{min}) = 9.921 \text{ kg/min} = 0.1654 \text{ kg/s}$$

To heat the water at this mass flow rate from 15°C to 65°C, heat must be supplied to the water at a rate of

$$\dot{Q} = \dot{m} c_p (T_e - T_i)$$
$$= (0.1654 \text{ kg/s})(4.179 \text{ kJ/kg·K})(65 - 15)°C$$
$$= 34.6 \text{ kJ/s} = 34.6 \text{ kW}$$

All of this energy must come from the resistance heater. Therefore, the power rating of the heater must be **34.6 kW**.

The surface temperature T_s of the tube at any location can be determined from

$$\dot{q}_s = h(T_s - T_m) \rightarrow T_s = T_m + \frac{\dot{q}_s}{h}$$

where h is the heat transfer coefficient and T_m is the mean temperature of the fluid at that location. The surface heat flux is constant in this case, and its value can be determined from

$$\dot{q}_s = \frac{\dot{Q}}{A_s} = \frac{34.6 \text{ kW}}{0.471 \text{ m}^2} = 73.46 \text{ kW/m}^2$$

To determine the heat transfer coefficient, we first need to find the mean velocity of water and the Reynolds number:

$$V_{\text{avg}} = \frac{\dot{V}}{A_c} = \frac{0.010 \text{ m}^3/\text{min}}{7.069 \times 10^{-4} \text{ m}^2} = 14.15 \text{ m/min} = 0.236 \text{ m/s}$$

$$\text{Re} = \frac{V_{\text{avg}} D}{\nu} = \frac{(0.236 \text{ m/s})(0.03 \text{ m})}{0.658 \times 10^{-6} \text{ m}^2/\text{s}} = 10{,}760$$

which is greater than 10,000. Therefore, the flow is turbulent, and the entry length is roughly

$$L_h \approx L_t \approx 10D = 10 \times 0.03 = 0.3 \text{ m}$$

which is much shorter than the total length of the tube. Therefore, we can assume fully developed turbulent flow in the entire tube and determine the Nusselt number from

$$\text{Nu} = \frac{hD}{k} = 0.023 \, \text{Re}^{0.8} \, \text{Pr}^{0.4} = 0.023 \, (10{,}760)^{0.8} \, (4.32)^{0.4} = 69.4$$

Then,

$$h = \frac{k}{D}\text{Nu} = \frac{0.631 \text{ W/m·K}}{0.03 \text{ m}}(69.4) = 1460 \text{ W/m}^2\text{·K}$$

and the inner surface temperature of the tube at the exit becomes

$$T_s = T_m + \frac{\dot{q}_s}{h} = 65°\text{C} + \frac{73{,}460 \text{ W/m}^2}{1460 \text{ W/m}^2\text{·K}} = \mathbf{115°C}$$

Discussion Note that the inner surface temperature of the tube will be 50°C higher than the mean water temperature at the tube exit. This temperature difference of 50°C between the water and the surface will remain constant throughout the fully developed flow region.

EXAMPLE 8–6   Heating of Water by Resistance Heaters with Transitional Flow in a Tube

Repeat Example 8–5 for a volume flow rate of 2.5 L/min (one-fourth of the initial value).

SOLUTION Same as Example 8–5 with a volume flow rate which is one-fourth of the initial value.
Assumptions Same as Example 8–5.
Properties Same as Example 8–5.
Analysis The cross-sectional and heat transfer surface areas are the same as in Example 8–5.

With the water volume flow rate of 2.5 L/min (one-fourth of the initial value), the mass flow rate becomes 0.04134 kg/s, and the velocity for this mass flow rate is 0.059 m/s.

To heat the water at this mass flow rate from 15°C to 65°C, heat must be supplied to the water from the resistance heater at a rate of **8.64 kW** (one-fourth of the initial value).

The surface heat flux is constant in this case, and its value is 18.34 kW/m² (one-fourth of the initial value).

Next, the Reynolds number and the convection heat transfer coefficient will be found.

$$\text{Re} = \frac{V_{\text{avg}}D}{\nu} = \frac{(0.059 \text{ m/s})(0.03 \text{ m})}{0.658 \times 10^{-6} \text{ m}^2/\text{s}} = 2690$$

which is between 2300 and 4000. Therefore, the flow is in the transitional region. With the Reynolds number known, it is possible to obtain the friction factor and the Nusselt number. The friction factor for transitional flow in a smooth tube with Re = 2690 is obtained from

$$f = 3.03 \times 10^{-12} \, \text{Re}^3 - 3.67 \times 10^{-8} \, \text{Re}^2 + 1.46 \times 10^{-4} \, \text{Re} - 0.151 = 0.0352$$

To calculate the transitional Nusselt number, as it was noted earlier, the most accurate way is to use Gnielinski's (2013) proposed linear interpolation in the transition region between the Nusselt numbers at Re = 2300 and Re = 4000. However, for this problem, we will use Gnielinski's (1976) fully developed turbulent flow heat transfer correlation, which is slightly less accurate since the lower Reynolds number limit of this equation is slightly higher than the Reynolds number of 2690 of this problem. The Nusselt number in the transitional flow with Re = 2690, Pr = 4.32, and $f = 0.0352$ is obtained from

$$\text{Nu} = \frac{(f/8)(\text{Re} - 1000)\text{Pr}}{1 + 12.7(f/8)^{0.5}(\text{Pr}^{2/3} - 1)} = 13.4$$

Then, from the Nusselt number, the convective heat transfer coefficient can be found,

$$h = \frac{k}{D}\,\text{Nu} = \frac{0.631 \text{ W/m·K}}{0.03 \text{ m}}(13.4) = 281.8 \text{ W/m}^2\text{·K}$$

and the inner surface temperature of the tube at the exit becomes

$$T_s = T_m + \frac{\dot{q}_s}{h} = 65°\text{C} + \frac{18,340 \text{ W/m}^2}{281.8 \text{ W/m}^2\text{·K}} = \mathbf{130.1°C}$$

Discussion Note that the inner surface temperature of the tube will be 65°C higher than the mean water temperature at the tube exit. This temperature difference of 65°C between the water and the surface will remain constant throughout the fully developed flow region. Also note that in comparison to Example 8–5, the convective heat transfer coefficient is much lower. This reflects the lower volume flow rate of water, which gives rise to a higher inner surface temperature at the exit.

PtD *EXAMPLE 8–7*   **Pipe Insulation for Thermal Burn Prevention**

A 10-m-long metal pipe ($k_{\text{pipe}} = 15$ W/m·K) with an inner diameter of 5 cm and an outer diameter of 6 cm is used for transporting hot saturated water vapor at a flow rate of 0.05 kg/s (Fig. 8–33). The water vapor enters and exits the pipe at 350°C and 290°C, respectively. To protect workers from thermal burns, the pipe is covered with a 2.25-cm-thick layer of insulation ($k_{\text{ins}} = 0.95$ W/m·K) to ensure that the outer surface temperature $T_{s,\,o}$ is below 45°C. Determine whether or not the thickness of the insulation is sufficient to alleviate the risk of thermal burns.

SOLUTION   In this example, the concepts of PtD are applied in conjunction with the concepts of internal forced convection and steady one-dimensional heat conduction. The inner pipe surface temperature $T_{s,\,i}$ is determined using the concept of internal forced convection. Having determined the inner surface temperature, we determine the outer surface temperature $T_{s,\,o}$ using one-dimensional heat conduction through the pipe wall and insulation.

Assumptions   **1** Steady operating conditions exist. **2** Radiation effects are negligible. **3** Convection effects on the outer pipe surface are negligible. **4** One-dimensional heat conduction through pipe wall and insulation. **5** The thermal conductivities of pipe wall and insulation are constant. **6** Thermal resistance at the interface is negligible. **7** The surface temperatures are uniform. **8** The inner surfaces of the tube are smooth.

Properties   The properties of saturated water vapor at $T_b = (T_i + T_e)/2 = 320°\text{C}$ are $c_p = 7900$ J/kg·K, $k = 0.0836$ W/m·K, $\mu = 2.084 \times 10^{-5}$ kg/m·s, and Pr = 1.97 (Table A–9).
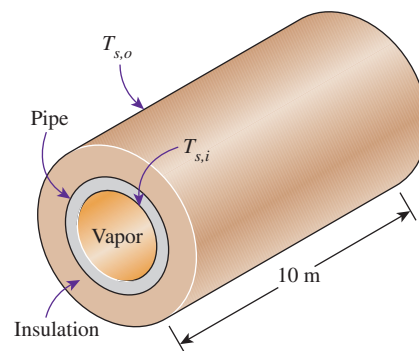
FIGURE 8–33
Schematic for Example 8–7.

The thermal conductivities of the pipe and the insulation are given to be $k_{pipe} = 15$ W/m·K and $k_{ins} = 0.95$ W/m·K, respectively.

Analysis The Reynolds number of the saturated water vapor flow in the pipe is

$$\text{Re} = \frac{4\dot{m}}{\pi D_i \mu} = \frac{4(0.05 \text{ kg/s})}{\pi (0.05 \text{ m})(2.084 \times 10^{-5} \text{ kg/m·s})} = 61{,}069 > 10{,}000$$

Therefore, the flow is turbulent, and the entry lengths in this case are roughly

$$L_h \approx L_t \approx 10D = 10(0.05 \text{ m}) = 0.5 \text{ m (assume fully developed turbulent flow)}$$

The Nusselt number can be determined from the Gnielinski correlation:

$$\text{Nu} = \frac{(f/8)(\text{Re} - 1000)\text{Pr}}{1 + 12.7(f/8)^{0.5}(\text{Pr}^{2/3} - 1)} = \frac{(0.02003/8)(61{,}096 - 1000)(1.97)}{1 + 12.7(0.02003/8)^{0.5}(1.97^{2/3} - 1)} = 217.45$$

where

$$f = (0.790 \ln \text{Re} - 1.64)^{-2} = 0.02003$$

Thus, the convection heat transfer coefficient for the saturated water vapor flow inside the pipe is

$$h = \frac{k}{D_i}\text{Nu} = \frac{0.0836 \text{ W/m·K}}{0.05 \text{ m}}(217.45) = 363.58 \text{ W/m}^2\text{·K}$$

The inner pipe surface temperature is

$$T_e = T_{s,i} - (T_{s,i} - T_i)\exp\left(-\frac{hA_s}{\dot{m}c_p}\right) \quad \longrightarrow \quad T_{s,i} = 271.52°\text{C}$$

where

$$A_s = \pi(0.05 \text{ m})(10 \text{ m}) = 1.571 \text{ m}^2$$

From Chap. 3, the thermal resistances for the pipe wall and the insulation are

$$R_{pipe} = \frac{\ln(D_{interface}/D_i)}{2\pi k_{pipe} L} = \frac{\ln(0.06/0.05)}{2\pi(15 \text{ W/m·K})(10 \text{ m})} = 1.9345 \times 10^{-4} \text{ K/W}$$

$$R_{ins} = \frac{\ln(D_o/D_{interface})}{2\pi k_{ins} L} = \frac{\ln(0.105/0.06)}{2\pi(0.95 \text{ W/m·K})(10 \text{ m})} = 9.3753 \times 10^{-3} \text{ K/W}$$

where $D_o = 0.06$ m $+ 2(0.0225$ m$) = 0.105$ m

The total thermal resistance and the rate of heat transfer are

$$R_{total} = R_{pipe} + R_{ins} = 9.5688 \times 10^{-3} \text{ K/W} \quad \text{and} \quad \dot{Q} = \frac{T_{s,i} - T_{s,o}}{R_{total}} = \dot{m}c_p(T_i - T_e)$$

Thus, the outer surface temperature is

$$T_{s,o} = T_{s,i} - R_{total}\dot{m}c_p(T_i - T_e)$$

$$= 271.52°\text{C} - (9.5688 \times 10^{-3} \text{ K/W})(0.05 \text{ kg/s})(7900 \text{ J/kg·K})(350 - 290)°\text{C}$$

$$= \mathbf{44.7°C}$$

Discussion The insulation thickness of 2.25 cm is just barely sufficient to keep the outer surface temperature below 45°C. To ensure that the outer surface is a few degrees below 45°C, the insulation thickness should be increased slightly to 2.3 cm, which would make $T_{s,o} = 41°$C.

EXAMPLE 8–8   Heat Loss from the Ducts of a Heating System

Hot air at atmospheric pressure and 80°C enters an 8-m-long uninsulated square duct of cross section 0.2 m × 0.2 m that passes through the attic of a house at a rate of 0.15 m³/s (Fig. 8–34). The duct is observed to be nearly isothermal at 60°C. Determine the exit temperature of the air and the rate of heat loss from the duct to the attic space.

SOLUTION   Heat loss from uninsulated square ducts of a heating system in the attic is considered. The exit temperature and the rate of heat loss are to be determined.
Assumptions   **1** Steady operating conditions exist. **2** The inner surfaces of the duct are smooth. **3** Air is an ideal gas.
Properties   We do not know the exit temperature of the air in the duct, and thus we cannot determine the bulk mean temperature of air, which is the temperature at which the properties are to be determined. The temperature of air at the inlet is 80°C, and we expect this temperature to drop somewhat as a result of heat loss through the duct whose surface is at 60°C. At 80°C and 1 atm, we read (Table A–15)

$$\rho = 0.9994 \text{ kg/m}^3 \qquad c_p = 1008 \text{ J/kg·K}$$

$$k = 0.02953 \text{ W/m·K} \quad \text{Pr} = 0.7154$$

$$\nu = 2.097 \times 10^{-5} \text{ m}^2/\text{s}$$

Analysis   The characteristic length (which is the hydraulic diameter), the mean velocity, and the Reynolds number in this case are

$$D_h = \frac{4A_c}{p} = \frac{4a^2}{4a} = a = 0.2 \text{ m}$$

$$V_{avg} = \frac{\dot{V}}{A_c} = \frac{0.15 \text{ m}^3/\text{s}}{(0.2 \text{ m})^2} = 3.75 \text{ m/s}$$

$$\text{Re} = \frac{V_{avg}D_h}{\nu} = \frac{(3.75 \text{ m/s})(0.2 \text{ m})}{2.097 \times 10^{-5} \text{ m}^2/\text{s}} = 35{,}765$$

which is greater than 10,000. Therefore, the flow is turbulent, and the entry lengths in this case are roughly

$$L_h \approx L_t \approx 10D = 10 \times 0.2 \text{ m} = 2 \text{ m}$$

which is much shorter than the total length of the duct. Therefore, we can assume fully developed turbulent flow in the entire duct and determine the Nusselt number from

$$\text{Nu} = \frac{hD_h}{k} = 0.023 \, \text{Re}^{0.8} \, \text{Pr}^{0.3} = 0.023 \, (35{,}765)^{0.8} \, (0.7154)^{0.3} = 91.4$$

Then,

$$h = \frac{k}{D_h}\text{Nu} = \frac{0.02953 \text{ W/m·K}}{0.2 \text{ m}}(91.4) = 13.5 \text{ W/m}^2\text{·K}$$

$$A_s = 4aL = 4 \times (0.2 \text{ m})(8 \text{ m}) = 6.4 \text{ m}^2$$

$$\dot{m} = \rho\dot{V} = (0.9994 \text{ kg/m}^3)(0.15 \text{ m}^3/\text{s}) = 0.150 \text{ kg/s}$$
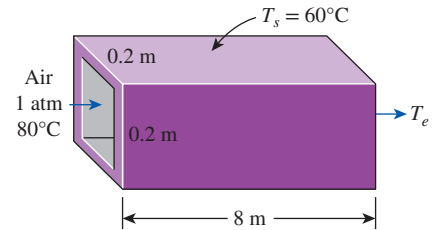
FIGURE 8–34
Schematic for Example 8–8.

Next, we determine the exit temperature of air from

$$T_e = T_s - (T_s - T_i) \exp(-hA_s/\dot{m}c_p)$$

$$= 60°C - [(60 - 80°C)] \exp\left[-\frac{(13.5 \text{ W/m}^2\text{·K})(6.4 \text{ m}^2)}{(0.150 \text{ kg/s})(1008 \text{ J/kg·K})}\right]$$

$$= \mathbf{71.3°C}$$

Then the log mean temperature difference and the rate of heat loss from the air become

$$\Delta T_{\text{lm}} = \frac{T_i - T_e}{\ln\dfrac{T_s - T_e}{T_s - T_i}} = \frac{80 - 71.3}{\ln\dfrac{60 - 71.3}{60 - 80}} = -15.2°C$$

$$\dot{Q} = hA_s\,\Delta T_{\text{lm}} = (13.5 \text{ W/m}^2\text{·K})(6.4 \text{ m}^2)(-15.2°C) = \mathbf{-1313 \text{ W}}$$

Therefore, air will lose heat at a rate of 1313 W as it flows through the duct in the attic.

Discussion   The average fluid temperature is $(80 + 71.3)/2 = 75.7°C$, which is sufficiently close to 80°C, at which we evaluated the properties of air. Therefore, it is not necessary to reevaluate the properties at this temperature and to repeat the calculations.

TOPIC OF SPECIAL INTEREST *

Transitional Flow in Tubes

An important design problem in industrial heat exchangers arises when flow inside the tubes falls into the transition region. In practical engineering design, the usual recommendation is to avoid design and operation in this region; however, this is not always feasible under design constraints. The usually cited transitional Reynolds number range of about 2300 (onset of turbulence) to 10,000 (fully turbulent condition) applies, strictly speaking, to a very steady and uniform entry flow with a rounded entrance. If the flow has a disturbed entrance typical of heat exchangers, in which there is a sudden contraction and possibly even a re-entrant entrance, the transitional Reynolds number range will be much different.

Ghajar and coworkers in a series of papers (listed in the references) have experimentally investigated the inlet configuration effects on the fully developed and developing transitional pressure drop under isothermal and heating conditions, as well as developing and fully developed transitional forced and mixed convection heat transfer in circular tubes. Based on their experimental data, they have developed practical and easy-to-use correlations for the friction coefficient and the Nusselt number in the transition region between laminar and turbulent flows. This section provides a brief summary of their work in the transition region.

---

*This section can be skipped without a loss of continuity.

Pressure Drop in the Transition Region

Pressure drops are measured in circular tubes for fully developed flows in the transition regime for three types of inlet configurations shown in Fig. 8–35: re-entrant (tube extends beyond tubesheet face into head of distributor), square-edged (tube end is flush with tubesheet face), and bell-mouth (a tapered entrance of tube from tubesheet face) under isothermal and heating conditions, respectively. The widely used expressions for the *friction factor f* (also called the *Darcy friction factor*) or the *friction coefficient C_f* (also called the *Fanning friction factor*) in laminar and turbulent flows with heating are

Inlet section
|← 23.5 cm →|

Test section

Flow
←1.93 cm

Re-entrant

Flow from calming section

Square-edged

Flow

Bell-mouth

FIGURE 8–35
Schematic of the three different inlet configurations.

$$f_{\text{lam}} = 4C_{f,\text{lam}} = 4\left(\frac{16}{\text{Re}}\right)\left(\frac{\mu_b}{\mu_s}\right)^m \tag{8–81}$$

$$f_{\text{turb}} = 4C_{f,\text{turb}} = 4\left(\frac{0.0791}{\text{Re}^{0.25}}\right)\left(\frac{\mu_b}{\mu_s}\right)^m \tag{8–82}$$

where the factors at the end account for the wall temperature effect on viscosity. The exponent *m* for laminar flows depends on a number of factors, while for turbulent flows the most typically quoted value for heating is -0.25. The transition friction factor is given as (Tam and Ghajar, 1997)

$$f_{\text{trans}} = 4C_{f,\text{trans}} = 4\left[1 + \left(\frac{\text{Re}}{A}\right)^B\right]^C\left(\frac{\mu_b}{\mu_s}\right)^m \tag{8–83}$$

where

$$m = m_1 - m_2 \text{Gr}^{m_3} \text{Pr}^{m_4} \tag{8–84}$$

and the Grashof number (Gr), which is a dimensionless number representing the ratio of the buoyancy force to the viscous force, is defined as $\text{Gr} = g\beta D^3 (T_s - T_b)/\nu^2$ (see Chap. 9 for more details). All properties appearing in the dimensionless numbers C_f, f, Re, Pr, and Gr are evaluated at the bulk fluid temperature T_b. The values of the empirical constants in Eqs. 8–83 and 8–84 are listed in Table 8–5. The range of application of Eq. 8–83 for the transition friction factor is as follows:

Re-entrant: $2700 \leq \text{Re} \leq 5500$, $16 \leq \text{Pr} \leq 35$, $7410 \leq \text{Gr} \leq 158{,}300$, $1.13 \leq \mu_b/\mu_s \leq 2.13$

Square-edged: $3500 \leq \text{Re} \leq 6900$, $12 \leq \text{Pr} \leq 29$, $6800 \leq \text{Gr} \leq 104{,}500$, $1.11 \leq \mu_b/\mu_s \leq 1.89$

Bell-mouth: $5900 \leq \text{Re} \leq 9600$, $8 \leq \text{Pr} \leq 15$, $11{,}900 \leq \text{Gr} \leq 353{,}000$, $1.05 \leq \mu_b/\mu_s \leq 1.47$

TABLE 8–5

Constants for transition friction coefficient correlation

Inlet Geometry	A	B	C	m_1	m_2	m_3	m_4
Re-entrant	5840	–0.0145	–6.23	–1.10	0.460	–0.133	4.10
Square-edged	4230	–0.1600	–6.57	–1.13	0.396	–0.160	5.10
Bell-mouth	5340	–0.0990	–6.32	–2.58	0.420	–0.410	2.46
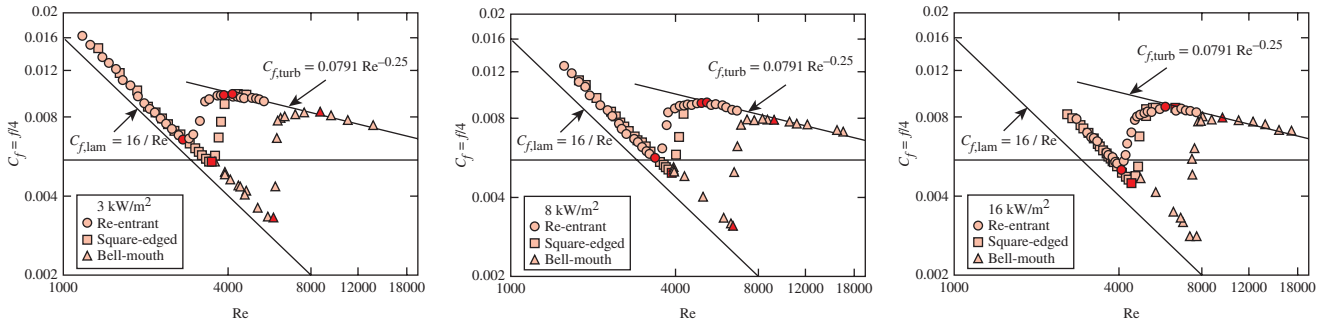
FIGURE 8–36

Fully developed friction coeffficients for three different inlet configurations and heat fluxes (filled symbols designate the start and end of the transition region for each inlet).

Source: Tam and Ghajar, 1997.

These correlations captured about 82 percent of measured data within an error band of $\pm10\%$, and 98 percent of measured data within $\pm20\%$. For laminar flows with heating, Tam and Ghajar (1997) give the following constants for determining the exponent m in Eq. 8–81: $m_1 = 1.65$, $m_2 = 0.013$, $m_3 = 0.170$, and $m_4 = 0.840$, which is applicable over the following range of parameters:

$$1100 \leq \text{Re} \leq 7400,\ 6 \leq \text{Pr} \leq 36,\ 17{,}100 \leq \text{Gr} \leq 95{,}600,$$
$$\text{and } 1.25 \leq \mu_b/\mu_s \leq 2.40.$$

The fully developed friction coefficient results for the three different inlet configurations shown in Fig. 8–36 clearly establish the influence of heating rate on the beginning and end of the transition regions for each inlet configuration. In the laminar and transition regions, heating seems to have a significant influence on the value of the friction coefficient. However, in the turbulent region, heating did not affect the magnitude of the friction coefficient. The significant influence of heating on the values of friction coefficient in the laminar and transition regions is directly due to the effect of secondary flow.

The isothermal friction coefficients for the three inlet types showed that the range of the Reynolds number values at which transition flow exists is strongly inlet-geometry dependent. Furthermore, heating caused an increase in the laminar and turbulent friction coefficients and an increase in the lower and upper limits of the isothermal transition regime boundaries. The friction coefficient transition Reynolds number ranges for the isothermal and nonisothermal (three different heating rates) and the three different inlets used in their study are summarized in Table 8–6.

TABLE 8–6

Transition Reynolds numbers for friction coefficient

Heat Flux	Re-entrant	Square-edged	Bell-mouth
0 kW/m^2 (isothermal)	2870 < Re < 3500	3100 < Re < 3700	5100 < Re < 6100
3 kW/m^2	3060 < Re < 3890	3500 < Re < 4180	5930 < Re < 8730
8 kW/m^2	3350 < Re < 4960	3860 < Re < 5200	6480 < Re < 9110
16 kW/m^2	4090 < Re < 5940	4450 < Re < 6430	7320 < Re < 9560

Figure 8–37 shows the influence of inlet configuration on the beginning and end of the isothermal fully developed friction coefficients in the transition region.

Note that the isothermal fully developed friction coefficients in the laminar, turbulent, and transition regions can be obtained easily from Eqs. 8–81, 8–82, and 8–83, respectively, by setting the viscosity ratio correction to unity (i.e., set m = 0).

The results presented so far were based on the experimental work of Tam and Ghajar (1997) for fully developed isothermal and nonisothermal friction factors. Ghajar and coworkers conducted similar experiments in the entrance (developing) region for square-edged and re-entrant inlets for laminar and transitional flows (Tam et al., 2013). The developing friction factor is referred to as the *apparent friction factor.* The apparent friction factor accounts for the combined effects of flow acceleration (variation in momentum flux) and surface shear forces.

For laminar developing friction factor in tubes with square-edged and re-entrant inlets, they recommended the following correlation:

$$f_{app,lam} = \left[\frac{1}{Re} \left(64 + \frac{0.01256}{4.836 \times 10^{-5} + 0.0609 \left(\frac{x/D}{Re} \right)^{1.28}} \right) \right] \left(\frac{\mu_b}{\mu_s} \right)^m \quad \textbf{(8–85)}$$

where $m = -5.06 + 0.84 \times Pr^{0.23} Gr^{0.09}$ for nonisothermal flow and $m = 0$ for isothermal flow.

The range of application of Eq. 8–85 is: $897 \leq Re \leq 2189, 7141 \leq Gr \leq 18{,}224, 1.27 \leq \mu_b/\mu_s \leq 1.56, 39 \leq Pr \leq 47$, and $3 \leq x/D \leq 200$.

For transitional developing friction factor in tubes, they recommended the following correlation:

$$f_{app,trans} = \left\{ \left(\frac{64}{Re} \right) [(1 + (0.0049 \, Re^{0.75})^a)^{1/a} + b] \left[1 + \left(\frac{c}{x/D} \right) \right] \right\} \left(\frac{\mu_b}{\mu_s} \right)^m \quad \textbf{(8–86)}$$

where the exponent *m* is obtained separately for each inlet for nonisothermal flow from Table 8–7 and is set to $m = 0$ for isothermal flow. The constants in Eq. 8–86 and its range of application for each inlet are also given in Table 8–7.
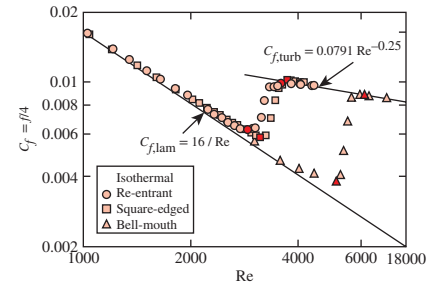
FIGURE 8–37

Influence of different inlet configurations on the isothermal fully developed friction coefficients (filled symbols designate the start and end of the transition region for each inlet).

Source: Tam and Ghajar, 1997.

TABLE 8–7

Constants and ranges of independent variables for transition friction factor correlation

Inlet Geometry	Constants and Ranges of Independent Variables
Re-entrant	$a = 0.52, b = -3.47, c = 4.8, m = -1.8 + 0.46 \, Gr^{-0.13} \, Pr^{0.41}$ $1883 < Re < 3262, 19.1 < Pr < 46.5, 4560 < Gr < 24{,}339,$ $1.12 < \mu_b/\mu_s < 1.54, 3 < x/D < 200$
Square-edged	$a = 0.50, b = -4.0, c = 3.0, m = -1.13 + 0.48 \, Gr^{-0.15} \, Pr^{0.55}$ $2084 < Re < 3980, 19.6 < Pr < 47.3, 6169 < Gr < 35{,}892,$ $1.10 < \mu_b/\mu_s < 1.54, 3 < x/D < 200$

EXAMPLE 8–9   Nonisothermal Fully Developed Friction Coefficient in the Transition Region

A tube with a bell-mouth inlet configuration is subjected to 8 kW/m^2 uniform wall heat flux. The tube has an inside diameter of 0.0158 m and a flow rate of 1.32×10^{-4} m^3/s. The liquid flowing inside the tube is an ethylene glycol–distilled water mixture with a mass fraction of 0.34. The properties of the ethylene glycol–distilled water mixture at the location of interest are Pr = 11.6, $\nu = 1.39 \times 10^{-6}$ m^2/s, and $\mu_b/\mu_s = 1.14$. Determine the fully developed friction coefficient at a location along the tube where the Grashof number is Gr = 60,800. What would the answer be if a square-edged inlet were used instead?

SOLUTION   A liquid mixture flowing in a tube is subjected to uniform wall heat flux. The friction coefficients are to be determined for the bell-mouth and square-edged inlet cases.

Assumptions   Steady operating conditions exist.

Properties   The properties of the ethylene glycol–distilled water mixture are given to be Pr = 11.6, $\nu = 1.39 \times 10^{-6}$ m^2/s, and $\mu_b/\mu_s = 1.14$.

Analysis   For the calculation of the nonisothermal fully developed friction coefficient, it is necessary to determine the flow regime before making any decision regarding which friction coefficient relation to use. The Reynolds number at the specified location is

$$\mathrm{Re} = \frac{(\dot{V}/A_c)D}{\nu} = \frac{[(1.32 \times 10^{-4}\ \mathrm{m^3/s})/(1.961 \times 10^{-4}\ \mathrm{m^2})](0.0158\ \mathrm{m})}{1.39 \times 10^{-6}\ \mathrm{m^2/s}} = 7651$$

since

$$A_c = \pi D^2/4 = \pi(0.0158\ \mathrm{m})^2/4 = 1.961 \times 10^{-4}\ \mathrm{m^2}$$

From Table 8–6, we see that for a bell-mouth inlet and a heat flux of 8 kW/m^2, the flow is in the transition region. Therefore, Eq. 8–83 applies. Reading the constants A, B, and C and m_1, m_2, m_3, and m_4 from Table 8–5, the friction coefficient is determined to be

$$
\begin{aligned}
C_{f,\,\mathrm{trans}} &= \left[1 + \left(\frac{\mathrm{Re}}{A}\right)^B\right]^C \left(\frac{\mu_b}{\mu_s}\right)^m \\
&= \left[1 + \left(\frac{7651}{5340}\right)^{-0.099}\right]^{-6.32} (1.14)^{-2.58 - 0.42 \times 60{,}800^{-0.41} \times 11.6^{2.46}} = \mathbf{0.010}
\end{aligned}
$$

Square-Edged Inlet Case   For this inlet shape, the Reynolds number of the flow is the same as that of the bell-mouth inlet (Re = 7651). However, it is necessary to check the type of flow regime for this particular inlet with 8 kW/m^2 of heating. From Table 8–6, the transition Reynolds number range for this case is 3860 < Re < 5200, which means that the flow in this case is turbulent, and Eq. 8–82 is the appropriate equation to use. It gives

$$C_{f,\,\mathrm{turb}} = \left(\frac{0.0791}{\mathrm{Re}^{0.25}}\right)\left(\frac{\mu_b}{\mu_s}\right)^m = \left(\frac{0.0791}{7651^{0.25}}\right)(1.14)^{-0.25} = \mathbf{0.0082}$$

Discussion   Note that the friction factors f can be determined by multiplying the friction coefficient values by 4.

Heat Transfer in the Transition Region

Ghajar and coworkers also experimentally investigated the inlet configuration effects on heat transfer in the transition region between laminar and turbulent flows in tubes for the same three inlet configurations shown in Fig. 8–35. They proposed some prediction methods for this regime to bridge between laminar methods and turbulent methods, applicable to forced and mixed convection in the entrance and fully developed regions for the three types of inlet configurations, which are presented next. For a detailed discussion on this topic, refer to Tam and Ghajar (2006). The local heat transfer coefficient in transition flow is obtained from the transition Nusselt number, Nu_{trans}, which is calculated as follows at a distance x from the entrance:

$$Nu_{trans} = Nu_{lam} + \{\exp[(a - Re)/b] + Nu_{turb}^c\}^c \tag{8–87}$$

where Nu_{lam} is the laminar flow Nusselt number for entrance region laminar flows with natural convection effects,

$$Nu_{lam} = 1.24 \left[\left(\frac{Re\,PrD}{x}\right) + 0.025(Gr\,Pr)^{0.75}\right]^{1/3} \left(\frac{\mu_b}{\mu_s}\right)^{0.14} \tag{8–88}$$

and Nu_{turb} is the turbulent flow Nusselt number with developing flow effects,

$$Nu_{turb} = 0.023Re^{0.8}\,Pr^{0.385}\left(\frac{x}{D}\right)^{-0.0054}\left(\frac{\mu_b}{\mu_s}\right)^{0.14} \tag{8–89}$$

The physical properties appearing in the dimensionless numbers Nu, Re, Pr, and Gr all are evaluated at the bulk fluid temperature T_b. The values of the empirical constants a, b, and c in Eq. 8–87 depend on the inlet configuration and are given in Table 8–8. The viscosity ratio accounts for the temperature effect on the process. The range of application of the heat transfer method based on their database of 1290 points (441 points for re-entrant inlet, 416 for square-edged inlet, and 433 points for bell-mouth inlet) is as follows:

Re-entrant: $3 \leq x/D \leq 192$, $1700 \leq Re \leq 9100$, $5 \leq Pr \leq 51$, $4000 \leq Gr < 210{,}000$, $1.2 < \mu_b/\mu_s < 2.2$

Square-edged: $3 \leq x/D \leq 192$, $1600 \leq Re \leq 10{,}700$, $5 \leq Pr \leq 55$, $4000 \leq Gr \leq 250{,}000$, $1.2 \leq \mu_b/\mu_s \leq 2.6$

Bell-mouth: $3 \leq x/D \leq 192$, $3300 \leq Re \leq 11{,}100$, $13 \leq Pr \leq 77$, $6000 \leq Gr \leq 110{,}000$, $1.2 \leq \mu_b/\mu_s \leq 3.1$

These correlations capture about 70 percent of measured data within an error band of $\pm 10\%$, and 97 percent of measured data within $\pm 20\%$, which is remarkable for transition flows. The individual expressions above for Nu_{lam} and Nu_{turb} can be used alone for developing flows in those respective regimes. The lower and upper limits of the heat transfer transition Reynolds number ranges for the three different inlets are summarized in Table 8–9. The results shown in this table indicate that the re-entrant inlet configuration causes the earliest transition from laminar flow into the transition regime (at about 2000), while the bell-mouth entrance retards this regime change (at about 3500). The square-edged entrance falls in between (at about 2400), which is close to the often-quoted value of 2300 in most textbooks.

TABLE 8–8

Constants for transition heat transfer correlation

Inlet Geometry	a	b	c
Re-entrant	1766	276	–0.955
Square-edged	2617	207	–0.950
Bell-mouth	6628	237	–0.980

TABLE 8–9

The lower and upper limits of the heat transfer transition Reynolds numbers

Inlet Geometry	Lower Limit	Upper Limit
Re-entrant	$Re_{lower} = 2157 - 0.65[192 - (x/D)]$	$Re_{upper} = 8475 - 9.28[192 - (x/D)]$
Square-edged	$Re_{lower} = 2524 - 0.82[192 - (x/D)]$	$Re_{upper} = 8791 - 7.69[192 - (x/D)]$
Bell-mouth	$Re_{lower} = 3787 - 1.80[192 - (x/D)]$	$Re_{upper} = 10{,}481 - 5.47[192 - (x/D)]$
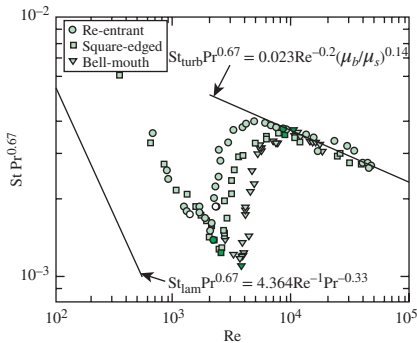
FIGURE 8–38

Influence of different inlets on the heat transfer transition region at $x/D = 192$ (filled symbols designate the start and end of the transition region for each inlet) between limits of Dittus–Boelter correlation ($Nu = 0.023\ Re^{0.8}\ Pr^n$) for fully developed turbulent flow (using $n = 1/3$ for heating) and $Nu = 4.364$ for fully developed laminar flow with a uniform heat flux boundary condition. Note buoyancy effect on the laminar flow data, giving the much larger mixed convection heat transfer coefficient.

Source: Ghajar and Tam, 1994.

Figure 8–38 clearly shows the influence of inlet configuration on the beginning and end of the heat transfer transition region. This figure plots the local average peripheral heat transfer coefficients in terms of the Colburn j factor ($j_H = St\ Pr^{0.67}$) versus local Reynolds number for all flow regimes at the length-to-diameter ratio of 192, and St is the Stanton number, which is also a dimensionless heat transfer coefficient (see Chapter 6 for more details), defined as $St = Nu/(Re\ Pr)$. The filled symbols in Fig. 8–38 represent the start and end of the heat transfer transition region for each inlet configuration. Note the large influence of natural convection superimposed on the forced convective laminar-flow heat transfer process ($Nu = 4.364$ for a fully developed laminar flow with a uniform heat-flux boundary condition without buoyancy effects), yielding a mixed convection value of about $Nu = 14.5$. Equation 8–88 includes this buoyancy effect through the Grashof number.

In a subsequent study, Tam and Ghajar (1998) experimentally investigated the behavior of local heat transfer coefficients in the transition region for a tube with a bell-mouth inlet. This type of inlet is used in some heat exchangers mainly to avoid the presence of eddies, which are believed to be one of the causes for erosion in the tube inlet region. For the bell-mouth inlet, the variation of the local heat transfer coefficient with length in the transition and turbulent flow regions is very unusual. For this inlet geometry, the boundary layer along the tube wall is at first laminar and then changes through a transition to the turbulent condition, causing a dip in the Nu versus x/D curve. In their experiments with a fixed inside diameter of 15.84 mm, the length of the dip in the transition region was much longer ($100 < x/D < 175$) than in the turbulent region ($x/D < 25$). The presence of the dip in the transition region has a significant influence on both the local and the average heat transfer coefficients. This is particularly important for heat transfer calculations in short tube heat exchangers with a bell-mouth inlet. Figure 8–39 shows the variation of local Nusselt number along the tube length in the transition region for the three inlet configurations at comparable Reynolds numbers.

As mentioned earlier, finned tubes (Fig. 8–30) enhance convection heat transfer. Single-phase liquid flow in internally enhanced tubes is becoming more important in commercial heating, ventilating, and air conditioning (HVAC) applications. One kind of internally enhanced tube is the spiral micro-fin tube (Fig. 8–40). The tube side roughening increases heat transfer surface area, resulting in high-efficiency heat exchangers. The increase in the surface area causes low flow rates in the heat exchanger tubes, resulting in flow at Reynolds numbers that are between laminar and turbulent, that is, in the transition region. Owing to the high efficiency requirements, it is
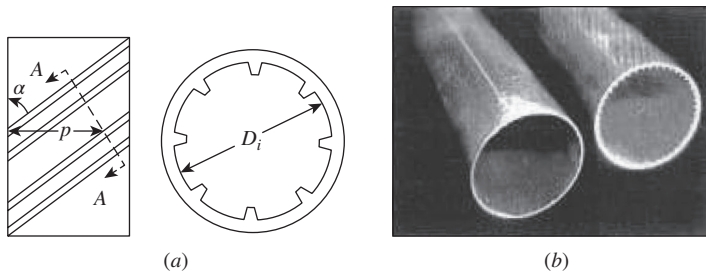
FIGURE 8–40

(*a*) Sectional view of the micro-fin tube; (*b*) The plain and micro-fin tubes.

(*a*) *Source: Tam et al., 2012.* (*b*) *©Afshin Ghajar*

likely that more HVAC units will operate in the transition region where the understanding of the pressure drop and heat transfer is limited. To respond to some of these challenges, Ghajar and coworkers extended their plain-tube studies presented earlier to finned tubes. They conducted pressure drop (friction factor) and heat transfer experiments in the transition region in three different micro-fin tubes and a plain tube with square-edged and re-entrant inlets (Tam et al., 2012). Table 8–10 shows the specifications of the plain and micro-fin tubes used in the studies of Tam et al. (2012).

Figure 8–41 represents the fully developed friction factor characteristics for the plain and different spiral-angle micro-fin tubes and different inlet configurations under the isothermal boundary condition. The plain tube behavior is similar to what was presented earlier (Fig. 8–37). However, for all the micro-fin tubes, a parallel shift from the classic laminar equation ($C_{f,\,lam} = 16/Re$) is observed regardless of the fin geometry and the type of inlet. In the transition region, it can be observed that the transition range of the micro-fin tubes is much wider than the plain tube transition range. The friction factor for all the micro-fin tubes goes through a steep increase followed by a relatively constant C_f section and then a parallel shift from the classical Blasius turbulent friction factor correlation ($C_{f,\,turb} = 0.0791\,Re^{-0.25}$). For the end of the transition for micro-fin tube, it is defined as the first point where the friction factor data become parallel to the Blasius correlation. Beyond this point, the flow is considered turbulent. With a higher spiral angle in the micro-fin tube, the increase of friction factor can be observed in the transition and turbulent regions. The
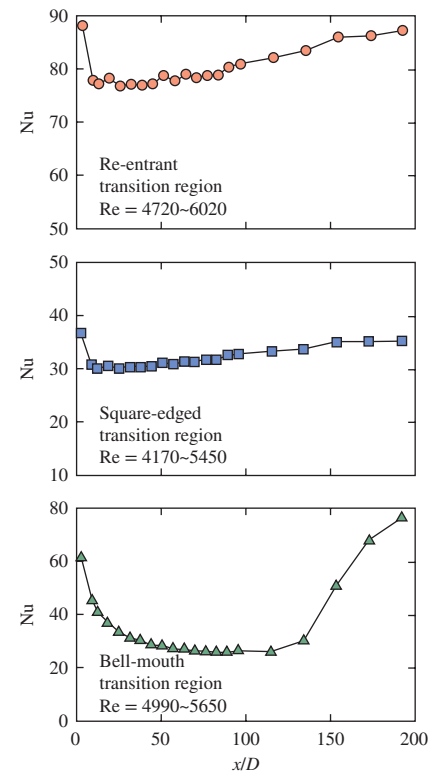
FIGURE 8–39

Variation of local Nusselt number with length for the re-entrant, square-edged, and bell-mouth inlets in the transition region.

Source: Tam and Ghajar, 1998.

TABLE 8–10

Specifications of the test tubes

Tube Type	Outer Dia., D_o (mm)	Inner Dia., D_i (mm)	Spiral Angle, α	Fin Height, e (mm)	Number of Start, N_s
Plain tube	15.9	14.9	—	—	—
Micro-fin tube #1	15.9	14.9	18°	0.5	25
Micro-fin tube #2	15.9	14.9	25°	0.5	25
Micro-fin tube #3	15.9	14.9	35°	0.5	25
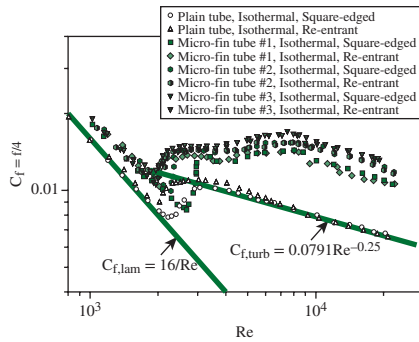
FIGURE 8–41
Fully developed friction factor characteristics for the plain and micro-fin tubes under isothermal boundary condition.
Source: Tam et al., 2012.
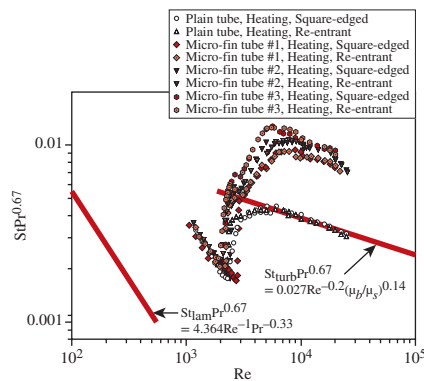
FIGURE 8–42
Fully developed heat transfer characteristics for the plain and micro-fin tubes under uniform wall heat flux boundary condition.
Source: Tam et al., 2012.

increase in the friction factor is caused by the stronger drag due to the larger spiral angle on the tube wall. From Fig. 8–41, it can be observed that the start of transition is inlet and spiral angle dependent. For all the micro-fin tubes, the square-edged inlet delays the start of transition. The micro-fin tube #3 with a larger spiral angle has an earlier start of transition. Moreover, it is also observed that a larger spiral angle in the micro-fin tube advances the end of transition for both inlet configurations.

Figure 8–42 shows that the heat transfer behavior in the upper transition region for the plain and micro-fin tubes is very different. For the plain tube, the heat transfer initially experienced an abrupt change in the lower transition region; this was followed by a moderate change in the upper transition, and finally the transition ended and the heat transfer data followed the Sieder and Tate correlation (1936) at a Reynolds number around 8000. The plain tube behavior is similar to what was presented earlier (Fig. 8–38). However, for the micro-fin tube, such a characteristic cannot be seen, and the abrupt change was observed in the entire transition region. When the Reynolds number is around 8000, a parallel shift of heat transfer data from the Sieder and Tate equation was observed. This increase in the Colburn j factor ($j_H = St\, Pr^{0.67}$) and the parallel shift from the Sieder and Tate correlation in the turbulent region is due to the swirling motion induced by the micro-fin. The larger spiral angle leads to a higher Colburn j factor. It is because the larger spiral angle increases the fluid mixing between the bulk fluid and the tube wall, and therefore the heat transfer is enhanced. Regarding the start and end of transition of heat transfer, it can be observed from Fig. 8–42 that the start of transition is defined as the critical point for the sudden change from the laminar region (the line parallel to Nu = 4.364) to the transition region. For the end of the transition for micro-fin tube, it is defined as the first point where the heat transfer data landed on a line parallel to the correlation proposed by Sieder and Tate (1936). As seen from Fig. 8–42, for the heat transfer, the transition is inlet dependent and the start and end of transition is spiral angle dependent. The delay of transition is obvious for smaller spiral angles, while an early transition occurred when larger spiral angle tubes were used.

EXAMPLE 8–10   **Heat Transfer in the Transition Region**

An ethylene glycol–distilled water mixture with a mass fraction of 0.6 and a flow rate of 2.6×10^{-4} m³/s flows inside a tube with an inside diameter of 0.0158 m subjected to uniform wall heat flux. For this flow, determine the Nusselt number at the location $x/D = 90$ if the inlet configuration of the tube is: (*a*) re-entrant, (*b*) square-edged, and (*c*) bell-mouth. At this location, the local Grashof number is Gr = 51,770. The properties of an ethylene glycol–distilled water mixture at the location of interest are Pr = 29.2, $\nu = 3.12 \times 10^{-6}$ m²/s, and $\mu_b/\mu_s = 1.77$.

SOLUTION   A liquid mixture flowing in a tube is subjected to uniform wall heat flux. The Nusselt number at a specified location is to be determined for three different tube inlet configurations.
Assumptions   Steady operating conditions exist.

Properties   The properties of the ethylene glycol–distilled water mixture are given to be $Pr = 29.2$, $\nu = 3.12 \times 10^{-6}$ m²/s, and $\mu_b/\mu_s = 1.77$.

Analysis   For a tube with a known diameter and volume flow rate, the type of flow regime is determined before making any decision regarding which Nusselt number correlation to use. The Reynolds number at the specified location is

$$\mathrm{Re} = \frac{(\dot{V}/A_c)D}{\nu} \frac{[(2.6 \times 10^{-4}\,\mathrm{m^3/s})/(1.961 \times 10^{-4}\,\mathrm{m^2})](0.0158\,\mathrm{m})}{3.12 \times 10^{-6}\,\mathrm{m^2/s}} = 6714$$

since

$$A_c = \pi D^2/4 = \pi(0.0158\,\mathrm{m})^2/4 = 1.961 \times 10^{-4}\,\mathrm{m^2}$$

Therefore, the flow regime is in the transition region for all three inlet configurations (thus use the information given in Table 8–9 with $x/D = 90$), and therefore Eq. 8–87 should be used with the constants *a, b, c* found in Table 8–8. However, Nu_{lam} and Nu_{turb} are the inputs to Eq. 8–87, and they need to be evaluated first from Eqs. 8–88 and 8–89, respectively. It should be mentioned that the correlations for Nu_{lam} and Nu_{turb} have no inlet dependency.

From Eq. 8–88:

$$Nu_{lam} = 1.24 \left[\left(\frac{\mathrm{Re}\,\mathrm{Pr}D}{x} \right) + 0.025\,(\mathrm{Gr}\,\mathrm{Pr})^{0.75} \right]^{1/3} \left(\frac{\mu_b}{\mu_s} \right)^{0.14}$$

$$= 1.24 \left[\left(\frac{(6714)(29.2)}{90} \right) + 0.025[(51{,}770)(29.2)]^{0.75} \right]^{1/3} (1.77)^{0.14} = 19.9$$

From Eq. 8–89:

$$Nu_{turb} = 0.023\,\mathrm{Re}^{0.8}\mathrm{Pr}^{0.385} \left(\frac{x}{D} \right)^{-0.0054} \left(\frac{\mu_b}{\mu_s} \right)^{0.14}$$

$$= 0.023(6714)^{0.8}(29.2)^{0.385}(90)^{-0.0054}(1.77)^{0.14} = 102.7$$

Then the transition Nusselt number can be determined from Eq. 8–87,

$$Nu_{trans} = Nu_{lam} + \{ \exp[(a - \mathrm{Re})/b] + Nu_{turb}^{c} \}^c$$

Case 1: For re-entrant inlet:

$$Nu_{trans} = 19.9 + \{ \exp[(1766 - 6714)/276] + 102.7^{-0.955} \}^{-0.955} = \mathbf{88.2}$$

Case 2: For square-edged inlet:

$$Nu_{trans} = 19.9 + \{ \exp[(2617 - 6714)/207] + 102.7^{-0.950} \}^{-0.950} = \mathbf{85.3}$$

Case 3: For bell-mouth inlet:

$$Nu_{trans} = 19.9 + \{ \exp[(6628 - 6714)/237] + 102.7^{-0.980} \}^{-0.980} = \mathbf{21.3}$$

Discussion   It is worth mentioning that, for the re-entrant and square-edged inlets, the flow behaves normally. For the bell-mouth inlet, the Nusselt number is low in comparison to the other two inlets. This is because of the unusual behavior of the bell-mouth inlet noted earlier (see Fig. 8–39); i.e., the boundary layer along the tube wall is at first laminar and then changes through a transition region to the turbulent condition.

Analogies Between Momentum and Heat Transfer in the Transition Region

Meyer and Everts (2018b) experimentally investigated the pressure drop and heat transfer characteristics of developing and fully developed flow in smooth tubes in the laminar, transitional, quasi-turbulent, and turbulent flow regimes. The Reynolds number was varied between 700 and 10,000 to ensure that the transitional and quasi-turbulent flow regimes, as well as sufficient parts of the laminar and turbulent flow regimes, were covered. It was found that the boundaries of the different flow regimes were the same for pressure drop and heat transfer, and that a direct relationship between pressure drop and heat transfer existed in the transitional flow regime as well. In the laminar flow regime, the relationship between pressure drop and heat transfer was a function of Grashof number (thus free convection effects), while it was a function of Reynolds number in the other three flow regimes. Correlations to predict the average friction factors as a function of average Nusselt number, as well as correlations to predict the average Nusselt number for developing and fully developed flow in all flow regimes, were also developed.

Pressure Drop in the Transition Region in Mini and Micro Tubes

Due to rapid advancement in fabrication techniques, the miniaturization of devices and components is ever increasing in many applications. Whether it is in the application of miniature heat exchangers, fuel cells, pumps, compressors, turbines, sensors, or artificial blood vessels, a sound understanding of fluid flow in microscale channels and tubes is required. To better understand the flow behavior in small tubes, Ghajar and coworkers extended their isothermal transitional pressure drop studies in standard-size tubes to mini- and microtubes. They performed a systematic and careful experimental study of friction factor in the transition region for single-phase water flow in 12 stainless steel tubes with diameters ranging from 2083 μm to 337 μm (Fig. 8–43). The pressure-drop measurements were carefully performed by paying particular attention to the sensitivity of the pressure-sensing diaphragms used in the pressure transducer. Experimental results indicated that the start and end of the transition region were influenced by the tube diameter (Table 8–11). The friction factor profile was not significantly affected for
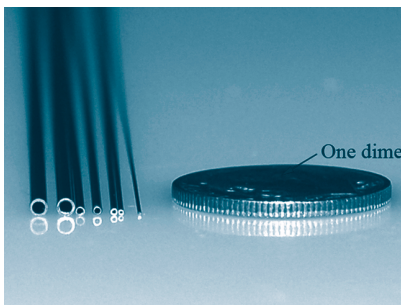
FIGURE 8–43
Representative mini/micro stainless steel tubes used in the experiments of Ghajar et al. (2010).

©Afshin Ghajar

TABLE 8–11

Summary of transition Reynolds number ranges for various stainless steel tube sizes

Tube I.D. [μm]	Transition Range	Tube I.D. [μm]	Transition Range
2083	1500 < Re < 4000	732	2200 < Re < 3000
1600	1700 < Re < 4000	667	2200 < Re < 3000
1372	1900 < Re < 4000	559	1900 < Re < 2500
1067	2000 < Re < 4000	508	1700 < Re < 2100
991	2000 < Re < 4000	413	1500 < Re < 1900
838	2200 < Re < 4000	337	1300 < Re < 1700

Source: Ghajar et al., 2010.

the tube diameters between 2083 μm and 1372 μm (Fig. 8–44). However, the influence of the tube diameter on the friction factor profile became noticeable as the diameter decreased from 838 μm to 337 μm (Fig. 8–45). The Reynolds number range for transition flow became narrower with decreasing tube diameter (Table 8–11). The results show that a decrease in tube diameter and an increase in relative roughness (ε/D), which is approximately within the range of $0.01 < \varepsilon/D < 0.04$, influence the friction factor, even in the laminar region. In addition, these factors cause the onset of transition from laminar flow to occur at lower Reynolds numbers.

REFERENCES

1. A. J. Ghajar and K. F. Madon. "Pressure Drop Measurements in the Transition Region for a Circular Tube with Three Different Inlet Configurations." *Experimental Thermal and Fluid Science,* Vol. 5 (1992), pp. 129–135.

2. A. J. Ghajar and L. M. Tam. "Heat Transfer Measurements and Correlations in the Transition Region for a Circular Tube with Three Different Inlet Configurations." *Experimental Thermal and Fluid Science,* Vol. 8 (1994), pp. 79–90.

3. A. J. Ghajar and L. M. Tam. "Flow Regime Map for a Horizontal Pipe with Uniform Wall Heat Flux and Three Inlet Configurations." *Experimental Thermal and Fluid Science,* Vol. 10 (1995), pp. 287–297.

4. A. J. Ghajar, L. M. Tam, and S. C. Tam. "Improved Heat Transfer Correlation in the Transition Region for a Circular Tube with Three Inlet Configurations Using Artificial Neural Networks." *Heat Transfer Engineering,* Vol. 25, No. 2 (2004), pp. 30–40.

5. A. J. Ghajar, C. C. Tang, and W. L. Cook. "Experimental Investigation of Friction Factor in the Transition Region for Water Flow in Minitubes and Microtubes." *Heat Transfer Engineering,* Vol. 31, No. 8 (2010), pp. 646–657.

6. L. M. Tam and A. J. Ghajar. "Effect of Inlet Geometry and Heating on the Fully Developed Friction Factor in the Transition Region of a Horizontal Tube." *Experimental Thermal and Fluid Science,* Vol. 15 (1997), pp. 52–64.

7. L. M. Tam and A. J. Ghajar. "The Unusual Behavior of Local Heat Transfer Coefficient in a Circular Tube with a Bell-Mouth Inlet." *Experimental Thermal and Fluid Science,* Vol. 16 (1998), pp. 187–194.

8. L. M. Tam and A. J. Ghajar. "Transitional Heat Transfer in Plain Horizontal Tubes." *Heat Transfer Engineering,* Vol. 27, No. 5 (2006), pp. 23–38.

9. L. M. Tam, A. J. Ghajar, and H. K. Tam. "Contribution Analysis of Dimensionless Variables for Laminar and Turbulent Flow Convection Heat Transfer in a Horizontal Tube Using Artificial Neural Network." *Heat Transfer Engineering,* Vol. 29, No. 9 (2008), pp. 793–804.

10. H. K. Tam, L. M. Tam, and A. J. Ghajar. "Effect of Inlet Geometries and Heating on the Entrance and Fully-Developed Friction Factors in the Laminar and Transition Regions of a Horizontal Tube." *Experimental Thermal and Fluid Science,* Vol. 44 (2013), pp. 680–696.

11. H. K. Tam, L. M. Tam, A. J. Ghajar, S. C. Tam, and T. Zhang. "Experimental Investigation of Heat Transfer, Friction Factor, and Optimal Fin Geometries for the Internally Microfin Tubes in the Transition and Turbulent Regions." *Journal of Enhanced Heat Transfer,* Vol. 19, No. 5 (2012), pp. 457–476. Reprinted with permission from Begell House, Inc.
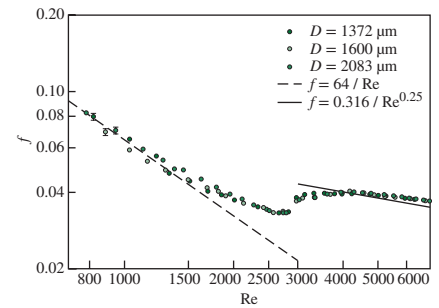
FIGURE 8–44

Transition region of stainless steel tubes with diameters from 2083 to 1372 μm.

Source: Ghajar et al., 2010.
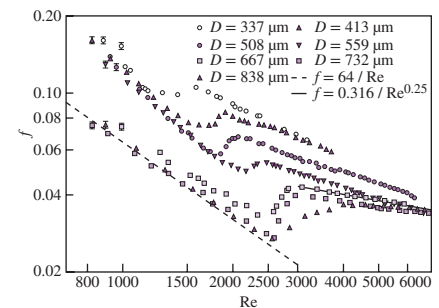
FIGURE 8–45

Transition region of stainless steel tubes with diameters from 838 to 337 μm.

Source: Ghajar et al., 2010.

SUMMARY

Internal flow is characterized by the fluid being completely confined by the inner surfaces of the tube. The mean or average velocity and temperature for a circular tube of radius R are expressed as

$$V_{avg} = \frac{2}{R^2}\int_0^R u(r)rdr \quad \text{and} \quad T_m = \frac{2}{V_{avg}R^2}\int_0^R u(r)T(r)rdr$$

The Reynolds number for internal flow and the hydraulic diameter are defined as

$$\text{Re} = \frac{\rho V_{avg}D}{\mu} = \frac{V_{avg}D}{\nu} \quad \text{and} \quad D_h = \frac{4A_c}{p}$$

The flow in a tube is laminar for $\text{Re} < 2300$, turbulent for about $\text{Re} > 10{,}000$, and transitional in between.

The length of the region from the tube inlet to the point at which the flow becomes fully developed is the *hydrodynamic entry length* L_h. The region beyond the entrance region in which the velocity profile is fully developed is the *hydrodynamically fully developed region.* The length of the region of flow over which the thermal boundary layer develops and reaches the tube center is the *thermal entry length* L_t. The region in which the flow is both hydrodynamically and thermally developed is the *fully developed flow region.* The entry lengths are given by

$$L_{h,\,laminar} \approx 0.05\,\text{Re}\,D$$

$$L_{t,\,laminar} \approx 0.05\,\text{Re}\,\text{Pr}\,D = \text{Pr}\,L_{h,\,laminar}$$

$$L_{h,\,turbulent} \approx L_{t,\,turbulent} = 10D$$

For $\dot{q}_s = $ constant, the rate of heat transfer is expressed as

$$\dot{Q} = \dot{q}_s A_s = \dot{m}c_p(T_e - T_i)$$

For $T_s = $ constant, we have

$$\dot{Q} = hA_s\Delta T_{lm} = \dot{m}c_p(T_e - T_i)$$

$$T_e = T_s - (T_s - T_i)\exp(-hA_s/\dot{m}c_p)$$

$$\Delta T_{lm} = \frac{T_i - T_e}{\ln[(T_s - T_e)/(T_s - T_i)]} = \frac{\Delta T_e - \Delta T_i}{\ln(\Delta T_e/\Delta T_i)}$$

The irreversible pressure loss due to frictional effects and the required pumping power to overcome this loss for a volume flow rate of $\dot{V}$ are

$$\Delta P_L = f\frac{L}{D}\frac{\rho V_{avg}^2}{2} \quad \text{and} \quad \dot{W}_{pump} = \dot{V}\Delta P_L$$

For *fully developed laminar flow* in a circular pipe, we have:

$$u(r) = 2V_{avg}\left(1 - \frac{r^2}{R^2}\right) = u_{max}\left(1 - \frac{r^2}{R^2}\right)$$

$$f = \frac{64\mu}{\rho DV_{avg}} = \frac{64}{\text{Re}}$$

$$\dot{V} = V_{avg}A_c = \frac{\Delta PR^2}{8\mu L}\pi R^2 = \frac{\pi R^4\Delta P}{8\mu L} = \frac{\pi R^4\Delta P}{128\mu L}$$

Circular tube, laminar ($\dot{q}_s = $ constant): $\text{Nu} = \dfrac{hD}{k} = 4.36$

Circular tube, laminar ($T_s = $ constant): $\text{Nu} = \dfrac{hD}{k} = 3.66$

For *developing laminar flow* in the entrance region with constant surface temperature, we have

Circular tube: $\text{Nu} = 3.66 + \dfrac{0.065(D/L)\text{Re}\,\text{Pr}}{1 + 0.04[(D/L)\text{Re}\,\text{Pr}]^{2/3}}$

Circular tube: $\text{Nu} = 1.86\left(\dfrac{\text{Re}\,\text{Pr}D}{L}\right)^{1/3}\left(\dfrac{\mu_b}{\mu_s}\right)^{0.14}$

Parallel plates: $\text{Nu} = 7.54 + \dfrac{0.03(D_h/L)\text{Re}\,\text{Pr}}{1 + 0.016[(D_h/L)\text{Re}\,\text{Pr}]^{2/3}}$

For *fully developed turbulent flow with smooth surfaces,* we have

$$f = (0.790\ln\text{Re} - 1.64)^{-2} \quad 10^4 < \text{Re} < 10^6$$

$$\text{Nu} = 0.125f\,\text{Re}\,\text{Pr}^{1/3}$$

$$\text{Nu} = 0.023\,\text{Re}^{0.8}\,\text{Pr}^{1/3} \quad \left(\begin{matrix}0.7 \le \text{Pr} \le 160 \\ \text{Re} > 10{,}000\end{matrix}\right)$$

$$\text{Nu} = 0.023\,\text{Re}^{0.8}\,\text{Pr}^n \text{ with } n = 0.4 \text{ for } \textit{heating} \text{ and } 0.3 \text{ for}$$
cooling of fluid

$$\text{Nu} = \frac{(f/8)(\text{Re} - 1000)\text{Pr}}{1 + 12.7(f/8)^{0.5}(\text{Pr}^{2/3} - 1)} \quad \left(\begin{matrix}0.5 \le \text{Pr} \le 2000 \\ 3\times10^3 < \text{Re} < 5\times10^6\end{matrix}\right)$$

The fluid properties are evaluated at the *bulk mean fluid temperature* $T_b = (T_i + T_e)/2$. For liquid metal flow in the range of $10^4 < \text{Re} < 10^6$ we have:

$T_s = $ constant: $\quad \text{Nu} = 4.8 + 0.0156\,\text{Re}^{0.85}\,\text{Pr}_s^{0.93}$

$\dot{q}_s = $ constant: $\quad \text{Nu} = 6.3 + 0.0167\,\text{Re}^{0.85}\,\text{Pr}_s^{0.93}$

For *fully developed turbulent flow with rough surfaces,* the friction factor f is determined from the Moody chart or

$$\frac{1}{\sqrt{f}} = -2.0 \log\left(\frac{\varepsilon/D}{3.7} + \frac{2.51}{\mathrm{Re}\sqrt{f}}\right) \approx -1.8 \log\left[\frac{6.9}{\mathrm{Re}} + \left(\frac{\varepsilon/D}{3.7}\right)^{1.11}\right]$$

For a *concentric annulus,* the hydraulic diameter is $D_h = D_o - D_i$, and the Nusselt numbers are expressed as

$$\mathrm{Nu}_i = \frac{h_i D_h}{k} \quad \text{and} \quad \mathrm{Nu}_o = \frac{h_o D_h}{k}$$

where the values for the Nusselt numbers are given in Table 8–4.

REFERENCES AND SUGGESTED READING

1. J. P. Abraham, E. M. Sparrow, and W. J. Minkowycz. "Internal-Flow Nusselt Numbers for the Low-Reynolds-Number End of the Laminar-to-Turbulent Transition Regime." *International Journal of Heat and Mass Transfer* 54 (2011), pp. 584–588.

2. J. P. Abraham, E. M. Sparrow, and J. C. K. Tong. "Heat Transfer in All Pipe Flow Regimes—Laminar, Transitional/Intermittent, and Turbulent." *International Journal of Heat and Mass Transfer* 52 (2009), pp. 557–563.

3. M. S. Bhatti and R. K. Shah. "Turbulent and Transition Flow Convective Heat Transfer in Ducts." In *Handbook of Single-Phase Convective Heat Transfer,* ed. S. Kakaç, R. K. Shah, and W. Aung. New York: Wiley Interscience, 1987.

4. Y. A. Çengel and J. M. Cimbala. *Fluid Mechanics: Fundamentals and Applications,* 4th ed. New York: McGraw-Hill Education, 2018.

5. A. P. Colburn. *Transactions of the AIChE* 26 (1933), p. 174.

6. C. F. Colebrook. "Turbulent Flow in Pipes, with Particular Reference to the Transition between the Smooth and Rough Pipe Laws." *Journal of the Institute of Civil Engineers London* 11 (1939), pp. 133–156.

7. R. G. Deissler. *Analysis of Turbulent Heat Transfer and Flow in the Entrance Regions of Smooth Passages.* Technical Note 3016. Washington, DC: National Advisory Committee for Aeronautics, 1953.

8. D. F. Dipprey and D. H. Sabersky. "Heat and Momentum Transfer in Smooth and Rough Tubes at Various Prandtl Numbers." *International Journal of Heat Mass Transfer* 6 (1963), pp. 329–353.

9. F. W. Dittus and L. M. K. Boelter. *University of California Publications on Engineering* 2 (1930), p. 433.

10. D. K. Edwards, V. E. Denny, and A. F. Mills. *Transfer Processes.* 2nd ed. Washington, DC: Hemisphere, 1979.

11. V. Gnielinski. "New Equations for Heat and Mass Transfer in Turbulent Pipe and Channel Flow." *International Chemical Engineering* 16 (1976), pp. 359–368.

12. V. Gnielinski. "Heat Transfer Coefficients for Turbulent Flow in Concentric Annular Ducts." *Heat Transfer Engineering* 30 (2009), pp. 431–436.

13. V. Gnielinski. "On Heat Transfer in Tubes." *International Journal of Heat and Mass Transfer* 63 (2013), pp. 134–140.

14. V. Gnielinski. "Turbulent Heat Transfer in Annular Spaces – A New Comprehensive Correlation." *Heat Transfer Engineering* 36 (2015), pp. 787–789.

15. S. E. Haaland. "Simple and Explicit Formulas for the Friction Factor in Turbulent Pipe Flow." *Journal of Fluids Engineering* (March 1983), pp. 89–90.

16. S. Kakaç, R. K. Shah, and W. Aung, eds. *Handbook of Single-Phase Convective Heat Transfer.* New York: Wiley Interscience, 1987.

17. W. M. Kays and M. E. Crawford. *Convective Heat and Mass Transfer.* 3rd ed. New York: McGraw-Hill, 1993.

18. W. M. Kays and H. C. Perkins. "Forced Convection, Internal Flow in Ducts." Chapter 7 in *Handbook of Heat Transfer,* ed. W. M. Rohsenow and J. P. Hartnett. New York: McGraw-Hill, 1972.

19. J. P. Meyer and M. Everts. "Single-Phase Mixed Convection of Developing and Fully Developed Flow in Smooth Horizontal Circular Tubes in the Laminar and Transitional Flow Regimes." *International Journal of Heat Mass Transfer* 117 (2018a) 1251–1273.

20. J. P. Meyer and M. Everts. "Relationship between Pressure Drop and Heat Transfer of Developing and Fully Developed Flow in Smooth Horizontal Circular Tubes in the Laminar, Transitional, Quasi-Turbulent and Turbulent Flow Regimes." *International Journal of Heat Mass Transfer* 117 (2018b) 1231–1250.

21. M. Molki and E. M. Sparrow. "An Empirical Correlation for the Average Heat Transfer Coefficient in Circular Tubes." *Journal of Heat Transfer* 108 (1986), pp. 482–484.

22. L. F. Moody. "Friction Factors for Pipe Flows." *Transactions of the ASME* 66 (1944), pp. 671–684.

23. R. H. Norris. "Some Simple Approximate Heat Transfer Correlations for Turbulent Flow in Ducts with Rough Surfaces." In *Augmentation of Convective Heat Transfer,* ed. A. E. Bergles and R. L. Webb. New York: ASME, 1970.

24. B. S. Petukhov. "Heat Transfer and Friction in Turbulent Pipe Flow with Variable Physical Properties." In *Advances in Heat Transfer,* ed. T. F. Irvine and J. P. Hartnett, Vol. 6. New York: Academic Press, 1970.

25. B. S. Petukhov and L. I. Roizen. "Generalized Relationships for Heat Transfer in a Turbulent Flow of a Gas in Tubes of Annular Section." *High Temperature* (USSR) 2 (1964), pp. 65–68.

26. O. Reynolds. "On the Experimental Investigation of the Circumstances Which Determine Whether the Motion of Water Shall Be Direct or Sinuous, and the Law of Resistance in Parallel Channels." *Philosophical Transactions of the Royal Society of London* 174 (1883), pp. 935–982.

27. H. Schlichting. *Boundary Layer Theory.* 7th ed. New York: McGraw-Hill, 1979.

28. R. K. Shah and M. S. Bhatti. "Laminar Convective Heat Transfer in Ducts." In *Handbook of Single-Phase Convective Heat Transfer,* ed. S. Kakaç, R. K. Shah, and W. Aung. New York: Wiley Interscience, 1987.

29. R. K. Shah and A. L. London. *Laminar Flow Forced Convection in Ducts.* New York: Academic Press, 1978.

30. H. Shokouhmand and K. Hooman. "An Exact Solution for Fully Developed Temperature Distribution in Laminar Steady Forced Convection Inside Circular Tubes with Uniform Wall Temperature." *Heat Transfer Research* 34 (2003), pp. 276–285.

31. E. N. Sieder and G. E. Tate. "Heat Transfer and Pressure Drop of Liquids in Tubes." *Industrial Engineering Chemistry* 28 (1936), pp. 1429–1435.

32. C. A. Sleicher and M. W. Rouse. "A Convenient Correlation for Heat Transfer to Constant and Variable Property Fluids in Turbulent Pipe Flow." *International Journal of Heat Mass Transfer* 18 (1975), pp. 1429–1435.

33. S. Whitaker. "Forced Convection Heat Transfer Correlations for Flow in Pipes, Past Flat Plates, Single Cylinders, and for Flow in Packed Beds and Tube Bundles." *AIChE Journal* 18 (1972), pp. 361–371.

34. W. Zhi-qing. "Study on Correction Coefficients of Laminar and Turbulent Entrance Region Effects in Round Pipes." *Applied Mathematical Mechanics* 3 (1982), p. 433.

PROBLEMS*

General Flow Analysis

8–1C Which fluid at room temperature requires a larger pump to move at a specified velocity in a given tube: water or engine oil? Why?

8–2C What do the average velocity V_{avg} and the mean temperature T_m represent in flow through circular tubes of constant diameter?

8–3C What is the generally accepted value of the Reynolds number above which the flow in smooth pipes is turbulent?

8–4C What is hydraulic diameter? How is it defined? What is it equal to for a circular tube of diameter D?

8–5C What fluid property is responsible for the development of the velocity boundary layer? For what kinds of fluids will there be no velocity boundary layer in a pipe?

8–6C In the fully developed region of flow in a circular tube, will the velocity profile change in the flow direction? How about the temperature profile?

8–7C Consider laminar flow in a circular tube. Will the friction factor be higher near the inlet of the tube or near the exit? Why? What would your response be if the flow were turbulent?

8–8C How does the friction factor f vary along the flow direction in the fully developed region in (*a*) laminar flow and (*b*) turbulent flow?

8–9C How does surface roughness affect the pressure drop in a tube if the flow is turbulent? What would your response be if the flow were laminar?

8–10C How is the hydrodynamic entry length defined for flow in a tube? Is the entry length longer in laminar or turbulent flow?

8–11C Consider the flow of oil in a tube. How will the hydrodynamic and thermal entry lengths compare if the flow is laminar? How would they compare if the flow were turbulent?

8–12C Consider the flow of mercury (a liquid metal) in a tube. How will the hydrodynamic and thermal entry lengths compare if the flow is laminar? How would they compare if the flow were turbulent?

8–13C How is the thermal entry length defined for flow in a tube? In what region is the flow in a tube fully developed?

*Problems designated by a "C" are concept questions, and students are encouraged to answer them all. Problems designated by an "E" are in English units, and the SI users can ignore them. Problems with the 🖥 icon are comprehensive in nature and are intended to be solved with appropriate software. Problems with the 🅿ᵗᴰ icon are Prevention through Design problems. Problems with the 🅲&ˢ icon are Codes and Standards problems.

8–14C Consider laminar forced convection in a circular tube. Will the heat flux be higher near the inlet of the tube or near the exit? Why?

8–15C Consider turbulent forced convection in a circular tube. Will the heat flux be higher near the inlet of the tube or near the exit? Why?

8–16C What does the logarithmic mean temperature difference represent for flow in a tube whose surface temperature is constant? Why do we use the logarithmic mean temperature instead of the arithmetic mean temperature?

8–17C Consider fluid flow in a tube whose surface temperature remains constant. What is the appropriate temperature difference for use in Newton's law of cooling with an average heat transfer coefficient?

8–18C What is the physical significance of the number of transfer units $NTU = hA_s/\dot{m}c_p$? What do small and large NTU values tell us about a heat transfer system?

8–19 Consider the velocity and temperature profiles for a fluid flow in a tube with a diameter of 50 mm that can be expressed as

$$u(r) = 0.05[1 - (r/R)^2]$$
$$T(r) = 400 + 80(r/R)^2 - 30(r/R)^3$$

with units in m/s and K, respectively. Determine the average velocity and the mean (average) temperature from the given velocity and temperature profiles.

8–20 Consider the velocity and temperature profiles for airflow in a tube with a diameter of 8 cm that can be expressed as

$$u(r) = 0.2[(1 - (r/R)^2)]$$
$$T(r) = 250 + 200(r/R)^3$$

with units in m/s and K, respectively. If the convection heat transfer coefficient is 100 W/m²·K, determine the mass flow rate and surface heat flux using the given velocity and temperature profiles. Evaluate the air properties at 20°C and 1 atm.

8–21 C&S Liquid water flows in a circular tube at a mass flow rate of 7 g/s. The water enters the tube at 5°C, and the average convection heat transfer coefficient for the internal flow is 20 W/m²·K. The tube is 3 m long and has an inner diameter of 25 mm. The tube surface is maintained at a constant temperature. The inner surface of the tube is lined with polyvinylidene chloride (PVDC) lining. According to the ASME Code for Process Piping (ASME B31.3-2014, Table A323.4.3), the recommended maximum temperature for PVDC lining is 79°C. If the water exits the tube at 15°C, determine the heat rate transferred to the water. Would the inner surface temperature of the tube exceed the recommended maximum temperature for PVDC lining?

8–22 C&S In a heating system, liquid water flows in a circular tube at a mass flow rate of 3.5 g/s. The water enters the tube at 5°C, where it is heated at a rate of 1 kW. The tube surface is maintained at a constant temperature. The

effectiveness of the system to heat water in the tube has been determined to have a number of transfer units of NTU = 2. According to the service restrictions of the ASME Boiler and Pressure Vessel Code (ASME BPVC.IV-2015, HG-101), hot water heaters should not be operating at temperatures exceeding 120°C at or near the heater outlet. The inner surface of the tube is lined with polyvinylidene chloride (PVDC) lining. According to the ASME Code for Process Piping (ASME B31.3-2014, Table A323.4.3), the recommended maximum temperature for PVDC lining is 79°C. To comply with both ASME codes, determine (*a*) Whether the water exiting the tube is at a temperature below 120°C. (*b*) Whether the inner surface temperature of the tube exceeds 79°C. Evaluate the fluid properties at 40°C. Is this an appropriate temperature to evaluate the fluid properties?

8–23 Air enters an 18-cm-diameter, 12-m-long underwater duct at 50°C and 1 atm at a mean velocity of 7 m/s and is cooled by the water outside. If the average heat transfer coefficient is 65 W/m²·K and the tube temperature is nearly equal to the water temperature of 10°C, determine the exit temperature of air and the rate of heat transfer. Evaluate air properties at a bulk mean temperature of 30°C. Is this a good assumption?

8–24 Combustion gases passing through a 5-cm-internal-diameter circular tube are used to vaporize wastewater at atmospheric pressure. Hot gases enter the tube at 115 kPa and 250°C at a mean velocity of 5 m/s and leave at 150°C. If the average heat transfer coefficient is 120 W/m²·K and the inner surface temperature of the tube is 110°C, determine (*a*) the tube length and (*b*) the rate of evaporation of water. Use air properties for the combustion gases.

8–25 Repeat Prob. 8–24 for a heat transfer coefficient of 40 W/m²·K.

8–26 Cooling water available at 10°C is used to condense steam at 30°C in the condenser of a power plant at a rate of 0.15 kg/s by circulating the cooling water through a bank of 5-m-long, 1.2-cm-internal-diameter thin copper tubes. Water enters the tubes at a mean velocity of 4 m/s and leaves at a temperature of 24°C. The tubes are nearly isothermal at 30°C. Determine the average heat transfer coefficient between the water, the tubes, and the number of tubes needed to achieve the indicated heat transfer rate in the condenser.

8–27 Repeat Prob. 8–26 for steam condensing at a rate of 0.60 kg/s.

8–28 Reconsider Prob. 8–26. Using appropriate software, investigate the effect of the cooling water average (mean) velocity on the number of tubes needed to achieve the indicated heat transfer rate in the condenser. By varying the cooling water average velocity from 0.3 to 6 m/s, plot the number of tubes as a function of the water average velocity.

8–29 Inside a condenser, there is a bank of seven copper tubes with cooling water flowing in them. Steam condenses at a rate of 0.6 kg/s on the outer surfaces of the tubes that are

at a constant temperature of 68°C. Each copper tube is 5 m long and has an inner diameter of 25 mm. Cooling water enters each tube at 5°C and exits at 60°C. Determine the average heat transfer coefficient of the cooling water flowing inside each tube and the cooling water mean velocity needed to achieve the indicated heat transfer rate in the condenser.

Steam
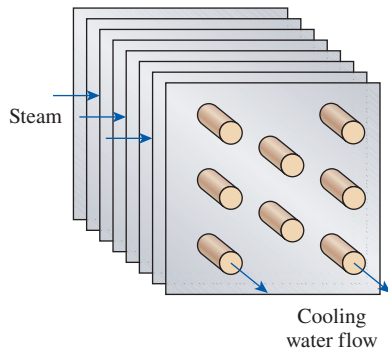
Cooling
water flow

FIGURE P8–29

8–30 Reconsider Prob. 8–29. Using appropriate software, evaluate the effect of the cooling water mean velocity on the rate of steam condensation in the condenser. By varying the cooling water mean velocity for $0 < V_{avg} \leq 2$ m/s, plot the steam condensation rate as a function of the water mean velocity.

8–31 In a gas-fired boiler, water is being boiled at 120°C by hot air flowing through a 5-m-long, 5-cm-diameter tube submerged in water. Hot air enters the tube at 1 atm and 300°C at a mean velocity of 7 m/s and leaves at 150°C. If the surface temperature of the tube is 120°C, determine the average convection heat transfer coefficient of the air and the rate of water evaporation, in kg/h.

Vent

Boiler

Water

120°C

Hot air
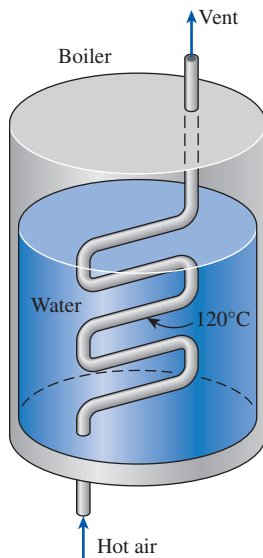
FIGURE P8–31

8–32 Reconsider Prob. 8–31. Using appropriate software, evaluate the effect of the tube length on the average convection heat transfer coefficient of air. By varying the tube length from 3 to 18 m, plot the average convection heat transfer coefficient as a function of the tube length.

8–33 Liquid water flows in fully developed conditions through a circular tube at a mass flow rate of 3.5 g/s. The water enters the tube at 5°C, and the average convection heat transfer coefficient for the internal flow is 20 W/m²·K. The tube is 3 m long and has an inner diameter of 25 mm. The tube surface is subjected to a constant heat flux at a rate of 300 W. The inner surface of the tube is lined with polyvinylidene chloride (PVDC) lining. According to the ASME Code for Process Piping (ASME B31.3-2014, Table A323.4.3), the recommended maximum temperature for PVDC lining is 79°C. Would the inner surface temperature of the tube exceed the recommended maximum temperature for PVDC lining? If so, determine the axial location along the tube where the tube's inner surface temperature reaches 79°C. Evaluate the fluid properties at 15°C. Is this an appropriate temperature at which to evaluate the fluid properties?

Laminar, Transitional, and Turbulent Flow in Tubes

8–34C Someone claims that the volume flow rate in a circular pipe with laminar flow can be determined by measuring the velocity at the centerline in the fully developed region, multiplying it by the cross-sectional area, and dividing the result by 2. Do you agree? Explain.

8–35C Someone claims that the average velocity in a circular pipe in fully developed laminar flow can be determined by simply measuring the velocity at $R/2$ (midway between the wall surface and the centerline). Do you agree? Explain.

8–36C How is the friction factor for flow in a tube related to the pressure drop? How is the pressure drop related to the pumping power requirement for a given mass flow rate?

8–37C Someone claims that in fully developed turbulent flow in a tube, the shear stress is a maximum at the tube surface. Do you agree with this claim? Explain.

8–38C Consider fully developed flow in a circular pipe with negligible entrance effects. If the length of the pipe is doubled, the pressure drop will (a) double, (b) more than double, (c) less than double, (d) reduce by half, or (e) remain constant.

8–39C Consider fully developed laminar flow in a circular pipe. If the diameter of the pipe is reduced by half while the flow rate and the pipe length are held constant, the pressure drop will (a) double, (b) triple, (c) quadruple, (d) increase by a factor of 8, or (e) increase by a factor of 16.

8–40C Consider fully developed laminar flow in a circular pipe. If the viscosity of the fluid is reduced by half by heating while the flow rate is held constant, how will the pressure drop change?

8–41 In fully developed laminar flow in a circular pipe, the velocity at $R/2$ (midway between the wall surface and the centerline) is measured to be 6 m/s. Determine the velocity at the center of the pipe. *Answer:* 8 m/s

8–42 The velocity profile in fully developed laminar flow in a circular pipe of inner radius $R = 10$ cm, in m/s, is given by $u(r) = 4(1 - r^2/R^2)$. Determine the mean and maximum velocities in the pipe, and determine the volume flow rate.

$$u(r) = 4\left(1 - \frac{r^2}{R^2}\right)$$

$R = 10$ cm
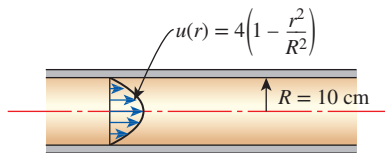
FIGURE P8–42

8–43 In fully developed laminar flow inside a circular pipe, the velocities at $r = 0.5R$ (midway between the wall surface and the centerline) are measured to be 3, 6, and 9 m/s. (*a*) Determine the maximum velocity for each of the measured midway velocities. (*b*) By varying r/R for $-1 \le r/R \le 1$, plot the velocity profile for each of the measured midway velocities with r/R as the *y*-axis and $V(r/R)$ as the *x*-axis.

8–44 Water is flowing in fully developed conditions through a 3-cm-diameter smooth tube with a mass flow rate of 0.02 kg/s at 15°C. Determine (*a*) the maximum velocity of the flow in the tube and (*b*) the pressure gradient for the flow.

8–45 Water at 15°C is flowing through a 5-cm-diameter smooth tube with a length of 200 m. Determine the Darcy friction factor and pressure loss associated with the tube for (*a*) mass flow rate of 0.02 kg/s and (*b*) mass flow rate of 0.5 kg/s.

8–46 Water at 10°C ($\rho = 999.7$ kg/m^3 and $\mu = 1.307 \times 10^{-3}$ kg/m·s) is flowing in a 0.20-cm-diameter, 15-m-long pipe steadily at an average velocity of 1.2 m/s. Determine (*a*) the pressure drop and (*b*) the pumping power requirement to overcome this pressure drop. Assume flow is fully developed. Is this a good assumption? *Answers: (a)* 188 kPa, *(b)* 0.71 W

8–47 Determine the hydrodynamic and thermal entry lengths for water, engine oil, and liquid mercury flowing through a 2.5-cm-diameter smooth tube with mass flow rate of 0.01 kg/s and temperature of 100°C.

8–48E Determine the average velocity and hydrodynamic and thermal entry lengths for water, engine oil, and liquid mercury flowing through a standard 2-in Schedule 40 pipe with a mass flow rate of 0.1 lbm/s and a temperature of 100°F.

8–49 An engineer is to design an experimental apparatus that consists of a 25-mm-diameter smooth tube, where different fluids at 100°C are to flow through in fully developed laminar flow conditions. For hydrodynamically and thermally fully developed laminar flow of water, engine oil, and liquid

mercury, determine (*a*) the minimum tube length and (*b*) the required pumping power to overcome the pressure loss in the tube at the largest allowable flow rate.

8–50 Consider a 25-mm-diameter and 15-m-long smooth tube that is used for heating fluids. The wall is heated electrically to provide a constant surface heat flux along the entire tube. Fluids enter the tube at 50°C and exit at 150°C. If the mass flow rate is maintained at 0.01 kg/s, determine the convection heat transfer coefficients at the tube outlet for water, engine oil, and liquid mercury.

8–51 C&S Liquid water flows in an ASTM B75 copper tube at a mass flow rate of 3.6 g/s. The water enters the tube at 40°C, and the tube surface is subjected to a constant heat flux at a rate of 1.8 kW. The tube is circular with an inner diameter of 25 mm and a length of 3 m. The maximum use temperature for ASTM B75 copper tube is 204°C (ASME Code for Process Piping, B31.3-2014, Table A-1M). Would the surface temperature of the tube exceed the maximum use temperature for the copper tube? If so, determine the axial location along the tube where the tube's surface temperature reaches 204°C. Evaluate the fluid properties at 100°C. Is this an appropriate temperature at which to evaluate the fluid properties?

8–52 Consider a 25-mm-diameter and 15-m-long smooth tube that is maintained at a constant surface temperature. Fluids enter the tube at 50°C with a mass flow rate of 0.01 kg/s. Determine the tube surface temperatures necessary to heat water, engine oil, and liquid mercury to the desired outlet temperature of 150°C.

8–53 C&S In a heating system, liquid water flows in a circular tube with a length of 3 m and an inner diameter of 12.5 mm. The water enters the tube at 15°C, where it is heated at a rate of 1.5 kW. The tube surface is maintained at a constant temperature. The flow is laminar, and it experiences a pressure loss of 5 Pa in the tube. According to the service restrictions of the ASME Boiler and Pressure Vessel Code (ASME BPVC.IV-2015, HG-101), hot water heaters should not be operating at temperatures exceeding 120°C at or near the heater outlet. The tube's inner surface is lined with polyvinylidene fluoride (PVDF) lining. According to the ASME Code for Process Piping (ASME B31.3-2014, Table A323.4.3), the recommended maximum temperature for PVDF lining is 135°C. To comply with both ASME codes, determine (*a*) whether the water exiting the tube is at a temperature below 120°C, and (*b*) whether the inner surface temperature of the tube exceeds 135°C. Evaluate the fluid properties at 80°C. Is this an appropriate temperature at which to evaluate the fluid properties?

8–54E In a chemical process plant, liquid isobutane at 50°F is being transported through a 30-ft-long standard 3/4-in Schedule 40 cast iron pipe with a mass flow rate of 0.4 lbm/s. Accuracy of the results is an important issue in this problem; therefore, use the most appropriate equation to determine

(a) the pressure loss and (b) the pumping power required to overcome the pressure loss. Assume flow is fully developed. Is this a good assumption?

8–55 Water at 15°C is flowing through a 200-m-long standard 1-in Schedule 40 cast iron pipe with a mass flow rate of 0.5 kg/s. If accuracy is an important issue, use the appropriate equation to determine (a) the pressure loss and (b) the pumping power required to overcome the pressure loss. Assume flow is fully developed. Is this a good assumption?

8–56 Reconsider Prob. 8–55. Using appropriate software, investigate the effect of the pipe roughness on the pumping power required to overcome the pressure loss. By varying the pipe roughness for $0.1 \leq \varepsilon \leq 0.26$ mm, plot the pumping power as a function of the pipe roughness.

8–57 Water at 15°C ($\rho = 999.1$ kg/m^3 and $\mu = 1.138 \times 10^{-3}$ kg/m·s) is flowing in a 4-cm-diameter and 25-m-long horizontal pipe made of stainless steel steadily at a rate of 7 L/s. Determine (a) the pressure drop and (b) the pumping power requirement to overcome this pressure drop. Assume flow is fully developed. Is this a good assumption?
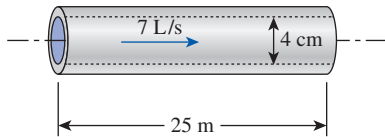
FIGURE P8–57

8–58 Reconsider Prob. 8–57. Using appropriate software, investigate the effect of the pipe diameter on the pumping power requirement to overcome the pressure loss. By varying the pipe diameter from 2 to 4 cm, plot the pumping power as a function of the pipe diameter.

8–59 Consider a fluid with mean inlet temperature T_i flowing through a tube of diameter D and length L, at a mass flow rate $\dot{m}$. The tube is subjected to a surface heat flux that can be expressed as $\dot{q}_s(x) = a + b \sin(x\pi/L)$, where a and b are constants. Determine an expression for the mean temperature of the fluid as a function of the x-coordinate.

8–60 A fluid is flowing in fully developed laminar conditions in a tube with diameter D and length L at a mass flow rate $\dot{m}$. The tube is subjected to a surface heat flux that can be expressed as $\dot{q}_s(x) = a \exp(-bx/2)$, where a and b are constants. Determine an expression for the difference in mean temperature at the tube inlet and outlet.

8–61 In a thermal system, water enters a 25-mm-diameter and 23-m-long circular tube with a mass flow rate of 0.1 kg/s at 25°C. The heat transfer from the tube surface to the water can be expressed in terms of heat flux as $\dot{q}_s(x) = ax$. The coefficient a is 400 W/m^3, and the axial distance from the tube inlet is x measured in meters. Determine (a) an expression for the mean temperature $T_m(x)$ of the water, (b) the outlet mean

temperature of the water, and (c) the value of a uniform heat flux $\dot{q}_s$ on the tube surface that would result in the same outlet mean temperature calculated in part (b). Evaluate water properties at 35°C.

8–62 Consider a 10-m-long smooth rectangular tube, with $a = 50$ mm and $b = 25$ mm, that is maintained at a constant surface temperature. Liquid water enters the tube at 20°C with a mass flow rate of 0.01 kg/s. Determine the tube surface temperature necessary to heat the water to the desired outlet temperature of 80°C.
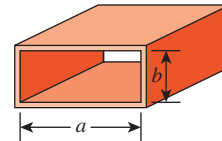
FIGURE P8–62

8–63 A 15-cm $\times$ 20-cm printed circuit board whose components are not allowed to come into direct contact with air for reliability reasons is to be cooled by passing cool air through a 20-cm-long channel of rectangular cross section 0.2 cm $\times$ 14 cm drilled into the board. The heat generated by the electronic components is conducted across the thin layer of the board to the channel, where it is removed by air that enters the channel at 15°C. The heat flux at the top surface of the channel can be considered to be uniform, and heat transfer through other surfaces is negligible. If the velocity of the air at the inlet of the channel is not to exceed 4 m/s and the surface temperature of the channel is to remain under 50°C, determine the maximum total power of the electronic components that can safely be mounted on this circuit board. As a first approximation, assume flow is fully developed in the channel. Evaluate properties of air at a bulk mean temperature of 25°C. Is this a good assumption?
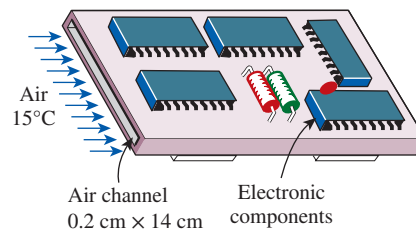
FIGURE P8–63

8–64 Repeat Prob. 8–63 by replacing air with helium, which has six times the thermal conductivity of air. Use the following properties for helium: $\rho = 0.1636$ kg/m^3, $k = 0.1502$ W/m·K, $\nu = 1.214 \times 10^{-4}$ m^2/s, $c_p = 5193$ J/kg·K, and Pr = 0.6867.

8–65 Reconsider Prob. 8–63. Using appropriate software, investigate the effects of air velocity at the inlet of

the channel and the maximum surface temperature on the maximum total power dissipation of electronic components. Let the air velocity vary from 1 m/s to 20 m/s and the surface temperature from 30°C to 90°C. Plot the power dissipation as functions of air velocity and surface temperature, and discuss the results.

8–66 A computer cooled by a fan contains eight printed circuit boards (PCBs), each dissipating 12 W of power. The height of the PCBs is 12 cm and the length is 15 cm. The clearance between the tips of the components on the PCB and the back surface of the adjacent PCB is 0.3 cm. The cooling air is supplied by a 10-W fan mounted at the inlet. If the temperature rise of air as it flows through the case of the computer is not to exceed 10°C, determine (a) the flow rate of the air that the fan needs to deliver, (b) the fraction of the temperature rise of air that is due to the heat generated by the fan and its motor, and (c) the highest allowable inlet air temperature if the surface temperature of the components is not to exceed 70°C anywhere in the system. As a first approximation, assume flow is fully developed in the channel. Evaluate properties of air at a bulk mean temperature of 25°C. Is this a good assumption?
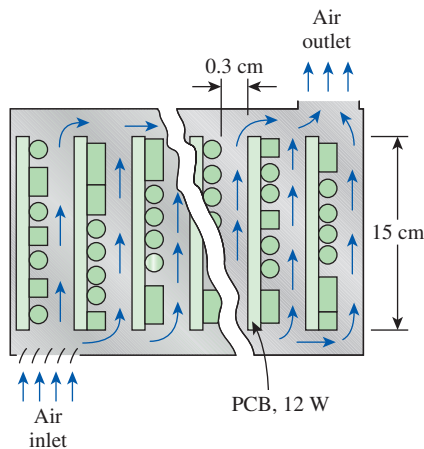
FIGURE P8–66

8–67 Liquid water is flowing between two very thin parallel 1-m-wide and 10-m-long plates with a spacing of 12.5 mm. The water enters the parallel plates at 20°C with a mass flow rate of 0.58 kg/s. The outer surface of the parallel plates is subjected to hydrogen gas (an ideal gas at 1 atm) flow width-wise in parallel over the upper and lower surfaces of the two plates. The free-stream hydrogen gas has a velocity of 5 m/s at a temperature of 155°C. Determine the outlet mean temperature of the water, the surface temperature of the parallel plates, and the total rate of heat transfer. Evaluate the properties for water at 30°C and the properties of H_2 gas at 100°C. Is this a good assumption?
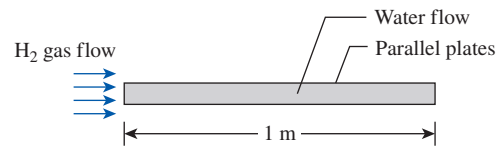
FIGURE P8–67

8–68 Reconsider Prob. 8–67. Using appropriate software, evaluate the effect of water mass flow rate on the free-stream H_2 gas velocity and the surface temperature of the parallel plates and the effect of the free-stream H_2 gas velocity on the total heat transfer rate. By varying the mass flow rate of water for $0 < \dot{m} \le 0.58$ kg/s, plot the free-stream H_2 gas velocity and the surface temperature of the plates as a function of the mass flow rate of water. Also, plot the total heat transfer rate as a function of the free-stream H_2 gas velocity.

8–69 Consider the flow of oil at 10°C in a 40-cm-diameter pipeline at an average velocity of 0.5 m/s. A 1500-m-long section of the pipeline passes through icy waters of a lake at 0°C. Measurements indicate that the surface temperature of the pipe is very nearly 0°C. Disregarding the thermal resistance of the pipe material, determine (a) the temperature of the oil when the pipe leaves the lake, (b) the rate of heat transfer from the oil, and (c) the pumping power required to overcome the pressure losses and to maintain the flow of oil in the pipe.

8–70 In a manufacturing plant that produces cosmetic products, glycerin is being heated by flowing through a 25-mm-diameter and 10-m-long tube. With a mass flow rate of 0.5 kg/s, the flow of glycerin enters the tube at 25°C. The tube surface is maintained at a constant surface temperature of 140°C. Determine the outlet mean temperature and the total rate of heat transfer for the tube. Evaluate the properties for glycerin at 30°C.

8–71 Liquid glycerin is flowing through a 25-mm-diameter and 10-m-long tube. The liquid glycerin enters the tube at 20°C with a mass flow rate of 0.5 kg/s. If the outlet mean temperature is 40°C and the tube surface temperature is constant, determine the surface temperature of the tube.

8–72 Liquid water flows in a thin-walled circular tube at a mass flow rate of 11 g/s. The water enters the tube at 60°C, where it is heated at a rate of 3.8 kW. The tube is circular with a length of 3 m and an inner diameter of 25 mm. The tube surface is maintained at a constant temperature. At the tube exit, a hydrogenated nitrile rubber (HNBR) o-ring is attached to the tube's outer surface. The maximum temperature permitted for the o-ring is 150°C (ASME Boiler and Pressure Vessel Code, BPVC.IV-2015, HG-360). Is the HNBR o-ring suitable for this operation? Evaluate the fluid properties at 100°C. Is this a reasonable temperature at which to evaluate the fluid properties?

8–73 Air at 20°C (1 atm) enters into a 5-mm-diameter and 10-cm-long circular tube at an average velocity of 5 m/s. The tube wall is maintained at a constant surface temperature of

160°C. Determine the convection heat transfer coefficient and the outlet mean temperature. Evaluate the air properties at 50°C.

8–74 Liquid methane flows at an average velocity of 1.7 mm/s between two isothermal parallel plates that are spaced 25 mm apart. The plates are made of ASTM A240 410S stainless steel, and each plate has a length of 2 m. The inlet temperature for the liquid methane is −150°C, and the liquid exits the parallel plates at −50°C. The minimum temperature suitable for ASTM A240 410S stainless steel plate is −30°C (ASME Code for Process Piping, ASME B31.3-2014, Table A-1M). To keep the plates from getting too cold, the plates are heated at 700 W/m². Determine the surface temperature of the plates. Are the ASTM A240 410S stainless steel plates suitable for this operation?

8–75 Glycerin is being heated by flowing between two parallel 1-m-wide and 10-m-long plates with 12.5-mm spacing. The glycerin enters the parallel plates with a temperature of 25°C and a mass flow rate of 0.7 kg/s. The plates have a constant surface temperature of 40°C. Determine the outlet mean temperature of the glycerin and the total rate of heat transfer. Evaluate the properties for glycerin at 30°C. Is this a good assumption?

8–76 Reconsider Prob. 8–75. Using appropriate software, evaluate the effect of the glycerin mass flow rate on the surface temperature of the parallel plates and the total rate of heat transfer necessary to keep the outlet mean temperature of the glycerin at 35°C. By varying the mass flow rate from 0.05 to 6 kg/s, plot the surface temperature of the parallel plates and the total rate of heat transfer as a function of the mass flow rate.

8–77 Glycerin is being heated by flowing between two very thin parallel 1-m-wide and 10-m-long plates with 12.5-mm spacing. The glycerin enters the parallel plates with a temperature 20°C and a mass flow rate of 0.7 kg/s. The outer surface of the parallel plates is subjected to hydrogen gas (an ideal gas at 1 atm) flow width-wise in parallel over the upper and lower surfaces of the two plates. The free-stream hydrogen gas has a velocity of 3 m/s and a temperature of 150°C. Determine the outlet mean temperature of the glycerin, the surface temperature of the parallel plates, and the total rate of heat transfer. Evaluate the properties for glycerin at 30°C and the properties of H_2 gas at 100°C. Are these good assumptions?
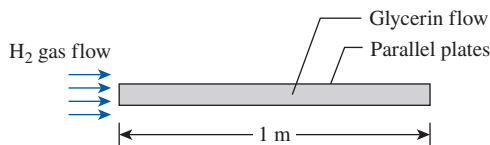
FIGURE P8–77

8–78 Reconsider Prob. 8–77. Using appropriate software, evaluate the effect of the glycerin mass flow rate on the free-stream velocity of the hydrogen gas needed to keep the outlet mean temperature of the glycerin at

40°C. By varying the mass flow rate of glycerin from 0.5 to 2.4 kg/s, plot the free-stream velocity of the hydrogen gas as a function of the mass flow rate of the glycerin.

8–79E Air flows in an isothermal tube under fully developed conditions. The inlet temperature is 60°F and the tube surface temperature is 120°F. The tube is 10 ft long, and the inner diameter is 2 in. The air mass flow rate is 18.2 lbm/h. Calculate the exit temperature of the air and the total rate of heat transfer from the tube wall to the air. Evaluate the air properties at a temperature 80°F. Is this a good assumption?

8–80 Water flows through a circular pipe. The pipe's inner diameter is 2 cm, and its length is 6 m. The average velocity of the water is 15 cm/s, and its inlet temperature is 20°C. Assuming that the heating is uniform and the flow is fully developed, what is the heat flux required to raise the water temperature by 1°C by the time it reaches the end of the pipe? What is the surface temperature of the pipe at the exit? Evaluate the properties of water at 20°C.

8–81 Air flows in a pipe under fully developed conditions with an average velocity of 1.25 m/s and a temperature of 20°C. The pipe's inner diameter is 4 cm, and its length is 4 m. The first half of the pipe is kept at a constant wall temperature of 100°C. The second half of the pipe is subjected to a constant heat flux of 200 W. Determine (*a*) the air temperature at the 2 m length, (*b*) the air temperature at the exit, (*c*) the total heat transfer to the air, and (*d*) the wall temperature at the exit of the tube. Evaluate the properties of air at 80°C.
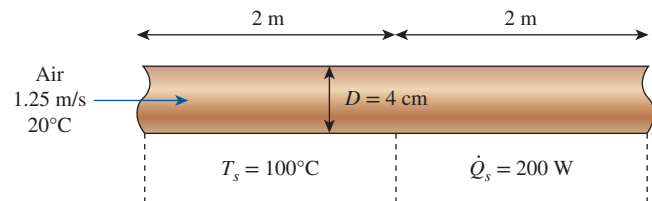
FIGURE P8–81

8–82E Air flows with an average velocity of 3 ft/s in a duct that is 1 ft wide and 1 in high and 40 ft long. The aspect ratio of the duct is very small (0.083), and the duct can be treated as a parallel-plate channel. The duct passes through a heated oven, and the temperature of the duct is approximately constant and equal to 100°F. The air enters the duct at 50°F. For fully developed flow of air in the duct, determine (*a*) the temperature of the air as it leaves the duct, (*b*) the rate of heat transfer from the duct to the air, and (c) the heat flux at the duct exit. Evaluate the properties of air at 75°F. Is this a good assumption?

8–83 Determine the convection heat transfer coefficient for the flow of (*a*) air and (*b*) water at a velocity of 5 m/s in an 8-cm-diameter and 10-m-long tube when the tube is subjected to uniform heat flux from all surfaces. Use fluid properties at 25°C.
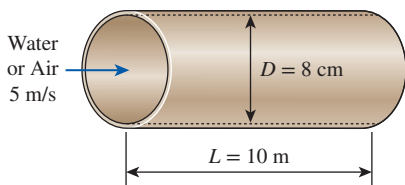
FIGURE P8−83

8–84 C&S Liquid water flows in a circular tube at a mass flow rate of 0.12 kg/s. The water enters the tube at 65°C, where it is heated at a rate of 5.5 kW. The tube is circular with a length of 3 m and an inner diameter of 25 mm. The tube surface is maintained isothermal. The inner surface of the tube is lined with polyvinylidene chloride (PVDC) lining. The recommended maximum temperature for PVDC lining is 79°C (ASME Code for Process Piping, ASME B31.3-2014, Table A323.4.3). Is the PVDC lining suitable for the tube under these conditions? Evaluate the fluid properties at 70°C. Is this an appropriate temperature at which to evaluate the fluid properties?

8–85 C&S Saturated liquid propane flows in a circular ASTM A268 TP443 stainless steel tube at a mass flow rate of 42 g/s. The liquid propane enters the tube at −50°C, and the tube surface is maintained isothermal. The tube has an inner diameter of 25 mm, and its length is 3 m. The inner surface of the tube has a relative surface roughness of 0.05. The ASME Code for Process Piping limits the minimum temperature suitable for using ASTM A268 TP443 stainless steel tube at −30°C(ASME B31.3-2014, Table A-1M). To keep the tube surface from getting too cold, the tube is heated at a rate of 1.3 kW. Determine the surface temperature of the tube. Is the ASTM A268 TP443 stainless steel tube suitable under these conditions? Evaluate the fluid properties at −40°C. Is this an appropriate temperature at which to evaluate the fluid properties?

8–86 Air at 10°C enters a 12-cm-diameter and 5-m-long pipe at a rate of 0.065 kg/s. The inner surface of the pipe has a roughness of 0.22 mm, and the pipe is nearly isothermal at 50°C. Determine the rate of heat transfer to air using the Nusselt number relation given by (*a*) Eq. 8–66 and (*b*) Eq. 8–71. Evaluate air properties at a bulk mean temperature of 20°C. Is this a good assumption?

8–87 C&S Liquid water flows in a thin-walled circular tube, where the pumping power required to overcome the turbulent flow pressure loss in the tube is 100 W. The water enters the tube at 10°C, where it is heated at a rate of 3.6 kW. The average convection heat transfer coefficient for the internal flow is 120 W/m²·K. The tube is 3 m long and has an inner diameter of 12.5 mm. The tube surface is maintained at a constant temperature. At the tube exit, an ethylene propylene diene (EPDM) rubber o-ring is attached to the tube's outer surface. The maximum temperature permitted for the o-ring is

150°C (ASME Boiler and Pressure Vessel Code, BPVC. IV-2015, HG-360). Is the EPDM o-ring suitable for this operation? Evaluate the fluid properties at 10°C. Is this an appropriate temperature at which to evaluate the fluid properties?

8–88 A 12-m-long and 12-mm-inner-diameter pipe made of commercial steel is used to heat a liquid in an industrial process. The liquid enters the pipe with $T_i = 25°C, V = 0.8$ m/s. A uniform heat flux is maintained by an electric resistance heater wrapped around the outer surface of the pipe so that the fluid exits at 75°C. Assuming fully developed flow and taking the average fluid properties to be $\rho = 1000$ kg/m³, $c_p = 4000$ J/kg·K, $\mu = 2 \times 10^{-3}$ kg/m·s, $k = 0.48$ W/m·K, and Pr = 10, determine:

(*a*) The required surface heat flux $\dot{q}_s$, produced by the heater
(*b*) The surface temperature at the exit, T_s
(*c*) The pressure loss through the pipe and the minimum power required to overcome the resistance to flow.

8–89 Water is to be heated from 10°C to 80°C as it flows through a 2-cm-internal-diameter, 13-m-long tube. The tube is equipped with an electric resistance heater, which provides uniform heating throughout the surface of the tube. The outer surface of the heater is well insulated, so in steady operation all the heat generated in the heater is transferred to the water in the tube. If the system is to provide hot water at a rate of 5 L/min, determine the power rating of the resistance heater. Also, estimate the inner surface temperature of the pipe at the exit.

8–90 Consider a fluid with a Prandtl number of 7 flowing through a smooth circular tube. Using the Colburn, Petukhov, and Gnielinski equations, determine the Nusselt numbers for Reynolds numbers at $3500, 10^4$, and 5×10^5. Compare and discuss the results.

8–91E The hot water needs of a household are to be met by heating water at 55°F to 180°F by a parabolic solar collector at a rate of 5 lbm/s. Water flows through a 1.25-in-diameter thin aluminum tube whose outer surface is anodized black in order to maximize its solar absorption ability. The centerline of the tube coincides with the focal line of the collector, and a glass sleeve is placed outside the tube to minimize the heat losses. If solar energy is transferred to water at a net rate of 350 Btu/h per ft length of the tube, determine the required length of the parabolic collector to meet the hot water requirements of this house. Also, determine the surface temperature of the tube at the exit.
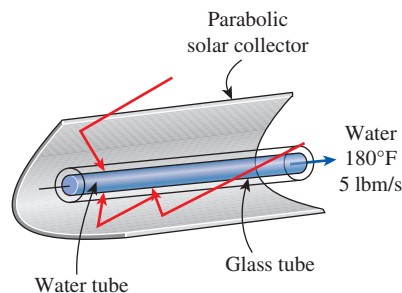
FIGURE P8−91E

8–92E Water at 60°F is heated by passing it through 0.75-in-internal-diameter thin-walled copper tubes. Heat is supplied to the water by steam that condenses outside the copper tubes at 250°F. If water is to be heated to 140°F at a rate of 0.4 lbm/s, determine (a) the length of the copper tube that needs to be used and (b) the pumping power required to overcome pressure losses. Assume the entire copper tube to be at the steam temperature of 250°F.

8–93 Air (1 atm) enters into a 5-cm-diameter circular tube at 20°C with an average velocity of 5 m/s. The tube wall is maintained at a constant surface temperature of 160°C, and the outlet mean temperature is 80°C. Estimate the length of the tube. Is the flow fully developed?

8–94 **PtD** In a food processing plant, hot liquid water is being transported in a pipe ($k = 15$ W/m·K, $D_i = 2.5$ cm, $D_o = 3$ cm, and $L = 10$ m.) The hot water flowing with a mass flow rate of 0.15 kg/s enters the pipe at 100°C and exits at 60°C. The plant supervisor thinks that since the hot water exits the pipe at 60°C, the pipe's outer surface temperature should be safe from thermal burn hazards. In order to prevent thermal burn upon accidental contact with skin tissue for individuals working in the vicinity of the pipe, the pipe's outer surface temperature should be kept below 45°C. Determine whether or not there is a risk of thermal burn on the pipe's outer surface. Assume the pipe outer surface temperature remains constant.

8–95 **PtD** Reconsider Prob. 8–94. The mass flow rate of the hot water can be varied between 0.05 and 0.5 kg/s. Using appropriate software, evaluate the effect of the hot water mass flow rate on the pipe's outer surface temperature. Plot the pipe's outer surface temperature as a function of the hot water mass flow rate for the water exit temperature of (a) 60°C and (b) 70°C. To prevent thermal burn on individuals working in the vicinity of the pipe, determine the condition of the hot water mass flow rate such that the pipe's outer surface temperature is below 45°C.

8–96 **PtD** A metal pipe ($k_{pipe} = 15$ W/m·K, $D_{i, pipe} = 5$ cm, $D_{o, pipe} = 6$ cm, and $L = 10$ m) situated in an engine room is used for transporting hot saturated water vapor at a flow rate of 0.03 kg/s. The water vapor enters and exits the pipe at 325°C and 290°C, respectively. Oil leakage can occur in the engine room, and when leaked oil comes in contact with hot spots above the oil's autoignition temperature, it can ignite spontaneously. To prevent any fire hazard caused by oil leakage on the hot surface of the pipe, determine the required insulation ($k_{ins} = 0.95$ W/m·K) layer thickness over the pipe for keeping the outer surface temperature below 180°C.

8–97 **PtD** Reconsider Prob. 8–96. Using appropriate software, evaluate the effect of the saturated water vapor mass flow rate on required insulation thickness for keeping the outer surface temperature below 180°C to prevent a fire hazard if oil leaks. By varying the mass flow rate from 0.01

to 0.1 kg/s, plot the insulation layer thickness as a function of the mass flow rate. If the flow rate of the saturated water vapor is adjusted between 0.03 and 0.1 kg/s, determine the insulation layer thickness that is suitable for this flow rate range.

8–98 **PtD** Exposure to high concentrations of gaseous ammonia can cause lung damage. To prevent gaseous ammonia from leaking out, ammonia is transported in its liquid state through a pipe ($k = 15$ W/m·K, $D_{i, pipe} = 5$ cm, $D_{o, pipe} = 6$ cm, and $L = 10$ m). The liquid ammonia enters the pipe at −30°C with a flow rate of 0.15 kg/s. Determine the insulation thickness for the pipe using a material with $k = 0.95$ W/m·K to keep the liquid ammonia's exit temperature at −20°C, while maintaining the insulated pipe outer surface temperature at 20°C.

8–99 **PtD** Reconsider Prob. 8–98. Using appropriate software, evaluate the effect of the liquid ammonia mass flow rate on the insulation thickness needed to keep the outer surface temperature at 20°C and the flow exit temperature at −20°C. By varying the mass flow rate from 0.02 to 0.2 kg/s, plot the insulation layer thickness as a function of the mass flow rate. If the flow rate of the liquid ammonia is adjusted between 0.04 and 0.2 kg/s, calculate the insulation layer thickness that is suitable for this range of flow rate.

8–100 An 8-m-long, uninsulated square duct of cross section 0.2 m × 0.2 m and relative roughness 10^{-3} passes through the attic space of a house. Hot air enters the duct at 1 atm and 80°C at a volume flow rate of 0.15 m³/s. The duct surface is nearly isothermal at 60°C. Determine the rate of heat loss from the duct to the attic space and the pressure difference between the inlet and outlet sections of the duct. Evaluate air properties at a bulk mean temperature of 80°C. Is this a good assumption?

8–101 Hot air at atmospheric pressure and 75°C enters a 10-m-long uninsulated square duct of cross section 0.15 m × 0.15 m that passes through the attic of a house at a rate of 0.2 m³/s. The duct is observed to be nearly isothermal at 70°C. Determine the exit temperature of the air and the rate of heat loss from the duct to the airspace in the attic. Evaluate air properties at a bulk mean temperature of 75°C. Is this a good assumption?
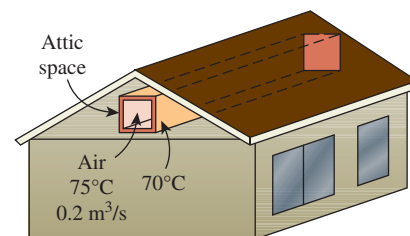
FIGURE P8−101

8–102 Reconsider Prob. 8–101. Using appropriate software, investigate the effect of the volume flow rate of air on the exit temperature of air and the rate of heat loss. Let the flow rate vary from 0.05 m^3/s to 0.15 m^3/s. Plot the exit temperature and the rate of heat loss as a function of flow rate, and discuss the results.

8–103 Hot air at 60°C leaving the furnace of a house enters a 12-m-long section of a sheet metal duct of rectangular cross section 20 cm × 20 cm at an average velocity of 4 m/s. The thermal resistance of the duct is negligible, and the outer surface of the duct, whose emissivity is 0.3, is exposed to the cold air at 10°C in the basement, with a convection heat transfer coefficient of 10 W/m²·K. Taking the walls of the basement to be at 10°C also, determine (*a*) the temperature at which the hot air will leave the basement and (*b*) the rate of heat loss from the hot air in the duct to the basement. Evaluate air properties at a bulk mean temperature of 50°C. Is this a good assumption?

10°C
$h_o = 10$ W/m²·K
12 m

Hot air
60°C
4 m/s

Air duct
20 cm × 20 cm
$\varepsilon = 0.3$
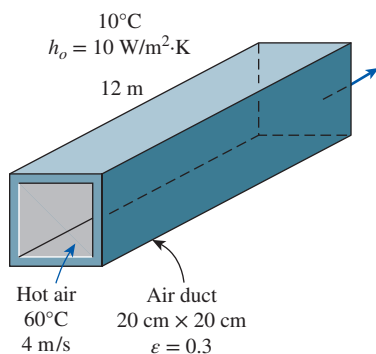
FIGURE P8–103

8–104 Reconsider Prob. 8–103. Using appropriate software, investigate the effect of air velocity and the surface emissivity on the exit temperature of air and the rate of heat loss. Let the air velocity vary from 1 m/s to 10 m/s and the emissivity from 0.1 to 1.0. Plot the exit temperature and the rate of heat loss functions of the air velocity and emissivity, and discuss the results.

8–105 The components of an electronic system dissipating 220 W are located in a 1-m-long horizontal duct whose cross section is 16 cm × 16 cm. The components in the duct are cooled by forced air, which enters at 27°C at a rate of 0.65 m^3/min. Assuming 85 percent of the heat generated inside is transferred to air flowing through the duct and the remaining 15 percent is lost through the outer surfaces of the duct, determine (*a*) the exit temperature of air and (*b*) the highest component surface temperature in the duct. As a first approximation, assume fully developed turbulent flow in the channel. Evaluate the properties of air at a bulk mean temperature of 35°C. Is this a good assumption?

8–106 Repeat Prob. 8–105 for a circular horizontal duct of 15 cm diameter.

8–107 A concentric annulus tube has inner and outer diameters of 25 mm and 100 mm, respectively. Liquid water flows at a mass flow rate of 0.05 kg/s through the annulus with the inlet and outlet mean temperatures of 20°C and 80°C, respectively. The inner tube wall is maintained with a constant surface temperature of 120°C, while the outer tube surface is insulated. Determine the length of the concentric annulus tube. Assume flow is fully developed.

T_s
Insulation
D_o
Water
D_i
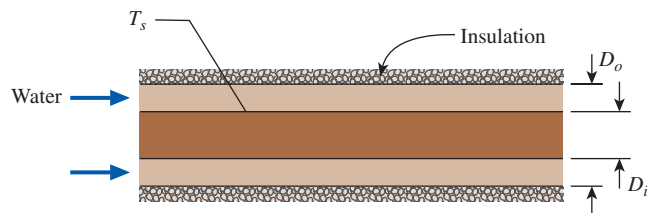
FIGURE P8–107

8–108 Liquid water flows at a mass flow rate of 0.7 kg/s through a concentric annulus tube with the inlet and outlet mean temperatures of 20°C and 80°C, respectively. The concentric annulus tube has inner and outer diameters of 10 mm and 100 mm, respectively. The inner tube wall is maintained with a constant surface temperature of 120°C, while the outer tube surface is insulated. Determine the length of the concentric annulus tube.

T_s
Insulation
D_o
Water
D_i
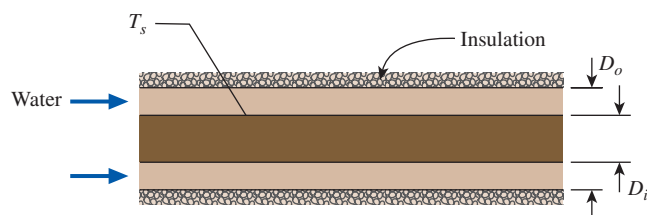
FIGURE P8–108

Special Topic: Transitional Flow

8–109 A tube with a bell-mouth inlet configuration is subjected to uniform wall heat flux of 3 kW/m². The tube has an inside diameter of 0.0158 m (0.622 in) and a flow rate of 1.43×10^{-4} m^3/s (2.27 gpm). The liquid flowing inside the tube is an ethylene glycol–distilled water mixture with a mass fraction of 2.27. Determine the fully developed friction coefficient at a location along the tube where the Grashof number is Gr = 16,600. The physical properties of the ethylene glycol–distilled water mixture at the location of interest are Pr = 14.85, $\nu = 1.93 \times 10^{-6}$ m²/s, and $\mu_b/\mu_s = 1.07$.

8–110 Reconsider Prob. 8–109. Calculate the fully developed friction coefficient if the volume flow rate is increased by 50 percent while the rest of the parameters remain unchanged.

8–111E A tube with a square-edged inlet configuration is subjected to uniform wall heat flux of 8 kW/m². The tube has an inside diameter of 0.622 in and a flow rate of 2.16 gpm. The liquid flowing inside the tube is an ethylene glycol–distilled water mixture with a mass fraction of 2.27. Determine the friction coefficient at a location along the tube where the Grashof number is Gr = 35,450. The physical properties of the ethylene glycol–distilled water mixture at the location of interest are Pr = 13.8, $\nu = 18.4 \times 10^{-6}$ ft²/s, and $\mu_b/\mu_s = 1.12$. Then recalculate the fully developed friction coefficient if the volume flow rate is increased by 50 percent while the rest of the parameters remain unchanged.

8–112 A 4-m-long tube is subjected to uniform wall heat flux. The tube has an inside diameter of 0.0149 m and a flow rate of 7.8×10^{-5} m³/s. The liquid flowing inside the tube is an ethylene glycol–distilled water mixture with a mass fraction of 0.5. Determine the apparent (developing) friction factor at the location $x/D = 20$ if the inlet configuration of the tube is: (*a*) re-entrant and (*b*) square-edged. At this location, the local Grashof number is Gr = 24,000, and the properties of the mixture of distilled water and ethylene glycol are: Pr = 20.9, $\nu = 2.33 \times 10^{-6}$ m²/s, and $\mu_b/\mu_s = 1.25$.

8–113 An ethylene glycol–distilled water mixture with a mass fraction of 0.72 and a flow rate of 2.05×10^{-4} m³/s flows inside a tube with an inside diameter of 0.0158 m and a uniform wall heat flux boundary condition. For this flow, determine the Nusselt number at the location $x/D = 10$ for the inlet tube configuration of (*a*) bell-mouth and (*b*) re-entrant. Compare the results for parts (*a*) and (*b*). Assume the Grashof number is Gr = 60,000. The physical properties of an ethylene glycol–distilled water mixture are Pr = 33.46, $\nu = 3.45 \times 10^{-6}$ m²/s, and $\mu_b/\mu_s = 2.0$.

8–114 Repeat Prob. 8–113 for the location $x/D = 90$.

Review Problems

8–115 The velocity profile in fully developed laminar flow in a circular pipe, in m/s, is given by $u(r) = 4(1 - 100\,r^2)$ where r is the radial distance from the centerline of the pipe in m. Determine (*a*) the radius of the pipe, (*b*) the mean velocity through the pipe, and (*c*) the maximum velocity in the pipe.

8–116E The velocity profile in fully developed laminar flow of water at 40°F in a 140-ft-long horizontal circular pipe, in ft/s, is given by $u(r) = 0.8(1 - 625\,r^2)$ where r is the radial distance from the centerline of the pipe in ft. Determine (*a*) the volume flow rate of water through the pipe, (*b*) the pressure drop across the pipe, and (*c*) the useful pumping power required to overcome this pressure drop.

8–117 Consider laminar flow of a fluid through a square channel maintained at a constant temperature. Now the mean velocity of the fluid is doubled. Determine the change in the pressure drop and the change in the rate of heat transfer between the fluid and the walls of the channel. Assume the flow regime remains unchanged. Assume fully developed flow, and disregard any changes in ΔT_{lm}.

8–118 Repeat Prob. 8–117 for turbulent flow.

8–119 A liquid hydrocarbon enters a 2.5-cm-diameter tube that is 5.0 m long. The liquid inlet temperature is 20°C and the tube wall temperature is 60°C. Average liquid properties are $c_p = 2.0$ kJ/kg·K, $\mu = 10$ mPa·s, and $\rho = 900$ kg/m³. At a flow rate of 1200 kg/h, the liquid outlet temperature is measured to be 30°C. Estimate the liquid outlet temperature when the flow rate is reduced to 400 kg/h. *Hint:* For heat transfer in tubes, Nu $\propto$ Re$^{1/3}$ in laminar flow and Nu $\propto$ Re$^{4/5}$ in turbulent flow.

8–120 A silicon chip is cooled by passing water through microchannels etched in the back of the chip, as shown in Fig. P8–120. The channels are covered with a silicon cap. Consider a 12-mm × 12-mm-square chip in which $N = 60$ rectangular microchannels, each of width $W = 50\ \mu$m and height $H = 200\ \mu$m, have been etched. Water enters the microchannels at a temperature $T_i = 290$ K and a total flow rate of 0.005 kg/s. The chip and cap are maintained at a uniform temperature of 350 K. Assuming that the flow in the channels is fully developed, all the heat generated by the circuits on the top surface of the chip is transferred to the water, and using circular tube correlations, determine:

(*a*) The water outlet temperature, T_e
(*b*) The chip power dissipation, $\dot{W}_e$

Evaluate liquid water properties at a bulk mean temperature of 298 K. Is this a good assumption?
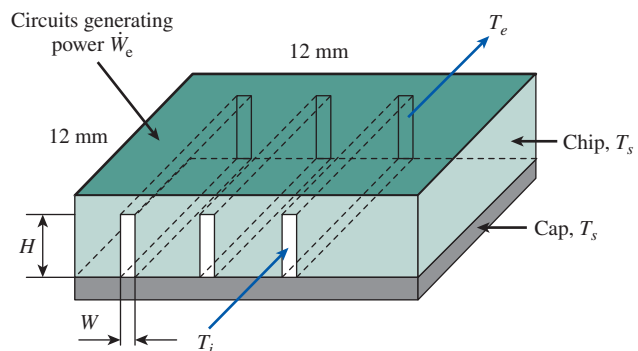
FIGURE P8–120

8–121 A fluid ($\rho = 1000$ kg/m³, $\mu = 1.4 \times 10^{-3}$ kg/m·s, $c_p = 4.2$ kJ/kg·K, and $k = 0.58$ W/m·K) flows with an average velocity of 0.3 m/s through a 14-m-long tube with inside diameter of 0.01 m. Heat is uniformly added to the entire tube at the rate of 1500 W/m². Determine (*a*) the value of convection heat transfer coefficient at the exit, (*b*) the value of $T_s - T_m$, and (*c*) the value of $T_e - T_i$.

8–122 Crude oil at 22°C enters a 20-cm-diameter pipe with an average velocity of 32 cm/s. The average pipe wall temperature is 2°C. Crude oil properties are as given below. Calculate the rate of heat transfer and the pipe length if the crude oil outlet temperature is 20°C.

T °C	ρ kg/m³	k W/m·K	μ mPa·s	c_p kJ/kg·K
2.0	900	0.145	60.0	1.80
22.0	890	0.145	20.0	1.90

8–123 Air (1 atm) enters a 5-mm-diameter circular tube at an average velocity of 5 m/s. The tube wall is maintained at a constant surface temperature. Determine the convection heat transfer coefficient for (a) a 10-cm-long tube and (b) a 50-cm-long tube. Evaluate the air properties at 50°C.

8–124 To cool a storehouse in the summer without using a conventional air-conditioning system, the owner decided to hire an engineer to design an alternative system that would make use of the water in the nearby lake. The engineer decided to flow air through a thin, smooth, 10-cm-diameter copper tube that is submerged in the lake. The water in the lake is typically at a constant temperature of 15°C and a convection heat transfer coefficient of 1000 W/m²·K. If air (1 atm) enters the copper tube at a mean temperature of 30°C with an average velocity of 2.5 m/s, determine the necessary copper tube length so that the outlet mean temperature of the air is 20°C.
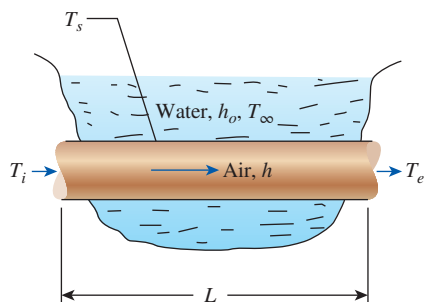
FIGURE P8−124

8–125 Liquid mercury is flowing at 0.6 kg/s through a 5-cm-diameter tube with inlet and outlet mean temperatures of 100°C and 200°C, respectively. The tube surface temperature is kept constant at 250°C. Determine the tube length using (a) the appropriate Nusselt number relation for liquid metals and (b) the Dittus-Boelter equation. (c) Compare the results of (a) and (b).

8–126 In the effort to find the best way to cool a smooth, thin-walled copper tube, an engineer decided to flow air either through the tube or across the outer tube surface. The tube has a diameter of 5 cm, and the surface temperature is held constant. Determine (a) the convection heat transfer coefficient when air is flowing through its inside at 25 m/s with a bulk mean temperature of 50°C and (b) the convection heat transfer coefficient when air is flowing across its outer surface at 25 m/s with a film temperature of 50°C.

8–127 Water is heated at a rate of 10 kg/s from a temperature of 15°C to 35°C by passing it through five identical tubes, each 5.0 cm in diameter, whose surface temperature is 60.0°C. Estimate (a) the steady rate of heat transfer and (b) the length of tubes needed to accomplish this task.

8–128 Repeat Prob. 8–127 for a flow rate of 20 kg/s.

8–129 Water at 1500 kg/h and 10°C enters a 10-mm-diameter smooth tube whose wall temperature is maintained at 49°C. Calculate (a) the tube length necessary to heat the water to 40°C, and (b) the water outlet temperature if the tube length is doubled. Assume average water properties to be the same as in (a).

8–130E The exhaust gases of an automotive engine leave the combustion chamber and enter an 8-ft-long and 3.5-in-diameter thin-walled steel exhaust pipe at 800°F and 15.5 psia at a rate of 0.05 lbm/s. The surrounding ambient air is at a temperature of 80°F, and the heat transfer coefficient on the outer surface of the exhaust pipe is 3 Btu/h·ft²·°F. Assuming the exhaust gases to have the properties of air, determine (a) the velocity of the exhaust gases at the inlet of the exhaust pipe and (b) the temperature at which the exhaust gases will leave the pipe and enter the air.

8–131E Air is flowing through a smooth, thin-walled, 4-in-diameter copper tube that is submerged in water. The water maintains a constant temperature of 60°F and a convection heat transfer coefficient of 176 Btu/h·ft²·R. If air (1 atm) enters the copper tube at a mean temperature of 90°F with an average velocity of 8 ft/s, determine the necessary copper tube length so that the outlet mean temperature of the air is 70°F.
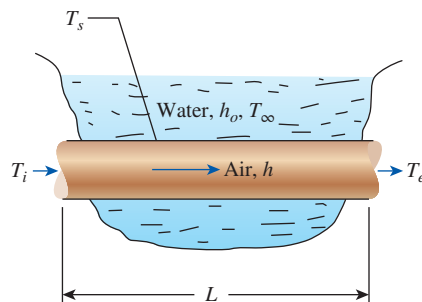
FIGURE P8−131E

8–132 Hot water at 90°C enters a 15-m section of a cast iron pipe ($k = 52$ W/m·K) whose inner and outer diameters are 4 and 4.6 cm, respectively, at an average velocity of 1.2 m/s. The

outer surface of the pipe, whose emissivity is 0.7, is exposed to the cold air at 10°C in a basement, with a convection heat transfer coefficient of 12 W/m²·K. Taking the walls of the basement to be at 10°C also, determine (*a*) the rate of heat loss from the water and (*b*) the temperature at which the water leaves the basement.

$T_{\text{ambient}} = 10°C$
$\varepsilon = 0.7$

Hot water 90°C 1.2 m/s

15 m
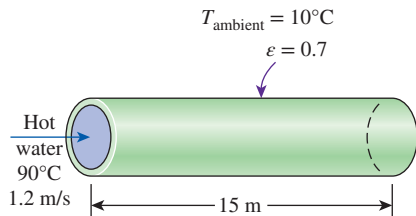
FIGURE P8–132

8–133 Repeat Prob. 8–132 for a pipe made of copper ($k = 386$ W/m·K) instead of cast iron.

8–134 Hot exhaust gases leaving a stationary diesel engine at 450°C enter a 15-cm-diameter pipe at an average velocity of 7.2 m/s. The surface temperature of the pipe is 180°C. Determine the pipe length if the exhaust gases are to leave the pipe at 250°C after transferring heat to water in a heat recovery unit. Use the properties of air for exhaust gases.

8–135 Geothermal steam at 165°C condenses in the shell side of a heat exchanger over the tubes through which water flows. Water enters the 4-cm-diameter, 14-m-long tubes at 20°C at a rate of 0.8 kg/s. Determine the exit temperature of water and the rate of condensation of geothermal steam.

8–136 Cold air at 5°C enters a 12-cm-diameter, 20-m-long isothermal pipe at a velocity of 2.5 m/s and leaves at 19°C. Estimate the surface temperature of the pipe.

8–137 100 kg/s of crude oil is heated from 20°C to 40°C through the tube side of a multitube heat exchanger. The crude oil flow is divided evenly among all 100 tubes in the tube bundle. The ID of each tube is 10 mm, and the inside tube-wall temperature is maintained at 100°C. Average properties of the crude oil are $\rho = 950$ kg/m³, $c_p = 1.9$ kJ/kg·K, $k = 0.25$ W/m·K, $\mu = 12$ mPa·s, and $\mu_w = 4$ mPa·s. Estimate the rate of heat transfer and the tube length.

8–138 Liquid water enters a 10-m-long smooth rectangular tube with $a = 50$ mm and $b = 25$ mm. The surface temperature is kept constant, and water enters the tube at 20°C with a mass flow rate of 0.25 kg/s. Determine the tube surface temperature necessary to heat the water to the desired outlet temperature of 80°C.

b

a
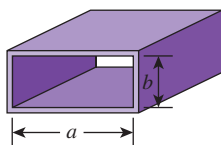
FIGURE P8–138

8–139 A geothermal district heating system involves the transport of geothermal water at 110°C from a geothermal well to a city at about the same elevation for a distance of 12 km at a rate of 1.5 m³/s in 60-cm-diameter stainless steel pipes. The fluid pressures at the wellhead and at the arrival point in the city are to be the same. The minor losses are negligible because of the large length-to-diameter ratio and the relatively small number of components that cause minor losses. (*a*) Assuming the pump-motor efficiency to be 65 percent, determine the electric power consumption of the system for pumping. (*b*) Determine the daily cost of power consumption of the system if the unit cost of electricity is $0.06/kWh. (*c*) The temperature of geothermal water is estimated to drop 0.5°C during this long flow. Determine if the frictional heating during flow can make up for this drop in temperature.

8–140 Repeat Prob. 8–139 for cast iron pipes of the same diameter.

8–141 A house built on a riverside is to be cooled in summer by utilizing the cool water of the river, which flows at an average temperature of 15°C. A 15-m-long section of a circular duct of 20 cm diameter passes through the water. Air enters the underwater section of the duct at 25°C at a velocity of 3 m/s. Assuming the surface of the duct to be at the temperature of the water, determine the outlet temperature of air as it leaves the underwater portion of the duct. Also, for an overall fan efficiency of 55 percent, determine the fan power input needed to overcome the flow resistance in this section of the duct.

Air 25°C, 3 m/s

15°C

Air

River, 15°C
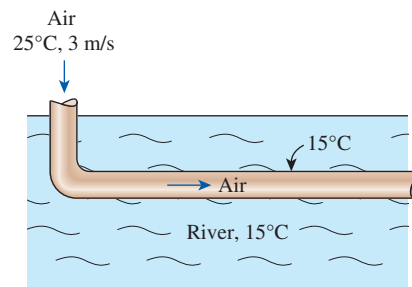
FIGURE P8–141

8–142 Repeat Prob. 8–141 assuming that a 0.25-mm-thick layer of mineral deposit ($k = 3$ W/m·K) formed on the inner surface of the pipe.

8–143 Oil at 15°C is to be heated by saturated steam at 1 atm in a double-pipe heat exchanger to a temperature of 25°C. The inner and outer diameters of the annular space are 3 cm and 5 cm, respectively, and oil enters with a mean velocity of 0.8 m/s. The inner tube may be assumed to be isothermal at 100°C, and the outer tube is well insulated. Assuming fully developed flow for oil, determine the tube length required to heat the oil to the indicated temperature. In reality, will you need a shorter or longer tube? Explain.

8–144E A concentric annulus tube has inner and outer diameters of 1 in and 4 in, respectively. Liquid water flows at a mass flow rate of 396 lbm/h through the annulus with the inlet and outlet mean temperatures of 68°F and 172°F, respectively. The inner tube wall is maintained with a constant surface temperature of 250°F, while the outer tube surface is insulated. Determine the length of the concentric annulus tube. Assume flow is fully developed.
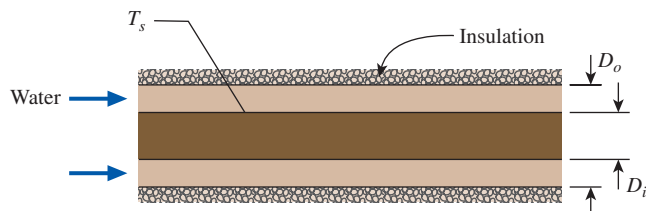
FIGURE P8–144E

Fundamentals of Engineering (FE) Exam Problems

8–145 Internal force flows are said to be fully developed once the _____ at a cross section no longer changes in the direction of flow.

 (*a*) temperature distribution
 (*b*) entropy distribution
 (*c*) velocity distribution
 (*d*) pressure distribution
 (*e*) none of the above

8–146 The bulk or mixed temperature of a fluid flowing through a pipe or duct is defined as

(*a*) $T_b = \dfrac{1}{A_c} \displaystyle\int_{A_c} T \, dA_c$

(*b*) $T_b = \dfrac{1}{\dot{m}} \displaystyle\int_{A_c} T \rho V \, dA_c$

(*c*) $T_b = \dfrac{1}{\dot{m}} \displaystyle\int_{A_c} h \rho V \, dA_c$

(*d*) $T_b = \dfrac{1}{A_c} \displaystyle\int_{A_c} h \, dA_c$

(*e*) $T_b = \dfrac{1}{\dot{V}} \displaystyle\int_{A_c} T \rho V \, dA_c$

8–147 Water ($\mu = 9.0 \times 10^{-4}$ kg/m·s, $\rho = 1000$ kg/m³) enters a 4-cm-diameter and 3-m-long tube whose walls are maintained at 100°C. The water enters this tube with a bulk temperature of 25°C and a volume flow rate of 3 m³/h. The Reynolds number for this internal flow is

 (*a*) 29,500　　(*b*) 38,200　　(*c*) 72,500
 (*d*) 118,100　　(*e*) 122,9000

8–148 Water enters a circular tube whose walls are maintained at constant temperature at a specified flow rate and temperature. For fully developed turbulent flow, the Nusselt number can be determined from $\mathrm{Nu} = 0.023\,\mathrm{Re}^{0.8}\mathrm{Pr}^{0.4}$. The correct temperature difference to use in Newton's law of cooling in this case is

 (*a*) The difference between the inlet and outlet water bulk temperatures.
 (*b*) The difference between the inlet water bulk temperature and the tube wall temperature.
 (*c*) The log mean temperature difference.
 (*d*) The difference between the average water bulk temperature and the tube temperature.
 (*e*) None of the above.

8–149 Air ($c_p = 1007$ J/kg·K) enters a 17-cm-diameter and 4-m-long tube at 65°C at a rate of 0.08 kg/s and leaves at 15°C. The tube is observed to be nearly isothermal at 5°C. The average convection heat transfer coefficient is

 (*a*) 24.5 W/m²·K　　(*b*) 46.2 W/m²·K
 (*c*) 53.9 W/m²·K　　(*d*) 67.6 W/m²·K
 (*e*) 90.7 W/m²·K

8–150 Water ($c_p = 4180$ J/kg·K) enters a 12-cm-diameter and 8.5-m-long tube at 75°C at a rate of 0.35 kg/s and is cooled by a refrigerant evaporating outside at -10°C. If the average heat transfer coefficient on the inner surface is 500 W/m²·K, the exit temperature of the water is

 (*a*) 18.4°C　　(*b*) 25.0°C　　(*c*) 33.8°C
 (*d*) 46.5°C　　(*e*) 60.2°C

8–151 Air enters a duct at 20°C at a rate of 0.08 m³/s, and it is heated to 150°C by steam condensing outside at 200°C. The error in calculating the rate of heat transfer to the air caused by using the arithmetic mean temperature difference instead of the logarithmic mean temperature difference is

 (*a*) 0%　　(*b*) 5.4%　　(*c*) 8.1%
 (*d*) 10.6%　　(*e*) 13.3%

8–152 Engine oil at 60°C ($\mu = 0.07399$ kg/m·s, $\rho = 864$ kg/m³) flows in a 5-cm-diameter tube with a velocity of 2.2 m/s. The pressure drop along a fully developed 6-m-long section of the tube is

 (*a*) 5.4 kPa　　(*b*) 8.1 kPa　　(*c*) 12.5 kPa
 (*d*) 18.4 kPa　　(*e*) 20.8 kPa

8–153 Engine oil flows in a 15-cm-diameter horizontal tube with a velocity of 1.3 m/s, experiencing a pressure drop of 12 kPa. The pumping power requirement to overcome this pressure drop is

 (*a*) 190 W　　(*b*) 276 W　　(*c*) 407 W
 (*d*) 655 W　　(*e*) 900 W

8–154 Water enters a 5-mm-diameter and 13-m-long tube at 15°C with a velocity of 0.3 m/s and leaves at 45°C. The tube is

subjected to a uniform heat flux of 2000 W/m^2 on its surface. The temperature of the tube surface at the exit is

(*a*) 48.7°C   (*b*) 49.4°C   (*c*) 51.1°C

(*d*) 53.7°C   (*e*) 55.2°C

(For water, use $k = 0.615$ W/m·K, Pr = 5.42, $\nu = 0.801 \times 10^{-6}$ m^2/s.)

8–155 Water enters a 5-mm-diameter and 13-m-long tube at 45°C with a velocity of 0.3 m/s. The tube is maintained at a constant temperature of 8°C. The exit temperature of the water is

(*a*) 4.4°C   (*b*) 8.9°C   (*c*) 10.6°C

(*d*) 12.0°C   (*e*) 14.1°C

(For water, use $k = 0.607$ W/m·K, Pr = 6.14, $\nu = 0.894 \times 10^{-6}$ m^2/s, $c_p = 4180$ J/kg·K, $\rho = 997$ kg/m^3.)

8–156 Water enters a 5-mm-diameter and 13-m-long tube at 45°C with a velocity of 0.3 m/s. The tube is maintained at a constant temperature of 5°C. The required length of the tube in order for the water to exit the tube at 25°C is

(*a*) 1.55 m   (*b*) 1.72 m   (*c*) 1.99 m

(*d*) 2.37 m   (*e*) 2.96 m

(For water, use $k = 0.623$ W/m·K, Pr = 4.83, $\nu = 0.724 \times 10^{-6}$ m^2/s, $c_p = 4178$ J/kg·K, $\rho = 994$ kg/m^3.)

8–157 Air enters a 7-cm-diameter and 4-m-long tube at 65°C and leaves at 15°C. The tube is observed to be nearly isothermal at 5°C. If the average convection heat transfer coefficient is 20 W/m^2·°C, the rate of heat transfer from the air is

(*a*) 491 W   (*b*) 616 W   (*c*) 810 W

(*d*) 907 W   (*e*) 975 W

8–158 Air ($c_p = 1000$ J/kg·K) enters a 16-cm-diameter and 19-m-long underwater duct at 50°C and 1 atm at an average velocity of 7 m/s and is cooled by the water outside. If the average heat transfer coefficient is 35 W/m^2·K and the tube temperature is nearly equal to the water temperature of 5°C, the exit temperature of the air is

(*a*) 6°C   (*b*) 10°C   (*c*) 18°C

(*d*) 25°C   (*e*) 36°C

8–159 Water enters a 2-cm-diameter and 3-m-long tube whose walls are maintained at 100°C with a bulk temperature of 25°C and a volume flow rate of 3 m^3/h. Neglecting the entrance effects and assuming turbulent flow, the Nusselt number can be determined from Nu = 0.023 Re$^{0.8}$ Pr$^{0.4}$. The convection heat transfer coefficient in this case is

(*a*) 4140 W/m^2·K   (*b*) 6160 W/m^2·K

(*c*) 8180 W/m^2·K   (*d*) 9410 W/m^2·K

(*e*) 2870 W/m^2·K

(For water, use $k = 0.610$ W/m·K, Pr = 6.0, $\mu = 9.0 \times 10^{-4}$ kg/m·s, $\rho = 1000$ kg/m^3.)

8–160 Air at 110°C enters an 18-cm-diameter and 9-m-long duct at a velocity of 4.5 m/s. The duct is observed to be nearly isothermal at 85°C. The rate of heat loss from the air in the duct is

(*a*) 760 W   (*b*) 890 W   (*c*) 1210 W

(*d*) 1370 W   (*e*) 1400 W

(For air, use $k = 0.03095$ W/m·K, Pr = 0.7111, $\nu = 2.306 \times 10^{-5}$ m^2/s, $c_p = 1009$ J/kg·K.)

8–161 Air at 10°C enters an 18-m-long rectangular duct of cross section 0.15 m × 0.20 m at a velocity of 4.5 m/s. The duct is subjected to uniform radiation heating throughout the surface at a rate of 400 W/m^2. The wall temperature at the exit of the duct is

(*a*) 58.8°C   (*b*) 61.9°C   (*c*) 64.6°C

(*d*) 69.1°C   (*e*) 75.5°C

(For air, use $k = 0.02551$ W/m·K, Pr = 0.7296, $\nu = 1.562 \times 10^{-5}$ m^2/s, $c_p = 1007$ J/kg·K, $\rho = 1.184$ kg/m^3.)

Design and Essay Problems

8–162 Electronic boxes such as computers are commonly cooled by a fan. Write an essay on forced air cooling of electronic boxes and on the selection of the fan for electronic devices.

8–163 Design a heat exchanger to pasteurize milk with steam in a dairy plant. Milk is to flow through a bank of 1.2-cm-internal-diameter tubes while steam condenses outside the tubes at 1 atm. Milk is to enter the tubes at 4°C, and it is to be heated to 72°C at a rate of 15 L/s. Making reasonable assumptions, you are to specify the tube length and the number of tubes and the pump for the heat exchanger.

8–164 A desktop computer is to be cooled by a fan. The electronic components of the computer consume 80 W of power under full-load conditions. The computer is to operate in environments at temperatures up to 50°C and at elevations up to 3000 m where the atmospheric pressure is 70.12 kPa. The exit temperature of air is not to exceed 60°C to meet the reliability requirements. Also, the average velocity of air is not to exceed 120 m/min at the exit of the computer case where the fan is installed; this is to keep the noise level down. Specify the flow rate of the fan that needs to be installed and the diameter of the casing of the fan.

NATURAL CONVECTION

I n Chaps. 7 and 8, we considered heat transfer by *forced convection,* where a fluid was *forced* to move over a surface or in a tube by external means such as a pump or a fan. In this chapter, we consider *natural convection,* alternatively called free convection, where any fluid motion occurs by natural means such as buoyancy. The fluid motion in forced convection is quite *noticeable,* since a fan or a pump can transfer enough momentum to the fluid to move it in a certain direction. The fluid motion in natural convection, however, is often not noticeable because of the low velocities involved.

The convection heat transfer coefficient is a strong function of *velocity:* the higher the velocity, the higher the convection heat transfer coefficient. The fluid velocities associated with natural convection are low, typically less than 1 m/s. Therefore, the heat transfer coefficients encountered in natural convection are usually much lower than those encountered in forced convection. Yet several types of heat transfer equipment are designed to operate under natural convection conditions instead of forced convection because natural convection does not require the use of a fluid mover.

We start this chapter with a discussion of the physical mechanism of *natural convection* and the *Grashof number.* We then present the correlations to evaluate heat transfer by natural convection for various geometries, including finned surfaces and enclosures. Finally, we discuss simultaneous forced and natural convection.

OBJECTIVES

When you finish studying this chapter, you should be able to:

- Understand the physical mechanism of natural convection,

- Derive the governing equations of natural convection, and obtain the dimensionless Grashof number by nondimensionalizing them,

- Evaluate the Nusselt number for natural convection associated with vertical, horizontal, and inclined plates as well as cylinders and spheres,

- Examine natural convection from finned surfaces, and determine the optimum fin spacing,

- Analyze natural convection inside enclosures such as double-pane windows, and

- Consider combined natural and forced convection, and assess the relative importance of each mode.
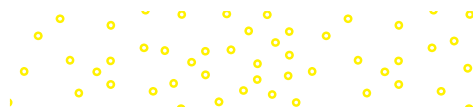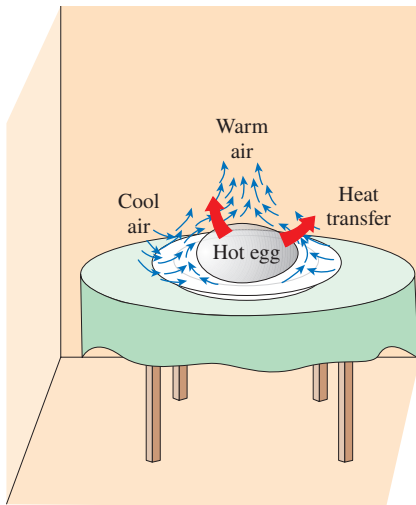
FIGURE 9–1

The cooling of a boiled egg in a cooler environment by natural convection.
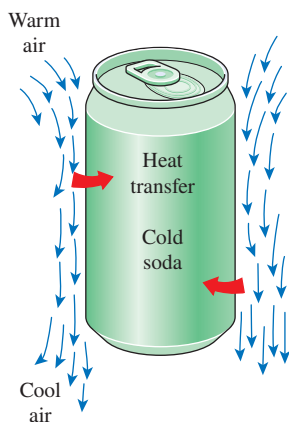
FIGURE 9–2

The warming up of a cold drink in a warmer environment by natural convection.

9–1 ▪ PHYSICAL MECHANISM OF NATURAL CONVECTION

Many familiar heat transfer applications involve natural convection as the primary mechanism of heat transfer. Some examples are cooling of electronic equipment such as power transistors, TVs, and DVDs; heat transfer from electric baseboard heaters or steam radiators; heat transfer from the refrigeration coils and power transmission lines; and heat transfer from the bodies of animals and human beings. Natural convection in gases is usually accompanied by radiation of comparable magnitude except for low-emissivity surfaces.

We know that a hot boiled egg (or a hot baked potato) on a plate eventually cools to the surrounding air temperature (Fig. 9–1). The egg is cooled by transferring heat by convection to the air and by radiation to the surrounding surfaces. Disregarding heat transfer by radiation, the physical mechanism of cooling a hot egg (or any hot object) in a cooler environment can be explained as follows:

As soon as the hot egg is exposed to cooler air, the temperature of the outer surface of the eggshell drops somewhat, and the temperature of the air adjacent to the shell rises as a result of heat conduction from the shell to the air. Consequently, the egg is surrounded by a thin layer of warmer air, and heat is then transferred from this warmer layer to the outer layers of air. The cooling process in this case is rather slow since the egg would always be blanketed by warm air, and it has no direct contact with the cooler air farther away. We may not notice any air motion in the vicinity of the egg, but careful measurements would indicate otherwise.

The temperature of the air adjacent to the egg is higher and thus its density is lower, since at constant pressure the density of a gas is inversely proportional to its temperature. Thus, we have a situation in which some low-density or "light" gas is surrounded by a high-density or "heavy" gas, and the natural laws dictate that the *light gas rise*. This is no different than the oil in a vinegar-and-oil salad dressing rising to the top (since $\rho_{\text{oil}} < \rho_{\text{vinegar}}$). This phenomenon is characterized incorrectly by the phrase "heat rises," which is understood to mean *heated air rises*. The space vacated by the warmer air in the vicinity of the egg is replaced by the cooler air nearby, and the presence of cooler air in the vicinity of the egg speeds up the cooling process. The rise of warmer air and the flow of cooler air into its place continues until the egg is cooled to the temperature of the surrounding air. The motion that results from the continual replacement of the heated air in the vicinity of the egg by the cooler air nearby is called a **natural convection current**, and the heat transfer that is enhanced as a result of this natural convection current is called **natural convection heat transfer**. Note that in the absence of natural convection currents, heat transfer from the egg to the air surrounding it would be by conduction only, and the rate of heat transfer from the egg would be much lower.

Natural convection is just as effective in the heating of cold surfaces in a warmer environment as it is in the cooling of hot surfaces in a cooler environment, as shown in Fig. 9–2. Note that the direction of fluid motion is reversed in this case.

In a gravitational field, there is a net force that pushes upward a light fluid placed in a heavier fluid. The upward force exerted by a fluid on a body completely or partially immersed in it is called the **buoyancy force**. The magnitude of the buoyancy force is equal to the weight of the *fluid displaced* by the body. That is,

$$F_{\text{buoyancy}} = \rho_{\text{fluid}}\, g V_{\text{body}} \tag{9–1}$$

where ρ_{fluid} is the average density of the *fluid* (not the body), *g* is the gravitational acceleration, and V_{body} is the volume of the portion of the body immersed in the fluid (for bodies completely immersed in the fluid, it is the total volume of the body). In the absence of other forces, the net vertical force acting on a body is the difference between the weight of the body and the buoyancy force. That is,

$$F_{\text{net}} = W - F_{\text{buoyancy}}$$
$$= \rho_{\text{body}}\, g V_{\text{body}} - \rho_{\text{fluid}}\, g V_{\text{body}}$$
$$= (\rho_{\text{body}} - \rho_{\text{fluid}})\, g V_{\text{body}} \qquad \textbf{(9–2)}$$

Note that this force is proportional to the difference in the densities of the fluid and the body immersed in it. Thus, a body immersed in a fluid will experience a "weight loss" in an amount equal to the weight of the fluid it displaces. This is known as *Archimedes' principle.*

To have a better understanding of the buoyancy effect, consider an egg dropped into water. If the average density of the egg is greater than the density of water (a sign of freshness), the egg settles at the bottom of the container. Otherwise, it rises to the top. When the density of the egg equals the density of water, the egg settles somewhere in the water while remaining completely immersed, acting like a "weightless object" in space. This occurs when the upward buoyancy force acting on the egg equals the weight of the egg, which acts downward.

The *buoyancy effect* has far-reaching implications in life. For one thing, without buoyancy, heat transfer between a hot (or cold) surface and the fluid surrounding it would be by *conduction* instead of by *natural convection.* The natural convection currents encountered in the oceans, lakes, and the atmosphere owe their existence to buoyancy. Also, light boats as well as heavy warships made of steel float on water because of buoyancy (Fig. 9–3). Ships are designed on the basis of the principle that the entire weight of a ship and its contents is equal to the weight of the water that the submerged volume of the ship can contain. The "chimney effect" that induces the upward flow of hot combustion gases through a chimney is also due to the buoyancy effect, and the upward force acting on the gases in the chimney is proportional to the difference between the densities of the hot gases in the chimney and the cooler air outside. Note that there is *no noticable gravity* in space, and thus there can be no natural convection heat transfer in a spacecraft, even if the spacecraft is filled with atmospheric air.

In heat transfer studies, the primary variable is *temperature,* and it is desirable to express the net buoyancy force (Eq. 9–2) in terms of temperature differences. But this requires expressing the density difference in terms of a temperature difference, which requires a knowledge of a property that represents the *variation of the density of a fluid with temperature at constant pressure. The property that provides that information is the* **volume expansion coefficient** β, defined as (Fig. 9–4)

$$\beta = \frac{1}{V}\left(\frac{\partial V}{\partial T}\right)_P = -\frac{1}{\rho}\left(\frac{\partial \rho}{\partial T}\right)_P \qquad (1/\text{K}) \qquad \textbf{(9–3)}$$

In natural convection studies, the condition of the fluid sufficiently far from the hot or cold surface is indicated by the subscript "infinity" to serve as a reminder that this is the value at a distance where the presence of the surface
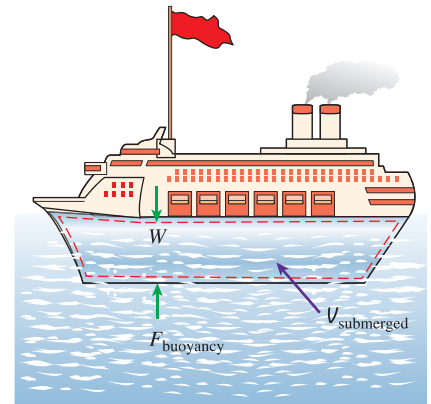
FIGURE 9–3
It is the buoyancy force that keeps the ships afloat in water ($W = F_{\text{buoyancy}}$ for floating objects).
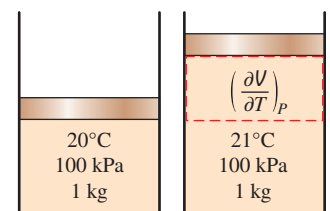
(*a*) A substance with a large β
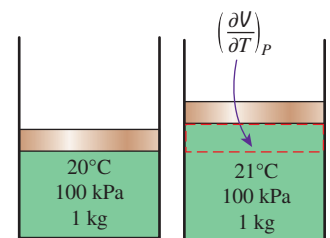
(*b*) A substance with a small β

FIGURE 9–4
The coefficient of volume expansion is a measure of the change in volume of a substance with temperature at constant pressure.

is not felt. In such cases, the volume expansion coefficient can be expressed approximately by replacing differential quantities with differences as

$$\beta \approx -\frac{1}{\rho}\frac{\Delta\rho}{\Delta T} = -\frac{1}{\rho}\frac{\rho_\infty - \rho}{T_\infty - T} \qquad \text{(at constant } P) \tag{9–4}$$

or

$$\rho_\infty - \rho = \rho\beta(T - T_\infty) \qquad \text{(at constant } P) \tag{9–5}$$

where ρ_∞ is the density and T_∞ is the temperature of the quiescent fluid away from the surface.

We can show easily that the volume expansion coefficient β of an *ideal gas* ($P = \rho RT$) at a temperature T is equivalent to the inverse of the temperature:

$$\beta_{\text{ideal gas}} = \frac{1}{T} \qquad (1/\text{K}) \tag{9–6}$$

where T is the *thermodynamic* temperature. Note that a large value of β for a fluid means a large change in density with temperature, and that the product $\beta\Delta T$ represents the fraction of volume change of a fluid that corresponds to a temperature change ΔT at constant pressure. Also note that the buoyancy force is proportional to the *density difference,* which is proportional to the *temperature difference* at constant pressure. Therefore, the larger the temperature difference between the fluid adjacent to a hot (or cold) surface and the fluid away from it, the *larger* the buoyancy force and the *stronger* the natural convection currents, and thus the *higher* the heat transfer rate.

The magnitude of the natural convection heat transfer between a surface and a fluid is directly related to the *flow rate* of the fluid. The higher the flow rate, the higher the heat transfer rate. In fact, it is the very high flow rates that increase the heat transfer coefficient by orders of magnitude when forced convection is used. In natural convection, no blowers are used, and therefore the flow rate cannot be controlled externally. The flow rate in this case is established by the dynamic balance of *buoyancy* and *friction.*

As we have discussed, the buoyancy force is caused by the density difference between the heated (or cooled) fluid adjacent to the surface and the fluid surrounding it, and it is proportional to this density difference and the volume occupied by the warmer fluid. It is also well known that whenever two bodies in contact (solid–solid, solid–fluid, or fluid–fluid) move relative to each other, a *friction force* develops at the contact surface in the direction opposite to that of the motion. This opposing force slows down the fluid and thus reduces the flow rate of the fluid. Under steady conditions, the airflow rate driven by buoyancy is established at the point where these two effects *balance* each other. The friction force increases as more and more solid surfaces are introduced, seriously disrupting the fluid flow and heat transfer. For that reason, heat sinks with closely spaced fins are not suitable for natural convection cooling.

Most heat transfer correlations in natural convection are based on experimental measurements. The instrument often used in natural convection experiments is the *Mach–Zehnder interferometer,* which gives a plot of isotherms in the fluid in the vicinity of a surface. The operation principle of interferometers is based on the fact that at low pressure, the lines of constant temperature for a gas correspond to the lines of constant density, and that the index of refraction of a gas is a function of its density. Therefore, the degree

(*a*) Laminar flow   (*b*) Turbulent flow

FIGURE 9–5

Isotherms in natural convection over a hot plate in air.

of refraction of light at some point in a gas is a measure of the temperature gradient at that point. An interferometer produces a map of interference fringes, which can be interpreted as lines of *constant temperature* as shown in Fig. 9–5. The smooth and parallel lines in (*a*) indicate that the flow is *laminar,* whereas the eddies and irregularities in (*b*) indicate that the flow is *turbulent.* Note that the lines are closest near the surface, indicating a *higher temperature gradient.*

9–2 ▪ EQUATION OF MOTION AND THE GRASHOF NUMBER

In this section we derive the equation of motion that governs the natural convection flow in laminar boundary layer. The conservation of mass and energy equations derived in Chap. 6 for forced convection are also applicable for natural convection, but the momentum equation needs to be modified to incorporate buoyancy.

Consider a vertical hot flat plate immersed in a quiescent fluid body. We assume the natural convection flow to be steady, laminar, and two-dimensional, and the fluid to be Newtonian with constant properties, including density, with one exception: the density difference $\rho - \rho_\infty$ is to be considered since it is this density difference between the inside and the outside of the boundary layer that gives rise to buoyancy force and sustains flow. (This is known as the *Boussinesq approximation.*) We take the upward direction along the plate to be *x,* and the direction normal to the surface to be *y,* as shown in Fig. 9–6. Therefore, gravity acts in the $-x$-direction. Noting that the flow is steady and two-dimensional, the *x*- and *y*-components of velocity within the boundary layer are $u = u(x, y)$ and $v = v(x, y)$, respectively.

The velocity and temperature profiles for natural convection over a vertical hot plate are also shown in Fig. 9–6. Note that as in forced convection, the thickness of the boundary layer increases in the flow direction. Unlike forced convection, however, the fluid velocity is *zero* at the outer edge of the velocity boundary layer as well as at the surface of the plate. This is expected since the fluid beyond the boundary layer is motionless. Thus, the fluid velocity increases with distance from the surface, reaches a maximum, and gradually decreases to zero at a distance sufficiently far from the surface. At the surface, the fluid temperature is equal to the plate temperature, and gradually decreases to the temperature of the surrounding fluid at a distance sufficiently far from the surface, as shown in the figure. In the case of *cold surfaces,* the shape of the velocity and temperature profiles remains the same, but their direction is reversed.

Consider a differential volume element of height *dx,* length *dy,* and unit depth in the *z*-direction (normal to the paper) for analysis. The forces acting on this volume element are shown in Fig. 9–7. Newton's second law of motion for this volume element can be expressed as

$$\delta m \cdot a_x = F_x \tag{9–7}$$

where $\delta m = \rho(dx \cdot dy \cdot 1)$ is the mass of the fluid within the volume element. The acceleration in the *x*-direction is obtained by taking the total differential of $u(x, y)$, which is $du = (\partial u/\partial x)dx + (\partial u/\partial y)dy$, and dividing it by *dt.* We get

$$a_x = \frac{du}{dt} = \frac{\partial u}{\partial x}\frac{dx}{dt} + \frac{\partial u}{\partial y}\frac{dy}{dt} = u\frac{\partial u}{\partial x} + v\frac{\partial u}{\partial y} \tag{9–8}$$
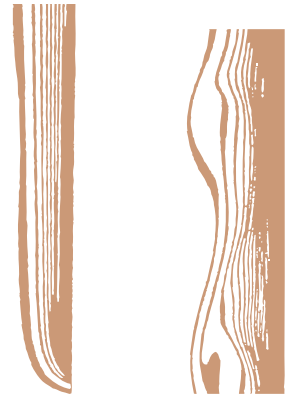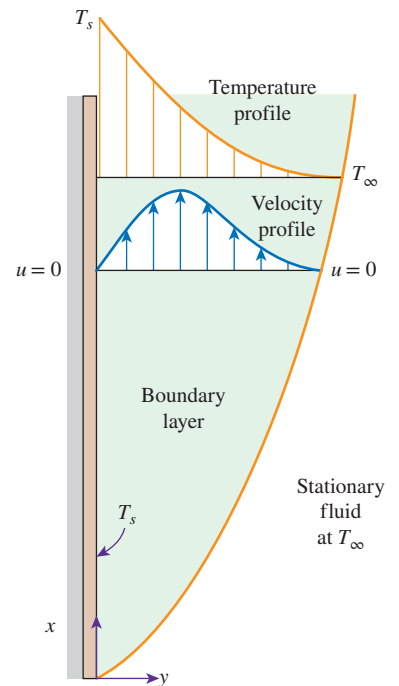
FIGURE 9–6

Typical velocity and temperature profiles for natural convection flow over a hot vertical plate at temperature T_s inserted in a fluid at temperature T_∞.
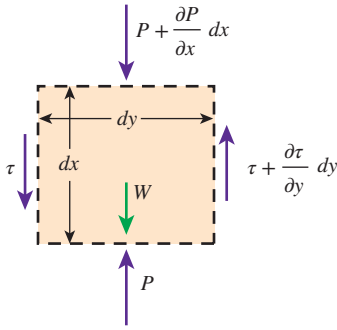
FIGURE 9–7
Forces acting on a differential volume element in the natural convection boundary layer over a vertical flat plate.

The forces acting on the differential volume element in the vertical direction are the pressure forces acting on the top and bottom surfaces, the shear stresses acting on the side surfaces (the normal stresses acting on the top and bottom surfaces are small and are disregarded), and the force of gravity acting on the entire volume element. Then the net surface force acting in the x-direction becomes

$$F_x = \left(\frac{\partial \tau}{\partial y}dy\right)(dx \cdot 1) - \left(\frac{\partial P}{\partial x}dx\right)(dy \cdot 1) - \rho g(dx \cdot dy \cdot 1)$$

$$= \left(\mu\frac{\partial^2 u}{\partial y^2} - \frac{\partial P}{\partial x} - \rho g\right)(dx \cdot dy \cdot 1) \tag{9–9}$$

since $\tau = \mu(\partial u/\partial y)$. Substituting Eqs. 9–8 and 9–9 into Eq. 9–7 and dividing by $\rho \cdot dx \cdot dy \cdot 1$ gives the *conservation of momentum* in the x-direction as

$$\rho\left(u\frac{\partial u}{\partial x} + v\frac{\partial u}{\partial y}\right) = \mu\frac{\partial^2 u}{\partial y^2} - \frac{\partial P}{\partial x} - \rho g \tag{9–10}$$

The x-momentum equation in the quiescent fluid outside the boundary layer can be obtained from the relation above as a special case by setting $u = 0$. It gives

$$\frac{\partial P_\infty}{\partial x} = -\rho_\infty g \tag{9–11}$$

which is simply the relation for the variation of hydrostatic pressure in a quiescent fluid with height, as expected. Also, noting that $v \ll u$ in the boundary layer and thus $\partial v/\partial x \approx \partial v/\partial y \approx 0$, and that there are no body forces (including gravity) in the y-direction, the force balance in that direction gives $\partial P/\partial y = 0$. That is, the variation of pressure in the direction normal to the surface is negligible, and for a given x the pressure in the boundary layer is equal to the pressure in the quiescent fluid. Therefore, $P = P(x) = P_\infty(x)$ and $\partial P/\partial x = \partial P_\infty/\partial x = -\rho_\infty g$. Substituting into Eq. 9–10,

$$\rho\left(u\frac{\partial u}{\partial x} + v\frac{\partial u}{\partial y}\right) = \mu\frac{\partial^2 u}{\partial y^2} + (\rho_\infty - \rho)g \tag{9–12}$$

The last term represents the net upward force per unit volume of the fluid (the difference between the buoyant force and the fluid weight). This is the force that initiates and sustains convection currents.

From Eq. 9–5, we have $\rho_\infty - \rho = \rho\beta(T - T_\infty)$. Substituting it into the last equation and dividing both sides by ρ gives the desired form of the x-momentum equation,

$$u\frac{\partial u}{\partial x} + v\frac{\partial u}{\partial y} = \nu\frac{\partial^2 u}{\partial y^2} + g\beta(T - T_\infty) \tag{9–13}$$

This is the equation that governs the fluid motion in the boundary layer due to the effect of buoyancy. Note that the momentum equation involves the temperature, and thus the momentum and energy equations must be solved simultaneously.

The complete set of conservation equations, continuity (Eq. 6–39), momentum (Eq. 9–13), and energy (Eq. 6–41) that govern natural convection flow over vertical isothermal plates are:

Continuity:
$$\frac{\partial u}{\partial x} + \frac{\partial v}{\partial y} = 0 \qquad \text{(Eq. 6–39)}$$

Momentum:
$$u\frac{\partial u}{\partial x} + v\frac{\partial u}{\partial y} = \nu\frac{\partial^2 u}{\partial y^2} + g\beta(T - T_\infty) \qquad \text{(Eq. 9–13)}$$

Energy:
$$u\frac{\partial T}{\partial x} + v\frac{\partial T}{\partial y} = \alpha\frac{\partial^2 T}{\partial y^2} \qquad \text{(Eq. 6–41)}$$

with the following boundary conditions (see Fig. 9–6):

At $y = 0$: $u(x, 0) = 0$, $v(x, 0) = 0$, $T(x, 0) = T_s$
At $y \to \infty$: $u(x, \infty) \to 0$, $T(x, \infty) \to T_\infty$
At $x = 0$: $u(0, y) = 0$, $T(0, y) = T_\infty$

The above set of three partial differential equations can be reduced to a set of two ordinary nonlinear differential equations by the introduction of a similarity variable. But the resulting equations must still be solved along with their transferred boundary conditions numerically (Ostrach, 1953). Interested readers are referred to advanced books on the topic for detailed discussions (e.g., Kays, Crawford, and Weigand, 2005).

The Grashof Number

The governing equations of natural convection and the boundary conditions can be nondimensionalized by dividing all dependent and independent variables by suitable constant quantities: all lengths by a characteristic length L_c, all velocities by an arbitrary reference velocity V (which, from the definition of Reynolds number, is taken to be $V = \text{Re}_L \nu/L_c$), and temperature by a suitable temperature difference (which is taken to be $T_s - T_\infty$) as

$$x^* = \frac{x}{L_c}, \quad y^* = \frac{y}{L_c}, \quad u^* = \frac{u}{V}, \quad v^* = \frac{v}{V}, \quad \text{and} \quad T^* = \frac{T - T_\infty}{T_s - T_\infty}$$

where asterisks are used to denote nondimensional variables. The nondimensionalized forms of continuity (Eq. 6–64) and energy (Eq. 6–66) equations derived in Chap. 6 are still applicable here. However, the nondimensionalized momentum equation due to buoyancy effects will be different. Nondimensionalizing the momentum equation (Eq. 9–13) with the preceding parameters and simplifying gives

$$u^*\frac{\partial u^*}{\partial x^*} + v^*\frac{\partial u^*}{\partial y^*} = \left[\frac{g\beta(T_s - T_\infty)L_c^3}{\nu^2}\right]\frac{T^*}{\text{Re}_L^2} + \frac{1}{\text{Re}_L}\frac{\partial^2 u^*}{\partial y^{*2}} \qquad \text{(9–14)}$$

The dimensionless parameter in the brackets represents the natural convection effects and is called the **Grashof number** Gr_L (Fig. 9–8),

$$\text{Gr}_L = \frac{g\beta(T_s - T_\infty)L_c^3}{\nu^2} \qquad \text{(9–15)}$$

FIGURE 9–8
Franz Grashof (1826–1893), a German engineer, was born at Düsseldorf, Germany. He was one of the founding leaders of the Society of German Engineers VDI (Verein Deutscher Ingenieure) and assumed an enormous load as author, editor, corrector, and dispatcher of publications, By 1863, Grashof's name was so esteemed that the Technical of Karlsruhe appointed him to be a successor Superintendent of the Engineering School. He also served as Professor of Applied Mechanics and Mechanical Engineering, where his renowned lectures included "Strength of Materials," "Hydraulics," "Theory of Heat," and "General Engineering." After Grashof's death, the Society of German Engineers honored his memory by instituting the Grashof Commemorative Medal as the highest distinction that the society could bestow for merit in the engineering skills. The dimensionless **Grashof number** representing the ratio of buoyant forces to viscous forces is named after him.

©Paul Fearn/Alamy
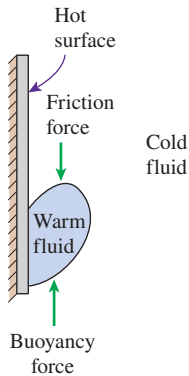
FIGURE 9–9
The Grashof number Gr is a measure of the relative magnitudes of the *buoyancy force* and the opposing *viscous force* acting on the fluid.
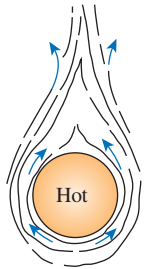
(*a*) Natural convection ($Gr_L / Re_L^2 \gg 1$)
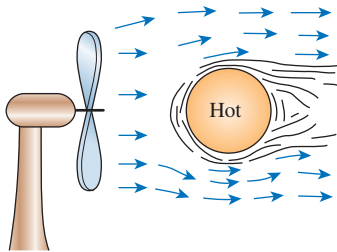
(*b*) Forced convection ($Gr_L / Re_L \ll 1$)
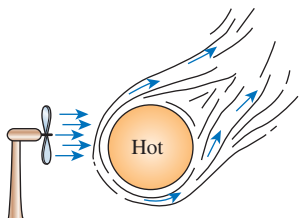
(*c*) Mixed convection ($Gr_L / Re_L^2 \approx 1$)

FIGURE 9–10
The relative importance of convection heat transfer regimes for flow near a hot sphere.

where

g = gravitational acceleration, m/s^2

β = coefficient of volume expansion, 1/K ($\beta = 1/T$ for ideal gases)

T_s = temperature of the surface, °C

T_∞ = temperature of the fluid sufficiently far from the surface, °C

L_c = characteristic length of the geometry, m

ν = kinematic viscosity of the fluid, m^2/s

We mentioned in the preceding chapters that the flow regime in forced convection is governed by the dimensionless *Reynolds number,* which represents the ratio of inertial forces to viscous forces acting on the fluid. The flow regime in natural convection is governed by the dimensionless *Grashof number,* which represents the ratio of the *buoyancy force* to the *viscous force* acting on the fluid (Fig. 9–9).

The role played by the Reynolds number in forced convection is played by the Grashof number in natural convection. As such, the Grashof number provides the main criterion in determining whether the fluid flow is laminar or turbulent in natural convection. For vertical plates, for example, the critical Grashof number is observed to be about 10^9. Therefore, the flow regime on a vertical plate becomes *turbulent* at Grashof numbers greater than 10^9.

When a surface is subjected to external flow, the problem involves both natural and forced convection. The relative importance of each mode of heat transfer is determined by the value of the coefficient Gr_L/Re_L^2, which appears in Eq. 9–14 (Fig. 9–10). If $Gr_L/Re_L^2 \gg 1$, inertia forces are negligible, and natural convection effects dominate. Conversely, if $Gr_L/Re_L^2 \ll 1$, buoyancy forces are negligible, and forced convection must be considered. For the case that $Gr_L/Re_L^2 \approx 1$, both inertia and buoyancy forces are equally present, and both natural and forced convection effects must be considered. In this case, the flow is referred to as **mixed convection**.

9–3 ■ NATURAL CONVECTION OVER SURFACES

Natural convection heat transfer on a surface depends on the geometry of the surface as well as its orientation. It also depends on the variation of temperature on the surface and the thermophysical properties of the fluid involved.

Although we understand the mechanism of natural convection well, the complexities of fluid motion make it very difficult to obtain simple analytical relations for heat transfer by solving the governing equations of motion and energy. Some analytical solutions exist for natural convection, but such solutions lack generality since they are obtained for simple geometries under some simplifying assumptions. Therefore, with the exception of some simple cases, heat transfer relations in natural convection are based on experimental studies. Of the many such correlations of varying complexity and claimed accuracy available in the literature for any given geometry, we present here the ones that are best known and most widely used.

The simple empirical correlations for the average *Nusselt number* Nu in natural convection are of the form (Fig. 9–11)

$$\text{Nu} = \frac{hL_c}{k} = C(\text{Gr}_L \, \text{Pr})^n = C \, \text{Ra}_L^n \tag{9–16}$$

where Ra_L is the **Rayleigh number** (Fig. 9–12), which is the product of the Grashof number, which describes the relationship between buoyancy and viscosity within the fluid, and the Prandtl number, which describes the relationship between momentum diffusivity and thermal diffusivity. Hence the Rayleigh number itself may also be viewed as the ratio of buoyancy forces and (the products of) thermal and momentum diffusitivities.

$$\text{Ra}_L = \text{Gr}_L \, \text{Pr} = \frac{g\beta(T_s - T_\infty)L_c^3}{\nu^2} \, \text{Pr} = \frac{g\beta(T_s - T_\infty)L_c^3}{\nu\alpha} \tag{9–17}$$

The values of the constants C and n depend on the *geometry* of the surface and the *flow regime,* which is characterized by the range of the Rayleigh number. The value of n is usually $\frac{1}{4}$ for laminar flow and $\frac{1}{3}$ for turbulent flow. The value of the constant C is normally less than 1.

Simple relations for the average Nusselt number for various geometries are given in Table 9–1, together with sketches of the geometries. Also given in this table are the characteristic lengths of the geometries and the ranges of Rayleigh number in which the relation is applicable. All fluid properties are to be evaluated at the film temperature $T_f = \frac{1}{2}(T_s + T_\infty)$.

When the average Nusselt number and thus the average convection coefficient is known, the rate of heat transfer by natural convection from a solid surface at a uniform temperature T_s to the surrounding fluid is expressed by Newton's law of cooling as

$$\dot{Q}_{\text{conv}} = hA_s(T_s - T_\infty) \qquad \text{(W)} \tag{9–18}$$

where A_s is the heat transfer surface area and h is the average heat transfer coefficient on the surface.

Vertical Plates (T_s = constant)

For a vertical flat plate, the characteristic length is the plate height L. In Table 9–1 we give three relations for the average Nusselt number for an isothermal vertical plate. The first two relations are very simple. Despite its complexity, we suggest using the third one (Eq. 9–21) recommended by Churchill and Chu (1975b) since it is applicable over the entire range of Rayleigh number. This relation is most accurate in the range of $10^{-1} < \text{Ra}_L < 10^9$.

Vertical Plates ($\dot{q}_s$ = constant)

In the case of constant surface heat flux, the rate of heat transfer is known (it is simply $\dot{Q} = \dot{q}_s A_s$), but the surface temperature T_s is not. In fact, T_s increases with height along the plate. It turns out that the Nusselt number
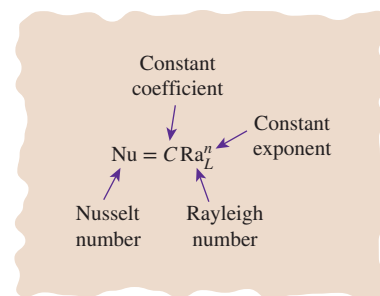
FIGURE 9–11
Natural convection heat transfer correlations are usually expressed in terms of the Rayleigh number raised to a constant *n* multiplied by another constant *C,* both of which are determined experimentally.
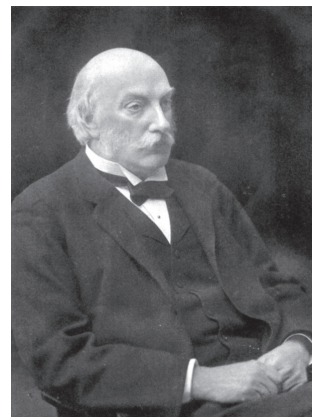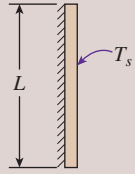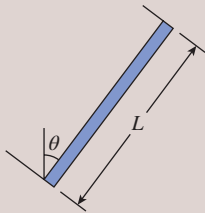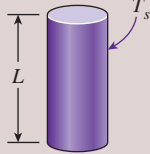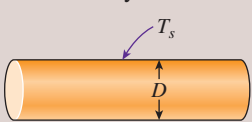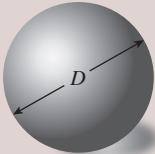
FIGURE 9–12
Lord Rayleigh (1842–1919), born John William Strutt, an English physicist, was born at Langford Grove, Maldon, Essex. He, with William Ramsay, discovered the element argon, an achievement for which he received the Nobel Prize for Physics in 1904. Rayleigh also discovered the phenomenon now called Rayleigh scattering, explaining why the sky is blue, and predicted the existence of the surface waves known as Rayleigh waves. The **Rayleigh number** is named after him.

TABLE 9–1

Empirical correlations for the average Nusselt number for natural convection over surfaces

Geometry	Characteristic Length L_c	Range of Ra	Nu	
Vertical plate	L	10^4–10^9 10^9–10^{13} Entire range	$\mathrm{Nu} = 0.59\,\mathrm{Ra}_L^{1/4}$ $\mathrm{Nu} = 0.1\,\mathrm{Ra}_L^{1/3}$ $\mathrm{Nu} = \left\{ 0.825 + \dfrac{0.387\,\mathrm{Ra}_L^{1/6}}{[1 + (0.492/\mathrm{Pr})^{9/16}]^{8/27}} \right\}^2$ (complex but more accurate)	(9–19) (9–20) (9–21)
Inclined plate	L		Use vertical plate equations for the upper surface of a cold plate and the lower surface of a hot plate Replace g with $g\cos\theta$ for $0 < \theta < 60°$	
Horizontal plate (surface area A and perimeter p) (*a*) Upper surface of a hot plate (or lower surface of a cold plate) (*b*) Lower surface of a hot plate (or upper surface of a cold plate)	A_s/p	10^4–10^7 10^7–10^{11} 10^5–10^{11}	(a) $\mathrm{Nu} = 0.54\,\mathrm{Ra}_L^{1/4}$ (a) $\mathrm{Nu} = 0.15\,\mathrm{Ra}_L^{1/3}$ (b) $\mathrm{Nu} = 0.27\,\mathrm{Ra}_L^{1/4}$	(9–22) (9–23) (9–24)
Vertical cylinder	L		A vertical cylinder can be treated as a vertical plate when $D \ge \dfrac{35L}{\mathrm{Gr}_L^{1/4}}$	
Horizontal cylinder	D	$\mathrm{Ra}_D \le 10^{12}$	$\mathrm{Nu} = \left\{ 0.6 + \dfrac{0.387\,\mathrm{Ra}_D^{1/6}}{[1 + (0.559/\mathrm{Pr})^{9/16}]^{8/27}} \right\}^2$	(9–25)
Sphere	D	$\mathrm{Ra}_D \le 10^{11}$ $(\mathrm{Pr} \ge 0.7)$	$\mathrm{Nu} = 2 + \dfrac{0.589\,\mathrm{Ra}_D^{1/4}}{[1 + (0.469/\mathrm{Pr})^{9/16}]^{4/9}}$	(9–26)

relations for the constant surface temperature and constant surface heat flux cases are nearly identical (Churchill and Chu, 1975b). Therefore, the relations for isothermal plates can also be used for plates subjected to constant heat flux, provided that the plate midpoint temperature $T_{L/2}$ is used for T_s in the evaluation of the film temperature, the Rayleigh number, and the Nusselt number. Noting that $h = \dot{q}_s/(T_{L/2} - T_\infty)$, the average Nusselt number in this case can be expressed as

$$\text{Nu} = \frac{hL}{k} = \frac{\dot{q}_s L}{k(T_{L/2} - T_\infty)} \qquad \text{(9–27)}$$

The midpoint temperature $T_{L/2}$ is determined by iteration so that the Nusselt numbers determined from Eqs. 9–21 and 9–27 match.

Vertical Cylinders

An outer surface of a vertical cylinder can be treated as a vertical plate when the diameter of the cylinder is large enough that the curvature effects are negligible. This condition is satisfied if

$$D \geq \frac{35L}{\text{Gr}_L^{1/4}} \qquad \text{(9–28)}$$

When this criterion is met, the relations for vertical plates can also be used for vertical cylinders. Nusselt number relations for slender cylinders that do not meet this criterion are available in the literature (e.g., Cebeci, 1974).

Inclined Plates

Consider an inclined hot plate that makes an angle θ from the vertical, as shown in Fig. 9–13, in a cooler environment. The net force $F = g(\rho_\infty - \rho)$ (the difference between the buoyancy and gravity) acting on a unit volume of the fluid in the boundary layer is always in the vertical direction. In the case of an inclined plate, this force can be resolved into two components: $F_x = F \cos \theta$ parallel to the plate that drives the flow along the plate, and $F_y = F \sin \theta$ normal to the plate. Noting that the force that drives the motion is reduced, we expect the convection currents to be weaker and the rate of heat transfer to be lower relative to the vertical plate case.

The experiments confirm what we suspect for the lower surface of a hot plate, but the opposite is observed on the upper surface. The reason for this curious behavior for the upper surface is that the force component F_y initiates upward motion in addition to the parallel motion along the plate, and thus the boundary layer breaks up and forms plumes, as shown in the figure. As a result, the thickness of the boundary layer and thus the resistance to heat transfer decreases, and the rate of heat transfer increases relative to the vertical orientation.

In the case of a cold plate in a warmer environment, the opposite occurs as expected: The boundary layer on the upper surface remains intact with weaker
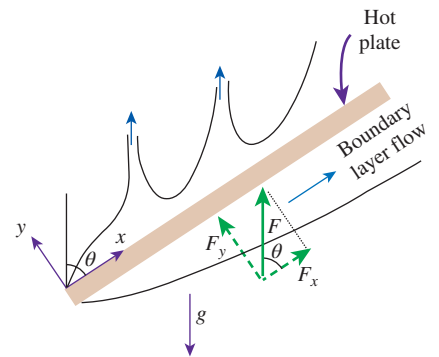
FIGURE 9–13
Natural convection flows on the upper and lower surfaces of an inclined hot plate.
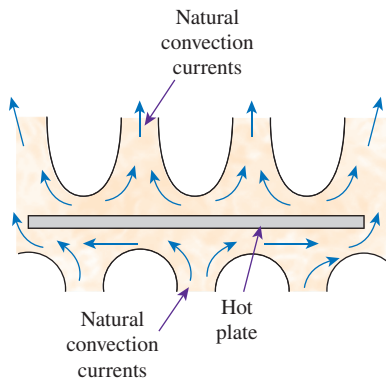
boundary layer flow and thus lower rate of heat transfer, and the boundary layer on the lower surface breaks apart (the colder fluid falls down) and thus enhances heat transfer.

When the boundary layer remains intact (the lower surface of a hot plate or the upper surface of a cold plate), the Nusselt number can be determined from the vertical plate relations provided that g in the Rayleigh number relation is replaced by $g\cos\theta$ for $\theta < 60°$. Nusselt number relations for the other two surfaces (the upper surface of a hot plate or the lower surface of a cold plate) are available in the literature (e.g., Fujii and Imura, 1972).

Horizontal Plates

The rate of heat transfer to or from a horizontal surface depends on whether the surface is facing upward or downward. For a hot surface in a cooler environment, the net force acts upward, forcing the heated fluid to rise. If the hot surface is facing upward, the heated fluid rises freely, inducing strong natural convection currents and thus effective heat transfer, as shown in Fig. 9–14. But if the hot surface is facing downward, the plate blocks the heated fluid that tends to rise (except near the edges), impeding heat transfer. The opposite is true for a cold plate in a warmer environment since the net force (weight minus buoyancy force) in this case acts downward, and the cooled fluid near the plate tends to descend.

The average Nusselt number for horizontal surfaces can be determined from the simple power-law relations given in Table 9–1. Depending on the Ra range, use either Eq. 9–22 or Eq. 9–23 for a horizontal plate with the hot surface facing up or Eq. 9–24 for a horizontal plate with the hot surface facing down. The characteristic length to be used in these equations for horizontal surfaces is calculated from

$$L_c = \frac{A_s}{p} \tag{9–29}$$

where A_s is the surface area and p is the perimeter. Note that $L_c = a/4$ for a horizontal square surface of length a and $D/4$ for a horizontal circular surface of diameter D.

Horizontal Cylinders and Spheres

The boundary layer over a hot horizontal cylinder starts to develop at the bottom, increasing in thickness along the circumference and forming a rising plume at the top, as shown in Fig. 9–15. Therefore, the local Nusselt number is highest at the bottom and lowest at the top of the cylinder when the boundary layer flow remains laminar. The opposite is true in the case of a cold horizontal cylinder in a warmer medium; the boundary layer in this case starts to develop at the top of the cylinder and ends with a descending plume at the bottom.

The average Nusselt number over the entire surface can be determined from Eq. 9–25 (Churchill and Chu, 1975a) for an isothermal horizontal cylinder and from Eq. 9–26 for an isothermal sphere (Churchill, 1983), both given in Table 9–1.

FIGURE 9–14
Natural convection flows on the upper and lower surfaces of a horizontal hot plate.

FIGURE 9–15
Natural convection flow over a horizontal hot cylinder.

FIGURE 9–16
Schematic for Example 9–1.

EXAMPLE 9–1   Heat Loss from Hot-Water Pipes

A 6-m-long section of an 8-cm-diameter horizontal hot-water pipe shown in Fig. 9–16 passes through a large room whose temperature is 20°C. If the outer surface temperature of the pipe is 70°C, determine the rate of heat loss from the pipe by natural convection.

SOLUTION   A horizontal hot-water pipe passes through a large room. The rate of heat loss from the pipe by natural convection is to be determined.

Assumptions   **1** Steady operating conditions exist. **2** Air is an ideal gas. **3** The local atmospheric pressure is 1 atm.

Properties   The properties of air at the film temperature of $T_f = (T_s + T_\infty)/2 = (70 + 20)/2 = 45°C$ and 1 atm are (Table A–15)

$$k = 0.02699 \text{ W/m·K} \qquad \text{Pr} = 0.7241$$

$$\nu = 1.750 \times 10^{-5} \text{ m}^2/\text{s} \qquad \beta = \frac{1}{T_f} = \frac{1}{318 \text{ K}}$$

Analysis   The characteristic length in this case is the outer diameter of the pipe, $L_c = D = 0.08$ m. Then the Rayleigh number becomes

$$\text{Ra}_D = \frac{g\beta(T_s - T_\infty)D^3}{\nu^2} \text{Pr}$$

$$= \frac{(9.81 \text{ m/s}^2)[1/(318 \text{ K})](70 - 20 \text{ K})(0.08 \text{ m})^3}{(1.750 \times 10^{-5} \text{ m}^2/\text{s})^2}(0.7241) = 1.867 \times 10^6$$

The natural convection Nusselt number in this case can be determined from Eq. 9–25 to be

$$\text{Nu} = \left\{ 0.6 + \frac{0.387 \text{ Ra}_D^{1/6}}{[1 + (0.559/\text{Pr})^{9/16}]^{8/27}} \right\}^2 = \left\{ 0.6 + \frac{0.387(1.867 \times 10^6)^{1/6}}{[1 + (0.559/0.7241)^{9/16}]^{8/27}} \right\}^2$$

$$= 17.39$$

Then,

$$h = \frac{k}{D}\text{Nu} = \frac{0.02699 \text{ W/m·K}}{0.08 \text{ m}}(17.39) = 5.867 \text{ W/m·K}$$

$$A_s = \pi DL = \pi(0.08 \text{ m})(6 \text{ m}) = 1.508 \text{ m}^2$$

and

$$\dot{Q} = hA_s(T_s - T_\infty) = (5.867 \text{ W/m}^2\text{·K})(1.508 \text{ m}^2)(70 - 20)°C = \mathbf{442 \text{ W}}$$

Therefore, the pipe loses heat to the air in the room at a rate of 442 W by natural convection.

Discussion   The pipe loses heat to the surroundings by radiation as well as by natural convection. Assuming the outer surface of the pipe to be black (emissivity $\varepsilon = 1$) and the inner surfaces of the walls of the room to be at room temperature, the radiation heat transfer is determined to be (Fig. 9–17)

$$\dot{Q}_{\text{rad}} = \varepsilon A_s \sigma(T_s^4 - T_{\text{surr}}^4)$$

$$= (1)(1.508 \text{ m}^2)(5.67 \times 10^{-8} \text{ W/m}^2\text{·K}^4)[(70 + 273 \text{ K})^4 - (20 + 273 \text{ K})^4]$$

$$= 553 \text{ W}$$

FIGURE 9–17
Radiation heat transfer is usually comparable to natural convection in magnitude and should be considered in heat transfer analysis.

90°C $T_\infty = 30°C$

$L = 0.6$ m

(*a*) Vertical

(*b*) Hot surface facing up

(*c*) Hot surface facing down
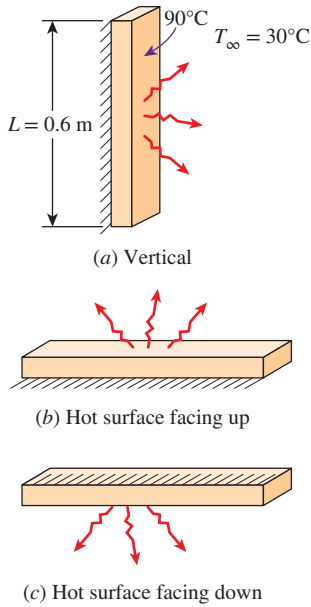
FIGURE 9–18
Schematic for Example 9–2.

which is larger than natural convection. The emissivity of a real surface is less than 1, and thus the radiation heat transfer for a real surface will be less. But radiation will still be significant for most systems cooled by natural convection. Therefore, a radiation analysis should normally accompany a natural convection analysis unless the emissivity of the surface is low.

EXAMPLE 9–2   Cooling of a Plate in Different Orientations

Consider a 0.6-m × 0.6-m thin square plate in a room at 30°C. One side of the plate is maintained at a temperature of 90°C, while the other side is insulated, as shown in Fig. 9–18. Determine the rate of heat transfer from the plate by natural convection if the plate is (*a*) vertical, (*b*) horizontal with hot surface facing up, and (*c*) horizontal with hot surface facing down.

SOLUTION   A hot plate with an insulated back is considered. The rate of heat loss by natural convection is to be determined for different orientations.
Assumptions   **1** Steady operating conditions exist. **2** Air is an ideal gas. **3** The local atmospheric pressure is 1 atm.
Properties   The properties of air at the film temperature of $T_f = (T_s + T_\infty)/2 = (90 + 30)/2 = 60°C$ and 1 atm are (Table A–15)

$$k = 0.02808 \text{ W/m·K} \qquad Pr = 0.7202$$

$$\nu = 1.896 \times 10^{-5} \text{ m}^2/\text{s} \qquad \beta = \frac{1}{T_f} = \frac{1}{333 \text{ K}}$$

Analysis   (*a*) *Vertical.* The characteristic length in this case is the height of the plate, which is $L = 0.6$ m. The Rayleigh number is

$$\text{Ra}_L = \frac{g\beta(T_s - T_\infty)L^3}{\nu^2} Pr$$

$$= \frac{(9.81 \text{ m/s}^2)[1/(333 \text{ K})](90 - 30 \text{ K})(0.6 \text{ m})^3}{(1.896 \times 10^{-5} \text{ m}^2/\text{s})^2}(0.7202) = 7.649 \times 10^8$$

Then the natural convection Nusselt number can be determined from Eq. 9–21 to be

$$\text{Nu} = \left\{ 0.825 + \frac{0.387 \text{ Ra}_L^{1/6}}{[1 + (0.492/Pr)^{9/16}]^{8/27}} \right\}^2$$

$$= \left\{ 0.825 + \frac{0.387(7.649 \times 10^8)^{1/6}}{[1 + (0.492/0.7202)^{9/16}]^{8/27}} \right\}^2 = 113.3$$

Note that the simpler relation Eq. 9–19 would give $\text{Nu} = 0.59 \text{ Ra}_L^{1/4} = 98.12$, which is 13 percent lower. Then,

$$h = \frac{k}{L}\text{Nu} = \frac{0.02808 \text{ W/m·K}}{0.6 \text{ m}}(113.3) = 5.302 \text{ W/m}^2\text{·K}$$

$$A_s = L^2 = (0.6 \text{ m})^2 = 0.36 \text{ m}^2$$

and

$$\dot{Q} = hA_s(T_s - T_\infty) = (5.302 \text{ W/m}^2\text{·K})(0.36 \text{ m}^2)(90 - 30)°C = \textbf{115 W}$$

(*b*) *Horizontal with hot surface facing up.* The characteristic length and the Rayleigh number in this case are

$$L_c = \frac{A_s}{p} = \frac{L^2}{4L} = \frac{L}{4} = \frac{0.6 \text{ m}}{4} = 0.15 \text{ m}$$

$$\text{Ra}_L = \frac{g\beta(T_s - T_\infty)L_c^3}{\nu^2} \text{Pr}$$

$$= \frac{(9.81 \text{ m/s}^2)[1/(333 \text{ K})](90 - 30 \text{ K})(0.15 \text{ m})^3}{(1.896 \times 10^{-5} \text{ m}^2/\text{s})^2}(0.7202) = 1.195 \times 10^7$$

The natural convection Nusselt number can be determined from Eq. 9–22 to be

$$\text{Nu} = 0.54 \text{ Ra}_L^{1/4} = 0.54(1.195 \times 10^7)^{1/4} = 31.75$$

Then,

$$h = \frac{k}{L_c}\text{Nu} = \frac{0.02808 \text{ W/m·K}}{0.15 \text{ m}}(31.75) = 5.944 \text{ W/m}^2\text{·K}$$

and

$$\dot{Q} = hA_s(T_s - T_\infty) = (5.944 \text{ W/m}^2\text{·K})(0.36 \text{ m}^2)(90 - 30)°\text{C} = \textbf{128 W}$$

Note that for the calculated Ra value in part (*b*), we could have used Eq. 9–23 given in Table 9–1. The results in this case would have been overpredicted by 8 percent, which is well within the accuracy of the relations given in the table.

(*c*) *Horizontal with hot surface facing down.* The characteristic length and the Rayleigh number in this case are the same as those determined in (*b*). But the natural convection Nusselt number is to be determined from Eq. 9–24,

$$\text{Nu} = 0.27 \text{ Ra}_L^{1/4} = 0.27(1.195 \times 10^7)^{1/4} = 15.87$$

Then,

$$h = \frac{k}{L_c}\text{Nu} = \frac{0.02808 \text{ W/m·K}}{0.15 \text{ m}}(15.87) = 2.971 \text{ W/m}^2\text{·K}$$

and

$$\dot{Q} = hA_s(T_s - T_\infty) = (2.971 \text{ W/m}^2\text{·K})(0.36 \text{ m}^2)(90 - 30)°\text{C} = \textbf{64.2 W}$$

Note that the natural convection heat transfer is the lowest in the case of the hot surface facing down. This is not surprising, since the hot air is "trapped" under the plate in this case and cannot get away from the plate easily. As a result, the cooler air in the vicinity of the plate will have difficulty reaching the plate, which results in a reduced rate of heat transfer.

Discussion The plate will lose heat to the surroundings by radiation as well as by natural convection. Assuming the surface of the plate to be black (emissivity $\varepsilon = 1$) and the inner surfaces of the walls of the room to be at room temperature, the radiation heat transfer in this case is determined to be

$$\dot{Q}_{\text{rad}} = \varepsilon A_s \sigma(T_s^4 - T_{\text{surr}}^4)$$
$$= (1)(0.36 \text{ m}^2)(5.67 \times 10^{-8} \text{ W/m}^2\text{·K}^4)[(90 + 273 \text{ K})^4 - (30 + 273 \text{ K})^4]$$
$$= 182 \text{ W}$$

which is larger than that for natural convection heat transfer for each case. Therefore, radiation can be significant and needs to be considered in surfaces cooled by natural convection.
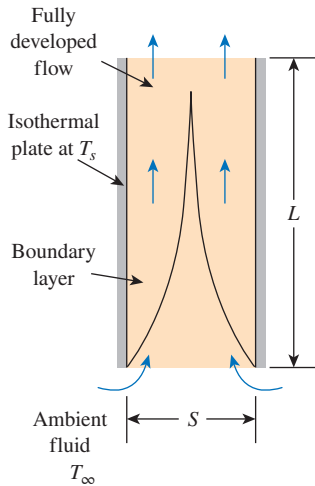
FIGURE 9–19
Natural convection flow through a channel between two isothermal vertical plates.

9–4 ▪ NATURAL CONVECTION FROM FINNED SURFACES AND PCBs

Natural convection flow through a channel formed by two parallel plates as shown in Fig. 9–19 is commonly encountered in practice. When the plates are hot ($T_s < T_\infty$), the ambient fluid at T_∞ enters the channel from the lower end, rises as it is heated under the effect of buoyancy, and the heated fluid leaves the channel from the upper end. The plates could be the fins of a finned heat sink or the PCBs (printed circuit boards) of an electronic device. The plates can be approximated as being isothermal (T_s = constant) in the first case and isoflux ($\dot{q}_s$ = constant) in the second case.

Boundary layers start to develop at the lower ends of opposing surfaces and eventually merge at the midplane if the plates are vertical and sufficiently long. In this case, we will have fully developed channel flow after the merger of the boundary layers, and the natural convection flow is analyzed as channel flow. But when the plates are short or the spacing is large, the boundary layers of opposing surfaces never reach each other, and the natural convection flow on a surface is not affected by the presence of the opposing surface. In that case, the problem should be analyzed as natural convection from two independent plates in a quiescent medium, using the relations given for surfaces, rather than natural convection flow through a channel.

Natural Convection Cooling of Finned Surfaces (T_s = constant)

Finned surfaces of various shapes, called *heat sinks,* are often used in the cooling of electronic devices. Energy dissipated by these devices is transferred to the heat sinks by conduction and from the heat sinks to the ambient air by natural or forced convection, depending on the power dissipation requirements. Natural convection is the preferred mode of heat transfer since it involves no moving parts, like the electronic components themselves. However, in the natural convection mode, the components are more likely to run at a higher temperature and thus undermine reliability. A properly selected heat sink may considerably lower the operation temperature of the components and thus reduce the risk of failure.

Natural convection from vertical finned surfaces of rectangular shape has been the subject of many studies, mostly experimental. Bar-Cohen and Rohsenow (1984) have compiled the available data under various boundary conditions and developed correlations for the Nusselt number and optimum spacing. The characteristic length for vertical parallel plates used as fins is usually taken to be the spacing between adjacent fins $S,$ although the fin height L could also be used. The Rayleigh number is expressed as

$$\text{Ra}_s = \frac{g\beta(T_s - T_\infty)S^3}{\nu^2}\text{Pr} \quad \text{and} \quad \text{Ra}_L = \frac{g\beta(T_s - T_\infty)L^3}{\nu^2}\text{Pr} = \text{Ra}_s\frac{L^3}{S^3} \quad \textbf{(9–30)}$$

The recommended relation for the average Nusselt number for vertical isothermal parallel plates is

T_s = constant: $\quad \text{Nu} = \dfrac{hS}{k} = \left[\dfrac{576}{(\text{Ra}_s S/L)^2} + \dfrac{2.873}{(\text{Ra}_s S/L)^{0.5}}\right]^{-0.5} \quad \textbf{(9–31)}$

A question that often arises in the selection of a heat sink is whether to select one with *closely packed* fins or *widely spaced* fins for a given base area (Fig. 9–20). A heat sink with closely packed fins will have greater surface area for heat transfer but a smaller heat transfer coefficient because of the extra resistance the additional fins introduce to fluid flow through the interfin passages. A heat sink with widely spaced fins, on the other hand, will have a higher heat transfer coefficient but a smaller surface area. Therefore, there must be an *optimum spacing* that maximizes the natural convection heat transfer from the heat sink for a given base area *WL,* where *W* and *L* are the width and height of the base of the heat sink, respectively, as shown in Fig. 9–21. When the fins are essentially isothermal and the fin thickness *t* is small relative to the fin spacing *S,* the optimum fin spacing for a vertical heat sink is determined by Bar-Cohen and Rohsenow to be

$$T_s = \text{constant:} \qquad S_{\text{opt}} = 2.714 \left(\frac{S^3 L}{\text{Ra}_s}\right)^{0.25} = 2.714 \frac{L}{\text{Ra}_L^{0.25}} \tag{9-32}$$

It can be shown by combining the three preceding equations that when $S = S_{\text{opt}}$, the Nusselt number is a constant and its value is 1.307,

$$S = S_{\text{opt}}: \qquad \text{Nu} = \frac{hS_{\text{opt}}}{k} = 1.307 \tag{9-33}$$

The rate of heat transfer by natural convection from the fins can be determined from

$$\dot{Q} = h(2nLH)(T_s - T_\infty) \tag{9-34}$$

where $n = W/(S + t) \approx W/S$ is the number of fins on the heat sink and T_s is the surface temperature of the fins. All fluid properties are to be evaluated at the average temperature $T_{\text{avg}} = (T_s + T_\infty)/2$.

Natural Convection Cooling of Vertical PCBs ($\dot{q}_s$ = constant)

Arrays of printed circuit boards used in electronic systems can often be modeled as parallel plates subjected to constant heat flux $\dot{q}_s$ (Fig. 9–22). The plate temperature in this case increases with height, reaching a maximum at the upper edge of the board. The modified Rayleigh number for constant heat flux on both plates is expressed as

$$\text{Ra}_s^* = \frac{g\beta\dot{q}_s S^4}{k\nu^2} \text{Pr} \tag{9-35}$$

The Nusselt number at the upper edge of the plate where maximum temperature occurs is determined from (Bar-Cohen and Rohsenow, 1984)

$$\text{Nu}_L = \frac{h_L S}{k} = \left[\frac{48}{\text{Ra}_s^* S/L} + \frac{2.51}{(\text{Ra}_s^* S/L)^{0.4}}\right]^{-0.5} \tag{9-36}$$

(*a*)

(*b*)
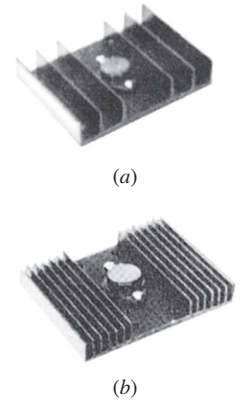
FIGURE 9–20
Heat sinks with (*a*) widely spaced and (*b*) closely packed fins.
©Yunus A. Cengel
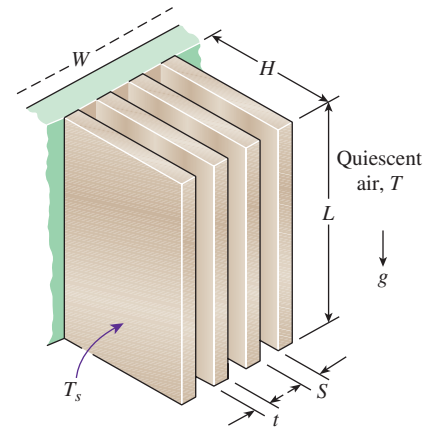
FIGURE 9–21
Various dimensions of a finned surface oriented vertically.
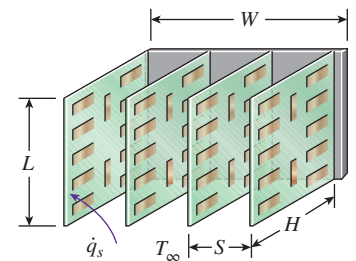
FIGURE 9–22
Arrays of vertical printed circuit boards (PCBs) cooled by natural convection.

The optimum fin spacing for the case of constant heat flux on both plates is given as

$$\dot{q}_s = \text{constant:} \qquad S_{\text{opt}} = 2.12 \left(\frac{S^4 L}{\text{Ra}_s^*} \right)^{0.2} \qquad \text{(9–37)}$$

The total rate of heat transfer from the plates is

$$\dot{Q} = \dot{q}_s A_s = \dot{q}_s (2nLH) \qquad \text{(9–38)}$$

where $n = W/(S + t) \approx W/S$ is the number of plates. The critical surface temperature T_L occurs at the upper edge of the plates, and it can be determined from

$$\dot{q}_s = h_L(T_L - T_\infty) \qquad \text{(9–39)}$$

All fluid properties are to be evaluated at the average temperature $T_{\text{avg}} = (T_L + T_\infty)/2$.

Mass Flow Rate Through the Space Between Plates

As we mentioned earlier, the magnitude of the natural convection heat transfer is directly related to the mass flow rate of the fluid, which is established by the dynamic balance of two opposing effects: *buoyancy* and *friction.*

The fins of a heat sink introduce both effects: *inducing extra buoyancy* as a result of the elevated temperature of the fin surfaces and *slowing down the fluid* by acting as an added obstacle on the flow path. As a result, increasing the number of fins on a heat sink can either enhance or reduce natural convection, depending on which effect is dominant. The buoyancy-driven fluid flow rate is established at the point where these two effects balance each other. The friction force increases as more and more solid surfaces are introduced, seriously disrupting fluid flow and heat transfer. Under some conditions, the increase in friction may more than offset the increase in buoyancy. This in turn will tend to reduce the flow rate and thus the heat transfer. For that reason, heat sinks with closely spaced fins are not suitable for natural convection cooling.

When the heat sink involves closely spaced fins, the narrow channels formed tend to block or "suffocate" the fluid, especially when the heat sink is long. As a result, the blocking action produced overwhelms the extra buoyancy and downgrades the heat transfer characteristics of the heat sink. Then, at a fixed power setting, the heat sink runs at a higher temperature relative to the no-shroud case. When the heat sink involves widely spaced fins, the shroud does not introduce a significant increase in resistance to flow, and the buoyancy effects dominate. As a result, heat transfer by natural convection may improve, and at a fixed power level the heat sink may run at a lower temperature.

When extended surfaces such as fins are used to enhance natural convection heat transfer between a solid and a fluid, the flow rate of the fluid in the vicinity of the solid adjusts itself to incorporate the changes in buoyancy and friction. It is obvious that this enhancement technique will work to advantage only when the increase in buoyancy is greater than the additional friction introduced. One does not need to be concerned with pressure drop or pumping power when studying natural convection since no pumps or blowers are

used in this case. Therefore, an enhancement technique in natural convection is evaluated on heat transfer performance alone.

The failure rate of an electronic component increases almost exponentially with operating temperature. The cooler the electronic device operates, the more reliable it is. A rule of thumb is that the semiconductor failure rate is halved for each 10°C reduction in junction operating temperature. The desire to lower the operating temperature without having to resort to forced convection has motivated researchers to investigate enhancement techniques for natural convection. Sparrow and Prakash (1980) have demonstrated that, under certain conditions, the use of discrete plates in lieu of continuous plates of the same surface area increases heat transfer considerably. In other experimental work, using transistors as the heat source, Çengel and Zing (1987) have demonstrated that temperature recorded on the transistor case dropped by as much as 30°C when a shroud was used, as opposed to the corresponding no-shroud case.

FIGURE 9–23
Schematic for Example 9–3.

■ *EXAMPLE 9–3*   **Optimum Fin Spacing of a Heat Sink**

A 12-cm-wide and 18-cm-high vertical hot surface in 30°C air is to be cooled by a heat sink with equally spaced fins of rectangular profile (Fig. 9–23). The fins are 0.1 cm thick and 18 cm long in the vertical direction and have a height of 2.4 cm from the base. Determine the optimum fin spacing and the rate of heat transfer by natural convection from the heat sink if the base temperature is 80°C.

SOLUTION   A heat sink with equally spaced rectangular fins is to be used to cool a hot surface. The optimum fin spacing and the rate of heat transfer are to be determined.
Assumptions   **1** Steady operating conditions exist. **2** Air is an ideal gas. **3** The atmospheric pressure at that location is 1 atm. **4** The thickness t of the fins is very small relative to the fin spacing S so that Eq. 9–32 for optimum fin spacing is applicable. **5** All fin surfaces are isothermal at base temperature.
Properties   The properties of air at the film temperature of $T_f = (T_s + T_\infty)/2$ $= (80 + 30)/2 = 55°C$ and 1 atm pressure are (Table A–15)

$$k = 0.02772 \text{ W/m·K} \qquad \text{Pr} = 0.7215$$
$$\nu = 1.847 \times 10^{-5} \text{ m}^2/\text{s} \qquad \beta = 1/T_f = 1/328 \text{ K}$$

Analysis   We take the characteristic length to be the length of the fins in the vertical direction (since we do not know the fin spacing). Then the Rayleigh number becomes

$$\text{Ra}_L = \frac{g\beta(T_s - T_\infty)L^3}{\nu^2}\text{Pr} = \frac{(9.81 \text{ m/s}^2)[1/(328 \text{ K})](80 - 30 \text{ K})(0.18 \text{ m})^3}{(1.847 \times 10^{-5} \text{ m}^2/\text{s})^2}(0.7215)$$
$$= 1.845 \times 10^7$$

The optimum fin spacing is determined from Eq. 9–32 to be

$$S_{\text{opt}} = 2.714\frac{L}{\text{Ra}_L^{0.25}} = 2.714\frac{0.18 \text{ m}}{(1.845 \times 10^7)^{0.25}} = 7.45 \times 10^{-3} \text{ m} = \textbf{7.45 mm}$$

which is about seven times the thickness of the fins. Therefore, the assumption of negligible fin thickness in this case is acceptable. The number of fins and the heat transfer coefficient for this optimum fin spacing case are

$$n = \frac{W}{S + t} = \frac{0.12 \text{ m}}{(0.00745 + 0.001) \text{ m}} \approx 14 \text{ fins}$$

The convection coefficient for this optimum fin spacing case is, from Eq. 9–33,

$$h = \text{Nu}_{\text{opt}} \frac{k}{S_{\text{opt}}} = 1.307 \frac{0.02772 \text{ W/m·K}}{0.00745 \text{ m}} = 4.863 \text{ W/m}^2\text{·K}$$

Then the rate of natural convection heat transfer becomes

$$\dot{Q} = hA_s(T_s - T_\infty) = h(2nLH)(T_s - T_\infty)$$
$$= (4.863 \text{ W/m}^2\text{·K})[2 \times 14(0.18 \text{ m})(0.024 \text{ m})](80 - 30)°\text{C} = \textbf{29.4 W}$$

Therefore, this heat sink can dissipate heat by natural convection at a rate of 29.4 W.
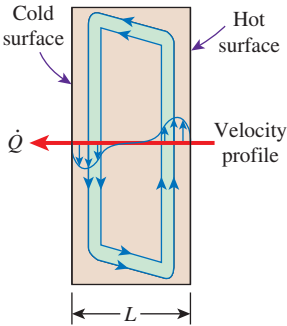
9–5 · NATURAL CONVECTION INSIDE ENCLOSURES

A considerable portion of heat loss from a typical residence occurs through the windows. We certainly would insulate the windows, if we could, in order to conserve energy. The problem is finding an insulating material that is transparent. An examination of the thermal conductivities of the insulating materials reveals that *air* is a *better insulator* than most common insulating materials. Besides, it is transparent. Therefore, it makes sense to insulate the windows with a layer of air. Of course, we need to use another sheet of glass to trap the air. The result is an *enclosure,* which is known as a *double-pane window* in this case. Other examples of enclosures include wall cavities, solar collectors, and cryogenic chambers involving concentric cylinders or spheres.

Enclosures are often encountered in practice, and heat transfer through them is of practical interest. Heat transfer in enclosed spaces is complicated by the fact that the fluid in the enclosure, in general, does not remain stationary. In a vertical enclosure, the fluid adjacent to the hotter surface rises and the fluid adjacent to the cooler one falls, setting off a rotationary motion within the enclosure that enhances heat transfer through the enclosure. Typical flow patterns in vertical and horizontal rectangular enclosures are shown in Figs. 9–24 and 9–25.

The characteristics of heat transfer through a horizontal enclosure depend on whether the hotter plate is at the top or at the bottom, as shown in Fig. 9–25. When the hotter plate is at the *top,* no convection currents develop in the enclosure, since the lighter fluid is always on top of the heavier fluid. Heat transfer in this case is by *pure conduction,* and we have Nu = 1. When the hotter plate is at the *bottom,* the heavier fluid will be on top of the lighter fluid, and there will be a tendency for the lighter fluid to topple the heavier fluid and rise to the top, where it comes in contact with the cooler plate and cools down. Until that happens, however, heat transfer is still by *pure conduction* and Nu = 1. When $\text{Ra}_L > 1708$, the buoyant force overcomes the fluid resistance and initiates natural convection currents, which are observed to be

FIGURE 9–24
Convective currents in a vertical rectangular enclosure.

(*a*) Hot plate at the top

(*b*) Hot plate at the bottom
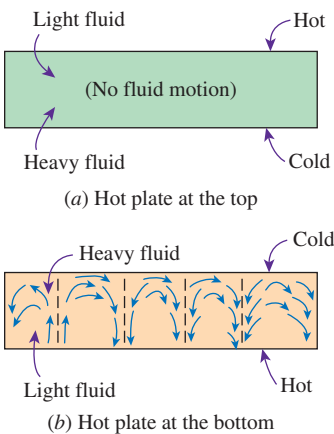
FIGURE 9–25
Convective currents in a horizontal enclosure with (*a*) hot plate at the top and (*b*) hot plate at the bottom.

in the form of hexagonal cells called *Bénard cells*. For $Ra_L > 3 \times 10^5$, the cells break down, and the fluid motion becomes turbulent.

The Rayleigh number for an enclosure is determined from

$$Ra_L = \frac{g\beta(T_1 - T_2)L_c^3}{\nu^2} Pr \qquad \text{(9–40)}$$

where the characteristic length L_c is the distance between the hot and cold surfaces, and T_1 and T_2 are the temperatures of the hot and cold surfaces, respectively. All fluid properties are to be evaluated at the average fluid temperature $T_{avg} = (T_1 + T_2)/2$.

Effective Thermal Conductivity

When the Nusselt number is known, the rate of heat transfer through the enclosure can be determined from

$$\dot{Q} = hA_s(T_1 - T_2) = kNuA_s\frac{T_1 - T_2}{L_c} \qquad \text{(9–41)}$$

since $h = kNu/L$. The rate of steady heat conduction across a layer of thickness L_c, area A_s, and thermal conductivity k is expressed as

$$\dot{Q}_{cond} = kA_s\frac{T_1 - T_2}{L_c} \qquad \text{(9–42)}$$

where T_1 and T_2 are the temperatures on the two sides of the layer. A comparison of this relation with Eq. 9–41 reveals that the convection heat transfer in an enclosure is analogous to heat conduction across the fluid layer in the enclosure provided that the thermal conductivity k is replaced by kNu. That is, *the fluid in an enclosure behaves like a fluid whose thermal conductivity is kNu as a result of convection currents.* Therefore, the quantity kNu is called the **effective thermal conductivity** of the enclosure. That is,

$$k_{eff} = kNu \qquad \text{(9–43)}$$

Note that for the special case of $Nu = 1$, the effective thermal conductivity of the enclosure becomes equal to the conductivity of the fluid. This is expected since this case corresponds to pure conduction (Fig. 9–26).

Natural convection heat transfer in enclosed spaces has been the subject of many experimental and numerical studies, and numerous correlations for the Nusselt number exist. Simple power-law-type relations in the form of $Nu = CRa_L^n$, where C and n are constants, are sufficiently accurate, but they are usually applicable to a narrow range of Prandtl and Rayleigh numbers and aspect ratios. The relations that are more comprehensive are naturally more complex. Next we present some widely used relations for various types of enclosures.

Horizontal Rectangular Enclosures

We need no Nusselt number relations for the case of the hotter plate being at the top, since there are no convection currents in this case and heat transfer is downward by conduction ($Nu = 1$). When the hotter plate is at the bottom, however, significant convection currents set in for $Ra_L > 1708$, and the rate of heat transfer increases (Fig. 9–27).
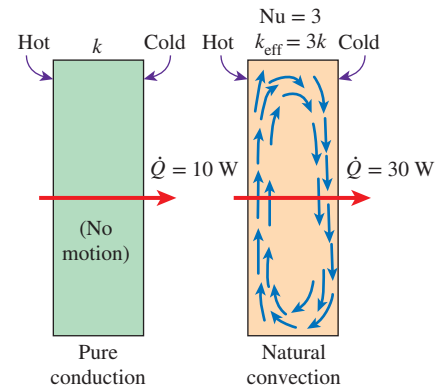
FIGURE 9–26
A Nusselt number of 3 for an enclosure indicates that heat transfer through the enclosure by *natural convection* is three times that by *pure conduction.*
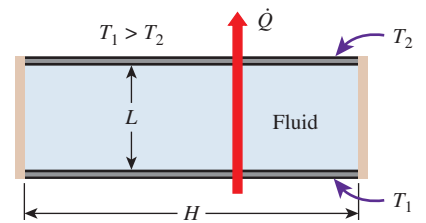
FIGURE 9–27
A horizontal rectangular enclosure with isothermal surfaces.

For horizontal enclosures that contain air, Jakob (1949) recommends the following simple correlations

$$\text{Nu} = 0.195 \, \text{Ra}_L^{1/4} \quad 10^4 < \text{Ra}_L < 4 \times 10^5 \tag{9–44}$$

$$\text{Nu} = 0.068 \, \text{Ra}_L^{1/3} \quad 4 \times 10^5 < \text{Ra}_L < 10^7 \tag{9–45}$$

These relations can also be used for other gases with $0.5 < \text{Pr} < 2$. Using water, silicone oil, and mercury in their experiments, Globe and Dropkin (1959) obtained this correlation for horizontal enclosures heated from below,

$$\text{Nu} = 0.069 \, \text{Ra}_L^{1/3} \, \text{Pr}^{0.074} \quad 3 \times 10^5 < \text{Ra}_L < 7 \times 10^9 \tag{9–46}$$

Based on experiments with air, Hollands et al. (1976) recommend this correlation for horizontal enclosures,

$$\text{Nu} = 1 + 1.44\left[1 - \frac{1708}{\text{Ra}_L}\right]^+ + \left[\frac{\text{Ra}_L^{1/3}}{18} - 1\right]^+ \quad \text{Ra}_L < 10^8 \tag{9–47}$$

The notation $[\ ]^+$ indicates that if the quantity in the bracket is negative, it should be set equal to zero. This relation also correlates data well for liquids with moderate Prandtl numbers for $\text{Ra}_L < 10^5$, and thus it can also be used for water.

Inclined Rectangular Enclosures

Airspaces between two inclined parallel plates are commonly encountered in flat-plate solar collectors (between the glass cover and the absorber plate) and the double-pane skylights on inclined roofs. Heat transfer through an inclined enclosure depends on the **aspect ratio** H/L as well as the tilt angle θ from the horizontal (Fig. 9–28).

For large aspect ratios ($H/L \geq 12$), this equation (Hollands et al., 1976) correlates experimental data extremely well for tilt angles up to 70°,

$$\text{Nu} = 1 + 1.44\left[1 - \frac{1708}{\text{Ra}_L \cos\theta}\right]^+ \left(1 - \frac{1708(\sin 1.8\theta)^{1.6}}{\text{Ra}_L \cos\theta}\right) + \left[\frac{(\text{Ra}_L \cos\theta)^{1/3}}{18} - 1\right]^+ \tag{9–48}$$

for $\text{Ra}_L < 10^5$, $0 < \theta < 70°$, and $H/L \geq 12$. Again, any quantity in $[\ ]^+$ should be set equal to zero if it is negative. This is to ensure that $\text{Nu} = 1$ for $\text{Ra}_L \cos\theta < 1708$. Note that this relation reduces to Eq. 9–47 for horizontal enclosures for $\theta = 0°$, as expected.

For enclosures with smaller aspect ratios ($H/L < 12$), the next correlation can be used, provided that the tilt angle is less than the critical value θ_{cr} listed in Table 9–2 (Catton, 1978)

$$\text{Nu} = \text{Nu}_{\theta=0°}\left(\frac{\text{Nu}_{\theta=90°}}{\text{Nu}_{\theta=0°}}\right)^{\theta/\theta_{cr}} (\sin\theta_{cr})^{\theta/(4\theta_{cr})} \quad 0° < \theta < \theta_{cr} \tag{9–49}$$

For tilt angles greater than the critical value ($\theta_{cr} < \theta < 90°$), the Nusselt number can be obtained by multiplying the Nusselt number for a vertical enclosure by $(\sin\theta)^{1/4}$ (Ayyaswamy and Catton, 1973),

$$\text{Nu} = \text{Nu}_{\theta=90°}(\sin\theta)^{1/4} \quad \theta_{cr} < \theta < 90°, \text{ any } H/L \tag{9–50}$$

FIGURE 9–28
An inclined rectangular enclosure with isothermal surfaces.

TABLE 9–2

Critical angles for inclined rectangular enclosures

Aspect Ratio, H/L	Critical Angle, θ_{cr}
1	25°
3	53°
6	60°
12	67°
>12	70°

For enclosures tilted more than 90°, the recommended relation is [Arnold et al. (1975)]

$$\text{Nu} = 1 + (\text{Nu}_{\theta=90°} - 1)\sin\theta \quad 90° < \theta < 180°, \text{ any } H/L \quad \textbf{(9–51)}$$

More recent but more complex correlations are also available in the literature (e.g., ElSherbiny et al., 1982).

Vertical Rectangular Enclosures

For vertical enclosures (Fig. 9–29), Catton (1978) recommends these two correlations due to Berkovsky and Polevikov (1977),

$$\text{Nu} = 0.18\left(\frac{\text{Pr}}{0.2 + \text{Pr}}\text{Ra}_L\right)^{0.29} \quad \begin{array}{l} 1 < H/L < 2 \\ \text{any Prandtl number} \\ \text{Ra}_L\text{Pr}/(0.2 + \text{Pr}) > 10^3 \end{array} \quad \textbf{(9–52)}$$

$$\text{Nu} = 0.22\left(\frac{\text{Pr}}{0.2 + \text{Pr}}\text{Ra}_L\right)^{0.28}\left(\frac{H}{L}\right)^{-1/4} \quad \begin{array}{l} 2 < H/L < 10 \\ \text{any Prandtl number} \\ \text{Ra}_L < 10^{10} \end{array} \quad \textbf{(9–53)}$$

For vertical enclosures with larger aspect ratios, the following correlations can be used (MacGregor and Emery, 1969)

$$\text{Nu} = 0.42\,\text{Ra}_L^{1/4}\,\text{Pr}^{0.012}\left(\frac{H}{L}\right)^{-0.3} \quad \begin{array}{l} 10 < H/L < 40 \\ 1 < \text{Pr} < 2 \times 10^4 \\ 10^4 < \text{Ra}_L < 10^7 \end{array} \quad \textbf{(9–54)}$$

$$\text{Nu} = 0.046\,\text{Ra}_L^{1/3} \quad \begin{array}{l} 1 < H/L < 40 \\ 1 < \text{Pr} < 20 \\ 10^6 < \text{Ra}_L < 10^9 \end{array} \quad \textbf{(9–55)}$$

Again, all fluid properties are to be evaluated at the average temperature $(T_1 + T_2)/2$.

Concentric Cylinders

Consider two long concentric horizontal cylinders maintained at uniform but different temperatures of T_i and T_o, as shown in Fig. 9–30. The diameters of the inner and outer cylinders are D_i and D_o, respectively, and the characteristic length is the spacing between the cylinders, $L_c = (D_o - D_i)/2$. The rate of heat transfer through the annular space between the cylinders by natural convection per unit length is expressed as

$$\dot{Q} = \frac{2\pi k_{\text{eff}}}{\ln(D_o/D_i)}(T_i - T_o) \quad \text{(W/m)} \quad \textbf{(9–56)}$$

The recommended relation for effective thermal conductivity is (Raithby and Hollands, 1975)

$$\frac{k_{\text{eff}}}{k} = 0.386\left(\frac{\text{Pr}}{0.861 + \text{Pr}}\right)^{1/4}(F_{\text{cyl}}\text{Ra}_L)^{1/4} \quad \textbf{(9–57)}$$
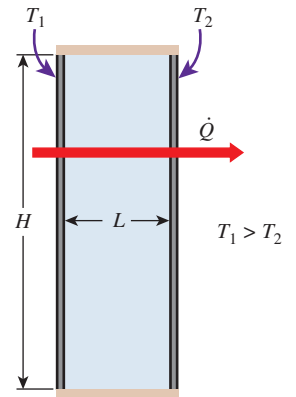
FIGURE 9–29
A vertical rectangular enclosure with isothermal surfaces.
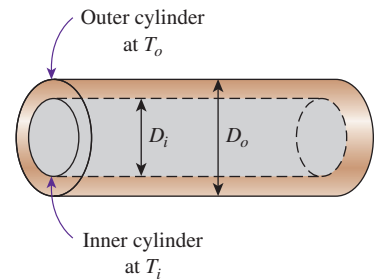
FIGURE 9–30
Two concentric horizontal isothermal cylinders.

where the geometric factor for concentric cylinders F_{cyl} is

$$F_{cyl} = \frac{[\ln(D_o/D_i)]^4}{L_c^3(D_i^{-3/5} + D_o^{-3/5})^5} \qquad \text{(9–58)}$$

The k_{eff} relation in Eq. 9–57 is applicable for $0.70 \le Pr \le 6000$ and $10^2 \le F_{cyl}Ra_L \le 10^7$. For $F_{cyl}Ra_L < 100$, natural convection currents are negligible, and thus $k_{eff} = k$. Note that k_{eff} cannot be less than k, and thus we should set $k_{eff} = k$ if $k_{eff}/k < 1$. The fluid properties are evaluated at the average temperature of $(T_i + T_o)/2$.

Concentric Spheres

For concentric isothermal spheres, the rate of heat transfer through the gap between the spheres by natural convection is expressed as (Fig. 9–31)

$$\dot{Q} = k_{eff}\frac{\pi D_i D_o}{L_c}(T_i - T_o) \qquad \text{(W)} \qquad \text{(9–59)}$$

FIGURE 9–31
Two concentric isothermal spheres.

where $L_c = (D_o - D_i)/2$ is the characteristic length. The recommended relation for effective thermal conductivity is (Raithby and Hollands, 1975)

$$\frac{k_{eff}}{k} = 0.74\left(\frac{Pr}{0.861 + Pr}\right)^{1/4}(F_{sph}Ra_L)^{1/4} \qquad \text{(9–60)}$$

where the geometric factor for concentric spheres F_{sph} is

$$F_{sph} = \frac{L_c}{(D_i D_o)^4(D_i^{-7/5} + D_o^{-7/5})^5} \qquad \text{(9–61)}$$

The k_{eff} relation in Eq. 9–60 is applicable for $0.70 \le Pr \le 4200$ and $10^2 \le F_{sph}Ra_L \le 10^4$. If $k_{eff}/k < 1$, we should set $k_{eff} = k$.

Combined Natural Convection and Radiation

Gases are nearly transparent to radiation, and thus heat transfer through a gas layer is by simultaneous convection (or conduction, if the gas is quiescent) and radiation. Natural convection heat transfer coefficients are typically very low compared to those for forced convection. Therefore, radiation is usually disregarded in forced convection problems, but it must be considered in natural convection problems that involve a gas. This is especially the case for surfaces with high emissivities. For example, about half of the heat transfer through the air space of a double-pane window is by radiation. The total rate of heat transfer is determined by adding the convection and radiation components,

$$\dot{Q}_{total} = \dot{Q}_{conv} + \dot{Q}_{rad} \qquad \text{(9–62)}$$

Radiation heat transfer from a surface at temperature T_s surrounded by surfaces at a temperature T_{surr} (both in K) is determined from

$$\dot{Q}_{rad} = \varepsilon\sigma A_s(T_s^4 - T_{surr}^4) \qquad \text{(W)} \qquad \text{(9–63)}$$

where ε is the emissivity of the surface, A_s is the surface area, and $\sigma = 5.67 \times 10^{-8}$ W/m²·K⁴ is the Stefan–Boltzmann constant.

When the end effects are negligible, radiation heat transfer between two large parallel plates at temperatures T_1 and T_2 is expressed as (see Chap. 13 for details)

$$\dot{Q}_{rad} = \frac{\sigma A_s(T_1^4 - T_2^4)}{1/\varepsilon_1 + 1/\varepsilon_2 - 1} = \varepsilon_{effective}\sigma A_s(T_1^4 - T_2^4) \qquad (W) \qquad \textbf{(9–64)}$$

where ε_1 and ε_2 are the emissivities of the plates, and $\varepsilon_{effective}$ is the *effective emissivity* defined as

$$\varepsilon_{effective} = \frac{1}{1/\varepsilon_1 + 1/\varepsilon_2 - 1} \qquad \textbf{(9–65)}$$

The emissivity of an ordinary glass surface, for example, is 0.84. Therefore, the effective emissivity of two parallel glass surfaces facing each other is 0.72. Radiation heat transfer between concentric cylinders and spheres is discussed in Chap. 13.

Note that in some cases the temperature of the surrounding medium may be below the surface temperature ($T_\infty < T_s$), while the temperature of the surrounding surfaces is above the surface temperature ($T_{surr} > T_s$). In such cases, convection and radiation heat transfers are subtracted from each other instead of being added since they are in opposite directions. Also, for a metal surface, the radiation effect can be reduced to negligible levels by polishing the surface and thus lowering the surface emissivity to a value near zero.

EXAMPLE 9–4   Heat Loss Through a Double-Pane Window

The vertical 0.8-m-high, 2-m-wide double-pane window shown in Fig. 9–32 consists of two sheets of glass separated by a 2-cm air gap at atmospheric pressure. If the glass surface temperatures across the air gap are measured to be 12°C and 2°C, determine the rate of heat transfer through the window.

SOLUTION Two glasses of a double-pane window are maintained at specified temperatures. The rate of heat transfer through the window is to be determined.
Assumptions **1** Steady operating conditions exist. **2** Air is an ideal gas. **3** Radiation heat transfer is not considered.
Properties The properties of air at the average temperature of $T_{avg} = (T_1 + T_2)/2 = (12 + 2)/2 = 7°C$ and 1 atm pressure are (Table A–15)

$$k = 0.02416 \text{ W/m·K} \qquad Pr = 0.7344$$
$$\nu = 1.400 \times 10^{-5} \text{ m}^2\text{/s} \qquad \beta = \frac{1}{T_{avg}} = \frac{1}{280 \text{ K}}$$

Analysis We have a rectangular enclosure filled with air. The characteristic length in this case is the distance between the two glasses, $L_c = L = 0.02$ m. Then the Rayleigh number becomes

$$Ra_L = \frac{g\beta(T_1 - T_2)L_c^3}{\nu^2} Pr$$

$$= \frac{(9.81 \text{ m/s}^2)[1/(280 \text{ K})](12 - 2 \text{ K})(0.02 \text{ m})^3}{(1.400 \times 10^{-5} \text{ m}^2\text{/s})^2}(0.7344) = 1.050 \times 10^4$$
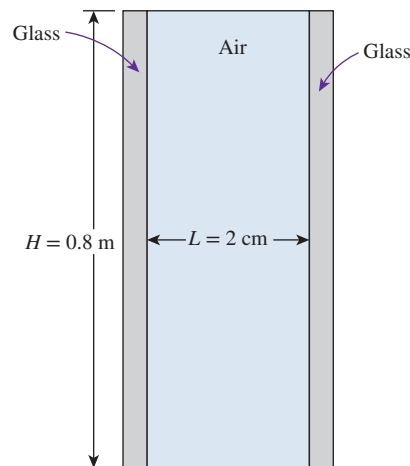
FIGURE 9–32
Schematic for Example 9–4.

$H = 0.8$ m $L = 2$ cm

Glass   Air   Glass

The aspect ratio of the geometry is $H/L = 0.8/0.02 = 40$. Then the Nusselt number in this case can be determined from Eq. 9–54 to be

$$\text{Nu} = 0.42 \, \text{Ra}_L^{1/4} \, \text{Pr}^{0.012} \left(\frac{H}{L} \right)^{-0.3}$$

$$= 0.42(1.050 \times 10^4)^{1/4}(0.7344)^{0.012} \left(\frac{0.8}{0.02} \right)^{-0.3} = 1.40$$

Then,

$$A_s = H \times W = (0.8 \text{ m})(2 \text{ m}) = 1.6 \text{ m}^2$$

and

$$\dot{Q} = hA_s(T_1 - T_2) = k\text{Nu}A_s \frac{T_1 - T_2}{L}$$

$$= (0.02416 \text{ W/m·K})(1.40)(1.6 \text{ m}^2)\frac{(12 - 2)°\text{C}}{0.02 \text{ m}} = \textbf{27.1 W}$$

Therefore, heat is lost through the window at a rate of 27.1 W.

Discussion   Recall that a Nusselt number of $\text{Nu} = 1$ for an enclosure corresponds to pure conduction heat transfer through the enclosure. The air in the enclosure in this case remains still, and no natural convection currents occur in the enclosure. The Nusselt number in our case is 1.40, which indicates that heat transfer through the enclosure is 1.40 times that by pure conduction. The increase in heat transfer is due to the natural convection currents that develop in the enclosure.

Outer cover
D_o, T_o

Spherical tank
D_i, T_i

L_c

Exothermic
reaction
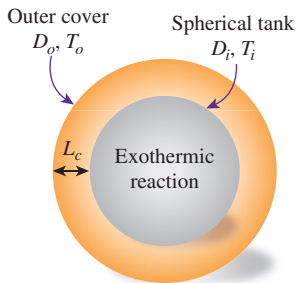
FIGURE 9–33
Schematic for Example 9–5.

PtD *EXAMPLE 9–5*   **Pipe Insulation for Thermal Burn Prevention**

In a chemical plant, a 3-m-diameter spherical tank contains a hot fluid that causes the surface temperature to be 150°C (Fig. 9–33). For safety purposes, the tank is enclosed by a 3.15-m-diameter concentric outer spherical cover. The concentric enclosure provides an air gap that serves as an insulation layer. To eliminate workplace hazards such as thermal burns on skin, the outer cover surface temperature should be kept below 45°C. The temperature of ambient air outside the tank is 20°C, and the surface of the tank's outer cover is covered with paint that gives an emissivity of 0.9. Determine whether the air gap is sufficient to keep the outer cover surface temperature below 45°C to prevent thermal burns. Assume that the properties of air in the enclosure and at the outer surface can be evaluated at 95°C and 30°C and 1 atm pressure, respectively.

SOLUTION   In this example, the concepts of PtD are applied in conjunction with the concepts of natural convection over a surface and in an enclosure.

Assumptions   **1** Steady operating conditions exist. **2** Surface temperatures are constant. **3** Air is an ideal gas with constant properties. **4** Heat loss by radiation is negligible. **5** The air pressure is at 1 atm. **6** The surrounding air temperature is $T_{\text{surr}} = T_\infty$.

Properties   The properties of air in the enclosure at the assumed average temperature $T_{\text{avg}} = (T_i + T_o)/2 = 95°\text{C}$ and 1 atm pressure are $k = 0.03060 \text{ W/m·K}$, $\nu = 2.254 \times 10^{-5} \text{ m}^2/\text{s}$, $\text{Pr} = 0.7122$ (Table A-15), and $\beta = 1/T_{\text{avg}} = 1/368 \text{ K}$.

The properties of air surrounding the outer surface at the assumed film temperature $T_f = (T_o + T_\infty)/2 = 30°C$ and 1 atm pressure are $k = 0.02588$ W/m·K, $\nu = 1.608 \times 10^{-5}$ m²/s, Pr = 0.7282 (Table A-15), and $\beta = 1/T_f = 1/303$ K. The emissivity of the outer surface is given as $\varepsilon = 0.9$.

Analysis For natural convection in the concentric enclosure, with the assumed $T_{avg} = 95°C$, the outer surface temperature is estimated as

$$T_o = 2T_{avg} - T_i = 2(95) - 150 = 40°C$$

The Rayleigh number is

$$\text{Ra}_L = \frac{g\beta(T_i - T_o)L_c^3}{\nu^2}\text{Pr}$$

$$= \frac{(9.81 \text{ m/s}^2)(95 + 273 \text{ K})^{-1}(150 - 40) \text{ K}(0.075 \text{ m})^3}{(2.254 \times 10^{-5} \text{ m}^2/\text{s})^2}(0.7122) = 1.7342 \times 10^6$$

where $L_c = (D_o - D_i)/2 = (3.15 - 3.0)/2 = 0.075$ m

The effective thermal conductivity is

$$F_{sph} = \frac{L_c}{(D_i D_o)^4(D_i^{-7/5} + D_o^{-7/5})^5}$$

$$= \frac{0.075 \text{ m}}{[(3.0 \text{ m})(3.15 \text{ m})]^4[(3.0 \text{ m})^{-7/5} + (3.15 \text{ m})^{-7/5}]^5} = 0.0007602$$

$$k_{eff} = 0.74k\left(\frac{\text{Pr}}{0.861 + \text{Pr}}\right)^{1/4}(F_{sph}\text{Ra})^{1/4}$$

$$= 0.74(0.03060 \text{ W/m·K})\left(\frac{0.7122}{0.861 + 0.7122}\right)^{1/4}[(0.0007602)(1.7342 \times 10^6)]^{1/4}$$

$$= 0.1119 \text{ W/m·K}$$

For natural convection at the outer surface with the surrounding air, the Rayleigh number is

$$\text{Ra}_D = \frac{g\beta(T_o - T_\infty)D_o^3}{\nu^2}\text{Pr}$$

$$= \frac{(9.81 \text{ m/s}^2)(30 + 273 \text{ K})^{-1}(40 - 20) \text{ K}(3.15 \text{ m})^3}{(1.608 \times 10^{-5} \text{ m}^2/\text{s})^2}(0.7282) = 5.6999 \times 10^{10}$$

The Nusselt number and the natural convection heat transfer coefficient at the outer surface are

$$\text{Nu} = 2 + \frac{0.589\text{Ra}_D^{1/4}}{\left[1 + \left(\frac{0.469}{\text{Pr}}\right)^{9/16}\right]^{4/9}} = 2 + \frac{0.589(5.6999 \times 10^{10})^{1/4}}{\left[1 + \left(\frac{0.469}{0.7282}\right)^{9/16}\right]^{4/9}} = 224.69$$

$$h = \frac{k}{D_o}\text{Nu} = \frac{0.02588 \text{ W/m·K}}{3.15 \text{ m}}(224.69) = 1.846 \text{ W/m}^2\text{·K}$$

The outer surface temperature can be solved from the rate of heat balance at the outer surface as

$$\dot{Q}_{encl} = \dot{Q}_{conv} + \dot{Q}_{rad}$$

$$k_{eff}\pi\left(\frac{D_i D_o}{L_c}\right)(T_i - T_o) = h(\pi D_o^2)(T_o - T_\infty) + \varepsilon\sigma(\pi D_o^2)(T_o^4 - T_{surr}^4) \rightarrow T_o = \textbf{40.6°C}$$

The assumed average temperature $T_{avg} = 95°C$ and film temperature $T_f = 30°C$ are appropriate for evaluating the air properties in the enclosure and at the outer surface, respectively. The determined $T_o = 40.6°C$ would give $T_{avg} = 95.3°C$ and $T_f = 30.3°C$.

Solar energy

Glass cover

70°F

4 in

2 in

Aluminum tube

Water
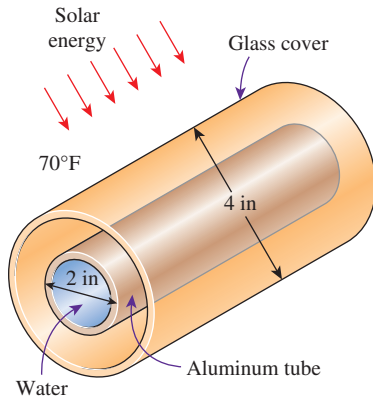
FIGURE 9–34
Schematic for Example 9–6.

EXAMPLE 9–6 Heating Water in a Tube by Solar Energy

A solar collector consists of a horizontal aluminum tube having an outer diameter of 2 in enclosed in a concentric thin glass tube of 4-in diameter (Fig. 9–34). Water is heated as it flows through the tube, and the annular space between the aluminum and the glass tubes is filled with air at 1 atm pressure. The pump circulating the water fails during a clear day, and the water temperature in the tube starts rising. The aluminum tube absorbs solar radiation at a rate of 30 Btu/h per foot length, and the temperature of the ambient air outside is 70°F. Disregarding any heat loss by radiation, determine the temperature of the aluminum tube when steady operation is established (i.e., when the rate of heat loss from the tube equals the amount of solar energy gained by the tube).

SOLUTION The circulating pump of a solar collector that consists of a horizontal tube and its glass cover fails. The equilibrium temperature of the tube is to be determined.

Assumptions **1** Steady operating conditions exist. **2** The tube and its cover are isothermal. **3** Air is an ideal gas. **4** Heat loss by radiation is negligible.

Properties The properties of air should be evaluated at the average temperature. But we do not know the exit temperature of the air in the duct, and thus we cannot determine the bulk fluid and glass cover temperatures at this point, and we cannot evaluate the average temperatures. Therefore, we assume the glass temperature to be 110°F, and we use properties at an anticipated average temperature of $(70 + 110)/2 = 90°F$ (Table A–15E),

$$k = 0.01505 \text{ Btu/h·ft·°F} \qquad \text{Pr} = 0.7275$$

$$\nu = 1.753 \times 10^{-4} \text{ ft}^2/\text{s} \qquad \beta = \frac{1}{T_{avg}} = \frac{1}{550 \ R}$$

Analysis We have a horizontal cylindrical enclosure filled with air at 1 atm pressure. The problem involves heat transfer from the aluminum tube to the glass cover and from the outer surface of the glass cover to the surrounding ambient air. When steady operation is reached, these two heat transfer rates must equal the rate of heat gain. That is,

$$\dot{Q}_{tube\text{-}glass} = \dot{Q}_{glass\text{-}ambient} = \dot{Q}_{solar \ gain} = 30 \text{ Btu/h} \qquad \text{(per foot of tube)}$$

The heat transfer surface area of the glass cover is

$$A_o = A_{glass} = (\pi D_o L) = \pi(4/12 \text{ ft})(1 \text{ ft}) = 1.047 \text{ ft}^2 \qquad \text{(per foot of tube)}$$

To determine the Rayleigh number, we need to know the surface temperature of the glass, which is not available. Therefore, it is clear that the solution will require a

trial-and-error approach. Assuming the glass cover temperature to be 110°F, the Rayleigh number, the Nusselt number, the convection heat transfer coefficient, and the rate of natural convection heat transfer from the glass cover to the ambient air are determined to be

$$\text{Ra}_{D_o} = \frac{g\beta(T_s - T_\infty)D_o^3}{\nu^2}\text{Pr}$$

$$= \frac{(32.2 \text{ ft/s}^2)[1/(550 \text{ R})](110 - 70 \text{ R})(4/12 \text{ ft})^3}{(1.753 \times 10^{-4} \text{ ft}^2/\text{s})^2}(0.7275) = 2.054 \times 10^6$$

$$\text{Nu} = \left\{0.6 + \frac{0.387 \text{ Ra}_D^{1/6}}{[1 + (0.559/\text{Pr})^{9/16}]^{8/27}}\right\}^2 = \left\{0.6 + \frac{0.387(2.054 \times 10^6)^{1/6}}{[1 + (0.559/0.7275)^{9/16}]^{8/27}}\right\}^2$$

$$= 17.89$$

$$h_o = \frac{k}{D_o}\text{Nu} = \frac{0.01505 \text{ Btu/h·ft·°F}}{4/12 \text{ ft}}(17.89) = 0.8077 \text{ Btu/h·ft}^2\text{·°F}$$

$$\dot{Q}_o = h_o A_o(T_o - T_\infty) = (0.8077 \text{ Btu/h·ft}^2\text{·°F})(1.047 \text{ ft}^2)(110 - 70)\text{°F}$$

$$= 33.8 \text{ Btu/h}$$

which is more than 30 Btu/h. Therefore, the assumed temperature of 110°F for the glass cover is high. Repeating the calculations with lower temperatures, the glass cover temperature corresponding to 30 Btu/h is determined to be 106°F.

The temperature of the aluminum tube is determined in a similar manner using the natural convection relations for two horizontal concentric cylinders. The characteristic length in this case is the distance between the two cylinders, which is

$$L_c = (D_o - D_i)/2 = (4 - 2)/2 = 1 \text{ in} = 1/12 \text{ ft}$$

We start the calculations by assuming the tube temperature to be 200°F, and thus an average temperature of $(106 + 200)/2 = 153$°F $= 613$ R. Using air properties at this temperature gives

$$\text{Ra}_L = \frac{g\beta(T_i - T_o)L_c^3}{\nu^2}\text{Pr}$$

$$= \frac{(32.2 \text{ ft/s}^2)[1/(613 \text{ R})](200 - 106 \text{ R})(1/12 \text{ ft})^3}{(2.117 \times 10^{-4} \text{ ft}^2/\text{s})^2}(0.7184) = 4.580 \times 10^4$$

The effective thermal conductivity is

$$F_{\text{cyl}} = \frac{[\ln(D_o/D_i)]^4}{L_c^3(D_i^{-3/5} + D_o^{-3/5})^5}$$

$$= \frac{[\ln(4/2)]^4}{(1/12 \text{ ft})^3[(2/12 \text{ ft})^{-3/5} + (4/12 \text{ ft})^{-3/5}]^5} = 0.1466$$

$$k_{\text{eff}} = 0.386k\left(\frac{\text{Pr}}{0.861 + \text{Pr}}\right)^{1/4}(F_{\text{cyl}}\text{Ra}_L)^{1/4}$$

$$= 0.386(0.01653 \text{ Btu/h·ft·°F})\left(\frac{0.7184}{0.861 + 0.7184}\right)^{1/4}$$

$$\times (0.1466 \times 4.580 \times 10^4)^{1/4}$$

$$= 0.04743 \text{ Btu/h·ft·°F}$$

Then the rate of heat transfer between the cylinders becomes

$$\dot{Q} = \frac{2\pi k_{\text{eff}}}{\ln(D_o/D_i)}(T_i - T_o)$$

$$= \frac{2\pi(0.04743 \text{ Btu/h·ft·°F})}{\ln(4/2)}(200 - 106)°F = 40.4 \text{ Btu/h}$$

which is more than 30 Btu/h. Therefore, the assumed temperature of 200°F for the tube is high. By trying other values, the tube temperature corresponding to 30 Btu/h is determined to be **180°F**. Therefore, the tube will reach an equilibrium temperature of 180°F when the pump fails.

Discussion Note that we have not considered heat loss by radiation in the calculations, and thus the tube temperature determined is probably too high. This problem is considered in Chap. 13 by accounting for the effect of radiation heat transfer.

9–6 ▪ COMBINED NATURAL AND FORCED CONVECTION

The presence of a temperature gradient in a fluid in a gravity field always gives rise to natural convection currents, and thus heat transfer by natural convection. Therefore, forced convection is always accompanied by natural convection.

We mentioned earlier that the convection heat transfer coefficient, natural or forced, is a strong function of the fluid velocity. Heat transfer coefficients encountered in forced convection are typically much higher than those encountered in natural convection because of the higher fluid velocities associated with forced convection. As a result, we tend to ignore natural convection in heat transfer analyses that involve forced convection, although we recognize that natural convection always accompanies forced convection. The error involved in ignoring natural convection is negligible at high velocities but may be considerable at low velocities. Therefore, it is desirable to have a criterion to assess the relative magnitude of natural convection in the presence of forced convection.

For a given fluid, it is observed that the parameter Gr/Re^2 represents the importance of natural convection relative to forced convection. This is not surprising since the convection heat transfer coefficient is a strong function of the Reynolds number Re in forced convection and the Grashof number Gr in natural convection.

A plot of the nondimensionalized heat transfer coefficient for combined natural and forced convection on a vertical plate is given in Fig. 9–35 for different fluids. We note from this figure that natural convection is negligible when $Gr/Re^2 < 0.1$, forced convection is negligible when $Gr/Re^2 > 10$, and neither is negligible when $0.1 < Gr/Re^2 < 10$. Therefore, both natural and forced convection must be considered in heat transfer calculations when the Gr and Re^2 are of the same order of magnitude (one is within a factor of 10 times the other). Note that forced convection is small relative to natural convection only in the rare case of extremely low forced flow velocities. From the preceding discussion and the Nusselt number correlations
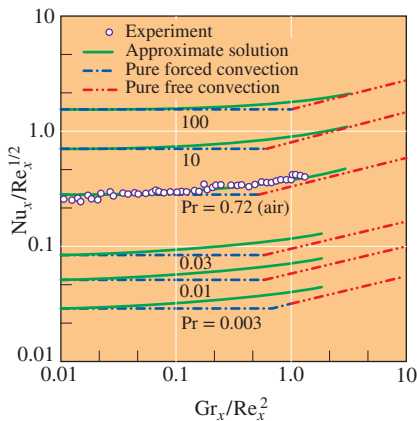
FIGURE 9–35
Variation of the local Nusselt number Nu_x for combined natural and forced convection from a hot isothermal vertical plate.
Source: Lloyd and Sparrow, 1970.
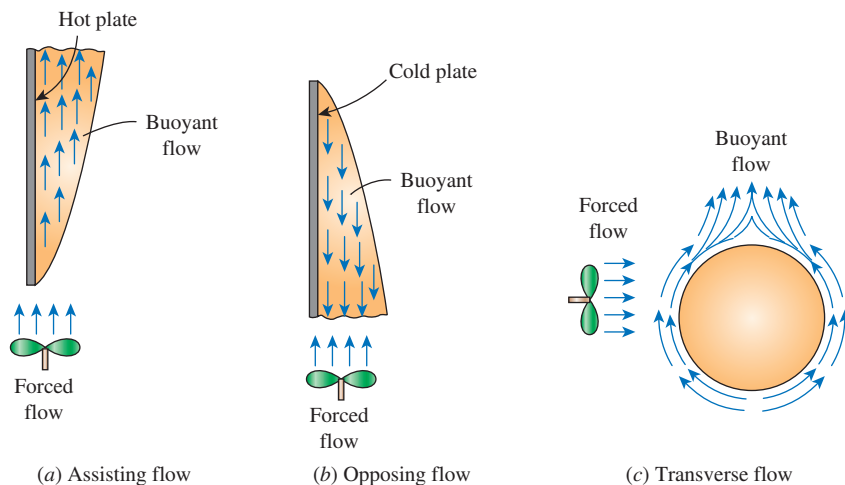
FIGURE 9–36
Natural convection can *enhance* or *inhibit* heat transfer, depending on the relative directions of *buoyancy-induced motion* and the *forced convection motion.*

presented in Chaps. 7 and 8 for external and internal forced convection, and Chap. 9 for natural convection, it can be concluded that for forced convection $\text{Nu} = f(\text{Re}_L, \text{Pr})$, for natural convection $\text{Nu} = f(\text{Gr}_L, \text{Pr})$, and for combined natural and forced (mixed) convection $\text{Nu} = f(\text{Re}_L, \text{Gr}_L, \text{Pr})$.

Natural convection may *help* or *hurt* forced convection heat transfer, depending on the relative directions of *buoyancy-induced* and *forced convection* motions (Fig. 9–36):

1. In *assisting flow,* the buoyant motion is in the *same* direction as the forced motion. Therefore, natural convection assists forced convection and *enhances* heat transfer. An example is upward forced flow over a hot surface (Fig. 9–36*a*).

2. In *opposing flow,* the buoyant motion is in the *opposite* direction to the forced motion. Therefore, natural convection resists forced convection and *decreases* heat transfer. An example is upward forced flow over a cold surface (Fig. 9–36*b*).

3. In *transverse flow,* the buoyant motion is *perpendicular* to the forced motion. Transverse flow enhances fluid mixing and thus *enhances* heat transfer. An example is horizontal forced flow over a hot or cold cylinder or sphere (Fig. 9–36*c*).

When determining heat transfer under combined natural and forced (mixed) convection conditions, it is tempting to add the contributions of natural and forced convection in assisting flows and to subtract them in opposing flows. However, the evidence indicates differently. A review of experimental data suggests a correlation of the form

$$\text{Nu}_{\text{combined}} = (\text{Nu}_{\text{forced}}^n \pm \text{Nu}_{\text{natural}}^n)^{1/n} \qquad \text{(9–66)}$$

where $\text{Nu}_{\text{forced}}$ and $\text{Nu}_{\text{natural}}$ are determined from the correlations for *pure forced* and *pure natural convection,* respectively. The plus sign is for *assisting* and *transverse* flows and the minus sign is for *opposing* flows. The value of

the exponent *n* varies between 3 and 4, depending on the geometry involved. It is observed that $n = 3$ often best correlates the experimental data, although larger *n* values of 3.5 and 4 are usually better suited for flows involving horizontal plates and cylinders (or spheres), respectively. An example of Eq. 9–66 is the mixed convection correlation developed by Tam and Ghajar (2006) for the calculation of Nusselt number in the transition region (Eq. 8–87).

A question that often arises in the cooling of heat-generating equipment such as electronic components is whether to use a fan or a pump (if the cooling medium is a liquid)—that is, whether to use *natural* or *forced* convection in the cooling of the equipment. The answer depends on the maximum allowable operating temperature. Recall that the convection heat transfer rate from a surface at temperature T_s in a medium at T_∞ is given by

$$\dot{Q}_{\text{conv}} = hA_s(T_s - T_\infty)$$

where *h* is the convection heat transfer coefficient and A_s is the surface area. Note that for a fixed value of power dissipation and surface area, *h* and T_s are *inversely proportional.* Therefore, the device operates at a *higher* temperature when *h* is low (typical of natural convection) and at a *lower* temperature when *h* is high (typical of forced convection).

Natural convection is the preferred mode of heat transfer, since no blowers or pumps are needed, and thus all the problems associated with these, such as noise, vibration, power consumption, and malfunctioning, are avoided. Natural convection is adequate for cooling *low-power-output* devices, especially when they are attached to extended surfaces such as heat sinks. For *high-power-output* devices, however, we have no choice but to use a blower or a pump to keep the operating temperature below the maximum allowable level. For *very-high-power-output* devices, even forced convection may not be sufficient to keep the surface temperature at the desirable levels. In such cases, we may have to use *boiling* and *condensation* to take advantage of the very high heat transfer coefficients associated with phase-change processes.

As mentioned earlier, natural convection is the preferred mode of heat transfer, since it does not require the use of a fluid mover (pump or blower). However, the major drawback for this mode of heat transfer is that the heat transfer coefficients encountered under normal operating conditions are typically much lower than those encountered in forced convection. The rates of heat transfer in natural convection can be made comparable to or even exceed the forced convection heat transfer rates by operating in the near-critical or supercritical regions of fluids. In these regions, fluids behave much differently than they do at states away from the critical point. Small changes in temperature or pressure in the vicinity of the critical point produce large changes in the fluid thermophysical properties (Fig. 9–37). A large change in fluid thermophysical properties can be associated with large changes in the rates of convective heat transfer. Simple yet highly accurate relations to predict the peculiar behavior of thermophysical properties of several fluids in the near-critical region are available in the literature (Najjar and Ghajar, 1983; Asgeirsson and Ghajar, 1986).

High rates of heat transfer in the near-critical and supercritical regions have become increasingly important in connection with applications like the use of near-critical helium to cool the coils of superconducting electromagnets and superconducting electronic or power-transmission equipment, the use of
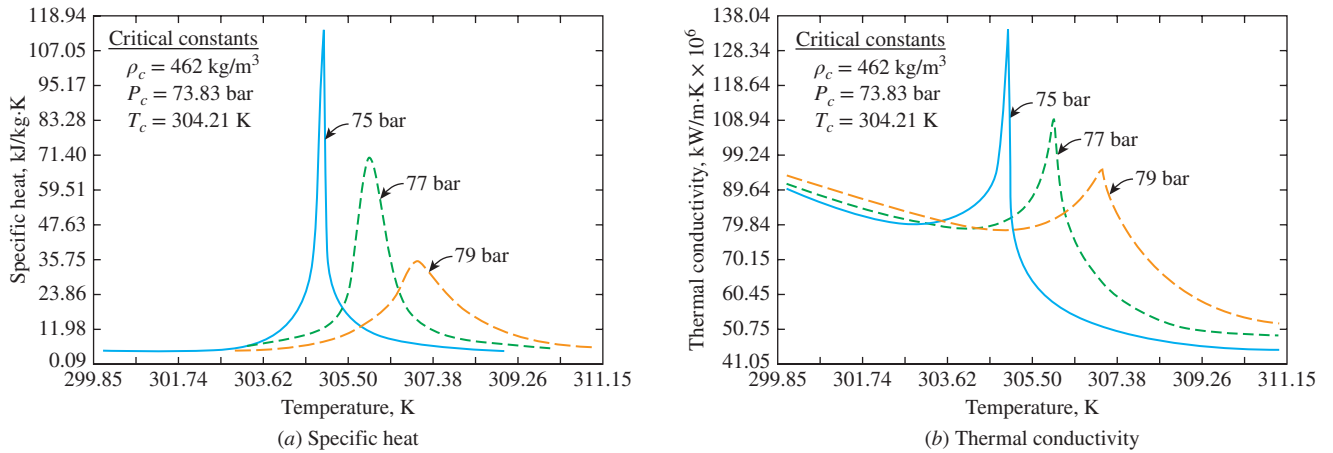
FIGURE 9–37
The variation of specific heat and thermal conductivity with temperature for carbon dioxide at different pressures.
Source: Ghajar and Asadi, 1986.

supercritical hydrogen as a working fluid for both chemical and nuclear rockets, the use of supercritical steam generators in electric utility plants, and the use of methane as a coolant and fuel for the supersonic transport. For horizontal wires and vertical plates, the following relation can be used to predict natural convection heat transfer in the near-critical region (Ghorbani-Tari and Ghajar, 1985)

$$\text{Nu}_\infty = a(\text{Gr}_\infty \text{Pr}_\infty)^b \left(\frac{\rho_w}{\rho_\infty}\right)^c \left(\frac{\bar{c}_p}{c_{p_\infty}}\right)^d \left(\frac{k_w}{k_\infty}\right)^e \left(\frac{\mu_w}{\mu_\infty}\right)^f$$

Here a, b, c, d, e, and f are curve-fitted constants, and the subscripts ∞ and w indicate properties to be evaluated at the free-stream and wall temperatures, respectively. The term $\bar{c}_p$ is the mean-integral heat capacity, which is the ratio of the difference of the enthalpies of the fluid evaluated at the free-stream and wall temperatures over the differences of the free-stream and wall temperatures. The correlation predicted the results of eight different experiments covering a Rayleigh number range of $0.2 < \text{Ra}_\infty < 4 \times 10^{13}$, with an absolute average deviation that ranged from 6.7 to 15.6 percent.

■ *EXAMPLE 9–7*   **Heat Transfer in the Presence of Assisting**
■ **and Opposing Flows (Vertical Plate)**

■ A 0.2-m × 0.2-m vertical plate has a surface temperature that is maintained at 40°C. Air at 20°C is flowing in parallel over the plate with a velocity of 0.4 m/s. Determine the Nusselt number for both assisting flow and opposing flow (Fig. 9–38).

SOLUTION   Air is flowing over a vertical plate. Nusselt numbers for both assisting and opposing flows are to be determined.
Assumptions   **1** Steady operating conditions exist. **2** Properties are constant. **3** The surface temperature is constant. **4** Air is an ideal gas. **5** Heat transfer by radiation is negligible.

Assisting
flow

Opposing
flow
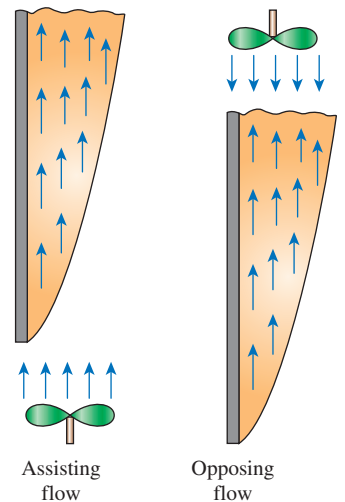
FIGURE 9–38
Schematic for Example 9–7.

Properties   The properties of air (1 atm) at 30°C are $\nu = 1.608 \times 10^{-5}$ m²/s, and Pr = 0.7282 (Table A–15). Also, $\beta = 1/T_f = 0.0033$ K⁻¹.

Analysis   The Reynolds and Grashof numbers are

$$\text{Re} = \frac{VL}{\nu} = \frac{(0.4 \text{ m/s})(0.2 \text{ m})}{1.608 \times 10^{-5} \text{ m}^2\text{/s}} = 4975$$

$$\text{Gr}_L = \frac{g\beta(T_s - T_\infty)L^3}{\nu^2} = \frac{(9.81 \text{ m/s}^2)(0.0033 \text{ K}^{-1})(40 - 20)\text{K}(0.2 \text{ m})^3}{(1.608 \times 10^{-5})^2 \text{ m}^4\text{/s}^2}$$

$$= 2.003 \times 10^7$$

Hence,

$$\frac{\text{Gr}_L}{\text{Re}^2} = \frac{2.003 \times 10^7}{(4975)^2} = 0.809$$

Noting that $\text{Gr}_L/\text{Re}^2 \approx 1$, both natural convection and forced convection are significant, and we have mixed flow. The Nusselt numbers for the natural and forced convection cases are determined from relevant relations to be

$$\text{Nu}_{\text{natural}} = 0.59 \text{ Ra}_L^{1/4} = 0.59(2.003 \times 10^7 \times 0.7282)^{1/4} = 36.46$$

$$\text{Nu}_{\text{forced}} = 0.664 \text{ Re}^{0.5}\text{Pr}^{1/3} = 0.664(4975)^{0.5}(0.7282)^{1/3} = 42.14$$

Finally, the combined Nusselt numbers for the cases of assisting flow (flowing upward) and opposing flow (flowing downward) become

Assisting flow: $\text{Nu}_{\text{combined}} = (\text{Nu}_{\text{forced}}^3 + \text{Nu}_{\text{natural}}^3)^{1/3} = (42.14^3 + 36.46^3)^{1/3} = \mathbf{49.8}$

Opposing flow: $\text{Nu}_{\text{combined}} = (\text{Nu}_{\text{forced}}^3 - \text{Nu}_{\text{natural}}^3)^{1/3} = (42.14^3 - 36.46^3)^{1/3} = \mathbf{29.8}$

Discussion   Note that the Nusselt number for the assisting flow is about 67 percent higher than that for the opposing flow. Therefore, natural convection must be taken into consideration when it is significant.
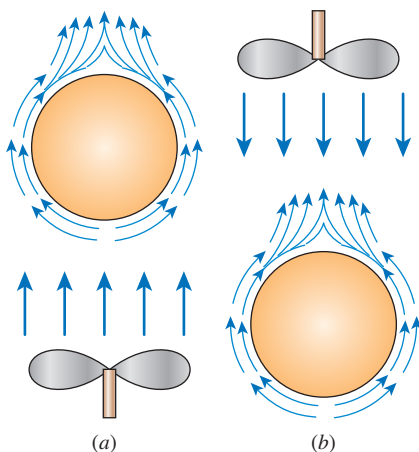
FIGURE 9–39
Schematic for Example 9-8.

EXAMPLE 9–8   **Heat Transfer in the Presence of Assisting and Opposing Flows (Horizontal Cylinder)**

A 15-cm-diameter horizontal cylinder has a surface temperature that is maintained at 120°C. Water at 40°C is flowing across the cylinder with a velocity of 0.2 m/s (Fig. 9–39). Determine the Nusselt number if the water is flowing (*a*) upward and (*b*) downward.

SOLUTION   Water is flowing across a horizontal cylinder. Nusselt numbers for water flowing *(a)* upward and *(b)* downward are to be determined.

Assumptions   **1** Steady operating conditions exist. **2** Properties are constant. **3** The surface temperature is constant. **4** Cylinder is oriented such that the characteristic length is its diameter. **5** Heat transfer by radiation is negligible.

Properties   The properties of water at $T_f = (T_s + T_\infty)/2 = (120 + 40)/2 = 80°C$ are (Table A–9)

$\rho = 971.8$ kg/m³, $\mu = 0.355 \times 10^{-5}$ kg/m·s,   Pr = 2.22,   and $\beta = 0.653 \times 10^{-3}$ K⁻¹.

Analysis To check if combined natural and forced convection exists, we find

$$\text{Re} = \frac{\rho V D}{\mu} = \frac{(971.8 \text{ kg/m}^3)(0.2 \text{ m/s})(0.15 \text{ m})}{0.355 \times 10^{-3} \text{ kg/m·s}} = 8.21 \times 10^4$$

$$\text{Gr}_D = \frac{g\beta(T_s - T_\infty)D^3}{(\mu/\rho)^2} = \frac{(9.81 \text{ m/s}^2)(0.653 \times 10^{-3} \text{ K}^{-1})(120 - 40) \text{ K}(0.15 \text{ m})^3}{(0.355 \times 10^{-3}/971.8)^2 \text{ m}^4/\text{s}^2}$$

$$= 1.296 \times 10^{10}$$

Hence,

$$\frac{\text{Gr}_D}{\text{Re}^2} = \frac{1.296 \times 10^{10}}{(8.21 \times 10^4)^2} = 1.92$$

Noting that $\text{Gr}_D/\text{Re}^2 \approx 1$, both natural convection and forced convection are significant, and we have mixed flow. The Nusselt numbers for the natural convection of a horizontal cylinder is

$$\text{Nu}_{\text{natural}} = \left\{ 0.6 + \frac{0.387 \text{ Ra}_D^{1/6}}{[1 + (0.559/\text{Pr})^{9/16}]^{8/27}} \right\}^2$$

$$= \left\{ 0.6 + \frac{0.387(1.296 \times 10^{10} \times 2.22)^{1/6}}{[1 + (0.559/2.22)^{9/16}]^{8/27}} \right\}^2 = 390$$

Then the Nusselt number for forced convection across a cylinder is calculated using the correlation listed in Table 7–1.

$$\text{Nu}_{\text{forced}} = 0.027 \text{ Re}^{0.805} \text{Pr}^{1/3} = 0.027(8.21 \times 10^4)^{0.805}(2.22)^{1/3} = 318$$

(*a*) For water flowing upward (assisting flow) the combined Nusselt number is (use $n = 4$ for horizontal cylinder)

$$\text{Nu}_{\text{combined}} = (\text{Nu}_{\text{forced}}^4 + \text{Nu}_{\text{natural}}^4)^{1/4} = (318^4 + 390^4)^{1/4} = \textbf{427}$$

(*b*) For water flowing downward (opposing flow) the combined Nusselt number is (use $n = 4$ for horizontal cylinder)

$$\text{Nu}_{\text{combined}} = (\text{Nu}_{\text{forced}}^4 - \text{Nu}_{\text{natural}}^4)^{1/4} = (318^4 - 390^4)^{1/4} = \textbf{337}$$

Discussion Note that the Nusselt number for the assisting flow is about 21 percent higher than that for the opposing flow. Therefore, natural convection must be taken into consideration when it is significant.

TOPIC OF SPECIAL INTEREST*

Heat Transfer Through Windows

Windows are *glazed apertures* in the building envelope that typically consist of single or multiple glazing (glass or plastic), framing, and shading. In a building envelope, windows offer the least resistance to heat transfer. In a typical house, about one-third of the total heat loss in winter occurs through the windows. Also, most air infiltration occurs at the edges of the windows.

---

* This section can be skipped without a loss of continuity.
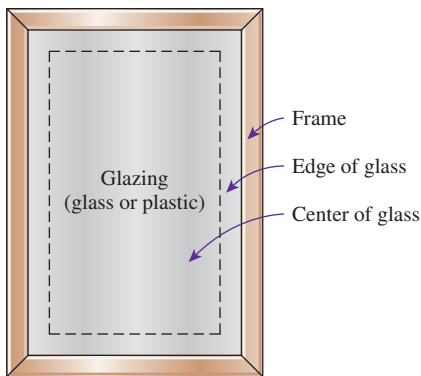
FIGURE 9–40
The three regions of a window considered in heat transfer analysis.

The solar heat gain through the windows is responsible for much of the cooling load in summer. The net effect of a window on the heat balance of a building depends on the characteristics and orientation of the window as well as the solar and weather data. Workmanship is very important in the construction and installation of windows to provide effective sealing around the edges while allowing them to be opened and closed easily.

Despite being so undesirable from an energy conservation point of view, windows are an essential part of any building envelope since they enhance the appearance of the building, allow daylight and solar heat to come in, and allow people to view and observe outside without leaving their home. For low-rise buildings, windows also provide easy exit areas during emergencies such as fire. Important considerations in the selection of windows are *thermal comfort* and *energy conservation.* A window should have a good light transmittance while providing effective resistance to heat transfer. The lighting requirements of a building can be minimized by maximizing the use of natural daylight. Heat loss in winter through the windows can be minimized by using airtight double- or triple-pane windows with spectrally selective films or coatings, and letting in as much solar radiation as possible. Heat gain and thus cooling load in summer can be minimized by using effective internal or external shading on the windows.

Even in the absence of solar radiation and air infiltration, heat transfer through the windows is more complicated than it appears to be. This is because the structure and properties of the frame are quite different than the glazing. As a result, heat transfer through the frame and the edge section of the glazing adjacent to the frame is two-dimensional. Therefore, it is customary to consider the window in three regions when analyzing heat transfer through it: (1) the *center-of-glass,* (2) the *edge-of-glass,* and (3) the *frame* regions, as shown in Fig. 9–40. Then the total rate of heat transfer through the window is determined by adding the heat transfer through each region as

$$\dot{Q}_{\text{window}} = \dot{Q}_{\text{center}} + \dot{Q}_{\text{edge}} + \dot{Q}_{\text{frame}}$$
$$= U_{\text{window}} A_{\text{window}} (T_{\text{indoors}} - T_{\text{outdoors}}) \tag{9–67}$$

where

$$U_{\text{window}} = (U_{\text{center}} A_{\text{center}} + U_{\text{edge}} A_{\text{edge}} + U_{\text{frame}} A_{\text{frame}})/A_{\text{window}} \tag{9–68}$$

is the *U*-**factor** or the **overall heat transfer coefficient** of the window; A_{window} is the window area; $A_{\text{center}}, A_{\text{edge}},$ and A_{frame} are the areas of the center, edge, and frame sections of the window, respectively; and $U_{\text{center}}, U_{\text{edge}},$ and U_{frame} are the heat transfer coefficients for the center, edge, and frame sections of the window. Note that $A_{\text{window}} = A_{\text{center}} + A_{\text{edge}} + A_{\text{frame}},$ and the overall *U*-factor of the window is determined from the area-weighed *U*-factors of each region of the window. Also, the inverse of the *U*-factor is the *R*-value, which is the unit thermal resistance of the window (thermal resistance for a unit area).

Consider steady one-dimensional heat transfer through a single-pane glass of thickness *L* and thermal conductivity *k*. The thermal resistance network of this problem consists of surface resistances on the inner and outer

surfaces and the conduction resistance of the glass in series, as shown in Fig. 9–41, and the total resistance on a unit area basis can be expressed as

$$R_{total} = R_{inside} + R_{glass} + R_{outside} = \frac{1}{h_i} + \frac{L_{glass}}{k_{glass}} + \frac{1}{h_o} \quad \text{(9–69)}$$

Using common values of 3 mm for the thickness and 0.92 W/m·K for the thermal conductivity of the glass and the winter design values of 8.29 and 34.0 W/m²·K for the inner and outer surface heat transfer coefficients, the thermal resistance of the glass is determined to be

$$R_{total} = \frac{1}{8.29 \text{ W/m}^2\text{·K}} + \frac{0.003 \text{ m}}{0.92 \text{ W/m·K}} + \frac{1}{34.0 \text{ W/m}^2\text{·K}}$$
$$= 0.121 + 0.003 + 0.029 = 0.153 \text{ m}^2\text{·K/W}$$

Note that the ratio of the glass resistance to the total resistance is

$$\frac{R_{glass}}{R_{total}} = \frac{0.003 \text{ m}^2\text{·K/W}}{0.153 \text{ m}^2\text{·K/W}} = 2.0\%$$

That is, the glass layer itself contributes about 2 percent of the total thermal resistance of the window, which is negligible. The situation would not be much different if we used acrylic, whose thermal conductivity is 0.19 W/m·K, instead of glass. Therefore, we cannot reduce the heat transfer through the window effectively by simply increasing the thickness of the glass. But we can reduce it by trapping still air between two layers of glass. The result is a **double-pane window**, which has become the norm in window construction.

The thermal conductivity of air at room temperature is $k_{air} = 0.025$ W/m·K, which is one-thirtieth that of glass. Therefore, the thermal resistance of 1-cm-thick still air is equivalent to the thermal resistance of a 30-cm-thick glass layer. Disregarding the thermal resistances of glass layers, the thermal resistance and U-factor of a double-pane window can be expressed as (Fig. 9–42)

$$\frac{1}{U_{double–pane (center region)}} \cong \frac{1}{h_i} + \frac{1}{h_{space}} + \frac{1}{h_o} \quad \text{(9–70)}$$

where $h_{space} = h_{rad, space} + h_{conv, space}$ is the combined radiation and convection heat transfer coefficient of the space trapped between the two glass layers.

Roughly half of the heat transfer through the airspace of a double-pane window is by radiation, and the other half is by conduction (or convection, if there is any air motion). Therefore, there are two ways to minimize h_{space} and thus the rate of heat transfer through a double-pane window:

1. *Minimize radiation heat transfer through the airspace.* This can be done by reducing the emissivity of glass surfaces by coating them with low-emissivity (or "low-e" for short) material. Recall that the *effective emissivity* of two parallel plates of emissivities ε_1 and ε_2 is given by

$$\varepsilon_{effective} = \frac{1}{1/\varepsilon_1 + 1/\varepsilon_2 - 1} \quad \text{(9–71)}$$
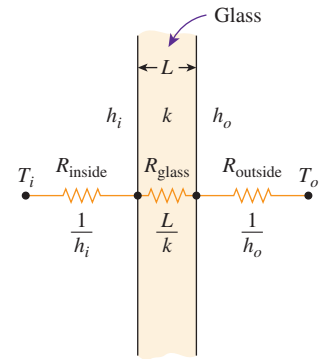
FIGURE 9–41
The thermal resistance network for heat transfer through a single glass.
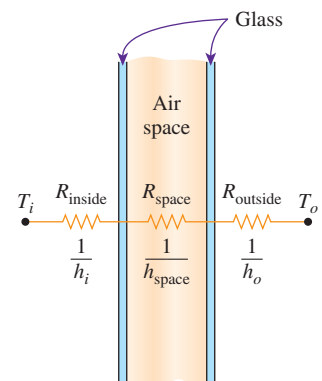
FIGURE 9–42
The thermal resistance network for heat transfer through the center section of a double-pane window (the resistances of the glasses are neglected).

TABLE 9–3

The heat transfer coefficient h_{space} for the airspace trapped between the two vertical parallel glass layers for 13-mm- and 6-mm-thick airspaces

(a) Airspace thickness = 13 mm						(b) Airspace thickness = 6 mm					
		h_{space}, W/m²·K*						h_{space}, W/m²·K*			
		$\varepsilon_{effective}$						$\varepsilon_{effective}$			
T_{avg}, °C	ΔT, °C	0.72	0.4	0.2	0.1	T_{avg}, °C	ΔT, °C	0.72	0.4	0.2	0.1
0	5	5.3	3.8	2.9	2.4	0	5	7.2	5.7	4.8	4.3
0	15	5.3	3.8	2.9	2.4	0	50	7.2	5.7	4.8	4.3
0	30	5.5	4.0	3.1	2.6	10	5	7.7	6.0	5.0	4.5
10	5	5.7	4.1	3.0	2.5	10	50	7.7	6.1	5.0	4.5
10	15	5.7	4.1	3.1	2.5	30	5	8.8	6.8	5.5	4.9
10	30	6.0	4.3	3.3	2.7	30	50	8.8	6.8	5.5	4.9
30	5	5.7	4.6	3.4	2.7	50	5	10.0	7.5	6.0	5.2
30	15	5.7	4.7	3.4	2.8	50	50	10.0	7.5	6.0	5.2
30	30	6.0	4.9	3.6	3.0						

Source: Building Materials and Structures, Report 151, U.S. Dept. of Commerce.
*Multiply by 0.176 to convert to Btu/h·ft²·°F.

The emissivity of an ordinary glass surface is 0.84. Therefore, the effective emissivity of two parallel glass surfaces facing each other is 0.72. But when the glass surfaces are coated with a film that has an emissivity of 0.1, the effective emissivity reduces to 0.05, which is one-fourteenth of 0.72. Then for the same surface temperatures, radiation heat transfer will also go down by a factor of 14. Even if only one of the surfaces is coated, the overall emissivity reduces to 0.1, which is the emissivity of the coating. Thus it is no surprise that about one-fourth of all windows sold for residences have a low-e coating. The heat transfer coefficient h_{space} for the airspace trapped between the two vertical parallel glass layers is given in Table 9–3 for 13-mm-$\left(\frac{1}{2}\text{-in}\right)$ and 6-mm-$\left(\frac{1}{4}\text{-in}\right)$ thick airspaces for various effective emissivities and temperature differences.

It can be shown that coating just one of the two parallel surfaces facing each other with a material of emissivity ε reduces the effective emissivity nearly to ε. Therefore, it is usually more economical to coat only one of the facing surfaces. Note from Fig. 9–43 that coating one of the interior surfaces of a double-pane window with a material having an emissivity of 0.1 reduces the rate of heat transfer through the center section of the window by half.

2. *Minimize conduction heat transfer through airspace.* This can be done by *increasing* the distance d between the two glasses. However, this cannot be done indefinitely, since increasing the spacing beyond a critical value initiates convection currents in the enclosed airspace, which increases the heat transfer coefficient and thus defeats the purpose. Besides, increasing the spacing also increases the thickness of the necessary framing and the cost of the window. Experimental studies have shown that when the spacing d is less than about 13 mm, there is no convection, and heat transfer through the air is by
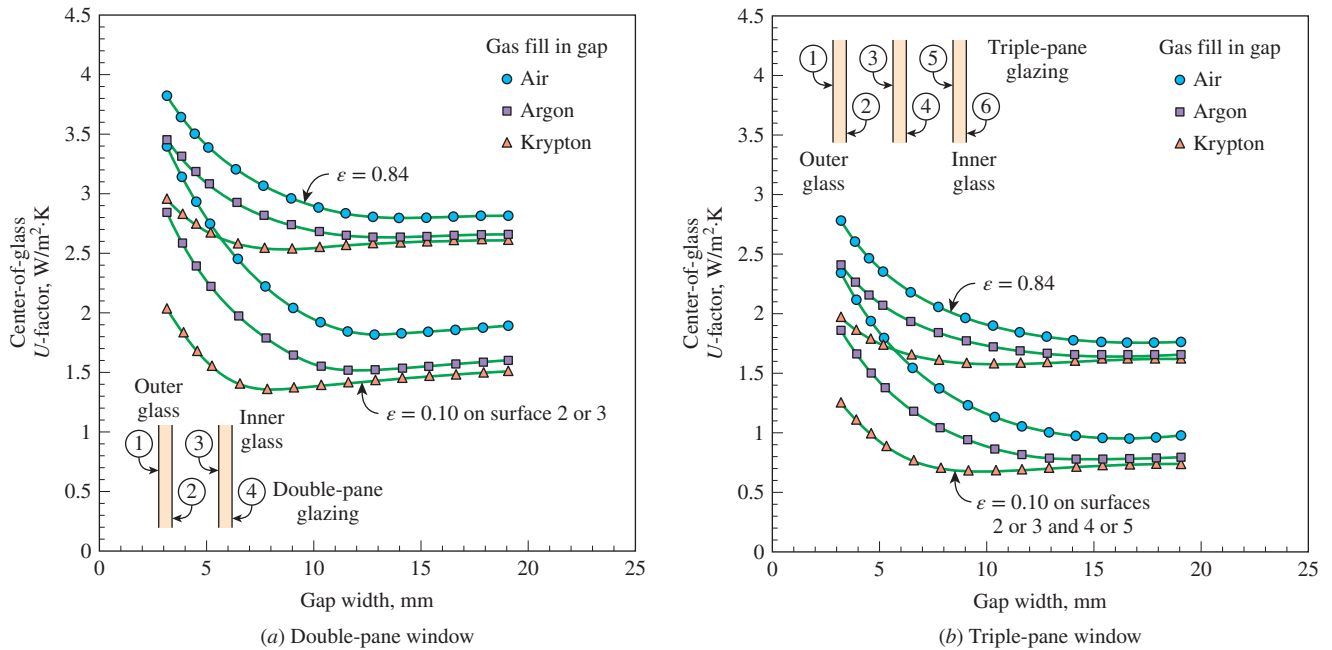
FIGURE 9–43

The variation of the *U*-factor for the center section of double- and triple-pane windows with uniform spacing between the panes.

Source: ASHRAE Handbook of Fundamentals*, Chap. 27, Fig. 1.*

conduction. But as the spacing is increased further, convection currents appear in the airspace, and the increase in heat transfer coefficient offsets any benefit obtained by the thicker air layer. As a result, the heat transfer coefficient remains nearly constant, as shown in Fig. 9–43. Therefore, it makes no sense to use an airspace thicker than 13 mm in a double-pane window unless a thin polyester film is used to divide the airspace into two halves to suppress convection currents. The film provides added insulation without adding much to the weight or cost of the double-pane window. The thermal resistance of the window can be increased further by using triple- or quadruple-pane windows whenever it is economical to do so. Note that using a triple-pane window instead of a double-pane reduces the rate of heat transfer through the center section of the window by about one-third.

Another way of reducing conduction heat transfer through a double-pane window is to use a *less-conducting fluid* such as argon or krypton to fill the gap between the glasses instead of air. The gap in this case needs to be well sealed to prevent the gas from leaking outside. Of course, another alternative is to evacuate the gap between the glasses completely, but it is not practical to do so.

Edge-of-Glass *U*-Factor of a Window

The glasses in double- and triple-pane windows are kept apart from each other at a uniform distance by **spacers** made of metals or insulators like aluminum, fiberglass, wood, and butyl. Continuous spacer strips are placed around the
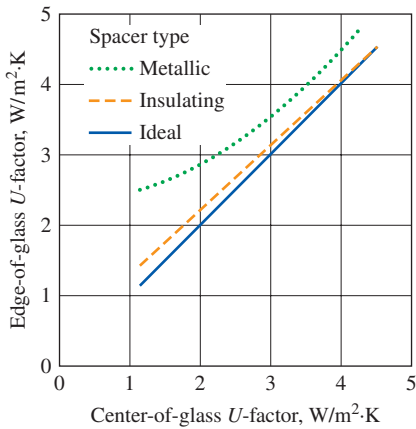
FIGURE 9–44

The edge-of-glass U-factor relative to the center-of-glass U-factor for windows with various spacers.

Source: ASHRAE Handbook of Fundamentals, *Chap. 27, Fig. 2.*

glass perimeter to provide an edge seal as well as uniform spacing. However, the spacers also serve as undesirable "thermal bridges" between the glasses, which are at different temperatures, and this short circuiting may increase heat transfer through the window considerably. Heat transfer in the edge region of a window is two-dimensional, and lab measurements indicate that the edge effects are limited to a 6.5-cm-wide band around the perimeter of the glass.

The U-factor for the edge region of a window is given in Fig. 9–44 relative to the U-factor for the center region of the window. The curve would be a straight diagonal line if the two U-values were equal to each other. Note that this is almost the case for insulating spacers such as wood and fiberglass. But the U-factor for the edge region can be twice that of the center region for conducting spacers such as those made of aluminum. Values for steel spacers fall between the two curves for metallic and insulating spacers. The edge effect is not applicable to single-pane windows.

Frame *U*-Factor

The framing of a window consists of the entire window except the glazing. Heat transfer through the framing is difficult to determine because of the different window configurations, different sizes, different constructions, and different combinations of materials used in the frame construction. The type of glazing such as single pane, double pane, and triple pane affects the thickness of the framing and thus heat transfer through the frame. Most frames are made of *wood, aluminum, vinyl,* or *fiberglass.* However, using a combination of these materials (such as aluminum-clad wood and vinyl-clad aluminum) is also common to improve appearance and durability.

Aluminum is a popular framing material because it is inexpensive, durable, and easy to manufacture, and it does not rot or absorb water like wood. However, from a heat transfer point of view, it is the least desirable framing material because of its high thermal conductivity. It will come as no surprise that the U-factor of solid aluminum frames is the highest, and thus a window with aluminum framing will lose much more heat than a comparable window with wood or vinyl framing. Heat transfer through the aluminum framing members can be reduced by using plastic inserts between components to serve as thermal barriers. The thickness of these inserts greatly affects heat transfer through the frame. For aluminum frames without the plastic strips, the primary resistance to heat transfer is due to the interior surface heat transfer coefficient. The U-factors for various frames are listed in Table 9–4 as a function of spacer materials and the glazing unit thicknesses. Note that the U-factor of metal framing and thus the rate of heat transfer through a metal window frame is more than three times that of a wood or vinyl window frame.

Interior and Exterior Surface Heat Transfer Coefficients

Heat transfer through a window is also affected by the convection and radiation heat transfer coefficients between the glass surfaces and surroundings. The effects of convection and radiation on the inner and outer

TABLE 9–4

Representative frame U-factors for fixed vertical windows

Frame Material	U-Factor, W/m^2·K*
Aluminum:	
Single glazing (3 mm)	10.1
Double glazing (18 mm)	10.1
Triple glazing (33 mm)	10.1
Wood or vinyl:	
Single glazing (3 mm)	2.9
Double glazing (18 mm)	2.8
Triple glazing (33 mm)	2.7

Source: ASHRAE Handbook of Fundamentals, *Chap. 27, Table 2.*

*Multiply by 0.176 to convert to Btu/h·ft^2·°F

surfaces of glazings are usually combined into the combined convection and radiation heat transfer coefficients h_i and h_o, respectively. Under still air conditions, the combined heat transfer coefficient at the inner surface of a vertical window can be determined from

$$h_i = h_{conv} + h_{rad} = 1.77(T_g - T_i)^{0.25} + \frac{\varepsilon_g \sigma(T_g^4 - T_i^4)}{T_g - T_i} \quad \text{(W/m}^2\text{·K)} \qquad \textbf{(9-72)}$$

where T_g = glass temperature in K, T_i = indoor air temperature in K, ε_g = emissivity of the inner surface of the glass exposed to the room (taken to be 0.84 for uncoated glass), and $\sigma = 5.67 \times 10^{-8}$ W/m²·K⁴ is the Stefan–Boltzmann constant. Here the temperature of the interior surfaces facing the window is assumed to be equal to the indoor air temperature. This assumption is reasonable when the window faces mostly interior walls, but it becomes questionable when the window is exposed to heated or cooled surfaces or to other windows. The commonly used value of h_i for peak load calculation is

$$h_i = 8.29 \text{ W/m}^2\text{·K} = 1.46 \text{ Btu/h·ft}^2\text{·°F} \quad \text{(winter and summer)}$$

which corresponds to the winter design conditions of $T_i = 22°C$ and $T_g = -7°C$ for uncoated glass with $\varepsilon_g = 0.84$. But the same value of h_i can also be used for summer design conditions as it corresponds to summer conditions of $T_i = 24°C$ and $T_g = 32°C$. The values of h_i for various temperatures and glass emissivities are given in Table 9–5. The commonly used values of h_o for peak load calculations are the same as those used for outer wall surfaces (34.0 W/m²·K for winter and 22.7 W/m²·K for summer).

Overall *U*-Factor of Windows

The overall *U*-factors for various kinds of windows and skylights are evaluated using computer simulations and laboratory testing for winter design conditions; representative values are given in Table 9–6. Test data may provide more accurate information for specific products and should be preferred when available. However, the values listed in the table can be used to obtain satisfactory results under various conditions in the absence of product-specific data. The *U*-factor of a fenestration product that differs considerably from the ones in the table can be determined by (1) determining the fractions of the area that are frame, center-of-glass, and edge-of-glass (assuming a 65-mm-wide band around the perimeter of each glazing), (2) determining the *U*-factors for each section (the center-of-glass and edge-of-glass *U*-factors can be taken from the first two columns of Table 9–6 and the frame *U*-factor can be taken from Table 9–5 or other sources), and (3) multiplying the area fractions and the *U*-factors for each section and adding them up.

Glazed wall systems can be treated as fixed windows. Also, the data for double-door windows can be used for single-glass doors. Several observations can be made from the data in the table:

1. Skylight *U*-factors are considerably greater than those of vertical windows. This is because the skylight area, including the curb, can be 13

TABLE 9–5

Combined convection and radiation heat transfer coefficient h_i at the inner surface of a vertical glass under still air conditions (in W/m²·K)*

T_i (°C)	T_g (°C)	Glass Emissivity, ε_g		
		0.05	0.20	0.84
20	17	2.6	3.5	7.1
20	15	2.9	3.8	7.3
20	10	3.4	4.2	7.7
20	5	3.7	4.5	7.9
20	0	4.0	4.8	8.1
20	−5	4.2	5.0	8.2
20	−10	4.4	5.1	8.3

*Multiply by 0.176 to convert to Btu/h·ft²·°F.

TABLE 9–6

Overall *U*-factors (heat transfer coefficients) for various windows and skylights in W/m²·K

Type →	Center-of-glass	Edge-of-glass		Fixed	Double door	Sloped skylight	Fixed		Double door		Sloped skylight	
				Glass Section (Glazing) Only	*Aluminum Frame (Without Thermal Break)*		*Wood or Vinyl Frame*					
Frame width →	(Not applicable)			32 mm ($1\frac{1}{4}$ in)	53 mm (2 in)	19 mm ($\frac{3}{4}$ in)	41 mm ($1\frac{5}{8}$ in)		88 mm ($3\frac{7}{18}$ in)		23 mm ($\frac{7}{8}$ in)	
Spacer type →	—	Metal	Insul.	All	All	All	Metal	Insul.	Metal	Insul.	Metal	Insul.
Glazing Type												
Single Glazing												
3 mm ($\frac{1}{8}$ in) glass	6.30	6.30	—	6.63	7.16	9.88	5.93	—	5.57	—	7.57	—
6.4 mm ($\frac{1}{4}$ in) acrylic	5.28	5.28	—	5.69	6.27	8.86	5.02	—	4.77	—	6.57	—
3 mm ($\frac{1}{8}$ in) acrylic	5.79	5.79	—	6.16	6.71	9.94	5.48	—	5.17	—	7.63	—
Double Glazing (no coating)												
6.4 mm airspace	3.24	3.71	3.34	3.90	4.55	6.70	3.26	3.16	3.20	3.09	4.37	4.22
12.7 mm airspace	2.78	3.40	2.91	3.51	4.18	6.65	2.88	2.76	2.86	2.74	4.32	4.17
6.4 mm argon space	2.95	3.52	3.07	3.66	4.32	6.47	3.03	2.91	2.98	2.87	4.14	3.97
12.7 mm argon space	2.61	3.28	2.76	3.36	4.04	6.47	2.74	2.61	2.73	2.60	4.14	3.97
Double Glazing [ε = 0.1, coating on one of the surfaces of airspace (surface 2 or 3, counting from the outside toward inside)]												
6.4 mm airspace	2.44	3.16	2.60	3.21	3.89	6.04	2.59	2.46	2.60	2.47	3.73	3.53
12.7 mm airspace	1.82	2.71	2.06	2.67	3.37	6.04	2.06	1.92	2.13	1.99	3.73	3.53
6.4 mm argon space	1.99	2.83	2.21	2.82	3.52	5.62	2.21	2.07	2.26	2.12	3.32	3.09
12.7 mm argon space	1.53	2.49	1.83	2.42	3.14	5.71	1.82	1.67	1.91	1.78	3.41	3.19
Triple Glazing (no coating)												
6.4 mm airspace	2.16	2.96	2.35	2.97	3.66	5.81	2.34	2.18	2.36	2.21	3.48	3.24
12.7 mm airspace	1.76	2.67	2.02	2.62	3.33	5.67	2.01	1.84	2.07	1.91	3.34	3.09
6.4 mm argon space	1.93	2.79	2.16	2.77	3.47	5.57	2.15	1.99	2.19	2.04	3.25	3.00
12.7 mm argon space	1.65	2.58	1.92	2.52	3.23	5.53	1.91	1.74	1.98	1.82	3.20	2.95
Triple Glazing [ε = 0.1, coating on one of the surfaces of airspaces (surfaces 3 and 5, counting from the outside toward inside)]												
6.4 mm airspace	1.53	2.49	1.83	2.42	3.14	5.24	1.81	1.64	1.89	1.73	2.92	2.66
12.7 mm airspace	0.97	2.05	1.38	1.92	2.66	5.10	1.33	1.15	1.46	1.30	2.78	2.52
6.4 mm argon space	1.19	2.23	1.56	2.12	2.85	4.90	1.52	1.35	1.64	1.47	2.59	2.33
12.7 mm argon space	0.80	1.92	1.25	1.77	2.51	4.86	1.18	1.01	1.33	1.17	2.55	2.28

From ASHRAE Handbook of Fundamentals, *Chap. 27, Table 5*
Notes:

(1) Multiply by 0.176 to obtain *U*-factors in Btu/h·ft²·°F.

(2) The *U*-factors in this table include the effects of surface heat transfer coefficients and are based on winter conditions of −18°C outdoor air and 21°C indoor air temperature, with 24 km/h (15 mph) winds outdoors and zero solar flux. Small changes in indoor and outdoor temperatures will not affect the overall *U*-factors much. Windows are assumed to be vertical, and the skylights are tilted 20° from the horizontal with upward heat flow. Insulation spacers are wood, fiberglass, or butyl. Edge-of-glass effects are assumed to extend the 65-mm band around the perimeter of each glazing. The product sizes are 1.2 m × 1.8 m for fixed windows, 1.8 m × 2.0 m for double-door windows, and 1.2 m × 0.6 m for the skylights, but the values given can also be used for products of similar sizes. All data are based on 3-mm ($\frac{1}{8}$ in) glass unless noted otherwise.

to 240 percent greater than the rough opening area. The slope of the skylight also has some effect.

2. The *U*-factor of multiple-glazed units can be reduced considerably by filling cavities with argon gas instead of dry air. The performance of CO_2-filled units is similar to those filled with argon. The *U*-factor can be reduced even further by filling the glazing cavities with krypton gas.

3. Coating the glazing surfaces with low-e (low-emissivity) films reduces the *U*-factor significantly. For multiple-glazed units, it is adequate to coat one of the two surfaces facing each other.

4. The thicker the airspace in multiple-glazed units, the lower the *U*-factor, for a thickness of up to 13 mm $\left(\frac{1}{2} \text{ in}\right)$ of airspace. For a specified number of glazings, the window with thicker air layers will have a lower *U*-factor. For a specified overall thickness of glazing, the higher the number of glazings, the lower the *U*-factor. Therefore, a triple-pane window with airspaces of 6.4 mm (two such airspaces) will have a lower *U*-value than a double-pane window with an airspace of 12.7 mm.

5. Wood or vinyl frame windows have a considerably lower *U*-value than comparable metal-frame windows. Therefore, wood or vinyl frame windows are called for in energy-efficient designs.

EXAMPLE 9–9   *U*-Factor for Center-of-Glass Section of Windows

Determine the *U*-factor for the center-of-glass section of a double-pane window with a 6-mm airspace for winter design conditions (Fig. 9–45). The glazings are made of clear glass that has an emissivity of 0.84. Take the average airspace temperature at design conditions to be 0°C.

SOLUTION   The *U*-factor for the center-of-glass section of a double-pane window is to be determined.
Assumptions   1 Steady operating conditions exist. 2 Heat transfer through the window is one-dimensional. 3 The thermal resistance of glass sheets is negligible.
Properties   The emissivity of clear glass is 0.84.
Analysis   Disregarding the thermal resistance of glass sheets, which are small, the *U*-factor for the center region of a double-pane window is determined from

$$\frac{1}{U_{\text{center}}} \cong \frac{1}{h_i} + \frac{1}{h_{\text{space}}} + \frac{1}{h_o}$$

where h_i, h_{space}, and h_o are the heat transfer coefficients at the inner surface of the window, the airspace between the glass layers, and the outer surface of the window, respectively. The values of h_i and h_o for winter design conditions were given earlier to be $h_i = 8.29 \text{ W/m}^2\cdot\text{K}$ and $h_o = 34.0 \text{ W/m}^2\cdot\text{K}$. The effective emissivity of the airspace of the double-pane window is

$$\varepsilon_{\text{effective}} = \frac{1}{1/\varepsilon_1 + 1/\varepsilon_2 - 1} = \frac{1}{1/0.84 + 1/0.84 - 1} = 0.72$$
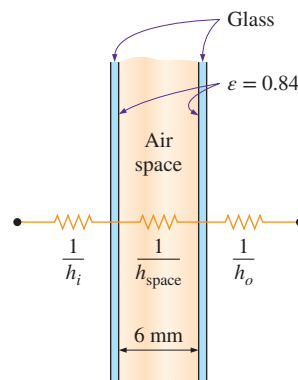
FIGURE 9–45
Schematic of Example 9–9.

For this value of emissivity and an average airspace temperature of 0°C, we read $h_{\text{space}} = 7.2$ W/m²·K from Table 9–3 for 6-mm-thick airspace. Therefore,

$$\frac{1}{U_{\text{center}}} = \frac{1}{8.29} + \frac{1}{7.2} + \frac{1}{34.0} \rightarrow U_{\text{center}} = \textbf{3.46 W/m}^2\textbf{·K}$$

Discussion The center-of-glass *U*-factor value of 3.24 W/m²·K in Table 9–6 (fourth row and second column) is obtained by using a standard value of $h_o = 29$ W/m²·K (instead of 34.0 W/m²·K) and $h_{\text{space}} = 6.5$ W/m²·K at an average airspace temperature of −15°C.
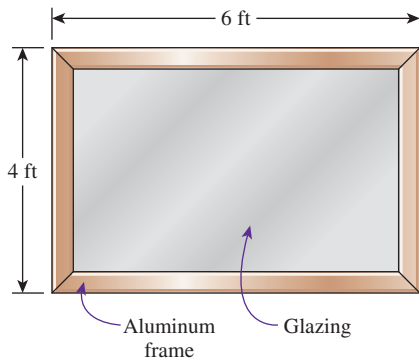
FIGURE 9–46
Schematic for Example 9–10.

EXAMPLE 9–10 **Heat Loss Through Aluminum-Framed Windows**

A fixed aluminum-framed window with glass glazing is being considered for an opening that is 4 ft high and 6 ft wide in the wall of a house that is maintained at 72°F (Fig. 9–46). Determine the rate of heat loss through the window and the inner surface temperature of the window glass facing the room when the outdoor air temperature is 15°F if the window is selected to be (*a*) $\frac{1}{8}$-in single glazing, (*b*) double glazing with an airspace of $\frac{1}{2}$ in, and (*c*) low-e-coated triple glazing with an airspace of $\frac{1}{2}$ in.

SOLUTION The rate of heat loss through an aluminum-framed window and the inner surface temperature are to be determined from the cases of single-pane, double-pane, and low-e triple-pane windows.

Assumptions **1** Steady operating conditions exist. **2** Heat transfer through the window is one-dimensional. **3** Thermal properties of the windows and the heat transfer coefficients are constant.

Properties The *U*-factors of the windows are given in Table 9–6.

Analysis The rate of heat transfer through the window can be determined from

$$\dot{Q}_{\text{window}} = U_{\text{overall}} A_{\text{window}} (T_i - T_o)$$

where T_i and T_o are the indoor and outdoor air temperatures, respectively; U_{overall} is the *U*-factor (the overall heat transfer coefficient) of the window; and A_{window} is the window area, which is determined to be

$$A_{\text{window}} = \text{Height} \times \text{Width} = (4 \text{ ft})(6 \text{ ft}) = 24 \text{ ft}^2$$

The *U*-factors for the three cases can be determined directly from Table 9–6 to be 6.63, 3.51, and 1.92 W/m²·K, respectively, to be multiplied by the factor 0.176 to convert them to Btu/h·ft²·°F. Also, the inner surface temperature of the window glass can be determined from

$$\dot{Q}_{\text{window}} = h_i A_{\text{window}} (T_i - T_{\text{glass}}) \longrightarrow T_{\text{glass}} = T_i - \frac{\dot{Q}_{\text{window}}}{h_i A_{\text{window}}}$$

where h_i is the heat transfer coefficient on the inner surface of the window, which is determined from Table 9–5 to be $h_i = 8.3$ W/m²·K = 1.46 Btu/h·ft²·°F.

Then the rate of heat loss and the interior glass temperature for each case are determined as follows:

(*a*) Single glazing:

$$\dot{Q}_{\text{window}} = (6.63 \times 0.176 \text{ Btu/h·ft}^2\text{·°F})(24 \text{ ft}^2)(72 - 15)\text{°F} = \textbf{1596 Btu/h}$$

$$T_{\text{glass}} = T_i - \frac{\dot{Q}_{\text{window}}}{h_i A_{\text{window}}} = 72\text{°F} - \frac{1596 \text{ Btu/h}}{(1.46 \text{ Btu/h·ft}^2\text{·°F})(24 \text{ ft}^2)} = \textbf{26.5°F}$$

(*b*) Double glazing ($\frac{1}{2}$ in airspace):

$$\dot{Q}_{\text{window}} = (3.51 \times 0.176 \text{ Btu/h·ft}^2\text{·°F})(24 \text{ ft}^2)(72 - 15)\text{°F} = \textbf{845 Btu/h}$$

$$T_{\text{glass}} = T_i - \frac{\dot{Q}_{\text{window}}}{h_i A_{\text{window}}} = 72\text{°F} - \frac{845 \text{ Btu/h}}{(1.46 \text{ Btu/h·ft}^2\text{·°F})(24 \text{ ft}^2)} = \textbf{47.9°F}$$

(*c*) Triple glazing ($\frac{1}{2}$ in airspace, low-e coated):

$$\dot{Q}_{\text{window}} = (1.92 \times 0.176 \text{ Btu/h·ft}^2\text{·°F})(24 \text{ ft}^2)(72 - 15)\text{°F} = \textbf{462 Btu/h}$$

$$T_{\text{glass}} = T_i - \frac{\dot{Q}_{\text{window}}}{h_i A_{\text{window}}} = 72\text{°F} - \frac{462 \text{ Btu/h}}{(1.46 \text{ Btu/h·ft}^2\text{·°F})(24 \text{ ft}^2)} = \textbf{58.8°F}$$

Therefore, heat loss through the window will be reduced by 47 percent in the case of double glazing and by 71 percent in the case of triple glazing relative to the single-glazing case. Also, in the case of single glazing, the low inner-glass surface temperature will cause considerable discomfort for the occupants because of the excessive heat loss from the body by radiation. It is raised from 26.5°F, which is below freezing, to 47.9°F in the case of double glazing and to 58.8°F in the case of triple glazing.

EXAMPLE 9–11   *U*-Factor of a Double-Door Window

Determine the overall *U*-factor for a double-door-type, wood-framed double-pane window with metal spacers, and compare your result to the value listed in Table 9–6. The overall dimensions of the window are 1.80 m × 2.00 m, and the dimensions of each glazing are 1.72 m × 0.94 m (Fig. 9–47).

SOLUTION The overall *U*-factor for a double-door-type window is to be determined, and the result is to be compared to the tabulated value.

Assumptions **1** Steady operating conditions exist. **2** Heat transfer through the window is one-dimensional.

Properties The *U*-factors for the various sections of windows are given in Tables 9–4 and 9–6.

Analysis The areas of the window, the glazing, and the frame are

$$A_{\text{window}} = \text{Height} \times \text{Width} = (1.8 \text{ m})(2.0 \text{ m}) = 3.60 \text{ m}^2$$

$$A_{\text{glazing}} = 2 \times (\text{Height} \times \text{Width}) = 2(1.72 \text{ m})(0.94 \text{ m}) = 3.23 \text{ m}^2$$

$$A_{\text{frame}} = A_{\text{window}} - A_{\text{glazing}} = 3.60 - 3.23 = 0.37 \text{ m}^2$$
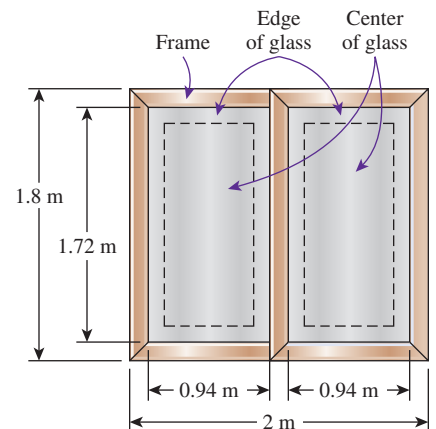
FIGURE 9–47
Schematic for Example 9–11.

The edge-of-glass region consists of a 6.5-cm-wide band around the perimeter of the glazings, and the areas of the center and edge sections of the glazing are determined to be

$$A_{\text{center}} = 2 \times (\text{Height} \times \text{Width}) = 2(1.72 - 0.13 \text{ m})(0.94 - 0.13 \text{ m}) = 2.58 \text{ m}^2$$

$$A_{\text{edge}} = A_{\text{glazing}} - A_{\text{center}} = 3.23 - 2.58 = 0.65 \text{ m}^2$$

The U-factor for the frame section is determined from Table 9–4 to be $U_{\text{frame}} = 2.8$ W/m²·K. The U-factors for the center and edge sections are determined from Table 9–6 (fifth row, second and third columns) to be $U_{\text{center}} = 3.24$ W/m²·K and $U_{\text{edge}} = 3.71$ W/m²·K. Then the overall U-factor of the entire window becomes

$$U_{\text{window}} = (U_{\text{center}}A_{\text{center}} + U_{\text{edge}}A_{\text{edge}} + U_{\text{frame}}A_{\text{frame}})/A_{\text{window}}$$

$$= (3.24 \times 2.58 + 3.71 \times 0.65 + 2.8 \times 0.37)/3.60 = \textbf{3.28 W/m}^2\textbf{·K}$$

The overall U-factor listed in Table 9–6 for the specified type of window is 3.20 W/m²·K, which is sufficiently close to the value obtained above.

SUMMARY

In this chapter, we have considered natural convection heat transfer where any fluid motion occurs by natural means such as buoyancy. The volume expansion coefficient of a substance represents the variation of the density of that substance with temperature at constant pressure, and for an ideal gas, it is expressed as $\beta = 1/T$, where T is the absolute temperature in K or R.

The flow regime in natural convection is governed by a dimensionless number called the *Grashof number,* which represents the ratio of the buoyancy force to the viscous force acting on the fluid and is expressed as

$$\text{Gr}_L = \frac{g\beta(T_s - T_\infty)L_c^3}{\nu^2}$$

where L_c is the *characteristic length,* which is the height L for a vertical plate and the diameter D for a horizontal cylinder. The correlations for the Nusselt number $\text{Nu} = hL_c/k$ in natural convection are expressed in terms of the *Rayleigh number* defined as

$$\text{Ra}_L = \text{Gr}_L \text{Pr} = \frac{g\beta(T_s - T_\infty)L_c^3}{\nu^2} \text{Pr}$$

Nusselt number relations for various surfaces are given in Table 9–1. All fluid properties are evaluated at the film temperature of $T_f = \frac{1}{2}(T_s + T_\infty)$. The outer surface of a vertical cylinder can be treated as a vertical plate when the curvature effects are negligible. The characteristic length for a horizontal surface is $L_c = A_s/p$, where A_s is the surface area and p is the perimeter.

The average Nusselt number for vertical isothermal *parallel plates* of spacing S and height L is given as

$$\text{Nu} = \frac{hS}{k} = \left[\frac{576}{(\text{Ra}_s S/L)^2} + \frac{2.873}{(\text{Ra}_s S/L)^{0.5}}\right]^{-0.5}$$

The optimum fin spacing for a vertical heat sink and the Nusselt number for optimally spaced fins is

$$S_{\text{opt}} = 2.714\left(\frac{S^3 L}{\text{Ra}_s}\right)^{0.25} = 2.714\frac{L}{\text{Ra}_L^{0.25}} \quad \text{and} \quad \text{Nu} = \frac{hS_{\text{opt}}}{k} = 1.307$$

In a *horizontal rectangular enclosure* with the hotter plate at the top, heat transfer is by pure conduction and $\text{Nu} = 1$. When the hotter plate is at the bottom, the Nusselt number is

$$\text{Nu} = 1 + 1.44\left[1 - \frac{1708}{\text{Ra}_L}\right]^+ + \left[\frac{\text{Ra}_L^{1/3}}{18} - 1\right]^+ \quad \text{Ra}_L < 10^8$$

The notation $[\ ]^+$ indicates that if the quantity in the bracket is negative, it should be set equal to zero. For *vertical rectangular enclosures,* the Nusselt number can be determined from

$$\text{Nu} = 0.18\left(\frac{\text{Pr}}{0.2 + \text{Pr}}\text{Ra}_L\right)^{0.29} \qquad \begin{array}{c} 1 < H/L < 2 \\ \text{any Prandtl number} \\ \text{Ra}_L\text{Pr}/(0.2 + \text{Pr}) > 10^3 \end{array}$$

$$\text{Nu} = 0.22\left(\frac{\text{Pr}}{0.2 + \text{Pr}}\text{Ra}_L\right)^{0.28}\left(\frac{H}{L}\right)^{-1/4} \qquad \begin{array}{c} 2 < H/L < 10 \\ \text{any Prandtl number} \\ \text{Ra}_L < 10^{10} \end{array}$$

For aspect ratios greater than 10, Eqs. 9–54 and 9–55 should be used. For inclined enclosures, Eqs. 9–48 through 9–51 should be used.

For *concentric horizontal cylinders,* the rate of heat transfer through the annular space between the cylinders by natural convection per unit length is

$$\dot{Q} = \frac{2\pi k_{\text{eff}}}{\ln(D_o/D_i)}(T_i - T_o)$$

where

$$\frac{k_{\text{eff}}}{k} = 0.386\left(\frac{\text{Pr}}{0.861 + \text{Pr}}\right)^{1/4}(F_{\text{cyl}}\text{Ra}_L)^{1/4}$$

and

$$F_{\text{cyl}} = \frac{[\ln(D_o/D_i)]^4}{L_c^3(D_i^{-3/5} + D_o^{-3/5})^5}$$

For a *spherical enclosure,* the rate of heat transfer through the space between the spheres by natural convection is expressed as

$$\dot{Q} = k_{\text{eff}}\frac{\pi D_i D_o}{L_c}(T_i - T_o)$$

where

$$\frac{k_{\text{eff}}}{k} = 0.74\left(\frac{\text{Pr}}{0.861 + \text{Pr}}\right)^{1/4}(F_{\text{sph}}\text{Ra}_L)^{1/4}$$

$$L_c = (D_o - D_i)/2$$

$$F_{\text{sph}} = \frac{L_c}{(D_i D_o)^4(D_i^{-7/5} + D_o^{-7/5})^5}$$

The quantity kNu is called the *effective thermal conductivity* of the enclosure, since a fluid in an enclosure behaves like a quiescent fluid whose thermal conductivity is kNu as a result of convection currents. The fluid properties are evaluated at the average temperature of $(T_i + T_o)/2$.

For a given fluid, the parameter Gr/Re^2 represents the importance of natural convection relative to forced convection. Natural convection is negligible when $\text{Gr}/\text{Re}^2 < 0.1$, forced convection is negligible when $\text{Gr}/\text{Re}^2 > 10$, and neither is negligible when $0.1 < \text{Gr}/\text{Re}^2 < 10$.

REFERENCES AND SUGGESTED READING

1. American Society of Heating, Refrigeration, and Air Conditioning Engineers. *Handbook of Fundamentals.* Atlanta, GA: ASHRAE, 1993.

2. J. N. Arnold, I. Catton, and D. K. Edwards. "Experimental Investigation of Natural Convection in Inclined Rectangular Regions of Differing Aspect Ratios." ASME Paper No. 75-HT-62, 1975.

3. L. S. Asgeirsson and A. J. Ghajar. "Prediction of Thermal Conductivity and Viscosity for Some Fluids in the Near-Critical Region." *Chemical Engineering Communications* 43, nos. 1–3 (1986), pp. 165–184.

4. P. S. Ayyaswamy and I. Catton. "The Boundary–Layer Regime for Natural Convection in a Differently Heated Tilted Rectangular Cavity." *Journal of Heat Transfer* 95 (1973), p. 543.

5. A. Bar-Cohen. "Fin Thickness for an Optimized Natural Convection Array of Rectangular Fins." *Journal of Heat Transfer* 101 (1979), pp. 564–566.

6. A. Bar-Cohen and W. M. Rohsenow. "Thermally Optimum Spacing of Vertical Natural Convection Cooled Parallel Plates." *Journal of Heat Transfer* 106 (1984), p. 116.

7. B. M. Berkovsky and V. K. Polevikov. "Numerical Study of Problems on High-Intensive Free Convection." In *Heat Transfer and Turbulent Buoyant Convection,* ed. D. B. Spalding and N. Afgan, pp. 443–445. Washington, DC: Hemisphere, 1977.

8. I. Catton. "Natural Convection in Enclosures." *Proceedings of Sixth International Heat Transfer Conference.* Toronto: Canada, 1978, Vol. 6, pp. 13–31.

9. T. Cebeci. "Laminar Free Convection Heat Transfer from the Outer Surface of a Vertical Slender Circular Cylinder." *Proceedings of Fifth International Heat Transfer Conference* paper NCI.4, 1974, pp. 15–19.

10. Y. A. Çengel and P. T. L. Zing. "Enhancement of Natural Convection Heat Transfer from Heat Sinks by Shrouding." *Proceedings of ASME/JSME Thermal Engineering Conference,* vol. 3. Honolulu: HI, 1987, pp. 451–475.

11. S. W. Churchill. "A Comprehensive Correlating Equation for Laminar Assisting Forced and Free Convection." *AIChE Journal* 23 (1977), pp. 10–16.

12. S. W. Churchill. "Free Convection Around Immersed Bodies." In *Heat Exchanger Design Handbook,* ed. E. U. Schlünder, Section 2.5.7. New York: Hemisphere, 1983.

13. S. W. Churchill. "Combined Free and Forced Convection Around Immersed Bodies." In *Heat Exchanger Design Handbook,* Section 2.5.9. New York: Hemisphere Publishing, 1986.

14. S. W. Churchill and H. H. S. Chu. "Correlating Equations for Laminar and Turbulent Free Convection from a Horizontal Cylinder." *International Journal of Heat Mass Transfer* 18 (1975a), p. 1049.

15. S. W. Churchill and H. H. S. Chu. "Correlating Equations for Laminar and Turbulent Free Convection from a Vertical Plate." *International Journal of Heat Mass Transfer* 18 (1975b), p. 1323.

16. E. R. G. Eckert and E. Soehngen. "Studies on Heat Transfer in Laminar Free Convection with Zehnder–Mach Interferometer." USAF Technical Report 5747, December 1948.

17. E. R. G. Eckert and E. Soehngen. "Interferometric Studies on the Stability and Transition to Turbulence of a Free Convection Boundary Layer." *Proceedings of General Discussion, Heat Transfer ASME-IME,* London, 1951.

18. S. M. ElSherbiny, G. D. Raithby, and K. G. T. Hollands. "Heat Transfer by Natural Convection Across Vertical and Inclined Air Layers." *Journal of Heat Transfer* 104 (1982), pp. 96–102.

19. T. Fujii and H. Imura. "Natural Convection Heat Transfer from a Plate with Arbitrary Inclination." *International Journal of Heat Mass Transfer* 15 (1972), p. 755.

20. A. J. Ghajar and A. Asadi, "Improved Forced Convective Heat Transfer Correlations for Liquids in the Near-Critical Region." *AIAA Journal* 24, No. 12 (1986), pp. 2030–2037.

21. S. Ghorbani-Tari and A. J. Ghajar. "Improved Free Convective Heat Transfer Correlations in the Near-Critical Region." *AIAA Journal* 23, no. 10 (1985), pp. 1647–1649.

22. S. Globe and D. Dropkin. "Natural Convection Heat Transfer in Liquids Confined between Two Horizontal Plates." *Journal of Heat Transfer* 81 (1959), pp. 24–28.

23. K. G. T. Hollands, T. E. Unny, G. D. Raithby, and L. Konicek. "Free Convective Heat Transfer Across Inclined Air Layers." *Journal of Heat Transfer* 98 (1976), pp. 182–193.

24. M. Jakob. *Heat Transfer.* New York: Wiley, 1949.

25. W. M. Kays, M. E. Crawford, and B. Weigand. *Convective Heat and Mass Transfer.* 4th ed. New York: McGraw-Hill, 2005.

26. Reprinted from J. R. Lloyd and E. M. Sparrow. "Combined Force and Free Convection Flow on Vertical Surfaces." *International Journal of Heat Mass Transfer* 13 copyright 1970, with permission from Elsevier.

27. R. K. MacGregor and A. P. Emery. "Free Convection Through Vertical Plane Layers: Moderate and High Prandtl Number Fluids." *Journal of Heat Transfer* 91 (1969), p. 391.

28. T. S. Najjar and A. J. Ghajar. "Prediction of Density and Constant Pressure Specific Heat for Several Fluids in the Near-Critical Region." AIAA paper No. 83-1476, *AIAA 18th Thermophysics Conference,* Montreal, Canada, June 1–3 (1983).

29. S. Ostrach. "An Analysis of Laminar Free Convection Flow and Heat Transfer About a Flat Plate Parallel to the Direction of the Generating Body Force." National Advisory Committee for Aeronautics, Report 1111, 1953.

30. G. D. Raithby and K. G. T. Hollands. "A General Method of Obtaining Approximate Solutions to Laminar and Turbulent Free Convection Problems." In *Advances in Heat Transfer,* vol. II, ed. F. Irvine and J. P. Hartnett, pp. 265–315. New York: Academic Press, 1975.

31. E. M. Sparrow and J. L. Gregg. "Laminar Free Convection from a Vertical Flat Plate." *Transactions of the ASME* 78 (1956), p. 438.

32. E. M. Sparrow and J. L. Gregg. "Laminar Free Convection Heat Transfer from the Outer Surface of a Vertical Circular Cylinder." *ASME* 78 (1956), p. 1823.

33. E. M. Sparrow and C. Prakash. "Enhancement of Natural Convection Heat Transfer by a Staggered Array of Vertical Plates." *Journal of Heat Transfer* 102 (1980), pp. 215–220.

34. E. M. Sparrow and S. B. Vemuri. "Natural Convection/Radiation Heat Transfer from Highly Populated Pin Fin Arrays." *Journal of Heat Transfer* 107 (1985), pp. 190–197.

35. L. M. Tam and A. J. Ghajar. "Transitional Heat Transfer in Plain Horizontal Tubes." *Heat Transfer Engineering* 27, no. 5 (2006), pp. 23–38.

PROBLEMS *

Physical Mechanism of Natural Convection

9–1C What is natural convection? How does it differ from forced convection? What force causes natural convection currents?

---

*Problems designated by a "C" are concept questions, and students are encouraged to answer them all. Problems designated by an "E" are in English units, and the SI users can ignore them. Problems with the 🖥 icon are comprehensive in nature and are intended to be solved with appropriate software. Problems with the PtD icon are Prevention through Design problems. Problems with the C&S icon are Codes and Standards problems.

9–2C In which mode of heat transfer is the convection heat transfer coefficient usually higher, natural convection or forced convection? Why?

9–3C Consider a hot boiled egg in a spacecraft that is filled with air at atmospheric pressure and temperature at all times. Will the egg cool faster or slower when the spacecraft is in space instead of on the ground? Explain.

9–4C When will the hull of a ship sink deeper in the water: when the ship is sailing in fresh water or in seawater? Why?

9–5C What is buoyancy force? Compare the relative magnitudes of the buoyancy force acting on a body immersed in

these media: (*a*) air, (*b*) water, (*c*) mercury, and (*d*) an evacuated chamber.

9–6C Consider a fluid whose volume does not change with temperature at constant pressure. What can you say about natural convection heat transfer in this medium?

9–7C Consider two fluids, one with a large coefficient of volume expansion and the other with a small one. In what fluid will a hot surface initiate stronger natural convection currents? Why? Assume the viscosity of the fluids to be the same.

9–8C Physically, what does the Grashof number represent? How does the Grashof number differ from the Reynolds number?

9–9 Show that the volume expansion coefficient of an ideal gas is $\beta = 1/T$, where T is the absolute temperature.

9–10 Using its definition and the values listed in Table A–9, determine the volume expression coefficient of saturated liquid water at 70°C. Compare the result with the value tabulated in Table A–9.

9–11 The density of liquid water can be correlated as $\rho(T) = 1000 - 0.0736\,T - 0.00355\,T^2$ where ρ and T are in kg/m^3 and °C, respectively. Determine the volume expansion coefficient at 70°C. Compare the result with the value tabulated in Table A–9.

9–12 A 10-cm × 10-cm plate has a constant surface temperature of 150°C. Determine the Grashof number if the chip is placed in the following fluids: air (1 atm, 30°C), liquid water (30°C), engine oil (10°C). Discuss how the Grashof number affects the natural convection flow.

9–13E A long 2-in-diameter rod with surface temperature of 200°F is submerged in a bath of fluid. Determine the Grashof and Rayleigh numbers if the fluid is (*a*) liquid water at 40°F, (*b*) liquid ammonia at 40°F, (*c*) engine oil at 50°F, and (*d*) air at 40°F (1 atm).

Natural Convection over Surfaces

9–14C How does the Rayleigh number differ from the Grashof number?

9–15C Will a hot horizontal plate whose back side is insulated cool faster or slower when its hot surface is facing down instead of up?

9–16C Consider laminar natural convection from a vertical hot plate. Will the heat flux be higher at the top or at the bottom of the plate? Why?

9–17C Under what conditions can the outer surface of a vertical cylinder be treated as a vertical plate in natural convection calculations?

9–18 A 0.2-m-long and 25-mm-thick vertical plate ($k = 15$ W/m·K) separates the hot water from the cold water. The plate surface exposed to the hot water has a temperature of 100°C, and the temperature of the cold water is 7°C. Determine the temperature of the plate surface exposed to the cold water ($T_{s,c}$). *Hint:* The $T_{s,c}$ has to be found iteratively. Start the iteration process with an initial guess of 53.5°C for the $T_{s,c}$.
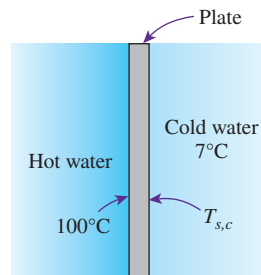
FIGURE P9–18

9–19 Reconsider Prob. 9–18. Using appropriate software, investigate the effect of the plate thermal conductivity on the surface temperature exposed to the cold water. By varying the plate thermal conductivity from 3 to 200 W/m·K, plot the plate surface temperature on the cold water side as a function of the plate thermal conductivity.

9–20 C&S A 0.5-m × 0.5-m vertical ASTM A203 B steel plate has one surface subjected to convection with cold, quiescent air at −70°C. The minimum temperature suitable for the steel plate is −30°C (ASME Code for Process Piping, ASME B31.3-2014, Table A-1M). Determine the heat addition rate needed to keep the plate surface temperature from dropping below the minimum suitable temperature.

9–21 C&S A 0.5-m × 0.5-m vertical ASTM B152 copper plate has one surface subjected to convection with hot, quiescent air. The maximum use temperature for the ASTM B152 copper plate is 260°C (ASME Code for Process Piping, ASME B31.3-2014, Table A-1M). If the rate of heat removal from the plate is 90 W, determine the maximum temperature that the air can reach without causing the surface temperature of the copper plate to increase above 260°C. Evaluate the properties of air at 300°C. Is this an appropriate temperature to evaluate the air properties?

9–22 A 0.2-m-long and 25-mm-thick vertical plate ($k = 1.5$ W/m·K) separates the hot water from the cold air at 2°C. The plate surface exposed to the hot water has a temperature of 100°C, and the surface exposed to the cold air has an emissivity of 0.73. Determine the temperature of the plate surface exposed to the cold air ($T_{s,c}$). *Hint:* The $T_{s,c}$ has to be found iteratively. Start the iteration process with an initial guess of 51°C for the $T_{s,c}$.
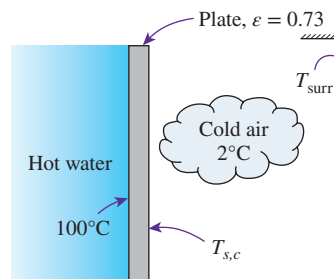
FIGURE P9–22

9–23 Reconsider Prob. 9–22. Using appropriate software, evaluate the effect of the plate thickness on the surface temperature exposed to the cold air. By varying the plate thickness from 0.01 to 0.1 m, plot the plate surface temperature on the cold air side as a function of the plate thickness.

9–24 **C&S** An ASTM F441 chlorinated polyvinyl chloride (CPVC) tube is embedded in a vertical concrete wall ($k = 1.4$ W/m·K). The wall has a height of 1 m, and one surface of the wall is subjected to convection with hot air at 140°C. The distance measured from the plate's surface that is exposed to the hot air to the tube surface is $d = 3$ cm. The ASME Code for Process Piping limits the maximum use temperature for ASTM F441 CPVC tube to 93.3°C (ASME B31.3-2014, Table B-1). If the concrete surface that is exposed to the hot air is at 100°C, would the CPVC tube embedded in the wall still comply with the ASME code?
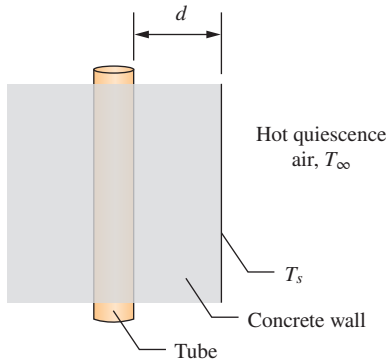
FIGURE P9–24

9–25 **C&S** A 0.5-m × 0.5-m vertical ASTM A240 410S stainless steel plate has one surface subjected to convection with a cold, quiescent gas at −70°C. The type of cold gas that the plate surface is exposed to alternates between carbon dioxide and hydrogen. The minimum temperature suitable for the stainless steel plate is −30°C(ASME Code for Process Piping, ASME B31.3-2014, Table A-1M). Determine the heat addition rate necessary for keeping the plate surface temperature from dropping below the minimum suitable temperature, such that it is applicable to both carbon dioxide gas and hydrogen gas.

9–26 A 0.5-m-long thin vertical plate is subjected to uniform heat flux on one side, while the other side is exposed to cool air at 5°C. The plate surface has an emissivity of 0.73, and its midpoint temperature is 55°C. Determine the heat flux on the plate surface.
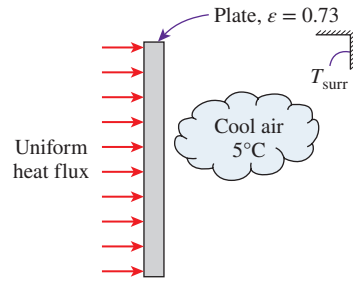
FIGURE P9–26

9–27 A 0.5-m-long thin vertical plate is subjected to a uniform heat flux of 1200 W/m² on one side, while the other side is exposed to hydrogen gas at 5°C. Assuming that the properties of the hydrogen gas can be evaluated at 50°C, determine the plate midpoint temperature $T_{L/2}$. Is 50°C an appropriate film temperature for evaluation of the properties of the hydrogen gas?
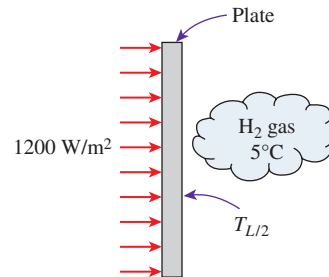
FIGURE P9–27

9–28 A 0.5-m-long thin vertical copper plate is subjected to a uniform heat flux of 1000 W/m² on one side, while the other side is exposed to air at 5°C. Determine the plate midpoint temperature for (*a*) a highly polished surface and (*b*) a black oxidized surface. *Hint:* The plate midpoint temperature ($T_{L/2}$) has to be found iteratively. Begin the calculations by using a film temperature of 30°C.
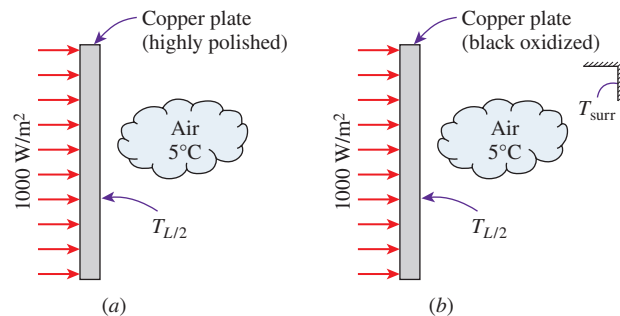
FIGURE P9–28

9–29 Reconsider Prob. 9–28. Using appropriate software, evaluate the effect of the uniform surface heat flux on the plate midpoint temperature for (*a*) the highly polished surface and (*b*) the black oxidized surface. By varying the surface heat flux from 500 to 1500 W/m², plot the plate midpoint temperature as a function of the surface heat flux.

9–30 A 0.2-m × 0.2-m street sign surface has an absorptivity of 0.6 and an emissivity of 0.7. Solar radiation is incident on the street sign at a rate of 200 W/m², and the surrounding quiescent air is at 25°C. Determine the surface temperature of the street sign. Assume the film temperature is 30°C.

$\varepsilon = 0.7$
$\alpha_s = 0.6$ Air, 25°C
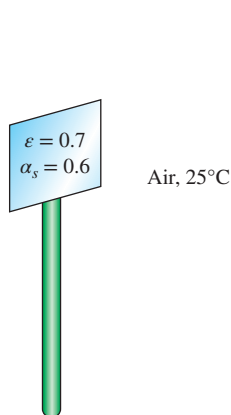
FIGURE P9–30

9–31 Consider a 1.2-m-high and 2-m-wide glass window with a thickness of 6 mm, thermal conductivity $k = 0.78$ W/m·K, and emissivity $\varepsilon = 0.9$. The room and the walls that face the window are maintained at 25°C, and the average temperature of the inner surface of the window is measured to be 5°C. If the temperature of the outdoors is −5°C, determine (*a*) the convection heat transfer coefficient on the inner surface of the window, (*b*) the rate of total heat transfer through the window, and (*c*) the combined natural convection and radiation heat transfer coefficient on the outer surface of the window. Is it reasonable to neglect the thermal resistance of the glass in this case?

Wall
Room 25°C
Glass
1.2 m
−5°C
5°C
$\varepsilon = 0.9$
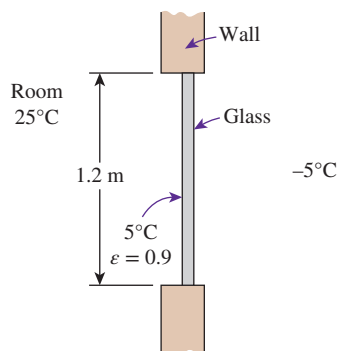
FIGURE P9–31

9–32E Consider a 2-ft × 2-ft thin square plate in a room at 75°F. One side of the plate is maintained at a temperature of 130°F, while the other side is insulated. Determine the rate of heat transfer from the plate by natural convection if the plate is (*a*) vertical, (*b*) horizontal with hot surface facing up, and (*c*) horizontal with hot surface facing down.

9–33E Reconsider Prob. 9–32E. Using appropriate software, plot the rate of natural convection heat transfer for different orientations of the plate as a function of the plate temperature as the temperature varies from 80°F to 180°F, and discuss the results.

9–34 The side surfaces of a 3-m-high cubic industrial furnace burning natural gas are not insulated, and the temperature at the outer surface of this section is measured to be 110°C. The temperature of the furnace room, including its surfaces, is 30°C, and the emissivity of the outer surface of the furnace is 0.7. It is proposed that this section of the furnace wall be insulated with glass wool insulation ($k = 0.038$ W/m·K) wrapped by a reflective sheet ($\varepsilon = 0.2$) in order to reduce the heat loss by 90 percent. Assuming the outer surface temperature of the metal section still remains at about 110°C, determine the thickness of the insulation that needs to be used.

The furnace operates continuously throughout the year and has an efficiency of 78 percent. The price of the natural gas is $1.10/therm (1 therm = 105,500 kJ of energy content). If the installation of the insulation will cost $550 for materials and labor, determine how long it will take for the insulation to pay for itself from the energy it saves.

Hot gases
30°C
3 m
Furnace
110°C
$\varepsilon = 0.7$
3 m
3 m
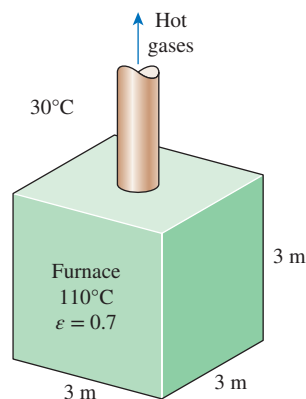
FIGURE P9–34

9–35 Consider a vertical plate with length *L,* placed in quiescent air. If the film temperature is 20°C and the average Nusselt number in natural convection is of the form $\mathrm{Nu} = C\mathrm{Ra}_L^n$, show that the average heat transfer coefficient can be expressed as

$$h = 1.51(\Delta T/L)^{1/4} \quad 10^4 < \mathrm{Ra}_L < 10^9$$
$$h = 1.19\,\Delta T^{1/3} \qquad 10^{10} < \mathrm{Ra}_L < 10^{13}$$

9–36 A 50-cm $\times$ 50-cm circuit board that contains 121 square chips on one side is to be cooled by combined natural convection and radiation by mounting it on a vertical surface in a room at 25°C. Each chip dissipates 0.18 W of power, and the emissivity of the chip surfaces is 0.7. Assuming the heat transfer from the back side of the circuit board to be negligible, and the temperature of the surrounding surfaces to be the same as the air temperature of the room, determine the surface temperature of the chips. Evaluate air properties at a film temperature of 30°C and 1 atm pressure. Is this a good assumption? *Answer:* 36.2°C

9–37 Repeat Prob. 9–36 assuming the circuit board to be positioned horizontally with (*a*) chips facing up and (*b*) chips facing down.

9–38 Consider a 15-cm $\times$ 20-cm printed circuit board (PCB) that has electronic components on one side. The board is placed in a room at 20°C. The heat loss from the back surface of the board is negligible. If the circuit board is dissipating 8 W of power in steady operation, determine the average temperature of the hot surface of the board, assuming the board is (*a*) vertical, (*b*) horizontal with hot surface facing up, and (*c*) horizontal with hot surface facing down. Take the emissivity of the surface of the board to be 0.8 and assume the surrounding surfaces to be at the same temperature as the air in the room. Evaluate air properties at a film temperature of 32.5°C and 1 atm pressure. Is this a good assumption? *Answers:* (*a*) 46.6°C, (*b*) 42.6°C, (*c*) 50.7°C
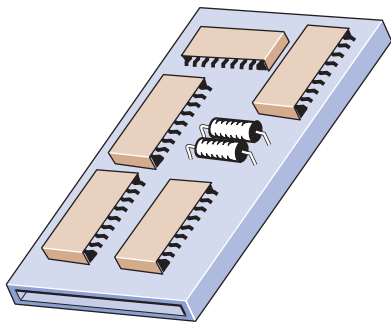
FIGURE P9–38

9–39 Reconsider Prob. 9–38. Using appropriate software, investigate the effects of the room temperature and the emissivity of the board on the temperature of the hot surface of the board for different orientations of the board. Let the room temperature vary from 5°C to 35°C and the emissivity from 0.1 to 1.0. Plot the hot surface temperature for different orientations of the board as the functions of the room temperature and the emissivity, and discuss the results.

9–40 [C&S] A 0.6-m $\times$ 0.6-m horizontal ASTM A240 410S stainless steel plate has its upper surface subjected to convection with cold, quiescent air. The minimum

temperature suitable for the stainless steel plate is −30°C (ASME Code for Process Piping, ASME B31.3-2014, Table A-1M). If heat is added to the plate at a rate of 70 W, determine the lowest temperature that the air can reach without causing the surface temperature of the plate to cool below the minimum suitable temperature. Evaluate the properties of air at −50°C. Is this an appropriate temperature at which to evaluate the air properties?

9–41 Consider a thin 24-cm-long and 20-cm-wide horizontal plate suspended in air at 20°C. The plate is equipped with electric resistance heating elements with a rating of 20 W. Now the heater is turned on and the plate temperature rises. Determine the temperature of the plate when steady operating conditions are reached. The plate has an emissivity of 0.90, and the surrounding surfaces are at 17°C. As an initial guess, assume a surface temperature of 50°C. Is this a good assumption?
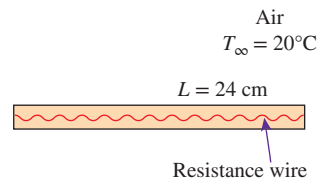
FIGURE P9–41

9–42 A manufacturer makes absorber plates that are 1.2 m $\times$ 0.8 m in size for use in solar collectors. The back side of the plate is heavily insulated, while its front surface is coated with black chrome, which has an absorptivity of 0.87 for solar radiation and an emissivity of 0.09. Consider such a plate placed horizontally outdoors in calm air at 25°C. Solar radiation is incident on the plate at a rate of 600 W/m². Taking the effective sky temperature to be 10°C, determine the equilibrium temperature of the absorber plate. What would your answer be if the absorber plate is made of ordinary aluminum plate that has a solar absorptivity of 0.28 and an emissivity of 0.07? Evaluate air properties at a film temperature of 70°C and 1 atm pressure. Is this a good assumption?
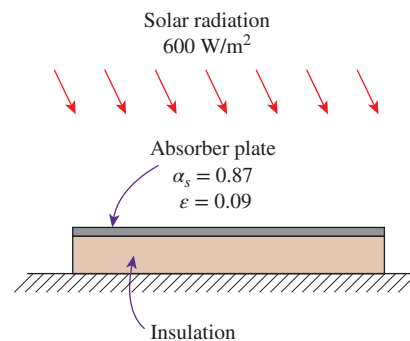
FIGURE P9–42

9–43 Repeat Prob. 9–42 for an aluminum plate painted flat black (solar absorptivity 0.98 and emissivity 0.98) and also for a plate painted white (solar absorptivity 0.26 and emissivity 0.90). Evaluate air properties at a film temperature of 45°C and 1 atm pressure. Is this a good assumption?

9–44 A 0.6-m × 0.6-m horizontal ASTM A203 B steel plate has its lower surface subjected to convection with cold, quiescent hydrogen gas at −70°C. The minimum temperature suitable for the steel plate is −30°C (ASME Code for Process Piping, ASME B31.3-2014, Table A-1M). The lower plate surface has an emissivity of 0.3, and thermal radiation exchange occurs between the lower plate surface and the surroundings at −70°C. Determine the heat addition rate necessary for keeping the lower plate surface temperature from dropping below the minimum suitable temperature.

9–45 Two 0.6-m × 0.6-m horizontal metal plates are secured together by a series of stainless steel bolts (ASTM A437 B4B). The bolts are leveled with the upper surface of the metal plate. The ASME Code for Process Piping limits the minimum suitable temperature for ASTM A437 B4B stainless steel bolts to −30°C (ASME B31.3-2014, Table A-2M). To prevent the bolts from being directly exposed to the cold, quiescent hydrogen gas at −60°C, a ceramic plate of the same size is attached to the metal plates. The ceramic plate has a thermal conductivity of 1.4 W/m·K, and its surface has an emissivity of 0.9. The upper surface of the ceramic plate is subjected to convection with a cold, quiescent hydrogen gas, and thermal radiation exchange occurs with the surroundings at −60°C. If the surface temperature of the ceramic plate is −40°C, determine the minimum thickness of the ceramic plate such that the stainless steel bolts are prevented from cooling below the minimum suitable temperature.
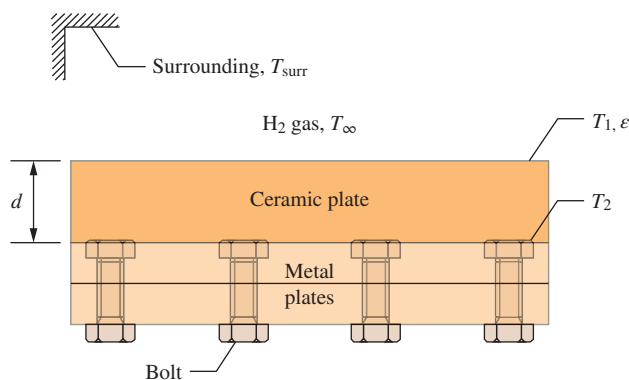
FIGURE P9-45

9–46 A circular grill of diameter 0.25 m has an emissivity of 0.8. If the surface temperature is maintained at 150°C, determine the required electrical power when the room air and surroundings are at 30°C.

9–47 A can of engine oil with a length of 150 mm and a diameter of 100 mm is placed vertically in the trunk of a car. On a hot summer day, the temperature in the trunk is 43°C. If the surface temperature of the can is 17°C, determine heat transfer rate from the can surface. Neglect the heat transfer from the ends of the can.

9–48 Flue gases from an incinerator are released to atmosphere using a stack that is 0.6 m in diameter and 10.0 m high. The outer surface of the stack is at 40°C and the surrounding air is at 10°C. Determine the rate of heat transfer from the stack, assuming (*a*) there is no wind and (*b*) the stack is exposed to 20 km/h winds.

9–49 Water is boiling in a 12-cm-deep pan with an outer diameter of 25 cm that is placed on top of a stove. The ambient air and the surrounding surfaces are at a temperature of 25°C, and the emissivity of the outer surface of the pan is 0.80. Assuming the entire pan to be at an average temperature of 98°C, determine the rate of heat loss from the cylindrical side surface of the pan to the surroundings by (*a*) natural convection and (*b*) radiation. (*c*) If water is boiling at a rate of 1.5 kg/h at 100°C, determine the ratio of the heat lost from the side surfaces of the pan to that by the evaporation of water. The enthalpy of vaporization of water at 100°C is 2257 kJ/kg. *Answers:* 46.2 W, 47.3 W, 0.099
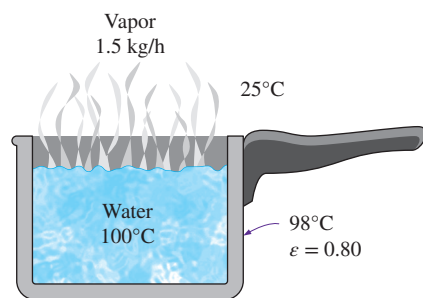
FIGURE P9−49

9–50 Repeat Prob. 9–49 for a pan whose outer surface is polished and has an emissivity of 0.1.

9–51 In a plant that manufactures canned aerosol paints, the cans are temperature-tested in water baths at 60°C before they are shipped to ensure that they withstand temperatures up to 55°C during transportation and shelving (as shown in Fig. P9–51). The cans, moving on a conveyor, enter the open hot water bath, which is 0.5 m deep, 1 m wide, and 3.5 m long, and they move slowly in the hot water toward the other end. Some of the cans fail the test and explode in the water bath. The water container is made of sheet metal, and the entire container is at about the same temperature as the hot water. The emissivity of the outer surface of the container is 0.7. If the temperature of the surrounding air and surfaces is 20°C, determine the rate

of heat loss from the four side surfaces of the container (disregard the top surface, which is open).

The water is heated electrically by resistance heaters, and the cost of electricity is $0.085/kWh. If the plant operates 24 h a day 365 days a year and thus 8760 h a year, determine the annual cost of the heat losses from the container for this facility.
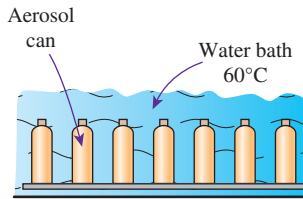
FIGURE P9–51

9–52 Reconsider Prob. 9–51. In order to reduce the heating cost of the hot water, it is proposed to insulate the side and bottom surfaces of the container with 5-cm-thick fiberglass insulation ($k = 0.035$ W/m·K) and to wrap the insulation with aluminum foil ($\varepsilon = 0.1$) in order to minimize the heat loss by radiation. An estimate is obtained from a local insulation contractor, who proposes to do the insulation job for $350, including materials and labor. Would you support this proposal? How long will it take for the insulation to pay for itself from the energy it saves? Evaluate air properties at a film temperature of 23°C and 1 atm pressure. Is this a good assumption?

9–53 A room is to be heated by a coal-burning stove, which is a cylindrical cavity with an outer diameter of 50 cm and a height of 120 cm. The rate of heat loss from the room is estimated to be 1.5 kW when the air temperature in the room is maintained constant at 24°C. The emissivity of the stove surface is 0.85, and the average temperature of the surrounding wall surfaces is 14°C. Determine the surface temperature of the stove. Neglect the heat transfer from the bottom surface and take the heat transfer coefficient at the top surface to be the same as that on the side surface.

The heating value of the coal is 30,000 kJ/kg, and the combustion efficiency is 65 percent. Determine the amount of coal burned in a day if the stove operates 14 h a day. Evaluate air properties at a film temperature of 77°C and 1 atm pressure. Is this a good assumption?

9–54 Consider a cylinder with a length of 15 cm and a diameter of 10 cm. The cylinder has a surface temperature of 43°C, while the room air temperature is 17°C. Determine whether placing the cylinder horizontally or vertically would achieve a higher heat transfer rate.

9–55 An aluminum soda can 150 mm in length and 60 mm in diameter is placed horizontally inside a refrigerator compartment that maintains a temperature of 4°C. If the surface temperature of the can is 36°C, estimate the heat transfer rate from the can. Neglect the heat transfer from the ends of the can.

9–56 **C&S** A boiler supplies hot water to a commercial dishwasher through a horizontal pipe with a surface temperature of 50°C. The hot water exits the boiler at 85°C, enters the pipe and is transported to the dishwasher. The outer diameter of the pipe is 20 mm, and the pipe distance between the boiler and the dishwasher is 20 m. The section of the pipe between the boiler and the dishwater is exposed to natural convection with air at an ambient temperature of 20°C. The hot water flows steadily in the pipe at 10 g/s, and its specific heat is 4.2 kJ/kg·K. The National Sanitation Foundation standard for commercial warewashing equipment (ANSI/NSF 3) requires that the final rinse water temperature be at least 82°C. Under these conditions, does the hot water entering the dishwasher meet the ANSI/NSF 3 standard? If not, discuss some possible ways to increase the temperature of the water entering the dishwasher.

9–57 Thermal energy generated by the electrical resistance of a 5-mm-diameter and 4-m-long bare cable is dissipated to the surrounding air at 20°C. The voltage drop and the electric current across the cable in steady operation are measured to be 60 V and 1.5 A, respectively. Disregarding radiation, estimate the surface temperature of the cable. Evaluate air properties at a film temperature of 60°C and 1 atm pressure. Is this a good assumption?

9–58 A 300-W cylindrical resistance heater is 0.75 m long and 0.5 cm in diameter. The resistance wire is placed horizontally in a fluid at 20°C. Determine the outer surface temperature of the resistance wire in steady operation if the fluid is (a) air and (b) water. Ignore any heat transfer by radiation. Use properties at 500°C for air and 40°C for water.

9–59 A 12-m-long section of a 5-cm-diameter horizontal hot-water pipe passes through a large room whose temperature is 27°C. If the temperature and the emissivity of the outer surface of the pipe are 73°C and 0.8, respectively, determine the rate of heat loss from the pipe by (a) natural convection and (b) radiation.

9–60 Thick fluids such as asphalt and waxes and the pipes in which they flow are often heated in order to reduce the viscosity of the fluids and thus to reduce the pumping costs. Consider the flow of such a fluid through a 100-m-long pipe of outer diameter 30 cm in calm, ambient air at 0°C. The pipe is heated electrically, and a thermostat keeps the outer surface temperature of the pipe constant at 25°C. The emissivity of the outer surface of the pipe is 0.8, and the effective sky temperature is −30°C. Determine the power rating of the electric resistance heater, in kW, that needs to be used. Also, determine the cost of electricity associated with heating the pipe during a 15-h period under the above conditions if the price of electricity is $0.09/kWh. *Answers:* 29.1 kW, $39.30

$T_{sky} = -30°C$

0°C

30 cm

$T_s = 25°C$
$\varepsilon = 0.8$

Asphalt   Resistance heater
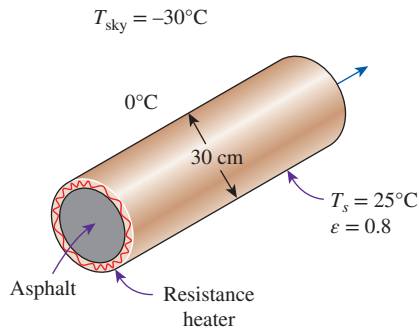
FIGURE P9–60

9–61 Reconsider Prob. 9–60. To reduce the cost of heating the pipe, it is proposed to insulate it with enough fiberglass insulation ($k = 0.035$ W/m·K) wrapped in aluminum foil ($\varepsilon = 0.1$) to cut down the heat losses by 85 percent. Assuming the pipe temperature must remain constant at 25°C, determine the thickness of the insulation that needs to be used. How much money will the insulation save during this 15-h period? Evaluate air properties at a film temperature of 5°C and 1 atm pressure. Is this a good assumption?   *Answers:* 1.3 cm, $33.40

9–62 **C & S** A boiler supplies hot water to equipment through a horizontal pipe. The hot water exits the pipe and enters the equipment at 98°C. The outer diameter of the pipe is 20 mm, and the pipe distance between the boiler and the equipment is 30 m. The section of the pipe between the boiler and the equipment is exposed to natural convection with air at an ambient temperature of 20°C. The hot water flows steadily in the pipe at 10 g/s, and its specific heat is 4.2 kJ/kg·K. The temperature at the pipe surface is 80°C, and the pipe has an emissivity of 0.6 that contributes to the thermal radiation with the surroundings at 20°C. According to the service restrictions of the ASME Boiler and Pressure Vessel Code (ASME BPVC.IV-2015, HG-101), hot water boilers should not be operating at temperatures exceeding 120°C at or near the boiler outlet. Determine whether the water temperature exiting the boiler is in compliance with the ASME Boiler and Pressure Vessel Code.

9–63 A 3-mm-diameter and 12-m-long electric wire is tightly wrapped with a 1.5-mm-thick plastic cover whose thermal conductivity and emissivity are $k = 0.20$ W/m·K and $\varepsilon = 0.9$. Electrical measurements indicate that a current of 10 A passes through the wire, and there is a voltage drop of 7 V along the wire. If the insulated wire is exposed to calm atmospheric air at $T_\infty = 30°C$, determine the temperature at the interface of the wire and the plastic cover in steady operation. Take the surrounding surfaces to be at about the same temperature as the air. Evaluate air properties at a film temperature of 40°C and 1 atm pressure. Is this a good assumption?

9–64 During a visit to a plastic sheeting plant, it was observed that a 45-m-long section of a 2-in nominal (6.03-cm-outer-diameter) steam pipe extended from one end of the plant to the other with no insulation on it. The temperature measurements

at several locations revealed that the average temperature of the exposed surfaces of the steam pipe was 170°C, while the temperature of the surrounding air was 20°C. The outer surface of the pipe appeared to be oxidized, and its emissivity can be taken to be 0.7. Taking the temperature of the surrounding surfaces to be 20°C also, determine the rate of heat loss from the steam pipe.

Steam is generated in a gas furnace that has an efficiency of 84 percent, and the plant pays $1.10 per therm (1 therm = 105,500 kJ) of natural gas. The plant operates 24 h a day, 365 days a year, and thus 8760 h a year. Determine the annual cost of the heat losses from the steam pipe for this facility.


170°C
20°C $\varepsilon = 0.7$
6.03 cm
45 m
Steam
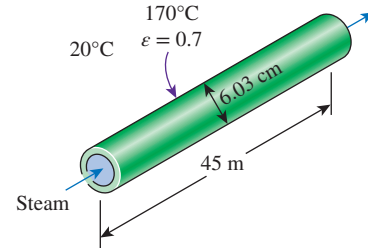
FIGURE P9–64

9–65 Reconsider Prob. 9–64. Using appropriate software, investigate the effect of the surface temperature of the steam pipe on the rate of heat loss from the pipe and the annual cost of this heat loss. Let the surface temperature vary from 100°C to 200°C. Plot the rate of heat loss and the annual cost as a function of the surface temperature, and discuss the results.

9–66 A 1.5-m-diameter, 4-m-long cylindrical propane tank is initially filled with liquid propane, whose density is 581 kg/m³. The tank is exposed to the ambient air at 25°C in calm weather. The outer surface of the tank is polished so that the radiation heat transfer is negligible. Now a crack develops at the top of the tank, and the pressure inside drops to 1 atm while the temperature drops to −42°C, which is the boiling temperature of propane at 1 atm. The heat of vaporization of propane at 1 atm is 425 kJ/kg. The propane is slowly vaporized as a result of the heat transfer from the ambient air into the tank, and the propane vapor escapes the tank at −42°C through the crack. Assuming the propane tank to be at about the same temperature as the propane inside at all times, determine how long it will take for the tank to empty if it is not insulated.

Propane vapor
25°C
1.5 m   Propane tank −42°C
4 m
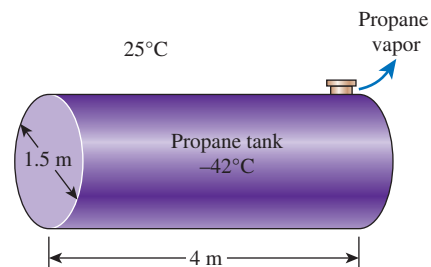
FIGURE P9–66

9–67 Hot water is being transported in a horizontal pipe ($k = 0.15$ W/m·K, $D_i = 2.5$ cm, $D_o = 4.5$ cm), where the pipe inner surface temperature is at 100°C. A length of 2 m of the pipe's outer surface is exposed to cool air at 12°C. Assuming that the properties of air can be evaluated at 40°C and 1 atm pressure, determine the outer surface temperature of the pipe. Is 40°C an appropriate film temperature for evaluation of the air properties?

9–68 [C&S] Water flows in a horizontal chlorinated polyvinyl chloride (CPVC) pipe with an inner and outer diameter of 15 mm and 20 mm, respectively. The thermal conductivity of the CPVC pipe is 0.136 W/m·K. The convection heat transfer coefficient at the inner surface of the pipe with the water flow is 50 W/m²·K. A section of the pipe is exposed to hot, quiescent air at 107°C, and the length of the pipe section in the hot air is 1 m. The recommended maximum temperature for CPVC pipe by the ASME Code for Process Piping is 93°C (ASME B31.3-2014, Table B-1). Determine the maximum temperature that the water flowing inside the pipe can be without causing the temperature of the CPVC pipe to go above 93°C.

9–69 Hot engine oil is being transported in a horizontal pipe ($k = 15$ W/m·K, $D_i = 5$ cm) with a wall thickness of 5 mm. The pipe is covered with a 5-mm-thick layer of insulation ($k = 0.15$ W/m·K). A length of 2 m of the outer surface is exposed to cool air at 10°C. If the pipe inner surface temperature is at 90°C, determine the outer surface temperature. *Hint:* The pipe outer surface temperature has to be found iteratively. Begin the calculations by using a film temperature of 50°C.

9–70 Reconsider Prob. 9–69. Using appropriate software, evaluate the effect of the insulation layer thickness on the outer surface temperature. By varying the insulation layer thickness from 5 to 15 mm, plot the outer surface temperature as a function of the thickness of the insulation layer.

9–71 A hot fluid ($k_{fluid} = 0.72$ W/m·K) is flowing as a laminar fully developed flow inside a pipe with an inner diameter of 35 mm and a wall thickness of 5 mm. The pipe is 10 m long, and the outer surface is exposed to air at 10°C. The average temperature difference between the hot fluid and the pipe inner surface is $\Delta T_{avg} = 10°C$, and the inner and outer surface temperatures are constant. Determine the outer surface temperature of the pipe. Evaluate the air properties at 50°C. Is this a good assumption?

9–72 A hot liquid ($c_p = 1000$ J/kg·K) flows at a flow rate of 0.05 kg/s inside a copper pipe with an inner diameter of 45 mm and a wall thickness of 5 mm. At the pipe exit, the liquid temperature decreases by 10°C from its temperature at the inlet. The outer surface of the 5-m-long copper pipe is black oxidized, which subjects the outer surface to radiation heat transfer. The air temperature surrounding the pipe is 10°C. Assuming that the properties of air can be evaluated at 35°C and 1 atm pressure, determine the outer surface temperature of

the pipe. Is 35°C an appropriate film temperature for evaluation of the air properties?

9–73 [PtD] A hot liquid ($c_p = 1000$ J/kg·K) flows at a flow rate of 0.028 kg/s inside a 5-m-long pipe with an inner diameter of 45 mm and a wall thickness of 5 mm. At the pipe exit, the liquid temperature decreases by 10°C from its inlet temperature. The pipe is located in surroundings with air at 10°C. To prevent thermal burn hazards, the pipe outer surface temperature should be at 45°C or lower. Instead of covering the pipe with insulation, a colleague has suggested painting the pipe outer surface with black paint ($\varepsilon = 0.88$). Determine whether or not painting the pipe outer surface black is sufficient to keep the temperature below 45°C. Evaluate the properties of air at 25°C and 1 atm pressure. Is this a good assumption?

9–74E An average person generates heat at a rate of 240 Btu/h while resting in a room at 70°F. Assuming one-quarter of this heat is lost from the head and taking the emissivity of the skin to be 0.9, determine the average surface temperature of the head when it is not covered. The head can be approximated as a 12-in-diameter sphere, and the interior surfaces of the room can be assumed to be at the room temperature.

9–75 An incandescent lightbulb is an inexpensive but highly inefficient device that converts electrical energy into light. It converts about 5 percent of the electrical energy it consumes into light while converting the remaining 95 percent into heat. The glass bulb of the lamp heats up very quickly as a result of absorbing all that heat and dissipating it to the surroundings by convection and radiation. Consider an 8-cm-diameter, 60-W lightbulb in a room at 25°C. The emissivity of the glass is 0.9. Assuming that 5 percent of the energy passes through the glass bulb as light with negligible absorption and the rest of the energy is absorbed and dissipated by the bulb itself by natural convection and radiation, determine the equilibrium temperature of the glass bulb. Assume the interior surfaces of the room to be at room temperature. *Answer:* 175°C
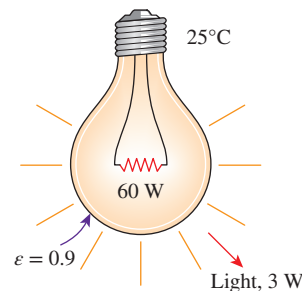
FIGURE P9–75

9–76 The water in a 40-L tank is to be heated from 15°C to 45°C by a 6-cm-diameter spherical heater whose surface temperature is maintained at 85°C. Determine how long the heater should be kept on.

9–77 A 2-m-diameter, thin-walled stainless steel spherical tank is filled with chemicals undergoing a reaction. The reaction releases heat through the tank, where the tank outer surface temperature is 50°C and is exposed to air at 20°C. The stainless steel surface of the tank has an emissivity of 0.35. Determine the rate of heat release from the chemical reaction inside the tank. Is the given emissivity value reasonable for a stainless steel surface? What is the contribution of natural convection to the overall rate of heat loss at the tank surface?

9–78 A hot liquid is poured into a spherical tank with an inner diameter of 3 m and a wall thickness of 3 cm. The tank wall is made of a material with a thermal conductivity of 0.15 W/m·K. The hot liquid in the tank causes the inner surface temperature to be 100°C, while the tank outer surface is exposed to air at 20°C and has an emissivity of 0.35. Determine the outer surface temperature of the tank. Assume that the properties of air can be evaluated at 40°C and 1 atm pressure. Is this a good assumption?

9–79 **PtD** A spherical stainless steel tank with an inner diameter of 3 m and a wall thickness of 10 mm is used to contain a solution undergoing an exothermic reaction that generates 450 W/m³ of heat. The tank is located in surroundings with air at 15°C. To prevent thermal burns to people working near the tank, the outer surface temperature should be at 45°C or lower. Determine whether the outer surface of the tank should be polished ($\varepsilon = 0.2$) or painted black ($\varepsilon = 0.88$). Evaluate the air properties at 30°C and 1 atm pressure. Is this a good assumption?

9–80 **PtD** A spherical tank ($k = 15$ W/m·K) with an inner diameter of 3 m and a wall thickness of 10 mm is used for storing hot liquid. The hot liquid inside the tank causes the inner surface temperature to be as high as 100°C. To prevent thermal burns to the people working near the tank, the tank is covered with a 7-cm-thick layer of insulation ($k = 0.15$ W/m·K), and the outer surface is painted to give an emissivity of 0.35. The tank is located in surroundings with air at 16°C. Determine whether or not the insulation layer is sufficient to keep the outer surface temperature below 45°C to prevent thermal burn hazards. Discuss ways to further decrease the outer surface temperature. Evaluate the air properties at 30°C and 1 atm pressure. Is this a good assumption?

Natural Convection from Finned Surfaces and PCBs

9–81C Why are finned surfaces frequently used in practice? Why are the finned surfaces referred to as heat sinks in the electronics industry?

9–82C Why are heat sinks with closely packed fins not suitable for natural convection heat transfer, although they increase the heat transfer surface area more?

9–83C Consider a heat sink with optimum fin spacing. Explain how heat transfer from this heat sink will be affected by (*a*) removing some of the fins on the heat sink and

(*b*) doubling the number of fins on the heat sink by reducing the fin spacing. The base area of the heat sink remains unchanged at all times.

9–84 Aluminum heat sinks of rectangular profile are commonly used to cool electronic components. Consider a 7.62-cm-long and 9.68-cm-wide commercially available heat sink whose cross section and dimensions are as shown in Fig. P9–84. The heat sink is oriented vertically and is used to cool a power transistor that can dissipate up to 125 W of power. The back surface of the heat sink is insulated. The surfaces of the heat sink are untreated, and thus they have a low emissivity (under 0.1). Therefore, radiation heat transfer from the heat sink can be neglected. During an experiment conducted in room air at 22°C, the base temperature of the heat sink was measured to be 120°C when the power dissipation of the transistor was 18 W. Assuming the entire heat sink to be at the base temperature, determine the average natural convection heat transfer coefficient for the case.
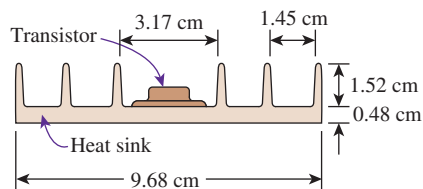
FIGURE P9–84

9–85 Reconsider the heat sink in Prob. 9–84. In order to enhance heat transfer, a shroud (a thin rectangular metal plate) whose surface area is equal to the base area of the heat sink is placed very close to the tips of the fins such that the inter-fin spaces are converted into rectangular channels. The base temperature of the heat sink in this case was measured to be 108°C. Noting that the shroud loses heat to the ambient air from both sides, determine the average natural convection heat transfer coefficient in this shrouded case. (For complete details, see Çengel and Zing, 1987.)
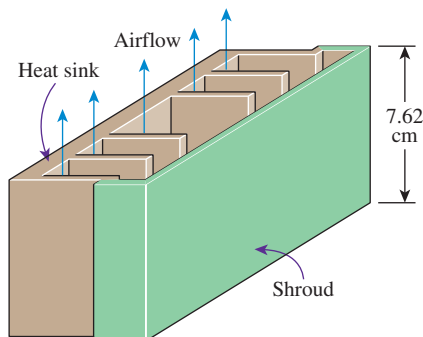
FIGURE P9–85

9–86 A 15-cm-wide and 18-cm-high vertical hot surface in 20°C air is to be cooled by a heat sink with equally spaced fins of rectangular profile. The fins are 0.1 cm thick, 4 cm wide, and 18 cm long in the vertical direction. Determine the optimum fin spacing and the rate of heat transfer by natural convection from the heat sink if the base temperature is 85°C.

9–87E A 6-in-wide and 8-in-high vertical hot surface in 78°F air is to be cooled by a heat sink with equally spaced fins of rectangular profile. The fins are 0.08 in thick and 8 in long in the vertical direction and have a height of 1.2 in from the base. Determine the optimum fin spacing and the rate of heat transfer by natural convection from the heat sink if the base temperature is 180°F.

9–88E Reconsider Prob. 9–87E. Using appropriate software, investigate the effect of the length of the fins in the vertical direction on the optimum fin spacing and the rate of heat transfer by natural convection. Let the fin length vary from 2 in to 10 in. Plot the optimum fin spacing and the rate of convection heat transfer as a function of the fin length, and discuss the results.

Natural Convection Inside Enclosures

9–89C The upper and lower compartments of a well-insulated container are separated by two parallel sheets of glass with an airspace between them. One of the compartments is to be filled with a hot fluid and the other with a cold fluid. If it is desired that heat transfer between the two compartments be minimal, would you recommend putting the hot fluid into the upper or the lower compartment of the container? Why?

9–90C Someone claims that the airspace in a double-pane window enhances the heat transfer from a house because of the natural convection currents that occur in the airspace and recommends that the double-pane window be replaced by a single sheet of glass whose thickness is equal to the sum of the thicknesses of the two glasses of the double-pane window to save energy. Do you agree with this claim?

9–91C Consider a double-pane window consisting of two glass sheets separated by a 1-cm-wide airspace. Someone suggests inserting a thin vinyl sheet between the two glass sheets to form two 0.5-cm-wide compartments in the window in order to reduce natural convection heat transfer through the window. From a heat transfer point of view, would you be in favor of this idea to reduce heat losses through the window?

9–92C What does the effective conductivity of an enclosure represent? How is the ratio of the effective conductivity to thermal conductivity related to the Nusselt number?

9–93 Show that the thermal resistance of a rectangular enclosure can be expressed as $R = L_c/(Ak\,\text{Nu})$, where k is the thermal conductivity of the fluid in the enclosure.

9–94 Consider a 3-m-high rectangular enclosure consisting of two surfaces separated by a 0.1-m air gap at 1 atm. If the surface temperatures across the air gap are 30°C and −10°C,

determine the ratio of the heat transfer rate for the horizontal orientation (with hotter surface at the bottom) to that for vertical orientation.
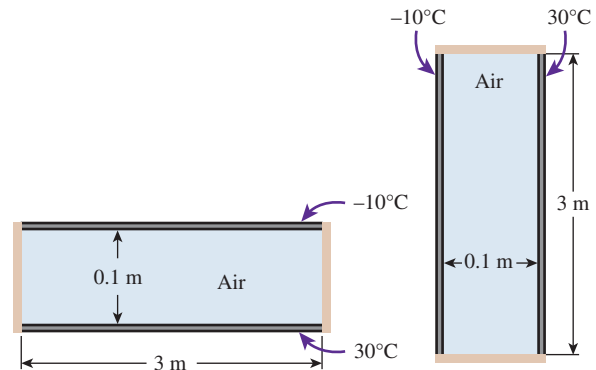
FIGURE P9–94

9–95 Flat-plate solar collectors are often tilted up toward the sun in order to intercept a greater amount of direct solar radiation. The tilt angle from the horizontal also affects the rate of heat loss from the collector. Consider a 1.5-m-high and 3-m-wide solar collector that is tilted at an angle θ from the horizontal. The back side of the absorber is heavily insulated. The absorber plate and the glass cover, which are spaced 2.5 cm from each other, are maintained at temperatures of 80°C and 40°C, respectively. Determine the rate of heat loss from the absorber plate by natural convection for $\theta = 0°$, 30°, and 90°.
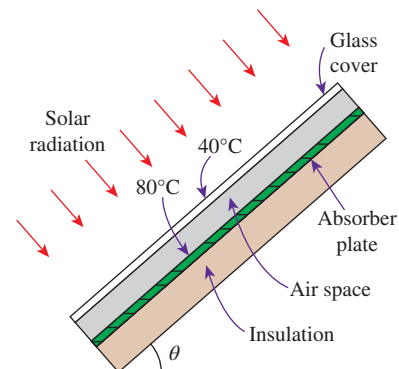
FIGURE P9–95

9–96 A vertical 1.5-m-high and 3.0-m-wide enclosure consists of two surfaces separated by a 0.4-m air gap at atmospheric pressure. If the surface temperatures across the air gap are measured to be 280 K and 336 K and the surface emissivities to be 0.15 and 0.90, determine the fraction of heat transferred through the enclosure by radiation. *Answer:* 0.30

9–97 A vertical 1.5-m-high, 2.8-m-wide double-pane window consists of two layers of glass separated by a 2.0-cm

air gap at atmospheric pressure. The room temperature is 26°C while the inner glass temperature is 18°C. Disregarding radiation heat transfer, determine the temperature of the outer glass layer and the rate of heat loss through the window by natural convection.

9–98E A vertical 4-ft-high and 6-ft-wide double-pane window consists of two sheets of glass separated by a 1-in air gap at atmospheric pressure. If the glass surface temperatures across the air gap are measured to be 65°F and 40°F, determine the rate of heat transfer through the window by (*a*) natural convection and (*b*) radiation. Also, determine the *R*-value of insulation of this window such that multiplying the inverse of the *R*-value by the surface area and the temperature difference gives the total rate of heat transfer through the window. The effective emissivity for use in radiation calculations between two large parallel glass plates can be taken to be 0.82.
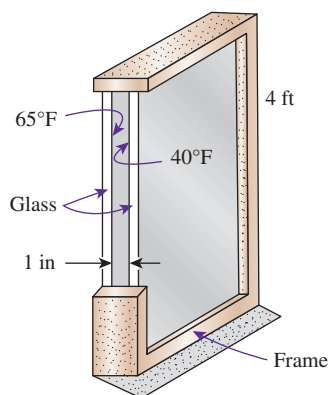
FIGURE P9–98E

9–99E Reconsider Prob. 9–98E. Using appropriate software, investigate the effect of the air gap thickness on the rates of heat transfer by natural convection and radiation and the *R*-value of insulation. Let the air gap thickness vary from 0.2 in to 2.0 in. Plot the rates of heat transfer by natural convection and radiation and the *R*-value of insulation as a function of the air gap thickness, and discuss the results.

9–100 A simple solar collector is built by placing a 5-cm-diameter clear plastic tube around a garden hose whose outer diameter is 1.6 cm. The hose is painted black to maximize solar absorption, and some plastic rings are used to keep the spacing between the hose and the clear plastic cover constant. During a clear day, the temperature of the hose is measured to be 65°C, while the ambient air temperature is 26°C. Determine the rate of heat loss from the water in the hose per meter of its length by natural convection. Also, discuss how the performance of this solar collector can be improved. Evaluate air properties at an average temperature of 50°C and 1 atm pressure. Is this a good assumption? *Answer: 8.2 W*
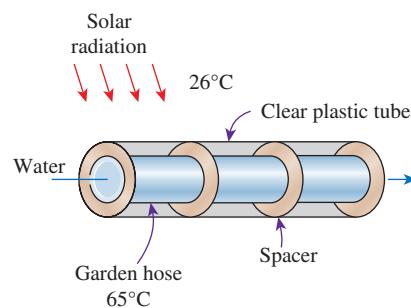
FIGURE P9–100

9–101 Reconsider Prob. 9–100. Using appropriate software, plot the rate of heat loss from the water by natural convection as a function of the ambient air temperature as the temperature varies from 4°C to 40°C, and discuss the results.

9–102 Consider two concentric horizontal cylinders of diameters 55 cm and 65 cm and length 125 cm. The surfaces of the inner and outer cylinders are maintained at 54°C and 106°C, respectively. Determine the rate of heat transfer between the cylinders by natural convection if the annular space is filled with (*a*) water and (*b*) air.

9–103 **PtD** A hot liquid ($c_p = 950$ J/kg·K) flows at a flow rate of 0.005 kg/s inside a tube with a diameter of 25 mm. At the tube exit, the liquid temperature decreases by 8°C from its temperature at the inlet. The hot liquid causes the tube surface temperature to be 120°C. To prevent thermal burn hazards, the tube is enclosed in a concentric outer cover 5 cm in diameter. Determine whether the outer cover temperature is below 45°C to prevent thermal burns to human skin. Evaluate the properties of air in the concentric enclosure at 80°C and 1 atm pressure. Is this a good assumption?
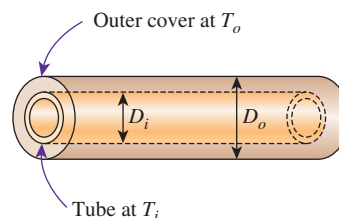
FIGURE P9–103

9–104 Two concentric spheres with diameters of 5 cm and 10 cm have their surface temperatures maintained at 100°C and 200°C, respectively. The enclosure between the two

concentric spherical surfaces is filled with nitrogen gas at 1 atm. Determine the rate of heat transfer through the enclosure.

$D_o = 10$ cm
$T_o = 200°C$

L_c

$D_i = 5$ cm
$T_i = 100°C$
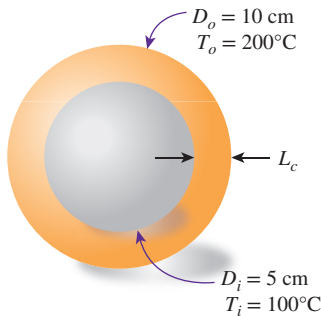
FIGURE P9–104

9–105 Two concentric spheres of diameters 15 cm and 25 cm are separated by air at 1 atm pressure. The surface temperatures of the two spheres enclosing the air are $T_1 = 350$ K and $T_2 = 275$ K, respectively. Determine the rate of heat transfer from the inner sphere to the outer sphere by natural convection.

9–106 Reconsider Prob. 9–105. Using appropriate software, plot the rate of natural convection heat transfer as a function of the hot surface temperature of the sphere as the temperature varies from 250 K to 450 K, and discuss the results.

9–107 Two concentric spheres of diameters $D_i = 20$ cm and $D_o = 30$ cm are separated by air at 1 atm pressure. The surface temperatures of the two spheres enclosing the air are $T_i = 320$ K and $T_o = 280$ K, respectively. Determine the rate of heat transfer from the inner sphere to the outer sphere by natural convection.

$D_o = 30$ cm
$T_o = 280$ K

$L_c = 5$ cm

$D_i = 20$ cm
$T_i = 320$ K
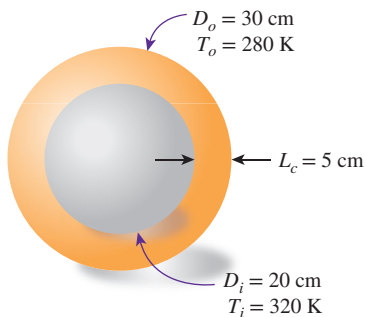
FIGURE P9–107

9–108 **PtD** A spherical tank with an inner diameter of 3 m is filled with a solution undergoing an exothermic reaction that generates 233 W/m³ of heat and causes the surface temperature to be 120°C. To prevent thermal burn hazards, the tank is enclosed by a concentric outer cover that

provides an air gap of 5 cm in the enclosure. Determine whether the air gap is sufficient to keep the outer cover temperature below 45°C to prevent thermal burns on human skin. Evaluate the properties of air in the enclosure at 80°C and 1 atm pressure. Is this a good assumption?

Outer cover
D_o, T_o

Spherical tank
D_i, T_i

L_c Exothermic
reaction
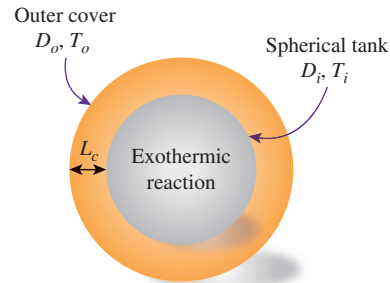
FIGURE P9–108

Combined Natural and Forced Convection

9–109C When is natural convection negligible and when is it not negligible in forced convection heat transfer?

9–110C Under what conditions does natural convection enhance forced convection, and under what conditions does it hurt forced convection?

9–111C When neither natural nor forced convection is negligible, is it correct to calculate each independently and add them to determine the total convection heat transfer?

9–112 Consider a 6-m-long vertical plate at 60°C in water at 25°C. Determine the forced motion velocity above which natural convection heat transfer from this plate is negligible.

9–113 In a production facility, thin square plates 3 m × 3 m in size coming out of the oven at 270°C are cooled by blowing ambient air at 18°C horizontally parallel to their surfaces. Determine the air velocity above which the natural convection effects on heat transfer are less than 10 percent and thus are negligible.

18°C

V

270°C

3 m

3 m

Hot
plates
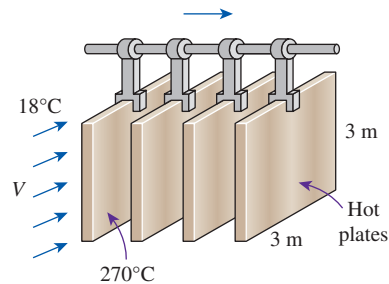
FIGURE P9–113

9–114 A 150-mm-diameter and 1-cm-long vertical rod has water flowing across its outer surface at a velocity of 0.5 m/s. The water temperature is uniform at 40°C, and the rod surface temperature

is maintained at 120°C. Under these conditions, are the natural convection effects important to the heat transfer process?

9–115 A 150-mm-diameter and 1-m-long rod is positioned horizontally and has water flowing across its outer surface at a velocity of 0.2 m/s. The water temperature is uniform at 40°C, and the rod surface temperature is maintained at 120°C. Under these conditions, are the natural convection effects important to the heat transfer process?

9–116 Consider a 5-m-long vertical plate at 85°C in air at 30°C. Determine the forced motion velocity above which natural convection heat transfer from this plate is negligible.

9–117 Reconsider Prob. 9–116. Using appropriate software, plot the forced motion velocity above which natural convection heat transfer is negligible as a function of the plate temperature as the temperature varies from 50°C to 150°C, and discuss the results.

9–118 A 12-cm-high and 20-cm-wide circuit board houses 100 closely spaced logic chips on its surface, each dissipating 0.05 W. The board is cooled by a fan that blows air over the hot surface of the board at 35°C at a velocity of 0.5 m/s. The heat transfer from the back surface of the board is negligible. Determine the average temperature on the surface of the circuit board assuming the air flows vertically upward along the 12-cm-long side by (*a*) ignoring natural convection and (*b*) considering the contribution of natural convection. Disregard any heat transfer by radiation. Evaluate air properties at a film temperature of 47.5°C and 1 atm pressure. Is this a good assumption?

9–119 A 0.25-m × 0.25-m horizontal square plate at 125°C is cooled by blowing 29°C air with a velocity of 0.1 m/s over the surface of the plate. Determine the Nusselt number for this case. Assume the back side of the plate is insulated.

FIGURE P9–119

Special Topic: Heat Transfer Through Windows

9–120C Why are the windows considered in three regions when analyzing heat transfer through them? Name those regions, and explain how the overall *U*-value of the window is determined when the heat transfer coefficients for all three regions are known.

9–121C Consider three similar double-pane windows with air gap widths of 5, 10, and 20 mm. For which case will the heat transfer through the window be a minimum?

9–122C In an ordinary double-pane window, about half of the heat transfer is by radiation. Describe a practical way of reducing the radiation component of heat transfer.

9–123C Consider a double-pane window whose airspace width is 20 mm. Now a thin polyester film is used to divide the airspace into two 10-mm-wide layers. How will the film affect (*a*) convection and (*b*) radiation heat transfer through the window?

9–124C Consider a double-pane window whose airspace is flashed and filled with argon gas. How will replacing the air in the gap with argon affect (*a*) convection and (*b*) radiation heat transfer through the window?

9–125C Is the heat transfer rate through the glazing of a double-pane window higher at the center or at the edge section of the glass area? Explain.

9–126C How do the relative magnitudes of *U*-factors of windows with aluminum, wood, and vinyl frames compare? Assume the windows are identical except for the frames.

9–127 Determine the *U*-factor for the center-of-glass section of a double-pane window with a 13-mm airspace for winter design conditions. The glazings are made of clear glass having an emissivity of 0.84. Take the average airspace temperature at design conditions to be 10°C and the temperature difference across the airspace to be 15°C.

9–128 The overall *U*-factor of a fixed wood-framed window with double glazing is given by the manufacturer to be $U = 2.76$ W/m²·K under the conditions of still air inside and winds of 12 km/h outside. What will the *U*-factor be when the wind velocity outside is doubled? *Answer:* 2.88 W/m²·K

9–129 The owner of an older house in Wichita, Kansas, is considering replacing the existing double-door-type wood-framed single-pane windows with vinyl-framed double-pane windows with an airspace of 6.4 mm. The new windows are of double-door type with metal spacers. The house is maintained at 22°C at all times, but heating is needed only when the outdoor temperature drops below 18°C because of the internal heat gain from people, lights, appliances, and the sun. The average winter temperature of Wichita is 7.1°C, and the house is heated by electric resistance heaters. If the unit cost of electricity is $0.085/kWh and the total window area of the house is 17 m², determine how much money the new windows will save the homeowner per month in winter.
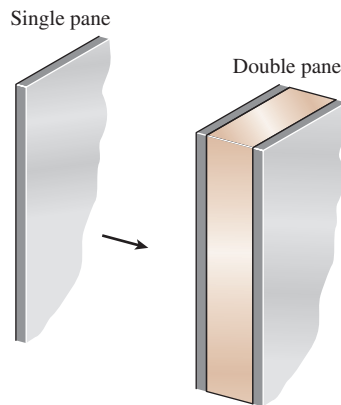
FIGURE P9–129

9–130 Consider a house in Atlanta, Georgia, that is maintained at 22°C and has a total of 14 m² of window area. The windows are double-door-type with wood frames and metal spacers. The glazing consists of two layers of glass with 12.7 mm of airspace with one of the inner surfaces coated with reflective film. The average winter temperature of Atlanta is 11.3°C. Determine the average rate of heat loss through the windows in winter. *Answer:* 319 W

9–131E Consider an ordinary house with *R*-13 walls (walls that have an *R*-value of 13 h·ft²·°F/Btu). Compare this to the *R*-value of the common double-door windows that are double pane with $\frac{1}{4}$ in of airspace and have aluminum frames. If the windows occupy only 20 percent of the wall area, determine if more heat is lost through the windows or through the remaining 80 percent of the wall area. Disregard infiltration losses.

9–132 A double-door wood-framed window with glass glazing and metal spacers is being considered for an opening that is 1.2 m high and 1.8 m wide in the wall of a house maintained at 20°C. Determine the rate of heat loss through the window and the inner surface temperature of the window glass facing the room when the outdoor air temperature is −8°C if the window is selected to be (*a*) 3-mm single glazing, (*b*) double glazing with an airspace of 13 mm, and (*c*) low-e-coated triple glazing with an airspace of 13 mm.
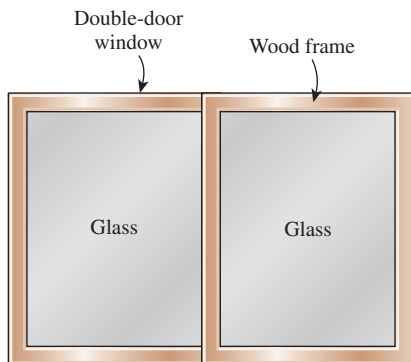
FIGURE P9–132

9–133 Determine the overall *U*-factor for a double-door-type wood-framed double-pane window with 13-mm airspace and metal spacers, and compare your result with the value listed in Table 9–6. The overall dimensions of the window are 2.00 m × 2.40 m, and the dimensions of each glazing are 1.92 m × 1.14 m.

Review Problems

9–134 An electric resistance space heater is designed such that it resembles a rectangular box 50 cm high, 80 cm long, and 15 cm wide filled with 45 kg of oil. The heater is to be placed against a wall, and thus heat transfer from its back surface is negligible. The surface temperature of the heater is not to exceed 75°C in a room at 25°C for safety considerations. Disregarding heat transfer from the bottom and top surfaces of

the heater in anticipation that the top surface will be used as a shelf, determine the power rating of the heater in W. Take the emissivity of the outer surface of the heater to be 0.8 and the average temperature of the ceiling and wall surfaces to be the same as the room air temperature.

Also, determine how long it will take for the heater to reach steady operation when it is first turned on (i.e., for the oil temperature to rise from 25°C to 75°C). State your assumptions in the calculations.
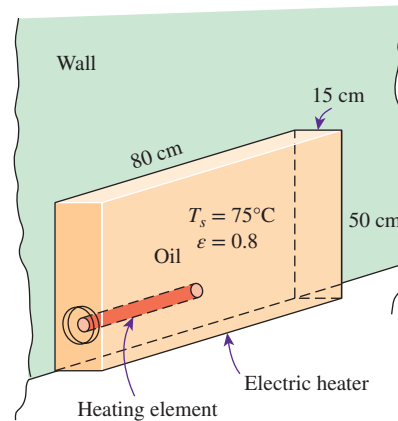
FIGURE P9–134

9–135 During a plant visit, it was observed that a 1.5-m-high and 1-m-wide section of the vertical front section of a natural gas furnace wall was too hot to touch. The temperature measurements on the surface revealed that the average temperature of the exposed hot surface was 110°C, while the temperature of the surrounding air was 25°C. The surface appeared to be oxidized, and its emissivity can be taken to be 0.7. Taking the temperature of the surrounding surfaces to be 25°C also, determine the rate of heat loss from this furnace.

The furnace has an efficiency of 79 percent, and the plant pays $1.20 per therm of natural gas. If the plant operates 10 h a day, 310 days a year, and thus 3100 h a year, determine the annual cost of the heat loss from this vertical hot surface on the front section of the furnace wall.

FIGURE P9–135

https://ebook2book.ir/

617
CHAPTER 9
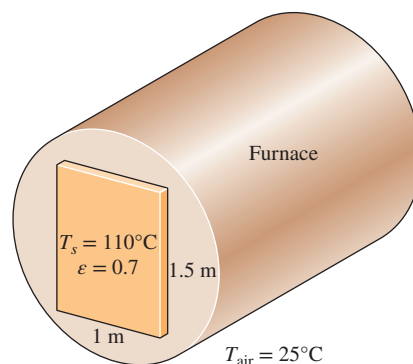
9–136 Consider a 2-m-high electric hot-water heater that has a diameter of 40 cm and maintains the hot water at 60°C. The tank is located in a small room at 20°C whose walls and ceiling are at about the same temperature. The tank is placed in a 44-cm-diameter sheet metal shell of negligible thickness, and the space between the tank and the shell is filled with foam insulation. The average temperature and emissivity of the outer surface of the shell are 40°C and 0.7, respectively. The price of electricity is $0.08/kWh. Hot-water tank insulation kits large enough to wrap the entire tank are available on the market for about $60. If such an insulation kit is installed on this water tank by the homeowner himself, how long will it take for this additional insulation to pay for itself? Disregard any heat loss from the top and bottom surfaces, and assume the insulation reduces the heat losses by 80 percent.
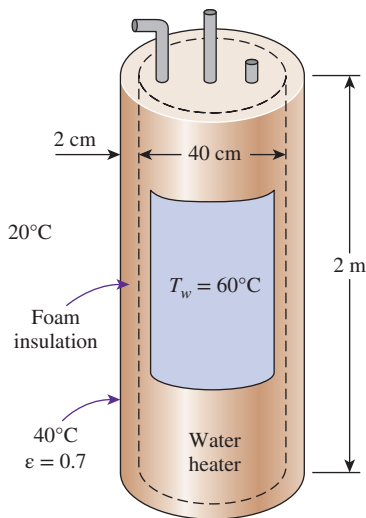
FIGURE P9–136

9–137 A plate (0.5 m × 0.5 m) is inclined at an angle of 30°. The top surface of the plate is well insulated. Estimate the rate of heat loss from the plate when the bottom surface is maintained at 60°C and the surrounding atmospheric quiescent air is at 0°C.

9–138 A group of 25 power transistors, dissipating 1.5 W each, are to be cooled by attaching them to a black-anodized square aluminum plate and mounting the plate on the wall of a room at 30°C. The emissivity of the transistor and the plate surfaces is 0.9. Assuming the heat transfer from the back side of the plate to be negligible and the temperature of the surrounding surfaces to be the same as the air temperature of the room, determine the size of the plate if the average surface temperature of the plate is not to exceed 50°C. *Answer:* 43 cm × 43 cm
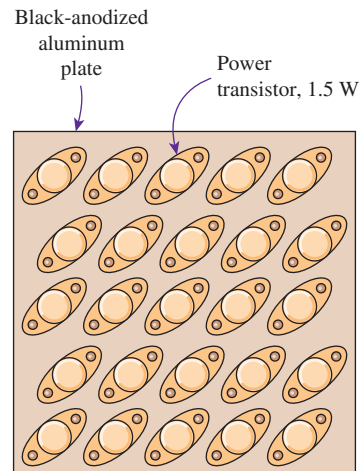
FIGURE P9–138

9–139 Repeat Prob. 9–138 assuming the plate to be positioned horizontally with (*a*) transistors facing up and (*b*) transistors facing down.

9–140 Consider an $L \times L$ horizontal plate that is placed in quiescent air with the hot surface facing up. If the film temperature is 20°C and the average Nusselt number in natural convection is of the form $Nu = CRa_L^n$, show that the average heat transfer coefficient can be expressed as

$$h = 1.95\,(\Delta T/L)^{1/4} \quad 10^4 < Ra_L < 10^7$$
$$h = 1.79\Delta T^{1/3} \quad\quad 10^7 < Ra_L < 10^{11}$$

9–141 Consider a flat-plate solar collector placed horizontally on the flat roof of a house. The collector is 1.5 m wide and 4.5 m long, and the average temperature of the exposed surface of the collector is 42°C. Determine the rate of heat loss from the collector by natural convection during a calm day when the ambient air temperature is 8°C. Also, determine the heat loss by radiation by taking the emissivity of the collector surface to be 0.85 and the effective sky temperature to be −15°C. *Answers:* 1314 W, 1762 W

9–142 Skylights or "roof windows" are commonly used in homes and manufacturing facilities since they let natural light in during daytime and thus reduce the lighting costs. However, they offer little resistance to heat transfer, and large amounts of energy are lost through them in winter unless they are equipped with a motorized insulating cover that can be used in cold weather and at nights to reduce heat losses. Consider a 1-m-wide and 2.5-m-long horizontal skylight on the roof of a house that is kept at 20°C. The glazing of the skylight is made of a single layer of 0.5-cm-thick glass ($k = 0.78$ W/m·K and $\varepsilon = 0.9$). Determine the rate of heat loss through the skylight when the air temperature outside is −10°C and

https://ebook2book.ir/

the effective sky temperature is $-30°C$. Compare your result with the rate of heat loss through an equivalent surface area of the roof that has a common R-5.34 construction in SI units (i.e., a thickness-to-effective-thermal-conductivity ratio of 5.34 m²·K/W). Evaluate air properties at a film temperature of $-7°C$ and 1 atm pressure. Is this a good assumption?

$T_{sky} = -30°C$
$T_{air} = -10°C$
Skylight
$\varepsilon = 0.9$
2.5 m 1 m
$T_{in} = 20°C$
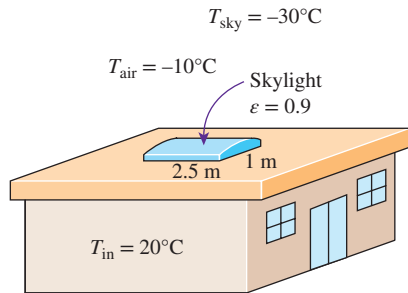
FIGURE P9–142

9–143 An electronic box that consumes 200 W of power is cooled by a fan blowing air into the box enclosure. The dimensions of the electronic box are 15 cm × 50 cm × 50 cm, and all surfaces of the box are exposed to the ambient environment except the base surface. Temperature measurements indicate that the box is at an average temperature of $32°C$ when the ambient temperature and the temperature of the surrounding walls are $25°C$. If the emissivity of the outer surface of the box is 0.75, determine the fraction of the heat lost from the outer surfaces of the electronic box.

25°C
32°C
$\varepsilon = 0.75$
15 cm
50 cm
50 cm
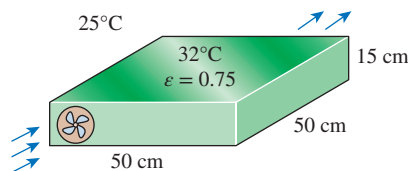
FIGURE P9–143

9–144E The components of an electronic system dissipating 150 W are located in a 5-ft-long horizontal duct whose cross section is 6 in × 6 in. The components in the duct are cooled by forced air, which enters at $85°F$ at a rate of 22 cfm and leaves at $100°F$. The surfaces of the sheet metal duct are not painted, and thus radiation heat transfer from the outer surfaces is negligible. If the ambient air temperature is $80°F$, determine (a) the heat transfer from the outer surfaces of the duct to the ambient air by natural convection and (b) the average temperature of the duct. Evaluate air properties at a film temperature of $100°F$ and 1 atm pressure. Is this a good assumption?

Natural convection
80°F 100°F
150 W
85°F 5 ft
22 cfm
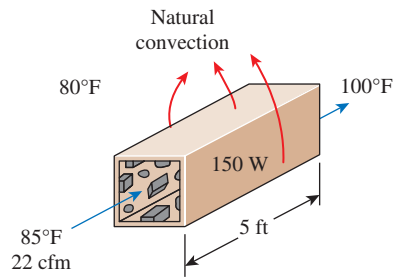
FIGURE P9–144E

9–145E Repeat Prob. 9–144E assuming the fan fails and thus all heat generated inside the duct must be rejected to the ambient air by natural convection through the outer surfaces of the duct. Evaluate air properties at a film temperature of $120°F$ and 1 atm pressure. Is this a good assumption?

9–146E Repeat Prob. 9–144E for a circular horizontal duct of diameter 4 in. Evaluate air properties at a film temperature of $115°F$ and 1 atm pressure. Is this a good assumption?

9–147 Exhaust gases from a manufacturing plant are being discharged through a 10-m-tall exhaust stack with outer diameter of 1 m. The exhaust gases are discharged at a rate of 0.125 kg/s, while temperature drop between inlet and exit of the exhaust stack is $30°C$, and the constant pressure-specific heat of the exhaust gases is 1600 J/kg·K. On a particular calm day, the surrounding quiescent air temperature is $33°C$. Solar radiation is incident on the exhaust stack outer surface at a rate of 500 W/m², and both the emissivity and solar absorptivity of the outer surface are 0.9. Determine the exhaust stack outer surface temperature. Assume the film temperature is $60°C$.

Exhaust gases
$\alpha_s = \varepsilon = 0.9$
Exhaust stack
Air, 33°C
$L = 10$ m
$T_{in} - T_{out} = 30°C$
Manufacturing plant
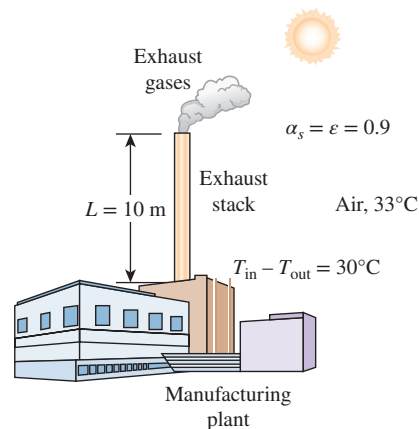
FIGURE P9–147

9–148 A 40-cm-diameter, 110-cm-high cylindrical hot-water tank is located in the bathroom of a house maintained at $20°C$. The surface temperature of the tank is measured to be $44°C$ and its emissivity is 0.4. Taking the surrounding surface temperature

to be also 20°C, determine the rate of heat loss from all surfaces of the tank by natural convection and radiation.

9–149 A 12-cm-diameter and 15-m-long cylinder with a surface temperature of 10°C is placed horizontally in air at 40°C. Calculate the steady rate of heat transfer for the cases of (*a*) free-stream air velocity of 10 m/s due to normal winds and (*b*) no winds and thus a free-stream velocity of zero.

9–150E Hot water is flowing at an average velocity of 4 ft/s through a cast iron pipe ($k = 30$ Btu/h·ft·°F) whose inner and outer diameters are 1.0 in and 1.2 in, respectively. The pipe passes through a 50-ft-long section of a basement whose temperature is 60°F. The emissivity of the outer surface of the pipe is 0.5, and the walls of the basement are also at about 60°F. If the inlet temperature of the water is 150°F and the heat transfer coefficient on the inner surface of the pipe is 30 Btu/h·ft²·°F, determine the temperature drop of water as it passes through the basement. Evaluate air properties at a film temperature of 105°C and 1 atm pressure. Is this a good assumption?

9–151E A 0.1-W small cylindrical resistor mounted on a lower part of a vertical circuit board is 0.3 in long and has a diameter of 0.2 in. The view of the resistor is largely blocked by another circuit board facing it, and the heat transfer through the connecting wires is negligible. The air is free to flow through the large parallel flow passages between the boards as a result of natural convection currents. If the air temperature near the resistor is 120°F, determine the approximate surface temperature of the resistor. Evaluate air properties at a film temperature of 170°F and 1 atm pressure. Is this a good assumption? *Answer:* 211°F
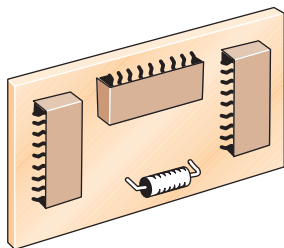
FIGURE P9–151E

9–152E Consider an industrial furnace that resembles a 13-ft-long horizontal cylindrical enclosure 8 ft in diameter whose end surfaces are well insulated. The furnace burns natural gas at a rate of 48 therms/h. The combustion efficiency of the furnace is 82 percent (i.e., 18 percent of the chemical energy of the fuel is lost through the flue gases as a result of incomplete combustion and the flue gases leaving the furnace at high temperature). If the heat loss from the outer surfaces of the furnace by natural convection and radiation is not to exceed 1 percent of the heat generated inside, determine the highest allowable surface temperature of the furnace. Assume the air and wall surface temperature of the room to be 75°F, and take the emissivity of the outer surface of the furnace to be 0.85.

If the cost of natural gas is $1.15/therm and the furnace operates 2800 h per year, determine the annual cost of this heat loss to the plant. Evaluate properties of air at a film temperature of 107.5°F and 1 atm pressure. Is this a good assumption?
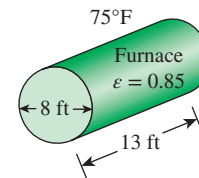
FIGURE P9–152E

9–153 A 6-m-internal-diameter spherical tank made of 1.5-cm-thick stainless steel ($k = 15$ W/m·K) is used to store iced water at 0°C in a room at 20°C. The walls of the room are also at 20°C. The outer surface of the tank is black (emissivity $\varepsilon = 1$), and heat transfer between the outer surface of the tank and the surroundings is by natural convection and radiation. Assuming the entire steel tank to be at 0°C and thus the thermal resistance of the tank to be negligible, determine (*a*) the rate of heat transfer to the iced water in the tank and (*b*) the amount of ice at 0°C that melts during a 24-h period. The heat of fusion of water is 333.7 kJ/kg. *Answers: (a)* 15.4 kW, *(b)* 3988 kg

9–154 A spherical vessel with a 30.0-cm outside diameter is used as a reactor for a slow endothermic reaction. The vessel is completely submerged in a large water-filled tank, held at a constant temperature of 30°C. The outside surface temperature of the vessel is 20°C. Calculate the rate of heat transfer in steady operation for the following cases: (*a*) the water in the tank is still, (*b*) the water in the tank is still (as in a part *a*), however, the buoyancy force caused by the difference in water density is assumed to be negligible, and (*c*) the water in the tank is circulated at an average velocity of 20 cm/s.

9–155 Consider a 1.2-m-high and 2-m-wide double-pane window consisting of two 3-mm-thick layers of glass ($k = 0.78$ W/m·K) separated by a 2.5-cm-wide airspace. Determine the steady rate of heat transfer through this window and the temperature of its inner surface for a day during which the room is maintained at 20°C while the temperature of the outdoors is 0°C. Take the heat transfer coefficients on the inner and outer surfaces of the window to be $h_1 = 10$ W/m²·K and $h_2 = 25$ W/m²·K, and disregard any heat transfer by radiation. Evaluate air properties at a film temperature of 10°C and 1 atm pressure. Is this a good assumption?

9–156 A solar collector consists of a horizontal copper tube of outer diameter 5 cm enclosed in a concentric thin glass tube of 9 cm diameter. Water is heated as it flows through the tube, and the annular space between the copper and glass tube is filled with air at 1 atm pressure. During a clear day, the temperatures of the tube surface and the glass cover are measured to be 60°C and 32°C, respectively. Determine the rate of heat

loss from the collector by natural convection per meter length of the tube.   *Answer:* 17.4 W
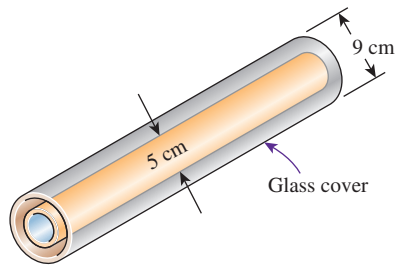
FIGURE P9−156

9–157   A solar collector consists of a horizontal aluminum tube of outer diameter 5 cm enclosed in a concentric thin glass tube of 7 cm diameter. Water is heated as it flows through the aluminum tube, and the annular space between the aluminum and glass tubes is filled with air at 1 atm pressure. The pump circulating the water fails during a clear day, and the water temperature in the tube starts rising. The aluminum tube absorbs solar radiation at a rate of 20 W per meter length, and the temperature of the ambient air outside is 30°C. Approximating the surfaces of the tube and the glass cover as being black (emissivity $\varepsilon = 1$) in radiation calculations and taking the effective sky temperature to be 20°C, determine the temperature of the aluminum tube when equilibrium is established (i.e., when the net heat loss from the tube by convection and radiation equals the amount of solar energy absorbed by the tube). For evaluation of air properties at 1 atm pressure, assume 33°C for the surface temperature of the glass cover and 45°C for the aluminum tube temperature. Are these good assumptions?

9–158   Two concentric spheres with diameters of 5 cm and 10 cm are having the surface temperatures maintained at 200°C and 100°C, respectively (see Fig. P9–158). The enclosure between the two concentric spherical surfaces is filled with nitrogen gas at 1 atm. If both concentric sphere surfaces are black ($\varepsilon = 1$), determine the rate of heat transfer on the inner surface.
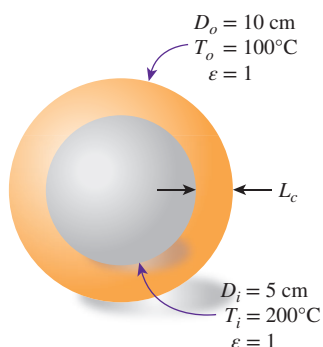
FIGURE P9−158

Fundamentals of Engineering (FE) Exam Problems

9–159   Consider a hot, boiled egg in a spacecraft that is filled with air at atmospheric pressure and temperature at all times. Disregarding any radiation effect, will the egg cool faster or slower when the spacecraft is in space instead of on the ground?
(*a*) faster   (*b*) no difference
(*c*) slower   (*d*) insufficient information

9–160   A hot object suspended by a string is to be cooled by natural convection in fluids whose volume changes differently with temperature at constant pressure. In which fluid will the rate of cooling be lowest? With increasing temperature, a fluid whose volume
(*a*) increases a lot   (*b*) increases slightly
(*c*) does not change   (*d*) decreases slightly
(*e*) decreases a lot

9–161   A spherical block of dry ice at −79°C is exposed to atmospheric air at 30°C. The general direction in which the air moves in this situation is
(*a*) horizontal   (*b*) up   (*c*) down
(*d*) recirculation around the sphere   (*e*) no motion

9–162   The primary driving force for natural convection is
(*a*) shear stress forces   (*b*) buoyancy forces
(*c*) pressure forces   (*d*) surface tension forces
(*e*) none of them

9–163   Consider a horizontal 0.7-m-wide and 0.85-m-long plate in a room at 30°C. The top side of the plate is insulated, while the bottom side is maintained at 0°C. The rate of heat transfer from the room air to the plate by natural convection is
(*a*) 36.8 W   (*b*) 43.7 W   (*c*) 128.5 W
(*d*) 92.7 W   (*e*) 69.7 W
(For air, use $k = 0.02476$ W/m·K, Pr = 0.7323, $\nu = 1.470 \times 10^{-5}$ m²/s)

9–164   A 4-m-long section of a 5-cm-diameter horizontal pipe in which a refrigerant flows passes through a room at 20°C. The pipe is not well insulated, and the outer surface temperature of the pipe is observed to be −10°C. The emissivity of the pipe surface is 0.85, and the surrounding surfaces are at 15°C. The fraction of heat transferred to the pipe by radiation is
(*a*) 0.24   (*b*) 0.30   (*c*) 0.37   (*d*) 0.48   (*e*) 0.58
(For air, use $k = 0.02401$ W/m·K, Pr = 0.735, $\nu = 1.382 \times 10^{-5}$ m²/s)

9–165   Consider a 0.2-m-diameter and 1.8-m-long horizontal cylinder in a room at 20°C. If the outer surface temperature of the cylinder is 40°C, the natural convection heat transfer coefficient is
(*a*) 2.9 W/m²·K   (*b*) 3.5 W/m²·K   (*c*) 4.1 W/m²·K
(*d*) 5.2 W/m²·K   (*e*) 6.1 W/m²·K

9–166   A 4-m-diameter spherical tank contains iced water at 0°C. The tank is thin-shelled, and thus its outer surface

temperature may be assumed to be same as the temperature of the iced water inside. Now the tank is placed in a large lake at 20°C. The rate at which the ice melts is

(*a*) 0.42 kg/s   (*b*) 0.58 kg/s   (*c*) 0.70 kg/s
(*d*) 0.83 kg/s   (*e*) 0.98 kg/s
(For lake water, use $k = 0.580$ W/m·K, Pr = 9.45, $\nu = 0.1307 \times 10^{-5}$ m²/s, $\beta = 0.138 \times 10^{-3}$K^{-1})

9–167 A vertical double-pane window consists of two sheets of glass separated by a 1.2-cm air gap at atmospheric pressure. The glass surface temperatures across the air gap are measured to be 278 K and 288 K. If it is estimated that the heat transfer by convection through the enclosure is 1.5 times that by pure conduction and that the rate of heat transfer by radiation through the enclosure is about the same magnitude as the convection, the effective emissivity of the two glass surfaces is

(*a*) 0.35   (*b*) 0.48   (*c*) 0.59   (*d*) 0.84   (*e*) 0.72

9–168 A horizontal 1.5-m-wide, 4.5-m-long double-pane window consists of two sheets of glass separated by a 3.5-cm gap filled with water. If the glass surface temperatures at the bottom and the top are measured to be 60°C and 40°C, respectively, the rate of heat transfer through the window is

(*a*) 27.6 kW   (*b*) 39.4 kW   (*c*) 59.6 kW
(*d*) 66.4 kW   (*e*) 75.5 kW
(For water, use $k = 0.644$ W/m·K, Pr = 3.55, $\nu = 0.554 \times 10^{-6}$ m²/s, $\beta = 0.451 \times 10^{-3}$K^{-1}. Also, the applicable correlation is Nu = 0.069 Ra$^{1/3}$Pr$^{0.074}$.)

9–169 A vertical 0.9-m-high and 1.5-m-wide double-pane window consists of two sheets of glass separated by a 2.0-cm air gap at atmospheric pressure. If the glass surface temperatures across the air gap are measured to be 20°C and 30°C, the rate of heat transfer through the window is

(*a*) 16.3 W   (*b*) 21.7 W   (*c*) 24.0 W
(*d*) 31.3 W   (*e*) 44.6 W
(For air, use $k = 0.02551$ W/m·K, Pr = 0.7296, $\nu = 1.562 \times 10^{-5}$ m²/s. Also, the applicable correlation is Nu = 0.42 Ra$^{1/4}$Pr$^{0.012}$ $(H/L)^{-0.3}$.)

9–170 Two concentric cylinders of diameters $D_i = 30$ cm and $D_o = 40$ cm and length $L = 5$ m are separated by air at 1 atm pressure. Heat is generated within the inner cylinder uniformly at a rate of 1100 W/m³, and the inner surface temperature of the outer cylinder is 300 K. The steady–state outer surface temperature of the inner cylinder is

(*a*) 402 K   (*b*) 415 K   (*c*) 429 K
(*d*) 442 K   (*e*) 456 K
(For air, use $k = 0.03095$ W/m·K, Pr = 0.7111, $\nu = 2.306 \times 10^{-5}$ m²/s)

Design and Essay Problems

9–171 Write a computer program to evaluate the variation of temperature with time of thin square metal plates that are removed from an oven at a specified temperature and placed vertically in a large room. The thickness, the size, the initial temperature, the emissivity, and the thermophysical properties of the plate as well as the room temperature are to be specified by the user. The program should evaluate the temperature of the plate at specified intervals and tabulate the results against time. The computer should list the assumptions made during calculations before printing the results.

For each step or time interval, assume the surface temperature to be constant and evaluate the heat loss during that time interval and the temperature drop of the plate as a result of this heat loss. This gives the temperature of the plate at the end of a time interval, which is to serve as the initial temperature of the plate for the beginning of the next time interval.

Try your program for 0.2-cm-thick vertical copper plates of 40 cm × 40 cm in size initially at 300°C cooled in a room at 25°C. Take the surface emissivity to be 0.9. Use a time interval of 1 s in calculations, but print the results at 10-s intervals for a total cooling period of 15 min.

9–172 Write a computer program to optimize the spacing between the two glass panes of a double-pane window. Assume the spacing is filled with dry air at atmospheric pressure. The program should evaluate the recommended practical value of the spacing to minimize the heat losses and list it when the size of the window (the height and the width) and the temperatures of the two panes are specified.

9–173 Contact a manufacturer of aluminum heat sinks and obtain its product catalog for cooling electronic components by natural convection and radiation. Write an essay on how to select a suitable heat sink for an electronic component when its maximum power dissipation and maximum allowable surface temperature are specified.

9–174 The top surfaces of practically all flat-plate solar collectors are covered with glass in order to reduce the heat losses from the absorber plate underneath. Although the glass cover reflects or absorbs about 15 percent of the incident solar radiation, it saves much more from the potential heat losses from the absorber plate, and thus it is considered to be an essential part of a well-designed solar collector. Inspired by the energy efficiency of double-pane windows, someone proposes to use double glazing on solar collectors instead of a single sheet of glass. Investigate if this is a good idea for the town in which you live. Use local weather data, and base your conclusion on heat transfer analysis and economic considerations.

BOILING AND CONDENSATION

We know from thermodynamics that when the temperature of a liquid at a specified pressure is raised to the saturation temperature T_{sat} at that pressure, *boiling* occurs. Likewise, when the temperature of a vapor is lowered to T_{sat}, *condensation* occurs. In this chapter we study the rates of heat transfer during such liquid-to-vapor and vapor-to-liquid phase transformations.

Although boiling and condensation exhibit some unique features, they are considered to be forms of *convection* heat transfer since they involve fluid motion (such as the rise of the bubbles to the top and the flow of condensate to the bottom). Boiling and condensation differ from other forms of convection in that they depend on the *latent heat of vaporization h_{fg}* of the fluid and the *surface tension σ* at the liquid–vapor interface, in addition to the properties of the fluid in each phase. Noting that under equilibrium conditions the temperature remains constant during a phase-change process at a fixed pressure, large amounts of heat (due to the large latent heat of vaporization released or absorbed) can be transferred during boiling and condensation essentially at constant temperature. In practice, however, it is necessary to maintain some difference between the surface temperature T_s and T_{sat} for effective heat transfer. Heat transfer coefficients h associated with boiling and condensation are typically much higher than those encountered in other forms of convection processes that involve a single phase.

We start this chapter with a discussion of the *boiling curve* and the modes of pool boiling such as *free convection boiling, nucleate boiling,* and *film boiling*. We then discuss boiling in the presence of forced convection. In the second part of this chapter, we describe the physical mechanism of *film condensation* and discuss condensation heat transfer in several geometrical arrangements and orientations. Finally, we introduce *dropwise condensation* and discuss ways of maintaining it.

OBJECTIVES

When you finish studying this chapter, you should be able to:

- Differentiate between evaporation and boiling, and gain familiarity with different types of boiling,

- Develop a good understanding of the boiling curve and the different boiling regimes corresponding to different regions of the boiling curve,

- Calculate the heat flux and its critical value associated with nucleate boiling, and examine the methods of boiling heat transfer enhancement,

- Derive a relation for the heat transfer coefficient in laminar film condensation over a vertical plate,

- Calculate the heat flux associated with condensation on inclined and horizontal plates, vertical and horizontal cylinders or spheres, and tube bundles,

- Examine dropwise condensation, and understand the uncertainties associated with them.
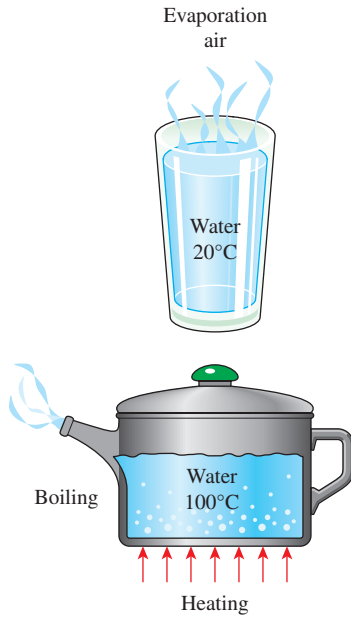
FIGURE 10–1

A liquid-to-vapor phase change process is called *evaporation* if it originates at a liquid–vapor interface and *boiling* if it occurs at a solid–liquid interface.
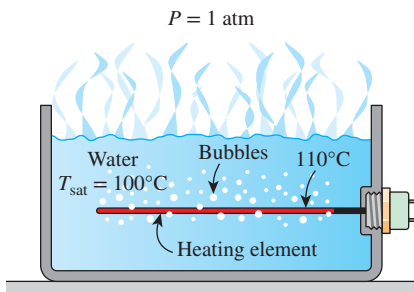
FIGURE 10–2

Boiling occurs when a liquid is brought into contact with a surface at a temperature above the saturation temperature of the liquid.

10–1 ▪ BOILING HEAT TRANSFER

Many familiar engineering applications involve condensation and boiling heat transfer. In a household refrigerator, for example, the refrigerant absorbs heat from the refrigerated space by boiling in the *evaporator* section and rejects heat to the kitchen air by condensing in the *condenser* section (the long coils behind or under the refrigerator). Also, in steam power plants, heat is transferred to the steam in the *boiler* where water is vaporized, and the waste heat is rejected from the steam in the *condenser* where the steam is condensed. Some electronic components are cooled by boiling by immersing them in a fluid with an appropriate boiling temperature.

Boiling is a liquid-to-vapor phase change process just like evaporation, but there are significant differences between the two. **Evaporation** occurs at the *liquid–vapor interface* when the vapor pressure is less than the saturation pressure of the liquid at a given temperature. Water in a lake at 20°C, for example, evaporates to air at 20°C and 60 percent relative humidity since the saturation pressure of water at 20°C is 2.3 kPa and the vapor pressure of air at 20°C and 60 percent relative humidity is 1.4 kPa (evaporation rates are determined in Chap. 14). Other examples of evaporation are the drying of clothes, fruits, and vegetables; the evaporation of sweat to cool the human body; and the rejection of waste heat in wet cooling towers. Note that evaporation involves no bubble formation or bubble motion (Fig. 10–1).

Boiling, on the other hand, occurs at the *solid–liquid interface* when a liquid is brought into contact with a surface maintained at a temperature T_s sufficiently above the saturation temperature T_{sat} of the liquid (Fig. 10–2). At 1 atm, for example, liquid water in contact with a solid surface at 110°C boils since the saturation temperature of water at 1 atm is 100°C. The boiling process is characterized by the rapid formation of *vapor bubbles* at the solid–liquid interface that detach from the surface when they reach a certain size and attempt to rise to the free surface of the liquid. When cooking, we do not say water is boiling until we see the bubbles rising to the top. Boiling is a complicated phenomenon because of the large number of variables involved in the process and the complex fluid motion patterns caused by the bubble formation and growth.

As a form of convection heat transfer, the *boiling heat flux* from a solid surface to the fluid is expressed from Newton's law of cooling as

$$\dot{q}_{boiling} = h(T_s - T_{sat}) = h\Delta T_{excess} \quad (\text{W/m}^2) \tag{10–1}$$

where $\Delta T_{excess} = T_s - T_{sat}$ is called the *excess temperature,* which represents the temperature excess of the surface above the saturation temperature of the fluid.

In the preceding chapters we considered forced and free convection heat transfer involving a single phase of a fluid. The analysis of such convection processes involves the thermophysical properties ρ, μ, k, and c_p of the fluid. The analysis of boiling heat transfer involves these properties of the liquid (indicated by the subscript l) or vapor (indicated by the subscript v) as well as the properties h_{fg} (the latent heat of vaporization) and σ (the surface tension). The h_{fg} represents the energy absorbed as a unit mass of liquid vaporizes at a specified temperature or pressure and is the primary quantity of energy transferred during boiling heat transfer. The h_{fg} values of water at various temperatures are given in Table A–9.

Bubbles owe their existence to the *surface-tension* σ at the liquid–vapor interface due to the attraction force on molecules at the interface toward the liquid phase. The surface tension decreases with increasing temperature and becomes zero at the critical temperature. This explains why no bubbles are formed during boiling at supercritical pressures and temperatures. Surface tension has the unit N/m.

The boiling processes in practice do not occur under *equilibrium* conditions, and normally the bubbles are not in thermodynamic equilibrium with the surrounding liquid. That is, the temperature and pressure of the vapor in a bubble are usually different than those of the liquid. The pressure difference between the liquid and the vapor is balanced by the surface tension at the interface. The temperature difference between the vapor in a bubble and the surrounding liquid is the driving force for heat transfer between the two phases. When the liquid is at a *lower temperature* than the bubble, heat is transferred from the bubble into the liquid, causing some of the vapor inside the bubble to condense and the bubble eventually to collapse. When the liquid is at a *higher temperature* than the bubble, heat is transferred from the liquid to the bubble, causing the bubble to grow and rise to the top under the influence of buoyancy.

Boiling is classified as *pool boiling* or *flow boiling,* depending on the presence of bulk fluid motion (Fig. 10–3). Boiling is called **pool boiling** in the absence of bulk fluid flow and **flow boiling** (or *forced convection boiling*) in the presence of it. In pool boiling, the fluid body is stationary, and any motion of the fluid is due to natural convection currents and the motion of the bubbles under the influence of buoyancy. The boiling of water in a pan on top of a stove is an example of pool boiling. Pool boiling of a fluid can also be achieved by placing a heating coil in the fluid. In flow boiling, the fluid is forced to move in a heated pipe or over a surface by external means such as a pump. Therefore, flow boiling is always accompanied by other convection effects.

Pool and flow boiling are further classified as *subcooled boiling* or *saturated boiling,* depending on the bulk liquid temperature (Fig. 10–4). Boiling is said to be **subcooled** (or *local*) when the temperature of the main body of the liquid is below the saturation temperature T_{sat} (i.e., the bulk of the liquid is subcooled) and **saturated** (or *bulk*) when the temperature of the liquid is equal to T_{sat} (i.e., the bulk of the liquid is saturated). At the early stages of boiling, the bubbles are confined to a narrow region near the hot surface. This is because the liquid adjacent to the hot surface vaporizes as a result of being heated above its saturation temperature. But these bubbles disappear soon after they move away from the hot surface as a result of heat transfer from the bubbles to the cooler liquid surrounding them. This happens when the bulk of the liquid is at a lower temperature than the saturation temperature. The bubbles serve as "energy movers" from the hot surface into the liquid body by absorbing heat from the hot surface and releasing it into the liquid as they condense and collapse. Boiling in this case is confined to a region in the locality of the hot surface and is appropriately called *local* or *subcooled* boiling. When the entire liquid body reaches the saturation temperature, the bubbles start rising to the top. We can see bubbles throughout the bulk of the liquid, and boiling in this case is called the *bulk* or *saturated* boiling. Next, we consider different boiling regimes in detail.

Heating   Heating
(*a*) Pool boiling   (*b*) Flow boiling
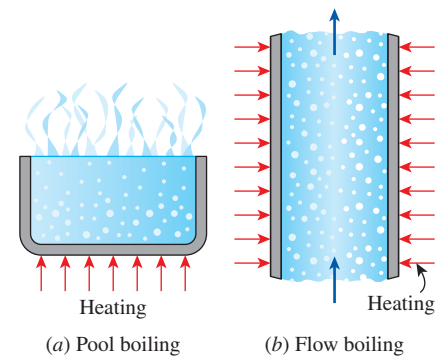
FIGURE 10–3
Classification of boiling on the basis of the presence of bulk fluid motion.

$P = 1$ atm $P = 1$ atm

Subcooled 80°C water   Saturated 100°C water
107°C   107°C
Bubble
Heating   Heating
(*a*) Subcooled boiling   (*b*) Saturated boiling
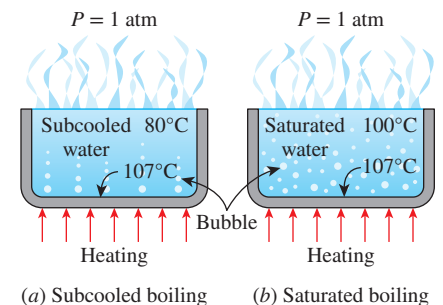
FIGURE 10–4
Classification of boiling on the basis of the presence of bulk liquid temperature.

10–2 ▪ POOL BOILING

So far we presented some general discussions on boiling. Now we turn our attention to the physical mechanisms involved in *pool boiling,* that is, the boiling of stationary fluids. In pool boiling, the fluid is not forced to flow by a mover such as a pump, and any motion of the fluid is due to natural convection currents and the motion of the bubbles under the influence of buoyancy.

As a familiar example of pool boiling, consider the boiling of tap water in a pan on top of a stove. The water is initially at about 15°C, far below the saturation temperature of 100°C at standard atmospheric pressure. At the early stages of boiling, you will not notice anything significant except some bubbles that stick to the surface of the pan. These bubbles are caused by the release of air molecules dissolved in liquid water and should not be confused with vapor bubbles. As the water temperature rises, you will notice chunks of liquid water rolling up and down as a result of natural convection currents, followed by the first vapor bubbles forming at the bottom surface of the pan. These bubbles get smaller as they detach from the surface and start rising, and eventually collapse in the cooler water above. This is *subcooled boiling* since the bulk of the liquid water has not reached saturation temperature yet. The intensity of bubble formation increases as the water temperature rises further, and you will notice waves of vapor bubbles coming from the bottom and rising to the top when the water temperature reaches the saturation temperature (100°C at standard atmospheric conditions). This full-scale boiling is the *saturated boiling.*

Boiling Regimes and the Boiling Curve

Boiling is probably the most familiar form of heat transfer, yet it remains the least understood form. After hundreds of papers written on the subject, we still do not fully understand the process of bubble formation, and we must still rely on empirical or semi-empirical relations to predict the rate of boiling heat transfer.

The pioneering work on boiling was done in 1934 by S. Nukiyama, who used electrically heated nichrome and platinum wires immersed in liquids in his experiments. Nukiyama noticed that boiling takes different forms, depending on the value of the excess temperature ΔT_{excess}. Four different boiling regimes are observed: *natural convection boiling, nucleate boiling, transition boiling,* and *film boiling* (Fig. 10–5). These regimes are illustrated on the **boiling curve** in Fig. 10–6, which is a plot of boiling heat flux versus the excess temperature. Although the boiling curve given in this figure is for water, the general shape of the boiling curve remains the same for different fluids. The specific shape of the curve depends on the fluid–heating surface material combination and the fluid pressure, but it is practically independent of the geometry of the heating surface. We now describe each boiling regime in detail.

Natural Convection Boiling (to Point *A* on the Boiling Curve)

We know from thermodynamics that a pure substance at a specified pressure starts boiling when it reaches the saturation temperature at that pressure. But in practice we do not see any bubbles forming on the heating surface until the liquid is heated a few degrees above the saturation temperature (about 2 to 6°C for water). Therefore, the liquid is slightly *superheated* in this case (a *metastable* condition) and evaporates when it rises to the free surface. The fluid motion in

(*a*) Natural convection boiling

(*b*) Nucleate boiling

(*c*) Transition boiling

(*d*) Film boiling

FIGURE 10–5
Different boiling regimes in pool boiling.
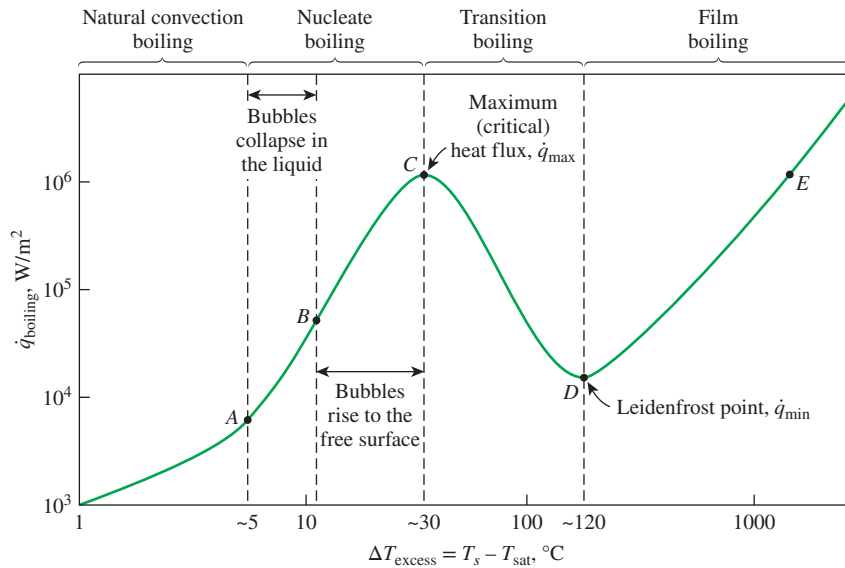
FIGURE 10–6
Typical boiling curve for water at
1 atm pressure.

this mode of boiling is governed by natural convection currents, and heat transfer from the heating surface to the fluid is by natural convection. For the conditions of Fig. 10–6, natural convection boiling ends at an excess temperature of about 5°C.

Nucleate Boiling (Between Points *A* and *C*)

The first bubbles start forming at point *A* of the boiling curve at various preferential sites on the heating surface. Point *A* is referred to as the ***onset of nucleate boiling (ONB)***. The bubbles form at an increasing rate at an increasing number of nucleation sites as we move along the boiling curve toward point *C*. From Fig. 10–6, nucleate boiling exists in the range from about 5°C to about 30°C.

The nucleate boiling regime can be separated into two distinct regions. In region *A–B* ($5°C \leq \Delta T_{excess} \leq 10°C$), *isolated bubbles* are formed at various preferential nucleation sites on the heated surface. But these bubbles are dissipated in the liquid shortly after they separate from the surface. The space vacated by the rising bubbles is filled by the liquid in the vicinity of the heater surface, and the process is repeated. The stirring and agitation caused by the entrainment of the liquid to the heater surface is primarily responsible for the increased heat transfer coefficient and heat flux in this region of nucleate boiling.

In region *B–C* ($10°C \leq \Delta T_{excess} \leq 30°C$), the heater temperature is further increased, and bubbles form at such great rates at such a large number of nucleation sites that they form numerous *continuous columns of vapor* in the liquid. These bubbles move all the way up to the free surface, where they break up and release their vapor content. The large heat fluxes obtainable in this region are caused by the combined effect of liquid entrainment and evaporation.

At large values of ΔT_{excess}, the rate of evaporation at the heater surface reaches such high values that a large fraction of the heater surface is covered by bubbles, making it difficult for the liquid to reach the heater surface and wet it. Consequently, the heat flux increases at a lower rate with increasing ΔT_{excess}, and it reaches a maximum at point *C*. The heat flux at this point is called the **critical** (or **maximum**) **heat flux** (**CHF**), $\dot{q}_{max}$. For water, the critical heat flux exceeds 1 MW/m². From Newton's law of cooling, the heat

(*a*)

(*b*)

FIGURE 10–7
Nature of bubble formation and bubble motion associated with boiling.

(*a*) ©*David Chasey/Getty Images*
(*b*) ©*McGraw-Hill Education/Stephen Frisch, photographer*
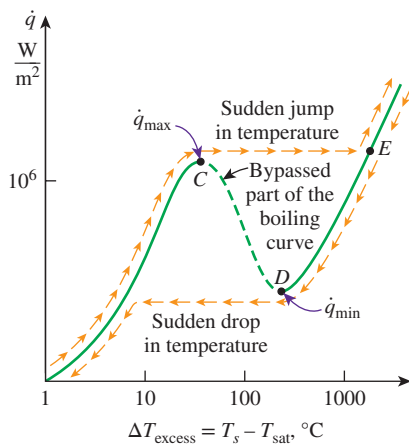
FIGURE 10–8
The actual boiling curve obtained with heated platinum wire in water as the heat flux is increased and then decreased.

transfer coefficient at point C is $h = \dot{q}_{max}/\Delta T_{excess} = (10^6 \text{ W/m}^2)/30 \text{ K} = 3.3 \times 10^4 \text{ W/m}^2\cdot\text{K}$. For the entire nucleate boiling range of Fig. 10–6, the heat transfer coefficient ranges from about 2000 to 30,000 W/m²·K, which is within the range of values tabulated in Table 1–5 for boiling.

Nucleate boiling is the most desirable boiling regime in practice because high heat transfer rates can be achieved in this regime with relatively small values of ΔT_{excess}, typically under 30°C for water. The photographs in Fig. 10–7 show the nature of bubble formation and bubble motion associated with boiling.

Transition Boiling (Between Points *C* and *D*)

As the heater temperature and thus the ΔT_{excess} is increased past point *C,* the heat flux decreases, as shown in Fig. 10–6. This is because a large fraction of the heater surface is covered by a vapor film, which acts as an insulation due to the low thermal conductivity of the vapor relative to that of the liquid. In the transition boiling regime, both nucleate and film boiling partially occur. Nucleate boiling at point *C* is completely replaced by film boiling at point *D.* Operation in the transition boiling regime, which is also called the *unstable film boiling regime,* is avoided in practice. For water, transition boiling occurs over the excess temperature range from about 30°C to about 120°C.

Film Boiling (Beyond Point *D*)

In this region, the heater surface is completely covered by a continuous stable vapor film. Point *D,* where the heat flux reaches a minimum, is called the **Leidenfrost point**, in honor of J. C. Leidenfrost, who observed in 1756 that liquid droplets on a very hot surface jump around and slowly boil away. The presence of a vapor film between the heater surface and the liquid is responsible for the low heat transfer rates in the film boiling region. The heat transfer rate increases with increasing excess temperature as a result of heat transfer from the heated surface to the liquid through the vapor film by radiation, which becomes significant at high temperatures.

A typical boiling process does not follow the boiling curve beyond point *C,* as Nukiyama has observed during his experiments. Nukiyama noticed, with surprise, that when the power applied to the nichrome wire immersed in water exceeded $\dot{q}_{max}$ even slightly, the wire temperature increased suddenly to the melting point of the wire (1500 K), and *burnout* occurred beyond his control. When he repeated the experiments with platinum wire, which has a much higher melting point (2045 K), he was able to avoid burnout and maintain heat fluxes higher than $\dot{q}_{max}$. When he gradually reduced power, he obtained the cooling curve shown in Fig. 10–8 with a sudden drop in excess temperature when $\dot{q}_{min}$ is reached. Note that the boiling process cannot follow the transition boiling part of the boiling curve past point *C* unless the power applied is reduced suddenly.

The *burnout phenomenon* in boiling can be explained as follows: In order to move beyond point *C* where $\dot{q}_{max}$ occurs, we must increase the heater surface temperature T_s. To increase T_s, however, we must increase the heat flux. But the fluid cannot receive this increased energy at an excess temperature just beyond point *C*. Therefore, the heater surface ends up absorbing the increased energy, causing the heater surface temperature T_s to rise. But the fluid can receive even less energy at this increased excess temperature, causing the heater surface temperature T_s to rise even further. This continues until the surface temperature reaches a point at which it no longer rises and the heat supplied can be transferred

to the fluid steadily. This is point *E* on the boiling curve, which corresponds to very high surface temperatures. Therefore, any attempt to increase the heat flux beyond $\dot{q}_{max}$ will cause the operation point on the boiling curve to jump suddenly from point *C* to point *E*. However, surface temperature that corresponds to point *E* is beyond the melting point of most heater materials, and *burnout* occurs. Therefore, point *C* on the boiling curve is also called the **burnout point**, and the heat flux at this point is the **burnout heat flux** (Fig. 10–9).

Most boiling heat transfer equipment in practice operates slightly below $\dot{q}_{max}$ to avoid any disastrous burnout. However, in cryogenic applications involving fluids with very low boiling points such as oxygen and nitrogen, point *E* usually falls below the melting point of the heater materials, and steady film boiling can be used in those cases without any danger of burnout.

Heat Transfer Correlations in Pool Boiling

Boiling regimes discussed above differ considerably in their character, and thus different heat transfer relations need to be used for different boiling regimes (Fig. 10–10). In the *natural convection boiling* regime ($\Delta T_{excess} \leq 5°C$), boiling is governed by natural convection currents, and heat transfer rates in this case can be determined accurately using natural convection relations presented in Chap. 9.

Nucleate Boiling

In the *nucleate boiling* regime ($5°C \leq \Delta T_{excess} \leq 30°C$), the rate of heat transfer strongly depends on the nature of nucleation (the number of active nucleation sites on the surface, the rate of bubble formation at each site, etc.), which is difficult to predict. The type and the condition of the heated surface also affect the heat transfer. These complications made it difficult to develop theoretical relations for heat transfer in the nucleate boiling regime, and we had to rely on relations based on experimental data. The most widely used correlation for the rate of heat transfer in the nucleate boiling regime was proposed in 1952 by Rohsenow and expressed as

$$\dot{q}_{nucleate} = \mu_l h_{fg} \left[\frac{g(\rho_l - \rho_v)}{\sigma}\right]^{1/2} \left[\frac{c_{pl}(T_s - T_{sat})}{C_{sf} h_{fg} Pr_l^n}\right]^3 \qquad \textbf{(10–2)}$$

where

$\dot{q}_{nucleate}$ = nucleate boiling heat flux, W/m^2

μ_l = viscosity of the liquid, kg/m·s

h_{fg} = enthalpy of vaporization, J/kg

g = gravitational acceleration, m/s^2

ρ_l = density of the liquid, kg/m^3

ρ_v = density of the vapor, kg/m^3

σ = surface tension of liquid–vapor interface, N/m

c_{pl} = specific heat of the liquid, J/kg·°C

T_s = surface temperature of the heater, °C

T_{sat} = saturation temperature of the fluid, °C

C_{sf} = experimental constant that depends on surface–fluid combination

Pr_l = Prandtl number of the liquid

n = experimental constant that depends on the fluid
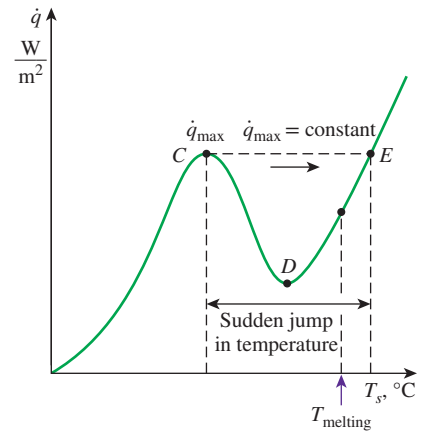
FIGURE 10–9
An attempt to increase the boiling heat flux beyond the critical value often causes the temperature of the heating element to jump suddenly to a value that is above the melting point, resulting in *burnout.*
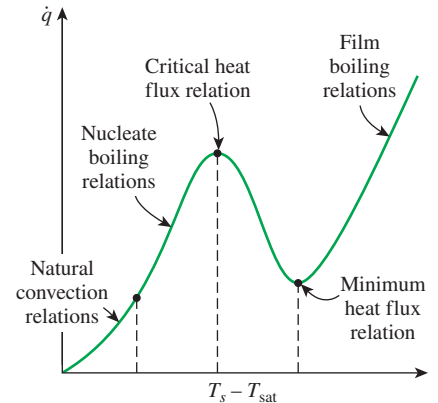
FIGURE 10–10
Different relations are used to determine the heat flux in different boiling regimes.

$$\dot{q} = \left(\frac{\text{kg}}{\text{m} \cdot \text{s}}\right)\left(\frac{\text{J}}{\text{kg}}\right)$$

$$\times \left(\frac{\dfrac{\text{m}}{\text{s}^2}\dfrac{\text{kg}}{\text{m}^3}}{\dfrac{\text{N}}{\text{m}}}\right)^{1/2}\left(\frac{\dfrac{\text{J}}{\text{kg} \cdot {}^{\circ}\text{C}}{}^{\circ}\text{C}}{\dfrac{\text{J}}{\text{kg}}}\right)^3$$

$$= \frac{\text{W}}{\text{m}}\left(\frac{1}{\text{m}^2}\right)^{1/2}(1)^3$$

$$= \text{W/m}^2$$

FIGURE 10–11
Equation 10–2 gives the boiling heat flux in W/m^2 when the quantities are expressed in the units specified in their descriptions.

TABLE 10–1

Surface tension of liquid–vapor interface for water

T, °C	σ, N/m*
0	0.0757
20	0.0727
40	0.0696
60	0.0662
80	0.0627
100	0.0589
120	0.0550
140	0.0509
160	0.0466
180	0.0422
200	0.0377
220	0.0331
240	0.0284
260	0.0237
280	0.0190
300	0.0144
320	0.0099
340	0.0056
360	0.0019
374	0.0

*Multiply by 0.06852 to convert to lbf/ft or by 2.2046 to convert to lbm/s².

It can be shown easily that using property values in the specified units in the Rohsenow equation produces the desired unit W/m^2 for the boiling heat flux, thus saving one from having to go through tedious unit manipulations (Fig. 10–11).

The surface tension at the vapor–liquid interface is given in Table 10–1 for water and Table 10–2 for some other fluids. Experimentally determined values of the constant C_{sf} and n (fluid-dependent experimental constant) are given in Table 10–3 for various fluid–surface combinations. These values can be used for *any geometry* since it is found that the rate of heat transfer during nucleate boiling is essentially independent of the geometry and orientation of the heated surface. The fluid properties in Eq. 10–2 are to be evaluated at the saturation temperature T_{sat}.

The *condition* of the heater surface greatly affects heat transfer, and the Rohsenow equation given above is applicable to *clean* and relatively *smooth* surfaces. The results obtained using the Rohsenow equation can be in error by $\pm100\%$ for the heat transfer rate for a given excess temperature and by $\pm30\%$ for the excess temperature for a given heat transfer rate. Therefore, care should be exercised in the interpretation of the results.

Recall from thermodynamics that the enthalpy of vaporization h_{fg} of a pure substance decreases with increasing pressure (or temperature) and reaches zero at the critical point. Noting that h_{fg} appears in the denominator of the Rohsenow equation, we should see a significant rise in the rate of heat transfer at *high pressures* during nucleate boiling. Values of h_{fg} for different substances are listed in Tables A–2 and A–9 to A–12.

Peak Heat Flux

In the design of boiling heat transfer equipment, it is extremely important for the designer to have a knowledge of the maximum heat flux in order to avoid the danger of burnout. The *maximum* (or *critical*) *heat flux* in nucleate pool boiling was determined theoretically by S. S. Kutateladze in Russia in 1948 and N. Zuber in the United States in 1958 using quite different approaches, and it is expressed as

$$\dot{q}_{\text{max}} = C_{cr} h_{fg}[\sigma g \rho_v^2 (\rho_l - \rho_v)]^{1/4} \tag{10–3}$$

where C_{cr} is a constant whose value depends on the heater geometry. Exhaustive experimental studies by Lienhard and his coworkers indicated that the value of C_{cr} is about 0.15. Specific values of C_{cr} for different heater geometries are listed in Table 10–4. Note that the heaters are classified as being large or small based on the value of the parameter L^*.

Equation 10–3 will give the maximum heat flux in W/m^2 if the properties are used *in the units specified* earlier in their descriptions following Eq. 10–2. The maximum heat flux is independent of the fluid–heating surface combination, as well as the viscosity, thermal conductivity, and the specific heat of the liquid.

Note that ρ_v increases but σ and h_{fg} decrease with increasing pressure, and thus the change in $\dot{q}_{\text{max}}$ with pressure depends on which effect dominates. The experimental studies of Cichelli and Bonilla indicate that $\dot{q}_{\text{max}}$ increases with pressure up to about one-third of the critical pressure and then starts to decrease and becomes zero at the critical pressure. Also note that $\dot{q}_{\text{max}}$ is proportional to h_{fg}, and large maximum heat fluxes can be obtained using fluids with a large enthalpy of vaporization, such as water.

TABLE 10–2

Surface tension of some fluids

Substance and Temp. Range	Surface Tension, σ, N/m* (T in °C)
Ammonia, -75 to -40°C :	$0.0264 + 0.000223T$
Benzene, 10 to 80°C :	$0.0315 - 0.000129T$
Butane, -70 to -20°C :	$0.0149 - 0.000121T$
Carbon dioxide, -30 to -20°C :	$0.0043 - 0.000160T$
Ethyl alcohol, 10 to 70°C :	$0.0241 - 0.000083T$
Mercury, 5 to 200°C :	$0.4906 - 0.000205T$
Methyl alcohol, 10 to 60°C :	$0.0240 - 0.000077T$
Pentane, 10 to 30°C :	$0.0183 - 0.000110T$
Propane, -90 to -10°C :	$0.0092 - 0.000087T$

Source: From Suryanarayana, 1995, originally based on data from Jasper, 1972.

*Multiply by 0.06852 to convert to lbf/ft or by 2.2046 to convert to lbm/s^2.

TABLE 10–3

Values of the coefficient C_{sf} and n for various fluid–surface combinations

Fluid–Heating Surface Combination	C_{sf}	n
Water–copper (polished)	0.0130	1.0
Water–copper (scored)	0.0068	1.0
Water–stainless steel (mechanically polished)	0.0130	1.0
Water–stainless steel (ground and polished)	0.0060	1.0
Water–stainless steel (Teflon pitted)	0.0058	1.0
Water–stainless steel (chemically etched)	0.0130	1.0
Water–brass	0.0060	1.0
Water–nickel	0.0060	1.0
Water–platinum	0.0130	1.0
n-Pentane–copper (polished)	0.0154	1.7
n-Pentane–chromium	0.0150	1.7
Benzene–chromium	0.1010	1.7
Ethyl alcohol–chromium	0.0027	1.7
Carbon tetrachloride–copper	0.0130	1.7
Isopropanol–copper	0.0025	1.7

TABLE 10–4

Values of the coefficient C_{cr} for use in Eq. 10–3 for maximum heat flux (dimensionless parameter $L^* = L[g(\rho_l - \rho_v)/\sigma]^{1/2}$)

Heater Geometry	C_{cr}	Charac. Dimension of Heater, L	Range of L^*
Large horizontal flat heater	0.149	Width or diameter	$L^* > 27$
Small horizontal flat heater[1]	$18.9K_1$	Width or diameter	$9 < L^* < 20$
Large horizontal cylinder	0.12	Radius	$L^* > 1.2$
Small horizontal cylinder	$0.12L^{*-0.25}$	Radius	$0.15 < L^* < 1.2$
Large sphere	0.11	Radius	$L^* > 4.26$
Small sphere	$0.227L^{*-0.5}$	Radius	$0.15 < L^* < 4.26$

[1]$K_1 = \sigma/[g(\rho_l - \rho_v)A_{heater}]$

Minimum Heat Flux

Minimum heat flux, which occurs at the Leidenfrost point, is of practical interest since it represents the lower limit for the heat flux in the film boiling regime. Using the stability theory, Zuber (1958) derived the following expression for the minimum heat flux for a *large horizontal plate,*

$$\dot{q}_{\min} = 0.09\rho_v h_{fg}\left[\frac{\sigma g(\rho_l - \rho_v)}{(\rho_l + \rho_v)^2}\right]^{1/4} \tag{10-4}$$

where the constant 0.09 was determined by Berensen in 1961. He replaced the theoretically determined value of $\frac{\pi}{24}$ with 0.09 to match the experimental data better. Still, this relation can be in error by 50 percent or more.

Operation in the *transition boiling* regime ($30°C \leq \Delta T_{\text{excess}} \leq 120°C$) is normally avoided in the design of heat transfer equipment, and thus no major attempt has been made to develop general correlations for boiling heat transfer in this regime. However, the upper (*peak heat flux, $\dot{q}_{\max}$*) and the lower (*minimum heat flux, $\dot{q}_{\min}$*) limits of this region are of interest to heat transfer equipment designers.

Film Boiling

Using an analysis similar to Nusselt's theory on filmwise condensation presented in the next section, Bromley (1950) developed a theory for the prediction of heat flux for stable film boiling on the outside of a horizontal cylinder. The heat flux for film boiling on a *horizontal cylinder* or *sphere* of diameter D is given by

$$\dot{q}_{\text{film}} = C_{\text{film}}\left[\frac{gk_v^3\rho_v(\rho_l - \rho_v)[h_{fg} + 0.4c_{pv}(T_s - T_{\text{sat}})]}{\mu_v D(T_s - T_{\text{sat}})}\right]^{1/4}(T_s - T_{\text{sat}}) \tag{10-5}$$

where k_v is the thermal conductivity of the vapor in W/m·K and

$$C_{\text{film}} = \begin{cases} 0.62 \text{ for horizontal cylinders} \\ 0.67 \text{ for spheres} \end{cases}$$

$P = 1$ atm

100°C

400°C

Vapor

$\dot{q}_{\text{film boiling}}$ $\dot{q}_{\text{rad}}$

Heating

FIGURE 10–12

At high heater surface temperatures, radiation heat transfer becomes significant during film boiling.

Other properties are as listed before in connection with Eq. 10–2. We used a modified latent heat of vaporization in Eq. 10–5 to account for the heat transfer associated with the superheating of the vapor.

The *vapor* properties are to be evaluated at the *film temperature* $T_f = (T_s + T_{\text{sat}})/2$, which is the *average temperature* of the vapor film. The liquid properties and h_{fg} are to be evaluated at the saturation temperature at the specified pressure. Again, this relation gives the film boiling heat flux in W/m² if the properties are used *in the units specified* earlier in their descriptions following Eq. 10–2.

At high surface temperatures (typically above 300°C), heat transfer across the vapor film by *radiation* becomes significant and needs to be considered (Fig. 10–12). Treating the vapor film as a transparent medium sandwiched between two large parallel plates and approximating the liquid as a blackbody, *radiation heat transfer* can be determined from

$$\dot{q}_{\text{rad}} = \varepsilon\sigma(T_s^4 - T_{\text{sat}}^4) \tag{10-6}$$

where ε is the emissivity of the heating surface and $\sigma = 5.67 \times 10^{-8}$ W/m²·K⁴ is the Stefan–Boltzmann constant. Note that the temperature in this case must be expressed in K, not °C, and that surface tension and the Stefan–Boltzmann constant share the same symbol.

You may be tempted to simply add the convection and radiation heat transfers to determine the total heat transfer during film boiling. However, these two mechanisms of heat transfer adversely affect each other, causing the total heat transfer to be less than their sum. For example, the radiation heat transfer from the surface to the liquid enhances the rate of evaporation, and thus the thickness of the vapor film, which impedes convection heat transfer. For $\dot{q}_{rad} < \dot{q}_{film}$, Bromley (1950) determined that the relation

$$\dot{q}_{total} = \dot{q}_{film} + \frac{3}{4}\dot{q}_{rad}$$

(10–7)

correlates experimental data well.

Note that the gravitational acceleration g, whose value is approximately 9.81 m/s^2 at sea level, appears in all of the preceding relations for boiling heat transfer. The effects of low and high gravity (as encountered in aerospace applications and turbomachinery) are studied experimentally. The studies confirm that the critical heat flux and heat flux in film boiling are proportional to $g^{1/4}$. However, they indicate that heat flux in nucleate boiling is practically independent of gravity g, instead of being proportional to $g^{1/2}$, as dictated by Eq. 10–2.

Enhancement of Heat Transfer in Pool Boiling

The pool boiling heat transfer relations given to this point apply to smooth surfaces. Next we discuss some methods to enhance heat transfer in pool boiling.

We pointed out earlier that the rate of heat transfer in the nucleate boiling regime strongly depends on the number of active nucleation sites on the surface and the rate of bubble formation at each site. Therefore, any modification that enhances *nucleation* on the heating surface will also enhance *heat transfer* in nucleate boiling. It is observed that *irregularities* on the heating surface, including roughness and dirt, serve as additional nucleation sites during boiling, as shown in Fig. 10–13. For example, the first bubbles in a pan filled with water are most likely to form at the *scratches* at the bottom surface. These scratches act like "nests" for the bubbles to form and thus increase the rate of bubble formation. Berensen has shown that heat flux in the nucleate boiling regime can be increased by a factor of 10 by *roughening* the heating surface. However, these high heat transfer rates cannot be sustained for long since the effect of surface roughness is observed to decay with time and the heat flux to drop eventually to values encountered on smooth surfaces. The effect of surface roughness is negligible on the maximum (critical) heat flux and the heat flux in film boiling.

Surfaces that provide enhanced heat transfer in nucleate boiling *permanently* are being manufactured and are available in the market. Enhancement in nucleation and thus heat transfer in such special surfaces is achieved either by *coating* the surface with a thin layer (much less than 1 mm) of very porous material or by *forming cavities* on the surface mechanically to facilitate continuous vapor formation. Such surfaces are reported to enhance heat transfer in the nucleate boiling regime by a factor of up to 10 and the maximum heat flux by a factor of 3. The enhancement provided by one such material prepared by machine roughening, the thermoexcel-E, is shown in Fig. 10–14. The use of finned surfaces is also known to enhance nucleate boiling heat transfer and the maximum heat flux.
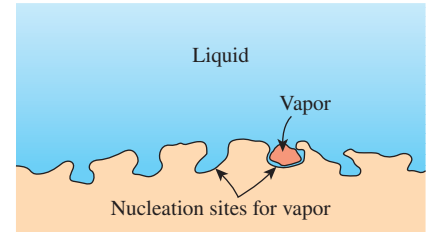
FIGURE 10–13
The cavities on a rough surface act as nucleation sites and enhance boiling heat transfer.
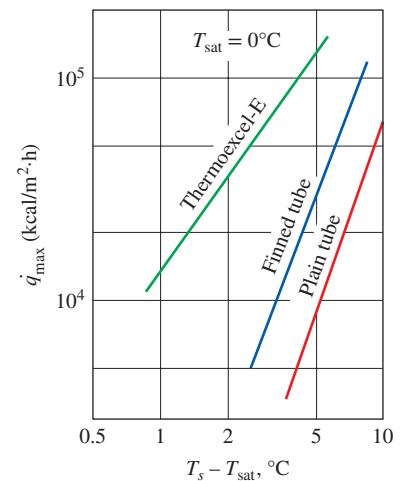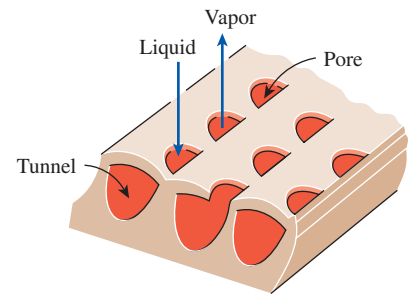
FIGURE 10–14
The enhancement of boiling heat transfer in Freon-12 by a mechanically roughened surface, thermoexcel-E.

Boiling heat transfer can also be enhanced by other techniques such as *mechanical agitation* and *surface vibration.* These techniques are not practical, however, because of the complications involved.

$P = 1$ atm

Water

100°C

108°C

Heating
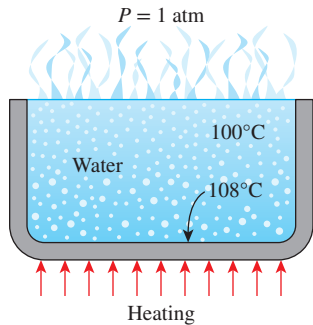
FIGURE 10–15
Schematic for Example 10–1.

EXAMPLE 10–1   Nucleate Boiling of Water in a Pan

Water is to be boiled at atmospheric pressure in a mechanically polished stainless steel pan placed on top of a heating unit, as shown in Fig. 10–15. The inner surface of the bottom of the pan is maintained at 108°C. If the diameter of the bottom of the pan is 30 cm, determine (*a*) the rate of heat transfer to the water and (*b*) the rate of evaporation of water.

SOLUTION   Water is boiled at 1 atm pressure on a stainless steel surface. The rate of heat transfer to the water and the rate of evaporation of water are to be determined.
Assumptions   **1** Steady operating conditions exist. **2** Heat losses from the heater and the pan are negligible.
Properties   The properties of water at the saturation temperature of 100°C are $\sigma = 0.0589$ N/m (Table 10–1) and, from Table A–9,

$$\rho_l = 957.9 \text{ kg/m}^3 \qquad h_{fg} = 2257 \times 10^3 \text{ J/kg}$$

$$\rho_v = 0.6 \text{ kg/m}^3 \qquad \mu_l = 0.282 \times 10^{-3} \text{ kg/m·s}$$

$$\text{Pr}_l = 1.75 \qquad c_{pl} = 4217 \text{ J/kg·K}$$

Also, $C_{sf} = 0.0130$ and $n = 1.0$ for the boiling of water on a mechanically polished stainless steel surface (Table 10–3). Note that we expressed the properties in units specified under Eq. 10–2 in connection with their definitions in order to avoid unit manipulations.
Analysis   (*a*) The excess temperature in this case is $\Delta T = T_s - T_{\text{sat}} = 108 - 100 = 8°C$, which is relatively low (less than 30°C). Therefore, nucleate boiling will occur. The heat flux in this case can be determined from the Rohsenow relation to be

$$\dot{q}_{\text{nucleate}} = \mu_l \, h_{fg} \left[\frac{g(\rho_l - \rho_v)}{\sigma} \right]^{1/2} \left[\frac{c_{pl}(T_s - T_{\text{sat}})}{C_{sf} \, h_{fg} \text{Pr}_l^n} \right]^3$$

$$= (0.282 \times 10^{-3})(2257 \times 10^3) \left[\frac{9.81 \times (957.9 - 0.6)}{0.0589} \right]^{1/2}$$

$$\times \left(\frac{4217(108 - 100)}{0.0130(2257 \times 10^3)\,1.75} \right)^3$$

$$= 7.21 \times 10^4 \text{ W/m}^2$$

The surface area of the bottom of the pan is

$$A = \pi D^2/4 = \pi(0.3 \text{ m})^2/4 = 0.07069 \text{ m}^2$$

Then the rate of heat transfer during nucleate boiling becomes

$$\dot{Q}_{\text{boiling}} = A\dot{q}_{\text{nucleate}} = (0.07069 \text{ m}^2)(7.21 \times 10^4 \text{ W/m}^2) = \mathbf{5097 \ W}$$

(*b*) The rate of evaporation of water is determined from

$$\dot{m}_{\text{evaporation}} = \frac{\dot{Q}_{\text{boiling}}}{h_{fg}} = \frac{5097 \text{ J/s}}{2257 \times 10^3 \text{ J/kg}} = \mathbf{2.26 \times 10^{-3} \ kg/s}$$

That is, water in the pan will boil at a rate of more than 2 grams per second.

FIGURE 10–16
Schematic for Example 10–2.

EXAMPLE 10–2 Peak Heat Flux in Nucleate Boiling

Water in a tank is to be boiled at sea level by a 1-cm-diameter nickel-plated steel heating element equipped with electrical resistance wires inside, as shown in Fig. 10–16. Determine the maximum heat flux that can be attained in the nucleate boiling regime and the surface temperature of the heater in that case.

SOLUTION Water is boiled at 1 atm pressure on a nickel-plated steel surface. The maximum heat flux and the surface temperature are to be determined.

Assumptions **1** Steady operating conditions exist. **2** Heat losses from the boiler are negligible.

Properties The properties of water at the saturation temperature of 100°C are $\sigma = 0.0589$ N/m (Table 10–1) and, from Table A–9,

$$\rho_l = 957.9 \text{ kg/m}^3 \qquad h_{fg} = 2257 \times 10^3 \text{ J/kg}$$

$$\rho_v = 0.6 \text{ kg/m}^3 \qquad \mu_l = 0.282 \times 10^{-3} \text{ kg/m·s}$$

$$\text{Pr}_l = 1.75 \qquad c_{pl} = 4217 \text{ J/kg·K}$$

Also, $C_{sf} = 0.0060$ and $n = 1.0$ for the boiling of water on a nickel-plated surface (Table 10–3). Note that we expressed the properties in units specified under Eqs. 10–2 and 10–3 in connection with their definitions in order to avoid unit manipulations.

Analysis The heating element in this case can be considered to be a short cylinder whose characteristic dimension is its radius. That is, $L = r = 0.005$ m. The dimensionless parameter L^* and the constant C_{cr} are determined from Table 10–4 to be

$$L^* = L \left[\frac{g(\rho_l - \rho_v)}{\sigma} \right]^{1/2} = (0.005) \left[\frac{(9.81)(957.9 - 0.6)}{0.0589} \right]^{1/2} = 2.00 > 1.2$$

which corresponds to $C_{cr} = 0.12$.

Then the maximum or critical heat flux is determined from Eq. 10–3 to be

$$\dot{q}_{\max} = C_{cr} h_{fg} [\sigma g \rho_v^2 (\rho_l - \rho_v)]^{1/4}$$

$$= 0.12(2257 \times 10^3)[0.0589 \times 9.81 \times (0.6)^2 (957.9 - 0.6)]^{1/4}$$

$$= \mathbf{1.017 \times 10^6 \text{ W/m}^2}$$

The Rohsenow relation, which gives the nucleate boiling heat flux for a specified surface temperature, can also be used to determine the surface temperature when the heat flux is given. Substituting the maximum heat flux into Eq. 10–2 together with other properties gives

$$\dot{q}_{\text{nucleate}} = \mu_l h_{fg} \left[\frac{g(\rho_l - \rho_v)}{\sigma} \right]^{1/2} \left[\frac{c_{pl}(T_s - T_{\text{sat}})}{C_{sf} h_{fg} \text{Pr}_l^n} \right]^3$$

$$1.017 \times 10^6 = (0.282 \times 10^{-3})(2257 \times 10^3) \left[\frac{9.81(957.9 - 0.6)}{0.0589} \right]^{1/2}$$

$$\times \left[\frac{4217(T_s - 100)}{0.0130 (2257 \times 10^3)1.75} \right]^3$$

$$T_s = \mathbf{119°C}$$

Discussion Note that heat fluxes on the order of 1 MW/m^2 can be obtained in nucleate boiling with a temperature difference of less than 20°C.
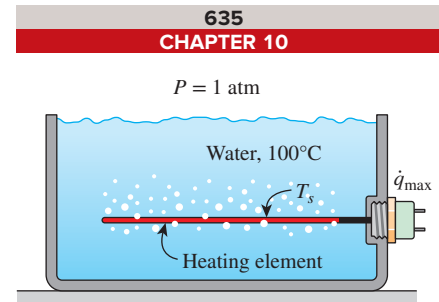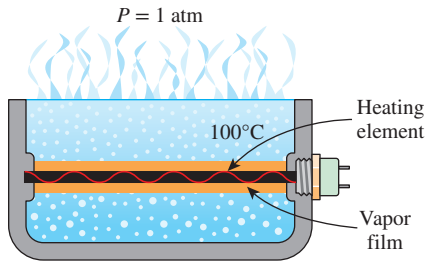
FIGURE 10–17
Schematic for Example 10–3.

EXAMPLE 10–3   Film Boiling of Water on a Heating Element

Water is boiled at atmospheric pressure by a horizontal polished copper heating element of diameter $D = 5$ mm and emissivity $\varepsilon = 0.05$ immersed in water, as shown in Fig. 10–17. If the surface temperature of the heating wire is 350°C, determine the rate of heat transfer from the wire to the water per unit length of the wire.

SOLUTION   Water is boiled at 1 atm by a horizontal polished copper heating element. The rate of heat transfer to the water per unit length of the heater is to be determined.

Assumptions   **1** Steady operating conditions exist. **2** Heat losses from the boiler are negligible.

Properties   The properties of water at the saturation temperature of 100°C are $h_{fg} = 2257 \times 10^3$ J/kg and $\rho_l = 957.9$ kg/m³ (Table A–9). The properties of vapor at the film temperature of $T_f = (T_{sat} + T_s)/2 = (100 + 350)/2 = 225°C$ are, from Table A–16,

$$\rho_v = 0.444 \text{ kg/m}^3 \qquad\qquad c_{pv} = 1951 \text{ J/kg·K}$$
$$\mu_v = 1.75 \times 10^{-5} \text{ kg/m·s} \qquad\qquad k_v = 0.0358 \text{ W/m·K}$$

Note that we expressed the properties in units that cancel each other in boiling heat transfer relations. Also note that we used vapor properties at 1 atm pressure from Table A–16 instead of the properties of saturated vapor from Table A–9 at 225°C since the latter are at the saturation pressure of 2.55 MPa.

Analysis   The excess temperature in this case is $\Delta T = T_s - T_{sat} = 305 - 100 = 250°C$, which is much larger than 30°C for water. Therefore, film boiling will occur. The film boiling heat flux in this case can be determined from Eq. 10–5 to be

$$\dot{q}_{\text{film}} = 0.62 \left[\frac{g k_v^3 \rho_v (\rho_l - \rho_v)[h_{fg} + 0.4 c_{pv}(T_s - T_{sat})]}{\mu_v D (T_s - T_{sat})} \right]^{1/4} (T_s - T_{sat})$$

$$= 0.62 \left[\frac{9.81(0.0358)^3 (0.444)(957.9 - 0.441)}{\begin{array}{c} \times [(2257 \times 10^3) + 0.4 \times 1951(250)] \end{array}}{(1.75 \times 10^{-5})(5 \times 10^{-3})(250)} \right]^{1/4} \times 250$$

$$= 5.93 \times 10^4 \text{ W/m}^2$$

The radiation heat flux is determined from Eq. 10–6 to be

$$\dot{q}_{\text{rad}} = \varepsilon \sigma (T_s^4 - T_{sat}^4)$$
$$= (0.05)(5.67 \times 10^{-8} \text{ W/m}^2\text{·K}^4)[(350 + 273 \text{ K})^4 - (100 + 273 \text{ K})^4]$$
$$= 372 \text{ W/m}^2$$

Note that heat transfer by radiation is negligible in this case because of the low emissivity of the surface and the relatively low surface temperature of the heating element. Then the total heat flux becomes (Eq. 10–7)

$$\dot{q}_{\text{total}} = \dot{q}_{\text{film}} + \frac{3}{4}\dot{q}_{\text{rad}} = 5.93 \times 10^4 + \frac{3}{4} \times 372 = 5.96 \times 10^4 \text{ W/m}^2$$

Finally, the rate of heat transfer from the heating element to the water is determined by multiplying the heat flux by the heat transfer surface area,

$$\dot{Q}_{total} = A\dot{q}_{total} = (\pi DL)\dot{q}_{total}$$
$$= (\pi \times 0.005 \text{ m} \times 1 \text{ m})(5.96 \times 10^4 \text{ W/m}^2)$$
$$= \textbf{936 W}$$

Discussion Note that the 5-mm-diameter copper heating element consumes about 1 kW of electric power per unit length in steady operation in the film boiling regime. This energy is transferred to the water through the vapor film that forms around the wire.

10–3 ▪ FLOW BOILING

The pool boiling we considered so far involves a pool of seemingly motionless liquid, with vapor bubbles rising to the top as a result of buoyancy effects. In **flow boiling**, the fluid is forced to move by an external source such as a pump as it undergoes a phase-change process. The boiling in this case exhibits the combined effects of convection and pool boiling. The flow boiling is also classified as either *external* or *internal flow boiling* depending on whether the fluid is forced to flow over a heated surface or inside a heated tube.

External flow boiling over a plate or cylinder is similar to pool boiling, but the added motion increases both the nucleate boiling heat flux and the maximum heat flux considerably, as shown in Fig. 10–18. Note that the higher the velocity, the higher the nucleate boiling heat flux and the maximum heat flux. In experiments with water, maximum heat flux values as high as 35 MW/m² have been obtained (compare this to the pool boiling value of 1.02 MW/m² at 1 atm pressure) by increasing the fluid velocity.

Internal flow boiling, commonly referred to as *two-phase flow,* is much more complicated in nature because there is no free surface for the vapor to escape, and thus both the liquid and the vapor are forced to flow together. The two-phase flow in a tube exhibits different flow boiling regimes, depending on the relative amounts of the liquid and the vapor phases. This complicates the analysis even further.

The different stages encountered in flow boiling in a heated tube are illustrated in Fig. 10–19 together with the variation of the heat transfer coefficient along the tube. Initially, the liquid is subcooled, and heat transfer to the liquid is by *forced convection.* Then bubbles start forming on the inner surfaces of the tube, and the detached bubbles are drafted into the mainstream. This gives the fluid flow a bubbly appearance, and thus the name *bubbly flow regime.* As the fluid is heated further, the bubbles grow in size and eventually coalesce into slugs of vapor. Up to half of the volume in the tube in this *slug-flow regime* is occupied by vapor. After a while the core of the flow consists of vapor only, and the liquid is confined only in the annular space between the vapor core and the tube walls. This is the *annular-flow regime,* and very high heat transfer coefficients are realized in this regime.
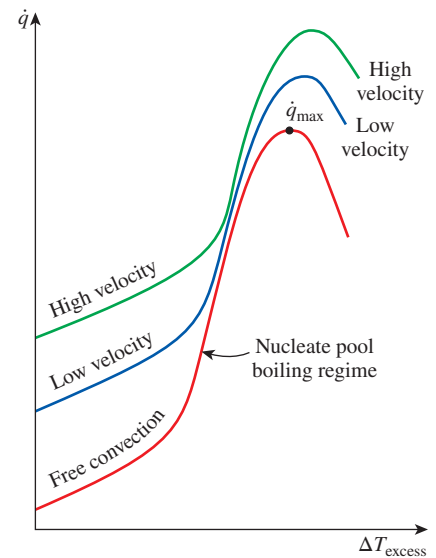
FIGURE 10–18
The effect of forced convection on external flow boiling for different flow velocities.

High   Low
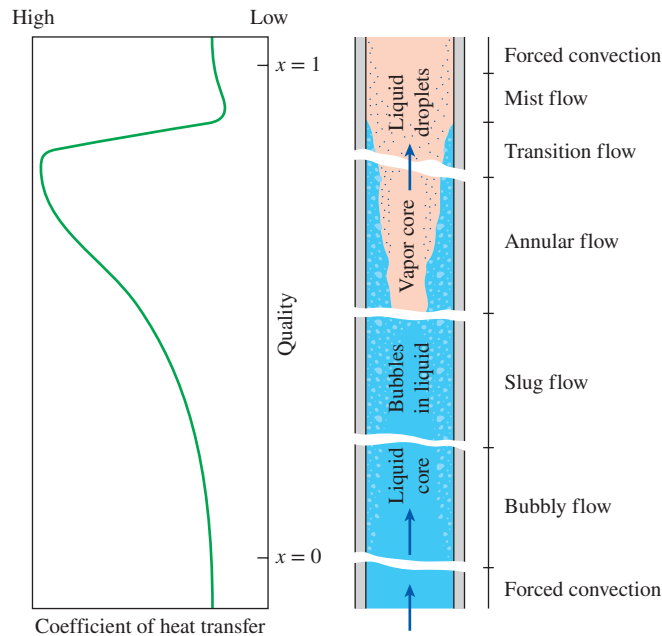
FIGURE 10–19
Different flow regimes encountered in flow boiling in a tube under forced convection.

As the heating continues, the annular liquid layer gets thinner and thinner, and eventually dry spots start to appear on the inner surfaces of the tube. The appearance of dry spots is accompanied by a sharp decrease in the heat transfer coefficient. This *transition regime* continues until the inner surface of the tube is completely dry. Any liquid at this moment is in the form of droplets suspended in the vapor core, which resembles a mist, and we have a *mist-flow regime* until all the liquid droplets are vaporized. At the end of the mist-flow regime we have saturated vapor, which becomes superheated with any further heat transfer.

Note that the tube contains a liquid before the bubbly flow regime and a vapor after the mist-flow regime. Heat transfer in those two cases can be determined using the appropriate relations for single-phase convection heat transfer. Many correlations are proposed for the determination of heat transfer in the two-phase flow (bubbly flow, slug-flow, annular-flow, and mist-flow) cases, but they are beyond the scope of this introductory text. A crude estimate for heat flux in flow boiling can be obtained by simply adding the forced convection and pool boiling heat fluxes.

10–4 ▪ CONDENSATION HEAT TRANSFER

Condensation occurs when the temperature of a vapor is reduced *below* its saturation temperature T_{sat}. This is usually done by bringing the vapor into contact with a solid surface whose temperature T_s is below the saturation temperature T_{sat} of the vapor. But condensation can also occur on the free surface of a liquid or even in a gas when the temperature of the liquid or the gas to which the vapor is exposed is below T_{sat}. In the latter case, the liquid droplets suspended in the gas form a fog. In this chapter, we consider condensation on solid surfaces only.

Two distinct forms of condensation are observed: *film condensation* and *dropwise condensation.* In **film condensation**, the condensate wets the surface and forms a liquid film on the surface that slides down under the influence of gravity. The thickness of the liquid film increases in the flow direction as more vapor condenses on the film. This is how condensation normally occurs in practice. In **dropwise condensation**, the condensed vapor forms droplets on the surface instead of a continuous film, and the surface is covered by countless droplets of varying diameters (Fig. 10–20).

In film condensation, the surface is blanketed by a liquid film of increasing thickness, and this "liquid wall" between the solid surface and the vapor serves as a *resistance* to heat transfer. The heat of vaporization h_{fg} released as the vapor condenses must pass through this resistance before it can reach the solid surface and be transferred to the medium on the other side. In dropwise condensation, however, the droplets slide down when they reach a certain size, clearing the surface and exposing it to vapor. There is no liquid film in this case to resist heat transfer. As a result, heat transfer rates that are more than 10 times larger than those associated with film condensation can be achieved with dropwise condensation. Therefore, dropwise condensation is the preferred mode of condensation in heat transfer applications, and people have long tried to achieve sustained dropwise condensation by using various vapor additives and surface coatings. These attempts have not been very successful, however, since the dropwise condensation achieved did not last long and converted to film condensation after some time. Therefore, it is common practice to be conservative and assume film condensation in the design of heat transfer equipment. For better heat transfer, it is desirable to use short surfaces because of the lower thermal resistance.
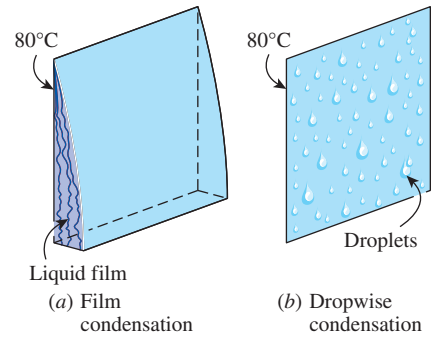
FIGURE 10–20
When a vapor is exposed to a surface at a temperature below T_{sat}, condensation in the form of a liquid film or individual droplets occurs on the surface.

10–5 ■ FILM CONDENSATION

We now consider film condensation on a vertical plate, as shown in Fig. 10–21. The liquid film starts forming at the top of the plate and flows downward under the influence of gravity. The thickness of the film δ *increases* in the flow direction x because of continued condensation at the liquid–vapor interface. Heat in the amount h_{fg} (the latent heat of vaporization) is released during condensation and is *transferred* through the film to the plate surface at temperature T_s. Note that T_s must be below the saturation temperature T_{sat} of the vapor for condensation to occur.

Typical velocity and temperature profiles of the condensate are also given in Fig. 10–21. Note that the *velocity* of the condensate at the wall is zero because of the "no-slip" condition and reaches a *maximum* at the liquid–vapor interface. The *temperature* of the condensate is T_{sat} at the interface and decreases gradually to T_s at the wall.

As was the case in forced convection involving a single phase, heat transfer in condensation also depends on whether the condensate flow is *laminar* or *turbulent.* Again the criterion for the flow regime is provided by the Reynolds number, which is defined as

$$\text{Re} = \frac{D_h \rho_l V_l}{\mu_l} = \frac{4A_c \rho_l V_l}{p\mu_l} = \frac{4\rho_l V_l \delta}{\mu_l} = \frac{4\dot{m}}{p\mu_l} \qquad \text{(10–8)}$$
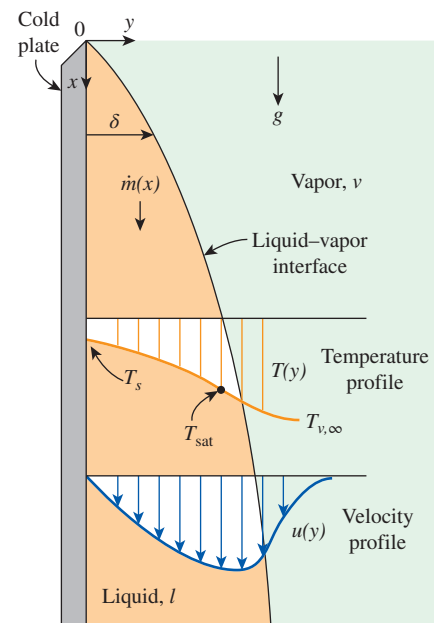
FIGURE 10–21
Film condensation on a vertical plate.

where

$D_h = 4A_c/p = 4\delta$ = hydraulic diameter of the condensate flow, m

p = wetted perimeter of the condensate, m

$A_c = p\delta$ = wetted perimeter × film thickness, m², cross-sectional area of the condensate flow at the lowest part of the flow

ρ_l = density of the liquid, kg/m³

μ_l = viscosity of the liquid, kg/m·s

V_l = average velocity of the condensate at the lowest part of the flow, m/s

$\dot{m} = \rho_l V_l A_c$ = mass flow rate of the condensate at the lowest part, kg/s

The evaluation of the hydraulic diameter D_h for some common geometries is illustrated in Fig. 10–22. Note that the hydraulic diameter is again defined such that it reduces to the ordinary diameter for flow in a circular tube, as was done in Chap. 8 for internal flow, and it is equivalent to four times the thickness of the condensate film at the location where the hydraulic diameter is evaluated. That is, $D_h = 4\delta$.

The latent heat of vaporization h_{fg} is the heat released as a unit mass of vapor condenses, and it normally represents the heat transfer per unit mass of condensate formed during condensation. However, the condensate in an actual condensation process is cooled further to some average temperature between T_{sat} and T_s, releasing more heat in the process. Therefore, the actual heat transfer will be larger. Rohsenow showed in 1956 that the cooling of the liquid below the saturation temperature can be accounted for by replacing h_{fg} with the **modified latent heat of vaporization** h_{fg}^*, defined as

$$h_{fg}^* = h_{fg} + 0.68c_{pl}(T_{sat} - T_s) \tag{10–9a}$$

where c_{pl} is the specific heat of the liquid at the average film temperature.

We can have a similar argument for vapor that enters the condenser as **superheated vapor** at a temperature T_v instead of as saturated vapor. In this case, the vapor must be cooled first to T_{sat} before it can condense, and this heat must be transferred to the wall as well. The amount of heat released as a unit mass of superheated vapor at a temperature T_v is cooled to T_{sat} is simply
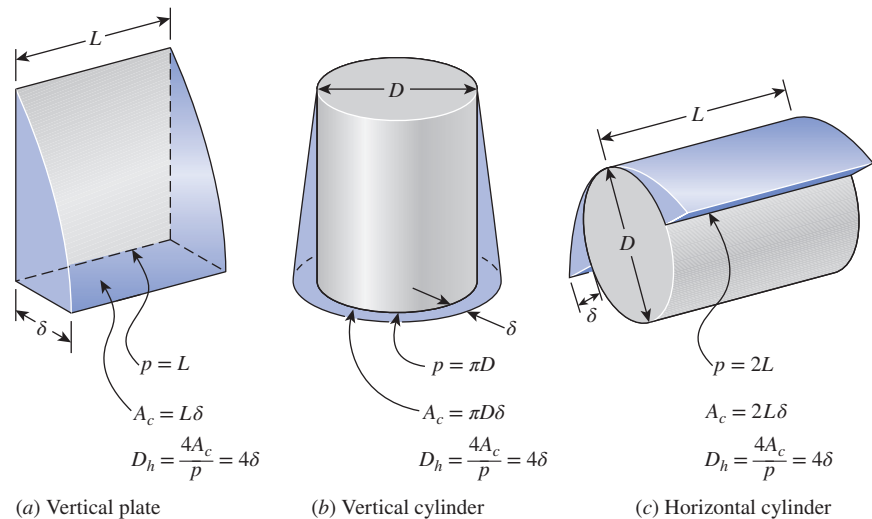
FIGURE 10–22

The wetted perimeter p, the condensate cross-sectional area A_c, and the hydraulic diameter D_h for some common geometries.

$p = L$

$A_c = L\delta$

$D_h = \dfrac{4A_c}{p} = 4\delta$

(a) Vertical plate

$p = \pi D$

$A_c = \pi D\delta$

$D_h = \dfrac{4A_c}{p} = 4\delta$

(b) Vertical cylinder

$p = 2L$

$A_c = 2L\delta$

$D_h = \dfrac{4A_c}{p} = 4\delta$

(c) Horizontal cylinder

$c_{pv}(T_v - T_{sat})$, where c_{pv} is the specific heat of the vapor at the average temperature of $(T_v + T_{sat})/2$. The modified latent heat of vaporization in this case becomes

$$h_{fg}^* = h_{fg} + 0.68c_{pl}(T_{sat} - T_s) + c_{pv}(T_v - T_{sat}) \qquad \textbf{(10–9b)}$$

With these considerations, the rate of heat transfer can be expressed as

$$\dot{Q}_{conden} = hA_s(T_{sat} - T_s) = \dot{m}h_{fg}^* \qquad \textbf{(10–10)}$$

where A_s is the heat transfer area (the surface area on which condensation occurs). Solving for $\dot{m}$ from the equation above and substituting it into Eq. 10–8 gives yet another relation for the Reynolds number,

$$Re = \frac{4\dot{Q}_{conden}}{p\mu_l h_{fg}^*} = \frac{4A_s h(T_{sat} - T_s)}{p\mu_l h_{fg}^*} \qquad \textbf{(10–11)}$$

This relation is convenient to use to determine the Reynolds number when the condensation heat transfer coefficient or the rate of heat transfer is known.

The temperature of the liquid film varies from T_{sat} on the liquid–vapor interface to T_s at the wall surface. Therefore, the properties of the liquid should be evaluated at the *film temperature* $T_f = (T_{sat} + T_s)/2$, which is approximately the *average* temperature of the liquid. The h_{fg}, however, should be evaluated at T_{sat} since it is not affected by the subcooling of the liquid.

Flow Regimes

The Reynolds number for condensation on the outer surfaces of vertical tubes or plates increases in the flow direction due to the increase of the liquid film thickness δ. The flow of liquid film exhibits *different regimes,* depending on the value of the Reynolds number. It is observed that the outer surface of the liquid film remains *smooth* and *wave-free* for about $Re \leq 30$, as shown in Fig. 10–23, and thus the flow is clearly *laminar.* Ripples or waves appear on the free surface of the condensate flow as the Reynolds number increases, and the condensate flow becomes fully *turbulent* at about $Re \approx 1800$. The condensate flow is called *wavy-laminar* in the range of $30 < Re < 1800$ and *turbulent* for $Re > 1800$. However, some disagreement exists about the value of Re at which the flow becomes wavy-laminar or turbulent.

Heat Transfer Correlations for Film Condensation

Next we discuss relations for the average heat transfer coefficient h for the case of *laminar* film condensation for various geometries.

1 Vertical Plates

Consider a vertical plate of height L and width b maintained at a constant temperature T_s that is exposed to vapor at the saturation temperature T_{sat}. The downward direction is taken as the positive x-direction with the origin placed at the top of the plate where condensation initiates, as shown in Fig. 10–24. The surface temperature is below the saturation temperature ($T_s < T_{sat}$) and thus the vapor condenses on the surface. The liquid film flows downward under the influence of gravity. The film thickness δ and thus the mass flow rate of the condensate increases with x as a result of continued condensation on the existing film. Then heat transfer from the vapor to the plate must occur through the film, which offers resistance to heat transfer. Obviously the thicker the film, the larger its thermal resistance and thus the lower the rate of heat transfer.
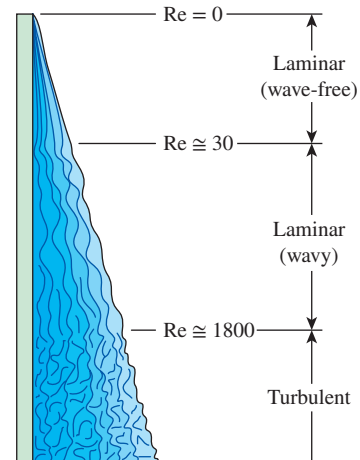
FIGURE 10–23
Flow regimes during film condensation on a vertical plate.
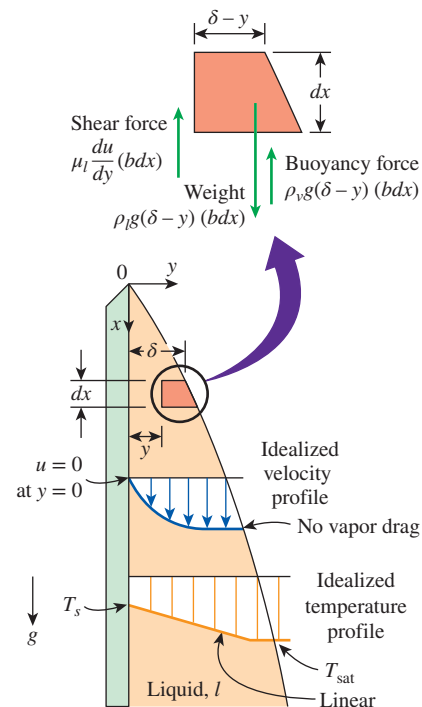
FIGURE 10–24
The volume element of condensate on a vertical plate considered in Nusselt's analysis.

The analytical relation for the heat transfer coefficient in film condensation on a vertical plate described above was first developed by Nusselt in 1916 under the following simplifying assumptions:

1. Both the plate and the vapor are maintained at *constant temperatures* of T_s and T_{sat}, respectively, and the temperature across the liquid film varies *linearly*.

2. Heat transfer across the liquid film is by pure *conduction* (no convection currents in the liquid film).

3. The velocity of the vapor is low (or zero) so that it exerts *no drag* on the condensate (no viscous shear on the liquid–vapor interface).

4. The flow of the condensate is *laminar* and the properties of the liquid are constant.

5. The acceleration of the condensate layer is negligible.

Then Newton's second law of motion for the volume element shown in Fig. 10–24 in the vertical *x*-direction can be written as

$$\sum F_x = ma_x = 0$$

since the acceleration of the fluid is zero. Noting that the only force acting downward is the weight of the liquid element, and the forces acting upward are the viscous shear (or fluid friction) force at the left and the buoyancy force, the force balance on the volume element becomes

$$F_{\text{downward} \downarrow} = F_{\text{upward} \uparrow}$$

Weight = Viscous shear force + Buoyancy force

$$\rho_l g(\delta - y)(bdx) = \mu_l \frac{du}{dy}(bdx) + \rho_v\, g(\delta - y)(bdx)$$

Canceling the plate width *b* and solving for *du/dy* gives

$$\frac{du}{dy} = \frac{g(\rho_l - \rho_v)(\delta - y)}{\mu_l}$$

Integrating from $y = 0$ where $u = 0$ (because of the no-slip boundary condition) to $y = y$ where $u = u(y)$ gives

$$u(y) = \frac{g(\rho_l - \rho_v)}{\mu_l}\left(y\delta - \frac{y^2}{2}\right) \tag{10–12}$$

The mass flow rate of the condensate at a location *x,* where the boundary layer thickness is δ, is determined from

$$\dot{m}(x) = \int_A \rho_l u(y)dA = \int_{y=0}^{\delta} \rho_l u(y)bdy \tag{10–13}$$

Substituting the *u(y)* relation from Eq. 10–12 into Eq. 10–13 gives

$$\dot{m}(x) = \frac{gb\rho_l(\rho_l - \rho_v)\delta^3}{3\mu_l} \tag{10–14}$$

whose derivative with respect to *x* is

$$\frac{d\dot{m}}{dx} = \frac{gb\rho_l(\rho_l - \rho_v)\delta^2}{\mu_l}\frac{d\delta}{dx} \tag{10–15}$$

which represents the rate of condensation of vapor over a vertical distance dx. The rate of heat transfer from the vapor to the plate through the liquid film is simply equal to the heat released as the vapor is condensed and is expressed as

$$d\dot{Q} = h_{fg}d\dot{m} = k_l(bdx)\frac{T_{\text{sat}} - T_s}{\delta} \quad \rightarrow \quad \frac{d\dot{m}}{dx} = \frac{k_l b}{h_{fg}}\frac{T_{\text{sat}} - T_s}{\delta} \qquad \textbf{(10–16)}$$

Equating Eqs. 10–15 and 10–16 for $d\dot{m}/dx$ to each other and separating the variables give

$$\delta^3 d\delta = \frac{\mu_l k_l(T_{\text{sat}} - T_s)}{g\rho_l(\rho_l - \rho_v)h_{fg}} dx \qquad \textbf{(10–17)}$$

Integrating from $x = 0$ where $\delta = 0$ (the top of the plate) to $x = x$ where $\delta = \delta(x)$, the liquid film thickness at any location x is determined to be

$$\delta(x) = \left[\frac{4\mu_l k_l(T_{\text{sat}} - T_s)x}{g\rho_l(\rho_l - \rho_v)h_{fg}}\right]^{1/4} \qquad \textbf{(10–18)}$$

The heat transfer rate from the vapor to the plate at a location x can be expressed as

$$\dot{q}_x = h_x(T_{\text{sat}} - T_s) = k_l\frac{T_{\text{sat}} - T_s}{\delta} \quad \rightarrow \quad h_x = \frac{k_l}{\delta(x)} \qquad \textbf{(10–19)}$$

Substituting the $\delta(x)$ expression from Eq. 10–18, the local heat transfer coefficient h_x is determined to be

$$h_x = \left[\frac{g\rho_l(\rho_l - \rho_v)h_{fg} k_l^3}{4\mu_l(T_{\text{sat}} - T_s)x}\right]^{1/4} \qquad \textbf{(10–20)}$$

The average heat transfer coefficient over the entire plate is determined from its definition by substituting the h_x relation and performing the integration. It gives

$$h = h_{\text{vert}} = \frac{1}{L}\int_0^L h_x dx = \frac{4}{3}h_{x=L} = 0.943\left[\frac{g\rho_l(\rho_l - \rho_v)h_{fg} k_l^3}{\mu_l(T_{\text{sat}} - T_s)L}\right]^{1/4} \qquad \textbf{(10–21)}$$

Equation 10–21, which is obtained with the simplifying assumptions stated earlier, provides good insight into the functional dependence of the condensation heat transfer coefficient. However, it is observed to underpredict heat transfer because it does not take into account the effects of the nonlinear temperature profile in the liquid film and the cooling of the liquid below the saturation temperature. Both of these effects can be accounted for by replacing h_{fg} with h_{fg}^* given by Eq. 10–9a. With this modification, the *average heat transfer coefficient* for laminar film condensation over a vertical flat plate of height L is determined to be

$$h_{\text{vert, laminar}} = 0.943\left[\frac{g\rho_l(\rho_l - \rho_v)h_{fg}^* k_l^3}{\mu_l(T_{\text{sat}} - T_s)L}\right]^{1/4} \quad (\text{W/m}^2\cdot\text{K}), \quad 0 < \text{Re} < 30 \qquad \textbf{(10–22)}$$

where

g = gravitational acceleration, m/s^2

ρ_l, ρ_v = densities of the liquid and vapor, respectively, kg/m^3

μ_l = viscosity of the liquid, kg/m·s

$h_{fg}^* = h_{fg} + 0.68c_{pl}(T_{\text{sat}} - T_s)$ = modified latent heat of vaporization, J/kg

k_l = thermal conductivity of the liquid, W/m·K

$$L = \text{height of the vertical plate, m}$$
$$T_s = \text{surface temperature of the plate, °C}$$
$$T_{\text{sat}} = \text{saturation temperature of the condensing fluid, °C}$$

At a given temperature, $\rho_v \ll \rho_l$ and thus $\rho_l - \rho_v \approx \rho_l$ except near the critical point of the substance. Using this approximation and substituting Eqs. 10–14 and 10–18 at $x = L$ into Eq. 10–8 by noting that $\delta_{x=L} = k/h_{x=L}$ and $h_{\text{vert}} = \frac{4}{3}h_{x=L}$ (Eqs. 10–19 and 10–21) give

$$\text{Re}_{\text{vert, laminar}} = \frac{4g\rho_l(\rho_l - \rho_v)\delta^3}{3\mu_l^2} = \frac{4g\rho_l^2}{3\mu_l^2}\left(\frac{k_l}{h_{x=L}}\right)^3 = \frac{4g}{3\nu_l^2}\left(\frac{k_l}{3h_{\text{vert}}/4}\right)^3 \quad \textbf{(10–23)}$$

Then the heat transfer coefficient h_{vert} in terms of Re becomes

$$h_{\text{vert, laminar}} \cong 1.47k_l\,\text{Re}^{-1/3}\left(\frac{g}{\nu_l^2}\right)^{1/3}, \qquad \begin{array}{l} 0 < \text{Re} < 30 \\ \rho_v \ll \rho_l \end{array} \quad \textbf{(10–24)}$$

The results obtained from the theoretical relations above are in excellent agreement with the experimental results. It can be shown easily that using property values in Eqs. 10–22 and 10–24 in the *specified units* gives the condensation heat transfer coefficient in W/m²·K, thus saving one from having to go through tedious unit manipulations each time (Fig. 10–25). This is also true for the equations below. All properties of the liquid are to be evaluated at the film temperature $T_f = (T_{\text{sat}} + T_s)/2$. The h_{fg} and ρ_v are to be evaluated at the saturation temperature T_{sat}.

Wavy Laminar Flow on Vertical Plates

At Reynolds numbers greater than about 30, it is observed that waves form at the liquid–vapor interface, although the flow in liquid film remains laminar. The flow in this case is said to be *wavy laminar*. The waves at the liquid–vapor interface tend to increase heat transfer. But the waves also complicate the analysis and make it very difficult to obtain analytical solutions. Therefore, we have to rely on experimental studies. The increase in heat transfer due to the wave effect is, on average, about 20 percent, but it can exceed 50 percent. The exact amount of enhancement depends on the Reynolds number. Based on his experimental studies, Kutateladze (1963) recommended the following relation for the average heat transfer coefficient in wavy laminar condensate flow for $\rho_v \ll \rho_l$ and $30 < \text{Re} < 1800$,

$$h_{\text{vert, wavy}} = \frac{\text{Re}\,k_l}{1.08\,\text{Re}^{1.22} - 5.2}\left(\frac{g}{\nu_l^2}\right)^{1/3}, \qquad \begin{array}{l} 30 < \text{Re} < 1800 \\ \rho_v \ll \rho_l \end{array} \quad \textbf{(10–25)}$$

A simpler alternative to the relation proposed by Kutateladze (1963) is

$$h_{\text{vert, wavy}} = 0.8\,\text{Re}^{0.11}\,h_{\text{vert (smooth)}} \quad \textbf{(10–26)}$$

which relates the heat transfer coefficient in wavy laminar flow to that in wave-free laminar flow. McAdams (1954) went even further and suggested accounting for the increase in heat transfer in the wavy region by simply increasing the heat transfer coefficient determined from Eq. 10–22 for the laminar case by 20 percent. It is also suggested that Eq. 10–22 can be used for the wavy region, with the understanding that this is a conservative approach that provides a safety margin in thermal design. In this book we use Eq. 10–25.

$$h_{\text{vert}} = \left(\dfrac{\dfrac{\text{m}}{\text{s}^2}\dfrac{\text{kg}}{\text{m}^3}\dfrac{\text{kg}}{\text{m}^3}\dfrac{\text{J}}{\text{kg}}\left(\dfrac{\text{W}}{\text{m·K}}\right)^3}{\dfrac{\text{kg}}{\text{m·s}}\cdot\text{K·m}}\right)^{1/4}$$

$$= \left[\dfrac{\text{m}}{\text{s}}\dfrac{1}{\text{m}^6}\dfrac{\text{W}^3}{\text{m}^3\cdot\text{K}^3}\dfrac{\text{J}}{\text{K}}\right]$$

$$= \left(\dfrac{\text{W}^4}{\text{m}^8\cdot\text{K}^4}\right)^{1/4}$$

$$= \text{W/m}^2\cdot\text{K}$$

FIGURE 10–25

Equation 10–22 gives the condensation heat transfer coefficient in W/m²·K when the quantities are expressed in the units specified in their descriptions.

A relation for the Reynolds number in the wavy laminar region can be determined by substituting the h relation in Eq. 10–25 into the Re relation in Eq. 10–11 and simplifying. It yields

$$\text{Re}_{\text{vert, wavy}} = \left[4.81 + \frac{3.70 \, L k_l (T_{\text{sat}} - T_s)}{\mu_l \, h_{fg}^*} \left(\frac{g}{\nu_l^2}\right)^{1/3}\right]^{0.820}, \qquad \rho_v \ll \rho_l \qquad \textbf{(10–27)}$$

Turbulent Flow on Vertical Plates

At a Reynolds number of about 1800, the condensate flow becomes turbulent. Several empirical relations of varying degrees of complexity are proposed for the heat transfer coefficient for turbulent flow. Again assuming $\rho_v \ll \rho_l$ for simplicity, Labuntsov (1957) proposed the following relation for the turbulent flow of condensate on *vertical plates:*

$$h_{\text{vert, turbulent}} = \frac{\text{Re} \, k_l}{8750 + 58 \, \text{Pr}_l^{-0.5}(\text{Re}^{0.75} - 253)} \left(\frac{g}{\nu_l^2}\right)^{1/3}, \qquad \begin{matrix} \text{Re} > 1800 \\ \rho_v \ll \rho_l \end{matrix} \qquad \textbf{(10–28)}$$

The physical properties of the condensate are again to be evaluated at the film temperature $T_f = (T_{\text{sat}} + T_s)/2$. The Re relation in this case is obtained by substituting the preceding h relation into the Re relation in Eq. 10–11, which gives

$$\text{Re}_{\text{vert, turbulent}} = \left[\frac{0.0690 \, L k_l \, \text{Pr}_l^{0.5} \, (T_{\text{sat}} - T_s)}{\mu_l \, h_{fg}^*} \left(\frac{g}{\nu_l^2}\right)^{1/3} - 151 \, \text{Pr}_l^{0.5} + 253\right]^{4/3} \qquad \textbf{(10–29)}$$

Nondimensionalized heat transfer coefficients for the wave-free laminar, wavy laminar, and turbulent flow of condensate on vertical plates are plotted in Fig. 10–26.

2 Inclined Plates

Equation 10–22 was developed for vertical plates, but it can also be used for laminar film condensation on the upper surfaces of plates that are *inclined* by an angle θ from the *vertical,* by replacing g in that equation with $g \cos \theta$
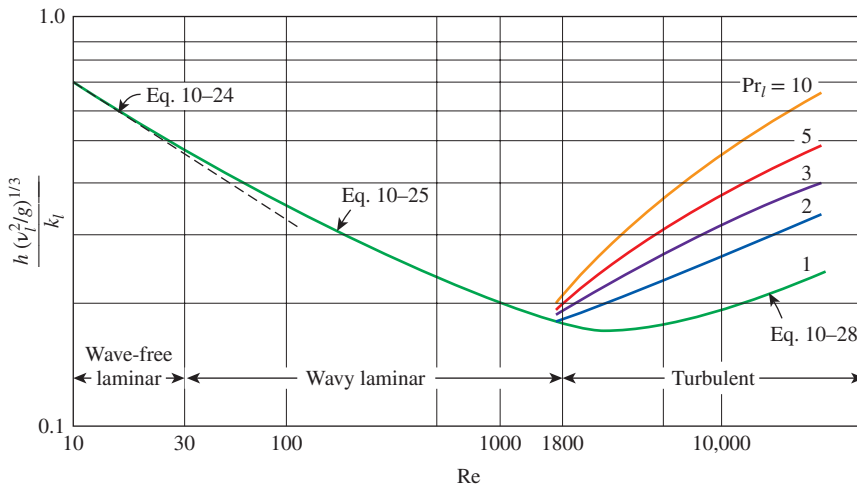
FIGURE 10–26

Nondimensionalized heat transfer coefficients for the wave-free laminar, wavy laminar, and turbulent flow of condensate on vertical plates.
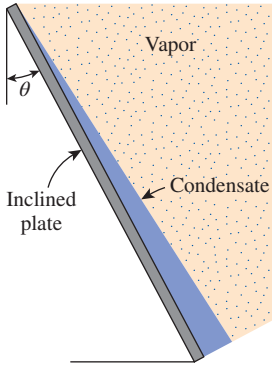
FIGURE 10–27
Film condensation on
an inclined plate.

(Fig. 10–27). This approximation gives satisfactory results, especially for $\theta \leq 60°$. Note that the condensation heat transfer coefficients on vertical and inclined plates are related to each other by

$$h_{\text{inclined}} = h_{\text{vert}}(\cos \theta)^{1/4} \qquad \text{(laminar)} \qquad \textbf{(10–30)}$$

Equation 10–30 is developed for laminar flow of condensate, but it can also be used for wavy laminar flows as an approximation.

3 Vertical Tubes

Equation 10–22 for vertical plates can also be used to calculate the average heat transfer coefficient for laminar film condensation on the outer surfaces of vertical tubes, provided that the tube diameter is large relative to the thickness of the liquid film ($D >> \delta$). In most of the problems encountered in this chapter, δ (the thickness of the liquid film at the bottom of the tube) can be calculated by combining Eqs. 10–19 and 10–21, which leads to $\delta = 4k_l/3h$.

4 Horizontal Tubes and Spheres

Nusselt's analysis of film condensation on vertical plates can also be extended to horizontal tubes and spheres. The average heat transfer coefficient for film condensation on the outer surfaces of a *horizontal tube* is determined to be

$$h_{\text{horiz}} = 0.729 \left[\frac{g\rho_l(\rho_l - \rho_v)h_{fg}^* k_l^3}{\mu_l(T_{\text{sat}} - T_s)D} \right]^{1/4} \quad \text{(W/m}^2\text{·K)} \qquad \textbf{(10–31)}$$

where D is the diameter of the horizontal tube. Equation 10–31 can easily be modified for a *sphere* by replacing the constant 0.729 by 0.815.

A comparison of the heat transfer coefficient relations for a vertical tube of height L (Eq. 10–22) and a horizontal tube of diameter D (Eq. 10–31) yields

$$\frac{h_{\text{vert}}}{h_{\text{horiz}}} = \frac{0.943/L^{1/4}}{0.729/D^{1/4}} = 1.29 \left(\frac{D}{L} \right)^{1/4} \qquad \textbf{(10–32)}$$

Setting $h_{\text{vert}} = h_{\text{horiz}}$ gives $L = 1.29^4 D = 2.77D$, which implies that for a tube whose length is 2.77 times its diameter, the average heat transfer coefficient for laminar film condensation will be the *same* whether the tube is positioned horizontally or vertically. For $L > 2.77D$, the heat transfer coefficient is higher in the horizontal position. Considering that the length of a tube in any practical application is several times its diameter, it is common practice to place the tubes in a condenser *horizontally* to maximize the condensation heat transfer coefficient on the outer surfaces of the tubes.

5 Horizontal Tube Banks

Horizontal tubes stacked on top of each other as shown in Fig. 10–28 are commonly used in condenser design. The average thickness of the liquid film at the lower tubes is much larger as a result of condensate falling on top of them from the tubes directly above. Therefore, the average heat transfer coefficient at the lower tubes in such arrangements is smaller. Assuming the condensate from the tubes above to the ones below drain smoothly, the average film condensation heat transfer coefficient for all tubes in a vertical tier can be expressed as

FIGURE 10–28
Film condensation on a vertical tier of
horizontal tubes.

$$h_{\text{horiz, } N\text{ tubes}} = 0.729 \left[\frac{g\rho_l(\rho_l - \rho_v)h_{fg}^* k_l^3}{\mu_l(T_{\text{sat}} - T_s)ND} \right]^{1/4} = \frac{1}{N^{1/4}}h_{\text{horiz, 1 tube}} \qquad \textbf{(10–33)}$$

Note that Eq. 10–33 can be obtained from the heat transfer coefficient relation for a horizontal tube (Eq. 10–31) by replacing D in that relation with ND, where N is the number of horizontal tubes in the tier. This relation does not account for the increase in heat transfer due to the ripple formation and turbulence caused during drainage, and thus generally yields conservative results.

Effect of Vapor Velocity

In the preceding analysis we assumed the vapor velocity to be small and thus the vapor drag exerted on the liquid film to be negligible, which is usually the case. However, when the vapor velocity is high, the vapor will "pull" the liquid at the interface along since the vapor velocity at the interface must drop to the value of the liquid velocity. If the vapor flows downward (i.e., in the same direction as the liquid), this additional force will increase the average velocity of the liquid and thus decrease the film thickness. This, in turn, will decrease the thermal resistance of the liquid film and thus increase heat transfer. Upward vapor flow has the opposite effects: the vapor exerts a force on the liquid in the opposite direction to flow, thickens the liquid film, and thus decreases heat transfer. Condensation in the presence of high vapor flow is studied (e.g., Shekriladze et al., 1966) and heat transfer relations are obtained, but a detailed analysis of this topic is beyond the scope of this introductory text.

The Presence of Noncondensable Gases in Condensers

Most condensers used in steam power plants operate at pressures well below the atmospheric pressure (usually under 0.1 atm) to maximize cycle thermal efficiency, and operation at such low pressures raises the possibility of air (a noncondensable gas) leaking into the condensers. Experimental studies show that the presence of noncondensable gases in the vapor has a detrimental effect on condensation heat transfer. Even small amounts of a noncondensable gas in the vapor cause significant drops in heat transfer coefficient during condensation. For example, the presence of less than 1 percent (by mass) of air in steam can reduce the condensation heat transfer coefficient by more than half. Therefore, it is common practice to periodically vent out the noncondensable gases that accumulate in the condensers to ensure proper operation.

The drastic reduction in the condensation heat transfer coefficient in the presence of a noncondensable gas can be explained as follows: When the vapor mixed with a noncondensable gas condenses, only the noncondensable gas remains in the vicinity of the surface (Fig. 10–29). This gas layer acts as a *barrier* between the vapor and the surface and makes it difficult for the vapor to reach the surface. The vapor now must diffuse through the noncondensable gas first before reaching the surface, and this reduces the effectiveness of the condensation process.

Experimental studies show that heat transfer in the presence of a noncondensable gas strongly depends on the nature of the vapor flow and the flow velocity. As you would expect, a *high flow velocity* is more likely to remove the stagnant noncondensable gas from the vicinity of the surface and thus *improve* heat transfer.
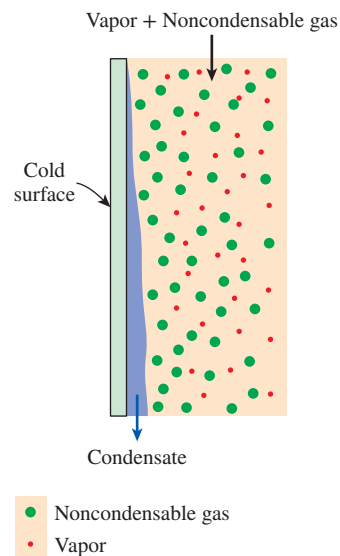
FIGURE 10–29
The presence of a noncondensable gas in a vapor prevents the vapor molecules from reaching the cold surface easily, and thus impedes condensation heat transfer.
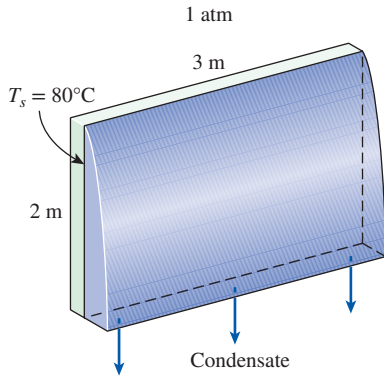
FIGURE 10–30
Schematic for Example 10–4.

EXAMPLE 10–4   **Condensation of Steam on a Vertical Plate**

Saturated steam at atmospheric pressure condenses on a 2-m-high and 3-m-wide vertical plate that is maintained at 80°C by circulating cooling water through the other side (Fig. 10–30). Determine (*a*) the rate of heat transfer by condensation to the plate and (*b*) the rate at which the condensate drips off the plate at the bottom.

SOLUTION   Saturated steam at 1 atm condenses on a vertical plate. The rates of heat transfer and condensation are to be determined.

Assumptions   **1** Steady operating conditions exist. **2** The plate is isothermal. **3** The condensate flow is wavy-laminar over the entire plate (will be verified). **4** The density of vapor is much smaller than the density of liquid, $\rho_v \ll \rho_l$.

Properties   The properties of water at the saturation temperature of 100°C are $h_{fg} = 2257 \times 10^3$ J/kg and $\rho_v = 0.60$ kg/m^3. The properties of liquid water at the film temperature of $T_f = (T_{sat} + T_s)/2 = (100 + 80)/2 = 90$°C are (Table A–9)

$$\rho_l = 965.3 \text{ kg/m}^3 \qquad\qquad c_{pl} = 4206 \text{ J/kg·K}$$
$$\mu_l = 0.315 \times 10^{-3} \text{ kg/m·s} \qquad k_l = 0.675 \text{ W/m·K}$$
$$\nu_l = \mu_l/\rho_l = 0.326 \times 10^{-6} \text{ m}^2/\text{s}$$

Analysis   (*a*) The modified latent heat of vaporization is

$$h_{fg}^* = h_{fg} + 0.68\, c_{pl}\, (T_{sat} - T_s)$$
$$= 2257 \times 10^3 \text{ J/kg} + 0.68 \times (4206 \text{ J/kg·K})(100 - 80)°\text{C}$$
$$= 2314 \times 10^3 \text{ J/kg}$$

For wavy-laminar flow, the Reynolds number is determined from Eq. 10–27 to be

$$\text{Re} = \text{Re}_{\text{vert, wavy}} = \left[4.81 + \frac{3.70\, L k_l (T_{sat} - T_s)}{\mu_l h_{fg}^*} \left(\frac{g}{\nu_l^2} \right)^{1/3} \right]^{0.820}$$

$$= \left[4.81 + \frac{3.70(2 \text{ m})(0.675 \text{ W/m·K})(100 - 80)°\text{C}}{(0.315 \times 10^{-3} \text{ kg/m·s})(2314 \times 10^3 \text{ J/kg})} \right.$$
$$\left. \times \left(\frac{9.81 \text{ m/s}^2}{(0.326 \times 10^{-6} \text{ m}^2/\text{s})^2} \right)^{1/3} \right]^{0.820}$$

$$= 1287$$

which is between 30 and 1800, and thus our assumption of wavy laminar flow is verified. Then the condensation heat transfer coefficient is determined from Eq. 10–25 to be

$$h = h_{\text{vert, wavy}} = \frac{\text{Re}\, k_l}{1.08 \text{ Re}^{1.22} - 5.2} \left(\frac{g}{\nu_l^2} \right)^{1/3}$$

$$= \frac{1287 \times (0.675 \text{ W/m·K})}{1.08\,(1287)^{1.22} - 5.2} \left(\frac{9.81 \text{ m/s}^2}{(0.326 \times 10^{-6} \text{ m}^2/\text{s})^2} \right)^{1/3} = 5850 \text{ W/m}^2\text{·K}$$

The heat transfer surface area of the plate is $A_s = W \times L = (3 \text{ m})(2 \text{ m}) = 6$ m^2. Then the rate of heat transfer during this condensation process becomes

$$\dot{Q} = h A_s (T_{sat} - T_s) = (5850 \text{ W/m}^2\text{·K})(6 \text{ m}^2)(100 - 80)°\text{C} = \mathbf{7.02 \times 10^5 \text{ W}}$$

(*b*) The rate of condensation of steam is determined from

$$\dot{m}_{\text{condensation}} = \frac{\dot{Q}}{h_{fg}^*} = \frac{7.02 \times 10^5 \text{ J/s}}{2314 \times 10^3 \text{ J/kg}} = \mathbf{0.303\ kg/s}$$

That is, steam will condense on the surface at a rate of 303 grams per second.

■ EXAMPLE 10–5 Condensation of Steam on a Tilted Plate

What would your answer be to the preceding example problem if the plate were tilted 30° from the vertical, as shown in Fig. 10–31?

SOLUTION (*a*) The heat transfer coefficient in this case can be determined from the vertical plate relation by replacing g with $g \cos\theta$. But we will use Eq. 10–30 instead since we already know the value for the vertical plate from the preceding example:

$$h = h_{\text{inclined}} = h_{\text{vert}}(\cos\theta)^{1/4} = (5850 \text{ W/m}^2\text{·K})(\cos 30°)^{1/4} = 5643 \text{ W/m}^2\text{·K}$$

The heat transfer surface area of the plate is still 6 m². Then the rate of condensation heat transfer in the tilted plate case becomes

$$\dot{Q} = hA_s(T_{\text{sat}} - T_s) = (5643 \text{ W/m}^2\text{·K})(6 \text{ m}^2)(100 - 80)°C = \mathbf{6.77 \times 10^5\ W}$$

(*b*) The rate of condensation of steam is again determined from

$$\dot{m}_{\text{condensation}} = \frac{\dot{Q}}{h_{fg}^*} = \frac{6.77 \times 10^5 \text{ J/s}}{2314 \times 10^3 \text{ J/kg}} = \mathbf{0.293\ kg/s}$$

Discussion Note that the rate of condensation decreased by about 3.3 percent when the plate was tilted.
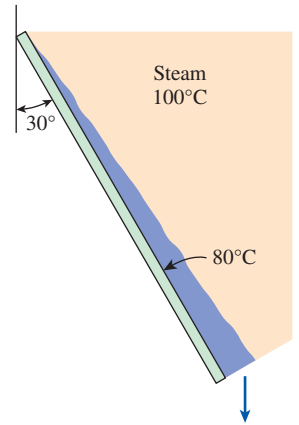
FIGURE 10–31
Schematic for Example 10–5.

■ EXAMPLE 10–6 Condensation of Steam on Horizontal Tubes

The condenser of a steam power plant operates at a pressure of 7.38 kPa. Steam at this pressure condenses on the outer surfaces of horizontal tubes through which cooling water circulates. The outer diameter of the pipes is 3 cm, and the outer surfaces of the tubes are maintained at 30°C (Fig. 10–32). Determine (*a*) the rate of heat transfer to the cooling water circulating in the tubes and (*b*) the rate of condensation of steam per unit length of a horizontal tube.

SOLUTION Saturated steam at a pressure of 7.38 kPa condenses on a horizontal tube at 30°C. The rates of heat transfer and condensation are to be determined.

Assumptions **1** Steady operating conditions exist. **2** The tube is isothermal.

Properties The properties of water at the saturation temperature of 40°C corresponding to 7.38 kPa are $h_{fg} = 2407 \times 10^3$ J/kg and $\rho_v = 0.05$ kg/m³. The properties of liquid water at the film temperature of $T_f = (T_{\text{sat}} + T_s)/2 = (40 + 30)/2 = 35°C$ are (Table A–9)

$$\rho_l = 994 \text{ kg/m}^3 \qquad c_{pl} = 4178 \text{ J/kg·K}$$
$$\mu_l = 0.720 \times 10^{-3} \text{ kg/m·s} \qquad k_l = 0.623 \text{ W/m·K}$$
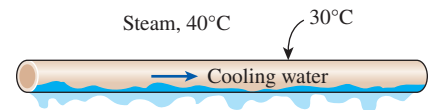
FIGURE 10–32
Schematic for Example 10–6.

Analysis (*a*) The modified latent heat of vaporization is

$$h_{fg}^* = h_{fg} + 0.68 \, c_{pl}(T_{\text{sat}} - T_s)$$
$$= 2407 \times 10^3 \text{ J/kg} + 0.68 \times (4178 \text{ J/kg·K})(40 - 30)°C$$
$$= 2435 \times 10^3 \text{ J/kg}$$

Noting that $\rho_v \ll \rho_l$ (since $0.05 \ll 994$), the heat transfer coefficient for condensation on a single horizontal tube is determined from Eq. 10–31 to be

$$h = h_{\text{horiz}} = 0.729 \left[\frac{g\rho_l(\rho_l - \rho_v)h_{fg}^* k_l^3}{\mu_l(T_{\text{sat}} - T_s)D}\right]^{1/4} \cong 0.729 \left[\frac{g\rho_l^2 h_{fg}^* k_l^3}{\mu_l(T_{\text{sat}} - T_s)D}\right]^{1/4}$$

$$= 0.729 \left[\frac{(9.81 \text{ m/s}^2)(994 \text{ kg/m}^3)^2 \, (2435 \times 10^3 \text{ J/kg})(0.623 \text{ W/m·K})^3}{(0.720 \times 10^{-3} \text{ kg/m·s})(40 - 30)°C \, (0.03 \text{ m})}\right]^{1/4}$$

$$= 9294 \text{ W/m}^2\text{·K}$$

The heat transfer surface area of the pipe per unit of its length is $A_s = \pi DL = \pi(0.03 \text{ m})(1 \text{ m}) = 0.09425 \text{ m}^2$. Then the rate of heat transfer during this condensation process becomes

$$\dot{Q} = hA_s(T_{\text{sat}} - T_s) = (9292 \text{ W/m}^2\text{·K})(0.09425 \text{ m}^2)(40 - 30)°C = \textbf{8760 W}$$

(*b*) The rate of condensation of steam is

$$\dot{m}_{\text{condensation}} = \frac{\dot{Q}}{h_{fg}^*} = \frac{8760 \text{ J/s}}{2435 \times 10^3 \text{ J/kg}} = \textbf{0.00360 kg/s}$$

Therefore, steam will condense on the horizontal tube at a rate of 3.6 g/s or 13.0 kg/h per meter of its length.

Condensate flow
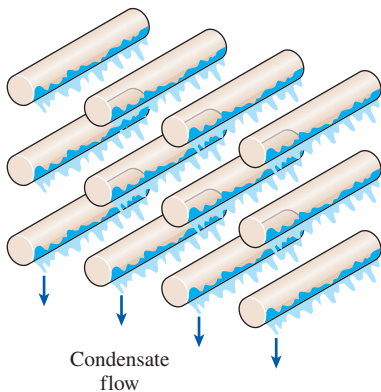
FIGURE 10–33
Schematic for Example 10–7.

EXAMPLE 10–7   **Condensation of Steam on Horizontal Tube Banks**

Repeat the preceding example problem for the case of 12 horizontal tubes arranged in a rectangular array of 3 tubes high and 4 tubes wide, as shown in Fig. 10–33.

SOLUTION (*a*) Condensation heat transfer on a tube is not influenced by the presence of other tubes in its neighborhood unless the condensate from other tubes drips on it. In our case, the horizontal tubes are arranged in four vertical tiers, each tier consisting of three tubes. The average heat transfer coefficient for a vertical tier of *N* horizontal tubes is related to the one for a single horizontal tube by Eq. 10–33 and is determined to be

$$h_{\text{horiz, N tubes}} = \frac{1}{N^{1/4}} h_{\text{horiz, 1 tube}} = \frac{1}{3^{1/4}}(9294 \text{ W/m}^2\text{·K}) = 7062 \text{ W/m}^2\text{·K}$$

Each vertical tier consists of three tubes, and thus the heat transfer coefficient determined above is valid for each of the four tiers. In other words, this value can be taken to be the average heat transfer coefficient for all 12 tubes.

The surface area for all 12 tubes per unit length of the tubes is

$$A_s = N_{total}\,\pi DL = 12\pi(0.03\text{ m})(1\text{ m}) = 1.1310\text{ m}^2$$

Then the rate of heat transfer during this condensation process becomes

$$\dot{Q} = hA_s(T_{sat} - T_s) = (7062\text{ W/m}^2\cdot\text{K})(1.131\text{ m}^2)(40 - 30)°\text{C} = \textbf{79,870 W}$$

(*b*) The rate of condensation of steam is again determined from

$$\dot{m}_{condensation} = \frac{\dot{Q}}{h_{fg}^*} = \frac{79,870\text{ J/s}}{2435 \times 10^3\text{ J/kg}} = \textbf{0.0328 kg/s}$$

Therefore, steam will condense on the horizontal pipes at a rate of 32.8 g/s per meter length of the tubes.

10–6 ▪ FILM CONDENSATION INSIDE HORIZONTAL TUBES

So far we have discussed film condensation on the *outer surfaces* of tubes and other geometries, which is characterized by negligible vapor velocity and the unrestricted flow of the condensate. Most condensation processes encountered in refrigeration and air-conditioning applications, however, involve condensation on the *inner surfaces* of horizontal or vertical tubes. Heat transfer analysis of condensation inside tubes is complicated by the fact that it is strongly influenced by the vapor velocity and the rate of liquid accumulation on the walls of the tubes (Fig. 10–34).

At high vapor velocities (Fig. 10–34*a*), the flow is characterized by two-phase annular conditions. The core of the annulus is occupied by the vapor, and its diameter decreases as the condensate thickness increases in the direction of the flow. At low vapor velocities (Fig. 10–34*b*), the condensate flow is from the upper portion of the tube to the bottom of the tube.

For *low vapor velocities,* Chato (1962) recommends this expression for condensation

$$h_{internal} = 0.555\left[\frac{g\rho_l(\rho_l - \rho_v)k_l^3}{\mu_l(T_{sat} - T_s)D}\left(h_{fg} + \frac{3}{8}c_{pl}(T_{sat} - T_s)\right)\right]^{1/4} \quad \textbf{(10–34)}$$

for

$$Re_{vapor} = \left(\frac{\rho_v V_v D}{\mu_v}\right)_{inlet} < 35,000 \quad \textbf{(10–35)}$$

where the Reynolds number of the vapor is to be evaluated at the tube *inlet* conditions using the internal tube diameter as the characteristic length. Heat transfer coefficient correlations for higher vapor velocities are given by Rohsenow (1973).

(*a*) High vapor velocities

(*b*) Low vapor velocities
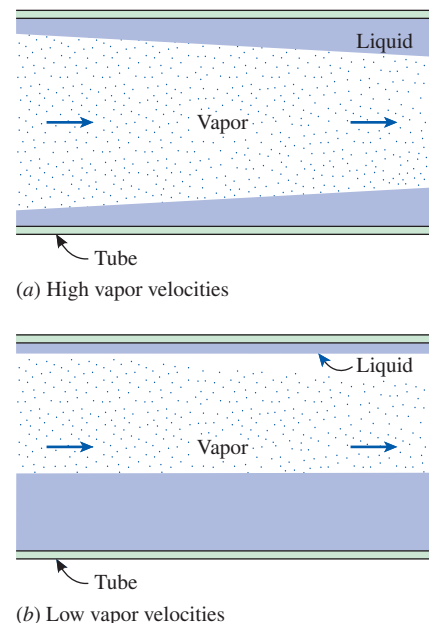
FIGURE 10–34
Condensate flow in a horizontal tube with high and low vapor velocities.

Liquid ammonia

Vapor ammonia
1003 kPa

Tube surface, 15°C
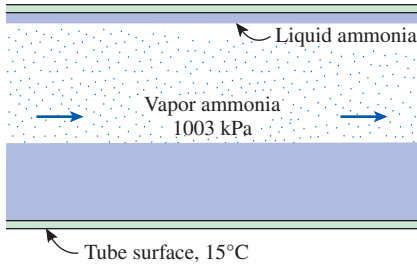
FIGURE 10–35
Schematic for Example 10–8.

PtD *EXAMPLE 10–8* **Prevention of Ammonia Gas Release by Condensing It to Liquid**

Exposure to high concentration of gaseous ammonia can cause respiratory tract and lung damage, and in some cases even death. One way of preventing the release of high concentration ammonia gas is storing it as liquid in pressurized vessels. Consider a process of condensing saturated ammonia vapor inside a horizontal tube. Saturated ammonia vapor enters a 25-mm-diameter tube with a length of 1.5 m, and it is condensed inside the tube at 1003 kPa. The surface temperature of the tube is maintained constant at 15°C (Fig. 10–35). To ensure that the ammonia is fully condensed to liquid at the exit of the 1.5-m-long tube, determine the flow rate of the ammonia entering the tube.

SOLUTION   In this example, the concepts of Prevention through Design (PtD) are applied in conjunction with the concept of condensation inside a horizontal tube to condense vapor ammonia.

Assumptions **1** Steady operating conditions exist. **2** Tube is isothermal. **3** The vapor velocity is low so that $Re_{vapor} < 35,000$ (will be verified).

Properties   The saturation temperature of ammonia at 1003 kPa is $T_{sat} = 25°C$ (Table A–11). The properties of saturated ammonia at $T_{sat} = 25°C$ are $h_{fg} = 1166 \times 10^3$ J/kg, $\rho_v = 7.809$ kg/m³, $\mu_v = 1.037 \times 10^{-5}$ kg/m·s. The properties of saturated ammonia at the film temperature of $T_f = (T_{sat} + T_s) = (25 + 15)/2 = 20°C$ are

$$\rho_l = 610.2 \text{ kg/m}^3$$
$$\mu_l = 1.519 \times 10^{-4} \text{ kg/m·s}$$
$$c_{pl} = 4745 \text{ J/kg·K}$$
$$k_l = 0.4927 \text{ W/m·K}$$

Analysis   The heat transfer coefficient for condensation inside a horizontal tube is

$$h = h_{internal} = 0.555 \left[\frac{g\rho_l(\rho_l - \rho_v)k_l^3}{\mu_l(T_{sat} - T_s)D} \left(h_{fg} + \frac{3}{8}c_{pl}(T_{sat} - T_s) \right) \right]^{1/4}$$

$$h = 0.555 \left[\frac{(9.81 \text{ m/s}^2)(610.2 \text{ kg/m}^3)(610.2 - 7.809) \text{ kg/m}^3(0.4927 \text{ W/m·K})^3}{(1.519 \times 10^{-4} \text{ kg/m·s})(25 - 15) \text{ K}(0.025 \text{ m})} \right.$$
$$\left. \times \left(1166 \times 10^3 \text{ J/kg} + \frac{3}{8}(4745 \text{ J/kg·K})(25 - 15)\text{K} \right) \right]^{1/4}$$
$$= 5976.3 \text{ W/m}^2\text{·K}$$

The heat transfer surface area of the tube is

$$A_s = \pi DL = \pi(0.025 \text{ m})(1.5 \text{ m}) = 0.11781 \text{ m}^2$$

Then the rate of heat transfer during this condensation process becomes

$$\dot{Q} = hA_s(T_{sat} - T_s) = (5976.3 \text{ W/m}^2\text{·K})(0.11781 \text{ m}^2)(25 - 15)\text{ K} = 7040.7 \text{ W}$$

The modified latent heat of vaporization in this case is

$$h_{fg}^* = h_{fg} + \frac{3}{8}c_{pl}(T_{sat} - T_s)$$
$$= 1166 \times 10^3 \text{ J/kg} + \frac{3}{8}(4745 \text{ J/kg·K})(25 - 15)\text{K} = 1183.8 \times 10^3 \text{ J/kg}$$

Then, the rate of condensation becomes

$$\dot{m}_{\text{condensation}} = \frac{\dot{Q}}{h_{fg}^*} = \frac{7040.7 \text{ J/s}}{1183.8 \times 10^3 \text{ J/kg}} = 0.005948 \text{ kg/s}$$

Thus, $\dot{m} \leq \textbf{0.00595 kg/s}$

Discussion To ensure that the saturated ammonia vapor is fully condensed to liquid inside the 1.5-m-long tube, the flow rate of the ammonia entering the tube must be lower than the rate of condensation inside the tube.

Note that the low vapor velocity assumption is appropriate for $\dot{m} \leq 0.005948$ kg/s, since

$$\text{Re}_{\text{vapor}} = \left(\frac{\rho_v V_v D}{\mu_v}\right)_{\text{inlet}} = \frac{4\dot{m}}{\pi D \mu_v} = \frac{4(0.005948 \text{ kg/s})}{\pi(0.025 \text{ m})(1.037 \times 10^{-5} \text{ kg/m·s})}$$
$$= 29{,}212 < 35{,}000$$

10–7 ▪ DROPWISE CONDENSATION

Dropwise condensation, characterized by countless droplets of varying diameters on the condensing surface instead of a continuous liquid film, is one of the most effective mechanisms of heat transfer, and extremely large heat transfer coefficients can be achieved with this mechanism (Fig. 10–36).

In dropwise condensation, the small droplets that form at the nucleation sites on the surface grow as a result of continued condensation, coalesce into large droplets, and slide down when they reach a certain size, clearing the surface and exposing it to vapor. There is no liquid film in this case to resist heat transfer. As a result, with dropwise condensation, heat transfer coefficients can be achieved that are more than 10 times larger than those associated with film condensation. Large heat transfer coefficients enable designers to achieve a specified heat transfer rate with a smaller surface area, and thus a smaller (and less expensive) condenser. Therefore, dropwise condensation is the preferred mode of condensation in heat transfer applications.

The challenge in dropwise condensation is not to achieve it, but rather, to *sustain* it for prolonged periods of time. Dropwise condensation is achieved by *adding* a promoting chemical into the vapor, *treating* the surface with a promoter chemical, or *coating* the surface with a polymer such as teflon or a noble metal such as gold, silver, rhodium, palladium, or platinum. The *promoters* used include various waxes and fatty acids such as oleic, stearic, and linoic acids. They lose their effectiveness after a while, however, because of fouling, oxidation, and the removal of the promoter from the surface. It is possible to sustain dropwise condensation for over a year by the combined effects of surface coating and periodic injection of the promoter into the vapor. However, any gain in heat transfer must be weighed against the cost associated with sustaining dropwise condensation.

Dropwise condensation has been studied experimentally for a number of surface–fluid combinations. Of these, the studies on the condensation of steam on copper surfaces has attracted the most attention because of their

FIGURE 10–36
Dropwise condensation of water on a vertical surface.
©Chris Young/Alamy

widespread use in steam power plants. P. Griffith (1983) recommends these simple correlations for dropwise condensation of *steam* on *copper surfaces:*

$$h_{\text{dropwise}} = \begin{cases} 51{,}104 + 2044 T_{\text{sat}}, & 22°C < T_{\text{sat}} < 100°C & \textbf{(10–36)} \\ 255{,}510, & T_{\text{sat}} > 100°C & \textbf{(10–37)} \end{cases}$$

where T_{sat} is in °C and the heat transfer coefficient h_{dropwise} is in W/m²·K.

The very high heat transfer coefficients achievable with dropwise condensation are of little significance if the material of the condensing surface is not a good conductor like copper or if the thermal resistance on the other side of the surface is too large. In steady operation, heat transfer from one medium to another depends on the sum of the thermal resistances on the path of heat flow, and a large thermal resistance may overshadow all others and dominate the heat transfer process. In such cases, improving the accuracy of a small resistance (such as one due to condensation or boiling) makes hardly any difference in overall heat transfer calculations.

EXAMPLE 10–9   Determination of Dropwise Condensation Rate

A can of beverage with a height of 123 mm and a diameter of 66 mm has a uniform temperature of 5°C when it is removed from the refrigerator. The can is placed on a table in a room and moist air condenses on the outer surface of the can (Fig. 10–37). Determine the dropwise condensation rate of the moisture in the air, if the saturation temperature is 25°C.

SOLUTION Beverage can at 5°C is placed in a room and condenses moist air at 25°C. The rate of dropwise condensation is to be determined.

Assumptions **1** Steady operating conditions exist. **2** The surface temperature of can is constant. **3** Condensation on top and bottom surface of the can is negligible.

Properties A required property of water at the saturation temperature $T_{\text{sat}} = 25°C$ is $h_{fg} = 2442 \times 10^3$ J/kg (Table A–9). A required property of liquid water at the film temperature $T_f = (T_{\text{sat}} + T_s)/2 = (25 + 5)/2 = 15°C$ is $c_{pl} = 4185$ J/kg·K (Table A–9).

Analysis The modified latent heat of vaporization is

$$h_{fg}^* = h_{fg} + 0.68\, c_{pl}\, (T_{\text{sat}} - T_s)$$
$$= 2442 \times 10^3 \text{ J/kg} + 0.68\,(4185 \text{ J/kg·K})(25 - 5)\,\text{K} = 2.4989 \times 10^6 \text{ J/kg}$$

The dropwise heat transfer coefficient, for $22°C < T_{\text{sat}} < 100°C$, is determined to be

$$h = h_{\text{dropwise}} = 51{,}104 + 2044\, T_{\text{sat}}$$
$$= 51{,}104 + 2044(25°C) = 102{,}204 \text{ W/m²·K}$$

The rate of heat transfer to the beverage can during this condensation process is

$$\dot{Q} = h\, A_s(T_{\text{sat}} - T_s) = h(\pi DL)(T_{\text{sat}} - T_s)$$
$$= (102{,}204 \text{ W/m²·K})\, \pi(0.066 \text{ m})(0.123 \text{ m})(25 - 5)\,\text{K} = 5.2131 \times 10^4 \text{ W}$$

Thus, the rate of condensation is

$$\dot{m} = \frac{\dot{Q}}{h_{fg}^*} = \frac{5.2131 \times 10^4 \text{ J/s}}{2.4989 \times 10^6 \text{ J/kg}} = \textbf{0.02086 kg/s}$$

Discussion The heat transfer rate during the dropwise condensation can be increased by increasing the surface area of the can, and thereby increasing the rate of condensation as well. Note that, if we had assumed film condensation in this case, the condensation rate estimate would be nearly 20 times less than the dropwise condensation.

FIGURE 10–37
Schematic for Example 10–9.
©belchonock/123RF

TOPIC OF SPECIAL INTEREST*

Non-Boiling Two-Phase Flow Heat Transfer

The different flow patterns (regimes) encountered in flow boiling (see Fig. 10–19) can also be observed in non-boiling two-phase flow in both vertical and horizontal tubes (Figs. 10–38 to 10–40). Non-boiling two-phase flow has many industrial applications, such as the flow of oil and natural gas in flow lines and wellbores, in which the knowledge of non-boiling two-phase, two-component (liquid and permanent gas) heat transfer is required. During the production of two-phase hydrocarbon fluids from an oil reservoir to the surface, the temperature of the hydrocarbon fluids changes due to the difference in temperatures of the oil reservoir and the surface. The change in temperature results in heat transfer between the hydrocarbon fluids and the earth surrounding the oil well, and the ability to estimate the flowing temperature profile is necessary to address several design problems in petroleum production engineering.

In subsea oil and natural gas production, hydrocarbon fluids may leave the reservoir with a temperature of 75°C and flow in subsea surroundings of 4°C. As a result of the temperature gradient between the reservoir and the surroundings, the knowledge of heat transfer is critical to prevent gas hydrate and wax deposition blockages. Wax deposition can result in problems that include a reduction of inner tube diameter causing blockage, an increase in surface roughness of the tube leading to restricted flow line pressure, and a decrease in production, along with various mechanical problems.

In situations where low-velocity flow is necessary while high heat transfer rates are desirable, heat transfer enhancement schemes such as coil-spring wire insert, twisted tape insert, and helical ribs are used to promote turbulence, thus enhancing heat transfer. Although these heat transfer enhancement schemes have been proven to be effective, they do come with drawbacks, such as fouling, an increase in pressure drop, and sometimes even blockage. An alternative approach to enhance heat transfer in tube flow is by injecting gas into liquid to promote turbulence.

In the assessment of non-boiling heat transfer, void fraction (the ratio of the volume of space occupied by the gas phase to the total volume of the system) and flow patterns (qualitatively defined based on the distribution of one phase with respect to another phase across the pipe cross section) are two critical parameters that need to be taken into consideration. In any gas–liquid system, void fraction has great effects on heat transfer, since the liquid phase generally has significantly larger thermal conductivity than the gas phase. The knowledge of flow patterns in gas–liquid systems is also critical in the assessment of non-boiling heat transfer. For example, heat transfer in slug flow (bubbles coalesce into gas slugs) is likely to be different than heat transfer in annular flow (core of the flow consists of gas phase with entrained liquid droplets from the surrounding liquid phase). Void fraction, flow pattern, and hence the heat transfer are also affected by the tube inclination. Bhagwat and Ghajar (2012) reported that

*This section can be skipped without a loss of continuity.
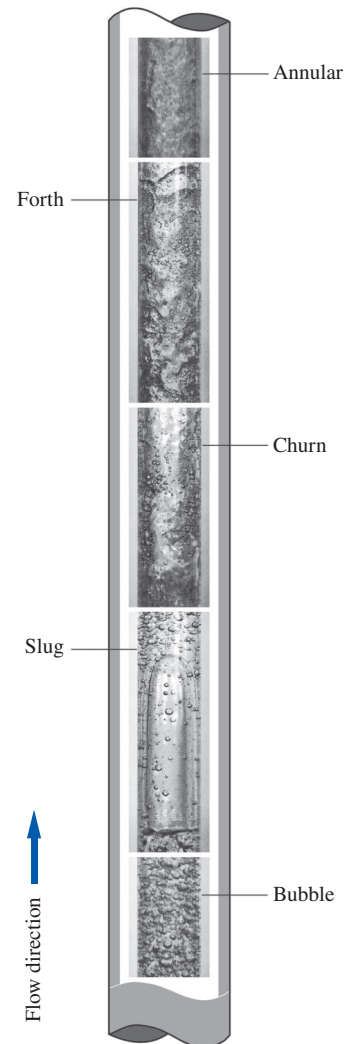
FIGURE 10–38
Flow patterns in upward vertical two-phase flow.
©*Ghajar and Tang, 2009*

Falling film

Bubble

Slug

Froth

Annular

Flow direction
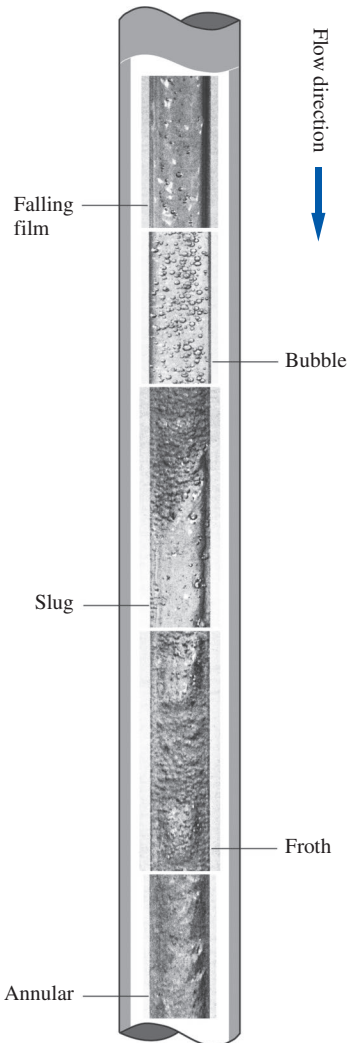
FIGURE 10–39
Flow patterns in downward vertical two-phase flow.
©*Ghajar and Tang, 2012*

in inclined and vertical upward and downward tubes, the hydrodynamics of two-phase flow is influenced by the balance between buoyancy and gravitational force. The influence of buoyancy and gravitational force affects the slippage between the gas and liquid phases, which in turn affects the void fraction. Tube inclination also affects the flow patterns, which is the reason for the difference in flow patterns between vertical and horizontal flows (see Figs. 10–38 through 10–40). The influence of tube inclination in the upward and downward directions on the hydrodynamics of two-phase flow also leads to its effect on heat transfer as reported by Bhagwat and Ghajar (2016 and 2017). Due to the complexity and the lack of fundamental understanding of void fraction, flow patterns, and non-boiling heat transfer in two-phase flow, the majority of the documented works, whether they are flow pattern maps or correlations for void fraction and heat transfer, are only applicable to selected flow conditions. Ghajar and co-workers have extensively studied flow patterns, void fraction, pressure drop, and non-boiling heat transfer in gas–liquid two-phase flow in various pipe inclinations, and the results of their studies are summarized in the second edition of *Handbook of Multiphase Flow;* see Ghajar and Bhagwat (2017). Based on a database of 986 points, Ghajar and Tang (2009) recommended the following general correlation for the non-boiling two-phase heat transfer coefficient h_{tp}, for a variety of gas–liquid flow patterns, fluid combinations, and tube inclinations. The correlation captures 90 percent of the measured data within an error band of $\pm 25\%$ and 94 percent of the measured data within an error band of $\pm 30\%$,

$$h_{tp} = F_p h_l \left[1 + 0.55 \left(\frac{x}{1-x} \right)^{0.1} \left(\frac{1 - F_p}{F_p} \right)^{0.4} \left(\frac{Pr_g}{Pr_l} \right)^{0.25} \left(\frac{\mu_l}{\mu_g} \right)^{0.25} (I^*)^{0.25} \right], \text{W/m}^2 \cdot \text{K}$$

(10–38)

where subscripts l and g refer to the liquid phase and gas phase, and

$$h_l = \text{liquid phase heat transfer coefficient}$$
$$= 0.027 Re_l^{4/5} Pr_l^{1/3} (k_l/D)(\mu_l/\mu_s)^{0.14}, \text{W/m}^2 \cdot \text{K}$$
$$Re_l = \text{in situ liquid Reynolds number} = 4\dot{m}_l/(\pi\sqrt{1-\alpha}\,\mu_l D)$$
$$x = \text{flow quality} = \dot{m}_g/(\dot{m}_g + \dot{m}_l)$$
$$I^* = \text{inclination factor} = 1 + \frac{(\rho_l - \rho_g)gD^2}{\sigma}|\sin\theta|$$
$$F_p = \text{flow pattern factor} = (1-\alpha) + \alpha \left[\frac{2}{\pi} \tan^{-1}\left(\sqrt{\frac{\rho_g(V_g - V_l)^2}{gD(\rho_l - \rho_g)}} \right) \right]^2$$

Here ρ is the density in kg/m³, V is the velocity in m/s, g is the gravitational acceleration in m/s², D is the tube diameter in m, $\dot{m}$ is the mass flow rate in kg/s, μ is the dynamic viscosity in kg/m·s, Pr is the Prandtl number, k is the thermal conductivity in W/m·K, σ is the surface tension in N/m, and θ is the inclination angle in radians.

Stratified   Slug   Slug/way   Wavy/annular

Plug   Wavy   Slug/bubbly   Annular

Flow direction →
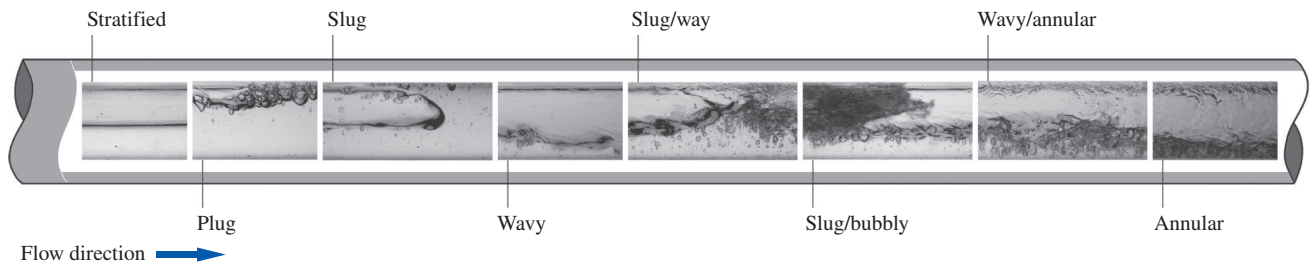
FIGURE 10–40
Flow patterns in horizontal two-phase flow.
©Ghajar and Tang, 2009

The void fraction α in Eq. 10–38 is to be determined from (Woldesemayat and Ghajar, 2007)

$$\alpha = \frac{V_{sg}}{C_o(V_{sg} + V_{sl}) + u_{gm}} \qquad (10\text{–}39)$$

where C_o = two-phase distribution coefficient

$$= \frac{V_{sg}}{V_{sg} + V_{sl}}\left[1 + (V_{sl}/V_{sg})^{(\rho_g/\rho_l)^{0.1}}\right]$$

and u_{gm} = gas drift velocity

$$= 2.9(1.22 + 1.22 \sin\theta)^{P_{atm}/P_{sys}}\left[\frac{gD\sigma(1 + \cos\theta)(\rho_l - \rho_g)}{\rho_l^2}\right]^{0.25}, \text{ m/s}$$

Here P_{sys} and P_{atm} are the system and atmosphere pressures in N/m^2, and V_{sl} and V_{sg} are the superficial liquid and gas velocities in m/s, respectively. In the preceding equations, all physical properties are evaluated at the *bulk mean temperature* $T_b = (T_i + T_e)/2$ except μ_s, which is evaluated at the surface temperature.

The non-boiling two-phase flow heat transfer correlation (Eq. 10–38) is based on 986 experimental data points (176 for horizontal flow, 555 for inclined flow, and 255 for upward vertical flow) and is applicable over the following range of parameters:

$$750 \le \mathrm{Re}_{sl} \le 127{,}000, \ 14 \le \mathrm{Re}_{sg} \le 209{,}000,$$

$$9.99 \times 10^{-3} \le \mathrm{Pr}_g/\mathrm{Pr}_l \le 148 \times 10^{-3},$$

and

$$3.64 \times 10^{-3} \le \mu_g/\mu_l \le 26.3 \times 10^{-3}$$

where Re_{sl} and Re_{sg} are the superficial liquid and gas Reynolds numbers.

The application of the general two-phase flow non-boiling heat transfer correlation given above is illustrated next with a practical example problem dealing with a mixture of air and liquid silicone.

EXAMPLE 10–10 **Air and Silicone (Dow Corning 200® Fluid, 5 cs) Flow in a Vertical Tube**

Liquid silicone such as the Dow Corning 200® Fluid, 5 cs, is used primarily as an ingredient in cosmetic and personal care products due to its high spreadability, low surface tension ($\sigma = 19.7 \times 10^{-3}$ N/m), nongreasy, soft feel, and subtle skin lubricity characteristics. A two-phase flow of air and silicone (Dow Corning 200® Fluid, 5 cs) is being transported in an 11.7-mm-internal-diameter vertical tube. The liquid phase consists of liquid silicone with dynamic viscosity of 45.7×10^{-4} kg/m·s, density of 913 kg/m³, thermal conductivity of 0.117 W/m·K, and Prandtl number of 64. The gas phase consists of air with dynamic viscosity of 18.4×10^{-6} kg/m·s, density of 1.19 kg/m³, and Prandtl number of 0.71. If the two-phase flow has flow quality of $x = 2.08 \times 10^{-5}$, void fraction of $\alpha = 0.011$, and liquid mass flow rate of $\dot{m}_l = 0.907$ kg/s, estimate the two-phase heat transfer coefficient h_{tp}. Assume the dynamic viscosity of liquid silicone evaluated at the tube surface temperature to be 39.8×10^{-4} kg/m·s.

SOLUTION A two-phase flow of air and silicone (Dow Corning 200® Fluid, 5 cs) is being transported in an 11.7-mm-diameter vertical tube. Using the non-boiling two-phase heat transfer correlation, the two-phase heat transfer coefficient h_{tp} is to be determined.

Assumptions **1** Steady operating conditions exist. **2** Two-phase flow is non-boiling, and it does not involve phase change. **3** Fluid properties are constant.

Properties The properties of liquid silicone (liquid) are given to be $\mu_l = 45.7 \times 10^{-4}$ kg/m·s, $\mu_s = 39.8 \times 10^{-4}$ kg/m·s, $\rho_l = 913$ kg/m³, $k_l = 0.117$ W/m·K, $\sigma = 19.7 \times 10^{-3}$ N/m, and $Pr_l = 64$. The properties of air (gas) are given to be $\mu_g = 18.4 \times 10^{-6}$ kg/m·s, $\rho_g = 1.19$ kg/m³, and $Pr_g = 0.71$.

Analysis With known liquid mass flow rate $\dot{m}_l$ and quality x, the gas mass flow rate $\dot{m}_g$ is determined using

$$\dot{m}_g = \frac{x}{1-x}\dot{m}_l = \frac{2.08 \times 10^{-5}}{1 - 2.08 \times 10^{-5}}(0.907 \text{ kg/s}) = 1.89 \times 10^{-5} \text{ kg/s}$$

From the gas and liquid mass flow rates, the superficial gas and liquid velocities can be calculated:

$$V_{sg} = \frac{\dot{m}_g}{\rho_g A} = \frac{4\dot{m}_g}{\rho_g \pi D^2} = \frac{4(1.89 \times 10^{-5} \text{ kg/s})}{(1.19 \text{ kg/m}^3)\pi(0.0117 \text{ m})^2} = 0.148 \text{ m/s}$$

$$V_{sl} = \frac{\dot{m}_l}{\rho_l A} = \frac{4\dot{m}_l}{\rho_l \pi D^2} = \frac{4(0.907 \text{ kg/s})}{(913 \text{ kg/m}^3)\pi(0.0117 \text{ m})^2} = 9.24 \text{ m/s}$$

Using the superficial velocities and void fraction, the gas and liquid velocities are found to be

$$V_g = \frac{V_{sg}}{\alpha} = \frac{0.148 \text{ m/s}}{0.011} = 13.5 \text{ m/s}$$

$$V_l = \frac{V_{sl}}{1 - \alpha} = \frac{9.24 \text{ m/s}}{1 - 0.011} = 9.34 \text{ m/s}$$

The flow pattern factor (F_p) can be calculated using

$$F_p = (1 - \alpha) + \alpha \left[\frac{2}{\pi}\tan^{-1}\left(\sqrt{\frac{\rho_g(V_g - V_l)^2}{gD(\rho_l - \rho_g)}}\right)\right]^2$$

$$= (1 - 0.011) + (0.011)\left[\frac{2}{\pi}\tan^{-1}\left(\sqrt{\frac{(1.19 \text{ kg/m}^3)(13.5 \text{ m/s} - 9.34 \text{ m/s})^2}{(9.81 \text{ m/s}^2)(0.0117 \text{ m})(913 \text{ kg/m}^3 - 1.19 \text{ kg/m}^3)}}\right)\right]^2$$

$$= 0.9898$$

The inclination factor (I^*) for a vertical tube ($\theta = 90°$) is calculated to be

$$I^* = 1 + \frac{(\rho_l - \rho_g)gD^2}{\sigma}|\sin \theta|$$

$$= 1 + \frac{(913 \text{ kg/m}^3 - 1.19 \text{ kg/m}^3)(9.81 \text{ m/s}^2)(0.0117 \text{ m})^2}{19.7 \times 10^{-3} \text{ N/m}}|\sin 90°|$$

$$= 63.16$$

The liquid phase heat transfer coefficient is calculated using:

$$h_l = 0.027\text{Re}_l^{4/5}\text{Pr}_l^{1/3}\left(\frac{k_l}{D}\right)\left(\frac{\mu_l}{\mu_s}\right)^{0.14}$$

$$= 0.027(21,718)^{4/5}(64)^{1/3}\left(\frac{0.117 \text{ W/m·K}}{0.0117 \text{ m}}\right)\left(\frac{45.7 \times 10^{-4} \text{ kg/m·s}}{39.8 \times 10^{-4} \text{ kg/m·s}}\right)^{0.14}$$

$$= 3246 \text{ W/m}^2\text{·K}$$

where the in *situ* liquid Reynolds number is

$$\text{Re}_l = \frac{4\dot{m}_l}{\pi\sqrt{1-\alpha}\,\mu_l D} = \frac{4(0.907 \text{ kg/s})}{\pi\sqrt{1-0.011}(45.7 \times 10^{-4} \text{ kg/m·s})(0.0117 \text{ m})}$$

$$= 21,718$$

Using the general two-phase flow heat transfer correlation, Eq. 10–38, the two-phase heat transfer coefficient is estimated to be

$$\frac{h_{tp}}{h_l} = F_p\left[1 + 0.55\left(\frac{x}{1-x}\right)^{0.1}\left(\frac{1-F_p}{F_p}\right)^{0.4}\left(\frac{\text{Pr}_g}{\text{Pr}_l}\right)^{0.25}\left(\frac{\mu_l}{\mu_g}\right)^{0.25}(I^*)^{0.25}\right]$$

$$= (0.9898)\left[1 + 0.55\left(\frac{2.08 \times 10^{-5}}{1-2.08 \times 10^{-5}}\right)^{0.1}\left(\frac{1-0.9898}{0.9898}\right)^{0.4}\left(\frac{0.71}{64}\right)^{0.25}\right.$$

$$\left.\times\left(\frac{45.7 \times 10^{-4} \text{ kg/m·s}}{18.4 \times 10^{-6} \text{ kg/m·s}}\right)^{0.25}(63.16)^{0.25}\right]$$

$$= 1.098$$

or

$$h_{tp} = 1.098\,h_l = 1.098(3246 \text{ W/m}^2\text{·K}) = \textbf{3560 W/m}^2\textbf{·K}$$

Discussion When compared with the two-phase heat transfer coefficient of 3480 W/m²·K measured by Rezkallah (1987) in similar flow conditions, the general two-phase flow heat transfer correlation, Eq. 10–38, over-predicted the measured value by 2.3 percent.

Application of Reynolds Analogy to Non-Boiling Two-Phase Flow

We have seen in Chap. 6 that using the concept of the Reynolds analogy, the single-phase heat transfer coefficient can be predicted from a knowledge of the single-phase friction coefficient. Tang and Ghajar (2011) extended the application of the Reynolds analogy concept and developed a correlation to predict the non-boiling two-phase heat transfer coefficient from the knowledge of two-phase frictional pressure drop in horizontal and upward inclined flows. The correlation predicts more than 87 percent of the 637 data points within $\pm 30\%$ error bands. The correlation is expressed in following form,

$$\frac{h_{tp}}{h_l} = F_p^m \left(\frac{\dot{m}_l}{\dot{m}}\right) \left(\frac{\rho_{tp}}{\rho_l}\right)^n \phi_l^p \qquad \text{(10–40)}$$

where the exponents m, n, and p have the values of 0.5, -0.5, and 0.2 respectively, and

h_l = liquid phase heat transfer coefficient

   = $0.027 \, \text{Re}_l^{4/5} \, \text{Pr}_l^{1/3} (k_l/D)(\mu_l/\mu_s)^{0.14}$, W/m²·K

F_p = flow pattern factor same as that used in Eq. 10–38

ρ_{tp} = two-phase mixture density = $(1 - \alpha)\rho_l + \alpha\rho_g$, kg/m³. The void fraction (α) can be determined using Woldesemayat and Ghajar (2007) correlation, Eq.10–39.

ϕ_l = two-phase frictional multiplier = $\sqrt{\dfrac{(dP/dL)_{f,tp}}{(dP/dL)_{f,l}}}$ (dimensionless quantity)

$(dP/dL)_{f,l}$ and $(dP/dL)_{f,tp}$ are the single-phase liquid and two-phase frictional pressure drop, respectively. The friction factor required for the single-phase liquid pressure drop calculation can be obtained using the Moody chart (Fig. A–20) or the Colebrook equation (Eq. 8–76). If the two-phase frictional pressure drop is not known, then correlations recommended by Ghajar and Bhagwat (2014) may be used. The two-phase heat transfer correlation based on the Reynolds analogy (Eq. 10–40) was developed using experimental data for horizontal, upward inclined, and vertical upward pipe orientations using air–water and air–glycerin fluid combinations and is applicable over the following range of parameters:

For air-water: $700 \leq \text{Re}_{sl} \leq 107{,}000$, $\quad 14 \leq \text{Re}_{sg} \leq 150{,}000$

For air-glycerin: $50 \leq \text{Re}_{sl} \leq 83{,}000$, $\quad 40 \leq \text{Re}_{sg} \leq 59{,}000$

where Re_{sl} and Re_{sg} are the superficial liquid and gas Reynolds numbers, respectively.

For vertical downward flow, Bhagwat et al. (2012) pointed out that the two-phase heat transfer coefficient is less than that measured in vertical upward flow at similar mass flow rates, while the two-phase pressure drop is considerably higher in the former orientation than in the latter. Thus Eq. 10–40 with fixed exponents doesn't give satisfactory performance in the

prediction of the two-phase heat transfer coefficient for vertical downward flow. Bhagwat et al. (2012) proposed the following form of the Reynolds analogy–based correlation that can be used for vertical downward flow:

$$\frac{h_{tp}}{h_l} = \phi_l^{0.55}$$

(10–41)

The single-phase heat transfer coefficient (h_l) and the two-phase frictional multiplier (ϕ_l) are calculated in the same way as in Eq. 10–40.

Equation 10–41 is based on the 165 data points measured in a vertically downward oriented, 0.0127-m stainless steel pipe using an air–water fluid combination. This correlation predicts more than 90 percent of the measured data points within $\pm 20\%$ error bands and is applicable for $1400 \leq$ Re$_{sl} \leq 29,000$ and $90 \leq$ Re$_{sg} \leq 18,000$.

It should be noted that both Eqs. (10–38) and (10–40) require accurate information for the void fraction. Ghajar and Bhagwat (2013, 2014) have evaluated several void fraction correlations available in the literature against air–water data (5162 data points for horizontal, upward, and downward inclinations) and refrigerant-vapor (645 data points for horizontal flow). They found the performance of the Woldesemayat and Ghajar (2007) correlation or a more recent correlation by Bhagwat and Ghajar (2014) for a wider range of gas–liquid two-phase flow are acceptable for general application with requisite accuracy. For more specific flow conditions, other top-performing void fraction correlations shortlisted by Ghajar and Bhagwat (2013, 2014) may be used.

REFERENCES

1. S. M. Bhagwat and A. J. Ghajar. "Similarities and Differences in the Flow Patterns and Void Fraction in Vertical Upward and Downward Two Phase Flow." *Experimental Thermal and Fluid Science* 39 (2012), pp. 213–227.

2. S. M. Bhagwat, M. Mollamahmutoglu, and A. J. Ghajar. "Experimental Investigation and Empirical Analysis of Non-Boiling Gas-Liquid Two Phase Heat Transfer in Vertical Downward Pipe Orientation." *Proceedings of the ASME 2012 Summer Heat Transfer Conference, Puerto Rico* (2012) HT2012-58072.

3. S. M. Bhagwat and A. J. Ghajar. "A Flow Pattern Independent Drift Flux Model Based Void Fraction Correlation for a Wide Range of Gas–Liquid Two Phase Flow." *International Journal of Multiphase Flow* 59 (2014), pp.186–205.

4. S. M. Bhagwat and A. J. Ghajar. "Experimental Investigation of Non-Boiling Gas-Liquid Two Phase Flow in Upward Inclined Pipes." *Experimental Thermal and Fluid Science* 79 (2016), pp. 301–318.

5. S. M. Bhagwat and A. J. Ghajar. "Experimental Investigation of Non-Boiling Gas–Liquid Two Phase Flow in Downward Inclined Pipes." *Experimental Thermal and Fluid Science* 89 (2017), pp. 219–237.

6. A. J. Ghajar and S. M. Bhagwat. "Effect of Void Fraction and Two-Phase Dynamic Viscosity Models on Prediction of Hydrostatic and Frictional Pressure Drop in Vertical Upward Gas-Liquid Two-Phase Flow." *Heat Transfer Engineering* 34, no. 13 (2013), pp. 1044–1059.

7. A. J. Ghajar and S. M. Bhagwat. "Flow Patterns, Void Fraction and Pressure Drop in Gas-Liquid Two Phase Flow at Different Pipe Orientations." In *Frontiers and Progress in Multiphase Flow I,* ed. L. Cheng, Chapter 4, pp. 157–212. Switzerland: Springer International Publishing, 2014.

8. A. J. Ghajar and S. M. Bhagwat. "Gas-Liquid Flow in Ducts." In *Handbook of Multiphase Flow,* 2nd ed., ed. E. E. Michaelides, C. T. Crowe, and J. D. Schwarzkopf, Chapter 3, pp. 287–356. Boca Raton, FL: CRC Press/Taylor & Francis, 2017.

9. A. J. Ghajar and C. C. Tang. "Advances in Void Fraction, Flow Pattern Maps and Non-Boiling Heat Transfer Two-Phase Flow in Pipes with Various Inclinations." In *Advances in Multiphase Flow and Heat Transfer,* Vol. 1, ed. L. Cheng and D. Mewes, pp. 1–52. Bentham Science Publishers, UK, 2009.

10. A. J. Ghajar, A. J. and C. C. Tang. "Void Fraction and Flow Patterns of Two-Phase Flow in Upward and Downward Vertical and Horizontal Pipes." In *Advances in Multiphase Flow and Heat Transfer,* Vol. 4, ed. L. Cheng and D. Mewes, pp. 175–201. Bentham Sciences Publishers, UK, 2012.

11. K. S. Rezkallah. "Heat Transfer and Hydrodynamics in Two-Phase Two-Component Flow in a Vertical Tube." Ph.D. thesis, University of Manitoba, Winnipeg, Manitoba, Canada, 1987.

12. C. C. Tang and A. J. Ghajar. "A Mechanistic Heat Transfer Correlation for Non-Boiling Two Phase Flow in Horizontal, Inclined and Vertical Pipes." *Proceedings of ASME/JSME 8th Thermal Engineering Joint Conference, Hawaii,* (2011) AJTEC2011-44114.

13. M. A. Woldesemayat and A. J. Ghajar. "Comparison of Void Fraction Correlations for Different Flow Patterns in Horizontal and Upward Inclined Pipes." *International Journal of Multiphase Flow* 33 (2007), pp. 347–370.

SUMMARY

Boiling occurs when a liquid is in contact with a surface maintained at a temperature T_s sufficiently above the saturation temperature T_{sat} of the liquid. Boiling is classified as *pool boiling* or *flow boiling,* depending on the presence of bulk fluid motion. Boiling is called *pool boiling* in the absence of bulk fluid flow and *flow boiling* (or *forced convection boiling*) in its presence. Pool and flow boiling are further classified as *subcooled boiling* and *saturated boiling,* depending on the bulk liquid temperature. Boiling is said to be *subcooled* (or *local*) when the temperature of the main body of the liquid is below the saturation temperature T_{sat} and *saturated* (or *bulk*) when the temperature of the liquid is equal to T_{sat}. Boiling exhibits different regimes depending on the value of the excess temperature ΔT_{excess}. Four different boiling regimes are observed: natural convection boiling, nucleate boiling, transition boiling, and film boiling. These regimes are illustrated on the *boiling curve.* The rate of evaporation and the rate of heat transfer in nucleate boiling increase with increasing ΔT_{excess} and reach a maximum at some point. The heat flux at this point is called the *critical* (or *maximum*) *heat flux,* $\dot{q}_{max}$. The rate of heat transfer in nucleate pool boiling is determined from

$$\dot{q}_{nucleate} = \mu_l h_{fg} \left[\frac{g(\rho_l - \rho_v)}{\sigma}\right]^{1/2} \left[\frac{c_{pl}(T_s - T_{sat})}{C_{sf} h_{fg} \mathrm{Pr}_l^n}\right]^3$$

The *maximum* (or *critical*) *heat flux* in nucleate pool boiling is determined from

$$\dot{q}_{max} = C_{cr} h_{fg} [\sigma g \rho_v^2 (\rho_l - \rho_v)]^{1/4}$$

where the value of the constant C_{cr} is about 0.15. The minimum heat flux is given by

$$\dot{q}_{min} = 0.09 \rho_v h_{fg} \left[\frac{\sigma g(\rho_l - \rho_v)}{(\rho_l + \rho_v)^2}\right]^{1/4}$$

The heat flux for stable *film boiling* on the outside of a *horizontal cylinder* or *sphere* of diameter D is given by

$$\dot{q}_{\text{film}} = C_{\text{film}} \left[\frac{gk_v^3 \rho_v (\rho_l - \rho_v) h_{fg} + 0.4 c_{pv}(T_s - T_{\text{sat}})}{\mu_v D(T_s - T_{\text{sat}})} \right]^{1/4}$$
$$\times (T_s - T_{\text{sat}})$$

where the constant $C_{\text{film}} = 0.62$ for horizontal cylinders and 0.67 for spheres. The *vapor* properties are to be evaluated at the *film temperature* $T_f = (T_{\text{sat}} + T_s)/2$, which is the *average temperature* of the vapor film. The liquid properties and h_{fg} are to be evaluated at the saturation temperature at the specified pressure.

Two distinct forms of condensation are observed in nature: film condensation and dropwise condensation. In *film condensation,* the condensate wets the surface and forms a liquid film on the surface that slides down under the influence of gravity. In *dropwise condensation,* the condensed vapor forms countless droplets of varying diameters on the surface instead of a continuous film.

The Reynolds number for the condensate flow is defined as

$$\text{Re} = \frac{D_h \rho_l V_l}{\mu_l} = \frac{4A_c \rho_l V_l}{p\mu_l} = \frac{4\dot{m}}{p\mu_l}$$

and

$$\text{Re} = \frac{4\dot{Q}_{\text{conden}}}{p\mu_l h_{fg}^*} = \frac{4A_s h(T_{\text{sat}} - T_s)}{p\mu_l h_{fg}^*}$$

where h_{fg}^* is the *modified latent heat of vaporization,* defined as

$$h_{fg}^* = h_{fg} + 0.68 c_{pl}(T_{\text{sat}} - T_s)$$

and represents heat transfer during condensation per unit mass of condensate.

Using some simplifying assumptions, the *average heat transfer coefficient* for smooth and wave-free laminar film condensation on a vertical plate of height L is determined to be

$$h_{\text{vert, laminar}} = 0.943 \left[\frac{g\rho_l(\rho_l - \rho_v) h_{fg}^* k_l^3}{\mu_l(T_{\text{sat}} - T_s)L} \right]^{1/4}$$

All properties of the *liquid* are to be evaluated at the film temperature $T_f = (T_{\text{sat}} + T_s)/2$. The h_{fg} and ρ_v are to be evaluated at T_{sat}. Condensate flow is *smooth* and *wave-free laminar* for about $\text{Re} \leq 30$, *wavy-laminar* in the range of $30 < \text{Re} < 1800$, and *turbulent* for $\text{Re} > 1800$. Heat transfer coefficients in the wavy-laminar and turbulent flow regions are determined from

$$h_{\text{vert, wavy}} = \frac{\text{Re} \, k_l}{1.08 \, \text{Re}^{1.22} - 5.2} \left(\frac{g}{\nu_l^2} \right)^{1/3}, \quad \begin{array}{l} 30 < \text{Re} < 1800 \\ \rho_v \ll \rho_l \end{array}$$

$$h_{\text{vert, turbulent}} = \frac{\text{Re} \, k_l}{8750 + 58 \, \text{Pr}^{-0.5}(\text{Re}^{0.75} - 253)} \left(\frac{g}{\nu_l^2} \right)^{1/3},$$
$$\text{Re} > 1800$$
$$\rho_v \ll \rho_l$$

Equations for vertical plates can also be used for laminar film condensation on the upper surfaces of the plates that are inclined by an angle θ from the vertical, by replacing g in that equation with $g \cos \theta$. Vertical plate equations can also be used to calculate the average heat transfer coefficient for laminar film condensation on the outer surfaces of vertical tubes, provided that the tube diameter is large relative to the thickness of the liquid film.

The average heat transfer coefficient for film condensation on the outer surfaces of a *horizontal tube* is determined to be

$$h_{\text{horiz}} = 0.729 \left[\frac{g\rho_l(\rho_l - \rho_v) h_{fg}^* k_l^3}{\mu_l(T_{\text{sat}} - T_s)D} \right]^{1/4}$$

where D is the diameter of the horizontal tube. This relation can easily be modified for a *sphere* by replacing the constant 0.729 with 0.815. It can also be used for *N horizontal tubes* stacked on top of each other by replacing D in the denominator with ND.

For low vapor velocities, film condensation heat transfer *inside horizontal tubes* can be determined from

$$h_{\text{internal}} = 0.555 \left[\frac{g\rho_l(\rho_l - \rho_v) k_l^3}{\mu_l(T_{\text{sat}} - T_s)D} \left(h_{fg} + \frac{3}{8} c_{pl}(T_{\text{sat}} - T_s) \right) \right]^{1/4}$$

$$\text{Re}_{\text{vapor}} = \left(\frac{\rho_v V_v D}{\mu_v} \right)_{\text{inlet}} < 35,000$$

where the Reynolds number of the vapor is to be evaluated at the tube inlet conditions using the internal tube diameter as the characteristic length. Finally, the heat transfer coefficient for *dropwise condensation* of steam on copper surfaces is given by

$$h_{\text{dropwise}} = \begin{cases} 51,104 + 2044 \, T_{\text{sat}}, & 22°C < T_{\text{sat}} < 100°C \\ 255,510, & T_{\text{sat}} > 100°C \end{cases}$$

where T_{sat} is in °C and the heat transfer coefficient h_{dropwise} is in W/m²·°C or its equivalent W/m²·K.

REFERENCES AND SUGGESTED READINGS

1. N. Arai, T. Fukushima, A. Arai, T. Nakajima, K. Fujie, and Y. Nakayama. "Heat Transfer Tubes Enhancing Boiling and Condensation in Heat Exchangers of a Refrigeration Machine." *ASHRAE Journal* 83 (1977), p. 58.

2. P. J. Berensen. "Film Boiling Heat Transfer for a Horizontal Surface." *Journal of Heat Transfer* 83 (1961), pp. 351–358.

3. P. J. Berensen. "Experiments in Pool Boiling Heat Transfer." *International Journal of Heat Mass Transfer* 5 (1962), pp. 985–999.

4. L. A. Bromley. "Heat Transfer in Stable Film Boiling." *Chemical Engineering Progress* 46 (1950), pp. 221–227.

5. J. C. Chato. "Laminar Condensation Inside Horizontal and Inclined Tubes." *ASHRAE Journal* 4 (1962), p. 52.

6. S. W. Chi. *Heat Theory and Practice.* Washington, DC: Hemisphere, 1976.

7. M. T. Cichelli and C. F. Bonilla. "Heat Transfer to Liquids Boiling Under Pressure." *Transactions of AIChE* 41 (1945), pp. 755–787.

8. R. A. Colclaser, D. A. Neaman, and C. F. Hawkins. *Electronic Circuit Analysis.* New York: John Wiley & Sons, 1984.

9. P. Griffith. "Dropwise Condensation." In *Heat Exchanger Design Handbook,* ed. E. U. Schlunder, Vol 2, Chapter 2.6.5. New York: Hemisphere, 1983.

10. H. Hampson and N. Özişik. "An Investigation into the Condensation of Steam." *Proceedings of the Institute of Mechanical Engineers,* London 1B (1952), pp. 282–294.

11. J. J. Jasper. "The Surface Tension of Pure Liquid Compounds." *Journal of Physical and Chemical Reference Data* 1, no. 4 (1972), pp. 841–1009.

12. S. S. Kutateladze. *Fundamentals of Heat Transfer.* New York: Academic Press, 1963.

13. S. S. Kutateladze. "On the Transition to Film Boiling Under Natural Convection." *Kotloturbostroenie* 3 (1948), p. 48.

14. D. A. Labuntsov. "Heat Transfer in Film Condensation of Pure Steam on Vertical Surfaces and Horizontal Tubes." *Teploenergetika* 4 (1957), pp. 72–80.

15. J. H. Lienhard and V. K. Dhir. "Extended Hydrodynamic Theory of the Peak and Minimum Pool Boiling Heat Fluxes." NASA Report NASA-CR-2270, July 1973.

16. J. H. Lienhard and V. K. Dhir. "Hydrodynamic Prediction of Peak Pool Boiling Heat Fluxes from Finite Bodies." *Journal of Heat Transfer* 95 (1973), pp. 152–158.

17. W. H. McAdams. *Heat Transmission.* 3rd ed. New York: McGraw-Hill, 1954.

18. W. M. Rohsenow. "A Method of Correlating Heat Transfer Data for Surface Boiling of Liquids." *ASME Transactions* 74 (1952), pp. 969–975.

19. W. M. Rohsenow. "Film Condensation." In *Handbook of Heat Transfer,* ed. W. M. Rohsenow and J. P. Hartnett, Chapter 12A. New York: McGraw-Hill, 1973.

20. I. G. Shekriladze, I. G. Gomelauri, and V. I. Gomelauri. "Theoretical Study of Laminar Film Condensation of Flowing Vapor." *International Journal of Heat Mass Transfer* 9 (1966), pp. 591–592.

21. N. V. Suryanarayana. *Engineering Heat Transfer.* St. Paul, MN: West Publishing, 1995.

22. J. W. Westwater and J. G. Santangelo. *Industrial Engineering Chemistry* 47 (1955), p. 1605.

23. N. Zuber. "On the Stability of Boiling Heat Transfer." *ASME Transactions* 80 (1958), pp. 711–720.

PROBLEMS*

Boiling Heat Transfer

10–1C What is boiling? What mechanisms are responsible for the very high heat transfer coefficients in nucleate boiling?

---

*Problems designated by a "C" are concept questions, and students are encouraged to answer them all. Problems designated by an "E" are in English units, and the SI users can ignore them. Problems with the 🖥 icon are comprehensive in nature and are intended to be solved with appropriate software. Problems with the 📵 icon are Prevention through Design problems. Problems with the 📘 icon are Codes and Standards problems.

10–2C Name the different boiling regimes in the order they occur in a vertical tube during flow boiling.

10–3C What is the difference between evaporation and boiling?

10–4C What is the difference between pool boiling and flow boiling?

10–5C Draw the boiling curve and identify the different boiling regimes. Also, explain the characteristics of each regime.

10–6C How does film boiling differ from nucleate boiling? Is the boiling heat flux necessarily higher in the stable film boiling regime than it is in the nucleate boiling regime?

10–7C Draw the boiling curve and identify the burnout point on the curve. Explain how burnout is caused. Why is the burnout point avoided in the design of boilers?

10–8C Discuss some methods of enhancing pool boiling heat transfer permanently.

10–9C Does the amount of heat absorbed as 1 kg of saturated liquid water boils at 100°C have to be equal to the amount of heat released as 1 kg of saturated water vapor condenses at 100°C?

10–10 Water is boiled at 120°C in a mechanically polished stainless-steel pressure cooker placed on top of a heating unit. The inner surface of the bottom of the cooker is maintained at 130°C. Determine the heat flux on the surface. *Answer:* 228.4 kW/m²

10–11 A platinum-plated rod with a diameter of 10 mm is submerged horizontally in water at atmospheric pressure. If the surface of the rod is maintained at 10°C above the saturation temperature, determine the nucleate pool boiling heat transfer rate per unit length and the rate of evaporation per unit length (in kg/s·m).

$P = 1$ atm

Water, 100°C

T_s

Platinum-plated rod
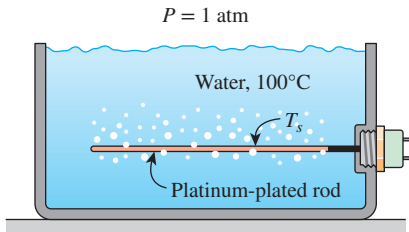
FIGURE P10–11

10–12 C&S Water is boiled at 361 kPa in a high-pressure system with an ASTM B371 brass rod. The ASTM B371 rod has a diameter and length of 5 mm and 15 cm, respectively. The rod is immersed in the water horizontally. The maximum use temperature for ASTM B371 brass rod is 149°C (ASME Code for Process Piping, ASME B31.3-2014, Table A-1M). The ASTM B371 rod is supplied with a heat transfer rate of 20 kW to boil the water. Determine if the supplied heat transfer rate would heat the rod surface temperature above the maximum use temperature.

10–13 A 65-cm-long, 2-cm-diameter brass heating element is to be used to boil water at 120°C. If the surface temperature of the heating element is not to exceed 125°C, determine the highest rate of steam production in the boiler, in kg/h. *Answer:* 19.4 kg/h

10–14 C&S An ASTM B75 copper tube sheaths a heating element that is used to boil water at 1254 kPa. The copper tube is immersed horizontally in the water, and its surface is polished. The tube diameter and length are 5 mm and 10 cm, respectively. The maximum use temperature for ASTM B75 copper tube is 204°C (ASME Code for Process Piping, ASME B31.3-2014, Table A-1M). Determine the highest evaporation rate of water that can be achieved by the heater without heating the tube surface above the maximum use temperature.

10–15 Water is to be boiled at atmospheric pressure in a mechanically polished steel pan placed on top of a heating unit. The inner surface of the bottom of the pan is maintained at 110°C. If the diameter of the bottom of the pan is 30 cm, determine (*a*) the rate of heat transfer to the water and (*b*) the rate of evaporation.
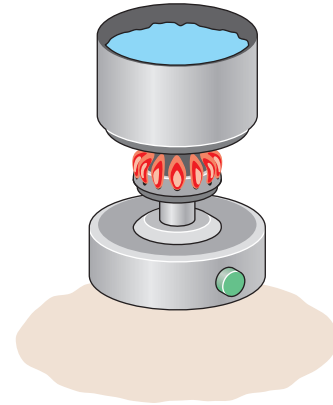
FIGURE P10–15

10–19 Water is boiled at atmospheric pressure by a horizontal platinum-plated rod with diameter of 10 mm. If the surface temperature of the rod is maintained at 110°C, determine the nucleate pool boiling heat transfer coefficient.
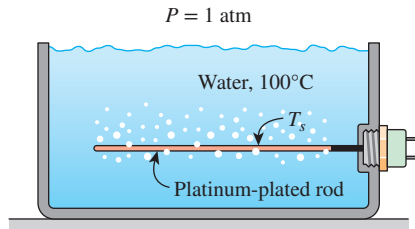
FIGURE P10–19

10–20 A 1-mm-diameter long electrical wire submerged in water at atmospheric pressure is dissipating 4100 W/m of heat, and the surface temperature reaches 128°C. If the experimental constant that depends on the fluid is $n = 1$, determine the nucleate boiling heat transfer coefficient and the value of the experimental constant C_{sf}.
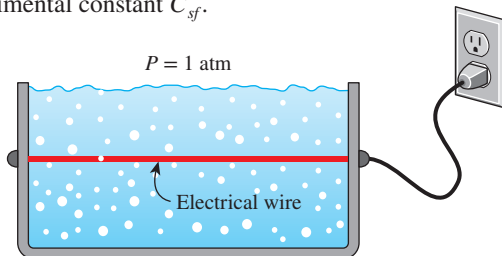
FIGURE P10–20

10–21 Water is boiled at sea level in a coffeemaker equipped with a 30-cm-long, 0.4-cm-diameter immersion-type electric heating element made of mechanically polished stainless steel. The coffeemaker initially contains 1 L of water at 14°C. Once boiling starts, it is observed that half of the water in the coffeemaker evaporates in 32 min. Determine the power rating of the electric heating element immersed in water and the surface temperature of the heating element. Also determine how long it will take for this heater to raise the temperature of 1 L of cold water from 14°C to the boiling temperature.
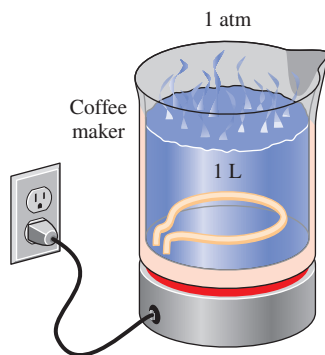
FIGURE P10–21

10–22 Repeat Prob. 10–21 for a copper heating element.

10–23 Water is boiled at 1 atm pressure in a 20-cm-internal-diameter Teflon®-pitted stainless steel pan on an electric range. If it is observed that the water level in the pan drops by 10 cm in 15 min, determine the inner surface temperature of the pan. *Answer:* 105.3°C

10–24 Repeat Prob. 10–23 for a polished copper pan.

10–25 Water is boiled at 120°C in a mechanically polished stainless steel pressure cooker placed on top of a heating unit. If the inner surface of the bottom of the cooker is maintained at 128°C, determine the boiling heat transfer coefficient.

10–26E Water is boiled at 250°F by a 2-ft-long and 0.25-in-diameter nickel-plated electric heating element maintained at 280°F. Determine (*a*) the boiling heat transfer coefficient, (*b*) the electric power consumed by the heating element, and (*c*) the rate of evaporation of water.

10–27E Repeat Prob. 10–26E for a platinum-plated heating element.

10–28E Reconsider Prob. 10–26E. Using appropriate software, investigate the effect of surface temperature of the heating element on the boiling heat transfer coefficient, the electric power, and the rate of evaporation of water. Let the surface temperature vary from 260°F to 300°F. Plot the boiling heat transfer coefficient, the electric power consumption, and the rate of evaporation of water as a function of the surface temperature, and discuss the results.

10–29 Mechanically polished, 5-cm-diameter, stainless steel ball bearings are heated to 125°C uniformly. The ball bearings are then submerged in water at 1 atm to be cooled. Determine the rate of heat that is removed from a ball bearing at the instant it is submerged in the water.

10–30 PtD A long, hot, mechanically polished stainless steel sheet ($c_p = 450$ J/kg·K, $\rho = 7900$ kg/m³) is being conveyed at 2 m/s through a water bath to be cooled. The 0.5-m-wide and 5-mm-thick stainless steel sheet has a temperature of 125°C as it enters the water bath. The length of the sheet submerged in water is 1 m as it is being conveyed through the water bath. As the hot sheet enters the water bath, boiling occurs at 1 atm. In order to prevent thermal burns to people handling the sheet, it must exit the water bath at a temperature below 45°C. Is the rate of heat that could be removed from the stainless steel sheet in the water bath sufficient to cool it to below 45°C as it leaves the water bath?
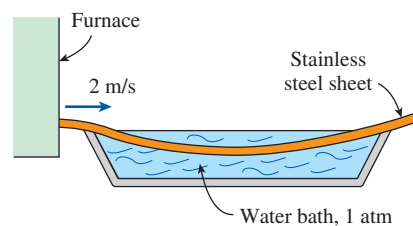
FIGURE P10–30

10–31 Water is boiled at 90°C by a horizontal brass heating element of diameter 8 mm. Determine the maximum heat flux that can be attained in the nucleate boiling regime.

10–32 A 1-mm-diameter nickel wire with electrical resistance of 0.129 Ω/m is submerged horizontally in water at atmospheric pressure. Determine the electrical current at which the wire would be in danger of burnout in nucleate boiling.

$P = 1$ atm

Nickel wire
0.129 Ω/m
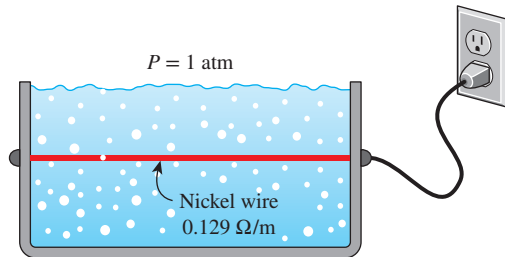
FIGURE P10–32

10–33 In a boiler, water is boiled at 100°C by hot gases flowing through a 10-m-long tube with an outer diameter of 5 cm that is submerged in the water. Determine the maximum rate of water vaporization that can be produced by the tube in the nucleate boiling regime.

10–34 Hot gases flow inside an array of tubes that are embedded in a 3-m × 3-m horizontal flat heater. The heater is used for boiling water in a tank at 160°C. In the interest of avoiding burnout, determine the maximum rate of water vaporization that can be achieved by the heater.

Water, 160°C
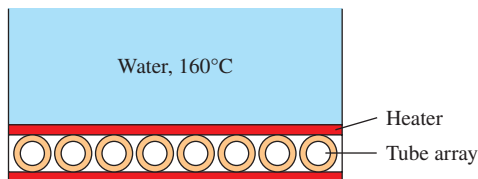
Heater
Tube array

FIGURE P10–34

10–35 Water is boiled by two heaters of different geometries: a spherical heater and a horizontal flat heater. Both heaters are submerged in water that boils at 1 atm. The spherical heater has a diameter of 1 m, and the horizontal flat heater has the same surface area as the spherical heater. Determine the maximum rate of water vaporization that can be achieved by each heater without reaching burnout. Which heater geometry would produce a higher maximum rate of vaporization?

10–36 Hot gases flow inside an array of tubes that are embedded in a 3-m × 3-m horizontal flat heater. The heater surface is nickel-plated and is used for generating steam by boiling water in the nucleate boiling regime at 180°C. Determine the surface temperature of the heater and the convection heat transfer coefficient that is necessary to achieve the maximum rate of steam generation.

10–37 Water is to be boiled at atmospheric pressure on a 2-cm-diameter mechanically polished steel heater. Determine the maximum heat flux that can be attained in the nucleate boiling regime and the surface temperature of the heater surface in that case.

10–38 Reconsider Prob. 10–37. Using appropriate software, investigate the effect of local atmospheric pressure on the maximum heat flux and the temperature difference $T_s - T_{sat}$. Let the atmospheric pressure vary from 70 kPa to 101.3 kPa. Plot the maximum heat flux and the temperature difference as a function of the atmospheric pressure, and discuss the results.

10–39 A 10-cm × 10-cm horizontal flat heater is used for vaporizing refrigerant-134a at 350 kPa. The heater is supplied with 0.35 MW/m² of heat flux, and the surface temperature of the heater is 25°C. If the experimental constant in the Rohsenow correlation is $n = 1.7$, determine the value of the coefficient C_{sf}. Discuss whether or not the Rohsenow correlation is applicable in this analysis.

10–40 In a gas-fired boiler, water is boiled at 150°C by hot gases flowing through 25-m-long, 5-cm-outer-diameter mechanically polished stainless steel pipes submerged in water. If the outer surface temperature of the pipes is 160°C, determine (a) the rate of heat transfer from the hot gases to water, (b) the rate of evaporation, (c) the ratio of the critical heat flux to the present heat flux, and (d) the surface temperature of the pipe at which critical heat flux occurs.

Vent
Boiler

150°C

Water
160°C

Hot gases
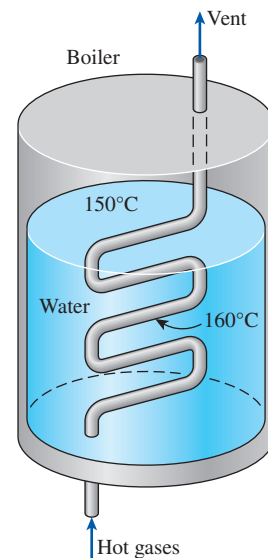
FIGURE P10–40

10–41 Repeat Prob. 10–40 for a boiling temperature of 155°C

10–42 A 1-m × 1-m horizontal flat heater is used for generating steam by boiling water at 1 atm. The boiling occurs at an excess temperature above 300°C, but it is maintained below

the burnout point. Determine the range of the steam generation rate that can be achieved by the heater.

10–43 Water is boiled at 90°C by a horizontal brass heating element of diameter 7 mm. Determine the surface temperature of the heater for the minimum heat flux case.

10–44 C&S An ASTM B165 nickel–copper alloy tube sheathes a heating element that is used to boil water at 1 atm. The tube is immersed horizontally in the water. The tube diameter and length are 5 mm and 15 cm, respectively. The maximum use temperature for ASTM B165 nickel–copper alloy tube is 260°C (ASME Code for Process Piping, ASME B31.3-2014, Table A-1M). Determine the highest evaporation rate of water that can be achieved by the heater without heating the tube surface above the maximum use temperature.

10–45 A 2-mm-diameter cylindrical metal rod with emissivity of 0.5 is submerged horizontally in water under atmospheric pressure. When electric current is passed through the metal rod, the surface temperature reaches 500°C. Determine the power dissipation per unit length of the metal rod.
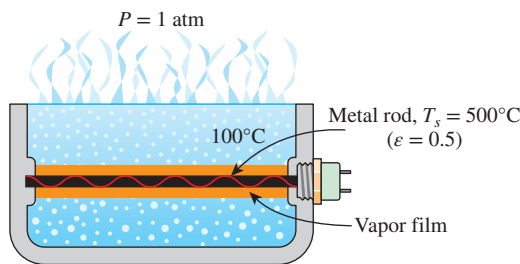
FIGURE P10–45

10–46E Water is boiled at atmospheric pressure by a horizontal polished copper heating element of diameter $D = 0.5$ in and emissivity $\varepsilon = 0.2$ immersed in water. If the surface temperature of the heating element is 788°F, determine the rate of heat transfer to the water per unit length of the heating element.

10–47E Repeat Prob. 10–46E for a heating element temperature of 988°F.

10–48 C&S An ASTM B335 nickel alloy rod, with a diameter of 5 mm and a length of 10 cm, is used to boil water at 1 atm. The rod is immersed in the water horizontally, and it has an emissivity of 0.3. The maximum use temperature for ASTM B335 nickel alloy rod is 427°C (ASME Code for Process Piping, ASME B31.3-2014, Table A-1M). Determine the highest rate of heat transfer that can be supplied from the ASTM B335 rod to boil the water without heating the rod surface above the maximum use temperature.

10–49 A 20-mm-diameter metal sphere has an emissivity of 0.75. The sphere was removed from a furnace when it reached a uniform temperature of 700°C and was suddenly submerged

in a water bath at atmospheric pressure. Estimate the initial heat transfer rate from the submerged metal sphere.

10–50 A 20-mm-diameter cylindrical steel rod with a length of 200 mm has an emissivity of 0.9. The steel rod was removed from a furnace when it reached a uniform temperature of 500°C and was suddenly submerged horizontally in a water bath at atmospheric pressure. Estimate the initial heat transfer rate from the submerged steel rod.

10–51 Water is boiled at 100°C by a spherical platinum heating element of diameter 15 cm and emissivity 0.10 immersed in the water. If the surface temperature of the heating element is 350°C, determine the rate of heat transfer from the heating element to the water.

10–52 Cylindrical stainless steel rods are heated to a uniform temperature of 700°C and then quenched in water at 1 atm. The rods are 25 cm in length, 25 mm in diameter, and their surface has an emissivity of 0.3. Determine the convection heat transfer coefficient and the total rate of heat removed from a rod at the instant it is submerged in the water during quenching.

10–53 PtD A long cylindrical stainless steel rod ($c_p = 450$ J/kg·K, $\rho = 7900$ kg/m³, $\varepsilon = 0.30$) with a mechanically polished surface is being conveyed through a water bath to be quenched. The 25-mm-diameter stainless steel rod has a temperature of 700°C as it enters the water bath. A length of 3 m of the rod is submerged in water as it is conveyed through the water bath during the quenching process. As the stainless steel rod enters the water bath, boiling occurs at 1 atm. In order to prevent thermal burns to people handling the rod, it must exit the water bath at a temperature below 45°C. Determine the speed of the rod being conveyed through the water bath so that it leaves the water bath without the risk of thermal burns.
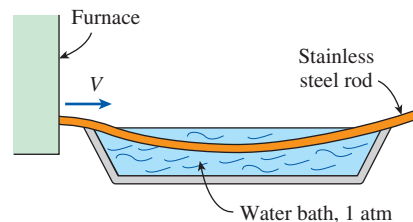
FIGURE P10–53

10–54 A cylindrical rod is used for boiling water at 1 atm. The rod has a diameter of 1 cm, and its surface has an emissivity of 0.3. Determine the film boiling convection heat transfer coefficient at the burnout point. Evaluate the properties of vapor at 1150°C. Discuss whether 1150°C is a reasonable film temperature for the vapor properties.

10–55 A 3-mm-diameter cylindrical heater is used for boiling water at 100°C. The heater surface is made of mechanically polished stainless steel with an emissivity of 0.3. Determine the boiling convection heat transfer coefficients at

the maximum heat flux for (*a*) nucleate boiling and (*b*) film boiling. For film boiling, evaluate the properties of vapor at 1150°C.

10–56   To understand the burnout phenomenon, boiling experiments are conducted in water at atmospheric pressure using an electrically heated 30-cm-long, 4-mm-diameter nickel-plated horizontal wire. Determine (*a*) the critical heat flux and (*b*) the increase in the temperature of the wire as the operating point jumps from the nucleate boiling to the film boiling regime at the critical heat flux. Take the emissivity of the wire to be 0.3.

10–57   Reconsider Prob. 10–56. Using appropriate software, investigate the effects of the local atmospheric pressure and the emissivity of the wire on the critical heat flux and the temperature rise of wire. Let the atmospheric pressure vary from 70 kPa to 101.3 kPa and the emissivity from 0.1 to 1.0. Plot the critical heat flux and the temperature rise as functions of the atmospheric pressure and the emissivity, and discuss the results.

Condensation Heat Transfer

10–58C   What is condensation? How does it occur?

10–59C   What is the difference between film and dropwise condensation? Which is a more effective mechanism of heat transfer?

10–60C   How does the presence of a noncondensable gas in a vapor influence the condensation heat transfer?

10–61C   What is the modified latent heat of vaporization? For what is it used? How does it differ from the ordinary latent heat of vaporization?

10–62C   Consider film condensation on a vertical plate. Will the heat flux be higher at the top or at the bottom of the plate? Why?

10–63C   Consider film condensation on the outer surfaces of four long tubes. For which orientation of the tubes will the condensation heat transfer coefficient be the highest: (*a*) vertical, (*b*) horizontal side by side, (*c*) horizontal but in a vertical tier (directly on top of each other), or (*d*) a horizontal stack of two tubes high and two tubes wide?

10–64C   In condensate flow, how is the wetted perimeter defined? How does wetted perimeter differ from ordinary perimeter?

10–65   The Reynolds number for condensate flow is defined as $\text{Re} = 4\dot{m}/p\,\mu_l$, where p is the wetted perimeter. Obtain simplified relations for the Reynolds number by expressing p and $\dot{m}$ by their equivalence for the following geometries: (*a*) a vertical plate of height L and width w, (*b*) a tilted plate of height L and width w inclined at an angle u from the vertical, (*c*) a vertical cylinder of length L and diameter D, (*d*) a horizontal cylinder of length L and diameter D, and (*e*) a sphere of diameter D.

10–66   A vertical 0.2-m × 0.2-m square plate is exposed to saturated water vapor at atmospheric pressure. If the surface temperature is 80°C and the flow is laminar, estimate the local heat transfer coefficients at the middle and at the bottom of the plate.

10–67   A vertical 0.5-m × 0.5-m square plate is used in a process to condense saturated water vapor. If the desired rate of condensation is 0.016 kg/s, determine the necessary surface temperature of the plate at atmospheric pressure. For this problem, as a first approximation, assume a film temperature of 90°C for the evaluation of the liquid properties and a surface temperature of 80°C for the evaluation of modified latent heat of vaporization. Are these good assumptions?

10–68   Saturated ammonia vapor at 30°C is passed over 30 vertical flat plates, each of which is 10 cm high and 25 cm wide. The average surface temperature of the plates is 10°C. Estimate the average heat transfer coefficient and the rate of ammonia condensation. Assume wavy-laminar flow. Is this a good assumption?

10–69   Saturated steam at 1 atm condenses on a 2-m-high and 10-m-wide vertical plate that is maintained at 90°C by circulating cooling water through the other side. Determine (*a*) the rate of heat transfer by condensation to the plate, and (*b*) the rate at which the condensate drips off the plate at the bottom. Assume wavy-laminar flow. Is this a good assumption?
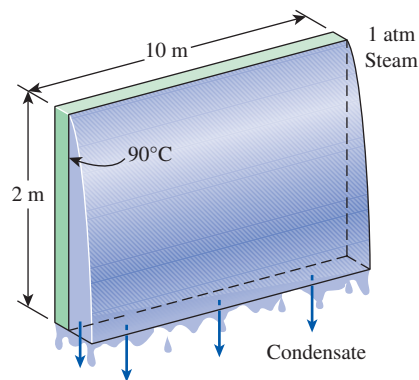
FIGURE P10–69

10–70   Repeat Prob. 10–69 for the case of the plate being tilted 60° from the vertical.

10–71   Saturated ammonia vapor in a pressurized system undergoes condensation at 190 kPa on a vertical plate. The plate is made of ASTM A240 410S stainless steel; it has a height of 2 m and a width of 1.5 m. According to the ASME Code for Process Piping, the minimum temperature suitable for ASTM A240 410S stainless steel plate is −30°C (ASME B31.3-2014, Table A-1M). Determine the highest rate of condensation that can be produced by the plate without cooling the plate below the minimum suitable

temperature set by the ASME Code for Process Piping. Assume wavy-laminar flow. Is this a good assumption?

10–72 Saturated steam at 100°C condenses on a 2-m × 2-m plate that is tilted 30° from the vertical. The plate is maintained at 80°C by cooling it from the other side. Determine (*a*) the average heat transfer coefficient over the entire plate and (*b*) the rate at which the condensate drips off the plate at the bottom. Assume wavy-laminar flow. Is this a good assumption?

10–73 Reconsider Prob. 10–72. Using appropriate software, investigate the effects of plate temperature and the angle of the plate from the vertical on the average heat transfer coefficient and the rate at which the condensate drips off. Let the plate temperature vary from 40°C to 90°C and the plate angle from 0° to 60°. Plot the heat transfer coefficient and the rate at which the condensate drips off as functions of the plate temperature and the tilt angle, and discuss the results.

10–74 Saturated steam at 30°C condenses on the outside of a 4-cm-outer-diameter, 2-m-long vertical tube. The temperature of the tube is maintained at 20°C by the cooling water. Determine (*a*) the rate of heat transfer from the steam to the cooling water, (*b*) the rate of condensation of steam, and (*c*) the approximate thickness of the liquid film at the bottom of the tube. Assume wavy-laminar flow and that the tube diameter is large relative to the thickness of the liquid film at the bottom of the tube. Are these good assumptions?
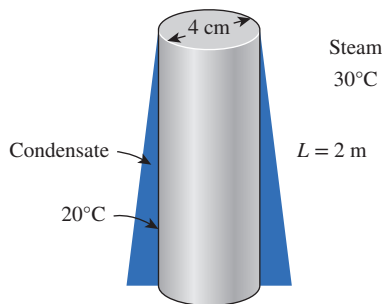
FIGURE P10–74

10–75 Saturated water vapor at atmospheric pressure condenses on the outer surface of a 0.1-m-diameter vertical pipe. The pipe is 1 m long and has a uniform surface temperature of 80°C. Determine the rate of condensation and the heat transfer rate by condensation. Discuss whether the pipe can be treated as a vertical plate. Assume wavy-laminar flow and that the tube diameter is large relative to the thickness of the liquid film at the bottom of the tube. Are these good assumptions?

10–76 Saturated steam at 55°C is to be condensed at a rate of 10 kg/h on the outside of a 3-cm-outer-diameter vertical tube whose surface is maintained at 45°C by the cooling water. Determine the required tube length. Assume wavy-laminar flow and that the tube diameter is large relative to the thickness of the liquid film at the bottom of the tube. Are these good assumptions?

10–77 Repeat Prob. 10–76 for a horizontal tube. *Answer:* 0.70 m

10–78 A 1.5-m-long vertical tube is used for condensing saturated steam at 60°C. The surface temperature of the tube is maintained at a uniform temperature of 40°C by flowing coolant inside the tube. Determine the heat transfer rate to the tube and the required tube diameter to condense 12 kg/h of steam during the condensation process. Assume wavy-laminar flow and that the tube diameter is large relative to the thickness of the liquid film at the bottom of the tube. Are these good assumptions?

10–79 Repeat Prob. 10–78 for a horizontal tube. Compare the required diameters between a vertical tube and a horizontal tube to condense 12 kg/h of steam during the condensation process.

10–80 Saturated ammonia vapor at 10°C condenses on the outside of a 4-cm-outer-diameter, 15-m-long horizontal tube whose outer surface is maintained at −10°C. Determine (*a*) the rate of heat transfer from the ammonia and (*b*) the rate of condensation of ammonia.

10–81 C & S Saturated refrigerant-134a vapor undergoes condensation on the outer surface of a horizontal ASTM A268 TP443 stainless steel tube at 133 kPa. The tube is 50 cm long and has a diameter of 15 mm. According to the ASME Code for Process Piping, the minimum temperature suitable for ASTM A268 TP443 stainless steel tube is −30°C (ASME B31.3-2014, Table A-1M). Determine whether the condensation of refrigerant-134a on the tube surface at a rate of 3 g/s would cool the surface below the minimum suitable temperature set by the ASME Code for Process Piping.

10–82 PtD A 3-m spherical tank storing cold fluid has a uniform surface temperature of 5°C. The lower temperature of the tank surface is causing condensation of moisture in the air at 25°C. The tank is situated in the vicinity of high-voltage devices, and water from the condensation on the tank surface can create an electrical hazard. To prevent an accident, a system is to be implemented to remove 0.5 kg/s of condensate from coming in contact with the high-voltage devices. Determine whether or not the preventive system can handle the rate of condensation from the tank surface.

10–83 Consider film condensation on the outer surfaces of *N* horizontal tubes arranged in a vertical tier. For what value of *N* will the average heat transfer coefficient for the entire stack of tubes be equal to half of what it is for a single horizontal tube?

10–84 A large heat exchanger has several columns of tubes, with 33 tubes in each column. The outer diameter of the tubes is 1.5 cm. Saturated steam at 50°C condenses on the outer surfaces of the tubes, which are maintained at 20°C. Determine (*a*) the average heat transfer coefficient and (*b*) the rate of condensation of steam per m length of a column.

10–85 The condenser of a steam power plant operates at a pressure of 4.25 kPa. The condenser consists of 144 horizontal

tubes arranged in a 12×12 square array. The tubes are 8 m long and have an outer diameter of 3 cm. If the tube surfaces are at 20°C, determine (a) the rate of heat transfer from the steam to the cooling water and (b) the rate of condensation of steam in the condenser. *Answers:* (a) 5060 kW, (b) 2.06 kg/s
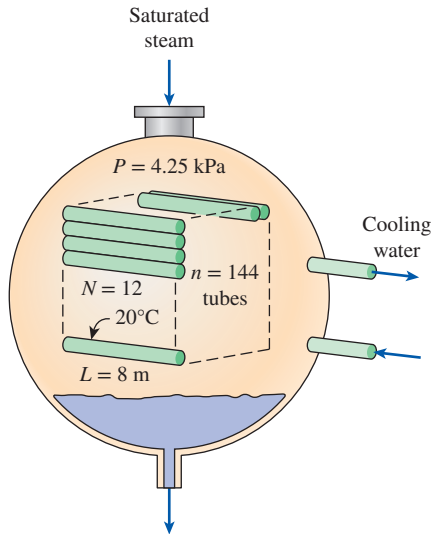
FIGURE P10–85

10–86 Reconsider Prob. 10–85. Using appropriate software, investigate the effect of the condenser pressure on the rate of heat transfer and the rate of condensation of the steam. Let the condenser pressure vary from 3 kPa to 15 kPa. Plot the rate of heat transfer and the rate of condensation of the steam as a function of the condenser pressure, and discuss the results.

10–87E Saturated steam at 95°F is condensed on the outer surfaces of an array of horizontal pipes through which cooling water circulates. The outer diameter of the pipes is 0.8 in and the outer surfaces of the pipes are maintained at 65°F. Determine (a) the rate of heat transfer to the cooling water circulating in the pipes and (b) the rate of condensation of steam per unit length of a single horizontal pipe.

10–88E Repeat Prob. 10–87E for the case of 32 horizontal pipes arranged in a rectangular array of 4 pipes high and 8 pipes wide.

10–89 A horizontal condenser uses a 4×4 array of tubes that have an outer diameter of 5.0 cm and length 2.0 m. Saturated steam at 101.3 kPa condenses on the outside tube surface held at a temperature of 80°C. Calculate the steady rate of steam condensation in kg/h.

10–90 C&S Four long ASTM A437 B4B stainless steel bolts are used to hold two separated plates together. The bolts are cylindrical, and each has a diameter of 13 mm. Between the two plates, the horizontal bolts are exposed to

saturated propane vapor. The length of each bolt between the plates is 15 cm. The bolts are arranged in a vertical tier, and condensation of saturated propane occurs on the bolts at 344 kPa. The minimum temperature suitable for ASTM A437 B4B stainless steel bolts is -30°C (ASME Code for Process Piping, ASME B31.3-2014, Table A-2M). Determine the highest rate of condensation that can occur on the bolts, without cooling the bolts below the minimum suitable temperature set by the ASME Code for Process Piping.
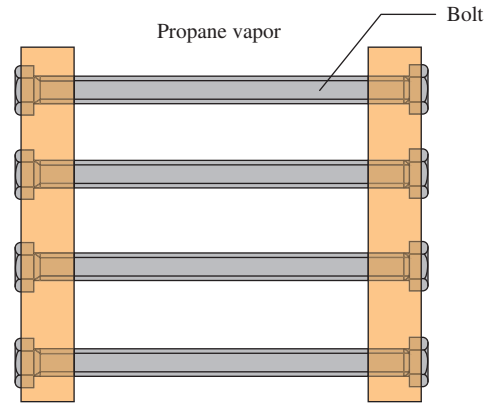
FIGURE P10–90

10–91 Saturated water vapor at a pressure of 12.4 kPa is condensed over 100 horizontal tubes in a rectangular array of 5 tubes high and 20 tubes wide, each with a diameter of 8 mm. If the tube surfaces are maintained with a uniform temperature of 30°C, determine the condensation rate per unit length (in kg/s·m) of the tubes.

10–92 Saturated water vapor at a pressure of 12.4 kPa is condensed over an array of 100 horizontal tubes, each with a diameter of 8 mm and a length of 1 m. The tube surfaces are maintained with a uniform temperature of 30°C. Determine the condensation rates of the tubes for (a) a rectangular array of 5 tubes high and 20 tubes wide and (b) a square array of 10 tubes high and 10 tubes wide. Compare and discuss the results of (a) and (b).

10–93 Saturated refrigerant-134a vapor at a pressure of 888 kPa is condensed as it is flowing through a 0.25-m-long tube with a diameter of 12 mm. The tube wall temperature is kept uniform at 15°C. If the vapor enters the tube at a flow rate of 0.003 kg/s, determine the flow rate of the vapor at the exit.

10–94 C&S Saturated ammonia vapor flows inside a horizontal tube with a length and an inner diameter of 1 m and 25 mm, respectively. The tube is made of ASTM A268 TP443 stainless steel. The ammonia vapor enters the tube at a flow rate of 5 g/s, and condensation occurs inside the tube at 190 kPa. The minimum temperature suitable for ASTM A268 TP443 stainless steel tube is -30°C (ASME Code for Process Piping, ASME B31.3-2014, Table A-1M). If the flow

rate of ammonia vapor at the tube exit is 0.5 g/s, would the temperature of the tube wall comply with the ASME Code?

10–95 Saturated ammonia vapor at a pressure of 1003 kPa is condensed as it flows through a 25-mm tube. The tube length is 0.5 m, and the wall temperature is kept uniform at 5°C. If the vapor exits the tube at a flow rate of 0.002 kg/s, determine the flow rate of the vapor at the inlet. Assume the Reynolds number of the vapor at the tube inlet is less than 35,000. Is this a good assumption?

10–96 A 10-m-long copper tube with a diameter of 25 mm is used for transporting cold coolant. The coolant flow inside the tube maintains the tube surface temperature at 5°C and causes moist air to condense on the outer surface. Determine the dropwise condensation rate of the moisture in the air if the saturation temperature is 25°C.

10–97 [PtD] A 10-m-long copper tube with a diameter of 25 mm is used for transporting cold fluid. The cold fluid flow inside the tube causes the tube surface temperature at 3°C to be colder than the ambient temperature. As a result, moist air condenses at 27°C on the tube outer surface. The tube is situated in the vicinity of high-voltage devices, and water from the condensation can cause an electrical hazard. It has been determined that both film condensation and dropwise condensation can occur on the tube surface. To prevent an electrical hazard, a system is to be implemented to remove the condensate and prevent it from coming in contact with the high-voltage devices. Size the system so that it is capable of handling the condensation rate from the tube surface.

Moist air, 27°C   Copper tube, 3°C

Cold fluid
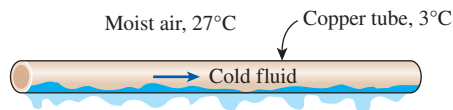
FIGURE P10–97

10–98 Steam is being condensed at 60°C by a 15-m-long horizontal copper tube with a diameter of 25 mm. The tube surface temperature is maintained at 40°C. Determine the condensation rate of the steam during (*a*) film condensation, and (*b*) dropwise condensation. Compare and discuss the results.

Special Topic: Non-Boiling Two-Phase Flow Heat Transfer

10–99 Consider a non-boiling gas–liquid two-phase flow in a tube, where the ratio of the mass flow rate is $\dot{m}_l/\dot{m}_g = 300$. Determine the flow quality (x) of this non-boiling two-phase flow.

10–100 Consider a non-boiling gas–liquid two-phase flow in a 102-mm diameter tube, where the superficial gas velocity is one-third that of the liquid. If the densities of the gas and liquid are $\rho_g = 8.5$ kg/m^3 and $\rho_l = 855$ kg/m^3, respectively, determine the flow quality and the mass flow rates of the gas and the liquid when the gas superficial velocity is 0.8 m/s.

10–101 A non-boiling two-phase flow of air and engine oil in a 25-mm-diameter tube has a bulk mean temperature of 140°C. If the flow quality is 2.1×10^{-3} and the mass flow rate of the engine oil is 0.9 kg/s, determine the mass flow rate of air and the superficial velocities of air and engine oil.

10–102 Consider a mixture of air–water flow in a tube. Suddenly the air flow is shut off, so that only water is flowing in the tube. Starting with the two-phase non-boiling heat transfer correlation, find the expression that is appropriate for this situation.

10–103 An air–water slug flows through a 25.4-mm-diameter horizontal tube in microgravity conditions (less than 1 percent of earth's normal gravity). The liquid phase consists of water with dynamic viscosity of $\mu_l = 85.5 \times 10^{-5}$ kg/m·s, density of $\rho_l = 997$ kg/m^3, thermal conductivity of $k_l = 0.613$ W/m·K, and Prandtl number of $\Pr_l = 5.0$. The gas phase consists of air with dynamic viscosity of $\mu_g = 18.5 \times 10^{-6}$ kg/m·s, density $\rho_g = 1.16$ kg/m^3, and Prandtl number $\Pr_g = 0.71$. At a superficial gas velocity of $V_{sg} = 0.3$ m/s, a superficial liquid velocity of $V_{sl} = 0.544$ m/s, and a void fraction of $\alpha = 0.27$, estimate the two-phase heat transfer coefficient h_{tp}. Assume the dynamic viscosity of water evaluated at the tube surface temperature to be 73.9×10^{-5} kg/m·s.

10–104 A two-phase flow mixture of air and silicone (Dow Corning 200® Fluid, 5 cs) is being transported in an 11.7-mm-diameter thin-walled horizontal tube. The liquid phase consists of liquid silicone with a surface tension (σ) of 19.7×10^{-3} N/m, dynamic viscosity (μ_l) of 45.7×10^{-4} kg/m·s, density (ρ_l) of 913 kg/m^3, thermal conductivity (k_l) of 0.117 W/m·K, and Prandtl number ($\Pr_l$) of 64. The dynamic viscosity of the liquid silicone evaluated at the tube surface temperature (μ_s) is 39.8×10^{-4} kg/m·s. The gas phase consists of air with dynamic viscosity (μ_g) of 18.4×10^{-6} kg/m·s, density (ρ_g) of 1.19 kg/m^3, and Prandtl number ($\Pr_g$) of 0.71. The two-phase flow has a flow quality (x) of 2.08×10^{-5}, void fraction (α) of 0.011, gas velocity (V_g) of 13.5 m/s, liquid velocity (V_l) of 9.34 m/s, and liquid mass flow rate ($\dot{m}_l$) of 0.907 kg/s. Moist air at a saturation temperature of 40°C condenses on the outer surface of the tube. The tube has a uniform surface temperature of 20°C. Determine the overall convection heat transfer coefficient (inside and outside) of the tube.

Moist air, 40°C

Air-silicone mixture

20°C
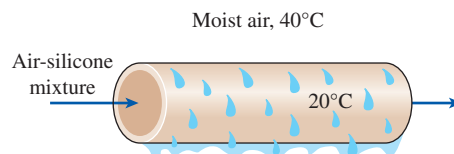
FIGURE P10–104

10–105 An air–water mixture is flowing in a 5° inclined tube that has a diameter of 25.4 mm. The two-phase mixture enters the tube at 25°C and exits at 65°C, while the tube surface

temperature is maintained at 80°C. If the superficial gas and liquid velocities are 1 m/s and 2 m/s, respectively, determine the two-phase heat transfer coefficient h_{tp}. Assume the surface tension is $\sigma = 0.068$ N/m and the void fraction is $\alpha = 0.33$.

10–106 A mixture of petroleum and natural gas is being transported in a pipeline with a diameter of 102 mm. The pipeline is located in a terrain that caused it to have an average inclination angle of $\theta = 10°$. The liquid phase consists of petroleum with dynamic viscosity of $\mu_l = 297.5 \times 10^{-4}$ kg/m·s, density of $\rho_l = 853$ kg/m³, thermal conductivity of $k_l = 0.163$ W/m·K, surface tension of $\sigma = 0.020$ N/m, and Prandtl number of $Pr_l = 405$. The gas phase consists of natural gas with dynamic viscosity of $\mu_g = 9.225 \times 10^{-6}$ kg/m·s, density of $\rho_g = 9.0$ kg/m³, and Prandtl number of $Pr_g = 0.80$. The liquid is flowing at a flow rate of 16 kg/s, while the gas is flowing at 0.055 kg/s. If the void fraction is $\alpha = 0.22$, determine the two-phase heat transfer coefficient h_{tp}. Assume the dynamic viscosity of liquid petroleum evaluated at the tube surface temperature to be 238×10^{-4} kg/m·s.

10–107 An air–water mixture is flowing in a tube with a diameter of 25.4 mm. The two-phase mixture enters the tube at 15°C and exits at 75°C, while the tube surface temperature is maintained at 80°C. If the superficial gas and liquid velocities are 1 m/s and 2 m/s, respectively, determine the two-phase heat transfer coefficient h_{tp} for (a) the horizontal tube ($\theta = 0°$) and (b) the vertical tube ($\theta = 90°$), and compare the two results. Assume the surface tension is $\sigma = 0.068$ N/m and the void fraction is $\alpha = 0.33$.

10–108 Consider a two-phase flow of air–water in a vertical upward stainless steel pipe with an inside diameter of 0.0254 m. The two-phase mixture enters the pipe at 25°C at a system pressure of 201 kPa. The superficial velocities of the water and air are 0.3 m/s and 23 m/s, respectively. The differential pressure transducer connected across the pressure taps set 1 m apart records a pressure drop of 2700 Pa, and the measured value of the void fraction is 0.86. Using the concept of the Reynolds analogy, determine the two-phase convective heat transfer coefficient. Use the following thermophysical properties for water and air: $\rho_l = 997.1$ kg/m³, $\mu_l = 8.9 \times 10^{-4}$ kg/m·s, $\mu_s = 4.66 \times 10^{-4}$ kg/m·s, $Pr_l = 6.26$, $k_l = 0.595$ W/m·K, $\sigma = 0.0719$ N/m, $\rho_g = 2.35$ kg/m³, and $\mu_g = 1.84 \times 10^{-5}$ kg/m·s.

Review Problems

10–109 Water is boiled at 120°C in a mechanically polished stainless steel pressure cooker placed on top of a heating unit. The inner surface of the bottom of the cooker is maintained at 130°C. The cooker that has a diameter of 20 cm and a height of 30 cm is half filled with water. Determine the time it will take for the tank to empty. *Answer:* 22.8 min

10–110 Water is to be boiled at sea level in a 30-cm-diameter mechanically polished AISI 304 stainless steel pan placed on top of a 3-kW electric burner. If 60 percent of the heat

generated by the burner is transferred to the water during boiling, determine the temperature of the inner surface of the bottom of the pan. Also, determine the temperature difference between the inner and outer surfaces of the bottom of the pan if it is 6 mm thick. Assume the boiling regime is nucleate boiling. Is this a good assumption?
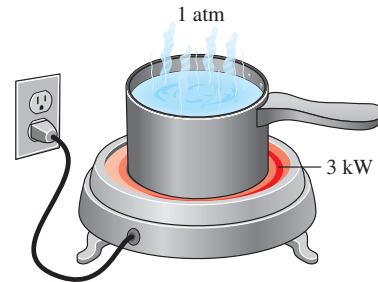
FIGURE P10–110

10–111 Repeat Prob. 10–110 for a location at an elevation of 1500 m where the atmospheric pressure is 84.5 kPa and thus the boiling temperature of water is 95°C.

10–112 A resistance heater made of 2-mm-diameter nickel wire is used to heat water at 1 atm pressure. Determine the highest temperature at which this heater can operate safely without the danger of burning out.

10–113 Water is boiled at 100°C electrically by an 80-cm-long, 2-mm-diameter horizontal resistance wire made of chemically etched stainless steel. Determine (a) the rate of heat transfer to the water and the rate of evaporation of water if the temperature of the wire is 115°C and (b) the maximum rate of evaporation in the nucleate boiling regime. *Answers:* (a) 2387 W, 3.81 kg/h, (b) 1280 kW/m²
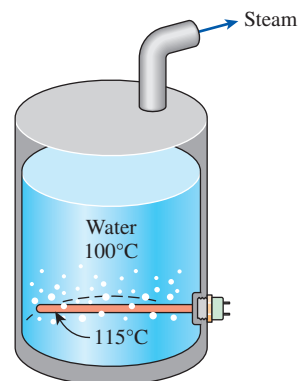
FIGURE P10–113

10–114 During a heat treatment process, a 20-mm-diameter cylindrical steel rod with a length of 200 mm was removed from a furnace when it reached a uniform temperature of

500°C and was suddenly submerged horizontally in a water bath at atmospheric pressure. If the steel rod has an emissivity of 0.9, determine the boiling heat transfer coefficient and the total heat transfer coefficient when it was initially submerged in the water bath.

10–115 Electric current is passed through a 2-mm-diameter cylindrical metal rod with emissivity of 0.5. The rod is submerged horizontally in water under atmospheric pressure, and the rod surface temperature reaches 500°C. Determine the boiling heat transfer coefficient and the total heat transfer coefficient.
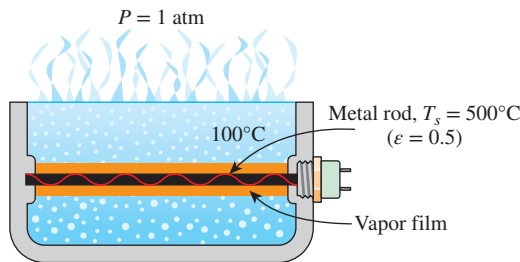
FIGURE P10–115

10–116 Water is boiled at 100°C by a spherical platinum heating element of diameter 8 cm and emissivity 0.10 immersed in the water. If the surface temperature of the heating element is 350°C, determine the convective boiling heat transfer coefficient.

10–117 In a heat treatment process, 20-mm-diameter steel ball bearings are being heated to a uniform temperature of 700°C. The ball bearings are then being removed and immediately submerged in a water bath at atmospheric pressure. If the steel ball bearings have an emissivity of 0.75, determine the boiling heat transfer coefficient and the total heat transfer coefficient when they were initially submerged in the water bath.

10–118E Saturated steam at 100°F is condensed on a 4-ft-high vertical plate that is maintained at 80°F. Determine the rate of heat transfer from the steam to the plate and the rate of condensation per foot width of the plate. Assume wavy-laminar flow. Is this a good assumption?

10–119 Saturated ammonia vapor at 25°C condenses on the outside of a 2-m-long, 3.2-cm-outer-diameter vertical tube maintained at 15°C. Determine (*a*) the average heat transfer coefficient, (*b*) the rate of heat transfer, and (*c*) the rate of condensation of ammonia. Assume turbulent flow and that the tube diameter is large, relative to the thickness of the liquid film at the bottom of the tube. Are these good assumptions?

10–120 Saturated refrigerant-134a vapor at 35°C is to be condensed on the outer surface of an 8-m-long, 1.2-cm-diameter horizontal tube that is maintained at a temperature of 25°C. Determine the rate at which the refrigerant will condense in kg/min.

10–121 Repeat Prob. 10–120 for a tube diameter of 3 cm.

10–122 Steam at 40°C condenses on the outside of a 3-cm-diameter thin horizontal copper tube by cooling water that enters the tube at 10°C at an average velocity of 2 m/s and leaves at 30°C. Determine the rate of condensation of steam, the average overall heat transfer coefficient between the steam and the cooling water, and the tube length.
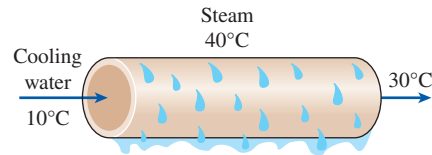
FIGURE P10–122

10–123 A 1.2-cm-diameter silver sphere initially at 25°C is suspended in a room filled with saturated steam at 100°C. Using the lumped system analysis, determine how long it will take for the temperature of the ball to rise to 50°C. Also determine the amount of steam that condenses during this process, and verify that the lumped system analysis is applicable.

10–124 Repeat Prob. 10–123 for a 3-cm-diameter copper ball.

10–125 Saturated isobutane vapor in a binary geothermal power plant is to be condensed outside an array of eight horizontal tubes. Determine the ratio of the condensation rate for the cases of the tubes being arranged in a horizontal tier versus in a vertical tier of horizontal tubes.

10–126E The condenser of a steam power plant operates at a pressure of 0.95 psia. The condenser consists of 100 horizontal tubes arranged in a 10×10 square array. The tubes are 15 ft long and have an outer diameter of 1.2 in. If the outer surfaces of the tubes are maintained at 80°F, determine (*a*) the rate of heat transfer from the steam to the cooling water and (*b*) the rate of condensation of steam in the condenser.

10–127E Repeat Prob. 10–126E for a tube diameter of 2 in.

10–128 Shown in Fig. P10–128 is the tube layout for a horizontal condenser that is used for liquefying 900 kg/h of saturated ammonia vapor at 37°C. There are 14 copper tubes, each with inner diameter $D_i = 3.0$ cm and outer diameter $D_o = 3.8$ cm. A coolant flows through the tubes at an average temperature of 20°C such that it yields a heat transfer coefficient of 4.0 kW/m²·K. For this condenser, estimate (*a*) the average value of the overall heat transfer coefficient and (*b*) the tube length. Assume a tube outer surface temperature of 31°C. Is this a good assumption?
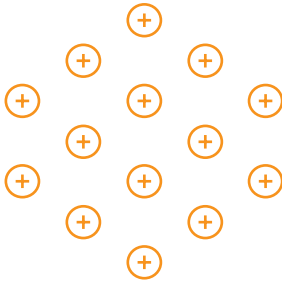
FIGURE P10–128

10–129 Saturated ammonia vapor at 25°C condenses on the outside surface of 16 thin-walled tubes, 2.5 cm in diameter, arranged horizontally in a 4×4 square array. Cooling water enters the tubes at 14°C at an average velocity of 2 m/s and exits at 17°C. Calculate (*a*) the rate of NH_3 condensation, (*b*) the overall heat transfer coefficient, and (*c*) the tube length.

10–130 Saturated steam at 270.1 kPa condenses inside a horizontal, 10-m-long, 2.5-cm-internal-diameter pipe whose surface is maintained at 110°C. Assuming low vapor velocity, determine the average heat transfer coefficient and the rate of condensation of the steam inside the pipe. *Answers: 8413 W/m²·K, 0.0608 kg/s*

Fundamentals of Engineering (FE) Exam Problems

10–131 When boiling a saturated liquid, one must be careful while increasing the heat flux to avoid burnout. Burnout occurs when the boiling transitions from _____ boiling.

(*a*) convection to nucleate   (*b*) convection to film
(*c*) film to nucleate   (*d*) nucleate to film
(*e*) none of them

10–132 Heat transfer coefficients for a vapor condensing on a surface can be increased by promoting

(*a*) film condensation   (*b*) dropwise condensation
(*c*) rolling action   (*d*) none of them

10–133 At a distance *x* down a vertical, isothermal flat plate on which a saturated vapor is condensing in a continuous film, the thickness of the liquid condensate layer is δ. The heat transfer coefficient at this location on the plate is given by

(*a*) k_l/δ (*b*) δh_f
(*c*) δh_{fg} (*d*) δh_g
(*e*) none of them

10–134 When a saturated vapor condenses on a vertical, isothermal flat plate in a continuous film, the rate of heat transfer is proportional to

(*a*) $(T_s - T_{sat})^{1/4}$ (*b*) $(T_s - T_{sat})^{1/2}$
(*c*) $(T_s - T_{sat})^{3/4}$ (*d*) $(T_s - T_{sat})$
(*e*) $(T_s - T_{sat})^{2/3}$

10–135 Saturated water vapor is condensing on a 0.5 m² vertical flat plate in a continuous film with an average heat transfer coefficient of 5 kW/m²·K. The temperature of the water is 80°C $(h_{fg} = 2309$ kJ/kg), and the temperature of the plate is 60°C. The rate at which condensate is being formed is

(*a*) 0.022 kg/s   (*b*) 0.048 kg/s   (*c*) 0.077 kg/s
(*d*) 0.16 kg/s   (*e*) 0.32 kg/s

10–136 Steam condenses at 50°C on a 1.2-m-high and 2.4-m-wide vertical plate that is maintained at 30°C. The condensation heat transfer coefficient is

(*a*) 4260 W/m²·K   (*b*) 4780 W/m²·K
(*c*) 5510 W/m²·K   (*d*) 6260 W/m²·K
(*e*) 6940 W/m²·K

(For water, use $\rho_l = 992.1$ kg/m³, $\mu_l = 0.653 \times 10^{-3}$ kg/m·s, $k_l = 0.631$ W/m·K, $c_{pl} = 4179$ J/kg·°C, $h_{fg@T_{sat}} = 2383$ kJ/kg)

10–137 An air conditioner condenser in an automobile consists of 2 m² of tubular heat exchange area whose surface temperature is 30°C. Saturated refrigerant-134a vapor at 50°C $(h_{fg} = 152$ kJ/kg) condenses on these tubes. What heat transfer coefficient must exist between the tube surface and condensing vapor to produce 1.5 kg/min of condensate?

(*a*) 95 W/m²·K   (*b*) 640 W/m²·K
(*c*) 727 W/m²·K   (*d*) 799 W/m²·K
(*e*) 960 W/m²·K

10–138 Saturated water vapor at 40°C is to be condensed as it flows through a tube at a rate of 0.2 kg/s. The condensate leaves the tube as a saturated liquid at 40°C. The rate of heat transfer from the tube is

(*a*) 34 kJ/s   (*b*) 268 kJ/s
(*c*) 453 kJ/s   (*d*) 481 kJ/s
(*e*) 515 kJ/s

10–139 Steam condenses at 50°C on the outer surface of a horizontal tube with an outer diameter of 6 cm. The outer surface of the tube is maintained at 30°C. The condensation heat transfer coefficient is

(*a*) 5493 W/m²·K   (*b*) 5921 W/m²·K
(*c*) 6796 W/m²·K   (*d*) 7040 W/m²·K
(*e*) 7350 W/m²·K

(For water, use $\rho_l = 992.1$ kg/m³, $\mu_l = 0.653 \times 10^{-3}$ kg/m·s, $k_l = 0.631$ W/m·K, $c_{pl} = 4179$ J/kg·°C, $h_{fg@T_{sat}} = 2383$ kJ/kg)

10–140 Steam condenses at 50°C on the tube bank consisting of 20 tubes arranged in a rectangular array of 4 tubes high and 5 tubes wide. Each tube has a diameter of 3 cm and a length of 5 m, and the outer surfaces of the tubes are maintained at 30°C. The rate of condensation of steam is

(*a*) 0.12 kg/s   (*b*) 0.28 kg/s
(*c*) 0.31 kg/s   (*d*) 0.45 kg/s
(*e*) 0.62 kg/s

(For water, use $\rho_l = 992.1$ kg/m³, $\mu_l = 0.653 \times 10^{-3}$ kg/m·s, $k_l = 0.631$ W/m·K, $c_{pl} = 4179$ J/kg·°C, $h_{fg@T_{sat}} = 2383$ kJ/kg)

Design and Essay Problems

10–141 Design the condenser of a steam power plant that has a thermal efficiency of 40 percent and generates 10 MW of net electric power. Steam enters the condenser as saturated vapor at 10 kPa, and it is to be condensed outside horizontal tubes through which cooling water from a nearby river flows. The temperature rise of the cooling water is limited to 8°C, and the velocity of the cooling water in the pipes is limited to 6 m/s to keep the pressure drop at an acceptable level. Specify the pipe diameter, the total pipe length, and the arrangement of the pipes to minimize the condenser volume.

10–142 The refrigerant in a household refrigerator is condensed as it flows through the coil that is typically placed behind the refrigerator. Heat transfer from the outer surface of the coil to the surroundings is by natural convection and radiation. Obtaining information about the operating conditions of the refrigerator, including the pressures and temperatures of the refrigerant at the inlet and the exit of the coil, show that the coil is selected properly, and determine the safety margin in the selection.

10–143 Water-cooled steam condensers are commonly used in steam power plants. Obtain information about water-cooled steam condensers by doing a literature search on the topic and also by contacting some condenser manufacturers. In a report, describe the various types, the way they are designed, the limitation on each type, and the selection criteria.

10–144 A manufacturing facility requires saturated steam at 120°C at a rate of 1.2 kg/min. Design an electric steam boiler for this purpose under these constraints:

- The boiler will be cylindrical with a height-to-diameter ratio of 1.5. The boiler can be horizontal or vertical.

- The boiler will operate in the nucleate boiling regime, and the design heat flux will not exceed 60 percent of the critical heat flux to provide an adequate safety margin.
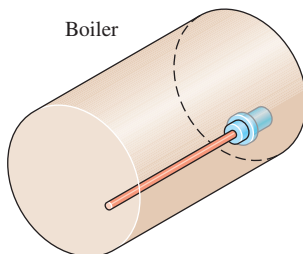
- A commercially available plug-in-type electrical heating element made of mechanically polished stainless steel will be used. The diameter of the heater cannot be between 0.5 cm and 3 cm.

- Half of the volume of the boiler should be occupied by steam, and the boiler should be large enough to hold enough water for a 2-h supply of steam. Also, the boiler will be well insulated.

You are to specify the following: (*a*) The height and inner diameter of the tank, (*b*) the length, diameter, power rating, and surface temperature of the electric heating element, (*c*) the maximum rate of steam production during short periods of overload conditions, and how it can be accomplished.

10–145 Repeat Prob. 10–144 for a boiler that produces steam at 150°C at a rate of 2.5 kg/min.

10–146 Conduct this experiment to determine the boiling heat transfer coefficient. You will need a portable immersion-type electric heating element, an indoor-outdoor thermometer, and metal glue (all can be purchased for about $15 in a hardware store). You will also need a piece of string and a ruler to calculate the surface area of the heater. First, boil water in a pan using the heating element and measure the temperature of the boiling water away from the heating element. Based on your reading, estimate the elevation of your location, and compare it to the actual value. Then glue the tip of the thermocouple wire of the thermometer to the midsection of the heater surface. The temperature reading in this case will give the surface temperature of the heater. Assuming the rated power of the heater to be the actual power consumption during heating (you can check this by measuring the electric current and voltage), calculate the heat transfer coefficients from Newton's law of cooling.
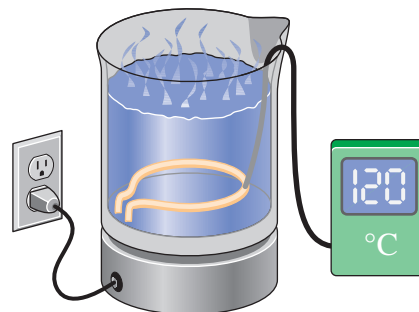
FIGURE P10–144

FIGURE P10–146

HEAT EXCHANGERS

Heat exchangers are devices that facilitate the *exchange of heat* between two fluids that are at different temperatures while keeping them from mixing with each other. Heat exchangers are commonly used in practice in a wide range of applications, from heating and air-conditioning systems in a household to chemical processing and power production in large plants. Heat exchangers differ from mixing chambers in that they do not allow the two fluids involved to mix.

Heat transfer in a heat exchanger usually involves *convection* in each fluid and *conduction* through the wall separating the two fluids. In the analysis of heat exchangers, it is convenient to work with an *overall heat transfer coefficient U* that accounts for the contribution of all these effects on heat transfer. The rate of heat transfer between the two fluids at a location in a heat exchanger depends on the magnitude of the temperature difference at that location, which varies along the heat exchanger.

Heat exchangers are manufactured in a variety of types, and thus we start this chapter with the *classification* of heat exchangers. We then discuss the determination of the overall heat transfer coefficient in heat exchangers, and the *log mean temperature difference* (LMTD) for some configurations. We then introduce the *correction factor F* to account for the deviation of the mean temperature difference from the LMTD in complex configurations. Next we discuss the effectiveness–NTU method, which enables us to analyze heat exchangers when the outlet temperatures of the fluids are not known. Finally, we discuss the selection of heat exchangers.

OBJECTIVES

When you finish studying this chapter, you should be able to:

- Recognize numerous types of heat exchangers, and classify them,
- Develop an awareness of fouling on surfaces, and determine the overall heat transfer coefficient for a heat exchanger,
- Perform a general energy analysis on heat exchangers,
- Obtain a relation for the logarithmic mean temperature difference for use in the LMTD method, and modify it for different types of heat exchangers using the correction factor,
- Develop relations for effectiveness, and analyze heat exchangers when outlet temperatures are not known using the effectiveness-NTU method,
- Know the primary considerations in the selection of heat exchangers.

11–1 ▪ TYPES OF HEAT EXCHANGERS

Different heat transfer applications require different types of hardware and different configurations of heat transfer equipment. The attempt to match the heat transfer hardware to the heat transfer requirements within the specified constraints has resulted in numerous types of innovative heat exchanger designs.

The simplest type of heat exchanger consists of two concentric pipes of different diameters, as shown in Fig. 11–1, called the **double-pipe** heat exchanger. One fluid in a double-pipe heat exchanger flows through the smaller pipe, while the other fluid flows through the annular space between the two pipes. Two types of flow arrangement are possible in a double-pipe heat exchanger: in **parallel flow**, both the hot and cold fluids enter the heat exchanger at the same end and move in the *same* direction. In **counterflow**, on the other hand, the hot and cold fluids enter the heat exchanger at opposite ends and flow in *opposite* directions.

Another type of heat exchanger, which is specifically designed to realize a large heat transfer surface area per unit volume, is the **compact** heat exchanger. The ratio of the heat transfer surface area of a heat exchanger to its volume is called the *area density* β. A heat exchanger with $\beta > 700 \text{ m}^2/\text{m}^3$ (or $200 \text{ ft}^2/\text{ft}^3$) is classified as being compact. Examples of compact heat exchangers are car radiators ($\beta \approx 1000 \text{ m}^2/\text{m}^3$), glass-ceramic gas turbine heat exchangers ($\beta \approx 6000 \text{ m}^2/\text{m}^3$), the regenerator of a Stirling engine ($\beta \approx 15{,}000 \text{ m}^2/\text{m}^3$), and the human lung ($\beta \approx 20{,}000 \text{ m}^2/\text{m}^3$). The flow passages in these compact heat exchangers are usually small, and the flow can be considered to be laminar. Compact heat exchangers enable us to achieve high heat transfer rates between
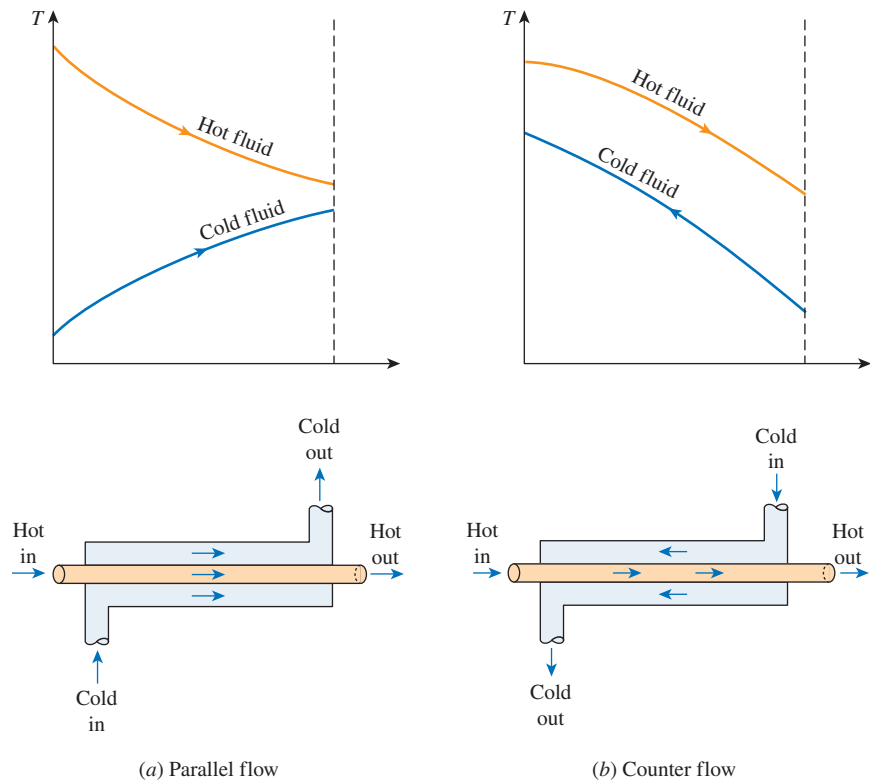
FIGURE 11–1
Different flow regimes and associated temperature profiles in a double-pipe heat exchanger.

(*a*) Parallel flow

(*b*) Counter flow

two fluids in a small volume, and they are commonly used in applications with strict limitations on the weight and volume of heat exchangers (Fig. 11–2).

The large surface area in compact heat exchangers is obtained by attaching closely spaced *thin plate* or *corrugated fins* to the walls separating the two fluids. Compact heat exchangers are commonly used in gas-to-gas and gas-to-liquid (or liquid-to-gas) heat exchangers to counteract the low heat transfer coefficient associated with gas flow with increased surface area. In a car radiator, which is a water-to-air compact heat exchanger, for example, it is no surprise that fins are attached to the air side of the tube surface.

Another example of compact heat exchangers widely used today in industrial applications such as chemical processing, fuel processing, waste heat recovery, and refrigeration is the **printed circuit heat exchanger** referred to as PCHE (Fig. 11–3). PCHE derives its name from the manufacturing process in which the flat metal plates that form the core of this heat exchanger are chemically etched to a depth of 1 to 3 mm. The chemically etched plates are then stacked together and joined by diffusion bonding. There may be different etching patterns on the plates to make the heat exchanger as a parallel, counter, or crossflow heat exchanger. Furthermore, Li et al. (2011) reported that unlike conventional heat exchangers with straight flow channels, the flow channels in PCHE can be made in zigzag, S-shape, or aero foil shape in order to induce flow turbulence and hence enhance the heat transfer coefficient. PCHEs have high surface density typically greater than 2500 m^2/m^3. The PCHEs are usually made from stainless steel, titanium, copper, nickel, and nickel alloys and can withstand operating pressures up to 500 bar. The major advantages of printed circuit heat exchangers are their wide operating temperature range, which is from $-250°C$ to $900°C$, very high heat transfer coefficients, and their size, which is about four to six times smaller and lighter than conventional heat exchangers. One of the major disadvantages of using PCHEs is very high pressure drop and that they require very clean fluid to be passed through them, otherwise blockages can occur easily in the fine channel spacing (0.5 to 2 mm).

In compact heat exchangers, the two fluids usually move *perpendicular* to each other, and such flow configuration is called **crossflow**. The crossflow is further classified as *unmixed* and *mixed flow,* depending on the flow configuration, as shown in Fig. 11–4. In (*a*) the crossflow is said to be *unmixed* since
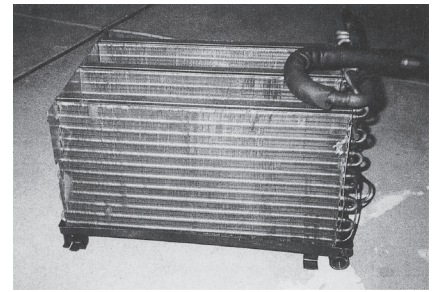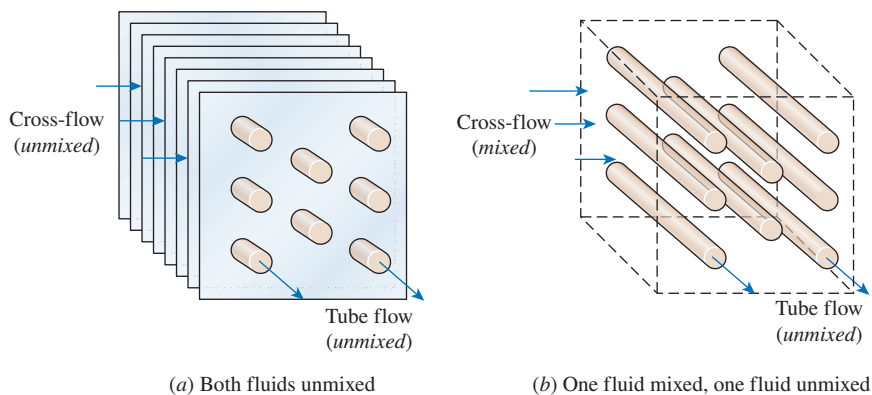
FIGURE 11–2
A gas-to-liquid compact heat exchanger for a residential air-conditioning system.
©Yunus A. Cengel
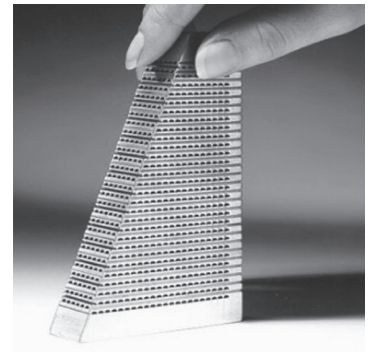
FIGURE 11–3
Photograph of a 'Core' section from a printed circuit heat exchanger (Heatric, a Meggitt Company, Dorset, UK).
©Heatric, a Meggitt Company, Dorset UK

Cross-flow
(*unmixed*)

Tube flow
(*unmixed*)

(*a*) Both fluids unmixed

Cross-flow
(*mixed*)

Tube flow
(*unmixed*)

(*b*) One fluid mixed, one fluid unmixed

FIGURE 11–4
Different flow configurations in cross-flow heat exchangers.
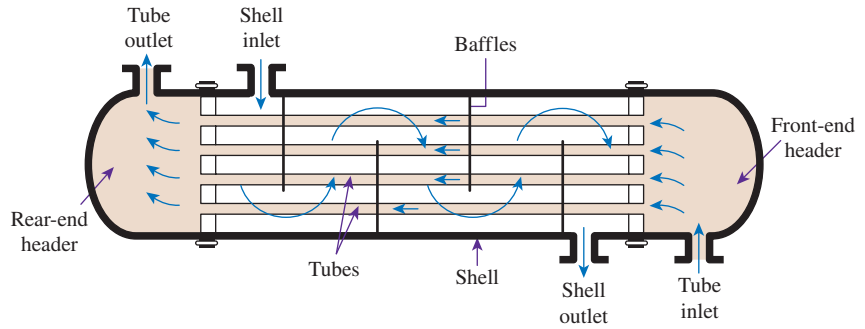
FIGURE 11–5
The schematic of a shell-and-tube heat exchanger (one-shell pass and one-tube pass).

the plate fins force the fluid to flow through a particular interfin spacing and prevent it from moving in the transverse direction (i.e., parallel to the tubes). The crossflow in (*b*) is said to be *mixed* since the fluid now is free to move in the transverse direction. Both fluids are unmixed in a car radiator. The presence of mixing in the fluid can have a significant effect on the heat transfer characteristics of the heat exchanger.

Perhaps the most common type of heat exchanger in industrial applications is the **shell-and-tube** heat exchanger, shown in Fig. 11–5. Shell-and-tube heat exchangers contain a large number of tubes (sometimes several hundred) packed in a shell with their axes parallel to that of the shell. Heat transfer takes place as one fluid flows inside the tubes while the other fluid flows outside the tubes through the shell. *Baffles* are commonly placed in the shell to force the shell-side fluid to flow across the shell to enhance heat transfer and to maintain uniform spacing between the tubes. Despite their widespread use, shell-and-tube heat exchangers are not suitable for use in automotive and aircraft applications because of their relatively large size and weight. Note that the tubes in a shell-and-tube heat exchanger open to some large flow areas called *headers* at both ends of the shell, where the tube-side fluid accumulates before entering the tubes and after leaving them.

Shell-and-tube heat exchangers are further classified according to the number of shell and tube passes involved. Heat exchangers in which all the tubes make one U-turn in the shell, for example, are called *one-shell-pass and two-tube-passes* heat exchangers. Likewise, a heat exchanger that involves two passes in the shell and four passes in the tubes is called a *two-shell-passes and four-tube-passes* heat exchanger (Fig. 11–6).

An innovative type of heat exchanger that has found widespread use is the **plate-and-frame** (or just plate) heat exchanger, which consists of a series of plates with corrugated flat flow passages (Fig. 11–7). The hot and cold fluids flow in alternate passages, and thus each cold fluid stream is surrounded by two hot fluid streams, resulting in very effective heat transfer. Also, plate heat exchangers can grow with increasing demand for heat transfer by simply mounting more plates. They are well suited for liquid-to-liquid heat exchange applications, provided that the hot and cold fluid streams are at about the same pressure.

Another type of heat exchanger that involves the alternate passage of the hot and cold fluid streams through the same flow area is the **regenerative** heat

(*a*) One-shell pass and two-tube passes

(*b*) Two-shell passes and four-tube passes
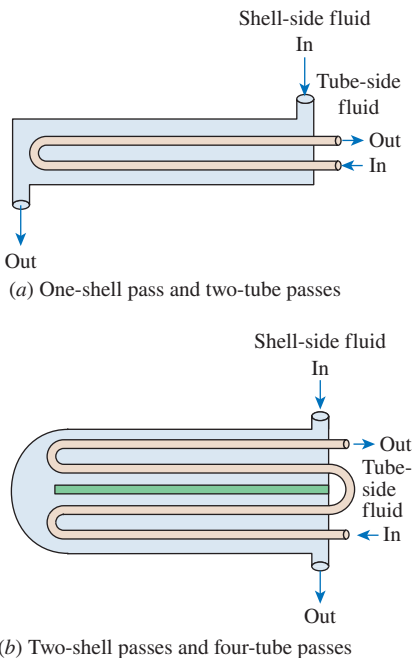
FIGURE 11–6
Multipass flow arrangements in shell-and-tube heat exchangers.
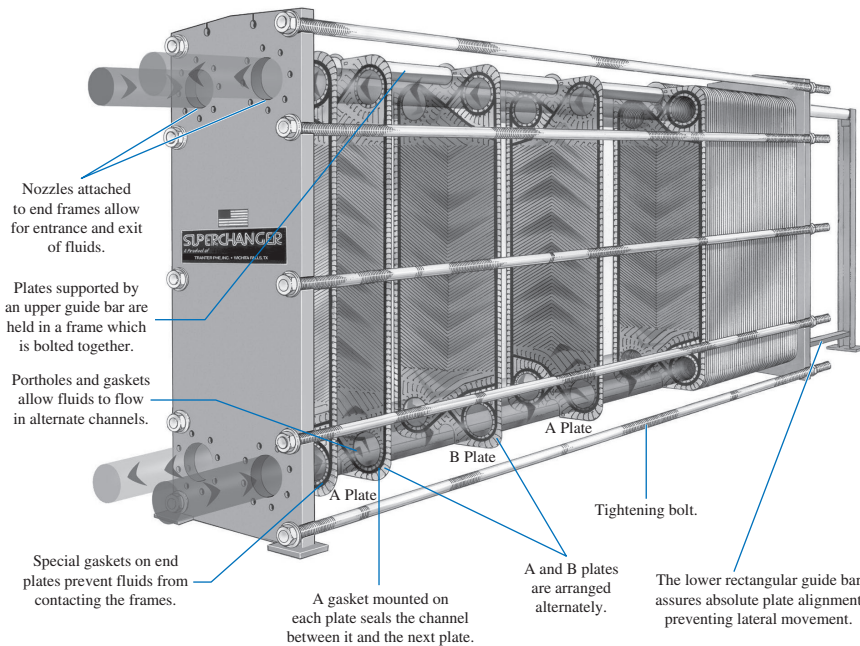
FIGURE 11–7
A plate-and-frame liquid-to-liquid heat exchanger.

exchanger. The *static*-type regenerative heat exchanger is basically a porous mass that has a large heat storage capacity, such as a ceramic wire mesh. Hot and cold fluids flow through this porous mass alternately. Heat is transferred from the hot fluid to the matrix of the regenerator during the flow of the hot fluid, and from the matrix to the cold fluid during the flow of the cold fluid. Thus, the matrix serves as a temporary heat storage medium.

The *dynamic*-type regenerator involves a rotating drum and continuous flow of the hot and cold fluid through different portions of the drum so that any portion of the drum passes periodically through the hot stream, storing heat, and then through the cold stream, rejecting this stored heat. Again the drum serves as the medium to transport the heat from the hot to the cold fluid stream.

Heat exchangers are often given specific names to reflect the specific application for which they are used. For example, a *condenser* is a heat exchanger in which one of the fluids is cooled and condenses as it flows through the heat exchanger. A *boiler* is another heat exchanger in which one of the fluids absorbs heat and vaporizes. A *space radiator* is a heat exchanger that transfers heat from the hot fluid to the surrounding space by radiation.

11–2 • THE OVERALL HEAT TRANSFER COEFFICIENT

A heat exchanger typically involves two flowing fluids separated by a solid wall. Heat is first transferred from the hot fluid to the wall by *convection,* through the wall by *conduction,* and from the wall to the cold fluid again by *convection.* Any radiation effects are usually included in the convection heat transfer coefficients.
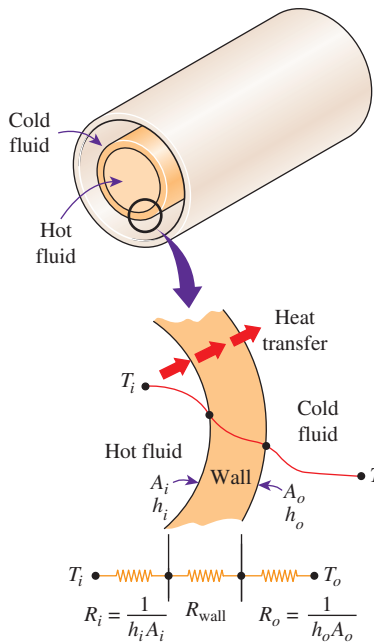
FIGURE 11–8
Thermal resistance network associated with heat transfer in a double-pipe heat exchanger.
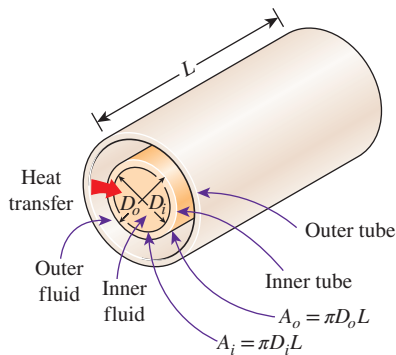
FIGURE 11–9
The two heat transfer surface areas associated with a double-pipe heat exchanger (for thin tubes, $D_i \approx D_o$ and thus $A_i \approx A_o$).

The thermal resistance network associated with this heat transfer process involves two convection resistances and one conduction resistance, as shown in Fig. 11–8. The analysis is very similar to the material presented in Chap. 3. Here the subscripts i and o represent the inner and outer surfaces of the inner tube. For a double-pipe heat exchanger, the *thermal resistance* of the tube wall is (also see Eq. 3–39)

$$R_{\text{wall}} = \frac{\ln(D_o/D_i)}{2\pi k L} \tag{11–1}$$

where k is the thermal conductivity of the wall material and L is the length of the tube. Then the *total thermal resistance* becomes (also see Eq. 3–43)

$$R = R_{\text{total}} = R_i + R_{\text{wall}} + R_o = \frac{1}{h_i A_i} + \frac{\ln(D_o/D_i)}{2\pi k L} + \frac{1}{h_o A_o} \tag{11–2}$$

The A_i is the area of the inner surface of the wall that separates the two fluids, and A_o is the area of the outer surface of the wall. In other words, A_i and A_o are surface areas of the separating wall wetted by the inner and the outer fluids, respectively. When one fluid flows inside a circular tube and the other outside of it, we have $A_i = \pi D_i L$ and $A_o = \pi D_o L$ (Fig. 11–9).

In the analysis of heat exchangers, it is convenient to combine all the thermal resistances in the path of heat flow from the hot fluid to the cold one into a single resistance R, and to express the rate of heat transfer between the two fluids as

$$\dot{Q} = \frac{\Delta T}{R} = U A_s \Delta T = U_i A_i \Delta T = U_o A_o \Delta T \tag{11–3}$$

where A_s is the surface area and U is the **overall heat transfer coefficient**, whose unit is W/m²·K, which is identical to the unit of the ordinary convection coefficient h. Canceling ΔT, Eq. 11–3 reduces to

$$\frac{1}{U A_s} = \frac{1}{U_i A_i} = \frac{1}{U_o A_o} = R = \frac{1}{h_i A_i} + R_{\text{wall}} + \frac{1}{h_o A_o} \tag{11–4}$$

Perhaps you are wondering why we have two overall heat transfer coefficients U_i and U_o for a heat exchanger. The reason is that every heat exchanger has two heat transfer surface areas A_i and A_o, which, in general, are not equal to each other.

Note that $U_i A_i = U_o A_o$, but $U_i \neq U_o$ unless $A_i = A_o$. Therefore, the overall heat transfer coefficient U of a heat exchanger is meaningless unless the area on which it is based is specified. This is especially the case when one side of the tube wall is finned and the other side is not, since the surface area of the finned side is several times that of the unfinned side.

When the wall thickness of the tube is small and the thermal conductivity of the tube material is high, as is usually the case, the thermal resistance of the tube is negligible ($R_{\text{wall}} \approx 0$) and the inner and outer surfaces of the tube are almost identical ($A_i \approx A_o \approx A_s$). Then Eq. 11–4 for the overall heat transfer coefficient simplifies to

$$\frac{1}{U} \approx \frac{1}{h_i} + \frac{1}{h_o} \tag{11–5}$$

https://ebook2book.ir/

where $U \approx U_i \approx U_o$. The individual convection heat transfer coefficients inside and outside the tube, h_i and h_o, are determined using the convection relations discussed in Chaps. 8 and 7 for internal and external forced convection flows, respectively.

The overall heat transfer coefficient U in Eq. 11–5 is dominated by the *smaller* convection coefficient, since the inverse of a large number is small. When one of the convection coefficients is *much smaller* than the other (say, $h_i \ll h_o$), we have $1/h_i \gg 1/h_o$, and thus $U \approx h_i$. Therefore, the smaller heat transfer coefficient creates a *bottleneck* on the path of heat transfer and seriously impedes heat transfer. This situation arises frequently when one of the fluids is a gas and the other is a liquid. In such cases, fins are commonly used on the gas side to enhance the product UA and thus the heat transfer on that side.

Representative values of the overall heat transfer coefficient U are given in Table 11–1. Note that the overall heat transfer coefficient ranges from about 10 W/m²·K for gas-to-gas heat exchangers to about 10,000 W/m²·K for heat exchangers that involve phase changes. This is not surprising, since gases have very low thermal conductivities, and phase-change processes involve very high heat transfer coefficients.

When the tube is *finned* on one side to enhance heat transfer, the total heat transfer surface area on the finned side becomes

$$A_s = A_{\text{total}} = A_{\text{fin}} + A_{\text{unfinned}} \tag{11–6}$$

TABLE 11–1

Representative values of the overall heat transfer coefficients in heat exchangers

Type of Heat Exchanger	U, W/m²·K*
Water-to-water	850–1700
Water-to-oil	100–350
Water-to-gasoline or kerosene	300–1000
Water-to-brine	600–1200
Feedwater heaters	1000–8500
Steam-to-light fuel oil	200–400
Steam-to-heavy fuel oil	50–200
Steam condenser	1000–6000
Freon condenser (water cooled)	300–1000
Ammonia condenser (water cooled)	800–1400
Alcohol condensers (water cooled)	250–700
Gas-to-gas	10–40
Gas-to-brine	10–250
Oil-to-oil	50–400
Organic vapors-to-water	700–1000
Organic solvents-to-organic solvents	100–300
Water-to-air in finned tubes (water in tubes)	30–60[†]
	400–850[‡]
Steam-to-air in finned tubes (steam in tubes)	30–300[†]
	400–4000[‡]

*Multiply the listed values by 0.176 to convert them to Btu/h·ft²·°F.
[†]Based on air-side surface area.
[‡]Based on water- or steam-side surface area.

https://ebook2book.ir/

where A_{fin} is the surface area of the fins and $A_{unfinned}$ is the area of the unfinned portion of the tube surface. For short fins of high thermal conductivity, we can use this total area in the convection resistance relation $R_{conv} = 1/hA_s$ since the fins in this case will be very nearly isothermal. Otherwise, we should determine the effective surface area from

$$A_s = A_{unfinned} + \eta_{fin}A_{fin} \tag{11-7}$$

where η_{fin} is the fin efficiency, which can be obtained from the relationships discussed in Chap. 3. This way, the temperature drop along the fins is accounted for. Note that $\eta_{fin} = 1$ for isothermal fins, and thus Eq. 11–7 reduces to Eq. 11–6 in that case. Note that for the finned surface, the relevant area (A_i or A_o) in Eq. 11–4 should be calculated from Eq. 11–7.

Fouling Factor

The performance of heat exchangers usually deteriorates with time as a result of accumulation of *deposits* on heat transfer surfaces. The layer of deposits represents *additional resistance* to heat transfer and causes the rate of heat transfer in a heat exchanger to decrease. The net effect of these accumulations on heat transfer is represented by a **fouling factor** R_f, which is a measure of the *thermal resistance* introduced by fouling.

The most common type of fouling is the *precipitation* of solid deposits in a fluid on the heat transfer surfaces. You can observe this type of fouling even in your house. If you check the inner surfaces of your teapot after prolonged use, you will probably notice a layer of calcium-based deposits on the surfaces at which boiling occurs. This is especially the case in areas where the water is hard. The scales of such deposits come off by scratching, and the surfaces can be cleaned of such deposits by chemical treatment. Now imagine those mineral deposits forming on the inner surfaces of fine tubes in a heat exchanger (Fig. 11–10) and the detrimental effect it may have on the flow passage area and the heat transfer. To avoid this potential problem, water in power and process plants is extensively treated, and its solid contents are removed before it is allowed to circulate through the system. The solid ash particles in the flue gases accumulating on the surfaces of air preheaters create similar problems.

Another form of fouling, which is common in the chemical process industry, is *corrosion* and other *chemical fouling*. In this case, the surfaces are fouled by the accumulation of the products of chemical reactions on the surfaces. This form of fouling can be avoided by coating metal pipes with glass or using plastic pipes instead of metal ones. Heat exchangers may also be fouled by the growth of algae in warm fluids. This type of fouling is called *biological fouling* and can be prevented by chemical treatment.

In applications where it is likely to occur, fouling should be considered in the design and selection of heat exchangers. In such applications, it may be necessary to select a larger and thus more expensive heat exchanger to ensure that it meets the design heat transfer requirements even after fouling occurs. The periodic cleaning of heat exchangers and the resulting downtime are additional penalties associated with fouling.

FIGURE 11–10
Precipitation fouling of ash particles on superheater tubes.

©From Steam: Its Generation, and Use, Babcock and Wilcox Co., 1978. Reprinted by permission.

The fouling factor is obviously zero for a new heat exchanger and increases with time as the solid deposits build up on the heat exchanger surface. The fouling factor depends on the *operating temperature* and the *velocity* of the fluids, as well as the length of service. Fouling increases with *increasing temperature* and *decreasing velocity*.

The overall heat transfer coefficient relation Eq. 11–4 or 11–5 for an unfinned double-pipe heat exchanger is valid for clean surfaces and needs to be modified to account for the effects of fouling on both the inner and the outer surfaces of the tube. For an unfinned double-pipe heat exchanger, it can be expressed as

$$\frac{1}{UA_s} = \frac{1}{U_i A_i} = \frac{1}{U_o A_o} = R = \frac{1}{h_i A_i} + \frac{R_{f,i}}{A_i} + \frac{\ln(D_o/D_i)}{2\pi kL} + \frac{R_{f,o}}{A_o} + \frac{1}{h_o A_o} \tag{11–8}$$

where $R_{f,i}$ and $R_{f,o}$ are the fouling factors at those surfaces.

Representative values of fouling factors are given in Table 11–2. More comprehensive tables of fouling factors are available in handbooks. As you would expect, considerable uncertainty exists in these values, and they should be used as a guide in the selection and evaluation of heat exchangers to account for the effects of anticipated fouling on heat transfer. Note that most fouling factors in the table are of the order of 10^{-4} m^2·K/W, which is equivalent to the thermal resistance of a 0.2-mm-thick limestone layer ($k = 2.9$ W/m·K) per unit surface area. Therefore, in the absence of specific data, we can assume the surfaces to be coated with 0.2 mm of limestone as a starting point to account for the effects of fouling.

TABLE 11–2

Representative fouling factors (thermal resistance due to fouling for a unit surface area)

Fluid	R_f, m^2·K/W
Distilled water, seawater, river water, boiler feedwater:	
Below 50°C	0.0001
Above 50°C	0.0002
Fuel oil	0.0009
Transformer, lubricating or hydraulic oil	0.0002
Quenching oil	0.0007
Vegetable oil	0.0005
Steam (oil-free)	0.0001
Steam (with oil traces)	0.0002
Organic solvent vapors, natural gas	0.0002
Engine exhaust and fuel gases	0.0018
Refrigerants (liquid)	0.0002
Refrigerants (vapor)	0.0004
Ethylene and methylene glycol (antifreeze) and amine solutions	0.00035
Alcohol vapors	0.0001
Air	0.0004

Source: Tubular Exchange Manufacturers Association.

EXAMPLE 11–1 Overall Heat Transfer Coefficient of a Heat Exchanger

Hot oil is to be cooled in a double-tube counterflow heat exchanger. The copper inner tubes have a diameter of 2 cm and negligible thickness. The inner diameter of the outer tube (the shell) is 3 cm. Water flows through the tube at a rate of 0.5 kg/s, and the oil flows through the shell at a rate of 0.8 kg/s. Taking the average temperatures of the water and the oil to be 45°C and 80°C, respectively, determine the overall heat transfer coefficient of this heat exchanger.

SOLUTION Hot oil is cooled by water in a double-tube counterflow heat exchanger. The overall heat transfer coefficient is to be determined.

Assumptions **1** The thermal resistance of the inner tube is negligible since the tube material is highly conductive and its thickness is negligible. **2** Both the oil and water flow are fully developed. **3** Properties of the oil and water are constant.

Properties The properties of water at 45°C are (Table A–9)

$$\rho = 990.1 \text{ kg/m}^3 \qquad \text{Pr} = 3.91$$
$$k = 0.637 \text{ W/m·K} \qquad \nu = \mu/\rho = 0.602 \times 10^{-6} \text{ m}^2/\text{s}$$

Hot oil
0.8 kg/s

Cold
water
→
↕2 cm   3 cm

0.5 kg/s
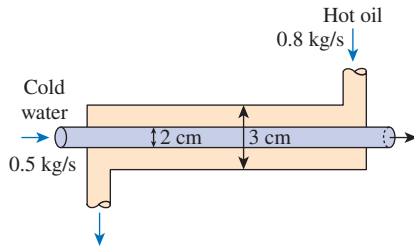
FIGURE 11–11
Schematic for Example 11–1.

The properties of oil at 80°C are (Table A–13)

$$\rho = 852 \text{ kg/m}^3 \qquad \text{Pr} = 499.3$$
$$k = 0.138 \text{ W/m·K} \qquad \nu = 3.794 \times 10^{-5} \text{ m}^2/\text{s}$$

Analysis The schematic of the heat exchanger is given in Fig. 11–11. The overall heat transfer coefficient U can be determined from Eq. 11–5:

$$\frac{1}{U} \approx \frac{1}{h_i} + \frac{1}{h_o}$$

where h_i and h_o are the convection heat transfer coefficients inside and outside the tube, respectively, which are to be determined using the forced convection relations.

The hydraulic diameter for a circular tube is the diameter of the tube itself, $D_h = D = 0.02$ m. The average velocity of water in the tube and the Reynolds number are

$$V = \frac{\dot{m}}{\rho A_c} = \frac{\dot{m}}{\rho(\frac{1}{4}\pi D^2)} = \frac{0.5 \text{ kg/s}}{(990.1 \text{ kg/m}^3)[\frac{1}{4}\pi(0.02 \text{ m})^2]} = 1.61 \text{ m/s}$$

and

$$\text{Re} = \frac{VD}{\nu} = \frac{(1.61 \text{ m/s})(0.02 \text{ m})}{0.602 \times 10^{-6} \text{ m}^2/\text{s}} = 53,490$$

which is greater than 10,000. Therefore, the flow of water is turbulent. Assuming the flow to be fully developed, the Nusselt number can be determined from

$$\text{Nu} = \frac{hD}{k} = 0.023 \text{ Re}^{0.8}\text{Pr}^{0.4} = 0.023(53,490)^{0.8}(3.91)^{0.4} = 240.6$$

Then,

$$h = \frac{k}{D}\text{Nu} = \frac{0.637 \text{ W/m·K}}{0.02 \text{ m}}(240.6) = 7663 \text{ W/m}^2\text{·K}$$

Now we repeat the analysis for oil.
The hydraulic diameter for the annular space is

$$D_h = D_o - D_i = 0.03 - 0.02 = 0.01 \text{ m}$$

The average velocity and the Reynolds number in this case are

$$V = \frac{\dot{m}}{\rho A_c} = \frac{\dot{m}}{\rho[\frac{1}{4}\pi(D_o^2 - D_i^2)]} = \frac{0.8 \text{ kg/s}}{(852 \text{ kg/m}^3)[\frac{1}{4}\pi(0.03^2 - 0.02^2)] \text{ m}^2} = 2.39 \text{ m/s}$$

and

$$\text{Re} = \frac{VD_h}{\nu} = \frac{(2.39 \text{ m/s})(0.01 \text{ m})}{3.794 \times 10^{-5} \text{ m}^2/\text{s}} = 630$$

which is less than 2300. Therefore, the flow of oil is laminar. Assuming fully developed flow, the Nusselt number on the tube side of the annular space

Nu_i corresponding to $D_i/D_o = 0.02/0.03 = 0.667$ can be determined from Table 11–3 by interpolation to be

$$Nu = 5.45$$

and

$$h_o = \frac{k}{D_h}Nu = \frac{0.138 \text{ W/m·K}}{0.01 \text{ m}}(5.45) = 75.2 \text{ W/m}^2\text{·K}$$

Then the overall heat transfer coefficient for this heat exchanger becomes

$$U = \frac{1}{\dfrac{1}{h_i} + \dfrac{1}{h_o}} = \frac{1}{\dfrac{1}{7663 \text{ W/m}^2\text{·K}} + \dfrac{1}{75.2 \text{ W/m}^2\text{·K}}} = \textbf{74.5 W/m}^2\textbf{·K}$$

Discussion Note that $U \approx h_o$ in this case, since $h_i \gg h_o$. This confirms our earlier statement that the overall heat transfer coefficient in a heat exchanger is dominated by the smaller heat transfer coefficient when the difference between the two values is large.

To improve the overall heat transfer coefficient and thus the heat transfer in this heat exchanger, we must use some enhancement techniques on the oil side, such as a finned surface.

TABLE 11–3

Nusselt number for fully developed laminar flow in a circular annulus with one surface insulated and the other isothermal

D_i/D_o	Nu_i	Nu_o
0.00	—	3.66
0.05	17.46	4.06
0.10	11.56	4.11
0.25	7.37	4.23
0.50	5.74	4.43
1.00	4.86	4.86

Kays and Perkins, 1972

EXAMPLE 11–2 **Effect of Fouling on the Overall Heat Transfer Coefficient**

A double-pipe (shell-and-tube) heat exchanger is constructed of a stainless steel ($k = 15.1$ W/m·K) inner tube of inner diameter $D_i = 1.5$ cm and outer diameter $D_o = 1.9$ cm and an outer shell of inner diameter 3.2 cm. The convection heat transfer coefficient is given to be $h_i = 800$ W/m²·K on the inner surface of the tube and $h_o = 1200$ W/m²·K on the outer surface. For a fouling factor of $R_{f,i} = 0.0004$ m²·K/W on the tube side and $R_{f,o} = 0.0001$ m²·K/W on the shell side, determine (*a*) the thermal resistance of the heat exchanger per unit length and (*b*) the overall heat transfer coefficients U_i and U_o based on the inner and outer surface areas of the tube, respectively.

SOLUTION The heat transfer coefficients and the fouling factors on the tube and shell sides of a heat exchanger are given. The thermal resistance and the overall heat transfer coefficients based on the inner and outer areas are to be determined.
Assumptions The heat transfer coefficients and the fouling factors are constant and uniform.
Analysis (*a*) The schematic of the heat exchanger is given in Fig. 11–12. The thermal resistance for an unfinned shell-and-tube heat exchanger with fouling on both heat transfer surfaces is given by Eq. 11–8 as

$$R = \frac{1}{UA_s} = \frac{1}{U_iA_i} = \frac{1}{U_oA_o} = \frac{1}{h_iA_i} + \frac{R_{f,i}}{A_i} + \frac{\ln(D_o/D_i)}{2\pi kL} + \frac{R_{f,o}}{A_o} + \frac{1}{h_oA_o}$$

Cold fluid
Outer layer of fouling
Tube wall
Hot fluid
Inner layer of fouling

Cold fluid

Hot fluid

$D_i = 1.5$ cm
$h_i = 800$ W/m²·K
$R_{f,i} = 0.0004$ m²·K/W

$D_o = 1.9$ cm
$h_o = 1200$ W/m²·K
$R_{f,o} = 0.0001$ m²·K/W
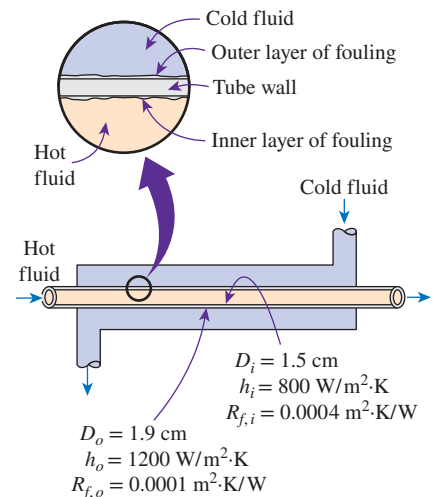
FIGURE 11–12
Schematic for Example 11–2.

where

$$A_i = \pi D_i L = \pi(0.015 \text{ m})(1 \text{ m}) = 0.0471 \text{ m}^2$$

$$A_o = \pi D_o L = \pi(0.019 \text{ m})(1 \text{ m}) = 0.0597 \text{ m}^2$$

Substituting, the total thermal resistance is determined to be

$$
R = \frac{1}{(800 \text{ W/m}^2 \cdot \text{K})(0.0471 \text{ m}^2)} + \frac{0.0004 \text{ m}^2 \cdot \text{K/W}}{0.0471 \text{ m}^2}
$$
$$
+ \frac{\ln(0.019/0.015)}{2\pi(15.1 \text{ W/m} \cdot \text{K})(1 \text{ m})}
$$
$$
+ \frac{0.0001 \text{ m}^2 \cdot \text{K/W}}{0.0597 \text{ m}^2} + \frac{1}{(1200 \text{ W/m}^2 \cdot \text{K})(0.0597 \text{ m}^2)}
$$
$$
= (0.02654 + 0.00849 + 0.0025 + 0.00168 + 0.01396)\text{K/W}
$$
$$
= \mathbf{0.0532°C/W}
$$

Note that about 19 percent of the total thermal resistance in this case is due to fouling and about 5 percent of it is due to the steel tube separating the two fluids. The rest (76 percent) is due to the convection resistances.

(*b*) Knowing the total thermal resistance and the heat transfer surface areas, the overall heat transfer coefficients based on the inner and outer surfaces of the tube are

$$U_i = \frac{1}{RA_i} = \frac{1}{(0.0532 \text{ K/W})(0.0471 \text{ m}^2)} = \mathbf{399 \ W/m^2 \cdot K}$$

and

$$U_o = \frac{1}{RA_o} = \frac{1}{(0.0532 \text{ K/W})(0.0597 \text{ m}^2)} = \mathbf{315 \ W/m^2 \cdot K}$$

Discussion   Note that the two overall heat transfer coefficients differ significantly (by 27 percent) in this case because of the considerable difference between the heat transfer surface areas on the inner and the outer sides of the tube. For tubes of negligible thickness, the difference between the two overall heat transfer coefficients would be negligible.

11–3 ▪ ANALYSIS OF HEAT EXCHANGERS

Heat exchangers are commonly used in practice, and an engineer often finds himself or herself in a position to *select a heat exchanger* that will achieve a *specified temperature change* in a fluid stream of known mass flow rate, or to *predict the outlet temperatures* of the hot and cold fluid streams in a *specified heat exchanger.*

In upcoming sections, we discuss the two methods used in the analysis of heat exchangers. Of these, the *log mean temperature difference* (or LMTD) method is best suited for the first task and the *effectiveness*–NTU (the number of transfer units) method for the second task. But first we present some general considerations.

Heat exchangers usually operate for long periods of time with no change in their operating conditions. Therefore, they can be modeled as *steady-flow* devices. As such, the mass flow rate of each fluid remains constant, and the fluid properties such as temperature and velocity at any inlet or outlet remain the same. Also, the fluid streams experience little or no change in their velocities and elevations, and thus the kinetic and potential energy changes are negligible. The specific heat of a fluid, in general, changes with temperature. But in a specified temperature range, it can be treated as a constant at some average value with little loss in accuracy. Axial heat conduction along the tube is usually insignificant and can be considered negligible. Finally, the outer surface of the heat exchanger is assumed to be *perfectly insulated,* so that there is no heat loss to the surrounding medium, and any heat transfer occurs between the two fluids only.

The idealizations stated above are closely approximated in practice, and they greatly simplify the analysis of a heat exchanger with little sacrifice in accuracy. Therefore, they are commonly used. Under these assumptions, the *first law of thermodynamics* requires that the rate of heat transfer from the hot fluid be equal to the rate of heat transfer to the cold one. That is,

$$\dot{Q} = \dot{m}_c c_{pc}(T_{c,\,\text{out}} - T_{c,\,\text{in}}) \qquad \textbf{(11–9)}$$

and

$$\dot{Q} = \dot{m}_h c_{ph}(T_{h,\,\text{in}} - T_{h,\,\text{out}}) \qquad \textbf{(11–10)}$$

where the subscripts c and h stand for *cold* and *hot* fluids, respectively, and

$$\dot{m}_c, \dot{m}_h = \text{mass flow rates}$$
$$c_{pc}, c_{ph} = \text{specific heats}$$
$$T_{c,\,\text{out}}, T_{h,\,\text{out}} = \text{outlet temperatures}$$
$$T_{c,\,\text{in}}, T_{h,\,\text{in}} = \text{inlet temperatures}$$

Note that the heat transfer rate $\dot{Q}$ is taken to be a positive quantity, and its direction is understood to be from the hot fluid to the cold one in accordance with the second law of thermodynamics.

In heat exchanger analysis, it is often convenient to combine the product of the mass flow rate and the specific heat of a fluid into a single quantity. This quantity is called the **heat capacity rate** and is defined for the hot and cold fluid streams as

$$C_h = \dot{m}_h c_{ph} \text{ and } C_c = \dot{m}_c c_{pc} \qquad \textbf{(11–11)}$$

The heat capacity rate of a fluid stream represents the rate of heat transfer needed to change the temperature of the fluid stream by 1°C as it flows through a heat exchanger. Note that in a heat exchanger, the fluid with a *large* heat capacity rate experiences a *small* temperature change, and the fluid with a *small* heat capacity rate experiences a *large* temperature change. Therefore, *doubling* the mass flow rate of a fluid while leaving everything else unchanged will *halve* the temperature change of that fluid.

Given the preceding definition of the heat capacity rate, Eqs. 11–9 and 11–10 can also be expressed as

$$\dot{Q} = C_c(T_{c,\,\text{out}} - T_{c,\,\text{in}}) \qquad \textbf{(11–12)}$$
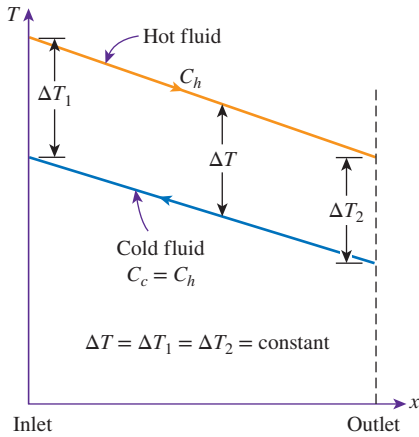
FIGURE 11–13
Two fluid streams that have the same capacity rates experience the same temperature change in a well-insulated heat exchanger.

(a) Condenser ($C_h \to \infty$)

(b) Boiler ($C_c \to \infty$)
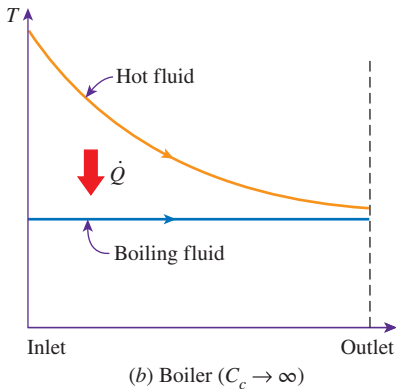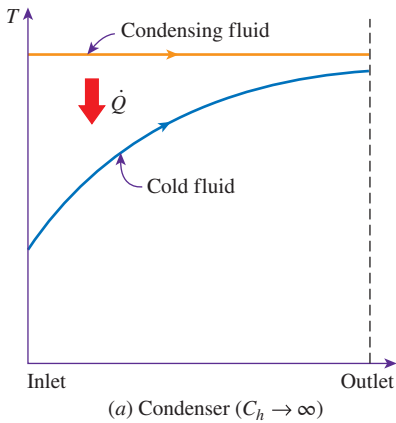
FIGURE 11–14
Variation of fluid temperatures in a heat exchanger when one of the fluids condenses or boils.

and

$$\dot{Q} = C_h(T_{h,\,\text{in}} - T_{h,\,\text{out}}) \tag{11–13}$$

That is, the heat transfer rate in a heat exchanger is equal to the heat capacity rate of either fluid multiplied by the temperature change of that fluid. Note that *the only time the temperature rise of a cold fluid is equal to the temperature drop of the hot fluid is when the heat capacity rates of the two fluids are equal to each other* (Fig. 11–13).

Two special types of heat exchangers commonly used in practice are *condensers* and *boilers.* One of the fluids in a condenser or a boiler undergoes a phase-change process, and the rate of heat transfer is expressed as

$$\dot{Q} = \dot{m} h_{fg} \tag{11–14}$$

where $\dot{m}$ is the rate of evaporation or condensation of the fluid and h_{fg} is the enthalpy of vaporization of the fluid at the specified temperature or pressure.

An ordinary fluid absorbs or releases a large amount of heat essentially at constant temperature during a phase-change process, as shown in Fig. 11–14. The heat capacity rate of a fluid during a phase-change process must approach infinity since the temperature change is practically zero. That is, $C = \dot{m} c_p \to \infty$ when $\Delta T \to 0$, so that the heat transfer rate $\dot{Q} = \dot{m} c_p \, \Delta T$ is a finite quantity. Therefore, in heat exchanger analysis, a condensing or boiling fluid is conveniently modeled as a fluid whose heat capacity rate is *infinity*.

The rate of heat transfer in a heat exchanger can also be expressed in an analogous manner to Newton's law of cooling as

$$\dot{Q} = U A_s \Delta T_m \tag{11–15}$$

where U is the overall heat transfer coefficient, A_s is the heat transfer surface area, and ΔT_m is an appropriate mean temperature difference between the two fluids. Here the surface area A_s can be determined precisely using the dimensions of the heat exchanger. However, the overall heat transfer coefficient U and the temperature difference ΔT between the hot and cold fluids, in general, may vary along the heat exchanger.

The average value of the overall heat transfer coefficient can be determined as described in Sec. 11–2 by using the average convection coefficients for each fluid. It turns out that the appropriate form of the average temperature difference between the two fluids is *logarithmic* in nature, and its determination is presented in Sec. 11–4. It should be noted that the mean temperature difference ΔT_m is dependent on the heat exchanger flow arrangement and its type of construction.

11–4 ▪ THE LOG MEAN TEMPERATURE DIFFERENCE METHOD

Earlier, we mentioned that the temperature difference between the hot and cold fluids varies along the heat exchanger, and it is convenient to have a *mean temperature difference* ΔT_m for use in the relation $\dot{Q} = U A_s \Delta T_m$.

In order to develop a relation for the equivalent average temperature difference between the two fluids, consider the *parallel-flow double-pipe* heat exchanger

shown in Fig. 11–15. Note that the temperature difference ΔT between the hot and cold fluids is large at the inlet of the heat exchanger but decreases exponentially toward the outlet. As you would expect, the temperature of the hot fluid decreases and the temperature of the cold fluid increases along the heat exchanger, but the temperature of the cold fluid can never exceed that of the hot fluid no matter how long the heat exchanger is.

Assuming the outer surface of the heat exchanger to be well insulated so that any heat transfer occurs between the two fluids, and disregarding any changes in kinetic and potential energy, an energy balance on each fluid in a differential section of the heat exchanger can be expressed as

$$\delta \dot{Q} = -\dot{m}_h c_{ph} \, dT_h \tag{11–16}$$

and

$$\delta \dot{Q} = \dot{m}_c c_{pc} \, dT_c \tag{11–17}$$

That is, the rate of heat loss from the hot fluid at any section of a heat exchanger is equal to the rate of heat gain by the cold fluid in that section. The temperature change of the hot fluid is a *negative* quantity, and so a *negative sign* is added to Eq. 11–16 to make the heat transfer rate $\dot{Q}$ a positive quantity. Solving the equations above for dT_h and dT_c gives

$$dT_h = -\frac{\delta \dot{Q}}{\dot{m}_h c_{ph}} \tag{11–18}$$

and

$$dT_c = \frac{\delta \dot{Q}}{\dot{m}_c c_{pc}} \tag{11–19}$$

Taking their difference, we get

$$dT_h - dT_c = d(T_h - T_c) = -\delta \dot{Q} \left(\frac{1}{\dot{m}_h c_{ph}} + \frac{1}{\dot{m}_c c_{pc}} \right) \tag{11–20}$$

The rate of heat transfer in the differential section of the heat exchanger can also be expressed as

$$\delta \dot{Q} = U(T_h - T_c) dA_s \tag{11–21}$$

Substituting this equation into Eq. 11–20 and rearranging give

$$\frac{d(T_h - T_c)}{T_h - T_c} = -U \, dA_s \left(\frac{1}{\dot{m}_h c_{ph}} + \frac{1}{\dot{m}_c c_{pc}} \right) \tag{11–22}$$

Integrating from the inlet of the heat exchanger to its outlet, we obtain

$$\ln \frac{T_{h,\text{out}} - T_{c,\text{out}}}{T_{h,\text{in}} - T_{c,\text{in}}} = -UA_s \left(\frac{1}{\dot{m}_h c_{ph}} + \frac{1}{\dot{m}_c c_{cp}} \right) \tag{11–23}$$

Finally, solving Eqs. 11–9 and 11–10 for $\dot{m}_c c_{pc}$ and $\dot{m}_h c_{ph}$ and substituting into Eq. 11–23 give, after some rearrangement,

$$\dot{Q} = UA_s \Delta T_{\text{lm}} \tag{11–24}$$
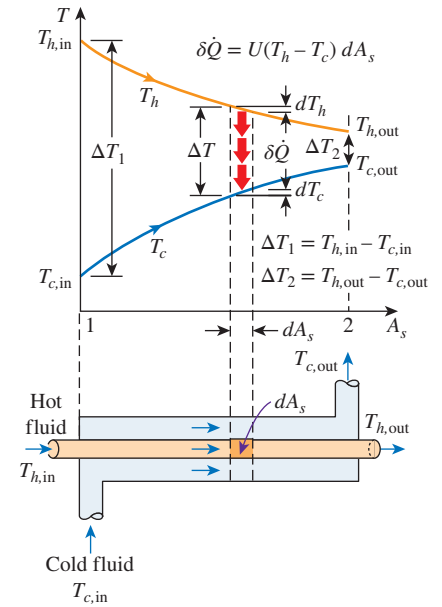
FIGURE 11–15
Variation of the fluid temperatures in a parallel-flow double-pipe heat exchanger.

(*a*) Parallel-flow heat exchangers

(*b*) Counter-flow heat exchangers
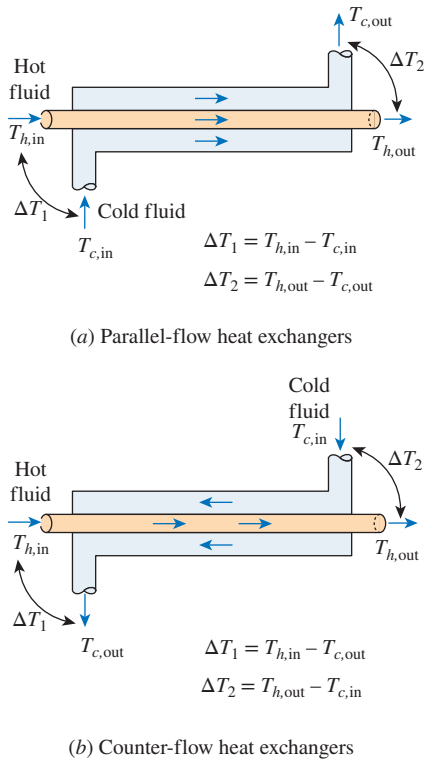
FIGURE 11–16
The ΔT_1 and ΔT_2 expressions in parallel-flow and counterflow heat exchangers.

where

$$\Delta T_{lm} = \frac{\Delta T_1 - \Delta T_2}{\ln(\Delta T_1/\Delta T_2)} \tag{11–25}$$

is the **log mean temperature difference**, which is the suitable form of the average temperature difference for use in the analysis of heat exchangers. Here ΔT_1 and ΔT_2 represent the temperature difference between the two fluids at the two ends (inlet and outlet) of the heat exchanger. It makes no difference which end of the heat exchanger is designated as the inlet or the outlet (Fig. 11–16). It should be noted that Eqs. 11–24 and 11–25 are good for any heat exchanger provided that the end point temperature differences are defined properly. For multipass and crossflow heat exchangers, as will be shown later, the log mean temperature difference should be corrected through a correction factor.

The temperature difference between the two fluids decreases from ΔT_1 at the inlet to ΔT_2 at the outlet. Thus, it is tempting to use the arithmetic mean temperature $\Delta T_{am} = \frac{1}{2}(\Delta T_1 + \Delta T_2)$ as the average temperature difference. The logarithmic mean temperature difference ΔT_{lm} is obtained by tracing the actual temperature profile of the fluids along the heat exchanger and is an *exact* representation of the *average temperature difference* between the hot and cold fluids. It truly reflects the exponential decay of the local temperature difference.

Note that ΔT_{lm} is always less than ΔT_{am}. Therefore, using ΔT_{am} in calculations instead of ΔT_{lm} will overestimate the rate of heat transfer in a heat exchanger between the two fluids. When ΔT_1 differs from ΔT_2 by no more than 40 percent, the error in using the arithmetic mean temperature difference is less than 1 percent. But the error increases to undesirable levels when ΔT_1 differs from ΔT_2 by greater amounts. Therefore, we should always use the *logarithmic mean temperature difference* when determining the rate of heat transfer in a heat exchanger.

Counterflow Heat Exchangers

The variation of temperatures of hot and cold fluids in a counterflow heat exchanger is given in Fig. 11–17. Note that the hot and cold fluids enter the heat exchanger from opposite ends, and the outlet temperature of the *cold fluid* in this case may exceed the outlet temperature of the *hot fluid.* In the limiting case, the cold fluid will be heated to the inlet temperature of the hot fluid. However, the outlet temperature of the cold fluid can *never* exceed the inlet temperature of the hot fluid, since this would be a violation of the second law of thermodynamics.

The relation already given for the log mean temperature difference is developed using a parallel-flow heat exchanger, but it can shown that the analysis is also applicable to counterflow heat exchangers. But this time, ΔT_1 and ΔT_2 are expressed as shown in Fig. 11–16.

For specified inlet and outlet temperatures, the log mean temperature difference for a counterflow heat exchanger is always greater than that for a parallel-flow heat exchanger. That is, $\Delta T_{lm, CF} > \Delta T_{lm, PF}$, and thus a smaller surface area (and thus a smaller heat exchanger) is needed to achieve a

specified heat transfer rate in a counterflow heat exchanger, assuming the same value of the overall heat transfer coefficient. Therefore, it is common practice to use counterflow arrangements in heat exchangers.

In a counterflow heat exchanger, the temperature difference between the hot and the cold fluids remains constant along the heat exchanger when the *heat capacity rates* of the two fluids are *equal* (that is, $\Delta T = $ constant when $C_h = C_c$ or $\dot{m}_h c_{ph} = \dot{m}_c c_{pc}$). Then we have $\Delta T_1 = \Delta T_2$, and the log mean temperature difference relation gives $\Delta T_{lm} = \frac{0}{0}$, which is indeterminate. It can be shown by the application of l'Hôpital's rule that in this case we have $\Delta T_{lm} = \Delta T_1 = \Delta T_2$, as expected.

A *condenser* or a *boiler* can be considered to be either a parallel- or counterflow heat exchanger since both approaches give the same result.

Multipass and Crossflow Heat Exchangers: Use of a Correction Factor

The log mean temperature difference ΔT_{lm} relation developed earlier is limited to parallel-flow and counterflow heat exchangers only. Similar relations are also developed for *crossflow* and *multipass shell-and-tube* heat exchangers, but the resulting expressions are too complicated because of the complex flow conditions.

In such cases, it is convenient to relate the equivalent temperature difference to the log mean temperature difference relation for the counterflow case as

$$\Delta T_{lm} = F \Delta T_{lm, CF} \tag{11–26}$$

where F is the **correction factor**, which depends on the *geometry* of the heat exchanger and the inlet and outlet temperatures of the hot and cold fluid streams. The $\Delta T_{lm, CF}$ is the log mean temperature difference for the case of a *counterflow* heat exchanger with the same inlet and outlet temperatures and is determined from Eq. 11–25 by taking $\Delta T_1 = T_{h, in} - T_{c, out}$ and $\Delta T_2 = T_{h, out} - T_{c, in}$ (Fig. 11–18).

The correction factor is less than unity for a crossflow and multipass shell-and-tube heat exchanger. That is, $F \le 1$. The limiting value of $F = 1$ corresponds to the counterflow heat exchanger. Thus, the correction factor F for a heat exchanger is *a measure of deviation of the* ΔT_{lm} *from the corresponding values for the counterflow case.*

The correction factor F for common crossflow and shell-and-tube heat exchanger configurations is given in Fig. 11–19 versus two temperature ratios P and R defined as

$$P = \frac{t_2 - t_1}{T_1 - t_1} \tag{11–27}$$

and

$$R = \frac{T_1 - T_2}{t_2 - t_1} = \frac{(\dot{m}c_p)_{\text{tube side}}}{(\dot{m}c_p)_{\text{shell side}}} \tag{11–28}$$

where the subscripts 1 and 2 represent the *inlet* and *outlet,* respectively. Note that for a shell-and-tube heat exchanger, T and t represent the *shell-* and *tube-side* temperatures, respectively, as shown in the correction factor charts.
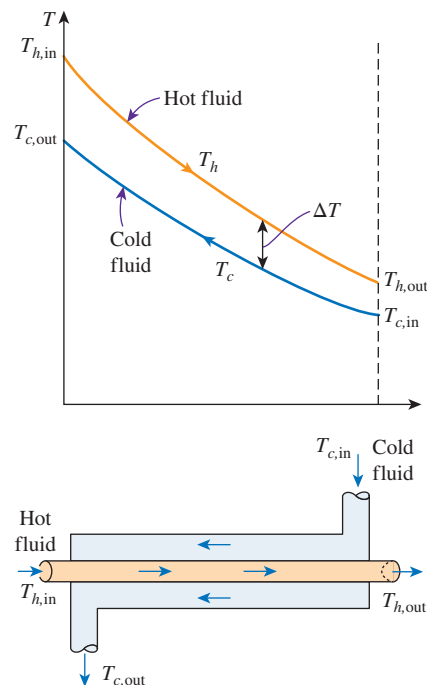
FIGURE 11–17

The variation of the fluid temperatures in a counterflow double-pipe heat exchanger.
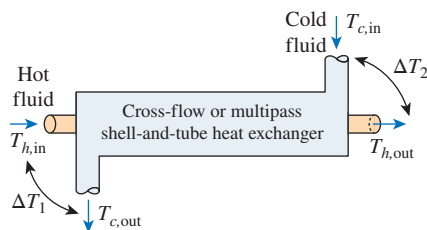
Heat transfer rate:
$$\dot{Q} = U A_s F \Delta T_{lm,CF}$$

where
$$\Delta T_{lm,CF} = \frac{\Delta T_1 - \Delta T_2}{\ln(\Delta T_1 / \Delta T_2)}$$

$$\Delta T_1 = T_{h,in} - T_{c,out}$$
$$\Delta T_2 = T_{h,out} - T_{c,in}$$

and $\quad F = \ldots$ (Fig. 11–19)

FIGURE 11–18

The determination of the heat transfer rate for crossflow and multipass shell-and-tube heat exchangers using the correction factor.
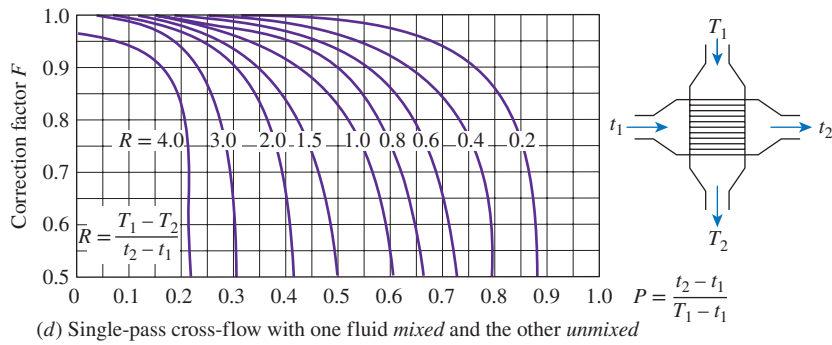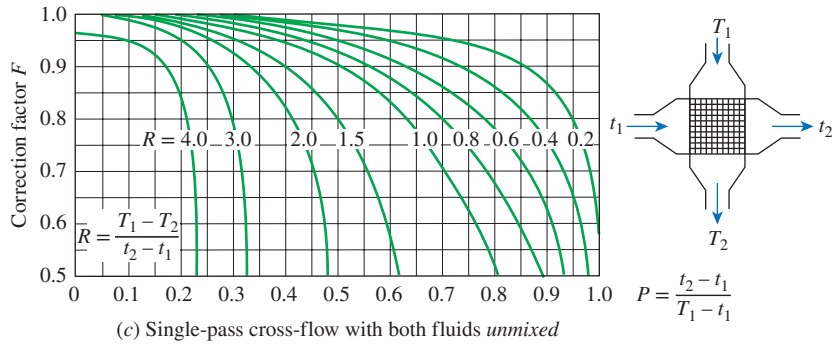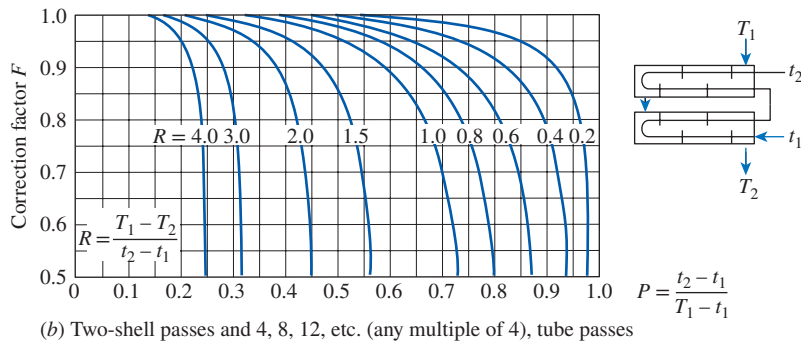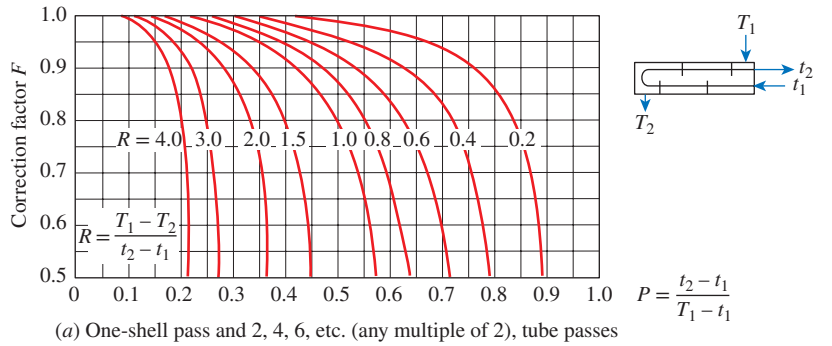
FIGURE 11–19

Correction factor F charts for common shell-and-tube and crossflow heat exchangers.

Source: Bowman, Mueller, and Nagle, 1940.

It makes no difference whether the hot or the cold fluid flows through the shell or the tube. The determination of the correction factor F requires the availability of the inlet and the outlet temperatures for both the cold and hot fluids.

Note that the value of P ranges from 0 to 1. The value of R, on the other hand, ranges from 0 to infinity, with $R = 0$ corresponding to the phase change (condensation or boiling) on the shell side and $R \rightarrow \infty$ to phase change on the tube side. The correction factor is $F = 1$ for both of these limiting cases. Therefore, the correction factor for a condenser or boiler is $F = 1$, regardless of the configuration of the heat exchanger.

EXAMPLE 11–3   The Condensation of Steam in a Condenser

Steam in the condenser of a power plant is to be condensed at a temperature of 30°C with cooling water from a nearby lake, which enters the tubes of the condenser at 14°C and leaves at 22°C. The surface area of the tubes is 45 m², and the overall heat transfer coefficient is 2100 W/m²·K. Determine the mass flow rate of the cooling water needed and the rate of condensation of the steam in the condenser.

SOLUTION   Steam is condensed by cooling water in the condenser of a power plant. The mass flow rate of the cooling water and the rate of condensation are to be determined.

Assumptions   **1** Steady operating conditions exist. **2** The heat exchanger is well insulated so that heat loss to the surroundings is negligible. **3** Changes in the kinetic and potential energies of fluid streams are negligible. **4** There is no fouling. **5** Fluid properties are constant.

Properties   The heat of vaporization of water at 30°C is $h_{fg} = 2431$ kJ/kg and the specific heat of cold water at the average temperature of 18°C is $c_p = 4184$ J/kg·K (Table A–9).

Analysis   The schematic of the condenser is given in Fig. 11–20. The condenser can be treated as a counterflow heat exchanger since the temperature of one of the fluids (the steam) remains constant.

The temperature difference between the steam and the cooling water at the two ends of the condenser is

$$\Delta T_1 = T_{h, \text{in}} - T_{c, \text{out}} = (30 - 22)°C = 8°C$$
$$\Delta T_2 = T_{h, \text{out}} - T_{c, \text{in}} = (30 - 14)°C = 16°C$$

That is, the temperature difference between the two fluids varies from 8°C at one end to 16°C at the other. The proper average temperature difference between the two fluids is the *log mean temperature difference* (not the arithmetic), which is determined from

$$\Delta T_{\text{lm}} = \frac{\Delta T_1 - \Delta T_2}{\ln(\Delta T_1/\Delta T_2)} = \frac{8 - 16}{\ln(8/16)} = 11.5°C$$

This is a little less than the arithmetic mean temperature difference of $\frac{1}{2}(8 + 16) = 12°C$. Then the heat transfer rate in the condenser is determined from

$$\dot{Q} = UA_s\Delta T_{\text{lm}} = (2100 \text{ W/m}^2\text{·K})(45 \text{ m}^2)(11.5°C) = 1.087 \times 10^6 \text{ W} = 1087 \text{ kW}$$
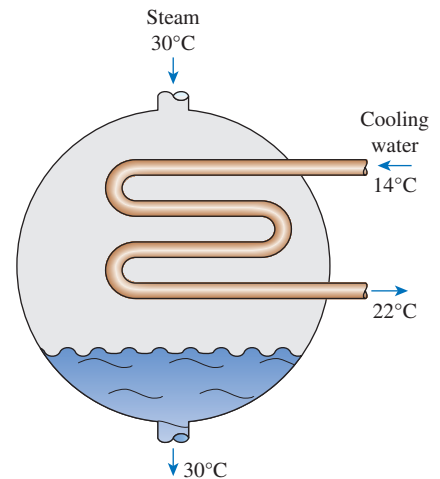
FIGURE 11–20
Schematic for Example 11–3.

Therefore, steam will lose heat at a rate of 1087 kW as it flows through the condenser, and the cooling water will gain practically all of it, since the condenser is well insulated.

The mass flow rate of the cooling water and the rate of the condensation of the steam are determined from $\dot{Q} = [\dot{m}c_p(T_{out} - T_{in})]_{cooling\ water} = (\dot{m}h_{fg})_{steam}$ to be

$$\dot{m}_{cooling\ water} = \frac{\dot{Q}}{c_p(T_{out} - T_{in})} = \frac{1087\ \text{kJ/s}}{(4.184\ \text{kJ/kg·K})(22 - 14)°\text{C}} = \textbf{32.5 kg/s}$$

and

$$\dot{m}_{steam} = \frac{\dot{Q}}{h_{fg}} = \frac{1087\ \text{kJ/s}}{2431\ \text{kJ/kg}} = \textbf{0.45 kg/s}$$

Therefore, we need to circulate about 72 kg of cooling water for each 1 kg of steam condensing to remove the heat released during the condensation process.

EXAMPLE 11–4   **Heating Water in a Counterflow Heat Exchanger**

A counterflow double-pipe heat exchanger is to heat water from 20°C to 80°C at a rate of 1.2 kg/s. The heating is to be accomplished by geothermal water available at 160°C at a mass flow rate of 2 kg/s. The inner tube is thin-walled and has a diameter of 1.5 cm. If the overall heat transfer coefficient of the heat exchanger is 640 W/m²·K, determine the length of the heat exchanger required to achieve the desired heating.

SOLUTION   Water is heated in a counterflow double-pipe heat exchanger by geothermal water. The required length of the heat exchanger is to be determined.
Assumptions   **1** Steady operating conditions exist. **2** The heat exchanger is well insulated so that heat loss to the surroundings is negligible. **3** Changes in the kinetic and potential energies of fluid streams are negligible. **4** There is no fouling. **5** Fluid properties are constant.
Properties   We take the specific heats of water and geothermal fluid to be 4.18 and 4.31 kJ/kg·K, respectively.
Analysis   The schematic of the heat exchanger is given in Fig. 11–21. The rate of heat transfer in the heat exchanger can be determined from

$$\dot{Q} = [\dot{m}c_p(T_{out} - T_{in})]_{water} = (1.2\ \text{kg/s})(4.18\ \text{kJ/kg·K})(80 - 20)°\text{C} = 301\ \text{kW}$$

Noting that all of this heat is supplied by the geothermal water, the outlet temperature of the geothermal water is determined to be

$$\dot{Q} = [\dot{m}c_p(T_{in} - T_{out})]_{geothermal} \longrightarrow T_{out} = T_{in} - \frac{\dot{Q}}{\dot{m}c_p}$$

$$= 160°\text{C} - \frac{301\ \text{kW}}{(2\ \text{kg/s})(4.31\ \text{kJ/kg·K})}$$

$$= 125°\text{C}$$

Hot geothermal water ↓160°C
2 kg/s

Cold water
→
20°C
1.2 kg/s

80°C

D = 1.5 cm

FIGURE 11–21
Schematic for Example 11–4.

Knowing the inlet and outlet temperatures of both fluids, the logarithmic mean temperature difference for this counterflow heat exchanger becomes

$$\Delta T_1 = T_{h,\,in} - T_{c,\,out} = (160 - 80)°C = 80°C$$
$$\Delta T_2 = T_{h,\,out} - T_{c,\,in} = (125 - 20)°C = 105°C$$

and

$$\Delta T_{lm} = \frac{\Delta T_1 - \Delta T_2}{\ln(\Delta T_1/\Delta T_2)} = \frac{80 - 105}{\ln(80/105)} = 91.9°C$$

Then the surface area of the heat exchanger is determined to be

$$\dot{Q} = UA_s\Delta T_{lm} \longrightarrow A_s = \frac{\dot{Q}}{U\Delta T_{lm}} = \frac{301,000 \text{ W}}{(640 \text{ W/m}^2\cdot\text{K})(91.9°C)} = 5.12 \text{ m}^2$$

To provide this much heat transfer surface area, the length of the tube must be

$$A_s = \pi DL \longrightarrow L = \frac{A_s}{\pi D} = \frac{5.12 \text{ m}^2}{\pi(0.015 \text{ m})} = \textbf{109 m}$$

Discussion The inner tube of this counterflow heat exchanger (and thus the heat exchanger itself) needs to be over 100 m long to achieve the desired heat transfer, which is impractical. In cases like this, we need to use a plate heat exchanger or a multipass shell-and-tube heat exchanger with multiple passes of tube bundles.

EXAMPLE 11–5   Heating of Glycerin in a Multipass Heat Exchanger

A two-shell-passes and four-tube-passes heat exchanger is used to heat glycerin from 20°C to 50°C by hot water, which enters the thin-walled 2-cm-diameter tubes at 80°C and leaves at 40°C (Fig. 11–22). The total length of the tubes in the heat exchanger is 60 m. The convection heat transfer coefficient is 25 W/m²·K on the glycerin (shell) side and 160 W/m²·K on the water (tube) side. Determine the rate of heat transfer in the heat exchanger (*a*) before any fouling and (*b*) after fouling with a fouling factor of 0.0006 m²·K/W occurs on the outer surfaces of the tubes.

SOLUTION Glycerin is heated in a two-shell-passes and four-tube-passes heat exchanger by hot water. The rate of heat transfer for the cases of fouling and no fouling are to be determined.
Assumptions **1** Steady operating conditions exist. **2** The heat exchanger is well insulated so that heat loss to the surroundings is negligible. **3** Changes in the kinetic and potential energies of fluid streams are negligible. **4** Heat transfer coefficients and fouling factors are constant and uniform. **5** The thermal resistance of the inner tube is negligible since the tube is thin-walled and highly conductive.
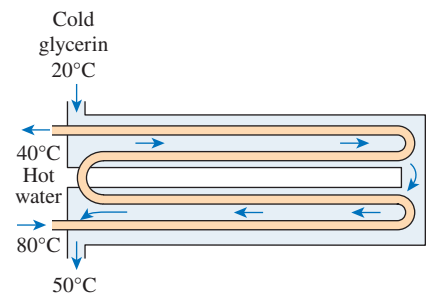
FIGURE 11–22
Schematic for Example 11–5.

Analysis The tubes are said to be thin-walled, and thus it is reasonable to assume the inner and outer surface areas of the tubes to be equal. Then the heat transfer surface area becomes

$$A_s = \pi DL = \pi(0.02 \text{ m})(60 \text{ m}) = 3.77 \text{ m}^2$$

The rate of heat transfer in this heat exchanger can be determined from

$$\dot{Q} = UA_s F \Delta T_{\text{lm, CF}}$$

where F is the correction factor and $\Delta T_{\text{lm, CF}}$ is the log mean temperature difference for the counterflow arrangement. These two quantities are determined from

$$\Delta T_1 = T_{h,\text{ in}} - T_{c,\text{ out}} = (80 - 50)°\text{C} = 30°\text{C}$$
$$\Delta T_2 = T_{h,\text{ out}} - T_{c,\text{ in}} = (40 - 20)°\text{C} = 20°\text{C}$$
$$\Delta T_{\text{lm, CF}} = \frac{\Delta T_1 - \Delta T_2}{\ln(\Delta T_1/\Delta T_2)} = \frac{30 - 20}{\ln(30/20)} = 24.7°\text{C}$$

and

$$\left.\begin{array}{l} P = \dfrac{t_2 - t_1}{T_1 - t_1} = \dfrac{40 - 80}{20 - 80} = 0.67 \\[2mm] R = \dfrac{T_1 - T_2}{t_2 - t_1} = \dfrac{20 - 50}{40 - 80} = 0.75 \end{array}\right\} F = 0.91 \qquad \text{(Fig. 11–19}b\text{)}$$

(*a*) In the case of no fouling, the overall heat transfer coefficient U is

$$U = \frac{1}{\dfrac{1}{h_i} + \dfrac{1}{h_o}} = \frac{1}{\dfrac{1}{160 \text{ W/m}^2\cdot\text{K}} + \dfrac{1}{25 \text{ W/m}^2\cdot\text{K}}} = 21.6 \text{ W/m}^2\cdot\text{K}$$

Then the rate of heat transfer becomes

$$\dot{Q} = UA_s F \Delta T_{\text{lm, CF}} = (21.6 \text{ W/m}^2\cdot\text{K})(3.77 \text{ m}^2)(0.91)(24.7°\text{C}) = \textbf{1830 W}$$

(*b*) When there is fouling on one of the surfaces, we have

$$U = \frac{1}{\dfrac{1}{h_i} + \dfrac{1}{h_o} + R_f} = \frac{1}{\dfrac{1}{160 \text{ W/m}^2\cdot\text{K}} + \dfrac{1}{25 \text{ W/m}^2\cdot\text{K}} + 0.0006 \text{ m}^2\cdot\text{K/W}}$$
$$= 21.3 \text{ W/m}^2\cdot\text{K}$$

and

$$\dot{Q} = UA_s F \Delta T_{\text{lm, CF}} = (21.3 \text{ W/m}^2\cdot\text{K})(3.77 \text{ m}^2)(0.91)(24.7°\text{C}) = \textbf{1805 W}$$

Discussion Note that the rate of heat transfer decreases as a result of fouling, as expected. The decrease is not dramatic, however, because of the relatively low convection heat transfer coefficients involved.

EXAMPLE 11–6   Cooling of Water in an Automotive Radiator

A test is conducted to determine the overall heat transfer coefficient in an automotive radiator that is a compact crossflow water-to-air heat exchanger with both fluids (air and water) unmixed (Fig. 11–23). The radiator has 40 tubes of internal diameter 0.5 cm and length 65 cm in a closely spaced plate-finned matrix. Hot water enters the tubes at 90°C at a rate of 0.6 kg/s and leaves at 65°C. Air flows across the radiator through the interfin spaces and is heated from 20°C to 40°C. Determine the overall heat transfer coefficient U_i of this radiator based on the inner surface area of the tubes.

SOLUTION During an experiment involving an automotive radiator, the inlet and exit temperatures of water and air and the mass flow rate of water are measured. The overall heat transfer coefficient based on the inner surface area is to be determined.

Assumptions **1** Steady operating conditions exist. **2** Changes in the kinetic and potential energies of fluid streams are negligible. **3** Fluid properties are constant.

Properties The specific heat of water at the average temperature of $(90 + 65)/2 = 77.5°C$ is 4.195 kJ/kg·K (Table A–9).

Analysis The rate of heat transfer in this radiator from the hot water to the air is determined from an energy balance on water flow,

$$\dot{Q} = [\dot{m}c_p(T_{in} - T_{out})]_{water} = (0.6 \text{ kg/s})(4.195 \text{ kJ/kg·K})(90 - 65)°C$$
$$= 62.93 \text{ kW}$$

The tube-side heat transfer area is the total surface area of the tubes and is determined from (where n is the number of tubes)

$$A_i = n\pi D_i L = (40)\pi(0.005 \text{ m})(0.65 \text{ m}) = 0.408 \text{ m}^2$$

Knowing the rate of heat transfer and the surface area, the overall heat transfer coefficient can be determined from

$$\dot{Q} = U_i A_i F \Delta T_{lm, CF} \longrightarrow U_i = \frac{\dot{Q}}{A_i F \Delta T_{lm, CF}}$$

where F is the correction factor and $\Delta T_{lm, CF}$ is the log mean temperature difference for the counterflow arrangement. These two quantities are found to be

$$\Delta T_1 = T_{h, in} - T_{c, out} = (90 - 40)°C = 50°C$$
$$\Delta T_2 = T_{h, out} - T_{c, in} = (65 - 20)°C = 45°C$$
$$\Delta T_{lm, CF} = \frac{\Delta T_1 - \Delta T_2}{\ln(\Delta T_1/\Delta T_2)} = \frac{50 - 45}{\ln(50/45)} = 47.5°C$$

and

$$\left.\begin{array}{l} P = \dfrac{t_2 - t_1}{T_1 - t_1} = \dfrac{65 - 90}{20 - 90} = 0.36 \\[2mm] R = \dfrac{T_1 - T_2}{t_2 - t_1} = \dfrac{20 - 40}{65 - 90} = 0.80 \end{array}\right\} F = 0.97 \qquad \text{(Fig. 11–19c)}$$

90°C

Air flow
(*unmixed*)
20°C

40°C

65°C
Water flow
(*unmixed*)
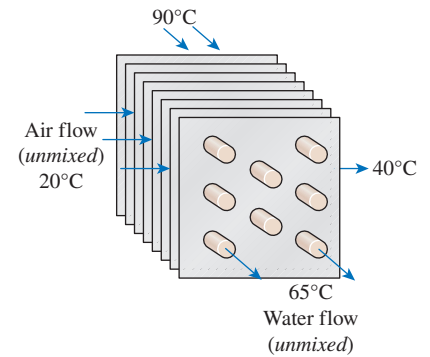
FIGURE 11–23
Schematic for Example 11–6.

Substituting, the overall heat transfer coefficient U_i is determined to be

$$U_i = \frac{\dot{Q}}{A_i F \Delta T_{\text{lm, CF}}} = \frac{62{,}930 \text{ W}}{(0.408 \text{ m}^2)(0.97)(47.5°\text{C})} = \mathbf{3347 \text{ W/m}^2 \cdot \text{K}}$$

Discussion   Note that the overall heat transfer coefficient on the air side will be much lower because of the large surface area involved on that side.

11–5 ▪ THE EFFECTIVENESS–NTU METHOD

The log mean temperature difference (LMTD) method discussed in Sec. 11–4 is easy to use in heat exchanger analysis when the inlet and the outlet temperatures of the hot and cold fluids are known or can be determined from an energy balance. Once ΔT_{lm}, the mass flow rates, and the overall heat transfer coefficient are available, the heat transfer surface area of the heat exchanger can be determined from

$$\dot{Q} = U A_s \Delta T_{\text{lm}}$$

Therefore, the LMTD method is very suitable for determining the *size* of a heat exchanger to realize prescribed outlet temperatures when the mass flow rates and the inlet and outlet temperatures of the hot and cold fluids are specified.

With the LMTD method, the task is to *select* a heat exchanger that will meet the prescribed heat transfer requirements. The procedure to be followed by the selection process is:

1. Select the type of heat exchanger suitable for the application.
2. Determine any unknown inlet or outlet temperature and the heat transfer rate using an energy balance.
3. Calculate the log mean temperature difference ΔT_{lm} and the correction factor *F,* if necessary.
4. Obtain (select or calculate) the value of the overall heat transfer coefficient *U.*
5. Calculate the heat transfer surface area A_s.

The task is completed by selecting a heat exchanger that has a heat transfer surface area equal to or larger than A_s.

A second kind of problem encountered in heat exchanger analysis is the determination of the *heat transfer rate* and the *outlet temperatures* of the hot and cold fluids for prescribed fluid mass flow rates and inlet temperatures when the *type* and *size* of the heat exchanger are specified. The heat transfer surface area of the heat exchanger in this case is known, but the *outlet temperatures* are not. Here the task is to determine the heat transfer performance of a specified heat exchanger or to determine if a heat exchanger available in storage will do the job.

The LMTD method could still be used for this alternative problem, but the procedure would require tedious iterations, and thus it is not practical. In an attempt to eliminate the iterations from the solution of such problems, Kays

and London came up with a method in 1955 called the **effectiveness–NTU method**, which greatly simplified heat exchanger analysis.

This method is based on a dimensionless parameter called the **heat transfer effectiveness** ε, defined as

$$\varepsilon = \frac{\dot{Q}}{\dot{Q}_{\text{max}}} = \frac{\text{Actual heat transfer rate}}{\text{Maximum possible heat transfer rate}} \quad \textbf{(11–29)}$$

The *actual* heat transfer rate in a heat exchanger can be determined from an energy balance on the hot or cold fluids and can be expressed as

$$\dot{Q} = C_c(T_{c,\,\text{out}} - T_{c,\,\text{in}}) = C_h(T_{h,\,\text{in}} - T_{h,\,\text{out}}) \quad \textbf{(11–30)}$$

where $C_c = \dot{m}_c c_{pc}$ and $C_h = \dot{m}_h c_{ph}$ are the heat capacity rates of the cold and hot fluids, respectively.

To determine the maximum possible heat transfer rate in a heat exchanger, we first recognize that the *maximum temperature difference* in a heat exchanger is the difference between the *inlet* temperatures of the hot and cold fluids. That is,

$$\Delta T_{\text{max}} = T_{h,\,\text{in}} - T_{c,\,\text{in}} \quad \textbf{(11–31)}$$

The heat transfer in a heat exchanger will reach its maximum value when (1) the cold fluid is heated to the inlet temperature of the hot fluid or (2) the hot fluid is cooled to the inlet temperature of the cold fluid. These two limiting conditions will not be reached simultaneously unless the heat capacity rates of the hot and cold fluids are identical (i.e., $C_c = C_h$). When $C_c \not\approx C_h$, which is usually the case, the fluid with the *smaller* heat capacity rate will experience a larger temperature change, and thus it will be the first to experience the maximum temperature, at which point the heat transfer will come to a halt. Therefore, the maximum possible heat transfer rate in a heat exchanger is (Fig. 11–24)

$$\dot{Q}_{\text{max}} = C_{\text{min}}(T_{h,\,\text{in}} - T_{c,\,\text{in}}) \quad \textbf{(11–32)}$$

where C_{min} is the smaller of C_h and C_c. This is further clarified by Example 11–7.
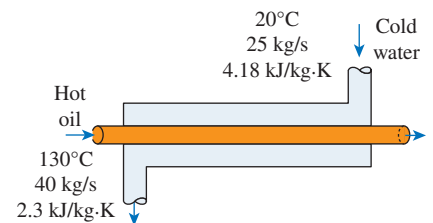
$C_c = \dot{m}_c c_{pc} = 104.5 \text{ kW/K}$

$C_h = \dot{m}_h c_{ph} = 92 \text{ kW/K}$

$C_{\text{min}} = 92 \text{ kW/K}$

$\Delta T_{\text{max}} = T_{h,\text{in}} - T_{c,\text{in}} = 110°C$

$\dot{Q}_{\text{max}} = C_{\text{min}}\,\Delta T_{\text{max}} = 10{,}120 \text{ kW}$

FIGURE 11–24
The determination of the maximum rate of heat transfer in a heat exchanger.

EXAMPLE 11–7 **Upper Limit for Heat Transfer in a Heat Exchanger**

Cold water enters a counterflow heat exchanger at 10°C at a rate of 8 kg/s, where it is heated by a hot-water stream that enters the heat exchanger at 70°C at a rate of 2 kg/s. Assuming the specific heat of water to remain constant at $c_p = 4.18$ kJ/kg·K, determine the maximum heat transfer rate and the outlet temperatures of the cold- and the hot-water streams for this limiting case.

SOLUTION Cold- and hot-water streams enter a heat exchanger at specified temperatures and flow rates. The maximum rate of heat transfer in the heat exchanger and the outlet temperatures are to be determined.

10°C
8 kg/s
Cold
water

Hot
water
→

70°C
2 kg/s
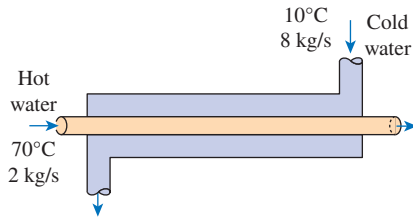
FIGURE 11–25
Schematic for Example 11–7.

Assumptions **1** Steady operating conditions exist. **2** The heat exchanger is well insulated so that heat loss to the surroundings is negligible. **3** Changes in the kinetic and potential energies of fluid streams are negligible. **4** Fluid properties are constant.

Properties The specific heat of water is given to be $c_p = 4.18$ kJ/kg·K.

Analysis A schematic of the heat exchanger is given in Fig. 11–25. The heat capacity rates of the hot and cold fluids are

$$C_h = \dot{m}_h c_{ph} = (2 \text{ kg/s})(4.18 \text{ kJ/kg·K}) = 8.36 \text{ kW/K}$$

and

$$C_c = \dot{m}_c c_{pc} = (8 \text{ kg/s})(4.18 \text{ kJ/kg·K}) = 33.4 \text{ kW/K}$$

Therefore,

$$C_{min} = C_h = 8.36 \text{ kW/K}$$

which is the smaller of the two heat capacity rates. Then the maximum heat transfer rate is determined from Eq. 11–32 to be

$$\dot{Q}_{max} = C_{min}(T_{h, in} - T_{c, in})$$
$$= (8.36 \text{ kW/K})(70 - 10)°C$$
$$= \mathbf{502 \text{ kW}}$$

That is, the maximum possible heat transfer rate in this heat exchanger is 502 kW. This value would be approached in a counterflow heat exchanger with a *very large* heat transfer surface area.

The maximum temperature difference in this heat exchanger is $\Delta T_{max} = T_{h, in} - T_{c, in} = (70 - 10)°C = 60°C$. Therefore, the hot water cannot be cooled by more than 60°C (to 10°C) in this heat exchanger, and the cold water cannot be heated by more than 60°C (to 70°C), no matter what we do. The outlet temperatures of the cold and the hot streams in this limiting case are determined to be

$$\dot{Q} = C_c(T_{c, out} - T_{c, in}) \longrightarrow T_{c, out} = T_{c, in} + \frac{\dot{Q}}{C_c} = 10°C + \frac{502 \text{ kW}}{33.4 \text{ kW/K}} = \mathbf{25°C}$$

$$\dot{Q} = C_h(T_{h, in} - T_{h, out}) \longrightarrow T_{h, out} = T_{h, in} - \frac{\dot{Q}}{C_h} = 70°C - \frac{502 \text{ kW}}{8.38 \text{ kW/K}} = \mathbf{10°C}$$

Discussion Note that the hot water is cooled to the limit of 10°C (the inlet temperature of the cold-water stream), but the cold water is heated to 25°C only when maximum heat transfer occurs in the heat exchanger. This is not surprising, since the mass flow rate of the hot water is only one-fourth that of the cold water, and, as a result, the temperature of the cold water increases by 0.25°C for each 1°C drop in the temperature of the hot water.

You may be tempted to think that the cold water should be heated to 70°C in the limiting case of maximum heat transfer. But this will require the temperature of the hot water to drop to −170°C (below 10°C), which is impossible. Therefore, heat transfer in a heat exchanger reaches its maximum value when the fluid with the smaller heat capacity rate (or the smaller mass flow rate when both fluids have the same specific heat value) experiences the maximum temperature change. This example explains why we use C_{min} in the evaluation of $\dot{Q}_{max}$ instead of C_{max}.

We can show that the hot water will leave at the inlet temperature of the cold water and vice versa in the limiting case of maximum heat transfer when the mass flow rates of the hot- and cold-water streams are identical (Fig. 11–26). We can also show that the outlet temperature of the cold water will reach the 70°C limit when the mass flow rate of the hot water is greater than that of the cold water.

$$\dot{Q} = \dot{m}_h\, c_{ph}\, \Delta T_h$$
$$= \dot{m}_c\, c_{pc}\, \Delta T_c$$

If $\quad \dot{m}_c\, c_{pc} = \dot{m}_h\, c_{ph}$

then $\quad \Delta T_h = \Delta T_c$

FIGURE 11–26
The temperature rise of the cold fluid in a heat exchanger will be equal to the temperature drop of the hot fluid when the heat capacity rates of the hot and cold fluids are identical.

The determination of $\dot{Q}_{max}$ requires the availability of the *inlet temperature* of the hot and cold fluids and their *mass flow rates,* which are usually specified. Then, once the effectiveness of the heat exchanger is known, the actual heat transfer rate $\dot{Q}$ can be determined from

$$\dot{Q} = \varepsilon \dot{Q}_{max} = \varepsilon C_{min}(T_{h,\,in} - T_{c,\,in}) \tag{11–33}$$

where

if $C_c = C_{min}$: $\qquad \varepsilon = \dfrac{\dot{Q}}{\dot{Q}_{max}} = \dfrac{C_c(T_{c,\,out} - T_{c,\,in})}{C_c(T_{h,\,in} - T_{c,\,in})} = \dfrac{T_{c,\,out} - T_{c,\,in}}{T_{h,\,in} - T_{c,\,in}}$

if $C_h = C_{min}$: $\qquad \varepsilon = \dfrac{\dot{Q}}{\dot{Q}_{max}} = \dfrac{C_h(T_{h,\,in} - T_{h,\,out})}{C_h(T_{h,\,in} - T_{c,\,in})} = \dfrac{T_{h,\,in} - T_{h,\,out}}{T_{h,\,in} - T_{c,\,in}}$

Therefore, the effectiveness of a heat exchanger enables us to determine the heat transfer rate without knowing the *outlet temperatures* of the fluids.

The effectiveness of a heat exchanger depends on the *geometry* of the heat exchanger as well as the *flow arrangement.* Therefore, different types of heat exchangers have different effectiveness relations. Next we illustrate the development of the effectiveness ε relation for the double-pipe *parallel-flow* heat exchanger.

Equation 11–23 developed in Sec. 11–4 for a parallel-flow heat exchanger can be rearranged as

$$\ln\frac{T_{h,\,out} - T_{c,\,out}}{T_{h,\,in} - T_{c,\,in}} = -\frac{UA_s}{C_c}\left(1 + \frac{C_c}{C_h}\right) \tag{11–34}$$

Also, solving Eq. 11–30 for $T_{h,\,out}$ gives

$$T_{h,\,out} = T_{h,\,in} - \frac{C_c}{C_h}(T_{c,\,out} - T_{c,\,in}) \tag{11–35}$$

Substituting this relation into Eq. 11–34 after adding and subtracting $T_{c,\,in}$ gives

$$\ln\frac{T_{h,\,in} - T_{c,\,in} + T_{c,\,in} - T_{c,\,out} - \dfrac{C_c}{C_h}(T_{c,\,out} - T_{c,\,in})}{T_{h,\,in} - T_{c,\,in}} = -\frac{UA_s}{C_c}\left(1 + \frac{C_c}{C_h}\right)$$

which simplifies to

$$\ln\left[1 - \left(1 + \frac{C_c}{C_h}\right)\frac{T_{c,\,\text{out}} - T_{c,\,\text{in}}}{T_{h,\,\text{in}} - T_{c,\,\text{in}}}\right] = -\frac{UA_s}{C_c}\left(1 + \frac{C_c}{C_h}\right) \tag{11–36}$$

We now manipulate the definition of effectiveness to obtain

$$\varepsilon = \frac{\dot{Q}}{\dot{Q}_{\text{max}}} = \frac{C_c(T_{c,\,\text{out}} - T_{c,\,\text{in}})}{C_{\text{min}}(T_{h,\,\text{in}} - T_{c,\,\text{in}})} \longrightarrow \frac{T_{c,\,\text{out}} - T_{c,\,\text{in}}}{T_{h,\,\text{in}} - T_{c,\,\text{in}}} = \varepsilon\frac{C_{\text{min}}}{C_c}$$

Substituting this result into Eq. 11–36 and solving for ε gives the following relation for the effectiveness of a *parallel-flow* heat exchanger:

$$\varepsilon_{\text{parallel flow}} = \frac{1 - \exp\left[-\dfrac{UA_s}{C_c}\left(1 + \dfrac{C_c}{C_h}\right)\right]}{\left(1 + \dfrac{C_c}{C_h}\right)\dfrac{C_{\text{min}}}{C_c}} \tag{11–37}$$

Taking either C_c or C_h to be C_{min} (both approaches give the same result), the preceding relation can be expressed more conveniently as

$$\varepsilon_{\text{parallel flow}} = \frac{1 - \exp\left[-\dfrac{UA_s}{C_{\text{min}}}\left(1 + \dfrac{C_{\text{min}}}{C_{\text{max}}}\right)\right]}{1 + \dfrac{C_{\text{min}}}{C_{\text{max}}}} \tag{11–38}$$

Again C_{min} is the *smaller* heat capacity rate and C_{max} is the larger one, and it makes no difference whether C_{min} belongs to the hot or cold fluid.

Effectiveness relations of the heat exchangers typically involve the *dimensionless* group UA_s/C_{min}. This quantity is called the **number of transfer units NTU** and is expressed as

$$\text{NTU} = \frac{UA_s}{C_{\text{min}}} = \frac{UA_s}{(\dot{m}c_p)_{\text{min}}} \tag{11–39}$$

where U is the overall heat transfer coefficient and A_s is the heat transfer surface area of the heat exchanger. Note that NTU is proportional to A_s. Therefore, for specified values of U and C_{min}, the value of NTU *is a measure of the heat transfer surface area A_s*. Thus, the larger the NTU, the larger the heat exchanger.

In heat exchanger analysis, it is also convenient to define another dimensionless quantity called the **capacity ratio** c as

$$c = \frac{C_{\text{min}}}{C_{\text{max}}} \tag{11–40}$$

It can be shown that the effectiveness of a heat exchanger is a function of the number of transfer units NTU and the capacity ratio c. That is,

$$\varepsilon = \text{function }(UA_s/C_{\text{min}},\ C_{\text{min}}/C_{\text{max}}) = \text{function (NTU, }c)$$

TABLE 11–4

Effectiveness relations for heat exchangers: $\text{NTU} = UA_s/C_{min}$ and $c = C_{min}/C_{max} = (\dot{m}c_p)_{min}/(\dot{m}c_p)_{max}$

Heat Exchanger Type	Effectiveness Relation
1 *Double pipe:* Parallel-flow	$\varepsilon = \dfrac{1 - \exp\,[-\text{NTU}(1 + c)]}{1 + c}$
Counterflow	$\varepsilon = \dfrac{1 - \exp\,[-\text{NTU}(1 - c)]}{1 - c\,\exp\,[-\text{NTU}(1 - c)]}$ (for $c < 1$)
	$\varepsilon = \dfrac{\text{NTU}}{1 + \text{NTU}}$ (for $c = 1$)
2 *Shell-and-tube:* One-shell pass 2, 4, . . . tube passes	$\varepsilon_1 = 2\left\{ 1 + c + \sqrt{1 + c^2}\,\dfrac{1 + \exp\left[-\text{NTU}_1\sqrt{1 + c^2}\right]}{1 - \exp\left[-\text{NTU}_1\sqrt{1 + c^2}\right]} \right\}^{-1}$
n-shell passes 2*n*, 4*n*, . . . tube passes	$\varepsilon = \left[\left(\dfrac{1 - \varepsilon_1 c}{1 - \varepsilon_1}\right)^n - 1\right]\left[\left(\dfrac{1 - \varepsilon_1 c}{1 - \varepsilon_1}\right)^n - c\right]^{-1}$
3 Crossflow (*single-pass*) Both fluids unmixed	$\varepsilon = 1 - \exp\left\{ \dfrac{\text{NTU}^{0.22}}{c}[\exp(-c\,\text{NTU}^{0.78}) - 1] \right\}$
C_{max} mixed, C_{min} unmixed	$\varepsilon = \dfrac{1}{c}(1 - \exp\{-c[1 - \exp(-\text{NTU})]\})$
C_{min} mixed, C_{max} unmixed	$\varepsilon = 1 - \exp\left\{ -\dfrac{1}{c}[1 - \exp(-c\,\text{NTU})] \right\}$
4 All heat exchangers with $c = 0$	$\varepsilon = 1 - \exp(-\text{NTU})$

Source: W. M. Kays and A. L. London. Compact Heat Exchangers, 3/e. McGraw-Hill, 1984.

Effectiveness relations have been developed for a large number of heat exchangers, and the results are given in Table 11–4. The effectivenesses of some common types of heat exchangers are also plotted in Fig. 11–27.

More extensive effectiveness charts and relations are available in the literature. The dashed lines in Fig. 11–27*f* are for the case of C_{min} unmixed and C_{max} mixed, and the solid lines are for the opposite case. The analytic relations for the effectiveness give more accurate results than the charts, since reading errors in charts are unavoidable, and the relations are very suitable for computerized analysis of heat exchangers.

We make these observations from the effectiveness relations and charts already given:

1. The value of the effectiveness ranges from 0 to 1. It increases rapidly with NTU for small values (up to about NTU = 1.5) but rather slowly for
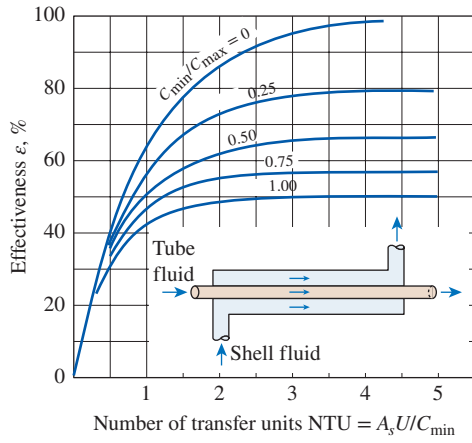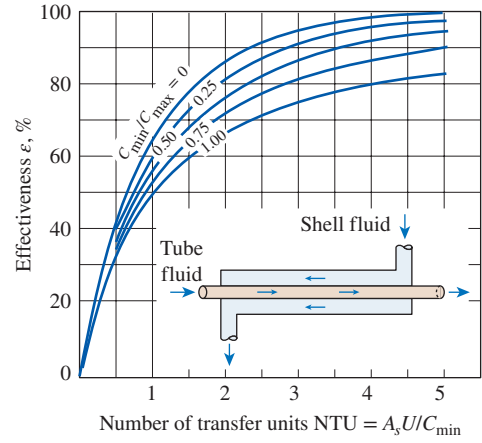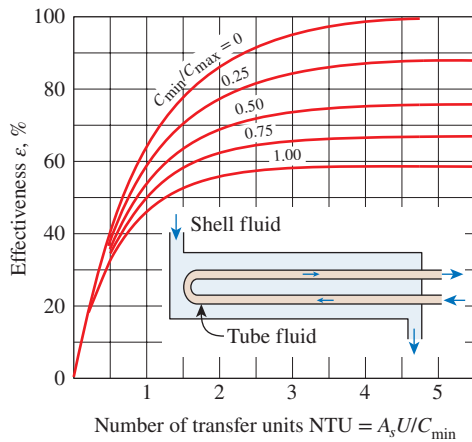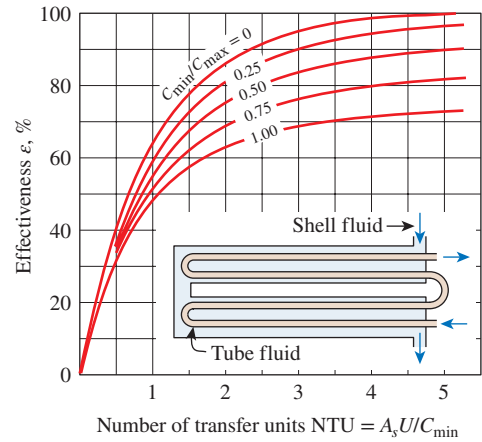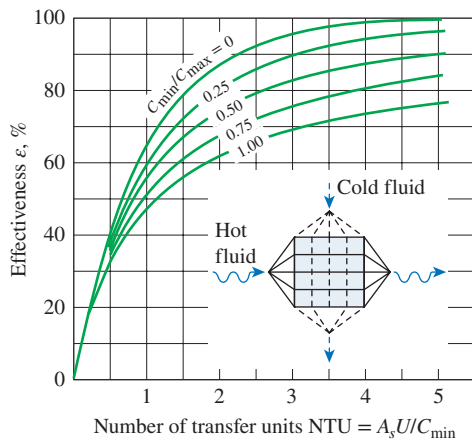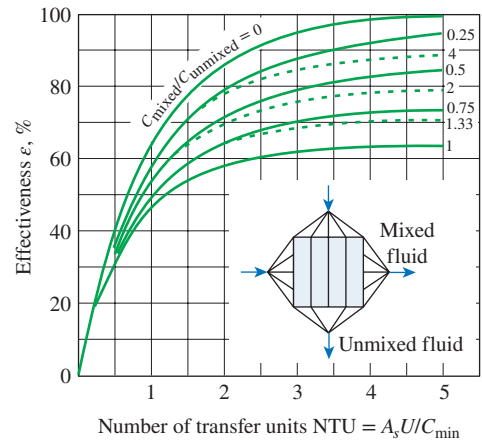
FIGURE 11–27
Effectiveness for heat exchangers.
Source: W. M. Kays and A. L. London. Compact Heat Exchangers, 3/e. McGraw-Hill, 1984.

larger values. Therefore, the use of a heat exchanger with a large NTU (usually larger than 3) and thus a large size cannot be justified economically, since a large increase in NTU in this case corresponds to a small increase in effectiveness. Thus, a heat exchanger with a very high effectiveness may be desirable from a heat transfer point of view but undesirable from an economical point of view.

2. For a given NTU and capacity ratio $c = C_{min}/C_{max}$, the *counterflow* heat exchanger has the *highest* effectiveness, followed closely by the cross-flow heat exchangers with both fluids unmixed. As you might expect, the lowest effectiveness values are encountered in parallel-flow heat exchangers (Fig. 11–28).

3. The effectiveness of a heat exchanger is independent of the capacity ratio c for NTU values of less than about 0.3.

4. The value of the capacity ratio c ranges between 0 and 1. For a given NTU, the effectiveness becomes a *maximum* for $c = 0$ and a *minimum* for $c = 1$. The case $c = C_{min}/C_{max} \to 0$ corresponds to $C_{max} \to \infty$, which is realized during a phase-change process in a *condenser* or *boiler.* All effectiveness relations in this case reduce to

$$\varepsilon = \varepsilon_{max} = 1 - \exp(-\text{NTU}) \tag{11–41}$$

regardless of the type of heat exchanger (Fig. 11–29). Note that the temperature of the condensing or boiling fluid remains constant in this case. The effectiveness is the *lowest* in the other limiting case of $c = C_{min}/C_{max} = 1$, which is realized when the heat capacity rates of the two fluids are equal. In industrial applications such as hot water cooling or chilled water heating pertaining to the heating, ventilating, and air conditioning (HVAC) industry, the hot or cold fluid is channeled from one location to another with the pipe immersed in ambient environment. Typical examples of this flow situation are the fluid-carrying heat exchanger pipe exposed to ambient air or submerged in large liquid media such as a lake. In such cases, since the effective change in reference temperature of the ambient environment is virtually zero and the relative mass of the ambient environment is infinitely large, the maximum heat capacity rate C_{max} is a very large number. Thus the capacity ratio, $c = C_{min}/C_{max} \to 0$ and hence Eq. 11–41 is applicable in cases when the heat exchanger is in contact with the ambient environment.

Once the quantities $c = C_{min}/C_{max}$ and $\text{NTU} = UA_s/C_{min}$ have been evaluated, the effectiveness ε can be determined from either the charts or the effectiveness relation for the specified type of heat exchanger. Then the rate of heat transfer $\dot{Q}$ and the outlet temperatures $T_{h,\,out}$ and $T_{c,\,out}$ can be determined from Eqs. 11–33 and 11–30, respectively. Note that the analysis of heat exchangers with unknown outlet temperatures is a straightforward matter with the effectiveness–NTU method but requires rather tedious iterations with the LMTD method.

We mentioned earlier that when all the inlet and outlet temperatures are specified, the *size* of the heat exchanger can easily be determined using the LMTD method. Alternatively, it can also be determined from the effectiveness–NTU method by first evaluating the effectiveness ε from its definition (Eq. 11–29) and then the NTU from the appropriate NTU relation in Table 11–5.
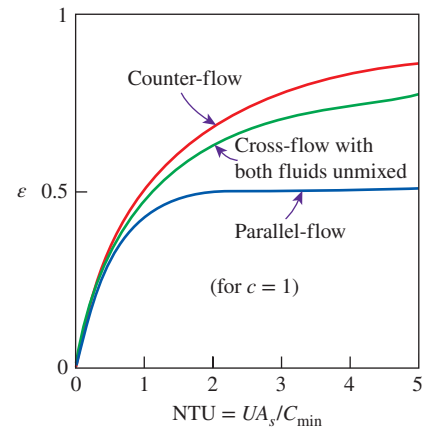
FIGURE 11–28
For a specified NTU and capacity ratio *c,* the counterflow heat exchanger has the highest effectiveness and the parallel-flow the lowest.
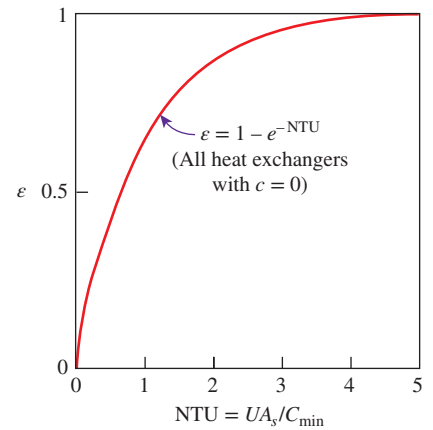
FIGURE 11–29
The effectiveness relation reduces to $\varepsilon = \varepsilon_{max} = 1 - \exp(-\text{NTU})$ for all heat exchangers when the capacity ratio $c = 0$.

TABLE 11–5

NTU relations for heat exchangers: $\text{NTU} = UA_s/C_{\min}$ and $c = C_{\min}/C_{\max} = (\dot{m}c_p)_{\min}/(\dot{m}c_p)_{\max}$

Heat Exchanger Type	NTU Relation
1 *Double-pipe:*	
Parallel-flow	$\text{NTU} = -\dfrac{\ln[1 - \varepsilon(1 + c)]}{1 + c}$
Counterflow	$\text{NTU} = \dfrac{1}{c - 1} \ln\left(\dfrac{\varepsilon - 1}{\varepsilon c - 1}\right)$ (for $c < 1$)
	$\text{NTU} = \dfrac{\varepsilon}{1 - \varepsilon}$ (for $c = 1$)

2   *Shell and tube:*
     One-shell pass
     2, 4, . . . tube passes
	$\text{NTU}_1 = -\dfrac{1}{\sqrt{1 + c^2}} \ln\left(\dfrac{2/\varepsilon_1 - 1 - c - \sqrt{1 + c^2}}{2/\varepsilon_1 - 1 - c - \sqrt{1 + c^2}}\right)$

n-shell passes 2n, 4n, . . . tube passes	$\text{NTU} = n(\text{NTU})_1$ To find effectiveness of the heat exchanger with one-shell pass use, $\varepsilon_1 = \dfrac{F - 1}{F - c}$ where $F = \left(\dfrac{\varepsilon c - 1}{\varepsilon - 1}\right)^{1/n}$
3 *Crossflow (single-pass):*	
$C_{\max}$ mixed, $C_{\min}$ unmixed	$\text{NTU} = -\ln\left[1 + \dfrac{\ln(1 + \varepsilon c)}{c}\right]$
$C_{\min}$ mixed, $C_{\max}$ unmixed	$\text{NTU} = -\dfrac{\ln[c \ln(1 - \varepsilon) + 1]}{c}$
4 All heat exchangers with $c = 0$	$\text{NTU} = -\ln(1 - \varepsilon)$

Source: W. M. Kays and A. L. London. Compact Heat Exchangers, 3/e. McGraw-Hill, 1984.

Note that the relations in Table 11–5 are equivalent to those in Table 11–4. Both sets of relations are given for convenience. The relations in Table 11–4 give the effectiveness directly when NTU is known, and the relations in Table 11–5 give the NTU directly when the effectiveness ε is known.

Hot geothermal brine   160°C
 2 kg/s

Cold water
 20°C
 1.2 kg/s

80°C

$D = 1.5$ cm
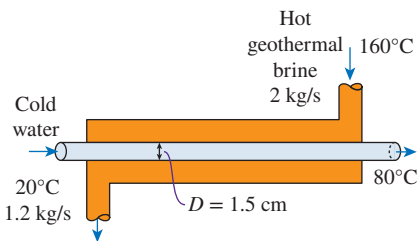
FIGURE 11–30
Schematic for Example 11–8.

EXAMPLE 11–8   **The Effectiveness-NTU Method**

A counterflow double-pipe heat exchanger is to heat water from 20°C to 80°C at a rate of 1.2 kg/s (Fig. 11–30). The heating is to be accomplished by geothermal water available at 160°C at a mass flow rate of 2 kg/s. The inner tube is thin-walled and has a diameter of 1.5 cm. The overall heat transfer coefficient of the heat exchanger is 640 W/m²·K. Using the effectiveness-NTU method, determine the length of the heat exchanger required to achieve the desired heating.

SOLUTION Water is heated in a counterflow double-pipe heat exchanger by geothermal water. Using the ε-NTU method, the required length of the heat exchanger is to be determined.

Analysis In the effectiveness-NTU method, we first determine the heat capacity rates of the hot and cold fluids and identify the smaller one.

$$C_h = \dot{m}_h c_{ph} = (2 \text{ kg/s})(4.31 \text{ kJ/kg·K}) = 8.62 \text{ kW/K}$$

$$C_c = \dot{m}_c c_{pc} = (1.2 \text{ kg/s})(4.18 \text{ kJ/kg·K}) = 5.02 \text{ kW/K}$$

Therefore,

$$C_{\min} = C_c = 5.02 \text{ kW/K}$$

and

$$c = C_{\min}/C_{\max} = 5.02/8.62 = 0.582$$

Then the maximum heat transfer rate is determined from Eq. 11–32 to be

$$\begin{aligned}
\dot{Q}_{\max} &= C_{\min}(T_{h,\text{in}} - T_{c,\text{in}}) \\
&= (5.02 \text{ kW/K})(160 - 20)°\text{C} \\
&= 702.8 \text{ kW}
\end{aligned}$$

That is, the maximum possible heat transfer rate in this heat exchanger is 702.8 kW. The actual rate of heat transfer is

$$\begin{aligned}
\dot{Q} &= [\dot{m}c_p(T_{\text{out}} - T_{\text{in}})]_{\text{water}} = (1.2 \text{ kg/s})(4.18 \text{ kJ/kg·K})(80 - 20)°\text{C} \\
&= 301.0 \text{ kW}
\end{aligned}$$

Thus, the effectiveness of the heat exchanger is

$$\varepsilon = \frac{\dot{Q}}{\dot{Q}_{\max}} = \frac{301.0 \text{ kW}}{702.8 \text{ kW}} = 0.428$$

Knowing the effectiveness, the NTU of this counterflow heat exchanger can be determined from Fig. 11–27*b* or the appropriate relation from Table 11–5 for $c < 1$. We choose the latter approach for greater accuracy:

$$\text{NTU} = \frac{1}{c-1}\ln\left(\frac{\varepsilon - 1}{\varepsilon c - 1}\right) = \frac{1}{0.582 - 1}\ln\left(\frac{0.428 - 1}{0.428 \times 0.582 - 1}\right) = 0.651$$

Then the heat transfer surface area becomes

$$\text{NTU} = \frac{UA_s}{C_{\min}} \longrightarrow A_s = \frac{\text{NTU}\, C_{\min}}{U} = \frac{(0.651)(5020 \text{ W/K})}{640 \text{ W/m}^2\text{·K}} = 5.11 \text{ m}^2$$

To provide this much heat transfer surface area, the length of the tube must be

$$A_s = \pi D L \longrightarrow L = \frac{A_s}{\pi D} = \frac{5.11 \text{ m}^2}{\pi(0.015 \text{ m})} = \textbf{108 m}$$

Discussion This problem was solved in Example 11–4 using the LMTD method. Note that we obtained practically the same result in a systematic and straightforward manner using the effectiveness–NTU method.
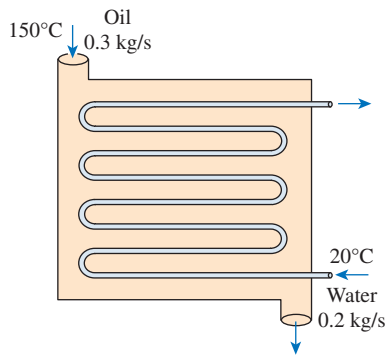
EXAMPLE 11–9   **Cooling Hot Oil by Water in a Multipass Heat Exchanger**

Hot oil is to be cooled by water in a one-shell-pass and eight-tube-passes heat exchanger. The tubes are thin-walled and are made of copper with an internal diameter of 1.4 cm. The length of each tube pass in the heat exchanger is 5 m, and the overall heat transfer coefficient is 310 W/m²·K. Water flows through the tubes at a rate of 0.2 kg/s and the oil through the shell at a rate of 0.3 kg/s. The water and the oil enter at temperatures of 20°C and 150°C, respectively. Determine the rate of heat transfer in the heat exchanger and the outlet temperatures of the water and the oil.

SOLUTION   Hot oil is to be cooled by water in a heat exchanger. The mass flow rates and the inlet temperatures are given. The rate of heat transfer and the outlet temperatures are to be determined.

Assumptions   **1** Steady operating conditions exist. **2** The heat exchanger is well insulated so that heat loss to the surroundings is negligible. **3** The thickness of the tube is negligible since it is thin-walled. **4** Changes in the kinetic and potential energies of fluid streams are negligible. **5** The overall heat transfer coefficient is constant and uniform.

Properties   We take the specific heats of water and oil to be 4.18 and 2.13 kJ/kg·°C, respectively.

Analysis   The schematic of the heat exchanger is given in Fig. 11–31. The outlet temperatures are not specified, and they cannot be determined from an energy balance. The use of the LMTD method in this case will involve tedious iterations, and thus the ε–NTU method is indicated. The first step in the ε–NTU method is to determine the heat capacity rates of the hot and cold fluids and identify the smaller one:

$$C_h = \dot{m}_h c_{ph} = (0.3 \text{ kg/s})(2.13 \text{ kJ/kg·°C}) = 0.639 \text{ kW/K}$$
$$C_c = \dot{m}_c c_{pc} = (0.2 \text{ kg/s})(4.18 \text{ kJ/kg·°C}) = 0.836 \text{ kW/K}$$

Therefore,

$$C_{\min} = C_h = 0.639 \text{ kW/K and } c = \frac{C_{\min}}{C_{\max}} = \frac{0.639}{0.836} = 0.764$$

Then the maximum heat transfer rate is determined from Eq. 11–32 to be

$$\dot{Q}_{\max} = C_{\min}(T_{h, \text{in}} - T_{c, \text{in}}) = (0.639 \text{ kW/K})(150 - 20)°C = 83.1 \text{ kW}$$

That is, the maximum possible heat transfer rate in this heat exchanger is 83.1 kW. The heat transfer surface area is

$$A_s = n(\pi DL) = 8\pi(0.014 \text{ m})(5 \text{ m}) = 1.76 \text{ m}^2$$

Then the NTU of this heat exchanger becomes

$$\text{NTU} = \frac{UA_s}{C_{\min}} = \frac{(310 \text{ W/m}^2\text{·K})(1.76 \text{ m}^2)}{639 \text{ W/K}} = 0.854$$

The effectiveness of this heat exchanger corresponding to $c = 0.764$ and NTU $= 0.854$ is determined from Fig. 11–27c to be

$$\varepsilon = 0.47$$

FIGURE 11–31
Schematic for Example 11–9.

We could also determine the effectiveness from the third relation in Table 11–4 more accurately but with more labor. Then the actual rate of heat transfer becomes

$$\dot{Q} = \varepsilon \dot{Q}_{max} = (0.47)(83.1 \text{ kW}) = \textbf{39.1 kW}$$

Finally, the outlet temperatures of the cold and the hot fluid streams are determined to be

$$\dot{Q} = C_c(T_{c,\,out} - T_{c,\,in}) \longrightarrow T_{c,\,out} = T_{c,\,in} + \frac{\dot{Q}}{C_c}$$

$$= 20°C + \frac{39.1 \text{ kW}}{0.836 \text{ kW/K}} = \textbf{66.8°C}$$

$$\dot{Q} = C_h(T_{h,\,in} - T_{h,\,out}) \longrightarrow T_{h,\,out} = T_{h,\,in} - \frac{\dot{Q}}{C_h}$$

$$= 150°C - \frac{39.1 \text{ kW}}{0.639 \text{ kW/K}} = \textbf{88.8°C}$$

Therefore, the temperature of the cooling water will rise from 20°C to 66.8°C as it cools the hot oil from 150°C to 88.8°C in this heat exchanger.

C&S *EXAMPLE 11–10* **Compliance of a Commercial Warewashing Equipment with the National Sanitation Foundation Standard**

Hot water for commercial warewashing equipment is generated by heat recovered from a furnace exhaust gas. A crossflow heat exchanger is used, with the hot gas (mixed) flowing over the tubes (Fig. 11–32). The hot gas (c_p = 1040 J/kg·K) enters the heat exchanger at 450°C with a flow rate of 2.5 kg/s. The water (c_p = 4200 J/kg·K) flows through the tubes unmixed at 4 kg/s. The tubes have negligible wall thickness, and each tube has a diameter and length of 25 mm and 2 m, respectively. The corresponding convection heat transfer coefficients on the outer and inner tube surfaces are 250 and 3300 W/m²·K, respectively. The National Sanitation Foundation (NSF) standard for commercial warewashing equipment (ANSI/NSF 3) requires that the final rinse water temperature be between 82 and 90°C. If the water enters the heat exchanger at 50°C, determine the number of tubes required in crossflow with the gas to heat the water to 86°C, so that it complies with the ANSI/NSF 3 standard.

SOLUTION In this example, the engineering codes developed by the National Sanitation Foundation (NSF) standard for commercial warewashing equipment (ANSI/NSF 3) are incorporated in a problem that involves the use of a crossflow heat exchanger to heat water for commercial warewashing equipment by heat recovered from a furnace exhaust gas. The concept of effectiveness-NTU method for heat exchanger analysis is used to determine the number of tubes required in crossflow with the gas such that the heat exchanger is in compliance with the ANSI/NSF 3 standard.

Gas flow (*mixed*)

Air flow (*unmixed*)
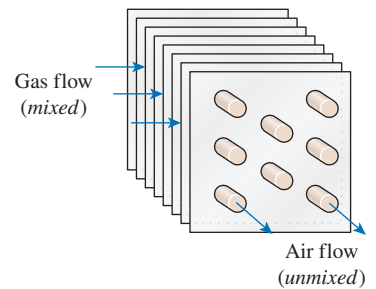
FIGURE 11–32
Schematic for Example 11–10.

Assumptions **1** Steady-state conditions. **2** The heat exchanger is well insulated so that heat loss to the surroundings is negligible, and thus heat transfer from the hot fluid is equal to the heat transfer to the cold fluid. **3** Properties of fluids are constant. **4** Negligible fouling factor.

Analysis The overall heat transfer coefficient for the heat exchanger is

$$U = \left(\frac{1}{h_i} + \frac{1}{h_o}\right)^{-1} = \left(\frac{1}{3300 \text{ W/m}^2\cdot\text{K}} + \frac{1}{250 \text{ W/m}^2\cdot\text{K}}\right)^{-1} = 232.39 \text{ W/m}^2\cdot\text{K}$$

The heat capacity rate for the cold fluid is

$$C_c = \dot{m}_c c_{pc} = (4 \text{ kg/s})(4200 \text{ J/kg}\cdot\text{K}) = 16{,}800 \text{ W/K}$$

The heat capacity rate for the hot fluid is

$$C_h = \dot{m}_h c_{ph} = (2.5 \text{ kg/s})(1040 \text{ J/kg}\cdot\text{K}) = 2600 \text{ W/K} = C_{\min}$$

The capacity ratio becomes

$$c = \frac{C_{\min}}{C_{\max}} = \frac{C_h}{C_c} = \frac{2600 \text{ W/K}}{16{,}800 \text{ W/K}} = 0.15476$$

The heat exchanger effectiveness is

$$\varepsilon = \frac{\dot{Q}}{\dot{Q}_{\max}} = \frac{C_c(T_{c,\text{out}} - T_{c,\text{in}})}{C_{\min}(T_{h,\text{in}} - T_{c,\text{in}})} = \frac{(16{,}800 \text{ W/K})(86 - 50) \text{ K}}{(2600 \text{ W/K})(450 - 50) \text{ K}} = 0.58154$$

The effectiveness–NTU relation for crossflow ($C_{\min}$ mixed, $C_{\max}$unmixed) heat exchanger from Table 11–5 is

$$\text{NTU} = -\frac{\ln[c\ln(1 - \varepsilon) + 1]}{c} = -\frac{\ln[(0.15476)\ln(1 - 0.58154) + 1]}{0.15476} = 0.93578$$

The total heat transfer surface area is

$$A_s = \text{NTU}\frac{C_{\min}}{U} = (0.93578)\frac{2600 \text{ W/K}}{232.39 \text{ W/m}^2\cdot\text{K}} = 10.47 \text{ m}^2$$

The heat transfer surface area is determined from the number of tubes, tube length, and tube diameter:

$$A_s = \pi DL \times \text{Number of tubes}$$

Thus, the number of tubes in crossflow with the hot gas is

$$\text{Number of tubes} = \frac{A_s}{\pi DL} = \frac{10.47 \text{ m}^2}{\pi(0.025 \text{ m})(2 \text{ m})} = 66.65 = \textbf{67 tubes}$$

Discussion To generate hot water by heat recovered from a furnace exhaust gas from 50 to 86°C (between 82 and 90°C required by the ANSI/NSF 3 standard), the crossflow heat exchanger would need 67 tubes in crossflow with the gas.

FIGURE 11–33
Schematic for Example 11–11.

PtD **EXAMPLE 11–11**   **Prevention of Fire Hazard by Cooling Ethanol to Below its Flash Point**

Ethanol is classified by the National Fire Protection Association (NFPA) as a flammable fluid because of its low flash point of 17°C. This means that at 17°C or higher, ethanol can vaporize and become a mixture in air that would ignite when an ignition source is present. Thus, in an environment where ignition sources are present, keeping ethanol at a temperature below its flash point can help to prevent fire hazard. Consider a process where ethanol is cooled by water in a one-shell-pass heat exchanger that can accommodate a maximum of 14 tube passes (Fig. 11–33). The tubes are made of copper and are thin-walled with an inner diameter of 1.5 cm. The length of each tube pass that can be fitted inside the heat exchanger is 3 m, and the overall heat transfer coefficient is 700 W/m²·K. Ethanol ($c_p = 2630$ J/kg·K) enters the heat exchanger at 55°C and flows through the shell at a rate of 0.28 kg/s. Water enters the heat exchanger at 2°C and flows through the tubes at a rate of 1.3 kg/s. To prevent fire hazard, the ethanol is to be cooled to 15°C, which is below its flash point. Determine the number of tube passes that is necessary inside the shell-and-tube heat exchanger to cool the ethanol to the prescribed temperature. Discuss whether or not this heat exchanger is suitable for this application. Evaluate any required property of water at 5°C. Is this a good assumption?

SOLUTION   In this example, the concepts of Prevention through Design (PtD) are applied in conjunction with the effectiveness–NTU method for heat exchanger analysis.
Assumptions   **1** Steady operating conditions exist. **2** The heat exchanger is well insulated so that heat loss to the surroundings is negligible. **3** Changes in the kinetic and potential energies of fluid streams are negligible. **4** Fluid properties are constant. **5** Thermal resistance of tube wall is negligible.
Properties   The specific heat of ethanol is given to be $c_{ph} = 2630$ J/kg·K. The specific heat of water at 5°C is $c_{pc} = 4205$ J/kg·K (Table A-9).
Analysis   In the effectiveness-NTU method, we first determine the heat capacity rates of the hot and cold fluids and identify the smaller one:

$$C_h = \dot{m}_h c_{ph} = (0.28 \text{ kg/s})(2630 \text{ J/kg·K}) = 736.4 \text{ W/K}$$
$$C_c = \dot{m}_c c_{pc} = (1.3 \text{ kg/s})(4205 \text{ J/Kg·K}) = 5466.5 \text{ W/K}$$

Therefore,

$$C_{\min} = C_h = 736.4 \text{ W/K}$$

and

$$c = C_{\min}/C_{\max} = 736.4/5466.5 = 0.1347$$

Then the maximum heat transfer rate is determined from Eq. 11–32 to be

$$\dot{Q}_{\max} = C_{\min}(T_{h,\text{ in}} - T_{c,\text{ in}}) = (736.4 \text{ W/K})(55 - 2)\text{K} = 39{,}029 \text{ W}$$

The actual rate of heat transfer is

$$\dot{Q} = C_h(T_{h,\text{ in}} - T_{h,\text{ out}}) = (736.4 \text{ W/K})(55 - 15)\text{K} = 29{,}456 \text{ W}$$

Thus, the effectiveness of the heat exchanger is

$$\varepsilon = \frac{\dot{Q}}{\dot{Q}_{\max}} = \frac{29{,}456}{39{,}029} = 0.7547$$
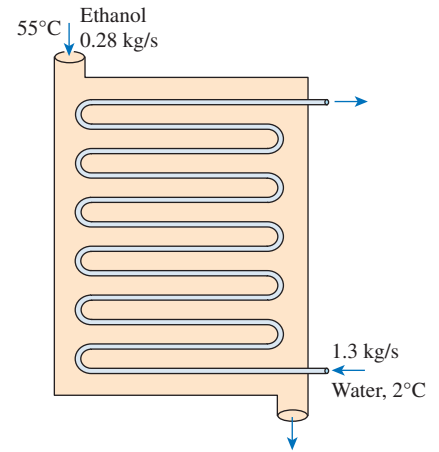
For this one-shell-pass heat exchanger, knowing the effectiveness (ε), the NTU of this heat exchanger can be determined from the appropriate relation from Table 11–5:

$$
\begin{aligned}
\text{NTU}_1 &= -\frac{1}{\sqrt{1+c^2}} \ln\left(\frac{2/\varepsilon_1 - 1 - c - \sqrt{1+c^2}}{2/\varepsilon_1 - 1 - c + \sqrt{1+c^2}}\right) \\
&= -\frac{1}{\sqrt{1+0.1347^2}} \ln\left(\frac{2/0.7547 - 1 - 0.1347 - \sqrt{1+0.1347^2}}{2/0.7547 - 1 - 0.1347 + \sqrt{1+0.1347^2}}\right) \\
&= 1.592
\end{aligned}
$$

Note that for this one-shell-pass heat exchanger, $\varepsilon_1 = \varepsilon$ and $\text{NTU}_1 = \text{NTU}$
Then the number of tube passes (n) can be determined using

$$
\text{NTU} = \frac{UA_s}{C_{min}} = \frac{U(\pi D L)n}{C_{min}} = 1.592
$$

Thus,

$$
n = \frac{C_{min}\text{NTU}}{U\pi DL} = \frac{(736.4 \text{ W/K})(1.592)}{(700 \text{ W/m}^2\cdot\text{K})\pi(0.015 \text{ m})(3 \text{ m})} = 11.8 \rightarrow \textbf{12 tube passes}
$$

Discussion To reduce the ethanol temperature from 55°C to 15°C, the one-shell-pass heat exchanger requires at least 12 tube passes of 1.5-cm-diameter and 3-m-long tubes. At 15°C, the temperature is below the flash point of ethanol, and the risk of fire hazard is alleviated.

The heat exchanger can accommodate up to 14 tube passes, so it is suitable for this application.

Note that the outlet temperature of water can be determined from

$$
\dot{Q} = C_c(T_{c,\,out} - T_{c,\,in}) \rightarrow T_{c,\,out} = \frac{\dot{Q}}{C_c} + T_{c,\,in} = \frac{29,456 \text{ W}}{5466.5 \text{ W/°C}} + 2°\text{C} = 7.4°\text{C}
$$

Then the bulk mean temperature for the water is $T_{c,\,b} = (T_{c,\,out} + T_{c,\,in})/2 = 4.7°\text{C}$. Thus, 5°C is an appropriate temperature for evaluating the specific heat of water.

11–6 ▪ SELECTION OF HEAT EXCHANGERS

Heat exchangers are complicated devices, and the results obtained with the simplified approaches presented previously should be used with care. For example, we assumed that the overall heat transfer coefficient U is constant throughout the heat exchanger and that the convection heat transfer coefficients can be predicted using the convection correlations. However, it should be kept in mind that the uncertainty in the predicted value of U can exceed 30 percent. Thus, it is natural to tend to overdesign the heat exchangers in order to avoid unpleasant surprises.

Heat transfer enhancement in heat exchangers is usually accompanied by *increased pressure drop,* and thus *higher pumping power.* Therefore, any gain from the enhancement in heat transfer should be weighed against the cost of the accompanying pressure drop. Also, some thought should be given to which fluid should pass through the tube side and which through the shell side. Usually, the *more viscous fluid is more suitable for the shell side* (larger passage area and thus lower pressure drop) and *the fluid with the higher pressure for the tube side.*

Engineers in industry often find themselves in a position to select heat exchangers to accomplish certain heat transfer tasks. Usually, the goal is to heat or cool a certain fluid at a known mass flow rate and temperature to a desired temperature. Thus, the *rate of heat transfer* in the prospective heat exchanger is

$$\dot{Q} = \dot{m}c_p(T_{\text{in}} - T_{\text{out}})$$

which gives the heat transfer requirement of the heat exchanger before we have any idea about the heat exchanger itself.

An engineer going through catalogs of heat exchanger manufacturers will be overwhelmed by the types and numbers of readily available off-the-shelf heat exchangers. The proper selection depends on several factors.

Heat Transfer Rate

This is the most important quantity in the selection of a heat exchanger. A heat exchanger should be capable of transferring heat at the specified rate in order to achieve the desired temperature change of the fluid at the specified mass flow rate.

Cost

Budgetary limitations usually play an important role in the selection of heat exchangers, except for some specialized cases where "money is no object." An off-the-shelf heat exchanger has a definite cost advantage over those made to order. However, in some cases, none of the existing heat exchangers will do, and it may be necessary to undertake the expensive and time-consuming task of designing and manufacturing a heat exchanger from scratch to suit the needs. This is often the case when the heat exchanger is an integral part of the overall device to be manufactured.

The operation and maintenance costs of the heat exchanger are also important considerations in assessing the overall cost.

Pumping Power

In a heat exchanger, both fluids are usually forced to flow by pumps or fans that consume electrical power. The annual cost of electricity associated with the operation of the pumps and fans can be determined from

Operating cost = (Pumping power, kW) × (Hours of operation, h)
× (Unit cost of electricity, $/kWh)

where the pumping power is the total electrical power consumed by the motors of the pumps and fans. For example, a heat exchanger that involves a 1-hp pump and a $\frac{1}{3}$-hp fan (1 hp = 0.746 kW) operating at full load 8 h a day and 5 days a week will consume 2069 kWh of electricity per year, which will cost $166 at an electricity cost of 8 cents/kWh.

Minimizing the pressure drop and the mass flow rate of the fluids will minimize the operating cost of the heat exchanger, but it will maximize the size of the heat exchanger and thus the initial cost. As a rule of thumb, doubling the mass flow rate will reduce the initial cost by *half* but will increase the pumping power requirements by a factor of roughly *eight.*

Typically, fluid velocities encountered in heat exchangers range between 0.7 and 7 m/s for liquids and between 3 and 30 m/s for gases. Low velocities are helpful in avoiding erosion, tube vibrations, and noise as well as pressure drop.

Size and Weight

Normally, the *smaller* and the *lighter* the heat exchanger, the better it is. This is especially the case in the *automotive* and *aerospace* industries, where size and weight requirements are most stringent. Also, a larger heat exchanger normally carries a higher price tag. The space available for the heat exchanger in some cases limits the length of the tubes that can be used.

Type

The type of heat exchanger to be selected depends primarily on the types of *fluids* involved, the *size* and *weight* limitations, and the presence of any *phase-change* processes. For example, a heat exchanger is suitable for cooling a liquid with a gas if the surface area on the gas side is many times that on the liquid side. On the other hand, a plate or shell-and-tube heat exchanger is very suitable for cooling a liquid with another liquid.

Materials

The materials used in the construction of the heat exchanger may be an important consideration in the selection of heat exchangers. For example, the thermal and structural *stress effects* need not be considered at pressures below 15 atm or temperatures below 150°C. But these effects are major considerations above 70 atm or 550°C and seriously limit the acceptable materials of the heat exchanger.

A temperature difference of 50°C or more between the tubes and the shell will probably pose *differential thermal expansion* problems and needs to be considered. In the case of corrosive fluids, we may have to select expensive *corrosion-resistant* materials such as stainless steel or even titanium if we are not willing to replace low-cost heat exchangers frequently.

Other Considerations

There are other considerations in the selection of heat exchangers that may or may not be important, depending on the application. For example, being *leak-tight* is an important consideration when *toxic* or *expensive* fluids are involved. Ease of servicing, low maintenance cost, and safety and reliability are some other important considerations in the selection process. Quietness is one of the primary considerations in the selection of liquid-to-air heat exchangers used in heating and air-conditioning applications.

EXAMPLE 11–12   **Installing a Heat Exchanger to Save Energy and Money**

In a dairy plant, milk is pasteurized by hot water supplied by a natural gas furnace. The hot water is then discharged to an open floor drain at 80°C at a rate of 15 kg/min. The plant operates 24 h a day and 365 days a year. The furnace has an efficiency of

80 percent, and the cost of the natural gas is $1.10 per therm (1 therm = 105,500 kJ). The average temperature of the cold water entering the furnace throughout the year is 15°C. The drained hot water cannot be returned to the furnace and recirculated because it is contaminated during the process.

To save energy, it is proposed that a water-to-water heat exchanger be installed to preheat the incoming cold water with the drained hot water. Assuming that the heat exchanger will recover 75 percent of the available heat in the hot water, determine the heat transfer rating of the heat exchanger that needs to be purchased, and suggest a suitable type. Also, determine the amount of money this heat exchanger will save the company per year by reducing its consumption of natural gas.

SOLUTION A water-to-water heat exchanger is to be installed to transfer energy from drained hot water to the incoming cold water to preheat it. The rate of heat transfer in the heat exchanger and the amounts of energy and money saved per year are to be determined.

Assumptions **1** Steady operating conditions exist. **2** The effectiveness of the heat exchanger remains constant.

Properties We use the specific heat of water at room temperature, $c_p = 4.18$ kJ/kg·°C, and treat it as a constant.

Analysis A schematic of the prospective heat exchanger is given in Fig. 11–34. The heat recovery from the hot water will be a maximum when it leaves the heat exchanger at the inlet temperature of the cold water. Therefore,

$$\dot{Q}_{max} = \dot{m}_h c_p (T_{h,\,in} - T_{c,\,in})$$
$$= \left(\frac{15}{60}\,\text{kg/s}\right)(4.18\,\text{kJ/kg·K})(80 - 15)°C$$
$$= 67.9\,\text{kJ/s}$$

That is, the existing hot-water stream has the potential to supply heat at a rate of 67.9 kJ/s to the incoming cold water. This value would be approached in a counterflow heat exchanger with a *very large* heat transfer surface area. A heat exchanger of reasonable size and cost can capture 75 percent of this heat transfer potential. Thus, the heat transfer rating of the prospective heat exchanger must be

$$\dot{Q} = \varepsilon\dot{Q}_{max} = (0.75)(67.9\,\text{kJ/s}) = \textbf{50.9 kJ/s}$$

That is, the heat exchanger should be able to deliver heat at a rate of 50.9 kJ/s from the hot to the cold water. An ordinary plate or *shell-and-tube* heat exchanger should be adequate for this purpose, since both sides of the heat exchanger involve the same fluid at comparable flow rates and thus comparable heat transfer coefficients. (Note that if we were heating air with hot water, we would have to specify a heat exchanger that has a large surface area on the air side.)

The heat exchanger will operate 24 h a day and 365 days a year. Therefore, the annual operating hours are

$$\text{Operating hours} = (24\,\text{h/day})(365\,\text{days/year}) = 8760\,\text{h/year}$$

Noting that this heat exchanger saves 50.9 kJ of energy per second, the energy saved during an entire year will be

$$\text{Energy saved} = (\text{Heat transfer rate})(\text{Operation time})$$
$$= (50.9\,\text{kJ/s})(8760\,\text{h/year})(3600\,\text{s/h})$$
$$= 1.605 \times 10^9\,\text{kJ/year}$$

80°C Hot water

Cold water
15°C
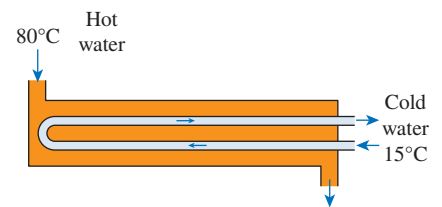
FIGURE 11–34
Schematic for Example 11–12.

The furnace is said to be 80 percent efficient. That is, for each 80 units of heat supplied by the furnace, natural gas with an energy content of 100 units must be supplied to the furnace. Therefore, the energy savings determined above result in fuel savings in the amount of

$$\text{Fuel saved} = \frac{\text{Energy saved}}{\text{Furnace efficiency}} = \frac{1.605 \times 10^9 \text{ kJ/year}}{0.80} \left(\frac{1 \text{ therm}}{105{,}500 \text{ kJ}} \right)$$
$$= 19{,}020 \text{ therms/year}$$

Noting that the price of natural gas is $1.10 per therm, the amount of money saved becomes

$$\text{Money saved} = (\text{Fuel saved}) \times (\text{Price of fuel})$$
$$= (19{,}020 \text{ therms/year})(\$1.10/\text{therm})$$
$$= \textbf{\$20{,}920/year}$$

Therefore, the installation of the proposed heat exchanger will save the company $20,920 a year, and the installation cost of the heat exchanger will probably be paid from the fuel savings in a short time.

TOPIC OF SPECIAL INTEREST*

FIGURE 11–35
Heat exchange between the human body and its environment by different mechanisms (conduction, convection, radiation, and evaporation).

The Human Cardiovascular System as a Countercurrent Heat Exchanger*

The human body experiences many mechanisms by which it gains or loses heat, including conduction (e.g., feet to concrete), convection (wind blowing past exposed skin), radiation (e.g., solar), and evaporation (Fig. 11–35), as described throughout Chap. 1. Additionally, the human body generates heat through metabolism; however, a significant amount of this heat can be lost to the surrounding environment through conduction and convection. In order to prevent the core body temperature from falling significantly, the cardiovascular system is organized as a countercurrent heat exchanger. This cardiovascular countercurrent mechanism plays a major role in human thermoregulation (Sec. 3–7). Recall from our previous discussion that the extremities tend to have a lower or higher temperature as compared with the core body and that this is partially due to external factors and activity levels. The core body temperature does not fluctuate significantly under normal conditions. In the cardiovascular system, the countercurrent design is composed of one artery that is always paired and adjacent to one vein (note that an artery transports blood away from the heart and generally toward the extremities, whereas a vein transports blood toward the heart and generally away from the extremities). It has been suggested that the salient physiological factor in reducing the amount of heat loss by the body to the environment, as measured by a blood flow temperature drop, is this very precise and very regular arrangement of the

*This section is contributed by Professor David A. Rubenstein, Department of Biomedical Engineering, Stony Brook University, Stony Brook, NY.

cardiovascular system as a countercurrent heat exchanger. This organization has been observed in many species (including all warm-blooded animals), and significant quantifiable heat transfer has been seen to occur and has been measured between these two vessels.

How does the countercurrent mechanism work in humans? Imagine a person who enters an environment colder than the body's core temperature (e.g., 37°C) from an environment that is approximately equal to the body's core temperature. Initially, the person's extremities (hands, fingers, toes, etc.) will be at a higher temperature than the environment. Thus, heat will flow from the extremities to the environment. This means that the temperature of the tissue in the extremity, and importantly the blood in the veins, will be lower than the temperature of blood in the arteries (Fig. 11–36). This is caused by the energy transfer to the environment if we remember that arteries feed tissue with blood, and it is the veins that remove blood from the tissue. With significant heat transfer between the artery and vein, the arterial blood temperature begins to fall, but at the same time, the venous blood begins to be rewarmed (remember that in warm-blooded animals, including humans, circulatory systems are closed). This results in the venous blood returning to the core at a higher temperature than it would have without the heat transfer between the artery and vein in a countercurrent mechanism. Furthermore, this warmed venous blood can continue to warm as it passes toward the heart, and thus it may be closer to the body's core temperature generated by metabolism once it returns to the heart. Therefore, the net heat transfer to the environment is reduced through the actions of the cardiovascular countercurrent heat exchanger. Part of the beauty of this system is that not only is the venous blood temperature altered so that it more closely matches the core body temperature, but the arterial blood temperature also changes to more closely match the environmental temperature. This effectively reduces the driving force for heat transfer at the extremities. Recall that with excessive heat lost to the environment, the human body will reduce the skin temperature and increase the rate of metabolic heat generation, as described in Chap. 1's Topic of Special Interest on Thermal Comfort. This mechanism plays a primary role when the external environmental temperature diverges significantly from the core body temperature in all warm-blooded animals (Fig. 11–36, shown for both a cold and a hot environment).

A simplified model of the cardiovascular countercurrent heat exchanger found in a limb can be depicted by Fig. 11–37. The heat transfer directions are denoted on this figure, but remember that temperature can increase or decrease (heat is gained or lost) primarily depending on the environmental temperature. Applying the conservation of energy to the system, we can see that energy is only transported by blood and the heat flux between the three systems (artery, vein, and external environment). The energy that is carried by the blood can be denoted as

$$\dot{Q}_{\text{blood}} = \dot{m}\frac{dh}{dx} = \dot{m}c_p\frac{dT}{dx} \qquad (11\text{–}42)$$
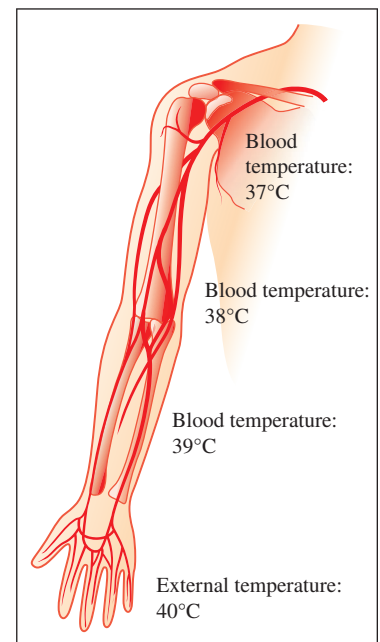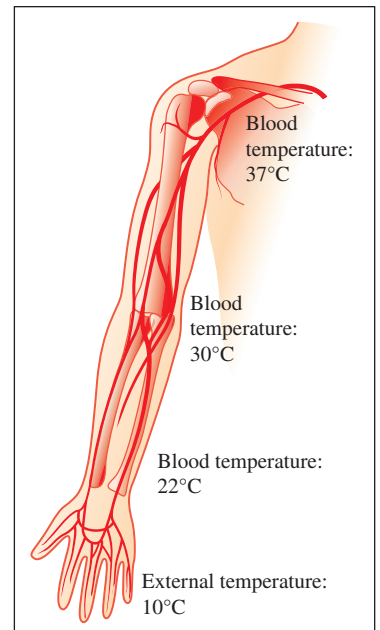
FIGURE 11–36
Blood temperature variation in the human arm for both a cold and a hot environment.

where $\dot{m}$ is the mass flow rate of the blood and h is the blood enthalpy. Furthermore, the heat transfer that occurs between the three systems can be described by

$$\dot{Q} = UA_s \Delta T_m \tag{11–15}$$

which has been used previously to describe the total heat transfer rate in a heat exchanger. Here we include multiple heat transfer occurrences into one global parameter to simplify the analysis. Therefore the total heat transfer rate of this system can be defined as

$$\dot{Q}_{\text{blood}} + \dot{Q} = \dot{m}c_p \frac{dT}{dx} + UA_s \Delta T_m \tag{11–43}$$

The preceding equation can be expanded for the arterial (denoted with a subscript A) and venous (denoted with a subscript V) systems as

$$\dot{m}c_p \frac{dT_A}{dx} + (UA_s)_{AV}(T_A - T_V) + (UA_s)_A(T_A - T_\infty) = 0 \quad \text{Artery}$$

$$\dot{m}c_p \frac{dT_V}{dx} + (UA_s)_{AV}(T_A - T_V) - (UA_s)_V(T_V - T_\infty) = 0 \quad \text{Vein} \tag{11–44}$$
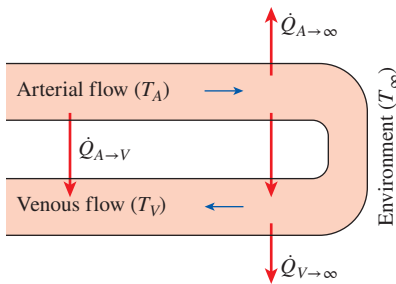
Equation 11–44 is a system of linear ordinary differential equations, which can be solved with any method that you are familiar with from a previous course in advanced mathematics. Before we continue, we want to point out that there are a few assumptions that have been incorporated in this model. The first assumption is that the temperature difference in the radial direction (r) and angular direction (ϕ) are negligible (please refer to the coordinate system discussion in Sec. 2–1, Fig. 2–3); the temperature is only a function of the flow direction (x). We can also expand this analysis to a more complicated vascular system if we know how each of the artery–vein pairs is related to the analyzed artery–vein pair (i.e., if all heat transfer properties are the same, then we can simply multiply by the number of vascular beds in the entire system to get the total heat transfer rate). We also assume that the heat transfer coefficients and all other thermal properties do not change along the flow direction within one vascular bed (i.e., the heat transfer coefficient between the artery and the vein are the same along the entire blood vessel length, which is not a great assumption since the biological tissue properties will change from the larger vessels to the smaller ones). That the flow rates within the arterial and venous circulation are the same (or very similar) will also be an underlying assumption of this model.

All methods that have been previously discussed in this section (the log mean temperature difference method or the effectiveness-NTU method) to analyze a countercurrent heat exchanger can be applied to the flow through the cardiovascular system. However, there are a couple of key points to remember which make these systems different than what we have discussed previously. First, the fluid is the same in both vessels, and we may be able to assume that the fluid properties (except for temperature) are very similar in each vessel. The bulk fluid viscosity and density are reasonably equal in arteries and veins, but in small vessels, the fluid properties may diverge.

FIGURE 11–37
Simplified extremity model for a countercurrent heat exchanger.

Furthermore, the outflow of the warmer vessel is connected to the inflow of the colder vessel, so we should have a similar mass flow rate through each tube, and $T_{h,\,out}$ may be assumed to equal $T_{c,\,in}$. This ignores that some fluid is lost along the length of the smallest blood vessels. Therefore, there is some additional coupling that may need to be considered in these cases.

The system of linear ordinary differential equations may be quite complex to analyze in practice. Therefore, there has been significant work on simplifying this analysis. The most applicable simplification came from Weinbaum and Jiji (1985) and can be represented as

$$\rho c_p \frac{\partial T}{\partial t} = \frac{\partial}{\partial x}\left(k_{\text{eff}}\frac{\partial T}{\partial x}\right) + \dot{e}_m \tag{11–45}$$

where $\dot{e}_m$ is the metabolic heat source term. Equation 11–45 is only valid if we can assume one-dimensional heat transfer. In fact, this equation can be derived from the bioheat transfer equation discussed in Chap. 3 (see Sec. 3–7). This model has been derived based on the temperature of the tissue only, assuming that the average blood temperature and the local tissue temperature will be similar. The difficulty with this analysis is that the effective conductivity term becomes quite complicated because Weinbaum and Jiji (1985) tried to incorporate the imperfections of the cardiovascular countercurrent heat exchanger design within this term. The effective conductivity can be represented as

$$k_{\text{eff}} = k + \frac{n\pi^2 r^4 \rho^2 c_p^2 V_{\text{avg}}^2}{S^2 k_b} \tag{11–46}$$

where S is the conduction shape factor of blood vessels, n is the number density of vessel pairs crossing the control volume, r is the artery radius, ρ is the blood density, V_{avg} is the average blood velocity, k is the thermal conductivity of the blood vessel, and k_b is the thermal conductivity of blood. The most critical finding from the Weinbaum and Jiji (1985) paper is that the design of the cardiovascular system in this manner effectively enhances the tissue conductivity. For the smallest vessels in the skin, the conductivity is approximately 5 percent larger than what would be anticipated without the countercurrent design. For larger vessels in the skin region, this enhancement can go as high as 70 percent, suggesting that the countercurrent cardiovascular mechanism is a very efficient design to rewarm blood before it enters the core of the body. The major assumptions in the Weinbaum and Jiji model are that the mean tissue temperature is equal to the average of the arterial blood temperature and the vein blood temperature at one particular cross section. Secondly, most of the heat conduction occurs between the artery and the vein, whereas minimal heat is lost to the surrounding tissue or the environment. There has been some computational and experimental work aimed at relieving the constraints of the models described above. For these methods, it was typical to take a volume averaging approach to derive the bioheat transfer equations and blood flow equations. These equations tend to ignore spatial inhomogeneities and the possibility of fluctuations with time. These models tend to be overly complicated without adding much accuracy.

EXAMPLE 11–13   Countercurrent Heat Exchanger in the Human Body

Blood is flowing through an artery and vein pair near an extremity of the human body. The artery has a diameter of 1 cm and the vein has a diameter of 1.5 cm. The length of each blood vessel is 100 cm. Blood is flowing through the artery at a mass flow rate of 2 g/s and is flowing through the vein at a mass flow rate of 1.8 g/s. The average temperature of blood in the artery is 34°C and the average temperature of blood in the vein is 32°C. The inflow temperature of the artery is 36°C and the external environment temperature is 20°C. Determine the overall heat transfer coefficient for blood and the change in temperature with respect to distance for these blood flow conditions.

SOLUTION   Blood in the artery is being cooled, while blood in the vein is being warmed. Blood flows in a countercurrent manner, and the overall heat transfer coefficient for blood and the change in temperature for these blood flow conditions are to be determined.

Assumptions   **1** The flow through each blood vessel is fully developed. **2** Properties of blood are constant and equal in the artery and the vein. **3** Constant surface heat flux. **4** The conductances to the environment from the artery and the vein are equal.

Properties   The properties of blood are as follows:

$$k = 0.67 \frac{W}{m \cdot K} \quad c_p = 3.475 \frac{kJ}{kg \cdot K}$$

$$\rho = 1050 \frac{kg}{m^3} \quad \mu = 0.035 \frac{g}{s \cdot cm}$$

Analysis   The schematic of the blood vessels is given in Fig. 11–37. The overall heat transfer coefficient can be calculated from

$$\frac{1}{U} = \frac{1}{h_{artery}} + \frac{1}{h_{vein}}$$

which is a modification of Eq. 11–5. The convection heat transfer coefficients can be determined using the forced convection relationships. Using Eq. 8–5, the Reynolds number for blood in the artery is

$$Re = \frac{4\dot{m}}{\mu \pi D} = \frac{4\left(2 \frac{g}{s}\right)}{\left(0.035 \frac{g}{s \cdot cm}\right)(\pi)(1 \text{ cm})} = 72.8$$

And the Reynolds number for blood in the vein is

$$Re = \frac{4\dot{m}}{\mu \pi D} = \frac{4\left(1.8 \frac{g}{s}\right)}{\left(0.035 \frac{g}{s \cdot cm}\right)(\pi)(1.5 \text{ cm})} = 43.7$$

The flow is laminar (Re < 2300) in both the artery and vein. Therefore, since the flow is fully developed laminar with constant surface heat flux boundary conditions, the Nusselt number for each of these flow conditions is 4.36 as given by Eq. 8–60.

The convection heat transfer coefficients can be calculated from

$$h_{artery} = \frac{k}{D} Nu = \frac{0.67 \dfrac{W}{m \cdot K}}{0.01 \text{ m}} (4.36) = 292 \frac{W}{m^2 \cdot K}$$

$$h_{vein} = \frac{k}{D} Nu = \frac{0.67 \dfrac{W}{m \cdot K}}{0.015 \text{ m}} (4.36) = 195 \frac{W}{m^2 \cdot K}$$

Therefore, the overall heat transfer coefficient is equal to

$$U = \frac{1}{\dfrac{1}{h_{artery}} + \dfrac{1}{h_{vein}}} = \frac{1}{\dfrac{1}{292.12 \dfrac{W}{m^2 \cdot K}} + \dfrac{1}{194.75 \dfrac{W}{m^2 \cdot K}}} = \mathbf{116.9 \; \frac{W}{m^2 \cdot K}}$$

If we solve Eq. 11–44, we get

$$\frac{T_A - T_\infty}{T_o - T_\infty} = \frac{\sqrt{1 + 2\left(\frac{N_i}{N_o}\right)} \cosh\left(N_o \sqrt{1 + 2\left(\frac{N_i}{N_o}\right)}\right)\left(1 - \frac{x}{L}\right) + \sinh\left(N_o \sqrt{1 + 2\left(\frac{N_i}{N_o}\right)}\right)\left(1 - \frac{x}{L}\right)}{\sqrt{1 + 2\left(\frac{N_i}{N_o}\right)} \cosh\left(N_o \sqrt{1 + 2\left(\frac{N_i}{N_o}\right)}\right) + \sinh\left(N_o \sqrt{1 + 2\left(\frac{N_i}{N_o}\right)}\right)}$$

$$\frac{T_V - T_\infty}{T_o - T_\infty} = \frac{\sqrt{1 + 2\left(\frac{N_i}{N_o}\right)} \cosh\left(N_o \sqrt{1 + 2\left(\frac{N_i}{N_o}\right)}\right)\left(1 - \frac{x}{L}\right) - \sinh\left(N_o \sqrt{1 + 2\left(\frac{N_i}{N_o}\right)}\right)\left(1 - \frac{x}{L}\right)}{\sqrt{1 + 2\left(\frac{N_i}{N_o}\right)} \cosh\left(N_o \sqrt{1 + 2\left(\frac{N_i}{N_o}\right)}\right) + \sinh\left(N_o \sqrt{1 + 2\left(\frac{N_i}{N_o}\right)}\right)}$$

where

$$N_o = \frac{(UA_s)_A L}{\dot{m}c_p} \cong \frac{(UA_s)_V L}{\dot{m}c_p} = 0.00132$$

$$N_i = \frac{(UA_s)_{AV} L}{\dot{m}c_p} = 1.06$$

where L is the total length of interest of the blood vessel and the subscripts either denote artery (A) or vein (V) or the combined vascular pair (AV). The solution to Eq. 11–44 follows a similar form to that discussed for the fin equation in Chap. 3 (see Sec. 3–6) and is closely related to the solution for convection from the fin tip. Solving the two preceding equations for our conditions, we get

$$\frac{T_A - 20°C}{36°C - 20°C}$$
$$= \frac{\sqrt{1 + 2\left(\frac{1.06}{0.00132}\right)} \cosh\left(0.00132 \sqrt{1 + 2\left(\frac{1.06}{0.00132}\right)}\right)\left(1 - \frac{x}{100 \text{ cm}}\right) + \sinh\left(0.00132 \sqrt{1 + 2\left(\frac{1.06}{0.00132}\right)}\right)\left(1 - \frac{x}{100 \text{ cm}}\right)}{\sqrt{1 + 2\left(\frac{1.06}{0.00132}\right)} \cosh\left(0.00132 \sqrt{1 + 2\left(\frac{1.06}{0.00132}\right)}\right) + \sinh\left(0.00132 \sqrt{1 + 2\left(\frac{1.06}{0.00132}\right)}\right)}$$

$$\frac{T_v - 20°C}{36°C - 20°C}$$
$$= \frac{\sqrt{1 + 2\left(\frac{1.06}{0.00132}\right)} \cosh\left(0.00132 \sqrt{1 + 2\left(\frac{1.06}{0.00132}\right)}\right)\left(1 - \frac{x}{100 \text{ cm}}\right) - \sinh\left(0.00132 \sqrt{1 + 2\left(\frac{1.06}{0.00132}\right)}\right)\left(1 - \frac{x}{100 \text{ cm}}\right)}{\sqrt{1 + 2\left(\frac{1.06}{0.00132}\right)} \cosh\left(0.00132 \sqrt{1 + 2\left(\frac{1.06}{0.00132}\right)}\right) + \sinh\left(0.00132 \sqrt{1 + 2\left(\frac{1.06}{0.00132}\right)}\right)}$$

Carrying out the algebraic operations, we can find an expression for the variation in temperature along the blood vessel length.

$$T_A = 16°C \left(1 - \frac{x}{100 \text{ cm}} \right) + 20°C$$

$$T_V = 15.97°C \left(1 - \frac{x}{100 \text{ cm}} \right) + 20°C$$

Discussion The temperature variation along the length of the blood vessel varies linearly with distance. We have encountered similar solutions for internal fully developed flow under constant surface heat flux boundary conditions (Fig. 8–11) and for heat exchangers with two fluid streams that have the same heat capacity (Fig. 11–13). We made the assumption that the fluid properties were the same in the artery and the vein and would change significantly with temperature. From the two temperature variation equations we can calculate the temperature along the blood vessel length. When $x = 0$ cm, the temperatures in the artery and vein are 36°C and 35.9°C, respectively (remember that the length would be relative to the inlet of the artery). When $x = 50$ cm, the temperatures in the artery and vein are 28°C and 27.9°C, respectively. Finally, when $x = 100$ cm, the temperature in the artery and the vein are equal and are 20°C, which is the environmental temperature.

In more recent work, it has been shown that the countercurrent organization of blood vessels has more significant physiological relevance than simply the warming/cooling of blood as it returns to the core body. The temperature of the brain is critical to many physiological processes, and one can imagine the harm that would occur if the brain temperature fluctuated significantly from its normal temperature. A recent paper identified that above a certain temperature threshold (in the range of 38.5°C), the increase in brain temperature does not match the increase in carotid artery (this is the blood vessel that supplies blood to the brain) blood temperature in sheep (Strauss et al., 2015). This group also illustrated that this mechanism was related to the hydration extent of the animal, and they proposed selective brain cooling as a mechanism to regulate the hydration of the animal. Under conditions when the sheep were dehydrated, selective brain cooling was used more frequently to manage the temperature of the brain, and this mechanism allowed the animals to save an average of 2.6 L of water per day. However, with those studies there was a significant amount of inter-animal variability. The point of this study was to illustrate additional physiological roles of the countercurrent heat exchange organization of the cardiovascular system.

REFERENCES

1. W. M. Strauss, R. S. Hetem, D. Mitchell, S. K. Maloney, L. C. R. Meyer, and A. Fuller. "Selective Brain Cooling Reduces Water Turnover in Dehydrated Sheep." *PLOS One* 10(2): 2015, pp. e0115514 (12 pages). doi: 10.1371/journal.pone.0115514.

2. S. Weinbaum and L. M. Jiji. "A New Simplified Bioheat Equation for the Effect of Blood Flow on Local Average Tissue Temperature." *Journal of Biomechanical Engineering* 107 (1985), pp. 131–139.

SUMMARY

Heat exchangers are devices that allow the exchange of heat between two fluids without allowing them to mix with each other. Heat exchangers are manufactured in a variety of types, the simplest being the *double-pipe* heat exchanger. In a *parallel-flow* type, both the hot and cold fluids enter the heat exchanger at the same end and move in the same direction, whereas in a *counterflow* type, the hot and cold fluids enter the heat exchanger at opposite ends and flow in opposite directions. In *compact* heat exchangers, the two fluids move perpendicular to each other, and such a flow configuration is called *crossflow*. Other common types of heat exchangers in industrial applications are the *plate* and the *shell-and-tube* heat exchangers.

Heat transfer in a heat exchanger usually involves convection in each fluid and conduction through the wall separating the two fluids. In the analysis of heat exchangers, it is convenient to work with an *overall heat transfer coefficient U* or a *total thermal resistance R,* expressed as

$$\frac{1}{UA_s} = \frac{1}{U_iA_i} = \frac{1}{U_oA_o} = R = \frac{1}{h_iA_i} + R_{\text{wall}} + \frac{1}{h_oA_o}$$

where the subscripts *i* and *o* stand for the inner and outer surfaces of the wall that separates the two fluids, respectively. When the wall thickness of the tube is small and the thermal conductivity of the tube material is high, the relation simplifies to

$$\frac{1}{U} \approx \frac{1}{h_i} + \frac{1}{h_o}$$

where $U \approx U_i \approx U_o$. The effects of fouling on both the inner and the outer surfaces of the tubes of a heat exchanger can be accounted for by

$$\frac{1}{UA_s} = \frac{1}{U_iA_i} = \frac{1}{U_oA_o} = R$$
$$= \frac{1}{h_iA_i} + \frac{R_{f,i}}{A_i} + \frac{\ln(D_o/D_i)}{2\pi kL} + \frac{R_{f,o}}{A_o} + \frac{1}{h_oA_o}$$

where $A_i = \pi D_i L$ and $A_o = \pi D_o L$ are the areas of the inner and outer surfaces and $R_{f,i}$ and $R_{f,o}$ are the fouling factors at those surfaces.

In a well-insulated heat exchanger, the rate of heat transfer from the hot fluid is equal to the rate of heat transfer to the cold one. That is,

$$\dot{Q} = \dot{m}_c c_{pc}(T_{c,\,\text{out}} - T_{c,\,\text{in}}) = C_c(T_{c,\,\text{out}} - T_{c,\,\text{in}})$$

and

$$\dot{Q} = \dot{m}_h c_{ph}(T_{h,\,\text{in}} - T_{h,\,\text{out}}) = C_h(T_{h,\,\text{in}} - T_{h,\,\text{out}})$$

where the subscripts *c* and *h* stand for the cold and hot fluids, respectively, and the product of the mass flow rate and the specific heat of a fluid $\dot{m}c_p$ is called the *heat capacity rate.*

Of the two methods used in the analysis of heat exchangers, the *log mean temperature difference* (or LMTD) method is best suited for determining the size of a heat exchanger when all the inlet and the outlet temperatures are known. The *effectiveness–NTU* method is best suited to predict the outlet temperatures of the hot and cold fluid streams in a specified heat exchanger. In the LMTD method, the rate of heat transfer is determined from

$$\dot{Q} = UA_s \Delta T_{\text{lm}}$$

where

$$\Delta T_{\text{lm}} = \frac{\Delta T_1 - \Delta T_2}{\ln(\Delta T_1/\Delta T_2)}$$

is the *log mean temperature difference,* which is the suitable form of the average temperature difference for use in the analysis of heat exchangers. Here ΔT_1 and ΔT_2 represent the temperature differences between the two fluids at the two ends (inlet and outlet) of the heat exchanger. For crossflow and multipass shell-and-tube heat exchangers, the logarithmic mean temperature difference is related to the counterflow one $\Delta T_{\text{lm, CF}}$ as

$$\Delta T_{\text{lm}} = F\Delta T_{\text{lm, CF}}$$

where *F* is the *correction factor,* which depends on the geometry of the heat exchanger and the inlet and outlet temperatures of the hot and cold fluid streams.

The *effectiveness* of a heat exchanger is defined as

$$\varepsilon = \frac{\dot{Q}}{\dot{Q}_{\text{max}}} = \frac{\text{Actual heat transfer rate}}{\text{Maximum possible heat transfer rate}}$$

where

$$\dot{Q}_{\text{max}} = C_{\text{min}}(T_{h,\,\text{in}} - T_{c,\,\text{in}})$$

and C_{min} is the smaller of $C_h = \dot{m}_h c_{ph}$ and $C_c = \dot{m}_c c_{pc}$. The effectiveness of heat exchangers can be determined from effectiveness relations or charts.

The selection or design of a heat exchanger depends on several factors such as the heat transfer rate, cost, pressure drop, size, weight, construction type, materials, and operating environment.

REFERENCES AND SUGGESTED READING

1. N. Afgan and E. U. Schlunder. *Heat Exchanger: Design and Theory Sourcebook.* Washington, DC: McGraw-Hill/Scripta, 1974.

2. R. A. Bowman, A. C. Mueller, and W. M. Nagle. "Mean Temperature Difference in Design." *Transactions of the ASME* 62 (1940), p. 283. Reprinted with permission of ASME International.

3. A. P. Fraas. *Heat Exchanger Design.* 2d ed. New York: John Wiley & Sons, 1989.

4. K. A. Gardner. "Variable Heat Transfer Rate Correction in Multipass Exchangers, Shell Side Film Controlling." *Transactions of the ASME* 67 (1945), pp. 31–38.

5. W. M. Kays and A. L. London. *Compact Heat Exchangers.* 3rd ed. New York: McGraw-Hill, 1984.

6. W. M. Kays and H. C. Perkins. "Forced Convection, Internal Flow in Ducts." In *Handbook of Heat Transfer,* ed. W. M. Rohsenow and J. P. Hartnett. New York: McGraw-Hill, 1972, Chap. 7.

7. Q. Li, G. Flamant, X. Yuan, P. Neveu and L. Luo. "Compact Heat Exchangers: A Review and Future Applications for a New Generation of High Temperature Solar Receivers." *Renewable and Sustainable Energy Reviews* 15 (2011), pp. 4855–4875.

8. A. C. Mueller. "Heat Exchangers." Chap. 18 in *Handbook of Heat Transfer,* ed. W. M. Rohsenow and J. P. Hartnett. New York: McGraw-Hill, 1972.

9. M. N. Özişik. *Heat Transfer—A Basic Approach.* New York: McGraw-Hill, 1985.

10. E. U. Schlunder. *Heat Exchanger Design Handbook.* Washington, DC: Hemisphere, 1982.

11. *Standards of Tubular Exchanger Manufacturers Association,* 9th ed. New York: Tubular Exchanger Manufacturers Association, 2007.

12. R. A. Stevens, J. Fernandes, and J. R. Woolf. "Mean Temperature Difference in One, Two, and Three Pass Crossflow Heat Exchangers." *Transactions of the ASME* 79 (1957), pp. 287–297.

13. J. Taborek, G. F. Hewitt, and N. Afgan. *Heat Exchangers: Theory and Practice.* New York: Hemisphere, 1983.

14. G. Walker. *Industrial Heat Exchangers.* Washington, DC: Hemisphere, 1982.

PROBLEMS*

Types of Heat Exchangers

11–1C Classify heat exchangers according to flow type, and explain the characteristics of each type.

11–2C When is a heat exchanger classified as being compact? Do you think a double-pipe heat exchanger can be classified as a compact heat exchanger?

11–3C What is a regenerative heat exchanger? How does a static type of regenerative heat exchanger differ from a dynamic type?

11–4C What is the role of the baffles in a shell-and-tube heat exchanger? How does the presence of baffles affect the heat transfer and the pumping power requirements? Explain.

11–5C Draw a one-shell-pass and six-tube-passes shell-and-tube heat exchanger. What are the advantages and disadvantages of using six tube passes instead of just two of the same diameter?

11–6C Draw a two-shell-passes and eight-tube-passes shell-and-tube heat exchanger. What is the primary reason for using so many tube passes?

11–7C How does a crossflow heat exchanger differ from a counterflow one? What is the difference between mixed and unmixed fluids in crossflow?

The Overall Heat Transfer Coefficient

11–8C What are the heat transfer mechanisms involved during heat transfer in a liquid-to-liquid heat exchanger from the hot to the cold fluid?

11–9C Under what conditions is the thermal resistance of the tube in a heat exchanger negligible?

11–10C Consider a double-pipe parallel-flow heat exchanger of length L. The inner and outer diameters of the inner tube are D_1 and D_2, respectively, and the inner diameter of the outer tube is D_3. Explain how you would determine the two heat transfer surface areas A_i and A_o. When is it reasonable to assume $A_i \approx A_o \approx A_s$?

*Problems designated by a "C" are concept questions, and students are encouraged to answer them all. Problems designated by an "E" are in English units, and the SI users can ignore them. Problems with the 💻 icon are comprehensive in nature and are intended to be solved with appropriate software. Problems with the PtD icon are Prevention through Design problems. Problems with the C&S icon are Codes and Standards problems.

11–11C How is the thermal resistance due to fouling in a heat exchanger accounted for? How do the fluid velocity and temperature affect fouling?

11–12C What are the restrictions on the relation $UA_s = U_iA_i = U_oA_o$ for a heat exchanger? Here A_s is the heat transfer surface area and U is the overall heat transfer coefficient.

11–13C In a thin-walled double-pipe heat exchanger, when is the approximation $U = h_i$ a reasonable one? Here U is the overall heat transfer coefficient and h_i is the convection heat transfer coefficient inside the tube.

11–14C What are the common causes of fouling in a heat exchanger? How does fouling affect heat transfer and pressure drop?

11–15C Under what conditions can the overall heat transfer coefficient of a heat exchanger be determined from $U = (1/h_i + 1/h_o)^{-1}$?

11–16E The tube in a heat exchanger has a 2-in inner diameter and a 3-in outer diameter. The thermal conductivity of the tube material is 0.5 Btu/h·ft·°F, while the inner surface heat transfer coefficient is 50 Btu/h · ft²·°F and the outer surface heat transfer coefficient is 10 Btu/h · ft²·°F. Determine the overall heat transfer coefficients based on the outer and inner surfaces.

11–17 A long, thin-walled double-pipe heat exchanger with tube and shell diameters of 1.0 cm and 2.5 cm, respectively, is used to condense refrigerant-134a with water at 20°C. The refrigerant flows through the tube, with a convection heat transfer coefficient of $h_i = 4100$ W/m²·K. Water flows through the shell at a rate of 0.3 kg/s. Determine the overall heat transfer coefficient of this heat exchanger.

11–18 Repeat Prob. 11–17 by assuming a 2-mm-thick layer of limestone ($k = 1.3$ W/m·K) forms on the outer surface of the inner tube.

11–19 Reconsider Prob. 11–18. Using appropriate software, plot the overall heat transfer coefficient as a function of the limestone thickness as it varies from 1 mm to 3 mm, and discuss the results.

11–20E Water at an average temperature of 180°F and an average velocity of 4 ft/s flows through a thin-walled $\frac{3}{4}$-in-diameter tube. The water is cooled by air that flows across the tube with a velocity of 12 ft/s at an average temperature of 80°F. Determine the overall heat transfer coefficient.

11–21 A jacketed-agitated vessel, fitted with a turbine agitator, is used for heating a water stream from 10°C to 54°C. The average heat transfer coefficient for water at the vessel's inner wall can be estimated from $\text{Nu} = 0.76\,\text{Re}^{2/3}\text{Pr}^{1/3}$. Saturated steam at 100°C condenses in the jacket, for which the average heat transfer coefficient in kW/m²·K is: $h_o = 13.1(T_g - T_w)^{-0.25}$. The vessel dimensions are: $D_t = 0.6$ m, $H = 0.6$ m, and $D_a = 0.2$ m. The agitator speed is 60 rpm. Calculate the mass rate of water that can be heated in this agitated vessel steadily.

11–22E A counterflow heat exchanger is stated to have an overall heat transfer coefficient based on outside tube area of 50 Btu/h·ft²·°F when operating at design and clean conditions. After a period of use, scale buildup in the heat exchanger gives a fouling factor of 0.002 h·ft²·°F/Btu. Determine (a) the overall heat transfer coefficient of the heat exchanger and (b) the percentage change in the overall heat transfer coefficient due to the scale buildup.

11–23 Water at an average temperature of 110°C and an average velocity of 3.5 m/s flows through a 7-m-long stainless steel tube ($k = 14.2$ W/m·K) in a boiler. The inner and outer diameters of the tube are $D_i = 1.0$ cm and $D_o = 1.4$ cm, respectively. If the convection heat transfer coefficient at the outer surface of the tube where boiling is taking place is $h_o = 7200$ W/m²·K, determine the overall heat transfer coefficient U_i of this boiler based on the inner surface area of the tube.

11–24 Repeat Prob. 11–23, assuming a fouling factor $R_{f,i} = 0.0005$ m²·K/W on the inner surface of the tube.

11–25 Reconsider Prob. 11–24. Using appropriate software, plot the overall heat transfer coefficient based on the inner surface as a function of fouling factor as it varies from 0.0001 m²·K/W to 0.0008 m²·K/W, and discuss the results.

11–26 A double-pipe heat exchanger is constructed of a copper ($k = 380$ W/m·K) inner tube of internal diameter $D_i = 1.2$ cm and external diameter $D_o = 1.6$ cm and an outer tube of diameter 3.0 cm. The convection heat transfer coefficient is reported to be $h_i = 800$ W/m²·K on the inner surface of the tube and $h_o = 240$ W/m²·K on its outer surface. For a fouling factor $R_{f,i} = 0.0005$ m²·K/W on the tube side and $R_{f,o} = 0.0002$ m²·K/W on the shell side, determine (a) the thermal resistance of the heat exchanger per unit length and (b) the overall heat transfer coefficients U_i and U_o based on the inner and outer surface areas of the tube, respectively.

11–27 Reconsider Prob. 11–26. Using appropriate software, investigate the effects of pipe conductivity and heat transfer coefficients on the thermal resistance of the heat exchanger. Let the thermal conductivity vary from 10 W/m·K to 400 W/m·K, the convection heat transfer coefficient from 500 W/m²·K to 1500 W/m²·K on the inner surface, and from 1000 W/m²·K to 2000 W/m²·K on the outer surface. Plot the thermal resistance of the heat exchanger as a function of thermal conductivity and heat transfer coefficients, and discuss the results.

11–28 Hot engine oil with a heat capacity rate of 4440 W/K (product of mass flow rate and specific heat) and an inlet temperature of 150°C flows through a double-pipe heat exchanger. The double-pipe heat exchanger is constructed of a 1.5-m-long copper pipe ($k = 250$ W/m·K) with an inner tube of inside diameter 2 cm and outside tube diameter of 2.25 cm. The inner diameter of the outer tube of the double-pipe heat exchanger is 6 cm. Oil flowing at a rate of 2 kg/s through the inner tube

exits the heat exchanger at a temperature of 50°C. The cold fluid, i.e., water, enters the heat exchanger at 20°C and exits at 70°C. Assuming the fouling factor on the oil side and water side to be 0.00015 m²·K/W and 0.0001 m²·K/W, respectively, determine the overall heat transfer coefficient on the inner and outer surfaces of the copper tube.

Analysis of Heat Exchangers

11–29C What are the common approximations made in the analysis of heat exchangers?

11–30C Under what conditions is the heat transfer relation

$$\dot{Q} = \dot{m}_c c_{pc}(T_{c,\,\text{out}} - T_{c,\,\text{in}}) = \dot{m}_h c_{ph}(T_{h,\,\text{in}} - T_{h,\,\text{out}})$$

valid for a heat exchanger?

11–31C Consider a condenser in which steam at a specified temperature is condensed by rejecting heat to the cooling water. If the heat transfer rate in the condenser and the temperature rise of the cooling water are known, explain how the rate of condensation of the steam and the mass flow rate of the cooling water can be determined. Also, explain how the total thermal resistance R of this condenser can be evaluated in this case.

11–32C What is the heat capacity rate? What can you say about the temperature changes of the hot and cold fluids in a heat exchanger if both fluids have the same capacity rate? What does a heat capacity of infinity for a fluid in a heat exchanger mean?

11–33C Under what conditions will the temperature rise of the cold fluid in a heat exchanger be equal to the temperature drop of the hot fluid?

11–34 Show that the temperature profiles of two fluid streams (hot and cold) that have the same heat capacity rates are parallel to each other at every section of the counterflow heat exchanger. *Hint:* Refer to the analysis presented in Secs. 11–3 and 11–4.

The Log Mean Temperature Difference Method

11–35C In the heat transfer relation $\dot{Q} = UA_s\,\Delta T_{\text{lm}}$ for a heat exchanger, what is ΔT_{lm} called? How is it calculated for a parallel-flow and a counterflow heat exchanger?

11–36C How does the log mean temperature difference for a heat exchanger differ from the arithmetic mean temperature difference? For specified inlet and outlet temperatures, which one of these two quantities is larger?

11–37C The temperature difference between the hot and cold fluids in a heat exchanger is given to be ΔT_1 at one end and ΔT_2 at the other end. Can the logarithmic temperature difference ΔT_{lm} of this heat exchanger be greater than both ΔT_1 and ΔT_2? Explain.

11–38C Can the outlet temperature of the cold fluid in a heat exchanger be higher than the outlet temperature of the hot fluid in a parallel-flow heat exchanger? How about in a counterflow heat exchanger? Explain.

11–39C Explain how the LMTD method can be used to determine the heat transfer surface area of a multipass shell-and-tube heat exchanger when all the necessary information, including the outlet temperatures, is given.

11–40C In the heat transfer relation $\dot{Q} = UA_s F\Delta T_{\text{lm}}$ for a heat exchanger, what is the quantity F called? What does it represent? Can F be greater than 1?

11–41C When the outlet temperatures of the fluids in a heat exchanger are not known, is it still practical to use the LMTD method? Explain.

11–42C For specified inlet and outlet temperatures, for what kind of heat exchanger will the ΔT_{lm} be greatest: double-pipe parallel-flow, double-pipe counterflow, crossflow, or multipass shell-and-tube heat exchanger?

11–43 A double-pipe parallel-flow heat exchanger is used to heat cold tap water with hot water. Hot water ($c_p = 4.25$ kJ/kg·K) enters the tube at 85°C at a rate of 1.4 kg/s and leaves at 50°C. The heat exchanger is not well insulated, and it is estimated that 3 percent of the heat given up by the hot fluid is lost from the heat exchanger. If the overall heat transfer coefficient and the surface area of the heat exchanger are 1150 W/m²·K and 4 m², respectively, determine the rate of heat transfer to the cold water and the log mean temperature difference for this heat exchanger.
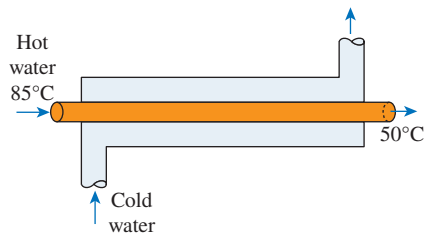
FIGURE P11–43

11–44 A stream of hydrocarbon ($c_p = 2.2$ kJ/kg·K) is cooled at a rate of 720 kg/h from 150°C to 40°C in the tube side of a double-pipe counterflow heat exchanger. Water ($c_p = 4.18$ kJ/kg·K) enters the heat exchanger at 10°C at a rate of 540 kg/h. The outside diameter of the inner tube is 2.5 cm, and its length is 6.0 m. Calculate the overall heat transfer coefficient.

11–45 A double-pipe parallel-flow heat exchanger is to heat water ($c_p = 4180$ J/kg·K) from 25°C to 60°C at a rate of 0.2 kg/s. The heating is to be accomplished by geothermal water ($c_p = 4310$ J/kg·K) available at 140°C at a mass flow rate of 0.3 kg/s. The inner tube is thin-walled and has a diameter of 0.8 cm. If the overall heat transfer coefficient of the heat exchanger is 550 W/m²·K, determine the length of the tube required to achieve the desired heating.

11–46 Reconsider Prob. 11–45. Using appropriate software, investigate the effects of temperature and mass flow rate of geothermal water on the length of the tube. Let the temperature vary from 100°C to 200°C, and the

mass flow rate from 0.1 kg/s to 0.5 kg/s. Plot the length of the tube as functions of temperature and mass flow rate, and discuss the results.

11–47 Glycerin (c_p = 2400 J/kg·K) at 20°C and 0.5 kg/s is to be heated by ethylene glycol (c_p = 2500 J/kg·K) at 70°C in a thin-walled double-pipe parallel-flow heat exchanger. The temperature difference between the two fluids is 15°C at the outlet of the heat exchanger. If the overall heat transfer coefficient is 240 W/m²·K and the heat transfer surface area is 3.2 m², determine (a) the rate of heat transfer, (b) the outlet temperature of the glycerin, and (c) the mass flow rate of the ethylene glycol.

11–48 A heat exchanger contains 400 tubes with inner diameter of 23 mm and outer diameter of 25 mm. The length of each tube is 3.7 m. The corrected log mean temperature difference is 23°C, while the inner surface convection heat transfer coefficient is 3410 W/m²·K and the outer surface convection heat transfer coefficient is 6820 W/m²·K. If the thermal resistance of the tubes is negligible, determine the heat transfer rate.

11–49E A single-pass heat exchanger is to be designed to heat 100,000 lbm of water in an hour from 60°F to 100°F by condensation of water vapor at 230°F on the shell side. Each tube has an inner diameter of 1.2 in and a wall thickness of 0.12 in. The inner surface convection heat transfer coefficient is 480 Btu/h·ft²·°F and the outer surface convection heat transfer coefficient is 2000 Btu/h·ft²·°F. If the inlet velocity of water (c_{pc} = 1 Btu/lbm·°F and ρ = 62.3 lbm/ft³) on the tube side is 4 ft/s, determine the required number of tubes and length of tubes. Assume the thermal resistance of the tubes is negligible.

11–50 Consider the flow of engine oil (c_p = 2048 J/kg·K) through a thin-walled copper tube at a rate of 0.3 kg/s. The engine oil that enters the copper tube at an inlet temperature of 80°C is to be cooled by cold water (c_p = 4180 J/kg·K) flowing at a temperature of 20°C. We wish to have the exit temperature of the engine oil not exceed 40°C. The individual convective heat transfer coefficients on oil and water sides are 750 W/m²·K and 350 W/m²·K, respectively. If a thermocouple probe installed on the downstream side of the cooling water measures a temperature of 32°C, for a double-pipe parallel-flow heat exchanger determine (a) the mass flow rate of the cooling water, (b) the log mean temperature difference, and (c) the area of the heat exchanger.

Hot oil
80°C

Cold water
20°C
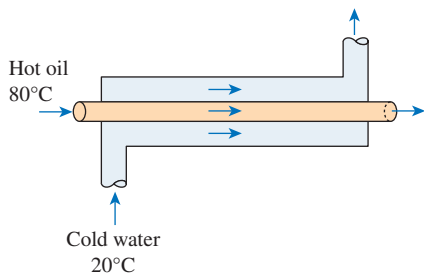
FIGURE P11–50

11–51 In a parallel-flow heat exchanger, hot fluid enters the heat exchanger at a temperature of 150°C and a mass flow rate of 3 kg/s. The cooling medium enters the heat exchanger at a temperature of 30°C with a mass flow rate of 0.5 kg/s and leaves at a temperature of 70°C. The specific heat capacities of the hot and cold fluids are 1150 J/kg·K and 4180 J/kg·K, respectively. The convection heat transfer coefficient on the inner and outer sides of the tube are 300 W/m²·K and 800 W/m²·K, respectively. For a fouling factor of 0.0003 m²·K/W on the tube side and 0.0001 m²·K/W on the shell side, determine (a) the overall heat transfer coefficient, (b) the exit temperature of the hot fluid, and (c) the surface area of the heat exchanger.

11–52 Ethylene glycol is heated from 25°C to 40°C at a rate of 2.5 kg/s in a horizontal copper tube (k = 386 W/m·K) with an inner diameter of 2.0 cm and an outer diameter of 2.5 cm. A saturated vapor (T_g = 110°C) condenses on the outside-tube surface with the heat transfer coefficient (in kW/m²·K) given by $9.2/(T_g - T_w)^{0.25}$, where T_w is the average outside-tube wall temperature. What tube length must be used? Take the properties of ethylene glycol to be ρ = 1109 kg/m³, c_p = 2428 J/kg·K, k = 0.253 W/m·K, μ = 0.01545 kg/m·s, and Pr = 148.5.

11–53 A counterflow heat exchanger is stated to have an overall heat transfer coefficient of 284 W/m²·K when operating at design and clean conditions. Hot fluid enters the tube side at 93°C and exits at 71°C, while cold fluid enters the shell side at 27°C and exits at 38°C. After a period of use, built-up scale in the heat exchanger gives a fouling factor of 0.0004 m²·K/W. If the surface area is 93 m², determine (a) the rate of heat transfer in the heat exchanger and (b) the mass flow rates of both hot and cold fluids. Assume both hot and cold fluids have a specific heat of 4.2 kJ/kg·K.

$T_{c,in}$

$T_{h,in}$

$T_{h,out}$

$T_{c,out}$
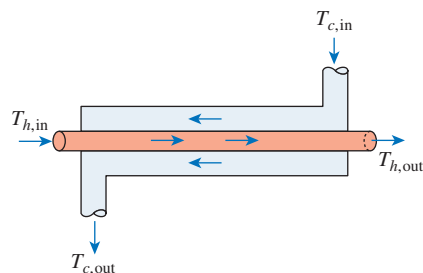
FIGURE P11–53

11–54 C&S A chemical process facility has a pipe system with the inner surface coated with polypropylene lining. The ASME Code for Process Piping limits the maximum use temperature for polypropylene lining to 107°C (ASME B31.3-2014, Table A323.4.3). A double-pipe counterflow heat exchanger is located upstream to reduce the hot fluid temperature before it flows into the pipe system coated with polypropylene lining. The inner tube of the heat exchanger has a negligible wall thickness, and its length and diameter are 5 m and 25 mm, respectively. The convection heat

transfer coefficients inside and outside of the heat exchanger inner tube are 1000 W/m²·K and 1500 W/m²·K, respectively. The hot fluid enters the heat exchanger at a heat capacity rate of 1 kW/K and 120°C. In the cold fluid stream, water enters the heat exchanger at 10°C and exits at 30°C. Determine the highest level of fouling factor that the heat exchanger can tolerate before it becomes unable to cool the hot fluid to 107°C at the outlet.

11–55 A thin-walled double-pipe counterflow heat exchanger is to be used to cool oil ($c_p = 2200$ J/kg·K) from 150°C to 50°C at a rate of 2.5 kg/s with water ($c_p = 4180$ J/kg·K) that enters at 22°C at a rate of 1.5 kg/s. The diameter of the tube is 2.5 cm, and its length is 6 m. Determine the overall heat transfer coefficient of this heat exchanger.

11–56 Reconsider Prob. 11–55. Using appropriate software, investigate the effects of oil exit temperature and water inlet temperature on the overall heat transfer coefficient of the heat exchanger. Let the oil exit temperature vary from 30°C to 70°C and the water inlet temperature from 5°C to 25°C. Plot the overall heat transfer coefficient as a function of the two temperatures, and discuss the results.

11–57 Engine oil ($c_p = 2100$ J/kg·K) is to be heated from 20°C to 60°C at a rate of 0.3 kg/s in a 2-cm-diameter thin-walled copper tube by condensing steam outside at a temperature of 130°C ($h_{fg} = 2174$ kJ/kg). For an overall heat transfer coefficient of 650 W/m²·K, determine the rate of heat transfer and the length of the tube required to achieve it. *Answers:* 25.2 kW, 7.0 m
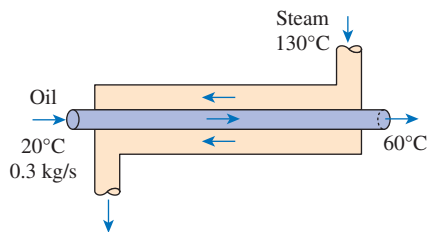
FIGURE P11–57

11–58E Geothermal water ($c_p = 1.03$ Btu/lbm·°F) is to be used as the heat source to supply heat to the hydronic heating system of a house at a rate of 40 Btu/s in a double-pipe counterflow heat exchanger. Water ($c_p = 1.0$ Btu/lbm·°F) is heated from 140°F to 200°F in the heat exchanger as the geothermal water is cooled from 270°F to 180°F. Determine the mass flow rate of each fluid and the total thermal resistance of this heat exchanger.

11–59 Cold water ($c_p = 4180$ J/kg·K) leading to a shower enters a thin-walled double-pipe counterflow heat exchanger at 15°C at a rate of 1.25 kg/s and is heated to 60°C by hot water ($c_p = 4190$ J/kg·K) that enters at 100°C at a rate of 4 kg/s. If the overall heat transfer coefficient is 880 W/m²·K, determine the rate of heat transfer and the heat transfer surface area of the heat exchanger.

11–60 A pipe system uses several ethylene propylene diene rubber (EPDM) O-rings in its various components. According to the ASME Boiler and Pressure Vessel Code (ASME BPVC.IV-2015, HG-360), the temperature limit for EPDM O-rings is 150°C. A double-pipe counterflow heat exchanger is placed upstream of the pipe system to reduce a hot fluid temperature before it flows into the pipe system. The hot fluid enters the heat exchanger with a heat capacity rate of 3 kW/K and 210°C. In the cold fluid stream, water enters the heat exchanger at 10°C and exits at 80°C. The overall heat transfer coefficient of the heat exchanger is estimated to be 2000 W/m²·K. The inner tube has a diameter of 25 mm and a length of 5 m. Determine whether the hot fluid temperature at the heat exchanger outlet is below the temperature limit for the O-rings. If not, determine the length of the heat exchanger necessary to cool the hot fluid below 150°C at the heat exchanger outlet, before it flows into the pipe system.

11–61E Steam is to be condensed on the shell side of a one-shell-pass and eight-tube-passes condenser, with 60 tubes in each pass at 90°F ($h_{fg} = 1043$ Btu/lbm). Cooling water ($c_p = 1.0$ Btu/lbm·°F) enters the tubes at 55°F and leaves at 70°F. The tubes are thin walled and have a diameter of 3/4 in and a length of 5 ft per pass. If the overall heat transfer coefficient is 600 Btu/h·ft²·°F, determine (*a*) the rate of heat transfer, (*b*) the rate of condensation of steam, and (*c*) the mass flow rate of the cold water.
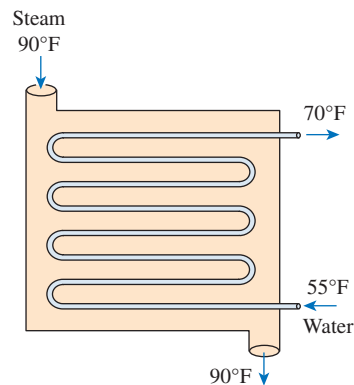
FIGURE P11–61E

11–62E Reconsider Prob. 11–61E. Using appropriate software, investigate the effect of the condensing steam temperature on the rate of heat transfer, the rate of condensation of steam, and the mass flow rate of the cold water. Let the steam temperature vary from 80°F to 120°F. Plot the rate of heat transfer, the condensation rate of steam, and the mass flow rate of the cold water as a function of steam temperature, and discuss the results.

11–63 Hot exhaust gases of a stationary diesel engine are to be used to generate steam in an evaporator. Exhaust gases ($c_p = 1051$ J/kg·K) enter the heat exchanger at 550°C at a

rate of 0.25 kg/s while water enters as saturated liquid and evaporates at 200°C ($h_{fg} = 1941$ kJ/kg). The heat transfer surface area of the heat exchanger based on the water side is 0.5 m², and the overall heat transfer coefficient is 1780 W/m²·K. Determine the rate of heat transfer, the exit temperature of the exhaust gases, and the rate of evaporation of the water.

11–64 ⌨ Reconsider Prob. 11–63. Using appropriate software, investigate the effect of the exhaust gas inlet temperature on the rate of heat transfer, the exit temperature of exhaust gases, and the rate of evaporation of water. Let the temperature of exhaust gases vary from 300°C to 600°C. Plot the rate of heat transfer, the exit temperature of exhaust gases, and the rate of evaporation of the water as a function of the temperature of the exhaust gases, and discuss the results.

11–65 In a textile manufacturing plant, the waste dyeing water ($c_p = 4295$ J/kg·K) at 80°C is to be used to preheat fresh water ($c_p = 4180$ J/kg·K) at 10°C at the same flow rate in a double-pipe counterflow heat exchanger. The heat transfer surface area of the heat exchanger is 1.65 m², and the overall heat transfer coefficient is 625 W/m²·K. If the rate of heat transfer in the heat exchanger is 35 kW, determine the outlet temperature and the mass flow rate of each fluid stream.
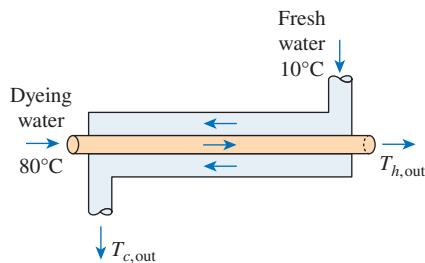
FIGURE P11–65

11–66 A performance test is being conducted on a double-pipe counterflow heat exchanger that carries engine oil and water at a flow rate of 2.5 kg/s and 1.75 kg/s, respectively. Since the heat exchanger has been in service for a long time, it is suspected that fouling might have developed inside the heat exchanger that could affect the overall heat transfer coefficient. The test to be carried out is such that, for a designed value of the overall heat transfer coefficient of 450 W/m²·K and a surface area of 7.5 m², the oil must be heated from 25°C to 55°C by passing hot water at 100°C ($c_p = 4206$ J/kg·K) at the flow rates mentioned above. Determine if the fouling has affected the overall heat transfer coefficient. If yes, then what is the magnitude of the fouling resistance?

11–67 In an industrial facility, a counterflow double-pipe heat exchanger uses superheated steam at a temperature of 250°C to heat feedwater at 30°C. The superheated steam experiences a temperature drop of 70°C as it exits the heat

exchanger. The water to be heated flows through the heat exchanger tube of negligible thickness at a constant rate of 3.47 kg/s. The convective heat transfer coefficient on the super-heated steam and water side is 850 W/m²·K and 1250 W/m²·K, respectively. To account for the fouling due to chemical impurities that might be present in the feedwater, use an appropriate fouling factor for the water side. Determine (*a*) the heat exchanger area required to maintain the exit temperature of the water to a minimum of 70°C, and (*b*) what would be the required heat exchanger area in the case of a parallel flow arrangement?
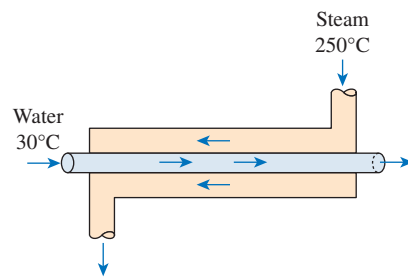
FIGURE P11–67

11–68 C&S A pipe system is mainly constructed with ASTM F441 CPVC pipes. The ASME Code for Process Piping (ASME B31.3-2014, Table B-1) recommends that the maximum temperature limit for CPVC pipes be 93.3°C. A double-pipe heat exchanger is located upstream of the pipe system to reduce the hot water temperature before it flows into the CPVC pipes. The inner tube of the heat exchanger has a negligible wall thickness, and its length and diameter are 5 m and 25 mm, respectively. The convection heat transfer coefficients inside and outside of the heat exchanger inner tube are 3600 W/m²·K and 4500 W/m²·K, respectively. The hot fluid enters the heat exchanger at 105°C with a flow rate of 0.75 kg/s. In the cold fluid stream, water enters the heat exchanger at 10°C and exits at 80°C. Determine whether this double-pipe heat exchanger should employ the parallel flow or the counterflow configuration to ensure that the hot water exiting the heat exchanger is 93.3°C or lower.

11–69 C&S A pipe system uses several hydrogenated nitrile rubber (HNBR) O-rings in its various connectors. The HNBR O-rings have a maximum temperature limit of 150°C set by the ASME Boiler and Pressure Vessel Code (ASME BPVC.IV-2015, HG-360). A double-pipe heat exchanger is located upstream to reduce the hot fluid temperature before it flows into the pipe system. The hot fluid enters the heat exchanger with a heat capacity rate of 1 kW/K and 180°C. In the cold fluid stream, water enters the heat exchanger at 10°C and exits at 30°C. The inner tube of the heat exchanger has a very thin wall, and its diameter and length are 25 mm and 5 m, respectively. The convection heat transfer coefficients

inside and outside of the heat exchanger inner tube are 1000 W/m²·K and 1500 W/m²·K, respectively. Determine whether a parallel flow or a counterflow configuration for this double-pipe heat exchanger would tolerate a higher level of fouling factor before it becomes unable to cool the hot fluid to 150°C at the outlet.

11–70 A test is conducted to determine the overall heat transfer coefficient in a shell-and-tube oil-to-water heat exchanger that has 24 tubes of internal diameter 1.2 cm and length 2 m in a single shell. Cold water ($c_p = 4180$ J/kg·K) enters the tubes at 20°C at a rate of 3 kg/s and leaves at 55°C. Oil ($c_p = 2150$ J/kg·K) flows through the shell and is cooled from 120°C to 45°C. Determine the overall heat transfer coefficient U_i of this heat exchanger based on the inner surface area of the tubes. *Answer:* 8.31 kW/m²·K

11–71 A shell-and-tube heat exchanger is used for heating 14 kg/s of oil ($c_p = 2.0$ kJ/kg·K) from 20°C to 46°C. The heat exchanger has one shell pass and six tube passes. Water enters the shell side at 80°C and leaves at 60°C. The overall heat transfer coefficient is estimated to be 1000 W/m²·K. Calculate the rate of heat transfer and the heat transfer area.

11–72E A one-shell-pass and eight-tube-passes heat exchanger is used to heat glycerin ($c_p = 0.60$ Btu/lbm·°F) from 80°F to 140°F by hot water ($c_p = 1.0$ Btu/lbm·°F) that enters the thin-walled 0.5-in-diameter tubes at 175°F and leaves at 120°F. The total length of the tubes in the heat exchanger is 400 ft. The convection heat transfer coefficient is 4 Btu/h·ft²·°F on the glycerin (shell) side and 50 Btu/h·ft²·°F on the water (tube) side. Determine the rate of heat transfer in the heat exchanger (*a*) before any fouling occurs and (*b*) after fouling with a fouling factor of 0.002 h·ft²·°F/Btu on the outer surfaces of the tubes.

11–73 A shell-and-tube heat exchanger with two shell passes and 12 tube passes is used to heat water ($c_p = 4180$ J/kg·K) with ethylene glycol ($c_p = 2680$ J/kg·K). Water enters the tubes at 22°C at a rate of 0.8 kg/s and leaves at 70°C. Ethylene glycol enters the shell at 110°C and leaves at 60°C. If the overall heat transfer coefficient based on the tube side is 280 W/m²·K, determine the rate of heat transfer and the heat transfer surface area on the tube side.

11–74 Reconsider Prob. 11–73. Using appropriate software, investigate the effect of the mass flow rate of water on the rate of heat transfer and the tube-side surface area. Let the mass flow rate vary from 0.4 kg/s to 2.2 kg/s. Plot the rate of heat transfer and the surface area as a function of the mass flow rate, and discuss the results.

11–75E Oil is being cooled from 180°F to 120°F in a one-shell and two-tube heat exchanger with an overall heat transfer coefficient of 40 Btu/h·ft²·°F. Water ($c_{pc} = 1.0$ Btu/lbm·°F) enters at 80°F and exits at 100°F with a mass flow rate of 20,000 lbm/h. Determine (*a*) the log mean temperature difference and (*b*) the surface area of the heat exchanger.
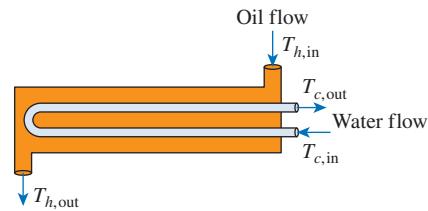
FIGURE P11–75E

11–76 A shell-and-tube heat exchanger with two shell passes and 12 tube passes is used to heat water ($c_p = 4180$ J/kg·K) in the tubes from 20°C to 70°C at a rate of 4.5 kg/s. Heat is supplied by hot oil ($c_p = 2300$ J/kg·K) that enters the shell side at 170°C at a rate of 10 kg/s. For a tube-side overall heat transfer coefficient of 350 W/m²·K, determine the heat transfer surface area on the tube side. *Answer:* 25.7 m²

11–77 Repeat Prob. 11–76 for a mass flow rate of 3 kg/s for water.

11–78 A shell-and-tube heat exchanger with two shell passes and eight tube passes is used to heat ethyl alcohol ($c_p = 2670$ J/kg·K) in the tubes from 25°C to 70°C at a rate of 2.1 kg/s. The heating is to be done by water ($c_p = 4190$ J/kg·K) that enters the shell side at 95°C and leaves at 45°C. If the overall heat transfer coefficient is 950 W/m²·K, determine the heat transfer surface area of the heat exchanger.
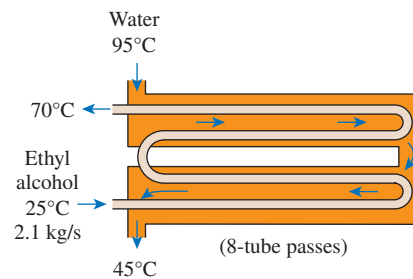
FIGURE P11–78

11–79 Consider a shell-and-tube heat exchanger in a milk pasteurizing unit in which the milk flowing is to be heated from 20°C by hot water initially at 140°C and flowing at a rate of 5 kg/s. The milk flows through 30 thin-walled tubes with an inside diameter of 20 mm, with each tube making 10 passes through the shell. The average convective heat transfer coefficients on the milk and water sides are 450 W/m²·K and 1100 W/m²·K, respectively. In order to complete the pasteurizing process and hence restrict the microbial growth in the milk, it is required to have the exit temperature of milk attain at least 70°C. As a design engineer, your job is to decide upon the shell width (tube length in each pass) so that the milk exit temperature of 70°C can be achieved. One of the design requirements is that the exit temperature of hot water should be at least 10°C higher than the exit temperature of milk.

Water
140°C, 5 kg/s

20°C
Milk
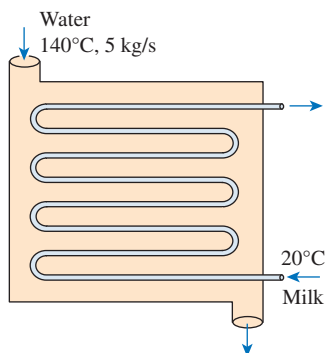
FIGURE P11–79

11–80E A single-pass crossflow heat exchanger is used to cool jacket water ($c_p = 1.0$ Btu/lbm·°F) of a diesel engine from 190°F to 140°F, using air ($c_p = 0.245$ Btu/lbm·°F) with an inlet temperature of 90°F. Both airflow and water flow are unmixed. If the water and air mass flow rates are 92,000 lbm/h and 400,000 lbm/h, respectively, determine the log mean temperature difference for this heat exchanger.

Air flow
(*unmixed*)

Water flow
(*unmixed*)
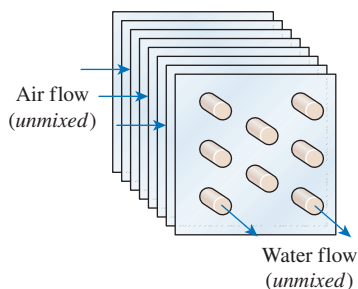
FIGURE P11–80E

11–81 A single-pass crossflow heat exchanger with both fluids unmixed has water entering at 16°C and exiting at 33°C, while oil ($c_p = 1.93$ kJ/kg·K and $\rho = 870$ kg/m³) flowing at 0.19 m³/min enters at 38°C and exits at 29°C. If the surface area of the heat exchanger is 20 m², determine the value of the overall heat transfer coefficient.

Oil flow
(*unmixed*)

Water flow
(*unmixed*)
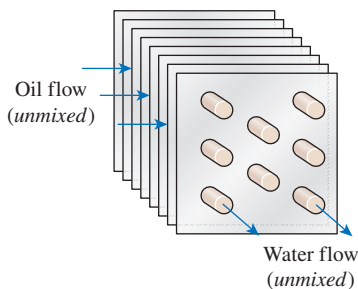
FIGURE P11–81

The Effectiveness–NTU Method

11–82C What does the effectiveness of a heat exchanger represent? Can effectiveness be greater than 1? On what factors does the effectiveness of a heat exchanger depend?

11–83C For a specified fluid pair, inlet temperatures, and mass flow rates, what kind of heat exchanger will have the highest effectiveness: double-pipe parallel-flow, double-pipe counterflow, crossflow, or multipass shell-and-tube heat exchanger?

11–84C Explain how you can evaluate the outlet temperatures of the cold and hot fluids in a heat exchanger after its effectiveness is determined.

11–85C Can the temperature of the hot fluid drop below the inlet temperature of the cold fluid at any location in a heat exchanger? Explain.

11–86C Can the temperature of the cold fluid rise above the inlet temperature of the hot fluid at any location in a heat exchanger? Explain.

11–87C Consider a heat exchanger in which both fluids have the same specific heats but different mass flow rates. Which fluid will experience a larger temperature change: the one with the lower or higher mass flow rate?

11–88C Explain how the maximum possible heat transfer rate $\dot{Q}_{max}$ in a heat exchanger can be determined when the mass flow rates, specific heats, and inlet temperatures of the two fluids are specified. Does the value of $\dot{Q}_{max}$ depend on the type of the heat exchanger?

11–89C Under what conditions can a counterflow heat exchanger have an effectiveness of 1? What would your answer be for a parallel-flow heat exchanger?

11–90C Consider a double-pipe counterflow heat exchanger. In order to enhance heat transfer, the length of the heat exchanger is now doubled. Do you think its effectiveness will also double?

11–91C Consider a shell-and-tube water-to-water heat exchanger with identical mass flow rates for both the hot- and cold-water streams. Now the mass flow rate of the cold water is reduced by half. Will the effectiveness of this heat exchanger increase, decrease, or remain the same as a result of this modification? Explain. Assume the overall heat transfer coefficient and the inlet temperatures remain the same.

11–92C Consider two double-pipe counterflow heat exchangers that are identical except that one is twice as long as the other one. Which heat exchanger is more likely to have a higher effectiveness?

11–93C How is the NTU of a heat exchanger defined? What does it represent? Is a heat exchanger with a very large NTU (say, 10) necessarily a good one to buy?

11–94C Consider a heat exchanger that has an NTU of 4. Someone proposes to double the size of the heat exchanger and

thus double the NTU to 8 in order to increase the effectiveness of the heat exchanger and thus save energy. Would you support this proposal?

11–95C Consider a heat exchanger that has an NTU of 0.1. Someone proposes to triple the size of the heat exchanger and thus triple the NTU to 0.3 in order to increase the effectiveness of the heat exchanger and thus save energy. Would you support this proposal?

11–96 The radiator in an automobile is a crossflow heat exchanger ($UA_s = 10$ kW/K) that uses air ($c_p = 1.00$ kJ/kg·K) to cool the engine-coolant fluid ($c_p = 4.00$ kJ/kg·K). The engine fan draws 22°C air through this radiator at a rate of 8 kg/s while the coolant pump circulates the engine coolant at a rate of 5 kg/s. The coolant enters this radiator at 80°C. Under these conditions, the effectiveness of the radiator is 0.4. Determine (*a*) the outlet temperature of the air and (*b*) the rate of heat transfer between the two fluids.

11–97 Consider an oil-to-oil double-pipe heat exchanger whose flow arrangement is not known. The temperature measurements indicate that the cold oil enters at 15°C and leaves at 55°C, while the hot oil enters at 80°C and leaves at 40°C. Do you think this is a parallel-flow or counterflow heat exchanger? Why? Assuming the mass flow rates of both fluids to be identical, determine the effectiveness of this heat exchanger.

11–98E Hot water enters a double-pipe counterflow water-to-oil heat exchanger at 190°F and leaves at 100°F. Oil enters at 70°F and leaves at 130°F. Determine which fluid has the smaller heat capacity rate, and calculate the effectiveness of this heat exchanger.

11–99 Glycerin ($c_p = 2400$ J/kg·K) at 20°C and 0.5 kg/s is to be heated by ethylene glycol ($c_p = 2500$ J/kg·K) at 60°C and the same mass flow rate in a thin-walled double-pipe parallel-flow heat exchanger. If the overall heat transfer coefficient is 380 W/m²·K and the heat transfer surface area is 6.5 m², determine (*a*) the rate of heat transfer and (*b*) the outlet temperatures of the glycerin and the glycol.

11–100 Hot water ($c_{ph} = 4188$ J/kg·K) with a mass flow rate of 2.5 kg/s at 100°C enters a thin-walled concentric tube counterflow heat exchanger with a surface area of 23 m² and an overall heat transfer coefficient of 1000 W/m²·K. Cold water ($c_{pc} = 4178$ J/kg·K) with a mass flow rate of 5 kg/s enters the heat exchanger at 20°C. Determine (*a*) the heat transfer rate for the heat exchanger and (*b*) the outlet temperatures of the cold and hot fluids. After a period of operation, the overall heat transfer coefficient is reduced to 500 W/m²·K, so determine (*c*) the fouling factor that caused the reduction in the overall heat transfer coefficient.

11–101 Water ($c_p = 4180$ J/kg·K) is to be heated by solar-heated hot air ($c_p = 1010$ J/kg·K) in a double-pipe counterflow heat exchanger. Air enters the heat exchanger at 90°C at a rate of 0.3 kg/s, while water enters at 22°C at a rate of 0.1 kg/s. The overall heat transfer coefficient based on the inner side of the tube is given to be 80 W/m²·K. The length of the tube is 12 m, and the internal diameter of the tube is 1.2 cm. Determine the outlet temperatures of the water and the air.

11–102 Reconsider Prob. 11–101. Using appropriate software, investigate the effects of the mass flow rate of water and the tube length on the outlet temperatures of water and air. Let the mass flow rate vary from 0.05 kg/s to 1.0 kg/s and the tube length from 5 m to 25 m. Plot the outlet temperatures of the water and the air as functions of the mass flow rate and the tube length, and discuss the results.

11–103 [C&S] A double-pipe heat exchanger is used to cool a hot fluid before it flows into a system of pipes. The inner surface of the pipes is primarily coated with polypropylene lining. The maximum use temperature for polypropylene lining is 107°C (ASME Code for Process Piping, ASME B31.3-2014, Table A323.4.3). The double-pipe heat exchanger has a thin-walled inner tube, with convection heat transfer coefficients inside and outside of the inner tube estimated to be 1400 W/m²·K and 1100 W/m²·K, respectively. The heat exchanger has a heat transfer surface area of 2.5 m², and the estimated fouling factor caused by the accumulation of deposit on the surface is 0.0002 m²·K/W. The hot fluid ($c_p = 3800$ J/kg·K) enters the heat exchanger at 200°C with a flow rate of 0.4 kg/s. In the cold side, cooling fluid ($c_p = 4200$ J/kg·K) enters the heat exchanger at 10°C with a mass flow rate of 0.5 kg/s.

11–104 Cold water ($c_p = 4180$ J/kg·K) leading to a shower enters a thin-walled double-pipe counterflow heat exchanger at 15°C at a rate of 0.25 kg/s and is heated to 45°C by hot water ($c_p = 4190$ J/kg·K) that enters at 100°C at a rate of 3 kg/s. If the overall heat transfer coefficient is 950 W/m²·K, determine the rate of heat transfer and the heat transfer surface area of the heat exchanger using the ε–NTU method.   *Answers:* 31.35 kW, 0.482 m²
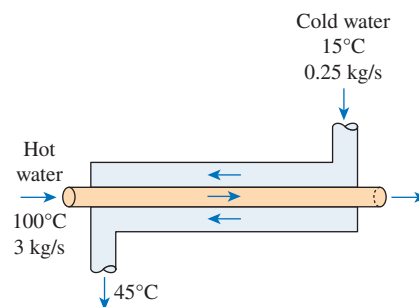
FIGURE P11–104

11–105 Reconsider Prob. 11–104. Using appropriate software, investigate the effects of the inlet temperature of hot water and the heat transfer coefficient on the rate of heat transfer and the surface area. Let the inlet temperature vary from 60°C to 120°C and the overall heat transfer

coefficient from 750 W/m²·K to 1250 W/m²·K. Plot the rate of heat transfer and surface area as functions of the inlet temperature and the heat transfer coefficient, and discuss the results.

11–106 C&S A double-pipe counterflow heat exchanger is used to cool a hot fluid before it flows into a pipe system. The pipe system is mainly constructed with ASTM F2389 polypropylene pipes. According to the ASME Code for Process Piping, the recommended maximum temperature for polypropylene pipes is 99°C (ASME B31.3-2014, Table B-1). The heat exchanger's inner tube has negligible wall thickness. The convection heat transfer coefficients inside and outside of the heat exchanger inner tube are 1500 W/m²·K and 1000 W/m²·K, respectively. The fouling factor estimated for the heat exchanger is 0.0001 m²·K/W. The hot fluid ($c_p = 3800$ J/kg·K) enters the heat exchanger at 150°C with a flow rate of 0.5 kg/s. In the cold side, cooling fluid ($c_p = 4200$ J/kg·K) enters the heat exchanger at 10°C with a mass flow rate of 0.75 kg/s. Determine the heat transfer surface area that the heat exchanger needs to cool the hot fluid to 99°C at the outlet so that it flows into the pipe system at a temperature not exceeding the recommended maximum temperature for polypropylene pipes.

11–107E A thin-walled double-pipe counterflow heat exchanger is to be used to cool oil ($c_p = 0.525$ Btu/lbm·°F) from 300°F to 105°F at a rate of 5 lbm/s with water ($c_p = 1.0$ Btu/lbm·°F) that enters at 70°F at a rate of 3 lbm/s. The diameter of the tube is 5 in, and its length is 200 ft. Determine the overall heat transfer coefficient of this heat exchanger using (*a*) the LMTD method and (*b*) the *ε*–NTU method.

11–108 In an industrial facility, a countercurrent double-pipe heat exchanger is used to heat the glycerin flowing at a rate of 1.5 kg/s from 10°C to 50°C by passing hot water at an inlet temperature of 120°C. The hot water experiences a temperature drop of 50°C as it flows through the heat exchanger. The overall heat transfer coefficient of the heat exchanger may be assumed to be 950 W/m²·K. A similar arrangement is to be installed at another location, and it is proposed to use two small heat exchangers of same surface area to be arranged in series instead of one single large heat exchanger. However, it is first necessary to compare the surface area of the two small heat exchangers against that of the single large heat exchanger, since the available space is a major constraint for the proposed design. The arrangement of the heat exchangers is as shown in Fig. P11–108. The water flow rate is split between the two heat exchangers such that 60 percent would go to the first heat exchanger and the remaining 40 percent would go to the second heat exchanger. The overall heat transfer coefficient of the two small heat exchangers is assumed to remain the same as that of the large heat exchanger. As a design engineer, for both cases determine the heat exchanger (*a*) effectiveness, (*b*) NTU, (*c*) surface area, and (*d*) choice of the heat exchanger if the construction cost of the smaller heat exchangers is about 15 percent higher than a single large heat exchanger per unit surface area.
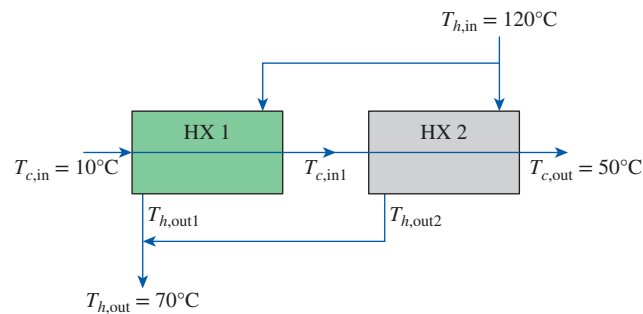
FIGURE P11–108

11–109E A one-shell and two-tube-type heat exchanger has an overall heat transfer coefficient of 300 Btu/h·ft²·°F. The shell-side fluid has a heat capacity rate of 20,000 Btu/h·°F, while the tube-side fluid has a heat capacity rate of 40,000 Btu/h·°F. The inlet temperatures on the shell side and tube side are 200°F and 90°F, respectively. If the total heat transfer area is 100 ft², determine (*a*) the heat transfer effectiveness and (*b*) the actual heat transfer rate in the heat exchanger.

11–110 In a one-shell and two-tube heat exchanger, cold water with inlet temperature of 20°C is heated by hot water supplied at the inlet at 80°C. The cold and hot water flow rates are 5000 kg/h and 10,000 kg/h, respectively. If the shell-and-tube heat exchanger has a UA_s value of 11,600 W/K, determine the cold water and hot water outlet temperatures. Assume $c_{pc} = 4178$ J/kg·K and $c_{ph} = 4188$ J/kg·K.

11–111 Hot oil ($c_p = 2200$ J/kg·K) is to be cooled by water ($c_p = 4180$ J/kg·K) in a 2-shell-passes and 12-tube-passes heat exchanger. The tubes are thin-walled and are made of copper with a diameter of 1.8 cm. The length of each tube pass in the heat exchanger is 3 m, and the overall heat transfer coefficient is 340 W/m²·K. Water flows through the tubes at a total rate of 0.1 kg/s, and the oil flows through the shell at a rate of 0.2 kg/s. The water and the oil enter at temperatures 18°C and 160°C, respectively. Determine the rate of heat transfer in the heat exchanger and the outlet temperatures of the water and the oil. *Answers:* 36.2 kW, 104.6°C, 77.7°C
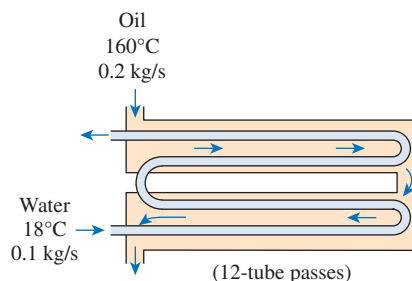
FIGURE P11–111

11–112E Oil is being cooled from 180°F to 120°F in a one-shell and two-tube heat exchanger with an overall heat transfer coefficient of 40 Btu/h·ft²·°F. Water ($c_{pc} = 1.0$ Btu/lbm·°F) enters at 80°F and exits at 100°F with a mass flow rate of 20,000 lbm/h. Determine (*a*) the NTU value and (*b*) the surface area of the heat exchanger.

Oil flow
$T_{h,in}$
$T_{c,out}$
Water flow
$T_{c,in}$
$T_{h,out}$
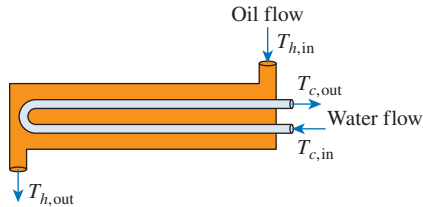
FIGURE P11–112E

11–113 A shell-and-tube heat exchanger with two shell passes and eight tube passes is used to heat ethyl alcohol ($c_p = 2670$ J/kg·K) in the tubes from 25°C to 70°C at a rate of 2.1 kg/s. The heating is to be done by water ($c_p = 4190$ J/kg·K) that enters the shell at 95°C and leaves at 60°C. If the overall heat transfer coefficient is 800 W/m²·K, determine the heat transfer surface area of the heat exchanger using (*a*) the LMTD method and (*b*) the ε–NTU method. *Answer: (a)* 11.4 m²

11–114 Cold water ($c_p = 4180$ J/kg·K) enters the tubes of a heat exchanger with two shell passes and 23 tube passes at 14°C at a rate of 3 kg/s, while hot oil ($c_p = 2200$ J/kg·K) enters the shell at 200°C at the same mass flow rate. The overall heat transfer coefficient based on the outer surface of the tube is 300 W/m²·K, and the heat transfer surface area on that side is 20 m². Determine the rate of heat transfer using (*a*) the LMTD method and (*b*) the ε–NTU method.

11–115 The National Sanitation Foundation (NSF) standard for commercial warewashing equipment (ANSI/NSF 3) requires that the final rinse water temperature be between 82 and 90°C. A shell-and-tube heat exchanger is to heat 0.5 kg/s of water ($c_p = 4200$ J/kg·K) from 48 to 86°C by geothermal brine flowing through a single shell pass. The heated water is then fed into commercial warewashing equipment. The geothermal brine enters and exits the heat exchanger at 98 and 90°C, respectively. The water flows through four thin-walled tubes, each with a diameter of 25 mm, with all four tubes making the same number of passes through the shell. The tube length per pass for each tube is 5 m. The corresponding convection heat transfer coefficients on the outer and inner tube surfaces are 1050 and 2700 W/m²·K, respectively. The estimated fouling factor caused by the accumulation of deposit from the geothermal brine is 0.0002 m²·K/W. Determine the number of passes required for the tubes inside the shell to heat the water to 86°C, within the temperature range required by the ANIS/NSF 3 standard.

11–116E In a one-shell and eight-tube-pass heat exchanger, the temperature of water flowing at rate of 50,000 lbm/h is

raised from 70°F to 150°F. Hot air ($c_p = 0.25$ Btu/lbm·°F) that flows on the tube side enters the heat exchanger at 600°F and exits at 300°F. If the convection heat transfer coefficient on the outer surface of the tubes is 30 Btu/h·ft²·°F, determine the surface area of the heat exchanger using both LMTD and ε–NTU methods. Account for the possible fouling resistance of 0.0015 and 0.001 h·ft²·°F/Btu on the water and air sides, respectively.

11–117 **C&S** A shell-and-tube (two shell passes) heat exchanger is to heat 0.5 kg/s of water ($c_p = 4200$ J/kg·K) by geothermal brine flowing through the shell passes. The heated water is then fed into commercial warewashing equipment. The National Sanitation Foundation (NSF) standard for commercial warewashing equipment (ANSI/NSF 3) requires that the final rinse water temperature be between 82 and 90°C. The geothermal brine enters and exits the heat exchanger at 98 and 90°C, respectively. The water flows through a thin-walled tube inside the shell passes. The tube diameter is 25 mm, and the tube length per pass is 4 m. The corresponding convection heat transfer coefficients on the outer and inner tube surfaces are 450 and 2700 W/m²·K, respectively. The estimated fouling factor caused by the accumulation of deposit from the geothermal brine is 0.0002 m²·K/W. If the water enters the heat exchanger at 20°C, determine the number of tube passes required inside each shell pass to heat the water to 86°C so that it complies with the ANSI/NSF 3 standard.

11–118 **C&S** A shell-and-tube (two shell passes, 12 tube passes in each shell) heat exchanger is used to cool a hot fluid before it flows into a pipe system. The pipe system is mainly constructed with ASTM B75 copper tubes. The maximum use temperature for ASTM B75 copper tubes is 204°C (ASME Code for Process Piping, ASME B31.3-2014, Table A-1M). The hot fluid is cooled by a heat transfer fluid ($c_p = 3$ kJ/kg·K) flowing at 1.4 kg/s through the shell passes. The heat transfer fluid enters and exits the heat exchanger at 50 and 200°C, respectively. The hot fluid flows through a thin-walled tube inside the shell passes. The tube diameter is 25 mm, and the corresponding convection heat transfer coefficients on the outer and inner tube surfaces are 2300 and 3000 W/m²·K, respectively. If the hot fluid enters the heat exchanger at 250°C, determine the tube length per pass required inside each shell pass to cool the hot fluid to 204°C, so that it complies with the ASME code.

11–119 Air ($c_p = 1005$ J/kg·K) enters a crossflow heat exchanger at 20°C at a rate of 3 kg/s, where it is heated by a hot water stream ($c_p = 4190$ J/kg·K) that enters the heat exchanger at 70°C at a rate of 1 kg/s. Determine the maximum heat transfer rate and the outlet temperatures of both fluids for that case.

11–120 A crossflow heat exchanger with both fluids unmixed has an overall heat transfer coefficient of 200 W/m²·K and a heat transfer surface area of 400 m². The hot fluid has a heat capacity of 40,000 W/K, while the cold fluid has a heat capacity of 80,000 W/K. If the inlet temperatures of both hot

and cold fluids are 80°C and 20°C, respectively, determine the exit temperature of the cold fluid.

11–121 A crossflow air-to-water heat exchanger with an effectiveness of 0.65 is used to heat water ($c_p = 4180$ J/kg·K) with hot air ($c_p = 1010$ J/kg·K). Water enters the heat exchanger at 20°C at a rate of 4 kg/s, while air enters at 100°C at a rate of 9 kg/s. If the overall heat transfer coefficient based on the water side is 260 W/m²·K, determine the heat transfer surface area of the heat exchanger on the water side. Assume both fluids are unmixed. *Answer:* 52.4 m²

11–122 Cold water ($c_p = 4.18$ kJ/kg·K) enters a crossflow heat exchanger at 14°C at a rate of 0.35 kg/s where it is heated by hot air ($c_p = 1.0$ kJ/kg·K) that enters the heat exchanger at 65°C at a rate of 0.8 kg/s and leaves at 25°C. Determine the maximum outlet temperature of the cold water and the effectiveness of this heat exchanger.

14°C
0.35 kg/s

Air
65°C
0.8 kg/s
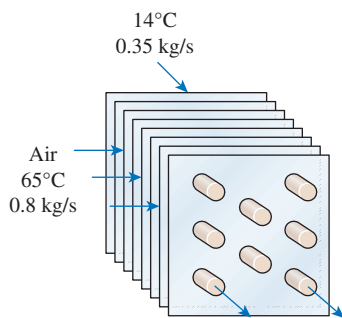
FIGURE P11–122

11–123 Oil in an engine is being cooled by air in a crossflow heat exchanger, where both fluids are unmixed. Oil ($c_{ph} = 2047$ J/kg·K) flowing with a flow rate of 0.026 kg/s enters the heat exchanger at 75°C, while air ($c_{pc} = 1007$ J/kg·K) enters at 30°C with a flow rate of 0.21 kg/s. The overall heat transfer coefficient of the heat exchanger is 53 W/m²·K and the total surface area is 1 m². Determine (*a*) the heat transfer effectiveness and (*b*) the outlet temperature of the oil.

Air flow
(*unmixed*)

Oil flow
(*unmixed*)
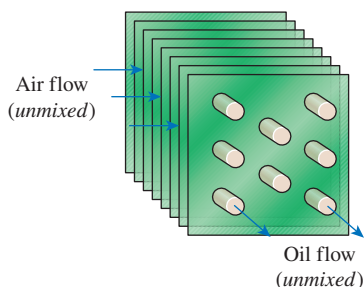
FIGURE P11–123

11–124 A crossflow heat exchanger consists of 80 thin-walled tubes of 3-cm diameter located in a duct of 1 m × 1 m cross section. There are no fins attached to the tubes. Cold

water ($c_p = 4180$ J/kg·K) enters the tubes at 18°C with an average velocity of 3 m/s, while hot air ($c_p = 1010$ J/kg·K) enters the channel at 130°C and 105 kPa at an average velocity of 12 m/s. If the overall heat transfer coefficient is 130 W/m²·K, determine the outlet temperatures of both fluids and the rate of heat transfer.

1 m

1 m

Hot air
130°C
105 kPa
12 m/s

Water
18°C
3 m/s
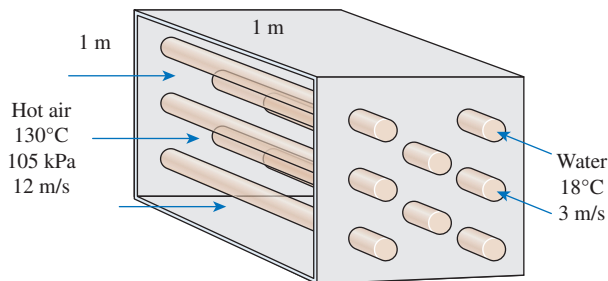
FIGURE P11–124

11–125 Consider a recuperative crossflow heat exchanger (both fluids unmixed) used in a gas turbine system that carries the exhaust gases at a flow rate of 7.5 kg/s and a temperature of 500°C. The air initially at 30°C and flowing at a rate of 15 kg/s is to be heated in the recuperator. The convective heat transfer coefficients on the exhaust gas and air sides are 750 W/m²·K and 300 W/m²·K, respectively. Due to long-term use of the gas turbine, the recuperative heat exchanger is subject to fouling on both gas and air sides that offers a resistance of 0.0004 m²·K/W each. Take the properties of exhaust gas to be the same as that of air ($c_p = 1069$ J/kg·K). If the exit temperature of the exhaust gas is 320°C, determine (*a*) if the air could be heated to a temperature of 150°C and (*b*) the area of the heat exchanger. (*c*) If the answer to part (*a*) is no, then determine what should be the air mass flow rate in order to attain the desired exit temperature of 150°C and (*d*) plot the variation of the exit air temperature over a range of 75°C to 300°C with the air mass flow rate, assuming all the other conditions remain the same.

Gas flow
(*unmixed*)

Air flow
(*unmixed*)
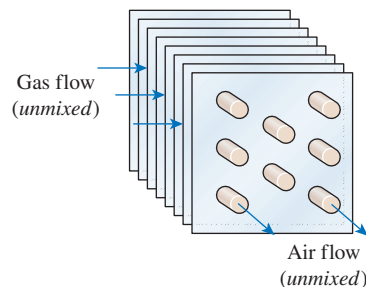
FIGURE P11–125

11–126 Consider the operation of a single-pass crossflow heat exchanger with water ($c_p = 4193$ J/kg·K) (mixed) and methanol ($c_p = 2577$ J/kg·K) (unmixed). Water entering and exiting the heat exchanger at 90°C and 60°C, respectively is

used to heat the methanol initially at 10°C. The overall heat transfer coefficient and the total heat transfer rate is estimated to be 650 W/m²·K and 250 kW, respectively. In order to achieve an effectiveness of at least 0.5, (*a*) what would be the mass flow rate of water and heat exchanger surface area? (*b*) If the mass flow rate of water is changed within ±30% of that determined in part (*a*) with the same surface area (A_s), plot the variation of heat transfer rate, methanol exit temperature, overall heat transfer coefficient, and the effectiveness of the heat exchanger with respect to change in the water flow rate.

11–127 Consider a crossflow engine oil heater that uses ethylene glycol flowing at a temperature of 110°C to heat the oil initially at 10°C. The ethylene glycol enters a tube bank consisting of copper tubes ($k = 250$ W/m·K) with staggered arrangement in a 0.5-m × 0.5-m plenum. The outside diameter of the 0.5-m-long copper tubes is 25 mm, and the wall thickness is 2 mm. The longitudinal and transverse pitch of the rod bundles is 0.035 m each. The engine oil to be heated flows inside the tubes with a mass flow rate of 4.05 kg/s. Take the heat transfer coefficient of the oil to be 2500 W/m²·K. If the minimum desired exit temperature of oil is 70°C and the measured exit temperature of ethylene glycol is 90°C, determine (*a*) the mass flow rate of ethylene glycol and (*b*) the number of tube rows. In your calculation, use the following properties for the ethylene glycol.

$$\rho = 1062 \text{ kg/m}^3 \qquad \mu = 2.499 \times 10^{-3} \text{ kg/m·s}$$
$$k = 0.262 \text{ W/m·K} \qquad c_p = 2742 \text{ J/kg·K}$$
$$\text{Pr} = 26.12 \qquad \text{Pr}_{s@40°C} = 96.97$$
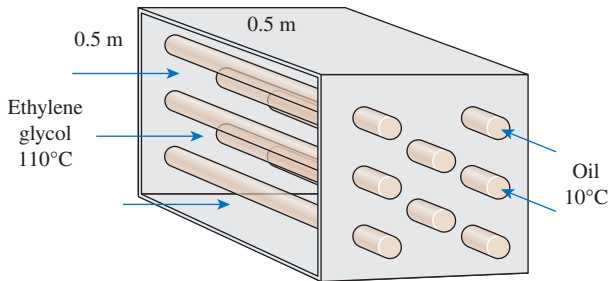
FIGURE P11–127

11–128 Water ($c_p = 4180$ J/kg·K) enters the 2.5-cm-internal-diameter tube of a double-pipe counterflow heat exchanger at 20°C at a rate of 2.2 kg/s. Water is heated by steam condensing at 120°C ($h_{fg} = 2203$ kJ/kg) in the shell. If the overall heat transfer coefficient of the heat exchanger is 700 W/m²·K, determine the length of the tube required in order to heat the water to 80°C using (*a*) the LMTD method and (*b*) the ε–NTU method.

11–129 Ethanol is vaporized at 78°C ($h_{fg} = 846$ kJ/kg) in a double-pipe parallel-flow heat exchanger at a rate of 0.04 kg/s by hot oil ($c_p = 2200$ J/kg·K) that enters at 115°C. If the heat

transfer surface area and the overall heat transfer coefficients are 6.2 m² and 320 W/m²·K, respectively, determine the outlet temperature and the mass flow rate of oil using (*a*) the LMTD method and (*b*) the ε–NTU method.
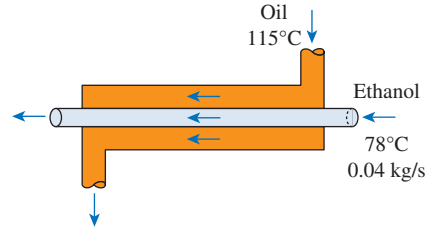
FIGURE P11–129

11–130 Saturated water vapor at 100°C condenses in a one-shell and two-tube heat exchanger with a surface area of 0.5 m² and an overall heat transfer coefficient of 2000 W/m²·K. Cold water ($c_{pc} = 4179$ J/kg·K) flowing at 0.5 kg/s enters the tube side at 15°C. Determine (*a*) the heat transfer effectiveness, (*b*) the outlet temperature of the cold water, and (*c*) the heat transfer rate for the heat exchanger.
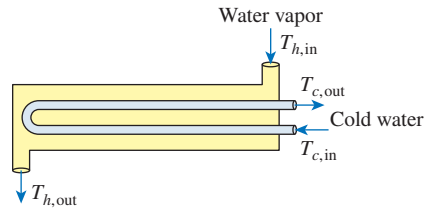
FIGURE P11–130

11–131 Steam is to be condensed on the shell side of a one-shell-pass and eight-tube-passes condenser, with 50 tubes in each pass, at 30°C ($h_{fg} = 2431$ kJ/kg). Cooling water ($c_p = 4180$ J/kg·K) enters the tubes at 18°C at a rate of 2200 kg/h. The tubes are thin-walled and have a diameter of 1.5 cm and a length of 2 m per pass. If the overall heat transfer coefficient is 3000 W/m²·K, determine (*a*) the rate of heat transfer and (*b*) the rate of condensation of steam.
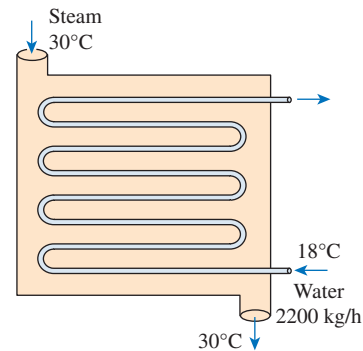
FIGURE P11–131

11–132 Reconsider Prob. 11–131. Using appropriate software, investigate the effects of the condensing steam temperature and the tube diameter on the rate of heat transfer and the rate of condensation of steam. Let the steam temperature vary from 20°C to 70°C and the tube diameter from 1.0 cm to 2.0 cm. Plot the rate of heat transfer and the rate of condensation as functions of steam temperature and tube diameter, and discuss the results.

11–133E Consider a closed-loop heat exchanger that carries exit water (c_p = 1 Btu/lbm·°F and ρ = 62.4 lbm/ft³) of a condenser side initially at 100°F. The water flows through a 500-ft-long stainless steel pipe of 1 in inner diameter immersed in a large lake. The temperature of lake water surrounding the heat exchanger is 45°F. The overall heat transfer coefficient of the heat exchanger is estimated to be 250 Btu/h·ft²·°F. What is the exit temperature of the water from the immersed heat exchanger if it flows through the pipe at an average velocity of 9 ft/s? Use the ε–NTU method for analysis.

11–134 Consider the flow of saturated steam at 270.1 kPa that flows through the shell side of a shell-and-tube heat exchanger while the water flows through four tubes of diameter 1.25 cm at a rate of 0.25 kg/s through each tube. The water enters the tubes of the heat exchanger at 20°C and exits at 60°C. Due to the heat exchange with the cold fluid, steam is condensed on the tube's external surface. The convection heat transfer coefficient on the steam side is 1500 W/m²·K, while the fouling resistance for the steam and water may be taken as 0.00015 and 0.0001 m²·K/W, respectively. Using the NTU method, determine (*a*) effectiveness of the heat exchanger, (*b*) length of the tube, and (*c*) rate of steam condensation.
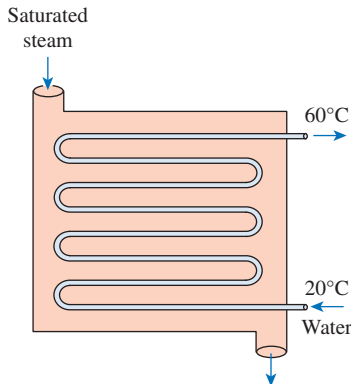
FIGURE P11−134

11–135 Consider a condenser unit (shell and tube heat exchanger) of an HVAC facility where saturated refrigerant R-134a at a saturation pressure of 1318.6 kPa and at a rate of 2.5 kg/s flows through thin-walled copper tubes. The refrigerant enters the condenser as saturated vapor and we wish to have a saturated liquid refrigerant at the exit. The cooling of refrigerant is carried out by cold water that enters the heat exchanger at 10°C and exits at 40°C. Assuming the initial overall heat transfer

coefficient of the heat exchanger to be 3500 W/m²·K, determine the surface area of the heat exchanger and the mass flow rate of cooling water for complete condensation of the refrigerant. In practice, over a long period of time, fouling occurs inside the heat exchanger that reduces its overall heat transfer coefficient and causes the mass flow rate of cooling water to increase. Increase in the mass flow rate of cooling water will require additional pumping power, making the heat exchange process uneconomical. To prevent the condenser unit from underperforming, assume that fouling has occurred inside the heat exchanger and has reduced its overall heat transfer coefficient by 20 percent. For the same inlet temperature and flow rate of refrigerant, determine the new flow rate of cooling water to ensure complete condensation of the refrigerant at the heat exchanger exit.

Selection of Heat Exchangers

11–136C There are two heat exchangers that can meet the heat transfer requirements of a facility. Both have the same pumping power requirements, the same useful life, and the same price tag. But one is heavier and larger. Under what conditions would you choose the smaller one?

11–137C There are two heat exchangers that can meet the heat transfer requirements of a facility. One is smaller and cheaper but requires a larger pump, while the other is larger and more expensive but has a smaller pressure drop and thus requires a smaller pump. Both heat exchangers have the same life expectancy and meet all other requirements. Explain which heat exchanger you would choose and under what conditions.

11–138C A heat exchanger is to be selected to cool a hot liquid chemical at a specified rate to a specified temperature. Explain the steps involved in the selection process.

11–139 A heat exchanger is to cool oil (c_p = 2200 J/kg·K) at a rate of 10 kg/s from 120°C to 40°C by air. Determine the heat transfer rating of the heat exchanger and propose a suitable type.

11–140 A shell-and-tube process heater is to be selected to heat water (c_p = 4190 J/kg·K) from 20°C to 90°C by steam flowing on the shell side. The heat transfer load of the heater is 600 kW. If the inner diameter of the tubes is 1 cm and the velocity of water is not to exceed 3 m/s, determine how many tubes need to be used in the heat exchanger.
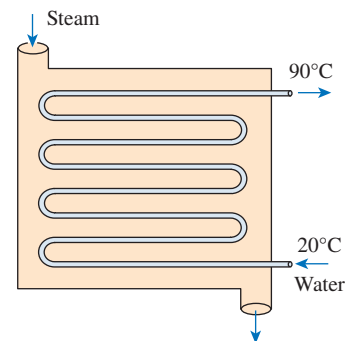
FIGURE P11−140

11–141 Reconsider Prob. 11–140. Using appropriate software, plot the number of tube passes as a function of water velocity as it varies from 1 m/s to 8 m/s, and discuss the results.

11–142 The condenser of a large power plant is to remove 125 MW of heat from steam condensing at 30°C ($h_{fg} = 2431$ kJ/kg). The cooling is to be accomplished by cooling water ($c_p = 4180$ J/kg·K) from a nearby river, which enters the tubes at 18°C and leaves at 26°C. The tubes of the heat exchanger have an internal diameter of 2 cm, and the overall heat transfer coefficient is 3500 W/m²·K. Determine the total length of the tubes required in the condenser. What type of heat exchanger is suitable for this task?

11–143 Repeat Prob. 11–142 for a heat transfer load of 50 MW.

11–144 A shell-and-tube heat exchanger is to be designed to cool down the petroleum-based organic vapor available at a flow rate of 5 kg/s and at a saturation temperature of 75°C. The cold water ($c_p = 4187$ J/kg·K) used for its condensation is supplied at a rate of 25 kg/s and a temperature of 15°C. The cold water flows through copper tubes with an outside diameter of 20 mm, a thickness of 2 mm, and a length of 5 m. The overall heat transfer coefficient is assumed to be 550 W/m²·K, and the latent heat of vaporization of the organic vapor may be taken to be 580 kJ/kg. Assuming negligible thermal resistance due to pipe wall thickness, determine the number of tubes required.

11–145E Water flowing through the tube side of a shell-and-tube crossflow heat exchanger at a rate of 40,000 lbm/h is heated from 80°F to 110°F. On the shell side, water at 175°F flows through one shell pass at a rate of 30,000 lbm/h and acts as a heating fluid. The overall heat transfer coefficient of the heat exchanger is 220 Btu/h·ft²·°F, and the average velocity of water flowing through a 0.75-in-inside-diameter pipe is 1.5 ft/s. Because of the space limitations, it is desired to limit the tube length to less than 8 ft. Calculate the number of tube passes, the number of tubes per pass, and the length of tubes that satisfy the space constraints.

11–146 Saturated liquid benzene flowing at a rate of 5 kg/s is to be cooled from 75°C to 45°C by using a source of cold water ($c_p = 4187$ J/kg·K) flowing at 3.5 kg/s and 15°C through a 20-mm-diameter tube of negligible wall thickness. The overall heat transfer coefficient of the heat exchanger is estimated to be 750 W/m²·K. If the specific heat of the liquid benzene is 1839 J/kg·K and assuming that the capacity ratio and effectiveness remain the same, determine the heat exchanger surface area for the following four heat exchangers: (*a*) parallel flow, (*b*) counterflow, (*c*) shell-and-tube with two shell passes and 40 tube passes, and (*d*) crossflow with one fluid mixed (liquid benzene) and other fluid unmixed (water).

Special Topic: The Human Cardiovascular System as a Countercurrent Heat Exchanger

11–147C Describe the cardiovascular countercurrent mechanism in the human body.

11–148C Discuss the differences between the cardiovascular countercurrent design and standard engineering countercurrent designs.

11–149C How do heavy clothing and extreme environmental conditions affect the cardiovascular countercurrent exchanger?

11–150 Calculate the total thermal resistance of the cardiovascular heat exchanger, assuming that the thermal conductivity of the system is $k = 0.670$ W/m·K and the convection heat transfer coefficients are $h_{artery} = 300$ W/m²·K and $h_{vein} = 190$ W/m²·K. The artery has an exterior diameter of 500 μm, the vein has an exterior diameter of 600 μm, and the length of both blood vessels is 50 cm.

11–151 Using the values discussed in Prob. 11–150, calculate the arterial and venous overall heat transfer coefficient.

11–152 How would the answer to Prob. 11–150 be altered if we tried to approximate the heat transfer loss through the blood vessel with a fouling factor to describe physiological inhomogeneities? Assume that the fouling factor for the artery is 0.0005 m²·K/W and the fouling factor for the vein is 0.0003 m²·K/W.

11–153 The cardiovascular countercurrent heat exchanger mechanism is to warm venous blood from 28°C to 35°C at a mass flow rate of 2 g/s. The artery inflow temperature is 37°C at a mass flow rate of 5 g/s. The average diameter of the vein is 5 cm and the overall heat transfer coefficient is 125 W/m²·K. Determine the overall blood vessel length needed to warm the venous blood to 35°C if the specific heat of both arterial and venous blood is constant and equal to 3475 J/kg·K.

11–154 The cardiovascular countercurrent heat exchanger has an overall heat transfer coefficient of 100 W/m²·K. Arterial blood enters at 37°C and exits at 27°C. Venous blood enters at 25°C and exits at 34°C. Determine the mass flow rates of the arterial blood and venous blood in g/s if the specific heat of both arterial and venous blood is constant and equal to 3475 J/kg·K, and the surface area of the heat transfer to occur is 0.15 cm².

Review Problems

11–155 Consider a water-to-water double-pipe heat exchanger whose flow arrangement is not known. The temperature measurements indicate that the cold water enters at 20°C and leaves at 50°C, while the hot water enters at 80°C and leaves at 45°C. Do you think this is a parallel-flow or counterflow heat exchanger? Explain.

11–156 By taking the limit as $\Delta T_2 \rightarrow \Delta T_1$, show that when $\Delta T_1 = \Delta T_2$ for a heat exchanger, the ΔT_{lm} relation reduces to $\Delta T_{lm} = \Delta T_1 = \Delta T_2$.

11–157E Water ($c_p = 1.0$ Btu/lbm·°F) is to be heated by solar-heated hot air ($c_p = 0.24$ Btu/lbm·°F) in a double-pipe counterflow heat exchanger. Air enters the heat exchanger at 190°F at a rate of 0.7 lbm/s and leaves at 135°F. Water enters at 70°F at a rate of 0.35 lbm/s. The overall heat transfer coefficient based on the inner side of the tube is given to be 20

Btu/h·ft^2·°F. Determine the length of the tube required for a tube internal diameter of 0.5 in.

11–158   A shell-and-tube heat exchanger with one shell pass and 14 tube passes is used to heat water in the tubes with geothermal steam condensing at 120°C ($h_{fg} = 2203$ kJ/kg) on the shell side. The tubes are thin-walled and have a diameter of 2.4 cm and a length of 3.2 m per pass. Water ($c_p = 4180$ J/kg·K) enters the tubes at 18°C at a rate of 6.2 kg/s. If the temperature difference between the two fluids at the exit is 46°C, determine (*a*) the rate of heat transfer, (*b*) the rate of condensation of steam, and (*c*) the overall heat transfer coefficient.

Steam
120°C

18°C
Water
(14 tubes)   6.2 kg/s
120°C
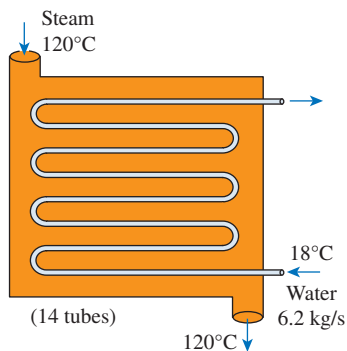
FIGURE P11–158

11–159   Hot water at 60°C is cooled to 36°C through the tube side of a one-shell-pass and two-tube-passes heat exchanger. The coolant is also a water stream, for which the inlet and outlet temperatures are 7°C and 31°C, respectively. The overall heat transfer coefficient and the heat transfer area are 950 W/m^2·K and 15 m^2, respectively. Calculate the mass flow rates of hot and cold water streams in steady operation.

11–160   Cold water ($c_p = 4180$ J/kg·K) enters the tubes of a heat exchanger with two shell passes and 20 tube passes at 15°C at a rate of 4 kg/s, while hot oil ($c_p = 2200$ J/kg·K) enters the shell at 130°C at the same mass flow rate and leaves at 60°C. If the overall heat transfer coefficient based on the outer surface of the tube is 220 W/m^2·K, determine (*a*) the rate of heat transfer and (*b*) the heat transfer surface area on the outer side of the tube.

Hot oil
130°C
4 kg/s

Cold water
15°C
4 kg/s
(20-tube passes)
60°C
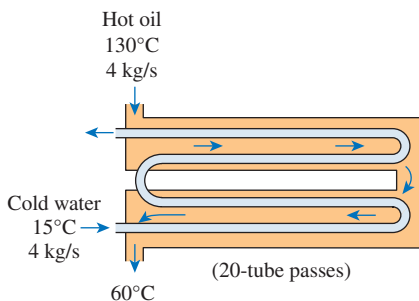
FIGURE P11–160

11–161   A shell-and-tube heat exchanger is used for cooling 47 kg/s of a process stream flowing through the tubes from 160°C to 100°C. This heat exchanger has a total of 100 identical tubes, each with an inside diameter of 2.5 cm and negligible wall thickness. The average properties of the process stream are: $\rho = 950$ kg/m^3, $k = 0.50$ W/m·K, $c_p = 3.5$ kJ/kg·K, and $\mu = 0.002$ kg/m·s. The coolant stream is water $c_p = 4.18$ kJ/kg·K at a flow rate of 66 kg/s and an inlet temperature of 10°C, which yields an average shell-side heat transfer coefficient of 4.0 kW/m^2·K. Calculate the tube length if the heat exchanger has (*a*) one shell pass and one tube pass and (*b*) one shell pass and four tube passes.

11–162   A two-shell-pass and four-tube-pass heat exchanger is used for heating a hydrocarbon stream ($c_p = 2.0$ kJ/kg·K) steadily from 20°C to 50°C. A water stream enters the shell side at 80°C and leaves at 40°C. There are 160 thin-walled tubes, each with a diameter of 2.0 cm and length of 1.5 m. The tube-side and shell-side heat transfer coefficients are 1.6 and 2.5 kW/m^2·K, respectively. (*a*) Calculate the rate of heat transfer and the mass rates of water and hydrocarbon streams. (*b*) With usage, the outlet hydrocarbon-stream temperature was found to decrease by 5°C due to the deposition of solids on the tube surface. Estimate the magnitude of the fouling factor.

11–163   A shell-and-tube heat exchanger with two shell passes and four tube passes is used for cooling oil ($c_p = 2.0$ kJ/kg·K) from 125°C to 55°C. The coolant is water, which enters the shell side at 25°C and leaves at 46°C. The overall heat transfer coefficient is 900 W/m^2·K. For an oil flow rate of 10 kg/s, calculate the cooling water flow rate and the heat transfer area.

11–164   Saturated water vapor at 100°C condenses in the shell side of a one-shell and two-tube heat exchanger with a surface area of 0.5 m^2 and an overall heat transfer coefficient of 2000 W/m^2·K. If cold water ($c_{pc} = 4179$ J/kg·K) flowing at 0.5 kg/s enters the tube side at 15°C, determine the outlet temperature of the cold water and the heat transfer rate for the heat exchanger.

Water vapor
$T_{h,in}$
$T_{c,out}$
Cold water
$T_{c,in}$
$T_{h,out}$
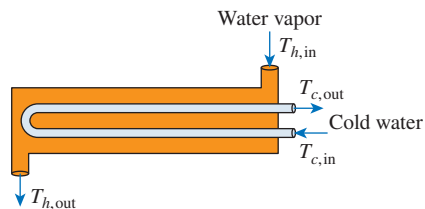
FIGURE P11–164

11–165   A single-pass crossflow heat exchanger uses hot air (mixed) to heat water (unmixed), flowing with a mass flow rate of 3 kg/s, from 30°C to 80°C. The hot air enters and exits the heat exchanger at 220°C and 100°C, respectively. If the overall heat transfer coefficient is 200 W/m^2·K, determine the required surface area.
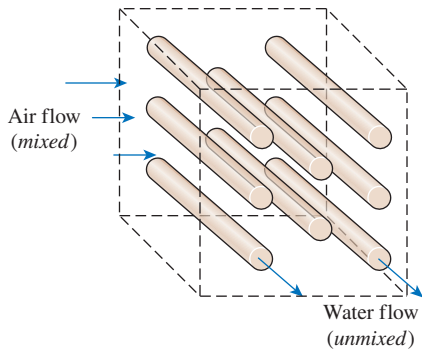
FIGURE P11–165

11–166 The condenser of a room air conditioner is designed to reject heat at a rate of 22,500 kJ/h from refrigerant-134a as the refrigerant is condensed at a temperature of 40°C. Air ($c_p = 1005$ J/kg·K) flows across the finned condenser coils, entering at 25°C and leaving at 32°C. If the overall heat transfer coefficient based on the refrigerant side is 150 W/m²·K, determine the heat transfer area on the refrigerant side.
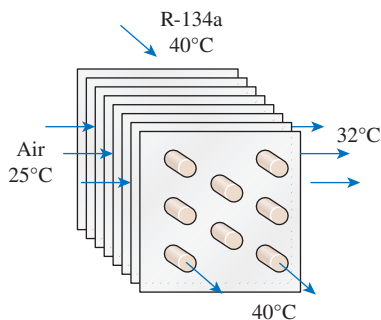
FIGURE P11–166

11–167 Oil in an engine is being cooled by air in a cross-flow heat exchanger, where both fluids are unmixed. Oil ($c_{ph} = 2047$ J/kg·K) flowing with a flow rate of 0.026 kg/s enters the tube side at 75°C, while air ($c_{pc} = 1007$ J/kg·K) enters the shell side at 30°C with a flow rate of 0.21 kg/s. The overall heat transfer coefficient of the heat exchanger is 53 W/m²·K, and the total surface area is 1 m². If the correction factor is $F = 0.96$, determine the outlet temperatures of the oil and air.
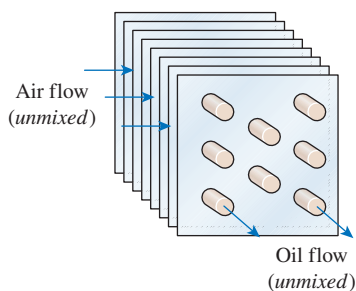
FIGURE P11–167

11–168 Consider a water-to-water counterflow heat exchanger with these specifications. Hot water enters at 90°C while cold water enters at 20°C. The exit temperature of the hot water is 15°C greater than that of the cold water, and the mass flow rate of the hot water is 50 percent greater than that of the cold water. The product of heat transfer surface area and the overall heat transfer coefficient is 2200 W/K. Taking the specific heat of both cold and hot water to be $c_p = 4180$ J/kg·K, determine (a) the outlet temperature of the cold water, (b) the effectiveness of the heat exchanger, (c) the mass flow rate of the cold water, and (d) the heat transfer rate.
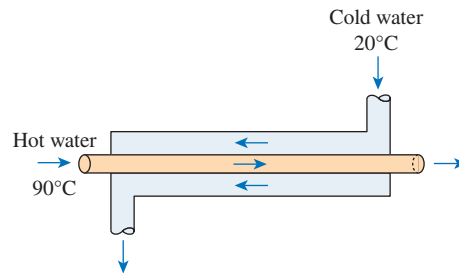
FIGURE P11–168

11–169 Geothermal water ($c_p = 4250$ J/kg·K) at 75°C is to be used to heat fresh water ($c_p = 4180$ J/kg·K) at 17°C at a rate of 1.2 kg/s in a double-pipe counterflow heat exchanger. The heat transfer surface area is 25 m², the overall heat transfer coefficient is 480 W/m²·K, and the mass flow rate of geothermal water is larger than that of fresh water. If the effectiveness of the heat exchanger must be 0.823, determine the mass flow rate of geothermal water and the outlet temperatures of both fluids.

11–170 A crossflow heat exchanger with both fluids unmixed has an overall heat transfer coefficient of 200 W/m²·K, and a heat transfer surface area of 400 m². The hot fluid has a heat capacity of 40,000 W/K, while the cold fluid has a heat capacity of 80,000 W/K. If the inlet temperatures of both hot and cold fluids are 80°C and 20°C, respectively, determine (a) the exit temperature of the hot fluid and (b) the rate of heat transfer in the heat exchanger.

11–171 In a chemical plant, a certain chemical is heated by hot water supplied by a natural gas furnace. The hot water ($c_p = 4180$ J/kg·K) is then discharged at 60°C at a rate of 8 kg/min. The plant operates 8 h a day, 5 days a week, 52 weeks a year. The furnace has an efficiency of 78 percent, and the cost of the natural gas is $1.00 per therm (1 therm = 105,500 kJ). The average temperature of the cold water entering the furnace throughout the year is 14°C. In order to save energy, it is proposed to install a water-to-water heat exchanger to preheat the incoming cold water with the drained hot water. Assuming that the heat exchanger will recover 72 percent of the available heat in the hot water, determine the heat transfer rating of the heat exchanger that needs to be purchased, and suggest a suitable type. Also, determine the amount of money this heat exchanger will save the company per year from natural gas savings.

11–172 A single-pass crossflow heat exchanger with both fluids unmixed has water entering at 16°C and exiting at 33°C, while oil ($c_p = 1.93$ kJ/kg·K and $\rho = 870$ kg/m³) flowing at 0.19 m³/min enters at 38°C and exits at 29°C. If the surface area of the heat exchanger is 20 m², determine (*a*) the NTU value and (*b*) the value of the overall heat transfer coefficient.

Oil flow (*unmixed*)

Water flow (*unmixed*)
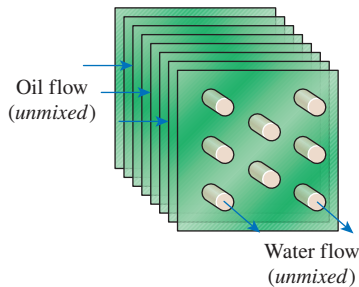
FIGURE P11–172

11–173 Air at 18°C ($c_p = 1006$ J/kg·K) is to be heated to 58°C by hot oil at 80°C ($c_p = 2150$ J/kg·K) in a crossflow heat exchanger with air mixed and oil unmixed. The product of the heat transfer surface area and the overall heat transfer coefficient is 750 W/K, and the mass flow rate of air is twice that of oil. Determine (*a*) the effectiveness of the heat exchanger, (*b*) the mass flow rate of air, and (*c*) the rate of heat transfer.

11–174 The mass flow rate, specific heat, and inlet temperature of the tube-side stream in a double-pipe, parallel-flow heat exchanger are 3200 kg/h, 2.0 kJ/kg·K, and 120°C, respectively. The mass flow rate, specific heat, and inlet temperature of the other stream are 2000 kg/h, 4.2 kJ/kg·K, and 20°C, respectively. The heat transfer area and overall heat transfer coefficient are 0.50 m² and 2.0 kW/m²·K, respectively. Find the outlet temperatures of both streams in steady operation using (*a*) the LMTD method and (*b*) the effectiveness–NTU method.

11–175 During an experiment, a plate heat exchanger that is used to transfer heat from a hot-water stream to a cold-water stream is tested, and the following measurements are taken:

	Hot-water stream	Cold-water stream
Inlet temperature, °C	38.9	14.3
Outlet temperature, °C	27.0	19.8
Volume flow rate, L/min	2.5	4.5

The heat transfer area is calculated to be 0.056 m².
(*a*) Calculate the rate of heat transfer to the cold water.
(*b*) Calculate the overall heat transfer coefficient.

(*c*) Determine if the heat exchanger is truly adiabatic. If it is not, determine the fraction of heat loss and calculate the heat transfer efficiency.
(*d*) Determine the effectiveness and the NTU values of the heat exchanger.

Also, discuss if the measured values are reasonable.

Fundamentals of Engineering (FE) Exam Problems

11–176 Saturated water vapor at 40°C is to be condensed as it flows through the tubes of an air-cooled condenser at a rate of 0.2 kg/s. The condensate leaves the tubes as a saturated liquid at 40°C. The rate of heat transfer to air is

(*a*) 34 kJ/s   (*b*) 268 kJ/s   (*c*) 453 kJ/s
(*d*) 481 kJ/s   (*e*) 515 kJ/s

11–177 Consider a double-pipe heat exchanger with a tube diameter of 10 cm and negligible tube thickness. The total thermal resistance of the heat exchanger was calculated to be 0.025 k/W when it was first constructed. After some prolonged use, fouling occurs at both the inner and outer surfaces with the fouling factors 0.00045 m²·K/W and 0.00015 m²·K/W, respectively. The percentage decrease in the rate of heat transfer in this heat exchanger due to fouling is

(*a*) 2.3%   (*b*) 6.8%   (*c*) 7.1%
(*d*) 7.6%   (*e*) 8.5%

11–178 Hot water coming from the engine is to be cooled by ambient air in a car radiator. The aluminum tubes in which the water flows have a diameter of 4 cm and negligible thickness. Fins are attached on the outer surface of the tubes in order to increase the heat transfer surface area on the air side. The heat transfer coefficients on the inner and outer surfaces are 2000 and 150 W/m²·K, respectively. If the effective surface area on the finned side is 12 times the inner surface area, the overall heat transfer coefficient of this heat exchanger based on the inner surface area is

(*a*) 760 W/m²·K   (*b*) 832 W/m²·K   (*c*) 947 W/m²·K
(*d*) 1075 W/m²·K   (*e*) 1210 W/m²·K

11–179 A heat exchanger is used to heat cold water entering at 12°C at a rate of 1.2 kg/s by hot air entering at 90°C at rate of 2.5 kg/s. The highest rate of heat transfer in the heat exchanger is

(*a*) 82 kW   (*b*) 156 kW   (*c*) 195 kW
(*d*) 224 kW   (*e*) 391 kW

11–180 Cold water ($c_p = 4.18$ kJ/kg·K) enters a heat exchanger at 15°C at a rate of 0.5 kg/s, where it is heated by hot air ($c_p = 1.0$ kJ/kg·K) that enters the heat exchanger at 50°C at a rate of 1.8 kg/s. The maximum possible heat transfer rate in this heat exchanger is

(*a*) 51.1 kW   (*b*) 63.0 kW   (*c*) 66.8 kW
(*d*) 73.2 kW   (*e*) 80.0 kW

11–181 Hot oil ($c_p = 2.1$ kJ/kg·K) at 110°C and 12 kg/s is to be cooled in a heat exchanger by cold water ($c_p = 4.18$ kJ/kg·K) entering at 10°C and at a rate of 2 kg/s. The lowest temperature that oil can be cooled in this heat exchanger is

(*a*) 10°C   (*b*) 24°C   (*c*) 47°C
(*d*) 61°C   (*e*) 77°C

11–182 Cold water ($c_p = 4.18$ kJ/kg·K) enters a counterflow heat exchanger at 18°C at a rate of 0.7 kg/s where it is heated by hot air ($c_p = 1.0$ kJ/kg·K) that enters the heat exchanger at 50°C at a rate of 1.6 kg/s and leaves at 25°C. The maximum possible outlet temperature of the cold water is

(*a*) 25.0°C   (*b*) 32.0°C   (*c*) 35.5°C
(*d*) 39.7°C   (*e*) 50.0°C

11–183 A heat exchanger is used to condense steam coming off the turbine of a steam power plant by cold water from a nearby lake. The cold water ($c_p = 4.18$ kJ/kg·K) enters the condenser at 16°C at a rate of 42 kg/s and leaves at 25°C, while the steam condenses at 45°C. The condenser is not insulated, and it is estimated that heat at a rate of 8 kW is lost from the condenser to the surrounding air. The rate at which the steam condenses is

(*a*) 0.228 kg/s   (*b*) 0.318 kg/s   (*c*) 0.426 kg/s
(*d*) 0.525 kg/s   (*e*) 0.663 kg/s

11–184 An air handler is a large unmixed heat exchanger used for comfort control in large buildings. In one such application, chilled water ($c_p = 4.2$ kJ/kg·K) enters an air handler at 5°C and leaves at 12°C with a flow rate of 1000 kg/h. This cold water cools 5000 kg/h of air ($c_p = 1.0$ kJ/kg·K) which enters the air handler at 25°C. If these streams are in counterflow and the water-stream conditions remain fixed, the minimum temperature at the air outlet is

(*a*) 5°C   (*b*) 12°C   (*c*) 19°C
(*d*) 22°C   (*e*) 25°C

11–185 An air handler is a large unmixed heat exchanger used for comfort control in large buildings. In one such application, chilled water ($c_p = 4.2$ kJ/kg·K) enters an air handler at 5°C and leaves at 12°C with a flow rate of 1000 kg/h. This cold water cools air ($c_p = 1.0$ kJ/kg·K) from 25°C to 15°C. The rate of heat transfer between the two streams is

(*a*) 8.2 kW   (*b*) 23.7 kW   (*c*) 33.8 kW
(*d*) 44.8 kW   (*e*) 52.8 kW

11–186 In a parallel-flow, liquid-to-liquid heat exchanger, the inlet and outlet temperatures of the hot fluid are 150°C and 90°C while those of the cold fluid are 30°C and 70°C, respectively. For the same overall heat transfer coefficient, the percentage decrease in the surface area of the heat exchanger if counterflow arrangement is used is

(*a*) 3.9%   (*b*) 9.7%   (*c*) 14.5%
(*d*) 19.7%   (*e*) 24.6%

11–187 A counterflow heat exchanger is used to cool oil ($c_p = 2.20$ kJ/kg·K) from 110°C to 85°C at a rate of 0.75

kg/s with cold water ($c_p = 4.18$ kJ/kg·K) that enters the heat exchanger at 20°C at a rate of 0.6 kg/s. If the overall heat transfer coefficient is 800 W/m²·K, the heat transfer area of the heat exchanger is

(*a*) 0.745 m²   (*b*) 0.760 m²   (*c*) 0.775 m²
(*d*) 0.790 m²   (*e*) 0.805 m²

11–188 The radiator in an automobile is a crossflow heat exchanger ($UA_s = 10$ kW/K) that uses air ($c_p = 1.00$ kJ/kg·K) to cool the engine coolant fluid ($c_p = 4.00$ kJ/kg·K). The engine fan draws 30°C air through this radiator at a rate of 12 kg/s while the coolant pump circulates the engine coolant at a rate of 5 kg/s. The coolant enters this radiator at 80°C. Under these conditions, what is the number of transfer units (NTU) of this radiator?

(*a*) 2.0   (*b*) 2.5   (*c*) 3.0
(*d*) 3.5   (*e*) 4.0

11–189 In a parallel-flow, water-to-water heat exchanger, the hot water enters at 75°C at a rate of 1.2 kg/s and cold water enters at 20°C at a rate of 0.9 kg/s. The overall heat transfer coefficient and the surface area for this heat exchanger are 750 W/m²·K and 6.4 m², respectively. The specific heat for both the hot and cold fluids may be taken to be 4.18 kJ/kg·K. For the same overall heat transfer coefficient and the surface area, the increase in the effectiveness of this heat exchanger if counterflow arrangement is used is

(*a*) 0.09   (*b*) 0.11   (*c*) 0.14
(*d*) 0.17   (*e*) 0.19

11–190 In a parallel-flow heat exchanger, the NTU is calculated to be 2.5. The lowest possible effectiveness for this heat exchanger is

(*a*) 10%   (*b*) 27%   (*c*) 41%
(*d*) 50%   (*e*) 92%

11–191 Cold water ($c_p = 4.18$ kJ/kg·K) enters a counterflow heat exchanger at 10°C at a rate of 0.35 kg/s, where it is heated by hot air ($c_p = 1.0$ kJ/kg·K) that enters the heat exchanger at 50°C at a rate of 1.9 kg/s and leaves at 25°C. The effectiveness of this heat exchanger is

(*a*) 0.50   (*b*) 0.63   (*c*) 0.72
(*d*) 0.81   (*e*) 0.89

11–192 Steam is to be condensed on the shell side of a two-shell-passes and eight-tube-passes condenser, with 20 tubes in each pass. Cooling water enters the tubes at a rate of 2 kg/s. If the heat transfer area is 14 m² and the overall heat transfer coefficient is 1800 W/m²·K, the effectiveness of this condenser is

(*a*) 0.70   (*b*) 0.80   (*c*) 0.90
(*d*) 0.95   (*e*) 1.0

11–193 Water is boiled at 150°C in a boiler by hot exhaust gases ($c_p = 1.05$ kJ/kg·°C) that enter the boiler at 540°C at a rate of 0.4 kg/s and leave at 200°C. The surface area of the heat exchanger is 0.64 m². The overall heat transfer coefficient of this heat exchanger is

(*a*) 880 W/m²·K   (*b*) 1120 W/m²·K
(*c*) 1350 W/m²·K   (*d*) 2120 W/m²·K
(*e*) 1840 W/m²·K

11–194 An air-cooled condenser is used to condense iso-butane in a binary geothermal power plant. The isobutane is condensed at 85°C by air ($c_p = 1.0$ kJ/kg·K) that enters at 22°C at a rate of 18 kg/s. The overall heat transfer coefficient and the surface area for this heat exchanger are 2.4 kW/m²·K and 2.6 m², respectively. The outlet temperature of the air is

(*a*) 35.6°C   (*b*) 40.5°C   (*c*) 52.1°C
(*d*) 58.5°C   (*e*) 62.8°C

Design and Essay Problems

11–195 Write an interactive computer program that will give the effectiveness of a heat exchanger and the outlet tempera-tures of both the hot and cold fluids when the types of fluids, the inlet temperatures, the mass flow rates, the heat transfer surface area, the overall heat transfer coefficient, and the type of heat exchanger are specified. The program should allow the user to select from the fluids water, engine oil, glycerin, ethyl alcohol, and ammonia. Assume constant specific heats at about room temperature.

11–196 Water flows through a shower head steadily at a rate of 8 kg/min. The water is heated in an electric water heater from 15°C to 45°C. In an attempt to conserve energy, it is pro-posed to pass the drained warm water at a temperature of 38°C through a heat exchanger to preheat the incoming cold water. Design a heat exchanger that is suitable for this task, and dis-cuss the potential savings in energy and money for your area.

11–197 Open the engine compartment of your car and search for heat exchangers. How many do you have? What type are they? Why do you think those specific types are selected? If you were redesigning the car, would you use different kinds? Explain.

11–198 Write an essay on the static and dynamic types of regenerative heat exchangers, and compile information about the manufacturers of such heat exchangers. Choose a few models by different manufacturers and compare their costs and performance.

11–199 Design a hydrocooling unit that can cool fruits and vegetables from 30°C to 5°C at a rate of 20,000 kg/h under the following conditions:

The unit will be of flood type that will cool the products as they are conveyed into the channel filled with water. The products will be dropped into the channel filled with water at one end and picked up at the other end. The channel can be as wide as 3 m and as high as 90 cm. The water is to be circulated and cooled by the evaporator section of a refrigera-tion system. The refrigerant temperature inside the coils is to be −2°C, and the water temperature is not to drop below 1°C and not to exceed 6°C.

Assuming reasonable values for the average product den-sity, specific heat, and porosity (the fraction of air volume in a box), recommend reasonable values for the quantities related to the thermal aspects of the hydrocooler, including (*a*) how long the fruits and vegetables need to remain in the channel, (*b*) the length of the channel, (*c*) the water velocity through the channel, (*d*) the velocity of the conveyor and thus the fruits and vegetables through the channel, (*e*) the refrigeration capacity of the refrigeration system, and (*f*) the type of heat exchanger for the evaporator and the surface area on the water side.

11–200 A company owns a refrigeration system whose refrig-eration capacity is 200 tons (1 ton of refrigeration $= 211$ kJ/min), and you are to design a forced-air cooling system for fruits whose diameters do not exceed 7 cm under the following conditions:

The fruits are to be cooled from 28°C to an average tem-perature of 8°C. The air temperature is to remain above −2°C and below 10°C at all times, and the velocity of air approach-ing the fruits must remain under 2 m/s. The cooling section can be as wide as 3.5 m and as high as 2 m.

Assuming reasonable values for the average fruit density, specific heat, and porosity (the fraction of air volume in a box), recommend reasonable values for the quantities related to the thermal aspects of the forced-air cooling, including (*a*) how long the fruits need to remain in the cooling sec-tion, (*b*) the length of the cooling section, (*c*) the air veloc-ity approaching the cooling section, (*d*) the product cooling capacity of the system, in kg fruit/h, (*e*) the volume flow rate of the air, and (*f*) the type of heat exchanger for the evapora-tor and the surface area on the air side.

11–201 A counterflow double-pipe heat exchanger with $A_s = 9.0$ m² is used for cooling a liquid stream ($c_p = 3.15$ kJ/kg·K) at a rate of 10.0 kg/s with an inlet temperature of 90°C. The coolant ($c_p = 4.2$ kJ/kg·K) enters the heat exchanger at a rate of 8.0 kg/s with an inlet temperature of 10°C. The plant data gave the following equation for the overall heat transfer coefficient in W/m²·K: $U = 600/(1/\dot{m}_c^{0.8} + 2/\dot{m}_h^{0.8})$, where $\dot{m}_c$ and $\dot{m}_h$ are the cold- and hot-stream flow rates in kg/s, respec-tively. (*a*) Calculate the rate of heat transfer and the outlet stream temperatures for this unit. (*b*) The existing unit is to be replaced. A vendor is offering a very attractive discount on two identical heat exchangers that are presently stocked in its warehouse, each with $A_s = 5$ m². Because the tube diameters in the existing and new units are the same, the preceding heat transfer coefficient equation is expected to be valid for the new units as well. The vendor is proposing that the two new units could be operated in parallel, such that each unit would pro-cess exactly one-half the flow rate of each of the hot and cold streams in a counterflow manner; hence, they together would meet (or exceed) the present plant heat duty. Give your recom-mendation, with supporting calculations, on this replacement proposal.

Design Element: C&S icon ©McGraw-Hill Education; PtD icon ©McGraw-Hill Education; laptop art ©McGraw-Hill Education".

FUNDAMENTALS OF THERMAL RADIATION

So far, we have considered the conduction and convection modes of heat transfer, which are related to the nature of the media involved and the presence of fluid motion, among other things. We now turn our attention to the third mechanism of heat transfer: *radiation,* which is characteristically different from the other two.

We start this chapter with a discussion of *electromagnetic waves* and the *electromagnetic spectrum,* with particular emphasis on *thermal radiation.* Then we introduce the idealized *blackbody, blackbody radiation,* and *blackbody radiation function,* together with the *Stefan–Boltzmann law, Planck's law,* and *Wien's displacement law.*

Radiation is emitted by every point on a plane surface in all directions into the hemisphere above the surface. The quantity that describes the magnitude of radiation emitted or incident in a specified direction in space is the *radiation intensity.* Various radiation fluxes such as *emissive power, irradiation,* and *radiosity* are expressed in terms of intensity. This is followed by a discussion of radiative properties of materials such as *emissivity, absorptivity, reflectivity,* and *transmissivity* and their dependence on wavelength, direction, and temperature. The *greenhouse effect* is presented as an example of the consequences of the wavelength dependence of radiation properties. We end this chapter with a discussion of *atmospheric* and *solar radiation.*

OBJECTIVES

When you finish studying this chapter, you should be able to:

- Classify electromagnetic radiation, and identify thermal radiation,

- Understand the idealized blackbody, and calculate the total and spectral blackbody emissive power,

- Calculate the fraction of radiation emitted in a specified wavelength band using the blackbody radiation functions,

- Understand the concept of radiation intensity, and define spectral directional quantities using intensity,

- Develop a clear understanding of the properties emissivity, absorptivity, reflectivity, and transmissivity on spectral, directional, and total basis,

- Apply Kirchhoff's law to determine the absorptivity of a surface when its emissivity is known,

- Model the atmospheric radiation by the use of an effective sky temperature, and appreciate the importance of the greenhouse effect.
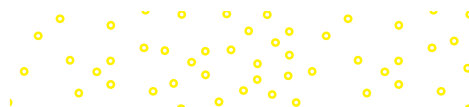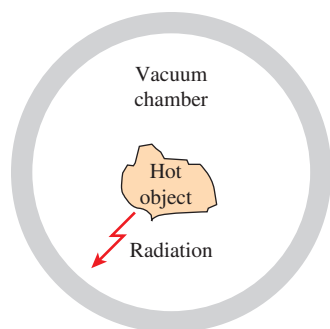
FIGURE 12–1
A hot object in a vacuum chamber loses heat by radiation only.
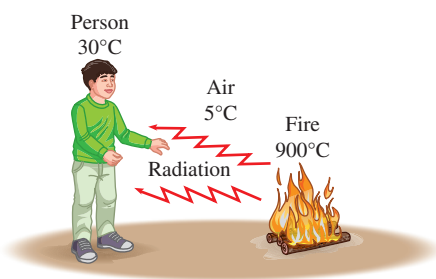
FIGURE 12–2
Unlike conduction and convection, heat transfer by radiation can occur between two bodies, even when they are separated by a medium colder than both.

12–1 ■ INTRODUCTION

Consider a hot object that is suspended in an evacuated chamber whose walls are at room temperature (Fig. 12–1). The hot object will eventually cool down and reach thermal equilibrium with its surroundings. That is, it will lose heat until its temperature reaches the temperature of the walls of the chamber. Heat transfer between the object and the chamber could not have taken place by conduction or convection, because these two mechanisms cannot occur in a vacuum. Therefore, heat transfer must have occurred through another mechanism that involves the emission of the internal energy of the object. This mechanism is *radiation.*

Radiation differs from the other two heat transfer mechanisms in that it does not require the presence of a material medium to take place. In fact, energy transfer by radiation is fastest (at the speed of light), and it suffers no attenuation in a *vacuum.* Also, radiation transfer occurs in solids as well as liquids and gases. In most practical applications, all three modes of heat transfer occur concurrently at varying degrees. But heat transfer through an evacuated space can occur only by radiation. For example, the energy of the sun reaches the earth by radiation.

You will recall that heat transfer by conduction or convection takes place in the direction of decreasing temperature; that is, from a high-temperature medium to a lower-temperature one. It is interesting that radiation heat transfer can occur between two bodies separated by a medium colder than both bodies (Fig. 12–2). For example, solar radiation reaches the surface of the earth after passing through cold air layers at high altitudes. Also, the radiation-absorbing surfaces inside a greenhouse reach high temperatures even when its plastic or glass cover remains relatively cool.

The theoretical foundation of radiation was established in 1864 by physicist James Clerk Maxwell, who postulated that accelerated charges or changing electric currents give rise to electric and magnetic fields. These rapidly moving fields are called **electromagnetic waves** or **electromagnetic radiation**, and they represent the energy emitted by matter as a result of the changes in the electronic configurations of the atoms or molecules. In 1887, Heinrich Hertz experimentally demonstrated the existence of such waves. Electromagnetic waves transport energy just like other waves, and all electromagnetic waves travel at the *speed of light* in a vacuum, which is $c_0 = 2.9979 \times 10^8$ m/s. Electromagnetic waves are characterized by their *frequency ν* or *wavelength λ*. These two properties in a medium are related by

$$\lambda = \frac{c}{\nu} \qquad (12\text{–}1)$$

where *c* is the speed of propagation of a wave in that medium. The speed of propagation in a medium is related to the speed of light in a vacuum by $c = c_0/n$, where *n* is the *index of refraction* of that medium. The refractive index is essentially unity for air and most gases, about 1.5 for glass, and 1.33 for water. The commonly used unit of wavelength is the *micrometer* (μm) or micron, where 1 μm = 10^{-6} m. Unlike the wavelength and the speed of propagation, the frequency of an electromagnetic wave depends only on the source and is independent of the medium through which the wave travels. The *frequency* (the number of oscillations per second) of an electromagnetic

wave can range from less than a million Hz to a septillion Hz or higher, depending on the source. Note from Eq. 12–1 that the wavelength and the frequency of electromagnetic radiation are inversely proportional.

It has proven useful to view electromagnetic radiation as the propagation of a collection of discrete packets of energy called **photons** or **quanta**, as proposed by Max Planck in 1900 in conjunction with his *quantum theory.* In this view, each photon of frequency ν is considered to have an energy of

$$e = h\nu = \frac{hc}{\lambda} \qquad \text{(12–2)}$$

where $h = 6.626069 \times 10^{-34}$ J·s is *Planck's constant.* Note from the second part of Eq. 12–2 that the energy of a photon is inversely proportional to its wavelength. Therefore, shorter-wavelength radiation possesses larger photon energies. It is no wonder that we try to avoid very-short-wavelength radiation such as gamma rays and X-rays since they are highly destructive.

12–2 ▪ THERMAL RADIATION

Although all electromagnetic waves have the same general features, waves of different wavelength differ significantly in their behavior. The electromagnetic radiation encountered in practice covers a wide range of wavelengths, varying from less than 10^{-10} μm for cosmic rays to more than 10^{10} μm for electrical power waves. The **electromagnetic spectrum** also includes gamma rays, X-rays, ultraviolet radiation, visible light, infrared radiation, thermal radiation, microwaves, and radio waves, as shown in Fig. 12–3.

Different types of electromagnetic radiation are produced through various mechanisms. For example, *gamma rays* are produced by nuclear reactions, *X-rays* by the bombardment of metals with high-energy electrons, *microwaves* by special types of electron tubes such as klystrons and magnetrons, and *radio waves* by the excitation of some crystals or by the flow of alternating current through electric conductors.

The short-wavelength gamma rays and X-rays are primarily of concern to nuclear engineers, while the long-wavelength microwaves and radio waves are of concern to electrical engineers. The type of electromagnetic radiation that is pertinent to heat transfer is the **thermal radiation** emitted as a result of energy transitions of molecules, atoms, and electrons of a substance. Temperature is a measure of the strength of these activities at the microscopic level, and the rate of thermal radiation emission increases with increasing temperature. Thermal radiation is continuously emitted by all matter whose temperature is above absolute zero. That is, everything around us, such as walls, furniture, and our friends constantly emits (and absorbs) radiation (Fig. 12–4). Thermal radiation is also defined as the portion of the electromagnetic spectrum that extends from about 0.1 to 100 μm, since the radiation emitted by bodies due to their temperature falls almost entirely into this wavelength range. Thus, thermal radiation includes the entire visible and infrared (IR) radiation bands as well as a portion of the ultraviolet (UV) radiation band.

What we call **light** is simply the *visible* portion of the electromagnetic spectrum that lies between 0.40 and 0.76 μm. Light is characteristically no different than other electromagnetic radiation, except that it happens to trigger the
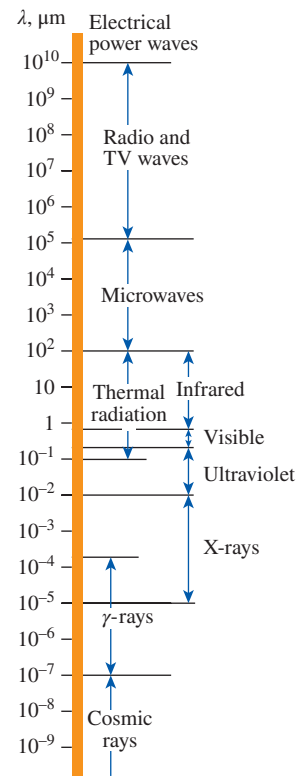
FIGURE 12–3
The electromagnetic wave spectrum.
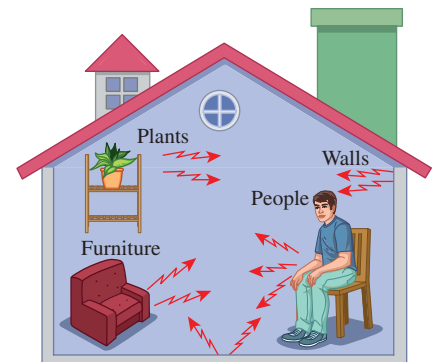
FIGURE 12–4
Everything around us constantly emits thermal radiation.

TABLE 12–1

The wavelength ranges of different colors

Color	Wavelength Band
Violet	0.40–0.44 μm
Blue	0.44–0.49 μm
Green	0.49–0.54 μm
Yellow	0.54–0.60 μm
Orange	0.60–0.67 μm
Red	0.63–0.76 μm

FIGURE 12–5

Food is heated or cooked in a microwave oven by absorbing the electromagnetic radiation energy generated by the magnetron of the oven.

sensation of seeing in the human eye. Light, or the visible spectrum, consists of narrow bands of color from violet (0.40–0.44 μm) to red (0.63–0.76 μm), as shown in Table 12–1.

A body that emits some radiation in the visible range is called a light source. The sun is obviously our primary light source. The electromagnetic radiation emitted by the sun is known as **solar radiation**, and nearly all of it falls into the wavelength band 0.3–3 μm. Almost *half* of solar radiation is light (i.e., it falls into the visible range), with the remaining portion being ultraviolet and infrared.

The radiation emitted by bodies at room temperature falls into the **infrared** region of the spectrum, which extends from 0.76 to 100 μm. Bodies start emitting noticeable visible radiation at temperatures above 800 K. The tungsten filament of a lightbulb must be heated to temperatures above 2000 K before it can emit any significant amount of radiation in the visible range.

The **ultraviolet** radiation includes the low-wavelength end of the thermal radiation spectrum and lies between the wavelengths 0.01 and 0.40 μm. Ultraviolet rays are to be avoided since they can kill microorganisms and cause serious damage to humans and other living beings. About 12 percent of solar radiation is in the ultraviolet range, and it would be devastating if it were to reach the surface of the earth. Fortunately, the ozone (O_3) layer in the atmosphere acts as a protective blanket and absorbs most of this ultraviolet radiation. The ultraviolet rays that remain in sunlight are still sufficient to cause serious sunburns to sun worshippers, and prolonged exposure to direct sunlight is the leading cause of skin cancer, which can be lethal. Recent discoveries of "holes" in the ozone layer have prompted the international community to ban the use of ozone-destroying chemicals such as the refrigerant Freon-12 in order to save the earth. Ultraviolet radiation is also produced artificially in fluorescent lamps for use in medicine as a bacteria killer and in tanning parlors as an artificial tanner.

Microwave ovens utilize electromagnetic radiation in the **microwave** region of the spectrum generated by microwave tubes called *magnetrons*. Microwaves in the range of 10^2–10^5 μm are very suitable for use in cooking since they are *reflected* by metals, *transmitted* by glass and plastics, and *absorbed* by food (especially water) molecules. Thus, the electric energy converted to radiation in a microwave oven eventually becomes part of the internal energy of the food. The fast and efficient cooking of microwave ovens has made them one of the essential appliances in modern kitchens (Fig. 12–5).

Radars and cordless telephones also use electromagnetic radiation in the microwave region. The wavelength of the electromagnetic waves used in radio and TV broadcasting usually ranges between 1 and 1000 m in the **radio wave** region of the spectrum.

In heat transfer studies, we are interested in the energy emitted by bodies because of their temperature only. Therefore, we limit our consideration to *thermal radiation,* which we simply call *radiation.* The relations developed below are restricted to thermal radiation only and may not be applicable to other forms of electromagnetic radiation.

The electrons, atoms, and molecules of all solids, liquids, and gases above absolute zero temperature are constantly in motion, and thus radiation is constantly emitted, as well as being absorbed or transmitted throughout the entire volume of matter. That is, radiation is a **volumetric phenomenon**. However,
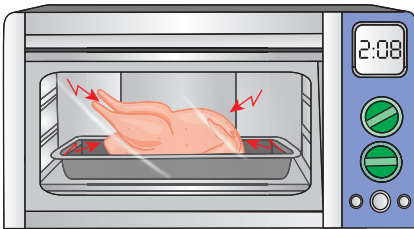
for opaque (nontransparent) solids such as metals, wood, and rocks, radiation is considered to be a **surface phenomenon**, since the radiation emitted by the interior regions can never reach the surface, and the radiation incident on such bodies is usually absorbed within a few microns from the surface (Fig. 12–6). Note that the radiation characteristics of surfaces can be changed completely by applying thin layers of coatings on them.

12–3 ▪ BLACKBODY RADIATION

A body at a thermodynamic (or absolute) temperature above zero emits radiation in all directions over a wide range of wavelengths. The amount of radiation energy emitted from a surface at a given wavelength depends on the material of the body and the condition of its surface as well as the surface temperature. Therefore, different bodies may emit different amounts of radiation per unit surface area, even when they are at the same temperature. Thus, it is natural to be curious about the *maximum* amount of radiation that can be emitted by a surface at a given temperature. Satisfying this curiosity requires the definition of an idealized body, called a *blackbody,* to serve as a standard against which the radiative properties of real surfaces may be compared.

A **blackbody** is defined as *a perfect emitter and absorber of radiation.* At a specified temperature and wavelength, no surface can emit more energy than a blackbody. A blackbody absorbs *all* incident radiation, regardless of wavelength and direction. Also, a blackbody emits radiation energy uniformly in all directions per unit area normal to direction of emission (Fig. 12–7). That is, a blackbody is a *diffuse* emitter. The term *diffuse* means "independent of direction."

The radiation energy emitted by a blackbody per unit time and per unit surface area was determined experimentally by Joseph Stefan in 1879 and expressed as

$$E_b(T) = \sigma T^4 \qquad (\text{W/m}^2) \tag{12–3}$$

where $\sigma = 5.670 \times 10^{-8}$ W/m^2·K^4 is the *Stefan–Boltzmann constant* and T is the absolute temperature of the surface in K. This relation was theoretically verified in 1884 by Ludwig Boltzmann. Equation 12–3 is known as the **Stefan–Boltzmann law** and E_b is called the **blackbody emissive power**. Note that the emission of thermal radiation is proportional to the *fourth power* of the absolute temperature.

Although a blackbody would appear *black* to the eye, a distinction should be made between the idealized blackbody and an ordinary black surface. Any surface that absorbs light (the visible portion of radiation) would appear black to the eye, and a surface that reflects it completely would appear white. Considering that visible radiation occupies a very narrow band of the spectrum from 0.4 to 0.76 μm, we cannot make any judgments about the blackness of a surface on the basis of visual observations. For example, snow and white paint reflect light and thus appear white. But they are essentially black for infrared radiation since they strongly absorb long-wavelength radiation. Surfaces coated with lampblack paint approach idealized blackbody behavior.

Another type of body that closely resembles a blackbody is a *large cavity with a small opening,* as shown in Fig. 12–8. Radiation coming in through the opening of area A undergoes multiple reflections, and thus it has several
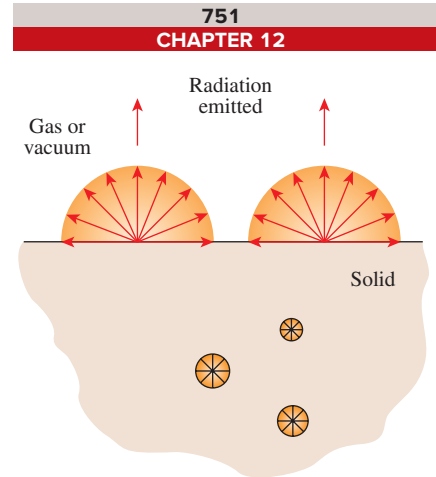
FIGURE 12–6
Radiation in opaque solids is considered a surface phenomenon since the radiation emitted only by the molecules at the surface can escape the solid.
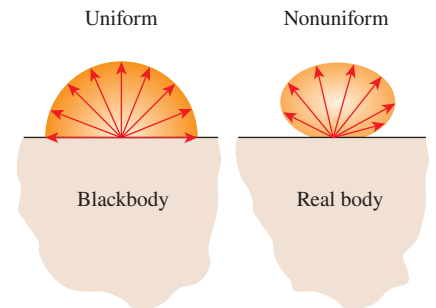
FIGURE 12–7
A blackbody is said to be a *diffuse* emitter since it emits radiation energy uniformly in all directions.
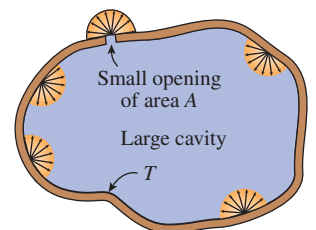
FIGURE 12–8
A large isothermal cavity at temperature T with a small opening of area A closely resembles a blackbody of surface area A at the same temperature.

chances to be absorbed by the interior surfaces of the cavity before any part of it can possibly escape. Also, if the surface of the cavity is isothermal at temperature *T,* the radiation emitted by the interior surfaces streams through the opening after undergoing multiple reflections, and thus it has a diffuse nature. Therefore, the cavity acts as a perfect absorber and perfect emitter, and the opening will resemble a blackbody of surface area *A* at temperature *T,* regardless of the actual radiative properties of the cavity.

The Stefan–Boltzmann law in Eq. 12–3 gives the *total* blackbody emissive power E_b, which is the sum of the radiation emitted over all wavelengths. Sometimes we need to know the **spectral blackbody emissive power**, which is *the amount of radiation energy emitted by a blackbody at a thermodynamic temperature T per unit time, per unit surface area, and per unit wavelength about the wavelength λ.* For example, we are more interested in the amount of radiation an incandescent lightbulb emits in the visible wavelength spectrum than we are in the total amount emitted.

The relation for the spectral blackbody emissive power $E_{b\lambda}$ was developed by Max Planck in 1901 in conjunction with his famous quantum theory. This relation is known as **Planck's law** and is expressed as

$$E_{b\lambda}(\lambda, T) = \frac{C_1}{\lambda^5 [\exp(C_2/\lambda T) - 1]} \quad (\text{W/m}^2 \cdot \mu\text{m}) \qquad \textbf{(12–4)}$$

where

$$C_1 = 2\pi h c_0^2 = 3.74177 \times 10^8 \ \text{W} \cdot \mu\text{m}^4/\text{m}^2$$

$$C_2 = h c_0/k = 1.43878 \times 10^4 \ \mu\text{m} \cdot \text{K}$$

Also, *T* is the absolute temperature of the surface, *λ* is the wavelength of the radiation emitted, and $k = 1.38065 \times 10^{-23}$ J/K is *Boltzmann's constant.* This relation is valid for a surface in a *vacuum* or a *gas.* For other media, it needs to be modified by replacing C_1 with C_1/n^2, where *n* is the index of refraction of the medium. Note that the term *spectral* indicates dependence on wavelength.

The variation of the spectral blackbody emissive power with wavelength is plotted in Fig. 12–9 for selected temperatures. Several observations can be made from this figure:

1. The emitted radiation is a continuous function of *wavelength.* At any specified temperature, it increases with wavelength, reaches a peak, and then decreases with increasing wavelength.

2. At any wavelength, the amount of emitted radiation *increases* with increasing temperature.

3. As temperature increases, the curves shift to the left to the shorter-wavelength region. Consequently, a larger fraction of the radiation is emitted at *shorter wavelengths* at higher temperatures.

4. The radiation emitted by the *sun,* which is considered to be a blackbody at 5780 K (or roughly at 5800 K), reaches its peak in the visible region of the spectrum. Therefore, the sun is in tune with our eyes. On the other hand, surfaces at $T \le 800$ K emit almost entirely in the infrared region and thus are not visible to the eye unless they reflect light coming from other sources.
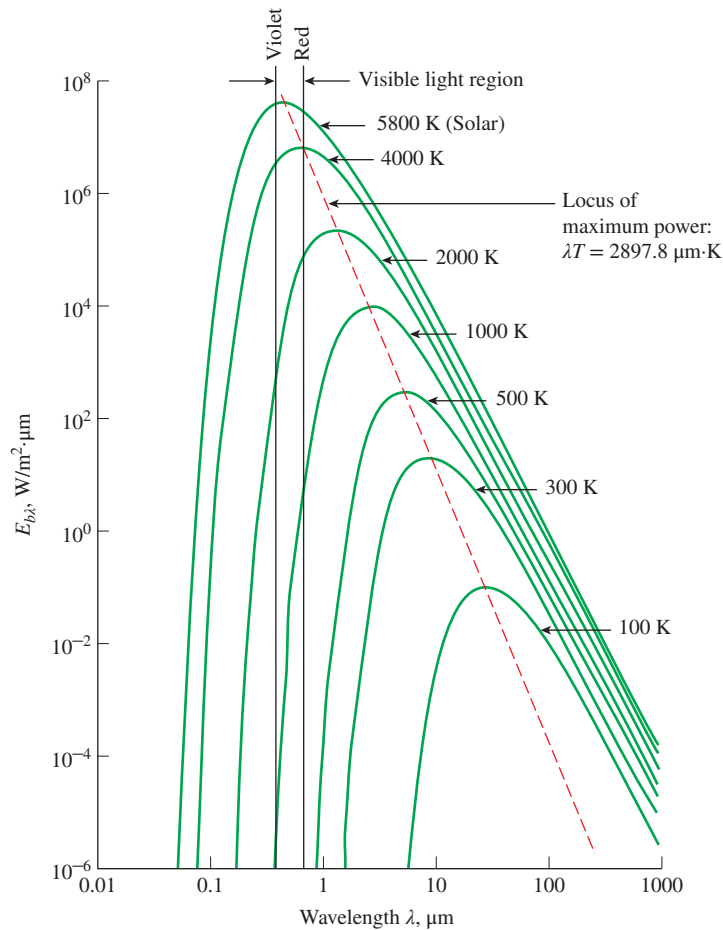
FIGURE 12–9
The variation of the blackbody emissive power with wavelength for several temperatures.

As the temperature increases, the peak of the curve in Fig. 12–9 shifts toward shorter wavelengths. The wavelength at which the peak occurs for a specified temperature is given by **Wien's displacement law** as

$$(\lambda T)_{\text{max power}} = 2897.8 \ \mu\text{m·K} \tag{12–5}$$

This relation was originally developed by Willy Wien in 1894 using classical thermodynamics, but it can also be obtained by differentiating Eq. 12–4 with respect to λ while holding T constant and setting the result equal to zero. A plot of Wien's displacement law, which is the locus of the peaks of the radiation emission curves, is also given in Fig. 12–9.

The peak of the solar radiation, for example, occurs at $\lambda = 2897.8/5780 = 0.50 \ \mu\text{m}$, which is near the middle of the visible range. The peak of the radiation emitted by a surface at room temperature ($T = 298$ K) occurs at 9.72 μm, which is well into the infrared region of the spectrum.

An electrical resistance heater starts radiating heat soon after it is plugged in, and we can feel the emitted radiation energy by holding our hands against the heater. But this radiation is entirely in the infrared region and thus cannot
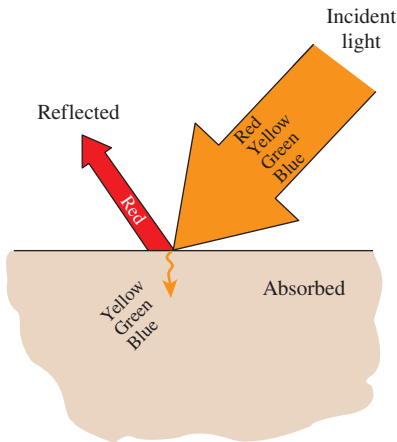
FIGURE 12–10
A surface that reflects red while absorbing the remaining parts of the incident light appears red to the eye.
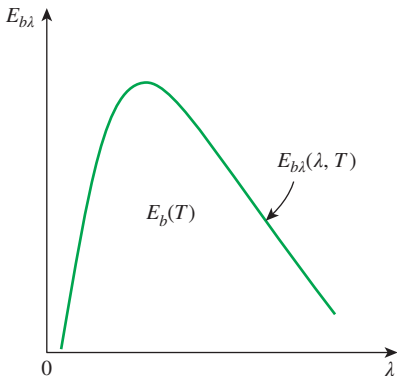
FIGURE 12–11
On an $E_{b\lambda}$–λ chart, the area under a curve for a given temperature represents the total radiation energy emitted by a blackbody at that temperature.

be sensed by our eyes. The heater will appear dull red when its temperature reaches about 1000 K, since it starts emitting a detectable amount (about 1 W/m²·μm) of visible red radiation at that temperature. As the temperature rises even more, the heater appears bright red and is said to be *red hot.* When the temperature reaches about 1500 K, the heater emits enough radiation in the entire visible range of the spectrum to appear almost *white* to the eye, and it is called *white hot.*

Although it cannot be sensed directly by the human eye, infrared radiation can be detected by infrared cameras, which transmit the information to microprocessors to display visual images of objects at night. *Rattlesnakes* can sense the infrared radiation or the "body heat" coming off warm-blooded animals, and thus they can see at night without using any instruments. Similarly, honeybees are sensitive to ultraviolet radiation. A surface that reflects all of the light appears *white,* while a surface that absorbs all of the light incident on it appears black. (Then how do we see a black surface?)

It should be clear from this discussion that the color of an object is not due to emission, which is primarily in the infrared region, unless the surface temperature of the object exceeds about 1000 K. Instead, the color of a surface depends on the absorption and reflection characteristics of the surface and is due to selective absorption and reflection of the incident visible radiation coming from a light source such as the sun or an incandescent lightbulb. A piece of clothing containing a pigment that reflects red while absorbing the remaining parts of the incident light appears "red" to the eye (Fig. 12–10). Leaves appear "green" because their cells contain the pigment chlorophyll, which strongly reflects green while absorbing other colors.

It is left as an exercise to show that integration of the *spectral* blackbody emissive power $E_{b\lambda}$ over the entire wavelength spectrum gives the *total* blackbody emissive power E_b:

$$E_b(T) = \int_0^\infty E_{b\lambda}(\lambda, T)\, d\lambda = \sigma T^4 \quad (\text{W/m}^2) \tag{12–6}$$

Thus, we obtained the Stefan–Boltzmann law (Eq. 12–3) by integrating Planck's law (Eq. 12–4) over all wavelengths. Note that on an $E_{b\lambda}$–λ chart, $E_{b\lambda}$ corresponds to any value on the curve, whereas E_b corresponds to the area under the entire curve for a specified temperature (Fig. 12–11). Also, the term *total* means "integrated over all wavelengths."

EXAMPLE 12–1   **Radiation Emission from a Black Ball**

Consider a 20-cm-diameter spherical ball at 800 K suspended in air as shown in Fig. 12–12. Assuming the ball closely approximates a blackbody, determine (*a*) the total blackbody emissive power, (*b*) the total amount of radiation emitted by the ball in 5 min, (*c*) the spectral blackbody emissive power at a wavelength of 3 μm, and (*d*) the wavelength for the maximum spectral blackbody emissive power at the ball surface temperature of 800 K.

SOLUTION   An isothermal sphere is suspended in air. The total blackbody emissive power, the total radiation emitted in 5 min, the spectral blackbody emissive power at 3 μm, and the wavelength for the maximum spectral blackbody emissive power at the ball surface temperature of 800 K are to be determined.
Assumptions   **1** The ball behaves as a blackbody. **2** Uniform surface temperature.

Analysis (*a*) The total blackbody emissive power is determined from the Stefan–Boltzmann law to be

$$E_b = \sigma T^4 = (5.67 \times 10^{-8} \text{ W/m}^2\cdot\text{K}^4)(800 \text{ K})^4 = \textbf{23.2 kW/m}^2$$

That is, the ball emits 23.2 kJ of energy in the form of electromagnetic radiation per second per m^2 of the surface area of the ball.

(*b*) The total amount of radiation energy emitted from the entire ball in 5 min is determined by multiplying the blackbody emissive power obtained above by the total surface area of the ball and the given time interval:

$$A_s = \pi D^2 = \pi (0.2 \text{ m})^2 = 0.1257 \text{ m}^2$$

$$\Delta t = (5 \text{ min})\left(\frac{60 \text{ s}}{1 \text{ min}}\right) = 300 \text{ s}$$

$$Q_{rad} = E_b A_s \Delta t = (23.2 \text{ kW/m}^2)(0.1257 \text{ m}^2)(300 \text{ s})\left(\frac{1 \text{ kJ}}{1 \text{ kW}\cdot\text{s}}\right)$$

$$= \textbf{875 kJ}$$

That is, the ball loses 875 kJ of its internal energy in the form of electromagnetic waves to the surroundings in 5 min, which is enough energy to heat 20 kg of water from 0°C to 100°C. Note that the surface temperature of the ball cannot remain constant at 800 K unless there is an equal amount of energy flow to the surface from the surroundings or from the interior regions of the ball through some mechanisms such as chemical or nuclear reactions.

(*c*) The spectral blackbody emissive power at a wavelength of 3 μm is determined from Planck's distribution law to be

$$E_{b\lambda} = \frac{C_1}{\lambda^5\left[\exp\left(\dfrac{C_2}{\lambda T}\right) - 1\right]} = \frac{3.74177 \times 10^8 \text{ W}\cdot\text{μm}^4/\text{m}^2}{(3 \text{ μm})^5\left[\exp\left(\dfrac{1.43878 \times 10^4 \text{ μm}\cdot\text{K}}{(3 \text{ μm})(800 \text{ K})}\right) - 1\right]}$$

$$= \textbf{3846 W/m}^2\cdot\textbf{μm}$$

(*d*) The wavelength for the maximum spectral blackbody emissive power at the ball surface temperature of 800 K is determined from Wien's displacement law to be

$$(\lambda T)_{\text{max power}} = 2897.8 \text{ μm}\cdot\text{K}$$

So,

$$\lambda_{\text{max power}} = \frac{2897.8 \text{ μm}\cdot\text{K}}{800 \text{ K}} = \textbf{3.62 μm}$$

Discussion The maximum spectral blackbody emmisive power at the $\lambda_{\text{max power}} = 3.62$ μm is 4229 W/m^2·μm. This is about 10 percent higher than the value calculated in part (*c*) for a wavelength of 3 μm.

FIGURE 12–12
The spherical ball considered in
Example 12–1.
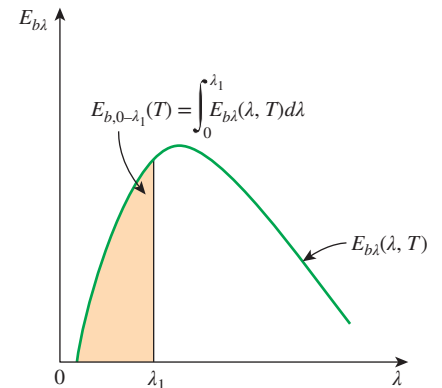
FIGURE 12–13
On an $E_{b\lambda}$–λ chart, the area under
the curve to the left of the $\lambda = \lambda_1$ line
represents the radiation energy emitted
by a blackbody in the wavelength
range 0–λ_1 for the given temperature.

The Stefan–Boltzmann law $E_b(T) = \sigma T^4$ gives the *total* radiation emitted by a blackbody at all wavelengths from $\lambda = 0$ to $\lambda = \infty$. But we are often interested in the amount of radiation emitted over *some wavelength band*. For example, an incandescent lightbulb is judged on the basis of the radiation it emits in the visible range rather than the radiation it emits at all wavelengths.

The radiation energy emitted by a blackbody per unit area over a wavelength band from $\lambda = 0$ to λ is determined from (Fig. 12–13)

$$E_{b,\,0-\lambda}(T) = \int_0^\lambda E_{b\lambda}(\lambda, T)d\lambda \quad (\text{W/m}^2) \tag{12–7}$$

It looks like we can determine $E_{b,\,0-\lambda}$ by substituting the $E_{b\lambda}$ relation from Eq. 12–4 and performing this integration. But it turns out that this integration does not have a simple closed-form solution, and performing a numerical integration each time we need a value of $E_{b,\,0-\lambda}$ is not practical. Therefore, we define a dimensionless quantity f_λ called the **blackbody radiation function** as

$$f_\lambda(T) = \frac{\int_0^\lambda E_{b\lambda}(\lambda, T)d\lambda}{\sigma T^4} \tag{12–8}$$

The function f_λ represents *the fraction of radiation emitted from a blackbody at temperature T in the wavelength band from $\lambda = 0$ to λ*. In reference to Fig. 12–13, f_λ can be interpreted as the ratio of the shaded region (radiation energy emitted by the blackbody in the wavelength range $0 - \lambda_1$) over the total area under the curve (total radiation energy emitted by the blackbody in the wavelength range $0 - \infty$). The values of f_λ are listed in Table 12–2 as a function of λT, where λ is in μm and T is in K.

TABLE 12–2

Blackbody radiation functions f_λ

λT, μm·K	f_λ	λT, μm·K	f_λ
200	0.000000	6200	0.754140
400	0.000000	6400	0.769234
600	0.000000	6600	0.783199
800	0.000016	6800	0.796129
1000	0.000321	7000	0.808109
1200	0.002134	7200	0.819217
1400	0.007790	7400	0.829527
1600	0.019718	7600	0.839102
1800	0.039341	7800	0.848005
2000	0.066728	8000	0.856288
2200	0.100888	8500	0.874608
2400	0.140256	9000	0.890029
2600	0.183120	9500	0.903085
2800	0.227897	10,000	0.914199
3000	0.273232	10,500	0.923710
3200	0.318102	11,000	0.931890
3400	0.361735	11,500	0.939959
3600	0.403607	12,000	0.945098
3800	0.443382	13,000	0.955139
4000	0.480877	14,000	0.962898
4200	0.516014	15,000	0.969981
4400	0.548796	16,000	0.973814
4600	0.579280	18,000	0.980860
4800	0.607559	20,000	0.985602
5000	0.633747	25,000	0.992215
5200	0.658970	30,000	0.995340
5400	0.680360	40,000	0.997967
5600	0.701046	50,000	0.998953
5800	0.720158	75,000	0.999713
6000	0.737818	100,000	0.999905

The fraction of radiation energy emitted by a blackbody at temperature T over a finite wavelength band from $\lambda = \lambda_1$ to $\lambda = \lambda_2$ is determined from (Fig. 12–14)

$$f_{\lambda_1 - \lambda_2}(T) = \frac{\int_0^{\lambda_2} E_{b\lambda}(\lambda, T)d\lambda - \int_0^{\lambda_1} E_{b\lambda}(\lambda, T)d\lambda}{\sigma T^4} = f_{\lambda_2}(T) - f_{\lambda_1}(T) \qquad \textbf{(12–9)}$$

where $f_{\lambda_1}(T)$ and $f_{\lambda_2}(T)$ are blackbody radiation functions corresponding to $\lambda_1 T$ and $\lambda_2 T$, respectively.
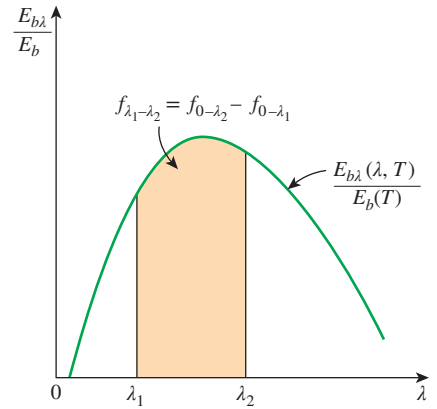
FIGURE 12–14
Graphical representation of the fraction of radiation emitted in the wavelength band from λ_1 to λ_2.

EXAMPLE 12–2 Light Emitted by the Sun and by a Lightbulb

Charge-coupled device (CCD) image sensors, which are common in modern digital cameras, respond differently to light sources with different spectral distributions. Daylight and incandescent light sources may be approximated as blackbodies at the effective surface temperatures of 5800 K and 2800 K, respectively. Determine the fraction of radiation emitted within the visible spectrum wavelengths, from 0.40 μm (violet) to 0.76 μm (red), for each of the lighting sources.

SOLUTION For specified blackbody temperatures, the fraction of visible radiation emitted by the sun and the filament of an incandescent lightbulb are to be determined.

Assumptions The sun and the incandescent light filament behave as blackbodies.

Analysis The visible range of the electromagnetic spectrum extends from $\lambda_1 = 0.40$ μm to $\lambda_2 = 0.76$ μm. For the sun at $T = 5800$ K, the blackbody radiation functions corresponding to $\lambda_1 T$ and $\lambda_2 T$ are determined from Table 12–2 to be (Fig. 12–15)

$$\lambda_1 T = (0.40 \text{ μm})(5800 \text{ K}) = 2320 \text{ μm·K} \rightarrow f_{\lambda_1, \text{ daylight}} = 0.124509$$
$$\lambda_2 T = (0.76 \text{ μm})(5800 \text{ K}) = 4408 \text{ μm·K} \rightarrow f_{\lambda_2, \text{ daylight}} = 0.550015$$

Then the fraction of visible radiation emitted by the sun becomes

$$f_{\lambda_1 - \lambda_2, \text{ daylight}} = 0.550015 - 0.124509 = \textbf{0.426} \text{ or } \textbf{42.6 percent}$$

For an incandescent lightbulb at $T = 2800$ K, the blackbody radiation functions corresponding to $\lambda_1 T$ and $\lambda_2 T$ are determined from Table 12–2 to be

$$\lambda_1 T = (0.40 \text{ μm})(2800 \text{ K}) = 1120 \text{ μm·K} \rightarrow f_{\lambda_1, \text{ incandescent}} = 0.001409$$
$$\lambda_2 T = (0.76 \text{ μm})(5800 \text{ K}) = 2128 \text{ μm·K} \rightarrow f_{\lambda_2, \text{ incandescent}} = 0.088590$$

Then the fraction of radiation the lightbulb emits in the visible range becomes

$$f_{\lambda_1 - \lambda_2, \text{ incandescent}} = 0.088590 - 0.001409 = \textbf{0.087} \text{ or } \textbf{8.7 percent}$$

Discussion Note that almost half of the radiation emitted by the sun is in the visible range, and thus the sun is a very efficient light source. But less than 10 percent of the radiation emitted by the incandescent lightbulb is in the form of visible light, and thus incandescent lightbulbs are inefficient as light sources. Consequently, they are being replaced by the highly efficient fluorescent and LED light sources.
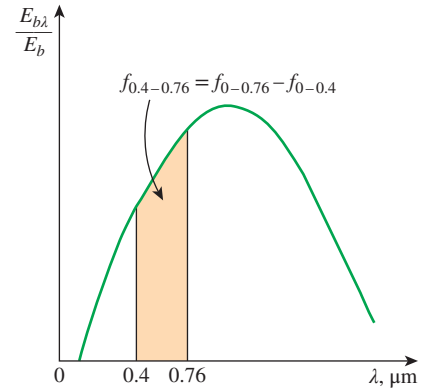
FIGURE 12–15
Graphical representation of the fraction of radiation emitted in the visible range in Example 12–2.
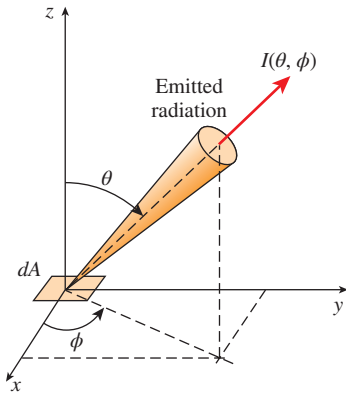
FIGURE 12–16
Radiation intensity is used to describe the variation of radiation energy with direction.

A slice of pizza of plane angle α

A slice of watermelon of solid angle ω

FIGURE 12–17
Describing the size of a slice of pizza by a plane angle and the size of a watermelon slice by a solid angle.

12–4 ▪ RADIATION INTENSITY

Radiation is emitted by all parts of a plane surface in all directions into the hemisphere above the surface, and the directional distribution of emitted (or incident) radiation is usually not uniform. Therefore, we need a quantity that describes the magnitude of radiation emitted (or incident) in a specified direction in space. This quantity is *radiation intensity,* denoted by *I*. Before we can describe a directional quantity, we need to specify direction in space. The direction of radiation passing through a point is best described in spherical coordinates in terms of the zenith angle θ and the azimuth angle ϕ, as shown in Fig. 12–16. Radiation intensity is used to describe how the emitted radiation varies with the zenith and azimuth angles.

If all surfaces emitted radiation uniformly in all directions, the *emissive power* would be sufficient to quantify radiation, and we would not need to deal with intensity. The radiation emitted by a blackbody per unit normal area is the same in all directions, and thus there is no directional dependence. But this is not the case for real surfaces. Before we define intensity, we need to quantify the size of an opening in space.

Solid Angle

Let us try to quantify the size of a slice of pizza. One way of doing that is to specify the arc length of the outer edge of the slice and to form the slice by connecting the end points of the arc to the center. A more general approach is to specify the angle of the slice at the center, as shown in Fig. 12–17. An angle of 90° (or $\pi/2$ radians), for example, always represents a quarter pizza, no matter what the radius is. For a circle of unit radius, the length of an arc is equivalent in magnitude to the *plane angle* it subtends (both are 2π for a complete circle of radius $r = 1$).

Now consider a watermelon, and let us attempt to quantify the size of a slice. Again we can do it by specifying the outer surface area of the slice (the green part) or by working with angles for generality. Connecting all points at the edges of the slice to the center in this case will form a three-dimensional body (like a cone whose tip is at the center), and thus the angle at the center in this case is properly called the **solid angle**. The solid angle is denoted by ω, and its unit is the *steradian* (sr). In analogy to plane angle, we can say that *the area of a surface on a sphere of unit radius is equivalent in magnitude to the solid angle it subtends* (both are 4π for a sphere of radius $r = 1$).

This can be shown easily by considering a differential surface area on a sphere $dS = r^2 \sin \theta \, d\theta \, d\phi$, as shown in Fig. 12–18, and integrating it from $\theta = 0$ to $\theta = \pi$, and from $\phi = 0$ to $\phi = 2\pi$. We get

$$S = \int_{\text{sphere}} dS = \int_{\phi=0}^{2\pi} \int_{\theta=0}^{\pi} r^2 \sin \theta \, d\theta d\phi = 2\pi r^2 \int_{\theta=0}^{\pi} \sin \theta \, d\theta = 4\pi r^2 \quad \text{(12–10)}$$

which is the formula for the area of a sphere. For $r = 1$ it reduces to $S = 4\pi$, and thus the solid angle associated with a sphere is $\omega = 4\pi$ sr. For a hemisphere, which is more relevant to radiation emitted or received by a surface, it is $\omega = 2\pi$ sr.
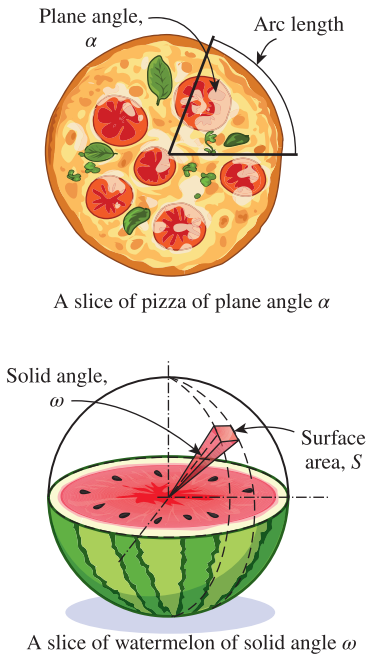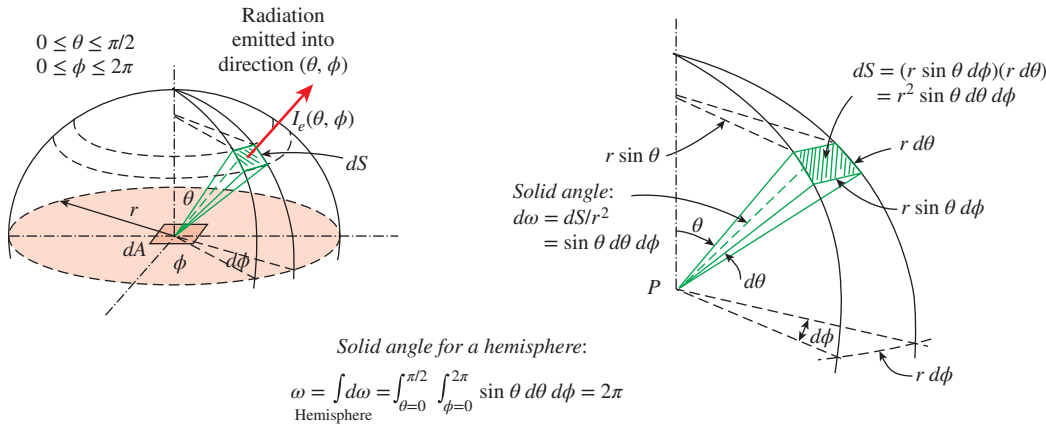
The differential solid angle $d\omega$ subtended by a differential area dS on a sphere of radius r can be expressed as

$$d\omega = \frac{dS}{r^2} = \sin\theta\, d\theta\, d\phi \qquad (12\text{–}11)$$

Note that the area dS is normal to the direction of viewing since dS is viewed from the center of the sphere. In general, the differential solid angle $d\omega$ subtended by a differential surface area dA when viewed from a point at a distance r from dA is expressed as

$$d\omega = \frac{dA_n}{r^2} = \frac{dA\cos\alpha}{r^2} \qquad (12\text{–}12)$$

where α is the angle between the normal of the surface and the direction of viewing, and thus $dA_n = dA\cos\alpha$ is the normal (or projected) area to the direction of viewing.

Small surfaces viewed from relatively large distances can approximately be treated as differential areas in solid angle calculations. For example, the solid angle subtended by a 5 cm^2 plane surface when viewed from a point at a distance of 80 cm along the normal of the surface is

$$\omega \cong \frac{A_n}{r^2} = \frac{5\text{ cm}^2}{(80\text{ cm})^2} = 7.81 \times 10^{-4}\text{ sr}$$

If the surface is tilted so that the normal of the surface makes an angle of $\alpha = 60°$ with the line connecting the point of viewing to the center of the surface, the projected area would be $dA_n = dA\cos\alpha = (5\text{ cm}^2)\cos 60° = 2.5\text{ cm}^2$, and the solid angle in this case would be half of the value just determined.

Intensity of Emitted Radiation

Consider the emission of radiation by a differential area element dA of a surface, as shown in Fig. 12–18. Radiation is emitted in all directions into the hemispherical space, and the radiation streaming though the surface area dS is proportional to the solid angle $d\omega$ subtended by dS. It is also proportional to the radiating area dA as seen by an observer on dS, which varies from a maximum of dA when dS is at the top directly above $dA(\theta = 0°)$ to a minimum of zero when dS is at the bottom ($\theta = 90°$). Therefore, the effective area of dA for emission in the direction of θ is the projection of dA on a plane normal to θ,

which is $dA \cos \theta$. Radiation intensity in a given direction is based on a unit area *normal* to that direction to provide a common basis for the comparison of radiation emitted in different directions.

The **radiation intensity** for emitted radiation $I_e(\theta, \phi)$ is defined as *the rate at which radiation energy $d\dot{Q}_e$ is emitted in the (θ, ϕ) direction per unit area normal to this direction and per unit solid angle about this direction.* That is,

$$I_e(\theta, \phi) = \frac{d\dot{Q}_e}{dA \cos \theta \cdot d\omega} = \frac{d\dot{Q}_e}{dA \cos \theta \sin \theta \, d\theta \, d\phi} \quad (\text{W/m}^2 \cdot \text{sr}) \qquad \textbf{(12–13)}$$

The *radiation flux* for emitted radiation is the **emissive power** E (the rate at which radiation energy is emitted per unit area of the emitting surface), which can be expressed in differential form as

$$dE = \frac{d\dot{Q}_e}{dA} = I_e(\theta, \phi) \cos \theta \sin \theta \, d\theta \, d\phi \qquad \textbf{(12–14)}$$

Noting that the hemisphere above the surface intercepts all the radiation rays emitted by the surface, the emissive power from the surface into the hemisphere surrounding it can be determined by integration as

$$E = \int_{\text{hemisphere}} dE = \int_{\phi=0}^{2\pi} \int_{\theta=0}^{\pi/2} I_e(\theta, \phi) \cos \theta \sin \theta \, d\theta \, d\phi \quad (\text{W/m}^2) \qquad \textbf{(12–15)}$$

The intensity of radiation emitted by a surface, in general, varies with direction (especially with the zenith angle θ). But many surfaces in practice can be approximated as being diffuse. For a *diffusely emitting* surface, the intensity of the emitted radiation is independent of direction and thus $I_e = $ constant. Noting that $\int_{\phi=0}^{2\pi} \int_{\theta=0}^{\pi/2} \cos \theta \sin \theta \, d\theta \, d\phi = \pi$, the emissive power relation in Eq. 12–15 reduces in this case to

Diffusely emitting surface: $\qquad\qquad E = \pi I_e \qquad (\text{W/m}^2) \qquad \textbf{(12–16)}$

Note that the factor in Eq. 12–16 is π. You might have expected it to be 2π since intensity is radiation energy per unit solid angle, and the solid angle associated with a hemisphere is 2π. The reason for the factor being π is that the emissive power is based on the *actual* surface area, whereas the intensity is based on the *projected* area (and thus the factor $\cos \theta$ that accompanies it), as shown in Fig. 12–19.

For a *blackbody,* which is a diffuse emitter, Eq. 12–16 can be expressed as

Blackbody: $\qquad\qquad\qquad E_b = \pi I_b \qquad\qquad \textbf{(12–17)}$

where $E_b = \sigma T^4$ is the blackbody emissive power. Therefore, the intensity of the radiation emitted by a blackbody at absolute temperature T is

Blackbody: $\qquad\qquad I_b(T) = \dfrac{E_b(T)}{\pi} = \dfrac{\sigma T^4}{\pi} \quad (\text{W/m}^2 \cdot \text{sr}) \qquad \textbf{(12–18)}$
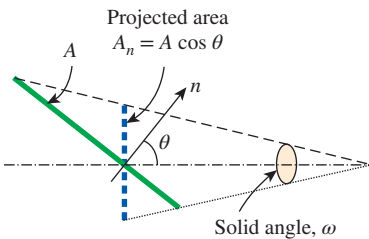
FIGURE 12–19
Radiation intensity is based on projected area, and thus the calculation of radiation emission from a surface involves the projection of the surface.

Incident Radiation

All surfaces emit radiation, but they also receive radiation emitted or reflected by other surfaces. The intensity of incident radiation $I_i(\theta, \phi)$ is defined as *the rate at which radiation energy dG is incident from the (θ, ϕ) direction per unit area of the receiving surface normal to this direction and per unit solid angle about this direction* (Fig. 12–20). Here θ is the angle between the direction of incident radiation and the normal of the surface.

The radiation flux incident on a surface from *all directions* is called **irradiation** G and is expressed as

$$G = \int_{\text{hemisphere}} dG = \int_{\phi=0}^{2\pi} \int_{\theta=0}^{\pi/2} I_i(\theta, \phi) \cos\theta \sin\theta \, d\theta \, d\phi \qquad (\text{W/m}^2) \qquad \textbf{(12–19)}$$

Therefore, irradiation represents the rate at which radiation energy is incident on a surface per unit area of the surface. When the incident radiation is diffuse and thus $I_i = $ constant, Eq. 12–19 reduces to

Diffusely incident radiation: $\qquad G = \pi I_i \qquad (\text{W/m}^2) \qquad \textbf{(12–20)}$

Again note that irradiation is based on the *actual* surface area (and thus the factor $\cos\theta$), whereas the intensity of incident radiation is based on the *projected* area.

FIGURE 12–20
Radiation incident on a surface in the direction (θ, ϕ).

Radiosity

Surfaces emit radiation as well as reflecting it, and thus the radiation leaving a surface consists of emitted and reflected components, as shown in Fig. 12–21. The calculation of radiation heat transfer between surfaces involves the *total* radiation energy streaming away from a surface, with no regard for its origin. Thus, we need to define a quantity that represents *the rate at which radiation energy leaves a unit area of a surface in all directions.* This quantity is called the **radiosity** J and is expressed as

$$J = \int_{\phi=0}^{2\pi} \int_{\theta=0}^{\pi/2} I_{e+r}(\theta, \phi) \cos\theta \sin\theta \, d\theta \, d\phi \qquad (\text{W/m}^2) \qquad \textbf{(12–21)}$$

where I_{e+r} is the sum of the emitted and reflected intensities. For a surface that is both a diffuse emitter and a diffuse reflector, $I_{e+r} = $ constant, and the radiosity relation reduces to

Diffuse emitter and reflector: $\qquad J = \pi I_{e+r} \qquad (\text{W/m}^2) \qquad \textbf{(12–22)}$

For a blackbody, radiosity J is equivalent to the emissive power E_b since a blackbody absorbs all radiation incident on it, and there is no reflected component in radiosity.

FIGURE 12–21
The three kinds of radiation flux (in W/m^2): emissive power, irradiation, and radiosity.

Spectral Quantities

So far we have considered *total* radiation quantities (quantities integrated over all wavelengths), and we have made no reference to wavelength dependence. This lumped approach is adequate for many radiation problems encountered

in practice. But sometimes it is necessary to consider the variation of radiation with wavelength as well as direction and to express quantities at a certain wavelength λ or per unit wavelength interval about λ. Such quantities are referred to as *spectral* quantities to draw attention to wavelength dependence. The modifier "spectral" is used to indicate "at a given wavelength."

The *spectral radiation intensity* $I_\lambda(\lambda, \theta, \phi)$, for example, is simply the total radiation intensity $I(\theta, \phi)$ per unit wavelength interval about λ. The **spectral intensity** for emitted radiation $I_{\lambda, e}(\lambda, \theta, \phi)$ can be defined as *the rate at which radiation energy* $d\dot{Q}_e$ *is emitted at the wavelength* λ *in the* (θ, ϕ) *direction per unit area normal to this direction, per unit solid angle about this direction,* and it can be expressed as

$I_{\lambda,e}$

Area $= \int_0^\infty I_{\lambda,e}\, d\lambda = I_e$

$I_{\lambda,e}$

$d\lambda$ $\qquad \lambda$

FIGURE 12–22
Integration of a "spectral" quantity for all wavelengths gives the "total" quantity.

$$I_{\lambda, e}(\lambda, \theta, \phi) = \frac{d\dot{Q}_e}{dA \cos \theta \cdot d\omega \cdot d\lambda} \quad \text{(W/m}^2\text{·sr·µm)} \tag{12–23}$$

Then the *spectral emissive power* becomes

$$E_\lambda = \int_{\phi=0}^{2\pi} \int_{\theta=0}^{\pi/2} I_{\lambda, e}(\lambda, \theta, \phi) \cos \theta \sin \theta \, d\theta \, d\phi \quad \text{(W/m}^2\text{)} \tag{12–24}$$

Similar relations can be obtained for spectral irradiation G_λ and spectral radiosity J_λ by replacing $I_{\lambda, e}$ in this equation with $I_{\lambda, i}$ and $I_{\lambda, e+r}$, respectively.

When the variation of spectral radiation intensity I_λ with wavelength λ is known, the total radiation intensity I for emitted, incident, and emitted + reflected radiation can be determined by integration over the entire wavelength spectrum as (Fig. 12–22)

$$I_e = \int_0^\infty I_{\lambda, e}\, d\lambda, \qquad I_i = \int_0^\infty I_{\lambda, i}\, d\lambda, \quad \text{and} \qquad I_{e+r} = \int_0^\infty I_{\lambda, e+r}\, d\lambda \tag{12–25}$$

These intensities can then be used in Eqs. 12–15, 12–19, and 12–21 to determine the emissive power E, irradiation G, and radiosity J, respectively.

Similarly, when the variations of spectral radiation fluxes E_λ, G_λ, and J_λ with wavelength λ are known, the total radiation fluxes can be determined by integration over the entire wavelength spectrum as

$$E = \int_0^\infty E_\lambda\, d\lambda, \qquad G = \int_0^\infty G_\lambda\, d\lambda, \quad \text{and} \qquad J = \int_0^\infty J_\lambda\, d\lambda \tag{12–26}$$

When the surfaces and the incident radiation are *diffuse,* the spectral radiation fluxes are related to spectral intensities as

$$E_\lambda = \pi I_{\lambda, e}, \qquad G_\lambda = \pi I_{\lambda, i}, \quad \text{and} \qquad J_\lambda = \pi I_{\lambda, e+r} \tag{12–27}$$

Note that the relations for spectral and total radiation quantities are of the same form.

The spectral intensity of radiation emitted by a blackbody at a thermodynamic temperature T at a wavelength λ was determined by Max Planck and is expressed as

$$I_{b\lambda}(\lambda, T) = \frac{2hc_0^2}{\lambda^5[\exp(hc_0/\lambda kT) - 1]} \quad \text{(W/m}^2\text{·sr·µm)} \tag{12–28}$$

where $h = 6.626069 \times 10^{-34}$ J·s is the Planck constant, $k = 1.38065 \times 10^{-23}$ J/K is the Boltzmann constant, and $c_0 = 2.9979 \times 10^8$ m/s is the speed of light in a vacuum. Then the spectral blackbody emissive power is, from Eq. 12–27,

$$E_{b\lambda}(\lambda, T) = \pi I_{b\lambda}(\lambda, T) \qquad \text{(12–29)}$$

A simplified relation for $E_{b\lambda}$ is given by Eq. 12–4.

$A_2 = 5 \text{ cm}^2$

$\theta_2 = 40°$

$\theta_1 = 55°$ $r = 75$ cm

$A_1 = 3 \text{ cm}^2$
$T_1 = 600$ K

FIGURE 12–23
Schematic for Example 12–3.

EXAMPLE 12–3   **Radiation Incident on a Small Surface**

A small surface of area $A_1 = 3 \text{ cm}^2$ emits radiation as a blackbody at $T_1 = 600$ K. Part of the radiation emitted by A_1 strikes another small surface of area $A_2 = 5 \text{ cm}^2$ oriented as shown in Fig. 12–23. Determine the solid angle subtended by A_2 when viewed from A_1, and the rate at which radiation emitted by A_1 strikes A_2.

SOLUTION   A surface is subjected to radiation emitted by another surface. The solid angle subtended and the rate at which emitted radiation is received are to be determined.

Assumptions   1 Surface A_1 emits diffusely as a blackbody. 2 Both A_1 and A_2 can be approximated as differential surfaces since both are very small compared to the square of the distance between them.

Analysis   Approximating both A_1 and A_2 as differential surfaces, the solid angle subtended by A_2 when viewed from A_1 can be determined from Eq. 12–12 to be

$$\omega_{2-1} \cong \frac{A_{n,2}}{r^2} = \frac{A_2 \cos \theta_2}{r^2} = \frac{(5 \text{ cm}^2) \cos 40°}{(75 \text{ cm})^2} = \mathbf{6.81 \times 10^{-4} \ sr}$$

since the normal of A_2 makes 40° with the direction of viewing. Note that the solid angle subtended by A_2 would be maximum if A_2 were positioned normal to the direction of viewing. Also, the point of viewing on A_1 is taken to be a point in the middle, but it can be any point since A_1 is assumed to be very small.

The radiation emitted by A_1 that strikes A_2 is equivalent to the radiation emitted by A_1 through the solid angle ω_{2-1}. The intensity of the radiation emitted by A_1 is

$$I_1 = \frac{E_b(T_1)}{\pi} = \frac{\sigma T_1^4}{\pi} = \frac{(5.67 \times 10^{-8} \text{ W/m}^2 \cdot \text{K}^4)(600 \text{ K})^4}{\pi} = 2339 \text{ W/m}^2 \cdot \text{sr}$$

This value of intensity is the same in all directions since a blackbody is a diffuse emitter. Intensity represents the rate of radiation emission per unit area normal to the direction of emission per unit solid angle. Therefore, the rate of radiation energy emitted by A_1 in the direction of θ_1 through the solid angle ω_{2-1} is determined by multiplying I_1 by the area of A_1 normal to θ_1 and the solid angle ω_{2-1}. That is,

$$\begin{aligned} \dot{Q}_{1-2} &= I_1 (A_1 \cos \theta_1) \omega_{2-1} \\ &= (2339 \text{ W/m}^2 \cdot \text{sr})(3 \times 10^{-4} \cos 55° \text{ m}^2)(6.81 \times 10^{-4} \text{ sr}) \\ &= \mathbf{2.74 \times 10^{-4} \ W} \end{aligned}$$

Therefore, the radiation emitted from surface A_1 will strike surface A_2 at a rate of 2.74×10^{-4} W.
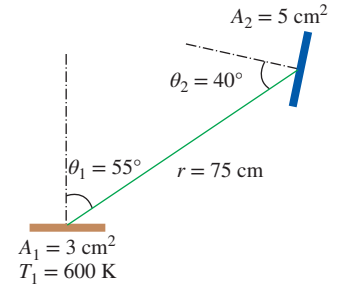
Discussion The total rate of radiation emission from surface A_1 is $\dot{Q}_e = A_1 \sigma T_1^4 = 2.204$ W. Therefore, the fraction of emitted radiation that strikes A_2 is $2.74 \times 10^{-4}/2.204 = 0.00012$ (or 0.012 percent). Noting that the solid angle associated with a hemisphere is 2π, the fraction of the solid angle subtended by A_2 is $6.81 \times 10^{-4}/(2\pi) = 0.000108$ (or 0.0108 percent), which is 0.9 times the fraction of emitted radiation. Therefore, the fraction of the solid angle a surface occupies does not represent the fraction of radiation energy the surface will receive even when the intensity of emitted radiation is constant. This is because radiation energy emitted by a surface in a given direction is proportional to the *projected area* of the surface in that direction and reduces from a maximum at $\theta = 0°$ (the direction normal to surface) to zero at $\theta = 90°$ (the direction parallel to surface).

12–5 ▪ RADIATIVE PROPERTIES

Most materials encountered in practice, such as metals, wood, and bricks, are *opaque* to thermal radiation, and radiation is considered to be a *surface phenomenon* for such materials. That is, thermal radiation is emitted or absorbed within the first few microns of the surface, and thus we speak of radiative properties of *surfaces* for opaque materials.

Some other materials, such as glass and water, allow visible radiation to penetrate to considerable depths before any significant absorption takes place. Radiation through such *semitransparent* materials obviously cannot be considered to be a surface phenomenon since the entire volume of the material interacts with radiation. On the other hand, both glass and water are practically opaque to infrared radiation. Therefore, materials can exhibit different behavior at different wavelengths, and the dependence on wavelength is an important consideration in the study of radiative properties such as emissivity, absorptivity, reflectivity, and transmissivity of materials.

In Sec. 12–4, we defined a *blackbody* as a perfect emitter and absorber of radiation and said that no body can emit more radiation than a blackbody at the same temperature. Therefore, a blackbody can serve as a convenient *reference* in describing the emission and absorption characteristics of real surfaces.

Emissivity

The **emissivity** of a surface represents *the ratio of the radiation emitted by the surface at a given temperature to the radiation emitted by a blackbody at the same temperature.* The emissivity of a surface is denoted by ε, and it varies between zero and one, $0 \le \varepsilon \le 1$. Emissivity is a measure of how closely a real surface approximates a blackbody, for which $\varepsilon = 1$.

The emissivity of a real surface is not a constant. Rather, it varies with the *temperature* of the surface as well as the *wavelength* and the *direction* of the emitted radiation. Therefore, different emissivities can be defined for a surface, depending on the effects considered. The most elemental emissivity of a surface at a given temperature is the **spectral directional emissivity**, which is defined as the ratio of the intensity of radiation emitted by the surface at a specified wavelength in a specified direction to the intensity of radiation emitted by a blackbody at the same temperature at the same wavelength. That is,

$$\varepsilon_{\lambda,\theta}(\lambda, \theta, \phi, T) = \frac{I_{\lambda,e}(\lambda, \theta, \phi, T)}{I_{b\lambda}(\lambda, T)} \tag{12–30}$$

where the subscripts λ and θ are used to designate *spectral* and *directional* quantities, respectively. Note that blackbody radiation intensity is independent of direction, and thus it has no functional dependence on θ and ϕ.

The **total directional emissivity** is defined in a like manner by using total intensities (intensities integrated over all wavelengths) as

$$\varepsilon_\theta(\theta, \phi, T) = \frac{I_e(\theta, \phi, T)}{I_b(T)} \qquad \text{(12–31)}$$

In practice, it is usually more convenient to work with radiation properties averaged over all directions, called *hemispherical properties.* Noting that the integral of the rate of radiation energy emitted at a specified wavelength per unit surface area over the entire hemisphere is *spectral emissive power,* the **spectral hemispherical emissivity** can be expressed as

$$\varepsilon_\lambda(\lambda, T) = \frac{E_\lambda(\lambda, T)}{E_{b\lambda}(\lambda, T)} \qquad \text{(12–32)}$$

Note that the emissivity of a surface at a given wavelength can be different at different temperatures since the spectral distribution of emitted radiation (and thus the amount of radiation emitted at a given wavelength) changes with temperature.

Finally, the **total hemispherical emissivity** is defined in terms of the radiation energy emitted over all wavelengths in all directions as

$$\varepsilon(T) = \frac{E(T)}{E_b(T)} \qquad \text{(12–33)}$$

Therefore, the total hemispherical emissivity (or simply the "average emissivity") of a surface at a given temperature represents the ratio of the total radiation energy emitted by the surface to the radiation emitted by a blackbody of the same surface area at the same temperature.

Noting from Eqs. 12–26 and 12–32 that $E = \int_0^\infty E_\lambda d\lambda$ and $E_\lambda(\lambda, T) = \varepsilon_\lambda(\lambda, T) E_{b\lambda}(\lambda, T)$, the total hemispherical emissivity can also be expressed as

$$\varepsilon(T) = \frac{E(T)}{E_b(T)} = \frac{\displaystyle\int_0^\infty \varepsilon_\lambda(\lambda, T) E_{b\lambda}(\lambda, T) d\lambda}{\sigma T^4} \qquad \text{(12–34)}$$

since $E_b(T) = \sigma T^4$. To perform this integration, we need to know the variation of spectral emissivity with wavelength at the specified temperature. The integrand is usually a complicated function, and the integration has to be performed numerically. However, the integration can be performed quite easily by dividing the spectrum into a sufficient number of *wavelength bands* and assuming the emissivity to remain constant over each band; that is, by expressing the function $\varepsilon_\lambda(\lambda, T)$ as a step function. This simplification offers great convenience for little sacrifice of accuracy, since it allows us to transform the integration into a summation in terms of blackbody emission functions.

As an example, consider the emissivity function plotted in Fig. 12–24. It seems like this function can be approximated reasonably well by a step function of the form

$$\varepsilon_\lambda = \begin{cases} \varepsilon_1 = \text{constant}, & 0 \le \lambda < \lambda_1 \\ \varepsilon_2 = \text{constant}, & \lambda_1 \le \lambda < \lambda_2 \\ \varepsilon_3 = \text{constant}, & \lambda_2 \le \lambda < \infty \end{cases} \qquad \text{(12–35)}$$
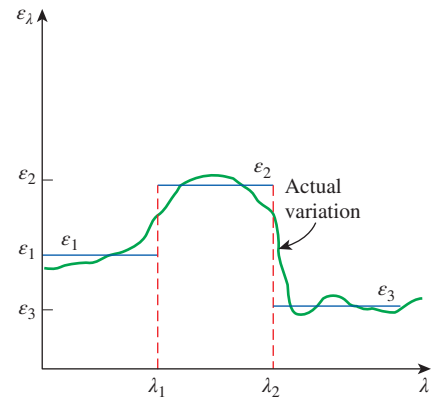
FIGURE 12–24

Approximating the actual variation of emissivity with wavelength by a step function.

Real surface:
  $\varepsilon_\theta \neq$ constant
  $\varepsilon_\lambda \neq$ constant

Diffuse surface:
  $\varepsilon_\theta =$ constant

Gray surface:
  $\varepsilon_\lambda =$ constant

Diffuse, gray surface:
  $\varepsilon = \varepsilon_\lambda = \varepsilon_\theta =$ constant

FIGURE 12–25
The effect of diffuse and gray approximations on the emissivity of a surface.
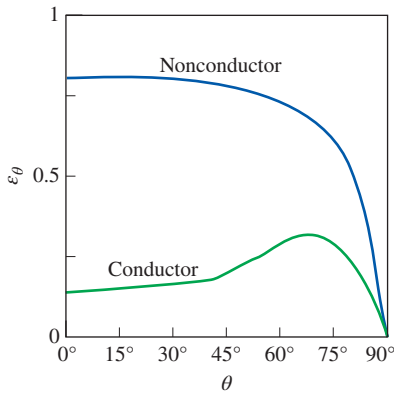
FIGURE 12–26
Typical variations of emissivity with direction for electrical conductors and nonconductors.

Then the average emissivity can be determined from Eq. 12–34 by breaking the integral into three parts and utilizing the definition of the blackbody radiation function as

$$\varepsilon(T) = \frac{\varepsilon_1 \displaystyle\int_0^{\lambda_1} E_{b\lambda} d\lambda}{E_b} + \frac{\varepsilon_2 \displaystyle\int_{\lambda_1}^{\lambda_2} E_{b\lambda} d\lambda}{E_b} + \frac{\varepsilon_3 \displaystyle\int_{\lambda_2}^{\infty} E_{b\lambda} d\lambda}{E_b} \qquad \text{(12–36)}$$

$$= \varepsilon_1 f_{0-\lambda_1}(T) + \varepsilon_2 f_{\lambda_1-\lambda_2}(T) + \varepsilon_3 f_{\lambda_2-\infty}(T)$$

Radiation is a complex phenomenon as it is, and the consideration of the wavelength and direction dependence of properties, assuming sufficient data exist, makes it even more complicated. Therefore, the *diffuse* and *gray* approximations are often used in radiation calculations. A surface is said to be *diffuse* if its properties are *independent of direction,* and *gray* if its properties are *independent of wavelength.* Therefore, the emissivity of a gray, diffuse surface is simply the total hemispherical emissivity of that surface because of independence of direction and wavelength (Fig. 12–25).

A few comments about the validity of the diffuse approximation are in order. Although real surfaces do not emit radiation in a perfectly diffuse manner as a blackbody does, they often come close. The variation of emissivity with direction for both electrical conductors and nonconductors is given in Fig. 12–26. Here θ is the angle measured from the normal of the surface, and thus $\theta = 0$ for radiation emitted in a direction normal to the surface. Note that ε_θ remains nearly constant for about $\theta < 40°$ for conductors such as metals and for $\theta < 70°$ for nonconductors such as plastics. Therefore, the directional emissivity of a surface in the normal direction is representative of the hemispherical emissivity of the surface. In radiation analysis, it is common practice to assume the surfaces to be diffuse emitters with an emissivity equal to the value in the normal ($\theta = 0$) direction.

The effect of the gray approximation on emissivity and emissive power of a real surface is illustrated in Fig. 12–27. Note that the radiation emission from a real surface, in general, differs from the Planck distribution, and the emission curve may have several peaks and valleys. A gray surface should emit as much

FIGURE 12–27
Comparison of the emissivity (*a*) and emissive power (*b*) of a real surface with those of a gray surface and a blackbody at the same temperature.
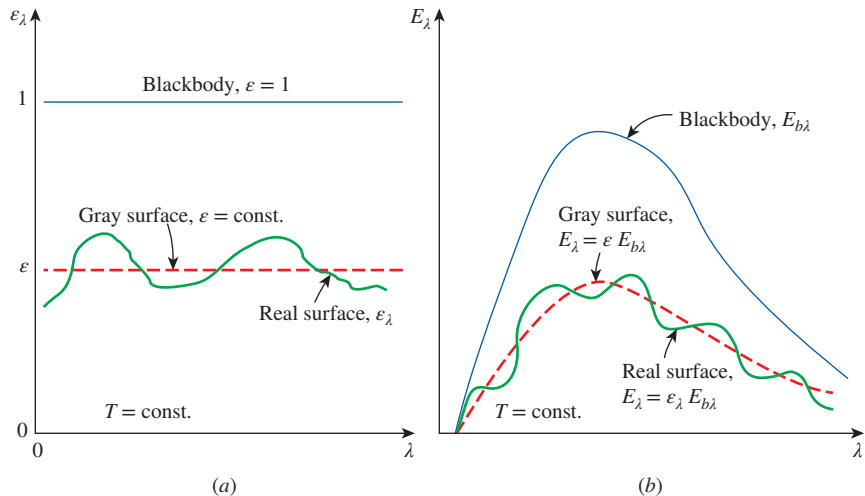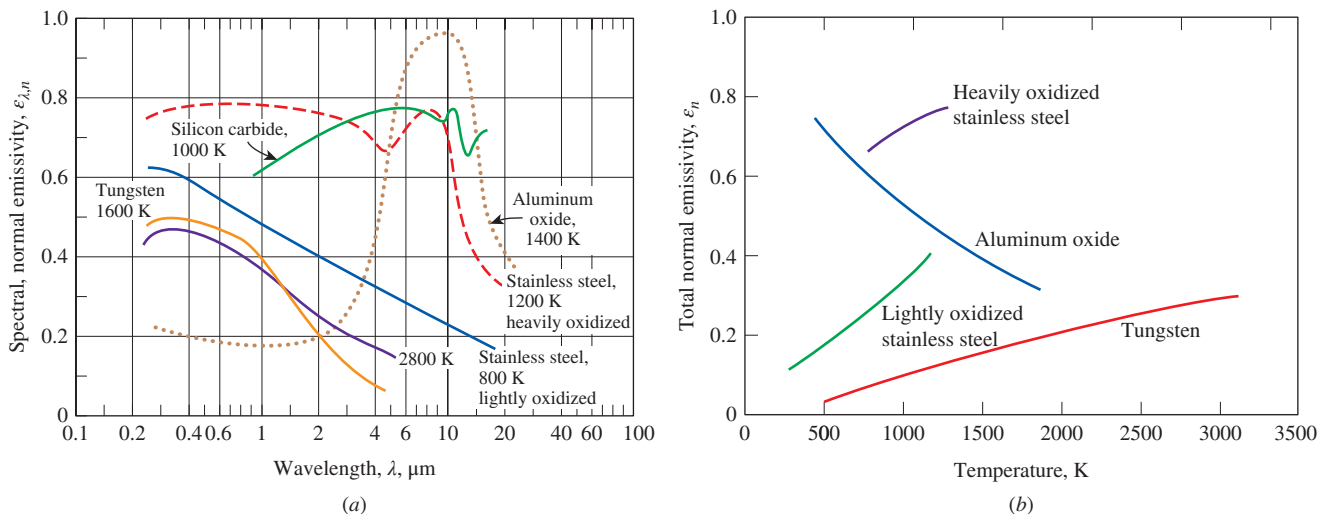
FIGURE 12–28
The variation of normal emissivity with (*a*) wavelength and (*b*) temperature for various materials.

radiation as the real surface it represents at the same temperature. Therefore, the areas under the emission curves of the real and gray surfaces must be equal.

The emissivities of common materials are listed in Tables A–18 and A–19, and the variation of emissivity with wavelength and temperature is illustrated in Fig. 12–28. Typical ranges of emissivity of various materials are given in Fig. 12–29. Note that metals generally have low emissivities, as low as 0.02 for polished surfaces, and nonmetals such as ceramics and organic materials have high ones. The emissivity of metals increases with temperature. Also, oxidation causes significant increases in the emissivity of metals. Heavily oxidized metals can have emissivities comparable to those of nonmetals.

Care should be exercised in the use and interpretation of radiation property data reported in the literature, since the properties strongly depend on the surface conditions such as oxidation, roughness, type of finish, and cleanliness. Consequently, there is considerable discrepancy and uncertainty in the reported values. This uncertainty is largely due to the difficulty in characterizing and describing the surface conditions precisely.
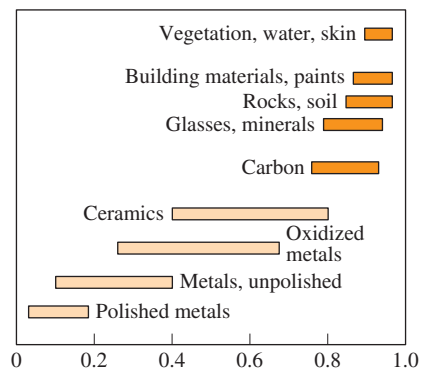
FIGURE 12–29
Typical ranges of emissivity for various materials.

■ **EXAMPLE 12–4**   **Emissivity of a Surface and Emissive Power**

The spectral emissivity function of an opaque surface at 800 K is approximated as (Fig. 12–30)

$$\varepsilon_\lambda = \begin{cases} \varepsilon_1 = 0.3, & 0 \le \lambda < 3 \ \mu m \\ \varepsilon_2 = 0.8, & 3 \ \mu m \le \lambda < 7 \ \mu m \\ \varepsilon_3 = 0.1, & 7 \ \mu m \le \lambda < \infty \end{cases}$$

Determine the average emissivity of the surface and its emissive power.

SOLUTION The variation of emissivity of a surface at a specified temperature with wavelength is given. The average emissivity of the surface and its emissive power are to be determined.
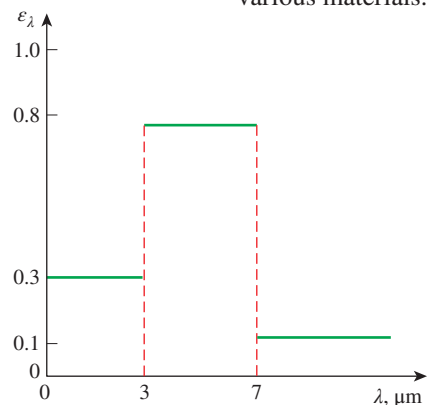
FIGURE 12–30
The spectral emissivity of the surface considered in Example 12–4.

Analysis The variation of the emissivity with wavelength is given as a step function. Therefore, the average emissivity of the surface can be determined from Eq. 12–34 by breaking the integral into three parts,

$$\varepsilon(T) = \frac{\varepsilon_1 \int_0^{\lambda_1} E_{b\lambda}\, d\lambda}{\sigma T^4} + \frac{\varepsilon_2 \int_{\lambda_1}^{\lambda_2} E_{b\lambda}\, d\lambda}{\sigma T^4} + \frac{\varepsilon_3 \int_{\lambda_2}^{\infty} E_{b\lambda}\, d\lambda}{\sigma T^4}$$

$$= \varepsilon_1 f_{0-\lambda_1}(T) + \varepsilon_2 f_{\lambda_1-\lambda_2}(T) + \varepsilon_3 f_{\lambda_2-\infty}(T)$$

$$= \varepsilon_1 f_{\lambda_1} + \varepsilon_2 (f_{\lambda_2} - f_{\lambda_1}) + \varepsilon_3 (1 - f_{\lambda_2})$$

where f_{λ_1} and f_{λ_2} are blackbody radiation functions and are determined from Table 12–2 to be

$$\lambda_1 T = (3\ \mu m)(800\ K) = 2400\ \mu m \cdot K \rightarrow f_{\lambda_1} = 0.140256$$
$$\lambda_2 T = (7\ \mu m)(800\ K) = 5600\ \mu m \cdot K \rightarrow f_{\lambda_2} = 0.701046$$

Note that $f_{0-\lambda_1} = f_{\lambda_1} - f_0 = f_{\lambda_1}$ since $f_0 = 0$, and $f_{\lambda_2-\infty} = f_\infty - f_{\lambda_2} = 1 - f_{\lambda_2}$ since $f_\infty = 1$. Substituting,

$$\varepsilon = 0.3 \times 0.140256 + 0.8(0.701046 - 0.140256) + 0.1(1 - 0.701046)$$
$$= \mathbf{0.521}$$

That is, the surface will emit as much radiation energy at 800 K as a gray surface having a constant emissivity of $\varepsilon = 0.521$. The emissive power of the surface is

$$E = \varepsilon \sigma T^4 = 0.521(5.67 \times 10^{-8}\ W/m^2 \cdot K^4)(800\ K)^4 = \mathbf{12{,}100\ W/m^2}$$

Discussion Note that the surface emits 12.1 kJ of radiation energy per second per m² area of the surface.

Absorptivity, Reflectivity, and Transmissivity

Everything around us constantly emits radiation, and the emissivity represents the emission characteristics of those bodies. This means that every body, including our own, is constantly bombarded by radiation coming from all directions over a range of wavelengths. Recall that radiation flux *incident on a surface* is called **irradiation** and is denoted by G.

When radiation strikes a surface, part of it is absorbed, part of it is reflected, and the remaining part, if any, is transmitted, as illustrated in Fig. 12–31. *The fraction of irradiation absorbed by the surface* is called the **absorptivity** α, *the fraction reflected by the surface* is called the **reflectivity** ρ, and *the fraction transmitted* is called the **transmissivity** τ. That is,

FIGURE 12–31
The absorption, reflection, and transmission of incident radiation by a semitransparent material.

Absorptivity: $\alpha = \dfrac{\text{Absorbed radiation}}{\text{Incident radiation}} = \dfrac{G_{\text{abs}}}{G}, \qquad 0 \le \alpha \le 1$ **(12–37)**

Reflectivity: $\rho = \dfrac{\text{Reflected radiation}}{\text{Incident radiation}} = \dfrac{G_{\text{ref}}}{G}, \qquad 0 \le \rho \le 1$ **(12–38)**

Transmissivity: $\tau = \dfrac{\text{Transmitted radiation}}{\text{Incident radiation}} = \dfrac{G_{\text{tr}}}{G}, \qquad 0 \le \tau \le 1$ **(12–39)**

where G is the radiation flux incident on the surface, and G_{abs}, G_{ref}, and G_{tr} are the absorbed, reflected, and transmitted portions of it, respectively. The first

law of thermodynamics requires that the sum of the absorbed, reflected, and transmitted radiation be equal to the incident radiation. That is,

$$G_{abs} + G_{ref} + G_{tr} = G$$

Dividing each term of this relation by G yields

$$\alpha + \rho + \tau = 1 \qquad \textbf{(12–40)}$$

For idealized blackbodies which are perfect absorbers, $\rho = 0$ and $\tau = 0$, and Eq. 12–40 reduces to $\alpha = 1$. For opaque surfaces such as most solids and liquids, $\tau = 0$, and thus

$$\alpha + \rho = 1 \qquad \textbf{(12–41)}$$

For most gases, the reflectance is absent, $\rho = 0$, and Eq. 12–40 reduces in this case to

$$\alpha + \tau = 1 \qquad \textbf{(12–42)}$$

The preceding two equations are important property relations since the knowledge of one property (either α or ρ in Eq. 12–41 and α or τ in Eq. 12–42) implies the knowledge of the other property.

These definitions are for *total hemispherical* properties, since G represents the radiation flux incident on the surface from all directions over the hemispherical space and over all wavelengths. Thus, α, ρ, and τ are the *average* properties of a medium for all directions and all wavelengths. However, like emissivity, these properties can also be defined for a specific wavelength and/or direction. For example, the **spectral directional absorptivity** and **spectral directional reflectivity** of a surface are defined, respectively, as the absorbed and reflected fractions of the intensity of radiation incident at a specified wavelength in a specified direction as

$$\alpha_{\lambda,\theta}(\lambda, \theta, \phi) = \frac{I_{\lambda, abs}(\lambda, \theta, \phi)}{I_{\lambda, i}(\lambda, \theta, \phi)} \qquad \text{and} \qquad \rho_{\lambda,\theta}(\lambda, \theta, \phi) = \frac{I_{\lambda, ref}(\lambda, \theta, \phi)}{I_{\lambda, i}(\lambda, \theta, \phi)} \qquad \textbf{(12–43)}$$

Likewise, the **spectral hemispherical absorptivity** and **spectral hemispherical reflectivity** of a surface are defined as

$$\alpha_\lambda(\lambda) = \frac{G_{\lambda, abs}(\lambda)}{G_\lambda(\lambda)} \qquad \text{and} \qquad \rho_\lambda(\lambda) = \frac{G_{\lambda, ref}(\lambda)}{G_\lambda(\lambda)} \qquad \textbf{(12–44)}$$

where G_λ is the spectral irradiation (in W/m²·μm) incident on the surface, and $G_{\lambda, abs}$ and $G_{\lambda, ref}$ are the reflected and absorbed portions of it, respectively.

Similar quantities can be defined for the transmissivity of semitransparent materials. For example, the **spectral hemispherical transmissivity** of a medium can be expressed as

$$\tau_\lambda(\lambda) = \frac{G_{\lambda, tr}(\lambda)}{G_\lambda(\lambda)} \qquad \textbf{(12–45)}$$

The average absorptivity, reflectivity, and transmissivity of a surface can also be defined in terms of their spectral counterparts as

$$\alpha = \frac{\int_0^\infty \alpha_\lambda\, G_\lambda\, d\lambda}{\int_0^\infty G_\lambda\, d\lambda}, \qquad \rho = \frac{\int_0^\infty \rho_\lambda\, G_\lambda\, d\lambda}{\int_0^\infty G_\lambda\, d\lambda}, \qquad \tau = \frac{\int_0^\infty \tau_\lambda\, G_\lambda\, d\lambda}{\int_0^\infty G_\lambda\, d\lambda} \qquad \textbf{(12–46)}$$
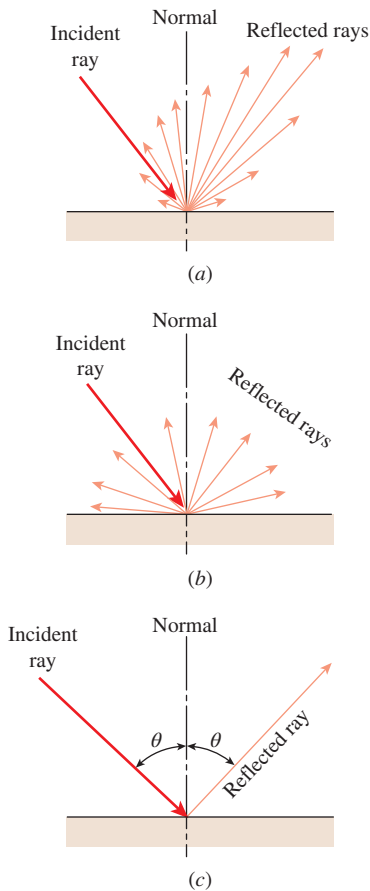
FIGURE 12–32

Different types of reflection from a surface: (*a*) actual or irregular, (*b*) diffuse, and (*c*) specular or mirrorlike.

The reflectivity differs somewhat from the other properties in that it is *bidirectional* in nature. That is, the value of the reflectivity of a surface depends not only on the direction of the incident radiation but also the direction of reflection. Therefore, the reflected rays of a radiation beam incident on a real surface in a specified direction form an irregular shape, as shown in Fig. 12–32. Such detailed reflectivity data do not exist for most surfaces, and even if they did, they would be of little value in radiation calculations since this would usually add more complication to the analysis.

In practice, for simplicity, surfaces are assumed to reflect in a perfectly *specular* or *diffuse* manner. In **specular** (or *mirrorlike*) **reflection**, *the angle of reflection equals the angle of incidence of the radiation beam.* In **diffuse reflection**, *radiation is reflected equally in all directions,* as shown in Fig. 12–32. Reflection from smooth and polished surfaces approximates specular reflection, whereas reflection from rough surfaces approximates diffuse reflection. In radiation analysis, smoothness is defined relative to wavelength. A surface is said to be *smooth* if the height of the surface roughness is much smaller than the wavelength of the incident radiation.

Unlike emissivity, the absorptivity of a material is practically independent of surface temperature. However, the absorptivity depends strongly on the temperature of the source from which the incident radiation is originating. This is also evident from Fig. 12–33, which shows the absorptivities of various materials at room temperature as functions of the temperature of the radiation source. For example, the absorptivity of the concrete roof of a house is about 0.6 for solar radiation (source temperature: 5780 K) and 0.9 for radiation originating from the surrounding trees and buildings (source temperature: 300 K), as illustrated in Fig. 12–34.

Notice that the absorptivity of aluminum increases with the source temperature, a characteristic for metals, and the absorptivity of electric nonconductors, in general, decreases with temperature. This decrease is most pronounced for
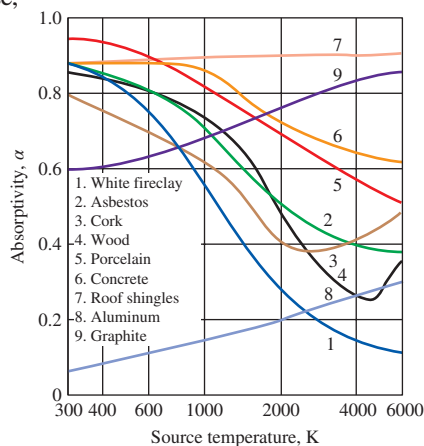
FIGURE 12–33

Variation of absorptivity with the temperature of the source of irradiation for various common materials at room temperature.
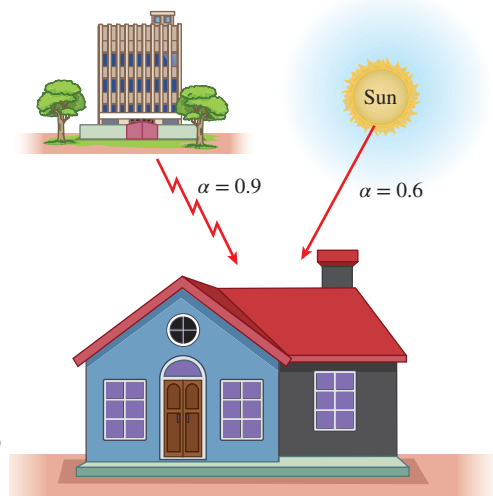
FIGURE 12–34

The absorptivity of a material may be quite different for radiation originating from sources at different temperatures.

surfaces that appear white to the eye. For example, the absorptivity of a white painted surface is low for solar radiation, but it is rather high for infrared radiation.

Kirchhoff's Law

Consider a small body of surface area A_s, emissivity ε, and absorptivity α at temperature T contained in a large isothermal enclosure at the same temperature, as shown in Fig. 12–35. Recall that a large isothermal enclosure forms a blackbody cavity regardless of the radiative properties of the enclosure surface, and the body in the enclosure is too small to interfere with the blackbody nature of the cavity. Therefore, the radiation incident on any part of the surface of the small body is equal to the radiation emitted by a blackbody at temperature T. That is, $G = E_b(T) = \sigma T^4$, and the radiation absorbed by the small body per unit of its surface area is

$$G_{\text{abs}} = \alpha G = \alpha \sigma T^4$$

The radiation emitted by the small body is

$$E_{\text{emit}} = \varepsilon \sigma T^4$$

Considering that the small body is in thermal equilibrium with the enclosure, the net rate of heat transfer to the body must be zero. Therefore, the radiation emitted by the body must be equal to the radiation absorbed by it:

$$A_s \varepsilon \sigma T^4 = A_s \alpha \sigma T^4$$

Thus, we conclude that for any surface in the enclosure,

$$\varepsilon(T) = \alpha(T) \qquad \text{(12–47)}$$

That is, *the total hemispherical emissivity of a surface at temperature T is equal to its total hemispherical absorptivity for radiation coming from a blackbody at the same temperature.* This relation, which greatly simplifies the radiation analysis, was first developed by Gustav Kirchhoff in 1860 and is now called **Kirchhoff's law**. Note that this relation is derived under the condition that the surface temperature is equal to the temperature of the source of irradiation, and the reader is cautioned against using it when considerable difference (more than a few hundred degrees) exists between the surface temperature and the temperature of the source of irradiation.

For any surface in the enclosure, the preceding derivation can also be repeated for radiation at a specified wavelength to obtain the *spectral* form of Kirchhoff's law:

$$\varepsilon_\lambda(T) = \alpha_\lambda(T) \qquad \text{(12–48)}$$

This relation is valid when the irradiation or the emitted radiation is independent of direction. The form of Kirchhoff's law that involves no restrictions is the *spectral directional* form expressed as $\varepsilon_{\lambda,\theta}(T) = \alpha_{\lambda,\theta}(T)$. That is, the emissivity of a surface at a specified wavelength, direction, and temperature is always equal to its absorptivity at the same wavelength, direction, and temperature.

It is very tempting to use Kirchhoff's law in radiation analysis since the relation $\varepsilon = \alpha$ together with $\rho = 1 - \alpha$ enables us to determine all three properties of an opaque surface from a knowledge of only *one* property.
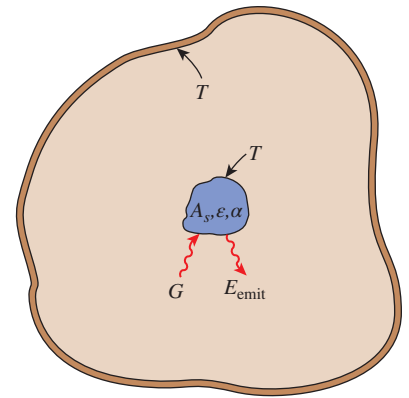
FIGURE 12–35
The small body contained in a large isothermal enclosure used in the development of Kirchhoff's law.

Although Eq. 12–47 gives acceptable results in most cases, in practice, care should be exercised when there is considerable difference between the surface temperature and the temperature of the source of incident radiation.
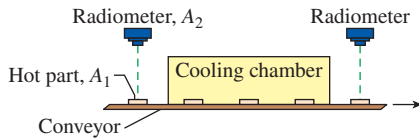
FIGURE 12–36
Schematic for Example 12–5.

PtD *EXAMPLE 12–5* **Prevention of Thermal Burn Hazard by Using Radiation Sensors to Monitor Temperatures of Parts on a Conveyor**

Hot opaque parts ($A_1 = 15$ cm^2, $m = 0.5$ kg, $c_v = 450$ J/kg·K, $\varepsilon = 0.85$), coming out of a production line and on their way to packaging, are cooled in an air-chilled chamber (Fig. 12–36). One of the reasons for cooling the parts prior to packing is to alleviate the risk of thermal burns. For the parts to be safe for handling by the operators, each part should be cooled to below $45°C$. To monitor the temperatures of the parts, two identical radiometers are placed at a distance of 1 m from the parts on the conveyor at the entrance and exit of the cooling chamber. Throughout the entire process, irradiation on the parts from the surroundings is estimated to be 300 W/m^2. Inside the cooling chamber, 215 W of heat is removed from each part in the duration of 1 minute. If the radiometer at the cooling chamber entrance detects an irradiation of 0.21 W/m^2, determine the irradiation that the radiometer at the cooling chamber exit would measure. Would the parts exiting the cooling chamber be safe for handling?

SOLUTION In this example, the concepts of Prevention through Design (PtD) are applied in conjunction with the concepts of radiation intensity and radiative properties.

Assumptions **1** Both part surface and radiometer can be approximated as differential surfaces since both are very small compared to the square of the distance between them. **2** Temperatures of parts are uniform. **3** Kirchhoff's law is applicable. **4** Parts are opaque and their properties are constant.

Properties The specific heat and the emissivity of the parts are given as $c_v = 450$ J/kg·K and $\varepsilon = 0.85$. The Stefan-Boltzmann constant is $\sigma = 5.67 \times 10^{-8}$ W/m^2·K^4.

Analysis From Kirchhoff's law, the emissivity of the parts is

$$\varepsilon = \alpha = 0.85$$

The parts are opaque ($\tau = 0$) and the reflectivity of the parts is

$$\rho = 1 - \alpha = 1 - 0.85 = 0.15$$

The solid angle subtended by both radiometers when viewed from the parts at the entrance and exit of the cooling chamber is

$$\omega_{2-1} \cong \frac{A_{n,2}}{L^2} = \frac{A_2 \cos \theta_2}{L^2}$$

The intensities of the radiation emitted and reflected (radiosity) by the parts A_1 at the entrance and exit of the cooling chamber are

$$I_{1,\text{in}} = \frac{J_{\text{in}}}{\pi} = \frac{E_{\text{in}} + G_{\text{ref}}}{\pi} = \frac{\varepsilon \sigma T_{1,\text{in}}^4 + \rho G_1}{\pi} \quad \text{and} \quad I_{1,\text{out}} = \frac{J_{\text{out}}}{\pi} = \frac{E_{\text{out}} + G_{\text{ref}}}{\pi} = \frac{\varepsilon \sigma T_{1,\text{out}}^4 + \rho G_1}{\pi}$$

The irradiations measured by the radiometers A_2 at the entrance and exit of the cooling chamber are

$$G_{2,\text{in}} = \frac{\dot{Q}_{1-2,\text{in}}}{A_2} = \frac{I_{1,\text{in}}(A_1\cos\theta_1)\omega_{2-1}}{A_2} = \frac{(\varepsilon\sigma T^4_{1,\text{in}} + \rho G_1)A_1(\cos\theta_1)(\cos\theta_2)}{\pi L^2}$$

and

$$G_{2,\text{out}} = \frac{\dot{Q}_{1-2,\text{out}}}{A_2} = \frac{I_{1,\text{out}}(A_1\cos\theta_1)\omega_{2-1}}{A_2} = \frac{(\varepsilon\sigma T^4_{1,\text{out}} + \rho G_1)A_1(\cos\theta_1)(\cos\theta_2)}{\pi L^2}$$

With both radiometers placed normal to the direction of viewing from each part that passes them ($\theta_1 = \theta_2 = 0°$), we have

$$G_{2,\text{in}} = \frac{(\varepsilon\sigma T^4_{1,\text{in}} + \rho G_1)A_1}{\pi L^2} \quad \text{and} \quad G_{2,\text{out}} = \frac{(\varepsilon\sigma T^4_{1,\text{out}} + \rho G_1)A_1}{\pi L^2}$$

From the given irradiation $G_{2,\text{in}}$ detected by the radiometer at the cooling chamber entrance, the temperature of the parts at that location is

$$T_{1,\text{in}} = \left[\left(\frac{G_{2,\text{in}}\pi L^2}{A_1} - \rho G_1\right)\left(\frac{1}{\varepsilon\sigma}\right)\right]^{1/4}$$

$$= \left\{\left[\frac{(0.21\text{ W/m}^2)\pi(1.5\text{ m})^2}{15\times10^{-4}\text{ m}^2} - (0.15)(300\text{ W/m}^2)\right]\frac{1}{(0.85)(5.67\times10^{-8}\text{ W/m}^2\cdot\text{K}^4)}\right\}^{1/4}$$

$$= 374\text{ K} = 101°\text{C}$$

The temperature of the parts at the exit of the cooling chamber can be determined from the change in the internal energy and the heat removed from the parts during the cooling process:

$$Q = \dot{Q}\Delta t = \Delta U = mc_v(T_{1,\text{in}} - T_{1,\text{out}}) \quad \text{or} \quad T_{1,\text{out}} = T_{1,\text{in}} - \frac{\dot{Q}\Delta t}{mc_v}$$

Thus,

$$T_{1,\text{out}} = 101°\text{C} - \frac{(215\text{ W})(60\text{ s})}{(0.5\text{ kg})(450\text{ J/kg}\cdot\text{K})} = \mathbf{43.7°C} < 45°\text{C}$$

Finally, the irradiation $G_{2,\text{out}}$ measured by the radiometer at the exit of the cooling chamber is

$$G_{2,\text{out}} = \frac{(\varepsilon\sigma T^4_{1,\text{out}} + \rho G_1)A_1}{\pi L^2}$$

$$= \frac{(0.85)(5.67\times10^{-8}\text{ W/m}^2\cdot\text{K}^4)(43.7+273)^4\text{ K}^4 + (0.15)(300\text{ W/m}^2)}{\pi(1.5\text{ m})^2}(15\times10^{-4}\text{ m}^2)$$

$$= \mathbf{0.112\text{ W/m}^2}$$

Discussion The temperature of the parts exiting the cooling chamber is below 45°C, and therefore they are safe for handling in the packing operation.

Having two radiometers monitoring the temperatures of the parts as they enter and exit the cooling chambers allows the engineers to determine the necessary cooling time for the parts. Therefore, the conveyor speed can be optimized while at the same time preventing thermal burn hazards.
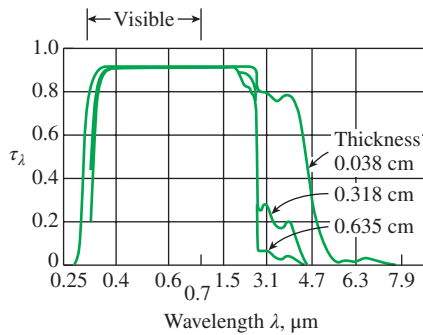
FIGURE 12–37

The spectral transmissivity of low-iron glass at room temperature for different thicknesses.
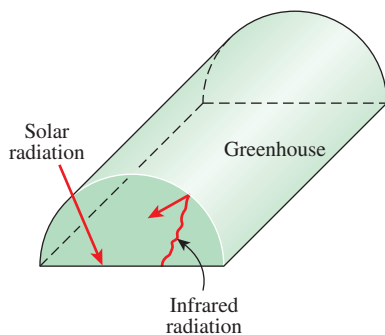
FIGURE 12–38

A greenhouse traps energy by allowing the solar radiation to come in but not allowing the infrared radiation to go out.

The Greenhouse Effect

You have probably noticed that when you leave your car under direct sunlight on a sunny day, the interior of the car gets much warmer than the air outside, and you may have wondered why the car acts like a *heat trap.* The answer lies in the spectral transmissivity curve of the *glass,* which resembles an inverted U, as shown in Fig. 12–37. We observe from this figure that glass at thicknesses encountered in practice transmits over 90 percent of radiation in the visible range and is practically opaque (nontransparent) to radiation in the longer-wavelength infrared regions of the electromagnetic spectrum (roughly $\lambda > 3$ μm). Therefore, glass has a transparent window in the wavelength range 0.3 μm $< \lambda < 3$ μm in which over 90 percent of solar radiation is emitted. On the other hand, the radiation emitted by surfaces at room temperature falls entirely in the infrared region. Consequently, glass allows the solar radiation to enter but does not allow the infrared radiation from the interior surfaces to escape. This causes a rise in the interior temperature as a result of the energy buildup in the car. This heating effect, which is due to the nongray characteristic of glass (or clear plastics), is known as the **greenhouse effect**, since it is used extensively in greenhouses (Fig. 12–38).

The greenhouse effect is also experienced on a larger scale on earth. The surface of the earth, which warms up during the day as a result of the absorption of solar energy, cools down at night by radiating its energy into deep space as infrared radiation. The combustion gases such as CO_2 and water vapor in the atmosphere transmit the bulk of the solar radiation but absorb the infrared radiation emitted by the surface of the earth. Thus, there is concern that the energy trapped on earth will eventually cause global warming and thus drastic changes in weather patterns.

In *humid* places such as coastal areas, there is not a large change between the daytime and nighttime temperatures because the humidity acts as a barrier on the path of the infrared radiation coming from the earth, and thus it slows down the cooling process at night. In areas with clear skies such as deserts, there is a large swing between the daytime and nighttime temperatures because of the absence of such barriers for infrared radiation.

12–6 ■ ATMOSPHERIC AND SOLAR RADIATION

The sun is our primary source of energy. The energy coming off the sun, called *solar energy,* reaches us in the form of electromagnetic waves after experiencing considerable interactions with the atmosphere. The radiation energy emitted or reflected by the constituents of the atmosphere form the *atmospheric radiation.* Here we give an overview of the solar and atmospheric radiation because of their importance and relevance to daily life. Also, our familiarity with solar energy makes it an effective tool in developing a better understanding for some of the new concepts introduced earlier. Detailed treatment of this exciting subject can be found in numerous books devoted to this topic.

The *sun* is a nearly spherical body that has a diameter of $D \approx 1.39 \times 10^9$ m and a mass of $m \approx 2 \times 10^{30}$ kg and is located at a mean distance of $L = 1.50 \times 10^{11}$ m from the earth. It emits radiation energy continuously at a rate of $E_{sun} \approx 3.8 \times 10^{26}$ W. Less than a billionth of this energy (about 1.7×10^{17} W)

strikes the earth, which is sufficient to keep the earth warm and to maintain life through the photosynthesis process. The energy of the sun is due to the continuous *fusion* reaction during which two hydrogen atoms fuse to form one atom of helium. Therefore, the sun is essentially a *nuclear reactor,* with temperatures as high as 40,000,000 K in its core region. The temperature drops to about 5800 K in the outer region of the sun, called the convective zone, as a result of the dissipation of this energy by radiation.

The solar energy reaching the earth's atmosphere is called the **total solar irradiance** G_s, whose value is

$$G_s = 1373 \text{ W/m}^2 \tag{12–49}$$

The total solar irradiance (also called the **solar constant**) represents *the rate at which solar energy is incident on a surface normal to the sun's rays at the outer edge of the atmosphere when the earth is at its mean distance from the sun* (Fig. 12–39).

The value of the total solar irradiance can be used to estimate the effective surface temperature of the sun from the requirement that

$$(4\pi L^2)G_s = (4\pi r^2)\sigma T_{sun}^4 \tag{12–50}$$

where L is the mean distance between the sun's center and the earth and r is the radius of the sun. The left-hand side of this equation represents the total solar energy passing through a spherical surface whose radius is the mean earth–sun distance, and the right-hand side represents the total energy that leaves the sun's outer surface. The conservation of energy principle requires that these two quantities be equal to each other, since the solar energy experiences no attenuation (or enhancement) on its way through the vacuum (Fig. 12–40). The **effective surface temperature** of the sun is determined from Eq. 12–50 to be $T_{sun} = 5780$ K. That is, the sun can be treated as a blackbody at a temperature of 5780 K. This is also confirmed by the measurements of the spectral distribution of the solar radiation just outside the atmosphere plotted in Fig. 12–41, which shows only small deviations from the idealized blackbody behavior.

The spectral distribution of solar radiation on the ground plotted in Fig. 12–41 shows that the solar radiation undergoes considerable *attenuation* as it passes through the atmosphere as a result of absorption and scattering. About 99 percent of the atmosphere is contained within a distance of 30 km from the earth's surface. The several dips on the spectral distribution of radiation on the earth's surface are due to *absorption* by the gases O_2, O_3 (ozone), H_2O, and CO_2. Absorption by *oxygen* occurs in a narrow band about $\lambda = 0.76$ μm. The *ozone* absorbs *ultraviolet* radiation at wavelengths below 0.3 μm almost completely, and radiation in the range 0.3–0.4 μm considerably. Thus, the ozone layer in the upper regions of the atmosphere protects biological systems on earth from harmful ultraviolet radiation. In turn, we must protect the ozone layer from the destructive chemicals commonly used as refrigerants, cleaning agents, and propellants in aerosol cans. The use of these chemicals is now banned. The ozone gas also absorbs some radiation in the visible range. Absorption in the infrared region is dominated by *water vapor* and *carbon dioxide*. The dust particles and other pollutants in the atmosphere also absorb radiation at various wavelengths.
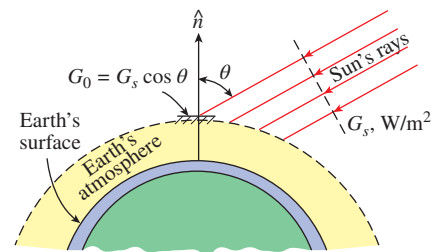
FIGURE 12–39
Solar radiation reaching the earth's atmosphere and the total solar irradiance.
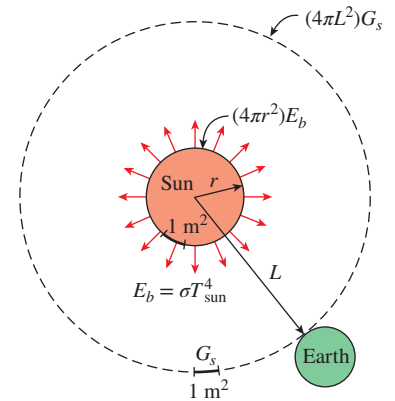
FIGURE 12–40
The total solar energy passing through concentric spheres remains constant, but the energy falling per unit area decreases with increasing radius.
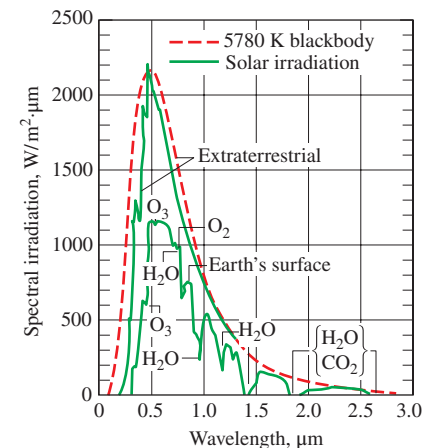
FIGURE 12–41
Spectral distribution of solar radiation just outside the atmosphere, at the surface of the earth on a typical day, and comparison with blackbody radiation at 5780 K.
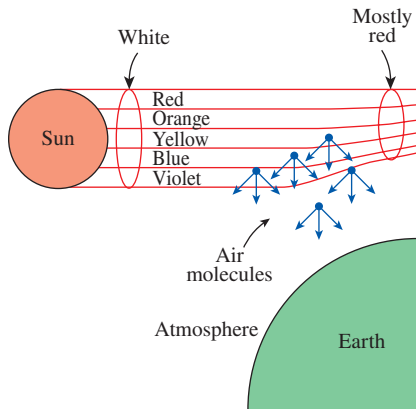
FIGURE 12–42
Air molecules scatter blue light much
more than they do red light. At sunset,
light travels through a thicker layer of
atmosphere, which removes much of
the blue from the natural light, allow-
ing the red to dominate.
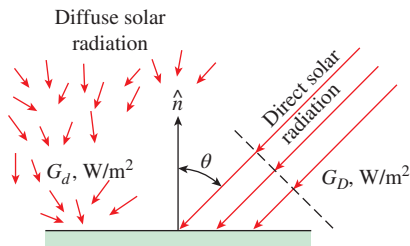
FIGURE 12–43
The direct and diffuse radiation inci-
dent on a horizontal surface on earth's
surface.

As a result of these absorptions, the solar energy reaching the earth's
surface is weakened considerably, to about 950 W/m^2 on a clear day and
much less on cloudy or smoggy days. Also, practically all of the solar
radiation reaching the earth's surface falls in the wavelength band from
0.3 to 2.5 μm.

Another mechanism that attenuates solar radiation as it passes through the
atmosphere is *scattering* or *reflection* by air molecules and the many other
kinds of particles such as dust, smog, and water droplets suspended in the
atmosphere. Scattering is mainly governed by the size of the particle relative
to the wavelength of radiation. The oxygen and nitrogen molecules primar-
ily scatter radiation at very short wavelengths, comparable to the sizes of the
molecules themselves. Therefore, radiation at wavelengths corresponding to
violet and blue colors is scattered the most. This molecular scattering in all
directions is what gives the sky its bluish color. The same phenomenon is
responsible for red sunrises and sunsets. Early in the morning and late in the
afternoon, the sun's rays pass through a greater thickness of the atmosphere
than they do at midday, when the sun is at the top. Therefore, the violet and
blue colors of the light encounter a greater number of molecules by the time
they reach the earth's surface, and thus a greater fraction of them are scattered
(Fig. 12–42). Consequently, the light that reaches the earth's surface consists
primarily of colors corresponding to longer wavelengths such as red, orange,
and yellow. The clouds appear in reddish-orange color during sunrise and
sunset because the light they reflect is reddish-orange at those times. For the
same reason, a red traffic light is visible from a longer distance than is a green
light under the same circumstances.

The solar energy incident on a surface on earth is considered to consist of
direct and *diffuse* parts. The part of solar radiation that reaches the earth's sur-
face without being scattered or absorbed by the atmosphere is called **direct
solar radiation** G_D. The scattered radiation is assumed to reach the earth's
surface uniformly from all directions and is called **diffuse solar radiation** G_d.
Then the *total* solar energy incident on the unit area of a *horizontal surface* on
the ground is (Fig. 12–43)

$$G_{solar} = G_D \cos \theta + G_d \quad (\text{W/m}^2) \tag{12–51}$$

where θ is the angle of incidence of direct solar radiation (the angle that the
sun's rays make with the normal of the surface). The diffuse radiation varies
from about 10 percent of the total radiation on a clear day to nearly 100 per-
cent on a totally cloudy day.

The gas molecules and the suspended particles in the atmosphere emit radi-
ation as well as absorbing it. The atmospheric emission is primarily due to the
CO_2 and H_2O molecules and is concentrated in the regions from 5 to 8 μm
and above 13 μm. Although this emission is far from resembling the distribu-
tion of radiation from a blackbody, it is convenient in radiation calculations to
treat the atmosphere as a blackbody at some lower fictitious temperature that
emits an equivalent amount of radiation energy. This fictitious temperature is
called the **effective sky temperature** T_{sky}. Then the radiation emission from
the atmosphere to the earth's surface is expressed as

$$G_{sky} = \sigma T_{sky}^4 \quad (\text{W/m}^2) \tag{12–52}$$

The value of T_{sky} depends on the atmospheric conditions. It ranges from about 230 K for cold, clear-sky conditions to about 285 K for warm, cloudy-sky conditions.

Note that the effective sky temperature does not deviate much from the room temperature. Thus, in the light of Kirchhoff's law, we can take the absorptivity of a surface to be equal to its emissivity at room temperature, $\alpha = \varepsilon$. Then the sky radiation absorbed by a surface can be expressed as

$$E_{sky, absorbed} = \alpha G_{sky} = \alpha \sigma T_{sky}^4 = \varepsilon \sigma T_{sky}^4 \quad (W/m^2) \tag{12–53}$$

The net rate of radiation heat transfer to a surface exposed to solar and atmospheric radiation is determined from an energy balance (Fig. 12–44):

$$\begin{aligned}
\dot{q}_{net, rad} &= \sum E_{absorbed} - \sum E_{emitted} \\
&= E_{solar, absorbed} + E_{sky, absorbed} - E_{emitted} \\
&= \alpha_s G_{solar} + \varepsilon \sigma T_{sky}^4 - \varepsilon \sigma T_s^4 \\
&= \alpha_s G_{solar} + \varepsilon \sigma (T_{sky}^4 - T_s^4) \quad (W/m^2)
\end{aligned} \tag{12–54}$$

where T_s is the temperature of the surface in K and ε is its emissivity at room temperature. A positive result for $\dot{q}_{net, rad}$ indicates a radiation heat gain by the surface and a negative result indicates a heat loss.

The absorption and emission of radiation by the *elementary gases* such as H_2, O_2, and N_2 at moderate temperatures are negligible, and a medium filled with these gases can be treated as a *vacuum* in radiation analysis. The absorption and emission of gases with *larger molecules* such as H_2O and CO_2, however, can be *significant* and may need to be considered when considerable amounts of such gases are present in a medium. For example, a 1-m-thick layer of water vapor at 1 atm pressure and 100°C emits more than 50 percent of the energy that a blackbody would emit at the same temperature.

In solar energy applications, the spectral distribution of incident solar radiation is very different than the spectral distribution of emitted radiation by the surfaces, since the former is concentrated in the short-wavelength region and the latter in the infrared region. Therefore, the radiation properties of surfaces are quite different for the incident and emitted radiation, and the surfaces cannot be assumed to be gray. Instead, the surfaces are assumed to have two sets of properties: one for solar radiation and another for infrared radiation at room temperature. Table 12–3 lists the *emissivity ε* and the *solar absorptivity α_s* of some common materials. Surfaces that are intended to *collect solar energy,* such as the absorber surfaces of solar collectors, are desired to have high α_s but low ε values to maximize the absorption of solar radiation and to minimize the emission of radiation. Surfaces that are intended to *remain cool* under the sun, such as the outer surfaces of fuel tanks and refrigerator trucks, are desired to have just the opposite properties. Surfaces are often given the desired properties by coating them with thin layers of *selective* materials. A surface can be kept cool, for example, by simply painting it white. In practice, engineers pay close attention to the ratio α_s/ε when selecting appropriate materials for the purpose of heat collection or heat rejection. For heat collection,
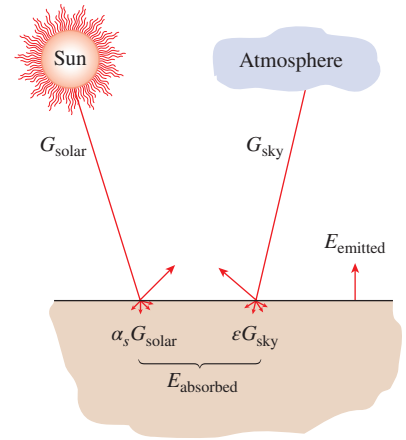
FIGURE 12–44
Radiation interactions of a surface exposed to solar and atmospheric radiation.

TABLE 12–3

Comparison of the solar absorptivity α_s of some surfaces with their emissivity ε at room temperature

Surface	α_s	ε
Aluminum		
Polished	0.09	0.03
Anodized	0.14	0.84
Foil	0.15	0.05
Copper		
Polished	0.18	0.03
Tarnished	0.65	0.75
Stainless steel		
Polished	0.37	0.60
Dull	0.50	0.21
Plated metals		
Black nickel oxide	0.92	0.08
Black chrome	0.87	0.09
Concrete	0.60	0.88
White marble	0.46	0.95
Red brick	0.63	0.93
Asphalt	0.90	0.90
Black paint	0.97	0.97
White paint	0.14	0.93
Snow	0.28	0.97
Human skin		
(Caucasian)	0.62	0.97
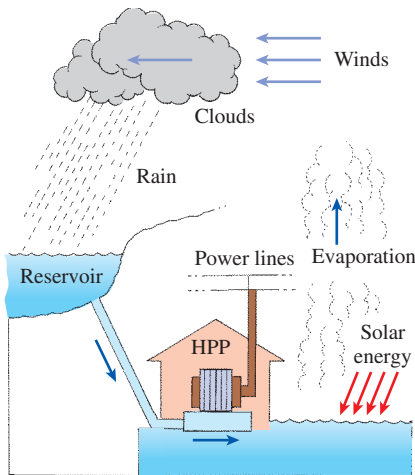
FIGURE 12–45
The cycle that water undergoes in a hydroelectric power plant.

materials with large values of α_s/ε (such as clean galvanized sheet metal with $\alpha_s/\varepsilon = 5.0$) are required. For heat rejection, on the other hand, materials with small values of α_s/ε (such as anodized aluminum with $\alpha_s/\varepsilon = 0.17$) are desirable. Values of α_s/ε together with solar absorptivity for selected materials are listed in Table A–19.

We close this section by pointing out that what we call *renewable energy* is usually nothing more than the manifestation of solar energy in different forms. Such energy sources include wind energy, hydroelectric power, ocean thermal energy, ocean wave energy, and wood. For example, no hydroelectric power plant can generate electricity year after year unless the water evaporates by absorbing solar energy and comes back as rainfall to replenish the water source (Fig. 12–45). Although solar energy is sufficient to meet all of the world's energy needs, currently it is not economical to do so because of the low concentration of solar energy on earth and the high capital cost of harnessing it.

EXAMPLE 12–6   **Selective Absorber and Reflective Surfaces**

Consider a surface exposed to solar radiation. At a given time, the direct and diffuse components of solar radiation are $G_D = 400$ and $G_d = 300$ W/m², and the direct radiation makes a 20° angle with the normal of the surface. The surface temperature is observed to be 320 K at that time. Assuming an effective sky temperature of 260 K, determine the net rate of radiation heat transfer for these cases (Fig. 12–46):

(a) $\alpha_s = 0.9$ and $\varepsilon = 0.9$ (gray absorber surface)
(b) $\alpha_s = 0.1$ and $\varepsilon = 0.1$ (gray reflector surface)
(c) $\alpha_s = 0.9$ and $\varepsilon = 0.1$ (selective absorber surface)
(d) $\alpha_s = 0.1$ and $\varepsilon = 0.9$ (selective reflector surface)

SOLUTION   A surface is exposed to solar and sky radiation. The net rate of radiation heat transfer is to be determined for four different combinations of emissivities and solar absorptivities.

Analysis   The total solar energy incident on the surface is

$$G_{\text{solar}} = G_D \cos\theta + G_d$$
$$= (400 \text{ W/m}^2) \cos 20° + (300 \text{ W/m}^2)$$
$$= 676 \text{ W/m}^2$$

Then the net rate of radiation heat transfer for each of the four cases is determined from:

$$\dot{q}_{\text{net, rad}} = \alpha_s G_{\text{solar}} + \varepsilon\sigma(T_{\text{sky}}^4 - T_s^4)$$

(a) $\alpha_s = 0.9$ and $\varepsilon = 0.9$ (gray absorber surface):

$$\dot{q}_{\text{net, rad}} = 0.9(676 \text{ W/m}^2) + 0.9(5.67 \times 10^{-8} \text{ W/m}^2\cdot\text{K}^4)[(260 \text{ K})^4 - (320 \text{ K})^4]$$
$$= \textbf{307 W/m}^2$$

(b) $\alpha_s = 0.1$ and $\varepsilon = 0.1$ (gray reflector surface):

$$\dot{q}_{\text{net, rad}} = 0.1(676 \text{ W/m}^2) + 0.1(5.67 \times 10^{-8} \text{ W/m}^2\cdot\text{K}^4)[(260 \text{ K})^4 - (320 \text{ K})^4]$$
$$= \textbf{34 W/m}^2$$

(c) $\alpha_s = 0.9$ and $\varepsilon = 0.1$ (selective absorber surface):

$$\dot{q}_{net,\,rad} = 0.9(676 \text{ W/m}^2) + 0.1(5.67 \times 10^{-8} \text{ W/m}^2\cdot\text{K}^4)[(260 \text{ K})^4 - (320 \text{ K})^4]$$
$$= \mathbf{575 \text{ W/m}^2}$$

(d) $\alpha_s = 0.1$ and $\varepsilon = 0.9$ (selective reflector surface):

$$\dot{q}_{net,\,rad} = 0.1(676 \text{ W/m}^2) + 0.9(5.67 \times 10^{-8} \text{ W/m}^2\cdot\text{K}^4)[(260 \text{ K})^4 - (320 \text{ K})^4]$$
$$= \mathbf{-234 \text{ W/m}^2}$$

Discussion   Note that the surface of an ordinary gray material of high absorptivity gains heat at a rate of 307 W/m^2. The amount of heat gain increases to 575 W/m^2 when the surface is coated with a selective material that has the same absorptivity for solar radiation but a low emissivity for infrared radiation. Also note that the surface of an ordinary gray material of high reflectivity still gains heat at a rate of 34 W/m^2. When the surface is coated with a selective material that has the same reflectivity for solar radiation but a high emissivity for infrared radiation, the surface loses 234 W/m^2 instead. Therefore, the temperature of the surface will decrease when a selective reflector surface is used.

FIGURE 12–46
Graphical representation of the spectral emissivities of the four surfaces considered in Example 12–6.

TOPIC OF SPECIAL INTEREST*

Solar Heat Gain Through Windows

The sun is the primary heat source of the earth, and the solar irradiance on a surface normal to the sun's rays beyond the earth's atmosphere at the mean earth–sun distance of 149.5 million km is called the total solar irradiance or solar constant. The accepted value of the solar constant is 1373 W/m^2 (435·4 Btu/h·ft^2), but its value changes by 3.5 percent from a maximum of 1418 W/m^2 on January 3 when the earth is closest to the sun, to a minimum of 1325 W/m^2 on July 4 when the earth is farthest away from the sun. The spectral distribution of solar radiation beyond the earth's atmosphere resembles the energy emitted by a blackbody at 5780°C, with about 9 percent of the energy contained in the ultraviolet region (at wavelengths between 0.29 to 0.4 µm), 39 percent in the visible region (0.4 to 0.7 µm), and the remaining 52 percent in the near-infrared region (0.7 to 3.5 µm). The peak radiation occurs at a wavelength of about 0.48 µm, which corresponds to the green color portion of the visible spectrum. Obviously a glazing material that transmits the visible part of the spectrum while absorbing the infrared portion is ideally suited for an application that calls for maximum daylight and minimum solar heat gain. Surprisingly, the ordinary window glass approximates this behavior remarkably well (Fig. 12–47).

Part of the solar radiation entering the earth's atmosphere is scattered and absorbed by air and water vapor molecules, dust particles, and water droplets in the clouds, and thus the solar radiation incident on earth's surface is less than the solar constant. The extent of the attenuation of solar radiation depends on the length of the path of the rays through the

* This section can be skipped without a loss of continuity.
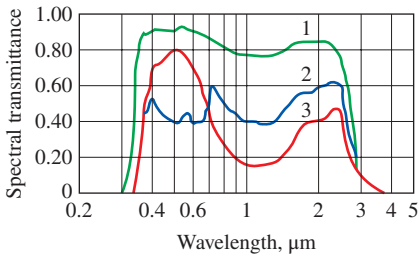
1. 3-mm regular sheet
2. 6-mm gray heat-absorbing plate/float
3. 6-mm green heat-absorbing plate/float

FIGURE 12–47

The variation of the transmittance of typical architectural glass with wavelength.

Source: ASHRAE Handbook of Fundamentals, *Chap. 27, Fig. 11.*
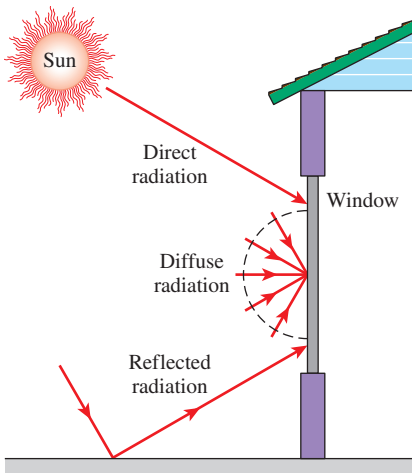
FIGURE 12–48

Direct, diffuse, and reflected components of solar radiation incident on a window.

atmosphere as well as the composition of the atmosphere (the clouds, dust, humidity, and smog) along the path. Most ultraviolet radiation is absorbed by the ozone in the upper atmosphere. At a solar altitude of 41.8°, the total energy of direct solar radiation incident at sea level on a clear day consists of about 3 percent ultraviolet, 38 percent visible, and 59 percent infrared radiation.

The part of solar radiation that reaches the earth's surface without being scattered or absorbed is the *direct radiation.* Solar radiation that is scattered or reemitted by the constituents of the atmosphere is the *diffuse radiation.* Direct radiation comes directly from the sun following a straight path, whereas diffuse radiation comes from all directions in the sky. The entire radiation reaching the ground on an overcast day is diffuse radiation. The radiation reaching a surface, in general, consists of three components: direct radiation, diffuse radiation, and radiation reflected onto the surface from surrounding surfaces (Fig. 12–48). Common surfaces such as grass, trees, rocks, and concrete reflect about 20 percent of the radiation while absorbing the rest. Snow-covered surfaces, however, reflect 70 percent of the incident radiation. Radiation incident on a surface that does not have a direct view of the sun consists of diffuse and reflected radiation. Therefore, at solar noon, solar radiations incident on the east, west, and north surfaces of a south-facing house are identical since they all consist of diffuse and reflected components. The difference between the radiations incident on the south and north walls in this case gives the magnitude of direct radiation incident on the south wall.

When solar radiation strikes a glass surface, part of it (about 8 percent for uncoated clear glass) is reflected back to outdoors, part of it (5 to 50 percent, depending on composition and thickness) is absorbed within the glass, and the remainder is transmitted indoors, as shown in Fig. 12–49. The conservation of energy principle requires that the sum of the transmitted, reflected, and absorbed solar radiations be equal to the incident solar radiation. That is,

$$\tau_s + \rho_s + \alpha_s = 1$$

where τ_s is the transmissivity, ρ_s is the reflectivity, and α_s is the absorptivity of the glass for solar energy, which are the fractions of incident solar radiation transmitted, reflected, and absorbed, respectively. The standard 3-mm(1/8-in)-thick single-pane double-strength clear window glass transmits 86 percent, reflects 8 percent, and absorbs 6 percent of the solar energy incident on it. The radiation properties of materials are usually given for normal incidence, but can also be used for radiation incident at other angles since the transmissivity, reflectivity, and absorptivity of the glazing materials remain essentially constant for incidence angles up to about 60° from the normal.

The hourly variation of solar radiation incident on the walls and windows of a house is given in Table 12–4. Solar radiation that is transmitted indoors is partially absorbed and partially reflected each time it strikes a surface, but all of it is eventually absorbed as sensible heat by the furniture,

walls, people, and so forth. Therefore, the solar energy transmitted inside a building represents a heat gain for the building. Also, the solar radiation absorbed by the glass is subsequently transferred to the indoors and outdoors by convection and radiation. The sum of the *transmitted* solar radiation and the portion of the *absorbed* radiation that flows indoors constitutes the **solar heat gain** of the building.

The fraction of incident solar radiation that enters through the glazing is called the **solar heat gain coefficient** (SHGC) and is expressed as

$$\text{SHGC} = \frac{\text{Solar heat gain through the window}}{\text{Solar radiation incident on the window}}$$

$$= \frac{\dot{q}_{\text{solar, gain}}}{\dot{q}_{\text{solar, incident}}} = \tau_s + f_i \alpha_s \tag{12–55}$$

where α_s is the solar absorptivity of the glass and f_i is the inward flowing fraction of the solar radiation absorbed by the glass. Therefore, the dimensionless quantity SHGC is the sum of the fractions of the directly transmitted (τ_s) and the absorbed and reemitted ($f_i \alpha_s$) portions of solar radiation incident on the window. The value of SHGC ranges from 0 to 1, with 1 corresponding to an opening in the wall (or the ceiling) with no glazing. When the SHGC of a window is known, the total solar heat gain through that window is determined from

$$\dot{Q}_{\text{solar, gain}} = \text{SHGC} \times A_{\text{glazing}} \times \dot{q}_{\text{solar, incident}} \qquad \text{(W)} \tag{12–56}$$

where A_{glazing} is the glazing area of the window and $\dot{q}_{\text{solar, incident}}$ is the solar heat flux incident on the outer surface of the window in W/m^2.

Another way of characterizing the solar transmission characteristics of different kinds of glazing and shading devices is to compare them to a well-known glazing material that can serve as a base case. This is done by taking the standard 3-mm(1/8-in)-thick double-strength clear window glass sheet whose SHGC is 0.87 as the *reference glazing* and defining a **shading coefficient** SC as

$$\text{SC} = \frac{\text{Solar heat gain of product}}{\text{Solar heat gain of reference glazing}}$$

$$= \frac{\text{SHGC}}{\text{SHGC}_{\text{ref}}} = \frac{\text{SHGC}}{0.87} = 1.15 \times \text{SHGC} \tag{12–57}$$

Therefore, the shading coefficient of a single-pane clear glass window is SC = 1.0. The shading coefficients of other commonly used fenestration products are given in Table 12–5 for summer design conditions. The values for winter design conditions may be slightly lower because of the higher heat transfer coefficients on the outer surface due to high winds and thus higher rate of outward flow of solar heat absorbed by the glazing, but the difference is small.

Note that the larger the shading coefficient, the smaller the shading effect, and thus the larger the amount of solar heat gain. A glazing material with a large shading coefficient allows a large fraction of solar radiation to come in.
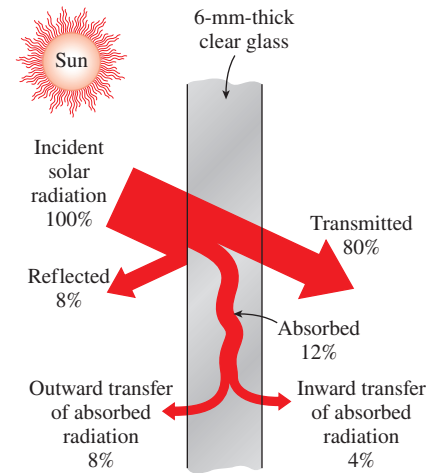
FIGURE 12–49
Distribution of solar radiation incident on a clear glass.

TABLE 12–4

Hourly variation of solar radiation incident on various surfaces and the daily totals throughout the year at 40° latitude

Date	Direction of Surface	Solar Radiation Incident on the Surface,* W/m²															Daily Total
		Solar Time															
		5	6	7	8	9	10	11	12 noon	13	14	15	16	17	18	19	
Jan.	N	0	0	0	20	43	66	68	71	68	66	43	20	0	0	0	446
	NE	0	0	0	63	47	66	68	71	68	59	43	20	0	0	0	489
	E	0	0	0	402	557	448	222	76	68	59	43	20	0	0	0	1863
	SE	0	0	0	483	811	875	803	647	428	185	48	20	0	0	0	4266
	S	0	0	0	271	579	771	884	922	884	771	579	271	0	0	0	5897
	SW	0	0	0	20	48	185	428	647	803	875	811	483	0	0	0	4266
	W	0	0	0	20	43	59	68	76	222	448	557	402	0	0	0	1863
	NW	0	0	0	20	43	59	68	71	68	66	47	63	0	0	0	489
	Horizontal	0	0	0	51	198	348	448	482	448	348	198	51	0	0	0	2568
	Direct	0	0	0	446	753	865	912	926	912	865	753	446	0	0	0	—
Apr.	N	0	41	57	79	97	110	120	122	120	110	97	79	57	41	0	1117
	NE	0	262	508	462	291	134	123	122	120	110	97	77	52	17	0	2347
	E	0	321	728	810	732	552	293	131	120	110	97	77	52	17	0	4006
	SE	0	189	518	682	736	699	582	392	187	116	97	77	52	17	0	4323
	S	0	18	59	149	333	437	528	559	528	437	333	149	59	18	0	3536
	SW	0	17	52	77	97	116	187	392	582	699	736	682	518	189	0	4323
	W	0	17	52	77	97	110	120	392	293	552	732	810	728	321	0	4006
	NW	0	17	52	77	97	110	120	122	123	134	291	462	508	262	0	2347
	Horizontal	0	39	222	447	640	786	880	911	880	786	640	447	222	39	0	6938
	Direct	0	282	651	794	864	901	919	925	919	901	864	794	651	282	0	—
July	N	3	133	109	103	117	126	134	138	134	126	117	103	109	133	3	1621
	NE	8	454	590	540	383	203	144	138	134	126	114	95	71	39	0	3068
	E	7	498	739	782	701	531	294	149	134	126	114	95	71	39	0	4313
	SE	2	248	460	580	617	576	460	291	155	131	114	95	71	39	0	3849
	S	0	39	76	108	190	292	369	395	369	292	190	108	76	39	0	2552
	SW	0	39	71	95	114	131	155	291	460	576	617	580	460	248	2	3849
	W	0	39	71	95	114	126	134	149	294	531	701	782	739	498	7	4313
	NW	0	39	71	95	114	126	134	138	144	203	383	540	590	454	8	3068
	Horizontal	1	115	320	528	702	838	922	949	922	838	702	528	320	115	1	3902
	Direct	7	434	656	762	818	850	866	871	866	850	818	762	656	434	7	—
Oct.	N	0	0	7	40	62	77	87	90	87	77	62	40	7	0	0	453
	NE	0	0	74	178	84	80	87	90	87	87	62	40	7	0	0	869
	E	0	0	163	626	652	505	256	97	87	87	62	40	7	0	0	2578
	SE	0	0	152	680	853	864	770	599	364	137	66	40	7	0	0	4543
	S	0	0	44	321	547	711	813	847	813	711	547	321	44	0	0	5731
	SW	0	0	7	40	66	137	364	599	770	864	853	680	152	0	0	4543
	W	0	0	7	40	62	87	87	97	256	505	652	626	163	0	0	2578
	NW	0	0	7	40	62	87	87	90	87	80	84	178	74	0	0	869
	Horizontal	0	0	14	156	351	509	608	640	608	509	351	156	14	0	0	3917
	Direct	0	0	152	643	811	884	917	927	917	884	811	643	152	0	0	—

*Multiply by 0.3171 to convert to Btu/h·ft².

Values given are for the 21st of the month for average days with no clouds. The values can be up to 15 percent higher at high elevations under very clear skies and up to 30 percent lower at very humid locations with very dusty industrial atmospheres. Daily totals are obtained using Simpson's rule for integration with 10-min time intervals. Solar reflectance of the ground is assumed to be 0.2, which is valid for old concrete, crushed rock, and bright green grass. For a specified location, use solar radiation data obtained for that location. The direction of a surface indicates the direction a vertical surface is facing. For example, W represents the solar radiation incident on a west-facing wall per unit area of the wall.

Solar time may deviate from the local time. Solar noon at a location is the time when the sun is at the highest location (and thus when the shadows are shortest). Solar radiation data are symmetric about the solar noon: the value on a west wall before the solar noon is equal to the value on an east wall two hours after the solar noon.

Source: ASHRAE Handbook of Fundamentals, Chap. 27, Table 15

Shading devices are classified as *internal shading* and *external shading,* depending on whether the shading device is placed *inside* or *outside.* External shading devices are more effective in reducing the solar heat gain since they intercept the sun's rays before they reach the glazing. The solar heat gain through a window can be reduced by as much as 80 percent by exterior shading. Roof overhangs have long been used for exterior shading of windows. The sun is high in the horizon in summer and low in winter. A properly sized roof overhang or a horizontal projection blocks off the sun's rays completely in summer while letting in most of them in winter, as shown in Fig. 12–50. Such shading structures can reduce the solar heat gain on the south, southeast, and southwest windows in the northern hemisphere considerably. A window can also be shaded from outside by vertical or horizontal architectural projections, insect or shading screens, and sun screens. To be effective, air must be able to move freely around the exterior device to carry away the heat absorbed by the shading and the glazing materials.

Some type of internal shading is used in most windows to provide privacy and aesthetic effects as well as some control over solar heat gain. Internal shading devices reduce solar heat gain by reflecting transmitted solar radiation back through the glazing before it can be absorbed and converted into heat in the building.

Draperies reduce the annual heating and cooling loads of a building by 5 to 20 percent, depending on the type and the user habits. In summer, they reduce heat gain primarily by reflecting back direct solar radiation (Fig. 12–51). The semiclosed airspace formed by the draperies serves as an additional barrier against heat transfer, resulting in a lower *U*-factor for the window and thus a lower rate of heat transfer in summer and winter. The solar optical properties of draperies can be measured accurately, or they can be obtained directly from the manufacturers. The shading coefficient of draperies depends on the openness factor, which is the ratio of the open area between the fibers that permits the sun's rays to pass freely, to the total area of the fabric. Tightly woven fabrics allow little direct radiation to pass through, and thus they have a small openness factor. The *reflectance* of the surface of the drapery facing the glazing has a major effect on the amount of solar heat gain. *Light-colored* draperies made of closed or tightly woven fabrics maximize the back reflection and thus minimize the solar gain. *Dark-colored* draperies made of open or semi-open woven fabrics, on the other hand, minimize the back reflection and thus maximize the solar gain.

The shading coefficients of drapes also depend on the way they are hung. Usually, the width of drapery used is twice the width of the draped area to allow folding of the drapes and to give them their characteristic "full" or "wavy" appearance. A flat drape behaves like an ordinary window shade. A flat drape has a higher reflectance and thus a lower shading coefficient than a full drape.

External shading devices such as overhangs and tinted glazings do not require operation, and they provide reliable service over a long time without significant degradation during their service life. Their operation does not depend on a person or an automated system, and these passive shading devices are considered fully effective when determining the peak cooling load and the

TABLE 12–5

Shading coefficient SC and solar transmissivity τ_{solar} for some common glass types for summer design conditions

Type of Glazing	Nominal Thickness mm	in	τ_{solar}	SC*
(*a*) Single Glazing				
Clear	3	$\frac{1}{8}$	0.86	1.0
	6	$\frac{1}{4}$	0.78	0.95
	10	$\frac{3}{8}$	0.72	0.92
	13	$\frac{1}{2}$	0.67	0.88
Heat absorbing	3	$\frac{1}{8}$	0.64	0.85
	6	$\frac{1}{4}$	0.46	0.73
	10	$\frac{3}{8}$	0.33	0.64
	13	$\frac{1}{2}$	0.24	0.58
(*b*) Double Glazing				
Clear in, clear out	3[a]	$\frac{1}{8}$	0.71[b]	0.88
	6	$\frac{1}{4}$	0.61	0.82
Clear in, heat absorbing out[c]	6	$\frac{1}{4}$	0.36	0.58

*Multiply by 0.87 to obtain SHGC.
[a]The thickness of each pane of glass.
[b]Combined transmittance for assembled unit.
[c]Refers to gray-, bronze-, and green-tinted heat-absorbing float glass.

Source: ASHRAE Handbook of Fundamentals, *Chap. 27, Table 11*
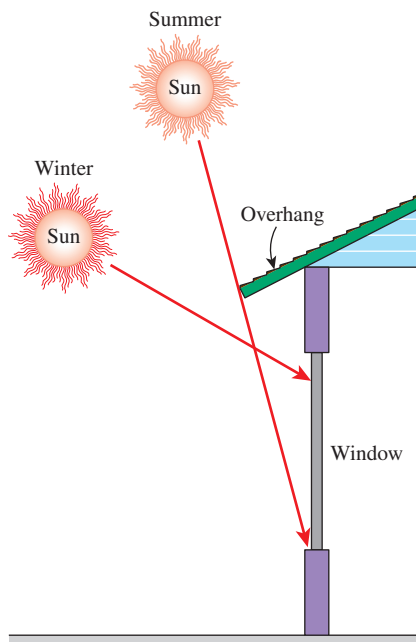
FIGURE 12–50
A properly sized overhang blocks off the sun's rays completely in summer while letting them in in winter.
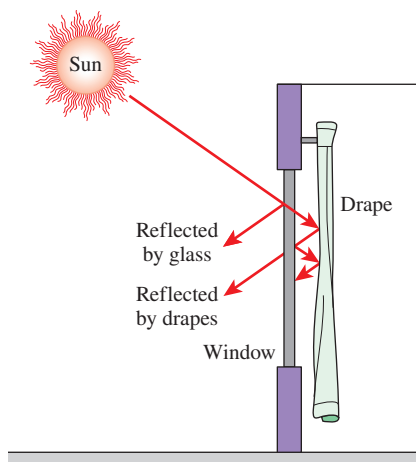
FIGURE 12–51
Draperies reduce heat gain in summer by reflecting back solar radiation and reduce heat loss in winter by forming an airspace before the window.

annual energy use. The effectiveness of manually operated shading devices, on the other hand, varies greatly depending on the user's habits, and this variation should be considered when evaluating performance.

The primary function of an indoor shading device is to provide *thermal comfort* for the occupants. An unshaded window glass allows most of the incident solar radiation in, and it also dissipates part of the solar energy it absorbs by emitting infrared radiation to the room. The emitted radiation and the transmitted direct sunlight may bother the occupants near the window. In winter, the temperature of the glass is lower than the room air temperature, causing excessive heat loss by radiation from the occupants. A shading device allows the control of direct solar and infrared radiation while providing various degrees of privacy and outward vision. The shading device is also at a higher temperature than the glass in winter and thus reduces radiation loss from occupants. *Glare* from draperies can be minimized by using off-white colors. Indoor shading devices, especially draperies made of a closed-weave fabric, are effective in reducing *sounds* that originate in the room, but they are not as effective against the sounds coming from outside.

The type of climate in an area usually dictates the types of windows to be used in buildings. In *cold climates* where the heating load is much larger than the cooling load, the windows should have the highest transmissivity for the entire solar spectrum, and a high reflectivity (or low emissivity) for the far infrared radiation emitted by the walls and furnishings of the room. Low-e windows are well suited for such heating-dominated buildings. Properly designed and operated windows allow more heat into the building over a heating season than it loses, making them energy contributors rather than energy losers. In *warm climates* where the cooling load is much larger than the heating load, the windows should allow the visible solar radiation (light) in but should block off the infrared solar radiation. Such windows can reduce the solar heat gain by 60 percent with no appreciable loss in daylighting. This behavior is approximated by window glazings that are coated with a heat-absorbing film outside and a low-e film inside (Fig. 12–52). Properly selected windows can reduce the cooling load by 15 to 30 percent compared to windows with clear glass.

Note that radiation heat transfer between a room and its windows is proportional to the emissivity of the glass surface facing the room, $\varepsilon_{\text{glass}}$, and can be expressed as

$$\dot{Q}_{\text{rad, room-window}} = \varepsilon_{\text{glass}} A_{\text{glass}} \sigma (T_{\text{room}}^4 - T_{\text{glass}}^4) \qquad \textbf{(12–58)}$$

Therefore, a low-e interior glass will reduce the heat loss by radiation in winter ($T_{\text{glass}} < T_{\text{room}}$) and heat gain by radiation in summer ($T_{\text{glass}} > T_{\text{room}}$).

Tinted glass and glass coated with reflective films reduce solar heat gain in summer and heat loss in winter. The conductive heat gains or losses can be minimized by using multiple-pane windows. Double-pane windows are usually called for in climates where the winter design temperature is less than $7°C(45°F)$. Double-pane windows with tinted or reflective films are commonly used in buildings with large window areas. Clear glass is preferred for showrooms since it affords maximum visibility from outside, but bronze-, gray-, and green-colored glass are preferred in office buildings since they provide considerable privacy while reducing glare.

EXAMPLE 12–7 Installing Reflective Films on Windows

A manufacturing facility located at 45°N latitude has a glazing area of 40 m^2 that consists of double-pane windows made of clear glass (SHGC = 0.766). To reduce the solar heat gain in summer, a reflective film that reduces the SHGC to 0.261 is considered. The cooling season consists of June, July, August, and September, and the heating season October through April. The average daily solar heat fluxes incident on the west side at this latitude are 1.86, 2.66, 3.43, 4.00, 4.36, 5.13, 4.31, 3.93, 3.28, 2.80, 1.84, and 1.54 kWh/day·m^2 for January through December, respectively. Also, the unit cost of electricity and natural gas are \$0.08/kWh and \$0.50/therm, respectively. If the coefficient of performance (COP) of the cooling system is 2.5 and efficiency of the furnace is 0.8, determine the net annual cost savings due to installing reflective coating on the windows. Also, determine the simple payback period if the installation cost of reflective film is \$20/m^2 (Fig. 12–53).

SOLUTION The net annual cost savings due to installing reflective film on the west windows of a building and the simple payback period are to be determined.

Assumptions **1** The calculations given below are for an average year. **2** The unit costs of electricity and natural gas remain constant.

Analysis Using the daily averages for each month and noting the number of days of each month, the total solar heat flux incident on the glazing during summer and winter months are determined to be

$$Q_{\text{solar, summer}} = 5.13 \times 30 + 4.31 \times 31 + 3.93 \times 31 + 3.28 \times 30 = 508 \text{ kWh/year}$$

$$\begin{aligned} Q_{\text{solar, winter}} &= 2.80 \times 31 + 1.84 \times 30 + 1.54 \times 31 + 1.86 \times 31 \\ &\quad + 2.66 \times 28 + 3.43 \times 31 + 4.00 \times 30 \\ &= 548 \text{ kWh/year} \end{aligned}$$

Then the decrease in the annual cooling load and the increase in the annual heating load due to the reflective film become

$$\begin{aligned} \text{Cooling load decrease} &= Q_{\text{solar, summer}} A_{\text{glazing}} (\text{SHGC}_{\text{without film}} - \text{SHGC}_{\text{with film}}) \\ &= (508 \text{ kWh/year})(40 \text{ m}^2)(0.766 - 0.261) \\ &= 10{,}262 \text{ kWh/year} \end{aligned}$$

$$\begin{aligned} \text{Heating load increase} &= Q_{\text{solar, winter}} A_{\text{glazing}} (\text{SHGC}_{\text{without film}} - \text{SHGC}_{\text{with film}}) \\ &= (548 \text{ kWh/year})(40 \text{ m}^2)(0.766 - 0.261) \\ &= 11{,}070 \text{ kWh/year} = 377.7 \text{ therms/year} \end{aligned}$$

since 1 therm = 29.31 kWh. The corresponding decrease in cooling costs and the increase in heating costs are

$$\begin{aligned} \text{Decrease in cooling costs} &= (\text{Cooling load decrease})(\text{Unit cost of electricity})/\text{COP} \\ &= (10{,}262 \text{ kWh/year})(\$0.08/\text{kWh})/2.5 = \$328/\text{year} \end{aligned}$$

$$\begin{aligned} \text{Increase in heating costs} &= (\text{Heating load increase})(\text{Unit cost of fuel})/\text{Efficiency} \\ &= (377.7 \text{ therms/year})(\$0.50/\text{therm})/0.80 = \$236/\text{year} \end{aligned}$$

Then the net annual cost savings due to the reflective film become

$$\begin{aligned} \text{Cost savings} &= \text{Decrease in cooling costs} - \text{Increase in heating costs} \\ &= \$328 - \$236 = \textbf{\$92/year} \end{aligned}$$

(*a*) Cold climates

(*b*) Warm climates
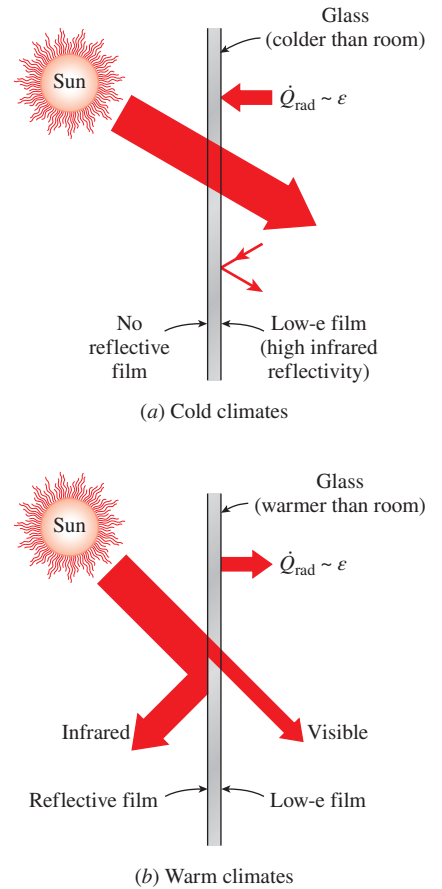
FIGURE 12–52
Radiation heat transfer between a room and its windows is proportional to the emissivity of the glass surface, and low-e coatings on the inner surface of the windows reduce heat loss in winter and heat gain in summer.
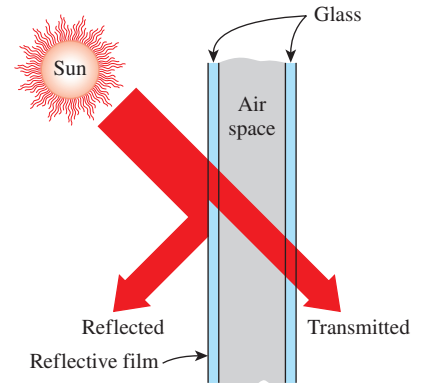
FIGURE 12–53
Schematic for Example 12–7.

The implementation cost of installing films is

$$\text{Implementation cost} = (\$20/\text{m}^2)(40 \text{ m}^2) = \$800$$

This gives a simple payback period of

$$\text{Simple payback period} = \frac{\text{Implementation cost}}{\text{Annual cost savings}} = \frac{\$800}{\$92/\text{year}} = \textbf{8.7 years}$$

Discussion The reflective film will pay for itself in this case in about nine years. This may be unacceptable to most manufacturers since they are not usually interested in any energy conservation measure that does not pay for itself within three years. But the enhancement in thermal comfort and thus the resulting increase in productivity often makes it worthwhile to install reflective film.

SUMMARY

Radiation propagates in the form of electromagnetic waves. The *frequency* ν and *wavelength* λ of electromagnetic waves in a medium are related by $\lambda = c/\nu$, where c is the speed of propagation in that medium. All matter continuously emits *thermal radiation* as a result of vibrational and rotational motions of molecules, atoms, and electrons of a substance.

A *blackbody* is defined as a perfect emitter and absorber of radiation. At a specified temperature and wavelength, no surface can emit more energy than a blackbody. A blackbody absorbs *all* incident radiation, regardless of wavelength and direction. The radiation energy emitted by a blackbody per unit time and per unit surface area is called the *blackbody emissive power* E_b and is expressed by the *Stefan–Boltzmann law* as

$$E_b(T) = \sigma T^4$$

where $\sigma = 5.670 \times 10^{-8} \text{ W/m}^2 \cdot \text{K}^4$ is the *Stefan–Boltzmann constant* and T is the absolute temperature of the surface in K. At any specified temperature, the spectral blackbody emissive power $E_{b\lambda}$ increases with wavelength, reaches a peak, and then decreases with increasing wavelength. The wavelength at which the peak occurs for a specified temperature is given by *Wien's displacement law* as

$$(\lambda T)_{\text{max power}} = 2897.8 \text{ μm} \cdot \text{K}$$

The *blackbody radiation function* f_λ represents the fraction of radiation emitted by a blackbody at temperature T in the wavelength band from $\lambda = 0$ to λ. The fraction of radiation energy emitted by a blackbody at temperature T over a finite wavelength band from $\lambda = \lambda_1$ to $\lambda = \lambda_2$ is determined from

$$f_{\lambda_1 - \lambda_2}(T) = f_{\lambda_2}(T) - f_{\lambda_1}(T)$$

where $f_{\lambda_1}(T)$ and $f_{\lambda_2}(T)$ are the blackbody radiation functions corresponding to $\lambda_1 T$ and $\lambda_2 T$, respectively.

The magnitude of a viewing angle in space is described by solid angle expressed as $d\omega = dA_n/r^2$. The *radiation intensity* for emitted radiation $I_e(\theta, \phi)$ is defined as the rate at which radiation energy is emitted in the (θ, ϕ) direction per unit area normal to this direction and per unit solid angle about this direction. The *radiation flux* for emitted radiation is the *emissive power E* and is expressed as

$$E = \int_{\text{hemisphere}} dE = \int_{\phi=0}^{2\pi} \int_{\theta=0}^{\pi/2} I_e(\theta, \phi) \cos \theta \sin \theta \, d\theta \, d\phi$$

For a *diffusely emitting* surface, intensity is independent of direction, and thus

$$E = \pi I_e$$

For a blackbody, we have

$$E_b = \pi I_b \quad \text{and} \quad I_b(T) = \frac{E_b(T)}{\pi} = \frac{\sigma T^4}{\pi}$$

The radiation flux incident on a surface from all directions is *irradiation G,* and for diffusely incident radiation of intensity I_i it is expressed as

$$G = \pi I_i$$

The rate at which radiation energy leaves a unit area of a surface in all directions is *radiosity J,* and for a surface that is both a diffuse emitter and a diffuse reflector it is expressed as

$$J = \pi I_{e+r}$$

where I_{e+r} is the sum of the emitted and reflected intensities. The spectral emitted quantities are related to total quantities as

$$I_e = \int_0^\infty I_{\lambda, e} \, d\lambda \quad \text{and} \quad E = \int_0^\infty E_\lambda \, d\lambda$$

They reduce for a diffusely emitting surface and for a black-body to

$$E_\lambda = \pi I_{\lambda, e} \quad \text{and} \quad E_{b\lambda}(\lambda, T) = \pi I_{b\lambda}(\lambda, T)$$

The *emissivity* of a surface represents the ratio of the radiation emitted by the surface at a given temperature to the radiation emitted by a blackbody at the same temperature. Different emissivities are defined as

Spectral directional emissivity:

$$\varepsilon_{\lambda, \theta}(\lambda, \theta, \phi, T) = \frac{I_{\lambda, e}(\lambda, \theta, \phi, T)}{I_{b\lambda}(\lambda, T)}$$

Total directional emissivity:

$$\varepsilon_\theta(\theta, \phi, T) = \frac{I_e(\theta, \phi, T)}{I_b(T)}$$

Spectral hemispherical emissivity:

$$\varepsilon_\lambda(\lambda, T) = \frac{E_\lambda(\lambda, T)}{E_{b\lambda}(\lambda, T)}$$

Total hemispherical emissivity:

$$\varepsilon(T) = \frac{E(T)}{E_b(T)} = \frac{\int_0^\infty \varepsilon_\lambda(\lambda, T) E_{b\lambda}(\lambda, T) d\lambda}{\sigma T^4}$$

Emissivity can also be expressed as a step function by dividing the spectrum into a sufficient number of *wavelength bands* of constant emissivity as, for example,

$$\varepsilon(T) = \varepsilon_1 f_{0-\lambda_1}(T) + \varepsilon_2 f_{\lambda_1-\lambda_2}(T) + \varepsilon_3 f_{\lambda_2-\infty}(T)$$

The *total hemispherical emissivity* ε of a surface is the average emissivity over all directions and wavelengths.

When radiation strikes a surface, part of it is absorbed, part of it is reflected, and the remaining part, if any, is transmitted. The fraction of incident radiation (intensity I_i or irradiation G) absorbed by the surface is called the *absorptivity,* the fraction reflected by the surface is called the *reflectivity,* and the fraction transmitted is called the *transmissivity.* Various absorptivities, reflectivities, and transmissivities for a medium are expressed as

$$\alpha_{\lambda, \theta}(\lambda, \theta, \phi) = \frac{I_{\lambda, \text{abs}}(\lambda, \theta, \phi)}{I_{\lambda, i}(\lambda, \theta, \phi)} \text{ and } \rho_{\lambda, \theta}(\lambda, \theta, \phi) = \frac{I_{\lambda, \text{ref}}(\lambda, \theta, \phi)}{I_{\lambda, i}(\lambda, \theta, \phi)}$$

$$\alpha_\lambda(\lambda) = \frac{G_{\lambda, \text{abs}}(\lambda)}{G_\lambda(\lambda)}, \rho_\lambda(\lambda) = \frac{G_{\lambda, \text{ref}}(\lambda)}{G_\lambda(\lambda)}, \text{ and } \tau_\lambda(\lambda) = \frac{G_{\lambda, \text{tr}}(\lambda)}{G_\lambda(\lambda)}$$

$$\alpha = \frac{G_{\text{abs}}}{G}, \rho = \frac{G_{\text{ref}}}{G}, \text{ and } \tau = \frac{G_{\text{tr}}}{G}$$

The consideration of wavelength and direction dependence of properties makes radiation calculations very complicated. Therefore, the *gray* and *diffuse* approximations are commonly utilized in radiation calculations. A surface is said to be *diffuse* if its properties are independent of direction and *gray* if its properties are independent of wavelength.

The sum of the absorbed, reflected, and transmitted fractions of radiation energy must be equal to unity,

$$\alpha + \rho + \tau = 1$$

For *opaque* surfaces $(\tau = 0)$: $\alpha + \rho = 1$

For surfaces with *no reflectance* $(\rho = 0)$: $\alpha + \tau = 1$

Surfaces are usually assumed to reflect in a perfectly *specular* or *diffuse* manner for simplicity. In *specular* (or *mirrorlike*) *reflection,* the angle of reflection equals the angle of incidence of the radiation beam. In *diffuse reflection,* radiation is reflected equally in all directions. Reflection from smooth and polished surfaces approximates specular reflection, whereas reflection from rough surfaces approximates diffuse reflection. *Kirchhoff's law* of radiation is expressed as

$$\varepsilon_{\lambda, \theta}(T) = \alpha_{\lambda, \theta}(T), \varepsilon_\lambda(T) = \alpha_\lambda(T), \text{ and } \varepsilon(T) = \alpha(T)$$

Gas molecules and the suspended particles in the atmosphere emit radiation as well as absorbing it. The atmosphere can be treated as a blackbody at some lower fictitious temperature, called the *effective sky temperature* T_{sky} that emits an equivalent amount of radiation energy,

$$G_{\text{sky}} = \sigma T_{\text{sky}}^4$$

The net rate of radiation heat transfer to a surface exposed to solar and atmospheric radiation is determined from an energy balance expressed as

$$\dot{q}_{\text{net, rad}} = \alpha_s G_{\text{solar}} + \varepsilon\sigma(T_{\text{sky}}^4 - T_s^4)$$

where T_s is the surface temperature in K, and ε is the surface emissivity at room temperature.

REFERENCES AND SUGGESTED READING

1. American Society of Heating, Refrigeration, and Air Conditioning Engineers. *Handbook of Fundamentals.* Atlanta, GA: ASHRAE, 1993.

2. A. G. H. Dietz. "Diathermanous Materials and Properties of Surfaces." In *Space Heating with Solar Energy,* ed. R. W. Hamilton. Cambridge, MA: MIT Press, 1954.

3. J. A. Duffy and W. A. Beckman. *Solar Energy Thermal Process.* New York: John Wiley & Sons, 1974.

4. H. C. Hottel. "Radiant Heat Transmission." In *Heat Transmission,* 3rd ed., ed. W. H. McAdams. New York: McGraw-Hill, 1954.

5. M. F. Modest. *Radiative Heat Transfer.* New York: McGraw-Hill, 1993.

6. M. Planck. *The Theory of Heat Radiation.* New York: Dover, 1959.

7. W. Sieber. *Zeitschrift für Technische Physics* 22 (1941), pp. 130–135.

8. R. Siegel and J. R. Howell. *Thermal Radiation Heat Transfer,* 3rd ed. Washington, DC: Hemisphere, 1992.

9. Y. S. Touloukian and D. P. DeWitt. "Nonmetallic Solids." In *Thermal Radiative Properties.* Vol. 8. New York: IFI/Plenum, 1970.

10. Y. S. Touloukian and D. P. DeWitt. "Metallic Elements and Alloys." In *Thermal Radiative Properties,* Vol. 7. New York: IFI/Plenum, 1970.

PROBLEMS*

Electromagnetic and Thermal Radiation

12–1C What is an electromagnetic wave? How does it differ from a sound wave?

12–2C By what properties is an electromagnetic wave characterized? How are these properties related to each other?

12–3C What is thermal radiation? How does it differ from the other forms of electromagnetic radiation?

12–4C How does microwave cooking differ from conventional cooking?

12–5C What is visible light? How does it differ from the other forms of electromagnetic radiation?

12–6C What is the cause of color? Why do some objects appear blue to the eye while others appear red? Is the color of a surface at room temperature related to the radiation it emits?

12–7C Why do skiers get sunburned so easily?

12–8C How do ultraviolet and infrared radiation differ? Do you think your body emits any radiation in the ultraviolet range? Explain.

12–9C Why is radiation usually treated as a surface phenomenon?

12–10 A cordless telephone is designed to operate at a frequency of 8.5×10^8 Hz. Determine the wavelength of these telephone waves.

12–11 Electricity is generated and transmitted in power lines at a frequency of 50 Hz (1 Hz = 1 cycle per second). Determine the wavelength of the electromagnetic waves generated by the passage of electricity in power lines.

12–12 The speed of light in vacuum is given to be 3.0×10^8 m/s. Determine the speed of light in air ($n = 1$), in water ($n = 1.33$), and in glass ($n = 1.5$).

12–13 A radio station is broadcasting radio waves at a wavelength of 150 m. Determine the frequency of these waves.

12–14 A microwave oven is designed to operate at a frequency of 2.2×10^9 Hz. Determine the wavelength of these microwaves and the energy of each microwave.

12–15 Consider a radio wave with a wavelength of 10^7 μm and a γ-ray with a wavelength of 10^{-7} μm. Determine the photon energies of the radio wave and the γ-ray, and the photon energy ratio of the γ-ray to the radio wave.

12–16 An electromagnetic wave with a wavelength of 0.5 μm is being propagated in different media: air, water, and glass. The refractive index of air, water, and glass are 1, 1.33, and 1.5 respectively. Determine the photon energy, in eV, of the electromagnetic wave in each medium (1 eV = 1.6022×10^{-19} J).

12–17 The electromagnetic spectrum that lies between 0.40 and 0.76 μm is what we call visible light. Within this spectrum, the color violet has the shortest wavelength while the color red has the longest wavelength. Determine which of these colors, violet ($\lambda = 0.40$ μm) or red ($\lambda = 0.76$ μm), propagates more photon energy.

Blackbody Radiation

12–18C What is a blackbody? Does a blackbody actually exist?

12–19C Define the total and spectral blackbody emissive powers. How are they related to each other? How do they differ?

12–20C Why did we define the blackbody radiation function? What does it represent? For what is it used?

12–21C Consider two identical bodies, one at 1000 K and the other at 1500 K. Which body emits more radiation in the shorter-wavelength region? Which body emits more radiation at a wavelength of 20 μm?

12–22 Consider a surface at a uniform temperature of 1000 K. Determine the maximum rate of thermal radiation that can be emitted by this surface, in W/m².

12–23 C&S A thin-walled tube has its inner surface coated with polypropylene lining. The ASME Code for Process Piping limits the maximum use temperature for polypropylene lining to 107°C (ASME B31.3-2014, Table A323.4.3). The tube has a diameter of 5 cm. Assume the tube behaves as a blackbody, and irradiation on the tube from the surroundings is negligible. Determine the maximum amount of total radiation emission rate per unit length of the tube that can be achieved without exceeding the maximum use temperature for polypropylene lining.

---

* Problems designated by a "C" are concept questions, and students are encouraged to answer them all. Problems designated by an "E" are in English units, and the SI users can ignore them. Problems with the 🖥 icon are comprehensive in nature and are intended to be solved with appropriate software. Problems with the **PtD** icon are Prevention through Design problems. Problems with the **C&S** icon are Codes and Standards problems.

12–24 Consider a 20-cm × 20-cm × 20-cm cubical body at 900 K suspended in the air. Assuming the body closely approximates a blackbody, determine (*a*) the rate at which the cube emits radiation energy in W and (*b*) the spectral blackbody emissive power at a wavelength of 4 μm.

12–25 A flame from a match may be approximated as a blackbody at the effective surface temperature of 1700 K, while moonlight may be approximated as a blackbody at the effective surface temperature of 4000 K, respectively. Determine the peak spectral blackbody emissive power for both lighting sources (match flame and moonlight).

12–26 C&S The maximum use temperature for an ASTM A479 904L stainless steel bar is 260°C (ASME Code for Process Piping, ASME B31.3-2014, Table A-1M). Assume the bar behaves as a blackbody and determine (*a*) the spectral blackbody emissive powers at the limits of the electromagnetic spectrum for thermal radiation at the maximum use temperature and (*b*) the maximum spectral blackbody emissive power that the bar can reach without exceeding its maximum use temperature.

12–27 At a wavelength of 0.7 μm, the blackbody emissive power is equal to 10^8 W/m³. Determine (*a*) the temperature of the blackbody and (*b*) the total emissive power at this temperature.

12–28 C&S The maximum use temperature for an ASTM A240 410S stainless steel plate is 649°C (ASME Code for Process Piping, ASME B31.3-2014, Table A-1M). The plate is used in a process where the maximum spectral blackbody emissive power from the plate surface is 9000 W/m²·μm. Assume the plate behaves as a blackbody, and determine whether the plate is suitable for this process.

12–29 The sun can be treated as a blackbody at 5780 K. Using appropriate software, calculate and plot the spectral blackbody emissive power $E_{b\lambda}$ of the sun versus wavelength in the range of 0.01 μm to 1000 μm. Discuss the results.

12–30 A small body is placed inside a spherical stainless steel chamber with a diameter of 3 m. The chamber is evacuated and has a constant surface temperature of 500 K. Determine the radiation incident on the surface of the small body inside the chamber if the interior surface of the chamber is (*a*) coated black and (*b*) well polished.

12–31 Consider a black spherical ball, with a diameter of 25 cm, that is suspended in air. Determine the surface temperature of the ball that should be maintained in order to heat 10 kg of air from 20 to 30°C in 5 minutes.

12–32 C&S A tube placed in a vacuum has an outer diameter of 5 cm, and its wall thickness is 1 cm. The tube wall has a thermal conductivity of 5 W/m·K. The tube inner surface is coated with polytetrafluoroethylene (PTFE) lining. The ASME Code for Process Piping limits the maximum use temperature for polypropylene lining to 260°C (ASME

B31.3-2014, Table A323.4.3). The total radiation emission rate per unit length of the tube from the tube outer surface is 680 W/m. Determine whether the use of PTFE lining is suitable for coating the tube's inner surface. Assume the tube behaves as blackbody and irradiation on the tube from the surroundings is negligible.

12–33 A thin vertical copper plate is subjected to a uniform heat flux of 1000 W/m² on one side, while the other side is exposed to ambient surroundings at 5°C. The surface of the plate is oxidized black and can be treated as a blackbody. The heat transfer coefficient due to natural convection on the plate surface is 5.3 W/m²·K. Determine the surface temperature of the plate. Discuss the contribution of the net radiation heat transfer on the total heat loss from the plate.
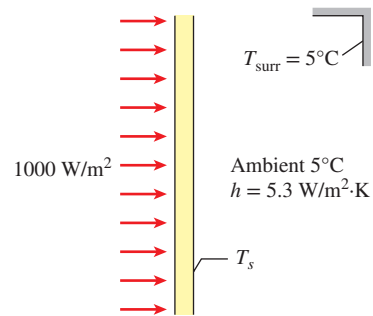
FIGURE P12–33

12–34 A circular ceramic plate that can be modeled as a blackbody is being heated by an electrical heater. The plate is 30 cm in diameter and is situated in a surrounding ambient temperature of 15°C where the natural convection heat transfer coefficient is 12 W/m²·K. If the efficiency of the electrical heater to transfer heat to the plate is 80 percent, determine the electric power that the heater needs to keep the surface temperature of the plate at 200°C.
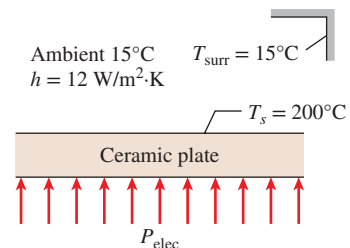
FIGURE P12–34

12–35 We wish an incandescent lightbulb to emit at least 15 percent of its energy at wavelengths shorter than 0.8 μm. Determine the minimum temperature to which the filament of the lightbulb must be heated.

12–36 The temperature of the filament of an incandescent lightbulb is 2500 K. Assuming the filament to be a blackbody,

determine the fraction of the radiant energy emitted by the filament that falls in the visible range. Also, determine the wavelength at which the emission of radiation from the filament peaks.

12–37 The temperature of the filament of an incandescent lightbulb is 2800 K. Treating the filament as a blackbody, determine the fraction of the radiant energy emitted by the filament that falls in the visible range. Also, determine the wavelength at which the emission of radiation from the filament peaks.

12–38 Reconsider Prob. 12–37. Using appropriate software, investigate the effect of temperature on the fraction of radiation emitted in the visible range. Let the surface temperature vary from 1000 K to 4000 K, and plot the fraction of radiation emitted in the visible range versus the surface temperature.

12–39E Consider a black surface at 2060°F. Determine the radiation energy emitted by the black surface per unit area (in Btu/h·ft^2) for $\lambda \geq 4$ μm.

12–40 It is desired that the radiation energy emitted by a light source reach a maximum in the blue range ($\lambda = 0.47$ μm). Determine the temperature of this light source and the fraction of radiation it emits in the visible range ($\lambda = 0.40 - 0.76$ μm).

12–41E The sun can be treated as a blackbody at an effective surface temperature of 10,400 R. Determine the rate at which infrared radiation energy ($\lambda = 0.76 - 100$ μm) is emitted by the sun, in Btu/h·ft^2.

12–42 A 3-mm-thick glass window transmits 90 percent of the radiation between $\lambda = 0.3$ and 3.0 μm and is essentially opaque for radiation at other wavelengths. Determine the rate of radiation transmitted through a 3-m × 3-m glass window from blackbody sources at (*a*) 5800 K and (*b*) 1000 K.

12–43 Daylight and candlelight may be approximated as a blackbody at the effective surface temperatures of 5800 K and 1800 K, respectively. Determine the radiation energy (in W/m^2) emitted by both lighting sources (daylight and candlelight) within the visible light region (0.40 to 0.76 μm).

12–44 C&S The maximum use temperature for an ASTM B335 nickel alloy rod is 427°C (ASME Code for Process Piping, ASME B31.3-2014, Table A-1M). Assume the rod behaves as a blackbody. Determine the highest radiation energy per unit area that can be emitted from the rod over a wavelength band from 2 to 10 μm, without exceeding the maximum use temperature.

12–45 Consider the sun, which is considered to be a blackbody with a surface temperature of roughly 5800 K. Determine the percentage of solar energy (*a*) in the visible range, (*b*) at wavelengths shorter than the visible range, and (*c*) at wavelengths longer than the visible range.

Radiation Intensity

12–46C What does a solid angle represent, and how does it differ from a plane angle? What is the value of a solid angle associated with a sphere?

12–47C For a surface, how is irradiation defined? For diffusely incident radiation, how is irradiation on a surface related to the intensity of incident radiation?

12–48C For a surface, how is radiosity defined? For diffusely emitting and reflecting surfaces, how is radiosity related to the intensities of emitted and reflected radiation?

12–49C When the variation of spectral radiation quantity with wavelength is known, how is the corresponding total quantity determined?

12–50C How is the intensity of emitted radiation defined? For a diffusely emitting surface, how is the emissive power related to the intensity of emitted radiation?

12–51 A small surface of area $A_1 = 3$ cm^2 emits radiation as a blackbody, and part of the radiation emitted by A_1 strikes another small surface of area $A_2 = 8$ cm^2 oriented as shown in Fig. P12-51. If the rate at which radiation emitted by A_1 that strikes A_2 is measured to be 274×10^{-6} W, determine the intensity of the radiation emitted by A_1, and the temperature of A_1.
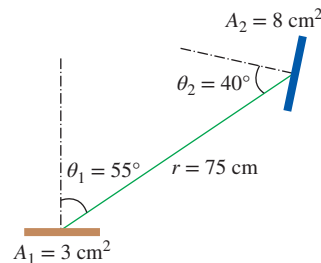
FIGURE P12–51

12–52 A small circular surface of area $A_1 = 2$ cm^2 located at the center of a 2-m-diameter sphere emits radiation as a blackbody at $T_1 = 1000$ K. Determine the rate at which radiation energy is streaming through a $D_2 = 1$-cm-diameter hole located (*a*) on top of the sphere directly above A_1 and (*b*) on the side of the sphere such that the line that connects the centers of A_1 and A_2 makes 45° with surface A_1.

12–53 Repeat Prob. 12–52 for a 4-m-diameter sphere.

12–54 A small surface of area $A_1 = 7$ cm^2 emits radiation as a blackbody at $T_1 = 800$ K. Part of the radiation emitted by A_1 strikes another small surface of area $A_2 = 7$ cm^2 oriented as shown in Fig. P12-54. Determine the solid angle subtended by A_2 when viewed from A_1, and the rate at which radiation emitted by A_1 strikes A_2 directly. What would your answer be if A_2 were directly above A_1 at a distance of 80 cm?
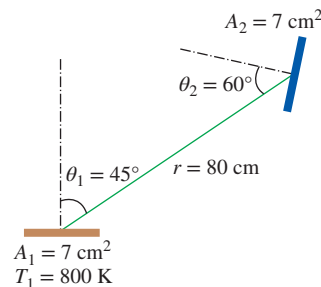
FIGURE P12–54

12–55 A small surface of area $A_1 = 1 \text{ cm}^2$ emits radiation as a blackbody at 2100 K. Determine the rate at which radiation energy is emitted through a band defined by $0 \leq \phi \leq 2\pi$ and $45 \leq \theta \leq 60°$, where θ is the angle a radiation beam makes with the normal of the surface and ϕ is the azimuth angle.

12–56 The intensity of solar radiation incident on earth's surface can be expressed as $I_i = 100 \cos\theta$, where I_i has the units of $\text{W/m}^2 \cdot \text{sr}$. Determine the peak value for the intensity of incident solar radiation and the solar irradiation on earth's surface.

12–57 A small surface of area $A_1 = 3 \text{ cm}^2$ emits radiation as a blackbody with total emissive power of $E_b = 5.67 \times 10^4 \text{ W/m}^2$. Part of the radiation emitted by A_1 strikes another small surface of area $A_2 = 8 \text{ cm}^2$ oriented as shown in Fig. P12-57. Determine the rate at which radiation emitted by A_1 strikes A_2, and the irradiation on A_2.
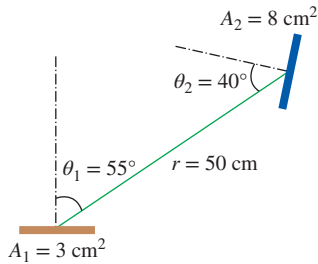
FIGURE P12–57

12–58 A small surface of area $A_1 = 3 \text{ cm}^2$ emits radiation as a blackbody at $T_1 = 1000 \text{ K}$. A radiation detector (A_2) is placed normal to the direction of viewing from surface A_1 at a distance L, as shown in Fig. P12-58. If the radiation detector is measuring an irradiation of 100 W/m^2, determine the distance between the radiation detector and the surface A_1.

FIGURE P12–58

12–59 A small surface of area $A_1 = 1 \text{ cm}^2$ is subjected to incident radiation of constant intensity $I_i = 2.2 \times 10^4 \text{ W/m}^2 \cdot \text{sr}$ over the entire hemisphere. Determine the rate at which radiation energy is incident on the surface through (a) $0 \leq \theta \leq 45°$ and (b) $45 \leq \theta \leq 90°$, where θ is the angle a radiation beam makes with the normal of the surface.

12–60 Consider an aperture of 10-mm diameter through which radiation is emitted as a blackbody with an emissive power of $2.87 \times 10^5 \text{ W/m}^2$. A radiation sensor is positioned with a 30° tilt off the normal direction of viewing, as shown in the figure. If the sensor is sensing an irradiation of 50 W/m^2, determine the distance between the aperture and the sensor.
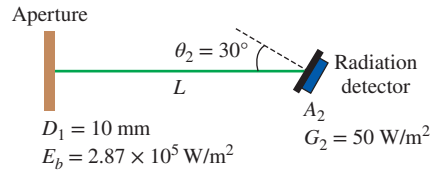
FIGURE P12–60

12–61 A small circular plate has a diameter of 2 cm and can be approximated as a blackbody. To determine the radiation from the plate, a radiometer is placed normal to the direction of viewing from the plate at a distance of 50 cm. If the radiometer measured an irradiation of 85 W/m^2 from the plate, determine the temperature of the plate.

12–62 **PtD** Heat dissipated from an engine in operation can cause hot spots on its surface. If the outer surface of an engine is situated in a place where oil leakage is possible, then when the leaked oil comes in contact with hot spots above the oil's autoignition temperature, it can ignite spontaneously. Consider an engine outer surface that can be approximated as a blackbody. To prevent fire hazard in the event of an oil leak on the engine's surface, the surface temperature of the engine should be kept below 180°C. A radiometer is placed normal to and at a distance of 1 m from the engine surface to monitor the surface temperature. The radiometer receives radiation from a target area of 1 cm^2 of the engine surface. If the radiometer detects an irradiation of 0.1 W/m^2, would there be any risk of fire hazard?

12–63 A radiometer can be used to determine the position of an approaching hot object by measuring the amount of irradiation it detects. Consider a radiometer placed at a distance $H = 0.5 \text{ m}$ from the x-axis used to measure the position of an approaching small blackbody object. If the radiometer is measuring 80 percent of the irradiation corresponding to the position of the object directly under the radiometer ($x = 0$), determine the position of the object L.
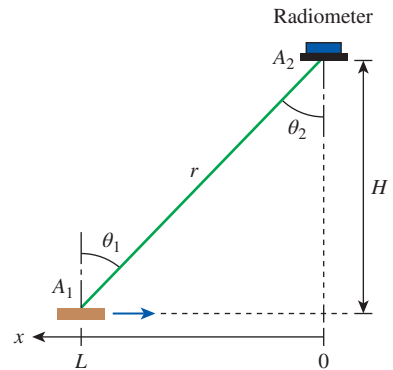
FIGURE P12–63

12–64 Reconsider Prob. 12–63. Using appropriate software, evaluate the effect of the position of the approaching object on the irradiation ratio $G_{2,x}/G_{2,0}$, where $G_{2,x}$ and $G_{2,0}$ are the irradiation on the radiometer when the

object is at position x and at $x = 0$, respectively. By varying x from 0 to 3 m with 0.2-m increments, plot the irradiation ratio $G_{2,x}/G_{2,0}$ as a function of the approaching object position x for the placement of the radiometer at $H = 0.5$, 1.0, and 1.5 m.

12–65 A small circular plate with a surface A_1 can be approximated as a blackbody. A radiometer with a surface A_2 is placed normal to the direction of viewing from the plate at a distance L. Would the irradiation on the radiometer from the plate decrease if the distance L were doubled, and if so, by how much?

12–66 A blackbody plate ($A_1 = 5$ cm^2) is subjected to a uniform heat flux of 1000 W/m^2 on the bottom, while the top surface is exposed to an ambient surrounding at 5°C. The heat transfer coefficient due to natural convection on the plate surface is 5 W/m^2·K. A radiometer is placed 1 m above the plate normal to the direction of viewing from the plate. Determine the irradiation that the radiometer would detect.

12–67 [PtD] A long metal sheet that can be approximated as a blackbody is being conveyed through a water bath to be cooled. In order to prevent thermal burns to people handling the sheet, it must exit the water bath at a temperature below 45°C. A radiometer is placed normal to and at a distance of 0.5 m from the sheet's surface to monitor the exit temperature. The radiometer receives radiation from a target area of 1 cm^2 of the metal sheet surface. When the radiometer detects that the metal sheet temperature is not below 45°C, an alarm will go off to warn that the sheet is not safe to touch. Determine the irradiation on the radiometer that should trigger the warning alarm.

12–68 [PtD] A radiometer is used to monitor the temperature of manufactured parts ($A_1 = 10$ cm^2) on a conveyor. The radiometer is placed at a distance of 1 m from and normal to the manufactured parts. When a part moves to the position normal to the radiometer, the sensor measures the radiation emitted from the part. In order to prevent thermal burns to people handling the manufactured parts at the end of the conveyor, the temperature of the parts should be below 45°C. An array of spray heads is programmed to discharge mist to cool the parts when the radiometer detects a temperature of 45°C or higher on a part. If the manufactured parts can be approximated as blackbodies, determine the irradiation on the radiometer that should trigger the spray heads to release cooling mist when the temperature is not below 45°C.
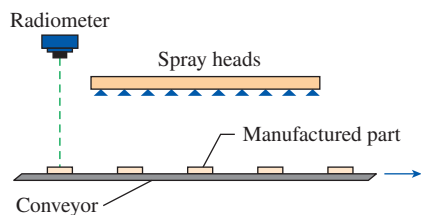
FIGURE P12–68

12–69 [PtD] A long metal bar ($c_p = 450$ J/kg·K, $\rho = 7900$ kg/m^3) is being conveyed through a water bath to be quenched. The metal bar has a cross section of 30 mm × 15 mm,

and it enters the water bath at 700°C. During the quenching process, 500 kW of heat is released from the bar in the water bath. In order to prevent thermal burns to people handling the metal bar, it must exit the water bath at a temperature below 45°C. A radiometer is placed normal to and at a distance of 1 m from the bar to monitor the exit temperature. The radiometer receives radiation from a target area of 1 cm^2 of the bar surface. An irradiation signal detected by the radiometer is used to control the speed of the bar being conveyed through the water bath so that the exit temperature is safe for handling. If the radiometer detects an irradiation of 0.015 W/m^2, determine the speed of the bar being conveyed through the water bath. Assume that the metal bar can be approximated as a blackbody.
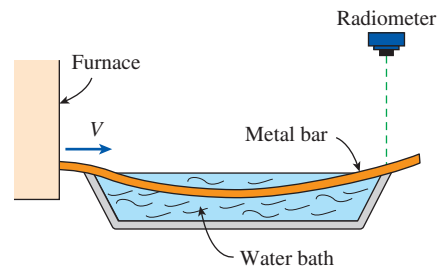
FIGURE P12–69

12–70 [C&S] A radiometer is placed normal to a CPVC pipe at a distance of 1 m to monitor the pipe surface temperature. The radiometer measures an irradiation of 500 μW/m^2 from a target area of 1 mm^2 on the CPVC pipe surface. The ASME Code for Process Piping specifies a maximum use temperature of 93.3°C for CPVC pipe (ASME B31.3-2014, Table A-1M). Determine whether the surface temperature of the CPVC pipe complies with the ASME code.

12–71 [C&S] A radiometer is placed normal to an ASTM A240 410S stainless steel sheet at a distance of 0.7 m to monitor the surface temperature. The maximum use temperature for an ASTM A240 410S stainless steel sheet is 649°C (ASME Code for Process Piping, ASME B31.3-2014, Table A-1M). The stainless steel sheet has an emissivity of 0.4, and an irradiation of 0.2 W/m^2 from a target area of 5 mm^2 is sensed by the radiometer. Determine whether the surface temperature of the stainless steel sheet complies with the ASME code.

Radiation Properties

12–72C What is a graybody? How does it differ from a blackbody? What is a diffuse gray surface?

12–73C Define the properties emissivity and absorptivity. When are these two properties equal to each other?

12–74C Define the properties reflectivity and transmissivity and discus the different forms of reflection.

12–75C What is the greenhouse effect? Why is it a matter of great concern among atmospheric scientists?

12–76C We can see the inside of a microwave oven during operation through its glass door, which indicates that visible

radiation is escaping the oven. Do you think that the harmful microwave radiation might also be escaping?

12–77E A 5-in-diameter spherical ball is known to emit radiation at a rate of 480 Btu/h when its surface temperature is 950 R. Determine the average emissivity of the ball at this temperature.

12–78 A small surface of area $A_1 = 5$ cm² emits radiation as a blackbody at $T_1 = 1000$ K. A radiation sensor of area $A_2 = 3$ cm² is placed normal to the direction of viewing from surface A_1 at a distance L. An optical filter with the following spectral transmissivity is placed in front of the sensor:

$$\tau_\lambda = \begin{cases} \tau_1 = 0, & 0 \le \lambda < 2\ \mu m \\ \tau_2 = 0.5, & 2\ \mu m \le \lambda < \infty \end{cases}$$

If the distance between the radiation sensor and surface A_1 is $L = 0.5$ m, determine the irradiation measured by the sensor.

12–79 [PtD] A tank is filled with chemicals undergoing an exothermic reaction. The reaction heats up the tank wall, and to prevent thermal burn on individuals, the tank's outer surface temperature should be below 45°C. The emissivity of the tank surface is 0.85, and irradiation on the tank surface from the surroundings is estimated to be 390 W/m². A radiometer is placed normal to and at a distance of 0.5 m from the tank surface to monitor the surface temperature. The radiometer receives radiation from a target area of 1 cm² of the tank surface. If the irradiation measured by the radiometer is 0.085 W/m², determine whether or not the tank surface is safe to touch.

12–80 A furnace that has a 40-cm × 40-cm glass window can be considered to be a blackbody at 1200 K. If the transmissivity of the glass is 0.7 for radiation at wavelengths less than 3 μm and zero for radiation at wavelengths greater than 3 μm, determine the fraction and the rate of radiation coming from the furnace and transmitted through the window.

12–81 The spectral emissivity function of an opaque surface at 1000 K is approximated as

$$\varepsilon_\lambda = \begin{cases} \varepsilon_1 = 0.4, & 0 \le \lambda < 3\ \mu m \\ \varepsilon_2 = 0.7, & 3\ \mu m \le \lambda < 6\ \mu m \\ \varepsilon_3 = 0.3, & 6\ \mu m \le \lambda < \infty \end{cases}$$

Determine the average emissivity of the surface and the rate of radiation emission from the surface, in W/m².

12–82 [C&S] The maximum use temperature for an ASTM A240 410S stainless steel plate is 649°C (ASME Code for Process Piping, ASME B31.3-2014, Table A-1M). The plate is treated such that it exhibits the following spectral emissivity:

$$\varepsilon_\lambda = \begin{cases} \varepsilon_1 = 0.8, & 0 \le \lambda < 3.25\ \mu m \\ \varepsilon_2 = 0.6, & 3.25\ \mu m \le \lambda < 10.3\ \mu m \\ \varepsilon_3 = 0.3, & 10.3\ \mu m \le \lambda < \infty \end{cases}$$

Determine the highest rate of radiation emission, in W/m², that the plate can achieve without violating the ASME code.

12–83 [C&S] A carbon steel (ASTM A992) plate has a maximum use temperature of 427°C specified by the

ASME Code for Process Piping (ASME B31.3-2014, Table A-1M). The plate was surface treated such that it exhibits the following spectral reflectivity:

$$\rho_\lambda = \begin{cases} \rho_1 = 0.2, & 0 \le \lambda < 4\ \mu m \\ \rho_2 = 0.5, & 4\ \mu m \le \lambda < 15\ \mu m \\ \rho_3 = 0.8, & 15\ \mu m \le \lambda < \infty \end{cases}$$

Assume the spectral form of Kirchhoff's law applies to the plate. Determine the highest rate of radiation emission, in W/m², that the plate can achieve without violating the ASME code.

12–84 The emissivity of a tungsten filament can be approximated to be 0.5 for radiation at wavelengths less than 1 μm and 0.15 for radiation at greater than 1 μm. Determine the average emissivity of the filament at (a) 1500 K and (b) 2500 K. Also, determine the absorptivity and reflectivity of the filament at both temperatures.

12–85 The variations of the spectral emissivity of two surfaces are as given in Fig. P12–85. Determine the average emissivity of each surface at $T = 3000$ K. Also, determine the average absorptivity and reflectivity of each surface for radiation coming from a source at 3000 K. Which surface is more suitable to serve as a solar absorber?
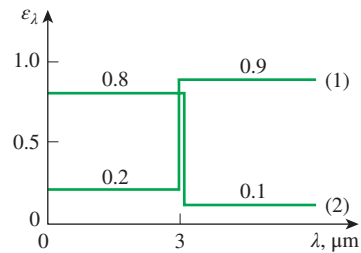
FIGURE P12–85

12–86 The emissivity of a surface coated with aluminum oxide can be approximated to be 0.15 for radiation at wavelengths less than 5 μm and 0.9 for radiation at wavelengths greater than 5 μm. Determine the average emissivity of this surface at (a) 5800 K and (b) 300 K. What can you say about the absorptivity of this surface for radiation coming from sources at 5800 K and 300 K? *Answers: (a) 0.154, (b) 0.89*

12–87 The variation of the spectral absorptivity of a surface is as given in Fig. P12–87. Determine the average absorptivity and reflectivity of the surface for radiation that originates from a source at $T = 2500$ K. Also, determine the average emissivity of this surface at 3000 K.
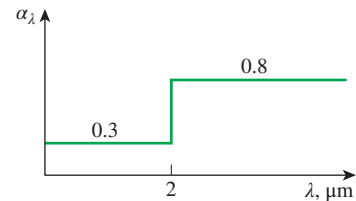
FIGURE P12–87

12–88 The reflectivity of aluminum coated with lead sulfate is 0.35 for radiation at wavelengths less than 3 μm and 0.95 for radiation greater than 3 μm. Determine the average reflectivity of this surface for solar radiation ($T \approx 5800$ K) and radiation coming from surfaces at room temperature ($T \approx 300$ K). Also, determine the emissivity and absorptivity of this surface at both temperatures. Do you think this material is suitable for use in solar collectors?

12–89 [C&S] The maximum use temperature for an ASTM A992 carbon steel plate is 427°C (ASME Code for Process Piping, ASME B31.3-2014, Table A-1M). The plate was surface treated such that it exhibits the following spectral reflectivity:

$$\rho_\lambda = \begin{cases} \rho_1 = 0.45, & 0 \le \lambda < 1 \text{ μm} \\ \rho_2 = 0.65, & 1 \text{ μm} \le \lambda < 6 \text{ μm} \\ \rho_3 = 0.80, & 6 \text{ μm} \le \lambda < \infty \end{cases}$$

Assume the spectral form of Kirchhoff's law applies to the plate. Solar irradiation ($T \approx 5800$ K) on the plate surface is 1000 W/m², and the net radiation heat flux leaving the plate surface is 6000 W/m². Determine whether the carbon steel plate is suitable for the given conditions so that it complies with the ASME code.

12–90 The variation of the spectral transmissivity of a 0.6-cm-thick glass window is as given in Fig. P12–90. Determine the average transmissivity of this window for solar radiation ($T \approx 5800$ K) and radiation coming from surfaces at room temperature ($T \approx 300$ K). Also, determine the amount of solar radiation transmitted through the window for incident solar radiation of 650 W/m². *Answers:* 0.870, 0.00016, 566 W/m²
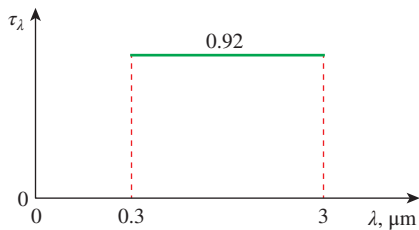
FIGURE P12–90

12–91 Consider an opaque horizontal plate that is well insulated on the edges and the lower surface. The plate is maintained at 500 K, has a total hemispherical absorptivity of 0.51, and has the following spectral emissivity function:

$$\varepsilon_\lambda = \begin{cases} \varepsilon_1 = 0.4, & 0 \le \lambda < 4 \text{ μm} \\ \varepsilon_2 = 0.8, & 4 \text{ μm} \le \lambda < \infty \end{cases}$$

If the plate is subjected to an irradiation of 5600 W/m², determine (*a*) the total hemispherical emissivity and (*b*) the radiosity of the plate surface.

12–92 An opaque horizontal plate is well insulated on the edges and the lower surface. The irradiation on the plate is 3000 W/m², of which 500 W/m² is reflected. The plate has a uniform temperature of 700 K and has an emissive power of 5000 W/m². Determine the total emissivity and absorptivity of the plate.
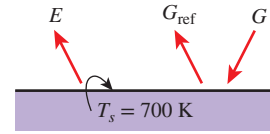
FIGURE P12–92

12–93 Irradiation on a semitransparent medium is at a rate of 520 W/m². If 160 W/m² of the irradiation is reflected from the medium and 130 W/m² is transmitted through the medium, determine the medium's absorptivity, reflectivity, transmissivity, and emissivity.

12–94 Consider an opaque horizontal plate that is well insulated on the edges and the lower surface. The plate is uniformly irradiated from above while air at $T_\infty = 300$ K flows over the surface, providing a uniform convection heat transfer coefficient of 40 W/m²·K. Under steady-state conditions, the surface has a radiosity of 4000 W/m², and the plate temperature is maintained uniformly at 350 K. If the total absorptivity of the plate is 0.40, determine (*a*) the irradiation on the plate, (*b*) the total reflectivity of the plate, (*c*) the emissive power of the plate, and (*d*) the total emissivity of the plate.
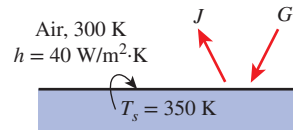
FIGURE P12–94

12–95 Consider an opaque plate that is well insulated on the edges and heated at the bottom with an electric heater. The plate has an emissivity of 0.67 and is situated in an ambient surrounding temperature of 7°C where the natural convection heat transfer coefficient is 7 W/m²·K. To maintain a surface temperature of 80°C, the electric heater supplies 1000 W/m² of uniform heat flux to the plate. Determine the radiosity of the plate under these conditions.

12–96 A horizontal plate is experiencing uniform irradiation on both upper and lower surfaces. The ambient air temperature surrounding the plate is 290 K with a convection heat transfer coefficient of 30 W/m²·K. Both upper and lower surfaces of the plate have a radiosity of 4000 W/m², and the plate temperature is maintained uniformly at 390 K. If the plate is not opaque and has an absorptivity of 0.527, determine the irradiation and emissivity of the plate.
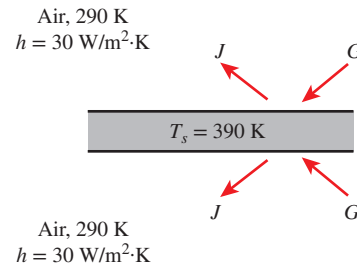
FIGURE P12–96

12–97 A semitransparent plate ($A_1 = 2$ cm^2) has an irradiation of 500 W/m^2, where 30 percent of the irradiation is reflected away from the plate and 50 percent of the irradiation is transmitted through the plate. A radiometer is placed 0.5 m above the plate normal to the direction of viewing from the plate. If the temperature of the plate is uniform at 350 K, determine the irradiation that the radiometer would detect.

Atmospheric and Solar Radiation

12–98C When the earth is closest to the sun, we have winter in the northern hemisphere. Explain why. Also explain why we have summer in the northern hemisphere when the earth is farthest away from the sun.

12–99C Explain why surfaces usually have quite different absorptivities for solar radiation and for radiation originating from the surrounding bodies.

12–100C You have probably noticed warning signs on the highways stating that bridges may be icy even when the roads are not. Explain how this can happen.

12–101C What changes would you notice if the sun emitted radiation at an effective temperature of 2000 K instead of 5762 K?

12–102C What is the solar constant? How is it used to determine the effective surface temperature of the sun? How would the value of the solar constant change if the distance between the earth and the sun doubled?

12–103C Explain why the sky is blue and the sunset is yellow-orange.

12–104C What is the effective sky temperature?

12–105E Solar radiation is incident on the outer surface of a spaceship at a rate of 400 Btu/h·ft^2. The surface has an absorptivity of $\alpha_s = 0.10$ for solar radiation and an emissivity of $\varepsilon = 0.6$ at room temperature. The outer surface radiates heat into space at 0 R. If there is no net heat transfer into the spaceship, determine the equilibrium temperature of the surface. *Answer:* 444 R

12–106 The air temperature on a clear night is observed to remain at about 4°C. Yet water is reported to have frozen that night due to radiation effect. Taking the convection heat transfer coefficient to be 18 W/m^2·K, determine the value of the maximum effective sky temperature that night.

12–107 A surface has an absorptivity of $\alpha_s = 0.72$ for solar radiation and an emissivity of $\varepsilon = 0.6$ at room temperature. The surface temperature is observed to be 350 K when the direct and the diffuse components of solar radiation are $G_D = 350$ and $G_d = 400$ W/m^2, respectively, and the direct radiation makes a 30° angle with the normal of the surface. Taking the effective sky temperature to be 280 K, determine the net rate of radiation heat transfer to the surface at that time.

12–108 The absorber surface of a solar collector is made of aluminum coated with black chrome ($\alpha_s = 0.87$ and $\varepsilon = 0.09$). Solar radiation is incident on the surface at a rate of 720 W/m^2.

The air and the effective sky temperatures are 25°C and 15°C, respectively, and the convection heat transfer coefficient is 10 W/m^2·K. For an absorber surface temperature of 70°C, determine the net rate of solar energy delivered by the absorber plate to the water circulating behind it.
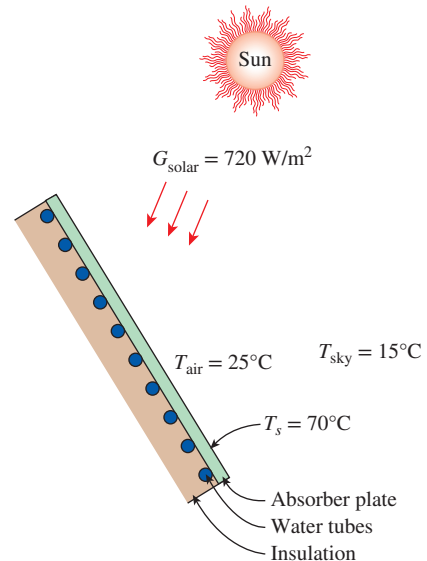
FIGURE P12–108

12–109 Determine the equilibrium temperature of the absorber surface in Prob. 12–108 if the back side of the absorber is insulated.

12–110 Reconsider Prob. 12–108. Using appropriate software, plot the net rate of solar energy transferred to water as a function of the absorptivity of the absorber plate. Let the absorptivity vary from 0.5 to 1.0, and discuss the results.

Special Topic: Solar Heat Gain Through Windows

12–111C What fraction of the solar energy is in the visible range (*a*) outside the earth's atmosphere and (*b*) at sea level on earth? Answer the same question for infrared radiation.

12–112C Describe the solar radiation properties of a window that is ideally suited for minimizing the air-conditioning load.

12–113C What is the effect of a low-e coating on the inner surface of a window glass on the (*a*) heat loss in winter and (*b*) heat gain in summer through the window?

12–114C What is a shading device? Is an internal or external shading device more effective in reducing the solar heat gain through a window? How does the color of the surface of a shading device facing outside affect the solar heat gain?

12–115C What does the SC (shading coefficient) of a device represent? How do the SCs of clear glass and heat-absorbing glass compare?

12–116C Define the SHGC (solar heat gain coefficient), and explain how it differs from the SC (shading coefficient). What are the values of the SHGC and SC of a single-pane clear-glass window?

12–117 Consider a building in New York (40°N latitude) that has 76 m² of window area on its south wall. The windows are double-pane heat-absorbing type and are equipped with light-colored venetian blinds with a shading coefficient of SC = 0.30. Determine the total solar heat gain of the building through the south windows at solar noon in April. What would your answer be if there were no blinds at the windows?
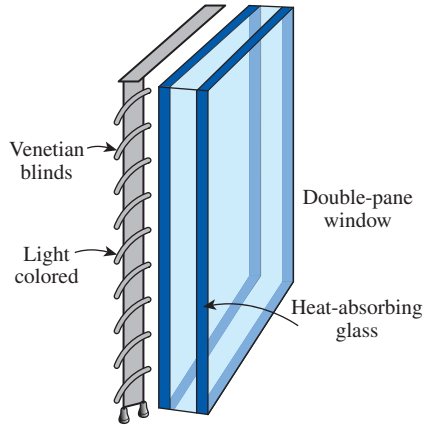
FIGURE P12–117

12–118 A typical winter day in Reno, Nevada (39°N latitude), is cold but sunny, and thus the solar heat gain through the windows can be more than the heat loss through them during daytime. Consider a house with double-door-type windows that are double paned with 3-mm-thick glasses and 6.4 mm of airspace and have aluminum frames and spacers. The house is maintained at 22°C at all times. Determine if the house is losing more or less heat than it is gaining from the sun through an east window on a typical day in January for a 24-h period if the average outdoor temperature is 10°C. *Answer:* less
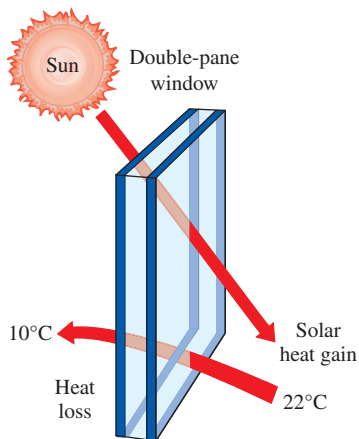
FIGURE P12–118

12–119 Repeat Prob. 12–118 for a south window.

12–120 Consider a building located near 40°N latitude that has equal window areas on all four sides. The building owner is considering coating the south-facing windows with reflective film to reduce the solar heat gain and thus the cooling load. But someone suggests that the owner will reduce the cooling load even more if she coats the west-facing windows instead. What do you think?

12–121E Determine the rate of net heat gain (or loss) through a 9-ft-high, 15-ft-wide, fixed $\frac{1}{8}$-in single-glass window with aluminum frames on the west wall at 3 PM solar time during a typical day in January at a location near 40°N latitude when the indoor and outdoor temperatures are 78°F and 20°F, respectively.

12–122 A manufacturing facility located at 32°N latitude has a glazing area of 60 m² facing west that consists of double-pane windows made of clear glass (SHGC = 0.766). To reduce the solar heat gain in summer, a reflective film that will reduce the SHGC to 0.35 is considered. The cooling season consists of June, July, August, and September, and the heating season is October through April. The average daily solar heat fluxes incident on the west side at this latitude are 2.35, 3.03, 3.62, 4.00, 4.20, 4.24, 4.16, 3.93, 3.48, 2.94, 2.33, and 2.07 kWh/day·m² for January through December, respectively. Also, the unit costs of electricity and natural gas are $0.15/kWh and $0.90/therm, respectively. If the coefficient of performance of the cooling system is 3.2 and the efficiency of the furnace is 0.90, determine the net annual cost savings due to installing reflective coating on the windows. Also, determine the simple payback period if the installation cost of reflective film is $15/m².

12–123 A house located in Boulder, Colorado (40°N latitude), has ordinary double-pane windows with 6-mm-thick glasses, and the total window areas are 8, 6, 6, and 4 m² on the south, west, east, and north walls, respectively. Determine the total solar heat gain of the house at 9:00, 12:00, and 15:00 solar time in July. Also, determine the total amount of solar heat gain per day for an average day in January.

12–124 Repeat Prob. 12–123 for double-pane windows that are gray-tinted.

Review Problems

12–125 A 1-m-diameter spherical cavity is maintained at a uniform temperature of 600 K. Now a 5-mm-diameter hole is drilled. Determine the maximum rate of radiation energy streaming through the hole. What would your answer be if the diameter of the cavity were 3 m?

12–126 Daylight and incandescent light may be approximated as blackbodies at the effective surface temperatures of 5800 K and 2800 K, respectively. Determine the wavelength at maximum emission of radiation for each of the lighting sources.

12–127 The human skin is "selective" when it comes to the absorption of the solar radiation that strikes it perpendicularly. The skin absorbs only 50 percent of the incident radiation with wavelengths between $\lambda_1 = 0.517\,\mu m$ and $\lambda_2 = 1.552\,\mu m$. The radiation with wavelengths shorter than λ_1 and longer than λ_2 is fully absorbed. The solar surface may be modeled as a blackbody with effective surface temperature of 5800 K. Calculate the fraction of the incident solar radiation that is absorbed by the human skin.

12–128 Consider a small black surface of area $A = 3.5\ cm^2$ maintained at 750 K. Determine the rate at which radiation energy is emitted by the surface through a ring-shaped opening defined by $0 \le \phi \le 2\pi$ and $40 \le \theta \le 50°$, where ϕ is the azimuth angle and θ is the angle a radiation beam makes with the normal of the surface.

12–129 A small surface of area $A = 3\ cm^2$ emits radiation with an intensity that can be expressed as $I_e(\theta, \phi) = 100\,\phi \cos\theta$ where I_e has the units of $W/m^2\cdot sr$. Determine the emissive power from the surface into the hemisphere surrounding it and the rate of radiation emission from the surface.

12–130 A radiation sensor and a small surface of area A_1 that emits radiation as a blackbody are oriented as shown in Fig. P12-130. Determine the distance L at which the sensor is measuring two-thirds of the radiation rate emitted from surface A_1 corresponding to the position directly under the sensor at $L = 0$.
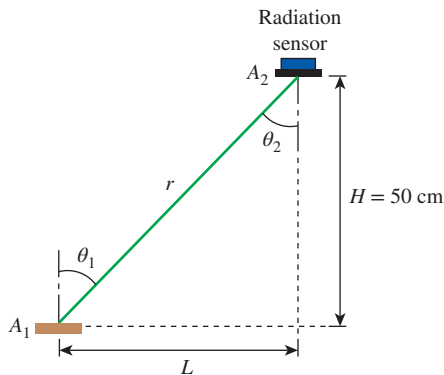
FIGURE P12−130

12–131 The spectral emissivity of an opaque surface at 1200 K is approximated as

$$\varepsilon_1 = 0 \quad \text{for} \quad \lambda < 2\,\mu m$$
$$\varepsilon_2 = 0.85 \quad \text{for} \quad 2 \le \lambda \le 6\,\mu m$$
$$\varepsilon_3 = 0 \quad \text{for} \quad \lambda > 6\,\mu m$$

Determine the total emissivity and the emissive flux of the surface.

12–132 The spectral absorptivity of an opaque surface is as shown in Fig. P12-132. Determine the absorptivity of the surface for radiation emitted by a source at (*a*) 1000 K and (*b*) 3000 K.
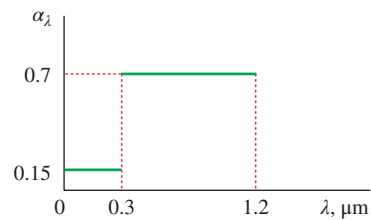
FIGURE P12−132

12–133 The surface in Prob. 12–132 receives solar radiation at a rate of 470 W/m^2. Determine the solar absorptivity of the surface and the rate of absorption of solar radiation.

12–134 The spectral transmissivity of a 3-mm-thick regular glass can be expressed as

$$\tau_1 = 0 \quad \text{for} \quad \lambda < 0.35\,\mu m$$
$$\tau_2 = 0.85 \quad \text{for} \quad 0.35 < \lambda < 2.5\,\mu m$$
$$\tau_3 = 0 \quad \text{for} \quad \lambda > 2.5\,\mu m$$

Determine the transmissivity of this glass for solar radiation. What is the transmissivity of this glass for light?

12–135 The spectral transmissivity of a glass cover used in a solar collector is given as

$$\tau_1 = 0 \quad \text{for} \quad \lambda < 0.3\,\mu m$$
$$\tau_2 = 0.9 \quad \text{for} \quad 0.3 < \lambda < 3\,\mu m$$
$$\tau_3 = 0 \quad \text{for} \quad \lambda > 3\,\mu m$$

Solar radiation is incident at a rate of 950 W/m^2, and the absorber plate, which can be considered to be black, is maintained at 340 K by the cooling water. Determine (*a*) the solar flux incident on the absorber plate, (*b*) the transmissivity of the glass cover for radiation emitted by the absorber plate, and (*c*) the rate of heat transfer to the cooling water if the glass cover temperature is also 340 K.

12–136 A small surface of area $A_1 = 3\ cm^2$ and a radiation sensor of area $A_2 = 1\ cm^2$ are oriented as shown in Fig. P12-136. Surface A_1 is opaque (diffuse emitter and reflector) and maintains a constant temperature of $T_1 = 400$ K. The absorptivity and emissivity of surface A_1 are 0.5 and 0.7, respectively. If surface A_1 is experiencing 2000 W/m^2 of irradiation, determine the rate at which radiation emitted from A_1 is intercepted by the sensor.
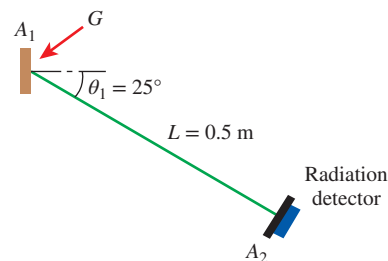
FIGURE P12−136

12–137 Solar radiation is incident on the front surface of a thin plate with direct and diffuse components of 300 and 250 W/m², respectively. The direct radiation makes a 30° angle with the normal of the surface. The plate surfaces have a solar absorptivity of 0.63 and an emissivity of 0.93. The air temperature is 5°C and the convection heat transfer coefficient is 20 W/m²·K. The effective sky temperature for the front surface is −33°C while the surrounding surfaces are at 5°C for the back surface. Determine the equilibrium temperature of the plate.
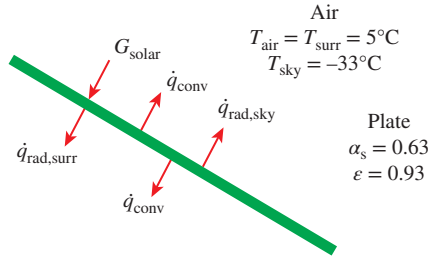
FIGURE P12−137

12–138 A horizontal opaque flat plate is well insulated on the edges and the lower surface. The top surface has an area of 5 m², and it experiences uniform irradiation at a rate of 5000 W. The plate absorbs 4000 W of the irradiation, and the surface is losing heat at a rate of 500 W by convection. If the plate maintains a uniform temperature of 350 K, determine the absorptivity, reflectivity, and emissivity of the plate.
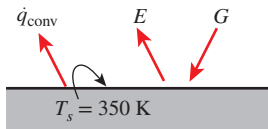
FIGURE P12−138

Fundamentals of Engineering (FE) Exam Problems

12–139 Consider a surface at −10°C in an environment at 25°C. The maximum rate of heat that can be emitted from this surface by radiation is

(a) 152 W/m²   (b) 176 W/m²   (c) 211 W/m²
(d) 271 W/m²   (e) 324 W/m²

12–140 Consider a surface at 900 K. The spectral blackbody emissive power at a wavelength of 50 μm is

(a) 3.2 W/m²·μm   (b) 9.6 W/m²·μm   (c) 24 W/m²·μm
(d) 76 W/m²·μm   (e) 108 W/m²·μm

12–141 The wavelength at which the blackbody emissive power reaches its maximum value at 300 K is

(a) 5.1 μm   (b) 9.7 μm   (c) 15.5 μm
(d) 38.0 μm   (e) 73.1 μm

12–142 A surface absorbs 10 percent of radiation at wavelengths less than 3 μm and 50 percent of radiation at wavelengths greater than 3 μm. The average absorptivity of this surface for radiation emitted by a source at 3000 K is

(a) 0.14   (b) 0.22   (c) 0.30   (d) 0.38   (e) 0.42

12–143 A surface at 300°C has an emissivity of 0.7 in the wavelength range of $0 - 4.4$ μm and 0.3 over the rest of the wavelength range. At a temperature of 300°C, 19 percent of the blackbody emissive power is in the wavelength range up to 4.4 μm. The total emissivity of this surface is

(a) 0.300 (b) 0.376 (c) 0.624 (d) 0.700 (e) 0.500

12–144 Consider a 4-cm-diameter and 6-cm-long cylindrical rod at 1200 K. If the emissivity of the rod surface is 0.75, the total amount of radiation emitted by all surfaces of the rod in 20 min is

(a) 88 kJ   (b) 118 kJ   (c) 6661 kJ
(d) 1064 kJ   (e) 1418 kJ

12–145 Solar radiation is incident on a semitransparent body at a rate of 500 W/m². If 150 W/m² of this incident radiation is reflected back and 225 W/m² is transmitted across the body, the absorptivity of the body is

(a) 0   (b) 0.25   (c) 0.30   (d) 0.45   (e) 1

12–146 Solar radiation is incident on an opaque surface at a rate of 400 W/m². The emissivity of the surface is 0.65 and the absorptivity to solar radiation is 0.85. The convection coefficient between the surface and the environment at 25°C is 6 W/m²·K. If the surface is exposed to atmosphere with an effective sky temperature of 250 K, the equilibrium temperature of the surface is

(a) 281 K   (b) 298 K   (c) 303 K   (d) 317 K   (e) 339 K

12–147 A surface is exposed to solar radiation. The direct and diffuse components of solar radiation are 480 and 250 W/m², and the direct radiation makes a 35° angle with the normal of the surface. The solar absorptivity and the emissivity of the surface are 0.24 and 0.41, respectively. If the surface is observed to be at 315 K and the effective sky temperature is 256 K, the net rate of radiation heat transfer to the surface is

(a) −79 W/m²   (b) −22 W/m²   (c) 25 W/m²
(d) 154 W/m²   (e) 643 W/m²

Design and Essay Problems

12–148 Write an essay on the radiation properties of selective surfaces used on the absorber plates of solar collectors. Find out about the various kinds of such surfaces, and discuss the performance and cost of each type. Recommend a selective surface that optimizes cost and performance.

12–149 According to an Atomic Energy Commission report, a hydrogen bomb can be approximated as a large fireball at a temperature of 7200 K. You are to assess the impact if such a bomb exploded 5 km above a city. Assume the diameter of the fireball to be 1 km and the blast to last 15 s. Investigate the level of radiation energy people, plants, and houses will be exposed to, and how adversely they will be affected by the blast.

CHAPTER

13

RADIATION HEAT TRANSFER

I n Chap. 12, we considered the fundamental aspects of radiation and the radiation properties of surfaces. We are now in a position to consider radiation exchange between two or more surfaces, which is the primary quantity of interest in most radiation problems.

We start this chapter with a discussion of view factors and the rules associated with them. View factor expressions and charts for some common configurations are given, and the crossed-strings method is presented. We then discuss radiation heat transfer, first between black surfaces and then between nonblack surfaces using the radiation network approach. We continue with radiation shields and discuss the radiation effect on temperature measurements and comfort. Finally, we consider gas radiation, and discuss the effective emissivities and absorptivities of gas bodies of various shapes. We also discuss radiation exchange between the walls of combustion chambers and the high-temperature emitting and absorbing combustion gases inside.

OBJECTIVES

When you finish studying this chapter, you should be able to:

- Define view factor, and understand its importance in radiation heat transfer calculations,

- Develop view factor relations, and calculate the unknown view factors in an enclosure by using these relations,

- Calculate radiation heat transfer between black surfaces,

- Determine radiation heat transfer between diffuse and gray surfaces in an enclosure using the concept of radiosity,

- Obtain relations for net rate of radiation heat transfer between the surfaces of a two-zone enclosure, including two large parallel plates, two long concentric cylinders, and two concentric spheres,

- Quantify the effect of radiation shields on the reduction of radiation heat transfer between two surfaces, and become aware of the importance of radiation effect in temperature measurements.
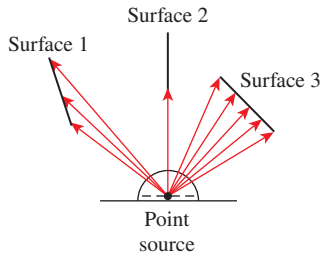
FIGURE 13–1
Radiation heat exchange between surfaces depends on the *orientation* of the surfaces relative to each other, and this dependence on orientation is accounted for by the *view factor.*

FIGURE 13–2
Geometry for the determination of the view factor between two surfaces.

13−1 ■ THE VIEW FACTOR

Radiation heat transfer between surfaces depends on the *orientation* of the surfaces relative to each other as well as their radiation properties and temperatures, as illustrated in Fig. 13–1. For example, a camper can make the most use of a campfire on a cold night by standing as close to the fire as possible and by blocking as much of the radiation coming from the fire by turning his or her front to the fire instead of the side. Likewise, a person can maximize the amount of solar radiation incident on him or her and take a sunbath by lying down on his or her back instead of standing.

To account for the effects of orientation on radiation heat transfer between two surfaces, we define a new parameter called the *view factor,* which is a purely geometric quantity and is independent of the surface properties and temperature. It is also called the *shape factor, configuration factor,* and *angle factor.* The view factor based on the assumption that the surfaces are diffuse emitters and diffuse reflectors is called the *diffuse view factor,* and the view factor based on the assumption that the surfaces are diffuse emitters but specular reflectors is called the *specular view factor.* In this book, we consider radiation exchange between diffuse surfaces only, and thus the term *view factor* simply means *diffuse view factor.*

The view factor from a surface i to a surface j is denoted by $F_{i \to j}$ or just F_{ij}, and is defined as

F_{ij} = *the fraction of the radiation leaving surface i that strikes surface j directly*

The notation $F_{i \to j}$ is instructive for beginners, since it emphasizes that the view factor is for radiation that travels from surface i to surface j. However, this notation becomes rather awkward when it has to be used many times in a problem. In such cases, it is convenient to replace it with its *shorthand* version F_{ij}.

The view factor F_{12} represents the fraction of radiation leaving surface 1 that strikes surface 2 directly, and F_{21} represents the fraction of radiation leaving surface 2 that strikes surface 1 directly. Note that the radiation that strikes a surface does not need to be absorbed by that surface. Also, radiation that strikes a surface after being reflected by other surfaces is not considered in the evaluation of view factors.

To develop a general expression for the view factor, consider two differential surfaces dA_1 and dA_2 on two arbitrarily oriented surfaces A_1 and A_2, respectively, as shown in Fig. 13–2. The distance between dA_1 and dA_2 is r, and the angles between the normals of the surfaces and the line that connects dA_1 and dA_2 are θ_1 and θ_2, respectively. Surface 1 emits and reflects radiation diffusely in all directions with a constant intensity of I_1, and the solid angle subtended by dA_2 when viewed by dA_1 is $d\omega_{21}$.

The rate at which radiation leaves dA_1 in the direction of θ_1 is $I_1 \cos \theta_1 dA_1$. Noting that $d\omega_{21} = dA_2 \cos \theta_2 / r^2$, the portion of this radiation that strikes dA_2 is

$$\dot{Q}_{dA_1 \to dA_2} = I_1 \cos \theta_1 \, dA_1 \, d\omega_{21} = I_1 \cos \theta_1 \, dA_1 \frac{dA_2 \cos \theta_2}{r^2} \quad \textbf{(13–1)}$$

The total rate at which radiation leaves dA_1 (via emission and reflection) in all directions is the radiosity (which is $J_1 = \pi I_1$) times the surface area,

$$\dot{Q}_{dA_1} = J_1 \, dA_1 = \pi I_1 \, dA_1 \quad \textbf{(13–2)}$$
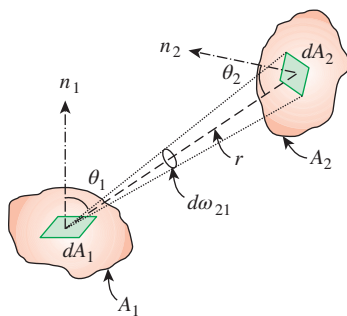
Then the *differential view factor* $dF_{dA_1 \to dA_2}$, which is the fraction of radiation leaving dA_1 that strikes dA_2 directly, becomes

$$dF_{dA_1 \to dA_2} = \frac{\dot{Q}_{dA_1 \to dA_2}}{\dot{Q}_{dA_1}} = \frac{\cos\theta_1 \cos\theta_2}{\pi r^2} dA_2 \qquad \text{(13–3)}$$

The differential view factor $dF_{dA_2 \to dA_1}$ can be determined from Eq. 13–3 by interchanging the subscripts 1 and 2.

The view factor from a differential area dA_1 to a finite area A_2 can be determined from the fact that the fraction of radiation leaving dA_1 that strikes A_2 is the sum of the fractions of radiation striking the differential areas dA_2. Therefore, the view factor $F_{dA_1 \to A_2}$ is determined by integrating $dF_{dA_1 \to dA_2}$ over A_2,

$$F_{dA_1 \to A_2} = \int_{A_2} \frac{\cos\theta_1 \cos\theta_2}{\pi r^2} dA_2 \qquad \text{(13–4)}$$

The total rate at which radiation leaves the entire area A_1 (via emission and reflection) in all directions is

$$\dot{Q}_{A_1} = J_1 A_1 = \pi I_1 A_1 \qquad \text{(13–5)}$$

The portion of this radiation that strikes dA_2 is determined by considering the radiation that leaves dA_1 and strikes dA_2 (given by Eq. 13–1), and integrating it over A_1,

$$\dot{Q}_{A_1 \to dA_2} = \int_{A_1} \dot{Q}_{dA_1 \to dA_2} = \int_{A_1} \frac{I_1 \cos\theta_1 \cos\theta_2 \, dA_2}{r^2} dA_1 \qquad \text{(13–6)}$$

Integration of this relation over A_2 gives the radiation that strikes the entire area A_2,

$$\dot{Q}_{A_1 \to A_2} = \int_{A_2} \dot{Q}_{A_1 \to dA_2} = \int_{A_2}\int_{A_1} \frac{I_1 \cos\theta_1 \cos\theta_2}{r^2} dA_1 \, dA_2 \qquad \text{(13–7)}$$

Dividing this by the total radiation leaving A_1 (from Eq. 13–5) gives the fraction of radiation leaving A_1 that strikes A_2, which is the view factor $F_{A_1 \to A_2}$ (or F_{12} for short),

$$F_{12} = F_{A_1 \to A_2} = \frac{\dot{Q}_{A_1 \to A_2}}{\dot{Q}_{A_1}} = \frac{1}{A_1}\int_{A_2}\int_{A_1} \frac{\cos\theta_1 \cos\theta_2}{\pi r^2} dA_1 \, dA_2 \qquad \text{(13–8)}$$

The view factor $F_{A_2 \to A_1}$ is readily determined from Eq. 13–8 by interchanging the subscripts 1 and 2,

$$F_{21} = F_{A_2 \to A_1} = \frac{\dot{Q}_{A_2 \to A_1}}{\dot{Q}_{A_2}} = \frac{1}{A_2}\int_{A_2}\int_{A_1} \frac{\cos\theta_1 \cos\theta_2}{\pi r^2} dA_1 \, dA_2 \qquad \text{(13–9)}$$

Note that I_1 is constant but $r, \theta_1,$ and θ_2 are variables. Also, integrations can be performed in any order since the integration limits are constants. These relations confirm that the view factor between two surfaces depends on their relative orientation and the distance between them.

(a) Plane surface

$F_{1 \to 1} = 0$

(b) Convex surface

$F_{2 \to 2} = 0$

(c) Concave surface

$F_{3 \to 3} \neq 0$
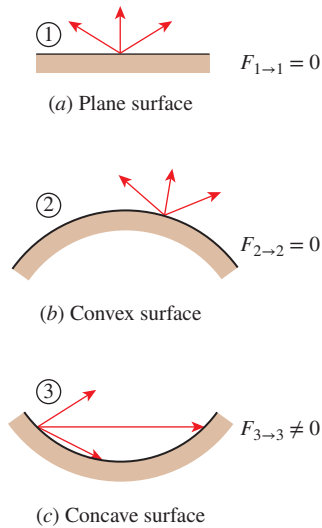
FIGURE 13–3

The view factor from a surface to itself is *zero* for *plane* or *convex* surfaces and *nonzero* for *concave* surfaces.

Outer sphere

②

Inner sphere

①
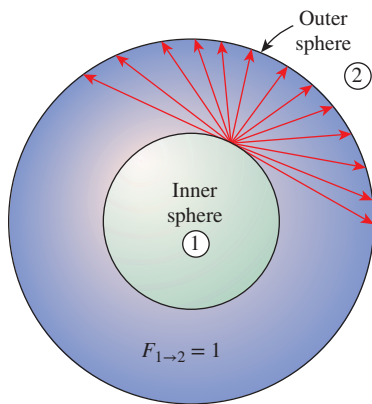
$F_{1 \to 2} = 1$

FIGURE 13–4

In a geometry that consists of two concentric spheres, the view factor $F_{1 \to 2} = 1$ since all radiation leaving the surface of the smaller sphere is intercepted by the larger sphere.

Combining Eqs. 13–8 and 13–9 after multiplying the former by A_1 and the latter by A_2 gives

$$A_1 F_{12} = A_2 F_{21} \qquad \text{(13–10)}$$

which is known as the **reciprocity relation** for view factors. It allows the calculation of a view factor from a knowledge of the other.

The view factor relations developed above are applicable to any two surfaces i and j provided that the surfaces are diffuse emitters and diffuse reflectors (so that the assumption of constant intensity is valid). For the special case of $j = i$, we have

$F_{i \to i}$ = *the fraction of radiation leaving surface i that strikes itself directly*

Noting that in the absence of strong electromagnetic fields radiation beams travel in straight paths, the view factor from a surface to itself is zero unless the surface "sees" itself. Therefore, $F_{i \to i} = 0$ for *plane* or *convex* surfaces and $F_{i \to i} \neq 0$ for concave surfaces, as illustrated in Fig. 13–3.
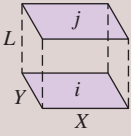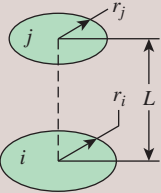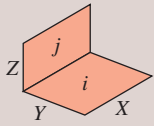
The value of the view factor ranges between *zero* and *one.* The limiting case $F_{i \to i} = 0$ indicates that the two surfaces do not have a direct view of each other, and thus radiation leaving surface i cannot strike surface j directly. The other limiting case $F_{i \to j} = 1$ indicates that surface j completely surrounds surface $i,$ so all radiation leaving surface i is intercepted by surface j. For example, in a geometry consisting of two concentric spheres, all radiation leaving the surface of the smaller sphere (surface 1) strikes the larger sphere (surface 2), and thus $F_{1 \to 2} = 1$, as illustrated in Fig. 13–4.

The view factor has proven to be very useful in radiation analysis because it allows us to express the *fraction of radiation* leaving a surface that strikes another surface in terms of the orientation of these two surfaces relative to each other. The underlying assumption in this process is that the radiation a surface receives from a source is directly proportional to the angle the surface subtends when viewed from the source. This would be the case only if the radiation coming off the source is *uniform* in all directions throughout its surface and the medium between the surfaces does not *absorb, emit,* or *scatter* radiation. That is, it is the case when the surfaces are *isothermal* and *diffuse* emitters and reflectors and the surfaces are separated by a *nonparticipating* medium such as a vacuum or air.

The view factor $F_{1 \to 2}$ between two surfaces A_1 and A_2 can be determined in a systematic manner first by expressing the view factor between two differential areas dA_1 and dA_2 in terms of the spatial variables and then by performing the necessary integrations. However, this approach is not practical, since even for simple geometries the resulting integrations are usually very complex and difficult to perform.

View factors for hundreds of common geometries are evaluated and the results given in analytical, graphical, and tabular form in several publications. Early tables and charts for simple configurations were given by Hamilton and Morgan (1952). Fairly extensive tabulations were given in the books by Siegel and Howell (2002) and Modest (2003). Siegel and Howell (2002) also give an exhaustive listing of sources for more involved view factors. The most complete tabulation is given in a catalog by Howell (1982). Some of the
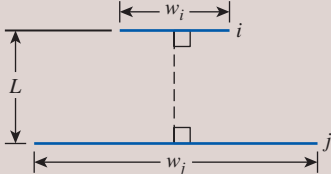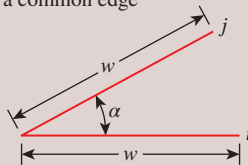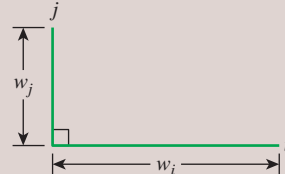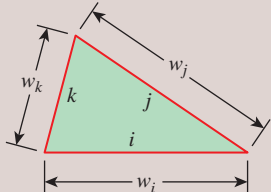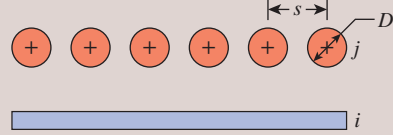
view factor expressions that appear in heat transfer books and catalogs are very difficult to use. Thyageswaran (2017) has derived an exact, closed-form and easy-to–use analytical expression to simplify view factor calculations for radiation exchange between a pair of directly opposed, unequal rectangles in parallel planes. View factors for selected geometries are given in Tables 13–1 and 13–2 in *analytical* form and in Figs. 13–5 to 13–8 in *graphical* form. The view factors in Table 13–1 are for three-dimensional geometries. The view factors in Table 13–2, on the other hand, are for geometries that are *infinitely long* in the direction perpendicular to the plane of the paper and are therefore two-dimensional.

TABLE 13–1

View factor expressions for some common geometries of finite size (3-D)

Geometry	Relation
Aligned parallel rectangles	$\overline{X} = X/L$ and $\overline{Y} = Y/L$ $F_{i \to j} = \dfrac{2}{\pi \overline{X} \overline{Y}} \left\{ \ln \left[\dfrac{(1 + \overline{X}^2)(1 + \overline{Y}^2)}{1 + \overline{X}^2 + \overline{Y}^2} \right]^{1/2} + \overline{X}(1 + \overline{Y}^2)^{1/2} \tan^{-1} \dfrac{\overline{X}}{(1 + \overline{Y}^2)^{1/2}} \right.$ $\left. + \overline{Y}(1 + \overline{X}^2)^{1/2} \tan^{-1} \dfrac{\overline{Y}}{(1 + \overline{X}^2)^{1/2}} - \overline{X} \tan^{-1} \overline{X} - \overline{Y} \tan^{-1} \overline{Y} \right\}$
Coaxial parallel disks	$R_i = r_i/L$ and $R_j = r_j/L$ $S = 1 + \dfrac{1 + R_j^2}{R_i^2}$ $F_{i \to j} = \dfrac{1}{2} \left\{ S - \left[S^2 - 4 \left(\dfrac{r_j}{r_i} \right)^2 \right]^{1/2} \right\}$ For $r_i = r_j = r$ and $R = r/L$: $\quad F_{i \to j} = F_{j \to i} = 1 + \dfrac{1 - \sqrt{4R^2 + 1}}{2R^2}$
Perpendicular rectangles with a common edge	$H = Z/X$ and $W = Y/X$ $F_{i \to j} = \dfrac{1}{\pi W} \left(W \tan^{-1} \dfrac{1}{W} + H \tan^{-1} \dfrac{1}{H} - (H^2 + W^2)^{1/2} \tan^{-1} \dfrac{1}{(H^2 + W^2)^{1/2}} \right.$ $+ \dfrac{1}{4} \ln \left\{ \dfrac{(1 + W^2)(1 + H^2)}{1 + W^2 + H^2} \left[\dfrac{W^2(1 + W^2 + H^2)}{(1 + W^2)(W^2 + H^2)} \right]^{W^2} \right.$ $\left. \left. \times \left[\dfrac{H^2(1 + H^2 + W^2)}{(1 + H^2)(H^2 + W^2)} \right]^{H^2} \right\} \right)$

TABLE 13–2

View factor expressions for some infinitely long (2-D) geometries

Geometry	Relation
Parallel plates with midlines connected by perpendicular line	$W_i = w_i/L$ and $W_j = w_j/L$ $F_{i \to j} = \dfrac{[(W_i + W_j)^2 + 4]^{1/2} - [(W_j - W_i)^2 + 4]^{1/2}}{2W_i}$
Inclined plates of equal width and with a common edge	$F_{i \to j} = 1 - \sin \dfrac{1}{2}\alpha$
Perpendicular plates with a common edge	$F_{i \to j} = \dfrac{1}{2} \left\{ 1 + \dfrac{w_j}{w_i} - \left[1 + \left(\dfrac{w_j}{w_i} \right)^2 \right]^{1/2} \right\}$
Three-sided enclosure	$F_{i \to j} = \dfrac{w_i + w_j - w_k}{2w_i}$
Infinite plane and row of cylinders	$F_{i \to j} = 1 - \left[1 - \left(\dfrac{D}{s} \right)^2 \right]^{1/2}$ $\qquad + \dfrac{D}{s} \tan^{-1} \left(\dfrac{s^2 - D^2}{D^2} \right)^{1/2}$

13–2 ▪ VIEW FACTOR RELATIONS

Radiation analysis on an enclosure consisting of N surfaces requires the evaluation of N^2 view factors, and this evaluation process is probably the most time-consuming part of a radiation analysis. However, it is neither practical nor necessary to evaluate all of the view factors directly. Once a sufficient
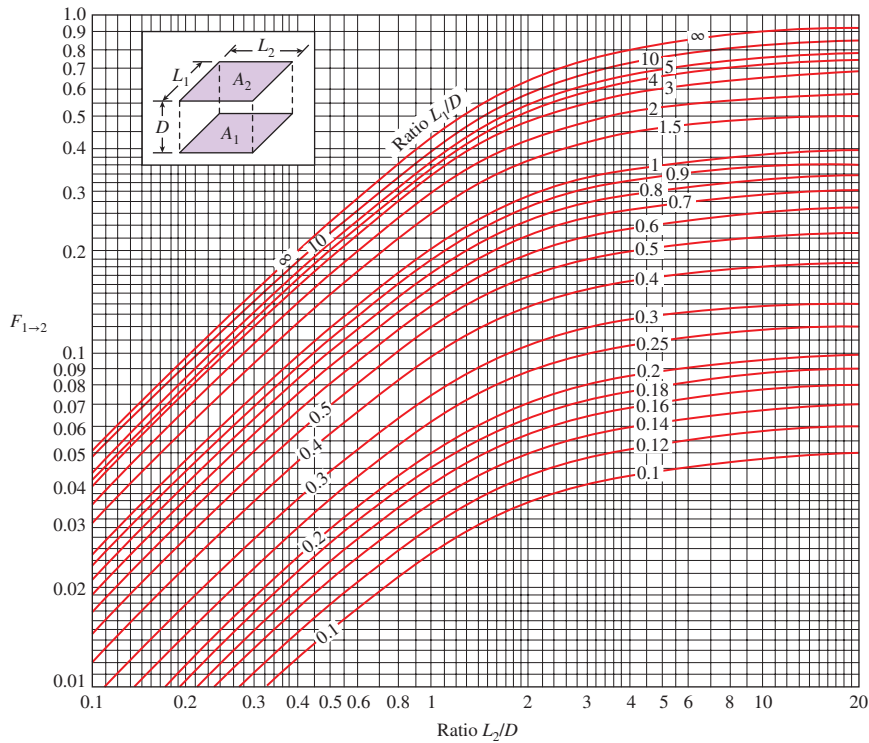
FIGURE 13–5
View factor between two aligned parallel rectangles of equal size.
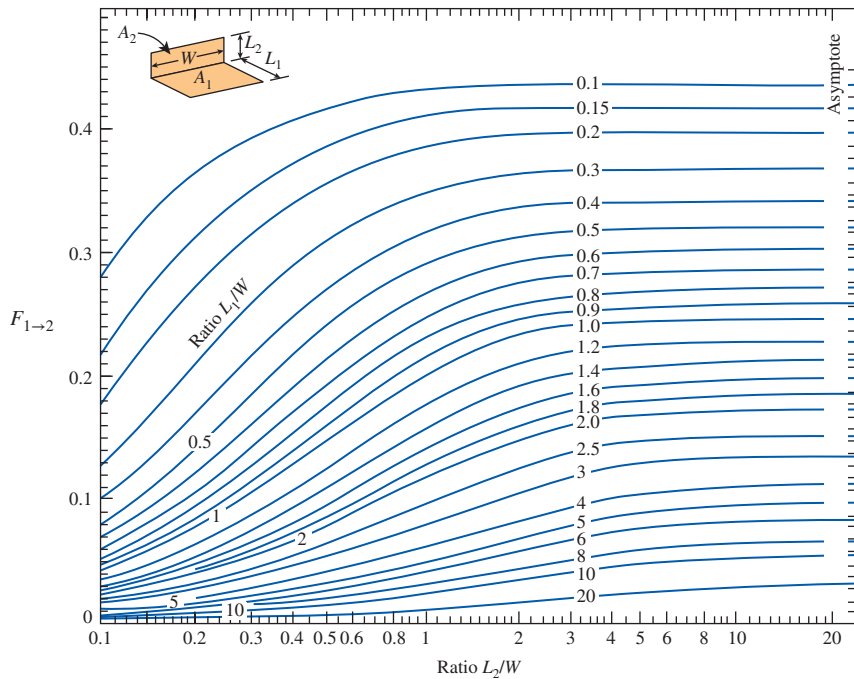
FIGURE 13–6
View factor between two perpendicular rectangles with a common edge.
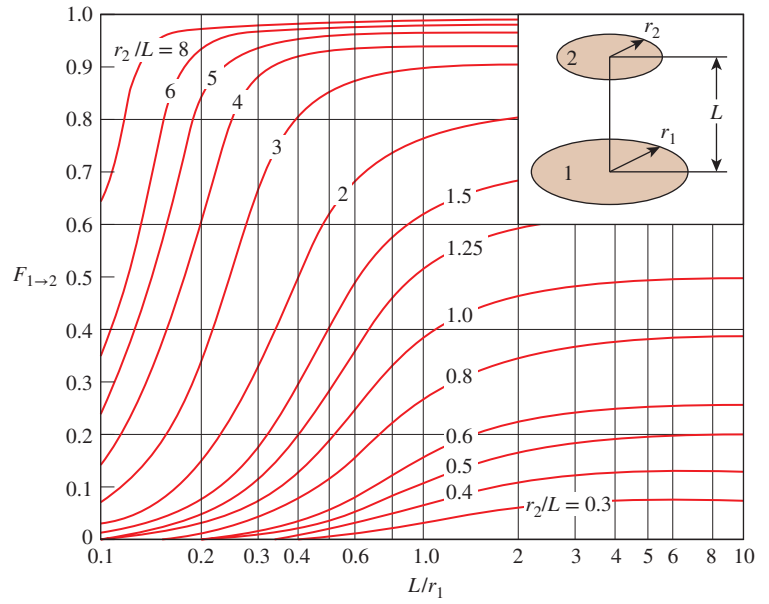
FIGURE 13–7
View factor between two coaxial parallel disks.
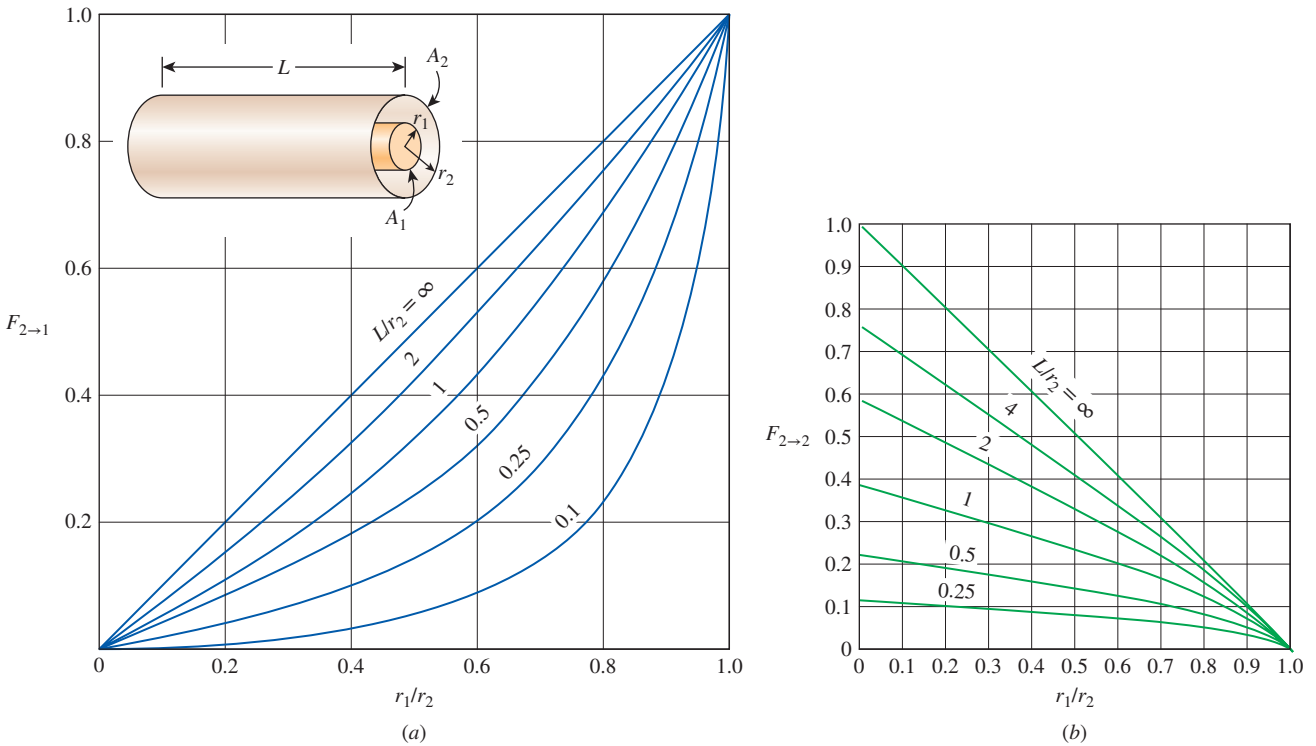
FIGURE 13–8
View factors for two concentric cylinders of finite length: (*a*) outer cylinder to inner cylinder; (*b*) outer cylinder to itself.

number of view factors are available, the rest of them can be determined by utilizing some fundamental relations for view factors, as discussed next.

1   The Reciprocity Relation

The view factors $F_{i \to j}$ and $F_{j \to i}$ are *not* equal to each other unless the areas of the two surfaces are. That is,

$$F_{j \to i} = F_{i \to j} \quad \text{when} \quad A_i = A_j$$
$$F_{j \to i} \neq F_{i \to j} \quad \text{when} \quad A_i \neq A_j$$

We have shown earlier that the pair of view factors $F_{i \to j}$ and $F_{j \to i}$ are related to each other by

$$A_i F_{i \to j} = A_j F_{j \to i} \tag{13–11}$$

This relation is referred to as the **reciprocity relation** or the **reciprocity rule**, and it enables us to determine the counterpart of a view factor from a knowledge of the view factor itself and the areas of the two surfaces. When determining the pair of view factors $F_{i \to j}$ and $F_{j \to i}$, it makes sense to evaluate first the easier one directly and then the more difficult one by applying the reciprocity relation.

2   The Summation Rule

The radiation analysis of a surface normally requires the consideration of the radiation coming in or going out in all directions. Therefore, most radiation problems encountered in practice involve enclosed spaces. When formulating a radiation problem, we usually form an *enclosure* consisting of the surfaces interacting radiatively. Even openings are treated as imaginary surfaces with radiation properties equivalent to those of the opening.

The conservation of energy principle requires that the entire radiation leaving any surface i of an enclosure be intercepted by the surfaces of the enclosure. Therefore, *the sum of the view factors from surface i of an enclosure to all surfaces of the enclosure, including to itself, must equal unity.* This is known as the **summation rule** for an enclosure and is expressed as (Fig. 13–9)

$$\sum_{j=1}^{N} F_{i \to j} = 1 \tag{13–12}$$

where N is the number of surfaces of the enclosure. For example, applying the summation rule to surface 1 of a three-surface enclosure yields

$$\sum_{j=1}^{3} F_{1 \to j} = F_{1 \to 1} + F_{1 \to 2} + F_{1 \to 3} = 1$$

The summation rule can be applied to each surface of an enclosure by varying i from 1 to N. Therefore, the summation rule applied to each of the N surfaces of an enclosure gives N relations for the determination of the view factors. Also, the reciprocity rule gives $\frac{1}{2}N(N-1)$ additional relations. Then the total number of view factors that need to be evaluated directly for an N-surface enclosure becomes

$$N^2 - [N + \tfrac{1}{2}N(N-1)] = \tfrac{1}{2}N(N-1)$$
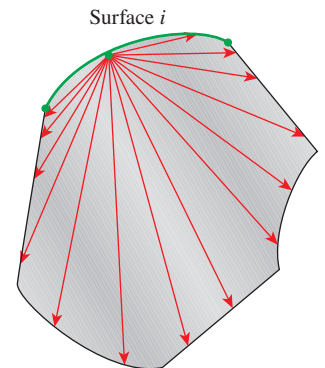
FIGURE 13–9

Radiation leaving any surface i of an enclosure must be intercepted completely by the surfaces of the enclosure. Therefore, the sum of the view factors from surface i to each one of the surfaces of the enclosure must be unity.

For example, for a six-surface enclosure, we need to determine only $\frac{1}{2} \times 6\,(6-1) = 15$ of the $6^2 = 36$ view factors directly. The remaining 21 view factors can be determined from the 21 equations that are obtained by applying the reciprocity and the summation rules.
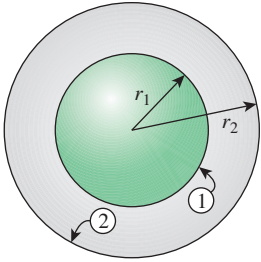
FIGURE 13–10
The geometry considered in
Example 13–1.

EXAMPLE 13–1   **View Factors Associated with Two Concentric Spheres**

Determine the view factors associated with an enclosure formed by two concentric spheres, shown in Fig. 13–10.

SOLUTION   The view factors associated with two concentric spheres are to be determined.
Assumptions   The surfaces are diffuse emitters and reflectors.
Analysis   The outer surface of the smaller sphere (surface 1) and the inner surface of the larger sphere (surface 2) form a two-surface enclosure. Therefore, $N = 2$, and this enclosure involves $N^2 = 2^2 = 4$ view factors, which are F_{11}, F_{12}, F_{21}, and F_{22}. In this two-surface enclosure, we need to determine only

$$\tfrac{1}{2}N(N-1) = \tfrac{1}{2} \times 2(2-1) = 1$$

view factor directly. The remaining three view factors can be determined by the application of the summation and reciprocity rules. But it turns out that we can determine not only one but *two* view factors directly in this case by a simple *inspection:*

$$F_{11} = 0, \qquad \text{since no radiation leaving surface 1 strikes itself}$$
$$F_{12} = 1, \qquad \text{since all radiation leaving surface 1 strikes surface 2}$$

Actually it would be sufficient to determine only one of these view factors by inspection, since we could always determine the other one from the summation rule applied to surface 1 as $F_{11} + F_{12} = 1$.

The view factor F_{21} is determined by applying the reciprocity relation to surfaces 1 and 2:

$$A_1 F_{12} = A_2 F_{21}$$

which yields

$$F_{21} = \frac{A_1}{A_2} F_{12} = \frac{4\pi r_1^2}{4\pi r_2^2} \times 1 = \left(\frac{r_1}{r_2}\right)^2$$

Finally, the view factor F_{22} is determined by applying the summation rule to surface 2:

$$F_{21} + F_{22} = 1$$

and thus

$$F_{22} = 1 - F_{21} = 1 - \left(\frac{r_1}{r_2}\right)^2$$

Discussion   Note that when the outer sphere is much larger than the inner sphere $(r_2 \gg r_1)$, F_{22} approaches one. This is expected, since the fraction of radiation leaving the outer sphere that is intercepted by the inner sphere will be negligible in that case. Also note that the two spheres considered above do not need to be concentric. However, the radiation analysis will be most accurate for the case of concentric spheres, since the radiation is most likely to be uniform on the surfaces in that case.

$$F_{1 \to (2,3)} = F_{1 \to 2} + F_{1 \to 3}$$

FIGURE 13–11

The view factor from a surface to a composite surface is equal to the sum of the view factors from the surface to the parts of the composite surface.

3 The Superposition Rule

Sometimes the view factor associated with a given geometry is not available in standard tables and charts. In such cases, it is desirable to express the given geometry as the sum or difference of some geometries with known view factors, and then to apply the **superposition rule**, which can be expressed as *the view factor from a surface i to a surface j is equal to the sum of the view factors from surface i to the parts of surface j.* Note that the reverse of this is not true. That is, the view factor from a surface *j* to a surface *i* is *not* equal to the sum of the view factors from the parts of surface *j* to surface *i*.

Consider the geometry in Fig. 13–11, which is infinitely long in the direction perpendicular to the plane of the paper. The radiation that leaves surface 1 and strikes the combined surfaces 2 and 3 is equal to the sum of the radiation that strikes surfaces 2 and 3. Therefore, the view factor from surface 1 to the combined surfaces of 2 and 3 is

$$F_{1 \to (2, 3)} = F_{1 \to 2} + F_{1 \to 3} \qquad \textbf{(13–13)}$$

Suppose we need to find the view factor $F_{1 \to 3}$. A quick check of the view factor expressions and charts in this section reveals that such a view factor cannot be evaluated directly. However, the view factor $F_{1 \to 3}$ can be determined from Eq. 13–13 after determining both $F_{1 \to 2}$ and $F_{1 \to (2, 3)}$ from the chart in Table 13–2. Therefore, it may be possible to determine some difficult view factors with relative ease by expressing one or both of the areas as the sum or differences of areas and then applying the superposition rule.

To obtain a relation for the view factor $F_{(2, 3) \to 1}$, we multiply Eq. 13–13 by A_1,

$$A_1 F_{1 \to (2, 3)} = A_1 F_{1 \to 2} + A_1 F_{1 \to 3}$$

and apply the reciprocity relation to each term to get

$$(A_2 + A_3)F_{(2, 3) \to 1} = A_2 F_{2 \to 1} + A_3 F_{3 \to 1}$$

or

$$F_{(2, 3) \to 1} = \frac{A_2 F_{2 \to 1} + A_3 F_{3 \to 1}}{A_2 + A_3} \qquad \textbf{(13–14)}$$

Areas that are expressed as the sum of more than two parts can be handled in a similar manner.

■ *EXAMPLE 13–2*   **Fraction of Radiation Leaving Through an Opening**

Determine the fraction of the radiation leaving the base of the cylindrical enclosure shown in Fig. 13–12 that escapes through a coaxial ring opening at its top surface. The radius and the length of the enclosure are $r_1 = 10$ cm and $L = 10$ cm, while the inner and outer radii of the ring are $r_2 = 5$ cm and $r_3 = 8$ cm, respectively.
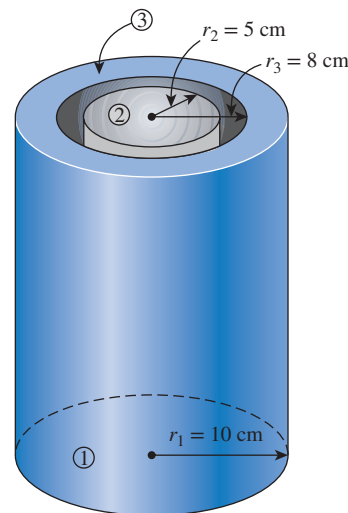
FIGURE 13–12

The cylindrical enclosure considered in Example 13–2.

SOLUTION The fraction of radiation leaving the base of a cylindrical enclosure through a coaxial ring opening at its top surface is to be determined.

Assumptions The base surface is a diffuse emitter and reflector.

Analysis We are asked to determine the fraction of the radiation leaving the base of the enclosure that escapes through an opening at the top surface. Actually, what we are asked to determine is simply the *view factor $F_{1 \to \text{ring}}$* from the base of the enclosure to the ring-shaped surface at the top.

We do not have an analytical expression or chart for view factors between a circular area and a coaxial ring, and so we cannot determine $F_{1 \to \text{ring}}$ directly. However, we do have a chart for view factors between two coaxial parallel disks, and we can always express a ring in terms of disks.

Let the base surface of radius $r_1 = 10$ cm be surface 1, the circular area of $r_2 = 5$ cm at the top be surface 2, and the circular area of $r_3 = 8$ cm be surface 3. Using the superposition rule, the view factor from surface 1 to surface 3 can be expressed as

$$F_{1 \to 3} = F_{1 \to 2} + F_{1 \to \text{ring}}$$

since surface 3 is the sum of surface 2 and the ring area. The view factors $F_{1 \to 2}$ and $F_{1 \to 3}$ are determined from the chart in Fig. 13–7.

$$\frac{L}{r_1} = \frac{10 \text{ cm}}{10 \text{ cm}} = 1 \quad \text{and} \quad \frac{r_2}{L} = \frac{5 \text{ cm}}{10 \text{ cm}} = 0.5 \xrightarrow{\text{(Fig. 13–7)}} = 0.11$$

$$\frac{L}{r_1} = \frac{10 \text{ cm}}{10 \text{ cm}} = 1 \quad \text{and} \quad \frac{r_3}{L} = \frac{8 \text{ cm}}{10 \text{ cm}} = 0.8 \xrightarrow{\text{(Fig. 13–7)}} = 0.28$$

Therefore,

$$F_{1 \to \text{ring}} = F_{1 \to 3} - F_{1 \to 2} = 0.28 - 0.11 = \mathbf{0.17}$$

which is the desired result. Note that $F_{1 \to 2}$ and $F_{1 \to 3}$ represent the fractions of radiation leaving the base that strike the circular surfaces 2 and 3, respectively, and their difference gives the fraction that strikes the ring area.

4 The Symmetry Rule

The determination of the view factors in a problem can be simplified further if the geometry involved possesses some sort of symmetry. Therefore, it is good practice to check for the presence of any *symmetry* in a problem before attempting to determine the view factors directly. The presence of symmetry can be determined *by inspection,* keeping the definition of the view factor in mind. Identical surfaces that are oriented in an identical manner with respect to another surface will intercept identical amounts of radiation leaving that surface. Therefore, the **symmetry rule** can be expressed as *two (or more) surfaces that possess symmetry about a third surface will have identical view factors from that surface* (Fig. 13–13).

The symmetry rule can also be expressed as *if the surfaces j and k are symmetric about the surface i then $F_{i \to j} = F_{i \to k}$.* Using the reciprocity rule, we can show that the relation $F_{j \to i} = F_{k \to i}$ is also true in this case.

$$F_{1 \to 2} = F_{1 \to 3}$$
(Also, $F_{2 \to 1} = F_{3 \to 1}$)

FIGURE 13–13
Two surfaces that are symmetric about a third surface will have the same view factor from the third surface.

EXAMPLE 13–3   View Factors Associated with a Tetragon

Determine the view factors from the base of the pyramid shown in Fig. 13–14 to each of its four side surfaces. The base of the pyramid is a square, and its side surfaces are isosceles triangles.

SOLUTION   The view factors from the base of a pyramid to each of its four side surfaces for the case of a square base are to be determined.

Assumptions   The surfaces are diffuse emitters and reflectors.

Analysis   The base of the pyramid (surface 1) and its four side surfaces (surfaces 2, 3, 4, and 5) form a five-surface enclosure. The first thing we notice about this enclosure is its symmetry. The four side surfaces are symmetric about the base surface. Then, from the *symmetry rule,* we have

$$F_{12} = F_{13} = F_{14} = F_{15}$$

Also, the *summation rule* applied to surface 1 yields

$$\sum_{j=1}^{5} F_{1j} = F_{11} + F_{12} + F_{13} + F_{14} + F_{15} = 1$$

However, $F_{11} = 0$, since the base is a *flat* surface. Then the two relations above yield

$$F_{12} = F_{13} = F_{14} = F_{15} = \mathbf{0.25}$$

Discussion   Note that each of the four side surfaces of the pyramid receive one-fourth of the entire radiation leaving the base surface, as expected. Also note that the presence of symmetry greatly simplified the determination of the view factors.
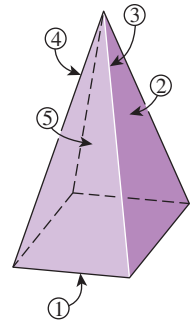
FIGURE 13–14
The pyramid considered
in Example 13–3.

EXAMPLE 13–4   View Factors Associated with a Triangular Duct

Determine the view factor from any one side to any other side of the infinitely long triangular duct whose cross section is given in Fig. 13–15.

SOLUTION   The view factors associated with an infinitely long triangular duct are to be determined.

Assumptions   The surfaces are diffuse emitters and reflectors.

Analysis   The widths of the sides of the triangular cross section of the duct are L_1, L_2, and L_3, and the surface areas corresponding to them are A_1, A_2, and A_3, respectively. Since the duct is infinitely long, the fraction of radiation leaving any surface that escapes through the ends of the duct is negligible. Therefore, the infinitely long duct can be considered to be a three-surface enclosure, $N = 3$.

This enclosure involves $N^2 = 3^2 = 9$ view factors, and we need to determine

$$\tfrac{1}{2}N(N - 1) = \tfrac{1}{2} \times 3(3 - 1) = 3$$

of these view factors directly. Fortunately, we can determine all three of them by inspection to be

$$F_{11} = F_{22} = F_{33} = 0$$

since all three surfaces are flat. The remaining six view factors can be determined by the application of the summation and reciprocity rules.
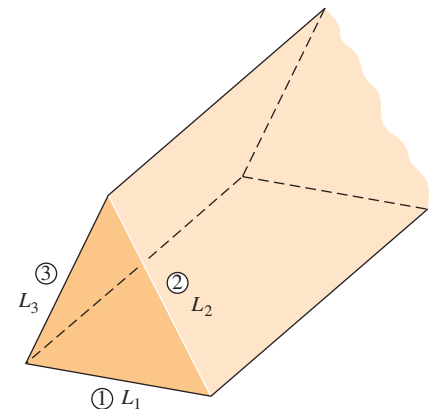
FIGURE 13–15
The infinitely long triangular duct
considered in Example 13–4.

Applying the summation rule to each of the three surfaces gives

$$F_{11} + F_{12} + F_{13} = 1$$
$$F_{21} + F_{22} + F_{23} = 1$$
$$F_{31} + F_{32} + F_{33} = 1$$

Noting that $F_{11} = F_{22} = F_{33} = 0$ and multiplying the first equation by A_1, the second by A_2, and the third by A_3 gives

$$A_1 F_{12} + A_1 F_{13} = A_1$$
$$A_2 F_{21} + A_2 F_{23} = A_2$$
$$A_3 F_{31} + A_3 F_{32} = A_3$$

Finally, applying the three reciprocity relations $A_1 F_{12} = A_2 F_{21}$, $A_1 F_{13} = A_3 F_{31}$, and $A_2 F_{23} = A_3 F_{32}$ gives

$$A_1 F_{12} + A_1 F_{13} = A_1$$
$$A_1 F_{12} + A_2 F_{23} = A_2$$
$$A_1 F_{13} + A_2 F_{23} = A_3$$

This is a set of three algebraic equations with three unknowns, which can be solved to obtain

$$F_{12} = \frac{A_1 + A_2 - A_3}{2A_1} = \frac{L_1 + L_2 - L_3}{2L_1}$$

$$F_{13} = \frac{A_1 + A_3 - A_2}{2A_1} = \frac{L_1 + L_3 - L_2}{2L_1} \qquad \text{(13–15)}$$

$$F_{23} = \frac{A_2 + A_3 - A_1}{2A_2} = \frac{L_2 + L_3 - L_1}{2L_2}$$

Discussion Note that we have replaced the areas of the side surfaces by their corresponding widths for simplicity, since $A = Ls$ and the length s can be factored out and canceled. We can generalize this result as *the view factor from a surface of a very long triangular duct to another surface is equal to the sum of the widths of these two surfaces minus the width of the third surface, divided by twice the width of the first surface.*
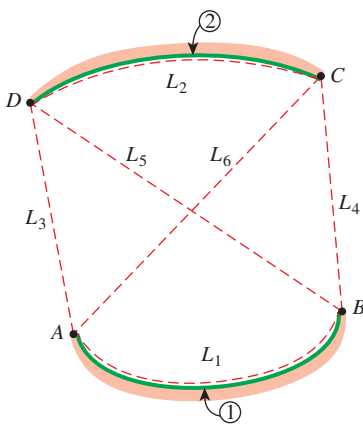
FIGURE 13–16
Determination of the view factor $F_{1 \to 2}$ by the application of the crossed-strings method.

View Factors Between Infinitely Long Surfaces: The Crossed-Strings Method

Many problems encountered in practice involve geometries of constant cross section such as channels and ducts that are *very long* in one direction relative to the other directions. Such geometries can conveniently be considered to be *two-dimensional,* since any radiation interaction through their end surfaces is negligible. These geometries can subsequently be modeled as being *infinitely long,* and the view factor between their surfaces can be determined by the amazingly simple *crossed-strings method* developed by H. C. Hottel in the 1950s. The surfaces of the geometry do not need to be flat; they can be convex, concave, or any irregular shape.

To demonstrate this method, consider the geometry shown in Fig. 13–16, and let us try to find the view factor $F_{1 \to 2}$ between surfaces 1 and 2. The first thing we do is identify the end points of the surfaces (the points *A, B, C,* and *D*)

and connect them to each other with tightly stretched strings, which are indicated by dashed lines. Hottel has shown that the view factor $F_{1 \to 2}$ can be expressed in terms of the lengths of these stretched strings, which are straight lines, as

$$F_{1 \to 2} = \frac{(L_5 + L_6) - (L_3 + L_4)}{2L_1} \tag{13–16}$$

Note that $L_5 + L_6$ is the sum of the lengths of the *crossed strings,* and $L_3 + L_4$ is the sum of the lengths of the *uncrossed strings* attached to the end points. Therefore, Hottel's crossed-strings method can be expressed verbally as

$$F_{i \to j} = \frac{\sum(\text{Crossed strings}) - \sum(\text{Uncrossed strings})}{2 \times (\text{Length of surface } i)} \tag{13–17}$$

The crossed-strings method is applicable even when the two surfaces considered share a common edge, as in a triangle. In such cases, the common edge can be treated as an imaginary string of zero length. The method can also be applied to surfaces that are partially blocked by other surfaces by allowing the strings to bend around the blocking surfaces.

EXAMPLE 13–5   The Crossed-Strings Method for View Factors

Two infinitely long parallel plates of widths $a = 12$ cm and $b = 5$ cm are located a distance $c = 6$ cm apart, as shown in Fig. 13–17. (*a*) Determine the view factor $F_{1 \to 2}$ from surface 1 to surface 2 by using the crossed-strings method. (*b*) Derive the crossed-strings formula by forming triangles on the given geometry and using Eq. 13–15 for view factors between the sides of triangles.

SOLUTION   The view factors between two infinitely long parallel plates are to be determined using the crossed-strings method, and the formula for the view factor is to be derived.
Assumptions   The surfaces are diffuse emitters and reflectors.
Analysis   (*a*) First we label the end points of both surfaces and draw straight dashed lines between the end points, as shown in Fig. 13–17. Then we identify the crossed and uncrossed strings and apply the crossed-strings method (Eq. 13–17) to determine the view factor $F_{1 \to 2}$:

$$F_{1 \to 2} = \frac{\sum(\text{Crossed strings}) - \sum(\text{Uncrossed strings})}{2 \times (\text{Length of surface 1})} = \frac{(L_5 + L_6) - (L_3 + L_4)}{2L_1}$$

where

$$L_1 = a = 12 \text{ cm} \qquad L_4 = \sqrt{7^2 + 6^2} = 9.22 \text{ cm}$$
$$L_2 = b = 5 \text{ cm} \qquad L_5 = \sqrt{5^2 + 6^2} = 7.81 \text{ cm}$$
$$L_3 = c = 6 \text{ cm} \qquad L_6 = \sqrt{12^2 + 6^2} = 13.42 \text{ cm}$$

Substituting,

$$F_{1 \to 2} = \frac{[(7.81 + 13.42) - (6 + 9.22)] \text{ cm}}{2 \times 12 \text{ cm}} = \mathbf{0.250}$$

(*b*) The geometry is infinitely long in the direction perpendicular to the plane of the paper, and thus the two plates (surfaces 1 and 2) and the two openings (imaginary

$b = L_2 = 5$ cm

$c = 6$ cm

$a = L_1 = 12$ cm
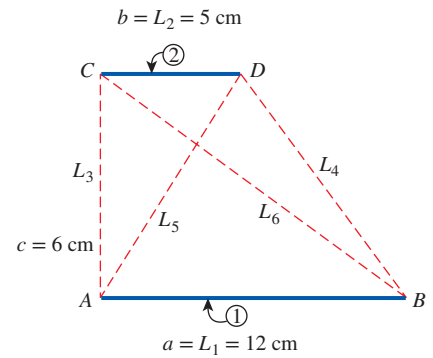
FIGURE 13–17
The two infinitely long parallel plates considered in Example 13–5.

surfaces 3 and 4) form a four-surface enclosure. Then applying the summation rule to surface 1 yields

$$F_{11} + F_{12} + F_{13} + F_{14} = 1$$

But $F_{11} = 0$ since it is a flat surface. Therefore,

$$F_{12} = 1 - F_{13} - F_{14}$$

where the view factors F_{13} and F_{14} can be determined by considering the triangles *ABC* and *ABD,* respectively, and applying Eq. 13–15 for view factors between the sides of triangles. We obtain

$$F_{13} = \frac{L_1 + L_3 - L_6}{2L_1}, \quad F_{14} = \frac{L_1 + L_4 - L_5}{2L_1}$$

Substituting,

$$F_{12} = 1 - \frac{L_1 + L_3 - L_6}{2L_1} - \frac{L_1 + L_4 - L_5}{2L_1}$$

$$= \frac{(L_5 + L_6) - (L_3 + L_4)}{2L_1}$$

which is the desired result. This is also a miniproof of the crossed-strings method for the case of two infinitely long plain parallel surfaces.

FIGURE 13–18
Two general black surfaces maintained at uniform temperatures T_1 and T_2.

13–3 ▪ RADIATION HEAT TRANSFER: BLACK SURFACES

So far, we have considered the nature of radiation, the radiation properties of materials, and the view factors, and we are now in a position to consider the rate of heat transfer between surfaces by radiation. The analysis of radiation exchange between surfaces, in general, is complicated because of reflection: a radiation beam leaving a surface may be reflected several times, with partial reflection occurring at each surface, before it is completely absorbed. The analysis is simplified greatly when the surfaces involved can be approximated as blackbodies because of the absence of reflection. In this section, we consider radiation exchange between *black surfaces* only; we extend the analysis to reflecting surfaces in the next section.

Consider two black surfaces of arbitrary shape maintained at uniform temperatures T_1 and T_2, as shown in Fig. 13–18. Recognizing that radiation leaves a black surface at a rate of $E_b = \sigma T^4$ per unit surface area and that the view factor $F_{1 \rightarrow 2}$ represents the fraction of radiation leaving surface 1 that strikes surface 2, and $F_{2 \rightarrow 1}$ represents the fraction of radiation leaving surface 2 that strikes surface 1. The *net* rate of radiation heat transfer from surface 1 to surface 2 can be expressed as

$$\dot{Q}_{1 \rightarrow 2} = \begin{pmatrix} \text{Radiation leaving} \\ \text{the entire surface 1} \\ \text{that strikes surface 2} \end{pmatrix} - \begin{pmatrix} \text{Radiation leaving} \\ \text{the entire surface 2} \\ \text{that strikes surface 1} \end{pmatrix}$$

$$= A_1 E_{b1} F_{1 \rightarrow 2} - A_2 E_{b2} F_{2 \rightarrow 1} \quad \text{(W)} \tag{13–18}$$

Applying the reciprocity relation $A_1 F_{1 \rightarrow 2} = A_2 F_{2 \rightarrow 1}$ yields

$$\dot{Q}_{1 \rightarrow 2} = A_1 F_{1 \rightarrow 2} \sigma (T_1^4 - T_2^4) \quad \text{(W)} \tag{13–19}$$

which is the desired relation. Eq. 13–19 provides the *net* rate at which radiation *leaves* surface 1 as a result of its interaction with surface 2, which is equal to the *net* rate at which surface 2 *gains* radiation due to its interaction with surface 1. A negative value for $\dot{Q}_{1 \rightarrow 2}$ indicates that *net* radiation heat transfer is from surface 2 to surface 1.

Now consider an *enclosure* consisting of *N black* surfaces maintained at specified temperatures. The *net* radiation heat transfer *from* any surface *i* of this enclosure is determined by adding up the net radiation heat transfers from surface *i* to each of the surfaces of the enclosure:

$$\dot{Q}_i = \sum_{j=1}^{N} \dot{Q}_{i \rightarrow j} = \sum_{j=1}^{N} A_i F_{i \rightarrow j} \sigma (T_i^4 - T_j^4) \qquad \text{(W)} \qquad \textbf{(13–20)}$$

Again a negative value for $\dot{Q}$ indicates that *net* radiation heat transfer is *to* surface *i* (i.e., surface *i gains* radiation energy instead of losing). Also, the *net* heat transfer from a surface to itself is zero, regardless of the shape of the surface.

EXAMPLE 13–6   Radiation Heat Transfer in a Black Furnace

Consider the 5-m × 5-m × 5-m cubical furnace shown in Fig. 13–19, whose surfaces closely approximate black surfaces. The base, top, and side surfaces of the furnace are maintained at uniform temperatures of 800 K, 1500 K, and 500 K, respectively. Determine (*a*) the net rate of radiation heat transfer between the base and the side surfaces, (*b*) the net rate of radiation heat transfer between the base and the top surface, and (*c*) the net radiation heat transfer from the base surface.

SOLUTION   The surfaces of a cubical furnace are black and are maintained at uniform temperatures. The *net* rate of radiation heat transfer between the base and side surfaces, between the base and the top surface, and from the base surface are to be determined.
Assumptions   The surfaces are black and isothermal.
Analysis   (*a*) The geometry involves six surfaces, and thus we may be tempted at first to treat the furnace as a six-surface enclosure. However, the four side surfaces possess the same properties, and thus we can treat them as a single side surface in radiation analysis. We consider the base surface to be surface 1, the top surface to be surface 2, and the side surfaces to be surface 3. Then the problem reduces to determining $\dot{Q}_{1 \rightarrow 3}$, $\dot{Q}_{1 \rightarrow 2}$, and $\dot{Q}_1$.

The *net* rate of radiation heat transfer $\dot{Q}_{1 \rightarrow 3}$ from surface 1 to surface 3 can be determined from Eq. 13–19, since both surfaces involved are black, by replacing the subscript 2 with 3:

$$\dot{Q}_{1 \rightarrow 3} = A_1 F_{1 \rightarrow 3} \sigma (T_1^4 - T_3^4)$$

But first we need to evaluate the view factor $F_{1 \rightarrow 3}$. After checking the view factor charts and tables, we realize that we cannot determine this view factor directly. However, we can determine the view factor $F_{1 \rightarrow 2}$ from Fig. 13–5 to be $F_{1 \rightarrow 2} = 0.2$, and we know that $F_{1 \rightarrow 1} = 0$ since surface 1 is a plane. Then applying the summation rule to surface 1 yields

$$F_{1 \rightarrow 1} + F_{1 \rightarrow 2} + F_{1 \rightarrow 3} = 1$$

or

$$F_{1 \rightarrow 3} = 1 - F_{1 \rightarrow 1} - F_{1 \rightarrow 2} = 1 - 0 - 0.2 = 0.8$$

Substituting,

$$\dot{Q}_{1 \rightarrow 3} = (25 \text{ m}^2)(0.8)(5.67 \times 10^{-8} \text{ W/m}^2 \cdot \text{K}^4)[(800 \text{ K})^4 - (500 \text{ K})^4]$$
$$= \textbf{394 kW}$$

*T*₂ = 1500 K ②

③ $T_3 = 500$ K

① $T_1 = 800$ K
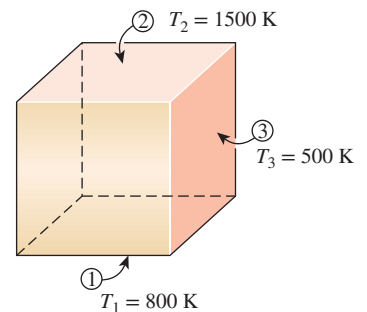
FIGURE 13–19
The cubical furnace of black surfaces considered in Example 13–6.

(*b*) The *net* rate of radiation heat transfer $\dot{Q}_{1 \to 2}$ from surface 1 to surface 2 is determined in a similar manner from Eq. 13–19 to be

$$\dot{Q}_{1 \to 2} = A_1 F_{1 \to 2} \sigma(T_1^4 - T_2^4)$$
$$= (25 \text{ m}^2)(0.2)(5.67 \times 10^{-8} \text{ W/m}^2\cdot\text{K}^4)[(800 \text{ K})^4 - (1500 \text{ K})^4]$$
$$= -1319 \text{ kW}$$

The negative sign indicates that *net* radiation heat transfer is from surface 2 to surface 1. (*c*) The *net* radiation heat transfer from the base surface $\dot{Q}_1$ is determined from Eq. 13–20 by replacing the subscript *i* with 1 and taking $N = 3$:

$$\dot{Q}_1 = \sum_{j=1}^{3} \dot{Q}_{1 \to j} = \dot{Q}_{1 \to 1} + \dot{Q}_{1 \to 2} + \dot{Q}_{1 \to 3}$$
$$= 0 + (-1319 \text{ kW}) + (394 \text{ kW})$$
$$= -925 \text{ kW}$$

Again the negative sign indicates that *net* radiation heat transfer is *to* surface 1. That is, the base of the furnace is gaining *net* radiation at a rate of 925 kW.

13–4 ▪ RADIATION HEAT TRANSFER: DIFFUSE, GRAY SURFACES

The analysis of radiation transfer in enclosures consisting of black surfaces is relatively easy, as we have seen, but most enclosures encountered in practice involve nonblack surfaces, which allow multiple reflections to occur. Radiation analysis of such enclosures becomes very complicated unless some simplifying assumptions are made.

To make a simple radiation analysis possible, it is common to assume the surfaces of an enclosure to be *opaque, diffuse,* and *gray.* That is, the surfaces are nontransparent, they are diffuse emitters and diffuse reflectors, and their radiation properties are independent of wavelength. Also, each surface of the enclosure is *isothermal,* and both the incoming and outgoing radiation are *uniform* over each surface. But first we review the concept of radiosity introduced in Chap. 12.

Radiosity

Surfaces emit radiation as well as reflect it, and thus the radiation leaving a surface consists of emitted and reflected parts. The calculation of radiation heat transfer between surfaces involves the *total* radiation energy streaming away from a surface, with no regard for its origin. The *total radiation energy leaving a surface per unit time and per unit area* is the **radiosity** and is denoted by *J* (Fig. 13–20).

For a surface *i* that is *gray* and *opaque* ($\varepsilon_i = \alpha_i$ and $\alpha_i + \rho_i = 1$), the radiosity can be expressed as

$$J_i = \begin{pmatrix} \text{Radiation emitted} \\ \text{by surface } i \end{pmatrix} + \begin{pmatrix} \text{Radiation reflected} \\ \text{by surface } i \end{pmatrix}$$
$$= \varepsilon_i E_{bi} + \rho_i G_i$$
$$= \varepsilon_i E_{bi} + (1 - \varepsilon_i)G_i \quad (\text{W/m}^2) \tag{13–21}$$

FIGURE 13–20
Radiosity represents the sum of the radiation energy emitted and reflected by a surface.

where $E_{bi} = \sigma T_i^4$ is the blackbody emissive power of surface i and G_i is irradiation (i.e., the radiation energy incident on surface i per unit time per unit area).

For a surface that can be approximated as a *blackbody* ($\varepsilon_i = 1$), the radiosity relation reduces to

$$J_i = E_{bi} = \sigma T_i^4 \qquad \text{(blackbody)} \tag{13–22}$$

That is, *the radiosity of a blackbody is equal to its emissive power.* This is expected, since a blackbody does not reflect any radiation, and thus radiation coming from a blackbody is due to emission only.

Net Radiation Heat Transfer to or from a Surface

During a radiation interaction, a surface *loses* energy by emitting radiation and *gains* energy by absorbing radiation emitted by other surfaces. A surface experiences a net gain or a net loss of energy, depending on which quantity is larger. The *net* rate of radiation heat transfer from a surface i of surface area A_i is denoted by $\dot{Q}_i$ and is expressed as

$$\dot{Q}_i = \begin{pmatrix} \text{Radiation leaving} \\ \text{entire surface } i \end{pmatrix} - \begin{pmatrix} \text{Radiation incident} \\ \text{on entire surface } i \end{pmatrix}$$

$$= A_i(J_i - G_i) \quad \text{(W)} \tag{13–23}$$

Solving for G_i from Eq. 13–21 and substituting into Eq. 13–23 yields

$$\dot{Q}_i = A_i\left(J_i - \frac{J_i - \varepsilon_i E_{bi}}{1 - \varepsilon_i}\right) = \frac{A_i \varepsilon_i}{1 - \varepsilon_i}(E_{bi} - J_i) \qquad \text{(W)} \tag{13–24}$$

In an electrical analogy to Ohm's law, this equation can be rearranged as

$$\dot{Q}_i = \frac{E_{bi} - J_i}{R_i} \qquad \text{(W)} \tag{13–25}$$

where

$$R_i = \frac{1 - \varepsilon_i}{A_i \varepsilon_i} \tag{13–26}$$

is the **surface resistance** to radiation. The quantity $E_{bi} - J_i$ corresponds to a *potential difference* and the net rate of radiation heat transfer corresponds to *current* in the electrical analogy, as illustrated in Fig. 13–21.

The direction of the net radiation heat transfer depends on the relative magnitudes of J_i (the radiosity) and E_{bi} (the emissive power of a blackbody at the temperature of the surface). It is *from* the surface if $E_{bi} > J_i$ and *to* the surface if $J_i > E_{bi}$. A negative value for $\dot{Q}_i$ indicates that heat transfer is *to* the surface. All of this radiation energy gained must be removed from the other side of the surface through some mechanism if the surface temperature is to remain constant.

The surface resistance to radiation for a *blackbody* is *zero* since $\varepsilon_i = 1$ and $J_i = E_{bi}$. The net rate of radiation heat transfer in this case is determined directly from Eq. 13–23.

Some surfaces encountered in numerous practical heat transfer applications are modeled as being *adiabatic* since their back sides are well insulated and the net heat transfer through them is zero. When the convection effects on the front (heat transfer) side of such a surface is negligible and steady-state
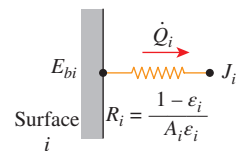
FIGURE 13–21
Electrical analogy of surface resistance to radiation.

conditions are reached, the surface must lose as much radiation energy as it gains, and thus $\dot{Q}_i = 0$. In such cases, the surface is said to *reradiate* all the radiation energy it receives, and such a surface is called a **reradiating surface**. Setting $\dot{Q}_i = 0$ in Eq. 13–25 yields

$$J_i = E_{bi} = \sigma T_i^4 \quad (\text{W/m}^2) \tag{13–27}$$

Therefore, the *temperature* of a reradiating surface under steady conditions can easily be determined from Eq. 13–27 once its radiosity is known. Note that the temperature of a reradiating surface is *independent of its emissivity.* In radiation analysis, the surface resistance of a reradiating surface is disregarded since there is no net heat transfer through it. (This is like the fact that there is no need to consider a resistance in an electrical network if no current is flowing through it.)

Net Radiation Heat Transfer Between Any Two Surfaces

Consider two diffuse, gray, and opaque surfaces of arbitrary shape maintained at uniform temperatures, as shown in Fig. 13–22. Recognizing that the radiosity J represents the rate of radiation leaving a surface per unit surface area and that the view factor $F_{i \to j}$ represents the fraction of radiation leaving surface i that strikes surface j, the *net* rate of radiation heat transfer from surface i to surface j can be expressed as

$$\dot{Q}_{i \to j} = \begin{pmatrix} \text{Radiation leaving} \\ \text{the entire surface } i \\ \text{that strikes surface } j \end{pmatrix} - \begin{pmatrix} \text{Radiation leaving} \\ \text{the entire surface } j \\ \text{that strikes surface } i \end{pmatrix}$$

$$= A_i J_i F_{i \to j} - A_j J_j F_{j \to i} \quad (\text{W}) \tag{13–28}$$

Applying the reciprocity relation $A_i F_{i \to j} = A_j F_{j \to i}$ yields

$$\dot{Q}_{i \to j} = A_i F_{i \to j} (J_i - J_j) \quad (\text{W}) \tag{13–29}$$

Again in analogy to Ohm's law, this equation can be rearranged as

$$\dot{Q}_{i \to j} = \frac{J_i - J_j}{R_{i \to j}} \quad (\text{W}) \tag{13–30}$$

where

$$R_{i \to j} = \frac{1}{A_i F_{i \to j}} \tag{13–31}$$

is the **space resistance** to radiation. Again the quantity $J_i - J_j$ corresponds to a *potential difference,* and the net rate of heat transfer between two surfaces corresponds to *current* in the electrical analogy, as illustrated in Fig. 13–22.

The direction of the net radiation heat transfer between two surfaces depends on the relative magnitudes of J_i and J_j. A positive value for $\dot{Q}_{i \to j}$ indicates that net heat transfer is *from* surface i *to* surface j. A negative value indicates the opposite.

In an *N*-surface enclosure, the conservation of energy principle requires that the net heat transfer from surface i be equal to the sum of the net heat transfers from surface i to each of the N surfaces of the enclosure. That is,
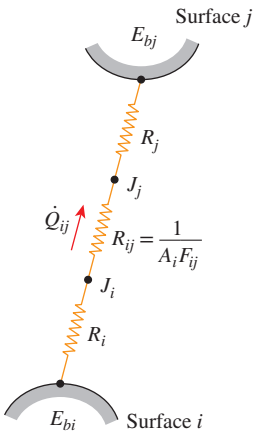
FIGURE 13–22
Electrical analogy of space resistance to radiation.

$$\dot{Q}_i = \sum_{j=1}^{N} \dot{Q}_{i \to j} = \sum_{j=1}^{N} A_i F_{i \to j}(J_i - J_j) = \sum_{j=1}^{N} \frac{J_i - J_j}{R_{i \to j}} \quad \text{(W)} \qquad \textbf{(13–32)}$$

The network representation of net radiation heat transfer from surface i to the remaining surfaces of an N-surface enclosure is given in Fig. 13–23. Note that $\dot{Q}_{i \to i}$ (the net rate of heat transfer from a surface to itself) is zero regardless of the shape of the surface. Combining Eqs. 13–25 and 13–32 gives

$$\frac{E_{bi} - J_i}{R_i} = \sum_{j=1}^{N} \frac{J_i - J_j}{R_{i \to j}} \quad \text{(W)} \qquad \textbf{(13–33)}$$

which has the electrical analogy interpretation that *the net radiation flow from a surface through its surface resistance is equal to the sum of the radiation flows from that surface to all other surfaces through the corresponding space resistances.*

FIGURE 13–23
Network representation of net radiation heat transfer from surface i to the remaining surfaces of an N-surface enclosure.

Methods of Solving Radiation Problems

In the radiation analysis of an enclosure, either the temperature or the net rate of heat transfer must be given for each of the surfaces to obtain a unique solution for the unknown surface temperatures and heat transfer rates. There are two methods commonly used to solve radiation problems. In the first method, Eqs. 13–32 (for surfaces with specified heat transfer rates) and 13–33 (for surfaces with specified temperatures) are simplified and rearranged as

Surfaces with specified net heat transfer rate $\dot{Q}$

$$\dot{Q}_i = A_i \sum_{j=1}^{N} F_{i \to j}(J_i - J_j) \qquad \textbf{(13–34)}$$

Surfaces with specified temperature T_i

$$\sigma T_i^4 = J_i + \frac{1 - \varepsilon_i}{\varepsilon_i} \sum_{j=1}^{N} F_{i \to j}(J_i - J_j) \qquad \textbf{(13–35)}$$

Note that $\dot{Q}_i = 0$ for insulated (or reradiating) surfaces, and $\sigma T_i^4 = J_i$ for black surfaces since $\varepsilon_i = 1$ in that case. Also, the term corresponding to $j = i$ drops out from either relation since $J_i - J_j = J_i - J_i = 0$ in that case.

The equations above give N linear algebraic equations for the determination of the N unknown radiosities for an N-surface enclosure. Once the radiosities $J_1, J_2, \ldots, J_N$ are available, the unknown heat transfer rates can be determined from Eq. 13–34, while the unknown surface temperatures can be determined from Eq. 13–35. The temperatures of insulated or reradiating surfaces can be determined from $\sigma T_i^4 = J_i$. A positive value for $\dot{Q}_i$ indicates net radiation heat transfer *from* surface i to other surfaces in the enclosure while a negative value indicates net radiation heat transfer *to* the surface.

The systematic approach described above for solving radiation heat transfer problems is very suitable for use with today's popular equation solvers such as EES, Mathcad, and Matlab, especially when there are a large number of surfaces, and it is known as the **direct method** (formerly the *matrix method,* since it resulted in matrices and the solution required a knowledge of linear algebra). The second method, which is described next, is called the **network method**, and it is based on the electrical network analogy.

The network method was first introduced by A. K. Oppenheim in the 1950s and found widespread acceptance because of its simplicity and emphasis on
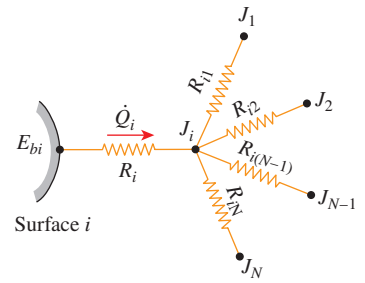
the physics of the problem. The application of the method is straightforward: Draw a surface resistance associated with each surface of an enclosure and connect them with space resistances. Then solve the radiation problem by treating it as an electrical network problem where the radiation heat transfer replaces the current and radiosity replaces the potential.

The network method is not practical for enclosures with more than three or four surfaces, however, because of the increased complexity of the network. Next we apply the method to solve radiation problems in two- and three-surface enclosures.

Radiation Heat Transfer in Two-Surface Enclosures

Consider an enclosure consisting of two opaque surfaces at specified temperatures T_1 and T_2, as shown in Fig. 13–24, and we try to determine the net rate of radiation heat transfer between the two surfaces with the network method. Surfaces 1 and 2 have emissivities ε_1 and ε_2 and surface areas A_1 and A_2 and are maintained at uniform temperatures T_1 and T_2, respectively. There are only two surfaces in the enclosure, and thus we can write

$$\dot{Q}_{12} = \dot{Q}_1 = -\dot{Q}_2$$

That is, the net rate of radiation heat transfer from surface 1 to surface 2 must equal the net rate of radiation heat transfer *from* surface 1 and the net rate of radiation heat transfer *to* surface 2.

The radiation network of this two-surface enclosure consists of two surface resistances and one space resistance, as shown in Fig. 13–24. In an electrical network, the electric current flowing through these resistances connected in series would be determined by dividing the potential difference between points A and B by the total resistance between the same two points. The net rate of radiation transfer is determined in the same manner and is expressed as

$$\dot{Q}_{12} = \frac{E_{b1} - E_{b2}}{R_1 + R_{12} + R_2} = \dot{Q}_1 = -\dot{Q}_2$$

or

$$\dot{Q}_{12} = \frac{\sigma(T_1^4 - T_2^4)}{\dfrac{1 - \varepsilon_1}{A_1\varepsilon_1} + \dfrac{1}{A_1 F_{12}} + \dfrac{1 - \varepsilon_2}{A_2\varepsilon_2}} \quad \text{(W)} \tag{13–36}$$

This important result is applicable to any two gray, diffuse, and opaque surfaces that form an enclosure. The view factor F_{12} depends on the geometry and must be determined first. Simplified forms of Eq. 13–36 for some familiar arrangements that form a two-surface enclosure are given in Table 13–3. Note that $F_{12} = 1$ for all of these special cases.
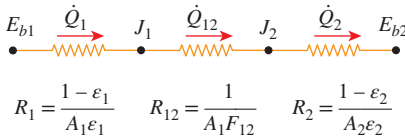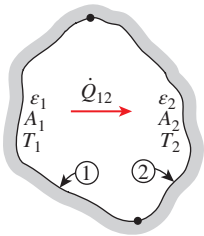
FIGURE 13–24
Schematic of a two-surface enclosure and the radiation network associated with it.
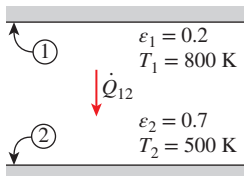
FIGURE 13–25
The two parallel plates considered in Example 13–7.

EXAMPLE 13–7   **Radiation Heat Transfer Between Parallel Plates**
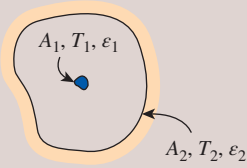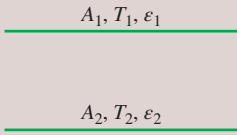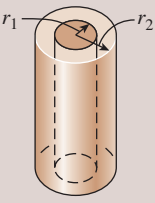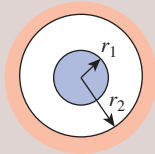
Two very large parallel plates are maintained at uniform temperatures $T_1 = 800$ K and $T_2 = 500$ K and have emissivities $\varepsilon_1 = 0.2$ and $\varepsilon_2 = 0.7$, respectively, as shown in Fig. 13–25. Determine the *net* rate of radiation heat transfer between the two surfaces per unit surface area of the plates.

SOLUTION   Two large parallel plates are maintained at uniform temperatures. The *net* rate of radiation heat transfer between the plates is to be determined.

Assumptions Both surfaces are opaque, diffuse, and gray.

Analysis The *net* rate of radiation heat transfer between the two plates per unit area is readily determined from Eq. 13–38 to be

$$\dot{q}_{12} = \frac{\dot{Q}_{12}}{A} = \frac{\sigma(T_1^4 - T_2^4)}{\dfrac{1}{\varepsilon_1} + \dfrac{1}{\varepsilon_2} - 1} = \frac{(5.67 \times 10^{-8} \text{ W/m}^2 \cdot \text{K}^4)[(800 \text{ K})^4 - (500 \text{ K})^4]}{\dfrac{1}{0.2} + \dfrac{1}{0.7} - 1}$$

$$= \textbf{3625 W/m}^2$$

Discussion Note that heat at a *net* rate of 3625 W is transferred from plate 1 to plate 2 by radiation per unit surface area of either plate.

TABLE 13–3

Radiation heat transfer relations for some familiar two-surface arrangements

Small object in a large cavity			
A_1, T_1, ε_1 A_2, T_2, ε_2	$\dfrac{A_1}{A_2} \approx 0$ $F_{12} = 1$	$\dot{Q}_{12} = A_1 \sigma \varepsilon_1 (T_1^4 - T_2^4)$	**(13–37)**
Infinitely large parallel plates			
A_1, T_1, ε_1 A_2, T_2, ε_2	$A_1 = A_2 = A$ $F_{12} = 1$	$\dot{Q}_{12} = \dfrac{A\sigma(T_1^4 - T_2^4)}{\dfrac{1}{\varepsilon_1} + \dfrac{1}{\varepsilon_2} - 1}$	**(13–38)**
Infinitely long concentric cylinders			
$r_1 \quad r_2$	$\dfrac{A_1}{A_2} = \dfrac{r_1}{r_2}$ $F_{12} = 1$	$\dot{Q}_{12} = \dfrac{A_1 \sigma (T_1^4 - T_2^4)}{\dfrac{1}{\varepsilon_1} + \dfrac{1 - \varepsilon_2}{\varepsilon_2}\left(\dfrac{r_1}{r_2}\right)}$	**(13–39)**
Concentric spheres			
$r_1 \quad r_2$	$\dfrac{A_1}{A_2} = \left(\dfrac{r_1}{r_2}\right)^2$ $F_{12} = 1$	$\dot{Q}_{12} = \dfrac{A_1 \sigma (T_1^4 - T_2^4)}{\dfrac{1}{\varepsilon_1} + \dfrac{1 - \varepsilon_2}{\varepsilon_2}\left(\dfrac{r_1}{r_2}\right)^2}$	**(13–40)**
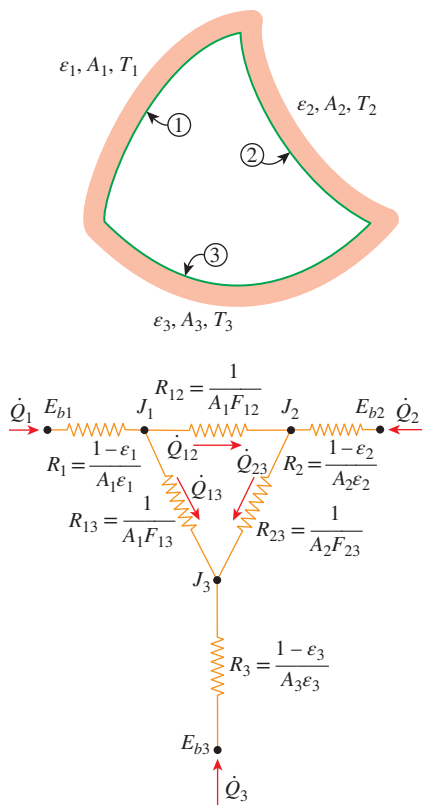
FIGURE 13–26
Schematic of a three-surface enclosure and the radiation network associated with it.

FIGURE 13–27
The cylindrical furnace considered in Example 13–8.

Radiation Heat Transfer in Three-Surface Enclosures

We now consider an enclosure consisting of three opaque, diffuse, and gray surfaces, as shown in Fig. 13–26. Surfaces 1, 2, and 3 have surface areas A_1, A_2, and A_3; emissivities ε_1, ε_2, and ε_3; and uniform temperatures T_1, T_2, and T_3, respectively. The radiation network of this geometry is constructed by following the standard procedure: draw a surface resistance associated with each of the three surfaces and connect these surface resistances with space resistances, as shown in the figure. Relations for the surface and space resistances are given by Eqs. 13–26 and 13–31. The three end point potentials E_{b1}, E_{b2}, and E_{b3} are considered known, since the surface temperatures are specified. Then all we need to find are the radiosities J_1, J_2, and J_3. The three equations for the determination of these three unknowns are obtained from the requirement that *the algebraic sum of the currents (net radiation heat transfer) at each node must equal zero.* That is,

$$\frac{E_{b1} - J_1}{R_1} + \frac{J_2 - J_1}{R_{12}} + \frac{J_3 - J_1}{R_{13}} = 0$$

$$\frac{J_1 - J_2}{R_{12}} + \frac{E_{b2} - J_2}{R_2} + \frac{J_3 - J_2}{R_{23}} = 0 \qquad \text{(13–41)}$$

$$\frac{J_1 - J_3}{R_{13}} + \frac{J_2 - J_3}{R_{23}} + \frac{E_{b3} - J_3}{R_3} = 0$$

Once the radiosities J_1, J_2, and J_3 are available, the net rate of radiation heat transfers at each surface can be determined from Eq. 13–32.

The set of equations above simplifies further if one or more surfaces are "special" in some way. For example, $J_i = E_{bi} = \sigma T_i^4$ for a *black* or *reradiating* surface. Also, $\dot{Q}_i = 0$ for a reradiating surface. Finally, when the *net* rate of radiation heat transfer $\dot{Q}_i$ is specified at surface i instead of the temperature, the term $(E_{bi} - J_i)/R_i$ should be replaced by the specified $\dot{Q}_i$.

EXAMPLE 13–8 **Radiation Heat Transfer in a Cylindrical Furnace**

Consider a cylindrical furnace with $r_o = H = 1$ m, as shown in Fig. 13–27. The top (surface 1) and the base (surface 2) of the furnace have emissivities $\varepsilon_1 = 0.8$ and $\varepsilon_2 = 0.4$, respectively, and are maintained at uniform temperatures $T_1 = 700$ K and $T_2 = 500$ K. The side surface closely approximates a blackbody and is maintained at a temperature of $T_3 = 400$ K. Determine the *net* rate of radiation heat transfer at each surface during steady operation, and explain how these surfaces can be maintained at specified temperatures.

SOLUTION The surfaces of a cylindrical furnace are maintained at uniform temperatures. The *net* rate of radiation heat transfer at each surface during steady operation is to be determined.

Assumptions **1** Steady operating conditions exist. **2** The surfaces are opaque, diffuse, and gray. **3** Convection heat transfer is not considered.

Analysis We will solve this problem systematically using the direct method to demonstrate its use. The cylindrical furnace can be considered to be a three-surface enclosure with surface areas of

$$A_1 = A_2 = \pi r_0^2 = \pi(1 \text{ m})^2 = 3.14 \text{ m}^2$$

$$A_3 = 2\pi r_o H = 2\pi(1 \text{ m})(1 \text{ m}) = 6.28 \text{ m}^2$$

The view factor from the base to the top surface is, from Fig. 13–7, $F_{12} = 0.38$. Then the view factor from the base to the side surface is determined by applying the summation rule to be

$$F_{11} + F_{12} + F_{13} = 1 \rightarrow F_{13} = 1 - F_{11} - F_{12} = 1 - 0 - 0.38 = 0.62$$

since the base surface is flat and thus $F_{11} = 0$. Noting that the top and bottom surfaces are symmetric about the side surface, $F_{21} = F_{12} = 0.38$ and $F_{23} = F_{13} = 0.62$. The view factor F_{31} is determined from the reciprocity relation,

$$A_1 F_{13} = A_3 F_{31} \rightarrow F_{31} = F_{13}(A_1/A_3) = (0.62)(0.314/0.628) = 0.31$$

Also, $F_{32} = F_{31} = 0.31$ because of symmetry. Now that all the view factors are available, we apply Eq. 13–35 to each surface to determine the radiosities:

Top surface $(i = 1)$: $\quad \sigma T_1^4 = J_1 + \dfrac{1 - \varepsilon_1}{\varepsilon_1}[F_{12}(J_1 - J_2) + F_{13}(J_1 - J_3)]$

Bottom surface $(i = 2)$: $\sigma T_2^4 = J_2 + \dfrac{1 - \varepsilon_2}{\varepsilon_2}[F_{21}(J_2 - J_1) + F_{23}(J_2 - J_3)]$

Side surface $(i = 3)$: $\quad \sigma T_3^4 = J_3 + 0$ (since surface 3 is black and thus $\varepsilon_3 = 1$)

Substituting the known quantities,

$$(5.67 \times 10^{-8} \text{ W/m}^2\cdot\text{K}^4)(700 \text{ K})^4 = J_1 + \frac{1 - 0.8}{0.8}[0.38(J_1 - J_2) + 0.62(J_1 - J_3)]$$

$$(5.67 \times 10^{-8} \text{ W/m}^2\cdot\text{K}^4)(500 \text{ K})^4 = J_2 + \frac{1 - 0.4}{0.4}[0.38(J_2 - J_1) + 0.62(J_2 - J_3)]$$

$$(5.67 \times 10^{-8} \text{ W/m}^2\cdot\text{K}^4)(400 \text{ K})^4 = J_3$$

Solving these equations for J_1, J_2, and J_3 gives

$$J_1 = 11{,}418 \text{ W/m}^2, \quad J_2 = 4562 \text{ W/m}^2, \quad \text{and} \quad J_3 = 1452 \text{ W/m}^2$$

Then the *net* rates of radiation heat transfer at the three surfaces are determined from Eq. 13–34 to be

$$\dot{Q}_1 = A_1[F_{1 \rightarrow 2}(J_1 - J_2) + F_{1 \rightarrow 3}(J_1 - J_3)]$$
$$= (3.14 \text{ m}^2)[0.38(11{,}418 - 4562) + 0.62(11{,}418 - 1452)] \text{ W/m}^2$$
$$= \textbf{27.6 kW}$$

$$\dot{Q}_2 = A_2[F_{2 \rightarrow 1}(J_2 - J_1) + F_{2 \rightarrow 3}(J_2 - J_3)]$$
$$= (3.14 \text{ m}^2)[0.38(4562 - 11{,}418) + 0.62(4562 - 1452)] \text{ W/m}^2$$
$$= \textbf{-2.13 kW}$$

$$\dot{Q}_3 = A_3[F_{3 \rightarrow 1}(J_3 - J_1) + F_{3 \rightarrow 2}(J_3 - J_2)]$$
$$= (6.28 \text{ m}^2)[0.31(1452 - 11{,}418) + 0.31(1452 - 4562)] \text{ W/m}^2$$
$$= \textbf{-25.5 kW}$$

Note that the direction of *net* radiation heat transfer is *from* the top surface *to* the base and side surfaces, and the algebraic sum of these three quantities must be equal to zero. That is,

$$\dot{Q}_1 + \dot{Q}_2 + \dot{Q}_3 = 27.6 + (-2.13) + (-25.5) \cong 0$$

Discussion   To maintain the surfaces at the specified temperatures, we must supply heat to the top surface continuously at a rate of 27.6 kW while removing 2.13 kW from the base and 25.5 kW from the side surfaces.

The direct method presented here is straightforward, and it does not require the evaluation of radiation resistances. Also, it can be applied to enclosures with any number of surfaces in the same manner.

EXAMPLE 13–9   **Radiation Heat Transfer in a Triangular Furnace**

A furnace is shaped like a long equilateral triangular duct, as shown in Fig. 13–28. The width of each side is 1 m. The base surface has an emissivity of 0.7 and is maintained at a uniform temperature of 600 K. The heated left-side surface closely approximates a blackbody at 1000 K. The right-side surface is well insulated. Determine the rate at which heat must be supplied to the heated side externally per unit length of the duct in order to maintain these operating conditions.

SOLUTION   Two of the surfaces of a long equilateral triangular furnace are maintained at uniform temperatures while the third surface is insulated. The external rate of heat transfer to the heated side per unit length of the duct during steady operation is to be determined.

Assumptions   **1** Steady operating conditions exist. **2** The surfaces are opaque, diffuse, and gray. **3** Convection heat transfer is not considered.

Analysis   The furnace can be considered to be a three-surface enclosure with a radiation network as shown in the figure, since the duct is very long and thus the end effects are negligible. We observe that the view factor from any surface to any other surface in the enclosure is 0.5 because of symmetry. Surface 3 is a reradiating surface since the net rate of heat transfer at that surface is zero. Then we must have $\dot{Q}_1 = -\dot{Q}_2$, since all heat lost by surface 1 must be gained by surface 2. The radiation network in this case is a simple series–parallel connection, and we can determine $\dot{Q}_1$ directly from

$$\dot{Q}_1 = \frac{E_{b1} - E_{b2}}{R_1 + \left(\dfrac{1}{R_{12}} + \dfrac{1}{R_{13} + R_{23}} \right)^{-1}} = \frac{E_{b1} - E_{b2}}{\dfrac{1 - \varepsilon_1}{A_1 \varepsilon_1} + \left(A_1 F_{12} + \dfrac{1}{1/A_1 F_{13} + 1/A_2 F_{23}} \right)^{-1}}$$

where

$$A_1 = A_2 = A_3 = wL = 1 \text{ m} \times 1 \text{ m} = 1 \text{ m}^2 \quad \text{(per unit length of the duct)}$$

$$F_{12} = F_{13} = F_{23} = 0.5 \quad \text{(symmetry)}$$

$$E_{b1} = \sigma T_1^4 = (5.67 \times 10^{-8} \text{ W/m}^2 \cdot \text{K}^4)(600 \text{ K})^4 = 7348 \text{ W/m}^2$$

$$E_{b2} = \sigma T_2^4 = (5.67 \times 10^{-8} \text{ W/m}^2 \cdot \text{K}^4)(1000 \text{ K})^4 = 56{,}700 \text{ W/m}^2$$

$T_2 = 1000$ K
Black

Insulated

$\varepsilon_1 = 0.7$
$T_1 = 600$ K

$\dot{Q}_1$ E_{b1} J_1 R_{12} $J_2 = E_{b2}$
R_1
$\dot{Q}_2 = -\dot{Q}_1$
R_{13} R_{23}
$(J_3 = E_{b3})$
$\dot{Q}_3 = 0$
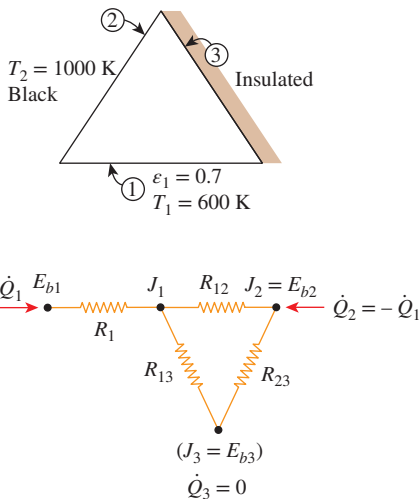
FIGURE 13–28
The triangular furnace considered in Example 13–9.

Substituting,

$$\dot{Q}_1 = \frac{(56{,}700 - 7348) \text{ W/m}^2}{\dfrac{1 - 0.7}{0.7 \times 1 \text{ m}^2} + \left[(0.5 \times 1 \text{ m}^2) + \dfrac{1}{1/(0.5 \times 1 \text{ m}^2) + 1/(0.5 \times 1 \text{ m}^2)}\right]^{-1}}$$

$$= \textbf{28.0 kW}$$

Therefore, heat at a rate of 28 kW must be supplied to the heated surface per unit length of the duct to maintain steady operation in the furnace.

EXAMPLE 13–10   Heat Transfer Through a Tubular Solar Collector

A solar collector consists of a horizontal aluminum tube having an outer diameter of 2 in enclosed in a concentric thin glass tube of 4-in diameter, as shown in Fig. 13–29. Water is heated as it flows through the tube, and the space between the aluminum and the glass tubes is filled with air at 1 atm pressure. The pump circulating the water fails during a clear day, and the water temperature in the tube starts rising. The aluminum tube absorbs solar radiation at a rate of 30 Btu/h per foot length, and the temperature of the ambient air outside is 70°F. The emissivities of the tube and the glass cover are 0.95 and 0.9, respectively. Taking the effective sky temperature to be 50°F, determine the temperature of the aluminum tube when steady operating conditions are established (i.e., when the rate of heat loss from the tube equals the amount of solar energy gained by the tube).

SOLUTION   The circulating pump of a solar collector that consists of a horizontal tube and its glass cover fails. The equilibrium temperature of the tube is to be determined.

Assumptions   **1** Steady operating conditions exist. **2** The tube and its cover are isothermal. **3** Air is an ideal gas. **4** The surfaces are opaque, diffuse, and gray for infrared radiation. **5** The glass cover is transparent to solar radiation.

Properties   The properties of air should be evaluated at the average temperature. But we do not know the exit temperature of the air in the duct, and thus we cannot determine the bulk fluid and glass cover temperatures at this point, so we cannot evaluate the average temperatures. Therefore, we assume the glass temperature to be 110°F, and we use properties at an anticipated average temperature of $(70 + 110)/2 = 90°F$ (Table A–15E),

$$k = 0.01505 \text{ Btu/h·ft·°F} \qquad \text{Pr} = 0.7275$$

$$\nu = 1.753 \times 10^{-4} \text{ ft}^2\text{/s} \qquad \beta = \frac{1}{T_{\text{avg}}} = \frac{1}{550 \text{ R}}$$

Analysis   This problem was solved in Chap. 9 by disregarding radiation heat transfer. Now we repeat the solution by considering natural convection and radiation occurring simultaneously.

We have a horizontal cylindrical enclosure filled with air at 1 atm pressure. The problem involves heat transfer from the aluminum tube to the glass cover and from

Solar energy

70°F

Glass cover
$\varepsilon = 0.9$

4 in

2 in

Aluminum tube
$\varepsilon = 0.95$

Water
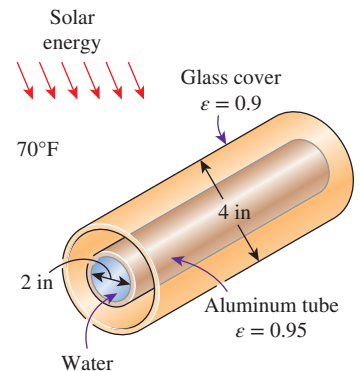
FIGURE 13–29
Schematic for Example 13–10.

the outer surface of the glass cover to the surrounding ambient air. When steady operation is reached, these two heat transfer rates must equal the rate of heat gain. That is,

$$\dot{Q}_{\text{tube-glass}} = \dot{Q}_{\text{glass-ambient}} = \dot{Q}_{\text{solar gain}} = 30 \text{ Btu/h} \qquad \text{(per foot of tube)}$$

The heat transfer surface area of the glass cover is

$$A_o = A_{\text{glass}} = (\pi D_o L) = \pi (4/12 \text{ ft})(1 \text{ ft}) = 1.047 \text{ ft}^2 \qquad \text{(per foot of tube)}$$

To determine the Rayleigh number, we need to know the surface temperature of the glass, which is not available. Therefore, it is clear that the solution requires a trial-and-error approach unless we use an appropriate equation solver. Assuming the glass cover temperature to be 110°F, the Rayleigh number, the Nusselt number, the convection heat transfer coefficient, and the rate of natural convection heat transfer from the glass cover to the ambient air are determined to be

$$\text{Ra}_{D_o} = \frac{g\beta(T_o - T_\infty)D_o^3}{\nu^2}\text{Pr}$$

$$= \frac{(32.2 \text{ ft/s}^2)[1/(550 \text{ R})](110 - 70 \text{ R})(4/12 \text{ ft})^3}{(1.753 \times 10^{-4} \text{ ft}^2/\text{s})^2}(0.7275) = 2.053 \times 10^6$$

$$\text{Nu} = \left\{ 0.6 + \frac{0.387 \, \text{Ra}_{D_o}^{1/6}}{[1 + (0.559/\text{Pr})^{9/16}]^{8/27}} \right\}^2 = \left\{ 0.6 + \frac{0.387 \, (2.053 \times 10^6)^{1/6}}{[1 + (0.559/0.7275)^{9/16}]^{8/27}} \right\}^2$$

$$= 17.88$$

$$h_o = \frac{k}{D_o}\text{Nu} = \frac{0.01505 \text{ Btu/h·ft·°F}}{4/12 \text{ ft}}(17.88) = 0.8073 \text{ Btu/h·ft}^2\text{·°F}$$

$$\dot{Q}_{o,\,\text{conv}} = h_o A_o (T_o - T_\infty) = (0.8073 \text{ Btu/h·ft}^2\text{·°F})(1.047 \text{ ft}^2)(110 - 70)\text{°F}$$

$$= 33.8 \text{ Btu/h}$$

Also,

$$\dot{Q}_{o,\,\text{rad}} = \varepsilon_o \sigma A_o (T_o^4 - T_{\text{sky}}^4)$$

$$= (0.9)(0.1714 \times 10^{-8} \text{ Btu/h·ft}^2\text{·R}^4)(1.047 \text{ ft}^2)[(570 \text{ R})^4 - (510 \text{ R})^4]$$

$$= 61.2 \text{ Btu/h}$$

Then the total rate of heat loss from the glass cover becomes

$$\dot{Q}_{o,\,\text{total}} = \dot{Q}_{o,\,\text{conv}} + \dot{Q}_{o,\,\text{rad}} = 33.8 + 61.2 = 95.0 \text{ Btu/h}$$

which is much larger than 30 Btu/h. Therefore, the assumed temperature of 110°F for the glass cover is high. Repeating the calculations with lower temperatures (including the evaluation of properties), the glass cover temperature corresponding to 30 Btu/h is determined to be 78°F (it would be 106°F if radiation were ignored).

The temperature of the aluminum tube is determined in a similar manner using the natural convection and radiation relations for two horizontal concentric cylinders. The characteristic length in this case is the distance between the two cylinders, which is

$$L_c = (D_o - D_i)/2 = (4 - 2)/2 = 1 \text{ in} = 1/12 \text{ ft}$$

Also,

$$A_i = A_{\text{tube}} = (\pi D_i L) = \pi(2/12 \text{ ft})(1 \text{ ft}) = 0.5236 \text{ ft}^2 \quad \text{(per foot of tube)}$$

We start the calculations by assuming the tube temperature to be 122°F, and thus an average temperature of $(78 + 122)/2 = 100°F = 560 \text{ R}$. Using properties at 100°F,

$$\text{Ra}_L = \frac{g\beta(T_i - T_o)L_c^3}{\nu^2}\text{Pr}$$

$$= \frac{(32.2 \text{ ft/s}^2)[1/(560 \text{ R})](122 - 78 \text{ R})(1/12 \text{ ft})^3}{(1.809 \times 10^{-4} \text{ ft}^2/\text{s})^2}(0.726) = 3.246 \times 10^4$$

The effective thermal conductivity is

$$F_{\text{cyl}} = \frac{[\ln(D_o/D_i)]^4}{L_c^3(D_i^{-3/5} + D_o^{-3/5})^5} = \frac{[\ln(4/2)]^4}{(1/12 \text{ ft})^3[(2/12 \text{ ft})^{-3/5} + (4/12 \text{ ft})^{-3/5}]^5} = 0.1466$$

$$k_{\text{eff}} = 0.386k\left(\frac{\text{Pr}}{0.861 + \text{Pr}}\right)^{1/4}(F_{\text{cyl}}\text{Ra}_L)^{1/4}$$

$$= 0.386(0.01529 \text{ Btu/h·ft·°F})\left(\frac{0.726}{0.861 + 0.726}\right)^{1/4}(0.1466 \times 3.248 \times 10^4)^{1/4}$$

$$= 0.04032 \text{ Btu/h·ft·°F}$$

Then the rate of heat transfer between the cylinders by convection becomes

$$\dot{Q}_{i, \text{conv}} = \frac{2\pi k_{\text{eff}}}{\ln(D_o/D_i)}(T_i - T_o)$$

$$= \frac{2\pi(0.04032 \text{ Btu/h·ft·°F})}{\ln(4/2)}(122 - 78)°F = 16.1 \text{ Btu/h}$$

Also,

$$\dot{Q}_{i, \text{rad}} = \frac{\sigma A_i(T_i^4 - T_o^4)}{\dfrac{1}{\varepsilon_i} + \dfrac{1 - \varepsilon_o}{\varepsilon_o}\left(\dfrac{D_i}{D_o}\right)}$$

$$= \frac{(0.1714 \times 10^{-8} \text{ Btu/h·ft}^2\text{·R}^4)(0.5236 \text{ ft}^2)[(582 \text{ R})^4 - (538 \text{ R})^4]}{\dfrac{1}{0.95} + \dfrac{1 - 0.9}{0.9}\left(\dfrac{2 \text{ in}}{4 \text{ in}}\right)}$$

$$= 25.1 \text{ Btu/h}$$

Then the total rate of heat loss from the glass cover becomes

$$\dot{Q}_{i,\,\text{total}} = \dot{Q}_{i,\,\text{conv}} + \dot{Q}_{i,\,\text{rad}} = 16.1 + 25.1 = 41.2 \text{ Btu/h}$$

which is larger than 30 Btu/h. Therefore, the assumed temperature of 122°F for the tube is high. By trying other values, the tube temperature corresponding to 30 Btu/h is determined to be **112°F** (it would be 180°F if radiation were ignored). Therefore, the tube will reach an equilibrium temperature of 112°F when the pump fails.

Discussion   It is clear from the results obtained that radiation should always be considered in systems that are heated or cooled by natural convection, unless the surfaces involved are polished and thus have very low emissivities.

13–5 · RADIATION SHIELDS AND THE RADIATION EFFECTS

Radiation heat transfer between two surfaces can be reduced greatly by inserting a thin, high-reflectivity (low-emissivity) sheet of material between the two surfaces. Such highly reflective thin plates or shells are called **radiation shields**. Multilayer radiation shields constructed of about 20 sheets per cm thickness separated by evacuated space are commonly used in cryogenic and space applications. Radiation shields are also used in temperature measurements of fluids to reduce the error caused by the radiation effect when the temperature sensor is exposed to surfaces that are much hotter or colder than the fluid itself. The role of the radiation shield is to reduce the rate of radiation heat transfer by placing additional resistances in the path of radiation heat flow. The lower the emissivity of the shield, the higher the resistance.

Radiation heat transfer between two large parallel plates of emissivities ε_1 and ε_2 maintained at uniform temperatures T_1 and T_2 is given by Eq. 13–38:

$$\dot{Q}_{12,\,\text{no shield}} = \frac{A\sigma(T_1^4 - T_2^4)}{\dfrac{1}{\varepsilon_1} + \dfrac{1}{\varepsilon_2} - 1}$$

Now consider a radiation shield placed between these two plates, as shown in Fig. 13–30. Let the emissivities of the shield facing plates 1 and 2 be $\varepsilon_{3,\,1}$ and $\varepsilon_{3,\,2}$, respectively. Note that the emissivity of different surfaces of the shield may be different. The radiation network of this geometry is constructed, as usual, by drawing a surface resistance associated with each surface and connecting these surface resistances with space resistances, as shown in the figure. The resistances are connected in series, and thus the rate of radiation heat transfer is

$$\dot{Q}_{12,\,\text{one shield}} = \frac{E_{b1} - E_{b2}}{\dfrac{1 - \varepsilon_1}{A_1\varepsilon_1} + \dfrac{1}{A_1 F_{13}} + \dfrac{1 - \varepsilon_{3,\,1}}{A_3\varepsilon_{3,\,1}} + \dfrac{1 - \varepsilon_{3,\,2}}{A_3\varepsilon_{3,\,2}} + \dfrac{1}{A_3 F_{32}} + \dfrac{1 - \varepsilon_2}{A_2\varepsilon_2}} \qquad \textbf{(13–42)}$$

(1)　　　　　　　　　　　Shield　　　　　　　　　　(2)

Noting that $F_{13} = F_{32} = 1$ and $A_1 = A_2 = A_3 = A$ for infinite parallel plates, Eq. 13–42 simplifies to

$$\dot{Q}_{12,\text{ one shield}} = \frac{A\sigma(T_1^4 - T_2^4)}{\left(\dfrac{1}{\varepsilon_1} + \dfrac{1}{\varepsilon_2} - 1\right) + \left(\dfrac{1}{\varepsilon_{3,1}} + \dfrac{1}{\varepsilon_{3,2}} - 1\right)} \tag{13–43}$$

where the terms in the second set of parentheses in the denominator represent the additional resistance to radiation introduced by the shield. The appearance of the equation above suggests that parallel plates involving multiple radiation shields can be handled by adding a group of terms like those in the second set of parentheses to the denominator for each radiation shield. Then the radiation heat transfer through large parallel plates separated by *N* radiation shields becomes

$$\dot{Q}_{12,\,N\text{ shields}} = \frac{A\sigma(T_1^4 - T_2^4)}{\left(\dfrac{1}{\varepsilon_1} + \dfrac{1}{\varepsilon_2} - 1\right) + \left(\dfrac{1}{\varepsilon_{3,1}} + \dfrac{1}{\varepsilon_{3,2}} - 1\right) + \cdots + \left(\dfrac{1}{\varepsilon_{N,1}} + \dfrac{1}{\varepsilon_{N,2}} - 1\right)} \tag{13–44}$$

If the emissivities of all surfaces are equal, Eq. 13–44 reduces to

$$\dot{Q}_{12,\,N\text{ shields}} = \frac{A\sigma(T_1^4 - T_2^4)}{(N+1)\left(\dfrac{1}{\varepsilon} + \dfrac{1}{\varepsilon} - 1\right)} = \frac{1}{N+1}\dot{Q}_{12,\text{ no shield}} \tag{13–45}$$

Therefore, when all emissivities are equal, 1 shield reduces the rate of radiation heat transfer to one-half, 9 shields reduce it to one-tenth, and 19 shields reduce it to one-twentieth (or 5 percent) of what it was when there were no shields.

The equilibrium temperature of the radiation shield T_3 in Figure 13–30 can be determined by expressing Eq. 13–43 for $\dot{Q}_{13}$ or $\dot{Q}_{23}$ (which involves T_3) after evaluating $\dot{Q}_{12}$ from Eq. 13–43 and noting that $\dot{Q}_{12} = \dot{Q}_{13} = \dot{Q}_{23}$ when steady conditions are reached.

Radiation shields used to reduce the rate of radiation heat transfer between concentric cylinders and spheres can be handled in a similar manner. In case of one shield, Eq. 13–42 can be used by taking $F_{13} = F_{32} = 1$ for both cases and by replacing the *A*'s with the proper area relations.
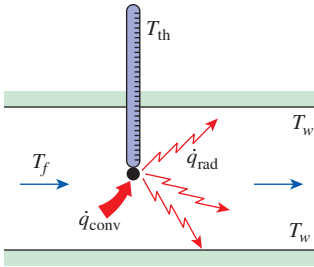
FIGURE 13–31
A thermometer used to measure the temperature of a fluid in a channel.

Radiation Effect on Temperature Measurements

A temperature measuring device indicates the temperature of its *sensor,* which is supposed to be, but is not necessarily, the temperature of the medium that the sensor is in contact with. When a thermometer (or any other temperature measuring device such as a thermocouple) is placed in a medium, heat transfer takes place between the sensor of the thermometer and the medium by convection until the sensor reaches the temperature of the medium. But when the sensor is surrounded by surfaces that are at a different temperature than the fluid, radiation exchange also takes place between the sensor and the surrounding surfaces. When the heat transfers by convection and radiation balance each other, the sensor indicates a temperature that falls between the fluid and surface temperatures. Next we develop a procedure to account for the radiation effect and to determine the actual fluid temperature.

Consider a thermometer that is used to measure the temperature of a fluid flowing through a large channel whose walls are at a lower temperature than the fluid (Fig. 13–31). Equilibrium will be established and the reading of the thermometer will stabilize when heat gain by convection, as measured by the sensor, equals heat loss by radiation (or vice versa). That is, on a unit-area basis,

$$\dot{q}_{\text{conv, to sensor}} = \dot{q}_{\text{rad, from sensor}}$$
$$h(T_f - T_{\text{th}}) = \varepsilon\sigma(T_{\text{th}}^4 - T_w^4)$$

or

$$T_f = T_{\text{th}} + \frac{\varepsilon\sigma(T_{\text{th}}^4 - T_w^4)}{h} \qquad (\text{K}) \qquad \textbf{(13–46)}$$

where

T_f = actual temperature of the fluid, K

T_{th} = temperature value measured by the thermometer, K

T_w = temperature of the surrounding surfaces, K

h = convection heat transfer coefficient, W/m²·K

ε = emissivity of the sensor of the thermometer

The last term in Eq. 13–46 is due to the *radiation effect* and represents the *radiation correction.* Note that the radiation correction term is most significant when the convection heat transfer coefficient is small and the emissivity of the surface of the sensor is large. Therefore, the sensor should be coated with a material of high reflectivity (low emissivity) to reduce the radiation effect.

Placing the sensor in a radiation shield without interfering with the fluid flow also reduces the radiation effect. The sensors of temperature measurement devices used outdoors must be protected from direct sunlight since the radiation effect in that case is sure to reach unacceptable levels.

The radiation effect is also a significant factor in *human comfort* in heating and air-conditioning applications. A person who feels fine in a room at a specified temperature may feel chilly in another room at the same temperature as a result of the radiation effect if the walls of the second room are at a considerably lower temperature. For example, most people feel comfortable in a room at 22°C if the walls of the room are also roughly at that temperature. When the wall temperature drops to 5°C for some reason, the interior temperature of the room must be raised to at least 27°C to maintain the same level

of comfort. Therefore, well-insulated buildings conserve energy not only by reducing the heat loss or heat gain, but also by allowing the thermostats to be set at a lower temperature in winter and at a higher temperature in summer without compromising the comfort level.

EXAMPLE 13–11   Radiation Shields

A thin aluminum sheet with an emissivity of 0.1 on both sides is placed between two very large parallel plates that are maintained at uniform temperatures $T_1 = 800$ K and $T_2 = 500$ K and have emissivities $\varepsilon_1 = 0.2$ and $\varepsilon_2 = 0.7$, respectively, as shown in Fig. 13–32. Determine the *net* rate of radiation heat transfer between the two plates per unit surface area of the plates, and compare the result to that without the shield.

SOLUTION   A thin aluminum sheet is placed between two large parallel plates maintained at uniform temperatures. The *net* rates of radiation heat transfer between the two plates with and without the radiation shield are to be determined.
Assumptions   The surfaces are opaque, diffuse, and gray.
Analysis   The *net* rate of radiation heat transfer between these two plates without the shield was determined in Example 13–7 to be 3625 W/m². Heat transfer in the presence of one shield is determined from Eq. 13–43 to be

$$\dot{q}_{12,\text{ one shield}} = \frac{\dot{Q}_{12,\text{ one shield}}}{A} = \frac{\sigma(T_1^4 - T_2^4)}{\left(\dfrac{1}{\varepsilon_1} + \dfrac{1}{\varepsilon_2} - 1\right) + \left(\dfrac{1}{\varepsilon_{3,1}} + \dfrac{1}{\varepsilon_{3,2}} - 1\right)}$$

$$= \frac{(5.67 \times 10^{-8} \text{ W/m}^2\cdot\text{K}^4)[(800 \text{ K})^4 - (500 \text{ K})^4]}{\left(\dfrac{1}{0.2} + \dfrac{1}{0.7} - 1\right) + \left(\dfrac{1}{0.1} + \dfrac{1}{0.1} - 1\right)}$$

$$= \textbf{806 W/m}^2$$

Discussion   Note that the rate of radiation heat transfer reduces to about one-fourth of what it was as a result of placing a radiation shield between the two parallel plates.
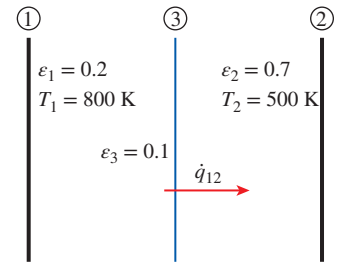
FIGURE 13–32
Schematic for Example 13–11.

PtD EXAMPLE 13–12   Prevention of Thermal Burn Hazards by Using Radiation Shields

Heat treatment of metals is commonly done using electrically heated draw batch furnaces. Consider a furnace that is situated in a room with surrounding air temperature of 30°C and an average convection heat transfer coefficient of 10 W/m²·K, as shown in Fig. 13–33. Convection and radiation heat transfer occur between the furnace outer surface and the surroundings. The furnace front is made of two parallel plates, where the inner plate has a temperature of 600°C. To ensure safety and prevent thermal burns to people working around the furnace, the outer surface of the furnace should be kept below 45°C. Based on the given information, determine the number of radiation shields that should be placed parallel in the furnace front. Assume all the surfaces have the same emissivity of 0.1.
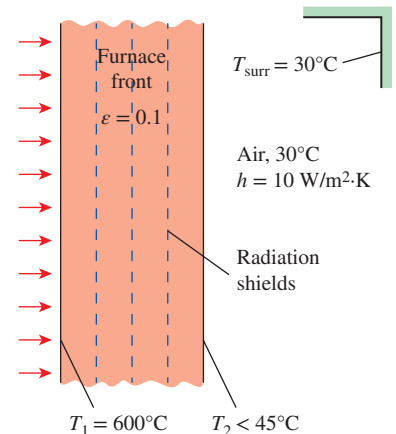
FIGURE 13–33
Schematic for Example 13–12.

SOLUTION In this example, the concepts of Prevention through Design (PtD) are applied in conjunction with the concepts of radiation shield and radiation heat transfer between surfaces.

Assumptions **1** Steady operating conditions exist. **2** The surfaces are opaque, diffuse, and gray. **3** Convection heat transfer in between the furnace front plates is not considered. **4** The ambient temperature is equal to the temperature of the surrounding surfaces, $T_\infty = T_{surr}$.

Properties The emissivity of all the surfaces is given as $\varepsilon = 0.1$.

Analysis The *net* radiation heat transfer between the parallel plates of the furnace front is

$$\dot{q}_{12} = \frac{\sigma(T_1^4 - T_2^4)}{(N+1)\left(\dfrac{1}{\varepsilon} + \dfrac{1}{\varepsilon} - 1\right)}$$

The convection and radiation heat transfer between the outer furnace front surface and the surroundings are

$$\dot{q}_{conv} = h(T_2 - T_{surr}) \qquad \text{and} \qquad \dot{q}_{rad} = \varepsilon\sigma(T_2^4 - T_{surr}^4)$$

Performing the energy balance on the outer surface, we have

$$\dot{q}_{12} = \dot{q}_{rad} + \dot{q}_{conv}$$

$$\frac{\sigma(T_1^4 - T_2^4)}{(N+1)\left(\dfrac{1}{\varepsilon} + \dfrac{1}{\varepsilon} - 1\right)} = h(T_2 - T_\infty) + \varepsilon\sigma(T_2^4 - T_{surr}^4)$$

Hence,

$$N = \left(\frac{1}{1/\varepsilon + 1/\varepsilon - 1}\right)\left[\frac{\sigma(T_1^4 - T_2^4)}{h(T_2 - T_\infty) + \varepsilon\sigma(T_2^4 - T_{surr}^4)}\right] - 1$$

$$= \left(\frac{1}{2/0.1 - 1}\right)$$

$$\left[\frac{(5.67 \times 10^{-8}\ \text{W/m}^2\cdot\text{K}^4)(873^4 - 318^4)\,\text{K}^4}{(10\ \text{W/m}^2\cdot\text{K})(318 - 303)\text{K} + (0.1)(5.67 \times 10^{-8}\ \text{W/m}^2\cdot\text{K}^4)(318^4 - 303^4)\,\text{K}^4}\right] - 1$$

$$= 9.63 \approx \mathbf{10}$$

Thus, placing 10 radiation shields inside the furnace front will keep the outer surface temperature below 45°C to prevent thermal burn hazards.

Discussion Without the radiation shield, the temperature of the furnace front outer surface will be 174°C. By placing radiation shields in the furnace front, heat transfer through the furnace front is reduced to 45°C as specified in the problem statement.

Air, T_f
Thermocouple
$T_{th} = 530$ K
$\varepsilon_1 = 0.7$
$\varepsilon_2 = 0.15$
$T_w = 380$ K
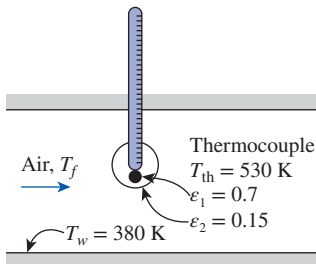
FIGURE 13–34
Schematic for Example 13–13.

EXAMPLE 13–13 Actual Gas Temperature Measurements With and Without Radiation Shield

A thermocouple shielded by aluminum foil of emissivity 0.15 is used to measure the temperature of hot gases flowing in a duct whose walls are maintained at $T_w = 380$ K. The thermocouple shows a temperature reading of $T_{th} = 530$ K (Fig. 13–34). Assuming the emissivity of the thermocouple junction to be 0.7 and the convection heat transfer coefficient to be 120 W/m²·K, determine the actual temperature of the gas. What would the actual temperature of the gas be if no radiation shield were used?

SOLUTION   The temperature of hot gas in a duct is measured by a thermocouple. The actual temperature of the gas is to be determined and compared with that without a radiation shield.

Assumptions   **1** The surfaces are opaque, diffuse, and gray. **2** The diameter of the thermocouple junction is very close to the diameter of the shield, $D_1 \approx D_2$, but they are not in contact. **3** The duct walls behave as a blackbody, $\varepsilon_w = 1.0$.

Properties   The emissivity of the thermocouple junction is $\varepsilon_1 = 0.7$, and the emissivity of the aluminum foil shield is $\varepsilon_2 = 0.15$.

Analysis   The radiation from the thermocouple junction to the duct walls, with the aluminum foil shield, is determined from Eq. 13–42

$$\dot{Q}_{\text{rad, from sensor}} = \frac{\sigma(T_{\text{th}}^4 - T_w^4)}{\dfrac{1-\varepsilon_1}{A_1\varepsilon_1} + \dfrac{1}{A_1 F_{12}} + \dfrac{1-\varepsilon_2}{A_2\varepsilon_2} + \dfrac{1-\varepsilon_2}{A_2\varepsilon_2} + \dfrac{1}{A_2 F_{2w}} + \dfrac{1-\varepsilon_w}{A_w\varepsilon_w}}$$

With $D_1 \approx D_2$, we have $A_1 \approx A_2$. Also, $\varepsilon_w = 1.0$, $F_{12} = F_{2w} = 1$, yields

$$\dot{q}_{\text{rad, from sensor}} = \frac{\dot{Q}_{\text{rad, from sensor}}}{A_1} = \frac{\sigma(T_{\text{th}}^4 - T_w^4)}{\dfrac{1-\varepsilon_1}{\varepsilon_1} + 1 + \dfrac{1-\varepsilon_2}{\varepsilon_2} + \dfrac{1-\varepsilon_2}{\varepsilon_2} + 1} = \frac{\sigma(T_{\text{th}}^4 - T_w^4)}{\dfrac{1}{\varepsilon_1} + 2\dfrac{1}{\varepsilon_2} - 1}$$

$$\dot{q}_{\text{rad, from sensor}} = \frac{(5.67 \times 10^{-8} \text{ W/m}^2\cdot\text{K}^4)[(530 \text{ K})^4 - (380 \text{ K})^4]}{\dfrac{1}{0.7} + 2\dfrac{1}{0.15} - 1} = 239.18 \text{ W/m}^2$$

Then the actual temperature of the gas can be determined from a heat transfer balance to be

$$\dot{q}_{\text{conv, to sensor}} = \dot{q}_{\text{rad, from sensor}}$$
$$h(T_f - T_{\text{th}}) = \dot{q}_{\text{rad, from sensor}}$$
$$T_f = T_{\text{th}} + \frac{\dot{q}_{\text{rad, from sensor}}}{h} = (530 \text{ K}) + \frac{239.18 \text{ W/m}^2}{120 \text{ W/m}^2\cdot\text{K}} = \textbf{532.0 K (with shield)}$$

Without the shield, the actual temperature of the gas is determined from Eq. 13–46 to be

$$T_f = T_{\text{th}} + \frac{\varepsilon_1\sigma(T_{\text{th}}^4 - T_w^4)}{h}$$
$$= (530 \text{ K}) + \frac{(0.7)(5.67 \times 10^{-8} \text{ W/m}^2\cdot\text{K}^4)[(530 \text{ K})^4 - (380 \text{ K})^4]}{120 \text{ W/m}^2\cdot\text{K}}$$
$$= \textbf{549.2 K (without shield)}$$

Discussion   With the radiation shield, the temperature of the thermocouple is only 2°C lower than the actual gas temperature. Without the radiation shield, the temperature of the thermocouple is 19.2°C lower than the actual gas temperature. Thus, the radiation shield minimizes the radiation effect on temperature measurement by the thermocouple, which gives a reading that is closer to the actual gas temperature.

13–6 ▪ RADIATION EXCHANGE WITH EMITTING AND ABSORBING GASES

So far we have considered radiation heat transfer between surfaces separated by a medium that does not emit, absorb, or scatter radiation—a nonparticipating medium that is completely transparent to thermal radiation. A vacuum satisfies this condition perfectly, and air at ordinary temperatures and pressures comes very close. Gases that consist of monatomic molecules such as Ar and He and symmetric diatomic molecules such as N_2 and O_2 are essentially transparent to radiation, except at extremely high temperatures at which ionization occurs. Therefore, atmospheric air can be considered to be a nonparticipating medium in radiation calculations.

Gases with asymmetric molecules such as H_2O, CO_2, CO, SO_2, and hydrocarbons $H_m C_n$ may participate in the radiation process by absorption at moderate temperatures, and by absorption and emission at high temperatures such as those encountered in combustion chambers. Therefore, air or any other medium that contains such gases with asymmetric molecules at sufficient concentrations must be treated as a participating medium in radiation calculations. Combustion gases in a furnace or a combustion chamber, for example, contain sufficient amounts of H_2O and CO_2, and thus the emission and absorption of gases in furnaces must be taken into consideration.

The presence of a participating medium complicates the radiation analysis considerably for several reasons:

- A participating medium emits and absorbs radiation throughout its entire volume. That is, gaseous radiation is a *volumetric phenomenon,* and thus it depends on the size and shape of the body. This is the case even if the temperature is uniform throughout the medium.

- Gases emit and absorb radiation at a number of narrow wavelength bands. This is in contrast to solids, which emit and absorb radiation over the entire spectrum. Therefore, the gray assumption may not always be appropriate for a gas even when the surrounding surfaces are gray.

- The emission and absorption characteristics of the constituents of a gas mixture also depend on the temperature, pressure, and composition of the gas mixture. Therefore, the presence of other participating gases affects the radiation characteristics of a particular gas.

The propagation of radiation through a medium can be complicated further by the presence of *aerosols* such as dust, ice particles, liquid droplets, and soot (unburned carbon) particles that *scatter* radiation. Scattering refers to the change of direction of radiation due to reflection, refraction, and diffraction. Scattering caused by gas molecules themselves is known as *Rayleigh scattering,* and it has a negligible effect on heat transfer. Radiation transfer in scattering media is considered in advanced books such as the ones by Modest (2003) and Siegel and Howell (2002).

The participating medium can also be semitransparent liquids or solids such as water, glass, and plastics. To keep complexities to a manageable level, we limit our consideration to gases that emit and absorb radiation. In particular, we consider the emission and absorption of radiation by H_2O and CO_2 only since they are the participating gases most commonly encountered in

practice (combustion products in furnaces and combustion chambers burning hydrocarbon fuels contain both gases at high concentrations), and they are sufficient to demonstrate the basic principles involved.

Radiation Properties of a Participating Medium

Consider a participating medium of thickness L. A spectral radiation beam of intensity $I_{\lambda, 0}$ is incident on the medium, which is attenuated as it propagates due to absorption. The decrease in the intensity of radiation as it passes through a layer of thickness dx is proportional to the intensity itself and the thickness dx. This is known as **Beer's law** and is expressed as (Fig. 13–35)

$$dI_\lambda(x) = -\kappa_\lambda I_\lambda(x)dx \tag{13–47}$$

where the constant of proportionality κ_λ is the **spectral absorption coefficient** of the medium whose unit is m^{-1} (from the requirement of dimensional homogeneity). This is just like the amount of interest earned by a bank account during a time interval being proportional to the amount of money in the account and the time interval, with the interest rate being the constant of proportionality.

Separating the variables and integrating from $x = 0$ to $x = L$ gives

$$\frac{I_{\lambda, L}}{I_{\lambda, 0}} = e^{-\kappa_\lambda L} \tag{13–48}$$

where we have assumed the absorptivity of the medium to be independent of x. Note that radiation intensity decays exponentially in accordance with Beer's law.

The **spectral transmissivity** of a medium can be defined as the ratio of the intensity of radiation leaving the medium to that entering the medium. That is,

$$\tau_\lambda = \frac{I_{\lambda, L}}{I_{\lambda, 0}} = e^{-\kappa_\lambda L} \tag{13–49}$$

Note that $\tau_\lambda = 1$ when no radiation is absorbed and thus radiation intensity remains constant. Also, the spectral transmissivity of a medium represents the fraction of radiation transmitted by the medium at a given wavelength.

Radiation passing through a nonscattering (and thus nonreflecting) medium is either absorbed or transmitted. Therefore $\alpha_\lambda + \tau_\lambda = 1$, and the **spectral absorptivity** of a medium of thickness L is

$$\alpha_\lambda = 1 - \tau_\lambda = 1 - e^{-\kappa_\lambda L} \tag{13–50}$$

From Kirchoff's law, the **spectral emissivity** of the medium is

$$\varepsilon_\lambda = \alpha_\lambda = 1 - e^{-\kappa_\lambda L} \tag{13–51}$$

Note that the spectral absorptivity, transmissivity, and emissivity of a medium are dimensionless quantities, with values less than or equal to 1. The spectral absorption coefficient of a medium (and thus ε_λ, α_λ, and τ_λ), in general, vary with wavelength, temperature, pressure, and composition.

For an *optically thick* medium (a medium with a large value of $\kappa_\lambda L$), Eq. 13–51 gives $\varepsilon_\lambda \approx \alpha_\lambda \approx 1$. For $\kappa_\lambda L = 5$, for example, $\varepsilon_\lambda = \alpha_\lambda = 0.993$. Therefore, an optically thick medium emits like a blackbody at the given wavelength. As a result, an optically thick absorbing-emitting medium with no significant scattering at a given temperature T_g can be viewed as a "black
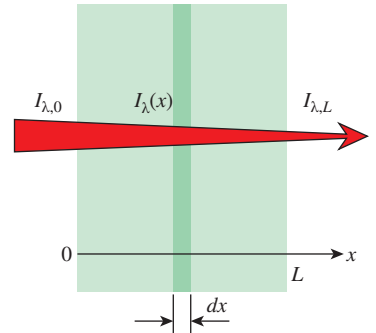
FIGURE 13–35
The attenuation of a radiation beam while passing through an absorbing medium of thickness L.

surface" at T_g since it will absorb essentially all the radiation passing through it, and it will emit the maximum possible radiation that can be emitted by a surface at T_g, which is $E_{b\lambda}(T_g)$.

Emissivity and Absorptivity of Gases and Gas Mixtures

The spectral absorptivity of CO_2 is given in Fig. 13–36 as a function of wavelength. The various peaks and dips in the figure together with discontinuities show clearly the band nature of absorption and the strong nongray characteristics. The shape and the width of these absorption bands vary with temperature and pressure, but the magnitude of absorptivity also varies with the thickness of the gas layer. Therefore, absorptivity values without specified thickness and pressure are meaningless.

The nongray nature of properties should be considered in radiation calculations for high accuracy. This can be done using a band model, and thus performing calculations for each absorption band. However, satisfactory results can be obtained by assuming the gas to be gray and using an effective total absorptivity and emissivity determined by some averaging process. Charts for the total emissivities of gases are first presented by Hottel (1954), and they have been widely used in radiation calculations with reasonable accuracy. Alternative emissivity charts and calculation procedures have been developed more recently by Edwards and Matavosian (1984). Here we present the Hottel approach because of its simplicity.

Even with gray assumption, the total emissivity and absorptivity of a gas depends on the geometry of the gas body as well as the temperature, pressure, and composition. Gases that participate in radiation exchange such as CO_2 and H_2O typically coexist with nonparticipating gases such as N_2 and O_2, and thus radiation properties of an absorbing and emitting gas are usually reported for a mixture of the gas with nonparticipating gases rather than the pure gas. The emissivity and absorptivity of a gas component in a mixture depend primarily on its density, which is a function of temperature and partial pressure of the gas.

The emissivity of H_2O vapor in a mixture of nonparticipating gases is plotted in Fig. 13–37a for a total pressure of $P = 1$ atm as a function of gas
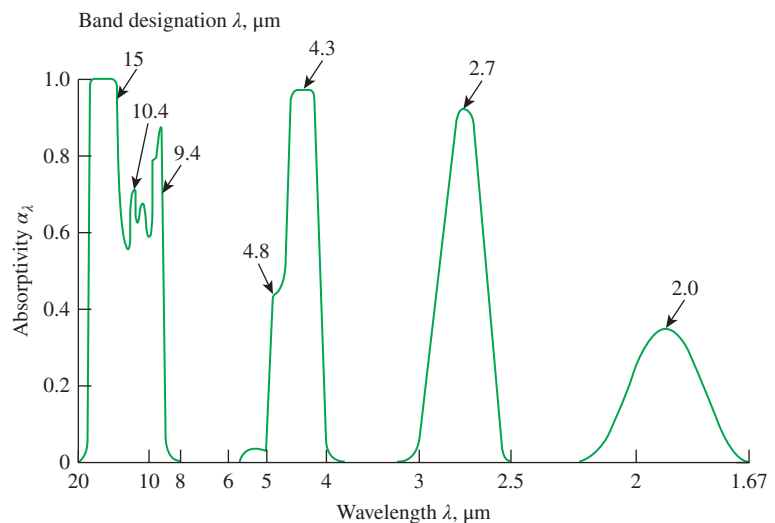
FIGURE 13–36
Spectral absorptivity of CO_2 at 830 K and 10 atm for a path length of 38.8 cm.
Source: Siegel and Howell, 2002.

temperature T_g for a range of values for $P_w L$, where P_w is the partial pressure of water vapor and L is the mean distance traveled by the radiation beam. Emissivity at a total pressure P other than $P = 1$ atm is determined by multiplying the emissivity value at 1 atm by a **pressure correction factor** C_w obtained from Fig. 13–38a for water vapor. That is,

$$\varepsilon_w = C_w \varepsilon_{w,\,1\text{ atm}} \qquad \textbf{(13–52)}$$

Note that $C_w = 1$ for $P = 1$ atm and thus $(P_w + P)/2 \cong 0.5$ (a very low concentration of water vapor is used in the preparation of the emissivity chart in Fig. 13–37a and thus P_w is very low). Emissivity values are presented in a similar manner for a mixture of CO_2 and nonparticipating gases in Figs. 13–37b and 13–38b.

Now the question that comes to mind is what will happen if the CO_2 and H_2O gases exist *together* in a mixture with nonparticipating gases. The emissivity of each participating gas can still be determined as explained above using its partial pressure, but the effective emissivity of the mixture cannot be determined by simply adding the emissivities of individual gases (although this would be the case if different gases emitted at different wavelengths). Instead, it should be determined from

$$\begin{aligned}\varepsilon_g &= \varepsilon_c + \varepsilon_w - \Delta\varepsilon \\ &= C_c \varepsilon_{c,\,1\text{ atm}} + C_w \varepsilon_{w,\,1\text{ atm}} - \Delta\varepsilon\end{aligned} \qquad \textbf{(13–53)}$$
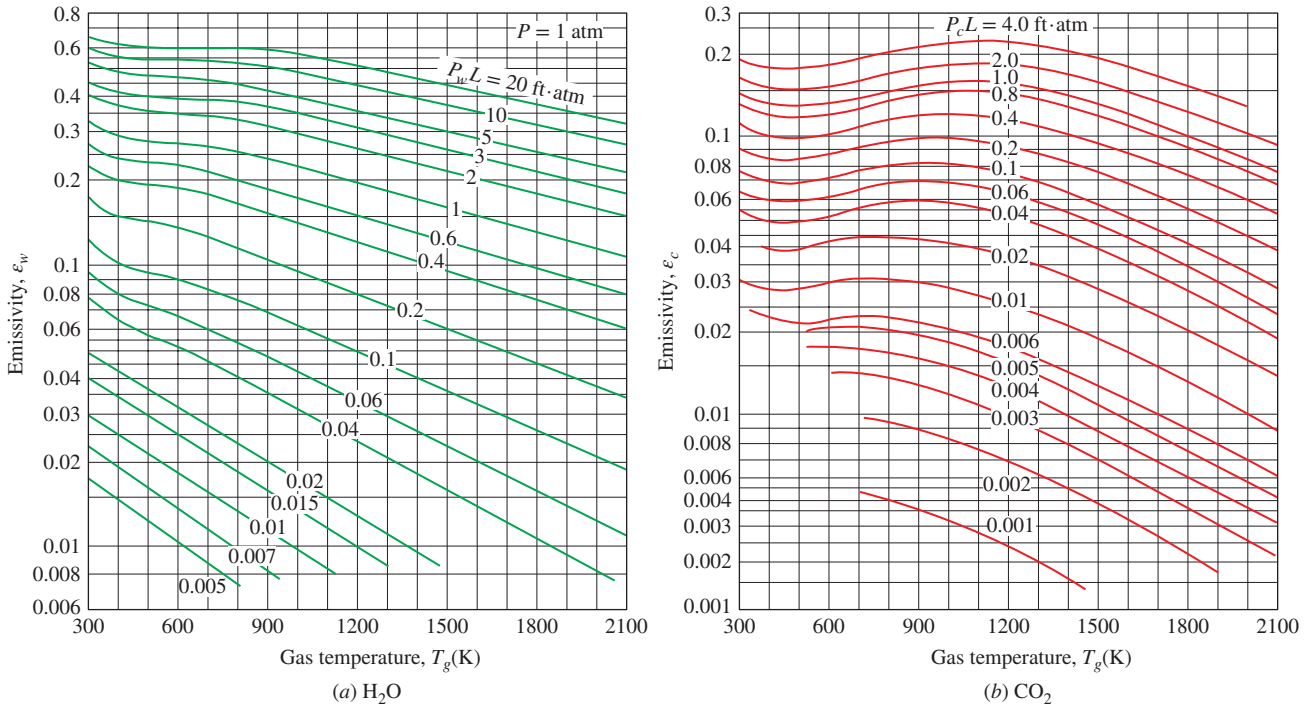
FIGURE 13–37

Emissivities of H_2O and CO_2 gases in a mixture of nonparticipating gases at a total pressure of 1 atm for a mean beam length of L (1 m·atm = 3.28 ft·atm).

Source: Hottel, 1954.
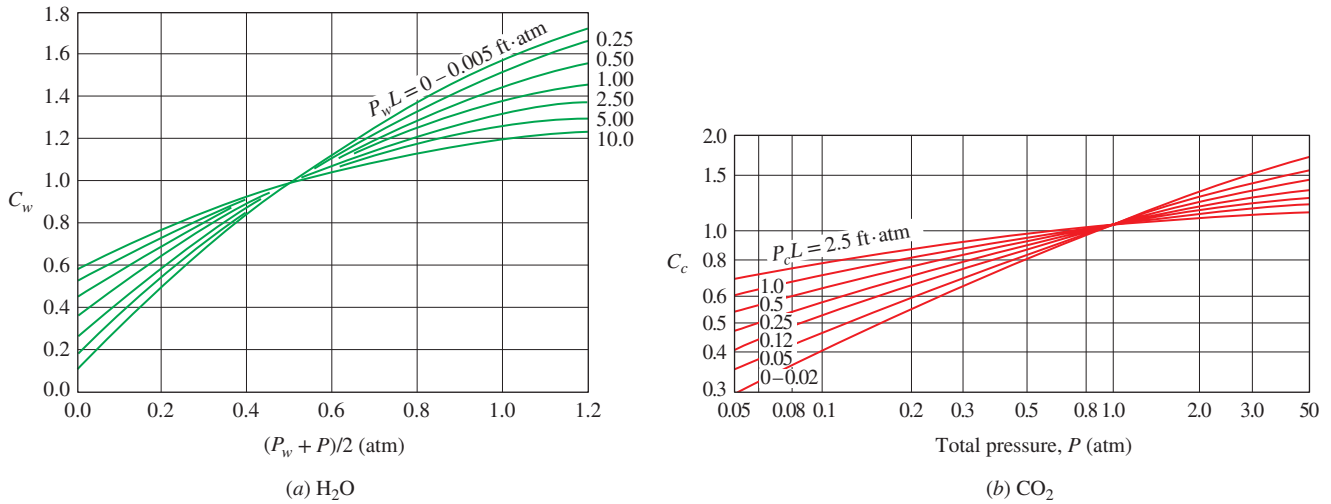
FIGURE 13−38
Correction factors for the emissivities of H_2O and CO_2 gases at pressures other than 1 atm for use in the relations $\varepsilon_w = C_w \varepsilon_{w, 1\,atm}$ and $\varepsilon_c = C_c \varepsilon_{c, 1\,atm}$ (1 m·atm = 3.28 ft·atm).
Source: Hottel, 1954.
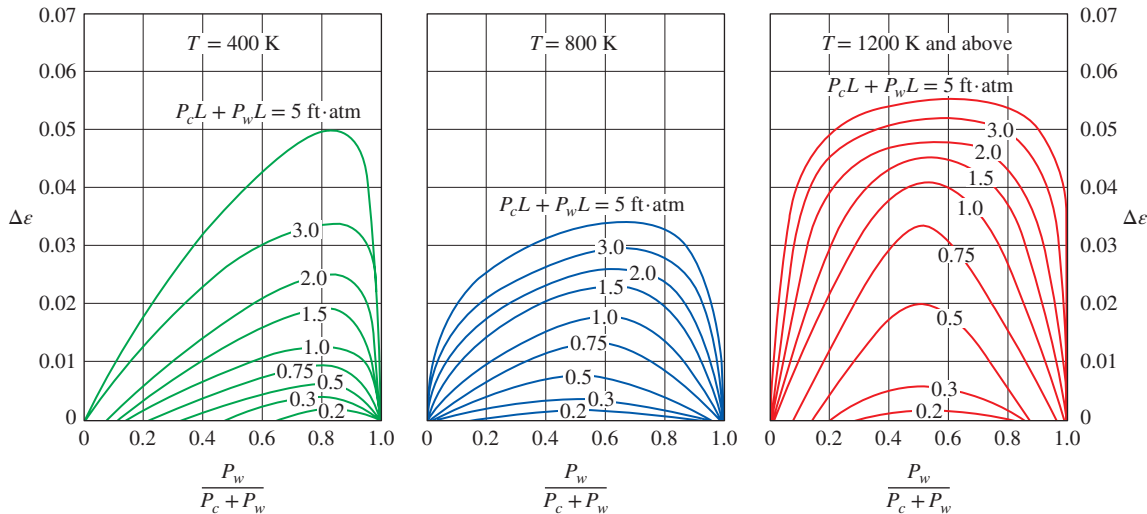
FIGURE 13−39
Emissivity correction $\Delta\varepsilon$ for use in $\varepsilon_g = \varepsilon_w + \varepsilon_c - \Delta\varepsilon$ when both CO_2 and H_2O vapor are present in a gas mixture (1 m·atm = 3.28 ft·atm).
Source: Hottel, 1954.

where $\Delta\varepsilon$ is the **emissivity correction factor**, which accounts for the overlap of emission bands. For a gas mixture that contains both CO_2 and H_2O gases, $\Delta\varepsilon$ is plotted in Fig. 13–39.

The emissivity of a gas also depends on the *mean length* an emitted radiation beam travels in the gas before reaching a bounding surface, and thus the shape and the size of the gas body involved. During their experiments in the 1930s, Hottel and his coworkers considered the emission of radiation from

TABLE 13–4

Mean beam length L for various gas volume shapes

Gas Volume Geometry	L
Hemisphere of radius R radiating to the center of its base	R
Sphere of diameter D radiating to its surface	$0.65D$
Infinite circular cylinder of diameter D radiating to curved surface	$0.95D$
Semi-infinite circular cylinder of diameter D radiating to its base	$0.65D$
Semi-infinite circular cylinder of diameter D radiating to center of its base	$0.90D$
Infinite semicircular cylinder of radius R radiating to center of its base	$1.26R$
Circular cylinder of height equal to diameter D radiating to entire surface	$0.60D$
Circular cylinder of height equal to diameter D radiating to center of its base	$0.71D$
Infinite slab of thickness D radiating to either bounding plane	$1.80D$
Cube of side length L radiating to any face	$0.66L$
Arbitrary shape of volume V and surface area A_s radiating to surface	$3.6\ V/A_s$

a hemispherical gas body to a small surface element located at the center of the base of the hemisphere. Therefore, the given charts represent emissivity data for the emission of radiation from a hemispherical gas body of radius L toward the center of the base of the hemisphere. It is certainly desirable to extend the reported emissivity data to gas bodies of other geometries, and this is done by introducing the concept of **mean beam length** L, which represents the radius of an equivalent hemisphere. The mean beam lengths for various gas geometries are listed in Table 13–4. More extensive lists are available in the literature such as (Hottel, 1954 and Siegel and Howell, 2002). The emissivities associated with these geometries can be determined from Figs. 13–37 through 13–39 by using the appropriate mean beam length.

Following a procedure recommended by Hottel, the absorptivity of a gas that contains CO_2 and H_2O gases for radiation emitted by a source at temperature T_s can be determined similarly from

$$\alpha_g = \alpha_c + \alpha_w - \Delta\alpha \qquad \textbf{(13–54)}$$

where $\Delta\alpha = \Delta\varepsilon$ and is determined from Fig. 13–39 at the source temperature T_s. The absorptivities of CO_2 and H_2O can be determined from the emissivity charts (Figs. 13–37 and 13–38) as

$$CO_2: \qquad \alpha_c = C_c \times (T_g/T_s)^{0.65} \times \varepsilon_c(T_s, P_c L T_s/T_g) \qquad \textbf{(13–55)}$$

and

$$H_2O: \qquad \alpha_w = C_w \times (T_g/T_s)^{0.45} \times \varepsilon_w(T_s, P_w L T_s/T_g) \qquad \textbf{(13–56)}$$

The notation indicates that the emissivities should be evaluated using T_s instead of T_g (both in K or R), $P_c L T_s/T_g$ instead of $P_c L$, and $P_w L T_s/T_g$ instead of $P_w L$. Note that the absorptivity of the gas depends on the source temperature T_s as well as the gas temperature T_g. Also, $\alpha = \varepsilon$ when $T_s = T_g$, as expected. The pressure correction factors C_c and C_w are evaluated using $P_c L$ and $P_w L$, as in emissivity calculations.

When the total emissivity of a gas ε_g at temperature T_g is known, the emissive power of the gas (radiation emitted by the gas per unit surface area) can be expressed as $E_g = \varepsilon_g \sigma T_g^4$. Then the rate of radiation energy emitted by a gas to a bounding surface of area A_s becomes

$$\dot{Q}_{g,e} = \varepsilon_g A_s \sigma T_g^4 \qquad (13\text{–}57)$$

If the bounding surface is black at temperature T_s, the surface will emit radiation to the gas at a rate of $A_s \sigma T_s^4$ without reflecting any, and the gas will absorb this radiation at a rate of $\alpha_g A_s \sigma T_s^4$, where α_g is the absorptivity of the gas. Then the *net* rate of radiation heat transfer between the gas and a black surface surrounding it becomes

Black enclosure: $\qquad \dot{Q}_{net} = A_s \sigma (\varepsilon_g T_g^4 - \alpha g T_s^4) \qquad (13\text{–}58)$

If the surface is not black, the analysis becomes more complicated because of the radiation reflected by the surface. But for surfaces that are nearly black with an emissivity $\varepsilon > 0.7$, Hottel (1954) recommends this modification,

$$\dot{Q}_{net,\,gray} = \frac{\varepsilon_s + 1}{2} \dot{Q}_{net,\,black} = \frac{\varepsilon_s + 1}{2} A_s \sigma (\varepsilon_g T_g^4 - \alpha_g T_s^4) \qquad (13\text{–}59)$$

The emissivity of wall surfaces of furnaces and combustion chambers are typically greater than 0.7, and thus the preceding relation provides great convenience for preliminary radiation heat transfer calculations.

EXAMPLE 13–14   Effective Emissivity of Combustion Gases

A cylindrical furnace whose height and diameter are 5 m contains combustion gases at 1200 K and a total pressure of 2 atm. The composition of the combustion gases is determined by volumetric analysis to be 80 percent N_2, 8 percent H_2O, 7 percent O_2, and 5 percent CO_2. Determine the effective emissivity of the combustion gases (Fig. 13–40).

SOLUTION   The temperature, pressure, and composition of a gas mixture is given. The emissivity of the mixture is to be determined.

Assumptions   **1** All the gases in the mixture are ideal gases. **2** The emissivity determined is the mean emissivity for radiation emitted to all surfaces of the cylindrical enclosure.

Analysis   The volumetric analysis of a gas mixture gives the mole fractions y_i of the components, which are equivalent to pressure fractions for an ideal gas mixture. Therefore, the partial pressures of CO_2 and H_2O are

$$P_c = y_{CO_2} P = 0.05(2 \text{ atm}) = 0.10 \text{ atm}$$
$$P_w = y_{H_2O} P = 0.08(2 \text{ atm}) = 0.16 \text{ atm}$$

The mean beam length for a cylinder of equal diameter and height for radiation emitted to all surfaces is, from Table 13–4,

$$L = 0.60D = 0.60(5 \text{ m}) = 3 \text{ m}$$

$H = 5$ m

$D = 5$ m $T_g = 1200$ K
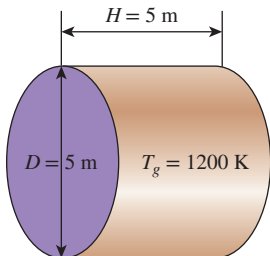
FIGURE 13–40
Schematic for Example 13–14.

Then,

$$P_c L = (0.10 \text{ atm})(3 \text{ m}) = 0.30 \text{ m·atm} = 0.98 \text{ ft·atm}$$
$$P_w L = (0.16 \text{ atm})(3 \text{ m}) = 0.48 \text{ m·atm} = 1.57 \text{ ft·atm}$$

The emissivities of CO_2 and H_2O corresponding to these values at the gas temperature of $T_g = 1200$ K and 1 atm are, from Fig. 13–37,

$$\varepsilon_{c, 1 \text{ atm}} = 0.16 \qquad \text{and} \qquad \varepsilon_{w, 1 \text{ atm}} = 0.23$$

These are the base emissivity values at 1 atm, and they need to be corrected for the 2 atm total pressure. Noting that $(P_w + P)/2 = (0.16 + 2)/2 = 1.08$ atm, the pressure correction factors are, from Fig. 13–38,

$$C_c = 1.1 \qquad \text{and} \qquad C_w = 1.4$$

Both CO_2 and H_2O are present in the same mixture, and we need to correct for the overlap of emission bands. The emissivity correction factor at $T = T_g = 1200$ K is, from Fig. 13–39,

$$\left.\begin{array}{l} P_c L + P_w L = 0.98 + 1.57 = 2.55 \\ \dfrac{P_w}{P_w + P_c} = \dfrac{0.16}{0.16 + 0.10} = 0.615 \end{array}\right\} \Delta\varepsilon = 0.048$$

Then the effective emissivity of the combustion gases becomes

$$\varepsilon_g = C_c \varepsilon_{c, 1 \text{ atm}} + C_w \varepsilon_{w, 1 \text{ atm}} - \Delta\varepsilon = 1.1 \times 0.16 + 1.4 \times 0.23 - 0.048 = \mathbf{0.45}$$

Discussion This is the average emissivity for radiation emitted to all surfaces of the cylindrical enclosure. For radiation emitted toward the center of the base, the mean beam length is $0.71D$ instead of $0.60D$, and the emissivity value would be different.

EXAMPLE 13–15   Radiation Heat Transfer in a Cylindrical Furnace

Reconsider the cylindrical furnace discussed in Example 13–14. For a wall temperature of 600 K, determine the absorptivity of the combustion gases and the rate of radiation heat transfer from the combustion gases to the furnace walls (Fig. 13–41).

SOLUTION The temperatures for the wall surfaces and the combustion gases are given for a cylindrical furnace. The absorptivity of the gas mixture and the rate of radiation heat transfer are to be determined.
Assumptions **1** All the gases in the mixture are ideal gases. **2** All interior surfaces of furnace walls are black. **3** Scattering by soot and other particles is negligible.
Analysis The average emissivity of the combustion gases at the gas temperature of $T_g = 1200$ K was determined in the preceding example to be $\varepsilon_g = 0.45$. For a source

$H = 5$ m

$D = 5$ m

$T_g = 1200$ K

$T_s = 600$ K

$\dot{Q}_{\text{net}}$
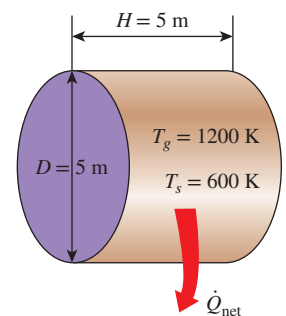
FIGURE 13–41
Schematic for Example 13–15.

temperature of $T_s = 600$ K, the absorptivity of the gas is again determined using the emissivity charts as

$$P_c L \frac{T_s}{T_g} = (0.10 \text{ atm})(3 \text{ m}) \frac{600 \text{ K}}{1200 \text{ K}} = 0.15 \text{ m·atm} = 0.49 \text{ ft·atm}$$

$$P_w L \frac{T_s}{T_g} = (0.16 \text{ atm})(3 \text{ m}) \frac{600 \text{ K}}{1200 \text{ K}} = 0.24 \text{ m·atm} = 0.79 \text{ ft·atm}$$

The emissivities of CO_2 and H_2O corresponding to these values at a temperature of $T_s = 600$ K and 1 atm are, from Fig. 13–37,

$$\varepsilon_{c,\, 1 \text{ atm}} = 0.11 \qquad \text{and} \qquad \varepsilon_{w,\, 1 \text{ atm}} = 0.25$$

The pressure correction factors were determined in the preceding example to be $C_c = 1.1$ and $C_w = 1.4$, and they do not change with surface temperature. Then the absorptivities of CO_2 and H_2O become

$$\alpha_c = C_c \left(\frac{T_g}{T_s} \right)^{0.65} \varepsilon_{c,\, 1 \text{ atm}} = (1.1) \left(\frac{1200 \text{ K}}{600 \text{ K}} \right)^{0.65} (0.11) = 0.19$$

$$\alpha_w = C_w \left(\frac{T_g}{T_s} \right)^{0.45} \varepsilon_{w,\, 1 \text{ atm}} = (1.4) \left(\frac{1200 \text{ K}}{600 \text{ K}} \right)^{0.45} (0.25) = 0.48$$

Also $\Delta\alpha = \Delta\varepsilon$, but the emissivity correction factor is to be evaluated from Fig. 13–39 at $T = T_s = 600$ K instead of $T_g = 1200$ K. There is no chart for 600 K in the figure, but we can read $\Delta\varepsilon$ values at 400 K and 800 K, and take their average. At $P_w/(P_w + P_c) = 0.615$ and $P_c L + P_w L = 2.55$ we read $\Delta\varepsilon = 0.027$. Then the absorptivity of the combustion gases becomes

$$\alpha_g = \alpha_c + \alpha_w - \Delta\alpha = 0.19 + 0.48 - 0.027 = \mathbf{0.64}$$

The surface area of the cylindrical surface is

$$A_s = \pi DH + 2 \frac{\pi D^2}{4} = \pi (5 \text{ m})(5 \text{ m}) + 2 \frac{\pi (5 \text{ m})^2}{4} = 118 \text{ m}^2$$

Then the *net* rate of radiation heat transfer from the combustion gases to the walls of the furnace becomes

$$\dot{Q}_{\text{net}} = A_s \sigma (\varepsilon_g T_g^4 - \alpha_g T_s^4)$$

$$= (118 \text{ m}^2)(5.67 \times 10^{-8} \text{ W/m}^2 \cdot \text{K}^4) [0.45 (1200 \text{ K})^4 - 0.64 (600 \text{ K})^4]$$

$$= \mathbf{5.69 \times 10^6 \text{ W}}$$

Discussion The heat transfer rate determined above is for the case of black wall surfaces. If the surfaces are not black but the surface emissivity ε_s is greater than 0.7, the heat transfer rate can be determined by multiplying the rate of heat transfer already determined by $(\varepsilon_s + 1)/2$.

TOPIC OF SPECIAL INTEREST*

Heat Transfer from the Human Body

The metabolic heat generated in the body is dissipated to the environment through the skin and the lungs by convection and radiation as *sensible heat* and by evaporation as *latent heat* (Fig. 13–42). Latent heat represents the heat of vaporization of water as it evaporates in the lungs and on the skin by absorbing body heat, and latent heat is released as the moisture condenses on cold surfaces. The warming of the inhaled air represents sensible heat transfer in the lungs and is proportional to the temperature rise of inhaled air. The total rate of heat loss from the body can be expressed as

$$\dot{Q}_{\text{body, total}} = \dot{Q}_{\text{skin}} + \dot{Q}_{\text{lungs}}$$
$$= (\dot{Q}_{\text{sensible}} + \dot{Q}_{\text{latent}})_{\text{skin}} + (\dot{Q}_{\text{sensible}} + \dot{Q}_{\text{latent}})_{\text{lungs}} \qquad \textbf{(13–60)}$$
$$= (\dot{Q}_{\text{convection}} + \dot{Q}_{\text{radiation}} + \dot{Q}_{\text{latent}})_{\text{skin}} + (\dot{Q}_{\text{convection}} + \dot{Q}_{\text{latent}})_{\text{lungs}}$$

Therefore, the determination of heat transfer from the body by analysis alone is difficult. Clothing further complicates the heat transfer from the body, and thus we must rely on experimental data. Under steady conditions, the total rate of heat transfer from the body is equal to the rate of metabolic heat generation in the body, which varies from about 100 W for light office work to roughly 1000 W during heavy physical work.

   Sensible heat loss from the skin depends on the temperatures of the skin, the environment, and the surrounding surfaces as well as the air motion. The *latent heat loss,* on the other hand, depends on the skin wettedness and the relative humidity of the environment as well. *Clothing* serves as insulation and reduces both the sensible and latent forms of heat loss. The heat transfer from the lungs through respiration obviously depends on the frequency of breathing and the volume of the lungs as well as the environmental factors that affect heat transfer from the skin.

   Sensible heat from the clothed skin is first transferred to the clothing and then from the clothing to the environment. The convection and radiation heat losses from the outer surface of a clothed body can be expressed as

$$\dot{Q}_{\text{conv}} = h_{\text{conv}} A_{\text{clothing}} (T_{\text{clothing}} - T_{\text{ambient}}) \quad \text{(W)} \qquad \textbf{(13–61)}$$
$$\dot{Q}_{\text{rad}} = h_{\text{rad}} A_{\text{clothing}} (T_{\text{clothing}} - T_{\text{surr}}) \qquad \textbf{(13–62)}$$

where

h_{conv} = convection heat transfer coefficient, as given in Table 13–5
h_{rad} = radiation heat transfer coefficient, 4.7 W/m²·K for typical indoor conditions; the emissivity is assumed to be 0.95, which is typical
A_{clothing} = outer surface area of a clothed person
T_{clothing} = average temperature of exposed skin and clothing
T_{ambient} = ambient air temperature
T_{surr} = average temperature of the surrounding surfaces

---

*This section can be skipped without a loss of continuity.
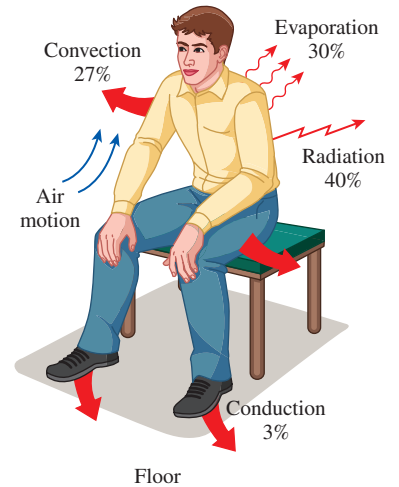
FIGURE 13–42
Mechanisms of heat loss from the human body and relative magnitudes for a resting person.

Convection heat transfer coefficients for a clothed body at 1 atm (V is in m/s) (compiled from various sources)

Activity	h_{conv},* W/m$^2\cdot$K
Seated in air moving at	
$0 < V < 0.2$ m/s	3.1
$0.2 < V < 4$ m/s	$8.3V^{0.6}$
Walking in still air at	
$0.5 < V < 2$ m/s	$8.6V^{0.53}$
Walking on treadmill	
in still air at	
$0.5 < V < 2$ m/s	$6.5V^{0.39}$
Standing in moving air at	
$0 < V < 0.15$ m/s	4.0
$0.15 < V < 1.5$ m/s	$14.8V^{0.69}$

* At pressures other than 1 atm, multiply by $P^{0.55}$, where P is in atm.
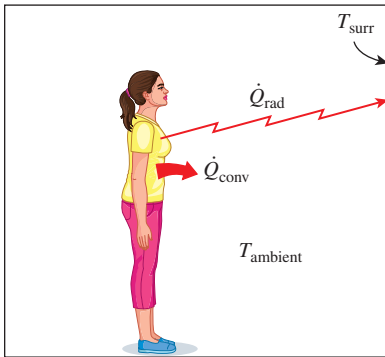
(a) Convection and radiation, separate
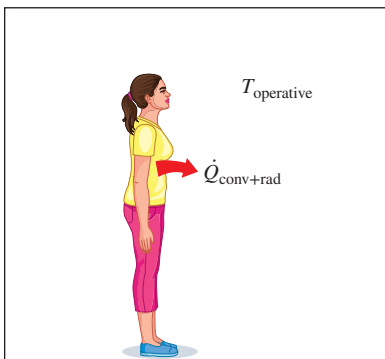
(b) Convection and radiation, combined

FIGURE 13–43

Heat loss by convection and radiation from the body can be combined into a single term by defining an equivalent operative temperature.

The convection heat transfer coefficients at 1 atm pressure are given in Table 13–5. Convection coefficients at pressures P other than 1 atm are obtained by multiplying the values at atmospheric pressure by $P^{0.55}$ where P is in atm. Also, it is recognized that the temperatures of different surfaces surrounding a person are probably different, and T_{surr} represents the **mean radiation temperature**, which is the temperature of an imaginary isothermal enclosure in which radiation heat exchange with the human body equals the radiation heat exchange with the actual enclosure. Noting that most clothing and building materials are very nearly black, the *mean radiation temperature* of an enclosure that consists of N surfaces at different temperatures can be determined from

$$T_{surr} \cong F_{person-1}T_1 + F_{person-2}T_2 + \ldots + F_{person-N}T_N \qquad \textbf{(13–63)}$$

where T_i is the *temperature of the surface i* and $F_{person-i}$ is the *view factor* between the person and surface i.

Total sensible heat loss can also be expressed conveniently by combining the convection and radiation heat losses as

$$\dot{Q}_{conv+rad} = h_{combined}A_{clothing}(T_{clothing} - T_{operative}) \qquad \textbf{(13–64)}$$

$$= (h_{conv} + h_{rad})A_{clothing}(T_{clothing} - T_{operative}) \quad \text{(W)} \qquad \textbf{(13–65)}$$

where the **operative temperature** $T_{operative}$ is the average of the mean radiant and ambient temperatures weighed by their respective convection and radiation heat transfer coefficients and is expressed as (Fig. 13–43)

$$T_{operative} = \frac{h_{conv}T_{ambient} + h_{rad}T_{surr}}{h_{conv} + h_{rad}} \cong \frac{T_{ambient} + T_{surr}}{2} \qquad \textbf{(13–66)}$$

Note that the operative temperature will be the arithmetic average of the ambient and surrounding surface temperatures when the convection and radiation heat transfer coefficients are equal to each other. Another environmental index used in thermal comfort analysis is the **effective temperature**, which combines the effects of temperature and humidity. Two environments with the same effective temperature evokes the same thermal response in people even though they are at different temperatures and humidities.

Heat transfer through the *clothing* can be expressed as

$$\dot{Q}_{conv+rad} = \frac{A_{clothing}(T_{skin} - T_{clothing})}{R_{clothing}} \qquad \textbf{(13–67)}$$

where $R_{clothing}$ is the **unit thermal resistance of clothing** in m$^2\cdot$K/W, which involves the combined effects of conduction, convection, and radiation between the skin and the outer surface of clothing. The thermal resistance of clothing is usually expressed in the unit **clo** where 1 clo = 0.155 m$^2\cdot$K/W = 0.880 ft$^2\cdot$°F·h/Btu. The thermal resistance of trousers, long-sleeve shirt, long-sleeve sweater, and T-shirt is 1.0 clo, or 0.155 m$^2\cdot$K/W. Summer clothing such as light slacks and short-sleeved shirt has an insulation value of 0.5 clo, whereas winter clothing such as heavy slacks, long-sleeve shirt, and a sweater or jacket has an insulation value of 0.9 clo.

Then the total sensible heat loss can be expressed in terms of the skin temperature instead of the inconvenient clothing temperature as (Fig. 13–44)

$$\dot{Q}_{\text{conv + rad}} = \frac{A_{\text{clothing}}(T_{\text{skin}} - T_{\text{operative}})}{R_{\text{clothing}} + \dfrac{1}{h_{\text{combined}}}} \tag{13–68}$$

At a state of thermal comfort, the average skin temperature of the body is observed to be 33°C (91.5°F). No discomfort is experienced as the skin temperature fluctuates by ±1.5°C (2.5°F). This is the case whether the body is clothed or unclothed.

Evaporative or **latent heat loss** from the skin is proportional to the difference between the water vapor pressure at the skin and the ambient air, and the skin wettedness, which is a measure of the amount of moisture on the skin. It is due to the combined effects of the *evaporation of sweat* and the *diffusion* of water through the skin, and can be expressed as

$$\dot{Q}_{\text{latent}} = \dot{m}_{\text{vapor}} h_{fg} \tag{13–69}$$

where

$\dot{m}_{\text{vapor}}$ = the rate of evaporation from the body, kg/s

h_{fg} = the enthalpy of vaporization of water = 2430 kJ/kg at 30°C

Heat loss by evaporation is maximum when the skin is completely wetted. Also, clothing offers resistance to evaporation, and the rate of evaporation in clothed bodies depends on the moisture permeability of the clothes. The maximum evaporation rate for an average man is about 1 L/h (0.3 g/s), which represents an upper limit of 730 W for the evaporative cooling rate. A person can lose as much as 2 kg of water per hour during a workout on a hot day, but any excess sweat slides off the skin surface without evaporating (Fig. 13–45).

During *respiration,* the inhaled air enters at ambient conditions and exhaled air leaves nearly saturated at a temperature close to the deep body temperature (Fig. 13–46). Therefore, the body loses both sensible heat by convection and latent heat by evaporation from the lungs, and these can be expressed as

$$\dot{Q}_{\text{conv, lungs,}} = \dot{m}_{\text{air, lungs}} c_{p, \text{air}}(T_{\text{exhale}} - T_{\text{ambient}}) \tag{13–70}$$

$$\dot{Q}_{\text{latent, lungs}} = \dot{m}_{\text{vapor, lungs}} h_{fg} = \dot{m}_{\text{air, lungs}}(\omega_{\text{exhale}} - \omega_{\text{ambient}}) h_{fg} \tag{13–71}$$

where

$\dot{m}_{\text{air, lungs}}$ = rate of air intake to the lungs, kg/s

$c_{p, \text{air}}$ = specific heat of air = 1.0 kJ/kg·K

T_{exhale} = temperature of exhaled air

ω = humidity ratio (the mass of moisture per unit mass of dry air)

The rate of air intake to the lungs is directly proportional to the metabolic rate $\dot{Q}_{\text{met}}$. The rate of total heat loss from the lungs through respiration can be expressed approximately as

$$\dot{Q}_{\text{conv + latent, lungs}} = 0.0014\dot{Q}_{\text{met}}(34 - T_{\text{ambient}}) + 0.0173\dot{Q}_{\text{met}}(5.87 - P_{v, \text{ambient}}) \tag{13–72}$$
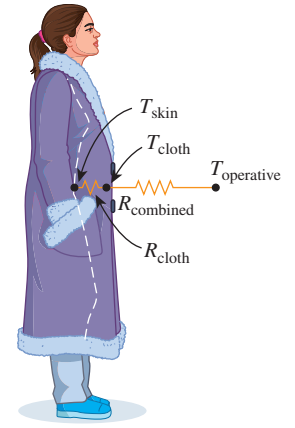
FIGURE 13–44
Simplified thermal resistance network for heat transfer from a clothed person.

$\dot{Q}_{\text{latent,max}} = \dot{m}_{\text{latent,max}} h_{fg @ 30°C}$
$= (0.3 \text{ g/s})(2430 \text{ kJ/kg})$
$= 729 \text{ W}$
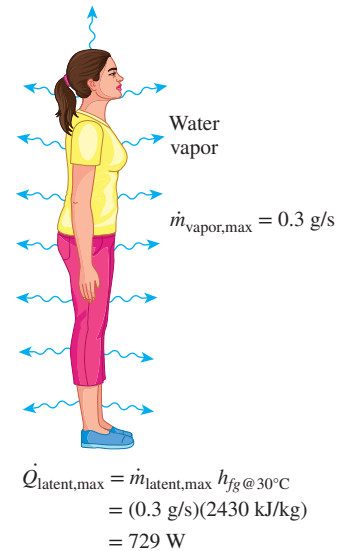
FIGURE 13–45
An average person can lose heat at a rate of up to 730 W by evaporation.
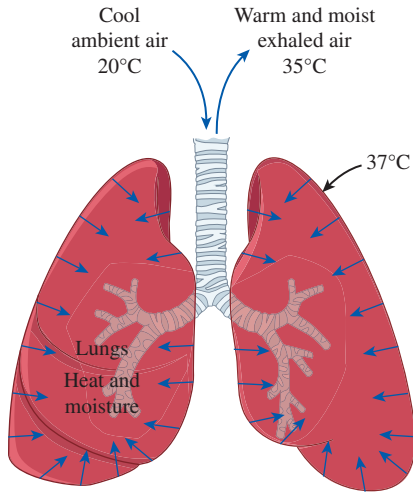
FIGURE 13–46
Part of the metabolic heat generated in the body is rejected to the air from the lungs during respiration.
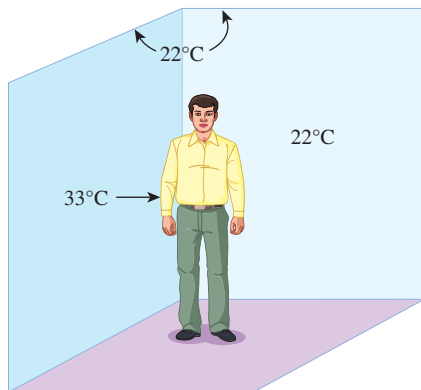
where $P_{v,\,\text{ambient}}$ is the vapor pressure of ambient air in kPa.

The fraction of sensible heat varies from about 40 percent in the case of heavy work to about 70 percent during light work. The rest of the energy is rejected from the body by perspiration in the form of latent heat.

EXAMPLE 13–16   Effect of Clothing on Thermal Comfort

It is well established that a clothed or unclothed person feels comfortable when the skin temperature is about 33°C. Consider an average man wearing summer clothes whose thermal resistance is 0.6 clo. The man feels very comfortable while standing in a room maintained at 22°C. The air motion in the room is negligible, and the interior surface temperature of the room is about the same as the air temperature. If this man were to stand in that room unclothed, determine the temperature at which the room must be maintained for him to feel thermally comfortable.

SOLUTION   A man wearing summer clothes feels comfortable in a room at 22°C. The room temperature at which this man would feel thermally comfortable when unclothed is to be determined.

Assumptions   **1** Steady conditions exist. **2** The latent heat loss from the person remains the same. **3** The heat transfer coefficients remain the same.

Analysis   The body loses heat in sensible and latent forms, and the sensible heat consists of convection and radiation heat transfer. At low air velocities, the convection heat transfer coefficient for a standing man is given in Table 13–5 to be 4.0 W/m²·K. The radiation heat transfer coefficient at typical indoor conditions is 4.7 W/m²·K. Therefore, the surface heat transfer coefficient for a standing person for combined convection and radiation is

$$h_{\text{combined}} = h_{\text{conv}} + h_{\text{rad}} = 4.0 + 4.7 = 8.7 \text{ W/m}^2\text{·K}$$

The thermal resistance of the clothing is given to be

$$R_{\text{clothing}} = 0.6 \text{ clo} = 0.6 \times 0.155 \text{ m}^2\text{·K/W} = 0.093 \text{ m}^2\text{·K/W}$$

Noting that the surface area of an average man is 1.8 m², the sensible heat loss from this person when clothed is determined to be (Fig. 13–47)

$$\dot{Q}_{\text{sensible, clothed}} = \frac{A_s(T_{\text{skin}} - T_{\text{ambient}})}{R_{\text{clothing}} + \dfrac{1}{h_{\text{combined}}}} = \frac{(1.8 \text{ m}^2)(33 - 22)°\text{C}}{0.093 \text{ m}^2\text{·°C/W} + \dfrac{1}{8.7 \text{ W/m}^2\text{·K}}}$$

$$= 95.2 \text{ W}$$

From a heat transfer point of view, taking the clothes off is equivalent to removing the clothing insulation or setting $R_{\text{clothing}} = 0$. The heat transfer in this case can be expressed as

$$\dot{Q}_{\text{sensible, unclothed}} = \frac{A_s(T_{\text{skin}} - T_{\text{ambient}})}{\dfrac{1}{h_{\text{combined}}}} = \frac{(1.8 \text{ m}^2)(33 - T_{\text{ambient}})°\text{C}}{\dfrac{1}{8.7 \text{ W/m}^2\text{·K}}}$$

FIGURE 13–47
Schematic for Example 13–16.

To maintain thermal comfort after taking the clothes off, the skin temperature of the person and the rate of heat transfer from him must remain the same. Then setting the equation above equal to 95.2 W gives

$$T_{\text{ambient}} = \textbf{26.9°C}$$

Therefore, the air temperature needs to be raised from 22 to 26.9°C to ensure that the person feels comfortable in the room after he takes his clothes off (Fig. 13–48).

Discussion   Note that the effect of clothing on latent heat is assumed to be negligible in the solution above. We also assumed the surface area of the clothed and unclothed person to be the same for simplicity, and these two effects should counteract each other.
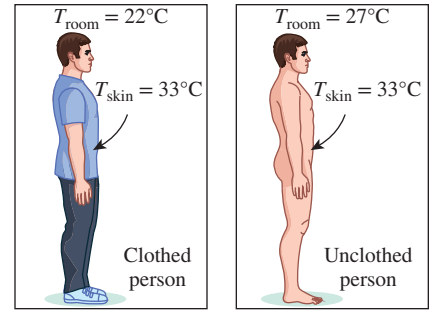
FIGURE 13–48
Clothing serves as insulation, and the room temperature needs to be raised when a person is unclothed to maintain the same comfort level.

SUMMARY

Radiation heat transfer between surfaces depends on the orientation of the surfaces relative to each other. In a radiation analysis, this effect is accounted for by the geometric parameter *view factor*. The *view factor* from a surface i to a surface j is denoted by $F_{i \to j}$ or F_{ij} and is defined as the fraction of the radiation leaving surface i that strikes surface j directly. The view factors between differential and finite surfaces are expressed as

$$dF_{dA_1 \to dA_2} = \frac{\dot{Q}_{dA_1 \to dA_2}}{\dot{Q}_{dA_1}} = \frac{\cos\theta_1 \cos\theta_2}{\pi r^2} dA_2$$

$$F_{dA_1 \to A_2} = \int_{A_2} \frac{\cos\theta_1 \cos\theta_2}{\pi r^2} dA_2$$

$$F_{12} = F_{A_1 \to A_2} = \frac{\dot{Q}_{A_1 \to A_2}}{\dot{Q}_{A_1}} = \frac{1}{A_1}\int_{A_2}\int_{A_1} \frac{\cos\theta_1 \cos\theta_2}{\pi r^2} dA_1\, dA_2$$

where r is the distance between dA_1 and dA_2, and θ_1 and θ_2 are the angles between the normals of the surfaces and the line that connects dA_1 and dA_2.

The view factor $F_{i \to i}$ represents the fraction of the radiation leaving surface i that strikes itself directly; $F_{i \to i} = 0$ for *plane* or *convex* surfaces and $F_{i \to i} \neq 0$ for *concave* surfaces. For view factors, the *reciprocity rule* is expressed as

$$A_i F_{i \to j} = A_j F_{j \to i}$$

The sum of the view factors from surface i of an enclosure to all surfaces of the enclosure, including to itself, must equal unity. This is known as the *summation rule* for an enclosure. The *superposition rule* is expressed as follows: The view factor from a surface i to a surface j is equal to the sum of the view factors from surface i to the parts of surface j. The symmetry rule is expressed as follows: If the surfaces j and k are symmetric about the surface i, then $F_{i \to j} = F_{i \to k}$.

The rate of *net* radiation heat transfer between two *black* surfaces is determined from

$$\dot{Q}_{1 \to 2} = A_1 F_{1 \to 2}\sigma(T_1^4 - T_2^4)$$

The *net* radiation heat transfer from any surface i of a *black* enclosure is determined by adding up the *net* radiation heat transfers from surface i to each of the surfaces of the enclosure:

$$\dot{Q}_i = \sum_{j=1}^{N} \dot{Q}_{i \to j} = \sum_{j=1}^{N} A_i F_{i \to j}\sigma(T_i^4 - T_j^4)$$

The total radiation energy leaving a surface per unit time and per unit area is called the *radiosity* and is denoted by J. The *net* rate of radiation heat transfer from a surface i of surface area A_i is expressed as

$$\dot{Q}_i = \frac{E_{bi} - J_i}{R_i}$$

where

$$R_i = \frac{1 - \varepsilon_i}{A_i \varepsilon_i}$$

is the *surface resistance* to radiation. The *net* rate of radiation heat transfer from surface i to surface j can be expressed as

$$\dot{Q}_{i \to j} = \frac{J_i - J_j}{R_{i \to j}}$$

where

$$R_{i \to j} = \frac{1}{A_i F_{i \to j}}$$

is the *space resistance* to radiation. The *network method* is applied to radiation enclosure problems by drawing a surface resistance associated with each surface of an enclosure and

connecting them with space resistances. Then the problem is solved by treating it as an electrical network problem where the radiation heat transfer replaces the current and the radiosity replaces the potential. The *direct method* is based on the following two equations:

Surfaces with specified net heat transfer rate $\dot{Q}_i$

$$\dot{Q}_i = A_i \sum_{j=1}^{N} F_{i \to j}(J_i - J_j)$$

Surfaces with specified temperature T_i

$$\sigma T_i^4 = J_i + \frac{1 - \varepsilon_i}{\varepsilon_i} \sum_{j=1}^{N} F_{i \to j}(J_i - J_j)$$

The first and the second groups of equations give N linear algebraic equations for the determination of the N unknown radiosities for an N-surface enclosure. Once the radiosities $J_1, J_2, \ldots, J_N$ are available, the unknown surface temperatures and heat transfer rates can be determined from the equations just shown.

The *net* rate of radiation transfer between any two gray, diffuse, opaque surfaces that form an enclosure is given by

$$\dot{Q}_{12} = \frac{\sigma(T_1^4 - T_2^4)}{\dfrac{1 - \varepsilon_1}{A_1 \varepsilon_1} + \dfrac{1}{A_1 F_{12}} + \dfrac{1 - \varepsilon_2}{A_2 \varepsilon_2}}$$

Radiation heat transfer between two surfaces can be reduced greatly by inserting between the two surfaces thin, high-reflectivity (low-emissivity) sheets of material called *radiation shields*. Radiation heat transfer between two large parallel plates separated by N radiation shields is

$$\dot{Q}_{12,\,N\text{ shields}} = \frac{A\sigma(T_1^4 - T_2^4)}{\left(\dfrac{1}{\varepsilon_1} + \dfrac{1}{\varepsilon_2} - 1\right) + \ldots + \left(\dfrac{1}{\varepsilon_{N,1}} + \dfrac{1}{\varepsilon_{N,2}} - 1\right)}$$

The radiation effect in temperature measurements can be properly accounted for by

$$T_f = T_{\text{th}} + \frac{\varepsilon\sigma(T_{\text{th}}^4 - T_w^4)}{h}$$

where T_f is the actual fluid temperature, T_{th} is the temperature value measured by the thermometer, and T_w is the temperature of the surrounding walls, all in K.

Gases with asymmetric molecules such as H_2O, CO_2 CO, SO_2, and hydrocarbons $H_n C_m$ participate in the radiation process by absorption and emission. The *spectral transmissivity, absorptivity,* and *emissivity* of a medium are expressed as

$$\tau_\lambda = e^{-\kappa_\lambda L}, \quad \alpha_\lambda = 1 - \tau_\lambda = 1 - e^{-\kappa_\lambda L}, \quad \text{and} \quad \varepsilon_\lambda = \alpha_\lambda = 1 - e^{-\kappa\lambda L}$$

where κ_λ is the *spectral absorption coefficient* of the medium.

The emissivities of H_2O and CO_2 gases are given in Fig. 13–36 for a total pressure of $P = 1$ atm. Emissivities at other pressures are determined from

$$\varepsilon_w = C_w \varepsilon_{w,\,1\text{ atm}} \quad \text{and} \quad \varepsilon_c = C_c \varepsilon_{c,\,1\text{ atm}}$$

where C_w and C_c are the *pressure correction factors*. For gas mixtures that contain both of H_2O and CO_2, the emissivity is determined from

$$\varepsilon_g = \varepsilon_c + \varepsilon_w - \Delta\varepsilon = C_c \varepsilon_{c,\,1\text{ atm}} + C_w \varepsilon_{w,\,1\text{ atm}} - \Delta\varepsilon$$

where $\Delta\varepsilon$ is the *emissivity correction factor,* which accounts for the overlap of emission bands. The gas absorptivities for radiation emitted by a source at temperature T_s are determined similarly from

$$\alpha_g = \alpha_c + \alpha_w - \Delta\alpha$$

where $\Delta\alpha = \Delta\varepsilon$ at the source temperature T_s and

CO_2: $\quad \alpha_c = C_c \times (T_g/T_s)^{0.65} \times \varepsilon_c(T_s, P_c L T_s/T_g)$

H_2O: $\quad \alpha_w = C_w \times (T_g/T_s)^{0.45} \times \varepsilon_w(T_s, P_w L T_s/T_g)$

The rate of radiation heat transfer between a gas and a surrounding surface is

Black enclosure: $\quad \dot{Q}_{\text{net}} = A_s \sigma(\varepsilon_g T_g^4 - \alpha_g T_s^4)$

Gray enclosure, with $\varepsilon_s > 0.7$: $\quad \dot{Q}_{\text{net, gray}} = \dfrac{\varepsilon_s + 1}{2} A_s \sigma(\varepsilon_g T_g^4 - \alpha_g T_s^4)$

REFERENCES AND SUGGESTED READING

1. D. K. Edwards. *Radiation Heat Transfer Notes.* Washington, DC: Hemisphere, 1981.

2. D. K. Edwards and R. Matavosian. "Scaling Rules for Total Absorptivity and Emissivity of Gases." *Journal of Heat Transfer* 106 (1984), pp. 684–689.

3. D. K. Edwards and R. Matavosian. "Emissivity Data for Gases." Section 5.5.5 in *Hemisphere Handbook of Heat Exchanger Design,* ed. G. F. Hewitt. New York: Hemisphere, 1990.

4. D. C. Hamilton and W. R. Morgan. "Radiation Interchange Configuration Factors." National Advisory Committee for Aeronautics, Technical Note 2836, 1952.

5. H. C. Hottel. "Radiant Heat Transmission." In *Heat Transmission,* 3rd ed., ed. W. H. McAdams. New York: McGraw-Hill, 1954.

6. H. C. Hottel. "Heat Transmission by Radiation from Non-Luminous Gases." *Transactions of the AIChE* 19 (1927), pp. 173–205.

7. H. C. Hottel and R. B. Egbert. "Radiant Heat Transmission from Water Vapor." *Transactions of the AIChE* 38 (1942), pp. 531–565.

8. J. R. Howell. *A Catalog of Radiation Configuration Factors.* New York: McGraw-Hill, 1982.

9. M. F. Modest. *Radiative Heat Transfer,* 2nd ed. New York: Academic Press, 2003.

10. A. K. Oppenheim. "Radiation Analysis by the Network Method." *Transactions of the ASME* 78 (1956), pp. 725–735.

11. R. Siegel and J. R. Howell. *Thermal Radiation Heat Transfer,* 4th ed. New York: Taylor & Francis, 2002.

12. S. Thyageswaran. "Radiation View Factor for Co-Axial and Unequal Rectangles in Parallel Planes." *Heat Transfer Engineering* 38 (2017), pp. 1522–1529.

PROBLEMS*

The View Factor

13–1C What does the view factor represent? When is the view factor from a surface to itself not zero?

13–2C How can you determine the view factor F_{12} when the view factor F_{21} and the surface areas are available?

13–3C What are the summation rule and the superposition rule for view factors?

13–4C What is the crossed-strings method? For what kinds of geometries is the crossed-strings method applicable?

13–5 Consider two coaxial parallel circular disks of equal diameter $D = 1$ m spaced apart by 1 m, and two aligned parallel square plates (1 m × 1 m) are also spaced apart by 1 m. Determine the view factors F_{12} between the circular disks and the square plates. Which of the two geometries has the higher view factor value?
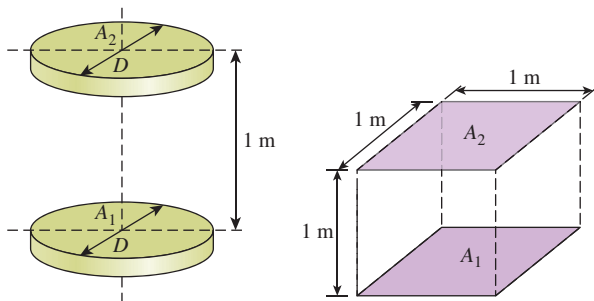
FIGURE P13–5

13–6 Consider two coaxial parallel circular disks of equal diameter D that are spaced apart by a distance L. If the view factor is $F_{12} = 0.1$, without altering the diameter of the disks, determine a solution that would increase the view factor F_{12} by a factor of 5.
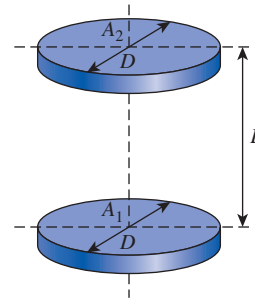
FIGURE P13–6

13–7 Cylindrical heaters are spaced equally at 5 cm apart in a row, and the heaters are positioned between two large parallel plates. If the diameter of the cylinders is 35 mm, determine the view factors between the plate and the row of cylinders, F_{12} and F_{32}.
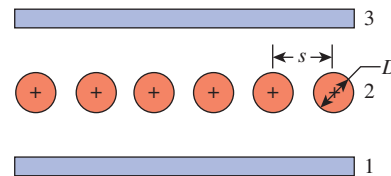
FIGURE P13–7

13–8 Consider an enclosure consisting of 13 surfaces. How many view factors does this geometry involve? How many of these view factors can be determined by the application of the reciprocity and the summation rules?

13–9 Consider an enclosure consisting of five surfaces. How many view factors does this geometry involve? How many of these view factors can be determined by the application of the reciprocity and summation rules?

*Problems designated by a "C" are concept questions, and students are encouraged to answer them all. Problems designated by an "E" are in English units, and the SI users can ignore them. Problems with the ⌨ icon are comprehensive in nature and are intended to be solved with appropriate software. Problems with the **PtD** icon are Prevention through Design problems. Problems with the **C&S** icon are Codes and Standards problems.

13–10 Consider a hemispherical furnace with a flat circular base of diameter D. Determine the view factor from the dome of this furnace to its base. *Answer:* 0.5

13–11 Consider a conical enclosure of height h and base diameter D. Determine the view factor from the conical side surface to a hole of diameter d located at the center of the base.
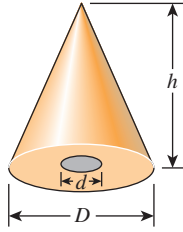
FIGURE P13–11

13–12 Determine the four view factors associated with an enclosure formed by two very long concentric cylinders of radii r_1 and r_2. Neglect the end effects.

13–13 Determine the view factors from the very long grooves shown in Fig. P13–13 to the surroundings without using any view factor tables or charts. Neglect end effects.
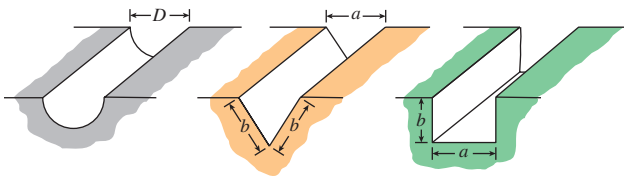
(*a*) Semicylindrical   (*b*) Triangular groove   (*c*) Rectangular groove

FIGURE P13–13

13–14 Consider a cylindrical enclosure with A_1, A_2, and A_3 representing the internal base, top, and side surfaces, respectively. Using the length-to-diameter ratio, $K = L/D$, determine (*a*) the expression for the view factor between the base and the side surface F_{13} in terms of K and (*b*) the value of the view factor F_{13} for $L = D$. *Answers:* (*a*) $F_{13} = 2K\sqrt{(K^2 + 1)} - 2K^2$, (*b*) 0.828
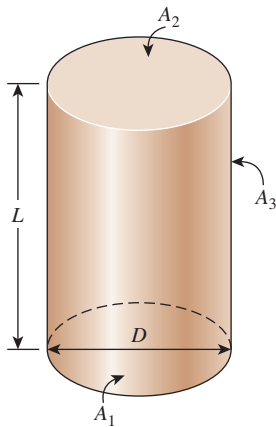
FIGURE P13–14

13–15 A circular cone of diameter D is positioned on a common axis with a circular disk, also of diameter, D, at a distance L, as shown in the figure. With a hypothetical area (A_3) corresponding to the opening of the cone, determine the values of F_{11} and F_{12} for $L = D = 100$ mm.
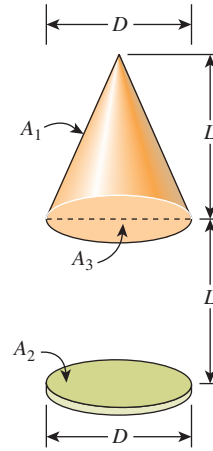
FIGURE P13–15

13–16 Consider a cylindrical surface and a disk oriented coaxially as shown in the figure. The cylinder has a diameter D and a length L. The disk of diameter D is placed coaxially with the cylinder at a distance L. If $L = 2D$, determine the view factor F_{12} between the cylindrical surface (1) and the disk (2) facing it.
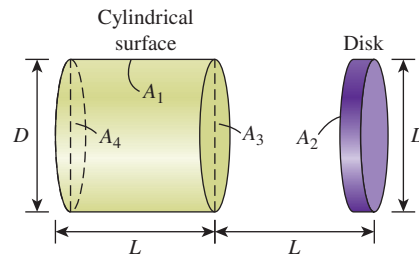
FIGURE P13–16

13–17 Repeat Prob. 13–16 with $L = D$.

13–18 A circular cone of diameter D with a length L is positioned on a common axis with a circular disk, also of diameter D, at a distance L (Fig. P13–18). A cylindrical surface of diameter D with a length L and a circular disk, of the same diameter D, are oriented coaxially at a distance L. Determine the view factors F_{12} for the two geometries. Which of the two geometries has the higher view factor value?
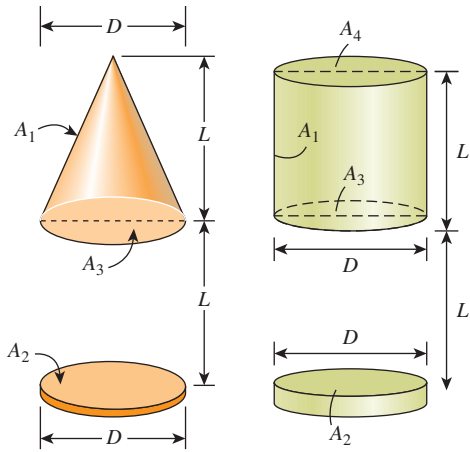
FIGURE P13−18

13–19 Determine the view factors from the base of a cube to each of the other five surfaces.

13–20 Determine the view factors F_{13} and F_{23} between the rectangular surfaces shown in Fig. P13–20.
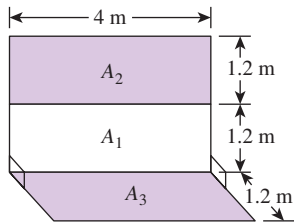
FIGURE P13−20

13–21 Determine the view factor F_{12} between the rectangular surfaces shown in Fig. P13–21.
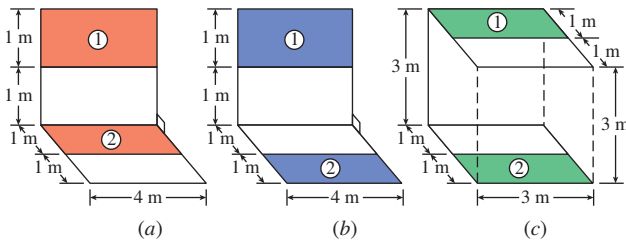
FIGURE P13−21

13–22 Consider a cylindrical enclosure whose height is twice the diameter of its base. Determine the view factor from the side surface of this cylindrical enclosure to its base surface.

13–23 For the internal surfaces of the right circular cylinder shown in Fig. P13–23, determine F_{13} and F_{33}.
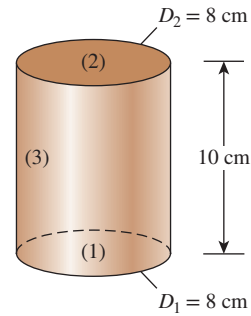
FIGURE P13−23

13–24 Two infinitely long parallel plates of width w are located at w distance apart, as shown in Fig. P13-24. Using the Hottel's crossed-strings method, determine the view factor F_{12}.
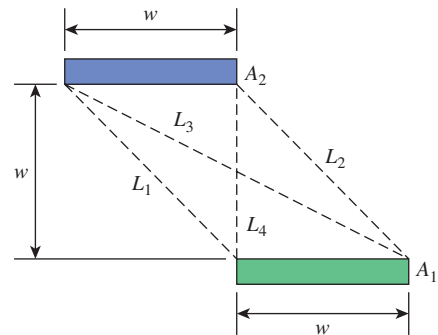
FIGURE P13−24

13–25 Two infinitely long parallel cylinders of diameter D are located a distance s apart from each other. Determine the view factor F_{12} between these two cylinders.

13–26 Two infinitely long parallel plates of width w are located at a distance of w apart, as shown in Fig. P13–26. Determine the view factors F_{12} and F_{21}.
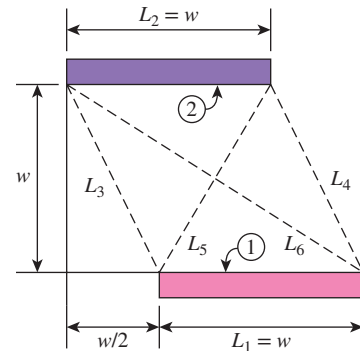
FIGURE P13−26

13–27 Determine the view factors F_{12} and F_{21} for the very long ducts shown in Fig. P13–27 without using any view factor tables or charts. Neglect end effects.
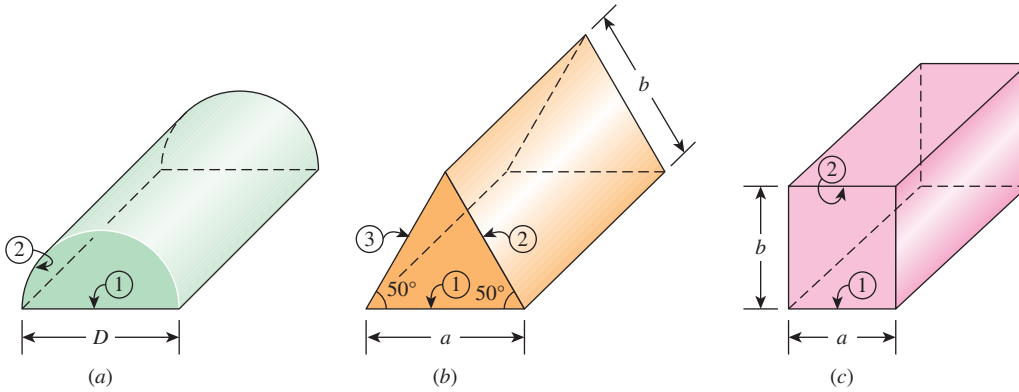
FIGURE P13–27

Radiation Heat Transfer Between Surfaces

13–28C Why is the radiation analysis of enclosures that consist of black surfaces relatively easy? How is the rate of radiation heat transfer between two surfaces expressed in this case?

13–29C How does radiosity for a surface differ from the emitted energy? For what kinds of surfaces are these two quantities identical?

13–30C What are the radiation surface and space resistances? How are they expressed? For what kinds of surfaces is the radiation surface resistance zero?

13–31C What is a reradiating surface? What simplifications does a reradiating surface offer in the radiation analysis?

13–32C What are the two methods used in radiation analysis? How do these two methods differ?

13–33 Consider a person whose exposed surface area is 1.9 m², emissivity is 0.85, and surface temperature is 30°C. Determine the rate of heat loss from that person by radiation in a large room whose walls are at a temperature of (a) 295 K and (b) 260 K.

13–34 Consider two black coaxial parallel circular disks of equal diameter D that are spaced apart by a distance L. The top and bottom disks have uniform temperatures of 500°C and 520°C, respectively. Determine the radiation heat transfer coefficient h_{rad} between the disks if they are spaced apart by $L = D$.
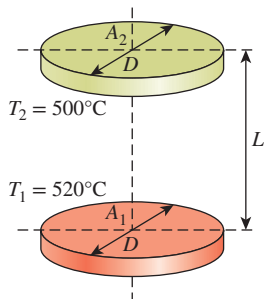
FIGURE P13–34

13–35 Reconsider Prob. 13–34. Using appropriate software, evaluate the effect of the distance L between the black coaxial parallel disks ($D = 1$ m) on the radiation heat transfer coefficient. By varying the distance L between the disks from 0.05 to 3 m, plot the radiation heat transfer coefficient h_{rad} as a function of the distance L between the disks.

13–36 Two coaxial parallel disks of equal diameter 1 m are originally placed at a distance of 1 m apart. If both disks behave as black surfaces, determine the new distance between the disks such that there is a 75 percent reduction in radiation heat transfer rate from the original distance of 1 m.
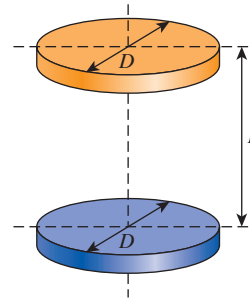
FIGURE P13–36

13–37 A row of tubes, equally spaced at a distance that is twice the diameter of the tubes, is positioned between two large parallel plates. The surface temperature of the tubes is constant at 10°C and the top and bottom plates are at constant temperatures of 100°C and 350°C, respectively. If the surfaces behave as blackbodies, determine the net radiation heat flux leaving the bottom plate.
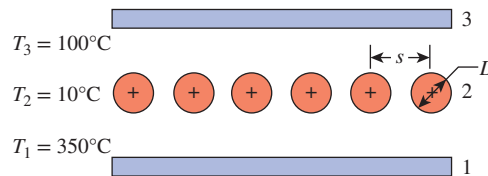
FIGURE P13–37

13–38 A row of long cylindrical power cables that are spaced 2 cm evenly apart are placed in parallel with a large wall. Each power cable is shielded with PVC insulation, and the diameter of each cable is 1 cm. The wall is at an elevated temperature of 100°C. The surfaces of the power cables and the wall can be approximated as blackbodies. According to the ASTM D2219-11 standard specification, PVC insulation is suitable for operation at temperatures up to 60°C. If the radiation heat transfer per unit area from the wall to the power cables is 200 W/m², determine whether the PVC insulation for the power cables would comply with the ASTM D2219-11 standard specification.
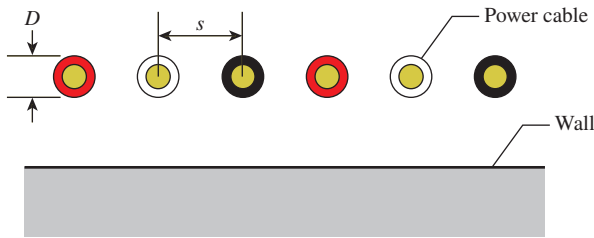
FIGURE P13−38

13–39 A row of long cylindrical power cables that are spaced 2 cm evenly apart are placed in parallel with a plate ($k = 15$ W/m·K). The plate has a thickness of 5 cm, and its lower and upper surface temperatures are $T_0 = 227°C$ and $T_1 = 207°C$, respectively. The power cables are shielded with polyethylene insulation, and the diameter of each cable is 1 cm. The opposite wall is at a temperature of $T_3 = 20°C$. The upper surface of the plate experiences convection with air at 20°C and a convection heat transfer coefficient of 20 W/m²·K. According to the ASTM D1351-14 standard specification, the polyethylene insulation is suitable for operation at temperatures up to 75°C. Determine whether the polyethylene insulation for the power cables would comply with the ASTM D1351-14 standard specification. All surfaces can be approximated as blackbodies.
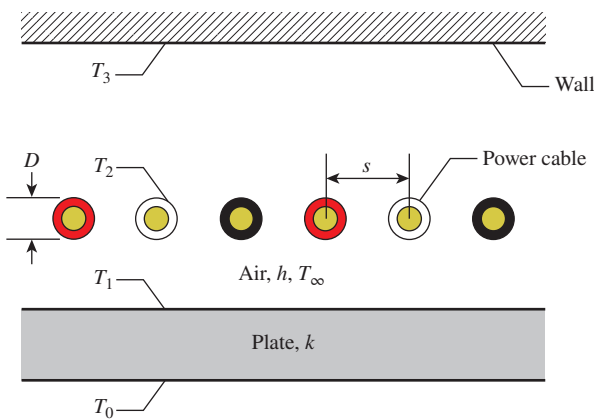
FIGURE P13−39

13–40E Two black parallel rectangles with dimensions 3 ft × 5 ft are spaced apart by a distance of 1 ft. The two parallel rectangles are experiencing radiation heat transfer as black surfaces, where the top rectangle receives a total of 180,000 Btu/h radiation heat transfer rate from the bottom rectangle. If the top rectangle has a uniform temperature of 60°F, determine the temperature of the bottom rectangle.
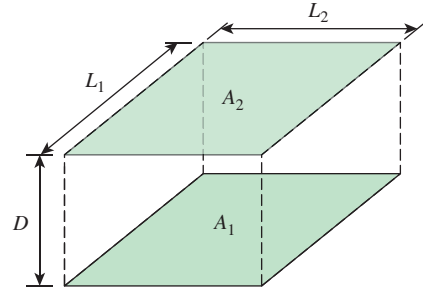
FIGURE P13−40E

13–41E The room shown in Fig. P13–41E is 20 ft by 20 ft wide and 9 ft high. The floor is at 100°F, the walls are at 60°F, and the ceiling is at 40°F. All surfaces are assumed to be black. Calculate the net radiation heat transfer (*a*) from floor to walls and (*b*) from floor to ceiling.
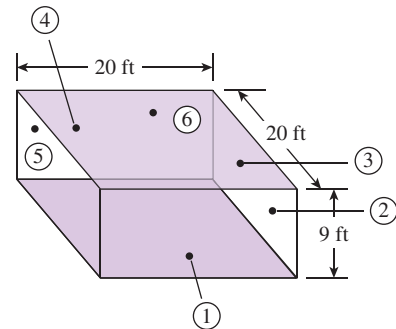
FIGURE P13−41E

13–42 Two aligned parallel rectangles with dimensions 6 m × 8 m are spaced apart by a distance of 2 m. If the two parallel rectangles are experiencing radiation heat transfer as black surfaces, determine the percentage of change in radiation heat transfer rate when the rectangles are moved 8 m apart.
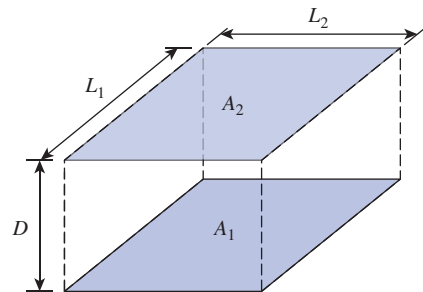
FIGURE P13−42

13–43 A dryer is shaped like a long semicylindrical duct of diameter 1.5 m. The base of the dryer is occupied with water-soaked materials to be dried. The base is maintained at a temperature of 370 K, while the dome of the dryer is maintained at 1000 K. If both surfaces behave as blackbodies, determine the drying rate per unit length experienced by the wet materials.
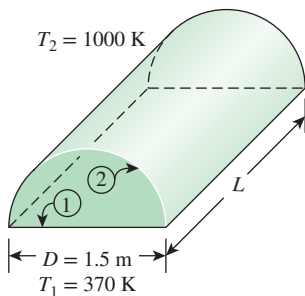
FIGURE P13−43

13–44 A furnace is of cylindrical shape with $R = H = 3$ m. The base, top, and side surfaces of the furnace are all black and are maintained at uniform temperatures of 500, 700, and 1400 K, respectively. Determine the net rate of radiation heat transfer to or from the top surface during steady operation.
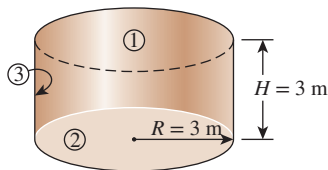
FIGURE P13−44

13–45 Two parallel disks of diameter $D = 0.6$ m separated by $L = 0.4$ m are located directly on top of each other. Both disks are black and are maintained at a temperature of 450 K. The back sides of the disks are insulated, and the environment that the disks are in can be considered to be blackbodies at 300 K. Determine the net rate of radiation heat transfer from the disks to the environment. *Answer:* 781 W

13–46 Consider a hemispherical furnace of diameter $D = 5$ m with a flat base, as shown in Fig. P13–46. The dome of the furnace is black, and the base has an emissivity of 0.7. The base and the dome of the furnace are maintained at uniform temperatures of 400 and 1000 K, respectively. Determine the net rate of radiation heat transfer from the dome to the base surface during steady operation. *Answer:* 759 kW

FIGURE P13−46

13–47 A dryer is shaped like a long semicylindrical duct of diameter 2 m. The base of the dryer is occupied with water-soaked materials that are to be dried. The dome of the dryer has a constant temperature of 500°C, while the materials at the base are at 40°C. Both surfaces can be approximated as blackbodies. Determine the length of the dryer so that the materials are dried at a rate of 0.1 kg/s.
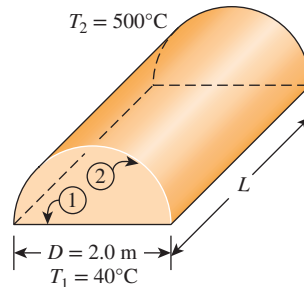
FIGURE P13−47

13–48 Two parallel black disks are positioned coaxially at a distance of 0.25 m apart in surroundings with a constant temperature of 300 K. The lower disk is 0.2 m in diameter and the upper disk is 0.4 m in diameter. If the lower disk is heated electrically at 100 W to maintain a uniform temperature of 500 K, determine the temperature of the upper disk.
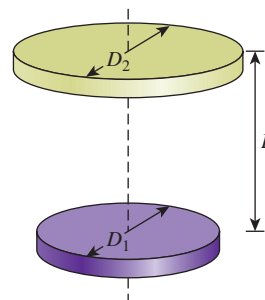
FIGURE P13−48

13–49E Two parallel disks of diameter $D = 3$ ft separated by $L = 2$ ft are located directly on top of each other. The disks are separated by a radiation shield whose emissivity is 0.15. Both disks are black and are maintained at temperatures of 1350 R and 650 R, respectively. The environment that the disks are in can be considered to be a blackbody at 540 R. Determine the net rate of radiation heat transfer through the shield under steady conditions.
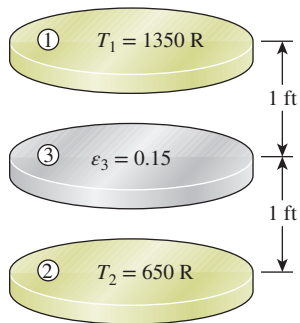
FIGURE P13–49E

13–50 Consider a hot cylindrical surface and a disk oriented as shown in the figure. Both the cylindrical surface and the disk behave as blackbodies. The cylinder has a diameter D and a length L of 0.2 m. The disk of diameter $D = 0.2$ m is placed coaxially with the cylinder at a distance of $L = 0.2$ m apart. The cylindrical surface and the disk are maintained at uniform temperatures of 1000 K and 300 K, respectively. Determine the rate of heat transfer by radiation from the cylindrical surface to the disk.
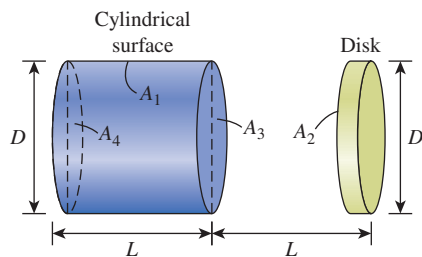
FIGURE P13–50

13–51 Two infinitely long parallel plates of width w are located at w distance apart, as shown in Fig. P13-51. The two plates behave as black surfaces, where surface A_1 has a temperature of 700 K and surface A_2 has a temperature of 300 K. Determine the radiation heat flux between the two surfaces.
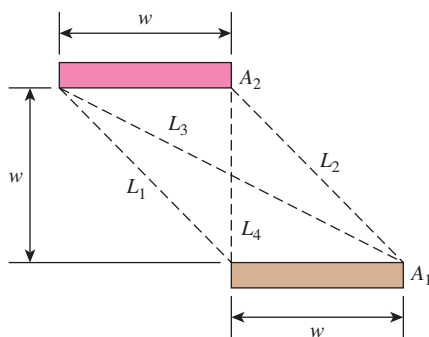
FIGURE P13–51

13–52 Two long, parallel 20-cm-diameter cylinders are located 30 cm apart from each other. Both cylinders are black and are maintained at temperatures 425 K and 275 K. The surroundings can be treated as a blackbody at 300 K. For a 1-m-long section of the cylinders, determine the rates of radiation heat transfer between the cylinders and between the hot cylinder and the surroundings.
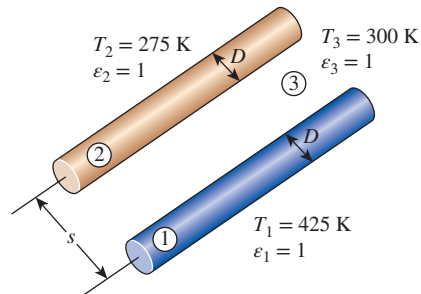
FIGURE P13–52

13–53 C&S A long cylindrical power cable is shielded with polyethylene insulation. The power cable is placed in parallel with a long cylindrical metal rod that is maintained at a temperature of 150°C. Both the power cable and the metal rod have the same diameter of 1 cm, and they are inside a blackbody surrounding at 27°C. Their distance apart from each other, measured from their centers, is 20 cm. The emissivity values for the metal rod and the polyethylene insulation are 0.33 and 0.95, respectively. According to the ASTM D1351-14 standard specification, the polyethylene insulation is suitable for operation at temperatures up to 75°C. If the radiation heat transfer per unit area from the metal rod is 445 W/m², determine whether the polyethylene insulation for the power cable would comply with the ASTM D1351-14 standard specification.

13–54 Two infinitely long parallel plates of width w are located at w distance apart, as shown in Fig. P13–54. The two plates behave as black surfaces, where surface 1 has a temperature of 500°C and surface 2 has a temperature of 50°C. Determine the radiation heat flux between the two surfaces.
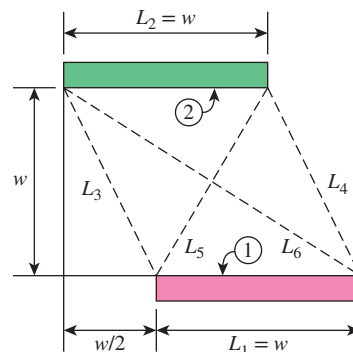
FIGURE P13–54

13–55 [C&S] A large ceramic plate that behaves as a blackbody is placed in parallel near a large ASTM A992 carbon steel plate. The ASME Code for Process Piping specifies the maximum use temperature suitable for ASTM A992 carbon steel to be 427°C (ASME B31.3-2014, Table A-1M). The ceramic plate has an elevated temperature of 700°C, and the steel plate has a reflectivity of 0.68. To keep the temperature of the steel plate from overheating, a cooling mechanism is in place to remove 2000 W/m² of heat from the steel plate. Under the given conditions, is the cooling mechanism removing enough heat by net radiation heat transfer between the two plates to keep the steel plate below 427°C?

13–56 Consider two rectangular surfaces perpendicular to each other with a common edge which is 1.6 m long. The horizontal surface is 0.8 m wide, and the vertical surface is 1.2 m high. The horizontal surface has an emissivity of 0.75 and is maintained at 450 K. The vertical surface is black and is maintained at 700 K. The back sides of the surfaces are insulated. The surrounding surfaces are at 290 K and can be considered to have an emissivity of 0.85. Determine the net rate of radiation heat transfer between the two surfaces and between the horizontal surface and the surroundings.
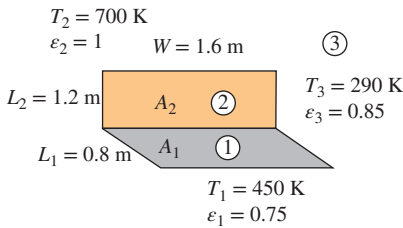
FIGURE P13–56

13–57 A furnace is shaped like a long equilateral-triangular duct where the width of each side is 2 m. Heat is supplied from the base surface, whose emissivity is $\varepsilon_1 = 0.8$, at a rate of 800 W/m² while the side surfaces, whose emissivities are 0.4, are maintained at 600 K. Neglecting the end effects, determine the temperature of the base surface. Can you treat this geometry as a two-surface enclosure?

13–58 [computer] Reconsider Prob. 13–57. Using appropriate software, investigate the effects of the rate of the heat transfer at the base surface and the temperature of the side surfaces on the temperature of the base surface. Let the rate of heat transfer vary from 500 W/m² to 1000 W/m² and the temperature from 300 K to 700 K. Plot the temperature of the base surface as functions of the rate of heat transfer and the temperature of the side surfaces, and discuss the results.

13–59 A solid sphere of 1 m diameter at 600 K is kept in an evacuated equilateral triangular enclosure (a tetrahedron) whose side length is L. Note that for the sphere to touch the tetrahedron's surfaces, the tetrahedron's side length should be $L = D\sqrt{6}$. The emissivity of the sphere is 0.45 and the temperature of the enclosure is 420 K. If heat is generated uniformly within the sphere at a rate of 3100 W, determine (a) the view factor from the enclosure to the sphere and (b) the emissivity of the enclosure.
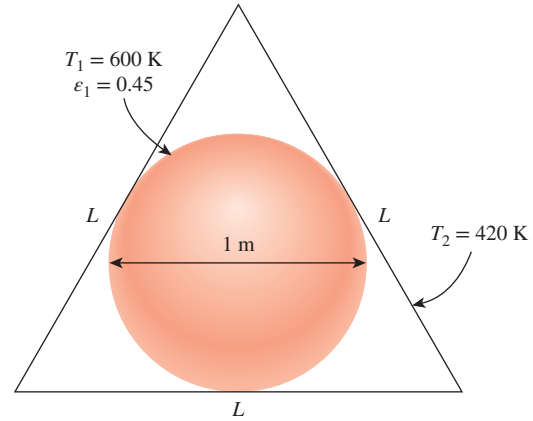
FIGURE P13–59

13–60 Consider a long semicylindrical duct of diameter 1.0 m. Heat is supplied from the base surface, which is black, at a rate of 1200 W/m², while the side surface with an emissivity of 0.4 is maintained at 650 K. Neglecting the end effects, determine the temperature of the base surface.

13–61 Consider a 30-cm-diameter hemispherical enclosure. The dome is maintained at 600 K, and heat is supplied from the dome at a rate of 65 W while the base surface with an emissivity of 0.55 is maintained at 400 K. Determine the emissivity of the dome.

13–62E A furnace is shaped like a long semicylindrical duct of diameter $D = 15$ ft. The base and the dome of the furnace have emissivities of 0.5 and 0.9 and are maintained at uniform temperatures of 550 and 1800 R, respectively. Determine the net rate of radiation heat transfer from the dome to the base surface per unit length during steady operation.
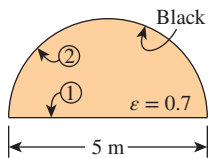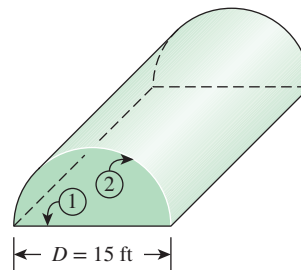

FIGURE P13–62E

13–63 This question deals with steady-state radiation heat transfer between a sphere ($r_1 = 30$ cm) and a circular disk ($r_2 = 120$ cm), which are separated by a center-to-center distance $h = 60$ cm. When the normal to the center of the disk passes through the center of the sphere, the radiation view factor is given by

$$F_{12} = 0.5\left\{ 1 - \left[1 + \left(\frac{r_2}{h} \right)^2 \right]^{-0.5} \right\}$$

Surface temperatures of the sphere and the disk are 600°C and 200°C, respectively; and their emissivities are 0.9 and 0.5, respectively.

(a) Calculate the view factors F_{12} and F_{21}.

(b) Calculate the net rate of radiation heat exchange between the sphere and the disk.

(c) For the given radii and temperatures of the sphere and the disk, the following four possible modifications could increase the net rate of radiation heat exchange: paint each of the two surfaces to alter their emissivities, adjust the distance between them, and provide an (refractory) enclosure. Calculate the net rate of radiation heat exchange between the two bodies if the *best values* are selected for each of the above modifications.
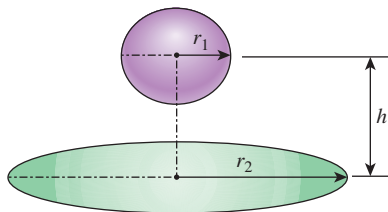
FIGURE P13–63

13–64 Two very large parallel plates are maintained at uniform temperatures of $T_1 = 600$ K and $T_2 = 400$ K and have emissivities $\varepsilon_1 = 0.5$ and $\varepsilon_2 = 0.9$, respectively. Determine the net rate of radiation heat transfer between the two surfaces per unit area of the plates.

13–65 Reconsider Prob. 13–64. Using appropriate software, investigate the effects of the temperature and the emissivity of the hot plate on the net rate of radiation heat transfer between the plates. Let the temperature vary from 500 K to 1000 K and the emissivity from 0.1 to 0.9. Plot the net rate of radiation heat transfer as functions of temperature and emissivity, and discuss the results.

13–66 Air is flowing between two infinitely large parallel plates. The upper plate is at 500 K and has an emissivity of 0.7, while the lower plate is a black surface with temperature at 330 K. If the air temperature is 290 K, determine the convection heat transfer coefficient associated with the air.
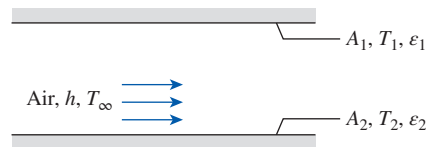
FIGURE P13–66

13–67 **C&S** A large ASTM B152 copper plate is placed in parallel near a large ceramic plate. The ceramic plate is at a temperature of 520°C. The copper and ceramic plates have emissivity values of 0.15 and 0.92, respectively. For the ASTM B152 copper plate, the ASME Code for Process Piping specifies the maximum use temperature at 260°C (ASME B31.3-2014, Table A-1M). If the net radiation heat flux between the two parallel plates is 2000 W/m², determine whether the ASTM B152 copper plate would comply with the ASME code.

13–68 Two very long concentric cylinders of diameters $D_1 = 0.35$ m and $D_2 = 0.5$ m are maintained at uniform temperatures of $T_1 = 950$ K and $T_2 = 500$ K and have emissivities $\varepsilon_1 = 1$ and $\varepsilon_2 = 0.55$, respectively. Determine the net rate of radiation heat transfer between the two cylinders per unit length of the cylinders.

13–69 A long cylindrical black surface fuel rod of diameter 25 mm is shielded by a surface concentric to the rod. The shield has a diameter of 50 mm, and its outer surface is exposed to surrounding air at 300 K with a convection heat transfer coefficient of 15 W/m²·K. Inner and outer surfaces of the shield have an emissivity of 0.05, and the gap between the fuel rod and the shield is a vacuum. If the shield maintains a uniform temperature of 320 K, determine the surface temperature of the fuel rod.
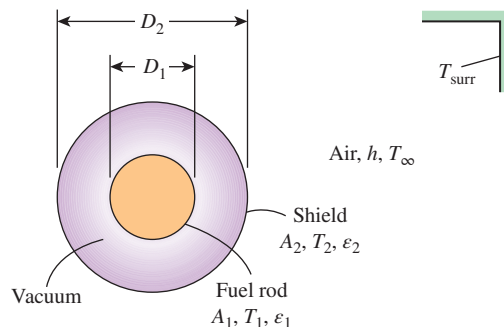
FIGURE P13–69

13–70 This experiment is conducted to determine the emissivity of a certain material. A long cylindrical rod of diameter $D_1 = 0.01$ m is coated with this new material and is placed in an evacuated long cylindrical enclosure of diameter $D_2 = 0.1$ m and emissivity $\varepsilon_2 = 0.95$, which is cooled externally and maintained at a temperature of 200 K at all times. The rod is heated

by passing electric current through it. When steady operating conditions are reached, it is observed that the rod is dissipating electric power at a rate of 12 W per unit of its length, and its surface temperature is 600 K. Based on these measurements, determine the emissivity of the coating on the rod.

13–71 PtD Liquid ammonia is being transported in an insulated tube with an outer diameter of $D_1 = 4$ cm, and the outer tube surface temperature is uniform at $T_1 = 0°C$. Exposure to high concentrations of gaseous ammonia can cause lung damage. To prevent gaseous ammonia from forming and leaking out, ammonia is transported in its liquid state inside the tube. In addition, the tube is enclosed by an outer concentric cylindrical shield with a diameter of $D_2 = 8$ cm, which gives a vacuumed gap in between the tube and the shield surfaces. Keeping the surface temperature of the shield uniform at 10°C or lower would prevent the liquid ammonia from vaporizing. Both the outer tube and the shield surfaces have the same emissivity of 0.33. The tube is situated in surroundings where the natural convection heat transfer coefficient is 3 W/m²·K, and both natural convection and radiation heat transfer occur at the outer shield surface. To keep the ammonia inside the tube in its liquid state, determine the surrounding temperature that would maintain temperatures of the outer tube and the shield at the specified values.

13–72 PtD A hot liquid is being transported inside a long tube with a diameter of 25 mm. The hot liquid causes the tube surface temperature to be 150°C. To prevent thermal burn hazards, the tube is enclosed by a concentric outer cylindrical cover of 5 cm in diameter, creating a vacuumed gap between the two surfaces. The concentric outer cover has an emissivity of 0.6, and the outer surface is exposed to natural convection with a heat transfer coefficient of 8 W/m²·K and radiation heat transfer with the surroundings at a temperature of 20°C. Determine the necessary emissivity of the inside tube so that the outer cover temperature remains below 45°C to prevent thermal burns.

13–73 C&S A long cylindrical fuel rod with a diameter of 25 mm is enclosed by a concentric tube with a diameter of 50 mm. The tube is an ASTM A249 904L stainless steel tube with a maximum use temperature of 260°C specified by the ASME Code for Process Piping (ASME B31.3-2014, Table A-1M). The gap between the fuel rod and the tube is a vacuum. The fuel rod has a surface temperature of 550°C. The emissivities of the fuel rod and the ASTM A249 904L tube are 0.97 and 0.33, respectively. Outside of the tube, convection with the ambient air and radiation with the surroundings occur. The convection heat transfer coefficient of the tube with the ambient air is 15 W/m²·K at 20°C. The temperature of the surroundings is the same as the ambient air temperature. Determine whether the temperature of the tube surface is below the maximum use temperature for ASTM A249 904L stainless steel tube.

13–74 C&S Cryogenic fluid flows inside a 10-mm-diameter metal tube. The metal tube is enclosed by a

concentric polypropylene tube with a diameter of 15 mm. The minimum temperature limit for polypropylene tube is −18°C, specified by the ASME Code for Process Piping (ASME B31.3-2014, Table B-1). The gap between the concentric tubes is a vacuum. The inner metal tube and the outer polypropylene tube have emissivity values of 0.5 and 0.97, respectively. The concentric tubes are placed in a vacuum environment, where the temperature of the surroundings is 0°C. Determine the lowest temperature that the inner metal tube can go without cooling the polypropylene tube below its minimum temperature limit of −18°C. Assume both tubes have thin walls.

13–75 Liquid nitrogen is stored in a spherical tank of 1 m diameter where the tank surface is maintained uniformly at 80 K. The spherical tank is enclosed by a 1.6-m-diameter concentric sphere with uniform surface temperature of 273 K. Both spherical surfaces have an emissivity of 0.01, and the gap between the inner sphere and outer sphere is vacuumed. Determine the rate of vaporization for the liquid nitrogen.
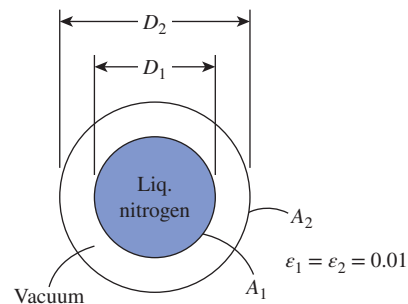
FIGURE P13–75

13–76 Two-phase gas–liquid oxygen is stored in a spherical tank of 1 m diameter, where it is maintained at its normal boiling point. The spherical tank is enclosed by a 1.6-m-diameter concentric spherical surface at 273 K. Both spherical surfaces have an emissivity of 0.01, and the gap between the inner sphere and the outer sphere is vacuumed. Assuming that the spherical tank surface has the same temperature as the oxygen, determine the heat transfer rate at the spherical tank surface.
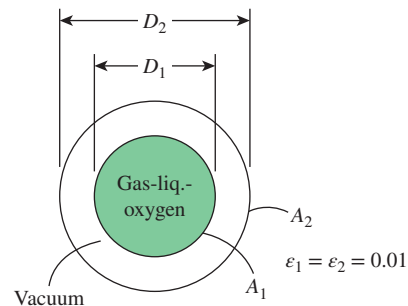
FIGURE P13–76

13–77 Two concentric spheres of diameters $D_1 = 0.3$ m and $D_2 = 0.6$ m are maintained at uniform temperatures $T_1 = 800$ K and $T_2 = 500$ K and have emissivities $\varepsilon_1 = 0.5$ and $\varepsilon_2 = 0.7$, respectively. Determine the net rate of radiation heat transfer between the two spheres. Also, determine the convection heat transfer coefficient at the outer surface if both the surrounding medium and the surrounding surfaces are at 30°C. Assume the emissivity of the outer surface is 0.35.

13–78 A spherical tank of diameter $D = 2$ m that is filled with liquid nitrogen at 100 K is kept in an evacuated cubic enclosure whose sides are 3 m long. The emissivities of the spherical tank and the enclosure are $\varepsilon_1 = 0.1$ and $\varepsilon_2 = 0.8$, respectively. If the temperature of the cubic enclosure is measured to be 240 K, determine the net rate of radiation heat transfer to the liquid nitrogen. *Answer:* 228 W

Liquid N_2
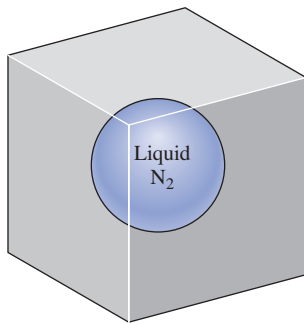
FIGURE P13–78

13–79 Repeat Prob. 13–78 by replacing the cubic enclosure with a spherical enclosure whose diameter is 3 m.

13–80 Reconsider Prob. 13–78. Using appropriate software, investigate the effects of the side length and the emissivity of the cubic enclosure, and the emissivity of the spherical tank on the net rate of radiation heat transfer. Let the side length vary from 2 m to 12 m and both emissivities from 0.1 to 0.9. Plot the net rate of radiation heat transfer as functions of side length and emissivities, and discuss the results.

13–81 **PtD** A 3-m spherical tank storing cold fluid has a uniform surface temperature of $T_1 = 5$°C. The lower temperature of the tank surface is causing condensation of moisture in the air at 13°C and a dew point at 10°C. If the outer surface temperature of the tank drops below the dew point, condensation can occur on the surface. The tank is situated in the vicinity of high-voltage devices, and water from the condensation on the tank surface can cause electrical hazards. In an attempt to remedy the situation, the tank is enclosed with a concentric outer cover that provides an evacuated gap in the enclosure. On the outer surface, the natural convection heat transfer coefficient is 3 W/m²·K, and radiation exchange with the surroundings is negligible. If the emissivity of the tank and the concentric outer cover is the same at 0.6, determine the

necessary gap of the vacuumed enclosure so that the outer cover surface temperature is not below the dew point of 10°C.

13–82 **PtD** A spherical tank, with an inner diameter of $D_1 = 3$ m, is filled with a solution undergoing an exothermic reaction that heats the surface to a uniform temperature of 120°C. To prevent thermal burn hazards, the tank is enclosed by a concentric outer cover that provides an evacuated gap of 5 cm in the enclosure. Both spherical surfaces have the same emissivity of 0.5, and the outer surface is exposed to natural convection with a heat transfer coefficient of 5 W/m²·K and radiation heat transfer with the surroundings at a temperature of 30°C. Determine whether or not the vacuumed gap is sufficient to keep the outer surface temperature below 45°C to prevent thermal burns. If not, propose a solution to keep the outer surface temperature below 45°C.

Air, 30°C
$h = 5$ W/m²·K

D_2
D_1

Chemical reaction

A_2
$\varepsilon_1 = \varepsilon_2 = 0.5$
A_1

Vacuum
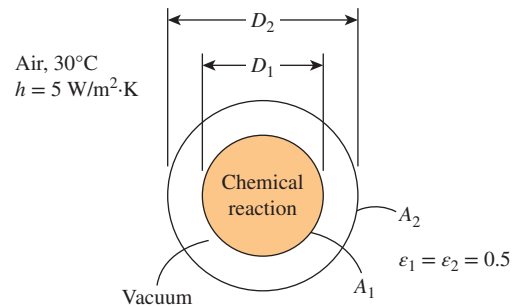
FIGURE P13–82

13–83E A 9-ft-high room with a base area of 12 ft × 12 ft is to be heated by electric resistance heaters placed on the ceiling, which is maintained at a uniform temperature of 90°F at all times. The floor of the room is at 65°F and has an emissivity of 0.8. The side surfaces are well insulated. Treating the ceiling as a blackbody, determine the rate of heat loss from the room through the floor.

13–84 Consider a 4-m × 4-m × 4-m cubical furnace whose floor and ceiling are black and whose side surfaces are reradiating. The floor and the ceiling of the furnace are maintained at temperatures of 550 K and 1100 K, respectively. Determine the net rate of radiation heat transfer between the floor and the ceiling of the furnace.

13–85 Consider a circular grill whose diameter is 0.3 m. The bottom of the grill is covered with hot coal bricks at 950 K, while the wire mesh on top of the grill is covered with steaks initially at 5°C. The distance between the coal bricks and the steaks is 0.20 m. Treating both the steaks and the coal bricks as blackbodies, determine the initial rate of radiation heat transfer from the coal bricks to the steaks. Also, determine the initial rate of radiation heat transfer to the steaks if the side opening of the grill is covered by aluminum foil, which can be approximated as a reradiating surface. *Answers:* 928 W, 2085 W
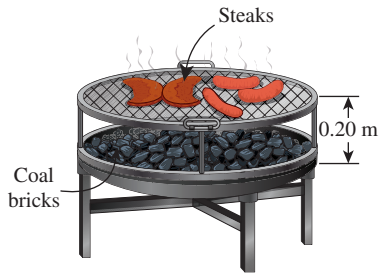
FIGURE P13–85

13–86E Consider a 10-ft × 10-ft × 10-ft cubical furnace whose top and side surfaces closely approximate black surfaces and whose base surface has an emissivity $\varepsilon = 0.4$. The base, top, and side surfaces of the furnace are maintained at uniform temperatures of 800 R, 1600 R, and 2400 R, respectively. Determine the net rate of radiation heat transfer between (*a*) the base and the side surfaces and (*b*) the base and the top surfaces. Also, determine the net rate of radiation heat transfer to the base surface.

13–87E Reconsider Prob. 13–86E. Using appropriate software, investigate the effect of base surface emissivity on the net rates of radiation heat transfer between the base and the side surfaces, between the base and top surfaces, and to the base surface. Let the emissivity vary from 0.1 to 0.9. Plot the rates of heat transfer as a function of emissivity, and discuss the results.

Radiation Shields and the Radiation Effect

13–88C What is a radiation shield? Why is it used?

13–89C What is the radiation effect? How does it influence the temperature measurements?

13–90C Give examples of radiation effects that affect human comfort.

13–91 A thin aluminum sheet with an emissivity of 0.15 on both sides is placed between two very large parallel plates, which are maintained at uniform temperatures $T_1 = 900$ K and $T_2 = 650$ K and have emissivities $\varepsilon_1 = 0.5$ and $\varepsilon_2 = 0.8$, respectively. Determine the net rate of radiation heat transfer between the two plates per unit surface area of the plates, and compare the result with that without the shield.
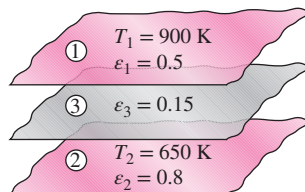
FIGURE P13–91

13–92 Reconsider Prob. 13–91. Using appropriate software, plot the net rate of radiation heat transfer between the two plates as a function of the emissivity of the aluminum sheet as the emissivity varies from 0.05 to 0.25, and discuss the results.

13–93 A radiation shield that has the same emissivity ε_3 on both sides is placed between two large parallel plates, which are maintained at uniform temperatures of $T_1 = 650$ K and $T_2 = 400$ K and have emissivities of $\varepsilon_1 = 0.6$ and $\varepsilon_2 = 0.9$, respectively. Determine the emissivity of the radiation shield if the radiation heat transfer between the plates is to be reduced to 15 percent of that without the radiation shield.

13–94 Reconsider Prob. 13–93. Using appropriate software, investigate the effect of the percent reduction in the net rate of radiation heat transfer between the plates on the emissivity of the radiation shields. Let the percent reduction vary from 40 to 95 percent. Plot the emissivity versus the percent reduction in heat transfer, and discuss the results.

13–95 A large ASTM B152 copper plate is placed in parallel near a large ceramic plate. The ceramic plate is at a temperature of 600°C. The ceramic and copper plates have emissivity values of 0.91 and 0.95, respectively. For the ASTM B152 copper plate, the ASME Code for Process Piping specifies the maximum use temperature at 260°C (ASME B31.3-2014, Table A-1M). A radiation shield is to be placed in parallel between the two plates to keep the temperature of the copper plate from exceeding its maximum use temperature. If the net radiation heat flux between the two parallel plates is 1000 W/m², determine the emissivity that the radiation shield needs to keep the copper plate surface from exceeding 260°C.

13–96 A large ASTM A992 carbon steel plate is placed in parallel near a large ceramic plate ($k = 10$ W/m·K). The ceramic plate has a thickness of 10 cm, with its lower surface at $T_0 = 800$°C and upper surface at $T_1 = 700$°C. The upper surface of the ceramic plate faces the carbon steel plate. Convection occurs on the upper surface of the ceramic plate with air at 20°C and a convection heat transfer coefficient of 12 W/m²·K. The ceramic and steel plates have emissivity values of 0.93 and 0.75, respectively. The ASME Code for Process Piping specifies the maximum use temperature suitable for ASTM A992 carbon steel to be 427°C (ASME B31.3-2014, Table A-1M). A radiation shield is to be placed in parallel between the two plates to keep the temperature of the steel plate from exceeding its maximum use temperature. Determine the emissivity that the radiation shield needs to keep the steel plate surface from exceeding 427°C.
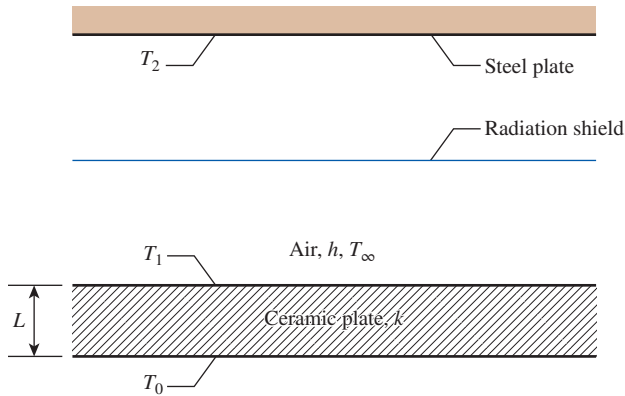
FIGURE P13−96

13–97 Two coaxial cylinders of diameters $D_1 = 0.10$ m and $D_2 = 0.50$ m and emissivities $\varepsilon_1 = 0.7$ and $\varepsilon_2 = 0.4$ are maintained at uniform temperatures of $T_1 = 750$ K and $T_2 = 500$ K, respectively. Now a coaxial radiation shield of diameter $D_3 = 0.20$ m and emissivity $\varepsilon_3 = 0.2$ is placed between the two cylinders. Determine the net rate of radiation heat transfer between the two cylinders per unit length of the cylinders, and compare the result with that without the shield.

13–98 Reconsider Prob. 13–97. Using appropriate software, investigate the effects of the diameter of the outer cylinder and the emissivity of the radiation shield on the net rate of radiation heat transfer between the two cylinders. Let the diameter vary from 0.25 m to 0.50 m and the emissivity from 0.05 to 0.35. Plot the rate of radiation heat transfer as functions of the diameter and the emissivity, and discuss the results.

13–99 C&S A long cylindrical fuel rod with a diameter of 3 cm is enclosed by a concentric tube with a diameter of 6 cm. The tube is an ASTM A249 904L stainless steel tube with a maximum use temperature of 260°C specified by the ASME Code for Process Piping (ASME B31.3-2014, Table A-1M). The gap between the fuel rod and the tube is a vacuum. The fuel rod has a surface temperature of 550°C. The emissivities of the fuel rod and the ASTM A249 904L tube are 0.97 and 0.33, respectively. The rate of radiation heat transfer per unit length from the fuel rod to the stainless steel tube is 120 W/m. A concentric radiation shield with a diameter of 45 mm is to be placed in between the fuel rod and the stainless steel tube to keep the temperature of the stainless steel tube from exceeding its maximum use temperature. Determine (a) the emissivity that the radiation shield needs to keep the stainless steel tube from exceeding 260°C and (b) the temperature of the stainless steel tube if there is no radiation shield.

13–100 Two very large parallel plates are maintained at uniform temperatures of $T_1 = 1100$ K and $T_2 = 700$ K and have emissivities of $\varepsilon_1 = \varepsilon_2 = 0.5$, respectively. It is desired to reduce the net rate of radiation heat transfer between the two plates to one-fifth by placing thin aluminum sheets with an emissivity of 0.1 on both sides between the plates. Determine the number of sheets that need to be inserted.

13–101 Five identical thin aluminum sheets with emissivities of 0.1 on both sides are placed between two very large parallel plates, which are maintained at uniform temperatures of $T_1 = 800$ K and $T_2 = 450$ K and have emissivities of $\varepsilon_1 = \varepsilon_2 = 0.1$, respectively. Determine the net rate of radiation heat transfer between the two plates per unit surface area of the plates, and compare the result to that without the shield.

13–102 Reconsider Prob. 13–101. Using appropriate software, investigate the effects of the number of the aluminum sheets and the emissivities of the plates on the net rate of radiation heat transfer between the two plates. Let the number of sheets vary from 1 to 10 and the emissivities of the plates from 0.1 to 0.9. Plot the rate of radiation heat transfer as functions of the number of sheets and the emissivities of the plates, and discuss the results.

13–103 Two thin radiation shields with emissivities of $\varepsilon_3 = 0.10$ and $\varepsilon_4 = 0.15$ on both sides are placed between two very large parallel plates, which are maintained at uniform temperatures $T_1 = 600$ K and $T_2 = 300$ K and have emissivities $\varepsilon_1 = 0.6$ and $\varepsilon_2 = 0.7$, respectively (Fig. P13–103). Determine the net rates of radiation heat transfer between the two plates with and without the shields per unit surface area of the plates, and the temperatures of the radiation shields in steady operation.
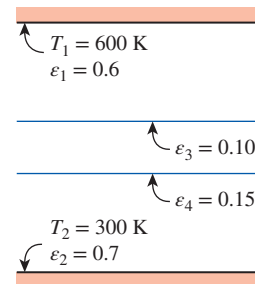
FIGURE P13−103

13–104 PtD Heat dissipated from an engine in operation can cause hot spots on its surface. If the outer surface of an engine is situated in a place where oil leakage is possible, then when leaked oil comes in contact with the hot spots above the oil's autoignition temperature, it can ignite spontaneously. Consider an engine cover that is made of two

large parallel plates. The heat flux from the engine is 125 W/m^2 and is heating the bottom plate to 300°C. To prevent fire hazard in the event of an oil leak on the engine cover, the top plate of the engine cover should be kept below 150°C. Determine whether the top plate of the engine cover is below 150°C, and if it is not, determine the number of radiation shields that should be positioned in parallel between the plates. Assume all the surfaces have the same emissivity of 0.3.
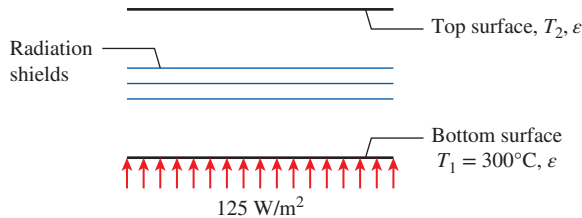
FIGURE P13–104

13–105 A thermocouple used to measure the temperature of hot air flowing in a duct whose walls are maintained at 400 K shows a temperature reading of 650 K. Assuming the emissivity of the thermocouple junction to be 0.6 and the convection heat transfer coefficient to be 80 W/m^2·K, determine the actual temperature of the air.
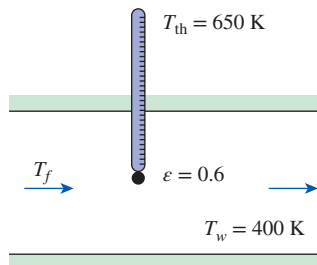
FIGURE P13–105

Radiation Exchange with Absorbing and Emitting Gases

13–106C How does radiation transfer through a participating medium differ from that through a nonparticipating medium?

13–107C Define the spectral transmissivity of a medium of thickness L in terms of (a) spectral intensities and (b) the spectral absorption coefficient.

13–108C How does the wavelength distribution of radiation emitted by a gas differ from that of a surface at the same temperature?

13–109C Define the spectral emissivity of a medium of thickness L in terms of the spectral absorption coefficient.

13–110 Consider an equimolar mixture of CO_2 and O_2 gases at 800 K and a total pressure of 0.5 atm. For a path length of 1.2 m, determine the emissivity of the gas.

13–111 A cylindrical container whose height and diameter are 8 m is filled with a mixture of CO_2 and N_2 gases at 600 K and 1 atm. The partial pressure of CO_2 in the mixture is 0.15 atm. If the walls are black at a temperature of 450 K, determine the rate of radiation heat transfer between the gas and the container walls.

13–112 Repeat Prob. 13–111 by replacing CO_2 with the H_2O gas.

13–113 A 5-m-diameter spherical furnace contains a mixture of CO_2 and N_2 gases at 1200 K and 1 atm. The mole fraction of CO_2 in the mixture is 0.15. If the furnace wall is black and its temperature is to be maintained at 600 K, determine the net rate of radiation heat transfer between the gas mixture and the furnace walls.

13–114 A cubic furnace whose side length is 6 m contains combustion gases at 1200 K and a total pressure of 1 atm. The composition of the combustion gases is 75 percent N_2, 9 percent H_2O, 6 percent O_2, and 10 percent CO_2. Determine the effective emissivity of the combustion gases.

13–115 In a cogeneration plant, combustion gases at 1 atm and 1000 K are used to preheat water by passing them through 6-m-long, 10-cm-diameter tubes. The inner surface of the tube is black, and the partial pressures of CO_2 and H_2O in combustion gases are 0.12 atm and 0.18 atm, respectively. If the tube temperature is 500 K, determine the rate of radiation heat transfer from the gases to the tube.

13–116 A flow-through combustion chamber consists of long, 15-cm-diameter tubes immersed in water. Compressed air is routed to the tube, and fuel is sprayed into the compressed air. The combustion gases consist of 70 percent N_2, 9 percent H_2O, 15 percent O_2, and 6 percent CO_2, and are maintained at 1 atm and 1500 K. The tube surfaces are near black, with an emissivity of 0.9. If the tubes are to be maintained at a temperature of 600 K, determine the rate of heat transfer from combustion gases to tube wall by radiation per m length of tube.

13–117 Repeat Prob. 13–116 for a total pressure of 3 atm.

13–118 A gas at 1200 K and 1 atm consists of 10 percent CO_2, 10 percent H_2O, 10 percent O_2, and 70 percent N_2 by volume. The gas flows between two large parallel black plates maintained at 600 K. If the plates are 20 cm apart, determine the rate of heat transfer from the gas to each plate per unit surface area.

Special Topic: Heat Transfer from the Human Body

13–119C Explain all the different mechanisms of heat transfer from the human body (a) through the skin and (b) through the lungs.

13–120C What is sensible heat? How is the sensible heat loss from a human body affected by (a) skin temperature, (b) environment temperature, and (c) air motion?

13–121C What is latent heat? How is the latent heat loss from the human body affected by (a) skin wettedness and (b) relative humidity of the environment? How is the rate of evaporation from the body related to the rate of latent heat loss?

13–122C How is the insulating effect of clothing expressed? How does clothing affect heat loss from the body by convection, radiation, and evaporation? How does clothing affect heat gain from the sun?

13–123C Consider a person who is resting or doing light work. Is it fair to say that roughly one-third of the metabolic heat generated in the body is dissipated to the environment by convection, one-third by evaporation, and the remaining one-third by radiation?

13–124C What is operative temperature? How is it related to the mean ambient and radiant temperatures? How does it differ from effective temperature?

13–125 The convection heat transfer coefficient for a clothed person while walking in still air at a velocity of 0.5 to 2 m/s is given by $h = 8.6V^{0.53}$, where V is in m/s and h is in W/m²·K. Plot the convection coefficient against the walking velocity, and compare the convection coefficients in that range to the average radiation coefficient of about 5 W/m²·K.

13–126 An average (1.82 kg or 4.0 lbm) chicken has a basal metabolic rate of 5.47 W and an average metabolic rate of 10.2 W (3.78 W sensible and 6.42 W latent) during normal activity. If there are 100 chickens in a breeding room, determine the rate of total heat generation and the rate of moisture production in the room. Take the heat of vaporization of water to be 2430 kJ/kg.

13–127 A person feels very comfortable in his house in light clothing when the thermostat is set at 22°C and the mean radiation temperature (the average temperature of the surrounding surfaces) is also 22°C. During a cold day, the average mean radiation temperature drops to 18°C. To what level must the indoor air temperature be raised to maintain the same level of comfort in the same clothing?

22°C

22°C
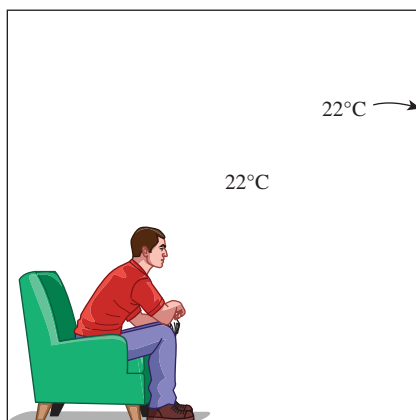
FIGURE P13–127

13–128 Repeat Prob. 13–127 for a mean radiation temperature of 10°C.

13–129 Consider a large classroom with 75 students on a hot summer day. All the lights with 2.0 kW of rated power are kept on. The room has no external walls, and thus heat gain through the walls and the roof is negligible. Chilled air is available at 15°C, and the temperature of the return air is not to exceed 25°C. The average rate of metabolic heat generation by a person sitting or doing light work is 115 W (70 W sensible and 45 W latent). Determine the required flow rate of air that needs to be supplied to the room.

13–130 A car mechanic is working in a shop whose interior space is not heated. Comfort for the mechanic is provided by two radiant heaters that radiate heat at a total rate of 4 kJ/s. About 5 percent of this heat strikes the mechanic directly. The shop and its surfaces can be assumed to be at the ambient temperature, and the emissivity and absorptivity of the mechanic can be taken to be 0.95 and the surface area to be 1.8 m². The mechanic is generating heat at a rate of 350 W, half of which is latent, and is wearing medium clothing with a thermal resistance of 0.7 clo. Determine the lowest ambient temperature in which the mechanic can work comfortably.

Radiant heater
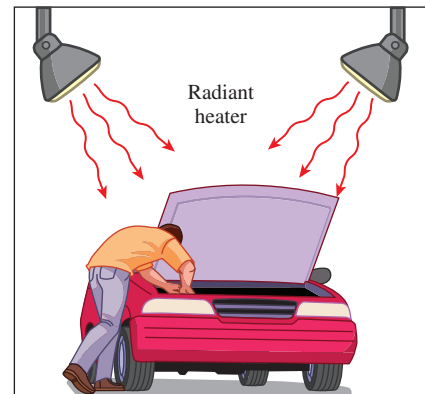
FIGURE P13–130

13–131E An average person produces 0.50 lbm of moisture while taking a shower and 0.12 lbm while bathing in a tub. Consider a family of four who shower once a day in a bathroom that is not ventilated. Taking the heat of vaporization of water to be 1050 Btu/lbm, determine the contribution of showers to the latent heat load of the air conditioner in summer per day.

13–132 A clothed or unclothed person feels comfortable when the skin temperature is about 33°C. Consider an average man wearing summer clothes whose thermal resistance is 1.1 clo. The man feels very comfortable while standing in a room maintained at 20°C. If this man were to stand in that room unclothed, determine the temperature at which the room must be maintained for him to feel thermally comfortable. Assume the latent heat loss from the person to remain the same. *Answer:* 27.8°C

Review Problems

13–133 Consider two diffuse surfaces A_1 and A_2 oriented on a spherical surface as shown in the figure. Determine (*a*) the expression for the view factor F_{12} in terms of A_2 and L, and (*b*) the value of the view factor F_{12} when $A_2 = 0.02$ m^2 and $L = 1$ m.
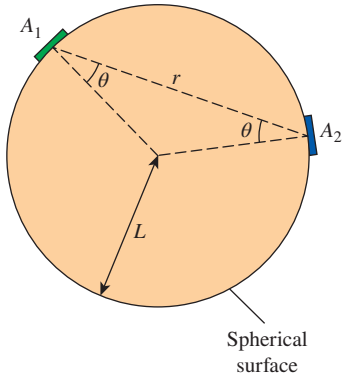
FIGURE P13–133

13–134 Consider an enclosure consisting of eight surfaces. How many view factors does this geometry involve? How many of these view factors can be determined by the application of the reciprocity and the summation rules?

13–135 Consider a cylindrical enclosure with A_1, A_2, and A_3 representing the internal base, top, and side surfaces, respectively. Using the length-to-diameter ratio, $K = L/D$, determine (*a*) the expression for the view factor from the side surface to itself F_{33} in terms of K and (*b*) the value of the view factor F_{33} for $L = D$.
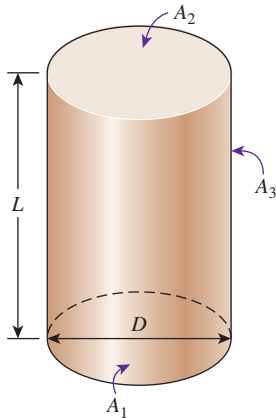
FIGURE P13–135

13–136 Two parallel black disks are positioned coaxially with a distance of 0.25 m apart. The lower disk is 0.2 m in diameter and the upper disk is 0.4 m in diameter. If the lower disk is heated electrically at 20 W to maintain a uniform temperature of 500 K, determine the temperature of the upper disk.
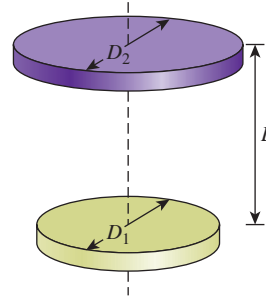
FIGURE P13–136

13–137 A simple solar collector is built by placing a 6-cm-diameter clear plastic tube around a garden hose whose outer diameter is 2 cm (Fig. P13–137). The hose is painted black to maximize solar absorption, and some plastic rings are used to keep the spacing between the hose and the clear plastic cover constant. The emissivities of the hose surface and the glass cover are 0.9, and the effective sky temperature is estimated to be 15°C. The temperature of the plastic tube is measured to be 40°C, while the ambient air temperature is 25°C. Determine the rate of heat loss from the water in the hose by natural convection and radiation per meter of its length under steady conditions.   *Answers:* 12.7 W, 26.1 W
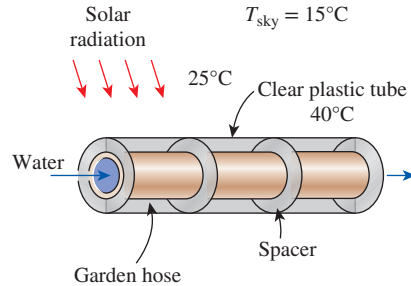
FIGURE P13–137

13–138 Two parallel concentric disks, 20 cm and 40 cm in diameter, are separated by a distance of 10 cm. The smaller disk ($\varepsilon = 0.80$) is at a temperature of 300°C. The larger disk ($\varepsilon = 0.60$) is at a temperature of 800°C.

(*a*) Calculate the radiation view factors.
(*b*) Determine the rate of radiation heat exchange between the two disks.
(*c*) Suppose that the space between the two disks is completely surrounded by a reflective surface. Estimate the rate of radiation heat exchange between the two disks.

13–139 A dryer is shaped like a long semicylindrical duct of diameter 1.5 m. The base of the dryer is occupied by water-soaked materials to be dried, and it is maintained at a temperature of 370 K and emissivity of 0.5. The dome of the dryer is maintained at 1000 K with emissivity of 0.8. Determine the drying rate per unit length experienced by the wet materials.
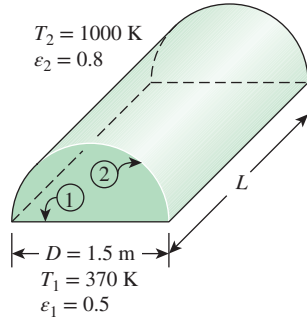
FIGURE P13–139

13–140 A large number of long tubes, each of diameter *D,* are placed parallel to each other and at a center-to-center distance of *s.* Since all of the tubes are geometrically similar and at the same temperature, these could be treated collectively as one surface (A_j) for radiation heat transfer calculations. As shown in Fig. P13–140, the tube bank (A_j) is placed opposite a large flat wall (A_i) such that the tube bank is parallel to the wall.

(*a*) Calculate the view factors F_{ij} and F_{ji} for $s = 3.0$ cm and $D = 1.5$ cm.

(*b*) Calculate the net rate of radiation heat transfer between the wall and the tube bank per unit area of the wall when $T_i = 900°C$, $T_j = 60°C$, $\varepsilon_i = 0.8$, and $\varepsilon_j = 0.9$.

(*c*) A fluid flows through the tubes at an average temperature of 40°C, resulting in a heat transfer coefficient of 2.0 kW/m²·K. Assuming $T_i = 900°C$, $\varepsilon_i = 0.8$ and $\varepsilon_j = 0.9$ (as above) and neglecting the tube wall thickness and convection from the outer surface, calculate the temperature of the tube surface in steady operation.
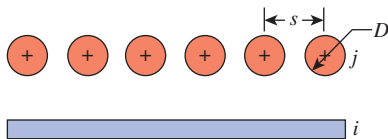
FIGURE P13–140

13–141 Consider the two parallel coaxial disks of diameters *a* and *b* shown in Fig. P13–141. For this geometry, the view factor from the smaller disk to the larger disk can be calculated from

$$F_{ij} = 0.5 \left(\frac{B}{A}\right)^2 \left\{ C - \left[C^2 - 4\left(\frac{A}{B}\right)^2\right]^{0.5} \right\}$$

where $A = a/2L$, $B = b/2L$, and $C = 1 + [(1 + A^2)/B^2]$. The diameter, emissivity, and temperature are 20 cm, 0.60, and 600°C, respectively, for disk *a,* and 40 cm, 0.80. and 200°C for disk *b.* The distance between the two disks is $L = 10$ cm.

(*a*) Calculate F_{ab} and F_{ba}.

(*b*) Calculate the net rate of radiation heat exchange between disks *a* and *b* in steady operation.

(*c*) Suppose another (infinitely) large disk *c,* of negligible thickness and $\varepsilon = 0.7$, is inserted between disks *a* and *b* such that it is parallel and equidistant to both disks. Calculate the net rate of radiation heat exchange between disks *a* and *c* and disks *c* and *b* in steady operation.
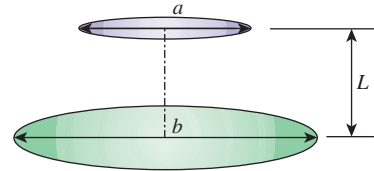
FIGURE P13–141

13–142 Two square plates, with the sides *a* and *b* (and $b > a$), are coaxial and parallel to each other, as shown in Fig. P13–142, and they are separated by a center-to-center distance of *L.* The radiation view factor from the smaller to the larger plate, F_{ab}, is given by

$$F_{ab} = \frac{1}{2A}\left\{ [(B+A)^2 + 4]^{0.5} - [(B-A)^2 + 4]^{0.5} \right\}$$

where, $A = a/L$ and $B = b/L$.

(*a*) Calculate the view factors F_{ab} and F_{ba} for $a = 20$ cm, $b = 60$ cm, and $L = 40$ cm.

(*b*) Calculate the net rate of radiation heat exchange between the two plates described above if $T_a = 800°C$, $T_b = 200°C$, $\varepsilon_a = 0.8$, and $\varepsilon_b = 0.4$.

(*c*) A large, square plate (with the side $c = 2.0$ m, $\varepsilon_c = 0.1$, and negligible thickness) is inserted symmetrically between the two plates such that it is parallel to and equidistant from them. For the data given above, calculate the temperature of this third plate when steady operating conditions are established.
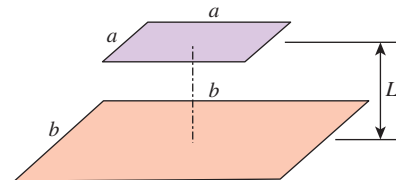
FIGURE P13–142

13–143 A vertical 2-m-high and 5-m-wide double-pane window consists of two sheets of glass separated by a 3-cm-thick air gap. In order to reduce heat transfer through the window,

the air space between the two glasses is partially evacuated to 0.3 atm pressure. The emissivities of the glass surfaces are 0.9. Taking the glass surface temperatures across the air gap to be 15°C and 5°C, determine the rate of heat transfer through the window by natural convection and radiation.
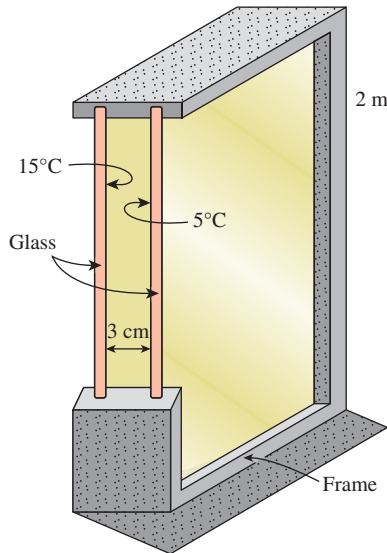
FIGURE P13–143

13–144 Consider a 1.5-m-high and 3-m-wide solar collector that is tilted at an angle 20° from the horizontal. The distance between the glass cover and the absorber plate is 3 cm, and the back side of the absorber is heavily insulated. The absorber plate and the glass cover are maintained at temperatures of 80°C and 32°C, respectively. The emissivity of the glass surface is 0.9 and that of the absorber plate is 0.8. Determine the rate of heat loss from the absorber plate by natural convection and radiation. *Answers:* 750 W, 1289 W
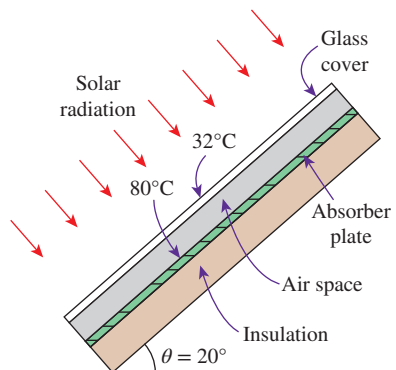
FIGURE P13–144

13–145 A 2-m-internal-diameter double-walled spherical tank is used to store iced water at 0°C. Each wall is 0.5 cm thick, and the 1.5-cm-thick airspace between the two walls of the tank is evacuated in order to minimize heat transfer. The surfaces surrounding the evacuated space are polished so that each surface has an emissivity of 0.15. The temperature of the outer wall of the tank is measured to be 20°C. Assuming the inner wall of the steel tank to be at 0°C, determine (*a*) the rate of heat transfer to the iced water in the tank and (*b*) the amount of ice at 0°C that melts during a 24-h period.
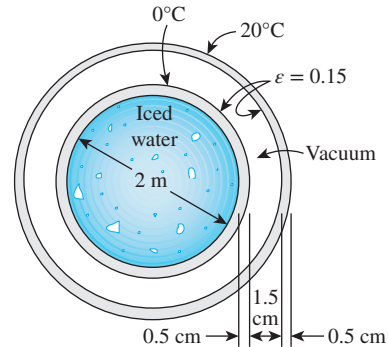
FIGURE P13–145

13–146 A solar collector consists of a horizontal copper tube of outer diameter 5 cm enclosed in a concentric thin glass tube of diameter 12 cm. Water is heated as it flows through the tube, and the annular space between the copper and the glass tubes is filled with air at 1 atm pressure. The emissivities of the tube surface and the glass cover are 0.85 and 0.9, respectively. During a clear day, the temperatures of the tube surface and the glass cover are measured to be 60°C and 40°C, respectively. Determine the rate of heat loss from the collector by natural convection and radiation per meter length of the tube.

13–147 Two concentric spheres of diameters $D_1 = 15$ cm and $D_2 = 25$ cm are separated by air at 1 atm pressure. The surface temperatures of the two spheres enclosing the air are $T_1 = 350$ K and $T_2 = 275$ K, respectively, and their emissivities are 0.75. Determine the rate of heat transfer from the inner sphere to the outer sphere by (*a*) natural convection and (*b*) radiation.

13–148E A solar collector consists of a horizontal aluminum tube having an outer diameter of 2.5 in enclosed in a concentric thin glass tube of diameter 5 in. Water is heated as it flows through the tube, and the annular space between the aluminum and the glass tube is filled with air at 0.5 atm pressure. The pump circulating the water fails during a clear day, and the water temperature in the tube starts rising. The aluminum tube absorbs solar radiation at a rate of 30 Btu/h per foot length, and the temperature of the ambient air outside is 75°F. The emissivities of the tube and the glass cover are 0.9. Taking the effective sky temperature to be 60°F, determine the temperature of the aluminum tube when thermal equilibrium is established (i.e., when the rate of heat loss from the tube equals the amount of solar energy gained by the tube).

13–149 A long cylindrical black surface fuel rod of diameter 25 mm is shielded by a surface concentric to the rod. The shield

has a diameter of 50 mm and a constant surface temperature of 320 K. Both inner and outer surfaces of the shield have an emissivity of 0.05, and the gap between the fuel rod and the shield is a vacuum. If the fuel rod is generating 0.5 MW/m³ of heat per unit length, determine the surface temperature of the fuel rod.
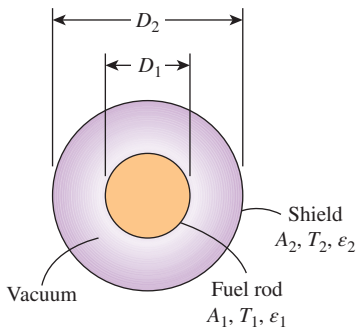
FIGURE P13−149

13–150 Consider a cubical furnace with a side length of 3 m. The top surface is maintained at 700 K. The base surface has an emissivity of 0.90 and is maintained at 950 K. The side surface is black and is maintained at 450 K. Heat is supplied from the base surface at a rate of 340 kW. Determine the emissivity of the top surface and the net rates of heat transfer between the top and the bottom surfaces and between the bottom and side surfaces.

13–151 A furnace is of cylindrical shape with a diameter of 1.2 m and a length of 1.2 m. The top surface has an emissivity of 0.60 and is maintained at 450 K. The bottom surface has an emissivity of 0.50 and is maintained at 800 K. The side surface has an emissivity of 0.40. Heat is supplied from the base surface at a net rate of 1400 W. Determine the temperature of the side surface and the net rates of heat transfer between the top and the bottom surfaces and between the bottom and side surfaces.
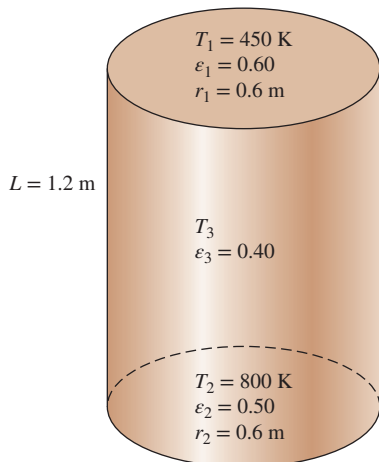
FIGURE P13−151

13–152 A thin aluminum sheet with an emissivity of 0.12 on both sides is placed between two very large parallel plates maintained at uniform temperatures of $T_1 = 750$ K and $T_2 = 400$ K. The emissivities of the plates are $\varepsilon_1 = 0.8$ and $\varepsilon_2 = 0.7$. Determine the net rate of radiation heat transfer between the two plates per unit surface area of the plates and the temperature of the radiation shield in steady operation.

13–153 A thermocouple used to measure the temperature of hot air flowing in a duct whose walls are maintained at $T_w = 500$ K shows a temperature reading of $T_{th} = 850$ K. Assuming the emissivity of the thermocouple junction to be $\varepsilon = 0.6$ and the convection heat transfer coefficient to be $h = 75$ W/m²·K, determine the actual temperature of air.
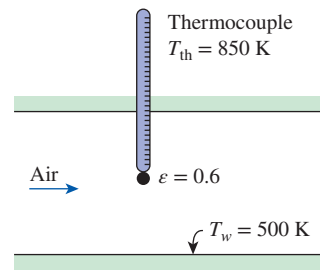
FIGURE P13−153

13–154 In a natural gas–fired boiler, combustion gases pass through 6-m-long,15-cm-diameter tubes immersed in water at 1 atm pressure. The tube temperature is measured to be 105°C, and the emissivity of the inner surfaces of the tubes is estimated to be 0.9. Combustion gases enter the tube at 1 atm and 1000 K at a mean velocity of 3 m/s. The mole fractions of CO_2 and H_2O in combustion gases are 8 percent and 16 percent, respectively. Assuming fully developed flow and using properties of air for combustion gases, determine (*a*) the rates of heat transfer by convection and by radiation from the combustion gases to the tube wall and (*b*) the rate of evaporation of water.

13–155 Repeat Prob. 13–154 for a total pressure of 3 atm for the combustion gases.

Fundamentals of Engineering (FE) Exam Problems

13–156 Consider an infinitely long three-sided triangular enclosure with side lengths 5 cm, 3 cm, and 4 cm. The view factor from the 5-cm side to the 4-cm side is

(*a*) 0.3   (*b*) 0.4   (*c*) 0.5
(*d*) 0.6   (*e*) 0.7

13–157 Consider a 15-cm-diameter sphere placed within a cubical enclosure with a side length of 15 cm. The view factor from any of the square-cube surfaces to the sphere is

(*a*) 0.09   (*b*) 0.26   (*c*) 0.52
(*d*) 0.78   (*e*) 1

13–158 A 90-cm-diameter flat black disk is placed in the center of the top surface of a 1-m $\times$ 1-m $\times$ 1-m black box. The view factor from the entire interior surface of the box to the interior surface of the disk is

(a) 0.07   (b) 0.13   (c) 0.26
(d) 0.32   (e) 0.50

13–159 Consider two concentric spheres with diameters 12 cm and 18 cm forming an enclosure. The view factor from the inner surface of the outer sphere to the inner sphere is

(a) 0   (b) 0.18   (c) 0.44
(d) 0.56   (e) 0.67

13–160 The number of view factors that need to be evaluated directly for a 10-surface enclosure is

(a) 1   (b) 10   (c) 22
(d) 34   (e) 45

13–161 Consider two concentric spheres forming an enclosure with diameters of 12 cm and 18 cm and surface temperatures 300 K and 500 K, respectively. Assuming that the surfaces are black, the net radiation exchange between the two spheres is

(a) 21 W   (b) 140 W   (c) 160 W
(d) 1275 W   (e) 3084 W

13–162 Consider a vertical 2-m-diameter cylindrical furnace whose surfaces closely approximate black surfaces. The base, top, and side surfaces of the furnace are maintained at 400 K, 600 K, and 1200 K, respectively. If the view factor from the base surface to the top surface is 0.2, the net radiation heat transfer between the base and the side surfaces is

(a) 73 kW   (b) 126 kW   (c) 215 kW
(d) 292 kW   (e) 344 kW

13–163 Consider a vertical 2-m-diameter cylindrical furnace whose surfaces closely approximate black surfaces. The base, top, and side surfaces of the furnace are maintained at 400 K, 600 K, and 900 K, respectively. If the view factor from the base surface to the top surface is 0.2, the net radiation heat transfer from the bottom surface is

(a) −93.6 kW   (b) −86.1 kW   (c) 0 kW
(d) 86.1 kW   (e) 93.6 kW

13–164 A solar flux of 1400 W/m^2 directly strikes a space-vehicle surface which has a solar absortivity of 0.4 and thermal emissivity of 0.6. The equilibrium temperature of this surface in space at 0 K is

(a) 300 K   (b) 360 K   (c) 410 K
(d) 467 K   (e) 510 K

13–165 A 70-cm-diameter flat black disk is placed at the center of the ceiling of a 1-m $\times$ 1-m $\times$ 1-m black box. If the temperature of the box is 620°C and the temperature of the disk is 27°C, the rate of heat transfer by radiation between the interior of the box and the disk is

(a) 2 kW   (b) 5 kW   (c) 8 kW
(d) 11 kW   (e) 14 kW

13–166 Consider two infinitely long concentric cylinders with diameters 20 and 25 cm. The inner surface is maintained at 700 K and has an emissivity of 0.40, while the outer surface is black. If the rate of radiation heat transfer from the inner surface to the outer surface is 2400 W per unit area of the inner surface, the temperature of the outer surface is

(a) 605 K   (b) 538 K   (c) 517 K
(d) 451 K   (e) 415 K

13–167 Consider a surface at 0°C that may be assumed to be a blackbody in an environment at 25°C. If 300 W/m^2 of radiation is incident on the surface, the radiosity of this black surface is

(a) 0 W/m^2 (b) 15 W/m^2 (c) 132 W/m^2
(d) 300 W/m^2 (e) 315 W/m^2

13–168 Consider a gray and opaque surface at 0°C in an environment at 25°C. The surface has an emissivity of 0.8. If the radiation incident on the surface is 240 W/m^2, the radiosity of the surface is

(a) 38 W/m^2 (b) 132 W/m^2 (c) 240 W/m^2
(d) 300 W/m^2 (e) 315 W/m^2

13–169 Consider a 3-m $\times$ 3-m $\times$ 3-m cubical furnace. The base surface is black and has a temperature of 400 K. The radiosities for the top and side surfaces are calculated to be 7500 W/m^2 and 3200 W/m^2, respectively. If the temperature of the side surfaces is 485 K, the emissivity of the side surfaces is

(a) 0.37   (b) 0.55   (c) 0.63
(d) 0.80   (e) 0.89

13–170 The base surface of a cubical furnace with a side length of 3 m has an emissivity of 0.80 and is maintained at 500 K. If the top and side surfaces also have an emissivity of 0.80 and are maintained at 900 K, the net rate of radiation heat transfer from the top and side surfaces to the bottom surface is

(a) 194 kW   (b) 233 kW   (c) 288 kW
(d) 312 kW   (e) 242 kW

13–171 Two gray surfaces that form an enclosure exchange heat with one another by thermal radiation. Surface 1 has a temperature of 400 K, an area of 0.2 m^2, and a total emissivity of 0.4. Surface 2 has a temperature of 600 K, an area of 0.3 m^2, and a total emissivity of 0.6. If the view factor F_{12} is 0.3, the rate of radiation heat transfer between the two surfaces is

(a) 135 W   (b) 223 W   (c) 296 W
(d) 342 W   (e) 422 W

13–172 The surfaces of a two-surface enclosure exchange heat with one another by thermal radiation. Surface 1 has a temperature of 400 K, an area of 0.2 m^2, and a total emissivity of 0.4. Surface 2 is black, has a temperature of 800 K, and has area of 0.3 m^2. If the view factor F_{12} is 0.3, the rate of radiation heat transfer between the two surfaces is

(*a*) 340 W   (*b*) 560 W   (*c*) 780 W
(*d*) 900 W   (*e*) 1160 W

13–173 Two concentric spheres are maintained at uniform temperatures $T_1 = 45°C$ and $T_2 = 280°C$ and have emissivities $\varepsilon_1 = 0.25$ and $\varepsilon_2 = 0.7$, respectively. If the ratio of the diameters is $D_1/D_2 = 0.30$, the net rate of radiation heat transfer between the two spheres per unit surface area of the inner sphere is

(*a*) 86 W/m²   (*b*) 1169 W/m²   (*c*) 1181 W/m²
(*d*) 2510 W/m²   (*e*) 3306 W/m²

13–174 Consider a 3-m × 3-m × 3-m cubical furnace. The base surface of the furnace is black and has a temperature of 550 K. The radiosities for the top and side surfaces are calculated to be 7500 W/m² and 3200 W/m², respectively. The net rate of radiation heat transfer to the bottom surface is

(*a*) 10 kW   (*b*) 54 kW   (*c*) 61 kW
(*d*) 113 kW   (*e*) 248 kW

13–175 Two very large parallel plates are maintained at uniform temperatures $T_1 = 750$ K and $T_2 = 500$ K and have emissivities $\varepsilon_1 = 0.85$ and $\varepsilon_2 = 0.7$, respectively. If a thin aluminum sheet with the same emissivity on both sides is to be placed between the plates in order to reduce the net rate of radiation heat transfer between the plates by 90 percent, the emissivity of the aluminum sheet must be

(*a*) 0.07   (*b*) 0.10   (*c*) 0.13
(*d*) 0.16   (*e*) 0.19

Design and Essay Problems

13–176 Consider an enclosure consisting of *N* diffuse and gray surfaces. The emissivity and temperature of each surface as well as the view factors between the surfaces are specified. Write a program to determine the net rate of radiation heat transfer for each surface.

13–177 Radiation shields are commonly used in the design of superinsulations for use in space and cryogenics applications. Write an essay on superinsulations and how they are used in different applications.

13–178 Thermal comfort in a house is strongly affected by the so-called radiation effect, which is due to radiation heat transfer between the person and the surrounding surfaces. A person feels much colder in the morning, for example, because of the lower surface temperature of the walls at that time, although the thermostat setting of the house is fixed. Write an essay on the radiation effect, how it affects human comfort, and how it is accounted for in heating and air-conditioning applications.

MASS TRANSFER

To this point we have restricted our attention to heat transfer problems that did not involve any mass transfer. However, many significant heat transfer problems encountered in practice involve mass transfer. For example, about one-third of the heat loss from a resting person is due to evaporation. It turns out that mass transfer is analogous to heat transfer in many respects, and there is close resemblance between heat and mass transfer relations. In this chapter we discuss the mass transfer mechanisms and develop relations for mass transfer rate for situations commonly encountered in practice.

Distinction should be made between *mass transfer* and the *bulk fluid motion* (or *fluid flow*) that occurs on a macroscopic level as a fluid is transported from one location to another. Mass transfer requires the presence of two regions at different chemical compositions, and mass transfer refers to the movement of a chemical species from a high-concentration region toward a lower concentration one. The primary driving force for fluid flow is the *pressure difference,* whereas for mass transfer it is the *concentration difference*.

We begin this chapter by pointing out numerous analogies between heat and mass transfer and draw several parallels between them. We then discuss boundary conditions associated with mass transfer and one-dimensional steady and transient mass diffusion, followed by a discussion of mass transfer in a moving medium. Finally, we consider convection mass transfer and simultaneous heat and mass transfer.

OBJECTIVES

When you finish studying this chapter, you should be able to:

- Understand the concentration gradient and the physical mechanism of mass transfer,
- Recognize the analogy between heat and mass transfer,
- Describe the concentration at a location on mass or mole basis, and relate the rate of diffusion to the concentration gradient by Fick's law,
- Calculate the rate of mass diffusion through a plane layer under steady conditions,
- Predict the migration of water vapor in buildings,
- Perform a transient mass diffusion analysis in large media,
- Calculate mass transfer by convection, and
- Analyze simultaneous heat and mass transfer.
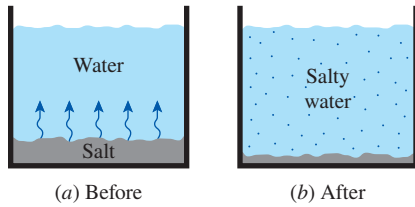
FIGURE 14–1
Whenever there is a concentration difference of a physical quantity in a medium, nature tends to equalize things by forcing a flow from the high- to the low-concentration region.

FIGURE 14–2
A tank that contains N_2 and air in its two compartments, and the diffusion of N_2 into the air (and the diffusion of O_2 into N_2) when the partition is removed.

14–1 ■ INTRODUCTION

It is a common observation that whenever there is an imbalance of a commodity in a medium, nature tends to redistribute it until a "balance" or "equality" is established. This tendency is often referred to as the *driving force,* which is the mechanism behind many naturally occurring transport phenomena.

If we define the amount of a commodity per unit volume as the **concentration** of that commodity, we can say that the flow of a commodity is always in the direction of decreasing concentration; that is, from the region of high concentration to the region of low concentration (Fig. 14–1). The commodity simply creeps away during redistribution, and thus the flow is a *diffusion process.* The rate of flow of the commodity is proportional to the *concentration gradient* dC/dx, which is the change in the concentration C per unit length in the flow direction $x,$ and the area A normal to flow direction, and is expressed as

$$\text{Flow rate} \propto (\text{Normal area})(\text{Concentration gradient})$$

or

$$\dot{Q} = -k_{\text{diff}} A \frac{dC}{dx} \tag{14–1}$$

Here the proportionality constant k_{diff} is the *diffusion coefficient* of the medium, which is a measure of how fast a commodity diffuses in the medium, and the negative sign is to make the flow in the positive direction a positive quantity (note that dC/dx is a negative quantity since concentration decreases in the flow direction). *Fourier's law of heat conduction, Ohm's law of electrical conduction,* and *Newton's law of viscosity* are all in the form of Eq. 14–1.

To understand the diffusion process better, consider a tank that is divided into two equal parts by a partition. Initially, the left half of the tank contains nitrogen N_2 gas, while the right half contains air (about 21 percent O_2 and 79 percent N_2) at the same temperature and pressure. The O_2 and N_2 molecules are indicated by dark and light circles, respectively. When the partition is removed, we know that the N_2 molecules will start diffusing into the air while the O_2 molecules diffuse into the N_2, as shown in Fig. 14–2. If we wait long enough, we will have a homogeneous mixture of N_2 and O_2 in the tank. This mass diffusion process can be explained by considering an imaginary plane indicated by the dashed line in the figure as: Gas molecules move randomly, and thus the probability of a molecule moving to the right or to the left is the same. Consequently, half of the molecules on one side of the dashed line at any given moment will move to the other side. Since the concentration of N_2 is greater on the left side than it is on the right side, more N_2 molecules will move toward the right than toward the left, resulting in a net flow of N_2 toward the right. As a result, N_2 is said to be *transferred* to the right. A similar argument can be given for O_2 being transferred to the left. The process continues until uniform concentrations of N_2 and O_2 are established throughout the tank so that the number of N_2 (or O_2) molecules moving to the right equals the number moving to the left, resulting in zero net transfer of N_2 or O_2 across an imaginary plane.

The molecules in a gas mixture continually collide with each other, and the diffusion process is strongly influenced by this collision process. The collision of like molecules is of little consequence since both molecules
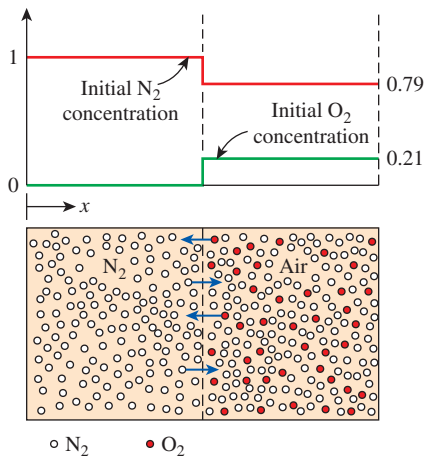
are identical, and it makes no difference which molecule crosses a certain plane. The collisions of unlike molecules, however, influence the rate of diffusion since unlike molecules may have different masses and thus different momentums, and thus the diffusion process is dominated by the heavier molecules. The diffusion coefficients and thus diffusion rates of gases depend strongly on *temperature* since the temperature is a measure of the average velocity of gas molecules. Therefore, the diffusion rates are higher at higher temperatures.

Mass transfer can also occur in liquids and solids as well as in gases. For example, a cup of water left in a room eventually evaporates as a result of water molecules diffusing into the air *(liquid-to-gas mass transfer)*. A piece of solid CO_2 (dry ice) also gets smaller and smaller in time as the CO_2 molecules diffuse into the air *(solid-to-gas mass transfer)*. A spoon of sugar in a cup of coffee eventually moves up and sweetens the coffee, although the sugar molecules are much heavier than the water molecules, and the molecules of a colored pencil inserted into a glass of water diffuse into the water as evidenced by the gradual spread of color in the water *(solid-to-liquid mass transfer)*. Of course, mass transfer can also occur from a gas to a liquid or solid if the concentration of the species is higher in the gas phase. For example, a small fraction of O_2 in the air diffuses into the water and meets the oxygen needs of marine animals. The diffusion of carbon into iron during case-hardening, doping of semiconductors for transistors, and the migration of doped molecules in semiconductors at high temperature are examples of solid-to-solid diffusion processes (Fig. 14–3).

Another factor that influences the diffusion process is the *molecular spacing*. The larger the spacing, in general, the higher the diffusion rate. Therefore, the diffusion rates are typically much higher in gases than they are in liquids and much higher in liquids than in solids. Diffusion coefficients in gas mixtures are a few orders of magnitude larger than these of liquid or solid solutions.

(*a*) Liquid to gas   (*b*) Solid to gas

(*c*) Solid to liquid   (*d*) Solid to solid

FIGURE 14–3
Some examples of mass transfer that involve a liquid and/or a solid.

14–2 ■ ANALOGY BETWEEN HEAT AND MASS TRANSFER

We have spent a considerable amount of time studying heat transfer, and we could spend just as much time studying mass transfer. However, the mechanisms of heat and mass transfer are analogous to each other, and thus we can develop an understanding of mass transfer in a short time with little effort by simply drawing *parallels* between heat and mass transfer. Establishing those "bridges" between the two seemingly unrelated areas will make it possible to use our heat transfer knowledge to solve mass transfer problems. Alternately, gaining a working knowledge of mass transfer will help us to better understand the heat transfer processes by thinking of heat as a massless substance as they did in the 19th century. The short-lived caloric theory of heat is the origin of most heat transfer terminology used today, and it served its purpose well until it was replaced by the kinetic theory. Mass is, in essence, energy since mass and energy can be converted to each other according to Einstein's formula $E = mc^2$, where c is the speed of light. Therefore, we can look at mass and heat as two different forms of energy and exploit this to advantage without going overboard.

FIGURE 14–4
Analogy between heat and mass transfer.
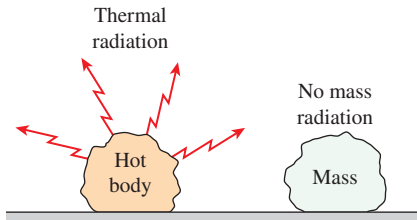
FIGURE 14–5
Unlike heat radiation, there is no such thing as mass radiation.
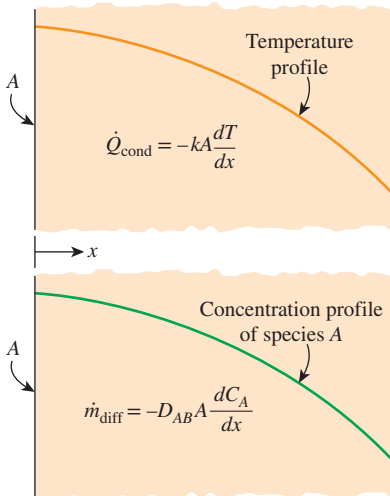
FIGURE 14–6
Analogy between heat conduction and mass diffusion.

Temperature

The driving force for heat transfer is the *temperature difference.* In contrast, the driving force for mass transfer is the *concentration difference.* We can view temperature as a measure of "heat concentration," and thus a high-temperature region is one that has a high heat concentration (Fig. 14–4). Therefore, both heat and mass are transferred from the more concentrated regions to the less concentrated ones. If there is no temperature difference between two regions, then there is no heat transfer. Likewise, if there is no difference between the concentrations of a species at different parts of a medium, there will be no mass transfer.

Conduction

You will recall that heat is transferred by conduction, convection, and radiation. Mass, however, is transferred by *conduction* (called diffusion) and *convection* only, and there is no such thing as "mass radiation" (unless there is something Scotty knows that we don't when he "beams" people to anywhere in space at the speed of light) (Fig. 14–5). The rate of heat conduction in a direction x is proportional to the temperature gradient dT/dx in that direction and is expressed by **Fourier's law of heat conduction** as

$$\dot{Q}_{cond} = -kA\frac{dT}{dx} \tag{14-2}$$

where k is the thermal conductivity of the medium and A is the area normal to the direction of heat transfer. Likewise, the rate of mass diffusion $\dot{m}_{diff}$ of a chemical species A in a stationary medium in the direction x is proportional to the concentration gradient dC/dx in that direction and is expressed by **Fick's law of diffusion** by (Fig. 14–6)

$$\dot{m}_{diff} = -D_{AB}A\frac{dC_A}{dx} \tag{14-3}$$

where D_{AB} is the **diffusion coefficient** (or *mass diffusivity*) of the species in the mixture and C_A is the concentration of the species in the mixture at that location.

It can be shown that the differential equations for both heat conduction and mass diffusion are of the same form. Therefore, the solutions of mass diffusion equations can be obtained from the solutions of corresponding heat conduction equations for the same type of boundary conditions by simply switching the corresponding coefficients and variables.

Heat Generation

Heat generation refers to the conversion of some form of energy such as electrical, chemical, or nuclear energy into *sensible thermal* energy in the medium. Heat generation occurs throughout the medium and exhibits itself as a rise in temperature. Similarly, some mass transfer problems involve chemical reactions that occur within the medium and result in the *generation of a species* throughout. Therefore, species generation is a *volumetric phenomenon,* and the rate of generation may vary from point to point in the medium. Such reactions that occur within the medium are called **homogeneous reactions** and

are analogous to internal heat generation. In contrast, some chemical reactions result in the generation of a species *at the surface* as a result of chemical reactions occurring at the surface due to contact between the medium and the surroundings. This is a *surface phenomenon,* and as such it needs to be treated as a boundary condition. In mass transfer studies, such reactions are called **heterogeneous reactions** and are analogous to *specified surface heat flux.*

Convection

You may recall that *heat convection* is the heat transfer mechanism that involves both *heat conduction* (molecular diffusion) and *bulk fluid motion.* Fluid motion enhances heat transfer considerably by removing the heated fluid near the surface and replacing it with the cooler fluid farther away. In the limiting case of no bulk fluid motion, convection reduces to conduction. Likewise, **mass convection** (or *convective mass transfer*) is the mass transfer mechanism between a surface and a moving fluid that involves both *mass diffusion* and *bulk fluid motion.* Fluid motion also enhances mass transfer considerably by removing the high-concentration fluid near the surface and replacing it with the lower-concentration fluid farther away. In mass convection, we define a *concentration boundary layer* in an analogous manner to the thermal boundary layer and define new dimensionless numbers that are counterparts of the Nusselt and Prandtl numbers.

The rate of heat convection for external flow was expressed conveniently by *Newton's law of cooling* as

$$\dot{Q}_{\text{conv}} = h_{\text{conv}} A_s (T_s - T_\infty) \tag{14-4}$$

where h_{conv} is the heat transfer coefficient, A_s is the surface area, and $T_s - T_\infty$ is the temperature difference across the thermal boundary layer. Likewise, the rate of mass convection can be expressed as (Fig. 14–7)

$$\dot{m}_{\text{conv}} = h_{\text{mass}} A_s (C_s - C_\infty) \tag{14-5}$$

where h_{mass} is the *mass transfer coefficient, A_s* is the surface area, and $C_s - C_\infty$ is a suitable concentration difference across the concentration boundary layer.

Various aspects of the analogy between heat and mass convection are explored in Sec. 14–9. The analogy is valid for *low mass transfer rate* cases in which the flow rate of species undergoing mass flow is low (under 10 percent) relative to the total flow rate of the liquid or gas mixture.

14–3 · MASS DIFFUSION

Fick's law of diffusion, proposed in 1855, states that the rate of diffusion of a chemical species at a location in a gas mixture (or liquid or solid solution) is proportional to the *concentration gradient* of that species at that location. Although a higher concentration for a species means more molecules of that species per unit volume, the concentration of a species can be expressed in several ways. Next we describe two common ways.

1 Mass Basis

On a *mass basis,* concentration is expressed in terms of **density** (or *mass concentration*), which is mass per unit volume. Considering a small volume V at
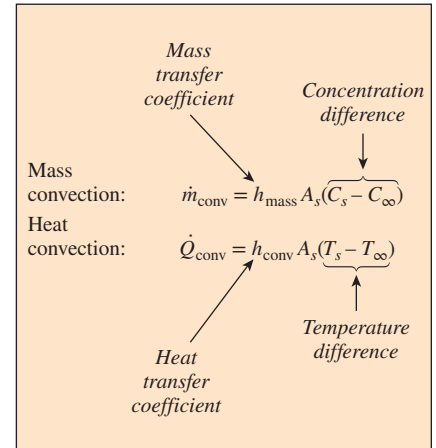
FIGURE 14–7
Analogy between convection heat transfer and convection mass transfer.

$A + B$ mixture

$V = V_A = V_B$

$m = m_A + m_B$

$\rho = \rho_A + \rho_B$

$C = C_A + C_B$
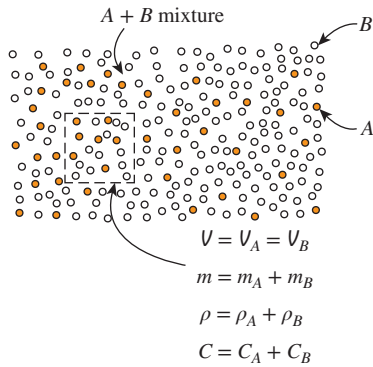
Mass basis:

$$\rho_A = \frac{m_A}{V}, \ \rho = \frac{m}{V}, \ w_A = \frac{\rho_A}{\rho}$$

Mole basis:

$$C_A = \frac{N_A}{V}, \ C = \frac{N}{V}, \ y_A = \frac{C_A}{C}$$

Relation between them:

$$C_A = \frac{\rho_A}{M_A}, \ w_A = y_A \frac{M_A}{M}$$

FIGURE 14–8

Different ways of expressing the concentration of species A of a binary mixture A and B.

a location within the mixture, the densities of a species (subscript i) and of the mixture (no subscript) at that location are given by (Fig. 14–8)

Partial density of species i: $\rho_i = m_i/V$ (kg/m³)

Total density of mixture: $\rho = m/V = \sum m_i/V = \sum \rho_i$

Therefore, the *density of a mixture* at a location is equal to the sum of the *densities of its constituents* at that location. Mass concentration can also be expressed in dimensionless form in terms of **mass fraction** w as

Mass fraction of species i: $w_i = \dfrac{m_i}{m} = \dfrac{m_i/V}{m/V} = \dfrac{\rho_i}{\rho}$ **(14–6)**

Note that the mass fraction of a species ranges between 0 and 1, and the conservation of mass requires that the sum of the mass fractions of the constituents of a mixture be equal to 1. That is, $\sum w_i = 1$. Also note that the density and mass fraction of a constituent in a mixture, in general, vary with location unless the concentration gradients are zero.

2   Mole Basis

On a *mole basis,* concentration is expressed in terms of **molar concentration** (or *molar density*), which is the amount of matter in kmol per unit volume. Again considering a small volume V at a location within the mixture, the molar concentrations of a species (subscript i) and of the mixture (no subscript) at that location are given by

Partial molar concentration of species i: $C_i = N_i/V$ (kmol/m³)

Total molar concentration of mixture: $C = N/V = \sum N_i/V = \sum C_i$

Therefore, the molar concentration of a mixture at a location is equal to the sum of the molar concentrations of its constituents at that location. Molar concentration can also be expressed in dimensionless form in terms of **mole fraction** y as

Mole fraction of species i: $y_i = \dfrac{N_i}{N} = \dfrac{N_i/V}{N/V} = \dfrac{C_i}{C}$ **(14–7)**

Again the mole fraction of a species ranges between 0 and 1, and the sum of the mole fractions of the constituents of a mixture is unity, $\sum y_i = 1$.

The mass m and mole number N of a substance are related to each other by $m = NM$ (or, for a unit volume, $\rho = CM$) where M is the *molar mass* (also called the *molecular weight*) of the substance. This is expected since the mass of 1 kmol of the substance is M kg, and thus the mass of N kmol is NM kg. Therefore, the mass and molar concentrations are related to each other by

$$C_i = \frac{\rho_i}{M_i} \quad \text{(for species } i) \quad \text{and} \quad C = \frac{\rho}{M} \quad \text{(for the mixture)} \qquad \textbf{(14–8)}$$

where M is the molar mass of the mixture, which can be determined from

$$M = \frac{m}{N} = \frac{\sum N_i M_i}{N} = \sum \frac{N_i}{N} M_i = \sum y_i M_i \qquad \textbf{(14–9)}$$

The mass and mole fractions of species i of a mixture are related to each other by

$$w_i = \frac{\rho_i}{\rho} = \frac{C_i M_i}{CM} = y_i \frac{M_i}{M} \qquad \text{(14–10)}$$

Two different approaches are presented above for the description of concentration at a location, and you may be wondering which approach is better to use. Well, the answer depends on the situation on hand. Both approaches are equivalent, and the better approach for a given problem is the one that yields the desired solution more easily.

Special Case: Ideal Gas Mixtures

At low pressures, a gas or gas mixture can conveniently be approximated as an ideal gas with negligible error. For example, a mixture of dry air and water vapor at atmospheric conditions can be treated as an ideal gas with an error much less than 1 percent. The total pressure of a gas mixture P is equal to the sum of the partial pressures P_i of the individual gases in the mixture and is expressed as $P = \sum P_i$. Here P_i is called the **partial pressure** of species i, which is the pressure species i would exert if it existed alone at the mixture temperature and volume. This is known as **Dalton's law of additive pressures**. Then using the ideal gas relation $PV = NR_u T$ where R_u is the universal gas constant for both the species i and the mixture, the **pressure fraction** of species i can be expressed as (Fig. 14–9)

$$\frac{P_i}{P} = \frac{N_i R_u T / V}{N R_u T / V} = \frac{N_i}{N} = y_i \qquad \text{(14–11)}$$

Therefore, the *pressure fraction* of species i of an ideal gas mixture is equivalent to the *mole fraction* of that species and can be used in place of it in mass transfer analysis.

Fick's Law of Diffusion: Stationary Medium Consisting of Two Species

We mentioned earlier that the rate of mass diffusion of a chemical species in a stagnant medium in a specified direction is proportional to the local concentration gradient in that direction. This linear relationship between the rate of diffusion and the concentration gradient proposed by Fick in 1855 is known as **Fick's law of diffusion** and can be expressed as

<div align="center">Mass flux = Constant of proportionality × Concentration gradient</div>

But the concentration of a species in a gas mixture or liquid or solid solution can be defined in several ways, such as density, mass fraction, molar concentration, and mole fraction, as already discussed, and thus Fick's law can be expressed mathematically in many ways. It turns out that it is best to express the concentration gradient in terms of the mass or mole fraction, and the most appropriate formulation of *Fick's law* for the diffusion of a species A in a stationary binary mixture of species A and B in a specified direction x is given by (Fig. 14–10)

$$\textit{Mass basis: } j_{\text{diff}, A} = \frac{\dot{m}_{\text{diff}, A}}{A} = -\rho D_{AB} \frac{d(\rho_A/\rho)}{dx} = -\rho D_{AB} \frac{dw_A}{dx} \quad \text{(kg/s·m}^2\text{)}$$

$$\text{(14–12)}$$

$$\textit{Mole basis: } \bar{j}_{\text{diff}, A} = \frac{\dot{N}_{\text{diff}, A}}{A} = -CD_{AB} \frac{d(C_A/C)}{dx} = -CD_{AB} \frac{dy_A}{dx} \quad \text{(kmol/s·m}^2\text{)}$$

2 mol A
6 mol B
$P = 120$ kPa
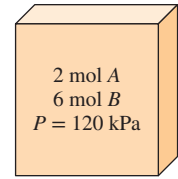
A mixture of two ideal gases A and B

$$y_A = \frac{N_A}{N} = \frac{2}{2+6} = 0.25$$

$$P_A = y_A P = 0.25 \times 120 = 30 \text{ kPa}$$

FIGURE 14–9
For ideal gas mixtures, pressure fraction of a gas is equal to its mole fraction.

Higher concentration of species A

Lower concentration of species A

slope $= \dfrac{dC_A}{dx}$

Area A

$C_A(x)$
Concentration profile of species A

x
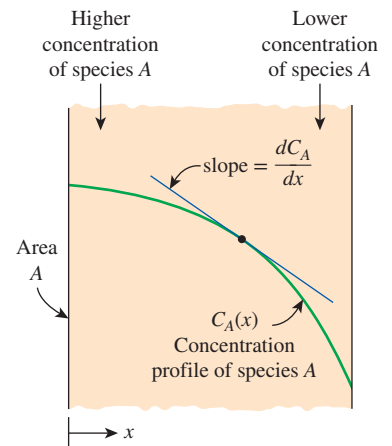
Mass basis:

$$\dot{m}_{\text{diff}} = -\rho A D_{AB} \frac{dw_A}{dx}$$

$$= -\rho A D_{AB} \frac{d(\rho_A/\rho)}{dx}$$

$$= -A D_{AB} \frac{d\rho_A}{dx} \text{ (if } \rho = \text{constant)}$$

Mole basis:

$$\dot{N}_{\text{diff}, A} = -CA D_{AB} \frac{dy_A}{dx}$$

$$= -CA D_{AB} \frac{d(C_A/C)}{dx}$$

$$= -A D_{AB} \frac{dC_A}{dx} \text{ (if } C = \text{constant)}$$

FIGURE 14–10
Various expressions of Fick's law of diffusion for a binary mixture.

Mass diffusion: $\dot{m}_A = -D_{AB}A\dfrac{d\rho_A}{dx}$

Heat conduction: $\dot{Q} = -kA\dfrac{dT}{dx}$
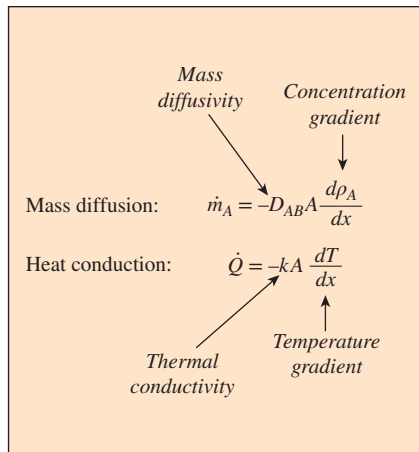
FIGURE 14–11
Analogy between Fourier's law of heat conduction and Fick's law of mass diffusion.

TABLE 14–1

Binary diffusion coefficients of some gases in air at 1 atm pressure

Binary Diffusion Coefficient,* $m^2/s \times 10^5$

T, K	O_2	CO_2	H_2	NO
200	0.95	0.74	3.75	0.88
300	1.88	1.57	7.77	1.80
400	5.25	2.63	12.5	3.03
500	4.75	3.85	17.1	4.43
600	6.46	5.37	24.4	6.03
700	8.38	6.84	31.7	7.82
800	10.5	8.57	39.3	9.78
900	12.6	10.5	47.7	11.8
1000	15.2	12.4	56.9	14.1
1200	20.6	16.9	77.7	19.2
1400	26.6	21.7	99.0	24.5
1600	33.2	27.5	125	30.4
1800	40.3	32.8	152	37.0
2000	48.0	39.4	180	44.8

Source: From Mills, 1995; Table A.17a, p. 869
*Multiply by 10.76 to convert to ft²/s.

Here $j_{\text{diff}, A}$ is the (**diffusive**) **mass flux** of species A (mass transfer by diffusion per unit time and per unit area normal to the direction of mass transfer, in kg/s·m²) and $\bar{j}_{\text{diff}, A}$ is the (**diffusive**) **molar flux** (in kmol/s·m²). The mass flux of a species at a location is proportional to the density of the mixture at that location. Note that $\rho = \rho_A + \rho_B$ is the density and $C = C_A + C_B$ is the molar concentration of the binary mixture, and in general, they may vary throughout the mixture. Therefore, $\rho d(\rho_A/\rho) \neq d\rho_A$ or $Cd(C_A/C) \neq dC_A$. But in the special case of constant mixture density ρ or constant molar concentration C, the relations above simplify to

Mass basis (ρ = constant): $\qquad j_{\text{diff}, A} = -D_{AB}\dfrac{d\rho_A}{dx}$ (kg/s·m²)

$$\text{(14–13)}$$

Mole basis (C = constant): $\qquad \bar{j}_{\text{diff}, A} = -D_{AB}\dfrac{dC_A}{dx}$ (kmol/s·m²)

The constant density or constant molar concentration assumption is usually appropriate for *solid* and *dilute liquid* solutions, but often this is not the case for gas mixtures or concentrated liquid solutions. Therefore, Eq. 14–12 should be used in the latter case. In this introductory treatment we limit our consideration to one-dimensional mass diffusion. For two- or three-dimensional cases, Fick's law can conveniently be expressed in vector form by simply replacing the derivatives in the preceding relations by the corresponding gradients (such as $\mathbf{j}_A = -\rho D_{AB}\nabla w_A$).

Remember that the constant of proportionality in Fourier's law was defined as the transport property *thermal conductivity*. Similarly, the constant of proportionality in Fick's law is defined as another transport property called the **binary diffusion coefficient** or **mass diffusivity**, D_{AB}. The unit of mass diffusivity is m²/s, which is the same as the units of *thermal diffusivity* or *momentum diffusivity* (also called *kinematic viscosity*) (Fig. 14–11).

Because of the complex nature of mass diffusion, the diffusion coefficients are usually determined experimentally. The kinetic theory of gases indicates that the diffusion coefficient for dilute gases at ordinary pressures is essentially independent of mixture composition and tends to increase with temperature while decreasing with pressure as

$$D_{AB} \propto \frac{T^{3/2}}{P} \quad \text{or} \quad \frac{D_{AB, 1}}{D_{AB, 2}} = \frac{P_2}{P_1}\left(\frac{T_1}{T_2}\right)^{3/2} \qquad \text{(14–14)}$$

This relation is useful in determining the diffusion coefficient for gases at different temperatures and pressures from a knowledge of the diffusion coefficient at a specified temperature and pressure. More general but complicated relations that account for the effects of molecular collisions are also available. The diffusion coefficients of some gases in air at 1 atm pressure are given in Table 14–1 at various temperatures.

The diffusion coefficients of solids and liquids also tend to increase with temperature while exhibiting a strong dependence on the composition. The diffusion process in solids and liquids is a great deal more complicated than that in gases, and the diffusion coefficients in this case are almost exclusively determined experimentally.

The binary diffusion coefficients for several binary gas mixtures and solid and liquid solutions are given in Tables 14–2 and 14–3. We make two observations from these tables:

1. The diffusion coefficients, in general, are *highest in gases* and *lowest in solids.* The diffusion coefficients of gases are several orders of magnitude greater than those of liquids.

2. Diffusion coefficients *increase with temperature.* The diffusion coefficient (and thus the mass diffusion rate) of carbon through iron during a hardening process, for example, increases by 6000 times as the temperature is raised from 500°C to 1000°C.

Due to its practical importance, the diffusion of *water vapor* in *air* has been the topic of several studies, and some empirical formulas have been developed for the diffusion coefficient $D_{H_2O–air}$. Marrero and Mason (1972) proposed this popular formula (Table 14–4):

$$D_{H_2O–air} = 1.87 \times 10^{-10} \frac{T^{2.072}}{P} \quad (m^2/s), \quad 280 \ K < T < 450 \ K \qquad (14–15)$$

where P is total pressure in atm and T is the temperature in K.

The primary driving mechanism of mass diffusion is the concentration gradient, and mass diffusion due to a concentration gradient is known as the **ordinary diffusion**. However, diffusion may also be caused by other effects. Temperature gradients in a medium can cause **thermal diffusion** (also called the **soret effect**), and pressure gradients may result in **pressure diffusion**. Both of these effects are usually negligible, however, unless the gradients are

TABLE 14–2

Binary diffusion coefficients of dilute gas mixtures at 1 atm

Substance A	Substance B	T, K	D_{AB} or D_{BA}, m²/s	Substance A	Substance B	T, K	D_{AB} or D_{BA}, m²/s
Air	Acetone	273	1.1×10^{-5}	Argon, Ar	Nitrogen, N_2	293	1.9×10^{-5}
Air	Ammonia, NH_3	298	2.6×10^{-5}	Carbon dioxide, CO_2	Benzene	318	0.72×10^{-5}
Air	Benzene	298	0.88×10^{-5}	Carbon dioxide, CO_2	Hydrogen, H_2	273	5.5×10^{-5}
Air	Carbon dioxide	298	1.6×10^{-5}	Carbon dioxide, CO_2	Nitrogen, N_2	293	1.6×10^{-5}
Air	Chlorine	273	1.2×10^{-5}	Carbon dioxide, CO_2	Oxygen, O_2	273	1.4×10^{-5}
Air	Ethyl alcohol	298	1.2×10^{-5}	Carbon dioxide, CO_2	Water vapor	298	1.6×10^{-5}
Air	Ethyl ether	298	0.93×10^{-5}	Hydrogen, H_2	Nitrogen, N_2	273	6.8×10^{-5}
Air	Helium, He	298	7.2×10^{-5}	Hydrogen, H_2	Oxygen, O_2	273	7.0×10^{-5}
Air	Hydrogen, H_2	298	7.2×10^{-5}	Oxygen, O_2	Ammonia	293	2.5×10^{-5}
Air	Iodine, I_2	298	0.83×10^{-5}	Oxygen, O_2	Benzene	296	0.39×10^{-5}
Air	Methanol	298	1.6×10^{-5}	Oxygen, O_2	Nitrogen, N_2	273	1.8×10^{-5}
Air	Mercury	614	4.7×10^{-5}	Oxygen, O_2	Water vapor	298	2.5×10^{-5}
Air	Napthalene	300	0.62×10^{-5}	Water vapor	Argon, Ar	298	2.4×10^{-5}
Air	Oxygen, O_2	298	2.1×10^{-5}	Water vapor	Helium, He	298	9.2×10^{-5}
Air	Water vapor	298	2.5×10^{-5}	Water vapor	Nitrogen, N_2	298	2.5×10^{-5}

Source: From Barrer, 1941; Geankoplis, 1972; Perry, 1963; and Reid et al., 1977
Note: The effect of pressure and temperature on D_{AB} can be accounted for through $D_{AB} \sim T^{3/2}/P$. Also, multiply D_{AB} values by 10.76 to convert them to ft²/s.

TABLE 14–3

Binary diffusion coefficients of dilute liquid solutions and solid solutions at 1 atm

(a) Diffusion Through Liquids				(b) Diffusion Through Solids			
Substance A (Solute)	Substance B (Solvent)	T, K	D_{AB}, m²/s	Substance A (Solute)	Substance B (Solvent)	T, K	D_{AB}, m²/s
Ammonia	Water	285	1.6×10^{-9}	Carbon dioxide	Natural rubber	298	1.1×10^{-10}
Benzene	Water	293	1.0×10^{-9}	Nitrogen	Natural rubber	298	1.5×10^{-10}
Carbon dioxide	Water	298	2.0×10^{-9}	Oxygen	Natural rubber	298	2.1×10^{-10}
Chlorine	Water	285	1.4×10^{-9}	Helium	Pyrex	773	2.0×10^{-12}
Ethanol	Water	283	0.84×10^{-9}	Helium	Pyrex	293	4.5×10^{-15}
Ethanol	Water	288	1.0×10^{-9}	Helium	Silicon dioxide	298	4.0×10^{-14}
Ethanol	Water	298	1.2×10^{-9}	Hydrogen	Iron	298	2.6×10^{-13}
Glucose	Water	298	0.69×10^{-9}	Hydrogen	Nickel	358	1.2×10^{-12}
Hydrogen	Water	298	6.3×10^{-9}	Hydrogen	Nickel	438	1.0×10^{-11}
Methane	Water	275	0.85×10^{-9}	Cadmium	Copper	293	2.7×10^{-19}
Methane	Water	293	1.5×10^{-9}	Zinc	Copper	773	4.0×10^{-18}
Methane	Water	333	3.6×10^{-9}	Zinc	Copper	1273	5.0×10^{-13}
Methanol	Water	288	1.3×10^{-9}	Antimony	Silver	293	3.5×10^{-25}
Nitrogen	Water	298	2.6×10^{-9}	Bismuth	Lead	293	1.1×10^{-20}
Oxygen	Water	298	2.4×10^{-9}	Mercury	Lead	293	2.5×10^{-19}
Water	Ethanol	298	1.2×10^{-9}	Copper	Aluminum	773	4.0×10^{-14}
Water	Ethylene glycol	298	0.18×10^{-9}	Copper	Aluminum	1273	1.0×10^{-10}
Water	Methanol	298	1.8×10^{-9}	Carbon	Iron (fcc)	773	5.0×10^{-15}
Chloroform	Methanol	288	2.1×10^{-9}	Carbon	Iron (fcc)	1273	3.0×10^{-11}

Source: From Barrer, 1941; Reid et al., 1977; Thomas, 1991; and Van Black, 1980

TABLE 14–4

In a binary ideal gas mixture of species A and B, the diffusion coefficient of A in B is equal to the diffusion coefficient of B in A, and both increase with temperature

T, °C	D_{H_2O-air} or D_{Air-H_2O} at 1 atm, in m²/s (from Eq. 14–15)
0	2.09×10^{-5}
5	2.17×10^{-5}
10	2.25×10^{-5}
15	2.33×10^{-5}
20	2.42×10^{-5}
25	2.50×10^{-5}
30	2.59×10^{-5}
35	2.68×10^{-5}
40	2.77×10^{-5}
50	2.96×10^{-5}
100	3.99×10^{-5}
150	5.18×10^{-5}

very large. In centrifuges, the pressure gradient generated by the centrifugal effect is used to separate liquid solutions and gaseous isotopes. An external force field such as an electric or magnetic field applied on a mixture or solution can be used successfully to separate electrically charged or magnetized molecules (as in an electrolyte or ionized gas) from the mixture. This is called **forced diffusion**. Also, when the pores of a porous solid such as silica gel are smaller than the mean free path of the gas molecules, the molecular collisions may be negligible, and a free molecule flow may be initiated. This is known as **Knudsen diffusion**. When the size of the gas molecules is comparable to the pore size, adsorbed molecules move along the pore walls. This is known as **surface diffusion**. Finally, particles whose diameter is under 0.1 µm such as mist and soot particles act like large molecules, and the diffusion process of such particles due to the concentration gradient is called **Brownian motion**. Large particles (those whose diameter is greater than 1 µm) are not affected by diffusion because the motion of such particles is governed by Newton's laws. In our elementary treatment of mass diffusion, we assume these additional effects to be nonexistent or negligible, as is usually the case, and refer the interested reader to advanced books on these topics.

EXAMPLE 14–1 Determining Mass Fractions from Mole Fractions

The composition of dry standard atmosphere is given on a molar basis to be 78.1 percent N_2, 20.9 percent O_2, and 1.0 percent Ar and small amounts of other constituents (Fig. 14–12). Treating other constituents as Ar, determine the mass fractions of the constituents of air.

SOLUTION The molar fractions of the constituents of air are given. The mass fractions are to be determined.
Assumptions The small amounts of other gases in air are treated as argon.
Properties The molar masses of N_2, O_2, and Ar are 28.0, 32.0, and 39.9 kg/kmol, respectively (Table A–1).
Analysis The molar mass of air is determined to be

$$M = \sum y_i M_i = 0.781 \times 28.0 + 0.209 \times 32.0 + 0.01 \times 39.9 = 29.0 \text{ kg/kmol}$$

Then the mass fractions of constituent gases are determined from Eq. 14–10 to be

N$_2$: $w_{N_2} = y_{N_2}\dfrac{M_{N_2}}{M} = (0.781)\dfrac{28.0}{29.0} = \mathbf{0.754}$

O$_2$: $w_{O_2} = y_{O_2}\dfrac{M_{O_2}}{M} = (0.209)\dfrac{32.0}{29.0} = \mathbf{0.231}$

Ar: $w_{Ar} = y_{Ar}\dfrac{M_{Ar}}{M} = (0.01)\dfrac{39.9}{29.0} = \mathbf{0.014}$

Therefore, the mass fractions of N_2, O_2, and Ar in dry standard atmosphere are 75.4 percent, 23.1 percent, and 1.4 percent, respectively.
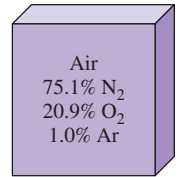
FIGURE 14–12
Schematic for Example 14–1.

14–4 ▪ BOUNDARY CONDITIONS

We mentioned earlier that the mass diffusion equation is analogous to the heat diffusion (conduction) equation, and thus we need comparable boundary conditions to determine the species concentration distribution in a medium. Two common types of boundary conditions are the (1) *specified species concentration,* which corresponds to specified temperature, and (2) *specified species flux,* which corresponds to specified heat flux.

Despite their apparent similarity, an important difference exists between temperature and concentration: temperature is necessarily a *continuous* function, but concentration, in general, is not. The wall and air temperatures at a wall surface, for example, are always the same. The concentrations of air on the two sides of a water–air interface, however, are obviously very different (in fact, the concentration of air in water is close to zero). Likewise, the concentrations of water on the two sides of a water–air interface are also different even when air is saturated (Fig. 14–13). Therefore, when specifying a boundary condition, specifying the location is not enough. We also need to specify the side of the boundary. To do this, we consider two imaginary surfaces on the two sides of the interface that are infinitesimally close to the interface. Whenever there is a doubt, we indicate the desired side of the interface by specifying its phase as a subscript. For example, the water (liquid or vapor)
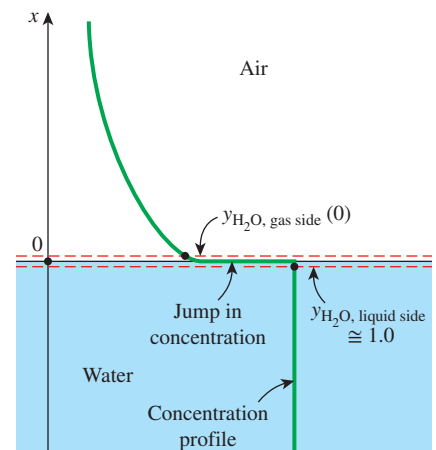
FIGURE 14–13
Unlike temperature, the concentration of species on the two sides of a liquid–gas (or solid–gas or solid–liquid) interface are usually not the same.
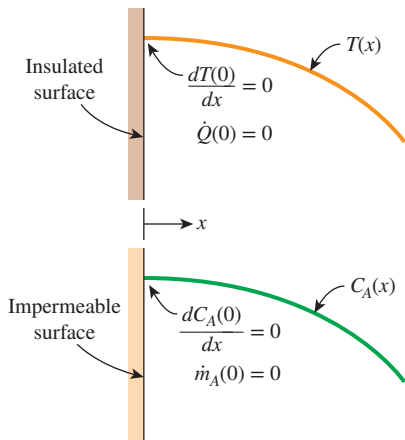
FIGURE 14–14

An impermeable surface in mass transfer is analogous to an insulated surface in heat transfer.

TABLE 14–5

Solubility of two inorganic compounds in water at various temperatures, in kg, in 100 kg of water

Temperature, K	Solute	
	Salt, (NaCl)	Calcium Bicarbonate, $Ca(HCO_3)_2$
273.15	35.7	16.15
280	35.8	16.30
290	35.9	16.53
300	36.2	16.75
310	36.5	16.98
320	36.9	17.20
330	37.2	17.43
340	37.6	17.65
350	38.2	17.88
360	38.8	18.10
370	39.5	18.33
373.15	39.8	18.40

Source: From Handbook of Chemistry *(New York: McGraw-Hill, 1961)*

concentration at the liquid and gas sides of a water–air interface at $x = 0$ can be expressed on a molar basis as

$$y_{H_2O,\ \text{liquid side}}(0) = y_1 \quad \text{and} \quad y_{H_2O,\ \text{gas side}}(0) = y_2 \qquad \textbf{(14–16)}$$

Using Fick's law, the constant species flux boundary condition for a diffusing species A at a boundary at $x = 0$ is expressed, in the absence of any blowing or suction, as

$$-CD_{AB}\frac{dy_A}{dx}\bigg|_{x=0} = \bar{j}_{A,\,0} \quad \text{or} \quad -\rho D_{AB}\frac{dw_A}{dx}\bigg|_{x=0} = j_{A,\,0} \qquad \textbf{(14–17)}$$

where $\bar{j}_{A,\,0}$ and $j_{A,\,0}$ are the specified mole and mass fluxes of species A at the boundary, respectively. The special case of zero mass flux ($\bar{j}_{A,\,0} = j_{A,\,0} = 0$) corresponds to an **impermeable surface** for which $dy_A(0)/dx = dw_A(0)/dx = 0$ (Fig. 14–14).

To apply the *specified concentration* boundary condition, we must know the concentration of a species at the boundary. This information is usually obtained from the requirement that *thermodynamic equilibrium* must exist at the interface of two phases of a species. In the case of air–water interface, the concentration values of water vapor in the air are easily determined from saturation data.

The situation is similar at *solid–liquid* interfaces. Again, at a given temperature, only a certain amount of solid can be dissolved in a liquid, and the solubility of the solid in the liquid is determined from the requirement that thermodynamic equilibrium exists between the solid and the solution at the interface. The **solubility** represents *the maximum amount of solid that can be dissolved in a liquid at a specified temperature* and is widely available in chemistry handbooks. In Table 14–5 we present sample solubility data for sodium chloride (NaCl) and calcium bicarbonate [$Ca(HCO_3)_2$] at various temperatures. For example, the solubility of salt (NaCl) in water at 310 K is 36.5 kg per 100 kg of water. Therefore, the mass fraction of salt in the brine at the interface is simply

$$w_{\text{salt, liquid side}} = \frac{m_{\text{salt}}}{m} = \frac{36.5\ \text{kg}}{(100 + 36.5)\ \text{kg}} = 0.267 \quad \text{(or 26.7 percent)}$$

whereas the mass fraction of salt in the pure solid salt is $w = 1.0$. Note that water becomes *saturated* with salt when 36.5 kg of salt are dissolved in 100 kg of water at 310 K.

Many processes involve the absorption of a gas into a liquid. Most gases are weakly soluble in liquids (such as air in water), and for such dilute solutions the mole fractions of a species i in the gas and liquid phases at the interface are observed to be proportional to each other. That is, $y_{i,\ \text{gas side}} \propto y_{i,\ \text{liquid side}}$ or $P_{i,\ \text{gas side}} \propto P\ y_{i,\ \text{liquid side}}$ since $y_{i,\ \text{gas side}} = P_{i,\ \text{gas side}}/P$ for ideal gas mixtures. This is known as **Henry's law** and is expressed as

$$y_{i,\ \text{liquid side}} = \frac{P_{i,\ \text{gas side}}}{H} \quad \text{(at interface)} \qquad \textbf{(14–18)}$$

where H is **Henry's constant**, which is the ratio of the partial pressure in the gas phase over the mole fraction of the liquid phase. For a given species, it is a function of temperature only and is practically independent of pressure for pressures under about 5 atm. Values of Henry's constant for a number of

TABLE 14–6

Henry's constant H (in bars) for selected gases in water at low to moderate pressures (for gas i, $H = P_{i, \text{gas side}}/y_{i, \text{water side}}$)

Solute	290 K	300 K	310 K	320 K	330 K	340 K
H_2S	440	560	700	830	980	1140
CO_2	1280	1710	2170	2720	3220	—
O_2	38,000	45,000	52,000	57,000	61,000	65,000
H_2	67,000	72,000	75,000	76,000	77,000	76,000
CO	51,000	60,000	67,000	74,000	80,000	84,000
Air	62,000	74,000	84,000	92,000	99,000	104,000
N_2	76,000	89,000	101,000	110,000	118,000	124,000

Source: From Mills, 1995; Table A.21

aqueous solutions are given in Table 14–6 for various temperatures. From this table and the equation above we make the following observations:

1. The concentration of a gas dissolved in a liquid is inversely proportional to Henry's constant. Therefore, the larger the Henry's constant, the smaller the concentration of dissolved gases in the liquid.

2. Henry's constant increases (and thus the fraction of a dissolved gas in the liquid decreases) with increasing temperature. Therefore, the dissolved gases in a liquid can be driven off by heating the liquid (Fig. 14–15).

3. The concentration of a gas dissolved in a liquid is proportional to the partial pressure of the gas. Therefore, the amount of gas dissolved in a liquid can be increased by increasing the pressure of the gas. This can be used to advantage in the carbonation of soft drinks with CO_2 gas.

Strictly speaking, the result obtained from Eq. 14–18 for the mole fraction of dissolved gas is valid for the liquid layer just beneath the interface and not necessarily the entire liquid. The latter will be the case only when thermodynamic phase equilibrium is established throughout the entire liquid body.
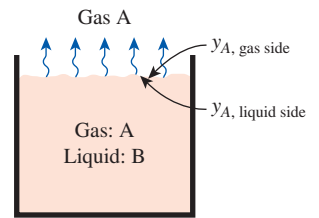
$y_{A, \text{gas side}} \propto y_{A, \text{liquid side}}$

or

$\dfrac{P_{A, \text{gas side}}}{P} \propto y_{A, \text{liquid side}}$

or

$P_{A, \text{gas side}} = H y_{A, \text{liquid side}}$

FIGURE 14–15
Dissolved gases in a liquid can be driven off by heating the liquid.

EXAMPLE 14–2   Mole Fraction of Dissolved Air in Water

Determine the mole fraction of air dissolved in water at the surface of a lake whose temperature is 17°C (Fig. 14–16). Take the atmospheric pressure at lake level to be 92 kPa.

SOLUTION The mole fraction of air dissolved in water at the surface of a lake is to be determined.
Assumptions   **1** Both the air and water vapor are ideal gases. **2** Air is weakly soluble in water so that Henry's law is applicable.
Properties   The saturation pressure of water at 17°C is 1.96 kPa (Table A–9). Henry's constant for air dissolved in water at 290 K is $H = 62,000$ bar (Table 14–6).
Analysis   This example is similar to the previous example. Again the air at the water surface is saturated, and thus the partial pressure of water vapor in the air at the lake surface is the saturation pressure of water at 17°C,

$$P_{\text{vapor}} = P_{\text{sat @ 17°C}} = 1.96 \text{ kPa}$$
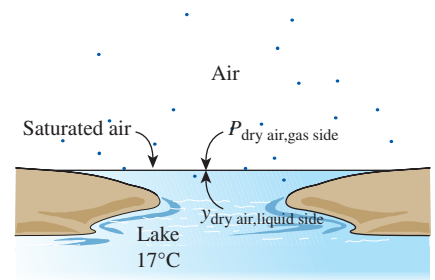
FIGURE 14–16
Schematic for Example 14–2.

Assuming both the air and vapor to be ideal gases, the partial pressure of dry air is determined to be

$$P_{\text{dry air}} = P - P_{\text{vapor}} = 92 - 1.96 = 90.04 \text{ kPa} = 0.9004 \text{ bar}$$

Note that with little loss in accuracy (an error of about 2 percent), we could have ignored the vapor pressure since the amount of vapor in air is so small. Then the mole fraction of air in the water becomes

$$y_{\text{dry air, liquid state}} = \frac{P_{\text{dry air, gas side}}}{H} = \frac{0.9004 \text{ bar}}{62,000 \text{ bar}} = \textbf{1.45} \times \textbf{10}^{-5}$$

which is very small, as expected. Therefore, the concentration of air in water just below the air–water interface is 1.45 moles per 100,0000 moles. But obviously this is enough oxygen for fish and other creatures in the lake. Note that the amount of air dissolved in water decreases with increasing depth.

We mentioned earlier that the use of Henry's law is limited to dilute gas–liquid solutions; that is, a liquid with a small amount of gas dissolved in it. Then the question that arises naturally is, what do we do when the gas is highly soluble in the liquid (or solid), such as ammonia in water? In this case the linear relationship of Henry's law does not apply, and the mole fraction of a gas dissolved in the liquid (or solid) is usually expressed as a function of the partial pressure of the gas in the gas phase and the temperature. An approximate relation in this case for the *mole fractions* of a species on the *liquid* and *gas sides* of the interface is given by **Raoult's law** as

$$P_{i, \text{ gas side}} = y_{i, \text{ gas side}} P = y_{i, \text{ liquid side}} P_{i, \text{ sat}}(T) \tag{14–19}$$

where $P_{i, \text{ sat}}(T)$ is the *saturation pressure* of the species i at the interface temperature and P is the *total pressure* on the gas phase side. Tabular data are available in chemical handbooks for common solutions such as the ammonia–water solution that is widely used in absorption-refrigeration systems.

Gases may also dissolve in *solids*, but the diffusion process in this case can be very complicated. The dissolution of a gas may be independent of the structure of the solid, or it may depend strongly on its porosity. Some dissolution processes (such as the dissolution of hydrogen in titanium, similar to the dissolution of CO_2 in water) are *reversible*, and thus maintaining the gas content in the solid requires constant contact of the solid with a reservoir of that gas. Some other dissolution processes are *irreversible*. For example, oxygen gas dissolving in titanium forms TiO_2 on the surface, and the process does not reverse itself.

The concentration of the gas species i in the solid at the interface $C_{i, \text{ solid side}}$ is proportional to the *partial pressure* of the species i in the gas $P_{i, \text{ gas side}}$ on the gas side of the interface and is expressed as

$$C_{i, \text{ solid side}} = \mathscr{S} \times P_{i, \text{ gas side}} \quad (\text{kmol/m}^3) \tag{14–20}$$

where $\mathscr{S}$ is the **solubility.** Expressing the pressure in bars and noting that the unit of molar concentration is kmol of species i per m^3, the unit of solubility is kmol/m^3·bar. Solubility data for selected gas–solid combinations are given in Table 14–7. The product of the *solubility* of a gas and the *diffusion coefficient*

TABLE 14–7

Solubility of selected gases and solids
(for gas i, $\mathscr{S} = C_{i, \text{ solid side}}/P_{i, \text{ gas side}}$)

Gas	Solid	T, K	$\mathscr{S}$, kmol/m³·bar
O_2	Rubber	298	0.00312
N_2	Rubber	298	0.00156
CO_2	Rubber	298	0.04015
He	SiO_2	293	0.00045
H_2	Ni	358	0.00901

Source: From Barrer, 1941

of the gas in a solid is referred to as the **permeability** $\mathscr{P}$, which is a measure of the ability of the gas to penetrate a solid. That is, $\mathscr{P} = \mathscr{L} D_{AB}$ where D_{AB} is the diffusivity of the gas in the solid. Permeability is inversely proportional to thickness and has the unit kmol/s·bar.

Finally, if a process involves the *sublimation* of a pure solid (such as ice or solid CO_2) or the *evaporation* of a pure liquid (such as water) in a different medium such as air, the mole (or mass) fraction of the substance in the liquid or solid phase is simply taken to be 1.0, and the partial pressure and thus the mole fraction of the substance in the gas phase can readily be determined from the saturation data of the substance at the specified temperature. Also, the assumption of thermodynamic equilibrium at the interface is very reasonable for pure solids, pure liquids, and solutions, except when chemical reactions are occurring at the interface.

■ **EXAMPLE 14–3**   **Diffusion of Hydrogen Gas into a Nickel Plate**

Consider a nickel plate that is in contact with hydrogen gas at 358 K and 300 kPa. Determine the molar and mass density of hydrogen in the nickel at the interface (Fig. 14–17).

SOLUTION   A nickel plate is exposed to hydrogen. The molar and mass density of hydrogen in the nickel at the interface are to be determined.
Assumptions   Nickel and hydrogen are in thermodynamic equilibrium at the interface.
Properties   The molar mass of hydrogen is $M = 2$ kg/kmol (Table A–1). The solubility of hydrogen in nickel at 358 K is 0.00901 kmol/m³·bar (Table 14–7).
Analysis   Noting that 300 kPa = 3 bar, the molar density of hydrogen in the nickel at the interface is determined from Eq. 14–20 to be

$$C_{H_2,\text{ solid side}} = \mathscr{L} \times P_{H_2,\text{ gas side}}$$
$$= (0.00901 \text{ kmol/m}^3\text{·bar})(3 \text{ bar}) = \mathbf{0.027 \text{ kmol/m}^3}$$

It corresponds to a mass density of

$$\rho_{H_2,\text{ solid side}} = C_{H_2,\text{ solid side}} M_{H_2}$$
$$= (0.027 \text{ kmol/m}^3)(2) = \mathbf{0.054 \text{ kg/m}^3}$$

That is, there will be 0.027 kmol (or 0.054 kg) of H_2 gas in each m³ volume of nickel adjacent to the interface.
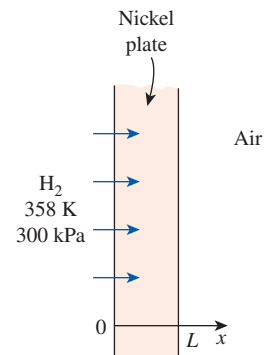
FIGURE 14–17
Schematic for Example 14–3.

■ **EXAMPLE 14–4**   **Gas Leak from a Vessel Through a Rubber Plug**

Consider a 4-L vessel filled with carbon dioxide gas at 25°C and 5 atm (Fig. 14–18). A 20-mm-diameter circular rubber plug with a thickness of 10 mm is used to contain the gas inside the vessel. Determine the rate of mass loss of carbon dioxide gas from the vessel through the rubber plug.

SOLUTION   A circular rubber plug with specified dimensions is used to contain carbon dioxide gas inside a vessel. The rate of gas loss from the vessel through the rubber plug is to be determined.
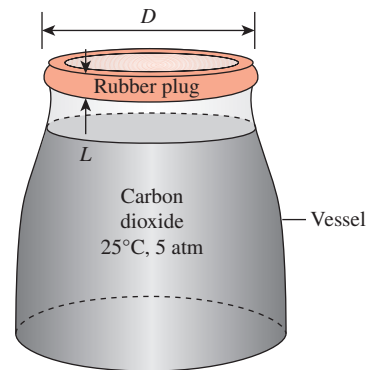
FIGURE 14–18
Schematic for Example 14–4.
Source: The McGraw-Hill Companies, Inc./Ken Karp photographer.

Assumptions **1** Mass diffusion is steady and one-dimensional. **2** There are no chemical reactions in the rubber plug that result in the generation or depletion of carbon dioxide.

Properties The binary diffusion coefficient for CO_2 in the rubber at 25°C or 298 K is $D_{AB} = 1.1 \times 10^{-10}$ m²/s (Table 14–3b). The molar mass of CO_2 is $M = 44.01$ kg/kmol (Table A–1). The solubility of CO_2 in the rubber at 25°C = 298 K is 0.04015 kmol/m³·bar (Table 14–7).

Analysis The mass density of CO_2 (for 5 atm) in the rubber at the interface is determined from

$$\rho_{A,1} = \mathcal{S}P_{A,1}$$

$$= (0.04015 \text{ kmol/m}^3\text{·bar})(5 \text{ atm})\left(\frac{44.01 \text{ kg}}{1 \text{ kmol}}\right)\left(\frac{1.01325 \text{ bar}}{1 \text{ atm}}\right)$$

$$= 8.952 \text{ kg/m}^2$$

On the opposite side, the mass density of CO_2 is zero, $\rho_{A,2} = 0$. Then the rate of carbon dioxide gas loss through the rubber plug becomes

$$\dot{m}_{\text{diff}} = D_{AB}A\frac{\rho_{A,1} - \rho_{A,2}}{L} = D_{AB}\left(\frac{\pi D^2}{4}\right)\frac{\rho_{A,1} - \rho_{A,2}}{L}$$

$$= (1.1 \times 10^{-10} \text{ m}^2\text{/s})\frac{\pi(0.02 \text{ m})^2}{4}\frac{(8.952 - 0)\text{ kg/m}^3}{0.01 \text{ m}}$$

$$= \mathbf{3.09 \times 10^{-11} \text{ kg/s}}$$

This corresponds to about 1 gram of CO_2 per year.

Discussion Using the ideal gas relation, the mass of CO_2 gas in the vessel can be shown to be 36 g. A loss of 1 g of CO_2 corresponds to about 3 percent of the total initial mass, which may be significant. Therefore, alternatives should be considered for long-term storage.

14–5 ▪ STEADY MASS DIFFUSION THROUGH A WALL

Many practical mass transfer problems involve the diffusion of a species through a plane-parallel medium that does not involve any homogeneous chemical reactions under *one-dimensional steady* conditions. Such mass transfer problems are analogous to the steady one-dimensional heat conduction problems in a plane wall with no heat generation and can be analyzed similarly. In fact, many of the relations developed in Chap. 3 can be used for mass transfer by replacing temperature with mass (or molar) fraction, thermal conductivity with ρD_{AB} (or CD_{AB}), and heat flux with mass (or molar) flux (Table 14–8).

Consider a solid plane wall (medium *B*) of area *A*, thickness *L*, and density ρ. The wall is subjected on both sides to different concentrations of a species *A* to which it is permeable. The boundary surfaces at $x = 0$ and $x = L$ are located within the solid adjacent to the interfaces, and the mass fractions of *A* at those surfaces are maintained at $w_{A,1}$ and $w_{A,2}$, respectively, at all times (Fig. 14–19). The mass fraction of species *A* in the wall varies in the *x*-direction only and can be expressed as $w_A(x)$. Therefore, mass transfer through the wall in this case can be modeled as *steady* and *one-dimensional*.

TABLE 14–8

Analogy between heat conduction and mass diffusion in a stationary medium

Heat Conduction	Mass Diffusion	
	Mass Basis	Molar Basis
T	w_i	y_i
k	ρD_{AB}	CD_{AB}
$\dot{q}$	j_i	$\bar{j}_i$
α	D_{AB}	D_{AB}
L	L	L

Here we determine the rate of mass diffusion of species *A* through the wall using a similar approach to that used in Chap. 3 for heat conduction.

The concentration of species *A* at any point does not change with time since operation is steady, and there is no production or destruction of species *A* since no chemical reactions are occurring in the medium. Then the **conservation of mass** principle for species *A* can be expressed as *the mass flow rate of species A through the wall at any cross section is the same.* That is

$$\dot{m}_{\text{diff}, A} = j_A A = \text{constant} \quad \text{(kg/s)}$$

Then Fick's law of diffusion becomes

$$j_A = \frac{\dot{m}_{\text{diff}, A}}{A} = -\rho D_{AB} \frac{dw_A}{dx} = \text{constant}$$

Separating the variables in this equation and integrating across the wall from $x = 0$, where $w(0) = w_{A,1}$, to $x = L$, where $w(L) = w_{A,2}$, we get

$$\frac{\dot{m}_{\text{diff}, A}}{A} \int_0^L dx = -\int_{w_{A,1}}^{w_{A,2}} \rho D_{AB}\, dw_A \tag{14–21}$$

where the mass transfer rate $\dot{m}_{\text{diff}, A}$ and the wall area *A* are taken out of the integral sign since both are constants. If the density ρ and the mass diffusion coefficient D_{AB} vary little along the wall, they can be assumed to be constant. The integration can be performed in that case to yield

$$\dot{m}_{\text{diff}, A, \text{wall}} = \rho D_{AB} A \frac{w_{A,1} - w_{A,2}}{L} = D_{AB} A \frac{\rho_{A,1} - \rho_{A,2}}{L} \quad \text{(kg/s)} \tag{14–22}$$

This relation can be rearranged as

$$\dot{m}_{\text{diff}, A, \text{wall}} = \frac{w_{A,1} - w_{A,2}}{L/\rho D_{AB} A} = \frac{w_{A,1} - w_{A,2}}{R_{\text{diff, wall}}} \tag{14–23}$$

where

$$R_{\text{diff, wall}} = \frac{L}{\rho D_{AB} A}$$

is the **diffusion resistance** of the wall, in s/kg, which is analogous to the electrical or conduction resistance of a plane wall of thickness *L* and area *A* (Fig. 14–20). Thus, we conclude that *the rate of mass diffusion through a plane wall is proportional to the average density, the wall area, and the concentration difference across the wall, but is inversely proportional to the wall thickness.* Also, once the rate of mass diffusion is determined, the mass fraction $w_A(x)$ at any location *x* can be determined by replacing $w_{A,2}$ in Eq. 14–22 with $w_A(x)$ and *L* with *x*.

The preceding analysis can be repeated on a molar basis with this result,

$$\dot{N}_{\text{diff}, A, \text{wall}} = C D_{AB} A \frac{y_{A,1} - y_{A,2}}{L} = D_{AB} A \frac{C_{A,1} - C_{A,2}}{L} = \frac{y_{A,1} - y_{A,2}}{\overline{R}_{\text{diff, wall}}} \tag{14–24}$$

where $\overline{R}_{\text{diff, wall}} = L/C D_{AB} A$ is the **molar diffusion resistance** of the wall in s/kmol. Note that mole fractions are accompanied by molar concentrations and mass fractions are accompanied by density. Either relation can be used to determine the diffusion rate of species *A* across the wall, depending on
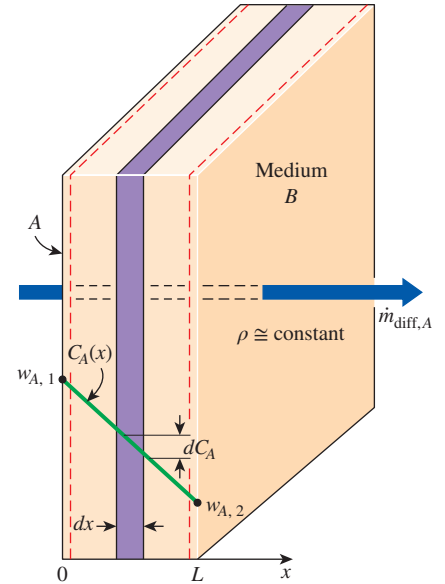
FIGURE 14–19
Schematic for steady one-dimensional mass diffusion of species *A* through a plane wall.

(*a*) Heat flow

$$\dot{Q} = \frac{T_1 - T_2}{R}$$

(*b*) Current flow

$$I = \frac{\mathbf{V}_1 - \mathbf{V}_2}{R_e}$$

(*c*) Mass flow

$$\dot{m}_{\text{diff}, A} = \frac{w_{A,1} - w_{A,2}}{R_{\text{mass}}}$$
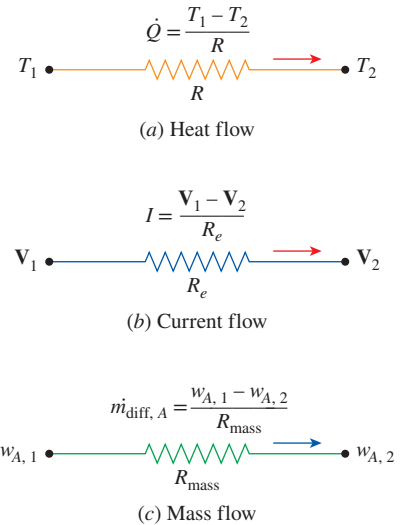
FIGURE 14–20
Analogy between thermal, electrical, and mass diffusion resistance concepts.
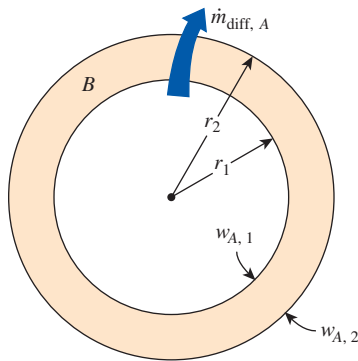
FIGURE 14–21
One-dimensional mass diffusion through a cylindrical or spherical shell.

whether the mass or molar fractions of species A are known at the boundaries. Also, the concentration gradients on both sides of an interface are different, and thus diffusion resistance networks cannot be constructed in an analogous manner to thermal resistance networks.

In developing these relations, we assumed the density and the diffusion coefficient of the wall to be nearly constant. This assumption is reasonable when a small amount of species A diffuses through the wall and thus *the concentration of A is small.* The species A can be a gas, a liquid, or a solid. Also, the wall can be a plane layer of a liquid or gas provided that it is *stationary.*

The analogy between heat and mass transfer also applies to *cylindrical* and *spherical* geometries. Repeating the approach outlined in Chap. 3 for heat conduction, we obtain the following analogous relations for steady one-dimensional mass transfer through nonreacting cylindrical and spherical layers (Fig. 14–21)

$$\dot{m}_{\text{diff}, A, \text{cyl}} = 2\pi L \rho D_{AB} \frac{w_{A, 1} - w_{A, 2}}{\ln(r_2/r_1)} = 2\pi L D_{AB} \frac{\rho_{A, 1} - \rho_{A, 2}}{\ln(r_2/r_1)} \qquad \textbf{(14–25)}$$

$$\dot{m}_{\text{diff}, A, \text{sph}} = 4\pi r_1 r_2 \rho D_{AB} \frac{w_{A, 1} - w_{A, 2}}{r_2 - r_1} = 4\pi r_1 r_2 D_{AB} \frac{\rho_{A, 1} - \rho_{A, 2}}{r_2 - r_1} \qquad \textbf{(14–26)}$$

or, on a molar basis,

$$\dot{N}_{\text{diff}, A, \text{cyl}} = 2\pi L C D_{AB} \frac{y_{A, 1} - y_{A, 2}}{\ln(r_2/r_1)} = 2\pi L D_{AB} \frac{C_{A, 1} - C_{A, 2}}{\ln(r_2/r_1)} \qquad \textbf{(14–27)}$$

$$\dot{N}_{\text{diff}, A, \text{sph}} = 4\pi r_1 r_2 C D_{Ab} \frac{y_{A, 1} - y_{A, 2}}{r_2 - r_1} = 4\pi r_1 r_2 D_{AB} \frac{C_{A, 1} - C_{A, 2}}{r_2 - r_1} \qquad \textbf{(14–28)}$$

Here, L is the length of the cylinder, r_1 is the inner radius, and r_2 is the outer radius for the cylinder or the sphere. Again, the boundary surfaces at $r = r_1$ and $r = r_2$ are located within the solid adjacent to the interfaces, and the mass fractions of A at those surfaces are maintained at $w_{A, 1}$ and $w_{A, 2}$, respectively, at all times. (We could make similar statements for the density, molar concentration, and mole fraction of species A at the boundaries.)

We mentioned earlier that the concentration of the gas species in a solid at the interface is proportional to the partial pressure of the adjacent gas and was expressed as $C_{A, \text{solid side}} = \mathscr{L}_{AB} P_{A, \text{gas side}}$ where $\mathscr{L}_{AB}$ is the *solubility* (in kmol/m³·bar) of the gas A in the solid B. We also mentioned that the product of solubility and the diffusion coefficient is called the *permeability,* $\mathscr{P}_{AB} = \mathscr{L}_{AB} D_{AB}$ (in kmol/m·s·bar). Then the molar flow rate of a gas through a solid under steady one-dimensional conditions can be expressed in terms of the partial pressures of the adjacent gas on the two sides of the solid by replacing C_A in these relations with $\mathscr{L}_{AB} P_A$ or $\mathscr{P}_{AB} P_A / D_{AB}$. In the case of a *plane wall,* for example, it gives (Fig. 14–22)

$$\dot{N}_{\text{diff}, A, \text{wall}} = D_{AB} \mathscr{L}_{AB} A \frac{P_{A, 1} - P_{A, 2}}{L} = \mathscr{P}_{AB} A \frac{P_{A, 1} - P_{A, 2}}{L} \quad \text{(kmol/s)} \quad \textbf{(14–29)}$$

where $P_{A, 1}$ and $P_{A, 2}$ are the *partial pressures* of gas A on the two sides of the wall. Similar relations can be obtained for cylindrical and spherical walls by following the same procedure. Also, if the permeability is given on a mass basis (in kg/m·s·bar), then Eq. 14–29 gives the diffusion mass flow rate.
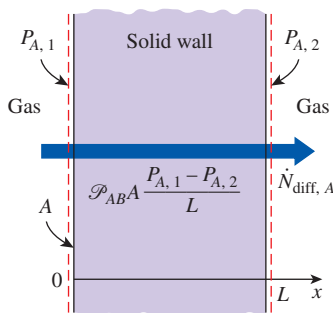
FIGURE 14–22
The diffusion rate of a gas species through a solid can be determined from a knowledge of the partial pressures of the gas on both sides and the permeability of the solid to that gas.

Noting that 1 kmol of an ideal gas at the standard conditions of 0°C and 1 atm occupies a volume of 22.414 m^3, the volume flow rate of the gas through the wall by diffusion can be determined from

$$\dot{V}_{\text{diff}, A} = 22.414\,\dot{N}_{\text{diff}, A} \quad \text{(standard m}^3\text{/s, at 0°C and 1 atm)}$$

The volume flow rate at other conditions can be determined from the ideal gas relation $P_A \dot{V} = \dot{N}_A R_u T$.

EXAMPLE 14–5   **Diffusion of Hydrogen Through a Spherical Container**

Pressurized hydrogen gas is stored at 358 K in a 4.8-m-outer-diameter spherical container made of nickel (Fig. 14–23). The shell of the container is 6 cm thick. The molar concentration of hydrogen in the nickel at the inner surface is determined to be 0.087 kmol/m³. The concentration of hydrogen in the nickel at the outer surface is negligible. Determine the mass flow rate of hydrogen by diffusion through the nickel container.

SOLUTION   Pressurized hydrogen gas is stored in a spherical container. The diffusion rate of hydrogen through the container is to be determined.
Assumptions   **1** Mass diffusion is *steady* and *one-dimensional* since the hydrogen concentration in the tank and thus at the inner surface of the container is practically constant, and the hydrogen concentration in the atmosphere and thus at the outer surface is practically zero. Also, there is thermal symmetry about the center. **2** There are no chemical reactions in the nickel shell that result in the generation or depletion of hydrogen.
Properties   The binary diffusion coefficient for hydrogen in the nickel at the specified temperature is 1.2×10^{-12} m²/s (Table 14–3*b*).
Analysis   We can consider the total molar concentration to be constant ($C = C_A + C_B \cong C_B = $ constant), and the container to be a *stationary* medium since there is no diffusion of nickel molecules ($\dot{N}_B = 0$) and the concentration of the hydrogen in the container is extremely low ($C_A \ll 1$). Then the molar flow rate of hydrogen through this spherical shell by diffusion can readily be determined from Eq. 14–28 to be

$$\dot{N}_{\text{diff}} = 4\pi r_1 r_2 D_{AB} \frac{C_{A,\,1} - C_{A,\,2}}{r_2 - r_1}$$

$$= 4\pi(2.34 \text{ m})(2.40 \text{ m})(1.2 \times 10^{-12} \text{ m}^2\text{/s})\frac{(0.087 - 0) \text{ kmol/m}^3}{(2.40 - 2.34) \text{ m}}$$

$$= 1.228 \times 10^{-10} \text{ kmol/s}$$

The mass flow rate is determined by multiplying the molar flow rate by the molar mass of hydrogen, which is $M = 2$ kg/kmol,

$$\dot{m}_{\text{diff}} = M\dot{N}_{\text{diff}} = (2 \text{ kg/kmol})(1.228 \times 10^{-10} \text{ kmol/s}) = \mathbf{2.46 \times 10^{-10}\,kg/s}$$

Therefore, hydrogen will leak out through the shell of the container by diffusion at a rate of 2.46×10^{-10} kg/s or 7.8 g/year. Note that the concentration of hydrogen in the nickel at the inner surface depends on the temperature and pressure of the hydrogen in the tank and can be determined as explained in Example 14–3. Also, the assumption of zero hydrogen concentration in nickel at the outer surface is reasonable since there is only a trace amount of hydrogen in the atmosphere (0.5 part per million by mole numbers).

$C_{A,1} = 0.087\,\dfrac{\text{kmol}}{\text{m}^3}$

$C_{A,2} = 0$

Pressurized
H_2 gas
358 K

$\dot{m}_{\text{diff}}$

Nickel
container
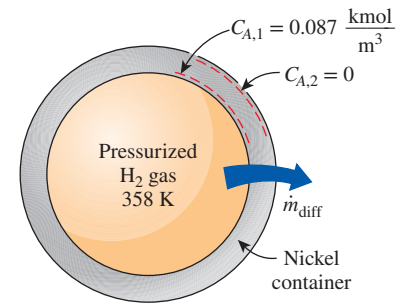
FIGURE 14–23
Schematic for Example 14–5.

14–6 ▪ WATER VAPOR MIGRATION IN BUILDINGS

Moisture greatly influences the performance and durability of building materials, and thus moisture transmission is an important consideration in the construction and maintenance of buildings.

The *dimensions* of wood and other hygroscopic substances change with moisture content. For example, a variation of 4.5 percent in moisture content causes the volume of white oak wood to change by 2.5 percent. Such cyclic changes of dimensions weaken the joints and can jeopardize the structural integrity of building components, causing "squeaking" at the minimum. Excess moisture can also cause changes in the *appearance* and *physical properties* of materials: *corrosion* and *rusting* in metals, *rotting* in woods, and *peeling of paint* on the interior and exterior wall surfaces. Soaked wood with a water content of 24 to 31 percent is observed to decay rapidly at temperatures 10 to 38°C. Also, *molds* grow on wood surfaces at relative humidities above 85 percent. The expansion of water during freezing may damage the cell structure of porous materials.
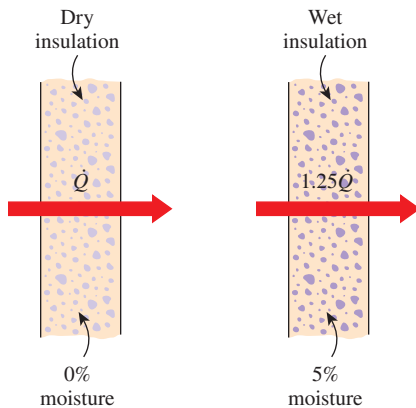
Moisture content also affects the *effective conductivity* of porous media such as soils, building materials, and insulations, and thus heat transfer through them. Several studies have indicated that heat transfer increases almost linearly with moisture content, at a rate of 3 to 5 percent for each percent increase in moisture content by volume. Insulation with 5 percent moisture content by volume, for example, increases heat transfer by 15 to 25 percent relative to dry insulation (ASHRAE *Handbook of Fundamentals,* 1993, Chap. 20) (Fig. 14–24). Moisture migration may also serve as a transfer mechanism for latent heat by alternate evaporation and condensation. During a hot and humid day, for example, water vapor may migrate through a wall and condense on the inner side, releasing the heat of vaporization, with the process reversing during a cool night. Moisture content also affects the *specific heat* and thus the heat storage characteristics of building materials.

Moisture migration in the walls, floors, or ceilings of buildings and in other applications is controlled by either **vapor barriers** or **vapor retarders**. *Vapor barriers* are materials that are impermeable to moisture, such as sheet metals, heavy metal foils, and thick plastic layers, and they effectively bar the vapor from migrating. *Vapor retarders,* on the other hand, *retard* or *slow down* the flow of moisture through the structures but do not totally eliminate it. Vapor retarders are available as solid, flexible, or coating materials, but they usually consist of a thin sheet or coating. Common forms of vapor retarders are *reinforced plastics or metals, thin foils, plastic films, treated papers, coated felts,* and *polymeric or asphaltic paint coatings.* In applications such as the building of walls where vapor penetration is unavoidable because of numerous openings such as electrical boxes, telephone lines, and plumbing passages, vapor retarders are used instead of vapor barriers to allow the vapor that somehow leaks in to exit to the outside instead of trapping it in. Vapor retarders with a permeance of 57.4×10^{-9} kg/s·m² are commonly used in residential buildings.

The insulation on *chilled water lines* and other impermeable surfaces that are always cold must be wrapped with a *vapor barrier jacket,* or such cold surfaces must be insulated with a material that is impermeable to moisture. This is because moisture that migrates through the insulation to the cold surface condenses and remains there indefinitely with no possibility of vaporizing

FIGURE 14–24
A 5 percent moisture content can increase heat transfer through wall insulation by 25 percent.

and moving back to the outside. The accumulation of moisture in such cases may render the insulation useless, resulting in excessive energy consumption.

Mechanical pipe insulation systems are commonly applied to cold piping surfaces in most industrial and commercial buildings in order to limit the heat losses and prevent water vapor condensation on the pipe exterior surfaces. Due to the fact that the surface temperature of these pipelines is normally below the ambient dew point temperature, water vapor diffuses inside the pipe insulation systems and often condenses when it reaches the pipe exterior surfaces. The water droplets accumulated in the pipe insulation system increase its overall thermal conductivity by thermally bridging the cells or the fibers of the insulation material. The moisture ingress into pipe insulation threatens the thermal performance and the overall efficiency of the building mechanical system. This phenomenon is also responsible for mold growth inside occupied spaces, and it causes pipelines to be more vulnerable to corrosion. Although a wide range of vapor barriers are used for preventing water vapor penetration into pipe insulation, common experience in the field shows that water vapor will inevitably ingress into the insulation materials from the end joints or from the cracks created during insulation installation. How to account for the moisture ingress on pipe insulation service life and thermal performance is still an open question.

Thermal conductivity is one of the most important properties for evaluating the thermal performance of the pipe insulation systems. The thermal performance of pipe insulation systems is affected by local ambient conditions and might vary gradually with time. Most published data are extrapolated from flat slab configurations of the insulation materials, but the measured thermal conductivity from flat slabs might over- or underestimate the actual thermal conductivity of cylindrical-shaped-pipe insulation systems due to radial configuration and longitudinal split joints. A methodology for measuring the thermal conductivity of cylindrical-shaped-pipe insulation systems exists in the ASTM standards, but it is based on a heated pipe approach with outward heat flow. If the average temperature of the pipe insulation system is below ambient temperature, then a more accurate prediction of the pipe insulation's actual thermal conductivity is needed for the design of insulation systems in chiller pipe applications. For a detailed review on pipe insulation thermal conductivity under dry and wet condensing conditions with moisture ingress, refer to Cai et al. (2014).

Cremaschi et al. (2012) at Oklahoma State University have developed a novel experimental apparatus to measure the thermal conductivity of pipe insulation systems at ambient and below-ambient conditions for dry noncondensing conditions and wet conditions with moisture ingress. The apparatus was validated for dry noncondensing conditions with two pipe insulation systems, cellular glass and polyisocyanurate (PIR), used to benchmark their measurements against data available in the public domain. The thermal conductivity of three additional pipe insulation materials, that is, fiberglass, flexible elastomeric, and phenolic, was also measured at several insulation temperatures at below-ambient and in dry noncondensing ambient conditions. Correlations of the pipe insulation thermal conductivity were developed based on insulation specimen average temperature and wall thicknesses. In subsequent series of experiments, Cai et al. (2012) measured the thermal conductivity of pipe insulation systems at below-ambient temperature in wet conditions with moisture ingress. Fiberglass and phenolic pipe insulation were tested to investigate the moisture effects on the material thermal conductivity. The data showed that these two types of pipe insulation systems had quite different water absorption

TABLE 14–9

Saturation pressure of water at various temperatures

Temperature, °C	Saturation Pressure, Pa
−40	13
−36	20
−32	31
−28	47
−24	70
−20	104
−16	151
−12	218
−8	310
−4	438
0	611
5	872
10	1228
15	1705
20	2339
25	3169
30	4246
35	5628
40	7384
50	12,350
100	101,330
200	1.55×10^6
300	8.58×10^6

rates due to different characteristics of the material and its structure. A serious degradation of fiberglass pipe insulation thermal performance was observed, and the thermal conductivity increased by as much as three times when the moisture content was about 12 percent in volume. Tested at a different condition, the thermal conductivity of phenolic pipe insulation increased to 1.6 times the original value, and the moisture content was 5 percent in volume.

Atmospheric air can be viewed as a mixture of dry air and water vapor, and the atmospheric pressure is the sum of the pressure of dry air and the pressure of water vapor, which is called the **vapor pressure** P_v. Air can hold a certain amount of moisture only, and the ratio of the actual amount of moisture in the air at a given temperature to the maximum amount air can hold at that temperature is called the **relative humidity** ϕ. The relative humidity ranges from 0 for dry air to 100 percent for *saturated* air (air that cannot hold any more moisture). The partial pressure of water vapor in saturated air is called the **saturation pressure** P_{sat}. Table 14–9 lists the saturation pressure at various temperatures.

The amount of moisture in the air is completely specified by the temperature and the relative humidity, and the vapor pressure is related to relative humidity ϕ by

$$P_v = \phi P_{sat} \tag{14–30}$$

where P_{sat} is the saturation (or boiling) pressure of water at the specified temperature. Then the mass flow rate of moisture through a plane layer of thickness L and normal area A can be expressed as

$$\dot{m}_v = \mathscr{P}A \frac{P_{v,1} - P_{v,2}}{L} = \mathscr{P}A \frac{\phi_1 P_{sat,1} - \phi_2 P_{sat,2}}{L} \quad \text{(kg/s)} \tag{14–31}$$

where $\mathscr{P}$ is the vapor permeability of the material, which is usually expressed on a mass basis in the unit ng/s·m·Pa, where ng $= 10^{-12}$ kg and 1 Pa $= 10^{-5}$ bar. Note that vapor migrates or diffuses from a region of higher vapor pressure toward a region of lower vapor pressure.

The permeability of most construction materials is usually expressed for a given thickness instead of per unit thickness. It is called the **permeance** $\mathscr{M}$, which is the ratio of the permeability of the material to its thickness. That is,

$$\text{Permeance} = \frac{\text{Permeability}}{\text{Thickness}}$$

$$\mathscr{M} = \frac{\mathscr{P}}{L} \quad \text{(kg/s·m}^2\text{·Pa)} \tag{14–32}$$

The reciprocal of permeance is called (unit) **vapor resistance** and is expressed as

$$\text{Vapor resistance} = \frac{1}{\text{Permeance}}$$

$$R_v = \frac{1}{\mathscr{M}} = \frac{L}{\mathscr{P}} \quad \text{(s·m}^2\text{·Pa/kg)} \tag{14–33}$$

Note that vapor resistance represents the resistance of a material to water vapor transmission.

It should be pointed out that the amount of moisture that enters or leaves a building by *diffusion* is usually negligible compared to the amount that enters with *infiltrating air* or leaves with *exfiltrating air*. The primary cause of interest in the moisture diffusion is its impact on the performance and longevity of building materials.

The overall vapor resistance of a *composite* building structure that consists of several layers in series is the sum of the resistances of the individual layers and is expressed as

$$R_{v,\,total} = R_{v,\,1} + R_{v,\,2} + \cdots + R_{v,\,n} = \sum R_{v,\,i} \qquad \textbf{(14–34)}$$

Then the rate of vapor transmission through a composite structure can be determined in an analogous manner to heat transfer from

$$\dot{m}_v = A\,\frac{\Delta P_v}{R_{v,\,total}} \quad \text{(kg/s)} \qquad \textbf{(14–35)}$$

Vapor permeance of common building materials is given in Table 14–10.

EXAMPLE 14–6   Condensation and Freezing of Moisture in Walls

The condensation and even freezing of moisture in walls without effective vapor retarders is a real concern in cold climates, and it undermines the effectiveness of insulations. Consider a wood frame wall that is built around 38-mm × 90-mm (2 × 4 nominal) wood studs. The 90-mm-wide cavity between the studs is filled with glass fiber insulation. The inside is finished with 13-mm gypsum wallboard and the outside with 13-mm wood fiberboard and 13-mm × 200-mm wood bevel lapped siding. Using manufacturers' data, the thermal and vapor resistances of various components for a unit wall area are determined to be

Construction	*R*-Value, m²·K/W	R_v-Value, s·m²·Pa/ng
1. Outside surface, 24 km/h wind	0.030	—
2. Painted wood bevel lapped siding	0.14	0.019
3. Wood fiberboard sheeting, 13 mm	0.23	0.0138
4. Glass fiber insulation, 90 mm	2.45	0.0004
5. Painted gypsum wallboard, 13 mm	0.079	0.012
6. Inside surface, still air	0.12	—
TOTAL	3.05	0.0452

The indoor conditions are 20°C and 60 percent relative humidity while the outside conditions are −16°C and 70 percent relative humidity. Determine if condensation or freezing of moisture will occur in the insulation.

SOLUTION   The thermal and vapor resistances of different layers of a wall are given. The possibility of condensation or freezing of moisture in the wall is to be investigated.

Assumptions   **1** Steady operating conditions exist. **2** Heat transfer through the wall is one-dimensional. **3** Thermal and vapor resistances of different layers of the wall and the heat transfer coefficients are constant.

Properties   The thermal and vapor resistances are as given in the problem statement. The saturation pressures of water at 20°C and −16°C are 2339 Pa and 151 Pa, respectively (Table 14–9).

Analysis   The schematic of the wall as well as the different elements used in its construction are shown in Fig. 14–25. Condensation is most likely to occur at the coldest part of insulation, which is the part adjacent to the exterior sheathing. Noting that the

TABLE 14–10

Typical vapor permeance of common building materials*

Materials and Their Thickness	Permeance ng/s·m²·Pa
Concrete (1:2:4 mix, 1 m)	4.7
Brick, masonry, 100 mm	46
Plaster on metal lath, 19 mm	860
Plaster on wood lath, 19 mm	630
Gypsum wall board, 9.5 mm	2860
Plywood, 6.4 mm	40–109
Still air, 1 m	174
Mineral wool insulation (unprotected), 1 m	245
Expanded polyurethane insulation board, 1 m	0.58–2.3
Aluminum foil, 0.025 mm	0.0
Aluminum foil, 0.009 mm	2.9
Polyethylene, 0.051 mm	9.1
Polyethylene, 0.2 mm	2.3
Polyester, 0.19 mm	4.6
Vapor retarder latex paint, 0.070 mm	26
Exterior acrylic house and trim paint, 0.040 mm	313
Building paper, unit mass of 0.16 − 0.68 kg/m²	0.1–2400

Source: From ASHRAE, 1993, Chap. 22, Table 9

*Data vary greatly. Consult manufacturer for more accurate data. Multiply by 1.41×10^{-6} to convert to lbm/s·ft²·psi. Also, 1 ng = 10^{-12} kg.

FIGURE 14–25
Schematic for Example 14–6.

total thermal resistance of the wall is 3.05 m²·K/W, the rate of heat transfer through a unit area $A = 1$ m² of the wall is

$$\dot{Q}_{\text{wall}} = A\frac{T_i - T_o}{R_{\text{total}}} = (1 \text{ m}^2)\frac{[20 - (-16)°\text{C}]}{3.05 \text{ m}^2\cdot\text{K/W}} = 11.8 \text{ W}$$

The thermal resistance of the exterior part of the wall beyond the insulation is $0.03 + 0.14 + 0.23 = 0.40$ m²·K/W. Then the temperature of the insulation–outer sheathing interface is

$$T_I = T_o + \dot{Q}_{\text{wall}}R_{\text{ext}} = -16°\text{C} + (11.8 \text{ W})(0.40 \text{ K/W}) = -11.3°\text{C}$$

The saturation pressure of water at $-11.3°$C is 234 Pa, as shown in Table 14–9, and if there is condensation or freezing, the vapor pressure at the insulation–outer sheathing interface will have to be this value. The vapor pressure at the indoors and the outdoors is

$$P_{v,1} = \phi_1 P_{\text{sat},1} = 0.60 \times (2340 \text{ Pa}) = 1404 \text{ Pa}$$

$$P_{v,2} = \phi_2 P_{\text{sat},2} = 0.70 \times (151 \text{ Pa}) = 106 \text{ Pa}$$

Then the rate of moisture flow through the interior and exterior parts of the wall becomes

$$\dot{m}_{v,\text{interior}} = A\left(\frac{\Delta P}{R_v}\right)_{\text{interior}} = A\frac{P_{v,I} - P_{v,l}}{R_{v,\text{interior}}}$$

$$= (1 \text{ m}^2)\frac{(1404 - 234) \text{ Pa}}{(0.012 + 0.0004) \text{ Pa}\cdot\text{m}^2\cdot\text{s/ng}} = 94{,}355 \text{ ng/s} = 94.4 \text{ μg/s}$$

$$\dot{m}_{v,\text{exterior}} = A\left(\frac{\Delta P}{R_v}\right)_{\text{exterior}} = A\frac{P_{v,I} - P_{v,2}}{R_{v,\text{exterior}}}$$

$$= (1 \text{ m}^2)\frac{(234 - 106) \text{ Pa}}{(0.019 + 0.0138) \text{ Pa}\cdot\text{m}^2\cdot\text{s/ng}} = 3902 \text{ ng/s} = 3.9 \text{ μg/s}$$

That is, moisture is flowing toward the interface at a rate of 94.4 μg/s but flowing from the interface to the outdoors at a rate of only 3.9 μg/s. Noting that the interface pressure cannot exceed 234 Pa, these results indicate that moisture is freezing in the insulation at a rate of

$$\dot{m}_{v,\text{freezing}} = \dot{m}_{v,\text{interior}} - \dot{m}_{v,\text{exterior}} = 94.4 - 3.9 = \mathbf{90.5 \text{ μg/s}}$$

Discussion This result corresponds to 7.82 g during a 24-h period, which can be absorbed by the insulation or sheathing, and then flows out when the conditions improve. However, excessive condensation (or frosting at temperatures below 0°C) of moisture in the walls during long cold spells can cause serious problems. This problem can be avoided or minimized by installing vapor barriers on the interior side of the wall, which will limit the moisture flow rate to 3.9 μg/s. Note that if there were no condensation or freezing, the flow rate of moisture through a 1 m² section of the wall would be 28.7 μg/s. (Can you verify this?)

14–7 ■ TRANSIENT MASS DIFFUSION

The steady analysis discussed earlier is useful when determining the leakage rate of a species through a stationary layer. But sometimes we are interested in the diffusion of a species into a body during a limited time before steady operating conditions are established. Such problems are studied using **transient analysis**. For example, the surface of a mild steel component is commonly hardened by packing the component in a carbonaceous material in a furnace at high temperature. During the short time period in the furnace, the carbon molecules diffuse through the surface of the steel component, but they penetrate to a depth of only a few millimeters. The carbon concentration decreases exponentially from the surface to the inner parts, and the result is a steel component with a very hard surface and a relatively soft core region (Fig. 14–26).

The same process is used in the gem industry to color clear stones. For example, a clear sapphire is given a brilliant blue color by packing it in titanium and iron oxide powders and baking it in an oven at about 2000°C for about a month. The titanium and iron molecules penetrate less than 0.5 mm into the sapphire during this process. Diffusion in solids is usually done at high temperatures to take advantage of the high diffusion coefficients at high temperatures and thus to keep the diffusion time at a reasonable level. Such diffusion or "doping" is also commonly practiced in the production of n- or p-type semiconductor materials used in the manufacture of electronic components. Drying processes such as the drying of coal, timber, food, and textiles constitute another major application area of transient mass diffusion.

Transient mass diffusion in a stationary medium is analogous to transient heat transfer provided that the solution is dilute and thus the density of the medium ρ is constant. In Chap. 4 we presented analytical solutions for one-dimensional transient heat conduction problems in solids with constant properties, no heat generation, and uniform initial temperature. The analogous one-dimensional transient mass diffusion problems satisfy these requirements:

1. The *diffusion coefficient is constant.* This is valid for an isothermal medium since D_{AB} varies with temperature (corresponds to constant thermal diffusivity).
2. There are *no homogeneous reactions* in the medium that generate or deplete the diffusing species A (corresponds to no heat generation).
3. Initially ($t = 0$) the concentration of species A is *constant* throughout the medium (corresponds to uniform initial temperature).

Then the solution of a mass diffusion problem can be obtained directly from the analytical solution of the corresponding heat conduction problem given in Chap. 4. The analogous quantities between heat and mass transfer are summarized in Table 14–11 for easy reference. For the case of a semi-infinite media with constant surface concentration, for example, the solution can be expressed in an analogous manner to Eq. 4–45 as

$$\frac{C_A(x, t) - C_{A, i}}{C_{A, s} - C_{A, i}} = \text{erfc}\left(\frac{x}{2\sqrt{D_{AB}t}}\right) \quad \text{(14–36)}$$

where $C_{A, i}$ is the initial concentration of species A at time $t = 0$ and $C_{A, s}$ is the concentration at the inner side of the exposed surface of the medium. By
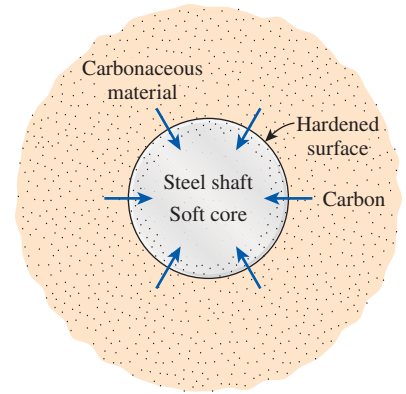
FIGURE 14–26
The surface hardening of a mild steel component by the diffusion of carbon molecules is a transient mass diffusion process.

TABLE 14–11

Analogy between the quantities that appear in the formulation and solution of transient heat conduction and transient mass diffusion in a stationary medium

Heat Conduction	Mass Diffusion
T	$C, y, \rho,$ or w
α	D_{AB}
$\theta = \dfrac{T(x, t) - T_\infty}{T_i - T_\infty},$	$\theta_{mass} = \dfrac{w_A(x, t) - w_{A, \infty}}{w_{A, i} - w_{A, \infty}}$
$\dfrac{T(x, t) - T_s}{T_i - T_s}$	$\dfrac{w_A(x,t) - w_A}{w_{A, i} - w_A}$
$\eta = \dfrac{x}{2\sqrt{\alpha t}}$	$\eta_{mass} = \dfrac{x}{2\sqrt{D_{AB}t}}$
$\text{Bi} = \dfrac{h_{conv} L}{k}$	$\text{Bi}_{mass} = \dfrac{h_{mass} L}{D_{AB}}$
$\tau = \dfrac{\alpha t}{L^2}$	$\tau = \dfrac{D_{AB}t}{L^2}$
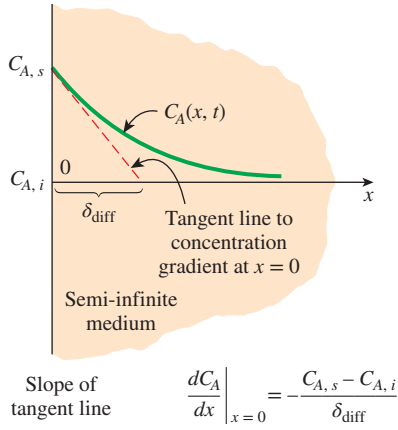
FIGURE 14–27
The concentration profile of species A in a semi-infinite medium during transient mass diffusion and the penetration depth.

using the definitions of molar fraction, mass fraction, and density, it can be shown that for dilute solutions,

$$\frac{C_A(x, t) - C_{A, i}}{C_{A, s} - C_{A, i}} = \frac{\rho_A(x, t) - \rho_{A, i}}{\rho_{A, s} - \rho_{A, i}} = \frac{w_A(x, t) - w_{A, i}}{w_{A, s} - w_{A, i}} = \frac{y_A(x, t) - y_{A, i}}{y_{A, s} - y_{A, i}} \quad \text{(14–37)}$$

since the total density or total molar concentration of dilute solutions is usually constant ($\rho = $ constant or $C = $ constant). Therefore, other measures of concentration can be used in Eq. 14–36.

A quantity of interest in mass diffusion processes is the depth of diffusion at a given time. This is usually characterized by the **penetration depth** defined as *the location x where the tangent to the concentration profile at the surface* ($x = 0$) *intercepts the* $C_A = C_{A, i}$ *line,* as shown in Fig. 14–27. Obtaining the concentration gradient at $x = 0$ by differentiating Eq. 14–36, the penetration depth is determined to be

$$\delta_{\text{diff}} = \frac{C_{A, s} - C_{A, i}}{-(dC_A/dx)_{x=0}} = \frac{C_{A, s} - C_{A, i}}{(C_{A, s} - C_{A, i})/\sqrt{\pi D_{AB}t}} = \sqrt{\pi D_{AB}t} \quad \text{(14–38)}$$

Therefore, the penetration depth is proportional to the square root of both the diffusion coefficient and time. The diffusion coefficient of zinc in copper at 1000°C, for example, is 5.0×10^{-13} m²/s (Table 14–3). Then the penetration depth of zinc in copper in 10 h is

$$\delta_{\text{diff}} = \sqrt{\pi D_{AB}t} = \sqrt{\pi(5.0 \times 10^{-13}\,\text{m}^2/\text{s})(10 \times 3600\,\text{s})}$$
$$= 0.00024 \text{ m} = 0.24 \text{ mm}$$

That is, zinc will penetrate to a depth of about 0.24 mm in an appreciable amount in 10 h, and there will hardly be any zinc in the copper block beyond a depth of 0.24 mm.

The diffusion coefficients in solids are typically very low (on the order of 10^{-9} to 10^{-15} m²/s), and thus the diffusion process usually affects a thin layer at the surface. A solid can conveniently be treated as a semi-infinite medium during transient mass diffusion regardless of its size and shape when the penetration depth is small relative to the thickness of the solid. When this is not the case, solutions for one-dimensional transient mass diffusion through a plane wall, cylinder, and sphere can be obtained from the solutions of analogous heat conduction problems using the one-term solutions presented in Chap. 4.
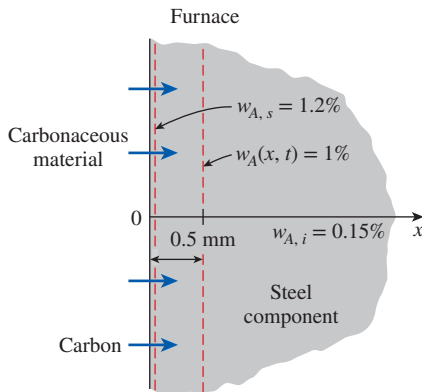
FIGURE 14–28
Schematic for Example 14–7.

EXAMPLE 14–7 **Hardening of Steel by the Diffusion of Carbon**

The surface of a mild steel component is commonly hardened by packing the component in a carbonaceous material in a furnace at a high temperature for a predetermined time. Consider such a component with a uniform initial carbon concentration of 0.15 percent by mass. The component is now packed in a carbonaceous material and is placed in a high-temperature furnace. The diffusion coefficient of carbon in steel at the furnace temperature is given to be 4.8×10^{-10} m²/s, and the equilibrium concentration of carbon in the iron at the interface is determined from equilibrium data to be 1.2 percent by mass. Determine how long the component should be kept in the furnace for the mass concentration of carbon 0.5 mm below the surface to reach 1 percent (Fig. 14–28).

SOLUTION A steel component is to be surface hardened by packing it in a carbonaceous material in a furnace. The length of time the component should be kept in the furnace is to be determined.

Assumptions Carbon penetrates into a very thin layer beneath the surface of the component, and thus the component can be modeled as a semi-infinite medium regardless of its thickness or shape.

Properties The relevant properties are given in the problem statement.

Analysis This problem is analogous to the one-dimensional transient heat conduction problem in a semi-infinite medium with specified surface temperature, and thus can be solved accordingly. Using mass fraction for concentration since the data are given in that form, the solution can be expressed as

$$\frac{w_A(x, t) - w_{A, i}}{w_{A, s} - w_{A, i}} = \text{erfc}\left(\frac{x}{2\sqrt{D_{AB}t}}\right)$$

Substituting the specified quantities gives

$$\frac{0.01 - 0.0015}{0.012 - 0.0015} = 0.81 = \text{erfc}\left(\frac{x}{2\sqrt{D_{AB}t}}\right)$$

The argument whose complementary error function is 0.81 is determined from Table 4–4 to be 0.17. That is,

$$\frac{x}{2\sqrt{D_{AB}t}} = 0.17$$

Then solving for the time t gives

$$t = \frac{x^2}{4 D_{AB}(0.17)^2} = \frac{(0.0005 \text{ m})^2}{4 \times (4.8 \times 10^{-10} \text{ m}^2/\text{s})(0.17)^2} = 4505 \text{ s} = \textbf{1 h 15 min}$$

Discussion The steel component in this case must be held in the furnace for 1 h and 15 min to achieve the desired level of hardening. The diffusion coefficient of carbon in steel increases exponentially with temperature, and thus this process is commonly done at high temperatures to keep the diffusion time at a reasonable level.

14−8 ▪ DIFFUSION IN A MOVING MEDIUM

To this point we have limited our consideration to mass diffusion in a *stationary medium,* and thus the only motion involved was the creeping motion of molecules in the direction of decreasing concentration, and there was no motion of the mixture as a whole. Many practical problems, such as the evaporation of water from a lake under the influence of the wind or the mixing of two fluids as they flow in a pipe, involve diffusion in a **moving medium** where the bulk motion is caused by an external force. Mass diffusion in such cases is complicated by the fact that chemical species are transported both by *diffusion* and by the bulk motion of the medium (i.e., *convection*). The velocities and mass flow rates of species in a moving medium consist of two components: one due to *molecular diffusion* and one due to *convection* (Fig. 14–29).

Diffusion in a moving medium, in general, is difficult to analyze since various species can move at different velocities in different directions. Turbulence complicates the things even more. To gain a firm understanding of the physical
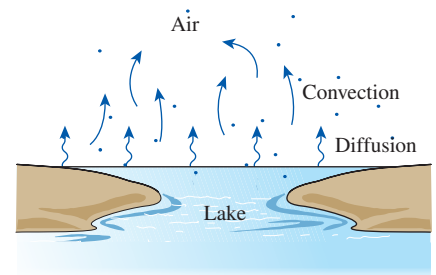
FIGURE 14−29
In a moving medium, mass transfer is due to both diffusion and convection.

mechanism while keeping the mathematical complexities to a minimum, we limit our consideration to systems that involve only *two components* (species *A* and *B*) in *one-dimensional flow* (velocity and other properties change in one direction only, say the *x*-direction). We also assume the total density (or molar concentration) of the medium remains constant. That is, $\rho = \rho_A + \rho_B =$ constant (or $C = C_A + C_B =$ constant) but the densities of species *A* and *B* may vary in the *x*-direction.

Several possibilities are summarized in Fig. 14–30. In the trivial case (case *a*) of a *stationary homogeneous mixture,* there will be no mass transfer by molecular diffusion or convection since there is no concentration gradient or bulk motion. The next case (case *b*) corresponds to the *flow of a well-mixed fluid mixture* through a pipe. Note that there are no concentration gradients and thus molecular diffusion in this case, and all species move at the bulk flow velocity of *V*. The mixture in the third case (case *c*) is *stationary* ($V = 0$), and thus it corresponds to ordinary molecular diffusion in stationary media, which we discussed before. Note that the velocity of a species at a location in this case is simply the **diffusion velocity**, which is the average velocity of a group of molecules at that location moving under the influence of concentration gradient. Finally, the last case (case *d*) involves both *molecular diffusion* and *convection,* and the velocity of a species in this case is equal to the sum of the bulk flow velocity and the diffusion velocity. Note that the flow and the diffusion velocities can be in the same or opposite directions, depending on

	● A ○ B	Species	Density	Velocity	Mass flow rate
(*a*) Homogeneous mixture without bulk motion (no concentration gradients and thus no diffusion)	$V = 0$	Species A	$\rho_A =$ constant	$V_A = 0$	$\dot{m}_A = 0$
		Species B	$\rho_B =$ constant	$V_B = 0$	$\dot{m}_B = 0$
		Mixture of A and B	$\rho = \rho_A + \rho_B$ = constant	$V = 0$	$\dot{m} = 0$
(*b*) Homogeneous mixture with bulk motion (no concentration gradients and thus no diffusion)	$\rightarrow V$	Species A	$\rho_A =$ constant	$V_A = V$	$\dot{m}_A = \rho_A V_A A$
		Species B	$\rho_B =$ constant	$V_B = V$	$m_B = \rho_B V_B A$
		Mixture of A and B	$\rho = \rho_A + \rho_B$ = constant	$V = V$	$\dot{m} = \rho V A$ $= \dot{m}_A + \dot{m}_B$
(*c*) Nonhomogeneous mixture without bulk motion (stationary medium with concentration gradients)	$V = 0$ $V_{\text{diff}, A} \rightarrow$ $\leftarrow V_{\text{diff}, B}$	Species A	$\rho_A \neq$ constant	$V_A = V_{\text{diff}, A}$	$\dot{m}_A = \rho_A V_{\text{diff}, A} A$
		Species B	$\rho_B \neq$ constant	$V_B = V_{\text{diff}, B}$	$\dot{m}_B = \rho_B V_{\text{diff}, B} A$
		Mixture of A and B	$\rho = \rho_A + \rho_B$ = constant	$V = 0$	$\dot{m} = \rho V A = 0$ (thus $\dot{m}_A = - \dot{m}_B$)
(*d*) Nonhomogeneous mixture with bulk motion (moving medium with concentration gradients)	$\rightarrow V$ $V_{\text{diff}, A} \rightarrow$ $\leftarrow V_{\text{diff}, B}$	Species A	$\rho_A \neq$ constant	$V_A = V + V_{\text{diff}, A}$	$\dot{m}_A = \rho_A V_A A$
		Species B	$\rho_B \neq$ constant	$V_B = V + V_{\text{diff}, B}$	$\dot{m}_B = \rho_B V_B A$
		Mixture of A and B	$\rho = \rho_A + \rho_B$ = constant	$V = V$	$\dot{m} = \rho V A$ $= \dot{m}_A + \dot{m}_B$

FIGURE 14–30

Various quantities associated with a mixture of two species *A* and *B* at a location *x* under one-dimensional flow or no-flow conditions. (The density of the mixture $\rho = \rho_A + \rho_B$ is assumed to remain constant.)

the direction of the concentration gradient. The diffusion velocity of a species is *negative* when the bulk flow is in the positive *x*-direction and the concentration gradient is positive (i.e., the concentration of the species increases in the *x*-direction).

Noting that the mass flow rate at any flow section is expressed as $\dot{m} = \rho V A$ where ρ is the density, *V* is the velocity, and *A* is the cross-sectional area, the conservation of mass relation for the flow of a mixture that involves two species *A* and *B* can be expressed as

$$\dot{m} = \dot{m}_A + \dot{m}_B$$

or

$$\rho V A = \rho_A V_A A + \rho_B V_B A$$

Canceling *A* and solving for *V* gives

$$V = \frac{\rho_A V_A + \rho_B V_B}{\rho} = \frac{\rho_A}{\rho} V_A + \frac{\rho_B}{\rho} V_B = w_A V_A + w_B V_B \quad \textbf{(14–39)}$$

where *V* is called the **mass-average velocity** of the flow, which is the velocity that would be measured by a velocity sensor such as a pitot tube, a turbine device, or a hot wire anemometer inserted into the flow.

The special case $V = 0$ corresponds to a **stationary medium**, which can now be defined more precisely as *a medium whose mass-average velocity is zero.* Therefore, mass transport in a stationary medium is by diffusion only, and zero mass-average velocity indicates that there is no bulk fluid motion.

When there is *no concentration gradient* (and thus no molecular mass diffusion) in the fluid, the velocity of all species will be equal to the *mass-average velocity of the flow.* That is, $V = V_A = V_B$. But when there is a concentration gradient, there will also be a simultaneous flow of species in the direction of decreasing concentration at a diffusion velocity of V_{diff}. Then the average velocity of the species *A* and *B* can be determined by superimposing the average flow velocity and the diffusion velocity as (Fig. 14–31)

$$\begin{aligned} V_A &= V + V_{\text{diff},A} \\ V_B &= V + V_{\text{diff},B} \end{aligned} \quad \textbf{(14–40)}$$

Similarly, we apply the superposition principle to the species mass flow rates to get

$$\begin{aligned} \dot{m}_A &= \rho_A V_A A = \rho_A (V + V_{\text{diff},A}) A = \rho_A V A + \rho_A V_{\text{diff},A} A = \dot{m}_{\text{conv},A} + \dot{m}_{\text{diff},A} \\ \dot{m}_B &= \rho_B V_B A = \rho_B (V + V_{\text{diff},B}) A = \rho_B V A + \rho_B V_{\text{diff},B} A = \dot{m}_{\text{conv},B} + \dot{m}_{\text{diff},B} \end{aligned} \quad \textbf{(14–41)}$$

Using Fick's law of diffusion, the total mass fluxes $j = \dot{m}/A$ can be expressed as

$$j_A = \rho_A V + \rho_A V_{\text{diff},A} = \frac{\rho_A}{\rho} \rho V - \rho D_{AB} \frac{dw_A}{dx} = w_A (j_A + j_B) - \rho D_{AB} \frac{dw_A}{dx}$$

$$\textbf{(14–42)}$$

$$j_B = \rho_B V + \rho_B V_{\text{diff},B} = \frac{\rho_B}{\rho} \rho V - \rho D_{BA} \frac{dw_B}{dx} = w_B (j_A + j_B) - \rho D_{BA} \frac{dw_B}{dx}$$

$V_{\text{diff},A} = 0$
$V_A = V$

(*a*) No concentration gradient

$V_{\text{diff},A} \neq 0$
$V_A = V + V_{\text{diff},A}$

(*b*) Mass concentration gradient and thus mass diffusion
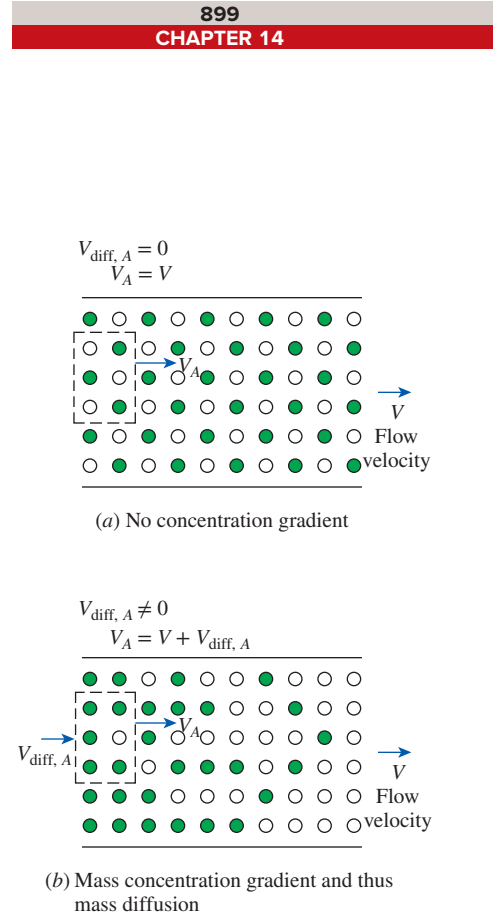
FIGURE 14–31

The velocity of a species at a point is equal to the sum of the bulk flow velocity and the diffusion velocity of that species at that point.

Note that the diffusion velocity of a species is negative when the molecular diffusion occurs in the negative x-direction (opposite to flow direction). The mass diffusion rates of the species A and B at a specified location x can be expressed as

$$\dot{m}_{\text{diff, }A} = \rho_A V_{\text{diff, }A} A = \rho_A(V_A - V)A$$
$$\dot{m}_{\text{diff, }B} = \rho_B V_{\text{diff, }B} A = \rho_B(V_B - V)A \tag{14-43}$$

By substituting the V relation from Eq. 14–39 into Eq. 14–43, it can be shown that at any cross section

$$\dot{m}_{\text{diff, }A} + \dot{m}_{\text{diff, }B} = 0 \rightarrow \dot{m}_{\text{diff, }A} = -\dot{m}_{\text{diff, }B} \rightarrow -\rho A D_{AB}\frac{dw_A}{dx} = \rho A D_{BA}\frac{dw_B}{dx} \tag{14-44}$$

which indicates that the rates of diffusion of species A and B must be equal in magnitude but opposite in sign. This is a consequence of the assumption $\rho = \rho_A + \rho_B =$ constant, and it indicates that *anytime the species A diffuses in one direction, an equal amount of species B must diffuse in the opposite direction to maintain the density (or the molar concentration) constant.* This behavior is closely approximated by dilute gas mixtures and dilute liquid or solid solutions. For example, when a small amount of gas diffuses into a liquid, it is reasonable to assume the density of the liquid remains constant.

Note that for a binary mixture, $w_A + w_B = 1$ at any location x. Taking the derivative with respect to x gives

$$\frac{dw_A}{dx} = -\frac{dw_B}{dx} \tag{14-45}$$

Thus we conclude from Eq. 14–44 that (Fig. 14–32)

$$D_{AB} = D_{BA} \tag{14-46}$$

That is, in the case of constant total concentration, the diffusion coefficient of species A into B is equal to the diffusion coefficient of species B into A.

We now repeat the analysis presented above with molar concentration C and the molar flow rate $\dot{N}$. The conservation of matter in this case is expressed as

$$\dot{N} = \dot{N}_A + \dot{N}_B$$

or

$$C\overline{V}A = C_A \overline{V}_A A + C_B \overline{V}_B A \tag{14-47}$$

Canceling A and solving for $\overline{V}$ gives

$$\overline{V} = \frac{C_A \overline{V}_A + C_B \overline{V}_B}{C} = \frac{C_A}{C}\overline{V}_A + \frac{C_B}{C}\overline{V}_B = y_A \overline{V}_A + y_B \overline{V}_B \tag{14-48}$$

where $\overline{V}$ is called the **molar-average velocity** of the flow. Note that $\overline{V} \neq V$ unless the mass and molar fractions are the same. The molar flow rates of species are determined similarly to be

$$\dot{N}_A = C_A V_A A = C_A(\overline{V} + \overline{V}_{\text{diff, }A})A = C_A \overline{V}A + C_A \overline{V}_{\text{diff, }A}A = \dot{N}_{\text{conv, }A} + \dot{N}_{\text{diff, }A}$$
$$\dot{N}_B = C_B V_B A = C_B(\overline{V} + \overline{V}_{\text{diff, }B})A = C_B \overline{V}A + C_B \overline{V}_{\text{diff, }B}A = \dot{N}_{\text{conv, }B} + \dot{N}_{\text{diff, }B} \tag{14-49}$$
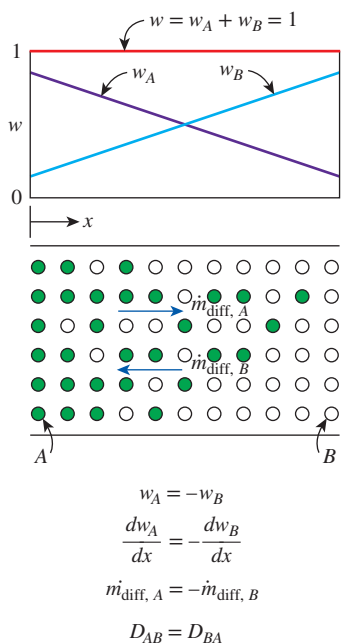
FIGURE 14–32

In a binary mixture of species A and B with $\rho = \rho_A - \rho_B =$ constant, the rates of mass diffusion of species A and B are equal magnitude and opposite in direction.

Using Fick's law of diffusion, the total molar fluxes $\bar{j} = \dot{N}/A$ and diffusion molar flow rates $\dot{N}_{\text{diff}}$ can be expressed as

$$\bar{j}_A = C_A \overline{V} + C_A \overline{V}_{\text{diff}, A} = \frac{C_A}{C} C \overline{V} - C D_{AB} \frac{dy_A}{dx} = y_A(\bar{j}_A + \bar{j}_B) - C D_{AB} \frac{dy_A}{dx}$$

$$\bar{j}_B = C_B \overline{V} + C_B \overline{V}_{\text{diff}, B} = \frac{C_B}{C} C \overline{V} - C D_{BA} \frac{dy_B}{dx} = y_B(\bar{j}_A + \bar{j}_B) - C D_{BA} \frac{dy_B}{dx}$$

$$\text{(14–50)}$$

and

$$\dot{N}_{\text{diff}, A} = C_A \overline{V}_{\text{diff}, A} A = C_A(V_A - \overline{V})A$$

$$\dot{N}_{\text{diff}, B} = C_B \overline{V}_{\text{diff}, B} A = C_B(V_B - \overline{V})A$$

$$\text{(14–51)}$$

By substituting the $\overline{V}$ relation from Eq. 14–48 into these two equations, it can be shown that

$$\dot{N}_{\text{diff}, A} + \dot{N}_{\text{diff}, B} = 0 \rightarrow \dot{N}_{\text{diff}, A} = -\dot{N}_{\text{diff}, B} \qquad \text{(14–52)}$$

which again indicates that the rates of diffusion of species *A* and *B* must be equal in magnitude but opposite in sign.

It is important to note that when working with molar units, a medium is said to be stationary when the *molar-average velocity* is zero. The average velocity of the molecules will be zero in this case, but the apparent velocity of the mixture as measured by a velocimeter placed in the flow will not necessarily be zero because of the different masses of different molecules. In a *mass-based stationary medium,* for each unit mass of species *A* moving in one direction, a unit mass of species *B* moves in the opposite direction. In a *mole-based stationary medium,* however, for each mole of species *A* moving in one direction, one mole of species *B* moves in the opposite direction. But this may result in a net mass flow rate in one direction that can be measured by a velocimeter since the masses of different molecules are different.

You may be wondering whether to use the mass analysis or molar analysis in a problem. The two approaches are equivalent, and either approach can be used in mass transfer analysis. But sometimes it may be easier to use one of the approaches, depending on what is given. When mass-average velocity is known or can easily be obtained, obviously it is more convenient to use the mass-based formulation. When the *total pressure* and *temperature* of a mixture are constant, however, it is more convenient to use the molar formulation, as explained in the following three cases: gas mixtures at constant pressure and temperature, Stefan flow, and equimolar counterdiffusion.

Special Case: Gas Mixtures at Constant Pressure and Temperature

Consider a gas mixture whose total pressure and temperature are constant throughout. When the mixture is homogeneous, the mass density ρ, the molar density (or concentration) C, the gas constant R, and the molar mass M of the mixture are the same throughout the mixture. But when the concentration of one or more gases in the mixture is not constant, setting the stage for mass diffusion, then the mole fractions y_i of the species will vary throughout the

mixture. As a result, the gas constant R, the molar mass M, and the mass density ρ of the mixture will also vary since, assuming ideal gas behavior,

$$M = \sum y_i M_i, \quad R = \frac{R_u}{M} \quad \text{and} \quad \rho = \frac{P}{RT}$$

where $R_u = 8.314$ kJ/kmol·K is the universal gas constant. Therefore, the assumption of *constant mixture density* ($\rho = $ constant) in such cases will not be accurate unless the gas or gases with variable concentrations constitute a very small fraction of the mixture. However, the *molar density C of a mixture remains constant* when the mixture pressure P and temperature T are constant since

$$P = \rho RT = \rho \frac{R_u}{M} T = CR_u T \tag{14–53}$$

$$C = \frac{P}{R_u T}$$

$$\rho = \frac{P}{RT} = \frac{P}{(R_u/M)T}$$

Depends on composition of mixture

FIGURE 14–33
When the total pressure P and temperature T of a binary mixture of ideal gases is held constant, then the molar concentration C of the mixture remains constant.

The condition $C = $ constant offers considerable simplification in mass transfer analysis, and thus it is more convenient to use the molar formulation when dealing with gas mixtures at constant total pressure and temperature (Fig. 14–33).

Diffusion of Vapor Through a Stationary Gas: Stefan Flow

Many engineering applications such as heat pipes, cooling ponds, and the familiar perspiration involve condensation, evaporation, and transpiration in the presence of a noncondensable gas, and thus the *diffusion* of a vapor through a stationary (or stagnant) gas. To understand and analyze such processes, consider a liquid layer of species A in a tank surrounded by a gas of species B, such as a layer of liquid water in a tank open to the atmospheric air (Fig. 14–34), at constant pressure P and temperature T. Equilibrium exists between the liquid and vapor phases at the interface ($x = 0$), and thus the vapor pressure at the interface must equal the saturation pressure of species A at the specified temperature. We assume the gas to be insoluble in the liquid and both the gas and the vapor to behave as ideal gases.

If the surrounding gas at the top of the tank ($x = L$) is not saturated, the vapor pressure at the interface will be greater than the vapor pressure at the top of the tank ($P_{A, 0} > P_{A, L}$ and thus $y_{A, 0} > y_{A, L}$ since $y_A = P_A/P$), and this pressure (or concentration) difference will drive the vapor upward from the air–water interface into the stagnant gas. The upward flow of vapor will be sustained by the evaporation of water at the interface. Under steady conditions, the molar (or mass) flow rate of vapor throughout the stagnant gas column remains constant. That is,

FIGURE 14–34
Diffusion of a vapor A through a stagnant gas B.

$$\bar{j}_A = \dot{N}_A/A = \text{constant (or } j_A = \dot{m}_A/A = \text{constant)}$$

The pressure and temperature of the gas–vapor mixture are said to be constant, and thus the molar density of the mixture must be constant throughout the mixture, as shown earlier. That is, $C = C_A + C_B = $ constant, and it is more convenient to work with mole fractions or molar concentrations in this case than with mass fractions or densities since $\rho \neq$ constant.

Noting that $y_A + y_B = 1$ and that $y_{A, 0} > y_{A, L}$, we must have $y_{B, 0} < y_{B, L}$. That is, the mole fraction of the gas must be decreasing downward by the same amount that the mole fraction of the vapor is increasing. Therefore, gas must

be diffusing from the top of the column toward the liquid interface. However, the gas is said to be *insoluble* in the liquid, and thus there can be no net mass flow of the gas downward. Then under steady conditions, there must be an *upward bulk fluid motion* with an average velocity V that is just large enough to balance the diffusion of air downward so that the net molar (or mass) flow rate of the gas at any point is zero. In other words, the upward bulk motion offsets the downward diffusion, and for each air molecule that moves downward, there is another air molecule that moves upward. As a result, the air appears to be *stagnant* (it does not move). That is,

$$\bar{j}_B = \dot{N}_B/A = 0 \ (\text{or } j_B = \dot{m}_B/A = 0)$$

The diffusion medium is no longer stationary because of the bulk motion. The implication of the bulk motion of the gas is that it transports vapor as well as the gas upward with a velocity of V, which results in *additional* mass flow of vapor upward. Therefore, the molar flux of the vapor can be expressed as

$$\bar{j}_A = \dot{N}_A/A = \bar{j}_{A,\text{conv}} + \bar{j}_{A,\text{diff}} = y_A(\bar{j}_A + \bar{j}_B) - CD_{AB}\frac{dy_A}{dx} \qquad \textbf{(14–54)}$$

Noting that $\bar{j}_B = 0$, it simplifies to

$$\bar{j}_A = y_A\bar{j}_A - CD_{AB}\frac{dy_A}{dx} \qquad \textbf{(14–55)}$$

Solving for $\bar{j}_A$ gives

$$\bar{j}_A = -\frac{CD_{AB}}{1-y_A}\frac{dy_A}{dx} \quad \rightarrow \quad -\frac{1}{1-y_A}\frac{dy_A}{dx} = \frac{\bar{j}_A}{CD_{AB}} = \text{constant} \qquad \textbf{(14–56)}$$

since $\bar{j}_A = \text{constant}, C = \text{constant},$ and $D_{AB} = \text{constant}$. Separating the variables and integrating from $x = 0$, where $y_A(0) = y_{A,0}$, to $x = L$, where $y_A(L) = y_{A,L}$ gives

$$-\int_{y_{A,0}}^{y_{A,L}} \frac{dy_A}{1-y_A} = \int_0^L \frac{\bar{j}_A}{CD_{AB}}dx \qquad \textbf{(14–57)}$$

Performing the integrations,

$$\ln\frac{1-y_{A,L}}{1-y_{A,0}} = \frac{\bar{j}_A}{CD_{AB}}L \qquad \textbf{(14–58)}$$

Then the molar flux of vapor A, which is the *evaporation rate of species A per unit interface area,* becomes

$$\bar{j}_A = \dot{N}_A/A = \frac{CD_{AB}}{L}\ln\frac{1-y_{A,L}}{1-y_{A,0}} \ (\text{kmol/s·m}^2) \qquad \textbf{(14–59)}$$

This relation is known as **Stefan's law**, and the *induced convective flow* described that enhances mass diffusion is called the **Stefan flow**. Noting that $y_A = P_A/P$ and $C = P/R_uT$ for an ideal gas mixture, the evaporation rate of species A can also be expressed as

$$\dot{N}_A = \frac{D_{AB}PA}{LR_uT}\ln\frac{P - P_{A,L}}{P - P_{A,0}} \ (\text{kmol/s}) \qquad \textbf{(14–60)}$$

An expression for the variation of the mole fraction of A with x can be determined by performing the integration in Eq. 14–57 to the upper limit of x where $y_A(x) = y_A$ (instead of to L where $y_A(L) = y_{A, L}$). It yields

$$\ln \frac{1 - y_A}{1 - y_{A, 0}} = \frac{\bar{j}_A}{CD_{AB}} x$$

Substituting the $\bar{j}_A$ expression from Eq. 14–59 into this relation and rearranging gives

$$\frac{1 - y_A}{1 - y_{A, 0}} = \left(\frac{1 - y_{A, L}}{1 - y_{A, 0}}\right)^{x/L} \quad \text{and} \quad \frac{y_B}{y_{B, 0}} = \left(\frac{y_{B, L}}{y_{B, 0}}\right)^{x/L} \tag{14–61}$$

The second relation for the variation of the mole fraction of the stationary gas B is obtained from the first one by substituting $1 - y_A = y_B$ since $y_A + y_B = 1$.

To maintain isothermal conditions in the tank during evaporation, heat must be supplied to the tank at a rate of

$$\dot{Q} = \dot{m}_A h_{fg, A} = j_A A_s h_{fg, A} = (\bar{j}_A M_A) A_s h_{fg, A} \quad \text{(kJ/s)} \tag{14–62}$$

where A_s is the surface area of the liquid–vapor interface, $h_{fg, A}$ is the latent heat of vaporization, and M_A is the molar mass of species A.

Equimolar Counterdiffusion

FIGURE 14–35
Equimolar isothermal counterdiffusion of two gases A and B.

Consider two large reservoirs connected by a channel of length L, as shown in Fig. 14–35. The entire system contains a binary mixture of gases A and B at a uniform temperature T and pressure P throughout. The concentrations of species are maintained constant in each of the reservoirs such that $y_{A, 0} > y_{A, L}$ and $y_{B, 0} < y_{B, L}$. The resulting concentration gradients will cause the species A to diffuse in the positive x-direction and the species B in the opposite direction. Assuming the gases to behave as ideal gases and thus $P = CR_uT$, the total molar concentration of the mixture C will remain constant throughout the mixture since P and T are constant. That is,

$$C = C_A + C_B = \text{constant} \quad \text{(kmol/m}^3\text{)}$$

This requires that for each molecule of A that moves to the right, a molecule of B moves to the left, and thus the molar flow rates of species A and B must be equal in magnitude and opposite in sign. That is,

$$\dot{N}_A = -\dot{N}_B \quad \text{or} \quad \dot{N}_A + \dot{N}_B = 0 \quad \text{(kmol/s)}$$

This process is called **equimolar counterdiffusion** for obvious reasons. The net molar flow rate of the mixture for such a process, and thus the molar-average velocity, is zero since

$$\dot{N} = \dot{N}_A + \dot{N}_B = 0 \quad \longrightarrow \quad C A \overline{V} = 0 \quad \longrightarrow \quad \overline{V} = 0$$

Therefore, the mixture is *stationary* on a molar basis and thus mass transfer is by diffusion only (there is no mass transfer by convection) so that

$$\bar{j}_A = \dot{N}_A/A = -CD_{AB} \frac{dy_A}{dx} \quad \text{and} \quad \bar{j}_B = \dot{N}_B/A = -CD_{BA} \frac{dy_B}{dx} \tag{14–63}$$

Under steady conditions, the molar flow rates of species A and B can be determined directly from Eq. 14–24 developed earlier for one-dimensional steady diffusion in a stationary medium, noting that $P = CR_uT$ and thus $C = P/R_uT$

for each constituent gas and the mixture. For one-dimensional flow through a channel of uniform cross sectional area A with no homogeneous chemical reactions, they are expressed as

$$\dot{N}_{\text{diff}, A} = CD_{AB}A\frac{y_{A, 1} - y_{A, 2}}{L} = D_{AB}A\frac{C_{A, 1} - C_{A, 2}}{L} = \frac{D_{AB}}{R_uT}A\frac{P_{A, 0} - P_{A, L}}{L}$$

$$\dot{N}_{\text{diff}, B} = CD_{BA}A\frac{y_{B, 1} - y_{B, 2}}{L} = D_{BA}A\frac{C_{B, 1} - C_{B, 2}}{L} = \frac{D_{BA}}{R_uT}A\frac{P_{B, 0} - P_{B, L}}{L}$$

$$\text{(14–64)}$$

These relations imply that the mole fraction, molar concentration, and the partial pressure of either gas vary linearly during equimolar counterdiffusion.

It is interesting to note that the mixture is *stationary* on a molar basis, but it is not stationary on a mass basis unless the molar masses of A and B are equal. Although the net molar flow rate through the channel is zero, the net mass flow rate of the mixture through the channel is not zero and can be determined from

$$\dot{m} = \dot{m}_A + \dot{m}_B = \dot{N}_A M_A + \dot{N}_B M_B = \dot{N}_A(M_A + M_B) \qquad \text{(14–65)}$$

since $\dot{N}_B = -\dot{N}_A$. Note that the direction of net mass flow rate is the flow direction of the gas with the larger molar mass. A velocity measurement device such as an anemometer placed in the channel will indicate a velocity of $V = \dot{m}/\rho_A$ where ρ is the total density of the mixture at the site of measurement.

■ **EXAMPLE 14–8**   **Venting of Helium into the Atmosphere by Diffusion**

■ The pressure in a pipeline that transports helium gas at a rate of 2 kg/s is maintained at 1 atm by venting helium to the atmosphere through a 5-mm-internal-diameter tube that extends 15 m into the air, as shown in Fig. 14–36. Assuming both the helium and the atmospheric air to be at 25°C, determine (*a*) the mass flow rate of helium lost to the atmosphere through the tube, (*b*) the mass flow rate of air that infiltrates into the pipeline, and (*c*) the flow velocity at the bottom of the tube where it is attached to the pipeline that will be measured by an anemometer in steady operation.

SOLUTION   The pressure in a helium pipeline is maintained constant by venting to the atmosphere through a long tube. The mass flow rates of helium and air through the tube and the net flow velocity at the bottom are to be determined.
Assumptions   **1** Steady operating conditions exist. **2** Helium and atmospheric air are ideal gases. **3** No chemical reactions occur in the tube. **4** Air concentration in the pipeline and helium concentration in the atmosphere are negligible, so the mole fraction of the helium is 1 in the pipeline and 0 in the atmosphere (we will check this assumption later).
Properties   The diffusion coefficient of helium in air (or air in helium) at normal atmospheric conditions is $D_{AB} = 7.2 \times 10^{-5}$ m²/s (Table 14–2). The molar masses of air and helium are 29 and 4 kg/kmol, respectively (Table A–1).
Analysis   This is a typical equimolar counterdiffusion process since the problem involves two large reservoirs of ideal gas mixtures connected to each other by
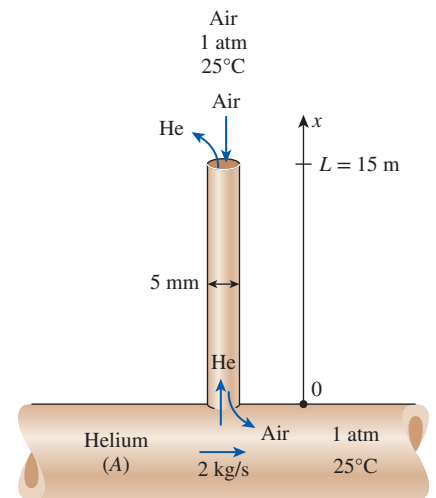
FIGURE 14–36
Schematic for Example 14–8.

a channel, and the concentrations of species in each reservoir (the pipeline and the atmosphere) remain constant.

(*a*) The flow area, which is the cross-sectional area of the tube, is

$$A = \pi D^2/4 = \pi(0.005 \text{ m})^2/4 = 1.963 \times 10^{-5} \text{ m}^2$$

Noting that the pressure of helium is 1 atm at the bottom of the tube ($x = 0$) and 0 at the top ($x = L$), its molar flow rate is determined from Eq. 14–64 to be

$$\dot{N}_{\text{helium}} = \dot{N}_{\text{diff}, A} = \frac{D_{AB} A}{R_u T} \frac{P_{A, 0} - P_{A, L}}{L}$$

$$= \frac{(7.20 \times 10^{-5} \text{ m}^2/\text{s})(1.963 \times 10^{-5} \text{ m}^2)}{(8.314 \text{ kPa·m}^3/\text{kmol·K})(298 \text{ K})}\left(\frac{1 \text{ atm} - 0}{15 \text{ m}}\right)\left(\frac{101.3 \text{ kPa}}{1 \text{ atm}}\right)$$

$$= 3.85 \times 10^{-12} \text{ kmol/s}$$

Therefore,

$$\dot{m}_{\text{helium}} = (\dot{N}M)_{\text{helium}} = (3.85 \times 10^{-12} \text{ kmol/s})(4 \text{ kg/kmol}) = \mathbf{1.54 \times 10^{-11} \text{ kg/s}}$$

which corresponds to about 0.5 g per year.

(*b*) Noting that $\dot{N}_B = -\dot{N}_A$ during an equimolar counterdiffusion process, the molar flow rate of air into the helium pipeline is equal to the molar flow rate of helium. The mass flow rate of air into the pipeline is

$$\dot{m}_{\text{air}} = (\dot{N}M)_{\text{air}} = (-3.85 \times 10^{-12} \text{ kmol/s})(29 \text{ kg/kmol}) = \mathbf{-112 \times 10^{-12} \text{ kg/s}}$$

The mass fraction of air in the helium pipeline is

$$w_{\text{air}} = \frac{|\dot{m}_{\text{air}}|}{\dot{m}_{\text{total}}} = \frac{112 \times 10^{-12} \text{ kg/s}}{(2 + 112 \times 10^{-12} - 1.54 \times 10^{-11}) \text{ kg/s}} = 5.6 \times 10^{-11} \approx 0$$

which validates our original assumption of negligible air in the pipeline.

(*c*) The net mass flow rate through the tube is

$$\dot{m}_{\text{net}} = \dot{m}_{\text{helium}} + \dot{m}_{\text{air}} = 1.54 \times 10^{-11} - 112 \times 10^{-12} = -9.66 \times 10^{-11} \text{ kg/s}$$

The mass fraction of air at the bottom of the tube is very small, as shown above, and thus the density of the mixture at $x = 0$ can simply be taken to be the density of helium, which is

$$\rho \cong \rho_{\text{helium}} = \frac{P}{RT} = \frac{101.325 \text{ kPa}}{(2.0769 \text{ kPa·m}^3/\text{kg·K})(298 \text{ K})} = 0.1637 \text{ kg/m}^3$$

Then the average flow velocity at the bottom part of the tube becomes

$$V = \frac{\dot{m}}{\rho A} = \frac{-9.66 \times 10^{-11} \text{ kg/s}}{(0.1637 \text{ kg/m}^3)(1.963 \times 10^{-5} \text{ m}^2)} = \mathbf{-3.01 \times 10^{-5} \text{ m/s}}$$

which is difficult to measure, even with the most sensitive velocity measurement devices. The negative sign indicates flow in the negative *x*-direction (toward the pipeline).

FIGURE 14–37
Schematic for Example 14–9.

EXAMPLE 14–9 **Measuring Diffusion Coefficient
by the Stefan Tube**

A 3-cm-diameter Stefan tube is used to measure the binary diffusion coefficient of water vapor in air at 20°C at an elevation of 1600 m where the atmospheric pressure is 83.5 kPa. The tube is partially filled with water, and the distance from the water surface to the open end of the tube is 40 cm (Fig. 14–37). Dry air is blown over the open end of the tube so that water vapor rising to the top is removed immediately and the concentration of vapor at the top of the tube is zero. In 15 days of continuous operation at constant pressure and temperature, the amount of water that has evaporated is measured to be 1.23 g. Determine the diffusion coefficient of water vapor in air at 20°C and 83.5 kPa.

SOLUTION The amount of water that evaporates from a Stefan tube at a specified temperature and pressure over a specified time period is measured. The diffusion coefficient of water vapor in air is to be determined.

Assumptions **1** Water vapor and atmospheric air are ideal gases. **2** The amount of air dissolved in liquid water is negligible. **3** Heat is transferred to the water from the surroundings to make up for the latent heat of vaporization so that the temperature of water remains constant at 20°C.

Properties The saturation pressure of water at 20°C is 2.34 kPa (Table A–9).

Analysis The vapor pressure at the air–water interface is the saturation pressure of water at 20°C, and the mole fraction of water vapor (species *A*) at the interface is determined from

$$y_{\text{vapor, 0}} = y_{A,\,0} = \frac{P_{\text{vapor, 0}}}{P} = \frac{2.34 \text{ kPa}}{83.5 \text{ kPa}} = 0.0280$$

Dry air is blown on top of the tube and, thus, $y_{\text{vapor, }L} = y_{A,\,L} = 0$. Also, the total molar density throughout the tube remains constant because of the constant temperature and pressure conditions and is determined to be

$$C = \frac{P}{R_u T} = \frac{83.5 \text{ kPa}}{(8.314 \text{ kPa·m}^3/\text{kmol·K})(293 \text{ K})} = 0.0343 \text{ kmol/m}^3$$

The cross-sectional area of the tube is

$$A = \pi D^2/4 = \pi(0.03 \text{ m})^2/4 = 7.069 \times 10^{-4} \text{ m}^2$$

The evaporation rate is given to be 1.23 g per 15 days. Then the molar flow rate of vapor is determined to be

$$\dot{N}_A = \dot{N}_{\text{vapor}} = \frac{\dot{m}_{\text{vapor}}}{M_{\text{vapor}}} = \frac{1.23 \times 10^{-3} \text{ kg}}{(15 \times 24 \times 3600 \text{ s})(18 \text{ kg/kmol})}$$

$$= 5.27 \times 10^{-11} \text{ kmol/s}$$
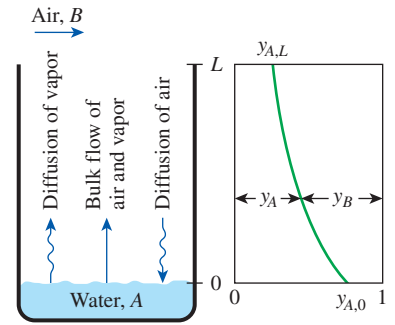
Finally, substituting the information above into Eq. 14–59 we get

$$\frac{5.27 \times 10^{-1} \text{ kmol/s}}{7.069 \times 10^{-4} \text{ m}^2} = \frac{(0.0343 \text{ kmol/m}^3) D_{AB}}{0.4 \text{ m}} \ln \frac{1-0}{1-0.028}$$

which gives

$$D_{AB} = \mathbf{3.06 \times 10^{-5} \text{ m}^2/\text{s}}$$

for the binary diffusion coefficient of water vapor in air at 20°C and 83.5 kPa.

Air, B →
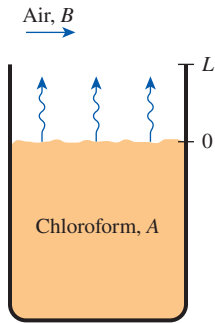
FIGURE 14–38
Schematic for Example 14–10.

PtD *EXAMPLE 14–10*   **Prevention of Health Hazards from Toxic Exposure**

Chloroform ($M = 119.38$ kg/kmol) is classified as a hazardous material because prolonged exposure to it is harmful to health. Inhalation of large amounts of chloroform may cause liver and kidney damage. The permissible exposure limit (PEL) of chloroform, established by the Occupational Safety and Health Administration (OSHA), is 240 mg/m^3. A lab technician, working in a lab space of 30 m^3, has poured liquid chloroform into 10 test tubes with inner diameter of 25 mm. Each test tube holds an equal amount of liquid chloroform at a level of 1 cm from the top (Fig. 14–38). The chloroform vapor pressure is 21 kPa, and evaporation of chloroform to the surrounding air is occurring at 25°C and 1 atm. If the diffusion coefficient of chloroform in air is $D_{AB} = 0.104$ cm^2/s, determine whether or not it is safe for the technician to remain in the lab for an hour during the evaporation of chloroform from the test tubes.

SOLUTION   In this example, the concepts of Prevention through Design (PtD) are applied in conjunction with the concepts of diffusion in a moving medium.
Assumptions   **1** Steady operating conditions exist. **2** Chloroform vapor and atmospheric air are ideal gases. **3** The amount of air dissolved in liquid chloroform is negligible. **4** Temperatures of air and chloroform remain constant at 25°C.
Properties   The molar mass of chloroform is given as $M = 119.38$ kg/kmol. The diffusion coefficient of chloroform in air is given as $D_{AB} = 0.104$ cm^2/s.
Analysis   The vapor pressure of chloroform at 25°C is given as $P_{A,0} = 21$ kPa, and the mole fraction of chloroform vapor (species A) at the interface is determined from

$$y_{A,0} = \frac{P_{A,0}}{P} = \frac{21 \text{ kPa}}{101.325 \text{ kPa}} = 0.20725$$

The total molar density throughout the tube remains constant because of the constant temperature and pressure conditions and is determined to be

$$C = \frac{P}{R_u T} = \frac{101.325 \text{ kPa}}{(8.314 \text{ kPa·m}^3/\text{kmol·K})(273 + 25)\text{K}} = 0.0409 \text{ kmol/m}^3$$

Then, the diffusion rate per unit interface area for one test tube is

$$\frac{\dot{N}_A}{A} = \frac{C D_{AB}}{L} \ln\left(\frac{1 - y_{A,L}}{1 - y_{A,0}}\right)$$

$$= \frac{(0.0409 \text{ kmol/m}^3)(0.104 \text{ cm}^2/\text{s})(1 \times 10^{-4} \text{ m}^2/\text{cm}^2)}{0.01 \text{ m}} \ln\left(\frac{1 - 0}{1 - 0.20725}\right)$$

$$= 9.8789 \times 10^{-6} \text{ kmol/s·m}^2$$

The evaporation rate of chloroform from one test tube is

$$\dot{m} = M D^2 \frac{\pi}{4} \frac{\dot{N}_A}{A}$$

$$= (119.38 \text{ kg/kmol})(0.025 \text{ m})^2 \frac{\pi}{4}(9.8789 \times 10^{-6} \text{ kmol/s·m}^2)$$

$$= 5.789 \times 10^{-7} \text{ kg/s}$$
$$= 34.734 \text{ mg/min}$$

The total rate of chloroform being evaporated from 10 test tubes to the surrounding air is

$$\dot{m}_{\text{total}} = 10(34.734 \text{ mg/min}) = 347.34 \text{ mg/min}$$

For a lab space of 30 m³, the time for the chloroform to reach the PEL (permissible exposure limit) from the evaporation is

$$\text{Time} = \text{PEL} \times \frac{\text{Lab space}}{\dot{m}_{\text{total}}} = (240 \text{ mg/m}^3)\left(\frac{30 \text{ m}^3}{347.34 \text{ mg/min}}\right) = \textbf{20.7 min} < 60 \text{ min}$$

Discussion It takes 20 minutes and 44 seconds for the evaporated chloroform to reach the PEL established by OSHA. Therefore, it would not be safe for the technician to remain in the lab for an hour. Substances that can release toxic vapors should be handled under a fume hood.

14–9 ■ MASS CONVECTION

So far we have considered *mass diffusion,* which is the transfer of mass due to a concentration gradient. Now we consider *mass convection* (or *convective mass transfer*), which is the transfer of mass between a surface and a moving fluid due to both *mass diffusion* and *bulk fluid motion.* We mentioned earlier that fluid motion enhances heat transfer considerably by removing the heated fluid near the surface and replacing it with the cooler fluid farther away. Likewise, fluid motion enhances mass transfer considerably by removing the high-concentration fluid near the surface and replacing it with the lower-concentration fluid farther away. In the limiting case of no bulk fluid motion, mass convection reduces to mass diffusion, just as convection reduces to conduction. The analogy between heat and mass convection holds for both *forced* and *natural* convection, *laminar* and *turbulent* flow, and *internal* and *external* flow.

Like heat convection, mass convection is also complicated because of the complications associated with fluid flow such as the *surface geometry, flow regime, flow velocity,* and the *variation of the fluid properties* and *composition.* Therefore, we have to rely on experimental relations to determine mass transfer. Also, mass convection is usually analyzed on a *mass basis* rather than on a molar basis. Therefore, we will present formulations in terms of mass concentration (density ρ or mass fraction w) instead of molar concentration (molar density C or mole fraction y). But the formulations on a molar basis can be obtained using the relation $C = \rho/M$ where M is the molar mass. Also, for simplicity, we will restrict our attention to convection in fluids that are (or can be treated as) *binary mixtures.*

Consider the flow of air over the free surface of a water body such as a lake under isothermal conditions. If the air is not saturated, the concentration of water vapor will vary from a maximum at the water surface where the air is always saturated to the free steam value far from the surface. In heat convection, we defined the region in which temperature gradients exist as the *thermal boundary layer.* Similarly, in mass convection, we define the region of the fluid in which concentration gradients exist as the **concentration boundary layer**, as shown in Fig. 14–39. In **external flow**, the thickness of the concentration boundary layer δ_c for a species A at a specified location on the surface is defined as the normal distance y from the surface at which

$$\frac{\rho_{A,s} - \rho_A}{\rho_{A,s} - \rho_{A,\infty}} = 0.99$$

where $\rho_{A,s}$ and $\rho_{A,\infty}$ are the densities of species A at the surface (on the fluid side) and the free stream, respectively.
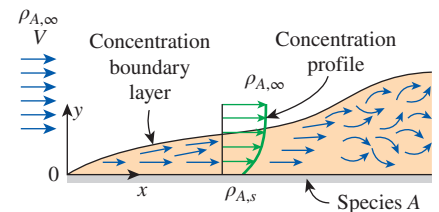
FIGURE 14–39
The development of a concentration boundary layer for species A during external flow on a flat surface.
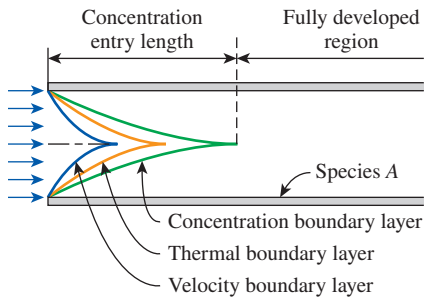
FIGURE 14–40
The development of the velocity, thermal, and concentration boundary layers in internal flow.

FIGURE 14–41
In mass transfer, the Schmidt number plays the role of the Prandtl number in heat transfer.

FIGURE 14–42
Ernst Heinrich Wilhelm Schmidt (1892–1975), a German engineer, was born at Vögelsen, Germany. One of his early research efforts was a careful measurement of the radiation properties of solids, which caused him to propose and develop the use of aluminum foil as an effective radiation shield. He was the first to measure the velocity and temperature field in a free convection boundary layer and the large heat-transfer coefficients occurring in droplet condensation. The dimensionless **Schmidt number** which characterizes fluid flows in which there are simultaneous momentum and mass diffusion convection processes was named after him.

In **internal flow**, we have a **concentration entrance region** where the concentration profile develops, in addition to the hydrodynamic and thermal entry regions (Fig. 14–40). The concentration boundary layer continues to develop in the flow direction until its thickness reaches the tube center and the boundary layers merge. The distance from the tube inlet to the location where this merging occurs is called the **concentration entry length** L_c, and the region beyond that point is called the **fully developed region**, which is characterized by

$$\frac{\partial}{\partial x}\left(\frac{\rho_{A,s} - \rho_A}{\rho_{A,s} - \rho_{A,b}}\right) = 0 \tag{14–66}$$

where $\rho_{A,b}$ is the *bulk mean density* of species A defined as

$$\rho_{A,b} = \frac{1}{A_c V_{avg}} \int_{A_c} \rho_A u \, dA_c \tag{14–67}$$

Therefore, the nondimensionalized concentration difference profile as well as the mass transfer coefficient remain constant in the fully developed region. This is analogous to the friction and heat transfer coefficients remaining constant in the fully developed region.

In heat convection, the relative magnitudes of momentum and heat diffusion in the velocity and thermal boundary layers are expressed by the dimensionless *Prandtl number,* defined as (Fig. 14–41)

Prandtl number: $$\text{Pr} = \frac{\nu}{\alpha} = \frac{\text{Momentum diffusivity}}{\text{Thermal diffusivity}} \tag{14–68}$$

The corresponding quantity in mass convection is the dimensionless **Schmidt number** (Fig. 14–42), defined as

Schmidt number: $$\text{Sc} = \frac{\nu}{D_{AB}} = \frac{\text{Momentum diffusivity}}{\text{Mass diffusivity}} \tag{14–69}$$

which represents the relative magnitudes of molecular momentum and mass diffusion in the velocity and concentration boundary layers, respectively.

The relative growth of the velocity and thermal boundary layers in laminar flow is governed by the Prandtl number, whereas the relative growth of the velocity and concentration boundary layers is governed by the Schmidt number. A Prandtl number of near unity ($\text{Pr} \approx 1$) indicates that momentum and heat transfer by diffusion are comparable, and velocity and thermal boundary layers almost coincide with each other. *A Schmidt number of near unity* ($\text{Sc} \approx 1$) *indicates that momentum and mass transfer by diffusion are comparable, and velocity and concentration boundary layers almost coincide with each other.*

It seems like we need one more dimensionless number to represent the relative magnitudes of heat and mass diffusion in the thermal and concentration boundary layers. That is the **Lewis number** (Fig. 14–43), defined as (Fig. 14–44)

Lewis number: $$\text{Le} = \frac{\text{Sc}}{\text{Pr}} = \frac{\alpha}{D_{AB}} = \frac{\text{Thermal diffusivity}}{\text{Mass diffusivity}} \tag{14–70}$$

The relative thicknesses of velocity, thermal, and concentration boundary layers in laminar flow are expressed as

$$\frac{\delta_{\text{velocity}}}{\delta_{\text{thermal}}} = \text{Pr}^n, \quad \frac{\delta_{\text{velocity}}}{\delta_{\text{concentration}}} = \text{Sc}^n, \quad \text{and} \quad \frac{\delta_{\text{thermal}}}{\delta_{\text{concentration}}} = \text{Le}^n \tag{14–71}$$

where $n = \frac{1}{3}$ for most applications in all three relations. These relations, in general, are not applicable to turbulent boundary layers since turbulent mixing in this case may dominate the diffusion processes.

Note that species transfer at the surface ($y = 0$) is by diffusion only because of the *no-slip boundary condition,* and mass flux of species A at the surface can be expressed by Fick's law as (Fig. 14–45)

$$\bar{j}_A = \dot{m}_A/A_s = -\rho D_{AB} \frac{\partial w_A}{\partial y}\bigg|_{y=0} = h_{\text{mass}}(w_{A,s} - w_{A,\infty}) \quad \text{(kg/s·m}^2) \qquad \textbf{(14–72)}$$

This is analogous to heat transfer at the surface being by conduction only and expressing it by Fourier's law.

The rate of heat convection for external flow was expressed conveniently by *Newton's law of cooling* as

$$\dot{Q}_{\text{conv}} = h_{\text{conv}} A_s (T_s - T_\infty)$$

where h_{conv} is the average heat transfer coefficient, A_s is the surface area, and $T_s - T_\infty$ is the temperature difference across the thermal boundary layer. Likewise, the rate of mass convection can be expressed as

$$\dot{m}_{\text{conv}} = h_{\text{mass}} A_s (\rho_{A,s} - \rho_{A,\infty}) = h_{\text{mass}} \rho A_s (w_{A,s} - w_{A,\infty}) \quad \text{(kg/s)} \qquad \textbf{(14–73)}$$

where h_{mass} is the average **mass transfer coefficient**, in m/s; A_s is the surface area; $\rho_{A,s} - \rho_{A,\infty}$ is the mass concentration difference of species A across the concentration boundary layer; and ρ is the average density of the fluid in the boundary layer. The product $h_{\text{mass}}\rho$, whose unit is kg/m²·s, is called the *mass transfer conductance.* For internal flow we have

$$\dot{m}_{\text{conv}} = h_{\text{mass}} A_s \frac{\Delta\rho_{A,e} - \Delta\rho_{A,i}}{\ln(\Delta\rho_{A,e}/\Delta\rho_{A,i})} \qquad \textbf{(14–74)}$$

where $\Delta\rho_{A,e} = \rho_{A,s} - \rho_{A,e}$ and $\Delta\rho_{A,i} = \rho_{A,s} - \rho_{A,i}$. If the local mass transfer coefficient varies in the flow direction, the *average mass transfer coefficient* can be determined from

$$h_{\text{mass, avg}} = \frac{1}{A_s} \int_{A_s} h_{\text{mass}} dA_s$$

In heat convection analysis, it is often convenient to express the heat transfer coefficient in a nondimensionalized form in terms of the dimensionless *Nusselt number,* defined as

Nusselt number: $$\text{Nu} = \frac{h_{\text{conv}} L_c}{k} \qquad \textbf{(14–75)}$$

where L_c is the characteristic length and k is the thermal conductivity of the fluid. The corresponding quantity in mass convection is the dimensionless **Sherwood number** (Fig. 14–46), defined as (Fig. 14–47)

Sherwood number: $$\text{Sh} = \frac{h_{\text{mass}} L_c}{D_{AB}} \qquad \textbf{(14–76)}$$

where h_{mass} is the mass transfer coefficient and D_{AB} is the mass diffusivity. The Nusselt and Sherwood numbers represent the effectiveness of heat and mass convection at the surface, respectively.
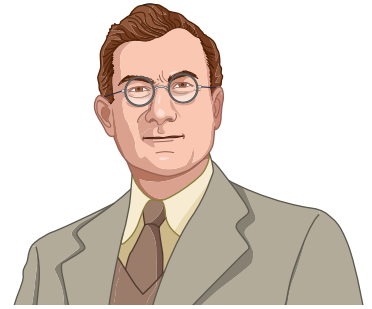
FIGURE 14–43
Warren Kendall Lewis (1882–1975), an American chemical engineer, was born in Laurel, Delaware. He was an MIT professor, and his coordination of chemistry, physics, and engineering into an independent discipline to serve the chemical industry led to his being called the father of modern chemical engineering. The dimensionless **Lewis number,** which characterizes fluid flows in which there are simultaneous heat and mass diffusion convection processes, was named after him.

FIGURE 14–44
Lewis number is a measure of heat diffusion relative to mass diffusion.
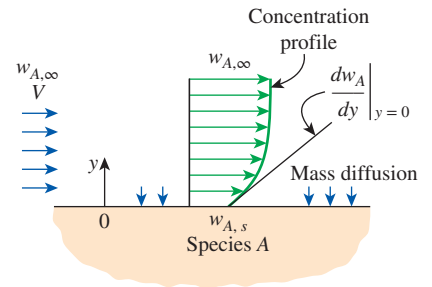
$$-\rho D_{AB} \frac{\partial w_A}{\partial y}\bigg|_{y=0} = h_{\text{mass}} \rho (w_{A,s} - w_{A,\infty})$$

FIGURE 14–45
Mass transfer at a surface occurs by diffusion because of the no-slip boundary condition, just like heat transfer occurring by conduction.

FIGURE 14–46
Thomas Kilgore Sherwood
(1903–1976), an American chemical engineer, was born in Columbus, Ohio. Sherwood came to MIT in 1923 for graduate work in the Chemical Engineering Department and completed his doctoral thesis under Warren K. Lewis. Sherwood's primary research area was mass transfer and its interaction with flow and with chemical reaction and industrial process operations in which those phenomena played an important part. He received numerous awards for his research contributions, such as the U.S. Medal for Merit and the Lewis Award. The dimensionless **Sherwood number,** which represents the ratio of convective to diffusive mass transport, was named after him.

FIGURE 14–47
In mass transfer, the Sherwood number plays the role the Nusselt number plays in heat transfer.

Sometimes it is more convenient to express the heat and mass transfer coefficients in terms of the dimensionless **Stanton number** as

Heat transfer Stanton number: $\qquad \text{St} = \dfrac{h_{\text{conv}}}{\rho V c_p} = \text{Nu} \dfrac{1}{\text{Re} \; \text{Pr}}$ (14–77)

and

Mass transfer Stanton number: $\qquad \text{St}_{\text{mass}} = \dfrac{h_{\text{mass}}}{V} = \text{Sh} \dfrac{1}{\text{Re} \; \text{Sc}}$ (14–78)

where V is the free-steam velocity in external flow and the bulk mean fluid velocity in internal flow.

For a given geometry, the average Nusselt number in forced convection depends on the Reynolds and Prandtl numbers, whereas the average Sherwood number depends on the Reynolds and Schmidt numbers. That is,

Nusselt number: $\qquad \text{Nu} = f(\text{Re}, \text{Pr})$
Sherwood number: $\qquad \text{Sh} = f(\text{Re}, \text{Sc})$

where the functional form of f is the same for both the Nusselt and Sherwood numbers in a given geometry, provided that the thermal and concentration boundary conditions are of the same type. Therefore, *the Sherwood number can be obtained from the Nusselt number expression by simply replacing the Prandtl number with the Schmidt number.* This shows what a powerful tool analogy can be in the study of natural phenomena (Table 14–12).

In *natural convection mass transfer,* the analogy between the Nusselt and Sherwood numbers still holds, and thus $\text{Sh} = f(\text{Gr}, \text{Sc})$. But the Grashof number in this case should be determined directly from

$$\text{Gr} = \frac{g(\rho_\infty - \rho_s)L_c^3}{\rho \nu^2} = \frac{g(\Delta\rho/\rho)L_c^3}{\nu^2}$$ (14–79)

which is applicable to both temperature- and/or concentration-driven natural convection flows. Note that in *homogeneous* fluids (i.e., fluids with no concentration gradients), density differences are due to temperature differences only, and thus we can replace $\Delta\rho/\rho$ with $\beta\Delta T$ for convenience, as we did in natural convection heat transfer. However, in *nonhomogeneous* fluids, density differences are due to the *combined effects* of *temperature* and *concentration differences,* and $\Delta\rho/\rho$ cannot be replaced by $\beta\Delta T$ in such cases, even when all we care about is heat transfer and we have no interest in mass transfer. For example, hot water at the bottom of a pond rises to the top. But when salt is placed at the bottom, as it is done in solar ponds, the salty water (brine) at the bottom will not rise because it is now heavier than the fresh water at the top (Fig. 14–48).

Concentration-driven natural convection flows are based on the densities of different species in a mixture being different. Therefore, at isothermal conditions, there will be no natural convection in a gas mixture that is composed of gases with identical molar masses. Also, the case of a hot surface facing up corresponds to diffusing fluid having a lower density than the mixture (and thus rising under the influence of buoyancy), and the case of a hot surface facing down corresponds to the diffusing fluid having a higher density. For example, the evaporation of water into air corresponds to a hot surface facing up since water vapor is lighter than the air and it tends to rise. But this is not

the case for gasoline unless the temperature of the gasoline–air mixture at the gasoline surface is so high that thermal expansion overwhelms the density differential due to higher gasoline concentration near the surface.

Analogy Between Friction, Heat Transfer, and Mass Transfer Coefficients

Consider the flow of a fluid over a flat plate of length L with free-stream conditions of T_∞, V, and $w_{A,\infty}$ (Fig. 14–49). Noting that convection at the surface ($y = 0$) is equal to diffusion because of the no-slip condition, the friction, heat transfer, and mass transfer conditions at the surface can be expressed as

Wall friction:
$$\tau_s = \mu \frac{\partial u}{\partial y}\bigg|_{y=0} = \frac{f}{2} \rho V^2 \tag{14–80}$$

Heat transfer:
$$\dot{q}_s = -k \frac{\partial T}{\partial y}\bigg|_{y=0} = h_{\text{heat}}(T_s - T_\infty) \tag{14–81}$$

Mass transfer:
$$j_{A,s} = -\rho D_{AB} \frac{\partial w_A}{\partial y}\bigg|_{y=0} = h_{\text{mass}} \rho(w_{A,s} - w_{A,\infty}) \tag{14–82}$$

These relations can be rewritten for internal flow by using *bulk mean properties* instead of free-stream properties. After some simple mathematical manipulations, the three relations above can be rearranged as

Wall friction:
$$\frac{d(u/V)}{d(y/L_c)}\bigg|_{y=0} = \frac{f}{2} \frac{\rho V L_c}{\mu} = \frac{f}{2} \text{Re} \tag{14–83}$$

Heat transfer:
$$\frac{d[(T - T_s)/(T_\infty - T_s)]}{d(y/L_c)}\bigg|_{y=0} = \frac{h_{\text{heat}} L_c}{k} = \text{Nu} \tag{14–84}$$

Mass transfer:
$$\frac{d[(w_A - w_{A,s})/(w_{A,\infty} - w_{A,s})]}{d(y/L_c)}\bigg|_{y=0} = \frac{h_{\text{mass}} L_c}{D_{AB}} = \text{Sh} \tag{14–85}$$

The left sides of these three relations are the slopes of the normalized velocity, temperature, and concentration profiles at the surface, and the right sides are the dimensionless numbers discussed earlier.

Special Case: Pr ≈ Sc ≈ 1 (Reynolds Analogy)

Now consider the hypothetical case in which the molecular diffusivities of momentum, heat, and mass are identical. That is, $\nu = \alpha = D_{AB}$ and thus $\text{Pr} = \text{Sc} = \text{Le} = 1$. In this case the normalized velocity, temperature, and concentration profiles will coincide, and thus the slope of these three curves at the surface (the left sides of Eqs. 14–83 through 14–85) will be identical (Fig. 14–50). Then we can set the right sides of those three equations equal to each other and obtain

$$\frac{f}{2} \text{Re} = \text{Nu} = \text{Sh} \quad \text{or} \quad \frac{f}{2} \frac{V L_c}{\nu} = \frac{h_{\text{heat}} L_c}{k} = \frac{h_{\text{mass}} L_c}{D_{AB}} \tag{14–86}$$

Noting that $\text{Pr} = \text{Sc} = 1$, we can also write this equation as

$$\frac{f}{2} = \frac{\text{Nu}}{\text{Re Pr}} = \frac{\text{Sh}}{\text{Re Sc}} \quad \text{or} \quad \frac{f}{2} = \text{St} = \text{St}_{\text{mass}} \tag{14–87}$$

TABLE 14–12

Analogy between the quantities that appear in the formulation and solution of heat convection and mass convection

Heat Convection	Mass Convection
T	C, y, ρ, or w
h_{conv}	h_{mass}
δ_{thermal}	$\delta_{\text{concentration}}$
$\text{Re} = \dfrac{V L_c}{\nu}$	$\text{Re} = \dfrac{V L_c}{\nu}$
$\text{Gr} = \dfrac{g\beta(T_s - T_\infty)L_c^3}{\nu^2}$	$\text{Gr} = \dfrac{g(\rho_\infty - \rho_s)L_c^3}{\rho\,\nu^2}$
$\text{Pr} = \dfrac{\nu}{\alpha}$	$\text{Sc} = \dfrac{\nu}{D_{AB}}$
$\text{St} = \dfrac{h_{\text{conv}}}{\rho V c_p}$	$\text{St}_{\text{mass}} = \dfrac{h_{\text{mass}}}{V}$
$\text{Nu} = \dfrac{h_{\text{conv}} L_c}{k}$	$\text{Sh} = \dfrac{h_{\text{mass}} L_c}{D_{AB}}$
$\text{Nu} = f(\text{Re}, \text{Pr})$	$\text{Sh} = f(\text{Re}, \text{Sc})$
$\text{Nu} = f(\text{Gr}, \text{Pr})$	$\text{Sh} = f(\text{Gr}, \text{Sc})$

20°C	Fresh water
No convection currents	Solar pond
70°C	$\rho_{\text{brine}} > \rho_{\text{water}}$ Brine
	Salt
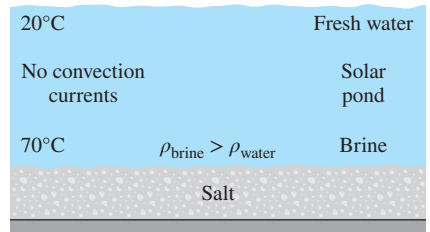
FIGURE 14–48
A hot fluid at the bottom will rise and initiate natural convection currents only if its density is lower.
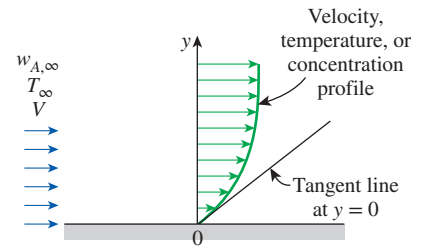
FIGURE 14–49
The friction, heat, and mass transfer coefficients for flow over a surface are proportional to the slope of the tangent line of the velocity, temperature, and concentration profiles, respectively, at the surface.

Reynolds analogy
$$\nu = \alpha = D_{AB}$$
(or Pr = Sc = Le)

FIGURE 14–50
When the molecular diffusivities of momentum, heat, and mass are equal to each other, the velocity, temperature, and concentration boundary layers coincide.

Chilton-Colburn Analogy
General:
$$h_{mass} = \frac{h_{heat}}{\rho c_p} \left(\frac{D_{AB}}{\alpha}\right)^{2/3}$$
$$= \frac{1}{2} fV \left(\frac{D_{AB}}{\nu}\right)^{2/3}$$
Special case: $\nu = \alpha = D_{AB}$
$$h_{mass} = \frac{h_{heat}}{\rho c_p} = \frac{1}{2} fV$$

FIGURE 14–51
When the friction or heat transfer coefficient is known, the mass transfer coefficient can be determined directly from the Chilton–Colburn analogy.

This relation is known as the **Reynolds analogy**, and it enables us to determine the seemingly unrelated friction, heat transfer, and mass transfer coefficients when only one of them is known or measured. (Actually the original Reynolds analogy proposed by O. Reynolds in 1874 is St = f/2, which is then extended to include mass transfer.) However, it should always be remembered that the analogy is restricted to situa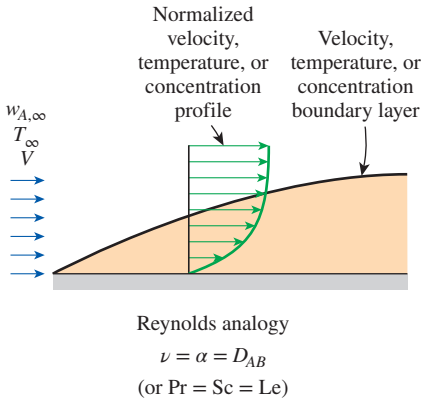tions for which Pr $\approx$ Sc $\approx$ 1. Of course the first part of the analogy between friction and heat transfer coefficients can always be used for gases since their Prandtl number is close to unity.

General Case: Pr ≠ Sc ≠ 1 (Chilton–Colburn Analogy)

The Reynolds analogy is a very useful relation, and it is certainly desirable to extend it to a wider range of Pr and Sc numbers. Several attempts have been made in this regard, but the simplest and the best known is the one suggested by Chilton and Colburn in 1934 as

$$\frac{f}{2} = \text{St Pr}^{2/3} = \text{St}_{mass} \text{Sc}^{2/3} \tag{14–88}$$

for $0.6 < \text{Pr} < 60$ and $0.6 < \text{Sc} < 3000$. This equation is known as the **Chilton–Colburn analogy**. Using the definition of heat and mass Stanton numbers, the analogy between heat and mass transfer can be expressed more conveniently as (Fig. 14–51)

$$\frac{\text{St}}{\text{St}_{mass}} = \left(\frac{\text{Sc}}{\text{Pr}}\right)^{2/3} \tag{14–89}$$

or

$$\frac{h_{heat}}{h_{mass}} = \rho c_p \left(\frac{\text{Sc}}{\text{Pr}}\right)^{2/3} = \rho c_p \left(\frac{\alpha}{D_{AB}}\right)^{2/3} = \rho c_p \text{Le}^{2/3}$$

For air–water vapor mixtures at 298 K, the mass and thermal diffusivities are $D_{AB} = 2.5 \times 10^{-5}$ m²/s and $\alpha = 2.18 \times 10^{-5}$ m²/s, and thus the Lewis number is Le $= \alpha/D_{AB} = 0.872$. (We simply use the α value of dry air instead of the moist air since the fraction of vapor in the air at atmospheric conditions is low.) Then $(\alpha/D_{AB})^{2/3} = 0.872^{2/3} = 0.913$, which is close to unity. Also, the Lewis number is relatively insensitive to variations in temperature. Therefore, for air–water vapor mixtures, the relation between heat and mass transfer coefficients can be expressed with good accuracy as

$$h_{heat} \cong \rho c_p h_{mass} \quad \text{(air–water vapor mixtures)} \tag{14–90}$$

where ρ and c_p are the density and specific heat of air at average conditions (or ρc_p is the specific heat of air per unit volume). Equation 14–90 is known as the **Lewis relation** and is commonly used in air-conditioning applications. Another important consequence of Le $\cong$ 1 is that the *wet-bulb* and *adiabatic saturation temperatures* of moist air are nearly identical. In *turbulent flow,* the Lewis relation can be used even when the Lewis number is not 1 since eddy mixing in turbulent flow overwhelms any molecular diffusion, and heat and mass are transported at the same rate.

The Chilton–Colburn analogy has been observed to hold quite well in laminar or turbulent flow over plane surfaces. But this is not always the case for

internal flow and flow over irregular geometries, and in such cases specific relations developed should be used. When dealing with flow over blunt bodies, it is important to note that *f* in these relations is the *skin friction coefficient,* not the total drag coefficient, which also includes the pressure drag.

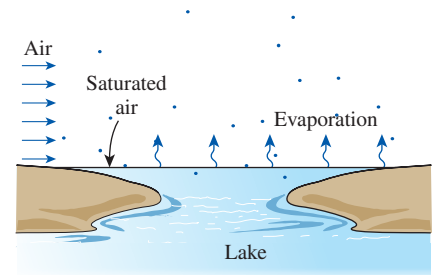## Limitation on the Heat–Mass Convection Analogy

Caution should be exercised when using the analogy in Eq. 14–88 since there are a few factors that cast some shadow on the accuracy of that relation. For one thing, the Nusselt numbers are usually evaluated for smooth surfaces, but many mass transfer problems involve wavy or roughened surfaces. Also, many Nusselt relations are obtained for constant surface temperature situations, but the concentration may not be constant over the entire surface because of the possible surface dryout. The blowing or suction at the surface during mass transfer may also cause some deviation, especially during high-speed blowing or suction.

Finally, the heat–mass convection analogy is valid for **low mass flux** cases in which the flow rate of species undergoing mass flow is low relative to the total flow rate of the liquid or gas mixture so that the mass transfer between the fluid and the surface does not affect the *flow velocity.* (Note that convection relations are based on *zero* fluid velocity at the surface, which is true only when there is no net mass transfer at the surface.) Therefore, the heat–mass convection analogy is not applicable when the rate of mass transfer of a species is high relative to the flow rate of that species.

Consider, for example, the evaporation and transfer of water vapor into air in an air washer, an evaporative cooler, a wet cooling tower, or just at the free surface of a lake or river (Fig. 14–52). Even at a temperature of 40°C, the vapor pressure at the water surface is the saturation pressure of 7.4 kPa, which corresponds to a mole fraction of 0.074 or a mass fraction of $w_{A,s} = 0.047$ for the vapor. Then the mass fraction difference across the boundary layer will be, at most, $\Delta w = w_{A,s} - w_{A,\infty} = 0.047 - 0 = 0.047$. For the evaporation of water into air, the error involved in the low mass flux approximation is roughly $\Delta w/2$, which is 2.5 percent in the worst case considered above. Therefore, in processes that involve the evaporation of water into air, we can use the heat–mass convection analogy with confidence. However, the mass fraction of vapor approaches 1 as the water temperature approaches the saturation temperature, and thus the low mass flux approximation is not applicable to mass transfer in boilers, condensers, and the evaporation of fuel droplets in combustion chambers. In this chapter, we limit our consideration to low mass flux applications.

FIGURE 14–52
Evaporation from the free surface of water into air.

Mass Convection Relations

Under low mass flux conditions, the mass convection coefficients can be determined by either (1) determining the friction or heat transfer coefficient and then using the Chilton–Colburn analogy or (2) picking the appropriate Nusselt number relation for the given geometry and analogous boundary conditions, replacing the Nusselt number with the Sherwood number and the Prandtl number with the Schmidt number, as shown in Table 14–13 for some representative cases. The first approach is obviously more convenient when the friction or heat transfer coefficient is already known. Otherwise,

the second approach should be preferred since it is generally more accurate, and the Chilton–Colburn analogy offers no significant advantage in this case. Relations for convection mass transfer in other geometries can be written similarly using the corresponding heat transfer relation in Chaps. 6 through 9.

TABLE 14–13

Sherwood number relations in mass convection for specified concentration at the surface corresponding to the Nusselt number relations in heat convection for specified surface temperature

Convective Heat Transfer	Convective Mass Transfer
1. *Forced Convection Over a Flat Plate* (*a*) Laminar flow (Re $< 5 \times 10^5$) $\mathrm{Nu} = 0.664\,\mathrm{Re}_L^{0.5}\,\mathrm{Pr}^{1/3}, \quad \mathrm{Pr} > 0.6$	$\mathrm{Sh} = 0.664\,\mathrm{Re}_L^{0.5}\,\mathrm{Sc}^{1/3}, \quad \mathrm{Sc} > 0.6$
(*b*) Turbulent flow ($5 \times 10^5 < \mathrm{Re} < 10^7$) $\mathrm{Nu} = 0.037\,\mathrm{Re}_L^{0.8}\,\mathrm{Pr}^{1/3}, \quad \mathrm{Pr} > 0.6$	$\mathrm{Sh} = 0.037\,\mathrm{Re}_L^{0.8}\,\mathrm{Sc}^{1/3}, \quad \mathrm{Sc} > 0.6$
(*c*) Combined laminar and turbulent flow ($5 \times 10^5 < \mathrm{Re} < 10^7$) $\mathrm{Nu} = (0.037\,\mathrm{Re}_L^{0.8} - 871)\,\mathrm{Pr}^{1/3}, \quad \mathrm{Pr} > 0.6$	$\mathrm{Sh} = (0.037\,\mathrm{Re}_L^{0.8} - 871)\,\mathrm{Sc}^{1/3}, \quad \mathrm{Sc} > 0.6$
2. *Forced Convection Over a Cylinder or a Sphere* (*a*) Cylinder (RePr > 0.2) $\mathrm{Nu} = 0.3 + \dfrac{0.62\,\mathrm{Re}^{1/2}\mathrm{Pr}^{1/3}}{[1 + (0.4/\mathrm{Pr})^{2/3}]^{1/4}}\left[1 + \left(\dfrac{\mathrm{Re}}{282{,}000}\right)^{5/8}\right]^{4/5}$	$\mathrm{Sh} = 0.3 + \dfrac{0.62\,\mathrm{Re}^{1/2}\mathrm{Sc}^{1/3}}{[1 + (0.4/\mathrm{Sc})^{2/3}]^{1/4}}\left[1 + \left(\dfrac{\mathrm{Re}}{282{,}000}\right)^{5/8}\right]^{4/5},$ $\mathrm{ReSc} > 0.2$
(*b*) Sphere ($3.5 < \mathrm{Re} < 8 \times 10^8$, $0.7 < \mathrm{Pr} < 380$, $1.0 < (\mu_\infty/\mu_s) < 3.2$) $\mathrm{Nu} = 2 + [0.4\,\mathrm{Re}^{1/2} + 0.06\,\mathrm{Re}^{2/3}]\,\mathrm{Pr}^{0.4}\left(\dfrac{\mu_\infty}{\mu_s}\right)^{1/4}$	$\mathrm{Sh} = 2 + [0.4\,\mathrm{Re}^{1/2} + 0.06\,\mathrm{Re}^{2/3}]\,\mathrm{Sc}^{0.4}\left(\dfrac{\mu_\infty}{\mu_s}\right)^{1/4},$ $0.7 < \mathrm{Sc} < 380$
3. *Fully Developed Flow in Smooth Circular Pipes* (*a*) Laminar flow (Re < 2300) $\mathrm{Nu} = 3.66$	$\mathrm{Sh} = 3.66$
(*b*) Turbulent flow (Re $> 10{,}000$) $\mathrm{Nu} = 0.023\,\mathrm{Re}^{0.8}\,\mathrm{Pr}^{0.4}, \quad 0.7 < \mathrm{Pr} < 160$	$\mathrm{Sh} = 0.023\,\mathrm{Re}^{0.8}\,\mathrm{Sc}^{0.4}, \quad 0.7 < \mathrm{Sc} < 160$
4. *Natural Convection Over Surfaces* (*a*) Vertical plate $\mathrm{Nu} = 0.59\,(\mathrm{Gr}\,\mathrm{Pr})^{1/4},\ 10^5 < \mathrm{Gr}\,\mathrm{Pr} < 10^9$ $\mathrm{Nu} = 0.1\,(\mathrm{Gr}\,\mathrm{Pr})^{1/3},\ \ 10^9 < \mathrm{Gr}\,\mathrm{Pr} < 10^{13}$	$\mathrm{Sh} = 0.59\,(\mathrm{Gr}\,\mathrm{Sc})^{1/4},\ 10^5 < \mathrm{Gr}\,\mathrm{Sc} < 10^9$ $\mathrm{Sh} = 0.1\,(\mathrm{Gr}\,\mathrm{Sc})^{1/3},\ \ 10^9 < \mathrm{Gr}\,\mathrm{Sc} < 10^{13}$
(*b*) Upper surface of a horizontal plate. Surface is hot ($T_s > T_\infty$) $\mathrm{Nu} = 0.54\,(\mathrm{Gr}\,\mathrm{Pr})^{1/4}, \quad 10^4 < \mathrm{Gr}\,\mathrm{Pr} < 10^7$ $\mathrm{Nu} = 0.15\,(\mathrm{Gr}\,\mathrm{Pr})^{1/3}, \quad 10^7 < \mathrm{Gr}\,\mathrm{Pr} < 10^{11}$	Fluid near the surface is light ($\rho_s < \rho_\infty$) $\mathrm{Sh} = 0.54\,(\mathrm{Gr}\,\mathrm{Sc})^{1/4}, 10^4 < \mathrm{Gr}\,\mathrm{Sc} < 10^7$ $\mathrm{Sh} = 0.15\,(\mathrm{Gr}\,\mathrm{Sc})^{1/3}, 10^7 < \mathrm{Gr}\,\mathrm{Sc} < 10^{11}$
(*c*) Lower surface of a horizontal plate. Surface is hot ($T_s > T_\infty$) $\mathrm{Nu} = 0.27\,(\mathrm{Gr}\,\mathrm{Pr})^{1/4}, \quad 10^5 < \mathrm{Gr}\,\mathrm{Pr} < 10^{11}$	Fluid near the surface is light ($\rho_s < \rho_\infty$) $\mathrm{Sh} = 0.27\,(\mathrm{Gr}\,\mathrm{Sc})^{1/4}, \quad 10^5 < \mathrm{Gr}\,\mathrm{Sc} < 10^{11}$

EXAMPLE 14–11   Mass Convection Over a Flat Plate

Dry air at 40°C and 0.85 atm flows over an 8-m-long wet flat surface with an average velocity of 2.5 m/s in order to dry the surface (Fig. 14–53). Using the analogy between heat and mass transfer, determine the mass transfer coefficient on the plate. Use dry air properties for the mixture at the specified temperature and pressure.

SOLUTION   A wet flat surface is dried by blowing air over it. The mass transfer coefficient is to be determined.

Assumptions   **1** The low mass flux model and thus the analogy between heat and mass transfer is applicable. **2** The critical Reynolds number for flow over a flat plate is 500,000.

Properties   Because of low mass flux conditions, we can use dry air properties for the mixture at the specified temperature of 40°C (313 K) and 1 atm from Table A–15, and correct for the pressure other than 1 atm. The kinematic viscosity of dry air at 0.85 atm is determined to be

$$\nu_{0.85\,atm} = \frac{\nu_{1\,atm}}{P(atm)} = \frac{1.702 \times 10^{-5}\ m^2/s}{0.85\ atm} = 2.0 \times 10^{-5}\ m^2/s$$

The mass diffusivity of water vapor in the air at 313 K is determined from Eq. 14–15 to be

$$D_{AB} = D_{H_2O\text{-air}} = 1.87 \times 10^{-10}\frac{T^{2.072}}{P} = 1.87 \times 10^{-10}\frac{(313\ K)^{2.072}}{0.85\ atm}$$

$$= 3.26 \times 10^{-5}\ m^2/s$$

Analysis   The Reynolds number for this external flow is

$$Re_L = \frac{VL}{\nu} = \frac{(2.5\ m/s)(8\ m)}{2.0 \times 10^{-5}\ m^2/s} = 1.0 \times 10^6 > Re_{cr} = 5 \times 10^5$$

Calculate the critical distance from the leading edge, $x_{cr} = \nu Re_{cr}/V = (2.0 \times 10^{-5}\ m^2/s)$ $(5 \times 10^5)/(2.5\ m/s) = 4\ m$. Thus we have combined laminar and turbulent flow over a flat plate. Using the analogy between heat and mass transfer, the mass transfer version of Eq. 7–24 for this case is (see Table 14–13)

$$Sh = \left(0.037\,Re_L^{0.8} - 871\right)Sc^{1/3} \quad \text{where } 5 \times 10^5 < Re_L < 10^7 \text{ and } Sc > 0.6$$

The Schmidt number in this case is

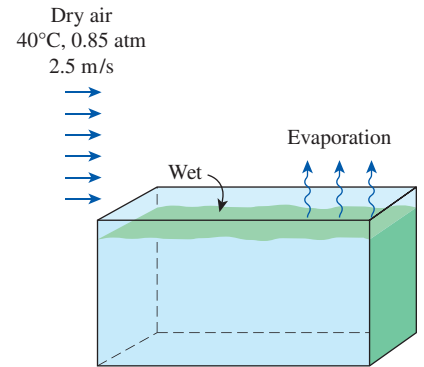$$Sc = \frac{\nu}{D_{AB}} = \frac{2.0 \times 10^{-5}\ m^2/s}{3.26 \times 10^{-5}\ m^2/s} = 0.614$$

And the Sherwood number is calculated to be

$$Sh = \left(0.037\,Re_L^{0.8} - 871\right)Sc^{1/3} = (0.037 \times 1,000,000^{0.8} - 871)(0.614)^{1/3} = 1244$$

Using the definition of Sherwood number, the mass transfer coefficient is determined to be

$$h_{mass} = \frac{Sh\,D_{AB}}{L} = \frac{(1244)(3.26 \times 10^{-5}\ m^2/s)}{8\ m} = \textbf{0.00507 m/s}$$

Discussion   Note that the Nusselt number relations in heat transfer can be used to determine the Sherwood number in mass transfer by replacing the Prandtl number with the Schmidt number.

Dry air
40°C, 0.85 atm
2.5 m/s

Evaporation

Wet

FIGURE 14–53
Schematic for Example 14–11.

Naphthalene
vapor

0.3 m²

Air

1 atm
$T_\infty = 25°C$
$V = 2$ m/s

Body covered
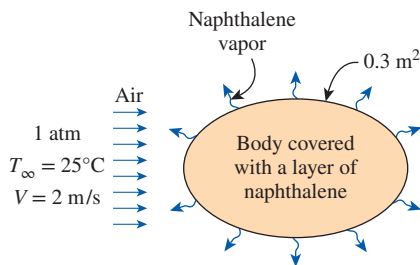with a layer of
naphthalene

FIGURE 14–54
Schematic for Example 14–12.

EXAMPLE 14–12   **Analogy Between Heat and Mass Transfer**

Heat transfer coefficients in complex geometries with complicated boundary conditions can be determined by mass transfer measurements on similar geometries under similar flow conditions using volatile solids such as naphthalene and dichlorobenzene and utilizing the Chilton–Colburn analogy between heat and mass transfer at low mass flux conditions. The amount of mass transfer during a specified time period is determined by weighing the model or measuring the surface recession.

During a certain experiment involving the flow of dry air at 25°C and 1 atm at a free-stream velocity of 2 m/s over a body covered with a layer of naphthalene, it is observed that 12 g of naphthalene has sublimated in 15 min (Fig. 14–54). The surface area of the body is 0.3 m². Both the body and the air were kept at 25°C during the study. The vapor pressure of naphthalene at 25°C is 11 Pa and the mass diffusivity of naphthalene in air at 25°C is $D_{AB} = 0.61 \times 10^{-5}$ m²/s. Determine the heat transfer coefficient under the same flow conditions over the same geometry.

SOLUTION   Air is blown over a body covered with a layer of naphthalene, and the rate of sublimation is measured. The heat transfer coefficient under the same flow conditions over the same geometry is to be determined.
Assumptions   **1** The low mass flux conditions exist so that the Chilton–Colburn analogy between heat and mass transfer is applicable (will be verified). **2** Both air and naphthalene vapor are ideal gases.
Properties   The molar mass of naphthalene is 128.2 kg/kmol. Because of low mass flux conditions, we can use dry air properties for the mixture at the specified temperature of 25°C and 1 atm, at which $\rho = 1.184$ kg/m³, $c_p = 1007$ J/kg·K, and $\alpha = 2.141 \times 10^{-5}$ m²/s (Table A–15).
Analysis   The incoming air is free of naphthalene, and thus the mass fraction of naphthalene at free stream conditions is zero, $w_{A,\infty} = 0$. Noting that the vapor pressure of naphthalene at the surface is 11 Pa, its mass fraction at the surface is determined to be

$$w_{A,s} = \frac{P_{A,s}}{p}\left(\frac{M_A}{M_{air}}\right) = \frac{11 \text{ Pa}}{101{,}325 \text{ Pa}}\left(\frac{128.2 \text{ kg/kmol}}{29 \text{ kg/kmol}}\right) = 4.8 \times 10^{-4}$$

which confirms that the low mass flux approximation is valid. The rate of evaporation of naphthalene in this case is

$$\dot{m}_{evap} = \frac{m}{\Delta t} = \frac{0.012 \text{ kg}}{(15 \times 60\text{s})} = 1.33 \times 10^{-5} \text{ kg/s}$$

Then the mass convection coefficient becomes

$$h_{mass} = \frac{\dot{m}}{\rho A_s(w_{A,s} - w_{A,\infty})} = \frac{1.33 \times 10^{-5} \text{ kg/s}}{(1.184 \text{ kg/m}^3)(0.3 \text{ m}^2)(4.8 \times 10^{-4} - 0)}$$
$$= 0.0780 \text{ m/s}$$

Using the analogy between heat and mass transfer, the average heat transfer coefficient is determined from Eq. 14–89 to be

$$h_{heat} = \rho c_p h_{mass}\left(\frac{\alpha}{D_{AB}}\right)^{2/3}$$

$$= (1.184 \text{ kg/m}^3)(1007 \text{ J/kg·K})(0.0780 \text{ m/s})\left(\frac{2.141 \times 10^{-5} \text{ m}^2/\text{s}}{0.61 \times 10^{-5} \text{ m}^2/\text{s}}\right)^{2/3}$$

$$= \textbf{215 W/m}^2\textbf{·K}$$

Discussion   Because of the convenience it offers, naphthalene has been used in numerous heat transfer studies to determine convection heat transfer coefficients.

14–10 ▪ SIMULTANEOUS HEAT AND MASS TRANSFER

Many mass transfer processes encountered in practice occur isothermally, and thus they do not involve any heat transfer. But some engineering applications involve the vaporization of a liquid and the diffusion of this vapor into the surrounding gas. Such processes require the transfer of the latent heat of vaporization h_{fg} to the liquid in order to vaporize it, and thus such problems involve simultaneous heat and mass transfer. To generalize, any mass transfer problem involving *phase change* (evaporation, sublimation, condensation, melting, etc.) must also involve *heat transfer,* and the solution of such problems needs to be analyzed by considering *simultaneous heat and mass transfer.* Some examples of simultaneous heat and mass problems are drying, evaporative cooling, transpiration (or sweat) cooling, cooling by dry ice, combustion of fuel droplets, and ablation cooling of space vehicles during reentry, and even ordinary events like rain, snow, and hail. In warmer locations, for example, the snow melts and the rain evaporates before reaching the ground (Fig. 14–55).

To understand the mechanism of simultaneous heat and mass transfer, consider the *evaporation of water* from a swimming pool into air. Let us assume that the water and the air are initially at the same temperature. If the air is saturated (a relative humidity of $\phi = 100$ percent), there will be no heat or mass transfer as long as the isothermal conditions remain. But if the air is not saturated ($\phi < 100$ percent), there will be a difference between the concentration of water vapor at the water–air interface (which is always saturated) and some distance above the interface (the concentration boundary layer). Concentration difference is the driving force for mass transfer, and thus this concentration difference drives the water into the air. But the water must vaporize first, and it must absorb the latent heat of vaporization in order to vaporize. Initially, the entire heat of vaporization comes from the water near the interface since there is no temperature difference between the water and the surroundings and thus there cannot be any heat transfer. The temperature of water near the surface must drop as a result of the sensible heat loss, which also drops the saturation pressure and thus vapor concentration at the interface.

This temperature drop creates temperature differences within the water at the top as well as between the water and the surrounding air. These temperature differences drive heat transfer toward the water surface from both the air and the deeper parts of the water, as shown in Fig. 14–56. If the evaporation rate is high and thus the demand for the heat of vaporization is higher than the amount of heat that can be supplied from the lower parts of the water body and the surroundings, the deficit is made up from the sensible heat of the water at the surface, and thus the temperature of water at the surface drops further. The process continues until the latent heat of vaporization equals the heat transfer to the water at the surface. Once the steady operation conditions are reached and the interface temperature stabilizes, the energy balance on a thin layer of liquid at the surface can be expressed as

$$\dot{Q}_{\text{sensible, transferred}} = \dot{Q}_{\text{latent, absorbed}} \quad \text{or} \quad \dot{Q} = \dot{m}_v h_{fg} \tag{14–91}$$

where $\dot{m}_v$ is the rate of evaporation and h_{fg} is the latent heat of vaporization of water at the surface temperature. Various expressions for $\dot{m}_v$ under various approximations are given in Table 14–14. The mixture properties such as the
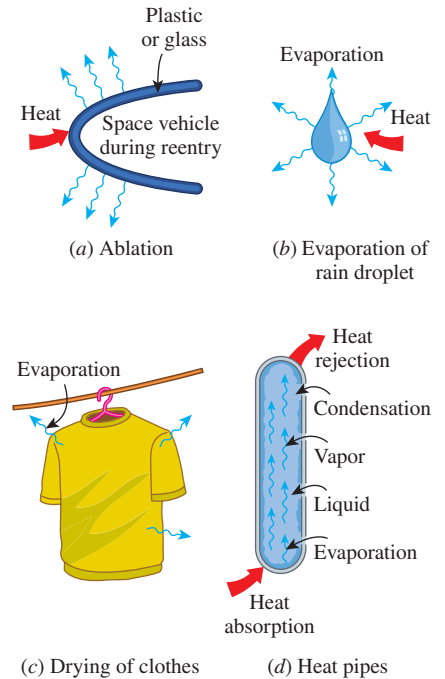

(*a*) Ablation   (*b*) Evaporation of rain droplet

(*c*) Drying of clothes   (*d*) Heat pipes

FIGURE 14–55
Many problems encountered in practice involve simultaneous heat and mass transfer.
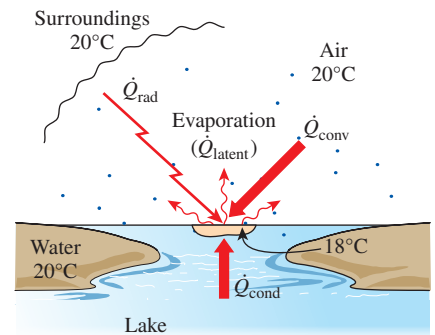

FIGURE 14–56
Various mechanisms of heat transfer involved during the evaporation of water from the surface of a lake.

TABLE 14–14

Various expressions for evaporation rate of a liquid into a gas through an interface area A_s under various approximations (subscript v stands for vapor, s for liquid–gas interface, and ∞ away from surface)

Assumption	Evaporation Rate
General	$\dot{m}_v = h_{mass}A_s(\rho_{v,s} - \rho_{v,\infty})$
Assuming vapor to be an ideal gas, $P_v = \rho_v R_v T$	$\dot{m}_v = \dfrac{h_{mass}A_s}{R_v}\left(\dfrac{P_{v,s}}{T} - \dfrac{P_{v,\infty}}{T_\infty}\right)$
Using Chilton–Colburn analogy, $h_{heat} = \rho c_p h_{mass}Le^{2/3}$	$\dot{m}_v = \dfrac{h_{heat}A_s}{\rho c_p Le^{2/3}R_v}\left(\dfrac{P_{v,s}}{T} - \dfrac{P_{v,\infty}}{T_\infty}\right)$
Using $\dfrac{1}{T_s} - \dfrac{1}{T_\infty} \approx \dfrac{1}{T}$, where $T = \dfrac{T_s + T_\infty}{2}$	$\dot{m}_v = \dfrac{h_{heat}A_s}{c_p Le^{2/3}}\dfrac{M_v}{M}\dfrac{P_{v,s} - P_{v,\infty}}{P}$

specific heat c_p and molar mass M should normally be evaluated at the *mean film composition* and *mean film temperature*. However, when dealing with air–water vapor mixtures at atmospheric conditions or other low mass flux situations, we can simply use the properties of the gas with reasonable accuracy.

The $\dot{Q}$ in Eq. 14–91 represents all forms of heat from all sources transferred to the surface, including convection and radiation from the surroundings and conduction from the deeper parts of the water due to the sensible energy of the water itself or due to heating the water body with a resistance heater, heating coil, or even chemical reactions in the water. If heat transfer from the water body to the surface as well as radiation from the surroundings is negligible, which is often the case, then the heat loss by evaporation must equal heat gain by convection. That is,

$$\dot{Q}_{conv} = \dot{m}_v h_{fg} \quad \text{or} \quad h_{conv}A_s(T_\infty - T_s) = \frac{h_{conv}A_s h_{fg}}{c_p Le^{2/3}}\frac{M_v}{M}\frac{P_{v,s} - P_{v,\infty}}{P}$$

Canceling $h_{conv}A_s$ from both sides of the second equation gives

$$T_s = T_\infty - \frac{h_{fg}}{c_p Le^{2/3}}\frac{M_v}{M}\frac{P_{v,s} - P_{v,\infty}}{P} \tag{14–92}$$

which is a relation for the temperature of the liquid under steady conditions.

1 atm
30°C
40% RH

Wet cloth

SODA
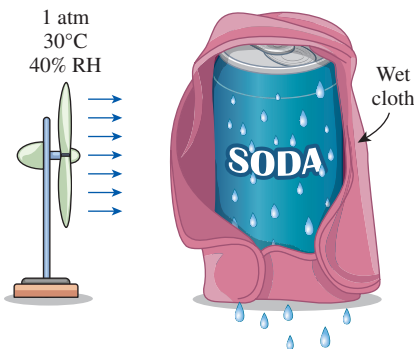
FIGURE 14–57
Schematic for Example 14–13.

EXAMPLE 14–13 **Evaporative Cooling of a Canned Drink**

During a hot summer day, a canned drink is to be cooled by wrapping it in a cloth that is kept wet continually, and blowing air to it by a fan (Fig. 14–57). If the environment conditions are 1 atm, 30°C, and 40 percent relative humidity, determine the temperature of the drink when steady conditions are reached.

SOLUTION Air is blown over a canned drink wrapped in a wet cloth to cool it by simultaneous heat and mass transfer. The temperature of the drink when steady conditions are reached is to be determined.

Assumptions **1** The low mass flux conditions exist so that the Chilton–Colburn analogy between heat and mass transfer is applicable since the mass fraction of vapor in the air is low (about 2 percent for saturated air at 25°C). **2** Both air and water vapor

at specified conditions are ideal gases (the error involved in this assumption is less than 1 percent). **3** Radiation effects are negligible.

Properties Because of low mass flux conditions, we can use dry air properties for the mixture at the average temperature of $(T_\infty + T_s)/2$ which cannot be determined at this point because of the unknown surface temperature T_s. We know that $T_s < T_\infty$ and, for the purpose of property evaluation, we take T_s to be 20°C. Then the properties of water at 20°C and the properties of dry air at the average temperature of 25°C and 1 atm are (Tables A–9 and A–15)

Water: $h_{fg} = 2454$ kJ/kg, $P_v = 2.34$ kPa; also, $P_v = 4.25$ kPa at 30°C

Dry air: $c_p = 1.007$ kJ/kg·°C, $\alpha = 2.141 \times 10^{-5}$ m²/s

The molar masses of water and air are 18 and 29 kg/kmol, respectively (Table A–1). Also, the mass diffusivity of water vapor in air at 25°C is $D_{H_2O\text{-air}} = 2.50 \times 10^{-5}$ m²/s (Table 14–4).

Analysis Utilizing the Chilton–Colburn analogy, the surface temperature of the drink can be determined from Eq. 14–92,

$$T_s = T_\infty - \frac{h_{fg}}{c_p \text{Le}^{2/3}} \frac{M_v}{M} \frac{P_{v,s} - P_{v,\infty}}{P}$$

where the Lewis number is

$$\text{Le} = \frac{\alpha}{D_{AB}} = \frac{2.141 \times 10^{-5} \text{ m}^2/\text{s}}{2.5 \times 10^{-5} \text{ m}^2/\text{s}} = 0.856$$

Note that we could take the Lewis number to be 1 for simplicity, but we chose to incorporate it for better accuracy.

The air at the surface is saturated, and thus the vapor pressure at the surface is simply the saturation pressure of water at the surface temperature (2.34 kPa). The vapor pressure of air away from the surface is

$$P_{v,\infty} = \phi P_{\text{sat} @ T_\infty} = (0.40) P_{\text{sat} @ 30°C} = (0.40)(4.25 \text{ kPa}) = 1.70 \text{ kPa}$$

Noting that the atmospheric pressure is 1 atm = 101.3 kPa, substituting gives

$$T_s = 30°C - \frac{2454 \text{ kJ/kg}}{(1.007 \text{ kJ/kg·K})(0.856)^{2/3}} \frac{18 \text{ kg/kmol}}{29 \text{ kg/kmol}} \frac{(2.34 - 1.70)\text{kPa}}{101.3 \text{ kPa}}$$

$$= \textbf{19.4°C}$$

Therefore, the temperature of the drink can be lowered to 19.4°C by this process.

EXAMPLE 14–14   Heat Loss from Uncovered Hot Water Baths

Hot water baths with open tops are commonly used in manufacturing facilities for various reasons. In a plant that manufactures spray paints, the pressurized paint cans are temperature tested by submerging them in hot water at 50°C in a 40-cm-deep rectangular bath and keeping them there until the cans are heated to 50°C to ensure that the cans can withstand temperatures up to 50°C during transportation and storage (Fig. 14–58). The water bath is 1 m wide and 3.5 m long, and its top surface is open to ambient air to facilitate easy observation for the workers. If the average conditions in the plant are 92 kPa, 25°C, and 52 percent relative humidity, determine the rate of
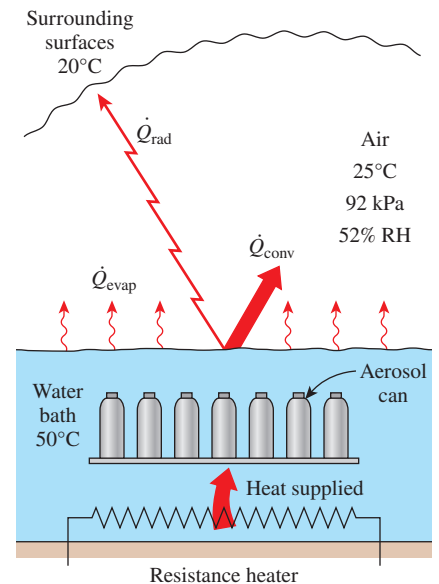
FIGURE 14–58
Schematic for Example 14–14.

heat loss from the top surface of the water bath by (*a*) radiation, (*b*) natural convection, and (*c*) evaporation. Assume the water is well agitated and maintained at a uniform temperature of 50°C at all times by a heater, and take the average temperature of the surrounding surfaces to be 20°C.

SOLUTION Spray paint cans are temperature tested by submerging them in an uncovered hot water bath. The rates of heat loss from the top surface of the bath by radiation, natural convection, and evaporation are to be determined.

Assumptions **1** The low mass flux conditions exist so that the Chilton–Colburn analogy between heat and mass transfer is applicable since the mass fraction of vapor in the air is low (about 2 percent for saturated air at 300 K). **2** Both air and water vapor at specified conditions are ideal gases (the error involved in this assumption is less than 1 percent). **3** Water is maintained at a uniform temperature of 50°C.

Properties Relevant properties for each mode of heat transfer are determined below in respective sections.

Analysis (*a*) The emissivity of liquid water is given in Table A–18 to be 0.95. Then the radiation heat loss from the water to the surrounding surfaces becomes

$$\dot{Q}_{\text{rad}} = \varepsilon A_s \sigma (T_s^4 - T_{\text{surr}}^4)$$
$$= (0.95)(3.5 \text{ m}^2)(5.67 \times 10^{-8} \text{ W/m}^2 \cdot \text{K}^4)[(323 \text{ K})^4 - (293 \text{ K})^4]$$
$$= \textbf{663 W}$$

(*b*) The air–water vapor mixture is dilute, and thus we can use dry air properties for the mixture at the average temperature of $(T_\infty + T_s)/2 = (25 + 50)/2 = 37.5$°C. Noting that the total atmospheric pressure is $92/101.3 = 0.9080$ atm, the properties of dry air at 37.5°C and 0.9080 atm are (Table A–15)

$$k = 0.02644 \text{ W/m·K}, \quad \text{Pr} = 0.7262 \text{ (independent of pressure)}$$
$$\alpha = (2.312 \times 10^{-5} \text{ m}^2/\text{s})/0.9080 = 2.546 \times 10^{-5} \text{ m}^2/\text{s}$$
$$\nu = (1.679 \times 10^{-5} \text{ m}^2/\text{s})/0.9080 = 1.849 \times 10^{-5} \text{ m}^2/\text{s}$$

The properties of water at 50°C are

$$h_{fg} = 2383 \text{ kJ/kg} \quad \text{and} \quad P_v = 12.35 \text{ kPa}$$

The air at the surface is saturated, and thus the vapor pressure at the surface is simply the saturation pressure of water at the surface temperature. The vapor pressure of air far from the water surface is

$$P_{v, \infty} = \phi P_{\text{sat @ } T_\infty} = (0.52)P_{\text{sat @ 25°C}} = (0.52)(3.17 \text{ kPa}) = 1.65 \text{ kPa}$$

Treating the water vapor and the air as ideal gases and noting that the total atmospheric pressure is the sum of the vapor and dry air pressures, the densities of the water vapor, dry air, and their mixture at the water–air interface and far from the surface are determined to be

At the surface:
$$\rho_{v, s} = \frac{P_{v, s}}{R_v T_s} = \frac{12.35 \text{ kPa}}{(0.4615 \text{ kPa·m}^3/\text{kg·K})(323 \text{ K})} = 0.0829 \text{ kg/m}^3$$

$$\rho_{a, s} = \frac{P_{a, s}}{R_a T_s} = \frac{(92 - 12.35) \text{ kPa}}{(0.287 \text{ kPa·m}^3/\text{kg·K})(323 \text{ K})} = 0.8592 \text{ kg/m}^3$$

$$\rho_s = \rho_{v, s} + \rho_{a, s} = 0.0829 + 0.8592 = 0.9421 \text{ kg/m}^3$$

Away from the surface: $\rho_{v,\infty} = \dfrac{P_{v,\infty}}{R_v T_\infty} = \dfrac{1.65 \text{ kPa}}{(0.4615 \text{ kPa·m}^3/\text{kg·K})(298 \text{ K})} = 0.0120 \text{ kg/m}^3$

$$\rho_{a,\infty} = \dfrac{P_{a,\infty}}{R_a T_\infty} = \dfrac{(92 - 1.65) \text{ kPa}}{(0.287 \text{ kPa·m}^3/\text{kg·K})(298 \text{ K})} = 1.0564 \text{ kg/m}^3$$

$$\rho_\infty = \rho_{v,\infty} + \rho_{a,\infty} = 0.0120 + 1.0564 = 1.0684 \text{ kg/m}^3$$

The area of the top surface of the water bath is $A_s = (3.5 \text{ m})(1 \text{ m}) = 3.5 \text{ m}^2$, and its perimeter is $p = 2(3.5 + 1) = 9$ m. Therefore, the characteristic length is

$$L_c = \frac{A_s}{p} = \frac{3.5 \text{ m}^2}{9 \text{ m}} = 0.3889 \text{ m}$$

Then using densities (instead of temperatures) since the mixture is not homogeneous, the Grashof number is

$$\text{Gr} = \frac{g(\rho_\infty - \rho_s)L_c^3}{\rho v^2}$$

$$= \frac{(9.81 \text{ m/s}^2)(1.0684 - 0.9421 \text{ kg/m}^3)(0.3889 \text{ m})^3}{[(0.9421 + 1.0684)/2 \text{ kg/m}^3](1.849 \times 10^{-5} \text{ m}^2/\text{s})^2}$$

$$= 2.121 \times 10^8$$

Recognizing that this is a natural convection problem with hot horizontal surface facing up, the Nusselt number and the convection heat transfer coefficients are determined to be

$$\text{Nu} = 0.15(\text{Gr Pr})^{1/3} = 0.15(2.121 \times 10^8 \times 0.7262)^{1/3} = 80.41$$

$$h_{\text{conv}} = \frac{\text{Nu}k}{L_c} = \frac{(80.41)(0.02644 \text{ W/m·K})}{0.3889 \text{ m}} = 5.47 \text{ W/m}^2\text{·K}$$

Then the natural convection heat transfer rate becomes

$$\dot{Q}_{\text{conv}} = h_{\text{conv}} A_s (T_s - T_\infty)$$

$$= (5.47 \text{ W/m}^2\text{·K})(3.5 \text{ m}^2)(50 - 25)°\text{C} = \textbf{479 W}$$

Note that the magnitude of natural convection heat transfer is comparable to that of radiation, as expected.

(*c*) Utilizing the analogy between heat and mass convection, the mass transfer coefficient is determined the same way by replacing Pr with Sc. The mass diffusivity of water vapor in air at the average temperature of 310.5 K is determined from Eq. 14–15 to be

$$D_{AB} = D_{\text{H}_2\text{O–air}} = 1.87 \times 10^{-10} \frac{T^{2.072}}{P} = 1.87 \times 10^{-10} \frac{310.5^{2.072}}{0.908}$$

$$= 3.00 \times 10^{-5} \text{ m}^2/\text{s}$$

The Schmidt number is

$$\text{Sc} = \frac{v}{D_{AB}} = \frac{1.849 \times 10^{-5} \text{ m}^2/\text{s}}{3.00 \times 10^{-5} \text{ m}^2/\text{s}} = 0.616$$

The Sherwood number and the mass transfer coefficients are determined to be

$$Sh = 0.15(Gr\ Sc)^{1/3} = 0.15(2.121 \times 10^8 \times 0.616)^{1/3} = 76.1$$

$$h_{mass} = \frac{Sh D_{AB}}{L_c} = \frac{(76.1)(3.00 \times 10^{-5}\ \text{m}^2/\text{s})}{0.3889\ \text{m}} = 0.00587\ \text{m/s}$$

Then the evaporation rate and the rate of heat transfer by evaporation become

$$\dot{m}_v = h_{mass} A_s(\rho_{v,s} - \rho_{v,\infty})$$
$$= (0.00587\ \text{m/s})(3.5\ \text{m}^2)(0.0829 - 0.0120)\ \text{kg/m}^3$$
$$= 0.00146\ \text{kg/s} = 5.24\ \text{kg/h}$$

$$\dot{Q}_{evap} = \dot{m}_v h_{fg} = (0.00146\ \text{kg/s})(2383\ \text{kJ/kg}) = 3.479\ \text{kW} = \mathbf{3479\ W}$$

which is more than seven times the rate of heat transfer by natural convection.

Finally, noting that the direction of heat transfer is always from high to low temperature, all forms of heat transfer determined above are in the same direction, and the total rate of heat loss from the water to the surrounding air and surfaces is

$$\dot{Q}_{total} = \dot{Q}_{rad} + \dot{Q}_{conv} + \dot{Q}_{evap} = 663 + 479 + 3479 = 4621\ \text{W}$$

Discussion Note that if the water bath is heated electrically, a 4.6-kW resistance heater will be needed just to make up for the heat loss from the top surface. The total heater size will have to be larger to account for the heat losses from the side and bottom surfaces of the bath as well as the heat absorbed by the spray paint cans as they are heated to 50°C. Also note that water needs to be supplied to the bath at a rate of 5.24 kg/h to make up for the water loss by evaporation. Also, in reality, the surface temperature will probably be a little lower than the bulk water temperature, and thus the heat transfer rates will be somewhat lower than indicated here.

SUMMARY

Mass transfer is the movement of a chemical species from a high-concentration region toward a lower-concentration one relative to the other chemical species present in the medium. Heat and mass transfer are analogous to each other, and several parallels can be drawn between them. The driving forces are the *temperature difference* in heat transfer and the *concentration difference* in mass transfer. Fick's law of mass diffusion is of the same form as Fourier's law of heat conduction. The species generation in a medium due to *homogeneous reactions* is analogous to heat generation. Also, mass convection due to bulk fluid motion is analogous to heat convection. Constant surface temperature corresponds to constant concentration at the surface, and an adiabatic wall corresponds to an impermeable wall. However, concentration is usually not a continuous function at a phase interface.

The concentration of a species A can be expressed in terms of density ρ_A or molar concentration C_A. It can also be expressed in dimensionless form in terms of *mass* or *molar fraction* as

Mass fraction of species A:
$$w_A = \frac{m_A}{m} = \frac{m_A/V}{m/V} = \frac{\rho_A}{\rho}$$

Mole fraction of species A:
$$y_A = \frac{N_A}{N} = \frac{N_A/V}{N/V} = \frac{C_A}{C}$$

In the case of an ideal gas mixture, the mole fraction of a gas is equal to its pressure fraction. *Fick's law* for the diffusion of a species A in a stationary binary mixture of species A and B in a specified direction x is expressed as

Mass basis:
$$j_{diff,A} = \frac{\dot{m}_{diff,A}}{A} = -\rho D_{AB} \frac{d(\rho_A/\rho)}{dx}$$
$$= -\rho D_{AB} \frac{dw_A}{dx}$$

Mole basis:
$$j_{diff,A} = \frac{\dot{N}_{diff,A}}{A} = -C D_{AB} \frac{d(C_A/C)}{dx}$$
$$= -C D_{AB} \frac{dy_A}{dx}$$

where D_{AB} is the *diffusion coefficient* (or *mass diffusivity*) of the species in the mixture, $j_{\text{diff}, A}$ is the diffusive *mass flux* of species A, and $\bar{j}_{\text{diff}, A}$ is the *molar flux.*

The mole fractions of a species i in the gas and liquid phases at the interface of a dilute mixture are proportional to each other and are expressed by *Henry's law* as

$$y_{i, \text{ liquid side}} = \frac{P_{i, \text{ gas side}}}{H}$$

where H is *Henry's constant.* When the mixture is not dilute, an approximate relation for the mole fractions of a species on the liquid and gas sides of the interface are expressed approximately by *Raoult's law* as

$$P_{i, \text{ gas side}} = y_{i, \text{ gas side}} P = y_{i, \text{ liquid side}} P_{i, \text{ sat}}(T)$$

where $P_{i, \text{ sat}}(T)$ is the saturation pressure of the species i at the interface temperature and P is the *total pressure* on the gas phase side.

The interface $C_{i, \text{ solid side}}$ is proportional to the *partial pressure* of the species i in the gas $P_{i, \text{ gas side}}$ on the gas side of the interface and is expressed as

$$C_{i, \text{ solid side}} = \mathscr{S} \times P_{i, \text{ gas side}}$$

where $\mathscr{S}$ is the *solubility.* The product of the *solubility* of a gas and the *diffusion coefficient* of the gas in a solid is referred to as the *permeability* $\mathscr{P}$, which is a measure of the ability of the gas to penetrate a solid.

In the absence of any chemical reactions, the mass transfer rates $\dot{m}_{\text{diff}, A}$ through a plane wall of area A and thickness L and cylindrical and spherical shells of inner and outer radii r_1 and r_2 under one-dimensional steady conditions are expressed as

$$\dot{m}_{\text{diff}, A, \text{ wall}} = \rho D_{AB} A \frac{w_{A, 1} - w_{A, 2}}{L} = D_{AB} A \frac{\rho_{A, 1} - \rho_{A, 2}}{L}$$

$$\dot{m}_{\text{diff}, A, \text{ cyl}} = 2\pi L \rho D_{AB} \frac{w_{A, 1} - w_{A, 2}}{\ln(r_2/r_1)} = 2\pi L D_{AB} \frac{\rho_{A, 1} - \rho_{A, 2}}{\ln(r_2/r_1)}$$

$$\dot{m}_{\text{diff}, A, \text{ sph}} = 4\pi r_1 r_2 \rho D_{AB} \frac{w_{A, 1} - w_{A, 2}}{r_2 - r_1}$$

$$= 4\pi r_1 r_2 D_{AB} \frac{\rho_{A, 1} - \rho_{A, 2}}{r_2 - r_1}$$

The flow rate of a gas through a solid plane wall under steady one-dimensional conditions can also be expressed in terms of the partial pressures of the adjacent gas on the two sides of the solid as

$$\dot{N}_{\text{diff}, A, \text{ wall}} = D_{AB} \mathscr{S}_{AB} A \frac{P_{A, 1} - P_{A, 2}}{L} = \mathscr{P}_{AB} A \frac{P_{A, 1} - P_{A, 2}}{L}$$

where $P_{A, 1}$ and $P_{A, 2}$ are the partial pressures of gas A on the two sides of the wall.

During mass transfer in a *moving medium,* chemical species are transported both by molecular diffusion and by the bulk fluid motion, and the velocities of the species are expressed as

$$V_A = V + V_{\text{diff}, A} \qquad V_B = V + V_{\text{diff}, B}$$

where V is the *mass-average velocity* of the flow. It is the velocity that would be measured by a velocity sensor and is expressed as

$$V = w_A V_A + w_B V_B$$

The special case $V = 0$ corresponds to a *stationary medium.* Using Fick's law of diffusion, the total mass fluxes $j = \dot{m}/A$ in a moving medium are expressed as

$$j_A = \rho_A V + \rho_A V_{\text{diff}, A} = w_A(j_A + j_B) - \rho D_{AB} \frac{dw_A}{dx}$$

$$j_B = \rho_B V + \rho_B V_{\text{diff}, B} = w_B(j_A + j_B) - \rho D_{BA} \frac{dw_B}{dx}$$

The *rate of mass convection* of species A in a binary mixture is expressed in an analogous manner to Newton's law of cooling as

$$\dot{m}_{\text{conv}} = h_{\text{mass}} A_s(\rho_{A, s} - \rho_{A, \infty}) = h_{\text{mass}} \rho A_s(w_{A, s} - w_{A, \infty})$$

where h_{mass} is the average *mass transfer coefficient,* in m/s.

The counterparts of the Prandtl and Nusselt numbers in mass convection are the *Schmidt number* Sc and the *Sherwood number* Sh, defined as

$$\text{Sc} = \frac{\nu}{D_{AB}} = \frac{\text{Momentum diffusivity}}{\text{Mass diffusivity}} \quad \text{and} \quad \text{Sh} = \frac{h_{\text{mass}} L_c}{D_{AB}}$$

The relative magnitudes of heat and mass diffusion in the thermal and concentration boundary layers are represented by the *Lewis number,* defined as

$$\text{Le} = \frac{\text{Sc}}{\text{Pr}} = \frac{\alpha}{D_{AB}} = \frac{\text{Thermal diffusivity}}{\text{Mass diffusivity}}$$

Heat and mass transfer coefficients are sometimes expressed in terms of the dimensionless *Stanton number,* defined as

$$\text{St} = \frac{h_{\text{conv}}}{\rho V c_p} = \text{Nu} \frac{1}{\text{Re Pr}} \quad \text{and} \quad \text{St}_{\text{mass}} = \frac{h_{\text{mass}}}{V} = \text{Sh} \frac{1}{\text{Re Sc}}$$

where V is the free-stream velocity in external flow and the bulk mean fluid velocity in internal flow. For a given geometry and boundary conditions, the Sherwood number in natural or forced convection can be determined from the corresponding Nusselt number expression by simply replacing the Prandtl number with the Schmidt number. But in natural convection, the Grashof number should be expressed in terms of density difference instead of temperature difference.

When the molecular diffusivities of momentum, heat, and mass are identical, we have $\nu = \alpha = D_{AB}$, and thus $\text{Pr} = \text{Sc} = \text{Le} = 1$. The similarity between momentum, heat, and mass transfer in this case is given by the *Reynolds analogy,* expressed as

$$\frac{f}{2} \text{Re} = \text{Nu} = \text{Sh} \quad \text{or}$$

$$\frac{f}{2} \frac{V_\infty L}{\nu} = \frac{h_{\text{heat}} L}{k} = \frac{h_{\text{mass}} L}{D_{AB}} \quad \text{or} \quad \frac{f}{2} = \text{St} = \text{St}_{\text{mass}}$$

For the general case of $\text{Pr} \neq \text{Sc} \neq 1$, it is modified as

$$\frac{f}{2} = \text{St Pr}^{2/3} = \text{St}_{\text{mass}} \text{Sc}^{2/3}$$

which is known as the *Chilton–Colburn analogy*. The analogy between heat and mass transfer is expressed more conveniently as

$$h_{\text{heat}} = \rho c_p \text{Le}^{2/3} \, h_{\text{mass}} = \rho c_p \, (\alpha/D_{AB})^{2/3} \, h_{\text{mass}}$$

For air–water vapor mixtures, $\text{Le}^{2/3} \cong 1$, and thus this relation simplifies further. The heat–mass convection analogy is limited to *low mass flux* cases in which the flow rate of species undergoing mass flow is low relative to the total flow rate of the liquid or gas mixture. The mass transfer problems that involve phase change (evaporation, sublimation, condensation, melting, etc.) also involve heat transfer, and such problems are analyzed by considering heat and mass transfer simultaneously.

REFERENCES AND SUGGESTED READING

1. American Society of Heating, Refrigeration, and Air Conditioning Engineers. *Handbook of Fundamentals.* Atlanta, GA: ASHRAE, 1993.

2. R. M. Barrer. *Diffusion In and Through Solids.* New York: Macmillan, 1941.

3. R. B. Bird. "Theory of Diffusion." *Advances in Chemical Engineering* 1 (1956), p. 170.

4. R. B. Bird, W. E. Stewart, and E. N. Lightfoot. *Transport Phenomena.* New York: John Wiley & Sons, 1960.

5. S. Cai, L. Cremaschi, and A. J. Ghajar. "Pipe Insulation Thermal Conductivity Under Dry and Wet Condensing Conditions with Moisture Ingress: A Critical Review." *HVAC&R Research* 20(4) (2014), pp. 458–479.

6. S. Cai, L. Cremaschi, and A. J. Ghajar. "Moisture Accumulation and Its Impact on the Thermal Performance of Pipe Insulation for Chilled Water Pipes in High Performance Buildings." *Proceedings of the International Refrigeration and Air Conditioning Conference at Purdue,* July 16–19, 2012.

7. L. Cremaschi, S. Cai, K. M. Worthington, and A. J. Ghajar. "Measurements of Pipe Insulation Thermal Conductivity at Below Ambient Temperatures Part 1: Experimental Methodology and Dry Tests." *ASHRAE Transactions* 118 (2012), pp. 1061–1076.

8. C. J. Geankoplis. *Mass Transport Phenomena.* New York: Holt, Rinehart, and Winston, 1972.

9. *Handbook of Chemistry and Physics,* 56th ed. Cleveland, OH: Chemical Rubber Publishing Co., 1976.

10. J. O. Hirshfelder, F. Curtis, and R. B. Bird. *Molecular Theory of Gases and Liquids.* New York: John Wiley & Sons, 1954.

11. *International Critical Tables.* Vol. 3. New York: McGraw-Hill, 1928.

12. W. M. Kays, M. E. Crawford, and B. Weigand. *Convective Heat and Mass Transfer,* 4th ed. New York: McGraw-Hill, 2005.

13. T. R. Marrero and E. A. Mason. "Gaseous Diffusion Coefficients." *Journal of Phys. Chem. Ref. Data* 1 (1972), pp. 3–118.

14. A. F. Mills. *Basic Heat and Mass Transfer.* Burr Ridge, IL: Richard D. Irwin, 1995.

15. J. H. Perry, ed. *Chemical Engineer's Handbook,* 4th ed. New York: McGraw-Hill, 1963.

16. R. D. Reid, J. M. Prausnitz, and T. K. Sherwood. *The Properties of Gases and Liquids,* 3rd ed. New York: McGraw-Hill, 1977.

17. A. H. P. Skelland. *Diffusional Mass Transfer.* New York: John Wiley & Sons, 1974.

18. D. B. Spalding. *Convective Mass Transfer.* New York: McGraw-Hill, 1963.

19. W. F. Stoecker and J. W. Jones. *Refrigeration and Air Conditioning.* New York: McGraw-Hill, 1982.

20. L. C. Thomas. *Mass Transfer Supplement—Heat Transfer.* Englewood Cliffs, NJ: Prentice Hall, 1991.

21. L. Van Black. *Elements of Material Science and Engineering.* Reading, MA: Addison-Wesley, 1980.

PROBLEMS*

*Problems designated by a "C" are concept questions, and students are encouraged to answer them all. Problems designated by an "E" are in English units, and the SI users can ignore them. Problems with the icon are comprehensive in nature and are intended to be solved with appropriate software. Problems with the PtD icon are Prevention through Design problems. Problems with the C&S icon are Codes and Standards problems.

Analogy Between Heat and Mass Transfer

14–1C How is the concentration of a commodity defined? How is the concentration gradient defined? How is the diffusion rate of a commodity related to the concentration gradient?

14–2C Give examples for (*a*) liquid-to-gas, (*b*) solid-to-liquid, (*c*) solid-to-gas, and (*d*) gas-to-liquid mass transfer.

14–3C What is the driving force for (*a*) heat transfer, (*b*) electric current flow, (*c*) fluid flow, and (*d*) mass transfer?

14–4C Both Fourier's law of heat conduction and Fick's law of mass diffusion can be expressed as $\dot{Q} = -kA(dT/dx)$. What do the quantities $\dot{Q}$, k, A, and T represent in (*a*) heat conduction and (*b*) mass diffusion?

14–5C How does mass transfer differ from bulk fluid flow? Can mass transfer occur in a homogeneous medium?

14–6C What do (*a*) homogeneous reactions and (*b*) heterogeneous reactions represent in mass transfer? To what do they correspond in heat transfer?

Mass Diffusion

14–7C Someone claims that the mass and the mole fractions for a mixture of CO_2 and N_2O gases are identical. Do you agree? Explain.

14–8C Mark these statements as being True or False for a binary mixture of substances *A* and *B*.

_____(*a*) The density of a mixture is always equal to the sum of the densities of its constituents.

_____(*b*) The ratio of the density of component *A* to the density of component *B* is equal to the mass fraction of component *A*.

_____(*c*) If the mass fraction of component *A* is greater than 0.5, then at least half of the moles of the mixture are component *A*.

_____(*d*) If the molar masses of *A* and *B* are equal to each other, then the mass fraction of *A* will be equal to the mole fraction of *A*.

_____(*e*) If the mass fractions of *A* and *B* are both 0.5, then the molar mass of the mixture is simply the arithmetic average of the molar masses of *A* and *B*.

14–9C Fick's law of diffusion is expressed on the mass and mole basis as $\dot{m}_{diff,\ A} = -\rho A D_{AB}(dw_A/dx)$ and $\dot{N}_{diff,\ A} = -CAD_{AB}(dy_A/dx)$, respectively. Are the diffusion coefficients D_{AB} in the two relations the same or different?

14–10C How does the mass diffusivity of a gas mixture change with (*a*) temperature and (*b*) pressure?

14–11C At a given temperature and pressure, do you think the mass diffusivity of air in water vapor will be equal to the mass diffusivity of water vapor in air? Explain.

14–12C At a given temperature and pressure, do you think the mass diffusivity of copper in aluminum will be equal to the mass diffusivity of aluminum in copper? Explain.

14–13C In a mass production facility, steel components are to be hardened by carbon diffusion. Would you carry out the hardening process at room temperature or in a furnace at a high temperature, say 900°C? Why?

14–14 Determine the maximum mass fraction of calcium bicarbonate $[Ca(HCO_3)_2]$ in water at 300 K.

14–15 The composition of moist air is given on a molar basis to be 78 percent N_2, 20 percent O_2, and 2 percent water vapor. Determine the mass fractions of the constituents of air. *Answers:* 76.4 percent N_2, 22.4 percent O_2, 1.2 percent H_2O

14–16 The molar analysis of a gas mixture at 290 K and 250 kPa is 65 percent N_2, 20 percent O_2, and 15 percent CO_2. Determine the mass fraction and partial pressure of each gas.

14–17E A gas mixture consists of 7 lbm of O_2, 8 lbm of N_2, and 10 lbm of CO_2. Determine (*a*) the mass fraction of each component, (*b*) the mole fraction of each component, and (*c*) the average molar mass of the mixture.

14–18 ⬛C&S The Environmental Protection Agency (EPA) sets the particle pollution level for the National Ambient Air Quality Standards (NAAQS) to protect the public health (40 CFR part 50). For atmospheric particulates that are less than 2.5 μm ($PM_{2.5}$), the NAAQS set the pollutant level in ambient air at 35 μg/m³ for an average time of one day. Beyond that level, $PM_{2.5}$ becomes a harmful pollutant to public health and the environment. If the mass fraction of $PM_{2.5}$ is 0.62 mg/kg in an ambient air at 0°C, determine whether the level of $PM_{2.5}$ is above the limit set by the NAAQS.

14–19 A gas mixture consists of 10 kmol of H_2 and 2 kmol of N_2. Determine the mass of each gas and the apparent gas constant of the mixture.

14–20 ⬛C&S The Clean Air Act requires the Environmental Protection Agency (EPA) to set the National Ambient Air Quality Standards (NAAQS) for harmful pollutants in ambient air (40 CFR part 50). Carbon monoxide (CO) is one of the principal pollutants listed by the NAAQS. For public health protection, the level of CO in ambient air set by the NAAQS is 35 parts per million (ppm) by volume for an average time of one hour. Beyond that level, CO is considered harmful to public health and the environment. If the partial pressures of CO and air is in the ratio of 0.01:0.99, determine whether the CO is at a level greater than 35 ppm set by the NAAQS.

14–21 ⬛C&S Lead (Pb) is one of the principal pollutants that the Clean Air Act (40 CFR part 50) requires the Environmental Protection Agency (EPA) to list in the National Ambient Air Quality Standards (NAAQS). The level of Pb in ambient air set by the NAAQS is 0.15 μg/m³ for an average time of three months to protect public health and the environment. Beyond that level, Pb is considered harmful to public health and the environment. If the level of Pb found in the ambient air of a residential place at 20°C is 0.005 mol/kmol for over a period of three months, determine whether the level of Pb is harmful. The molar mass of Pb is 207.2 kg/kmol.

14–22 ⬛C&S The Environmental Protection Agency (EPA) sets the particle pollution level for the National Ambient Air Quality Standards (NAAQS) to protect public health and the environment (40 CFR part 50). For

atmospheric particulates that are less than 10 µm (PM_{10}), the NAAQS set the pollutant level in ambient air at 150 µg/m³ for an average time of one day. Beyond that level, PM_{10} becomes a harmful pollutant to public health and the environment. Consider an environment where the PM_{10} soot particulate molar concentration is found to be 0.01 mol/m³ in ambient air at 20°C. Determine whether the level of PM_{10} soot particulates is harmful. The molar mass of soot is 12.01 kg/kmol.

14–23 C&S Sulfur dioxide (SO_2) is one of the principal pollutants that the Environmental Protection Agency (EPA) has listed in the National Ambient Air Quality Standards (NAAQS), as required by the Clean Air Act (40 CFR part 50). The level of SO_2 in ambient air set by the NAAQS is 0.5 parts per million (ppm) by volume for an average time of 3 h to protect public welfare. Beyond that level the SO_2 becomes a harmful pollutant to the environment. If the mass fraction of SO_2 in an ambient air at 20°C is 0.5 mg/kg, determine whether the level of SO_2 is above the limit set by the NAAQS.

14–24 Determine the binary diffusion coefficient of CO_2 in air at (*a*) 200 K and 1 atm, (*b*) 400 K and 0.5 atm, and (*c*) 600 K and 5 atm.

14–25 Repeat Prob. 14–24 for O_2 in N_2.

14–26 Determine the binary diffusion coefficient for (*a*) carbon dioxide in nitrogen, (*b*) carbon dioxide in oxygen, and (*c*) carbon dioxide in hydrogen at 320 K and 2 atm.

14–27 The diffusion coefficient of hydrogen in steel is given as a function of temperature as

$$D_{AB} = 1.65 \times 10^{-6} \exp(-4630/T) \ (\text{m}^2/\text{s})$$

where *T* is in K. Determine the diffusion coefficients at 300 K, 500 K, 1000 K, and 1500 K.

14–28 Reconsider Prob. 14–27. Using appropriate software, plot the diffusion coefficient as a function of the temperature in the range of 200 K to 1200 K.

Boundary Conditions

14–29C Consider the free surface of a lake exposed to the atmosphere. If the air at the lake surface is saturated, will the mole fraction of water vapor in air at the lake surface be the same as the mole fraction of water in the lake (which is nearly 1)?

14–30C When prescribing a boundary condition for mass transfer at a solid–gas interface, why do we need to specify the side of the surface (whether the solid or the gas side)? Why did we not do it in heat transfer?

14–31C Write three boundary conditions for mass transfer (on a mass basis) for species A at $x = 0$ that correspond to specified temperature, specified heat flux, and convection boundary conditions in heat transfer.

14–32C What is an impermeable surface in mass transfer? How is it expressed mathematically (on a mass basis)? To what does it correspond in heat transfer?

14–33C Using solubility data of a solid in a specified liquid, explain how you would determine the mass fraction of the solid in the liquid at the interface at a specified temperature.

14–34C Using Henry's constant data for a gas dissolved in a liquid, explain how you would determine the mole fraction of the gas dissolved in the liquid at the interface at a specified temperature.

14–35C Using properties of saturated water, explain how you would determine the mole fraction of water vapor at the surface of a lake when the temperature of the lake surface and the atmospheric pressure are specified.

14–36C Using solubility data of a gas in a solid, explain how you would determine the molar concentration of the gas in the solid at the solid–gas interface at a specified temperature.

14–37C What is permeability? How is the permeability of a gas in a solid related to the solubility of the gas in that solid?

14–38 Determine the mole fraction of carbon dioxide (CO_2) dissolved in water at the surface of water at 300 K. The mole fraction of CO_2 in air is 0.006, and the local atmosphere pressure is 100 kPa.

14–39E Water is sprayed into air at 80°F and 14.3 psia, and the falling water droplets are collected in a container on the floor. Determine the mass and mole fractions of air dissolved in the water.

14–40 Consider a glass of water in a room at 15°C and 97 kPa. If the relative humidity in the room is 100 percent and the water and the air are in thermal and phase equilibrium, determine (*a*) the mole fraction of the water vapor in the air and (*b*) the mole fraction of air in the water.

14–41E Determine the mole fraction of the water vapor at the surface of a lake whose temperature at the surface is 70°F, and compare it to the mole fraction of water in the lake. Take the atmospheric pressure at lake level to be 13.8 psia.

14–42 Determine the mole fraction of dry air at the surface of a lake whose temperature is 18°C. Take the atmospheric pressure at lake level to be 100 kPa.

14–43 Reconsider Prob. 14–42. Using appropriate software, plot the mole fraction of dry air at the surface of the lake as a function of the lake temperature as the temperature varies from 5°C to 30°C, and discuss the results.

14–44 Consider a carbonated drink in a bottle at 37°C and 130 kPa. Assuming the gas space above the liquid consists of a saturated mixture of CO_2 and water vapor and treating the drink as water, determine (*a*) the mole fraction of the water vapor in the CO_2 gas and (*b*) the mass of dissolved CO_2 in a 200-ml drink. *Answers: (a)* 4.9 percent, *(b)* 0.28 g
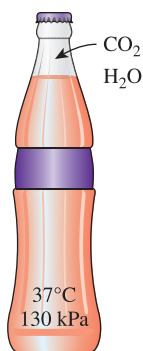
FIGURE P14–44

14–45 Consider a rubber plate that is in contact with nitrogen gas at 298 K and 250 kPa. Determine the molar and mass densities of nitrogen in the rubber at the interface. *Answers:* 0.0039 kmol/m³, 0.1092 kg/m³

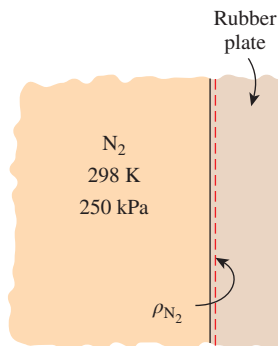**FIGURE P14–45**

14–46 A wall made of natural rubber separates O_2 and N_2 gases at 25°C and 750 kPa. Determine the molar concentrations of O_2 and N_2 in the wall.

14–47 Hydrogen gas at 750 kPa and 85°C is stored in a spherical nickel vessel. The vessel is situated in a surrounding of atmospheric air at 1 atm. Determine the molar and mass concentrations of hydrogen in the nickel at the inner and outer surfaces of the vessel.

14–48 Pure nitrogen gas at 200 kPa and 25°C is flowing inside a long circular rubber pipe. The atmospheric air surrounding the pipe is at 1 atm and 25°C, with 79 percent nitrogen and 21 percent oxygen. Determine the molar concentrations of (*a*) nitrogen and (*b*) oxygen in the rubber at the inner and outer surfaces of the pipe.

14–49 Consider a nickel wall separating hydrogen gas that is maintained on one side at 5 atm and on the opposite at 3 atm.

If the temperature is constant at 85°C, determine (*a*) the mass densities of hydrogen gas in the nickel wall on both sides and (*b*) the mass densities of hydrogen outside the nickel wall on both sides.
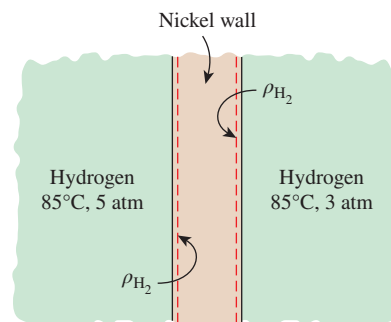

FIGURE P14–49

14–50 Consider a rubber membrane separating carbon dioxide gas that is maintained on one side at 2 atm and on the opposite at 1 atm. If the temperature is constant at 25°C, determine (*a*) the molar densities of carbon dioxide in the rubber membrane on both sides and (*b*) the molar densities of carbon dioxide outside the rubber membrane on both sides.
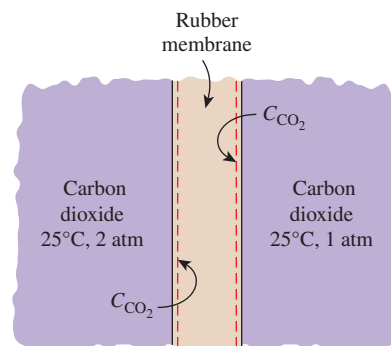

FIGURE P14–50

14–51 A 2-mm-thick, 5-L vessel made of nickel is used to store hydrogen gas at 358 K and 300 kPa. If the total inner surface area of the vessel is 1600 cm², determine the rate of gas loss from the nickel vessel via mass diffusion. Also, determine the fraction of the hydrogen lost by mass diffusion after one year of storage.

14–52 Hydrogen gas at 85°C is maintained at constant pressures of 5 atm and 3 atm on opposite sides of a 0.1-mm-thick nickel wall. Determine the molar diffusion rate per unit area through the nickel wall.
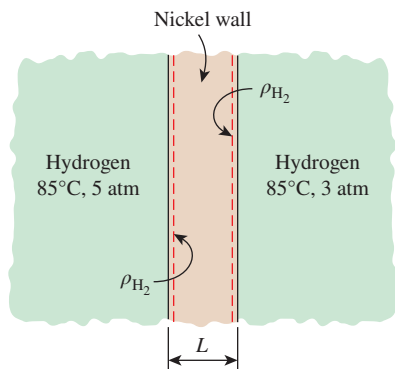
FIGURE P14–52

14–53 During cold weather periods, vapor in a room diffuses through the dry wall and condenses in the adjoining insulation. This process decreases the thermal resistance and degrades the insulation. Consider a condition at which the vapor pressure in the air at 25°C inside a room is 3 kPa, and the vapor pressure in the insulation is negligible. The 3-m-high and 10-m-wide dry wall is 12 mm thick with a solubility of water vapor in the wall material of approximately 0.007 kmol/m³·bar, and the diffusion coefficient of water vapor in the wall is 0.2×10^{-9} m²/s. Determine the mass diffusion rate of water vapor through the wall.
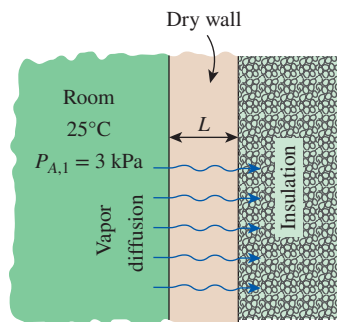

FIGURE P14–53

Steady Mass Diffusion Through a Wall

14–54C Consider one-dimensional mass diffusion of species *A* through a plane wall. Does the species *A* content of the wall change during steady mass diffusion? How about during transient mass diffusion?

14–55C Write down the relations for steady one-dimensional heat conduction and mass diffusion through a plane wall, and identify the quantities in the two equations that correspond to each other.

14–56C Consider steady one-dimensional mass diffusion through a wall. Mark these statements as being True or False.
_____(*a*) Other things being equal, the higher the density of the wall, the higher the rate of mass transfer.

_____(*b*) Other things being equal, doubling the thickness of the wall will double the rate of mass transfer.
_____(*c*) Other things being equal, the higher the temperature, the higher the rate of mass transfer.
_____(*d*) Other things being equal, doubling the mass fraction of the diffusing species at the high concentration side will double the rate of mass transfer.

14–57 A thin plastic membrane separates hydrogen from air. The molar concentrations of hydrogen in the membrane at the inner and outer surfaces are determined to be 0.045 and 0.002 kmol/m³, respectively. The binary diffusion coefficient of hydrogen in plastic at the operation temperature is 5.3×10^{-10} m²/s. Determine the mass flow rate of hydrogen by diffusion through the membrane under steady conditions if the thickness of the membrane is (*a*) 2 mm and (*b*) 0.5 mm.

14–58 [PtD] Exposure to high concentrations of gaseous ammonia can cause lung damage. The acceptable short-term ammonia exposure level set by the Occupational Safety and Health Administration (OSHA) is 35 ppm for 15 min. Consider a vessel filled with gaseous ammonia at 30 mol/L, and a 10-cm-diameter circular plastic plug with a thickness of 2 mm is used to contain the ammonia inside the vessel. The ventilation system is capable of keeping the room safe with fresh air, provided that the rate of ammonia being released is below 0.2 mg/s. If the diffusion coefficient of ammonia through the plug is 1.3×10^{-10} m²/s, determine whether or not the plug can safely contain the ammonia inside the vessel.

14–59 The solubility of hydrogen gas in steel in terms of its mass fraction is given as $w_{H_2} = 2.09 \times 10^{-4} \exp(-3950/T) P_{H_2}^{0.5}$ where P_{H_2} is the partial pressure of hydrogen in bars and *T* is the temperature in K. If natural gas is transported in a 1-cm-thick, 3-m-internal-diameter steel pipe at 500 kPa pressure and the mole fraction of hydrogen in the natural gas is 8 percent, determine the highest rate of hydrogen loss through a 100-m-long section of the pipe at steady conditions at a temperature of 293 K if the pipe is exposed to air. Take the diffusivity of hydrogen in steel to be 2.9×10^{-13} m²/s. *Answer:* 3.98×10^{-14} kg/s

14–60 [💻] Reconsider Prob. 14–59. Using appropriate software, plot the highest rate of hydrogen loss as a function of the mole fraction of hydrogen in natural gas as the mole fraction varies from 5 to 20 percent, and discuss the results.

14–61 Pure hydrogen gas, at 25°C, is flowing through an iron pipe with an inner diameter of 25 mm. The iron pipe is 10 m long and has a wall thickness of 5 mm. If the concentration of hydrogen in the iron pipe at the inner surface is 0.1 kmol/m³ and negligible at the outer surface, determine the diffusion rate of hydrogen through the pipe wall, in kg/s.

14–62 [💻] Reconsider Prob. 14–61. Using appropriate software, evaluate the effect of pipe wall thickness on the diffusion rate of hydrogen through the pipe wall. By varying the pipe wall thickness from 0.5 to 10 mm, plot the diffusion rate of hydrogen through the pipe wall as a function of wall thickness.

14–63 Pure helium gas is stored at 20°C in the cylindrical Pyrex tank of 2 m in length with an inner diameter of 12 cm and a wall thickness of 2.5 mm. A helium detector situated beside the tank has detected a steady leakage of helium at 1.8×10^{-6} g over the duration of an hour. Assume that both ends of the tank are impermeable surfaces and the concentration of helium at the tank outer surface is negligible. Determine the concentration of helium at the inner surface of the tank.

14–64 Helium gas is stored at 293 K in a 3-m-outer-diameter spherical container made of 3-cm-thick Pyrex. The molar concentration of helium in the Pyrex is 0.00069 kmol/m³ at the inner surface and negligible at the outer surface. Determine the mass flow rate of helium by diffusion through the Pyrex container.
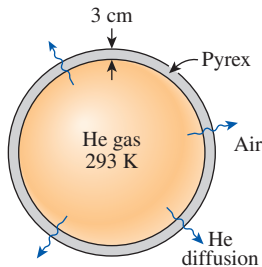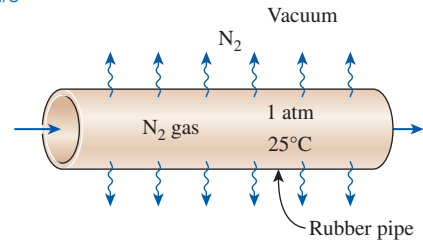

FIGURE P14–64

14–65 **PtD** Hydrogen can cause fire hazards, and hydrogen gas leaking into surrounding air can lead to spontaneous ignition with extremely hot flames. Even at very low leakage rate, hydrogen can sustain combustion causing extended fire damages. Hydrogen gas is lighter than air, so if a leakage occurs it accumulates under roofs and forms explosive hazards. To prevent such hazards, buildings containing source of hydrogen must have adequate ventilation system and hydrogen sensors. Consider a metal spherical vessel, with an inner diameter of 5 m and a thickness of 3 mm, containing hydrogen gas at 2000 kPa. The vessel is situated in a room with atmospheric air at 1 atm. The ventilation system for the room is capable of keeping the air fresh, provided that the rate of hydrogen leakage is below 5 μg/s. If the diffusion coefficient and solubility of hydrogen gas in the metal vessel are 1.5×10^{-12} m²/s and 0.005 kmol/m³·bar, respectively, determine whether or not the vessel is safely containing the hydrogen gas.

14–66 Helium gas is stored at 293 K and 500 kPa in a 1-cm-thick, 2-m-inner-diameter spherical tank made of fused silica (SiO_2). The area where the container is located is well ventilated. Determine (a) the mass flow rate of helium by diffusion through the tank and (b) the pressure drop in the tank in one week as a result of the loss of helium gas.

14–67 Pure N_2 gas at 1 atm and 25°C is flowing through a 10-m-long, 3-cm-inner diameter pipe made of 2-mm-thick rubber. Determine the rate at which N_2 leaks out of the pipe if the medium surrounding the pipe is (a) a vacuum and (b)

atmospheric air at 1 atm and 25°C with 21 percent O_2 and 79 percent N_2. *Answers:* (a) 2.28×10^{-10} kmol/s, (b) 4.78×10^{-11} kmol/s

FIGURE P14–67

14–68 You probably have noticed that balloons inflated with helium gas rise in the air the first day during a party but they fall down the next day and act like ordinary balloons filled with air. This is because the helium in the balloon slowly leaks out through the wall while air leaks in by diffusion.

Consider a balloon that is made of 0.2-mm-thick soft rubber and has a diameter of 15 cm when inflated. The pressure and temperature inside the balloon are initially 120 kPa and 25°C. The permeability of rubber to helium, oxygen, and nitrogen at 25°C are $9.4 \times 10^{-13}, 7.05 \times 10^{-13}$, and 2.6×10^{-13} kmol/m·s·bar, respectively. Determine the initial rates of diffusion of helium, oxygen, and nitrogen through the balloon wall and the mass fraction of helium that escapes the balloon during the first 5 h, assuming the helium pressure inside the balloon remains nearly constant. Assume air to be 21 percent oxygen and 79 percent nitrogen by mole numbers, and take the room conditions to be 100 kPa and 25°C.

FIGURE P14–68

14–69 Reconsider the balloon discussed in Prob. 14–68. Assuming the volume to remain constant and disregarding the diffusion of air into the balloon, obtain a relation for the variation of pressure in the balloon with time. Using the results

obtained and the numerical values given in the problem, determine how long it will take for the pressure inside the balloon to drop to 100 kPa.

Water Vapor Migration in Buildings

14–70C What are the adverse effects of excess moisture on the wood and metal components of a house and the paint on the walls?

14–71C How does the condensation or freezing of water vapor in the wall affect the effectiveness of the insulation in the wall? How does the moisture content affect the effective thermal conductivity of soil?

14–72C Moisture migration in the walls, floors, and ceilings of buildings is controlled by vapor barriers or vapor retarders. Explain the difference between the two, and discuss which is more suitable for use in the walls of residential buildings.

14–73C Why are the insulations on the chilled water lines always wrapped with vapor barrier jackets?

14–74C Consider a tank that contains moist air at 3 atm and whose walls are permeable to water vapor. The surrounding air at 1 atm pressure also contains some moisture. Is it possible for the water vapor to flow into the tank from surroundings? Explain.

14–75C Explain how vapor pressure of the ambient air is determined when the temperature, total pressure, and relative humidity of the air are given.

14–76C Express the mass flow rate of water vapor through a wall of thickness L in terms of the partial pressure of water vapor on both sides of the wall and the permeability of the wall to the water vapor.

14–77 A glass of milk left on top of a counter in the kitchen at 15°C, 88 kPa, and 50 percent relative humidity is tightly sealed by a sheet of 0.009-mm-thick aluminum foil whose permeance is 2.9×10^{-12} kg/s·m²·Pa. The inner diameter of the glass is 12 cm. Assuming the air in the glass to be saturated at all times, determine how much the level of the milk in the glass will recede in 12 h. *Answer:* 0.0011 mm
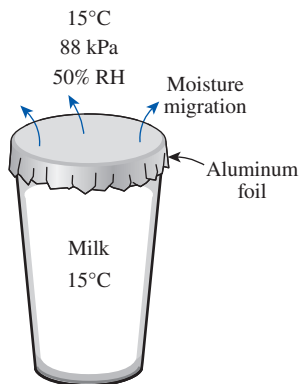

15°C
88 kPa
50% RH
Moisture migration

Aluminum foil

Milk
15°C

FIGURE P14–77

14–78 Consider a 20-cm-thick brick wall of a house. The indoor conditions are 25°C and 40 percent relative humidity, while the outside conditions are 50°C and 40 percent relative humidity. Assuming that there is no condensation or freezing within the wall, determine the amount of moisture flowing through a unit surface area of the wall during a 24-h period.

14–79 The roof of a house is 15 m × 8 m and is made of a 30-cm-thick concrete layer. The interior of the house is maintained at 25°C and 50 percent relative humidity and the local atmospheric pressure is 100 kPa. Determine the amount of water vapor that will migrate through the roof in 24 h if the average outside conditions during that period are 3°C and 30 percent relative humidity. The permeability of concrete to water vapor is 24.7×10^{-12} kg/s·m·Pa.

14–80 Reconsider Prob. 14–79. Using appropriate software, investigate the effects of temperature and relative humidity of air inside the house on the amount of water vapor that will migrate through the roof. Let the temperature vary from 10°C to 30°C and the relative humidity from 30 to 70 percent. Plot the amount of water vapor that will migrate as functions of the temperature and the relative humidity, and discuss the results.

14–81 Reconsider Prob. 14–79. In order to reduce the migration of water vapor, the inner surface of the wall is painted with vapor retarder latex paint whose permeance is 26×10^{-12} kg/s·m²·Pa. Determine the amount of water vapor that will diffuse through the roof in this case during a 24-h period.

14–82 The diffusion of water vapor through plaster boards and its condensation in the wall insulation in cold weather are of concern since they reduce the effectiveness of insulation. Consider a house that is maintained at 20°C and 60 percent relative humidity at a location where the atmospheric pressure is 97 kPa. The inside of the walls is finished with 9.5-mm-thick gypsum wallboard. Taking the vapor pressure at the outer side of the wallboard to be zero, determine the maximum amount of water vapor that will diffuse through a 3-m × 8-m section of a wall during a 24-h period. The permeance of the 9.5-mm-thick gypsum wallboard to water vapor is 2.86×10^{-9} kg/s·m²·Pa.
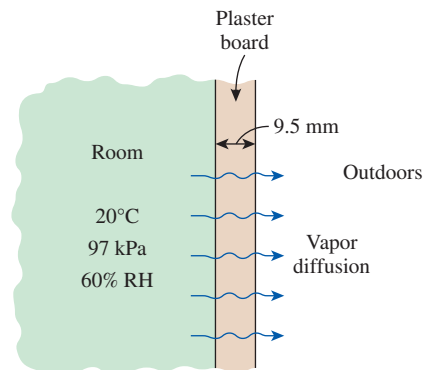

Plaster board

9.5 mm

Room

Outdoors

20°C
97 kPa
60% RH

Vapor diffusion

FIGURE P14–82

14–83 Reconsider Prob. 14–82. In order to reduce the migration of water vapor through the wall, it is proposed to use a 0.051-mm-thick polyethylene film with a permeance of 9.1×10^{-12} kg/s·m²·Pa. Determine the amount of water vapor that will diffuse through the wall in this case during a 24-h period. *Answer:* 26.4 g

Transient Mass Diffusion

14–84C In transient mass diffusion analysis, can we treat the diffusion of a solid into another solid of finite thickness (such as the diffusion of carbon into an ordinary steel component) as a diffusion process in a semi-infinite medium? Explain.

14–85C When the density of a species A in a semi-infinite medium is known at the beginning and at the surface, explain how you would determine the concentration of the species A at a specified location and time.

14–86C Define the penetration depth for mass transfer, and explain how it can be determined at a specified time when the diffusion coefficient is known.

14–87 A thick wall made of natural rubber is exposed to pure oxygen gas on one side of its surface. Both the wall and oxygen gas are isothermal at 25°C, and the oxygen concentration at the wall surface is constant. Determine the time required for the oxygen concentration at $x = 5$ mm to reach 5 percent of its concentration at the wall surface.
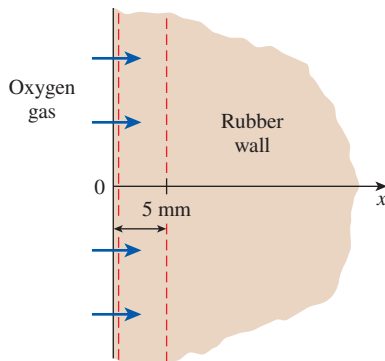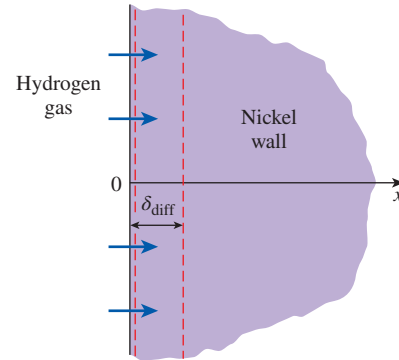

FIGURE P14–87

14–88 Reconsider Prob. 14–87. Using appropriate software, evaluate the oxygen concentration with varying time and distance from the wall surface. By varying the distance from the wall surface for $0 \le x \le 2$ cm, for $t = 10{,}000$ s, $50{,}000$ s, and $150{,}000$ s, plot the oxygen concentration ratio, $C_A(x,t)/C_{A,s}$, as a function of the distance from the surface, x.

14–89 Consider a piece of steel undergoing a decarburization process at 925°C. The mass diffusivity of carbon in steel at 925°C is 1×10^{-7} cm²/s. Determine the depth below the surface of the steel at which the concentration of carbon is reduced to 40 percent from its initial value as a result of

the decarburization process for (*a*) an hour and (*b*) 10 hours. Assume the concentration of carbon at the surface is zero throughout the decarburization process.

14–90 A thick nickel wall is exposed to pure hydrogen gas at 165°C on one side of its surface. The hydrogen concentration at the wall surface is constant. Determine the hydrogen concentration at the penetration depth in percentage of its concentration at the wall surface.

FIGURE P14–90

14–91 Reconsider Prob. 14–90. Using appropriate software, evaluate the hydrogen concentration with varying time and distance from the wall surface. By varying the elapsed time for $0 \le t \le 150{,}000$ s, for $x = 0.5$, 1.0, and 2.0 mm, plot the hydrogen concentration ratio, $C_A(x,t)/C_{A,s}$, as a function of the elapsed time.

14–92 A long nickel bar with a diameter of 5 cm has been stored in a hydrogen-rich environment at 358 K and 300 kPa for a long time, and thus it contains hydrogen gas throughout uniformly. Now the bar is taken into a well-ventilated area so that the hydrogen concentration at the outer surface remains at almost zero at all times. Determine how long it will take for the hydrogen concentration at the center of the bar to drop by half. The diffusion coefficient of hydrogen in the nickel bar at the room temperature of 298 K can be taken to be $D_{AB} = 1.2 \times 10^{-12}$ m²/s. *Answer:* 3.3 years

14–93 **PtD** When handling corrosive and toxic substances, chemical-resistant gloves should be worn. When selecting gloves to handle a substance, the suitability of the gloves should be considered. Depending on the material of the gloves, they could be easily permeable by some substances. An employee is handling tetrachloroethylene solution for a metal-cleaning process. Dermal exposure to tetrachloroethylene can cause skin irritation, and long-term exposure to it can have adverse neurological effects on humans. As a protective measure, the employee wears rubber-blend gloves while handling the tetrachloroethylene solution. The average thickness of the gloves is 0.67 mm, and the mass diffusivity of tetrachloroethylene in the gloves is 3×10^{-8} m²/s. Estimate how long the

employee's hand can be in contact with the tetrachloroethylene solution before the concentration of the solution at the inner glove surface reaches 1 percent of the concentration at the outer surface. Is this type of glove suitable for handling tetrachloroethylene solution?

14–94 A layer of glucose is submerged under a deep layer of water at 25°C. As the layer of glucose dissolves in the water, its density at the glucose-water interface is maintained constant. Determine (a) the time required for the glucose concentration at $x = 1$ cm to reach 1 percent of its concentration at the glucose–water interface and (b) the penetration depth of glucose in water in the duration of time calculated in part (a).
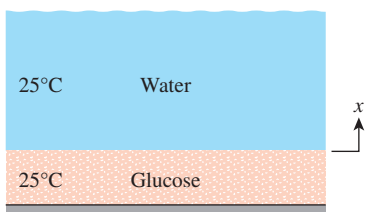

FIGURE P14–94

14–95 An accidental leakage caused benzene to spill into a water reservoir. A layer of benzene is formed on the surface of the water at 20°C. As the layer of benzene dissolves in the water, its concentration at the benzene–water interface remains constant. The equilibrium mass concentration of benzene at the benzene–water interface is 5 kg/m³. The Environmental Protection Agency (EPA) sets the standards for the National Primary Drinking Water Regulations (NPDWR) that apply to public water systems. The drinking water regulations limit the levels of contaminants in drinking water to protect public health. The maximum contaminant level for benzene in drinking water, set by the NPDWR, is 0.005 mg/L. Determine the time duration for the benzene concentration to reach the maximum contaminant level set by the NPDWR at a water depth of $x = 10$ cm measured from the benzene–water interface.

14–96 Benzene is spilled over the floor of a tiny room at 25°C. As the layer of benzene dissolves in the air inside the tiny room, its concentration at the benzene–air interface remains constant. The equilibrium concentration of benzene at the benzene–air interface is 2 percent by mass. Benzene is considered a toxic and hazardous substance by the Occupational Safety and Health Administration (OSHA). According to OSHA's Occupational Safety and Health Standards (1910.1028 App A), the maximum short-term exposure limit is 5 parts of benzene vapor per million parts of air for any 15-minute period. Determine the time duration for the

benzene concentration to reach the maximum short-term exposure limit set by OSHA at a height of $x = 1.5$ m measured from the benzene–air interface. The molar mass of benzene is 78.11 kg/kmol.

14–97 A steel part whose initial carbon content is 0.10 percent by mass is to be case-hardened in a furnace at 1150 K by exposing it to a carburizing gas. The diffusion coefficient of carbon in steel is strongly temperature dependent, and at the furnace temperature it is given to be $D_{AB} = 7.2 \times 10^{-12}$ m²/s. Also, the mass fraction of carbon at the exposed surface of the steel part is maintained at 0.011 by the carbon-rich environment in the furnace. If the hardening process is to continue until the mass fraction of carbon at a depth of 0.6 mm is raised to 0.32 percent, determine how long the part should be held in the furnace.
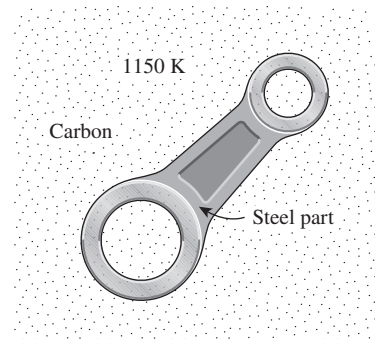

FIGURE P14–97

14–98 Repeat Prob. 14–97 for a furnace temperature of 500 K at which the diffusion coefficient of carbon in steel is $D_{AB} = 2.1 \times 10^{-20}$ m²/s.

14–99 A pond with an initial oxygen content of zero is to be oxygenated by forming a tent over the water surface and filling the tent with oxygen gas at 25°C and 110 kPa. Determine the mole fraction of oxygen at a depth of 0.8 cm from the surface after 24 h.
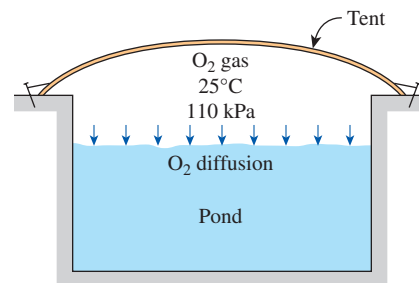

FIGURE P14–99

14–100 A heated piece of steel, with a uniform initial carbon concentration of 0.20 percent by mass, was exposed to a carburizing atmosphere for an hour. Throughout the entire process, the carbon concentration on the surface was 0.70 percent. If the mass diffusivity of carbon in steel in this process was uniform at 1×10^{-11} m²/s, determine the percentage of mass concentration of carbon at 0.2 mm and 0.4 mm below the surface after the process. *Answers:* 0.428 percent, 0.268 percent

14–101 A large pond, at a temperature of 25°C, has an initial uniform oxygen density of 2 kg/m³. During an aeration process, the pond surface has its oxygen density suddenly increased to 9 kg/m³. Determine the oxygen density at 5 cm below the pond surface after 100 h of aeration.

Diffusion in a Moving Medium

14–102C What is diffusion velocity? How does it affect the mass-average velocity? Can the velocity of a species in a moving medium relative to a fixed reference point be zero in a moving medium? Explain.

14–103C What is the difference between mass-average velocity and mole-average velocity during mass transfer in a moving medium? If one of these velocities is zero, will the other also necessarily be zero? Under what conditions will these two velocities be the same for a binary mixture?

14–104C Define the following terms: mass-average velocity, diffusion velocity, stationary medium, and moving medium.

14–105C Consider one-dimensional mass transfer in a moving medium that consists of species A and B with $\rho = \rho_A + \rho_B = $ constant. Mark these statements as being True or False.
_____(*a*) The rates of mass diffusion of species A and B are equal in magnitude and opposite in direction.
_____(*b*) $D_{AB} = D_{BA}$.
_____(*c*) During equimolar counterdiffusion through a tube, equal numbers of moles of A and B move in opposite directions, and thus a velocity measurement device placed in the tube will read zero.
_____(*d*) The lid of a tank containing propane gas (which is heavier than air) is left open. If the surrounding air and the propane in the tank are at the same temperature and pressure, no propane will escape the tank, and no air will enter.

14–106C What is Stefan flow? Write the expression for Stefan's law and indicate what each variable represents.

14–107 A researcher is using a 5-cm-diameter Stefan tube to measure the mass diffusivity of chloroform in air at 25°C and 1 atm. Initially, the liquid chloroform surface was 7.00 cm from the top of the tube; after 10 h elapsed, the liquid chloroform surface was 7.44 cm from the top of the tube, which corresponds to 222 g of chloroform being diffused. At 25°C, the chloroform vapor pressure is 0.263 atm, and the concentration of chloroform is zero at the top of the tube. If the molar mass of chloroform is 119.39 kg/kmol, determine the mass diffusivity of chloroform in air.
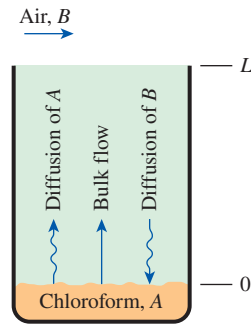

Air, B

Diffusion of A — Bulk flow — Diffusion of B

— L

— 0

Chloroform, A

FIGURE P14−107

14–108E A 1-in-diameter Stefan tube is used to measure the binary diffusion coefficient of water vapor in air at 80°F and 13.8 psia. The tube is partially filled with water with a distance from the water surface to the open end of the tube of 10 in. Dry air is blown over the open end of the tube so that water vapor rising to the top is removed immediately and the concentration of vapor at the top of the tube is zero. During 10 days of continuous operation at constant pressure and temperature, the amount of water that has evaporated is measured to be 0.0025 lbm. Determine the diffusion coefficient of water vapor in air at 80°F and 13.8 psia.

14–109 [PtD] Benzene is classified by the U.S. Department of Health and Human Services (DHHS) as a carcinogen. Exposure to benzene increases the risk of cancer and other illnesses in humans. The Occupational Safety and Health Administration (OSHA) has established that action should be taken when the benzene level in air reaches 0.5 ppm. A lab technician has poured liquid benzene ($M = 78.11$ kg/kmol) into 10 test tubes with an inner diameter of 25 mm. Each test tube holds an equal amount of liquid benzene at a level of 1 cm from the top. The benzene vapor pressure is 10 kPa, and evaporation of benzene to the surrounding air is occurring at 25°C and 1 atm. The HVAC system for the laboratory is capable of keeping the air fresh, provided that the rate of benzene vapor being evaporated is below 3 g/h. Determine whether or not the benzene evaporation rate from all 10 test tubes would present health risks to the people in the laboratory.

14–110 The mass diffusivity of ethanol ($\rho = 789$ kg/m³ and $M = 46$ kg/kmol) through air was determined in a Stefan tube. The tube has a uniform cross-sectional area of 0.8 cm². Initially, the ethanol surface was 10 cm from the top of the tube; after 10 hours elapsed, the ethanol surface was 25 cm from the top of the tube, which corresponds to 0.0445 cm³ of ethanol being evaporated. The ethanol vapor pressure is 0.0684 atm, and the concentration of ethanol is zero at the top of the tube. If the entire process was operated at 24°C and 1 atm, determine the mass diffusivity of ethanol in air.
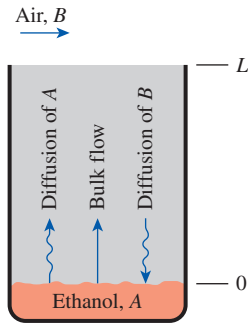
Air, B

FIGURE P14–110

14–111 Methanol ($\rho = 791$ kg/m^3 and $M = 32$ kg/kmol) undergoes evaporation in a vertical tube with a uniform cross-sectional area of 0.8 c m^2. At the top of the tube, the methanol concentration is zero, and its surface is 30 cm from the top of the tube (Fig. P14–111). The methanol vapor pressure is 17 kPa, with a mass diffusivity of $D_{AB} = 0.162$ cm^2/s in air. The evaporation process is operated at 25°C and 1 atm. (*a*) Determine the evaporation rate of the methanol in kg/h and (*b*) plot the mole fraction of methanol vapor as a function of the tube height, from the methanol surface ($x = 0$) to the top of the tube ($x = L$).
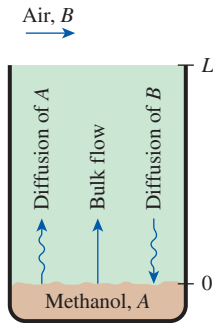
Air, B

FIGURE P14–111

14–112 A tank with a 2-cm-thick shell contains hydrogen gas at the atmospheric conditions of 25°C and 90 kPa. The charging valve of the tank has an internal diameter of 3 cm and extends 8 cm above the tank. If the lid of the tank is left open so that hydrogen and air can undergo equimolar counterdiffusion through the 10-cm-long passageway, determine the mass flow rate of hydrogen lost to the atmosphere through the valve at the initial stages of the process. *Answer:* 4.20 × 10^{-8} kg/s

14–113 Reconsider Prob. 14–112. Using appropriate software, plot the mass flow rate of hydrogen lost as a function of the diameter of the charging valve as the diameter varies from 1 cm to 10 cm, and discuss the results.

14–114 An 8-cm-internal-diameter, 30-cm-high pitcher half-filled with water is left in a dry room at 10°C and 0.92 atm

with its top open. If the water is maintained at 10°C at all times also, determine how long it will take for the water to evaporate completely.

FIGURE P14–114
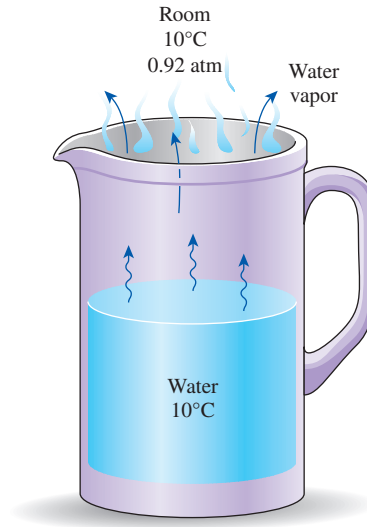
14–115 A large tank containing ammonia at 1 atm and 25°C is vented to the atmosphere through a 2-m-long tube whose internal diameter is 1.5 cm. Determine the rate of loss of ammonia and the rate of infiltration of air into the tank.

14–116E The pressure in a pipeline that transports helium gas at a rate of 7 lbm/s is maintained at 14.5 psia by venting helium to the atmosphere through a 0.4-in-internal-diameter tube that extends 30 ft into the air. Assuming both the helium and the atmospheric air to be at 80°F, determine (*a*) the mass flow rate of helium lost to the atmosphere through the tube, (*b*) the mass flow rate of air that infiltrates into the pipeline, and (*c*) the flow velocity at the bottom of the tube where it is attached to the pipeline that will be measured by an anemometer in steady operation.
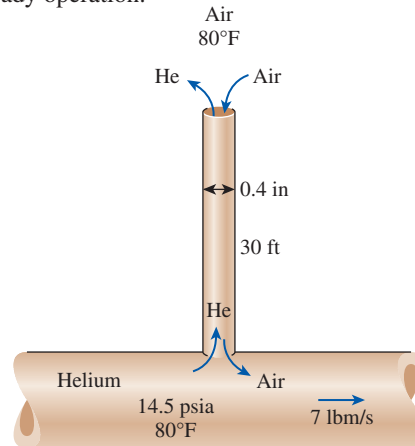

FIGURE P14–116E

14–117E Repeat Prob. 14–116E for a pipeline that transports carbon dioxide instead of helium.

Mass Convection

14–118C What is a concentration boundary layer? How is it defined for flow over a plate?

14–119C What is the physical significance of the Schmidt number? How is it defined? To what dimensionless number does it correspond in heat transfer? What does a Schmidt number of 1 indicate?

14–120C What is the physical significance of the Lewis number? How is it defined? What does a Lewis number of 1 indicate?

14–121C Under what conditions will the normalized velocity, thermal, and concentration boundary layers coincide during flow over a flat plate?

14–122C Heat convection is expressed by Newton's law of cooling as $\dot{Q} = hA_s(T_s - T_\infty)$. Express mass convection in an analogous manner on a mass basis, and identify all the quantities in the expression and state their units.

14–123C What is the physical significance of the Sherwood number? How is it defined? To what dimensionless number does it correspond in heat transfer? What does a Sherwood number of 1 indicate for a plane fluid layer?

14–124C In natural convection mass transfer, the Grashof number is evaluated using density difference instead of temperature difference. Can the Grashof number evaluated this way be used in heat transfer calculations also?

14–125C What is the relation $(f/2)$ Re = Nu = Sh known as? Under what conditions is it valid? What is the practical importance of it?

14–126C What is the name of the relation $f/2 = \text{St Pr}^{2/3} = \text{St}_{\text{mass}} \text{Sc}^{2/3}$, and what are the names of the variables in it? Under what conditions is it valid? What is the importance of it in engineering?

14–127C Using the analogy between heat and mass transfer, explain how the mass transfer coefficient can be determined from the relations for the heat transfer coefficient.

14–128C What is the relation $h_{\text{heat}} = \rho c_p h_{\text{mass}}$ known as? For what kind of mixtures is it valid? What is the practical importance of it?

14–129C What is the low mass flux approximation in mass transfer analysis? Can the evaporation of water from a lake be treated as a low mass flux process?

14–130 A flat plate made of rubber separates carbon dioxide gas at 25°C from air. On the surface exposed to air, there is mass convection. Determine the mass concentration gradient of carbon dioxide at the plate surface that is exposed to air, if the mass flux of CO_2 through the rubber plate is 4.43×10^{-11} kmol/s·m².

14–131 Consider a wet concrete patio covered with a thin film of water. At the surface, mass convection of water to air occurs at an average mass transfer coefficient of 0.03 m/s. If the air is at 1 atm, 15°C and 35 percent relative humidity, determine the mass fraction concentration gradient of water at the surface.

14–132 A fluid with a free stream velocity of 2 m/s is flowing over a surface of a body with characteristic length of 2 m. The flow conditions are maintained at 298 K and 1 atm, and the average mass transfer convection is 0.015 m/s. Determine the average Reynolds number, Schmidt number, Sherwood number, and friction coefficient for (*a*) air flowing over the surface coated with water (evaporation) and (*b*) air flowing over the surface coated with naphthalene (sublimation). Assume the mass diffusivity of naphthalene in air is 0.61×10^{-5} m²/s.

14–133 The average heat transfer coefficient for airflow over an odd-shaped body is to be determined by mass transfer measurements and using the Chilton–Colburn analogy between heat and mass transfer. The experiment is conducted by blowing dry air at 1 atm at a free-stream velocity of 2 m/s over a body covered with a layer of naphthalene. The surface area of the body is 0.75 m², and it is observed that 100 g of naphthalene has sublimated in 45 min. During the experiment, both the body and the air were kept at 25°C, at which the vapor pressure and mass diffusivity of naphthalene are 11 Pa and $D_{AB} = 0.61 \times 10^{-5}$ m²/s, respectively. Determine the heat transfer coefficient under the same flow conditions over the same geometry.
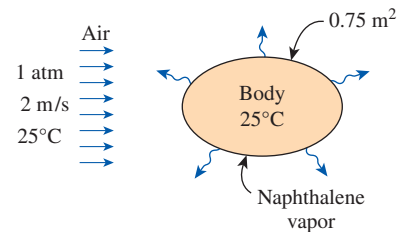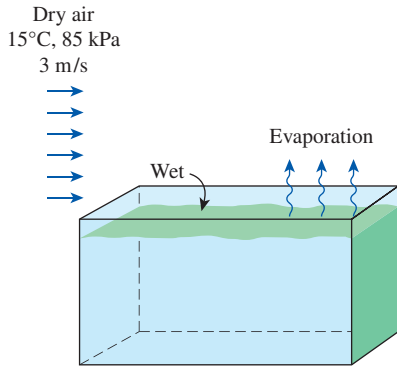

FIGURE P14–133

14–134 The local convection heat transfer coefficient for air flowing parallel over a 1-m-long plate with irregular surface topology is experimentally determined to be $h_x = 0.5 + 12x - 0.7x^3$, where h_x is in W/m²·K. If the plate surface is coated with water, determine the corresponding average mass convection coefficient over the entire plate. Assume properties can be evaluated at 298 K and 1 atm.

14–135 Ethyl alcohol is spilled and spread over a flat table into a layer approximately 1 m in diameter. Dry air at 25°C and 1 atm flows over the ethyl alcohol surface with a free-stream velocity of 1 m/s. Determine the average mass transfer coefficient of ethyl alcohol in air.

14–136 Dry air at 15°C and 85 kPa flows over a 2-m-long wet surface with a free-stream velocity of 3 m/s. Determine the average mass transfer coefficient.   *Answer:* 0.00463 m/s

FIGURE P14–136

14–137 A thin slab of solid salt (NaCl) with dimensions of $0.15 \text{ m} \times 0.15 \text{ m}$ is being dragged through seawater ($\nu = 1.022 \times 10^{-6} \text{ m}^2/\text{s}$) at an average relative velocity of 0.6 m/s. The seawater at 18°C has a salt concentration of 31 kg/m^3, while the salt slab has a concentration of $35,000 \text{ kg/m}^3$. If the diffusion coefficient of salt in seawater is $1.2 \times 10^{-9} \text{ m}^2/\text{s}$, determine the mass convection rate of salt being dissolved in the seawater.

14–138 In a manufacturing facility, 50-cm × 50-cm wet brass plates coming out of a water bath are to be dried by passing them through a section where dry air at 1 atm and 25°C is blown parallel to their surfaces at 6 m/s. If the plates are at 15°C and there are no dry spots, determine the rate of evaporation from both sides of a plate.
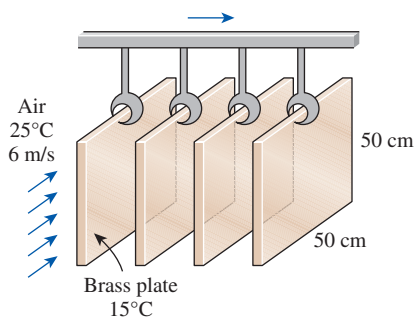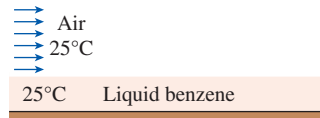

FIGURE P14–138

14–139E Air at 80°F, 1 atm, and 30 percent relative humidity is blown over the surface of a 15-in × 15-in square pan filled with water at a free stream velocity of 10 ft/s. If the water is maintained at a uniform temperature of 80°F, determine the rate of evaporation of water and the amount of heat that needs to be supplied to the water to maintain its temperature constant.

14–140E Repeat Prob. 14–139E for a temperature of 60°F for both the air and water.

14–141 Consider a 5-m × 5-m wet concrete patio with an average water film thickness of 0.2 mm. Now wind at 50 km/h is blowing over the surface. If the air is at 1 atm, 15°C, and 35 percent relative humidity, determine how long it will take for the patio to dry completely.

14–142 [PtD] Benzene ($M = 78.11$ kg/kmol) is a carcinogen, and exposure to benzene increases the risk of cancer and other illnesses in humans. A truck transporting liquid benzene was involved in an accident that spilled the liquid on a flat highway. The liquid benzene formed a pool approximately 10 m in diameter on the highway. On this particular windy day at 25°C and 1 atm with an average wind velocity of 10 m/s, the liquid benzene surface is experiencing mass transfer to air by convection. Nearby is a residential area that is downwind and could be affected by the benzene vapor. Local health officials say that if the benzene level in the air reaches 500 kg within an hour of the spill, residents should be evacuated from the area. If the benzene vapor pressure is 10 kPa, estimate the mass transfer rate of benzene being convected to the air, and determine whether the residents should be evacuated or not.

FIGURE P14–142

14–143 Air at 40°C and 1 atm flows over an 8-m-long wet plate with an average velocity of 2.5 m/s in order to dry the surface. Using the analogy between heat and mass transfer, determine the mass transfer coefficient on the plate.

14–144E A 2-in-diameter spherical naphthalene ball is suspended in a room at 1 atm and 80°F. Determine the average mass transfer coefficient between the naphthalene and the air if air is forced to flow over naphthalene with a free-stream velocity of 15 ft/s. The Schmidt number of naphthalene in air at room temperature is 2.35.   *Answer:* 0.0524 ft/s

14–145 Consider a 3-mm-diameter raindrop that is falling freely in atmospheric air at 25°C. Taking the temperature of the raindrop to be 9°C, determine the terminal velocity of the raindrop at which the drag force equals the weight of the drop and the average mass transfer coefficient at that time.

14–146E Consider a circular pipe of inner diameter $D = 0.7$ in whose inner surface is covered with a thin layer of liquid water as a result of condensation. In order to dry the pipe, air at 540 R and 1 atm is forced to flow through it with an

average velocity of 6 ft/s. Using the analogy between heat and mass transfer, determine the mass transfer coefficient inside the pipe for fully developed flow. *Answer: 0.017 ft/s*

14–147 Consider a circular pipe of inner diameter $D = 0.015$ m whose inner surface is covered with a layer of liquid water as a result of condensation. In order to dry the pipe, air at 300 K and 1 atm is forced to flow through it with an average velocity of 1.2 m/s. Using the analogy between heat and mass transfer, determine the mass transfer coefficient inside the pipe for fully developed flow.
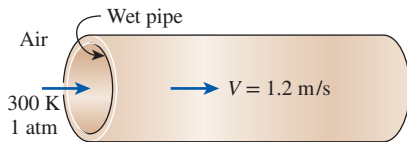

FIGURE P14–147

14–148 Consider a 12-cm-internal-diameter, 14-m-long circular duct whose interior surface is wet. The duct is to be dried by forcing dry air at 1 atm and 15°C through it at an average velocity of 3 m/s. The duct passes through a chilled room, and it remains at an average temperature of 15°C at all times. Determine the mass transfer coefficient in the duct.

14–149 Reconsider Prob. 14–148. Using appropriate software, plot the mass transfer coefficient as a function of the air velocity as the velocity varies from 1 m/s to 8 m/s, and discuss the results.

14–150 **C&S** The Environmental Protection Agency (EPA) sets the standards for the National Primary Drinking Water Regulations (NPDWR) that apply to public water systems. The drinking water regulations limit the levels of contaminants in drinking water to protect public health. The maximum contaminant level for lead in drinking water, set by the NPDWR, is 0.015 mg/L. Above that, additional steps are required to treat the water before it is considered safe for the public. A circular metal pipe with an inner diameter of 2 cm and a length of 100 m is used to transport drinking water. Water flows in the pipe at an average velocity of 0.1 m/s at 20°C. The pipe contains traces of lead, where at the inner pipe surface the mass concentration of lead in water is 5 g/m³. Determine whether the water from the pipe has a safe level of lead as per the NPDWR. The diffusion coefficient for lead in water is 3.6×10^{-10} m²/s.

14–151 **C&S** A circular copper tube with an inner diameter of 2 cm and a length of 100 m is used to transport drinking water. Water flows in the tube at an average velocity of 0.11 m/s at 20°C. At the inner tube surface, the mass concentration of copper in water is 50 g/m³. The Environmental Protection Agency (EPA) sets the standards for the National Primary Drinking Water Regulations (NPDWR) that apply to public water systems. The drinking water

regulations limit the levels of contaminants in drinking water to protect public health. The maximum contaminant level for copper in drinking water, set by the NPDWR, is 1.3 mg/L. Above that, additional steps are required to treat the water before it is considered safe for the public. Determine whether the water from the tube has a safe level of copper as per the NPDWR. The diffusion coefficient for copper in water is 1.5×10^{-9} m²/s.

Simultaneous Heat and Mass Transfer

14–152C Does a mass transfer process have to involve heat transfer? Describe a process that involves both heat and mass transfer.

14–153C During evaporation from a water body to air, under what conditions will the latent heat of vaporization be equal to convection heat transfer from the air?

14–154C Consider a shallow body of water. Is it possible for this water to freeze during a cold and dry night even when the ambient air and surrounding surface temperatures never drop to 0°C? Explain.

14–155E During a hot summer day, a 2-L bottle drink is to be cooled by wrapping it in a cloth kept wet continually and blowing air to it with a fan. If the environment conditions are 1 atm, 80°F, and 30 percent relative humidity, determine the temperature of the drink when steady conditions are reached.

14–156 Jugs made of porous clay were commonly used to cool water in the past. A small amount of water that leaks out keeps the outer surface of the jug wet at all times, and hot and relatively dry air flowing over the jug causes this water to evaporate. Part of the latent heat of evaporation comes from the water in the jug, and the water is cooled as a result. If the environment conditions are 1 atm, 32°C, and 40 percent relative humidity, determine the temperature of the water when steady conditions are reached.
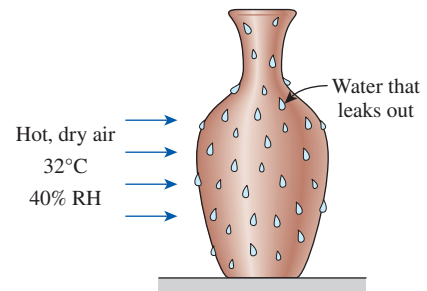

FIGURE P14–156

14–157 Reconsider Prob. 14–156. Using appropriate software, plot the water temperature as a function of the relative humidity of air as the relative humidity varies from 10 to 100 percent, and discuss the results.

14–158 A soaked sponge is experiencing dry air flowing over its surface. The air is at 1 atm and zero relative humidity. Determine the difference in the air temperature and the surface temperature of the sponge, $T_\infty - T_s$, when steady-state conditions are reached, if the sponge is soaked with (*a*) water, $D_{AB} = 2.42 \times 10^{-5}$ m²/s, and (*b*) ammonia, $D_{AB} = 2.6 \times 10^{-5}$ m²/s. Evaluate the properties of air, water, and ammonia at $20°C, 10°C$, and $-40°C$, respectively.

14–159 A water-soaked 10-cm × 10-cm-square sponge is experiencing parallel dry airflow over its surface. The average convection heat transfer coefficient of dry air at 20°C flowing over the sponge surface is estimated to be 30 W/m²·K, and the sponge surface is maintained at 30°C. If the sponge is placed under an array of radiant lamps, determine (*a*) the rate of evaporation of water from the sponge and (*b*) the net radiation heat transfer rate.
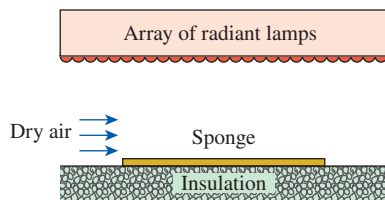

FIGURE P14–159

14–160 Consider a thin layer of liquid water on a concrete surface. The surrounding air is dry with a convection heat transfer coefficient of 50 W/m²·K. The liquid water has an emissivity of 0.95, and the air and surrounding temperature is 30°C. If the layer of liquid water has a uniform temperature of 20°C, determine the conduction heat flux through the concrete.
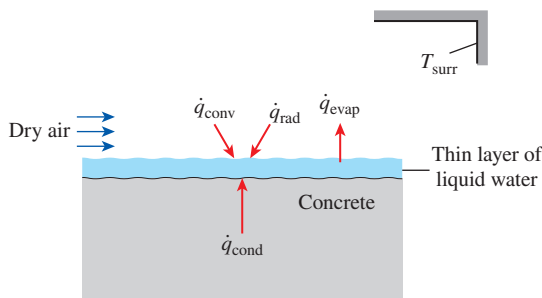

FIGURE P14–160

14–161 One way of increasing heat transfer from the head on a hot summer day is to wet it. This is especially effective in windy weather, as you may have noticed. Approximating the head as a 30-cm-diameter sphere at 30°C with an emissivity of 0.95, determine the total rate of heat loss from the head at ambient air conditions of 1 atm, 25°C, 30 percent relative humidity, and 25 km/h winds if the head is (*a*) dry and (*b*) wet. Take the surrounding temperature to be 25°C. *Answers:* (*a*) 40.5 W, (*b*) 385 W
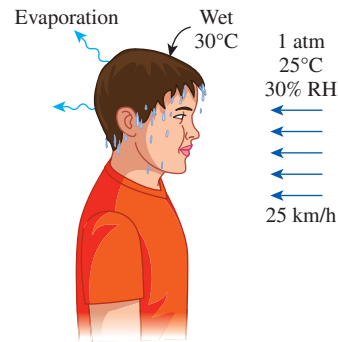

FIGURE P14–161

14–162 A 1.5-m-deep, 25-m × 25-m heated swimming pool is maintained at a constant temperature of 30°C at a location where the atmospheric pressure is 1 atm. If the ambient air is at 20°C and 60 percent relative humidity and the effective sky temperature is 0°C, determine the rate of heat loss from the top surface of the pool by (*a*) radiation, (*b*) natural convection, and (*c*) evaporation. (*d*) Assuming the heat losses to the ground to be negligible, determine the size of the heater.

14–163 Repeat Prob. 14–162 for a pool temperature of 25°C.

14–164 A glass bottle washing facility uses a well-agitated hot water bath at 50°C with an open top that is placed on the ground. The bathtub is 1 m high, 2 m wide, and 4 m long and is made of sheet metal so that the outer side surfaces are also at about 50°C. The bottles enter at a rate of 800 per minute at ambient temperature and leave at the water temperature. Each bottle has a mass of 150 g and removes 0.6 g of water as it leaves the bath wet. Makeup water is supplied at 15°C. If the average conditions in the plant are 1 atm, 25°C, and 50 percent relative humidity, and the average temperature of the surrounding surfaces is 15°C, determine (*a*) the amount of heat and water removed by the bottles themselves per second, (*b*) the rate of heat loss from the top surface of the water bath by radiation, natural convection, and evaporation, (*c*) the rate of heat loss from the side surfaces by natural convection and radiation, and (*d*) the rate at which heat and water must be supplied to maintain steady operating conditions. Disregard heat loss through the bottom surface of the bath, and take the emissivities of sheet metal and water to be 0.61 and 0.95, respectively.

14–165 Repeat Prob. 14–164 for a water bath temperature of 55°C.

Review Problems

14–166 Determine the mole fraction of the water vapor at the surface of a lake whose temperature is 15°C and compare it to the mole fraction of water in the lake. Take the atmospheric pressure at lake level to be 92 kPa.
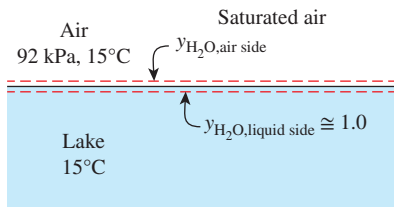
FIGURE P14–166

FIGURE P14–174

14–167 Show that for an ideal gas mixture maintained at a constant temperature and pressure, the molar concentration C of the mixture remains constant, but this is not necessarily the case for the density ρ of the mixture.

14–168E A gas mixture in a tank at 550 R and 25 psia consists of 1 lbm of CO_2 and 3 lbm of CH_4. Determine the volume of the tank and the partial pressure of each gas.

14–169 Dry air whose molar analysis is 78.1 percent N_2, 20.9 percent O_2, and 1 percent Ar flows over a water body until it is saturated. If the pressure and temperature of air remain constant at 1 atm and 25°C during the process, determine (*a*) the molar analysis of the saturated air and (*b*) the density of air before and after the process. What do you conclude from your results?

14–170 The diffusion coefficient of carbon in steel is given as

$$D_{AB} = 2.67 \times 10^{-5} \exp(-17{,}400/T) \ \ (\text{m}^2/\text{s})$$

where T is in K. Determine the diffusion coefficient from 200 K to 1200 K in 100-K increments, and plot the results.

14–171 Consider a 30-cm-diameter pan filled with water at 15°C in a room at 20°C, 1 atm, and 30 percent relative humidity. Determine (*a*) the rate of heat transfer by convection, (*b*) the rate of evaporation of water, and (*c*) the rate of heat transfer to the water needed to maintain its temperature at 15°C. Disregard any radiation effects.

14–172 Repeat Prob. 14–171 assuming a fan blows air over the water surface at a velocity of 5 m/s. Take the radius of the pan to be the characteristic length.

14–173 Using Henry's law, show that the dissolved gases in a liquid can be driven off by heating the liquid.

14–174 Consider a glass of water in a room at 20°C and 100 kPa. If the relative humidity in the room is 70 percent and the water and the air are at the same temperature, determine (*a*) the mole fraction of the water vapor in the room air, (*b*) the mole fraction of the water vapor in the air adjacent to the water surface, and (*c*) the mole fraction of air in the water near the surface. *Answers:* (*a*) 1.64 percent, (*b*) 2.34 percent, (*c*) 0.0015 percent
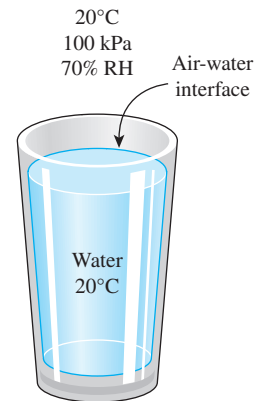
14–175 A membrane made of 0.15-mm-thick soft rubber separates pure O_2 at 1 atm and 25°C from air at 5 atm pressure. Determine the mass flow rate of O_2 through the membrane per unit area and the direction of flow.

14–176 Consider a brick house that is maintained at 20°C and 60 percent relative humidity at a location where the atmospheric pressure is 85 kPa. The walls of the house are made of 20-cm-thick brick whose permeance is 23×10^{-12} kg/s·m²·Pa. Taking the vapor pressure at the outer side of the wallboard to be zero, determine the maximum amount of water vapor that will diffuse through a 3-m × 5-m section of a wall during a 24-h period.

14–177 A thick part made of nickel is put into a room filled with hydrogen at 3 atm and 85°C. Determine the hydrogen concentration at a depth of 2 mm from the surface after 24 h. *Answer:* 4.1×10^{-7} kmol/m³

14–178 A tanker truck carrying liquid herbicide overturned and caused a spill over a field. The liquid herbicide remained on the soil for 30 min before evaporating into the air. The mass diffusivity of the liquid herbicide in the soil is 2×10^{-8} m²/s. If a concentration of 0.1 percent by weight will destroy most life, determine the depth of the soil at which plant and insect life is likely to be affected by the spill.

14–179 Oxygen gas is forced into an aquarium at 1 atm and 25°C, and the oxygen bubbles are observed to rise to the free surface in 4 s. Determine the penetration depth of oxygen into water from a bubble during this time period.

14–180 In an experiment, a sphere of crystalline sodium chloride (NaCl) was suspended in a stirred tank filled with water at 20°C. Its initial mass was 100 g. In 10 minutes, the mass of the sphere was found to have decreased by 10 percent. The density of NaCl is 2160 kg/m³. Its solubility in water at 20°C is 320 kg/m³. Use these results to obatin an average value for the mass transfer coefficient.

14–181 Liquid toluene ($C_6H_5CH_3$) was stored at 6.4°C in an open-top 30-cm-diameter cylindrical container. The vapor

pressure of toluene at 6.4°C is 10 mm Hg. A gentle stream of fresh air at 6.4°C and 101.3 kPa was allowed to flow over the open end of the container. The rate of evaporation of toluene into air was measured to be 80 g/day. Estimate the concentration of toluene (in g/m^3) at exactly 10 mm above the liquid surface. The diffusion coefficient of toluene at 25°C is $D_{AB} = 0.084 \times 10^{-4} \ m^2/s$.

14–182 Liquid methanol is accidentally spilled on a 1-m × 1-m laboratory bench and covers the entire bench surface. A fan is providing a 20 m/s airflow parallel over the bench surface. The air is maintained at 25°C and 1 atm, and the concentration of methanol in the free stream is negligible. If the methanol vapor at the air–methanol interface has a pressure of 4000 Pa and a temperature of 25°C, determine the evaporation rate of methanol on a molar basis.

14–183E The top section of an 8-ft-deep, 100-ft × 100-ft heated solar pond is maintained at a constant temperature of 80°F at a location where the atmospheric pressure is 1 atm. If the ambient air is at 70°F and 100 percent relative humidity and wind is blowing at an average velocity of 40 mph, determine the rate of heat loss from the top surface of the pond by (a) forced convection, (b) radiation, and (c) evaporation. Take the average temperature of the surrounding surfaces to be 60°F.

14–184E Repeat Prob. 14-183E for a solar pond surface temperature of 90°F. *Answers: (a)* 1,060,000 Btu/h, *(b)* 299,400 Btu/h, *(c)* 3,410,000 Btu/h

14–185E A swimmer extends his wet arms into the windy air outside at 1 atm, 40°F, 50 percent relative humidity, and 20 mph. If the average skin temperature is 80°F, determine the rate at which water evaporates from both arms and the corresponding rate of heat transfer by evaporation. The arm can be modeled as a 2-ft-long and 3-in-diameter cylinder with adiabatic ends.

14–186 A sphere of ice, 5 cm in diameter, is exposed to 65 km/h wind with 15 percent relative humidity. Both the ice sphere and air are at −1°C and 90 kPa. Predict the rate of evaporation of the ice in g/h by use of the following correlation for single spheres: Sh = $[4.0 + 1.21 (ReSc)^{2/3}]^{0.5}$. Data at −1°C and 90 kPa: $D_{air-H_2O} = 2.5 \times 10^{-5} \ m^2/s^3$, kinematic viscosity (air) = $1.32 \times 10^{-7} \ m^2/s$, vapor pressure ($H_2O$) = 0.56 kPa and density (ice) = 915 kg/m^3.

14–187 Benzene-free air at 25°C and 101.3 kPa enters a 5-cm-diameter tube at an average velocity of 5 m/s. The inner surface of the 6-m-long tube is coated with a thin film of pure benzene at 25°C. The vapor pressure of benzene (C_6H_6) at 25°C is 13 kPa, and the solubility of air in benzene is assumed to be negligible. Calculate (a) the average mass transfer coefficient in m/s, (b) the molar concentration of benzene in the outlet air, and (c) the evaporation rate of benzene in kg/h.

14–188 Air at 52°C, 101.3 kPa, and 20 percent relative humidity enters a 5-cm-diameter tube with an average velocity

of 6 m/s. The tube inner surface is wetted uniformly with water, whose vapor pressure at 52°C is 13.6 kPa. While the temperature and pressure of air remain constant, the partial pressure of vapor in the outlet air is increased to 10 kPa. Detemine (a) the average mass transfer coefficient in m/s, (b) the log-mean driving force for mass transfer in molar concentration units, (c) the water evaporation rate in kg/h, and (d) the length of the tube.

Fundamentals of Engineering (FE) Exam Problems

14–189 The basic equation describing the diffusion of one medium through another stationary medium is

(a) $j_A = -C D_{AB} \dfrac{d(C_A/C)}{dx}$

(b) $j_A = -D_{AB} \dfrac{d(C_A/C)}{dx}$

(c) $j_A = -k \dfrac{d(C_A/C)}{dx}$

(d) $j_A = -k \dfrac{dT}{dx}$

(e) none of them

14–190 For the absorption of a gas (like carbon dioxide) into a liquid (like water) Henry's law states that partial pressure of the gas is proportional to the mole fraction of the gas in the liquid–gas solution with the constant of proportionality being Henry's constant. A bottle of soda pop (CO_2-H_2O) at room temperature has a Henry's constant of 17,100 kPa. If the pressure in this bottle is 140 kPa and the partial pressure of the water vapor in the gas volume at the top of the bottle is neglected, the concentration of the CO_2 in the liquid H_2O is

(a) 0.004 mol-CO_2/mol
(b) 0.008 mol-CO_2/mol
(c) 0.012 mol-CO_2/mol
(d) 0.024 mol-CO_2/mol
(e) 0.035 mol-CO_2/mol

14–191 A rubber object is in contact with nitrogen (N_2) at 298 K and 250 kPa. The solubility of nitrogen gas in rubber is 0.00156 $kmol/m^3$·bar. The mass density of nitrogen at the interface is

(a) 0.049 kg/m^3
(b) 0.064 kg/m^3
(c) 0.077 kg/m^3
(d) 0.092 kg/m^3
(e) 0.109 kg/m^3

14–192 Nitrogen gas at high pressure and 298 K is contained in a 2-m × 2-m × 2-m cubical container made of natural rubber whose walls are 3 cm thick. The concentration of nitrogen in the rubber at the inner and outer surfaces are 0.067 kg/m^3 and 0.009 kg/m^3, respectively. The diffusion coefficient of nitrogen through rubber is $1.5 \times 10^{-10} \ m^2/s$. The mass flow rate of nitrogen by diffusion through the cubical container is

(a) 8.1×10^{-10} kg/s
(b) 3.2×10^{-10} kg/s
(c) 3.8×10^{-9} kg/s
(d) 7.0×10^{-9} kg/s
(e) 1.60×10^{-8} kg/s

14–193 A recent attempt to circumnavigate the world in a balloon used a helium-filled balloon whose volume was 7240 m^3 and surface area was 1800 m^2. The skin of this balloon is 2 mm thick and is made of a material whose helium diffusion coefficient is 1×10^{-9} m^2/s. The molar concentration of the helium at the inner surface of the balloon skin is 0.2 kmol/m^3 and the molar concentration at the outer surface is extremely small. The rate at which helium is lost from this balloon is

(a) 0.26 kg/h
(b) 1.5 kg/h
(c) 2.6 kg/h
(d) 3.8 kg/h
(e) 5.2 kg/h

14–194 Carbon at 1273 K is contained in a 7-cm-inner-diameter cylinder made of iron whose thickness is 1.2 mm. The concentration of carbon in the iron at the inner surface is 0.5 kg/m^3 and the concentration of carbon in the iron at the outer surface is negligible. The diffusion coefficient of carbon through iron is 3×10^{-11} m^2/s. The mass flow rate of carbon by diffusion through the cylinder shell per unit length of the cylinder is

(a) 2.8×10^{-9} kg/s
(b) 5.4×10^{-9} kg/s
(c) 8.8×10^{-9} kg/s
(d) 1.6×10^{-8} kg/s
(e) 5.2×10^{-8} kg/s

14–195 The surface of an iron component is to be hardened by carbon. The diffusion coefficient of carbon in iron at 1000°C is given to be 3×10^{-11} m^2/s. If the penetration depth of carbon in iron is desired to be 1.0 mm, the hardening process must take at least

(a) 1.10 h
(b) 1.47 h
(c) 1.86 h
(d) 2.50 h
(e) 2.95 h

14–196 A natural gas (methane, CH_4) storage facility uses 3-cm-diameter by 6-m-long vent tubes on its storage tanks to keep the pressure in these tanks at atmospheric value. If the diffusion coefficient for methane in air is 0.2×10^{-4} m^2/s and the temperature of the tank and environment is 300 K, the rate at which natural gas is lost from a tank through one vent tube is

(a) 13×10^{-5} kg/day
(b) 3.2×10^{-5} kg/day
(c) 8.7×10^{-5} kg/day
(d) 5.3×10^{-5} kg/day
(e) 0.12×10^{-5} kg/day

14–197 Saturated water vapor at 25°C ($P_{sat} = 3.17$ kPa) flows in a pipe that passes through air at 25°C with a relative humidity of 40 percent. The vapor is vented to the atmosphere through a 9-mm internal-diameter tube that extends 10 m into the air. The diffusion coefficient of vapor through air is 2.5×10^{-5} m^2/s. The amount of water vapor lost to the atmosphere through this individual tube by diffusion is

(a) 1.7×10^{-6} kg
(b) 2.3×10^{-6} kg
(c) 3.8×10^{-6} kg
(d) 5.0×10^{-6} kg
(e) 7.1×10^{-6} kg

14–198 When the _____ number is unity, one can expect the momentum and mass transfer by diffusion to be the same.

(a) Grashof
(b) Reynolds
(c) Lewis
(d) Schmidt
(e) Sherwood

14–199 Air flows in a 4-cm-diameter wet pipe at 20°C and 1 atm with an average velocity of 4 m/s in order to dry the surface. The Nusselt number in this case can be determined from $Nu = 0.023 Re^{0.8} Pr^{0.4}$ where $Re = 10{,}550$ and $Pr = 0.731$. Also, the diffusion coefficient of water vapor in air is 2.42×10^{-5} m^2/s. Using the analogy between heat and mass transfer, the mass transfer coefficient inside the pipe for fully developed flow becomes

(a) 0.0918 m/s
(b) 0.0408 m/s
(c) 0.0366 m/s
(d) 0.0203 m/s
(e) 0.0022 m/s

14–200 Air flows through a wet pipe at 298 K and 1 atm, and the diffusion coefficient of water vapor in air is 2.5×10^{-5} m^2/s. If the heat transfer coefficient is determined to be 80 W/m^2·K, the mass transfer coefficient is

(a) 0.0022 m/s
(b) 0.036 m/s
(c) 0.074 m/s
(d) 0.092 m/s
(e) 0.13 m/s

Design and Essay Problems

14–201 Write an essay on diffusion caused by effects other than the concentration gradient such as thermal diffusion, pressure diffusion, forced diffusion, Knudsen diffusion, and surface diffusion.

14–202 One way of generating electricity from solar energy involves the collection and storage of solar energy in large artificial lakes a few meters deep, called solar ponds. Solar energy is stored at the bottom part of the pond at temperatures close to boiling, and the rise of hot water to the top is prevented by

planting salt in the bottom of the pond. Write an essay on the operation of solar pond power plants, and find out how much salt is used per year per m^2. If the cost is not a factor, can sugar be used instead of salt to maintain the concentration gradient? Explain.

14–203 The condensation and even freezing of moisture in building walls without effective vapor retarders is a real concern in cold climates because it undermines the effectiveness of the insulation. Investigate how the builders in your area are coping with this problem, whether they are using vapor retarders or vapor barriers in the walls, and where they are located in the walls. Prepare a report on your findings, and explain the reasoning for the current practice.

14–204 You are asked to design a heating system for a swimming pool that is 2 m deep, 25 m long, and 25 m wide. Your client desires that the heating system be large enough to raise the water temperature from 20°C to 30°C in 3 h. The heater must also be able to maintain the pool at 30°C at the outdoor design conditions of 15°C, 1 atm, 35 percent relative humidity,

40 mph winds, and effective sky temperature of 10°C. Heat losses to the ground are expected to be small and can be disregarded. The heater considered is a natural gas furnace whose efficiency is 80 percent. What heater size (in Btu/h input) would you recommend that your client buy?
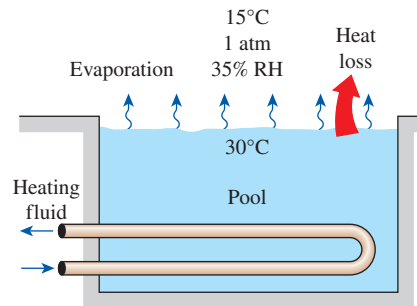
FIGURE P14–204

PROPERTY TABLES AND CHARTS (SI UNITS)

TABLE A–1

Molar mass, gas constant, and ideal-gas specific heats of some substances

Substance	Molar Mass M, kg/kmol	Gas Constant R, kJ/kg·K*	Specific Heat Data at 25°C		
			c_p, kJ/kg·K	c_v, kJ/kg·K	$k = c_p/c_v$
Air	28.97	0.2870	1.005	0.7180	1.400
Ammonia, NH_3	17.03	0.4882	2.093	1.605	1.304
Argon, Ar	39.95	0.2081	0.5203	0.3122	1.667
Bromine, Br_2	159.81	0.05202	0.2253	0.1732	1.300
Isobutane, C_4H_{10}	58.12	0.1430	1.663	1.520	1.094
n-Butane, C_4H_{10}	58.12	0.1430	1.694	1.551	1.092
Carbon dioxide, CO_2	44.01	0.1889	0.8439	0.6550	1.288
Carbon monoxide, CO	28.01	0.2968	1.039	0.7417	1.400
Chlorine, Cl_2	70.905	0.1173	0.4781	0.3608	1.325
Chlorodifluoromethane (R-22), $CHClF_2$	86.47	0.09615	0.6496	0.5535	1.174
Ethane, C_2H_6	30.070	0.2765	1.744	1.468	1.188
Ethylene, C_2H_4	28.054	0.2964	1.527	1.231	1.241
Fluorine, F_2	38.00	0.2187	0.8237	0.6050	1.362
Helium, He	4.003	2.077	5.193	3.116	1.667
n-Heptane, C_7H_{16}	100.20	0.08297	1.649	1.566	1.053
n-Hexane, C_6H_{14}	86.18	0.09647	1.654	1.558	1.062
Hydrogen, H_2	2.016	4.124	14.30	10.18	1.405
Krypton, Kr	83.80	0.09921	0.2480	0.1488	1.667
Methane, CH_4	16.04	0.5182	2.226	1.708	1.303
Neon, Ne	20.183	0.4119	1.030	0.6180	1.667
Nitrogen, N_2	28.01	0.2968	1.040	0.7429	1.400
Nitric oxide, NO	30.006	0.2771	0.9992	0.7221	1.384
Nitrogen dioxide, NO_2	46.006	0.1889	0.8060	0.6171	1.306
Oxygen, O_2	32.00	0.2598	0.9180	0.6582	1.395
n-Pentane, C_5H_{12}	72.15	0.1152	1.664	1.549	1.074
Propane, C_3H_8	44.097	0.1885	1.669	1.480	1.127
Propylene, C_3H_6	42.08	0.1976	1.531	1.333	1.148
Steam, H_2O	18.015	0.4615	1.865	1.403	1.329
Sulfur dioxide, SO_2	64.06	0.1298	0.6228	0.4930	1.263
Tetrachloromethane, CCl_4	153.82	0.05405	0.5415	0.4875	1.111
Tetrafluoroethane (R-134a), $C_2H_2F_4$	102.03	0.08149	0.8334	0.7519	1.108
Trifluoroethane (R-143a), $C_2H_3F_3$	84.04	0.09893	0.9291	0.8302	1.119
Xenon, Xe	131.30	0.06332	0.1583	0.09499	1.667

*The unit kJ/kg·K is equivalent to kPa·m³/kg·K. The gas constant is calculated from $R = R_u/M$, where $R_u = 8.31447$ kJ/kmol·K is the universal gas constant and M is the molar mass.

Source: Specific heat values are obtained primarily from the property routines prepared by The National Institute of Standards and Technology (NIST), Gaithersburg, MD.

TABLE A–2

Boiling and freezing point properties

Substance	Boiling Data at l atm		Freezing Data		Liquid Properties		
	Normal Boiling Point, °C	Latent Heat of Vaporization h_{fg}, kJ/kg	Freezing Point, °C	Latent Heat of Fusion h_{if}, kJ/kg	Temperature, °C	Density ρ, kg/m³	Specific Heat c_p, kJ/kg·K
Ammonia	−33.3	1357	−77.7	322.4	−33.3	682	4.43
					−20	665	4.52
					0	639	4.60
					25	602	4.80
Argon	−185.9	161.6	−189.3	28	−185.6	1394	1.14
Benzene	80.2	394	5.5	126	20	879	1.72
Brine (20% sodium chloride by mass)	103.9	—	−17.4	—	20	1150	3.11
n-Butane	−0.5	385.2	−138.5	80.3	−0.5	601	2.31
Carbon dioxide	−78.4*	230.5 (at 0°C)	−56.6		0	298	0.59
Ethanol	78.2	838.3	−114.2	109	25	783	2.46
Ethyl alcohol	78.6	855	−156	108	20	789	2.84
Ethylene glycol	198.1	800.1	−10.8	181.1	20	1109	2.84
Glycerin	179.9	974	18.9	200.6	20	1261	2.32
Helium	−268.9	22.8	—	—	−268.9	146.2	22.8
Hydrogen	−252.8	445.7	−259.2	59.5	−252.8	70.7	10.0
Isobutane	−11.7	367.1	−160	105.7	−11.7	593.8	2.28
Kerosene	204–293	251	−24.9	—	20	820	2.00
Mercury	356.7	294.7	−38.9	11.4	25	13,560	0.139
Methane	−161.5	510.4	−182.2	58.4	−161.5	423	3.49
					−100	301	5.79
Methanol	64.5	1100	−97.7	99.2	25	787	2.55
Nitrogen	−195.8	198.6	−210	25.3	−195.8	809	2.06
					−160	596	2.97
Octane	124.8	306.3	−57.5	180.7	20	703	2.10
Oil (light)					25	910	1.80
Oxygen	−183	212.7	−218.8	13.7	−183	1141	1.71
Petroleum	—	230–384			20	640	2.0
Propane	−42.1	427.8	−187.7	80.0	−42.1	581	2.25
					0	529	2.53
					50	449	3.13
Refrigerant-134a	−26.1	216.8	−96.6	—	−50	1443	1.23
					−26.1	1374	1.27
					0	1295	1.34
					25	1207	1.43
Water	100	2257	0.0	333.7	0	1000	4.22
					25	997	4.18
					50	988	4.18
					75	975	4.19
					100	958	4.22

*Sublimation temperature. (At pressures below the triple-point pressure of 518 kPa, carbon dioxide exists as a solid or gas. Also, the freezing-point temperature of carbon dioxide is the triple-point temperature of −56.5°C.)

TABLE A–3

Properties of solid metals

Composition	Melting Point, K	Properties at 300 K				Properties at Various Temperatures (K), k(W/m·K)/c_p(J/kg·K)					
		ρ kg/m^3	c_p J/kg·K	k W/m·K	$\alpha \times 10^6$ m^2/s	100	200	400	600	800	1000
Aluminum:											
Pure	933	2702	903	237	97.1	302	237	240	231	218	
						482	798	949	1033	1146	
Alloy 2024-T6 (4.5% Cu, 1.5% Mg, 0.6% Mn)	775	2770	875	177	73.0	65	163	186	186		
						473	787	925	1042		
Alloy 195, Cast (4.5% Cu)		2790	883	168	68.2			174	185		
Beryllium	1550	1850	1825	200	59.2	990	301	161	126	106	90.8
						203	1114	2191	2604	2823	3018
Bismuth	545	9780	122	7.86	6.59	16.5	9.69	7.04			
						112	120	127			
Boron	2573	2500	1107	27.0	9.76	190	55.5	16.8	10.6	9.60	9.85
						128	600	1463	1892	2160	2338
Cadmium	594	8650	231	96.8	48.4	203	99.3	94.7			
							198	222	242		
Chromium	2118	7160	449	93.7	29.1	159	111	90.9	80.7	71.3	65.4
						192	384	484	542	581	616
Cobalt	1769	8862	421	99.2	26.6	167	122	85.4	67.4	58.2	52.1
						236	379	450	503	550	628
Copper:											
Pure	1358	8933	385	401	117	482	413	393	379	366	352
						252	356	397	417	433	451
Commercial bronze (90% Cu, 10% Al)	1293	8800	420	52	14		42	52	59		
							785	160	545		
Phosphor gear bronze (89% Cu, 11% Sn)	1104	8780	355	54	17		41	65	74		
							—	—	—		
Cartridge brass (70% Cu, 30% Zn)	1188	8530	380	110	33.9	75	95	137	149		
							360	395	425		
Constantan (55% Cu, 45% Ni)	1493	8920	384	23	6.71	17	19				
						237	362				
Germanium	1211	5360	322	59.9	34.7	232	96.8	43.2	27.3	19.8	17.4
						190	290	337	348	357	375
Gold	1336	19,300	129	317	127	327	323	311	298	284	270
						109	124	131	135	140	145
Iridium	2720	22,500	130	147	50.3	172	153	144	138	132	126
						90	122	133	138	144	153
Iron:											
Pure	1810	7870	447	80.2	23.1	134	94.0	69.5	54.7	43.3	32.8
						216	384	490	574	680	975
Armco (99.75% pure)		7870	447	72.7	20.7	95.6	80.6	65.7	53.1	42.2	32.3
						215	384	490	574	680	975
Carbon steels:											
Plain carbon (Mn ≤ 1% Si ≤ 0.1%)		7854	434	60.5	17.7			56.7	48.0	39.2	30.0
								487	559	685	1169
AISI 1010		7832	434	63.9	18.8			58.7	48.8	39.2	31.3
								487	559	685	1168
Carbon- silicon (Mn ≤ 1% 0.1% < Si ≤ 0.6%)		7817	446	51.9	14.9			49.8	44.0	37.4	29.3
								501	582	699	971

TABLE A–3

Properties of solid metals (*Continued*)

Composition	Melting Point, K	Properties at 300 K				Properties at Various Temperatures (K), k(W/m·K)/c_p(J/kg·K)					
		ρ kg/m^3	c_p J/kg·K	k W/m·K	$\alpha \times 10^6$ m^2/s	100	200	400	600	800	1000
Carbon–manganese–silicon (1% < Mn < 1.65% 0.1% < Si < 0.6%)		8131	434	41.0	11.6			42.2 487	39.7 559	35.0 685	27.6 1090
Chromium (low) steels:											
$\frac{1}{2}$Cr−$\frac{1}{4}$Mo−Si (0.18% C, 0.65% Cr, 0.23% Mo, 0.6% Si)		7822	444	37.7	10.9			38.2 492	36.7 575	33.3 688	26.9 969
1 Cr−$\frac{1}{2}$Mo (0.16% C, 1% Cr, 0.54% Mo, 0.39% Si)		7858	442	42.3	12.2			42.0 492	39.1 575	34.5 688	27.4 969
1 Cr–V (0.2% C, 1.02% Cr, 0.15% V)		7836	443	48.9	14.1			46.8 492	42.1 575	36.3 688	28.2 969
Stainless steels:											
AISI 302		8055	480	15.1	3.91			17.3 512	20.0 559	22.8 585	25.4 606
AISI 304	1670	7900	477	14.9	3.95	9.2 272	12.6 402	16.6 515	19.8 557	22.6 582	25.4 611
AISI 316		8238	468	13.4	3.48			15.2 504	18.3 550	21.3 576	24.2 602
AISI 347		7978	480	14.2	3.71			15.8 513	18.9 559	21.9 585	24.7 606
Lead	601	11,340	129	35.3	24.1	39.7 118	36.7 125	34.0 132	31.4 142		
Magnesium	923	1740	1024	156	87.6	169 649	159 934	153 1074	149 1170	146 1267	
Molybdenum	2894	10,240	251	138	53.7	179 141	143 224	134 261	126 275	118 285	112 295
Nickel:											
Pure	1728	8900	444	90.7	23.0	164 232	107 383	80.2 485	65.6 592	67.6 530	71.8 562
Nichrome (80% Ni, 20% Cr)	1672	8400	420	12	3.4			14 480	16 525	21 545	
Inconel X-750 (73% Ni, 15% Cr, 6.7% Fe)	1665	8510	439	11.7	3.1	8.7 —	10.3 372	13.5 473	17.0 510	20.5 546	24.0 626
Niobium	2741	8570	265	53.7	23.6	55.2 188	52.6 249	55.2 274	58.2 283	61.3 292	64.4 301
Palladium	1827	12,020	244	71.8	24.5	76.5 168	71.6 227	73.6 251	79.7 261	86.9 271	94.2 281
Platinum: Pure	2045	21,450	133	71.6	25.1	77.5 100	72.6 125	71.8 136	73.2 141	75.6 146	78.7 152
Alloy 60Pt–40Rh (60% Pt, 40% Rh)	1800	16,630	162	47	17.4			52 —	59 —	65 —	69 —
Rhenium	3453	21,100	136	47.9	16.7	58.9 97	51.0 127	46.1 139	44.2 145	44.1 151	44.6 156
Rhodium	2236	12,450	243	150	49.6	186 147	154 220	146 253	136 274	127 293	121 311

TABLE A–3

Properties of solid metals (*Concluded*)

Composition	Melting Point, K	Properties at 300 K				Properties at Various Temperatures (K), k(W/m·K)/c_p(J/kg·K)					
		ρ kg/m³	c_p J/kg·K	k W/m·K	$\alpha \times 10^6$ m²/s	100	200	400	600	800	1000
Silicon	1685	2330	712	148	89.2	884	264	98.9	61.9	42.4	31.2
						259	556	790	867	913	946
Silver	1235	10,500	235	429	174	444	430	425	412	396	379
						187	225	239	250	262	277
Tantalum	3269	16,600	140	57.5	24.7	59.2	57.5	57.8	58.6	59.4	60.2
						110	133	144	146	149	152
Thorium	2023	11,700	118	54.0	39.1	59.8	54.6	54.5	55.8	56.9	56.9
						99	112	124	134	145	156
Tin	505	7310	227	66.6	40.1	85.2	73.3	62.2			
						188	215	243			
Titanium	1953	4500	522	21.9	9.32	30.5	24.5	20.4	19.4	19.7	20.7
						300	465	551	591	633	675
Tungsten	3660	19,300	132	174	68.3	208	186	159	137	125	118
						87	122	137	142	146	148
Uranium	1406	19,070	116	27.6	12.5	21.7	25.1	29.6	34.0	38.8	43.9
						94	108	125	146	176	180
Vanadium	2192	6100	489	30.7	10.3	35.8	31.3	31.3	33.3	35.7	38.2
						258	430	515	540	563	597
Zinc	693	7140	389	116	41.8	117	118	111	103		
						297	367	402	436		
Zirconium	2125	6570	278	22.7	12.4	33.2	25.2	21.6	20.7	21.6	23.7
						205	264	300	332	342	362

Source: Frank P. Incropera and David P. DeWitt, *Fundamentals of Heat and Mass Transfer, 3rd ed.,* 1990.

TABLE A–4

Properties of solid nonmetals

Composition	Melting Point, K	Properties at 300 K				Properties at Various Temperatures (K), k(W/m·K)/c_p(J/kg·K)					
		ρ kg/m^3	c_p J/kg·K	k W/m·K	$\alpha \times 10^6$ m^2/s	100	200	400	600	800	1000
Aluminum oxide, sapphire	2323	3970	765	46	15.1	450 —	82 —	32.4 940	18.9 1110	13.0 1180	10.5 1225
Aluminum oxide, polycrystalline	2323	3970	765	36.0	11.9	133 —	55 —	26.4 940	15.8 1110	10.4 1180	7.85 1225
Beryllium oxide	2725	3000	1030	272	88.0			196 1350	111 1690	70 1865	47 1975
Boron	2573	2500	1105	27.6	9.99	190 —	52.5 —	18.7 1490	11.3 1880	8.1 2135	6.3 2350
Boron fiber epoxy (30% vol.) composite	590	2080									
k, ‖ to fibers				2.29		2.10	2.23	2.28			
k, ⊥ to fibers				0.59		0.37	0.49	0.60			
c_p			1122			364	757	1431			
Carbon, amorphous	1500	1950	—	1.60	—	0.67 —	1.18 —	1.89 —	21.9 —	2.37 —	2.53 —
Diamond, type IIa insulator	—	3500	509	2300		10,000 21	4000 194	1540 853			
Graphite, pyrolytic	2273	2210									
k, ‖ to layers				1950		4970	3230	1390	892	667	534
k, ⊥ to layers				5.70		16.8	9.23	4.09	2.68	2.01	1.60
c_p			709			136	411	992	1406	1650	1793
Graphite fiber epoxy (25% vol.) composite	450	1400									
k, heat flow ‖ to fibers				11.1		5.7	8.7	13.0			
k, heat flow ⊥ to fibers			0.87		0.46	0.68	1.1				
c_p			935			337	642	1216			
Pyroceram, Corning 9606	1623	2600	808	3.98	1.89	5.25 —	4.78 —	3.64 908	3.28 1038	3.08 1122	2.96 1197
Silicon carbide	3100	3160	675	490	230			— 880	— 1050	— 1135	87 1195
Silicon dioxide, crystalline (quartz)	1883	2650									
k, ‖ to c-axis				10.4		39	16.4	7.6	5.0	4.2	
k, ⊥ to c-axis				6.21		20.8	9.5	4.70	3.4	3.1	
c_p			745			—	—	885	1075	1250	
Silicon dioxide, polycrystalline (fused silica)	1883	2220	745	1.38	0.834	0.69 —	1.14 —	1.51 905	1.75 1040	2.17 1105	2.87 1155
Silicon nitride	2173	2400	691	16.0	9.65	— —	— 578	13.9 778	11.3 937	9.88 1063	8.76 1155
Sulfur	392	2070	708	0.206	0.141	0.165 —	0.185 403	606			
Thorium dioxide	3573	9110	235	13	6.1			10.2 255	6.6 274	4.7 285	3.68 295
Titanium dioxide, polycrystalline	2133	4157	710	8.4	2.8			7.01 805	5.02 880	8.94 910	3.46 930

TABLE A–5

Properties of building materials (at a mean temperature of 24°C)

Material	Thickness, L mm	Density, ρ kg/m³	Thermal Conductivity, k W/m·K	Specific Heat, c_p kJ/kg·K	R-value (for listed thickness, L/k), K·m²/W
Building Boards					
Asbestos–cement board	6 mm	1922	—	1.00	0.011
Gypsum of plaster board	10 mm	800	—	1.09	0.057
	13 mm	800	—	—	0.078
Plywood (Douglas fir)	—	545	0.12	1.21	—
	6 mm	545	—	1.21	0.055
	10 mm	545	—	1.21	0.083
	13 mm	545	—	1.21	0.110
	20 mm	545	—	1.21	0.165
Insulated board and sheathing	13 mm	288	—	1.30	0.232
(regular density)	20 mm	288	—	1.30	0.359
Hardboard (high density, standard					
tempered)	—	1010	0.14	1.34	—
Particle board:					
Medium density	—	800	0.14	1.30	—
Underlayment	16 mm	640	—	1.21	0.144
Wood subfloor	20 mm	—	—	1.38	0.166
Building Membrane					
Vapor-permeable felt	—	—	—	—	0.011
Vapor seal (2 layers of mopped					
0.73 kg²/m² felt)	—	—	—	—	0.021
Flooring Materials					
Carpet and fibrous pad	—	—	—	1.42	0.367
Carpet and rubber pad	—	—	—	1.38	0.217
Tile (asphalt, linoleum, vinyl)	—	—	—	1.26	0.009
Masonry Materials					
Masonry units:					
Brick, common		1922	0.72	—	—
Brick, face		2082	1.30	—	—
Brick, fire clay		2400	1.34	—	—
		1920	0.90	0.79	—
		1120	0.41	—	—
Concrete blocks (3 oval cores,	100 mm	—	0.77	—	0.13
sand and gravel aggregate)	200 mm	—	1.0	—	0.20
	300 mm	—	1.30	—	0.23
Concretes:					
Lightweight aggregates, (including		1920	1.1	—	—
expanded shale, clay, or slate;		1600	0.79	0.84	—
expanded slags; cinders;		1280	0.54	0.84	—
pumice; and scoria)		960	0.33	—	—
	940	0.18	—	—	—
Cement/lime, mortar, and stucco		1920	1.40	—	—
		1280	0.65	—	—
Stucco		1857	0.72	—	—

TABLE A–5

Properties of building materials (at a mean temperature of 24°C)   (*Concluded*)

Material	Thickness, L mm	Density, ρ kg/m³	Thermal Conductivity, k W/m·K	Specific Heat, c_p kJ/kg·K	R-value (for listed thickness, L/k), K·m²/W
Roofing					
Asbestos-cement shingles		1900	—	1.00	0.037
Asphalt roll roofing		1100	—	1.51	0.026
Asphalt shingles		1100	—	1.26	0.077
Built-in roofing	10 mm	1100	—	1.46	0.058
Slate	13 mm	—	—	1.26	0.009
Wood shingles (plain and plastic/film faced)		—	—	1.30	0.166
Plastering Materials					
Cement plaster, sand aggregate	19 mm	1860	0.72	0.84	0.026
Gypsum plaster:					
Lightweight aggregate	13 mm	720	—	—	0.055
Sand aggregate	13 mm	1680	0.81	0.84	0.016
Perlite aggregate	—	720	0.22	1.34	—
Siding Material (on flat surfaces)					
Asbestos-cement shingles	—	1900	—	—	0.037
Hardboard siding	11 mm	—	—	1.17	0.12
Wood (drop) siding	25 mm	—	—	1.30	0.139
Wood (plywood) siding lapped	10 mm	—	—	1.21	0.111
Aluminum or steel siding (over sheeting):					
Hollow backed	10 mm	—	—	1.22	0.11
Insulating-board backed	10 mm	—	—	1.34	0.32
Architectural glass	—	2530	1.0	0.84	0.018
Woods					
Hardwoods (maple, oak, etc.)	—	721	0.159	1.26	—
Softwoods (fir, pine, etc.)	—	513	0.115	1.38	—
Metals					
Aluminum (1100)	—	2739	222	0.896	—
Steel, mild	—	7833	45.3	0.502	—
Steel, Stainless	—	7913	15.6	0.456	—

Source: Table A–5 and A–6 are adapted from *ASHRAE, Handbook of Fundamentals* (Atlanta, GA: American Society of Heating, Refrigerating, and Air-Conditioning Engineers, 1993), Chap. 22, Table 4. Used with permission.

TABLE A–6

Properties of insulating materials (at a mean temperature of 24°C)

Material	Thickness, L mm	Density, ρ kg/m³	Thermal Conductivity, k W/m·K	Specific Heat, c_p kJ/kg·K	R-value (for listed thickness, L/k), K·m²/W
Blanket and Batt					
Mineral fiber (fibrous form	50 to 70 mm	4.8–32	—	0.71–0.96	1.23
processed from rock, slag,	75 to 90 mm	4.8–32	—	0.71–0.96	1.94
or glass)	135 to 165 mm	4.8–32	—	0.71–0.96	3.32
Board and Slab					
Cellular glass		136	0.055	1.0	—
Glass fiber (organic bonded)		64–144	0.036	0.96	—
Expanded polystyrene (molded beads)		16	0.040	1.2	—
Expanded polyurethane (R-11 expanded)		24	0.023	1.6	—
Expanded perlite (organic bonded)		16	0.052	1.26	—
Expanded rubber (rigid)		72	0.032	1.68	—
Mineral fiber with resin binder		240	0.042	0.71	—
Cork		120	0.039	1.80	—
Sprayed or Formed in Place					
Polyurethane foam		24–40	0.023–0.026	—	—
Glass fiber		56–72	0.038–0.039	—	—
Urethane, two-part mixture (rigid foam)		70	0.026	1.045	—
Mineral wool granules with asbestos/					
inorganic binders (sprayed)		190	0.046	—	—
Loose Fill					
Mineral fiber (rock, slag, or glass)	~75 to 125 mm	9.6–32	—	0.71	1.94
	~165 to 222 mm	9.6–32	—	0.71	3.35
	~191 to 254 mm	—	—	0.71	3.87
	~185 mm	—	—	0.71	5.28
Silica aerogel		122	0.025	—	—
Vermiculite (expanded)		122	0.068	—	—
Perlite, expanded		32–66	0.039–0.045	1.09	—
Sawdust or shavings		128–240	0.065	1.38	—
Cellulosic insulation (milled paper or wood pulp)		37–51	0.039–0.046	—	—
Roof Insulation					
Cellular glass	—	144	0.058	1.0	—
Preformed, for use above deck	13 mm	—	—	1.0	0.24
	25 mm	—	—	2.1	0.49
	50 mm	—	—	3.9	0.93
Reflective Insulation					
Silica powder (evacuated)		160	0.0017	—	—
Aluminum foil separating fluffy glass mats; 10–12 layers					
(evacuated); for cryogenic applications (150 K)		40	0.00016	—	—
Aluminum foil and glass paper laminate; 75–150					
layers (evacuated); for cryogenic applications (150 K)		120	0.000017	—	—

Source: Table A–5 and A–6 are adapted from *ASHRAE, Handbook of Fundamentals* (Atlanta, GA: American Society of Heating, Refrigerating, and Air-Conditioning Engineers, 1993), Chap. 22, Table 4. Used with permission.

TABLE A–7

Properties of common foods
(a) Specific heats and freezing-point properties

Food	Water content[a] % (mass)	Freezing point[a] °C	Specific heat[b] kJ/kg·K — Above Freezing	Specific heat[b] kJ/kg·K — Below Freezing	Latent Heat of Fusion[c] kJ/kg
Vegetables					
Artichokes	84	−1.2	3.65	1.90	281
Asparagus	93	−0.6	3.96	2.01	311
Beans, snap	89	−0.7	3.82	1.96	297
Broccoli	90	−0.6	3.86	1.97	301
Cabbage	92	−0.9	3.92	2.00	307
Carrots	88	−1.4	3.79	1.95	294
Cauliflower	92	−0.8	3.92	2.00	307
Celery	94	−0.5	3.99	2.02	314
Corn, sweet	74	−0.6	3.32	1.77	247
Cucumbers	96	−0.5	4.06	2.05	321
Eggplant	93	−0.8	3.96	2.01	311
Horseradish	75	−1.8	3.35	1.78	251
Leeks	85	−0.7	3.69	1.91	284
Lettuce	95	−0.2	4.02	2.04	317
Mushrooms	91	−0.9	3.89	1.99	304
Okra	90	−1.8	3.86	1.97	301
Onions, green	89	−0.9	3.82	1.96	297
Onions, dry	88	−0.8	3.79	1.95	294
Parsley	85	−1.1	3.69	1.91	284
Peas, green	74	−0.6	3.32	1.77	247
Peppers, sweet	92	−0.7	3.92	2.00	307
Potatoes	78	−0.6	3.45	1.82	261
Pumpkins	91	−0.8	3.89	1.99	304
Spinach	93	−0.3	3.96	2.01	311
Tomatos, rIpe	94	−0.5	3.99	2.02	314
Turnips	92	−1.1	3.92	2.00	307
Fruits					
Apples	84	−1.1	3.65	1.90	281
Apricots	85	−1.1	3.69	1.91	284
Avocados	65	−0.3	3.02	1.66	217
Bananas	75	−0.8	3.35	1.78	251
Blueberries	82	−1.6	3.59	1.87	274
Cantaloupes	92	−1.2	3.92	2.00	307
Cherries, sour	84	−1.7	3.65	1.90	281
Cherries, sweet	80	−1.8	3.52	1.85	267
Figs, dried	23	—	—	1.13	77
Figs, fresh	78	−2.4	3.45	1.82	261
Grapefruit	89	−1.1	3.82	1.96	297
Grapes	82	−1.1	3.59	1.87	274
Lemons	89	−1.4	3.82	1.96	297
Olives	75	−1.4	3.35	1.78	251
Oranges	87	−0.8	3.75	1.94	291
Peaches	89	−0.9	3.82	1.96	297
Pears	83	−1.6	3.62	1.89	277
Pineapples	85	−1.0	3.69	1.91	284
Plums	86	−0.8	3.72	1.92	287
Quinces	85	−2.0	3.69	1.91	284
Raisins	18	—	—	1.07	60
Strawberries	90	−0.8	3.86	1.97	301
Tangerines	87	−1.1	3.75	1.94	291
Watermelon	93	−0.4	3.96	2.01	311
Fish/Seafood					
Cod, whole	78	−2.2	3.45	1.82	261
Halibut, whole	75	−2.2	3.35	1.78	251
Lobster	79	−2.2	3.49	1.84	264
Mackerel	57	−2.2	2.75	1.56	190
Salmon, whole	64	−2.2	2.98	1.65	214
Shrimp	83	−2.2	3.62	1.89	277
Meats					
Beef carcass	49	−1.7	2.48	1.46	164
Liver	70	−1.7	3.18	1.72	234
Round, beef	67	—	3.08	1.68	224
Sirloin, beef	56	—	2.72	1.55	187
Chicken	74	−2.8	3.32	1.77	247
Lamb leg	65	—	3.02	1.66	217
Port carcass	37	—	2.08	1.31	124
Ham	56	−1.7	2.72	1.55	187
Pork sausage	38	—	2.11	1.32	127
Turkey	64	—	2.98	1.65	214
Other					
Almonds	5	—	—	0.89	17
Butter	16	—	—	1.04	53
Cheese,					
Cheddar	37	−12.9	2.08	1.31	124
Cheese, Swiss	39	−10.0	2.15	1.33	130
Chocolate milk	1	—	—	0.85	3
Eggs, whole	74	−0.6	3.32	1.77	247
Honey	17	—	—	1.05	57
Ice cream	63	−5.6	2.95	1.63	210
Milk, whole	88	−0.6	3.79	1.95	294
Peanuts	6	—	—	0.92	20
Peanuts, roasted	2	—	—	0.87	7
Pecans	3	—	—	0.87	10
Walnuts	4	—	—	0.88	13

Sources: [a]Water content and freezing-point data are from ASHRAE, *Handbook of Fundamentals*, SI version (Atlanta, GA: American Society of Heating, Refrigerating and Air–Conditioning Engineers, Inc., 1993), Chap. 30. Table 1.

[b]Specific heat data are based on the specific heat values of a water and ice at 0°C and are determined from Siebel's formulas: $c_{p,\,fresh} = 3.35 \times$ (Water content) + 0.84, above freezing, and $c_{p,\,frozen} = 1.26 \times$ (Water content) + 0.84, below freezing.

[c]The latent heat of fusion is determined by multiplying the heat of fusion of water (334 kJ/kg) by the water content of the food.

TABLE A–7

Properties of common foods
(*b*) Other properties

Food	Water Content,% (mass)	Temperature, T °C	Density, ρ kg/m³	Thermal Conductivity, k W/m·K	Thermal Diffusivity, α m²/s	Specific Heat c_p kJ/kg·K
Fruits/Vegetables						
Apple juice	87	20	1000	0.559	0.14×10^{-6}	3.86
Apples	85	8	840	0.418	0.13×10^{-6}	3.81
Apples, dried	41.6	23	856	0.219	0.096×10^{-6}	2.72
Apricots, dried	43.6	23	1320	0.375	0.11×10^{-6}	2.77
Bananas, fresh	76	27	980	0.481	0.14×10^{-6}	3.59
Broccoli	—	26	560	0.385	—	—
Cherries, fresh	92	0–30	1050	0.545	0.13×10^{-6}	3.99
Figs	40.4	23	1241	0.310	0.096×10^{-6}	2.69
Grape juice	89	20	1000	0.567	0.14×10^{-6}	3.91
Peaches	89	2–32	960	0.526	0.14×10^{-6}	3.91
Plums	—	−16	610	0.247	—	—
Potatoes	78	0–70	1055	0.498	0.13×10^{-6}	3.64
Raisins	32	23	1380	0.376	0.11×10^{-6}	2.48
Meats						
Beef, ground	67	6	950	0.406	0.13×10^{-6}	3.36
Beef, lean	74	3	1090	0.471	0.13×10^{-6}	3.54
Beef fat	0	35	810	0.190	—	—
Beef liver	72	35	—	0.448	—	3.49
Cat food	39.7	23	1140	0.326	0.11×10^{-6}	2.68
Chicken breast	75	0	1050	0.476	0.13×10^{-6}	3.56
Dog food	30.6	23	1240	0.319	0.11×10^{-6}	2.45
Fish, cod	81	3	1180	0.534	0.12×10^{-6}	3.71
Fish, salmon	67	3	—	0.531	—	3.36
Ham	71.8	20	1030	0.480	0.14×10^{-6}	3.48
Lamb	72	20	1030	0.456	0.13×10^{-6}	3.49
Pork, lean	72	4	1030	0.456	0.13×10^{-6}	3.49
Turkey breast	74	3	1050	0.496	0.13×10^{-6}	3.54
Veal	75	20	1060	0.470	0.13×10^{-6}	3.56
Other						
Butter	16	4	—	0.197	—	2.08
Chocolate cake	31.9	23	340	0.106	0.12×10^{-6}	2.48
Margarine	16	5	1000	0.233	0.11×10^{-6}	2.08
Milk, skimmed	91	20	—	0.566	—	3.96
Milk, whole	88	28	—	0.580	—	3.89
Olive oil	0	32	910	0.168	—	—
Peanut oil	0	4	920	0.168	—	—
Water	100	0	1000	0.569	0.14×10^{-6}	4.217
	100	30	995	0.618	0.15×10^{-6}	4.178
White cake	32.3	23	450	0.082	0.10×10^{-6}	2.49

Source: Data obtained primarily from ASHRAE, *Handbook of Fundamentals,* SI version (Atlanta, GA: American Society of Heating, Refrigerating and Air-Conditioning Engineers, Inc., 1993), Chap. 30, Tables 7 and 9. Used with permission.

Most specific heats are calculated from $c_p = 1.68 + 2.51 \times$ (Water content), which is a good approximation in the temperature range of 3 to 32°C. Most thermal diffusivities are calculated from $\alpha = k/\rho c_p$. Property values given here are valid for the specific water content.

TABLE A–8

Properties of miscellaneous materials
(Values are at 300 K unless indicated otherwise)

Material	Density, ρ kg/m^3	Thermal Conductivity, k W/m·K	Specific Heat, c_p J/kg·K	Material	Density, ρ kg/m^3	Thermal Conductivity, k W/m·K	Specific Heat, c_p J/kg·K
Asphalt	2115	0.062	920	Ice			
Bakelite	1300	1.4	1465	273 K	920	1.88	2040
Brick, refractory				253 K	922	2.03	1945
Chrome brick				173 K	928	3.49	1460
473 K	3010	2.3	835	Leather, sole	998	0.159	—
823 K	—	2.5	—	Linoleum	535	0.081	—
1173 K	—	2.0	—		1180	0.186	—
Fire clay, burnt 1600 K				Mica	2900	0.523	—
				Paper	930	0.180	1340
773 K	2050	1.0	960	Plastics			
1073 K	—	1.1	—	Plexiglass	1190	0.19	1465
1373 K	—	1.1	—	Teflon			
Fire clay, burnt 1725 K				300 K	2200	0.35	1050
				400 K	—	0.45	—
773 K	2325	1.3	960	Lexan	1200	0.19	1260
1073 K	—	1.4	—	Nylon	1145	0.29	—
1373 K	—	1.4	—	Polypropylene	910	0.12	1925
Fire clay brick				Polyester	1395	0.15	1170
478 K	2645	1.0	960	PVC, vinyl	1470	0.1	840
922 K	—	1.5	—	Porcelain	2300	1.5	—
1478 K	—	1.8	—	Rubber, natural	1150	0.28	—
Magnesite				Rubber, vulcanized			
478 K	—	3.8	1130	Soft	1100	0.13	2010
922 K	—	2.8	—	Hard	1190	0.16	—
1478 K	—	1.9	—	Sand	1515	0.2–1.0	800
Chicken meat,				Snow, fresh	100	0.60	—
white (74.4%				Snow, 273 K	500	2.2	—
water content)				Soil, dry	1500	1.0	1900
198 K	—	1.60	—	Soil, wet	1900	2.0	2200
233 K	—	1.49	—	Sugar	1600	0.58	—
253 K	—	1.35	—	Tissue, human			
273 K	—	0.48	—	Skin	—	0.37	—
293 K	—	0.49	—	Fat layer	—	0.2	—
Clay, dry	1550	0.930	—	Muscle	—	0.41	—
Clay, wet	1495	1.675	—	Vaseline	—	0.17	—
Coal, anthracite	1350	0.26	1260	Wood, cross-grain			
Concrete (stone				Balsa	140	0.055	—
mix)	2300	1.4	880	Fir	415	0.11	2720
Cork	86	0.048	2030	Oak	545	0.17	2385
Cotton	80	0.06	1300	White pine	435	0.11	—
Fat	—	0.17	—	Yellow pine	640	0.15	2805
Glass				Wood, radial			
Window	2800	0.7	750	Oak	545	0.19	2385
Pyrex	2225	1–1.4	835	Fir	420	0.14	2720
Crown	2500	1.05	—	Wool, ship	145	0.05	—
Lead	3400	0.85	—				

Source: Compiled from various sources.

TABLE A–9

Properties of saturated water

Temp. T, °C	Saturation Pressure P_{sat}, kPa	Density ρ, kg/m³		Enthalpy of Vaporization h_{fg}, kJ/kg	Specific Heat c_p, J/kg·K		Thermal Conductivity k, W/m·K		Dynamic Viscosity μ, kg/m·s		Prandtl Number Pr		Volume Expansion Coefficient β, 1/K
		Liquid	Vapor		Liquid	Vapor	Liquid	Vapor	Liquid	Vapor	Liquid	Vapor	Liquid
0.01	0.6113	999.8	0.0048	2501	4217	1854	0.561	0.0171	1.792×10^{-3}	0.922×10^{-5}	13.5	1.00	-0.068×10^{-3}
5	0.8721	999.9	0.0068	2490	4205	1857	0.571	0.0173	1.519×10^{-3}	0.934×10^{-5}	11.2	1.00	0.015×10^{-3}
10	1.2276	999.7	0.0094	2478	4194	1862	0.580	0.0176	1.307×10^{-3}	0.946×10^{-5}	9.45	1.00	0.733×10^{-3}
15	1.7051	999.1	0.0128	2466	4185	1863	0.589	0.0179	1.138×10^{-3}	0.959×10^{-5}	8.09	1.00	0.138×10^{-3}
20	2.339	998.0	0.0173	2454	4182	1867	0.598	0.0182	1.002×10^{-3}	0.973×10^{-5}	7.01	1.00	0.195×10^{-3}
25	3.169	997.0	0.0231	2442	4180	1870	0.607	0.0186	0.891×10^{-3}	0.987×10^{-5}	6.14	1.00	0.247×10^{-3}
30	4.246	996.0	0.0304	2431	4178	1875	0.615	0.0189	0.798×10^{-3}	1.001×10^{-5}	5.42	1.00	0.294×10^{-3}
35	5.628	994.0	0.0397	2419	4178	1880	0.623	0.0192	0.720×10^{-3}	1.016×10^{-5}	4.83	1.00	0.337×10^{-3}
40	7.384	992.1	0.0512	2407	4179	1885	0.631	0.0196	0.653×10^{-3}	1.031×10^{-5}	4.32	1.00	0.377×10^{-3}
45	9.593	990.1	0.0655	2395	4180	1892	0.637	0.0200	0.596×10^{-3}	1.046×10^{-5}	3.91	1.00	0.415×10^{-3}
50	12.35	988.1	0.0831	2383	4181	1900	0.644	0.0204	0.547×10^{-3}	1.062×10^{-5}	3.55	1.00	0.451×10^{-3}
55	15.76	985.2	0.1045	2371	4183	1908	0.649	0.0208	0.504×10^{-3}	1.077×10^{-5}	3.25	1.00	0.484×10^{-3}
60	19.94	983.3	0.1304	2359	4185	1916	0.654	0.0212	0.467×10^{-3}	1.093×10^{-5}	2.99	1.00	0.517×10^{-3}
65	25.03	980.4	0.1614	2346	4187	1926	0.659	0.0216	0.433×10^{-3}	1.110×10^{-5}	2.75	1.00	0.548×10^{-3}
70	31.19	977.5	0.1983	2334	4190	1936	0.663	0.0221	0.404×10^{-3}	1.126×10^{-5}	2.55	1.00	0.578×10^{-3}
75	38.58	974.7	0.2421	2321	4193	1948	0.667	0.0225	0.378×10^{-3}	1.142×10^{-5}	2.38	1.00	0.607×10^{-3}
80	47.39	971.8	0.2935	2309	4197	1962	0.670	0.0230	0.355×10^{-3}	1.159×10^{-5}	2.22	1.00	0.653×10^{-3}
85	57.83	968.1	0.3536	2296	4201	1977	0.673	0.0235	0.333×10^{-3}	1.176×10^{-5}	2.08	1.00	0.670×10^{-3}
90	70.14	965.3	0.4235	2283	4206	1993	0.675	0.0240	0.315×10^{-3}	1.193×10^{-5}	1.96	1.00	0.702×10^{-3}
95	84.55	961.5	0.5045	2270	4212	2010	0.677	0.0246	0.297×10^{-3}	1.210×10^{-5}	1.85	1.00	0.716×10^{-3}
100	101.33	957.9	0.5978	2257	4217	2029	0.679	0.0251	0.282×10^{-3}	1.227×10^{-5}	1.75	1.00	0.750×10^{-3}
110	143.27	950.6	0.8263	2230	4229	2071	0.682	0.0262	0.255×10^{-3}	1.261×10^{-5}	1.58	1.00	0.798×10^{-3}
120	198.53	943.4	1.121	2203	4244	2120	0.683	0.0275	0.232×10^{-3}	1.296×10^{-5}	1.44	1.00	0.858×10^{-3}
130	270.1	934.6	1.496	2174	4263	2177	0.684	0.0288	0.213×10^{-3}	1.330×10^{-5}	1.33	1.01	0.913×10^{-3}
140	361.3	921.7	1.965	2145	4286	2244	0.683	0.0301	0.197×10^{-3}	1.365×10^{-5}	1.24	1.02	0.970×10^{-3}
150	475.8	916.6	2.546	2114	4311	2314	0.682	0.0316	0.183×10^{-3}	1.399×10^{-5}	1.16	1.02	1.025×10^{-3}
160	617.8	907.4	3.256	2083	4340	2420	0.680	0.0331	0.170×10^{-3}	1.434×10^{-5}	1.09	1.05	1.145×10^{-3}
170	791.7	897.7	4.119	2050	4370	2490	0.677	0.0347	0.160×10^{-3}	1.468×10^{-5}	1.03	1.05	1.178×10^{-3}
180	1,002.1	887.3	5.153	2015	4410	2590	0.673	0.0364	0.150×10^{-3}	1.502×10^{-5}	0.983	1.07	1.210×10^{-3}
190	1,254.4	876.4	6.388	1979	4460	2710	0.669	0.0382	0.142×10^{-3}	1.537×10^{-5}	0.947	1.09	1.280×10^{-3}
200	1,553.8	864.3	7.852	1941	4500	2840	0.663	0.0401	0.134×10^{-3}	1.571×10^{-5}	0.910	1.11	1.350×10^{-3}
220	2,318	840.3	11.60	1859	4610	3110	0.650	0.0442	0.122×10^{-3}	1.641×10^{-5}	0.865	1.15	1.520×10^{-3}
240	3,344	813.7	16.73	1767	4760	3520	0.632	0.0487	0.111×10^{-3}	1.712×10^{-5}	0.836	1.24	1.720×10^{-3}
260	4,688	783.7	23.69	1663	4970	4070	0.609	0.0540	0.102×10^{-3}	1.788×10^{-5}	0.832	1.35	2.000×10^{-3}
280	6,412	750.8	33.15	1544	5280	4835	0.581	0.0605	0.094×10^{-3}	1.870×10^{-5}	0.854	1.49	2.380×10^{-3}
300	8,581	713.8	46.15	1405	5750	5980	0.548	0.0695	0.086×10^{-3}	1.965×10^{-5}	0.902	1.69	2.950×10^{-3}
320	11,274	667.1	64.57	1239	6540	7900	0.509	0.0836	0.078×10^{-3}	2.084×10^{-5}	1.00	1.97	
340	14,586	610.5	92.62	1028	8240	11,870	0.469	0.110	0.070×10^{-3}	2.255×10^{-5}	1.23	2.43	
360	18,651	528.3	144.0	720	14,690	25,800	0.427	0.178	0.060×10^{-3}	2.571×10^{-5}	2.06	3.73	
374.14	22,090	317.0	317.0	0	—	—	—	—	0.043×10^{-3}	4.313×10^{-5}			

Note 1: Kinematic viscosity ν and thermal diffusivity α can be calculated from their definitions, $\nu = \mu/\rho$ and $\alpha = k/\rho c_p = \nu/\text{Pr}$. The temperatures 0.01°C, 100°C, and 374.14°C are the triple-, boiling-, and critical-point temperatures of water, respectively. The properties listed above (except the vapor density) can be used at any pressure with negligible error except at temperatures near the critical-point value.

Note 2: The unit kJ/kg·°C for specific heat is equivalent to kJ/kg·K, and the unit W/m·°C for thermal conductivity is equivalent to W/m·K.

Source: Viscosity and thermal conductivity data are from J. V. Sengers and J. T. R. Watson, *Journal of Physical and Chemical Reference Data* 15 (1986), pp. 1291–1322. Other data are obtained from various sources or calculated.

TABLE A–10

Properties of saturated refrigerant-134a

Temp. T, °C	Saturation Pressure P, kPa	Density ρ, kg/m³		Enthalpy of Vaporization h_{fg}, kJ/kg	Specific Heat c_p, J/kg·K		Thermal Conductivity k, W/m·K		Dynamic Viscosity μ, kg/m·s		Prandtl Number Pr		Volume Expansion Coefficient β, 1/K	Surface Tension, N/m
		Liquid	Vapor		Liquid	Vapor	Liquid	Vapor	Liquid	Vapor	Liquid	Vapor	Liquid	
−40	51.2	1418	2.773	225.9	1254	748.6	0.1101	0.00811	4.878×10^{-4}	2.550×10^{-6}	5.558	0.235	0.00205	0.01760
−35	66.2	1403	3.524	222.7	1264	764.1	0.1084	0.00862	4.509×10^{-4}	3.003×10^{-6}	5.257	0.266	0.00209	0.01682
−30	84.4	1389	4.429	219.5	1273	780.2	0.1066	0.00913	4.178×10^{-4}	3.504×10^{-6}	4.992	0.299	0.00215	0.01604
−25	106.5	1374	5.509	216.3	1283	797.2	0.1047	0.00963	3.882×10^{-4}	4.054×10^{-6}	4.757	0.335	0.00220	0.01527
−20	132.8	1359	6.787	213.0	1294	814.9	0.1028	0.01013	3.614×10^{-4}	4.651×10^{-6}	4.548	0.374	0.00227	0.01451
−15	164.0	1343	8.288	209.5	1306	833.5	0.1009	0.01063	3.371×10^{-4}	5.295×10^{-6}	4.363	0.415	0.00233	0.01376
−10	200.7	1327	10.04	206.0	1318	853.1	0.0989	0.01112	3.150×10^{-4}	5.982×10^{-6}	4.198	0.459	0.00241	0.01302
−5	243.5	1311	12.07	202.4	1330	873.8	0.0968	0.01161	2.947×10^{-4}	6.709×10^{-6}	4.051	0.505	0.00249	0.01229
0	293.0	1295	14.42	198.7	1344	895.6	0.0947	0.01210	2.761×10^{-4}	7.471×10^{-6}	3.919	0.553	0.00258	0.01156
5	349.9	1278	17.12	194.8	1358	918.7	0.0925	0.01259	2.589×10^{-4}	8.264×10^{-6}	3.802	0.603	0.00269	0.01084
10	414.9	1261	20.22	190.8	1374	943.2	0.0903	0.01308	2.430×10^{-4}	9.081×10^{-6}	3.697	0.655	0.00280	0.01014
15	488.7	1244	23.75	186.6	1390	969.4	0.0880	0.01357	2.281×10^{-4}	9.915×10^{-6}	3.604	0.708	0.00293	0.00944
20	572.1	1226	27.77	182.3	1408	997.6	0.0856	0.01406	2.142×10^{-4}	1.075×10^{-5}	3.521	0.763	0.00307	0.00876
25	665.8	1207	32.34	177.8	1427	1028	0.0833	0.01456	2.012×10^{-4}	1.160×10^{-5}	3.448	0.819	0.00324	0.00808
30	770.6	1188	37.53	173.1	1448	1061	0.0808	0.01507	1.888×10^{-4}	1.244×10^{-5}	3.383	0.877	0.00342	0.00742
35	887.5	1168	43.41	168.2	1471	1098	0.0783	0.01558	1.772×10^{-4}	1.327×10^{-5}	3.328	0.935	0.00364	0.00677
40	1017.1	1147	50.08	163.0	1498	1138	0.0757	0.01610	1.660×10^{-4}	1.408×10^{-5}	3.285	0.995	0.00390	0.00613
45	1160.5	1125	57.66	157.6	1529	1184	0.0731	0.01664	1.554×10^{-4}	1.486×10^{-5}	3.253	1.058	0.00420	0.00550
50	1318.6	1102	66.27	151.8	1566	1237	0.0704	0.01720	1.453×10^{-4}	1.562×10^{-5}	3.231	1.123	0.00455	0.00489
55	1492.3	1078	76.11	145.7	1608	1298	0.0676	0.01777	1.355×10^{-4}	1.634×10^{-5}	3.223	1.193	0.00500	0.00429
60	1682.8	1053	87.38	139.1	1659	1372	0.0647	0.01838	1.260×10^{-4}	1.704×10^{-5}	3.229	1.272	0.00554	0.00372
65	1891.0	1026	100.4	132.1	1722	1462	0.0618	0.01902	1.167×10^{-4}	1.771×10^{-5}	3.255	1.362	0.00624	0.00315
70	2118.2	996.2	115.6	124.4	1801	1577	0.0587	0.01972	1.077×10^{-4}	1.839×10^{-5}	3.307	1.471	0.00716	0.00261
75	2365.8	964	133.6	115.9	1907	1731	0.0555	0.02048	9.891×10^{-5}	1.908×10^{-5}	3.400	1.612	0.00843	0.00209
80	2635.2	928.2	155.3	106.4	2056	1948	0.0521	0.02133	9.011×10^{-5}	1.982×10^{-5}	3.558	1.810	0.01031	0.00160
85	2928.2	887.1	182.3	95.4	2287	2281	0.0484	0.02233	8.124×10^{-5}	2.071×10^{-5}	3.837	2.116	0.01336	0.00114
90	3246.9	837.7	217.8	82.2	2701	2865	0.0444	0.02357	7.203×10^{-5}	2.187×10^{-5}	4.385	2.658	0.01911	0.00071
95	3594.1	772.5	269.3	64.9	3675	4144	0.0396	0.02544	6.190×10^{-5}	2.370×10^{-5}	5.746	3.862	0.03343	0.00033
100	3975.1	651.7	376.3	33.9	7959	8785	0.0322	0.02989	4.765×10^{-5}	2.833×10^{-5}	11.77	8.326	0.10047	0.00004

Note 1: Kinematic viscosity ν and thermal diffusivity α can be calculated from their definitions, $\nu = \mu/\rho$ and $\alpha = k/\rho\, c_p = \nu/\text{Pr}$. The properties listed here (except the vapor density) can be used at any pressures with negligible error except at temperatures near the critical-point value.

Note 2: The unit kJ/kg·°C for specific heat is equivalent to kJ/kg·K, and the unit W/m·°C for thermal conductivity is equivalent to W/m·K.

Source: Data generated from the EES software developed by S. A. Klein and F. L. Alvarado. Original sources: R. Tillner-Roth and H. D. Baehr, "An International Standard Formulation for the Thermodynamic Properties of 1,1,1,2-Tetrafluoroethane (HFC-134a) for Temperatures from 170 K to 455 K and Pressures up to 70 MPa," *J. Phys. Chem. Ref. Data,* Vol. 23, No. 5, 1994; M.J. Assael, N. K. Dalaouti, A. A. Griva, and J. H. Dymond, "Viscosity and Thermal Conductivity of Halogenated Methane and Ethane Refrigerants," *IJR,* Vol. 22, pp. 525–535, 1999; NIST REFPROP 6 program (M. O. McLinden, S. A. Klein, E. W. Lemmon, and A. P. Peskin, Physical and Chemical Properties Division, National Institute of Standards and Technology, Boulder, CO 80303, 1995).

TABLE A–11

Properties of saturated ammonia

Temp. T, °C	Saturation Pressure P, kPa	Density ρ, kg/m³ Liquid	Density ρ, kg/m³ Vapor	Enthalpy of Vaporization h_{fg}, kJ/kg	Specific Heat c_p, J/kg·K Liquid	Specific Heat c_p, J/kg·K Vapor	Thermal Conductivity k, W/m·K Liquid	Thermal Conductivity k, W/m·K Vapor	Dynamic Viscosity μ, kg/m·s Liquid	Dynamic Viscosity μ, kg/m·s Vapor	Prandtl Number Pr Liquid	Prandtl Number Pr Vapor	Volume Expansion Coefficient β, 1/K Liquid	Surface Tension, N/m
−40	71.66	690.2	0.6435	1389	4414	2242	—	0.01792	2.926×10^{-4}	7.957×10^{-6}	—	0.9955	0.00176	0.03565
−30	119.4	677.8	1.037	1360	4465	2322	—	0.01898	2.630×10^{-4}	8.311×10^{-6}	—	1.017	0.00185	0.03341
−25	151.5	671.5	1.296	1345	4489	2369	0.5968	0.01957	2.492×10^{-4}	8.490×10^{-6}	1.875	1.028	0.00190	0.03229
−20	190.1	665.1	1.603	1329	4514	2420	0.5853	0.02015	2.361×10^{-4}	8.669×10^{-6}	1.821	1.041	0.00194	0.03118
−15	236.2	658.6	1.966	1313	4538	2476	0.5737	0.02075	2.236×10^{-4}	8.851×10^{-6}	1.769	1.056	0.00199	0.03007
−10	290.8	652.1	2.391	1297	4564	2536	0.5621	0.02138	2.117×10^{-4}	9.034×10^{-6}	1.718	1.072	0.00205	0.02896
−5	354.9	645.4	2.886	1280	4589	2601	0.5505	0.02203	2.003×10^{-4}	9.218×10^{-6}	1.670	1.089	0.00210	0.02786
0	429.6	638.6	3.458	1262	4617	2672	0.5390	0.02270	1.896×10^{-4}	9.405×10^{-6}	1.624	1.107	0.00216	0.02676
5	516	631.7	4.116	1244	4645	2749	0.5274	0.02341	1.794×10^{-4}	9.593×10^{-6}	1.580	1.126	0.00223	0.02566
10	615.3	624.6	4.870	1226	4676	2831	0.5158	0.02415	1.697×10^{-4}	9.784×10^{-6}	1.539	1.147	0.00230	0.02457
15	728.8	617.5	5.729	1206	4709	2920	0.5042	0.02492	1.606×10^{-4}	9.978×10^{-6}	1.500	1.169	0.00237	0.02348
20	857.8	610.2	6.705	1186	4745	3016	0.4927	0.02573	1.519×10^{-4}	1.017×10^{-5}	1.463	1.193	0.00245	0.02240
25	1003	602.8	7.809	1166	4784	3120	0.4811	0.02658	1.438×10^{-4}	1.037×10^{-5}	1.430	1.218	0.00254	0.02132
30	1167	595.2	9.055	1144	4828	3232	0.4695	0.02748	1.361×10^{-4}	1.057×10^{-5}	1.399	1.244	0.00264	0.02024
35	1351	587.4	10.46	1122	4877	3354	0.4579	0.02843	1.288×10^{-4}	1.078×10^{-5}	1.372	1.272	0.00275	0.01917
40	1555	579.4	12.03	1099	4932	3486	0.4464	0.02943	1.219×10^{-4}	1.099×10^{-5}	1.347	1.303	0.00287	0.01810
45	1782	571.3	13.8	1075	4993	3631	0.4348	0.03049	1.155×10^{-4}	1.121×10^{-5}	1.327	1.335	0.00301	0.01704
50	2033	562.9	15.78	1051	5063	3790	0.4232	0.03162	1.094×10^{-4}	1.143×10^{-5}	1.310	1.371	0.00316	0.01598
55	2310	554.2	18.00	1025	5143	3967	0.4116	0.03283	1.037×10^{-4}	1.166×10^{-5}	1.297	1.409	0.00334	0.01493
60	2614	545.2	20.48	997.4	5234	4163	0.4001	0.03412	9.846×10^{-5}	1.189×10^{-5}	1.288	1.452	0.00354	0.01389
65	2948	536.0	23.26	968.9	5340	4384	0.3885	0.03550	9.347×10^{-5}	1.213×10^{-5}	1.285	1.499	0.00377	0.01285
70	3312	526.3	26.39	939.0	5463	4634	0.3769	0.03700	8.879×10^{-5}	1.238×10^{-5}	1.287	1.551	0.00404	0.01181
75	3709	516.2	29.90	907.5	5608	4923	0.3653	0.03862	8.440×10^{-5}	1.264×10^{-5}	1.296	1.612	0.00436	0.01079
80	4141	505.7	33.87	874.1	5780	5260	0.3538	0.04038	8.030×10^{-5}	1.292×10^{-5}	1.312	1.683	0.00474	0.00977
85	4609	494.5	38.36	838.6	5988	5659	0.3422	0.04232	7.646×10^{-5}	1.322×10^{-5}	1.338	1.768	0.00521	0.00876
90	5116	482.8	43.48	800.6	6242	6142	0.3306	0.04447	7.284×10^{-5}	1.354×10^{-5}	1.375	1.871	0.00579	0.00776
95	5665	470.2	49.35	759.8	6561	6740	0.3190	0.04687	6.946×10^{-5}	1.389×10^{-5}	1.429	1.999	0.00652	0.00677
100	6257	456.6	56.15	715.5	6972	7503	0.3075	0.04958	6.628×10^{-5}	1.429×10^{-5}	1.503	2.163	0.00749	0.00579

Note 1: Kinematic viscosity ν and thermal diffusivity α can be calculated from their definitions, $\nu = \mu/\rho$ and $\alpha = k/\rho\, c_p = \nu/\text{Pr}$. The properties listed here (except the vapor density) can be used at any pressures with negligible error except at temperatures near the critical-point value.

Note 2: The unit kJ/kg·°C for specific heat is equivalent to kJ/kg·K, and the unit W/m·°C for thermal conductivity is equivalent to W/m·K.

Source: Data generated from the EES software developed by S. A. Klein and F. L. Alvarado. Original sources: Tillner-Roth, Harms-Watzenberg, and Baehr, "Eine neue Fundamentalgleichung fur Ammoniak," DKV-Tagungsbericht 20:167–181, 1993; Liley and Desai, "Thermophysical Properties of Refrigerants," *ASHRAE,* 1993, ISBN 1-1883413-10-9.

TABLE A–12

Properties of saturated propane

Temp. T, °C	Saturation Pressure P, kPa	Density ρ, kg/m³ Liquid	Density ρ, kg/m³ Vapor	Enthalpy of Vaporization h_{fg}, kJ/kg	Specific Heat c_p, J/kg·K Liquid	Specific Heat c_p, J/kg·K Vapor	Thermal Conductivity k, W/m·K Liquid	Thermal Conductivity k, W/m·K Vapor	Dynamic Viscosity μ, kg/m·s Liquid	Dynamic Viscosity μ, kg/m·s Vapor	Prandtl Number Pr Liquid	Prandtl Number Pr Vapor	Volume Expansion Coefficient β, 1/K Liquid	Surface Tension, N/m
−120	0.4053	664.7	0.01408	498.3	2003	1115	0.1802	0.00589	6.136×10^{-4}	4.372×10^{-6}	6.820	0.827	0.00153	0.02630
−110	1.157	654.5	0.03776	489.3	2021	1148	0.1738	0.00645	5.054×10^{-4}	4.625×10^{-6}	5.878	0.822	0.00157	0.02486
−100	2.881	644.2	0.08872	480.4	2044	1183	0.1672	0.00705	4.252×10^{-4}	4.881×10^{-6}	5.195	0.819	0.00161	0.02344
−90	6.406	633.8	0.1870	471.5	2070	1221	0.1606	0.00769	3.635×10^{-4}	5.143×10^{-6}	4.686	0.817	0.00166	0.02202
−80	12.97	623.2	0.3602	462.4	2100	1263	0.1539	0.00836	3.149×10^{-4}	5.409×10^{-6}	4.297	0.817	0.00171	0.02062
−70	24.26	612.5	0.6439	453.1	2134	1308	0.1472	0.00908	2.755×10^{-4}	5.680×10^{-6}	3.994	0.818	0.00177	0.01923
−60	42.46	601.5	1.081	443.5	2173	1358	0.1407	0.00985	2.430×10^{-4}	5.956×10^{-6}	3.755	0.821	0.00184	0.01785
−50	70.24	590.3	1.724	433.6	2217	1412	0.1343	0.01067	2.158×10^{-4}	6.239×10^{-6}	3.563	0.825	0.00192	0.01649
−40	110.7	578.8	2.629	423.1	2258	1471	0.1281	0.01155	1.926×10^{-4}	6.529×10^{-6}	3.395	0.831	0.00201	0.01515
−30	167.3	567.0	3.864	412.1	2310	1535	0.1221	0.01250	1.726×10^{-4}	6.827×10^{-6}	3.266	0.839	0.00213	0.01382
−20	243.8	554.7	5.503	400.3	2368	1605	0.1163	0.01351	1.551×10^{-4}	7.136×10^{-6}	3.158	0.848	0.00226	0.01251
−10	344.4	542.0	7.635	387.8	2433	1682	0.1107	0.01459	1.397×10^{-4}	7.457×10^{-6}	3.069	0.860	0.00242	0.01122
0	473.3	528.7	10.36	374.2	2507	1768	0.1054	0.01576	1.259×10^{-4}	7.794×10^{-6}	2.996	0.875	0.00262	0.00996
5	549.8	521.8	11.99	367.0	2547	1814	0.1028	0.01637	1.195×10^{-4}	7.970×10^{-6}	2.964	0.883	0.00273	0.00934
10	635.1	514.7	13.81	359.5	2590	1864	0.1002	0.01701	1.135×10^{-4}	8.151×10^{-6}	2.935	0.893	0.00286	0.00872
15	729.8	507.5	15.85	351.7	2637	1917	0.0977	0.01767	1.077×10^{-4}	8.339×10^{-6}	2.909	0.905	0.00301	0.00811
20	834.4	500.0	18.13	343.4	2688	1974	0.0952	0.01836	1.022×10^{-4}	8.534×10^{-6}	2.886	0.918	0.00318	0.00751
25	949.7	492.2	20.68	334.8	2742	2036	0.0928	0.01908	9.702×10^{-5}	8.738×10^{-6}	2.866	0.933	0.00337	0.00691
30	1076	484.2	23.53	325.8	2802	2104	0.0904	0.01982	9.197×10^{-5}	8.952×10^{-6}	2.850	0.950	0.00358	0.00633
35	1215	475.8	26.72	316.2	2869	2179	0.0881	0.02061	8.710×10^{-5}	9.178×10^{-6}	2.837	0.971	0.00384	0.00575
40	1366	467.1	30.29	306.1	2943	2264	0.0857	0.02142	8.240×10^{-5}	9.417×10^{-6}	2.828	0.995	0.00413	0.00518
45	1530	458.0	34.29	295.3	3026	2361	0.0834	0.02228	7.785×10^{-5}	9.674×10^{-6}	2.824	1.025	0.00448	0.00463
50	1708	448.5	38.79	283.9	3122	2473	0.0811	0.02319	7.343×10^{-5}	9.950×10^{-5}	2.826	1.061	0.00491	0.00408
60	2110	427.5	49.66	258.4	3283	2769	0.0765	0.02517	6.487×10^{-5}	1.058×10^{-5}	2.784	1.164	0.00609	0.00303
70	2580	403.2	64.02	228.0	3595	3241	0.0717	0.02746	5.649×10^{-5}	1.138×10^{-5}	2.834	1.343	0.00811	0.00204
80	3127	373.0	84.28	189.7	4501	4173	0.0663	0.03029	4.790×10^{-5}	1.249×10^{-5}	3.251	1.722	0.01248	0.00114
90	3769	329.1	118.6	133.2	6977	7239	0.0595	0.03441	3.807×10^{-5}	1.448×10^{-5}	4.465	3.047	0.02847	0.00037

Note 1: Kinematic viscosity ν and thermal diffusivity α can be calculated from their definitions, $\nu = \mu/\rho$ and $\alpha = k/\mu c_p = \nu/\text{Pr}$. The properties listed here (except the vapor density) can be used at any pressures with negligible error except at temperatures near the critical-point value.

Note 2: The unit kJ/kg·°C for specific heat is equivalent to kJ/kg·K, and the unit W/m·°C for thermal conductivity is equivalent to W/m·K.

Source: Data generated from the EES software developed by S. A. Klein and F. L. Alvarado. Original sources: Reiner Tillner-Roth, "Fundamental Equations of State," Shaker, Verlag, Aachan, 1998; B. A. Younglove and J. F. Ely, "Thermophysical Properties of Fluids. II Methane, Ethane, Propane, Isobutane, and Normal Butane," *J. Phys. Chem. Ref. Data,* Vol. 16, No. 4, 1987; G.R. Somayajulu, "A Generalized Equation for Surface Tension from the Triple-Point to the Critical-Point," *International Journal of Thermophysics,* Vol. 9, No. 4, 1988.

TABLE A–13

Properties of liquids

Temp. T, °C	Density ρ, kg/m³	Specific Heat c_p, J/kg·K	Thermal Conductivity k, W/m·K	Thermal Diffusivity α, m²/s	Dynamic Viscosity μ, kg/m·s	Kinematic Viscosity ν, m²/s	Prandtl Number Pr	Volume Expansion Coeff. β, 1/K
				Methane $[CH_4]$				
−160	420.2	3492	0.1863	1.270×10^{-7}	1.133×10^{-4}	2.699×10^{-7}	2.126	0.00352
−150	405.0	3580	0.1703	1.174×10^{-7}	9.169×10^{-5}	2.264×10^{-7}	1.927	0.00391
−140	388.8	3700	0.1550	1.077×10^{-7}	7.551×10^{-5}	1.942×10^{-7}	1.803	0.00444
−130	371.1	3875	0.1402	9.749×10^{-8}	6.288×10^{-5}	1.694×10^{-7}	1.738	0.00520
−120	351.4	4146	0.1258	8.634×10^{-8}	5.257×10^{-5}	1.496×10^{-7}	1.732	0.00637
−110	328.8	4611	0.1115	7.356×10^{-8}	4.377×10^{-5}	1.331×10^{-7}	1.810	0.00841
−100	301.0	5578	0.0967	5.761×10^{-8}	3.577×10^{-5}	1.188×10^{-7}	2.063	0.01282
−90	261.7	8902	0.0797	3.423×10^{-8}	2.761×10^{-5}	1.055×10^{-7}	3.082	0.02922
				Methanol $[CH_3(OH)]$				
20	788.4	2515	0.1987	1.002×10^{-7}	5.857×10^{-4}	7.429×10^{-7}	7.414	0.00118
30	779.1	2577	0.1980	9.862×10^{-8}	5.088×10^{-4}	6.531×10^{-7}	6.622	0.00120
40	769.6	2644	0.1972	9.690×10^{-8}	4.460×10^{-4}	5.795×10^{-7}	5.980	0.00123
50	760.1	2718	0.1965	9.509×10^{-8}	3.942×10^{-4}	5.185×10^{-7}	5.453	0.00127
60	750.4	2798	0.1957	9.320×10^{-8}	3.510×10^{-4}	4.677×10^{-7}	5.018	0.00132
70	740.4	2885	0.1950	9.128×10^{-8}	3.146×10^{-4}	4.250×10^{-7}	4.655	0.00137
				Isobutane (R600a)				
−100	683.8	1881	0.1383	1.075×10^{-7}	9.305×10^{-4}	1.360×10^{-6}	12.65	0.00142
−75	659.3	1970	0.1357	1.044×10^{-7}	5.624×10^{-4}	8.531×10^{-7}	8.167	0.00150
−50	634.3	2069	0.1283	9.773×10^{-8}	3.769×10^{-4}	5.942×10^{-7}	6.079	0.00161
−25	608.2	2180	0.1181	8.906×10^{-8}	2.688×10^{-4}	4.420×10^{-7}	4.963	0.00177
0	580.6	2306	0.1068	7.974×10^{-8}	1.993×10^{-4}	3.432×10^{-7}	4.304	0.00199
25	550.7	2455	0.0956	7.069×10^{-8}	1.510×10^{-4}	2.743×10^{-7}	3.880	0.00232
50	517.3	2640	0.0851	6.233×10^{-8}	1.155×10^{-4}	2.233×10^{-7}	3.582	0.00286
75	478.5	2896	0.0757	5.460×10^{-8}	8.785×10^{-5}	1.836×10^{-7}	3.363	0.00385
100	429.6	3361	0.0669	4.634×10^{-8}	6.483×10^{-5}	1.509×10^{-7}	3.256	0.00628
				Glycerin				
0	1276	2262	0.2820	9.773×10^{-8}	10.49	8.219×10^{-3}	84,101	
5	1273	2288	0.2835	9.732×10^{-8}	6.730	5.287×10^{-3}	54,327	
10	1270	2320	0.2846	9.662×10^{-8}	4.241	3.339×10^{-3}	34,561	
15	1267	2354	0.2856	9.576×10^{-8}	2.496	1.970×10^{-3}	20,570	
20	1264	2386	0.2860	9.484×10^{-8}	1.519	1.201×10^{-3}	12,671	
25	1261	2416	0.2860	9.388×10^{-8}	0.9934	7.878×10^{-4}	8,392	
30	1258	2447	0.2860	9.291×10^{-8}	0.6582	5.232×10^{-4}	5,631	
35	1255	2478	0.2860	9.195×10^{-8}	0.4347	3.464×10^{-4}	3,767	
40	1252	2513	0.2863	9.101×10^{-8}	0.3073	2.455×10^{-4}	2,697	
				Engine Oil (unused)				
0	899.0	1797	0.1469	9.097×10^{-8}	3.814	4.242×10^{-3}	46,636	0.00070
20	888.1	1881	0.1450	8.680×10^{-8}	0.8374	9.429×10^{-4}	10,863	0.00070
40	876.0	1964	0.1444	8.391×10^{-8}	0.2177	2.485×10^{-4}	2,962	0.00070
60	863.9	2048	0.1404	7.934×10^{-8}	0.07399	8.565×10^{-5}	1,080	0.00070
80	852.0	2132	0.1380	7.599×10^{-8}	0.03232	3.794×10^{-5}	499.3	0.00070
100	840.0	2220	0.1367	7.330×10^{-8}	0.01718	2.046×10^{-5}	279.1	0.00070
120	828.9	2308	0.1347	7.042×10^{-8}	0.01029	1.241×10^{-5}	176.3	0.00070
140	816.8	2395	0.1330	6.798×10^{-8}	0.006558	8.029×10^{-6}	118.1	0.00070
150	810.3	2441	0.1327	6.708×10^{-8}	0.005344	6.595×10^{-6}	98.31	0.00070

Source: Data generated from the EES software developed by S. A. Klein and F. L. Alvarado. Originally based on various sources.

TABLE A–14

Properties of liquid metals

Temp. T, °C	Density ρ, kg/m³	Specific Heat c_p, J/kg·K	Thermal Conductivity k, W/m·K	Thermal Diffusivity α, m²/s	Dynamic Viscosity μ, kg/m·s	Kinematic Viscosity ν, m²/s	Prandtl Number Pr	Volume Expansion Coeff. β, 1/K
				Mercury (Hg) Melting Point: −39°C				
0	13595	140.4	8.18200	4.287×10^{-6}	1.687×10^{-3}	1.241×10^{-7}	0.0289	1.810×10^{-4}
25	13534	139.4	8.51533	4.514×10^{-6}	1.534×10^{-3}	1.133×10^{-7}	0.0251	1.810×10^{-4}
50	13473	138.6	8.83632	4.734×10^{-6}	1.423×10^{-3}	1.056×10^{-7}	0.0223	1.810×10^{-4}
75	13412	137.8	9.15632	4.956×10^{-6}	1.316×10^{-3}	9.819×10^{-8}	0.0198	1.810×10^{-4}
100	13351	137.1	9.46706	5.170×10^{-6}	1.245×10^{-3}	9.326×10^{-8}	0.0180	1.810×10^{-4}
150	13231	136.1	10.07780	5.595×10^{-6}	1.126×10^{-3}	8.514×10^{-8}	0.0152	1.810×10^{-4}
200	13112	135.5	10.65465	5.996×10^{-6}	1.043×10^{-3}	7.959×10^{-8}	0.0133	1.815×10^{-4}
250	12993	135.3	11.18150	6.363×10^{-6}	9.820×10^{-4}	7.558×10^{-8}	0.0119	1.829×10^{-4}
300	12873	135.3	11.68150	6.705×10^{-6}	9.336×10^{-4}	7.252×10^{-8}	0.0108	1.854×10^{-4}
				Bismuth (Bi) Melting Point: 271°C				
350	9969	146.0	16.28	1.118×10^{-5}	1.540×10^{-3}	1.545×10^{-7}	0.01381	
400	9908	148.2	16.10	1.096×10^{-5}	1.422×10^{-3}	1.436×10^{-7}	0.01310	
500	9785	152.8	15.74	1.052×10^{-5}	1.188×10^{-3}	1.215×10^{-7}	0.01154	
600	9663	157.3	15.60	1.026×10^{-5}	1.013×10^{-3}	1.048×10^{-7}	0.01022	
700	9540	161.8	15.60	1.010×10^{-5}	8.736×10^{-4}	9.157×10^{-8}	0.00906	
				Lead (Pb) Melting Point: 327°C				
400	10506	158	15.97	9.623×10^{-6}	2.277×10^{-3}	2.167×10^{-7}	0.02252	
450	10449	156	15.74	9.649×10^{-6}	2.065×10^{-3}	1.976×10^{-7}	0.02048	
500	10390	155	15.54	9.651×10^{-6}	1.884×10^{-3}	1.814×10^{-7}	0.01879	
550	10329	155	15.39	9.610×10^{-6}	1.758×10^{-3}	1.702×10^{-7}	0.01771	
600	10267	155	15.23	9.568×10^{-6}	1.632×10^{-3}	1.589×10^{-7}	0.01661	
650	10206	155	15.07	9.526×10^{-6}	1.505×10^{-3}	1.475×10^{-7}	0.01549	
700	10145	155	14.91	9.483×10^{-6}	1.379×10^{-3}	1.360×10^{-7}	0.01434	
				Sodium (Na) Melting Point: 98°C				
100	927.3	1378	85.84	6.718×10^{-5}	6.892×10^{-4}	7.432×10^{-7}	0.01106	
200	902.5	1349	80.84	6.639×10^{-5}	5.385×10^{-4}	5.967×10^{-7}	0.008987	
300	877.8	1320	75.84	6.544×10^{-5}	3.878×10^{-4}	4.418×10^{-7}	0.006751	
400	853.0	1296	71.20	6.437×10^{-5}	2.720×10^{-4}	3.188×10^{-7}	0.004953	
500	828.5	1284	67.41	6.335×10^{-5}	2.411×10^{-4}	2.909×10^{-7}	0.004593	
600	804.0	1272	63.63	6.220×10^{-5}	2.101×10^{-4}	2.614×10^{-7}	0.004202	
				Potassium (K) Melting Point: 64°C				
200	795.2	790.8	43.99	6.995×10^{-5}	3.350×10^{-4}	4.213×10^{-7}	0.006023	
300	771.6	772.8	42.01	7.045×10^{-5}	2.667×10^{-4}	3.456×10^{-7}	0.004906	
400	748.0	754.8	40.03	7.090×10^{-5}	1.984×10^{-4}	2.652×10^{-7}	0.00374	
500	723.9	750.0	37.81	6.964×10^{-5}	1.668×10^{-4}	2.304×10^{-7}	0.003309	
600	699.6	750.0	35.50	6.765×10^{-5}	1.487×10^{-4}	2.126×10^{-7}	0.003143	
				Sodium-Potassium (%22Na-%78K) Melting Point: −11°C				
100	847.3	944.4	25.64	3.205×10^{-5}	5.707×10^{-4}	6.736×10^{-7}	0.02102	
200	823.2	922.5	26.27	3.459×10^{-5}	4.587×10^{-4}	5.572×10^{-7}	0.01611	
300	799.1	900.6	26.89	3.736×10^{-5}	3.467×10^{-4}	4.339×10^{-7}	0.01161	
400	775.0	879.0	27.50	4.037×10^{-5}	2.357×10^{-4}	3.041×10^{-7}	0.00753	
500	751.5	880.1	27.89	4.217×10^{-5}	2.108×10^{-4}	2.805×10^{-7}	0.00665	
600	728.0	881.2	28.28	4.408×10^{-5}	1.859×10^{-4}	2.553×10^{-7}	0.00579	

Source: Data generated from the EES software developed by S. A. Klein and F. L. Alvarado. Originally based on various sources.

TABLE A–15

Properties of air at 1 atm pressure

Temp. T, °C	Density ρ, kg/m³	Specific Heat c_p, J/kg·K	Thermal Conductivity k, W/m·K	Thermal Diffusivity α, m²/s	Dynamic Viscosity μ, kg/m·s	Kinematic Viscosity ν, m²/s	Prandtl Number Pr
−150	2.866	983	0.01171	4.158×10^{-6}	8.636×10^{-6}	3.013×10^{-6}	0.7246
−100	2.038	966	0.01582	8.036×10^{-6}	1.189×10^{-5}	5.837×10^{-6}	0.7263
−50	1.582	999	0.01979	1.252×10^{-5}	1.474×10^{-5}	9.319×10^{-6}	0.7440
−40	1.514	1002	0.02057	1.356×10^{-5}	1.527×10^{-5}	1.008×10^{-5}	0.7436
−30	1.451	1004	0.02134	1.465×10^{-5}	1.579×10^{-5}	1.087×10^{-5}	0.7425
−20	1.394	1005	0.02211	1.578×10^{-5}	1.630×10^{-5}	1.169×10^{-5}	0.7408
−10	1.341	1006	0.02288	1.696×10^{-5}	1.680×10^{-5}	1.252×10^{-5}	0.7387
0	1.292	1006	0.02364	1.818×10^{-5}	1.729×10^{-5}	1.338×10^{-5}	0.7362
5	1.269	1006	0.02401	1.880×10^{-5}	1.754×10^{-5}	1.382×10^{-5}	0.7350
10	1.246	1006	0.02439	1.944×10^{-5}	1.778×10^{-5}	1.426×10^{-5}	0.7336
15	1.225	1007	0.02476	2.009×10^{-5}	1.802×10^{-5}	1.470×10^{-5}	0.7323
20	1.204	1007	0.02514	2.074×10^{-5}	1.825×10^{-5}	1.516×10^{-5}	0.7309
25	1.184	1007	0.02551	2.141×10^{-5}	1.849×10^{-5}	1.562×10^{-5}	0.7296
30	1.164	1007	0.02588	2.208×10^{-5}	1.872×10^{-5}	1.608×10^{-5}	0.7282
35	1.145	1007	0.02625	2.277×10^{-5}	1.895×10^{-5}	1.655×10^{-5}	0.7268
40	1.127	1007	0.02662	2.346×10^{-5}	1.918×10^{-5}	1.702×10^{-5}	0.7255
45	1.109	1007	0.02699	2.416×10^{-5}	1.941×10^{-5}	1.750×10^{-5}	0.7241
50	1.092	1007	0.02735	2.487×10^{-5}	1.963×10^{-5}	1.798×10^{-5}	0.7228
60	1.059	1007	0.02808	2.632×10^{-5}	2.008×10^{-5}	1.896×10^{-5}	0.7202
70	1.028	1007	0.02881	2.780×10^{-5}	2.052×10^{-5}	1.995×10^{-5}	0.7177
80	0.9994	1008	0.02953	2.931×10^{-5}	2.096×10^{-5}	2.097×10^{-5}	0.7154
90	0.9718	1008	0.03024	3.086×10^{-5}	2.139×10^{-5}	2.201×10^{-5}	0.7132
100	0.9458	1009	0.03095	3.243×10^{-5}	2.181×10^{-5}	2.306×10^{-5}	0.7111
120	0.8977	1011	0.03235	3.565×10^{-5}	2.264×10^{-5}	2.522×10^{-5}	0.7073
140	0.8542	1013	0.03374	3.898×10^{-5}	2.345×10^{-5}	2.745×10^{-5}	0.7041
160	0.8148	1016	0.03511	4.241×10^{-5}	2.420×10^{-5}	2.975×10^{-5}	0.7014
180	0.7788	1019	0.03646	4.593×10^{-5}	2.504×10^{-5}	3.212×10^{-5}	0.6992
200	0.7459	1023	0.03779	4.954×10^{-5}	2.577×10^{-5}	3.455×10^{-5}	0.6974
250	0.6746	1033	0.04104	5.890×10^{-5}	2.760×10^{-5}	4.091×10^{-5}	0.6946
300	0.6158	1044	0.04418	6.871×10^{-5}	2.934×10^{-5}	4.765×10^{-5}	0.6935
350	0.5664	1056	0.04721	7.892×10^{-5}	3.101×10^{-5}	5.475×10^{-5}	0.6937
400	0.5243	1069	0.05015	8.951×10^{-5}	3.261×10^{-5}	6.219×10^{-5}	0.6948
450	0.4880	1081	0.05298	1.004×10^{-4}	3.415×10^{-5}	6.997×10^{-5}	0.6965
500	0.4565	1093	0.05572	1.117×10^{-4}	3.563×10^{-5}	7.806×10^{-5}	0.6986
600	0.4042	1115	0.06093	1.352×10^{-4}	3.846×10^{-5}	9.515×10^{-5}	0.7037
700	0.3627	1135	0.06581	1.598×10^{-4}	4.111×10^{-5}	1.133×10^{-4}	0.7092
800	0.3289	1153	0.07037	1.855×10^{-4}	4.362×10^{-5}	1.326×10^{-4}	0.7149
900	0.3008	1169	0.07465	2.122×10^{-4}	4.600×10^{-5}	1.529×10^{-4}	0.7206
1000	0.2772	1184	0.07868	2.398×10^{-4}	4.826×10^{-5}	1.741×10^{-4}	0.7260
1500	0.1990	1234	0.09599	3.908×10^{-4}	5.817×10^{-5}	2.922×10^{-4}	0.7478
2000	0.1553	1264	0.11113	5.664×10^{-4}	6.630×10^{-5}	4.270×10^{-4}	0.7539

Note: For ideal gases, the properties c_p, k, μ, and Pr are independent of pressure. The properties ρ, ν, and α at a pressure P (in atm) other than 1 atm are determined by multiplying the values of P at the given temperature by ρ and by dividing ν and α by P.

TABLE A–16

Properties of gases at 1 atm pressure

Temp. T, °C	Density ρ, kg/m³	Specific Heat c_p, J/kg·K	Thermal Conductivity k, W/m·K	Thermal Diffusivity α, m²/s	Dynamic Viscosity μ, kg/m·s	Kinematic Viscosity ν, m²/s	Prandtl Number Pr
			Carbon Dioxide, CO_2				
−50	2.4035	746	0.01051	5.860×10^{-6}	1.129×10^{-5}	4.699×10^{-6}	0.8019
0	1.9635	811	0.01456	9.141×10^{-6}	1.375×10^{-5}	7.003×10^{-6}	0.7661
50	1.6597	866.6	0.01858	1.291×10^{-5}	1.612×10^{-5}	9.714×10^{-6}	0.7520
100	1.4373	914.8	0.02257	1.716×10^{-5}	1.841×10^{-5}	1.281×10^{-5}	0.7464
150	1.2675	957.4	0.02652	2.186×10^{-5}	2.063×10^{-5}	1.627×10^{-5}	0.7445
200	1.1336	995.2	0.03044	2.698×10^{-5}	2.276×10^{-5}	2.008×10^{-5}	0.7442
300	0.9358	1060	0.03814	3.847×10^{-5}	2.682×10^{-5}	2.866×10^{-5}	0.7450
400	0.7968	1112	0.04565	5.151×10^{-5}	3.061×10^{-5}	3.842×10^{-5}	0.7458
500	0.6937	1156	0.05293	6.600×10^{-5}	3.416×10^{-5}	4.924×10^{-5}	0.7460
1000	0.4213	1292	0.08491	1.560×10^{-4}	4.898×10^{-5}	1.162×10^{-4}	0.7455
1500	0.3025	1356	0.10688	2.606×10^{-4}	6.106×10^{-5}	2.019×10^{-4}	0.7745
2000	0.2359	1387	0.11522	3.521×10^{-4}	7.322×10^{-5}	3.103×10^{-4}	0.8815
			Carbon Monoxide, CO				
−50	1.5297	1081	0.01901	1.149×10^{-5}	1.378×10^{-5}	9.012×10^{-6}	0.7840
0	1.2497	1048	0.02278	1.739×10^{-5}	1.629×10^{-5}	1.303×10^{-5}	0.7499
50	1.0563	1039	0.02641	2.407×10^{-5}	1.863×10^{-5}	1.764×10^{-5}	0.7328
100	0.9148	1041	0.02992	3.142×10^{-5}	2.080×10^{-5}	2.274×10^{-5}	0.7239
150	0.8067	1049	0.03330	3.936×10^{-5}	2.283×10^{-5}	2.830×10^{-5}	0.7191
200	0.7214	1060	0.03656	4.782×10^{-5}	2.472×10^{-5}	3.426×10^{-5}	0.7164
300	0.5956	1085	0.04277	6.619×10^{-5}	2.812×10^{-5}	4.722×10^{-5}	0.7134
400	0.5071	1111	0.04860	8.628×10^{-5}	3.111×10^{-5}	6.136×10^{-5}	0.7111
500	0.4415	1135	0.05412	1.079×10^{-4}	3.379×10^{-5}	7.653×10^{-5}	0.7087
1000	0.2681	1226	0.07894	2.401×10^{-4}	4.557×10^{-5}	1.700×10^{-4}	0.7080
1500	0.1925	1279	0.10458	4.246×10^{-4}	6.321×10^{-5}	3.284×10^{-4}	0.7733
2000	0.1502	1309	0.13833	7.034×10^{-4}	9.826×10^{-5}	6.543×10^{-4}	0.9302
			Methane, CH_4				
−50	0.8761	2243	0.02367	1.204×10^{-5}	8.564×10^{-6}	9.774×10^{-6}	0.8116
0	0.7158	2217	0.03042	1.917×10^{-5}	1.028×10^{-5}	1.436×10^{-5}	0.7494
50	0.6050	2302	0.03766	2.704×10^{-5}	1.191×10^{-5}	1.969×10^{-5}	0.7282
100	0.5240	2443	0.04534	3.543×10^{-5}	1.345×10^{-5}	2.567×10^{-5}	0.7247
150	0.4620	2611	0.05344	4.431×10^{-5}	1.491×10^{-5}	3.227×10^{-5}	0.7284
200	0.4132	2791	0.06194	5.370×10^{-5}	1.630×10^{-5}	3.944×10^{-5}	0.7344
300	0.3411	3158	0.07996	7.422×10^{-5}	1.886×10^{-5}	5.529×10^{-5}	0.7450
400	0.2904	3510	0.09918	9.727×10^{-5}	2.119×10^{-5}	7.297×10^{-5}	0.7501
500	0.2529	3836	0.11933	1.230×10^{-4}	2.334×10^{-5}	9.228×10^{-5}	0.7502
1000	0.1536	5042	0.22562	2.914×10^{-4}	3.281×10^{-5}	2.136×10^{-4}	0.7331
1500	0.1103	5701	0.31857	5.068×10^{-4}	4.434×10^{-5}	4.022×10^{-4}	0.7936
2000	0.0860	6001	0.36750	7.120×10^{-4}	6.360×10^{-5}	7.395×10^{-4}	1.0386
			Hydrogen, H_2				
−50	0.11010	12635	0.1404	1.009×10^{-4}	7.293×10^{-6}	6.624×10^{-5}	0.6562
0	0.08995	13920	0.1652	1.319×10^{-4}	8.391×10^{-6}	9.329×10^{-5}	0.7071
50	0.07603	14349	0.1881	1.724×10^{-4}	9.427×10^{-6}	1.240×10^{-4}	0.7191
100	0.06584	14473	0.2095	2.199×10^{-4}	1.041×10^{-5}	1.582×10^{-4}	0.7196
150	0.05806	14492	0.2296	2.729×10^{-4}	1.136×10^{-5}	1.957×10^{-4}	0.7174
200	0.05193	14482	0.2486	3.306×10^{-4}	1.228×10^{-5}	2.365×10^{-4}	0.7155

TABLE A–16

Properties of gases at 1 atm pressure (*Concluded*)

Temp. T, °C	Density ρ, kg/m³	Specific Heat c_p, J/kg·K	Thermal Conductivity k, W/m·K	Thermal Diffusivity α, m²/s	Dynamic Viscosity μ, kg/m·s	Kinematic Viscosity ν, m²/s	Prandtl Number Pr
300	0.04287	14481	0.2843	4.580×10^{-4}	1.403×10^{-5}	3.274×10^{-4}	0.7149
400	0.03650	14540	0.3180	5.992×10^{-4}	1.570×10^{-5}	4.302×10^{-4}	0.7179
500	0.03178	14653	0.3509	7.535×10^{-4}	1.730×10^{-5}	5.443×10^{-4}	0.7224
1000	0.01930	15577	0.5206	1.732×10^{-3}	2.455×10^{-5}	1.272×10^{-3}	0.7345
1500	0.01386	16553	0.6581	2.869×10^{-3}	3.099×10^{-5}	2.237×10^{-3}	0.7795
2000	0.01081	17400	0.5480	2.914×10^{-3}	3.690×10^{-5}	3.414×10^{-3}	1.1717
Nitrogen, N_2							
−50	1.5299	957.3	0.02001	1.366×10^{-5}	1.390×10^{-5}	9.091×10^{-6}	0.6655
0	1.2498	1035	0.02384	1.843×10^{-5}	1.640×10^{-5}	1.312×10^{-5}	0.7121
50	1.0564	1042	0.02746	2.494×10^{-5}	1.874×10^{-5}	1.774×10^{-5}	0.7114
100	0.9149	1041	0.03090	3.244×10^{-5}	2.094×10^{-5}	2.289×10^{-5}	0.7056
150	0.8068	1043	0.03416	4.058×10^{-5}	2.300×10^{-5}	2.851×10^{-5}	0.7025
200	0.7215	1050	0.03727	4.921×10^{-5}	2.494×10^{-5}	3.457×10^{-5}	0.7025
300	0.5956	1070	0.04309	6.758×10^{-5}	2.849×10^{-5}	4.783×10^{-5}	0.7078
400	0.5072	1095	0.04848	8.727×10^{-5}	3.166×10^{-5}	6.242×10^{-5}	0.7153
500	0.4416	1120	0.05358	1.083×10^{-4}	3.451×10^{-5}	7.816×10^{-5}	0.7215
1000	0.2681	1213	0.07938	2.440×10^{-4}	4.594×10^{-5}	1.713×10^{-4}	0.7022
1500	0.1925	1266	0.11793	4.839×10^{-4}	5.562×10^{-5}	2.889×10^{-4}	0.5969
2000	0.1502	1297	0.18590	9.543×10^{-4}	6.426×10^{-5}	4.278×10^{-4}	0.4483
Oxygen, O_2							
−50	1.7475	984.4	0.02067	1.201×10^{-5}	1.616×10^{-5}	9.246×10^{-6}	0.7694
0	1.4277	928.7	0.02472	1.865×10^{-5}	1.916×10^{-5}	1.342×10^{-5}	0.7198
50	1.2068	921.7	0.02867	2.577×10^{-5}	2.194×10^{-5}	1.818×10^{-5}	0.7053
100	1.0451	931.8	0.03254	3.342×10^{-5}	2.451×10^{-5}	2.346×10^{-5}	0.7019
150	0.9216	947.6	0.03637	4.164×10^{-5}	2.694×10^{-5}	2.923×10^{-5}	0.7019
200	0.8242	964.7	0.04014	5.048×10^{-5}	2.923×10^{-5}	3.546×10^{-5}	0.7025
300	0.6804	997.1	0.04751	7.003×10^{-5}	3.350×10^{-5}	4.923×10^{-5}	0.7030
400	0.5793	1025	0.05463	9.204×10^{-5}	3.744×10^{-5}	6.463×10^{-5}	0.7023
500	0.5044	1048	0.06148	1.163×10^{-4}	4.114×10^{-5}	8.156×10^{-5}	0.7010
1000	0.3063	1121	0.09198	2.678×10^{-4}	5.732×10^{-5}	1.871×10^{-4}	0.6986
1500	0.2199	1165	0.11901	4.643×10^{-4}	7.133×10^{-5}	3.243×10^{-4}	0.6985
2000	0.1716	1201	0.14705	7.139×10^{-4}	8.417×10^{-5}	4.907×10^{-4}	0.6873
Water Vapor, H_2O							
−50	0.9839	1892	0.01353	7.271×10^{-6}	7.187×10^{-6}	7.305×10^{-6}	1.0047
0	0.8038	1874	0.01673	1.110×10^{-5}	8.956×10^{-6}	1.114×10^{-5}	1.0033
50	0.6794	1874	0.02032	1.596×10^{-5}	1.078×10^{-5}	1.587×10^{-5}	0.9944
100	0.5884	1887	0.02429	2.187×10^{-5}	1.265×10^{-5}	2.150×10^{-5}	0.9830
150	0.5189	1908	0.02861	2.890×10^{-5}	1.456×10^{-5}	2.806×10^{-5}	0.9712
200	0.4640	1935	0.03326	3.705×10^{-5}	1.650×10^{-5}	3.556×10^{-5}	0.9599
300	0.3831	1997	0.04345	5.680×10^{-5}	2.045×10^{-5}	5.340×10^{-5}	0.9401
400	0.3262	2066	0.05467	8.114×10^{-5}	2.446×10^{-5}	7.498×10^{-5}	0.9240
500	0.2840	2137	0.06677	1.100×10^{-4}	2.847×10^{-5}	1.002×10^{-4}	0.9108
1000	0.1725	2471	0.13623	3.196×10^{-4}	4.762×10^{-5}	2.761×10^{-4}	0.8639
1500	0.1238	2736	0.21301	6.288×10^{-4}	6.411×10^{-5}	5.177×10^{-4}	0.8233
2000	0.0966	2928	0.29183	1.032×10^{-3}	7.808×10^{-5}	8.084×10^{-4}	0.7833

Note: For ideal gases, the properties c_p, k, μ, and Pr are independent of pressure. The properties ρ, ν, and α at a pressure P (in atm) other than 1 atm are determined by multiplying the values of P at the given temperature by ρ and by dividing ν and α by P.

Source: Data generated from the EES software developed by S. A. Klein and F. L. Alvarado. Originally based on various sources.

TABLE A–17

Properties of the atmosphere at high altitude

Altitude, z, m	Temperature, T, °C	Pressure, P, kPa	Gravity g, m/s^2	Speed of Sound, c, m/s	Density, ρ, kg/m^3	Viscosity μ, kg/m·s	Thermal Conductivity, k, W/m·K
0	15.00	101.33	9.807	340.3	1.225	1.789×10^{-5}	0.0253
200	13.70	98.95	9.806	339.5	1.202	1.783×10^{-5}	0.0252
400	12.40	96.61	9.805	338.8	1.179	1.777×10^{-5}	0.0252
600	11.10	94.32	9.805	338.0	1.156	1.771×10^{-5}	0.0251
800	9.80	92.08	9.804	337.2	1.134	1.764×10^{-5}	0.0250
1000	8.50	89.88	9.804	336.4	1.112	1.758×10^{-5}	0.0249
1200	7.20	87.72	9.803	335.7	1.090	1.752×10^{-5}	0.0248
1400	5.90	85.60	9.802	334.9	1.069	1.745×10^{-5}	0.0247
1600	4.60	83.53	9.802	334.1	1.048	1.739×10^{-5}	0.0245
1800	3.30	81.49	9.801	333.3	1.027	1.732×10^{-5}	0.0244
2000	2.00	79.50	9.800	332.5	1.007	1.726×10^{-5}	0.0243
2200	0.70	77.55	9.800	331.7	0.987	1.720×10^{-5}	0.0242
2400	−0.59	75.63	9.799	331.0	0.967	1.713×10^{-5}	0.0241
2600	−1.89	73.76	9.799	330.2	0.947	1.707×10^{-5}	0.0240
2800	−3.19	71.92	9.798	329.4	0.928	1.700×10^{-5}	0.0239
3000	−4.49	70.12	9.797	328.6	0.909	1.694×10^{-5}	0.0238
3200	−5.79	68.36	9.797	327.8	0.891	1.687×10^{-5}	0.0237
3400	−7.09	66.63	9.796	327.0	0.872	1.681×10^{-5}	0.0236
3600	−8.39	64.94	9.796	326.2	0.854	1.674×10^{-5}	0.0235
3800	−9.69	63.28	9.795	325.4	0.837	1.668×10^{-5}	0.0234
4000	−10.98	61.66	9.794	324.6	0.819	1.661×10^{-5}	0.0233
4200	−12.3	60.07	9.794	323.8	0.802	1.655×10^{-5}	0.0232
4400	−13.6	58.52	9.793	323.0	0.785	1.648×10^{-5}	0.0231
4600	−14.9	57.00	9.793	322.2	0.769	1.642×10^{-5}	0.0230
4800	−16.2	55.51	9.792	321.4	0.752	1.635×10^{-5}	0.0229
5000	−17.5	54.05	9.791	320.5	0.736	1.628×10^{-5}	0.0228
5200	−18.8	52.62	9.791	319.7	0.721	1.622×10^{-5}	0.0227
5400	−20.1	51.23	9.790	318.9	0.705	1.615×10^{-5}	0.0226
5600	−21.4	49.86	9.789	318.1	0.690	1.608×10^{-5}	0.0224
5800	−22.7	48.52	9.785	317.3	0.675	1.602×10^{-5}	0.0223
6000	−24.0	47.22	9.788	316.5	0.660	1.595×10^{-5}	0.0222
6200	−25.3	45.94	9.788	315.6	0.646	1.588×10^{-5}	0.0221
6400	−26.6	44.69	9.787	314.8	0.631	1.582×10^{-5}	0.0220
6600	−27.9	43.47	9.786	314.0	0.617	1.575×10^{-5}	0.0219
6800	−29.2	42.27	9.785	313.1	0.604	1.568×10^{-5}	0.0218
7000	−30.5	41.11	9.785	312.3	0.590	1.561×10^{-5}	0.0217
8000	−36.9	35.65	9.782	308.1	0.526	1.527×10^{-5}	0.0212
9000	−43.4	30.80	9.779	303.8	0.467	1.493×10^{-5}	0.0206
10,000	−49.9	26.50	9.776	299.5	0.414	1.458×10^{-5}	0.0201
12,000	−56.5	19.40	9.770	295.1	0.312	1.422×10^{-5}	0.0195
14,000	−56.5	14.17	9.764	295.1	0.228	1.422×10^{-5}	0.0195
16,000	−56.5	10.53	9.758	295.1	0.166	1.422×10^{-5}	0.0195
18,000	−56.5	7.57	9.751	295.1	0.122	1.422×10^{-5}	0.0195

Source: U.S. Standard Atmosphere Supplements, U.S. Government Printing Office, 1966.

TABLE A–18

Emissivities of surfaces
(*a*) Metals

Material	Temperature, K	Emissivity, ε	Material	Temperature, K	Emissivity, ε
Aluminum			Magnesium, polished	300–500	0.07–0.13
Polished	300–900	0.04–0.06	Mercury	300–400	0.09–0.12
Commercial sheet	400	0.09	Molybdenum		
Heavily oxidized	400–800	0.20–0.33	Polished	300–2000	0.05–0.21
Anodized	300	0.8	Oxidized	600–800	0.80–0.82
Bismuth, bright	350	0.34	Nickel		
Brass			Polished	500–1200	0.07–0.17
Highly polished	500–650	0.03–0.04	Oxidized	450–1000	0.37–0.57
Polished	350	0.09	Platinum, polished	500–1500	0.06–0.18
Dull plate	300–600	0.22	Silver, polished	300–1000	0.02–0.07
Oxidized	450–800	0.6	Stainless steel		
Chromium, polished	300–1400	0.08–0.40	Polished	300–1000	0.17–0.30
Copper			Lightly oxidized	600–1000	0.30–0.40
Highly polished	300	0.02	Highly oxidized	600–1000	0.70–0.80
Polished	300–500	0.04–0.05	Steel		
Commercial sheet	300	0.15	Polished sheet	300–500	0.08–0.14
Oxidized	600–1000	0.5–0.8	Commercial sheet	500–1200	0.20–0.32
Black oxidized	300	0.78	Heavily oxidized	300	0.81
Gold			Tin, polished	300	0.05
Highly polished	300–1000	0.03–0.06	Tungsten		
Bright foil	300	0.07	Polished	300–2500	0.03–0.29
Iron			Filament	3500	0.39
Highly polished	300–500	0.05–0.07	Zinc		
Case iron	300	0.44	Polished	300–800	0.02–0.05
Wrought iron	300–500	0.28	Oxidized	300	0.25
Rusted	300	0.61			
Oxidized	500–900	0.64–0.78			
Lead					
Polished	300–500	0.06–0.08			
Unoxidized, rough	300	0.43			
Oxidized	300	0.63			

TABLE A–18

Emissivities of surfaces
(*b*) Nonmetals (*Concluded*)

Material	Temperature, K	Emissivity, ε	Material	Temperature, K	Emissivity, ε
Alumina	800–1400	0.65–0.45	Paper, white	300	0.90
Aluminum oxide	600–1500	0.69–0.41	Plaster, white	300	0.93
Asbestos	300	0.96	Porcelain, glazed	300	0.92
Asphalt pavement	300	0.85–0.93	Quartz, rough, fused	300	0.93
Brick			Rubber		
Common	300	0.93–0.96	Hard	300	0.93
Fireclay	1200	0.75	Soft	300	0.86
Carbon filament	2000	0.53	Sand	300	0.90
Cloth	300	0.75–0.90	Silicon carbide	600–1500	0.87–0.85
Concrete	300	0.88–0.94	Skin, human	300	0.95
Glass			Snow	273	0.80–0.90
Window	300	0.90–0.95	Soil, earth	300	0.93–0.96
Pyrex	300–1200	0.82–0.62	Soot	300–500	0.95
Pyroceram	300–1500	0.85–0.57	Teflon	300–500	0.85–0.92
Ice	273	0.95–0.99	Water, deep	273–373	0.95–0.96
Magnesium oxide	400–800	0.69–0.55	Wood		
Masonry	300	0.80	Beech	300	0.94
Paints			Oak	300	0.90
Aluminum	300	0.40–0.50			
Black, lacquer, shiny	300	0.88			
Oils, all colors	300	0.92–0.96			
Red primer	300	0.93			
White acrylic	300	0.90			
White enamel	300	0.90			

TABLE A–19

Solar radiative properties of materials

Description/composition	Solar Absorptivity, α_s	Emissivity, ε, at 300 K	Ratio, α_s/ε	Solar Transmissivity, τ_s
Aluminum				
Polished	0.09	0.03	3.0	
Anodized	0.14	0.84	0.17	
Quartz-overcoated	0.11	0.37	0.30	
Foil	0.15	0.05	3.0	
Brick, red (Purdue)	0.63	0.93	0.68	
Concrete	0.60	0.88	0.68	
Galvanized sheet metal				
Clean, new	0.65	0.13	5.0	
Oxidized, weathered	0.80	0.28	2.9	
Glass, 3.2-mm thickness				
Float or tempered				0.79
Low iron oxide type				0.88
Marble, slightly off-white (nonreflective)	0.40	0.88	0.45	
Metal, plated				
Black sulfide	0.92	0.10	9.2	
Black cobalt oxide	0.93	0.30	3.1	
Black nickel oxide	0.92	0.08	11	
Black chrome	0.87	0.09	9.7	
Mylar, 0.13-mm thickness				0.87
Paints				
Black (Parsons)	0.98	0.98	1.0	
White, acrylic	0.26	0.90	0.29	
White, zinc oxide	0.16	0.93	0.17	
Paper, white	0.27	0.83	0.32	
Plexiglas, 3.2-mm thickness				0.90
Porcelain tiles, white (reflective glazed surface)	0.26	0.85	0.30	
Roofing tiles, bright red				
Dry surface	0.65	0.85	0.76	
Wet surface	0.88	0.91	0.96	
Sand, dry				
Off-white	0.52	0.82	0.63	
Dull red	0.73	0.86	0.82	
Snow				
Fine particles, fresh	0.13	0.82	0.16	
Ice granules	0.33	0.89	0.37	
Steel				
Mirror-finish	0.41	0.05	8.2	
Heavily rusted	0.89	0.92	0.96	
Stone (light pink)	0.65	0.87	0.74	
Tedlar, 0.10-mm thickness				0.92
Teflon, 0.13-mm thickness				0.92
Wood	0.59	0.90	0.66	

Source: V. C. Sharma and A. Sharma, "Solar Properties of Some Building Elements," *Energy* 14 (1989), pp. 805–810, and other sources.
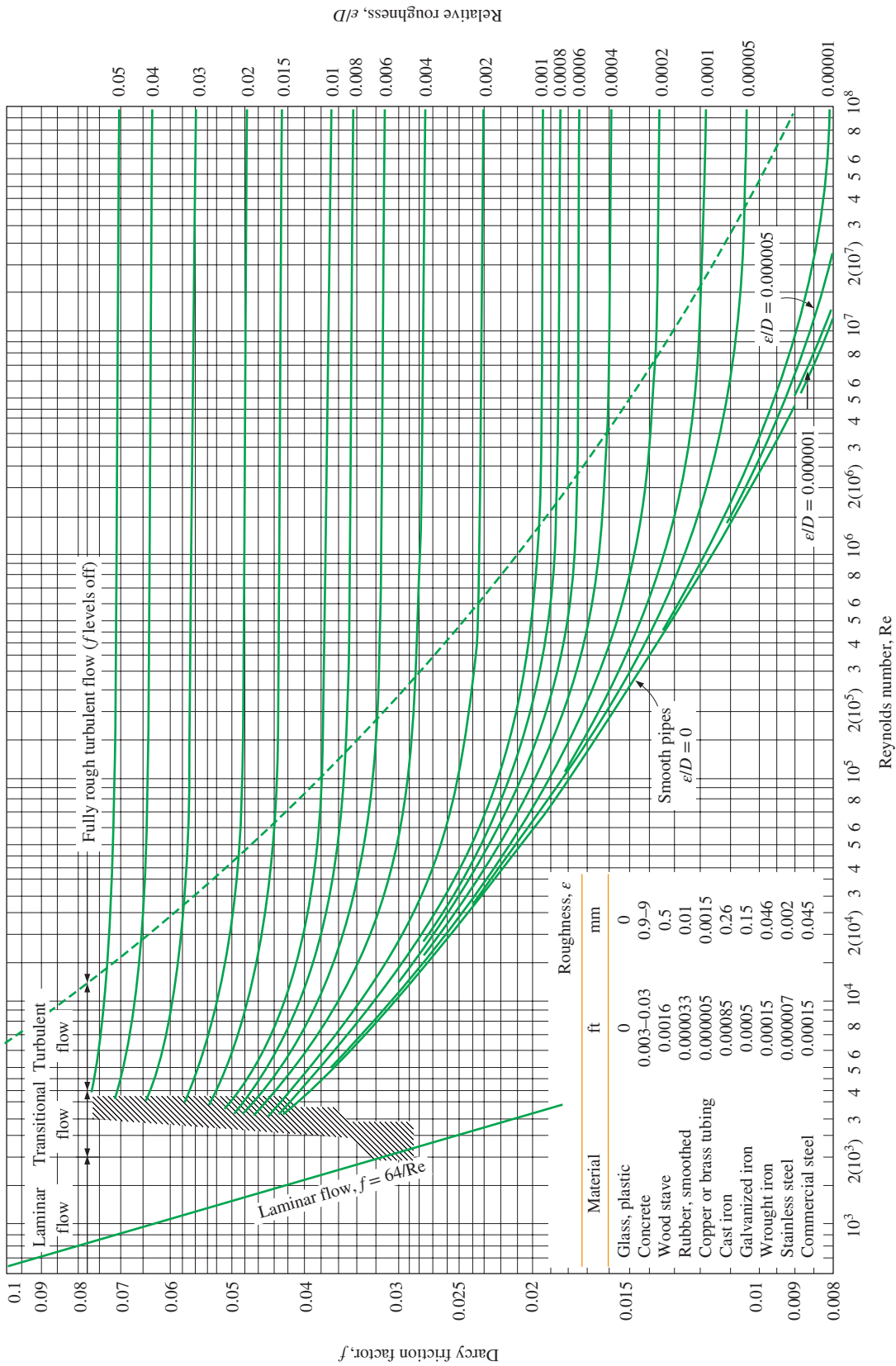
FIGURE A–20

The Moody chart for the friction factor for fully developed flow in circular pipes for use in the head loss relation $\Delta P_L = f \dfrac{L}{D} \dfrac{\rho V^2}{2}$. Friction factors in the turbulent flow are evaluated from the Colebrook equation $\dfrac{1}{\sqrt{f}} = -2 \log_{10} \left(\dfrac{\varepsilon/D}{3.7} + \dfrac{2.51}{\mathrm{Re}\,\sqrt{f}} \right)$.

Relative roughness, ε/D

	Roughness, ε	
Material	ft	mm
Glass, plastic	0	0
Concrete	0.003–0.03	0.9–9
Wood stave	0.0016	0.5
Rubber, smoothed	0.000033	0.01
Copper or brass tubing	0.000005	0.0015
Cast iron	0.00085	0.26
Galvanized iron	0.0005	0.15
Wrought iron	0.00015	0.046
Stainless steel	0.000007	0.002
Commercial steel	0.00015	0.045

Darcy friction factor, f

Reynolds number, Re

PROPERTY TABLES AND CHARTS (ENGLISH UNITS)

TABLE A–1E

Molar mass, gas constant, and ideal-gas specific heats of some substances

| Substance | Molar Mass, M, lbm/lbmol | Gas Constant R* | | Specific Heat Data at 77°F | | |
		Btu/ lbm·R	psia·ft³/ lbm·R	c_p, Btu/lbm·R	c_v, Btu/lbm·R	$k = c_p/c_v$
Air	28.97	0.06855	0.3704	0.2400	0.1715	1.400
Ammonia, NH_3	17.03	0.1166	0.6301	0.4999	0.3834	1.304
Argon, Ar	39.95	0.04970	0.2686	0.1243	0.07457	1.667
Bromine, Br_2	159.81	0.01242	0.06714	0.0538	0.04137	1.300
Isobutane, C_4H_{10}	58.12	0.03415	0.1846	0.3972	0.3631	1.094
n-Butane, C_4H_{10}	58.12	0.03415	0.1846	0.4046	0.3705	1.092
Carbon dioxide, CO_2	44.01	0.04512	0.2438	0.2016	0.1564	1.288
Carbon monoxide, CO	28.01	0.07089	0.3831	0.2482	0.1772	1.400
Chlorine, Cl_2	70.905	0.02802	0.1514	0.1142	0.08618	1.325
Chlorodifiuoromethane (R-22), $CHClF_2$	86.47	0.02297	0.1241	0.1552	0.1322	1.174
Ethane, C_2H_6	30.070	0.06604	0.3569	0.4166	0.3506	1.188
Ethylene, C_2H_4	28.054	0.07079	0.3826	0.3647	0.2940	1.241
Fluorine, F_2	38.00	0.05224	0.2823	0.1967	0.1445	1.362
Helium, He	4.003	0.4961	2.681	1.2403	0.7442	1.667
n-Heptane, C_7H_{16}	100.20	0.01982	0.1071	0.3939	0.3740	1.053
n-Hexane, C_6H_{14}	86.18	0.02304	0.1245	0.3951	0.3721	1.062
Hydrogen, H2	2.016	0.9850	5.323	3.416	2.431	1.405
Krypton, Kr	83.80	0.02370	0.1281	0.05923	0.03554	1.667
Methane, CH_4	16.04	0.1238	0.6688	0.5317	0.4080	1.303
Neon, Ne	20.183	0.09838	0.5316	0.2460	0.1476	1.667
Nitrogen, N_2	28.01	0.07089	0.3831	0.2484	0.1774	1.400
Nitric oxide. NO	30.006	0.06618	0.3577	0.2387	0.1725	1.384
Nitrogen dioxide, NO_2	46.006	0.04512	0.2438	0.1925	0.1474	1.306
Oxygen, O_2	32.00	0.06205	0.3353	0.2193	0.1572	1.395
n-Pentane, C_5H_{12}	72.15	0.02752	0.1487	0.3974	0.3700	1.074
Propane, C_3H_8	44.097	0.04502	0.2433	0.3986	0.3535	1.127
Propylene, C_3H_6	42.08	0.04720	0.2550	0.3657	0.3184	1.148
Steam, H_2O	18.015	0.1102	0.5957	0.4455	0.3351	1.329
Sulfur dioxide, SO_2	64.06	0.03100	0.1675	0.1488	0.1178	1.263
Tetrachloromethane, CCl_4	153.82	0.01291	0.06976	0.1293	0.1164	1.111
Tetrafluoroethane (R-134a), $C_2H_2F_4$	102.03	0.01946	0.1052	0.1991	0.1796	1.108
Trifluoroethane (R-143a), $C_2H_3F_3$	84.04	0.02363	0.1277	0.2219	0.1983	1.119
Xenon, Xe	131.30	0.01512	0.08173	0.03781	0.02269	1.667

*The gas constant is calculated from $R = R_u/M$, where $R_u = 1.9859$ Btu/lbmol·R $= 10.732$ psia·ft³/lbmol·R is the universal gas constant and M is the molar mass.

Source: Specific heat values are mostly obtained from the property routines prepared by The National Institute of Standards and Technology (NIST), Gaithersburg, MD.

TABLE A–2E

Boiling and freezing point properties

Substance	Boiling Data at 1 atm		Freezing Data		Liquid Properties		
	Normal Boiling Point, °F	Latent Heat of Vaporization h_{fg}, Btu/lbm	Freezing Point, °F	Latent Heat of Fusion h_{if}, Btu/lbm	Tempera- ture, °F	Density ρ, lbm/ft^3	Specific Heat c_p, Btu/lbm·R
Ammonia	−27.9	24.54	−107.9	138.6	−27.9	42.6	1.06
					0	41.3	1.083
					40	39.5	1.103
					80	37.5	1.135
Argon	−302.6	69.5	−308.7	12.0	−302.6	87.0	0.272
Benzene	176.4	169.4	41.9	54.2	68	54.9	0.411
Brine (20% sodium							
chloride by mass)	219.0	—	0.7	—	68	71.8	0.743
n-Butane	31.1	165.6	−217.3	34.5	31.1	37.5	0.552
Carbon dioxide	−109.2*	99.6 (at 32°F)	−69.8	—	32	57.8	0.583
Ethanol	172.8	360.5	−173.6	46.9	77	48.9	0.588
Ethyl alcohol	173.5	368	−248.8	46.4	68	49.3	0.678
Ethylene glycol	388.6	344.0	12.6	77.9	68	69.2	0.678
Glycerin	355.8	419	66.0	86.3	68	78.7	0.554
Helium	−452.1	9.80	—	—	−452.1	9.13	5.45
Hydrogen	−423.0	191.7	−434.5	25.6	−423.0	4.41	2.39
Isobutane	10.9	157.8	−255.5	45.5	10.9	37.1	0.545
Kerosene	399–559	108	−12.8	—	68	51.2	0.478
Mercury	674.1	126.7	−38.0	4.90	77	847	0.033
Methane	−258.7	219.6	296.0	25.1	−258.7	26.4	0.834
					−160	20.0	1.074
Methanol	148.1	473	−143.9	42.7	77	49.1	0.609
Nitrogen	−320.4	85.4	−346.0	10.9	−320.4	50.5	0.492
					−260	38.2	0.643
Octane	256.6	131.7	−71.5	77.9	68	43.9	0.502
Oil (light)	—	—			77	56.8	0.430
Oxygen	−297.3	91.5	−361.8	5.9	−297.3	71.2	0.408
Petroleum	—	99–165			68	40.0	0.478
Propane	−43.7	184.0	−305.8	34.4	−43.7	36.3	0.538
					32	33.0	0.604
					100	29.4	0.673
Refrigerant-134a	−15.0	93.2	−141.9	—	−40	88.5	0.283
					−15	86.0	0.294
					32	80.9	0.318
					90	73.6	0.348
Water	212	970.5	32	143.5	32	62.4	1.01
					90	62.1	1.00
					150	61.2	1.00
					212	59.8	1.01

*Sublimation temperature. (At pressures below the triple-point pressure of 75.1 psia, carbon dioxide exists as a solid or gas. Also, the freezing-point temperature of carbon dioxide is the triple-point temperature of −69.8°F.)

TABLE A–3E

Properties of solid metals

Composition	Melting Point, R	Properties at 540 R ρ lbm/ft³	c_p(Btu/ lbm·R)	k(Btu/ h·ft·R)	$\alpha \times 10^6$ ft²/s	Properties at Various Temperatures (R), k(Btu/h·ft·R)/c_p(Btu/lbm·R) 180	360	720	1080	1440	1800
Aluminum	1679	168	0.216	137	1045	174.5	137	138.6	133.4	126	
Pure						0.115	0.191	0.226	0.246	0.273	
Alloy 2024-T6	1395	173	0.209	102.3	785.8	37.6	94.2	107.5	107.5		
(4.5% Cu, 1.5% Mg, 0.6% Mn)						0.113	0.188	0.22	0.249		
Alloy 195, cast (4.5% Cu)		174.2	0.211	97	734		100.5	106.9			
Beryllium	2790	115.5	0.436	115.6	637.2	572	174	93	72.8	61.3	52.5
						0.048	0.266	0.523	0.621	0.624	0.72
Bismuth	981	610.5	0.029	4.6	71	9.5	5.6	4.06			
						0.026	0.028	0.03			
Boron	4631	156	0.264	15.6	105	109.7	32.06	9.7	6.1	5.5	5.7
						0.03	0.143	0.349	0.451	0.515	0.558
Cadmium	1069	540	0.055	55.6	521	117.3	57.4	54.7			
						0.047	0.053	0.057			
Chromium	3812	447	0.107	54.1	313.2	91.9	64.1	52.5	46.6	41.2	37.8
						0.045	0.091	0.115	0.129	0.138	0.147
Cobalt	3184	553.2	0.101	57.3	286.3	96.5	70.5	49.3	39	33.6	80.1
						0.056	0.09	0.107	0.12	0.131	0.145
Copper	2445	559	0.092	231.7	1259.3	278.5	238.6	227.07	219	212	203.4
Pure						0.06	0.085	0.094	0.01	0.103	0.107
Commercial bronze	2328	550	0.1	30	150.7	24.3	30	34			
(90% Cu, 10% Al)						0.187	0.109	0.130			
Phosphor gear bronze	1987	548.1	0.084	31.2	183	23.7	37.6	42.8			
(89% Cu, 11% Sn)						—	—	—			
Cartridge brass	2139	532.5	0.09	63.6	364.9	43.3	54.9	79.2	86.0		
(70% Cu, 30% Zn)						0.09	0.09	0.101			
Constantan	2687	557	0.092	13.3	72.3	9.8	1.1				
(55% Cu, 45% Ni)						0.06	0.09				
Germanium	2180	334.6	0.08	34.6	373.5	134	56	25	15.7	11.4	10.05
						0.045	0.069	0.08	0.083	0.085	0.089
Gold	2405	1205	0.03	183.2	1367	189	186.6	179.7	172.2	164.09	156
						0.026	0.029	0.031	0.032	0.033	0.034
Iridium	4896	1404.6	0.031	85	541.4	99.4	88.4	83.2	79.7	76.3	72.8
						0.021	0.029	0.031	0.032	0.034	0.036
Iron:	3258	491.3	0.106	46.4	248.6	77.4	54.3	40.2	31.6	25.01	19
Pure						0.051	0.091	0.117	0.137	0.162	0.232
Armco		491.3	0.106	42	222.8	55.2	46.6	38	30.7	24.4	18.7
(99.75% pure)						0.051	0.091	0.117	0.137	0.162	0.233
Carbon steels		490.3	0.103	35	190.6			32.8	27.7	22.7	17.4
Plain carbon (Mn ≤ 1%, Si ≤ 0.1%)								0.116	0.113	0.163	0.279
AISI 1010		489	0.103	37	202.4			33.9	28.2	22.7	18
								0.116	0.133	0.163	0.278
Carbon-silicon		488	0.106	30	160.4			28.8	25.4	21.6	17
(Mn ≤ 1%, 0.1% < Si ≤ 0.6%)								0.119	0.139	0.166	0.231
Carbon-manganese-silicon		508	0.104	23.7	125			24.4	23	20.2	16
(1% < Mn ≤ 1.65%, 0.1% < Si ≤ 0.6%)								0.116	0.133	0.163	0.260
Chromium (low) steels:		488.3	0.106	21.8	117.4			22	21.2	19.3	15.6
$\frac{1}{2}$ Cr–$\frac{1}{4}$ Mo–Si								0.117	0.137	0.164	0.23
(0.18% C, 0.65% Cr, 0.23% Mo, 0.6% Si)											
1 Cr –$\frac{1}{2}$ Mo (0.16% C,		490.6	0.106	24.5	131.3			24.3	22.6	20	15.8
1% Cr, 0.54% Mo, 0.39% Si)								0.117	0.137	0.164	0.231
1 Cr–V		489.2	0.106	28.3	151.8			27.0	24.3	21	16.3
(0.2% C, 1.02% Cr, 0.15% V)								0.117	0.137	0.164	0.231

TABLE A–3E

Properties of solid metals   (*Concluded*)

Composition	Melting Point, R	ρ lbm/ft³	c_p(Btu/ lbm·R)	k(Btu/ h·ft·R)	$\alpha \times 10^6$ ft²/s	Properties at Various Temperatures (R), k(Btu/h·ft·R)/c_p(Btu/lbm·R)					
						180	360	720	1080	1440	1800
Stainless steels:		503	0.114	8.7	42			10	11.6	13.2	14.7
AISI 302								0.122	0.133	0.140	0.144
AISI 304	3006	493.2	0.114	8.6	42.5	5.31	7.3	9.6	11.5	13	14.7
						0.064	0.096	0.123	0.133	0.139	0.145
AISI 316		514.3	0.111	7.8	37.5			8.8	10.6	12.3	14
						0.12	0.131	0.137	0.143		
AISI 347		498	0.114	8.2	40			9.1	1.1	12.7	14.3
								0.122	0.133	0.14	0.144
Lead	1082	708	0.03	20.4	259.4	23	21.2	19.7	18.1		
						0.028	0.029	0.031	0.034		
Magnesium	1661	109	0.245	90.2	943	87.9	91.9	88.4	86.0	84.4	
						0.155	0.223	0.256	0.279	0.302	
Molybdenum	5209	639.3	0.06	79.7	578	1034	82.6	77.4	72.8	68.2	64.7
						0.038	0.053	0.062	0.065	0.068	0.070
Nickel:	3110	555.6	0.106	52.4	247.6	94.8	61.8	46.3	37.9	39	41.4
Pure						0.055	0.091	0.115	0.141	0.126	0.134
Nichrome	3010	524.4	0.1	6.9	36.6			8.0	9.3	12.2	
(80% Ni, 20% Cr)							0.114	0.125	0.130		
Inconel X-750	2997	531.3	0.104	6.8	33.4	5	5.9	7.8	9.8	11.8	13.9
(73% Ni, 15% Cr, 6.7% Fe)						—	0.088	0.112	0.121	0.13	0.149
Niobium	4934	535	0.063	31	254	31.9	30.4	32	33.6	35.4	32.2
						0.044	0.059	0.065	0.067	0.069	0.071
Palladium	3289	750.4	0.058	41.5	263.7	44.2	41.4	42.5	46	50	54.4
						0.04	0.054	0.059	0.062	0.064	0.067
Platinum:	3681	1339	0.031	41.4	270	44.7	42	41.5	42.3	43.7	45.5
Pure						0.024	0.03	0.032	0.034	0.035	0.036
Alloy 60Pt-40Rh	3240	1038.2	0.038	27.2	187.3			30	34	37.5	40
(60% Pt, 40% Rh)								—	—	—	
Rhenium	6215	1317.2	0.032	27.7	180	34	30	26.6	25.5	25.4	25.8
						0.023	0.03	0.033	0.034	0.036	0.037
Rhodium	4025	777.2	0.058	86.7	534	107.5	89	84.3	78.5	73.4	70
						0.035	0.052	0.06	0.065	0.069	0.074
Silicon	3033	145.5	0.17	85.5	960.2	510.8	152.5	57.2	35.8	24.4	18.0
						0.061	0.132	0.189	0.207	0.218	0.226
Silver	2223	656	0.056	248	1873	257	248.4	245.5	238	228.8	219
						0.044	0.053	0.057	0.059	0.062	0.066
Tantalum	5884	1036.3	0.033	33.2	266	34.2	33.2	33.4	34	34.3	34.8
						0.026	0.031	0.034	0.035	0.036	0.036
Thorium	3641	730.4	0.028	31.2	420.9	34.6	31.5	31.4	32.2	32.9	32.9
						0.024	0.027	0.029	0.032	0.035	0.037
Tin	909	456.3	0.054	38.5	431.6	49.2	42.4	35.9			
						0.044	0.051	0.058			
Titanium	3515	281	0.013	12.7	100.3	17.6	14.2	11.8	11.2	11.4	12
						0.071	0.111	0.131	0.141	0.151	0.161
Tungsten	6588	1204.9	0.031	100.5	735.2	120.2	107.5	92	79.2	72.2	68.2
						0.020	0.029	0.032	0.033	0.034	0.035
Uranium	2531	1190.5	0.027	16	134.5	12.5	14.5	17.1	19.6	22.4	25.4
						0.022	0.026	0.029	0.035	0.042	0.043
Vanadium	3946	381	0.117	17.7	110.9	20.7	18	18	19.3	20.6	22.0
						0.061	0.102	0.123	0.128	0.134	0.142
Zinc	1247	445.7	0.093	67	450	67.6	68.2	64.1	59.5		
						0.07	0.087	0.096	0.104		
Zirconium	3825	410.2	0.067	13.1	133.5	19.2	14.6	12.5	12	12.5	13.7
						0.049	0.063	0.072	0.77	0.082	0.087

Source: Tables A–3E and A–4E are obtained from the respective tables in SI units in Appendix 1 using proper conversion factors.

TABLE A–4E

Properties of solid nonmentals

Composition	Melting Point, R	ρ lbm/ft³	c_p(Btu/ lbm·R)	k(Btu/ h·ft·R)	$\alpha \times 10^6$ ft²/s	180	360	720	1080	1440	1800
		Properties at 540 R				*Properties at Various Temperatures (R),* $k(Btu/h\cdot ft\cdot R)/c_p(Btu/lbm\cdot R)$						
Aluminum oxide,	4181	247.8	0.182	26.6	162.5	260	47.4	18.7	11	7.5	6
sapphire						—	—	0.224	0.265	0.281	0.293
Aluminum oxide	4181	247.8	0.182	20.8	128	76.8	31.7	15.3	9.3	6	4.5
polycrystalline								0.244	0.265	0.281	0.293
Beryllium oxide	4905	187.3	0.246	157.2	947.3			113.2	64.2	40.4	27.2
								0.322	0.40	0.44	0.459
Boron	4631	156	0.264	16	107.5	109.8	30.3	10.8	6.5	4.6	3.6
								0.355	0.445	0.509	0.561
Boron fiber epoxy	1062	130									
(30% vol.) composite											
k, ∥ to fibers				1.3		1.2	1.3	1.31			
k, ⊥ to fibers				0.34		0.21	0.28	0.34			
c_p			0.268			0.086	0.18	0.34			
Carbon	2700	121.7	—	0.92	—	0.38	0.68	1.09	1.26	1.36	1.46
Amorphous diamond,	—	219	0.121	1329	—	5778	2311.2	889.8			
type lla								0.005	0.046	0.203	
insulator	4091	138									
Graphite, pyrolytic				1126.7		2871.6	1866.3	803.2	515.4	385.4	308.5
k, ∥ to layers				3.3		9.7	5.3	2.4	1.5	1.16	0.92
k, ⊥ to layers			0.169			0.32	0.098	0.236	0.335	0.394	0.428
c_p											
Graphite fiber epoxy	810	87.4									
(25% vol.) composite											
k, heat flow ∥ to fibers				6.4		3.3	5.0	7.5			
k, heat flow ⊥ to fibers				0.5	5	0.4	0.63				
c_p			0.223			0.08	0.153	0.29			
	2921	162.3	0.193	2.3	20.3	3.0	2.3	2.1	1.9	1.7	1.7
Pyroceram, Corning 9606	5580	197.3	0.161	283.1	2475.7			—	—	—	50.3
Silicon carbide								0.210	0.25	0.27	0.285
Silicon dioxide,											
crystalline (quartz)	3389	165.4									
k , ∥ to c-axis				6		22.5	9.5	4.4	2.9	2.4	
k , ⊥ to c-axis				3.6		12.0	5.9	2.7	2	1.8	
c_p			0.177					0.211	0.256	0.298	
Silicon dioxide,	3389	138.6	0.177	0.79	9	0.4	0.65	0.87	1.01	1.25	1.65
polycrystalline (fused silica)					—	—	—	0.216	0.248	0.264	0.276
Silicon nitride	3911	150	0.165	9.2	104	—	—	8.0	6.5	5.7	5.0
						—	0.138	0.185	0.223	0.253	0.275
Sulfur	706	130	0.169	0.1	1.51	0.095	0.1				
						0.962	0.144				
Thorium dioxide	6431	568.7	0.561	7.5	65.7			5.9	3.8	2.7	2.12
								0.609	0.654	0.680	0.704
Titanium dioxide,	3840	259.5	0.170	4.9	30.1			4.0	2.9	2.3	2
polycrystalline								0.192	0.210	0.217	0.222

Source: Tables A–3E and A–4E are obtained from the respective tables in SI units in Appendix 1 using proper conversion factors.

TABLE A–5E

Properties of building materials
(at a mean temperature of 75°F)

Material	Thickness, L in	Density, ρ lbm/ft^3	Thermal Conductivity, k Btu·in/h·ft^2·°F	Specific Heat, c_p Btu/lbm·R	R-value (for listed thickness, L/k), °F·h·ft^2/Btu
Building Boards					
Asbestos–cement board	¼ in.	120	—	0.24	0.06
Gypsum of plaster board	⅜ in.	50	—	0.26	0.32
	½ in.	50	—	—	0.45
Plywood (Douglas fir)	—	34	0.80	0.29	—
	¼ in.	34	—	0.29	0.31
	⅜ in.	34	—	0.29	0.47
	½ in.	34	—	0.29	0.62
	¾ in.	34	—	0.29	0.93
Insulated board and sheathing	½ in.	18	—	0.31	1.32
(regular density)	²⁵⁄₃₂ in.	18	—	0.31	2.06
Hardboard (high density, standard					
tempered)	—	63	1.00	0.32	—
Particle board					
Medium density	—	50	0.94	0.31	—
Underlayment	⅝ in.	40	—	0.29	0.82
Wood subfloor	¾ in.	—	—	0.33	0.94
Building Membranes					
Vapor-permeable felt	—	—	—	—	0.06
Vapor seal (2 layers of mopped					
17.3 lbm/ft^2 felt)	—	—	—	—	0.12
Flooring Materials					
Carpet and fibrous pad	—	—	—	0.34	2.08
Carpet and rubber pad	—	—	—	0.33	1.23
Tile (asphalt, linoleum, vinyl)	—	—	—	0.30	0.05
Masonry Materials					
Masonry units:					
Brick, common		120	5.0	—	—
Brick, face		130	9.0	—	—
Brick, fire clay		150	9.3	—	—
		120	6.2	0.19	—
		70	2.8	—	—
Concrete blocks (3 oval cores,					
sand and gravel aggregate)	4 in.	—	5.34	—	0.71
	8 in.	—	6.94	—	1.11
	12 in.	—	9.02	—	1.28
Concretes					
Lightweight aggregates		120	5.2	—	—
(including expanded shale,		100	3.6	0.2	—
clay, or slate, expanded slags,		80	2.5	0.2	—
cinders; pumice; and scoria)		60	1.7	—	—
		40	1.15	—	—
Cement/lime, mortar, and stucco		120	9.7	—	—
		80	4.5		
Stucco		116	5.0		

TABLE A–5E

Properties of building materials (*Concluded*)
(at a mean temperature of 75°F)

Material	Thickness, L in	Density, ρ lbm/ft^3	Thermal Conductivity, k Btu·in/h·ft^2·°F	Specific Heat, c_p Btu/lbm·R	R-value (for listed thickness, L/k), °F·h·ft^2/Btu
Roofing					
Asbestos-cement shingles		120	—	0.24	0.21
Asphalt roll roofing		70	—	0.36	0.15
Asphalt shingles		70	—	0.30	0.44
Built-in roofing	⅜ in.	70	—	0.35	0.33
Slate	½ in.	—	—	0.30	0.05
Wood shingles (plain and plastic film faced)		—	—	0.31	0.94
Plastering Materials					
Cement plaster, sand aggregate	¾ in.	1.16	5.0	0.20	0.15
Gypsum plaster					
Lightweight aggregate	½ in.	45	—	—	0.32
Sand aggregate	½ in.	105	5.6	0.20	0.09
Perlite aggregate	—	45	1.5	0.32	—
Siding Material (on flat surfaces)					
Asbestos-cement shingles	—	120	—	—	0.21
Hardboard siding	⁷⁄₁₆ in.	—	—	0.28	0.67
Wood (drop) siding	1 in.	—	—	0.31	0.79
Wood (plywood) siding, lapped	⅜ in.	—	—	0.29	0.59
Aluminum or steel siding (over sheeting):					
Hollow backed	⅜ in.	—	—	0.29	0.61
Insulating-board backed	⅜ in.	—	—	0.32	1.82
Architectural glass	—	158	6.9	0.21	0.10
Woods					
Hardwoods (maple, oak, etc.)	—	45	1.10	0.30	—
Softwoods (fir, pine, etc.)	—	32	0.80	0.33	—
Metals					
Aluminum (1100)	—	171	1536	0.214	—
Steel, mild	—	489	314	0.120	—
Steel, stainless	—	494	108	0.109	—

Source: Tables A-5E and A-6E are adapted from *ASHRAE, Handbook of Fundamentals* (Atlanta, GA: American Society of Heating, Refrigerating, and Air-Conditioning Engineers, 1993), Chap. 22, Table 4. Used with permission.

TABLE A–6E

Properties of insulating materials
(at a mean temperature of 75°F)

Material	Thickness, L in	Density, ρ lbm/ft^3	Thermal Conductivity, k Btu·in/h·ft^2·°F	Specific Heat, c_p Btu/lbm·R	R-value (for listed thickness, L/k) °F·h·ft^2/Btu
Blanket and Batt					
Mineral fiber (fibrous form	~ 2 to 2¾ in	0.3–2.0	—	0.17–0.23	7
processed from rock, slag,	~ 3 to 3½ in	0.3–2.0	—	0.17–0.23	11
or glass)	~ 5¼ to 6½ in	0.3–2.0	—	0.17–0.23	19
Board and Slab					
Cellular glass		8.5	0.38	0.24	—
Glass fiber (organic bonded)		4–9	0.25	0.23	—
Expanded polystyrene (molded beads)		1.0	0.28	0.29	—
Expanded polyurethane (R-11 expanded)		1.5	0.16	0.38	—
Expanded perlite (organic bonded)		1.0	0.36	0.30	—
Expanded rubber (rigid)		4.5	0.22	0.40	—
Mineral fiber with resin binder		15	0.29	0.17	—
Cork		7.5	0.27	0.43	—
Sprayed or Formed in Place					
Polyurethane foam		1.5–2.5	0.16–0.18	—	—
Glass fiber		3.5–4.5	0.26–0.27	—	—
Urethane, two-part mixture (rigid foam)		4.4	0.18	0.25	—
Mineral wool granules with asbestos/inorganic binders (sprayed)		12	0.32	—	—
Loose Fill					
Mineral fiber (rock, slag,	~ 3.75 to 5 in	0.6–0.20	—	0.17	11
or glass)	~ 6.5 to 8.75 in	0.6–0.20	—	0.17	19
	~ 7.5 to 10 in	—	—	0.17	22
	~ 7.25 in	—	—	0.17	30
Silica aerogel		7.6	0.17	—	—
Vermiculite (expanded)		7–8	0.47	—	—
Perlite, expanded		2–4.1	0.27–0.31	—	—
Sawdust or shavings		8–15	0.45	—	—
Cellulosic insulation (milled paper or wood pulp		0.3–3.2	0.27–0.32	—	—
Cork, granulated		10	0.31	—	—
Roof Insulation					
Cellular glass		9	0.4	0.24	—
Preformed, for use above deck	½ in	—	—	0.24	1.39
	1 in	—	—	0.50	2.78
	2 in	—	—	0.94	5.56
Reflective Insulation					
Silica powder (evacuated)		10	0.0118	—	—
Aluminum foil separating fluffy glass mats; 10–12 layers (evacuated); for cryogenic applications (270 R)		2.5	0.0011	—	—
Aluminum foil and glass paper laminate; 75–150 layers (evacuated); for cryogenic applications (270 R)		7.5	0.00012	—	—

TABLE A–7E

Properties of common foods
(a) Specific heats and freezing-point properties

Food	Water Content[a] % (mass)	Freezing Point[a] °F	Specific Heat[b] Btu/lbm·°F Above Freezing	Below Freezing	Latent Heat of Fusion[c] Btu/lbm
Vegetables					
Artichokes	84	30	0.873	0.453	121
Asparagus	93	31	0.945	0.481	134
Beans, snap	89	31	0.913	0.468	128
Broccoli	90	31	0.921	0.471	129
Cabbage	92	30	0.937	0.478	132
Carrots	88	29	0.905	0.465	126
Cauliflower	92	31	0.937	0.478	132
Celery	94	31	0.953	0.484	135
Corn, sweet	74	31	0.793	0.423	106
Cucumbers	96	31	0.969	0.490	138
Eggplant	93	31	0.945	0.481	134
Horseradish	75	29	0.801	0.426	108
Leeks	85	31	0.881	0.456	122
Lettuce	95	32	0.961	0.487	136
Mushrooms	91	30	0.929	0.474	131
Okra	90	29	0.921	0.471	129
Onions, green	89	30	0.913	0.468	128
Onions, dry	88	31	0.905	0.465	126
Parsley	85	30	0.881	0.456	122
Peas, green	74	31	0.793	0.423	106
Peppers, sweet	92	31	0.937	0.478	132
Potatoes	78	31	0.825	0.435	112
Pumpkins	91	31	0.929	0.474	131
Spinach	93	31	0.945	0.481	134
Tomatos, ripe	94	31	0.953	0.484	135
Turnips	92	30	0.937	0.478	132
Fruits					
Apples	84	30	0.873	0.453	121
Apricots	85	30	0.881	0.456	122
Avocados	65	31	0.721	0.396	93
Bananas	75	31	0.801	0.426	108
Blueberries	82	29	0.857	0.447	118
Cantaloupes	92	30	0.937	0.478	132
Cherries, sour	84	29	0.873	0.453	121
Cherries, sweet	80	29	0.841	0.441	115
Figs, dried	23	—	—	0.270	33
Figs, fresh	78	28	0.825	0.435	112
Grapefruit	89	30	0.913	0.468	128
Grapes	82	29	0.857	0.447	118
Lemons	89	29	0.913	0.468	128
Olives	75	29	0.801	0.426	108
Oranges	87	31	0.897	0.462	125
Peaches	89	30	0.913	0.468	128
Pears	83	29	0.865	0.450	119
Pineapples	85	30	0.881	0.456	122
Plums	86	31	0.889	0.459	124
Quinces	85	28	0.881	0.456	122
Raisins	18	—	—	0.255	26
Strawberries	90	31	0.921	0.471	129
Tangerines	87	30	0.897	0.462	125
Watermelon	93	31	0.945	0.481	134
Fish/Seafood					
Cod, whole	78	28	0.825	0.435	112
Halibut, whole	75	28	0.801	0.426	108
Lobster	79	28	0.833	0.438	113
Mackerel	57	28	0.657	0.372	82
Salmon, whole	64	28	0.713	0.393	92
Shrimp	83	28	0.865	0.450	119
Meats					
Beef carcass	49	29	0.593	0.348	70
Liver	70	29	0.761	0.411	101
Round, beef	67	—	0.737	0.402	96
Sirloin, beef	56	—	0.649	0.369	80
Chicken	74	27	0.793	0.423	106
Lamb leg	65	—	0.721	0.396	93
Pork carcass	37	—	0.497	0.312	53
Ham	56	29	0.649	0.369	80
Pork sausage	38	—	0.505	0.315	55
Turkey	64	—	0.713	0.393	92
Other					
Almonds	5	—	—	0.216	7
Butter	16	—	—	0.249	23
Cheese, cheddar	37	9	0.497	0.312	53
Cheese, Swiss	39	14	0.513	0.318	56
Chocolate, milk	1	—	—	0.204	1
Eggs, whole	74	31	0.793	0.423	106
Honey	17	—	—	0.252	24
Ice cream	63	22	0.705	0.390	90
Milk, whole	88	31	0.905	0.465	126
Peanuts	6	—	—	0.219	9
Peanuts, roasted	2	—	—	0.207	3
Pecans	3	—	—	0.210	4
Walnuts	4	—	—	0.213	6

Source: [a]Water content and freezing point data are from ASHRAE, *Handbook of Fundamentals*, I-P version (Atlanta, GA: American Society of Heating, Refrigerating, and Air-Conditioning Engineers, Inc., 1993), Chap. 30, Table 1. Used with permission.

[b]Specific heat data are based on the specific heat values of water and ice at 32°F and are determined from Siebel's formulas: $c_{p,fresh} = 0.800 \times$ (Water content) + 0.200, above freezing, and $c_{p,frozen} = 0.300 \times$ (Water content) + 0.200, below freezing.

[c]The latent heat of fusion is determined by multiplying the heat of fusion of water (143 Btu/lbm) by the water content of the food.

TABLE A–7E

Properties of common foods (*Concluded*)
(*b*) Other properties

Food	Water Content, % (mass)	Temperature, T °F	Density, ρ lbm/ft^3	Thermal Conductivity, k Btu/h·ft·°F	Thermal Diffusivity, α ft^2/s	Specific Heat, c_p Btu/lbm·R
Fruits/Vegetables						
Apple juice	87	68	62.4	0.323	1.51×10^{-6}	0.922
Apples	85	32–86	52.4	0.242	1.47×10^{-6}	0.910
Apples, dried	41.6	73	53.4	0.127	1.03×10^{-6}	0.650
Apricots, dried	43.6	73	82.4	0.217	1.22×10^{-6}	0.662
Bananas, fresh	76	41	61.2	0.278	1.51×10^{-6}	0.856
Broccoli	—	21	35.0	0.223	—	—
Cherries, fresh	92	32–86	65.5	0.315	1.42×10^{-6}	0.952
Figs	40.4	73	77.5	0.179	1.03×10^{-6}	0.642
Grape juice	89	68	62.4	0.328	1.51×10^{-6}	0.934
Peaches	36–90	2–32	59.9	0.304	1.51×10^{-6}	0.934
Plums	—	3	38.1	0.143	–	—
Potatoes	32–158	0–70	65.7	0.288	1.40×10^{-6}	0.868
Raisins	32	73	86.2	0.217	1.18×10^{-6}	0.592
Meats						
Beef, ground	67	43	59.3	0.235	1.40×10^{-6}	0.802
Beef, lean	74	37	68.0	0.272	1.40×10^{-6}	0.844
Beef fat	0	95	50.5	0.110	—	—
Beef liver	72	95	—	0.259	—	0.832
Cat food	39.7	73	71.2	0.188	1.18×10^{-6}	0.638
Chicken breast	75	32	65.5	0.275	1.40×10^{-6}	0.850
Dog food	30.6	73	77.4	0.184	1.18×10^{-6}	0.584
Fish, cod	81	37	73.7	0.309	1.29×10^{-6}	0.886
Fish, salmon	67	37	—	0.307	—	0.802
Ham	71.8	72	64.3	0.277	1.51×10^{-6}	0.831
Lamb	72	72	64.3	0.263	1.40×10^{-6}	0.832
Pork, lean	72	39	64.3	0.263	1.40×10^{-6}	0.832
Turkey breast	74	37	65.5	0.287	1.40×10^{-6}	0.844
Veal	75	72	66.2	0.272	1.40×10^{-6}	0.850
Other						
Butter	16	39	—	0.114	—	0.496
Chocolate cake	31.9	73	21.2	0.061	1.29×10^{-6}	0.591
Margarine	16	40	62.4	0.135	1.18×10^{-6}	0.496
Milk, skimmed	91	72	—	0.327	—	0.946
Milk, whole	88	82	—	0.335	—	0.928
Olive oil	0	90	56.8	0.097	—	—
Peanut oil	0	39	57.4	0.097	—	—
Water	100	0	62.4	0.329	1.51×10^{-6}	1.000
	100	30	59.6	0.357	1.61×10^{-6}	1.000
White cake	32.3	73	28.1	0.047	1.08×10^{-6}	0.594

Source: Data obtained primarily from ASHRAE, *Handbook of Fundamentals,* I-P version (Atlanta, GA: American Society of Heating, Refrigerating, and Air-Conditioning Engineers, Inc., 1993), Chap. 30, Tables 7 and 9. Used with permission.

Most specific heats are calculated from $c_p = 0.4 + 0.6 \times$ (Water content), which is a good approximation in the temperature range of 40 to 90°F. Most thermal diffusivities are calculated from $\alpha = k/\rho c_p$. Property values given above are valid for the specified water content.

TABLE A–8E

Properties of miscellaneous materials
(values are at 540 R unless indicated otherwise)

Material	Density, ρ lbm/ft^3	Thermal Conductivity, k Btu/h·ft·R	Specific Heat, c_p Btu/lbm·R	Material	Density, ρ lbm/ft^3	Thermal Conductivity, k Btu/h·ft·R	Specific Heat, c_p Btu/lbm·R
Asphalt	132.0	0.036	0.220	Ice			
Bakelite	81.2	0.81	0.350	492 R	57.4	1.09	0.487
Brick, refractory				455 R	57.6	1.17	0.465
Chrome brick				311 R	57.9	2.02	0.349
851 R	187.9	1.33	0.199	Leather, sole	62.3	0.092	—
1481 R	—	1.44	—	Linoleum	33.4	0.047	—
2111 R	—	1.16	—		73.7	0.11	—
Fire clay, burnt 2880 R				Mica	181.0	0.30	—
				Paper	58.1	0.10	0.320
1391 R	128.0	0.58	0.229	Plastics			
1931 R	—	0.64	—	Plexiglass	74.3	0.11	0.350
2471 R	—	0.64	—	Teflon			
Fire clay, burnt 3105 R				540 R	137.3	0.20	0.251
				720 R	—	0.26	—
1391 R	145.1	0.75	0.229	Lexan	74.9	0.11	0.301
1931 R	—	0.81	—	Nylon	71.5	0.17	—
2471 R	—	0.81	—	Polypropylene	56.8	0.069	0.388
Fire clay brick				Polyester	87.1	0.087	0.279
860 R	165.1	0.58	0.229	PVC, vinyl	91.8	0.058	0.201
1660 R	—	0.87	—	Porcelain	143.6	0.87	—
2660 R	—	1.04	—	Rubber, natural	71.8	0.16	—
Magnesite				Rubber, vulcanized			
860 R	—	2.20	0.270	Soft	68.7	0.075	0.480
1660 R	—	1.62	—	Hard	74.3	0.092	—
2660 R	—	1.10	—	Sand	94.6	0.1–0.6	0.191
Chicken meat,				Snow, fresh	6.24	0.35	—
white (74.4%				Snow 492 R	31.2	1.27	—
water content)				Soil, dry	93.6	0.58	0.454
356 R	—	0.92	—	Soil, wet	118.6	1.16	0.525
419 R	—	0.86	—	Sugar	99.9	0.34	—
455 R	—	0.78	—	Tissue, human			
492 R	—	0.28	—	Skin	—	0.21	—
527 R	—	0.28	—	Fat layer	—	0.12	—
Clay, dry	96.8	0.54	—	Muscle	—	0.24	—
Clay, wet	93.3	0.97	—	Vaseline	—	0.098	—
Coal, anthracite	84.3	0.15	0.301	Wood, cross-grain			
Concrete (stone mix)	143.6	0.81	0.210	Balsa	8.74	0.032	—
Cork	5.37	0.028	0.485	Fir	25.9	0.064	0.650
Cotton	5.0	0.035	0.311	Oak	34.0	0.098	0.570
Fat	—	0.10	—	White pine	27.2	0.064	—
Glass				Yellow pine	40.0	0.087	0.670
Window	174.8	0.40	0.179	Wood, radial			
Pyrex	138.9	0.6–0.8	0.199	Oak	34.0	0.11	0.570
Crown	156.1	0.61	—	Fir	26.2	0.081	0.650
Lead	212.2	0.49	—	Wool, ship	9.05	0.029	—

TABLE A–9E

Properties of saturated water

Temp. T, F°	Saturation Pressure P_{sat}, psia	Density ρ, lbm/ft³ Liquid	Density ρ, lbm/ft³ Vapor	Enthalpy of Vaporization h_{fg}, Btu/lbm	Specific Heat c_p, Btu/lbm·R Liquid	Specific Heat c_p, Btu/lbm·R Vapor	Thermal Conductivity k, Btu/h·ft·R Liquid	Thermal Conductivity k, Btu/h·ft·R Vapor	Dynamic Viscosity μ, lbm/ft·s Liquid	Dynamic Viscosity μ, lbm/ft·s Vapor	Prandtl Number Pr Liquid	Prandtl Number Pr Vapor	Volume Expansion Coefficient β, 1/R Liquid
32.02	0.0887	62.41	0.00030	1075	1.010	0.446	0.324	0.0099	1.204×10^{-3}	6.194×10^{-6}	13.5	1.00	-0.038×10^{-3}
40	0.1217	62.42	0.00034	1071	1.004	0.447	0.329	0.0100	1.308×10^{-3}	6.278×10^{-6}	11.4	1.01	A0.003 $\times 10^{-3}$
50	0.1780	62.41	0.00059	1065	1.000	0.448	0.335	0.0102	8.781×10^{-4}	6.361×10^{-6}	9.44	1.01	0.047×10^{-3}
60	0.2563	62.36	0.00083	1060	0.999	0.449	0.341	0.0104	7.536×10^{-4}	6.444×10^{-6}	7.95	1.00	0.080×10^{-3}
70	0.3632	62.30	0.00115	1054	0.999	0.450	0.347	0.0106	6.556×10^{-4}	6.556×10^{-6}	6.79	1.00	0.115×10^{-3}
80	0.5073	62.22	0.00158	1048	0.999	0.451	0.352	0.0108	5.764×10^{-4}	6.667×10^{-6}	5.89	1.00	0.145×10^{-3}
90	0.6988	62.12	0.00214	1043	0.999	0.453	0.358	0.0110	5.117×10^{-4}	6.778×10^{-6}	5.14	1.00	0.174×10^{-3}
100	0.9503	62.00	0.00286	1037	0.999	0.454	0.363	0.0112	4.578×10^{-4}	6.889×10^{-6}	4.54	1.01	0.200×10^{-3}
110	1.2763	61.86	0.00377	1031	0.999	0.456	0.367	0.0115	4.128×10^{-4}	7.000×10^{-6}	4.05	1.00	0.224×10^{-3}
120	1.6945	61.71	0.00493	1026	0.999	0.458	0.371	0.0117	3.744×10^{-4}	7.111×10^{-6}	3.63	1.00	0246×10^{-3}
130	2.225	61.55	0.00636	1020	0.999	0.460	0.375	0.0120	3.417×10^{-4}	7.222×10^{-6}	3.28	1.00	0.267×10^{-3}
140	2.892	61.38	0.00814	1014	0.999	0.463	0.378	0.0122	3.136×10^{-4}	7.333×10^{-6}	2.98	1.00	0.287×10^{-3}
150	3.722	61.19	0.0103	1008	1.000	0.465	0.381	0.0125	2.889×10^{-4}	7.472×10^{-6}	2.73	1.00	0.306×10^{-3}
160	4.745	60.99	0.0129	1002	1.000	0.468	0.384	0.0128	2.675×10^{-4}	7.583×10^{-6}	2.51	1.00	0.325×10^{-3}
170	5.996	60.79	0.0161	996	1.001	0.472	0.386	0.0131	2.483×10^{-4}	7.722×10^{-6}	2.90	1.00	0.346×10^{-3}
180	7.515	60.57	0.0199	990	1.002	0.475	0.388	0.0134	2.317×10^{-4}	7.833×10^{-6}	2.15	1.00	0.367×10^{-3}
190	9.343	60.35	0.0244	984	1.004	0.479	0.390	0.0137	2.169×10^{-4}	7.972×10^{-6}	2.01	1.00	0.382×10^{-3}
200	11.53	60.12	0.0297	978	1.005	0.483	0.391	0.0141	2.036×10^{-4}	8.083×10^{-6}	1.88	1.00	0.395×10^{-3}
210	14.125	59.87	0.0359	972	1.007	0.487	0.392	0.0144	1.917×10^{-4}	8.222×10^{-6}	1.77	1.00	0.412×10^{-3}
212	14.698	59.82	0.0373	970	1.007	0.488	0.392	0.0145	1.894×10^{-4}	8.250×10^{-6}	1.75	1.00	0.417×10^{-3}
220	17.19	59.62	0.0432	965	1.009	0.492	0.393	0.0148	1808×10^{-4}	8.333×10^{-6}	1.67	1.00	0.429×10^{-3}
230	20.78	59.36	0.0516	959	1.011	0.497	0.394	0.0152	1.711×10^{-4}	8.472×10^{-6}	1.58	1.00	0.443×10^{-3}
240	24.97	59.09	0.0612	952	1.013	0.503	0.394	0.0156	1.625×10^{-4}	8.611×10^{-6}	1.50	1.00	0.462×10^{-3}
250	29.82	58.82	0.0723	946	1.015	0.509	0.395	0.0160	1.544×10^{-4}	8.611×10^{-6}	1.43	1.00	0.480×10^{-3}
260	35.42	58.53	0.0850	939	1.018	0.516	0.395	0.0164	1.472×10^{-4}	8.861×10^{-6}	1.37	1.00	0.497×10^{-3}
270	41.85	58.24	0.0993	932	1.020	0.523	0.395	0.0168	1.406×10^{-4}	9.000×10^{-6}	1.31	1.01	0.514×10^{-3}
280	49.18	57.94	0.1156	926	1.023	0.530	0.395	0.0172	1.344×10^{-4}	9.111×10^{-6}	1.25	1.01	0.532×10^{-3}
290	57–53	57.63	0.3390	918	1.026	0.538	0.395	0.0177	1.289×10^{-4}	9.250×10^{-6}	1.21	1.01	0.549×10^{-3}
300	66.98	57.31	0.1545	910	1.029	0.547	0.394	0.0182	1.236×10^{-4}	9.389×10^{-6}	1.16	1.02	0.566×10^{-3}
320	89.60	56.65	0.2033	895	1.036	0.567	0.393	0.0191	1.144×10^{-4}	9.639×10^{-6}	1.09	1.03	0.636×10^{-3}
340	117.93	55.95	0.2637	880	1.044	0.590	0.391	0.0202	1.063×10^{-4}	9.889×10^{-6}	1.02	1.04	0.656×10^{-3}
360	152.92	56.22	0.3377	863	1.054	0.617	0.389	0.0213	9.972×10^{-5}	1.013×10^{-5}	0.973	1.06	0.681×10^{-3}
380	195.60	54.46	0.4275	845	1.065	0.647	0.385	0.0224	9.361×10^{-5}	1.041×10^{-5}	0.932	1.08	0.720×10^{-3}
400	241.1	53.65	0.5359	827	1.078	0.683	0.382	0.0237	8.833×10^{-5}	1.066×10^{-5}	0.893	1.11	0.771×10^{-3}
450	422.1	51.46	0.9082	775	1.121	0.799	0.370	0.0271	7.722×10^{-5}	1.130×10^{-5}	0.842	1.20	0.912×10^{-3}
500	680.0	48.95	1.479	715	1.188	0.972	0.352	0.0312	6.833×10^{-5}	1.200×10^{-5}	0.830	1.35	1.111×10^{-3}
550	1046.7	45.96	4.268	641	1.298	1.247	0.329	0.0368	6.083×10^{-5}	1.280×10^{-5}	0.864	1.56	1.445×10^{-3}
600	1541	42.32	3.736	550	1.509	1.759	0.299	0.0461	5.389×10^{-5}	1.380×10^{-5}	0.979	1.90	1.883×10^{-3}
650	2210	37.31	6.152	422	2.086	3.103	0.267	0.0677	4.639×10^{-5}	1.542×10^{-5}	1.30	2.54	
700	3090	27.28	13.44	168	13.80	25.90	0.254	0.1964	3.417×10^{-5}	2.044×10^{-5}	6.68	9.71	
705.44	3204	19.79	19.79	0	∞	∞	∞	∞	2.897×10^{-5}	2.897×10^{-5}			

Note 1: Kinematic viscosity ν and thermal diffusivity α can be calculated from their definitions, $\nu = \mu/\rho$ and $\alpha = k/\rho c_\rho = \nu/Pr$. The temperatures 32.02°F, 212°F, and 705.44°F are the triple-, boiling-, and critical-point temperatures of water, respectively. All properties listed above (except the vapor density) can be used at any pressures with negligible error except at temperatures near the critical-point value.

Note 2: The unit Btu/lbm·°F for specific heat is equivalent to Btu/lbm·R, and the unit Btu/h·ft·°F for thermal conductivity is equivalent to Btu/h·ft·R.

Source: Viscosity and thermal conductivity data are from J. V. Sengers and J. T. T. Watson, *Journal of Physical and Chemical Reference Data* 15 (1986), pp. 1291–1322. Other data are obtained from various sources or calculated.

TABLE A–10E

Properties of saturated refrigerant-134a

Temp. T, F°	Saturation Pressure P_{sat}, psia	Density ρ, lbm/ft³ Liquid	Vapor	Enthalpy of Vaporization h_{fg}, Btu/lbm	Specific Heat c_p, Btu/lbm·R Liquid	Vapor	Thermal Conductivity k, Btu/h·ft·R Liquid	Vapor	Dynamic Viscosity μ, lbm/ft·s Liquid	Vapor	Prandtl Number Pr Liquid	Vapor	Volume Expansion Coefficient β, 1/R Liquid	Surface Tension lbf/ft
−40	7.4	88.51	0.1731	97.1	0.2996	0.1788	0.0636	0.00466	3.278×10^{-4}	1.714×10^{-6}	5.558	0.237	0.00114	0.001206
−30	9.9	87.5	0.2258	95.6	0.3021	0.1829	0.0626	0.00497	3.004×10^{-4}	2.053×10^{-6}	5.226	0.272	0.00117	0.001146
−20	12.9	86.48	0.2905	94.1	0.3046	0.1872	0.0613	0.00529	2.762×10^{-4}	2.433×10^{-6}	4.937	0.310	0.00120	0.001087
−10	16.6	85.44	0.3691	92.5	0.3074	0.1918	0.0602	0.00559	2.546×10^{-4}	2.856×10^{-6}	4.684	0.352	0.00124	0.001029
0	21.2	84.38	0.4635	90.9	0.3103	0.1966	0.0589	0.00589	2.345×10^{-4}	3.314×10^{-6}	4.463	0.398	0.00128	0.000972
10	26.6	83.31	0.5761	89.3	0.3134	0.2017	0.0576	0.00619	2.181×10^{-4}	3.811×10^{-4}	4.269	0.447	0.00132	0.000915
20	33.1	82.2	0.7094	87.5	0.3167	0.2070	0.0563	0.00648	2.024×10^{-4}	4.342×10^{-6}	4.098	0.500	0.00132	0.000859
30	40.8	81.08	0.866	85.8	0.3203	0.2127	0.0550	0.00676	1.883×10^{-4}	4.906×10^{-6}	3.947	0.555	0.00142	0.000803
40	49.8	79.92	1.049	83.9	0.3240	0.2188	0.0536	0.00704	1.752×10^{-4}	5.494×10^{-6}	3.814	0.614	0.00149	0.000749
50	60.2	78.73	1.262	82.0	0.3281	0.2253	0.0522	0.00732	1.633×10^{-4}	6.103×10^{-6}	3.697	0.677	0.00156	0.000695
60	72.2	77.51	1.509	80.0	0.3325	0.2323	0.0507	0.00758	1.522×10^{-4}	6.725×10^{-6}	3.594	0.742	0.00163	0.000642
70	85.9	76.25	1.794	78.0	0.3372	0.2398	0.0492	0.00785	1.420×10^{-4}	7.356×10^{-6}	3.504	0.810	0.00173	0.000590
80	101.4	74.94	2.122	75.8	0.3424	0.2481	0.0476	0.00810	1.324×10^{-4}	7.986×10^{-6}	3.425	0.880	0.00183	0.000538
90	119.1	73.59	2.5	73.5	0.3481	0.2572	0.0460	0.00835	1.234×10^{-4}	8.611×10^{-6}	3.357	0.955	0.00195	0.000488
100	138.9	72.17	2.935	71.1	0.3548	0.2674	0.0444	0.00860	1.149×10^{-4}	9.222×10^{-6}	3.303	1.032	0.00210	0.000439
110	161.2	70.69	3.435	68.5	0.3627	0.2790	0.0427	0.00884	1.068×10^{-4}	9.814×10^{-6}	3.262	1.115	0.00227	0.000391
120	186.0	69.13	4.012	65.8	0.3719	0.2925	0.0410	0.00908	9.911×10^{-5}	1.038×10^{-5}	3.235	1.204	0.00248	0.000344
130	213.5	67.48	4.679	62.9	0.3829	0.3083	0.0392	0.00931	9.175×10^{-5}	1.092×10^{-5}	3.223	1.303	0.00275	0.000299
140	244.1	65.72	5.455	59.8	0.3963	0.3276	0.0374	0.00954	8.464×10^{-5}	1.144×10^{-5}	3.229	1.416	0.00308	0.000255
150	277.8	63.83	6.367	56.4	0.4131	0.3520	0.0355	0.00976	7.778×10^{-5}	1.195×10^{-5}	3.259	1.551	0.00351	0.000212
160	314.9	61.76	7.45	52.7	0.4352	0.3839	0.0335	0.00998	7.108×10^{-5}	1.245×10^{-5}	3.324	1.725	0.00411	0.000171
170	355.8	59.47	8.762	48.5	0.4659	0.4286	0.0314	0.01020	6.450×10^{-5}	1.298×10^{-5}	3.443	1.963	0.00498	0.000132
180	400.7	56.85	10.4	43.7	0.5123	0.4960	0.0292	0.01041	5.792×10^{-5}	1.366×10^{-5}	3.661	2.327	0.00637	0.000095
190	449.9	53.75	12.53	38.0	0.5929	0.6112	0.0267	0.01063	5.119×10^{-5}	1.431×10^{-5}	4.090	2.964	0.00891	0.000061
200	504.0	49.75	15.57	30.7	0.7717	0.8544	0.0239	0.01085	4.397×10^{-5}	1.544×10^{-5}	5.119	4.376	0.01490	0.000031
210	563.8	43.19	21.18	18.9	1.4786	1.6683	0.0199	0.01110	3.483×10^{-5}	1.787×10^{-5}	9.311	9.669	0.04021	0.000006

Note 1: Klnematic viscosity ν and thermal diffusivity α can be calculated from their definitions, $\nu = \mu/\rho$ and $\alpha = k/\rho c_p = \nu/Pr$. The properties listed here (except the vapor density) can be used at any pressures with negligible error except at temperatures near the critical-point value.

Note 2: The unit Btu/lbm·°F for specific heat is equivalent to Btu/lbm·R, and the unit Btu/h·ft·°F for thermal conductivity is equivalent to Btu/h·ft·R.

Source: Data generated from the EES software developed by S. A. Klein and F. L. Alvarado. Original sources: R. Tilner-Roth and H. D. Baehr, "An International Standard Formulation for the Thermodynamic Properties of 1,1,1,2-Tetrafluorethane (HFC-134a) for Temperatures from 170 K to 455 K and Pressures up to 70 Mpa," *J. Phys. Chem. Ref. Data,* Vol. 23, No.5, 1994: M. J. Assael, N. K. Dalaouti, A. A. Griva, and J. H. Dymond, "Viscosity and Thermal Conductivity of Halogenated Methane and Ethane Refrigerants," *IJR,* Vol. 22, pp. 525–535, 1999: NIST REPROP 6 program (M. O. McLinden, S. A. Klein, E. W. Lemmon, and A. P. Peskin, Phyisical and Chemical Properties Division, National Institute of Standards and Technology, Boulder, CO 80303. 1995).

TABLE A–11E

Properties of saturated ammonia

Temp. T, F°	Saturation Pressure P_{sat}, psia	Density ρ, lbm/ft³ Liquid	Vapor	Enthalpy of Vaporization h_{fg}, Btu/lbm	Specific Heat c_p, Btu/lbm·R Liquid	Vapor	Thermal Conductivity k, Btu/h·ft·R Liquid	Vapor	Dynamic Viscosity μ, lbm/ft·s Liquid	Vapor	Prandtl Number Pr Liquid	Vapor	Volume Expansion Coefficient β, 1/R Liquid	Surface Tension lbf/ft
−40	10.4	43.08	0.0402	597.0	1.0542	0.5354	–	0.01026	1.966×10^{-4}	5.342×10^{-6}	–	1.003	0.00098	0.002443
−30	13.9	42.66	0.0527	590.2	1.0610	0.5457	–	0.01057	1.853×10^{-4}	5.472×10^{-6}	–	1.017	0.00101	0.002357
−20	18.3	42.33	0.0681	583.2	1.0677	0.5571	0.3501	0.01089	1.746×10^{-4}	5.600×10^{-6}	1.917	1.031	0.00103	0.002272
−10	23.7	41.79	0.0869	575.9	1.0742	0.5698	0.3426	0.01121	1.645×10^{-4}	5.731×10^{-6}	1.856	1.048	0.00106	0.002187
0	30–4	41.34	0.1097	568.4	1.0807	0.5838	0.3352	0.01154	1.549×10^{-4}	5.861×10^{-6}	1.797	1.068	0.00109	0.002103
10	38.5	40.89	0.1370	560.7	1.0873	0.5992	0.3278	0.01187	1.458×10^{-4}	5.994×10^{-6}	1.740	1.089	0.00112	0.002018
20	48.2	40.43	0.1694	552.6	1.0941	0.6160	0.3203	0.01220	1.371×10^{-4}	6.125×10^{-6}	1.686	1.113	0.00116	0.001934
30	59.8	39.96	0.2075	544.4	1.1012	0.6344	0.3129	0.01254	1290×10^{-4}	6.256×10^{-6}	1.634	1.140	0.00119	0.001850
40	73.4	39.48	0.2521	535.8	1.1087	0.6544	0.3055	0.01288	1.213×10^{-4}	6.389×10^{-6}	1.585	1.168	0.00123	0.001767
50	89.2	38.99	0.3040	526.9	1.1168	0.6762	0.2980	0.01323	1.140×10^{-4}	6.522×10^{-6}	1.539	1.200	0.00128	0.001684
60	107.7	38.50	0.3641	517.7	1.1256	0.6999	0.2906	0.01358	1.072×10^{-4}	6.656×10^{-6}	1.495	1.234	0.00132	0.001601
70	128.9	37.99	0.4332	508.1	1.1353	0.7257	0.2832	0.01394	1.008×10^{-4}	6.786×10^{-6}	1.456	1.272	0.00137	0.001518
80	153.2	37.47	0.5124	498.2	1.1461	0.7539	0.2757	0.01431	9.486×10^{-5}	6.922×10^{-6}	1.419	1.313	0.00143	0.001436
90	180.8	36.94	0.6029	487.8	1.1582	0.7846	0.2683	0.01468	8.922×10^{-5}	7.056×10^{-6}	1.387	1.358	0.00149	0.001354
100	212.0	36.40	0.7060	477.0	1.1719	0.8183	0.2609	0.01505	8.397×10^{-5}	7.189×10^{-6}	1.358	1.407	0.00156	0.001273
110	247.2	35.83	0.8233	465.8	1.1875	0.8554	0.2535	0.01543	7.903×10^{-5}	7.325×10^{-6}	1.333	1.461	0.00164	0.001192
120	286.5	35.26	0.9564	454.1	1.2054	0.8965	0.2460	0.01582	7.444×10^{-5}	7.458×10^{-6}	1.313	1.522	0.00174	0.001111
130	330.4	34.66	1.1074	441.7	1.2261	0.9425	0.2386	0.01621	7.017×10^{-5}	7.594×10^{-6}	1.298	1.589	0.00184	0.001031
140	379.4	34.04	1.2786	428.8	1.2502	0.9943	0.2312	0.01661	6.617×10^{-5}	7.731×10^{-6}	1.288	1.666	0.00196	0.000951
150	433.2	33.39	1.4730	415.2	1.2785	1.0533	0.2237	0.01702	6.244×10^{-5}	7.867×10^{-4}	1.285	1.753	0.00211	0.000872
160	492.7	32.72	1.6940	400.8	1.3120	1.1214	0.2163	0.01744	5.900×10^{-5}	8.006×10^{-6}	1.288	1.853	0.00228	0.000794
170	558.2	32.01	1.9460	385.4	1.3523	1.2012	0.2089	0.01786	5.578×10^{-5}	8.142×10^{-6}	1.300	1.971	0.00249	0.000716
180	630.1	31.26	2.2346	369.1	1.4015	1.2965	0.2014	0.01829	5.278×10^{-5}	8.281×10^{-6}	1.322	2.113	0.00274	0.000638
190	708.5	30.47	2.5670	351.6	1.4624	1.4128	0.1940	0.01874	5.000×10^{-5}	8.419×10^{-6}	1.357	2.286	0.00306	0.000562
200	794.4	29.62	2.9527	332.7	1.5397	1.5586	0.1866	0.01919	4.742×10^{-5}	8.561×10^{-6}	1.409	2.503	0.00348	0.000486
210	887.9	28.70	3.4053	312.0	1.6411	1.7473	0.1791	0.01966	4.500×10^{-5}	8.703×10^{-6}	1.484	2.784	0.00403	0.000411
220	989.5	27.69	3.9440	289.2	1.7798	2.0022	0.1717	0.02015	4.275×10^{-5}	8.844×10^{-6}	1.595	3.164	0.00480	0.000338
230	1099.0	25.57	4.5987	263.5	1.9824	2.3659	0.1643	0.02065	4.064×10^{-5}	8.989×10^{-6}	1.765	3.707	0.00594	0.000265
240	1219.4	25.28	5.4197	234.0	2.3100	2.9264	0.1568	0.02119	3.864×10^{-5}	9.136×10^{-6}	2.049	4.542	0.00784	0.000194

Note 1: Kinematic viscosity ν and thermal diffusivity α can be calculated from their definitions, $\nu = \mu/\rho$ and $\alpha = k/\rho\, c_\rho = \nu/\mathrm{Pr}$. The properties listed here (except the vapor density) can be used at any pressures with negligible error except at temperatures near the critical-point value.

Note 2: The unit Btu/lbm·°F for specific heat is equivalent to Btu/lbm·R, and the unit Btu/lbm·F, for thermal conductivity is equivalent to Btu/h·ft·R.

Source: Data generated from the EES software developed by S. A. Klein and F. L. Alvarado. Orginal sources: Tillner-Roth, Harms-Watzenterg, and Baehr, "Eine neue Fundamentalgleichung fur Ammoniak," *DKV-Tagungsbericht* 20: 167–181, 1993; Liley and Desai, "Thermophysical Properties of Refrigerants," *ASHRAE,* 1993, ISBN 1-1883413-10-9.

TABLE A–12E

Properties of saturated propane

Temp. T, °F	Saturation Pressure P_{sat}, psia	Density ρ, lbm/ft³ Liquid	Density ρ, lbm/ft³ Vapor	Enthalpy of Vaporization h_{fg}, Btu/lbm	Specific Heat c_p, Btu/lbm·R Liquid	Specific Heat c_p, Btu/lbm·R Vapor	Thermal Conductivity k, Btu/h·ft·R Liquid	Thermal Conductivity k, Btu/h·ft·R Vapor	Dynamic Viscosity μ, lbm/ft·s Liquid	Dynamic Viscosity μ, lbm/ft·s Vapor	Prandtl Number Pr Liquid	Prandtl Number Pr Vapor	Volume Expansion Coefficient β, 1/R Liquid	Surface Tension lbf/ft
−200	0.0201	42.06	0.0003	217.7	0.4750	0.2595	0.1073	0.00313	5.012×10^{-4}	2.789×10^{-6}	7.991	0.833	0.00083	0.001890
−180	0.0752	41.36	0.0011	213.4	0.4793	0.2680	0.1033	0.00347	3.941×10^{-4}	2.975×10^{-6}	6.582	0.826	0.00086	0.001780
−160	0.2307	40.65	0.0032	209.1	0.4845	0.2769	0.0992	0.00384	3.199×10^{-4}	3.164×10^{-6}	5.626	0.821	0.00088	0.001671
−140	0.6037	39.93	0.0078	204.8	0.4907	0.2866	0.0949	0.00423	2.660×10^{-4}	3.358×10^{-6}	4.951	0.818	0.00091	0.001563
−120	1.389	39.20	0.0170	200.5	0.4982	0.2971	0.0906	0.00465	2.252×10^{-4}	3.556×10^{-6}	4.457	0.817	0.00094	0.001455
−100	2.878	38.46	0.0334	196.1	0.5069	0.3087	0.0863	0.00511	1.934×10^{-4}	3.756×10^{-6}	4.087	0.817	0.00097	0.001349
−90	4.006	38.08	0.0453	193.9	0.5117	0.3150	0.0842	0.00534	1.799×10^{-4}	3.858×10^{-6}	3.936	0.819	0.00099	0.001297
−80	5.467	37.70	0.0605	191.6	0.5169	0.3215	0.0821	0.00559	1.678×10^{-4}	3.961×10^{-6}	3.803	0.820	0.00101	0.001244
−70	7.327	37.32	0.0793	189.3	0.5224	0.3284	0.0800	0.00585	1.569×10^{-4}	4.067×10^{-6}	3.686	0.822	0.00104	0.001192
−60	9.657	36.93	0.1024	186.9	0.5283	0.3357	0.0780	0.00611	1.469×10^{-4}	4.172×10^{-6}	3.582	0.825	0.00106	0.001140
−50	12.54	36.54	0.1305	184.4	0.5345	0.3433	0.0760	0.00639	1.378×10^{-4}	4.278×10^{-6}	3.490	0.828	0.00109	0.001089
−40	16.05	36.13	0.1641	181.9	0.5392	0.3513	0.0740	0.00568	1.294×10^{-4}	4.386×10^{-6}	3.395	0.831	0.00112	0.001038
−30	20.29	35.73	0.2041	179.3	0.5460	0.3596	0.0721	0.00697	1.217×10^{-4}	4.497×10^{-6}	3.320	0.835	0.00115	0.000987
−20	25.34	35.31	0.2512	176.6	0.5531	0.3684	0.0702	0.00728	1.146×10^{-4}	4.611×10^{-6}	3.253	0.840	0.00119	0.000937
−10	31.3	34.89	0.3063	173.8	0.5607	0.3776	0.0683	0.00761	1.079×10^{-4}	4.725×10^{-6}	3.192	0.845	0.00123	0.000887
0	38.28	34.46	0.3703	170.9	0.5689	0.3874	0.0665	0.00794	1.018×10^{-4}	4.842×10^{-6}	3.137	0.850	0.00127	0.000838
10	46.38	34.02	0.4441	167.9	0.5775	0.3976	0.0647	0.00829	9.606×10^{-5}	4.961×10^{-6}	3.088	0.857	0.00132	0.000789
20	55.7	33.56	0.5289	164.8	0.5867	0.4084	0.0629	0.00865	9.067×10^{-5}	5.086×10^{-6}	3.043	0.864	0.00138	0.000740
30	66.35	33.10	0.6259	161.6	0.5966	0.4199	0.0512	0.00903	8.561×10^{-5}	5.211×10^{-6}	3.003	0.873	0.00144	0.000692
40	78.45	32.62	0.7365	158.1	0.6072	0.4321	0.0595	0.00942	8.081×10^{-5}	5.342×10^{-6}	2.967	0.882	0.00151	0.000644
50	92.12	32.13	0.8621	154.6	0.6187	0.4452	0.0579	0.00983	7.631×10^{-5}	5.478×10^{-6}	2.935	0.893	0.00159	0.000597
60	107.5	31.63	1.0046	150.8	0.6311	0.4593	0.0563	0.01025	7.200×10^{-5}	5.617×10^{-6}	2.906	0.906	0.00168	0.000551
70	124.6	31.11	1.1659	146.8	0.6447	0.4746	0.0547	0.01070	6.794×10^{-5}	5.764×10^{-6}	2.881	0.921	0.00179	0.000505
80	143.7	30.56	1.3484	142.7	0.6596	0.4915	0.0532	0.01116	6.406×10^{-5}	5.919×10^{-6}	2.860	0.938	0.00191	0.000460
90	164.8	30.00	1.5549	138.2	0.6762	0.5103	0.0517	0.01165	6.033×10^{-5}	6.081×10^{-6}	2.843	0.959	0.00205	0.000416
100	188.1	29.41	1.7887	133.6	0.6947	0.5315	0.0501	0.01217	5.675×10^{-5}	6.256×10^{-6}	2.831	0.984	0.00222	0.000372
120	241.8	28.13	2.3562	123.2	0.7403	0.5844	0.0472	0.01328	5.000×10^{-6}	6.644×10^{-6}	2.825	1.052	0.00267	0.000288
140	306.1	26.69	3.1003	111.1	0.7841	0.6613	0.0442	0.01454	4.358×10^{-5}	7.111×10^{-6}	2.784	1.164	0.00338	0.000208
160	382.4	24.98	4.1145	96.4	0.8696	0.7911	0.0411	0.01603	3.733×10^{-5}	7.719×10^{-6}	2.845	1.371	0.00459	0.000133
180	472.9	22.79	5.6265	77.1	1.1436	1.0813	0.0376	0.01793	3.083×10^{-5}	8.617×10^{-6}	3.380	1.870	0.00791	0.000065

Note 1: Kinematic viscosity ν and thermal diffusivity α can be calculated from their definitions, $\nu = \mu/\rho$ and $\alpha = k/\rho\,c_p = \nu/Pr$. The properties listed here (except the vapor density) can be used at any pressures with negligible error at temperatures near the critical-point value.

Note 2: The unit Btu/lbm·°F for specific heat is equivalent to Btu/lbm·°R, and the unit Btu/h·ft·°F for thermal conductivity is equivalent to Btu/h·ft·R.

Source: Data generated from the EES software developed by S. A. Klein and F. L. Alvarado. Original sources: Reiner Tillner-Roth, "Fundamental Equations of State," Shaker, Verlag, Aachan, 1998; B. A. Younglove and J. F. Ely. "Thermophysical Properties of Fluids. II Methane, Ethane, Propane, Isobutane, and Normal Butane," *J. Phys. Chem. Ref. Data,* Vol. 16, No. 4, 1987; G. R. Somayajulu, "A Generalized Equation for Surface Tension from the Triple-Point to the Critical-Point," *International Journal of Thermophysics,* Vol. 9, No. 4, 1988.

TABLE A–13E

Properties of liquids

Temp. T, F°	Density ρ, lbm/ft³	Specific Heat c_p, Btu/lbm·R	Thermal Conductivity k, Btu/h·ft·R	Thermal Diffusivity α, ft²/s	Dynamic Viscosity μ, lbm/ft·s	Kinematic Viscosity ν, ft²/s	Prandtl Number Pr	Volume Expansion Coeff. β, 1/R
				Methane (CH_4)				
−280	27.41	0.8152	0.1205	1.497×10^{-6}	1.057×10^{-4}	3.857×10^{-6}	2.575	0.00175
−260	26.43	0.8301	0.1097	1.389×10^{-6}	8.014×10^{-5}	3.032×10^{-6}	2.183	0.00192
−240	25.39	0.8523	0.0994	1.276×10^{-6}	6.303×10^{-5}	2.482×10^{-6}	1.945	0.00215
−220	24.27	0.8838	0.0896	1.159×10^{-6}	5.075×10^{-5}	2.091×10^{-6}	1.803	0.00247
−200	23.04	0.9314	0.0801	1.036×10^{-6}	4.142×10^{-5}	1.798×10^{-6}	1.734	0.00295
−180	21.64	1.010	0.0709	9.008×10^{-7}	3.394×10^{-5}	1.568×10^{-6}	1.741	0.00374
−160	19.99	1.158	0.0616	7.397×10^{-7}	2.758×10^{-5}	1.379×10^{-6}	1.865	0.00526
−140	17.84	1.542	0.0518	5.234×10^{-7}	2.168×10^{-5}	1.215×10^{-6}	2.322	0.00943
				Methanol $[CH_3(OH)]$				
70	49.15	0.6024	0.1148	1.076×10^{-6}	3.872×10^{-4}	7.879×10^{-3}	7.317	0.000656
90	48.50	0.6189	0.1143	1.057×10^{-6}	3.317×10^{-4}	6.840×10^{-6}	6.468	0.000671
110	47.85	0.6373	0.1138	1.036×10^{-6}	2.872×10^{-4}	6.005×10^{-6}	5.793	0.000691
130	47.18	0.6576	0.1133	1.014×10^{-6}	2.513×10^{-4}	5.326×10^{-6}	5.250	0.000716
150	46.50	0.6796	0.1128	9.918×10^{-7}	2.218×10^{-4}	4.769×10^{-6}	4.808	0.000749
170	45.80	0.7035	0.1124	9.687×10^{-7}	1.973×10^{-4}	4.308×10^{-6}	4.447	0.000789
				Isobutane (R600a)				
−150	42.75	0.4483	0.0799	1.157×10^{-6}	6.417×10^{-4}	1.500×10^{-5}	12.96	0.000785
−100	41.06	0.4721	0.0782	1.120×10^{-3}	3.669×10^{-4}	8.939×10^{-6}	7.977	0.000836
−50	39.31	0.4986	0.0731	1.036×10^{-6}	2.376×10^{-4}	6.043×10^{-6}	5.830	0.000908
0	37.48	0.5289	0.0664	9.299×10^{-7}	1.651×10^{-4}	4.406×10^{-6}	4.738	0.001012
50	35.52	0.5643	0.0591	8.187×10^{-7}	1.196×10^{-4}	3.368×10^{-6}	4.114	0.001169
100	33.35	0.6075	0.0521	7.139×10^{-7}	8.847×10^{-5}	2.653×10^{-3}	3.716	0.001421
150	30.84	0.6656	0.0457	6.188×10^{-7}	6.558×10^{-5}	2.127×10^{-6}	3.437	0.001883
200	27.73	0.7635	0.0400	5.249×10^{-7}	4.750×10^{-5}	1.713×10^{-6}	3.264	0.002970
				Glycerin				
32	79.65	0.5402	0.163	1.052×10^{-6}	7.047	0.08847	84101	
40	79.49	0.5458	0.1637	1.048×10^{-3}	4.803	0.06042	57655	
50	79.28	0.5541	0.1645	1.040×10^{-6}	2.850	0.03594	34561	
60	79.07	0.5632	0.1651	1.029×10^{-6}	1.547	0.01956	18995	
70	78.86	0.5715	0.1652	1.018×10^{-6}	0.9422	0.01195	11730	
80	78.66	0.5794	0.1652	1.007×10^{-6}	0.5497	0.00699	6941	
90	78.45	0.5878	0.1652	9.955×10^{-7}	0.3756	0.004787	4809	
100	78.24	0.5964	0.1653	9.841×10^{-7}	0.2277	0.00291	2957	
				Engine Oil (unused)				
32	56.12	0.4291	0.0849	9.792×10^{-7}	2.563	4.566×10^{-2}	46636	0.000389
50	55.79	0.4395	0.08338	9.448×10^{-7}	1.210	2.169×10^{-2}	22963	0.000389
75	55.3	0.4531	0.08378	9.288×10^{-7}	0.4286	7.751×10^{-3}	8345	0.000389
100	54.77	0.4669	0.08367	9.089×10^{-7}	0.1630	2.977×10^{-3}	3275	0.000389
125	54.24	0.4809	0.08207	8.740×10^{-7}	7.617×10^{-2}	1.404×10^{-3}	1607	0.000389
150	53.73	0.4946	0.08046	8.411×10^{-7}	3.833×10^{-2}	7.135×10^{-4}	848.3	0.000389
200	52.68	0.5231	0.07936	7.999×10^{-7}	1.405×10^{-2}	2.668×10^{-4}	333.6	0.000389
250	51.71	0.5523	0.07776	7.563×10^{-7}	6.744×10^{-3}	1.304×10^{-4}	172.5	0.000389
300	50.63	0.5818	0.07673	7.236×10^{-7}	3.661×10^{-3}	7.232×10^{-5}	99.94	0.000389

Source: Data generated from the EES software developed by S. A. Klein and F. L. Alvarado. Originally based on various sources.

TABLE A–14E

Properties of liquid metals

Temp. T, F°	Density ρ, lbm/ft^3	Specific Heat c_p, Btu/lbm·R	Thermal Conductivity k, Btu/h·ft·R	Thermal Diffusivity α, ft^2/s	Dynamic Viscosity μ, lbm/ft·s	Kinematic Viscosity ν, ft^2/s	Prandtl Number Pr	Volume Expansion Coeff. β, 1/R
Mercury (Hg) Melting Point: −38°F
32	848.7	0.03353	4.727	4.614×10^{-5}	1.133×10^{-3}	1.335×10^{-6}	0.02895	1.005×10^{-4}
50	847.2	0.03344	4.805	4.712×10^{-5}	1.092×10^{-3}	1.289×10^{-6}	0.02737	1.005×10^{-4}
100	842.9	0.03319	5.015	4.980×10^{-5}	9.919×10^{-4}	1.176×10^{-6}	0.02363	1.005×10^{-4}
150	838.7	0.03298	5.221	5.244×10^{-5}	9.122×10^{-4}	1.087×10^{-6}	0.02074	1.005×10^{-4}
200	834.5	0.03279	5.422	5.504×10^{-5}	8.492×10^{-4}	1.017×10^{-6}	0.01849	1.005×10^{-4}
300	826.2	0.03252	5.815	6.013×10^{-5}	7.583×10^{-4}	9.180×10^{-7}	0.01527	1.005×10^{-4}
400	817.9	0.03236	6.184	6.491×10^{-5}	6.972×10^{-4}	8.524×10^{-7}	0.01313	1.008×10^{-4}
500	809.6	0.03230	6.518	6.924×10^{-5}	6.525×10^{-4}	8.061×10^{-7}	0.01164	1.018×10^{-4}
600	801.3	0.03235	6.839	7.329×10^{-5}	6.186×10^{-4}	7.719×10^{-7}	0.01053	1.035×10^{-4}
Bismuth (Bi) Melting Point: 520°F
700	620.7	0.03509	9.361	1.193×10^{-4}	1.001×10^{-3}	1.614×10^{-6}	0.01352	
800	616.5	0.03569	9.245	1.167×10^{-4}	9.142×10^{-4}	1.482×10^{-6}	0.01271	
900	612.2	0.0363	9.129	1.141×10^{-4}	8.267×10^{-4}	1.350×10^{-6}	0.01183	
1000	608.0	0.0369	9.014	1.116×10^{-4}	7.392×10^{-4}	1.215×10^{-6}	0.0109	
1100	603.7	0.0375	9.014	1.105×10^{-4}	6.872×10^{-4}	1.138×10^{-6}	0.01029	
Lead (Pb) Melting Point: 621°F
700	658	0.03797	9.302	1.034×10^{-4}	1.612×10^{-3}	2.450×10^{-6}	0.02369	
800	654	0.03750	9.157	1.037×10^{-4}	1.453×10^{-3}	2.223×10^{-6}	0.02143	
900	650	0.03702	9.013	1.040×10^{-4}	1.296×10^{-3}	1.994×10^{-6}	0.01917	
1000	645.7	0.03702	8.912	1.035×10^{-4}	1.202×10^{-3}	1.862×10^{-6}	0.01798	
1100	641.5	0.03702	8.810	1.030×10^{-4}	1.108×10^{-3}	1.727×10^{-6}	0.01676	
1200	637.2	0.03702	8.709	1.025×10^{-4}	1.013×10^{-3}	1.590×10^{-6}	0.01551	
Sodium (Na) Melting Point: 280°F
300	57.13	0.3258	48.19	7.192×10^{-4}	4.136×10^{-4}	7.239×10^{-6}	0.01007	
400	56.28	0.3219	46.58	7.142×10^{-4}	3.572×10^{-4}	6.350×10^{-6}	0.008891	
500	55.42	0.3181	44.98	7.087×10^{-4}	3.011×10^{-4}	5.433×10^{-6}	0.007667	
600	54.56	0.3143	43.37	7.026×10^{-4}	2.448×10^{-4}	4.488×10^{-6}	0.006387	
800	52.85	0.3089	40.55	6.901×10^{-4}	1.772×10^{-4}	3.354×10^{-6}	0.004860	
1000	51.14	0.3057	38.12	6.773×10^{-4}	1.541×10^{-4}	3.014×10^{-6}	0.004449	
Potassium (K) Melting Point: 147°F
300	50.40	0.1911	26.00	7.500×10^{-4}	2.486×10^{-4}	4.933×10^{-6}	0.006577	
400	49.58	0.1887	25.37	7.532×10^{-4}	2.231×10^{-4}	4.500×10^{-6}	0.005975	
500	48.76	0.1863	24.73	7.562×10^{-4}	1.976×10^{-4}	4.052×10^{-6}	0.005359	
600	47.94	0.1839	24.09	7.591×10^{-4}	1.721×10^{-4}	3.589×10^{-6}	0.004728	
800	46.31	0.1791	22.82	7.643×10^{-4}	1.210×10^{-4}	2.614×10^{-6}	0.003420	
1000	44.62	0.1791	21.34	7.417×10^{-4}	1.075×10^{-4}	2.409×10^{-6}	0.003248	
Sodium-Potassium (%22Na-%78K) Melting Point: 12°F
200	52.99	0.2259	14.79	3.432×10^{-4}	3.886×10^{-4}	7.331×10^{-6}	0.02136	
300	52.16	0.2230	14.99	3.580×10^{-4}	3.467×10^{-4}	6.647×10^{-6}	0.01857	
400	51.32	0.2201	15.19	3.735×10^{-4}	3.050×10^{-4}	5.940×10^{-6}	0.0159	
600	49.65	0.2143	15.59	4.070×10^{-4}	2.213×10^{-4}	4.456×10^{-6}	0.01095	
800	47.99	0.2100	15.95	4.396×10^{-4}	1.539×10^{-4}	3.207×10^{-6}	0.007296	
1000	46.36	0.2103	16.20	4.615×10^{-4}	1.353×10^{-4}	2.919×10^{-6}	0.006324	

Source: Data generated from the EES software developed by S. A. Klein and F. L. Alvarado. Originally based on various sources.

TABLE A–15E

Properties of air at 1 atm pressure

Temp. T, F°	Density ρ, lbm/ft³	Specific Heat c_p, Btu/lbm·R	Thermal Conductivity k, Btu/h·ft·R	Thermal Diffusivity α, ft²/s	Dynamic Viscosity μ, lbm/ft·s	Kinematic Viscosity ν, ft²/s	Prandtl Number Pr
−300	0.24844	0.5072	0.00508	1.119×10^{-5}	4.039×10^{-6}	1.625×10^{-5}	1.4501
−200	0.15276	0.2247	0.00778	6.294×10^{-5}	6.772×10^{-6}	4.433×10^{-5}	0.7042
−100	0.11029	0.2360	0.01037	1.106×10^{-4}	9.042×10^{-6}	8.197×10^{-5}	0.7404
−50	0.09683	0.2389	0.01164	1.397×10^{-4}	1.006×10^{-5}	1.039×10^{-4}	0.7439
0	0.08630	0.2401	0.01288	1.726×10^{-4}	1.102×10^{-5}	1.278×10^{-4}	0.7403
10	0.08446	0.2402	0.01312	1.797×10^{-4}	1.121×10^{-5}	1.328×10^{-4}	0.7391
20	0.08270	0.2403	0.01336	1.868×10^{-4}	1.140×10^{-5}	1.379×10^{-4}	0.7378
30	0.08101	0.2403	0.01361	1.942×10^{-4}	1.158×10^{-5}	1.430×10^{-4}	0.7365
40	0.07939	0.2404	0.01385	2.016×10^{-4}	1.176×10^{-5}	1.482×10^{-4}	0.7350
50	0.07783	0.2404	0.01409	2.092×10^{-4}	1.194×10^{-5}	1.535×10^{-4}	0.7336
60	0.07633	0.2404	0.01433	2.169×10^{-4}	1.212×10^{-5}	1.588×10^{-4}	0.7321
70	0.07489	0.2404	0.01457	2.248×10^{-4}	1.230×10^{-5}	1.643×10^{-4}	0.7306
80	0.07350	0.2404	0.01481	2.328×10^{-4}	1.247×10^{-5}	1.697×10^{-4}	0.7290
90	0.07217	0.2404	0.01505	2.409×10^{-4}	1.265×10^{-5}	1.753×10^{-4}	0.7275
100	0.07088	0.2405	0.01529	2.491×10^{-4}	1.281×10^{-5}	1.809×10^{-4}	0.7260
110	0.06963	0.2405	0.01552	2.575×10^{-4}	1.299×10^{-5}	1.866×10^{-4}	0.7245
120	0.06843	0.2405	0.01576	2.660×10^{-4}	1.316×10^{-5}	1.923×10^{-4}	0.7230
130	0.06727	0.2405	0.01599	2.746×10^{-4}	1.332×10^{-5}	1.981×10^{-4}	0.7216
140	0.06615	0.2406	0.01623	2.833×10^{-4}	1.349×10^{-5}	2.040×10^{-4}	0.7202
150	0.06507	0.2406	0.01646	2.921×10^{-4}	1.365×10^{-5}	2.099×10^{-4}	0.7188
160	0.06402	0.2406	0.01669	3.010×10^{-4}	1.382×10^{-5}	2.159×10^{-4}	0.7174
170	0.06300	0.2407	0.01692	3.100×10^{-4}	1.398×10^{-5}	2.220×10^{-4}	0.7161
180	0.06201	0.2408	0.01715	3.191×10^{-4}	1.414×10^{-5}	2.281×10^{-4}	0.7148
190	0.06106	0.2408	0.01738	3.284×10^{-4}	1.430×10^{-5}	2.343×10^{-4}	0.7136
200	0.06013	0.2409	0.01761	3.377×10^{-4}	1.446×10^{-5}	2.406×10^{-4}	0.7124
250	0.05590	0.2415	0.01874	3.857×10^{-4}	1.524×10^{-5}	2.727×10^{-4}	0.7071
300	0.05222	0.2423	0.01985	4.358×10^{-4}	1.599×10^{-5}	3.063×10^{-4}	0.7028
350	0.04899	0.2433	0.02094	4.879×10^{-4}	1.672×10^{-5}	3.413×10^{-4}	0.6995
400	0.04614	0.2445	0.02200	5.419×10^{-4}	1.743×10^{-5}	3.777×10^{-4}	0.6971
450	0.04361	0.2458	0.02305	5.974×10^{-4}	1.812×10^{-5}	4.154×10^{-4}	0.6953
500	0.04134	0.2472	0.02408	6.546×10^{-4}	1.878×10^{-5}	4.544×10^{-4}	0.6942
600	0.03743	0.2503	0.02608	7.732×10^{-4}	2.007×10^{-5}	5.361×10^{-4}	0.6934
700	0.03421	0.2535	0.02800	8.970×10^{-4}	2.129×10^{-5}	6.225×10^{-4}	0.6940
800	0.03149	0.2568	0.02986	1.025×10^{-3}	2.247×10^{-5}	7.134×10^{-4}	0.6956
900	0.02917	0.2599	0.03164	1.158×10^{-3}	2.359×10^{-5}	8.087×10^{-4}	0.6978
1000	0.02718	0.2630	0.03336	1.296×10^{-3}	2.467×10^{-5}	9.080×10^{-4}	0.7004
1500	0.02024	0.2761	0.04106	2.041×10^{-3}	2.957×10^{-5}	1.460×10^{-3}	0.7158
2000	0.01613	0.2855	0.04752	2.867×10^{-3}	3.379×10^{-5}	2.095×10^{-3}	0.7308
2500	0.01340	0.2922	0.05309	3.765×10^{-3}	3.750×10^{-5}	2.798×10^{-3}	0.7432
3000	0.01147	0.2972	0.05811	4.737×10^{-3}	4.082×10^{-5}	3.560×10^{-3}	0.7516
3500	0.01002	0.3010	0.06293	5.797×10^{-3}	4.381×10^{-5}	4.373×10^{-3}	0.7543
4000	0.00889	0.3040	0.06789	6.975×10^{-3}	4.651×10^{-5}	5.229×10^{-3}	0.7497

Note: For ideal gases, the properties c_p, k, μ, and Pr are independent of pressure. The properties ρ, ν, and α at a pressure P (in atm) other than 1 atm are determined by multiplying the values of ρ at the given temperature by P and by dividing ν and α by P.

Source: Data generated from the EES software developed by S. A. Klein and F. L. Alvarado. Original sources: Keenan, Chao, Keyes, Gas Tables, Wiley, 1984; and *Thermophysical Properties of Matter,* Vol. 3: *Thermal Conductivity,* Y. S. Touloukian, P. E. Liley, S. C. Saxena, Vol. 11: *Viscosity,* Y. S. Touloukian, S. C. Saxena, and P. Hestermans, IFI/Plenun, NY, 1970, ISBN 0-306067020-8.

TABLE A–16E

Properties of gases at 1 atm pressure

Temp. T, F°	Density ρ, lbm/ft^3	Specific Heat c_p, Btu/lbm·R	Thermal Conductivity k, Btu/h·ft·R	Thermal Diffusivity α, ft^2/s	Dynamic Viscosity μ, lbm/ft·s	Kinematic Viscosity ν, ft^2/s	Prandtl Number Pr
			Carbon Dioxide, CO_2				
−50	0.14712	0.1797	0.00628	6.600×10^{-5}	7.739×10^{-6}	5.261×10^{-5}	0.7970
0	0.13111	0.1885	0.00758	8.522×10^{-5}	8.661×10^{-6}	6.606×10^{-5}	0.7751
50	0.11825	0.1965	0.00888	1.061×10^{-4}	9.564×10^{-6}	8.086×10^{-5}	0.7621
100	0.10769	0.2039	0.01017	1.286×10^{-4}	1.045×10^{-5}	9.703×10^{-5}	0.7543
200	0.09136	0.2171	0.01273	1.784×10^{-4}	1.217×10^{-5}	1.332×10^{-4}	0.7469
300	0.07934	0.2284	0.01528	2.341×10^{-4}	1.382×10^{-5}	1.743×10^{-4}	0.7445
500	0.06280	0.2473	0.02027	3.626×10^{-4}	1.696×10^{-5}	2.700×10^{-4}	0.7446
1000	0.04129	0.2796	0.03213	7.733×10^{-4}	2.381×10^{-5}	5.767×10^{-4}	0.7458
1500	0.03075	0.2995	0.04281	1.290×10^{-3}	2.956×10^{-5}	9.610×10^{-4}	0.7445
2000	0.02450	0.3124	0.05193	1.885×10^{-3}	3.451×10^{-5}	1.408×10^{-3}	0.7474
			Carbon Monoxide, CO				
−50	0.09363	0.2571	0.01118	1.290×10^{-4}	9.419×10^{-6}	1.005×10^{-4}	0.7798
0	0.08345	0.2523	0.01240	1.636×10^{-4}	1.036×10^{-5}	1.242×10^{-4}	0.7593
50	0.07526	0.2496	0.01359	2.009×10^{-4}	1.127×10^{-5}	1.498×10^{-4}	0.7454
100	0.06854	0.2484	0.01476	2.408×10^{-4}	1.214×10^{-5}	1.772×10^{-4}	0.7359
200	0.05815	0.2485	0.01702	3.273×10^{-4}	1.379×10^{-5}	2.372×10^{-4}	0.7247
300	0.05049	0.2505	0.01920	4.217×10^{-4}	1.531×10^{-5}	3.032×10^{-4}	0.7191
500	0.03997	0.2567	0.02331	6.311×10^{-4}	1.802×10^{-5}	4.508×10^{-4}	0.7143
1000	0.02628	0.2732	0.03243	1.254×10^{-3}	2.334×10^{-5}	8.881×10^{-4}	0.7078
1500	0.01957	0.2862	0.04049	2.008×10^{-3}	2.766×10^{-5}	1.413×10^{-3}	0.7038
2000	0.01559	0.2958	0.04822	2.903×10^{-3}	3.231×10^{-5}	2.072×10^{-3}	0.7136
			Methane, CH_4				
−50	0.05363	0.5335	0.01401	1.360×10^{-4}	5.861×10^{-6}	1.092×10^{-4}	0.8033
0	0.04779	0.5277	0.01616	1.780×10^{-4}	6.506×10^{-6}	1.361×10^{-4}	0.7649
50	0.04311	0.5320	0.01839	2.228×10^{-4}	7.133×10^{-6}	1.655×10^{-4}	0.7428
100	0.03925	0.5433	0.02071	2.698×10^{-4}	7.742×10^{-6}	1.972×10^{-4}	0.7311
200	0.03330	0.5784	0.02559	3.690×10^{-4}	8.906×10^{-6}	2.674×10^{-4}	0.7245
300	0.02892	0.6226	0.03077	4.748×10^{-4}	1.000×10^{-5}	3.457×10^{-4}	0.7283
500	0.02289	0.7194	0.04195	7.075×10^{-4}	1.200×10^{-5}	5.244×10^{-4}	0.7412
1000	0.01505	0.9438	0.07346	1.436×10^{-3}	1.620×10^{-5}	1.076×10^{-3}	0.7491
1500	0.01121	1.1162	0.10766	2.390×10^{-3}	1.974×10^{-5}	1.760×10^{-3}	0.7366
2000	0.00893	1.2419	0.14151	3.544×10^{-3}	2.327×10^{-5}	2.605×10^{-3}	0.7353
			Hydrogen, H_2				
−50	0.00674	3.0603	0.08246	1.110×10^{-3}	4.969×10^{-6}	7.373×10^{-4}	0.6638
0	0.00601	3.2508	0.09049	1.287×10^{-3}	5.381×10^{-6}	8.960×10^{-4}	0.6960
50	0.00542	3.3553	0.09818	1.500×10^{-3}	5.781×10^{-6}	1.067×10^{-3}	0.7112
100	0.00493	3.4118	0.10555	1.742×10^{-3}	6.167×10^{-6}	1.250×10^{-3}	0.7177
200	0.00419	3.4549	0.11946	2.295×10^{-3}	6.911×10^{-6}	1.652×10^{-3}	0.7197
300	0.00363	3.4613	0.13241	2.924×10^{-3}	7.622×10^{-6}	2.098×10^{-3}	0.7174
500	0.00288	3.4572	0.15620	4.363×10^{-3}	8.967×10^{-6}	3.117×10^{-3}	0.7146
1000	0.00189	3.5127	0.20989	8.776×10^{-3}	1.201×10^{-5}	6.354×10^{-3}	0.7241
1500	0.00141	3.6317	0.26381	1.432×10^{-2}	1.477×10^{-5}	1.048×10^{-2}	0.7323
2000	0.00112	3.7656	0.31923	2.098×10^{-2}	1.734×10^{-5}	1.544×10^{-2}	0.7362
			Nitrogen, N_2				
−50	0.09364	0.2320	0.01176	1.504×10^{-4}	9.500×10^{-6}	1.014×10^{-4}	0.6746
0	0.08346	0.2441	0.01300	1.773×10^{-4}	1.043×10^{-5}	1.251×10^{-4}	0.7056
50	0.07527	0.2480	0.01420	2.113×10^{-4}	1.134×10^{-5}	1.507×10^{-4}	0.7133

TABLE A–16E

Properties of gases at 1 atm pressure (*Concluded*)

Temp. T, F°	Density ρ, lbm/ft^3	Specific Heat c_p, Btu/lbm·R	Thermal Conductivity k, Btu/h·ft·R	Thermal Diffusivity α, ft^2/s	Dynamic Viscosity μ, lbm/ft·s	Kinematic Viscosity ν, ft^2/s	Prandtl Number Pr
100	0.06854	0.2489	0.01537	2.502×10^{-4}	1.221×10^{-5}	1.783×10^{-4}	0.7126
200	0.05815	0.2487	0.01760	3.379×10^{-4}	1.388×10^{-5}	2.387×10^{-4}	0.7062
300	0.05050	0.2492	0.01970	4.349×10^{-4}	1.543×10^{-5}	3.055×10^{-4}	0.7025
500	0.03997	0.2535	0.02359	6.466×10^{-4}	1.823×10^{-5}	4.559×10^{-4}	0.7051
1000	0.02628	0.2697	0.03204	1.255×10^{-3}	2.387×10^{-5}	9.083×10^{-4}	0.7232
1500	0.01958	0.2831	0.04002	2.006×10^{-3}	2.829×10^{-5}	1.445×10^{-3}	0.7202
2000	0.01560	0.2927	0.04918	2.992×10^{-3}	3.212×10^{-5}	2.059×10^{-3}	0.6882
Oxygen, O$_2$							
−50	0.10697	0.2331	0.01216	1.355×10^{-4}	1.104×10^{-5}	1.032×10^{-4}	0.7622
0	0.09533	0.2245	0.01346	1.747×10^{-4}	1.218×10^{-5}	1.277×10^{-4}	0.7312
50	0.08598	0.2209	0.01475	2.157×10^{-4}	1.326×10^{-5}	1.543×10^{-4}	0.7152
100	0.07830	0.2200	0.01601	2.582×10^{-4}	1.429×10^{-5}	1.826×10^{-4}	0.7072
200	0.06643	0.2221	0.01851	3.484×10^{-4}	1.625×10^{-5}	2.446×10^{-4}	0.7020
300	0.05768	0.2262	0.02096	4.463×10^{-4}	1.806×10^{-5}	3.132×10^{-4}	0.7018
500	0.04566	0.2352	0.02577	6.665×10^{-4}	2.139×10^{-5}	4.685×10^{-4}	0.7029
1000	0.03002	0.2520	0.03698	1.357×10^{-3}	2.855×10^{-5}	9.509×10^{-4}	0.7005
1500	0.02236	0.2626	0.04701	2.224×10^{-3}	3.474×10^{-5}	1.553×10^{-3}	0.6985
2000	0.01782	0.2701	0.05614	3.241×10^{-3}	4.035×10^{-5}	2.265×10^{-3}	0.6988
Water Vapor, H$_2$O							
−50	0.06022	0.4512	0.00797	8.153×10^{-5}	4.933×10^{-6}	8.192×10^{-5}	1.0050
0	0.05367	0.4484	0.00898	1.036×10^{-4}	5.592×10^{-6}	1.041×10^{-4}	1.0049
50	0.04841	0.4472	0.01006	1.291×10^{-4}	6.261×10^{-6}	1.293×10^{-4}	1.0018
100	0.04408	0.4473	0.01121	1.579×10^{-4}	6.942×10^{-6}	1.574×10^{-4}	0.9969
200	0.03740	0.4503	0.01372	2.263×10^{-4}	8.333×10^{-6}	2.228×10^{-4}	0.9845
300	0.03248	0.4557	0.01648	3.093×10^{-4}	9.756×10^{-6}	3.004×10^{-4}	0.9713
500	0.02571	0.4707	0.02267	5.204×10^{-4}	1.267×10^{-5}	4.931×10^{-4}	0.9475
1000	0.01690	0.5167	0.04134	1.314×10^{-3}	2.014×10^{-5}	1.191×10^{-3}	0.9063
1500	0.01259	0.5625	0.06315	2.477×10^{-3}	2.742×10^{-5}	2.178×10^{-3}	0.8793
2000	0.01003	0.6034	0.08681	3.984×10^{-3}	3.422×10^{-5}	3.411×10^{-3}	0.8563

Note: For ideal gases, the properties c_p, k, μ, and Pr are independent of pressure. The properties ρ, ν, and α at a pressure P (in atm) other than 1 atm are determined by multiplying the values of ρ at the given temperature by P and by dividing ν and α by P.

Source: Data generated from the EES software developed by S. A. Klein and F. L. Alvarado. Originally based on various sources.

TABLE A–17E

Properties of the atmosphere at high altitude

Altitude, z, ft	Temperature T, °F	Pressure, ρ, psia	Gravity g, ft/s^2	Speed of Sound c, ft/s	Density ρ, lbm/ft^3	Viscosity μ, lbm/ft·s	Thermal Conductivity, k, Btu/h·ft·R
0	59.00	14.7	32.174	1116	0.07647	1.202×10^{-5}	0.0146
500	57.22	14.4	32.173	1115	0.07536	1.199×10^{-5}	0.0146
1000	55.43	14.2	32.171	1113	0.07426	1.196×10^{-5}	0.0146
1500	53.65	13.9	32.169	1111	0.07317	1.193×10^{-5}	0.0145
2000	51.87	13.7	32.168	1109	0.07210	1.190×10^{-5}	0.0145
2500	50.09	13.4	32.166	1107	0.07104	1.186×10^{-5}	0.0144
3000	48.30	13.2	32.165	1105	0.06998	1.183×10^{-5}	0.0144
3500	46.52	12.9	32.163	1103	0.06985	1.180×10^{-5}	0.0143
4000	44.74	12.7	32.162	1101	0.06792	1.177×10^{-5}	0.0143
4500	42.96	12.5	32.160	1099	0.06690	1.173×10^{-5}	0.0142
5000	41.17	12.2	32.159	1097	0.06590	1.170×10^{-5}	0.0142
5500	39.39	12.0	32.157	1095	0.06491	1.167×10^{-5}	0.0141
6000	37.61	11.8	32.156	1093	0.06393	1.164×10^{-5}	0.0141
6500	35.83	11.6	32.154	1091	0.06296	1.160×10^{-5}	0.0141
7000	34.05	11.3	32.152	1089	0.06200	1.157×10^{-5}	0.0140
7500	32.26	11.1	32.151	1087	0.06105	1.154×10^{-5}	0.0140
8000	30.48	10.9	32.149	1085	0.06012	1.150×10^{-5}	0.0139
8500	28.70	10.7	32.148	1083	0.05919	1.147×10^{-5}	0.0139
9000	26.92	10.5	32.146	1081	0.05828	1.144×10^{-5}	0.0138
9500	25.14	10.3	32.145	1079	0.05738	1.140×10^{-5}	0.0138
10,000	23.36	10.1	32.145	1077	0.05648	1.137×10^{-5}	0.0137
11,000	19.79	9.72	32.140	1073	0.05473	1.130×10^{-5}	0.0136
12,000	16.23	9.34	32.137	1069	0.05302	1.124×10^{-5}	0.0136
13,000	12.67	8.99	32.134	1065	0.05135	1.117×10^{-5}	0.0135
14,000	9.12	8.63	32.131	1061	0.04973	1.110×10^{-5}	0.0134
15,000	5.55	8.29	32.128	1057	0.04814	1.104×10^{-5}	0.0133
16,000	+1.99	7.97	32.125	1053	0.04659	1.097×10^{-5}	0.0132
17,000	−1.58	7.65	32.122	1049	0.04508	1.090×10^{-5}	0.0132
18,000	−5.14	7.34	32.119	1045	0.04361	1.083×10^{-5}	0.0130
19,000	−8.70	7.05	32.115	1041	0.04217	1.076×10^{-5}	0.0129
20,000	−12.2	6.76	32.112	1037	0.04077	1.070×10^{-5}	0.0128
22,000	−19.4	6.21	32.106	1029	0.03808	1.056×10^{-5}	0.0126
24,000	−26.5	5.70	32.100	1020	0.03553	1.042×10^{-5}	0.0124
26,000	−33.6	5.22	32.094	1012	0.03311	1.028×10^{-5}	0.0122
28,000	−40.7	4.78	32.088	1003	0.03082	1.014×10^{-5}	0.0121
30,000	−47.8	4.37	32.082	995	0.02866	1.000×10^{-5}	0.0119
32,000	−54.9	3.99	32.08	987	0.02661	0.986×10^{-5}	0.0117
34,000	−62.0	3.63	32.07	978	0.02468	0.971×10^{-5}	0.0115
36,000	−69.2	3.30	32.06	969	0.02285	0.956×10^{-5}	0.0113
38,000	−69.7	3.05	32.06	968	0.02079	0.955×10^{-5}	0.0113
40,000	−69.7	2.73	32.05	968	0.01890	0.955×10^{-5}	0.0113
45,000	−69.7	2.148	32.04	968	0.01487	0.955×10^{-5}	0.0113
50,000	−69.7	1.691	32.02	968	0.01171	0.955×10^{-5}	0.0113
55.000	−69.7	1.332	32.00	968	0.00922	0.955×10^{-5}	0.0113
60,000	−69.7	1.048	31.99	968	0.00726	0.955×10^{-5}	0.0113

Source: U.S. Standard Atmosphere Supplements, U.S. Government Printing Office, 1966.

I N D E X

A_s	Surface area, m^2		M	Molar mass, kg/kmol
A_c	Cross-sectional area, m^2		N	Number of moles, kmol
Bi	Biot number		NTU	Number of transfer units
C	Molar concentration rate, kmol/m^3		Nu	Nusselt number
c	Specific heat, kJ/kg·K		p	Perimeter, m
C_c, C_h	Heat capacity rate, W/K		P	Pressure, kPa
C_D	Drag coefficient		P_v	Vapor pressure, kPa
C_f	Friction coefficient		Pr	Prandtl number
c_p	Constant pressure specific heat, kJ/kg·K		$\dot{q}$	Heat flux, W/m^2
c_υ	Constant volume specific heat, kJ/kg·K		Q	Total heat transfer, kJ
COP	Coefficient of performance		$\dot{Q}$	Heat transfer rate, kW
d, D	Diameter, m		r_{cr}	Critical radius of insulation
D_{AB}	Diffusion coefficient		R	Gas constant, kJ/kg·K
D_h	Hydraulic diameter, m		R, r_o	Radius, m
e	Specific total energy, kJ/kg		R	Thermal resistance, K/W
$\dot{e}_{gen}$	Heat generation rate, W/m^3		R_c	Thermal contact resistance, m^2·K/W
erfc	Complementary error function		R_f	Fouling factor
E	Total energy, kJ		R_u	Universal gas constant, kJ/kmol·K
$\dot{E}_{gen}$	Total heat generation rate, W		R-value	R-value of insulation
E_b	Blackbody emissive flux		Ra	Rayleigh number
$E_{b\lambda}$	Spectral blackbody emissive flux		Re	Reynolds number
f	Friction factor		S	Conduction shape factor
f_λ	Blackbody radiation function		Sc	Schmidt number
F	Force, N		Sh	Sherwood number
F_D	Drag force, N		St	Stanton number
$F_{ij}, F_{i \to j}$	View factor		SC	Shading coefficient
Fo	Fourier number		SG	Specific gravity
g	Gravitational acceleration, m/s^2		SHGC	Solar heat gain coefficient
G	Incident radiation, W/m^2		t	Time, s
Gr	Grashof number		t	Thickness, m
h	Convection heat transfer coefficient, W/m^2·K		T	Temperature, °C or K
h	Specific enthalpy, $u + Pv$, kJ/kg		T_b	Bulk fluid temperature, °C or K
h_c	Thermal contact conductance, W/m^2·K		T_f	Film temperature, °C or K
h_{fg}	Latent heat of vaporization, kJ/kg		T_{sat}	Saturation temperature, °C or K
I	Electric current, A		T_s	Surface temperature, °C or K
I	Modified Bessel function of the first kind		u	Specific internal energy, kJ/kg
I	Radiation intensity, W/m^2·sr		u, v	x- and y-components of velocity, m/s
j	Diffusive mass flux, kg/s·m^2		U	Overall heat transfer coefficient, W/m^2·K
J	Radiosity, W/m^2; Bessel function		υ	Specific volume, m^3/kg
k	Thermal conductivity, W/m·K		V	Voltage, volt
k_{eff}	Effective thermal conductivity, W/m·K		$\mathcal{V}$	Total volume, m^3
K	Modified Bessel function of the second kind		$\dot{\mathcal{V}}$	Volume flow rate, m^3/s
L	Length; half thickness of a plane wall		V	Velocity, m/s
L_c	Characteristic or corrected length		V_{avg}	Average velocity, m/s
L_h	Hydrodynamic entry length		w	Mass fraction
L_t	Thermal entry length		$\dot{W}$	Power, kW
m	Mass, kg		y	Mole fraction
$\dot{m}$	Mass flow rate, kg/s			

Greek Letters

α	Absorptivity
α	Thermal diffusivity, m^2/s
α_s	Solar absorptivity
β	Volume expansivity, $1/\text{K}$
δ	Velocity boundary layer thickness, m
δ_t	Thermal boundary layer thickness, m
ΔP	Pressure drop, Pa
ΔT_{lm}	Log mean temperature difference
ε	Emissivity; heat exchanger or fin effectiveness
ε	Roughness size, m
η_{fin}	Fin efficiency
η_{th}	Thermal efficiency
θ	Total energy of a flowing fluid, kJ/kg
μ	Dynamic viscosity, kg/m·s or N·s/m^2
ν	Kinematic viscosity $= \mu/\rho$, m^2/s
ν	Frequency, l/s
ρ	Density, kg/m^3
σ	Stefan–Boltzmann constant
σ_n	Normal stress, N/m^2
σ_s	Surface tension, N/m
τ	Shear stress, N/m^2
τ	Transmissivity; Fourier number
τ_s	Wall shear stress, N/m^2
ϕ	Relative humidity
θ	Dimensionless temperature
ω	Specific or absolute humidity, kg H_2O/kg dry air

Subscripts

atm	Atmospheric
avg	Average
b	Boundary, bulk fluid
cond	Conduction
conv	Convection
cyl	Cylinder
e	Exit conditions
f	Saturated liquid; film

i	Inlet, initial, or indoor conditions
i	ith component
l	Liquid
m	Mixture
o	Outlet or outdoor conditions
rad	Radiation
s	Surface
surr	Surrounding surfaces
sat	Saturated
semi-inf	Semi-infinite medium
sph	Sphere
sys	System
v	Water vapor
1	Initial or inlet state
2	Final or exit state
∞	Far from a surface; free-flow conditions

Superscripts

· (over dot)	Quantity per unit time
¯ (over bar)	Quantity per unit mole

Conversion Factors

DIMENSION	METRIC	METRIC/ENGLISH
Acceleration	$1 \text{ m/s}^2 = 100 \text{ cm/s}^2$	$1 \text{ m/s}^2 = 3.2808 \text{ ft/s}^2$ $1 \text{ ft/s}^2 = 0.3048^* \text{ m/s}^2$
Area	$1 \text{ m}^2 = 10^4 \text{ cm}^2 = 10^6 \text{ mm}^2$ $= 10^{-6} \text{ km}^2$	$1 \text{ m}^2 = 1550 \text{ in}^2 = 10.764 \text{ ft}^2$ $1 \text{ ft}^2 = 144 \text{ in}^2 = 0.09290304^* \text{ m}^2$
Density	$1 \text{ g/cm}^3 = 1 \text{ kg/L} = 1000 \text{ kg/m}^3$	$1 \text{ g/cm}^3 = 62.428 \text{ lbm/ft}^3 = 0.036127 \text{ lbm/in}^3$ $1 \text{ lbm/in}^3 = 1728 \text{ lbm/ft}^3$ $1 \text{ kg/m}^3 = 0.062428 \text{ lbm/ft}^3$
Energy, heat, work, internal energy, enthalpy	$1 \text{ kJ} = 1000 \text{ J} = 1000 \text{ Nm} = 1 \text{ kPa·m}^3$ $1 \text{ kJ/kg} = 1000 \text{ m}^2/\text{s}^2$ $1 \text{ kWh} = 3600 \text{ kJ}$ $1 \text{ cal}^\dagger = 4.184 \text{ J}$ $1 \text{ IT cal}^\dagger = 4.1868 \text{ J}$ $1 \text{ Cal}^\dagger = 4.1868 \text{ kJ}$	$1 \text{ kJ} = 0.94782 \text{ Btu}$ $1 \text{ Btu} = 1.055056 \text{ kJ}$ $= 5.40395 \text{ psia·ft}^3 = 778.169 \text{ lbf·ft}$ $1 \text{ Btu/lbm} = 25{,}037 \text{ ft}^2/\text{s}^2 = 2.326^* \text{ kJ/kg}$ $1 \text{ kJ/kg} = 0.430 \text{ Btu/lbm}$ $1 \text{ kWh} = 3412.14 \text{ Btu}$ $1 \text{ therm} = 10^5 \text{ Btu} = 1.055 \times 10^5 \text{ kJ (natural gas)}$
Force	$1 \text{ N} = 1 \text{ kg·m/s}^2 = 10^5 \text{ dyne}$ $1 \text{ kgf} = 9.80665 \text{ N}$	$1 \text{ N} = 0.22481 \text{ lbf}$ $1 \text{ lbf} = 32.174 \text{ lbm·ft/s}^2 = 4.44822 \text{ N}$
Heat flux	$1 \text{ W/cm}^2 = 10^4 \text{ W/m}^2$	$1 \text{ W/m}^2 = 0.3171 \text{ Btu/h·ft}^2$
Heat generation rate	$1 \text{ W/cm}^3 = 10^6 \text{ W/m}^3$	$1 \text{ W/m}^3 = 0.09665 \text{ Btu/h·ft}^3$
Heat transfer coefficient	$1 \text{ W/m}^2\text{·°C} = 1 \text{ W/m}^2\text{·K}$	$1 \text{ W/m}^2\text{·°C} = 0.17612 \text{ Btu/h·ft}^2\text{·°F}$
Length	$1 \text{ m} = 100 \text{ cm} = 1000 \text{ mm}$ $1 \text{ km} = 1000 \text{ m}$	$1 \text{ m} = 39.370 \text{ in} = 3.2808 \text{ ft} = 1.0926 \text{ yd}$ $1 \text{ ft} = 12 \text{ in} = 0.3048^* \text{ m}$ $1 \text{ mile} = 5280 \text{ ft} = 1.6093 \text{ km}$ $1 \text{ in} = 2.54^* \text{ cm}$
Mass	$1 \text{ kg} = 1000 \text{ g}$ $1 \text{ metric ton} = 1000 \text{ kg}$	$1 \text{ kg} = 2.2046226 \text{ lbm}$ $1 \text{ lbm} = 0.45359237^* \text{ kg}$ $1 \text{ ounce} = 28.3495 \text{ g}$ $1 \text{ slug} = 32.174 \text{ lbm} = 14.5939 \text{ kg}$ $1 \text{ short ton} = 2000 \text{ lbm} = 907.1847 \text{ kg}$
Power, heat transfer rate	$1 \text{ W} = 1 \text{ J/s}$ $1 \text{ kW} = 1000 \text{ W} = 1.341 \text{ hp}$ $1 \text{ hp}^\ddagger = 745.7 \text{ W}$	$1 \text{ kW} = 3412.14 \text{ Btu/h}$ $= 737.56 \text{ lbf·ft/s}$ $1 \text{ hp} = 550 \text{ lbf·ft/s} = 0.7068 \text{ Btu/s}$ $= 42.41 \text{ Btu/min} = 2544.5 \text{ Btu/h}$ $= 0.74570 \text{ kW}$ $1 \text{ boiler hp} = 33{,}475 \text{ Btu/h}$ $1 \text{ Btu/h} = 1.055056 \text{ kJ/h}$ $1 \text{ ton of refrigeration} = 200 \text{ Btu/min}$
Pressure	$1 \text{ Pa} = 1 \text{ N/m}^2$ $1 \text{ kPa} = 10^3 \text{ Pa} = 10^{-3} \text{ MPa}$ $1 \text{ atm} = 101.325 \text{ kpa} = 1.01325 \text{ bars}$ $= 760 \text{ mm Hg at } 0\text{°C}$ $= 1.03323 \text{ kgf/cm}^2$ $1 \text{ mm Hg} = 0.1333 \text{ kPa}$	$1 \text{ Pa} = 1.4504 \times 10^{-4} \text{ psia}$ $= 0.020886 \text{ lbf/ft}^2$ $1 \text{ psia} = 144 \text{ lbf/ft}^2 = 6.894757 \text{ kPa}$ $1 \text{ atm} = 14.696 \text{ psia} = 29.92 \text{ in Hg at } 30\text{°F}$ $1 \text{ in Hg} = 3.387 \text{ kPa}$
Specific heat	$1 \text{ kJ/kg·°C} = 1 \text{ kJ/kg·K} = 1 \text{ J/g·°C}$	$1 \text{ Btu/lbm·°F} = 4.1868 \text{ kJ/kg·°C}$ $1 \text{ Btu/lbmol·R} = 4.1868 \text{ kJ/kmol·K}$ $1 \text{ kJ/kg·°C} = 0.23885 \text{ Btu/lbm·°F}$ $= 0.23885 \text{ Btu/lbm·R}$

*Exact conversion factor between metric and English units.

†Calorie is originally defined as the amount of heat needed to raise the temperature of 1 g of water by 1°C, but it varies with temperature. The international steam table (IT) calorie (generally preferred by engineers) is exactly 4.1868 J by definition and corresponds to the specific heat of water at 15°C. The thermochemical calorie (generally preferred by physicists) is exactly 4.184 J by definition and corresponds to the specific heat of water at room temperature. The difference between the two is about 0.06 percent, which is negligible. The capitalized Calorie used by nutritionists is actually a kilocalorie (1000 IT calories).

1017

DIMENSION	METRIC	METRIC/ENGLISH
Specific volume	$1 \ m^3/kg = 1000 \ L/kg = 1000 \ cm^3/g$	$1 \ m^3/kg = 16.02 \ ft^3/lbm$ $1 \ ft^3/lbm = 0.062428 \ m^3/kg$
Temperature	$T(K) = T(°C) + 273.15$ $\Delta T(K) = \Delta T(°C)$	$T(R) = T(°F) + 459.67 = 1.8 \ T(K)$ $T(°F) = 1.8 \ T(°C) + 32$ $\Delta T(°F) = \Delta T(R) = 1.8\Delta T(K)$
Thermal conductivity	$1 \ W/m·°C = 1 \ W/m·K$	$1 \ W/m·°C = 0.57782 \ Btu/h·ft·°F$
Thermal resistance	$1°C/W = 1 \ K/W$	$1 \ K/W = 0.52750°F·h/Btu$
Velocity	$1 \ m/s = 3.60 \ km/h$	$1 \ m/s = 3.2808 \ ft/s = 2.237 \ mi/h$ $1 \ mi/h = 1.46667 \ ft/s$ $1 \ mi/h = 1.609 \ km/h$
Viscosity, dynamic	$1 \ kg/m·s = 1 \ N·s/m^2 = 1 \ Pa·s = 10 \ poise$	$1 \ kg/m·s = 2419.1 \ lbm/ft·h$ $= 0.020886 \ lbf·s/ft^2$ $= 0.67197 \ lbm/ft·s$
Viscosity, kinematic	$1 \ m^2/s = 10^4 \ cm^2/s$ $1 \ stoke = 1 \ cm^2/s = 10^{-4} \ m^2/s$	$1 \ m^2/s = 10.764 \ ft^2/s = 3.875 \times 10^4 \ ft^2/h$ $1 \ m^2/s = 10.764 \ ft^2/s$
Volume	$1 \ m^3 = 1000 \ L = 10^6 \ cm^3 \ (cc)$	$1 \ m^3 = 6.1024 \times 10^4 in^3 = 35.315 \ ft^3$ $= 264.17 \ gal \ (U.S.)$ $1 \ U.S. \ gallon = 231 \ in^3 = 3.7854 \ L$ $1 \ fl \ ounce = 29.5735 \ cm^3 = 0.0295735 \ L$ $1 \ U.S. \ gallon = 128 \ fl \ ounces$
Volume flow rate	$1 \ m^3/s = 60,000 \ L/min = 10^6 \ cm^3/s$	$1 \ m^3/s = 15,850 \ gal/min \ (gpm) = 35.315 \ ft^3/s$ $= 2118.9 \ ft^3/min \ (cfm)$

‡Mechanical horsepower. The electrical horsepower is taken to be exactly 746 W.

Some Physical Constants

Universal gas constant	$R_u = 8.31447 \ kJ/kmol·K$ $= 8.31447 \ kPa·m^3/kmol·K$ $= 0.0831447 \ bar·m^3/kmol·K$ $= 82.05 \ L·atm/kmol·K$ $= 1.9858 \ Btu/lbmol·R$ $= 1545.35 \ ft·lbf/lbmol·R$ $= 10.73 \ psia·ft^3/lbmol·R$
Standard acceleration of gravity	$g = 9.80665 \ m/s^2$ $= 32.174 \ ft/s^2$
Standard atmospheric pressure	$1 \ atm = 101.325 \ kPa$ $= 1.01325 \ bar$ $= 14.696 \ psia$ $= 760 \ mm \ Hg \ (0°C)$ $= 29.9213 \ in \ Hg \ (32°F)$ $= 10.3323 \ m \ H_2O \ (4°C)$

Some Physical Constants

Stefan–Boltzmann constant	$\sigma = 5.670 \times 10^{-8} \ W/m^2·K^4$ $= 0.1714 \times 10^{-8} \ Btu/h·ft^2·R^4$
Boltzmann's constant	$k = 1.380650 \times 10^{-23} \ J/K$
Speed of light in vacuum	$c = 2.9979 \times 10^8 \ m/s$ $= 9.836 \times 10^8 \ ft/s$
Speed of sound in dry air at 0°C and 1 atm	$c = 331.36 \ m/s$ $= 1089 \ ft/s$
Heat of fusion of water at 1 atm	$h_{if} = 333.7 \ kJ/kg$ $= 143.5 \ Btu/lbm$
Enthalpy of vaporization of water at 1 atm	$h_{fg} = 2256.5 \ kJ/kg$ $= 970.12 \ Btu/lbm$